

Handbook of Chlor-Alkali Technology

Volume I: Fundamentals



Thomas F. O'Brien, Tilak V. Bommaraju,
and Fumio Hine

Uploaded by:

Ebooks Chemical Engineering

(<https://www.facebook.com/pages/Ebooks-Chemical-Engineering/238197077030>)

For More Books, softwares & tutorials Related to Chemical Engineering

Join Us

@google+: <http://gplus.to/ChemicalEngineering>

@facebook: <https://www.facebook.com/AllAboutChemicalEngineering>

@facebook: <https://www.facebook.com/groups/10436265147/>

@facebook: <https://www.facebook.com/pages/Ebooks-Chemical-Engineering/238197077030>

Handbook of Chlor-Alkali Technology

Handbook of Chlor-Alkali Technology

Volume I: Fundamentals

Thomas F. O'Brien

*Independent Consultant
Media, Pennsylvania*

Tilak V. Bommaraju

*Independent Consultant
Grand Island, New York*

and

Fumio Hine

*Professor Emeritus
Nagoya Institute of Technology
Nagoya, Japan*

 Springer

Library of Congress Cataloging-in-Publication Data

O'Brien, Thomas, 1934–

Handbook of chlor-alkali technology/Thomas F. O'Brien, Tilak V. Bommaraju, Fumio Hine.

p. cm.

Includes bibliographical references and index.

ISBN 0-306-48618-0 (v. 1) — ISBN 0-306-48649-9 (v. 2) — ISBN 0-306-48620-2 (v. 3) — ISBN 0-306-48621-0 (v. 4) — ISBN 0-306-48622-9 (v. 5) — ISBN 0-306-48623-7 (indivisible set) — ISBN 0-306-48624-5 (eBook)

1. Chlorine industry—Handbooks, manuals, etc. 2. Alkali industry and trade—Handbooks, manuals, etc. 3. Electrochemistry, Industrial—Handbooks, manuals, etc. I. Bommaraju, Tilak V. II. Hine, Fumio. III. Title.

TP245.C5O34 2005

2004051611

ISBN: 0-306-48618-0

eISBN: 0-306-48624-5

Set ISBN: 0-306-48623-7

©2005 Springer Science+Business Media, Inc.

All rights reserved. This work may not be translated or copied in whole or in part without the written permission of the publisher (Springer Science+Business Media, Inc., 233 Spring Street, New York, NY 10013, USA), except for brief excerpts in connection with reviews or scholarly analysis. Use in connection with any form of information storage and retrieval, electronic adaptation, computer software, or by similar or dissimilar methodology now known or hereafter developed is forbidden.

The use in this publication of trade names, trademarks, service marks and similar terms, even if they are not identified as such, is not to be taken as an expression of opinion as to whether or not they are subject to proprietary rights.

Printed in the United States of America

9 8 7 6 5 4 3 2 1

springeronline.com

Foreword

It is surprising that we had to wait so long for a new book that gives a comprehensive treatment of chlor-alkali manufacturing technology. Technologists are largely still making do with the classical book edited by Sconce, but that is more than thirty years old. At the time of its publication, metal anodes were just beginning to appear, and ion-exchange membrane technology was confined to laboratories. The various encyclopedias of industrial technology have more up-to-date information, but they are necessarily limited in their scope. Schmittinger recently provided an excellent shorter treatment of the broad field of chlorine technology and applications. After discussing electrolysis and the principal types of cell, this, too, gives rather brief coverage to brine and product processing. It then follows on with descriptions of the major derivatives and direct uses of chlorine and a discussion of environmental issues.

The last feature named above has relieved the authors of this work of the obligation to cover applications in any detail. Instead, they provide a concentrated treatment of all aspects of technology and handling directly related to the products of electrolysis. It covers the field from a history of the industry, through the fundamentals of thermodynamics and electrochemistry, to the treatment and disposal of the waste products of manufacture. Membrane cells are considered the state of the art, but the book does not ignore mercury and diaphragm cells. They are considered both from a historical perspective and as examples of current technology that is still evolving and improving. Dear to the heart of a director of Euro Chlor, the book also pays special attention to safe handling of the products, the obligations of Responsible Care[®], and process safety management.

Other major topics include corrosion, membranes, electrolyzer design, brine preparation and treatment, and the design and operation of processing facilities. Perhaps uniquely, the book also includes a chapter on plant commissioning. The coverage of membranes is both fundamental and applied. The underlying transport processes and practical experience with existing types of membrane both are covered. The same is true of electrolyzer design. The book explores the basic electrode processes and the fundamentals of current distribution in electrolyzers as well as the characteristics of the leading cell designs. The chapter on brine production and treatment first covers the sources of salt and the techniques used to prepare brine. It then explains the mechanisms by which brine impurities affect cell performance and outlines the processes by which they can be removed or controlled. While pointing out the lack of fundamental science in much of

the process, it describes the various unit operations phenomenologically and discusses methods for sizing equipment and choosing materials of construction. The chapter on processing and handling of products is similarly comprehensive. Again, it is good to see that the authors have included a lengthy discussion of safe methods and facilities for the handling of the products, particularly liquid chlorine. While the discussion of the various processing steps includes the topic of process control, there is also a separate chapter on instrumentation which is more hardware oriented.

Other chapters deal with utility systems, cell room design and arrangement (with an emphasis on direct current supply), alternative processes for the production of either chlorine or caustic without the other, the production of hypochlorite, industrial hygiene, and speculations on future developments in technology. There is an Appendix with selected physical property data.

The authors individually have extensive experience in chlor-alkali technology but with diverse backgrounds and fields of specialization. This allows them to achieve both the breadth and the depth which are offered here.

The work is divided into five volumes, successively treating fundamentals, brine preparation and treatment, production technology, support systems such as utilities and instrumentation, and ancillary topics. Anyone with interest in the large field of chlor-alkali manufacture and distribution, and indeed in industrial electrochemistry in general, will find something useful here. The work is recommended to students; chlor-alkali technologists; electrochemists; engineers; and producers, shippers, packagers, distributors, and consumers of chlorine, caustic soda, and caustic potash.

This book is thoroughly up to date and should become the standard reference in its field.

Barrie S. Gilliatt
Executive Director
Euro Chlor
March, 2004

Preface

Despite commercial setbacks in recent years, the production of chlorine and alkalis still is of enormous importance, and chlorine and caustic soda both are among the ten largest-volume chemical products in the world. The number of final end uses for the products of a chlor-alkali plant perhaps cannot be matched by any other single plant.

There is no comprehensive modern treatment of the chlor-alkali manufacturing process. The authors therefore saw a need for a book on the subject, focusing on chlorine and the alkali products themselves and providing full detail on basic electrochemistry, thermodynamics, and the processing and handling of raw materials and products. Product applications are not covered in any detail. The anticipated audience includes students, electrochemists, all engineers and scientists involved in chlor-alkali technology, and those with a lively interest in an important segment of industry.

This work is divided into five volumes. Volume I contains introductory and historical information, followed by the fundamentals of electrochemistry pertinent to chlor-alkali cells. The topics addressed include thermodynamics, kinetics of electrode reactions and electrocatalysis, experimental techniques, energy consumption and its components, and the basic aspects of mercury, diaphragm, and membrane cells. The importance of brine purification, the influence of brine impurities on electrolysis, and the methods used for their removal are presented in Volume II. This volume also discusses the three major processes used for electrolysis (diaphragm, mercury, and membrane cells) and offers comparisons of the individual cell technologies employed. Volume III covers the practical aspects of plant engineering and operation. Subject matter includes cell room design and engineering and the processing of chlorine, hydrogen, and caustic soda or potash. There is also an extensive discussion of the safe storage and handling of the products. Volume IV deals with support systems such as plant utilities and instrumentation hardware and systems. It also contains a chapter dedicated to the commissioning and operation of plants, with an emphasis on membrane cell rooms. Volume V rounds out the presentation by treating a variety of topics. These include the fundamentals of corrosion; alternative processes for chlorine and caustic, each without the other as co-product; the manufacture of hypochlorites; general safety information (chemical hazards, industrial hygiene, safety programs, waste disposal or minimization); and possible future technological developments in the industry. An Appendix gives some of the physical and chemical properties of relevant materials.

Particularly in Volumes II and III, we present examples and discuss specifics of design. These are not to be taken as recommendations for any particular apparatus or

technology. They are offered knowing that many alternatives exist in practice and that some readers may have their own preferred solutions. The authors feel that it is better to provide some practical feel for students and technologists who are unfamiliar with the subject than it is to hesitate because others approaches exist.

The authors expect that the typical reader will most frequently consult individual sections of most interest to him or her. Relatively few will read all five volumes consecutively. We have therefore not hesitated to repeat basic information in order to provide quicker understanding of the subject at hand. There are also many cross-references between sections. These will assist the reader seeking broader coverage.

The book does not cover first aid or medical practice, nor does it supply complete details on safe handling of materials. Readers must refer to the literature, material safety data sheets, suppliers, and users of the various chemicals and equipment that are discussed. While there are summaries of material specifications and suggested analytical schedules, there is likewise not a section on analytical procedures.

Safety is of primary importance in manufacture of chemicals. This book therefore makes frequent reference to good practice in design, construction, and operation of chlor-alkali plants. The authors frequently refer to the subject and to various safety codes. We note here that no one code or set of practices may be best in all circumstances, and we take no position in this matter. When specific practices are discussed, it is not to say that they are the best or the only way. Rather, they are offered as possible approaches to specific problems when their inclusion seems to add value to the work. They are not all-inclusive, and as time goes on some will be supplanted by new codes and regulations.

Every effort has been made in preparing these volumes to provide information that is accurate and that will be useful to those involved in the chlor-alkali industry. The publisher and the authors jointly and severally make no guarantee and assume no liability in connection with any of the aforesaid information.

A NOTE ON USAGE

Generally, this book uses metric units, and the authors assume that technologists everywhere are familiar and comfortable with these units. Strict SI practice is not observed, some published data being kept in units that may be more familiar to those in the chlor-alkali industry.

The language and spelling are intended to be standard American, and American usage (barring the use of metric units) prevails. Thus, an “electrolyser” is an “electrolyzer.”

ACKNOWLEDGEMENTS

The authors wish to acknowledge first the sizable contributions of Thomas A. Weedon, Jr., of Information Technology, Inc., and Dr. Gary M. Shannon, of INEOS Chlor Limited, principal authors, respectively, of Chapters 11 and 13. John M. Lucas made important contributions to the sections on electrical systems.

Euro Chlor and The Chlorine Institute generously made many of their publications available to the authors, and both organizations also granted permission to reproduce or

adapt a number of their illustrations. Dr. Barrie S. Gilliatt of Euro Chlor also contributed the Foreword. The authors are grateful to Steve Fitzgerald of Occidental Chemical Corporation and Dr. Kenzo Yamaguchi of Chlorine Engineers Corporation for providing us with their endorsements of the book.

Other contributors of material or technical assistance included:

Robert A. Arnold, Jamestown Chemical
Steve Brien, Mary Blackburn, Chemical Marketing Associates, Inc
Dr. Chao-Peng Chen, Headway Technology - A TDK group company
Thomas F. Florkiewicz, Donald J. Groszek, Richard L. Romine and Charles D. Schultz, ELTECH Systems Corporation
David Francis, DE NORA ELETTRODI S.p.A.,
Brent Hardman and members of staff, Powell Fabrication and Manufacturing, Inc.
Glenn M. Hymel, Occidental Chemical Corporation
Adam Jacobsen, Dorr-Oliver EIMCO
Dr. James T. Keating, E.I. duPont de Nemours and Co, Inc.
Charles J. Kotzo and Norbert Eckert, Chemetics
Library, University of Dortmund
Dr. Eric Linak, SRI Consulting
Dr. Benno Lüke and K. Sambamurty, Uhde GmbH
A. Stuart Middleton, Agra Simons
C. E. "Skip" Niman, Cargill Salt Company
Dr. S. Sarangapani, ICET, Inc.
Roger E. Shamel, Consulting Resources Corporation
Janet L. White, USFilter Corporation
Dr. James R. Wilson, FMC Corporation
Dr. Kenzo Yamaguchi, Chlorine Engineers Corporation

Reviewers of the material included:

Dr. Harry S. Burney Jr., Dow Chemical Corporation
Prof. Brian E. Conway, University of Ottawa
Dr. Yoshio Harada, Mitsubishi Heavy Industries, Ltd.
Glenn M. Hymel, Occidental Chemical Corporation
Jeffrey Jones, INEOS Chlor Limited
Dr. James T. Keating, Jeffrey L. Jones, Robert D. Theobald, E.I. duPont de Nemours and Co, Inc.
Thomas A. Liederbach, Electrode Corporation
Thomas J. Navin, Consultant
Masao Ohkubo, Sumitomo Chemical Company
Dr. Francis Otto, Jr., Alfa Laval Biokinetics
Richard L. Romine, Dr. Kenneth L. Hardee, ELTECH Systems Corporation
Philip H. Sears, Chlorine Solutions LLC (ex Vulcan Chemical)
Dr. Ian F. White, Advanced Optimax Consulting, Ltd.
Dr. Harry C. Williford, Catalytic, Inc.
Dr. Kenzo Yamaguchi, Chlorine Engineers Corporation

The authors would like to thank Mike Smith for the excellent graphics and his patience in putting up with the constant changes. Finally, Tilak V. Bommaraju would like to acknowledge his wife, Savithri and his daughters, Sudha and Uma for their encouragement during the course of this effort, with special thanks to his daughter, Sudha, for her help in typing from hand written drafts and page-proofing.

Contents

Volume I: Fundamentals

Chapter 1. Introduction	1
1.1. Purpose and Scope of the Book	1
1.2. Origin of the Importance of Chlorine and Caustic	2
1.3. End Uses of Chlorine	4
1.3.1. Organic Chemicals	4
1.3.2. Inorganic Chemicals	11
1.4. End Uses of Sodium Hydroxide	11
1.4.1. Organic Chemicals	14
1.4.2. Inorganic Chemicals	15
1.5. End Uses of Potassium Hydroxide	15
References	16
Chapter 2. History of the Chlor-Alkali Industry	17
2.1. Diaphragm-Cell Technology Development	18
2.1.1. Vertical Diaphragm Cells	22
2.1.2. Developments in Anodes and Diaphragms	24
2.1.3. Diaphragm-Cell Technologies	26
2.1.4. Bipolar Diaphragm Cells	27
2.2. Mercury-Cell Technology	28
2.3. Membrane-Cell Technology	31
2.4. Caustic Soda	34
2.4.1. Lime Soda Process	35
2.4.2. Electrolytic Process	35
2.5. Future Developments	35
References	35
Chapter 3. Overview of the Chlor-Alkali Industry	37
3.1. Introduction	37
3.2. Overall Process	37

3.2.1.	Electrolyzers	37
3.2.2.	Chlorine Processing	40
3.2.3.	Hydrogen Processing	40
3.2.4.	Caustic Soda Process	41
3.2.5.	Brine Process	43
3.3.	Growth of the Chlor-Alkali Industry	46
3.3.1.	World	47
3.3.2.	United States	52
3.3.3.	Chlor-Alkali Industry in Canada	59
3.3.4.	Chlor-Alkali Industry in Mexico and Brazil	60
3.3.5.	Chlor-Alkali Industry in Western Europe	60
3.3.6.	Chlor-Alkali Industry in Eastern Europe	64
3.3.7.	Chlor-Alkali Industry in The Middle East	64
3.3.8.	Chlor-Alkali Industry in Japan	64
3.3.9.	Chlor-Alkali Industry in Korea, Taiwan, China, and India	65
3.3.10.	Chlorine and Caustic Prices	65
3.4.	Environmental Considerations Affecting the Growth of the Chlor-Alkali Industry	66
3.4.1.	Organic Chemicals	67
3.4.2.	Inorganic Chemicals and Direct Application	72
	References	74
Chapter 4. Chemistry and Electrochemistry of the Chlor-Alkali Process		75
4.1.	Thermodynamics	75
4.1.1.	Free Energy and Its Significance	75
4.1.2.	Nernst Equation	78
4.1.3.	Reversible Electrode Potentials	81
4.1.4.	Thermodynamic Decomposition Voltage	89
4.1.5.	Galvanic vs Electrolytic Cells	89
4.1.6.	Measurement of Standard Single Electrode Reduction Potentials	90
4.1.7.	Standard Reference Electrodes	92
	References	94
4.2.	Kinetics	95
4.2.1.	Introduction	95
4.2.2.	Electrochemical Rate Equation	96
4.2.3.	Tafel Slope and Exchange Current Density	99
4.2.4.	Rate Equation Under Mass Transfer Control	104
4.2.5.	Electrocatalysis	107
	References	125
4.3.	Electrochemical Techniques	127
4.3.1.	Introduction	127
4.3.2.	Steady-State Techniques	128
4.3.3.	Non-Steady-State Techniques	142
4.3.4.	Supporting Techniques	150
4.3.5.	Conductivity Measurements	150
	References	160

4.4. Energy Consumption	163
4.4.1. Faraday's Law	163
4.4.2. Energy Consumption Calculations	165
4.4.3. Current Efficiency	167
4.4.4. Cell Voltage and Its Components	195
References	210
4.5. Anodes	211
4.5.1. Introduction	211
4.5.2. Electrode Preparation	212
4.5.3. Other Patented Anode Compositions	213
4.5.4. Physical Characteristics and Morphology of RuO ₂ + TiO ₂ -Based Electrodes	214
4.5.5. Electrochemical Behavior of RuO ₂ + TiO ₂ -Based Coatings	217
4.5.6. Cell Performance Characteristics with RuO ₂ + TiO ₂ -Based Anodes	224
4.5.7. Anode Failure Mechanisms	224
4.5.8. Anode Structures	232
4.5.9. Anode Costs and Manufacturers	234
4.5.10. Alternate Anode Compositions	237
References	238
4.6. Cathodes	241
4.6.1. Introduction	241
4.6.2. Criteria for Low Overvoltage Hydrogen Cathode	244
4.6.3. Methods Employed to Realize High Surface Area	251
4.6.4. Cathode Materials and Compositions	252
4.6.5. HER Mechanisms on Low Overvoltage Cathodes	261
4.6.6. Cathode Deactivation	263
4.6.7. Current Status	265
References	266
4.7. Diaphragms	271
4.7.1. Introduction	271
4.7.2. Asbestos Diaphragms	272
4.7.3. Transport Characteristics of Diaphragms	274
4.7.4. Mass Transfer through Diaphragms	279
4.7.5. Modified Asbestos Diaphragms	290
4.7.6. Non-Asbestos Diaphragms	293
4.7.7. Diaphragm Deposition	295
4.7.8. Effect of Shutdowns on the Performance of Diaphragms	300
References	303
4.8. Ion-Exchange Membranes	306
4.8.1. Introduction	306
4.8.2. Chemical Structure and Synthesis of Perfluorinated Membranes	306

4.8.3. Physicochemical Properties	310
4.8.4. Transport Characteristics	323
4.8.5. Performance Characteristics of Membranes	341
4.8.6. Membrane Damage	350
4.8.7. Brine Purity Specifications	352
4.8.8. High Performance Membranes—New Developments	355
References	370
4.9. Amalgam Decomposition	375
4.9.1. Introduction	375
4.9.2. Design Aspects of the Amalgam Decomposer	378
4.9.3. Graphite Packings	386
References	386

Volume II: Brine Treatment and Cell Operation

Chapter 5. Chlor-Alkali Technologies	387
5.1. Introduction	387
5.2. Cell Types—Bipolar and Monopolar	388
5.2.1. Origin of Parasitic Currents	391
5.2.2. Modeling	394
5.2.3. Experimental Determination of Leakage Currents	397
5.2.4. Minimization of Leakage Currents	398
5.3. Mercury-Cell Technologies	398
5.3.1. DeNora Mercury Cells	400
5.3.2. Uhde Mercury Cells	402
5.3.3. Krebskosmo Mercury Cells	403
5.3.4. Olin Mercury Cells	403
5.3.5. Amalgam Decomposers	404
5.4. Diaphragm-Cell Technologies	405
5.4.1. Bipolar Filter-Press Cells	405
5.4.2. Vertical Diaphragm Cells	408
5.5. Membrane-Cell Technologies	413
5.5.1. Guidelines for Choosing Cell Technologies	413
5.5.2. Electrolyzer Technologies: General	426
5.5.3. Commercial Electrolyzers	426
References	439
Chapter 6. Process Overview	443
6.1. General Introduction	443
6.2. Brine Preparation and Treatment	443
6.3. Electrolysis	446

6.4. Product Recovery	449
6.4.1. Chlorine	449
6.4.2. Hydrogen	451
6.4.3. Caustic	451
6.5. Mass Balances	453
6.6. Process Design	458
6.6.1. Cell Room Operating Variables	458
6.6.2. Process Control	459
6.6.3. Cell-to-Cell Variation	463
References	464
Chapter 7. Brine Preparation and Treatment	465
7.1. Sources of Salt	465
7.1.1. General	465
7.1.2. Rock Salt	466
7.1.3. Solar Salt	469
7.1.4. Other Sources	475
7.1.5. Refining of Salt	478
7.1.6. Potassium Chloride	487
7.1.7. Storage of Salt	492
7.2. Preparation of Brine	495
7.2.1. Salt Handling	495
7.2.2. Salt Dissolving	509
7.3. Brine Storage and Transfer	525
7.3.1. Storage of Brine	525
7.3.2. Transfer of Brine	527
7.4. The Role of Brine Purification	529
7.4.1. Composition of Salts and Brines	529
7.4.2. Effects of Brine Impurities	529
7.5. The Brine Treatment Process	543
7.5.1. Brine Specifications and Treatment Techniques	543
7.5.2. Chemical Treatment	545
7.5.3. Clarification and Thickening	564
7.5.4. Filtration	587
7.5.5. Ion Exchange	606
7.5.6. Acidification of Feed Brine	626
7.5.7. Control of Sulfates	634
7.5.8. Control of Other Brine Impurities	649
7.5.9. Removal of Dissolved Chlorine and Chlorate	665
References	696

Volume III: Facility Design and Product Handling

Chapter 8. Cell-Room Design	705
8.1. Introduction	705

8.2.	Building Considerations	706
8.2.1.	Outdoor vs Indoor Installation	706
8.2.2.	Electrolyzer and Building Arrangements	706
8.2.3.	Building Ventilation	712
8.3.	Electrical Systems	713
8.3.1.	Supply of Direct Current	713
8.3.2.	Electrical Supply Efficiency	736
8.4.	Cell-Room Auxiliaries	745
8.4.1.	Piping	745
8.4.2.	Cell-Room Process Control	749
8.4.3.	Cell Renewal Activities	753
8.5.	Cell-Room Hazards	755
8.5.1.	Electrical Hazards	755
8.5.2.	Chemical and Explosion Hazards	761
	References	762
Chapter 9. Product Handling		765
9.1.	Chlorine	765
9.1.1.	Introduction	765
9.1.2.	Materials of Construction	767
9.1.3.	Cooling	771
9.1.4.	Drying	792
9.1.5.	Mist Elimination	805
9.1.6.	Compression	807
9.1.7.	Liquefaction	829
9.1.8.	Storage and Handling of Chlorine	847
9.1.9.	Handling of Liquefaction Tail Gas	884
9.1.10.	Safety Devices	895
9.1.11.	Explosion Hazards	909
9.1.12.	Evacuation and Sniff Systems	925
9.2.	Hydrogen	927
9.2.1.	Cathode Construction	927
9.2.2.	Uses of Hydrogen	928
9.2.3.	Compression	934
9.2.4.	Cooling	936
9.2.5.	Purification of Hydrogen	939
9.2.6.	Hazards	943
9.3.	Caustic Soda and Potash	944
9.3.1.	Products of the Various Cells	944
9.3.2.	Processing of Caustic Liquors	947
9.3.3.	Evaporation	968
9.3.4.	Purification of Caustic	983
9.3.5.	Solid Caustic	987
9.3.6.	Caustic Product Handling	990
9.4.	Byproduct Utilization	995
9.4.1.	Evaporator Salt	995
9.4.2.	Sodium Sulfate	997

9.4.3. Amalgam	1003
9.4.4. Calcium Carbonate	1006
References	1006

Volume IV: Plant Commissioning and Support Systems

Chapter 10. Chemical Engineering Principles	1013
10.1. Introduction	1013
10.2. Material and Energy Balance	1013
10.2.1. Thermodynamics	1014
10.2.2. Energy Balance in Electrochemical Processes	1023
References	1031
10.3. Current Distribution	1031
10.3.1. Primary Current Distribution	1031
10.3.2. Secondary Current Distribution	1036
10.3.3. Tertiary Current Distribution	1039
10.3.4. Numerical Methods	1040
10.3.5. Some Examples	1040
References	1047
10.4. Fluid Processing	1048
10.4.1. Fluid Dynamics	1048
10.4.2. Removal of Solids	1057
10.4.3. Compression and Liquefaction	1058
References	1062
10.5. Transport Operations	1062
10.5.1. Heat Transfer	1063
10.5.2. Gas Absorption	1067
10.5.3. Adsorption and Ion Exchange	1074
10.5.4. Distillation	1081
References	1087
Chapter 11. Instrumentation and Control Systems	1089
11.1. Introduction	1089
11.1.1. General	1089
11.1.2. Design Coordination	1091
11.1.3. Control System Selection	1092
11.2. Brine Systems	1092
11.2.1. Modes of Control	1092
11.2.2. Membrane-Cell Brine Systems	1093
11.3. Chlorine Systems	1113
11.3.1. Background	1113
11.3.2. Operating Systems	1113

11.4. Hydrogen Systems	1134
11.4.1. Introduction	1134
11.4.2. Membrane- and Mercury-Cell Hydrogen Systems	1135
11.4.3. Diaphragm-Cell Hydrogen Systems	1147
11.5. Caustic Systems	1149
11.5.1. Mercury-Cell Caustic Systems	1149
11.5.2. Diaphragm-Cell Caustic Systems	1151
11.5.3. Membrane-Cell Caustic Systems	1152
11.6. Caustic Evaporation Systems	1159
11.6.1. Membrane-Cell Caustic Evaporation	1159
11.6.2. Diaphragm-Cell Caustic Evaporation	1166
References	1168
Chapter 12. Utilities	1169
12.1. Introduction	1169
12.2. Electricity	1170
12.3. Steam and Condensate	1171
12.3.1. Steam Systems	1171
12.3.2. Steam Condensate	1173
12.3.3. Cogeneration Systems	1174
12.4. Water Systems	1177
12.4.1. Sources of Water and General Plant Use	1177
12.4.2. Water as Heat Sink	1180
12.4.3. Purified Water	1191
12.5. Air Systems	1196
12.5.1. Plant or Utility Air	1196
12.5.2. Purified Air	1198
12.5.3. Nitrogen	1201
12.5.4. Backup Systems	1201
12.6. Vacuum Systems	1201
12.6.1. Sources of Vacuum	1202
12.6.2. Vapor Condensers	1208
12.6.3. Process Control	1210
12.7. Utility Piping and Connections	1211
12.7.1. Utility Piping and Headers	1211
12.7.2. Utility-Process Connections	1212
References	1216
Chapter 13. Plant Commissioning and Operation	1217
13.1. Introduction	1217
13.2. Commissioning Organization and Planning	1218
13.2.1. Systems Approach and Personnel	1218
13.2.2. Planning	1219

13.3.	Training	1220
13.4.	Documentation	1223
13.4.1.	Operating Manual	1223
13.4.2.	Maintenance Manual	1225
13.4.3.	Analytical Manual	1225
13.5.	General Precommissioning	1226
13.5.1.	Flushing and Cleaning	1226
13.5.2.	Pressure Testing	1227
13.5.3.	Punch Lists	1229
13.5.4.	Control Systems and Equipment Packages	1230
13.6.	System Commissioning	1231
13.6.1.	Commissioning Procedures	1232
13.6.2.	General Notes on Commissioning of Instrumentation	1232
13.6.3.	Brine System	1234
13.6.4.	Catholyte System	1237
13.6.5.	Chlorine System	1238
13.6.6.	Hydrogen System	1243
13.6.7.	Caustic Evaporation System	1244
13.6.8.	Rectifier/Transformers	1247
13.7.	Electrolyzer Assembly, Testing, and Installation	1247
13.7.1.	Membrane Handling	1247
13.7.2.	Membrane Installation	1249
13.7.3.	Electrolyzer Testing	1253
13.7.4.	Storage and Berthing	1254
13.7.5.	Record Keeping	1255
13.8.	Plant Operation	1256
13.8.1.	Initial Plant Startup	1256
13.8.2.	Normal Cell Room Operation	1261
13.8.3.	Electrolyzer Shutdowns	1264
13.8.4.	Normal Electrolyzer Startup	1267
13.9.	Plant Performance Testing	1268
13.10.	Cell Room Operating Specifications	1271
13.10.1.	Product Quality	1271
13.10.2.	Electrolyzer Voltage and Energy Consumption	1272
13.10.3.	Membrane Operating Conditions	1273
13.10.4.	Cell Room Material Specifications	1276
13.10.5.	Sources and Effects of Impurities	1277
13.10.6.	Cell Operating Conditions	1283
13.11.	Routine Monitoring and Analysis	1286
13.11.1.	Recording of Operating Parameters	1286
13.11.2.	Analytical Program	1287
13.11.3.	Current Efficiency Determination	1288
13.11.4.	Voltage Monitoring	1290
13.12.	Decommissioning of Mercury-Cell Plants	1290
	References	1293

Volume V: Corrosion, Environmental Issues, and Future Development

Chapter 14. Corrosion	1295
14.1. Introduction	1295
14.2. Origin of Corrosion	1297
14.2.1. Free Energy Considerations	1297
14.2.2. Kinetics	1303
14.2.3. Corrosion Prevention	1308
14.2.4. Corrosion Rates	1311
14.3. Manifestations of Corrosion	1312
14.3.1. Uniform or General Corrosion	1313
14.3.2. Galvanic or “Two-Metal” Corrosion	1313
14.3.3. Crevice Corrosion	1314
14.3.4. Pitting Corrosion	1317
14.3.5. Intergranular Corrosion	1318
14.3.6. Selective Leaching or Dealloying	1319
14.3.7. Erosion Corrosion	1319
14.3.8. Stress Corrosion	1320
14.3.9. Corrosion Fatigue	1323
14.3.10. High-Temperature Corrosion	1323
14.3.11. Failure of Nonmetallic Materials	1325
14.4. Material Selection	1325
14.5. Corrosion In Chlor-Alkali Operations	1328
14.5.1. General Aspects	1328
14.5.2. Materials of Construction in Chlor-Alkali Operation	1328
References	1347
Chapter 15. Alternative Processes	1349
15.1. Introduction	1349
15.2. Production of Chlorine without Caustic	1351
15.2.1. Oxidation Processes	1351
15.2.2. Electrochemical Methods for Producing Chlorine	1361
15.3. Production of Hypochlorite	1372
15.3.1. Electrochemical Production of Hypochlorite	1373
15.3.2. Chemical Production of Hypochlorite	1378
15.3.3. Miscellaneous Applications	1388
15.3.4. Calcium Hypochlorite	1389
15.4. Production of Caustic without Chlorine	1389
15.4.1. Causticization of Soda Ash	1389
15.4.2. Salt Splitting by Ion Exchange	1392
15.4.3. Electrochemical Methods	1393
References	1396

Chapter 16. Environmental Safety and Industrial Hygiene	1401
16.1. General Introduction	1401
16.2. Materials Hazards	1402
16.2.1. Chlorine and Hypochlorites	1403
16.2.2. Caustic Soda and Potash	1407
16.2.3. Hydrogen	1407
16.2.4. Hydrochloric Acid	1407
16.2.5. Sulfuric Acid	1408
16.2.6. Mercury	1408
16.2.7. Asbestos	1413
16.2.8. Nitrogen Trichloride	1415
16.2.9. Other Materials	1416
16.3. Process Hazards	1419
16.4. Prevention and Mitigation	1421
16.4.1. Safety Equipment	1421
16.4.2. Safety-Oriented Programs	1422
16.4.3. Mitigation of Effects of Release of Chlorine	1438
16.5. Waste Minimization and Disposal	1445
16.5.1. Solids	1445
16.5.2. Liquids	1448
16.5.3. Vapors and Gases	1451
16.5.4. Retired Brine Caverns	1452
16.5.5. Mercury-Containing Wastes	1452
References	1459
Chapter 17. Future Developments	1463
17.1. Introduction	1463
17.2. Cell Operation	1464
17.2.1. Increased Current Density	1464
17.2.2. Depolarized Cathodes and Fuel Cells	1466
17.2.3. Membranes	1473
17.3. Auxiliary Operations	1474
17.3.1. Back-Pulse Filtration	1475
17.3.2. DC Power Supply	1477
17.4. Chlorine Processing	1478
17.4.1. Integrated Production of Ethylene Dichloride	1478
17.4.2. Chlorine Recovery	1478
17.5. Speculations	1480
17.5.1. Improved Electrodes	1480
17.5.2. Operation under Pressure	1480
References	1487
Appendix	1491
A. Universal Constants	1491

B.	Conversion Factors	1491
C.	Dimensionless Groups	1495
D.	Nomenclature in Appendix C	1496
E.	Correlations	1496
F.	Sodium Chloride	1502
G.	Potassium Chloride	1510
H.	Sodium Hydroxide	1516
I.	Potassium Hydroxide	1525
J.	Chlorine	1532
K.	Hydrogen	1539
L.	Sulfuric Acid	1543
M.	Hydrochloric Acid	1546
N.	NaOH + NaCl Mixtures	1552
O.	Bleach	1552
P.	Sodium Carbonate	1553
Q.	Water	1554
R.	Miscellaneous	1556
Index		1561

1

Introduction

1.1. PURPOSE AND SCOPE OF THE BOOK

The chlor-alkali industry is one of the largest electrochemical operations in the world, the main products being chlorine and sodium hydroxide generated simultaneously by the electrolysis of sodium chloride solutions. The chlor-alkali industry serves the commodity chemical business, chlorine and sodium hydroxide (also called caustic soda) being indispensable intermediates in the chemical industry [1–10].

The purpose of this handbook is to elucidate the basic chemistry and chemical engineering principles involved in the chlor-alkali technologies, and to thoroughly discuss the various operations involved in manufacturing chlorine and caustic. The status of the chlor-alkali industry is also discussed along with issues relevant to the future growth of the industry and the environmental concerns.

There is no other single book currently available that addresses the fundamentals of chlor-alkali technology or the engineering principles involved in design of a chlor-alkali plant, although there are seminars and symposia proceedings published by the Chlorine Institute, Consulting Resources Corporation, ELTECH Systems Corporation, Japan Soda Industry Association, Krupp Uhde, Tecnon, the Electrochemical Society, and the Society of Chemical Industry which cover some specific topics. The book entitled *Chlorine: Its Manufacture, Properties and Uses*, edited by Sconce [3], was published in 1962, and since then there have been significant developments in the technology. Stanford Research Institute Consulting's Process Economics Program reports cover the process economics of the chlor-alkali technologies, and are updated periodically for the clients funding this effort [4]. Market analyses and forecasts are also available to clients from Chemical Marketing Associates, Inc., and Kline & Company.

This handbook will attempt to consolidate the concepts presented at the various meetings and symposia and address the relevant chemistry and engineering concepts, so that it is useful not only to the personnel involved with the chlor-alkali industry, but also to the junior and senior chemical engineering and chemistry students who wish to join the industry or pursue academic careers. With this thought in the background, the first three chapters introduce the reader to the chlor-alkali industry. The fundamental principles associated with the chemistry and electrochemistry of the chlor-alkali processes and the components involved in the electrolytic cells are discussed in Chapter 4.

The need for brine purification for the three chlor-alkali cell technologies is addressed in Volume II, Chapter 7, along with the pertinent chemistry involved in the removal of impurities and the relevant engineering aspects. The designs of the various cell technology suppliers are discussed in detail in Chapter 5 of Volume II, followed by the future expansions and conversions from the current to the modern cell technologies. Chapter 6 provides a general overview of the chlor-alkali process.

Volume III is devoted to facility design and product handling. Chapter 8 addresses cell room design and Chapter 9 provides a thorough discussion of handling the products of electrolysis.

Volume IV covers support systems and commissioning. Chapter 10 discusses some chemical engineering principles required for design of a chlorine plant, and examples are provided explaining how these fundamental concepts are translated into practice. Instrumentation and control systems required for the various unit operations are addressed in Chapter 11 and the utilities needed for running the plant are presented in Chapter 12. Details pertinent to plant commissioning and operation are treated in Chapter 13.

Volume V addresses corrosion, environmental issues, and future developments. Chapter 14 covers the principles of corrosion and how to minimize corrosion in chlor-alkali operations, exemplified by case studies. Alternate processes for producing chlorine and caustic are outlined in Chapter 15.

Mercury and asbestos, used in the chlor-alkali process, are health hazards. These and the other related environmental issues, safety, and industrial hygiene aspects are discussed in Chapter 16. Chapter 17 addresses concepts that may lead to the next generation of chlor-alkali technologies, having significant cost and energy benefits.

Physicochemical data related to Cl_2 , NaOH , NaCl , and other materials encountered in chlor-alkali operations are presented in the Appendix in Volume V.

1.2. ORIGIN OF THE IMPORTANCE OF CHLORINE AND CAUSTIC

Chlorine and sodium hydroxide (or caustic soda) are among the top 10 chemicals produced in the world, and are involved in the manufacturing of a myriad of products that are used in day-to-day life. These products include pharmaceuticals, detergents, deodorants, disinfectants, herbicides, pesticides, and plastics.

The first observation of a possible application of chlorine was its bleaching effect on vegetable matter, discovered by Carl Wilhelm Scheele in 1774 while investigating in detail the reactivity of the greenish yellow gas generated during the reaction between pyrolusite (manganese dioxide) and hydrochloric acid [5,7]. The generation of the corrosive, suffocating greenish-yellow fumes of chlorine had been observed ever since the 13th century, when chemists became aware of aqua regia. A *flatus incoercible* (forcible release of chlorine) formed when ammonium chloride was reacted with nitric acid in 1668 [8]. Berthollet, in 1785, tried without success to use elemental chlorine to replace the existing solar bleaching process (also called grassing or crofting) for textiles. The elemental chlorine caused discomfort to the workers, corroded metal parts, and softened the fabrics. The first use of chlorine in the form of potassium hypochlorite, formed by absorbing chlorine in a potash solution on an industrial scale, for bleaching purposes, dates back to 1789, and was credited to McPherson. Renant replaced the potash solution

with milk of lime to produce calcium hypochlorite solution, for which a patent was granted in 1798. The first bleaching powder patent was issued in 1789 to Tennant. It was only in 1808 that this greenish-yellow gas was characterized as an element and was named chlorine from the Greek $\chi\lambda\omega\rho\sigma\zeta$, meaning green, by Davy.

The development of chemical bleaching with chlorine and the discovery of calcium hypochlorite bleaching powder as a practical mode of transporting chlorine was of great significance as these technologies made a marked impact on the textile bleaching operations in Great Britain and Europe, who were in the middle of industrial revolution with an expanding population, and hence, the demand for textiles. The invention of the power loom provided the means to produce textiles. However, bleaching by spreading the cloth in open fields required months and became increasingly expensive because of soaring land values. The chlorine bleaching process not only shortened the operations from months to a few days but also freed vast areas for more productive use [9]. Based on the greatly improved efficiency of textile bleaching, the pulp and paper industry also began using bleaching powder [10].

Following the discovery that bacteria were responsible for the transmission of certain diseases, several investigators [10] studied the chlorination of both sewage and potable water in the 1890s. By 1912, the use of chlorine for water treatment had become a practice [11] and there was significant reduction in the incidence of waterborne diseases such as typhoid [12]. There were 549 cases during the “winter typhoid” reported in Montreal, Canada during the months of October to December 1909, and after the chlorination of drinking water in 1910, only 170 cases were reported during the same time period [13]. During the period of 1756 to 1932, the use of chlorine in the pulp-making industry made inroads, as chlorine in the form of hypochlorites removed the color or color-producing materials from the cellulosic fibers, without undue degradation of the fibers. Thus, water disinfection operations and the pulp and paper industry consumed virtually all the chlorine manufactured during the 19th century. The first use of chlorine for disinfection dates back to 1823, when it was used in hospitals. Chlorine water was employed in obstetric wards to prevent puerperal fever in 1826, and fumigation with chlorine was practiced during the great European cholera epidemic.

Dichloroethane was produced in 1795, and chloroform was synthesized in 1831. By 1848, the anesthetic properties of chloroform were recognized and used in surgical practice [14,15].

A major turning point for the industry was the use of chlorine for water purification during the typhoid epidemic, in Niagara Falls in 1912, although, bleaching powder was used in 1897 to clean the polluted mains during a typhoid out-break in England. Many new uses of chlorine were developed during World War I, when the US chemical industry started to become independent of the European chemical industry.

Many new applications for chlorine (e.g., manufacture of ethylene glycol, chlorinated solvents, vinyl chloride, and others), were developed between 1920 and 1940. The war period triggered the development of new uses for chlorine for military needs, and the trend continued to produce new products for civilian use following World War II. Progress in synthetic organic chemistry in the 19th century had led to the preparation of substitutes for natural products and entirely new and useful compounds including intermediates and final products. Chlorine, because of its reactivity, unique properties,

and low price, was used in many of these, including solvents, pharmaceuticals, and dyes [9,13,14].

Chlorine and caustic are used for manufacturing many products routinely used in all walks of life. The following sections discuss some of the end uses of chlorine, caustic soda, and potassium hydroxide. For an almost complete listing of the end products involving chlorine and caustic, the reader is referred to references [2,16], where the intermediates formed from chlorine and the final products and end uses are compiled.

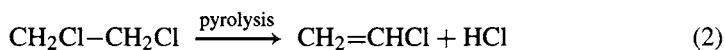
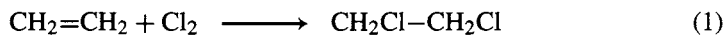
1.3. END USES OF CHLORINE

The major end uses of chlorine are described in Table 1.1. Chlorine is used either directly or indirectly in the manufacture of organic and inorganic chemicals. The primary market is in the production of organic chemicals, described in Section 1.3.1. Section 1.3.2 discusses the inorganic chemicals.

Direct use of chlorine is in pulp and paper manufacturing and water treatment operations. Chlorine is used in the pulp and paper industry to bleach the pulp to produce a high-quality whitened material, devoid of dark lignin and any other undesirable residuals. Chlorine has been the most common disinfectant and is still used by municipalities and others to treat potable, process, and waste water streams. Because of this specific use of chlorine, waterborne diseases such as typhoid and cholera have been eradicated in the industrialized world. Chlorine also removes hydrogen sulfide, iron compounds, and organic species that are responsible for objectionable tastes or odor associated with water.

1.3.1. Organic Chemicals

The major use of chlorine is in the manufacture of organic chemicals; the largest volume product is polyvinyl chloride (PVC), produced via ethylene dichloride (EDC) and vinyl chloride monomer (VCM) as described by reactions (1) and (2) respectively. PVC is a very versatile thermoplastic. Rigid PVC is used for piping, siding, windows, bottles, and packaging sheeting. Flexible (plasticized) PVC is used for floor coverings, film and sheet, wire and cable insulation, and a myriad of other applications. In general, PVC is used judiciously to replace metals.



Propylene oxide, made by reacting propylene with chlorine to form propylene chlorohydrin which is then dehydrochlorinated with caustic soda or lime (Eqs. 3–5), is used in the production of polyether polyols used for producing urethane foam. It also finds use in propylene glycol for making unsaturated polyester resins and in the pharmaceutical and food industries. Epichlorohydrin (EPI), formed by chlorination of propylene to allyl chloride and then dehydrochlorination (Eqs. 6 and 7), is used to make epoxy resins for producing laminates, fiber-reinforced composites, protective coatings, and adhesives.

TABLE 1.1. End Uses of Chlorine (with permission from SRI Consulting)

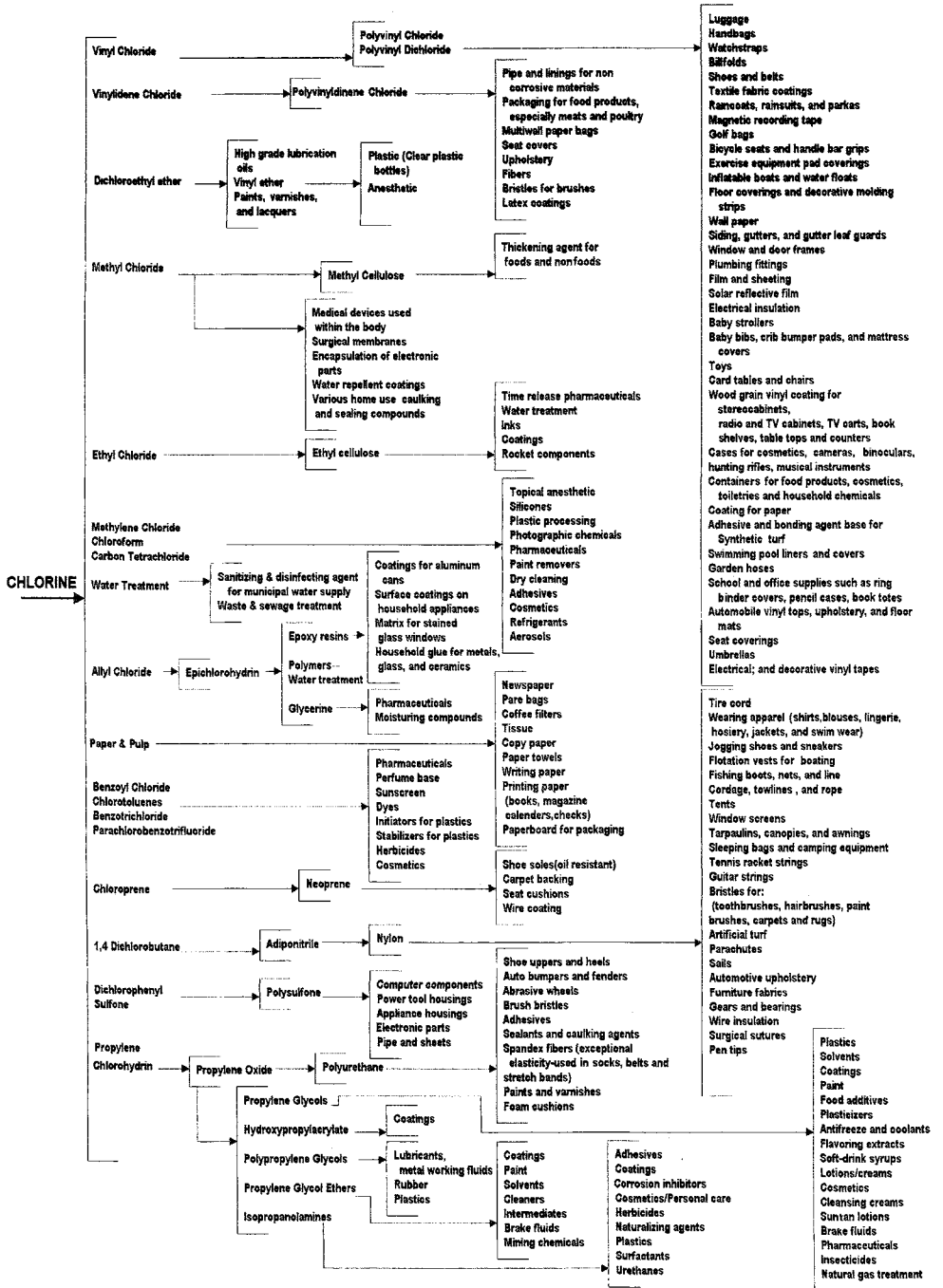
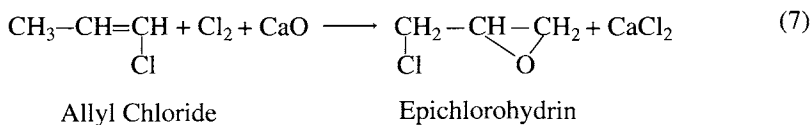
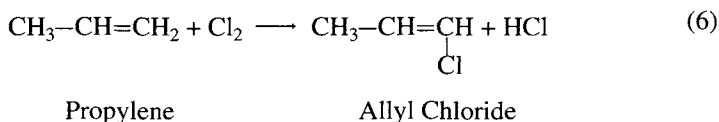
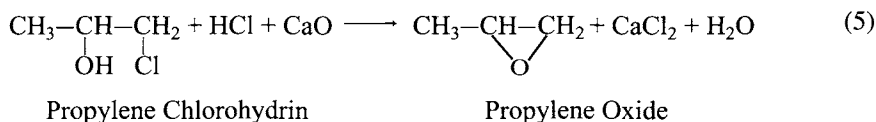
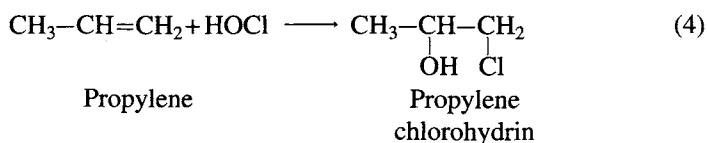
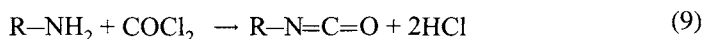


TABLE 1.1. (continued)

Hydrochloric Acid	<p>Food processing</p> <p>Desulfurization agent for petroleum</p> <p>Production of alkyl chlorides</p> <p>Oil well acidizing</p> <p>Production of metallic chlorides</p> <p>Pickling in steel manufacture</p> <p>Production of hydrochlorides</p> <p>Latex coagulating agent</p>	<p>Sugar refining</p> <p>Corn syrup</p> <p>Gelatin</p> <p>Monosodium glutamate</p> <p>Brewing</p> <p>Electronic silicones</p> <p>Photoflash bulbs</p> <p>Refractories</p> <p>Alloys</p> <p>Pyrotechnics</p> <p>Rubber accelerator</p> <p>Plastics stabilizer</p> <p>Rocket propellants</p> <p>Pharmaceuticals</p>
Chloroacetic Acid	<p>Liniments and pharmaceuticals</p>	<p>Permanent wave solutions and hair care products</p> <p>2, 4, D and other herbicides</p> <p>Synthetic caffeine</p> <p>Vinyl stabilizer</p> <p>Pharmaceuticals</p>
Tetrachlorophthalic anhydride	<p>Highway stripe paint</p> <p>High pressure lubricants</p> <p>Fireproofing agent for textiles</p> <p>Pesticide for polyvinyl chlorides</p> <p>Detergents</p>	<p>Flame retardant for plastics</p>
Chlorinated Paraffins	<p>Highway stripe paint</p> <p>High pressure lubricants</p> <p>Fireproofing agent for textiles</p> <p>Pesticide for polyvinyl chlorides</p> <p>Detergents</p>	<p>Photographic chemicals</p> <p>Dyes</p> <p>Rubber antioxidants</p> <p>Purifying sugar juices</p> <p>Band Aids</p> <p>Erasers</p> <p>Oil additives</p> <p>Pacemaker batteries</p> <p>Fungicides</p>
Sulfur Dichloride Sulfur Monochloride Thionyl Chloride Sulfuryl Chloride	<p>Gasoline additives</p> <p>Hydraulic fluids</p> <p>Semiconductor manufacture</p> <p>Fire retarding agents</p> <p>Herbicide</p>	<p>Photography</p> <p>Etching and engraving</p> <p>Printed circuitry</p> <p>Pharmaceuticals</p> <p>Water and sewage treatment</p>
Phosphorus Trichloride Phosphorus Pentachloride Phosphorus Oxychloride	<p>Gasoline additives</p> <p>Hydraulic fluids</p> <p>Semiconductor manufacture</p> <p>Fire retarding agents</p> <p>Herbicide</p>	<p>Soldering fluxes</p> <p>Deodorant preparations</p> <p>Dental cements and dentifrices</p>
Ferric Chloride	<p>Silvering mirrors</p> <p>Stabilizer for perfume</p> <p>In soaps</p>	<p>Bleaching pulp, paper and textiles</p> <p>Water purification</p> <p>Pharmaceuticals</p> <p>Household bleach</p> <p>Disinfectant for swimming pools</p>
Stannous Chloride	<p>Silvering mirrors</p> <p>Stabilizer for perfume</p> <p>In soaps</p>	<p>Paper deinker</p> <p>Transformer fluid</p> <p>Circuit boards</p> <p>Drain cleaners</p> <p>Textile manufacture</p> <p>Leather finishing</p> <p>Pigments</p> <p>Dyes</p> <p>Refrigerants</p> <p>Spot remover</p> <p>Insecticides</p> <p>Pesticides</p> <p>Solvents</p> <p>Adhesives</p> <p>Degreaser</p> <p>Dry cleaning</p>
Zinc Chloride	<p>Sanitizers for swimming pools</p> <p>Household and commercial bleaches</p> <p>Detergents for automatic dishwashers</p> <p>Scouring powders</p>	<p>Paper deinker</p> <p>Transformer fluid</p> <p>Circuit boards</p> <p>Drain cleaners</p> <p>Textile manufacture</p> <p>Leather finishing</p> <p>Pigments</p> <p>Dyes</p> <p>Refrigerants</p> <p>Spot remover</p> <p>Insecticides</p> <p>Pesticides</p> <p>Solvents</p> <p>Adhesives</p> <p>Degreaser</p> <p>Dry cleaning</p>
Sodium Hypochlorite	<p>Algaecide</p> <p>Bactericide</p> <p>Deodorant</p> <p>Potable water purification</p> <p>Disinfectant for swimming pools</p>	<p>Electrical components</p> <p>Semiconductors</p> <p>Corrosion resistant paint</p> <p>Synthetic gem stones</p> <p>Catalyst</p> <p>Paint pigments</p>
Calcium Hypochlorite	<p>Algaecide</p> <p>Bactericide</p> <p>Deodorant</p> <p>Potable water purification</p> <p>Disinfectant for swimming pools</p>	<p>Electrical components</p> <p>Semiconductors</p> <p>Corrosion resistant paint</p> <p>Synthetic gem stones</p> <p>Catalyst</p> <p>Paint pigments</p>
Titanium Dioxide	<p>Algaecide</p> <p>Bactericide</p> <p>Deodorant</p> <p>Potable water purification</p> <p>Disinfectant for swimming pools</p>	<p>Electrical components</p> <p>Semiconductors</p> <p>Corrosion resistant paint</p> <p>Synthetic gem stones</p> <p>Catalyst</p> <p>Paint pigments</p>
1,1,1 Trichloroethane Perchloroethylene Ethylene Dichloride Trichloroethylene	<p>Algaecide</p> <p>Bactericide</p> <p>Deodorant</p> <p>Potable water purification</p> <p>Disinfectant for swimming pools</p>	<p>Electrical components</p> <p>Semiconductors</p> <p>Corrosion resistant paint</p> <p>Synthetic gem stones</p> <p>Catalyst</p> <p>Paint pigments</p>



Phosgene produced by chlorinating carbon monoxide is used as a carbonylating agent to convert amines to isocyanates, as shown by reactions (8) and (9). Thus, the reaction of phosgene with diphenylmethane diamine results in the formation of methylene diphenyl diisocyanate (MDI), and with toluenediamine to form toluene diisocyanate (TDI). The isocyanates are used to produce polyurethanes for flexible and rigid foams, elastomers, coatings, and adhesives, for the construction and automotive industries.



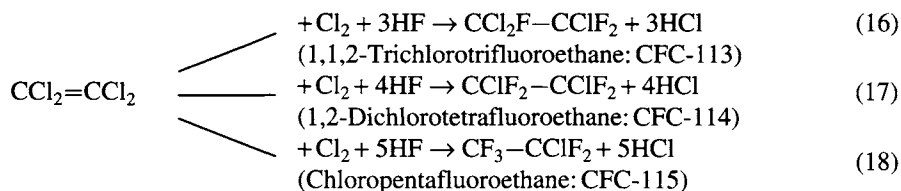
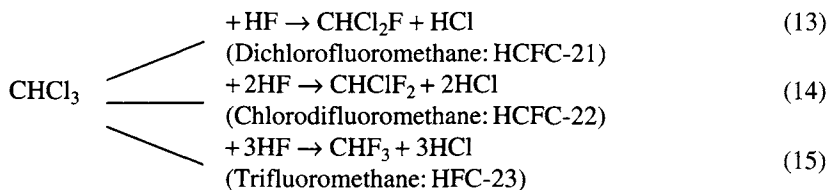
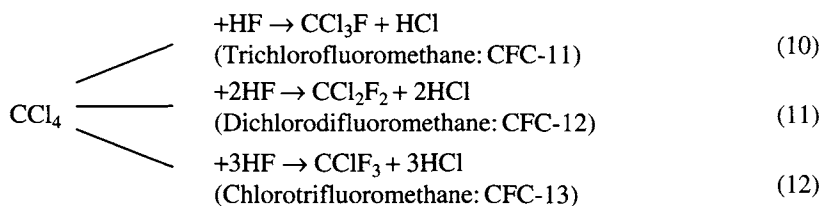
Amine Phosgene Isocyanate

Chlorinated solvents made from EDC and VCM include perchloroethylene (PCE), used for dry cleaning, and 1,1,1-trichloroethane and trichloroethylene (TCE), used in vapor degreasing operations. Chlorofluorocarbons (CFCs), used as solvents, blowing agents, and refrigerants for household and commercial air conditioners, are made by reacting HF with carbon tetrachloride (CCl_4) (to form CFC-11 and -12) and with PCE

to produce CFC-113, -114, and -115. Hydrochlorofluorocarbon HCFC-22, which is less harmful than CFCs to the ozone layer, is derived from chloroform and is used not only for air-conditioning but also as an intermediate in the production of tetrafluoroethylene for manufacturing polytetrafluoroethylene (PTFE) and other fluoropolymers. HCFC-142b, made from 1,1,1-trichloroethane, is used as a blowing agent for polystyrene and as raw material for vinylidene fluoride that is used in the production of fluoroplastics and fluoroelastomers.

HFC-134a, a substitute for CFC-12 in the production of refrigerants, contains no chlorine, and is environmentally benign. It is made from chlorinated organic intermediates. Reaction schemes involved in the production of these fluorinated compounds from CCl_4 , chloroform (CHCl_3), and PCE ($\text{CCl}_2=\text{CCl}_2$) are shown in Eqs. (10) to (18). Figure 1.1 illustrates the fluorinated compounds made with C-2 compounds.

Methyl chloride is used in the production of chlorosilanes which are intermediates in the production of silicone fluids, elastomers, and resins. Methylene chloride finds use in film processing, paint removing, metal cleaning, urethane foam blowing, and the electronic and pharmaceutical industries. Household food wraps such as Saran[®] are made from VCM and vinylidene chloride. The latter is made by chlorinating EDC to 1,1,2-trichloroethane, followed by dehydrochlorination with caustic soda.



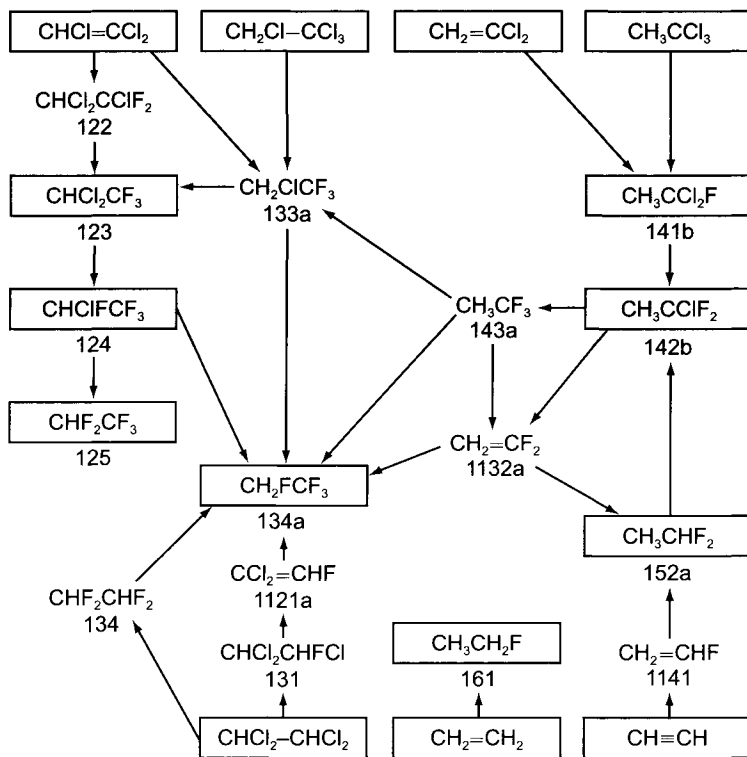
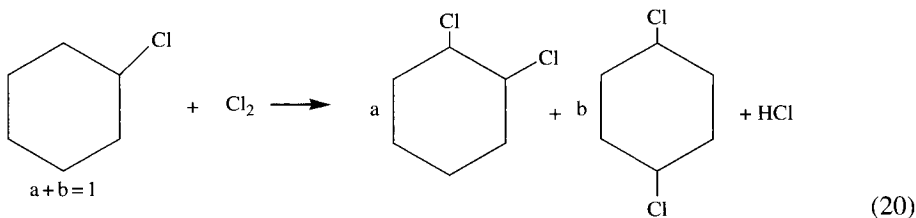
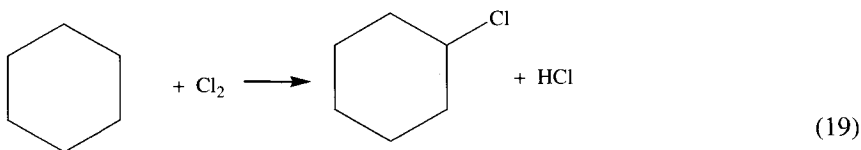


FIGURE 1.1. C₂-HCFCs and HFCs and their precursors.

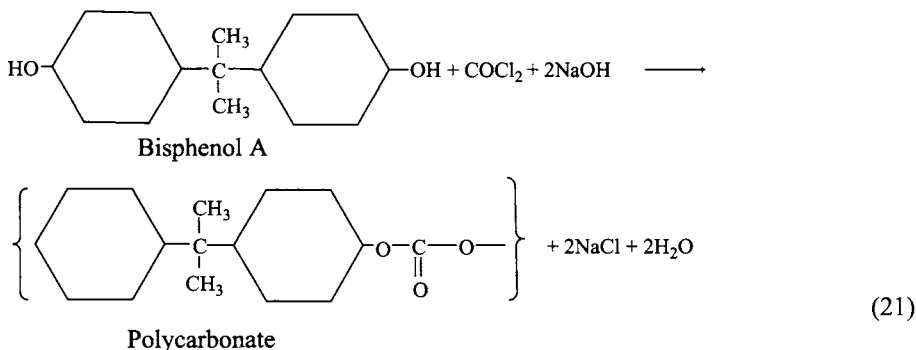
Chlorination of benzene in the presence of a metal catalyst such as FeCl₃ or AlCl₃ leads to the formation of chlorobenzenes as shown by Eqs. (19) and (20).



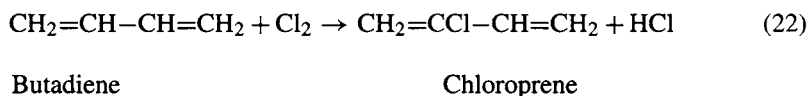
Monochlorobenzene is used in the production of nitrochlorobenzenes which are intermediates for making rubber chemicals, antioxidants, dyes and pigments, and of diphenyl ether, a component of heat transfer fluids. Dichlorobenzenes are used for producing mothballs, dye intermediates, and process solvents.

Synthetic glycerin, produced by the chlorination of allyl alcohol to form dichlorohydrin followed by hydrolysis, is the raw material in the manufacture of allyl resins and the production of nitroglycerine and other explosives. It is also used as a humectant in tobacco processing and as a plasticizer in cellophane manufacturing.

Polycarbonate resins, formed by using phosgene as a carbonylating agent for bisphenol A (Eq. 21), are used in automotive parts, appliances, power tools, and glazing, among many other applications.



Chloroprene, used to manufacture neoprene, which is an elastomer with high resilience and resistance to ozone, flame, and weathering, is produced by the reaction of chlorine with butadiene (Eq. 22).



Chlorine-based intermediates including methyl chloride, 1,1,1-Trichloroethane, and chlorobenzenes are used in the production of a wide spectrum of pesticides (including herbicides, insecticides, fumigants) and fungicides. Pentachlorophenol is used as a wood preservative.

There are several straight-chain saturated hydrocarbons in the C₁₀–C₃₀ range, which are directly chlorinated to produce chlorinated paraffins, used as coolants and lubricants for metal-working compounds and also as plasticizers and flame retardants.

Controlled chlorination of cyanuric acid results in the formation of di- and trichloroisocyanuric acids containing more than 90% available chlorine, which are used in dishwashing detergents and industrial and commercial laundries for their effective bleaching and disinfecting properties. They can be dry-packaged for domestic use and compete with the commonly used sodium hypochlorite.

Cyanuric chloride, formed by the reaction of chlorine with hydrogen cyanide, is used to produce herbicides, optical brighteners, pharmaceuticals, explosives, and surfactants. Ethyl chloride, made by reacting ethylene with HCl, was used to make tetraethyl lead.

Other products involving chlorine in their manufacturing processes include epoxy resins, polyurethanes, chlorinated solvents, refrigerants, process solvents, cellophane, wood preservatives, flame retardants, herbicides, pharmaceuticals, and explosives.

1.3.2. Inorganic Chemicals

Chlorine is also used in the production of many inorganic chemicals. The major product is titanium dioxide, which is made by reacting rutile (92–96% TiO_2) or a mixture of ilmenite (40–55% TiO_2) and rutile with chlorine to form TiCl_4 which is then purified and oxidized to TiO_2 . TiO_2 is used as a pigment for paints, paper, plastics, and rubber.

Bromine, which finds use in flame retardants, fire extinguishing agents, drilling fluids (calcium and zinc bromides), and fumigants to kill pests in soil and in buildings, is produced by treating hot brine containing bromide ion with chlorine. High-purity hydrochloric acid, made by burning H_2 and Cl_2 , is used in the food, electronics, and pharmaceutical industries. Also, a large amount of hydrochloric acid or gaseous hydrogen chloride is recovered from various hydrocarbon chlorination processes.

Hypochlorites of sodium, calcium, and lithium, and chlorinated trisodium phosphate involve chlorine in their production. Sodium hypochlorite of about 5% strength finds extensive use in the household bleach market and in residential swimming pools, and 15% sodium hypochlorite, an industrial bleach, is used for water treatment in municipal and industrial plants. Sodium hypochlorite is made by reacting chlorine with caustic soda. Calcium hypochlorite is mainly used as a swimming pool chemical. Aluminum chloride, produced from chlorine and aluminum or alumina, is used as a catalyst (for alkyl and ethyl benzenes, dyestuffs, ethyl chloride, and hydrocarbon resin production) and also in the production of pharmaceuticals and titanium dioxide.

Exotic metals such as titanium and zirconium are produced from their respective chlorides, which are formed by reacting chlorine with the oxides. Thus, metallic titanium is produced by reacting TiCl_4 with molten sodium or magnesium, while metallic zirconium is made by reaction of ZrCl_4 with magnesium. Molten salt electrolysis of magnesium chloride generates magnesium metal and chlorine, and fused salt electrolysis of sodium chloride and calcium chloride mixtures produces metallic sodium.

1.4. END USES OF SODIUM HYDROXIDE

The end uses of caustic soda, shown in Table 1.2, are more varied than the uses of chlorine. The origin of its extensive use lies in its ability to neutralize acids, as it is a strong base, and its ability to react with some metals and oxides, such as aluminum or Al_2O_3 to form anionic aluminates.

Caustic soda is used either directly or indirectly in the production of organic and inorganic chemicals, described below.

The direct use of caustic is in the pulp and paper industry, soap and detergent manufacturing, petroleum and natural gas operations, and alumina. Wood pulp, used for producing paper and paperboard, rayon, and cellulose ester plastics, among others, is made from small wood chips from either hardwood or softwood logs, which are digested with steam and white liquor containing caustic soda and sodium sulfide. Following the dissolution of lignin and conversion of the wood chips into pulp, the pulp is washed and separated from the black liquor, which is a mixture of spent pulping chemicals, degraded lignin byproducts, etc. The pulp at this stage is dark brown and is treated

TABLE 1.2. End Uses of Sodium Hydroxide (with permission from SRI Consulting)

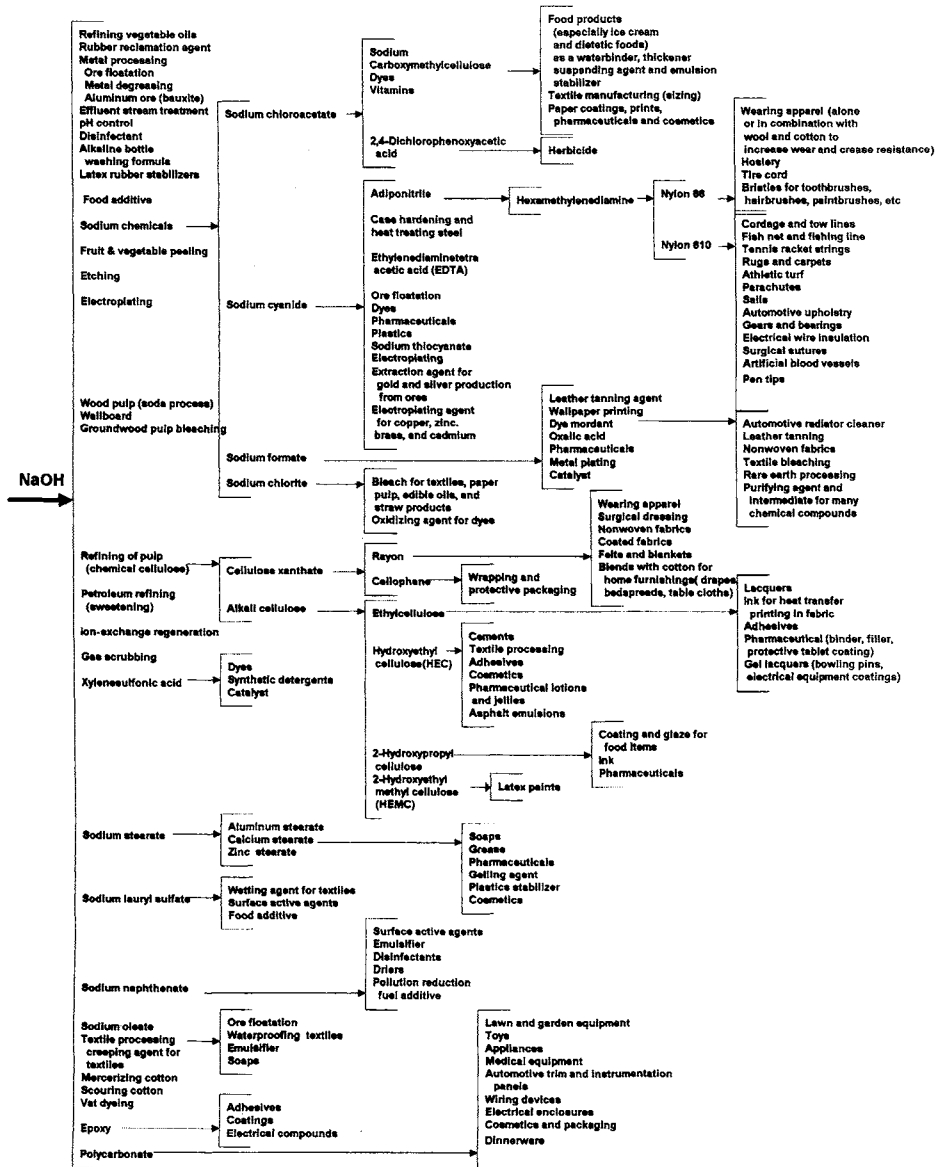


TABLE 1.2. (continued)

Sodium propionate	Mold preventive for food	
Sodium phenolate		Antiseptics Asprin (salicylic acid)
Sodium metasilicate	Dye intermediate	Blueprint paper Dye mordants Ceramics and glass Tin electroplating Textile fireproofing Stabilizer for hydrogen peroxide
Sodium orthosilicate	Zeolites	
Sodium picramate	Detergents	
Sodium stannate		
Sodium polysulfides	Sulfur dyes	Sulfur dyes Synthetic rubber Petroleum additives Electroplating
Sodium sulfite		
Sodium arsenite	Textile desizer	
Sodium bromite		Fungicide Activator for rubber vulcanization
Sodium dimethyl dithiocarbamate	Zinc dimethyl dithiocarbamate	
Sodium dinitro <i>O</i> -cresylate	Herbicide Control agent for fruit setting fungicide	
Sodium diuranate	Rodenticide	
Sodium tungstate		
Sodium fluoroacetate		
Sodium formaldehyde sulfoxylate	Textile stripping Bleaching agent for molasses and soap	
Monosodium glutamate	Flavor enhancer	
Sodium molybdate	Pharmaceuticals Paint pigments Fertilizer	Paint pigment Perfumes Cosmetics Pharmaceuticals Batteries (especially for miniaturized equipment) Polishing compounds
Cupric hydroxide	Pigment for fabrics	
Manganous Hydroxide	Ceramics	
Mercuric oxide		
Nickel hydroxide	Refining of beet sugar	Refining of beet sugar Manufacture of oil and grease additives Steel carbonizing agent Glass manufacture
Beryllium hydroxide	Manufacture of oil and grease additives	
Barium hydroxide	Steel carbonizing agent	
	Glass manufacture	
Cadmium hydroxide	Cadmium plating	
Cobalt hydroxide		
Lead hydroxide		
Amyl alcohol	Pharmaceuticals	
Acrylonitrile	ABS resins Automotive body parts Telephones Shoe heels Luggage Shower stalls Boats Radiator grills Business machines Electronic equipment housings Toys Nitrile rubber Softdrink bottles	Rocket propellant Pharmaceuticals Polymerization catalyst Blowing agent Spandex fibers (imparts elasticity to garments such as socks and special hosiery) Photographic developers Plating metals on glass Fuel cells Buoyancy agent for undersea salvage
Hydrazine		
Vanillin	Flavors Perfumes	

further to remove the remnant lignin, and is brightened by bleaching with chlorine or other oxidizers to produce a whitened pulp to produce high quality, white paper.

Soaps are primarily the sodium salts of fatty acids (and contain small quantities of ingredients such as perfumes, whitening agents, and builders, which complex calcium and magnesium ions). Stearic acid, present in tallow, oleic acids, and coconut oil, is a typical fatty acid. Detergents, constituting a large market for caustic, contain surface active agents, corrosion inhibitors, sud regulators, and other additives. The surfactants are made by reaction of caustic with linear alkyl sulfonates, alcohol sulfates, and ether sulfates. Caustic soda is used to saponify oils, fatty acids, and waxes to produce cosmetics, greases, and other products.

Caustic is used in the petroleum and natural gas industry as an additive to drilling mud, which is circulated to provide cooling and lubrication and to decrease the corrosion caused by acidic species. Addition of caustic not only minimizes the corrosion of drilling materials, but also enhances petroleum recovery by solubilizing the drilling mud components at high pH and by reducing the interfacial tension between oil, water, and rock, thereby facilitating the recovery of oil during the chemical flooding operation. Furthermore, caustic acts as a bactericide. The use of caustic in the oil and gas industry is associated with the removal of H_2S from crude hydrocarbons and extraction of nonvolatile components such as phenols, cresols, fatty acids, and naphthenic acids from hydrocarbon streams. Cresols, used in the production of resins, are recovered from the spent caustic from scrubbing the petroleum distillates.

One of the major direct uses of caustic is the manufacture of alumina from bauxite by the Bayer process. Bauxite, an ore containing hydrated alumina and various impurities such as iron and silica, is treated with caustic to solubilize alumina as sodium aluminate. The solution is filtered to remove the insolubles. The sodium aluminate solution is then hydrolyzed and cooled to form aluminum hydroxide, which is calcined to form pure alumina, from which metallic aluminum is produced by electrolysis.

1.4.1. Organic Chemicals

Caustic soda is used in the manufacture of organic chemicals for neutralization of acids, pH control, off-gas scrubbing, and dehydrochlorination. In addition, it can act as a catalyst and as a source of sodium during chemical reactions. Thus, propylene oxide, a raw material for polyether polyols used in flexible and rigid urethane foams, elastomers, coatings, and injection molding polymers, is made by the dehydrochlorination of propylene chlorohydrin with lime or caustic soda. Caustic is also used in the manufacture of EPI and the dehydrochlorination stage of epoxy resin production—the epoxy resins being used to make protective coatings, laminates, and fiber-reinforced plastics. Hydrolysis of EPI with caustic results in the formation of glycerin used in the pharmaceutical, tobacco, cosmetic, and food and beverage industries.

Chelating agents used to sequester metal ions such as calcium, magnesium, iron, and copper, are made by reacting caustic with ethylene diamine tetraacetic acid, hydroxy ethylenediamine triacetic acid, nitrilotriacetic acid, citric acid, gluconic acid, and diethylene triamine pentaacetic acid. Cellulose ether, which alters the flow characteristics of organic and inorganic solutions (e.g., oil drilling muds, pharmaceuticals, foods, and detergents) is made by reacting caustic with cellulose and sodium monochloroacetate.

Hydroxy ethyl cellulose, carboxymethyl hydroxyethyl cellulose, and methyl cellulose use caustic in their manufacture. Several other applications of caustic are summarized in Table 1.2.

1.4.2. Inorganic Chemicals

Caustic soda is used mainly in the manufacture of various sodium-containing compounds and sodium salts of acids, as well as in other applications where a high pH should be maintained. The major use of caustic soda in inorganic chemicals is the production of sodium hypochlorite for household and industrial bleaching purposes. Sodium-containing compounds used in the pulp and paper industry include: sodium hydrosulfide, sodium hydrosulfite (a bleaching agent for mechanical pulp), sodium sulfide, and sodium sulfite, which is also a raw material for making sodium thiosulfate. Sodium cyanide, made with caustic and hydrogen cyanide, is used in electroplating and chemical synthesis, the largest use being the extraction of gold from ores. Zeolites, which are hydrated aluminosilicates of alkali and alkaline earth metals, are used as detergent builders, catalysts, and adsorbents. Zeolites are made either by the hydrogel process, involving slow crystallization of an amorphous gel formed by reacting sodium aluminate with sodium silicate to form an orderly structure of sodium cations and aluminate and silicate anions, or by the kaolin conversion process where caustic is reacted with kaolin from clay.

Sodium silicates, produced by reacting caustic or dry soda ash with silica, are non-crystalline solid solutions that find use in adhesives, cleaners, catalysts, and detergents. Sodium phosphates, produced by reacting phosphoric acid with caustic, are used in detergents and cleaners. Caustic is also used in several food processing applications, including the removal of skins from produce items (potatoes, tomatoes, etc.).

1.5. END USES OF POTASSIUM HYDROXIDE

Potassium hydroxide, like its sodium counterpart, is a versatile intermediate in the production of chemicals. Because KOH is more expensive, NaOH dominates in large-scale uses, and potassium chemicals are largely restricted to specialty markets. They are often more soluble and more reactive than the corresponding sodium chemicals, and this fact is responsible for many of their applications. Widely used derivatives include acetate, bicarbonate, bromide, cyanide, ferrocyanide, oxalate, permanganate, and phosphate. The derivative with the greatest market probably is potassium carbonate, which is discussed in Section 7.5.2.2A.

The largest end-use for KOH is the production of soaps and detergents. The cost handicap, again, does not prevent the use of KOH in specialty products, primarily liquid soaps, detergents, and shampoos. KOH is also used in glassmaking, in petroleum refineries for the removal of sulfides and mercaptans, in fertilizers, and in many other products.

Worldwide capacity for production of KOH is about 1.7×10^6 tons/yr. Production is expected to grow by 4–5% per year from the 1.4×10^6 tons produced in 2001 [17].

The excess capacity should then disappear within a few years, but it is not known how much “swing” capacity exists that can easily be switched from NaOH to KOH production.

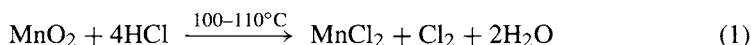
REFERENCES

1. S. Brien, *Paper presented at the 1999 World Petrochemical Conference*, Houston, TX, March 24–25 (1999).
2. E. Linak and Y. Inui *CEH Marketing Report: Chlorine/Sodium Hydroxide*, SRI International, Menlo Park, CA (2002).
3. J.S. Sconce (ed), *Chlorine: Its Manufacture, Properties and Uses*, Reinhold Publishing Corp., New York (1962).
4. Y.C. Chen, *Process Economics Program Report*, Stanford Research Institute, Menlo Park, CA, #61 (1970); #61A (1974); #61B (1978); #61C (1982); #61D (1992).
5. C.W. Scheele, *Brusten, eller Magnesia och dess Egenskaper*, Kong, Stockholm, Vetenskaps Academiens Handlingen XXXV (1774).
6. P. Schmittinger, *Chlorine, Principles and Industrial Practice*, Wiley-VCH, New York (2000).
7. I. Eidem and L. Lundevall, Chlorine-Glimpses from its History. In T.C. Jeffery, P.A. Danna, and H.S. Holden (eds), *Chlorine Bicentennial Symposium*, The Electrochemical Society, Princeton, NJ (1974), p. 20.
8. J.B. Van Helmont, *De Flatibus in Ortus Medicinae* (1668).
9. H. Ashworth, *Chem. News* **4**, 169 (1861).
10. R.T. Baldwin, *J. Chem. Ed.* **4**, 454 (1927).
11. J. Race, *Can. Eng.* **23**, 255 (1912).
12. J. Race, *Chlorination of Water*, John Wiley, New York (1918).
13. J.O. Meadows, *Eng. News* **65**, 80 (1911).
14. J.T. Conroy, *Trans. Amer. Electrochem. Soc.* **49**, 209 (1929).
15. V.R. Kokatura, *Chem. Mat. Eng.* **19**, 667 (1918).
16. *The Global Chlor-alkali Industry—Strategic Implications and Impacts; Final Report, Volume IV/Product Trees*, SRI International Multi-client Project #2437 (1993).
17. R.E. Shamel, Consulting Resources Corp., Personal communication (2002).

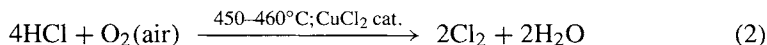
2

History of the Chlor-Alkali Industry

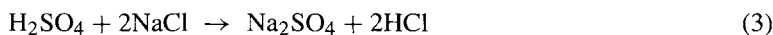
During the last half of the 19th century, chlorine, used almost exclusively in the textile and paper industry, was made [1] by reacting manganese dioxide with hydrochloric acid



Recycling of manganese improved the overall process economics, and the process became known as the Weldon process [2]. In the 1860s, the Deacon process, which generated chlorine by direct catalytic oxidation of hydrochloric acid with air according to Eq. (2) was developed [3].



The HCl required for reactions (1) and (2) was available from the manufacture of soda ash by the LeBlanc process [4,5].



Utilization of HCl from reaction (3) eliminated the major water and air pollution problems of the LeBlanc process and allowed the generation of chlorine. By 1900, the Weldon and Deacon processes generated enough chlorine for the production of about 150,000 tons per year of bleaching powder in England alone [6].

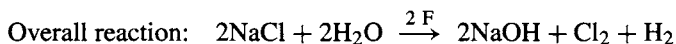
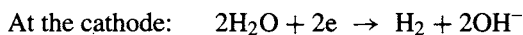
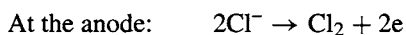
An important discovery during this period was the fact that steel is immune to attack by dry chlorine [7]. This permitted the first commercial production and distribution of dry liquid chlorine by Badische Anilin-und-Soda Fabrik (BASF) of Germany in 1888 [8,9]. This technology, using H_2SO_4 for drying followed by compression of the gas and condensation by cooling, is much the same as is currently practiced.

In the latter part of the 19th century, the Solvay process for caustic soda began to replace the LeBlanc process. The resulting shortage of HCl made it necessary to find another route to chlorine.

Although the first formation of chlorine by the electrolysis of brine was attributed to Cruikshank [10] in 1800, it was 90 years later that the electrolytic method was used successfully on a commercial scale. In 1833, Faraday formulated the laws that governed the electrolysis of aqueous solutions, and patents were issued to Cook and Watt in 1851 and to Stanley in 1853 for the electrolytic production of chlorine from brine [11].

2.1. DIAPHRAGM-CELL TECHNOLOGY DEVELOPMENT

During the electrolysis of NaCl brine, chlorine is generated at the anode and sodium hydroxide is produced at the cathode.



The main difficulty during the electrolysis of NaCl solutions was that of achieving continuous separation of chlorine generated at the anode and sodium hydroxide produced at the cathode. While it was easy to keep the chlorine and hydrogen gases in U-shaped tubes, the sodium hydroxide formed at the cathode reacted with chlorine to form sodium hypochlorite. The British scientist Charles Watt devised the concept of a current-permeable separator, which allowed the electric current to pass but kept the anode and cathode products separated. Thus, the diaphragm cell was invented in 1851. The major drawback to the use of the Watt cell was the lack of electrical generation capacity. The development of the dynamo around 1865 allowed Edison, Siemens, Varley, Wheatstone, and others to invent generators of electricity with sufficient capacity and efficiency to make electrolytic production of chlorine and caustic soda feasible.

Following the breakthroughs in electricity generation, parallel developments in diaphragm cells were made in many countries. The credit for the first commercial cell for chlorine production goes to the Griesheim Company in Germany, in 1888. This non-percolating diaphragm cell, used predominantly for Cl₂ production in the early 1900s, was based on the use of porous cement diaphragms, invented by Brauer in 1886 and made by mixing Portland cement with brine acidified with HCl, followed by setting and soaking in water to remove the soluble salts. The cell, termed the Griesheim Elektron cell [12, 13] and shown in Fig. 2.1, consists of an iron box with a steam jacket and is mounted on insulation blocks. Each unit contains six rectangular boxes made of cement about 1 cm thick. The cement boxes act as diaphragms and contain the anodes made of magnetite or graphite. The outer box forms the cathodes, and cathode plates are also provided in the form of iron sheets placed between anode compartments and reach the bottom of the cell. The cell was operated at 2.5 kA, batchwise, with saturated potassium chloride solutions for 3 days until a concentration of 7% KOH was obtained, at a current density of 100–200 A/m² at 80–90°C; the cell voltage is about 4 V and the current efficiency 70–80%. It is very interesting to note that the best operating conditions for this cell were

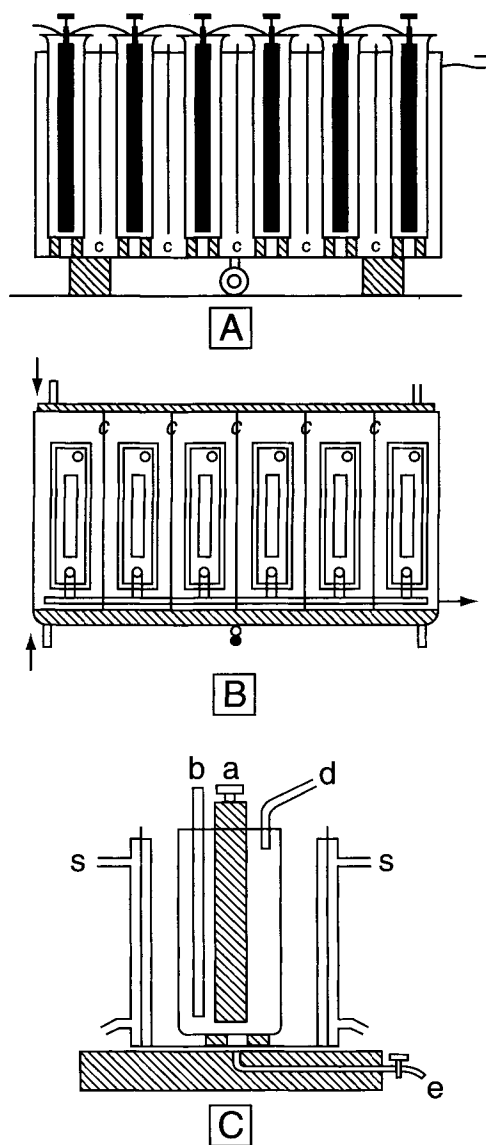


FIGURE 2.1. A and B: Griesheim Electrolysis cell bank; C: Cross-section of Griesheim Electrolysis cell. a: anode; b: brine inlet; c: cathode; d: brine outlet; e: caustic outlet; s: steam.

found to be: (1) anodes preferably of magnetite, to obtain pure chlorine without any CO_2 in the anode gas, (2) high concentration of brine, and (3) a temperature of $80\text{--}90^\circ\text{C}$, to reduce the cell voltage. Items (2) and (3) are still the desired parameters for optimal cell operation.

The first diaphragm cell developed in Great Britain was the Hargreaves–Bird cell, operated in 1890 by the United Alkali Company. Each cell consisted of a rectangular iron box lined with cement. The box was 10 ft long, 4–5 ft deep, and 2 ft wide, divided into

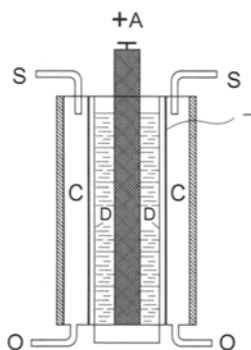


FIGURE 2.2. Hargreaves–Bird cell. A: anodes; C: cathodes; D: diaphragms; O: outlet pipes for brine mixed with sodium carbonate; S: outlets for CO_2 and steam.

three parts of two separate asbestos sheet diaphragms. Six carbon anodes were placed in the anode compartment, and the cathode was a copper gauze attached to the diaphragms. This basic approach of anchoring the diaphragm onto the cathode is still used in modern diaphragm cells. The cell design is shown in Fig. 2.2.

The anode compartment was filled with saturated brine, and during electrolysis chlorine evolved at the anode. The sodium ions, along with sodium chloride and water, percolated through the diaphragm into the cathode compartment. Back migration of hydroxyl ions was suppressed by injecting CO_2 and steam into the cathode compartment to form sodium carbonate. The major contribution of this cell was its vertical diaphragm configuration, which is the basis of modern cells.

Twelve cells were run in series at 2 kA, which corresponds to a current density of 200 A/m^2 , at 4 to 4.5 V, when 60% of the salt is converted to sodium carbonate.

The cell, used in France and Italy, was the Outhenin–Chalandre cell [13], which consisted of an iron box divided into three compartments; the outer ones contained the cathode liquor, and the inner one had the graphite anodes in strong brine. The diaphragm was made from cylindrical unglazed porcelain tubes, cemented together into dividing walls of the cell. This cell was more complex than the Griesheim cell and required considerable attention.

In the United States, LeSueur [14–17] developed and operated a cell in 1890, employing a percolating horizontal diaphragm (Fig. 2.3A). This design permitted brine to flow from the anolyte through the diaphragm continuously to achieve a higher efficiency than the contemporary nonpercolating diaphragm cells in Germany and Great Britain. LeSueur's percolating diaphragm cell, which is the basis for all diaphragm chlor-alkali cells in use today, shown in Fig. 2.3B, is an improved version of the cell depicted in Fig. 2.3A.

The LeSueur cell was made of iron and divided into two compartments separated by a diaphragm, which was deposited on an iron-gauze cathode. The anode was graphite, and the anode compartment was sealed to avoid the release of chlorine. The liquid level in the anode compartment was higher than the level in the cathode compartment, and the caustic flowed out of the cell continuously. This was the first cell to use the percolation method for caustic withdrawal.

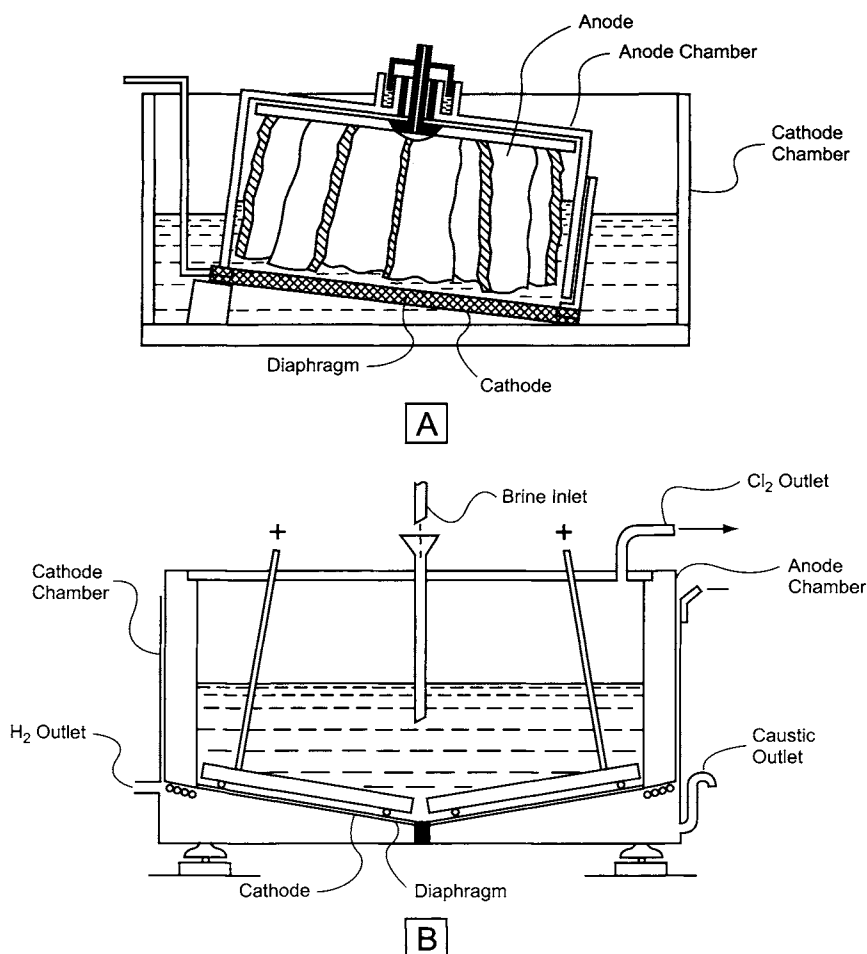


FIGURE 2.3. A: original LeSueur cell; B: modified LeSueur cell.

During the 1920s, the Billiter cell was developed in Germany [13]. This cell was similar to the LeSueur cell, and the original design had a flat electrode and a horizontal diaphragm. By modifying the cathode to a corrugated shape, current loads were increased from 12 kA to 24 kA (Figs. 2.4A and B). The diaphragm was a closed woven steel screen covered with a mixture of long fiber asbestos wool and barium sulfate. Asbestos became the primary component of the diaphragm for the next 80 years.

There was significant cell development activity during the period 1890–1910, following LeSueur's and Hargreaves–Bird cell with a vertical diaphragm, and the development of synthetic graphite independently by Castner and Vaughn, and Acheson [18], who also developed a method for producing synthetic graphite anodes. The cell designs focused on heavy concrete housing, either cylindrical or vertical, with graphite anodes entering through the top and the cathode plates bolted on the side. The basic types of

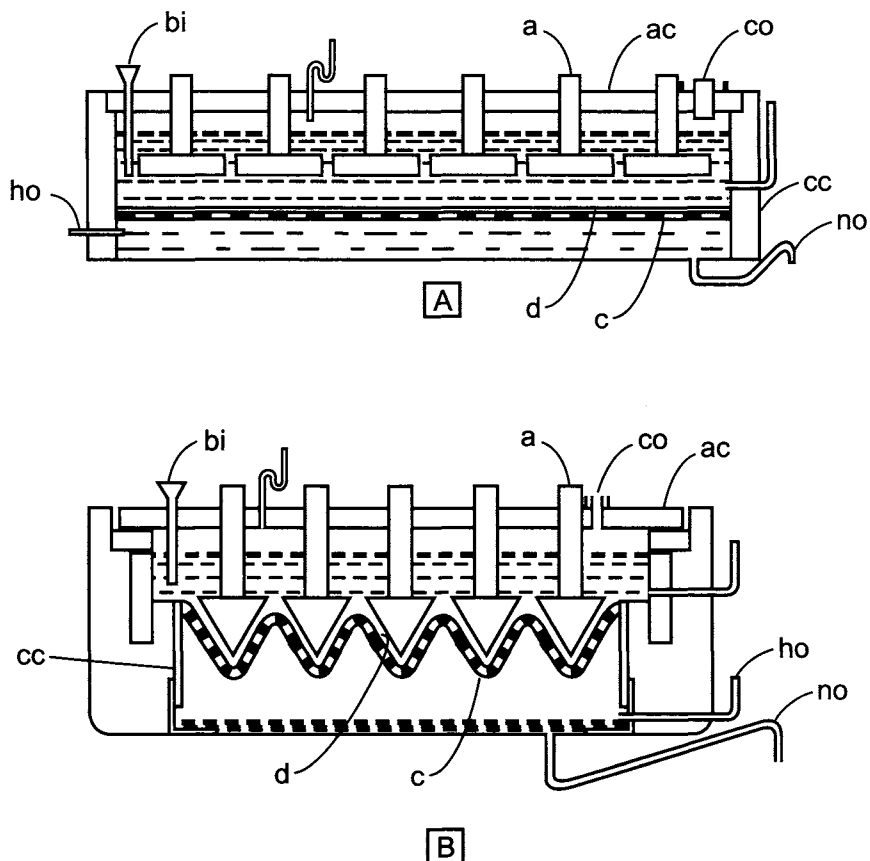


FIGURE 2.4. Billiter cell. A: flat cathode; B: corrugated cathode. a: anode; c: cathode; d: diaphragm; ac: anode chamber; cc: cathode chamber; bi: brine inlet; co: chlorine outlet; no: caustic outlet; ho: hydrogen outlet.

cells developed were rectangular vertical cells, cylindrical cells, and bipolar filter-press type cells, as shown in Fig. 2.5.

2.1.1. Vertical Diaphragm Cells

Of the various vertical diaphragm cells shown in Fig. 2.5, the Townsend cell was the forerunner of the modern diaphragm cells. The cell design of the early 1900s had poor efficiency as the chlorine was reacting with the back-migrating caustic. This problem was addressed in the Townsend process by covering the caustic with a film of kerosene. The first plant employing the Townsend cell was built in Niagara Falls, and had 68 2-kA cells, producing chlorine and caustic soda with low hypochlorite and chlorate. One of the important developments that took place around this period was feeding the saturated brine through orifices to maintain the desired brine level in the cell, thereby eliminating expensive overflow controls [19].

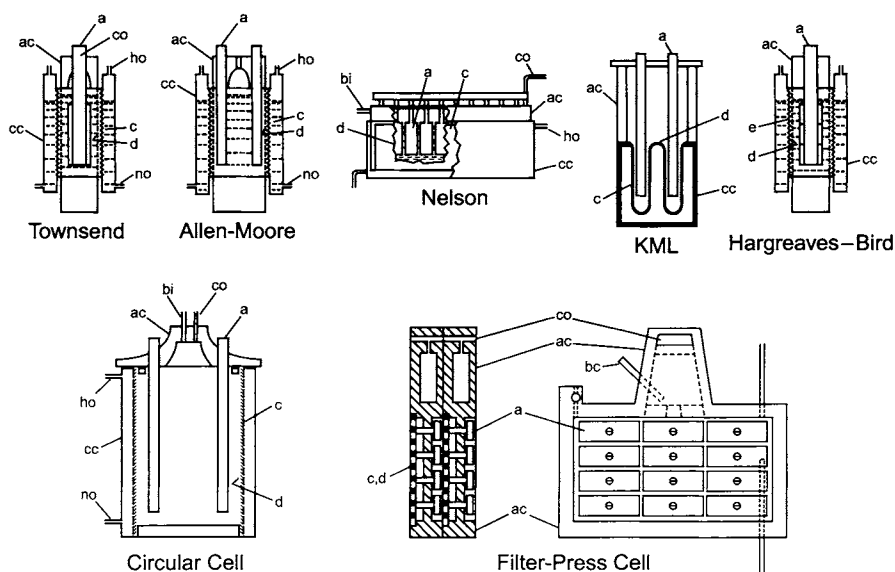


FIGURE 2.5. Schematic of historical diaphragm cells. The symbols are the same as in Fig. 2.4.

Clarence Marsh improved the design of the Townsend cell in 1913 by installing side-entering cathodes and anodes and corrugated finger cathode plates. This design was the forerunner of the cathode used in Hooker Type S cell with asbestos paper folded to fit the corrugations, the edges being protected by putty. However, the cell putty disintegrated exposing the bare cathode surface and thereby reducing the cell current efficiency. In 1925, Stuart solved the problem of completely covering the round cathode pieces by mixing asbestos fiber in dilute caustic liquor and sucking the asbestos mixture onto the cathode by applying a vacuum. The asbestos then formed a tight coating on the cathode, conforming perfectly to the contours of the cathode figures. This technique of vacuum deposition of asbestos is one of the most important developments in the history of chlor-alkali cells [19]. The Marsh cell, before and after diaphragm deposition, is shown in Fig. 2.6.

Following the invention of deposited asbestos diaphragms, Stuart developed the Hooker “S” cell, which had vertical cathode fingers with deposited diaphragms. These “S” cells were very popular after World War II and were phased into operation throughout the world. In 1960, almost 60% of the chlorine production in the United States was in Hooker cells.

While Hooker pioneered the development of vertical diaphragm cells, Diamond Alkali Company developed an alternate cell design. In 1959, Diamond licensed a cell with cathode fingers, which run continuously from one side of the cell to the other. The support of the cathode fingers at both ends (as opposed to Hooker’s cantilevered construction with support only at one end) helped ensure the stability of anode–cathode alignment. Also, the fingers are oriented parallel to the cell circuit to accommodate thermal expansion during operation, and realize voltage savings via the reduced current path. This feature

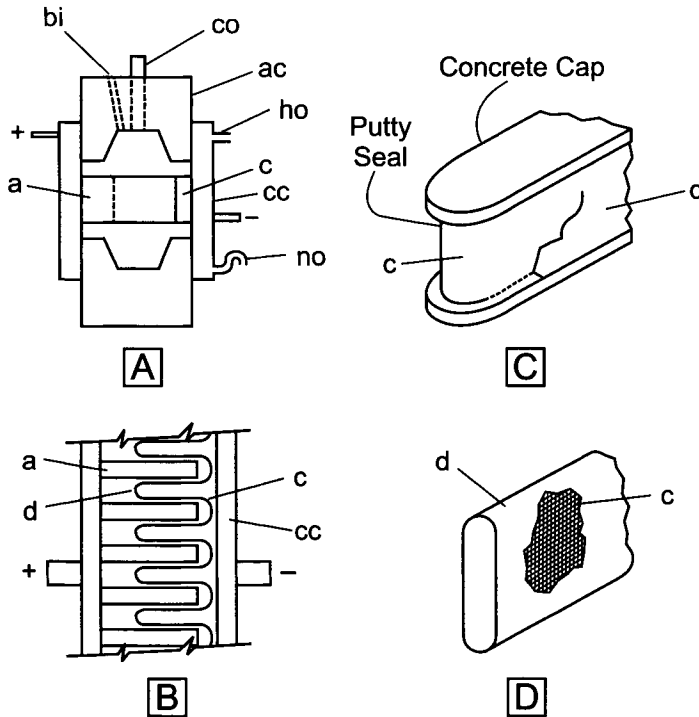


FIGURE 2.6. Marsh cell. A: vertical section; B: plan, sectional diagram; C: original cathode with asbestos paper diaphragm; D: asbestos deposited cathode finger. The symbols are the same as in Fig. 2.4.

has been adopted in almost all modern cells including some Hooker types described in Russian patents. The alternative cathode finger supports are shown in Fig. 2.7.

2.1.2. Developments in Anodes and Diaphragms

During the early 1900s, the anode used for chlorine generation was either platinum or magnetite. However, because of the high cost of platinum and the current density limitation (0.4 kA/m^2) with the magnetite, graphite became the predominantly used anode material from 1913 to the mid-1970s.

Artificial graphite anodes were developed by Acheson and, in 1919, Wheeler improved their performance by impregnation with linseed oil. Periodic replacement of anodes was nevertheless necessary, as the graphite blades wore away resulting in higher cell voltage, due to the increased anode-cathode gap. This motivated the search for dimensionally stable anode structures to replace graphite. Platinum and Pt/Ir activated titanium was found to offer excellent corrosion resistance in brine electrolysis service. However, these anodes suffered from either a short life or a high cost.

Henri Bernard Beer developed and applied for two patents [20] issued in 1965 and 1967 that revolutionized the chlor-alkali industry. These patents described thermal decomposition techniques to coat titanium substrates with mixed crystals of valve metal

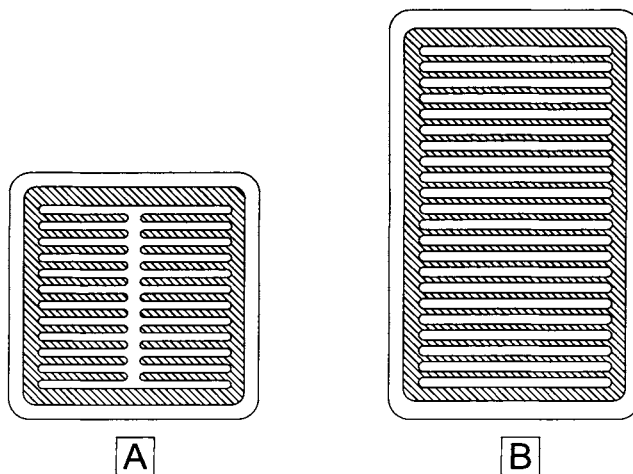


FIGURE 2.7. Comparison of Hooker and Diamond cathode designs. A: finger type construction (Hooker type "S" cell); B: flattened tube-type construction (Columbia-Hooker Diamond, Hooker type "T").

oxides and platinum group metal oxides—the valve-metal oxide content in these coatings being more than 50%. These anodes were initially used in DeNora mercury cells, and they exhibited low cell voltage and a long life. Over the next few years, most diaphragm-cell plants throughout the world were converted to these anodes, which were given the registered trademark DSA[®], for dimensionally stable anodes [21]. All the technology suppliers, to realize the benefits of the low energy consumption offered by the metal anodes, changed their cell configurations to incorporate the metal anode.

After the development of dimensionally stable anodes, the focus shifted to improvements in asbestos diaphragms. Replacement of concrete tops with fiberglass-reinforced polyester cell tops improved diaphragm life and voltage by eliminating the degradation products of concrete. Still, the asbestos diaphragms swelled during operation, resulting in increased cell voltage. Diamond Shamrock examined the behavior of these asbestos diaphragms and developed a modified composition by mixing asbestos and polytetrafluoroethylene (PTFE), which, on heating, resulted in a dimensionally stable diaphragm [22]. This diaphragm showed improved cell voltage in commercial tests in 1972, and made possible the use of expandable anodes, also developed by Diamond [23]. At the same time, Hooker developed a stabilized diaphragm, HAPP (Hooker Asbestos Plus Polymer), which did not swell. This diaphragm was formed by mixing a polymer into the asbestos slurry before deposition and baking at the fusion point of the polymer [24].

A major concern with continued exposure to asbestos is its toxicological effect on the human body resulting in diseases—such as asbestosis, which becomes significant 15 to 20 years after first exposure. As a result, the EPA has banned its use in roofing felts, flooring felts, vinyl-asbestos floor tile, asbestos cement pipe and fittings, and heat-resistant clothing. Although the chlorine industry in the USA is currently exempt, allowing continued use of asbestos as diaphragm material, it is believed that environmental pressures will ultimately force the industry to adopt non-asbestos diaphragm technology. Some

countries have already banned asbestos or defined preferred technology as asbestos-free. Anticipating the potential replacement of asbestos, there has been a flurry of activity to develop non-asbestos diaphragms. These include the microporous diaphragm, which is either a PTFE sheet containing sodium carbonate as a pore former [25] or a mixture of PTFE fibers and zirconia [26], vacuum-depositable non-asbestos fibers called Polyramix [27] and Tephram [28]. Details related to these technologies are addressed in Section 4.7.

2.1.3. Diaphragm-Cell Technologies

As mentioned previously, the vacuum-deposited diaphragm developed in 1928, coupled with the vertical finger anode–cathode construction, initiated the Hooker “S” series cell. The “S” type cell continued until 1966, when the single C-60 cell was introduced. In 1970, the “H” series cell was introduced, with metal anodes replacing the graphite anodes. A summary of the major innovations in Hooker diaphragm-cell design is presented in Table 2.1.

Diamond Alkali developed cells very similar to the Hooker cells and began licensing the technology in 1959. Its main cell during the late 1950s and the early 1960s was the D-3 cell operating at 33 kA. As noted earlier, the D-3 had cathode fingers secured on both sides of the cathode assembly, which was a rectangular steel can with a

TABLE 2.1. Summary of Major Changes in Hooker Diaphragm Technology

Date	Cell	Key innovation
1928–48	S-1	First successful deposited diaphragm cell. Consistent increases in the allowable amperage with minor electrical circuit changes
1948	S-3	Doubled the anode and cathode areas of S-1 to double capacity
1951	S-3A	Conductor sizes increased to permit greater current density
1956	S-3B	Increased Cl ₂ and H ₂ disengaging space to permit greater chlorine production
1960	S-3C	Redesigned conductors for optimum economic current density
1963	S-4	Increased anode and cathode height and added five rows of electrodes over S-3C to increase cell output
1964	S-4B	Decreased grid height to decrease cost without affecting cathode area. Disengaging space increased accordingly
1966	C-60	Redesigned cathode to reduce copper content without increasing voltage
1970	H-1	Substituted metal anodes for graphite anodes in S-4B to increase current density and cell life
1970	H-2, 2A	Increased cathode and base copper to carry large currents on basic S-4 and C-60 designs
1971	HC-4B	Substituted metal anodes for graphite anodes in S-3C to increase current density and cell life
1972	H-4	Increased anode and cathode area to increase capacity
1978	H-4M	Added polymer to asbestos to create a stable, resistant diaphragm with reduced energy consumption
1979	H-4/84 (or LCD)	The LCD (low current density) cell operated with about 12% lower current density by reducing the anode–cathode gap, and allowing for more anode and cathode fingers in the shell of the H-4 cathode

deposited asbestos diaphragm. A concrete head on top of the cathode assembly completed the cell.

Later models of Diamond cells include the DS-31, DS-45, and DS-85, which used metal anodes. The DS-85 model allows amperage up to 150 kA. The base or cell “bottom” features a patented design consisting of a welded steel structure supporting a flat copper grid, which carries current to the anodes. A corrosion-resistant mat covers the grid to protect the copper from attack by the anolyte and the vertically disposed metal anodes are simply bolted to the base through the mat. As in Hooker designs, the cover or cell head is made of proprietary polyester resin instead of concrete. This type of cover avoids the anolyte contamination resulting from attack on the concrete (as experienced in earlier cells), and this, in turn, reduces the frequency of blockage of the diaphragm.

ELTECH System Corporation currently markets both the Hooker cells and Diamond cells. Other diaphragm-cell technologies developed during the 1970s include the Hooker–Uhde cell and the ICI–Solvay cell. These cell designs are addressed in Chapter 5.

2.1.4. Bipolar Diaphragm Cells

The filter-press cell for producing chlorine and caustic was designed by several early investigators. However, it was Dow who pioneered the development of bipolar filter-press cells over several years in view of the advantages, which included minimization of the bus between the cells and floor space, and low capital cost. The original patents of Dow were issued in 1911 and 1913 [29]. The filter-press cell design, patented in 1921 [30], shown in Fig. 2.5, comprises concrete filter-press units with graphite rods embedded and extending into the anode compartment, and the cathode screen on the other side.

An improved bipolar design of Dow is described in U.S. patent 2,282,058 (1942) by Hunter-Otis and Blue, where a graphite dividing wall was cast into the concrete filter-press frame with graphite anodes projecting vertically from the backing plate. The cathode fingers were made of steel wire screen wrapped with asbestos paper and fastened to a screen backing plate of the adjacent unit cell. Lucas and Armstrong [31] made additional improvements to this cell by using bipolar units, which slip into grooves in a cell box, which eliminated the sealing problems. The cathode fingers of steel wire screen and graphite anodes project vertically from a steel base plate, thereby constituting an integral electrode unit. Figures 2.8 and 2.9 describe the cell designs of Hunter-Otis and Blue, and of Lucas and Armstrong. These cells have been modernized with metal anodes and modified diaphragms in recent years.

PPG and DeNora jointly developed a bipolar filter-press diaphragm cell called the Glanor[®] electrolyzer [32]. The central design feature is the bipolar electrode where one side acts as an anode and the other as a cathode. The electrode consists of a steel plate to which anode fingers are connected on one side and cathode fingers on the other.

The electrode is set into a bipolar element, which consists of a channel frame surrounding the anodes, lined with titanium for protection against corrosion in the anolyte environment. The elements, with the anode side of one facing the cathode side of another, thereby forming a cell, are clamped together with tie-rods. The resulting assemblage has the appearance of a plate and frame filter-press—a commonly used piece of equipment for filtration operations. Hence, the term “bipolar filter-press cell.”

Bipolar cell designs and their performance characteristics are discussed in Chapter 5.

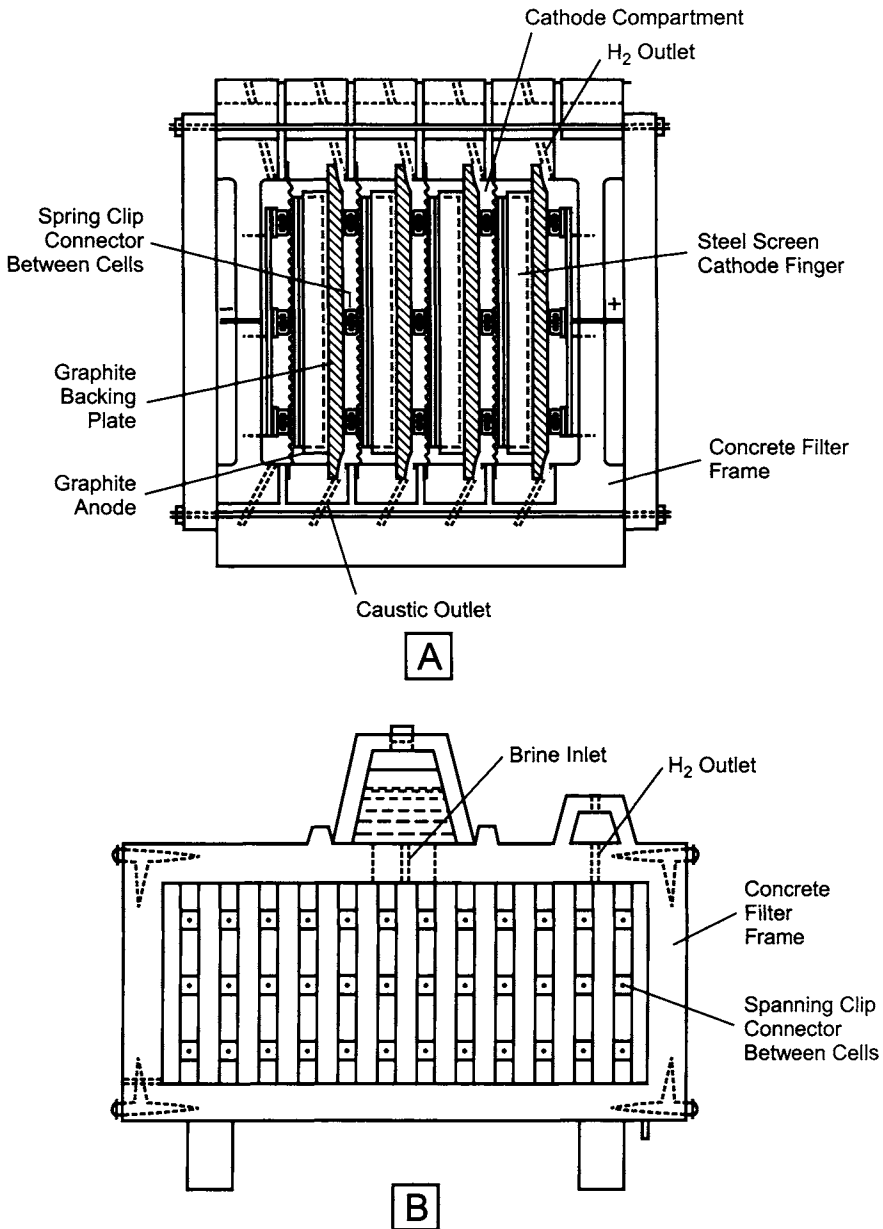


FIGURE 2.8. Dow filter-press cell of Hunter-Otis and Blue. A: basic cell configuration; B: horizontal cross-sectional view.

2.2. MERCURY-CELL TECHNOLOGY

An alternative method of producing chlorine and caustic soda involves the use of mercury cells, whose cathode reactions differ from those occurring in diaphragm cells.

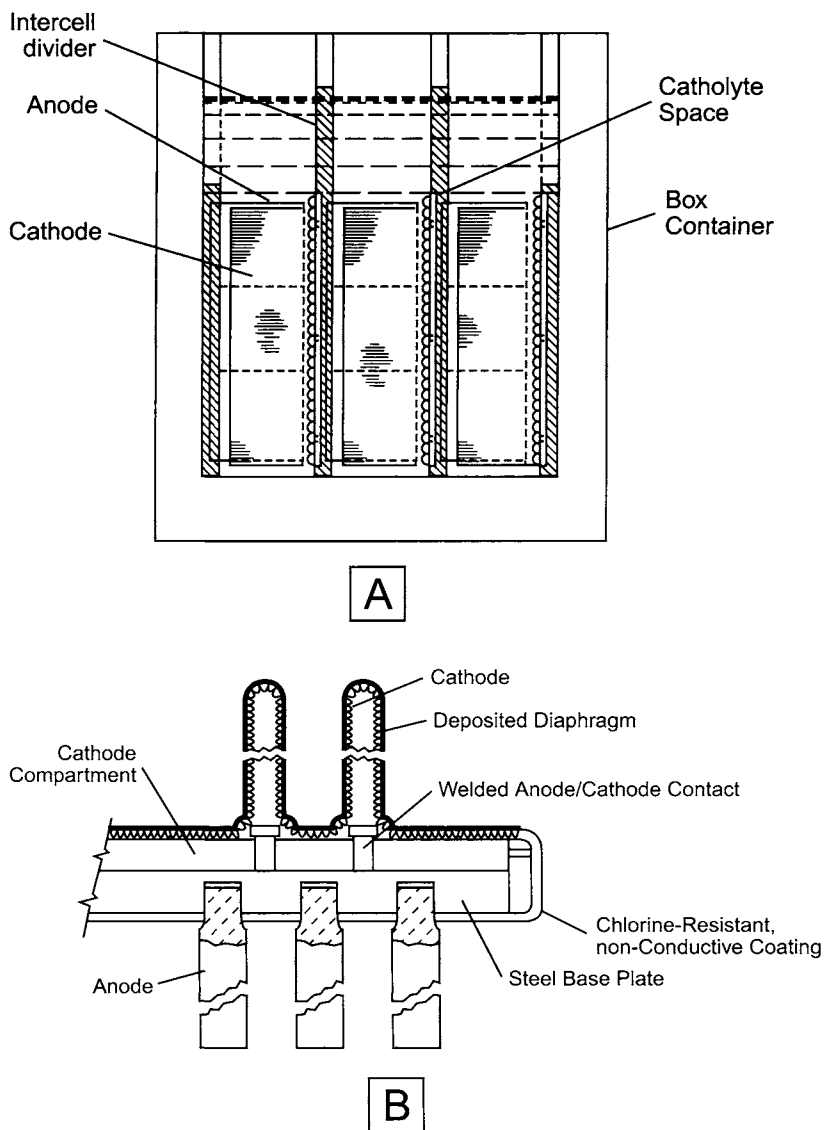
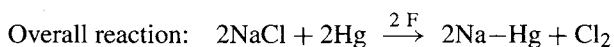
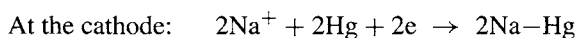
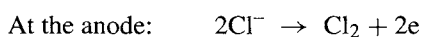
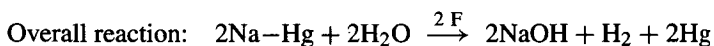
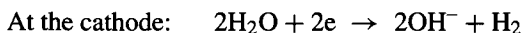
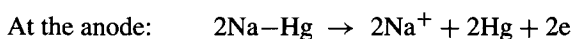


FIGURE 2.9. Dow box cell of Lucas and Armstrong. A: Dow box cell; B: horizontal section of bipolar electrode.

The mercury cell consists of two primary units—the electrolyzer and the decomposer or denuder. The principal electrochemical reactions are as follows:
In the electrolyzer:



In the decomposer:



The overall process involves a flow of purified, saturated brine through an elongated, slightly inclined trough between a shallow cocurrent stream of mercury and an assembly of electrodes (graphite or metal), the lower surfaces of which are close to the mercury surface and parallel to it. The cell trough is provided with a gas-tight cover, which also serves to support the anodes. During electrolysis, chlorine is liberated at the anodes, while the sodium ions are discharged at the surface of the mercury cathode to form a low concentration sodium amalgam (0.10–0.30% sodium by weight). Thus, the sodium ions are almost entirely prevented from reacting with the aqueous electrolyte to form caustic soda, or with dissolved chlorine to re-form sodium chloride. The amalgam reacts with water in the decomposer to form pure concentrated caustic.

The mercury-cell process for producing chlorine and caustic was developed by Hamilton Y. Castner, an American, and Karl Kellner, an Austrian, in 1892, although the first patent dealing with mercury cell was British patent 4349, issued in 1882, to Nolf. Following patent disputes, Castner and Kellner combined their efforts and sold their combined patent rights to Solvay et Cie. The first mercury cell of Castner consisted of a stationary, thick cast-iron base in which cylinders were bored for the ram pumps employed to circulate the amalgam. There were two anode compartments for electrolysis and an intermediate compartment for amalgam decomposition to generate caustic. This cell suffered from seizure of the ram pumps, as a result of the growth of caustic soda deposits. Castner overcame the problem of pumping mercury by using a rocking cell (Fig. 2.10), which was built in 1894 in England. A similar plant was built in 1895 in

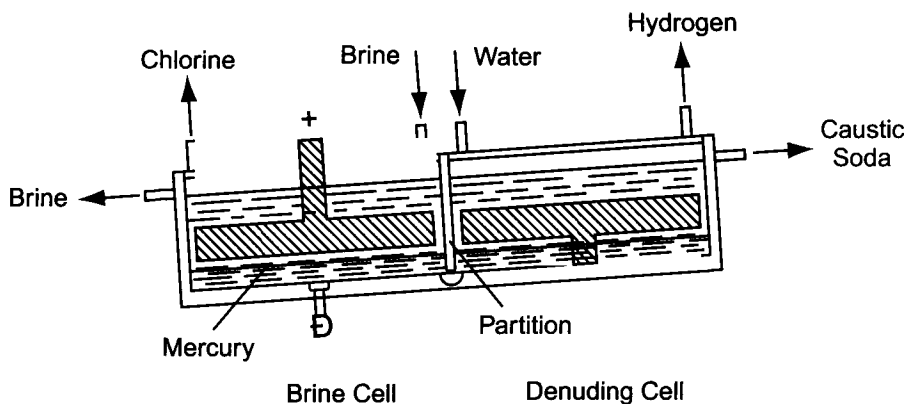


FIGURE 2.10. Schematic of original mercury cell.

Saltville, VA, and the Mathieson Alkali Company adopted this process in 1897. The Castner–Kellner Alkali Company started production in Weston Point, Runcorn, in 1897, and the Mathieson Alkali works began production in the same year at Niagara Falls.

The success of the latter venture was evidenced by the fact that the capacity of the plant was greatly enlarged, and except for minor changes, the old Castner “rocking cells” were in continuous operation from 1897 to 1960 [33]. They were finally replaced by 100 kA Olin Mathieson cells.

Parallel to this development in the United States, Brichaux and W. Wilsing of Solvay built the first “long” cell, in Germany, in 1898. This cell had the modern characteristics of forced mercury circulation.

With the growth of synthetic fibers, such as rayon, a tremendous demand for very pure (salt free) caustic soda developed. A significant number of mercury-cell plants were built in the years around World War II.

Cell capacities increased progressively after 1945, from about 10 kA to 200–300 kA. Suppliers of this technology include De Nora, Hoechst–Uhde, Krebs, Krebskosmo, BASF, Kureha, Olin–Mathieson, Solvay, Toyo Soda, and Asahi Glass. The increased capacity of the mercury cell depended on the use of efficient silicon rectifiers, which replaced the old mercury-arc rectifiers. The distinguishing differences in these mercury-cell technologies lie in several design factors which include the manner by which mercury is fed to the electrolyzer (e.g., gravity flow vs forced flow), decomposer design, support structure for the anodes and the cathodes, types of cell cover, and mercury inventory requirements, the main motivation being improved economics. These technologies are outlined in Chapter 5.

The primary cell technology used for producing chlorine and caustic, in the world and in United States, is the diaphragm-cell process, which had a 37% share of world chlorine production. In the United States, the diaphragm cell contributed 67% of chlorine production [34]. The mercury-cell technology had a dominating share initially. However, following the mercury poisoning cases in Minamata and Niigata, both in Japan, in 1972, there has been a declining trend away from this technology for chlorine production. Japan was the first country to change from mercury-cell technology, and currently there is no mercury-cell operation in Japan. In Western Europe, mercury-cell technology is more widely practiced. The mercury-cell technology still accounts for 18% share in 2001, in the world. Mercury cells generate 11% of the chlorine produced in the United States. This situation is unlikely to dramatically change in the near future. The environmental issues and concerns related to the mercury-cell process are discussed in Chapter 16.

2.3. MEMBRANE-CELL TECHNOLOGY

An alternative to diaphragm and mercury cells is the membrane cell. Actually, the membrane cell is a modification of the diaphragm cell wherein the diaphragm is replaced with a permselective ion-exchange membrane. The membrane inhibits the passage of negative chloride ions but allows positive sodium ions to move through freely.

In the membrane-cell process, sodium or potassium chloride brine is fed to the cell and distributed equally among the anode compartments, while water fed into a second header flows into the cathode compartments or into an externally recirculating stream

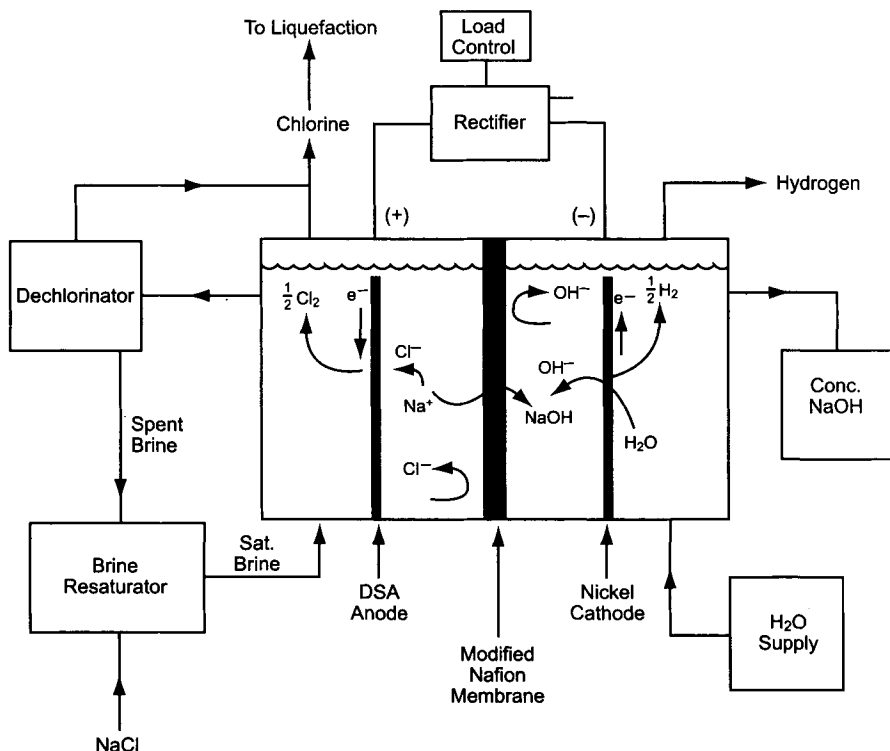


FIGURE 2.11. Schematic of ion-exchange membrane cell. (Reproduced with permission of the Society of Chemical Industry.)

of catholyte. The electrode reactions are the same as in a diaphragm cell. The depleted brine, or anolyte, overflows with the chlorine gas into an anolyte header and the caustic soda liquor overflows with the hydrogen gas into a catholyte header. Figure 2.11 is a schematic diagram of the membrane-cell process.

Several firms participated in the development of the membrane cell. Conceptual studies of permselective membranes began in the mid-1940s. W. Juda *et al.* of Ionics Corporation, and S.G. Osborne of Hooker Chemical hold early patents (1950s) on the membrane-cell process [35].

Diamond and Ionics mounted a joint effort to develop the membrane cell from the mid-1950s to the early 1960s [36]. This work demonstrated the feasibility of the concept, but serious problems developed, including erosion of carbon anodes, high cell voltage, and very short membrane life. The project was dormant for about 10 years.

In the late 1960s, concern over environmental problems associated with mercury-cell plants initiated a revival of interest in the membrane-cell technology. Initial problems associated with membrane cells were steadily being alleviated in the early 1970s. The development of metal anodes negated problems associated with graphite anode erosion. As a spin-off of the space program, DuPont developed a perfluorinated ion-exchange

membrane while performing fuel cell research. This membrane was initially called “XR” and was later trademarked as “Nafion.” Nafion[®] membranes were found to have good ion-exchange properties as well as high resistance to the harsh environment of the chlor-alkali cell.

After DuPont introduced Nafion[®] membranes, Diamond Shamrock intensified its research efforts in membrane-cell technology. Initial research tests with the membranes began in 1970 using laboratory cells. In 1972, a commercial-size electrolyzer and pilot plant were placed in operation in Painesville, Ohio. Four years later, a 20-ton per day demonstration plant was built in Muscle Shoals, Alabama. This unit was integrated with an existing mercury-cell plant.

Diamond’s first commercial membrane cell was its “DM-14 Electrolyzer,” a monopolar cell. A number of individual membranes are held between anode and cathode frames bolted together in a “filter-press” configuration. Each electrolyzer unit (anode, membrane, and cathode) has an active electrode area of 1.41 m². A current density of 3.1 kA/m² produces 0.14 metric ton of caustic per unit per day. The number of unit cells bolted together determines the operating amperage of the electrolyzer, ranging from 5 kA to over 150 kA. Because of the monopolar arrangement of the cells, the voltage of the electrolyzer is independent of the number of membranes installed in the electrolyzer [36]. The DM-14 operated at 3.9 V at a current density of 3.1 kA/m².

Like Diamond, Hooker Chemicals demonstrated an interest in ion-exchange membranes since the mid-1940s. S.G. Osborne *et al.* of Hooker Chemical Corporation hold the original patent for the first membrane cell [36]. This patent was filed on January 23, 1952. With this patent, Hooker embarked upon a major development program until 1957. Following a period of relative inactivity, the Nafion[®] membrane rekindled interest in membrane-cell technology.

Research during the early 1970s culminated in the licensing of the MX cell of Hooker Chemicals to Reed Paper Ltd., a firm that built a 45-ton per day membrane plant at Dryden, Ontario. Actually, these membrane cells replaced 13-year-old mercury cells that were being phased out because of growing concern over mercury pollution problems in Canada. The plant was brought on stream on November 19, 1975.

Around the same period, Asahi Chemical started a pilot plant operation with ion-exchange membrane cells, using DuPont’s Nafion[®]. In 1975, a commercial plant was commissioned, producing about 10 tons of caustic/day, at Nobeoka in Japan.

Since then, several membrane-cell technologies were developed in Japan, as a pollution-free chlor-alkali process. Japanese contributions include composite membranes and several electrolyzer designs. Japan was the first major chlorine producing country to convert entirely to membrane cell technology. As of January 2003, ~35% of world production of chlorine is by membrane-cell technology, generating ~52,000 metric tons caustic/day.

Many chlor-alkali producers and technology licensing companies have refined and optimized membrane cell designs to realize low energy consumption and long life. The new cell designs incorporated the zero-gap concept, which eliminated the electrolyte gap between the electrodes and the membrane.

Two types of electrolyzers were developed, and are labeled monopolar or bipolar. In the monopolar type, all of the anode and the cathode elements are arranged electrically in

parallel, constituting an electrolyzer operating at high amperage and low voltage. In the bipolar type, the cathode of a cell is connected to the anode of an adjoining cell, so that the cells are in series and the resulting electrolyzer has low amperage and high voltage. The advantages and disadvantages associated with these electrolyzer configurations are addressed in Chapter 5.

Membrane-cell technologies were developed for licensing by Asahi Chemical Industry, Asahi Glass, Chlorine Engineers, ICI, Lurgi, DeNora, Uhde, ELTECH, PPG, and Tokuyama Soda. Presently, there are only five major suppliers of cell technology and they are: Asahi Kasei Corporation (Asahi Chemical Industry), Chlorine Engineers, ELTECH Systems Corporation, INEOS Chlor (formerly ICI), and Uhde. Chlorine Engineers Corporation still makes available the technology of Asahi Glass, and Uhde and DeNora have combined their technical efforts. The performance characteristics and the distinguishing features in these cell technologies of the bipolar and monopolar type are discussed in Chapter 5.

Another development worth noting was the diaphragm retrofit technology, where ion-exchange membranes replace the asbestos diaphragms in an existing cell. During the retrofitting operation, the membranes are shaped and heat sealed to cover the electrodes, thereby replacing asbestos. Chlorine Engineers applied this approach to the DS cells and Kanegafuchi Chemical to H-series cells [37]. The diaphragm retrofit technology was proven by several companies, including Mitsui Chemical, Tokuyama Soda, and Toyo Soda [38,39].

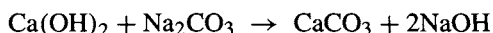
The first membranes, made from the perfluorosulfonate polymer Nafion[®] [40–42], were practical only at low caustic concentrations, as the caustic efficiency decreased significantly at high caustic strengths. To overcome this problem, asymmetric membranes having sulfonic acid groups on the anode side and converted groups on the cathode side were developed. Later, a perfluorocarboxylate membrane, Flemion [43], which exhibited better resistance to caustic back-migration was produced. The low electrical resistivity of persulfonate-based membranes and the low caustic back-migration characteristics of perfluorocarboxylate membranes were coupled by converting the sulfonic acid groups of Nafion[®] to carboxylate groups on the cathode side to realize the beneficial properties of both the membrane types. Today's membranes comprise a perfluorosulfonate polymer layer, a PTFE reinforcing fabric and a perfluorocarboxylate polymer, all bonded together. The performance of these composite membranes is discussed in Section 4.8.

2.4. CAUSTIC SODA

In the early 1900s, caustic soda was manufactured by the lime-soda process (Section 2.4.1), even when caustic was available from the chlor-alkali electrolysis process, as there was not much demand for chlorine. During World War I, chlorine demand dramatically increased to provide chlorine for the production of various chemicals. This led to an increased share of the market for caustic from the electrolytic process. World War II had a similar effect. Nowadays, nearly all caustic soda is a coproduct of electrolytic chlorine.

2.4.1. Lime Soda Process

This process involves reaction of lime with sodium carbonate as follows:



Calcium carbonate precipitates from the calcium hydroxide solution, as it has a lower solubility than that of calcium hydroxide. The optimum reaction temperature is 80 to 90°C. The calcium carbonate is settled, and the overflow is a weak caustic soda, which is concentrated by evaporation.

2.4.2. Electrolytic Process

Caustic soda is produced as a coproduct of chlorine in the sodium chloride brine electrolytic process employing diaphragm cells, mercury cells, and membrane cells.

The diaphragm cell produces caustic soda containing 11% caustic soda and 15% salt, with a low concentration of sodium chlorate. This solution, called cell liquor, is evaporated to produce 50% caustic soda. During evaporation, salt crystallizes as the caustic concentration increases. About 1% salt is present in the 50% caustic soda solution.

The mercury cell produces 50% caustic, and it can also produce up to 70% caustic soda. This is a highly pure caustic with a few ppm of salt and less than 5 ppm of sodium chlorate. However, it carries trace amounts of mercury, and hence, many customers do not accept the caustic soda from mercury cells.

The membrane cell produces about 35% caustic soda, which is concentrated by evaporation to 50%. Membrane cell caustic soda is the preferred product compared to the diaphragm and mercury-cell caustic soda.

2.5. FUTURE DEVELOPMENTS

Significant studies were made in the chlor-alkali technologies during the last century to economically and optimally produce chlorine and caustic soda in an environmentally safe manner, complying with all government regulations. The energy consumed has decreased from about 4,000 AC kWh/ton of caustic in the 1950s to about 2,500 AC kWh during 1998 with the advent of the dimensionally stable anodes and optimal cell design/operation. Additional improvements such as the incorporation of fuel cell concepts and electrocatalyst development, will further reduce the energy consumption and hence, the cost for producing chlorine and caustic.

REFERENCES

1. *The Early History of Chlorine, Alembic Club Reprints #13*. Edinburgh (1905).
2. W. Weldon, *Chem. News* **20**, 109 (1869).
3. L. Mond, *J. Soc. Chem. Ind.* **15**, 713 (1896).
4. M. Gossage, *Chem. News* **4**, 172 (1861).
5. I. Hurter, *J. Soc. Chem. Ind.* **2**, 103 (1883).

6. R.T. Baldwin, *J. Chem. Ed.* **4**, 454 (1927).
7. H.W. Schultze, In T.C. Jeffery, P.A. Danna, and H.S. Holden (eds.), *Chlorine Bicentennial Symposium*, The Electrochemical Society, Princeton, NJ (1974), p. 1.
8. G. Ornstein, *Trans. Am. Electrochem. Soc.* **29**, 529 (1916).
9. J.L.K. Snyder and H.P. Wells, *Trans. Am. Inst. Chem. Eng.* **14**, 145 (1921–1922).
10. L.D. Vorce, *Trans. Electrochem. Soc.* **86**, 69 (1944).
11. R.T. Baldwin, *J. Chem. Ed.* **4**, 313 (1927).
12. V. Engelhardt, *Handbuch der Technischen Elektrochemie*, vol. 2, Leipzig Akademische Verlagsgesellschaft (1933).
13. A.J. Hale, *The Applications of Electrolysis in Chemical Industry*, Longmans, Green & Co, New York (1918), p. 90.
14. C.R. Barton, *Trans. Am. Inst. Chem. Eng.* **13**, 1 (1920).
15. E.A. LeSueur, *Trans. Electrochem. Soc.* **63**, 187 (1933).
16. L.E. Vaaler, *Trans. Electrochem. Soc.* **107**, 691 (1960).
17. E.A. LeSueur, *U.S. Patent* 723, 398 (1903).
18. M.S. Kircher, Electrolysis of Brines in Diaphragm Cells. In J.S. Sconce (ed.), *Chlorine: Its Manufacture, Properties and Use*, Reinhold Publishing Corp., New York (1962), p. 81.
19. R.E. Thomas, *Salt & Water, Power & People*, Hooker Electrochemical Co., Niagara Falls, New York (1955).
20. H.B. Beer, British Patents, 1,147,442 (1965); 1,195,871 (1967).
21. V. deNora and J.-W. Kuhn von Burgsdorff, *Chem. Ing. Tech.* **47**, 125 (1975).
22. R.W. Fenn III, E.J. Pless, R.L. Harris, and K.J. O'Leary, *U.S. Patent* 4,410,411 (1983).
23. E.I. Fogelman, *U.S. Patent* 3,674,676 (1972).
24. J.E. Currey, *Diaphragm Cells for Chlorine Production*, Proceedings of a symposium held at the City University, London, June 1976, The Society of Chemical Industry, London (1977), p. 79.
25. E.H. Cook and M.P. Grotheer, Energy Savings Developments for Diaphragm Cells and Caustic Evaporators, *23rd Chlorine Institute Plant Managers Seminar*, New Orleans, LA (1980).
26. R.N. Beaver and C.W. Becker, *U.S. Patents*, 4,093,533 (1978), 4,142,951 (1979).
27. T. Florkiewicz and L.C. Curlin, Polyramix™ Diaphragm: A Commercial Reality. In T.C. Wellington (ed.), *Modern Chlor-Alkali Technology*, vol. 5, Elsevier Applied Science, London (1992), p. 209.
28. P.C. Foller, D.W. DuBois, and J. Hutchins, PPG's Tephram Diaphragm: The Adaptable Non-Asbestos Diaphragm. In S. Sealy (ed.), *Modern Chlor-Alkali Technology*, vol. 7, Royal Society of Chemistry, Cambridge, UK (1998), p. 163.
29. T. Griswold, Jr., *U.S. Patents*, 987,717 (1911); 1,070,454 (1913).
30. L.E. Ward, *U.S. Patent* 1,365,875 (1921).
31. J.L. Lucas and B.J. Armstrong, *U.S. Patent* 2,858,263 (1958).
32. T.C. Jeffery and R.J. Scott, *Diaphragm Cells for Chlorine Production*, Proceedings of a symposium held at the City University, London, June 1976, The Society of Chemical Industry, London (1977), p. 67.
33. D.W.F. Hardie, *Electrolytic Manufacture of Chemicals from Salt*, The Chlorine Institute, Inc., New York (1959).
34. M. Blackburn. Personal Communication (2003).
35. J.C. Iverstine, J.L. Kinard, and R.M. Cudd, *Technological Response to Environmental Protection Regulations and Energy Price/Supply Structure: A Case Study of Chlorine/Caustic Soda Manufacturing*, Report PB83-114751 to National Science Foundation (1981).
36. K.J. O'Leary, *Diaphragm Cells for Chlorine Production*, Proceedings of a symposium held at the City University, London, June 1976, The Society of Chemical Industry, London (1977), p. 103.
37. T. Iijima, T. Yamamoto, K. Kishimoto, T. Komabashiri, and T. Kano, *U.S. Patent* 4,268,265 (1981).
38. M. Esayan and J.H. Austin, *Membrane Technology for existing Chlor-Alkali plants, 27th Chlorine Plant Operations Seminar*, Washington (1984).
39. I. Kumagai, T. Ichisaka, and K. Yamaguchi, *Diaphragm Cell Retrofitting, 27th Chlorine Plant Operations Seminar*, Washington (1984).
40. *DM-14 Membrane Electrolyzer*, Brochure of Diamond Shamrock Corp.
41. *Nafion Perfluorinated Membranes for KOH production*, Nafion® Product Bulletin, E.I. duPont de Nemours & Co., Inc., Wilmington (1988).
42. *Nafion Perfluorinated Membranes, Introduction*, E.I. duPont de Nemours & Co., Inc., Wilmington (1987).
43. *Asahi Chemical Membrane Chlor-Alkali Process*, Asahi Chemical Industry Co., Ltd., Tokyo (1987).

3

Overview of the Chlor-Alkali Industry

3.1. INTRODUCTION

The world production capacity of chlorine reached 53 million tons in 2002 from approximately 22 million tons in 1970 [1–7] and is expected to increase to 65 million tons by the year 2015 [8]. In this chapter, the major manufacturing processes and the factors affecting the growth pattern of the chlor-alkali industry are presented.

Chlorine is sold as a gas or a liquid, and caustic soda is sold as 50% or 73% solution, or as anhydrous beads or flakes. There is also a significant market for caustic soda in the concentration range of 10–25%. The caustic soda product is designated by the manufacturing technology used, namely mercury, diaphragm, or membrane cells. More than 95% of the chlorine and 99.5% of the caustic in the world are produced by these cell technologies. About 0.5% of caustic soda is made chemically from soda ash, and KOH accounts for 2.5% of the caustic produced in the world.

An overview of the three chlor-alkali technologies is presented in this chapter, and the process details are addressed in Volumes II and III. The terminology and the overall processes discussed in this chapter should enable the reader to relate the process steps to the electrochemical and chemical engineering principles discussed in Chapters 4 and 10.

3.2. OVERALL PROCESS

3.2.1. *Electrolyzers*

As stated in Chapter 2, chlorine and caustic soda are produced by the electrolysis of sodium chloride solutions. The electrical energy required to operate the electrolytic cells constitutes a major portion of the operating cost in producing chlorine. The current efficiency of the electrolyzers can be as high as 98% or as low as 85%, depending on the technology used, the operation of the electrolyzers, and the purity of the brine used in the process. Schematics of the cell technologies are shown in Fig. 3.1.

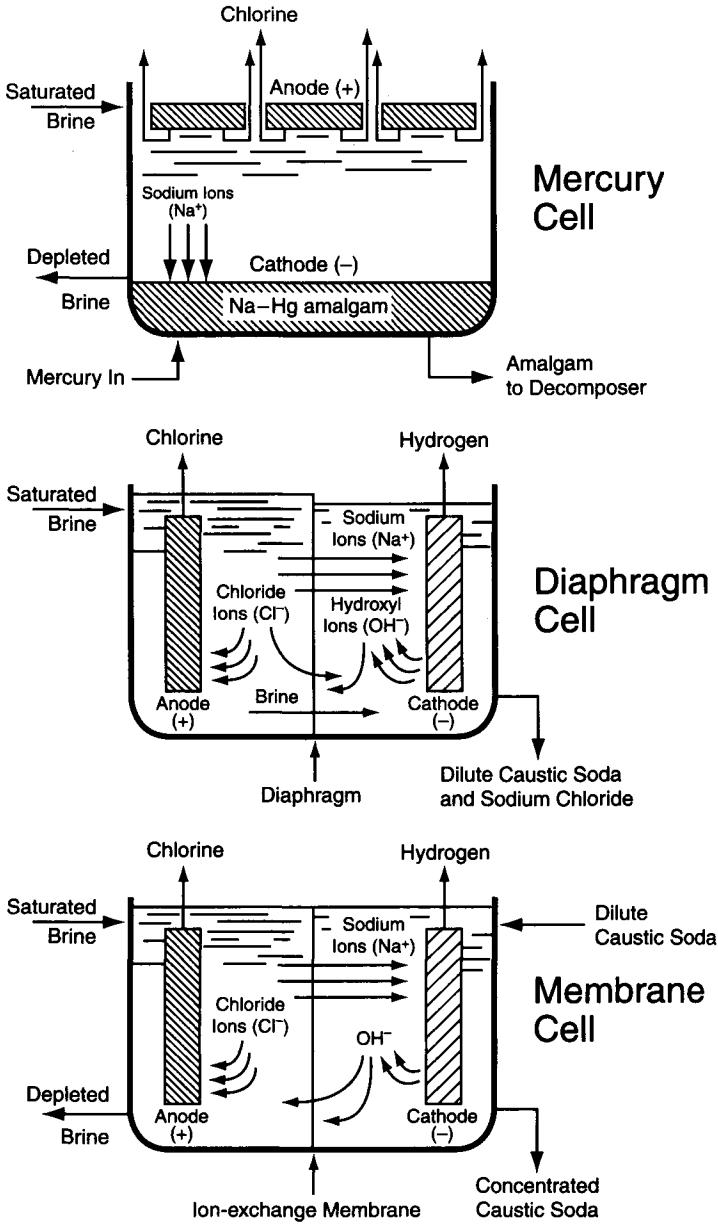


FIGURE 3.1. Schematics of mercury, diaphragm, and membrane chlor-alkali cells.

3.2.1.1. Mercury Cells. The mercury cell has a steel bottom with rubber-coated steel sides, as well as the boxes for brine and mercury feed and exit streams, with a flexible rubber or rubber-lined steel cover. Horizontal, adjustable metal anodes hang from the top, and mercury flows on the inclined bottom. The current flows from the steel bottom to the flowing mercury.

Saturated brine fed from the end box is electrolyzed at the anode to produce chlorine, and the depleted brine flows from the top portion of the trough. The cation, be it sodium or potassium, reacts with the mercury to form an amalgam, which flows out of the end box to a vertical cylindrical tank. Approximately 0.10–0.30% sodium or potassium amalgam is produced in the cell. The amalgam reacts with water in the decomposer, packed with graphite particles, and produces caustic soda or potash and hydrogen. Hydrogen saturated with water vapor exits from the top, along with the mercury vapors. The concentration out of the decomposer is either 48–50 wt% caustic soda or 45–50 wt% caustic potash. The depleted brine flows out of the exit end box. Some cells are designed with chlorine and anolyte outlets from the end box, which are separated in the depleted brine tank. The mercury from the decomposer is pumped back to the cell.

3.2.1.2. Diaphragm Cells. The diaphragm cell is a rectangular box with metal anodes supported from the bottom with copper base plates. The cathodes are vertical screens or punched plates connected from one end to the other end of the rectangular tank. The cathodes are vacuum-deposited with asbestos dispersed as a slurry in a bath. Saturated brine enters the anode compartment, and the chlorine gas is liberated at the anode during electrolysis. The chlorine gas is saturated with water vapor at the vapor pressure of the anolyte. The sodium ion from the anode compartment is transported to the cathode compartment, where it combines with the hydroxyl ion generated at the cathode during the formation of hydrogen from the water molecules to form caustic soda. The diaphragm resists the back migration of the hydroxyl ions, which would otherwise react with the chlorine in the anode compartment. The concentrations are about 12% NaOH and 14% NaCl in the cathode compartment. There is also some sodium chlorate formed in the anolyte compartment, dependent upon the pH of the anolyte. There are non-asbestos separators that have been commercially proven, and a number of asbestos-based cell circuits have been converted to these non-asbestos diaphragms.

3.2.1.3. Membrane Cells. In a membrane cell, an ion-exchange membrane separates the anode and cathode compartments. The separator is generally a bilayer membrane made of perfluorocarboxylic and perfluorosulfonic acid-based films, sandwiched between the anode and the cathode. The saturated brine is fed to the anolyte compartment where chlorine is liberated at the anode, and the sodium ion migrates to the cathode compartment. In contrast to the diaphragm cells, only sodium ions and water molecules are transported across the membrane. The unreacted NaCl and other inert species remain in the anolyte compartment. About 30–32% caustic soda is fed to the catholyte compartment, where sodium ions combine with hydroxyl ions produced during the course of the H₂ evolution from the water molecules. This forms caustic, which increases the concentration to 32–35%. The hydrogen gas, saturated with water, exits from the catholyte. Part of the caustic soda product is withdrawn from the catholyte compartment and the remaining caustic is diluted and returned.

Thus, all three basic cell technologies for producing chlorine generate chlorine at the anode, and hydrogen along with NaOH or KOH at the cathode. The distinguishing difference lies in the manner in which the anolyte and the catholyte are prevented from

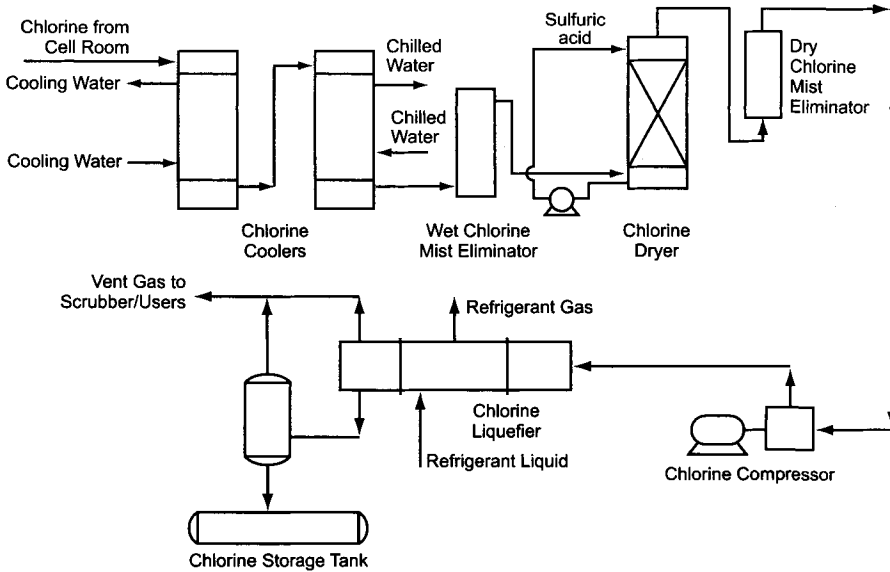


FIGURE 3.2. Process scheme for producing chlorine from cell gas.

mixing with each other. Separation is achieved in a diaphragm cell by a porous separator and in a membrane cell by an ion-exchange membrane. In mercury cells, the cathode itself acts as a separator by forming sodium amalgam, which is subsequently reacted with water to form sodium hydroxide.

3.2.2. Chlorine Processing

The chlorine gas contains moisture, byproduct oxygen, and some hydrogen. In addition, it also contains carbon dioxide and some oxygen and nitrogen from the air leakage via the process or pipelines. A simple schematic of the process to produce either dry chlorine or liquid chlorine from the cell gas is shown in Fig. 3.2.

Chlorine is first cooled and passed through demisters to remove the water droplets and the particulates of salt. The cooled gas goes to sulfuric acid circulating towers, which are operated in series. Commonly, three towers are used for the removal of moisture. This stream often goes through dry demisters and then to compressors. The compressed gas is then liquefied at a low temperature. The noncondensed gas, called snift gas, is used for producing hypochlorite or hydrochloric acid. If there is no market for hydrochloric acid, the snift gas is neutralized with caustic soda or lime to form hypochlorite. The hypochlorite is either sold as bleach or decomposed to form salt and oxygen.

3.2.3. Hydrogen Processing

The processing steps involved in treating the hydrogen from the electrolytic cells are shown in Fig. 3.3.

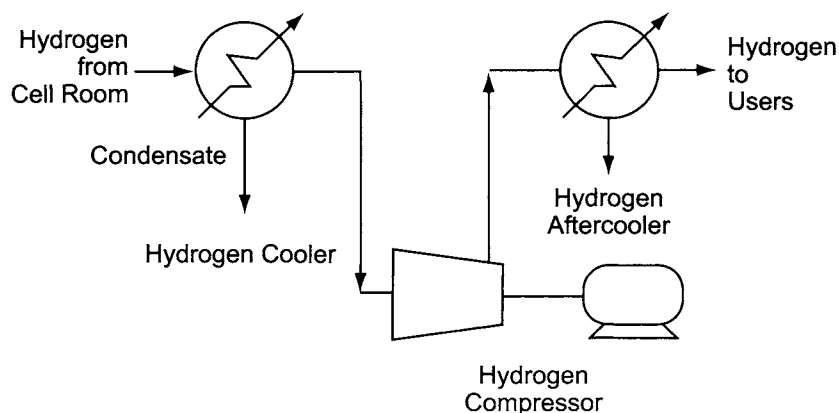


FIGURE 3.3. Process scheme for treating hydrogen from the electrolytic cells.

The hydrogen gas from the chlor-alkali cells is normally used for the production of hydrochloric acid, or used as a fuel to produce steam. Hydrogen from the mercury cell is first cooled, and the condensed mercury is then returned to the cells. Usually, a secondary treatment is used to remove the trace levels of mercury in the hydrogen. The gas is then compressed. If there is a customer available in need of pure hydrogen containing low amounts of oxygen, some plants heat the hydrogen over a platinum catalyst to remove oxygen, cool and compress the diaphragm and membrane cell hydrogen, and then supply it to the customer. The heat value in the hydrogen cell gas can be recovered by cross-exchanging the hydrogen vapor with the brine that is fed to the cells.

3.2.4. Caustic Soda Process

Caustic soda is marketed as 50% and 73% solution and as anhydrous beads and flakes. Mercury cells can produce 50% and 70% caustic directly. This is a high-purity caustic compared with the membrane- or diaphragm-cell caustic. The caustic from the decomposer is cooled and passed once or twice through an activated carbon filter. After filtration, the mercury concentration is lowered to ppm levels. This is still unacceptable to some customers, who have switched to using membrane grade caustic soda. The mercury cell caustic soda has a few ppm salt and <5 ppm sodium chlorate. If trace concentrations of mercury are tolerable in the end use of caustic, then the mercury cell caustic will be the highest purity caustic that can be made electrolytically.

The membrane-cell caustic is concentrated in an evaporator, following the scheme in Fig. 3.4. The multiple-effect evaporator yields a high steam economy. The 50% caustic from the membrane cell generally has 30 ppm salt and 5–10 ppm sodium chlorate.

The catholyte from the diaphragm cells contains 12% caustic, 0.25–0.3% sodium sulfate, and 0.15–0.2% sodium chlorate. The catholyte is evaporated, as shown in Fig. 3.5. When the caustic concentration reaches 50%, most of the salt separates and about 1% salt remains in the solution. The 50% caustic also has a high chlorate concentration

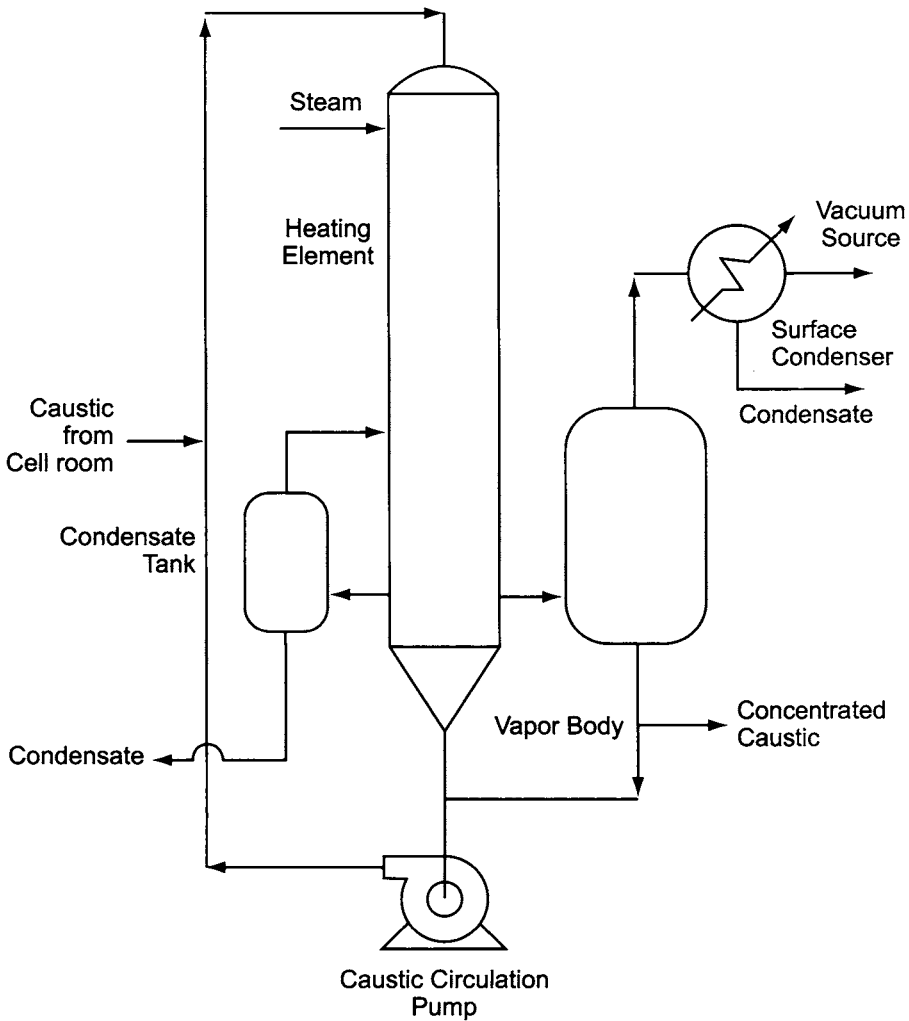


FIGURE 3.4. Process scheme for concentrating membrane-cell caustic.

compared with the product of membrane and mercury cells. The salt separated from the caustic during evaporation is used to resaturate the brine fed to the cells.

The 73% caustic is made by feeding steam instead of water to the decomposer, and also by evaporation of 50% caustic. Anhydrous caustic is produced in a rising film evaporator, operating at 385°C under vacuum.

Caustic from the mercury-cell process is called Rayon-grade caustic. Rayon-grade caustic and membrane-grade caustic are referred to as “low salt” caustic soda, which is a premium product.

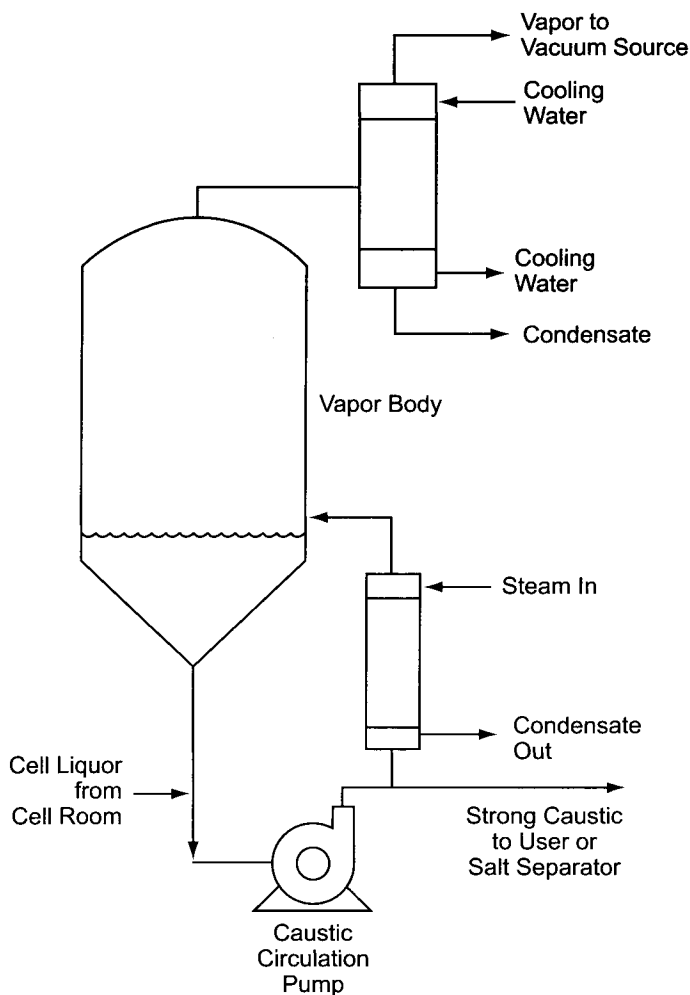


FIGURE 3.5. Process scheme for concentrating diaphragm-cell caustic.

3.2.5. Brine Process

Sodium chloride is available in the form of solid salt, mined by excavation or produced by evaporating seawater. It is also available as an aqueous solution from solution mining. The salt has varying concentrations of impurities, which should be removed to operate the electrolytic cells at a high current efficiency. The major impurities are calcium, magnesium, and sulfates. Minor impurities, which are undesirable depending upon the type of chlor-alkali process selected, are barium, strontium, manganese, aluminum, silica, iron, vanadium, chromium, molybdenum, titanium, etc. The brine processing steps are shown in Figs. 3.6–3.8.

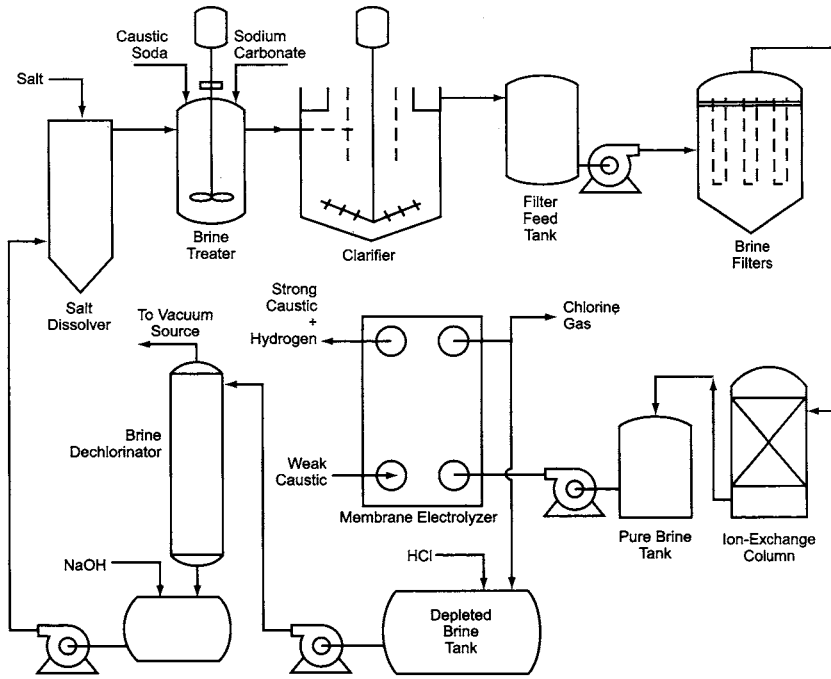


FIGURE 3.6. Brine processing scheme for membrane-cell operations.

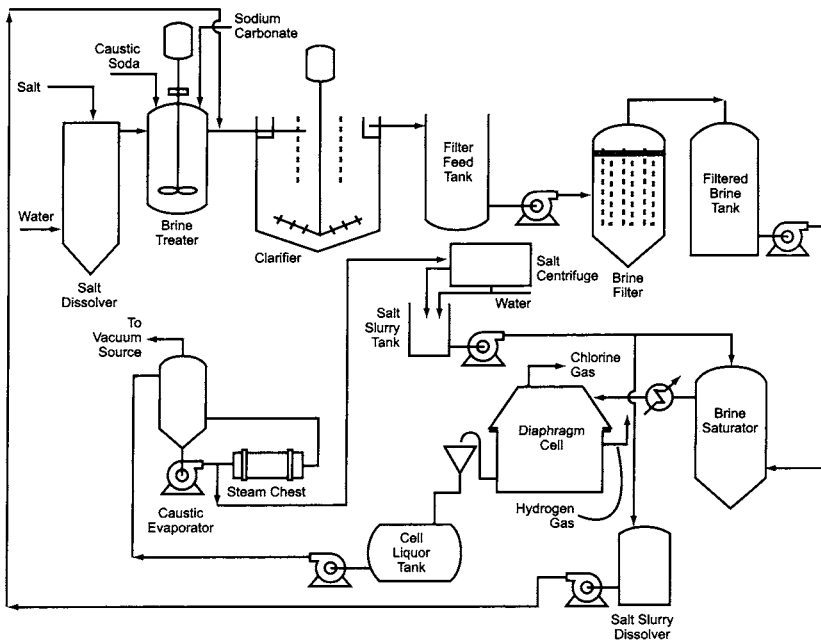


FIGURE 3.7. Brine processing scheme for diaphragm-cell operations.

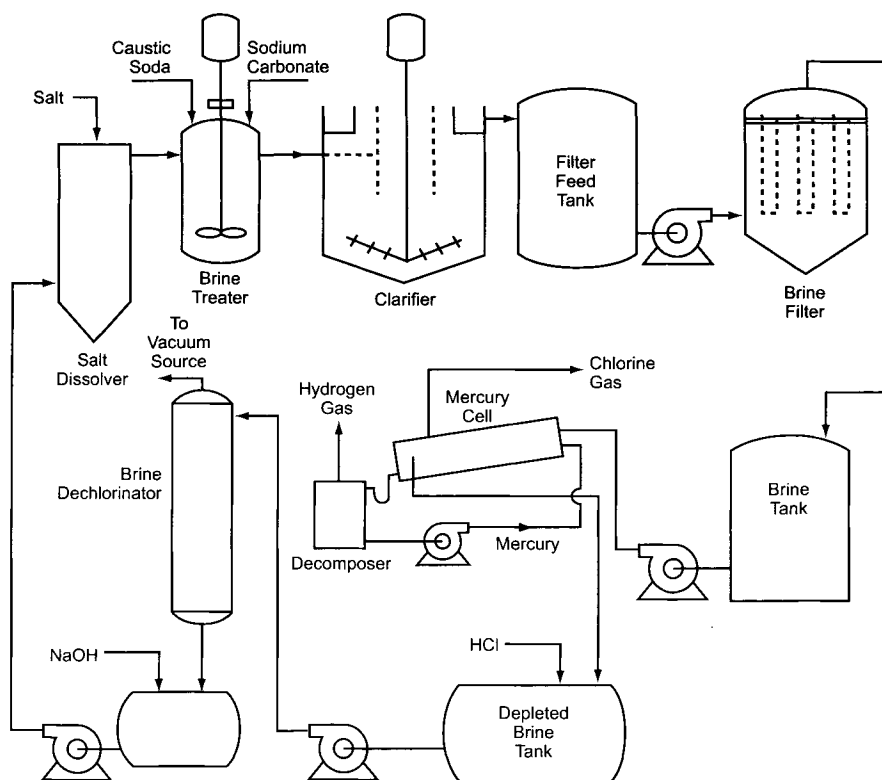
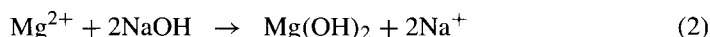
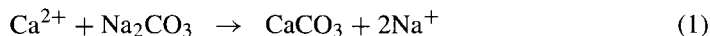


FIGURE 3.8. Brine processing scheme for mercury-cell operations.

Brine is treated in a reactor with sodium carbonate and caustic soda to precipitate calcium carbonate and magnesium hydroxide, as shown in Eqs. (1) and (2).



These precipitates are settled and removed as a slurry, which is pumped to a filter to remove it as sludge. Sometimes, it is disposed of, along with the rest of the liquid effluent, from the plant. The calcium carbonate precipitate is heavy and carries the hydroxides of aluminum, magnesium, strontium, etc., with it. The overflow from the settler, which carries 10–50 ppm of suspended solids, is filtered. For the mercury and the diaphragm cell process, this brine is adequate and can be fed to the electrolyzers. In the case of the diaphragm cell process, the filtered brine is heated and passed through a bed of salt in a saturator in order to increase the salt concentration before feeding it to the electrolyzers. In some plants, the feed brine is acidified to improve the cell current efficiency. The acidification reduces the alkalinity, which would otherwise react with the chlorine in the anolyte compartment, forming hypochlorite and

chlorate. In the case of the mercury cell process, the brine is acidified and fed directly to the cells.

In the membrane cell process, the brine specifications are more stringent than in the mercury and diaphragm processes, and this calls for impurities to be at the ppb level. Filtering the brine in a precoat-type secondary filter, and then using an ion-exchange resin to remove the calcium, magnesium, barium, and iron impurities, accomplishes this. It is also possible to remove aluminum by ion exchange. Aluminum and silica can also be removed by adding magnesium chloride in the brine exiting from the salt dissolver.

The depleted brine from the membrane and mercury cell processes carries dissolved chlorine. This brine is acidified to reduce the chlorine solubility, and then dechlorinated in a vacuum brine dechlorinator. The dechlorinated brine is returned to the brine wells for solution mining, or to the salt dissolver. If the membrane and diaphragm processes coexist at a given location, the dechlorinated brine is sent for re-saturation before being fed to the diaphragm cells.

3.3. GROWTH OF THE CHLOR-ALKALI INDUSTRY

The chlor-alkali industry is a commodity chemical business involving Cl_2 and NaOH consumption in a wide variety of products that are used in daily life. The growth of the chlor-alkali industry has been primarily dictated by market demand, environmental concerns and constraints, and energy prices, and will continue to be governed by these factors in the future. These issues are intertwined making it difficult to understand the growth of the industry in the past, as well as to forecast the future in a simple manner. An overall perspective of the industry is presented in this section, by outlining the global growth, end uses and environmental considerations that have influenced the growth of the industry [2-7,9,10].

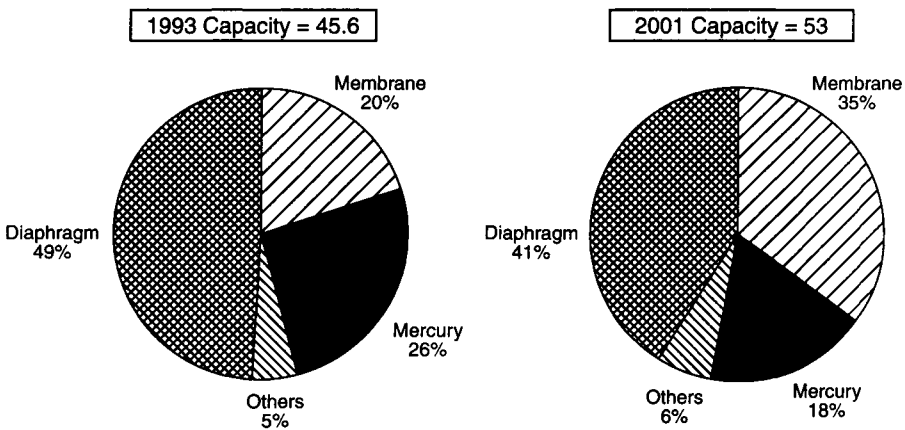


FIGURE 3.9. World capacity for chlorine (in MM tons/year) listed by cell technologies (plotted from the data in [1,2,4,6]).

3.3.1. World

As noted earlier, chlorine and caustic are produced electrolytically using mercury, diaphragm, and membrane technologies. While diaphragm-cell technology continues to be important in the industry, mercury-cell technology is slowly declining and is being replaced by membrane-cell technology. This is due to lower operating costs and the absence of any environmental issues, like those associated with mercury and asbestos. Figure 3.9 depicts the distribution of the individual cell technologies [1,2]. The market share of the cell technologies in individual regions in the world is shown in Fig. 3.10 [5]. It is interesting to note that in the year 2001, 11% of the capacity in North America and approximately 18% in the world, was based on mercury cells. These plants will continue to operate as long as the economics are favorable and the operations are not constrained by local government regulations. Operation of the diaphragm cells in the United States and in the world will be dictated by economics and profit margins.

The world capacity for chlorine from the year 1970, depicted in Fig. 3.11, grew from 22 MM tons per year to 53 MM tons per year in 2002 [6,7,9,10]. Of the world chlorine capacity, 26% was installed in the United States, while 22% was installed in Western Europe, 10% in Japan, 13% in China, and 6% in Eastern Europe.

The great disadvantage of electrolysis to the global economy is the fixed ratio of production of the major products. Thus, 1.13 tons of NaOH or 1.58 tons of KOH accompany production of 1 ton of chlorine. The former combination, for convenience, is often referred to as an “electrochemical unit” or ecu.

Since markets do not consider the laws of stoichiometry, the electrolytic chlor-alkali industry is in a state of perpetual imbalance. Nearly always, either chlorine or caustic soda is in long supply, while there is a shortage of the other. This situation is reflected in spot market prices, which can fluctuate wildly over short periods, usually in opposite directions for the two products. The combined price of an ecu is less volatile, and “ecu customers” who take nearly equivalent amounts of chlorine and caustic soda are a stabilizing influence in the industry. KOH, as a relatively minor product, is somewhat immune to these problems. Total KOH production is free to respond to market pressures; the amount of chlorine produced along with KOH is a small part of the total and not a large factor in the market. The KOH producer who is also a chlorine merchant, however, is still subject to the fluctuating market prices of chlorine.

In the early days of the electrolytic process, the demand for NaOH was much greater than that for chlorine. Chemical production of NaOH was necessary to fill the market. With the great surge in petrochemical and synthetic organic chemical production that followed World War II, the demand for chlorine grew very rapidly and began to outstrip the demand for caustic soda. In the years from 1945 to 1970, for example, chlorine production increased more than 10-fold. Even with the virtual abandonment of chemical caustic, shortages in chlorine supply became frequent. Replacement of soda ash in some of its traditional applications with caustic soda increased the consumption of caustic and allowed more production of chlorine. Still, shortages persisted and the trend seemed to indicate development of a chronic shortage in chlorine. This increased interest in the manufacture of chlorine without caustic as a coproduct. Section 15.2 covers some of the available processes.

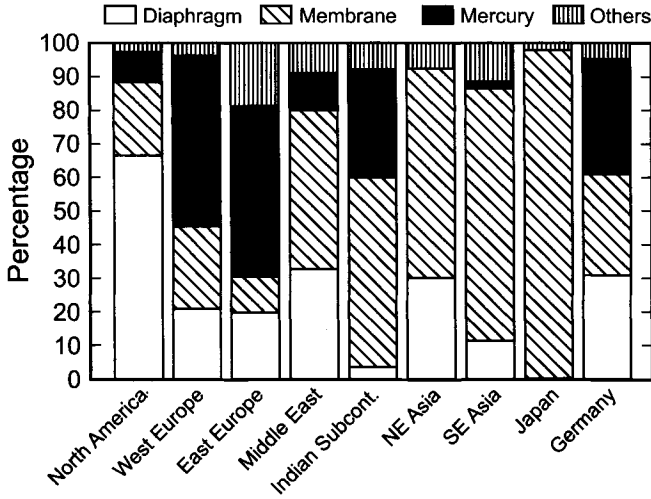


FIGURE 3.10. Cell technology distribution in the various regions in the world in 2001.

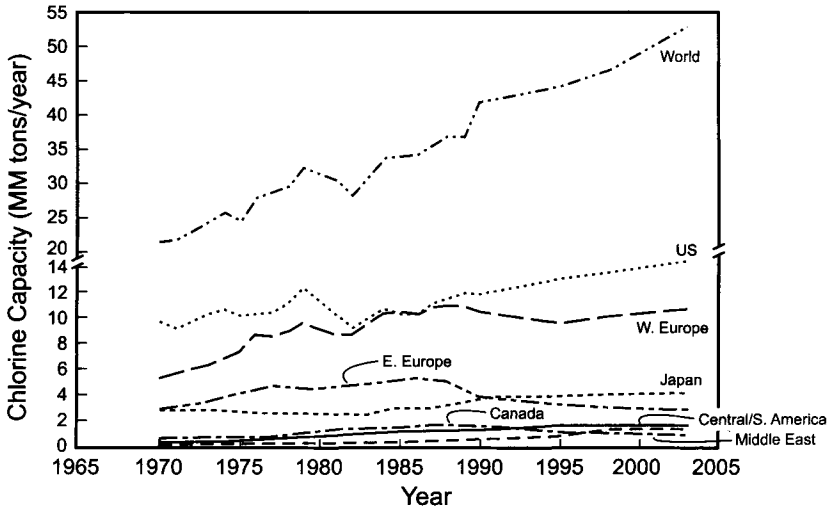


FIGURE 3.11. Growth of chlorine in the world and in various regions of the world (plotted from the data in [2,7,9]).

More recently, environmental problems have caused certain applications of chlorine to be phased out. Imagined problems have foreclosed its use in other applications. The use of chlorine in the pulp and paper industry and in the production of solvents, which constitute 12% of the total chlorine demand, has declined because of: (1) the “cluster” rules in the pulp and paper industry mandating chlorine-free bleaching, and (2) the Montreal Protocol, calling for elimination or the reduced production of chlorinated solvents.

TABLE 3.1. World Chlorine Demand

	(-000- Metric tons)				AAGR% 2000-2010
	1995	2000	2005	2010	
Chlorinated intermediates	3,131	3,155	3,215	3,353	0.6
Vinyls	12,074	14,832	15,824	18,446	2.4
Organics	6,678	8,492	9,609	10,945	2.9
Pulp & paper	3,024	2,352	1,753	1,696	-2.8
Water treatment	1,962	2,455	2,836	3,283	3.4
Inorganics	813	1,027	1,045	1,055	0.3
Others	11,133	12,600	14,566	16,134	2.8
Total demand	38,815	44,913	48,848	54,912	2.2

Note: AAGR: Average aggregate growth rate.

Organics include propylene oxide, epichlorohydrin, and the phosgene based chemicals, TDI, MDI, and polycarbonates.

Inorganics include titanium dioxide, bromine.

Others include water treatment chemicals, agricultural chemicals, HCl, bleach, and other miscellaneous chlorine end-uses.

(With permission from Chemical Marketing Associates, Inc.)

The reverse trend in product utilization seemed to have arrived, and several plants for the chemical production of caustic soda were built in conjunction with the Wyoming trona deposits. With that, the market for certain chlorine derivatives, most notably polyvinyl chloride (PVC), began to increase more rapidly. With the increased availability of electrolytic caustic soda, some of the new caustic capacity was temporarily shut down.

Recent years have seen a precarious and shifting balance between the chlorine and caustic soda markets. While caustic soda has retained its extraordinarily wide range of applications, the uses of chlorine have become more and more concentrated in certain products. PVC now consumes approximately 40% of the total production of chlorine and has continued to grow in importance. We should note that there is a proliferation of HCl usage in the production of EDC and VCM by oxychlorination. This has impacted the industry both by reducing the chlorine demand and by providing an outlet for HCl byproduct.

In recent years, the demand for chlorine has been relatively good, and the total demand over the period 1993-2003 has tracked the world gross domestic product (GDP) index (Fig. 3.12). An annual growth of 3% for Cl₂ resulted from increases [4] in most of its uses (Fig. 3.13). The growth of the chlor-alkali industry in the United States and the world is shown in Fig. 3.14. The overall supply/demand scenario is depicted in Fig. 3.15. Table 3.1 shows the growth rate of chlorine market segments during the period 2000-2010 [11]. The chlorine demand is projected to increase to 55 million tons per year by 2010 [6], with most of the increase occurring in Asia.

The world demand for caustic soda is shown in Fig. 3.16, along with its growth in various countries. Table 3.2 depicts the caustic demand during the period 1995-2010 [6]. Its use in the manufacture of various segments is illustrated in Fig. 3.17. The global caustic demand is projected to increase by 2.3% per year through the year 2010, primarily because of its demand in the production of alumina, soaps, detergents and

textiles, organic chemicals, and water treatment. Figure 3.18 depicts the capacity-demand profile for caustic through 2003.

The major chlorine-producing regions in the world are North America, Western Europe, and China, constituting 61% of the total capacity in 2001 [2]. About 6% of the total production is from Eastern Europe, 10% from Japan, and 14% from Asia, excluding

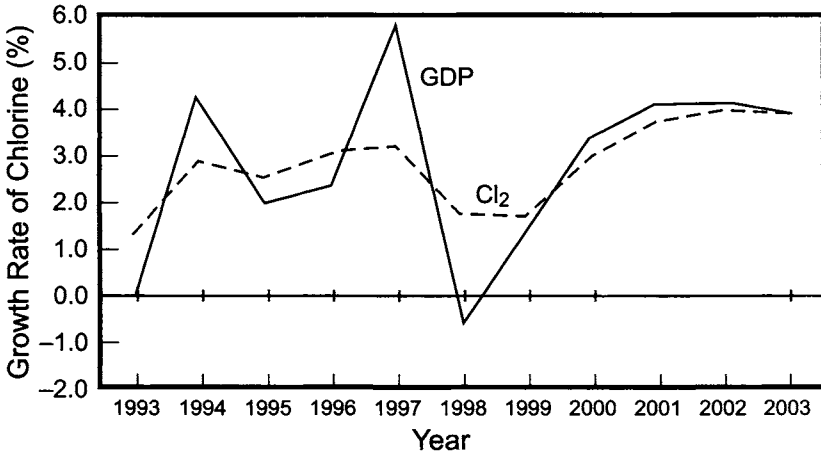


FIGURE 3.12. Variation of the growth profile of the chlorine industry with the gross domestic product [1].

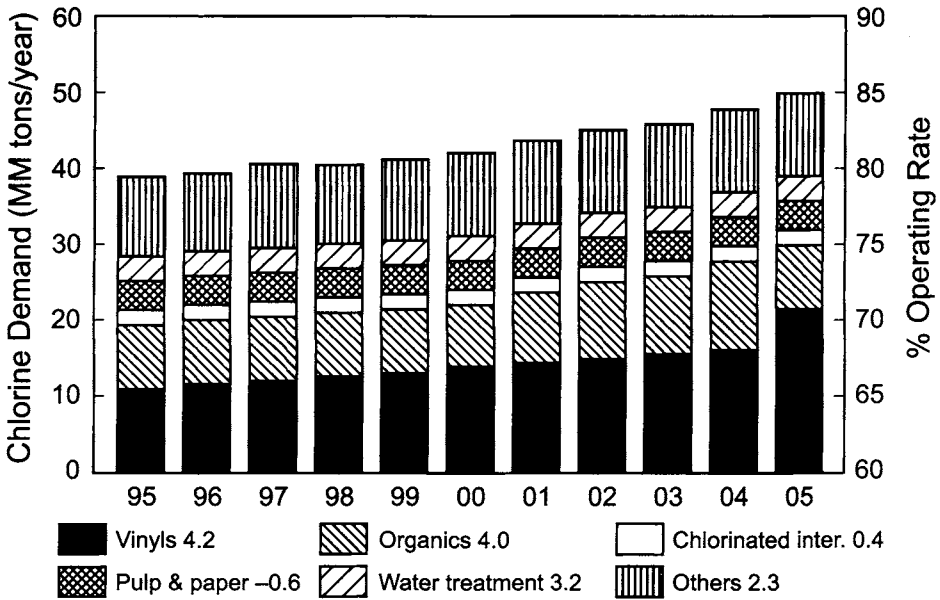


FIGURE 3.13. World chlorine demand [4]. The number next to the group of chemicals noted below the figure refers to the average aggregate growth rate in %.

China. In 2002, more than 500 companies produced chlorine and caustic at over 650 sites located throughout the world. Approximately half of the plants, generally small, are located in Asia. A total of eleven producers account for 40% of the total capacity, the six leading companies being Dow Chemical, Occidental Chemical, PPG Industries, Formosa Plastics, Solvay, and Bayer. The growth of the chlor-alkali industry, in major chlorine-producing regions in the world, is discussed in the following sections.

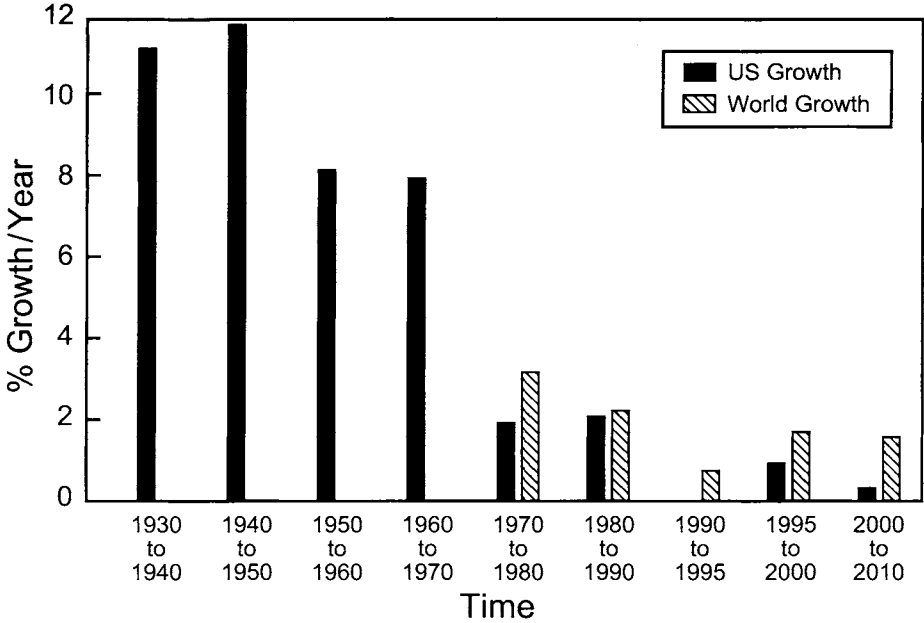


FIGURE 3.14. Historical growth profile of the chlorine industry (plotted from the data in [2,7,9]).

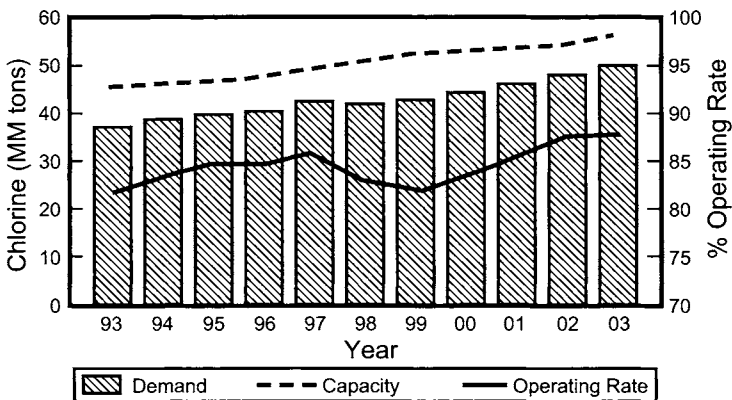


FIGURE 3.15. Demand, capacity, and operating rates for chlorine in the world [6].

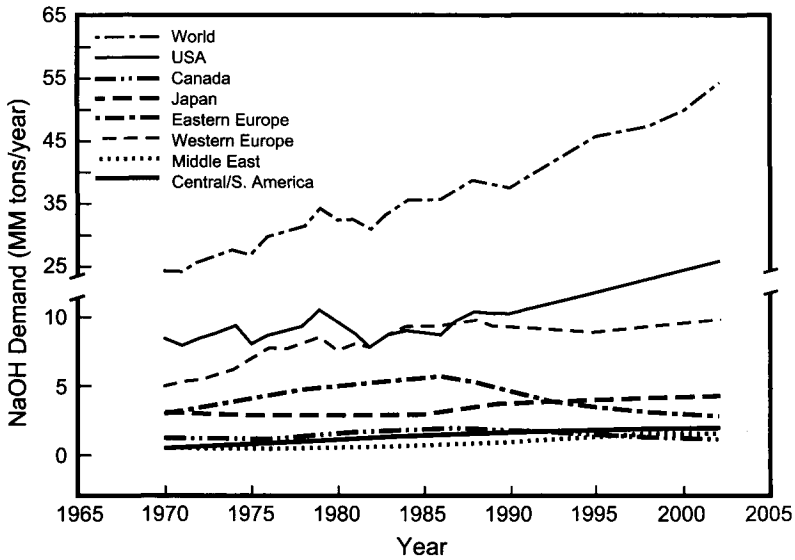


FIGURE 3.16. Growth of caustic soda in the world and in other regions of the world (plotted from the data in [2,7,9]).

TABLE 3.2. World Caustic Soda Demand

	(-000- Metric tons)				AAGR% 2000-2010
	1995	2000	2005	2010	
Pulp & paper	7,800	8,179	8,262	8,868	0.8
Alumina	3,337	4,045	4,536	5,274	3.0
Soaps/detergents/textiles	5,163	5,807	6,572	7,673	3.2
Organics	7,027	8,479	9,216	10,278	2.1
Inorganics	6,347	6,945	7,357	8,022	1.6
Water treatment	1,945	2,155	2,431	2,864	3.3
Others	8,836	11,686	12,862	14,972	2.8
Total demand	40,455	47,296	51,236	57,951	2.3

Note: Organics include TDI, MDI, polycarbonate and other organic chemicals such as synthetic glycerin, sodium formate.
 Inorganics include titanium dioxide and other inorganic chemicals such as sodium silicate and sodium cyanide.
 Others include agricultural chemicals, swing demand from other alkali sources, monosodium glutamate.
 (With permission from Chemical Marketing Associates, Inc.)

3.3.2. United States

3.3.2.1. Chlorine. Figure 3.19 shows the production and capacity profile for chlorine since the 1930s and Fig. 3.14 shows the growth rate pattern during these years. The chlor-alkali industry enjoyed strong growth during the 1950s and 1960s, the demand for

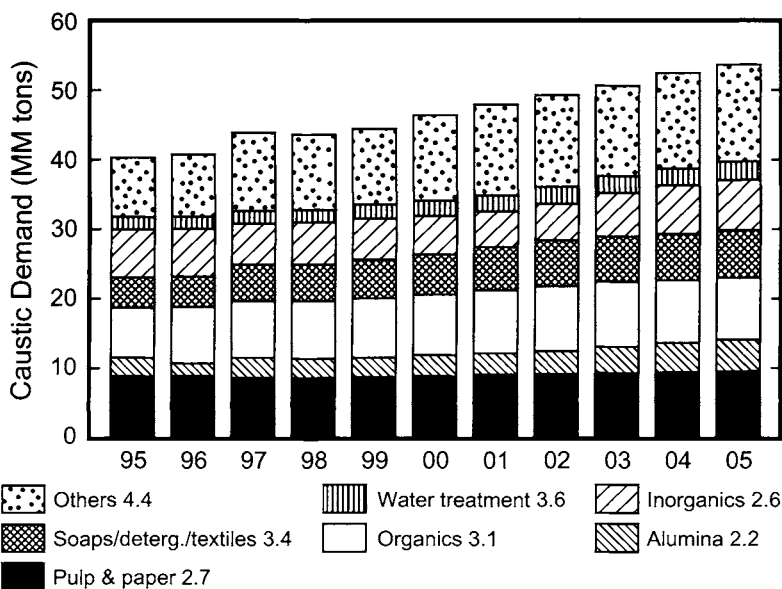


FIGURE 3.17. World caustic demand [4]. The number next to the group of chemicals noted below the figure refers to the average aggregate growth rate in %.

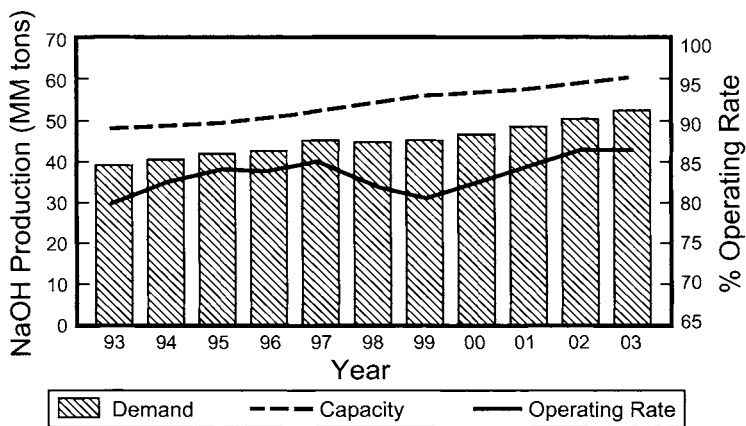


FIGURE 3.18. Demand, capacity, and operating rates for caustic soda in the world [6].

chlorine growing at a rate of 8% per year and the plants operating at greater than 90% capacity.

The growth during the 1950s and 1960s was led by chlorinated derivatives and intermediates such as chlorinated pesticides (e.g., DDT), used in agriculture, and chlorinated solvents, mainly chlorinated ethanes, which replaced flammable hydrocarbons in many cleaning and degreasing applications. Use of chlorinated methanes, as intermediates, increased in the manufacture of organo-silicones, tetramethyl lead gasoline additives,

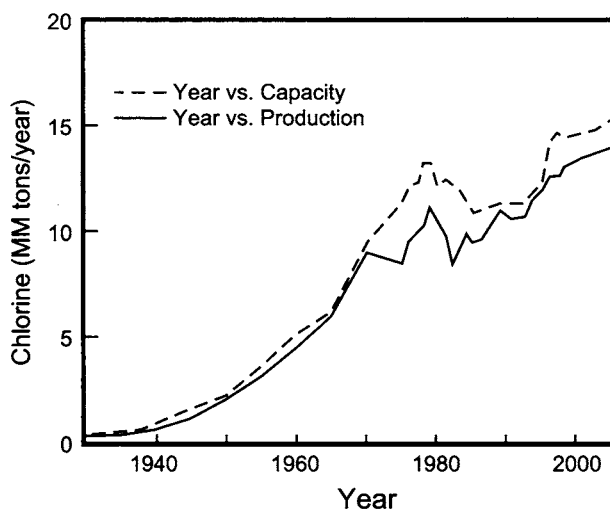


FIGURE 3.19. Historical chlorine capacity and production profile in the US (plotted from the data in [2,7,9]).

and fluorocarbons used in aerosol propellants and refrigerants. PVC plastics, ethylene oxide, and propylene oxide (PO), made by processes using chlorinated intermediates, grew 14% per year. In the 1970s, chlorine growth slowed down to 2% per year because of environmental concerns that brought about restrictions for the uses of solvents and pesticides such as DDT, kepone, dieldrin, and endrin. The carcinogenic characteristics of trichloroethylene, polychlorinated biphenyls (PCBs), and similar compounds also contributed to the decline in growth rate. In 1978, the use of fluorocarbon propellants for aerosols was banned by the Environmental Protection Agency (EPA) because of fears related to the depletion of the ozone in the upper atmosphere. The passage of clean water legislation also had an adverse impact on a variety of end uses. As a result, the paper industry implemented changes in bleaching technologies by increasing the use of ClO_2 , O_2 , and H_2O_2 as replacements for chlorine bleaching. During this period, many chemical processes using chlorine, particularly ethylene oxide and PO production, were converted to non-chlorine consuming processes [12,13].

Ethylene oxide was conventionally prepared by reacting Cl_2 , ethylene, and water to produce chlorohydrin, which is further treated with caustic to generate the oxide. This process was superseded by the direct oxidation of ethylene in the presence of silver catalysts with air or oxygen. The isobutane process displaced the route from propylene chlorohydrin to produce PO. Another significant loss was the conversion of DuPont's hexamethylene diamine process from butadiene to a non-chlorine-based technology. All these changes led to a loss of 140 000 tons of market demand for chlorine.

The chlor-alkali producers, in spite of these environmental concerns, continued to project a growth of 4–6% per year because of the anticipated chlorine demand from exports, particularly the Far East. An additional capacity 15 000 tons day^{-1} was added between 1975 and 1980 to meet this anticipated demand.

Around the 1980s, environmental constraints impacted the downstream use of chlorine. Operating costs increased because of the energy crisis, which, in turn, increased

the cost of electricity. In addition, exports declined because of new ethylene dichloride plants coming on-stream overseas. As a result, demand declined, and the industry operated at only 64% of its capacity. Overcapacity, slow growth, and high energy costs forced chlor-alkali producers to put a large number of production facilities, accounting for 1.2 MM tons, on standby. The restructuring that occurred in the industry resulted in an operating capacity of 12.8 MM tons/year at the end of 1986, operating at a 91% effective rate.

In the late 1980s, the chlorine industry recovered from the decline in the consumption pattern experienced earlier and enjoyed banner years in 1987 and 1988. Annual increases of 4–5% resulted from a strong economy, which were manifested by the increased demand for PVC and pulp and paper products, as well as increased exports of chlorine derivatives through the 1990s. However, during the very late 1990s and the early 2000s, the economy took a downturn because of the financial crisis in Asia. This was compounded by the after-effects of the 9/11 incident and increased energy and fuel prices. As a result, the chlorine demand fell by an estimated 1.6 MM tons between 2000 and 2003, and operating rates declined to approximately 86%. However, as the economy improves, increased chlorine consumption in seasonal demand segments such as water treatment, agricultural products, TiO₂, etc., is expected to result in increased operating rates of about 96% over the years 2003–2013 [11,14].

In 2002, approximately 67% of the chlorine in the United States was produced using the diaphragm-cell technology, 20% by the membrane-cell technology, and 10% by the mercury-cell technology. Five companies—Dow Chemical, Occidental Chemical Corporation, PPG Industries, Olin Corporation, and Formosa Plastics Corporation—manufacture 79% of the chlorine. Twenty-eight percent of the total US chlorine production was by Dow Chemical, whereas twenty-two percent of the production was by Occidental Chemical. PPG, Olin, and Formosa Plastics produce 12%, 9%, and 7% of the chlorine production in the United States, respectively.

The projections for increase in demand for chlorine during the years 1995–2010 [6,11], vary from zero to 1.3% through 2010. The optimistic projections predict an overall increase in the growth of chlorine-based products, although some market segments, such as solvents and phosgene, are expected to decline. The zero growth scenario assumes declining demand for vinyls and water treatment [6], and is presented in Table 3.3. A brief discussion of the state of the various market segments is presented here [8,11].

3.3.2.1A. Organic Chemicals.

PVC: While the PVC market is expected to decline through 2010, growth is also forecasted for the following: PO, used in making urethane foam; propylene glycol, used in producing unsaturated polyesters; pharmaceuticals and foods; isocyanates, used in the manufacture of products used in the construction and automobile industries; and epoxy resins, made by reacting bisphenol A with epichlorohydrin.

Chlorinated Ethanes: The use of 1,1,1-trichloroethane (1,1,1-TCA) or methyl chloroform, used in metal cleaning, increased from 1970. However, its production has been phased out since 1996 because of its contribution to ozone depletion. The use of 1,1,1-TCA in the production of HCFC-141b and -142b will also be phased out by the

year 2005, according to the Montreal Protocol. Perchloroethylene (PCE) and trichloroethylene (TCE) have been classified as hazardous air pollutants by the 1990 Clean Air Act Amendments.

Chlorofluorocarbons: Approximately 46 000 tons of chlorine were used in 1995 to produce CFC-11 through CFC-13. All the CFCs were phased out in 1996, although small amounts are still used as polymer precursors, and in specialized applications. The HCFC category of alternate CFCs deplete the ozone layer to a much smaller degree than CFCs, and are transitional substitutes for CFCs until they are phased out between 2015 and 2030. HFCs, containing no chlorine and made using TCE and PCE, are not subject to being phased out.

HCFC-22 and HCFC-142b are used in the production of tetrafluoroethylene and vinylidene fluoride, respectively. They are used for producing fluoroplastics and fluoroelastomers and the use of chlorine in this market segment will continue to increase.

Chlorinated Methanes: While methyl chloride, used mainly to make silicones, will grow marginally, the market for methylene chloride will decline because of environmental and occupational concerns calling for restricted emissions and limited use, and worker exposure.

Polycarbonates, Vinylidene Chloride (VDC), and Synthetic Glycerin: Annual growth of polycarbonates is projected to be 6.0% through the year 2006 [2], because of its use in glazing and sheet, and automotive and power tools. VDC is expected to grow 1.5% per year through 2006, because of its use in the production of household wraps (e.g., Saran Wrap), although there is some concern about the leaching of VCM into food following prolonged exposure. The growth of the synthetic glycerin market depends on the internal needs of Dow, the sole manufacturer of synthetic glycerin.

Chlorobenzenes: Monochlorobenzene is an intermediate in the production of nitrochlorobenzenes, which are precursors for rubber chemicals, antioxidants, dyes and pigments, and diphenyl ether, which is used in making heat transfer fluids. This market is projected to decline as the customers shift to alternative processes.

Pesticides: A wide variety of pesticides, which include herbicides, insecticides, and fumigants, are made from methyl chloride, 1,1,1-TCA, chlorobenzenes, and PCl_3 .

TABLE 3.3. United States Chlorine Demand

	(-000- Metric tons)				AAGR% 1995-2010
	1995	2000	2005	2010	
Chlorinated intermediates	1,187	1,278	1,187	1,160	-0.2
Vinyls	4,414	4,997	4,652	4,340	-0.1
Organics	2,420	3,295	3,162	3,445	2.8
Pulp & paper	750	313	82	82	-5.9
Water treatment	545	583	633	691	1.8
Inorganics	534	654	639	640	1.3
Others	2,275	1,969	1,637	1,776	-1.5
Total demand	12,125	13,089	11,992	12,134	0.0

Source: With permission from Chemical Marketing Associates, Inc.

The use of chlorinated pesticides is expected to decline because of environmental concerns. The toxic effects associated with pentachlorophenol will impact its production and, in turn, the chlorine consumption in this market. The use of chlorine in producing chlorinated isocyanurates, chlorinated paraffins, and ethyleneamines is projected to grow over the next several years. However, the market for cyanuric chloride is expected to decline as a result of the flat demand for its primary derivative, triazine herbicides.

3.3.2.1B. Inorganic Chemicals. The major use of chlorine in inorganic chemical production is in the manufacture of TiO_2 , HCl , hypochlorites, phosphorous chloride, ferric chloride, and aluminum chloride. All these markets are growth areas with no environmental or safety-related problems facing them. The only segment that will be adversely affected is the ethylene dibromide market, which is used as a lead scavenger in leaded gasoline and as a fumigant. The phasing out of lead in gasoline will reduce the need for ethylene dibromide in antiknock mixes over the next several years. The elimination of ethylene dibromide as a fumigant, as well as methyl bromide, is expected.

3.3.2.1C. Direct Application. The direct application market for chlorine has been in the pulp and paper industry and for water treatment, which has been under great scrutiny because of environmental concerns. Chlorine is used in the paper industry as a bleaching agent to produce clean, white, strong pulp, free of lignin, for making high-quality paper. This leads to the formation of various chlorinated species including dioxin, which is a carcinogen found in wastewater effluent. This has prompted legislation limiting the level of chlorinated organics in mill effluents. The pulp and paper industry has reduced contaminant levels by using other bleaching agents. These include chlorine dioxide, hydrogen peroxide, oxygen, ozone, and bio-bleaching enzymes, which, besides reducing pollution, increase the capacity of the mill to recover the extraction liquors. The elemental chlorine-free (ECF) process involves, at present, the use of chlorine dioxide, produced by the reduction of sodium chlorate. In contrast, the total chlorine-free bleaching (TCF) involves using a combination of ozone, hydrogen peroxide, and oxygen. The EPA's cluster rules in 1998 allowed the substitution of chlorine dioxide for chlorine over TCF bleaching.

The US pulp and paper mills have conformed to the 'cluster rules' that combine water and air quality regulations, which are based on the total conversion of pulping and bleaching mills to oxygen delignification, and the total chlorine dioxide substitution of chlorine.

Water disinfection by chlorination has dramatically reduced the incidence of infectious diseases since the early part of the 20th century. However, during the chlorination process, trihalomethanes (THMs) are formed by the reaction of chlorine with the organics present in the water. In 1979, the US EPA adopted a THM regulation, setting the maximum level of THM in drinking water. While this regulation is unlikely to affect the use of chlorine in water treatment, many options are being pursued to remove the THMs and their precursors. These methods are effective but expensive. Thus, the use of chlorine in

the pulp and paper industry and in water treatment will continue to decline through the year 2006 and probably beyond in the United States.

3.3.2.2. Caustic. Caustic is used in manufacturing a wide variety of chemicals and end products. Table 3.4, depicting the US demand of caustic in 2000–2010, shows the caustic market growing by 0.3% through 2010 [6]. Figure 3.20 illustrates the various market segments utilizing caustic soda.

Caustic soda is used in the manufacture of a large number of organic chemicals, for dehydrochlorination, acid neutralization, as a catalyst, and as a source of sodium. In inorganic chemical manufacture, caustic is mainly used to produce sodium-containing

TABLE 3.4. United States Caustic Soda Demand

	(-000- Metric tons)				AAGR% 1995–2010
	1995	2000	2005	2010	
Pulp & paper	2,693	2,707	2,415	2,480	-0.5
Alumina	333	339	339	343	0.2
Soaps/detergents/textiles	1,140	1,192	1,210	1,236	0.6
Organics	2,236	2,902	2,871	3,077	2.5
Inorganics	2,352	2,743	2,827	3,018	1.9
Water treatment	250	272	286	313	1.7
Others	2,347	2,018	1,245	1,403	-2.7
Total demand	11,351	12,173	11,193	11,870	0.3

Source: With permission from Chemical Marketing Associates, Inc.

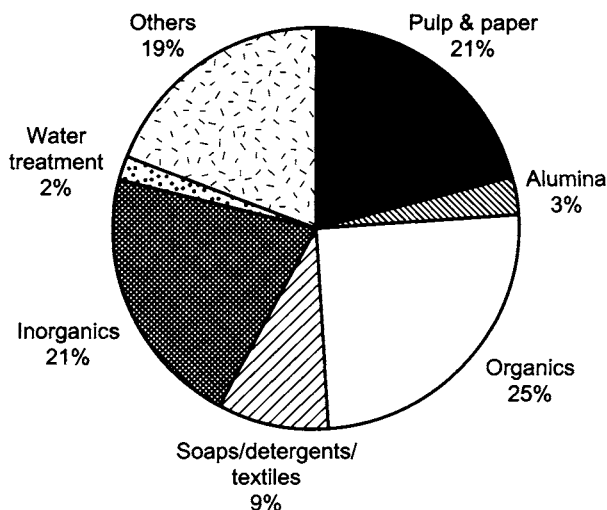


FIGURE 3.20. End-use profile of caustic soda.

TABLE 3.5. Canadian Chlorine and Caustic Soda Demand

	(-000- Metric tons)				AAGR% 1995-2010
	1995	2000	2005	2010	
<i>A. Chlorine</i>					
Chlorinated intermediates	9	0	0	0	0.0
Vinyls	432	438	318	396	-0.6
Pulp & paper	134	60	26	3	-6.5
Water treatment	66	73	80	88	2.2
Inorganics	7	8	7	7	0.0
Others	129	175	203	223	4.9
Total demand	777	754	634	717	-0.5
<i>B. Caustic soda</i>					
Pulp & paper	801	868	864	942	1.2
Alumina	85	99	103	105	1.6
Soaps/detergents/textiles	93	108	121	137	3.2
Organics	55	80	95	110	6.7
Inorganics	73	83	92	104	2.8
Water treatment	50	54	58	63	1.7
Others	103	74	91	101	-0.1
Total demand	1,260	1,366	1,424	1,562	1.6

Source: With permission from Chemical Marketing Associates, Inc.

compounds. All these applications are expected to grow as the caustic consumption follows the GDP, which is forecasted to increase through the year 2006. The only markets where its use is declining are the chloroprene market and the pulp and paper industry. Chloroprene is used to produce neoprene, which is used as an elastomer with excellent resistance to ozone, flame, and weathering. However, lower priced elastomers are expected to compete with neoprene. As a result, neoprene consumption is expected to decrease by 2.5% in the next 5 years. The pulp and paper industry consumes 20% of the caustic produced in the United States. The pulp production declined in the United States in 1998, due to lowered pulp exports and increased paper imports. The slight decline in caustic consumption in the pulp and paper industry is believed to be offset by the growth in organic chemicals, which will support a net increased demand for caustic.

3.3.3. Chlor-Alkali Industry in Canada

Canada produced 754,000 tons of chlorine in 2000 [6]. More than 50% of it was used to produce EDC, VCM, and PVC. While 27% of the chlorine was used in the pulp and paper industry in 1995, the Clean Water Law of that year required mills to reduce emissions of absorbable organic halogens (AOXs) by the end of 1999. In addition, the province of Ontario mandated phasing out of chlorinated organics by 2002. Substitution of ClO₂ for Cl₂ in pulp bleaching decreased the demand for Cl₂ in pulp manufacturing. This decline in the chlorine consumption in pulp mills offset the growth in EDC, the result being a decline in chlorine demand through the year 2010 [6]. Table 3.5 illustrates the chlorine and caustic demand through 2010.

Of the 1,366,000 tons of caustic consumed in 2000, more than 60% of it was used in the pulp and paper industry. This demand may decline when the industry starts implementing technologies that reduce the demand for caustic [2].

Diaphragm-cell technology contributes 62% of the total chlorine produced in Canada, while membrane- and mercury-cell technologies produce 36% and 2% chlorine, respectively. Dow Chemical Canada, Nexen Chemicals, PCI Chemicals Canada, and PPG Canada are the major producers of chlorine.

3.3.4. Chlor-Alkali Industry in Mexico and Brazil

In 2000, Mexico produced 340,000 tons of chlorine and Brazil produced 1,196,000 tons. Approximately 86% of the chlorine in Mexico was produced in diaphragm cells and about 7% in mercury cells, while 79% of the chlorine in Brazil was manufactured in diaphragm cells and 17% in mercury cells.

About 28% of the chlorine consumed in Mexico was used for PVC production and 36% for manufacturing hydrochloric acid. Twenty-eight percent of the caustic was consumed for producing organic chemicals. The demand for chlorine and caustic was estimated to increase by about 2.5% per year through 2010 [6].

The major use of chlorine in Brazil was for PVC (38%) and PO (22%) production, while chemical manufacturing and the pulp and paper industry consumed 31% and 19% of caustic. The demand for chlorine and caustic is estimated to grow by 0.8% and 4.5%, respectively, by 2010 [6].

Tables 3.6 and 3.7 show the demand for chlorine and caustic in Mexico and Brazil through the year 2010.

3.3.5. Chlor-Alkali Industry in Western Europe

Western Europe, consisting of Austria, Belgium, Finland, France, Germany, Greece, Ireland, Italy, the Netherlands, Norway, Portugal, Spain, Sweden, Switzerland, and the United Kingdom, produced 23% of the world chlorine in 2002. The 10 largest chlor-alkali producers, accounting for 70% of the Western European chlorine capacity, are noted in Table 3.8.

Approximately 54% of the chlorine in Western Europe was manufactured using mercury-cell technology, while the diaphragm-cell process contributes 23% of the total capacity in year 2000. Both these technologies will be gradually changed to membrane-cell technology. All the mercury-cell plants in Western Europe have complied with the Paris Marine Commission's (PARCOM) mandated limit on mercury emissions (2 g emission to air, water, and products/ton of chlorine produced). The long-term PARCOM recommendation is to close all the mercury plants by 2010. The primary driving force for the change to membrane-cell operations is the cost of energy in Europe and the low profit margin of the chlorine-based markets in Europe with the current technologies.

3.3.5.1. Chlorine. In 2001, 9.72 MM tons of chlorine was consumed in Western Europe. Chlorine consumption is projected to increase by 0.2% per year through 2010 [6].

Most of this chlorine is used in PVC manufacturing and the C₁ and C₂ chlorinated solvents. The EDC, VCM, and PVC market segments consumed about 38% of the chlorine produced during 2000, and are not expected to grow through 2010, because of potential regulations related to the use of plastic. The PO and phosgene markets are projected to grow annually by 1.4% and 2%, respectively.

Production of chlorinated solvents, which include carbon tetrachloride, methylene chloride, 1,1,1-trichloroethane, PCE, and TCE, is expected to decline because of environmental concerns. The demand for methyl chloride will also decrease, as Bayer has developed a new process for producing silicones, where the byproduct hydrochloric acid is fed back to the system, regenerating methyl chloride.

Epichlorohydrin, used in the manufacture of epoxy resins, is expected to grow, while the use of monochloroacetic acid and benzyl chloride is expected to remain at the same levels as in 1996. The use of chlorine for the production of chloroprene is expected to decline because of competition from low-cost elastomers.

The chlorobenzene market will decline in Western Europe because of competition from Eastern Europe and the declining end-use applications. The major outlet for monochlorobenzene is nitrochlorobenzene, which will be produced outside Western Europe.

Chlorine demand for ethyl chloride declined by 13% per year through the year 2000 because of the decreased production of tetraethyl lead.

The major markets for chlorine containing inorganic chemicals are hypochlorites, hydrochloric acid, phosphorous chloride, cyanuric chloride, titanium dioxide, and aluminum chloride. All these markets are projected to grow except for cyanuric chloride,

TABLE 3.6. Mexican Chlorine and Caustic Soda Demand

	(-000- Metric tons)				AAGR% 1995-2010
	1995	2000	2005	2010	
<i>A. Chlorine</i>					
Chlorinated intermediates	22	0	0	0	-6.7
Vinyls	112	96	207	250	8.2
Organics	16	15	0	0	-6.7
Pulp & paper	14	16	10	9	-2.4
Water treatment	24	30	38	46	6.1
Inorganics	44	58	57	30	-2.1
Others	117	125	130	150	1.9
Total demand	349	340	442	485	2.6
<i>B. Caustic soda</i>					
Pulp & paper	34	39	36	62	5.5
Soaps/detergents/textiles	63	80	91	109	4.9
Organics	119	140	150	1,265	64.2
Inorganics	73	88	93	93	1.8
Water treatment	48	60	69	84	5.0
Others	85	92	102	126	3.2
Total demand	422	499	541	639	3.4

Source: With permission from Chemical Marketing Associates, Inc.

TABLE 3.7. Brazilian Chlorine and Caustic Soda Demand

	(-000- Metric tons)				AAGR% 1995-2010
	1995	2000	2005	2010	
<i>A. Chlorine</i>					
Chlorinated intermediates	64	48	36	23	-4.3
Vinyls	432	451	398	442	0.2
Organics	277	321	364	385	2.6
Pulp & paper	59	59	29	27	-3.6
Water treatment	35	44	51	53	3.4
Others	231	273	283	295	1.8
Total demand	1,098	1,196	1,161	1,225	0.8
<i>B. Caustic soda</i>					
Pulp & paper	178	220	340	324	5.5
Alumina	191	338	377	539	12.1
Soaps/detergents/textiles	147	165	181	199	2.4
Organics	343	383	415	455	2.2
Inorganics	154	165	179	196	1.8
Water treatment	41	44	48	53	2.0
Others	154	163	190	213	2.6
Total demand	1,208	1,478	1,730	1,979	4.3

Source: With permission from Chemical Marketing Associates, Inc.

TABLE 3.8. Largest Chlorine Producers in Western Europe in 2002 (Thousands of Tons of Chlorine)

	Quantity	% of total
Dow	1,351	12
Solvay	1,239	11
Bayer	1,013	9
INEOS Chlor	1,013	9
ATOFINA	900	8
Akzo Nobel	675	6
EniChem	563	5
BASF	450	4
Aragonesas	337	3
LaRoche	337	3
Others	3,377	30
Total	11,259	100

which is used for agricultural chemicals, dyestuffs, and enhancement of optical brightness. This is a result of a decline in agricultural production in Western Europe and exports to Asian countries, which are producing cyanuric chloride to meet domestic demand.

There is no direct use of chlorine in pulp and paper bleaching as of 1996, since all the Western European paper mills have shifted their bleaching operations to the

TABLE 3.9. Western European Chlorine Demand

	(-000- Metric tons)				AAGR% 1995-2010
	1995	2000	2005	2010	
Chlorinated intermediates	956	973	911	894	-0.4
Vinyls	3,470	3,760	3,480	3,400	-0.1
Organics	2,501	2,849	3,041	3,191	1.8
Pulp & paper	18	5	5	5	-4.8
Water treatment	200	208	213	219	0.6
Inorganics	71	94	84	86	1.4
Others	1,877	1,832	1,715	1,556	-1.1
Total demand	9,093	9,721	9,449	9,351	0.2

Source: With permission from Chemical Marketing Associates, Inc.

TABLE 3.10. Western European Caustic Soda Demand

	(-000- Metric tons)				AAGR% 1995-2010
	1995	2000	2005	2010	
Pulp & paper	1,155	1,248	1,234	1,351	1.1
Alumina	277	307	301	298	0.5
Soaps/detergents/textiles	746	767	783	801	0.5
Organics	2,298	2,581	2,680	2,856	1.6
Inorganics	2,109	2,143	2,222	2,349	0.8
Water treatment	390	397	405	417	0.5
Others	1,596	2,365	1,998	1,654	0.2
Total demand	8,571	9,808	9,623	9,726	0.9

Source: With permission from Chemical Marketing Associates, Inc.

use of chlorine dioxide or hydrogen peroxide. Chlorine will continue to be used for water treatment. However, the use of chlorine in water treatment has decreased because of the toxicological and environmental issues related to the formation of halogenated byproducts. Hence, the chlorine use for this end application will remain flat through the year 2006. Table 3.9 shows the chlorine demand forecast through the year 2010.

3.3.5.2. Sodium Hydroxide. The Western European consumption of sodium hydroxide in 2000 was 9.80 MM tons, the projected growth rate through 2010 being 0.9% (Table 3.10). The demand for NaOH for producing major organic chemicals will increase by 0.9% from a 2001 market of 2.581 MM tons. However, the use of caustic for sodium hypochlorite will decline 0.7% per year through 2006, while its use in producing sodium cyanide is expected to be flat.

The direct application of caustic in pulp and paper will increase in line with the output of pulp, and in the de-inking process for waste paper processing, as the use of recycled fiber in paper production will continue to grow in Western Europe.

3.3.6. Chlor-Alkali Industry in Eastern Europe

Eastern Europe, comprised of Albania, Armenia, Azerbaijan, Bulgaria, Bosnia-Herzegovina, Croatia, Czech Republic, Hungary, Macedonia, Poland, Romania, Russia, Serbia, Slovakia, Tajikistan, Ukraine, and Yugoslavia, produced 6% of the total world chlorine in 2002. The chlorine production in this region has decreased because of political and economic instability. Russia is the largest chlorine consuming country in Eastern Europe, accounting for 41% of the total.

The main use of chlorine in Eastern Europe is for the production of PVC and organic chemicals, which include PO, chlorinated solvents, phosgene, and chlorobenzene. Chlorine is also used to produce hydrochloric acid and hypochlorite.

The major end use of caustic in Eastern Europe is the production of rayon fibers, accounting for 10–12% of the region's caustic soda demand. This may be compared with the world average of 4%. Other applications include wood pulping, petroleum processing, and the production of alumina.

3.3.7. Chlor-Alkali Industry in The Middle East

The Middle East, comprised of Egypt, Iran, Iraq, Israel, Jordan, Kuwait, Oman, Pakistan, Qatar, Saudi Arabia, Syria, Turkey, and the United Arab Emirates, manufactures 3% of the world's chlorine. Approximately 71% of the chlorine in this region is produced using membrane-cell technology, while mercury- and diaphragm-cell technologies contribute 24% and 4%, respectively. Chlorine consumption is expected to grow by 8% per year through 2006, because of the growing demand for the vinyl chain products. The EDC nameplate capacity will increase from 2.4 MM metric tons in 2001 to about 3.4 MM in 2006.

Most of the chlorine is used to make EDC, some of which is utilized in PVC production and the remaining for exports. The major local outlet for caustic is for petroleum and natural gas processing, but most of the caustic is exported to Australia and other regions. The Middle East is a significant net exporter of caustic.

3.3.8. Chlor-Alkali Industry in Japan

Japan produced 10% of the world's chlorine in 2001. The capacity for chlorine and caustic increased by 7% through the period 1998–2002 as a result of increases in the pulp and paper industry, PVC, TDI, MDI, and other organic and inorganic chemicals.

Consumption of chlorine and caustic has decreased annually during 1997–2001 by 1.7% and 0.6% respectively, because of the weak economy and environmental concerns. The chlorine demand is expected to decline during 2001–2006 at an annual rate of 0.1%, while the caustic demand is projected to grow annually by 1.2% during the same period.

Historically, the Japanese chlor-alkali industry started in 1881, when the LeBlanc process was used to produce caustic soda. Osaka Soda and Hodogaya Chemical commercialized the mercury- and diaphragm-cell technologies in 1915. Asahi Glass started the Solvay process soon after. By 1973, 95% of the chlorine was produced by the mercury-cell process and 5% by diaphragm cells. In 1973, mercury pollution issues

forced the government to mandate conversion to non-mercury-cell technologies. As a result, two thirds of the mercury-cell capacity was converted to diaphragm-cell technology during 1975–1976, and during 1983–1986 the remaining were converted to the membrane-cell processes. By the end of 1999, all the diaphragm cells were converted to membrane cells, with technologies developed in Japan by Asahi Glass, Asahi Chemical, Tokuyama Soda, and Chlorine Engineers.

3.3.9. Chlor-Alkali Industry in Korea, Taiwan, China, and India

Korea produced 1.035 million tons of chlorine in 2002 and added another 650,000 tons of capacity in 2003. More than 50% of the chlorine produced was used for VCM manufacture and the remainder was for food uses, steel production, ferric chloride, and sodium glutamate. Most other chlorine derivatives were imported from the United States and Western Europe.

Taiwan's production of chlorine in 2002 was 987,000 tons, 79% of which was used for manufacturing EDC. Chlorine consumption is expected to rise by 5–6% per year during the next 5 years.

China produced 6.2 MM tons of chlorine in 2001. About 72% of the capacity was based on diaphragm cells, 26% on membrane cells, and the rest by the lime-soda process. China produced over 100 chlorinated organics, 50 chlorinated inorganics, and 30 chlorine-based agricultural chemicals. Consumption of chlorine is projected to grow by 5% per year to 7.9 MM tons in 2006.

India produced 2.05 MM tons of chlorine in 2001, membrane cells holding a share of 68%, mercury cells at 31%, and diaphragm cells at 1%.

3.3.10. Chlorine and Caustic Prices

The price of chlorine and liquid caustic has constantly changed, unlike that of solid caustic, over the past 25 years. The US spot price variations are presented in Fig. 3.21. The United States is the largest merchant market for chlorine in the world, and is also the main exporter of chlorine derivatives.

The price of chlorine and caustic generally fluctuates, as the chlorine market is heavily dependent on the PVC industry, which fluctuates with swings in the economy. Caustic is generally more recession-proof as it is generally a utility chemical in manufacturing (i.e., much like water, steam, etc.), unlike chlorine. As a result, there is price elasticity in caustic usage. When caustic pricing is low, demand grows from alkali substitution from soda ash. The opposite is true when caustic soda pricing is high. Thus, the supply/demand profile plays a critical role in chlorine pricing as the ability to store chlorine is limited.

The price of chlorine was on an increasing trend from 1970 to 1980, and then decreased to ~\$90–105 per ton during 1981 and 1982. The prices increased from 1983 until ~1988, when the prices fell to \$35 per ton in 1992 due to an overall weak economy. The caustic prices also dropped to \$220 per ton in 1992. The pricing took an upward trend in 1993 from \$215 per ton to \$270 per ton and continued to increase due to the strong EDC, VCM, and PVC markets.

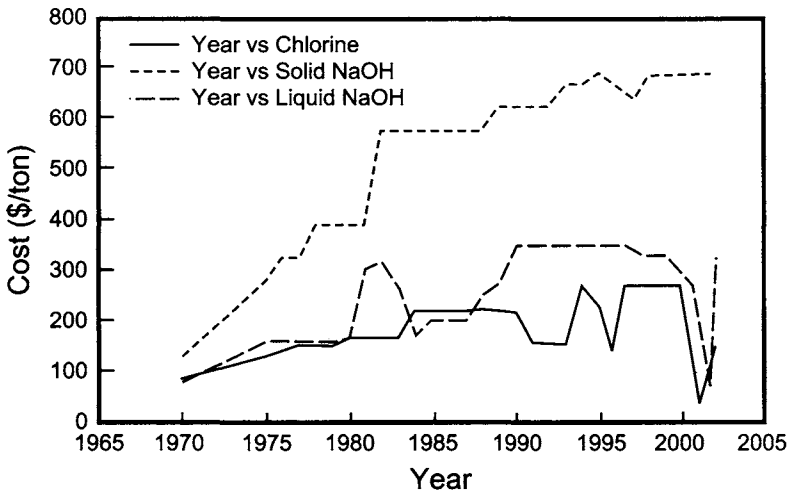


FIGURE 3.21. Chlorine and caustic list prices from 1970 to present (plotted from the data in [2,7,9]).

The chlorine price at the start of 1998 was \$220 per ton, but it had decreased to \$60 per ton by the end of 1998 mainly due to increased world capacity and a lower than expected demand for chlorine derivatives as a result of the Asian situation at that time.

The chlorine prices started increasing toward the end of 1999, as the Asian situation improved, and the industry restructured to make its operations profitable. The spot price of chlorine in the United States in 1997 was \$260 per ton and had fallen to ~\$32 per ton in 2001 as a result of the financial problems in Asia, slow growth in the rest of the world, economic echoes of the 9/11 terrorist acts, increased energy costs and fuel prices, coupled with an increased world capacity. Since then, the industry has restructured its operations and chlorine prices increased to ~\$240 per ton in late 2002. It should be noted that most chlorine is sold under contract prices, which do not bounce around, unlike the spot market prices that vary with market demands.

It is important to note that the philosophy of production, transportation, and storage of chlorine has changed drastically following the 9/11 incident. Heightened security measures by the producers and the consumers have added significant costs to the industry. The consideration of relocation of consumers to nearby chlorine production facilities has received attention. The development of security regulations will impact the chlor-alkali industry in the future.

3.4. ENVIRONMENTAL CONSIDERATIONS AFFECTING THE GROWTH OF THE CHLOR-ALKALI INDUSTRY

The environmental issues that constantly threatened the chlor-alkali industry can be classified into two categories, one related to the process and the technology, and the other, dictated by the end-use applications. The process and technology issues are addressed in Chapter 16. The product-related concerns are discussed here.

Chlorine is used to produce organic and inorganic chemicals, besides being directly employed in the pulp and paper and water treatment operations. Chlorine, itself, is acutely toxic to humans, animals, and plants, but it does not accumulate in the human body and has no long-term effects. Hence, precautions are in place for transporting chlorine in liquid form by choosing proper containers and selecting proper valves and piping materials. Leaks from chlorine containers will allow the gas under pressure to escape as a yellow cloud, forcing the evacuation of the people within the vicinity. This is part of the Community Awareness and Emergency Response (CAER) program in "Responsible Care."

3.4.1. Organic Chemicals

3.4.1.1. EDC/VCM/PVC. Most of the chlorine produced in the world is used to manufacture PVC and its intermediates. These plastics are used widely in many applications, especially in the construction industry. Western Europe was the largest producer of PVC in the 1990s, followed by Asia and North America.

There are four major environmental concerns regarding the use of PVC that are still being debated by the environmental agencies and the PVC manufacturers. These are: (1) the formation of toxic dioxins, furans, and HCl during the incineration of PVC either in building fires or municipal waste incinerators, (2) the presence of lead and cadmium in the toxic fly ash formed during the incineration of PVC containing metal stabilizers, (3) the presence of phthalate plasticizers which are suspected carcinogens, and (4) the non-degradability of chlorinated plastics in landfills. Until now, there have been no laws or regulations restricting the use of PVC. Nevertheless, environmental groups are attacking its use. As a result, some local restrictions have been imposed, especially in Germany. In the packaging sector, some countries have banned PVC for bottle production and PVC sheets for food packaging. The issue of HCl and dioxin emissions is not as serious because the fugitive emissions can be minimized via improved waste incineration technologies. The use of Pb- and Cd-based stabilizers has declined in favor of Zn- and Ca-based stabilizers. Flexible PVC-containing dioctylphthalate plasticizers has been banned in children's toys. The phthalates have been replaced by phosphate esters. It is worth noting that dioctylphthalate was recently found not to be as carcinogenic as was originally thought.

VCM used in the production of PVC is a carcinogen, and the regulations call for a threshold limit value of 3–5 ppm in air. PVC manufacturers have conformed to these limits and the carcinogenic issue related to VCM has been well under control for this end product.

3.4.1.2. Propylene Chlorohydrin. Propylene chlorohydrin is one of the most important intermediates used in the production of PO, which is a raw material for producing propylene glycols and urethane polyether polyols. The United States and Western Europe are the largest producers of propylene chlorohydrin, accounting for 74% of the world's production. The main environmental issues relate to the chlorinated waste generated in the process and the disposal of the byproduct calcium chloride sludge. The formation of

the calcium chloride sludge can be avoided by using caustic soda. However, the use of caustic depends on the price of caustic vs the CaCl_2 sludge disposal costs.

Olin has developed a new process for manufacturing PO by direct oxidation of propylene. There are also several peroxidation technologies for production of PO. Possible breakthroughs in the non-propylene chlorohydrin-based routes could reduce the demand for chlorine for making PO.

3.4.1.3. Chlorination Technologies. Chlorine is used in the manufacture of several large-volume products, which include chlorobenzene, chlorophenols, and chloroacetic acids. The other chlorinating agents used in the production of intermediates are hydrochloric acid, thionyl chloride, chlorosulfonic acid, phosphorous tri- and pentachloride, and phosphorous oxychloride. One of the issues being considered during the course of these chlorination reactions is the formation of HCl gas, which can be mitigated by installing exhaust gas containment devices. The other environmental concern is the contamination of solid waste and wastewater with organic and inorganic impurities, which, when burnt, release highly toxic dioxins. While complete thermal decomposition by high-temperature burners can avoid this problem, the public acceptance of this practice is a major concern in the industry.

Since the 1980s, several European and Japanese chemical companies have instituted stringent safety standards, well ahead of governmental regulations. This investment towards environmental and safety measures has reduced waste emissions significantly.

3.4.1.4. Phosgene. Phosgene, a major chlorine consumer and an intermediate in the production of isocyanates, is used in the manufacture of polyurethanes, polycarbonates, and pesticides, and chloroformates and carbonates, for producing pharmaceuticals. The United States and Western Europe each account for 41% of the total world phosgene production, and Japan generates 12% of the total.

Phosgene is highly toxic and there are legislative restrictions on production, consumption, and transportation. Phosgene manufacturing facilities have incorporated all the safety measures, properly conforming to the mandated standards. However, public perception of risks may limit its production in neighborhoods that are highly populated, or where environmental standards are very high.

3.4.1.5. Chlorine-Based Pesticides. There are about 100 chlorine-based compounds used in several hundred pesticides. Of these, more than 40% have insecticidal activity, 30% have fungicidal activity, and 15% have herbicidal activity, and are used extensively in the agricultural industry. The major herbicides, fungicides, and insecticides used in some regions in the world are shown in Table 3.11 [9].

The need for these chemicals depends on the specific market of importance in any given country. Thus, cotton, cereal, and vegetables are the important markets in Europe, while maize and soybeans are important in the United States. Protection of rice crops is in demand in Japan and Hong Kong, where the use of pesticides to protect fruits and vegetables is also growing. Major agricultural markets in other countries include maize

TABLE 3.11. Major Chlorine Containing Herbicides, Fungicides, and Insecticides with Regional Importance

	Major end uses	United States	Western Europe	East Asia
<i>A. Herbicide</i>				
Acetochlor	Corn	X		
Alachlor	Corn, soybeans	X		X
Atrazine	Corn	X	X	X
Bentazon	Soybeans	X	X	
Chloramben	Soybeans	X		
Chlorsulfuron	Wheat	X		
Cyanazine	Corn, cotton	X	X	
2,4 D	Corn, cotton	X	X	X
Dicyclofop-methyl	Wheat	X		
MCPA	Wheat	X	X	X
Metalochlor	Corn	X		
Metribuzin	Soybeans	X	X	
Triallate	Wheat, oilseed, beet, maize	X	X	
Trifluralin	Corn, cotton, soybeans	X	X	X
<i>B. Fungicide</i>				
Anilazine	Nonagriculture	X		X
Captan	Vegetables, nonagriculture	X	X	X
Carboxin	Peanuts	X	X	X
Chloroneb	Nonagriculture			
Chlorothalonil	Peanuts, potatoes, vegetables, nonagriculture	X	X	X
Etridiazol	Nonagriculture	X		
Iprodione	Stone fruit, nuts, rice, vegetables, nonagriculture	X	X	X
Maneb	Potatoes, fruits, vegetables		X	X
Metalaxyl	Nuts, potatoes, tobacco, vegetables, nonagriculture	X		
Metiram	Potatoes	X	X	
PCNB	Peanuts	X	X	X
Propiconazole	Small grain, nonagriculture	X		X
Thiram	Nonagriculture	X		X
Vinclozolin	Vegetables, nonagriculture	X		
Ziram	Apples, stone fruit	X		
<i>C. Insectide</i>				
Carbofuran	Corn, fruit, nuts, maize, beets	X	X	X
Chlorpyrifos	Corn	X	X	
Cloethocarb	Corn	X		
Dicofol	Cotton, citrus, fruit	X	X	X
Dimethoate	Fruit, vegetables, wheat		X	X
Endosulfan	Corn, fruit, raps	X	X	X
Fonofos	Corn	X		
Formetanate hydrochloride	Beet, fruit, vines	X	X	
Lindane	Corn	X	X	
Methoxychlor	Nonagricultural	X		
Thiodicarb	Cotton, soybeans	X	X	

Source: With permission from SRI Consulting.

in South Africa, cereals and cotton in Australia, fruits and vines in Chile, and rice and cotton in Colombia.

While the pesticides control pest infestation and disease, they can adversely affect the plants and the environment via ground water contamination, besides causing adverse side effects in humans. This has led to regulations by the EPA in the United States to curtail the use of pesticides that leach into the ground water. Triazines, a group commonly present in pesticides, have antibacterial and anti-protozoan activity, and are used in the production of atrazine, which is a controversial weed-control chemical.

There is no general agreement on the maximum allowable atrazine level. However, world health organizations have set the level at $2 \mu\text{g L}^{-1}$, while the US EPA has set the limit at $3 \mu\text{g L}^{-1}$ of daily intake as acceptable. In Europe, atrazine is not regulated, but the European communities' drinking water directive has set a maximum allowable concentration of $0.1 \mu\text{g L}^{-1}$ for each individual pesticide and $0.5 \mu\text{g L}^{-1}$ for all pesticides combined. Still, debates and lobbying continue to change some of these regulations.

Fungicides causing environmental pressure are chlorine-containing dithiocarbamate-based and heterocyclic nitrogen-based compounds, and include maneb, metiram, and thioram for apples, and ziram, folpet, maneb, and thiram for stone fruit use. Regulations in the United States have discontinued use of prochloraz, mancozeb, and maneb for barley, oat, rye, and wheat crops.

The first insecticide banned by the EPA in 1970 for safety reasons was DDT, which was used to control malaria and the typhus epidemic, saving thousands of lives. Other insecticides include: aldrin, dieldrin, chlordane, and heptachlor, which were banned because of the health hazards associated with them. 1,4-Dichlorobenzene, toxaphene, and 1,3-dichloroprene are classified by the US National Toxicological Program as suspected human carcinogens, although the last two chemicals are under special review by the EPA. Production of 2,4,5-trichlorophenoxy acetic acid herbicides and 2,4,5-trichlorophenol fungicides has been discontinued in most regions, as they have low biodegradability and accumulate in the food chain.

Environmental and health hazards associated with chlorine-based herbicides have impacted the production of these chemicals, and the consumption of chlorinated hydrocarbon insecticides has decreased by more than 95% since 1974. However, as this market segment constitutes <1% of the total chlorine consumption, the chlorine industry is unlikely to be affected by the restrictions on the Cl_2 -based agricultural chemicals, although debates and discussions on the pesticides have created a bad public image for the chemical industry.

3.4.1.6. Chlorine Derivatives. Certain chlorine derivatives pose major risks to the environment because their emissions can destroy the ozone layer and add to the greenhouse effect. Table 3.12 shows the "Ozone Depletion Potential" (ODP) and the "Global Warming Potential" (GWP) of various chlorine-based chemicals [15]. ODP values are compared with CFC-11 with a value of 1.0, and GWP values are compared with CO_2 with a value of 1. The time period for the GWP indicates when the greenhouse effect will disappear, and the lifetime in the atmosphere reflects the time for decomposition for the given species. Table 3.13, describing the major greenhouse gases and their contribution to the greenhouse effect [15].

TABLE 3.12. Climatic Effects of Chlorine Derivatives

Product	Life time in atmosphere (yr)	Ozone depletion potential (ODP)	Global warming potential (GWP) time horizon			
			20 yr	100 yr	500 yr	
CO ₂	120	—	1	1	1	
<i>CFCs</i>						
11	CCl ₃ F	60	1	4,500	3,500	1,500
12	CCl ₂ F ₂	130	0.96	7,100	7,300	4,500
113	F ₂ ClC-CCl ₂ F	90	0.85	4,500	4,200	2,100
114	F ₂ CIC-CClF ₂	200	0.71	6,000	6,900	5,500
115	F ₂ CIC-CF ₃	400	0.4	5,500	6,900	7,400
<i>HCFCs</i>						
22	HCClF ₂	15	0.05	4,100	1,500	510
123	HCl ₂ C-CF ₃	1.6	0.02	310	85	29
124	HClFC-CF ₃	6.6	0.02	1,500	430	150
141b	H ₃ C-CCl ₂ F	13	0.15	1,500	430	150
142b	H ₃ C-CClF ₂	19	0.05	3,700	1,600	540
<i>HFCs</i>						
125	HF ₂ C-CF ₃	28	0	4,700	2,500	860
134a	H ₂ FC-CF ₃	16	0	3,200	1,200	420
143a	H ₃ C-CF ₃	41	0	4,500	2,900	1,000
152a	H ₃ C-CHF ₂	1.7	0	510	140	47
<i>CCs</i>						
CCl ₄		50	1.13	1,900	1,300	460
CCl ₃ CH ₃		6	0.12	350	100	34

Source: With permission from SRI Consulting.

TABLE 3.13. Greenhouse Effect

	CO ₂	CH ₄	N ₂ O	Ozone	CFC 11	CFC 12
Concentration in the atmosphere (ppm)	354	1.72	0.31	0.03	0.00028	0.00048
Time in the atmosphere (yrs)	120	10	150	0.1	60	30
Increment (%/yr)	0.5	1	0.25	0.5	5	3
Relative global warming potential; CO ₂ = 1 (v/v)	1	21	206	2,000	12,400	15,800
Relative global warming potential; CO ₂ = 1 (w/w)	1	58	206	1,800	3,970	5,750
Contribution to incremental greenhouse effect in the 80s (%)	50	13	5	7	5	12

Source: With permission from SRI Consulting.

Attempts to reduce the ozone layer depletion and the emission of greenhouse gases, under the auspices of the United Nations, resulted in the Montreal Protocol in 1987. Table 3.14 shows the CFC-phase out plans adopted in 1990 [15]. Industry has volunteered to recover CFCs from old refrigeration units, complying with the Montreal Protocol.

3.4.1.7. Chlorinated Solvents. The chlorinated solvents of relevance include all chloromethanes and the chlorinated C₂ hydrocarbons, perchloroethylene (PCE), trichloroethylene (TCE), and 1,1,1-trichloroethane (1,1,1-TCA), which are produced in large volumes throughout the world. All these products are under great pressure from stringent government regulations all over the world, and their production will significantly decrease over the next few decades.

All chlorinated solvents are regarded as either atmospheric pollutants, or potentially hazardous chemicals for occupational exposure. Hence, government regulations have had a significant impact on their use over the past 25 years. Laboratory tests on animals also indicate that these solvents have the potential for chronic effects on humans [15].

The second Montreal Protocol (1990) restricted the production and use of 1,1,1-TCA because of its high ODP, ultimately leading to its phase out by 2005. Metal cleaning is one of the important end uses of C₂ chlorinated solvents, and emission of these solvents is a major issue. The metal industry has improved operations to recover these solvents and minimize emissions into the atmosphere. A similar trend is ongoing in dry cleaning operations to reduce the use of PCE. Phase-out of PCE is well underway.

3.4.2. Inorganic Chemicals and Direct Application

3.4.2.1. Bromine. Bromine is highly toxic, but bromine-based compounds are not. However, fire fighting gases, such as halons, exhibit ODP, and lead antiknocks cause soil and air pollution, both being restricted by the Montreal Protocol. Therefore, regulations will be enforced on bromine-based compounds, particularly in developed countries.

3.4.2.2. Water Treatment. Five to six percent of the world chlorine consumption is for the treatment of potable, process, and wastewater streams. Disinfection of drinking water with chlorine, a practice dating back to the mid-1800s, has eradicated deaths from typhoid and many other infectious diseases. However, during the chlorination process, halogenated organic compounds, including chloroform, are formed.

As these species are human carcinogens, the US EPA and the environmental agencies in other countries are seeking to limit the use of chlorine in drinking water. In the United States, Canada, and Western Europe, chlorine consumption will decrease as water treatment operations switch to different disinfectant technologies. However, chlorine consumption will increase in less-developed countries as more water treatment plants go in.

3.4.2.3. Pulp and Paper Industry. The major issue related to the use of chlorine in the pulp industry is the formation of AOXs during the bleaching sequence with chlorine

TABLE 3.14. Phasing Out of Ozone Killers

	Montreal Protocol 1987	London Protocol 1990	Suggested
<i>CFCs</i>			
11,12,113,114,115	1990: freeze on 1986 level 1994: 20% red 1999: 50% red	1991–1990: freeze on 1986 level 1995: 50% red 2000: 100% red	1997: 100% red ^a
<i>CFCs</i>	—	1992: freeze on 1988 level 1997: 85% red 2000: 100% red	1997: 100% red ^a
13,111,112,211, 212,213,214,215,216,217			
<i>Halones</i>	1992: freeze on 1986 level	1992: freeze on 1986 level 1995: 50% red 2000: 100% red	1997: 100% red ^a
1211,1301,2402			
<i>CCs</i>			
<i>CCl₄</i>	—	1995: 50% red 2000: 100% red	1997: 100% red ^a
1,1,1-Trichloroethane	—	1995: 30% red 2000: 50% red 2005: 100% red	1997: 100% red ^a
<i>HCFCs, FCs</i>	—		2005: 100% red ^b

Notes: Red: reduction from current levels.

^aGerman companies stopped production in domestic plants.

^b100% red of HCFC 22 by 2000.

Source: With permission from SRI Consulting.

or chlorine-containing bleaches. These toxic AOXs leave the pulp mill in air, water, and the bleached pulp. As a result, the use of chlorine has significantly declined for pulp bleaching. Restrictions are in place in Canada, the United States, Japan, and Europe to reduce the AOX levels from 8 kg ton⁻¹ of pulp to 0.5 kg ton⁻¹ of pulp.

3.4.2.4. Dioxins and Furans. Dioxins and furans are formed [15,16] during the incineration of chlorine-containing materials, and also during the bleaching operations in pulp and paper plants. Dioxins are defined as tetrachlorodibenzo dioxidines, and furans with chlorine atoms on at least 2,3,7 and 8, as well as coplanar PCBs. This group of *n*-chlorodibenzo-*p*-dioxins, particularly 2,3,7,8-tetrachlorodibenzo-*p*-dioxin (TCDD) is highly toxic and carcinogenic to humans, the exposure path being via meat, dairy products, and fish. While dioxins were found at 40–50 ppt levels in human blood in 1994, the mechanism by which these dioxins will induce toxicity is still unknown. The fears about dioxins started when maximum exposure of TCDD in Agent Orange occurred during the Vietnam War. The “psychological fear” and the uncertainty about the true toxicity to humans resulted in a ban on sales of products or processes in which TCDD was present at more than trace levels.

According to the United Nations Environment Program (UNEP) London directives, the sale of products are prohibited if the TCDD content is >0.002 mg kg⁻¹ and if any

of the following compounds exceed 0.005 mg kg^{-1} , whereas the German Hazardous Products Regulations limit the total PCDD at the 5 ppb level.

1,2,3,7,8 Penta-CDD	Polychlorodibenzo-p-dioxin (PCDD)
1,2,3,7,8,9 Hexa-CDD	2,3,4,7,8-Penta-CDF
1,2,3,6,7,8 Hexa-CDD	2,3,7,8-Tetrachlorobenzofurane
1,2,3,4,7,8 Hexa-CDD	1,2,3,6,7,8-Hexa CDF

REFERENCES

1. S. Brien, *Paper presented at the 1999 World Petrochemical Conference*, Houston (1999).
2. E. Linak and Y. Inui, *CEH Marketing Research Report, Chlorine/Sodium Hydroxide, Chemical Economics Handbook*, SRI International, 733.1000A (2002).
3. C. Fryer, *Chlor-Alkali Conference 2002, Tecnon OrbiChem*, Naples, FL.
4. T.V. Bommaraju, B. Lüke, G. Dammann, T.F. O'Brien, and M.C. Blackburn, *Chlorine in Kirk-Othmer Encyclopedia of Chemical Technology, on-line version*, John Wiley & Sons, Inc., New York (2002).
5. H.-J. Hartz and J. Marciniak, *11th Krupp Uhde Chlorine Symposium*, Forum ThyssenKrupp (2001).
6. M.C. Blackburn, Chemical Marketing Associates, Inc., Personal Communication (2004).
7. M.C. Blackburn, *Paper presented at the 1999 World Petrochemical Conference*, Houston (1999).
8. R.E. Shamel, Consulting Resources Corporation, Personal Communication (2004).
9. *The Global Chlor-Alkali Industry—Strategic Implications and Impacts, Final Report, Volume III/Chapter 6–7*, SRI International Multi-client Project #2437 (1993).
10. S. Berthiaume, E. Linak, P. Yau, A. Leder, and K. Miyashita, *CEH Marketing Research Report, Chlorine/Sodium Hydroxide, Chemical Economics Handbook*, SRI International, 733.1000A (1996).
11. R. Peterson, Chlorine, Caustic, and Derivatives: Insights and Outlook, *Chlor-Alkali Summit 2004*, Consulting Resources Corporation, Houston (2004).
12. W.P. Fiedler and L.A. Zengirski, *Paper presented at the American Paper Institute Conference on Energy and Materials* (1984).
13. C.J. Verbanic, *Chemical Business*, Sept. 1985, Sept. 1990.
14. <http://www.consultingresources.net/chloralkalis.html> (Feb. 13, 2004).
15. *The Global Chlor-Alkali Industry, Strategic Implications and Impacts, Final Report, Chapter 3*, SRI International, Multi-client Project #2437 (1993) Menlo Park, CA.
16. B. Hileman, J.R. Long, and E.M. Kirschner, *Chem. & Eng. News*. 21 (Nov. 21, 1994).

4

Chemistry and Electrochemistry of the Chlor-Alkali Process

4.1. THERMODYNAMICS

4.1.1. Free Energy and Its Significance

Thermodynamics is a powerful tool for the study of chemical reactions and is intimately related to the atomic and molecular description of the species participating in these reactions. The transformation of energy involved in the reactions depends on the thermodynamic conditions of the reaction, and can be expressed in terms of various thermodynamic functions. One such function is the Gibbs free energy [1–4], expressed by Eq. (1):

$$G = H - TS \quad (1)$$

H in Eq. (1) refers to the heat content or enthalpy at temperature T , and S refers to the entropy. Equation (1) can be rewritten as:

$$\Delta G = \Delta H - T \Delta S \quad (2)$$

which describes the energy changes in the system and the surroundings. In a process where the enthalpy decreases, the decrease in the enthalpy of the system is due to (1) the heat that must be released to the thermal surroundings to balance the decrease in the entropy of the system and so preserve the state of balance, and (2) the work delivered to the mechanical surroundings. Thus, the entropy decrease in a system must be compensated for before the system is free to perform any work.

The concept described above will now be elaborated upon by examining the effect of expansion for a reversible process. Defining $H = U + PV$, where U refers to internal energy, T to temperature and P to pressure, and substituting it in Eq. (1) results in:

$$G = U + PV - TS \quad (3)$$

For infinitesimal changes in G ,

$$dG = dU + P dV + V dP - T dS - S dT \quad (4)$$

At constant temperature and pressure, Eq. (4) reduces to:

$$dG = dU + P dV - T dS \quad (5)$$

Since

$$dU = \delta q + \delta w$$

where q refers to the heat absorbed by the system and w the work done by the system,

$$dG = \delta q + \delta w + P dV - T dS \quad (6)$$

The work done by the system, $-\delta w$, consists of the work of expansion, $P dV$, and useful work, $-\delta w'$. Hence

$$-\delta w = P dV - \delta w' \quad (7)$$

or

$$\delta w = \delta w' - P dV$$

It follows from Eqs. (6) and (7) that

$$dG = \delta q - T dS + \delta w' \quad (8)$$

For a reversible process,

$$dq/T = dS \quad (9)$$

and therefore, at constant temperature and pressure,

$$-dG = -\delta w' \quad (10)$$

Thus, the decrease in free energy for a reaction is the maximum work that could be obtained at constant temperature and pressure. Therefore, reactions exhibiting a negative ΔG are those that can be harnessed to do work.

ΔG for a given reaction can be positive, negative, or zero. If $\Delta G = 0$, the system is in equilibrium. If ΔG is negative, the reaction can proceed spontaneously as written, and if it is positive, the reaction will not proceed unless driven by an external force, such as the application of voltage during electrolysis.

Electrical work is equal to the product of the total charge needed to drive an Avogadro number (i.e., a mole) of electrons and the voltage through which the charge is

driven. The charge required to drive a mole of electrons is 96,485 C, which is a Faraday, F . When the cell voltage, E , drives n moles of electrons, the electrical work is equal to nFE . This energy is equal to the decrease in the free energy of reaction. Thus,

$$\Delta G = -nFE \quad (11)$$

where E is the reversible electromotive force (EMF) of the cell. Note that the negative sign of E corresponds to the spontaneous direction of the reaction.

The Gibbs free energy is a function of temperature, pressure, and the chemical potential of the species involved in the reaction, and it can be written in general [1] as:

$$dG = -S dT + V dP + \sum \mu_i dn_i \quad (12)$$

where μ_i refers to the chemical potential of a species and n_i to the number of moles. At constant temperature and pressure, Eq. (12) becomes

$$dG = \sum \mu_i dn_i \quad (13)$$

Integration of Eq. (13) leads to

$$G_{T,P,n} = \sum n_i \mu_i \quad (14)$$

and differentiation of Eq. (14) results in

$$(dG)_{T,P} = \sum (n_i d\mu_i + \mu_i dn_i) \quad (15)$$

or

$$\sum n_i d\mu_i = 0 \quad (16)$$

when coupled with Eq. (13), at constant temperature and pressure. One can now use Eq. (17), obtained from Eq. (14), to calculate the changes in the free energy of a reaction of the type expressed by the scheme in (18).

$$\Delta G = \sum \nu_i \mu_i \quad (17)$$

ν refers to the stoichiometric coefficients in the reaction.

Let us now consider a chemical reaction between A and B to form C and D as:



For example, for the reaction: $\text{Zn} + \text{Cl}_2 \rightarrow \text{Zn}^{2+} + 2 \text{Cl}^-$, $A = \text{Zn}$; $B = \text{Cl}_2$; $C = \text{Zn}^{2+}$; $D = \text{Cl}^-$; $\nu_1 = 1$; $\nu_2 = 1$; $\nu_3 = 1$; and $\nu_4 = 2$.

The free energy change, ΔG , for this reaction is given as:

$$\Delta G = G_{\text{products}} - G_{\text{reactants}} \quad (19)$$

where

$$G_{\text{products}} = \nu_3 \mu_C - \nu_4 \mu_D \quad (20)$$

and

$$G_{\text{reactants}} = \nu_1 \mu_A - \nu_2 \mu_B \quad (21)$$

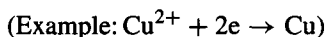
The μ in Eqs. (20) and (21) refers to the chemical potential (i.e., partial molar free energy) of the species denoted in the subscript, which can be calculated from:

$$\mu = \mu^0 + RT \ln a_i \quad (22)$$

μ^0 in the above equation is called the standard Gibbs free energy of formation at unit activity, a_i . For the purpose of the present discussion, let us assume the activity of a solid to be unity, the activity of the dissolved electrolytes to be their concentrations (expressed in g-mol L^{-1}) and the activity of the gases to be equal to their partial pressures (expressed in atmospheres). Theoretically, however, one has to correct the concentration to activity, using the published activity coefficient data. Values of μ^0 are available in the published literature [6], and some typical values are given in Table 4.1.1.

4.1.2. Nernst Equation

Let us now examine the case of an electrochemical reaction given by:



where, [ox] stands for the oxidized species, [red] for the reduced species, and n for the number of Faradays involved in the reaction. Since Eq. (23) should be at equilibrium ($\Delta G = 0$) for the calculation of E_0 , the following relationship is applicable.

$$\nu_{\text{red}} \mu_{\text{red}} - \nu_{\text{ox}} \mu_{\text{ox}} - n \mu_e = 0 \quad (24)$$

TABLE 4.1.1 Free Energies of Formation

Species	Gibbs Free Energy of formation (kcal/g-mol)
$\text{Cl}_2, \text{H}_2(\text{gas})$	0
Zn, Cu	0
Cl^-	-31.35
NaCl(aqueous)	-93.94

μ_e is defined as

$$\mu_e = -FE \quad (25)$$

Substituting Eqs. (22) and (25) into (24), we have

$$nFE_0 = [v_{\text{ox}} \mu_{\text{ox}}^0 - v_{\text{red}} \mu_{\text{red}}^0] + RT \ln \frac{(a_{\text{ox}})^{v_{\text{ox}}}}{(a_{\text{red}})^{v_{\text{red}}}}$$

or

$$E_0 = E^0 + \frac{RT}{nF} \ln \frac{(a_{\text{ox}})^{v_{\text{ox}}}}{(a_{\text{red}})^{v_{\text{red}}}} \quad (26)$$

where

$$E^0 = \left\{ \frac{v_{\text{ox}} \mu_{\text{ox}}^0 - v_{\text{red}} \mu_{\text{red}}^0}{nF} \right\} \quad (27)$$

In the above equation, E^0 is the standard electrode potential $[a_{\text{ox}}] = [a_{\text{red}}] = 1$, R refers to the gas constant $1.987 \text{ cal (g-mol)}^{-1} \text{ K}^{-1}$, T to the absolute temperature in degrees Kelvin, and F to Faraday's constant ($F = 23.06 \text{ kcal (g-equivalent)}^{-1} \text{ V}^{-1}$). Equation (26) is called the Nernst equation relating the electrode potential to the concentrations, and it is one of the most important relationships in electrochemistry. E^0 values for various reactions are presented in Table 4.1.2.

It should be emphasized here that the sign of the potential depends on the manner in which a given reaction is written. The values given in the table refer to the reduction reactions as given by Eq. (23). However, if the reaction is written as $v_{\text{red}}[\text{red}] \rightarrow v_{\text{ox}}[\text{ox}] + ne$, the E^0 value will be positive, representing the oxidation process. In thermodynamics, the oxidation process is treated as the forward direction, whereas in electrochemistry, the reduction process is regarded as the forward direction, following the convention adopted by the International Union of Pure and Applied Chemistry (IUPAC) (see Section 4.1.6).

The following example illustrates the methodology described above by calculating the E^0 for the reaction $\text{Cl}_2 + 2e \rightarrow 2\text{Cl}^-$, given $\mu_{\text{Cl}_2}^0 = 0$ and $\mu_{\text{Cl}^-}^0 = -31.35 \text{ kcal (g-mol)}^{-1}$.

$$\begin{aligned} E^0 &= - \left\{ \frac{2\mu_{\text{Cl}^-}^0 - \mu_{\text{Cl}_2}^0}{2F} \right\} \\ &= - \frac{2 \left(-31.35 \frac{\text{kcal}}{\text{g-mol}} \right)}{\left(2 \frac{\text{g-equivalents}}{\text{g-mol}} \right) \left(23.06 \frac{\text{kcal}}{\text{g-equivalent V}} \right)} \\ &= 1.3595 \text{ V} \end{aligned}$$

TABLE 4.1.2 Standard Electrode Potentials at 25°C

Electrode reaction	Standard reversible potential, volt vs Standard Hydrogen Electrode (SHE)
$2\text{H}_2\text{O} = \text{H}_2\text{O}_2 + 2\text{H}^+ + 2\text{e}$	1.770
$\text{Au} = \text{Au}^+ + \text{e}$	1.680
$\text{Au} = \text{Au}^{3+} + 3\text{e}$	1.500
$\text{Pb}^{2+} + 2\text{H}_2\text{O} = \text{PbO}_2 + 4\text{H}^+ + 2\text{e}$	1.455
$2\text{Cl}^- = \text{Cl}_2 + 2\text{e}$	1.359
$2\text{H}_2\text{O} = \text{O}_2 + 4\text{H}^+ + 4\text{e}$	1.229
$2\text{Br}^- = \text{Br}_2 + 2\text{e}$	1.065
$\text{Pd} = \text{Pd}^{2+} + 2\text{e}$	0.987
$\text{Ag} = \text{Ag}^+ + \text{e}$	0.799
$2\text{Hg} = \text{Hg}_2^{2+} + 2\text{e}$	0.789
$\text{Fe}^{2+} = \text{Fe}^{3+} + \text{e}$	0.771
$\text{H}_2\text{O}_2 = \text{O}_2 + 2\text{H}^+ + 2\text{e}$	0.682
$2\text{Ag} + \text{SO}_4^{2-} = \text{Ag}_2\text{SO}_4 + 2\text{e}$	0.653
$2\text{I}^- = \text{I}_2 + 2\text{e}$	0.535
$\text{Cu} = \text{Cu}^+ + \text{e}$	0.521
$\text{Fe}(\text{CN})_6^{4-} = \text{Fe}(\text{CN})_6^{3-} + \text{e}$	0.360
$\text{Cu} = \text{Cu}^{2+} + 2\text{e}$	0.337
$\text{Ag} + \text{Cl}^- = \text{AgCl} + \text{e}$	0.222
$\text{Cu}^+ = \text{Cu}^{2+} + \text{e}$	0.153
$\text{H}_2 = 2\text{H}^+ + 2\text{e}$	0.000
$\text{Pb} = \text{Pb}^{2+} + 2\text{e}$	-0.126
$\text{Sn} = \text{Sn}^{2+} + 2\text{e}$	-0.136
$\text{Mo} = \text{Mo}^{3+} + 3\text{e}$	-0.200
$\text{Ni} = \text{Ni}^{2+} + 2\text{e}$	-0.250
$\text{Co} = \text{Co}^{2+} + 2\text{e}$	-0.277
$\text{Pb} + \text{SO}_4^{2-} = \text{PbSO}_4 + 2\text{e}$	-0.356
$\text{Fe} = \text{Fe}^{2+} + 2\text{e}$	-0.440
$\text{Cd} = \text{Cd}^{2+} + 2\text{e}$	-0.453
$2\text{Nb} + 5\text{H}_2\text{O} = \text{Nb}_2\text{O}_5 + 10\text{H}^+ + 10\text{e}$	-0.650
$\text{Cr} = \text{Cr}^{3+} + 3\text{e}$	-0.740
$\text{Zn} = \text{Zn}^{2+} + 2\text{e}$	-0.763
$\text{Zr} = \text{Zr}^{4+} + 4\text{e}$	-1.530
$\text{Ti} = \text{Ti}^{3+} + 3\text{e}$	-1.630
$\text{Al} = \text{Al}^{3+} + 3\text{e}$	-1.660
$\text{Mg} = \text{Mg}^{2+} + 2\text{e}$	-2.370
$\text{Na} = \text{Na}^+ + \text{e}$	-2.714
$\text{K} = \text{K}^+ + \text{e}$	-2.925
$\text{Li} = \text{Li}^+ + \text{e}$	-3.045

The reversible potential E_0 for the above reaction at 2M NaCl, $p_{\text{Cl}_2} = 600$ mm Hg, and $T = 298$ K, assuming the activity coefficient of Cl^- to be unity, can be calculated as follows.

$$\begin{aligned}
 E_0 &= E^0 - \frac{RT}{2F} \ln \left[\frac{(a_{\text{Cl}^-})^2}{a_{\text{Cl}_2}} \right] \\
 &= 1.359 - \frac{2.303RT}{2F} \log \left[\frac{(a_{\text{Cl}^-})^2}{a_{\text{Cl}_2}} \right] \\
 &= 1.359 - \left(\frac{2.303 \left(1.987 \frac{\text{cal}}{\text{g.mol K}} \right) 298 \text{ K}}{\left(2 \frac{\text{g.mol}}{\text{g-mol}} \right) \left(23,060 \frac{\text{cal}}{\text{g.mol V}} \right)} \right) \log \left(\frac{2^2}{600/760} \right) \\
 &= 1.359 - 0.0296 \log (5.066) \\
 &= 1.338 \text{ V vs SHE}
 \end{aligned}$$

where SHE refers to the standard hydrogen electrode (Section 4.1.6 and Table 4.1.2).

4.1.3. Reversible Electrode Potentials

4.1.3.1. *The Chlorine Electrode Process.* Chlorine exists in various oxidation states [5–7] as shown in Table 4.1.3. Of these, the chloride ion and elemental chlorine couple



TABLE 4.1.3 Oxidation States of Chlorine

Oxidation number	Examples
-1	Chloride ion Cl^-
0	Elemental chlorine Cl_2
1	Hypochlorous acid/Hypochlorite HClO/OCl^-
	Chlorine oxide Cl_2O
3	Chlorous acid/Chlorite $\text{HClO}_2/\text{ClO}_2^-$
4	Chlorine dioxide ClO_2
5	Chlorate ClO_3^-
6	Chlorine trioxide ClO_3
7	Perchlorate ClO_4^-
	Chlorine heptoxide Cl_2O_7
8	Chlorine tetroxide ClO_4

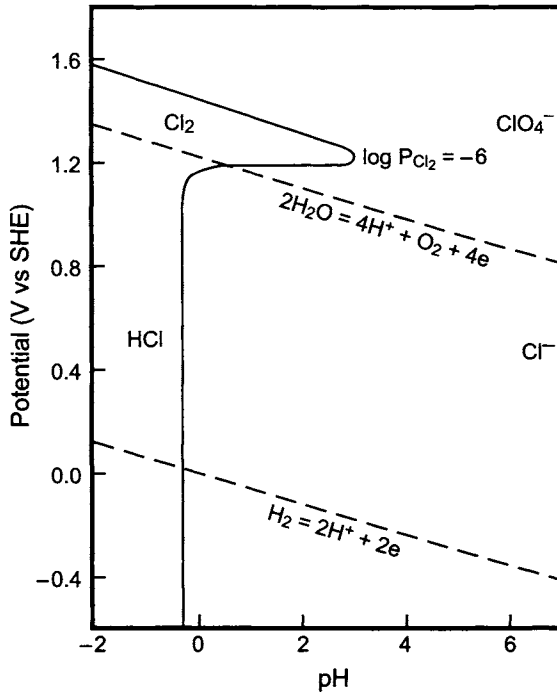
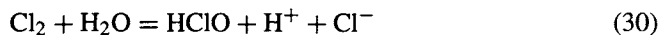


FIGURE 4.1.1. Potential-pH diagram for the chlorine-water system at 25°C [6]. (With permission from NACE and CEBELCOR).

are important in the context of chlor-alkali technology. Its reversible potential is represented by Eq. (29):

$$E_0 = E_{\text{Cl}^-/\text{Cl}_2}^0 + \frac{RT}{2F} \ln \frac{p_{\text{Cl}_2}}{(a_{\text{Cl}^-})^2} \quad (29)$$

where $E_{\text{Cl}^-/\text{Cl}_2}^0$ is the standard potential, p_{Cl_2} is the partial pressure of chlorine in the gas phase and a_{Cl^-} is the activity of the chloride ion. Figure 4.1.1 is a potential/pH diagram for the chlorine-water system [6]. It should be noted that chlorine is hydrated and hence has a finite solubility in aqueous solutions. The solubility increases with increasing pH, as the dissolved chlorine forms HOCl and OCl⁻, following the reaction schemes (30) and (31), illustrated in Fig. 4.1.2.



The standard potential $E_{\text{Cl}^-/\text{Cl}_2}^0$ of reaction (28) is available from a number of publications [6, 8–11]. Fanta and coworkers [12] measured the standard potential of

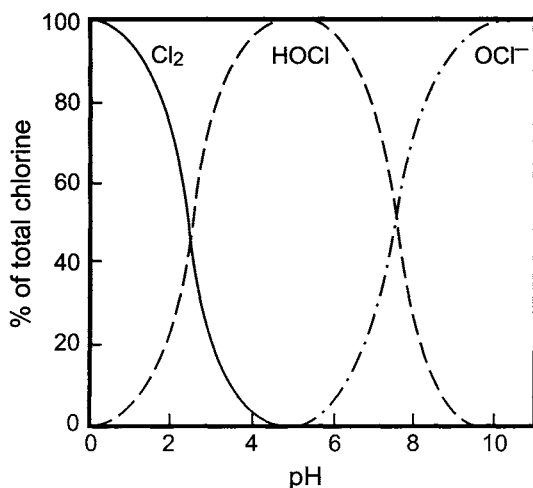
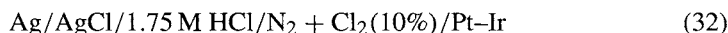


FIGURE 4.1.2. Distribution of the components of active chlorine in the brine as a function of pH at 25°C.

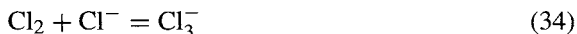
a Cl_2/Cl^- electrode in the temperature range 25–80°C, using the cell:



and found the potential to vary with temperature as:

$$E^0 = 1.47252 + (4.82271 \times 10^{-4}) T - (2.90055 \times 10^{-6}) T^2 \quad (33)$$

These authors used low-pressure chlorine during the experiments to minimize the deviation of the Cl^- activity, caused by the formation of trichloride ions:



Comparison of Eq. (33) with that proposed by Mussini and Longhi [11] in Eq. (35) showed the differences to be minor, within 0.05 V.

$$E^0 = 1.484867 + 3.958492 \times 10^{-4} T - 2.750639 \times 10^{-6} T^2 \quad (35)$$

4.1.3.2. The Hydrogen Electrode Process. There are three oxidation states of hydrogen, as shown in Table 4.1.4. The hydrogen–water couple in solution at pH = 0, in contact with hydrogen gas at a partial pressure of 1 atm at a given temperature, is called the SHE. The electrode reaction is given by Eq. (36):



TABLE 4.1.4 Oxidation States of Hydrogen

Oxidation number	Examples	
-1	Metal hydride	MeH
	Hydride	H
0	Elemental hydrogen	H ₂
1	Water	H ₂ O
	Hydroxide ion	OH ⁻
	Hydrogen ion	H ⁺

The Nernst equation for the hydrogen electrode reaction (36) is

$$E_H = E_H^0 + \frac{RT}{2F} \ln \frac{(a_{H^+})^2}{p_{H_2}} \quad (37)$$

By convention, $E_H^0 = 0$. Assuming $p_{H_2} = 1$ atm, we have

$$E_H = -\frac{2.303RT}{F}(\text{pH}) \quad (38)$$

since

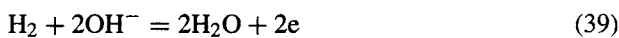
$$\text{pH} = -\log a_{H^+}$$

At 25°C,

$$E_H = -0.059 \text{ pH}$$

The reversible hydrogen electrode potential decreases by 0.059 V with each unit of increasing pH, as shown by the dashed line in Fig. 4.1.1.

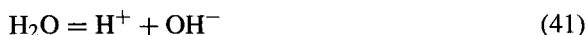
In alkaline media, the H⁺ concentration is low and hence, the potential-controlling reaction is:



When $p_{H_2} = 1$ atm and the activity of water is unity, the Nernst equation for reaction (39) at 25°C in 1N NaOH solutions, assuming the activity coefficient for 1N NaOH solution to be unity, is:

$$\begin{aligned} E_{H^+/H_2} &= E_{H^+/H_2}^0 + 0.0591 \log a_{OH^-} \\ &= -0.828 \text{ V vs SHE} \end{aligned} \quad (40)$$

The reversible potential for reaction (39) can also be calculated from Eq. (38) as follows. The dissociation constant of K_w for reaction (41)



at 25°C is 10^{-14} , and thus the H^+ concentration in 1 M NaOH is estimated to be 10^{-14} M. Substituting $\text{pH} = 14$ into Eq. (38) results in:

$$E_{\text{H}^+/\text{H}_2} = -0.0591 \times 14 = -0.8274 \text{ V vs SHE} \quad (42)$$

which agrees with the value of $E_{\text{H}^+/\text{H}_2}^0$ calculated using Eq. (40). Thus, the reactions (36) and (39) are equivalent and the hydrogen electrode process can proceed through these alternative routes, depending on the operating conditions. In concentrated alkali solutions, there is no doubt that reaction (39) is operative. Also, reaction (39) may occur in dilute acid solutions at high current densities, when the transport of H^+ from the bulk of solution to the cathode surface becomes a limiting factor [13].

4.1.3.3. The Amalgam Electrode Process. Sodium and other alkali metals have three oxidation states: hydride (NaH , -1), metal (Na , 0) and cation (Na^+ , $+1$), where -1 , 0 , $+1$ in the parentheses are the oxidation numbers. The reversible potential of the sodium hydride–sodium ion couple, given by Eq. (43), is -1.162 V vs SHE . It is more positive than the Na/Na^+ couple, represented by reaction (44) and illustrated in Fig. 4.1.3.

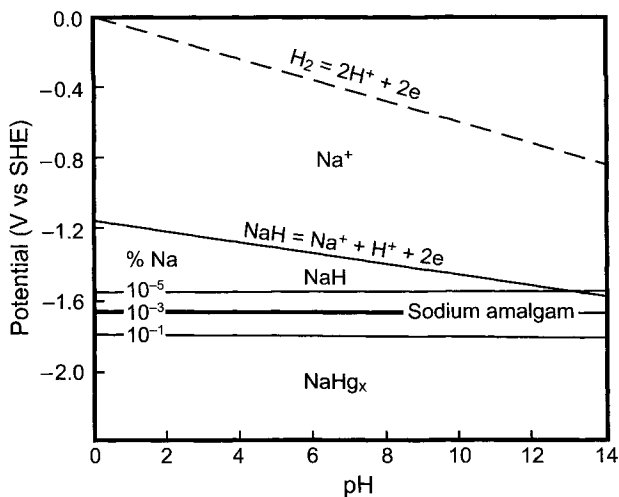
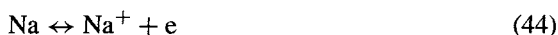
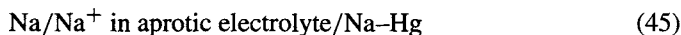


FIGURE 4.1.3. Potential-pH diagram of sodium amalgam in 108 g L^{-1} sodium chloride solution at 25°C [6]. (Courtesy of Marcel Dekker Inc.)

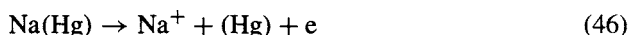


Since metallic sodium is unstable in aqueous solutions, the measurement of the reversible potential for reaction (44) is difficult. This was, however, overcome by measuring the voltage of a cell with sodium metal and amalgam as the electrode in an aprotic electrolyte, to ensure stability of sodium, as:



The potential of the Na-Hg electrode was then measured in a separate cell containing the aqueous solution of sodium salt. The standard potential for reaction (44) thus obtained was -2.714 V [6, 8, 9] or -2.71324 V [14] at 25°C . The standard potentials for the reaction (44) in the temperature range of 5 – 40°C were also reported [14].

The reversible potential of the sodium amalgam electrode



in the concentration range of 0.00001 – 0.74 wt% Na in 108 g L^{-1} NaCl is described by Eq. (47):

$$E_{\text{Na-Hg}} = -2.71 + 0.0591 \log \frac{a_{\text{Na}^+}}{a_{\text{Na}}} \quad (47)$$

where a_{Na^+} and a_{Na} are the activities of Na^+ and Na, respectively [15]. These values are depicted in Fig. 4.1.4 for various %Na levels in the amalgam.

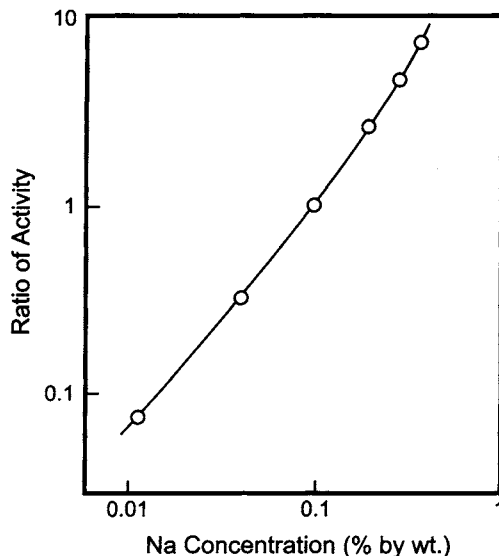
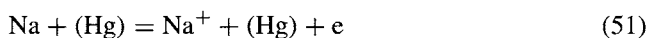


FIGURE 4.1.4. Ratio of the Na ion activity to that in 0.1% sodium amalgam at 80°C . Plotted from the data in [15].

Two other approaches [15] to determine the reversible potential for reaction (46) are as follows. The reversible potential for reaction (46) is given by Eq. (48).

$$E_{\text{Na(Hg)}} = E_{\text{Na(Hg)}}^0 + \frac{RT}{F} \ln \frac{a_{\text{Na}^+}}{a_{\text{Na(Hg)}}} \quad (48)$$

The standard potential for the reaction (46), $E_{\text{Na(Hg)}}^0$, can be determined from the component reactions describing the overall reaction (46) as shown by the schemes (49) and (50).



Reaction (49) represents the dissolution of sodium into the mercury, and reaction (50) describes the charge transfer process between Na and Na^+ . Thus, we can obtain ΔG for reaction (50) as the difference of the ΔG 's of reactions (49) and (51).

Alternatively, we may follow a different approach. When sodium amalgam, having the activity of $[a_{\text{Na(Hg)}}]_0$, is in contact with a sodium chloride solution of unit activity, $a_{\text{Na}^+} = 1$, the reversible potential of reaction (46) is given by Eq. (52) or (53).

$$E_{\text{Na(Hg)}_0} = E_{\text{Na(Hg)}}^0 + \frac{RT}{F} \ln \frac{1}{[a_{\text{Na(Hg)}}]_0} \quad (52)$$

$$E_{\text{Na(Hg)}} = E_{\text{Na(Hg)}_0} + \frac{RT}{F} \ln \frac{a_{\text{Na}^+}}{Y} \quad (53)$$

where

$$Y = \frac{a_{\text{Na(Hg)}}}{[a_{\text{Na(Hg)}}]_0} \quad (54)$$

Equation (53) represents the reversible potential of the sodium amalgam electrode at any concentration, with respect to the same electrode at a specific concentration or activity. For example, the potential of the 0.1 w/o Na amalgam at 80°C is:

$$E_{\text{Na(Hg)}}^0 = -1.834 \text{ V vs SHE} \quad (55)$$

The relative activity of the sodium amalgam Y , with respect to 0.1 w/o Na–Hg at 80°C, is shown in Fig. 4.1.5. In a practical cell, the amalgam concentration is in the range 0.1–0.3 w/o Na, mostly 0.2 w/o. At 0.2 w/o Na, $Y \approx 3.8$. Fig. 4.1.5 shows the activity coefficient of NaCl solutions. Thus,

$$E_{\text{Na(Hg)}}^0 = -1.834 + \frac{1.987 \times 353.15}{23,060} \ln \frac{4.032}{3.8} = -1.822 \text{ V vs SHE} \quad (56)$$

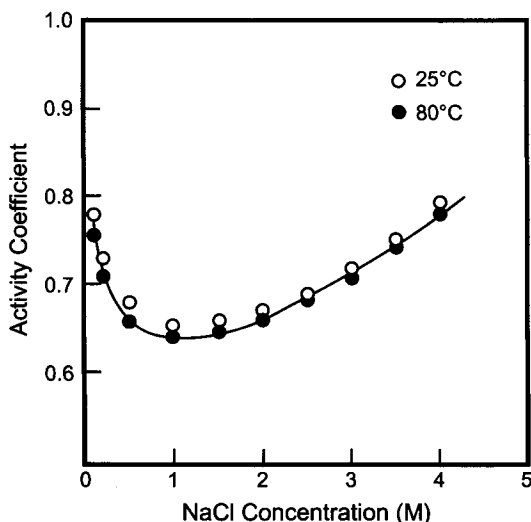


FIGURE 4.1.5. Mean activity coefficient of NaCl solutions [15].

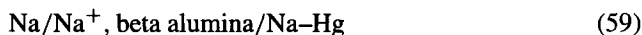
The reversible potential can be evaluated from the Gibbs free energy [10,11,16]. Although thermodynamic data at 25°C are abundant, corresponding values at high temperatures are relatively few. DeBethune and coworkers published very useful papers on the temperature coefficients of electrode potential [17] and of enthalpy, entropy, Gibbs free energy, and specific heat at constant pressure [9].

Balej and coworkers published a number of papers on the thermodynamics and the reversible potential of sodium amalgam in contact with Na^+ [18–27]. They measured the reversible potential of electrochemical cells consisting of



(PC = very dry propylene carbonate)

and



and calculated the equilibrium constant of the reaction:



where Na-Hg_m is an intermetallic compound of Na and Hg. They estimated m to be 4, 5, 6, 7, 8, 9, 10, 12, and 14 with decreasing sodium content. The amalgam in a chlorine cell, which contains <0.3 w/o Na in general, is thus estimated to be a mercury solution of Na-Hg_4 . They evaluated the standard potential $E_{\text{Na-Hg}/\text{Na}^+}^0$ to be

equal to -1.95584 V vs SHE at 25°C by extrapolating the potential vs concentration curve to zero concentration. The activity coefficient $\gamma_{\text{Na-Hg}}$ of Na in the amalgam was found to be:

$$\log \gamma_{\text{Na-Hg}} = 16.393 x_{\text{Na}} \quad (61)$$

where x_{Na} is the mole fraction of Na. Balej also studied the temperature dependence of the potential difference of the cell (Eq. 59) in the temperature range 25 – 165°C and obtained

$$\begin{aligned} \Delta E(T) = & 0.84855 - 3.0326 \times 10^{-4} T - (2.3026RT/F) \\ & \times [\log x_{\text{Na}} + (20.8369 - 1.5737 \times 10^{-2} T)x_{\text{Na}}] \end{aligned} \quad (62)$$

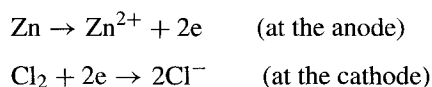
with a mean deviation of $\pm 0.54\%$.

4.1.4. Thermodynamic Decomposition Voltage

In any electrochemical system, there are two electrodes, an anode and a cathode. During electrolysis, electrons are consumed at the cathode while they are generated at the anode. The reactions occurring at the individual electrodes are usually called the component electrochemical reactions, the combination being termed a redox, or oxidation–reduction, reaction system. Let us now examine the component electrochemical reactions involved in the overall reaction.



This redox reaction comprises two reactions involving the exchange of electrons:



A general rule that is particularly useful in computing the thermodynamic decomposition voltage, E_{rev} , of an electrolytic cell is:

$$E_{\text{rev}} = E_{0,\text{a}} - E_{0,\text{c}} \quad (64)$$

where $E_{0,\text{a}}$ and $E_{0,\text{c}}$ are the equilibrium single electrode reduction potentials at the anode and the cathode, respectively.

4.1.5. Galvanic vs Electrolytic Cells

Galvanic processes are spontaneous ($\Delta G < 0$) when the reaction proceeds as written. Batteries and corrosion are examples of galvanic cells. Processes in electrolytic cells are not spontaneous and an external voltage must be applied to make the reaction proceed in

TABLE 4.1.5 Distinguishing Features of Galvanic Cells and Electrolytic Cells

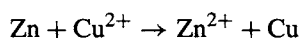
Type of cell	Reaction at the more positive electrode	Reaction at the more negative electrode
Galvanic cell (produces electricity from chemicals)	Reduction (cathode)	Oxidation (anode)
Electrolytic cell (produces chemicals from electricity)	Oxidation (anode)	Reduction (cathode)

the desired direction. The differences between galvanic and electrolytic cells are noted in Table 4.1.5.

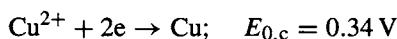
Unlike the case of electrolytic cells, E_{rev} for battery systems is expressed as:

$$E_{\text{rev}} = E_{0,c} - E_{0,a} \quad (65)$$

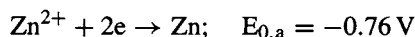
Assuming unit activities at 298 K, E for the following reaction may now be calculated



At the cathode:



At the anode:



Hence,

$$E_{\text{rev}} = 0.34 - (-0.76) = 1.10 \text{ V} \quad (66)$$

A more general definition applicable for any cell is:

$$E_{\text{rev}} = (\text{reduction potential at the more positive electrode in the external circuit}) \\ - (\text{reduction potential at the negative electrode in the external circuit})$$

4.1.6. Measurement of Standard Single Electrode Reduction Potentials

The single electrode reduction potentials are measured with respect to the SHE. The SHE, which is based on the reaction, $2\text{H}^+ + 2e \leftrightarrow \text{H}_2$ on platinumized platinum, is assigned the reduction potential of zero when the activity of the hydrogen ion is unity and the pressure of H_2 is 1 atm. Figure 4.1.6 illustrates the schematic for measuring the standard single reduction potential of Cu^{2+}/Cu and Zn^{2+}/Zn systems.

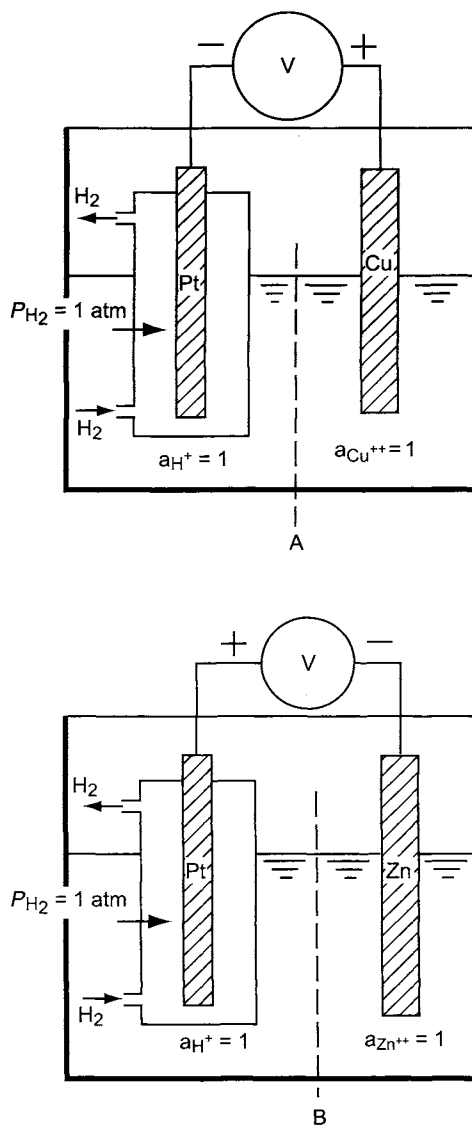


FIGURE 4.1.6. Electric circuit for measurement of electrode potentials. A: Voltmeter reads +0.337 V at 25°C. Copper electrode is positive with respect to SHE; B: Voltmeter reads -0.76 V at 25°C. Zinc electrode is negative with respect to SHE.

The IUPAC has adopted the following conventions [2] for determining the electrode potentials.

1. The cell implicit in the measurement of a standard electrode potential should be arranged so that the SHE is on the left (Fig. 4.1.6).
2. The measured potential difference across such a cell gives the magnitude of the standard electrode potential.

3. The polarity of the electrode on the right, that is, the sign of the charge on the electrode, serves to define the sign that is affixed to the E^0 value.
4. The charge-transfer reaction implicit in the statement of a standard potential is a reduction reaction, for example, $\text{Cl}_2 + 2e \rightarrow 2\text{Cl}^-$.

4.1.7. Standard Reference Electrodes

The measurement of an electrode potential requires the use of a reference electrode [2,28] to complete the electrical circuit (Fig. 4.1.6). The SHE is chosen as the primary reference electrode and its equilibrium potential is assigned the value of zero when the activities of H^+ and $\text{H}_2(\text{g})$ are unity. Thus, the equilibrium single electrode potential values in Table 4.1.2 are relative, as they are measured with respect to the SHE, and are not absolute.

One of the important attributes of a reference electrode is the “reversibility” (i.e., high i_0 [Section 4.2]) associated with the electrochemical reaction setting up the potential. Thus, Pt is reversible for the reaction $2\text{H}^+ + 2e \leftrightarrow \text{H}_2$ and a Pt-Ir electrode is reversible for the reaction $\text{Cl}_2 + 2e \leftrightarrow 2\text{Cl}^-$. Reversibility implies that the Nernst equation is obeyed by the given system and that there are no parasitic reactions. The reference electrodes should have chemical stability in the electrolyte medium; that is, they should not corrode or deteriorate in the given medium.

1. Standard Hydrogen Electrode: The construction of a SHE is simple as shown in Fig. 4.1.6. It consists of a platinized platinum electrode immersed in a solution of $\text{pH} = 0$. H_2 is bubbled continuously through the solution at atmospheric pressure. The equilibrium potential for the SHE described above for the reaction $2\text{H}^+ + 2e \leftrightarrow \text{H}_2$ is given as:

$$E_0 = \frac{RT}{2F} \ln \left[\frac{p_{\text{H}_2}}{(a_{\text{H}^+})^2} \right] = 0 \text{ (V)} \quad (\text{pH} = 0, p_{\text{H}_2} = 1) \quad (67)$$

If the platinized Pt electrode is immersed in a solution whose $\text{pH} = 14$, the equilibrium electrode potential would then be calculated as:

$$\begin{aligned} E_0 &= \frac{RT}{2F} \ln \left[\frac{1}{a_{\text{H}^+}^2} \right] = -0.0591 \text{ pH} \\ &= -0.0591 \times 14 = -0.828 \text{ V vs SHE at } 25^\circ\text{C} \end{aligned} \quad (68)$$

Single electrode potentials for other couples, however, cannot always be measured with a SHE. This problem may be overcome by using other reference electrodes.

2. Calomel Electrode: The most frequently used secondary reference electrode, because of its availability at a modest price, is the calomel electrode, shown in Fig 4.1.7. The electrode reaction responsible for the potential of a calomel

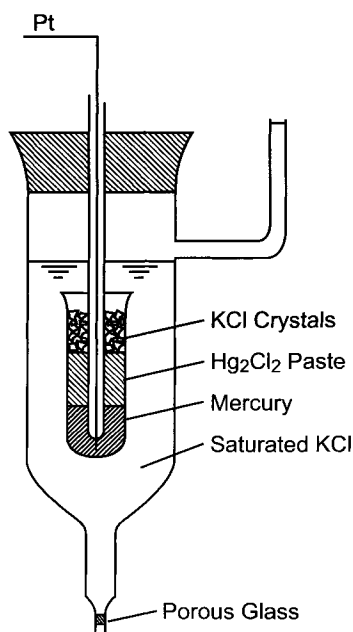


FIGURE 4.1.7. Schematic of a calomel electrode.

electrode is given by



The Nernst equation describing reaction (69) is

$$E_0 = 0.268 - \frac{RT}{2F} \ln \left[\frac{a_{\text{Cl}^-}^2 \cdot a_{\text{Hg}}^2}{a_{\text{Hg}_2\text{Cl}_2}} \right] \quad (70)$$

Since $a_{\text{Hg}} = a_{\text{Hg}_2\text{Cl}_2} = 1$,

$$\begin{aligned} E_0 &= 0.268 - \frac{RT}{F} \ln(a_{\text{Cl}^-}) \\ &= 0.241 \text{ V (at } 25^\circ\text{C for a saturated calomel system)} \end{aligned}$$

3. Silver–Silver Chloride Electrode: Another commonly used reference electrode is the Ag/AgCl electrode. The potential-determining electrode reaction for this electrode is given as:



— the Nernst equation being:

$$E_0 = 0.222 - \frac{RT}{F} \ln a_{\text{Cl}^-} \quad (72)$$

The reader is referred to ref. [28] which describes several other reference electrodes such as Hg/HgO electrode and glass electrode, which are useful in some applications.

REFERENCES

1. G. Kortüm and J.O'M. Bockris, *Text Book of Electrochemistry*, Vol. 1, Elsevier Publishing Company, New York (1951).
2. J.O'M. Bockris and A.K.N. Reddy, *Modern Electrochemistry*, Vols. 1 and 2, Plenum Press, New York (1970).
3. G.M. Barrow, *Physical Chemistry*, 4th Edition, McGraw-Hill Book Company, New York (1979).
4. R. Parsons, Equilibrium Properties of Electrified Interfaces. In J.O'M. Bockris and B.E. Conway (eds), *Modern Aspects of Electrochemistry*, Butterworths Scientific Publications, London (1954), p. 103.
5. W.W. Smith, Chapter 2, Chlorine. In *Supplement to Mellor's Comprehensive Treatise on Inorganic and Theoretical Chemistry*, Vol. 2, Supplement 1, Longmans, London (1965), p. 262.
6. M. Pourbaix, *Atlas of Electrochemical Equilibria in Aqueous Solutions*, Pergamon Press, Oxford (1966).
7. A.J. Downs and C.J. Adams. Chlorine, Bromine, Iodine, and Astatine. In A.F.T. Dickerson (ed.) *Comprehensive Inorganic Chemistry*, Vol. 2, Pergamon Press, Oxford (1970), p. 107.
8. W.M. Latimer, *The Oxidation Potentials of the Elements and Their Potentials in Aqueous Solutions*, Prentice-Hall, Englewood Cliffs (1961).
9. A.J. deBethune and N.A.S. Loud, *Standard Aqueous Electrode Potentials and Temperature Coefficients at 25°C*, Clifford A. Hampel, Skokie, IL (1964).
10. T. Mussini and G. Faita, Chlorine. In A.J. Bard (ed.), *Encyclopedia of Electrochemistry of the Elements*, Vol. 1, Marcel Dekker, New York (1973). p. 1.
11. T. Mussini and P. Longhi, Chlorine. In, A.J. Bard, R. Parsons, and J. Jordan (eds), *Standard Potentials in Aqueous Solutions*, Marcel Dekker, New York (1985), p. 70.
12. G. Faita, P. Longhi, and T. Mussini, *J. Electrochem. Soc.* **114**, 340 (1967).
13. F. Hine, *Boshoku Gijutsu (Corrosion Engineering)* **19**, 513 (1970).
14. R.F. Scarr, Alkali Metals. In A.J. Bard (ed.), *Encyclopedia of Electrochemistry of the Elements*, Vol. 9B, Marcel Dekker, New York (1986), p. 2.
15. F. Hine, *Electrode Processes and Electrochemical Engineering*, Plenum Press, New York (1985), p. 26.
16. I. Barin and O. Knacke, *Thermochemical Properties of Inorganic Substances*, Springer-Verlag, Berlin (1973).
17. A.J. deBethune, T.S. Licht, and N. Swendeman, *J. Electrochem. Soc.* **106**, 616 (1959).
18. J. Balej, *Collection Czechoslov. Chem. Commun.* **40**, 2257 (1975).
19. J. Balej, *Chem. Zvesti.* **22**(6), 767 (1975).
20. J. Balej, *Electrochim. Acta* **21**, 953 (1976).
21. J. Balej, *Electrochim. Acta* **22**, 1105 (1977).
22. J. Balej, F.P. Dousek, and J. Jansta, *Collection Czechoslov. Chem. Commun.* **42**, 2737 (1977).
23. J. Balej and J. Birosov, *Collection Czechoslov. Chem. Commun.* **43**, 2834 (1978).
24. J. Balej, *J. Electroanal. Chem.* **94**, 13 (1978).
25. J. Balej, F.P. Dousek, and J. Jansta, *Collection Czechoslov. Chem. Commun.* **43**, 3123 (1978).
26. J. Balej, *Chem. Zvesti.* **33**(5), 585 (1979).
27. J. Balej, *Electrochim. Acta* **26**, 719 (1981).
28. D.V.G. Ives and G.J. Janz, *Reference Electrodes*, Academic Press, New York (1961).

4.2. KINETICS

4.2.1. Introduction

Treatments of all chemical reactions are based on both thermodynamic principles and kinetics, and electrochemical reactions are no exception. The latter are heterogeneous catalytic processes, accompanied by charge transfer at an electrode immersed in an electrolyte.

The rate of a chemical reaction, ν , represented by Eq. (1),



can be described, following the Theory of Absolute Reaction Rates [1], as

$$\nu = dC_C/dt = (kTC_A/h) \exp(\Delta G^{0\ddagger}/RT) \quad (2)$$

where

k = Boltzmann's constant (cal K⁻¹ or J K⁻¹);

T = temperature (K);

h = Planck's constant (cal sec or J sec);

C = concentration of the species noted in the subscript (mol cm⁻³);

$\Delta G^{0\ddagger}$ = free energy of activation (cal mol⁻¹ or J mol⁻¹);

t = time(sec).

Equation (2) can be recast as:

$$\nu = k^*C_A \quad (3)$$

where

$$k^* = (kT/h) \exp(\Delta G^{0\ddagger}/RT) \quad (4)$$

k^* in Eq. (4) is the concentration-independent rate constant in units of per second and the reaction rate ν has the dimensions of moles per second per cubic centimeter. In electrochemical reactions or electrode processes, the chemical reaction takes place only at the electrode-electrolyte interface, and is two dimensional, unlike the three-dimensional conventional chemical reactions. Therefore, the rate of an electrochemical reaction is represented by the conversion of chemical species per unit area of the electrode surface per second. Hence, the electrochemical rate constant has the dimensions of centimeter per second instead of per second.

An understanding of the nature of chemical reactions requires the details of the elementary-reaction steps in which, the molecules come together, rearrange, and leave as species that differ from the reactants. There are two descriptions that deal with the rates of chemical reactions. The collision theory considers the concept that the reaction of molecules can occur only as a result of collision of the reactant molecules. The transition-state theory focuses on the species that corresponds to the maximum-energy stage in the reaction process. This species is called the activated complex or transition state. The transition state, denoted by the symbol A^\ddagger for reaction (1), is a short-lived species, which is converted to C. The reader is referred to [1-10] for a thorough discussion of the energetics involved in chemical reactions.

4.2.2. Electrochemical Rate Equation

The rates of electrochemical reactions are directly measurable as currents, I . These rates are related to the chemical reaction rate ν by

$$i = zF\nu \quad (5)$$

where

ν = reaction velocity ($\text{mol cm}^{-2} \text{s}^{-1}$)

z = number of electrons involved in the reaction

F = Faraday constant

The current density i is related to the measured current I by

$$i = I/A \quad (6)$$

where A is the electrochemically active area.

The kinetics of electrochemical reactions distinguish themselves from the kinetics of other reactions by their dependence on the potential, V , of the electrode referred to that of a reference electrode in the same electrolyte. Thus, when a potential is applied to a metal in contact with an electrolyte, the energy of the initial state of the ion or molecule and the electron in the metal at the Fermi level is changed by $\pm eV$ or VF per mole of electrons (i.e., 96,485 C), and the activation energy is altered by a fraction β of $\pm VF$.

β is around 0.5 ± 0.1 for many charge-transfer processes and is termed "the symmetry factor." The significance [11] of changing VF in relation to β , illustrated in the schematic energy diagram Fig. 4.2.1, shows its effect on the activation energy ΔE^\ddagger or ΔG^\ddagger for the Gibbs free energy involved in the rate equation. β represents a fraction of the field which changes the potential energy of the activated state when there is an applied potential V across the interface. Thus,

$$\Delta G_V^\ddagger = \Delta G_0^\ddagger \pm \beta VF \quad (7)$$

over a wide range of V .

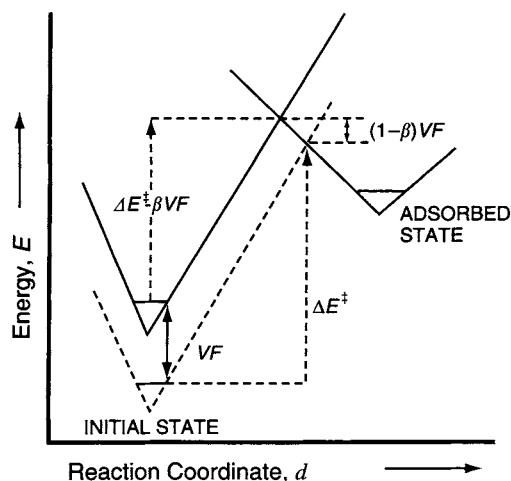


FIGURE 4.2.1. Effect of change of electrode potential, as VF , on energy of activation, ΔE^\ddagger , of an electron transfer reaction in relation to the barrier symmetry factor, β [11].

Let us now examine the rate equation for an electrochemical reaction involving the discharge of H^+ ions on a metal electrode surface, M , to form a $M-H$ species, as:



The basic equation for such a reaction can be written in the form:

$$\frac{i}{zF} = \bar{k}_f C_{H^+,S} (1 - \theta_H) \exp(-\beta VF/RT) - \bar{k}_b \theta_H \exp[(1 - \beta)VF/RT] \quad (9)$$

where

i = current sustained by the reaction (8)

θ_H = coverage of the electrode surface by the product of discharge, H

$C_{H^+,S}$ = local concentration of H^+ at electrode surface in the Helmholtz compact-layer region of the double layer

\bar{k} = rate constant for the process at a hypothetical $V = 0$

f and b = forward and backward reactions, respectively.

This equation is generally called the “Butler–Volmer equation.”

The single electrode potential, V , cannot be measured. However, a practical scale of potentials can be defined if V is referred to the potential of a reference electrode in the same solution. A convenient reference electrode is one that employs the same reaction as the one under consideration, at reversible equilibrium. Then the V scale becomes an overvoltage (η) scale, given by the equation (10).

$$\eta = V - V_{rev} \quad (10)$$

The overvoltage is the driving force that pushes the reaction in a net forward direction. Substituting Eq. (10) into Eq. (9) results in:

$$i = zF \left[k_f C_{H^+,S} (1 - \theta_H) \exp\left(\frac{-\beta \eta F}{RT}\right) - k_b \theta_H \exp\left(\frac{(1 - \beta) \eta F}{RT}\right) \right] \quad (11)$$

where $k_f = \bar{k}_f \exp(-\beta V_{rev} F/RT)$; $k_b = \bar{k}_b \exp((1 - \beta) V_{rev} F/RT)$, k_f and k_b being the electrochemical rate constants for the forward and backward reactions respectively.

Equation (11) can be recast as (for $z = 1$):

$$i = i_0 \left[\exp\left(\frac{-\beta \eta F}{RT}\right) - \exp\left(\frac{(1 - \beta) \eta F}{RT}\right) \right] \quad (12)$$

where

$$i_0 = k_f C_{H^+,S} (1 - \theta_H) = k_b \theta_H$$

i_0 is called the exchange current density and is the anodic and the cathodic current passing reversibly at the equilibrium potential (i.e., $\eta = 0$). It is of great significance to note here

that the rate of an electrochemical reaction, besides being dependent on the temperature as in chemical reactions, is proportional to the exponential of the term containing the overvoltage. Thus, at 300 K and $\beta = 1/2$, a change of 1 V results in a change of the rate constant by a factor of 10^9 , or a change in the overvoltage by 118 mV will change the rate by a factor of 10. It may be noted that η is negative for a cathodic process by convention.

4.2.2.1. *Limiting Cases of Eq. (12) when $\theta_H \ll 1$.* At small overpotentials, say, $\eta < 5$ mV, and near-equilibrium conditions, the exponential terms in Eq. (12) may be linearized in a Taylor series expansion, leading to:

$$i = i_0[-\eta F/RT] \quad (13)$$

Hence,

$$\frac{-di}{d\eta} = \frac{i_0 F}{RT} \quad (14)$$

Under these conditions, the “microscopic polarization” curve shows a linear dependence of i on η , the reciprocal of the slope corresponding to an electrochemical reaction resistance, called the Faradaic resistance, having the dimensions of ohm square centimeter.

When the forward rate of the reaction (8) is predominant at appreciable values of η , the backward reaction rate can be neglected. This leads to:

$$i = i_0 \exp(-\beta\eta F/RT) \quad (15)$$

Equation (15), called the Tafel relation (after Tafel’s work in 1905), can be recast as:

$$\eta = \frac{RT}{\beta F} [\ln i_0 - \ln i] = a + b \ln i \quad (16)$$

or

$$\eta = \frac{2.303RT}{\beta F} [\log i_0 - \log i] = a' + b' \log i \quad (17)$$

where

$$a = \frac{RT}{\beta F} \ln i_0 \quad \text{and} \quad b = -\frac{RT}{\beta F}$$

or

$$a' = 2.303a \quad \text{and} \quad b' = 2.303b$$

The derivative

$$b = -\frac{\partial \eta}{\partial \ln i} \quad \text{or} \quad b' = -\frac{\partial \eta}{\partial \log i} \quad (18)$$

is called the Tafel slope. The slope $|b'|$ on a $\log i$ basis is about 120 mV at $T = 298$ K and $\beta = 0.5$, for a simple discharge reaction of the type depicted by Eq. (8).

The magnitude of the Tafel slope depends on the rate-controlling step during the course of the Faradaic reaction and is generally of the form $(2.303RT/(n + \beta)F)$ or $(2.303RT/mF)$, where n and m are integers. The former dependence arises when desorption of an adsorbed intermediate is rate determining via a further electron transfer step and the coverage of the intermediate is potential-dependent and follows an electro-sorption isotherm. The latter is a consequence of a nonelectrochemical desorption step involving the recombination of adsorbed intermediates or dissociation of a radical. The value of n can range from 1 to 2 and m can vary from 2 to 4. When coverage by an adsorbed intermediate is potential-dependent, the Tafel slope can be written in the form:

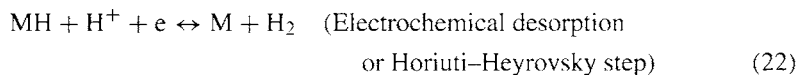
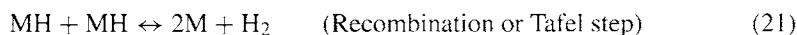
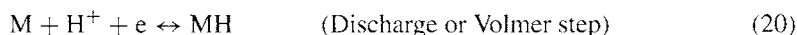
$$\frac{d \log i}{dV} = \frac{1}{b'} = \frac{d \log \theta}{dV} + \frac{\beta F}{2.303 RT} \quad (19)$$

where the first term is the logarithmic derivative of the adsorption isotherm and the second term arises from the potential dependence of electron charge transfer through the symmetry barrier.

4.2.3. Tafel Slope and Exchange Current Density

A knowledge of the magnitude of the Tafel slope and the exchange current density for any given electrochemical reaction on a given substrate is essential not only for understanding the mechanistic aspects of the electrochemical reaction but also for designing electrode structures and compositions to achieve low cell voltages. For the latter purpose, it is desirable to have high i_0 and low Tafel slope, as this would permit operation at high current densities without significant voltage penalties. In this section, the Tafel slope expression for the hydrogen evolution reaction (HER) will be deduced on planar surfaces and porous matrices, followed by a discussion of the complexities associated with the Tafel slope.

4.2.3.1. Tafel Slopes for the Hydrogen Evolution Reaction (HER) on Planar Surfaces and Porous Surfaces. The HER is generally believed to follow the reaction pathways noted below.



The initial step, reaction (20), in the HER is charge transfer, leading to the formation of an adsorbed intermediate MH containing the metal M. The MH can either recombine to form molecular hydrogen by reaction (21) or interact with H^+ and an electron to form hydrogen by reaction (22). The former step is termed the recombination or Tafel reaction and the latter, the electrochemical desorption or Horiuti–Heyrovsky mechanism.

The rates of reactions (20)–(22) can be written as:

$$v_1 = k_1 C_H (1 - \theta) e^{\beta_1 h E} e^{\beta_1 g \theta} - k_{-1} \theta e^{-(1-\beta_1) h E} e^{-(1-\beta_1) g \theta} \quad (23)$$

$$= k_1 C_H e^{\beta_1 h E} e^{-\beta_1 g \theta} (Y - \theta) \quad (24)$$

where

$$Y = 1 - \frac{k_{-1} \theta}{k_1 C_H} e^{-h E} e^{g \theta} \quad (25)$$

$$v_2 = k_2 \theta^2 e^{2g \theta} - k_{-2} (1 - \theta)^2 e^{-2g \theta} \quad (26)$$

$$= k_2 e^{2g \theta} (\theta^2 - X) \quad (27)$$

where

$$X = \frac{k_{-2}}{k_2} (1 - \theta)^2 e^{-4g \theta} \quad (28)$$

$$v_3 = k_3 C_H \theta e^{\beta_3 h E} e^{\beta_3 g \theta} - k_{-3} (1 - \theta) e^{-(1-\beta_3) h E} e^{-(1-\beta_3) g \theta} \quad (29)$$

$$= k_3 C_H e^{\beta_3 h E} e^{\beta_3 g \theta} (\theta - A) \quad (30)$$

$$A = \frac{k_{-3}}{k_3 C_H} (1 - \theta) e^{-h E} e^{-g \theta} \quad (31)$$

where v_1 , v_2 , and v_3 represent the electrochemical reaction rates for the reaction pathways (20), (21), and (22), respectively. In these equations, F/RT is written as h , and C_H refers to the concentration of the reactant H^+ ions. The k s in the above expressions refer to the rate constants for Eqs. (20)–(22), the negative sign representing the backward reaction step, and are equal to $k_i^0 \exp(\beta_i h E_{rev})$, E to the electrode potential, and β_1 and β_3 to the symmetry factors for the forward reactions of (20) and (22), respectively. The exponential terms in the rate equations have been written with a positive argument for the cathodic direction of the HER, for the sake of convenience. The quantity g in Eqs. (23)–(31) represents, in RT units, the change of the free energy of adsorption under Temkin isotherm conditions of adsorption [12], which accounts for the heterogeneity of the surface with no molecular interactions between the molecules.

The total current density, i , can be described under steady-state conditions, based on charge and material considerations, as:

$$\frac{i}{F} = v_1 + v_3 = 2(v_2 + v_3) \quad (32)$$

One can now define the Tafel slope, b , as:

$$\frac{1}{b} = \left(\frac{\partial \ln i}{\partial E} \right)_{C_H} = \frac{1}{i} \left(\frac{\partial i}{\partial E} \right)_{C_H} \quad (33)$$

Using Eqs. (32) and (33), the expression for the Tafel slope may be written in the form:

$$\frac{1}{b} = \frac{\{ [(\partial v_1/\partial E)_\theta + (\partial v_3/\partial E)_\theta]_{C_H} + [(\partial v_1/\partial \theta)_E + (\partial v_3/\partial \theta)_E]_{C_H} (\partial \theta/\partial E)_{C_H} \}}{v_1 + v_3} \quad (34)$$

where $(\partial \theta/\partial E)_{C_H}$ can be obtained by the steady-state material balance Eq. (35) for the adsorbed intermediates, for the reaction scheme represented by Eqs. (20)–(22).

$$\gamma \frac{\partial \theta}{\partial t} = 0 = v_1 - 2v_2 - v_3 \quad (35)$$

$$\gamma = q_{\max}/F$$

q_{\max} in the above equation refers to the saturation coverage ($\mu\text{C cm}^{-2}$), by the adsorbed H species.

Equation (34) shows the expression for the Tafel slope to be complex, its value depending on the characterizing parameters involved in the various reaction steps. However, one can obtain limiting values by making assumptions regarding the magnitude of the symmetry factor, the interaction energy between the adsorbed MH species and the magnitude of the coverage by the adsorbed MH intermediate. Reference [13] gives the detailed derivation of the generalized expressions for the Tafel slope and reaction order for the HER.

The limiting expression when the recombination reaction (the Tafel step) is the rate-determining step can be shown to be:

$$b = \frac{RT}{F} \left[\frac{1 + g\theta(1 - \theta)}{2(1 + g\theta)(1 - \theta)} \right] \quad (36)$$

when $g = 0$ and $\theta \rightarrow 0$, $b = RT/2F$ and when $\theta \rightarrow 1$, $b \rightarrow \infty$.

When the electrochemical desorption mechanism (the Horiuti–Heyrovsky step) becomes rate controlling,

$$b = \frac{RT}{F} \left[\frac{1 + g\theta(1 - \theta)}{\beta + (1 - \theta)(1 + g\theta)} \right] \quad (37)$$

Thus, when $g = 0$ and $\beta = 0.5$, $b = 2RT/3F$ for $\theta \rightarrow 0$, and $b = 2RT/F$ for $\theta \rightarrow 1$.

Schematic Tafel relations when each of the steps noted in Eqs. (20)–(22) becomes rate determining are depicted in Fig. 4.2.2. The Tafel relationships deduced here describe the current–voltage behavior when the HER is proceeding on a planar surface. However,

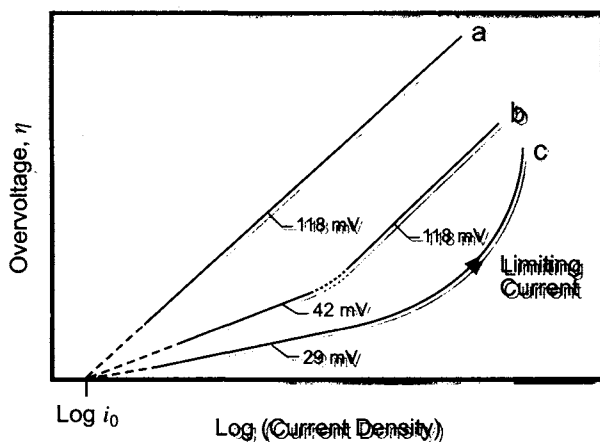


FIGURE 4.2.2. Schematic Tafel relations for rate controlling: (a), H^+ discharge; (b), electrochemical desorption; and (c) recombination at $25^\circ C$ [11].

TABLE 4.2.1 Limiting Values of Tafel Slopes on Planar and Porous Electrodes for Various Reaction Schemes

Reaction scheme	Planar electrodes		Porous electrodes	
	$\theta \rightarrow 0$	$\theta \rightarrow 1$	$\theta_f \rightarrow 1$	$\theta_f \rightarrow 1$
$A^+ + e \xrightarrow{\text{slow}} A_{\text{ads}}$	$2RT/F$	$2RT/3F$	$4RT/F$	$4RT/3F$
$A_{\text{ads}} + e \rightleftharpoons B$				
$A^+ + e \rightleftharpoons A_{\text{ads}}$	$RT/2F$	∞^a	RT/F	Non-Tafel: $i \propto \eta^{0.5}$
$2A_{\text{ads}} \xrightarrow{\text{slow}} B$				
$A^+ + e \rightleftharpoons A_{\text{ads}}$	$2RT/3F$	$2RT/F$	$4RT/3F$	$4RT/F$
$A_{\text{ads}} + A + e \xrightarrow{\text{slow}} B$				
$A^+ + e \rightleftharpoons A_{\text{ads}}$	RT/F	∞^a	$2RT/F$	Non-Tafel: $i \propto \eta^{0.5}$
$A_{\text{ads}} \xrightarrow{\text{slow}} B$				

Note:

^a"Saturation" or potential independent limit.

Source: Reproduced by permission from The Electrochemical Society, Inc.

if the HER is occurring on a porous matrix, the current-voltage relationship will be more complex. Nevertheless, it is possible to derive the limiting characteristics, employing a homogeneous model [14] for the porous electrode. These results, presented in Table 4.2.1, show doubling of the Tafel slopes when the slow step involves an electron-transfer step, and "quadratic" behavior, or linearity of η in i^2 , when a chemical step becomes rate controlling.

The discussion presented above assumes that the same mechanism prevails whether the reaction is occurring on a planar or a porous surface. However, it is possible that the mechanism or the slow step on a porous or a high surface area electrode is different,

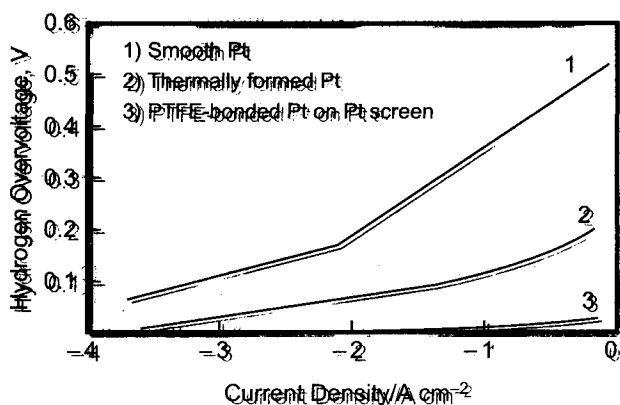


FIGURE 4.2.3. Comparison of the polarization data for the HER on three types of Pt: smooth Pt and two high-area materials. [15].

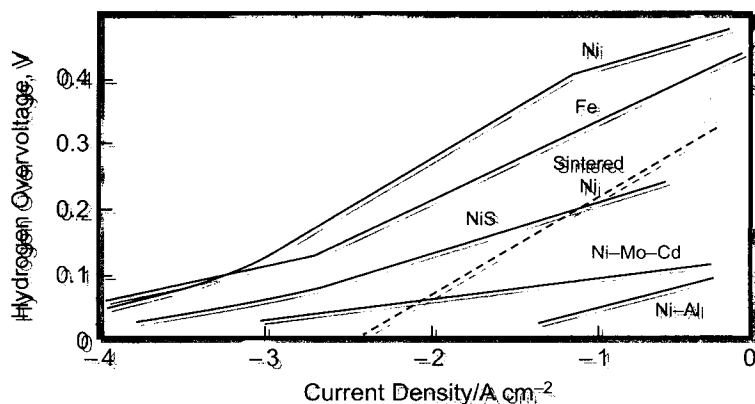


FIGURE 4.2.4. Comparison of polarization data for HER on various Ni electrodes and pure Fe [15].

resulting in a different value for the Tafel slope. This behavior is exemplified in Figs. 4.2.3 and 4.2.4 for the HER in alkaline media.

Thus, as shown above, the magnitude of the Tafel slope depends on the surface morphology of the electrode material and the reaction mechanism. In addition, it is also a function of the temperature, deviating from the expected direct proportionality and exhibiting decreasing Tafel slopes with increasing temperature (e.g., HER on Ni-Mo-Cd in alkaline media) or being independent of temperature (e.g., Br₂ evolution on pyrolytic graphite from (n-Pt)₄NBr solutions). A detailed discussion of this issue is beyond the scope of this chapter and the reader is referred to the excellent discussion by Conway [15].

The purpose of addressing these variations of Tafel slopes is to emphasize that it is safer to experimentally determine the magnitude of the Tafel slope under the desired conditions than to take them from the literature. Extrapolations can result in erroneous values, leading to errors in estimating the cell voltage from its components.

4.2.4. Rate Equation Under Mass Transfer Control :

The electrochemical rate equation presented in Sections 4.2.2 and 4.2.3 is applicable when the electrochemical reactions are under activation or kinetic control. However, when mass transfer of the electroactive species becomes rate controlling, the rate equation requires modification, as shown below.

The mass transfer of an ionic species M^+ from the bulk of the solution to the cathode surface during its reduction, is controlled by two factors, migration and diffusion [16]. Thus,

$$v = v_m + v_d \quad (38)$$

$$v_m = \frac{\lambda C}{\kappa} \frac{i}{F} = t \frac{i}{F} \quad (39)$$

$$v_d = -D \frac{dC}{dx} \quad (40)$$

where

v = flux or reaction rate ($\text{mol cm}^{-2} \text{s}^{-1}$)

t = transport number

x = distance (cm)

C = concentration (mol cm^{-3})

D = diffusion coefficient ($\text{cm}^2 \text{s}^{-1}$)

λ = equivalent conductance ($\text{mho cm}^{-2} \text{g eq}^{-1}$)

κ = conductivity of the solution (mho cm^{-1})

m and d (in the subscripts) = migration and diffusion, respectively.

When the solution contains supporting electrolyte, the contribution of migration to mass transfer is small. Hence, the flux, v , or the current density, i , is a result of diffusion, since the charge-transfer step is considered to be fast. The M^+ concentration at the cathode surface, C_S , decreases under these conditions as shown in Fig. 4.2.5. Assuming a linear distribution of concentration in the diffusion layer thickness δ , we have, at steady state:

$$v = D \left(\frac{C - C_S}{\delta} \right) \quad (41)$$

Equation (41) shows that the reaction rate is highest when C_S approaches zero. Since $i = nFv$, Eq. (41) can be rewritten as:

$$i_d = nFD \left(\frac{C - C_S}{\delta} \right) \quad (42)$$

and the maximum current density is

$$i_L = nFD \left(\frac{C}{\delta} \right) \quad (43)$$

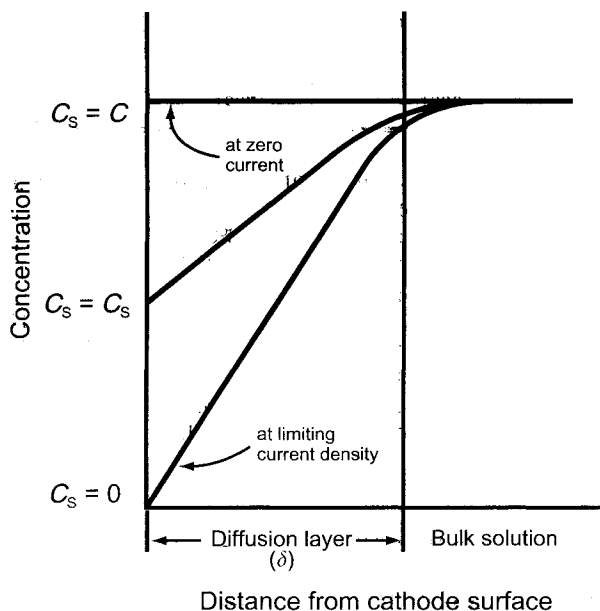


FIGURE 4.2.5. Concentration of species near the diffusion layer.

Thus,

$$\frac{i_d}{i_L} = 1 - \frac{C_s}{C} \quad (44)$$

where i_d is the current density controlled by diffusion. It is clear that i_L is the maximum current density when $C_s = 0$, and this is called the limiting current density.

Since the charge-transfer step is assumed to be nearly reversible, the Nernst equation can be applied:

$$E = E^0 + \frac{RT}{nF} \ln C \quad \text{at } i = 0$$

$$E' = E^0 + \frac{RT}{nF} \ln C_s \quad \text{at } i = i_d$$

By convention,

$$\eta = E' - E = \frac{RT}{nF} \ln \left(\frac{C_s}{C} \right) \quad (45)$$

Substituting Eq. (44) in Eq. (45) results in:

$$\eta = \frac{RT}{nF} \ln \left(1 - \frac{i_d}{i_L} \right) \quad (46)$$

This equation shows that η becomes infinite when i_d approaches i_L . Substituting the following data for the cathodic deposition of copper from acidified copper sulfate solution,

$$\begin{aligned} i_L &= 0.12 \text{ A cm}^{-2}, & C &= 10^{-3} \text{ mol cm}^{-3} \\ D &= 10^{-5} \text{ cm}^2 \text{ s}^{-1}, & nF &= 2 \times 96,500 \text{ A s mol}^{-1} \end{aligned}$$

in Eq. (43), we can calculate the thickness of the diffusion layer δ as

$$\delta = \frac{2 \times 96,500 \times 10^{-5} \times 10^{-3}}{0.12} \approx 1.6 \times 10^{-2} \text{ cm}$$

The thickness of the diffusion layer is generally in the range 10^{-4} – 10^{-2} cm, depending on the hydrodynamic conditions at the electrode-electrolyte interface.

We may now consider the effect of migration on the current density, which can be described as follows. Since the contribution to the total current is from diffusion and migration,

$$i = i_m + i_d = nFD \left(\frac{nFC\phi}{RT} - \frac{dC}{dx} \right) \quad (47)$$

where i_m and i_d are the currents associated with migration and diffusion, respectively, and ϕ is the electric field in volts per centimeter. The current density, i , can also be described by the conventional rate equation, without any coverage effects, as:

$$i = \frac{i_d}{1-t} = i_0 \left(\frac{C_S}{C} \right) [\exp(f\eta) - \exp(-f'\eta)] \quad (48)$$

where $t = i_m/i$ is the transport number, and C_S is the concentration of the ionic species of interest at the electrode surface. Also, $f = \alpha F/RT$, and $f' = (1-\alpha)F/RT$.

Substituting $\frac{C_S}{C} = 1 - \frac{(1-t)i}{i_L}$ in Eq. (48) results in:

$$i = \frac{i_0 [\exp(f\eta) - \exp(-f'\eta)]}{1 + (1-t)(i_0/i_L) [\exp(f\eta) - \exp(-f'\eta)]} \quad (49)$$

If mass transfer is fast, and the reaction step is slow, Eq. (49) becomes:

$$i = i_0 [\exp(f\eta) - \exp(-f'\eta)] \quad (50)$$

when $(1-t) \frac{i_0}{i_L} \exp(-f\eta) \ll 1$, which agrees with Eq. (12). On the contrary, for a mass transfer-controlled process, when $(1-t) \frac{i_0}{i_L} \exp(-f\eta) \gg 1$, and $f + f' = F/RT$,

$$i = \frac{-i_L}{1-t} \left[\exp\left(\frac{F\eta}{RT}\right) - 1 \right] \quad (51)$$

or

$$\eta \equiv \frac{RT}{F} \ln \left[1 - (1-t) \frac{i}{i_0} \right] \quad (52)$$

when $t \equiv 0$, Eq. (51) becomes Eq. (46).

4.2.5. Electrocatalysis

The electrochemical reactions of relevance to chlor-alkali operations are the Cl_2 evolution reaction, the H_2 evolution reaction, the O_2 evolution and reduction reactions, and the OCl^- and ClO_3^- reduction reactions. It is important to understand the mechanistic factors involved in these reactions on the substrates that are currently used in the industry, to permit optimization of the pertinent reaction rates, and to aid in the further development of cost-effective electrode materials. In this context, it is relevant to examine the electrocatalytic effects involved for a given electrochemical reaction.

Electrocatalysis may in general be described as the ability of the electrode surface to alter the rates of the reactions, as reflected by the changes in the magnitude of the exchange current density with the type and nature of the substrate in a given medium. This section will present the current status of our understanding of the electrocatalysis of the reactions of interest to us [(8, 17-20)].

It must be emphasized that elucidation of the reaction mechanism requires a knowledge of various parameters, including the Tafel slopes, reaction orders, and stoichiometric numbers, complemented by an independent determination of the surface coverage by the adsorbed intermediates. All these parameters should be consistent with the postulated mechanism. However, most kinetic investigations focus on one parameter to propose the reaction mechanism, more specifically, the rate-determining step involved in the overall reaction. This approach would certainly lead to dubious conclusions.

4.2.5.1. The Hydrogen Evolution Reaction (HER). The HER is the most thoroughly examined reaction from a fundamental viewpoint and, as noted earlier, it is generally accepted to follow the pathways described by Eqs. (20-22). Starting from the basic electrochemical rate equations, it can be shown that the exchange current density is related to the free energy of activation of H_2 on a given metal surface, and the free energy of activation at the reversible potential, ΔG_r^0 ,

$$i_0 = k\theta^{*\beta}(1-\theta^*)^{(1-\beta)}e^{\Delta G_r^0} \quad (53)$$

where k is a constant, β is the symmetry factor, and θ^* is the value of the coverage, θ , at the reversible potential, governed by the adsorption isotherm. Under Langmuir isotherm conditions, the isotherm is given by

$$\left(\frac{\theta^*}{1-\theta^*} \right)^2 = p_{\text{H}_2} \exp(-\Delta g^0/kT) \quad (54)$$

where p_{H_2} is the hydrogen pressure and Δg° is the standard free energy of the reaction:



From Eqs. (53) and (54), it follows that:

$$i_0 = k \left[p_{\text{H}_2}^{1/2} \exp\left(\frac{-\Delta g^\circ}{2kt}\right) \right]^\beta \left[1 + p_{\text{H}_2}^{1/2} \exp\left(\frac{-\Delta g^\circ}{2kt}\right) \right]^{-1} \Delta G_r^0 \quad (56)$$

Equation (56) shows that the i_0 value depends solely on the coverage by the adsorbed H intermediates, which is related to the free energy of adsorption of H on the metal, M. When H is bound to the metal strongly (i.e., Δg° is negative) or when the H is weakly bound (i.e., Δg° is positive), the i_0 or the reaction rate at equilibrium becomes small, the maximum i_0 value being realized when $\Delta g^\circ = 0$. These conclusions of Parsons [21] were shown to be in agreement with experimental data (see Fig. 4.2.6) when the i_0 values were plotted as a function of the M–H bond strength. Thus, the Pt group metals, having $\theta \rightarrow 0$, exhibit maximum i_0 values, the sp metals with very weak affinity for H showing the lowest i_0 values. The $d^{10}s^1$ metals, Cu, Ag, and Au and the transition metals, Fe, Co, and Ni, at which an oxide film forms, inhibit the adsorption of H, and thereby, show

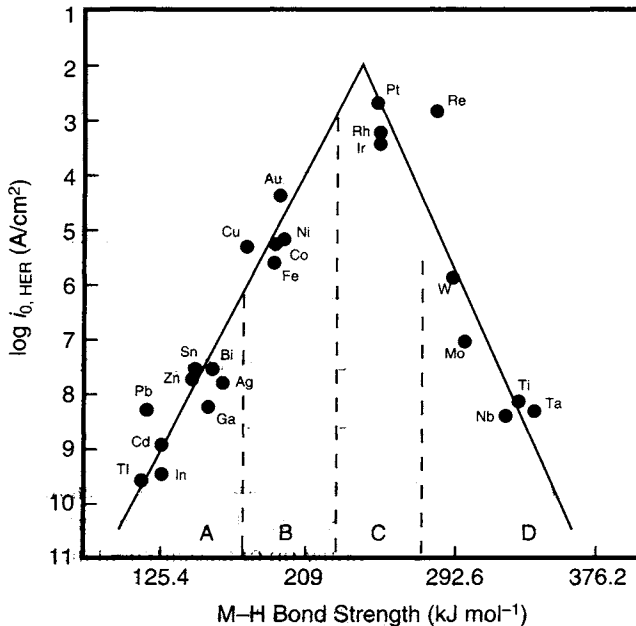
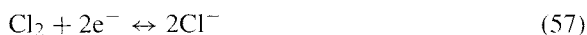


FIGURE 4.2.6. Volcano plot for $\log i_0$ values for the HER as a function of M–H bond strength [20]. A: p-block and d-electron rich metals; weak adsorption of H to form under potential deposited H (UPD H). B: Fe-group and noble metals; stronger adsorption of H than on group A metals. C: Pt-group metals; weak adsorption of H on UPD H. D: valve metals; strong adsorption of H and interstitial absorption of H forming hydrides. (With permission from Elsevier.)

intermediate i_0 values. The metals on which the HER occurs at the metal-hydride phase, covered by barrier layer oxide films (Ti, Ta, etc.), also show low i_0 values, as H is too strongly bound to the metal surface. The plot shown in Fig. 4.2.6 is called a volcano plot. These plots have several implications as to the mechanism of the reaction [19–21].

A casual look at the volcano plots for the HER leads to the temptation of developing a catalyst by mixing the metals on either side of the volcano curve to mimic the performance of the Pt-group metals. Qualitative concepts about electron “spill-over” from one component to the other at the monocrystal grain boundaries, or transfer of adsorbed intermediates from one side to the other, could suggest the possibility of such an effect. However, the theoretical analysis of Parsons [22] showed that, for practical applications, almost no such benefits accrue. It was concluded, based on a rigorous analysis, that it is almost impossible to produce a good electrocatalyst from two poor ones when only one adsorbed intermediate is involved in the overall reaction. This appears to be generally true based on experimental observations in the case of nickel during the course of the HER in alkaline media, as no enhancement in i_0 was observed when nickel was alloyed with various Pt-group metals, transition metals, and others. It should be emphasized that these evaluations should be made on a common basis, ensuring that the surface morphology and the surface area are the same on all the electrode matrices.

4.2.5.2. The Chlorine Evolution Reaction. The anodic reaction of most interest to the chlor-alkali industry is the chlorine evolution reaction. The thermodynamics of the $\text{Cl}_2\text{--Cl}^-$ reaction at equilibrium



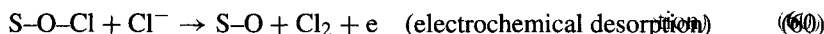
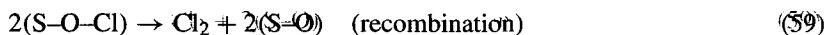
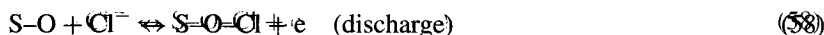
are well established [23]. Detailed data for this reaction at various temperatures and for other equilibria involving Cl_2 , Cl^- , and oxy anions of chlorine are found in refs. [24,25] and also in Section 4.1.

Oxygen, with a lower standard reversible potential, should evolve before chlorine. However, the exchange current densities of the Cl_2 evolution reaction on noble metals [26] are usually substantially greater than those of O_2 evolution. Hence, Cl_2 evolution is the predominant reaction during the electrolysis of saturated aqueous chloride solution in the pH range of 2–5. Furthermore, the chlorine evolution reaction always proceeds, in aqueous media, at electrode surfaces that are covered either partially or completely with an oxide film. Therefore, the state of the oxide film on which chlorine is generated and its properties (i.e., growth characteristics, Cl^- ion adsorbability, conductivity, and catalytic influence) play a critical role during the course of the chlorine evolution reaction.

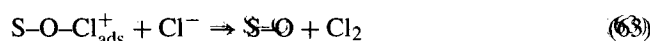
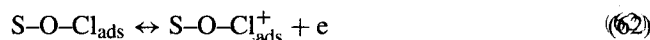
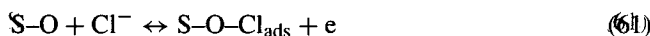
Several reviews addressing the polarization behavior, Cl^- adsorption, competition between Cl^- adsorption and OH^- codeposition, oxide film formation and Cl^- ion discharge, as well as the kinetic aspects on oxide-covered and oxide-free surfaces have been published. Section 4.5 reviews the mechanistic aspects of chlorine evolution, focusing on the nature and characterization of the adsorbed intermediates [26,27].

The chlorine evolution reaction proceeds on an oxidic surface covering the base metal substrate. Denoting the substrate covered with an oxide film as S–O, the various

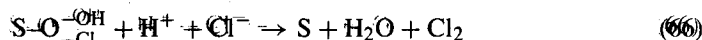
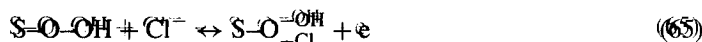
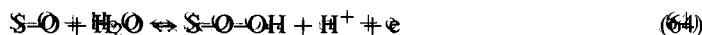
steps involved during the discharge of Cl^- ions are noted below, along with the terminology describing them.



These pathways are essentially the same as those proposed for the HER. However, the possible slow steps described by the reaction schemes (59) and (60) cannot explain the reaction order of 1 with respect to the Cl^- ion observed experimentally with the $\text{RuO}_2 + \text{TiO}_2$ electrodes, and hence, this scheme was abandoned. An alternative pathway [28] that explains the first-order reaction with respect to the chloride ion involves the adsorbed intermediate $\text{S-O-Cl}_{\text{ads}}^+$.



Reaction schemes proposed to explain the similar chloride ion reaction order [27,32] are discussed in Section 4.5. However, additional investigations [27–31] have revealed decreasing currents with decreasing pH, implying a reaction order of -1 to -2 with respect to H^+ , which lead to the suggestion of the following mechanism on RuO_2 -based oxide electrodes:



The observation of the negative reaction order for the chlorine evolution reaction with respect to the H^+ ions is a questionable issue [33].

A wide variety of oxide materials have been examined as substrates for the chlorine evolution reaction from a fundamental viewpoint, to establish the mechanistic pathways during the course of this reaction. Some of these results obtained in NaCl solutions are presented in Table 4.2.2, along with the postulated rate-determining step.

Irrespective of which reaction scheme (58–66) is the rate-controlling step during the Cl_2 evolution reaction, it is obvious that the “ S-O-Cl ” species is involved in the rate-controlling path, as Cl_2 evolution always occurs on a surface that is covered by an oxide film, with anions adsorbed on it. It is therefore reasonable, as in the case of the HER, to relate the i_0 for the Cl_2 evolution reaction to the bond strength of the adsorbed intermediate, which presumably is the S-O-Cl species. Table 4.2.3 shows a comparison

TABLE 4.2.2 Kinetic Parameters for the Chlorine Evolution Reaction (from 5M NaCl Solutions at 25°C.)

Electrode material	i_0 (A cm ⁻²)	Tafel slope (mV)	Refs	Postulated mechanism (Reaction #)
Pt	8.5×10^{-3}	72	34	59 or 60
Ir	6.4×10^{-3}	76	34	59 or 60
Rh	5.9×10^{-3}	90	34	59 or 60
Pt-Ir	0.85×10^{-3}	86	34	59 or 60
(70:30; smooth)				
Pt-Ir (70:30; thermally formed)	3.75×10^{-3}	36	34	59 or 60
Ru	0.2×10^{-3}	38-40	34	59 or 60
TiO ₂ + RuO ₂ on Ti	1.25×10^{-3}	40	34	59 or 60
Vitreous carbon	0.3×10^{-3}	120	34	58
Graphite	1.2×10^{-3}	40-120	34	59 or 60
Fe ₃ O ₄	5.5×10^{-8}	85	35	
TiO ₂	4.0×10^{-5}	30-120 at high overvoltages	36	58?
IrO ₂	1.17×10^{-3}	40	37	60
RuO ₂ (30) + Co ₃ O ₄ (10)+ TiO ₂ (60 mol%)	$\sim 10^{-4}$	~ 40	38	
Ru _{0.3} Pt _{0.3} Ce _{0.4} O ₂	3.0×10^{-3}	32	39	66
Ru _{0.3} Pt _{0.7} O ₂	1.0×10^{-2}	31	40	66
Co ₃ O ₄ (thermally formed)	8.5×10^{-6}	40	41	S-OH ₂ ⁺ + Cl ⁻ = S-OH ₂ Cl S-OH ₂ Cl = S-OHCl + H ⁺ + e S-OHCl → S-(OHCl) ⁺ + e S-(OHCl) ⁺ + Cl ⁻ = S-OH ₂ ⁺ + Cl ₂

TABLE 4.2.3 Comparison of Some i_0 Values for the Chlorine Evolution Reaction and ΔH Values for Cl Bonding (From Ref. 26)

Substrate	ΔH_{SO-Cl} (kcal mol ⁻¹)	ΔH_{M-Cl} (kcal mol ⁻¹)	$\Delta H_{measured}$ (kcal mol ⁻¹)	log i_0 (A cm ⁻²)
IrO ₂	21	91	65.127	-1.4
MnO ₂	64	87		-2.2
RuO ₂	30	80	256	-2.2
TiO ₂	115	109	15	-4.4
C (graphite)			31-35	-3.6

of log i_0 values and ΔH_{SO-Cl} and ΔH_{M-Cl} , calculated using Pauling's formula, with the electronegativity values for binary oxides estimated by

$$\Delta H_{M-Cl} = \frac{1}{2}(D_{MM} + D_{ClCl}) + 23.06(\chi_M - \chi_{Cl})^2 \tag{67}$$

where D_{MM} and D_{ClCl} refer to the dissociation energies of the metal lattice and of Cl₂, respectively, and χ refers to the electronegativities. The electronegativity of the oxide is

calculated from

$$\chi_{M_3O_2} = \frac{y\chi_M + z\chi_O}{y + z} \quad (68)$$

The calculated ΔH_{M-Cl} and ΔH_{SO-Cl} values are compared [26] in Table 4.2.3 with the experimentally determined values of heats of adsorption of Cl_2 on various materials using flash desorption spectrometry. The lack of agreement between the experiment and the calculations clearly indicates that the substrate–chloride interactions are more complex in character than presumed here, and that there is no obvious correlation relating the electrochemical characteristics to the simple metal oxide–chloride interactions.

Several electrocatalytic correlations have been developed based on limited experimental data. These include the dependence of the rates of the Cl_2 evolution reaction on $M-Cl$ dissociation energy [42] (Fig. 4.2.7) and d-band vacancy [43] (Fig. 4.2.8), of Pt + noble metal alloys.

In addition, a qualitative description [37,42] was also proposed, hoping to find a relationship between the Cl_2 evolution mechanism and the catalytic activities of oxide electrodes (e.g., RuO_2 , IrO_2 , WO_3 , and Ti/PtO_2) by taking into account the chemical and physical properties of these oxide electrodes. It was proposed that the active site on the electrode is a Ru center and that a Cl^- ion is adsorbed on the “Ru–OH” site, thus completing the Ru^{3+} coordination shell. The Cl_2 evolution mechanism involved the interaction of the electrode surface with adsorbed Cl atoms. Thus, if the electrode contains a transition metal cation with partially filled t_{2g} levels and empty e_g levels, as in the case of RuO_2 and IrO_2 , electrochemical desorption (Eq. 60) becomes the rate-determining step. However, if the transition metal cation has a half or just filled t_{2g} , and partially filled e_g levels, as in the case of TiO_2 –“ PtO_2 ,” it is suggested that the recombination step (Eq. 59) becomes rate-limiting. Table 4.2.4 depicts these conclusions for some metal oxides during the Cl_2 evolution reaction.

Summing up, there is no satisfactory relationship as yet relating the i_0 to either the mechanism or the chemical nature of the oxide and the “oxide-adsorbed intermediates”

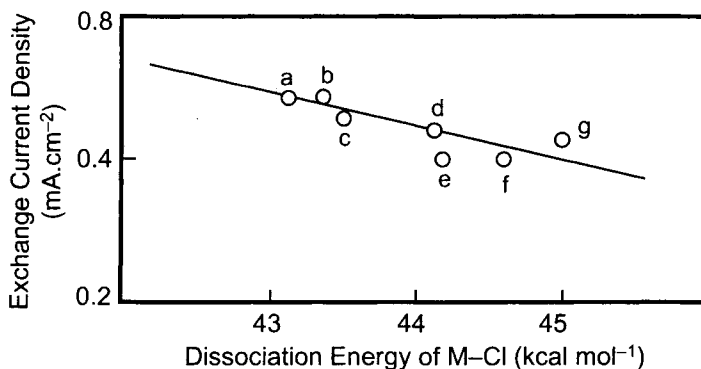


FIGURE 4.2.7. Relationship between exchange current density for chlorine evolution and the dissociation energy of metal chlorides. (a) Pt; (b) Pt/Ir 10.1%; (c) Pt/Ir 15.2%; (d) Pt/Ru 17.6%; (e) Pt/Ru 17%; (f) Pt/Pd 24%; (g) Pt/Rh 32.4% [42]. (With permission from Elsevier.)

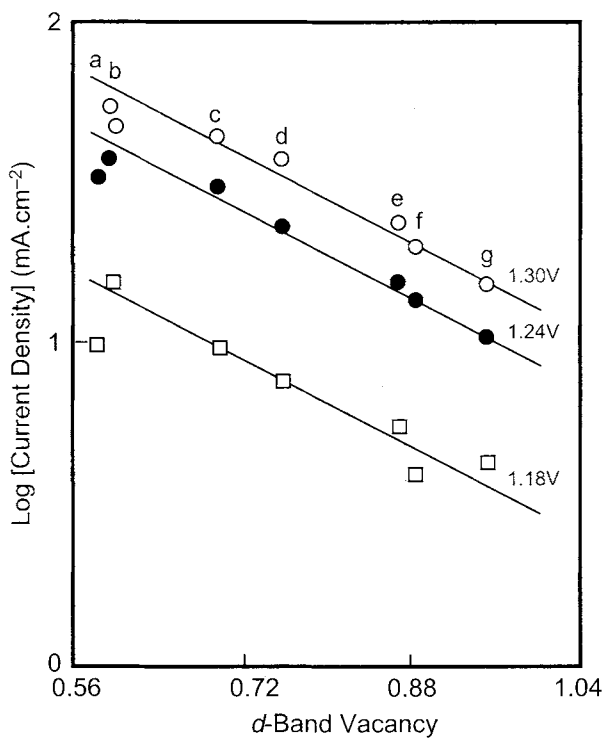


FIGURE 4.2.8. Dependence of the rates of chlorine evolution on *d*-band vacancy at various Pt alloy surfaces at three potentials (V vs SCE). (a) Pt; (b) Pt/Ir 10.1%; (c) Pt/Ir 15.2%; (d) Pt/Ru 17.6%; (e) Pt/Ru 17%; (f) Pt/Pd 24%; (g) Pt/Rh 32.4% [42]. (With permission from Elsevier.)

TABLE 4.2.4 Summary of the Reaction Mechanisms and *i*₀ Values^a for the Chlorine Evolution Reaction as a Function of *d*-Electron Configurations at Various Electrocatalysts

Electrode	Tafel slope	Slow step (equation #)	<i>d</i> -Electron configuration	<i>i</i> ₀ (mA/100 μF)
RuO ₂	2RT/3F	60	(<i>t</i> _{2g}) ⁴	0.118
IrO ₂	2RT/3F	60	(<i>t</i> _{2g}) ⁵	0.39
Eu _{0.3} WO ₃	2RT/3F	60	<i>d</i> ⁰ or (<i>t</i> _{2g}) ^x	0.019
Graphite	2RT/3F	59		
Pt-MnO ₂	RT/2F	59	(<i>e</i> _g) ¹	0.41
Ti-PtO ₂	RT/2F	59	(<i>e</i> _g) ^x	0.55
La _{0.6} Sr _{0.4} CoO ₃	RT/2F	59	(<i>e</i> _g) ^{0.4}	0.433
LaNiO ₃	RT/2F	59	(<i>e</i> _g) ¹	0.144

Note:

^a*i*₀ expressed as mA/100 μF of double layer capacitance and hence real area.

Source: With permission from Elsevier.

participating in the Cl_2 evolution reaction. Furthermore, the mechanism of this reaction is yet to be elucidated in an unequivocal manner, as there are several questions that need to be clarified, even though the $\text{RuO}_2\text{-TiO}_2$ -based anodes have been in commercial use for many years, and have been the focus of fundamental investigations [27,32,33].

4.2.5.3. The Sodium Amalgam Reaction. The deposition of sodium ions onto mercury from a concentrated NaCl solution, given by Eq. (69), proceeds rapidly at low overvoltages [43], as can be seen in Fig. 4.2.9.



However, at very high current densities, the forward and backward reactions of Eq. (69), that is, the anodic and cathodic reactions, are limited by the diffusion of Na and Na^+ in the amalgam and the solution, respectively.

A schematic profile of the concentration of Na and Na^+ under these conditions is shown in Fig. 4.2.10. Thus, when the amalgam electrode is polarized cathodically, one will observe limiting currents, as may be seen with the data for the 0.0002% Na in the amalgam. During anodic polarization [44] of the sodium amalgam, the sodium ion concentration, $C_{\text{Na}}(S)$, decreases with increasing current density, ultimately reaching zero at the maximum current density, $i_L(a)$, as:

$$i_L(a) = \frac{F D_{\text{Na}} C_{\text{Na}}}{\delta_{\text{Na}}} \tag{70}$$

On the other hand, during the cathodic reduction of Na^+ , the surface concentration of Na^+ ion, $N_{\text{Na}^+}(S)$, diminishes and approaches zero at the current density $i_L(c)$, which

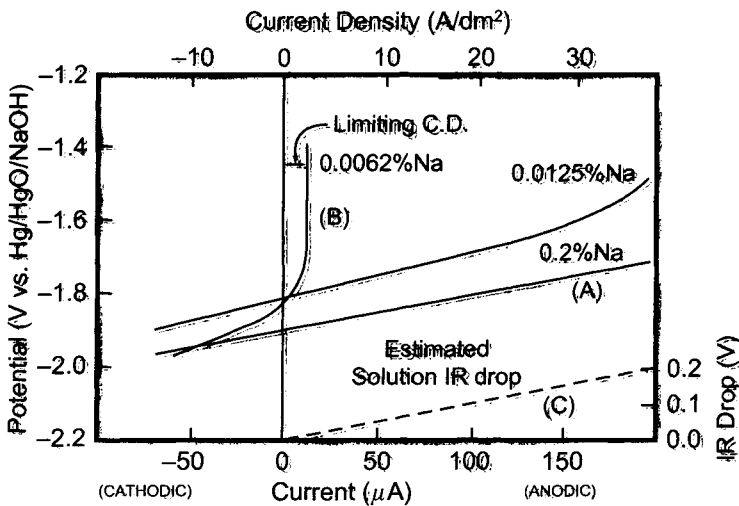


FIGURE 4.2.9. Polarization curves of sodium amalgam electrode in 50% NaOH [42].

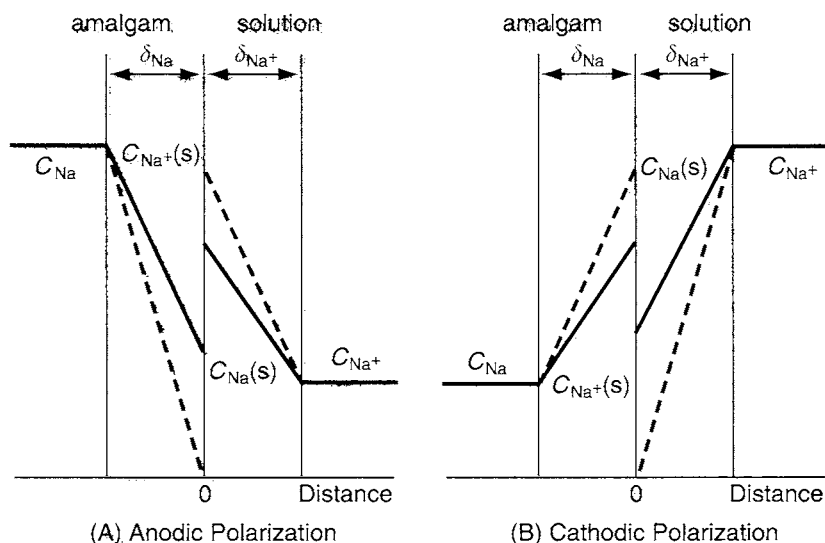


FIGURE 4.2.10. Concentration profile of Na and Na⁺ near the interface between sodium amalgam and NaCl solution.

is expressed by the equation:

$$i_L(c) = \frac{FD_{Na^+}C_{Na^+}}{\delta_{Na^+}} \tag{71}$$

where D is the diffusion coefficient and δ is the diffusion layer thickness, the subscripts Na and Na⁺ representing the amalgam and solution, respectively.

Since Na⁺ ion deposition onto a mercury cathode is a mass-transfer controlled reaction, the overpotential for Na⁺ deposition is (cf. Eq. (46))

$$\eta = \frac{RT}{F} \ln \left(1 - \frac{i}{i_L} \right) \tag{72}$$

At a constant potential, $1 - (i/i_L)$ is constant, that is,

$$1 - i/i_L = k \tag{73}$$

or

$$i = (1 - k)i_L \tag{74}$$

Since the thickness of the diffusion layer, δ , near the working electrode is inversely proportional to the square root of the Reynolds number, Re , or the flow velocity, u , in a pipe, we have:

$$i_L = \frac{nFC}{\delta} \propto nFC Re^{1/2} \propto nFCu^{1/2} \tag{75}$$

Hence,

$$i = k^* C \text{Re}^{1/2} = k^{**} C u^{1/2} \quad (76)$$

where k^* and k^{**} are constants and $\text{Re} = ud/\nu$, d being the diameter of the pipe and ν being the kinematic viscosity.

The current is proportional to the square root of the flow rate of the mercury in the amalgam type mercury cell [43–46]. In practical cells, mercury flows on a steel plate bed from the inlet to the outlet along the trough as illustrated in Fig. 4.2.11. The velocity of mercury flow is almost zero at the cathode bed because of wetting of the steel by the amalgam. Therefore, there is a rapid variation of flow velocity in the mercury perpendicular to the steel plate, causing vigorous agitation of the amalgam and enhancing mass transfer of the Na^+ ions to the amalgam interface, as well as the mass transfer of Na in the amalgam cathode.

4.2.5.4. The Oxygen Evolution Reaction (OER). The OER is the primary electrochemical reaction in water electrolysis, metal electrowinning, and recharging of metal-air cells. The standard electrode potential for this reaction at 25°C is 1.299 V vs the normal hydrogen electrode (NHE) in acid media and 0.401 V in alkaline media. The pertinent reactions are

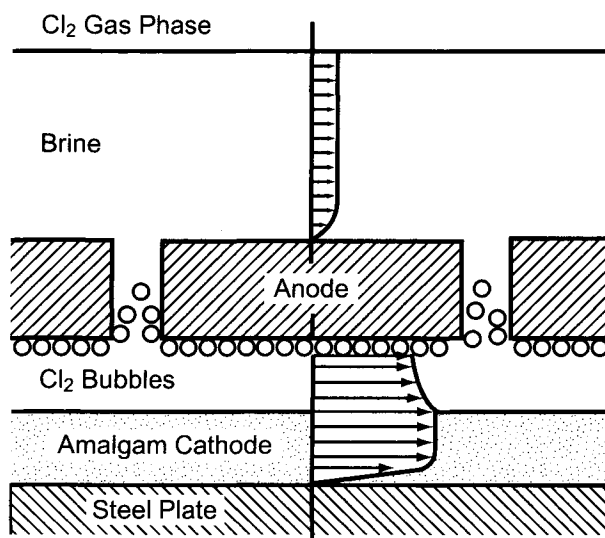
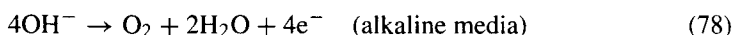
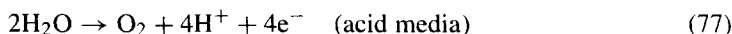
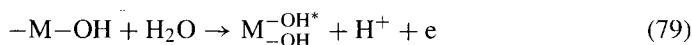


FIGURE 4.2.11. Flow patterns of brine and the amalgam cathode.

Depending on the pH, one of these reactions occurs during the course of the chlorine evolution reaction. The OER then becomes a parallel, unwanted reaction, and it lowers the current efficiency for the generation of chlorine. The OER, like the chlorine evolution reaction, proceeds over a potential region where the surface of the electrode is covered fully or partially by an oxide film with adsorption and catalytic properties substantially differing from those of the corresponding bulk oxides.

The kinetics of the OER were extensively examined [47–49] on various metal substrates and on metal oxides formed by thermal decomposition techniques. The polarization data for the OER on thermally formed metal oxides [50,51] in 4M KOH at 22°C are shown in Fig. 4.2.12. Generally, the Tafel slope is about 40mV for RuO₂ in alkaline and acidic media, IrO₂, and PdO₂, but varies [27,32] from 30 mV on RuO₂ to 120 mV on PtO₂.

Based on Tafel slope values, a generalized mechanism was proposed [52–54] for the OER on all oxide materials where the initial step involved the discharge of water molecules (in acidic media) or of OH⁻ ions (in alkaline medium) as:



where the asterisk denotes the “oxidized” surface state. This intermediate is subsequently converted to an “oxide”:

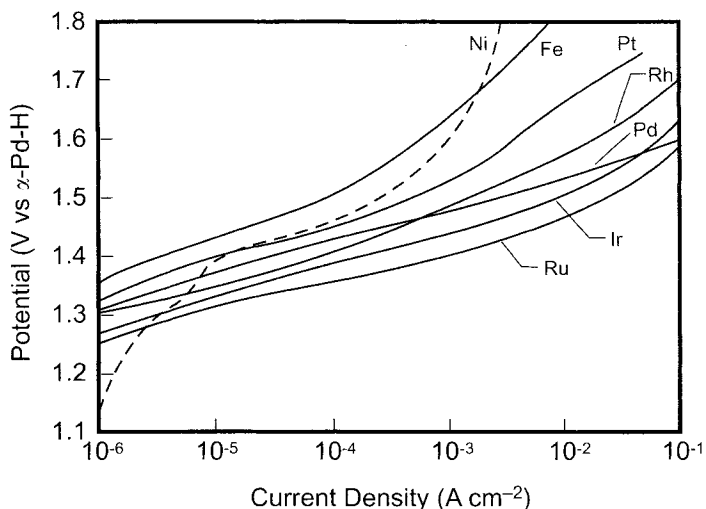
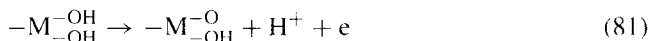
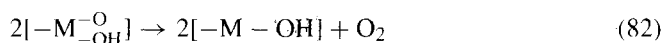


FIGURE 4.2.12. Polarization curves for oxygen generation in 4M KOH at 22°C on various metal oxides formed by thermal decomposition of their salts on a titanium substrate [51]. (Reproduced by permission of The Electrochemical Society, Inc.)

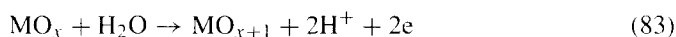
The M_{-OH}^{-O} species, being unstable, decomposes to form O_2 :



The expected Tafel slope, when or if, each of these steps becomes the rate-controlling pathway, is shown below.

Equation #	Tafel slope (mV)
79	120
80	60
81	40

The main feature involved in all these steps is the formation of a higher oxide and its subsequent decomposition to form O_2 :



Therefore, it is the bond strength of the oxide surface and its higher oxidation state, which can be related to the standard enthalpy of the lower to higher oxide transition that dictates the kinetics of the OER. The involvement of the OH or OH species [52–57] and higher oxidation states of metal ions of the oxide or oxide film, acting as a mediator species in the mechanism of the OER, thus becomes an important issue in electrocatalysis of the OER.

Figure 4.2.13 illustrates the dependence of the overpotential for the OER reaction on the standard enthalpy of the lower to higher oxide transition (Table 4.2.5). It may be noted that the adsorption of an oxygenated intermediate on the surface of an oxide is equivalent to oxidation of the metal cation on the oxide surface from a lower to a higher valent state. Oxides with small heat of transition adsorb the intermediate weakly and oxides with high heat of transition adsorb the intermediate too strongly. Both these situations lead to high overpotentials. Oxide showing high oxygen overpotential on the ascending branch of the volcano plot in Fig. 4.2.13 is PbO_2 , and Co_3O_4 and Fe_3O_4 on the descending branch exhibit high overpotentials. Oxides providing low overpotentials are PtO_2 , MnO_2 , RuO_2 and IrO_2 .

The kinetics of oxygen evolution during the course of the Cl_2 evolution reaction was not thoroughly investigated, although some basic studies were performed [58,59]. These are not definitive, and there are many unanswered questions with respect to the proposed mechanism and the current efficiency for Cl_2 evolution (Section 4.5). Nevertheless, it appears that the mechanism for the OER is the same as that occurring during the course of the Cl_2 evolution reaction, the rate being lowered by the decreased exchange current density for the OER (Table 4.2.6) via doping the RuO_2 -based coatings with HfO_2 and SnO_2 .

4.2.5.5. The Hypochlorite and Chlorate Reduction Reactions. There are two parasitic, parallel reactions occurring during the course of the HER, these reactions being the

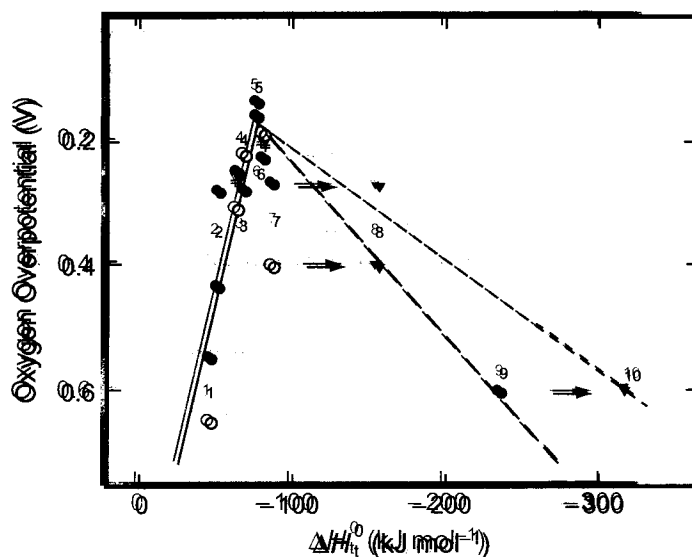


FIGURE 4.2.13. Oxygen overpotential on different oxides as a function of the enthalpy of lower \rightarrow higher oxide transition. (1) PbO_2 ; (2) Ni_2O_3 ; (3) PtO_2 ; (4) MnO_2 ; (5) RuO_2 ; (6) IrO_2 ; (7,8) Co_3O_4 ; (9,10) Fe_3O_4 ; Closed circles: acid solutions; open circles: alkaline solutions; closed triangles: different sets of data points [57]. (With permission from Elsevier.)

TABLE 4.2.5 Standard Enthalpy of Lower \rightarrow Higher Oxide Transition^a

Oxide	Transition	ΔH_1^0 (kJ mol ⁻¹ O-atoms)
RuO_2	$\text{Ru}_2\text{O}_3 \rightarrow$	79.5 ^b
IrO_2	$\text{Ir}_2\text{O}_3 \rightarrow$	88.4
Fe_3O_4	$\rightarrow \text{Fe}_2\text{O}_3$	238.5
	$\text{FeO} \rightarrow$	317.6
Co_3O_4	$\rightarrow \text{Co}_2\text{O}_3$	90
	$\text{CoO} \rightarrow$	160.7
PtO_2	$\text{Pt}_3\text{O}_4 \rightarrow$	67
PtO_2	$\text{Pt}_2\text{O}_3 \rightarrow$	48.1
MnO_2	$\text{Mn}_2\text{O}_3 \rightarrow$	74.1
Ni_2O_3	$\text{NiO} \rightarrow$	54.4

Note:

^aCalculated for the reaction scheme in such a way that only one O-atom appears on the left-hand side.

^bFrom ΔG_1^0 corrected for ΔS_1^0 .

cathodic reduction of the OCl^- and ClO_3^- ions:

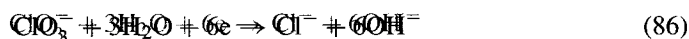
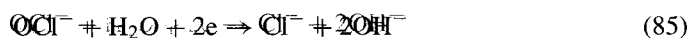


TABLE 4.2.6 Kinetic Parameters for RuO₂-based coatings

Electrode	Cl ₂ evolution		O ₂ evolution	
	Tafel slope (mV)	<i>i</i> ₀ (mA cm ⁻²)	Tafel slope (mV)	<i>i</i> ₀ (mA cm ⁻²)
RuO ₂ -TiO ₂	28	1.65	128	0.1
Ru : Hf				
25 : 75	54	0.38	125	0.034
50 : 50	34	1	122	0.029
66 : 34	27	1	132	0.034
Ru : Sn				
25 : 75	37	0.6	125	0.024
75 : 25	37	0.9	132	0.029

Source: Reproduced by permission of The Electrochemical Society, Inc.

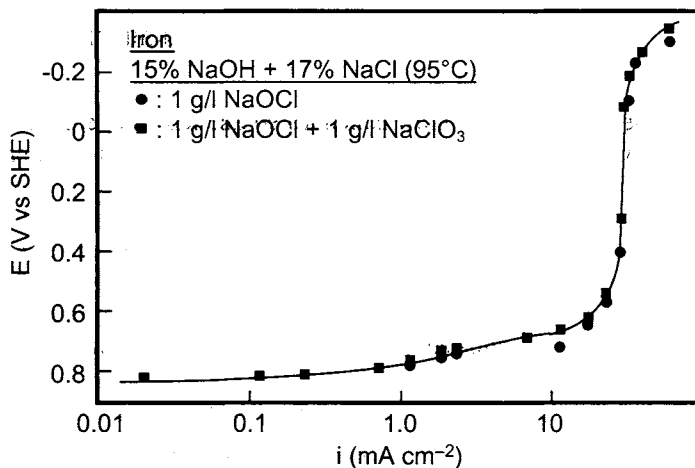


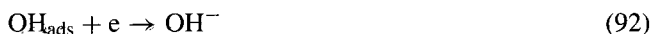
FIGURE 4.2.14. Current–voltage profile on a rotating Fe disc electrode in the presence of OCl⁻ with and without chlorate in 15% NaOH + 17% NaCl at 95°C at 2,000 rpm [58]. (Reproduced by permission of The Electrochemical Society, Inc.)

The cathodic reduction [58] of OCl⁻ is a diffusion-controlled reaction on iron, exhibiting limiting currents, as may be seen from the polarization data in Fig. 4.2.14. Hence, the current efficiency for the HER will be reduced at low current densities, while the caustic current efficiency is unaffected (see also Section 4.4.3.2G).

Mechanistic studies [59,60] have shown that OCl⁻ reduction follows the reaction scheme:



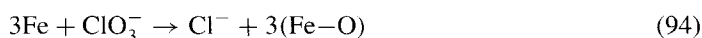
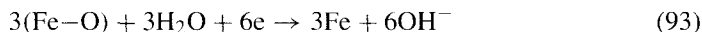
where the first step is the rate-controlling path. This explains the experimentally observed Tafel slope of 120 mV and the first-order dependence of the rate on the OCl^- ion concentration. An alternative sequence of steps was also proposed [61] involving the reactions (89)–(92), where the step (90) was identified as the slow step.



Basic investigations [58] have shown that the cathodic reduction of ClO_3^- in alkaline media is an activation-controlled process proceeding at very low rates. Mass balance studies have shown that the ClO_3^- ion can indeed be reduced to chloride, the reaction being favored only on “Fe” surfaces, and not on metals such as Co, Ni, Mo, Ti, Hg, and carbon, in smooth form (Fig. 4.2.15). The exact mechanism leading to this specificity is not clear and more fundamental studies are required to decipher the pathways controlling the chlorate reduction process.

The surface state of Fe appears to play a critical role in enhancing the rate of the ClO_3^- reduction reaction. Studies [58,62] performed with porous Fe_2O_3 , Fe_3O_4 , and FeO, and steel wool oxidized by washing with NaOCl showed that surface oxides of Fe participate in chlorate reduction (Figs. 4.2.16, 4.2.17).

A mechanism involving surface oxides of Fe during the cathodic reduction of ClO_3^- ion follows the scheme in Eqs. (93) and (94),



according to which ClO_3^- reduction takes place by the formation and decomposition of “labile” surface oxides of iron [63].

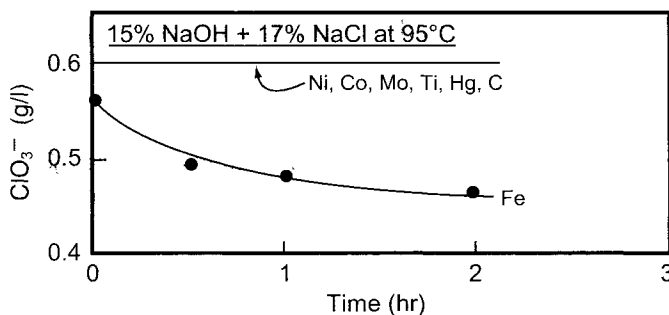


FIGURE 4.2.15. Variation of the concentration of chlorate ion with time on various electrode materials at a current density of 15 mA cm^{-2} [58]. (Reproduced by permission of The Electrochemical Society, Inc.)

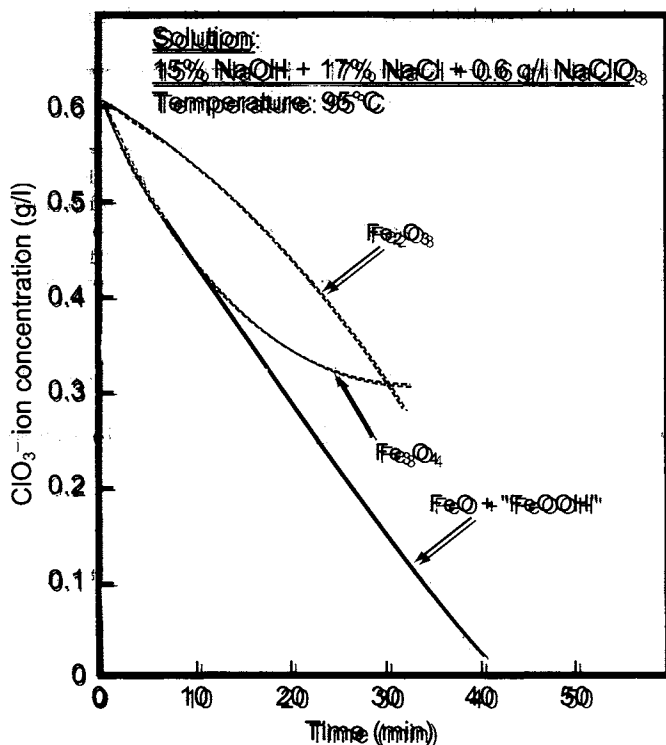


FIGURE 4.2.16. Variation of the concentration of chlorate ion with time at a current density of 70 mA cm^{-2} on various Fe-oxides [58]. (Reproduced by permission of The Electrochemical Society, Inc.)

The specificity associated with Fe-oxides in facilitating the ClO_3^- reduction process must be taken into consideration when non-Fe-based materials are selected as potential alternatives to the Fe cathodes. Furthermore, as the reduction of chlorate is more efficient at low current densities, one may prefer to design a cathode with areas that are nearly "blind" to the current. This, however, will lead to the corrosion of the cathode during operation, as these areas are not cathodically protected.

4.2.5.6. The Oxygen Reduction Reaction. One of the future technologies of importance to realize low energy consumption for producing Cl_2 and NaOH is the oxygen cathode technology, where the conventional H_2 -evolving cathodes can be replaced with O_2 cathodes. This should lower the cell voltage, in principle, by 1.23 V and hence, save $840\text{--}850 \text{ kW hr ton}^{-1}$ of chlorine produced. The oxygen reduction reaction involved in O_2 cathode technology has been extensively studied over the past 25–30 years in connection with the development of fuel cells to generate electricity.

The oxygen reduction reaction occurs in both acid and alkaline media, the latter being of relevance to the development of the oxygen cathodes for chlor-alkali cells. The pathways involved in O_2 reduction are very complex [64–71]. The simplified reaction schemes are presented here.

The generally acknowledged reaction schemes involved in the oxygen reduction reaction are: (1) the direct four-electron scheme, and (2) the peroxide pathway. The best

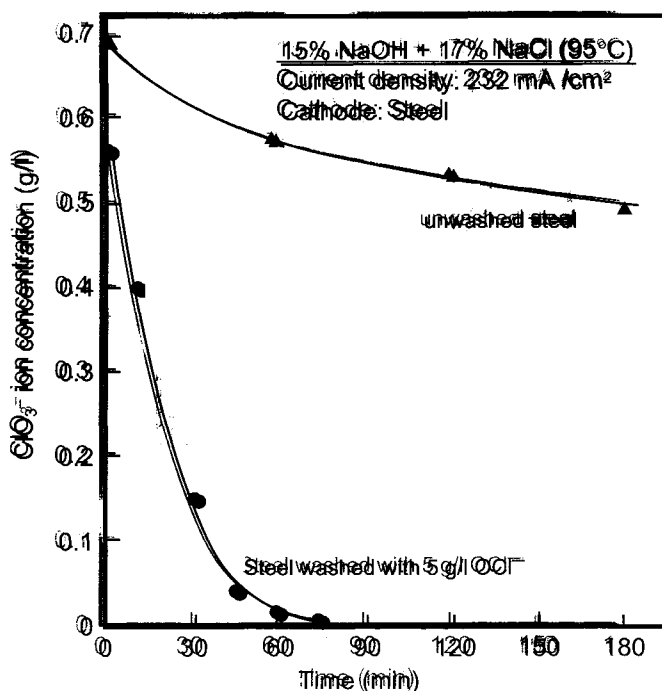
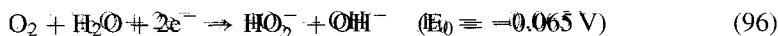


FIGURE 4.2.17. Variation of the concentration of chlorate ion with time on treated and untreated steel [58]. (Reproduced by permission of The Electrochemical Society, Inc.)

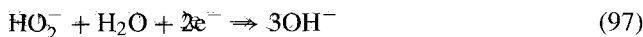
catalyst materials on which the four-electron pathway, depicted by Eq. (95), proceeds, are pure Pt and Pt-black.



However, on Pt-C composites (i.e., Pt loaded on carbon), the predominant reaction (95) proceeds on Pt-sites, while the peroxide pathway is the dominant scheme on carbon sites. The peroxide reaction, in alkaline solution, is believed to proceed as follows.



followed by,



or



Although both the pathways yield the same end result, the peroxide pathway results in a thermodynamic voltage penalty of 465 mV. The kinetic losses for both reactions have to

TABLE 4.2.7 Kinetic Parameters for the Oxygen Reduction Reaction in Acid and Alkaline Solutions

Material	Acid				Alkaline ^a			
	Medium (temp.) ^a	i_0 (A cm ⁻²)	Tafel slope (mV)	Refs.	Medium (temp.) ^a	i_0 (A cm ⁻²)	Tafel slope (mV)	Refs.
Pt	HClO ₂ (pH ~ 1.0)	3.0×10^{-10}	60	73	NaOH (pH ~ 13)	1.0×10^{-11}	65	73
Ir	HClO ₄ (pH ~ 0.2)	1.0×10^{-11}	105	74	KOH (pH ~ 13)	1.0×10^{-11}	100	74
Rh	HClO ₄ (pH ~ 0.2)	1.0×10^{-11}	65	74	KOH (pH ~ 13)	1.2×10^{-12}	55	74
Au	0.1N HClO ₄	1.5×10^{-11}	120	75	0.1N NaOH	1.8×10^{-4} (for O ₂ /HO ₂ ⁻ couple)	120	80
Pd	HClO ₄ (pH ~ 1.0)	3.0×10^{-11}	60	75	NaOH (pH ~ 13)	1.2×10^{-11}	55	81
Ag					NaOH (pH ~ 13)	1.5×10^{-9}	110	84
Fe					NaOH (pH ~ 13)	4.3×10^{-10}	120	81
Ni					NaOH (pH ~ 13)	4.3×10^{-10}	120	81
Pt Black	50% H ₃ PO ₄ (70°C)	4.0×10^{-10}	60	76	30% KOH (70°C)	4.0×10^{-10}	50	76
Pt	85% H ₃ PO ₄ (25°C)	1.2×10^{-11}	125	77				
Active Pt	85% H ₃ PO ₄ (22°C)	2.7×10^{-10}	106	71				
Pt crystallites (on Pt)					0.1 NaOH	4.5×10^{-7}	120	82

Note:

^a Values of i_0 refer to room temperature unless otherwise stated.

Source: Reprinted by permission of John Wiley & Sons, Inc.

be taken into account when factoring the kWh ton^{-1} of caustic produced. Of the two electrochemical reactions shown above, Eq. (96) is very fast on most electrode materials, and Eq. (97) is extremely slow, occurring rarely, if at all, except on Au-Fe complexes. The most favored scheme for the decomposition of HO_2^- is reaction (98), the known catalysts being carbon, heavy metals, Ag, RuO_2 , Co-spinels, and the Pt-group metals. Note that the oxygen generated by the decomposition reaction is available right at the catalytic site and is efficiently recycled. An efficient peroxide decomposition is a must for the longevity of the electrode, since accumulation of peroxide may result in increased corrosion of the carbon in the electrode. Table 4.2.7 shows some kinetic data for the O_2 -reduction reaction in alkaline media [69,72-81]. The current status of the development of O_2 cathode technology is described in Chapter 17.

REFERENCES

1. S. Glasstone, K. Laidler, and H. Eyring, *The Theory of Rate Processes*, McGraw-Hill Book Co., New York (1941).
2. F.R. Cruickshank, J. Hyde, and D. Pugh, *J. Chem. Educ.* **54**, 289 (1977).
3. R.D. Levine and R.B. Bernstein, *Molecular Reaction Dynamics*, Oxford University Press, New York (1974).
4. A.A. Frost and R.G. Pearson, *Kinetics and Mechanism: A Study of Homogeneous Chemical Reactions*, 2nd Edition, John Wiley & Sons, New York (1961).
5. G.M. Barrow, *Physical Chemistry*, McGraw-Hill Book Co., New York (1979).
6. J.O'M. Bockris and S.U.M. Khan, *Quantum Electrochemistry*, Plenum Press, New York (1979).
7. B.E. Conway, *Theory and Principles of Electrode Processes*, Ronald Press, New York (1964).
8. J.O'M. Bockris and A.K.N. Reddy. Vols. 1 and 2, *Modern Electrochemistry*, Plenum Press, New York (1970).
9. J. Albery, *Electrode Kinetics*, Clarendon Press, Oxford (1975).
10. K. Vetter, *Electrochemical Kinetics: Theoretical Aspects*, Academic Press, New York (1967).
11. B.E. Conway, *Electrochemical Supercapacitors: Scientific Principles and Technological Applications*, Kluwer Academic/Plenum Publishers, New York (1999).
12. B.E. Conway and E. Gileadi, *Trans. Faraday Soc.* **58**, 2493 (1962).
13. B.V. Tilak and C.P. Chen, *J. Appl. Electrochem.* **23**, 631 (1993).
14. B.V. Tilak, S. Venkatesh, and S.K. Rangarajan, *J. Electrochem. Soc.* **136**, 1977 (1989).
15. B.E. Conway, The Temperature and Potential Dependence of Electrochemical Reaction Rates, and the Real Form of the Tafel Equation, In B.E. Conway, R.E. White, J.O'M. Bockris (eds), *Modern Aspects of Electrochemistry*, Vol. 16, Plenum Publishing Corp, New York (1985), p. 103.
16. F. Hine, *Electrode Processes and Electrochemical Engineering*, Plenum Press, New York (1985), p. 59.
17. A.J. Appleby, H. Kita, M. Chemla, and G. Bronöel, Hydrogen. In A.J. Bard (ed.), *Encyclopedia of Electrochemistry of the Elements*, Vol. IX, Part A, Marcel Dekker, New York (1982), p. 384.
18. A.J. Appleby, Electrocatalysis. In B.E. Conway, J.O'M. Bockris, E. Yeager, S.U.M. Khan, and R.E. White (eds), *Comprehensive Treatise of Electrochemistry*, Vol. 7, Plenum Press, New York (1983), p. 173.
19. J.O'M. Bockris, A.K.N. Reddy, and M. Gamboa-Aldeco, *Modern Electrochemistry 2A: Fundamentals of Electrodes*, 2nd Edition, Kluwer Academic/Plenum Publishers, New York (2000).
20. B.E. Conway and G. Jerkiewicz, *Electrochim. Acta* **45**, 4075 (2000).
21. R. Parsons, *Trans. Faraday Soc.* **34**, 1053 (1958).
22. R. Parsons, *Surface Science* **18**, 28 (1969).
23. *Reference Electrodes*, D.J. Ives and G.I. Janz (eds), Ch. II, Academic Press, New York (1961), p. 111.
24. J. Mussini and G. Faita, Chlorine. In A.J. Bard (ed.), *Encyclopedia of Electrochemistry of the Elements*, Ch. I, Tables 1.2.1, 1.2.4, Marcel Dekker, New York (1973).
25. H.S. Harned and M.A. Cook, *J. Am. Chem. Soc.* **59**, 1290, 1903 (1937).

26. D.M. Novak, B.V. Tilak and B.E. Conway, Anodic Chlorine Production: Fundamental and Applied Aspects, In J.O.M. Bockris, B.E. Conway and R.E. White (eds), *Modern Aspects of Electrochemistry*, Vol. 14, Plenum Press, New York (1982), p. 249.
27. S. Trasatti, Transition Metal Oxides: Versatile Materials for Electrocatalysis, In J. Lipkowski and R.N. Ross (eds), *The Electrochemistry of Novel Materials*, Ch. 5, VCH Publishers, New York (1974), p. 207.
28. R.G. Erenberg, L.I. Khristalik, and I.P. Yaroskevskaya, *Soviet Electrochem.* **11**, 989 (1975).
29. R.G. Erenberg, L.I. Khristalik, and N.P. Bobozhima, *Soviet Electrochem.* **20**, 1089 (1984).
30. L.D. Burke and J.P. O'Neill, *J. Electroanal. Chem.* **101**, 341 (1979).
31. V. Consonni, S. Trasatti, F.H. Pollack, and W.E. O'Grady, Extended Abstracts, *Electrochemical Society Meeting*, Vol. 86-1, Abstract # 510, The Electrochemical Society, Pennington, NJ (1986).
32. B.E. Conway and B.V. Tilak, Behavior and Characterization of Kinetically Involved Chemisorbed Intermediates in Electrocatalysis of Gas Evolution Reactions, In D.D. Eley, H. Pines, and R.B. Weisz (eds), *Advances in Catalysis*, Vol. 38, Academic Press, Inc., New York (1992), p. 1.
33. E.J. Kelley, D.E. Heatherly, C.E. Vallat, and C.W. White, *J. Electrochem. Soc.* **134**, 1667 (1987).
34. B.V. Tilak, *J. Electrochem. Soc.* **126**, 1343 (1979).
35. F. Hine and M. Yasuda, *J. Electrochem. Soc.* **121**, 1289 (1974).
36. A.T. Kuhn and C.J. Mortimer, *J. Electrochem. Soc.* **120**, 231 (1973).
37. T. Arikado, C. Iwakura, and H. Tamura, *Electrochim. Acta* **23**, 9 (1978).
38. Y. Liguang and W. Mingxian, *Electrochemistry (China)*, **2**, 285 (1996).
39. L.A. DeFaria, J.F.C. Boodts, and S. Trasatti, *Electrochim. Acta* **42**, 3525 (1997).
40. T.A.F. Lassali, J.F.C. Boodts, and S. Trasatti, *Electrochim. Acta* **39**, 1545 (1994).
41. R. Boggio, A. Carozzi, G. Lodi, and S. Trasatti, *J. Appl. Electrochem.* **15**, 335 (1985).
42. T. Arikado, C. Iwakura, and H. Tamura, *Electrochim. Acta* **22**, 229 (1977).
43. F. Hine, M. Okada, and S. Yoshizawa, *Denkí Kagaku (J. Electrochem. Soc.)*, **27**, 419 (1959); F. Hine, *Soda-to-Enso (Soda and Chlorine)*, **31**, 135 (1980).
44. F. Hine, *Electrode Processes and Electrochemical Engineering*, Plenum Press, New York (1985), p. 58.
45. G.I. Volkov and Y.V. Lyadin, *Soviet Electrochem.* **5**, 979 (1969).
46. Y.V. Lyadin and G.I. Volkov, *Soviet Electrochem.* **6**, 1291 (1970).
47. S. Trasatti and G. Lodi, Properties of Conductive Transition Metal Oxides with Rutile-Type Structure, In S. Trasatti (ed.), *Electrodes of Conductive Metallic Oxide, Part A*, Ch. 7, Elsevier, New York (1980), p. 301.
48. S. Trasatti and G. Lodi, Oxygen and Chlorine Evolution At Conductive Metallic Oxide Anodes, In S. Trasatti (ed.), *Electrodes of Conductive Metallic Oxide, Part B*, Ch. 10, Elsevier, New York (1981), p. 521.
49. L.D. Burke, Oxide Growth and Oxygen Evolution on Noble Metals, In S. Trasatti (ed.), *Electrodes of Conductive Metallic Oxide, Part A*, Ch. 3, Elsevier, New York (1980) p. 1.
50. W. O'Grady, C. Iwakura, and E. Yeager, *Proc. Intersoc. Conf. Environ. Syst., Amer. Soc. Mech. Eng.*, San Diego (1976), pp. 37-48.
51. W. O'Grady, C. Iwakura, J. Huang, and E. Yeager, Ruthenium Oxide Catalysis For The Oxygen Electrode, In M. Breiter (ed.), *Electrocatalysis*, *Electrochem. Soc. Princeton, NJ* (1976), p. 286.
52. S. Trasatti, *Electrochim. Acta* **36**, 225 (1991).
53. L.I. Khristalik, *Electrochim. Acta* **26**, 329 (1981).
54. B.N. Efremov and M.R. Tarasovich, *Soviet Electrochem.* **17**, 1392 (1981).
55. B.E. Conway and P.L. Bourgault, *Trans. Faraday Soc.* **58**, 593 (1962).
56. A.C.C. Tseung and P. Rasaiiah, *J. Electrochem. Soc.* **131**, 803 (1984).
57. S. Trasatti, *J. Electroanal. Chem.* **111**, 125 (1980).
58. B.V. Tilak, K. Tari, and C.L. Hoxter, *J. Electrochem. Soc.* **135**, 1386 (1988).
59. A.I. Onuchukwu and S. Trasatti, *J. Appl. Electrochem.* **21**, 858 (1991).
60. F. Hine and M. Yasuda, *J. Electrochem. Soc.* **118**, 170 (1971).
61. J. Wu, *J. Electrochem. Soc.* **134**, 1462 (1987).
62. T.V. Bommaraju and C.G. Rader, *U.S. Patent* 4,444,631 (1984).
63. I.E. Veselovskaya, E.M. Kuchinskii, and L.V. Morochko, *Zhur. Priklad. Khim.* **37**, 76 (1964).
64. J.P. Hoar, *The Electrochemistry of Oxygen*, Interscience, New York (1968).
65. A. Damjanovic and A.T. Ward, Some Aspects of Electrocatalysis of Oxygen Reactions at Bare and Oxide-Covered Electrodes with a View on the Future, In H. Blum and E. Gutmarm (eds), *Electrochemistry*, Plenum Press, New York (1977), p. 89.

66. E. Yeager, Oxygen Electrodes for Industrial Electrolysis and Electrochemical Power Generation. In U. Landau, E. Yeager, and D. Kortan (eds), *Electrochemistry in Industry*, Plenum Press, New York (1982), p. 29.
67. M.R. Tarasevich, A. Sadkowski, and E. Yeager, Oxygen Electrochemistry. In B.E. Conway, J.O'M. Bockris, E. Yeager, S.U.M. Khan, and R.E. White (eds), *Comprehensive Treatise of Electrochemistry*, Vol. 7, Plenum Press, New York (1983), p. 301.
68. E. Yeager, *Oxygen Cathodes for Energy Conversion and Storage*, Annual Report from Oct. 1, 1977 Sept. 30, 1978, DOE Contract # DE-AC02-77ET25502 (1980).
69. J.O'M. Bockris and S. Srinivasan, *Fuel Cells: Their Electrochemistry*, McGraw-Hill Book Co., New York (1969).
70. K. Kinoshita, *Electrochemical Oxygen Technology*, John Wiley & Sons, New York (1992).
71. A.J. Appleby, Electrocatalysis, In B.E. Conway and J.O'M. Bockris (eds), *Modern Aspects of Electrochemistry* Vol 9, Plenum Press, New York (1974), p. 369.
72. B.V. Tilak, S. Sarangapani, and N.L. Weinberg, Electrode Materials, In N.L. Weinberg and B.V. Tilak (eds), *Techniques of Chemistry, Vol. V, Part III: Techniques of Electroorganic Synthesis- Scale-Up and Engineering Aspects*, John Wiley & Sons, New York (1982), p. 195.
73. A. Damjanovic and V. Brusic, *Electrochim. Acta* **12**, 615 (1967).
74. A. Damjanovic, A. Dey, and J.O'M. Bockris, *J. Electrochem. Soc.* **113**, 739 (1966).
75. A. Damjanovic and V. Brusic, *Electrochim. Acta* **12**, 1171 (1967).
76. W.M. Vogel, and J.T. Lundquist, *J. Electrochem. Soc.* **117**, 1512 (1970).
77. E. Yeager, *EPRI Report No: EPRI-EM-505: Research Project 634-1*, June, 1977.
78. E. Yeager, *EPRI Report, EM-505*, June, 1979.
79. P.N. Ross, *EPRI Report No: EPRI-EM-1553, Project 1200-5*, Sept., 1980.
80. R.W. Zurilla, R.K. Sen, and E. Yeager, *J. Electrochem. Soc.* **125**, 1103 (1978).
81. P. Bindra and E. Yeager, O₂ Reduction on Electrodeposited Pt Crystallites in Sodium Hydroxide Solution, *Abstract # 28, Extended Abstracts*, Electrochemical Society Meeting, Vol. 79-1, Boston, MA (1979).

4.3. ELECTROCHEMICAL TECHNIQUES

4.3.1. Introduction

Industrial electrochemical cells are generally operated at a constant load or amperage, as this is a direct measure of the production rate. The amperage is a function of the terminal voltage, V_T :

$$\text{Amperage} = \frac{V_T - E_d}{R_c} \quad (1)$$

where E_d is the thermodynamic decomposition voltage, and $(V_T - E_d)$ is the driving force, in volts. The cell resistance, R_c , is composed of the polarization resistance at the anode and the cathode, the ohmic resistance of the electrolytic solution, the separator (be it an asbestos diaphragm or an ion-exchange membrane), and the metal hardware between the cells. While the ohmic resistance is independent of the current or voltage, the polarization resistance associated with the kinetics of the electrode reactions at the anode and cathode is a nonlinear function of the current, I , passing through the cell. Thus, the voltage across a cell is composed of various factors described by Eq. (2),

$$V_T = E_A + \eta_A - E_C - (-\eta_C) + IR_{sol} + IR_S + IR_M \quad (2)$$

$$= E_d + (\eta_A + \eta_C) + IR_{sol} + IR_S + IR_M$$

$$E_d = E_A - E_C \quad (3)$$

where E_A and E_C are the equilibrium potentials for the anodic and cathodic processes, and η_A and η_C are the overvoltages at the anode and cathode, respectively. The decomposition voltage is the minimum voltage required to drive the reaction in a forward direction, and is the difference of the reversible potentials of the two electrodes, as given by Eq. (3). The IR terms with the subscripts sol, S, and M refer to the ohmic voltage across the solution, separator, and the metal hardware. A detailed discussion of the cell voltage and its components is presented in Section 4.4. The overvoltage is the excess voltage needed to drive the electrochemical reaction in the direction of interest at a desirable rate, and is a measure of the deviation of the actual electrode potential from the equilibrium potential for the electrode process under discussion. It is a function of the current density or the reaction rate per unit area of electrode.

Thus, the parameters related to the cell voltage include the overvoltage and ohmic drop terms, which can be experimentally measured. The electrode material and the electrochemical reaction under study dictate the magnitude of the overvoltage. Therefore, it is important to characterize the electrode material and the pertinent electrochemical reaction, especially the mechanistic aspects, as this knowledge can lead to developing more energy-efficient electrodes.

The kinetic parameters required to characterize an electrode reaction are reaction order, rate constant or exchange current density, symmetry factor, stoichiometric coefficient, and the standard heat and entropy of activation. These basic parameters can be measured using electrochemical techniques, some of which are discussed in this chapter. The interested reader is referred to refs. [1–12] for a detailed discussion of the various electrochemical and physicochemical techniques available at present to characterize the electrode surfaces and the electrochemical reactions.

The techniques for characterizing the kinetics of electrode reactions can be classified into steady-state and transient methods. The steady-state methods involve the measurement of the current–potential relationships at constant current (galvanostatic control) or constant potential (potentiostatic control) conditions and measuring the response, which is either the potential or the current after a steady state is achieved. The non-steady-state methods involve the perturbation of the system from an equilibrium or a steady-state condition, and follow the response of the system as a function of time using current, potential, charge, impedance, or any other accessible property of the interface. Relaxation methods are a subclass of perturbation methods.

4.3.2. Steady-State Techniques

Conventional polarization measurements are performed in a cell containing the working electrode, counter electrode, and a reference electrode, as shown in Fig. 4.3.1. The working and counter electrodes are connected to a DC power source through an ammeter. The potential of the working electrode is measured with respect to a reference electrode, using a high input impedance voltmeter to ensure that the reference electrode is not polarized. The potential difference between the working electrode and the reference electrode comprises not only the potential of the working electrode but also an ohmic drop from the solution between the reference and working electrodes. This additional ohmic drop can be minimized by using a proper probe, and it can be measured using the current interruption technique (Section 4.3.2.3).

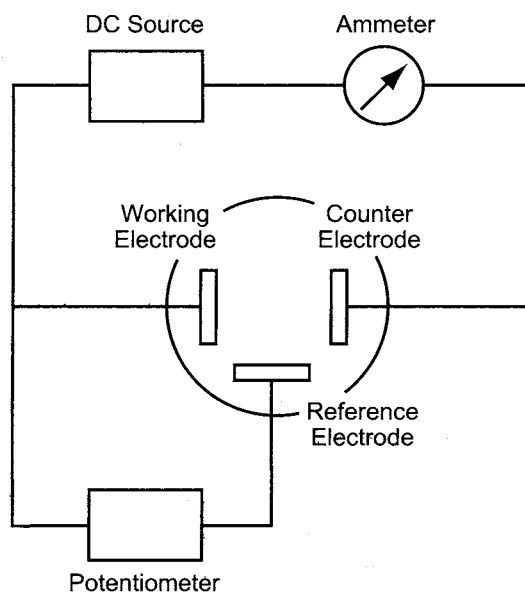


FIGURE 4.3.1. Conventional circuit for polarization measurements.

4.3.2.1. *Reference Electrodes.* The requirements for a reference electrode are:

1. It is a non-polarizable electrode, exhibiting a high exchange current density.
2. Its potential is well established, stable, and reproducible.
3. It contains the same electrolyte as the solution in the cell under study, so that liquid junction potentials are avoided.
4. It is maintained at the same temperature as the electrolyte under study in order to eliminate the deviation of the potential caused by the difference in the temperature.

4.3.2.1A. *Hydrogen Electrode.* By convention, the hydrogen electrode is the primary standard for measuring the electrode potentials. The HER proceeding on an electrochemically active metal electrode, such as a platinized platinum sheet, fulfills all the requirements shown above. The HER is represented by Eq. (4), and its reversible potential by Eq. (5).



$$E_{\text{H}} = (RT/F) \ln \frac{a_{\text{H}^+}}{(p_{\text{H}_2})^{1/2}} \quad (5)$$

When $p_{\text{H}_2} = 1$, we have

$$E_{\text{H}} = -(2.303RT/F)\text{pH} \quad (6)$$

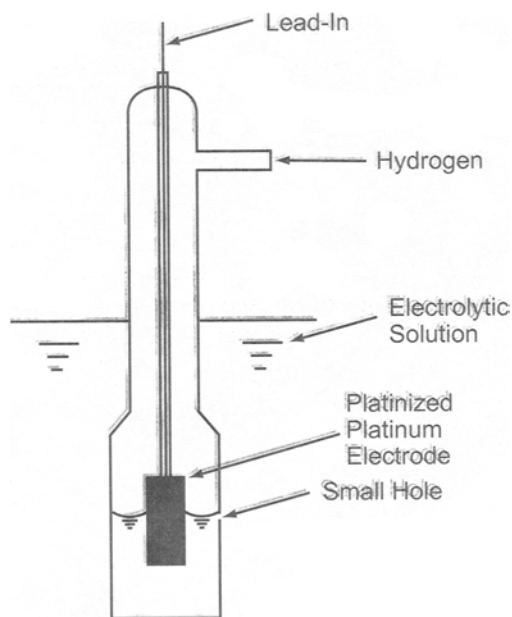
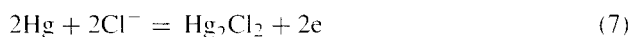


FIGURE 4.3.2. Hydrogen reference electrode.

Equation (4) shows that hydrogen gas and hydrogen ions must be present to establish the hydrogen electrode. Figure 4.3.2 illustrates an example of the hydrogen reference electrode. Purified hydrogen is passed through a glass tube with a platinized platinum sheet immersed in an oxygen-free electrolytic solution, and gas bubbles escape from the tube through small holes located at about the center of the Pt electrode. This establishes an interface with three phases: metal electrode, electrolytic solution, and hydrogen gas. A platinized platinum sheet or spiral wire, immersed in an aqueous solution saturated with hydrogen by bubbling hydrogen directly in the solution, can also provide a simple reversible hydrogen electrode. Platinized platinum is chemically active, and thus, is easily poisoned by trace impurities, including dissolved oxygen in the solution. Measurements should always be made on fresh electrodes.

Although the reversible hydrogen electrode is the primary standard, there are several other reference electrodes that are used in practice. Some of these secondary reference electrodes are described below (see also Section 4.1.7).

4.3.2.1B. Calomel Electrode and Other Mercury-Based Electrodes. The calomel electrode consists of mercurous chloride (calomel, Hg_2Cl_2) in contact with liquid mercury in the presence of a chloride solution, as $\text{Hg}/\text{Hg}_2\text{Cl}_2/\text{KCl}$. The electrode reaction is:



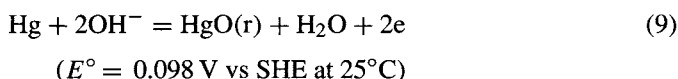
Mercurous chloride is an insoluble compound having a solubility product of 2×10^{-18} at 25°C [13], and the reversible potential of the calomel electrode, E_{cal} , is represented

by the Nernst equation as follows:

$$E_{\text{cal}} = E_{\text{cal}}^{\circ} - (RT/F) \ln a_{\text{Cl}^-} \quad (8)$$

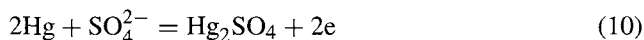
where E_{cal}° is the standard potential for the calomel electrode. The primary electrochemical reaction here is: $2\text{Hg} \leftrightarrow \text{Hg}_2^{2+} + 2e$, but the electrode measures the Cl^- ion activity because of the equilibrium reaction: $\text{Hg}_2^{2+} + 2\text{Cl}^- \leftrightarrow \text{Hg}_2\text{Cl}_2$. The reversible potential of the calomel electrode at various KCl concentrations and temperatures is shown in Table 4.3.1 [14]. Various types of calomel electrodes are available.

Calomel electrodes are not stable in concentrated NaOH solutions because the permeation of caustic into the electrode structure alters the potential. In alkaline solutions, the recommended electrode is the mercuric oxide electrode, whose standard electrode potential is dictated by reaction (9):



where $\text{HgO}(\text{r})$ denotes red HgO and SHE refers to the standard hydrogen electrode.

Another commonly used electrode is the mercury–mercurous sulfate electrode, represented by Eq. (10):



and having an E° of 0.6051 V vs SHE at 25°C . This reference electrode is preferred for electrode potential measurements in sulfate solutions.

TABLE 4.3.1 Standard Potential of the Calomel Electrode as a Function of the KCl Concentration and Temperature

Temperature (°C)	Saturated KCl (V)	3.5N KCl (V)	1.0N KCl (V)	0.1N KCl (V)
0	0.2602		0.2854	0.3338
10	0.2541		0.2839	0.3343
15	0.2509			
20	0.2477		0.2815	0.3340
25	0.2444		0.2801	0.3337
30	0.2411		0.2786	0.3332
35	0.2377			
40	0.2343	0.2466	0.2753	0.3316
50	0.2272	0.2428	0.2716	0.3296
60	0.2199	0.2377	0.2673	0.3229
70	0.2124	0.2331	0.2622	0.3236
80	0.2047	0.2277		
90	0.1967	0.2237		
100	0.1885			

4.3.2.1C. Silver–Silver Chloride Electrode. Although the mercury–mercury compound electrodes are useful, the toxicity of mercury compounds is a concern with regard to their use and disposal. This is overcome by using silver–silver chloride electrodes. The electrode reaction responsible for the potential of the Ag/AgCl electrode is:



The standard potential for this reaction [15] at 25°C is 0.2223 V vs SHE. The silver–silver chloride electrode must be used in a dark environment to prevent instability and irreproducibility arising from the photochemical reactions of AgCl.

4.3.2.1D. Copper–Cupric Sulfate Electrode. This electrode is composed of a copper rod immersed in a saturated cupric sulfate solution, leading to the establishment of the reaction:



The thermodynamic potential is estimated to be 0.295 V at 25°C, the standard potential being 0.337 V vs SHE in saturated solutions of CuSO₄. However, experimental results showed a value of 0.3160 V, which was about 20 mV more positive than estimated, probably because of the effect of dissolved oxygen [16]. In spite of this, copper–cupric sulfate electrodes of various types are widely used in the cathodic protection equipment for steel structures, because of their stable potential and simple construction.

Useful literature devoted to the various reference electrodes are [8–22] where the electrode processes and the thermodynamic potentials are discussed and summarized. The reference electrodes used for nonaqueous solutions are noted in refs. [23–27], for fused salt in refs. [24,28], for solid electrolytes in ref. [29], for soil and seawater in ref. [30], and for high-temperature and high-pressure operations in refs. [31,32].

4.3.2.2. *Luggin–Haber Probe*. The static potential or the reversible potential of a working electrode, shown in Fig. 4.3.1, can be measured with respect to a reference electrode. The reference electrode is generally placed in a separate compartment and is connected to the cell, the connecting tube being drawn out to a small capillary so that its tip is very near the electrode. The capillary tube is called the Luggin probe or the Luggin–Haber probe.

When there is no current flow, the measured value is independent of the position of the reference electrode since the potential in the electrolytic solution is equal across the cell. The potential of the working electrode is either the static potential or a reversible potential, E .

When a direct current, i , is applied to the cell, both the anode and the cathode are polarized. E' in Fig. 4.3.3 illustrates the polarization potential of the working electrode under study, which is the sum of the static potential E and the overvoltage η . However, the measured potential difference between the working electrode and the reference electrode contains the solution ohmic drop, $i\rho x$, since the Luggin tip is located far from the electrode surface by the distance x . ρ refers to the specific resistivity of the electrolytic

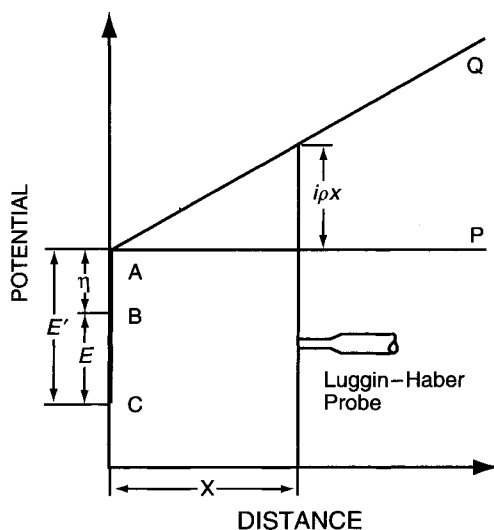


FIGURE 4.3.3. Schematic of the potential vs distance profile in front of a working electrode.

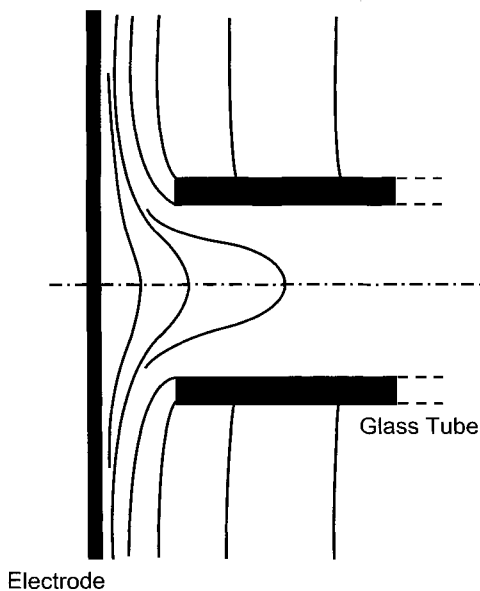


FIGURE 4.3.4. Deformation of equipotential lines by the presence of glass tube [33].

solution. The solution ohmic drop is large in solutions having large resistivity and at high current densities. It is possible to eliminate the solution ohmic drop by extrapolating line AQ to $x = 0$ if that profile can be obtained [33].

A problem that arises when the Luggin probe is positioned close to the metal/solution interface is the nonuniform current distribution (Fig. 4.3.4) near the

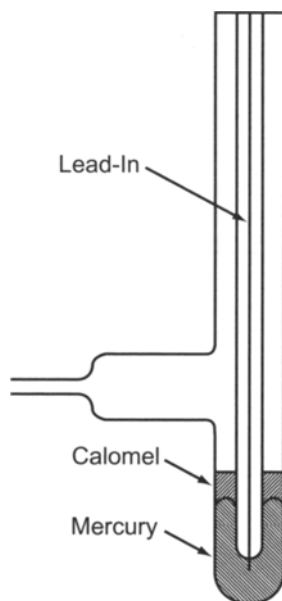


FIGURE 4.3.5. A Luggin-Haber probe combined with the calomel reference electrode.

working electrode, which alters the local current density and hence, the electrode potential. To overcome this problem, the Luggin-Haber probe connected with the reference electrode was designed (Fig. 4.3.5). This design minimizes the distortion of the current distribution near the working electrode, because the tip is small, about 1 mm in diameter.

Piontelli and coworkers [34–36], Barnett [37], and others [31] investigated the current distribution near a flat plate electrode with a Luggin-Haber probe, and showed that the capillary tip of the Luggin-Haber probe had to be removed from the electrode surface by more than twice the diameter of the tip to minimize its adverse effects. However, at very high current densities, this design does not eliminate the solution ohmic drop. Hine and coworkers utilized the Luggin-Haber probe supported with an arm which could be moved three dimensionally, with a micrometer in front of the working electrode, and obtained curves of the potential vs distance. The procedure was useful in investigations with gas-evolving electrodes, as with chlorine evolution, where bubbles become dispersed in the electrolytic solution, resulting in a gradual change of electrical resistance [33,38–40]. Figure 4.3.6 depicts examples of the potential vs distance curves obtained by this procedure [38], showing least interference from the gas bubbles during the potential measurements when the horizontal plate electrode is facing upward. This is also reflected in the current-potential curve in Fig. 4.3.7, which shows linearity of the potential with the logarithm of the current density, as theoretically anticipated.

4.3.2.3. Current Interruption Technique. As discussed in the previous section, proper choice and positioning of the Luggin probe will minimize the contribution of the ohmic drop to the measured electrode potential. One can also correct the measured electrode

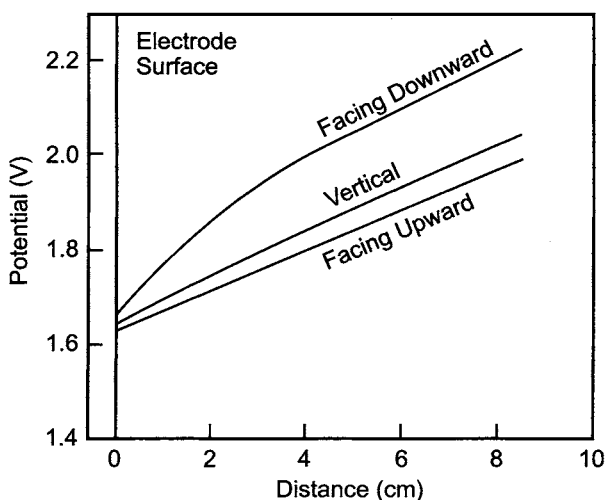


FIGURE 4.3.6. Potential vs distance variations in front of the working electrode in 20% NaOH at 15°C and 2 A dm^{-2} [38].

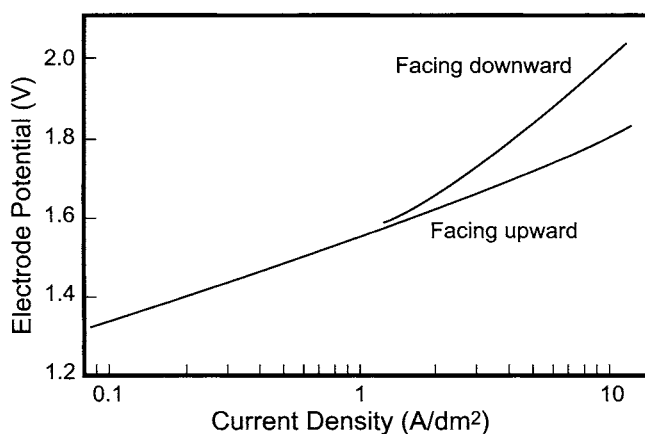


FIGURE 4.3.7. Polarization curves in 20% NaOH at 15°C and 2 A dm^{-2} [38].

potential for the ohmic potential still present by extrapolation, provided the distance between the Luggin tip and the electrode is accurately known. This can be avoided by using the current interruption technique [41,42] during potential measurements when a constant current is applied. Figure 4.3.8 shows a conventional circuit employed for polarization studies, and Fig. 4.3.9 shows a typical potential–time profile, following the application of a constant current to an electrolytic cell. After the potential has reached steady state, the current is interrupted, for example with a mercury-wetted switch, ensuring that the current is cut off in $\ll 10^{-6} \text{ s}$, and the variation of the potential with time is recorded using an oscilloscope, or by digitization. When the current is interrupted at

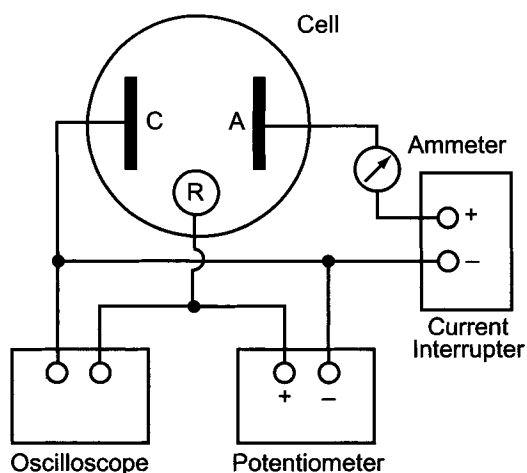


FIGURE 4.3.8. Circuit for polarization measurements. A: Anode; C: Cathode; R: Reference electrode.

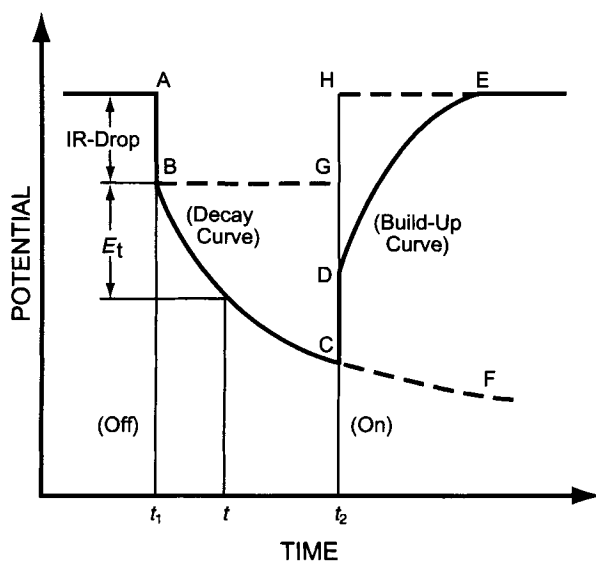


FIGURE 4.3.9. Potential vs. time profile following current interruption [44]. (Reproduced by permission of The Electrochemical Society, Inc.)

time, t_1 , the potential drops from A to B instantaneously and then decreases with time as indicated by curve BC, because of the discharge of the double layer capacity at the electrode surface. The potential will approach the static or reversible potential of the working electrode after a long time, as shown by the dashed line CF. If the current is switched on at time t_2 , the potential jumps immediately, and then approaches a steady-state value at the given current density, as shown by the curve DE. We may call the curves BC and DE the “decay” and the “build-up” curves, respectively. In this figure, E_t is the potential at

the time t . The reason for the instantaneous fall or rise when the current is interrupted or applied is that pure ohmic drops do not have “decay” or “rise” times, unless coupled with a capacitance or an inductance. The slow decay of the potential, represented by the curve BC, is a result of the discharge of the double layer and the pseudocapacitance. The theoretical basis for the potential-relaxation method and an analysis of the potential decay curves is reviewed by Conway and Tilak [43].

Thus, the IR drop between the working electrode and the reference electrode can be measured and eliminated from the measured potential difference. However, the IR drop (AB) should be as small as possible, to improve experimental accuracy. The differential capacitance, C_d , of the electrode surface and the Tafel slope, b , of the kinetic-controlled process, can be obtained from the potential–time transients by Eqs. (13) and (14).

$$C_d = i / (dE_t/dt) \quad (13)$$

$$b = dE_t / d \log t \quad (14)$$

where i is the current density and E_t is the electrode potential at time t [42]. Figure 4.3.10 shows an example of an oscilloscope trace obtained with a pure mercury cathode in 0.2N HCl at 1.5 A dm^{-2} [44].

4.3.2.4. Galvanostatic and Potentiostatic Polarization Measurements. Electrode processes may be classified into two types: reaction or charge-transfer controlled, and diffusion or mass-transfer controlled. The electrode processes in diaphragm and membrane chlor-alkali cells are charge-transfer controlled. On the other hand, the formation of sodium amalgam on a mercury cathode, is diffusion-controlled.

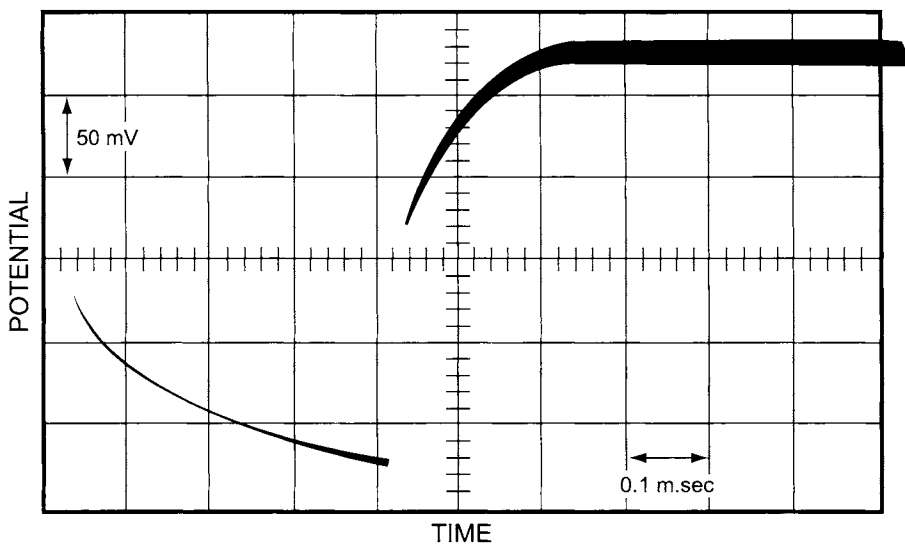


FIGURE 4.3.10. Oscillographic trace of a potential–time profile on a pure mercury cathode in 0.2N HCl at 1.5 A cm^{-2} and -1.169 V (SHE) [44]. (Reproduced by permission of The Electrochemical Society, Inc.)

The rate equation for a charge-transfer process is (see Section 4.2 for details):

$$i = i_0 \{ \exp(\alpha F \eta / RT) - \exp[-(1 - \alpha) F \eta / RT] \} \quad (15)$$

where i is the current density, i_0 is the exchange current density, η is the overvoltage, and α is the transfer coefficient, which is about 0.5. When $|\eta|$ is greater than ~ 0.07 V, Eq. (15) can be approximated by:

$$|\eta| = (RT/F) [\ln |i| - \ln i_0] \quad (16)$$

Thus, the overvoltages, both anodic and cathodic, are linear with the logarithm of current density, as shown in Fig. 4.3.11 [45]. From this plot, the exchange current density can be estimated by extrapolation to $|\eta| = 0$, and the slope of the η vs $\log i$ curve provides the value of the Tafel slope, $b = 2.303 RT / \alpha F$, from which the transfer coefficient can also be evaluated.

When the overvoltage is less than 20 mV, Eq. (15) can be linearized, resulting in:

$$i = i_0 (F \eta / RT) \quad (17)$$

Thus, at low overvoltages, the current density is directly proportional to the overvoltage, as shown in Fig. 4.3.12, giving the Faradaic reaction resistance treated in

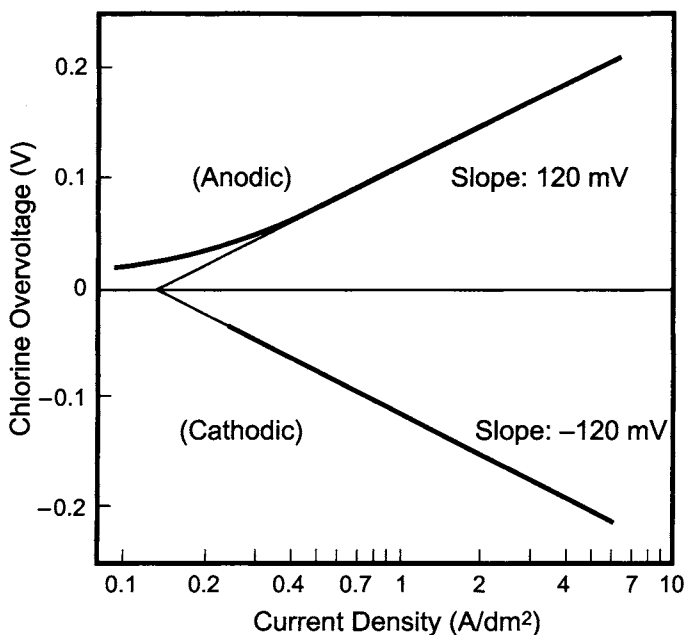


FIGURE 4.3.11. Anodic and cathodic polarization curves for graphite in saturated NaCl solutions (pH ca.0.5) at 50°C and $p_{\text{Cl}_2} = \text{ca.}1$ atm [45]. (Reproduced by permission of The Electrochemical Society, Inc.)

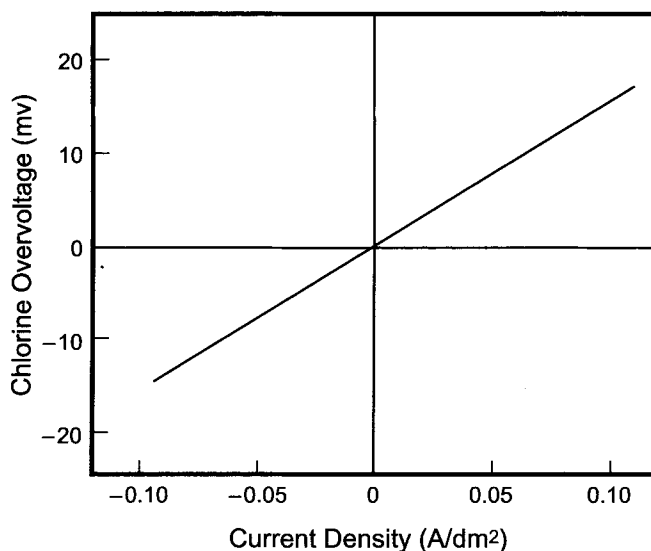


FIGURE 4.3.12. Plot of overvoltage vs current density in the low current density region for graphite in saturated NaCl solutions (pH ca.0.5) at 50°C and $p_{\text{Cl}_2} = \text{ca.1 atm}$ [45]. (With permission from The Electrochemical Society.)

Section 4.2.2. The exchange current density can also be evaluated from the slope of the linear plot.

Current-overvoltage data can be obtained galvanostatically by applying a constant current and measuring the potential under steady-state conditions, or potentiostatically, by imposing a constant potential and recording the current. Current is applied stepwise, both in the upward and downward directions, to establish reproducibility. The galvanostatic method is simpler than the potentiostatic method, but modern instruments can employ either method.

The polarization curve can also be obtained by the potential sweep method, employing a potentiostat and a function generator at low sweep rates of about 20 mV min^{-1} . However, preliminary experiments at various sweep rates are recommended to obtain a quasi-steady-state polarization curve, which is close to the true steady-state curve.

A typical diffusion-controlled reaction is the cathodic deposition of copper from acidified solutions of cupric sulfate. Under agitation, at relatively high current densities, the rate equation is:

$$\eta = \frac{RT}{F} \ln \left[1 - \frac{i}{i_L} \right] \quad (18)$$

where i_L is the limiting current density. The overvoltage on the copper cathode increases linearly with increasing current density. Near the limiting current density, it increases abruptly, as shown in Fig. 4.3.13 [46]. For these types of systems, potentiostatic

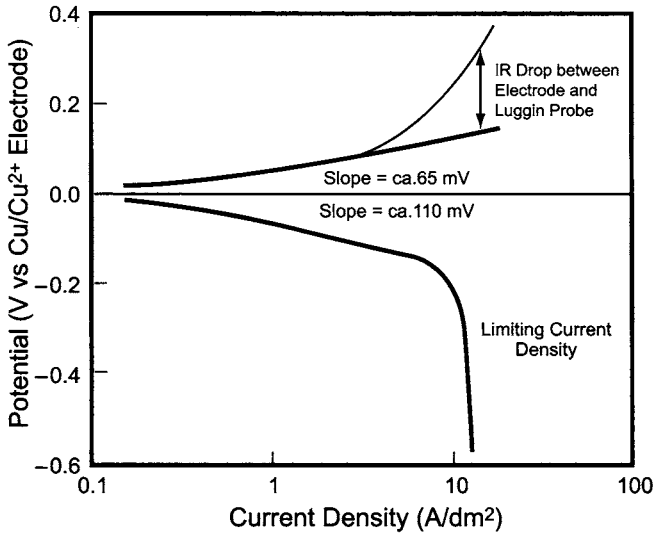


FIGURE 4.3.13. Polarization data for a copper electrode in 1M CuSO_4 at 40°C under free convection [46].

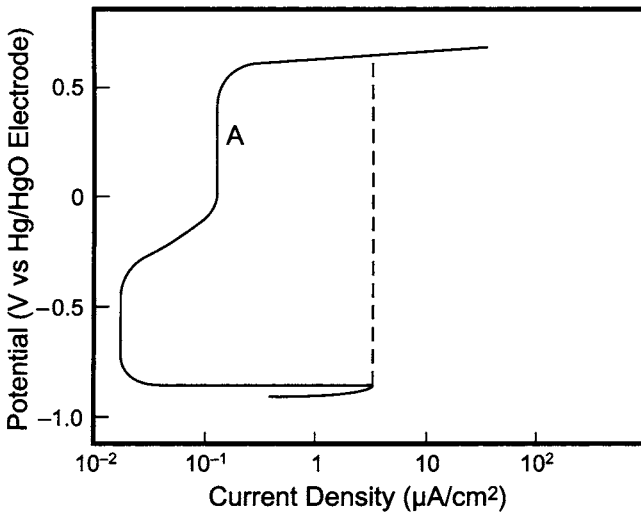


FIGURE 4.3.14. Polarization curve for a carbon steel anode in 2M NaOH at 40°C obtained by the potential step method [47].

measurement is preferred over the galvanostatic method to determine the polarization behavior of a given electrode.

Another example of a polarization curve is the anodic polarization behavior of metals and alloys in aqueous solutions when they are passivated. Figure 4.3.14 shows the polarization curve of a carbon steel in dilute NaOH solution, obtained by using the potential step method. The anodic current density increased with increasing polarization

potential, starting from the rest potential of about -0.9 V vs Hg/HgO [47]. When the polarization potential exceeded the Flade potential at about -0.83 V, the current suddenly decreased by two orders of magnitude, and remained almost unchanged up to about -0.3 V. The potential corresponding to the maximum in the current–potential curve is called the passivation potential, and the Flade potential is the potential value anodic to the passivation potential. The Flade potential is a well-characterized feature representing the transition of metals between passive and active states at a given pH. As the current density increased slightly in the potential range of 0 – 0.5 V, further oxidation of the anodic film from ferrous oxide to magnetite Fe_3O_4 occurred, and oxygen evolved at potentials higher than 0.6 V. If the galvanostatic method is used in such a system, the anode potential jumps from the Flade potential to the oxygen evolution directly, as shown by the dashed line, and the curve A is no longer accessible. Sometimes this causes the onset of oscillations of potential at constant current.

4.3.2.5. Rotating Electrodes. One of the problems that arises during polarization studies is the concentration polarization in quiescent solutions, which affects the current–voltage characteristics. This can be avoided by employing a rotating disc electrode (RDE). Levich [48] has shown that the RDE in a liquid medium has uniform accessibility to diffusing species, and that the current at the RDE rapidly attains a steady state [49,50]. Solution of the convection–diffusion equation gives the diffusion layer thickness, δ , as a function of the rotational speed:

$$\delta = [1.6\nu^{1/6}D^{1/3}]\omega^{-1/2} \quad (19)$$

where ω is the rotation speed in radians per second ($\omega = 2\pi f$, where f is the rotational speed in revolutions per second), D is the diffusion coefficient, and ν is the kinematic viscosity, defined as viscosity/density. Thus, by simply changing the rotational speed of the RDE, the thickness of the diffusion layer can be controlled precisely. If the current–voltage curve is independent of the rotational speed, one can rely on those data to deduce the kinetic parameters for the electrochemical reaction under study.

There are several variations of the RDE system, including rotating hemispherical electrodes [51] and rotating cylinder or cone electrodes [52,53]. The rotating cylinder electrode (RCE) is particularly useful if one wants to measure corrosion rates at high-flow velocities that are generally encountered in practice. Use of the RCE, with accurate measurement of a soluble species by conventional analytical techniques, gives results that can be converted into corrosion rates. Note that the data generated at the RCE can be directly correlated [54] with the flow velocities in a tube, since

$$\log \text{Re}_{\text{tube}} = 0.670 + 0.0833 \log \text{Re}_{\text{cyl}} \quad (20)$$

where Re represents the Reynolds number for the tube (denoted by the subscript tube) and the rotating cylinder (denoted by the subscript cyl) and is equal to Ud/ν , where U refers to the flow velocity in centimeters per second and d the characteristic length in centimeters.

The RDE is constructed from a disc of the electrode material of interest mounted on a metal shaft, usually made of stainless steel or brass and covered with a cylindrical shroud of PTFE, polychlorotrifluoroethylene (PCTFE) or epoxy, ensuring that the metal shaft and the disc edge of the electrode are not in contact with the solution. These electrodes are available commercially from various suppliers, the most popular being the one produced by Pine Instruments Company [55].

These electrodes are inserted into a rotator, constructed with a variable speed synchronous motor drive controlled by a feedback system sensing the rotational velocity. The velocity of rotation is controlled to $\pm 1\%$.

4.3.3. Non-Steady-State Techniques

In non-steady-state methods [56,57], the system is perturbed by a signal and then allowed to relax to the equilibrium value or to another steady state. During these measurements, the double layer is charged first, as any change in the electrical state of an electrochemical system results in the rearrangement of charges at the electrical double layer. The resulting displacement current density can be expressed by:

$$i_{dl} = \frac{\partial q}{\partial t} = \frac{\partial}{\partial t} \int_{E_z}^E C dE \quad (21)$$

where q is the charge per unit area, t is time, C is the differential capacity/unit area, E_z is the potential of zero charge and i_{dl} is the current required to charge the double layer. For small amplitude perturbations, where the potential dependence of the capacitance is not significant, Eq. (21) may be replaced by Eq. (22),

$$i_{dl} = C \frac{dE}{dt} \quad (22)$$

Following the charging of the double layer, the Faradaic process will respond to the perturbation imposed on the system.

Transient techniques were developed to investigate the kinetics of electrochemical reactions, and they are summarized in ref. [8]. Rangarajan [58] analyzed the rationale behind these relaxation techniques and showed that they are all equivalent in that the desired kinetic information can be derived from any input–output response. However, what makes one method preferable to another is the ease with which it can be set up and used. Two techniques that are widely used in chlor-alkali studies are presented here.

4.3.3.1. Cyclic Voltammetry. In this method, the potential of the working electrode is varied linearly with time from an initial potential of E_i to a final value of E_f , and then reversed from E_f to E_i at the same rate, as shown in Fig. 4.3.15. The resulting current is measured as a function of time or potential. This scheme can be used as a single sweep or a multisweep, as used in cyclic voltammetry. The potential range is generally selected to suit the reaction under study.

This method can be classified by the values of the potential sweep rates. At a low sweep rate, the current–potential relation is the same as that obtained under steady-state

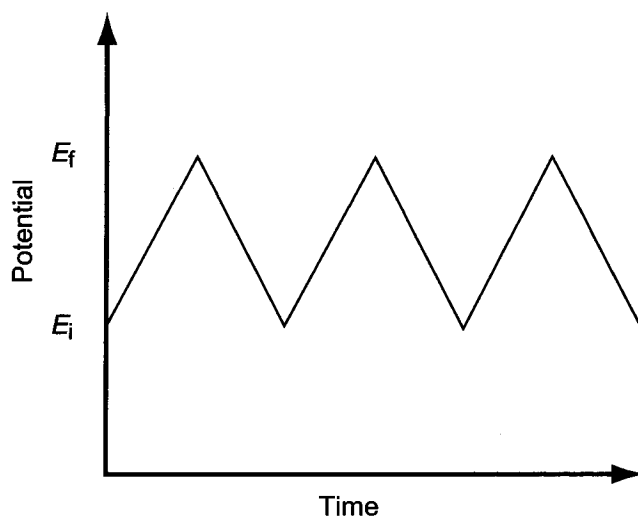


FIGURE 4.3.15. Variation of potential with time in a multisweep.

conditions by the galvanostatic or potentiostatic methods. Since this is not a true steady state, results should be confirmed by conventional measurements.

At intermediate sweep rates, the steady-state behavior is perturbed by diffusion to or away from the electrode, and by the possible slow adsorption/desorption equilibrium.

At sufficiently high sweep rates, one can measure currents used to charge the double layer, and for the processes of adsorption or desorption of reactants or intermediates involved in the charge-transfer step. The latter current is called the pseudocapacitive current.

Cyclic voltammetry offers several advantages, which include rapid acquisition of the current–overpotential variations under quasi-steady-state conditions and the ease with which the experiment can be performed. A block diagram of the circuit used for this method is presented in Fig. 4.3.16.

At moderate sweep rates, the current–potential profile passes through a maximum, as shown in Fig. 4.3.17. The peak current I_p occurring at a potential E_p is due to the maximal transport of the oxidant, Ox, from the bulk of the solution to the cathode surface. Since the electrode process under discussion



is fast, the electrode potential can be represented by the Nernst equation (24):

$$E'(t) = E_1 - vt = E + \ln \frac{RT}{nF} \frac{C_{\text{Ox}}(t)}{C_{\text{Red}}(t)} \quad (24)$$

where $E'(t)$ is the electrode potential at time t_1 , v is the rate of potential sweep, E is the reversible potential or the formal potential, and C is the concentration of the

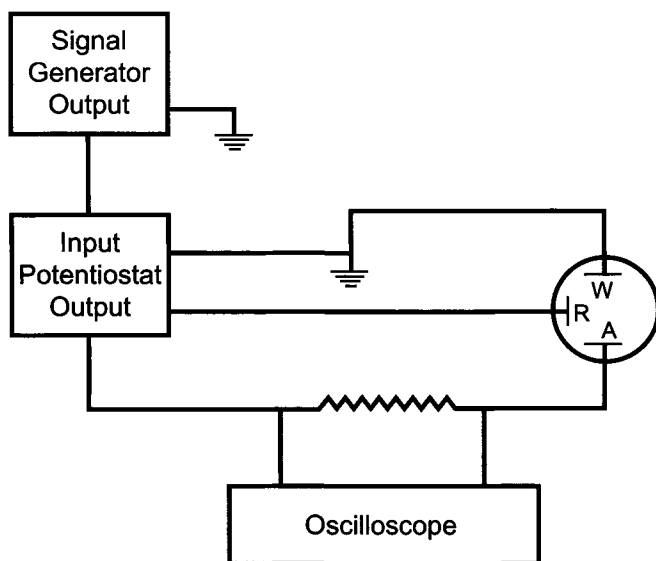


FIGURE 4.3.16. Block diagram of the circuit for cyclic voltammetry. A: Auxiliary electrode; W: Working electrode; R: Reference electrode.

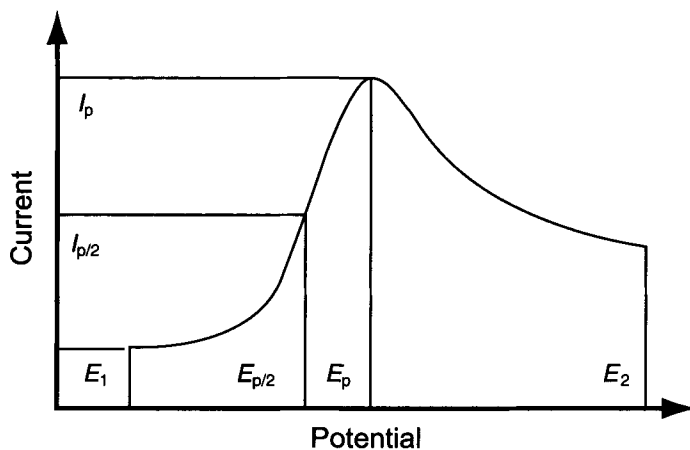


FIGURE 4.3.17. A schematic of the potential sweep polarization curve.

chemical species at the electrode surface. The cathodic current I_C can be represented from Faraday's law as

$$I_C t = n F V C_{ox}(t) \quad (25)$$

or

$$I_C = n F V \frac{dC_{ox}}{dt}$$

where V is the solution volume. At the beginning, C_{red} is zero while C_{ox} is large. When the potential is scanned in the cathodic direction, C_{ox} decreases and C_{red} increases because of slow mass transfer, and the current increases exponentially to the half-peak potential, $I_{p/2}$. With further polarization in the cathodic direction, C_{ox} becomes small, while C_{red} increases, and the increment of current decreases. At the peak potential, E_p , the current reaches the maximum, I_p . The diffusion of the oxidant no longer increases. The mass transport of the reductant from the electrode surface to the bulk of the solution also decreases because the concentration of the reductant in the solution increases, which results in a gradual decrease in the current.

For a reversible reaction, occurring under diffusion-controlled conditions [6], I_p is given by:

$$I_p = kn^{3/2}AD^{1/2}C_R^0v^{1/2} \quad (26)$$

where $k = 2.72 \times 10^5 \text{ A s mol}^{-1} \text{ V}^{1/2}$, n is the number of electrons transferred in the overall reaction, A is the effective area of electrode in centimeters, D is the diffusion coefficient in square centimeter per second, C_R^0 is the bulk concentration of the reactant in moles per cubic centimeter, and $v = dV/dt$ is the sweep rate in volts per second. The potential at which the current is maximum is expressed by the relationship:

$$E_p = E_{1/2} - \frac{1.1RT}{nF} \quad (27)$$

where $E_{1/2}$ is the polarographic half-wave potential. The positive sign applies to an anodic reaction and the negative sign to a cathodic reaction. Thus, the peak current is proportional to the square of the sweep rate and varies linearly with the concentration of the reactant, while the peak potential is independent of the sweep rate.

In the case of an irreversible reaction, the peak current and the peak potential are

$$I_p = k_1 A n F \left(\frac{\alpha n F}{RT} \right)^{1/2} D_o^{1/2} C_R^0 v^{1/2} \quad (28)$$

$$E_p = E_i + \frac{RT}{\alpha n F} \left[k_2 + \ln \frac{k}{D_R^{1/2}} - \frac{1}{2} \ln \left(\frac{\alpha n F}{RT} v \right) \right] \quad (29)$$

where $k_1 = (3-5) \times 10^{-5}$, $k_2 \approx 0.77$, and k is the reaction rate constant.

Thus, the peak current is proportional to $v^{1/2}$ and C_R^0 , while E_p varies logarithmically with the sweep rate. Additional information related to other cases is found in refs. [11,12,59-61].

At high sweep rates, one can examine the surface electrochemical processes, including the double layer charging process occurring prior to the Faradaic reactions. Figure 4.3.18 is the cyclic voltammogram recorded at 0.10 Vs^{-1} sweep rate, of a clean Pt electrode in $0.5\text{M H}_2\text{SO}_4$ at 25°C [62]. The data were developed in the voltage region of $0.1-1.3 \text{ V}$ vs NHE, prior to the H_2 evolution on the cathodic side and O_2 discharge on the anodic side. The current-voltage profile reveals hydrogen adsorption and desorption in the potential region of $0.1-0.3$, double layer charging in the potential range of

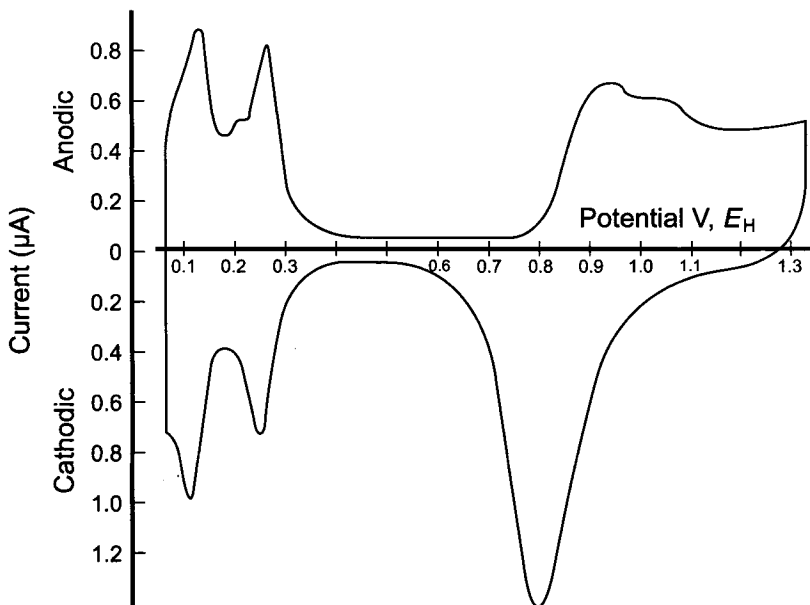
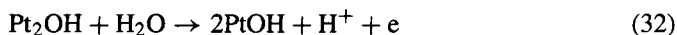
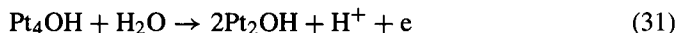
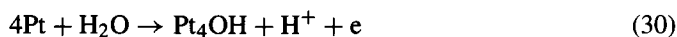


FIGURE 4.3.18. Potentiodynamic current–voltage profile for a clean Pt electrode in 0.5M H₂SO₄ at room temperature [62]. (With permission from Elsevier.)

0.4–0.6 V, and oxide formation and reduction in the voltage region of 0.6–1.3 V. The maxima observed in the potential of 0.1–0.3 V were attributed to two clearly resolved redox processes corresponding to the formation and removal of weakly and strongly bonded hydride on the surface of Pt, prior to the discharge of H₂. The appearance of humps in the anodic current profile in the voltage region of 0.8–1.3 V has been attributed [62] to the formation of PtO, following the reaction scheme noted below.



where each step contributed to a maximum in the current–voltage profile.

Theoretical analysis [63,64] has shown that when a surface reaction of the type $\text{M} + \text{A}^- \leftrightarrow \text{MA} + e$ is proceeding reversibly, one will observe a maximum in the current–voltage profile, with

$$i_M = \frac{k^*F}{4RT} \cdot v \quad (34)$$

at a peak potential of

$$E_p = -\frac{RT}{F} \ln k_1^* \quad (35)$$

where k^* refers to the maximum surface charge for the formation of a monolayer of the adsorbed species (in $\mu\text{C cm}^{-2}$), and k_1^* to the ratio of the forward and the backward rate constants of the reaction noted above.

However, if the reaction is irreversible and can be described by the Tafel approximation, then

$$i_p \approx \frac{k^* F v}{5.4 RT} \quad (36)$$

and

$$E_p = \frac{RT}{\beta F} \ln \frac{k^* \beta F}{k_1 RT} + \frac{RT}{\beta F} \ln v \quad (37)$$

where β is the symmetry factor and k_1 is the forward rate constant of the reaction $M + A^- \rightarrow MA + e^-$.

4.3.3.2. AC Impedance. Impedance spectroscopy has been developed in recent years to study the characteristics of electrochemical reactions at metal/solution interfaces. In all electrochemical techniques, one is examining the impedance behavior, either directly or indirectly. The impedance at an interface is dictated by the reaction mechanism and is characterized by a nonlinear current-voltage relationship.

The electrical behavior of an electrode-solution interface and the processes that take place due to an electrochemical reaction can be treated in terms of an equivalent circuit [1,65,66]. It has been shown that when a Faradaic reaction is occurring at low overpotentials, without the involvement of adsorbed intermediates, the equivalent circuit may be expressed as shown in Fig. 4.3.19A.

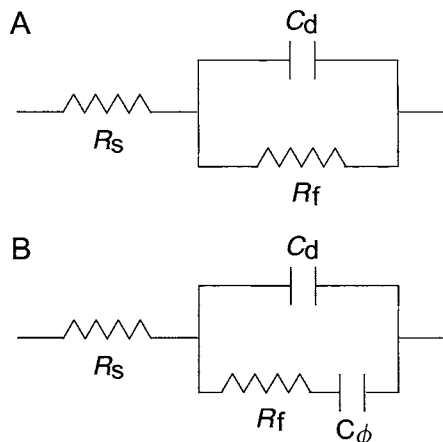


FIGURE 4.3.19. Equivalent circuit representation of an electrode-solution interface for a simple charge-transfer process. (A) Without adsorbed intermediates, and (B) with adsorbed intermediates.

Thus, the equivalent circuit consists of a solution resistance, R_S , in series with the double layer capacitance, C_{dl} , and R_F , the Faradaic resistance associated with the charge-transfer process. However, if an adsorbed intermediate is involved in the charge-transfer process, such as:



the equivalent circuit contains an added capacitance, C_ϕ , associated with the potential dependence of the coverage by the adsorbed intermediate (Fig. 4.3.19B). These "circuits" exhibit frequency-dependent impedance and it is this that is measured in the AC impedance measurements. The impedance associated with the equivalent circuit in Fig. 4.3.19A can be written as:

$$\frac{1}{Z} = \frac{1}{R_f} + j\omega C_d \quad (39)$$

where $j = (-1)^{1/2}$ and ω is the frequency of the AC signal.

When the reaction is under charge-transfer control, the reaction rate is given by the Butler–Volmer equation (see Section 4.2.2)

$$i = i_o[\exp(\alpha nF/RT) - \exp\{-(1 - \alpha)nF\eta/RT\}] \quad (40)$$

where i is the current density, i_o is the exchange current density, α is the transfer coefficient, and η is the overvoltage. At small perturbations in potential, for example, $\eta < 10$ mV, Eq. (40) can be approximated as follows:

$$i = i_o F \eta / RT \quad \text{or} \quad R_f = RT / F i_o \quad (41)$$

$RT / F i_o$ is called the polarization resistance. Substituting Eq. (41) into Eq. (39) results in:

$$\frac{1}{Z} = \frac{F i_o}{RT} + j\omega C_d \quad (42)$$

or

$$Z = Z_r + Z_i \quad (43)$$

where,

$$Z_r = \frac{F i_o RT}{(F i_o)^2 + (\omega C_d RT)^2}$$

$$Z_i = -j \frac{\omega C_d (RT)^2}{(F i_o)^2 + (\omega C_d RT)^2}$$

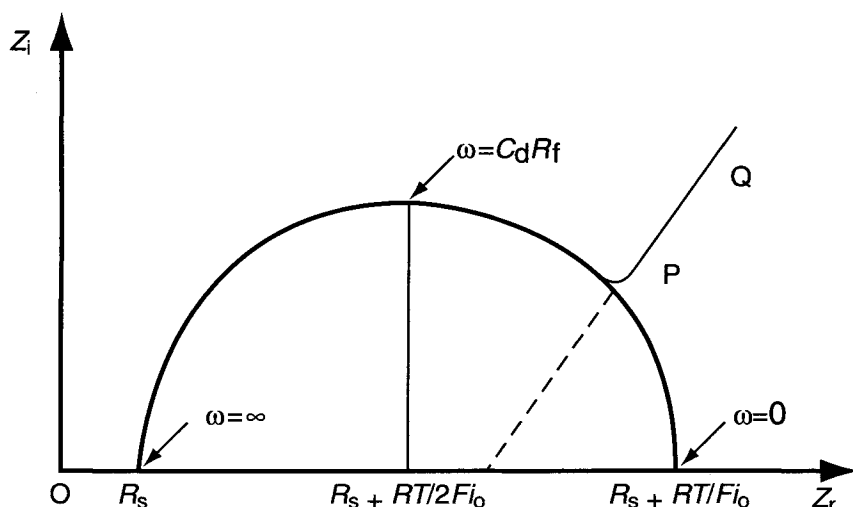


FIGURE 4.3.20. Complex plane representation of a charge-transfer controlled process.

Z_r and Z_i are the real and imaginary parts of a complex function Z . Eliminating ω from these equations leads to:

$$[Z_r - (RT/2i_0F)]^2 + Z_i^2 = (RT/2i_0F)^2 \quad (44)$$

Thus, a plot of Z_r vs Z_i shows a semicircle of $RT/2i_0F$ in radius, with the center located at the coordinates, $RT/2i_0F$ and 0, as shown in Fig. 4.3.20.

When the electrode reaction is controlled by the charge-transfer and the mass-transfer steps, the plot at low frequencies deviates from the semicircle, as illustrated by line PQ. In fact, the Z_r vs Z_i plots, called the Cole-Cole plots or the Nyquist plots, are often skewed and the simple model shown above is inadequate.

The experimental setup for measuring the AC impedance basically involves the measurement of the magnitude and the phase of an AC current generated in response to an applied low-amplitude (~ 5 mV) alternating voltage and recording using phase-sensitive instrumentation. Two commercially available instruments popularly used are the Solatron Frequency Response Analyzer system, made in England, or the EG&G system, available in North America.

The analysis and interpretation of the AC response usually follow this procedure.

1. The observed frequency-response behavior is fitted to that expected of equivalent circuit models that simulate the behavior of the actual system.
2. The frequency-response behavior is interpreted in an analytical, mathematical manner, based on electrochemical kinetic reaction mechanisms, together with a double layer capacitance. It must be emphasized that a given reaction mechanism dictates the equivalent circuit expected of it. However, fitting the experimental data to the theoretical impedance behavior is generally difficult and hence, great

caution has to be exercised in the impedance analysis. Computer programs are available for this purpose, for example, *Z*-plot.

There are basically three ways of representing the AC impedance results. The first one involves plotting the modulus of impedance as a function of frequency. These plots, called Bode plots, reveal one or more inflections over the characteristic frequency ranges, corresponding to the frequencies of various electrode-kinetic relaxation processes. The second is the phase angle plot of ϕ vs log frequency, which can exhibit phase angle values of -90° to 0° for simple RC circuits or positive values when an inductive element is present in the equivalent circuit. The more popular way of representation is a plot of the imaginary vs the real components of the impedance at a constant potential, each point on the curve corresponding to a given frequency. These are called Nyquist plots. A useful summary of the frequency response of various equivalent circuits is available in refs. [65,67–70].

4.3.4. Supporting Techniques

Electrode performance is greatly influenced by the structure, morphology, and chemical composition of the electrode surface, which can be examined and characterized by a wide variety of physical techniques in addition to the electrochemical methods outlined in this chapter. These techniques [71,72] are noted in Table 4.3.2. Table 4.3.3 gives the sensitivity and response time for various groups of methods. Table 4.3.4 and Fig. 4.3.21 give characteristics, detection limits [73], and applications for various types of surface analyses. Of these, scanning tunneling microscopy (STM) and atomic force microscopy (AFM) have received great attention in recent years as methods for examination of surfaces at an atomic scale [74–76]. Figure 4.3.22 is an example of an AFM profile of a $\text{RuO}_2 + \text{TiO}_2$ anode [77].

4.3.5. Conductivity Measurements

A knowledge of the conductivity of the electrolyte solutions, diaphragms and ion-exchange membranes is essential to calculate the ohmic drop in a cell, and thus to evaluate the dissipative energy losses in cell operation. Some definitions pertinent to this topic are noted below.

1. Specific resistance: Specific resistance, ρ , is defined as the resistance between two electrodes of 1 cm^2 area each, separated by 1 cm. Then,

$$R_s = \frac{\rho l}{A} \quad (45)$$

where R_s refers to the solution resistance in ohms (Ω), l refers to the electrode-electrode distance in centimeters, and A to the geometric area of the electrode in square centimeters. From Eq. (45), it follows that ρ has the units of ohm-centimeter. Thus, the inverse, or specific conductivity σ , has the units of mho per centimeter. The specific resistance of metals is in the range of 10^{-2} – $10^{-6} \Omega \text{ cm}$

TABLE 4.3.2 Modern Techniques for Surface Analysis

Microscopy	
Transmission Electron Microscopy	TEM
Scanning Electron Microscopy	SEM
Field Ion Microscopy	FIM
Atomic Force Microscopy	AFM
Scanning Tunneling Microscopy	STM
High Resolution STM	HRSTM
X-ray Fluorescence Microscopy	XFM
Spectroscopy	
Primary spectrum	
<i>Scattering spectrum</i>	
High Energy Electron Diffraction	HEED
Small Angle X-ray Scattering	SAXS
Small Angle Neutron Scattering	SANS
Inelastic Neutron Scattering	INS
Electron Loss Spectroscopy	ELS
<i>Absorption spectrum</i>	
Fourier Transform Infrared	FTIR
X-ray Absorption Near Edge Structure	XANES
Extended X-ray Absorption Fine Structure	EXAFS
Secondary spectrum	
Infrared Spectroscopy	IR
X-ray Photoelectron Spectroscopy	XPS
Electron Spectroscopy for Chemical Analysis	ESCA
Auger Electron Spectroscopy	AES
X-ray Emission Spectroscopy	XES
Electron Impact Desorption	EID

TABLE 4.3.3 Sensitivity and Response Time of Various Techniques

Technique	Sensitivity (g)	Response time (s)
Atomic absorption spectroscopy		
Flame	10^{-6}	1
Graphite tube	10^{-8}	>100
Polarography		
Conventional	10^{-10}	100
Modern	10^{-14}	>100
Photoelectron spectroscopy	10^{-8}	100
Electrochemical quartz crystal balance	10^{-8}	0.1
Cyclic voltammetry	10^{-9}	500
Impedance spectroscopy	10^{-8}	>100
Potentiostatic pulsed measurements	10^{-8}	10^{-4}

TABLE 4.3.4 Surface Analytical Techniques: Applications and Detection Limits

Analytical technique	Typical applications	Signal detected	Detection limits	Depth/analysis resolution	Lateral resolution/probe size
SIMS (Magnetic sector) Secondary Ion Mass Spectrometry	Dopant and impurity depth profiling, surface and microanalysis	Secondary ions	10^{12} – 10^{16} atoms/cm ³ (ppb-ppm)	50–300 Å	1.0 μm (imaging) ≥30 μm (depth profiling)
SIMS (Quadrupole) Quadrupole Sims	Dopant and impurity depth profiling, surface and microanalysis, insulator analysis	Secondary ions	10^{12} – 10^{16} atoms	<50 Å	<5 μm (imaging) ≥30 μm (depth profiling)
TOF-SIMS Time-of-flight SIMS	Surface microanalysis of organic/molecular and elemental species	Secondary ions and molecules	<1 ppm 10^8 at/cm ²	1–3 monolayers	0.10 μm
XPS/ESCA	Surface analysis of organic and inorganic materials	Photoelectrons	0.01–1 at%	10–100 Å	10 μm–10 mm
AUGER Auger Electron Spectroscopy	Surface analysis and high resolution depth profiling	Auger electrons from near surface atoms	0.1–1 at%	<20 Å	≥1,000 Å
FE AUGER Field Emission Auger Electron Spectroscopy	Surface analysis, microanalysis, microarea depth profiling	Auger electrons from near surface atoms	0.01–1 at%	20–60 Å	<150 Å
TXRF Total Reflection X-ray Fluorescence	Metallic contamination on semiconductor wafers	Fluorescent X-rays	10^9 – 10^{12} at/cm ²	10–1000 Å	10 mm
RBS Rutherford Backscattering Spectroscopy	Quantitative thin film composition and thickness	Backscattered He atoms	0.001–10 at%	20–200 Å	2 mm
SEM/EDS Scanning Electron Microscopy Energy Dispersive X-ray Spectroscopy	Imaging and elemental microanalysis	Secondary and backscattered electrons and characteristic X-rays	0.1–1 at%	1–5 μm (EDS)	45 Å (SEM) 1 μm (EDS)
AFM/SPM Atomic Force Microscopy Scanning Probe Microscopy	Surface imaging with near atomic spatial resolution	Atomic scale morphology		0.1 Å	50 Å

Source: Courtesy of Charles Evans & Associates.

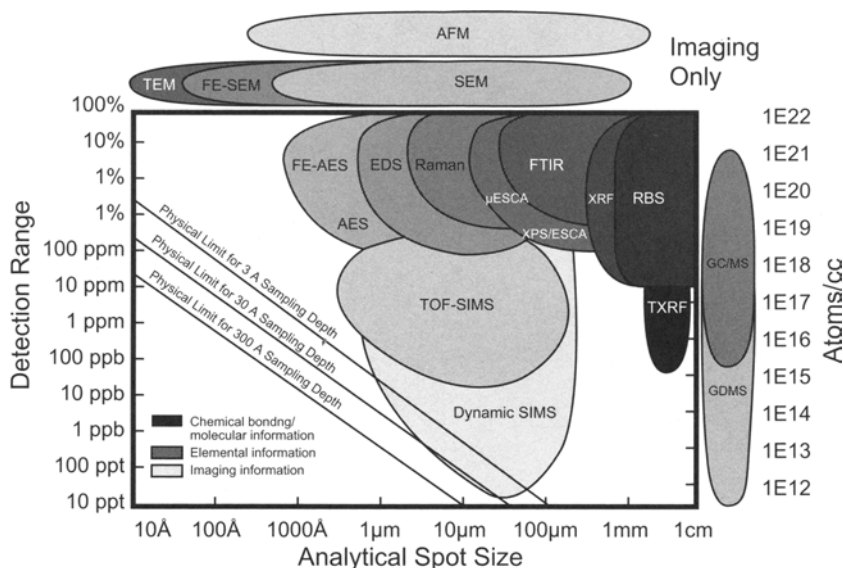


FIGURE 4.3.21. Analytical resolution vs sensitivity of various surface and bulk analytical techniques [73]. (With permission from Charles Evans & Associates.)

(Table 4.3.5), which may be compared to the resistance of 1–100 Ω cm for electrolytic solutions.

2. Molal conductance: When two electrodes are placed 1 cm apart with such an area that the solution between them contains 1 mol of the given electrolyte, the conductance of such a system is termed molal conductance, λ_m , defined by Eq. (46)

$$\lambda_m = \frac{1000\sigma}{C} \tag{46}$$

where C refers to the concentration of the electrolyte in moles per liter. If one equivalent of the electrolyte is present between the two electrodes, instead of 1 mol, then the conductance would be the equivalent conductance, λ_e , defined by

$$\lambda_e = \frac{1,000\sigma}{N} \tag{47}$$

where N refers to the normality. λ_m and λ_e have the dimensions of mho per square centimeter.

4.3.5.1. Measurement of Resistance. The resistance of a conducting system can be measured by a Wheatstone resistance bridge, shown in Fig. 4.3.23. Current from a DC power supply passes to node A, where the circuit branches. A fraction goes through R_x .

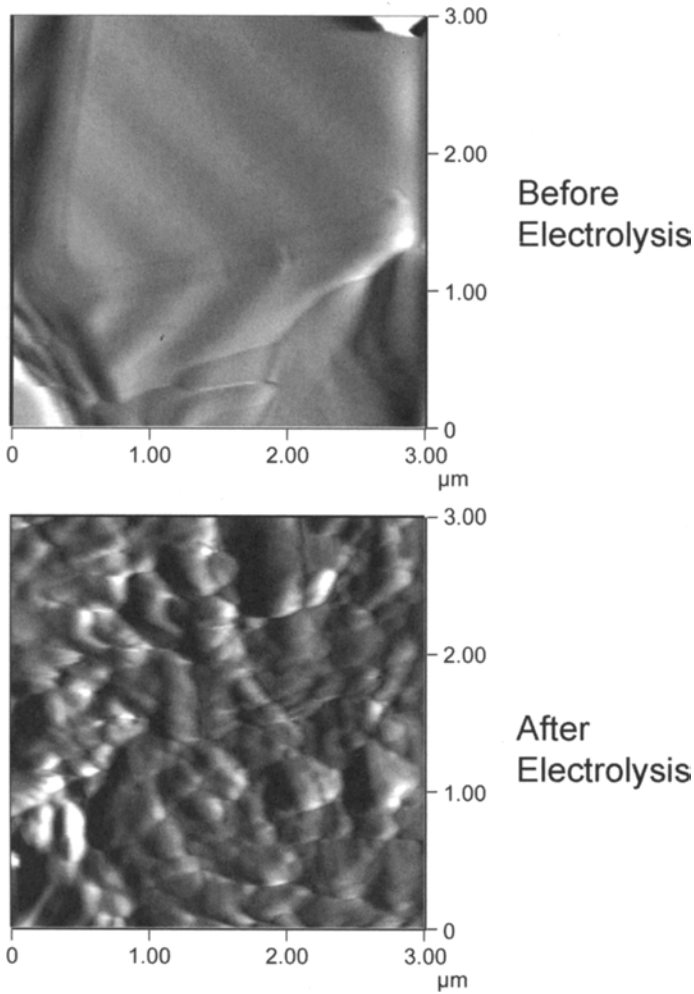


FIGURE 4.3.22. AFM images of $\text{RuO}_2 + \text{TiO}_2$ anode before and after electrolysis [77]. (With permission from C. Vallet.)

This may go through D (in either direction), and the rest passes through R_2 . The balance of the total current passes through the two known resistances, R_3 and R_4 . A current indicator D (e.g., a galvanometer) is connected between point F and junction B. When zero current passes through D, by appropriate adjustments of R_2 , the following relationship holds true:

$$\frac{R_x}{R_3} = \frac{R_2}{R_4} \quad (48)$$

Since R_2 , R_3 , and R_4 are known, R_x may be computed from Eq. (48).

TABLE 4.3.5 Resistivities of Some Common Materials at 25°C

Material	Resistivity (Ω cm)	Reference
Al	2.826×10^{-6} (20°C)	78
Au	2.44×10^{-6}	78
Ag	1.60×10^{-6}	78
Cu	1.72×10^{-6}	78
Fe	9.2×10^{-6}	79
Hg	95.78×10^{-6}	78
Ir	6.1×10^{-6} (20°C)	78
Nb	13.2×10^{-6}	79
Ni	7.8×10^{-6} (20°C)	78
Pd	11×10^{-6}	78
Pt	10×10^{-6}	78
Sn	11.5×10^{-6}	78
Ta	15.5×10^{-6} (20°C)	78
Ti	55×10^{-6}	79
W	5.5×10^{-6}	78
Zn	5.8×10^{-6}	78
Graphite	$0.3-3 \times 10^{-3}$	79
Fe ₃ O ₄	3.96×10^{-3}	79
PbO ₂	9.08×10^{-5}	79
Rh ₂ O ₃	130	80
RuO ₂	2×10^{-5}	80
IrO ₂	3×10^{-5}	80
Pt ₃ O ₄	4×10^{-3}	80
α -PtO ₂	1×10^{-6}	80
β -PtO ₂	$\sim 6 \times 10^{-4}$	80
MnO ₂	10	81
SiO ₂	3×10^4 (27°C)	82
SnO ₂	4×10^6 (20°C)	82
WO ₃	2×10^5	82
TiO	$\sim 8 \times 10^{-3}$	83
TiO ₂	$> 10^{13}$	82

4.3.5.2. *Measurement of Solution Conductivity.* A typical cell for measuring solution conductivity is shown in Fig. 4.3.24. The cell is provided with inlets B and C, to fill it with the given electrolyte, and electrodes E and E' , which are preferably platinized platinum. Electrical contact is made through the wires sealed in the glass wall. These electrical leads are also in contact with mercury in tubes A and D. The cross-sectional areas of the electrodes and the distance between them must be accurately determined in order to calculate the specific conductance. These precision measurements may be avoided by filling the cell compartment with solution of known specific conductance (usually a KCl solution of known concentration), and measuring the overall resistance, R_s .

This permits the definition of cell constant as $b = l/A = R_s \sigma$. By measuring R_s , the cell constant may be calculated, since the value of σ is known for the reference

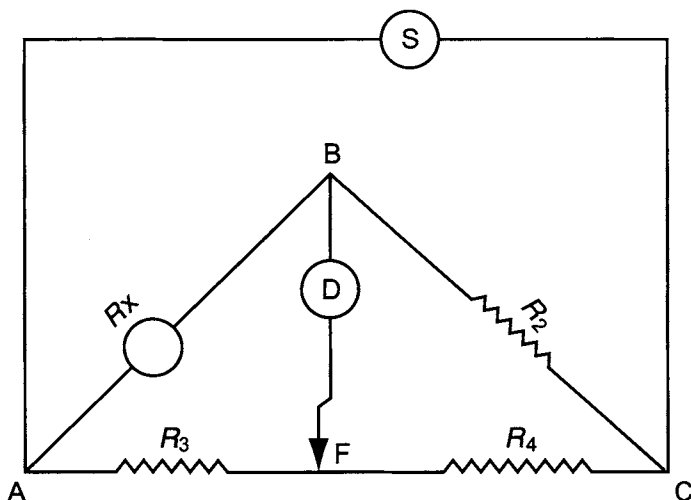


FIGURE 4.3.23. Schematic of a Wheatstone bridge for the measurement of resistance.

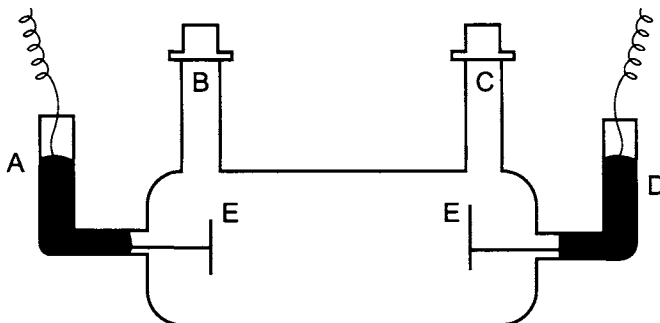


FIGURE 4.3.24. Schematic of a conductivity cell.

solution. Once the cell constant is determined, the specific conductance of any solution can be obtained by simply measuring the resistance and calculating σ from Eq. (49):

$$\sigma = \frac{b}{R_s} \quad (49)$$

4.3.5.3. Diaphragm Resistance. The calculation of the resistance across a separator, such as an asbestos or a polymeric diaphragm, is identical to the method employed to determine the resistance of an electrolyte between two parallel plates. However, the distance between the two faces of a separator is not equal to its thickness, as the liquid path in the separator is tortuous and the area is restricted by the finite porosity. Therefore, the l/A term in the parallel plate configuration should be modified to read as $[\text{tortuosity} \times \text{length}]/[\text{porosity} \times \text{area}]$ or as the ratio of tortuosity to porosity, which is called the MacMullin number. The MacMullin number, characterizing a

porous separator, can be obtained experimentally from the resistances measured with and without the separator. The experimental test cell (Fig. 4.3.25A) is comprised of two platinized platinum electrodes placed in a two-compartment cell filled with 1M K_2CO_3 solution. The resistance is measured using the procedure outlined earlier with and without the test material placed between the electrodes. The distance between the electrodes is measured using a micrometer gauge or a cathetometer.

Let the resistance with no separator be R_1 , and the distance between the electrodes be x_1 . Then, the resistance per unit length of solution, ρ , is

$$\rho = \frac{R_1}{x_1} (\Omega \text{ cm}^{-1}) \quad (50)$$

Let the resistance with a separator of thickness δ be R_2 . Then, the tortuosity will be given by:

$$\frac{\text{Tortuosity}}{\text{Porosity}} = \frac{R_2 - \rho(x_2 - \delta)}{\rho\delta} \quad (51)$$

This approach will yield a conservative measure of the tortuosity/porosity ratio for a given diaphragm.

4.3.5.4. Membrane Resistance. The resistance of an ion-exchange membrane can be measured directly by the cell shown in Fig. 4.3.25A with and without the electrolyte. The membrane resistance is:

$$R_m = R_{\text{cell with membrane}} - R_{\text{cell without membrane}} \quad (52)$$

An alternative approach is to place Au or Pt electrodes directly in contact with the membrane and measure the resistance using the cell presented in Fig. 4.3.25B. This method may include the contact resistance between the metal and the membrane, and hence mercury electrodes are preferred.

One can also measure the potential drop across the membrane in a cell [84] depicted in Fig. 4.3.25C, where current is passed through large electrodes and the ohmic drop is measured between the Luggin probes placed close to the membrane so that the IR drop between the Luggin tip and the membrane is negligible. From the measured drop, the resistance could be calculated using Ohm's law.

The resistance of membranes can be measured by AC impedance methods [85,86], using the four-point-probe technique. The test membrane is placed in a cell consisting of two Pt-foil electrodes, spaced 3 cm apart, to feed the current to a sample of $3 \times 1 \text{ cm}^2$ and two platinum needles placed 1 cm apart, to measure the potential drop (see Fig. 4.3.26). The cell is placed in a vessel maintained at constant temperature by circulating water. The impedance measurements are then carried out at 1–10 kHz using a frequency-response analyzer (e.g., Solatron Model 1255HF frequency analyzer). After ensuring that there are no parasitic processes (from the phase angle measurements, which should be zero), one can measure the resistance directly. The membrane resistance can also be obtained directly from the real part of the impedance (see typical data in Fig. 4.3.27).

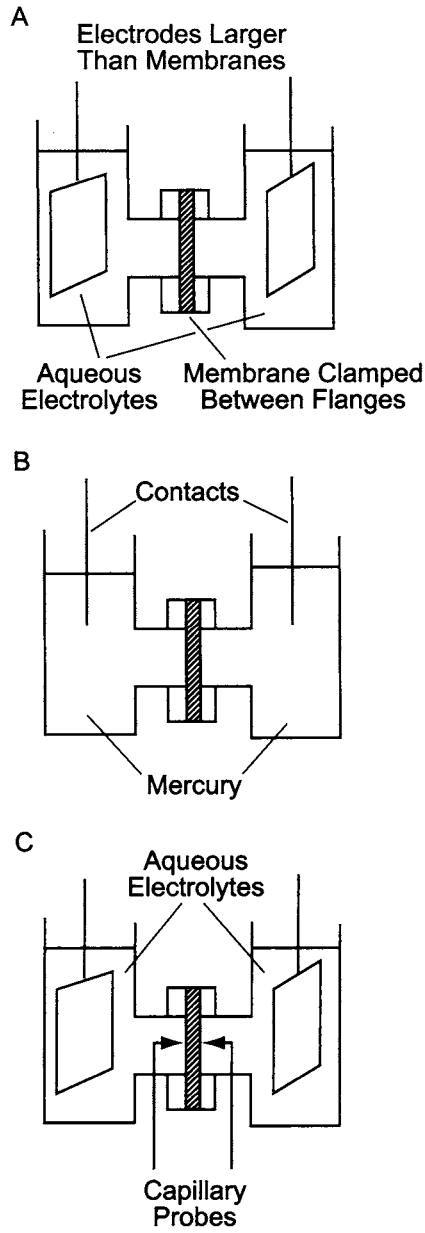


FIGURE 4.3.25. Schematic of cells for measuring the resistivity of membranes. Use of the three arrangements is described in the text.

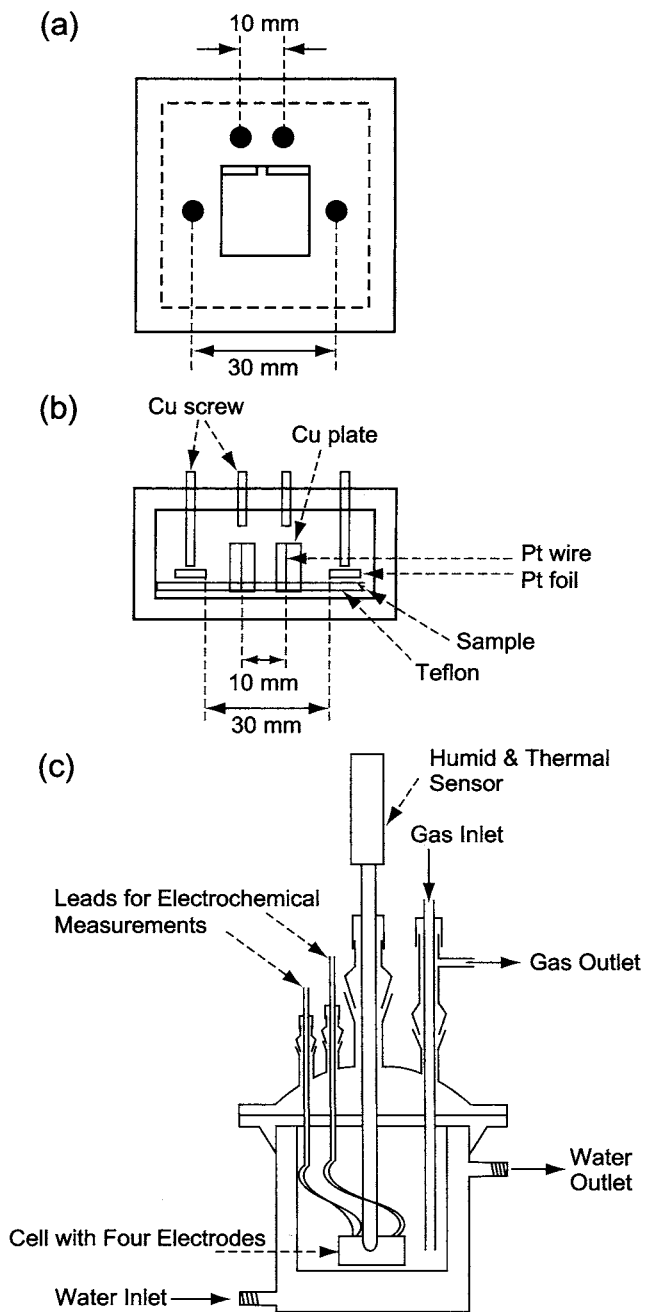


FIGURE 4.3.26. Apparatus for measuring conductivity [86]. (a) Cell top with four Pt electrodes; (b) cell bottom; and (c) the cell. (Reproduced by permission of The Electrochemical Society, Inc.)

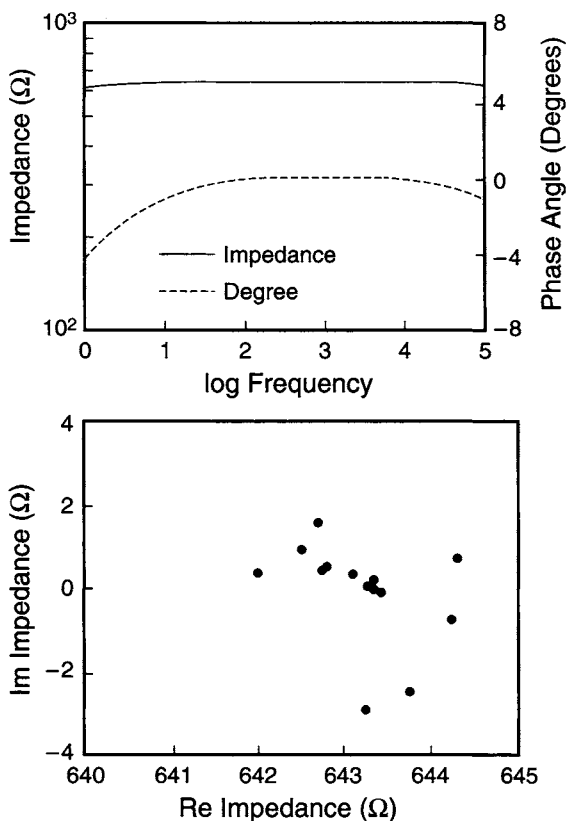


FIGURE 4.3.27. Typical data for impedance analysis using the four-electrode impedance method on Bode type plot (top) and Cole–Cole type plot (bottom) [86]. (Reproduced by permission of The Electrochemical Society, Inc.)

REFERENCES

1. A.J. Bard and L.R. Faulkner, *Electrochemical Methods*, John Wiley & Sons Inc., New York (1980).
2. D.T. Sawyer and J.L. Roberts, *Experimental Electrochemistry for Chemists*, John Wiley & Sons Inc., New York (1974).
3. P.A. Christensen and A. Hammet, *Techniques and Mechanisms in Electrochemistry*, Blackie Academic & Professional, New York (1994).
4. E. Gileadi, E. Kirova-Eisner, and J. Penciner, *Interfacial Electrochemistry: An Experimental Approach*, Addison-Wesley, New York (1975).
5. B.E. Conway, *Theory and Principles of Electrode Processes*, Ronald Press, New York (1965).
6. P. Delahay, *New Instrumental Methods in Electrochemistry*, Wiley-Interscience, New York (1954).
7. Southampton Electrochemistry Group, *Instrumental Methods in Electrochemistry*, Ellis Horwood, Chichester, UK (1985).
8. *Comprehensive Treatise of Electrochemistry*, Vol. 9, *Electrode Processes: Experimental Techniques*, E. Yeager, J.O'M. Bockris, B.E. Conway, and S. Sarangapani (eds), Plenum Press, New York (1984).
9. *Comprehensive Treatise of Electrochemistry*, Vol. 8, *Experimental Methods in Electrochemistry*, R.E. White, J.O'M. Bockris, B.E. Conway, and E. Yeager (eds), Plenum Press, New York (1984).
10. K. Vetter, *Electrochemical Kinetics*, Academic Press, New York (1967), p. 219.

11. H.R. Thirsk and J.A. Harrison, *A Guide to the Study of Electrode Kinetics*, Academic Press, New York (1972), pp. 61–62.
12. J. Headridge, *Electrochemical Techniques for Inorganic Chemists*, Academic Press, London (1969), p. 42.
13. *Kagaku Binran (Handbook of Chemistry)*, Edited by the Chemical Society of Japan, Maruzen Publ., Tokyo (1958), p. 640.
14. D.J.G. Ives and G.J. Janz, The Calomel Electrode and Other Mercury-Mercurous Salt Electrodes. In D.J.G. Ives and G.J. Janz (eds), *Reference Electrodes*, Academic Press, New York (1961), p. 127.
15. N.A. Shumilova and G.V. Zhutaeva, Silver. In A.J. Bard (ed.) *Encyclopedia of Electrochemistry of the Elements*, Vol. 8, Marcel Dekker, New York (1978), p. 1.
16. F. Hine, *Fushoku Kagaku no Gaiyo (Outline of Corrosion Engineering)*, Kagaku Dojin, Kyoto (1981), p. 63.
17. D.J.G. Ives and G.J. Janz, *Reference Electrodes*, Academic Press, New York (1961).
18. W.M. Latimer, *Oxidation Potentials*, Prentice Hall, Englewood Cliffs, NJ (1961).
19. A.J. deBethune and N.A.S. Loud, *Standard Aqueous Electrode Potentials and Temperature Coefficients at 25°C*, Clifford A. Hampel, Skokie, IL (1964).
20. M. Pourbaix, *Atlas of Electrochemical Equilibria in Aqueous Solutions*, Pergamon Press, Oxford (1966).
21. *Encyclopedia of Electrochemistry of the Elements*, Vols. 1–15, A.J. Bard (ed.), Marcel Dekker, New York (1973–1984).
22. *Standard Potentials in Aqueous Solutions*, A.J. Bard, R. Parsons, and J. Jordan, Marcel Dekker, New York (1985).
23. G.J. Hills, Reference Electrodes in Non-Aqueous Solutions. In D.J.G. Ives and G.J. Janz (eds), *Reference Electrodes*, Academic Press, New York (1961), p. 433.
24. R.W. Laity, Electrodes in Fused Salt Systems. In D.J.G. Ives and G.J. Janz (eds), *Reference Electrodes*, Academic Press, New York (1961), p. 524.
25. *Kiso Denki-Kagaku Sokutei-ho (Basic Method of Electrochemical Measurements)*, Electrochemical Society, Japan (1988).
26. *Zoku Kiso-Kagaku Sokutei-ho (Method of Electrochemical Measurements, Supplemental)*, Electrochemical Society, Japan (1996).
27. K. Izutsu and T. Nakamura, Reference Electrodes in Non-Aqueous Solutions. In *Kiso Denki-Kagaku Sokutei-ho (Basic Method of Electrochemical Measurements)*, Electrochemical Society, Japan (1988), p. 7.
28. K. Niki, Reference Electrodes in Fused Salts. In *Zoku Kiso-Kagaku Sokutei-ho (Method of Electrochemical Measurements, Supplemental)*, Electrochemical Society, Japan (1996), p. 147.
29. J. Mizusaki, Reference Electrodes Used in Solid Electrolyte. In *Zoku Kiso-Kagaku Sokutei-ho (Method of Electrochemical Measurements, Supplemental)*, Electrochemical Society, Japan (1996), p. 150.
30. T. Yamada, Reference Electrodes in Soils and Seawater. In *Zoku Kiso-Kagaku Sokutei-ho (Method of Electrochemical Measurements, Supplemental)*, Electrochemical Society, Japan (1996), p. 156.
31. P.E. Morris, New Electrochemical Techniques for High Temperature Aqueous Environments. In R. Baboian (ed.), *Electrochemical Techniques for Corrosion*, National Association of Corrosion Engineers, Houston (1977), p. 66.
32. T. Fujii, Reference Electrodes Under High Temperature and High Pressure Environments. In *Kiso Denki-Kagaku Sokutei-ho (Basic Method of Electrochemical Measurements)*, Electrochemical Society, Japan (1988), p. 13.
33. F. Hine, *Denki Kagaku (Journal of Electrochemistry Society of Japan)* **26**, 139 (1958).
34. R. Piontelli, G. Bianchi, and R. Aletti, *Zeit. Elektrochem.* **56**, 86 (1952).
35. R. Piontelli, G. Bianchi, U. Bertocci, C. Guerci, and B. Rivoltai, *Zeit Elektrochem.* **58**, 54 (1954).
36. R. Piontelli, G. Bianchi, U. Bertocci, C. Guerci, and G. Poli, *Zeit Elektrochem.* **58**, 86 (1954).
37. S. Barnett, *J. Electrochem. Soc.* **108**, 102 (1961).
38. F. Hine, S. Yoshizawa, and S. Okada, *Denki Kagaku (Journal of Electrochemistry Society of Japan)* **24**, 370 (1956).
39. S. Okada, S. Yoshizawa, F. Hine, and Z. Takehara, *Denki Kagaku (Journal of Electrochemistry Society of Japan)* **26**, 165, 211 (1958).
40. S. Yoshizawa, F. Hine, Z. Takehara, and M. Yamashita, *Denki Kagaku (Journal of Electrochemistry Society of Japan)* **28**, 205 (1960).
41. E. Yeager and F. Hovorka, *J. Electrochem. Soc.* **98**, 69 (1951).

42. J.O'M. Bockris and E.C. Potter, *J. Electrochem. Soc.* **99**, 169 (1952).
43. B.E. Conway and B.V. Tilak, Behavior and Characterization of Kinetically Involved Chemisorbed Intermediates in Electrocatalysis of Gas Evolution Reactions, In D.D. Eley, H. Pines, and P.B. Weisz (eds), *Advances in Catalysis*, vol. 38, Academic Press, Inc., New York (1992), p. 1.
44. F. Hine, S. Matsuura, and S. Yoshizawa, *Electrochem. Technol.* **5**, 251 (1967).
45. F. Hine and M. Yasuda, *J. Electrochem. Soc.* **121**, 1289 (1974).
46. F. Hine, *Electrode Processes and Electrochemical Engineering*, Plenum Press, New York (1985), p. 51.
47. F. Hine, *Fushoku Kogaku no Gaiyo (Outline of Corrosion Engineering)*, Kagaku Dojin, Kyoto (1981), p. 86.
48. V.I. Levich, *Physicochemical Hydrodynamics*, Prentice-Hall, Englewood Cliffs, NJ (1962).
49. Y.V. Pleskov and V.Y. Filinovskii, *The Rotating Disc Electrode*, Consultants Bureau, New York (1976).
50. V.Y. Filinovskii and Y.V. Pleskov, Rotating disk and Ring-Disk electrodes, In E. Yeager, J.O'M. Bockris, B.E. Conway, and S. Sarangapani (eds), *Comprehensive Treatise of Electrochemistry*, Vol. 9, *Electrode Processes: Experimental Techniques*, Plenum Press, New York (1984), Chapter 5, p. 293.
51. D.T. Chin, Theory and Experimental Aspects of the Rotating Hemispherical Electrode, In H. Gerischer and C.W. Tobias (eds), *Advances in Electrochemical Science and Engineering*, Vol. 1, VCH Publishers, New York (1990), p. 171.
52. D.R. Gabe, *J. Appl. Electrochem.* **4**, 91 (1974).
53. D.R. Gabe and F.C. Walsh, *J. Appl. Electrochem.* **13**, 3 (1983).
54. G. Karlsberg and G. Wranglen, *Proceedings of the 7th Scandinavian Corrosion Congress*, Trondheim, (1975), p. 154.
55. *Pine Instrument Company*, 101 Industrial Drive, Grove City, PA (2003).
56. E. Yeager and J. Kuta, Techniques for the Study of Electrode Processes, In H. Eyring, D. Henderson, and W. Jost (eds), *Physical Chemistry*, Vol. 9A, Academic Press, New York (1970), p. 345.
57. J. Kuta and E. Yeager, Overpotential Measurements, In E. Yeager and A.J. Salkind (eds), *Techniques of Electrochemistry*, Vol. 1, Wiley Interscience, New York (1972), p. 141.
58. S.K. Rangarajan, *J. Electroanal. Chem.* **41**, 459 (1973).
59. I. Epelboin, C. Gabrielli, and M. Keddam, Non-Steady State Techniques. In E. Yeager, J.O'M. Bockris, B.E. Conway, and S. Sarangapani (eds), *Comprehensive Treatise of Electrochemistry*, Vol. 9, *Electrode Processes: Experimental Techniques*, Plenum Press, New York (1984).
60. V.D. Parker, Linear Sweep and Cyclic Voltammetry. In C.H. Bamford and R.G. Compton (eds), *Chemical Kinetics*, Elsevier, Amsterdam (1986), p. 145.
61. J.O'M. Bockris and S.U.M. Khan, *Surface Electrochemistry*, Plenum Press, New York (1993), p. 223.
62. H.A. Kozłowska, B.E. Conway, and W.B.A. Sharp, *J. Electroanal. Chem.* **43**, 9 (1973).
63. E. Gileadi and S. Srinivasan, *Electrochim. Acta* **11**, 321 (1966).
64. E. Gileadi and B.E. Conway, *J. Chem. Phys.* **39**, 3420 (1963); B.E. Conway and E. Gileadi, *Electrochim. Acta* **4**, 325 (1961).
65. B.E. Conway, *Electrochemical Capacitors: Scientific Fundamentals and Technological Applications*, Kluwer Academic/Plenum Publishers, New York (1999).
66. B.V. Tilak, C.-P. Chen, and S.K. Rangarajan, *J. Electroanal. Chem.* **324**, 405 (1992).
67. C. Gabrielli, *Identification of Electrochemical Processes by Frequency Response Analysis*, The Solatron Electronic Group Ltd., Farnborough, Hampshire, UK (1980).
68. I. Epelboin, C. Gabrielli, and M. Keddam, Non-steady State Techniques, In E. Yeager, J.O'M. Bockris, B.E. Conway, and S. Sarangapani (eds), *Comprehensive Treatise of Electrochemistry*, Vol. 9, *Electrode Processes: Experimental Techniques*, Plenum Press, New York (1984), p. 62.
69. M. Sluyters-Rehbach and J.H. Sluyters, A.C. Techniques, In E. Yeager, J.O'M. Bockris, B.E. Conway, and S. Sarangapani (eds), *Comprehensive Treatise of Electrochemistry*, Vol. 9, *Electrode Processes: Experimental Techniques*, Plenum Press, New York (1984), p. 177.
70. J.R. McDonald, *Electrochim. Acta* **35**, 1483 (1990).
71. D.P. Woodruff and T.A. Delchar, *Modern Techniques of Surface Science*, Cambridge University Press, Cambridge (1986).
72. M. Lobregel and K. Kluger, *Soviet Electrochem.* **29**, 117 (1998).
73. Charles Evans Labs, Brochure entitled *Analytical Services* (2000).
74. K. Ogaki and K. Itaya, *Electrochim. Acta* **40**, 1249 (1995).
75. D.O. Wipf and A.J. Bard, *J. Electrochem. Soc.* **138**, 14 (1991).
76. C. Wei and A.J. Bard, *J. Electrochem. Soc.* **142**, 2523 (1995).

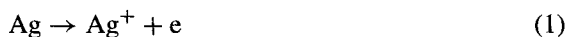
77. C.E. Vallet, B.V. Tilak, R.A. Zuhr and C.-P. Chen, A study of the Failure Mechanism of Chlorine Anodes, In J.B. Talbot, B.E. Conway, J.M. Fenton, and B.V. Tilak (eds), *Proceedings of the Symposia on Fundamentals Electrochemical Process Design: A Tutorial and Anodic Processes: Fundamental and Applied Aspects*, Proc. Vol. 95–11, The Electrochemical Society Inc., Pennington, NJ (1995); C.E. Vallet, *Appl. Phys.* **A65**, 387 (1997).
78. *Handbook of Chemistry and Physics*, C.D. Hodgman (ed.) 36th edition, Chemical Rubber Publishing Co., Cleveland (1954).
79. K.B. Keating, Electrode Selection for Electrochemical Processes, Paper #40A, *Presented at the 78th National AIChE Meeting*, Salt Lake City, Utah (1974).
80. V.B. Lazarev and I.S. Shaplygin, *Russ. J. Inorg. Chem.* **23**, 163 (1978).
81. C.N.R. Rao and G.V. Subba Rao, *Phys. Stat. Sol A*, **1**, 597 (1970).
82. G.V. Samsonov, *The Oxide Handbook*, Plenum Press, New York (1973).
83. R.W. Vest and J.M. Honig, Highly Conducting Ceramics and The Conductor–Insulator Transition, In N.M. Tallan (ed.), *Electrical Conduction in Ceramics and Glass*, part B, Marcel Dekker, New York (1974), p. 343.
84. T.A. Davis, J.D. Genders, and D. Pletcher, *A First Course in Ion-Permeable Membranes*, Alresford Press Ltd., Alresford, Hants, UK (1977).
85. R.P. Buck, *Electrochim. Acta* **35**, 1609 (1990).
86. Y. Sone, P. Ekdung, and D. Simonsson, *J. Electrochem. Sol.* **143**, 1254 (1996).

4.4. ENERGY CONSUMPTION

Electrochemical technologists routinely perform energy consumption calculations to understand and improve the economics of electrochemical operations and to compare alternative routes to products of interest. It is usually expressed in AC or DC kilowatt hours (kW hr) per unit weight of the substance produced electrochemically. Note that the electric utility companies charge the customers for the AC kWhr consumed in their operations.

4.4.1. Faraday's Law

When current is passed across a metal/electrolyte interface, it results in an electrochemical reaction. An electrode at which an oxidation reaction takes place is termed an anode. An electrode at which a reduction reaction takes place is called a cathode (Fig. 4.4.1). Thus, dissolution of Ag to form Ag^+ ion is accompanied by the release of an electron. This is an example of an oxidation reaction, as shown in Eq. (1), where e refers to an electron.



Correspondingly, when silver is deposited from Ag^+ ions, electrons are consumed. This is a reduction reaction as depicted by Eq. (2).



When a current passes through an electrolytic cell containing an anode and a cathode, oxidation reaction(s) and the corresponding reduction reaction(s) must take place at the respective electrodes, in order to ensure electroneutrality in the system.

Positively charged ions are called cations (e.g., Ca^{2+} , Mg^{2+} , etc.). Cations tend to travel toward the cathode. Negatively charged ions are called anions (e.g., Cl^- , F^- , etc.). Anions tend to travel toward the anode. Anions can react at the cathode and cations at

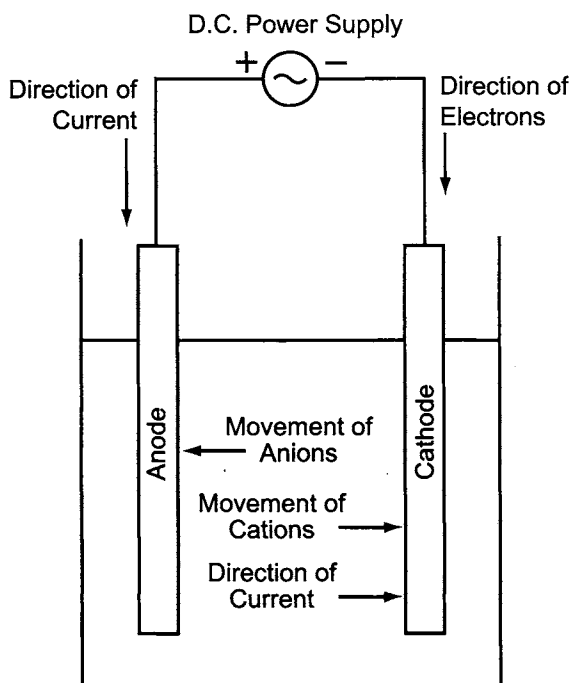


FIGURE 4.4.1. Schematic of an electrolysis setup.

the anode. This often leads to confusion since the tendency is to think of anions always reacting at the anode.

By convention, current is considered to flow in the opposite direction of anion (and electron) movement as shown below.

→ Negative ion flow	→ Positive ion flow
← Current flow	→ Current flow

Figure 4.4.1 summarizes the concepts introduced above.

4.4.1.1. Faraday's Law: Definition. "The number of equivalents of any substance liberated or deposited at an electrode is exactly proportional to the quantity of electricity which passes across the metal-electrolyte junction." This is Faraday's law, which is among the most exact in all of nature. It is independent of the shape of the electrode, temperature, the nature of the electrode, and the rate of current passage.

One gram-equivalent of an oxidizing agent is defined as the weight of a substance that picks up an Avogadro number of electrons ($\sim 6 \times 10^{23}$) in a given reaction. By the same token, one gram-equivalent of a reducing agent is defined as the weight of a substance that releases an Avogadro number of electrons. One Avogadro number of

electrons is called the Faraday, described in Eq. (3):

$$\begin{aligned}
 F &= N_A \varepsilon_e \\
 \text{Faraday} &= \text{Avogadro number} \times \text{charge of an electron} \\
 &= 6.064 \times 10^{23} \times 1.591 \times 10^{-19} \text{ C} \\
 &= 96500 \text{ C}
 \end{aligned}
 \tag{3}$$

where C = coulomb and is defined as one ampere of current passed for one second.

Based on the above definitions, Faraday's law can be restated as follows: one Faraday of electricity produces or consumes one equivalent of any substance. For example, in the reaction of Al and O₂ to produce Al₂O₃, aluminum changes valence from 0 to +3, and oxygen changes valence from 0 to -2. Each atom of Al releases three electrons and hence, one gram-atom of Al releases three times the Avogadro number of electrons. Thus, the equivalent weight of Al is 9 g. For oxygen, the equivalent weight is 8 g. The following example illustrates the use of Faraday's law in estimating the yield of chlorine, when Y amps are passed over t min, during the electrolysis of a sodium chloride solution. The number of coulombs passed = $Y \times t \times 60$.

$$\begin{aligned}
 \text{Hence, the number of Faradays} &= \frac{Y \times t \times 60}{96,500} \\
 &= Y \times t \times 6.21 \times 10^{-4} \text{ Faradays}
 \end{aligned}$$

The electrochemical reaction involved during the generation of chlorine is:



Therefore, two Faradays produce a mole of chlorine gas.

Hence, $Y \times t \times 6.2176 \times 10^{-4} \text{ F}$ will generate $Y \times t \times 3.1088 \times 10^{-4} \text{ mol}$ or $Y \times t \times 4.414 \times 10^{-2} \text{ g}$ of chlorine.

4.4.2. Energy Consumption Calculations

By definition, power expressed in watts is equal to amperes \times volts, and energy expressed in watt-hours is equal to amperes \times volts \times time (in hours). Therefore, the calculation of energy consumption requires a knowledge of the overall reaction and the number of Faradays required to produce the desired product, the operating cell voltage, and the cell current efficiency, which is illustrated here for the case of electrolytic chlorine production. The main anodic electrochemical reaction during the electrolysis of brine is the discharge of the chloride ions to produce chlorine, as described by reaction (4). When the chlorine current efficiency, ξ_{Cl_2} , is 100%, one Faraday of electricity will produce

0.5 mol or 35.45 g of chlorine. Therefore, the number of coulombs required to produce 1 ton of chlorine will be:

$$\frac{1,000 \text{ kg}}{\text{ton}} \times \frac{1,000 \text{ g}}{\text{kg}} \times \frac{96,500 \text{ C}}{35.45 \text{ g}} = \frac{2.722 \times 10^9 \text{ C}}{\text{ton of chlorine}}$$

Hence,

$$\begin{aligned} \frac{\text{Energy consumption}}{\text{ton of chlorine}} &= P_{\text{Cl}_2} = \text{Number of coulombs} \times \text{cell voltage} \\ &= 2.722 \times 10^9 \times E (\text{A} \times \text{V} \times \text{s ton}^{-1} = \text{W s ton}^{-1}) \\ &= 2.722 \times 10^6 \times E (\text{kW s ton}^{-1}) \\ &= 756.1 \times E (\text{kW hr ton}^{-1}) \end{aligned}$$

If the cell current efficiency is less than 1, and has a value of ξ_{Cl_2} , then

$$P_{\text{Cl}_2} = \frac{756.1E}{\xi_{\text{Cl}_2}} (\text{kW hr/ECU}) \quad (5)$$

Note that ECU stands for Electrochemical Unit or 1 ton of chlorine and an equivalent weight of NaOH. Table 4.4.1 gives the theoretical coefficients needed to calculate the energy consumption per short ton and metric ton of chlorine, NaOH, and KOH.

The units of the energy consumption figures calculated using Eq. (5) are in DC kWhr/unit product. However, some chlor-alkali plants require data on the energy consumption expressed in AC kW hr/unit product, in which case the rectifier efficiency, $\xi_{\text{rectifier}}$, has to be taken into account:

$$P_{\text{Cl}_2}^* (\text{AC kW hr/unit product}) = \frac{756.1E}{\xi_{\text{Cl}_2} \xi_{\text{rectifier}}} (\text{kW hr/ECU}) \quad (6)$$

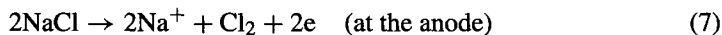
Equations (5) and (6) will permit the calculation of the energy consumption of a given electrolytic cell operation. For calculating the overall process efficiency, it is necessary to account for the chlorine recovered during dechlorination. This is done by dividing Eq. (6) by the dechlorinator efficiency, which is generally in the range of 98–99%. Thus, the energy consumption for producing chlorine or caustic can be calculated using Eq. (5) or (6), with a knowledge of the cell current efficiency and the cell voltage.

TABLE 4.4.1 Theoretical Coefficients for Calculating Energy Consumption

	Value for short ton	Value for metric ton
Cl ₂	685.8	756.1
NaOH	607.9	670.2
KOH	433.4	477.8

4.4.3. Current Efficiency

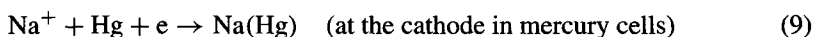
4.4.3.1. *Process Chemistry.* The main electrochemical reactions occurring in chlor-alkali cells [1–4] are:



and

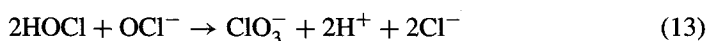
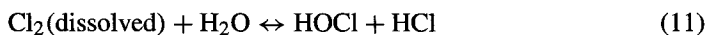


or

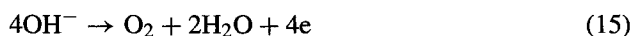


Thus, chloride ions are discharged at the anode to form chlorine, and sodium ions are transported through a separator to form NaOH with the hydroxyl ions generated at the cathode. In mercury cells, the sodium ions are discharged at the cathode to form sodium amalgam, which is subsequently decomposed with water to generate NaOH.

When a cation exchange membrane is ideal, the caustic current efficiency of the electrolyzer, ξ_{OH} , should be 100%, whereas the gaseous chlorine current efficiency, ξ_{Cl_2} , is expected to be less than 100% because of: (1) chlorine losses arising from the finite solubility of chlorine in the brine and the several reactions involving the dissolved chlorine:



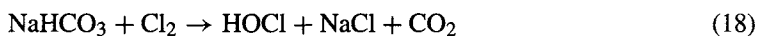
and (2) anodic oxygen evolution from the discharge of either the water molecules or the hydroxyl ions, following reaction (14) or (15):



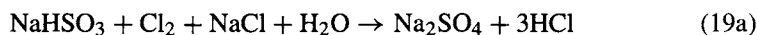
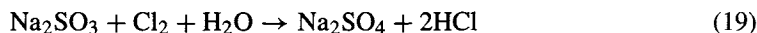
It may be noted that the oxygen evolution reaction (14) or (15) is thermodynamically favored over the chlorine evolution reaction. It results in the generation of electrons at the anode. Hence, the chlorine efficiency will be lower than the caustic efficiency. It is interesting to mention here that the caustic efficiency will never be 100% because of the oxygen evolution reaction, as the H^+ generated via Eq. (14) must react with the OH^- ions generated at the cathode to preserve the electroneutrality of the system.

The presence of OCl^- , HOCl , and ClO_3^- in the anode compartment is not only a result of reactions (11–13) but also a consequence of the presence of NaOH, NaHCO_3 ,

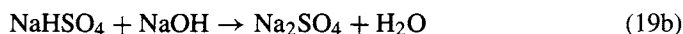
and Na_2CO_3 in the feed brine. These react with dissolved chlorine in the anolyte to form HOCl and OCl^- by reactions (16–18). Some of the HOCl goes on to form chlorate by reactions (12) and (13).



Another species in the feed brine to the membrane cells that consumes Cl_2 in the anolyte is Na_2SO_3 , via Eq. (19), which is generally added to remove the active chlorine in the feed brine to the ion-exchange columns in order to prevent the degradation of the ion-exchange resin by the hypochlorite [1].



While reactions (19) and (19a) are important, the presence of Na_2SO_3 or NaHSO_3 is not considered in the material balance equations described below, since their levels in the feed brine are generally controlled in the range of 1–10 ppm. However, when the feed brine or the anolyte pH is less than three, it is essential that the material balance accounts for the HSO_4^- species because of reaction (19b).



Note that the HSO_4^- ion concentration varies with pH since $\log ([\text{SO}_4^{2-}]/[\text{HSO}_4^-]) = -2.86 + \text{pH}$ at 90°C [5]. The corresponding expression for the $\text{SO}_3^{2-}/\text{HSO}_3^-$ equilibrium [5] at 90°C is $\log ([\text{SO}_3^{2-}]/[\text{HSO}_3^-]) = -7.72 + \text{pH}$, which indicates the predominant species to be HSO_3^- below pH 7 at 90°C .

4.4.3.2. Generalized Caustic and Chlorine Current Efficiency Expressions. The caustic current efficiency can be directly determined by the caustic collection technique, using the amount of caustic produced over a certain period of time, a knowledge of the number of coulombs passed during the same period, and Faraday's law. However, this is a tedious and time-consuming method. On the other hand, direct measurement of the chlorine produced is much more difficult for practical reasons. Hence, the chlor-alkali industry relies on indirect methods that provide rapid and accurate current efficiency values. The theory underlying the indirect methods is discussed in this section.

A generalized material balance approach [2] is outlined here involving the molar flow rates of Cl_2 , Cl , Na^+ , and OH^- species across the electrolyzer, and the conventional

definition of the gaseous chlorine (ξ_{Cl_2}) and caustic efficiency (ξ_{OH}), expressed as:

$$\xi_{Cl_2} = \frac{J_{Cl_2}^0}{I/2F} \tag{20}$$

$$\xi_{OH} = 1 - \frac{J_{OH}^{c \rightarrow a}}{I/F} = \frac{J_{Na^+}^{a \rightarrow c}}{I/F} \tag{21}$$

according to which the chlorine current efficiency is the ratio of the amount of chlorine leaving the electrolyzer to the theoretically expected quantity of chlorine produced. Equation (21) defines caustic current efficiency as the ratio of the amount of caustic collected from the electrolyzer to the theoretical amount of caustic generated, which is also equal to the amount of sodium ions that have migrated from the anode compartment to the cathode compartment, divided by the amount of caustic expected from Faraday's law.

One can now derive the current efficiency expressions for Cl_2 and $NaOH$ from the material balance (i.e., input + generation - loss = output) of the Cl , Cl_2 , OH^- (from the catholyte to the anolyte) and Na^+ (from the anolyte to the catholyte), following the schematic in Fig. 4.4.2, and Eqs. (20) and (21).

The material balances for the Cl , Cl_2 , Na^+ and OH^- are as follows from Fig. 4.4.2. In these expressions, the term J refers to the molar flow rate of the species (noted

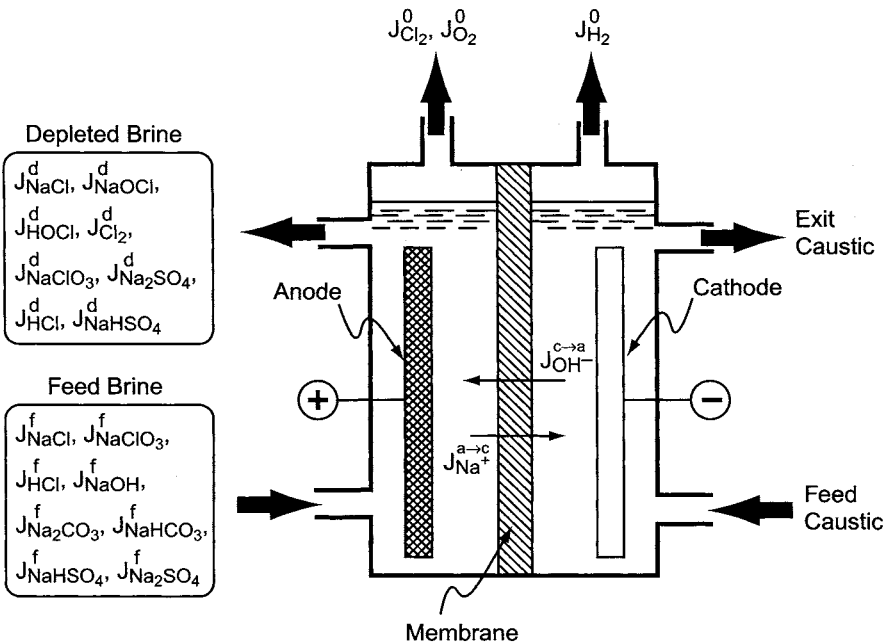


FIGURE 4.4.2. Schematic of the ion-exchange membrane cell describing the material balance around the electrolyzer [2].

in the subscripts) in the source stream (noted in the superscripts). An explanation of superscripts, subscripts, and other symbols used in these equations is as follows.

$J_{\text{Species}}^{\text{Source}}$	Molar flow rate of species (noted in the subscript), in the source stream (noted in the superscript), moles per second.
$C_{\text{Species}}^{\text{Source}}$	Concentration of species (noted in the subscript) in the source stream (noted in the superscript) (moles per liter).
P_{sp}	Energy consumption of species (sp) stated in the subscript.
$\Delta J_{\text{Species}}$	$= J_{\text{Species}}^f - J_{\text{Species}}^d = pC_{\text{Species}}^f - qC_{\text{Species}}^d$
a	anolyte
c	catholyte
ch	chemical
d	depleted brine for membrane cells or cell liquor for diaphragm cells
D	diaphragm
e	electrochemical
f	feed brine
o	gases leaving the electrolytic cell
'	feed catholyte
"	exit catholyte
ξ_{Cl_2}	Membrane cell chlorine current efficiency
$\xi_{\text{Cl}_2}^a$	Chlorine efficiency losses from the formation of HOCl, OCl^- , ClO_3^- , and soluble chlorine in the anolyte
ξ_{OH}^a	Caustic efficiency losses from the formation of HOCl, OCl^- , and ClO_3^- in the anolyte, and neutralization of feed brine acidity
$\xi_{\text{Cl}_2}^D$	Diaphragm cell chlorine current efficiency
$\xi_{\text{Cl}_2}^p$	Process chlorine efficiency for diaphragm cells
$\xi_{\text{H}_2}^D$	Diaphragm cell hydrogen current efficiency
ξ_{OH}	Membrane cell caustic efficiency
ξ_{OH}^D	Diaphragm cell caustic efficiency
$\xi_{\text{Cl}_2}^m$	Mercury cell chlorine current efficiency
ξ_{NaHg}	Amalgam formation current efficiency
ξ_{NaOH}^m	Caustic current efficiency of mercury cells
p	Feed brine flow rate (liters per second)
q	Depleted brine flow rate for membrane cells or cell liquor flow rate for diaphragm cells (liters per second)
R^*	$= q/p$
F	Faraday (96,487 A s or C)
I	Total current or load (amperes)

4.4.3.2A. Cl Balance. The material balance for the Cl species is described by Eqs. (22) to (24).

$$\text{Input} = J_{\text{NaCl}}^f + 2J_{\text{Cl}_2}^f + J_{\text{HOCl}}^f + J_{\text{NaOCl}}^f + J_{\text{NaClO}_3}^f + J_{\text{HCl}}^f \quad (22)$$

$$\text{Generation} = \text{Loss} = 0 \quad (23)$$

$$\text{Output} = J_{\text{NaCl}}^d + 2J_{\text{Cl}_2}^o + 2J_{\text{Cl}_2}^d + J_{\text{HOCl}}^d + J_{\text{NaOCl}}^d + J_{\text{NaClO}_3}^d + J_{\text{HCl}}^d \quad (24)$$

From Eqs. (20) and (22) to (24), the chlorine current efficiency, ξ_{Cl_2} , can be deduced as:

$$\xi_{\text{Cl}_2} = \frac{\Delta \text{Cl}}{I/F} \quad (25)$$

where

$$\Delta \text{Cl} = \text{Cl}^f - \text{Cl}^d \quad (26)$$

$$= \Delta(J_{\text{NaCl}} + J_{\text{HOCl}} + J_{\text{NaClO}_3} + 2J_{\text{Cl}_2} + J_{\text{HCl}} + J_{\text{NaOCl}}) \quad (27)$$

$$\text{Cl}^f = J_{\text{NaCl}}^f + 2J_{\text{Cl}_2}^f + J_{\text{HOCl}}^f + J_{\text{NaOCl}}^f + J_{\text{NaClO}_3}^f + J_{\text{HCl}}^f \quad (27a)$$

$$\text{Cl}^d = J_{\text{NaCl}}^d + 2J_{\text{Cl}_2}^d + J_{\text{HOCl}}^d + J_{\text{NaOCl}}^d + J_{\text{NaClO}_3}^d + J_{\text{HCl}}^d \quad (27b)$$

4.4.3.2B. Cl_2 Balance. The material balance for the Cl_2 -based species is given by Eqs. (28) to (31).

$$\text{Input} = J_{\text{Cl}_2}^f + J_{\text{HOCl}}^f + J_{\text{NaOCl}}^f + 3J_{\text{NaClO}_3}^f \quad (28)$$

$$\text{Generation} = J_{\text{Cl}_2}^e = (I/2F) - 2J_{\text{O}_2}^e \quad (29)$$

$$\text{Loss} = J_{\text{O}_2}^{\text{ch}} \quad (30)$$

$$\text{Output} = J_{\text{Cl}_2}^d + J_{\text{HOCl}}^d + J_{\text{NaOCl}}^d + 3J_{\text{NaClO}_3}^d + J_{\text{Cl}_2}^0 \quad (31)$$

The total amount of O_2 generated is, from the electrochemical and chemical reactions, as described by Eqs. (14), (15) and (32).



Hence,

$$J_{\text{O}_2}^0 = J_{\text{O}_2}^e + J_{\text{O}_2}^{\text{ch}} \quad (33)$$

From Eqs. (28) to (31), (33) and (20), it follows that:

$$\xi_{\text{Cl}_2} = \frac{1 + (2F/I)\Delta \text{Cl}_2}{1 + 2(\% \text{O}_2 / \% \text{Cl}_2)} \quad (34)$$

where,

$$\begin{aligned} \Delta \text{Cl}_2 &= \text{Cl}_2^f - \text{Cl}_2^d \\ &= \Delta(J_{\text{Cl}_2} + J_{\text{HOCl}} + J_{\text{NaOCl}} + 3J_{\text{NaClO}_3}) \end{aligned} \quad (35)$$

$$\text{Cl}_2^f = J_{\text{Cl}_2}^f + J_{\text{HOCl}}^f + J_{\text{NaOCl}}^f + 3J_{\text{NaClO}_3}^f \quad (35a)$$

$$\text{Cl}_2^d = J_{\text{Cl}_2}^d + J_{\text{HOCl}}^d + J_{\text{NaOCl}}^d + 3J_{\text{NaClO}_3}^d \quad (35b)$$

The term, $\%O_2/\%Cl_2$, in Eq. (34) arises from the fact that the mole fraction is equal to the volume fraction in a gas.

Equation (34) requires a knowledge of the applied load, which can be avoided by using Eq. (36), which can be derived by substituting Eq. (25) into Eq. (34), followed by rearranging the terms.

$$\xi_{Cl_2} = \frac{1}{1 + (\%O_2/\%Cl_2) - 2(\Delta Cl_2/\Delta Cl)} \quad (36)$$

4.4.3.2C. Na Balance. The Na material balance is described by Eqs. (37) to (39).

$$\begin{aligned} \text{Input} &= J_{NaCl}^f + J_{NaClO_3}^f + J_{NaOH}^f + 2J_{Na_2CO_3}^f \\ &+ J_{NaHCO_3}^f + J_{NaOCl}^f + J_{NaHSO_4}^f + 2J_{Na_2SO_4}^f \end{aligned} \quad (37)$$

$$\text{Generation} = \text{Loss} = 0 \quad (38)$$

$$\begin{aligned} \text{Output} &= J_{NaCl}^d + J_{NaClO_3}^d + J_{NaOH}^d + 2J_{Na_2CO_3}^d \\ &+ J_{NaHCO_3}^d + J_{NaOCl}^d + J_{NaHSO_4}^d \\ &+ 2J_{Na_2SO_4}^d + J_{Na^{a \rightarrow c}}^- \end{aligned} \quad (39)$$

From Eqs. (21) and (37) to (39), ξ_{OH} can be expressed as:

$$\xi_{OH} = \frac{\Delta Na}{I/F} \quad (40)$$

where

$$\begin{aligned} \Delta Na &= Na^f - Na^d \\ &= \Delta (J_{NaCl} + J_{NaClO_3} + J_{NaOH} + 2J_{Na_2CO_3} + J_{NaHCO_3} + J_{NaOCl} \\ &+ J_{NaHSO_4} + 2J_{Na_2SO_4}) \end{aligned} \quad (41)$$

$$\begin{aligned} Na^f &= J_{NaCl}^f + J_{NaClO_3}^f + J_{NaOH}^f + 2J_{Na_2CO_3}^f \\ &+ J_{NaHCO_3}^f + J_{NaOCl}^f + J_{NaHSO_4}^f + 2J_{Na_2SO_4}^f \end{aligned} \quad (41a)$$

$$\begin{aligned} Na^d &= J_{NaCl}^d + J_{NaClO_3}^d + J_{NaOH}^d + 2J_{Na_2CO_3}^d \\ &+ J_{NaHCO_3}^d + J_{NaOCl}^d + J_{NaHSO_4}^d + 2J_{Na_2SO_4}^d \end{aligned} \quad (41b)$$

4.4.3.2D. OH Balance. From the material balance for the hydroxide species given through Eqs. (42) to (45), the caustic current efficiency can be deduced,

as expressed by Eq. (46).

$$\begin{aligned} \text{Input} = & J_{\text{OH}}^{\text{c}\rightarrow\text{a}} + J_{\text{HOCl}}^{\text{f}} + 2J_{\text{NaOCl}}^{\text{f}} \\ & + 6J_{\text{NaClO}_3}^{\text{f}} + 2J_{\text{Na}_2\text{CO}_3}^{\text{f}} + J_{\text{NaHCO}_3}^{\text{f}} + J_{\text{NaOH}}^{\text{f}} - J_{\text{HCl}}^{\text{f}} - J_{\text{NaHSO}_4}^{\text{f}} \end{aligned} \quad (42)$$

$$\text{Generation} = 0 \quad (43)$$

$$\text{Loss} = 4J_{\text{O}_2}^{\text{ch}} + 4J_{\text{O}_2}^{\text{e}} \quad (44)$$

$$\begin{aligned} \text{Output} = & J_{\text{HOCl}}^{\text{d}} + 2J_{\text{NaOCl}}^{\text{d}} + 6J_{\text{NaClO}_3}^{\text{d}} \\ & + 2J_{\text{Na}_2\text{CO}_3}^{\text{d}} + J_{\text{NaHCO}_3}^{\text{d}} + J_{\text{NaOH}}^{\text{d}} - J_{\text{HCl}}^{\text{d}} - J_{\text{NaHSO}_4}^{\text{d}} \end{aligned} \quad (45)$$

$$\xi_{\text{OH}} = 1 - 2 \left(\frac{\% \text{O}_2}{\% \text{Cl}_2} \right) \xi_{\text{Cl}_2} + \frac{F}{I} \Delta \text{OH} \quad (46)$$

where

$$\begin{aligned} \Delta \text{OH} = & \text{OH}^{\text{f}} - \text{OH}^{\text{d}} \\ = & \Delta (J_{\text{HOCl}} + 2J_{\text{NaOCl}} + 6J_{\text{NaClO}_3} + 2J_{\text{Na}_2\text{CO}_3} + J_{\text{NaHCO}_3} + J_{\text{NaOH}} \\ & - J_{\text{HCl}} - J_{\text{NaHSO}_4}) \end{aligned} \quad (47)$$

$$\begin{aligned} \text{OH}^{\text{f}} = & J_{\text{HOCl}}^{\text{f}} + 2J_{\text{NaOCl}}^{\text{f}} + 6J_{\text{NaClO}_3}^{\text{f}} + 2J_{\text{Na}_2\text{CO}_3}^{\text{f}} \\ & + J_{\text{NaHCO}_3}^{\text{f}} + J_{\text{NaOH}}^{\text{f}} - J_{\text{HCl}}^{\text{f}} - J_{\text{NaHSO}_4}^{\text{f}} \end{aligned} \quad (47\text{a})$$

$$\begin{aligned} \text{OH}^{\text{d}} = & J_{\text{HOCl}}^{\text{d}} + 2J_{\text{NaOCl}}^{\text{d}} + 6J_{\text{NaClO}_3}^{\text{d}} + 2J_{\text{Na}_2\text{CO}_3}^{\text{d}} \\ & + J_{\text{NaHCO}_3}^{\text{d}} + J_{\text{NaOH}}^{\text{d}} - J_{\text{HCl}}^{\text{d}} - J_{\text{NaHSO}_4}^{\text{d}} \end{aligned} \quad (47\text{b})$$

It may be noted that the last term in Eq. (42) is a result of OH^- consumption by Eq. (19b). Elimination of the F/I term, using Eq. (40) and the ξ_{Cl_2} term with Eq. (36) in Eq. (46), leads to:

$$\xi_{\text{OH}} = \frac{1 - 2(\Delta \text{Cl}_2 / \Delta \text{Cl})}{(1 - \Delta \text{OH} / \Delta \text{Na})[1 + 2(\% \text{O}_2 / \% \text{Cl}_2) - 2(\Delta \text{Cl}_2 / \Delta \text{Cl})]} \quad (48)$$

The chlor-alkali producers sometimes prefer this version of the caustic current efficiency equation since it avoids the need for measuring the applied load.

Since the current efficiency can be described based on the material balances for Cl , Cl_2 , OH^- and Na^+ , there will be four seemingly different equations providing the same value. The various forms of general equations for Cl_2 and NaOH efficiencies are

described by Eqs. (49) to (53).

$$\xi_{\text{Cl}_2} = \frac{1 + (2F/I)\Delta\text{Cl}_2}{1 + 2(\%O_2/\%Cl_2)} \quad (49)$$

$$= \frac{\Delta\text{Cl}}{(\Delta\text{Cl} - 2\Delta\text{Cl}_2) + 2(\%O_2/\%Cl_2)\Delta\text{Cl}} \quad (50)$$

$$= \frac{1}{1 + 2(\%O_2/\%Cl_2) - 2(\Delta\text{Cl}_2/\Delta\text{Cl})} \quad (51)$$

$$\xi_{\text{OH}} = \xi_{\text{Cl}_2} + \frac{F}{I}(\Delta\text{OH} - 2\Delta\text{Cl}_2) \quad (52)$$

$$= \frac{\Delta\text{Na}}{(\Delta\text{Cl} - 2\Delta\text{Cl}_2) + 2(\%O_2/\text{Cl}_2)\Delta\text{Cl}} \quad (53)$$

where

$$\Delta\text{Cl} = \Delta(J_{\text{NaCl}} + J_{\text{HOCl}} + J_{\text{NaClO}_3} + 2J_{\text{Cl}_2} + J_{\text{HCl}} + J_{\text{NaOCl}})$$

$$\Delta\text{Cl}_2 = \Delta(J_{\text{Cl}_2} + J_{\text{HOCl}} + J_{\text{NaOCl}} + 3J_{\text{NaClO}_3})$$

$$\Delta\text{Na} = \Delta(J_{\text{NaCl}} + J_{\text{NaClO}_3} + J_{\text{NaOH}} + 2J_{\text{Na}_2\text{CO}_3} + J_{\text{NaHCO}_3} \\ + J_{\text{NaOCl}} + J_{\text{NaHSO}_4} + 2J_{\text{Na}_2\text{SO}_4})$$

$$\Delta\text{OH} = \Delta(J_{\text{HOCl}} + 2J_{\text{NaOCl}} + 6J_{\text{NaClO}_3} + 2J_{\text{Na}_2\text{CO}_3} \\ + J_{\text{NaHCO}_3} + J_{\text{NaOH}} - J_{\text{HCl}} - J_{\text{NaHSO}_4})$$

The Δ s in the above expressions refer to the differences in the mass flow rates of the relevant species in the equations. Equations (49) and (51) can be reduced to the various versions of the efficiency equations published in the literature [6–10] with the appropriate assumptions [2].

4.4.3.2E. Disparity between Chlorine and Caustic Inefficiencies. From Eqs. (25 and 34) it can be shown that:

$$\frac{I}{F} = \Delta\text{Cl} + \frac{2\%O_2}{\%Cl_2} - 2\Delta\text{Cl}_2 \quad (54)$$

or

$$1 = \xi_{\text{Cl}_2} + \xi_{\text{O}_2} + \xi_{\text{Cl}_2}^a \quad (55)$$

In other words, the chlorine current inefficiency is a result of O_2 evolution and the formation of ClO_3^- , OCl^- , HOCl , and dissolved chlorine in the anolyte.

The origin of caustic current inefficiency can be traced by rearranging Eqs. (40) and (46), which results in Eq. (56).

$$\frac{I}{F} = \Delta\text{Na} + \left(\frac{2\%O_2}{\%Cl_2} \right) \Delta\text{Cl} - \Delta\text{OH} \quad (56)$$

or

$$1 = \xi_{\text{OH}} + \xi_{\text{O}_2} + \xi_{\text{OH}}^a \quad (57)$$

Thus, the caustic inefficiency is a result of a loss of hydroxyl ions to the anode chamber resulting in (1) the generation of oxygen, (2) the formation of ClO_3^- , OCl^- and HOCl in the anolyte, and (3) the neutralization of the feed brine acidity.

The factors contributing to these inefficiencies may be deciphered by the rearrangement of Eqs. (34), (35), (46), and (47) in terms of the feed and depleted mass flow rates for the various pertinent components. When the feed brine contains no active chlorine species, and when there is no acid fed to the brine,

$$\begin{aligned} \xi_{\text{Cl}_2} = 1 - 2 \left(\frac{\%O_2}{\%Cl_2} \right) \xi_{\text{Cl}_2} + \frac{2F}{I} \\ \times \left[3pC_{\text{NaClO}_3}^f - q \left(C_{\text{Cl}_2}^d + C_{\text{HOCl}}^d + C_{\text{NaOCl}}^d + 3C_{\text{NaClO}_3}^d \right) \right] \end{aligned} \quad (58)$$

and

$$\begin{aligned} \xi_{\text{OH}} = 1 - 2 \left(\frac{\%O_2}{\%Cl_2} \right) \xi_{\text{Cl}_2} \\ + \frac{F}{I} \left[p \left(6C_{\text{NaClO}_3}^f + 2C_{\text{Na}_2\text{CO}_3}^f + C_{\text{NaHCO}_3}^f + C_{\text{NaOH}}^f - C_{\text{NaHSO}_4}^f \right) \right. \\ \left. - q \left(C_{\text{HOCl}}^d + 2C_{\text{NaOCl}}^d + 6C_{\text{NaClO}_3}^d - C_{\text{NaHSO}_4}^d \right) \right] \end{aligned} \quad (59)$$

It follows from Eq. (58) that the chlorine current efficiency decreases with increasing formation of active chlorine species and chlorate in the anolyte, the increasing active chlorine species being formed not only by the reaction involving Cl_2 , and OH^- species, but also by interaction between Cl_2 and alkalinity (i.e., Na_2CO_3 , NaHCO_3 , and NaOH) present in the feed brine. Hence, lowering the alkalinity of the feed brine, by acid addition, should improve the chlorine efficiency.

The disparity between the chlorine and caustic current efficiencies can be quantitatively estimated from Eqs. (25) and (40) as:

$$\xi_{\text{OH}} - \xi_{\text{Cl}_2} = \frac{F}{I} \Delta \left(J_{\text{NaOH}} + 2J_{\text{Na}_2\text{CO}_3} + J_{\text{NaHCO}_3} - J_{\text{HOCl}} - J_{\text{HCl}} - 2J_{\text{Cl}_2} \right) \quad (60)$$

Eq. (60) reiterates that the disparity between the Cl_2 and NaOH current efficiencies is a result of the alkalinity in the feed brine and the active chlorine species in the anolyte. If the feed brine is neutral and there is no active chlorine in the anolyte, it can be seen that

$$\xi_{\text{OH}} - \xi_{\text{Cl}_2} = 0 \quad (61)$$

4.4.3.2F. Current Efficiency Equation for Membrane Cells. The chlorine and caustic efficiency expressions derived from the material balance for the various pertinent species across the electrolyzer are given by Eqs. (49) to (53). These equations need further simplification to eliminate the F/I term and the brine flow rate terms, especially the depleted brine flow rate q , because of the practical difficulties associated with its measurement.

The ratio of the feed brine flow rate to the depleted brine flow rate can be determined from the various material balances described earlier. Thus, ΔNa can be expressed in terms of ΔCl , ΔCl_2 and ΔOH , employing Eqs. (25), (40), (46) and (54) as:

$$\Delta\text{Na} = \Delta\text{Cl} - 2\Delta\text{Cl}_2 + \Delta\text{OH} \quad (62)$$

since

$$\begin{aligned} \Delta\text{Cl} &= p[\text{Cl}]^f - q[\text{Cl}]^d; & \Delta\text{Cl}_2 &= p[\text{Cl}_2]^f - q[\text{Cl}_2]^d; \\ \Delta\text{Na} &= p[\text{Na}]^f - q[\text{Na}]^d; & \Delta\text{OH} &= p[\text{OH}]^f - q[\text{OH}]^d \end{aligned}$$

where $[\]^f$ and $[\]^d$ terms refer to the concentration of the non-bracketed molar flow rates described in Eqs. (27a), (27b), (35a), (35b), (41a), (41b), (47a), and (47b).

Hence, Eq. (62) becomes:

$$R^* = \frac{q}{p} = \frac{[\text{Na}]^f - [\text{Cl}]^f + 2[\text{Cl}_2]^f - [\text{OH}]^f}{[\text{Na}]^d - [\text{Cl}]^d + 2[\text{Cl}_2]^d - [\text{OH}]^d} \quad (63)$$

Following proper substitution of the terms in brackets, using Eqs. (27), (35), (41), and (47), R^* can be shown to be

$$R^* = \frac{C_{\text{NaHSO}_4}^f + C_{\text{Na}_2\text{SO}_4}^f}{C_{\text{NaHSO}_4}^d + C_{\text{Na}_2\text{SO}_4}^d} \quad (64)$$

expressed as a ratio of the $[\text{NaHSO}_4] + [\text{Na}_2\text{SO}_4]$ in the feed and depleted brine, given by Eq. (64). This result should not be surprising since the transport of SO_4^{2-} into the catholyte was not allowed in the material balance.

It should be noted that anions such as Cl^- , SO_4^{2-} and ClO_3^- are transported through the membrane into the catholyte by diffusion and electro-osmosis. However, this driving force is negated by migration, an electric field effect. Theoretical calculations [11] and experimental studies [12] show that while the transport of these anions is suppressed during normal operation, maximum carryover of anions into the catholyte occurs when

the applied load is zero. The magnitude of the transport of SO_4^{2-} and ClO_3^- was noted to be proportional to the corresponding anolyte concentrations, whereas the Cl^- content in the catholyte was found to decrease with increasing Cl^- concentration in the anolyte. Overall, the concentration of Cl^- , SO_4^{2-} , and ClO_3^- in the catholyte is in the ppm range, even though they are in the grams per liter range in the anolyte and hence, were not considered in the overall material balance, although their presence can easily be incorporated in the formulation.

Use of the SO_4^{2-} ratio to estimate the ratio of the depleted brine flow rate and the feed brine flow rate, needed for calculating the efficiencies, requires accurate measurement of SO_4^{2-} in the range of 2–15 g L⁻¹ in NaCl solutions of 200–300 g L⁻¹. Gravimetric analysis by precipitation of SO_4^{2-} as BaSO_4 should, in principle, provide an accuracy of $\pm 0.01\%$. Inductively coupled plasma analysis and ion chromatographic techniques for sulfate, on the other hand, involve dilution factors of the order of about 10, and provide an accuracy of only 2–3%. Thus, while the use of a “sulfate ratio” to arrive at the ratio of q/p is simple, it may not be a reliable method to estimate the efficiencies unless a practical and accurate method is available for determining SO_4^{2-} in brines. Issues related to the adverse effect of SO_4^{2-} on the membrane performance, disclosed in the literature, should be paid close attention to while considering sulfate additions to the feed brine [13,14] to determine the ratio of the feed and depleted brine flow rates.

Another approach to arrive at the magnitude of the q/p term is by a Na or Cl material balance. Thus, the Na material balance from Eq. (41) leads to

$$R^* = \frac{q}{p} = \frac{[\text{Na}]^f}{[\text{Na}]^d} - \frac{I\xi_{\text{OH}}}{pF[\text{Na}]^d} \quad (65)$$

or

$$R^* = L - M \left(\frac{I\xi_{\text{OH}}}{pF} \right) \quad (66)$$

where $L = [\text{Na}]^f/[\text{Na}]^d$ and $M = 1/[\text{Na}]^d$. Similarly, the Cl balance results in

$$R^* = \frac{q}{p} = \frac{[\text{Cl}]^f}{[\text{Cl}]^d} - \frac{I\xi_{\text{Cl}_2}}{pF[\text{Cl}]^d} \quad (67)$$

or

$$R^* = X - Y \left(\frac{I\xi_{\text{Cl}_2}}{pF} \right) \quad (68)$$

where $X = [\text{Cl}]^f/[\text{Cl}]^d$ and $Y = 1/[\text{Cl}]^d$. Substitution of Eqs. (66) and (68) in Eqs. (34) and (46), followed by algebraic manipulations, leads to the caustic current

efficiency expression as:

$$\xi_{\text{OH}} = \frac{1 - (F/I)p \left[2(1 - C)(\text{LCl}_2^{\text{d}} - \text{Cl}_2^{\text{f}}) + C(\text{LOH}^{\text{d}} - \text{OH}^{\text{f}}) \right]}{C - M \left[2(1 - C)\text{Cl}_2^{\text{d}} + \text{COH}^{\text{d}} \right]} \quad (69)$$

where $C = 1 + 2(\% \text{O}_2 / \% \text{Cl}_2)$.

Similarly, substitution of Eq. (68) in Eq. (34) leads to

$$\xi_{\text{Cl}_2} = \frac{1 - (2F/I)p \left(X\text{Cl}_2^{\text{d}} - \text{Cl}_2^{\text{f}} \right)}{C - 2Y\text{Cl}_2^{\text{d}}} \quad (70)$$

Equation (70) provides an estimate of the cell efficiency for chlorine and accounts for the dissolved chlorine in the anolyte, which is generally recovered during dechlorination operations.

The process chlorine efficiency, $\xi_{\text{Cl}_2}^{\text{p}}$, can be determined from Eq. (71) assuming 100% recovery of the dissolved chlorine and the active Cl_2 species from the depleted brine, when the terms involving the dissolved Cl_2 and the active chlorine are omitted from Eq. (70).

$$\xi_{\text{Cl}_2}^{\text{p}} = \frac{1 - (2F/I)p \left[X_0 \left(3C_{\text{NaClO}_3}^{\text{d}} \right) - \text{Cl}_2^{\text{f}} \right]}{C - 2Y_0 \left(3C_{\text{NaClO}_3}^{\text{d}} \right)} \quad (71)$$

where

$$X_0 = \left(C_{\text{NaCl}}^{\text{f}} + C_{\text{NaClO}_3}^{\text{f}} \right) / (Y_0)^{-1}$$

$$Y_0 = \left(C_{\text{NaCl}}^{\text{d}} + C_{\text{NaClO}_3}^{\text{d}} + 10^{-\text{pH}} \right)^{-1}$$

Thus, from Eqs. (69) to (71), the chlorine and caustic current efficiencies of membrane cells can be determined without any ambiguity in the choice of operating parameters. The reader is referred to ref. [9] for estimating the concentration of dissolved chlorine in NaCl solutions required for calculating the chlorine and caustic current efficiencies using Eqs. (69) and (70).

It is important to note that the process chlorine efficiency is essentially the same as the cell caustic efficiency since, from Eq. (60), it can be seen that:

$$\xi_{\text{OH}} - \xi_{\text{Cl}_2}^{\text{p}} = \frac{F}{I} \Delta (J_{\text{NaOH}} + J_{\text{Na}_2\text{CO}_3} + J_{\text{NaHCO}_3} - J_{\text{HCl}}) \quad (72)$$

The difference between ξ_{OH} and $\xi_{\text{Cl}_2}^{\text{p}}$ is approximately 0.7% under normal operating conditions.

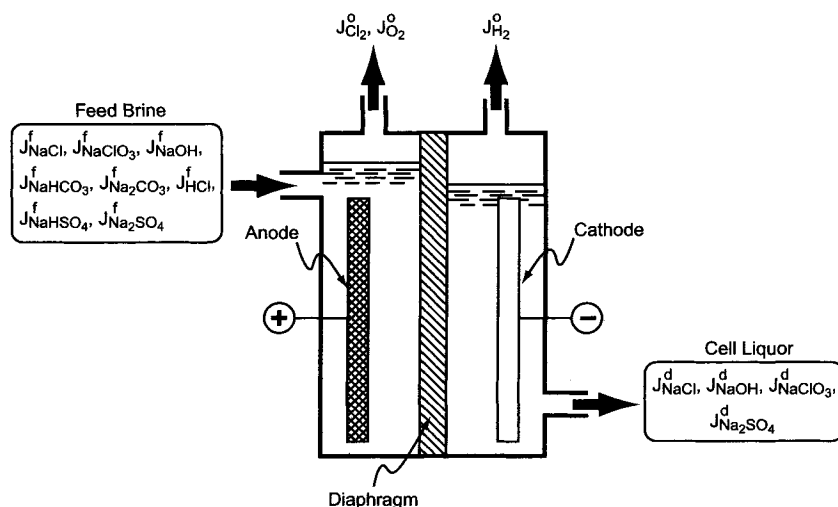


FIGURE 4.4.3. Schematic of the diaphragm cell describing the material balance around the electrolyzer [2].

4.4.3.2G. Current Efficiency Equations for Diaphragm Cells. In a diaphragm cell, the anolyte percolates through a porous separator into the catholyte, whereas in a membrane cell, Na^+ and H_2O are the only major species transported from the anolyte to the catholyte. The chlorine current efficiency may now be determined from the material balance of the chlorine tracking species,* shown in Fig. 4.4.3, and described through Eqs. (73) to (76).

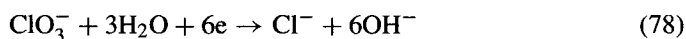
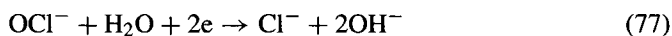
$$\text{Input} = 3J_{NaClO_3}^f \quad (73)$$

$$\text{Output} = 3J_{NaClO_3}^d + J_{Cl_2}^o \quad (74)$$

$$\text{Generation} = I/2F - 2J_{O_2}^e \quad (75)$$

$$\text{Loss} = 2J_{O_2}^{ch} + (1 - \xi_{H_2}^D) I/2F \quad (76)$$

The loss term, represented by Eq. (76), accounts for the oxygen generated chemically via Eq. (8), and for the blind current losses (BCLs) arising from the thermodynamically favored cathodic reduction of OCl^- and ClO_3^- , as described by reactions (77) and (78).



*Generally, the feed brine to the diaphragm cells and the exiting caustic liquor do not contain any active chlorine species. However, if these species (i.e., Cl_2 , $HOCl$, OCl^-) are present in the feed brine or cell liquor, the material balance can easily be modified to account for their presence.

These cathodic reactions affect only the amount of current used for the H_2 evolution reaction and not the hydroxyl ion formation rate. Hence, the magnitude of these BCLs can be quantified from the moles of H_2 evolved, which is equal to $(I - \xi_{H_2}^D) I/2F$. Since,

$$\xi_{Cl_2}^D = \frac{J_{Cl_2}^0}{I/2F} \quad (79)$$

and

$$J_{O_2}^0 = J_{O_2}^c + J_{O_2}^{ch} = \left(\frac{\%O_2}{\%Cl_2} \right) \left(\frac{I}{2F} \right) \xi_{Cl_2}^D \quad (80)$$

it can be shown, from Eqs. (73) to (76), that:

$$\xi_{Cl_2}^D = \frac{\xi_{H_2}^D + (6F/I)\Delta J_{NaClO_3}}{1 + 2(\%O_2/\%Cl_2)} \quad (81)$$

The caustic current efficiency expression for diaphragm cells can be derived from the NaOH material balance in a similar way, employing Eqs. (82) to (86) (see Fig. 4.4.3 for a schematic of the material balance across the cell, taking into account the BCLs). Thus,

$$\begin{aligned} \text{Input} = & J_{NaOH}^f - J_{HCl}^f + 2J_{Na_2CO_3}^f \\ & + J_{NaHCO_3}^f + 6J_{NaClO_3}^f - J_{NaHSO_4}^f \end{aligned} \quad (82)$$

$$\text{Output} = J_{NaOH}^d + 6J_{NaClO_3}^d \quad (83)$$

$$\text{Generation} = I/F \quad (84)$$

$$\begin{aligned} \text{Loss} = & 4J_{O_2}^{ch} + 4J_{O_2}^c + (1 - \xi_{H_2}^D) I/F \\ = & 4J_{O_2}^0 + (1 - \xi_{H_2}^D) I/F \end{aligned} \quad (85)$$

Since,

$$\xi_{OH}^D = \frac{J_{NaOH}^d}{I/F} \quad (86)$$

it can be shown from Eqs. (82) to (85) that:

$$\begin{aligned} \xi_{OH}^D = & \xi_{H_2}^D - 2 \left(\frac{\%O_2}{\%Cl_2} \right) \xi_{Cl_2}^D \\ & + \frac{F}{I} \left(\Delta 6J_{NaClO_3} + 2J_{Na_2CO_3}^f + J_{NaHCO_3}^f \right. \\ & \left. - J_{HCl}^f + J_{NaOH}^f - J_{NaHSO_4}^f \right) \end{aligned} \quad (87)$$

Elimination of $\xi_{\text{Cl}_2}^{\text{D}}$ from Eq. (87), using Eq. (81), results in:

$$\xi_{\text{OH}}^{\text{D}} = \xi_{\text{Cl}_2}^{\text{D}} + \frac{F}{I} \left(J_{\text{NaOH}}^{\text{f}} + 2J_{\text{Na}_2\text{CO}_3}^{\text{f}} + J_{\text{NaHCO}_3}^{\text{f}} - J_{\text{HCl}}^{\text{f}} - J_{\text{NaHSO}_4}^{\text{f}} \right) \quad (88)$$

Thus, Eqs. (81) and (88) represent the chlorine and caustic efficiency expressions derived rigorously from the appropriate material balances while accounting for the BCLs. Equations (81) and (88) can be simplified, by expressing the depleted brine flow rate in terms of caustic current efficiency as:

$$q = \frac{I}{F} \frac{\xi_{\text{OH}}^{\text{D}}}{C_{\text{NaOH}}^{\text{d}}} \quad (89)$$

Thus, the equations describing the caustic and chlorine current efficiency for diaphragm cells are given by Eqs. (90) and (91).

$$\xi_{\text{OH}}^{\text{D}} = \frac{\xi_{\text{H}_2}^{\text{D}} + (F/I)p \left\{ 6C_{\text{NaClO}_3}^{\text{f}} + [1 + 2(\% \text{O}_2/\% \text{Cl}_2)]G \right\}}{1 + 2(\% \text{O}_2/\% \text{Cl}_2) + 6(C_{\text{NaClO}_3}^{\text{d}}/C_{\text{NaOH}}^{\text{d}})} \quad (90)$$

$$\xi_{\text{Cl}_2}^{\text{D}} = \frac{\xi_{\text{H}_2}^{\text{D}} + (6F/I)p \left\{ C_{\text{NaClO}_3}^{\text{f}} - (C_{\text{NaClO}_3}^{\text{d}}/C_{\text{NaOH}}^{\text{d}})G \right\}}{1 + 2(\% \text{O}_2/\% \text{Cl}_2) + 6(C_{\text{NaClO}_3}^{\text{d}}/C_{\text{NaOH}}^{\text{d}})} \quad (91)$$

$$G = (C_{\text{NaOH}}^{\text{f}} + 2C_{\text{Na}_2\text{CO}_3}^{\text{f}} + C_{\text{NaHCO}_3}^{\text{f}} - C_{\text{HCl}}^{\text{f}} - C_{\text{NaHSO}_4}^{\text{f}})$$

where the hydrogen current efficiency, $\xi_{\text{H}_2}^{\text{D}}$, can be shown to be: $\xi_{\text{H}_2}^{\text{D}} = 1 - 2(C_{\text{av,Cl}_2}^{\text{a}}/C_{\text{NaOH}}^{\text{d}})$ (see Appendix 4.4.1). Note that the hydrogen inefficiency arises from the BCLs due to the discharge of the available chlorine at the cathode. However, the chlor-alkali industry routinely measures only the chlorine current efficiency of diaphragm cells using the relationship in Eq. (92) detailed in [1,7,13].

$$\xi_{\text{Cl}_2}^{\text{D}} = \frac{1}{1 + 2(\% \text{O}_2/\% \text{Cl}_2) + \alpha} \quad (92)$$

where

$$\alpha = \frac{6(C_{\text{NaClO}_3}^{\text{a}} - C_{\text{NaClO}_3}^{\text{f}})}{C_{\text{NaOH}}^{\text{d}}} \quad (93)$$

An alternate expression for α used by some chlor-alkali producers is

$$\alpha = \frac{x C_{\text{NaClO}_3}^{\text{d}}}{C_{\text{NaOH}}^{\text{d}}} \quad (94)$$

where x has values varying from 2 to 8.

Comparison of Eq. (94) with Eq. (91) clearly shows that Eq. (92) is a “crude” approximation for estimating the chlorine current efficiency of diaphragm cells operating with acidic or basic feed brine. Calculations show that the “six equation” (Eq. 93) overestimates the efficiency by 1–2% compared with the rigorous Eq. (91).

The F/I term in the numerators of Eqs. (90) and (91) can, in principle, be eliminated using the Cl or Na material balance across the diaphragm cell, given by Eqs. (95) and (96).

$$\xi_{\text{Cl}_2}^{\text{D}} = \left(\frac{F}{I} \right) \frac{\Delta \text{Cl}^*}{\xi_{\text{H}_2}^{\text{D}}} \quad (95)$$

where

$$\Delta \text{Cl}^* = \Delta (J_{\text{NaCl}} + J_{\text{NaClO}_3} + J_{\text{HCl}})$$

and

$$\xi_{\text{OH}}^{\text{D}} = \left(\frac{F}{I} \right) \frac{\Delta \text{Na}^*}{\xi_{\text{H}_2}^{\text{D}}} \quad (96)$$

where

$$\begin{aligned} \Delta \text{Na}^* = & \Delta (J_{\text{NaCl}} + J_{\text{NaClO}_3} + 2J_{\text{Na}_2\text{SO}_4}) + J_{\text{NaOH}}^{\text{f}} \\ & + J_{\text{NaHCO}_3}^{\text{f}} + 2J_{\text{Na}_2\text{CO}_3}^{\text{f}} + J_{\text{NaHSO}_4}^{\text{f}} \end{aligned}$$

However, the resulting expressions will be unwieldy because the cell liquor flow rate term, q , required for expanding $\Delta(\text{species})$ involves the I/F terms via Eq. (89). Equations (90) and (91) can be rearranged to arrive at Eq. (93) with $\alpha = 6C_{\text{NaClO}_3}^{\text{d}}/C_{\text{NaOH}}^{\text{d}}$, only when the feed brine is devoid of NaClO_3 , NaOH , Na_2CO_3 , NaHCO_3 , NaHSO_4 , and HCl , that is, when the feed brine is neutral and does not contain NaClO_3 , and the BCLs are negligible. Feed brine alkalinity and chlorates can be best accounted for only by employing Eq. (90) or (91) for calculating the caustic or chlorine current efficiency.

4.4.3.2H. Current Efficiency Equations for Mercury Cells. A schematic of the mercury cell is depicted in Fig. 4.4.4. As stated earlier, the cathodic reaction in the mercury cell is the discharge of the Na^+ ions to form sodium amalgam as described by reaction (9). The material balance for the Cl_2 and the Cl species for the mercury cells are the same as in the membrane cells and hence, the chlorine current efficiency of the mercury cells, $\xi_{\text{Cl}_2}^{\text{m}}$, is given by Eq. (49), which can be simplified by using Eq. (97) obtained from Eq. (25) to result in Eq. (98). (See ref. [15] for details.)

$$p(\text{Cl}^{\text{f}}) = q(\text{Cl})^{\text{d}} + \frac{\xi_{\text{Cl}_2}}{F/I} \quad (97)$$

$$\xi_{\text{Cl}_2}^{\text{m}} = \frac{(1 + F/I)p \left[6C_{\text{NaClO}_3}^{\text{f}} + 2C_{\text{av.Cl}_2}^{\text{f}} - (\text{Cl}^{\text{f}}/\text{Cl}^{\text{d}}) \left(6C_{\text{NaClO}_3}^{\text{d}} + 2C_{\text{av.Cl}_2}^{\text{d}} \right) \right]}{1 + (2\% \text{O}_2/\% \text{Cl}_2) - (1/(\text{Cl})^{\text{d}}) \left(6C_{\text{NaClO}_3}^{\text{d}} + 2C_{\text{av.Cl}_2}^{\text{d}} \right)} \quad (98)$$

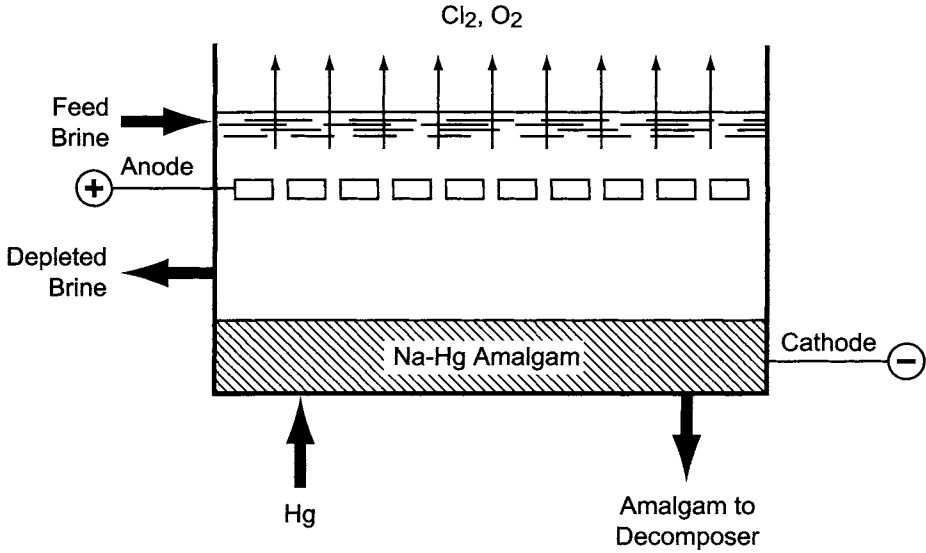


FIGURE 4.4.4. Schematic of the mercury cell.

Equation (98) can be further simplified. The feed brine flow rate is almost equal to the depleted brine flow rate, since the water loss in the cell is about 0.5 kg min^{-1} . Hence, $p = q$. Thus, $\xi_{\text{Cl}_2}^m$ can be rewritten as:

$$\xi_{\text{Cl}_2}^m = \frac{1}{1 + (2\% \text{O}_2 / \% \text{Cl}_2) - ((6\Delta \text{NaClO}_3 + 2\Delta \text{Cl}_2) / \Delta \text{Cl})} \quad (99)$$

All the parameters in Eq. (99) are experimentally accessible except $C_{\text{av-Cl}_2}^f$ and $C_{\text{av-Cl}_2}^d$ in the ΔCl term. These values can be calculated using the correlations given in Appendix 4.4.2 [16].

Sodium amalgam formation efficiency, ξ_{NaHg} , is defined as:

$$\xi_{\text{NaHg}} = \frac{J_{\text{NaHg}}^d - J_{\text{NaHg}}^f}{I/F} \quad (100)$$

The “Na” material balance across the cell can now be formulated as follows:

$$\text{Input} = J_{\text{NaCl}}^f + J_{\text{NaClO}_3}^f + J_{\text{NaHg}}^f + J_{\text{NaOCl}}^f \quad (101)$$

$$\text{Output} = J_{\text{NaCl}}^d + J_{\text{NaClO}_3}^d + J_{\text{NaHg}}^d + J_{\text{NaOCl}}^d \quad (102)$$

$$\text{Generation} = \text{Loss} = 0 \quad (103)$$

Defining

$$\text{Na}^f = J_{\text{NaCl}}^f + J_{\text{NaClO}_3}^f + J_{\text{NaOCl}}^f \quad (104)$$

and

$$\text{Na}^d = J_{\text{NaCl}}^d + J_{\text{NaClO}_3}^d + J_{\text{NaOCl}}^d \quad (105)$$

and rearranging the terms in Eqs. (100) to (105) results in:

$$\xi_{\text{NaOH}}^m = \frac{J_{\text{NaHg}}^d - J_{\text{NaHg}}^f}{I/F} = \frac{(\text{Na}^f - \text{Na}^d)}{I/F} \quad (106)$$

Equation (106) assumes that all the sodium amalgam is decomposed to form caustic, and that there are no caustic losses during caustic collection. Rearrangement of Eq. (106) with $p = q$ leads to the caustic current efficiency expression (107) for the mercury cells.

$$\xi_{\text{NaOH}}^m = p \left(\frac{\Delta C_{\text{NaCl}} + \Delta C_{\text{NaClO}_3} + \Delta C_{\text{NaOCl}}}{I/F} \right) \quad (107)$$

Elimination of the $p/(I/F)$ term, using Eq. (25) and the identity $p = q$, leads to Eq. (108),

$$\xi_{\text{NaOH}}^m = \left(\frac{\Delta C_{\text{NaCl}} + \Delta C_{\text{NaClO}_3} + \Delta C_{\text{NaOCl}}}{\text{Cl}^f - \text{Cl}^d} \right) \xi_{\text{Cl}_2}^m \quad (108)$$

which will permit the calculation of caustic efficiency from the chlorine current efficiency calculated using Eq. (99).

All the sodium in the sodium amalgam formed in the cell is converted to caustic in the decomposer. However, all of the caustic generated in the decomposer is not collected, as some slips back to the cell. Hence, the measured caustic efficiency ξ_{NaOH}^{m*} will be equal to:

$$\xi_{\text{NaOH}}^{m*} = \xi_{\text{NaOH}}^m - \xi_{\text{NaOH}}^s \quad (109)$$

where

$$\xi_{\text{NaOH}}^s = \frac{J_{\text{NaOH}}^s}{I/F} \quad (109a)$$

J_{NaOH}^s is the amount of caustic slipped back to the cell measured in units of moles of caustic per liter of mercury, and can be experimentally determined by taking a known amount of Hg (50 ml) going back to the cell, mixing with 50 ml deionized water, and measuring the pH of the resulting water. From this measured pH value, pH^m , the amount of caustic slipped can be calculated by:

$$J_{\text{NaOH}}^s = p^* \left(\frac{K_w 10^{\text{pH}^m} Y^*}{X^*} \right) = p^* \left(\frac{Y^* 10^{(\text{pH}^m - 14)}}{X^*} \right) \quad (110)$$

where X^* and Y^* are the amounts of mercury and water used (in liters) in the above test, p^* is the flow rate of mercury to the cell in units of liters per second, and K_w is the dissociation constant of water, which is 10^{-14} at 25°C .

There is yet another way to calculate the caustic current efficiency based on the charge balance. The cathodic current constitutes the current used for Na^+ ion deposition to form sodium amalgam, and the current for H_2 evolution reaction. Hence,

$$\xi_{\text{NaOH}}^m = 1 - \frac{J_{\text{H}_2}^0}{I/2F} \quad (111)$$

Substituting Eq. (20) in Eq. (111) results in:

$$\xi_{\text{NaOH}}^m = 1 - \frac{J_{\text{H}_2}^0 \xi_{\text{Cl}_2}^m}{J_{\text{Cl}_2}^0} \quad (112)$$

Since the mole fraction is equal to the volume fraction, Eq. (112) becomes:

$$\xi_{\text{NaOH}}^m = 1 - \frac{\xi_{\text{Cl}_2}^m \% \text{H}_2}{\% \text{Cl}_2} \quad (113)$$

Thus, it follows from Eqs. (109) and (113) that

$$\xi_{\text{NaOH}}^{m*} = 1 - \frac{\xi_{\text{Cl}_2}^m \% \text{H}_2}{\% \text{Cl}_2} - \xi_{\text{NaOH}}^s \quad (114)$$

ξ_{NaOH}^{m*} can be determined from ξ_{NaOH}^s , expressed by Eq. (109a), and a knowledge of I/F , and $\% \text{H}_2/\% \text{Cl}_2$.

4.4.3.2I. Errors Involved in the Energy Consumption and Efficiency Calculations. Error analysis using the "propagation of errors" technique, in Appendix 4.4.3, shows the error associated with the process chlorine efficiency to be $\pm 0.25\%$ and the error in the energy consumption, ΔP , calculation to be $\pm 15 \text{ kW hr ton}^{-1}$ of Cl_2 as shown in Table 4.4.2. The analytical method, along with its precision is detailed in Table 4.4.3.

4.4.3.3. Sources of Current Inefficiency. The primary sources of chlorine current efficiency are: (1) oxygen generated during chlorine evolution, be it chemical from the decomposition of HOCl or OCl^- or electrochemical as described by the reactions (14) or (15), and (2) formation of OCl^- , HOCl , and ClO_3^- by reaction schemes (10)–(13) and (16)–(18). On the other hand, the main reason for the caustic inefficiency in membrane and diaphragm cells is the back-migration of caustic leading to the same inefficiencies noted above. However, with mercury cells, the cathodic inefficiency is a consequence of the hydrogen evolution reaction (HER), initiated by impurities in the feed brine. The fundamental factors associated with these inefficient reactions are addressed in this section.

TABLE 4.4.2 Error Analysis for Current Efficiency and Energy Consumption

Current efficiency (%)		Energy consumption (kW hr ton ⁻¹ Cl ₂)	
ξ_{Cl_2}	$\Delta\xi_{\text{Cl}_2}$	P	ΔP
<i>Diaphragm cell data from plant A</i>			
98.39	0.17	2,634	12
95.84	0.17	2,623	12
90.34	0.14	2,694	12
<i>Membrane cell data from plant A</i>			
95.33	0.21	2,626	13
93.62	0.22	2,727	14
90.34	0.22	2,741	14

TABLE 4.4.3 Analytical Methods for Calculating the Current Efficiency

Item	Analytical method	Precision
<i>a. Feed brine</i>		
NaCl	AgNO ₃ titration-Na ₂ CrO ₄ indicator	± 2.5 gpl
NaClO ₃	Mixed acid-FeSO ₄ titration	± 0.005 gpl
NaOH	Autotitrator-potentiometric	± 10 ppm
Na ₂ CO ₃	Autotitrator-potentiometric	± 10 ppm
Flow rate	Cell rotameter	± 0.15 L/min
<i>b. Depleted brine</i>		
NaCl	AgNO ₃ titration-Na ₂ CrO ₄ indicator	± 2.5 gpl
NaClO ₃	Mixed acid-FeSO ₄ titration	± 0.02 gpl
NaOCl	Titration-KI starch indicator	± 0.05 gpl
pH	Orion-double electrodes	± 0.1 unit
<i>c. Cell liquor</i>		
NaOCl	Titration-KI starch indicator	± 0.5 gpl
NaClO ₃	Mixed acid-FeSO ₄ titration	± 0.02 gpl
NaOH	Autotitrator-potentiometric	± 1.5 gpl
<i>d. Cell gas</i>		
% O ₂	Gas chromatography—direct with standard	± 0.05%
% Cl ₂	Gas chromatography—by difference, no standard	± 0.20%

4.4.3.3A. Oxygen Evolution

Electrochemical Oxygen Evolution. Thermodynamically, the oxygen evolution reaction is favoured over the chlorine evolution reaction in aqueous solutions because the standard reversible potential is 1.23 V for the oxygen evolution reaction and 1.35 V for the chlorine evolution reaction. However, because of the slow kinetics of the oxygen evolution

reaction compared with the chlorine evolution reaction, chloride ion discharge predominates. This is schematically illustrated in Fig. 4.4.5, which shows that because of the high exchange current density and the low Tafel slope for the electrochemical discharge of the chloride ions to form chlorine on RuO₂-based electrodes, the ratio of current producing chlorine to that generating oxygen is high. At low overvoltages, the ratio is smaller, as a result of which the %O₂ in Cl₂ increases.

These qualitative statements can be quantified by examining the relevant kinetic equations. Thus, when two electrochemical reactions are simultaneously occurring under activation-controlled conditions, as in the case of O₂ discharge during the course of the Cl₂ evolution reaction, the total current, i , may be represented as the sum of the contributions from the individual reactions as:

$$i = i_{\text{Cl}_2} + i_{\text{O}_2} \quad (115)$$

The partial currents, i_{Cl_2} and i_{O_2} , may be expressed in the Tafel form as:

$$i_{\text{Cl}_2} = i_{0,\text{Cl}_2} \cdot A \cdot \exp(k\eta_{\text{Cl}_2}) \quad (116)$$

$$i_{\text{O}_2} = i_{0,\text{O}_2} \cdot A \cdot \exp(k'(\eta_{\text{Cl}_2} + \Delta E)) \quad (117)$$

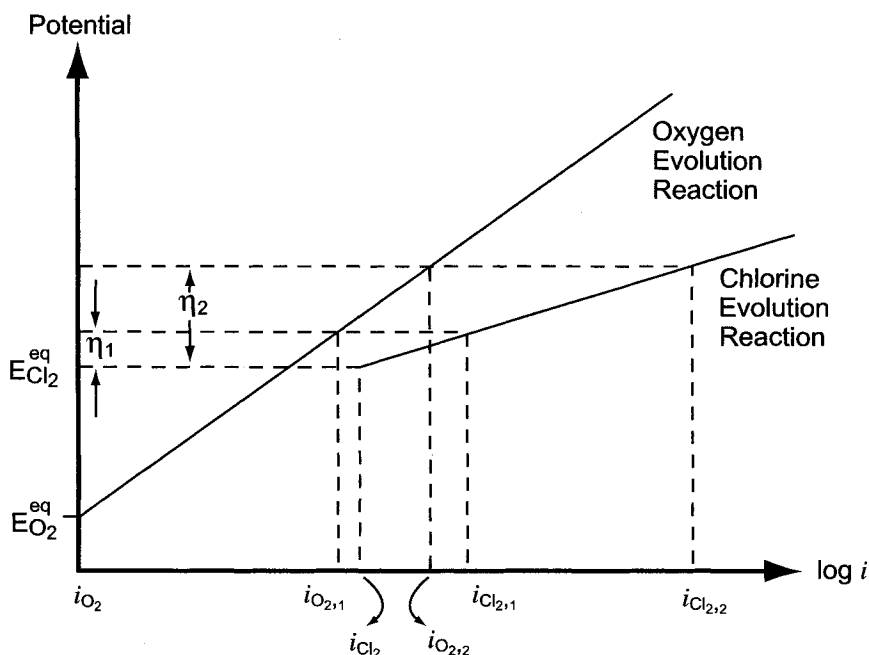


FIGURE 4.4.5. Schematic of the polarization behavior of the oxygen and the chlorine evolution reactions. Note that $i_{\text{Cl}_2,2}/i_{\text{O}_2,2} \gg i_{\text{Cl}_2,1}/i_{\text{O}_2,1}$ at η_1 because the Tafel slope for the oxygen evolution reaction is higher than that for the chlorine evolution reaction. Therefore, the %O₂ in chlorine is higher at low current densities.

where

i_{Cl_2} partial current for the chlorine evolution reaction

i_{O_2} partial current for the oxygen evolution reaction

A surface area of the electrode

η_{Cl_2} chlorine overpotential.

Defining the chlorine current efficiency, ξ_{Cl_2} , as:

$$\xi_{\text{Cl}_2} = \frac{i_{\text{Cl}_2}}{i} \quad (118)$$

ξ_{Cl_2} can now be expressed in terms of the kinetic parameters characterizing the electrochemical reactions contributing to the total current as:

$$\xi_{\text{Cl}_2} = \frac{1}{1 + \delta \xi_{\text{Cl}_2}^{-z} i^{-z}} = \frac{1}{1 + \delta^* \xi_{\text{Cl}_2}^{-z} i^{-z} 10^{\beta \text{pH}}} \quad (119)$$

where $z = (k - k')/k$ where k and k' refer to the inverse Tafel slopes of the chlorine and oxygen evolution reactions, respectively.

$$\delta = \frac{i_{0,\text{O}_2}}{i_{0,\text{Cl}_2}} \cdot \exp(k' \Delta E) \cdot (i_{0,\text{Cl}_2} \cdot A)^z = \delta^* 10^{\beta \text{pH}} \quad (120)$$

$$k' = \beta F / RT \quad (121)$$

$$\Delta E^{\text{Eq}} = \left(E_{\text{Cl}_2}^0 - E_{\text{O}_2}^0 \right) + \frac{RT}{2F} \ln \frac{p_{\text{Cl}_2}}{a_{\text{Cl}^-}^2} - \frac{RT}{4F} \ln \frac{p_{\text{O}_2}}{a_{\text{H}_2\text{O}}^2} \quad (122)$$

$$\Delta E = \Delta E^{\text{Eq}} + 2.303 \frac{RT}{F} \text{pH} \quad (122a)$$

where $E_{\text{Cl}_2}^0$, $E_{\text{O}_2}^0$ refer to the standard electrode potentials of the couple Cl_2/Cl^- and $\text{O}_2/\text{H}_2\text{O}$ couple respectively, p_{Cl_2} to the partial pressure of chlorine, p_{O_2} to the partial pressure of oxygen, R to the gas constant, and T to the temperature in Kelvin.

It follows from Eq. (119) that ξ_{Cl_2} is a strong function of δ , i , z and pH, and will increase with increasing current density when $k > k'$, which is the case for the present system, as the Tafel slope for the Cl_2 evolution reaction is ~ 40 mV and the corresponding value for the O_2 evolution reaction is ~ 130 mV at 95°C . From Eqs. (115), (118) and (123),

$$J_{\text{Cl}_2}^0 = \frac{i_{\text{Cl}_2}}{2F}; \quad J_{\text{O}_2}^0 = \frac{i_{\text{O}_2}}{4F} \quad (123)$$

it can be shown that the % O_2 in gaseous Cl_2 is

$$\% \text{O}_2 = (1 - \xi_{\text{Cl}_2}) / (1 + \xi_{\text{Cl}_2}) \quad (124)$$

The dependence of %O₂ on pH and current density for various ratios of $i_{0,O_2}/i_{0,Cl_2}$ and i , is shown in Figs. 4.4.6 and 4.4.7. Thus, the %O₂ generated is a function of the pH at the electrode surface, the current density, and the ratio of the exchange current densities of the O₂ evolution reaction and the Cl₂ evolution reaction, and it varies as $10^{0.5pH^e}$, pH^e being the pH value at the electrode surface [17–19].

The pH at the anode surface is not the same as in the bulk because the H⁺ ions generated at the anode by reaction (14) are transported to the bulk by diffusion. Thus,

$$J_{H^+} = -D_{H^+} \left(\frac{dC_{H^+}}{dx} \right)_{x=0} \quad (125)$$

where J_{H^+} refers to the flux of H⁺ ions, C_{H^+} to the concentration of H⁺ ions, and x to the distance coordinate.

Approximating,

$$-\left(\frac{dC_{H^+}}{dx} \right) = \frac{C_{H^+}^e - C_{H^+}^b}{\delta^*}$$

where the superscripts e and b refer to the electrode surface and the bulk respectively, and δ^* to the diffusion layer thickness, and expressing

$$\frac{i_{O_2}}{F} = J_{H^+} \quad (126)$$

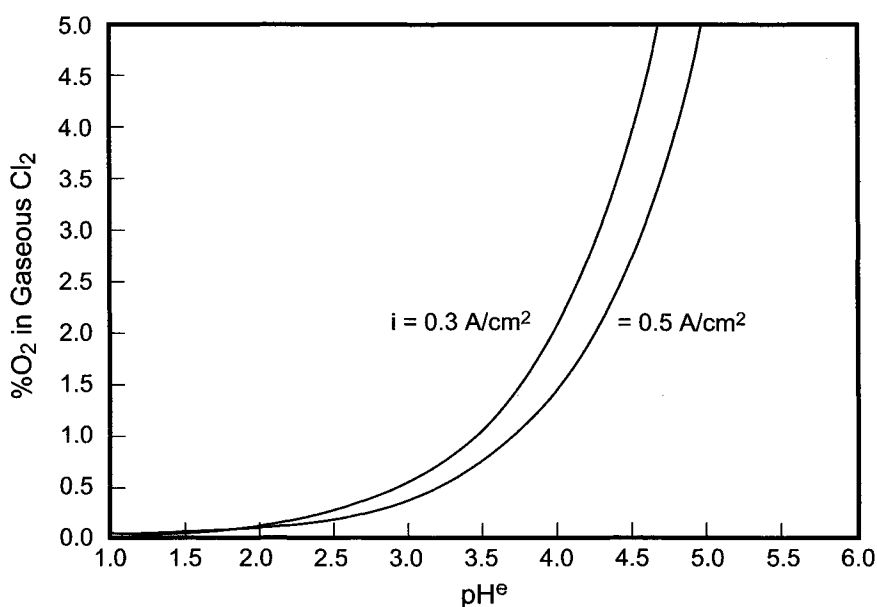


FIGURE 4.4.6. Calculated variation of the %O₂ with the pH at the electrode surface, pH^e, using Eq. (124) for $i_{0,Cl_2} = 1 \text{ mA cm}^{-2}$ and $i_{0,O_2}/i_{0,Cl_2} = 0.001$ at 95°C.

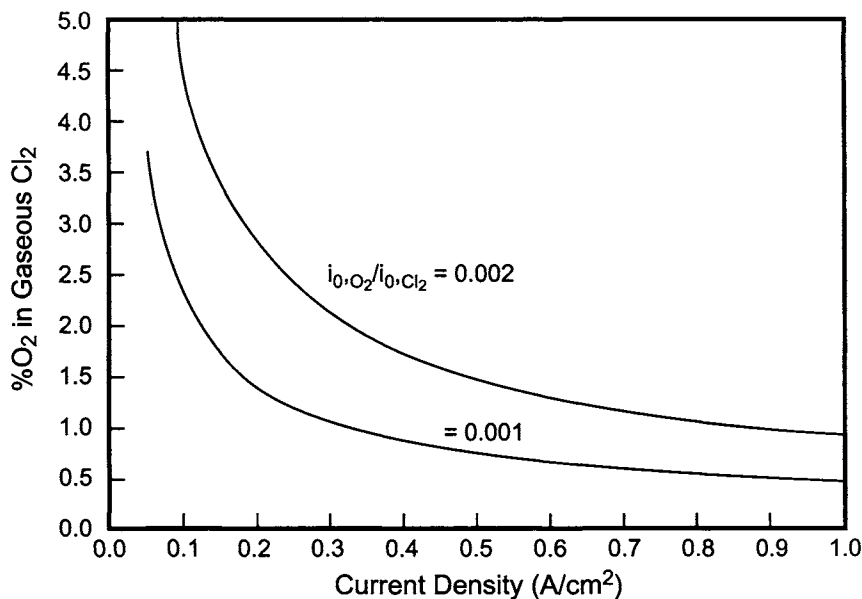


FIGURE 4.4.7. Calculated variation of the %O₂ with current density for various ratios of $i_{0,O_2}/i_{0,Cl_2}$ using Eq. (124) for $i_{0,Cl_2} = 1 \text{ mA cm}^{-2}$ and $\text{pH}^e = 3.5$ at 95°C .

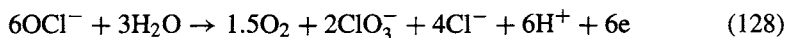
the pH at the electrode surface, pH^e , can be related to the bulk pH, pH^b , as:

$$\text{pH}^e = \text{pH}^b - \log \left\{ 1 + \left(\frac{i_{O_2}}{10^{-\text{pH},b}} \right) \left(\frac{1}{10^{-3} F K_m^{\text{H}^+}} \right) \right\} \quad (127)$$

where

$$K_m^{\text{H}^+} = D_{\text{H}^+} / \delta^*$$

The factor 10^{-3} in Eq. (127) arises because the units of C_{H^+} are in mol/liter. It follows from Eq. (127) that pH^e is a function of the current used for oxygen evolution, and that the value of the pH^e will be low even though the bulk pH is high. Figure 4.4.8 illustrates the variation of %O₂ with the bulk pH for various boundary layer thickness values. Another possible source of oxygen is the direct electrochemical oxidation of OCl^- to ClO_3^- .



Equation (128) was proposed as one of the causes of the presence of O₂ in electrolytic sodium chlorate operations using graphite anodes. However, there is no evidence for its participation in chlor-alkali cells because (1) the anolyte pH in these cells is ca. 3–5 where hypochlorite is not a major species and (2) the anode potentials are much lower than that required for reaction (128) to take place at any measurable rate.

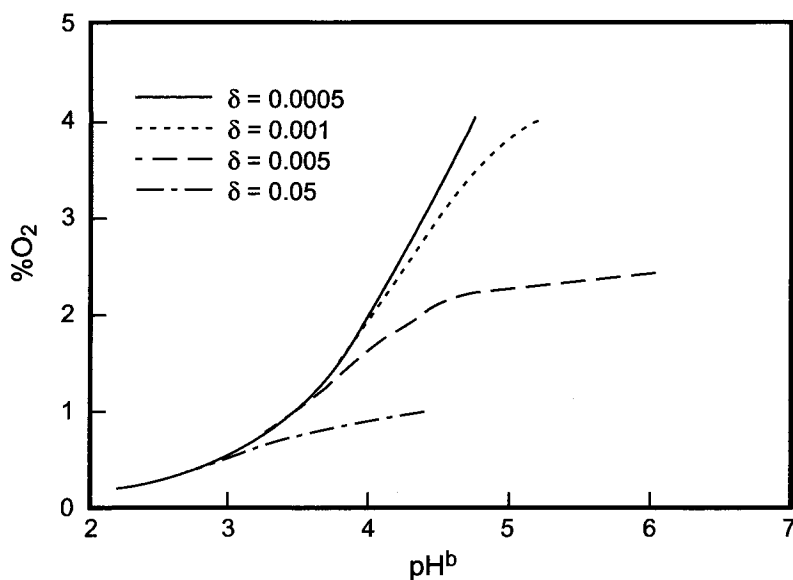


FIGURE 4.4.8. Calculated variation of the %O₂ with the bulk pH, pH^b, for various diffusion layer thickness values using Eqs. (124) and (127) for $i = 0.3 \text{ A cm}^{-2}$; $i_{0,\text{Cl}_2} = 1 \text{ mA cm}^{-2}$; $i_{0,\text{O}_2} = 1 \text{ mA cm}^{-2}$ at 95°C.

Chemical Oxygen Evolution. The other source of O₂ during Cl₂ evolution is the decomposition of OCl⁻ and HOCl as:



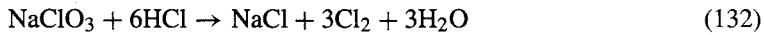
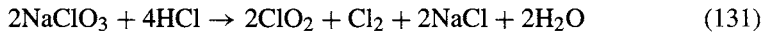
However, the reaction rate of $2.04 \times 10^{-3} \text{ min}^{-1}$ [20] for reaction (129) and $5.64 \times 10^{-6} \text{ L mol}^{-1} \text{ s}^{-1}$ [21] for reaction (129) at 95°C will lead to unreasonable values of %O₂, in contrast to the observations which show a $10^{0.5\text{pH}^b}$ dependency of %O₂ at pH values > 5. Hence, it appears that while these reactions are possible, they may not be proceeding at measurable rates in commercial operations.

It should be noted that the rates of Eqs. (129) and (130) are enhanced by cations such as Ni²⁺, Co²⁺, and Cu²⁺. Therefore, it is prudent to exclude these cations from the feed brine.

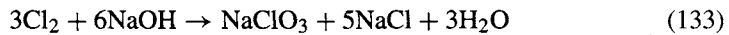
Thus, the primary and major reaction contributing to the %O₂ in Cl₂ is the electrochemical formation of O₂ from H₂O molecules or OH⁻ ions. The %O₂ can be reduced to very low levels by the proper choice of anode materials, and by adding HCl to lower the pH, as a result of which ξ_{Cl_2} will be higher than that achieved by suppressing reactions (11) and (13).

4.4.3.3B. Chlorate Formation. The soluble chlorine-based species in the anolyte, leading to the chlorine current inefficiency, are dissolved chlorine, HOCl, OCl⁻, and ClO₃⁻.

The first three are generally recovered by HCl addition at the dechlorination stage, which will force the reactions (11) and (12) backward to release molecular chlorine. The chlorine values in the chlorate can also be recovered following the reaction schemes (131 and 131a) or (132) to improve the process efficiency.



However, this is not universally practiced because of the cost of additional equipment required for this operation and the corrosive nature of the medium. As a result, the chlorine current efficiency is decreased to the extent that is consumed by chlorine during the formation of chlorate, which can be described by the reaction scheme (133).



It is stated [22] that the %O₂ and the chlorate levels in the anolyte are functions of the nature and composition of the anode coating. It should, however, be emphasized that while the %O₂ is indeed a function of the anode coating composition, the ratio of the exchange current densities of the oxygen and chlorine evolution reactions and the surface pH at the anode. The rate of chlorate formation, Γ , is solely dictated by the bulk pH, pH^b [15,23], as given by the relationship (134), and as shown in Fig. 4.4.9.

$$\Gamma = \frac{r}{kVC_t^3} = \left(\frac{K_a 10^{-2\text{pH}}}{(K_a + 10^{-\text{pH}})^3} \right) \quad (134)$$

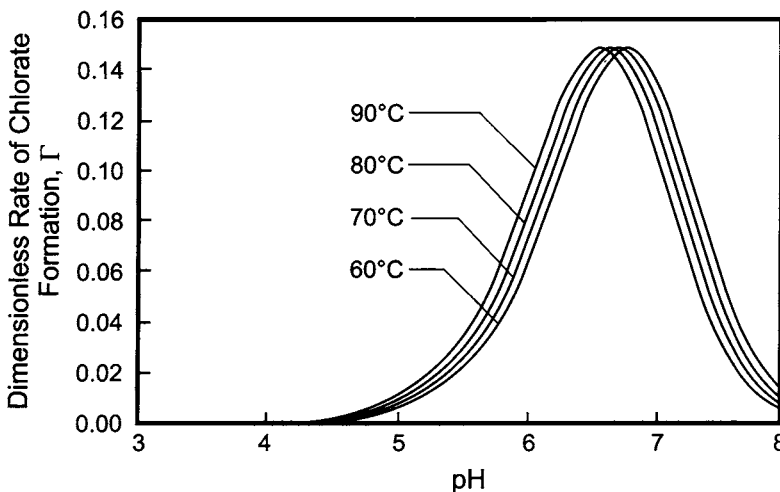


FIGURE 4.4.9. Dimensionless rate of chlorate formation as a function of pH.

where

$$r = kV[\text{HOCl}]^2 [\text{OCl}^-]$$

V = Volume of the reactor vessel

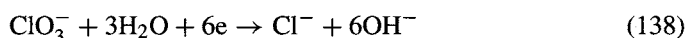
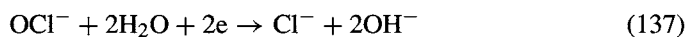
$$C_t = [\text{HOCl}] + [\text{OCl}^-]$$

$$k = \text{Rate constant for reaction (13)} = 8.509 \times 10^5 e^{-4777/T}$$

$$K_a = \text{Equilibrium constant for reaction (12)} = 3.04 \times 10^{-5} e^{-2000/T}$$

High %O₂ and low anolyte chlorate levels are self-consistent as, at high %O₂ levels, the bulk pH is low and hence, the chlorate formation rate is minimized and vice versa. Anode composition and its electrochemical characteristics influence the amount of chlorate formed only via the pH in the bulk, which is dictated by the %O₂ generated at the anode.

4.4.3.3C. Parasitic Reactions at the Cathode. The anolyte in all three chlor-alkali technologies contains dissolved Cl₂, HOCl, OCl⁻ and ClO₃⁻. All these species can be reduced at the cathode



as they are thermodynamically favored. Reactions (135)–(137) are mass-transfer controlled, and reaction (138) takes place under kinetic control [17]. Since the product of reactions (136)–(138) is the hydroxyl ion, the caustic efficiency is not affected by these reactions. However, the current efficiency for hydrogen will be lowered by the extent to which these reactions take place. As the caustic efficiency is unaffected by these parasitic reactions, which are consuming part of the cathodic current, these inefficiencies are called “blind current losses” or BCLs, introduced in Section 4.4.3.2G. This is not the situation in mercury cells where the main cathodic reaction is the discharge of Na⁺ to form sodium amalgam. The amalgam formation efficiency will indeed be reduced, but only to a very small extent since the hypochlorite reduction reaction proceeds under diffusion limited conditions, the limiting current density being about 1.4 A m⁻² (at a NaOCl concentration of 5 g L⁻¹ and a diffusion layer thickness of 0.01 cm).

The reaction that adversely influences the amalgam formation efficiency is the HER at the cathode in the mercury cells. Sodium ions are discharged at the mercury cathode to form a dilute sodium amalgam, the reversible potential for the 0.2% sodium amalgam being about 1.85 V vs standard hydrogen electrode (SHE) in concentrated NaCl solution [24]. On the other hand, the reversible potential for hydrogen evolution, at pH = 9, which is the solution pH near the cathode surface, is 0.54 V vs SHE. Hence, the HER is the favored reaction. However, the hydrogen evolution does not take place on sodium amalgam because the hydrogen overvoltage on mercury is high (Fig. 4.4.10). The hydrogen overvoltage on sodium amalgam [24] is presented in Fig. 4.4.10.

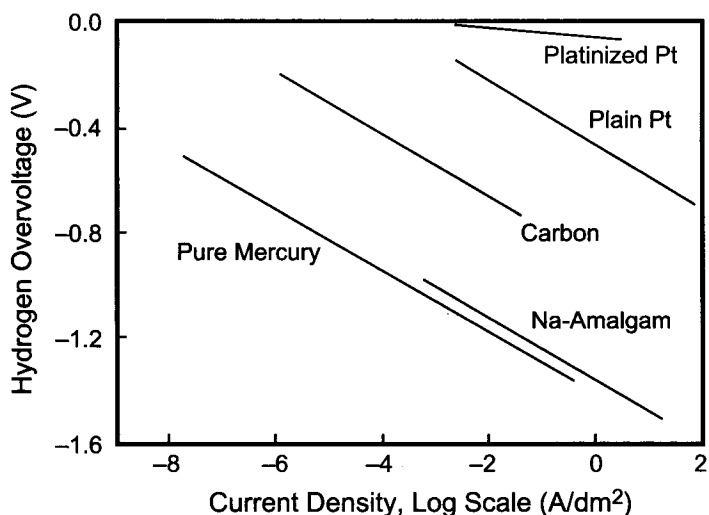


FIGURE 4.4.10. Hydrogen overvoltage on various cathodes [24].

An examination of the hydrogen overvoltage on various metals shows that most exhibit lower hydrogen overvoltage than mercury, and therefore, impurities in brine play a dominant role in promoting the HER. The brine impurities can promote [25–32] the HER by (1) direct discharge of H^+ ions or by decreasing the hydrogen overvoltage on the sodium amalgam, and (2) decomposing the sodium amalgam as it is formed by a local corrosion mechanism involving the anodic dissolution of Na amalgam and cathodic reduction of an ionic species.

Thus, V, Cr, and Mo ions promote the HER even at concentrations below 1 ppm, whereas Mg and Ca ions form colloidal precipitates on the cathode surface on which the hydrogen discharge is initiated. Impurities such as Ag, Pb, and Zn form a relatively uniform amalgam and may not promote hydrogen evolution on an amalgam cathode. Others, such as Fe, Ni, and C are not soluble in mercury but form “amalgam butter” on which the HER is favored. Thus, according to MacMullin [32], V, Mo, Cr, Ti, Ta, and (Mg + Fe) are harmful; Ni, Co, Fe, and W are moderately harmful; Ca, Ba, Cu, Al, Mg, and graphite are slightly harmful; and Ag, Pb, Zn, and Mn have no effect during sodium amalgam formation. It was also observed that a combination of two or more impurities often is more harmful than either impurity by itself, a typical example being Mg + Fe. Al was found to have no effect, but colloidal $Al(OH)_3$ was undesirable as it occluded impurities and led to the formation of amalgam butter. Table 4.4.4 shows the maximum allowable concentration of impurities in the brine to form 0.3% H_2 in Cl_2 gas [25].

Amalgam butter—a commonly used term in mercury cell operations—is a multiphase material, which has not been characterized thoroughly. The butter formed with Fe, Ni, and C consists of finely divided metal particles dispersed in mercury, whereas graphite butter is shiny and foamy. Ca butter is hard and compact, while Fe butter is blackish.

TABLE 4.4.4 Effect of Metallic Impurities on Hydrogen Evolution at the Cathode of a Mercury Cell Operated at 4 kA m^{-2} and at 80°C

Metal	Concentration (mg L^{-1})
Ca	100
Mg	1
Fe	0.3
Ti	0.1
Mo	0.001–0.010
Cr	0.001–0.010
V	0.001–0.010
Very harmful	V, Mo, Cr, Ti, Ta, (Mg + Fe)
Moderately harmful	Ni, Co, Fe, W
Slightly harmful	Ca, Ba, Cu, Al, Mg, graphite
No effect	Ag, Pb, Zn, Mn

There have been attempts to mitigate the influence of impurities by complexing them through the addition of silicate, borate, or pyrophosphate to the brine [33–36]. To the knowledge of the authors, this is not done in commercial operation.

High chlorine efficiency in all of the three cell technologies can be realized by (1) lowering the alkalinity of the feed brine to negate the formation of OCl^- , HOCl , and ClO_3^- via reactions (16)–(18), and by (2) adding HCl to the feed brine, in order to reverse the equilibrium reaction (11) to liberate more gaseous Cl_2 from the anolyte. The other advantages associated with acid addition to the feed brine are:

1. high chlorine quality because of low $\% \text{O}_2$;
2. high ξ_{Cl_2} and low energy consumption for Cl_2 production;
3. high caustic current efficiency;
4. long anode life due to less O_2 evolution at the anode (see Section 4.5 for details).

The economic benefits, however, are dependent on the price of acid, power, Cl_2 , and NaOH , and hence, a comprehensive cost–benefit analysis should precede the implementation of the acid addition.

4.4.4. Cell Voltage and Its Components

The theoretical energy requirement for chlorine and caustic production was shown in Section 4.4.2 to be:

$$P = x E_{\text{rev}} \quad (139)$$

The values of x for Cl_2 , NaOH , and KOH are given in Table 4.4.1. E_{rev} in Eq. (139) refers to the thermodynamic decomposition voltage to produce the given product, which can be calculated from the free energy change involved in the overall reaction describing

the generation of chlorine. Thus, for the overall reaction (140),



The free energy change, ΔG , is related to the thermodynamic decomposition voltage, E_{rev} , as:

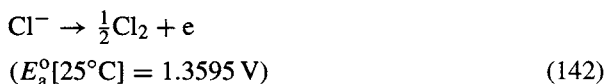
$$\Delta G = -zFE_{\text{rev}} \quad (141)$$

E_{rev} can be calculated from Eq. (141) or from the $E_{\text{o},i}$ values of the component electrochemical reactions constituting the overall reaction (140).

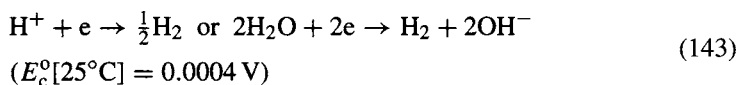
4.4.4.1. Thermodynamic Decomposition Voltage for Membrane and Diaphragm Cells.

The primary anodic and cathodic reactions associated with the reaction scheme (140) are:

Anodic reaction:



Cathodic reaction:



The E_{a}° and E_{c}° values shown in parentheses are the equilibrium electrode potentials for reactions (142) and (143) at 25°C and with reactants and products at unit activity. In practice, chlor-alkali cells operate at different temperatures and concentrations, hence, the E_{a}° and E_{c}° terms should be properly corrected using the Nernst equation. Typical conditions encountered in diaphragm-type chlor-alkali cells are as follows:

Anolyte: 267 g L^{-1} NaCl (4.56M at 96.4°C); pH = 3.5–4

Catholyte: 140 g L^{-1} NaOH (3.5M) + 150 g L^{-1} NaCl at 101.6°C ; pH ~ 14

The Nernst equation for the anodic reaction can be written as:

$$E_{\text{o},\text{a}} = E_{\text{a}}^{\circ}(t) + \frac{2.303RT}{F} \log \left[(p_{\text{Cl}_2})^{1/2} / (\text{NaCl}) \right] \quad (144)$$

where

$$E_{\text{a}}^{\circ}(t) = E_{\text{a}}^{\circ}(25^{\circ}\text{C}) + \left(\frac{dE^{\circ}}{dT} \right)_{\text{isoth}} (t - 25) + \frac{1}{2} \left(\frac{d^2E^{\circ}}{dT^2} \right)_{\text{isoth}} (t - 25)^2 \quad (145)$$

Substituting the values of dE°/dT and d^2E°/dT^2 from ref. [36], in Eq. (145), gives:

$$E_a^{\circ}(t) = E_a^{\circ}(\text{at } 25^{\circ}\text{C}) - 0.00126(t - 25) \quad (146)$$

where t is expressed in degrees centigrade and T in Kelvin. p_{Cl_2} in Eq. (144) refers to the partial pressure of chlorine, which is equal to the total pressure minus the vapor pressure of water at a given temperature and the electrolyte concentration minus the partial pressure of other gases (e.g., O_2). The reader should refer to Appendix for the partial pressure data for various concentrations of NaCl and temperatures. The term $[\text{NaCl}]$ refers to the concentration of NaCl in moles per liter. Hence, the standard equilibrium anode potential $E_a^{\circ}(t)$ at 96.4°C is:

$$\begin{aligned} E_a^{\circ}(96.4^{\circ}\text{C}) &= E_a^{\circ}(25^{\circ}\text{C}) - 0.00126(96.4 - 25) \\ &= 1.3595 - 0.0899 = 1.27 \text{ V} \end{aligned} \quad (147)$$

Substituting the E_a° value in Eq. (144) provides the reversible anode potential, $E_{\text{o,a}}$ as:

$$\begin{aligned} E_{\text{o,a}} &= 1.27 + 0.07329 \log \left(\frac{254}{760} \right)^{1/2} - 0.07329 \log 4.56 \\ &= 1.205 \text{ V} \end{aligned} \quad (148)$$

The term $2.303RT/F$ in Eq. (144) is equal to 0.07329 V at 96.4°C , R/F being 8.6166×10^{-5} .

The cathodic reaction proceeds in diaphragm cells at 101.6°C at pH 14. The Nernst equation for the cathodic reaction can be written as:

$$E_{\text{o,c}} = E_c^{\circ}(t) - \frac{2.303RT}{F} \log(p_{\text{H}_2})^{1/2} + \frac{2.303RT}{F} \log a_{\text{H}^+} \quad (149)$$

$$= E_c^{\circ}(t) - \frac{2.303RT}{F} \log(p_{\text{H}_2})^{1/2} - \frac{2.303RT}{F} \text{pH} \quad (150)$$

where

$$E_c^{\circ}(t) = E_c^{\circ}(25^{\circ}\text{C}) - 0.000033(t - 25) \quad (151)$$

$$= 0.0004 - 0.000033(101.6 - 25) \quad (152)$$

$$= -0.002128 \text{ V} \quad (153)$$

p_{H_2} can be calculated in a manner similar to that used for the p_{Cl_2} calculation. The vapor pressure data in pure caustic solution are provided in Appendix, and the vapor pressure

data in NaOH + NaCl mixtures can be calculated using Eq. (154) [3,37].

$$p_{\text{H}_2} = 1 - (M - 3)(0.0019772 - 0.00001193t) + 0.035M - (174 - t) \left(a + bN + C(N)^2 + \frac{d}{n} \right) + 0.0317Np_{\text{H}_2\text{O}} \quad (154)$$

where

$$a = -8.6715 \times 10^{-5}; b = 3.368 \times 10^{-5}; c = -1.354 \times 10^{-6}; d = 7.88 \times 10^{-5};$$

N = molality of NaOH; M = molality of NaCl; T = temperature in degrees centigrade;

$p_{\text{H}_2\text{O}}$ = vapor pressure in units of torr.

Inserting the appropriate value of p_{H_2} in Eq. (149) yields the reversible cathode potential as:

$$E_{\text{o,c}} = -0.002128 - 0.07433 \log \left(\frac{216}{760} \right)^{1/2} - 0.07433 \times 14$$

$$= -1.022 \text{ V} \quad (155)$$

Since,

$$E_{\text{rev}} = E_{\text{o,a}} - E_{\text{o,c}}$$

the thermodynamic decomposition voltage of a diaphragm cell becomes $1.205 - (-1.0224) = 2.227 \text{ V}$, at the operating conditions stated above.

The thermodynamic decomposition voltage of a membrane cell can be calculated in a similar manner as that shown for the diaphragm cells. Typical operating conditions in a membrane cell are

Anolyte: 200 g L⁻¹ NaCl (3.42 M at 90.0°C); pH = 3.5–4

Catholyte: 32% NaOH (at 90°C); pH ~ 14

Substituting the appropriate values in Eqs. (144) and (149) results in $E_{\text{o,a}} = 1.2322 \text{ V}$ and $E_{\text{o,c}} = -0.9944 \text{ V}$. Hence, the thermodynamic decomposition voltage of a membrane cell is 2.226 V at the operating conditions noted above.

4.4.4.2. Thermodynamic Decomposition Voltage for Mercury Cells. While the anodic reaction in mercury cells is the same as in diaphragm and membrane cells, the cathodic reaction in mercury cells is the discharge of Na⁺ ions to form sodium amalgam as given by Eq. (9). The sodium concentration in the sodium amalgam is generally in the range of 0.2–0.4%, as at 0.6%, the sodium amalgam is a solid at room temperature.

The equilibrium potential for the sodium amalgam with respect to SHE can be obtained from Table 4.4.5 or from Fig. 4.4.11 for various combinations of sodium amalgam strength, sodium chloride concentration, and temperature [3,38].

TABLE 4.4.5 Equilibrium Potentials of Sodium Amalgam [3] (volts)

NaCl (gpl)	% Na in the amalgam										Temperature (°C)	
	0.01	0.05	0.1	0.15	0.2	0.25	0.3	0.35	0.4	0.5		
120	1.734	1.793	1.816	1.831	1.843	1.853	1.861	1.869	1.877	1.886	40	
160	1.726	1.806	1.820	1.834	1.844	1.852	1.852	1.860	1.867	1.878		
200	1.718	1.774	1.812	1.824	1.834	1.834	1.843	1.851	1.858	1.870		
220	1.714	1.769	1.790	1.806	1.818	1.828	1.837	1.845	1.853	1.866		
240	1.710	1.764	1.786	1.801	1.813	1.823	1.833	1.841	1.849	1.862		
260		1.760	1.781	1.796	1.809	1.819	1.828	1.837	1.845	1.859		
280		1.755	1.776	1.792	1.803	1.814	1.823	1.833	1.841	1.854		
300		1.750	1.770	1.786	1.799	1.810	1.819	1.828	1.837	1.851		
120	1.763	1.784	1.805	1.823	1.838	1.849	1.859	1.868	1.876	1.888		60
160	1.752	1.774	1.796	1.815	1.830	1.841	1.851	1.860	1.867	1.879		
200	1.742	1.765	1.787	1.804	1.819	1.830	1.839	1.848	1.856	1.870		
220	1.737	1.759	1.781	1.798	1.813	1.824	1.833	1.842	1.850	1.864		
240	1.733	1.755	1.776	1.794	1.808	1.820	1.829	1.838	1.846	1.858		
260	1.729	1.750	1.770	1.789	1.804	1.815	1.825	1.833	1.841	1.854		
280	1.725	1.746	1.767	1.785	1.800	1.811	1.820	1.829	1.836	1.848		
300	1.718	1.741	1.762	1.780	1.793	1.804	1.814	1.823	1.831	1.845		
120	1.754	1.776	1.797	1.818	1.834	1.845	1.853	1.862	1.870	1.887	80	
160	1.745	1.766	1.788	1.808	1.824	1.834	1.843	1.852	1.860	1.878		
200	1.733	1.756	1.779	1.800	1.816	1.826	1.834	1.843	1.852	1.869		
220	1.729	1.751	1.773	1.795	1.811	1.822	1.830	1.838	1.847	1.863		
240	1.723	1.746	1.768	1.789	1.807	1.817	1.825	1.834	1.842	1.859		
260	1.718	1.741	1.763	1.784	1.801	1.812	1.821	1.829	1.838	1.855		
280	1.711	1.734	1.758	1.779	1.796	1.804	1.816	1.824	1.832	1.849		
300	1.704	1.728	1.752	1.773	1.790	1.802	1.810	1.819	1.828	1.845		

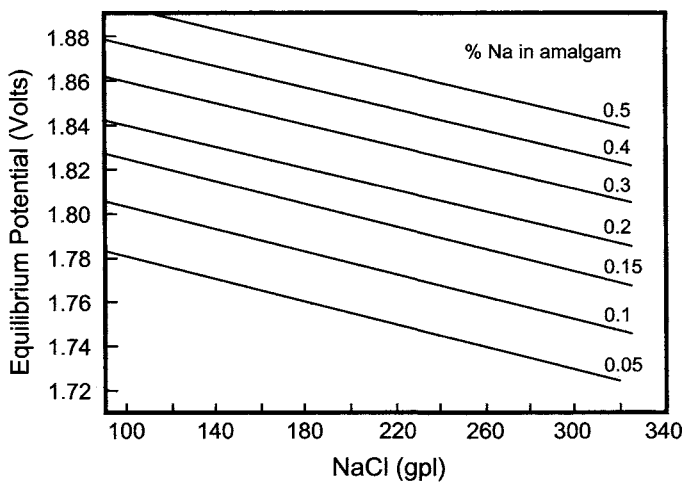


FIGURE 4.4.11. Equilibrium potentials of sodium amalgam vs NaCl concentration at various amalgam concentrations at 80°C [3]. (Courtesy of Marcel Dekker, Inc.)

Equation (156) also may be used [25] to calculate the equilibrium potential for the cathodic reaction.

$$E_{\text{Na}/\text{Hg}_x/\text{Na}^+} = \left[E_{\text{Na}/\text{Hg}_x/\text{Na}^+}^{\circ} \right] + \left[\frac{RT}{F} \ln \frac{a_{\text{Na}^+}}{Y} \right] \quad (156)$$

$E_{\text{Na}/\text{Hg}_x/\text{Na}^+}^{\circ}$ is the potential of a 0.1% amalgam with $a_{\text{Na}^+} = 1$, which is -1.834 V . a_{Na^+} in Eq. (7) refers to the activity of Na^+ ions, which can be calculated using the activity coefficient data in Fig. 4.1.5, and Y is the ratio of the Na activity in the sodium amalgam at 80°C referred to 0.1% Na amalgam (Fig. 4.1.4). Thus, the reversible potential for 0.2% Na amalgam in 4.8M NaCl ($\sim 281 \text{ g L}^{-1}$ NaCl) at 80°C can be calculated using Eq. (156) as:

$$E_{\text{o,NaHg}_x} = -1.834 + \frac{1.987 \times 353.15}{23,060} \ln \frac{4.032}{3.8} \quad (157)$$

$$= -1.832 \text{ V vs SHE} \quad (158)$$

Hence, the thermodynamic decomposition voltage of a mercury cell operating at 80°C with 0.2% Na amalgam is equal to 3.058 V as shown below.

$$E_{\text{rev}} = E_{\text{o,a}} - E_{\text{o,NaHg}_x} \quad (159)$$

$$= 1.226 - (-1.832) = 3.058 \text{ V} \quad (160)$$

$E_{\text{o,a}}$ of 1.226 V is calculated for 4.8M NaCl solutions at 80°C using Eq. (144).

The thermodynamic decomposition voltages calculated above are the equilibrium cell voltages when there is no applied current. When current passes, the system departs from equilibrium conditions to drive the reactions. The cell voltage will then be higher than the thermodynamic decomposition voltage because of the overvoltages associated with the anodic and cathodic reactions and the ohmic drops.

4.4.4.3. Cell Voltage. When a current passes through an electrochemical cell, the cell voltage is the sum of the individual components

$$E = E_{\text{o,a}} - E_{\text{o,c}} + \eta_{\text{a}} - \eta_{\text{c}} + iR_{\text{sol}} + iR_{\text{sep}} + iR_{\text{hw}} \quad (161)$$

where η_{a} and η_{c} are the anodic and cathodic overvoltages, respectively, and i is the current density. The R terms refer to the ohmic drops in solution, separator (either a diaphragm or a membrane), and hardware, represented by sol, sep, and hw, respectively, in the subscript. η_{c} is negative for cathodic processes and η_{a} is positive for anodic processes.

4.4.4.3A. Overvoltages. Overvoltage is the driving force for the reaction to proceed in a given direction, and it is defined as the difference between the electrode potential at a given current density and the equilibrium potential for the same reaction in the same solution. Overvoltage is measured by using a reference electrode, which is reversible

to the same ions under study (i.e., Cl^-/Cl_2 or H^+/H_2 or $\text{NaHg}_x/\text{Na}^+$ electrodes in the given medium). The overvoltage corresponds to the electrical energy that is irreversibly converted into heat and arises from the irreversible phenomena occurring at or near the electrode surface, of which activation polarization plays a major role.

Overvoltage arises from the kinetic limitations or from the inherent rate of the electrode reaction on a given material. The magnitude of the overvoltage is expressed by the Tafel relationship:

$$\eta = k \log(i/i_0) \quad (162)$$

where k refers to the slope of the η vs $\log i$ curve, i to the applied current density and i_0 to the exchange current density of the reaction. The values of k and i_0 depend on the nature of the metal or coating on a given substrate, composition and pH of the solution, and the surface characteristics of a given surface. This phenomenon, which is called "electrocatalysis", is addressed in Section 4.2.

Typical values of k and i_0 are presented in Table 4.4.6 for the chlorine evolution reaction on $\text{RuO}_2 + \text{TiO}_2$ based anodes [39], HER on steel [40], and Na amalgam formation [25], based on Figs. 4.4.12–4.4.14. It should be cautioned that these values vary depending on the composition of the anode for the chlorine evolution reaction and the nature of the cathode material for the HER. The exact values for a given operating condition are best determined by conducting the classical polarization studies. The overvoltages at these electrodes, calculated using Eq. (160), are noted in Table 4.4.6.

4.4.4.3B. Ohmic Drops. Another irreversible contribution to the measured cell voltage is the ohmic drop across the electrolyte, separator, and cell hardware. The potential drop across the electrolyte can be calculated using Ohm's law if the medium is homogenous. In a gas-evolving system, such as a chlor-alkali cell, however, the gases generated at the electrode(s) may be partially dispersed in the electrolyte between the electrodes. Since the current lines have to go around the insulating gas bubbles, the specific conductivity of the medium decreases. This results in an increased ohmic drop. If the volume fraction of the gas bubbles is small compared with the total volume of the electrolyte between the electrodes, the specific resistivity of the gas + electrolyte mixture, ρ_{mix} , may be

TABLE 4.4.6 Values of k and i_0 for Various Reactions

Electrode reaction	Electrode material	k (V)	i_0 (mA cm ⁻²)	Current	
				Overvoltage(V)	Density(A cm ⁻²)
Chlorine evolution	RuO ₂ + TiO ₂ based anode	0.03	1.2	0.068	0.23
				0.074	0.35
				0.087	1.00
Hydrogen evolution	Steel	0.125	0.251	0.371	0.23
	Bare nickel	0.115	0.0075	0.536	0.35
	Ni coated with 10 μm Ni-Al	0.05	3	0.103	0.35
Amalgam formation	Mercury	0.07	50	0.091	1.00

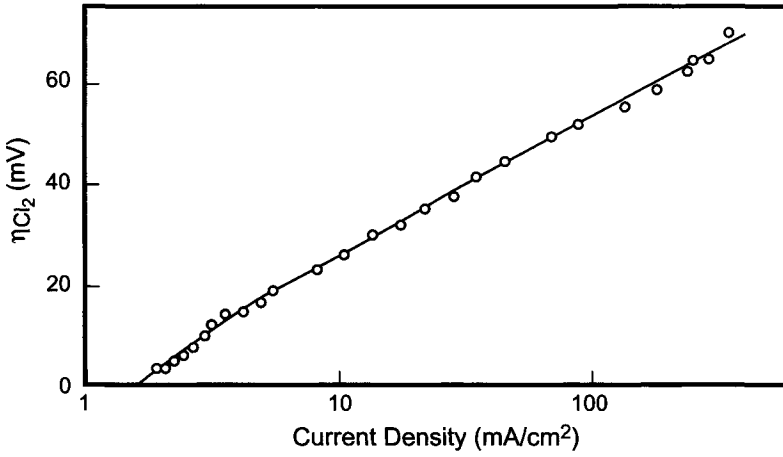


FIGURE 4.4.12. Chlorine overvoltage variation with current density in 5M NaCl solutions (pH = 3.5) at 95°C [39].

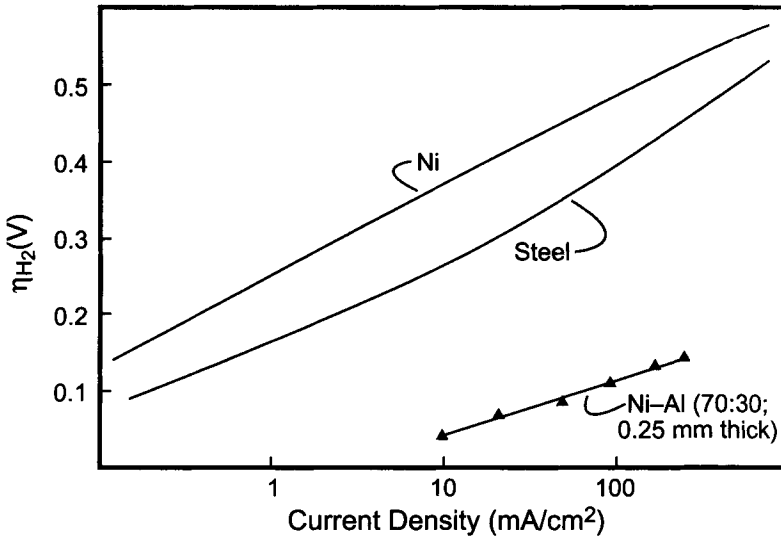


FIGURE 4.4.13. Hydrogen overvoltage on Ni, steel, and 0.25 mm thick Ni-Al plasma sprayed coating on Ni in 15% NaCl+17% NaOH solutions at 95°C [39].

estimated using the LaRue and Tobias [41,42] equation.

$$\frac{\rho_{mix}}{\rho} = (1 - \epsilon)^{-1.5} \tag{163}$$

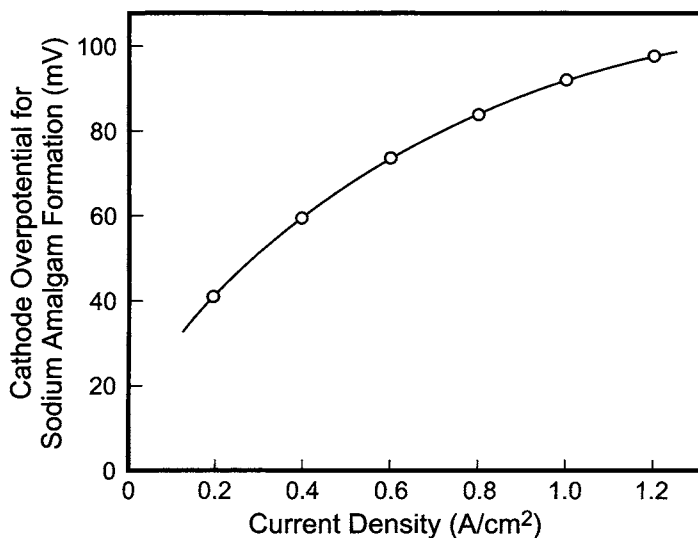


FIGURE 4.4.14. Cathodic polarization data for sodium amalgam formation (plotted from the data in ref. [25]).

where ε is the gas void fraction defined as the ratio of the volume of the gas to the volume of the gas + the volume of the electrolyte and ρ to the specific resistance of the electrolyte. When ε is small (i.e., < 0.1), Eq. (163) may be approximated by:

$$\frac{\rho_{\text{mix}}}{\rho} = 1 + 1.5\varepsilon + 2\varepsilon^2 \quad (164)$$

Equation (164) is accurate to within 2% for values $\varepsilon = 0.2$. However, when the solution is completely dispersed with gas bubbles, the electrode or separator may be completely covered with the bubbles resulting in what is usually termed as “gas blinding.” This condition produces excessive cell voltages.

Electric conductance of an electrolytic solution is governed by the transport of anions and cations in the solution. It is not electronic in nature, but Ohm’s law applies. Let us examine the case of a rectangular cell containing a pair of parallel, flat plate electrodes, each having an area A (cm^2), the interelectrode distance being L (cm). When the cell is filled with an electrolytic solution having a resistivity of ρ ($\Omega \text{ cm}$), the electric resistance between the two electrodes is

$$R = \rho L/A = L/\kappa A \quad (165)$$

where κ is the reciprocal of ρ , and is called the electric conductivity in units of $\Omega^{-1} \text{ cm}^{-1}$ or S cm^{-1} ($\text{S} = \text{siemen or mho}$). The conductivity of electrolytic solutions used in industrial electrochemical processes is generally in the range of $0.1\text{--}10 \text{ S cm}^{-1}$. The conductivity is a function of the solution composition. Generally, the higher the concentration or the number of the ionic species, the larger the magnitude of electric conductivity. However, because of the differences in the transport characteristics of hydrated ions, which

have a larger diameter than less hydrated species, the conductivity vs concentration curve often exhibits a maximum conductivity at a certain concentration. This pattern is not observed with KCl or NaCl solutions, which is why concentrated brine is fed to the electrolyzers. The conductivity of electrolytic solutions increases with increasing temperature, unlike the conductivity of metals.

Another complication that may interfere with estimating the ohmic drops is the cell geometry. The electrodes do not always extend from one side of the cell wall to the other, and they may have differing geometries and sizes. Under these conditions, Eq. (165) is not directly applicable. Thus, when two concentric cylindrical electrodes are used, the electric resistance in a narrow gap, dR , between the cylinders is:

$$dR = (\rho/2\pi r) dr$$

Integrating the above expression between the limits r_1 and r_2 leads to:

$$R = (\rho/2\pi) \ln(r_2/r_1)$$

For more complex domains, sophisticated mathematical treatments such as conformal transformation or computer simulation must be employed to calculate the resistance.

In the case of a diaphragm or membrane chlor-alkali cell, there are three ohmic drops to consider: anode to separator, cathode to separator, and across the separator. The anode to cathode distance in ELTECH's H-4 cell is 7.74 mm, the thickness of the diaphragm is 3.05 mm, and the cathode to diaphragm distance is negligible. The anode to diaphragm ohmic drop, $iR_{A/S}$, may now be estimated from the conductivity data of the electrolytes, which are presented in the appendix to this section.

Relevant conductivity values are noted below:

Saturated brine = $0.59 \Omega^{-1} \text{ cm}^{-1}$ at 95°C ;
 15% NaOH + 17% NaCl = $0.72 \Omega^{-1} \text{ cm}^{-1}$ at 95°C .

The calculation of the distance between the anode and the separator is slightly complex as the asbestos diaphragm is deposited on the cathode screen, and the anode blade is located 4–5 mm from the diaphragm with the anolyte in between, and contains dispersed chlorine gas bubbles. The gas–solution mixture is circulated effectively by the convection of the two-phase flow resulting in a relatively low gas void fraction in the electrolysis zone. The superficial resistivity, ρ_{mix} , based on Eq. (163), would be about 1.2 times the resistivity of the solution free of gas bubbles, which is $1.2/0.59 = 2.03 \Omega \text{ cm}$. The ohmic drop between the anode and the diaphragm can then be calculated from Eq. (165) and the current as:

$$iR_{A/S} = 0.232 (\text{A cm}^{-2}) \times 2.03 (\Omega \text{ cm}) \times (0.774 - 0.305) (\text{cm}) = 0.221 \text{ V} \quad (166)$$

The calculation of the ohmic drop across a separator, iR_{sep} , is similar to the method used to estimate the ohmic drop between two parallel plates with a diaphragm having a finite porosity. MacMullin and coworkers [43] have shown that the relative resistivity, R_{sep}/R or ρ_{sep}/ρ , is a function of the permeability, P (in m^2), the void fraction, ϵ , and

the relative surface area, S (in m^2/m^3) of the diaphragm, and is independent of the nature of the materials.

Thus:

$$N_M = R_{\text{sep}}/R = m^2/kP \quad (167)$$

$$m = \varepsilon/S \quad (168)$$

$$k = 3.666 \pm 0.098$$

where m is the hydrodynamic radius in meters, which contains the porosity and the tortuosity of the micropores in the diaphragm. N_M is the MacMullin number.

Studies addressing mass transport and solution concentration profiles across diaphragms (Section 4.7) have shown that when the anolyte is at a pH of 2–3 and saturated with chlorine and the catholyte is a mixture of NaCl and NaOH, the neutral zone is located in the vicinity of the diaphragm surface facing the anolyte. In other words, the diaphragm is almost filled with an alkaline medium, whose composition varies with position in the diaphragm. If it is assumed that the average conductivity of the solution in the diaphragm is $(0.59 + 0.72)/2 = 0.655 \text{ mho cm}^{-1}$, and the MacMullin number for Hooker asbestos plus polymer (HAPP) diaphragms is 3.5, the superficial resistivity of the diaphragm can be estimated to be $3.5/0.655 = 5.34 \text{ } \Omega \text{ cm}$. Substituting this value into Eq. (165) results in:

$$i R_{\text{sep}} = 0.232 \text{ (A cm}^{-2}\text{)} \times 5.34 \text{ (}\Omega \text{ cm)} \times 0.305 \text{ (cm)} = 0.378 \text{ (V)}$$

The ohmic drop of the hardware depends on the nature of the materials used, and the intercell design configuration. These values have been found to be about 0.25 V for H-4 type diaphragm chlor-alkali cells, at a load of 150 kA or 2.32 kA m^{-2} .

The ohmic drop across an ion-exchange membrane can be calculated using Eq. (165) and the specific resistance and thickness of the membrane. Unfortunately, the resistivity data of ion-exchange membranes in caustic solutions is not available in the open literature. However, one may make an approximate calculation based on the data in refs. [11,12], which shows the resistance of Nafion NX961 to be about $0.833 \text{ } \Omega \text{ cm}^2$. It should be cautioned that the calculations shown here are strictly for illustrating the methodology and one should determine these resistivity values for the specific membrane used in a given operation. Thus, the ohmic drop across Nafion NX961 at 3.5 kA m^{-2} , would be:

$$0.833 \times 0.35 = 0.291 \text{ V}$$

The component terms constituting the cell voltage are presented in Table 4.4.7 for the three technologies.

Thus, the cell voltage can be calculated using the procedures discussed above. However, as the individual values of the voltage components are dependent on several variables, it is prudent that these estimates are made for the specific situation under consideration with data that is experimentally determined.

TABLE 4.4.7 Components of the Voltage of Diaphragm, Membrane and Mercury Cells

	Diaphragm cell operating at 2.32 kA m^{-2}	Membrane cell operating at 3.5 kA m^{-2}	Mercury cell operating at 10 kA m^{-2}
$E_{o,a}$	1.205 V	1.205 V	1.226 V
$E_{o,c}$	1.022 V	1.022 V	1.832 V
η_a	0.068 V	0.074 V	0.087 V
η_c	0.371 V (with steel cathode)	0.536 V (bare Ni cathode); 0.103 V (with Ni-Al based cathode)	0.091 V
iR_{sol}	0.221 V (4.69 mm gap)	0 (zero gap cell)	0.406 V (2 mm gap)
iR_{sep}	0.38 V	0.291	—
iR_{hw}	0.25 V	0.37 V	0.2 V
Total cell voltage	3.51 V	3.498 V (bare Ni cathode) 3.065 V (Ni-Al based cathode)	3.843 V

4.4.4.4. k -Factor. A popular diagnostic parameter that is measured and used in the chlor-alkali industry to monitor the performance of mercury and membrane electrolyzers and to control (manually or automatically) the anode–cathode gap in the mercury cells is the k -factor. The k -factor is the slope of the current density–voltage curve, plotted from the cell voltages measured at different loads.

Theoretical Significance of k . The voltage–current relationship of a chlor-alkali cell described by Eq. (161) can be recast as

$$E = E^{\circ} + \eta_a - \eta_c + iR_{sol} + iR_{sep} + iR_{hw} \quad (169)$$

where E is the measured cell voltage (V), and E° is the thermodynamic decomposition voltage, which is the algebraic sum of the reversible potentials of the anodic and cathodic reactions, $E_{o,a}$ and $E_{o,c}$.

Equation (169) does not take into account the concentration overvoltages, which depend on the concentration of NaCl and NaOH in the anolyte and the catholyte.

Under Tafel conditions, the overvoltages are expressed by Eq. (162). Substitution of Eq. (162) into Eq. (169) results in:

$$E = E^{\circ} - k_a \log i_{o,a} + k_c \log i_{o,c} + (k_a - k_c) \log i + (R_{sol} + R_{sep} + R_{hw})i \quad (170)$$

where the subscripts a and c to the k and the i_0 terms refer to the anodic and cathodic reactions, respectively. Equation (170) can be recast as

$$E = E^* + (k_a - k_c) \log i + (R_{sol} + R_{sep} + R_{hw})i \quad (171)$$

where

$$E^* = E^{\circ} - k_a \log i_{o,a} + k_c \log i_{o,c}$$

Clearly, according to Eq. (171), the E - i relationship is not linear, contrary to experimental observations. However, when the $\log i$ term is approximated [44] as:

$$\log i/i = k^* \quad (172)$$

the E - i variations follow a linear relationship. This approximation is good within a few percent over the current density range of 2 – 5 kA m^{-2} .

The slope and the intercept of these plots are related to the basic parameters characterizing the anode, cathode, membrane, and the electrolyte as:

$$\text{Slope} = k^*(k_a - k_c) + R_{\text{sol}} + R_{\text{sep}} + R_{\text{hw}} \quad (173)$$

$$\text{Intercept} = E^0 - k_a \log i_{o,a} - k_c \log i_{o,c} \quad (174)$$

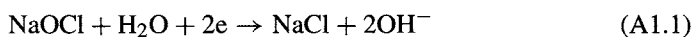
Use of k -factors to monitor the electrolytic cells is a good practice. However, caution has to be exercised in attributing the variations in k to the failure of the membrane or electrodes with membrane cells. In the case of mercury cells, the data interpretation is straightforward as there is no membrane to contend with.

Instead of employing Eq. (173) to interpret the k -factors, one can curve-fit [44] the experimentally observed linear E - i data to the nonlinear Eq. (170). This approach requires high accuracy in the data to draw valid conclusions.

It should be noted that the large error in the linearization of the $\log(i)$ term makes it impossible to calculate the exact values of the terms in Eqs. (173) and (174). Furthermore, Eq. (170) was based on the assumption that the overvoltages follow a simple Tafel relationship, and that the resistance of the membrane [45] and the gas-solution mixture follow Ohm's law. Both these simplifications are questionable as discussed in Sections 4.2 and 4.4. A rigorous analysis of the k -factors requires a proper description of the overpotential-current variations on a given substrate and the conductivity characteristics of the membranes. If the commercial electrolyzers are of the monopolar type, one has to be more cautious while interpreting the k -factors, as these electrolyzers contain cells connected in parallel. Therefore, all the cells operate at the same voltage, even though the resistance of each cell in the electrolyzer is different. The k -factor in this case reflects only the variations in the electrolyzer.

APPENDIX 4.4.1: DERIVATION OF HYDROGEN CURRENT EFFICIENCY

Hydrogen current inefficiency arises from the blind current losses (BCLs) from the discharge of available chlorine at the cathode, forming NaCl and NaOH.



The BCL can be estimated to be

$$\text{BCL} = 2FqC_{\text{av.Cl}_2}^a \quad (\text{A1.2})$$

Available chlorine constitutes dissolved chlorine, HOCl and OCl⁻. Since the cell liquor flow rate, q , can be expressed as

$$q = \left(\frac{I}{F} \right) \frac{\xi_{\text{OH}}^{\text{D}}}{C_{\text{NaOH}}^{\text{d}}} \quad (\text{A1.3})$$

Equation (A1.2) becomes:

$$\text{BCL} = 2C_{\text{av.Cl}_2}^{\text{a}} \frac{I\xi_{\text{OH}}^{\text{D}}}{C_{\text{NaOH}}^{\text{d}}} \quad (\text{A1.4})$$

The hydrogen inefficiency can be written as:

$$1 - \xi_{\text{H}_2}^{\text{D}} = \frac{\text{BCL}/2}{I\xi_{\text{OH}}^{\text{D}}/2} \quad (\text{A1.5})$$

Substitution of Eq. (A1.4) into Eq. (A1.5) gives

$$\xi_{\text{H}_2}^{\text{D}} = 1 - 2 \left(\frac{C_{\text{av.Cl}_2}^{\text{a}}}{C_{\text{NaOH}}^{\text{d}}} \right) \quad (\text{A1.6})$$

APPENDIX 4.4.2: SOLUBILITY OF CHLORINE IN BRINE

NaCl system

$$C_{\text{av.Cl}_2}^{\text{f}} \text{ or } C_{\text{av.Cl}_2}^{\text{d}} = 1.408 \times 10^{-5} P_{\text{Cl}_2} [(1.567 - 0.002822[\text{NaCl}]^{\text{d}})10^{1000/T} + 70906 \times 10^{(\text{pH}-A)}]$$

where:

$$A = 6.01 + 0.001(T-273.15) - 0.00044 [\text{NaCl}]^{\text{d}};$$

G = specific gravity of depleted brine;

pH = depleted brine pH;

T = anolyte temperature (K);

$[\text{NaCl}]^{\text{d}}$ = depleted brine concentration (g L⁻¹);

P_{Cl_2} = partial pressure of chlorine gas (atm) = Fraction of chlorine in dry gas (1 - $P_{\text{H}_2\text{O}}$);

$P_{\text{H}_2\text{O}}$ = water vapor pressure of depleted brine (atm) = (1 - $R \times S$) $P_{\text{H}_2\text{O}}^{\circ}$;

$P_{\text{H}_2\text{O}}^{\circ}$ = vapor pressure of pure water (atm) = $\left(\frac{1}{760} \right) 10^{(7.95190 - (1659.793/T - 45.854))}$;

$R = (S - 3)[1.9772 \times 10^{-3} - 1.193 \times 10^{-5}(T - 273.15)] + 0.035$;

$S = \frac{[\text{NaCl}]^{\text{d}}}{58.44} \left(\frac{1000}{1000G - [\text{NaCl}]^{\text{d}}} \right)$.

KCl system

$$C_{av.Cl_2}^f \text{ or } C_{av.Cl_2}^d = 1.408 \times 10^{-5} P_{Cl_2} [(1.567 - 0.002822[KCl]^d) 10^{1000/T} + 70906 \times 10^{(pH-A)}]$$

where:

$$A = 6.01 + 0.001(T - 273.15) - 0.00044 [KCl]^d;$$

G = special gravity of depleted brine;

pH = depleted brine pH ;

T = anolyte temperature (K);

$[KCl]^d$ = depleted brine concentration ($g L^{-1}$);

P_{Cl_2} = partial pressure of chlorine gas (atm) = Fraction of chlorine in dry gas $(1 - P_{H_2O})$;

P_{H_2O} = water vapor pressure of depleted brine (atm) = $(1 - R \times S) P_{H_2O}^o$;

$P_{H_2O}^o$ = vapor pressure of pure water (atm) = $\left(\frac{1}{760}\right) 10^{(7.95190 - (1659.793/T - 45.854))}$;

$R = 7 \times 10^{-4}(S - 2) + 0.0317$;

$S = ([KCl]^d / 74.55) (1000 / 1000G - [KCl]^d)$.

APPENDIX 4.4.3: PROPAGATION OF ERRORS TECHNIQUE

We consider a quantity Q which is to be calculated from several observed quantities a, b, c, \dots

$$Q = f(a, b, c, \dots) \tag{A3.1}$$

$$\Delta Q = \left(\frac{\partial Q}{\partial a}\right) \Delta a + \left(\frac{\partial Q}{\partial b}\right) \Delta b + \left(\frac{\partial Q}{\partial c}\right) \Delta c \dots \tag{A3.2}$$

and the standard deviation σ_Q resulting from standard deviations $\sigma_a, \sigma_b, \dots$ can be written as:

$$\sigma_Q = \sqrt{\left(\frac{\partial Q}{\partial a}\right)^2 \sigma_a^2 + \left(\frac{\partial Q}{\partial b}\right)^2 \sigma_b^2 + \left(\frac{\partial Q}{\partial c}\right)^2 \sigma_c^2 + \dots} \tag{A3.3}$$

For simplicity, Eq. (A3.2) is used to estimate the errors in the chlorine process efficiency and energy consumption calculations. The equation used for the energy consumption calculation is given by

$$\frac{AC \text{ kWh}}{\text{Ton } Cl_2} = \frac{685.834 \times \text{cell voltage}}{\xi_{Cl_2} \times \xi_{\text{rectifier}} \times \xi_{\text{liquefaction}}}$$

Typical rectifier and liquefaction efficiencies are 0.975 and 0.992, respectively. $\xi_{\text{Liquefaction}}$ refers to the liquefaction efficiency.

REFERENCES

1. L.C. Curlin, T.V. Bommaraju, and C.B. Hansson, Chlorine and Sodium Hydroxide, In *Kirk-Othmer Encyclopedia of Chemical Technology*, Vol. 1, John Wiley & Sons, Inc., New York (1991), p. 938.
2. C-P. Chen, B.V. Tilak, and J.W. Quigley, *J. Appl. Electrochem.* **25**, 95 (1995).
3. J.E. Currey and G.G. Pumplun, Chlorine, In J.J. McKetta and W.A. Cunningham (eds), *Encyclopedia of Chemical Processing and Design*, vol. 7, Marcel Dekker, New York (1978), p. 305.
4. D.L. Caldwell, Production of Chlorine, In J.O'M. Bockris, B.E. Conway, E.A. Yeager, and R.E. White (eds), *Comprehensive Treatise of Electrochemistry*, vol. 2, chapter 2, Plenum Press, New York, (1981).
5. HSC Chemistry Software, Versions 3 and 4, Outokumpu Research Oy (1999).
6. H.S. Burney, Membrane Chlor-Alkali Process, In R.E. White, B.E. Conway, and J.O'M. Bockris (eds), *Modern Aspects of Electrochemistry*, vol. 24, Plenum Press, New York, (1993), p. 393.
7. B.V. Tilak, S.R. Fitzgerald, and C.L. Hoover, *J. Appl. Electrochem.* **18**, 699 (1988).
8. G.W. Cowell, A.D. Martin, and B.K. Revill, A New Improved Method for the Determination of Sodium Hydroxide Efficiency in Membrane Cells. In T.C. Wellington (ed.), *Modern Chlor-Alkali Technology*, vol. 5, Elsevier Applied Science, New York (1992), p. 143.
9. D. Bergner, M. Hartmann, and F. Wergel, *Dechema Monographien*, VCH-Verlagsgesellschaft, Weinheim, **125**, 121 (1992).
10. N. Masuko and M. Takahashi, *Soda to Enso*. **41**, 185 (1990).
11. C-P. Chen and B.V. Tilak, *J. Appl. Electrochem.* **26**, 235 (1996).
12. *DuPont Technical Bulletins* 92-2, 88-1, and 84-3.
13. B.V. Tilak and S.D. Fritts, *J. Appl. Electrochem.* **22**, 675 (1992).
14. J.T. Keating, *Electrochemical Engineering in the Chlor-Alkali and Chlorate Industries*, The Electrochemical Society, Pennington, NJ, PV 88-2 (1988), pp. 311-328; *DuPont Technical Information Bulletin*, 91-08 (1991).
15. C-P. Chen and B.V. Tilak, *J. Appl. Electrochem.* **27**, 1300 (1997).
16. N. Yokota, *Kagaku Kogaku (J. Chem. Eng.)* **22**, 476 (1958).
17. B.V. Tilak, K. Tari, and C.L. Hoover, *J. Electrochem. Soc.* **135**, 1386 (1988).
18. C-P. Chen and B.V. Tilak, Unpublished Results (2001).
19. M. Takahashi and N. Masuko, *Soda to Enso* **7**, 232 (1990).
20. M.W. Lister, *Can. J. Chem.* **30**, 879 (1952).
21. M.W. Lister and R.C. Peterson, *Can. J. Chem.* **40**, 729 (1962).
22. R.C. Carlson, The Effect of Brine Impurities on DSA[®] Electrodes, *14th Annual Chlorine/Chlorate Seminar*, ELTECH Systems Corp., Cleveland, OH (1998).
23. J.E. Colman and B.V. Tilak, Sodium Chlorate, *Encyclopedia of Chemical Processing and Design*, vol. 51, Marcel Dekker, New York (1995), p. 126.
24. F. Hine, *Muki Kogyo Kagaku (Industrial Inorganic Chemistry)* Asakura, Tokyo (1967), p. 21.
25. F. Hine, *Electrode Processes and Electrochemical Engineering*, Plenum Press, New York, (1985).
26. F. Hine, B.V. Tilak, and K. Viswanathan, Chemistry and Chemical Engineering in the Chlor-Alkali Industry, In R.E. White, J.O'M. Bockris and B.E. Conway (eds), *Modern Aspects of Electrochemistry*, vol. 18, Plenum Press, New York (1986), p. 249.
27. G. Angel and T. Lunden, *J. Electrochem. Soc.* **99**, 432, 435 (1952); **100**, 39 (1953); **102**, 124 (1955); and **104**, 167 (1957).
28. W.E. Cowley, B. Lott, and J.H. Entwisle, *Trans. Inst. Chem. Eng.* **41**, 372 (1963).
29. K. Hass, *Electrochem. Technol.* **5**, 246 (1967).
30. F. Hine, S. Matsuura, and S. Yoshizawa, *Electrochem. Technol.* **5**, 251 (1967).
31. F. Hine, M. Yasuda, F. Wang, and K. Yamakawa, *Electrochim. Acta* **16**, 1519 (1971).
32. R.B. MacMullin, *Chlorine*, *ACS Monograph 154*, J.S. Sconce (ed.), Reinhold Publishing Co., New York (1962), p. 151.
33. G. Angel, T. Lunden, and R. Brännland, *J. Electrochem. Soc.* **100**, 39 (1953).
34. G. Angel, T. Lunden, S. Dahlerus, and R. Brännland, *J. Electrochem. Soc.* **102**, 124 (1955); **102**, 246 (1955).
35. G. Angel, R. Brännland, and S. Dahlerus, *J. Electrochem. Soc.* **104**, 167 (1957).
36. A.J. deBethune and N.A.S. Loud, *Standard Aqueous Electrode Potentials and Temperature Coefficients at 25°C*, Clifford A. Hampel, Skokie, IL (1964).

37. R.B. MacMullin, *J. Electrochem. Soc.* **116**, 416 (1969).
38. T. Sugino and K. Aoki, *J. Electrochem. Soc. Japan* **27** (1–3), E17 (1959).
39. B.V. Tilak, Unpublished Results.
40. B.V. Tilak, A.C.R. Murty, and B.E. Conway, *Proc. Indian Acad. Sci. (Chem. Sci.)* **97**, 359 (1986).
41. R.M. LaRue and C.W. Tobias, *J. Electrochem. Soc.* **106**, 827 (1959).
42. I. Rousar, V. Cezner, M. Vender, M. Kroutil, and J. Vachuda, *Chemicky Prumysl.* **17/42**, 466 (1967).
43. R.B. MacMullin and G.A. Muccini, *AIChE J.* **2**, 393 (1956).
44. D. Bergner, M. Hartmann, and H. Kirsch, Voltage–Current Curves: Application to Membrane Cells. In N.M. Prout and J.S. Moorhouse (eds), *Modern Chlor-Alkali Technology*, vol. 4, Elsevier Applied Science, London (1900), p. 158.
45. K.L. Hardee, A Simple Procedure for Evaluation of Membrane Electrolyzer Performance. In R.W. Curry (ed.), *Modern Chlor-Alkali Technology*, vol. 6, The Royal Society of Chemistry, London (1995), p. 234.

4.5. ANODES

4.5.1. Introduction

The conditions prevailing in the anode compartment during the chlorine evolution reaction impose stringent requirements on the anode material, including

1. Stability toward electrochemical oxidation and chemical attack by NaCl, KCl, HCl, Cl₂, HOCl, ClO₃⁻, and O₂;
2. Maintenance of conductivity of the surface layers formed at potentials where chlorine is generated, the general tendency being either the dissolution or formation of insulating surface films;
3. Electrocatalysis to achieve low anodic overvoltage.

Platinum, magnetite, and carbon were the first anode materials [1–3] employed in the electrolytic production of chlorine. Platinum was expensive, and the magnetite anode suffered from difficulties in fabrication, poor machinability, fragility, and poor conductivity. The conductivity of magnetite was only 5% of that of graphite [3], and the maximum anode current density was only 0.4 kA m⁻². This led to the extensive use of graphite from the 1900s to the late 1960s, following the synthetic graphite manufacturing process, independently innovated by Castner and Chas, and Acheson [4,5]. Graphite anodes, however, posed several problems such as:

1. Short life (6–24 months) due to the consumption of 1–3 kg graphite per ton of chlorine by abrasion by the anode gases and oxidation of C to CO₂.
2. Contamination of the product stream with chlorinated hydrocarbons.
3. Adverse influence of the graphite particles on the performance of the diaphragm.
4. Difficulties associated with the machinability and installation of electrodes in the cells.

In addition, anode wear caused the anode–cathode gap to increase with time, resulting in increased cell voltage and energy consumption. Various attempts to reduce the degradation of graphite were not completely successful [4].

It is well known that the platinum group metals are electrically conductive and stable in the anolyte environment described above, and that the valve metals belonging

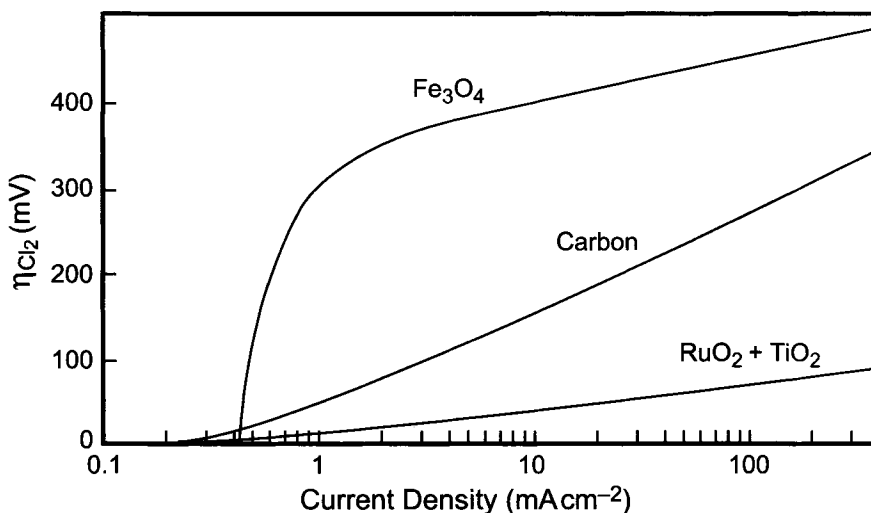


FIGURE 4.5.1. Variation of the chlorine overvoltage, η_{Cl_2} , with current density on various anodes in 5M NaCl solutions at 95°C at pH = 3.5 [20].

to the periodic groups IVB, VB, and VIB develop tightly adherent, insulating oxide films that protect them from corrosion. Efforts to combine these two features to form an anode structure started in 1913 with the development of Pt-coated tungsten anodes by Stevens [6]. Platinum-coated Ti anodes were tested in the early 1960s but were not successful. The platinum wear rates were unacceptably high, and the electrodes were prone to premature coating losses, especially in mercury cells. Nevertheless, continued studies by Cotton *et al.* [7] and Beer [8] resulted in the discovery of (RuO₂ + TiO₂)-based coatings on titanium substrates. These are termed Dimensionally Stable Anodes (or DSA[®] electrodes) because of their resistance to degradation. Information related to Beer's RuO₂-based coatings was first published in *South African Patents* 662,667 (1966), 680,034 (1968), and in the United States (covering RuO₂ + TiO₂ solid solutions and other features) in *U.S. Patents* 3,214,110 (1966), 3,632,498 (1972), 3,711,385 (1973), and 3,751,291 (1973). The solid solution RuO₂ + TiO₂ coating was further developed and commercialized by DeNora [9] and licensed globally by Diamond Shamrock Technologies, S.A. of Geneva.

DSA[®] electrodes exhibited low overvoltage (Fig. 4.5.1) resulting in a savings of about 0.3 V and a long life (about 8 years in diaphragm cells and about 2 years in mercury cells). These advantages, coupled with escalating energy and maintenance costs, have forced the complete replacement of graphite by metal anodes.

4.5.2. Electrode Preparation

Basically, the DSA[®] electrode is a titanium substrate coated with a TiO₂ + RuO₂ mixture containing up to 50 mol% of precious metal oxide, the precious metal loading varying from 5 to 20 g m⁻². These coatings are generally prepared by the thermal decomposition technique described below, following the "recipes" published in the patent literature.

This procedure, originally described by Beer in *South African Patent* 680,834, consists of an initial treatment of the substrate (Grade 1 or 2 titanium) in hot aqueous oxalic acid, followed by ultrasonic cleaning in water. After the electrode is dried, it is coated with a butyl alcohol solution, containing about 0.5 M HCl and Ru as RuCl_3 and Ti as butyl titanate. The ratio of Ru : Ti in the solution is the same as the value desired in the coating. It is then heated in air at a temperature of 300–500°C for 1–5 min to form a coating of $\text{TiO}_2 + \text{RuO}_2$ on the titanium substrate.

Another electrode preparation [10] is a $\text{RuO}_2 + \text{TiO}_2 + \text{SnO}_2$ “mixed-crystal” coating, which is used in diaphragm cells. It is cost effective (because of reduced Ru loading) and generates 22–25% less O_2 than does the $\text{RuO}_2 + \text{TiO}_2$ coating on titanium. The mole ratio of $\text{TiO}_2/(\text{SnO}_2 + \text{RuO}_2)$ is 1.5–2.5 and SnO_2 constitutes 35–50 mol% of the combined level of $\text{RuO}_2 + \text{SnO}_2$. This electrode is prepared by coating a clean titanium surface with a solution of RuCl_3 , SnCl_2 , butyl titanate, and HCl in butanol, and heating it in air at 450°C for 7 min. This procedure is repeated 10 times to achieve a final loading of about 17 g m^{-2} of $\text{RuO}_2 + \text{SnO}_2$.

DSA[®] electrodes generally exhibit a long life in commercial chlor-alkali cells. Nevertheless, a rejuvenation procedure has also been developed to enable anodes to be reused and consists of either cleaning [11] in a 2 : 1 $\text{NaNO}_3 + \text{NaOH}$ melt at 450°C prior to recoating or removing [12] the loose material and etching in 20% HCl for 5 min at 100°C prior to recoating with Ru-containing solutions (see ref. [13], which also covers other rejuvenation techniques).

4.5.3. Other Patented Anode Compositions

As described earlier, the DSA[®] electrode is typically a valve metal substrate coated with a noble-metal-based composition. Either to circumvent the basic Beer patents or to achieve better and less expensive anode compositions, considerable efforts have been devoted to the development of novel anode coatings. A wide variety of compositions [14] have been described in the literature, and it is beyond the scope of this chapter to review these developments individually. A generalized formulation of anode materials can be schematically described as Sub/VM + NM + NNM, where Sub refers to the substrate, VM to the valve metal, NM to the noble metal, and NNM to the non-noble metal. The compositions cited in the literature include the following in various combinations:

Sub: Ti, Zr, Hf, Nb, Ta, W, Al, Bi, C, Fe_3O_4 , etc., either singly or in combination, or as alloys of one with another.

VM + NM + NNM: oxides, carbides, borides, nitrides, oxychlorides, fluorides, silicides, phosphides, arsenides, etc., of valve metals (Ti, Zr, Hf, Nb, Ta, W, Al, Bi) + noble metals (Pt, Ir, Rh, Ru, Os, Pd) + non-noble metals (Cu, Ag, Au, Fe, Co, Ni, Sn, Si, Pb, Sb, As, Cr, Mn, etc.) at various loadings of each component. The oxides examined include spinels ($A\text{B}_2\text{O}_4$), perovskites ($A\text{BO}_3$), pyrochlores ($A_2\text{B}_2\text{O}_{7-y}$), and delafossites ($A\text{BO}_2$), where A can be a noble metal and B, a valve or non-noble metal. Sometimes, the general structures stated above are further coated with other oxides (e.g., SiO_2 in *U.S. Patent* 3,677,815) or formed in layers as Sub/NM/VM.

Some anode compositions are presented in Table 4.5.1 to illustrate the directions followed to develop alternate anode coatings. It should be noted that this is not a complete list and that more details are available [15–20].

TABLE 4.5.1 Some Patented Anode Compositions

Coating composition	Patent #
Solid solution of Ti, Ru–Sn	U.S. 3,776,834
$M_xPt_3O_4$, where M is Li, Na, K, Ag, or Cu and $x = 0.4–0.6$	U.S. 4,042,484
Precious metal coating—PdO + precious metal oxide + 31–25% of AB_2O_4 spinel, where $A = Fe, Co, Ni$; $B = Fe, Co, Ni, Al, Cr, Mn$	U.S. 3,677,917
Noble metals or their oxycompounds and noble-metal-based spinels $M_1M_2O_4$, where $M_1 = Mg, Zn, Co$; $M_2 = Cd, Co, Ni$	U.S. 3,711,397
Pyrochlores of the type $A_2B_2O_7-y$, where $B = Ru, Rh, Ir, Pt, Ru-Pb$ and $1 > y > 0$	U.S. 4,146,548
ABO_4 , where $A = Rh, Al, Ga, La$ and $B = Sb, Nb, Ta$	German (DE-MS) 2,333,485
Delafossites (ABO_2), where $A = Pd, Pt, Ag, Cu$ and $B = Cr, Fe, Co, Rh$; Examples: $PtCoO_2, PdCoO_2$	U.S. 3,804,740
$M_xCo_3O_4$, where $x = 0.1–1$ and $M = \text{group IB, IIA, or IIB elements}$	U.S. 4,061,549
A_2BO_6 or $A_2BO_6 + MO_2$, where $A = Rh, Fe$ and $B = W, Te$ and $M = Ru, Ir$; Examples: $Rh_2WO_6, RhSbO_2$	German patent, 2,136,391
Co_3O_4 -based coatings	U.S. 3,977,958; 4,142,005; 4,061,549

TABLE 4.5.2 Key Anode Patents

General description	U.S. Patent #	Expiration year
Method of application	3,864,163	1992
Two-component coatings	3,711,385	1989
Three-component coatings	3,948,751	1993
	4,003,817	1994
	4,070,504	1995
	4,318,795	1999

There are thousands of patents describing various anode compositions, yet only “Beer patents” were commercialized. The “valid” patents are noted in Table 4.5.2 along with their current status. The key patents in Table 4.5.2 all have expired.

4.5.4. Physical Characteristics and Morphology of $RuO_2 + TiO_2$ -Based Electrodes

RuO_2 -based coatings prepared by thermal decomposition have been examined by various techniques and some important features emerging from these studies are presented here.

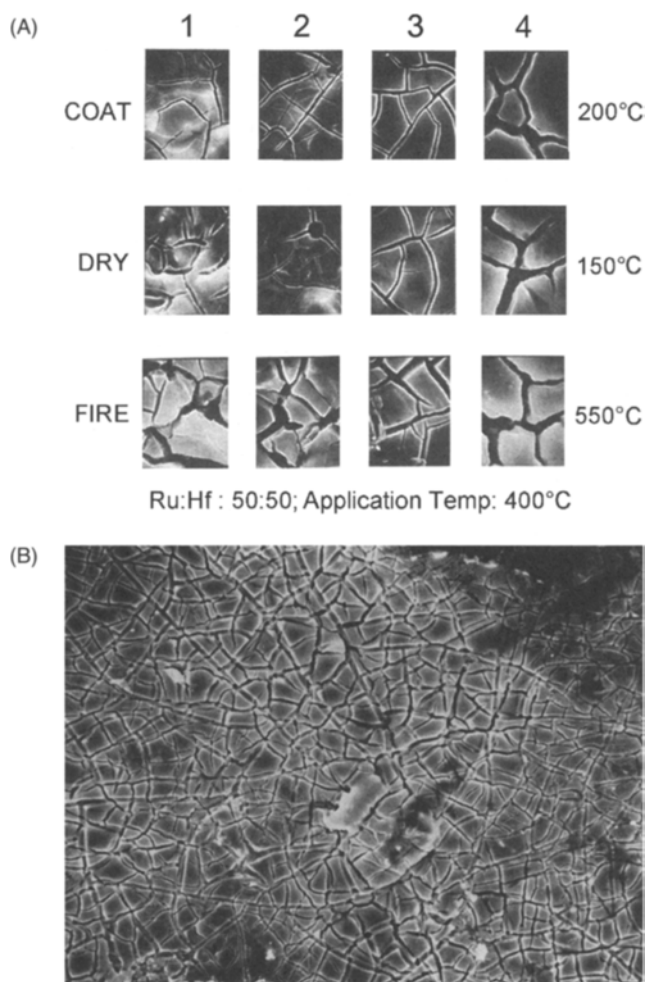


FIGURE 4.5.2. (A) SEM images of RuO₂-HfO₂ coatings (application temperature: 400°C; drying temperature: 150°C; final firing temperature: 550°C; number of coats are stated on the top) [21]. (Reproduced by permission of The Electrochemical Society, Inc.) (B) SEM image after final firing [20].

(RuO₂ + TiO₂)-based coatings are polycrystalline and structurally complex, and their structure depends on the variables involved in the preparation of the coatings. These variables include the nature of the solvent used to mix the precursors, the method of application (e.g., brushing or spraying), the temperature and time variations during application, drying, and final firing, and the number of coatings applied to obtain the desired final loading of Ru. Scanning electron microscope images [21] show progressive development of surface roughness and mud-cracked structure (Fig. 4.5.2) with the formation of crystallites.

The catalytic layer is essentially a mixture of TiO₂ and RuO₂ existing as Ti_(1-n)Ru_nO₂. RuO₂ and TiO₂ form a solid solution in the catalytic layer since,

TABLE 4.5.3 Some Crystallographic Features of RuO₂, TiO₂, Ti, and Ru

Property	TiO ₂	RuO ₂
Symmetry group	P4 ₂ /mnm	P _{mmm}
Crystal habit	Tetragonal	Tetragonal
Crystal structure	Rutile	Rutile
a ₀	0.4594 nm	0.4490 nm
c ₀	0.2958 nm	0.3195 nm
V	0.062 nm ³	0.062 nm ³
	Ti	Ru
Ionic radius	0.068 nm	0.065 nm
Electronegativity	1.5	1.8
Valence	4	4

structurally, they are rutiles with “identical” crystallographic characteristics following the Hume–Rothery rules (Table 4.5.3). Solid solutions form at 400°C on Ti supports over the entire compositional range, although it is reported [22,23] that they are metastable phases.

X-ray diffraction and micro-X-ray spectroscopic examination of the RuO₂–TiO₂–Cl system [23,24] shows that it coexists with an anatase solid solution on the TiO₂ side (depending on the conditions of preparation) and with a pure RuO₂ on the RuO₂ side, the phase exhibiting a defect structure and low degree of crystallinity.

The coatings exhibit a crystallite size of 1–5 μm [25] in the firing temperature range of 300–700°C, and BET and electrochemical surface area measurements [21,26] show high surface area of the order of 200 cm² per apparent square centimeter, the exact value being a function of the variables involved in preparing the coating and the composition of the coating. X-ray photoelectron spectroscopic studies [26] of RuO₂ and RuO₂ + TiO₂ film electrodes before and after anodic polarization in 4M NaCl solutions reveal a defect structure with two different species, Cl⁻ and adsorbed atomic Cl, on these surfaces.

SEM studies show (Fig. 4.5.2) a microcracked surface composed of discrete islands (a “mud-cracked” structure), which is, again, a function of the variables involved in the preparation of the sample. This structure is a possible consequence of the volume contraction arising from differences in thermal expansion coefficients and is probably responsible for the large surface area and the microcrystallinity of the coatings.

Pure RuO₂ is a metallic conductor with a conductivity of 2–3 × 10⁴ Ω⁻¹ cm⁻¹ at room temperature, whereas TiO₂ is an insulator with a room temperature conductivity of 10⁻¹³ Ω⁻¹ cm⁻¹. The RuO₂ + TiO₂ mixtures appear to vary in their conductivity characteristics from those of metals [27] to those of n-type semiconductors.

The conductivity of RuO₂ + TiO₂ mixtures varies with the RuO₂ content as shown in Fig. 4.5.3, which has been compiled from the conductivity data published in refs. [28–32]. These results show that the conductivity is high beyond 25 mol% RuO₂ and decreases to very low values at less than 20 mol% RuO₂. It is for this reason that the commercial DSA composition contains up to 70–80% of TiO₂. While the theory of the metal–non-metal variations involved in the insulator–conductor mixtures is complex and

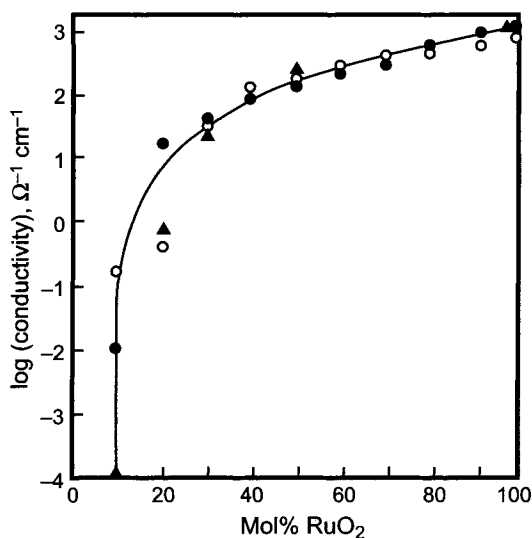


FIGURE 4.5.3. Variation of conductivity with mol% RuO₂ in RuO₂ + TiO₂ coatings. (●: direct resistance measurement [29]; ○: impedance measurement [30]; ▲: direct measurement [28]) [104]. (Reproduced with permission of The Society of Chemical Industry.)

still being debated [33], the high conductivity of the mixtures containing >25% RuO₂ has been attributed [34–36] to the formation of an infinite chain of RuO₂ clusters in the TiO₂ matrix. The breakdown of this chain has resulted in the poor conductivity of mixtures with <25% RuO₂.

Surface characterization of mixed oxide coatings [37] by spectroscopic techniques shows surface enrichment with one of the metals. The surface of (Ti + Ru)O₂ appears to be enriched with Ti [38,39], and that of (Ru + Ir)O₂ with Ir [40–42]. The degree of enrichment depends on the method of preparation [40,43]. SIMS analysis, however, does not reveal the surface enrichment of Ti in the commercial RuO₂ + TiO₂ coatings [44].

4.5.5. Electrochemical Behavior of RuO₂ + TiO₂-Based Coatings

The electrochemical behavior of RuO₂-based electrodes has been thoroughly investigated by several workers and summarized in various publications [19,20,45–49]. Particular mention should be made of refs. [20] and [47], where the equilibrium and nonequilibrium electrochemical properties of oxide electrodes prepared by various methods were analyzed, and to refs. [49] and [50], where the mechanistic aspects of the chlorine evolution reaction were critically addressed.

RuO₂ exhibits a rest potential of 0.65 V with respect to the reversible hydrogen electrode (RHE) in the same solution [51]. The rest potentials of thermally-formed RuO₂ films measured with respect to a saturated calomel electrode (SCE) change linearly with pH with a slope of 0.059 V/pH unit in the pH range of 0–14 (Fig. 4.5.4). This has been

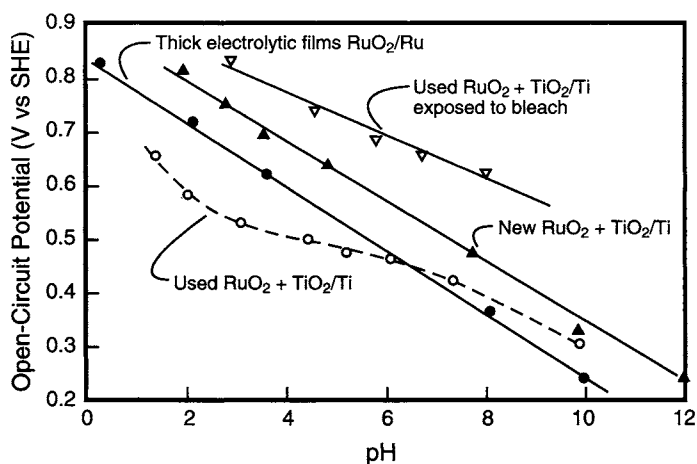
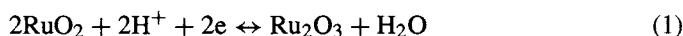


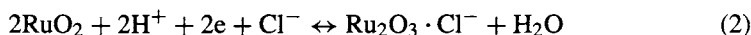
FIGURE 4.5.4. Variation of the open circuit potential of RuO_2 electrodes vs pH at 25°C . The $\text{RuO}_2 + \text{TiO}_2/\text{Ti}$ electrodes were thermally formed [53].

attributed [52] to the reaction:



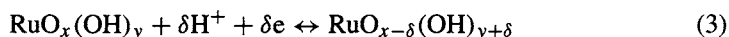
on the electrode surface.

Freshly prepared $\text{RuO}_2 + \text{TiO}_2$ coatings containing 30 mol% RuO_2 also exhibit the same slope of 60 mV/pH, whereas “used” ($\text{RuO}_2 + \text{TiO}_2$) electrodes deviate [53] from this pattern, as shown in Fig. 4.5.4. However, when the used electrodes are exposed to NaOCl solutions, the electrodes, again, show a slope of 60 mV, suggesting Cl^- ion participation in the open circuit behavior as



These observations can be used to predict the cell voltage behavior when the current is interrupted (e.g., during shutdowns).

Cyclic voltammetric curves [54–60] in the potential range of 1.2 to 0.4 V in acid and alkaline solutions, as shown in Fig. 4.5.5, reveal a featureless profile in acidic solutions, and a well-developed peak in alkaline solutions, prior to oxygen evolution. The voltammetric behavior of RuO_2 electrodes has been attributed [54,61] to a reversible oxidation–reduction reaction through a mechanism involving proton exchange with the solution as



It is this reaction that contributes to the significant pseudocapacitance associated with RuO_2 electrodes, which are used to produce capacitor devices. The monograph by Conway [62] elaborated the fundamental and practical application of these pseudocapacitors.

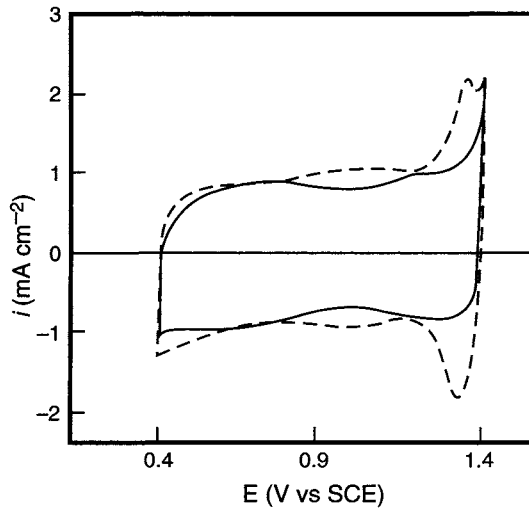


FIGURE 4.5.5. Typical voltammetric curves of RuO_2 electrode in 1M solutions of HClO_4 (solid lines) and KOH (dotted lines) at a sweep rate of 20 mV s^{-1} at 25°C [58]. (With permission from Elsevier.)

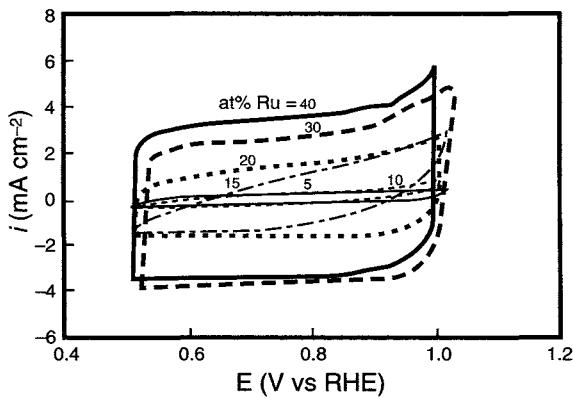


FIGURE 4.5.6. Cyclic voltammetry of fresh Ru-Ti electrodes of $2 \mu\text{m}$ thickness with different Ru contents in 5M NaCl ($\text{pH}=3.5$) at 100 mV s^{-1} at 90°C [63]. (Reproduced by permission of The Electrochemical Society, Inc.)

Cyclic voltammetric curves [63] in Fig. 4.5.6 show that the current at a given potential varies with the Ru content of the coating. This property can be used as a diagnostic tool to characterize the anodes during service.

The polarization behavior of the $\text{RuO}_2 + \text{TiO}_2$ electrode in 5M NaCl solutions [63] during the course of the chlorine evolution is presented in Fig. 4.5.7. The Tafel slopes of these electrodes show a value of $30\text{--}40 \text{ mV}$ at high Ru levels and a value ca. 120 mV with electrodes containing $<10 \text{ at}\%$ Ru . The exchange current density, i_0 , for the Cl_2

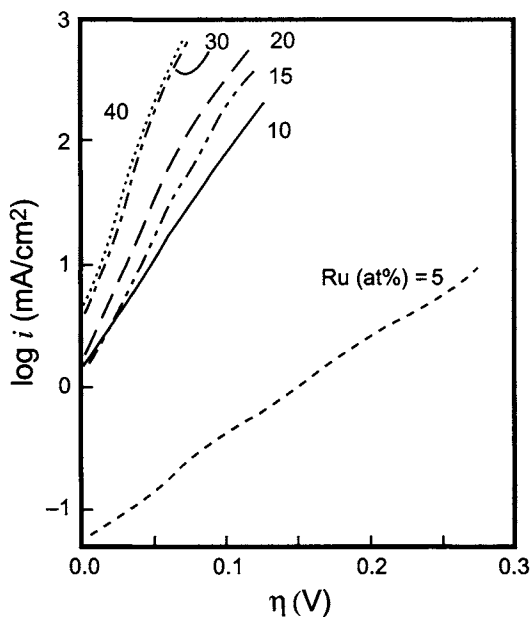
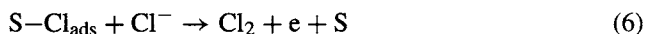
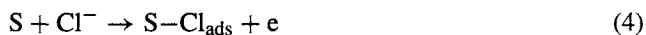


FIGURE 4.5.7. Effect of Ru content on the Tafel plot of fresh Ru-Ti electrodes in 5M NaCl (pH = 3.5) at room temperature [63]. (Reproduced by permission of The Electrochemical Society, Inc.)

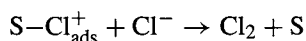
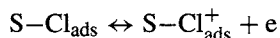
evolution reaction, in Fig. 4.5.8 (calculated from the data in Fig. 4.5.7) shows that i_0 decreases with decreasing %Ru in the coating [64].

Kinetic investigations with $\text{RuO}_2 + \text{TiO}_2$ electrodes containing >25 at% Ru during the course of the chlorine evolution [49,50,65,66] reveal: (1) a Tafel slope of 40 mV or $(2RT/3F)$, (2) a reaction order of 1 with respect to the chloride ion, and (3) a stoichiometric number of 1. These observations cannot be explained by the conventional pathways, that are shown in Eqs. (4–6):



S in Eqs. (4)–(6) represents a state of the oxide film surface and not of the anode metal.

Reaction mechanisms proposed to account for the experimental observations include:



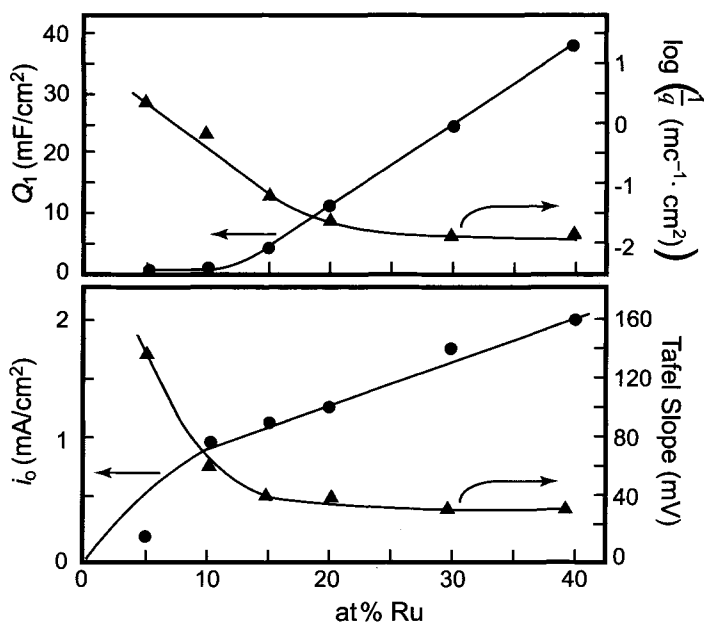
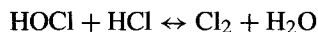
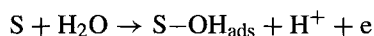
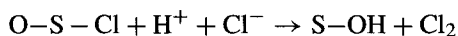
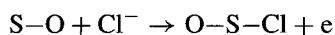


FIGURE 4.5.8. Variation of electrochemical characteristics of Ru-Ti oxide films: Top: Capacitance (Q_1) and voltammetric charge (q) as a function of at% Ru; Bottom: i_0 and Tafel slope as a function of at% Ru [64]. (With permission from NRC Research Press.)

and



However, the unexpected observation [50,67] of a reaction order of -1 with respect to H^+ led to the reaction scheme:



This scheme accounts for the reaction order of -1 , but it requires the rate of the chlorine evolution reaction to decrease with decreasing pH, which contradicts actual industrial observations [50] (Fig. 4.5.9). Thus, the mechanistic aspects of the chlorine evolution reaction are not yet unambiguously understood. (See refs. [49] and [50] for details related

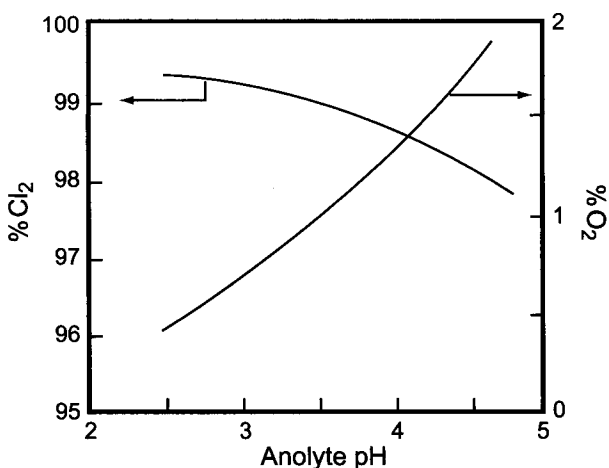


FIGURE 4.5.9. Variation of %Cl₂ and %O₂ at RuO₂ + TiO₂ anodes with anolyte pH in an industrial cell at 0.232 A cm⁻² [50]. (With permission from Elsevier.)

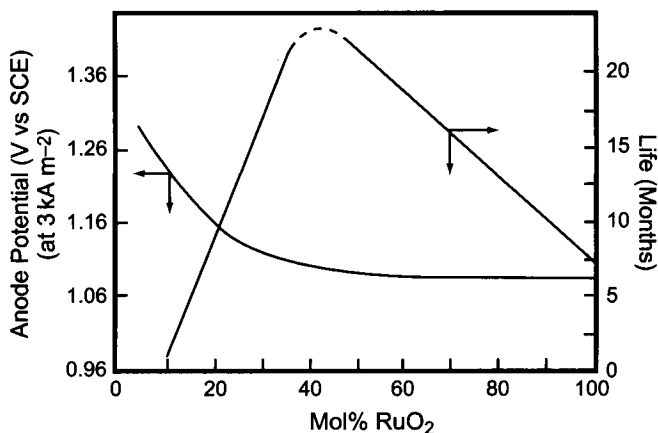


FIGURE 4.5.10. Variation of the anode potential and the operating anode life with mol% RuO₂ in the anode coating (plotted from the data in ref. [68]). Operating life was determined by tests in 300 gpl NaCl at 3 kA m⁻² (pH = 2.0–2.5; temperature = 80°C) with coatings containing 5 gms of Ru per m².

to the mechanisms proposed for the chlorine evolution reaction on RuO₂ and RuO₂-based coatings.)

Basic kinetic electrochemical studies show that RuO₂ + TiO₂ electrodes containing more than 25% RuO₂ exhibit low Tafel slope and high exchange current density for the chlorine evolution reaction. However, the performance of these electrodes depends on the method of preparation as well as the RuO₂ content and the Ru metal loading in the coatings. The chlorine overvoltage increases when the mole% Ru decreases below 20 or the Ru loading is less than 4 g m⁻² for a 40 mol% Ru electrode [68]. This results in a shorter anode life, as shown in Figs. 4.5.10 and 4.5.11.

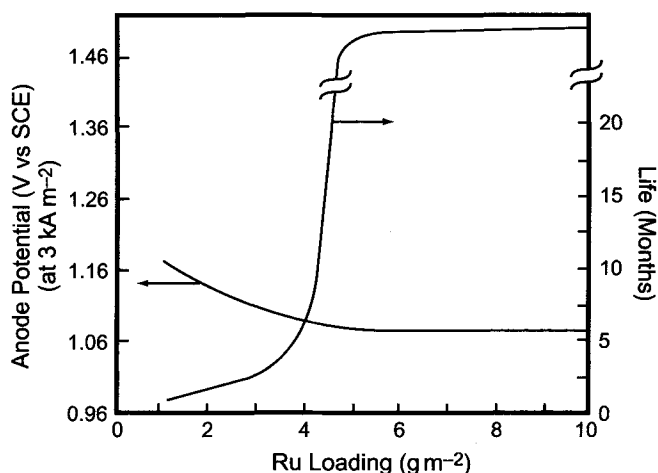


FIGURE 4.5.11. Variation of the anode potential and the operating anode life with 40 mol% Ru electrode as a function of Ru loading (plotted from the data in ref. [68]). Operating life was determined in 300 gpl NaCl at 3 kA m⁻² (pH = 2.0–2.5; temperature = 80°C). The break in the life curve indicates a rapid increase in life beyond a loading of 4 g m⁻².

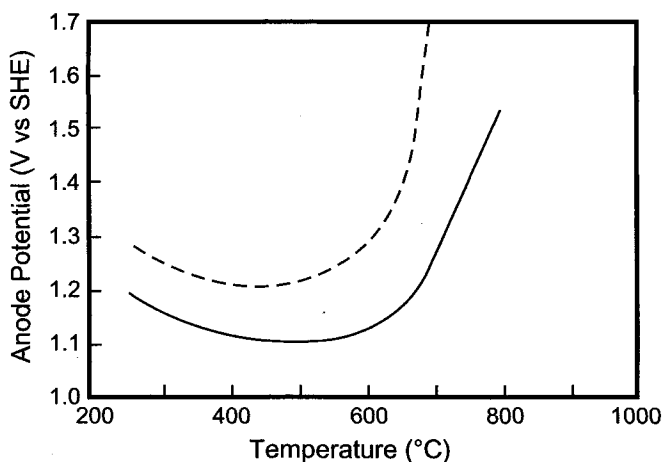


FIGURE 4.5.12. Variation of the anode potential at 3.0 kA m⁻² with the baking temperature. Solid line: 40 mol% RuO₂ electrode in 300 gpl NaCl (pH = 2.0–2.5) at 80°C [68]; dashed line: 33 mol% RuO₂ electrode at a loading of 2 g m⁻² in saturated brine at pH = 0.9 at 40°C [27].

Furthermore, the thermal decomposition temperature dictates [27,68] the magnitude of the chlorine overpotential, η_{Cl_2} , the minimal η_{Cl_2} being achieved by baking at 400–500°C over a 1 hr duration (Fig. 4.5.12). Overtreating irreversibly produces high overvoltage. It should be emphasized that the high η_{Cl_2} values, resulting from less than 20 mol% Ru in the coating are a direct result of the lowered conductivity of the coating (Fig. 4.5.3). The effects of the lower mol% Ru, Ru loading, and improper baking

conditions are revealed in the service life, and not in the initial η_{Cl_2} values (Figs. 4.5.10 and 4.5.11). Thus, for a long service life, the optimal ruthenium content is more than 25 mol% in the coating at a Ru loading of more than 2 g m^{-2} .

4.5.6. Cell Performance Characteristics with $\text{RuO}_2 + \text{TiO}_2$ -Based Anodes

Anode performance depends on the brine quality and the operating parameters such as pH, current density, NaCl concentration, and NaOH concentration (in diaphragm and membrane cells). The contribution of the anode to the cell inefficiency, as mentioned in Section 4.4, is directly related to the losses arising from the oxygen evolution reaction, and indirectly by chlorate formation. Thus, as the % O_2 increases, the pH at the anode–solution interface decreases, and hence, the amount of chlorate formed will decrease as the bulk pH is lowered. The amount of O_2 generated at the anode is a function of the current density, pH, the composition and surface area of the anode coating, and the salt concentration.

pH: The anode efficiency is high at low anolyte pH values because of low chlorate and oxygen levels. The diaphragm cell efficiency increases from about 88% to 98% when the pH is lowered from 4.8 to 3.35. DSA[®] manufacturers recommend a maximum pH of 12 and minimum pH of 2 for the anodes because of potential dissolution of the coating at high pH values and Ti dissolution at low pH values.

Current Density. The current efficiency increases with increasing current density for the reasons discussed in Section 4.4. Thus, at 95°C and a caustic strength of 150 g L^{-1} NaOH, diaphragm cell efficiency is about 91% at 1.55 kA m^{-2} and 94–95% at 2.32 kA m^{-2} .

Brine Concentration. With diaphragm cells, the anode efficiency decreases with decreasing NaCl concentration—the optimal feed brine concentration being 315 g L^{-1} and the minimal brine strength being 285 g L^{-1} . The efficiency decreases as the salt strength goes below 285 g L^{-1} , which is a direct result of increased oxygen evolution.

With membrane cells, the feed brine concentration is usually about 300 g L^{-1} , and the recommended minimum salt concentration in the depleted brine is 170 g L^{-1} .

NaOH Concentration. The anodic cell efficiency decreases with increasing NaOH strength in diaphragm cells and with increased back-migration of OH^- in membrane cells.

Temperature. Temperature affects the cell voltage and not the cell efficiency. The optimal anolyte temperature at 2.52 kA m^{-2} in diaphragm cells is about 96°C .

4.5.7. Anode Failure Mechanisms

The DSAs used for chlorine generation are titanium substrates (Grade 1 or 2) [69] coated with $\text{RuO}_2 + \text{TiO}_2$ mixtures containing at least 25% RuO_2 . SnO_2 and IrO_2 are sometimes added to these coatings for use in diaphragm cells and membrane

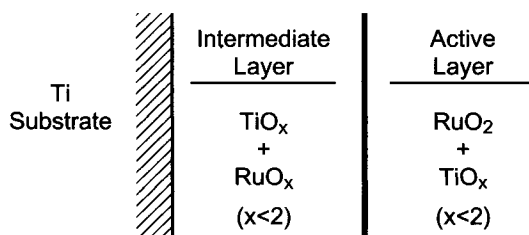


FIGURE 4.5.13. Schematic of the cross-section of $\text{RuO}_2 + \text{TiO}_2$ coatings on Ti.

cells, respectively. The coatings are generally prepared by thermal decomposition of RuCl_3 /butyl titanate/butanol mixtures at $400\text{--}450^\circ\text{C}$. The coatings are $10\text{--}15\ \mu\text{m}$ thick, with a roughness factor (real area/geometric area) of $200\text{--}300$ depending on the conditions of thermal decomposition. The Ru loading in these anodes varies from 4 to $5\ \text{g m}^{-2}$ in diaphragm cells and from $10\text{--}15\ \text{g m}^{-2}$ in membrane and mercury cells.

The anode potential of new or re-coated anodes, with respect to the SCE, is generally $1.06\text{--}1.08\ \text{V}$ at $3\text{--}4\ \text{kA m}^{-2}$, corresponding to a η_{Cl_2} of $95\text{--}115\ \text{mV}$. When the anode potential increases by $200\text{--}300\ \text{mV}$, the anode is regarded as electrocatalytically inactive. The anode potential increases with time in operating electrolytic cells. However, if it happens during the initial stages, it can be a consequence of poor anode manufacturing techniques. Figure 4.5.13 is a schematic of the cross-section of an anode coated with the electrocatalytic composition.

Inadequate surface preparation of titanium before coating can result in surface oxides of Ti with the “O” content approaching two. Also, if the anode potential is high, the oxide films on the Ti can break down, leading to the anodic dissolution of Ti. It is essential to ensure that the intermediate layer containing mixed oxides of Ti and Ru is conductive. This can be done by proper thermal treatment of the coating. Otherwise, the anode potential will be high from the start.

The η_{Cl_2} and the life of the anode as judged from accelerated tests (at $30\ \text{kA m}^{-2}$ in $30\ \text{gpl NaCl}$ solution), are functions of the mol% RuO_2 [68] and the grams of Ru per square meter [68] in the coating (Figs. 4.5.10 and 4.5.11). Below $20\ \text{mol}\%$ RuO_2 , the anode potential increases and the life decreases. When the mol% RuO_2 approaches 100 , the anode is, again, unstable even though its potential is unaffected. Similarly, the Ru loadings of less than $2\ \text{g m}^{-2}$ reduce the anode life when compared with coatings containing greater than $4\text{--}5\ \text{g m}^{-2}$ of Ru. Note that the loading required for long life varies with mol% RuO_2 , the presence of other dopants (e.g., SnO_2), and the application and firing temperatures used in the preparation of these mixed oxide coatings.

The increase in anode potential as the ruthenium content decreases (at constant loading) is a consequence of two factors:

1. As the mol% RuO_2 decreases, the conductivity of the mixed oxide decreases (Fig. 4.5.3). The reason for this transition in conduction from that of metal to that of an insulator is associated with changes in physical properties and in the nature of the chemical bonding [33].

2. As the mol% RuO₂ decreases, the mechanism of the chlorine evolution (Fig. 4.5.7) changes from one involving adsorbed intermediates to a slow electron transfer step, presumably because of the limited number of electrocatalytic sites available for the reaction. Note that if adsorbed intermediates participate, the Tafel slope is 30–40 mV, and when the charge transfer step is slow, the Tafel slope is 120 mV [70].

Since the Tafel slope increases as the mol% RuO₂ decreases (Fig. 4.5.7), the %O₂ generated will also increase with decreasing mol% RuO₂, as schematically illustrated in Fig. 4.5.14. Observation of high %O₂ in real situations will happen only when all the anodes, connected in parallel in a monopolar cell, exhibit Tafel slopes of greater than 120 mV. If only part of the anode is deactivated due to either low mol% RuO₂ or surface blockage, the rest of the active surface will operate at a high current density leading to low %O₂.

The increase in anode potential with decreasing RuO₂ loading (at constant at% Ru in the coating) is a result of a change in the mechanism of the chlorine evolution reaction.

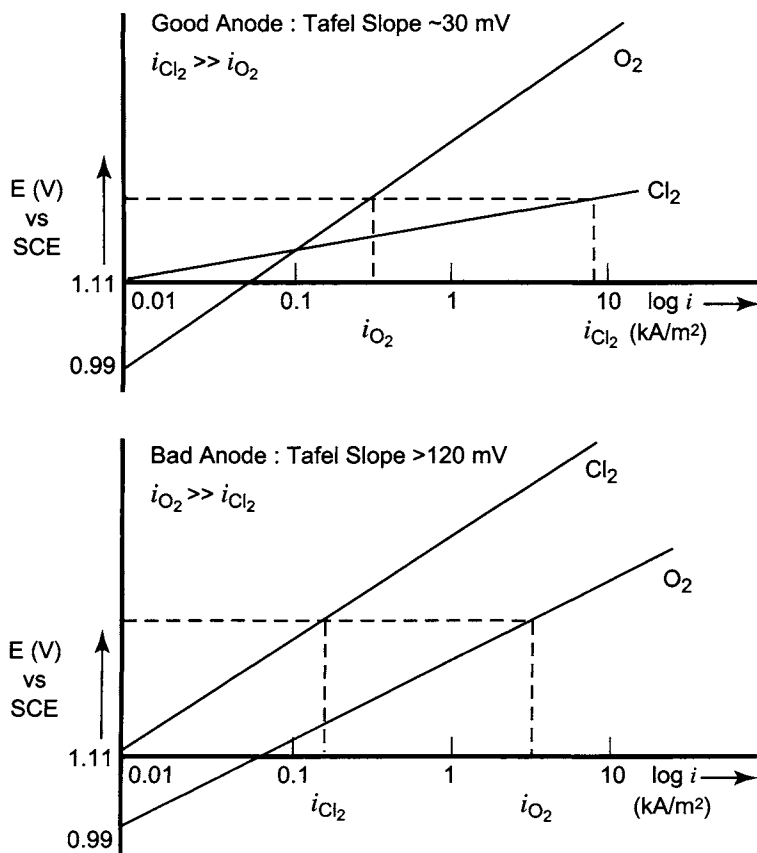
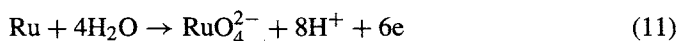


FIGURE 4.5.14. Schematic explaining high %O₂ in chlorine with deactivated anodes.

The reduction in the anode life with low initial RuO₂ loading coating arises from the lack of compactness of the coating in the thin layers, as a result of which the Ti substrate will develop a TiO₂ layer, contributing to the escalating anode potential.

Chlorine overpotential also may increase as a result of the contamination of the active surface by impurities such as MnO₂, SiO₂, BaSO₄, Fe₂O₃, etc. These contaminants can increase the anode potential by blocking the active surface or, in the case of Fe₂O₃, by interaction with RuO₂ and TiO₂, leading to the surface enrichment of TiO₂ as follows:



Surface blockage is a result of deposition of insoluble species or adsorption of organic compounds. Impurities adversely affecting the anodes are noted in Table 4.5.4.

Note that if the reason for the high anode potential is simple blockage, chemical or physical cleaning should rejuvenate the deactivated anode. When the Tafel slope is greater than 120 mV on these anodes that are completely covered with impurities, O₂ evolution can take over the chlorine evolution reaction resulting in high %O₂.

The deleterious effects arising from the surface deposits can be offset to some extent by judiciously cleaning with appropriate media such as HCl for Fe deposits and NaOH for "SiO₂" deposits. However, when the loading decreases to <2 g m⁻² or when the mol% RuO₂ in the coating, especially in the top surface layers, drops below 20%, the anode requires recoating, preceded by stripping the old coating, in order to optimize the anode potentials and performance.

4.5.7.1. Reasons for Lowered RuO₂ Loading and Mol% RuO₂. Erosion by the gases evolving at an anode can progressively strip the active layers of the coating and so reduce

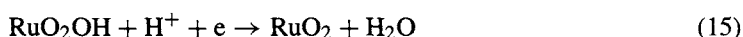
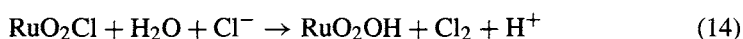
TABLE 4.5.4 Effect of Impurities in Brine on Anodes [71,72]

Impurity	Maximum allowed concentration (ppm)	Effect at greater concentrations
Ba	0.4	BaSO ₄ deposition
Mn	0.01	MnO ₂ deposition
Co	0.02	Co-oxide formation
Sr, Si	0.03	Anode blinding via the formation of SrSO ₄ and SiO ₂ deposits
Hg	0.04	Formation of calomel
Ti hydrides		Formation of TiO ₂
Fe		Formation of Fe oxides
TOC	5-10	Anode deactivation
F ⁻	1	Attacks Ti to form soluble Ti-fluorides

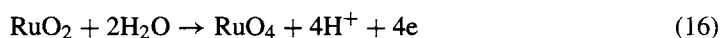
the loading. At the same time, chlorine evolution, shutdowns, and oxygen generation can cause RuO_2 to dissolve selectively. This will change the composition of the surface layers.

Decreased mol% RuO_2 in the surface layers[†] of the coating is a direct result of RuO_2 dissolution during: (1) chlorine evolution, (2) shutdowns, and (3) oxygen generation.

It should be emphasized that thermodynamically [73,74], RuO_2 can oxidize to RuO_4^- or RuO_4^{2-} (in alkaline solutions). RuO_2 can be leached from the anode during the course of the chlorine evolution reaction via the loss of the unstable adsorbed intermediates or the oxidized surface oxides formed during the discharge of the chloride ions as described by the reaction schemes (13)–(15).



or



Ruthenium losses arising from the erosion and the dissolution of the adsorbed intermediates formed during the course of the chlorine evolution reaction, and the surface oxides [75], are depicted in Fig. 4.5.15. These results [76] show the dissolution rate (V_c in $\text{g cm}^{-2} \text{hr}^{-1}$) of Ru to be high initially and decrease rapidly with time (t in hr). Thus,

$$V_c = 2.5 \times 10^{-6} t^{-1.2} \quad (18)$$

RuO_2 also dissolves during shutdowns [77], as shown in Fig. 4.5.16. The reasons for the enhanced RuO_2 losses during this process are not clearly addressed in the literature. One contribution to these RuO_2 losses can be the reverse currents arising from the cathodic reduction of sodium hypochlorite in the anolyte, which make the anode cathodic and reduce the RuO_2 to Ru or some lower oxide (e.g., RuO_x where $x < 2$), that is oxidized during electrolysis to a soluble Ru species such as H_2RuO_3 or H_2RuO_5 or RuO_4^{2-} . Alternately, the surface oxidation state of RuO_2 can be modified during the current interruptions to an unstable intermediate, leading to its dissolution in the anolyte. The reaction schemes leading to Ru dissolution closely follow Eqs. (11) and (17). The enhanced Ru losses with current interruptions are a consequence of the changes in the composition of the surface oxide following each cathodic pulse (because of reverse currents) and anodic pulse (after electrolysis is resumed) that dissolves at a faster rate than the original oxide that is thermally formed.

Depletion of RuO_2 can also result from oxygen generation. It was shown [78] that the concentration of Ru sites on the surface of the anode, as reflected in the overall

[†]Surface enrichment of TiO_2 was noted [78] from ESCA studies.

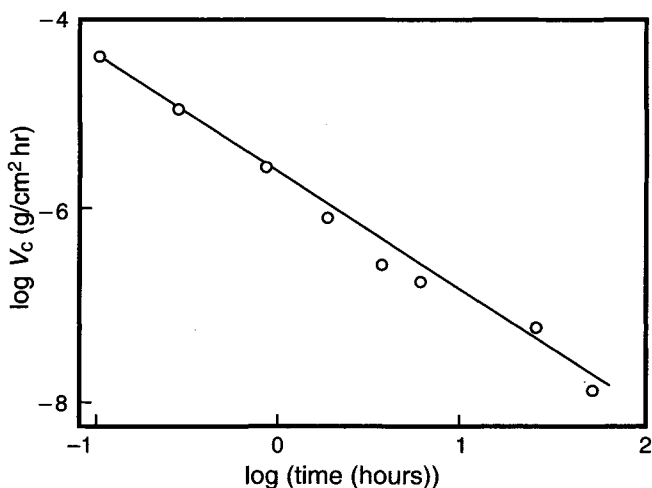


FIGURE 4.5.15. Ruthenium losses arising from erosion and general dissolution with 30% RuO₂ + 70% TiO₂ electrode at 2 kA m⁻² in 300 gpl NaCl at 70°C (plotted from the data in ref. [75]).

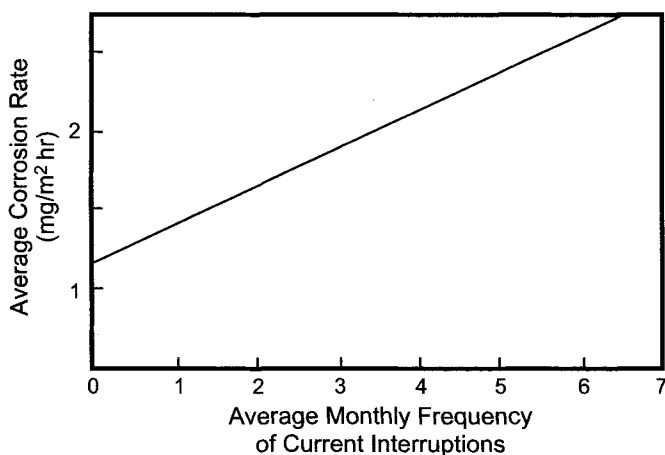


FIGURE 4.5.16. Dependence of corrosion rate RuO₂ + TiO₂ anode on the frequency of shutdowns [77].

capacitance[‡] of the system, first increased and then decreased as the anode potential increased to unacceptable values (Fig. 4.5.17). The initial increase of RuO₂ sites is a consequence of the opening of pores on the surface, and the final decrease is a result of the depletion of Ru sites. When pores develop on the surface, electrolysis of NaCl continues in the pores and, at some stage, when all the chloride ions are depleted, O₂ evolution takes over in the pore. It has been shown [60] that oxygen evolution from a

[‡]The capacitance of the oxide/solution interface reflects the electrical characteristics of the system [62,79].

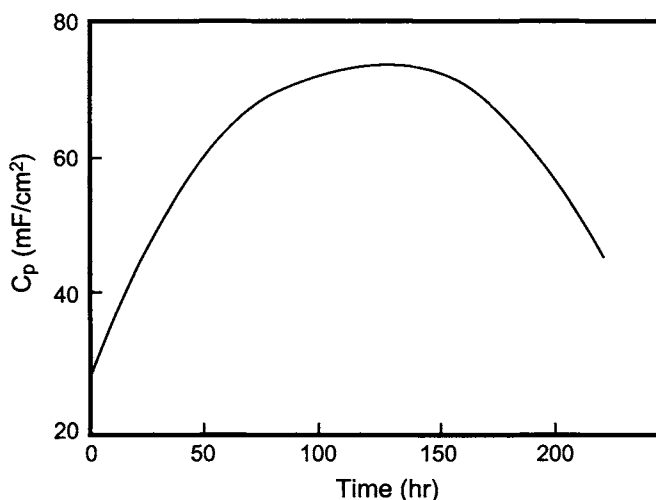
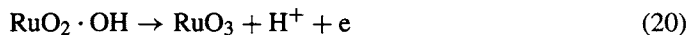
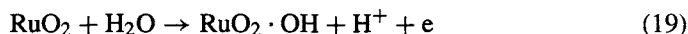


FIGURE 4.5.17. Time dependence of the pseudocapacitance, C_p , reflecting anode failure [78]. (Reproduced with permission of The Society of Chemical Industry.)

RuO₂ surface involves the RuO₂ · OH and RuO₃ species as:



RuO₂ losses can occur via the dissolution of the intermediates in the above reactions. However, the published corrosion data for Ru from O₂ evolution are not reliable as the data forecast Ru losses as high as 40 g m⁻² hr⁻¹ [80], which are inconsistent with the observations in diaphragm chlor-alkali cell operations.

The %O₂ from the anode generally:

1. increases with increasing %RuO₂ in the coating, increasing surface area of the coating, decreasing current density, and increasing pH (but is insensitive to pH values below 2), and
2. decreases with increasing Cl⁻ ion concentration (the recommended level: 280–315 g L⁻¹) and with the addition of dopants such as SnO₂ and HfO₂ to the coating [21,81].

It is easy to comprehend the anode potential escalation arising from the impurities and loss of Ru loadings to <2 g m⁻². However, the anode deactivation observed when the Ru loadings are >2 g m⁻² is difficult to rationalize.

The mechanisms involved in the deactivation of RuO₂/TiO₂-based anodes during the course of the chlorine and oxygen evolution reactions have been the subject of several recent reviews [18,72,82,83], and various publications [39,68,76–78,84–101]. It is unequivocally agreed that, during electrolysis, some RuO₂ does dissolve

electrochemically (although the magnitude of the rate of dissolution is not known with certainty), and that some of it is also lost by erosion [84,86]. The corrosion rate of RuO_2 is minimal, around pH 1–2 [91,94], and increases below a pH of ~ 0.2 (forming RuOHCl_5^{2-}) [91] and above a pH of ~ 4 (forming RuO_4^{2-} and gaseous RuO_4 [76,87,96,102]). The RuO_2 dissolution rate increases with increasing current density [76,88], increasing $\% \text{O}_2$ generation [85,95,96], decreasing NaCl concentration [90,97,98], and an increasing number of shutdowns of operating cells [76,77]. TiO_2 dissolution is believed to be chemical [93], resulting in the formation of TiO^{2+} .

While it is accepted that RuO_2 coatings dissolve during operation in both NaCl and H_2SO_4 solutions, the relationship between this loss and the mechanism of deactivation of $\text{RuO}_2/\text{TiO}_2$ anodes is still not very clear. Some studies [39,78,88,91,100,103–105] attribute the deactivation solely to the surface depletion of RuO_2 , resulting in the development of a high resistivity $\text{RuO}_2 + \text{TiO}_2$ composition when the Ru content is $< 20\%$.

Others [87–89,101] consider the buildup of a TiO_2 layer at the TiO_2 -coating interface to be the cause of the anode failure. The porous nature of the coatings will contribute to the rate of TiO_2 growth, as will the dissolution of the active coating with time. This failure mode is consistent with that for other coatings on titanium, especially iridium oxide-based coatings, where surface depletion is not a significant factor [101,106]. For $\text{RuO}_2/\text{TiO}_2$ coatings, the actual failure mode may be a combination of the two phenomena: Ru loss and growth of a TiO_2 layer.

4.5.7.2. Strategies to Prevent the Loss of Ru. As shown above, the lowered proportion of RuO_2 in the outer region of the coating causes the anode potential to reach unacceptable values. The decreasing Ru levels on the surface are a consequence of shutdowns, loss of Ru-based adsorbed intermediates involved in the chlorine and oxygen evolution reactions, erosion, and the blockage of the active anode surface by the impurities in the solution. The last, which causes localized high current densities, can be minimized by using high quality brine, devoid of impurities such as SiO_2 or SiO_3^{2-} , Mn^{2+} , Ba^{2+} , and Fe^{2+} or Fe^{3+} . The Ru losses, arising from erosion by the chlorine gas generated at the anode, can be lowered by operating at a low current density, or by designing the anodes to reduce the gas velocities. However, the reduction in current density is not a practical option, as the present trend is to operate the cells at the highest current density as the system permits. The loss of Ru during shutdowns can be substantially reduced by minimizing the number of shutdowns, or by negating their effect by cathodic protection or by rapid removal of hypochlorite from the cells. This would preserve the surface compositional integrity of the anode coating. In addition, operating the cells at pH 2–3 would also be beneficial in two ways. First, electrolysis at a low pH would dissolve TiO_2 , resulting in minimal changes in the surface composition of the coating. Second, in the low pH region, less oxygen would evolve at the anode and less ruthenium would be lost through the oxygen evolution reaction.

Another option to lower the Ru losses is to dope the anode coatings with IrO_2 , which has been shown to markedly decrease the Ru corrosion rate during electrolysis in NaCl solutions. This would minimize the surface depletion of Ru and thus extend the operating life of the anodes. The Ru : Ir ratio in the coating is 1 : 1 on either a weight or mole basis.

4.5.7.3. Rejuvenation of Deactivated RuO₂ Anodes. If the Ru loss in the deactivated anode is a result of a uniform dissolution across the entire coating layer, resulting in a Ru loading of less than 2 g m⁻², the anode must be recoated to regain its electrocatalytic activity. Under these conditions, the remaining coating must be stripped off before recoating. However, if surface depletion of Ru is the cause for the increased anode potential, then replenishment of these surface sites should result in the rejuvenation of the deactivated anodes.

Recent studies performed with deactivated anodes [100,103] show that electroless or electrolytic platinum deposition on failed anodes not only lowered the polarization behavior of these anodes, but also demonstrated lifetimes equal to those of new anodes in accelerated life tests in sulfuric acid solutions [100]. These results demonstrated that the deactivation of anodes whose Ru loading was still high was a direct consequence of the depletion of Ru from the outer region of the coating. Note that this process of surface enrichment by conducting electroactive species will not reactivate a failed anode if there is a TiO₂ buildup at the Ti substrate-coating interface.

4.5.8. Anode Structures

In the 1960s, the technology of choice to produce chlorine was the mercury cell, in part because of its ability to operate at high current densities. Therefore, DSAs first operated commercially in mercury cells, where rapid gas release was very important. The anode designs [107] used in mercury cells to accomplish the quick release of chlorine, so that the anode-cathode gap could be lowered and the NaCl strength in this space maintained at high levels, are shown in Fig. 4.5.18. Baffles on the back of the active anode surface are claimed [108] to provide sufficient gas lift to force the brine into the space between the anode and cathode.

Figure 4.5.19 depicts the schematics of the mercury cell anodes with an expanded titanium mesh [109]. Other types of mercury cell anodes use small diameter titanium rods or thin titanium blades. Electrical connection in the cell is made through the boss using solid copper rods protected with a riser tube of titanium. A typical arrangement of anodes in a mercury cell is shown in Fig. 4.5.20.

The two basic anode designs used [69,108,109] in diaphragm cells are box anodes and expandable anodes. Figure 4.5.21 illustrates the box anode, which was designed as a direct replacement for graphite anodes. The active surface is the coated expanded titanium mesh and a copper-cased titanium conductor bar which carries current. The expandable anode, presented in Fig. 4.5.22, contains clips that hold the anodes prior to cell assembly to ensure that the asbestos diaphragm is not damaged. After positioning the cathode and placing the 3 mm diameter spacers over the cathode, the clips are removed from the anode. The spring-activated anode surfaces then close in, providing a uniform and narrow anode-cathode gap.

Membrane-cell anodes are coated expanded titanium mesh type or louvered type [110], and the anode is generally in contact with the membrane. The anode surface has to be absolutely smooth to ensure that no pinholes are created in the membranes [69]. It is claimed that punched steel metal is superior to a flattened expanded metal as the anode substrate [111].

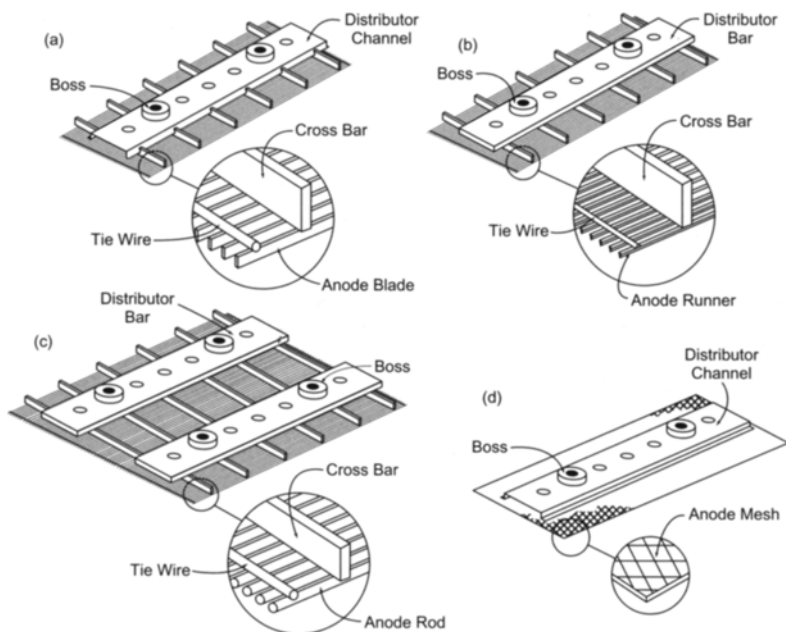


FIGURE 4.5.18. Configurations of mercury cell anodes: (a) blade type; (b) runner type; (c) rod type; (d) mesh type [106]. (Reprinted by permission of John Wiley & Sons, Inc.)

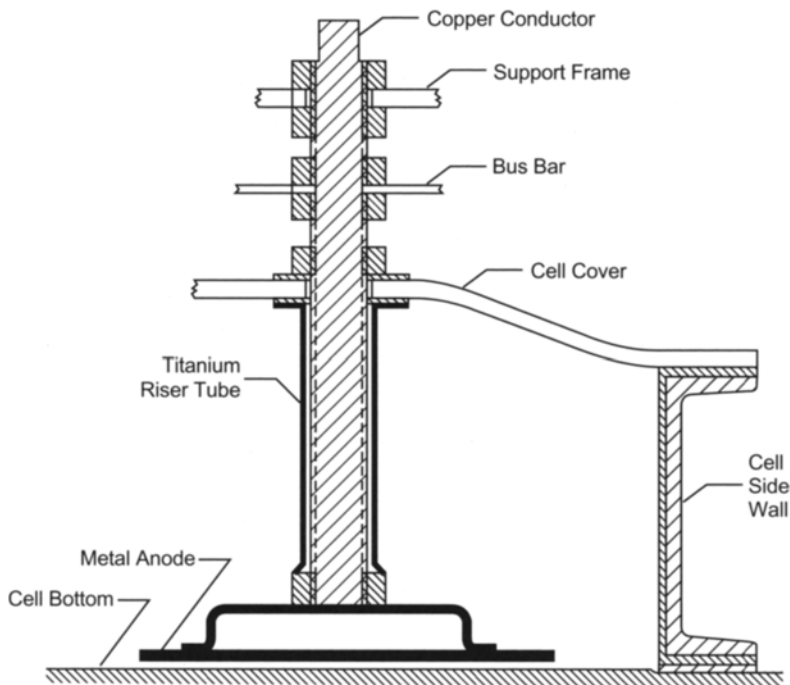


FIGURE 4.5.19. Method for making electrical connections to a metal anode in mercury cells [106]. (Reprinted by permission of John Wiley & Sons, Inc.)

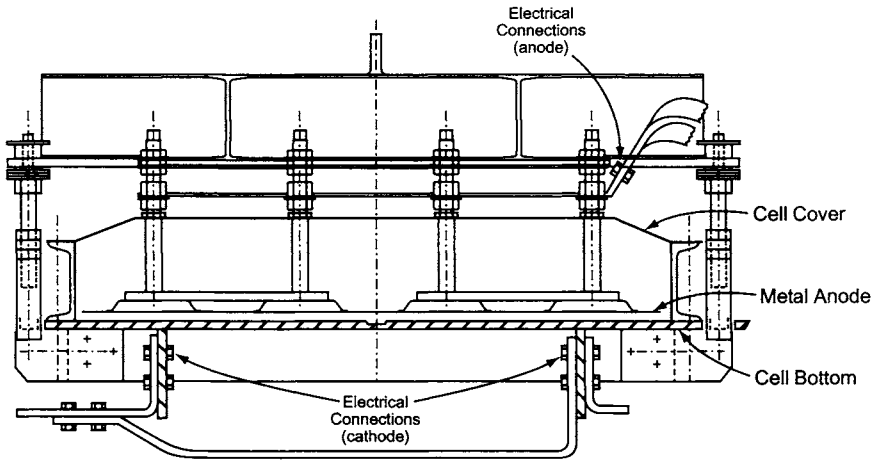


FIGURE 4.5.20. End view of a mercury cell showing typical arrangement of metal anodes [106]. (Reprinted with permission of John Wiley & Sons, Inc.)

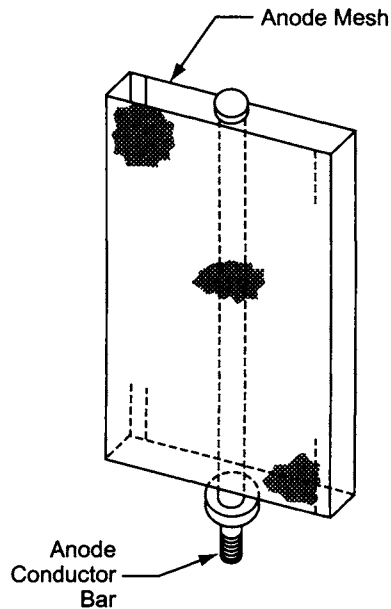


FIGURE 4.5.21. Typical diaphragm cell box anode [71]. (Reprinted with permission of John Wiley & Sons, Inc.)

The lifetimes [69] of RuO_2 -based anodes under normal operating conditions are shown in Table 4.5.5.

4.5.9. Anode Costs and Manufacturers

The cost of an anode is a function of the anode configuration and the coating technology and coating composition. It can easily be calculated from the labor and chemical costs

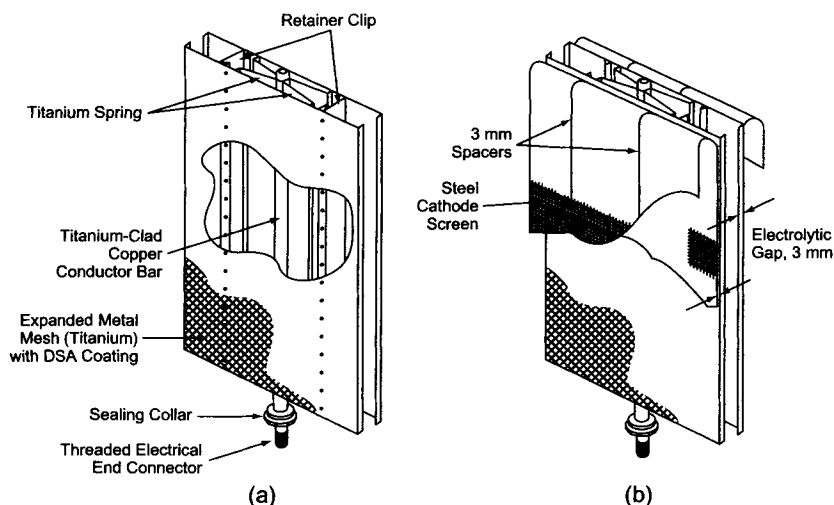


FIGURE 4.5.22. Expandable anode for diaphragm cells: (a) clamped; (b) expanded [106,108]. (Reprinted with permission of John Wiley & Sons, Inc.)

TABLE 4.5.5 Average Lifetimes of RuO₂-Based Anodes

Cell type	Average current density (kA m ⁻²)	Coating composition	Ru loading (g m ⁻²)	Typical life (years)
Mercury Diaphragm	10	RuO ₂ + TiO ₂	10–15	1.5–2.5 (or 180 tons Cl ₂ /m ²)
Diaphragm	2	RuO ₂ + TiO ₂ + SnO ₂	4–7 (mole ratio: 3Ru : 2Sn : 1Ti)	10 (or >200 tons Cl ₂ /m ²)
Membrane	4	RuO ₂ + TiO ₂ + IrO ₂	4–5 (Ru : Ir = equimolar or equal weight)	7 (expected) (or 300 tons Cl ₂ /m ²)

involved in the application of the coatings. Generally, they lie in the range of 30–40 times the cost of the noble metal used in the coating by the thermal decomposition techniques, or \$75–100 g⁻¹ of noble metal [112]. The variability in the multiplication factor arises from the nature of the anode base, the extent of repair, labor cost, and the ease with which the coating can be applied.

Figure 4.5.23 shows a typical anode coating process [107]. Appendix 4.5.1 describes the individual steps.

Anode coating suppliers include Chemapol Industries (India), ELTECH (US), Electrode Products Inc. (US), DeNora (US), Huron (Canada), Permelec (Japan), INEOS (UK), Magneto-Chemie (Holland), Permelec (Italy), Team (India), Titan (India), and many others.

Several RuO₂-based compositions are available for use in the chlor-alkali service. The anodes marketed [113] by ELTECH Systems Corporation are shown in Table 4.5.6.

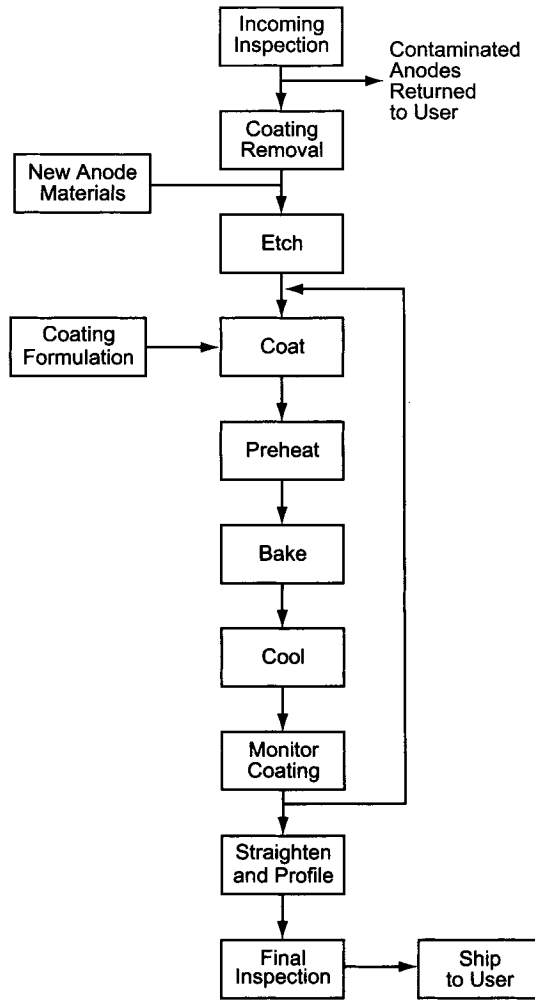


FIGURE 4.5.23. Metal anode coating process [108]. (Reprinted with permission of John Wiley & Sons, Inc.)

TABLE 4.5.6 ELTECH's Anodes for Chlor-Alkali Service

Designation	Primary components	Applications
EC 100	Ru, Ti	Mercury
EC 107	Ru, Ti	Diaphragm
EC 150	Ru, Ti	Membrane
EC 200	Ru, Ti, Sn	Diaphragm
EC 300	Ru, Ti, Ir	Membrane
EC 301	Ru, Ti, Ir	Mercury
800 Series	Proprietary	Customer specified formulations

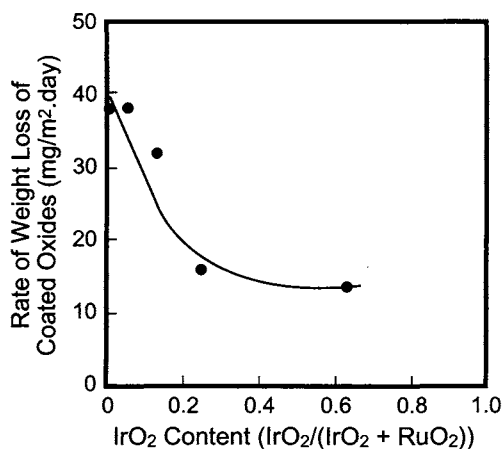


FIGURE 4.5.24. Weight loss of anode coatings with varying IrO₂ content. Anode: 50 mol% TiO₂ at 10 g m⁻² prepared at a firing temperature of 400°C; Electrolysis conditions: 210 gpl NaCl at 90°C, pH = 3.0; current density: 20 kA m⁻² [121]. (With permission from The Electrochemical Society of Japan.)

4.5.10. Alternate Anode Compositions

Several anode coatings not mentioned in Table 4.5.6 have been examined for use in chlor-alkali cells. The interesting compositions are Pt–Ir on titanium [114,115], cobalt spinels [116–118], PdO-based coatings [111], and platinates [119,120].

To the knowledge of the authors, these coatings have found only limited application. A promising composition that has made inroads in membrane cell applications is Ru–Ti–Ir, as the incorporation of iridium oxide reduces corrosion during operation (Fig. 4.5.24) and shutdowns [121,122].

APPENDIX 4.5.1: RuO₂ + TiO₂ COATINGS ON TITANIUM

Substrate preparation

1. Solvent cleaning
 - (a) Acetone soak and dry
 - (b) Methylene chloride soak and dry
2. Surface etching
 - (a) Hydrochloric acid and oxalic acid etch solution
18% HCl + 10% by weight H₂C₂O₄
 - (b) Etch procedure
 - (i) Heat solution to 95°C with stirring
 - (ii) Soak titanium substrate in hot solution for 15–30 min (ensure that the etch is uniform and the surface has dull gray matte finish)
 - (iii) Repeat Step (ii) if necessary
 - (iv) Rinse with distilled water or ultrapure water
 - (v) Rinse and store in methanol.

Coatings application and conversion

1. Coating application

(a) Coating techniques:

Brushing, spraying, dipping

(b) Solution composition (this solution should not be exposed to moisture)

(i) Ruthenium chloride (RuCl_3), 18.2 g(ii) Tetrabutyl titanate ($\text{Ti}[\text{O}(\text{CH}_2)_3\text{CH}_3]_4$), 45 cc

(iii) Hydrochloric acid (HCl—37%), 6 cc

(iv) Butyl alcohol ($\text{CH}_3(\text{CH}_2)_3\text{OH}$), 93 cc

2. Thermal conversion

(a) Heat in air to $\sim 100^\circ\text{C}$ at $5\text{--}10^\circ\text{C min}^{-1}$. Maintain at 100°C for ~ 15 min.(b) Heat further to $435\text{--}450^\circ\text{C}$ in air at $\sim 10^\circ\text{C min}^{-1}$, hold for 30 min.

(c) Remove and cool to room temperature

(d) Depending on the coating thickness desired, repeat the coating procedure 10–15 times to achieve the desired loading of about 10 g m^{-2} of Ru.

REFERENCES

1. V. Englehardt, *Handbuch der Technischen Electrochemie*, Vol. 2, (1), Leipzig Academische Verlagsgesellschaft (1993).
2. J. Billiter, *Die Technische Elektrolyse der Nichtmetalle*, Springer-Verlag, Wien (1954), p. 358.
3. F. Jeitner, *Chem. Ing. Tech.* **34**, 353 (1962).
4. A.T. Kuhn, *Industrial Electrochemical Processes*, Elsevier Publishing Co., New York (1971).
5. S. Puschaver, *Chem. Ind.* **15**, 236.
6. R.H. Stevens, *U.S. Patent* 1,077,894 (1913).
7. J.B. Cotton, E.C. Williams, and A.H. Barber, *British Patent* 877,901 (1961).
8. H.B. Beer, *Neth. Pat. Appl.* 216,199 (1957); 3,236,756 (1966).
9. O. DeNora, *Chem. Ing. Tech.* **42**, 222 (1970); **43**, 182 (1971).
10. K.J. O'Leary, *U.S. Patent* 3,776,834 (1973).
11. H.B. Beer, *U.S. Patent* 3,573,100 (1971).
12. V. DeNora, L. Meyer, and A. Barbato, *U.S. Patent* 3,684,543 (1972).
13. *U.S. Patents* 3,706,600 and 3,706,644; *French Patents* 2,075,006 and 2,096,044; *Belgian Patent* 781,798; and *German Patent* 2,008,335.
14. F.I.L. Vovich and V.V. Avksent'yev, *Abroad* **69–71**, 469–551 (1973).
15. Yen-chin Yin, Reports No. 61, 61A, 61B, *Process Economics Program*, SRI International, Menlo Park, CA (1978).
16. H.V.K. Udupa, R. Thangappan, B.R. Yadav, and P. Subbiah, *Chem. Age. India*, **23**, 545 (1975).
17. J.A.M. LeDuc, *International Electrochemistry Institute*, Milburn, NJ, **3** (1976); **6** (1977).
18. E.N. Balko, *Studies in Inorganic Chemistry* **11**, 267 (1991).
19. *Electrodes of Conductive Metallic Oxides*, Parts A and B, S. Trasatti (ed.), Elsevier Publishing Co., New York (1980).
20. D.M. Novak, B.V. Tilak, and B.E. Conway, Anodic Chlorine Production: Fundamental and Applied Aspects, In J.O'M. Bockris, B.E. Conway and R.E. White (eds), *Modern Aspects of Electrochemistry*, vol. 14, Plenum Publishing Corp., New York (1982), p. 249.
21. B.V. Tilak, K. Tari, and C.L. Hoover, *J. Electrochem. Soc.* **135**, 1386 (1988).
22. Yu.E. Roginskaya, B.Sh. Galyamov, V.M. Lebedev, I.D. Belova, and Yu.N. Venetsev, *Zh. Neorg. Khim.* **22**, 499 (1977).

23. V.M. Lebedev, Yu.E. Roginskaya, N.L. Klimasenko, V.I. Bystrov, and Yu.N. Venetsev, *Russ. J. Inorg. Chem.* **21**, 1380 (1976).
24. U.E. Roginskaya, V.I. Bystrov, and D.M. Shub, *Russ. J. Inorg. Chem.* **22**, 110 (1977).
25. K.J. O'Leary and T.J. Navin, Morphology of Dimensionally Stable Anodes, In *Chlorine Bicentennial Symposium*, T.C. Jeffrey, P.A. Dana and H.S. Holden (eds), The Electrochemical Society, Princeton, NJ (1974), p. 174.
26. J. Augustynski, L. Balsene, and J. Hinden, *J. Electrochem. Soc.* **125**, 1093 (1978).
27. F. Hine, M. Yasuda, and T. Yoshida, *J. Electrochem. Soc.* **124**, 500 (1977).
28. W.A. Gerrard and B.C.H. Steele, *J. Appl. Electrochem.* **8**, 417 (1978).
29. P.H. Duvigneaud and A. Coussment, *J. Solid State Chem.* **52**, 22 (1984).
30. E.K. Spasskaya, Yu.B. Makarychev, A.A. Yakovleva, and L.M. Yakimenko, *Electrokhimiya* **13**, 327 (1977).
31. C.E. Vallet, D.E. Heatherly, and C.W. White, *J. Electrochem. Soc.* **137**, 579 (1990).
32. C.E. Vallet, *J. Electrochem. Soc.* **138**, 1234 (1991).
33. P.P. Edwards, T.V. Ramakrishnan and C.N.R. Rao, *J. Phys. Chem.* **99**, 5228 (1995).
34. B.Sh. Galyamov, Yu.E. Roginskaya, R.M. Lazorenko-Manevich, K.B. Kozhevnikov, M.I. Yanovskaya, and Ya.M. Kolotyrim, *Mater. Chem. Phys.* **11**, 525 (1984).
35. N.C. Halder, *Electrocomp. Sci. Technol.* **11**, 21 (1983).
36. J.V. Biggers, J.R. McKelvey, and W.A. Schultze, *Commun. Am. Ceram. Soc.* **C13** (1982).
37. R. Kötz. Photoelectron Spectroscopy of Practical Electrode Materials, In H. Gerischer and C.W. Tobias (eds), *Advances in Electrochemical Science and Engineering* vol. 1, VCH Publishers, New York (1990), p. 75.
38. A. DeBattisti, G. Lodi, M. Cappadonia, G. Battaglin, and R. Kötz, *J. Electrochem. Soc.* **136**, 2596 (1989).
39. V.V. Gorodetskii, P.N. Zorin, M.M. Pecherskii, V.B. Busse-Machukas, V.L. Kubasov, and Yu.Ya. Tomashpolskii, *Soviet Electrochem.* **17**, 66 (1981).
40. C. Angelinetta, S. Trasatti, L.J.D. Atanasoska, Z.S. Minovski, and R.T. Atanasoski, *Mater. Chem. Phys.* **22**, 231 (1989).
41. C. Angelinetta, S. Trasatti, L.J.D. Atanasoska, and R.T. Atanasoski, *J. Electroanal. Chem.* **214**, 535 (1986).
42. R. Hutchings, K. Müller, R. Kötz and S. Stucki, *J. Mater. Sci.* **19**, 3987 (1984).
43. R. Kötz and S. Stucki, *Electrochim. Acta* **31**, 1311 (1986).
44. B.V. Tilak, Unpublished investigations.
45. T. Mussini and G. Fanta. Chlorine, In A.J. Bard (ed.), *Encyclopedia of Electrochemistry of Elements*, Chapter 1, Table 1.2.1, Marcel Dekker, New York (1973).
46. S. Trasatti and G. Lodi, Oxygen and Chlorine Evolution at Conductive Metallic Oxide Anodes, Chapter 10 in ref. 19, Part B.
47. S. Trasatti and W.E. O'Grady, Properties and Applications of RuO₂-Based Electrodes, In H. Gerischer and C.W. Tobias (Eds), *Advances in Electrochemistry and Electrochemical Engineering*, vol. 12 (1981), p. 177.
48. E.J.M. O'Sullivan and E.J. Calvo, *Comphr., Chem. Kinetics.* **27**, 247 (1987).
49. S. Trasatti, *Electrochim. Acta* **32**, 369 (1987).
50. B.E. Conway and B.V. Tilak, Behavior and Characterization of Kinetically Involved Chemisorbed Intermediates in Electrocatalysis of Gas Evolution Reactions, In D.D. Eley, H. Pines, and P.B. Weisz (eds), *Advances in Catalysis*, vol. 38, Academic Press, New York (1992).
51. J.G.D. Haenen, W. Visscher, and E. Barendrecht, *J. Appl. Electrochem.* **15**, 29 (1985).
52. G. Lodi, E. Sivieri, A. DeBattisti, and S. Trasatti, *J. Appl. Electrochem.* **8**, 135 (1978).
53. B.V. Tilak and C.P.-Chen, Unpublished investigations.
54. S. Trasatti and G. Buzzanca, *J. Electroanal. Chem.* **29**, App. 1 (1971).
55. W.E. O'Grady, C. Iwakura, J. Huang, and E. Yeager, Ruthenium Oxide Catalysis for the Oxygen Electrode, In *Electrocatalysis*, The Electrochemical Society Inc. Princeton, NJ (1974), p. 286.
56. I.R. Burrows, J.H. Entwisle, and J.A. Harrison, *J. Electroanal. Chem.* **27**, 21 (1977).
57. D. Galizziolo, F. Tantardini, and S. Trasatti, *J. Appl. Electrochem.* **4**, 57 (1974); **5**, 203 (1975).
58. S. Ardizzone, G. Fregnora, and S. Trasatti, *Electrochim. Acta* **35**, 263 (1990).
59. T. Arikado, C. Iwakura, and H. Tamura, *Electrochim. Acta* **22**, 513 (1977).
60. L.D. Burke, O.J. Murphy, J.F. O'Neill, and S. Venkatesan, *J. Chem., Soc., Faraday Trans 1.* **73**, 1659 (1977).

61. K. Döblhofer, M. Metikoš, Z. Ogumi, and H. Gerischer, *Ber. Bunsenges. Phys. Chem.* **82**, 1046 (1978).
62. B.E. Conway, *Electrochemical Supercapacitors*, Kluwer Academic/Plenum Publishers, New York (1999).
63. B.V. Tilak, V.I. Birss, and S.K. Rangarajan, Deactivation of Thermally Formed Ru/Ti oxide Electrodes: An a.c Impedance Characterization Study, In H.S. Burney, N. Furuya, F. Hine, and K-I. Ota (eds), *Chlor-Alkali and Chlorate Technology: R.B. MacMullin Symposium*, Proc. vol. 99-21, The Electrochemical Society Inc., Pennington, NJ (1999), p. 58.
64. B.V. Tilak, C.-P. Chen, V.I. Birss, and J. Wang, *Can J. Chem.* **75**, 1773 (1997).
65. R.G. Erenburg, L.I. Khristalik, and I.P. Yaroskevskaya, *Soviet Electrochem.* **11**, 989 (1975).
66. D.A. Denton, J.A. Harrison, and R.I. Knowles, *Electrochim. Acta* **24**, 521 (1979).
67. R.G. Erenburg, *Soviet Electrochem.* **20**, 1481 (1984).
68. M.D. Spasojevic, N.V. Krstajic, and M.M. Jaksic, *J. Res. Inst. Catalysis, Hokkaido Univ.* **31**, 77 (1984).
69. P. Schmittinger, L.C. Curlin, T. Asawa, S. Kotowski, H.B. Beer, A.M. Greenberg, E. Zelfel, and R. Breitstadt, Chlorine, In *Ullmann's Encyclopedia of Industrial Chemistry*, vol. A6 (1986), p. 399.
70. B.V. Tilak and C.-P. Chen, *J. Appl. Electrochem.* **23**, 631 (1993).
71. L.C. Curlin, T.V. Bommaraju, and C.B. Hansson, Chlorine and Sodium hydroxide in *Kirk-Othmer Encyclopedia of Chemical Technology*, 4th ed., Vol. 1, John Wiley & Sons, New York (1991), p. 938.
72. R.C. Carlson, The Effect of Brine Impurities on DSA[®] Electrodes, *Paper presented at the 7th Annual Chlorine/Chlorate Seminar*, Cleveland (1991).
73. M. Pourbaix, I. Van Molyder, and N. dezoubov, *Platinum Metals Review* #3. (1959); p. 100. G. Barral, J.P. Diard, and C. Montella, *Electrochim. Acta* **31**, 277 (1986).
74. F. Hine, *Electrode Processes and Electrochemical Engineering*, Chapter 12, Plenum Press, New York (1985).
75. S.V. Evdokimov and K.A. Mishenina, *Electrokhimiya* **25**, 1439 (1989).
76. V.V. Gorodetskii, M.M. Pecherskii, V.B. Yanke, D.M. Shub, and V.V. Losev, *Soviet Electrochem.* **15**, 471 (1979).
77. V.I. Eberil, N.V. Zhinkin, V.P. Archakov, R.I. Izosenkov, V.B. Busse-Machukas, and A.F. Mazanko, *Soviet Electrochem.* **22**, 428 (1986).
78. S. Manli and C. Yanxi. The Mechanism of the Activity Loss of RuO₂ – TiO₂ Anodes in Saturated NaCl solution, In N.M. Prout and J.S. Moorhouse (eds), *Modern Chlor-Alkali Technology*, vol. 4, Elsevier Appl., Sci., New York (1990), p. 149.
79. B.V. Tilak, C.-P. Chen, and S.K. Rangarajan, *J. Electroanal. Chem.* **324**, 405 (1992); **356**, 319 (1993).
80. M.M. Pecherskii, V.V. Gorodetskii, N.Ya. Bune, and V.V. Losev, *Soviet Electrochem.* **18**, 367 (1982).
81. A.I. Onuchukwu and S. Trasatti, *J. Appl. Electrochem.* **21**, 858 (1991).
82. S. Trasatti, Transition Metal Oxides: Versatile Materials for Electrocatalysis, In J. Lipkowski and P.N. Ross (eds), *The Electrochemistry of Novel Materials*, VCH Publishers, New York (1994), p. 207.
83. B.E. Conway and B.V. Tilak. Involvement of Oxide Films and their Surfaces in Anodic Faradaic Reactions: A Review, In J.B. Talbot, B.E. Conway, J.M. Fenton, and B.V. Tilak (eds), *Proc. Symp. Fundamentals of Electrochemical Process Design: A Tutorial and Anodic Processes: Fundamental and Applied Aspects*, vol. 95-11, The Electrochemical Society Inc., Pennington, NJ (1995), p. 319.
84. Yu.B. Makarychev, E.K. Spassakaya, S.D. Khodkevich, and L.M. Yakimenko, *Soviet Electrochem.* **12**, 921 (1976).
85. T. Loucka, *J. Appl. Electrochem.* **7**, 211 (1977).
86. A.A. Uzbekov, V.G. Lambrev, I.F. Yazikov, N.N. Rodin, L.M. Zabrodskaya, V.S. Klement'eva, and Yu.M. Vlodov, *Soviet Electrochem.* **14**, 997 (1978).
87. F. Hine, M. Yasuda, T. Noda, T. Yoshida, and J. Okuda, *J. Electrochem. Soc.* **126**, 1439 (1979).
88. C. Iwakura, M. Inai, M. Manabe, and T. Tamura, *Denki Kagaku.* **48**, 91 (1980).
89. T. Loucka, *J. Appl. Electrochem.* **11**, 143 (1981).
90. V.V. Gorodetskii, M.M. Pecherskii, V.B. Yanke, N.Ya. Bun'e, V.B. Busse-Machukas, V.L. Kubasov, and V.V. Losev, *Soviet Electrochem.* **17**, 421 (1981).
91. A.A. Uzbekov and V.S. Klement'eva, *Soviet Electrochem.* **21**, 698 (1985).
92. C. Iwakura and K. Sakamoto, *J. Electrochem. Soc.* **132**, 2420 (1985).
93. V.S. Klement'eva and A.A. Uzbekov, *Soviet Electrochem.* **21**, 736 (1985).
94. M.M. Pecherskii, V.V. Gorodetskii, N.Ya. Bun'e, and V.V. Losev, *Soviet Electrochem.* **22**, 615 (1986).

95. N.V. Zhinkin, E.A. Novikov, N.S. Fedotova, V.I. Eberil, and V.B. Busse-Macukas, *Soviet Electrochem.* **25**, 980 (1989).
96. S.V. Evdokimov and K.A. Mishenina, *Soviet Electrochem.* **25**, 1439 (1989).
97. E.A. Novikov, N.V. Zhinkin, V.I. Eberil, and V. Busse-Macukas, *Soviet Electrochem.* **26**, 228 (1990).
98. E.V. Novikov and V. Busse-Macukas, *Soviet Electrochem.* **27**, 108 (1991).
99. A.S. Pilla, E.O. Cobo, M.M.E. Duarte, and D.R. Salinas, *J. Appl. Electrochem.* **27**, 1283 (1997).
100. C.E. Vallet, B.V. Tilak, R.A. Zuhr, and C.-P. Chen, *J. Electrochem. Soc.* **144**, 1289 (1997).
101. K.L. Hardee and R.A. Kus. Evidence for the Passivation of the Coating/Substrate Interface in Chlorine Evolving Anodes, In S. Sealey (ed.) *Modern Chlor-Alkali Technology*, Vol. 7, Royal Society of Chemistry, Cambridge, (1998), p. 43.
102. M. Pourbaix, *Atlas of Electrochemical Equilibria in Aqueous Solutions*, NACE, Houston (1974).
103. C.-P. Chen and T.V. Bommaraju, *U.S. Patent* 5,948,222 (1999); 6,156,185 (2000).
104. T.V. Bommaraju, C.-P. Chen, and V.I. Birss. Deactivation of Thermally formed RuO₂ + TiO₂ Coatings During Chlorine Evolution: Mechanisms and Reactivation Measures, In J. Moorhouse (ed.), *Modern Chlor-Alkali Technology*, Vol. 8, Chapter 5 Society for Chemical Industry, London (2001), p. 57.
105. B.V. Tilak, V.I. Birss, J. Wang, C.-P. Chen, and S.K. Rangarajan, *J. Electrochem. Soc.* **148**, D112 (2001); **148**, L10 (2001).
106. S. Kotowski and B. Busse. Titanium Anodes for Steel Strip Electrogalvanizing, In F. Hine, B.V. Tilak, J.M. Denton, J.D. Lisius (eds), *Performances of Electrodes for Industrial Electrochemical Processes*, The Electrochemical Society Inc., Pennington, NJ, 245 (1989).
107. T.A. Liederbach, Metal Anodes, in *Kirk-Othmer Encyclopedia of Chemical Technology*, 4th ed., Vol. 16, John Wiley & Sons, New York (1995), p. 244.
108. A. Pellegrini, Oronzio DeNora Impianti Elettrochimici, S.P.A., *British Patent* 2,051,131 (1980).
109. H.S. Holden and J.M. Kolb, Metal Anodes, in *Kirk-Othmer Encyclopedia of Chemical Technology*, 3rd ed., Vol. 15, John Wiley & Sons, New York (1981), p. 172.
110. H. Schmitt, H. Schurig and W. Strewe, *German Patent* 3,219,704 (1982).
111. S. Saito. Development of a New Anode for Chlor-Alkali Production, In M.O. Coulter (ed.), *Modern Chlor-Alkali Technology*, Ellis Horwood, Chichester (1980), p. 137.
112. M. Saraiya, Chemapol Industries, India, Private Communication (1995).
113. R.C. Carlson, *Effects of Brine Impurities on Dimensionally Stable Anodes*, in *14th Annual Chlorine-Chlorate Seminar*, Eltech Systems Corporation, Chardon, OH (1998).
114. C.H. Angell and M.G. Deriaz, *British Patent* 885,891 (1961); 984,973 (1965).
115. C.H. Angell, S. Coldfield, and M.G. Deniaz, *U.S. Patent* 3,177,131 (1965).
116. D.L. Caldwell and R.J. Fuchs, *U.S. Patent* 3,977,958 (1976).
117. D.L. Caldwell and M.J. Hazelrigg, *U.S. Patent* 4,142,005 (1979).
118. M.J. Hazelrigg and D.L. Caldwell, *U.S. Patent* 4,061,549 (1977).
119. G. Thiele, D. Zöllner, and K. Koziol, *German Patent* 1,813,944 (1968).
120. K. Koziol, K.-H. Sieberer, and H.C. Rathjen, *German Patent* 2,255,690 (1972).
121. R. Kötz and S. Stucki, *Electrochim. Acta* **31**, 1311 (1986).
122. T. Morimoto, T. Matsubara, and S. Ohashi, *Denki Kagaku.* **60**, 649 (1992).

4.6. CATHODES

4.6.1. Introduction

The primary electrochemical reaction at the cathode in diaphragm and membrane cells is hydrogen evolution from alkaline solutions. The cathode is carbon steel in diaphragm cells and usually nickel in membrane cells. An examination of the components of cell voltage of these cells shows the cathode overvoltage to be in the range of 0.2–0.3 V in the current density range of 2–4 kA m⁻² on steel substrates, and slightly higher on nickel substrates.

One of the major achievements in the chlor-alkali industry in the early 1960s was the introduction of metal anodes. The changeover from carbon to noble metal coated anodes resulted in a voltage savings of over 0.2 V, longer anode life, better cell gas (i.e., higher current efficiency), and permitted operation of the cells at higher loads without significant voltage penalties. Commercialization of DSA[®] anodes worldwide provided impetus in the water electrolysis industry [1,2] to develop materials such as mixed oxides as anodes and high surface area nickel-based electrodes as cathodes to reduce energy consumption.

The hydrogen overvoltage at the cathode is the difference between the operating voltage of the hydrogen-producing cathode and the reversible hydrogen discharge potential in the given electrolyte. Under industrial conditions, hydrogen overvoltage normally follows the Tafel equation:

$$\eta = b \ln \left(\frac{I}{i_0 A} \right) \quad (1)$$

where η refers to the hydrogen overvoltage, b to the Tafel slope, A to the surface area, i_0 to the exchange current density in amperes per square centimeter of the real surface area, and I to the total current (i.e., $I = iA$, i being the real current density in amperes per square centimeter of the electrochemically active surface area). i_0 and b are constants that depend on the rate of the hydrogen evolution reaction (HER) on the given substrate and the mechanism of the HER. The Tafel slope b is approximately 120 mV on most smooth metal surfaces, at 25°C in alkaline solutions.

The overvoltage for hydrogen discharge on mercury is very high, which makes the mercury cathode-based chlorine cell a viable concept. In a typical mercury cell, the cathode potential is about 1.8 V more cathodic than the reversible hydrogen electrode potential. An average chlorine gas sample from such a cell may contain 0.5% H₂, indicating that 0.5% of the cathodic current is carried by the hydrogen ion, the other 99.5% being carried by the sodium ion. The sodium overvoltage at the mercury cathode is quite small, of the order of 10–20 mV.

The traditional cathode material for diaphragm cells is low-carbon steel which exhibits low hydrogen overvoltage and high durability in sodium hydroxide solutions and is available at low cost in a wide variety of structural shapes. It is cathodically protected from corrosion during operation and, with proper care, produces 250–300 tons of NaOH/m² of the cathode area. Although steel is a relatively good electrocatalyst for hydrogen evolution, its overvoltage in diaphragm chlorine cells is typically 300 mV, the exact value depending on the state of the cathode surface (Fig. 4.6.1). Furthermore, iron will dissolve as ferrate, HFeO₂⁻ in hot concentrated caustic solutions at the open circuit potential, as expected from the Pourbaix diagram [3] of Fig. 4.6.2. This situation also arises when the cell is short-circuited during shutdowns, as the cathode surface, free of any oxide, is suddenly polarized anodically.

Nickel, which is not as electrocatalytically active as iron toward the HER, exhibits excellent corrosion resistance in hot, concentrated, alkaline solutions. Motivated by the stability of Ni in caustic solutions (Fig. 4.6.3) and the extensive investigations by the water electrolysis industry to develop Ni-based cathodes, significant efforts have been made to develop catalytic cathodes for application in chlor-alkali cells.

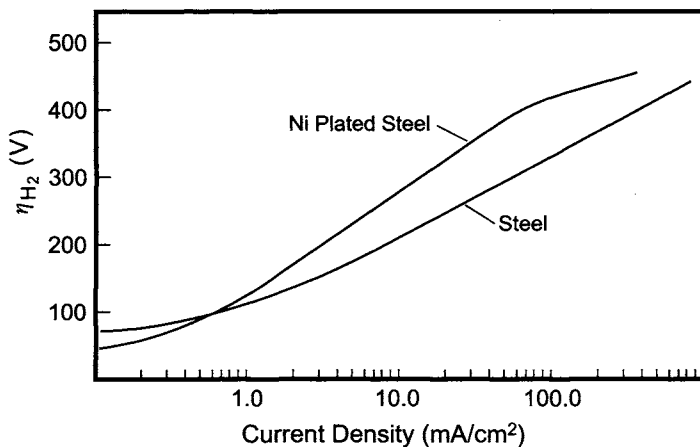


FIGURE 4.6.1. Polarization data for the HER on steel and Ni plated steel in 15% NaOH + 17% NaCl solutions at 95°C [10]. (With permission from the Indian Academy of Sciences.)

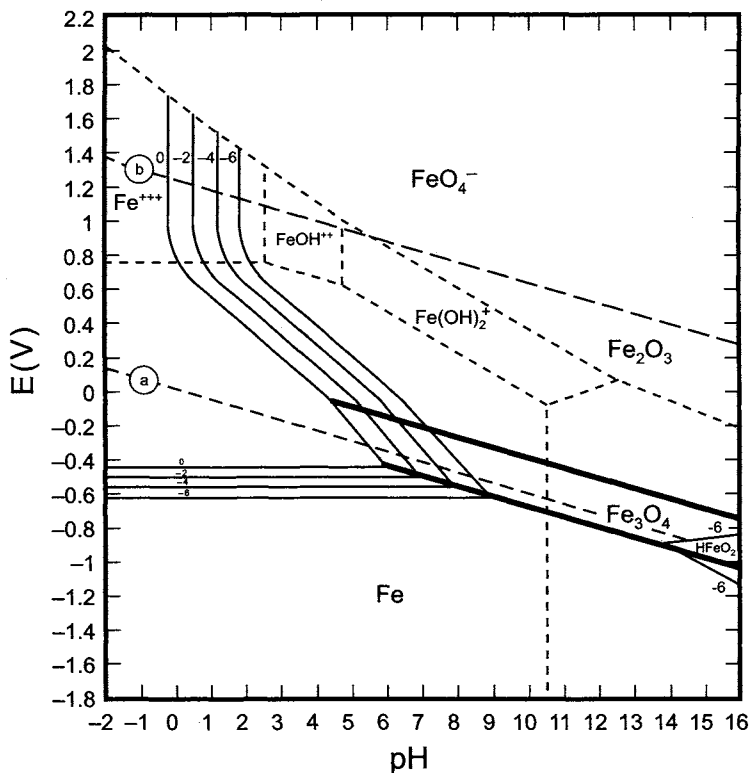


FIGURE 4.6.2. Potential-pH diagram for the Fe-H₂O system at 25°C [3]. The region between the lines (a) and (b) represents the domain of the thermodynamic stability of water. The numbers on the lines represent the logarithm of the activity of the species. (M. Pourbaix, *Atlas of Electrochemical Equilibria in Aqueous Solutions*, Publishers: NACE and CEBELCOR.)

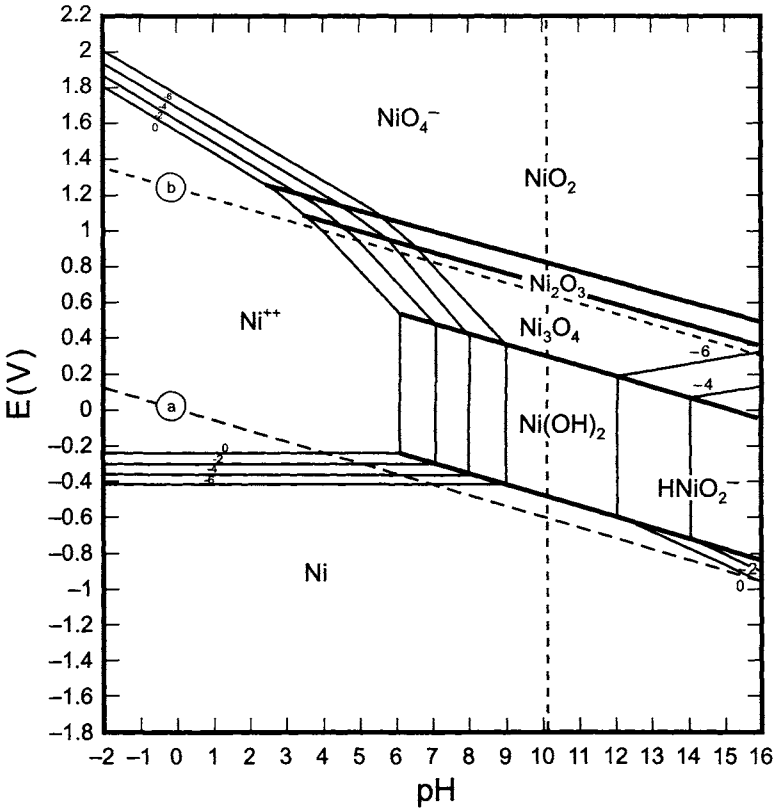


FIGURE 4.6.3. Potential-pH diagram for the Ni-H₂O system at 25°C [3]. The region between the lines (a) and (b) represents the domain of the thermodynamic stability of water. The numbers on the lines represent the logarithm of the activity of the species. (M. Pourbaix, *Atlas of Electrochemical Equilibria in Aqueous Solutions*, Publishers: NACE and CEBELCOR).

4.6.2. Criteria for Low Overvoltage Hydrogen Cathode

The strategy to obtain high performance materials for the discharge of hydrogen from high alkaline media has been two-fold:

- I. Selection of materials with high i_0 and low b .
- II. Enhancement of the surface area.

The preferred materials are those exhibiting high i_0 and low b , since high operating current densities can be achieved without significant increase in the overvoltage, as shown qualitatively in Fig. 4.6.4. Kinetic treatment of the generally accepted pathways during the HER shows that participation of adsorbed intermediates in the slow step during the HER results in low Tafel slopes (Table 4.6.1) [4-9].

Since the atomic hydrogen participating in the slow step diffuses into the bulk metal, metals exhibiting low Tafel slopes act as sinks for adsorbed hydrogen, resulting in hydrogen embrittlement via lattice expansion/distortion [5,7]. While the presence of adsorbed

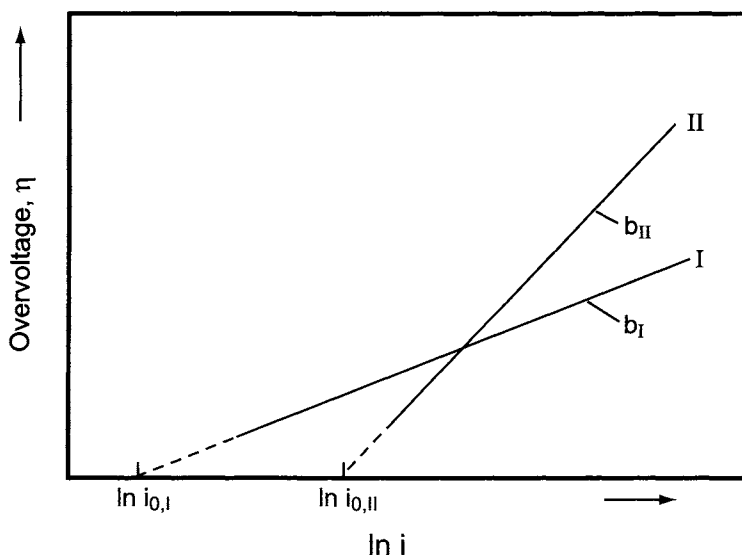


FIGURE 4.6.4. Schematic of the polarization data when two activation controlled reactions with different Tafel slopes proceed.

TABLE 4.6.1 Pathways Involved in the H₂ Evolution Reaction

Mechanism	$Fd\eta/RTd \ln i$	Comments
Discharge $M + H^+ + e \rightarrow MH$	2	Non-embrittling
Recombination $MH + MH \rightarrow M + H_2$	$0.5 (1 - \theta)$	Hydrogen embrittlement possible
Electrochemical desorption $MH + H^+ + e \rightarrow 2M + H_2$	$1/(1.5 - \theta)$	Hydrogen embrittlement possible

Note: θ in the above table refers to the coverage by the adsorbed H intermediate.

hydrogen is advantageous under some conditions (e.g., “buffering” the “reverse currents” encountered during shutdowns), it is most deleterious to the structural integrity of the metal. Hence, the ideal material would be one exhibiting a high i_0 for the HER, with discharge as the slow step. Another obvious, but a nontrivial factor, is the enhancement of the area, which brings about a decrease in the overvoltage as shown by Eq. (1).

The main technical criteria for selection of a high-performance cathode material include

1. cost/life;
2. electrocatalytic activity;
3. stability under open circuit conditions;
4. coating technique *vis-à-vis* cell design/cathode geometry;
5. product purity.

4.6.2.1. *Cost/Life.* If one assumes that a catalytic cathode provides a savings of $100 \text{ kW hr ton}^{-1}$ of chlorine, the cost savings, at $\$0.035 \text{ kW hr}^{-1}$ and an operating current density of 3 kA m^{-2} over a 5-year period at 360 days per year at 100% efficiency will be $\$600$. At a cathode coating cost of $\$600 \text{ m}^{-2}$, the payback period is 5 years. The payback time T can be calculated using the following relationship.

$$T = 31.5P/LEDSC$$

T = Payback time, yr

L = Operating load, $\text{kA} \cdot \text{m}^{-2}$

E = Current efficiency, fraction

D = On-line factor, $\text{days} \cdot \text{yr}^{-1}$

S = Energy saving, $\text{kW hr} \cdot \text{ton}^{-1}$

C = Cost of DC power, $\$ \cdot \text{kW hr}^{-1}$

P = Coating cost, $\$ \cdot \text{m}^{-2}$

This simple expression shows that the cost is a function of several parameters like current density, energy savings, cost of power, and operating life, not excluding the downtime costs, if the cathode has to be changed or replaced.

4.6.2.2. *Electrocatalytic Activity.* As discussed in Section 4.2, there are no simple predictive tools for selection of a cathode composition that will provide low overvoltages in alkaline solutions. Table 4.6.2 shows the exchange current density and the Tafel slope for the HER on various metals, and Figs. 4.6.5 and 4.6.6 depict the cathodic polarization of some metals in $\text{NaOH} + \text{NaCl}$ solutions, at 95°C [10]. These data, obtained on planar surfaces, reveal that the hydrogen overpotential on all these metals is in the range of $300\text{--}350 \text{ mV}$ at $200\text{--}300 \text{ mA cm}^{-2}$, similar to the hydrogen overvoltage on steel.

As nickel is most stable in caustic solutions, there has been significant focus on imparting catalytic activity to nickel, by alloying with other metals and nonmetals. The concept behind this approach is the possibility of inducing electrocatalysis to nickel toward the HER, by incorporating metals which fall on either side of the volcano curve (Section 4.2), constructed based on the heats of formation of metal-hydrogen bonds [11], in the nickel matrix. Studies with various nickel alloys and other compounds (Figs. 4.6.7 and 4.6.8) reveal the effect of alloying. Figure 4.6.7 shows best activity from $10\% \text{ Co} + 90\% \text{ Ni}$. Ni-Sn alloy behaved more like nickel, but NiTi and NiTi_2 showed dramatic effects by exhibiting low overvoltages in the high current density region. These alloys, however, disintegrated after a few hours because of the formation of Ti hydrides and associated lattice expansion. Ni-Ir , Ni-W , and Ni-Co alloys exhibited overpotentials which were high compared to those presently used in the industry.

The influence of B, P, Bi, S, SiC, Si, and ZrO_2 in the nickel matrix on the current-voltage curves is depicted in Fig. 4.6.8. The enhancement in catalytic activity was significant, but the overvoltages were still high except on NiSi and NiSi_2 , which showed

TABLE 4.6.2 Kinetic Data for the Hydrogen Evolution Reaction in Alkaline Media (Compiled from refs. [2,8–10])

Metal	Medium/(temp.°C)	i_0 (A cm ⁻²) ^a	Tafel slope (mV) ^b
Ag	1N NaOH/(30)	3.16×10^{-7}	120
Au	0.1N NaOH/(25)	10^{-5} to 10^{-7}	71–120
C	40% NaOH/(40)	2.95×10^{-5}	148
C (vitreous)	15% NaOH + 17% NaCl/(95)	7×10^{-3}	700(?)
Co	15% NaOH + 7% NaCl/(95)	10^{-8}	135
	6N NaOH/(25)	5×10^{-5}	140
Cu	0.1N NaOH/(25)	10^{-7}	120
Cd	6N NaOH/(25)	4×10^{-7}	160
Cr	6N NaOH/(25)	1.6×10^{-6}	120
Fe	15% NaOH + 17% NaCl/(95)	2.4×10^{-4}	150
	0.1N NaOH/(25)	1.6×10^{-6}	120
Hg	0.1N NaOH/(25)	3×10^{-15}	120
Ir	0.1N NaOH/(25)	45×10^{-4}	125
	15% NaOH + 17% NaCl/(95)	2×10^{-5}	110
Mo	15% NaOH + 17% NaCl/(95)	10^{-5}	120
	0.1N NaOH/(25)	5×10^{-7} to 5×10^{-8}	80–116
Nb	1.0N NaOH/(25)	3.2×10^{-8}	140
Ni	0.5N NaOH/(25)	8×10^{-7}	96
	15% NaOH + 17% NaCl/(95)	3×10^{-6}	100
Pb	0.5N NaOH/(25)	3.2×10^{-7}	130
Pd	0.1N NaOH/(25)	10^{-5}	125
Pt	0.1N NaOH/(25)	7×10^{-5}	114
	15% NaOH + 17% NaCl/(95)	8×10^{-4}	170
Re	15% NaOH + 17% NaCl/(95)	1×10^{-3}	160
Rh	0.1N NaOH/(25)	10^{-4}	118
	15% NaOH + 17% NaCl/(95)	10^{-3}	170
Ru	15% NaOH + 17% NaCl/(95)	10^{-8}	155–45(?)
Sn	6N NaOH/(25)	3.2×10^{-7}	150
	15% NaOH + 17% NaCl/(95)	2×10^{-8}	140
Ti	6N NaOH/(25)	10^{-6}	140
	15% NaOH + 17% NaCl/(95)	8×10^{-4}	240
W	0.5N NaOH/(25)	2×10^{-7} to 3×10^{-8}	80–100
	15% NaOH + 17% NaCl/(95)	5×10^{-4}	200
Zn	0.1N NaOH/(25)	4×10^{-7}	210

Note:

^aExtrapolated from the high current density region.

^bFrom the data in the high current density region.

high I_0 values (defined as $i_0 A$) and low Tafel slopes. The enhanced activity was a result of the high surface area generated by the leaching of Si from the matrix of NiSi and NiSi₂. It is interesting to compare these low Tafel slopes of 20–30 mV to the Tafel slope value of ~110 mV observed with the smooth nickel surfaces. This realization of low overvoltages has prompted extensive investigations to prepare nickel-based electrodes with large surface areas.

There are several techniques available to generate large surface areas, the most popular and practical being plasma or thermal spraying, thermal decomposition, and

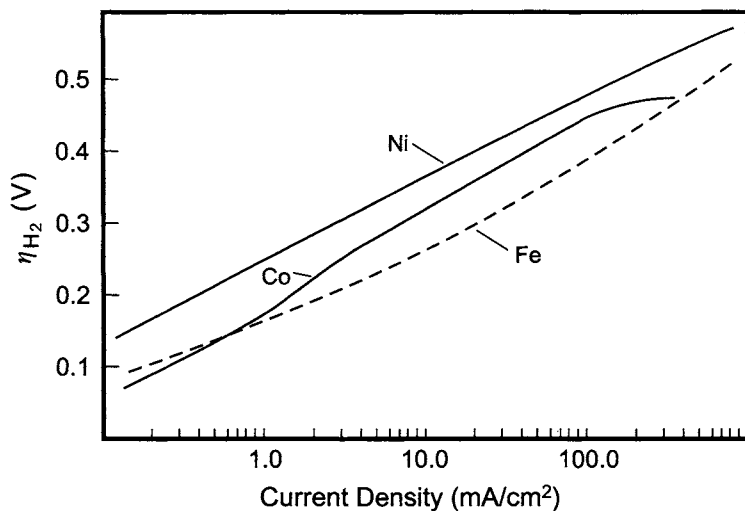


FIGURE 4.6.5. Polarization data for the HER on Fe, Co, and Ni electrodes in 15% NaOH + 17% NaCl solutions at 95°C [10]. (With permission from the Indian Academy of Sciences.)

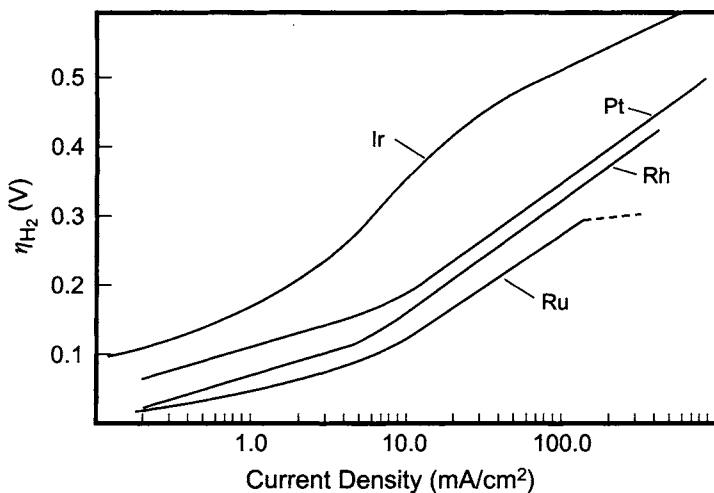


FIGURE 4.6.6. Polarization data for the HER on Pt, Ir, Rh, and Ru electrodes in 15% NaOH + 17% NaCl solutions at 95°C [10]. (With permission from the Indian Academy of Sciences.)

electrodeposition. These can produce pure nickel coatings and composites that contain nickel and a component leachable in caustic solutions (e.g., Zn, Al, S, Mo, and Si). The various composites examined are discussed in Section 4.6.3.

4.6.2.3. Stability Under Open-Circuit Conditions. Most metals remain stable when cathodically protected. However, many of them are unstable in hot concentrated caustic

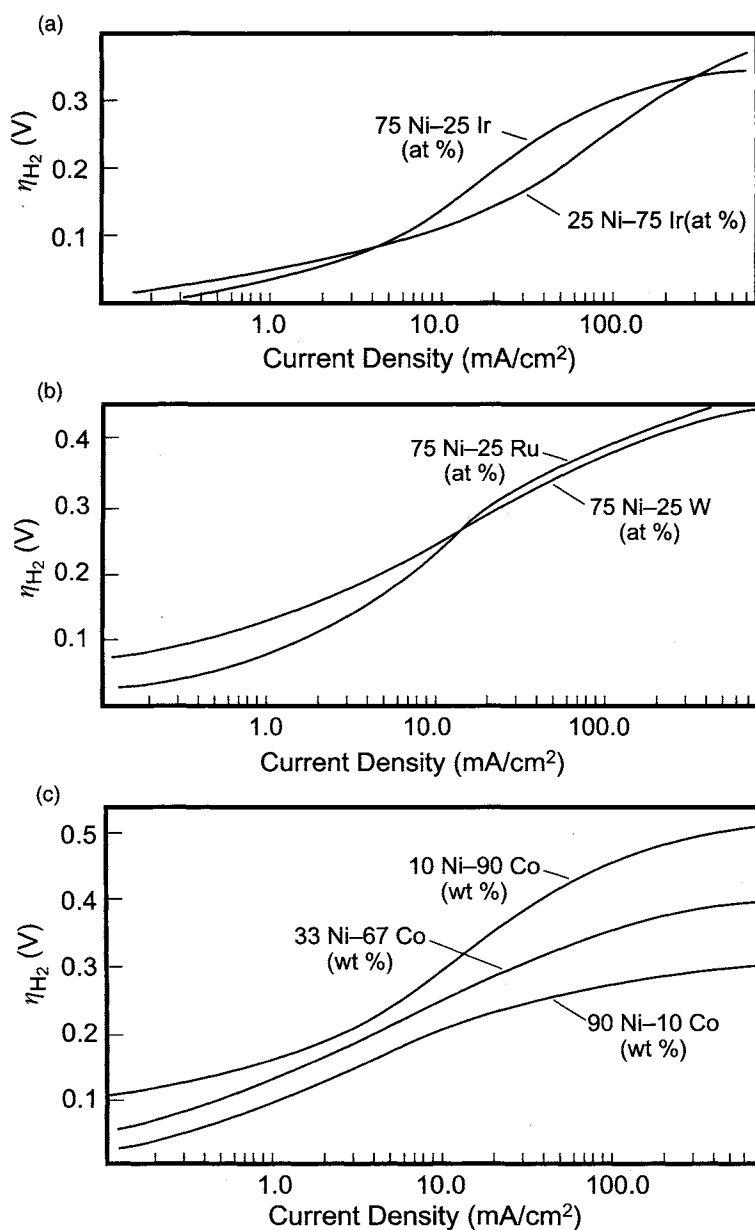


FIGURE 4.6.7. Polarization data for the HER on (a) Ni-Ir alloys, (b) Ni-Ru alloys, and (c) Ni-Co alloys in 15% NaOH + 17% NaCl solutions at 95°C [10]. (With permission from the Indian Academy of Sciences.)

solutions. Thus, iron cathodes in NaOH solution exhibit an open circuit potential that is negative with respect to the reversible hydrogen electrode in the same solution. Thus a corrosion potential arises from the anodic dissolution of Fe as $HFeO_2^-$. The corresponding reduction reaction is the discharge of H_2O molecules to form hydrogen, or the

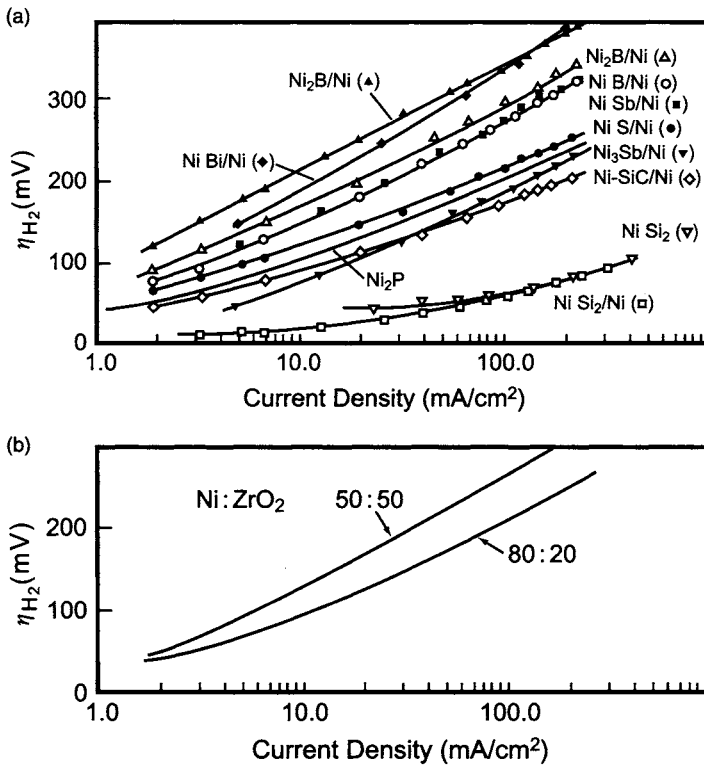
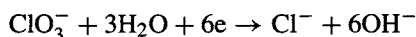
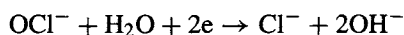


FIGURE 4.6.8. Polarization data for the HER on (a) various Ni-based compounds and (b) Ni-ZrO₂ mixtures plasma sprayed on Ni substrates in 15% NaOH + 17% NaCl solutions at 95°C [10]. (With permission from the Indian Academy of Sciences.)

reduction of other catholyte species such as OCI^- and ClO_3^- . While the corrosion of iron arising from the former can be controlled by appropriately manipulating the pH of the medium, the forced instability of Fe by the cathodic reduction of OCI^- or ClO_3^- can not be easily avoided. It is thus essential that any cathode material chosen for operation in chlor-alkali cells not only be stable in highly alkaline NaOH solutions, but also be able to resist oxidation by the OCI^- and ClO_3^- reduction reactions.

4.6.2.4. Selection of the Coating Technique. Several methods, such as plasma spraying, thermospraying, electrodeposition, and thermal decomposition, are available for generating high-surface area coatings on iron or nickel substrates. However, it is necessary to consider the operating temperature and to examine the complexity of the cathode structure before choosing the coating technology, because of the limited “throwing power” of the various coating methods. Thus, coating an entire cathode finger in the highly complex diaphragm cell *in situ* would be extremely difficult. Furthermore, the tolerances involved in the fabrication of the cathodes are so stringent that any coating technique that requires operations at high temperatures is likely to distort the cathode. This, in turn, skews the current distribution in the cell and increase the structural ohmic drop.

4.6.2.5. *Product Purity.* In chlor-alkali cells, there are two parasitic cathode reactions, which lead to “blind” current efficiency losses:



It is known that OCl^- is reduced at the cathode under limiting current density conditions on all metals, whereas the cathodic reduction of ClO_3^- to Cl^- is kinetically slow and proceeds only on iron-based surfaces at low current densities [12]. Since chlorate is an undesirable impurity in caustic for some end uses, this would be an advantage for iron-based cathodes. The disadvantages of iron cause nickel to be the metal of choice for membrane-cell cathodes. In future developments, electrocatalytic activity toward chlorate reduction would be a useful goal.

4.6.3. *Methods Employed to Realize High Surface Area*

As discussed earlier, cathodes of pure metals or alloys are not electrocatalytically better than steel or nickel. Low cathode overvoltages are realized only when the cathode surface area is large. This is why efforts to achieve low cathodic overvoltages have focused on cathode surface coatings. Techniques for the generation of high surface area coatings include: (1) plasma or thermal spraying, (2) thermal decomposition, (3) electrodeposition, and (4) *in situ* activation.

Plasma and thermal spraying techniques [13,14] involve degreasing a nickel substrate, followed by sandblasting with 20-mesh alumina to generate a surface that can provide good adhesion of the coating. Nickel and sometimes a second constituent such as Zn, Al, Si, or Mo in a powder form (–200 to +325 mesh) are mixed and fed to a plasma gun, powered at 30–40 kW to a temperature of about 5,000°C in an argon atmosphere. The substrates are maintained at 200–300°C by external cooling, and the mixtures are sprayed at a rate of 25 μm per pass until the desired thickness is achieved. The second component is subsequently leached out in NaOH solutions to generate a high surface area. Alternatively, one may employ an electroarc wire spray process [15] to achieve the desired surface area.

The thermal decomposition method involves either spraying or painting the substrate with a solution of the chloride salt of the appropriate metal dissolved in HCl or a solvent such as isopropyl alcohol, followed by a high temperature treatment in air to form the corresponding oxide. This is quite similar to the process for forming anode coatings on titanium substrates. In some instances, the oxides are reduced to a metallic form by heating in the presence of hydrogen with an optional sintering procedure. Metals that can be applied by this method include Ni, Co, Ru, Zn, Rh, and Ir.

Electroplating, or in some instances electroless plating of a metal or an alloy, can also generate high surface areas. Plating typically involves a ferrous substrate (steel) or nickel on which metals such as Ni, Mo, Co, Cd, and W, or their alloys, have been deposited. A variation of the plating scheme involves codeposition of elements such as Zn or Al with Ni (or other metals or metal oxide powders) and a subsequent chemical leaching treatment to form a high-surface area porous matrix, if required. Other options

include the deposition of a thin layer of a noble metal such as Pt on an intermediate nonporous Ni layer formed on steel substrates.

Ni-S, Ni-Zn, Ni-Re, Ni-Mo, Ni-Mo-Cd, and Ni-Sn coatings can be deposited onto nickel substrates by electroplating. Nickel substrates are initially degreased in trichloroethylene at room temperature for 30 min, followed by rinsing in acetone-ethyl alcohol and then in water. The substrates are then activated in a 1:1 mixture of concentrated HNO₃ and glacial acetic acid for 5 min prior to plating. Ni-S coatings [16] can be deposited from a modified Watts nickel bath containing 150 g L⁻¹ NiSO₄, 47.5 g L⁻¹ NiCl₂, 30 g L⁻¹ H₃BO₃, and 30 g L⁻¹ KSCN (pH ≈ 4) at 45°C and at a current density of 20 mA cm⁻² for 1 hr. Ni-Zn coatings are prepared from solutions containing 330 g L⁻¹ NiSO₄, 45 g L⁻¹ NiCl₂, 37.5 g L⁻¹ H₃BO₃, and 20 g L⁻¹ ZnCl₂ (pH ~ 4.5) at 50°C and at a current density of 3 mA cm⁻² for 1 hr. Plating conditions and baths employed for electrodepositing Ni-Re [17,18], Ni-Mo [19], Ni-Mo-Cd [20], and Ni-Sn [21] are noted in the references cited.

In situ activation to achieve low cathodic overvoltages was motivated by the studies of Riley and Moran [22], who found reduced cathode potentials on pure nickel by the addition of small quantities of iron to the catholyte, as a result of the deposition of Fe in a high surface area form. Scanning electron microscope studies confirmed the enhancement in the surface area. Similar *in situ* activation of nickel and cobalt cathodes was noticed [23] by the addition of Na₂MoO₄ to 30 wt% KOH at 70°C—the activation being optimal at an Mo concentration of 0.004 M, added as MoO₄⁻. Addition of chloroplatinic acid to the catholyte of a chlor-alkali cell was found to result in lowered cathode potentials and this was the basis of a patent [24]. This approach is attractive, as it does not involve the costs associated with a coating process. However, caution is necessary as the unreacted chloroplatinic acid may adversely affect the product or its end uses, or it may cause galvanic corrosion.

4.6.4. Cathode Materials and Compositions

A wide variety of materials and coatings have been evaluated for use as cathodes in diaphragm and membrane cells, most of them nickel-based. Some of the compositions disclosed in the patent literature are presented in Table 4.6.3, and Trasatti [13] and Conway and Tilak [4] have reviewed kinetic factors involved during the course of the HER on various materials in alkaline media. Various activation procedures have been employed to modify the surface morphology of nickel to increase the active surface area. Although many promising compositions and methods were reported [25–186], most were not tested in commercial chlorine cells. This section discusses selected compositions and techniques of particular interest. Section 4.6.7 addresses the coatings that have been used in commercial operations.

4.6.4.1. Raney Nickel. Raney nickel was first used as a catalyst for the hydrogenation of hydrocarbons, and Justi *et al.* [25] suggested it as an electrocatalyst for the HER in 1954. Several procedures are available for applying Raney nickel coatings on a given substrate. These include plasma spraying, sintering of metal powders, plating from molten salt, electroplating from aqueous solutions, and dispersion plating. Ni-Al and Ni-Zn alloys are obtained by the first three methods, whereas electroplating from aqueous solutions

TABLE 4.6.3 Catalytic Cathode Patent Literature

Patent assignee	Elements in the coating/ coating technique	Patent #
PPG Industries	Hydroxy carboxylic or aromatic acid addition to the catholyte	U.S. 3,854,581 (1976)
Diamond Shamrock	Co-ZrO ₂ /Flame spraying	U.S. 3,992,278 (1976)
Diamond Shamrock	Ni-Zn/Electroplating	U.S. 4,104,133 (1978)
Olin Chemicals	Noble metal addition to the catholyte	Ger. Offen. 2,818,306 (1978)
Tokuyama Soda	Ni, S/Electroplating	Ger. Offen. 2,811,472 (1978)
PPG Industries	W and Ni and/or Co/ Electroless plating	U.S. 4,086,149 (1979)
Osaka Soda	Ni, Mn/ Electroplating, Thermal	Japan 79,38,277 (1979)
Showa Denko	Ni, Al/ Electroplating	Japan 79,71,184 (1979)
Showa Denko	Ni, Co, P, Se/ Electroplating	Japan 79,75,481 (1979)
Showa Denko	Fe/Oxide formation	Japan 79,80,282 (1979)
Tokuyama Soda	Ni, Ru, Ir/Electroplating	Japan 79,90,080 (1979)
Chlorine Engineers	Ni, Noble metals/Electroplating, Flame spraying	Japan 79,110,983 (1979)
Metallgesellschaft	Fe, Co, Ni, Ag/Thermal spraying	Ger. Offen. 2,829,901 (1980)
PPG Industries	Ni, P, Fe/Electroplating	U.S. 4,184,941 (1980)
British Petroleum Co.	Co, Fe, Ni, Mo, W, V/Thermal process	Euro Pat. Appl. 9,406(1980)
PPG Industries	Ni, Mo/Flame spraying	U.S. 4,248,679 (1981)
Hooker Chemical	Ni, Zn/Electroplating	U.S. 4,314,893 (1982)
Occidental Chemical	Ni, Mo, Cd/Electroplating	U.S. 4,354,715 (1982)
Occidental Chemical	Cd, Pt,Pd /Electroplating	U.S. 4,377,454 (1983)
Occidental Chemical	Ni, Mo, Cd/Electroplating	U.S. 4,414,064 (1983)
Solvay & Cie	Co, Fe, Ru, Ni/Thermal decomposition	U.S. 4,394,231 (1983)
Occidental Chemical	Ni, Mo, Cd/Electroplating	U.S. 4,421,626 (1983)
Chlorine Engineers	Ni, Pt/Electroplating,	U.S. 4,465,580 (1984)
Chlorine Engineers	Ni, RuO ₂ /Electroplating, Thermal decomposition	U.S. 4,543,265 (1985)
Solvay & Cie	Ni, Co/Electroplating	U.S. 4,555,317 (1985)
Dow Chemical	Ru, Ni/Thermal decomposition	U.S. 4,572,770 (1986)
ICI	Ni with Pt group metals/Electroplating	U.S. 4,586,998 (1986)
Asahi Kasei	Ni, Co, Cr/Melt spraying	U.S. 4,605,484 (1986)
Oronzio de Nora	Ni, Ru oxide/Electroplating	U.S. 4,618,404 (1986)
Oronzio de Nora	Ni, RuO ₂ /Electroplating	U.S. 4,648,946 (1987)
Oronzio de Nora	Ni, RuO ₂ /Electroplating	U.S. 4,668,370 (1987)
Oronzio de Nora	Ni, RuO ₂ /Electroplating	U.S. 4,724,052 (1988)
Dow Chemical	Ni, Ru oxide/Thermal decomposition	U.S. 4,760,041 (1988)
Johnson Matthey	Pt, Ru with Au or Ag/Electroplating	U.S. 4,784,730 (1988)
DeNora Permelec	Ceramic/Thermal deposition	U.S. 4,975,161 (1990)
Dow Chemical	Pd with Pt, Ni/Electroplating	U.S. 5,066,380 (1991)
Dow Chemical	Pd with Pt, Ni/Electroplating	U.S. 5,104,062 (1992)
Moltech	Ceramic/Combination synthesis	U.S. 5,316,718 (1994)
Wilson Greatbatch	Ag with V/Thermal decomposition	U.S. 5,389,472 (1995)
ICI	Ce with group VIII metals/Plasma spraying	U.S. 5,492,732 (1996)

forms Ni-Zn alloys. These deposits are treated with hot, concentrated caustic soda to leach aluminum or zinc, and the porous layer obtained is electrocatalytically active to the hydrogen electrode process, depending on the chemical composition of precursor alloy and other factors. However, the coating is generally mechanically weak, because the bonding of the porous layer to the substrate is weakened during the leaching process. Also, post-treatment of the waste solutions is a concern in this approach.

The Ni–Al type Raney nickel alloys have been examined extensively [24–32] for use in chlor-alkali cells. There are three intermediate compounds of nickel and aluminum (Fig. 4.6.9), as noted below.

Ni	α -phase, f.c.c	100% Ni
Ni ₃ Al	α' -phase, f.c.c	86.71% Ni
NiAl	β' -phase, b.c.c	68.51% Ni
Ni ₂ Al ₃	hexagonal	42.03% Ni
Al	c.c.p.	100% Al

f.c.c refers to a face-centered cubic structure, b.c.c to a body-centered cubic, and c.c.p to a cubic closest packed arrangement.

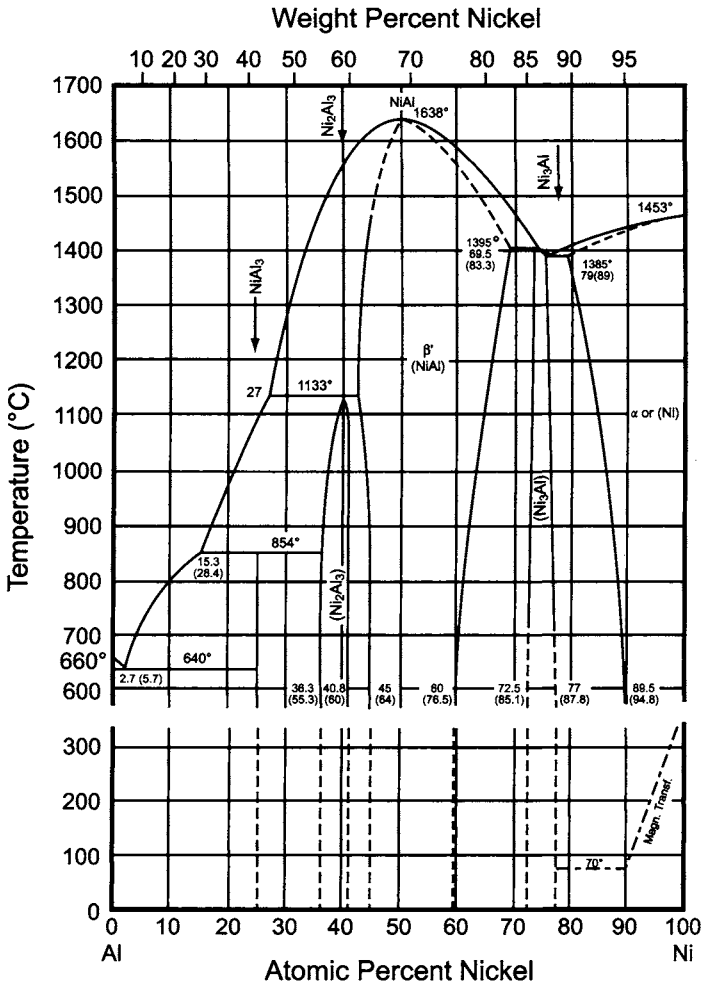


FIGURE 4.6.9. Phase diagram of the Al–Ni system [32]. (With permission from McGraw Hill.)

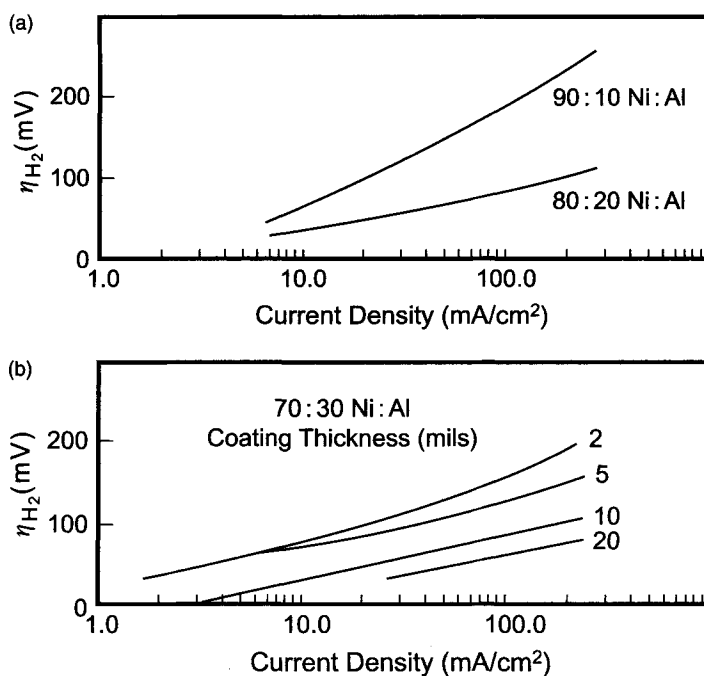
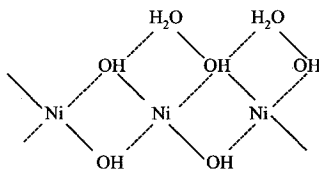


FIGURE 4.6.10. Polarization data for the HER on plasma sprayed Ni-Al composites with (a) varying Ni:Al ratio and (b) thickness in 15% NaOH + 17% NaCl solutions at 95°C [10]. (With permission from the Indian Academy of Sciences.)

Aluminum is preferentially leached out from Ni_2Al_3 and Ni_3Al by hot caustic solutions. The mixture of these compounds, applied by the plasma spraying technique, was found to be active for the hydrogen electrode process, the best results being observed at Ni/Al = 65/35 [33,34].

Typical polarization data of Ni-Al composites is shown in Fig. 4.6.10. These electrodes exhibit a Tafel slope of 40–60 mV in the low current density region and 120 mV in the high current density region [10,46,50–52].

Raney nickel-based electrodes are prone to deactivate for several reasons, one of them being the formation of α -Ni(OH)₂, which is catalytically active but thermodynamically unstable. The long-term performance of this Raney nickel electrode is found to be significantly improved by the *in situ* formation of β -Ni(OH)₂, which is thermodynamically stable, but is inactive electrochemically [41,53–55]. Korovin *et al.* [56] suggested that while Ni(OH)₂·*n*H₂O is unstable, its cross-linked structure, noted below, may prevent further oxidation and poisoning of the electrode surface.



Another Raney Ni preparation that has been studied by many investigators is that formed from Ni–Zn alloys that are prepared either by plasma spraying Ni and Zn powders or by electrolytic methods. Electroplating of Ni–Zn alloys [57–65] results in the formation of various alloys such as NiZn, NiZn₃, and Ni₃Zn₂, which are treated with NaOH to dissolve Zn as a soluble zincate ion, in order to develop a porous matrix with a large area and exhibiting low hydrogen overvoltage in chlor-alkali cells [66,67].

The preparation and electrochemical characterization of plasma sprayed coatings of Raney nickel and nickel powders with additions of Cr, Co, Ti, W, Mo, and Fe is described in [37–52, 74–77], and electrodeposited alloys of Ni–Zn and Co are discussed in [68–72].

4.6.4.2. Ni–Mo-Based Coatings. Ni–Mo-based coatings have been examined extensively. Inclusion of Mo in the nickel coatings to achieve catalysis was probably motivated by the use of molybdenized graphite to enhance the decomposition of sodium or potassium amalgams in the chlor-alkali industry [78]. Although Mo is not

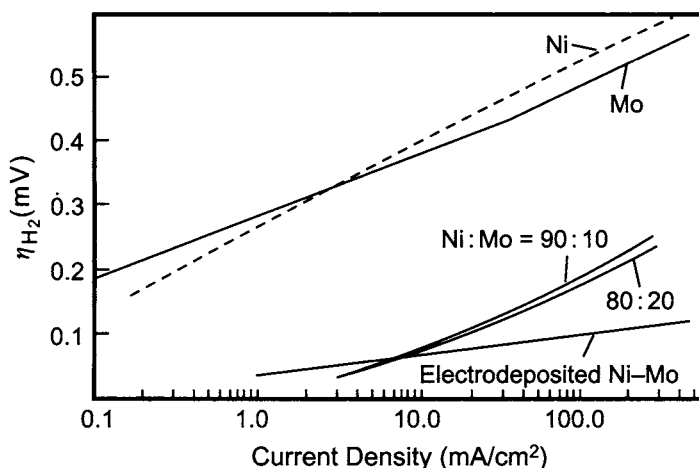


FIGURE 4.6.11. Polarization data for the HER on plasma sprayed Ni, Mo; plasma sprayed Ni : Mo composites at varying Ni : Mo ratios; and electrodeposited Ni–Mo in 15% NaOH + 17% NaCl solutions at 95°C [10]. (With permission from the Indian Academy of Sciences.)

TABLE 4.6.4 Characteristics of the Ni–Mo-based Alloy Cathodes for Hydrogen Evolution in 6M KOH at 80°C [93]

Material	Tafel slope		Overvoltage at 300 mA cm ⁻²
	at <50 mA cm ⁻²	at >50 mA cm ⁻²	
Ni–Mo–Fe	115	165	187
Ni–Mo–Cu	28	180	190
Ni–Mo–Zn	24	116	220
Ni–Mo–W	28	150	286
Ni–Mo–Co	26	140	270
Ni–Mo–Cr	32	165	350
Steel	135	125	540

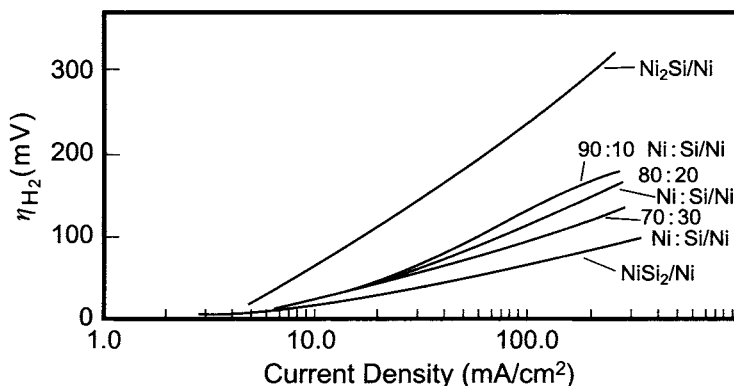


FIGURE 4.6.12. Polarization data for the HER on plasma sprayed Ni:Si composites at varying Ni:Si ratios, Ni_2Si and NiSi_2 on Ni substrates in 15% NaOH + 17% NaCl solutions at 95°C [10]. (With permission from the Indian Academy of Sciences.)

electrocatalytically active for the HER, Ni–Mo alloys formed electrolytically or by plasma spraying show low overvoltages, as depicted in Fig. 4.6.11. It is interesting to note that bulk alloys of Ni–Mo do not exhibit low overvoltages [10]. Various minor additives, such as V, Ti, W, Cd, Re, Fe, Co, Cr, and Cu, when incorporated in the basic Ni–Mo composites, improved performance [73,79–92] (Table 4.6.4). The catalytic activity of the Ni–Mo alloy cathode varies greatly with the chemical composition and the method of preparation [87–92]. The 60Ni–40Mo (in at%) alloy showed high catalytic activity [91].

An interesting patented composition, studied in detail [93,94] from a fundamental viewpoint, was the Ni–Mo–Cd coating formed electrolytically on nickel substrates, which exhibited a Tafel slope of about 40 mV in the current density range of 0.1–0.3 A cm^{-2} . These coatings were found to be more active than Ni–Mo layers, the activity being attributed to the presence of Cd, which imparted a hydrogen absorbing ability or modulated the properties of the hydrogen phase on the surface [93–95]. Coatings based on Ni–Mo–Fe are described in [93–99].

4.6.4.3. Other Ni-Based Materials. The Ni–Sn (5.9–37 at% Sn) alloy formed by electroplating from a bath containing NiCl_2 , pyrophosphate, and SnCl_2 , showed low hydrogen overvoltage in 28% KOH at 20°C , with a Tafel slope of 52 mV [100]. On the other hand, an electrodeposited Ni–Mn alloy did not exhibit low overvoltages for the HER [101]. It is interesting to note that Ni–Si based coatings showed low overvoltages and low Tafel slopes (Fig. 4.6.12). The activity exhibited by these electrodes is a direct consequence of the high surface area generated by leaching of Si with NaOH [10].

The hydrogen overvoltages on Ni–Co–P, Ni–P, and Co–P prepared by electroless plating were relatively low in KOH solutions—the Tafel slope being 120 mV. The hydrogen overvoltage increased with increase in the P content [102] of the coating.

Other compositions studied include: high surface area cobalt coatings [103–113], amorphous alloys of Ni, Co, Si, and B [114,115], Ni + AlPO_4 + LaPO_4 composites [116–123], PTFE bonded metal powders [125–128], nickel coatings modified with heteropolyacids [134,135], AB_5 -type cathodes (e.g., $\text{LaNi}_{4.7}\text{O}_{0.3}$) [130,143–145], electrodeposited Fe, Ni, Mo layers co-formed with W or W/Mo [132–142], spinels of Ni, Co, Fe, Mn [159,160] and La, Zr, Al [161], and Co_3O_4 [162].

4.6.4.4. *Oxides.* Another class of compounds investigated as cathode materials are the oxides of noble metals. These oxides are thermodynamically prone to reduction [146]. However, the kinetics of reduction will dictate their stability when used as cathodes for the HER. Thus, RuO_2 is stable during long-term electrolysis, when used as a cathode with no bulk reduction of the oxide, although RuO_2 can be reduced by hydrogen at high temperatures [145].

A number of noble metal coatings, including $\text{RuO}_2\text{-TiO}_2$, were examined in alkaline solutions [147,149–157]. The hydrogen overvoltage of these materials was low because of their large surface area, which is due to their composition and the method of preparation. For example, the physicochemical properties of IrO_2 prepared by thermal oxidation of IrCl_3 at temperatures lower than 350°C differed from those fired at higher temperatures [156], the optimal temperature for perfect oxidation of IrCl_3 being ca. 500°C [150].

The Tafel slope for the hydrogen electrode reaction on a thermally deposited RuO_2 cathode is 40–50 mV at low current densities and 120 mV at high current densities. Also, the cathodic reduction of ClO_3^- occurred on the RuO_2 -coated cathode in chlorate solutions [155].

A composite porous layer of Ni plus RuO_2 , having a high catalytic activity for the hydrogen evolution reaction, was obtained by dispersion electroplating from a Watts-type bath containing RuO_2 powder [154]. A coating of thermally formed RuO_2 on a nickel substrate, modified by a top layer of electroless nickel [158], operated at 250 mV less than a smooth nickel electrode (Fig. 4.6.13) for more than 2.5 years and was relatively insensitive to the presence of iron.

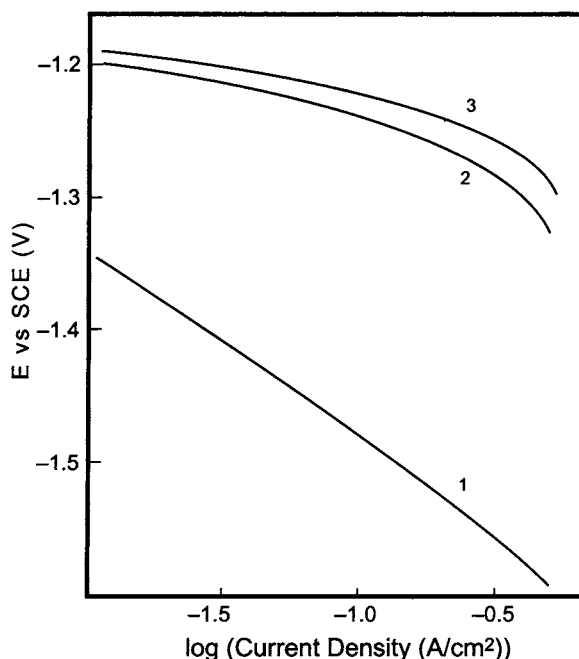


FIGURE 4.6.13. Polarization data for the HER in 35 wt% NaOH at 85°C on (1) electroless Ni coating; (2) thermally formed RuO_2 ; and (3) RuO_2 with electroless Ni coating [158]. (With permission from Elsevier.)

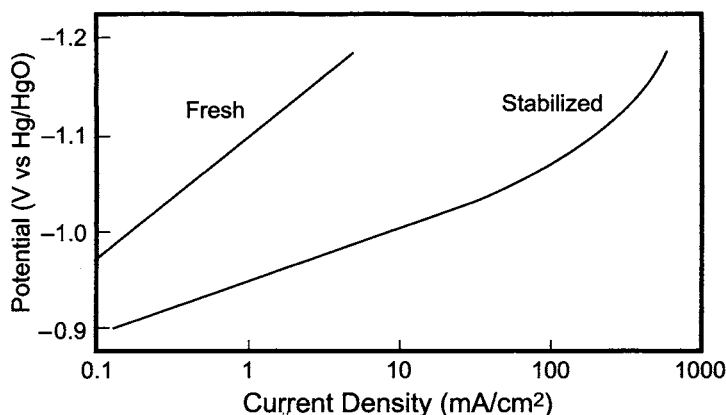


FIGURE 4.6.14. Polarization data for the HER in 1M NaOH at 25°C on NiS_x electrode [174].

4.6.4.5. Sulfides. Sulfur-activated cathodes were first developed in the late 1970s for water electrolysis [163–166], and later extended for use in chlor-alkali cells [167–186]. While FeS_x , CoS_x , and NiCoS_x have been examined, NiS_x is the compound most extensively studied.

NiS_x can be formed in a variety of ways which include: (1) electrodeposition [108,165] from the Watts bath containing sulfur compounds such as thiourea or thiocyanates, (2) electroless plating [169,170] in the presence of dithionite, (3) dispersion plating [171] from the Watts bath with NiS_x powders, and (4) sulfidation of NiO [172]. The sulfur content in the deposit increases with increasing concentration of thiourea in the plating solution [173]. The hydrogen overvoltage decreases as sulfur content increases, the optimum being 12% [174].

The steady-state polarization curves of the NiS_x cathode in alkaline solutions show two Tafel regions with different slopes, which vary with the method of preparation and the sulfur content. Figure 4.6.14 illustrates the polarization characteristics of the NiS_x cathode [174]. The overvoltage of a fresh cathode was significantly high, with a Tafel slope of about 120 mV. The overvoltage decreased gradually during electrolysis, and stabilized after about 200 hr [175]. The Tafel slope decreased to 60 mV at low current densities, while it was still high at high current densities.

The NiS_x cathodes were irreversibly deactivated in the presence of S^{2-} , Cu^{2+} , and Fe^{2+} [180,181] as the adsorption of H intermediates on the cathode surface was retarded by these impurities [18,173].

The NiS_x electrodeposited layer was modified by the addition of other elements to mitigate degradation and deactivation. Addition of molybdenum imparted resistance to the impurities, especially Fe, primarily because of the large surface area [183]. Other sulfur-based compositions studied are activated NiS [173] and Teflon-bonded NiCo_2S_4 [185,186].

4.6.4.6. In Situ Activation. The various cathode coatings examined for application in industrial chlor-alkali cells, and discussed above, have to be applied on to a nickel or steel cathode substrate by electroplating or thermal procedures. This step involves significant cost, depending on the technique employed for laying the active coating,

and can be avoided if an electrocatalytically active material can be deposited, *in situ*, by adding the precursor to the catholyte in the membrane cells or to the anolyte in the diaphragm cells, which will be reduced to the metallic state under cathodic polarization conditions. Of the various additives examined, chloroplatinic acid is promising based on a cost-benefit analysis. Doping of the catholyte with a few ppm of H_2PtCl_6 will yield a voltage savings of 100–150 mV, which can last over 2–3 months depending on the nature and amount of impurities present in the catholyte stream, especially iron.

The kinetic data and the overvoltages of various alloys and composites [10] are presented in Table 4.6.5.

TABLE 4.6.5 Comparison of Hydrogen Overvoltage on Metals/Coatings in 15% NaOH + 17% NaCl at 95°C at a Current Density of 200 mA cm⁻²

Material	Tafel slope ^a (mV)	Overvoltage (mV)	Material	Tafel slope ^a (mV)	Overvoltage (mV)
Ru	45	300	NiB	140	318 ^b
Rh	170	381	Ni ₃ B	130	337 ^b
Pt	170	400	Ni ₂ B	135	381 ^b
Ir	110	540	NiBi	150	393 ^b
Fe	150	440	Ni : ZrO ₂ (80 : 20)	130	250 ^b
Co	40	465	Ni : Al (80 : 20)	63	140 ^b
Ni	100	518	Ni : Al (90 : 10)	162	243 ^b
WC	160	481	Ni : Al (2mils)	100	187 ^b
W	200	531	Ni : Al (5mils)	86	156 ^b
Ti	240	531	Ni : Al (10mils)	53	106 ^b
Vitreous C	700	1087	Ni : Al (20mils)	53	75 ^b
Steel	121	375	NiSi ₂	80	73 ^b
Ni-plated steel	85	440	Ni : Si (70 : 30)	86	118 ^b
Pt implanted steel	150	481	Ni : Si (80 : 20)	100	156 ^b
			Ni : Si (90 : 10)	100	169 ^b
Ni : Ir (75 : 25)	60	310	Ni ₂ Si	200	300 ^b
Ni : Ir (25 : 75)	140	329	Ni : Re (15 : 85)	25	100 ^b
Ni : W (75 : 25)	110	400	Ni : Re (50 : 50)	25	108 ^b
Ni : Ru (75 : 25)	80	416	Ni : Re (84 : 16)	166	325 ^b
Ni : Co (90 : 10)	75	283	Re	350	383
Ni : Co (33 : 67)	60	371	Ni : Mo	30	100
Ni : Co (10 : 90)	50	487	Electroplated		
Ni : Sn (35 : 65): Electroplated	130	691	Ni : Mo(80 : 20)	115	200 ^b
NiT ₂	100	100	Ni : Mo(90 : 10)	115	216 ^b
NiT	90	150	Mo	140	508 ^b
NiSi ₂	170	94	Ni : Al (Raney)	60	59 ^b
Ni : SiC	100	200 ^b	Ni : Mo : Cd Electroplated	30	100
Ni ₃ Sb	120	237 ^b	NiS	110	242
NiS	105	253 ^b	Sintered Ni	180	275
Ni ₂ P	100	240	Thermally formed Pt	83	133
			Teflon bonded Pt	30	41

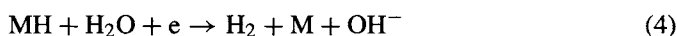
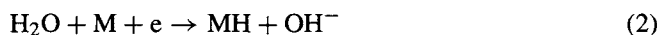
Note:

^aObtained from the high current density region.

^bCoatings were formed by plasma spraying on Ni substrates.

4.6.5. HER Mechanisms on Low Overvoltage Cathodes

The reaction pathways involved in the course of the HER on smooth metals are described in Section 4.2. The generally accepted mechanism of the HER in alkaline solutions involves water molecules as a source of protons, which discharge on the cathode surface, M, to form an M–H bond, as in Eq. (2) (Table 4.6.1). The adsorbed H can either combine with another H to form H₂ (Eq. 3) or react with a water molecule to form H₂ (Eq. 4).



Whenever adsorbed intermediates are involved in the slow step of the HER, the Tafel slopes assume low values, as shown theoretically and depicted in Table 4.6.1. However, mechanisms that give rise to low Tafel slopes, because of the dependence of coverage by the adsorbed intermediates on the potential, may have a disadvantage on metals, as hydrogen embrittlement [5] can occur because of the diffusion of adsorbed H into the metal. Thus, while the low Tafel slopes are advantageous from a voltage viewpoint, they can have a serious adverse influence on long-term performance.

A comparison of polarization data on high surface area preparations, with the same metal in the bulk form, shows that as the surface area increases, the Tafel slope decreases [10,187]. Thus, the Tafel slope on smooth Ni in alkaline solutions decreases from about 100 mV to 30–40 mV with Raney Ni and various other compositions (Fig. 4.6.15). This behavior is not unique to Ni, but is also observed on Pt during the course of the HER in alkaline solutions (Fig. 4.6.16).

As the HER occurred on high-surface area matrices, the effect of the porous structure on the Tafel slope behavior was examined [188] by assuming a homogeneous elementary flooded pore model and deducing the current–voltage relationships, taking into account the backward rate and the coverage dependence on potential. This analysis showed that

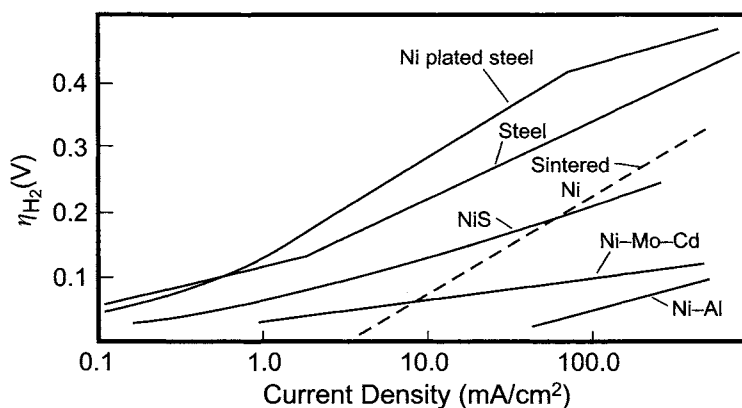


FIGURE 4.6.15. Polarization data for the HER on various Ni-based compositions in 15% NaOH + 17% NaCl solutions at 95°C [10]. (With permission from the Indian Academy of Sciences.)

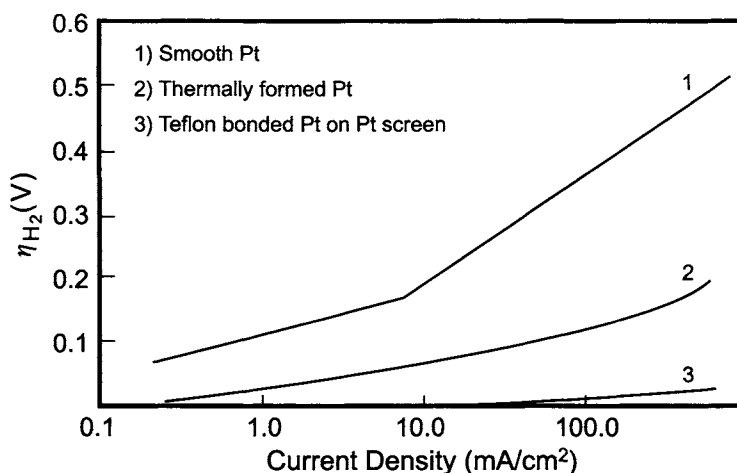
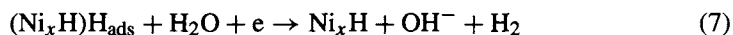
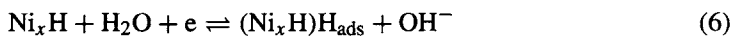
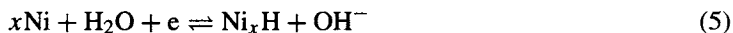


FIGURE 4.6.16. Polarization data for the HER on smooth and high surface area Pt in 15% NaOH + 17% NaCl solutions at 95°C [10]. (With permission from the Indian Academy of Sciences.)

when the rate-determining step is discharge or electrochemical desorption, the Tafel slopes change from $2RT/F$ and $2RT/3F$, respectively to $4RT/F$ at high overvoltages. However, when recombination is the slow step, the Tafel slope changes from $RT/2F$ to a non-Tafel characteristic where $I \propto \sqrt{\eta}$. Thus, it is not the porous nature of the surface structure that is responsible for the low Tafel slopes observed with high surface composites.

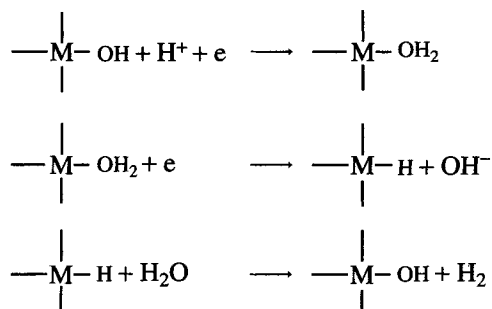
Another explanation [95], based on an analysis of the decay in potential after the interruption of current, involves the possible formation of a three-dimensional hydride lattice (on high area nickel surfaces formed by leaching of plasma sprayed Ni–Al coatings, and electrodeposited Ni–Mo–Cd coatings), on which the HER proceeds, as described below.



While the two quasi-equilibria, Eqs. (5 and 6), preceding the slow-step will indeed give low Tafel slopes, it is difficult to comprehend hydride formation only on high surface area matrices and not on smooth electrodes. Furthermore, as noted earlier, this behavior is not unique to nickel, as similar behavior was observed on Pt electrodes (Fig. 6.4.16).

Since high-surface electrodes have “active sites” with varying energetics, it is conceivable that the activation energy is altered, resulting in mechanistic changes. However, the role of the surface area in inducing mechanistic variations is yet to be clearly understood. Any proposed model should involve a “surface-area related factor” in the exponential term $\beta\eta F/RT$.

In the RuO₂-based electrodes, the mechanism of the hydrogen evolution leading to low Tafel slopes of 40–50 mV is believed [13,189] to be as follows:



This mechanism allows the oxide state to remain unchanged.

4.6.6. Cathode Deactivation

Cathode potentials can increase for many different reasons. These include blockage by H₂ gas bubbles [176–178], organic impurities [179], and inorganic impurities such as silicate in diaphragm cells [180], deposition of high overvoltage metals [e.g., Hg, Cd] on the cathode substrate [181–186,190], and corrosion of the catalytic coatings during (1) shutdowns (because of reverse currents flowing under those conditions), (2) attack by hypochlorite, and (3) formation of hydride, followed by spalling of the coatings or the substrate.

Studies have shown that Cr, Ni, Hg, Fe, and organic compounds containing N or S adversely affect the cathode potential [186,190] of steel. Iron was found to be particularly harmful to the performance of activated cathodes (Fig. 4.6.17). Pt-Ru coated cathodes [191] are affected at Fe levels as low as 3 ppm Fe in the solution. However, with smooth Ni or Ti cathodes, Fe was found to lower the cathode potential [181,182], as the deposits formed on the cathode had a large surface area.

Another reason for cathode deactivation is the progressive leaching of one of the components of the cathode coating. Thus, an NiS_x cathode is gradually deactivated [181–183] by the dissolution of S in alkaline solutions. Similar behavior may be anticipated when one of the components in the coating is thermodynamically unstable in a NaOH solution (e.g., Mo in Ni–Mo-based coatings). Hence, it is important that the inherent thermodynamic stability of the various components in the coating and the substrate be initially assessed to a first approximation from the Pourbaix diagrams. This analysis can provide insights into probable mechanisms for increase in overvoltage.

The cathode coating and substrate should also be resistant to hypochlorite and the reverse currents encountered during shutdowns. Whenever the current is interrupted, a reverse current flows through the cell because of the presence of the active chlorine species in the anolyte. As a result, the cathode becomes anodic for a brief period until all the active chlorine species are reduced to chloride. Also, following a shutdown, the hypochlorite in the anolyte is transported into the catholyte, raising its hypochlorite level to 5–30 ppm in membrane cells, and 300–5,000 ppm in diaphragm cells. Reduction of

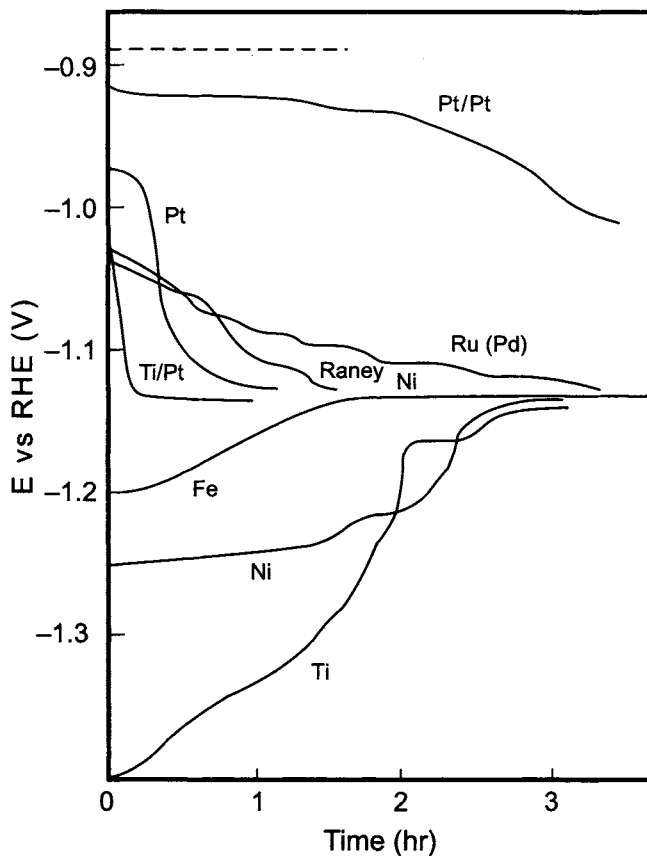
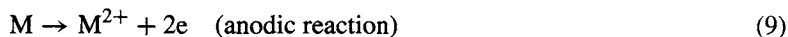
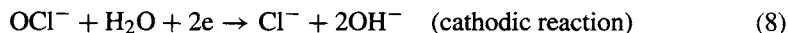


FIGURE 4.6.17. Variation of the cathode potential with time during the course of the HER from 33% NaOH at 90°C and 3 kA m^{-2} in the presence of 10 ppm Fe. The dashed line represents the reversible potential [188]. (Reproduced by permission of The Electrochemical Society, Inc.)

hypochlorite leads to the oxidation of the metal, as described by the equations,



Thus, the primary reason for the deactivation of cathode coatings is the presence of impurities and OCl^- in the catholyte. Highly porous coatings with a large surface area can minimize the effects of poisoning by the impurities because the electrode offers a significant area for the HER even after a fraction of the surface becomes unavailable. Porosity can thus serve as a sponge for the impurities, depending on the morphology of the active layer. It should be noted that there is no catalytic cathode coating immune to the impurity effects, since the impurities will either deposit or physically block the surface. If the hydrogen overvoltage is high on these deposited species, the overvoltage can increase and negate the intended effects. If the cathode coatings are oxides or sulfides, it is possible that the impurities may not deposit on these “nonmetallic” surfaces [182–186].

The adverse effects from the dissolved chlorine in the anolyte can be eliminated either by destroying hypochlorite when the current is interrupted or by cathodically protecting the cathode during shutdowns. Hypochlorite removal can be achieved by flushing the anolyte or by reacting it with a sulfite or H_2O_2 . If the cathode material is unstable in the pH region of 3–7, the pH must simultaneously be brought into the alkaline region. This step must be implemented as quickly as possible.

4.6.7. Current Status

A number of active cathode materials have been investigated and developed within the past 30 years, following the energy crisis and the skyrocketing electricity prices of the mid-1970s. Among them, nickel and nickel-plated steel cathodes coated with electrocatalytically active and porous layers have been commercialized in the chlor-alkali industry. Table 4.6.3 describes the various compositions developed for chlor-alkali applications, and Table 4.6.5 gives kinetic parameters of some of the coatings. Activated cathodes developed by various technology suppliers are described below.

Tosoh Co. developed a Ni–Fe alloy cathode containing 20–85 at% Fe in the alloy. This coating, formed by electroplating [190], showed a hydrogen overvoltage of about 120 mV at 4 kA m^{-2} in 32.5% NaOH at 90°C. It was claimed to offer resistance to current interruptions, based on the constancy of the voltage of a bipolar electrolyzer (BiTAC) at 3.23–3.25 V over 250 days with 4 shutdowns.

Asahi Kasei's electrolyzers use NiO cathodes that are resistant to impurities and current interruptions [191]. They are prepared by plasma spraying a mixture of NiO and Cr_2O_3 or a TiO_2 promoter onto nickel-plated steel. The loading of the catalyst mixture is 0.10–0.15 g cm^{-2} . This cathode has been used for more than 15 years in commercial operations.

INEOS chlor offers both precious metal and nickel alloy coatings [192]. The precious metal coatings are deposited on a nickel substrate, and the electrocatalytically active layers are applied to the surface by thermal deposition or electroplating. Thermal spraying or vacuum deposition techniques form the nickel-alloy coating. These materials have been used in the FM 21 electrolyzers for over four membrane cycles.

Dow uses a porous cathode coating activated with RuO_2 on a woven nickel wire screen [193]. The active layer is prepared by painting a mixture of ruthenium chloride and palladium chloride, followed by heating at 300–500°C, in order to deposit the oxides. A thin layer of electroless nickel strengthens the cathode coating structure. This electrode is resistant to iron as the hydrogen overvoltage increases only by 10 mV during electrolysis with solutions contaminated with Fe.

Tokuyama Soda Company developed NiS_x and Ni–Sn alloy coated cathodes [194–197]. The hydrogen overvoltage of the electroplated Ni–Sn alloy cathode, with a nickel content of 40–80 wt%, in a mixed solution of NaOH and NaCl at 90°C, was about 100 mV. The Ni–Sn cathodes were used in retrofit-type membrane cells and filter press-type electrolyzers, both operating at 4 kA m^{-2} and 80°C. The cell voltages were constant for over 8 years.

Toagosei Chemical Company and Chlorine Engineers Corporation jointly developed Ni–C dispersion electroplated cathodes, named TWAC, in the 1980s [198–200]. The Ni–C composite layer is applied to the nickel plated type 304 stainless steel substrate by dispersion electroplating. The Watts-type plating bath contains

a small amount of CuSO_4 , as well as carbon powder, to improve the electrocatalytic activity for the HER. The coated layer is then overlaid with electrodeposited Ni-S to improve the mechanical strength. The two-step electroplating process is repeated three times to obtain a large surface area. Antimony trioxide is added to modify the TWAC coating. The hydrogen overvoltage of TWAC, in alkaline solutions under chlor-alkali operating conditions, is about the same as that of a rhodium-coated cathode. TWAC is also resistant to solution impurities and shutdowns.

Asahi Glass Company prepared a modified Raney nickel-coated cathode for their AZEC chlor-alkali electrolyzers [201–206]. While the Raney Ni catalyst is active to the hydrogen electrode process, it is also sensitive to solution impurities and oxidation, caused by short-circuiting. AGC applied the Ni-based composite layer on the cathode substrate by dispersion electroplating. The plating bath contains the Raney Ni powder and hydrogen-storing alloy powder, which are codeposited with the Ni matrix. The coated layer is resistant to erosion due to the rapid flow of gas-solution mixture. The third constituent absorbs and stores a large amount of hydrogen during cell operation, and discharges during shutdowns when the cell is virtually short-circuited. Hydrogen is electrochemically oxidized at low potentials and hence, the Raney nickel and the Ni matrix are prevented from oxidation. The hydrogen overvoltage of this material remains constant at ca. 100 mV, for several days online even when the electrolyzer is shut down.

ELTECH Systems Corporation supplies a Voltage Reduction Solution (VRS) [207], which is essentially a solution of chloroplatinic acid. When added to the catholyte, it is electrodeposited in a high surface form and reduces cathodic overvoltage. This *in situ* activation is claimed to be very economical and convenient as long as the residual platinum species in the catholyte caustic has no adverse effect on the end use of the caustic soda.

REFERENCES

1. T. Ohta, J.E. Funk, J.D. Porter, and B.V. Tilak, *Int. J. Hydrogen Energy* **10**, 571 (1985).
2. B.V. Tilak, P.W.T. Lu, J.E. Colman, and S. Srinivasan. Electrolytic Production of Hydrogen, In J.O'M. Bockis, B.E. Conway, E. Yeager, and R.E. White (eds), *Comprehensive Treatise of Electrochemistry*, Vol. 2, Plenum Press, New York (1981), p. 1.
3. M. Pourbaix, *Atlas of Electrochemical Equilibria in Aqueous Solutions*, Pergamon Press, Oxford (1960), p. 312.
4. B.E. Conway and B.V. Tilak, *Adv. Catalysis* **38**, 1 (1992).
5. J.O'M. Bockris and P.K. Subramanian, *Electrochim. Acta* **16**, 2169 (1971).
6. B.V. Tilak and C.P. Chen, *J. Appl. Electrochem.* **23**, 631 (1993).
7. H.F. Flitt and J.O'M. Bockris, *Int. J. Hydrogen Energy* **7**, 411 (1982).
8. H. Kita, *J. Electrochem. Soc.* **113**, 1095 (1966).
9. A.T. Kuhn. Surveying Electrocatalysis, In H. Bloom and F. Gutmann (eds), *Electrochemistry—The Past Thirty and the Next Thirty Years*, Plenum Press, New York (1977).
10. B.V. Tilak, A.C.R. Murty, and B.E. Conway, *Proc. Indian Acad. Sci.* **97**, 359 (1986).
11. R. Parsons, *Surface Science* **18**, 28 (1969).
12. B.V. Tilak, K. Tari, and C.L. Hoover, *J. Electrochem. Soc.* **135**, 1386 (1988).
13. S. Trasatti. Electrocatalysis of Hydrogen Evolution: Progress in Cathode Activation, In H. Gerischer and C.W. Tobias (eds), *Advances in Electrochemical Science and Engineering*, Vol. 2, VCH Publishers, New York (1992), p. 1.
14. Heany Industries Brochure (1999).

15. C. Welch, C.N. Hughes, R.A. Crawford, and D.W. DuBois, Electroarc-Produced Raney Nickel Alloy-Coated Cathodes for Chlor-Alkali cells, In M.M. Silver and E.M. Spore (eds), *Proceedings of Symposium on Advances in the Chlor-Alkali and Chlorate Industry*, Vol. 84-11, In The Electrochemical Society Inc., Princeton, NJ (1984), p. 192.
16. F. Hine, M. Yasuda and M. Watanabe, *Denki Kagaku. J. Electrochem. Soc. Japan.* **47**, 401 (1979).
17. L.E. Hetherington and M.L. Holt, *J. Electrochem. Soc.* **98**, 106 (1951).
18. L. Komnikov, *Metal Finishing* **62**, 49 (1964).
19. N.W. Hovey, A. Krohn, and G.M. Hanneken Jr., *J. Electrochem. Soc.* **110**, 362 (1963).
20. J.Z.O. Stachurski, D. Pouli, J. Ripa, and G.F. Pokrzyk, *U.S. Patent* 4,354,915 (1982).
21. J.E. Bennett and H.G. Tompkins, *J. Electrochem. Soc.* **123**, 999 (1976).
22. M.A. Riley and P.J. Moran, *J. Electrochem. Soc.* **133**, 760 (1988).
23. J.Y. Huot and L. Bossard, *Surf. Coat. Tech.* **34**, 373 (1988); *Int. J. Hydrogen Energy* **12**, 821 (1987); **14**, 229 (1989); *J. Appl. Electrochem.* **18**, 815 (1988).
24. *Ger. Offen*, 2,818,306 (1978).
25. E. Justi, W. Scheibe, and A. Winsel, *German Patent* DPB 1 101 361 1954.
26. N.V. Korovin, V.N. Savel'eva, Yu.I. Shishkov, and E.I. Mingulina, *Soviet Electrochem.* **8**, 533 (1972).
27. J. Balej, *Int. J. Hydrogen Energy* **10**, 89 (1985).
28. T. Kenjo, *Electrochim. Acta* **33**, 41 (1988).
29. *U.S. Patent* 4,248,679 (1981).
30. *U.S. Patent* 4,251,478 (1981).
31. *U.S. Patent* 4,323,595 (1982); *U.S. Patent* 4,396,473 (1983).
32. M. Hansen, *Constitution of Binary Alloys*, McGraw-Hill Book Company, New York (1958), p. 119.
33. K. Subramanian, V. Arumugan, K. Asokan, P. Subbiah, and S. Krishnamurthy, *Bull. Electrochem.* **7**, 271 (1991).
34. A.T. Skiarov, F.V. Kupovich, V. Busse-Macukus, and A.F. Mazanko, *Soviet Electrochem.* **27**, 1405 (1991).
35. P. Los, A. Rami, and A. Lasia, *J. Appl. Electrochem.* **23**, 135 (1993).
36. L. Chen and A. Lasia, *J. Electrochem.* **140**, 246 (1993).
37. H. Kronberger, Ch. Farian, and G. Frithum, *Int. J. Hydrogen Energy* **16**, 219 (1991).
38. A. Kayser, V. Borck, M. von Bradke, R. Henne, W.A. Kaysser, and G. Schiller, *Zeit. Metallkd.* **83**, 565 (1992).
39. *U.S. Patent* 4,024,044 (1997).
40. *British Patent* 1,533,758 (1978).
41. Y. Choquette, H. Menard, and L. Brossard, *Int. J. Hydrogen Energy* **15**, 21 (1990).
42. A. Dang, A. Capuano, J.M. Chapuzel, and J. Lassard, *Int. J. Hydrogen Energy* **18**, 41 (1993).
43. R.W. Brennecke and H.H. Ewe, *Energy Commercial Manage.* **31**, 85 (1991).
44. N. Korovin and E. Udris, *Int. J. Hydrogen Energy* **17**, 929 (1992).
45. H. Wendt, H. Hofmann, and V. Plzak, *Mat. Chem. Phys.* **22**, 27 (1989).
46. K. Lohrberg and P. Kohl, *Electrochim. Acta* **29**, 1557 (1984).
47. L. Brossard, *Int. J. Hydrogen Energy* **13**, 315 (1988).
48. Y. Choquette, H. Menard, and L. Brossard, *Int. J. Hydrogen Energy* **14**, 637 (1989); Y. Choquette, L. Brossard, and H. Menard, *J. Appl. Electrochem.* **20**, 855 (1990).
49. S. Pushpavanam, M. Pushpavanam, S.R. Natarajan, K.C. Narasimham, and S. Chinnasamy, *Int. J. Hydrogen Energy* **18**, 277 (1993).
50. A.G. Pshenichnikov, *Int. J. Hydrogen Energy* **7**, 51 (1982).
51. A.G. Pshenichnikov, *Mat. Chem. Phys.* **22**, 121 (1989).
52. J. Divisek, J. Mergel, and H. Schmitz, *Int. J. Hydrogen Energy* **7**, 695 (1982).
53. K. Schultze and H. Bartelt, *Int. J. Hydrogen Energy* **17**, 711 (1992).
54. H. Bode, K. Dehmelt, and J. Witte, *Electrochim. Acta* **11**, 1079 (1966).
55. J. Huot and L. Brossard, *Int. J. Hydrogen Energy* **12**, 821 (1987).
56. N.V. Korovin, J. Udris, and M. Yu. Khodos, *Soviet Electrochem.* **29**, 631 (1993).
57. M. Hansen, *Constitution of Binary Alloys*, McGraw-Hill Book Company, New York (1958), p. 1059.
58. L. Domnikov, *Metal Finishing*. p. 49, August 1963.
59. L. Domnikov, *Metal Finishing*. p. 63, March 1965.
60. A. Knodler and S. Gmund, *Metalloberflach.* **21**, 321 (1967).
61. K.N. Rao, M.I.A. Siddiqi, and C.V. Suryanarayana, *Electrochim. Acta* **10**, 577 (1965).

62. J.W. Dini and H.R. Johnson, *Metal Finishing*, (August 1979), p. 31.
63. J.W. Dini, H.R. Johnson, and J.A. Brooks, *Metal Finishing* (Feb. 1979), p. 99.
64. M. Yunus, C. Capel-Boute, and C. Decroly, *Electrochim. Acta* **10**, 885 (1965).
65. J. Mindowicz, C. Capel-Boute, and C. Decroly, *Electrochim. Acta* **10**, 901 (1965).
66. T.A. Liederbach, A.M. Greenberg, and V.H. Thomas. Commercial Application of Cathode Coatings in Electrolytic Chlorine Cells, Commercial Application of Cathode Coatings in Electrolytic Chlorine Cells, In M.O. Coulter (ed.), *Modern Chlor-Alkali Technology*, Ellis Horwood, Chichester, (1980), p. 145.
67. *U.S. Patent* 4,104,133 (1978).
68. R.Ku. Burshstein, V.E. Kazarinov, A.G. Pshenichnikov, I.E. Barbasheva, G.A. Gafarova, and I.V. Obrushnikova, *Soviet Electrochem.* **23**, 674 (1987).
69. M.J. DeGiz, S.a.S. Machado, L.A. Avaca, and E.R. Gonzalez, *J. Appl. Electrochem.* **22**, 973 (1992).
70. M.J. DeGiz, G. Tremiilliosi-Filho, and E.R. Gonzalez, *Electrochim. Acta* **39**, 1775 (1994).
71. L. Chen and A. Lasia, *J. Electrochem. Soc.* **138**, 3321 (1991).
72. L. Chen and A. Lasia, *J. Electrochem. Soc.* **139**, 3214 (1992).
73. A. Rami and A. Lasia, *J. Appl. Electrochem.* **22**, 376 (1992).
74. M. Okido, J.K. Depo, and G.A. Capuano, *J. Electrochem. Soc.* **140**, 127 (1993).
75. H. Wendt and V. Plzak, *Electrochim. Acta* **28**, 27 (1983).
76. P. Ekdunge, K. Juttner, and G. Kresya, *J. Electrochem. Soc.* **138**, 2660 (1991).
77. S.F. Chenyshov, Yu.I. Kryukov, and A.G. Pschenichnikov, *Soviet Electrochem.* **28**, 317 (1992).
78. M.M. Jaksic and I.M. Csonka, *Electrochem. Technol.* **4**, 49 (1966).
79. G. Imarisio, *Int. J. Hydrogen Energy* **2**, 53 (1977).
80. C. Baileux, A. Damien, and A. Montet, *Int. J. Hydrogen Energy* **8**, 529 (1983).
81. I.A. Raj and V.K. Venkatesan, *Int. J. Hydrogen Energy* **13**, 215 (1988).
82. M. Bonner, T. Botts, J. McBreen, A. Mezzina, F. Salzano, and C. Yang, *Int. J. Hydrogen Energy* **9**, 265 (1984).
83. M.V. Ananth and N.V. Parthasarathy, *Int. J. Hydrogen Energy* **15**, 193 (1990).
84. I.A. Raj, R. Pattabiraman, S. Dheenadayalan, R. Chandrasakaran, and V.K. Venkatesan, *Bull. Electrochem.* **2**, 477 (1986).
85. I.A. Raj and K.I. Vasu, *J. Appl. Electrochem.* **20**, 32 (1990).
86. A. Nidola, *Int. J. Hydrogen Energy* **9**, 367 (1984).
87. V. Arumugan, K. Subramanian, and K.I. Vasu, *Bull. Electrochem.* **4**, 965 (1988).
88. J.Y. Huot, M.I. Trudeau, and R. Schultz, *J. Electrochem. Soc.* **138**, 1316 (1991).
89. C. Fan, D.L. Piron, and M. Roias, *Int. J. Hydrogen Energy* **19**, 29 (1994).
90. C. Fan, D.L. Piron, A. Sleb, and P. Paradis, *J. Electrochem. Soc.* **141**, 382 (1994).
91. S. Anderson, D.E. Brown, S.M. Hall, M.M. Mahmood, M.C.M. Man, A.K. Turner, and D. Wood, An Electro-catalyst for Hydrogen Electrodes, *Electrochem. Soc. Meeting, Extended Abstracts*, Vol. 81-1 (1981), p. 1254.
92. J. Divisek, H. Schitz, and J. Balej, *J. Appl. Electrochem.* **19**, 519 (1989).
93. I.A. Raj, *Int. J. Hydrogen Energy* **17**, 413 (1992); *J. Mater. Sci.* **28**, 4375 (1993); I.A. Raj and K.I. Vasu *J. Appl. Electrochem.* **22**, 471 (1992).
94. B.E. Conway and L. Bai, *Int. J. Hydrogen Energy* **11**, 533 (1986).
95. B.E. Conway, H.A. Kozłowska, M.A. Sattar, and B.V. Tilak, *J. Electrochem. Soc.* **130**, 1825 (1983).
96. R. Simpraga, L. Bai, and B.E. Conway, *J. Electrochem. Soc.* **25**, 628 (1995).
97. J. DeCarvalho, G.T. Filho, and E.R. Gonzalez, *Int. J. Hydrogen Energy* **14**, 161 (1989).
98. H.J. Miao and D.L. Piron, *Electrochim. Acta* **38**, 1079 (1993).
99. L. Brossard, *Int. J. Hydrogen Energy* **16**, 13 (1991).
100. M.F.B. Santos, E.P. deSilva, R. Andrade, Jr., and J.A.F. Dias, *Electrochim. Acta* **37**, 29 (1992).
101. M.V. Ananth and N.V. Parthasarathy, *Bull. Electrochem.* **6**, 40 (1990).
102. J.J. Podesta, R.C.V. Piatti, A.J. Arvia, P. Ekdunge, K. Juttner, and G. Kresya, *Int. J. Hydrogen Energy* **17**, 9 (1992).
103. S.P. Jiang, Y.Z. Chen, J.K. You, T.X. Chen, and A.C. C. Tsueng, *J. Electrochem. Soc.* **137**, 3374 (1990).
104. S.P. Jiang, and A.C.C. Tsueng, *J. Electrochem. Soc.* **137**, 3381 (1990).
105. S.P. Jiang, and A.C.C. Tsueng, *J. Electrochem. Soc.* **137**, 3387 (1990).
106. S.P. Jiang, and A.C.C. Tsueng, *J. Electrochem. Soc.* **138**, 1216 (1991).
107. S.P. Jiang, C.Q. Cui, and A.C.C. Tsueng, *J. Electrochem. Soc.* **138**, 3599 (1991).
108. C.Q. Cui, S.P. Jiang, and A.C.C. Tsueng, *J. Electrochem. Soc.* **139**, 60 (1991).
109. C.Q. Cui, S.P. Jiang, and A.C.C. Tsueng, *J. Electrochem. Soc.* **139**, 1276 (1992).

110. C.Q. Cui, S.P. Jiang, and A.C.C. Tsueng, *J. Electrochem. Soc.* **139**, 1535 (1992).
111. M. Rojas, C.L. Fan, H.J. Maio, and D.L. Piron, *J. Appl. Electrochem.* **22**, 1135 (1992).
112. C.L. Fan, D.L. Piron, H.J. Maio, and M. Rojas, *J. Appl. Electrochem.* **23**, 985 (1993).
113. C.L. Fan, D.L. Piron, M. Meilleur, and L.P. Marin, *Can. J. Chem. Engg.* **71**, 570 (1993).
114. K. Lian, D.W. Kirk, and S.J. Thorpe, *Electrochim. Acta* **36**, 537 (1991).
115. L.J. Vracar and B.E. Conway, *Int. J. Hydrogen Energy* **15**, 701 (1990).
116. E. Potvin, H. Menard, and J.M. Lalancette, *J. Appl. Electrochem.* **20**, 252 (1990).
117. E. Potvin, H. Menard, L. Brossard, and J.M. Lalancette, *Int. J. Hydrogen Energy* **15**, 843 (1990).
118. E. Potvin, A. Lasia, H. Menard, and L. Brossard, *J. Electrochem. Soc.* **138**, 900 (1991).
119. H. Dumont, P. Los, L. Brossard, A. Lasia, and H. Menard, *J. Electrochem. Soc.* **139**, 2143 (1992).
120. H. Dumont, P. Los, A. Lasia, H. Menard, and L. Brossard, *J. Appl. Electrochem.* **23**, 684 (1993).
121. H. Dumont, P. Los, L. Brossard, and H. Menard, *J. Electrochem. Soc.* **141**, 1225 (1994).
122. H. Dumont, P. Los, H. Menard, L. Brossard, B. Salvato, and O. Vittori, *Int. J. Hydrogen Energy* **18**, 719 (1993).
123. P. Los, A. Lasia, H. Menard, and L. Brossard, *J. Electroanal. Chem.* **360**, 101 (1993).
124. A. Anani, Z. Mao, S. Srinivasan, and A.J. Appleby, *J. Appl. Electrochem.* **21**, 683 (1991).
125. P.R. Vassie and A.C.C. Tseung, *Electrochim. Acta* **20**, 759 (1975).
126. P.R. Vassie and A.C.C. Tseung, *Electrochim. Acta* **20**, 763 (1975).
127. A.C.C. Tseung and P.R. Vassie, *Electrochim. Acta* **21**, 763 (1976).
128. J.J. Borodzinski and A. Lasia, *Int. J. Hydrogen Energy* **18**, 985 (1993).
129. A.C. Chialvo and M.R.G. deChialvo, *J. Appl. Electrochem.* **21**, 440 (1991).
130. D.E. Hall, J.M. Sarver, and D.O. Gothard, Hydrogen Evolution with AB₅-Catalyzed Coatings, In F. Hine, R.E. White, W.B. Darlington, and R.D. Varjian (eds), *Proceedings on Electrochemical Engineering in the Chlor-Alkali and Chlorate Industries*, Vol. 88-2, The Electrochemical Society Inc., Princeton, NJ (1988), p. 184.
131. O.A. Petrii, K.N. Semenenko, I.I. Korobov, S. Ya. Vasima, I.V. Kovrigina, and V.V. Burnasheva, *J. Less. Common Mat.* **136**, 121 (1987).
132. O. Savadogo and C. Alard, *J. Appl. Electrochem.* **21**, 71 (1991).
133. O. Savadogo and S. Levesque, *J. Appl. Electrochem.* **21**, 457 (1991).
134. O. Savadogo, *Electrochim. Acta* **37**, 1457 (1992).
135. O. Savadogo and F. Carrier, *J. Appl. Electrochem.* **22**, 437 (1992).
136. K. Amuzgare and O. Savadogo, *J. Appl. Electrochem.* **21**, 519 (1992).
137. O. Savadogo and G. Bartolacci, *Int. J. Hydrogen Energy* **17**, 109 (1992).
138. O. Savadogo and H. Lavoie, *Int. J. Hydrogen Energy* **17**, 473 (1992).
139. E. Nuzzebei and O. Savadogo, *Int. J. Hydrogen Energy* **17**, 751 (1992).
140. O. Savadogo and E. Nuzzebei, *J. Appl. Electrochem.* **22**, 915 (1992).
141. O. Savadogo, F. Carrier, and E. Forget, *Int. J. Hydrogen Energy* **19**, 429 (1994).
142. E. Nuzzebei and O. Savadogo, *Int. J. Hydrogen Energy* **19**, 687 (1994).
143. M.M. Jaksic, *Electrochim. Acta* **29**, 1539 (1984).
144. M.M. Jaksic, *Int. J. Hydrogen Energy* **11**, 519 (1986).
145. M.M. Jaksic, *High Temperature Sci.* **30**, 19 (1990).
146. G. Barnel, J.P. Diard, and C. Montella, *Electrochim. Acta* **31**, 277 (1986).
147. E.R. Kotz and S. Stucki, *J. Appl. Electrochem.* **17**, 1190 (1987).
148. Y.C. Lang, Z.D. Zhang, K. Dwight, and A. Wold, *Mat. Res. Bull.* **23**, 631 (1988).
149. D. Galizzioli, F. Tantardini, and S. Trasatti, *J. Appl. Electrochem.* **5**, 203 (1975).
150. G.W. Jang and K. Rajehwar, *J. Electrochem. Soc.* **134**, 1830 (1987).
151. J.F.C. Boodts and S. Trasatti, *J. Appl. Electrochem.* **19**, 255 (1989).
152. J.F.C. Boodts, G. Fregonara, and S. Trasatti. Hydrogen Evolution on Oxide Cathodes, In F. Hine, B.V. Tilak, M. Fenton, and J.D. Lisius (eds), *Symposium on Performance of Electrodes for Industrial Electrochemical Processes*, The Electrochemical Society Inc., Princeton, NJ (1989), p. 135.
153. S. Trasatti, Hydrogen Evolution on Oxide Electrodes, In T.C. Wellington (ed.), *Modern Chlor-Alkali Technology*, Vol. 5, Elsevier, London, (1992), p. 281.
154. C. Iwakura, N. Furukawa, and M. Tanaka, *Electrochim. Acta* **37**, 757 (1992).
155. A. Cornell and D. Simonson, *J. Electrochem. Soc.* **140**, 3123 (1993).
156. H. Chen and S. Trasatti, *J. Appl. Electrochem.* **23**, 559 (1993).
157. I.M. Kodintsev and S. Trasatti, *Electrochim. Acta* **39**, 1803 (1994).
158. M. Jaccoud, F. Leroux, and J.C. Millet, *Mat. Chem. Phys.* **22**, 105 (1989).

159. W.B. Darlington, Activated Cathodes for Reduced Power Consumption in Electrolytic Cells, In O. DeNora (ed.), *Proceedings of the DeNora Symposium on Chlorine Technology*, Venice, (1979), p. 30.
160. E. Nicholas, *Fr. Appl.* 7917441(1979).
161. A.S. Ivanova, V.A. Dzisko, E.M. Moroz, and S.P. Noskova, *Kinet. Katal.* **26**, 1193 (1985); **27**, 428 (1986).
162. E. Veggetti and S. Trasatti, Unpublished results (ref. 483 in ref. 13).
163. P.M. Spaziante, *Ing. Chim. Ital.* **11**, 155 (1975).
164. *Industrial Water Electrolysis*. S. Srinivasan, F.J. Salzano, and A.R. Landgrebe (eds), The Electrochemical Society Inc., Princeton, NJ (1977).
165. H. Vandendorre, Ph.Vermeiren, and R. Laysen, *Electrochim. Acta* **29**, 297 (1984).
166. H. Vandendorre, R. Laysen, H. Nackaerts, and Ph.van Asbroeck, *Int. J. Hydrogen Energy* **9**, 277 (1984).
167. K. Yamakawa, H. Tubakino, K. Akiyoshi, H. Inoue, and K. Yoshimoto. Ni-S Amorphous Alloy as Cathode Material in Chlorine Cell, In F. Hine, R.E. White, W.B. Burlington, and R.D. Varjian (eds), *Electrochemical Engineering in the Chlor-Alkali Industry*, The Electrochemical Society Inc., Princeton, NJ (1988), p. 174.
168. A. Nidola and R. Schira, *Int. J. Hydrogen Energy* **11**, 449 (1986).
169. A.C.C. Tseung, J.A.A. Antonian, and D.B. Hibbert, *Chem. Ind.* **2**, 54 (1984).
170. R. Kh. Burshtein, V.E. Kazarinov, O.A. Gafarova, I.E. Barbasheva, Ya.S. Lapin, and N.P. Kuznetsova, *Soviet Electrochem.* **24**, 1335 (1988).
171. A. Nidola and A. Schira. In T.N. Veziroglu and J.B. Taylor (eds), *Hydrogen Energy Progress V*, Vol. 2, Pergamon Press, New York, (1984), p. 909.
172. A.J. Onuchukwu, *Electrochim. Acta* **27**, 529 (1982).
173. R. Sabela and I. Paseka, *J. Appl. Electrochem.* **29**, 500 (1990).
174. T.C. Wen, S.M. Lin, and J.M. Tsai, *J. Appl. Electrochem.* **24**, 233 (1994).
175. E.R. Gonzalez, L.A. Avaca, G. Tremiliosi-Filho, S.A.S. Machado, and M. Ferreira, *Int. J. Hydrogen Energy* **19**, 17 (1994).
176. P. Gallone, G. Modica, and S. Trasatti, *J. Electroanal. Chem.* **180**, 421 (1984).
177. J. Dukovic and C.W. Tobias, *J. Electrochem. Soc.* **134**, 331 (1987).
178. J.Y. Huot, *J. Appl. Electrochem.* **19**, 453 (1989).
179. A.A. Kuznetsov and Yu.V. Federov, *Soviet Electrochem.* **18**, 738 (1982).
180. A.E. Avrushchhenko, B.N. Yanchuk, N.V. Korovin, and L.G. Ganichenko, *Soviet Electrochem.* **22**, 1186 (1986).
181. C. Baillieux, A. Damien, and A. Montet, *Int. J. Hydrogen Energy* **8**, 529 (1983).
182. A. Nidola and R. Schira. Deactivation of Low Hydrogen Overvoltage Cathodes in Chlor-Alkali Membrane Cell Technology by Metallic Impurities, In M.M. Silver and E.M. Spore (eds), *Advances in the Chlor-Alkali and Chlorate Industry*, The Electrochemical Society Inc., Princeton, NJ (1984), p. 206.
183. A. Nidola. In P. Vincenzini (ed.), *High Tech Ceramics*, Elsevier, Amsterdam (1987), p. 2191.
184. E.R. Kotz and S. Stucki, *J. Appl. Electrochem.* **17**, 1190 (1987).
185. S. Ardrizzone, A. Carugati, G. Lodi, and S. Trasatti, *J. Electrochem. Soc.* **129**, 1689 (1982).
186. S. Ardrizzone, G. Fregonara, and S. Trasatti, *Electrochim. Acta* **35**, 263 (1990).
187. B.E. Conway. The Temperature and Potential Dependence of Electrochemical Reaction Rates, and the Real Form of the Tafel Equation, In B.E. Conway, R.E. White, and J.O'M. Bockris (eds), *Modern Aspects of Electrochemistry*, Vol. 16, Plenum Press, New York (1985), p. 103.
188. B.V. Tilak, S. Venkatesh, and S.K. Rangarajan, *J. Electrochem. Soc.* **136**, 1977 (1989).
189. J.C.F. Boodts and S. Trasatti, *J. Appl. Electrochem.* **19**, 255 (1989).
190. K. Suetsugu, T. Sakaki, K. Yoshimitsu, K. Yamaguchi, A. Kawashima, and K. Hashimoto, Ni-Fe Alloy Cathodes for Chlor-Alkali Electrolysis, In *Proc. Vol. 99-21*, The Electrochemical Society Inc., Princeton, NJ (1999), p. 169.
191. H. Houda, Y. Naoki, and H. Obanawa, Characteristics of Plasma-Sprayed NiO Cathode and Mechanism of Hydrogen Evolution Reaction at its surface, In *Proc. Vol. 98-10*, The Electrochemical Society Inc. (1998), p. 329.
192. J.F. Cairns, M.R. Cook, P.M. Hayes, D.R. Hodgson, P.A. Izzard, M.J. Mockford, E. Paul, and F. Rourke, Advances In ICI's Activated Cathode Technology for Chlor-Alkali Production, In *Proc. Vol. 98-10*, The Electrochemical Society Inc. Princeton, NJ (1998), p. 289.
193. Yu-Min Tsou, Novel High performance Hydrogen Cathode Coating, In *Proc. Vol. 99-21*, The Electrochemical Society Inc., Princeton, NJ (1999), p. 160.

194. Y. Yamakawa, H. Tubakino, K. Akiyoshi, H. Inoue, and K. Yoshimoto, *Proc. Vol. 88-2*, The Electrochemical Society Inc., Princeton, NJ (1988), p. 174.
195. H. Yamashita, T. Yamamura, and K. Yoshimoto, *J. Electrochem. Soc.* **140**, 2238 (1993).
196. H. Yamashita, T. Yamamura, and K. Yoshimoto, *Denki Kagaku (J. Electrochem. Soc. Japan)*. **62**, 48 (1994).
197. M. Fukouka, H. Yamashita, and K. Yoshimoto, Ni-Sn Alloy Activated Cathodes for Chlor-Alkali Process, In *Proc. Vol. 98-10*, The Electrochemical Society Inc., Princeton, NJ (1989), p. 305.
198. K. Yamaguchi, A. Senda, and A. Sakata, *J. Electrochem. Soc.* **137**, 1419 (1990).
199. A. Senda and K. Yamaguchi, Development of TWAC Activated Cathode, In *Proc. Vol. 89-10*, The Electrochemical Society Inc., Princeton, NJ (1989), p. 111.
200. K. Hayashi and K. Yamaguchi, Additional Effect of Antimony Trioxide to the TWAC Activated Cathode, In *Proc. Vol. 89-10*, The Electrochemical Society Inc., Princeton, NJ (1989), p. 341.
201. E. Endoh, H. Otouma, T. Morimoto, and Y. Oda, *Int. J. Hydrogen Energy* **12**, 473 (1987).
202. E. Endoh, H. Otouma, and T. Morimoto, *Int. J. Hydrogen Energy* **13**, 207 (1988).
203. N. Yoshida, M. Yoshitake, E. Endoh, and T. Morimoto, *Int. J. Hydrogen Energy* **14**, 137 (1989).
204. E. Endoh, M. Nakao, and Y. Takechi, Raney Nickel Dispersion-plated Low Hydrogen Overvoltage Cathode, In *Proc. Vol. 99-21*, The Electrochemical Society Inc., Princeton, NJ (1999), p. 245.
205. E. Endoh, Development and performance of the Raney Nickel Dispersion-plated Cathodes for Chlor-Alkali Process, In *Proc. Vol. 98-10*, The Electrochemical Society Inc., Princeton, NJ (1998), p. 317.
206. N. Yoshida, M. Yoshitake, E. Endoh, and T. Morimoto, Development of Highly Durable Low Hydrogen Overvoltage Cathode in Chlor-Alkali Cells, In *Proc. Vol. 98-10*, The Electrochemical Society Inc., Princeton, NJ (1998) p. 125.
207. ELTECH Systems Corporation Brochure (2000).

4.7. DIAPHRAGMS

4.7.1. Introduction

In the early days, as discussed in Chapter 3, sodium chloride solution was electrolyzed in an undivided cell to produce chlorine and caustic soda. The bell jar cell, illustrated in Fig. 4.7.1, was provided with an anode in the bell-type compartment, and a number

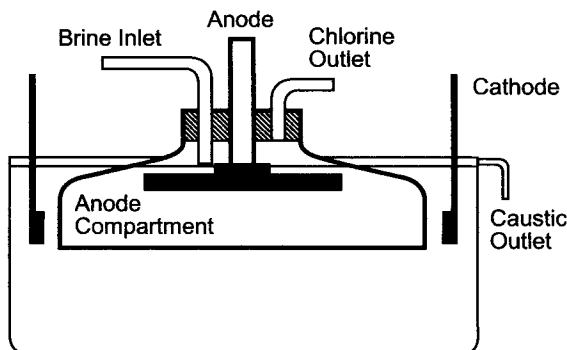


FIGURE 4.7.1. Bell Jar cell.

of cathode blades were positioned around the outside of the bell jar. Chlorine evolved at the anode, left the top of the jar, and the caustic solution overflowed from the cell. In this arrangement, the chlorine did not mix with the catholyte, since the brine fed to the cathode flowed to the cell top, thereby restricting the diffusion of caustic toward the anode side. This is why this cell is classified as a “moving electrolyte-type” [1]. A small amount of chlorine, dissolved in the anolyte, flowed to the cathode side and reacted with the caustic solution to form hypochlorite, resulting in current inefficiency. Another problem of this cell was the large gap between the anode and the cathode, which resulted in a high cell voltage, especially at high current densities.

The performance of this “chlor-alkali” cell was substantially improved by introducing a porous separator between the two electrodes to prevent the mixing of the products generated at the cathode and the anode. The separator material was an asbestos mat, in the form of a paper or vacuum-deposited felt [1–5]. Pores in the separator allow passage of electricity and electrolyte between the anode and the cathode compartments. The properties of the diaphragm determine the cell efficiency, the range of caustic strengths obtainable from the cell, and to a large extent, the cell voltage. Since the introduction of metal anodes, it has also been the life-limiting component of the diaphragm cell.

Chrysotile asbestos was determined in the late 1880s to be a material from which satisfactory diaphragms could be produced. Since that time asbestos has been the basic diaphragm material. Earlier electrolytic cells used asbestos paper, which was hand-fitted to simple cathode shapes. Later, Hooker Chemicals developed the technique of making diaphragms on intricate surfaces by vacuum depositing the asbestos from a bath containing asbestos fibers and the cell liquor. Standard asbestos diaphragms, now in use in most cells, may account for 0.1–0.3 V of the cell voltage when new, and probably twice as much before their replacement because of swelling and plugging.

Since 1972, modified diaphragms with plastic reinforcement have been used to enhance the performance of cells. The improvement consists of adding a corrosion-resistant fluorocarbon polymer to the asbestos slurry to give a diaphragm containing particles and fibers of both asbestos and polymer. The cathode is then heated, first evaporating the water and finally softening or melting the polymer, thereby cementing the asbestos fibers into a tough leather-like diaphragm material. The asbestos still determines the performance of the diaphragm. The addition of polymer reduces swelling, improves mechanical strength, allows the formation of thinner diaphragms, and reduces the dissolution and erosion of the asbestos. This technology has been refined through extensive development programs, resulting in better control of the diaphragm characteristics, greater uniformity, and lower voltages. This development also made possible the reduction of the anode–cathode gap, further reducing energy consumption.

4.7.2. Asbestos Diaphragms

4.7.2.1. Physical and Chemical Properties. Asbestos is a generic term for a variety of hydrated silicate minerals (see Table 4.7.1), which are characterized by their fibrous structure [6–8]. Although there are six different asbestos minerals and several have found use in cell separators, chrysotile predominates as a chlorine cell diaphragm material. Chrysotile fibers consist of bundles of parallel fibrils. These fibrils are hollow needles with an outer diameter of about 30 nm and an inner diameter of 4 nm, and consist of

TABLE 4.7.1 Types of Asbestos

Variety	Chemical composition
<i>Amphibole class</i>	
Amosite	$(\text{FeMg})_7\text{Si}_8\text{O}_{22}(\text{OH})_2$
Crocidolite-“Blue”	$\text{Na}_2(\text{Fe(II)Mg})_3\text{Fe(III)Si}_8\text{O}_{22}(\text{OH})_2$
Anthophyllite	$(\text{MgFe})_7\text{Si}_8\text{O}_{22}(\text{OH})_2$
Tremolite	$\text{Ca}_2\text{Mg}_5\text{Si}_8\text{O}_{22}(\text{OH})_2$
Actinolite	$\text{Ca}_2(\text{FeMg})_5\text{Si}_8\text{O}_{22}(\text{OH})_2$
<i>Serpentine class</i>	
Chrysotile	$\text{Mg}_3\text{Si}_2\text{O}_5(\text{OH})_4$ (or $3\text{MgO} \cdot 2\text{SiO}_2 \cdot 2\text{H}_2\text{O}$)

alternate layers of $\text{Mg}(\text{OH})_2$ and SiO_2 . The number of fibrils in a fiber varies widely, and the fibers exhibit considerable variance in diameter and length. In preparing commercial diaphragms, the fibers are slurried in a suitable liquid medium and sucked by vacuum onto the outer surface of the foraminous cathode. The cathode is then heated to drive off the water, leaving the diaphragm as a fibrous mat. It is the void space between the fibers that provides the electrolyte path, and not the tiny pores in the center of the fibrils. It should be apparent that these voids exhibit no geometric regularity and their mathematical description is a formidable task. The reader is referred to references [9–19], which are devoted to the fundamentals.

Chrysotile asbestos is not chemically stable in chlorine cells. $\text{Mg}(\text{OH})_2$ is soluble in acid solutions and stable in basic solutions; the reverse is true for SiO_2 . When a cell is energized, a chrysotile diaphragm will become SiO_2 enriched on its acidic, anolyte face. The flow through the diaphragm will flush Mg^{2+} ions from the anolyte site toward the catholyte, where they precipitate as $\text{Mg}(\text{OH})_2$. This precipitate will constrict the flow channels and decrease the flow rate and efficiency. As a result, the caustic strength and the voltage drop across the diaphragm increases. The diaphragm is then characterized as “tightened.” After a period in service, the diaphragm reaches a state of equilibrium with its surroundings and its characteristics are stabilized. However, any drastic change in operating conditions will cause the dissolution-precipitation process to start again.

4.7.2.2. Sources. The world asbestos production for 1999 is given in Table 4.7.2. Russia leads with 36.8% and Canada is second with 18.6% of the world’s output. Both countries mine only chrysotile asbestos, and most of the fiber comes from the Urals and Quebec. The third leading asbestos producer is China followed by Brazil. These four countries furnished 79.6% of the world’s chrysotile asbestos in 1999.

The Vermont Asbestos Group (VAG) formerly supplied most of the asbestos to the chlor-alkali industry in the United States and many other parts of the world. The VAG mine closed in the mid-1980s. Asbestos from the following suppliers is now used in many plants throughout the world.

1. JM Asbestos Inc., Asbestos, Quebec; Grades: Chlor-5; 4D-12.
2. Lab Chrysotile, Inc., Thetford Mines, Quebec; Grades: Chryso-Cell 1; Chryso-Cell 2.

TABLE 4.7.2 World Production of Chrysotile Asbestos in 1999

Country	Production (metric tons)	% Total production
Russia	683,000	36.8
Canada	345,000	18.6
China	250,000	13.5
Brazil	200,000	10.7
Zimbabwe	137,000	7.4
Kazakistan	105,000	5.7
Greece	50,000	3.7
India	25,000	1.3
Swaziland	20,000	1.1
South Africa	18,000	1
Colombia	8,000	0.4
United States	7,000	0.4
Others	10,000	0.5
Total	1,858,000	

3. Zambezi Resources, Zimbabwe; Grades: Z1B; Z-2.

Chapter 16 addresses the medical and regulatory aspects of asbestos.

4.7.3. Transport Characteristics of Diaphragms

The principles involved in the brine flow across a vacuum-deposited asbestos diaphragm in a chlor-alkali cell are similar to those for filtration operations. When the flow is laminar (the typical brine velocity in diaphragm cells is $\sim 10^{-3} \text{ cm s}^{-1}$), and the porous mat does not deform during operation, the Hagen–Poiseuille flow theory applies and the pressure drop across the separator is:

$$\Delta p \cdot g_c = \frac{32\mu Lv}{d^2} = \frac{128\mu LV}{\pi d^4} \quad (1)$$

where μ refers to viscosity, L to the thickness of the porous mat, and d to the pore diameter.

According to Eq. (1) the pressure drop, Δp , across the diaphragm is proportional to the average flow velocity, v , or the volumetric rate, V .

The Fanning Equation

$$\Delta p \cdot g_c = 4f \left(\frac{L}{d} \right) \left(\frac{v^2}{2} \right) \rho \quad (2)$$

applies to a liquid passing through a porous medium over a wide range of flow rates, including turbulent flow. In Eq. (2), g_c is the gravity conversion factor and ρ refers to density. The term f in Eq. (2), is the Fanning friction factor [20,21]. Eq. (2) is also called the Darcy equation when f' is substituted for $4f$.

From Eqs. (1) and (2), we have, in laminar flow,

$$f = 16/Re \quad (3)$$

where Re , the Reynolds number, is defined as:

$$Re = dv\rho/\mu \quad (4)$$

It is useful to describe a parameter, m , called the hydraulic radius of the bed, which is defined by:

$$m = \frac{\text{Cross-sectional area of the conduit}}{\text{Wetted perimeter}} \quad (5)$$

$$= \frac{\text{Volume of the voids in the packed bed}}{\text{Total area of the porous bed}} \\ = \frac{AL\varepsilon}{ALS(1-\varepsilon)} = \frac{\varepsilon}{S(1-\varepsilon)} \quad (6)$$

S in Eq. (6) refers to the total surface area per unit bed volume, and the liquid void fraction or porosity, ε , is given by the ratio of the superficial velocity, v or V/A (where A is the sectional area in m^2) to the effective flow velocity, v_e , in the pores as:

$$\varepsilon = \frac{v}{v_e} \quad (7)$$

Substituting m into Eqs. (1) and (2), and v_e into v , results in:

$$Re = \frac{mv_e\rho}{\mu} = \frac{v\rho}{S\mu(1-\varepsilon)} \quad (8)$$

and

$$\Delta p \cdot g_c = 2f \left(\frac{(1-\varepsilon)LSv^2\rho}{\varepsilon^3} \right) \quad (9)$$

According to Carman [22],

$$2f \cong k_1/Re \quad (10)$$

in the range of $Re < 2$, where k_1 is a coefficient. Substituting Eq. (10) into Eq. (9), leads to:

$$\Delta p \cdot g_c = \frac{\mu v L}{P} \quad (11)$$

where P , the permeability of the porous bed (in m^2), is given by:

$$P = \frac{\varepsilon^3}{k_1 S^2 (1 - \varepsilon)^2} \quad (12)$$

k_1 being in the range generally between 5–5.5.

From Eqs. (6) and (12), it can be shown that:

$$\frac{m^2}{P} = \frac{k_1}{\varepsilon} \quad (13)$$

MacMullin and coworkers [23] measured the electric resistance of a porous bed filled with electrolytic solution under various conditions, and concluded that the “Bruggemann” equation given below

$$R/R^0 = \varepsilon^{-2/3} \quad (14)$$

gave consistently low values of R/R^0 , but it was good up to within about 4% for packed beds of glass spheres [24]. R refers to the electric resistance of the porous bed filled with an electrolytic solution and R^0 is the resistance of the same volume without any nonconductive packing. Assuming,

$$R/R^0 = k_2/\varepsilon \quad (15)$$

and substituting it into Eq. (12) results in MacMullin’s basic equation [23]:

$$\frac{m^2}{P} = k \left(\frac{R}{R^0} \right) = \left(\frac{k_1}{\tau} \right) \left(\frac{\tau}{\varepsilon} \right) \quad (16)$$

where,

$$k = k_1/k_2 \quad \text{and} \quad \tau = \text{tortuosity}$$

Detailed studies by MacMullin *et al.* [23], showed that the value of k_1/τ for many porous beds is 3.666 ± 0.098 . Therefore, the model describing the porous beds is applicable for the separators used in diaphragm-type chlor-alkali cells. The tortuosity of a porous asbestos diaphragm is about 1.5, and hence, k_1 is about 5.5.

There are several models [25–33] available for describing the tortuosity factor, and two of these are briefly addressed here. Spiegler [27] measured the interdiffusion of a mixed gas of oxygen and argon through a porous glass disc filled with a dilute KCl solution, and the electric resistance of the same medium, and found the formation factor, F_f , for gas diffusion to agree with that for electric conductance within 10% deviation. He proposed the “Spaghetti model” consisting of n_j tubes in a unit volume, all with a length of χ and radius, r_j . The porosity, ε , for this geometry is given by:

$$\varepsilon = \sum n_j r_j^2 \pi \chi \quad (17)$$

where χ is the hydraulic length, which is larger than L . Expressing the ratio of the resistances and the formation factor by Eqs. (18) and (19):

$$R/R^0 = \chi / \sum n_j r_j^2 \pi \quad (18)$$

$$N_M = R/R^0 = \chi^2 / \varepsilon \quad (19)$$

where N_M is called the MacMullin number.

It can be shown that $\chi^2 = k_2$ from Eqs. (15) and (19). Also, from Eqs. (13–19), we have,

$$P = \frac{\varepsilon m^2}{k \chi} \quad (20)$$

Since $\chi/L = \tau$, the tortuosity factor is the ratio of the effective length of micropores to the thickness of the diaphragm mat.

Matsuno calculated [28] the statistical mean length, \bar{l} , of micropores having an inclination to the surface of the diaphragm as:

$$\bar{l} = \frac{\int_0^{\pi/2} l \sin \theta \sin \theta 2\pi \cos \theta d\theta}{\int_0^{\pi/2} 2\pi \cos \theta d\theta} = \frac{l}{3} \quad (21)$$

and showed that the true length l of the micropores is approximately three times the thickness of the diaphragm. Experimental results revealed that R/R^0 was in the range of 2–3, and nearly independent of the nature of the diaphragm materials. Note that the resistance ratio R/R^0 is N_M , as shown in Eq. (17), but not dependent on χ . Matsuno's model is based on the length of micropores, where Spiegler's spaghetti model is based on the volume of the bundles of capillary tubes of radius r_j , and length, m . Thus, the definition of tortuosity varies depending on the model used for its description. While tortuosity is a valuable factor for characterizing porous media, the MacMullin number is preferred as a characteristic value for a diaphragm, as it can be obtained directly from the measured resistances. N_M describes the hydraulic mean length and the porosity for any geometry of the porous medium.

Chirkov examined various models for the calculation of the electric resistance of porous electrodes for fuel cells and air cells [29,30], which are useful to describe the diaphragms. Experiments [31] on diffusion of gas across porous media consisting of nickel particles of different sizes (1–5 μm and 50 μm) and shapes showed that the area for gas diffusion across the hydrophilic porous media depended only on the pressure drop.

It is clear that from the above discussion that any simple modeling of the diaphragm is limited, because both the porosity (30–60% open) and the size of capillary tubes (1–100 μm) vary widely, and the configuration of the porous bed is complex [32].

The flow velocity, v , can be expressed as a function of the pressure drop, Δp , when the electrolyte flow through the diaphragm is assumed to be analogous to filtration, as:

$$v = \frac{P}{\mu L} \Delta p \cdot g_c \quad (22)$$

If the filter medium is compressible, the permeability, P , depends on the pressure drop, Δp . Hence,

$$\log \left(\frac{v}{v^0} \right) = (1 - s) \log(\Delta p \cdot g_c) \quad (23)$$

where s is the compressibility factor, and v^0 is the flow velocity at $P = 1$.

Studies of the flow of sodium chloride solutions through deposited asbestos mats at constant pressure showed the slope of the log-log plots of v vs Δp to be about 0.8 (Fig. 4.7.2), and hence, $s \approx 0.2$ [34]. Thus, as the viscosity of the electrolyte increases, the flow velocity decreases with increasing NaOH concentration in the mixed solution of NaOH and NaCl. The ratio P/L is almost constant over a wide range of the concentrations, as shown in Fig. 4.7.3.

Although the model for porous beds is applicable to porous asbestos diaphragms under "static" conditions, complications arise during electrolysis. Asbestos fiber consists of $\sim 40\%$ SiO_2 and $\sim 40\%$ MgO . This fiber dissolves readily in acid media, while it is resistant to caustic at low temperatures [34]. During electrolysis, the magnesium layer is believed to dissolve preferentially on the anolyte side and reprecipitate within the diaphragm. Thus, a used diaphragm consists of a silica-rich layer on the anolyte side of the diaphragm and a magnesium-rich layer on the catholyte side.

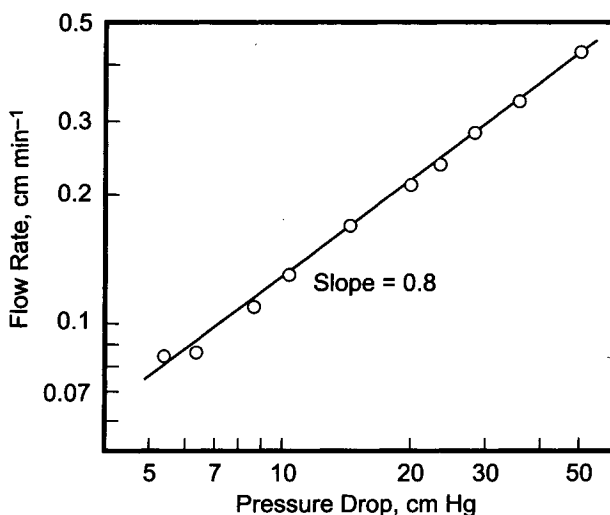


FIGURE 4.7.2. Flow rate vs pressure drop curve of a 2–3 mm thick deposited asbestos bed at 20°C in NaCl solutions [34]. (With permission from Elsevier.)

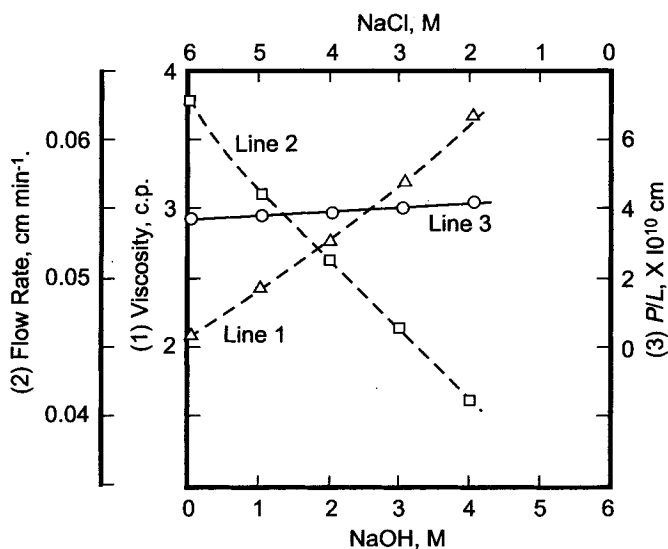


FIGURE 4.7.3. Flow rate, viscosity and P/L as a function of catholyte composition at 20°C for a diaphragm thickness of 2 mm and at a pressure drop of 4.5 cm Hg [34]. (With permission from Elsevier.)

It is well known that the flow rate through the asbestos diaphragm is significantly reduced when the current is switched on. MacMullin [35] attributed this effect to electrokinetic phenomena. However, experimental results [36] did not support this hypothesis since the brine strength is near its saturation limit. Hine and Yasuda [36] showed that the reduction in flow rate is caused by the penetration of hydrogen bubbles into the diaphragm. When the asbestos separator is placed away from the cathode, the brine flow rate is unaffected when the current is switched on. Regular asbestos diaphragms swell and in extreme cases, touch the anodes, resulting in high cell voltages. This can be prevented by thermally setting the asbestos mat with small amounts of PTFE (polytetrafluoroethylene) or Halar powder, without any adverse effects on the flow characteristics. Thus, the structure of the mat is unaffected by the heat treatment while the polymer contributes to set the fiber. Repeated current interruptions should not result in any chemical changes of the asbestos mat if these additives cover the asbestos fibers and impart chemical stability. In such a case, these additives should minimize “diaphragm tightening,” normally observed with pure asbestos diaphragms.

4.7.4. Mass Transfer through Diaphragms

During electrolysis, hydroxyl ions are generated at the cathode and transported to the anode compartment by migration and diffusion, even while opposed by the anolyte flow through the diaphragm. Convection and migration, in general, depend on diaphragm properties, electrolysis, and flow conditions, which vary over the height of the diaphragm because the pressure difference increases linearly with the distance from the catholyte level (Fig. 4.7.4). Because the anolyte density and the catholyte density are nearly the

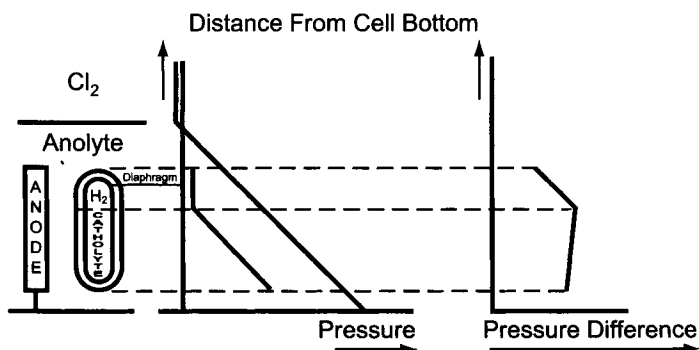


FIGURE 4.7.4. Variation of the pressure difference over the height of the diaphragm [37]. (Reproduced with permission of the Society of Chemical Industry.)

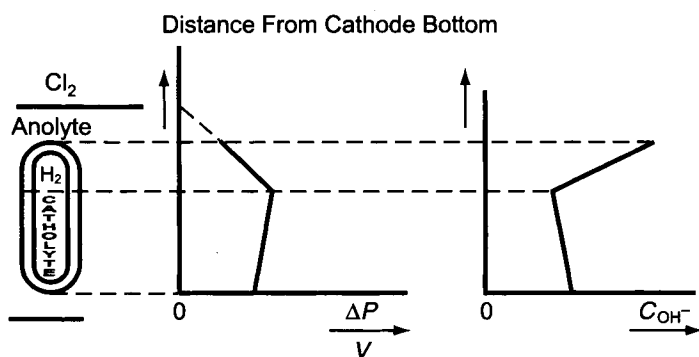


FIGURE 4.7.5. Variation of the pressure difference, volume flow, and caustic concentration across the diaphragm [37]. (Reproduced with permission of the Society of Chemical Industry.)

same, the pressure differences in the lower section can be considered constant. Below the catholyte level, convection will be much greater than migration and diffusion, because of a relatively high liquid volume flow rate and a low caustic concentration. In the upper part of the diaphragm, conditions are favorable for migration and diffusion because of relatively low flow rates and high caustic concentrations (Fig. 4.7.5), resulting in low efficiencies compared to that in the lower section. Also, in the upper section, there is a higher degree of degradation of asbestos fibers because of high caustic concentrations, giving rise to sharper pH gradients through the diaphragm [37].

Furthermore, as mentioned earlier, the magnesium in the chrysotile asbestos dissolves in the acidic anolyte during electrolysis. As a result, the diaphragm becomes enriched in SiO_2 on the anolyte face. The Mg^{2+} ions from the anolyte side, transported to the catholyte by convective flow, precipitate as $\text{Mg}(\text{OH})_2$ on the catholyte side of the diaphragm. At the same time, hydrogen bubbles penetrate the diaphragm in the anode direction, and increase the voltage drop. The diaphragm then becomes tighter during operation, and drastic changes in the operating conditions further tighten the diaphragm

as the dissolution–precipitation process is repeated. Thus, the asbestos mat changes during electrolysis from a single matrix to a “dual matrix” of asbestos on the anolyte side, and $\text{Mg}(\text{OH})_2$ -impregnated asbestos on the catholyte side.

4.7.4.1. Theoretical Modeling. Mass transfer through the separators used in diaphragm cells has been studied by many authors [38–57]. The general one-dimensional model (Fig. 4.7.6) that has been used extensively to describe the transport of hydroxyl ions across the diaphragm is presented here. This model assumes plug flow, uniform pore distribution within the diaphragm and no hydrogen bubble penetration into the diaphragm.

Anolyte flows from the anode compartment through the diaphragm under a hydrostatic head with a velocity of v . Hydroxyl ions generated in the cathode compartment move into the anolyte through the diaphragm by diffusion and migration. On the other hand, H^+ and dissolved Cl_2 (i.e., $\text{Cl}_2 + \text{HOCl}$) move into the cathode compartment, establishing a neutral zone at a distance δ from the anolyte/diaphragm interface. Experimental studies have shown [58–60] that δ is small, around 10^{-3} cm, and the neutral zone is located at $x = L$, that is, at the anolyte/diaphragm interface.

The hydroxyl ion flux, J , expressed in $\text{kg mol m}^{-2} \text{s}^{-1}$, is composed of contributions from diffusion, J_d , migration, J_m , and convection, J_c , as:

$$J = J_d + J_m + J_c \quad (24)$$

J_d in (24) is given by:

$$J_d = -D \frac{dC}{dx} \quad (25)$$

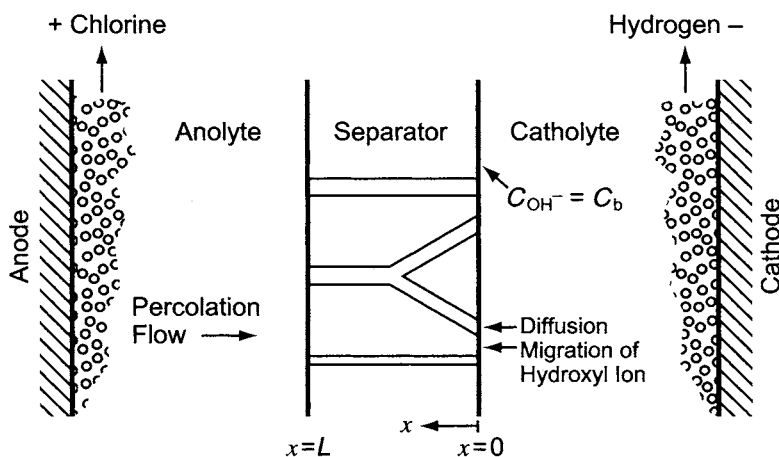


FIGURE 4.7.6. Mass transfer through the separator in a diaphragm type chlor-alkali cell.

where D is the diffusion coefficient of the OH^- ions through the porous diaphragm having a porosity, ε , and C is the concentration of the OH^- ions. D can be obtained from the diffusion coefficient of OH^- in the bulk, D^0 , as:

$$N_M = \frac{R}{R^0} = \frac{D^0}{D} \quad (26)$$

The migration and convection terms [61] are given by:

$$J_m = -\frac{F}{R^*T} D C \frac{d\phi}{dx} \quad (27)$$

$$J_c = -Cv \quad (28)$$

where F is the Faraday constant, R^* is the gas constant, T is temperature, and $\frac{d\phi}{dx}$ is the potential gradient in V m^{-1} .

If uniform properties are assumed to prevail in the diaphragm, then

$$\frac{d\phi}{dx} = \frac{-i}{\chi} \quad (29)$$

where i refers to current density and χ to the conductivity of the medium in the diaphragm. Equation (27) can now be written as:

$$J_m = \frac{F}{R^*T} \frac{DC}{\chi} i \quad (30)$$

Substituting Eqs. (25), (28), and (30), into Eq. (24) results in:

$$J = -D \frac{dC}{dx} + \frac{F}{R^*T} \frac{DC}{\chi} i - vC \quad (31)$$

Eq. (31) represents the loss of hydroxyl ions caused by migration and diffusion of hydroxyl ions to the anolyte compartment and hence, the loss in caustic current efficiency, η . Therefore, Eq. (31) can be alternatively expressed as:

$$J = \frac{i}{F} (1 - \eta) \quad (32)$$

where i/F represents the amount of OH^- ions formed in the catholyte.

Equation (31) can be recast as:

$$J = -D \frac{dC}{dx} + uC \quad (33)$$

where

$$u = \frac{DFi}{RT\chi} - v \quad (34)$$

Equation (33) can now be solved using the boundary conditions:

$$C = C_b \text{ at } x = 0$$

$$C = C_o \text{ at } x = L$$

Thus,

$$J = \frac{uC_b}{1 - \exp(-uL/D)} \quad (35)$$

Hence,

$$\frac{C}{C_b} = \frac{1 - \exp(-u(L-x)/D)}{1 - \exp(-uL/D)} \quad (36)$$

Since

$$J = \text{theoretical amount of caustic formed} - \text{the actual amount of caustic collected} \quad (37)$$

$$J = \frac{I}{F} - C_b \cdot v \quad (38)$$

It follows that

$$\eta = \frac{C_b v}{I/F} = \frac{1}{1 + J/C_b v} \quad (39)$$

Therefore, the caustic current efficiency, η , is, given by:

$$\eta = \frac{1}{1 + (u/v)(1/[1 - \exp(-uL/D)])} \quad (40)$$

u in Eq. (40) represents the difference between the migration term and the convective term, describing the difference in the migration velocity and the percolation velocity. Hence, with thick separators, $u > 0$ because the convective flow is very small, and the C vs x curve is convex. When $u < 0$, the C vs x curve is concave, as shown in Figs. 4.7.7 and 4.7.8, which is the pattern observed in industrial cells.

The model described above was first proposed by Mukaibo [38] and was found to agree well with experimental data by Hine *et al.* [58–60]. It is important to emphasize that the values of D , C , and χ in the transport equations shown above are not the bulk properties, but those prevailing in the diaphragm, which are generally obtained

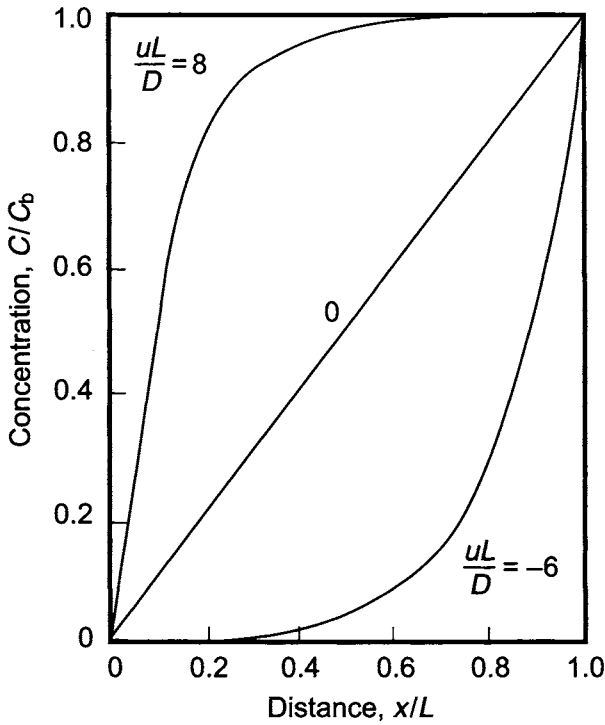


FIGURE 4.7.7. OH^- ion concentration profile in the diaphragm showing the functional dependence of C_{OH} on uL/D_{OH} using Eq. (36).

from the bulk values by employing Eq. (26). There are several factors that should, in principle, be incorporated in a proper formulation. These include replacing the concentration with activity, coupling the concentrations of various species participating during the transport across the diaphragm, and considering nonuniformities in the composition and physicochemical properties of the diaphragm. Nevertheless, the corrections to the equations deduced above do not alter the basic predictions and conclusions of Mukaibo's description of the transport across the diaphragms.

Eq. (40) can be recast as:

$$\eta = \frac{1 - \exp(-uL/D)}{u/v + 1 - \exp(-uL/D)} \quad (41)$$

Defining

$$\gamma_1 = \frac{DFi}{RT\chi v} = \frac{u}{v} + 1$$

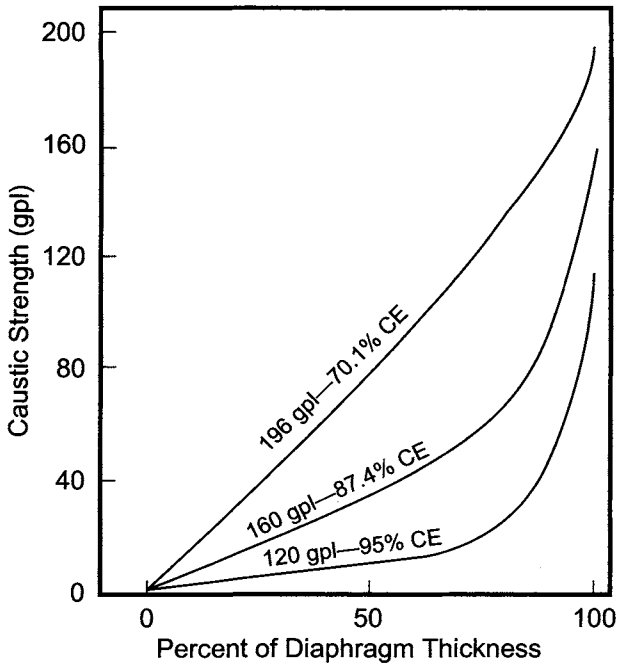


FIGURE 4.7.8. Theoretical profiles of hydroxyl concentration across the diaphragm using Eq. (40).

which represents the ratio of migration to convection, and

$$\gamma_2 = \frac{vL}{D}$$

depicting the ratio of convection to diffusion, Eq. (41) can now be rewritten as:

$$\eta = \frac{1 - \exp(\gamma_2 - \gamma_1\gamma_2)}{\gamma_1 - \exp(\gamma_2 - \gamma_1\gamma_2)} \tag{42}$$

This result is the same as that obtained by various authors if the γ_1 and γ_2 are properly identified as shown below.

1. Mukaibo *et al.* [38], Stender *et al.* [39]

$$\gamma_1 = \frac{FDi}{RT\chi v}; \quad \gamma_2 = \frac{vL}{D}$$

2. Chandran *et al.* [49]

$$\gamma_1 = \frac{FDi_e}{RT\chi v_e}; \quad \gamma_2 = \frac{v_e L_e}{D}$$

where

$$i_e = i \left(\frac{\tau}{\varepsilon} \right); \quad v_e = v \left(\frac{\tau}{\varepsilon} \right); \quad L_e = L/\tau;$$

τ = tortuosity and ε = porosity.

3. Van Zee *et al.* [51]

$$\gamma_1 = \frac{FD_e i}{RT \chi_e v}; \quad \gamma_2 = \frac{vL}{D_e}$$

where

$$D_e = \frac{D}{N_M}; \quad \chi_e = \frac{\chi}{N}; \quad N = \frac{\tau}{\varepsilon};$$

N_M = MacMullin number.

Van Zee *et al.* [50–57] extended the model described in this section representing the various parameters involved in terms of dimensionless groups. This treatment is presented in Appendix 4.7.1.

In Eqs. (25) to (40), the diffusion term is related to the bulk diffusion coefficient, D^0 , and the formation factor, F_f , shown by Eq. (20). On the other hand, the migration term is governed by the solution composition and the operating conditions, such as temperature and the potential gradient. Since J_m in Eq. (27) contains D_i , it is a function of the physical properties of the diaphragm. However, $D_i(d\phi/dx)$ is constant even if the porosity of the diaphragm mat varies over a wide range, because the potential gradient increases with decreasing porosity and diffusivity. Consequently, the migration term is almost independent of the configuration of the diaphragm. The hydraulic flux, J_c , is a function of the flow velocity, v , or the pressure drop, Δp_{gc} , across the diaphragm as shown in Eqs. (22) and (23). The relationship between v and Δp_{gc} is related to the hydraulic characteristics and the configuration of the diaphragm, as shown by Eqs. (12) and (13), and to the solution viscosity and the density as revealed by Eqs. (11) and (22).

4.7.4.2. Highlights of the Theoretical Modeling Studies

4.7.4.2A. Dependence of Caustic Efficiency on Caustic Strength and Flow Velocity.

The caustic strength plays an important role in determining the current efficiency for a given diaphragm thickness. For an efficient diaphragm, u should be greater than zero throughout the thickness of the diaphragm, and hence, the minimum percolation velocity to achieve high efficiency should satisfy the condition:

$$u = v - (u_{OH} Fi / \varepsilon \chi) > 0 \quad (43)$$

The percolation velocity in a commercial ELTECH H-4 cell is $8.67 \times 10^{-4} \text{ cm s}^{-1}$, which may be compared with the migration velocity of $7.6 \times 10^{-4} \text{ cm s}^{-1}$ (see Appendix 4.7.2 for details).

The maximum caustic strength that can be produced with a high efficiency is possible only when $u = 0$ at the anolyte surface of the diaphragm, when the percolation velocity equals the migration velocity, given by $(u_{\text{OH}} - iF)/\epsilon\chi$.

From the percolation velocity, one can calculate the catholyte flow by subtracting the water that is decomposed by electrolysis and the water that has evaporated. The maximum caustic strength

$$C_{\text{max}} = \frac{i}{F \times \text{catholyte flow}} \quad (44)$$

varies between 170 and 180 g L⁻¹. At higher caustic strengths, the efficiency should fall steeply regardless of the thickness of the diaphragm (Figs 4.7.9–4.7.11). The caustic efficiency vs NaOH concentration diagram is called the Angel curve, in honor of its first investigator [62,63].

4.7.4.2B. Effect of Current Density. When the current density is decreased, the flow per unit area of the separator must decrease if the anolyte and catholyte concentrations are fixed. Hence, the value of u decreases by the same factor as the current density. The thickness of the membrane must increase by the same factor so that the voltage drop remains the same. The percolation velocity has to decrease with decreasing current density, and this requires a thick separator.

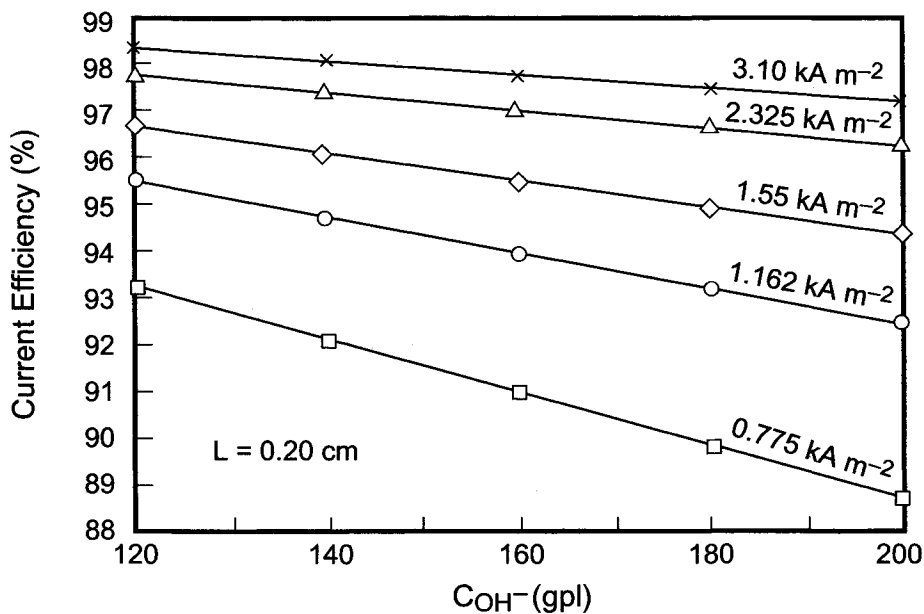


FIGURE 4.7.9. Variation of caustic current efficiency with caustic concentration at various current densities for a diaphragm thickness of 0.2 cm, calculated using Eq. (40).

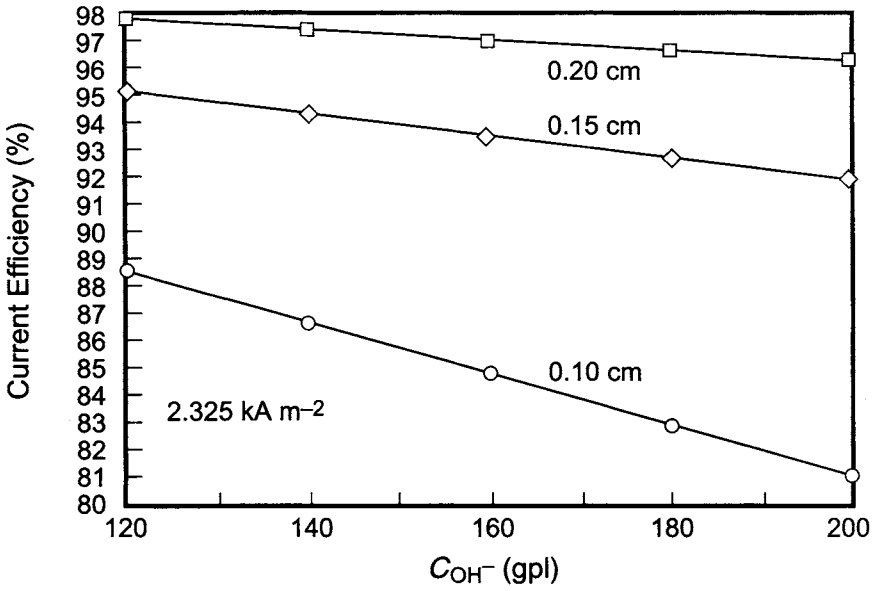


FIGURE 4.7.10. Variation of caustic current efficiency with caustic concentration at various diaphragm thicknesses at a current density of 2.325 kA m^{-2} , calculated using Eq. (40).

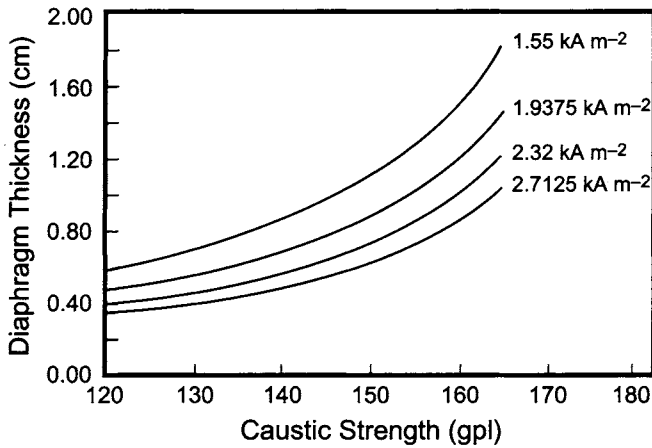


FIGURE 4.7.11. Diaphragm thickness vs caustic concentration to achieve a caustic current efficiency of 95% at various current densities, calculated using Eq. (40).

Thus, for a given diaphragm thickness, the current efficiency usually falls with decreasing current densities, at a fixed catholyte caustic strength. Furthermore, the model predicts that in order to produce the same caustic strength at a given caustic current efficiency at any current density, the thickness of the diaphragm must vary in such a

way that ΔV is approximately the same at all current densities. This is because both V and u decrease by the same factor as the current density decreases, and the thickness of diaphragm increases correspondingly.

4.7.4.2C. Voltage Drop Across the Separator. The voltage drop across the diaphragm, ΔV is:

$$\Delta V = \frac{iL}{\varepsilon\chi} \quad (45)$$

Thus, when $L = 0.35$ cm, $\chi = 0.64 \Omega^{-1} \text{ cm}^{-1}$, and $\varepsilon = 0.75$, $\Delta v = 170$ mV. The thickness of the diaphragm, L , can be estimated from Eqs. (32) and (35):

$$L = -\frac{D}{u} \ln \left[1 - \frac{uC_b}{(i/F)(1-\eta)} \right] \quad (46)$$

4.7.4.2D. Examples of Thickness and Voltage Drop Calculations. Experiments have shown that the hydroxyl ion concentration in the middle of the diaphragm is very low for the efficient operation of the cell. This suggests that the average composition within the diaphragm consists of at least 75% anolyte and 25% catholyte. The thickness of the separator and the voltage drop across it for three combinations of anolyte and catholyte in the diaphragm, simulating the possible composition in the diaphragm, are illustrated here.

Case 1: 75% anolyte + 25% catholyte

Case 2: 80% anolyte + 20% catholyte

Case 3: 85% anolyte + 15% catholyte

The values of u obtained for these cases are shown in Table 4.7.3, assuming the current efficiency to be 95%, at a temperature of 90°C, with a diaphragm porosity of 0.75. The catholyte composition for all these cases was 150 g L⁻¹ NaOH and 181.5 g L⁻¹, the anolyte analyzing 264 g L⁻¹ NaCl.

The equivalent conductivities of ions are noted below, along with the interpolated values at 90°C.

Ion	Published values			Interpolated values
	75°C	100°C	128°C	90°C
Na ⁺	116	155	203	139.4
Cl ⁻	160	207	264	188.2
OH ⁻	360	439	525	407.4

From the values of catholyte flow, percolation flow and the percolation velocity (see Appendix 4.7.2 for details) and the u_{OH^-} and D_{OH^-} values calculated using the

following equations [64], the voltage drop across the diaphragm is estimated and shown in Table 4.7.4.

$$\lambda = \beta\lambda^{\circ}$$

where λ is the equivalent conductivity and λ° is its value at infinite dilution, $\beta = 1.1 - 0.33 C^{1/2}$, C being expressed in mol L^{-1} .

$$u_i = \frac{\lambda_i}{|z_i|F^2} \quad \text{and} \quad D_i = \frac{RT\lambda_i}{|z_i|F^2} \quad (47)$$

The term z in the above equation refers to the valence of the ionic species under consideration.

4.7.5. Modified Asbestos Diaphragms

Asbestos diaphragms are formed on the cathode structure by immersing it in a vessel containing asbestos slurred in catholyte liquor and applying vacuum to deposit a mat onto the cathode screen. Vacuum, time of application, and composition of the slurry control the thickness of the deposit. The procedures and the variables involved in the deposition of asbestos diaphragms are discussed in Section 4.7.7.

As mentioned earlier, asbestos diaphragms are prone to swelling because of dissolution of the magnesium present in the fiber and its redeposition as $\text{Mg}(\text{OH})_2$ on the catholyte side, and also by the penetration of the hydrogen bubbles into the diaphragm, and subsequent loosening of the mat. This process results in increased voltage drop across the diaphragm, limiting the useful life of asbestos diaphragms to 6–8 months.

A wide variety of techniques and modifiers have been investigated to impart dimensional stability to asbestos diaphragms. The techniques examined include heat-treating the diaphragm at 500–600°C instead of 450°C, using crocidolite asbestos and mixing

TABLE 4.7.3 Values of U for Three Assumed Electrolyte Compositions in the Diaphragm

Case #	NaCl (mol L^{-1})	NaOH (mol L^{-1})	$u(\text{cm s}^{-1})$
1	4.16	0.9375	$(8.57-6.98) \times 10^{-4}$
2	4.23	0.75	$(8.57-7.288) \times 10^{-4}$
3	4.3	0.563	$(8.57-7.624) \times 10^{-4}$

TABLE 4.7.4 Voltage Drop, ΔV , Across a Diaphragm

Case #	$u(\text{cm s}^{-1})$	$D_{\text{OH}}(\text{cm}^2 \text{s}^{-1})$	$L(\text{cm})$	$\Delta V(V)$
1	1.59×10^{-4}	4.69×10^{-5}	0.526	0.245
2	1.282×10^{-4}	4.80×10^{-5}	0.602	0.286
3	0.946×10^{-4}	4.91×10^{-5}	0.712	0.345

chrysotile with amphibole asbestos. Inorganic binders examined include silicic acid, sodium silicate, BaSO_4 , calcium titanate, ZrO_2 , and TiO_2 . Various polymeric materials were also tested to achieve chemical stability of the asbestos diaphragms, and included chloroprene rubber, chlorinated rubber, PVC, polyethylene, polypropylene, and polyurethane. However, significant improvements were achieved only with fluorinated polymers. Although a wide variety of fluorinated polymeric materials were patented [65], currently there are only four compositions that are used in the industry. All these polymer-modified diaphragms are presently licensed by ELTECH Systems.

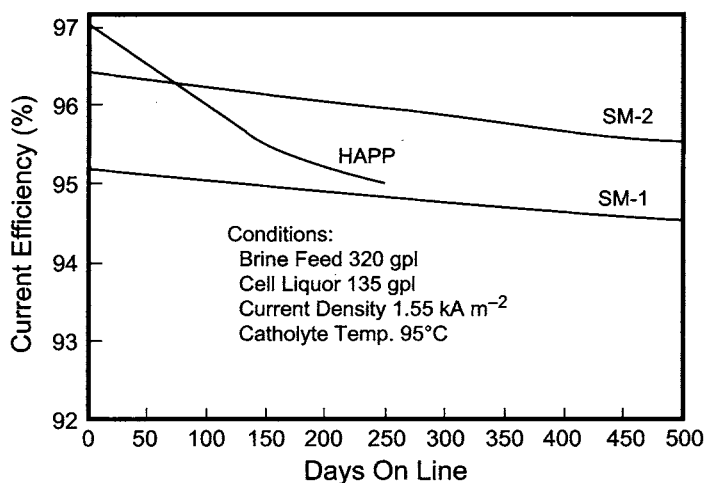


FIGURE 4.7.12. Comparison of current efficiency data with HAPP, SM-1, and SM-2 diaphragms vs time [72]. (With permission from ELTECH Systems Corporation.)

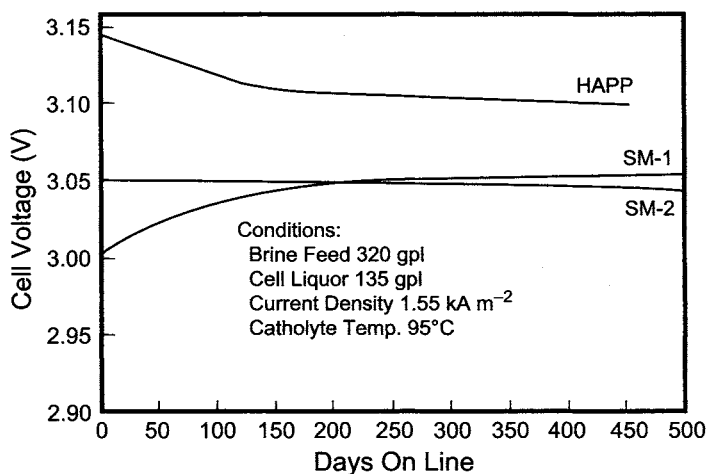


FIGURE 4.7.13. Comparison of cell voltage data with HAPP, SM-1 and SM-2 diaphragms vs time [72]. (With permission from ELTECH Systems Corporation.)

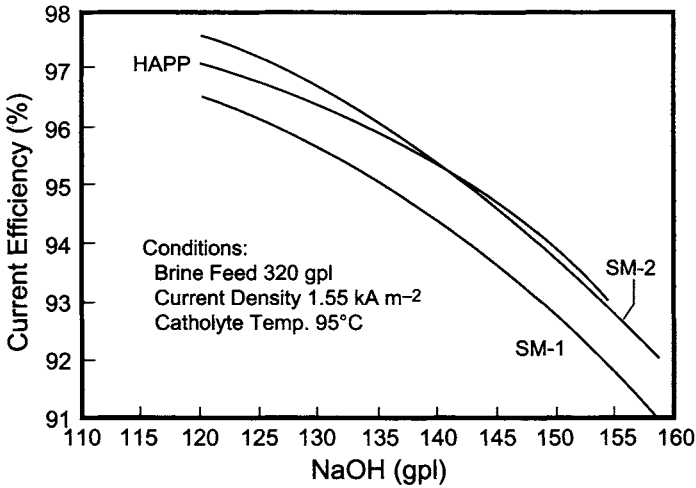


FIGURE 4.7.14. Current efficiency vs caustic strength for HAPP, SM-1 and SM-2 diaphragms [72]. (With permission from ELTECH Systems Corporation.)

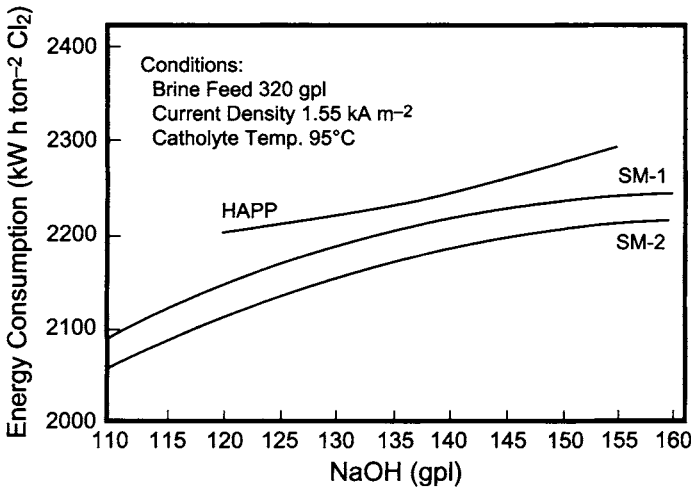


FIGURE 4.7.15. Comparison of energy consumption at various caustic strengths with HAPP, SM-1 and SM-2 diaphragms [72]. (With permission from ELTECH Systems Corporation.)

The four modifiers are Halar [66], SM-1 [67], SM-2 [68], and SM-3 [69]. Halar-modified diaphragms are called HAPP diaphragms (i.e., Hooker Asbestos Plus Polymer) [70]. These contain about 5% of a predominantly alternating E-CTFE copolymer. The commercial resin melts at about 245°C and contains 82% alternating units, 8% ethylene blocks, and 10% chlorotrifluoroethylene blocks [71]. SM-1 is an extruded PTFE fiber

cut to a specific length, and SM-2 is a branched fiber. SM-3 is 80% SM-2 with 20% perfluoroalkoxy (PFA) powder.

Halar, SM-2, and SM-3 adhere to the asbestos when fused, and SM-1 fiber shrinks during fusion and tightens the mat. SM-based diaphragms typically contain 20% modifier, and the polymer weight, excluding the salt, is included in the total weight of the diaphragm. Comparative performance characteristics of Halar, SM-1, and SM-2 diaphragms [72] are presented in Figs. 4.7.12 to 4.7.15, which show that while Halar diaphragms offer stable performance initially, the SM-based diaphragms exhibit long-term stability. The short life associated with Halar-modified diaphragms is believed to stem from the disappearance of Halar with time, because of either chemical attack or thermal instability. Note that the SM-based diaphragms are baked at 340–370°C, while HAPP diaphragms are baked at 270°C. SM-based diaphragms provide higher energy savings when compared with the performance of HAPP diaphragms. However, the PTFE-based compositions are more expensive. Each specific case should be analyzed to minimize the life-cycle cost.

4.7.6. Non-Asbestos Diaphragms

40% of the chlorine in the world is produced from cells with polymer-modified asbestos (PMA) diaphragms. Asbestos presents a health hazard. Nevertheless, proper handling of equipment and procedures and use of prepackaged containers to prepare the asbestos slurry have reduced operator exposure. As a result, there is less regulatory pressure in the United States to eliminate the use of asbestos in chlor-alkali operations. However, the environmental regulations in other countries are more stringent, and countries such as France and Brazil have proposed legislation to ban the use of asbestos. The ban on asbestos started in the year 2003 in France, and in the year 2010 in the rest of Europe. The state of Rio de Janeiro in Brazil has banned the production of caustic in cells using either mercury or asbestos [73,74].

Anticipating regulatory pressures, chlor-alkali technology suppliers began research to develop substitutes for asbestos in the 1970s. Using perfluorocarbon-based materials, synthetic diaphragms were made with controlled porosity, using pore formers (e.g., CaCO_3) that were subsequently leached out. The diaphragms were prepared in sheet form placed over the cathode structure [75] or slurried and vacuum deposited on the cathode as in the conventional process. The materials examined earlier include: PTFE [76,77], PVDF + K_2CO_3 [78], zirconium oxides [79], PTFE powder + K-titanate [80], and Ti screens bombarded by plasma of Ba powder [81]. However, none of these have achieved commercial status.

In recent years, ELTECH Systems and PPG Industries have made significant progress. ELTECH Systems developed a non-asbestos diaphragm [82–84] called Polyramix (PMX) with a porosity similar to that of asbestos and which can be directly deposited on the cathode. Polyramix™ is a fibrous composite material of ZrO_2 or TiO_2 and PTFE. The PMX fiber is 10–100 μm in diameter, and 1000–7000 μm long. Chrysotile fibers, for comparison, are 0.1–0.3 μm in diameter and 0.1–6.0 μm long. These fiber characteristics make Polyramix noncarcinogenic [83]. While the conditions for preparing the bath and applying it to deposit diaphragms are different because of the differences in the fiber characteristics, the deposition methodology is the same as that employed to form

TABLE 4.7.5 Comparison of the Operating Cost^a of PMA and PMX Diaphragms [74] in MDC-55 Cells at 2.55 kA m^{-2}

	PMA diaphragm	PMX diaphragm	
Life (years)	0.75	3	5
Operating costs (\$/ton of Cl_2)			
No voltage savings	\$4.13	\$4.21	\$2.53
0.1 V savings vs PMA diaphragm	\$4.13	\$2.11	\$0.43

Note: ^a energy cost = $\$0.03(\text{kW h})^{-1}$

the regular and modified asbestos diaphragms. The weight of the PMX diaphragm is about 4.5 kg m^{-2} of the cathode area, compared to 2 kg m^{-2} required with a polymer modified asbestos diaphragm [82].

PPG Industries has also developed a non-asbestos diaphragm, Tephram[®], which has three components: basecoat, topcoat, and dopant [85]. The basecoat, containing PTFE fiber, PTFE microfiber, Nafion[®] ion-exchange resin, and other constituents, is vacuum deposited on the cathode screen. PTFE fiber forms the base mat and the microfiber provides a suitable porosity. The Nafion resin contributes to the wettability of the PTFE mat. The topcoat, with inorganic particles, is applied on the basecoat by vacuum deposition to achieve adequate permeability and uniformity. The third component, which contains soluble and insoluble materials, is added to the anolyte during start-up and also intermittently during operation, to form a gel layer in the micropores of the diaphragm mat to improve the performance of the diaphragm. Tephram, like polyramix, is expensive compared to the regular asbestos diaphragm, and hence, the cell must operate for 3–4 years to reduce the unit cost of production.

The tensile strength of the PMX diaphragm is about 10 kg cm^{-2} compared with $1\text{--}3 \text{ kg cm}^{-2}$ of the polymer bonded asbestos mat, and hence, the PMX diaphragm is not susceptible to erosion by the gas–solution mixture along the surface [74].

These diaphragms are generally treated with muriatic acid when they are plugged with Ca, Mg, Fe, and Ni precipitates. Unlike asbestos, the PMX fiber is stable to HCl. The longer service life of the PMX diaphragms justifies its higher cost. ELTECH's evaluation of the PMX diaphragm showed better operating cost savings when the service life exceeded 5 years, depending on the electricity price and the operating conditions. The economic evaluation and the case history in the United States and Europe are described in refs [84,85]. Table 4.7.5 shows an economic comparison of the Polymer Modified Asbestos (PMA) and PMX diaphragms.

There have been various reports comparing costs of polymer-modified asbestos diaphragms and non-asbestos diaphragms. The non-asbestos diaphragm is not economical for low current density operations. At higher current densities, the life of the diaphragm should be substantially more than three years to be economically attractive, as evident from the cost comparison developed by PPG [85], and presented in Table 4.7.6.

TABLE 4.7.6 Operating Cost (\$/Ton of Cl₂) of Diaphragm in MDC-55 Cells Operating at 120 kA and 95% Current Efficiency

	SM-2	Tephram	Polyramix
Life (months)	12	36	36
Cost of diaphragm and cell renewal	2.66	2.06	4.76
Other costs ^a	0.29	2.27	0.1
Total cost	2.95	4.33	4.86

Note: ^a Fees, equipment cost, lost production and waste disposal

Rhone Poulenc Chemie developed “Built-in Precathode Diaphragms” in the early 1990s [86]. These consist of two layers, both vacuum deposited on the cathode. The first layer, the precathode, is made of a conducting fibrous material, an electrocatalyst (e.g., Raney Ni), a pore-forming agent, and a fluoropolymer. The second layer is a PTFE-based composition with a pore-forming agent. It is claimed, based on test results in MDC-55 cells, that this diaphragm provides energy savings of up to 200 kW hr ton⁻¹ of chlorine at 2.64 kA m⁻², with lowered chlorates in caustic and <0.1% of H₂ in Cl₂.

There has been significant commercial experience with various non-asbestos diaphragms. The non-asbestos diaphragm technology could become competitive over conversion to the membrane technology, because of the high conversion cost of diaphragm cells to membrane cells, as the life of the diaphragms improves and the regulatory agencies mandate the elimination of asbestos.

4.7.7. Diaphragm Deposition

The theoretical description of transport across diaphragms in Sections 4.7.3 and 4.7.4 shows that a given diaphragm (with a specific L and τ/ε or weight and tortuosity/porosity, respectively) will provide the highest caustic efficiency at only one caustic strength and current density. There is no single, universal diaphragm that will give high current efficiency at all caustic strengths and current densities. The diaphragm must be designed and optimized for each case. Any change in operating parameters will then lower the efficiency. It is these factors that make the diaphragm deposition a “delicate/sensitive” process, and hence, it is essential that proper approaches and precautions are followed to consistently achieve a uniform diaphragm. Thus, diaphragm deposition is an “art”, as there are several variables involved in the deposition of asbestos or asbestos-based diaphragms. These are noted in Tables 4.7.7 and 4.7.8, along with the factors influenced by the performance of the diaphragm.

The primary variables [87,88] in depositing a diaphragm are the asbestos type and bath composition, rate of deposition, and baking, which are elaborated below. The guidelines discussed here are applicable with all the modifiers, although the precise values of the operating variables depend on the requirements at a given site.

4.7.7.1. Asbestos Type. The primary source of chrysotile asbestos used worldwide is Zambezi asbestos. Zambezi fibers are mechanically processed and are soft with consistent length. Zambezi asbestos yields uniform diaphragms that are not prone to webs or bridging between the cathode fingers. However, they tend to form pinholes, especially on old cathodes.

One of the characteristics of asbestos is the rapid surface area (RSA) factor. A low RSA fiber will permit rapid drainage of liquid and hence, lower drying vacuums and bath operating levels. All varieties of asbestos come in long and short fibers. The long : short fiber ratio in the bath generally is in the range 2 : 1 to 4 : 1 depending on the source of asbestos. The ratio varies depending on the load and the desired caustic strength. Generally, increased fiber ratios will lead to fewer holes and increased bridging of the fibers.

4.7.7.2. Bath Composition. The asbestos slurry bath is prepared by mixing asbestos with catholyte cell liquor. The fiber concentration of the bath is in the range of 12 to 15 gpl; at higher concentrations there is a tendency to form bridges and holes. The

TABLE 4.7.7 Influence of Depositing Variables on Diaphragm Characteristics [87,88]

Variable	Units	Range	Comments
<i>Diaphragm</i>			
Asbestos			
Diaphragm weight	kg m ⁻²	1.5–2.0	Chrysotile Increases cell voltage, current efficiency and bridging at >2.0 kg m ⁻² .
Long : short fiber ratio		2 : 1 to 4 : 1	Hole formation decreases and bridging increases at > 4:1 ratio.
Modifier (Halar, SM-1, SM-2, SM-3)	%	5–25	Increases stability and porosity at >25%, resulting in a tightened diaphragm.
<i>Depositing profile</i>			
Fiber concentration	gpl	12–20	At >20 gpl, bridging is enhanced.
NaCl concentration	gpl	120–170	Salt reduces the settling rate of the fibers. Increased salt levels provide diaphragm uniformity, and low salt levels lead to the settling of fibers during deposition.
NaOH concentration	gpl	120–140	Caustic reacts with fibers and allows them to swell, reducing the porosity of the diaphragm. Very high levels of caustic result in the formation of silica gel in the bath.
Bath temperature	°C	20–25	Increases diaphragm tightness and decreased bridging at >25°C.
Mix time	min	4–20	Decreases porosity and bridging results if mixed for long times and causes diaphragm tightening.
Cathode agitation amplitude	cm	10–40	At > 100 cm, bridging decreases and the diaphragm tightens.
Cathode agitation frequency	# min ⁻¹	1–4	At > 4 min ⁻¹ , bridging decreases and the diaphragm tightens.

TABLE 4.7.7 (continued)

<i>Depositing profile</i>	
1st stage	Average slurry flow rate should be $5.7\text{--}8.2\text{ L m}^{-2}\text{ min}^{-1}$ of cathode area; cathode agitation 1 min^{-1} to 0.5 min^{-1} . Increase in vacuum will result in holes in the first stage.
2nd stage	Applied vacuum increased in increments of 7–13 cm of Hg/increments until 50–70% of the total volume of the deposit passes through the diaphragm. Agitation of the slurry increased to 1/30 s to 1/60 s, when the formation of the bridges is minimized.
3rd stage	Applied vacuum is maximum, at least 25 cm of mercury, prior to removing the cathode.
Draw down	Cathode removed and air allowed to pass for 20 min to 1 hr, when the wet diaphragm is compressed. Air drying vacuum should be 30–45 cm of Hg. Higher drying vacuums of >65 cm of Hg are indicative of tight diaphragms.
<i>Curing/Baking</i>	
Step 1—Ramping	Air temperature increased to 90–95°C at rate of 2°C min^{-1} , when all the moisture is removed from the diaphragm over 4–8 hr. Temperature held at 100°C until the diaphragm is completely dry. Incomplete water removal results in blisters in the diaphragm.
Step 2—Drying	Oven air temperature increased to 100°C.
Step 3—Fusion	Temperature further increased at 2°C min^{-1} to 229–241°C for Halar based diaphragms and to 375°C for SM based diaphragms for ~1 hr to bond the polymer to the fibers.
Step 4—Cool down	Allowed to cool with fans operating over 2 h before the cathode is taken out.

fiber concentration must be maintained constant to realize a consistent weight of the diaphragm. Modifiers such as Halar, SM-1, SM-2, and SM-3, are then added to the bath—the Halar level being 5–10% and SM-based modifier levels being 15–25% of the total dry weight.

The NaOH concentration in the depositing bath must be held in the range of 120–160 gpl. The caustic reacts with the silica layers of the asbestos fibers. The fibers will swell and reduce the porosity of the diaphragm. The higher caustic concentration in the bath will degrade the asbestos fiber and form a silica gel in the bath.

NaCl is added to the bath to increase its specific gravity and to reduce the settling rate of the fibers. At salt concentrations below 120 gpl, the fibers will settle, and at concentrations above 180 gpl, the diaphragm will tend to be porous, leading to high levels of hydrogen in chlorine during operation.

Viscosity and fiber concentration should be measured before each deposit. Monitoring the slurry composition will allow the determination of the weight of the diaphragm, and the viscosity measurement will indicate changes in fiber properties.

4.7.7.3. Deposition Sequence. The diaphragms are formed by applying vacuum to the cathode to draw the slurry uniformly from the bath, and this is done in three stages.

After asbestos is added to the bath, the slurry is well mixed. This is achieved by blowing compressed air through spargers located in the bottom of the tank or by employing a vacuum compressor to pull air through bottom connections to the tank. The mix

TABLE 4.7.8 Diaphragm Cell Variables

Cell data	Operating data
Deposit date	Date
Bath number	Cell location
Deposit number	
Cathode comments	Voltage
	Intercell voltage
Asbestos type	Anolyte position
Asbestos quantity	Perc pipe position
Modifier type	Catholyte temperature
Modifier quantity	Circuit voltage
Wetting agent type	Operating data comments
Wetting agent quantity	
	Catholyte caustic
Mix time	Catholyte chlorate
Temperature	Catholyte salt
Slurry viscosity	Catholyte hypo
Caustic concentration	Hydrogen
Salt concentration	Oxygen (air free)
Carbonate concentration	Chlorine
Fiber concentration	Nitrogen
Start level	Carbon dioxide
End level	Feed salt
Vacuum profile	Feed pH
Flow profile	Feed temperature
Low vacuum time	Feed carbonate
Total deposit time	Feed bicarbonate
Final deposit time	Feed free acid
Drying vacuum	Feed flow rate
Drying time	
Deposit comments	Doping records
	Repair data
Oven	Technician surveys
Drying time	Test identification
	Connecting buss voltage
Post bake comments	Circuit efficiencies
Anode set	Significant events
Anode potential data	
Base number	
Cathode number	
Cathode quality rating	
Installation location	
Installation comments	
Removal comments	

time is typically 6–10 min. It should be noted that with longer mix times the diaphragm tightens, lowering its permeability. The bath temperature should be maintained in the range of 20–25°C. At high temperatures, while bridging is decreased, there is an increasing tendency for the diaphragm to become tight, as caustic attacks the fibers more rapidly to form a gelatinous matter.

In the first stage, when a base layer of fiber is set, the average slurry flow rate is maintained in the range of $5.7\text{--}8.2\text{ L m}^{-2}\text{ min}^{-1}$ of cathode area by controlling the system vacuum, until the sight glass in the depositing line is clear. This takes about 18–20 min and ensures that the mat is compact and free of holes. During this period, 20–30% of the total volume is pulled through the cathode structure. It is critical that the depositing sight glass is clear at this stage. This ensures the formation of a uniform mat without holes. Raising the vacuum before the sight glass is clear results in holes in the diaphragm. Gentle agitation of the asbestos slurry, by raising and lowering the cathode through 25–100 cm once every minute or two is also suggested, in order to maintain the mechanical integrity of the asbestos fibers and to produce a smooth, uniform mat on the cathode.

The second stage involves applying vacuum in stepwise increments of 7–13 cm of mercury, pausing each time until the sight glass is clear. During this period, 50–70% of the total volume of the deposit passes through the diaphragm. The slurry is agitated once every 30 to 60 s to minimize bridge or web formation. The cathode must remain deeply immersed in the bath during agitation.

In the final stage of deposition, application of maximum vacuum compacts the diaphragm before it is taken out of the bath. 10–30% of the volume of the deposit forms on the cathode in this stage. It is necessary to maintain a differential of at least 25 cm of Hg across the diaphragm so that the liquid inside the cathode does not push the diaphragm away from the cathode screen.

The cathode is held at an angle as it is removed from the depositing tank. The liquid drains, and air passes through the deposit more rapidly. As a result, the diaphragm is tightened and the porosity lowered. Air drying time is normally 20–60 min.

The diaphragm is inspected at this stage, and any holes are plugged with asbestos fiber. The air drying vacuum should be between 45 and 50 cm of mercury for SM-2 diaphragms, 65 cm for Halar diaphragms, and 15–20 cm for SM-1 diaphragms. This is an important parameter that should be monitored, as it reflects the porosity of the diaphragm. Low drying vacuums generally provide an acceptable startup level, quickly approaching the target caustic strength. High drying vacuums of >65 cm of mercury are indicative of low porosity. Soaking them in brine over 24 hr can rejuvenate the low porosity diaphragms.

4.7.7.4. Baking. After air drying, it is necessary to cure the diaphragm. Successful curing requires proper temperature distribution in the assembly. This is achieved in five stages, in an oven with properly located thermocouples around the cathode to monitor air and cathode temperatures. The temperature profile and the heat treatment times in these various stages are shown in Fig. 4.7.16 for the SM-2 diaphragms.

- A. *Ramping*: During the first stage, termed ramping, the diaphragm is cured in three steps, by increasing the oven temperature to 90–95°C, then to 330°C, and finally to 365°C, at a rate of about 2°C min^{-1} .
- B. *Drying*: Maintaining the temperature at 100°C for 4 to 8 hr removes the moisture from the asbestos mat. Drying above the boiling temperature results in formation of blisters and powdering of the diaphragm.

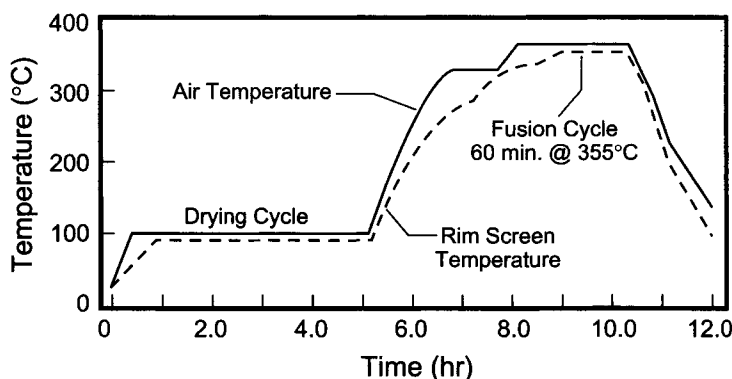


FIGURE 4.7.16. Typical SM-2 diaphragm cycle [87]. (With permission from ELTECH Systems Corporation.)

- C. *Heat Sink Plateau*: This is the second plateau of the process, at an air temperature of 330°C for about 40 min. During this time, the diaphragm temperature reaches the temperature of the air.
- D. *Fusion Cycle*: This is the third and last plateau of the process. The temperature maintained during this regime depends on the fusion temperature of the chosen polymer, when the polymer is softened to a state where it bonds to the asbestos without decomposing. HAPP diaphragms require a temperature of 240°C for 1 hr (Halar melts at 230–240°C and decomposes at >350°C). SM-2 and SM-3 diaphragms are normally fused at 350°C for 1 hr.
- E. *Cool Down Segment*: The oven's heating elements are shut off and the fans are allowed to operate for about 2 hr to cool the diaphragm and the cathode gradually, before removal from the oven.

The fused diaphragms are ready to be installed in the cells, and it is preferable to use them within 2 days in order to minimize corrosion of the cathode, unless precautions are taken to ensure that the diaphragm is dry. It is essential that all the procedures and the specifications be adhered to in order to realize reproducible and optimal diaphragms. Run charts are suggested to monitor the various parameters discussed in this section.

4.7.8. Effect of Shutdowns on the Performance of Diaphragms

As discussed earlier, the performance of asbestos diaphragms and non-asbestos diaphragms depends on several variables, which include composition of the baths used, method of forming the diaphragms, follow-up thermal treatment, and brine quality. Another factor that can adversely affect performance is the shutdown procedure followed during current interruptions. A proper procedure calls for rapidly destroying the hypochlorite in the anolyte and increasing its pH to 10–12. This ensures the absence of hypochlorite and acidity, which corrode steel cathodes. When corrosion occurs, iron oxides form in the alkaline medium in the vicinity of the cathode and plug the diaphragm.

This results in tighter diaphragms, higher caustic strength, and lower efficiency. Sometimes, depending on the residual hypo level, these oxides grow as dendrites and penetrate the diaphragm. When the cell is energized, the iron oxides are reduced to the metal and become sites for the hydrogen evolution reaction. This leads to increased hydrogen levels in chlorine. Temporary measures to clean the diaphragms include flushing with brine at a pH of 2–3, sugar doping and selectively solubilizing the iron oxides with complexing agents such as gluconate. However, with asbestos diaphragms, the acid dissolving the iron oxides will also leach out magnesium that will be redeposited on the cathode side as $Mg(OH)_2$ and tighten it again. Diaphragms that are extensively plugged up with iron oxides therefore cannot be acid cleaned effectively because of potential corrosion of steel cathodes, and must be replaced.

APPENDIX 4.7.1: DIAPHRAGM MODELLING BY VAN ZEE ET AL. [50–57]

The flux of OH^- in the porous diaphragm is represented by Eq. (A1.1):

$$N_1 = -\frac{D_1}{N_M} \frac{dC_1}{dx} - \frac{D_1}{\kappa_{avg}} \frac{Fi}{RT} C_1 + vC_1 \quad (A1.1)$$

where C refers to the concentration of the OH^- ions, D to the diffusion coefficient, κ_{avg} to the solution conductivity, N_M to the MacMullin number, F to the Faraday constant, R to gas constant, T to the temperature, v to the percolation velocity, x to the coordinate across the diaphragm and subscript 1 represents OH^- . This equation is the same as Eq. (31), except that the diffusion coefficient of OH^- ions in the first term of the right-hand side is divided by N_M , since OH^- can pass only through the micropores. The current density, i , in the second term, is also a function of N_M , as:

$$i = -\frac{\kappa_{avg}}{N_M} \frac{d\phi}{dx} \quad (A1.2)$$

where $d\phi/dx$ refers to the potential gradient. Under steady state conditions, when the OH^- flow along the coordinate x remains constant, $dN_i/dx = 0$. Substituting this condition and Eq. (A1.2) in Eq. (A1.1), a second order differential equation, which governs the OH^- concentration in the diaphragm, is obtained: Thus,

$$\frac{D_1}{N_M} \frac{d^2C_1}{dx^2} + \left(\frac{D_1 Fi}{\kappa_{avg} RT} - v \right) \frac{dC_1}{dx} = 0 \quad (A1.3)$$

Integrating it with proper boundary conditions gives the OH^- concentration, $C_1(x)$.

$$C_1(x) = \frac{(i/vF)(1 - \exp(A_1x))}{(FiD_1/RT\kappa_{avg}v) - \exp(A_1t)} \quad (A1.4)$$

where

$$A_1 = \frac{-FiN_M}{RT\kappa_{\text{avg}}} + \frac{vN_M}{D_1} \quad (\text{A1.5})$$

t = thickness of the diaphragm.

These equations for the OH^- concentration, current efficiency, η , and the voltage drop, $\Delta\phi$, can be recast using the dimensionless groups [51], as:

Current Efficiency

$$\eta = \frac{1 - \exp(\text{Pe} + \Delta\phi)}{(-\Delta\phi/\text{Pe}) - \exp(\text{Pe} + \Delta\phi)} \quad (\text{A1.6})$$

where

$$\text{Pe} = \frac{vN_M t}{D_1} \quad (\text{Peclet number}) \quad (\text{A1.7})$$

Voltage Drop

$$-\Delta\phi = \frac{F}{RT} [\phi_{(x=t)} - \phi_{(x=0)}] = \frac{FiN_M t}{RT\kappa_{\text{avg}}} \quad (\text{A1.8})$$

OH^- Concentration

$$\psi_1(\xi) = \frac{C_1(\xi)}{C_F} = \frac{(\text{Pe}_c/\text{Pe})[1 - \exp\{(\text{Pe} + \Delta\phi)(\xi)\}]}{(-\Delta\phi/\text{Pe}) - \exp(\text{Pe} + \Delta\phi)} \quad (\text{A1.9})$$

C_F in Eq. (A1.9) refers to the NaCl concentration in the feed brine, Pe_c to the Peclet number at current density, i , $\psi_1(\xi)$ to the dimensionless OH^- concentration, and ξ being the dimensionless diaphragm coordinate.

$$\text{Pe}_c = \frac{(i/F)C_F}{(D_1/N_M t)} \quad (\text{A1.10})$$

Equations (A1.5) through (A1.10) show that the current efficiency depends on the product of N_M and t . From Eqs. A1.7 and A1.10, a new dimensionless number, N_H , the Hine number, can be defined as:

$$N_H = \frac{\text{Pe}_c}{\text{Pe}} = \frac{i/(FC_F)}{v} \quad (\text{A1.11})$$

which represents the contribution of the ratio of current density to the flow rate of brine, i/Fv , and to the OH^- concentration.

APPENDIX 4.7.2: CALCULATION OF PERCOLATION AND MIGRATION VELOCITIES

Cell:	ELTECH H-4
Load, I	150 KA at 90°C
Current efficiency, η :	90% at 150 g L ⁻¹ NaOH
Porosity, ε :	0.75
Flow Area:	64.5 m ² (same as anode area)
Catholyte Flow:	$\frac{I\eta}{FC_{OH}^0} = \frac{22.4 L}{\text{min}}$
Percolation Flow:	Catholyte flow + H ₂ O decomposed + H ₂ O evaporated by H ₂
H ₂ O Decomposed:	1 F → 1 mol of H ₂ O → 1 mol OH ⁻
H ₂ O carried by H ₂ = f (temp) =	~22 kg H ₂ O kg ⁻¹ of H ₂ at 90°C = 25.2 l min ⁻¹

$$\text{Percolation Velocity: } \frac{\text{Percolation Flow}}{\text{Flow Area} \times \text{Porosity}} = 8.67 \times 10^{-4} \text{ cm s}^{-1}$$

$$\text{Migration Velocity} = v_m = F \cdot \frac{U_{OH}}{\varepsilon \chi} \cdot i = \frac{F}{RT} \frac{D_{OH}}{\varepsilon \chi} \frac{\text{load}}{\text{flowarea}}$$

$$F = 23,060 \text{ cal V}^{-1} (\text{g-equivalent})^{-1}$$

$$R = 1.987 \text{ cal mol}^{-1} \text{ K}^{-1}$$

$$T = 363 \text{ K (90°C)}$$

$$D_{OH} = 4.91 \times 10^{-5} \text{ cm s}^{-1}$$

$$\chi = 0.64 \Omega^{-1} \text{ cm}^{-1} \text{ for } 150 \text{ g L}^{-1} \text{ NaOH} + 182 \text{ g L}^{-1} \text{ NaCl}$$

$$A = 6.452 \times 10^5 \text{ cm}^2$$

Substituting these values into the above equation results in $v_m = 7.6 \times 10^{-4} \text{ cm s}^{-1}$.

REFERENCES

1. C.L. Mantell, *Industrial Electrochemistry*, 2nd Edition, McGraw-Hill Book Co., New York (1940), p. 332.
2. C.L. Mantell, *Electrochemical Engineering*, 4th Edition, McGraw-Hill Book Co., New York, (1960), p. 277.
3. M.S. Kircher, Electrolysis of Brines in Diaphragm Cells. In J.S. Sconce *Chlorine—Its Manufacture, Properties, and Uses*, ACS Monograph 154 (ed.), Reinhold Publishing Co., New York (1962), p. 81.
4. D.W.F. Hardie, *Electrolytic Manufacture of Chemicals From Salt*, W.W. Smith (ed.), The Chlorine Institute, New York (1975), p. 75.
5. J.E. Currey and G.G. Pumplun, Chlor-Alkali. In *Encyclopedia of Chemical Processing and Design*, Vol. 7, Marcel Dekker, New York (1978), p. 305.
6. L. Michaels, and S.S. Chissick (eds.), *Asbestos: Properties, Applications, and Hazards, Vol. 1*, John Wiley & Sons, Inc., New York (1979).
7. R.J. Levine, M.D. Gidley, M. Feuerstein, M. Chesney, and P.M. Giever, Asbestos-Related Diseases Part 5: The prevention of Asbestos-Related Diseases, in Ref. 6, p. 485.
8. J.A. Moore, *Proceedings of the NBS Workshop on Asbestos: Definitions and Measurement Methods*, Gaithersburg, MD (1977).

9. T.F. Gates, L.B. Sand, and J.F. Mink, *Science* **111**, 512 (1950).
10. B. Nagy and T.F. Bates, *Am. Mineralogist* **37**, 1055 (1952).
11. E.J.W. Whittaker, *Acta Cryst.* **6**, 747 (1953).
12. A.C. Zettlemoyer, G.J. Young, J.J. Chessick, and F.H. Healey, *J. Phys. Chem.* **57**, 647 (1952).
13. G.J. Young and F.H. Healey, *J. Phys. Chem.* **58**, 881 (1954).
14. F.L. Pundsack, *J. Phys. Chem.* **59**, 892 (1955); **60**, 361 (1956).
15. F.L. Pundsack and G. Reimschuessel, *J. Phys. Chem.* **60**, 1218 (1956).
16. S.G. Clark and P.F. Holt, *Nature* **185**, 237 (1960).
17. E. Martinez and G.L. Zucker, *J. Phys. Chem.* **64**, 924 (1960).
18. I. Choi and R.W. Smith, *J. Colloid and Interface Sci.* **10**, 253 (1972).
19. T. Otouma and S. Take, *J. Chem. Soc. Japan* **10**, 1897 (1974).
20. J.H. Perry, *Chemical Engineers' Handbook*, 4th Edition, McGraw-Hill Book Co., New York (1960), pp. 19–55.
21. S. Kamei, *Kagaku Kikai no Riron to Keisan (Theory and Calculation of Chemical Process Equipment)*, Sangyo Tosho, Tokyo (1959).
22. P.C. Carman, *Trans. Inst. Chem. Eng. (London)* **23**, 150 (1937).
23. R.B. MacMullin and G.A. Muccini, *AIChE J.* **2**, 393 (1956).
24. R.E. De La Rue and C.W. Tobias, *J. Electrochem. Soc.* **106**, 827 (1959).
25. M. Yasuda, *Soda to Enso (Soda and Chlorine)* **25**, 225 (1974).
26. F.A.L. Dullien, *AIChE J.* **21**, 820 (1975).
27. K.S. Spiegler, *J. Electrochem. Soc.* **113**, 161 (1966).
28. T. Matsuno, *Kogyo Butsuri-Kagaku (Industrial Physical Chemistry)*, Vol. 2, Corona Publ., Tokyo (1948), p. 107.
29. Yu.C. Chirkov, *Soviet Electrochem.* **7**, 1462, 1622 (1971); **8**, 549, 723 (1972).
30. Yu.C. Chirkov, *Soviet Electrochem.* **8**, 1042, 1156 (1972).
31. V.N. Zhuravleva, V.S. Markin, A.G. Pshenichnikov, and Yu.C. Chirkov, *Soviet Electrochem.* **13**, 135 (1977).
32. H. Kaden and A. Pohl, *Chem. Techn.* **30**, 25 (1978).
33. Yu.L. Golin, V.E. Karynkin, B.S. Pospelov, and V.I. Seredkin, *Soviet Electrochem.* **28**, 87 (1992).
34. F. Hine, M. Yasuda, and T. Tanaka, *Electrochim. Acta* **22**, 429 (1977).
35. R.B. MacMullin, Private Communication (1990).
36. F. Hine and M. Yasuda, *J. Electrochem. Soc.* **118**, 166 (1971).
37. G. van der Heiden, Diaphragm Cells for Chlorine Production, *Proc. Symp. held at the City University, London* (1976), Society of Chemical Industry, London (1977), p. 33; *J. Appl. Electrochem.* **19**, 571 (1989).
38. T. Mukaibo, *Denki Kagaku (J. Electrochem. Soc. Japan)* **20**, 482 (1952).
39. V.V. Stender, O.S. Ksenzhek, and V.N. Lazarev, *Zh. Prikl. Khim.* **40**, 1293 (1967).
40. P. Gallone and E. Rubino, *Annali di Chimica.* **66**, 103 (1976).
41. L.I. Kheifets and A.B. Goldberg, *Soviet Electrochem.* **12**, 1525 (1976).
42. A.B. Goldberg and L.I. Kheifets, *Soviet Electrochem.* **12**, 1555 (1976).
43. A.B. Goldberg and L.I. Kheifets, *Soviet Electrochem.* **13**, 123 (1977).
44. V.L. Kubasov, *Soviet Electrochem.* **12**, 72 (1976).
45. O.S. Ksenzhek and V.M. Serebriskii, *Soviet Electrochem.* **4**, 1294 (1968).
46. V.M. Serebriskii and O.S. Ksenzhek, *Soviet Electrochem.* **7**, 1592 (1971).
47. G. Matic, P.M. Robertson, and N. Ibl, *Electrochim. Acta* **25**, 487 (1980).
48. P.M. Robertson, R. Cherlin, and N. Ibl, *Electrochim. Acta* **26**, 941 (1981).
49. R.R. Chandran, D.T. Chin, and K. Viswanathan, *J. Applied Electrochem.* **14**, 511 (1984).
50. R.E. White, J.S. Beckerdite, and J. Van Zee, A Simple Model of a Diaphragm-Type Chlorine Cell. In R.E. White (ed.), *Plenum Press, Electrochemical Cell Design*, New York (1984) p. 28.
51. J. Van Zee and R.E. White, *J. Electrochem. Soc.* **132**, 818 (1985).
52. J. Van Zee, R.E. White, and A.T. Watson, *J. Electrochem. Soc.* **133**, 501 (1986).
53. J. Van Zee and R.E. White, *J. Electrochem. Soc.* **133**, 508 (1989).
54. J. Van Zee and T.H. Teng, The Effect of Acidic Brine on the Dynamic Behavior of Chlorine/Caustic Diaphragm-Type Electrolyzers. In U. Landau, R.E. White, and R.D. Varjian (eds), *Engineering of Industrial Electrolytic Processes*, PV 86-8, Electrochem. Society, Princeton, NJ, (1986), p. 219.

55. J. Van Zee and B. Tamtasna, Nonlinear Potential Gradients in Chlorine/Caustic Diaphragm-Type Electrolyzers. In J. Van Zee, R.E. White, K. Kinoshita and H.B. Burney (eds), *Diaphragms, Separators, and Ion Exchange Membranes*, PV 86-13, Electrochem. Society, Princeton, NJ (1986), p. 60.
56. S.A. McCluney and J. van Zee, *J. Electrochem. Soc.* **136**, 2556 (1989).
57. D.L. Caldwell, K.A. Poush, J.W. Van Zee, and R.E. White, Mathematical Model of the Chlorine Cell Diaphragm. In R.C. Alkire, T.R. Beck, and R.D. Varjian (eds), *Electrochemical Process and Plant Design* PV 83-6, Electrochem. Society, Princeton, NJ (1983), p. 216.
58. F. Hine and K. Murakami, *J. Electrochem. Soc.* **127**, 292 (1980).
59. F. Hine and M. Yasuda, *J. Electrochem. Soc.* **118**, 171 (1971).
60. F. Hine and M. Yasuda, *J. Electrochem. Soc.* **118**, 183 (1971).
61. J.S. Newman, *Electrochemical Systems*, Prentice Hall, Englewood Cliffs, NJ (1973), p. 3.
62. G. Angel, Electrolysis of Alkali Metal Salts in Diaphragm-Equipped Baths (Russian Translation), *ONTI Khintoret*, Moscow (1935), p. 7.
63. V.B. Vorob'eva, V.L. Kubasov, and L.I. Yurkov, *Soviet Electrochem.* **14**, 812 (1978).
64. V.L. Kubasov, *Soviet Electrochem.* **9**(12), 1680 (1973).
65. *U.S. Patents* 3,928,166 (1975); 3,980,613 (1976); 4,260,453 (1981); 4,189,369 (1980); 4,187,390 (1970); 4,031,041 (1977); 3,853,721 (1974); 3,945,910 (1976); *French Patent*, 2,300,145 (1976); *British Patents*, 1,410,313 (1975); 1,473,963 (1977); *Japanese Kokai*, 52-142695 (1977); 52-23870 (1978); 52-23900 (1978).
66. *U.S. Patents* 4,410,411 (1983); 4,489,025 (1984); 4,701,250 (1987).
67. *U.S. Patent* 3,928,166 (1975).
68. *U.S. Patent* 4,444,640 (1984).
69. *U.S. Patents* 4,447,566 (1984); 4,563,260 (1986); 4,665,120 (1987).
70. J.V. Winings and D.H. Porter, Evolutionary Developments in Hooker Diaphragm Cells. In M.O. Coulter (ed.), *Modern Chlor-Alkali Technology*, Society of Chemical Industry, London (1980), p. 27.
71. A. Bruce Robertson, *Appl. Polymer Symposium*, **21**, 89 (1973).
72. R. Romine, ELTECH Systems Corporation, Private Communication, 2000.
73. J. Faravarque, A New Life for the Diaphragm Process, *Info Chemie*, March 1999.
74. T.F. Florkiewicz, Long-Life Diaphragm Cell. In S. Sealey (ed.), *Modern Chlor-Alkali Technology*, Vol. 7, Society of Chemical Industry, London, Special Publication, #121 (1998), p. 171.
75. J.E. Currey and W. Strewé, *Chem. Ing. Techn.* **47**, 145 (1975).
76. *French Patent* 2,324,781 (1977).
77. *U.S. Patent* 4,003,818 (1977).
78. *Japanese Kokai* 51-80699 (1976).
79. *British Patent* 1,482,749 (1977).
80. *Japanese Kokai* 53-23900 (1978).
81. *Japanese Kokai* 50-40473 (1975).
82. T.F. Florkiewicz and R.C. Matousek, *Polyramix*[®]: A Depositible Replacement for Asbestos Diaphragms in *Chlorine Institute 31st Plant Manager's Seminar*, New Orleans, LA, 1988.
83. L.C. Curlin, T.F. Florkiewicz, and R.C. Matousek, *Polyramix*[®]: A Depositible Replacement for Asbestos Diaphragms, In N.M. Prout and J.S. Moorhouse (eds), *Modern Chlor-Alkali Technology*, Vol. 4, Elsevier, London (1990), p. 333.
84. T.F. Florkiewicz and L.C. Curlin, *Polyramix*[®]: A Commercial Reality. In T.C. Wellington (ed.), *Modern Chlor-Alkali Technology*, Vol. 5, Elsevier, London (1992), p. 209.
85. P.C. Foller, D.W. DuBois, and J. Hutchins, PPG's Tephram[®] Diaphragm, The Adaptable Non-Asbestos Diaphragm. In S. Sealey (ed.), *Modern Chlor-Alkali Technology*, Vol. 7, Royal Society of Chemistry, Cambridge, UK (1988), p. 162.
86. F. Kuntzburger, D. Horbez, J.G. LeHelloco, and J.M. Perineau, New Developments in Built-in Precathode Diaphragm Technology. In *Modern Chlor-Alkali Technology*, Vol. 7, Society of Chemical Industry, London (1998), p. 181.
87. L.C. Curlin and E.S. Kazimir, Diaphragm Depositing and Cell Renewal Fundamentals, in *Electrode Corporation's 12th Annual Chlorine/Chlorate Seminar*, 1966, Cleveland, Ohio.
88. R. Gritte, Optimizing Diaphragms to Match Plant Objectives, in *Electrode Corporation's 14th Annual Chlorine/Chlorate Seminar*, 1998, Cleveland, Ohio.

4.8. ION-EXCHANGE MEMBRANES

4.8.1. Introduction

Ion-exchange membranes were first developed for electro dialysis applications such as desalination of seawater or brackish water, where an impure stream is electrolyzed in a dialyzer consisting of an anode and cathode assembly, between which a stack of anion and cation-exchange membranes is placed. During electrolysis, the field across the membranes allows the transfer of anions and cations, thereby producing dilute and concentrated brine streams.

The chlor-alkali industry's development of ion-exchange membrane-based electrolytic cells in the early 1970s was driven by environmental concerns associated with mercury and asbestos and the desire to reduce energy costs associated with electrolysis and caustic evaporation [1] (Table 4.8.1).

The first commercial membrane cells [2] started in 1975 (by Asahi Chemical at Nobeoka, Japan, and Hooker Chemicals at Dryden, Ontario, Canada), while the evolution of chlor-alkali membrane technology presumably began with the invention of Teflon in 1938. The first ion-exchange membranes developed were hydrocarbon-based, for the electro dialysis of saline water. They are unstable in chlor-alkali cells because of oxidation by the dissolved chlorine in the anolyte and chemical attack by the hot, concentrated caustic in the catholyte. Grot and coworkers [3–7] of DuPont developed perfluorinated polymers, utilizing the advantages of Teflon and ion-exchange technologies, following the discovery of a new copolymer described in *U.S. Patent 3,282,875* in 1972, which today is known as Nafion[®]. Although the first generation of ion-exchange membranes were capable of directly producing 2–40% caustic, the efficiencies generally were very low, and highest in the range of 10–15%. The first commercial installation produced 10% caustic, with current efficiencies of about 85%. Today, membranes are capable of producing 32% caustic at efficiencies of about 97%. Research efforts are continuing to perfect a membrane that will allow direct production of 50% caustic at high efficiencies and exhibit a long life.

4.8.2. Chemical Structure and Synthesis of Perfluorinated Membranes

Ion-exchange membranes are designed to selectively allow the passage of either cations or anions and are therefore known as cation- or anion-permeable or exchange membranes.

TABLE 4.8.1 Energy Consumption of Operating Cells (kW hr ton⁻¹ of Chlorine)

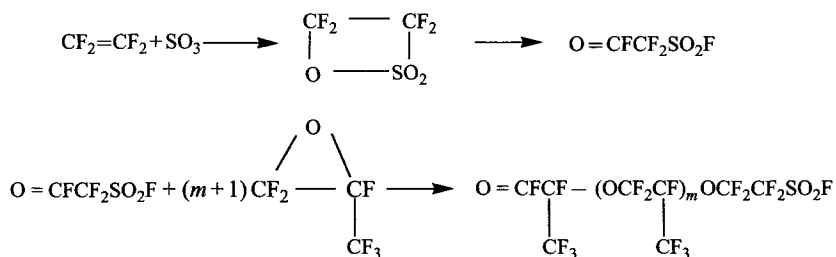
Energy	Cell type		
	Diaphragm	Mercury	Membrane
Electricity for electrolysis	2800–3000	3200–3600	2600–2800
Steam ^a	600–800	0	200–300
Total	3400–3800	3200–3600	2800–3100

Note: ^a 1 ton of steam is assumed to be ~250–300 kWh.

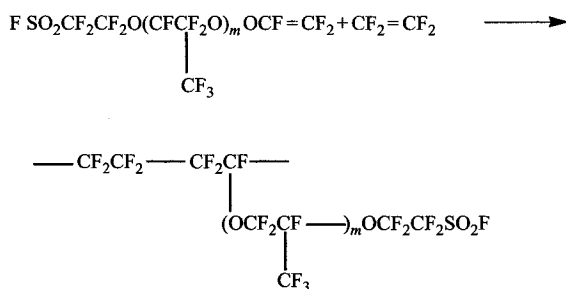
These membranes are produced from organic polymers containing a significant concentration of covalently bonded fixed ionic groups, and are 50 to 200 μm thick. The polymeric matrix contains fixed ionic groups or functional sites, and their charges are compensated by counter ions or mobile ions, which can be exchanged with the medium that is in contact with the membrane. The fixed sites of cation-exchange membranes are sulfonate or carboxylate acid groups, while anion-exchange membranes contain amine or quaternary ammonium groups in their fixed sites. The perfluorinated membranes developed for use in chlor-alkali cells exhibit superselectivity and high thermal and chemical stability, which are not found in other classes of polymeric ion-selective membranes. The three commercial perfluorinated membranes that have been extensively studied and used include:

1. Nafion[®] (perfluorosulfonate membrane produced by DuPont)
2. Flemion[®] (perfluorocarboxylate membrane produced by Asahi Glass), and
3. Aciplex[®] (bilayered perfluorosulfonate and carboxylate membrane developed by Asahi Chemical (now Asahi Kasei)).

The first perfluorinated ion-exchange membrane was Nafion[®] perfluoroionomer with sulfonate functionality. It is synthesized [8–12] by reacting tetrafluoroethylene with SO_3 to form a cyclic sulfone. Following rearrangement, it is then reacted with hexafluoropropylene oxide to generate sulfonyl fluoride adducts, with $m > 1$.

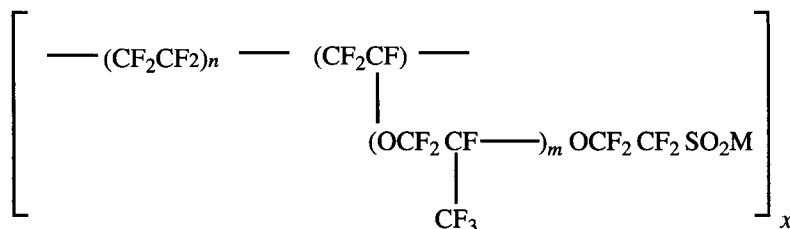


These adducts are heated with Na_2CO_3 to form a sulfonyl fluoride vinyl ether, which is subsequently copolymerized with tetrafluoroethylene to form XR resin as:



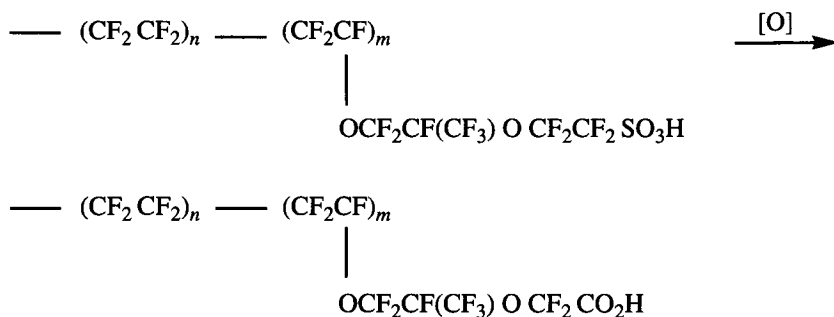
The polymer in this sulfonyl fluoride form is thermoplastic and can be melt processed with conventional fluoropolymer processing equipment. For use in chlor-alkali electrolyzers, the polymer is extruded to film form and reinforced, if necessary, with

fluoropolymer fabric. To make the polymer, it is hydrolyzed to form the chemical structure shown below, where M is sodium or potassium.



In commercial membranes, m is usually one, and n varies from about 5 to 11. This generates an equivalent weight (EW) ranging from 1000 to 1500 g of polymer, in its dry hydrogen ion form. Equivalent weight is defined as the weight of ionomer in grams that will neutralize one g-mole of a base, such as sodium hydroxide.

Asahi Kasei has developed [13–16] a modified membrane by treating the cathode side surface of the sulfonate ionomer to convert the sulfonate functional groups at and near the surface to carboxylate functional groups. It was found that the carboxyl ionomer of this structure was not sufficiently long-lived in the chlor-alkali environment and more stable carboxyl ionomer structures were developed.



Asahi Glass membranes are prepared [17–23] by copolymerization of tetrafluoroethylene with molecules such as perfluoro- δ -butyrolactone and hexafluoropropylene oxide to form $\text{CF}_2=\text{CFOCF}_2\text{CF}_2\text{CF}_2\text{CO}_2\text{CH}_3$. This is then polymerized with tetrafluoroethylene and a larger monomer and hydrolyzed to form the perfluorocarboxylate polymer. The carboxyl ionomer gives superior current efficiency and the ability to make strong caustic, about 32 wt%, in the electrolyzer. Because of its greater cost, lower conductivity, and susceptibility to become nonconductive at low pH, the carboxylate ionomer is generally used with the sulfonate ionomer in a “bilayer” membrane. This membrane may be made by laminating films of the respective ionomers, or by coextruding them to make the bilayer membrane in a single step. The membrane is then hydrolyzed.

4.8.2.1. Structure of Perfluorinated Membranes. It is generally accepted that the fluorocarbon polymers undergo phase separation on a molecular scale when swollen by

contact with water, resulting in distinct hydrophobic zones (based on the fluorocarbon chains) and hydrophilic zones (constituting the fixed ionic groups). These ionic groups hydrate and attract more water, thus forming channels through which the cations migrate when an electric field is applied.

Many experimental techniques have been used to examine the detailed structure of perfluorinated polymeric membranes. These include transmission electron microscopy [23], small angle X-ray scattering [24], Infra Red spectroscopy [25,26], neutron diffraction [27], Nuclear Magnetic Resonance [26,28], mechanical and dielectric relaxation [25,29], X-ray diffraction, and transport measurements. All these methods show convincing evidence for the existence of two phases in the perfluorosulfonate and perfluorocarboxylate polymers. One phase has crystallinity and a structure close to that of polytetrafluoroethylene (PTFE), and the other is an aqueous phase containing ionic groups.

Based on the various results, several descriptions have been proposed for characterizing the perfluoro-based polymers. Some of these models are: Ion-Dipole Cluster Model [30–33], Cluster-Network Model [23,34,35], Core-Shell and Lamellar Spacing Model [36,37], and Tortuous Pore Network Model [38,39]. The Cluster-Network Model, proposed by Gierke, provides a general picture of the structure of the aqueous domain constituting the membrane matrix. The model (Fig. 4.8.1) assumes that the ions and the sorbed solutions are all in clusters, the cluster diameter varying from 3 to 5 nm for a 1200 EW polymer and the average cluster containing approximately 70 ion-exchange sites and 1,000 water molecules. The counter ions, the fixed sites, and the swelling water phase are separated from the fluorocarbon matrix into spherical domains connected by short narrow channels. The fixed sites are embedded in the water phase very near to the water/fluorocarbon interface. The diameter of the channels, estimated from hydraulic permeability data, is ~ 1 nm. Assuming that the Bragg spacing (~ 5 nm from SAXS data) represents the distance between the clusters, the variations of cluster diameter and the number of ion-exchange sites per cluster are correlated to the water content (Fig. 4.8.2),

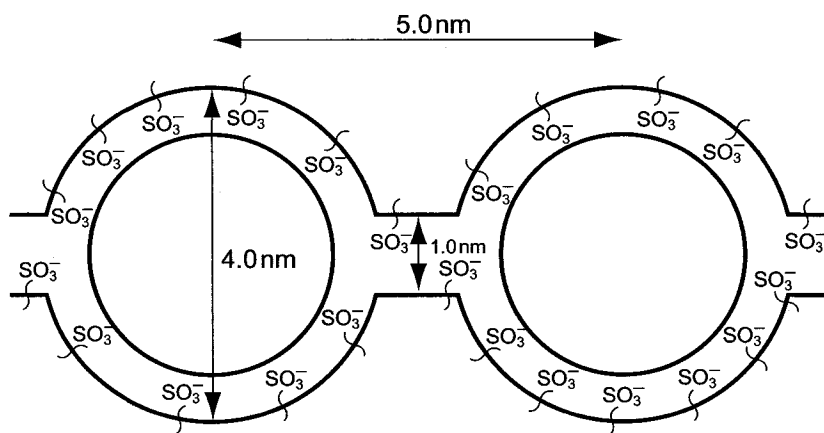


FIGURE 4.8.1. Cluster network model for Nafion[®] perfluorosulfonic acid membrane [24]. (With permission from Elsevier.)

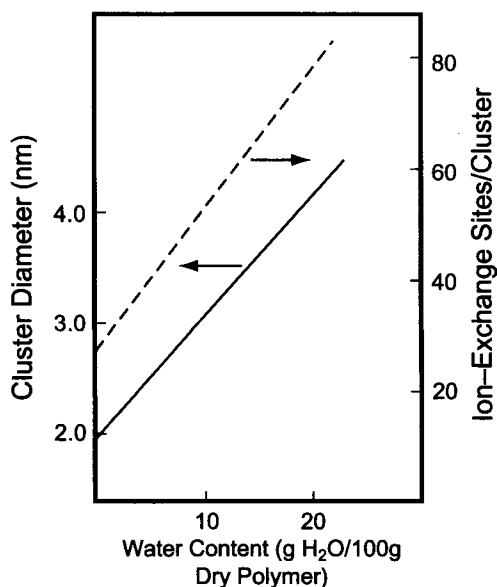


FIGURE 4.8.2. Variation of the cluster diameter and number of ion-exchange sites per cluster with water content in Nafion[®] 1200 EW polymer [24]. (With permission from Elsevier.)

and it was established that the pore diameter decreases with an increase in the EW. The size of the ionic clusters was shown to be dependent on the EW, the nature of the cations and the fixed sites, and also on the temperature.

The reasons for the success of this model are elaborated in the next section, which also addresses the physicochemical and transport properties of Nafion[®]. It may be noted that the existence of cluster networks in the perfluorinated membranes was demonstrated by Gierke *et al.* [40] by transmission electron microscopy.

4.8.3. Physicochemical Properties

4.8.3.1. Water Uptake. The physical and transport properties of perfluorinated polymeric cation-exchange membranes are greatly influenced by the amount of water and electrolyte uptake, which depends on the polymer EW, the nature of the electrolyte, and the pretreatment procedures. The water uptake increases [41] with increasing temperature, as shown in Fig. 4.8.3.

Figure 4.8.4 shows that water absorption also depends on the NaOH concentration [41,42]. The water absorption in perfluorocarboxylate membranes is lower than that in perfluorosulfonate membranes, and it decreases with increasing EW. The latter effect is a result of the lower concentration of ionic groups. Both sulfonate and carboxylate membranes sorb large amounts of electrolytes [43] and other solvents, particularly alcohols and other protic solvents [44]. Figure 4.8.5, illustrating the number of water molecules attached to each ionic group, shows that the water absorption depends not only on the hydration of the fixed ionic groups and their counter ions, but also on other interactions (such as cation–cation and anion–anion repulsions), which will result

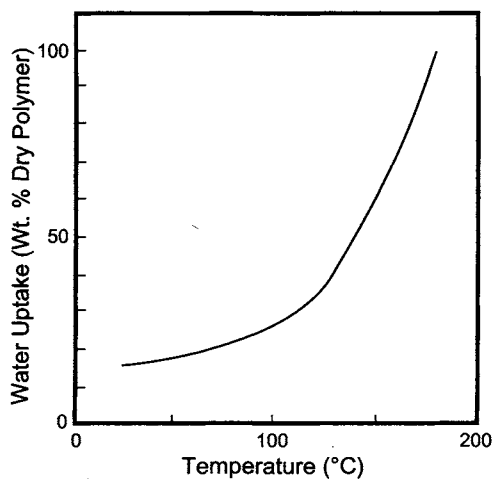


FIGURE 4.8.3. Water uptake for H⁺ form of Nafion[®] 1200 EW as a function of temperature [41]. (Reproduced by permission from The Electrochemical Society, Inc.)

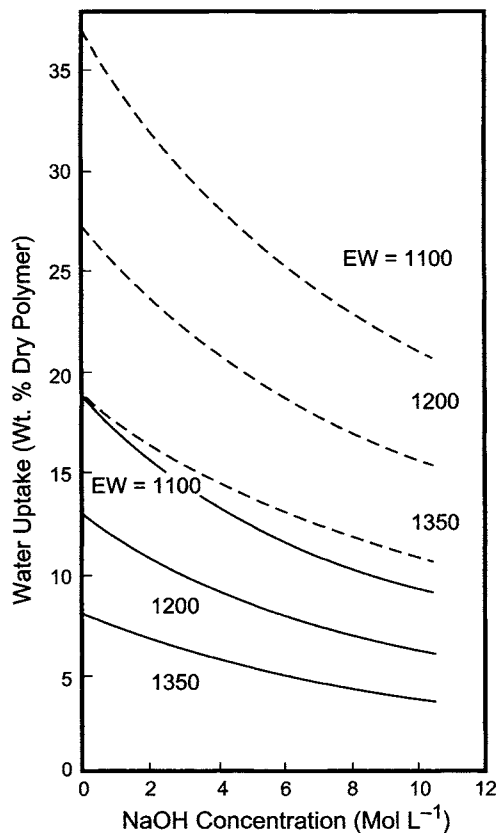


FIGURE 4.8.4. Water uptake for perfluorinated membranes for various EW as a function of NaOH concentration: (---) sulfonate and (—) carboxylate [42]. (Reprinted with permission from the American Chemical Society.)

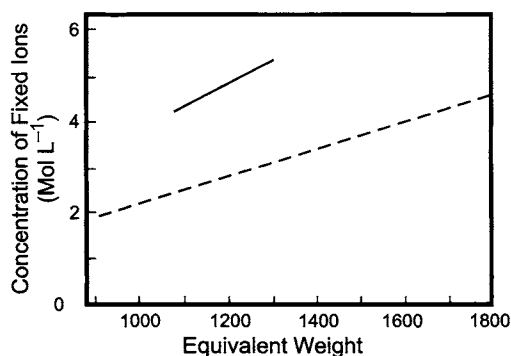


FIGURE 4.8.5. Calculated concentration of fixed ion for Nafion[®] of various EW in equilibrium with water at 25°C. (—) As received and (---) expanded by exposing to water at 100°C [48]. (Reproduced with permission of The Electrochemical Society, Inc.)

in increased water absorption beyond that needed for the primary hydration shell of the ions [45].

The state of water in Nafion[®] was examined by several authors, employing a multitude of techniques. Dielectric relaxation studies [46], neutron scattering data [47], and infrared data [48] showed that 20–24% of the water is in the organic phase. The rest is in the ion clusters, where its physical properties differ from those of bulk water.

Differential scanning calorimetric studies have shown that Nafion[®] contains at least three types of water—one tightly bound to the ions, one weakly bound in the secondary hydration shell to the ion or another component of the fluorocarbon polymer (e.g., to the ether oxygens), and one free from strong interactions with ions or polymer chains. Thus, the K⁺ form of Nafion contains ~3.8 water molecules per fixed ionic group in the primary hydration shell, 0.15 molecules as loosely bound water, and 3.8 water molecules as free water per each ionic group [49].

This tendency to absorb water results in the swelling of the membrane. The perfluorinated membranes swell by 10–20% from the dry state when exposed to an aqueous solution, and swelling can be followed by monitoring the thickness of the membrane. This process occurs in the electrolytic cell in three dimensions and hence, great caution has to be exercised to preserve dimensional integrity and to avoid shrinking and wrinkling of the membrane. Various procedures have been developed to treat and handle the membranes, and they will be discussed in Section 4.8.5.

4.8.3.2. Ion-Exchange Capacity. The ion-exchange capacity is usually expressed as the millimoles of charge associated with the fixed ionic groups per gram of the polymer. It is a measure of the number of fixed ionic groups per unit weight or volume of the membrane polymer, which is dictated by the synthesis procedure. Note that the ion-exchange capacity depends predominantly on the ratio of substituted to unsubstituted fluoroethylenes in the polymer chain and, to a lesser extent, on the length on the side chains.

The ion-exchange capacity of perfluorinated membranes is generally about 0.85 mmol g⁻¹ of dry membrane polymer, although it can be fabricated over a range of 0.5–1.2 mmol g⁻¹.

The terminology used to describe the ion-exchange capacities in the industry is the equivalent weight (EW), which is the weight of the polymer in the H^+ form that is neutralized by one equivalent of alkali and is the reciprocal of the ion-exchange capacity (EC in $mg\ eq\ g^{-1}$ dry resin).

$$EW(g\ eq^{-1}) = \frac{1000}{EC(mg\ eq\ g^{-1})} \quad (1)$$

The concentration of fixed ions (in $mol\ liter^{-1}$), or exchange sites, \bar{C}_f , is dependent on the EW as:

$$\bar{C}_f = \frac{EC f_i}{V_w f_w} = \frac{1000 d_e}{EW \cdot W_e} \left(\frac{f_i}{f_w} \right) \quad (2)$$

where W_e and d_e refer to the weight fraction and density of the electrolyte absorbed by the membrane, respectively, V_w to the volume of the electrolyte absorbed by the membrane, f_i to the fraction of the ionic groups in the ion cluster, and f_w to the fraction of the electrolyte solution in the ion clusters. The value of f_i varies from 0.4 to 1.0, while f_w varies in the range of 0.76 to 1.0 [47,48]. Hence, the ratio of f_i/f_w varies from 0.4 to 1.32. Thus, the fraction of water in the clusters depends on the fraction of ionic groups in the cluster. The calculated values [48] of \bar{C}_f as a function of the EW of Nafion[®], with $f_i/f_w = 1$, in Fig. 4.8.5, shows that the concentration of fixed sites increases with increasing EW . This is because, as the EW increases, the V_w decreases more significantly than the decrease in the ionic groups expected from the increased EW . The \bar{C}_f also increases with electrolyte concentration (Fig. 4.8.6) because of ion-cluster morphology [50]. In NaOH solutions, the concentration of the fixed ions is 50% less than those expected from Eq. (2), because of ion-pair formation and a strong association in the ion-clusters.

As the ion-exchange capacity increases, the water content increases [51], as shown in Fig. 4.8.7, the sulfonate membranes having a higher equilibrium water content compared to the carboxylate membrane. Shorter chain lengths in carboxylate membranes also result in lower water content.

4.8.3.3. Selectivity. The desired characteristic of a cation-exchange membrane is the ability to repel anions and allow only cation transport. This exclusion of co-ions results from their repulsion by the fixed ionic groups and the co-ions of the same electrical charge. Hence, the extent of the exclusion of co-ions depends on how closely the ions of like charge are located in the membrane and how many of them are available to repel the incoming co-ions. It must be appreciated here that increasing the concentration of fixed ionic groups proportionally increases the water capacity. The higher EC allows more water absorption, which swells the membrane, and decreases the concentration of fixed ionic groups.

The extent of the ingress of co-ions into the membrane polymer may be discussed quantitatively from a thermodynamic viewpoint, as follows. When an ion-exchange membrane with pendant groups such as $-SO_3Na$ is immersed in a NaCl solution of concentration, C , an equilibrium is established between the Na^+ and Cl^- ions in the solution

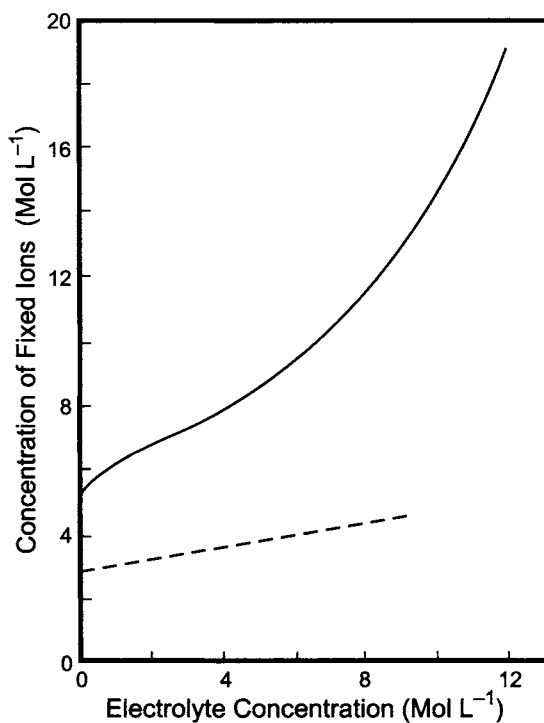


FIGURE 4.8.6. Calculated concentration of fixed ions for Nafion[®]. (—) As received and (---) expanded by exposing to water at 100°C for various EW and for varying HCl concentrations at 25°C [50]. (Reproduced with permission of The Electrochemical Society, Inc.)

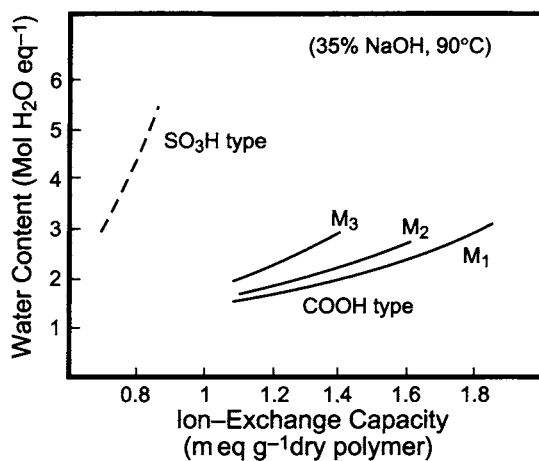


FIGURE 4.8.7. Dependence of water content on the ion-exchange capacity of membranes [51]. The subscripts 1, 2 and 3 to M, the membrane, refer to the length of the side chain. Membranes with shorter side chain length exhibit lower equilibrium water content. (With permission from Elsevier.)

and the Na^+ , Cl^- , and SO_3^- ions in the membrane. At equilibrium, the electrochemical potential of Na^+ and Cl^- in the membrane and solution become equal.

The electrochemical potential of an ion, μ_i^e , is defined as:

$$\mu_i^e = \mu_i^0 + RT \ln C_i + z_i F \phi + P V_i^m \quad (3)$$

where μ_i^0 is the chemical potential of the ion in its standard state, z_i is the ionic charge, F is the Faraday constant, ϕ is the potential of the phase, P is the pressure, V_i^m is the partial molar volume of the ion, and C_i is the concentration of the ion in the given phase (i.e., either the solution or the membrane). Expressing the above terms with bars for the membrane phase and equating the electrochemical potentials, assuming that $\bar{P} - P$ is small, the μ_i^0 terms are the same in the solution and the membrane phase, and $z = 1$, it can be shown that:

$$\phi_d = \bar{\phi}_{\text{mem}} - \phi_{\text{sol}} = \frac{RT}{F} \ln \frac{C_{\text{Na}^+}}{C_{\text{Na}^+}} \quad (4)$$

and

$$\phi_d = -\frac{RT}{F} \ln \frac{C_{\text{Cl}^-}}{C_{\text{Cl}^-}} \quad (5)$$

ϕ_d refers to the Donnan potential [52], which is the potential that is established between the membrane and the solution and is one of the components of the voltage across the membrane. Equating (4) and (5) results in:

$$\frac{\bar{C}_{\text{Na}^+}}{C_{\text{Na}^+}} = \frac{C_{\text{Cl}^-}}{\bar{C}_{\text{Cl}^-}} \quad (6)$$

Charge neutrality dictates that in the solution,

$$C_{\text{Na}^+} = C_{\text{Cl}^-} \quad (7)$$

and, in the membrane,

$$\bar{C}_{\text{Na}^+} = \bar{C}_{\text{Cl}^-} + \bar{C}_{\text{SO}_3^-} \quad (8)$$

Hence,

$$\frac{\bar{C}_{\text{Cl}^-}}{C_{\text{Cl}^-}} = \frac{C_{\text{Cl}^-}}{\bar{C}_{\text{Cl}^-} + \bar{C}_{\text{SO}_3^-}} \quad (9)$$

or

$$C_{\text{Cl}^-}^2 = \bar{C}_{\text{Cl}^-} \left[\bar{C}_{\text{Cl}^-} + \bar{C}_{\text{SO}_3^-} \right] \left[\frac{\bar{\gamma}}{\gamma} \right]^2 \quad (10)$$

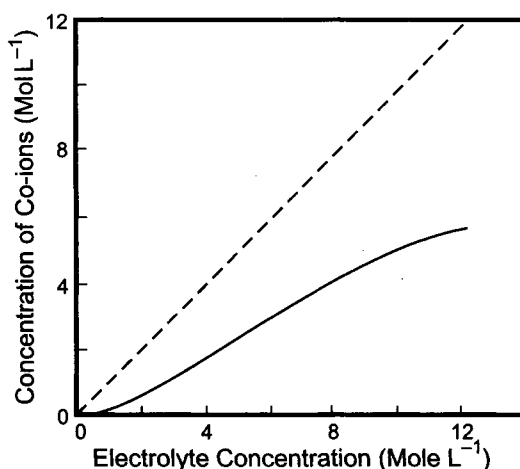


FIGURE 4.8.8. Concentration of co-ions in as received Nafion[®] of 1200 EW in equilibrium with various HCl electrolytes at 25°C. (---) no Donnan effect (—) calculated using Eq. (10). [50]. (Reproduced with permission of The Electrochemical Society, Inc.)

when the activity coefficient in the membrane phase, $\bar{\gamma}$, and the solution phase, γ , are taken into account [53]. Assuming $\bar{\gamma}/\gamma$ to be 1, Eq. (9) predicts that the concentration of the co-ions (i.e., Cl^- in the membrane phase) is proportional to the concentration of Cl^- in the solution, when $\bar{C}_{\text{SO}_3^-} = 0$, and that the ratio, $\bar{C}_{\text{Cl}^-}/C_{\text{Cl}^-}$, in the solution decreases as the concentration of the fixed ionic group (i.e., SO_3^- groups in the membrane) increases. However, experimental results in Fig. 4.8.8 show marked deviation [50] from the expectation of Eq. (10), that is, good permselectivity in dilute solutions and no permselectivity in concentrated solution. Data observed with perfluorosulfonate and carboxylate membranes [54] in NaOH solutions (Table 4.8.2) showed significant pick up of NaOH by the membrane, even though these membranes exhibited substantial resistance to the back migration of OH^- ions. Thus, permselectivity of Nafion[®] prevails beyond the Donnan limit and is referred to as superselectivity [55]. It is this characteristic that provides enhanced current efficiency with these membranes, and it is attributed to the unusual ion-cluster morphology in these materials. Thus, it is the sulfonate group concentration at the necks between the clusters, beyond what is present in the cluster, that acts as barrier to the OH^- back migration. It may be noted that the lower pick up of NaOH by the carboxylate membrane, seen in Table 4.8.2, arises from the lower water content [54].

4.8.3.4. Conductivity. Nafion[®] membrane behaves as an insulator when dry. However, it becomes conductive when hydrated, absorbing six molecules of water for each SO_3^{2-} group in it. The conductivity of the H^+ form of a membrane is an inherent characteristic that stems from the strong acidic groups present in the membrane. Its high intrinsic conductivity, coupled with its hydrophobicity, make Nafion[®] a “solid electrolyte.” Hence, it replaces the conventional electrolyte in several electrochemical applications.

TABLE 4.8.2 Water Contents and Absorbed NaOH Concentrations (Based on the Volume of Water in the Pores) Within Perfluorinated Polymers with an Equivalent Weight of 1200 at 90°C^a

	$C_{\text{NaOH}}(\text{M})$	$\text{H}_2\text{O}(\text{g/g dry polymer})$	$C_{\text{NaOH}}(\text{M})$
-SO ₃ ⁻	0	0.172	0
	5.1	0.109	1.8
	8.2	0.086	4
	10.7	0.076	5.5
-COO ⁻	0	0.14	0
	5.1	0.1	2.1
	8.2	0.072	3.9
	10.7	0.052	3.6

Note: ^a With permission from the American Chemical Society.

The membrane is a heterogeneous material with conductive ion clusters scattered randomly in an insulating fluorocarbon matrix. Its conductivity of 6–13 S m⁻¹ is due to the 10–20% aqueous H₂SO₄ present in 80–90% of the insulator matrix.

Gierke and Hsu [23] proposed, based on the cluster-network model, that the conductivity of the perfluorinated polymeric membranes can be described by the equation:

$$k_m = k_m^0 (C - C_0)^n \quad (11)$$

where k_m refers to the membrane conductivity, k_m^0 to the specific conductivity of the conducting phase, C to the volume fraction of the solution phase, and C_0 to the critical volume fraction (a threshold value at which the percolation model followed to describe Eq. (11) is not applicable). n is a constant, which is 1.5 based on a site percolation model. Figure 4.8.9 shows that Eq. (11) is a good description of the conductivity of Nafion[®] membranes. The empirical value of C_0 of 10% was less than the ideal value of 15% estimated by Gierke *et al.* for a completely random system. The value of n was reported to be 1.53 for H⁺, 1.51 for K⁺, 1.51 for Li⁺, and 1.43 for Na⁺. Hsu and Gierke [24] found n to be 1.5 for Nafion[®] 125 (with EW = 1200), equilibrated with Na⁺ ions. Equation (11) is valid only at moderate water contents. It does not apply at high water contents since the percolation model is not valid when there are no more isolated domains [56, 57].

The conductivity of sulfonic acid membranes in the H⁺ form is a function of temperature and water content as shown in Figs. 4.8.10 and 4.8.11. The conductivity increases with temperatures up to 57°C. Its decrease at higher temperatures is attributed to incomplete ionization [58].

Comparison of the conductivity of two perfluorosulfonic acid membranes in Fig. 4.8.11 shows that the conductivity increases [59] with increasing water content and also increasing ion-exchange capacity or concentration of fixed ionic groups. The Dow membrane has a higher EC and a shorter side-chain length than Nafion[®].

The conductivity is a strong function of the nature of the cation and increases with increasing water content until it reaches a plateau. The decreasing conductivity

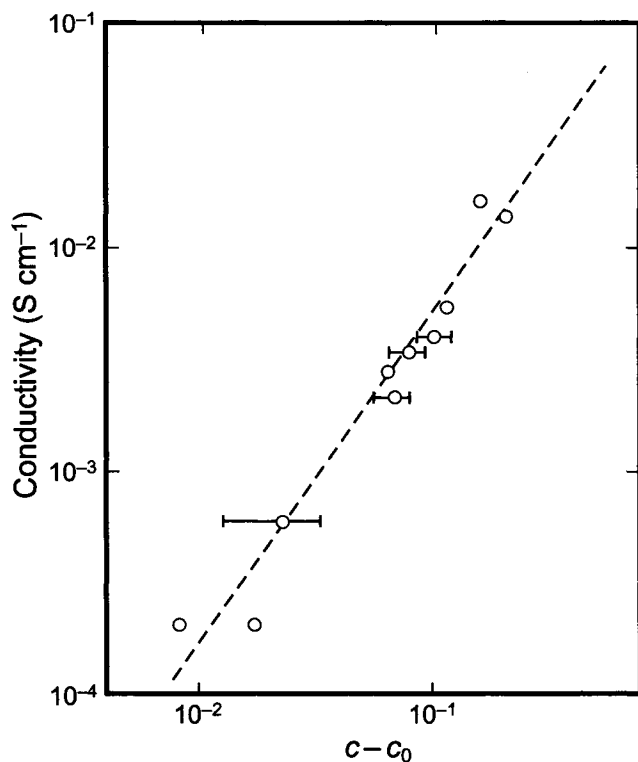


FIGURE 4.8.9. Log-log plot of conductivity vs excess volume fraction ($C - C_0$) of the aqueous phase with the cluster-network model [23]. (Reprinted with permission from the American Chemical Society.)

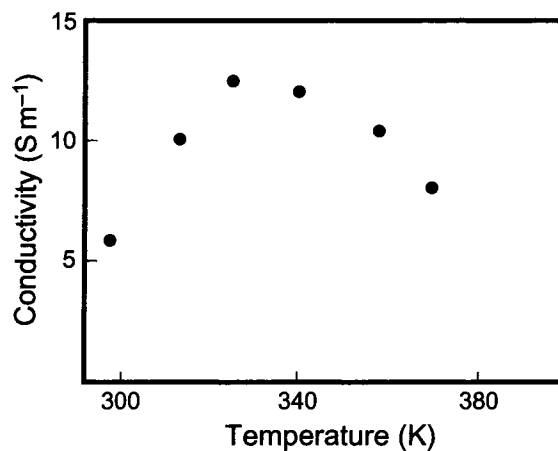


FIGURE 4.8.10. Conductivity of Nafion® of EW 1100 in the hydrogen form as a function of temperature [58]. (With permission from Elsevier.)

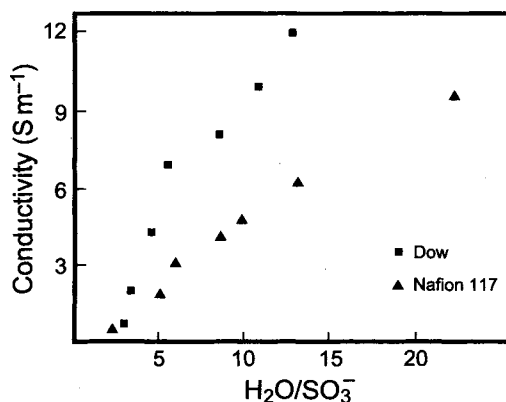


FIGURE 4.8.11. Variation of proton conductivity of perfluorosulfonic acid membranes with water content at 30°C. ■ Dow ▲ DuPont Nafion[®] 117 (revised from the figure in [59]).

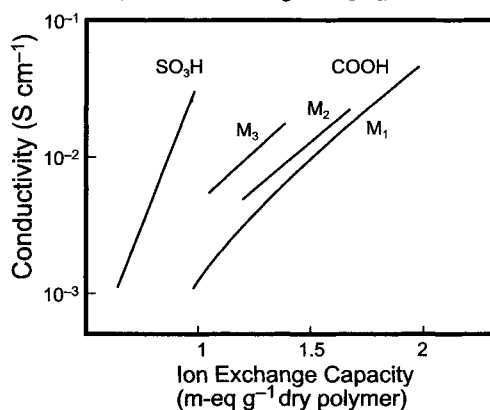


FIGURE 4.8.12. Variation of conductivity of membranes with ion-exchange capacity [51]. (Description of the terminology is same as in Fig. 4.8.7.) (With permission from Elsevier.)

observed with cations of higher valence states reflects their lower ionic mobilities and the extent of interaction between the counter ions and the fixed ionic groups in the perfluoropolymer.

The conductivity of Nafion[®] in alkaline solutions has been extensively investigated and was generally found to be one order of magnitude smaller than in pure water or acidic electrolytes because of lowered electrolyte absorption. Both sulfonic acid and carboxylic acid membranes exhibit increasing conductivity [51] with increasing ion-exchange capacity (EC) (Fig. 4.8.12). Since carboxylic acid has a lower dissociation constant than sulfonic acid, carboxylate membranes show lower conductivity at a given EC. The membrane conductivity varies with NaOH concentration in a manner similar to that of the free electrolyte and exhibits a maximum at ~20% NaOH. The conductivity decrease is more drastic in membranes than in solutions of the same concentrations and is attributed to the less hydrated state of the membrane and stronger binding of the mobile ions by the matrix at a lower water content in the matrix [60].

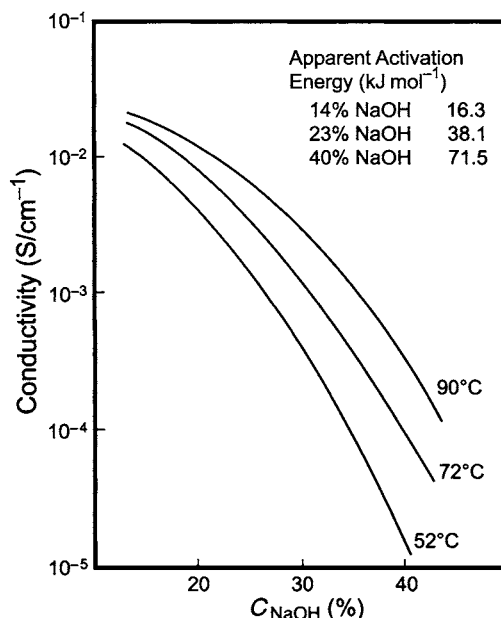


FIGURE 4.8.13. Dependence of conductivity of carboxylate membranes on caustic concentration [51]. (With permission from Elsevier.)

The carboxylic acid membrane behaves differently [51], as the maximum appears at 12% NaOH concentration and the conductivity then decreases with increasing NaOH strength (Fig. 4.8.13). This is attributed to the loss of the water in the membrane and hence, decreased ionic mobility. These factors arise from the strong interactions between the fixed ions in the membrane and the counter ions.

It is important to recognize that the conductivity of Nafion[®] in alkaline media strongly depends on the pretreatment history of the membrane. Thus, higher conductivities result when the membranes are equilibrated in NaOH solutions rather than in KOH solutions [61,62], and better conductivity can be achieved with thinner, low EW membranes. It was also reported that the conductivity of the membranes is increased by soaking the membranes in water at high temperatures and at elevated pressures (Table 4.8.3 [63]). Table 4.8.4 describes the Nafion[®] membrane conductivity data at various concentrations of HCl and NaOH [43].

4.8.3.5. Diffusivity. The self-diffusion coefficient values for Na⁺ are presented in Fig. 4.8.14 for perfluorocarboxylate and perfluorosulfonate membranes [64,65]. These data show the self-diffusion coefficient to be lower in NaOH and also in NaCl solutions in the perfluorocarboxylate membranes compared to the same in the perfluorosulfonate membranes. This behavior reflects the high activation energy [65] for the perfluorocarboxylate membranes, as shown in Fig. 4.8.15.

In perfluorocarboxylate membranes, the apparent diffusion coefficient of Na⁺ in NaOH is five times larger than that in 3.5N NaCl, while the diffusion coefficient values in NaCl and NaOH are similar, at about 10⁻⁵ cm² s⁻¹, in aqueous solutions.

TABLE 4.8.3 Effect of Pretreatment on Conductivity of Nafion[®] Membrane in 40% KOH

Temperature (°C)	Pressure (atm)	W _e (wt%)	κ (Ω ⁻¹ cm ⁻¹)
100	1	28.2	1.15 × 10 ⁻⁴
150	4.9	38.8	0.011
150	35.2	86.4	0.046
175	35.2	116.2	0.071
200	703	370	0.2

TABLE 4.8.4 Conductivity of Nafion[®] Membrane of 1200 EW in Various Electrolytes^c

Electrolyte concentration	Electrolyte uptake (%)	Conductivity at 25°C (× 10 ³ Ω ⁻¹ cm ⁻¹)	E _a ^a
H ₂ O	7.8	22.8	9.46
H ₂ O	17	52.2	9.46
H ₂ O	30	68	9.37
5% HCl	12.9	58.8	10.33
10% HCl	11.9	62.5	11.59
15% HCl	10.5	46	10.75
22% HCl	8.8	23	11.59
26% HCl	7.8	14.3	16.95
30% HCl	6.8	6.8	13.47
37% HCl	4.8	3.9	15.69
4.5% KCl	7	3.93	12.07
25% NaCl	10	5.3	17.74
5.4% KOH	6	1.7	25.02
0.4% NaOH	—	5.7	—
5% NaOH	12.8	6	15.43
10% NaOH	12.1	9.3	14.86
20% NaOH	9.6	9.7	13.08
30% NaOH	8.4	6	15.43
40% NaOH	8.3	1	17.79
17% NaOH	—	—	10 ^b
30% NaOH	—	—	10 ^b

Notes:

^a E_a is the activation energy (kJ mol⁻¹).^b For Nafion of 1150 EW at 100–180°C.^c With permission from Elsevier.

Conductivity and diffusion are governed by the mobility of a given ion and are related to the concentration of the mobile ions as:

$$C_i = \frac{1000k}{D} \cdot \frac{RT}{F^2} \quad (12)$$

where k is the equivalent conductance and D is the diffusion coefficient. Comparison of the C_i values deduced from Eq. (12) with those from Eq. (2), showed good agreement,

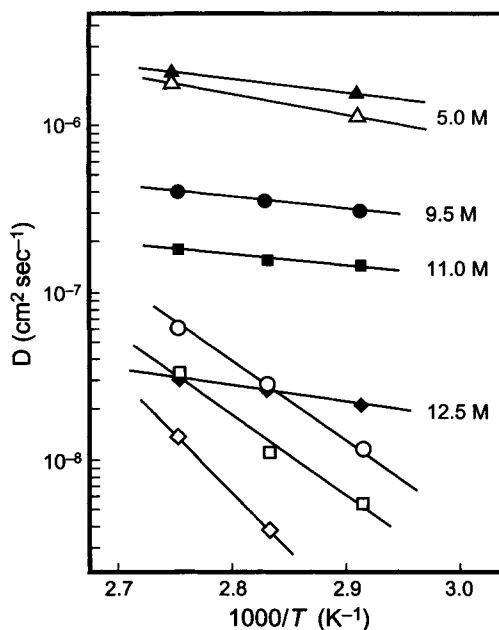


FIGURE 4.8.14. Variation of sodium ion diffusion coefficient with temperature for perfluorocarboxylate (open symbols) and perfluorosulfonate (dark symbols) polymers in concentrated NaOH solutions [65]. The concentration of NaOH in moles liter⁻¹ is noted in the figure. (Reproduced with permission from The Electrochemical Society, Inc.)

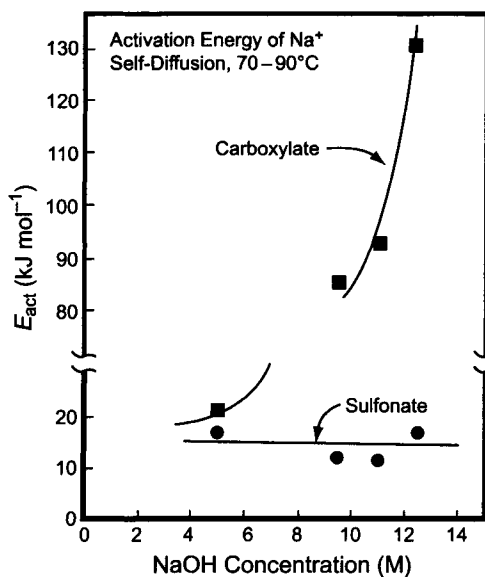


FIGURE 4.8.15. Activation energy of Na⁺ ion diffusion in perfluorinated ionomer membranes vs concentration of NaOH in the temperature range of 70–90°C [65]. (Reproduced with permission of The Electrochemical Society, Inc.)

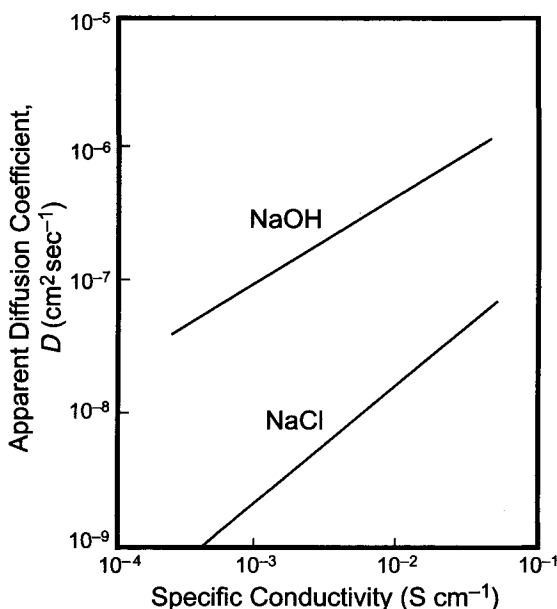


FIGURE 4.8.16. Correlation between diffusion coefficient and membrane conductivity [51]. D values refer to the system: $3.5 \text{ mol}^{-1} \text{ L NaCl/membrane/35\% NaOH}$ at 90°C and χ values to 35% NaOH at 90°C . (With permission from Elsevier.)

thus establishing the validity of Eq. (12). Figure 4.8.16 shows the correlation developed using the perfluorocarboxylate polymers.

4.8.3.6. Permeation of H_2 , O_2 and Cl_2 . The permeability of H_2 [66], O_2 [66], and Cl_2 through the membrane is an important consideration, as it may influence the gas purity and operating safety considerations. The permeation rates for H_2 and O_2 increase with increasing water content, temperature, and with thinner membranes.

The values of the diffusion coefficients for H_2 , O_2 , and Cl_2 in the perfluorosulfonate and carboxylate membranes are presented in Table 4.8.5.

4.8.4. Transport Characteristics

4.8.4.1. Na^+ Ion Transport

4.8.4.1A. General. Preferential transport of selected species is the primary characteristic property of membranes. In a chlor-alkali cell, for example, one equivalent of cation will pass across the cation-exchange membrane for each Faraday of electricity if the selectivity is perfect. In practice, some OH^- passes through the membrane in the opposite direction, resulting in current inefficiency. The membrane selectivity, therefore, directly determines the caustic current efficiency of the process.

TABLE 4.8.5 Diffusion Coefficients for Gases Through Ion-Exchange Membranes

Species	Membrane	Diffusion coefficient, D ($10^{11} D(\text{m}^2 \text{s}^{-1})$)	References
H ₂	H ⁺ Nafion [®] 120	6.9	[67]
O ₂	H ⁺ Nafion 120 [®] (EW 1200)	18	[68]
	H ⁺ Nafion 117 [®] (EW 1100)	30	[68]
	K ⁺ Nafion [®] 120	2.2	[69]
Cl ₂	Na ⁺ Asahi Glass perfluoro carboxylate (EW 1300)	0.1	[70]
	H ⁺ Nafion [®] 120	3.5	[71]

Let us consider a cell with two compartments separated by a cation-exchange membrane. Both compartments are filled with NaCl solution. The respective concentrations on the left-hand and right-hand sides of the membrane are C_1 and C_2 with $C_1 > C_2$. We expect Na⁺ to diffuse from left to right, and we define this as the forward direction. The flux j_i of species i is represented by the Nernst–Planck equation:

$$j_i = j_d + j_m + j_c = -D_i \partial C_i / \partial x - n_i u_i C_i \partial \varphi / \partial x + C_i v \quad (13)$$

where

j_d, j_m, j_c = fluxes due to diffusion, migration, and convection

D_i = diffusion coefficient

C_i = concentration

n_i = valency of ionic species

u_i = ionic mobility

φ = electrical potential

x = distance

v = velocity of liquid

We will neglect j_c for simplicity. In our example, Na⁺ and Cl⁻ move in opposite directions because their charges are opposite in sign. The overall current passing through the membrane is represented by the sum of the flows of Na⁺ and Cl⁻ multiplied by F , the Faraday constant. Therefore, the contribution of species i is as follows:

$$t_i = i_i / \sum i_i = n_i F j_i / F \sum n_i j_i = n_i j_i / \sum n_i j_i \quad (14)$$

t being the transport number. For pure NaCl solutions,

$$t_{\text{Na}^+} = j_{\text{Na}^+} / (j_{\text{Na}^+} + j_{\text{Cl}^-}) \quad \text{and} \quad t_{\text{Cl}^-} = j_{\text{Cl}^-} / (j_{\text{Na}^+} + j_{\text{Cl}^-})$$

Therefore,

$$t_{\text{Na}^+} + t_{\text{Cl}^-} = 1$$

or, in general,

$$\sum t_i = 1 \quad (15)$$

Since an ideal permselective membrane does not permit Cl^- to pass through, t_{Cl^-} is equal to zero and t_{Na^+} is equal to unity. Thus, the current efficiency for Na^+ is 100%.

While an ideal ion-exchange membrane should have a sodium ion transport number of unity, the question arises of whether it is possible to ever realize this goal? There appear to be at least two factors that one must consider. First, by judicious choice of the polymer and its chemistry, proper design of the membrane with optimized reinforcements and composites, and efficient catholyte mixing [72], it may be possible to reach a t_{Na^+} of unity. The second factor that would prevent reaching the ideal situation is the fact that during the course of NaCl electrolysis, oxygen evolution, a parasitic anode reaction, generates protons.



These protons will be transported to the cathode side, lowering the caustic efficiency. Thus, as long as O_2 evolution is occurring at the anode, it appears impossible to achieve 100% caustic efficiency, even though one may approach it.

4.8.4.1B. Historical. As stated in Section 4.8.1 the impetus to produce chlorine and caustic using ion-exchange membrane-based cells is to directly produce concentrated caustic free of chloride, in addition to replacing the mercury and asbestos-based chlorine cells. The ion-exchange membrane for chlor-alkali production should be chemically and physically stable and provide high current efficiency, low electrical resistance, and negligible electrolyte diffusion. Such a membrane based on perfluorinated materials was first developed in the 1970s, with pendant sulfonate groups. However, because of poor hydroxyl ion rejection, these membranes produced only 10% caustic, at efficiencies of ~70–80% (Fig. 4.8.17). This was a consequence of the low fixed-ion concentration in the sulfonate membranes soaked in NaOH , under equilibrium conditions (Fig. 4.8.18), and hence, high OH^- ion pick-up by the perfluorosulfonate membranes (Fig. 4.8.19). Because of the high concentration of OH^- ions, these membranes allowed OH^- ions to be transported from the catholyte to the anolyte.

Comparison of the fixed-ion concentration and OH^- pick-up data [51] by the perfluorocarboxylate membranes soaked in NaOH solution (Figs. 4.8.18 and 4.8.19) show that, while the fixed-ion concentration is high in these membranes, the OH^- pick-up is small, thereby allowing fewer OH^- ions to pass through during electrolysis to realize high efficiencies. This high fixed-ion concentration in the perfluorocarboxylate membranes is attributed to the shorter side-chain length in these fluoropolymers and also in part to the lower hydration of the carboxylic groups. Note that the fixed-ion concentration can be varied by adjusting the EC also. Typical efficiency data of perfluorocarboxylate acid membranes is shown in Fig. 4.8.20.

Thus, the perfluorosulfonate membranes provide low caustic efficiencies at high caustic strengths, while the perfluorocarboxylate membranes offer high current

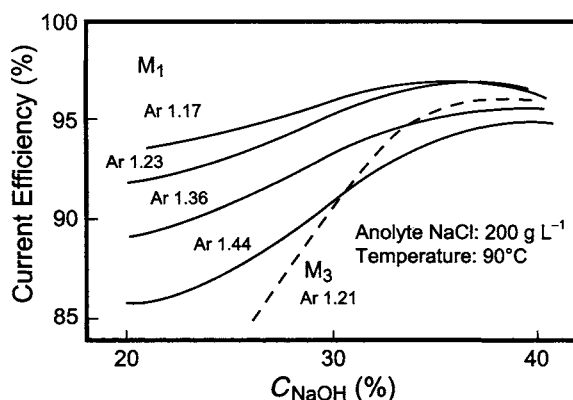


FIGURE 4.8.17. Influence of caustic concentration on current efficiency (C.E) [51]. Ar = m eq g^{-1} polymer; the side chain length in membrane M_1 is shorter than in membrane M_3 . (With permission from Elsevier.)

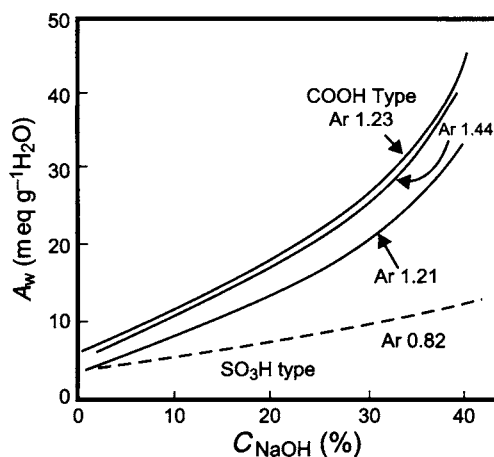


FIGURE 4.8.18. Influence of caustic concentration on fixed ion concentration, A_w [49]. $A_w = Ar/W$; $A_w = \text{m eq g}^{-1} \text{H}_2\text{O}$; Ar = m eq g^{-1} polymer; W = $\text{g H}_2\text{O/g polymer}$ (With permission from Elsevier).

efficiencies at high caustic strengths. On the other hand, the sulfonate membranes, with their high water content [73,74], have lower electrical resistance, as shown in Figs. 4.8.21 and 4.8.22. It is for these reasons that bilayer membranes, with the sulfonic acid side facing the anolyte side and the carboxylic acid side facing the catholyte, were developed in order to realize high efficiency and low resistance or low cell voltage. The thickness of the carboxylate layer only needs to be 6–7 μm to achieve high caustic efficiencies without incurring a voltage penalty. Another important reason for the manner in which the two layers are put together lies in the chemical stability of these membranes. Sulfonic acid has a pK_a of <1 and hence, is stable in acidic media. However, carboxylic acid has a pK_a of 2–3 and therefore, while it is stable in the anolyte pH range of 3–5 during the course of electrolysis, it protonates at $\text{pH} < 2$, resulting in increased resistance (Fig. 4.8.20).

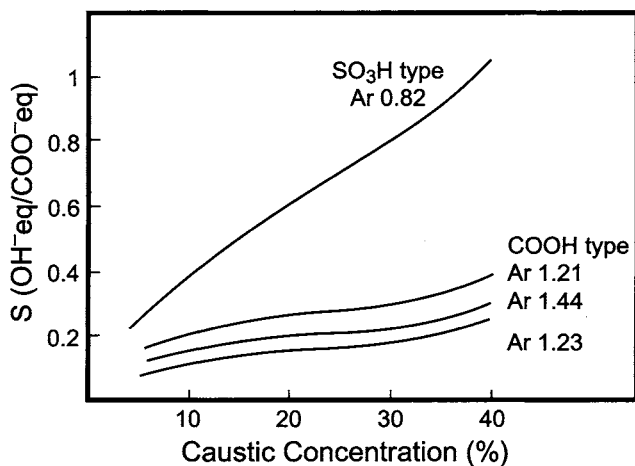


FIGURE 4.8.19. *S* value and caustic concentration. *S* refers to the ratio of hydroxyl ion concentration (in Donnan equilibrium with caustic solutions) to the COO⁻ concentration in the membranes [51]. (With permission from Elsevier.)

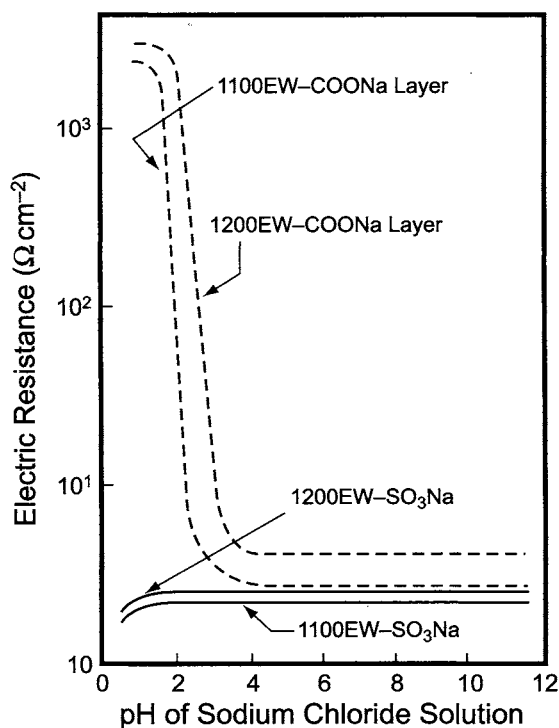


FIGURE 4.8.20. Variation of electrical resistance of membranes with pH of NaCl solutions at 25°C [69]. (Reproduced with permission of the Society of Chemical Industry.)

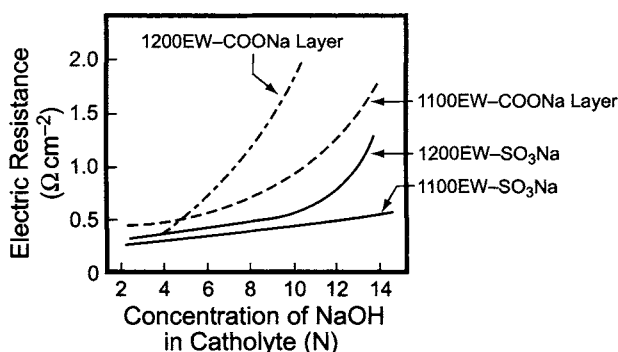


FIGURE 4.8.21. Variation of electric resistance of membranes with caustic concentration at 80°C [69]. (Reproduced with permission of the Society of Chemical Industry.)

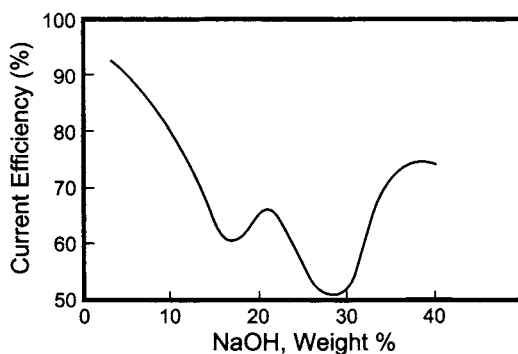


FIGURE 4.8.22. Current efficiency vs caustic strength for Nafion 427 perfluorosulfonate membrane [69, 74]. (Reproduced with permission of The Electrochemical Society, Inc.)

These composite membranes are prepared either by lamination of the perfluorocarboxylate and perfluorosulfonate films [75–77] or by the chemical conversion [78–80] of one surface of the perfluorosulfonic acid to perfluorocarboxylic acid to realize a carboxylate layer thickness of 5–10 μm .

Several approaches have been followed to understand the transport phenomena occurring in perfluoropolymeric membranes, and these include irreversible thermodynamics, use of the Nernst–Planck transport equation (Eq.13), and various descriptions (e.g., free-volume model, lattice model, quasi-crystalline model) coupling the morphological and chemical properties of the membranes. The reader is referred to the references and citations in the reviews [81–87] for more details related to these models.

Based on the cluster-network model, the dependence of current efficiency on the polymer structure was first developed by Gierke [34]. This postulates that clusters with diameters of 4 nm are distributed throughout the matrix and connected to each other by short narrow channels 1 nm in diameter—the cluster separation distance being 5 nm. It should be noted that this structure was developed based on experimental evidence [23]. High caustic current efficiency, according to this model, is a result of the repulsive electrostatic interaction between the OH^- ions and the fixed ionic charges on the surface

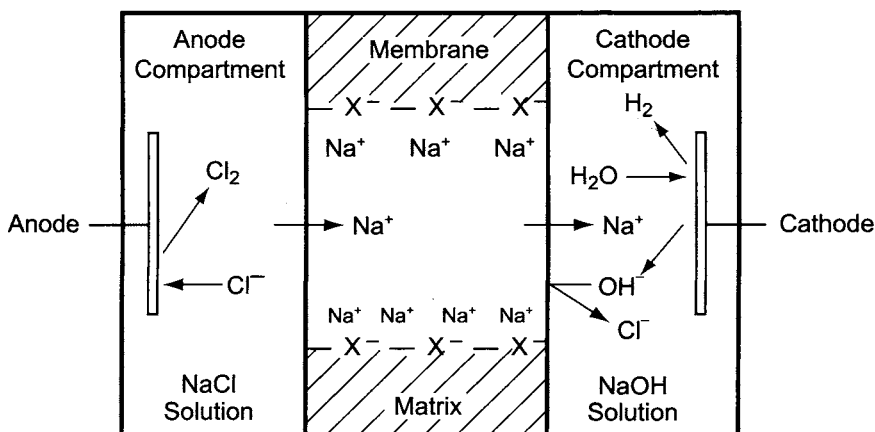


FIGURE 4.8.23. Profile of a cation-exchange membrane.

of the clusters and the connecting channels, over an effective range of 0–5 nm. Hence, migration of OH^- ions from one cluster to another is difficult, as it has to overcome a large electrostatic barrier in the channel. This results in high caustic current efficiency.

Based on this qualitative description, an expression for the current efficiency was derived and shown to explain the increasing current efficiency with increasing EW of the polymer. However, new experimental evidence showed the shortcomings of Gierke's approach, and hence, various other approaches were pursued. All these studies [31–33, 50,55] basically suggest that it is the high local concentration of fixed ions that provides an excellent selectivity to membranes. A combination of differences in morphology and water absorption results in fixed ion–water interactions that alter the OH^- ion rejection characteristics.

It should be mentioned here that there was significant activity toward understanding the transport phenomena in these membranes prior to the development of bilayer membranes. Since then, the membrane manufacturers have developed composite membranes exhibiting a long life and efficiencies as high as 96–98% (see section 4.8.5). At the same time, theoretical efforts to understand these molecular interactions have waned.

4.8.4.1C. Maximum Current Density. When a direct current is applied to a two-compartment cell divided by an ion-exchange membrane, as illustrated in Fig. 4.8.23, ionic species may flow across the membrane. Equation (13) gives the flux of species i . The three terms on the right-hand side of this equation are the components associated with diffusion, migration, and convection, respectively.

Diffusion results from the concentration gradient dC/dx in the medium and hence, occurs when the NaCl concentration in the anode compartment differs from that in the cathode compartment. In a chlor-alkali cell, the anolyte is nearly a saturated NaCl solution, whereas the catholyte contains only traces of NaCl. Although Cl^- ion is subjected to the same diffusional driving force as Na^+ ion, it is rejected by the fixed anions in the membrane, which also retard the transport of Na^+ to some degree to maintain the charge balance.

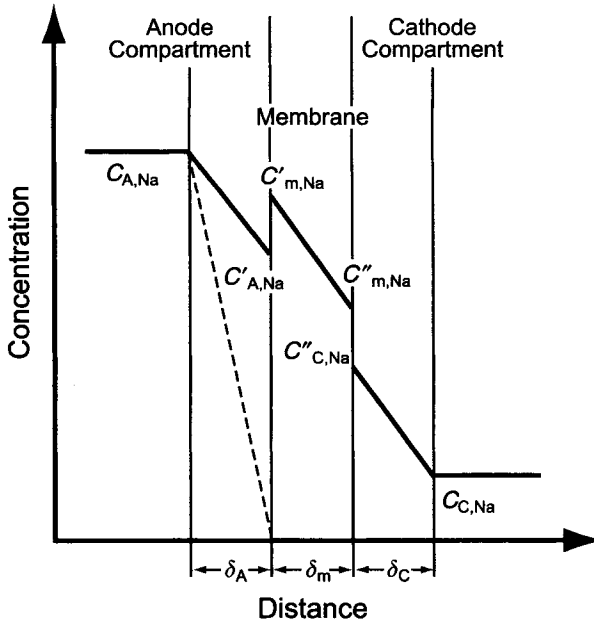


FIGURE 4.8.24. Concentration distribution of Na^+ in a cation-exchange membrane.

There are boundary layers at each side of the membrane where the Na^+ concentration differs from the bulk concentration because of insufficient mixing of the solution. Figure 4.8.24 illustrates this concept. C denotes the concentration, δ the distance, the subscripts A, C and m to the anolyte, catholyte, and the membrane respectively, ' and '' refer to the solution-membrane interfaces. Omitting the subscript Na, the diffusional flux is given as:

$$k_A (C_A - C'_A) = k_M (C'_m - C''_m) = k_C (C''_C - C_C) \quad (17)$$

where

$$k_i = D_i / \delta_i$$

It is worth noting that the Na^+ concentration in the membrane is always higher than the concentration in the adjacent solution, because the fixed charges on the ion-exchange membrane allow relatively large quantities of Na^+ to enter the membrane. Now we may assume that the Na^+ concentration in the membrane is proportional to the Na^+ concentration in the solution as:

$$C'_m = \alpha C'_A \quad (18)$$

and

$$C''_m = \alpha C''_C$$

where α is a coefficient depending on the characteristics of the membrane. Substituting into Eq. (17), we have:

$$j = K(C_A - C_C) \quad (19)$$

$$1/K = 1/k_A + 1/\alpha k_m + 1/k_C \quad (20)$$

It is clear from the above equation that the concentration gradients in the boundary layers and the membrane increase when the flux or the current density increases. Finally, the concentration at the anolyte–membrane interface reaches zero, as shown by the dotted line in Fig. 4.8.24. The same phenomenon also occurs at the cathode surface. In other words, the reaction rate in a membrane–cell system is greatly affected by diffusion, and the maximum or limiting current density is represented by:

$$i_L = nFJ_L = zFD_{A,Na}C_{A,Na}/\delta_A \quad (21)$$

The subscript L denotes the limiting condition. Thus, each membrane has a specific limiting current density, and we cannot operate it beyond this point.

The bulk concentration of anolyte, $C_{A,Na}$, is almost unchanged under normal operations. However, δ_A is a function of the flow rate and of the surface roughness of the membrane. Chlorine bubbles, generated at the anode, agitate the anolyte solution near the membrane. As bubble action becomes more intense, the diffusional boundary layers become thinner. The membrane surface itself is not flat. Industrial membranes are normally reinforced with PTFE fiber or cloth. A metal oxide coating on zero-gap membranes improves their hydrophilicity and allows easier detachment of chlorine bubbles. These coatings also affect the thickness of the diffusion layer and the limiting current density.

The limiting current density depends on the cell design, the membranes, and the operating conditions. Note that at the current density, i_L , the Na^+ concentration at the membrane surface is zero and that higher current densities beyond this value cannot be sustained by the anodic discharge of the chloride ions. We can make a practical estimate of the limiting current density by substituting typical values in Eq. (21). We know that $n = 1$ and $F \cong 10^5 \text{ A s mol}^{-1}$. The diffusivity is about $10^{-5} \text{ cm}^2 \text{ s}^{-1}$, and a typical anolyte concentration is about 4 M, or $4 \times 10^{-3} \text{ mol cm}^{-3}$. The thickness of the diffusion layer is usually estimated to lie between 10^{-2} and 10^{-3} cm. Using the former value, we have:

$$i_L = (10^5 \times 10^{-5} \times 4 \times 10^{-3})/10^{-2} = 0.4 \text{ A cm}^{-2}$$

This is 4 kA m^{-2} , which, for several years was regarded as a practical maximum current density for membrane cells. The latest generation of cells, designed for improved internal circulation, operates above this value, and the diffusion layers, therefore, must be less than 0.01 cm thick. If we use a thickness of 0.001 cm in our estimate, the limiting current density becomes about 40 kA m^{-2} , which, in a practical sense in today's technology, is no limit at all.

The transport of ionic species by convection, which is shown by the third term on the right-hand side of Eq. (13) is zero if water does not move across the membrane.

Water does in fact pass through the membrane by osmosis, and the osmotic pressure, p , is proportional to the solution concentration:

$$p = CRT \quad (22)$$

The pressure difference across the membrane is a driving force for water transport. Water is also transported by electroosmosis under the influence of the electric field, the electroosmotic velocity of water being given as:

$$v = u_0 d\phi/dx \quad (23)$$

$$u_0 = \xi D_E 4\pi \eta \quad (24)$$

where

u_0 = electroosmotic mobility (flow rate under unit potential gradient)

ξ = zeta (electrokinetic) potential

D_E = dielectric constant of the medium

η = viscosity of the medium

$d\phi/dx$ = potential gradient

The volume of water passing through the membrane with each coulomb of electricity is:

$$V_0 = Av/I\theta = u_0/\kappa \quad (25)$$

where

V_0 = volumetric flow of water

A = area

I = current

θ = time

κ = conductivity

Three to four molecules of water of hydration, depending on the operating conditions, are transported with each sodium ion from the anode side to the cathode side. Hence, only a relatively small amount of water needs to be added to the catholyte loop in order to adjust NaOH concentration in a chlor-alkali cell. In KCl electrolysis, each cation carries only two to three molecules of water. The water balance of a cell alters, and both anolyte and catholyte flows must respond to the change.

The extent of absorption and rate of transport are important properties of a membrane. Physicochemical characteristics such as electrical conductivity and ion selectivity are closely related to the amount of water sorption. On the other hand, mass transport in solutions next to membranes depends on the buildup of the hydrodynamic boundary layers, especially at high current densities. Therefore, the maximum current density is determined by the diffusion of chemical species through the boundary layers outside the membrane and not so much by processes that occur inside the membrane. The limiting current density, therefore, is not strongly affected by the water content of the membrane or by the processes of water transport through it.

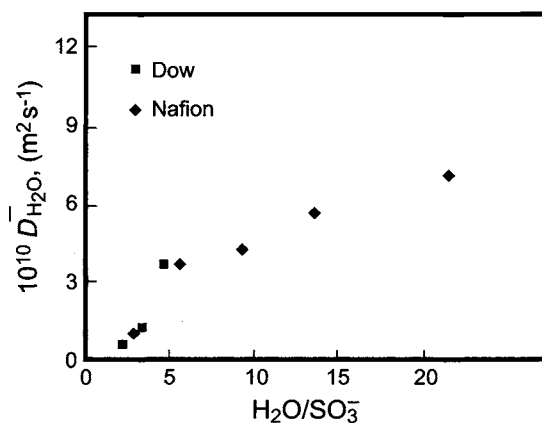


FIGURE 4.8.25. Diffusion coefficient of water as a function of water content for two perfluorinated membranes from DuPont and Dow at 30°C. (Modified figure from [59].)

4.8.4.2. Water Transport. The presence of water and its transport across the membrane are vital if the membrane is to function with excellent conductivity and selectivity. Because of their importance, the transport characteristics of water have been studied extensively both theoretically [88] and experimentally. Water transport numbers in chlor-alkali cell environments have been studied by several workers [64,88–92].

Figure 4.8.25 shows the variation of the diffusion coefficient of water with water content for two perfluorinated membranes in H⁺ form [45]. The diffusion coefficient of water in Nafion[®] (EW 1200) in Na⁺ form was reported to be $2.6 \times 10^{-10} \text{ m}^2 \text{ s}^{-1}$ and the activation energy was 21.4 kJ mol^{-1} [93]. The effect of applied pressure on the water flux with Nafion[®] showed the flux of water to decrease with increasing weight of the counter ion as: $\text{Li}^+ > \text{Na}^+ > \text{K}^+ > \text{Cs}^+$; the difference in the flux for a pressure difference of 50 kPa ($\sim 0.5 \text{ atm}$) being $\sim 3.6 \text{ cm}^3 \text{ m}^{-2} \text{ hr}^{-1}$ [94]. The decrease in the water flux with increasing weight of the cation reflects the reduced hydration of the larger cations.

4.8.4.3. Anion Transport. The anions of concern for caustic purity that are transported from the anolyte to the catholyte during electrolysis are Cl^- and ClO_3^- . These species cannot be easily removed by simple chemical treatment of the caustic from a membrane cell. However, one can optimize the membrane cell operations to minimize the ingress of these ions into the caustic.

The mass transport of anions across a membrane [95] is governed by diffusion, migration, and electroosmotic water convection and can be described using the Nernst–Planck equation.

$$N = -D \frac{dC}{dx} - \frac{zF}{RT} DC \frac{d\phi}{dx} + Cv \quad (26)$$

where

N = flux of species

D = diffusion coefficient

$\frac{dC}{dx}$ = concentration gradient at distance x

$\frac{d\phi}{dx}$ = potential gradient

z = charge of species

F = Faraday constant

C = concentration of species

v = electroosmotic water velocity across the membrane.

The voltage gradient, $d\phi/dx$, is related to the current density, i ($A\ cm^{-2}$), and membrane conductivity, κ ($\Omega^{-1}\ cm^{-1}$), by:

$$\frac{d\phi}{dx} = -\frac{i}{\kappa} \quad (27)$$

Substituting Eq. (27) into (26) gives:

$$N = -D\frac{dC}{dx} - (u - v)C \quad (28)$$

where

$$u = -zDFi/RT\kappa$$

The steady state flux of the ionic species across the membrane can be obtained by solving Eq. (24) with the boundary conditions: $x = 0$, $C = C_b$ and $x = \delta$, $C = C_o$ as:

$$N = (u - v) \left[\frac{\gamma C_b - C}{1 - \gamma} \right] \quad (29)$$

where δ is the thickness of the membrane (in cm), C_o and C_b = concentration of the species in the cathode and anode compartments, respectively (in mol cm^{-3})

$$\gamma = \exp(-(u - v)\delta/D)$$

From the material balance of the species around the cathode compartment: $qC_o = pC_i + NS$ (Fig. 4.8.26), the concentration of the species of interest in the caustic product, C_o , can now be expressed as

$$C_o = \frac{(1 - \gamma)pC_i + \gamma(u - v)SC_b}{(1 - \gamma)q + (u - v)S} \quad (30)$$

where p and q are the feed and exit flow rates of the caustic ($\text{cm}^3\ \text{sec}^{-1}$), S is the total surface area of the membrane in the electrolyzer (cm^2) and C_i is the concentration of the anionic impurity in the feed caustic.

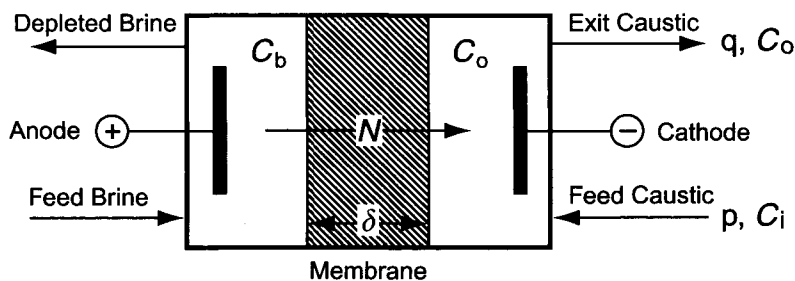


FIGURE 4.8.26. Schematic of an ion-exchange membrane cell describing the material balance around the electrolyzer. The symbols are described in the text.

It follows from Eq. (28) that anions such as Cl^- and ClO_3^- , present at high concentrations in the anolyte, are transported to the cathode compartment by diffusion and electroosmotic flow and repelled by the potential gradient. We can now examine the effect of current density, anolyte chloride and chlorate concentration, and the anolyte temperature on the extent of transport of these anions into the cathode chamber, based on the transport characteristics of a given membrane.

Unfortunately, all the properties required for these calculations are not available in the open literature for the membranes that are used commercially. Therefore, some simplified descriptions and assumptions are employed here to show the trends expected of a membrane under given operating conditions. One can refine these calculations with more precise data, when made available by the membrane suppliers.

The electroosmotic water velocity, v , was calculated by

$$v = \frac{1.8 \times 10^4 i W \eta}{F(10^3 d - C_S)} \quad (31)$$

where d is the specific gravity of the anolyte (g cm^{-3}) and η is the caustic efficiency. The water transport number for sodium (W in moles of H_2O per mole of Na^+), was estimated from the empirical Eq. (32) by DuPont [96],

$$W = 11.612 - 5.886 \times 10^{-2} C_S + 1.14 \times 10^{-4} C_S^2 \quad (32)$$

where C_S is the anolyte salt strength in g dm^{-3} . Equation (32) applies to cells operating at 3.1 kA m^{-2} and 90°C at a catholyte strength of 32% NaOH, with Nafion[®] 901 membrane. Water transport was nearly constant over the current density range of 1.5 to 4 kA m^{-2} . No membrane swelling was observed in the temperature range of 80 to 95°C . The water transport characteristics of Nafion[®] 90209 membranes are very similar to those of Nafion[®] 901 series membranes [96]. The water transport number is dependent on the catholyte caustic concentration [97]. However, this dependency was not incorporated in Eq. (32), since the caustic strength was fixed at a value of 32%.

The values of the other parameters [95] employed in these calculations are noted in Table 4.8.6.

TABLE 4.8.6 Values of Parameters Used for Calculating the Impurity Levels in Caustic

Parameter ^a	Value
Membrane thickness (δ)	1.4×10^{-2} cm
Membrane surface area (S)	2.4×10^5 cm ²
Membrane conductivity (κ)	$145.76 \exp(-4000/T)$ Ω^{-1} cm ⁻¹
Diffusivity of chloride (D_{Cl^-})	$4.27 \times 10^{-3} \exp(-4000/T)$ cm ² sec ⁻¹
Diffusivity of chlorate ($D_{\text{ClO}_3^-}$)	$4.27 \times 10^{-3} \exp(-4000/T)$ cm ² sec ⁻¹
Feed caustic flow rate (p)	820 cm ³ sec ⁻¹
Exit caustic flow rate (q)	779 cm ³ sec ⁻¹

^a It is important to point out that there is a need to measure these values for each membrane as no such information is presently available in the open literature.

The membrane conductivity data used in the present calculation are those for a carboxylic acid membrane [97–99], as the overall conductivity of a composite membrane is dictated by the carboxylic layer. Diffusion coefficient data for chloride and chlorate ions across the commercial composite membranes are not available. Hence, an average of the diffusion coefficient data for the chloride ion for carboxylic acid membranes [100,101] was used, assuming the same temperature dependence as that of membrane conductivity. The diffusion coefficient of the chlorate ion was assumed to be the same as that of the chloride ion. Variations in D_{Cl^-} and κ with anolyte concentration, under commercial operating conditions, were reported [102] to be weak, and hence, these dependencies were not considered here.

4.8.4.3A. Effect of Current Density

1. $i \rightarrow 0$ (i.e., during circuit shutdown).

It can be shown from Eq. (30) that as $i \rightarrow 0$,

$$N = D \left(\frac{C_b - C_o}{\delta} \right) \quad (33)$$

Hence,

$$C_o = \frac{p\delta C_i + DC_b S}{q\delta + DS} \quad (34)$$

Thus, during a cell shutdown, the transport of anions is solely governed by diffusion (Fig. 4.8.27). The flow of anions into the cathode compartment can be minimized by lowering the cell operating temperature before shutdown, as is evident from Eq. (33), via the variations in D with cell temperature, T . Because of this effect of maximal carryover of anions at $i \rightarrow 0$, it is important that the cells be designed so that the ratio of active membrane area to the peripheral inactive area is high in order to achieve low anionic impurity content in the caustic product.

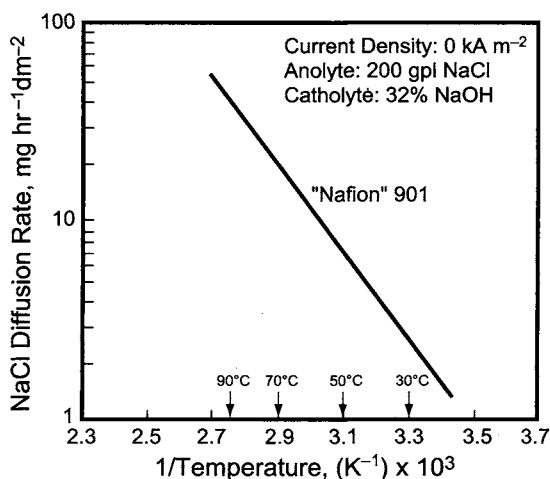


FIGURE 4.8.27. Diffusion rate of NaCl vs temperature [96]. (With permission from E.I. duPont de Nemours & Co, Inc.)

2. $i \rightarrow$ very high (high current density operation).

At high current densities, Eq. (30) can be reduced to:

$$N = -(u - v)C_o \quad (35)$$

$$C_o = \frac{pC_i}{q + (u - v)S} \quad (36)$$

At high current densities, the effect of diffusion is negated by the migration and electroosmotic water flow, resulting in minimal carry over of anions to the catholyte, as shown in Figs. 4.8.28 and 4.8.29. It should be noted that the maximal current density that can be practically employed depends on the cell design and the specifications set by the membrane supplier. The trends depicted in Figs. 4.8.28 and 4.8.29 are in general agreement with the published data [96,98].

In commercial chlor-alkali membranes the current distribution is non-uniform because of the presence of non-conductive reinforcing filaments. The current density is greater in the openings between the filaments, and less where the filaments obstruct the flow of ionic current through the membrane. Therefore, during operation, anions tend to accumulate near the filaments because the local current density is small, tending to zero. Since the local concentration of anions is high in this region, precipitation of insoluble products of anions with cations such as sodium occurs near the filaments. This was seen [102] as a whitened or frosty area on the cathode side in thick, heavily reinforced membranes, and confirmed by X-ray analysis. Whitening arises because of the disruption of the polymer on the cathode side of the membrane by these precipitates.

4.8.4.3B. Effect of Anolyte Cl^- and ClO_3^- Concentration. As the chlorate concentration in the anolyte increases, the diffusion of chlorate ions to the cathode compartment is enhanced. However, a similar pattern does not prevail with chloride ions since

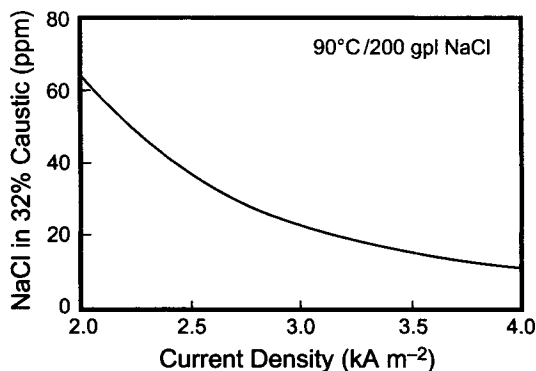


FIGURE 4.8.28. Effect of current density on the NaCl concentration in the caustic product at 90°C and 200 gpl NaCl in the anolyte, calculated using Eq. (30) [95].

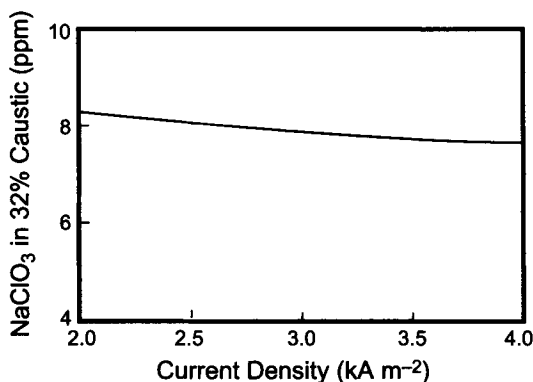


FIGURE 4.8.29. Effect of current density on the NaClO₃ concentration in the caustic product at 90°C and 4 gpl NaClO₃ in the anolyte, calculated using Eq. (30) [95].

the electroosmotic water flow decreases as the anolyte salt strength increases (Fig. 4.8.30), resulting in reduced carry-over of chloride ions into the cathode compartment (Figs. 4.8.31 and 4.8.32). The lack of significant variation of the catholyte ClO₃⁻ level, with changes in the anolyte chlorate level, is a result of lower chlorate ion concentration in the anolyte in contrast to the anolyte chloride level, which is 70 times higher in molar concentration.

4.8.4.3C. Effect of Operating Temperature. Increase in temperature lowers the electric field-driven migration rate and increases the diffusion rate. Hence, the chloride and chlorate concentrations in the caustic product will increase at elevated temperatures as shown in Figs. 4.8.31 and 4.8.32. Note that the activation energy for the diffusion of Cl⁻ ions is about 10 kcal mol⁻¹, implying that the Cl⁻ levels decrease by about 30% for every 10°C decrease in the temperature.

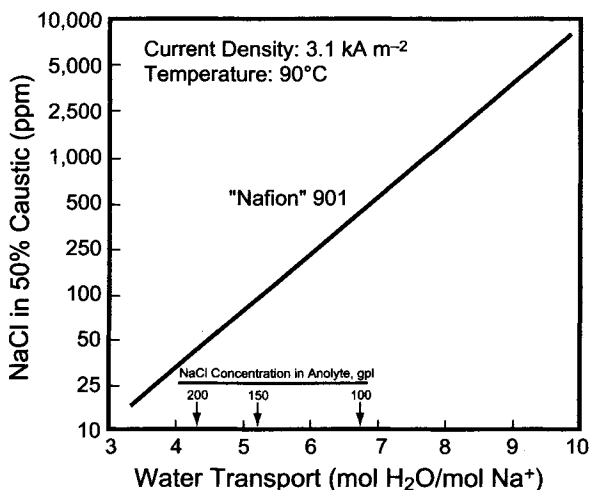


FIGURE 4.8.30. Dependence of NaCl in caustic on the water transport across Nafion® membrane [96]. (Reproduced with permission of the Society of Chemical Industry.)

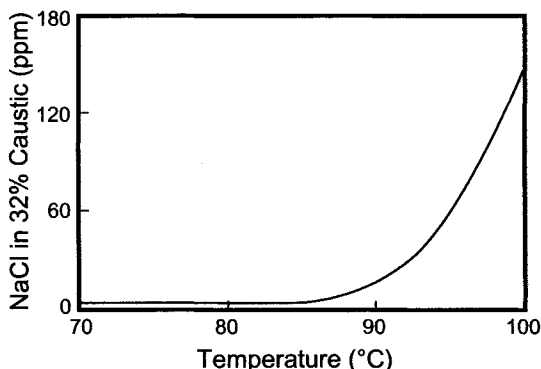


FIGURE 4.8.31. Effect of anolyte NaCl strength on the NaCl concentration in the caustic product at 90°C and at a current density of 3.5 kA m⁻², calculated using Eq. (30).

4.8.4.3D. Caustic Quality in NaOH vs KOH Systems. Chloride and chlorate levels in the caustic are expected to be lower during the electrolysis of KCl as compared to the NaCl system because of the lower water transport number of 2 to 3 during KCl electrolysis [96] compared to ~4 during NaCl electrolysis. Calculations using the water transport number only showed the Cl⁻ and ClO₃⁻ levels in the KOH product to be about 2 to 3 ppm, still exhibiting a dependency on current density, temperature, and anolyte concentration. This influence should be cautiously interpreted since the D_{Cl^-} , $D_{ClO_3^-}$, and κ values in the calculations are those for the NaCl/NaOH system and not for the KCl/KOH system for which relevant data are not available.

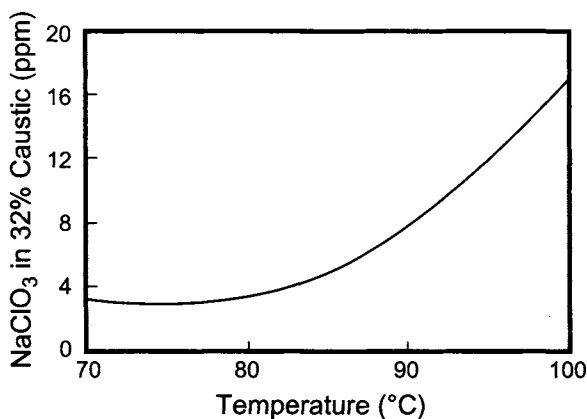


FIGURE 4.8.32. Effect of anolyte NaClO_3 concentration on the NaClO_3 level in the caustic product at 90°C and at a current density of 3.5 kA m^2 , calculated using Eq. (30).

4.8.4.3E. $\% \text{H}_2$ in Cl_2 . Since the water transport number of Na^+ ions, during NaCl electrolysis is ~ 4 vs $2\text{--}3$ during KCl electrolysis, there is greater liquid flow in an NaCl system than in a KCl system. As a result, there is a greater force opposing hydrogen transport during NaCl electrolysis. This gives a lower $\% \text{H}_2$ in Cl_2 during NaCl electrolysis, by at least 50%, based on the number of water molecules moving into the catholyte.

Thus, the caustic product quality from the membrane electrolyzers can be adeptly manipulated by adjusting the cell operating conditions. The chloride content in the caustic can be reduced by (1) increasing the current density, (2) increasing the anolyte salt strength, and (3) decreasing the cell operating temperature. The chlorate levels in the caustic can be reduced by (1) increasing the current density, (2) decreasing the chlorate concentration in the anolyte, and (3) decreasing the cell temperature. In addition, the cell operating temperature must be lowered prior to the circuit shutdown to minimize the diffusion rate of the chloride and chlorate ions. Another important, but neglected outcome of this study is the influence of the electrolyzer design. They should be configured in such a way that the ratio of the active membrane area to peripheral inactive area is high. This is an important factor to consider when evaluating cell technologies. A related issue addressing the minimization of the “current-blind” areas in the membrane is ensuring the absence of stagnant regions in the anode and cathode compartments by reducing the gas space at the top of the cell by maintaining a differential pressure between the catholyte and anolyte in order to minimize the transport of chlorine across the membrane.

Lastly, it is critical that a rigid planar membrane surface be maintained during electrolysis, as any wrinkles in the membrane will lead to stagnation of the electrolyte. This, in turn, will cause further distortion of the membrane by creating nonuniform current distribution and affecting the brine strength and, therefore, the water content in the membrane. This type of problem is generally alleviated by properly attaching and supporting the membrane. While this improves the mechanical properties of the membrane, it can retard the ionic flux across the membrane and offer a high resistance. Thus, as shown in Fig. 4.8.33, increasing the carboxylate layer thickness will lower the

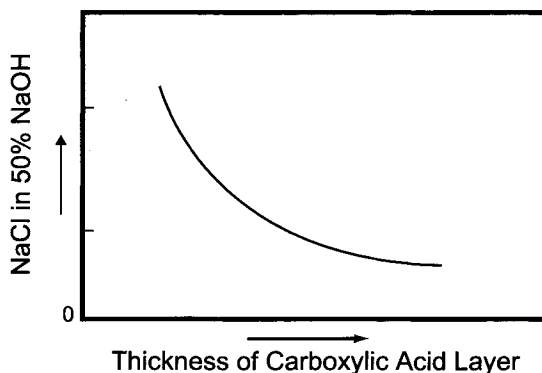


FIGURE 4.8.33. Dependence of amount of NaCl in 50% caustic on the thickness of the carboxylic layer [98]. (Reproduced with permission of the Society of Chemical Industry.)

Cl^- ion flux into the catholyte, at the expense of an increased membrane resistance and cell voltage.

4.8.5. Performance Characteristics of Membranes

4.8.5.1. Effects of Impurities

4.8.5.1A. General. When a high-performance cation-exchange membrane separates pure aqueous NaCl in the anolyte from aqueous NaOH in the catholyte, hydrated sodium ions pass through the membrane from the anode side to the cathode side during the course of electrolysis. Some water molecules also pass in the same direction by electroosmosis, at a rate depending on the NaCl concentration in the anolyte. The cation-exchange membrane rejects hydroxyl ions trying to move in the anode direction by diffusion and migration. The membrane also prevents chloride ions in the anolyte from passing through to the catholyte. The potential gradient drives the OH^- ions from the cathode side to the anode side. Chlorine generated at the anode dissolves in the anolyte solution to form hypochlorous acid and hypochlorite ions. The membrane also prevents the passage of these species.

This is an ideal representation that approximates the real behavior of a membrane cell. A variety of ionic and neutral species besides Na^+ , Cl^- , and OH^- exist both in the anolyte and in the catholyte, and these impurities also affect the performance of the cell. Consequently, the effects of these impurities on membrane-cell behavior have been investigated extensively in order to determine the allowable limits of impurity concentrations and develop industrial procedures for the removal of these impurities from the electrolysis system.

Crude salt, whether it be rock or sea salt, contains a number of chemical constituents (see Table 5.1). The saturated NaCl solution prepared from these salts must be treated to remove impurities before going to a cell. Brine specifications depend on the type of cell used (diaphragm, mercury, or membrane) and the operating conditions. Water is transported from the anolyte to the catholyte through the membrane, as stated above, but more is required to maintain the water balance in the cathode compartment.

Process water for brine treatment and catholyte adjustment may also contain impurities. On the catholyte side, the likely impurities are silica from the water supply and iron and nickel from metallic corrosion. However, the catholyte is removed continuously from the system, and while the presence of impurities may be of concern, they are not permitted to accumulate to high concentrations. On the other side, the anolyte is recirculated between the brine-treatment plant and the electrolyzers, allowing the accumulation of trace impurities to undesirable levels.

Brine impurities originate from various sources and their effects on cell performance differ. We can classify them into several groups: cationic impurities such as Mg^{2+} and Ca^{2+} , anionic impurities such as sulfate and halides other than chloride, and nonionic impurities such as alumina and silica. The effects of the interactions of certain combinations of impurities must also be considered.

Before discussing impurity effects, let us examine the pH profile across the membrane during the course of electrolysis. Using experimental data from a laboratory cell, Ogata and coworkers [18,103] and Obanawa and coworkers [104] found the pH in a sulfonate-carboxylate bilayer to be in the range 9–12 over the bulk of the membrane with the exception of narrow regions near the membrane/solution interfaces. On the anode side, the pH decreased steeply to about 3, while on the cathode side, it increased to 14. Thus, the pH of ~ 9 –12 in the membrane can indeed force the precipitation of metal hydroxides [105] when the metal ion concentration exceeds the dictates of the solubility product (Fig. 4.8.34). It should be noted that Hg and Fe are electrodeposited on the cathode and oxides of Mn, Pb, and Fe are formed on the anode as a result of oxidation of the relevant ionic species by the active chlorine in the anolyte.

4.8.5.1B. Formation of Hydroxides. The effects of impurities on membranes are classified as chemical or physical in nature. When the micropores are plugged by insolubles, the ionic and water fluxes become limited, resulting in increased resistance in those regions. As a result, heat is generated and the vapor pressure of the water increases.

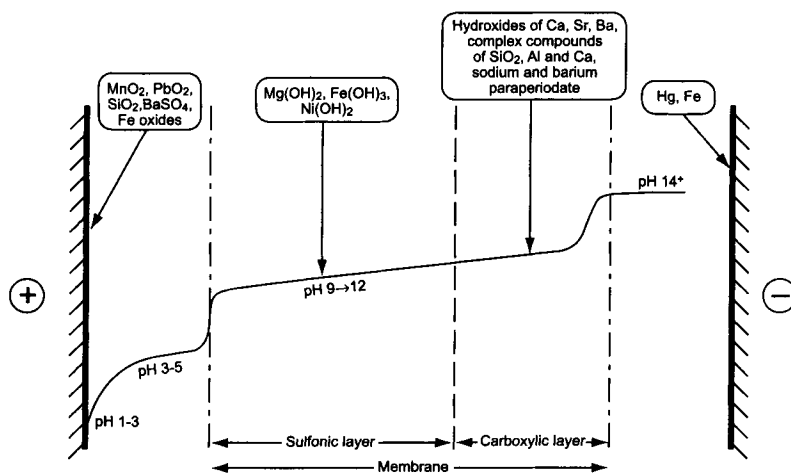


FIGURE 4.8.34. The pH profile in the membrane cell and its importance during the precipitation of impurities in the membrane.

This leads to mechanical damage and the formation of blisters. The voltage across the membrane increases and the current efficiency decreases.

Impurities such as Ni and Mg, whose hydroxides have low solubilities, tend to precipitate near the membrane surface on the anode side, causing an increase in the ohmic drop across the membrane. On the other hand, impurities such as Ca, Sr, and Ba, with higher solubilities, are prone to deposit on the cathode side of the membrane in the carboxylate layer, leading to the formation of large voids and therefore, to decreased current efficiencies. The actual situation may be more complex because of mutual interactions of impurities to form complex species.

Calcium in the brine is particularly harmful because of the moderate solubility product of its hydroxide ($\sim 10^{-6}$). Calcium ions penetrate the membrane and precipitate as hydroxide near the membrane-catholyte interface or at the interface of the sulfonate and carboxylate layers. The voltage drop increases greatly when $\text{Ca}(\text{OH})_2$ accumulates to a concentration of about 1 mg cm^{-2} [18].

The time-to-failure (TTF) of a membrane is inversely proportional to the IC in the feed brine:

$$TTF = a/(IC)^b \quad (37)$$

where a and b are coefficients that depend on the impurity and IC refers to the impurity content. Figure 4.8.35 [18] shows that b is nearly unity for the alkaline earth metals. Calcium is most harmful, followed by magnesium, strontium, and barium. Table 4.8.7 shows the solubility products of the hydroxides [18,106–108]. The TTF , and hence, the value of a in Eq. (37), follows the sequence of solubility, except in the case of $\text{Mg}(\text{OH})_2$. It is likely that Mg^{2+} in the anolyte precipitates in colloidal form and that only a small fraction penetrates the membrane before precipitating. Scanning Electron Microscopy (SEM) images show that precipitation extends throughout most of the sulfonate layer, but only small amounts of $\text{Mg}(\text{OH})_2$ are found in the carboxylate layer. Magnesium hydroxide molecules are small, and hence, less harmful to the microstructure of the membrane than the other hydroxides.

Ferrous iron in the anolyte is oxidized to Fe^{3+} by dissolved chlorine. Since the solubility product of ferric hydroxide is very small ($\sim 10^{-40}$), iron deposits on the membrane surface before it can penetrate the membrane. Iron, therefore, does not affect the selectivity of the membrane but may increase the voltage drop by reducing the effective area. Nickel has similar effects. Iron is generally less harmful because of very low solubility. However, it was reported [109] that in the presence of iron contamination, the current efficiency of Asahi Chemical cells with Aciplex membranes decreased by 2%. The cell voltage, on the other hand, was unaffected over 50 months of operation. The source of the iron was potassium ferrocyanide, an anticaking agent in the evaporated salt used as the raw material.

4.8.5.1C. Sulfate. Besides the chloride ion that is present at high concentrations, the anolyte contains anions such as bromide, iodide, and sulfate in small quantities, and hypochlorite at a $3\text{--}5 \text{ g L}^{-1}$ level, from the reaction of water with dissolved chlorine. The bromide and iodide ions from the anolyte are transported to the catholyte by the same driving force as discussed earlier. The mass transport of sulfate ions in the

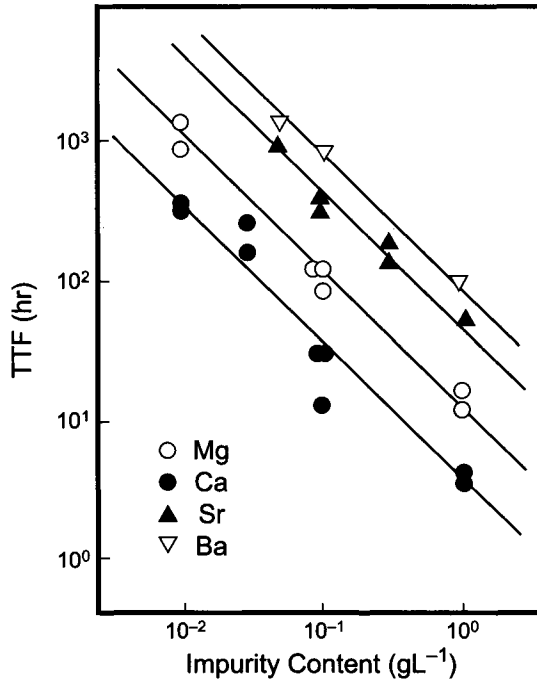


FIGURE 4.8.35. Time-to-Failure (TTF) as a function of the impurity content in the brine [103].

TABLE 4.8.7 Solubility Product of the Hydroxides of Alkaline Earth Metals [18, 101–103]

	Temperature				Composition of hydroxide
	25°C	60°C	80°C	90°C	
Mg	5.60×10^{-12}	4.86×10^{-12}	4.32×10^{-12}	4.11×10^{-12}	Mg(OH) ₂
Ca	4.68×10^{-6}	2.02×10^{-6}	1.21×10^{-6}	9.33×10^{-7}	Ca(OH) ₂
Sr	5.67×10^{-5a}	3.44×10^{-3a}	4.77×10^{-2a}	5.67×10^{-5}	Sr(OH) ₂ · 8H ₂ O
Ba	2.55×10^{-4}	1.97×10^{-1a}	$2.24 \times 10^{+1a}$	2.55×10^{-4}	Ba(OH) ₂ · 8H ₂ O

Notes:

^a Calculated from the solubility data assuming the activity coefficient of the ions to be 0.3.

membrane is small because of its low diffusion coefficient (ca. $10^{-7} \text{ cm}^2 \text{ s}^{-1}$) [100]. The membrane tolerates relatively high levels, in the g L^{-1} range. However, because the solubility of sulfate decreases at high NaOH concentrations, it precipitates as the double salt $\text{Na}_2\text{SO}_4 \cdot x \text{ NaOH}$ and the triple salt $\text{Na}_2\text{SO}_4 \cdot x \text{ NaOH} \cdot y \text{ NaCl}$ in the membrane [110,111].

The transport behavior of sulfate is unusual [112,113] as the rate of transport increases with the current density and the thickness of the membrane at a constant current density. Sulfate deposits everywhere in the membrane, preferentially in the regions of low current density. However, no sulfate deposits were found in areas where there was no flow of current. Photographs of the cross-sections of degraded Nafion[®] 901 showed

sulfate damage at the cathode side behind the PTFE reinforcement. It was shown [114] that with the less mobile sulfate ions, migration was relatively small compared to diffusion and convection, and hence, the overall flux of the sulfate ions was in the direction of the cathode rather than the anode.

4.8.5.1D. Silica. Silica is a nonionic impurity, with low solubility in the slightly acidic anolyte and high solubility in the alkaline catholyte, where it exists as HSiO_3^- and SiO_3^{2-} . It is difficult to remove silica from either the brine or the caustic. Silica, alone, may not affect the cell performance, but it will precipitate when combined with ionic species such as Ca^{2+} and Al^{3+} . The transport mechanism of silica was examined extensively [115–120], and it is generally accepted that silica accompanies the water flux into the membrane where it forms silicate in the alkaline environment prevailing in the membrane. Silicate ions in the catholyte, on the other hand, are transported to the membrane by migration. As a result, a maximum silica/silicate concentration is reached near the cathode surface of the membrane (Fig. 4.8.36). Reaction of Al^{3+} , AlO_2^- , Ca^{2+} , etc. with silicate in this region results in the precipitation [117] of complex sodium–aluminum silicates such as faujasite $(\text{Na}_2, \text{Ca}, \text{Mg})\text{Al}_2\text{Si}_4\text{O}_{12} \cdot 8\text{H}_2\text{O}$, sodalite $[3(\text{Na}_2\text{Al}_2\text{Si}_2\text{O}_8) \cdot 2\text{NaCl}]$, and $\text{Na}_2\text{Ca}_2\text{Si}_2\text{O}_7 \cdot \text{H}_2\text{O}$. The SiO_2 and NaCl concentrations of 50% NaOH solution are related to the SiO_2 concentration in the brine in ppm, the thickness of the membrane (T) in microns, and the current density (CD) in kA m^{-2} as:

$$[\text{SiO}_2/50\% \text{NaOH}] = k_1[\text{SiO}_2]^{0.5}[CD]^{0.75}[T]^{0.5} \quad (38)$$

$$[\text{NaCl}/50\% \text{NaOH}] = k_2[CD]^{-1.0}[T]^{-1.4} \quad (39)$$

It is interesting to note that while the NaCl content of the product caustic decreases with increasing membrane thickness and current density, according to Eq. (39), the silica content, as shown by Eq. (38) behaves differently and increases with all three variables. The transport mechanism of SiO_2 is the same as that described above for sulfate.

The exact location where these complex silicates are deposited depends on the operating conditions and the impurity concentrations in the various streams feeding the cell. Thus, Bissot's studies [117] showed calcium silicate of a different composition on the cathode side (Fig. 4.8.36), compared to the $\text{Ca}_2\text{SiO}_4 \cdot \text{H}_2\text{O}$ and $\text{Ca}(\text{OH})_2$ formed on the anode side of the membrane and the absence of any precipitates on the cathode side in Hine's studies [120]. It was suggested [119, 120] that this might be due to higher levels of calcium when it precipitated as calcium silicate closer to the anode side.

The difference in the chemical composition of calcium silicate precipitates is not a surprising observation, as the phase diagrams of the silicate systems are complex and become even more so when other constituents, such as alkali metals and aluminum associate with silica [121].

In conclusion, the alkaline earth metal ions, precipitated in the membrane, affect both current efficiency and cell voltage. At sufficiently high concentrations, they physically distort the membrane structure. The effects of the anions, such as sulfate, and nonionic species, such as silica, are relatively minor, but these impurities often form insoluble compounds with other chemical species entering the membrane, thereby seriously affecting the membrane structure.

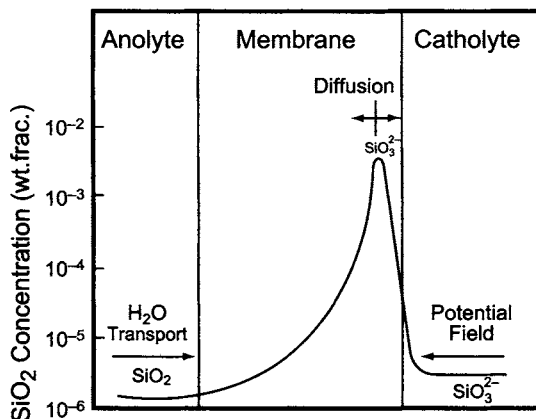
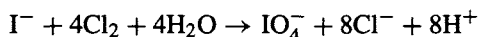


FIGURE 4.8.36. Concentration distribution of silica in the membrane [119]. (With permission from E.I. duPont de Nemours & Co, Inc.)

4.8.5.1E. Iodide. Iodide present in the feed brine is oxidized to periodate inside the membrane by the dissolved chlorine in the anolyte:



The IO_4^- ion goes through the membrane towards the high pH zone and becomes paraperiodate, which precipitates as $\text{Na}_3\text{H}_2\text{IO}_6$ in the carboxylate acid layer and reduces the current efficiency by as much as 3% during the first 100 days or so of operation. However, in the presence of Ba^{2+} , iodide exhibits synergistic behavior. At levels of < 1 ppm Ba^{2+} , and 0.5 to 1 gpl of SO_4^{2-} , the adverse influence of I^- on the current efficiency is negated, I^- being evenly distributed in the sulfonic acid layer as a Ba-I compound. At higher levels of Ba^{2+} (> 1 ppm) and Na_2SO_4 levels of 2–7 gpl, two distinct precipitates of Ba-I compounds—one fine and the other large, form in the sulfonate and carboxylate layers with no effect on efficiency. When the sulfate levels exceed 10 gpl, a fine precipitate of Na_2SO_4 is formed near the carboxylate/sulfonate interface in the membrane and on the PTFE reinforcement, resulting in lowered efficiency. Thus, the adverse effect of iodide on the current efficiency can be offset depending on the sulfate level in the brine (Fig. 4.8.37) [122].

4.8.5.2. *Effects of Operating Conditions* Membranes function over a wide range of conditions, allowing chlor-alkali producers to select electrolyzer designs and process conditions. However, if membranes are operated outside the recommended ranges, their performance may be adversely affected. The effects of the electrolyzer, anolyte, and catholyte operating conditions on membrane performance are addressed here.

4.8.5.2A. Electrolyzer Conditions

1. *Current density*: As current density increases, the cell voltage increases linearly, and the current efficiency and the water transport coefficient remain essentially constant.

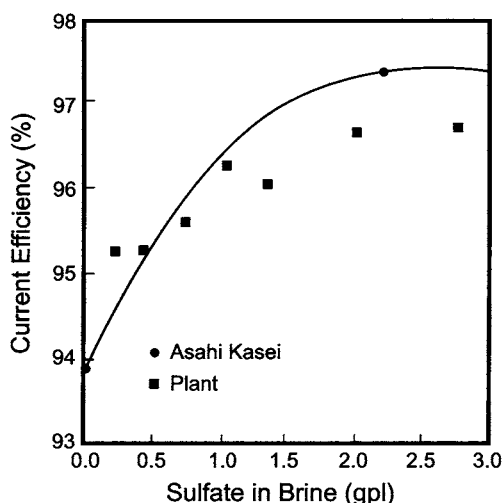


FIGURE 4.8.37. Variation of current efficiency with the sulfate content in the brine (plotted from data in [122]). ●: Asahi Kasei Chemical laboratory data with brine containing 0.5 ppm Ba^{2+} and 0.6 ppm I^- at 4 kA m^{-2} , 90°C , 33% NaOH using Aciplex F-4100 membrane over 30 days on line. ■: Plant data over 30–40 days on line with brine containing 20–30 ppb Ba^{2+} , 500 ppb I^- , and 1–2 gpl sulfate at 3.5 kA m^{-2} and 33% NaOH.

However, when the current density is cycled to capitalize on off-peak power rates, the anolyte and caustic concentrations must be carefully controlled to prevent upsets in membrane equilibration. Successful performance at a higher current density requires careful design to avoid localized brine depletion and to achieve efficient gas disengagement, minimizing bubble entrapment and avoiding pressure surges.

2. *Temperature*: As temperature increases in the range $80\text{--}90^\circ\text{C}$, the voltage decreases by $5\text{--}10 \text{ mV}/^\circ\text{C}$ depending on the current density. The current efficiency is unchanged. Membranes are thermally stable in the chlor-alkali environment up to 105°C , but performance data are not available at temperatures above 95°C .

3. *Electrode gap*: When the gap between the anode and the cathode is reduced, the voltage decreases because of the reduced electrolyte resistance. For gaps less than 2–3 mm, membranes have been designed to avoid gas blinding at the membrane surface (which increases the cell voltage), by coating the catholyte side of the membrane with a ZrO_2 -based or SiC -based composition.

4. *Differential pressure*: Higher hydrostatic pressure on the catholyte side of the membrane is recommended, the allowable differential pressure across the membrane being based on the electrolyzer design. The correct differential pressure immobilizes the membrane and minimizes flutter and vibration, which, over extended periods, can cause abrasion or flex-fatigue. Pressure changes due to surging, loss of electrolyte in one chamber, or plugging of an exit line may cause cuts or tears in a membrane. Excessive pressure differential may deform the membrane by forcing it into anode openings (depending on the cell design), leading to increased voltage and inadequate replenishment of the depleted brine between anodes and membranes.

4.8.5.2B. Anolyte Conditions

1. *Anolyte concentration*: NaCl concentrations of less than 170 gpl in the anolyte can permanently damage the membrane (i.e., blistering) and result in increased voltage. Blistering most commonly involves a separation of sulfonate and carboxylate layers, as shown in Fig. 4.8.38. These layers, bonded in the manufacturing process, remain intact under normal operating conditions. However, internal forces beyond the strength of the interlayer bond can cause blisters. Blisters increase the electrical resistance and force more current through the unblistered areas. If the carboxylate layer remains intact, there should be little effect on current density. Backward mounting of the membrane accidentally can also result in blistering. As shown in Fig. 4.8.39, the property sensitive to anolyte strength is the water transport, expressed as the number of moles of water per sodium ion passing through the membrane, which increases as the NaCl strength decreases. When the water transport capability of the sulfonic layer exceeds that of the carboxylic layer, fluid will accumulate, causing separation of the layers. In addition, localized brine depletion will lead to increased water transport, which will result in lowered mechanical strength.

2. *Acidity*: The minimum recommended anolyte pH is 2. Hydrochloric acid is sometimes added to the brine to neutralize the hydroxyl ions back-migrating across the membrane. This reduces oxygen generation and extends the life of the anode. Excessive acid addition or poor mixing can acidify the carboxylate layer of the membrane and destroy its functional conductivity, resulting in membrane damage and high voltage. When membranes are operating at high current efficiency (96%), little or no acid is needed. If membranes in separate electrolyzers are operating at different values of current efficiency, acid addition in the brine feed should be based on the membranes operating at the highest current efficiency, unless separate acid feed and anolyte pH measurement systems are employed. This will prevent over-acidification of higher efficiency membranes.

3. *Brine impurities*: Soluble impurities in the anolyte can diffuse into the membrane, assisted by the electric field or water transport through the membrane. The impurities may pass harmlessly through the membrane, selectively displace sodium, reducing the

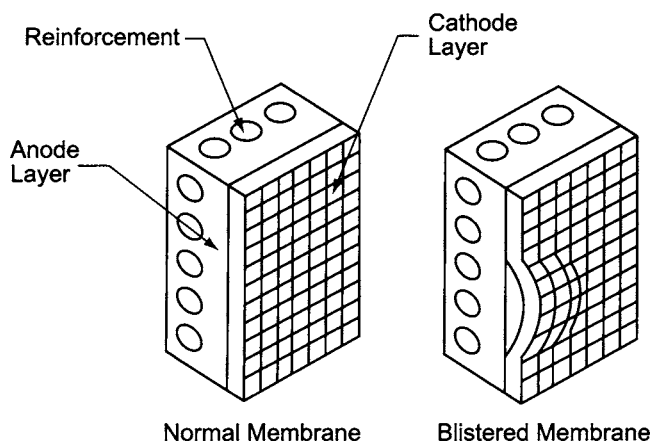


FIGURE 4.8.38. Schematic of the formation of blisters in membranes.

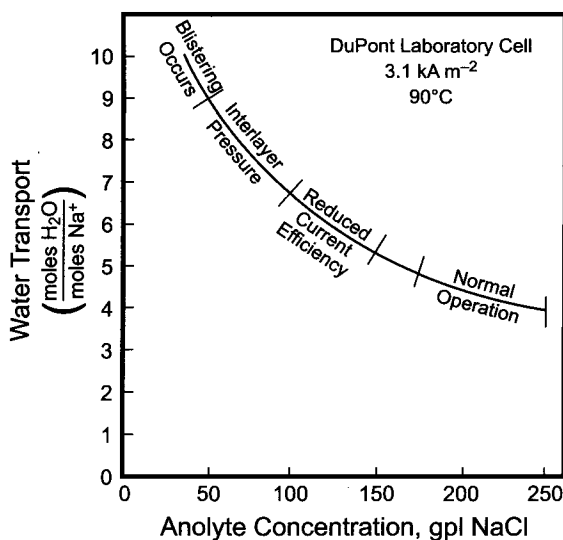


FIGURE 4.8.39. Dependence of water transport on the NaCl concentration in the anolyte [131]. (Reproduced with permission of the Society of Chemical Industry.)

number of active sites available for ion transport, or precipitate and physically disrupt the membrane. Many species soluble in the acidic anolyte form insoluble compounds in an alkaline environment, often near the cathode-side surface, which is the current efficiency-controlling layer. The precipitated material permanently damages the membrane, causing an irreversible decline in current efficiency. Performance may be reduced during brine purity upsets, and the original performance may not be completely recovered after returning to normal conditions. For example, spiking brine feed with 5 ppm calcium for 24 hr can substantially reduce the current efficiency and raise the voltage by 100 mV or more. Restoring the brine quality can recover the losses in efficiency only to some extent. Damage is cumulative. The recommended levels of impurities and the rationale behind these choices are outlined in Section 4.8.6.

4.8.5.2C. Catholyte Conditions

1. *Caustic concentration:* The recommended caustic concentration for a bilayer membrane is generally 30–35 wt%, 32–35% NaOH providing the minimum energy consumption. Minor excursions outside the 30–35% range will cause temporary decreases in current efficiency. Above 37%, the current efficiency decline may be permanent. During start-ups, the target concentration should be 30–33% NaOH to minimize the risk of exposing the membrane to higher caustic concentrations. Current efficiency peaks at 34–35%, while cell voltage increases linearly with increasing caustic concentration. Above 30% NaOH, water transport through the membrane does not change significantly with caustic concentration.

2. *Caustic purity:* The recommended feed water quality is a resistance of greater than 200,000 ohm-cm (or less than 0.5 ppm calcium). However, impurities entering the catholyte compartment generally impose fewer problems than those entering the anolyte.

Chloride concentrations are typically less than 50 ppm (as NaCl on 50% NaOH basis). The chloride content decreases as current density increases, electrolyzer temperature decreases, caustic concentration increases, or anolyte concentration increases. During current interruptions, the rate of chloride diffusion through a membrane is about five times higher than during operation. Cooling the electrolyzer is the most effective way to reduce the diffusion of chloride ions during shutdowns. These measures are also helpful in controlling the chlorate levels in the catholyte.

4.8.6. Membrane Damage

The composite membranes used in membrane cells are prone to damage for a variety of reasons [123,124], some of which are discussed in Section 4.8.5. Obvious forms of physical damage are tears, pinholes, and blisters. However, physical damage can also arise from brine impurity precipitation and void damage from “low conductivity” operation.

Tears are developed by improper handling of the membranes and by rough anode and cathode surfaces. Pinholes are formed either by exposure to rough spots during handling or because of excessive differential pressure fluctuations fatiguing the membrane and weakening it. The extent of caustic leakage from pinholes can be determined from the amount of caustic in the brine when the cell is not energized.

Blisters, visible to the naked eye, are formed in the membrane because of poor operating conditions resulting in localized delamination of the sulfonate and carboxylate layers. These blisters are generally greater than 5 mm in diameter in the electrochemically active areas. Smaller blisters, called microblisters or voids, are formed in the inactive areas. The primary reason for blister formation is the imbalance in the transport of water across the two layers of the membrane resulting in either accumulation or depletion of water in the membrane. Thus, when the salt strength is low, more water is transported across the sulfonate layer. This results in fluid accumulation in the membrane when the carboxylate layer cannot allow the passage of more water. This generates high internal pressures and delaminates the membrane. When the salt strength is 40 gpl and the caustic strength is 32%, for example, the fluid accumulation of $1 \text{ ml hr}^{-1} \text{ m}^{-2}$ leads to an internal pressure of 120 kg m^{-2} . This pressure is more than sufficient to cause delamination.

There are three types of blisters, water, salt, and others. Water blisters are formed when there is high water transport across the layers. Salt blisters result from localized heating of the membrane because of high local current density or nonuniform current distribution. Proper cell design can alleviate this problem (Chapter 5). The other type of blister arises when the acidity of the anolyte is high. When the anolyte pH is below 2, the carboxylate layer protonates to a nonconductive carboxylic acid. This will increase the voltage and the internal vapor pressure, and finally result in the formation of voids in the carboxylate layer.

To summarize, the three mechanisms proposed for the formation of blisters are as follows.

1. Delamination by high internal pressure by backward installation of the membranes, reverse water transport during shutdowns, and excessive anolyte depletion.

2. Voids resulting from poor conductivity as a result of high anolyte acidity, low temperature of brine or caustic, high caustic strength, and high local current density.
3. Voids by precipitation in the carboxylate layer because of anode-side blinding and impurity deposits. When a nonporous material such as a gasket or grease blinds the anode side of the membrane, water will diffuse through the non-blinded areas, while caustic dehydrates the membranes in the blinded region. As a result, the salt is concentrated and precipitates in the carboxylate layer, creating voids and hence, holes in the membrane. This is called anode-side blinding and is observed near the anode welds and along the perimeter in the gasket area. Perimeter blistering occurs in the gas phase at the top of the electrolyzer and can be avoided by keeping the cell flooded all times.

Membrane blistering can also occur during shutdowns, when reverse currents flow and water is transported from the cathode side to the anode side. A similar situation arises when a membrane is installed backward. The accumulation of water in the membranes leads to void formation. It is, therefore, essential that the reverse currents be suppressed by flushing the cell to remove the hypochlorite, by lowering the temperature to lower the diffusion rates, and by maintaining the same electrolyte concentrations in both the compartments. Dilution of the catholyte, or continuous flow of the anolyte is necessary to reduce diffusion/anolyte dehydration with salt deposits on the anode face of the membrane.

Voids are formed when the temperature is low and when the caustic strength is high. Since the water content of the membrane decreases with decreasing temperature and increasing caustic concentration, it is necessary that the water content of the membrane be maintained at a given temperature by choosing the appropriate caustic strength. For example, at 70°C or less, the suggested caustic strength is 28–30%. Departure from this condition may lead to the formation of voids as a result of localized increase in the resistance of the membrane (because of low water content at low temperatures) and therefore, local overheating during operation. It might be worth noting that the membrane conductivity is also related to temperature (Fig. 4.8.40).

Precipitation of impurities in the sulfonate or the carboxylate layer disrupts the transport properties of water and sodium ions. Impurity precipitation usually roughens

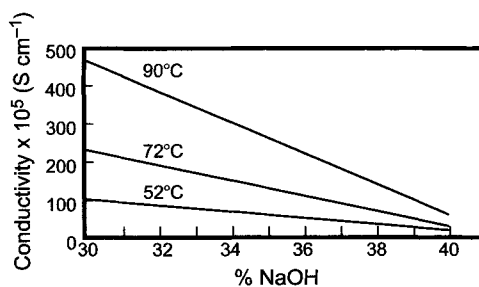


FIGURE 4.8.40. Variation of membrane conductivity with caustic concentration and temperature [123]. (With permission from E.I. duPont de Nemours & Co., Inc.)

the cathode layer through the formation of mini voids, which can enhance the back migration of hydroxyl ions. This roughening does not lead to a weak membrane and pinholes. Impurity precipitation can also tie up exchange sites and increase voltage.

4.8.7. Brine Purity Specifications

As briefly stated in Section 4.8.5, the impurity specifications imposed on the brine are dictated by the very nature of the structural features of the membrane. Thus, it is generally acknowledged that the membranes are composed of a backbone structure with crystalline PTFE segments and clusters containing the ion-exchange groups. The “heart” of the membrane is these clusters, 5 nm in diameter and connected to each other by narrow channels of 1 nm in diameter. It is through these structures that the ionic species and water molecules are transported during electrolysis.

Keating [119] has estimated the brine flow over a 28-month time span to be about 200,000 kg m⁻² of membrane, at a brine flow rate of 200–250 kg day⁻¹ and at a current density of 5 kA m⁻². If the impurity concentration is 1 ppm, then the amount of impurities that are lodged in the membrane can be as much as 200 g. This is 50% of the total membrane weight of 400 g m⁻². If the total weight of the impurities in the membrane is to be restricted to a number of grams, the impurity levels must be in the ppb range.

One also can estimate the number of ion-exchange sites in a membrane by assuming a cluster diameter of 5 nm and a membrane thickness of 250 μm. The number of clusters for this case will be 3.6 × 10²¹ m⁻². With 10 exchange sites per cluster, the total number is 3.6 × 10²² m⁻². At a brine flow of 200 kg day⁻¹, with 10 ppb of Ca of which 10% of it is blocking the sites, it can be shown that it takes less than a year to block all the sites in the membrane, rendering it ineffective for ion exchange. This calculation is not precise and has been made with several assumptions. Nevertheless, it emphasizes the fact that there are a finite number of sites available for exchange of ions in any given membrane and very low impurity levels in the brine can very quickly block them.

The exact specifications depend on the membrane, cell design, and operating conditions [125–127]. The brine specifications recommended by membrane suppliers are shown in Table 4.8.8, and Table 4.8.9 describes the impurities and possible mechanisms of membrane damage. The reader is referred to the Appendix, where the effects of impurities are summarized along with the recommended analytical methods suggested by the membrane manufacturers. References [128–131] provide a discussion on brine treatment costs vs membrane costs.

Electrochemical experiments to measure cell voltage and current efficiency are simple, direct, and useful for the investigation of membrane performance. Visual and microscopic observations are indispensable. Visual inspection is the principal method used for determining the soundness of the membrane surface. SEM is quite useful for the inspection of morphology of the surface or cross-sections. It can be used to identify deposits of impurities. XRD and X-ray fluorescence spectroscopy (XRF) are useful for the semiquantitative determination of impurity accumulation and distribution [126]. Table 4.8.10 [132] summarizes the recommended methods for detecting the physical and chemical damage to membranes.

TABLE 4.8.8 Brine Specifications for Membrane Electrolyzers

	Units	Nafion®			Aciplex™			Flemion™
		≤4 kA m ⁻²	4-6 kA m ⁻²	≤4 kA m ⁻²	4-5 kA m ⁻²	5-6 kA m ⁻²	6 kA m ⁻²	
<i>Feed Brine</i>								
Ca + Mg	mg kg ⁻¹ (as Ca)	<0.03	<0.02	<0.03	<0.02	<0.02	<0.02	<0.02
Sr	mg kg ⁻¹	<0.5	<0.4	<0.5	<0.4	<0.5	<0.5	<0.5
SiO ₂	mg kg ⁻¹	<10.0	<6.0	<5.0	<5.0	<5.0	<5.0	<15.0
Al	mg kg ⁻¹	<0.1	<0.1	<0.1	<0.1	<0.1	<0.1	<0.1
Mn	mg kg ⁻¹	<i>a</i>	<i>a</i>	<0.05	<0.05	<0.05	<0.05	<0.05
Pb	mg kg ⁻¹	<i>a</i>	<i>a</i>	<0.05	<0.05	<0.05	<0.05	<0.05
Fe	mg kg ⁻¹	<i>a</i>	<i>a</i>	<0.2 ^e	<0.15 ^e	<0.15 ^e	<0.15	<0.15
Ni	mg kg ⁻¹	<i>a</i>	<i>a</i>	<0.10	<0.10	<0.10	<0.10	<0.10
Hg	mg kg ⁻¹	<i>a</i>	<i>a</i>	<0.5	<0.5	<0.5	<0.5	<0.5
Ba	mg kg ⁻¹	<1.0	<0.5	<0.5	<0.5	<0.5	<0.5	<1.0 (I < 0.1 mg kg ⁻¹) <0.5 (I < 0.2 mg kg ⁻¹)
Total heavy metals (Mn, Pb, Cu, Cr, Ti only)	mg kg ⁻¹ (as Pb)							<0.1
Na ₂ SO ₄	gpl (23°C)	<10.0	<8.0 (max) >4.0 (min)	<9.6	<9.6	<9.6	<9.6	<10.4(max); > 5.9(min) <1.0
Suspended solids	mg kg ⁻¹							
Total iodine ^c	mg kg ⁻¹	<1.0	<0.2	<0.2 (Ba < 0.3 mg kg ⁻¹) <0.1 (Ba > 0.3 mg kg ⁻¹)	<0.1	<0.1	<0.1	<0.2
NaClO ₃	gpl (23°C)				<31.9			<19.1
Organics					^d			
<i>Depleted brine</i>								
F ⁻	mg kg ⁻¹				< 1.0			< 1.0

Notes:
^a Nafion® has no specification for depleted brine or for Mn, Pb, Hg, Fe, and Ni in the feed brine.
^b The minimum level of sulfate for Aciplex™ and Flemion™ can be relaxed during startup and shutdown, but must be maintained during normal operation.
^c All iodine compounds are expressed as the element.
^d The effect of organics depends on the type and amount of the organics in the brine.
^e The Fe specification for Aciplex™ with acidified brine is 0.05 mg/kg.
 Nafion® : Trademark of E.I. DuPont de Nemours & Company; Aciplex™ : Trademark of Asahi Kasei Corporation; Flemion™: Trademark of Asahi Glass Company Ltd.

TABLE 4.8.9 Adverse Effects of Brine Impurities on Membrane Performance (From Ref. [127]; Summary of Findings by Japan Soda Industry Association, as Modified by Asahi Kasei-Based Experience and Investigations)

Impurity (specs)	Intramembrane precipitate	Membrane		Electrodes		Observations
		CE	CV	Ano	Cat	
Ca (30 ppb)	Ca(OH) ₂	**	o	o	o	Large effect, worsens with SiO ₂ .
Mg	Mg(OH) ₂	x	**	o	o	Large rise in cell voltage, small effect on current efficiency.
Sr (500 ppb)	Sr(OH) ₂ H ₂ O	**	o	o	o	Effect worsens with SiO ₂ .
Ba (1000 ppb)	Ba(OH) ₂ H ₂ O	o	o	**	o	Small effect by itself, large effect with iodide.
Al (100 ppb)	Al(OH) ₃	x	o	o	o	No effect alone, some effect with SiO ₂ .
Fe (<0.2 ppm)	Fe(OH) ₃	o	**	**	**	Deposits on the anode face of the membrane.
Ni (<0.1 ppm)	Ni ₃ O ₄ , Ni ₂ O ₃ , NiO(OH)	o	**	o	o	Deposits in the anode side of the membrane and in contact with Ni-based activated cathodes.
Hg (<15 ppm)		o	o	o	**	Increase the cathodic overvoltage, effect generally reversible.
F		o	o	**	o	No effect on membrane.
I (10 ppm)	Na ₃ H ₂ IO ₆	**	**	o	o	Effect aggravated with Ba.
SiO ₂ (10 ppm)		**	o	o	o	Effect worse with Ca, Sr, or Al
SO ₄ (10 gpl)	Na ₂ SO ₄	**	o	**	o	Low levels reduce the effect of Ba ²⁺ ; high levels result in precipitates, lowers CE.
NaClO ₃ (<20 gpl)		o	o	o	o	Diffuses through membrane, affects product caustic quality.
Ca + SiO ₂	Na ₂ Ca ₂ Si ₂ O ₇ · H ₂ O	**	o	o	o	Large effect on CE.
Ba ²⁺ + I ⁻	Ba ₃ H ₄ (IO ₆) ₂	**	o	**	o	Affects CE (fine particles precipitate in the membrane).
Al + SiO ₂	Na ₂ Al ₂ Si ₃ O ₁₀ · H ₂ O	**	o	o	o	Forms complexes and precipitate in the membrane.
C + Al + SiO ₂		**	o	o	o	Zeolite like precipitates in the membrane.
Suspended solids		**	**	o	o	Dissolves in the electrolyzer, releasing Ca, Mg, and other impurities.

Note: CE: current efficiency; CV: cell voltage; Ano: anode; Cat: cathode; **: clear adverse effect; x: small effect; o: no observed effect

TABLE 4.8.10 Methods for the Determination of Pores, Holes, and Tears in the Membrane [130]

Method of detection	Advantages	Disadvantages
Gas analysis of H ₂ and O ₂ in the anode gases	<ol style="list-style-type: none"> 1. Possible during cell operations 2. Use of online analyzers 3. Locates damaged electrolyzer 4. Detects large holes 	<ol style="list-style-type: none"> 1. Dilution by anode gas from other cells 2. Does not locate damaged membranes
Titration of anolyte caustic content	<ol style="list-style-type: none"> 1. Fast 2. Use of online analyzers 3. Locates damaged electrolyzer 4. Detects large holes 	<ol style="list-style-type: none"> 1. Only possible during shutdown 2. Dilution by anolyte from other cells 3. Does not locate damaged membranes
Cell voltage measurement at low current density	<ol style="list-style-type: none"> 1. Fast 2. Locates damaged membranes 3. Detects large holes 	<ol style="list-style-type: none"> 1. Only possible during startup 2. Only possible with bipolar electrolyzers
Determination of N ₂ flow through membranes	<ol style="list-style-type: none"> 1. Locates all damaged membranes 	<ol style="list-style-type: none"> 1. Only possible with drained electrolyzers 2. Single cells must be accessible 3. Slow

4.8.8. High Performance Membranes—New Developments

4.8.8.1. *Design of Membranes: General Aspects.* Ideal membranes would have high chemical and physical stability, uniform strength and flexibility, high current efficiency, low electrical resistance, and low rates of electrolyte diffusion. These characteristics have been the subject of a great deal of research and developmental effort. The highlights are noted below.

4.8.8.1A. *Exchange Groups.* The original membranes developed by DuPont in the 1960s and 1970s contained only sulfonate groups. Sulfonic acid is a strong acid and absorbs water, which reduces current efficiency by allowing increased back-flow of hydroxyl ions from the catholyte to the anolyte. All sulfonic group-based membranes have desired properties such as chemical stability and low electrical resistance (Table 4.8.11). Asahi Chemical discovered that membranes with only carboxylic acid groups show a much higher efficiency since they hold less water. The low dissociation constant of the carboxylic acid, however, gives them low electrical conductivity. Electrical resistance increases linearly as thickness increases, but efficiency improvements level off at a thickness of about 7 μm . For this reason, it is advantageous to utilize

TABLE 4.8.11 Membrane Properties Classified by Ion-Exchange Group and Membrane Structure [42]

Ion-exchange group	$R_f\text{SO}_3\text{H}$	$R_f\text{SO}_2\text{NHR}$	$R_f\text{COOH}$	$R_f\text{SO}_3\text{H}/R_f\text{COOH}$
pK_a	<1	8–9	2–3	2–3/<1
Hydrophilicity	High	Very low	Low	Low/High
Water content	High	Very low	Low	Low/High
Current efficiency(%); 8N NaOH	75	88	96	96
Electric resistance	Low	Very high	High	Low
Chemical stability	Very high	Low	High	High
Handling condition (pH)	>1	>10	>3	>3
pH of anolyte	>1	>10	>3	>1
Neutralization of OH^- by HCl	Applicable	Impossible	Impossible	Applicable
O_2 in product Cl_2	<0.5%	>2%	>2%	<0.5%
Anode life	Long	Short	Short	Long
Current density	High	Low	Low	High
Necessary number of cells	Large	Large	Large	Small

a multilayer membrane, containing both carboxylate and sulfonate layers. Important considerations in the design of the multilayer membrane are as follows:

1. The presence of a thin carboxylate layer in the membrane surface facing the catholyte is effective for realizing low unit energy consumption, as it results in high efficiency and low electrical resistance. The minimum thickness of the carboxylic acid layer is related to the ion-exchange capacity. In the normal range of ion-exchange capacities, a 10 μm thickness is sufficient. With a thickness greater than 10 μm , little change in current efficiency occurs, but the resistance increases.
2. Increasing the thickness of the carboxylic acid layer can effectively decrease the chloride content in the product caustic soda. Beyond a certain thickness this effect diminishes. Hence, a proper choice of thickness is critical to achieve high product quality without paying an energy penalty.
3. Increasing the thickness of the carboxylic acid layer tends to alleviate mechanical damage and stress on the membrane. Beyond a certain thickness, however, this effect diminishes and an optimum thickness also exists in this regard.
4. Addition of HCl to the anolyte increases the purity of the product chlorine and increases the service life of anode as well. Because of the high pK_a of the carboxylic acid group, it is impossible to add HCl to completely neutralize the hydroxyl ion diffusing from the catholyte. Therefore, it would be difficult to obtain an oxygen content of less than 1.5% in the product chlorine. With the membrane containing both sulfonic and carboxylic acid groups, sufficient addition of acid becomes possible and an oxygen content of 0.5% or less can be obtained in the product chlorine. This also results in prolonged life of the anode.

4.8.8.1B. Exchange Capacity. The degree of ionic permselectivity of the membrane is determined by the number of exchange groups and hence, the fixed-ion concentration in the membrane. During electrolysis, the water content of the membrane decreases with increasing caustic soda concentration. The fixed-ion concentration thus increases,

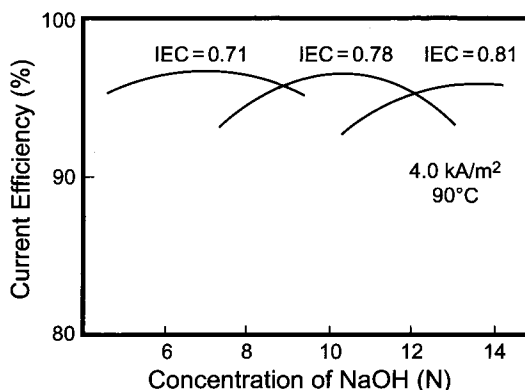


FIGURE 4.8.41. Variation of current efficiency with caustic strength for a bilayer membrane (prepared by chemical modification) at various ion-exchange capacities [98]. (Reproduced with permission of the Society of Chemical Industry.)

leading to the maximum level of current efficiency. This level varies with ion-exchange capacity and the optimum ion-exchange capacity of caustic soda to be obtained from the catholyte compartment. The ion-exchange capacity must also be selected to result in the long-term stability of the cell voltage. Figure 4.8.41 shows the relationship between caustic soda concentration, ion-exchange capacity, and current efficiency. The designed ion-exchange capacity of the sulfonic acid layer is higher than that of the carboxylic acid layer.

4.8.8.1C. Anolyte Concentration. The concentration of NaCl in the anolyte directly influences cell voltage, current efficiency, and NaCl content in the caustic soda. The NaCl concentration is chosen to provide the optimum of these three characteristics. It must be above 180 g L^{-1} to avoid irreversible membrane damage. For stable current efficiency, the concentration must be above 200 g L^{-1} .

4.8.8.1D. Catholyte Concentration. The membrane's performance is strongly affected by the caustic concentration in the catholyte, and its composition is designed to give low unit energy consumption at the desired caustic concentration. Each type of membrane has its own optimum catholyte concentration, at which it operates at a minimum energy consumption. In addition to unit energy consumption, factors such as product quality, mechanical strength, and long-term stability of performance are considered in the ultimate determination of the membrane composition.

4.8.8.1E. Factors Determining the Chloride Content in Caustic Soda. Quality requirements for product caustic soda depend on the intended use. The effect of sodium chloride content varies considerably among fields of use such as papermaking, fiber and textiles, food products, and pharmaceuticals. In some of these, even trace amounts of chloride ions may lead to difficulties. Membrane design and electrolysis conditions are properly

chosen to obtain low Cl^- levels in caustic by using thick membrane and carboxylic layers, which tend to increase the cell voltage. This requires, again, the judicious choice of the membrane characteristics. Another problem arises when chloride ions diffuse through membranes at shutdown. KOH is more susceptible than NaOH to this problem.

4.8.8.1F. Influence of Reinforcing Material. Vigorous agitation is necessary in the anolyte to ensure the transport of ions across the boundary layer near the membrane, and a rigid planar membrane surface must be maintained during electrolysis. Any curvature in the surface will lead to local stagnation of the electrolyte and polarization, which in turn will distort the membrane surface and reduce local current density. To obtain a rigid planar membrane surface, dimensionally stable PTFE woven reinforcing cloth is used to reinforce the membrane. Reinforcement is also necessary to prevent damage or tearing of the membrane. The mechanical properties of the membrane, particularly its tensile and tear strength, are greatly improved by reinforcement. However, the reinforcing material also increases the resistance of the membrane as shown in Figs. 4.8.42 A and B, depending on the reinforcement and the type of weave.

4.8.8.1G. Physical Relaxation. One of the major objectives in ion-exchange membrane development is the elimination of the decline in current efficiency due to physical relaxation. This phenomenon cannot be completely avoided with the present ion-exchange membranes, regardless of their carboxylic acid layer thickness. The ion-exchange membrane contains three types of domains. In the first type, the C-F regions exhibit a strong degree of intermolecular attraction and clustering with crystalline characteristics. The second type is marked by the presence of hydrophilic exchange groups that exert a strong swelling effect. The third domain contains a small number of exchange groups and has intermediate characteristics. The performance of the membrane depends on the relative ratio of these domains. In long-term operations, the intermediate domain undergoes changes due to microphase separation, resulting in a shift in the optimum operating conditions and a consequent decline in current efficiency. Inappropriate use of the membrane will also accelerate this decline. This shift includes an increase in the optimum caustic soda concentration, aggravating the microphase separation. Thus, it is possible to maintain a high level of current efficiency in long-term operation by appropriate upward adjustment of the operating caustic soda concentration [133].

4.8.8.2. Operation of Membranes. Bilayer membranes separate Cl_2 and NaOH very efficiently. The best performance from these membranes can be sustained over a long period of time only when the physical, chemical, and mechanical integrity of the membrane is preserved. As discussed in earlier sections, the physical characteristics of the membranes depend not only on their architecture, but also on the water content. The latter should be kept unaltered over the entire surface of the membrane, both during electrolysis and when the power is off. The membrane must be taut, free of pinholes, and not subjected to any variation in pressure or water content that will change the localized water content and not cause wrinkles in the membrane. Any local depletion of the brine concentration will cause wrinkles to form, where either a tear can develop or pinholes

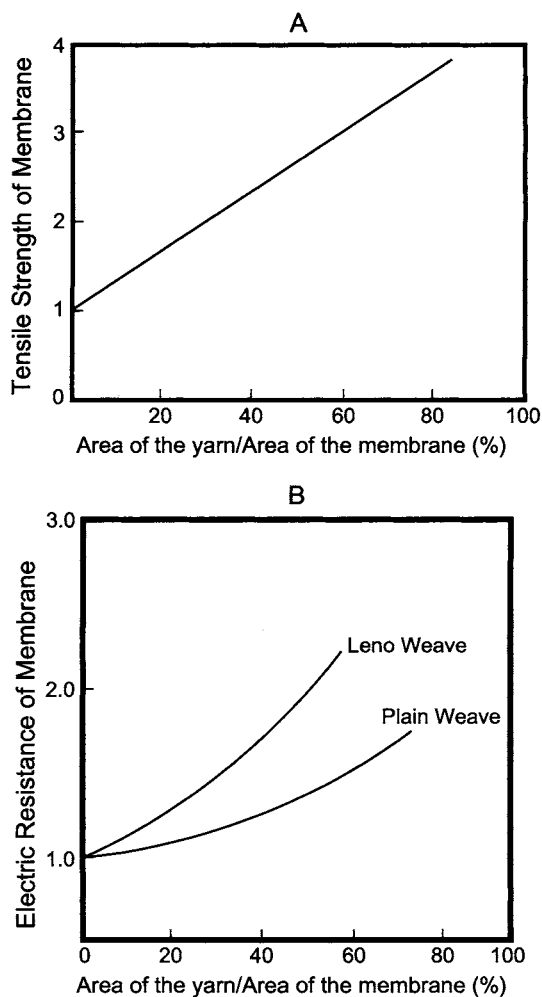


FIGURE 4.8.42. A: Tensile strength vs area of membrane reinforcement (taking the tensile strength of unreinforced membrane to be one). B: Electric resistance vs area of membrane reinforcement (taking the electric resistance of unreinforced membrane to be one). In Leno weave, the vertical strands are double twisted and the horizontal strands are single twisted. (With permission from E.I. duPont de Nemours & Co, Inc.)

can form. It is for this reason that all membrane cell technology suppliers have modified their cells to provide good mass transfer in the cells via internal or external circulation.

In addition, the membrane is prone to develop salt blisters in (1) the gas zone in the anolyte compartment, (2) gasket areas, and (3) regions where gas bubbles adhere to the membrane. The term "salt blister" describes the deposition of salt in the membrane because of a localized increase in the salt concentration. Complete flooding of the electrolyzers and proper gasket assembly prevent the formation of salt blisters. Gas bubble adhesion is suppressed by pressuring the cell (to lower the void fraction and gas

bubble size), and by coating both sides of the membrane with valve metal oxide in order to prevent the sticking of gas bubbles.

Finally, as mentioned above, it is imperative that the brine quality is excellent so that no impurities are deposited in the membrane, disrupting its structure and its chemical integrity. Thus, all efforts, be they operations-related or design-related, should preserve the physical, mechanical, and chemical properties of the membrane during electrolysis to realize sustained maximal performance from the membrane.

4.8.8.3. Membrane Technology Developments. The three major membrane suppliers are DuPont, Asahi Glass, and Asahi Kasei. All these manufacturers are constantly striving to improve membranes to achieve low energy consumption, long life, and insensitivity to impurities and upsets in operation.

Asahi Glass developed Flemion[®] membranes [134–141] exhibiting high ion-exchange capacity and permselectivity for Na^+ . Early versions showed increased voltage at a low anode–cathode gap due to the gas blinding effect. This led to the development of Flemion DX for use in their zero-gap electrolyzer, AZEC, which eliminated the void fraction-related effect by applying a nonconductive metal oxide to the membrane in order to induce hydrophilicity (Fig. 4.8.43) [135,136]. Figure 4.8.43 shows DX723 and DX753, which are not discussed here.

A low-resistance membrane, F-8934, recently developed by Asahi Glass [141], has operated at a current density of 8 kA m^{-2} , at $2300 \text{ DC kWh ton}^{-1}$. Its resistance was reported to be 25% lower than the F-893 membrane, and it gave an energy reduction of $30\text{--}40 \text{ kWh ton}^{-1}$ compared to the F-893 membrane at $3\text{--}4 \text{ kA m}^{-2}$.

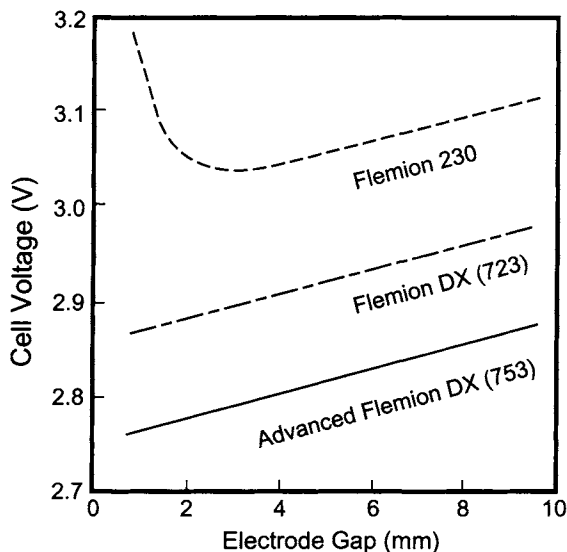


FIGURE 4.8.43. Cell voltage vs electrode gap with anolyte containing 200 gpl NaCl and catholyte containing 35% NaOH at 90°C and at 2 kA m^{-2} [135]. (Reproduced with permission of the Society of Chemical Industry.)

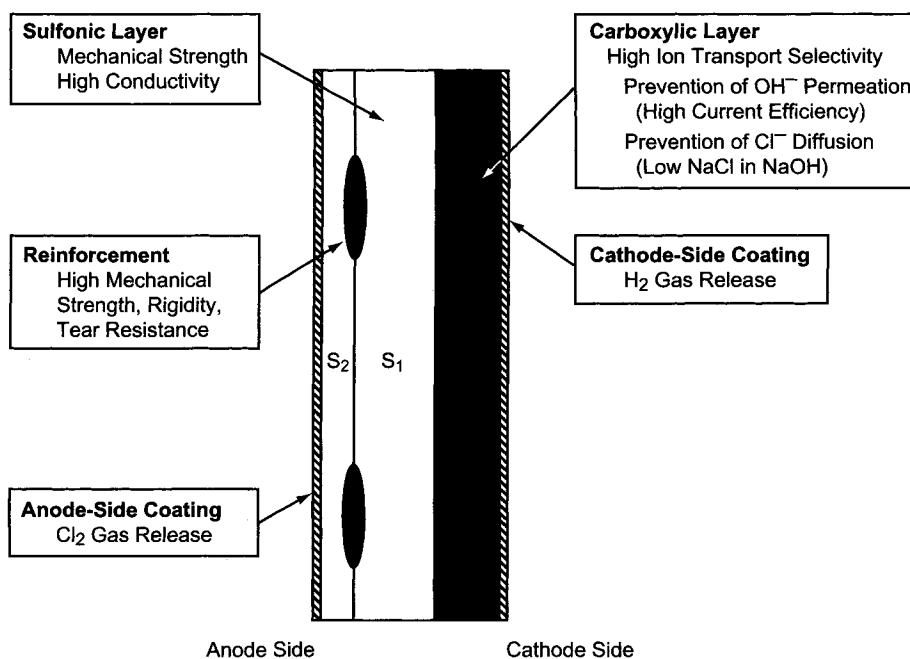


FIGURE 4.8.44. Role of the components constituting an ion exchange membrane [127]. S₁ and S₂ refer to sulfonic layers of different thicknesses and equivalent weights. (With permission from ELTECH Systems Corporation.)

A newer membrane, AG 8020, is claimed to exhibit resistance to iodide in the feed brine and the results from tests at an unidentified plant over a period of 1 year at $\sim 4 \text{ kA m}^{-2}$ have shown no decline in efficiency.

The membranes developed by Asahi Kasei are called Aciplex[®]-F membranes and the typical structure is shown in Fig. 4.8.44 [127]. There are two classes of Asahi Kasei membranes available, depending on the desired caustic strength. F-2200 series membranes (i.e., F2202, F2201, F2204, and F2205) are suitable for producing 20–24% caustic at high efficiencies. For operation to generate 30–34% caustic, three series of membranes were developed. All are designed to offer high tolerance to the impurities in brine, the distinguishing feature between them being the incorporation of sacrificial threads that provide high openness in the membranes. F-4100 series (i.e., F4101, F4111, and F4112) membranes contain no sacrificial threads and are non-coated, whereas the F-4200 series (i.e., F4201, F4202, and F4203) are coated membranes with no sacrificial threads. These membranes exhibit high mechanical strength and offer low cell voltage.

The F-4400 series of Asahi Kasei contain sacrificial threads and coatings on either side of the membranes that facilitate gas release. Besides providing mechanical strength and low voltage, these membranes (F4402X, F4401C, and F4401) are designed to operate at high current densities with a low energy consumption. The F-4400 series are resistant to brine impurities, and F4401, in particular, was shown to be resistant to iodide in the brine in operating plants over 2 years. Tables 4.8.12 and 4.8.13 summarize the developments of Asahi Kasei.

TABLE 4.8.12 Description of Asahi Kasei Membranes

Membrane type	Surface modification	Features
F2200	F2202 F2204 F2205x	For low concentration caustic production, no sacrificial threads.
F4100	F4111 F4112	For finite gap cells, non-coated, no sacrificial threads.
F4200	F4201 F4202 F4203	For high concentration caustic production in finite and zero-gap cells, coated, no sacrificial threads.
F4400	F4401 F4401c F4402	For high concentration caustic production in finite and zero-gap cells, coated with sacrificial threads.

TABLE 4.8.13 Laboratory Cell Performance Data^a for Asahi Kasei Membranes

Membrane type	Finite gap cells	
	Cell voltage (V)	Current efficiency (%)
F2202	3.1	97
F2204	3.02	97.5
F2205x	2.95	97
F4111	3.2	97.5
F4112	3.12	97
F4201	3.1	97
F4202	3.02	97
F4203	2.97	97
F4401	2.92	97.5
F4401c	2.95	98
F4402	2.95	97

^aNote:

current density: $4 \text{ kA} \cdot \text{m}^{-2}$; 32% NaOH (23% for F-2200 series);
205 g l^{-1} anolyte NaCl; 90°C; 1.5 mm gap; activated cathode.

DuPont's bilayer membranes generally comprise the elements shown in Fig. 4.8.45 [105,142–144], the first bilayer membrane introduced in 1982 being N901. Several modifications and improvements were made to this basic structure, and this series of membranes is shown in Tables 4.8.14 and 4.8.15.

One of the changes in the design of these membranes is the nature of the reinforcement (Fig. 4.8.45). The earlier DuPont membranes had a twisted PTFE ribbon behind which the impurities lodged in the sulfonate layer. Replacement with a PTFE filament not only retained the mechanical strength but also reduced the “shadow” area behind the filament. This increased the active area, which reflected in improved current distribution and water influx, and increased tolerance to impurities.

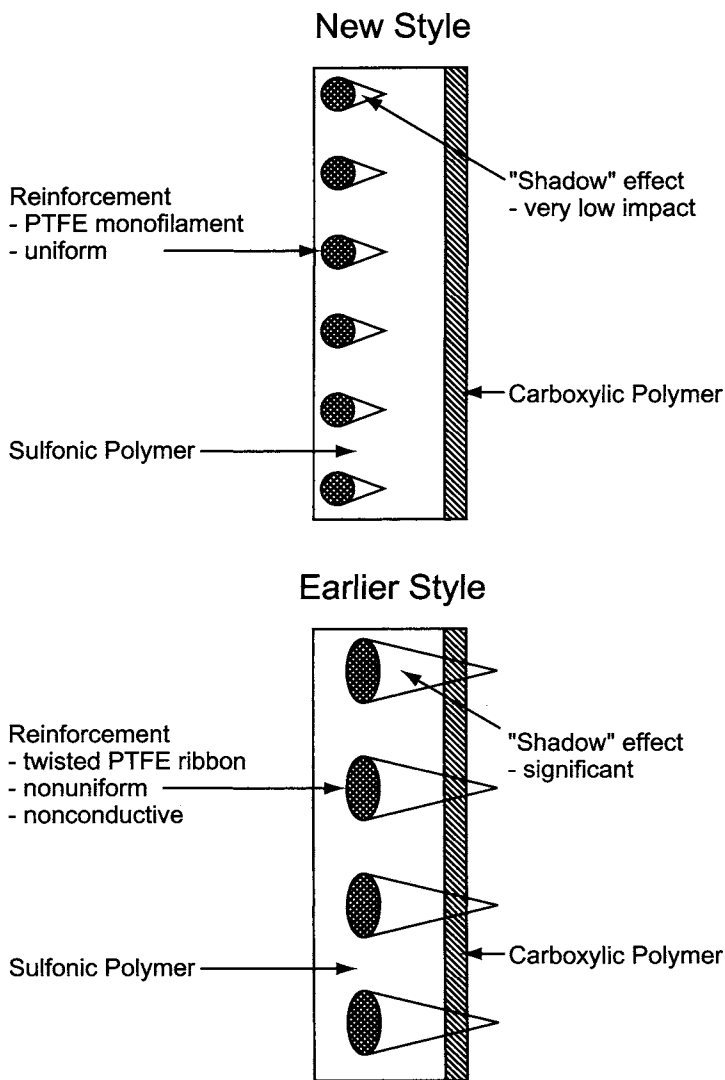


FIGURE 4.8.45. Shadow minimization with changing reinforcement configuration [144]. (With permission from E.I. duPont de Nemours & Co, Inc.)

Another important development is the nature of the fabric architecture. Figure 4.8.46 classifies the various membranes according to the type of polymer and the number of reinforcing fibers used. The use of more and thinner fibers increases mechanical strength (Table 4.8.16), besides providing low voltage and high efficiency. Thus, Nafion[®] 2002 showed 120 mV less than N90209, and 110 mV less than N960 membrane, at a current efficiency of >96% at the same current density. The NE 2010, which is the next generation of NX 982, was found to offer a voltage savings of 50 mV compared to 981, with significant resistance to Ni, Mg, and I in plant tests.

TABLE 4.8.14 Description of DuPont Membranes

Membrane type	Surface modification	Cell gap	Features
N90209	None	Finite	Introduced in 1982, still widely used in many types of cells.
N954	Cathode side	Finite and narrow	Cathode side surface modification allowed narrow gap cell operation to realize lower voltage than N90209.
N961	Cathode side	Finite and narrow	Introduced in 1985, provides low voltage.
N962	Anode and cathode side	Finite and narrow	Anode side modified version of N961 for better voltage stability.
N966	Anode and cathode side	Finite and narrow	Very high strength allows easier handling and more resistance to operational upsets.
NX2002	Anode and cathode side	Finite and narrow	Lower voltage but similar in strength to N966.
N981	Anode and cathode side	Finite and narrow	Lower voltage and improved brine imputity resistance achieved by polymer reinforcement and architecture modifications.
NX982	Anode and cathode side	Finite and narrow	Same performance as N981 with a stronger fabric.
NX2010	Anode and cathode side	Finite and narrow	Lower voltage with the same strength as NX982.

TABLE 4.8.15 Laboratory Cell Performance Data for Nafion[®] Membranes Noted in Table 4.8.14

Membrane type	Finite gap cell ^a		Narrow gap cell ^b	
	Cell voltage (V)	Current efficiency(%)	Cell voltage (V)	Current efficiency(%)
N90209	3.43	>95	—	—
N954	3.38	>95	3.15	>95
N961	—	—	3.05	>95
N962	—	—	3.05	>95
N966	3.4	>95	3.15	>95
NX2002	—	—	3	>95
N981	—	—	2.95	>95
NX982	—	—	2.95	>95
NX2010	—	—	2.92	>95

Notes:

^aConditions: 3 mm gap, DSA anode, bare Ni cathode, 32% NaOH, 200 gpl anolyte, 90°C, 3.1 kA m⁻².

^bConditions: 0 mm gap, DSA anode, activated Ni cathode, 32% NaOH, 200 gpl anolyte, 90°C, 3.1 kA m⁻².

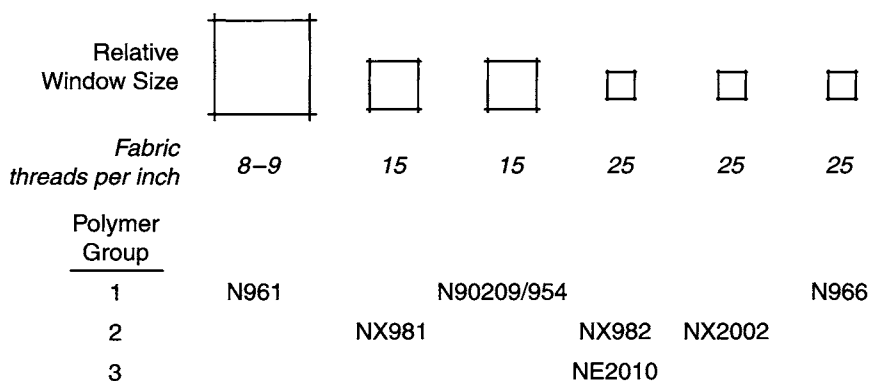


FIGURE 4.8.46. Fabric architecture of Nafion membranes [144]. (With permission from E.I. duPont de Nemours & Co, Inc.)

TABLE 4.8.16 Physical Properties of DuPont Membranes

	961	981	90209/954	982/2010	966/2002
Threads cm^{-1}	3.3	5.9	5.9	9.8	9.8
Denier	200	100	200	100	200
Tenacity (g d^{-1})	3	3	3	3	3
Tear (kgf)	0.8	1.5	2.5	2.4	5
Tensile strength (kg cm^{-1})	3.5	3	5.6	4	7.5

Thus, all the membrane manufacturers are focusing on a new class of structured membranes to achieve energy savings and tolerance to operational upsets.

Presently, commercial cells operate at caustic strengths of 32–35%, which require evaporation to produce the 50% product. Generally, the current efficiency vs NaOH concentration curves exhibit a maximum, which moves in the direction of higher concentration as the ion-exchange capacity increases to 0.8 m.eq g^{-1} dry resin [42,98,122,145–148]. Efforts will be in the direction of generating higher percentage caustic (at higher efficiency) in the future.

APPENDIX 4.8.1: EFFECTS OF IMPURITIES ON THE PERFORMANCE OF MEMBRANES (REPRODUCED FROM NAFION® TECHNICAL INFORMATION BULLETIN 91-08, BY PERMISSION OF THE DUPONT COMPANY)

Calcium (Ca)

Effect on Membrane: Calcium deposits as hydroxide, silicate, aluminate, and other compounds in the cathode layer of the membrane, and causes physical disruption (holes). Current efficiency can decline to as low as 85%.

Mechanism of Damage: Calcium salts deposit as large crystals in the carboxyl polymer near the cathode surface of the membrane. This causes physical disruption of the otherwise smooth polymer layer. Electron micrographs show craters and holes in the membrane surface.

Control Method—Commercial Experience: Calcium can effectively be removed from brine by ion-exchange treatment. Levels below 20 ppb are routinely achieved and values below 10 ppb have been reported.

Research Results: In a laboratory cell, brine, spiked with 5 ppm Ca^{2+} , lowered the current efficiency to ~90% in 90 days. The current efficiency (CE) decline at various levels of Ca^{2+} is noted below.

Ca^{2+} (ppb)	% loss in CE	Time (days)
1000	6	50
500	6	13
400	3.5	12
200	2.5	35

Recommended Analytical Methods

1. Colorimetry with a spectrophotometer and Hach reagents (Hach Company, *Handbook of Brine Analysis*, 2nd Edition, p. 9). Note: Detects Ca + Mg.
2. Inductively coupled plasma (ICP) chromatography or AA graphite furnace.

Magnesium (Mg)

Effect on Membrane: Magnesium in brine will increase voltage, but does not affect the current efficiency. A level of 5 ppm Mg in brine will increase the voltage by 100 mV in 2 days, 200 mV in 4 days.

Mechanism of Damage: Magnesium has low solubility at high pH, and will deposit as a fine particulate hydroxide primarily on the anode side of the membrane.

Control Method—Commercial Experience: Magnesium is present in most brines and is usually considered together with calcium as hardness, because the colorimetric analysis used does not distinguish between the cations. However, the ratio of calcium to magnesium influences the efficacy of the treatment of the brine, where the calcium carbonate and the magnesium hydroxide are made insoluble by the addition of soda ash and caustic soda to the raw brine. The efficiency with which those insolubles settle depends on the ratio of calcium to magnesium. If the ratio is two or greater, settling will usually occur unassisted. At lower ratios, a flocculating agent (acrylamides and acrylic acid) is added to facilitate settling. It is also important to prevent temperature-induced convection in the settling tank from disturbing the settling or redepositing of the precipitates. Efficient precipitation of the magnesium hydroxide in the primary treatment stage is necessary because at the high pH of brine, the hydroxide remains unionized and passes through the ion-exchange columns as a suspension in the brine. The more soluble calcium is removed by releasing the magnesium ion, which can enter the membrane and raise the voltage, if present, in sufficient quantity.

Recommended Analytical Methods: To analyze electrolyzer feed brine after the ion-exchanger, it is advisable to acidify the sample before testing. This will dissolve any magnesium hydroxide precipitates and make it detectable by colorimeter analysis. Such analysis will reveal any magnesium breakthrough because of upsets in the primary treatment.

1. Colorimetry with a spectrophotometer and Hach reagents (Hach Company, *Handbook of Brine Analysis*, 2nd Edition, p. 9). Note: Detects Ca + Mg.
2. ICP chromatography or AA graphite furnace.

Strontium (Sr)

Effect on Membrane: Excessive strontium in the brine raises the voltage and decreases the current efficiency. DuPont laboratory tests have shown that a voltage rise of 50 mV and a current efficiency decline of 3% can occur with large strontium excursions (e.g., 5 ppm for 1 month).

Mechanism of Damage: Strontium belongs to the alkaline earth family along with Mg, Ca, and Ba. Solubility of strontium hydroxide is greater than that of magnesium and calcium hydroxides (The order of solubility of the alkaline earth hydroxides is $Mg < Ca < Sr < Ba$). Consequently, strontium hydroxide will deposit near the cathode side of the membrane and cause physical damage to the polymer.

Control Method—Commercial Experience: Strontium is adsorbed on ion-exchange columns, but not as strongly as calcium. Furthermore, if an ion-exchange column is saturated with strontium, incoming calcium will displace strontium and release it to the brine system. Therefore, if strontium is known to be a significant impurity in the brine, the ion-exchange columns should be monitored for breakthrough of this ion, as well as calcium, and should be regenerated on that basis.

Recommended Analytical Methods:

1. ICP chromatography.
2. AA graphite furnace.

Barium (Ba)

Effect on Membrane: Barium, which precipitates as hydroxide or with iodine as paraperiodate, $Ba_3(H_2IO_6)_2$, slightly reduces current efficiency (0.5–1.0%) and causes small voltage increases (approximately 50 mV).

Mechanism of Damage: Barium will form finely divided periodate salts that deposit throughout the membrane.

Control Method—Commercial Experience: Barium can be removed by ion-exchange similar to calcium and behaves like Sr. If an ion-exchange column is saturated with barium, the incoming calcium will displace barium and release it to the brine system. Therefore, the ion-exchange columns should be monitored for breakthrough of this ion, as well as calcium, and should be regenerated on that basis.

Recommended Analytical Methods:

1. ICP chromatography.
2. AA graphite furnace.

Nickel (Ni)

Effect on Membrane: Nickel precipitates as Ni-oxides on the anode side of the membrane, resulting in increased cell voltage. The voltage escalation (ΔV), arising from the Ni levels in brine is shown below:

Ni (ppb)	ΔV (mV after 50 days)
10	90
25	120
100	170

Mechanism of Damage: Ni species from the brine or from the caustic side where it exists as HNiO_2^- can form Ni-oxides in the sulfonate layer and/or the sulfonate/carboxylate interface.

Control Method—Commercial Experience: Ni can be removed as Ni-oxide by reacting the raw brine with hypochlorite, followed by filtration or by ion-exchange with Duolite 467 resin at pH 2–3 to achieve levels of <2 ppb.

Recommended Analytical Methods: Extraction with methyl isobutyl ketone by complexing it with ammonium pyrrolidine dithiocarbonate, followed by evaporation to dryness, dissolving the residue in 5% HNO_3 , and analyzing by ICP technique.

Iodine (I)

Effect on Membrane: Iodine is sometimes present as an impurity in the raw salt and brine as iodide or iodate. It can precipitate as insoluble sodium paraperiodate near the membrane cathode layer, reducing the current efficiency.

Mechanism of Damage: The mechanism of iodine damage is known from DuPont research on brine impurity effects. Iodine, which is present as iodide, is oxidized to iodate, IO_3^- , in the anolyte. A fraction of the iodate passes into the membrane, where it is oxidized to periodate, IO_4^- . The sodium salt of periodate is only slightly soluble in alkaline solution. If the periodate concentration is high enough, sodium paraperiodate, $\text{Na}_3\text{H}_2\text{IO}_6$, precipitates, damaging the cathode layer and reducing current efficiency. Periodate in the membrane reacts with calcium and barium and other alkaline earth cations to form precipitates. The precipitates are finely divided and do not damage the membrane physically, and do not affect current efficiency or voltage. Iodide is not reported to be a problem in KCl electrolysis. This is probably a result of the increased solubility of potassium periodate with pH, unlike the sodium periodate whose solubility decreases with increasing pH.

Control Method—Commercial Experience: There is no effective method to chemically remove iodine from brine. However, ion-exchange methods are being developed to remove I_2 generated by treating the brine with chlorine (see Chapter 5 for details).

Recent Research: With brine containing 1 ppm iodide and 20–30 ppb calcium, iodine accumulates at the rate of $\sim 10 \text{ mg dm}^2 \text{ year}^{-1}$ with no change in current efficiency or voltage. This rate of accumulation will not affect performance in commercial use, as experience has demonstrated. However, at iodine levels above 1 ppm and at

normal hardness levels, current efficiency may decline through formation of sodium paraperiodate. The current efficiency loss at 10 ppm level is ~4% after 20 days and 10% at 100 ppm level in 10 days.

Recommended Analytical Methods: Colorimetry using Hach reagents (Hach Company, *Handbook of Brine Analysis*, 2nd Edition, p. 29).

Sodium Sulfate (Na₂SO₄)

Effect on Membrane: Sodium sulfate or its triple salt with NaOH and NaCl deposits in the membrane near the cathode side and reduces the current efficiency to ~93%. In the presence of Ba²⁺, BaSO₄ will form and coat the anode, which will increase the cell voltage.

Mechanism of Damage: Sodium sulfate deposits cause an interruption of the normally smooth cathode surface layer and thus, reduce the OH⁻ ion rejection capacity. The damage is similar to that observed with Ca deposits but occurs at much higher salt levels.

Control Method—Commercial Experience: Sodium sulfate concentration in the solution-mined brine is suppressed by additives that reduce the solubility of anhydrite. Sodium sulfate can be precipitated from brine with barium or calcium ions, and its concentration can be controlled by purging the brine system (see Chapter 7.5.7.2A for additional details).

References: Research from DuPont and others on sulfate in brine and its behavior in chlor-alkali membranes can be found in references [112,113] and

A. Herrera and H.L. Yeager, *J. Electrochem. Soc.* **134**, 2445 (1987).

Recommended Analytical Methods:

1. Gravimetric procedure as BaSO₄ precipitate.
2. ICP chromatography.

Aluminum (Al)

Effect on Membrane: Aluminum forms sodium aluminosilicates, which precipitate near the membrane cathode layer, causing physical damage to the polymer and reducing the current efficiency.

Mechanism of Damage: The source of aluminum, during the primary brine treatment, is from the clay in the salt. If filtration fails, the clay reaches the anolyte and dissolves, releasing the aluminum ions. The aluminum cations will pass into the membrane and change to the anionic form as they move toward the cathode side. The anionic aluminum will accumulate in the membrane by combining with other anions, such as silicates, and/or cations such as Na⁺, forming compounds that are precipitated, thereby damaging the membrane and reducing the current efficiency.

Control Method—Commercial Experience: Clarification and filtration of the brine can eliminate suspended clay. Also, it can be removed by ion-exchange in the acidic medium, using the cation-exchange resins such as Duolite-467 or precipitated as magnesium–aluminum silicate during the primary brine treatment.

Recommended Analytical Methods:

1. Colorimetry using Hach reagents (Hach Company, *Handbook of Brine Analysis*, 2nd Edition, p. 15).
2. ICP chromatography.
3. AA graphite furnace.

Silica (SiO₂)

Effect on Membrane: Silica in the membrane forms calcium silicate, which is less soluble than Ca(OH)₂, and precipitates near the membrane cathode surface, thus reducing the current efficiency.

Mechanism of Damage: Silica enters the membrane as a neutral or cationic species and becomes a soluble anion as the pH increases in the region closer to the cathode. Silica can then trap calcium and precipitate as calcium silicate. It can also react with aluminum to precipitate as sodium aluminosilicate. These precipitates can form large crystals near the membrane cathode surface, causing physical damage to the normally smooth surface and reduce the OH⁻ rejection capacity.

Control Method—Commercial Experience: Silica is present in some salt sources and also in the water used in making brine. It can normally be controlled in the feed water by ion-exchange or removed as solids during the primary brine treatment by reacting it with MgCl₂ (without upsetting the Ca : Mg ratio) to form Mg silicates, which can be carried out along with CaCO₃ and Mg(OH)₂.

Recommended Analytical Methods:

1. Colorimetry using Hach reagents (Hach Company, *Handbook of Brine Analysis*, 2nd Edition, p. 37).
2. AA graphite furnace.

REFERENCES

1. L.C. Curlin, T.V. Bommaraju, and C.B. Hansson, Chlorine and Sodium Hydroxide, In *Kirk-Othmer Encyclopedia of Chemical Technology*, 4th Edition, Vol. 1, John Wiley & Sons, New York (1991), p. 938.
2. F. Hine, B.V. Tilak, and K. Viswanathan, Chemistry and Chemical Engineering in the Chlor-Alkali Industry, In R.E. White, J.O'M. Bockris and B.E. Conway (eds), *Modern Aspects of Electrochemistry*, Vol. 18, Plenum Publishing Corp., New York (1986), p. 249.
3. W.G. Grot, *Chem. Ing. Techn.* **44**, 167 (1972).
4. W.G. Grot, *Chem. Ing. Techn.* **50**, 299 (1978).
5. W.G. Grot, *Chem. Ind. (London)*, (1980), p. 647.
6. W.G. Grot, V. Mehra, G.E. Munn, and J.C. Solenberger, Nafion[®] Electrolytic Separators, *Abstract # 344, Electrochemical Society Meeting*, Toronto, (1975).
7. W.G. Grot, *Chem. Ing. Techn.* **47**, 617 (1975).
8. O.D. Bonner and L.L. Smith, *J. Phys. Chem.* **61**, 326 (1957).
9. O.D. Bonner, W.L. Argensinger, and A.W. Davidson, *J. Am. Chem. Soc.* **74**, 1044 (1952).
10. D.J. Vaughan, *Dupont Innovation* **4**(3),10 (1973).
11. W.G. Grot, Discovery and Development of Nafion Perfluorinated Membranes: The SCI. Castner Medal Lecture. In K. Wall (ed.), *Modern Chlor-Alkali Technology*, Ellis Horwood Ltd, Chichester, Vol. 3, (1986), p. 122.
12. D.E. Maloney, Fluorocarbon Membranes for Chlor-Alkali Industry. In M.O. Coulter (ed.) *Modern Chlor-Alkali Technology*, Ellis Horwood Ltd, Chichester, Vol. 1 (1980), p. 173.
13. M. Seko, Ion Exchange Membranes for the Chlor-Alkali Electrolysis, *Abstract # 417, Electrochemical Society Meeting*, Minneapolis, MN, May 1981.

14. M. Seko, S. Ogawa, and K. Kimoto, Perfluorocarboxylic Acid Membranes and Membrane Chlor-Alkali Process Developed by Asahi Chemical Industry. In A. Eisenberg and H.L. Yeager (eds), *Perfluorinated Ionomer Membranes*, ACS Symposium Series 180, American Chemical Society (1982), p. 365.
15. M. Seko, New Development of the Asahi Chemical Membrane Chlor-Alkali Process. In *Proceedings of the Oronzio DeNora Symposium: Chlorine Technology*, Venice (1979), p. 141.
16. M. Seko, Ion-Exchange Membrane for the Chlor-Alkali process, ACS Polymer Division Workshop on Perfluorinated Ionomer Membranes, American Chemical Society, Lake Buena Vista, Florida, Feb 1982.
17. H. Ukihashi and M. Yamabe, Perfluorocarboxylate Polymer Membranes. In A. Eisenberg and H.L. Yeager (eds), *Perfluorinated Ionomer Membranes*, ACS Symposium Series 180, American Chemical Society (1982), p. 427.
18. Y. Ogata, T. Kojima, S. Uchida, M. Yasuda, and F. Hine, *J. Electrochem. Soc.* **136**, 91 (1989).
19. *U.S. Patent* 4,138,373 (1979).
20. *Japanese Patent* 116,790 (1977); 81,485; 76,282.
21. *British Patent* 1,522,877; 1,523,047
22. H. Ukihashi, *Chem. Tech.* Feb 1980.
23. T.D. Gierke and W.Y. Hsu, The Cluster Network Model of Ion Clustering in Perfluorosulfonated Membranes. In A. Eisenberg and H.L. Yeager (eds), *Perfluorinated Ionomer Membranes*, ACS Symposium Series 180, American Chemical Society (1982), p. 283.
24. W.Y. Hsu and T.D. Gierke, *J. Membrane Sci.* **13**, 307 (1983).
25. M. Falk, Infrared Spectra of Perfluorinated Polymers and of Water. In A. Eisenberg and H.L. Yeager (eds), *Perfluorinated Ionomer Membranes*, ACS Symposium Series 180, American Chemical Society (1982), p. 139.
26. S.J. Sondheimer, N.J. Bunce, and C.A. Fyfe, *Rev. Macromol. Chem. Phys.* **C26**, 353 (1986).
27. M. Pineri, R. Duplessix, and F. Volino, Neutron Studies of Perfluorinated Polymer Structure. In A. Eisenberg and H.L. Yeager (eds), *Perfluorinated Ionomer Membranes*, ACS Symposium Series, 180, American Chemical Society (1982), p. 249.
28. R.A. Komoroski and K.A. Mauritz, Nuclear Magnetic Resonance Studies and the Theory of Ion Pairing. In A. Eisenberg and H.L. Yeager (eds), *Perfluorinated Ionomer Membranes*, ACS Symposium Series, 180, American Chemical Society (1982), p. 113.
29. T. Kyu and A. Eisenberg, Mechanical Relaxations in Perfluorosulfonate Ionomer Membranes. In A. Eisenberg and H.L. Yeager (eds), *Perfluorinated Ionomer Membranes*, ACS Symposium Series, 180, American Chemical Society (1982), p. 79.
30. A.J. Hopfinger and K.A. Mauritz, Theory of Structures of Ionomeric Membranes. In J.O'M. Bockris, B.E. Conway, E. Yeager, and R.E. White (eds), *Comprehensive Treatise of Electrochemistry*, Vol. 2, Plenum Press, New York (1981), p. 521.
31. K.A. Mauritz and A.J. Hopfinger, Structural Properties of Membrane Ionomers. In J.O'M. Bockris, B.E. Conway, and R.E. White (eds), *Modern Aspects of Electrochemistry*, Vol. 14, Plenum Press, New York (1982), p. 425.
32. K.A. Mauritz, C.J. Hora, and A.J. Hopfinger, Theoretical Model for the Structures of Ionomers. In U. Landau, E. Yeager, and D. Kortan (eds), *Electrochemistry in Industry*, Plenum Press, New York (1982), p. 89.
33. A.J. Hopfinger, C.J. Hora, and K.A. Mauritz, Prediction of the Molecular Structure of Nafion[®] under Different Physicochemical Conditions, *Abstract # 439, Electrochemical Society Meeting*, Atlanta, Oct. 1977.
34. T.D. Gierke, Ionic Clustering in Nafion[®] Perfluorosulfonic Acid Membranes and its Relationship to Hydroxyl Rejection and Chlor-Alkali Current Efficiency, *Abstract # 438, Electrochemical Society Meeting*, Atlanta, GA (1977).
35. T.D. Gierke, G.E. Munn, and F.C. Wilson, Morphology of Perfluorosulfonated Membrane Products. In A. Eisenberg and H.L. Yeager (eds), *Perfluorinated Ionomer Membranes*, ACS Symposium Series 180, American Chemical Society (1982), p. 195.
36. M. Fujimura, T. Hashimoto, and H. Kawai, *Macromolecules* **14**, 1309 (1981); **15**, 136 (1982).
37. G.G. Sherer and P.P. Fluger, ESCA Investigation of Nafion Membranes. In J.W. VanZee, R.E. White, K. Kinoshita and H.S. Burney (eds), *Diaphragms, Separators and Ion-Exchange Membranes*, PV 86-13, The Electrochemical Society, Pennington, NJ (1986), p. 52.
38. M.V. Verbrugge and R.F. Hill, *J. Electrochem. Soc.* **137**, 886, 893 (1990).
39. E.H. Cwirko and R.B. Carbonell, *J. Membrane Sci.* **67**, 211, 227 (1992).
40. T.D. Gierke, G.E. Munn, and F.C. Wilson, *J. Polym. Sci. Phys. Edu.* **19**, 1987 (1980).

41. W.G. Grot, G.E. Munn, and P.N. Walmsley, Perfluorinated Ion Exchange Membranes (XR membranes), Abstract # 154 *Electrochemical Society Meeting*, Houston, TX (1972).
42. M. Seko, S. Ogawa, and K. Kimito, Perfluorocarboxylic Acid Membrane and Membrane Chlor-Alkali Process Developed by Asahi Chemical Industry, In A. Eisenberg and H.L. Yeager (eds), *Polyfluorinated Ionomer Membranes*, ACS Symposium Series # 180 (1982), p. 365.
43. R.S. Yeo, Intrinsic Conductivity of Perfluorosulfonic Acid Membranes and its Implication to the Solid Polymer Electrolyte (SPE) Technology, In R.S. Yeo, T. Katan, and D.T. Chin (eds), *Transport Processes in Electrochemical Systems*, Electrochemical Society, Pennington, NJ (1982), p. 178.
44. R.S. Yeo, *Polymer* **21**, 432 (1980).
45. T.A. Davis, J.D. Genders, and D. Fletcher, *A First Course in Ion Permeable Membranes*, The Electrochemical Consultancy, Alresford, Hants, U.K. (1977).
46. R.S. Yeo and A. Eisenberg, *J. Appl. Polym. Sci.* **21**, 875 (1977).
47. E.J. Roche, M. Pineri, and R. Duplessix, *J. Polym. Sci. Phys. Ed.* **20**, 101 (1982).
48. M. Falk, *Can. J. Chem.* **58**, 1495 (1980).
49. H. Yoshida and Y. Miura, *J. Membrane Sci.* **68**, 1 (1992).
50. R.S. Yeo, *J. Electrochem. Soc.* **130**, 533 (1983).
51. H. Ukihashi, M. Yamabe, and H. Miyake, *Prog. Polym. Sci.* **12**, 229 (1986).
52. T. Hanai, *Maku to Ion (Membranes and Ions)*, Kagaku Dojin, Kyoto (1978), p. 161.
53. F.G. Donnan and E.A. Guggenheim, *Z. Phys. Chem.* **A162**, 346 (1932).
54. K. Kimito, *J. Electrochem. Soc.* **130**, 334 (1983).
55. H. Riess and I.C. Bassigana, *J. Membrane Sci.* **11**, 219 (1982).
56. W.Y. Hsu, J.R. Barkley, and P. Meakin, *Macromolecules* **13**, 198 (1980).
57. C. Gavach, G. Pamboutzoglou, M. Nedyalkov, and G. Pourcelly, *J. Membrane Sci.* **45**, 37 (1989).
58. P.C. Rieke and N. Vanderborgh, *J. Membrane Sci.* **32**, 313 (1987).
59. T.A. Zawardowski, T.E. Springer, J. Davey, R. Jestel, C. Lopez, J. Valerio, and S. Gottesfeld, *J. Electrochem. Soc.* **140**, 1981 (1993).
60. N.I. Menshakava, V.L. Kubasov, and L.I. Khristalik, *Soviet Electrochemistry* **17**, 228 (1981).
61. B. Rodmacq, J.M. Coey, M. Escoubes, E. Roche, R. Duplessix, A. Eisenberg, and M. Pineri, Water Absorption in Neutralized Nafion Membranes, In S.P. Powland (ed.), *Water in Polymers*, ACS Symposium Series, **127** (1980), p. 487.
62. R.S. Yeo, J. McBreen, G. Kissel, F. Kulesa, and S. Srinivasan, *J. Appl. Electrochem.* **10**, 741 (1980).
63. R.L. Coalson and W.G. Grot, *U.S. Patent* 3,684,747 (1972).
64. T. Zwardowski, H.L. Yeager, and B. O'Dell, *J. Electrochem. Soc.* **129**, 328 (1982).
65. H.L. Yeager, Sodium Ion Diffusion and Migration in Perfluorinated Ionomer Membranes, In E.B. Yeager, B. Schumm, Jr., K. Mauritz, K. Abbey, D. Blankenship, and J. Akridge (eds.) *Membranes and Ionic and Electronic Conducting Polymers*, PV 83-3, The Electrochemical Society, Pennington, NJ (1982), p. 134.
66. A.B. LaConti, A.R. Fragale, and J.R. Boyack, Solid Polymer Electrolyte Electrochemical Cells: Electrode and Other Materials Considerations, In J.D.E. McIntyre, S. Srinivasan, and F.G. Will (eds), *Electrode Materials and Processes for Energy Conservation*, PV 77-6, The Electrochemical Society, Pennington, NJ (1977), p. 354.
67. R.S. Yeo and J. McBreen, *J. Electrochem. Soc.* **126**, 1682 (1979).
68. F.N. Buchi, M. Wakizoe, and S. Srinivasan, *J. Electrochem. Soc.* **143**, 927 (1996).
69. Z. Ogumi, Z. Takehara, and S. Yoshizawa, *J. Electrochem. Soc.* **131**, 769 (1984).
70. Y.T. Lee, K. Iwamoto, and M. Seno, *J. Membrane. Sci.* **49**, 85 (1990).
71. T. Sakai, H. Takenaka, and E. Torikai, *J. Electrochem. Soc.* **133**, 88 (1986).
72. H.L. Yeager and A.A. Gronowski, Factors Which Influence the Permselectivity of High Performance Chlor-Alkali Membranes, In T.C. Welligton (ed.), *Modern Chlor-Alkali Technology*, Vol. 5, Society of Chemical Industry, London (1992), p. 81.
73. T. Sata, K. Motani, and Y. Ohashi. Perfluorinated ion Exchange Membrane. Neosepta-F and its properties. In D.S. Flett (ed.), *Ion Exchange Membranes*, Society of Chemical Industry, London (1983), p. 137.
74. E.J. Hora and D.E. Maloney, Chemically Modified Nafion® Perfluorosulfonic Acid Membranes as Separators in Chlor-Alkali Cells, Abstract # 441, *Electrochemical Society Meeting*, Atlanta, GA (1977).
75. M. Seko, *U.S. Patent* 4,178,218 (1979).
76. C.J. Molnar, E.H. Price, and T. Gunjima, *U.S. Patent* 4,176,215 (1977).
77. T. Asawa, Y. Oda, and T. Gunjima, *Japanese Patent Appl.* 52-36589 (1977).

78. M. Seko, Y. Yamakoshi, H. Miyauchi, M. Fukomoto, K. Kimoto, I. Watanabe, T. Hane, and S. Tsushima, *U.S. Patent* 4,151,053 (1979).
79. W.G. Grot, C.J. Molnar, and P.R. Resnick, *Belgian Patent* 866122 (1978).
80. T. Sata, A. Nakahara, and J. Ito, *Japanese Patent Appl.* 53-137888 (1978).
81. K.A. Mauritz and A.J. Hopfinger, Structural Properties of Membrane Ionomers. In J.O'M. Bockris, B.E. Conway, and R.E. White (eds), *Modern Aspects of Electrochemistry*, Vol. 14, Plenum Press, New York (1982), p. 425.
82. D.N. Bennion, Experimental Measurement and Theoretical Interpretation of Membrane Transport of Concentrated Electrolytic Solutions, In E.B. Yeager, B. Schuum, K. Mauritz, K. Abbey, D. Blankenship, and J. Akridge (eds), *Proceedings Symposium on Membranes and Ionic and Electronic Conducting Polymers*, PV 83-3, The Electrochemical Society Inc. (1983), p. 78.
83. A. Eisenberg and H.L. Yeager (eds), *Perfluorinated Ionomer Membranes*, ACS Symposium Series, 180, American Chemical Society, Washington, D.C (1982).
84. E. Riande, Transport Phenomena in Ion-Exchange Membranes, In H. Jean (ed.), *Physical Electrolytes*, Academic Press, New York (1972), p. 401.
85. H.P. Gregor, *Pure and Appl. Chem.* **16**(2-3), 329 (1968).
86. Y. Mizutani, *J. Membrane Sci.* **49**, 121 (1990).
87. M.W. Verbrugge and P.N. Pintauro, Transport Models for Ion-Exchange Membranes, In B.E. Conway, J.O'M. Bockris and R.E. White (eds), *Modern Aspects of Electrochemistry*, vol 19, Plenum Press, New York (1989), p. 1.
88. C.A. Kruissink, *J. Membrane Sci.* **14**, 331 (1983).
89. R.L. Dotson, R.W. Lynch, and G.E. Hillard, Transport of Water Molecules and Sodium Ions Through Nafion[®] Ion Exchange Membranes, In R.S. Yeo and R.P. Buck (eds), *Ion-Exchange: Transport and Interfacial Properties*, PV 81-2, The Electrochemical Society, Pennington, NJ, (1981), p. 268.
90. R.L. Dotson and K.E. Woodard, Electrosynthesis with Perfluorinated Ionomer Membranes in Chlor-Alkali Cells. In A. Eisenberg and H.L. Yeager (eds), *Perfluorinated Ionomer Membranes*, ACS Symposium Series, 180, American Chemical Society, Washington, D.C (1982), p. 311.
91. R.A. Komoroski. In A.E. Eisenberg (ed.), *Ions in Polymers*, ACS Advances in Chemistry Series, 187 (1980), p. 155.
92. H.L. Yeager, B.O'Dell, and T. Zwardowski, *J. Electrochem. Soc.* **129**, 85 (1982).
93. H.L. Yeager, Transport Properties of Perfluorosulfonate Polymer Membranes. In A. Eisenberg and H.L. Yeager (eds), *Perfluorinated Ionomer Membranes*, ACS Symposium Series, 180, American Chemical Society, Washington, D.C (1982), p. 41.
94. C. Fabiani, S. Scuppa, L. Bimbi, and M. deFrancesco, *J. Electrochem. Soc.* **130**, 583 (1982).
95. C.P. Chen and B.V. Tilak, *J. Appl. Electrochem.* **26**, 235 (1996).
96. *DuPont Technical Bulletin*, 84-3 (1984); 88-1 (1989); 92-2 (1992).
97. J.T. Keating, Understanding Membrane Operating Conditions. In T.C. Wellington (ed.) *Modern Chlor-Alkali Technology*, Vol. 5, Elsevier Applied Science, London, (1992), p. 69.
98. M. Seko, J. Omura, and M. Yoshida, Recent Developments in Ion Exchange Membranes for Chlor-Alkali Electrolysis. In K. Wall (ed.) *Modern Chlor-Alkali Technology*, Vol. 3, Ellis Horwood, Chichester, (1986), p. 178.
99. H. Miyake, N. Sugaya, and M. Yamabe, *Reports Res. Lab. Asahi Glass Co. Ltd.* **37**, 241 (1987).
100. A. Herrera and H.L. Yeager, *J. Electrochem. Soc.* **134**, 2446 (1987).
101. H. Ukihashi, M. Yamabe, and H. Miyake, *Prog. Polym. Sci.* **12**, 229 (1986).
102. J.T. Keating, Personal Communication (1995).
103. Y. Ogata, S. Uchiyama, M. Hayashi, M. Yasuda, and F. Hine, *J. Appl. Electrochem.* **20**, 555 (1990).
104. H. Obanawa, H. Naoki, H. Takei, and H. Hoda, Simulation of Ion Behavior in Ion Exchange Membranes. In S. Sealy (ed.) *Modern Chlor-Alkali Technology*, Vol. 7, Royal Society of Chemistry, Cambridge (1998), p. 113.
105. S. Banerjee, Understanding Membrane Operating Conditions, In *ELTECH Chlorine/Chlorate Seminar*, ELTECH Systems Corp., Cleveland, OH, Sept. 1999.
106. W.F. Linke, *Solubilities*, originated by A. Seidell, 4th Edition, Vol. 1, p. 379; Vol. 2, p. 1513, American Chemical Society, Washington, D.C 1958 and 1965.
107. D.D. Wagman, W.H. Evans, V.B. Parker, R.H. Schumm, I. Halow, S.M. Barriley, K.L. Churney, and R.L. Nuttall, *J. Phys. Chem. Ref. Data* **11**, suppl. 2 (1982).

108. G.N. Lewis and M. Randall, *Thermodynamics*, 2nd Edition, Revised by K.S. Pitzer and L. Brewer, McGraw-Hill Book Co., New York (1961).
109. J.H.G. Van der Stegen and P. Breuning, The Formation of Precipitates of Iron Ions Inside Perfluorinated Membranes During Chlor-Alkali Electrolysis. In S. Sealy (ed.) *Modern Chlor-Alkali Technology*, vol. 7, Royal. Soc. Chem. Cambridge (1995), p. 123.
110. *Supplement to Mellor's Comprehensive Treatise on Inorganic and Theoretical Chemistry*, vol. 2, Supplement 2, The Alkali Metals, Part 1, Longmans, London (1964), p. 1018.
111. W.F. Linke (ed.) *Solubilities—Inorganic and Metal Organic Compounds*, vol. 2, 4th ed, American Chemical Society, Washington, D.C (1965), p. 1130.
112. J.T. Keating, Sulfate Deposition and Current Distribution in Membranes for Chlor-Alkali Cells. In F. Hine, W.B. Darlington, R.E. White, and R.D. Varjian (eds), *Electrochemical Engineering in the Chlor-Alkali and Chlorate Industries*, PV 88-2, The Electrochemical Society Pennington, NJ (1988), p. 311.
113. T.C. Bissot, Sulfate Ion Transport Through Perfluorinated Chlor-Alkali Membranes. In U. Landau, R.E. White, and R.D. Varjian (eds), *Engineering of Industrial Electrolytic Processes*, PV 86-8, The Electrochemical Society, Pennington, NJ (1986), p. 194.
114. E.A. Zezina, Yu.M. Popkov and S.F. Timashev, *Russian J. Electrochem.* **34**, 946 (1998).
115. D.C. Brandt, The Economics of Producing High-Strength Caustic Soda in Membrane Cells, 32nd Chlorine Institute Plant Managers Seminar, Washington, D.C (1989).
116. T.C. Bissot, Mechanism of Silica Damage to Chlor-Alkali Membranes, *Abstract # 439, Electrochemical Society Meeting*, Boston, MA, May 1986.
117. T.C. Bissot, Mechanism of Silicate Damage to Chlor-Alkali Membranes. In J.W. Van Zee, R.F. White, K. Kinoshita, and H.S. Burney (eds), *Diaphragms, Separators and Ion Exchange Membranes*, PV86-13, Electrochemical Society Pennington, NJ (1986), p. 42.
118. D.L. Liczwek, Impurity Damage to Chlor-Alkali Membranes. In F. Hine, W.B. Darlington, R.E. White, and R.D. Varjian (eds), *Chlor-Alkali and Chlorate Industries*, PV 88-2, The Electrochemical Society, Pennington, NJ (1988), p. 284.
119. J.T. Keating and K.J. Behling, Brine Impurities and Membrane Cell Performance. In N.M. Prout and J.S. Moorhouse (eds) *Modern Chlor-Alkali Technology*, Vol. 4, Elsevier Applied Science, London (1990), p. 125.
120. F. Hine, T. Ohtsuka, M. Hayashi, K. Suzuki, and Y. Ogata, *J. Appl. Electrochem.* **21**, 781 (1991).
121. E.G. Rochow, Silicon. In J.C. Bailar, H.J. Emeleus, R. Nyholm, and A.F. Trotman-Dickerson (eds) *Comprehensive Inorganic Chemistry*, Vol. 1, Pergamon Press, Oxford (1973), p. 1323.
122. H. Shiroki, T. Hiyoshi, and T. Ohta, Recent Development and Operation Dynamics of New Ion Exchange Series Aciplex[®]-F from Asahi Chemical. In T.C. Wellington (ed.), *Modern Chlor-Alkali Technology*, Vol. 5, Elsevier Applied Science, London (1992), p. 117.
123. *Nafion[®] Technical Bulletin*, 91-09, DuPont Co (2000).
124. *Nafion[®] Technical Bulletin*, 88-06, DuPont Co (1988).
125. K. Yamaguchi, T. Ichisaka, and I. Kumagai, The Control of Brine Impurities in the Membrane Process in the Chlor-Alkali Industry. In *Chlorine Institute's 29th Plant Operation Seminar*, Tampa, FL (1986).
126. *Nafion[®] Technical Bulletin*, 91-08, DuPont Co. (1991).
127. H. Obanawa, Effect of Brine Impurities and Blisters and Membrane Service Life. In *ELTECH's 16th Annual Chlorine/Chlorate Seminar*, ELTECH Systems Corporation, Cleveland, OH (2000).
128. H.M.B. Gerner and R.D. Theobald, Global Operating Experience With Ion-Exchange Membranes, in *Modern Chlor-Alkali Technologies*. In R.W. Curry (ed.), *Modern Chlor-Alkali Technology*, Vol. 6, Royal. Society of Chemistry, Cambridge (1995), p. 173.
129. D.L. Peet, Membrane Durability in Chlor-Alkali Plants, In F. Hine, W.B. Darlington, R.E. White, and R.D. Varjian (eds), *Electrochemical Engineering in Chlor-Alkali and Chlorate Industries*, PV 88-2, Electrochemical Society (1988), p. 329.
130. J.T. Keating and H.M.B. Gerner, High Current Density Operation—The Behavior of Ion Exchange Membranes in Chlor-Alkali Electrolyzers. In S. Sealy (ed.), *Modern Chlor-Alkali Technology*, Vol. 7, Royal. Society of Chemistry, Cambridge (1995), p. 135.
131. J.H. Austin, Nafion[®] Perfluorinated Membranes Operation in Chlor-Alkali Plants. In K. Wall (ed.) *Modern Chlor-Alkali Technology*, Vol. 3, Ellis Horwood, Chichester (1986), p. 131.
132. D. Bergner and M. Hartmann, *J. Appl. Electrochem.* **24**, 1201 (1994).
133. M. Seko, J. Omura, and M. Yoshida, Recent Developments in Ion Exchange Membranes for Chlor-Alkali Electrolysis. In K. Wall, (ed.), *Modern Chlor-Alkali Technology*, Vol. 3, Ellis Horwood Ltd, Chichester (1986), p. 178.

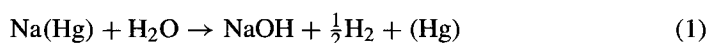
134. M. Nagamura, H. Ukihashi, and O. Shiragami, Chlor-Alkali Process with Flemion[®]. In M.O. Coulter, (ed.), *Modern Chlor-Alkali Technology*, Ellis Horwood Ltd, Chichester (1980), p. 195.
135. M. Nagamura, H. Ukihashi, and O. Shiragami, AZEC System—New Ion Exchange Membrane Chlor-Alkali Process. In C. Jackson, (ed.), *Modern Chlor-Alkali Technology*, Vol. 2, Ellis Horwood Ltd, Chichester (1983), p. 61.
136. T. Yamashita, Y. Sajima, and H. Ukihashi, The Design and Operating Experiences of AZEC Electrolyzers and Recent Development of Flemion Membranes. In N.M. Prout and J.S. Moorhouse (eds) *Modern Chlor-Alkali Technology*, Vol. 4, Elsevier Applied Science, London (1990), p. 109.
137. H. Miyake, The Design and Development of Flemion Membranes. In T.C. Wellington (ed.) *Modern Chlor-Alkali Technology*, Vol. 5, Elsevier Applied Science, London (1992), p. 59.
138. Y. Sajima, M. Nakao, T. Shimohira, and H. Miyake, Advances in Flemion Membranes for Chlor-Alkali Production. In T.C. Wellington (ed.), *Modern Chlor-Alkali Technology*, Vol. 5, Elsevier Applied Science, London (1992), p. 159.
139. M. Nakao and H. Miyake, Advanced Cell Operations with Flemion Membranes. In R.W. Curry (ed.), *Modern Chlor-Alkali Technology*, Vol. 6, Royal Society of Chemistry, Cambridge (1994), p. 185.
140. N. Nakao, T. Shimohira, and Y. Takechi, High Performance Operation with Flemion Membranes and the AZEC Electrolyzer. In S. Sealey (ed.), *Modern Chlor-Alkali Technology*, Vol. 7, Royal Society Chemistry, Cambridge (1998).
141. T. Shimohira, T. Kimura, T. Uchibori, and H. Takeda, Advanced Cell Technology with Flemion[®] Membranes and the AZEC[®] Bipolar Electrolyzer. In J. Moorhouse (ed.), *Modern Chlor-Alkali Technology*, Vol. 8, Society of Chemical Industry, Blackwell Science, Oxford (2001), p. 237.
142. *DuPont Bulletin # 97-01*, Rev. 10/13/00 (2000).
143. P. Sedor, *DuPont Presentation, Membrane development review to customers* (2001).
144. C. Bricker, *DuPont Presentation, Membrane development review to customers* (2001).
145. M. Seko, H. Miyauchi, and O. Shiragami, New Development of the Asahi Chemical Membrane Chlor-Alkali Process. In M.O. Coulter (ed.), *Modern Chlor-Alkali Technology*, Ellis Horwood, Chichester (1980), p. 195.
146. Y. Sajima, M. Nakao, T. Shimohira, and H. Miyake, Advances in Flemion Membranes for Chlor-Alkali Production. In T.C. Wellington (ed.), *Modern Chlor-Alkali Technology*, Vol. 5, Elsevier Applied Science, London (1992), p. 159.
147. K.-J. Behling and D.L. Peet, Influence of System Design and Operation Parameters on Membrane Performance. In N.M. Prout and J.S. Moorhouse (eds), *Modern Chlor-Alkali Technology*, Vol. 4, Elsevier Applied Science, London (1990), p. 63.
148. T. Shimohira, Y. Saito, K. Saito, and H. Miyake, *Reports Res. Lab. Asahi Glass Co. Ltd.* **43**(2), 119 (1993).

4.9. AMALGAM DECOMPOSITION

4.9.1. Introduction

The three major steps in the amalgam chlor-alkali process, shown in Fig. 4.9.1, are brine treatment, electrolysis, and amalgam decomposition. Purified brine is sent to the electrolyzer to produce chlorine and sodium amalgam at the anode and cathode, respectively. The sodium amalgam is then sent to the amalgam decomposer to produce caustic soda of 50% concentration. Mercury, after decomposition, is recycled to the top of the cell.

The overall process of amalgam decomposition can be described as:



This reaction is facilitated by contacting the sodium amalgam with graphite, as illustrated in Fig. 4.9.2. The amalgam decomposition reaction is an electrochemical process

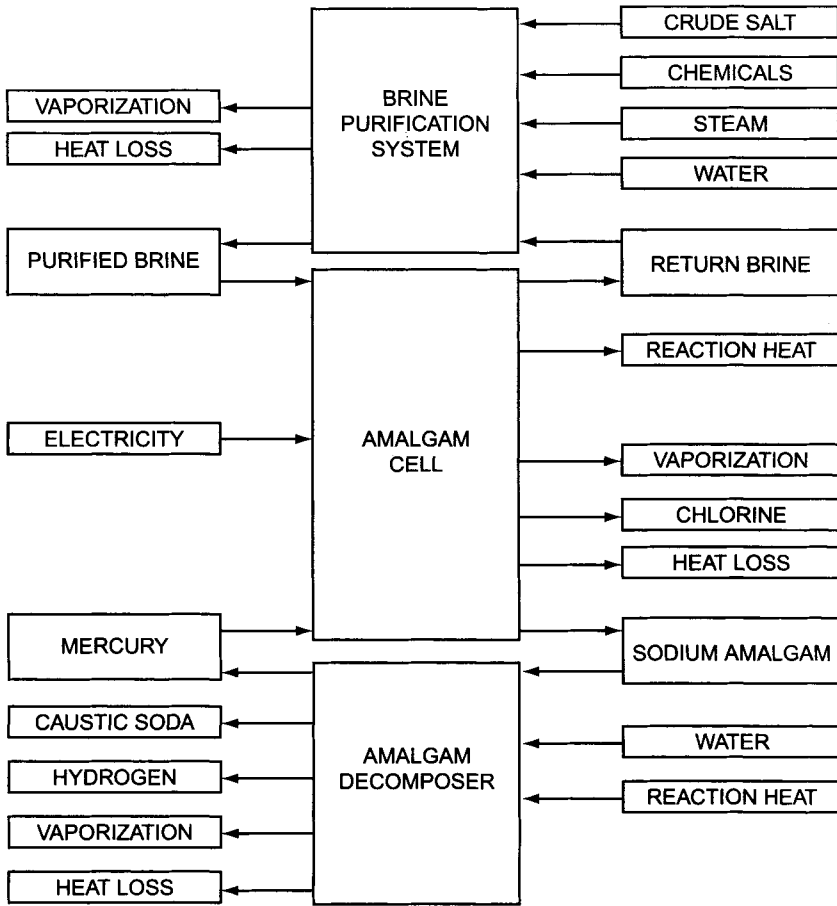


FIGURE 4.9.1. Material and energy balance in an amalgam chlorine plant.

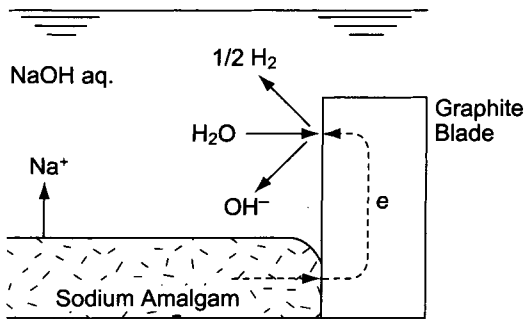
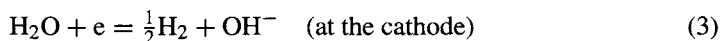
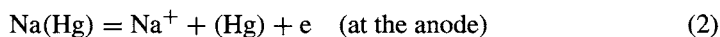


FIGURE 4.9.2. Schematic of the amalgam decomposition process.

consisting of the anodic dissolution of Na from the amalgam anode, and the cathodic discharge of hydrogen at the graphite surface, under short-circuiting conditions in caustic solutions, as shown by Eqs. (2) and (3).



The electrode potential for reaction (1) is given as:

$$E_f = E_f^0 + \frac{RT}{F} \ln \frac{a_{\text{Na(Hg)}} a_{\text{H}_2\text{O}}}{a_{\text{NaOH}} \sqrt{p_{\text{H}_2}}} \quad (4)$$

where E_f^0 is the standard electrode potential, which is a function of temperature, $a_{\text{Na(Hg)}}$ is the activity of sodium amalgam, which depends on the amalgam concentration and temperature, $a_{\text{H}_2\text{O}}$ and a_{NaOH} are the activities of H_2O and NaOH , respectively, which are functions of the NaOH concentration and temperature, and p_{H_2} is the partial pressure of hydrogen, which is assumed here to be constant. Thus, E_f is a function of the amalgam concentration and the NaOH concentration at a given temperature. E_f is composed of the sum of the overvoltages of anodic and cathodic processes (2) and (3), and the solution IR drop. The overvoltage of the amalgam anode is very small (Fig. 4.9.3 and Section 4.2.5). The hydrogen overvoltage on the graphite cathode is almost independent of the caustic concentration and is a linear function of current density below 0.5 kA m^{-2} .

In the original design, a horizontal trough is annexed to a horizontal electrolyzer in parallel. The mercury flows through the cell by gravity, and the sodium concentration in the amalgam increases during electrolysis to about 0.2% by weight. The concentrated amalgam is brought to the second trough with a number of graphite combs, where a

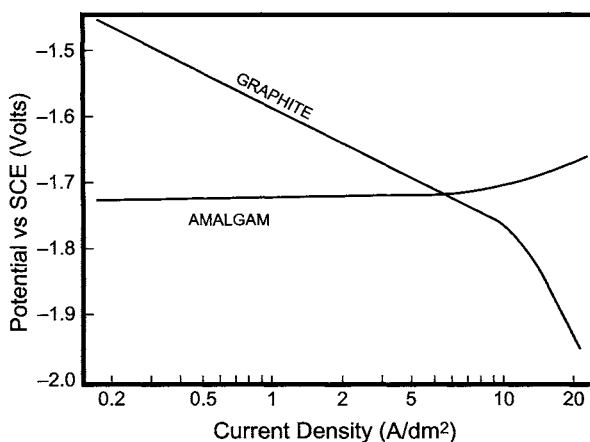


FIGURE 4.9.3. Anodic and cathodic polarization data in 40 w/o caustic solutions at 80°C . Concentration of Na in the amalgam: 0.2 w/o [1].

short-circuited galvanic cell composed of the amalgam anode and graphite blade (hydrogen cathode) is established, as illustrated in Fig. 4.9.2, and the amalgam is decomposed on the way back to the lower end of the trough, also by gravity. The mercury or very dilute amalgam, after decomposition, is then pumped up to the top end box of the electrolyzer, located just 20–40 cm above, depending on the cell design.

The vertical amalgam decomposer, packed with graphite lumps, was developed in the 1960s. A tower about a meter high is located at the lower end of the electrolyzer, and the sodium amalgam decomposes as it flows through the packed column by gravity. Mercury is recycled to the cell top. The head of mercury is high compared with the horizontal decomposer, and specially designed mercury pumps are required. Nevertheless, the use of the decomposition tower optimizes the floor space in the electrolysis area.

4.9.2. Design Aspects of the Amalgam Decomposer

We may now consider the energy and material balance [2] associated with the decomposition tower, shown in Fig. 4.9.4. The voltage balance of the tower can be represented as:

$$E_h = E_f - \Delta E_h = -\eta_c + IR \text{ (solution)} \quad (5)$$

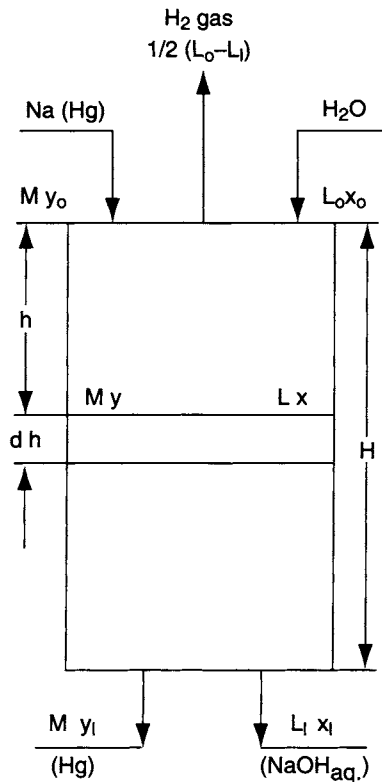


FIGURE 4.9.4. Material balance in the amalgam decomposer [1].

where E_h is the effective EMF, ΔE_h is the intercept of the potential vs current density plot at $i = 0$, η_c is the hydrogen overvoltage, and IR (solution) is the solution IR drop. The current per unit height of the tower, I , is:

$$\begin{aligned} I &= K_H F S (-\eta_c) \quad (\text{cathode process}) \\ &= K_F F S \kappa [E_h - (-\eta_c)] \quad (\text{solution IR}) \\ &= K F S E_h \quad (\text{overall}) \end{aligned} \quad (6)$$

where S is the cross-sectional area of the tower, F is the Faraday constant, K_H , K_F , and K are the coefficients, and κ is the conductivity of the caustic soda solution. Hence,

$$\frac{1}{K} = \frac{1}{K_H} + \frac{1}{\kappa K_F} \quad (7)$$

The amount of caustic produced, dw , in a small section of height, dh , is:

$$dw = -M dy = d(Lx) = -dL \quad (8)$$

By Faraday's law, we have,

$$dw = \frac{I}{F} dh \quad (9)$$

From Eqs. (8) and (9),

$$d(Lx) = K E_h S dh \quad (10)$$

or

$$-M dy = K E_h S dh \quad (11)$$

where M is the mercury flow (kg mol hr^{-1}), L is the water flow (kg mol hr^{-1}), y is the Na concentration ($\text{kg mol Na/kg mol Hg}$), and x is the NaOH concentration ($\text{kg mol NaOH/kg mol H}_2\text{O}$). By integration,

$$SH = \int_{L_0 x_0}^{L_1 x_1} \frac{d(Lx)}{K E_h} \quad (12)$$

and

$$\frac{SH}{M} = - \int_{y_0}^{y_1} \frac{dy}{K E_h} = - \frac{1}{K} \int_{y_0}^{y_1} \frac{dy}{E_h} \quad (13)$$

where 0 and 1 denote the top and the bottom of the tower, respectively, and H is the height of the tower. Equation (13) can be used to calculate the required volume of the amalgam decomposer.

Chilton and Colburn have employed the idea of the number of transfer units (NTU) and the height of the transfer unit (HTU) to describe packed columns [3] according to which the height, H , is represented by the product:

$$H = (\text{HTU})(\text{NTU}) \quad (14)$$

where HTU has the dimensions of length and NTU is dimensionless.

Since K is independent of y , due to the negligibly small polarization of the anode (see Section 4.2.5), Eq. (13) can be recast as:

$$\text{NTU} = - \int_{y_0}^{y_1} \frac{dy}{E_h} \quad (15)$$

$$\text{HTU} = M/KS \quad (16)$$

The value of NTU can be evaluated using Eq. (15), if the concentration of caustic soda solution and the operating temperature are kept constant.

An empirical relation, obtained with laboratory and plant data [2], relating E_h to the various operating parameters, is given by

$$E_h = -0.910x + 11.0y - 270.0y^2 + 0.9060 + 0.0005(70 - t) - 15.977t^{-0.928} \quad (17)$$

where t is the temperature in degrees celsius. This relationship is valid for 10–50% NaOH, 0–0.25% Na in the amalgam, and 50–90°C.

Substituting Eq. (17) into (15), results in:

$$\text{NTU} = \frac{2}{F(x, t)} \left[\tan^{-1} \frac{11 - 540y}{F(x, t)} \right]_{y_0}^{y_1} \quad (18)$$

$$[F(x, t)]^2 = 1099.48 + 0.54(70 - t) - 17280t^{-0.928} - 982.8x \quad (19)$$

where $F(x, t)$ is a function of x and t . $F(x, t)$, since it depends on temperature and caustic concentration, is called the “operation factor.” Figure 4.9.5 graphs the relationship of Eq. (19). $F(x, t)$ can be combined with amalgam concentrations in Eq. (18) to calculate the number of transfer units required. Figure 4.9.6 also shows the value of NTU as a function of the concentration of the amalgam and of the operation factor when $y_1 = 0$.

Next, the value of HTU must be determined. This may be represented as a function of the flow of mercury and of the specific conductivity of the caustic soda solution in the tower.

It is desirable to maximize the overall mass transfer coefficient, K . The relationship between K and the flow rate of mercury, measured experimentally at 50°C with 25% NaOH using 10 mm diameter spheres as the packing medium [1,2], is shown in Fig. 4.9.7. These results reveal the proper flow rate to be in the range of 300–450 kg mol hr⁻¹ m⁻² or 80–110 L min⁻¹ m⁻².

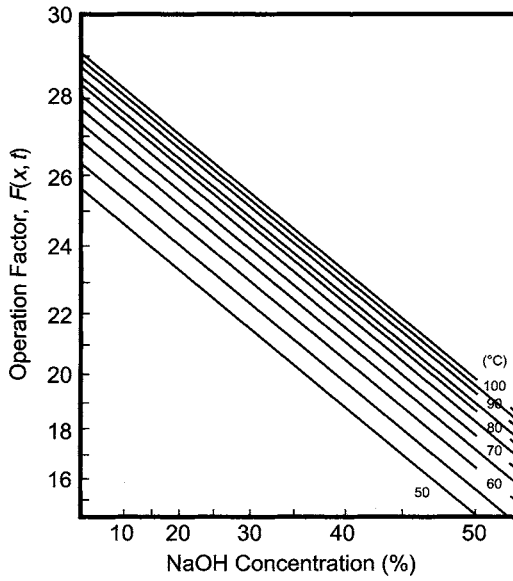


FIGURE 4.9.5. Operation factor as a function of caustic soda solutions at various temperatures [1].

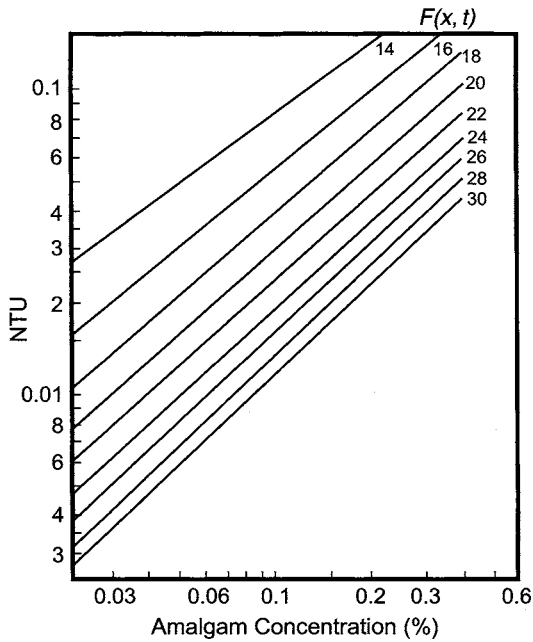


FIGURE 4.9.6. NTU of the amalgam decomposition tower as a function of the amalgam concentration and of the operation factor under the condition of $y_1 = 0$ [1].

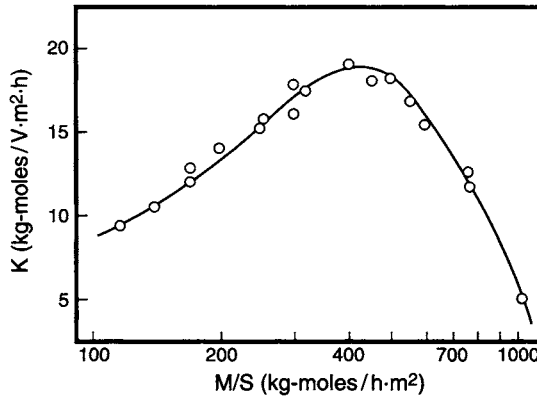


FIGURE 4.9.7. Relationship between K and M/S in 25% caustic soda at 50°C with packed spheres of 10-mm diameter [1].

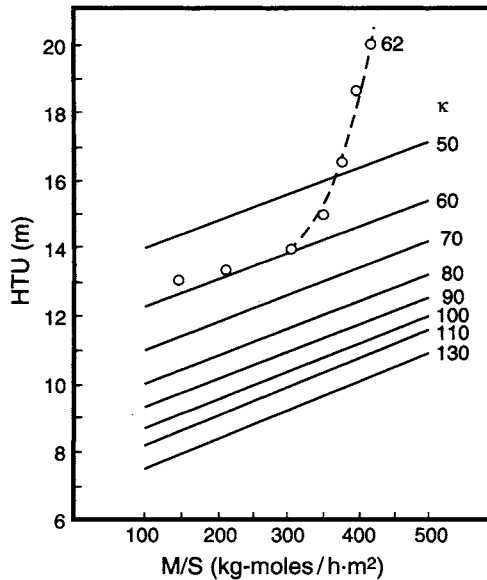


FIGURE 4.9.8. HTU of the amalgam decomposer tower as a function of the flow velocity of mercury and the specific conductivity of the caustic soda solution. κ refers to the conductivity of NaOH solution in mho m^{-1} [1].

Values of HTU as a function of the flow velocity of mercury, M/S , and the specific conductivity of caustic soda, κ , are shown in Fig. 4.9.8. It may be noted that, in practice, poor distribution occurs at low values of M/S , and flooding takes place at large mercury flow rates. An example of the flooding of mercury, observed during a field test, is shown by the dashed line labeled $\kappa = 62$ in Fig. 4.9.8. There was reasonable agreement with the solid line, $\kappa = 60$, up to $M/S = 300$, above which the tower was considered to have been flooded. The important factors for avoiding flooding are: uniform flow distribution

of amalgam and the shape of the packings. Proper attention to these allows operating the decomposer without flooding, even at $M/S = 400$.

A sample calculation is provided here for the conditions noted below.

Total current	100 k A
Concentration of amalgam	
At top	0.21%
At bottom	0.01%
Concentration of product caustic	50%
Operating temperature	90°C.

Minimum sectional area: The flow rate of mercury is 52.7 L min^{-1} or $213 \text{ kg mol hr}^{-1}$. A value of $99 \text{ L min}^{-1} \text{ m}^{-2}$ ($400 \text{ kg mol hr}^{-1} \text{ m}^{-2}$) is assumed for M/S . Hence, the minimum area should be:

$$S = \frac{52.7}{99} = 53.3 \times 10^{-2} (\text{m}^2)$$

Thus, the diameter of the column is 0.83 m.

Minimum height: The specific conductivity of 50% caustic soda solution at 90°C is 100.2 mho m^{-1} , hence, from Fig. 4.9.8, the value of HTU at $M/S = 400$ is about 11.10. From Fig. 4.9.5, the operation factor is obtained as $F(x, t) = 19.5$. Therefore, the NTU from Fig. 4.9.6 is 5.8×10^{-2} , and the minimum height is:

$$H = (\text{HTU})(\text{NTU}) = 11.10 \times 5.8 \times 10^{-2} = 0.644 \text{ m}$$

Table 4.9.1 shows that the exothermic heat of reaction is slightly more than $7,000 \text{ kcal hr}^{-1}$. This supplies the heat of formation of the caustic solution and then contributes about $5,000 \text{ kcal hr}^{-1}$ to the sensible heat of the flowing mercury. Therefore, the operating temperature, t , of the amalgam decomposition tower depends on the flow rate and the incoming temperature of mercury or amalgam, $t_{\text{Na-Hg}}$. A typical temperature increase is about 20°C.

An empirical equation (20) developed to estimate the temperature [2], is shown below

$$t = [t_{\text{Na-Hg}} + (377 - 2.48p)\Delta q] \left[1 - \frac{55.4}{p} \Delta q \right] \quad (20)$$

$$\Delta q = q_0 - q_1$$

where p is the NaOH concentration in percent by weight and q is the Na concentration in the amalgam in percent by weight. At $t_{\text{Na-Hg}} = 80^\circ\text{C}$, $p = 50\%$, and $\Delta q = 0.2\%$, the operating temperature is estimated to be 102°C .

TABLE 4.9.1 An Example of Heat Balance in the Amalgam Decomposer

	kcal hr ⁻¹
Input	
Sensible heat of mercury flow	28,118
Sensible heat of water	702
Heat of reaction	7,171
Total	35,991
Output	
Sensible heat of mercury flow	33,364
Sensible heat of caustic soda	2,363
Sensible heat of hydrogen gas	95
Latent heat of water	129
Heat loss	40
Total	35,991

Conversion factors required for these calculations are noted below.

$$M = 4.04Q \quad \begin{array}{l} M = \text{Hg, kg mol hr}^{-1} \\ Q = \text{Hg, L min}^{-1} \end{array} \quad (21)$$

$$x = \frac{0.45p}{100 - p} \quad \begin{array}{l} x = \text{NaOH, kg mol/kg mol H}_2\text{O} \\ p = \text{NaOH in percent by weight} \end{array} \quad (22)$$

$$y = 8.75 \times 10^{-2}q \quad \begin{array}{l} y = \text{Na, kg mol/kg mol Hg} \\ q = \text{Na in percent by weight in the amalgam} \end{array} \quad (23)$$

$$Q = \frac{0.1056J}{q_0 - q_1} \quad J = \text{total current of the electrolyzer in kA} \quad (24)$$

Figures 4.9.9 and 4.9.10 depict the minimum height of a decomposer column as a function of the operating temperature and the Na concentration in the amalgam, respectively. These plots show that a tall tower is needed when the amalgam concentration is high, as the NTU is large and the decomposer must be operated at high temperatures to let the reaction proceed effectively. Cooling the decomposer leads to the incomplete decomposition of the amalgam, which in turn affects the performance of the electrolyzer. Lowering the temperature of the decomposer lowers the efficiency, since the mass transfer coefficient is lowered, and thereby leads to an increase in the overall energy consumption of the process. Thus, it is essential to operate the decomposers at a uniform flow rate of mercury, and at high temperatures to ensure complete decomposition of the amalgam. Optimization of a given decomposer was achieved in Japan when employing two separate baskets (with space between the basket and the wall for hydrogen escape), which closely adhered to the design parameters shown in Fig. 4.9.9.

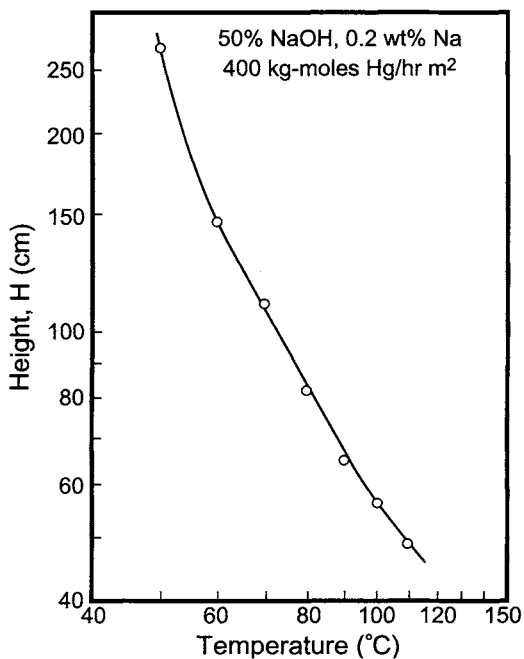


FIGURE 4.9.9. Minimum height vs temperature in the decomposition tower [1].

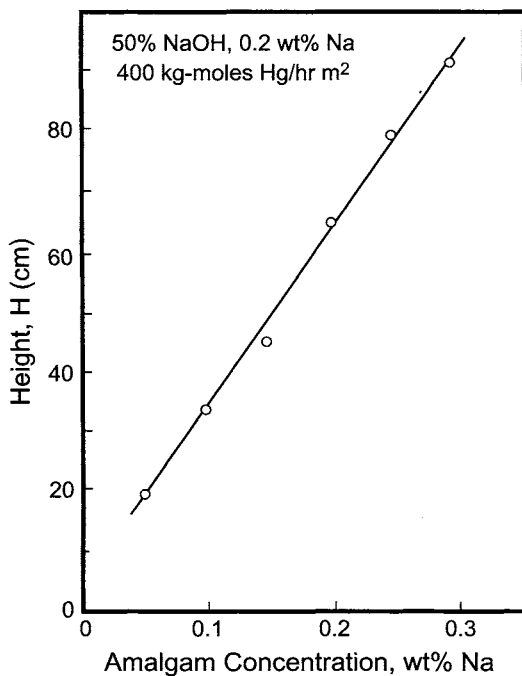


FIGURE 4.9.10. Minimum height vs amalgam concentration in the decomposition tower [1].

4.9.3. Graphite Packings

In the United States and Europe, many plants employ graphite lumps, while the usage of graphite balls is popular in Japan—the optimal diameter of the graphite ball being 15 mm, and the average diameter of the graphite lumps being 10–20 mm. It may be pointed out that the maximum mass transfer coefficient is a weak function of the diameter of graphite packing and varies with the amalgam concentration and the temperature. Hence, the height of the column would be the same as with graphite spheres of 10–15 mm diameter. It is worth noting that the diameter of the amalgam drop is 0.1–2.0 mm, and therefore, the current distribution is determined by the size of the mercury drop rather than the graphite.

Graphite is degraded in the decomposer by erosion, and hence the tower should be washed every 3 years. These packings can then be properly segregated and reused. The tower wall is inspected carefully for corrosion, and the vessel is filled with dilute NaOH to prevent rusting during shutdowns.

The hydrogen overvoltage on the graphite cathode has a major effect on amalgam decomposition kinetics, and several efforts have been made to improve the characteristics of the graphite surface. Sintered mixtures of graphite and iron exhibited low overvoltage and improved the contact resistance between the graphite and the amalgam. However, this surface was amalgamated and deactivated within several hours and was prone to Fe dissolution. The only successful additive to achieve low hydrogen overvoltage appears to be molybdate solution. However, one has to be careful with respect to the contamination of brine with molybdate which can result in H₂ discharge on the cathode.

REFERENCES

1. F. Hine, *Electrode Processes and Electrochemical Engineering*, Plenum Press, New York (1985), p. 143.
2. F. Hine, *Electrochem. Technol.* **2**, 79 (1964).
3. T.H. Chilton & A.P. Colburn, *Ind. Eng. Chem.* **27**, 255 (1935).

5

Chlor-Alkali Technologies

5.1. INTRODUCTION

About 97% of the chlorine and nearly 100% of the caustic soda in the world are produced electrolytically from sodium chloride, while the rest of the chlorine is manufactured by the electrolysis of KCl, HCl, chlorides of Ti and Mg, and by the chemical oxidation of chlorides [1]. The electrolytic technologies currently used are mercury, diaphragm, and ion-exchange membrane cells. Figures 5.1 and 3.10 show the distribution of these cell technologies in the world and on a regional basis [2]. Mercury cells had a world share of 45% in 1984 and declined to 18% in 2001 because of the health and environmental concerns associated with mercury. However, it is still the leading technology in Europe.

Diaphragm cells held a 67% market share in the United States, vs 37% in the world in 2003. The emerging cell technology is the membrane process, which had a world market share of 30% in 1999 and 40% in 2003.

A wide variety of designs have been developed for each of these three cell processes and have been installed in commercial plants. However, only a few of those cell designs

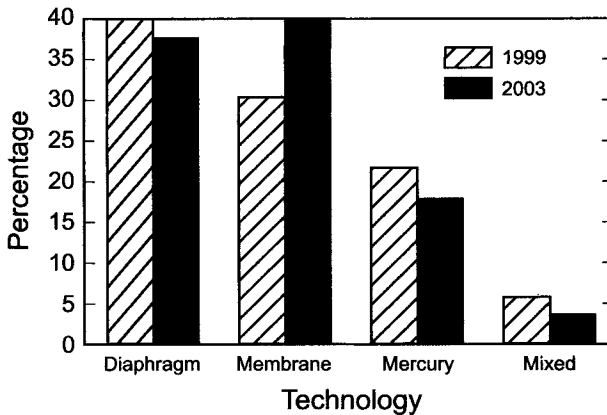


FIGURE 5.1. Breakdown of world chlorine market share based on technology [2].

have captured significant shares of the market, withstanding the test of time and market vulnerabilities. This chapter will address those cell technologies that are currently available in the market. Pertinent references are provided for readers interested in prior chlor-alkali cell configurations.

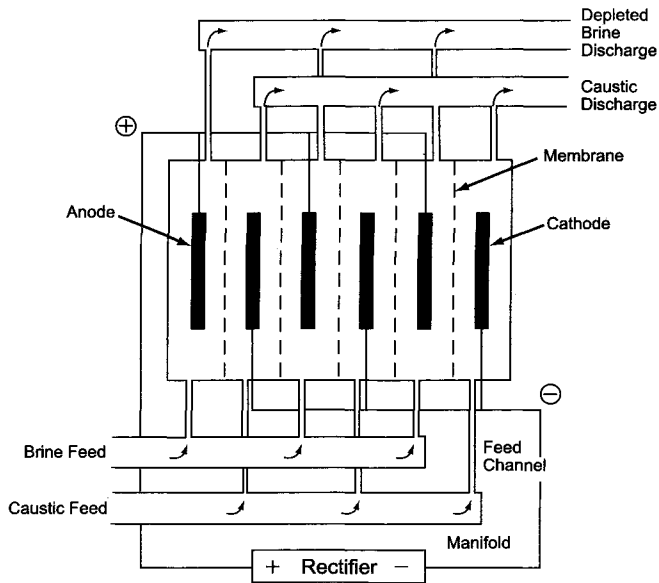
5.2. CELL TYPES—BIPOLAR AND MONOPOLAR

Electrochemical cells, be they for electrolysis to generate products or for producing electricity (e.g., batteries, fuel cells), fall into two broad categories with respect to the electrode configuration, monopolar and bipolar cells. In a monopolar cell, there are typically many anode and cathode assemblies that are electrically in parallel with each other. Thus, a monopolar cell is typically a high current cell compared to most bipolar cells. In the typical DC circuit configuration, monopolar cells are connected in series by intercell conductors.

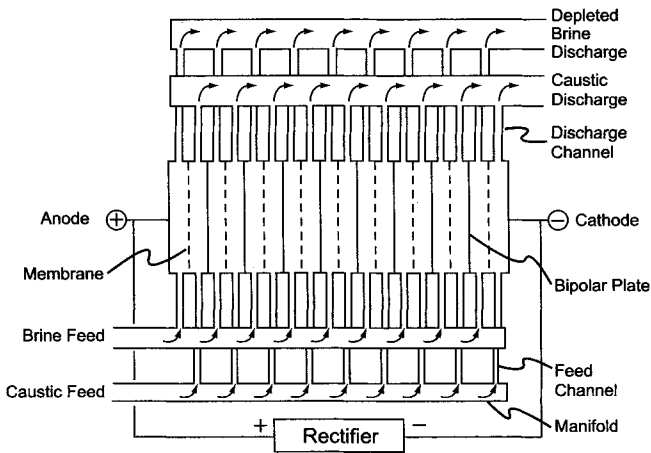
On the other hand, in bipolar cells, only the terminal cells are connected by intercell conductors, and there are typically many unit cells electrically in series between the terminal cells (Fig. 5.2). The two basic types of bipolar cells are the flat plate cell and the finger type cell. A group of bipolar cells that have a common piping system for the fluids, via manifolds, is referred to as an electrolyzer or sometimes a series or a stack. Within a single bipolar electrolyzer, there are sometimes more than one set of terminal cells. Bipolar electrolyzers can be connected via an external bus within a DC circuit in series or in parallel, but usually not both. Furthermore, in the case of mercury-cell plant conversions to membrane cells, the electrolyzers are connected electrically in parallel as shown in Fig. 5.3.

Historically, the concept of arranging the cells in bipolar and monopolar fashion was known before 1800, when Volta assembled batteries [3]. There are several advantages and disadvantages associated with the construction and operation of monopolar and bipolar cells [4,5]. They are noted in Table 5.1.

One significant difference between the two cell arrangements is the capital cost associated with the cells and the electrical supply system constituting rectifiers and transformers. The most expensive components of the cells are the membranes and electrodes. Therefore, their cost becomes lower as the current density increases and allows the use of less electrode and membrane area. In recent years, membranes that can operate successfully above 4 kA m^{-2} have been developed. As explained in Section 8.3.1.3, bipolar cells are better suited to take advantage of this development. This explains the current trend favoring bipolar systems. A recent comprehensive cost analysis [6], taking into account the cost of the cells and rectifiers, penalties arising from the lower efficiency of the bipolar cells, and higher downtime production losses compared to monopolar cells, showed (Fig. 5.4) favorable economics for monopolar cells operating below a current density of about 4 kA m^{-2} and for bipolar cells operating at higher current densities. This critical current density varies with the parameters chosen for the cost calculations. When investment capital is scarce, the choice of bipolar cell technologies makes good economic sense. The structural IR of flat plate type bipolar cells is typically less than for monopolar cells, because the current path through the metal



A. Monopolar arrangement



B. Bipolar arrangement (filter-press type electrolyzer)

FIGURE 5.2. Schematic of cell assemblies.

structure is shorter. Less busbar and fewer busbar connections for bipolar cells also save some voltage and some capital.

The other cost difference between the monopolar and bipolar cell arrangements is in the electrical supply system. The monopolar connection calls for a high current and low voltage while the bipolar connection allows a low current and high voltage. The capital cost of transformers decreases with increasing voltage, although high current needs increase the cost by about 30%. However, the rectifier costs decrease with decreasing

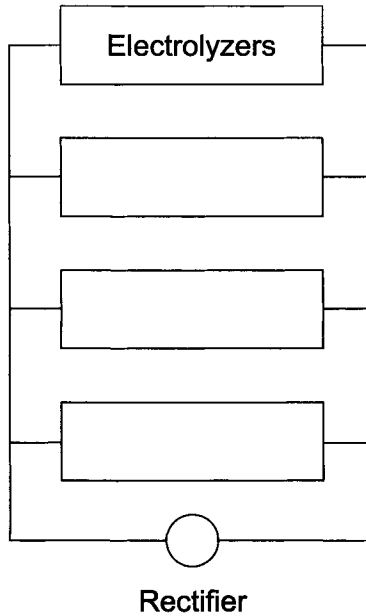


FIGURE 5.3. Conversion of mercury electrolyzers to membrane electrolyzers.

TABLE 5.1. Comparison of Monopolar and Bipolar Cells

Advantages	Disadvantages
<i>Monopolar cells</i>	
Simple and rugged design	Heavy and more numerous intercell connectors
Relatively inexpensive parts	Higher unit cell voltages
Simple fabrication techniques	Each cell requires operator attention
Individual cells can be easily monitored	More instrumentation required
Cells can be easily isolated with minimum disruption to production	More electrolytic cells in system
Rectifiers optimized for large scale plants	
<i>Bipolar cells</i>	
Lower unit cell voltage	Higher parasitic currents that lower current efficiency and cause corrosion
Intercell busbars greatly reduced	Malfunction of a unit cell can be difficult to locate
Rectifier costs more easily optimized for small to medium size plants	No flow measurements to the individual cells
Less instrumentation needed	Repairs to an unit cell require shutdown of entire electrolyzer, thereby reducing production
Fewer electrolyzers in the system	
Higher capacities for electrolyzer	

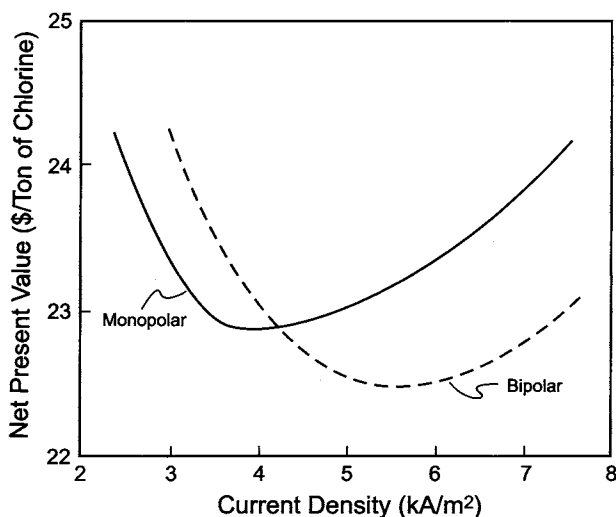


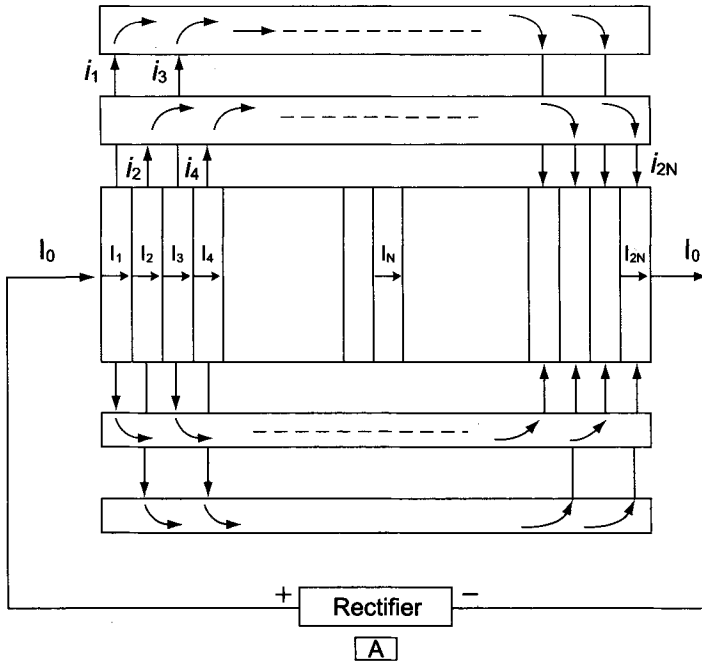
FIGURE 5.4. Comparison of costs with monopolar and bipolar cells (Power cost: $\$0.025 \text{ kW hr}^{-1}$; Discount rate: 20%; Amortization: 20 years; Membrane: $\$780 \text{ m}^{-2}$; Anode: $\$800 \text{ m}^{-2}$; Current efficiency: 95%; Bipolar costs include a lost production penalty of $\$1.35 \text{ ton}^{-1}$ of chlorine) [7].

amperage. While these costs for a small size plant show that low amperage/high voltage rectifiers cost 40–50% less than high amperage/low voltage systems for the same kilowatts [7], the cost differential becomes less or even reverses in large scale plants. This cost advantage, however, is negated by (a) the lower efficiency of the bipolar systems (which we will address later), (b) safety aspects related to operating high voltage stacks and (c) downtime production losses during shutdowns.

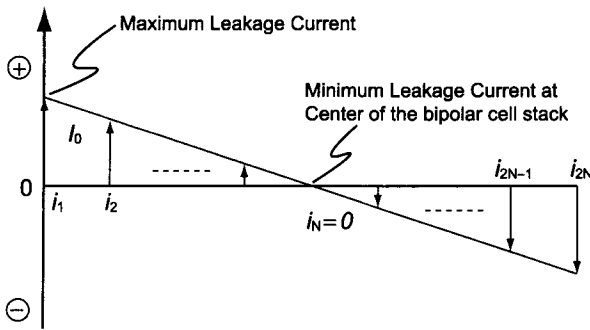
5.2.1. Origin of Parasitic Currents

As noted in Fig. 5.2B, a bipolar electrolyzer consists of a multitude of unit cells, each containing an anode and a cathode, sometimes separated by an ion-exchange membrane and feed and discharge tubing connected to common headers or manifolds. With divided cells, there will be separate feed and discharge piping to each of the anode and cathode compartments. When electrical current is fed to the terminal cells of a bipolar electrolyzer, most of the supplied current will flow from an end anode to the opposite end cathode through the bipolar cells in the stack. But some current will also flow through the electrolyte in the feed and discharge manifolds and the connecting piping to the cells. The current flowing in this piping is known as parasitic current, shunt current, bypass current, or leakage current. The current flowing in the electrolytes within the manifolds and connecting piping is ionic (as in between the anode and cathode), whereas the conduction through metallic conductors is electronic.

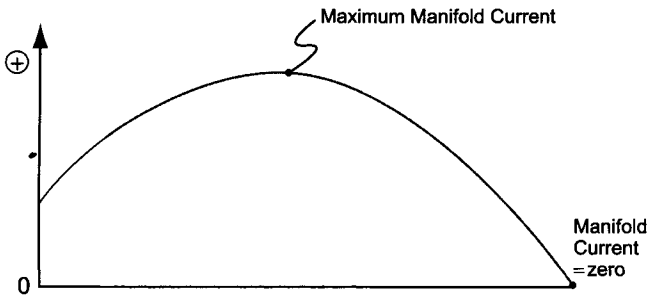
The simplest explanation for shunt currents is that the electrolytes in the manifolds, or the manifolds themselves if they are metallic, provide parallel paths to the current flowing in the cells. Thus, with few exceptions, some shunt currents will flow in the connecting piping of bipolar cell stacks. As shown in Fig. 5.5A, the distribution of shunt



Leakage Current



Manifold Current



B

FIGURE 5.5. A. Schematic of the current flow in bipolar electrolyzer. B. Schematic of the distribution of leakage current and manifold current in a bipolar electrolyzer.

currents is typically symmetrical with respect to the total number of cells in a DC circuit. Shunt currents leave the cells in the positive half of the circuit, “bypass” the “center” cells via the piping, and then re-enter the cells in the negative half of the circuit. From Fig. 5.5B, it can be seen that the unit cells at the center of the electrolyzer have the lowest current, whereas the terminal cells, which are connected to the negative and positive poles of the rectifier, have the highest current. Figure 5.5B also shows that the magnitude of the shunt currents in the connecting piping is highest near the ends of the electrolyzer and lowest at the center.

It must be emphasized that this symmetry exists over all cells connected in series between the negative and positive poles of the rectifier, not just the cells in a single electrolyzer. Thus, if two bipolar electrolyzers are connected in series in a single DC circuit, the bipolar unit cells with the lowest current will typically be those located near the center of the DC circuit, not those cells at the center of the two electrolyzers. Likewise, if each half of a single electrolyzer is connected in a parallel DC circuit, then the bipolar unit cells with the lowest current will be those located in the center of each half of the electrolyzer, not the ones located in the centers of the electrolyzers. It should be mentioned that leakage currents are also present in monopolar cell circuits. However, their magnitude is very small.

The typical problems associated with shunt currents include:

1. lost production
2. corrosion
3. reverse currents during off-line periods
4. generation of impurity gases

Not all the shunt current returns to the electrolyzer. Some leaks from the system and does not take part in electrolysis. Since the production rate depends on the current supplied, there is a production loss caused by shunt currents. In order to accurately determine current efficiency, the actual current received by each cell in the circuit needs to be known. One of the uses of shunt current models, discussed in the next section, is the estimation of the shunt currents as well as the current in each cell. For well-designed chlor-alkali plants, the shunt current loss will usually be less than 2% and frequently less than 1%. The shunt currents that “bypass” the “center” cells do no useful electrolysis, but will cause IR heating of the electrolytes. For production of molten metals, where shunt current loss could be much higher than 2% because of the high conductivity, such IR heating could be of some benefit, but the economic trade-off between the choice of bipolar and monopolar cells for such an application needs to be carefully considered [8].

Failure to understand the nature of shunt currents in bipolar cell stacks frequently leads to corrosion problems. Corrosion occurs most frequently where shunt currents leave a metal component of the cells or piping system, but corrosion can also occur where the shunt currents re-enter a metal component. Such corrosion can occur at nearly any metal component of an electrolyzer, but the following are the most common: cell nozzles, manifold ports, edges of the main cathode in a unit cell adjacent to an inlet or outlet, metal cell components electronically in contact with the cathode and adjacent to an inlet or outlet of the catholyte compartment, and pipe walls adjacent to the flanges of a manifold when these manifold flanges are located near the center of a DC circuit.

A possible consequence of piping or cell nozzle corrosion failure is a fire caused by escaping hydrogen. Another consequence is that corrosion of the main electrode in a unit cell could cause failure of the separator. Failure of the separator could lead to an H_2-Cl_2 explosion. However, because of the presence of significant amounts of water vapor in the H_2-Cl_2 mixture, explosions rarely occur.

The accumulation of gas impurities generated by the electrochemical reactions associated with shunt currents are typically not a problem for a correctly designed electrolyzer during normal operation because they are diluted by the large amounts of H_2 and Cl_2 produced by the cells. During normal operation, impure gases are hydrogen in the chlorine and oxygen in the hydrogen. Following shutdown of bipolar electrolyzers, reverse currents at the main electrodes of the cells typically occur, and the cells act as a stack of batteries. Even in the case where electrical switches are opened between the electrolyzer and the rectifier, there is a path for the discharge of electrical current through the electrolytes in the connecting piping and manifolds. Note that this path for discharge currents is the same as that defined above for shunt currents. The main sources of the charge or driving force for such reverse currents are the active chlorine species in the anolyte such as OCl^- and to a lesser degree other species such as adsorbed H_2 on the cathode.

So one concern with bipolar cell stacks, especially following shutdown but also during startup, is the generation and accumulation of impure gases in the top of the cells and in the outlet piping of the cell stacks. Unless some action is taken, such as adding a diluent gas, the hydrogen concentration can exceed the explosive limit of about 4–5 volume percent. Because reverse currents can cause corrosion problems with the main electrodes, especially activated cathodes, and the corrosion products from the cathode can then enter, precipitate, and accumulate in the separator, a polarization rectifier or cathodic protection rectifier is sometimes used during shutdowns and prior to startups for bipolar chlor-alkali circuits.

The generation of impure gases is greater during the use of a polarization rectifier. Also, because the production rate of product gases at the main electrodes of the cells is usually quite small when a polarization rectifier is used, accumulation of explosive gas mixtures becomes an even greater possibility unless some action is taken, such as adding a diluent gas. One use of shunt current models, discussed in the next section, is to estimate the amount of diluent gas that is needed to maintain the impure gas levels below the explosive limit. It is interesting to note that during the use of a polarization rectifier prior to startups or following shutdowns, the percent shunt current loss can easily exceed 50% and may approach 80%.

5.2.2. Modeling

Bipolar cell configurations have been examined and are used in various electrochemical operations which include fuel cells [9,10], batteries [11–20], electrochemical capacitors [21], chlorate and chlor-alkali cells [22–27], electrowinning of metals [28–30], fused salt electrolysis of Al and Mg [31–36], electro dialysis [37], and electroorganic processes [38].

A typical bipolar electrolyzer stack, with each cell containing an anode and a cathode separated by an ion-exchange membrane, and the current pathways through

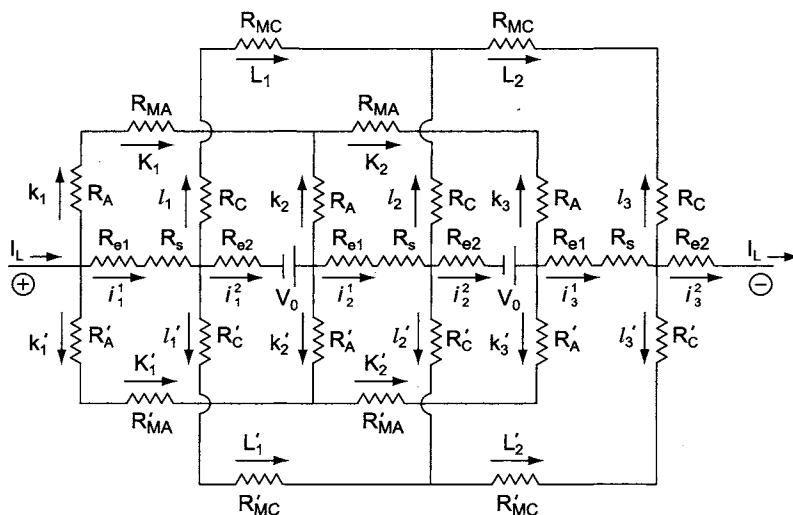


FIGURE 5.6. Equivalent circuit for the bipolar stack in Fig. 5.7A. (Manifold resistances: R_{MA}, R_{MC} ; bypass channel resistances: R_A, R_C, R'_A, R'_C ; cell resistances: R_{e1}, R_s, R_{e2} ; load: I_L ; open circuit potential: V_0 ; number of cells: N ; leakage [channel] currents: $k_1, k_2, k_3, l_1, l_2, l_3, k'_1, k'_2, k'_3, l'_1, l'_2, l'_3$; manifold currents: $K_1, K_2, K'_1, K'_2, L_1, L_2, L'_1, L'_2$; cell currents: $i_1^1, i_1^2, i_2^1, i_2^2, i_3^1, i_3^2$.)

the electrolyte and the cells are shown in Fig. 5.5A. As noted in Fig. 5.5A, the current flow is mainly via two streams—one through the electrode compartments and the other through the electrolyte manifolds via bypass channels (i.e., the path from the cell to the feed and discharge manifolds).

The complex analog model of the circuit in Fig. 5.6 representing the current pathways can be simplified [39,40] by (1) assuming the electrolyte resistance in the cells, bypass channels and the manifolds to be the same, (2) lumping the resistance of the membrane with that of the electrolyte, and (3) using linear kinetic resistance at both the electrodes. These approaches, however, ignore the effects imposed by the nonuniform geometry of the channels, concentration gradients in the cells, and the potential dependent kinetic resistance at the electrodes.

The simplifications noted above have been well recognized in the literature leading to equivalent circuit descriptions. An equivalent circuit model is a schematic of the input–output mode of the bipolar assembly describing the apportioning of the overall cell voltage as well as branching of the currents. The complications introduced by asymmetrical geometries and the varied boundary conditions are transferred to the specifications of the effective parameters (i.e., resistances of the bypass channel, manifolds). The details that are explicitly included in this model can vary depending on the specific situation.

The equivalent circuit, which is essentially a resistive network, provides a set of simultaneous equations derived by applying Kirchoff's node and loop laws. Thus, at a node, the algebraic sum of electric currents flowing in and out is zero, and in a closed circuit of network, the sum of the ohmic voltages (with respect to the direction of the current) is equal to the sum of the voltage sources. These equations, expressed in

a finite difference form, can be solved using a power law solution technique [41–43] or replaced by a differential equation, which is solved to yield a solution containing exponential terms [44–54]. Other numerical approaches used to solve these equations include: piecewise linear method (PLM), iterative-piecewise linear method (IPLM), non-perturbative adomian decomposition method (ADM) and piecewise linear continuum method. Of these, IPLM and ADM converged rapidly to identical values and ADM had a better range of convergence. The reader is referred to reference [51,52] where the pertinent references to these numerical techniques are outlined.

A more elegant way of estimating the leakage currents is to use the continuum model by solving the Laplace equation. Comparison [55] of the equivalent circuit model (ecm) calculations, obtained under linear polarization conditions, with the Laplace solution using the finite element approach (fea), showed the former to provide higher values for the leakage currents. The ratio of the ecm/fea currents was reported to be 1.1 (at a ratio of the resistance of the solution to the bipolar plate of 10, when the leakage currents are large).

The calculation of manifold leakage currents j_k essentially involves solving Eq. (1) with η_k described by the Butler–Volmer equation, following the equivalent circuit model.

$$R_b j_{k+1} - (2R_b + R_c + R_m)j_k + R_b j_{k-1} = -U_0 - \eta_k \quad (1)$$

where

$$U_0 = E_e + I_0 R_c$$

and

m = total number of electrolytic compartments of a bipolar cell

$k = 0, 1 \dots m$: the numbering of electrodes

E_k = emf of the k th-electrode at a given polarized condition

I_k = electrolytic currents flowing through the 0th electrode

i_k = currents flowing through the k th bypass channel with a resistance of R_b

j_k = currents flowing through the k th manifold

R_b, R_c, R_m = resistance of the bypass channel, electrolyte in the cell, electrolyte in the manifolds between every two sets of bypass channels

E_e = emf of the galvanic cell of formation of electrolyzed substance

I_0 = applied current

U_0 = cell voltage.

Several authors have used limiting forms of η_k as function of I_k , and solved for j_k using various numerical techniques. The intent here is not to compare the numerical techniques but to discuss the limitations of using the approximate versions of the rate equation to describe η_k as a function of I_k for an evaluation of the magnitude of j_k . Highlights [51,52] of comparison of the Tafel vs the exact equation are noted below.

1. The Tafel approximation underestimates the leakage currents (by $\sim 6\%$ in the middle compartment) except at the end electrodes. This effect is lessened as the I_0 increases, other parameters remaining the same.
2. Under linear conditions, the leakage currents follow the same behavior as above.

3. Under linear conditions, when $\varepsilon = 0$, that is, when the resistance in the bypass channel is much greater than the combined resistance of the electrolyte in the cell manifold and the kinetic resistance associated with the anode and the cathode reactions, the bypass percentage index, $J\%$ is given as [51,52,56–58]:

$$j_k = \frac{U_0}{2R_b}k(m - k) \quad (2)$$

$$J\% = 100 \left(\frac{U_0}{6R_b I_0} \right) (m^2 - 1) \quad (3)$$

5.2.3. Experimental Determination of Leakage Currents

Three different approaches [59] are available to determine the magnitude of the leakage currents in bipolar electrolytic cells. The direct method involves placing annular magnetic field detectors around the electrolyte feed or exit piping and measuring the current [12,58]. However, this method suffers from interference from the magnetic field in the circuit, which is not easy to overcome. The second method [53] involves direct measurement of the individual cell efficiency and then calculating the magnitude of the leakage currents. This approach works well with metal deposition or dissolution reactions but is practically limited with gas evolution reactions as each cell has to have separate feed and discharge piping.

A more practical approach was developed by Rousar [54,60] involving inserting platinized platinum probes into the feed or discharge pipes and calculating the current from the measured potential difference. In addition, one may insert reference or nonpolarizable electrode probes into the lines near the metallic areas to determine the value of potential established at the metal/solution interface from which the potential for corrosion can be evaluated. Placement of the probes in a single-phase flow region will provide reliable values. In all membrane chlorine cells, the feed and discharge pipes (and hoses and tubes) are made of some type of polytetrafluoroethylene (PTFE). Another way to estimate the shunt current flow in such a PTFE pipe/hose is to measure the voltage drop from the metal cell nozzle to the metal manifold port to which the hose is attached. From the geometry of the hose, the resistance of the electrolyte in the hose can be calculated. With resistance and voltage drop known, the shunt current can be calculated. If the voltage drop is measured at the terminal cells of a production size electrolyzer, there is sufficient voltage drop (typically >100 V and sometimes >200 V), therefore it is not necessary to measure the potential drop of the electrolyte. This method requires no special hardware and can only be done accurately for inlet hoses, which do not contain gas. With the inlet hose shunt current known, the accuracy/readability of a clip-on ammeter can then be checked and determined within the magnetic field of the electrolyzer. The clip-on ammeter can then be used to measure the shunt current at a terminal cell outlet hose. The voltage drop across the outlet hose is also measured. With the current and voltage known, the resistance of the fluid (gas and electrolyte) in the outlet hose can then be calculated. With terminal cell currents known and the outlet hose resistances indirectly measured, the shunt current model can then be used to calculate the remaining shunt currents, cell currents, and lost production due to the shunt currents.

5.2.4. Minimization of Leakage Currents

The key to minimizing the leakage currents is to increase the resistance of the bypass channels and the manifold for a given number of cells in the bipolar stack, acknowledging that the leakage current increases approximately as m^2 , where m refers to the number of cells. Limiting the number of cells in a given stack and circuit is another option that should be considered. j_k can be lowered [26,55,61] by increasing the specific resistance of the electrolyte and the length of the pipe and by decreasing the area of cross section of the pipe (i.e., narrow tubes). In addition, increasing the number of plates for a given cell thickness reduces the bypass currents [55].

One of the concepts described in the patent literature is to increase the electrolyte resistance in the pipes by gas-injection [62], which will increase the resistivity of the electrolyte. Making the electrolyte path longer will produce the same result. Interrupting the electrolyte path so that the current is broken is also practiced [22]. Methods used to break the path include the introduction of freely rotating, plastic water wheels in the electrolyte path and siphon pouring into a common path [63]. Potential corrosion at the edges of the electrodes in the bipolar H_2/O_2 fuel cells is avoided by providing an edge seal so that the electrodes are impervious to the reactant gases [10].

Leakage currents can be short circuited [64] or biased by placing an opposite current via electrodes placed in the piping [40] or reacted at sacrificial electrodes located in the manifolds [65]. These concepts have been used in the manifolds of MBC electrolyzers of Chlorine Engineers and also in the design of the CME and BiTac cells. Corrosion of catalytic cathodes used in bipolar water electrolyzers during shutdowns is prevented by cathodic protection [9].

5.3. MERCURY-CELL TECHNOLOGIES

Castner demonstrated the first mercury cell in 1894, and by 1967 there were 14 cell technologies available for licensing [66–69]. These cells operated at high loads, in the range of 70 to 450 kA. In the early 1970s, conversion to metal anodes started, along with computer-controlled anode adjustment and computer monitoring to lower the energy consumption and minimize short circuits within the cell. In addition, devices were also developed to reduce mercury emissions. However, following the Minamata disaster, stringent regulations were placed on the operation of mercury cells. As a result, there was a significant shift from mercury-cell technology to diaphragm- and membrane-cell technologies.

Presently, there are five mercury-cell technologies [70,71] practiced in the world, and their operating characteristics are summarized in Table 5.2. The only technology supplier that is active in optimizing the cell design and the cell operations to achieve negligible mercury emissions is DeNora [72].

A mercury cell consists of three major elements: (1) a cell with inlet and outlet end boxes, anodes, connecting buses, short-circuiting switches, and inlet and outlet piping for gases, water and brine; (2) a vertical or a horizontal decomposer, located beneath the cell or at the lower end of the cell, where the amalgam is stripped to form sodium hydroxide and hydrogen, and (3) a mercury pump to recycle the mercury from the bottom of the decomposer to the high end of the cell, as shown schematically in Fig. 5.7.

TABLE 5.2. Operating Characteristics of Modern Mercury Cells

Characteristic	Manufacturer				
	Uhde	DeNora	Krebskosmo	Olin	Solvay
Cell type	300-100	24M2	232-270	E 812	MAT 17
Cathode area, m ²	30.74	26.4	23.2	28.8	17
Cathode dimensions, l × b, m ²	14.6 × 2.1	12.6 × 2.1	14.4 × 1.61	14.8 × 1.94	12.6 × 1.8
Slope of cell base, %	1.5	2.0	1.8	1.5	1.7
Rated current, kA	350	270	300	288	170
Maximum current density, kA m ⁻²	12.5	13	13	10	10
Cell voltage at 10 kA m ⁻² , V	4.25	3.95	4.25	4.24	4.10
Number of anodes	54	48	36	96	96
Stems per anode	4	4	4	2	1
Number of intercell bus bars	36	32	18	24	24
Quantity of mercury per cell, kg	5,000	4,550	2,750	3,800	
Energy consumption per ton of Cl ₂ , DC kW hr	3,300	3,080	3,300	3,300	3,200

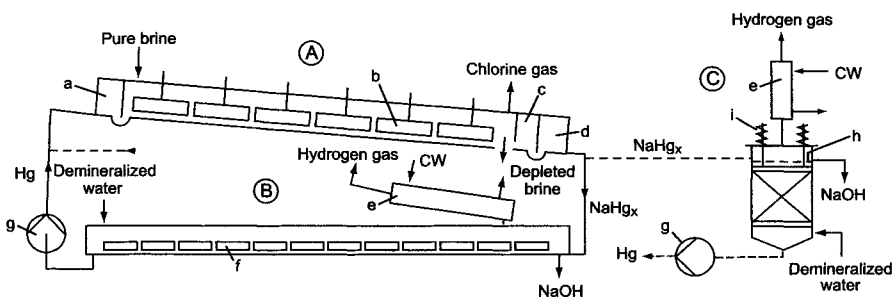


FIGURE 5.7. Schematic of a mercury cell with decomposer [71]. (A) Mercury cell: (a) Mercury inlet box; (b) Anodes; (c) End box; (d) Wash box. (B) Horizontal decomposer: (e) Hydrogen gas cooler; (f) Graphite blades; (g) Mercury pump. (C) Vertical decomposer: (e) Hydrogen gas cooler; (g) Mercury pump; (h) Mercury distributor; (i) Packing pressing springs; CW: cold water. (With permission from John Wiley & Sons, Inc.)

In all these cells, the mercury flows over a sloped (by 1.0–2.5%) steel base, and the flanged sidewalls are rubber-lined. The cell cover is steel lined with rubber or titanium on the underside or made of rubberized fabrics, and is fixed to the side walls by clamps.

The anodes are titanium coated with oxides of Ru, Ir, and Ti and are placed in groups from carrying devices with the ability to change the height (and hence the anode–cathode gap) manually, hydraulically, or by motor. Each cell can be short-circuited externally by a switch. The cell bus bars are generally copper but

sometimes aluminum (Section 8.3.1.4). The anodes are protected from internal short circuiting by electronic monitoring.

The distinguishing differences in these various cell designs lie in the manner by which the anodes are assembled, placed in the cell through the cell cover, and operated to achieve minimal inter-electrode gaps, the decomposer design, the cathode area and the current densities. These aspects are noted below.

5.3.1. DeNora Mercury Cells

The DeNora cells [68,72] have cathode areas ranging from 4.5 to 36 m², operating at 10–11 kA m⁻². These cells are covered with a flexible, multilayer sheet of an elastomer, which is supported by the anode rods. DSA anodes, with four stems per anode, are suspended in frames supported from the cells.

The cells are equipped for automatic anode adjustment in groups, by electric motors, with short-circuit protection. The anodes are not individually adjustable in the support frames. Flexible copper straps to the anode bus bars connect the anode rods individually, and the cathode current is carried by a cathode plate and copper bus bars. Figure 5.8 is a cross-sectional view of the DeNora mercury cell.

Several modifications have been made in recent years to achieve low energy consumption and to minimize mercury losses to the environment. The inlet and outlet end boxes were redesigned (Figs. 5.9 and 5.10) to be air-tight, and the use of wash water was eliminated or reduced. The inlet end box has been equipped with a cell bottom cleaning

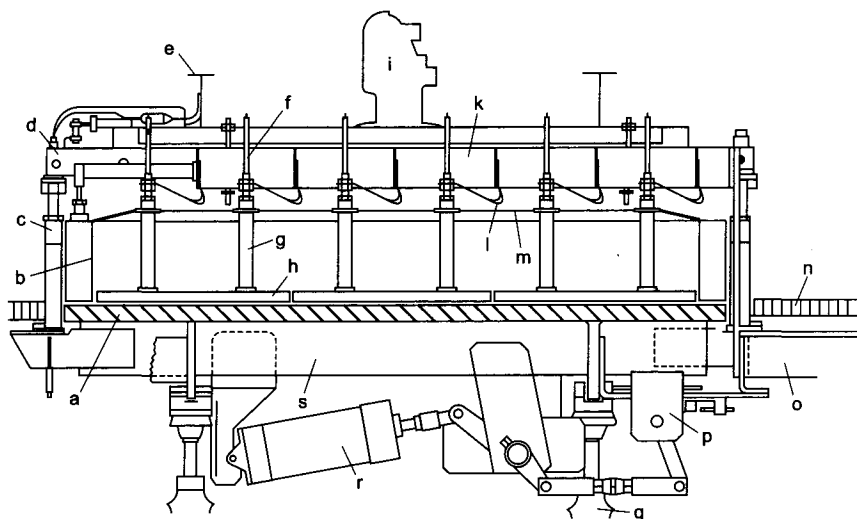


FIGURE 5.8. Cross section of the DeNora mercury cell [71]. (a) Cell base (steel); (b) Side wall (rubber-lined steel); (c) Lifting gear; (d) Transverse support; (e) Lengthwise support; (f) Anode carrier; (g) Anode rod; (h) Anode surface; (i) Adjustment motor; (k) Bus bar; (l) Flexible anode current strap; (m) Multilayer cell cover; (n) Service walkway; (o) Intercell bus bar; (p) Switch; (q) Insulator; (r) Switch drive; (s) Support. (With permission from John Wiley & Sons, Inc.)

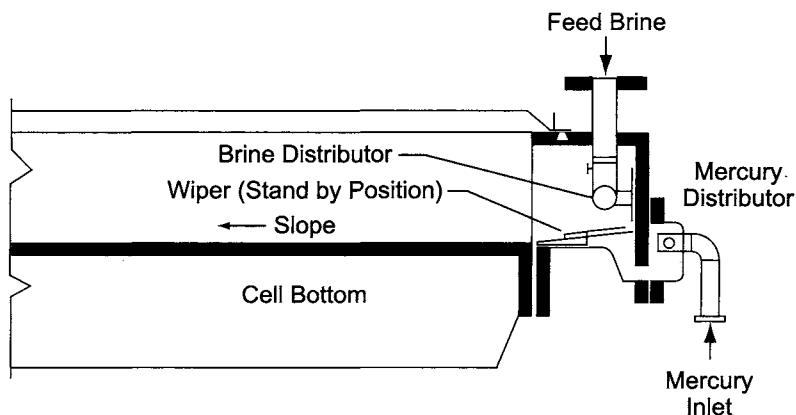


FIGURE 5.9. Inlet end box with Wiper® [72]. (With permission from DE NORA ELETTRODI S.p.A., Milan.)

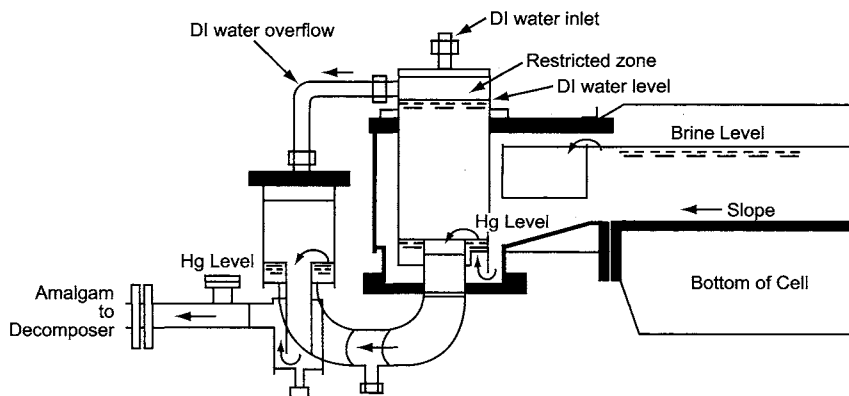


FIGURE 5.10. Outlet end box [72]. (With permission from DE NORA ELETTRODI S.p.A., Milan.)

device, called a wiper, to allow periodic cleaning of the cell bottom without opening the cell cover.

In the outlet end box, wash water is fed only to the restricted zone, since the “beach” and the double hydraulic seal configuration prevent carryover of salt with the amalgam. This results in low chloride levels in the caustic and reduces the wash water needs from 3 L hr^{-1} to 0.9 L hr^{-1} for DeNora’s 24H5 cell. The extended beach area also allows dampening of the speed of mercury within the end box, thus maintaining the level of mercury lower than on the cell base. This static mercury area inside the end box reduces the transport of brine with the amalgam and eliminates the buildup of mercury in the end rows of the anodes.

DeNora also developed a new anode design, called the Runner anode, with the THM (Titanium Hydrodynamic Means) configuration (Fig. 5.11) which utilized the gas lifting force to improve mixing of the brine, thereby eliminating the concentration gradient of brine from the bulk to the mercury interface. This allowed the operation of the cells at the

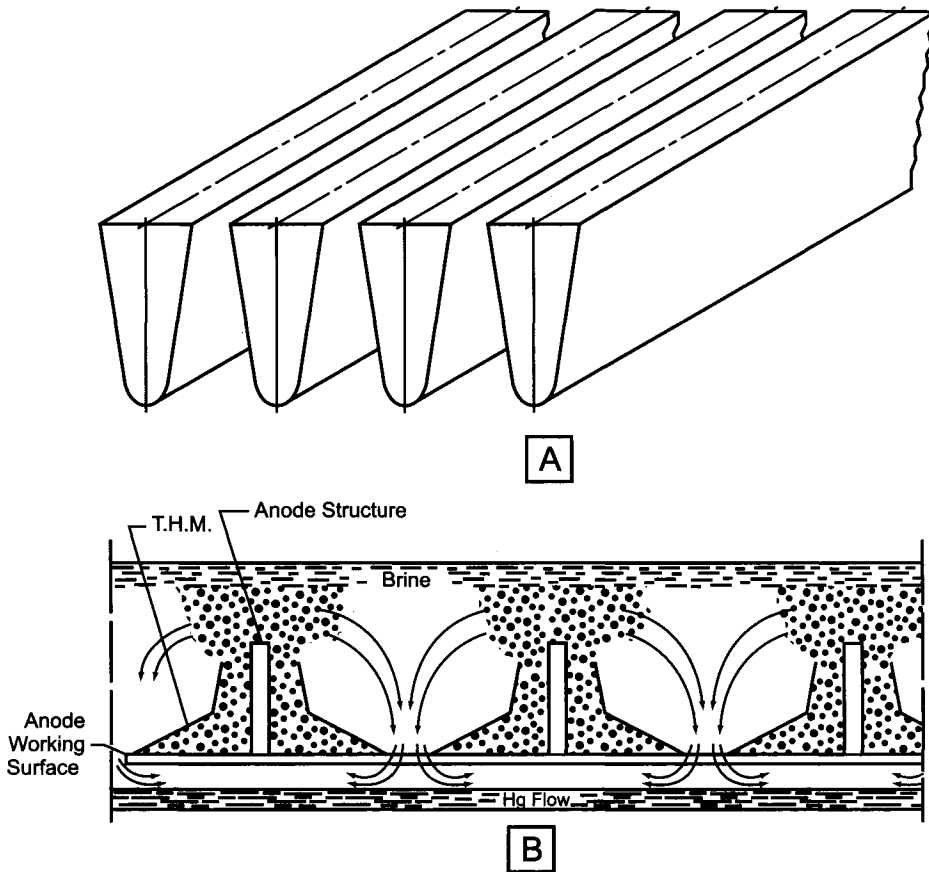


FIGURE 5.11. (A) Runner anode configuration; (B) Brine circulation profile [72]. (With permission from DE NORA ELETTRODI S.p.A., Milan.)

depleted brine levels as low as 225–230 gpl without any effect on the current efficiency. The reduced brine flow also lowered the burden on the settlers and the brine filters, as well as the carryover of mercury into the brine sludge.

Other improvements include automatic control and protection devices to achieve low inter-electrode gaps and motorized anode frames to permit independent movement of each row of anodes. This allows fine adjustment of the electrode gap. As a result, a k -factor of $0.005 \text{ V m}^2 \text{ kA}^{-1}$ is achieved at a current efficiency of $96 \pm 1\%$.

5.3.2. Uhde Mercury Cells

The Uhde cells [68,73] have a cathode surface area of $4\text{--}30 \text{ m}^2$. They have a machined steel cell bottom with rubber-lined sidewalls and end boxes. The inlet end box, through

which the brine is fed to the cell, has two pipes for removing the chlorine. The anodes are suspended in groups in carrying frames, which are supported on transverse girds with lifting gear. The anodes are individually adjustable by raising or lowering them within the bellows seal. The current is fed to anode rods using flexible copper straps, which are bolted on. The compressed air switches are located beneath the cells. Copper bus bars are employed to carry large currents. Shunt current measurements allow computer control of the adjustment of the anodes to operate at an optimal k -factor and to protect the anodes from short-circuiting. Short copper busbars between the cells allow shunt measurements of the anode currents.

Vertical decomposers, situated at the end of each cell, are provided with hydrogen coolers. The flow of the amalgam into the decomposer is by gravity. A two-compartment rubber-lined end box cleans the amalgam off the entrained brine before it enters the decomposer.

5.3.3. *Krebskosmo Mercury Cells*

The Krebskosmo cells [74] have steel bottoms with rubber-lined side channels, and brine flows over a weir to distribute it uniformly across the width of the cell. The anode stems are made of copper and are individually sealed to the rubber-lined steel top, using PTFE bellows. The anodes are supported in groups from steel frames, which may be adjusted manually or by electric motors. A pressure-operated switch in the mercury return line from the decomposer can shut the cells down, if the mercury pump fails.

Copper or aluminum bus bars carry the electric current to the cell covers, and then by flexible copper straps to the anode rods. The short-circuiting switches are located beneath the cells and when the cell is short-circuited, the cell bottom also acts as a current conductor. A vertical amalgam decomposer is located at the end of each cell.

5.3.4. *Olin Mercury Cells*

Olin cells have a number of unique features in size, arrangement, and adjustment of anodes for voltage regulation. Olin pioneered the development of vertical decomposers, which reduce the mercury inventory required by the cells.

The Olin cells [68] have machined steel cell bottom units with rubber-lined steel side channels and steel tops. The anode stems are sealed through individual flexible rubber sleeves and are suspended from a copper channel, which also carries the current from the flexible buses to the anodes. Olin has developed a novel system to mount and adjust the anode–cathode gaps. The U-shaped copper or aluminum bus bar, located above each row of anodes, provides support to the anode lifting gear and current to the anodes, which are bolted to it. The anodes can be adjusted manually or electronically with the remote computerized anode adjusted (RCAA) system.

The RCAA system generates current signals and anode–cathode voltage signals, which are fed to a console that displays the currents and voltages for each bus in a given cell. The computer analyzes the data and automatically raises or lowers each

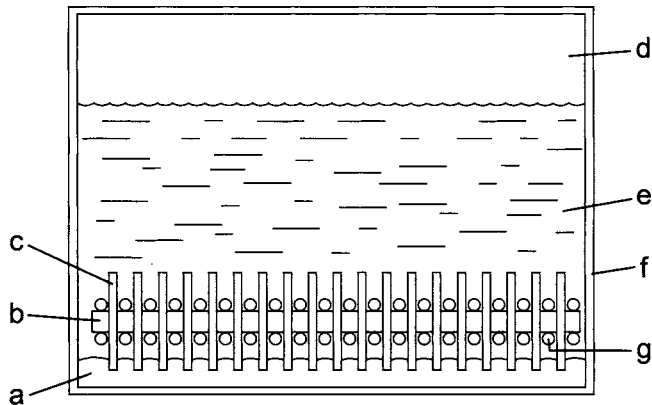


FIGURE 5.12. Cross section through a horizontal decomposer [71]. (a) Amalgam; (b) Bolt; (c) Graphite cathodes; (d) Hydrogen; (e) NaOH solution; (f) Decomposer casing; (g) Spacers. (With permission from John Wiley & Sons, Inc.)

anode set. Short circuits are sensed and avoided by using reed switches, which sense an approaching short and activate the motor controls to raise the anodes. The reed signals cannot be overridden manually or electronically. All the cells are protected by reed switches [75].

5.3.5. Amalgam Decomposers

There are two types of industrial decomposers, horizontal and vertical. Horizontal decomposers are ducts with rectangular channels (Fig. 5.12) located below the cells with a 1.0–2.5% slope. The amalgam flows with a depth of 10 mm, and the catalyst is in the form of graphite blades 4–6 mm thick, immersed in the amalgam.

The amalgam reacts with demineralized water in counterflow. Horizontal decomposers require about 30–40% of the space required for the cells. Horizontal decomposers produce caustic with a low mercury content. However, they are difficult to service and maintain. They are obsolete and have been replaced by vertical decomposers.

Vertical decomposers are towers packed with graphite spheres or particles 8–20 mm in diameter. A typical cross section is 0.35 m² per 100 kA of cell load. The amalgam flows from the top and water is fed into the bottom of the tower. Since the volume of the decomposer is small, it is necessary to cool the hydrogen generated during the course of the amalgam decomposition reaction. The mercury inventory is small with the vertical decomposer. However, the caustic contains more mercury.

DeNora [72] has improved the vertical decomposer design by employing a basket (Fig. 5.13), which allows packing the graphite outside the decomposer. A vibrating table is used to pack the graphite, thereby reducing the channeling in the decomposer and increasing the life of the catalyst. A spring-loaded graphite compression system allows uniform compactness of the graphite bed over 12–16 months. A mercury distribution plate achieves uniform amalgam distribution. The graphite catalyst is activated by molybdate impregnation, which allows reduced maintenance and a long life.

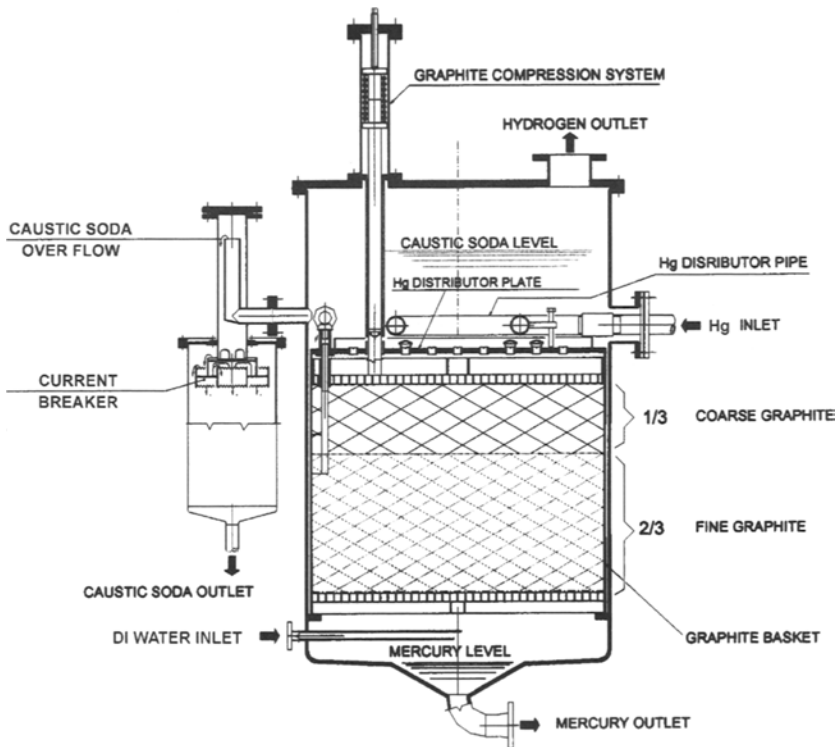


FIGURE 5.13. Modified decomposer of DeNora [72]. (With permission from DE NORA ELETTRODI S.p.A., Milan.)

5.4. DIAPHRAGM-CELL TECHNOLOGIES

Electrolysis of sodium chloride solutions to generate and continuously separate the chlorine and the caustic using a porous diaphragm was first described in a patent issued in 1851 to Charles Watt. However, it was only in the 1890s that E.A. LeSueur designed and operated a chlorine cell with a percolating asbestos diaphragm, realizing high chlorine efficiencies. Over the next 50 years, various designs of diaphragm cells were developed, which can be classified into three groups: horizontal diaphragm cells, vertical diaphragm cells, and bipolar filter-press cells.

An example of the horizontal cell is the Billiter cell, which employed a corrugated steel cathode covered with a mixture of long fiber asbestos and barium sulfate paste. These cells were used in Germany between the world wars and were completely replaced later by vertical diaphragm cells.

5.4.1. Bipolar Filter-Press Cells

There are two bipolar filter-press cell designs for manufacturing chlorine, the Dow cell and the Glanor cell. Both use finger-type electrodes, as opposed to flat plates. The Dow cells, developed over the past eighty years [76–79] are simple and rugged. They employ

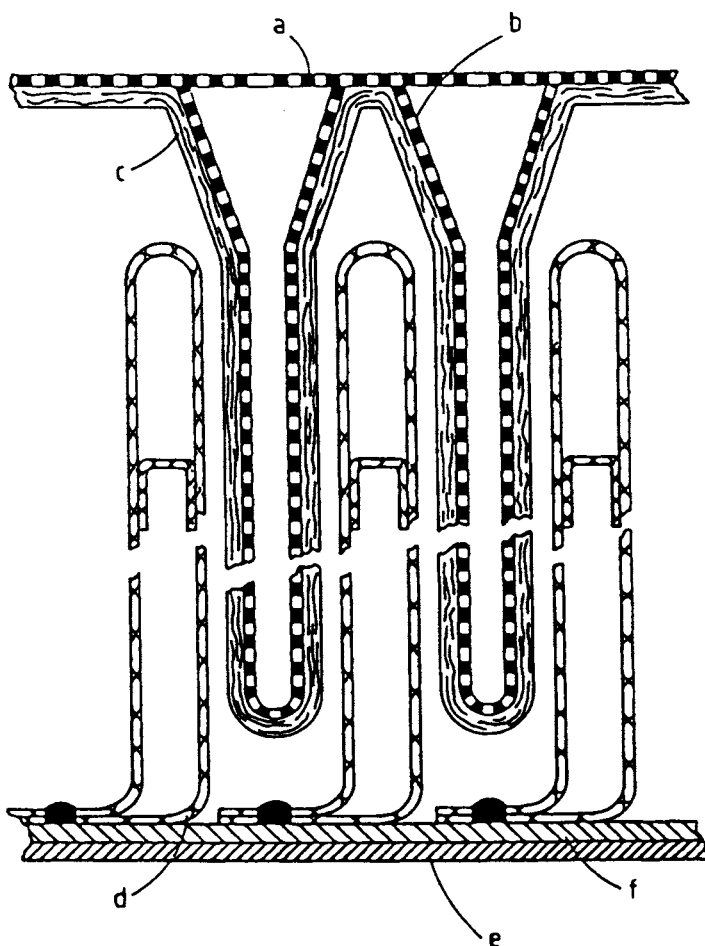


FIGURE 5.14. Dow Diaphragm-cell sectional view: (a) Perforated steel back plate; (b) Cathode pocket; (c) Asbestos diaphragm; (d) DSA anode; (e) Copper back plate; (f) Titanium back plate [85]. (With permission from John Wiley & Sons, Inc.)

vertical coated titanium anodes and mild steel cathodes with mesh bolted to a perforated steel back plate. Copper springs are attached to the back of the perforated cathode plate and the anode of the adjoining cell. This electrical connection is immersed in the catholyte during operation. Figure 5.14 depicts the internals of the cell. Each bipolar element can have an active area of 100 m^2 . These cells operate at current densities of about 0.5 kA m^{-2} .

The Dow electrolyzers have 50 or more cells in one unit and each electrical circuit may consist of only two of these units. The cells operate at about 80°C , allowing the use of vinyl ester resins and other plastics for cell construction. Because of the low operating current density, the cell voltage is only 300–400 mV above the thermodynamic

decomposition voltage. Dow neither license their diaphragm-cell technology nor discuss their operating data in open forum.

The Glanor electrolyzer [80–82], developed jointly by PPG Industries and DeNora, consists of a series of bipolar cells clamped between two end plates by tie-rods to constitute an electrolyzer. Each electrolyzer contains up to 11 cells. The bipolar electrode consists of a steel plate with a titanium lining to which the anode fingers are connected on one side and the cathode fingers on the other. The electrode is set into a bipolar element (Fig. 5.15) consisting of channel frame around the anodes, lined with titanium to protect it from corrosion arising from the chlorine containing acidic anolyte. These elements are then clamped together, the anode of one facing the cathode side of another, to form a cell.

A unique feature of the cathode design is the extension of the cathode fingers from the back plate, which allows easy inspection of the cathode surfaces, and the adaptability to use synthetic separators with minor modifications. The anolyte compartment is connected to an independent brine feed tank by flanged connections and chlorine leaves from the top, through the brine feed tank and then to the chlorine header. Each electrolyzer is fitted with a level alarm, which monitors the level of all the cells in the unit. Figure 5.16 is an isometric cutaway of a Glanor V Type 1144 electrolyzer.

There are two versions of the Glanor electrolyzer: V-1144 containing 11 cells, each having an area of 35 m², and V-1161 containing 11 cells, having an area of 49 m² per cell. The Glanor cells are currently used only by PPG Industries in the United States, Mexico, and Russia.

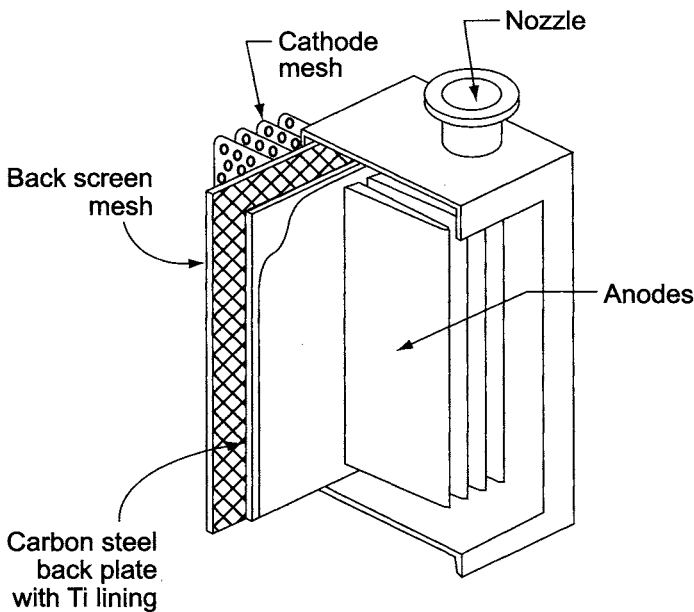


FIGURE 5.15. Glanor[®] bipolar element. (With permission from John Wiley & Sons, Inc.)

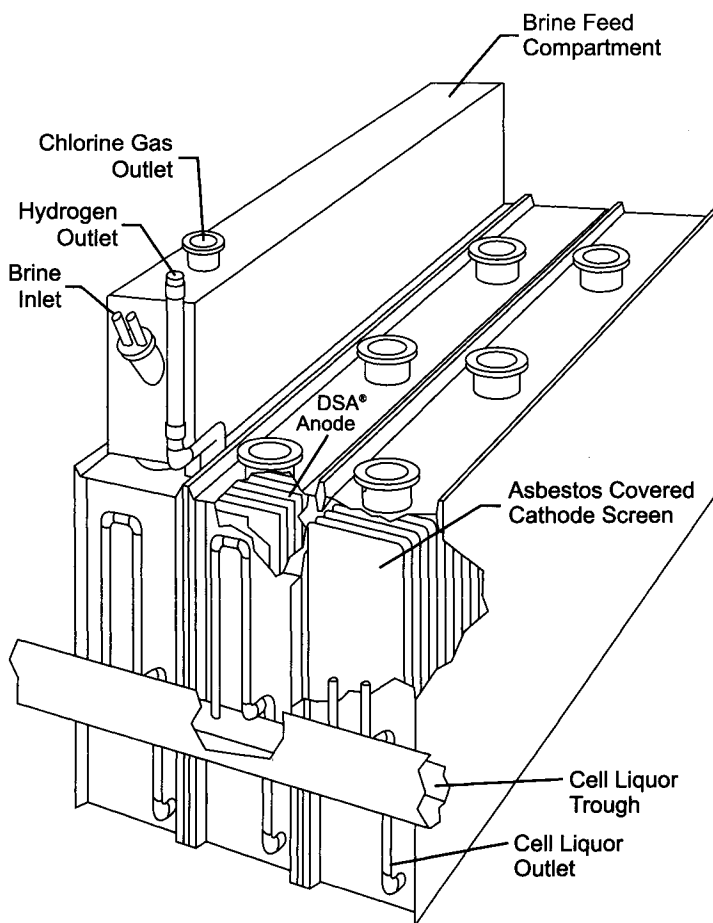


FIGURE 5.16. Glanor V Type 1144 Electrolyzer. (With permission from John Wiley & Sons, Inc.)

5.4.2. Vertical Diaphragm Cells

Vertical diaphragm cells are either cylindrical or rectangular. The cylindrical cells include the Gibbs, Moore, and Wheeler cells [83,84]. The rectangular cell designs are the Allen Moore, Townsend, Nelson, Hooker, Diamond, Solvay & Cie, Kureha Chemical, Nippon Soda, Showa Denka, and ICI cells. The only supplier of diaphragm cells today is ELTECH, who provides the Hooker H-Type and Diamond MDC-type electrolyzers. The reader is referred to Chapter 3 and the literature [66–68,71,85] for details related to the Hooker-Uhde cells and the earlier versions of the S- and H-type cells.

The major workhorse of the diaphragm-cell electrolysis is the ELTECH electrolyzer, H-4 and MDC-55. There are several common features in these cell designs, as can be seen in Fig. 5.17. The base of the cell is a copper plate with spot faced holes to anchor the anodes (Fig. 5.18). It also acts as a current conductor. Either a sheet rubber cover or a titanium base cover using rubber rings around the anode posts protects the copper base.

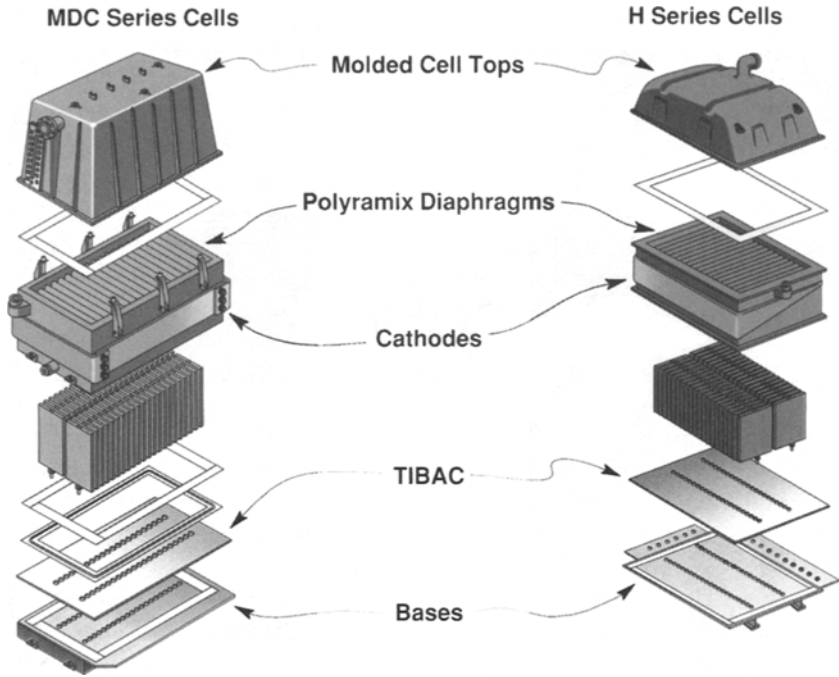


FIGURE 5.17. ELTECH's MDC and H series cells. (With permission from ELTECH Systems Corporation.)

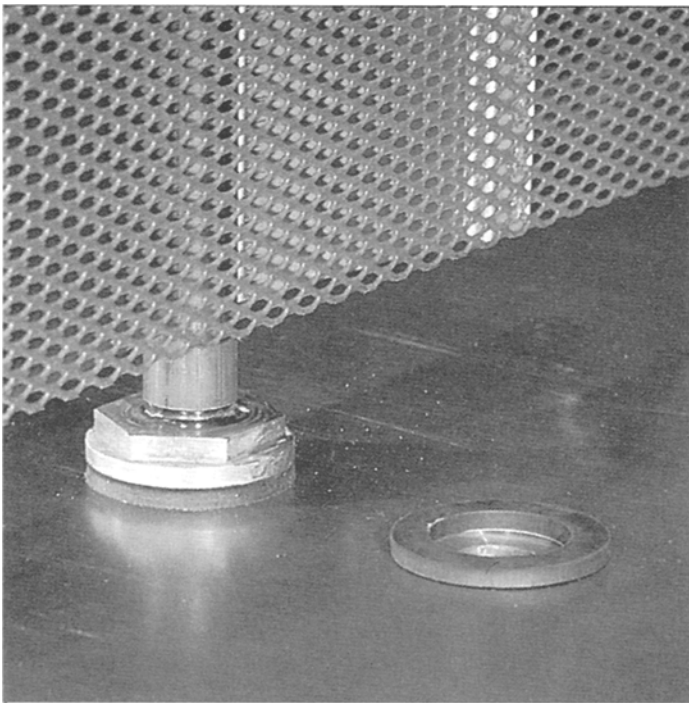


FIGURE 5.18. Anode base plate. (With permission from ELTECH Systems Corporation.)

The cathode structure is complex and generally consists of an inner assembly and the shell. The former is made of cathode tubes, fabricated out of perforated steel plates in H-cells and wire mesh in MDC cells. The cathode tubes are held together on each side by a tube sheet in MDC cells. Stiffener straps provide structural support and vertical screens and horizontal rim screens complete the inner assembly. Thus, the components of the cathode shell are its side plates, rear end plate, gird bar, end connectors, side and end bars, lifting lugs, and hydrogen outlet, which are welded together. The cathode tubes run parallel to the current flow in both these cells.

The major difference between the MDC and H-type cells is the manner in which the current is distributed over the cathode. In the MDC cells, current distribution bars carry the current directly from the side plate to the tube sheet. A copper gird bar is then bonded to the steel side plate by silver brazing or explosion bonding, thereby providing a greater cross-sectional area for the current to travel into the shell (Fig. 5.19). On the other hand, the copper gird bar in H-4 cells is perimeter welded to the steel shell, forcing all the current to pass via the copper welds. Corrugated supports, welded to the side plate, carry the current to the fingers. The H-4 cathode has copper rods embedded in the valleys of steel corrugations (Figs. 5.20 and 5.21) to provide a lower cell structural voltage drop.

Recently, ELTECH made a series of improvements to both series of cells to reduce the voltage and to achieve a longer diaphragm life. ELTECH's Advanced Diaphragm Cell Technology, ADCT™, includes Polyramix® diaphragms and Energy Saving Anodes, in addition to the modifications made to the cathode structure. The anodes were designed with heavy expanders to lower the structural ohmic drop. The use of fine, unflattened mesh installed over traditional flattened mesh allowed zero-gap operation with the Polyramix diaphragms. The H-4-75, H2-A-42, and MDC-55 cells were reconfigured with more surface area by decreasing the cathode tube spacing and installing more anodes.

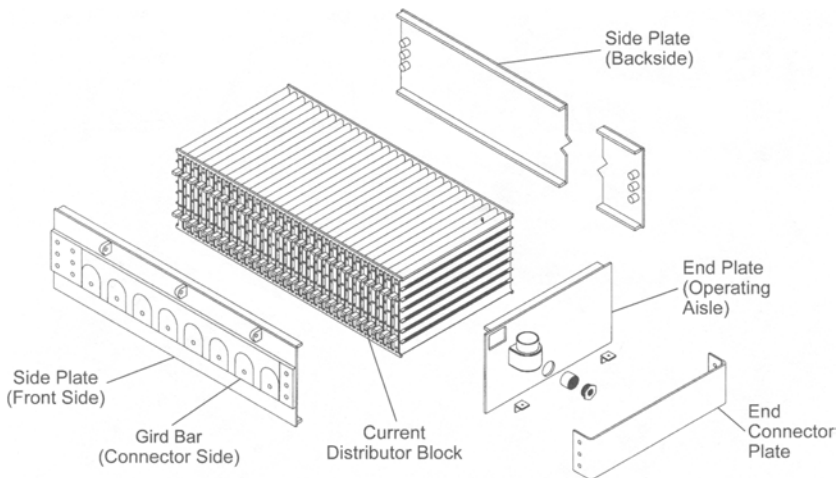


FIGURE 5.19. MDC-55 cathode assembly showing current distributor blocks. (With permission from ELTECH Systems Corporation.)

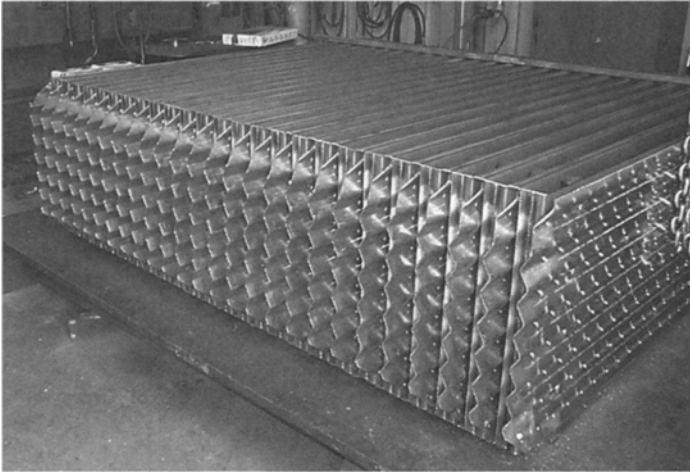


FIGURE 5.20. Current distributor bars of MDC series cells. (With permission from ELTECH Systems Corporation.)

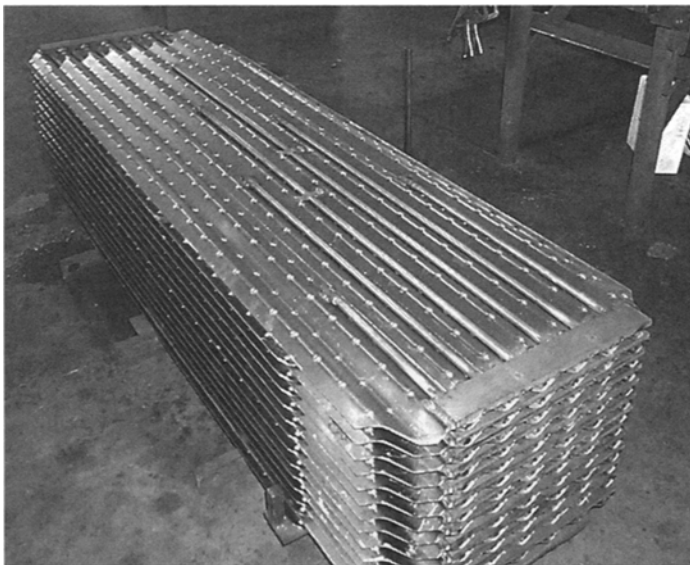


FIGURE 5.21. Current distributor bars of H series cells. (With permission from ELTECH Systems Corporation.)

The latter was made possible by redrilling the base plate to accommodate a closer anode spacing. As a result, the cell designations have been changed as: MDC-55 to MDC-66, H2-A-42 to H2-A-50, and H-4-75 to H-4-93. Substitution of copper for steel in the design of the cathode tube supports is another change instituted in the ADCT™.

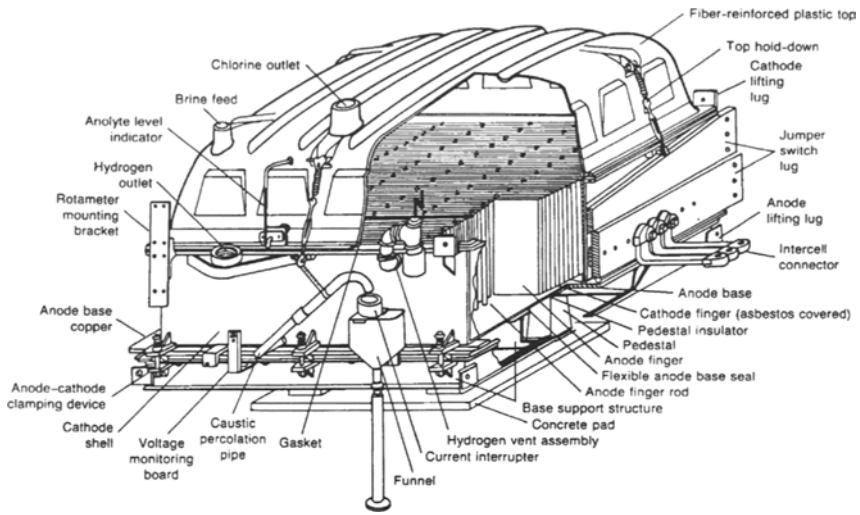


FIGURE 5.22. Cut view of ELTECH's H-4 diaphragm cell. (With permission from ELTECH Systems Corporation.)

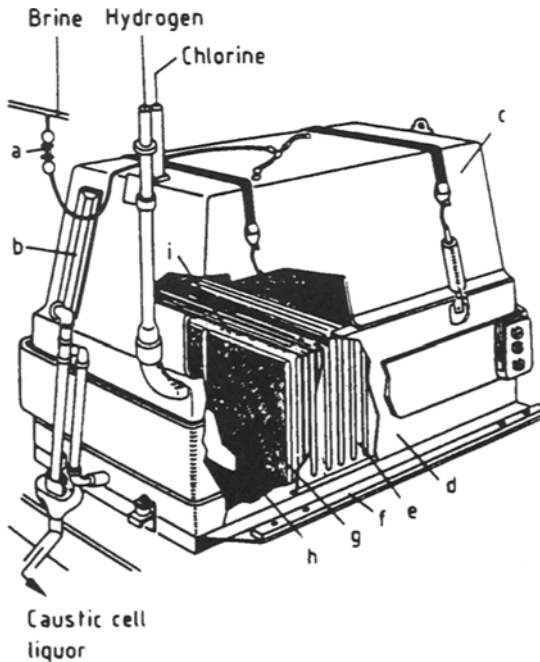


FIGURE 5.23. ELTECH's MDC cell: (a) Brine feed rotameter; (b) Head sight glass; (c) Cell head; (d) Cathode assembly; (e) Tube sheet; (f) Grid plate; (g) Cathode tube; (h) Grid protector; (i) DSA expandable anode. (With permission from ELTECH Systems Corporation.)

TABLE 5.3. Operating Characteristics of ELTECH Diaphragm Cells

Characteristics	Standard design			ADCT™ design ^e		
	MDC-29	MDC-55	H-2A	H-4	MDC-66	H-4-93
Current capacity, kA	80	150	80	165	180	200
Cl ₂ capacity, t day ⁻¹	2.43	4.55	2.42	5.00	5.45	6.06
Caustic capacity, t day ⁻¹	2.74	5.14	2.73	5.64	6.16	6.85
H ₂ capacity, m ³ day ⁻¹	798	1497	798	1647	1796	2000
Current density, kA m ⁻²	2.76	2.74	2.21	2.56	2.74	2.56
Voltage, V (includes intercells)	3.60	3.60	3.35	3.40	3.10	3.06
Energy consumption, DC kW hr ton ⁻¹ of Cl ₂	2847	2839	2655	2694	2454	2423
Diaphragm life, days	200 ^a	200 ^b	300 ^c	275 ^b	3–5 years ^c	3–5 years ^c
Anode life, years	8–10	8–10	8–10	8–10	8–10	8–10
Cathode life, years	5–8	5–8	5–8	5–8	5–8	5–8
Distance between cells ^d , m	1.60	2.13	2.32	3.05	2.13	3.05

Notes:^a SM-2 diaphragm.^b HAPP diaphragm.^c Polyramix® non-asbestos diaphragm.^d Distance is measured from center line to center line with intercell bus connected.^e ADCT includes increased active area, Advanced technology cathodes (ATC™), Energy saving anodes (ESA™), Polyramix™ diaphragms, zero-gap operation, titanium base covers (Tibac™) and Telene™ cell tops.

The sealing medium for both MDC and H series cells is either cell putty or elastomer gaskets. The use of cell putty on gaskets limits the life of a diaphragm. The typical operating life of cell putty is 9–18 months.

The cell top is a clamshell molding and has been FRP based since 1969. However, injection-molded Telene tops have been gaining prominence since 1990. Telene™ is a polydicyclopentadiene thermoset polymer made by Cymetech. Figures 5.22 and 5.23 show the cell designs of the MDC and H series diaphragm cells. Table 5.3 depicts the comparative performance characteristics of these electrolyzers with standard design and ADCT design [86–88].

5.5. MEMBRANE-CELL TECHNOLOGIES

5.5.1. Guidelines for Choosing Cell Technologies

In the early 1990s, membrane-cell technology was available from seven or eight suppliers. However, there are now only five suppliers of ion-exchange membrane cells. They are Asahi Kasei, Chlorine Engineers, ELTECH, Uhde, and INEOS Chlor (formerly ICI). Both monopolar and bipolar cells are available from these cell manufacturers, but bipolar cells have become more popular in recent years.

Significant developments have been made in all designs; as a result the cells operate at an energy consumption of 2000–2100 kW hr ton⁻¹ of NaOH at 5 kA m⁻². The key design modifications closing any technical gap between these cell designs include: internal anolyte circulation, ensuring that the cell is full and all the membrane is wet all the time without any stagnated regions where the gases contact the membrane, uniform current and salt distribution in the anode compartment, absence of fluttering of the membrane during startup and steady-state operation, improved gasket designs and materials, and minimal ohmic drops. Granting that the differences between the electrolyzer designs have narrowed and that the cells are technically sound, it becomes onerous to the chlor-alkali producer to select the most appropriate cell technology from among those available.

The choice is generally based on overall capital costs, energy consumption, and operating costs over the life of the cell. These issues are discussed below.

The dominant role of energy consumption in chlor-alkali economics makes it the most important aspect of cell performance. If one type of cell can offer substantially lower energy consumption than others, it will have a major advantage in any techno-economic comparison. This fact is the single most important reason for the ongoing conversion of the industry to membrane cells.

Any membrane-cell design with a clear advantage in energy performance will no doubt be recommended over others. During the rapid evolution of membrane-cell technology over the past 25 years, there have been times when such differences existed. With the trend toward higher operating current densities, we have already noted the advantages of bipolar designs in this regard (Section 5.2). It is also true that refinements in bipolar cell design have removed many sources of inefficiency and that the differences in performance among the leading electrolyzer designs have become relatively small.

A glance at Table 5.4 shows this to be the case. While the percentage differences in energy requirements may be small, we have seen examples in this book of the economic importance of some of these small differences. A change of 20 kW hr ton⁻¹ in an 800-tpd plant operating 350 days/year represents 5.6 GW hr year. At \$30 MW hr⁻¹, the cost is \$168,000/year.

Still, a small relative difference in performance between two types of cell or two different proposals raises the question of its sustainability. The discussion of membrane performance in Section 4.8.5 makes it clear that performance deteriorates with time. The rate or extent of deterioration becomes just as important as the initial performance. It is essential for anyone studying the justification for a new membrane-cell installation or evaluating the differences between offers to understand this and to quantify it to some degree. The following are important factors:

1. Extent and quality of field experience (Where is the membrane/cell combination used? Has experience been good or bad at startup and after extended operation?).
2. Company/site experience with membrane cells (veterans or beginners?).
3. Commissioning assistance available.
4. Anticipated quality of technical service.

Sources of information include:

1. membrane suppliers
2. technology licensors

TABLE 5.4. Comparison of Bipolar Membrane Cell Technologies

Cell component	Asahi-Kasei	Chlorine Engineers	ELTECH	INEOS Chlor Ltd	Uhde
Cell designation	ML32, ML60	BiTAC-880	ExL ^B	BiChlor	BL-2.7
# of cells/electrolyzer	150	6 min, 90 max	60	Up to 160	160
Current density (kA m ⁻²)	2-6	1.5-6.5	1.5-7	1.5-8.0	6
Energy consumption (kW hr ton ⁻¹ of caustic)	2100 (@ 5 kA m ⁻²)	2050 (@ 5 kA m ⁻²)	2100 (@ 5 kA m ⁻²)	2200 (@ 6 kA m ⁻²)	2100 (@ 4 kA m ⁻²)
Outside dimensions (m)					
Length		4.85 (for 80 elements)	4.11 (60 cells)	18 (over the steel work)	14.5
Width	2.59, 3.86	2.38	1.46	3.04 (over the steel work)	8
Height	1.32, 1.67	1.6	2.56	2.28 (including foot insulator)	
Weight of electrolyzer (empty and full)		20,700 kg (empty)	9,700 kg (full) (60 cells)	65 tons (empty); 110 tons (full)	50 tons (empty); 95 tons (full)
Electrolyte volume (per unit cell)		36,000 kg (full)			200L/element
Operating conditions (Temp, Pressure, and electrolyte concentrations)		88°C, 0-330 mbar, 200-220 gpl NaCl, ca.32% NaOH	Temp: Normal/Max: 85/90°C	Temp: 90°C; Pressure: 0-250 mbar; Feed brine: 300 gpl; Exit brine: 200 gpl; 32% NaOH (or KOH)	Temp: 90°C; Pressure: 200-240 mbarg; Exit brine: 220 gpl; Exit NaOH: 32.5%
Unit cell	Single element consists of an anode and cathode bonded together	Single element consists of an anode and a cathode bonded together	Single cell consists of anode/cathode/membrane gaskets held together by 8 bolts	Nestpak (single cell) consists of anode/cathode/membrane	Individually bolted/sealed single elements consisting of anode/cathode/membrane

TABLE 5.4. continued

Cell component	Asahi-Kasei	Chlorine Engineers	ELTECH	INEOS Chlor Ltd	Uhde
Anode/cathode bonding		Assembled as unitary bipolar elements		Not applicable	Laser welded support/current conducting sheet metal
Anode compartment to cathode compartment electrical connection	Ti/Ag/Ni; Ag or Ag alloy Explosion bonded metal	Ti/Ag/Ni; Ag or Ag alloy	Nickel reticulate between cell packs held together by tie rods and low internal pressure	Proprietary	Cathode back pressed to anode back, use welded contact strips to minimize voltage drop
Anode/Membrane gap	1–2 mm physical gap achieved by gasket	Narrow physical gap	Membrane gap: achieved by pressure operation; needs minimum 14 kPa for good contact to the reticulate; Actual pressure: 28 kPa	Zero	Membrane suspended by mesh type anode (overpressure on cathode side; 40 mbarg); Defined gap maintained by 17 vertical PTFE strips clamped to cathode distributed over the width of the cell.
Anode gasket	PTFE/EPDM	EPDM	Rubber/FEP		PTFE
Cathode gasket	EPDM	EPDM	Rubber		PTFE
Anode coating		All use Ti/Ru/Ir based coatings			

Cathode coating	Plasma sprayed "NiO"	Special nickel plating	Plasma sprayed Ni-Al	Pt based	Plasma sprayed Ni-Ir-Ru
Cathodic Protection	No	Yes	Yes	Yes	Yes
Anode/cathode structure	Expanded mesh	Expanded mesh rigidly attached	Expanded Ti/Ni metal	Expanded mesh	Mesh-type anode and louver-type cathode; welds to support sheet metal covered by spacer strips
Anode mesh contact	Welded		Free floating	Welded to current carriers	
Anode pan to mesh contact	Welded to standoffs located $\sim 7''$ apart	Spot welded waveform pan structure	Welded to standoffs located at $\sim 1\ 3/4''$ apart	Current carriers welded to pan at $6''$ intervals	17 vertical metal sheets; laser welded semi-shell to the anode
Pan thickness (cm)	>2.5	2.5	<2.5	0.16 cm thick material, module length: 9.5 cm	2 mm (material thickness)
Electrode size (m ²)	2.7/5.1	3,276	1.5	2.9	2.7
Membrane	Aciplex	Various	Nafion	Nafion/Aciplex/Flemion	Nafion
Control of electrolyte feed rate		Flow control to each individual circuit	Rotameters (optional vortex)	Flow control to individual electrolyzers; electrolyzer feed header (individual packs) distributes flow via 8 mm id long tubes	Flow meter in electrolyzer feed line
Method of control of electrolyte level in the cell		Overflow	Gravity feed overflow	Gravity overflow ensuring membrane fully wetted	Hydrostatic balance inside the single element

TABLE 5.4. continued

Cell component	Asahi-Kasei	Chlorine Engineers	ELTECH	INEOS Chlor Ltd	Uhde
Electrolyte feed			All feed the brine from the bottom		
Gas Disengagement	Depleted brine comes from the top; two-phase flow through clear tubing (Fig. 5.36A1)	Two-phase flow from top through a tube (Fig. 5.36B1)	In the manifold (Fig. 5.36C1)	Each Nestpak has an external exit header (Fig. 5.36D1)	Within the cells; two-phase discharge downward through an internal vertical PTFE stand pipe; all headers are located underneath the electrolyzer (Fig. 5.36E1)
Internal/Natural recirculation	(Fig. 5.36A2)	(Fig. 5.36B2)	Cells fed from the bottom with distribution by stand-off holes (Fig. 5.36C2)	Internal circulation (Fig. 5.36D2)	Inclined upper baffle plate ensures good anolyte supply to the upper membrane section (See Fig. 5.36E2); Vertical lower baffle plate promotes uniform distribution of concentration and temperature
Gaskets	Picture frame/PTFE, EPDM (Fig. 5.36A3)	Picture frame, EPDM (Fig. 5.36B3)	Double gasketing (Fig. 5.36C3)	Picture frame/PTFE protected EPDM (Fig. 5.36D3)	Membrane/PTFE gasket/Gore-Tex Bead (Fig. 5.36E3)
Anode side pans/cell flange	Pure Ti (Grade 2)	Pan is made of Ti and the flange is coated	Ti Grade 11 or 27 for crevice corrosion protection	Pure Ti (grade 1) with flanges coated for corrosion protection; Anode pan volume: 112 L; cathode pan volume: 153 L	Titanium

Current leakage prevention	Sacrificial target in the anolyte exit flange	DSA coat the areas where the electrolyte comes in contact with the metal	DSA coat the areas where the electrolyte first contacts Ti metal; Spiral manifolds or tubing act as current breakers	Coated Ti current collectors in brine and exit collectors to nestpaks; Ni current collector in caustic outlet	Long feed and discharge hoses/pipes; two-phase flow in discharge pipes; electrolyzer isolation from ground, earthing only feed and discharge lines with shared piping
Current leakage (magnitude)		Typically <0.2%		5 amp. max per header to ground	0.05–0.1%
Perimeter damage	Gasket stops at the same place as membrane (Fig. 5.36A4)	Minimized by central electrolyte connections (Fig. 5.36B4)	Membrane extends past gasket area. (Fig. 5.36C4); mesh extended to side of pan for smooth transition in perimeter area	None; fully wetted (Fig. 5.36D4)	None (Fig 5.36E4)
Differential Pressure across membranes (Allowable range; set point)					40 mbar
Membrane flutter	Two-phase flow out of the top of the cells/Yes	Design of overflow assures smooth operation and lack of membrane flutter	Better with ExL cells; positive pressure against the anode assures no fluttering	No; zero gap	Eliminated because of differential pressure and clamping the membrane in 18 sections

TABLE 5.4. continued

Cell component	Asahi-Kasei	Chlorine Engineers	ELTECH	INEOS Chlor Ltd	Uhde
Salt/caustic/temperature distribution in the cells	3-5 to 1; recirculation rate/good	Optimized by waveform structure for increased circulation	Stand-offs promote good mixing	Caustic flow rate is 1-1.5 times the brine flow rate to maintain temperatures	Optimized because of baffle plates for increased circulation
Sealing force for gaskets	Hydraulic	14 tie-rods	6 tie-rods	32 compression screw jacks	27 tie-rods/electrolyzer rack
Pressure operation	20 psi; pr. differential: 15.24 cm	Atmospheric presence preferred but operation can be at 200-300 mbarg	20-35 kPa; pr. differential: 15 cm. (Cl ₂ /H ₂)-0.21/0.225 kg cm ⁻² gauge		240 mbarg for H ₂ and 200 mbarg for Cl ₂ ; can be increased to 400 mbarg
Caustic recirculation Internal or external		External	Yes; Gravity flow to caustic tank with pumped loop back to the cells which includes heat adjustment	External	External dilution of feed caustic

N.B.: All the information in this table was provided by the technology suppliers.

3. contractors and technologists
4. operating companies
5. literature
6. grapevine

Much of the available literature deals with the progress of membrane technology and describes performance under well-controlled laboratory conditions. Other reports describe the effects of artificial disturbances, which usually are made in order to accelerate rates of deterioration. There is no scientific way at present to calculate the effects of likely plant disturbances on cell performance and component life. In this situation, the relative importance of other components of the life-cycle cost increases. Some of these are hard to quantify, but this is no reason to ignore them.

Pearson [89] presented a method for the evaluation of these factors. This was intended for use by those who are considering adopting membrane-cell technology, and we approach the subject from the same viewpoint. Pearson's outline included the following:

Technical Criteria

- Membranes
- Energy consumption
- Materials
- Products
- Operating characteristics
- Maintenance

Commercial Considerations

- Engineering capability
- License terms and conditions
- Operational support capability
- Licensors background

Evaluation

Intangibles

5.5.1.1. Membranes. Membrane costs are considerable, about $\$10\text{ton}^{-1}$ of product in many cases. In most evaluations, membranes are assigned an average useful life, frequently an integral number of years. The same is true of other components such as electrodes, their coatings, and gaskets. A long-range evaluation should consider the interactions among the various numbers. Assume, for example, that membranes have a 3-year life and gaskets a 5-year life. Assume further that changing gaskets requires the membranes to be discarded and replaced, and that the service lives mentioned are precise numbers rather than statistically distributed averages. The average membrane life becomes 2.5 years, and the cost of their replacement is 20% higher. It may be better to change the gaskets each time the membranes are removed, incurring a 40% loss in attainable gasket life.

Most producers will want to establish more than one source of supply of membranes. Many will want to have several different types of membranes at startup in order to begin comparative evaluations. It is important to discuss this with the cell supplier and

to determine any effects on required operating conditions, contractual terms, patent indemnities, and technical service policies.

It is always physically possible to install different types of membrane, but when different operating conditions are necessary for the different types, or when their presence complicates contractual matters or makes guarantee provisions less clear, this option becomes less practical.

Membranes do not fail suddenly. However, because of surges of brine impurities, excursions in electrolyte composition, over-acidification of the feed brine, or mechanical damage, sudden failures do occur, the usual situation being a gradual deterioration in performance. The decision to replace a membrane should be based on a balance between the costs of replacement and power cost. The rate of deterioration determines the average performance during the life of a membrane. This information, not the initial operating data, should be used in an economic evaluation of the cell technology.

5.5.1.2. Energy Consumption. The basis on which energy consumption is quoted must be clear and unequivocal. An electrolyzer supplier will quote only on DC consumption but may base the number on energy consumed within the cells or may provide data across the circuit including any intercell losses. At a minimum, the evaluation should include all losses between rectifier terminals. Ultimately, the AC requirement must be stated or estimated. The actual characteristics of rectifiers should be used in this determination. Evaluators should allow for conversion losses, based on efficiencies that represent rectifiers that may be operating below their full design load, and for equipment necessary to maintain a high power factor and control harmonics within allowable limits (e.g., capacitor banks).

There are also differences in the specified electrolyte concentrations into and out of the cells. The resulting differences in flows affect pumping costs and the size and operating cost of treating systems.

Undue emphasis on electrical energy consumption can result in quotes based on caustic concentrations less than the optimum. Unless all cell operating data are based on the same caustic concentration, differences in the cost of evaporation must be included in the evaluation.

5.5.1.3. Auxiliary Materials. There are some differences between suppliers that are related to the details of brine specifications, which may make the treating requirements more onerous in particular cases, and translate into increased capital or operating costs. When treatment needs add to the difficulty of operation and the probability of failure, evaluation becomes more elusive. There are also differences in requirements for the auxiliary materials. Chapter 9 will show that there is not strong agreement on the amounts of chemicals required for primary brine treatment. Chapter 9 will also show that ion-exchange regenerant requirements are substantial and will vary from one technology to the next.

5.5.1.4. Products. Product quality is another important aspect for which one usually can expect to see few superficial differences among the various offers. One aspect of

gas “quality” that must be considered is the operating pressure. Various references in Chapters 9 and 17 describe the efficiencies and lower costs offered by delivering gas under positive pressure. Otherwise, there will be little to choose in hydrogen quality. Chlorine quality is affected by subatmospheric pressure between the cells and the compressors and by current inefficiency. Poor quality translates into high processing cost. It also reduces the efficiency of liquefaction or requires the application of more severe conditions to achieve a certain liquid recovery.

The most important impurity in chlorine is oxygen, particularly so in its major application, the synthesis of ethylene dichloride. As discussed in Section 9.6.1 and in parts of Chapter 11, acidification of feed brine is a common practice that helps to reduce the oxygen content of the cell gas. The acid of choice is HCl, and this is frequently produced on site from the cell product gases.

Use of brine acidification requires proper accounting for the cost of HCl. This is straightforward when acid is purchased from an outside source. Internal production of acid brings in several options. First, a project definition may provide for production of a certain amount of chlorine from the cells. In this case, the production of HCl for use in the process directly reduces the amounts of chlorine and hydrogen available for other uses. It also reduces the amount of caustic product available. This is a result of the addition of HCl to the brine. It increases the efficiency of production of chlorine by the cell but has no effect on the amount of caustic produced. The higher yield of chlorine means that the amperage can be reduced, saving on the electrical cost but also producing less NaOH or KOH. The reduction in the amount of product available for external use is an important economic consideration. Second, if the project definition provides instead for a certain amount of chlorine available after production of internally consumed HCl, the amount of gas produced must increase. This can increase the electrical cost substantially but also gives more caustic product. The value of this depends on market conditions. The costing of the chlorine used to produce HCl may reflect the difficulty of liquefaction of an equal amount. Section 9.1.7 points out that the severity of liquefaction must increase as recovery becomes greater. The incremental energy cost increases rapidly as the concentration of noncondensable gases in the chlorine mounts. Chlorine that is present in the tail gas, the usual source of manufactured HCl, is less valuable than chlorine that is present in more concentrated streams.

The quality of caustic from membrane cells depend on the relative rates of transport of various species across the membrane. The user should be aware that the rates of transport of anions are less sensitive to the current density than is the rate of transport of Na^+ or K^+ . When production is curtailed or stopped, the concentrations of anions such as Cl^- and ClO_3^- increase. This becomes an important effect when there are tight product specifications. This situation is more likely in the case of KOH production. Not all membranes are equal when it comes to rejecting Cl^- and ClO_3^- .

5.5.1.5. Operating Characteristics. Operating characteristics in Pearson’s scheme of things include system considerations such as control of the cells, operating dynamics, and analytical requirements. One control aspect that deserves some attention is the acceptable range in differential pressure across the membranes. This is an important parameter because excessive swings in differential pressure allow the membrane to shift

its position between the electrodes. This movement can lead to mechanical fatigue, and so rapid fluctuations in pressure are especially dangerous. The requirements for process control must be judged in terms of the operating pressure. Allowable differential pressure is a small fraction of absolute operating pressure. Operating the cells under positive pressure aggravates the control problem, and Section 11.4.2.1 discusses this issue.

5.5.1.6. Evaluation and Commercial Considerations. The evaluation that follows collection of the data can profitably use a method of differences. Each technology is evaluated for each factor against a base case. The technology most familiar to the evaluators (or for which the most reliable information is available) is a natural choice for the base case. The relative capital costs of all candidate processes are then assembled, area-by-area. The comparison must not be confined to the electrolyzers and their auxiliaries but should include the differences seen in the following:

1. brine preparation and treatment
2. chlorine processing
3. hydrogen handling
4. caustic evaporation and handling
5. utilities
6. waste treatment
7. auxiliaries
8. other costs (e.g., design, site development, acquisition of permits, etc.)

The analysis of operating costs should be on a similar basis. Small differences in unit consumption rates can become quite important.

Commercial considerations are beyond the scope of this book, but they are extremely important in financial analysis. The financial criteria must be clearly stated before analysis begins. The discounting philosophy or the rate of return to be used in judging incremental investments should be shared with bidders. This will then allow and require them to provide the best balance between capital and operating costs in determining, for example, the current density on which to base their offers.

Finally, there are the ubiquitous intangibles such as corporate agreements or “deals” between the chlor-alkali producer and the cell technology supplier or its parent organization, the membrane supplier, and the anode vendor. This is sometimes a reality, in which case the cell technology comparison may become moot.

The many factors that seem to defy rigorous analysis can be quantified in different ways. One would involve probabilistic estimates and assign hard numerical values to each factor. The size and quality of the reliable database, however, do not support this approach. It becomes a judgmental exercise. Another is to prepare a matrix of the various factors considered to be important in a given analysis. Some of these factors might be:

1. safety;
2. licensor's field experience;
 - (a) with membrane offered
 - (b) with cell configuration offered

- (c) at similar plant capacities
- (d) at similar current densities
- 3. other field experience with membrane in cells of similar configuration
- 4. ease of cell handling and renewal
 - (a) types of labor required and size of crew
 - (b) sophistication
- 5. uniformity of current distribution
 - (a) between electrolyzers
 - (b) between electrodes in given electrolyzer
 - (c) across face of electrodes
- 6. quality of performance guarantee (not specific data, but evaluator's assessment of reliability)
- 7. expected quality of technical service
- 8. patent indemnities

Each item selected for evaluation is given a weighting factor reflecting its importance. The fact that evaluators expect to see small differences in certain areas should not cause them to proclaim these items of little importance and to assign low weighting factors. There is a certain esthetic appeal in having the values of all the weighting factors add up to 100 or 1,000. Finally comes the evaluation of the various offers. Each is assigned a score based on narrow consideration of the issue at hand. For example, take item #4, the ease of cell handling and renewal. This should not include the time expended, the production lost while changing amperage or while the electrolyzer berth is empty, or the cost of performing a normal cell renewal. These are quantifiable and should be in the comparative cost analysis. This item relates instead to the disruption of normal labor assignments (how many people are required during peak handling/renewal activity? where do they come from?) and to the complexity of the renewal process (what training is required? what is the likelihood of error?).

The scores assigned should be on a uniform scale for each factor analyzed (e.g., 0–10). Any other scale can be used, but the use of more than one significant figure, or “1.3” significant figures with half-points allowed, usually is not justified by the quality of the information available and the different perceptions of various evaluators. Weighting factors and scores are then multiplied together and the products added to give final totals. The method is also consistent with the use of “go/no go” criteria, where options that do not meet preset conditions are rejected. It can also create go/no go levels, for example, the rejection of a design that is clearly rated less safe than others, without consideration of its merits.

It is difficult to agree on what is perfect in any item. Rather than assign 10 as a perfect score and deal with the variability in opinion on how far an offer falls short, it may be more convenient to rate the best candidate at 10 and then to evaluate the others by comparison. A similar approach would take up Pearson's suggestion to choose the most familiar or best-documented technology as a base case with scores of zero or ten and to rate all others by direct comparison.

This procedure has the advantage of bringing essentially qualitative judgments together in the form of a single number. Perhaps it is unnecessary to point out that the method has little value unless the weighting factors are agreed upon before doing the analysis.

5.5.2. *Electrolyzer Technologies: General*

Electrolyzers are classified as monopolar or bipolar, depending on the manner in which an electrical connection is made between the electrolyzer elements. In the monopolar type, all anode and cathode elements are arranged in parallel (Fig. 5.2A). Such an electrolyzer will operate at a high amperage and low voltage. While the amperage is set by the number of elements in an electrolyzer, the voltage depends on how many electrolyzers are in an electric circuit. In a bipolar configuration, the cathode of one cell is connected to the anode of the next cell, and thus the cells are configured in series (Fig. 5.2B). This scheme of cell assembly results in operation of the electrolyzers at low amperage and high voltage. The bipolar arrangement gives a low voltage drop between the cells. However, problems associated with current leakage and corrosion arise in bipolar operations, since the feed and discharge streams of electrolytes having different electrical potentials are hydraulically connected through common manifolds and collectors. These problems can be avoided by limiting the number of elements per electrolyzer to limit the overall stack voltage to an acceptable value. The monopolar design, on the other hand, suffers from the voltage losses in the inter-electrolyzer bus bars. This inevitable drawback can be minimized by a conservative design. While the bipolar systems allow shutdown for maintenance of a single electrolyzer unit, independently from the rest of the plant, monopolar electrolyzers have to be designed in such a way that an individual electrolyzer can be short-circuited, enabling maintenance and membrane replacement without shutting down the entire circuit. It is also possible to combine these two configurations in a hybrid electrolyzer arrangement. This has been used in conversion projects where the electrolyzers had to be configured properly to integrate with the existing rectifiers and their performance.

5.5.3. *Commercial Electrolyzers*

All membrane electrolyzers have common general design features such as vertical arrangement of membranes, stacked elements, and usage of similar materials of construction. Nevertheless, there are quite substantial differences in the cell design.

One difference is the manner of achieving effective sealing of the electrolyzer. The most common version is the filter-press arrangement, where tightness is achieved by pressing together all elements of the electrolyzer from both ends. The relatively high sealing forces are produced by hydraulic devices or tie rods. A different approach is the single element design, first developed and applied by Uhde, where each element is individually sealed by a flanged connection between the cathode and the anode semi-shell. The pre-assembled elements are stacked to form an electrolyzer, but only moderate forces are applied to ensure electrical contact.

As membrane development allows increasing current densities, electrolyzer internals have to meet the related effects. Essential design targets are the minimization of

structural voltage losses, homogenization of electrolyte concentration and temperature, and measures to counter problems related to the increased gas evolution.

All the technology cell suppliers claim that their cells can operate at current densities greater than 5 kA m^{-2} with an energy consumption of $2,000\text{--}2,100 \text{ kW hr ton}^{-1}$ of caustic at 5 kA m^{-2} . They also claim that their designs have addressed and solved many of the problems observed during their operation. Details are in their publications and promotional literature.

The key component of a membrane cell is the ion-exchange membrane, which determines the performance characteristics of the cell, reckoned in terms of cell voltage, current efficiency, product purity, and the active life of the cell. The ion-exchange membrane operates best if it maintains its dimensional and structural integrity in the cell during startup, shutdown, and operation. It is essential that the membrane is fully stretched in the cell without any folds or wrinkles and is not subjected to physical wear or fluttering. Furthermore, the entire surface of the membrane should be exposed to a constant flux of sodium ions and water molecules during operation.

The prerequisites for realizing a constant and uniform flux are: uniform current density, temperature, and electrolyte concentrations. Uniform current density across the membrane requires proper geometry of the electrodes and an efficient design for delivering current to the anode and cathode structures and distributing it to the faces of the electrodes. Another factor that will skew the current and concentration distributions is the presence of gas bubbles in the anolyte facing the membrane. Achieving uniform concentration of salt at a constant temperature across the face of the entire membrane requires efficient circulation in the cells by natural or forced circulation. Ensuring the absence of gas bubbles that will cause local blinding of the membrane and local depletion of salt depends on effective removal of gas bubbles from the top of the cell and where the gas is disengaged from the anolyte. How each technology achieves the above needs to keep the membrane "happy" depends on the specific design features in the cell. A detailed knowledge of these features will allow the technology users to evaluate the appropriate one that would be comfortable to them. These cell design features are not always clearly elaborated in the cell description brochures. Summing up, the questions that should be asked by the buyer are as follows.

1. Electrolyte feed: How uniform is the electrolyte distribution in a given cell and in the electrolyzer stack? Is the same amount of brine going through each cell? How does the given cell design accomplish this uniformity in concentration within the cell and across the cell stack?
2. Gas outlets: How well are the gases taken out of the cell without any surging, and ensuring that the entire membrane is completely wet?
3. How good is the internal circulation in the cell? What specific feature of the cell design allows uniform distribution of reactants and temperature within the system? Reactants include protons!
4. How well are the membranes supported to minimize flutter during startup, shutdown, and load fluctuations, without causing any stress on them?
5. What specific anode and cathode geometry and membrane structure ensure that there are no electrically dead zones in the membranes?

6. How uniform is the current distribution across the membrane and between the cells?
7. What is the voltage drop across the intercell connectors (in a monopolar cell) or the connecting strips (in bipolar cells)? What specific design feature allows minimization of these voltage drops?
8. How difficult are assembly and disassembly? Ease includes simplicity and minimal manpower requirement.
9. How difficult is it to replace a cell or a cell stack?
10. How complex are maintenance and repair?
11. How complex and expensive is the cell renewal process?
12. How difficult is it to identify and reach a damaged cell?
13. Is individual cell voltage monitoring available?

The following section addresses the actual electrolyzer designs of the suppliers.

5.5.3.1. Asahi Kasei Chemicals. Asahi Kasei's electrolyzer (Acilyzer-ML[®]) [90–93] is a filter-press type bipolar cell holding a series of cell frames up to a total of 180. The right side of Fig. 5.24 shows a front view of the cell frame and the bipolar cell element. The left side shows a cross-sectional view of two cell frames with the membrane in between. Various components are labeled. A unit cell consists of the anode compartment from one bipolar cell frame, a membrane, and the cathode compartment of a second bipolar cell frame.

The anode compartment is titanium and the cathode compartment is nickel. Both of these compartments are combined onto a partition wall made of an explosion-bonded titanium-steel plate. Anodes and cathodes are spot-welded onto the ribs of each

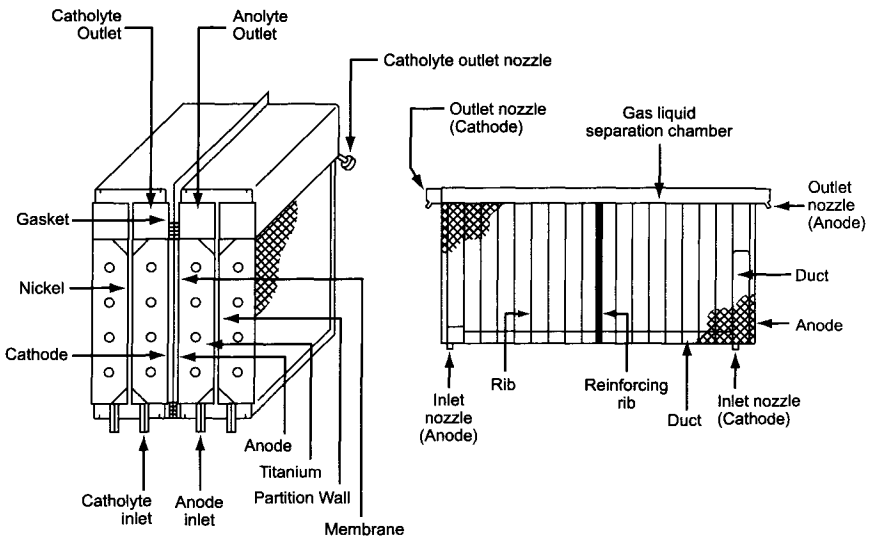


FIGURE 5.24. Schematic of Asahi Kasei's ML32NC and ML60NC cells. (With permission from Asahi Kasei Chemicals.)

compartment. Each compartment has an electrolyte inlet at the bottom and gas/liquid outlet at the top. These are connected to the inlet and outlet headers by PFA hoses. AKI's activated cathode does not require the installation of a polarization rectifier. The anolyte headers are titanium and the catholyte headers are nickel. Supporting arms on both sides allow the cell frames to hang on the side bars of the filter press.

The model ML32 with an effective membrane area of 2.7 m² has an annual production capacity of about 15,000 tons of NaOH (100% basis) with 100 cells. ML60 has an effective area of 5.05 m² and an annual production capacity of 30,000 tons of NaOH (100% basis).

The Asahi Kasei electrolyzer can operate at pressures up to 100 kPa. Its structure is strong enough to allow an operator to stand on top of the cell frame during maintenance, thereby eliminating the need for a separate maintenance area.

Both anolyte and catholyte are circulated in the cell chambers. Uniform concentration is achieved by forced or natural circulation as shown in Fig. 5.25.

As of 2002, a total production capacity of about 6,820,000 tons of caustic per year was in operation or under construction with Asahi Kasei technology.

5.5.3.2. Chlorine Engineers Electrolyzers. Chlorine Engineers Corporation (CEC), a subsidiary of Mitsui and Company, produces the filter-press type, monopolar membrane electrolyzer shown in Fig. 5.26 [94]. Uniform electrical current travels into each anode element through titanium-clad, copper-cored conductor rods and current distributors. The current distributor also serves as a downcomer, which promotes circulation

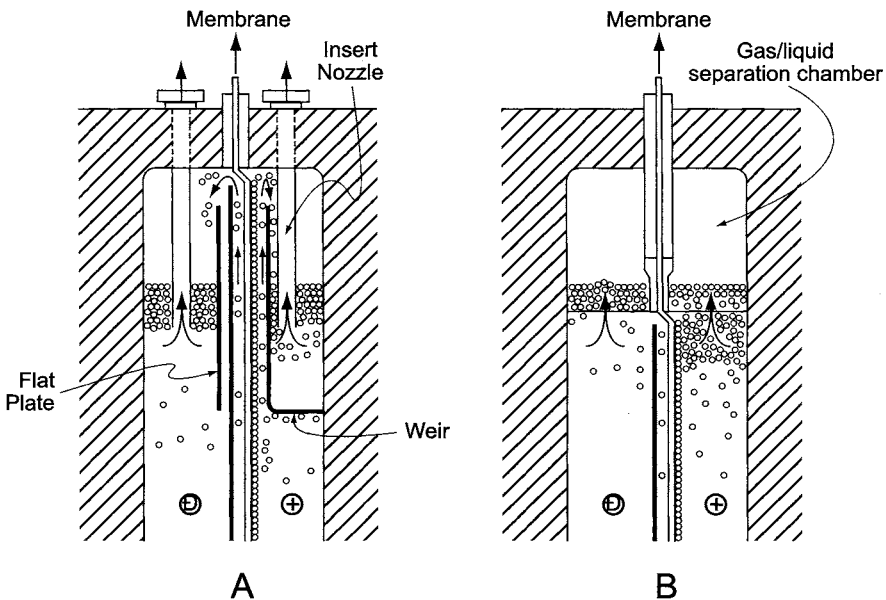
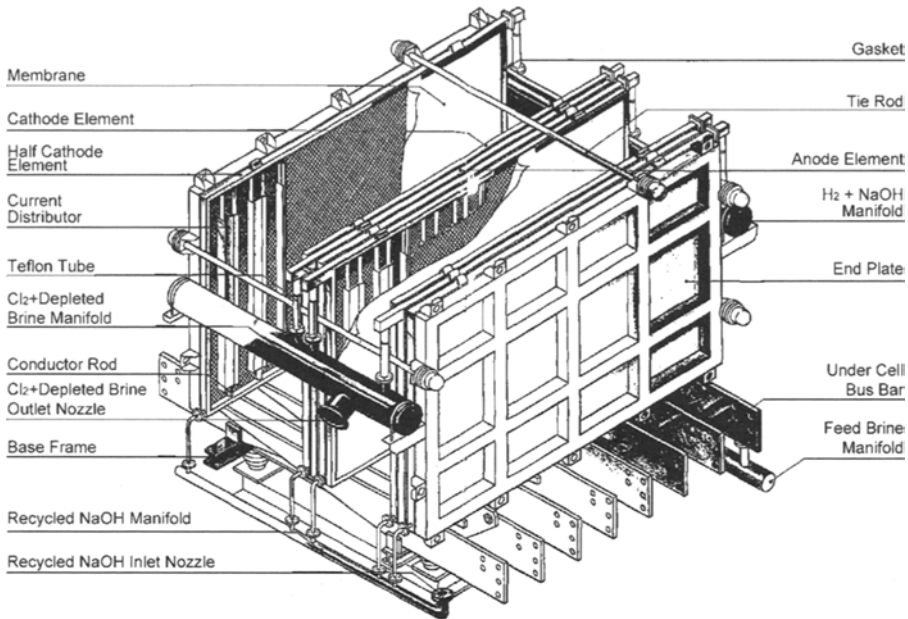
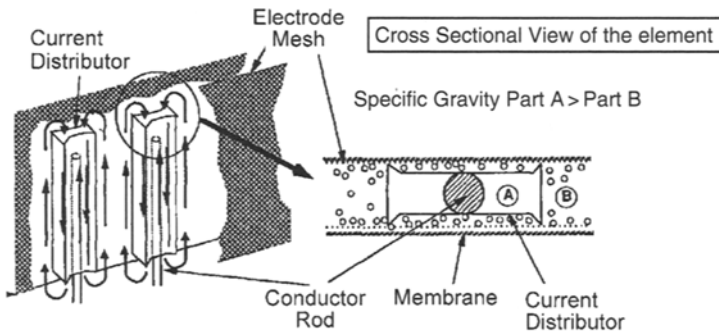


FIGURE 5.25. Forced (A) and natural (B) circulation in Asahi Kasei cells. (With permission from Asahi Kasei Chemicals.)



CME Structure



Internal Circulation in CME Cell

FIGURE 5.26. CME monopolar electrolyzer showing bus bar alignment and internal circulation. (With permission from Chlorine Engineers Corporation.)

of the electrolyte within the cell to maintain uniform concentration and efficient gas release. The internal circulation is intended to eliminate the necessity for an external forced recirculation system.

The gasket thickness sets the electrode spacing, and either finite- or narrow-gap configuration is possible. The anode frame is titanium and the cathode frame is stainless steel or nickel. The anolyte volume is larger than it is in competing elements, therefore, the electrolyte gas void fraction is smaller. This feature also reduces the change in liquid

levels during shutdowns. CEC offers electroplated activated cathodes. Gas and liquid leave the cell in the stratified overflow mode, as the liquid level is maintained in the upper cell frame. Semitransparent PTFE tubes are used to monitor the operation visually. The bus bars are installed beneath and at a right angle to the cell elements, requiring no equalizer between electrolyzers (see detail in Fig. 5.27). The bus bar can be used as a short-circuiting element by changing the connections.

Chlorine Engineers also developed a bipolar electrolyzer, BiTAC[®]-800, with Tosoh Corporation. The electrolyzer [95–97] is of the filter-press type and has an effective membrane area of about 3.3 m². Up to 100 elements can be assembled together by spring-loaded tie rods. The electrode frames are made of a special titanium alloy on the anode side and nickel on the cathode side. The wave-like structure of the cathode and anode pans serves the combined function of partition plates and conductor ribs, as shown in Fig. 5.27.

The current is led to the anode mainly through nickel to avoid the ohmic losses from the poor electrical conductivity of titanium. The exit streams leave the cells by overflowing into the collecting pipes located at each side of the electrolyzer via external flexible

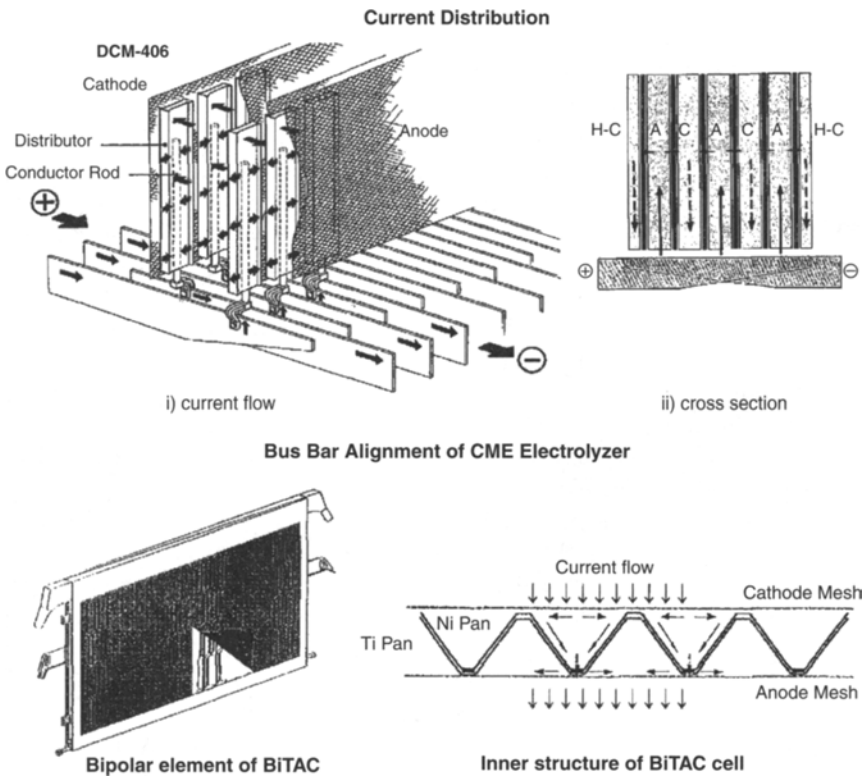


FIGURE 5.27. Current distribution in CME electrolyzer and bipolar element of BiTAC and cross-sectional view of the BiTAC[®] cell element showing current path. (With permission from Chlorine Engineers Corporation.)

hoses. The membrane–cathode gap can be adjusted from a narrow to a finite value, to meet the requirements of various commercial membranes. BiTAC[®] electrolyzers have been operating at 5 kA m^{-2} since 1994, and at 6.5 kA m^{-2} since 1999. As of 2003, the installed capacity with these cells was 2,370,000 tpy of NaOH.

Chlorine Engineers Corporation also provides the hardware for the Asahi Glass cells. Asahi Glass Company was a major supplier of cell technology [85], but they are no longer involved in the development of chlorine cells. Asahi Glass remains in the membrane business and is still a major manufacturer of chlorine.

Asahi Glass Company developed monopolar and bipolar cells. The bipolar electrolyzer, AZEC IB1-75, has 75 unit cells and operates in the current density range of $1.5\text{--}6.0 \text{ kA m}^{-2}$, the energy consumption at 5 kA m^{-2} being $2,100 \text{ kW hrt}^{-1}$ caustic, at $80\text{--}90^\circ\text{C}$, 5 kPa, and 32% caustic. Each unit cell is a single element consisting of a Ru–Ir–Ti-coated titanium anode and a Raney-nickel coated nickel cathode, which are bonded together. The electrode size is 2.88 m^2 . The anode mesh is welded to the stand offs located at 17.8 cm apart in the anode pan. Brine is fed from the bottom and controlled by a rotameter. The gases are disengaged from the top through a tube. The anode and cathode gaskets are made of EPDM. The differential pressure prevents flutter across the Flemion membrane.

5.5.3.3. ELTECH ExL Electrolyzers. ELTECH offers three electrolyzers designated ExL^M, ExL^B, and ExL^{DP} [98]. These are 1.5 m^2 cells operating in monopolar, bipolar, and dense pak, “orientations” respectively. The monopolar ExL^M is the modified version of the earlier MGC (membrane gap cell) electrolyzer. The general cell design is of the filter-press type, where the elements are pressed together by tie rods using copper distributors or nickel reticulate between elements. The intercell connections are from the sides, and the support for the electrolyzer is the copper current redistribution bus bar between electrolyzers. The feed streams and products enter and leave the elements via the attached manifold devices, thereby allowing gravity flow to the inlet from the head tank and from the outlet to caustic circulation and depleted brine tanks.

Improvements have been made to the anode and cathode design and fabrication techniques, as well as to the gasket and manifold materials. These have resulted in a uniform current distribution across the active membrane area and increased internal circulation. In addition, the use of modular bipolar “paks” with the use of only eight bolts reduces cell renewal time.

One of the main features of this cell is the double-gasket design. The cathode O-ring is located closer to the liquid than the anode O-ring, which is not in permanent contact with the chlorinated brine, thereby serving as a well-protected back-up seal. Rounded corners in the anode and cathode pans eliminate gas stagnation in the corners of the cell.

In the monopolar orientation, up to 30 membranes, with an effective area of about 1.5 m^2 each, can be put together to achieve a production capacity of 9.3 tons of NaOH per day (100% basis) at a current density of 6 kA m^{-2} . The ExL^B (Fig. 5.28) is the bipolar version of the ExL^M. The bipolar arrangement is realized by pressing the nickel cathode pan onto the nickel plated back of the anode pan. Up to 60 elements can be combined in one electrolyzer, to realize a production capacity of 22 tons of NaOH per day at a current density of 7 kA m^{-2} . The ExL^{DP} electrolyzer (dense pak) represents

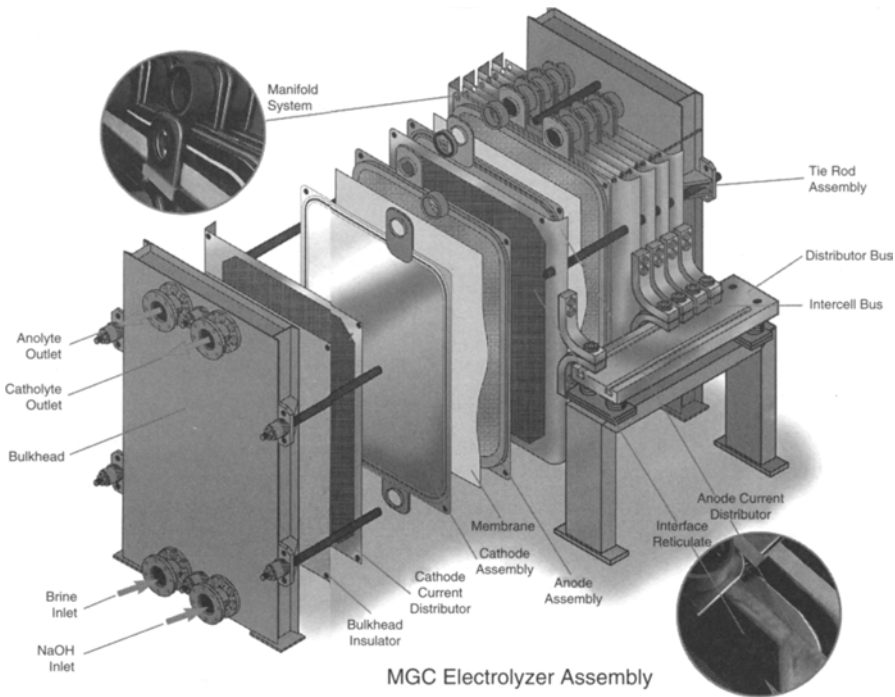


FIGURE 5.28. ELTECH ExL^B electrolyzer. (With permission from ELTECH Systems Corporation.)

a hybrid cell-arrangement, combining multiple ExL^B blocks, each containing two to ten elements, in one electrolyzer unit. The blocks are electrically separated from each other using standard monopolar components. ELTECH is developing a 3.1 m² version of the ExL bipolar design consisting of 80 elements for a production capacity of 60 tpd at 7 kA m⁻² [99].

As of 2003, the total installed capacity with these cells was 1,000,000 tpy.

5.5.3.4. INEOS Electrolyzers. INEOS' FM21-SP monopolar electrolyzer (Fig. 5.29) uses stamped electrodes. The anode is a 2-mm thick titanium panel between compression-molded joints of a special cross-linked EPDM elastomer. The cathode is a 2-mm thick nickel panel between compression molded EPDM joints.

The anodes and cathodes are assembled between two end plates, up to 60 anodes in the FM21-SP and up to 90 anodes in the larger FM-1500. A key feature of both designs is the elimination of any external piping to the individual cell compartments by the use of a simple but effective internal manifold arrangement. As shown in Fig. 5.30, the anode and cathode panels are designed to form feed and discharge channels when assembled.

The electrolyzer has coated titanium anodes, while the cathodes are made of pure nickel, either plain or coated with activated coatings. Both electrodes are pressed from integral sheets of pure metal, and this makes recoating of the electrodes simple and cost-effective. The upper left side of Fig. 5.29 shows electrical connectors attached to the tops

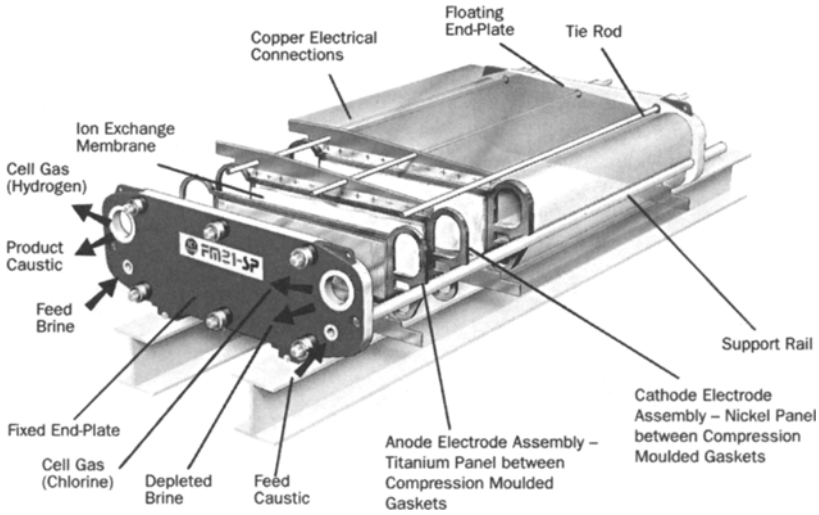


FIGURE 5.29. INEOS FM21-SP monopolar electrolyzer. (With permission from INEOS Chlor Ltd.)

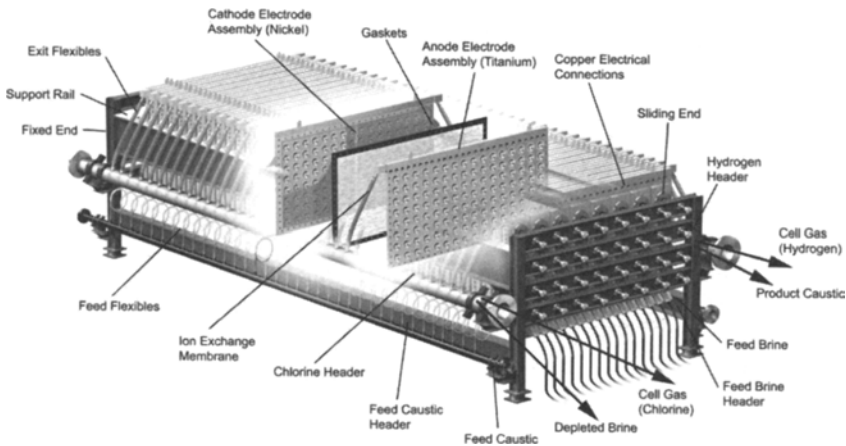


FIGURE 5.30. INEOS BiChlor™ electrolyzer. (With permission from INEOS Chlor Ltd.)

of the cathodes. There are similar attachments to the bottoms of the anodes. Flexible copper strips, formed of many thin copper leaves, link the cathodes of one cell to the anodes of an adjacent cell. Each strip normally connects two cathodes to two anodes. Recoated structures can be sent to the site before electrolyzer refurbishment from a pool of electrodes kept in stock by the electrode supplier. The removed electrodes are recoated without interfering with plant operations and are added to the pool of electrodes.

The effective electrode area of one monopolar cell is 0.21 m^2 , which makes this electrolyzer very compact [100]. The individual, lightweight electrodes are readily handled without the need for lifting devices, allowing the electrolyzer to be rebuilt or refurbished by a small crew in a short time.

The INEOS BiChlor™ electrolyzer [101–103], shown in Fig. 5.30, is a modular bipolar design that uses the unit-cell principle. Each module is termed “Nestpak,” consisting of an anode, a membrane, and a cathode. Anodes and cathodes are both expanded mesh. The anode mesh is welded to current carriers that, in turn, are welded to the anode pan at certain intervals. Current transfer to the electrode meshes is through multi-legged spiders. The configuration and spacing of the spiders are chosen to provide even current flow across the whole membrane area. In the standard design with a cross-sectional area of about 2.9 m^2 , the legs of the spiders effectively provide 32 electrical conductors in parallel on each side of the membrane (Fig. 5.31).

The anode and cathode pans have dimples that give them their characteristic shape. The dimples interlock when an electrode pack is assembled. Figure 5.31 shows that the

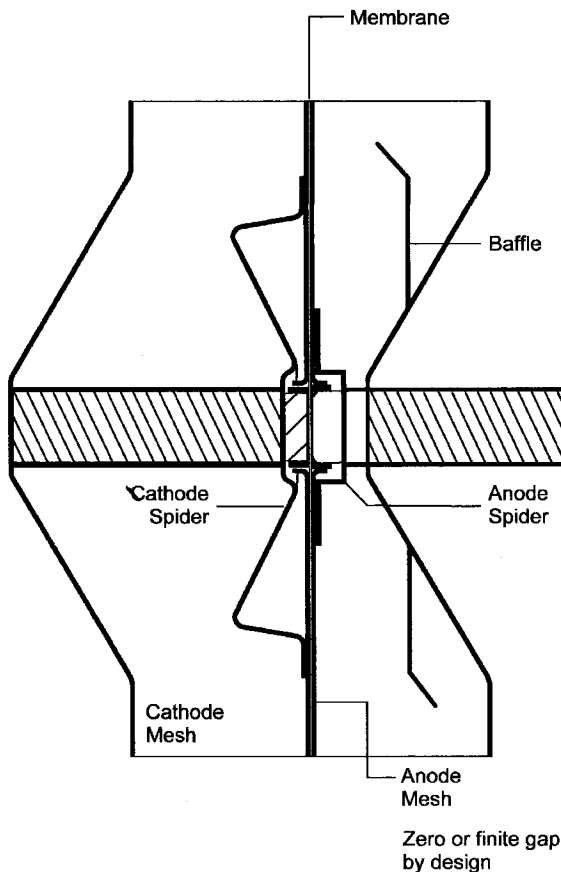


FIGURE 5.31. Current distribution to mesh electrodes in the BiChlor cell. (With permission from INEOS Chlor Ltd.)

anode-pan dimples closely approach the anode mesh and the membrane. Cathode-pan dimples protrude away from the membrane. This leaves the cathode spider some distance from the pan. Metal strips are added to provide a connection with high conductivity.

Internal mixing of electrolytes is driven by gas lift. Feed headers run the full width of the electrodes, giving even distribution of electrolyte flows. Internal baffles complete the process by preventing channeling of the gas flow. One intent of these design features is to permit controlled acid injection into the brine in order to limit the oxygen content of the chlorine gas, without the need for extensive recirculation devices. Internal circulation is promoted by the use of a split baffle.

Similarly, gas leaves the compartment along its entire length. This minimizes pressure drop and, with an elevated discharge header, keeps the entire surface of the membrane wet. Tests with a demonstration electrolyzer showed a cell voltage of 3.02–3.05 V (depending on the membrane) at a current efficiency of 96–97% at 6 kA m^{-2} .

5.5.3.5. Uhde Bipolar Electrolyzers, Single Element Design. The characteristic feature of the Uhde membrane electrolyzer is its single-element design [104–108]. Each element consists mainly of anode and cathode semi-shells separated by an ion-exchange membrane. Unlike the filter-press design used in other electrolyzers, each element is individually sealed by a separately bolted flange with a gasket. This enables long-term storage of fully assembled elements in working order. The elements are suspended on

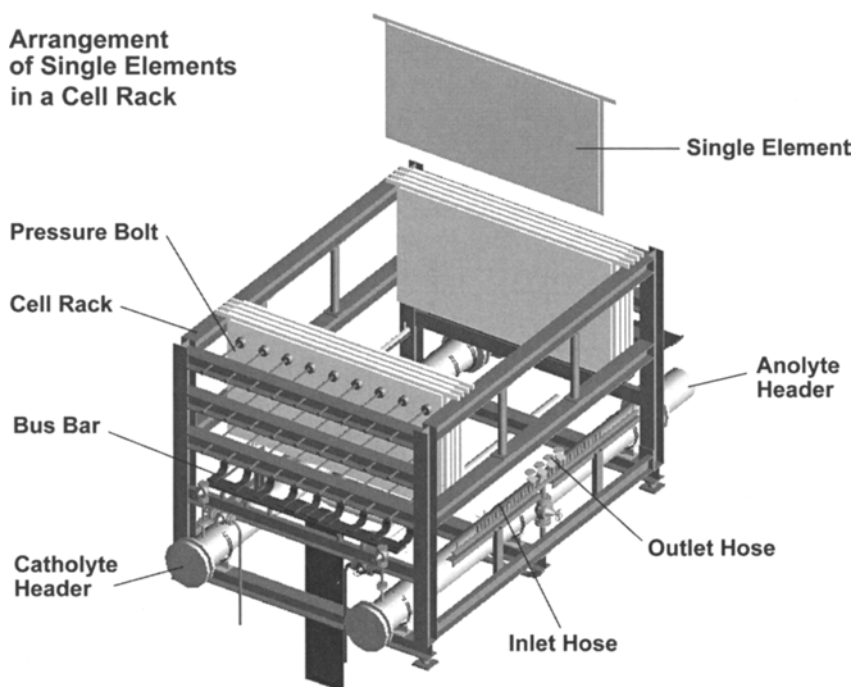


FIGURE 5.32. Uhde BM-2.7 electrolyzer. (With permission from Uhde GmbH.)

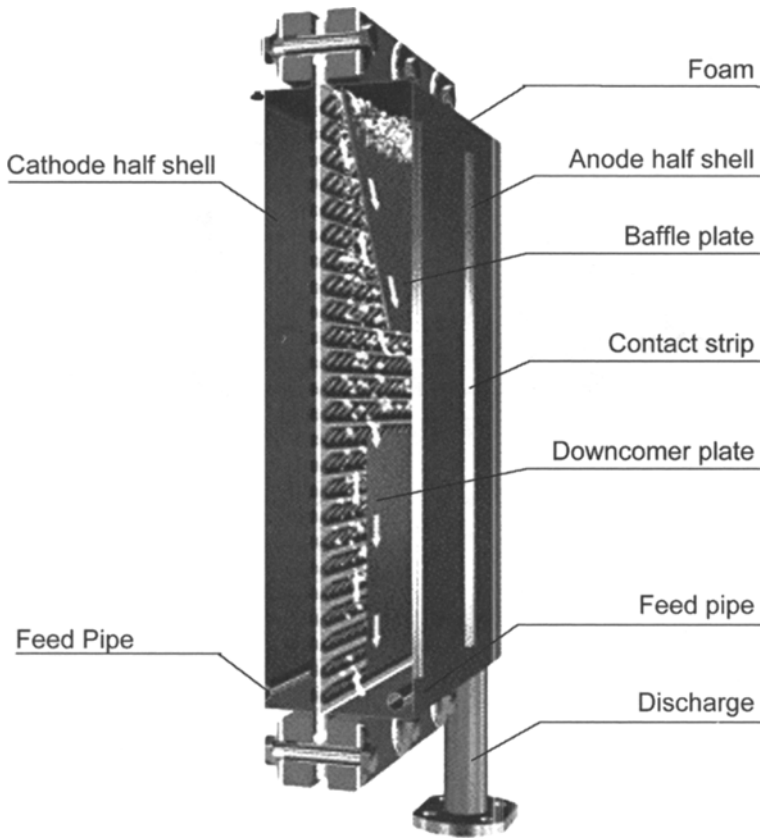


FIGURE 5.33. Uhde single element, 3rd generation. (With permission from Uhde GmbH.)

a steel rack and are pressed together to establish good electrical contacts. High forces are not required to achieve effective sealing in the single-element concept. Up to 160 elements can be combined in one electrolyzer, as shown in Fig. 5.32. Currently, single elements of the third generation, as shown in Figs. 5.33 and 5.34, are used. The standard electrolyzer configuration is the bipolar arrangement, although monopolar or hybrid arrangements can be made, as needed by the customer.

The current passes from the back of the cathode wall from one element to the back of the anode wall of the subsequent element by a series of contact strips. Voltage losses are kept low by a laser-welded, direct connection between the outer contact strips and by vertical inner current-conducting plates and the electrodes (Fig. 5.35). Both brine and caustic enter the element through flexible hoses leading to horizontal inner distribution pipes. These provide uniform feed concentration profiles inside the compartments. Internal circulation is enhanced by two baffle plates located in the anode compartment. The upper, inclined baffle plate provides a constant exposure of brine to the membrane, thereby avoiding gas-phase blistering of the membrane. In addition, the vertical

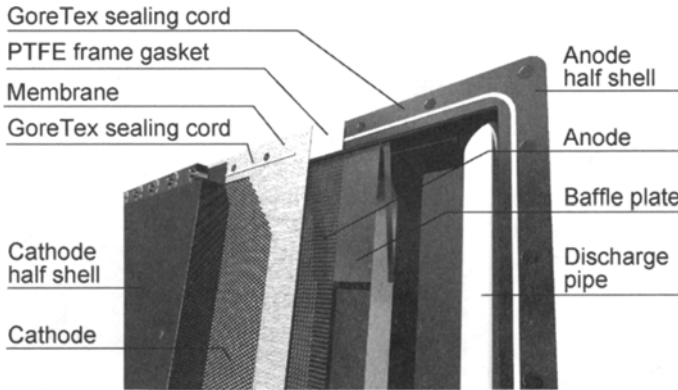


FIGURE 5.34. Components of Uhde single element. (With permission from Uhde GmbH.)

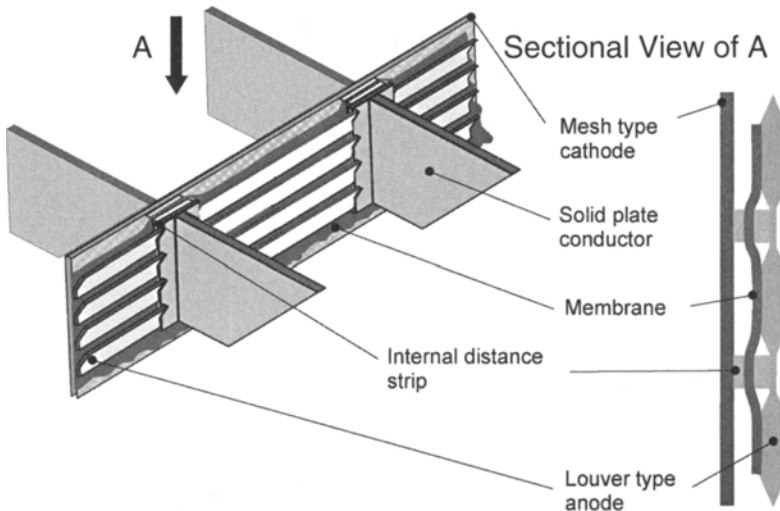


FIGURE 5.35. Current contacts in Uhde single element. (With permission from Uhde GmbH.)

baffle plate contributes to the uniformity of both temperature and concentration in the compartment.

The product gases leave the elements together with the electrolytes downward through vertical discharge pipes, the collectors, and flexible PTFE hoses. All inlet and outlet connections are located at the bottom of the electrolyzer, releasing the space above the cell for maintenance access. The mesh-type anode serves as a support for the membrane, while a defined gap can be maintained between the louver type cathode and the membrane by spacing devices.

The typical electrode active area is 2.7 m^2 (1.8 m^2 is also available), and the annual electrolyzer production capacity can be up to 28,000 tons of NaOH (100% basis, with electrolyzers having 160 elements at 6.0 kA m^{-2}). In 2002, Uhde had 70 plants with

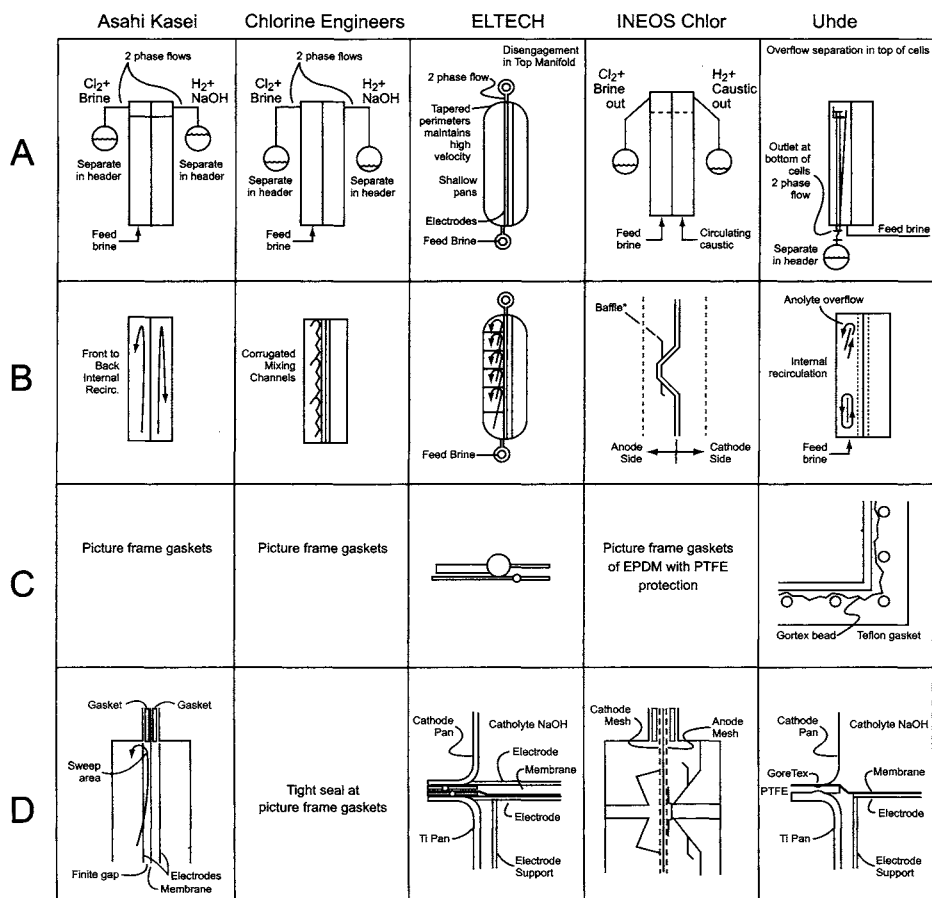


FIGURE 5.36. Schematic comparison of key features of the five cell technologies. A: Cell inlet and outlet location; B: Internal circulation pattern; C: Gasket design; D: Membrane disposition.

a total annual capacity of approximately 4,800,000 tons of NaOH (100% basis) commissioned or under construction. About one third of this capacity came from conversion projects from mercury or diaphragm plants to membrane technology [108].

5.5.3.6. *Summary.* An attempt is made to summarize the distinguishing characteristics of the five leading electrolyzer technologies in Table 5.4 and Fig. 5.36, based on the information provided by the technology suppliers and in Refs [109] and [110].

REFERENCES

1. T.V. Bommaraju, B. Lüke, G. Dammann, T.F. O'Brien, and M. Blackburn, Chlorine. *Kirk-Othmer Encyclopedia of Chemical Technology*, John Wiley & Sons, Inc., New York (2003).

2. H.-J. Hartz and J. Marciniak, Krupp Uhde, Technology Partner for the Chlor-Alkali Industry. *11th Krupp Uhde Chlorine Symposium*, Dortmund, Germany (2001).
3. G.W. Vinal, A. Volta. In C.A. Hampel (ed.), *Encyclopedia of Electrochemistry*, Reinhold Publishing Co., New York (1964), p. 1154.
4. J.E. Colman. Electrolytic Production of Sodium Chlorate. In R. Alkire and T. Beck (eds.), *Tutorial Lectures in Electrochemical Engineering and Technology*, AIChE Symposium Series 204, vol. 77, American Institute of Chemical Engineers, New York (1981), p. 244.
5. T.A. Ross, Monopolar or Bipolar?—The Current Debate, Reprint from *Process Industry J.* Feb. 1990.
6. T. Navin, OxyTech Systems Inc., Private Communication (1998).
7. M. Quissek, Asea Brown Boveri Industrie AG, Private Communication (1998).
8. T.R. Beck, I. Rousar, and J. Thonstad, *J. Light Metals* **485** (1993).
9. U. Bossel, *German Patent Application* WO-94-EP2181 (1994).
10. A. Kaufman and J. Werth, *European Patent Application*: EP-85-306022 850823 (1985).
11. M. Yang, H. Wu, and J. Selman, *J. Appl. Electrochem.* **19**, 247 (1989).
12. H.N. Sieger, *J. Electrochem. Soc.* **133**, 2002 (1986).
13. Y. Yoshida, *GS News Tech. Rep.* **44**, 28 (1985).
14. G. Codina, J.R. Perez, M. Lopez-Atalaya, J.L. Vazquez, and A. Aldaz, *J. Power Sources* **48**, 293 (1994).
15. M.A. Manzo, R.F. Gahn, O.D. Ganzalez-Somabria, R.L. Cataldo, and R.P. Gemeiner, *Proc. Inter. Soc. Energy Convers. Eng. Conf.* **22**(22), 864 (1987), *NASA Tech. Memo, Issue NASA-TM-89907*, E-3600 (1987).
16. P. Grimes, R. Bellows, and P. Malacheskyy, *Proc. Symp. Eng. Ind. Electrolytic Processes*, PV 86–88, The Electrochemical Society, Pennington, NJ (1986) p. 142.
17. J.R. Driscoll, R. Pollard, J.J. Smith, and S. Szpak, *Proc. Inter. Soc. Energy Convers. Eng. Conf.* **20**(2), 2.55–2.62 (1985).
18. K. Nozaki, H. Kaneko, A. Negishi, K. Kanari, and T. Ozawa, *Proc. Inter. Soc. Energy Convers. Eng. Conf.* **19**(2), 844 (1984).
19. R.I. Cataldo, *Proc. Inter. Soc. Energy Convers. Eng. Conf.* **18**(4), 1561 (1983).
20. R.J. Bellows, H. Einstein, P. Grimes, E. Kantner, K. Newby, and J.A. Shropshire, *Proc. Inter. Soc. Energy Convers. Eng. Conf.* **15**(2), 1465 (1980).
21. S. Sarangapani, J.A. Kosek, and A.B. LaConti, Proton Conducting Electrochemical Capacitors with Solid Polymer Electrolyte. In M.Z.A. Munshi (ed.), *Handbook—Solid State Batteries and Capacitors*, World Scientific, Singapore (1995), p. 601.
22. Y. Kakiyama, S. Mataga, and M. Murata, *Japanese Patent* JP 61001513 (1986).
23. M. Yoshitake, Y. Nakamura, and Z. Kamio, *Japanese Patent* JP 60181288 (1985).
24. E. Balko, M. Nicholas, and L.C. Mouthrop, *FR 2491957* (1982).
25. T. Morokuma, H. Yoshida, A. Hiroyuki, and J. Akazawa, *Japanese Patent* JP 48042559 (1973).
26. G.O. Westerlund, *Canadian Patent* 892733 (1972).
27. R.E. White, C. Walton, H.S. Burney, and R.N. Beaver, *J. Electrochem. Soc.* **133**, 485 (1986).
28. B.J. Scheiner, D.L. Pool, R.E. Lindstrom, and G.E. McClelland, Prototype Commercial Electrooxidation Cell for the Recovery of Molybdenum and Rhenium from Molybdate Concentrates. *Reno Metall. Res. Cent., Bur. Mines, Reno*, Report Issue: BM-RI-8357 (1979).
29. R. Collini, *PCT Int. Appl.* WO 8707652 (1987).
30. G. Zhao, S. Duan, Q. Tian, and T. Wu, *Metall Trans B.* **21B**, 783 (1990).
31. T.R. Beck, I. Rousar, and I. Thonstad, *Metall Trans B.* **25B**, 661 (1994).
32. N. Feng, Z. Qiu, G. Kai, and H.K. Zjotheim, *J. Light Met.* **379** (1990).
33. N. Hoy-Patterson, T. Aune, T. Vralstad, K. Andreassen, D. Qymo, T. Haugerod, and O. Skaane, Magnesium. In *Ullmanns Encyclopedia of Industrial Chemistry*, vol. A15, Wiley-VCH Verlag GmbH, Weinheim, Germany (1990), p. 559.
34. O.G. Sivillotti and A. Briand, *U.S. Patent* 3,396,094 (1968).
35. O.G. Sivillotti, *U.S. Patent* 4,055,474 (1977).
36. H. Ishizuka, *U.S. Patents* 4,495,037 (1985); 4,647,355 (1987).
37. W.G.B. Mandersloot and R.E. Hickes, *Desalination* **1**, 178 (1966).
38. C.J.H. King and D.E. Danly, Experimental Measurement of Current Leakage in a Commercial Scale Bipolar Cell Stack, Abstract #392, *Electrochemical Society Meeting*, Montreal (1982).
39. E.A. Kaminski and R.F. Savinell, *J. Electrochem. Soc.* **130**, 1103 (1983).

40. M. Zahn, P.G. Grimes, and R.I. Bellows, *U.S. Patent* 4,197,169 (1980).
41. P.G. Grimes, M. Zahn, and R. Bellows, *U.S. Patent* 4,312,735 (1982).
42. P.G. Grimes, *U.S. Patent* 4,377,445 (1983).
43. P.G. Grimes, R.J. Bellows, and M. Zahn, Shunt Current Control in Electrochemical Systems—Theoretical Analysis. In R.E. White (ed.), *Electrochemical Cell Design*, Plenum Press, New York (1984), p. 259.
44. V.B. Kogan and R.-R. Ousepyan, *Khim-Prom.* **8**, 463 (1954).
45. A.S. Bogoslovskii, *Tsvetnye Metally* **29**(4), 57 (1956).
46. O.S. Ksenzhek and N.D. Koshel, *Soviet Electrochem.* **7**, 331 (1971).
47. V.A. Onishchuk, *Soviet Electrochem.* **8**, 681 (1972).
48. B.P. Nestevrov, G.A. Karnzelev, V.P. Gerasimenko, and N.V. Koronin, *Soviet Electrochem.* **9**, 1091 (1973).
49. W. Thiele, M. Schleiff, and H. Matschiner, *Electrochim. Acta* **26**, 1005 (1981).
50. G. Zhao, S. Duan, Q. Tian, and T. Wu, *Metall. Trans. B.* **21B**, 784 (1990).
51. S.K. Rangarajan and V. Yegnanarayanan, *Electrochim. Acta* **42**, 153 (1997).
52. S.K. Rangarajan, V. Yegnanarayanan, and M. Muthukumar, *Electrochim. Acta* **44**, 491 (1998).
53. J. Yang, Q. Zhang, H. Wang, and Y. Liu, *Trans NFsoc.* **5**, 29 (1995).
54. I. Rousar, *J. Electrochem. Soc.* **116**, 676 (1969).
55. J.W. Holmes and R.E. White, A Finite Element Model of Bipolar Plate Cells. In R.E. White (ed.), *Electrochemical Cell Design*, Plenum Press, New York (1984), p. 311.
56. G. Bonvin and Ch. Comminellis, *J. Appl. Electrochem.* **24**, 469 (1994).
57. J.C. Burnett and D.E. Danly, Current Bypass in Electrochemical Cell Assemblies. In M. Krumplett, E.Y. Weissmann, and R.C. Alkire (eds), *Electro-Organic Synthesis Technology*, AIChE Symp. Series 185, vol. 75, American Institute of Chemical Engineers, New York (1979), p. 8.
58. P.P. Pirotskii and N.N. Shvetsov, *Ismeri-Tel'naya Tekhnika* **12**, 43 (1961).
59. A.T. Kuhn and J.S. Booth, *J. Appl. Electrochem.* **10**, 233 (1980).
60. I. Rousar and V. Cezner, *J. Electrochem. Soc.* **121**, 648 (1974).
61. *French Patent* 2,114,043 (1972).
62. *Japanese Patent* 7,342,559 (1973).
63. *Japanese Patent* 7,757,086 (1977).
64. *German Patent* 2,556,065 (1976).
65. R.N. Beaver and G.E. Newman, *PCT Int. Appl.* WO 9404719 (1994).
66. C.L. Mantell, *Electrochemical Engineering*, 4th Edition, McGraw-Hill Book Company, Inc., New York (1960), p. 248.
67. R.B. MacMullin, Electrolysis of Brines in Mercury Cells. In J.S. Sconce (ed.), *Chlorine: Its Manufacture, Properties and Uses*, R.E. Kreiger Publishing Company, Huntington, New York (1972), p. 127.
68. J.E. Currey and G.G. Pumphlin. Chlorine. In J.J. McKetta and W.A. Cunningham (eds), *Encyclopedia of Chemical Processing and Design*, vol. 7, Marcel Dekker Inc., New York (1978), p. 305.
69. H.A. Sommers, *Electrochem. Technol.* **5**, 108 (1967).
70. Y. Chin, *Process Economics Program: Chlorine Report 61D*, SRI International, Menlo Park, CA (1992).
71. P. Schmittinger, T. Florkiewicz, L.C. Curlin, B. Lüke, R. Scanelli, T. Navin, E. Zelfel, and R. Bartsch, Chlorine. In *Ullmann's Encyclopedia of Industrial Chemistry*, 6th Edition, Wiley-VCH Verlag GmbH, Weinheim, Germany (1999), p. 1.
72. D. Francis, *DeNora's Cell Room Technology Enhancements to Reduce Mercury Emissions*, paper produced at the Chlorine Institute Conference, New Orleans (2001).
73. Uhde: *Alkali Chloride Electrolyse nach dem Quecksilberverfahren*.
74. Krebskosmo, *Chlor-Alkali-Anlage*.
75. R.W. Ralston, *U.S. Patent* 4,004,989A (1977).
76. *U.S. Patents* 1,365,875 (1921); 2,282,085 (1924).
77. P.J. Kienholz, Bipolar Chlorine Cell Development. In *Chlorine Bicentennial Symposium*, The Electrochemical Society, Princeton, NJ (1974), p. 198.
78. R.N. Beaver and C.W. Becker, *U.S. Patents* 4,093,533 (1978); 4,142,951 (1979).
79. H.D. Dang, R.N. Beaver, F.W. Spillers, and M.J. Hazelrigg, Jr., *U.S. Patent* 4,497,112 (1985).
80. V. DeNora, *Chem-Ing.-Tech.* **47**, 141 (1975).
81. Brochure from PPG Industries, *Glanor V Type 1144 Electrolyzer* (1976).

82. T.C. Jeffery and R.J. Scott, The Glanor[®] Electrolyzer—The New Look in Chlorine Production. In *Diaphragm Cells for Chlorine Production*, Proceedings. Symposium at The City University, London, Society of Chemical Industry (1977), p. 67.
83. *Chlorine Institute*, North American Chlor-Alkali Plants, Pamphlet #10; Chlor-Alkali Producers Outside North America, Pamphlet # 16, New York (1976).
84. K. Hass, *Chem.-Ing.-Tech.* **47**, 121 (1975).
85. L.C. Curlin, T.V. Bommaraju, and C.B. Hansson, *Chlorine and Sodium Hydroxide*. In *Kirk-Othmer Encyclopedia of Chemical Technology*, 4th Edition, vol. 1, John Wiley & Sons, Inc., New York (1991), p. 938.
86. R. Romine and R. Matousek, New and Improved Diaphragm Cell Hardware Designs. *Electrode Corporation Chlorine/Chlorate Seminar*, ELTECH Systems Corporation, Chardon, OH (1998).
87. E.S. Kazimir, Monopolar Cathode Design Improvements and Other Diaphragm Cell Component Advances. *Electrode Corporation Chlorine/Chlorate Seminar*, ELTECH Systems Corporation, Chardon, OH (1999).
88. T. Florkiewicz, *Diaphragm Cell Improvements*, 44th *Chlorine Institute Plant Managers Seminar*, New Orleans (2001).
89. E. Pearson, Criteria for the Selection of Membrane Cell Technology. In C. Jackson (ed.), *Modern Chlor-Alkali Technology*, vol. 2, Ellis Horwood, Chichester (1983), p. 177.
90. H. Shiroki, Y. Noaki, M. Katayose, and A. Kashiwada, Improvement of Electrolyzer and Ion Exchange Membrane for High Efficiency Chlorine and Caustic Soda Production. In R.W. Curry (ed.), *Modern Chlor-Alkali Technology*, vol. 6, The Royal Society of Chemistry, Cambridge (1995), p. 222.
91. Y. Noaki and S. Okamoto, *U.S. Patent* 5,225,060 (1993).
92. M. Yoshida and Y. Tamura, *U.S. Patent* 4,557,816 (1985).
93. M. Seko, S. Ogawa, N. Ajiki, and M. Yoshida, *U.S. Patent* 4,111,789 (1978).
94. *CME Chlorine Engineers Membrane Electrolyzer*, Chlorine Engineers Corp. Ltd., Tokyo, Japan (1989).
95. A. Hironaga, M. Okura, S. Katayama, and Y. Take, Development of the Advanced Bipolar Membrane Electrolyzer (BiTACTM), In R.W. Curry (ed.), *Modern Chlor-Alkali Technology*, vol. 6, The Royal Society of Chemistry, Cambridge (1995), p. 205.
96. S. Katayama and Y. Take, *U.S. Patent* 5,314,591 (1994).
97. S. Katayama, *U.S. Patent* 5,484,514 (1996).
98. Brochure on ExL and Dense Pak Cells, *OxyTech Systems Inc*, Chardon, OH (1998).
99. C.D. Schulz, ELTECH Systems Corp., Chardon, Personal Communication (2003).
100. *FM-21 SP Series Membrane Electrolyzer*, ICI PLC, Northwich, Cheshire, (1989).
101. S. Collings, Chlor-Alkali Membrane Electrolyzer. In J. Moorhouse (ed.), *Modern Chlor-Alkali Technology*, vol. 8, Chap. 18, Society of Chemical Industry, London (2001), p. 225.
102. INEOS Chlor brochure, *Chlor-Alkali Electrolyzer Technology* (2003).
103. M.A. Cook, *INEOS Chlor Ltd.*, Personal Communication (2003).
104. *Alkaline Chloride Electrolysis by the Membrane Process*, Krupp Uhde GmbH, Dortmund, Germany (2001).
105. M. Hartmann, D. Bergner, and K. Hannessen, *U.S. Patent* 5,194,132 (1993).
106. T. Borucinski and K. Schneiders, A New Generation of the Krupp Uhde Single-Element Design. In S. Sealy (ed.), *Modern Chlor-Alkali Technology*, vol. 7, The Royal Society of Chemistry, Cambridge, UK (1998), p. 105.
107. R. Beckmann and B. Lüke, Know-How and Technology-Improving the Return on Investment for Conversions, Expansions and New Chlorine Plants. In J. Moorhouse (ed.), *Modern Chlor-Alkali Technology*, Society of Chemical Industry, London (2001), p. 196.
108. G. Dammann, *Krupp Uhde GmbH*, Dortmund, Germany, Personal Communication (2003).
109. H.S. Burney, Past, Present, and Future of the Chlor-Alkali Industry. In H.S. Burney, N. Furuya, F. Hine, and K.-I. Ota (eds), *Chlor-Alkali and Chlorate Technology: R.B. MacMullin Memorial Symposium*, Proc. vol. 99-21, The Electrochemical Society Inc., Pennington, NJ (1999), p. 105.
110. *Soda Handbook*, Japan Soda Industry Association, Tokyo (1998).

6

Process Overview

6.1. GENERAL INTRODUCTION

This chapter presents a general overview of the processing steps in a typical chlor-alkali plant. As shown in Fig. 6.1, we can divide the process into three major steps. These are the preparation of purified brine, electrolysis, and processing of the crude products of electrolysis. The figure also subdivides brine preparation into its main elements. Later sections present flowsheets in block form for each of the process steps. A discussion of the differences among the various types of electrolyzer technology accompanies each flow diagram. Separate flowsheets for the complete processes for the three electrolyzer technologies are also available in the literature [1,2].

6.2. BRINE PREPARATION AND TREATMENT

The brine process includes the supply of salt, its dissolution, and purification of the resulting brine to the standards required by the cell technology. The brine-making function may be on or off site. In other words, the chlor-alkali producer may receive the basic raw material as solid salt or as a solution. When using solid salt, the mercury- or membrane-cell operator can resaturate circulating depleted brine for recycle to the cells. When salt is supplied in the form of brine, this is no longer possible. Unless weak caustic is produced or the process is changed by addition of evaporative capacity, water will accumulate in the system. The problem is that with NaCl, for example, each weight of salt entering the plant is accompanied by about 2.75 weights of water. Only about one weight is consumed by the reaction or exported with the 50% NaOH product. Evaporation within the membrane-cell process accounts for another 1.25 weights of water. This includes water vapor accompanying the hydrogen and chlorine evolved by the cells as well as that removed in the caustic evaporators. Even after this water is used outside the process or properly treated for disposal, 0.5 weights or about 20% of the total accumulates, an inoperable situation.

By contrast, in the diaphragm-cell process, more than enough water will be removed in the evaporators. Therefore, one of the advantages of this process is its ability to accept a brine feed, which is usually cheaper than solid salt.

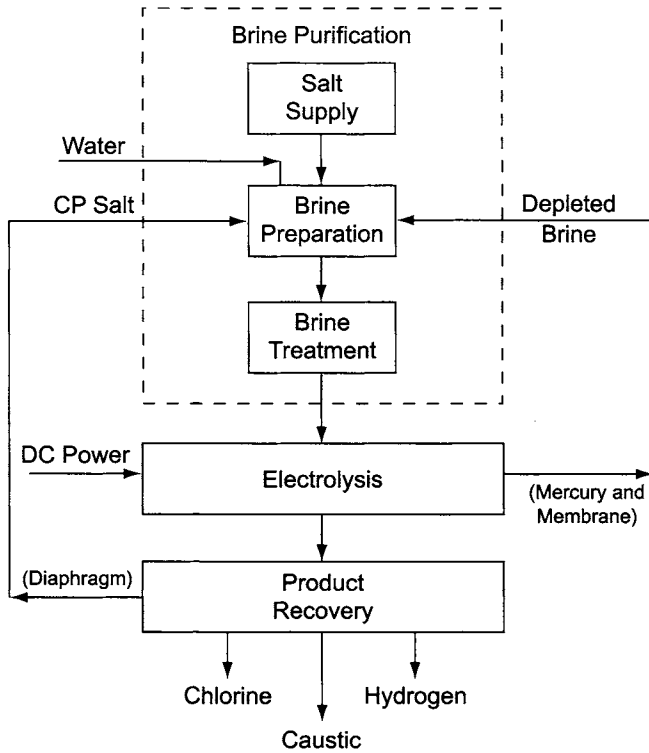


FIGURE 6.1. Major components of electrolytic chlor-alkali process.

The brine-treatment block of Fig. 6.1 is expanded in Fig. 6.2 to show its component steps. The first step is the removal of hardness and heavy metals by precipitation with OH^- and CO_3^{2-} . The precipitates form a sludge, removed by settling in a clarifier. Addition of a polymeric flocculation aid sometimes helps the separation in the clarifier. The sludge is a waste product, frequently concentrated by filtration before disposal as landfill. The clarifier overflow will have some residual suspended solids which are removed by filtration. The two types of filter commonly found in the chlor-alkali industry are the solid-bed filter and the leaf or candle filter. The first relies on the low porosity of a bed of fine particles to remove solids from the brine. Sand is the fill commonly used in the industry, but it is not suitable with all cells because of the possibility of dissolving too much silica. Anthracite, similar to sand in its particle size and pressure-drop characteristics, is a typical substitute. Pressure-leaf filters, which rely on woven filter elements, have long been used as alternatives or adjuncts to "sand" filters. They use a filter aid to provide a tighter filtering surface. Classically, the filter aid has been diatomaceous earth. Again, membrane cells require a substitute not based on silica. Cellulosic filter aids are the usual choice. Vertical candle filters or rotating-disc filters sometimes appear as substitutes for leaf filters. The candle filters in particular have found a growing use in newer (i.e., membrane) plants.

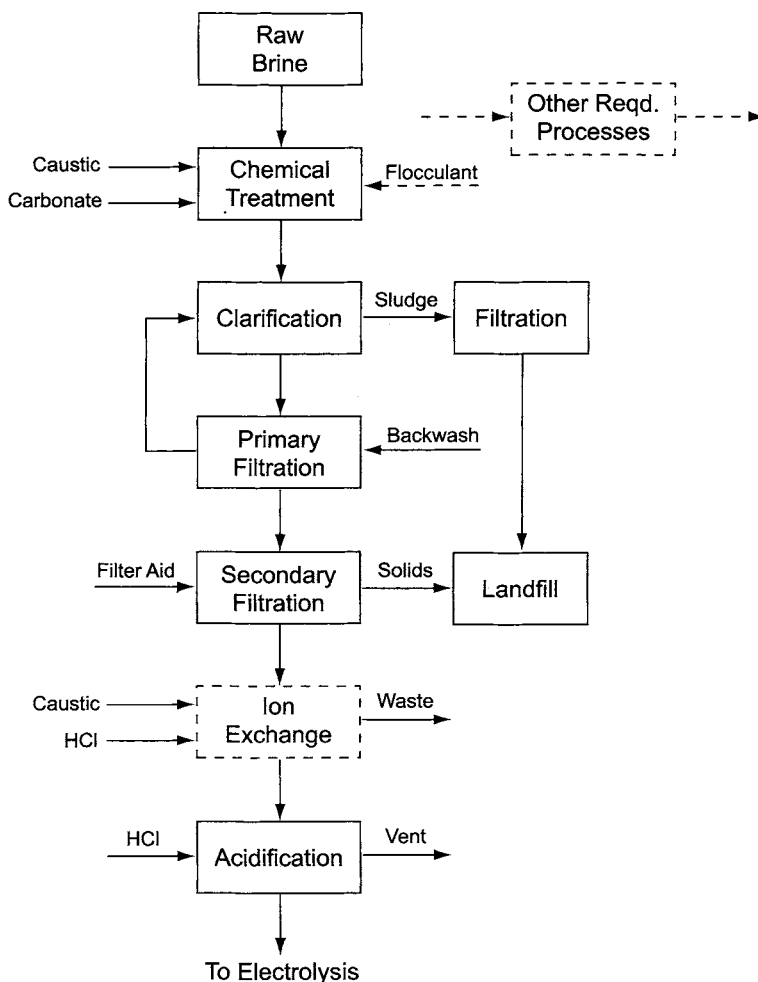


FIGURE 6.2. Brine treatment flow diagram.

There are other impurities that may have to be removed from the brine. Sulfate is a frequent example. The techniques used are varied and are applied at different areas of the flowsheet. Therefore, they are not shown as part of the normal sequence in this basic flow diagram.

The process as discussed so far produces brine suitable for use in diaphragm or mercury cells. Residual hardness levels may be in the range 2–10 ppm. This is not acceptable in membrane cells. Hardness is reduced to less than 20 ppb by ion exchange, using resins developed specifically for this purpose. These require periodic regeneration with caustic and HCl. Regeneration produces a waste for recycle or disposal. It should be noted when considering brine specifications that some are given on a weight–volume basis, as milligrams per liter or ppm (w/v). Others are on a weight basis, as milligrams

per kilogram or ppm (w/w). The two bases differ by a density factor of about 1.2, but common usage sometimes is careless of the difference.

The final step in brine preparation is acidification. This is truly not a purification step and is not an essential part of the chlor-alkali process, but it offers several improvements in cell performance. These are discussed in Section 7.5.6. The acid used is HCl, often produced by reacting together some of the chlorine and hydrogen produced in the plant.

6.3. ELECTROLYSIS

Purified brine and DC power are the inputs to the electrolysis section (Fig. 6.1). The next three diagrams cover the three different cell processes. Diaphragm cells, with only one liquid-phase output, have the simplest diagram and are shown in Fig. 6.3. Electrolysis of the brine produces chlorine gas and an anolyte in which roughly half the NaCl has reacted. The anolyte flows in bulk through the diaphragm into the cathode chamber (dashed line). Electrolysis is completed here by converting water into hydrogen and hydroxyl ions. The catholyte, or cell liquor, resulting from this leaves the cell. It contains all the unconverted NaCl as well as the NaOH produced in the cells. Its processing by evaporation is discussed below in Section 6.4.3. Chlorine and hydrogen gases go off to their separate processing lines, discussed in Sections 6.4.1 and 6.4.2.

The anode reaction in a diaphragm cell is



The circuit is completed when two electrons are consumed at the cathode in the electrolysis of water:

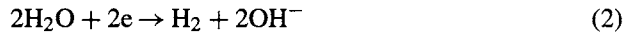


Figure 6.4 shows the operation of the mercury, or amalgam, cells. The anodic process is the same as that in the diaphragm cells. Again, chlorine gas generated by electrolysis goes on to product recovery. Unlike the situation in the diaphragm cell,

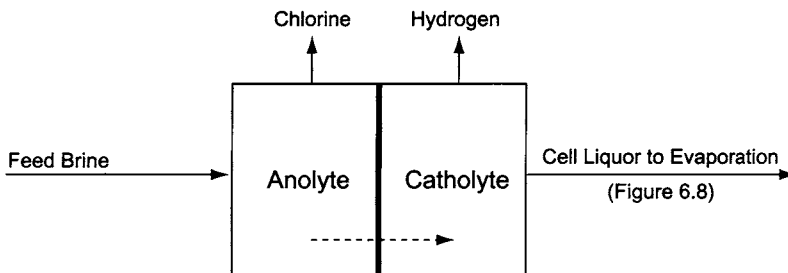


FIGURE 6.3. Electrolysis area flow diagram—Diaphragm cells.

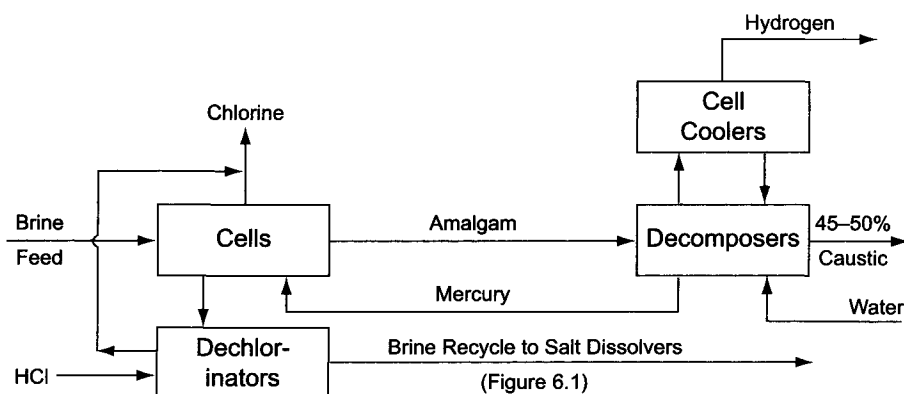


FIGURE 6.4. Electrolysis area flow diagram—Mercury cells.

however, the cathode in a mercury cell is not enclosed in a separate chamber. The brine traveling through the cell is exposed to a flowing mercury cathode. The cathode reaction is completely different:



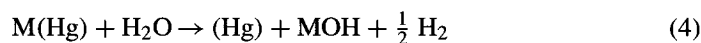
where M = alkali metal, Na or K

M(Hg)=dilute alkali metal amalgam

The anolyte leaves the cell as depleted brine. This must be recycled to the cells to prevent a massive loss of salt, and it must be resaturated with salt to keep the current efficiency of the cells high. Technically, it is possible to operate with once-through brine. While losing salt, this option eliminates handling and treatment of the recycle stream. This practice was fairly common in the past but is almost unknown in today's mercury-cell plants. The overriding issue is not the loss of salt but rather the escape of mercury from the system.

Recycled anolyte must first be dechlorinated for recycle to the brine plant. Most commonly, this involves acidification with HCl and removal of the evolved chlorine under vacuum. The chlorine goes to the cell gas header for processing.

The amalgam leaves the cells, which are sloped to permit gravity flow. Each mercury cell has a companion "denuder" or "decomposer." This is a short-circuited cell, usually packed with graphite, in which amalgam decomposition in the presence of added water regenerates the mercury and forms caustic soda or potash:



The mercury returns to the cell, and the caustic liquor is ready for processing. By controlling the amount of water fed to the decomposer, the operator can control the strength of a mercury-cell product and can produce commercial concentrations directly.

These are usually 48–50% NaOH and 45–50% KOH. This is a unique advantage of the mercury cell. Another advantage of mercury cells is the purity of the caustic product. High purity requires a high grade of water, and demineralized water is the standard material here.

Energy consumption is usually somewhat lower in KOH cells. When reported on an alkali weight basis, it is lower because of the higher equivalent weight of KOH. With generally lower voltages, it is also true on a molar basis. This is in spite of lower current efficiency. A typical voltage difference of about 0.2 outweighs a current efficiency penalty of about 2%. The lower current efficiency carries other penalties with it. The increase in hydrogen content of the chlorine makes gas processing less efficient and can be more hazardous.

When both NaOH and KOH are made in the same plant, the ease of conversion of some number of cells from one service to the other may be an issue. This is another advantage of the mercury cell. Switching between the two products is not especially difficult. Loss of mercury and cross-contamination are the significant problems that need to be overcome.

The hydrogen gas is usually cooled at each cell as it leaves the decomposer. This condenses most of the water and, more importantly, most of the mercury from the gas. The hydrogen then goes into a common header for final processing.

Finally, we consider the membrane cells in Fig. 6.5. The electrode processes are the same as those in the diaphragm cells (Eqs. 1 and 2). Anolyte processing is quite similar to that practiced with mercury cells. We saw above in the discussion on brine treatment that membrane cells had stricter requirements. The same is true regarding dechlorination of the depleted brine. After vacuum dechlorination, the residual active chlorine content is high enough to damage the ion-exchange resin in the brine purification

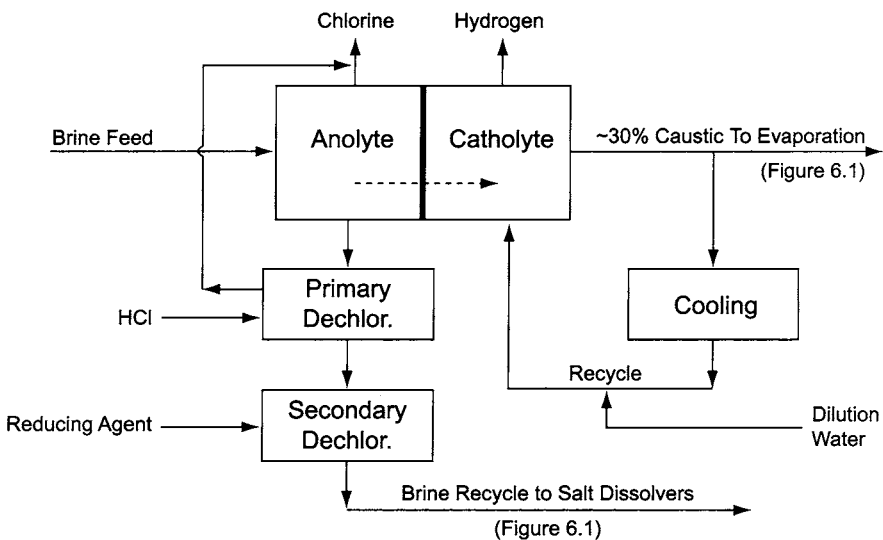


FIGURE 6.5. Electrolysis area flow diagram—Membrane cells.

plant. A “secondary” dechlorination is necessary, in which addition of a reducing agent or contact with a catalyst converts the oxidized chlorine to the innocuous chloride ion.

The equipment in the brine recycle loop is much smaller in a membrane-cell plant. This is because the depleted brine concentration is lower (about 200–220 gpl NaCl vs about 270 gpl NaCl in a mercury-cell plant) and therefore the per-pass conversion of chloride is higher. With both technologies, there may also be some direct recycle of depleted brine around the cells. With mercury cells, this provides a smaller temperature gradient along the cells. It is most useful at high loads. Recycle is much more common with membrane cells. They characteristically have more backmixing, and variations in conditions within the cells are less extreme. In the most modern designs, however, depleted brine recycle still may be used to reduce the temperature and concentration gradients and to allow deeper acidification of the feed brine. This technique reduces the oxygen content of the chlorine gas and makes it more acceptable for direct use in processes such as the chlorination of ethylene.

The caustic liquor produced in a membrane cell is weaker than that from a mercury cell. Typical concentrations are 30–35% NaOH and 28–32% KOH. The net production of caustic solution goes to evaporation and final processing. The caustic solution also recycles around the catholyte side of the cells. This allows control of both temperature and concentration. A cooler removes the waste heat generated in the cells, and water addition keeps the catholyte concentration at the desired level.

Membrane cells, like mercury cells, can switch back and forth between NaOH and KOH production. This operation is much more complex in the membrane-cell case when different types of membrane are recommended for the two different services. We have seen (Chapter 5) that removal and replacement of cells is more or less complicated and time-consuming. Providing separate brine and caustic piping headers to a number of cell berths is also more difficult, because of the much more compact layout of a membrane-cell room.

6.4. PRODUCT RECOVERY

6.4.1. Chlorine

Full processing of chlorine gas (Fig. 6.6) takes a hot, wet vapor at approximately atmospheric pressure and converts it to a cold, dry liquid under significant positive pressure. The common processing steps therefore are cooling, drying, compression, and liquefaction. The severity of the two latter processes depends on the desired degree of recovery of chlorine as the liquid and on the composition of the gas produced in the cells. The major impurities in this gas will be:

1. oxygen, the major product of electrochemical inefficiencies;
2. water, at its vapor pressure over the anolyte;
3. carbon dioxide, from decomposition of carbonates in the feed brine;
4. air, introduced with the brine or by leakage into sections under vacuum;
5. hydrogen, from the cathode chambers or by production at cathodic areas on the anodes;
6. bromine and other products of electrolysis of brine impurities;

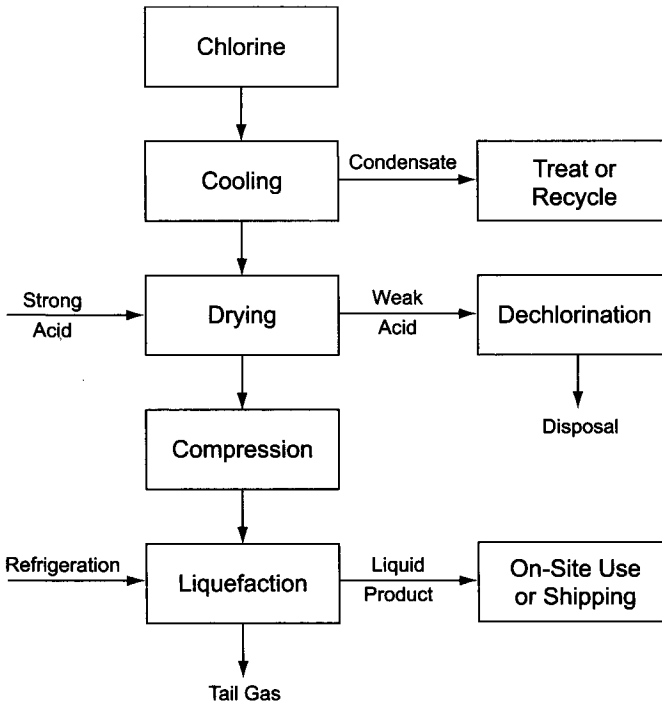


FIGURE 6.6. Chlorine processing flow diagram.

7. chlorinated organics, from the reaction of chlorine with other components of the brine or with cell construction materials (e.g., diaphragm-cell putty);
8. salt, by entrainment of liquor from the anolyte compartments; and
9. mercury vapor, from the cathodes of mercury cells.

The cooling step removes most of the water vapor. The condensate, saturated with chlorine, requires treatment. Figures 6.4 and 6.5 showed that membrane- and mercury-cell plants require facilities for removal of dissolved chlorine from depleted brine. With proper design, those facilities can also accept the condensate from the chlorine cooling plant. A common practice in diaphragm-cell plants is to strip the condensate, after acidification, with steam. The chlorine, again, can return to the main gas header, and the stripped condensate becomes a process waste.

The success of the cooling process in removing water from the gas depends on the available cooling water temperature. To improve results, many plants include a second stage using chilled water to reduce the temperature of the gas below that of the cooling water supply. Cooling may take place in a surface exchanger or by direct contact in a column. In the latter case, use of process fluids allows some heat economization. Exchange between chlorine and purified brine in a diaphragm-cell plant is also a way of keeping most of the chlorinated condensate within the process.

Regardless of the type of cell, chlorine after cooling is still too wet for processing in ferrous-metal equipment. The next step in its processing therefore is drying with

sulfuric acid. There are several different approaches to the process, but the essentials are simply staged contact of the gas with acid of increasing strength, up to 96–98%. The strong desiccant action of the acid reduces the moisture content of the gas to a few tens of ppm. The dilute acid produced is essentially a waste product. After dechlorination, usually by stripping with air, it is used in plant neutralization systems or returned to the supplier for upgrading. On-site reconcentration is difficult and expensive and so is seldom practiced in the industry.

The dry gas is usually compressed before use. The level of compression depends on the application. A large fraction of the world's output of chlorine is consumed on site. The production of ethylene dichloride (EDC) is the single largest-volume use. The dry gas supply pressure then is determined by the needs of the EDC process. Merchant chlorine will be liquefied. The choice of compressor output pressure is then an economic/technical balance with the requirements of the liquefaction process. Because some of the impurities in the chlorine gas are noncondensables, a chlorine-containing tail gas always results. Some of this chlorine value can be recovered directly or in the form of various byproducts. A system is also required for safe disposal of any unrecovered chlorine as well as any released from the process during emergencies.

6.4.2. Hydrogen

Electrolytic hydrogen is quite pure and is acceptable for most applications. The only major distinguishing features of the three processes are the presence or absence of mercury and the wide variation in water content of the gas.

Normal processing, shown in Fig. 6.7, involves cooling, which may also serve to remove entrained caustic, and compression. Hydrogen frequently is cooled by direct contact with brine. This is a simple matter of heat economization. Entrained caustic is removed by this operation but may be replaced by salt or brine mist. Process design must take into account the water condensed into the brine. The condensate from mercury-cell hydrogen will also contain mercury, both as a separate phase and in a dissolved form. After decantation from the metallic mercury, the liquid phase requires treatment before it can be discharged.

The extent of compression depends on the application. Much of the hydrogen is used as fuel or as raw material for the production of HCl. Only modest pressures are required, within the capability of simple rotary blowers. In the membrane-cell process, it is sometimes possible to operate the cells under positive pressure and eliminate the need for a blower. Other applications require higher pressure and the installation of compressors. The synthesis of ammonia is an example. Operating pressures range up to 30,000 kPa. Recent developments have lowered this to about 3,000 kPa in some plants. Less frequently, hydrogen is compressed to high pressure and packaged in cylinders. For high-grade chemical applications, oxygen and traces of chlorine may also be removed.

6.4.3. Caustic

A major differentiator among the various chlor-alkali cells is the quality of their product caustic solutions. Diaphragm cells produce a liquor containing about 11% NaOH and

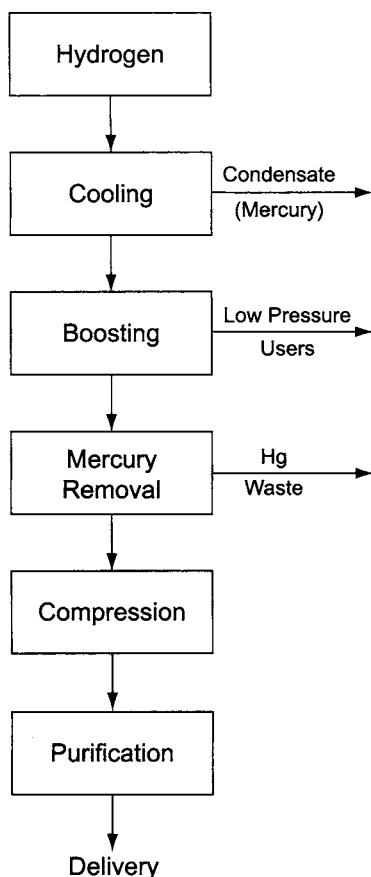


FIGURE 6.7. Hydrogen processing flow diagram.

15% NaCl. In addition, all the feed brine impurities and any chlorate produced in the anode compartments are carried through by bulk flow of the anolyte into the cell liquor. Unless special steps are taken to remove them, they appear in the final product.

The strength of the caustic produced in membrane cells depends on the type of membrane chosen. Since membranes ideally pass only water and alkali metal ions, chloride, chlorate, and sulfate in the caustic are measured in parts per million. The highest-grade caustic solutions (barring mercury contamination) are produced in amalgam cells. Through control of the rate of addition of water to the amalgam decomposer, these cells can also produce caustic directly at commercial concentrations (50% for NaOH and 45–50% for KOH). These differences result in the separate flow lines of Fig. 6.8.

It is usually necessary to concentrate diaphragm- and membrane-cell caustic by evaporation. Simple concentrating evaporators suffice in membrane-cell service, but diaphragm-cell evaporators reject most of the dissolved salt in the process of concentration. This salt must be removed from the resultant slurry, and it is used to prepare

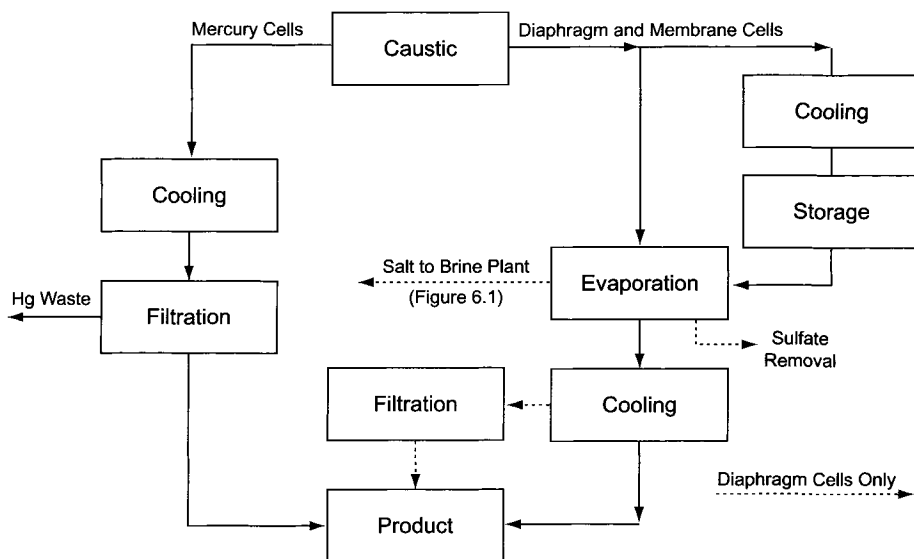


FIGURE 6.8. Caustic processing flow diagram.

and resaturate brine (Fig. 6.1). The sulfate carried through the diaphragms can also be removed in the evaporation plant. Most plants have substantial intermediate storage for cell liquor. This uncouples the electrolysis and evaporation processes.

In all cases, caustic at essentially its final concentration is cooled before storage and shipping. In the diaphragm-cell process, this cooling causes another small quantity of salt to drop from solution. This is removed by filtration, and the resulting 50% NaOH solution still contains 1.0–1.1% NaCl. Processes for removal of this salt are available but are not commonly applied. Section 9.3.4 discusses the most frequently used process. A number of plants operate diaphragm cells in conjunction with one of the other types. When the higher-purity product commands a premium price, most of these plants have separate storage and handling systems for the two grades of NaOH.

Sometimes, caustic solutions are processed to higher concentrations. NaOH is often shipped at 73%. Both NaOH and KOH are also sold as nearly anhydrous material in several different physical forms. Section 9.3.5 treats this subject.

6.5. MASS BALANCES

To provide a feel for the quantities involved in a chlor-alkali plant and to allow us to illustrate the size of some of the key equipment, we adopt here a reference plant based on the use of membrane cells and calculate an approximate electrolysis area mass balance. The characteristics of this plant serve as reference material for the specific examples used in later chapters. We defer energy considerations to those later chapters, but we list here all the relevant parameters.

Nominal capacity of plant	800 tpd NaOH
Chlorine usage	Merchant
Current efficiency of cells	94%
Average cell voltage	3.2
Water transport coefficient	4.0 moles F^{-1}
Concentration of cell product caustic	32% NaOH
Concentration of cell feed caustic	30.3% NaOH
Feed brine concentration	300 gpl NaCl
Depleted brine concentration	220 gpl
Cell operating temperature	88°C
Cathode-side pressure	105 kPa
Differential pressure across membranes	4 kPa
Type of electrolyzer	Bipolar
Cross-sectional area	2.5 m ²
Current density	5.5 kA m ⁻²
Sulfuric acid supply concentration	96%
Spent sulfuric acid concentration	78%
Hydrochloric acid concentration (plant is to be self-sufficient)	31.5%
Source of carbonate	Soda ash slurry
Reducing agent	Solid Na ₂ SO ₃
Nonhazardous solid disposal	Landfill (50% min. solids)
Salt supply	Washed solar salt
Method of delivery	100-ton rail cars
Salt analysis (dry basis)	
NaCl	99.63%
CaSO ₄	0.17%
CaCl ₂	0.04%
MgCl ₂	0.03%
Insolubles	0.13%
Water content	4.5% max
Bulk density	1,080 kg m ⁻³
Plant location	Coastal
Altitude	Near sea level
Ambient temperatures	
Maximum	40°C
Minimum	-5°C
Ambient pressure, minimum	95 kPa
Cooling water temp.	
Design max.	30°C
Minimum	5°C
Steam supply pressure	1,150 kPa
Steam temperature	10°C superheat

This book is not a design manual. We provide examples to illustrate the points under discussion and not to serve collectively as a coordinated design. Safety factors and

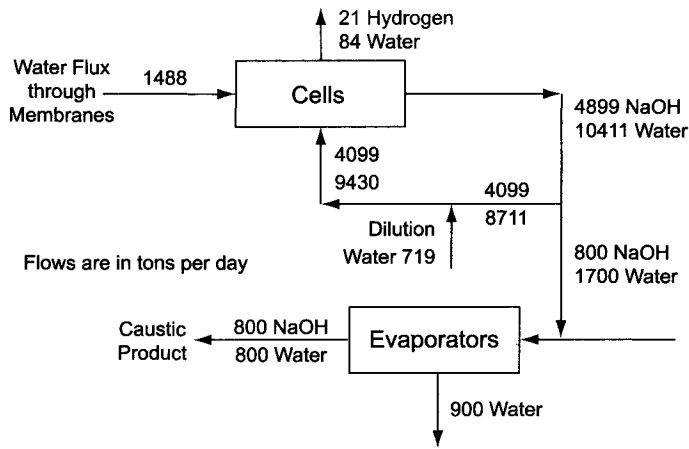


FIGURE 6.9. Cathode-side mass balance.

design contingencies are necessary to the latter objective. They differ from plant to plant, and their consistent inclusion here would add little to the reader's understanding of the technology. For the same reason, detailed calculations do not accompany all examples.

Figure 6.9 shows the cathode-side balance. There are several interesting features:

1. The water flux through the membranes is much greater than the amount of water that must be evaporated. In volumetric terms, it is greater than the output of 50% caustic soda. In KOH electrolysis, the water flux is much smaller.
2. The amount of water evaporated is greater than the amount of dilution water required. It is therefore possible to use evaporator condensate in the caustic recycle system and not introduce new water. This has the benefit of freedom from any contaminants that might enter with the water supply but adds the possibility of contamination by metallic impurities picked up in the evaporator system.
3. The ratio of caustic flow from the cells to net production is about 5.5:1. This is a result of the assumptions of 30.3% NaOH in and 32% out. Some operators or suppliers may specify other concentrations, and the recycle flow of caustic soda is quite sensitive to this variable. With 30% NaOH entering the cells, for example, the ratio is 4.77; with 30.5% NaOH, it becomes 6.11, or 28% greater. Some producers or licensors may specify the recycle ratio directly. Higher recycle flows add to the pumping and capital costs but reduce the temperature and concentration gradients in the catholyte.

Note that the current efficiency used for the calculations is 94%. At startup, it usually will be 96% or more. With time and the gradual deterioration of the membranes, the current efficiency will decline. Membranes are often removed when the current efficiency reaches an arbitrary value of about 93%. Cell room auxiliary equipment often is designed for this condition. However, all cells usually do not reach low current efficiency simultaneously. Cell renewal should begin before all membranes have reached

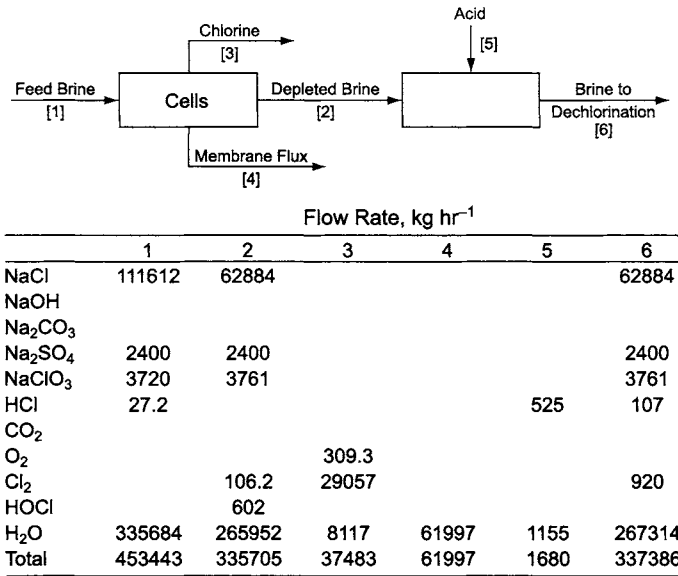


FIGURE 6.10. Anode-side mass balance.

the change-out point. We adopt 94% here as a reasonable design case, recognizing that the time-weighted average is higher.

Figure 6.10 shows the anolyte balance. The sulfate flow into and out of the electrolyzers is an arbitrary but reasonable number chosen to suit a typical membrane supplier's specification. The balance ignores any flow of sulfate out of the anolyte. Sulfate in some form is known to penetrate the membrane (therefore the need to limit its concentration). The rate of penetration is so small, however, that the assumption of zero flux is the basis for one method of estimating current efficiency [3]. The chlorate flows are in the same category as the sulfate flows. There is a small difference between the flows out and in, representing the rate of chlorate production in the cells. This amount would be removed by purging or by deliberate destruction in the brine process.

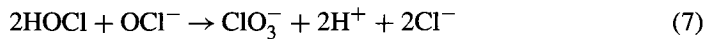
Analysis of the chlorine flows shows that the anode current efficiency is different from the cathode current efficiency. The "current efficiency" commonly used in discussing membrane cells is the caustic current efficiency, determined by the amount of hydroxide ion lost by leakage through the membranes into the anolyte. The hydrogen current efficiency, on the other hand, is nearly 100%. In other words, the electrode process is nearly quantitative, but the membranes allow some of the product of electrolysis to escape.

On the anode side, the electrode process itself is less than quantitative because of the formation of oxygen, and there is also some internal loss of the chlorine generated at the anodes. Some of the chlorine remains in solution rather than leaving the cell as a gas, and some hydrolyzes by the equilibrium reaction

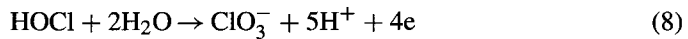


The acid formed here explains the low pH of the anolyte in all types of cell. Acidification of mercury- or membrane-cell anolyte after it leaves the cells reverses the hydrolysis and allows recovery of some of this chlorine value.

Hypochlorous acid can continue to react, disproportionating to chlorate and chloride. This is usually written in two steps



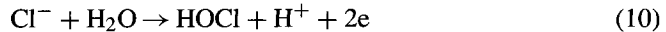
Chlorate can also form electrochemically by the anodic oxidation of HOCl:



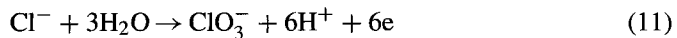
Finally, the anode can produce the direct electrochemical oxidation of water



This is not a chemical yield loss, since no chloride is involved, but is an irreversible faradaic loss. By consuming chlorine produced at the anode, the other reactions also waste some of the current. If we add Eq. (5) for the formation of HOCl to the fundamental anode reaction of Eq. (1), we have



Similarly, the formation of chlorate can be rolled back to chloride ions by combining Eq. (10)—three times—with Eqs. (6) and (7):

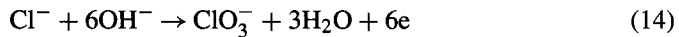
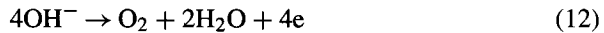


Combining Eq. (10) with the electrolytic formation of chlorate by Eq. (8) also results in Eq. (11). Each mole of chlorate therefore represents the loss of 6 F.

Therefore, the recognized products of the major anode inefficiencies are oxygen, HOCl, and NaClO₃ (or KClO₃), and their stoichiometry and electron transfer requirements are shown in Eqs. (9) through (11).

Each of these reactions produces hydrogen ions. If the anolyte were totally isolated from the catholyte, the inefficiencies would be self-limiting. The H⁺ produced by the electrolytic reaction (9) would reduce the amount of other impurities by reversing the hydrolysis reaction (5). In the real case, the catholyte continues to contribute hydroxide ions by leakage through the membrane. This OH⁻ flux ties up the H⁺ ions and permits the reactions to continue. In our example, the catholyte contributes about 2.8 moles of OH⁻ to each liter of anolyte leaving the cell. Since the OH⁻ supply is orders of magnitude greater than the standing population of hydrogen ions in the anolyte, the extent of the reactions is nearly totally determined by the amount of hydroxide back-migration. In other words, the anode current efficiency is closely related to the cathode current efficiency.

Equations (6) through (9) show the paths the anode current losses are assumed to take. Including the hydroxide ions that remove the hydrogen ions produced by these reactions as they form, the stoichiometry becomes



These equations are part of the basis for our material balance.

Equation (13) has another important consequence. It consumes one hydroxyl ion and therefore wastes only one cathodic electron transfer. On the other hand, it accounts for the generation of two electrons at the anode. In this reaction scheme, derived for a membrane cell, the anode and cathode current efficiencies therefore are not equal. The anode efficiency fundamentally should be the lower of the two. In our example, it is about 1% lower than the cathode efficiency. The chlorine in the cell gas represents an efficiency slightly less than 93%; adding the dissolved chlorine to this brings the efficiency slightly above 93%. The remaining difference is the chlorine content of the HOCl. The distribution of byproducts, furthermore, is not a unique function of the amount of hydroxide leakage. The hydroxide flux depends on the type of membrane used, but the various reactions summarized above are competitive, and the relative amounts of chlorate and oxygen formed depend on the anode. Anodes can be designed with higher than normal oxygen overvoltages, for example. This inhibits reaction (9) or its equivalent given in Eq. (12). This result is the formation of less oxygen and more chlorate, with the same total electrical inefficiency.

In practice, the anode current efficiency of a membrane cell can be manipulated and may be either higher or lower than the cathode current efficiency. Leaving aside the question of recovery of some of the chlorine value after the anolyte leaves the cell, the manipulation usually takes the form of acid addition along with the feed brine. This combines with some of the hydroxide ion and reduces its ability to degrade the anode process. Discussion of the techniques, limitations, and practicality of acid addition is not part of this chapter.

6.6. PROCESS DESIGN

6.6.1. Cell Room Operating Variables

No chemical plant can be designed to operate only at its standard process flow diagram conditions. Chlor-alkali plants in particular are subject to a number of perturbations that affect the requirements of the process.

The operating voltage and current efficiency of a cell fix its unit DC power requirement. This varies with time, usually in the direction of increasing power consumption, and so cells and their auxiliaries must be designed with this fact in mind. In a diaphragm or membrane cell, performance declines over the lifetime of the anolyte/catholyte separator, usually as a result of the accumulation of impurities. The performance of a mercury cell

is also affected by the presence of certain impurities in the brine and by the accumulation of mercury butter (Section 7.4.2.1).

When current efficiency declines, higher amperage is necessary to maintain production. The resistive losses within the electrolyzers increase, and this in turn increases the operating voltage and the duties of the process coolers. Brine, caustic, and chlorine flows are not greatly affected, but the hydrogen flow increases nearly in inverse proportion to the current efficiency. The most serious effect of lower current efficiency is the increased production of impurities. Oxygen usually is the most troublesome. It can interfere with downstream use of chlorine or make liquefaction less efficient (Section 9.1.7.2). As explained in Section 6.5, the operator has some control over oxygen production through acidification of the brine.

Higher voltage (and therefore higher power consumption) in itself has no effect on the cell mass balance if control of other operating variables is maintained. It does influence the heat load, and the cell room heat exchange system must have the capacity to operate at a chosen maximum voltage. Likewise, the electrical supply system must be designed to operate at currents and voltages higher than their start-up values.

Cell temperature and operating pressure can have large effects on the mass and heat balances. This is especially so on the anolyte side. Dissolved alkali chlorides do not greatly depress the vapor pressure of water. Since the cells operate at temperatures fairly close to the atmospheric boiling point, small changes in the cell temperature or the ambient pressure can produce large changes in the water content of the chlorine gas leaving the cells. These, in turn, change the duty of the chlorine coolers.

The water content of the hydrogen gas is lower because of the presence of caustic in the catholyte or decomposer. Differences among the various types of cells are greater than in the case of chlorine because of the large differences in caustic concentration.

Changes in the design concentrations of the solutions entering and leaving the cells affect the required electrolyte flow rates. In a mercury cell, this statement applies only to brine flows. Water is in almost all cases the feed stream to the decomposer, and the product caustic concentration usually is fixed and closely controlled. In a diaphragm cell, the situation is a bit more complex if one thinks of controlling both anolyte and catholyte concentrations, because of the interrelationship caused by flow of the anolyte through the diaphragm. In a membrane cell, there is a similar effect due to water flux through the membranes, but this varies little from day to day. Practically, the electrolyte concentrations in these cells can be considered independent of each other.

6.6.2. Process Control

Under the working assumption that the catholyte is perfectly uniform, changes in the feed concentration *per se* have no effect on the process. The dilution value of the recycle stream in Fig. 6.9 is then proportional to the difference between its concentration and that of the catholyte. On a weight basis, the required flow rate is inversely proportional to the same quantity.

When the catholyte concentration is changed at a constant feed concentration, the situation is different. The mass and energy balance in the catholyte chamber will change. As the catholyte concentration goes down, more dilution is required in order to reach the lower concentration. At the same time, the amount of water evaporated into the hydrogen

stream increases because of the higher vapor pressure. This must be replaced by adding more recycle. The calculated recycle flow therefore is more sensitive in this mode.

Example. Figure 6.9 shows a flow of about 489 tph, or $377 \text{ m}^3 \text{ hr}^{-1}$, of 30.3% NaOH to the cells in order to produce 800 tpd of NaOH in 32% solution. Changes in the feed concentration, as stated in the text, require inverse changes in the inlet flow rate. Increasing the feed concentration to 30.5%, for example, requires a flow of $489 \times (32 - 30.3)/(32 - 30.5) = 555$ tph. Variations in the outlet concentration require greater changes. The tabulation below shows the flows required for other outlet concentrations, along with approximations made by assuming that the flow rate is inversely proportional to the difference between caustic feed and product concentrations. The inlet concentration in all cases is 30.3% NaOH.

% NaOH in product	Dilute NaOH rate, tph	Estimated rate, tph
31.0	1309	1188
31.4	802	756
31.7	612	594
32.0	489	—
32.5	359	378
33.0	277	309
33.5	220	260

The actual changes here are about 18% greater than those estimated.

The example assumed a constant water transport coefficient (WTC). This is not a realistic assumption, because the coefficient depends, among other things, on the NaOH concentration. The extent of this dependence is a function of other variables and on the type of membrane used. A single relationship between WTC and operating variables cannot be assumed.

The effect of a change in the water transport coefficient can, however, be evaluated separately. The required recycle flow varies linearly and inversely with the water transport coefficient. The relationship is a strong one:

$$\partial Q / \partial W = -(M_w / M_c) P C_o / \xi (C_o - C_i) \quad (15)$$

where

- Q = inlet flow rate, weight/time
- W = water transport coefficient
- M_w = molecular weight of water
- M_c = molecular weight of caustic
- P = production rate of caustic, same units as Q
- C_o = concentration of caustic leaving cells
- C_i = concentration of caustic entering cells
- ξ = cathode current efficiency

In our reference plant model, Eq. (15) shows that a reduction of one unit in WTC requires an increase of about 300 tph in recycle flow. This information is of value primarily to the designer. The operator seldom is directly aware of the value of the water transport coefficient in the plant, and the rate of caustic recycle to an electrolyzer is not often manipulated in response to small changes in performance. Instead, the inlet concentration of caustic is allowed to float. The most important consideration is rapid dispersal of the solution entering a cell to achieve homogeneity. A high circulation rate, within design limits in order to avoid excessive turbulence at the membrane surface, both increases the rate of mixing and reduces concentration gradients by keeping the inlet concentration close to the average concentration in the cell.

Section 6.5 mentioned that the transport coefficients are much lower in KOH service than in NaOH production. KOH production therefore requires higher recirculation pumping rates. In NaOH service, the water transport coefficient is higher, but it depends on a number of variables, not least the type of membrane. Membrane suppliers are the best source of information on water transport coefficients. In the extreme case of a reduction from 4.0 to 2.0, the required brine feed rate increases by about 25% and that of 30.3% caustic more than doubles.

From a physical standpoint, the role of the WTC in the anolyte and catholyte water balances explains its effects in process control. Electrolysis tends to increase the strength of the catholyte, which then requires dilution in order to maintain the proper concentration. The water added to the circulating caustic and the water flux through the membranes provide this dilution. When one source diminishes, the other must increase. Therefore, a reduction in the WTC requires an increase in the flow of dilution water.

With more dilution water entering the caustic, either the strength of the recirculating stream will be lower or the rate of recirculation of cell product must increase to hold that concentration and reduce the concentration change across the cells. The increased flow rate enhances mixing of the recycle stream in the cells, and there is probably some economic optimum of the circulating rate and solution concentration. Intuitively, that optimum seems to be on the side of holding the concentration steady. This is the method usually adopted in practice.

An opposite effect holds on the brine side. Electrolysis continuously depletes the anolyte. The brine feed, which is more concentrated, serves to keep the concentration at the chosen level. Transportation of water through the membranes also helps to keep the concentration higher. As the water transport coefficient becomes smaller, less water leaves the anolyte through the membranes, reducing this contribution to a higher concentration. More strong brine is then necessary to offset this effect. A reduction in WTC therefore requires higher inlet flows on both sides of the cell.

Valves in the gas headers control the pressures on the cells. In the usual case where pressures are close to atmospheric, pressure drops everywhere must be kept very low. Each header is sized generously in order to keep the gas pressure essentially equal on every cell in the line. The two gas pressures can be controlled independently. However, the differential pressure between the cathode and anode chambers may be more important than the individual header pressures. In a membrane cell, for example, fluctuations in differential pressure cause vibration of the membranes. This can lead to physical damage, sometimes allowing passage of cell fluids, and to early failure. A frequent practice is to control the differential pressure directly, forcing any pressure fluctuations on the two

systems to be in phase. The discussion in Sections 11.3.2 and 11.4.2 describe more fully the other approach in which the two header pressures are controlled directly.

The hydrogen pressure is greater than the chlorine pressure. One advantage is that this makes it easier to hold a positive pressure throughout the low-pressure hydrogen system. This prevents infiltration by air. In membrane cells, this arrangement also keeps the membranes pressed against the anodes, which is the preferred arrangement. In diaphragm cells, even though the hydrogen pressure has the higher control point, the pressure on the diaphragms actually is higher on the chlorine side. This is due to the hydraulic gradient used to push anolyte through the diaphragms, and again the pressure differential helps to hold the separator in place.

Control of cell temperatures refers to the temperatures of the anolyte and catholyte. In diaphragm cells, separate control is not possible. In mercury cells, the decomposer and cell temperatures usually are different. In membrane cells, it is possible to maintain different temperatures. Heat transfer through the membrane, or rather unsymmetrical flow of the heat generated in the membrane, tends to limit any difference. This is of no great practical importance, for there is little reason to strive for widely different temperatures. The target temperatures, as often as not, are the same on both sides.

Temperature control usually is indirect. The temperature of the brine or caustic fed to the cells actually is controlled. The temperature of the liquor leaving the cells is monitored and used to reset the control point if necessary. This approach has two advantages:

1. Control dynamics are better, because the dead time associated with the cells and piping is eliminated.
2. The cells do not all have the same characteristics and therefore do not all operate at the same temperatures. Below, Section 6.6.3 discusses this aspect of cell-to-cell variation, along with the advantages of having some individual cell control.

There are similarities between temperature and concentration control. The proper cell concentrations result when the right combination of solution feed rate and concentration exists. With all three types of cell, the feed brine concentration usually is set and controlled in the brine plant. Specifications imposed by the various technologies on the feed brine concentration allow only limited control to be exercised from that source. The feed rate is the variable usually manipulated in the cell room. In a mercury cell, the caustic product concentration is determined by the rate of feed of water to the decomposer. This must be proportioned to the rate of production of amalgamated alkali metal, or essentially to the operating load. In a membrane cell installation, the concentration of the recirculating caustic usually is continuously controlled by the addition of water. Again, the right combination of flow rate and inlet concentration produces the desired outlet concentration. In fact, the material balance on the catholyte is determined simply by the rate of addition of dilution water, and the concentration/flow rate combination of the recycle stream must conform to this requirement. With the proper model of cell room operation built into a control computer, one can control the average catholyte concentration directly by manipulation of the water makeup rate. It is therefore possible to inject water directly into the cells and avoid caustic recycle, provided that mixing of the water is rapid and that the catholyte heat balance can be maintained.

Normal operation of diaphragm cells does not permit independent control of anolyte and catholyte concentrations or temperatures. The catholyte composition is the more important, since it has a greater effect on cell operating efficiency and also determines the load on the caustic evaporators. The anolyte concentration must remain above some minimum, and this can become a constraint on the catholyte concentration.

6.6.3. Cell-to-Cell Variation

The discussion so far has tacitly assumed that all cells are operating at the same concentrations and temperatures. The reality is quite different, and operating characteristics vary from cell to cell. The conventional process for depositing diaphragms, for example, is inexact, and membrane cells require manual assembly with its inherent variability. The characteristics of new cells at startup will vary about their means. Aging of the components, primarily diaphragms and membranes, also will not be uniform. Even if all cells operated at the same current, there would still be differences in their voltages and current efficiencies. From a process control standpoint, the most important variation is that in voltage. This affects the heat balance on a cell, and a higher voltage means an increase in the cooling load. To the extent that an increased voltage is part of an overall cell room trend, a change in electrolyte feed temperature, for instance, can offset some of the increased demand. Operating temperature also is partially self-regulating. At higher temperatures, more water vaporizes and carries with it some of the increased heat flux. In the end, however, an increase in feed rate is necessary to maintain temperature control. This changes the mass balance as well.

With a diaphragm cell, an increase in brine flow rate means a decrease in the concentration of NaOH and the NaOH/NaCl ratio in the catholyte. Those two parameters then move away from what were presumably optimum values. Cell performance suffers and evaporation load increases. The latter effect can be avoided by maintaining the same total flow to the cell room. The small change that adjustment of the flow to one cell causes in the performance of the other cells is not measurable, but the accumulated change becomes significant as more and more cells require special attention. Eventually a cell reaches some operating limit (voltage; production of chlorate, oxygen, or hydrogen; position of overflow pipe) and must be removed in order to replace the diaphragm. Opposite adjustments are necessary after installation of the new cell. Because of variations in diaphragm quality, these cannot be predicted with great confidence, and the new cell will require close attention and possibly some adjustments before settling in to steady operation.

In a mercury cell, adjustments to the brine and caustic loops are independent but subject to the same sorts of fluctuation. Anode adjustment and the occasional stoppage to remove mercury butter can offset changes in mercury cell performance.

Membrane cells follow the diaphragm-cell pattern, with the need to consider anodic and cathodic processes separately. An increase in brine flow increases the depleted brine concentration. This has no particular deleterious effect on cell performance, but allowing for higher flow throughout the brine recycle system adds to the plant cost. On the cathode side, an increase in net flow through the cells would reduce the product concentration and perhaps move it away from the economic optimum. Eventually, membrane cells must also be renewed. Their operating cycles are longer, averaging several years against

normally less than one year in the case of modified asbestos diaphragms. There is somewhat less variability in the performance of new cells. Observation of membrane- and diaphragm-cell circuits at startup indicates that, at the same average voltage, the center and low-voltage end of the voltage frequency distribution are much the same. Membrane installations have the advantage of less skewness and fewer high-voltage outriders.

REFERENCES

1. T.V. Bommaraju, B. Lüke, G. Dammann, T.F. O'Brien, and M.C. Blackburn, Chlorine. In *Kirk-Othmer Encyclopedia of Chemical Technology*, on-line edition, John Wiley and Sons, Inc., New York (2002).
2. P. Schmittinger, *Chlorine—Principles and Industrial Practice*, Wiley-VCH, Weinheim (2000), pp. 20–22.
3. G.W. Cowell, A.D. Martin, and B.K. Reville, A New Improved Method for the Determination of Sodium Hydroxide Current Efficiency in Membrane Cells. In T.C. Wellington (ed.), *Modern Chlor-Alkali Technology*, vol. 5, Elsevier Applied Science, London (1992), p. 143.

7

Brine Preparation and Treatment

This chapter considers the preparation of brine from solid salt and the design and operation of each of the major units in a brine purification system. The discussion begins with the sources of electrolysis salts (both sodium and potassium chlorides; both natural and refined) and the methods of handling and storing them and then dissolving them to prepare brine. There is also a brief discussion of the storage and handling of brine. The rest of the chapter is then devoted to the treatment of brine to reach the purity demanded by the various types of cell. The sequence of the discussion follows the flow diagrams of Figs. 6.1 and 6.2.

7.1. SOURCES OF SALT

7.1.1. General

The classical work on salt is Kaufmann's ACS Monograph 145, *Sodium Chloride*. Although first published in 1960, it is an unmatched overview of all aspects of salt technology and still has much useful material.

Salt is an ubiquitous mineral and perhaps history's most important mineral. In an age when most of the developed world worries about too much salt intake, it is sometimes hard to remember that salt is an essential component of the human diet and that throughout most of history it has been in short supply. Salt deficiencies that are less than fatal still can interfere seriously with bodily functions. Thousands of Napoleon's soldiers, faced with a lack of salt in their diet and as a disinfectant, died during the retreat from Moscow because their wounds could not heal. Access to salt or the salt trade has played a large part in shaping the history of nations. The long-lasting alliance between England and Portugal was originally based on trading naval protection for a source of salt [1].

The very word "salary" reflects the importance of salt in the days of the Roman Empire. A soldier's pay was his *salarium argentum*, or his salt money. The same origin tells us that a useful man is "worth his salt," and we say that good people are the "salt of the earth." Plato referred to salt as "a substance dear to the gods."

There are large underground deposits of salt, usually in the form of the cubic crystal halite, in many parts of the world, and the oceans themselves contain about 2.7% NaCl. Each cubic kilometer of seawater therefore contains more than 27 million tons of NaCl.

This is enough to meet the world's demand for salt for seven or eight weeks. Since the seas contain about 1.35 billion cubic kilometers, the present rate of use would consume their chloride in about 180 million years. Solid deposits of salt, measured only in the billions of tons, add very little to this. Since over the course of 180 million years, a very high percentage of the chloride used will have found its way back to the seas, this situation is less alarming than it might appear.

The salt found in underground deposits is usually referred to as rock salt. It is recovered both by classical mechanical mining and by forcing an aqueous stream down into the deposit and back to the surface through a pipe (solution mining). Seawater and saline brines are the other major sources. These are allowed to evaporate in large ponds, precipitating the salt for mechanical recovery. The product is usually referred to as sea salt or solar salt. A relatively minor source is the occasional near-surface pool of brine or low-lying surface deposit. The latter is often in the form of loose particles which can simply be dredged and then washed.

Salt mining is a large-scale specialized activity. Few chlorine producers mine salt or have much control over the process. Section 7.1.2 therefore gives only a brief review of the subject of mechanical mining of rock salt. Solar salt production, on the other hand, is closely tied to chlorine plants in some parts of the world. A fuller description of its production seems appropriate and appears in Section 7.1.3.

While the natural salts predominate in the NaCl market, the chlor-alkali industry also uses quantities of processed and byproduct NaCl. Several techniques, discussed in Section 7.1.5, are used to upgrade both rock and solar salts in order to reduce the cost of on-site treatment. In other cases, byproduct brines are available from chlorine consumers. These usually result from the neutralization of HCl produced in phosgenation or chlorination processes (Section 7.1.4).

KCl is much less plentiful than NaCl. Its molar concentration in seawater is only one fiftieth that of NaCl. It is obtained chiefly from mineral deposits and again is not so widespread as NaCl. Much of the KCl, moreover, exists in mixed ores such as sylvinite, a combination of NaCl and KCl. KCl is discussed separately in Section 7.1.6.

Any chlor-alkali producer whose operation is based on the solid raw material will find it necessary to store salt. Section 7.1.7 addresses this topic.

7.1.2. Rock Salt

Rock salts are those formed by evaporation of inland seas over a broad range of geologic time, ranging from the Precambrian through the Quaternary. They abound in many parts of the world and are used extensively in chlor-alkali production. Less than half the total salt used is rock salt. In Canada and the United States, rock salt is the primary source for the chlor-alkali industry, outweighing solar salt by about 5:1. Rock salt is recovered by subsurface mining. Certain applications, including chlor-alkali manufacture, can use the NaCl solution obtained directly from rock salt by forcing water into the deposit to dissolve the salt. This technique, solution mining, is regarded as a brine preparation process and treated in Section 7.2.2.4.

Most rock salt mining involves undercutting of a deposit, drilling, and blasting. Usually, mining advances by undercutting the salt to a distance of about 5 m from the

face. The miners then drill a series of holes of the same length in the face of the deposit and charge them with an explosive. The explosive most often used is ANFO, a mixture of fertilizer-grade ammonium nitrate with No. 2 fuel oil. Exact procedures and the amount of salt that can be released by a blast depend on the geometry and physical characteristics of the deposit.

There are two principal types of deposit. In one, the salt exists in bedded, relatively horizontal strips or strata, separated by layers of shale, limestone, or gypsum. The extent of some of these deposits is huge. The salt zone in eastern North America extends about 2,500 km east to west (equivalent to Paris–Moscow) and more than 600 km north to south (equivalent to Hamburg–Vienna). The top of a deposit may lie 100 m or more than 1 km below the surface. Each stratum of salt is mined individually, usually by excavating rooms about 15 m wide and up to 8 m high. Mine shafts, typically 6 m in diameter, are excavated to the depth of the deposit. Many shafts are lined with concrete through the overburden. Mining usually progresses by drilling holes for placement of the explosive across the entire face of the salt in a room. Several hundred tons of salt may be released by each blast. The rooms are interconnected by crosscuts at certain intervals. Recovery of the salt is incomplete, because some of it is left in place as pillars that provide support for the overburden. Under the high loads that many mines support, salt undergoes plastic deformation. Over a long period of time, the mine floor and roof can converge. Proper sizing of the rooms and pillars, based on the principles of rock mechanics, allows convergence without failure of the roof or floor [2].

Salt also occurs in large deposits of great thickness, called “domes.” These apparently formed by the plastic flow of salt from great depths up through weak sections in the surrounding rock. Figure 7.1 shows a typical sequence. Salt domes occur in parts of Europe and on the Gulf Coast of North America and often have diameters of more than a kilometer. Figure 7.2 shows the outline of a typical dome in Avery Island, Louisiana [3]. Assuming a circular cross-section, the amount of salt shown here could supply the world with chlorine at its present rate of production for over 600 years. The largest domes may contain hundreds of billions of tons. Mining can be more efficient in domes, because the operation is less constrained by the dimensions of the salt face. Holes still may be drilled across the width of a cavern but only to a certain height. Much larger quantities of salt can be released. In a large mine, a single blast might release more than 30,000 tons [4]. While mining in stratified deposits is usually at a single level in each stratum, dome mining proceeds more gradually, with the levels stoped.

Mined salt must be crushed to a usable particle size. Three stages of crushing are typical, with at least the first performed underground to eliminate the need to handle meter-sized chunks and raise them to the surface. The maximum size from this stage is typically about 250 mm. Final grinding reduces the maximum particle size to something on the order of 30 mm. Screening then produces several cuts, which are intended for different uses. While several auxiliary crushing and screening operations are employed with recycle streams, the major screening operation can be divided into two steps. Primary screening produces three fractions. The oversize material is sent to a recrushing system and is then screened again. The destinations of the three fractions from this operation are the same as those from the primary screener. In one version, the

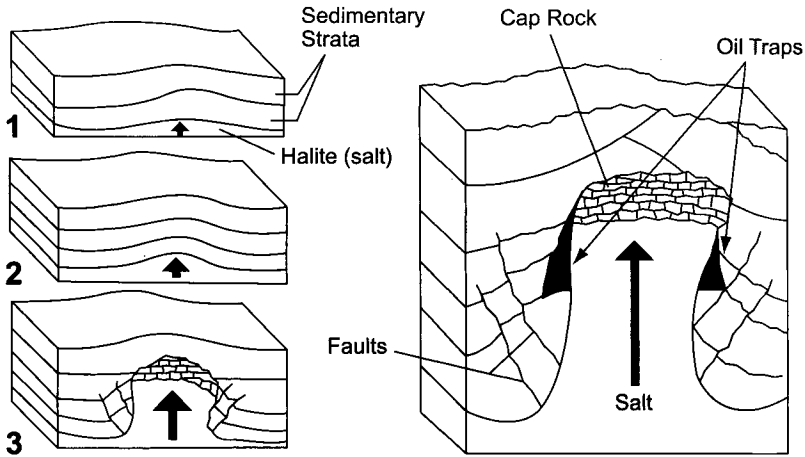


FIGURE 7.1. Progressive formation of a salt dome. (With permission of Compton's NewMedia.)

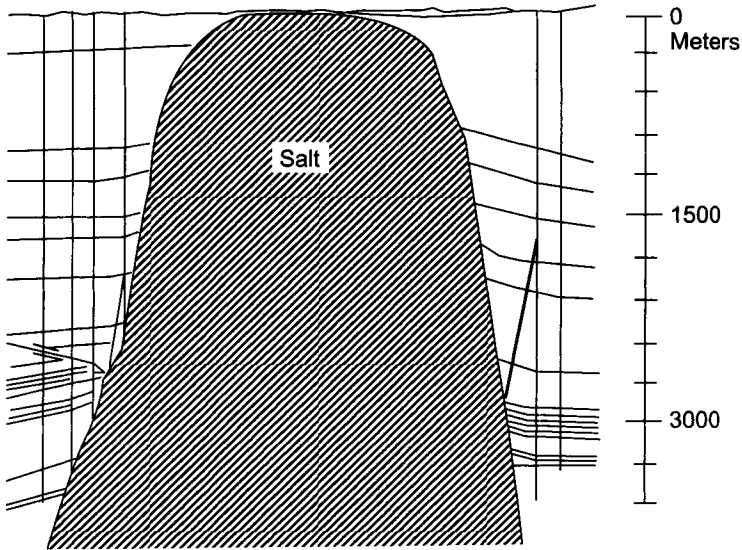


FIGURE 7.2. Cross-section of a salt dome. (Avery Island, LA) (After J.B. Carser, *Bull. Am. Assoc. Petrol. Geol.* (1950).)

center cut, sized from about 9 to 15 mm, is sent to storage as a product referred to as “#2.” The undersize from the primary screening is sent to a tails screener. The oversize from this screen, sized from about 6 to 10 mm, is another product, #1. The center cut is sized from about 3 to 6.5 mm. This is known as coarse crystal, or “CC.” The undersize, below 3 mm, is fine crystal, or “FC.” Alternatively, grades are designated by descriptive

terms as in the following tabulation:

Fine	0.2–2.8 mm
Medium	0.4–4.0 mm
Coarse	2–8 mm
Extra Coarse	1–11 mm

Screens are usually made of stainless steel or Monel, at least in the finer sizes. Coarse, heavy-duty screens may be made of hot-dipped galvanized steel.

The finest particles (<600 μm) are hard to handle, cake easily, and have the least commercial value. They often are used for maintenance inside the mine, as in road building and repair, and to build temporary barriers. The latter often are erected between pillars for control of ventilation.

At some stage in the size-reduction process, the broken salt is transported to the surface. Belt conveyors are used in the crushing and screening operation. Various types of vehicles, suited to the characteristics of individual mines, deliver the salt to the primary crusher or the shafts, for hoisting to the surface. Vehicles include front-end loaders and diesel trucks. Low-profile end-loaders of relatively small capacity are used when roofs are low. Load-haul-dump (LHD) units, needing only one operator/driver, can collect, transport, and deliver salt to a crusher.

Continuous mining machines have rotating moveable heads with carbide cutting edges. They are used more extensively in mine development than in production.

Major considerations in mine engineering are safety, ventilation, the working environment, and transportation of salt and workers. Drainage is of critical concern, because water accumulated in the process or leaked into mine shafts from the surface or water-bearing strata can damage the unmined columns of salt that are used as structural support. Shafts and mine superstructures are built mostly of concrete and heavy structural steel. The latter requires painting and constant maintenance. The worst area for corrosion is at the head of the mineshaft. The atmosphere there includes moisture condensed by cold mine ventilating air; salt dust; gases such as H_2S , CH_4 , and CO_2 released from occlusions in the salt; and the products of combustion from blasting. Normal practice is to monitor the air in the mine for carbon monoxide released by combustion and for the toxic gases associated with the salt deposit and the methods of mining.

7.1.3. Solar Salt

7.1.3.1. Production from Seawater

7.1.3.1A. Principles. Solar salt results from natural evaporation of seawater or brine in large ponds. Its production is a slow process. The retention time from intake of seawater to harvesting of salt is usually several years. Even brine from wells, which is much more concentrated to begin with, requires a year or more. Because the rate of evaporation and the success of salt production depend on local weather patterns, it is an uncertain business and one that must follow a yearly cycle. Many solar salt plants make product during only part of the year.

Because of the complex constitution of seawater, many species other than NaCl can precipitate from solution. Therefore, the production of solar salt involves a sequence of

fractional crystallizations. Total crystallization of the dissolved solids from seawater [5,6] would produce a salt of this approximate and unattractive composition:

NaCl	77.8% (w/w)
MgCl ₂	10.9
MgSO ₄	4.7
CaSO ₄	3.6
KCl	2.5
CaCO ₃	0.3
MgBr ₂	0.2

The list refers to anhydrous species. Allowing for hydration of magnesium and calcium compounds, the solid salt actually would contain about 65% NaCl. Baseggio [7] also reported the analysis of salt obtained by the evaporation of seawater taken from the Caribbean Sea (Inagua, Bahamas). He grouped the solids somewhat differently and ignored the presence of carbonate. Adjusting the data in all three references [5–7] to an ionic basis shows that they are in close agreement.

As evaporation proceeds, fortunately, the dissolved salts tend to precipitate sequentially, and so it is possible to harvest NaCl selectively. With the composition given, CaSO₄ and the carbonate will precipitate first and will be followed by NaCl. Magnesium compounds precipitate later than NaCl. Each species precipitates over a certain range in brine strength, and there are no sharp demarcations. Thus, precipitation of NaCl begins before precipitation of calcium compounds is complete and continues into the magnesium-precipitation phase. Optimum separation of these overlapping processes is part of the art of solar salt production.

The first salt produced by solar evaporation, many centuries ago, would have had approximately the composition tabulated above. Its taste would have been very bitter. Technology began to advance when someone noticed that the taste deteriorated rapidly toward the end of the evaporation. By draining off the last small volume of brine and harvesting the salt already formed, the solution responsible for the bitterness, still referred to as “bitterns,” was isolated. Similarly, someone noticed at some point that the first material precipitated was not salt. By making a cut on the front end, transferring the brine after the onset of NaCl precipitation to another pond, the amount of gypsum in the product was also reduced. This simple technique is the essence of the methods used today.

Baseggio evaporated the seawater and reported its composition as a function of density, noting the onsets of gypsum and salt crystallization. The water used was about 10% more concentrated than water from the open oceans (3.76% total salts vs 3.42%) but was identical in salt composition. Evaporation continued until the density of the remaining brine reached 1.25, just at the onset of magnesium precipitation. The volume by then had been reduced to about 3.5% of its starting value; salt precipitation did not begin until the volume was reduced by about 89%.

The curves of Fig. 7.3 qualitatively show the course of precipitation of the solids. From the onset of NaCl crystallization until the final density is reached, about 77% of the salt precipitated in Baseggio’s work, the rest remaining with the bitterns. The CaSO₄ crystallizing along with the salt represents a dry-basis concentration of 0.6%. This can

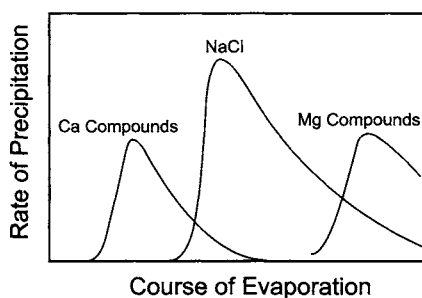


FIGURE 7.3. Course of precipitation of solids from seawater.

be reduced by delaying the start of the product cut. In commercial operation, evaporation proceeds until the brine density reaches 1.25 or 1.26. This corresponds to precipitation of 72–79% of the NaCl [2]. These numbers vary in practice, as commercial operations may continue evaporation in order to improve the salt yield. The exigencies of production will make the boundaries between stages of precipitation less precise, and economic optimization of the operation may call for greater production of salt at the expense of purity. Most solar salt on the commercial market does in fact contain significant amounts of magnesium compounds.

Because of the importance of climatic conditions, solar salt plants are largely confined to warm or dry parts of the world. Where concentrated natural brines are available, there are exceptions. In the United States, for example, a solar salt plant once operated in Syracuse, New York, a city renowned among Americans for its annual snowfall.

Each plant will follow a yearly program. Productive operation typically ceases during the winter months. “Winter” is a relative term here; the length of the unproductive period is highly variable. It may be as much a question of wet and dry seasons as a change in average temperature. When operation begins again, the objective will be to deliver saturated brine as soon as possible to the part of the plant in which NaCl is precipitated. Toward this end, the salt plant will be divided into a number of ponds, each of which is intended for brine of a certain density. The brine being processed flows from one pond to another, finally reaching the end of the cascade where solid salt is produced. There are four groups of ponds with different functions:

1. the concentrators or condensers, which remove suspended solids and concentrate the brine to saturation;
2. the lime ponds, which allow further evaporation and the crystallization of calcium compounds;
3. the crystallizers, in which evaporation of the brine produces salt crystals;
4. the bitterns-holding ponds, which hold highly concentrated solutions of magnesium salts.

At the end of a yearly production period, the various ponds are more or less full of brine at different stages of concentration. Maintaining a profile of concentration will help the restart in the next production period. Doing this in the face of wintertime rainfall requires some management. Adding residual brine or wash brine from the crystallizers can offset

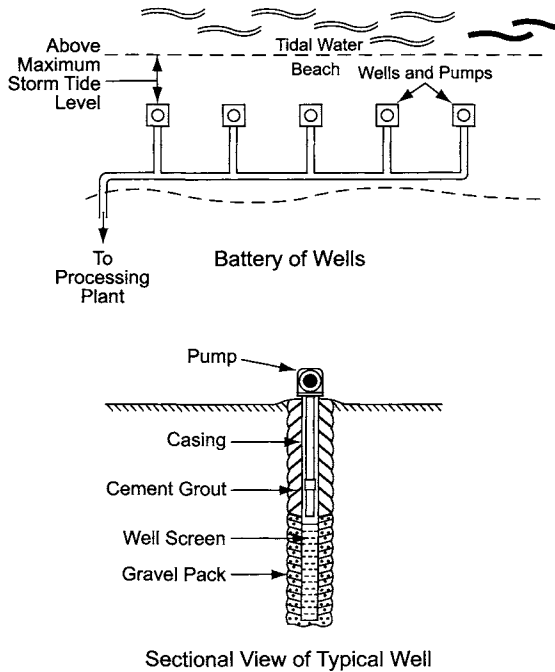


FIGURE 7.4. Beach well system to supply solar salt plant.

a rigid launching frame. The pipe ends in a riser that carries the suction clear of the floor of the sea.

7.1.3.1C. Evaporation. Seawater collected in a pond is allowed to sit and evaporate. Tidal gates, which are always closed during low tide to prevent backflow of brine, can be kept closed to prevent dilution until a certain amount of water has evaporated and the partly evaporated brine has been transferred to another pond. Alternatively, seawater can be allowed to enter the first pond along with the tides in order to keep the front-end productivity at a maximum.

Eventually, a cascade of ponds operating at different brine strengths emerges. The art of solar salt production consists in management of the concentrations and proper staging of the brine flow. Depending on the terrain, transfer from pond to pond can be by gravity or by pumping. Addition of new brine to a pond dilutes the contents of that pond and can disrupt the concentration profile in the cascade. Dividing a pond can offset this effect and force the brine to flow in a pattern that is closer to plug flow. This raises the average surface concentration and lowers the overall evaporation rate. Furthermore, in dividing the pond, one spends money to reduce the total area available for evaporation. This approach therefore requires close attention to brine hydraulics and the optimization of the number and arrangement of subdivisions [9,10].

As the brine becomes more concentrated, its vapor pressure and rate of evaporation become less. By the end of NaCl precipitation, the rate will have dropped nearly by

half. Joshi and Bhatt [11] divided the evaporation into 10 stages, determined by the density of the brine. For each stage, they estimated the rate of evaporation by applying a correction factor for vapor pressure. These factors are based on the average density in each stage [12]. Using fixed limits for brine densities in and out of the last stage, they provided a formula for its area. Applying a small degree of conservatism, this becomes

$$A = 0.9 T / DE \quad (1)$$

where

A = area of last compartment, hectares

T = tons per year of salt production

D = crystallizing days per year

E = evaporation rate of fresh water, mm per day

E is determined for each site by applying a correction factor to the results of tests in a standard evaporimeter. For large ponds, the factor is 0.7. This and the vapor pressure correction already alluded to are built into Eq. (1), whose results agree with those published by See [13] for operations in California.

Joshi and Bhatt derived the areas required in each stage and expressed them as fractions of the area of the final (crystallization) stage. The total area amounted to more than 13 times the area of the crystallizer. This is typical; See reports a range of 10 to 15. Since the depth of brine also varies from stage to stage, being typically 400 mm in the front end and 100–200 mm toward the end of the cascade, the volume of the crystallizing stage may be only about 3% of the total.

Example. Our reference plant, as shown by a later example in Section 7.1.7, requires a supply of about 1,300 tpd of salt. Operation for 350 days a year would consume $1300 \times 350 = 455,000$ tons annually. A solar salt plant operating for 200 days a year with an average evaporimeter rate of 10 mm per day requires a crystallizer area of about $(0.9 \times 455,000) / (200 \times 0.7 \times 10) = 292$ ha. The multipliers given in the text then suggest that the total area dedicated to supplying our plant must be 38 km^2 . This is a rather good productivity. Bertram [2] notes that a 400,000 tpy plant can require 40 km^2 or more.

7.1.3.1D. Percolation. Percolation of brine through the walls and bottoms of the ponds can be a significant yield loss. Sandy beaches are obviously poor candidates for brine ponds. There is always an attempt to locate a solar salt plant on less permeable soil. According to the Karman equations, permeability increases with the square of the average particle size and decreases with approximately the 1.75 power of the uniformity coefficient. The latter is a descriptive index calculated by dividing the size of an opening passing 60% of the soil by the size of one passing 10%. Fine soils therefore are desirable, and a wide particle size distribution (PSD) allows better packing, as the finest particles can fill the interstices among the larger particles. Clay serves much better than sand or loosely packed soil. The ponds as constructed are often lined with clay to reduce permeation. Synthetic liners fabricated from thermoplastics are also sometimes used.

The precipitated matter itself also helps to seal the ponds. A permanent salt floor of 200–250 mm acts as a seal and also prevents inclusions of dirt and clay in the harvested salt. Fresh salt then accumulates to a thickness of 100–200 mm before harvesting.

Permeation losses become more important as the brine becomes more concentrated. The crystallizing ponds are obviously the most important of all, and the strength of their surfaces is another major consideration. The bottom of a crystallizing pond must be able to support harvesting equipment and must be able to withstand damage from its movement and operation.

7.1.3.1E. *Energy Efficiency.* The amount of energy transferred in solar ponds can be huge. A good site should produce a noontime flux of more than $80 \text{ kJ m}^{-2} \text{ min}^{-1}$ [14]. The energy transferred at this rate in 1 ha is equivalent to burning about 40 tons of coal per day. Butts [15] presents data from a Northern Hemisphere site that in July evaporates 55 tons of water daily from 1 ha. In 81 km^2 , this plant can evaporate about 450,000 tons of water each day. This is more than is evaporated in all the world's caustic soda evaporators combined.

7.1.3.2. *Production from Inland Sources.* Inland sources of brine are valuable when their locations reduce transportation expense and when they are much more concentrated than ocean water. Famous examples of the latter effect are the Dead Sea and the Great Salt Lake. These may be regarded in terms of salt production as enormous condenser ponds. Other sources may be springs or subsurface streams.

The composition of inland sources is variable and may be quite different from seawater. Other minerals may be more important than the salt. The Dead Sea, for example, is a major source of magnesium and bromine. Various parts of the world have deposits of mixed sodium and potassium chlorides; the potash is the more valuable component of these deposits, and the NaCl is often a waste product. Its disposal then can become an environmental problem [16].

The techniques used to produce salt are the same as those above, but the details of plant arrangement and operation may be radically different, reflecting the composition of the brine. Condenser ponds will be much less extensive. The relative size and importance of lime ponds will depend on the calcium content of the source. The ponding operation extends beyond NaCl recovery when other products are to be recovered.

7.1.4. *Other Sources*

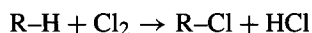
7.1.4.1. *Vacuum Pan Salt.* “Vacuum pan” is the name given to the evaporative process for recovery of solid salt from brines. The process is the source of a substantial amount of salt, and it is one of great historical interest. It has been a common practice to evaporate natural brine from more or less shallow iron pans that were directly fired. The use of open pans is mentioned in Agricola's *De Re Metallica*. This situation evolved through various stages of sophistication in evaporator design, the introduction of multiple effects, and the use of vacuum to allow better energy economy. The use of vacuum became common in the 19th century, and the first multiple-effect salt evaporator went into operation in 1899 [17]. Most facilities were small and intended to supply local markets. Calandria evaporators

with central downcomers were common. Tube lengths were limited in order to prevent excessive boiling point elevation due to hydrostatic pressure. Most new evaporators are forced-circulation, vertical tube units (Section 9.3.3.2), and the use of Monel as a material of construction is widespread.

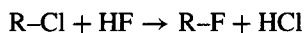
Some multiple units operate in cascade, with the brine following any of several paths through the unit. When nearly saturated brine is the feed solution, there is less to be gained by staging the brine, and parallel feed is common.

Today's standard vacuum evaporators are far removed from open pans. The so-called grainer process actually is closer to the original vacuum-pan process [17,18]. It was displaced by developments in the vacuum-pan process. It survives as a minor source thanks largely to the unique particle characteristics of its product. These are due to slow rates of evaporation from large, quiescent brine surface areas. A flow of air across the brine surface keeps the evaporation temperature at 90–95°C. Surface tension keeps afloat the flakes that initially form. Growth continues, mostly on the underside, until the hollow, pyramidal particles reach a size where they sink to the bottom. The process obviously is energy-intensive, and this fact accounts for its commercial demise [2].

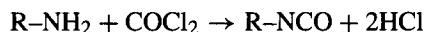
7.1.4.2. Byproduct Salt. One of the major uses of chlorine is in substitution chlorination of hydrocarbons:



Some of these products go into the preparation of fluorocarbons:



Another intermediate prepared from chlorine is phosgene, which then goes into the production of isocyanates:



All these have in common the production of HCl as a byproduct. Much of it is recovered as such for direct use, sale, or conversion back to chlorine. Some of it is neutralized to NaCl and supplied to a chlorine plant as byproduct brine.

Polycarbonates are produced by interfacial polycondensation of the sodium salt of bisphenol A with phosgene. The aqueous phase from this process therefore always contains NaCl.

Depending on the source of process water, byproduct brine may have the advantage of lower concentrations of some of the classical salt impurities. On the other hand, it often introduces the new problem of the presence of various organics.

The influence of organics on the electrolytic process is highly variable and of most concern in membrane cells. Application of byproduct brine must be studied on a case-by-case basis, and it may be necessary to treat the brine to reduce the organic content.

7.1.4.3. *Concentrated Seawater.* Seawater increasingly is used as a source of drinking water. Evaporation, multistage flash distillation, or RO can produce water of satisfactorily low salt content. All these processes reject a concentrated salt solution whose strength depends on the amount of purified water recovered from the seawater.

Most of the concentrate is returned to the sea, but some plants process it further to produce salt. Since the recovery by RO is often less than 50%, salt production is not often combined with RO. With the development of higher-pressure membranes and increasing restrictions on effluent, this combination may become more important in the future [19].

Seawater evaporation plants with more concentrated blowdown are more amenable to the addition of salt production. Salt production usually is a separate operation, receiving concentrated seawater from the desalination plant. Further evaporation of this solution produces solid salt. As is the case in a solar salt plant, gypsum precipitates before NaCl and must be removed from the system. It is taken off as a slurry, part of which returns to the evaporators as seed crystal. The salt as produced, is contaminated with magnesium salts. By recovering the salt from its slurry in pusher centrifuges, the operator can greatly reduce the quantity of occluded magnesium-rich liquor. Because the precipitated magnesium concentrates at the surfaces of the particles, much of it also can be removed by washing the centrifuge cake. This phenomenon also accounts for the success of the salt washing process described in Section 7.1.5.1.

Evaporation of seawater down to solid salt produces a huge concentration factor for trace impurities. The effects of this will vary greatly with locality. So too will the measures necessary to prevent fouling and foaming in the evaporators.

We should also consider a variation on solar salt production in which the ponds are preconcentrators, with final salt production in conventional evaporators. Figure 7.5 shows the steam required to produce a ton of dry NaCl in a triple-effect evaporator as a function of the incoming seawater concentration.

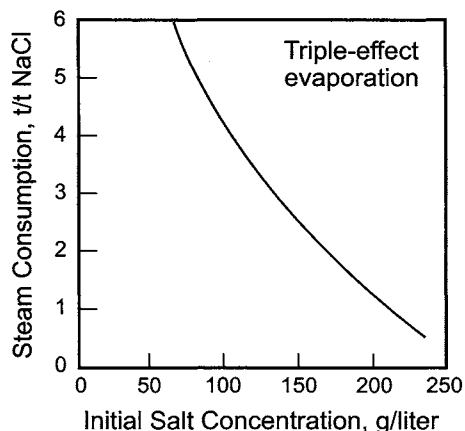


FIGURE 7.5. Steam required to produce salt from concentrated seawater.

Seawater can also be concentrated by electro dialysis. An expenditure of about 150 kWh ton^{-1} of NaCl can bring the NaCl concentration up to 200 gpl [20]. This process has not found commercial application as an intermediate step in the production of large quantities of industrial salt. Where there is more value added on a smaller scale and not much competition from large producers, as in the production of table salt in Japan, it can operate successfully.

7.1.5. Refining of Salt

Natural salts are often processed to remove some of their impurities before sale. All food-grade and certain chemical applications require this. In the chlor-alkali industry, it is necessary at some point to convert crude salt as mined or produced into a material suitable for use in electrolysis. Whether this occurs at the salt producer's site or in the chlor-alkali plant is fundamentally irrelevant. For economic or technical reasons, the salt supplier often undertakes a certain amount of upgrading. The most important processes are salt washing, brine evaporation, and salt recrystallization.

7.1.5.1. Washing. For reasons explained below, washing salt to remove its impurities is easier with solar salts. While this is an operation that can be performed by the supplier, it is also a frequent practice in the chlor-alkali industry for the user to install and operate salt-washing facilities.

By the nature of the process of their formation, particles of solar salt are not uniform in composition. From Fig. 7.3, one can construct an accurate idea of the structure of a particle. The first overlap between curves shows that precipitation of NaCl begins before CaSO_4 is exhausted and that CaSO_4 precipitation continues well into the NaCl phase. Economically, collection of product must begin while CaSO_4 is still precipitating. One therefore expects that CaSO_4 will be found throughout the salt particle, perhaps at higher concentrations in the interior. Magnesium precipitation begins after about 75% of the NaCl has precipitated, and the process may end at about 85% recovery. In an idealized model, then, all the magnesium appears in the outer 4% of the depth of a particle. Liquid occlusions between particles are also high in magnesium.

This picture is consistent with observed differences between solar and rock salts. The ability to reject calcium and magnesium impurities by controlled fractional crystallization means that good solar salts are on the whole purer than rock salt. The high concentration of magnesium compounds at the surface makes the salt more hygroscopic. Solar salts may have higher overall concentrations of magnesium and usually have higher ratios of magnesium to calcium impurities. The latter fact, for reasons discussed in Section 7.5.2.1, creates problems in brine processing by making it more difficult to remove precipitated impurities from treated brine. Finally, when a batch of solar salt dissolves, the first solution that appears is rich in magnesium.

The last fact means that solar salt will release high concentrations of magnesium when small amounts are dissolved. Rainfall onto a pile of solar salt will produce a high-magnesium runoff, and this along with drainage from the pile may be considered part of the first step in refining.

If a fresh shipment of solar salt is added as a batch to a salt dissolver, there will be a surge in magnesium content of the brine being manufactured. This can upset the performance of the brine treatment system and eventually of the cells. Many plants

therefore have systems to isolate these fractions, the bitterns, for special treatment or gradual blending into the main brine stream.

The heterogeneous structure of solar salts can be turned to an advantage. It makes it possible to improve quality by a simple washing process. Rapid washing of solar salt removes magnesium selectively while dissolving a relatively small amount of NaCl. It is more difficult to remove calcium from rock or solar salt by washing. Results in this case are improved by selective rupturing of the salt particles. If salt is milled, it will tend to fracture at the calcium sulfate inclusions. This opens the inclusions to the action of the washer, and they tend to be swept away. Because of their irregular shape, the sulfate inclusions are slower to settle than halite crystals. Therefore, after release, they can be removed from the undissolved salt by elutriation.

There are several commercial versions of the salt-washing process. Figure 7.6 is a generic illustration. Essential features are the limitation of the amount of salt dissolved and countercurrent exposure of the salt to any fresh water input. The flowsheet shows slurry transfer of salt from one section to another. The brine carrier in each case returns to the source. By grouping sets of equipment in order to eliminate the recycle lines, Fig. 7.7 brings out the simple countercurrent nature of the process more clearly.

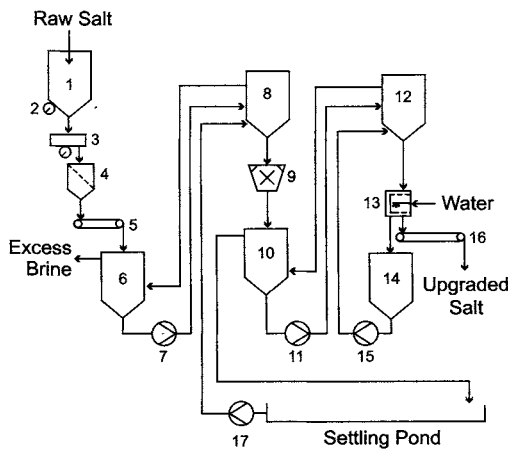


FIGURE 7.6. Salt washing process. 1. Feed hopper; 2. Vibrator; 3. Vibrating feeder; 4. Screener; 5. Belt conveyor; 6. Slurring vessel; 7. Slurry pump; 8. Thickener; 9. Hydromill; 10. Elutriator; 11. Slurry pump; 12. Thickener; 13. Centrifuge; 14. Filtrate vessel; 15. Filtrate pump; 16. Belt conveyor; 17. Rework pump.

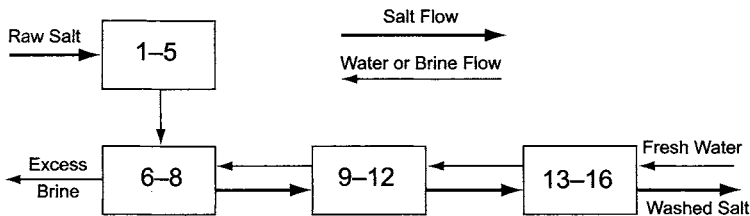


FIGURE 7.7. Countercurrent nature of flows in salt-washing plant. (Numbers refer to equipment in Fig. 7.6.)

Design data from one solar salt washing plant follow:

	Feed salt analysis	Product analysis
NaCl	97.85% (w/w)	99.45
MgCl ₂	0.78	0.10
MgSO ₄	0.33	0.04
CaSO ₄	0.75	0.29
Insolubles	0.29	0.12

The feed salt analysis is equivalent to 0.22% Ca, 0.27% Mg, and 0.79% SO₄. Washing removes about 8% of the NaCl value, along with nearly 90% of the magnesium and 65% of the calcium, and about 60% of the insolubles. For each 100 parts of NaCl forwarded to the chlor-alkali plant, the washing process rejects 8.7 parts NaCl, 0.77 MgCl₂, 0.33 MgSO₄, 0.54 CaSO₄, and 0.20 insolubles. This is a nonhazardous effluent that amounts to about 175 kg of total solids per ton of chlorine. Unless aerated, its corrosivity also is low, with pH = 6.5 to 8 [21].

In this example, removal of the impurities reduces the consumption of treating chemicals by 0.78 kg NaOH and 0.37 kg Na₂CO₃ per 100 kg NaCl. Reducing the on-site consumption of NaOH improves its effective plant yield by about 1.2%. If the NaOH equivalent of the carbonate is included, this increases to 1.5%.

The savings of chemicals listed above are based on stoichiometry. The assumed excess concentrations are unchanged. Sometimes it is argued that with less danger of a magnesium “spike”, the excess NaOH concentration can be reduced as well. Since the excess concentration is never very great, it does not provide any protection against a sizable spike, and this argument may be discounted.

A significant benefit of salt washing sometimes is the change in the Ca/Mg ratio. It has already been mentioned that low ratios can lead to difficulties in phase separation in the chemical treatment of brine. In our example, the ratio improved from 0.83 to 2.5. This would be of substantial, if hard to quantify, benefit.

7.1.5.2. Brine Evaporation. Brine evaporation is a technique for closing the water balance in certain plants and a method for removal of impurities such as sulfate from the process [22]. Later sections of this volume discuss these applications. Most brine evaporation, however, is aimed at the production of higher grades of solid salt for commercial sale. Food-grade salt, for instance, is almost exclusively the product of evaporation of NaCl brine. After evaporation, this salt is recovered in centrifuges and then dried to less than 0.05% moisture [2]. Two particular grades of evaporated salt are most important to the chlor-alkali industry. In one, evaporative crystallization of raw brine gives purity substantially better than the salt that was the basis for the brine. Any version of the vacuum-pan process (Section 7.1.4.1) enhances salt quality by leaving impurities behind in solution. The second grade, vacuum purified salt, is the commercial ultimate in purity. This grade is produced from chemically purified brine. After removal of most of the impurities by methods described in Section 7.5, brine is evaporated to

TABLE 7.1. Comparison of Purity of Various Types of Salt (wt.% on dry basis)

Component	Rock salt	Washed solar salt	Vacuum salt
NaCl	93–99	99	99.95
Sulfate	0.2–1	0.2	0.04
Calcium	0.056–0.4	0.04	0.0012
Magnesium	0.01–0.1	0.01	0.0001
Iron	0.05–0.5	0.03	0.0001

Source: Akzo Zout Chemie Booklet *Electrolysis Salt (Sodium Chloride)*.

TABLE 7.2. Hardness of Industrial Brines

Type of salt	ppm Ca + Mg (as calcium)	Dry sludge (kg ton ⁻¹ salt)
Vacuum purified	5–25	nil
Common purified	100–400	nil
Coarse solar	150–700	0.4–1
Coarse southern US rock	400–1,300	2–4
Medium northern US rock	–	5–15

crystallize the salt. This two-step purification yields a product of more than 99.9% NaCl. The use of vacuum purified salt for large-scale chlor-alkali production is most common in Europe.

Table 7.1 compares the composition of typical rock, washed solar, and vacuum-purified salts. The quality of the salt is directly reflected in the brine that it produces. Table 7.2 shows typical values of hardness in brines produced from several grades of salt [23]. All cases involved wet salt storage in a downflow brinemaker. The last column of the table also shows the amounts of insoluble material accumulated. These do not include residual NaCl, which varies with the operation. A good result would be about 30% NaCl in the total solids before washing. The southern rock salt used as an example is a high-purity grade. This was chosen to show, along with the data on sludge formation by the northern salt, the wide compositional range of rock salt.

Evaporation is energy-intensive. The latent heat associated with separation of a ton of dry NaCl from saturated solution is about 6.5 GJ. With KCl, the equivalent figure depends more on the temperature assumed for the brine as produced but is in the range of 3.5–4 GJ. Energy economization is therefore a major consideration in evaporation process design. Two different approaches are in widespread use, multiple-effect evaporation and vapor recompression.

7.1.5.2A. Multiple-Effect Evaporation. The fundamental idea of multiple-effect evaporation is that a vapor produced from a solution can itself be used as a source of heat. In a simple single-vessel process, the latent heat of this vapor is removed in a condenser by cooling water and becomes waste heat. Condensing it instead in the heating

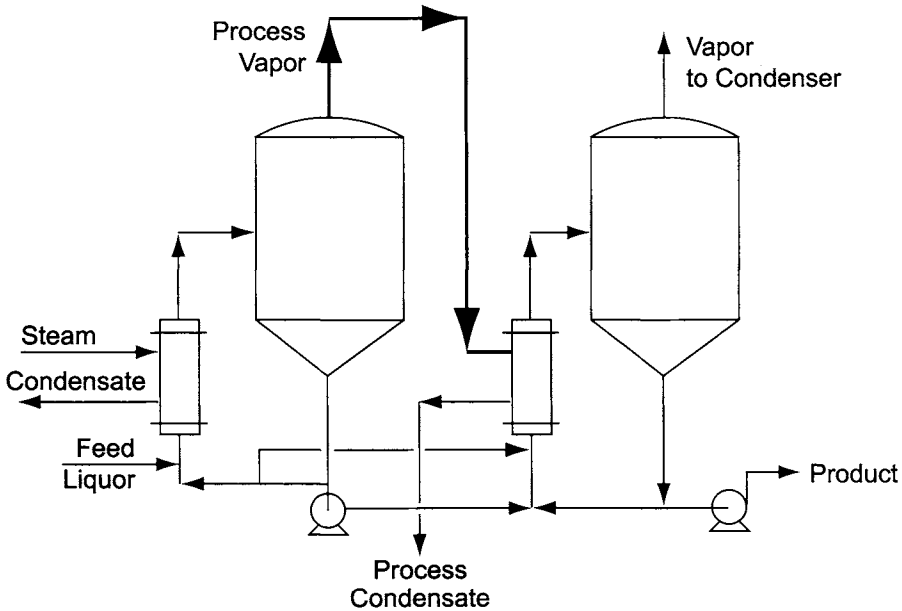


FIGURE 7.8. Use of process vapor in multiple-effect evaporation.

zone of another evaporator transfers its latent heat into the solution being concentrated, producing another increment of vapor. In a sense, some of the latent heat of the outside steam supply is used more than once. Figure 7.8 is an example. Here, a solution has some of its water evaporated by heating it with steam in the first effect. After separation from the remaining liquid, the vapor becomes the source of heat in the second evaporation effect. In principle, the second-effect vapor could be used similarly to produce even more evaporation in a third effect, and so on. The total amount of water evaporated in all the effects divided by the amount of primary steam consumed is referred to as the “steam economy.”

In a completely reversible process using steam to evaporate pure, saturated water, the number of effects could be increased almost without limit, and the steam economy could be very high. It would in fact approach the value N in an N -effect system. A real system never reaches this ideal. Heat loss to the surroundings is an obvious reason, but this loss is controllable in design and is not usually a large factor. Another loss in economy sometimes results from the need to supply sensible heat to bring the feed solution to its boiling point. Again, good design can reduce this loss by interchanging the feed with a hotter stream.

Other limitations on the utilization of the available temperature potential are more fundamental than the factors mentioned above. The total temperature potential available to the designer can be taken as the condensing temperature of the available steam minus the temperature that can be achieved in the condenser of the last effect. Both these temperatures are limited. The practicalities of design limit steam temperature and

pressure. Available coolant temperature and the expense of producing deeper vacuums limit condenser temperature.

When a practical value of available ΔT is selected, the use of multiple effects divides it into N parts. The driving force for heat transfer in each effect then is only about $1/N$ times as great as in the single-effect case. This alone means that the total heat-transfer area in an N -effect system will be about N times that required by a single effect. Next, the boiling point rise (BPR) of the solution in each effect must be subtracted from the total driving force to give the total useful temperature difference. Not all the available temperature potential can be consumed by the BPR. Some must be reserved for the temperature differentials for heat transfer. To a first approximation, the required heat transfer surface will be proportional to the number of effects divided by this residual temperature differential.

Figure 7.9 shows how the available temperature driving force typically is divided between useful potential and the BPR [24]. The example is a forward-feed evaporator concentrating sodium chloride brine with low-pressure steam (140 kPag), using from one to four effects. It is clear that as the number of effects increases, the driving force available for heat transfer declines. The more effective use of steam and the possibility of using a smaller boiler or releasing some boiler capacity for other uses must be balanced against the cost of providing more evaporator bodies and a greater total exchange surface area. Table 7.3 shows relative values of available ΔT and required surface area for different numbers of effects. The last column is based on the approximation noted in the preceding paragraph.

Use of higher-pressure steam would increase the total available ΔT without changing the number of degrees lost to the BPR. The percentage effects would be less severe than those listed above, and a larger number of effects might be used economically.

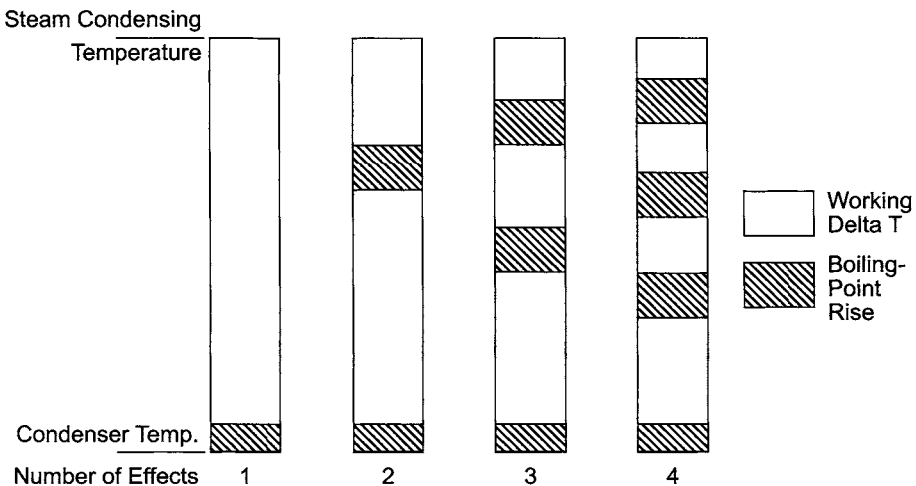


FIGURE 7.9. Allocation of temperature potential in multiple-effect evaporation. (Evaporation of NaCl brine; forward feed.)

TABLE 7.3. Effect of Evaporator Staging on Required Heat-Transfer Area

Number of effects	Available driving force (%)	Area required (%)
1	100	100
2	86	230
3	77	390
4	65	610

In-process economization also would reduce the amount of heat to be transferred in the evaporators themselves. There would be less steam required and, along with it, less heat-transfer surface. In any event, adding more effects and reducing the available temperature drop eventually becomes counterproductive. One rule of thumb is that it is seldom desirable to use an effective temperature drop of less than five or six degrees in each stage [25]. In brine evaporation, consideration of all these factors usually leads to a design containing three to six effects.

7.1.5.2B. Vapor-Recompression Evaporation. The existence of the BPR in a solution means that the condensing temperature of the vapor raised in an evaporator will be lower than the boiling point of the solution from which it came. In other words, the vapor as it forms is superheated. When the vapor is used in another effect, the superheat provides very little thermal energy, and the vapor temperature quickly drops to the saturation temperature of pure water at the operating pressure.

The value of that vapor would be increased if it were boosted to higher pressure and higher condensing temperature. It could then be used in place of steam to produce more evaporation. This is the fundamental idea of vapor-recompression evaporation. If the vapor produced by evaporation has its pressure increased by the black box in Fig. 7.10, it can be returned to the heating zone of the same effect.

When the black box is a compressor, it is mechanical energy that makes the vapor more valuable, and the technique is referred to as mechanical vapor recompression (MVR). The steam temperature in the heating element of the evaporator must give a reasonable ΔT for heat transfer. This sets the condensing pressure, and the vapor from the evaporator must be compressed at least to that pressure. There is an economic balance to be struck between energy cost and evaporator surface area. Low compression ratios reduce compressor energy consumption but provide smaller temperature differentials and therefore require more heat-transfer surface.

Example. The normal boiling point of saturated NaCl brine is 108.7°C. If we are to provide a temperature differential of 10°C, the steam must condense at 118.7°C, or at 190.3 kPa. Taking compression to be a constant-entropy process, we can follow its course on a Mollier diagram or in the steam tables. Increasing the pressure of the cogenerated steam from atmospheric requires an increase in enthalpy of 118 kJ kg⁻¹ and produces a vapor temperature of 196.5°C (78° superheat). We can perform similar calculations for

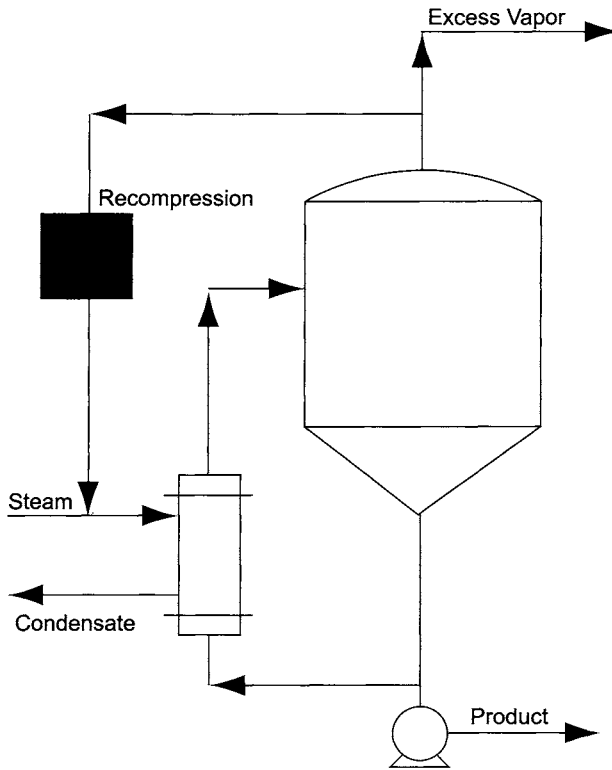


FIGURE 7.10. Vapor-recompression evaporation.

other sets of conditions. Comparing a temperature differential of 5°C with the numbers above gives us the following:

Temperature differential, $^{\circ}\text{C}$	5	10
Condensing temperature, $^{\circ}\text{C}$	113.7	118.7
Required pressure, kPa	162.0	190.3
Increased enthalpy, kJ kg^{-1}	83.3	118.0
Compressor input, kJ kg^{-1}	111.0	177.3
Compressed vapor temperature, $^{\circ}\text{C}$	168.4	196.5
Superheat produced, $^{\circ}\text{C}$	54.7	77.8
Relative power demand, %	70	100
Relative surface requirement, %	200	100

The power demand with the lower temperature differential is 30% less, but this reduction requires twice as much heat-transfer surface.

Steam economy in a mechanical recompression system can be very high, equivalent to that obtained in a 10- or 20-effect system. It may be limited by the fact that less vapor

is generated from the process fluid than is condensed on the steam side. The difference must be made up with fresh steam. The steam delivery system must also be sized to allow operation at some level without the compressor. This covers startups as well as compressor downtime.

The capability of compressors is a limitation on the practical application of MVR. Single-stage machinery is most economical. Standard centrifugal and rotary lobe compressors operate at compression ratios below two. High-speed centrifugal machines can deliver compression ratios of perhaps 2.5. Higher ratios require expenditure on a second stage or the use of special high-speed centrifugal or screw compressors.

The mechanical supply of energy makes electricity the major cost component in MVR. At the same time, it makes it possible to improve a plant's overall power factor. The vapor compressors are large consumers of energy. Outfitting them with synchronous motors can reduce the total energy demand. Increasing the field current on a synchronous motor causes the current drawn to lead the supply voltage. This characteristic is opposite to the normal lagging characteristic of induction motors and offsets their reduction of the power factor.

When high-pressure steam is available, it can be used to replace electrical power in mechanical recompression if a steam turbine drive is provided. This is most effective when the heating value of the motive steam then can be used elsewhere. An alternative to mechanical compression is the use of steam in a booster jet to bring the process vapor back to condensing-side pressure. The black box of Fig. 7.10 becomes a jet with high-pressure steam input. This process is referred to as thermal vapor recompression (TVR). The motive steam picks up vapor from the vapor/liquid separator of the evaporator. High velocity is converted to pressure energy in a venturi. Depending on the ratio of steam to vapor, the outlet pressure can be anywhere between process pressure and steam supply pressure. Since steam is consumed in the booster, the true steam economy in thermal recompression is lower than it is in mechanical recompression. A single-stage evaporator, for example, may have the steam economy of a conventional two-stage system. Thermal recompression, in compensation, has a substantially lower capital cost.

Again, there is a tradeoff between steam consumption and heat-transfer area. Use of more motive steam allows operation at higher pressure. The higher condensing temperature translates into less area. There will also be an excess of vapor available. Some systems use this in a sort of hybrid operation by adding a second evaporation effect, driven by the excess steam.

Steam-jet ejectors must transfer work to the low-pressure fluid, and so there is a loss of enthalpy from the system. The overall mechanical efficiency of a well-designed jet is usually about 85%. Section 12.6.1.2 includes an analysis of the operating losses in a typical steam jet.

7.1.5.2C. Materials of Construction. Evaporator materials of construction and their costs play a large role in determining the optimum compression ratio. Monel is a standard material of construction for brine evaporator bodies. Stabilized titanium (e.g., Grade 12) is a frequent choice for heater tubing and Type 316 stainless steel for the circulating pumps. The evaporator normally will be of the forced-circulation type described in Section 9.3.3.2. It will either contain a number of effects or operate with vapor recompression. Salt-recovery centrifuges may be Monel or stainless steel.

In membrane-cell plants fed with well brine, evaporation of depleted brine can be used to remove the excess water and maintain a water balance. This approach does not require a crystallizing evaporator. The solids-recovery section of a salt evaporator also is not required, and evaporator design is simpler. However, the problem of sulfates in the brine remains, and the materials of construction mentioned above may not be suitable. Free chlorine should be scrupulously removed from the depleted brine before it enters an evaporator, and even the chlorate that forms in the cells can be a problem. The working materials may have to be upgraded to types with higher nickel contents. Thus, the evaporator bodies and liquor-handling components may be upgraded from Monel to one of the Incolloys, which contain about 20% chromium and up to 45% nickel.

7.1.5.3. Recrystallization. Solid impure salt, as mined or crudely crystallized by other means, can be upgraded by recrystallization [26]. The process involves addition of solid salt to a circulating brine, which is heated by the injection of steam. Flashing the hot brine under vacuum, after removal of insoluble material by settling and filtration, allows the salt to crystallize from solution. Recovery of the salt releases the brine carrier for recycle to the process.

Theilgard [27] describes a similar approach that specifically rejects sulfate. When salt is dissolved and then recrystallized, certain impurities remain behind in the mother liquor. The inverse solubility of some forms of calcium sulfate enhances the separation that can be made between it and NaCl. As a salt is dissolved at higher temperatures, the solubility of NaCl increases and that of CaSO₄ drops. Some of the selective dissolving techniques of Section 7.2.2.5 may also help the efficiency of separation and produce a high chloride/sulfate ratio. When the resulting low-sulfate solution evaporates at lower temperature under vacuum, the solubility of CaSO₄ increases and that of NaCl decreases. NaCl is then produced as refined crystals. These are recovered by centrifugation, washed to remove surface contamination and occluded impurities, and dried for shipment to customers. Figure 7.11 illustrates the process.

Evaporation can be multiple-effect, to conserve energy, and some of the vapor generated can be used to heat the salt slurry before dissolving. In either approach, the steam consumption is less than 1 ton per ton salt (say, 0.7–1.0).

7.1.6. Potassium Chloride

Discussions of chlor-alkali technology and production usually focus on the production of caustic soda from NaCl. The use of KCl to produce caustic potash, an application that accounts for only a few percent of chlorine production, is often ignored. The authors have made a conscious attempt not to do this. Therefore, this section discusses sources and recovery of KCl. The comprehensive discussion of the potash industry and the processing of ore to commercial forms of KCl by Zandon, Schoeld, and McManus [28] is the basis for much of what follows.

7.1.6.1. Sources. The world produces about 30 million tons of potash each year. This is expressed as K₂O and includes all primary potassium mineral products. Besides KCl, these include the sulfate and mixed potassium–magnesium sulfates. The major outlet for potash and agricultural fertilizers accounts for about 95% of production. Known

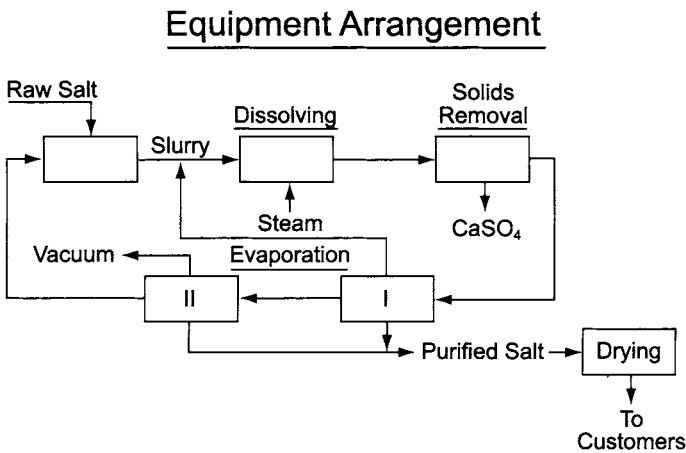
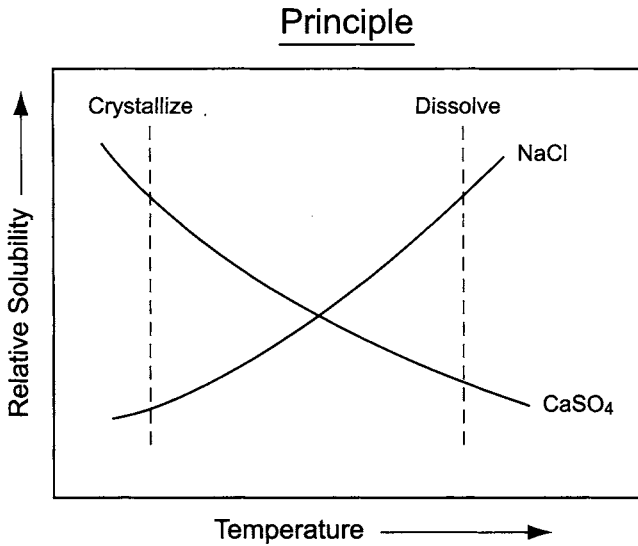


FIGURE 7.11. Salt recrystallization process.

deposits of potash amount to about 10^{11} tons. Ninety-eight percent of this occurs in Canada, the former Soviet Union, and Germany. The first two account for about 40% each and Germany for about 18%. The same three areas lead in potash production, with about 80% of the world's total. France, the United States, and the Dead Sea region comprise a second tier of producers who rely more heavily on natural brines and lake deposits.

KCl is the most important form of potash and is our main interest here. While deposits of sodium chloride are essentially crystalline NaCl with accompanying impurities, potassium chloride frequently exists in mixed ores. Much of it occurs as sylvinite, a mechanical mixture of sylvite (KCl) and halite (NaCl). Sylvite crystals are quite similar

to halite. Both are cubic with four molecules in a unit cell. The lattice length is greater in sylvite, 0.628 vs 0.5628 nm. The crystal density of sylvite should therefore be 91.8% of that of halite, and handbook data are very close to this. Other potassium ores contain major amounts of other components. Examples are the German ore Hartsalz, a mechanical mixture of sylvite, halite, anhydrite (CaSO_4), and kieserite (MgSO_4). In all ores, the levels of impurities vary.

Underground deposits of KCl, like those of NaCl, are of marine origin. They occur in nearly horizontal strata anywhere from 300 meters to more than two kilometers below the surface. The analogies to NaCl continue: mechanical mining is widely used and can follow standard coal-mining practice, the first stage of size reduction often takes place underground, and solution mining may be favored for deeper deposits. Regarding size reduction, it should be noted that some continuous mining machines produce ore in sizes less than 50 mm. The product of these machines can be conveyed immediately to the surface without underground crushing.

Lake deposits may be in the form of brine or of crystallized salts. Pure KCl seldom is obtained from any of these, and the same sorts of beneficiation are used for all materials regardless of their sources.

Section 7.1.3.1 on solar NaCl salt mentioned that the evaporation of some brines rich in KCl continues past the NaCl harvesting stage. Residual magnesium and potassium concentrations are high, and continued evaporation produces first a sylvinite material and then carnallite ($\text{KCl}\cdot\text{MgCl}_2\cdot 6\text{H}_2\text{O}$) with some uncombined KCl and a trace of NaCl. The sylvinite is beneficiated by flotation. The carnallite is debrined on a filter. Partial decomposition of the filter cake with water tends to give MgCl_2 brine and a KCl/NaCl cake.

Some mined ores are rich in sulfate, and K_2SO_4 is their primary product. Langbeinite ($\text{K}_2\text{SO}_4\cdot 2\text{MgSO}_4$) is an example. Ores that yield KCl include carnallite, mentioned above as a product of solar evaporation, and kainite ($\text{KCl}\cdot\text{MgSO}_4\cdot 3\text{H}_2\text{O}$). The former is mined in Germany as a mixture with sylvite. Thermal leaching of KCl and recovery by vacuum crystallization yield a low-grade (<80%) material that is suitable for agriculture. It is upgraded to 95% for sale as KCl by further leaching and recrystallization. Kainite usually is processed to recover K_2SO_4 .

7.1.6.2. Beneficiation

7.1.6.2A. Flotation. When potash ores are mechanical mixtures of pure crystals, it is possible to separate the components by flotation. This is reputed to be the first use of the flotation principle on water-soluble ores. A hydrophobic agent (the collector) that attaches itself selectively to one component allows that component to be wet by air rather than brine. Introduction of air bubbles then causes that component to float to the top of a pool of brine while the other component, wet by the liquid, drops toward the bottom. In modern potash processing, which is principally of sylvinite ore, it is invariably the KCl that is selected for flotation. Collectors are primary amines with 16 to 18 carbon atoms. Beef tallow is the major source; the mixture is often hydrogenated to remove double bonds and thus to increase its hydrophobicity. Usually, 50 to 150 ppm of the collector, based on the weight of the ore, is applied to a slurry of the ore in a conditioning tank. The tank must provide enough retention time to allow complete coverage of the particles.

Most of the air for flotation is brought into the mass by the action of agitators. It may be supplemented by addition of compressed air.

Several other treating agents may appear in a flotation process. The effectiveness of these agents, and even the need for some of them, depend greatly on the nature of the ore and the intended application of the product. Clay, for example, can adsorb the amine collector and interfere with its operation. To remove clay, slurried ore is scrubbed by vigorous agitation in agitated tanks or rotating cylinders to break up agglomerates. With the help of dispersants, clay (and fine particles of ore) forms a slime that can be removed in classifiers or hydroseparators. Other materials (depressants) prevent the adsorption of the collector by the wrong mineral. Flotation aids, mostly oils, enhance the action of the collectors; froth modifiers inhibit the formation of excessive froth; etc. Accordingly, there are many variations in the flotation process [28]. There is no attempt to cover them here.

7.1.6.2B. Crystallization. Since flotation is a mechanical separation of particles, it does little to remove impurities occluded in the KCl crystals. These include iron compounds, which impart a characteristic red color, as well as the familiar list of calcium, magnesium, sulfate, and bromide. KCl beneficiated by flotation alone therefore is more suitable for agricultural application than for electrolysis. Higher purity results when an ore is refined by crystallization, applied alone or in combination with flotation. The combination of flotation and crystallization is often useful when the KCl liberation characteristics of the ore are variable. Crystals then are produced mainly from dissolved fines, and the KCl recovery in the plant will be more than 90%, as opposed to the more typical 85–87% reported by Zandon *et al.*

Figure 7.12 shows the mutual solubilities of NaCl and KCl in saturated brine. The solubility of KCl, shown in the lower field, is much more sensitive to temperature than is the solubility of NaCl. Therefore, dissolving a mixed ore such as sylvinites at high

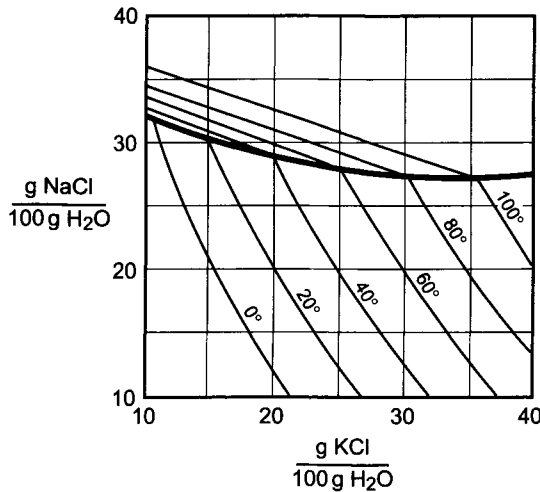


FIGURE 7.12. Mutual solubilities in water—NaCl and KCl.

temperature and crystallizing at low temperature can yield solid KCl of high purity. This effect and the more uniform PSD make the crystallized product superior to mechanically beneficiated material as feed to an electrolysis plant. The typical process uses a series of vacuum crystallizers. Evaporation of water cools the mixture, and progressive steps are at deeper vacuums and lower temperatures. The ore fed to the dissolvers and the mother liquor recovered from crystallization are heated by steam, at least some of which may be taken from the ejectors used to provide vacuum at the crystallizers. KCl crystals from the different effects are brought together and recovered by thickening, filtration or centrifugation, washing, and drying.

Although the solubility of NaCl on a unit water basis increases stage by stage (Fig. 7.12), the loss of water through evaporation would be sufficient to allow NaCl to crystallize along with KCl. Replacement of some of the evaporated water reduces the amount of NaCl that precipitates. The addition of water to a crystallizing stage also increases the amount of mother liquor produced and reduces the yield of solids. Table 7.4 compares the material balances for 1 ton of feed solution in a crystallizer stage with and without water addition. In both cases, the feed liquor is at 102°C and contains 19.9% KCl and 15.7% NaCl. The crystallizer temperature is 25°C, giving a mother liquor composition of 10.45% KCl and 18.0% NaCl. To simplify the comparison, the water added in the last column is assumed to be at the crystallizer temperature. The recovery of KCl drops by 5% in absolute terms, and there is nearly a 25% increase in the ratio of mother liquor to solid KCl. On the other hand, the purity of the crystals is greatly enhanced. Water added to the process therefore acts as a crystal-purifying agent, at the cost of less-efficient recovery, and its addition can be optimized to give the best combination of purity and recovery. Further treatment beyond that assumed above is necessary to reach typical sales specifications of 62–62.5% K₂O.

It is also important to control the degree of supersaturation in order to produce crystals of a useful size. This involves heavy recirculation of a slurry, usually maintained at about 20% solids in suspension. Draft-tube crystallizers with mechanical agitation are a commonly used design. Mother liquor is then withdrawn from a baffled zone and crystal slurry from the bottom of a vessel. Since separation is not perfect, the mother liquor transferred from stage to stage contains some quantity of fine crystal that acts as

TABLE 7.4. KCl Crystallization from Sylvinites—Effects of Addition of Water to Crystallizing Stage

Water added	0	70
Water evaporated	111	111
Mother liquor	745	843
KCl in mother liquor	78	88
NaCl in mother liquor	134	152
Crystal produced	144	116
KCl in crystal	121	111
NaCl in crystal	23	5
% recovery of KCl	60.8	55.8
% K ₂ O in crystal	53.1	60.5

Note: All weights are kg per ton of feed solution.

seed in the next stage and increases the crystal population. An occasional phenomenon in KCl production, then, is a reduction in particle size and an increase in the amount of fine material produced in the later stages. This effect can be offset with a “fines killing” arrangement in which the fines are dissolved by mixing the dilution water with the mother liquor before subjecting the mixture to crystallizing conditions.

Foreign ions can build up in the process through recycle of the mother liquor. These ions can alter solubility relationships and distort crystal formation. Most plants therefore include a purge of liquor in order to keep the concentrations of these species under control.

7.1.6.2C. Materials of Construction. KCl is noncorrosive when dry, but once exposed to the atmosphere, it is quite hygroscopic. Exposed steel surfaces in a KCl plant should be coated with an epoxy or a good enamel. There should be special efforts to keep electrical equipment dry and free of dust.

The corrosiveness of aqueous KCl systems increases with aeration, agitation, and higher temperature. The common material of construction for vessels in most beneficiation plants is rubber-lined steel, but this can not be used with certain flotation oils. Concrete lining on expanded metal is a popular substitute.

The hot brine found in crystallization plants can be quite corrosive. Inconel, Monel, and stainless steel are used in most of the major equipment. Nonmetallic piping, including FRP, is common, within its serviceable temperature range, and Schedule 80 carbon steel pipe is often used in pump lines. The soil in a salt-processing plant can itself become corrosive as a result of spillage. Underground carbon steel lines therefore are protected by sacrificial anodes of magnesium or zinc or by application of direct electrical current.

7.1.7. Storage of Salt

Purified grades of NaCl and most KCl may be stored in specially designed facilities or in process tanks, sparger cars, etc. Most NaCl is stored outdoors. This is the cheapest approach, and with even minimal design effort it offers easy access to the salt. The salt should be placed on a pad designed to withstand traffic of the handling equipment as well as the load of the salt itself. Asphalt and concrete are the most frequently used materials. Salt brine can damage concrete and cause spalling if it is allowed to penetrate. The Salt Institute [29] recommends high-quality air-entrained concrete treated with sealants or asphaltic coatings. Plastic or elastomeric liners may be used for added protection.

The chief concerns in the storage area are the potential for environmental pollution, caking, and the loss of salt. Caking is not usually a serious problem at a chlor-alkali plant when outdoor storage is applied wisely. The finest (often, the purest) salts usually have the greatest caking tendency. When their generally higher costs also are considered, they become poor candidates for open storage.

Caking often is a serious problem when salt is dissolved directly from the pile. Intermittent dissolving in fact aggravates the caking phenomenon by leaving insoluble matter on the surface of the pile and by producing fines that drop into interstices between larger particles. The results are the formation of an impervious surface, channeling, and undersaturated brine. Section 7.2.2.3 on brine preparation points out that from a technical

standpoint this is an inferior process. More frequently, the salt is in intermediate storage and must be moved as the solid to a dissolver. This involves the use of mobile equipment that generally is equipped to break up a crusty surface as well as to lift the salt.

Any loss of salt from a pile must be regarded as a form of pollution. Salt, however, is quite benign and is not deemed a serious pollutant. Handling of solid salt, especially in windy conditions, produces a fine dust. This "drift" is one consideration in siting a salt storage pile. The wind-blown salt can be a nuisance in process areas and usually ends up in the plant's effluent water system. Salt dissolved from the pile (e.g., by rainfall) can be recovered by collection in a sump and returned to the process.

Salt piles can be covered in order to reduce losses. Commonly used materials are tarpaulins and PVC or reinforced polyethylene sheets. Covers are used mostly on inactive piles and sometimes have the incidental advantage of preventing contamination of the salt by windborne particles. Sometimes, sections of a large open pile are effectively inactive. Some parts of the pile are more easily accessible than others, and it is easier to withdraw salt as needed from these sections. An inactive section, after long exposure to weather, may have a composition and angle of repose that are significantly different from the original values. The angle of repose is defined as the constant angle to the horizontal assumed by a cone-like pile of solid. A variable composition can upset brine treatment. The angle may increase to the point where one sees operators of mobile salt movers working in a pile with an overhang of salt, an obviously hazardous situation.

Salt is also lost in rainwater runoff. Crusting of the surface of the pile by accumulation of insolubles actually helps to limit this loss. The storage pad should be sloped at least 1–2% to remove drainage to a catchment efficiently and to prevent accumulation of surface water [29]. At the same time, the slope should be limited to about 5% [30], above which operation of equipment like front-end loaders can become unstable. On large pads, ditches and pipes can improve drainage. The drainage should be away from any adjacent ground-water system. Otherwise, it can follow the terrain.

At the chlor-alkali plant, storage usually is in conical piles or windrows. The volume of a cone is one third that of a cylinder with the same diameter and height. The height of the cone in this case is related to its diameter by the angle of repose of the salt:

$$h/D = 0.5 \tan \theta \quad (2)$$

where

h = height of pile, m

D = diameter of pile, m

θ = base angle (assumed equal to angle of repose)

The volume therefore can be expressed in terms of either one of the principal dimensions. For example,

$$V = (\pi D^3/24) \tan \theta \quad (3)$$

where V is the volume of the salt pile, m³

When height is restricted, an expression in terms of the height of the cone is more useful:

$$V = \pi h^3 / (3 \tan^2 \theta) \quad (4)$$

The angles of repose used in design of salt-handling equipment are usually 45° or 60°. These values are deliberately high in order to promote flow of the salt. Using them in one of the above equations will give an incorrect estimate. The true angle of repose for most salts is 30–40°. Many are close to 32°, at which angle the volume of a pile is approximately 0.0818 D^3 or 2.682 h^3 , and $h = 0.3124d$. The exposed area of such a pile is very nearly equal to the square of its diameter.

A windrow can be regarded as two halves of a cone separated by a triangular prismatic pile. The volume of the prism is $Lwh/2$, where L is its length and w its width. The width is equal to the diameter of the cone, and the height of the pile is of course the same as that of the cone. The volume of this section, which must be added to the volume of the cone from Eq. (3) or (4), is

$$V = (LD^2/4) \tan \theta \quad (5)$$

or

$$V = Lh^2 / \tan \theta \quad (6)$$

When the base angle is 32°, these become 0.1562 LD^2 and 1.6 Lh^2 . The exposed area per meter of running length is about 1.2 D .

Example. The salt equivalent to 800 tpd NaOH is 1,169 tpd. To calculate the need for raw salt, we allow 0.37% for impurities, 4.5% for water, and 1% for in-process loss. This gives us 1,241 tpd. We must also allow for in-process use of NaOH if we are to have 800 tpd available for sale. A 3% allowance raises our salt requirement to 1,280 tpd. We round this up, to allow for extra mechanical downtime and to provide some spare capacity, to 1,500 tpd.

With the given bulk density of 1,080 kg m^{-3} , the volume equivalent to a week's supply of salt is 9,722 m^3 . First we calculate the dimensions of a single conical pile. Using a 32° angle of repose, we have approximately

$$\begin{aligned} V &= 0.08 D^3 & D &= 49.6 \text{ m} \\ \text{or } V &= 2.6 h^3 & h &= 15.6 \text{ m} \end{aligned}$$

This could be acceptable. The entire facility, with room for access, could fit into a 60-meter square. The exposed area of the pile is about 2,500 m^2 .

If delivery were less reliable, or if it depended on infrequent delivery to a port, we might require a month's supply of salt in storage. The volume required then is 42,300 cu m , and the diameter of a single pile is greater than 80 m. Perhaps more importantly, the height is more than 25 m. So, we consider the windrow. Possible dimensions,

where length means total length including the conical ends, are:

Length (m)	Width (m)	Height (m)
188	40	12.5
116	55	17.2
140	48	15

The last combination was chosen to keep the height no more than 15 m. The best combination depends on site constraints, but the plot requirements are substantial. The shape of the pile is never ideal, and so some extra allowance of space is necessary. The true exposed surface area, calculated from the dimensions given to be 7,000–8,700 m², is also larger than that of a uniform pile.

When salt is handled or stored, it tends to segregate by particle size. If the PSD is wide and salt is dumped onto a pile, the finest material will tend to be in the center, while the coarsest will be low in the pile and nearer the periphery. This segregation sometimes causes problems in handling and can increase the salt's tendency to cake.

A subtler problem is the effect of particle-size segregation on salt analyses. The composition of salt is not uniform, and it is found in particular with rock salts that purity is a function of particle size. In a rock salt deposit, anhydrite is present as layers and as inclusions in particles of salt. It is less friable than salt, and so regions of high salt content tend to crush more easily and form finer particles. Whether these segregate from the associated insolubles is open to question, and Sutter [31] reports that screening has little effect on the insoluble impurity content of a sample. On the other hand, soluble impurities tend to be more concentrated in the finer salt. This phenomenon is less likely to be a problem with solar salt or processed grades.

The analysis of salt for its major impurities is straightforward. The real problem in obtaining reliable data is one of sampling. Careless sampling always results in a non-representative PSD. This can lead to a faulty analysis and improper conclusions. These subjects are beyond the scope of this book, but there is an extensive literature available including methods specifically recommended for salt. The American Waterworks Association publishes one set of methods in AWWA B200-49T.

A minor note on salt analyses is that wet methods assay the concentrations of ions. Impurities are present in salt as minerals, and so standard wet analyses do not unequivocally identify all the solid compounds present. While this fact is worth noting, it is usually not of immediate interest to the chlor-alkali plant operator.

7.2. PREPARATION OF BRINE

7.2.1. Salt Handling

Salt is delivered by ship, barge, train, and truck. Bulk solids unloading is by various methods, usually labor-intensive, which are not discussed here. Vibration during transit can pack the salt to the point where it resists flow. When mechanical flow aids are called for, Kaufmann [32] recommends heavy-duty large-amplitude vibrators.

Many different methods are used to transfer the unloaded salt to the process. Most coarse salt handles well, and most of the common types of conveyor are used where appropriate. This section reviews some of the characteristics of the different salts and describes the types of conveying equipment found most often in chlor-alkali plants. First, we consider some of the properties that are important to the design and operation of conveying systems.

7.2.1.1. Physical Properties and Particle Size Distributions. Kaufmann [33] gives an extensive compilation of the physical and chemical properties of salt, and the various suppliers issue data sheets specific to their own products. Most commercial salts are pure enough that all grades have essentially the same inherent physical properties. Bulk and surface properties, on the other hand, are less constant. The handling properties, in particular, are highly variable, and this variability is primarily related to the particle size distribution (PSD).

The PSD of a given salt is a function of the processing it has undergone. Most potash and the vacuum-purified salts of sodium are prepared by mechanical crystallization and have relatively fine, well-formed particles. Diaphragm-cell evaporator salts are similar, but they seldom appear as items of commerce. Solar salts are formed by very slow crystallization under uncontrolled conditions. They have larger and more irregular particles. These tend to crystallize as large pyramidal aggregates that are more fragile than rock salt; the particle size of a solar salt as delivered therefore is a function of its handling subsequent to its formation. Compared to vacuum salts, solar salts are large and have a wide PSD. Rock salts appear in a variety of sizes. This is a result of their processing, which includes mining, milling, and screening. Particles tend to be relatively large and variable in size, but the screening operation allows some control and also truncates the PSD.

Figure 7.13 shows PSDs for several salts typical of the various classes. Curve 1 is a Canadian potash. Curve 2 is an Italian vacuum salt. Curves 3 and 4 are two samples of the same Bahamian solar salt from two different final suppliers. Curve 5 is a typical dissolver-grade rock salt. All distributions depart from true lognormal by the presence of too much fine material. As shown by the uniformity coefficients, the solar salts have the widest PSDs and the vacuum salt the narrowest. Figure 7.14 shows the variation in PSD caused by screening. All three curves are for rock salt from Weeks Island (United States). These are well-screened fractions whose distributions are closer to lognormal. The uniformity coefficients are about 1.5.

The crystal density of NaCl is about 2.16 and that of KCl is about 1.98. As pointed out in Section 7.1.6.1, this difference of 9% is consistent with reported dimensions of the crystals. Bulk densities of NaCl as supplied run from 1.1 to 1.3. The finer grades have higher bulk densities. Thus, most rock and solar salts have bulk densities less than 1.15; vacuum salts normally range up to about 1.25. KCl with its lower particle density is lighter, size for size, than NaCl. Since much of the KCl used in the industry is supplied in the finer grades, the difference in particle density is largely offset. One should be careful not to confuse reported bulk densities obtained by two different methods. The “loose” bulk density results when salt is simply poured into a container. The “tight” or “packed” bulk density is measured after tamping the sample to induce settling and is usually 3–6% higher.

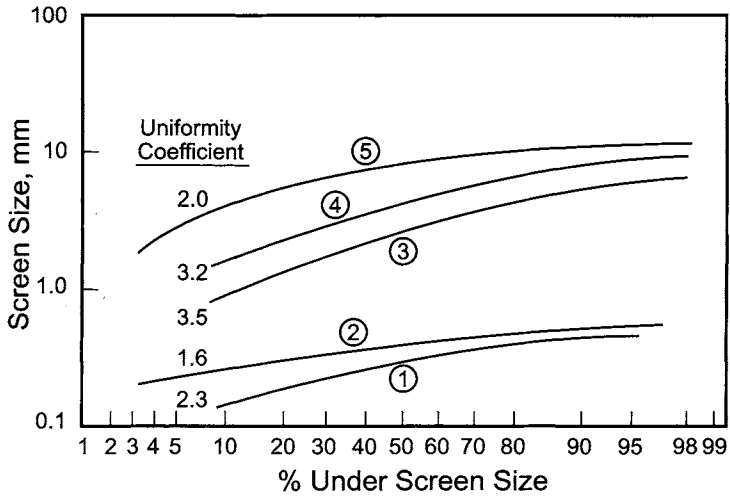


FIGURE 7.13. Particle size distributions of representative salts. Refer to text for identification of curves 1–5.

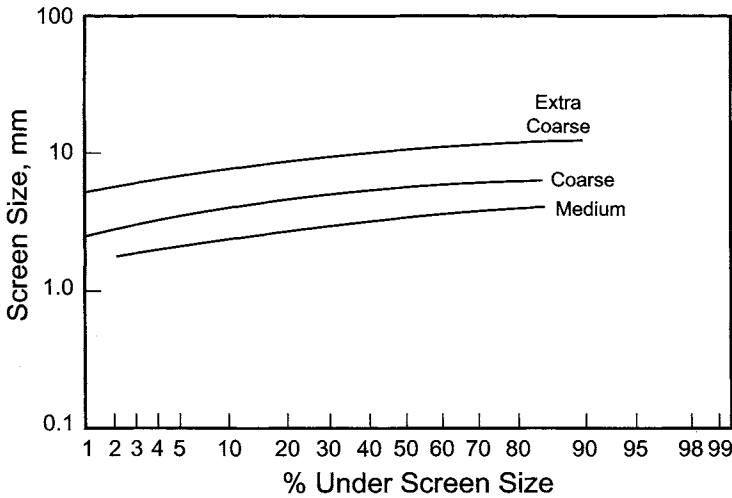


FIGURE 7.14. Particle size distributions of screened rock salt fractions.

The handling properties of a salt and the capacity of a storage bin or area are related to the angle of repose. This is also a function of the PSD, but it is heavily influenced by surface moisture. Salt merchants can supply this information on the salt as supplied, but the user should be aware that the angle of repose is not a fundamental property independent of in-plant handling.

Suppliers usually publish particle-size data as the fraction or percentage of a sample retained by each screen in a graded pack. Data may be on either a differential

or a cumulative basis. Screens are usually identified by mesh number, which in the English-speaking world represents the number of openings per lineal inch. Since wire diameters vary from one standard group of screens to another, so too do the sizes of the openings. Identification of the standard used in screening therefore is essential in careful work.

Commonly used standards in the United States are Tyler screens and US Standard screens (American Society for Testing and Materials). Similar standards in the United Kingdom are British Standard screens and Institute of Mining and Metallurgy (IMM) screens. The dimensions of the screens are widely published and it is a simple matter to assemble PSD curves such as those in Figs 7.13 and 7.14. A recent correlation mathematizing all these standards may still be useful for drawing comparisons [34]. The correlating equation takes the form

$$d = a/M^b \quad (7)$$

where

d = particle size, mm

M = mesh number

a, b = constants for each standard

The constants with their ranges of applicability are in Table 7.5. The maximum size (minimum mesh number) covered by these correlations is within the range of interest with the coarser salts. The commonly used standards change their identification systems in this range and report particle sizes (e.g., 3/8-inch) rather than mesh number.

Only the IMM scale retains geometric similarity. The others use standard wire diameters that become larger relative to the mesh openings as size decreases. Another European (French) standard uses a direct rather than inverse scale to characterize particle size. The nominal diameter is given by

$$d_F = 0.0008 \times 10^{0.1M} \quad (8)$$

Like the other scales, this increases nominal size approximately in multiples of $2^{0.25}$.

As the constants in the table show, there is not a great difference in particle sizes at a given US Standard and Tyler mesh number, and in common usage they are regarded as nearly interchangeable.

TABLE 7.5. Empirical Constants for Screen Sizes

Screens	a	b	Range (mesh numbers)	Range, sizes (mm)
ASTM	23.5	1.090	3.5–400	0.038–5.66
Tyler	20.9	1.070	2.5–400	0.038–8.00
BSS	17.2	1.024	4–350	0.044–4.00
IMM	12.3	1.000	5–200	0.063–2.54

For use in Eq. (7).

7.2.1.2. *The Phenomena of Caking and Freezing*

7.2.1.2A. **Caking.** Most of the problems that arise in storage and subsequent transport of salt are related to caking, which is the result of localized alternate dissolving and drying. Salt, being hygroscopic, can pick up moisture from humid air. Saturated brine then collects on the surfaces of the salt and by capillary action forms links between particles. If this solution dries by evaporation when the surrounding humidity decreases, the links become solid. When the humidity cycles, the process repeats. With each cycle, the links between particles become larger and stronger, and the ultimate result is caking of the salt. Over time, the surface of a pile of salt may become impervious and extremely hard to break. It also shields the interior of the pile so that caking is partly self-limiting.

Since saturated NaCl brine has a vapor pressure approximately 75% of that of water, a relative humidity greater than 75% will cause condensation onto the salt. This is known as the critical humidity. KCl solutions have higher vapor pressures and therefore higher critical humidity. Because KCl also has a higher temperature coefficient of solubility, the concentration of saturated solutions increases more rapidly with temperature. The critical humidity therefore is not so nearly constant as is the case with NaCl, and it decreases with increasing temperature. At most ambient temperatures, the critical humidity of KCl is 85% or higher.

If the critical humidity is exceeded permanently, a salt dissolves in its own water of absorption. If the humidity never exceeds the critical value, very little water is taken up, and the salt remains dry. In dry climates, caking of salt may therefore be unknown.

Since caking is a surface phenomenon, impurities in the salt can have a disproportionate effect. Section 7.1.5.1 referred to the fact that the magnesium chloride impurity in solar salts tends to be at the surfaces of the particles. With its low critical humidity (~29%), MgCl_2 is more likely than NaCl to attract moisture from the air. The surfaces of solar salt particles, even if initially dry, tend to be wet when stored in the open. This does not necessarily mean that solar salts have more tendency to cake; that requires humidity cycles. If the humidity seldom drops below the critical level, caking will not occur. Calcium chloride, with a critical humidity of about 35%, acts the same way and is added to certain specialty salts by spraying onto the surface partly to achieve this effect. Because the impurity is concentrated at the surface but at a low overall concentration, the absorption of water is limited, and the particles do not dissolve but maintain their wet feel and resist caking.

Small particles, with their high surface/volume ratio, pick up water more readily and are especially liable to caking. Vacuum salts and potash, as suggested by Fig. 7.13, are therefore the most sensitive. They are frequently treated with an anticaking additive before shipping. The one most widely used is sodium ferrocyanide, or yellow prussiate of soda (YPS). By the nature of the addition process, YPS also tends to concentrate at the surfaces of the particles. Therefore, when a batch of treated salt is dissolved, the first brine formed has a high concentration of YPS. Rain also selectively removes YPS from the salt, and this is one reason not to store such salts in the open.

Rock salt, with its more or less uniform composition and its relatively large particle size, is less susceptible to caking. Outdoor storage of rock salt is a common and successful technique.

A related phenomenon with rock salt is caking at the mine head. A hot, humid climate often produces dew points of 25°C. There will be rapid condensation of water onto salt brought to the surface at lower temperature. This can lead to caking as the salt weathers.

Wide PSD and storage of large quantities in deep beds or piles also aggravate caking tendencies. When the PSD is wide, fine particles find their way into the interstices among the large particles. This fact increases the number of interparticle contact points. Also, thermodynamically, the solubility of the smaller particles is greater [35]. There is a tendency for small particles to dissolve and for the salt to redeposit onto the larger particles and so provide another opportunity to form solid bridges. The effect of a deep bed is simply one of pressure. Pressure in the lower levels not only favors the cementing of the particles together but also increases the solubility of the salt slightly and promotes the formation of bridges of concentrated solution.

7.2.1.2B. Freezing. Salt is used in large quantities to de-ice highways and is added to some bulk materials to prevent their freezing. Almost paradoxically, salt itself may freeze when stored in outdoor piles. The phenomenon can be understood by studying the NaCl–water phase diagram of Fig. 7.15. This shows that a hydrate, NaCl · 2H₂O, forms close to the freezing point of water (actually at 0.1°C). This hydrate is the stable form of solid for solution concentrations to the right of the eutectic. The saturated brine that forms

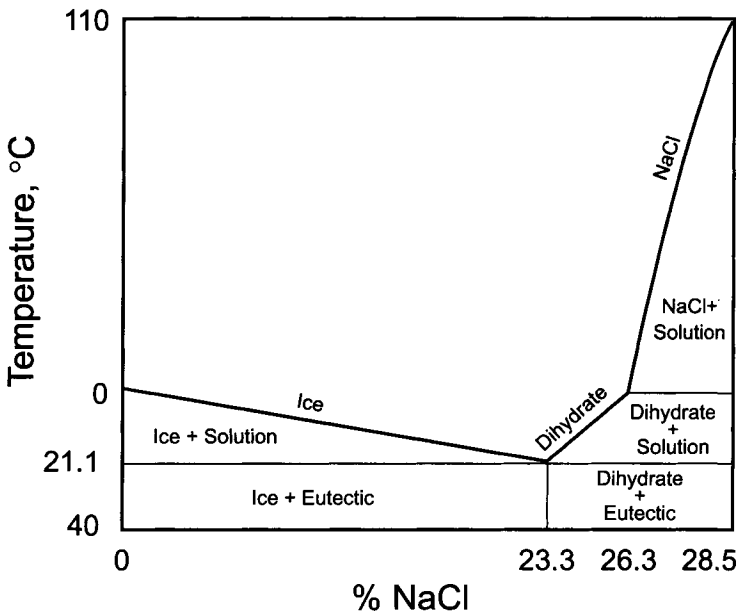


FIGURE 7.15. Sodium chloride–water phase diagram.

on the surfaces of salt particles is in this region, and so when the temperature drops below the saturation curve, the dihydrate begins to deposit as a solid and to form salt bridges between particles. Since this solid contains more than 60% NaCl, the concentration of the surface brine decreases. More salt then goes into solution. The process repeats until all the water has been consumed, and the result is the formation of about 2.6 parts of hydrate for every part of water originally present. All this occurs at the freezing point of the hydrate, not at the eutectic temperature of about -20°C . Fine particle sizes aggravate freezing problems by their speed of response. The initial moisture content of the particles is the other important variable determining the rates of solution and subsequent freezing.

7.2.1.3. Transport of Salt. Large quantities of salt are moved by road, rail, barge, and ship. This section does not cover these modes of transport but is limited to the more common systems used for intrasite transfer. Most salts convey well, and most common types of conveyor are suitable for their transport. In many conveyor installations, the best arrangement does not simply follow a straight line. Smaller local conveyors are also required. At some stage, the conveying equipment must be protected by separators or magnets that remove tramp metal, fragments of blasting caps, wire, etc.

Engineering handbooks and vendors' literature contain descriptions and design details for most types of conveyor. This section gives equations for the capacity of certain types and for the amount of power that they consume. These are empirical and derived from handbook and catalog data. They should not be used in place of specific information given by equipment suppliers. They are supplied here once again to give the reader a practical feel for the systems used in chlor-alkali operation.

7.2.1.3A. Belt Conveyors. Belt conveyors are sometimes used to transport solids over quite long distances. They are used mostly for horizontal transport and are also capable of moving material at angles up to about 20° above the horizontal.

For transfer of salt, belts almost exclusively are made of rubber. Other components in contact with the salt are stainless steel or resistant plastic. The supporting structure and bearings are steel. Rain covers are common.

There are many different methods for addition of salt to a conveyor. When the salt drops from some distance, there are usually a metal skirt plate and a rubber sealing mechanism.

Rubber belts are reinforced with fabric or wire cable in multi-ply construction. They are supported by idler bearings, usually arranged to "trough" the belt at an angle of about 20° to increase its holding capacity and to prevent spills. Idlers are covered with rubber or enamel to prevent corrosion and resist the buildup of salt on their surfaces. The drive may be at either end of the conveyor. The speed depends on the size of the belt and on the

application. In long-distance salt conveying, as from a dock to a storage facility, 100 or 150 m min⁻¹ is a representative speed. The maximum speed used is about 170 m min⁻¹. For belts less than a meter wide, maximum speed is listed as an irregular function of width; conceptually, the speed is approximately $35 + 140w$, w being the width of the belt in meters. Within process areas, a maximum speed on the order of 75 m min⁻¹ is usually observed.

The load, the temperature, and even the humidity can affect the length of a belt. Some take-up device therefore is necessary to keep the proper tension on the belt. Gravity take-ups are sometimes used, especially when a belt is in nearly continuous service. In this case, the return belt is diverted over a pulley hanging from a sliding frame. Weights suspended from the pulley fix the tension on the belt.

When salt is to be delivered to a single point, it can simply be allowed to fall from the end of the conveyor. In cases where the salt is delivered to more than one point, for example to a number of silos or dissolvers, the conveyor must be unloaded at intermediate points as well as at the end of the belt. This can be done by arranging the supporting idlers to let the belt run flat at the unloading point and installing a baffle or scraper at approximately a 45° angle across the belt. This adds to the wear on the belt and allows some of the salt to spill before it reaches the scraper. A more expensive but more positive approach is to use a belt tripper. This is a mechanism that forces the belt to run over another pair of pulleys. The first is at an elevation higher than that of the main belt; the second is placed lower than the first and farther back along the direction of belt travel. The belt therefore doubles back, spilling the salt, which is collected by a chute and delivered to the side of the belt. A tripper consumes power and adds 1.5–2 m lift but offers convenience and flexibility of operation. Its movement along the line of travel of the belt is through a gear that is operated by belt motion and so from the main drive. A tripper mounted on rails can move to serve several hoppers at discrete positions or to shift the unloading point for a long storage bin or salt pile back and forth.

The capacity of a belt conveyor is related to its width and its speed. A belt is sized on the basis of the volumetric flow that it must handle. Manufacturers' ratings and the methods approved by the Conveying Equipment Manufacturers Association or similar authority should always be used for accurate design. For convenience, we also present methods for rapid approximation, which are adapted from the data presented in *Marks' Handbook* [36]. For a given load, the width of the belt required can be estimated by

$$w = f\sqrt{Q/S'} \quad (9)$$

where

w = width of belt, m

Q = salt flow, m³ hr⁻¹

S' = speed of belt, m hr⁻¹

and

$$f = 3.71 - 1.3\sqrt{Q/S'} + 0.6Q/S' \quad (10)$$

The power required can be estimated by the equation

$$P = 0.003[FL'(T + 7wS) + TH] \quad (11)$$

where

P = power required, kW

F = constant (0.05 for standard bearings; 0.03 for antifriction bearings)

L' = adjusted length, m (add 30.5 m to length of belt between terminal pulleys for standard bearings; add 46 m for antifriction bearings)

T = salt flow, t hr^{-1}

S = speed of belt, m min^{-1}

H = vertical lift, m

Operation of a tripper will add P_T kilowatts to the load, where

$$P_T = aS + bT \quad (12)$$

The constants a and b are given approximately by

$$a = 0.012w + 0.0047w^2 \quad (13)$$

$$b = 0.023 + 0.0009w + 0.0012w^2 \quad (14)$$

7.2.1.3B. Bucket Elevators. Elevators are used when a material is to be lifted without significant horizontal travel. The type of most interest in salt transport is the bucket elevator, in which a number of buckets are attached to a continuous belt or chain. As they travel, the buckets receive their load through a chute or scoop it from a hopper at the foot of the elevator. Because of the potential for corrosion of metal drive chains when service is intermittent, salt elevators in chlor-alkali plants tend to be belt-driven.

Elevators are usually classified as continuous discharge or centrifugal discharge. Continuous-discharge elevators have closely spaced buckets and operate at relatively low speeds. As the buckets pass over the top sprocket, they tip and allow their load to tumble out over the preceding bucket and into a discharge chute. Centrifugal-discharge elevators operate at higher speeds, and the load is flung out by centrifugal force. More space is allowed between buckets.

Continuous discharge is appropriate for fragile materials and very high capacities. Since the salt supply to a chlor-alkali plant has neither of these characteristics, the cheaper centrifugal-discharge approach is the norm. It has an operating/maintenance advantage because of the lower probability of salt becoming wedged between the bucket and belt.

Buckets are highly irregular in shape. Still, we can quite easily estimate the amount of material carried by a bucket as a function of the top dimensions of the bucket. For a wide range of sizes, the effective depth of the solids (volume of solids divided by the open area at the top) in one industrial line was found to be 45–50% of the smaller dimension at the top of the bucket [37].

The spacing between buckets is usually $2\frac{1}{2}$ –3 times the bucket width. Speed will depend on the sizes of the belt and the buckets; a typical value when handling salt is

80 m min⁻¹. Operating capacity is based on the buckets being 2/3–3/4 full. The drive power required by a bucket elevator when a feeding device delivers the salt to the buckets can be estimated by

$$P = 0.006 TH \quad (15)$$

where

P = delivered power, kW

T = capacity, ton hr⁻¹

H = lift, m

A feeder should meet the elevator buckets head-on to prevent side forces that might make operation unbalanced and less stable. Loading buckets by dragging through the salt in the elevator boot requires an allowance for the added force. This must be determined empirically or estimated by experience with the specific design being used. A rough, usually conservative estimate of the force required is

$$F_d = D_p W/d \quad (16)$$

where

F_d = digging force

D_p = diameter of boot pulley

W = weight carried by a bucket

d = distance between buckets

This can be reduced if the salt is not lumpy and can be cut in half for continuous discharge.

Buckets usually are made of Type 316 stainless steel or heavy-duty carbon steel. Nylon also is used in some small units. Belts will be of fabric-reinforced rubber, and there will be provision to adjust the position of this belt and its tension. The unit should be totally enclosed, with removable access panels. Desirable features are a jogging mechanism on the drive to allow the buckets and belt to be inspected from a single position, an automatic stop when the unit becomes jammed, an emergency stop device available to the operator at all positions, and prevention of reverse movement when the belt stops.

The discharge chute at the top of an elevator should have a slope of at least 60°. The top elevation must be sufficient to allow the salt to drop to its destination at this angle. If the salt is delivered by rail in hopper cars, the bottom of the elevator should be in a pit deep enough to hold a delivery hopper, usually a feeder, and a short conveyor to the elevator boot. A typical depth is 6 or 7 m [38].

7.2.1.3C. Screw Conveyors. Salt can also be moved by screw conveyors. These are very compact units that require little headroom and no return mechanism. Screws provide some mixing action, which is useful in some phases of salt processing. Since the torque developed on the shaft limits the length of a screw, they are used mostly for short-distance conveying in the vicinity of processing equipment. Internal bearings allow the use of

longer units, but this is not a recommended practice when handling salt. Multiple units are preferred.

Allowable torque also limits screws to a maximum of 500–600 mm in diameter. Screw conveyors are used for nearly horizontal transport. While they are able to lift solids at an angle, the particles begin to fall back along the flights of the screw, and efficiency drops off rapidly as the slope increases. At an inclination of 15–20°, the capacity of a screw can be cut by 50%. Specially designed units can operate vertically. These can replace short elevators in small plants.

The ability of screw conveyors to handle lumps is limited. When a small unit is specified for service with a very lumpy salt, this aspect should be checked. Screws also are not self-cleaning, and those in intermittent service require frequent washing to remove any buildup of salt and contaminants such as rust. “Horizontal” conveyors should actually have a slight pitch and a drain plug at the lower end, in order to allow washing.

The simplest arrangement and easiest duty for a screw conveyor is a direct, metered feed at one end of the screw. When the screw is used to initiate flow along a line rather than from a point, as for instance at the bottom of a wide bin, the pitch of the screw should be varied within the feed zone, becoming wider as it progresses in the direction of flow. With tall bins, side inlets to the conveyor have the advantage of not putting all the weight of the salt in the bin directly onto the feed zone of the screw.

The screw will be helicoidal and will be enclosed in a covered U-shaped trough. Both screw and trough are usually of stainless steel or heavy-duty carbon steel. In wet salt service, Monel is preferred. Rotational rates are modest. Large screw conveyors in salt service will rotate at less than 50 rpm; small units (<200 mm) may approach 100 rpm. The conveying capacity of a screw depends on its size and its rate of rotation:

$$Q = 13 ND^3 \quad (17)$$

where

Q = volumetric flow rate, $\text{m}^3 \text{hr}^{-1}$

N = rotational speed, rpm

D = diameter of screw, m

The constant in Eq. (17) corresponds to the operation with about 28% of the cross-section being full. This is slightly conservative, a typical estimate being 31%. The power required is given by

$$P = 0.0033TL \quad (18)$$

where

P = power required, kW

T = salt flow, tons hr^{-1}

L = length of screw, m

Example. We base our design on moving an average of 1,500 tpd of salt. To allow for car movements and discontinuous deliveries, we assume a conveying time of only

12 hr a day. The instantaneous design capacity is then 125 tph or $116 \text{ m}^3 \text{ hr}^{-1}$. Since our basis assumes 100-ton hopper cars, we assume two unloading points for each car, each dropping salt into a below-grade bifurcated hopper. Each spot should unload 62.5 tph, but we allow for uneven delivery and the occasional failure by designing each branch for 80 tph, or $74 \text{ m}^3 \text{ hr}^{-1}$. From each hopper, we feed a bucket elevator by way of two screw conveyors.

We calculate the required diameter of the screw conveyors by Eq. (17). Using a rotational speed of 40 rpm,

$$D^3 = 37/13/40 = 0.0712 \quad D = 0.414, \text{ say } 0.45 \text{ or } 0.5 \text{ m.}$$

The power requirement to move the salt 10 m comes from Eq. (18):

$$P = 0.0033 \times 40 \times 10 = 1.5 \text{ kW for each of four screws}$$

The recommended maximum speed for a screw of this size is about 45–50 rpm, so 40 rpm is acceptable. The power requirement is modest. The screws can be installed at a slight upward angle if desired, and the drive requirements can be estimated at 10 kW.

The elevators lift the salt from a pit to the main conveyor belt. We assume that the belt runs about 2 m above grade, where it can be observed from a low walkway. We take the feed point for the elevators to be 6 m below grade. Allowing approximately 3 m between the elevator and conveyor, the top of the transfer chute must be 5 m above the delivery point in order to provide a 60° angle. One meter should be a sufficient allowance for the connections. The design lift therefore is 14 m. From Eq. (15), we obtain for each elevator

$$P = 0.006 TH = 0.006 \times 80 \times 14 = 6.72 \text{ kW}$$

The digging force for any of the likely models is only a few kilograms, adding a fraction of a kilowatt to the load. The total required by each elevator is therefore about 8 kW, and so we provide drives rated for at least 10–15 kW.

We operate the belt conveyor at 75 m min^{-1} , or $4,500 \text{ m hr}^{-1}$. The required width, using Eqs. (9) and (10), is

$$w = f \sqrt{116/4500} = 0.16 f$$

$$f = 3.71 - 1.3(0.16) + 0.6(0.026) = 3.52$$

The required width is about 0.565 m; we shall use 0.6. The recommended maximum speed is about 120 m min^{-1} , well above our 75. We arbitrarily take the length of the belt conveyor to be 300 m. It could be quite different in a real plant. We assume, equally arbitrarily, that the conveyor must lift the salt 5 m. Then, with antifriction bearings, we have from Eq. (11)

$$P = 0.003[0.03(L + 46)(T + 7wS) + TH]$$

$$= 0.003[0.03(346)(125 + 315) + 125(5)] = 15.6 \text{ kW}$$

This delivers the salt to the vicinity of the storage pile. Another elevator and more conveyors are necessary, but it would not be instructive to continue this example. It might be worthwhile to include the calculation of the power required by a tripper. With salt stored in a windrow, a tripper could profitably be used with a longitudinal belt conveyor. With the same 0.6 m belt width, the constants of Eqs. (13) and (14) are

$$a = 0.012(0.6) + 0.0047(0.36) = 0.0089$$

$$b = 0.023 + 0.0009(0.6) + 0.0012(0.36) = 0.024$$

The power required, by Eq. (12), is

$$P_T = aS + bT = 0.0089(75) + 0.024(125) = 3.7 \text{ kW}$$

The total conveyor power requirement is then $15.6 + 3.7 = 19.3 \text{ kW}$. A 25-kW drive might be appropriate if it meets the requirements of the next subsection.

7.2.1.3D. Conveyor Drive Systems. As the example above shows, salt conveying devices are not large power consumers, and drive requirements are modest from that standpoint. They also are not high-speed devices, and some kind of speed reduction is always present. Motors and speed reducers must be protected from damage when conveyors jam or become overloaded. Elevators and positively inclined conveyors must be protected from reversal when drives stop. The nature of the starting load is a special consideration. Conveyors must at times be started when loaded with material. At least the larger units, such as high-capacity belts and elevators, should have motors with high starting torques. Double-squirrel-cage motors generally have favorable characteristics.

While motors themselves conventionally have overload protection, one must also consider the possibility of damage to the conveyor by inertia of the rotating motor. Shear pins uncoupling the drive from the member can prevent this.

Finally, the size or at least the orientation of a conveyor may require operators to be in the vicinity of the conveyor but far from the drive and its controls. Emergency trip devices should be provided wherever this presents a hazardous situation. Since most conveying systems have multiple members, a trip of any one member should automatically shut down others, at least on the upstream side.

7.2.1.3E. Feeders. Conveyors work best with even, continuous feed. Salt is not simply dropped to a conveyor but is collected into a hopper and then delivered to the conveyor by a feeder. Also, when salt must be fed at a regulated or uniform rate over a short distance, a feeder may be used. Screw conveyors sometimes serve as feeders; otherwise a specialized device is chosen. One type is the reciprocating plate feeder, mounted on wheels and driven by an eccentrically mounted rod. Speeds of 60–70 strokes per minute are common. The salt moves forward with the plate, but at each retraction a certain amount falls from the end of the plate into a delivery chute. Electrically vibrated feeders are also used. These usually slope down at slight angles, typically 6–10°. Since the

slope is less than the angle of repose of the salt, vibration is necessary to move the load along. The range of frequencies is from 15 to 30 Hz, and the higher frequencies correspond to more gradual slopes. Higher capacities usually are associated with lower frequencies and higher amplitudes of vibration. The connection between the storage hopper and the feeder is enclosed to prevent dusting and loss of salt. A flexible rubber section 80–100 mm long helps to isolate the hopper from the vibrations.

Even the reciprocating-plate feeder, because of its rapid oscillation, is essentially a constant-feed device. Other types are intermittent. The gate-swing feeder and the undercut-gate feeder can have strokes timed, for example, to meet the buckets of an elevator.

7.2.1.3F. **Pneumatic Conveying.** Salt can also be conveyed pneumatically. This is associated most frequently with truck deliveries. A truck that carries its own blower can be brought close to the receiving vessel. The method is most easily adaptable to small plants, and the relatively high power consumption of a pneumatic system is less of a disadvantage in that situation. When there is no easy truck access to the process area, it is better to locate the salt receiver in a convenient spot and produce brine close to the delivery spot than to attempt to convey solid salt over a long distance. This remark may well be extended to large plants and to other modes of delivery and conveying.

7.2.1.3G. **Slurry Transfer.** Slurry transfer, in which salt can be dumped from a truck or hopper car into a pit where a brine carrier picks it up, is another option. Losses of salt are very small, and so this method is especially suited to the more expensive materials. The brine circulates by overflowing a wet salt storage tank into a fabricated or lined pit below the unloading spot. It picks up salt as it discharges, and the mixture returns to the storage tank through a slurry pump. Some of the circulating brine can be sent to the transport container to help along the flow of salt. Figure 7.16 is a simple flowsheet of this operation.

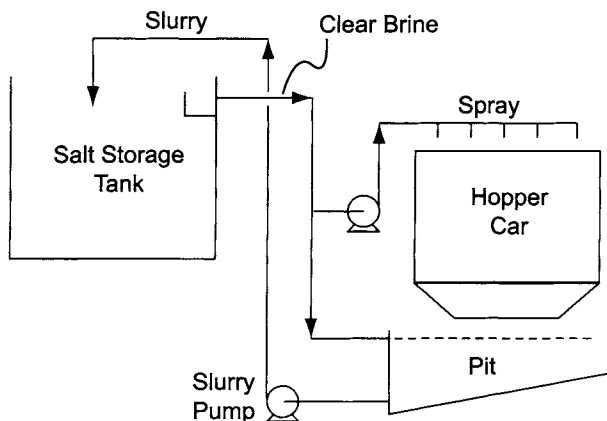


FIGURE 7.16. Slurry transfer of salt in hopper-car unloading.

The circulating pump should be designed for slurry service. Horizontal centrifugal pumps are best, with straight suction connections and, in the case of fine salts, open impellers. With rock salts, closed or semi-open impellers may be suitable. The pump seal must be flushed with clear water. Pipeline design should follow good practice for slurry service, with straight runs and gradual bends. Velocities of at least 3 m s^{-1} may be necessary to prevent settling of coarse salts. With evaporated salts, it may be possible to drop the velocity down close to 2 m s^{-1} . Slurry concentrations may be as high as 25–30% (w/w) solids. As in all wet-storage systems, addition of a new lot of salt will displace brine and can cause an overflow. There must be provisions to handle this overflow, either in a surge tank or by transferring it to the process.

7.2.2. Salt Dissolving

In this section, we consider the dissolving of NaCl and KCl to produce solutions for the production of chlorine and the corresponding alkali. These solutions are referred to as “brines.” The emphasis will be on in-plant dissolving in static beds of salt, usually confined in vessels known as “dissolvers,” but there will also be a short discussion of underground dissolving, or “solution mining.” Salt may be dissolved with water to produce new brine, or with dilute brine to bring its concentration back to saturation. In the latter case, the dissolver may be referred to as a “saturator” or a “resaturator.” The liquid traffic in the vessel increases, but the operation is the same.

Many processes in many different industries use salt in quantities much smaller than those used in chlor-alkali manufacture. Proprietary systems are available for dissolving salt in these applications and for producing brine for prewetting highway salt, but they are not considered here.

7.2.2.1. Process Basics. NaCl dissolving is a slightly endothermic process. The solubility increases only slowly with temperature, as shown in Fig. 7.17. Saturated solutions, furthermore, have concentrations slightly greater than those specified for the brine to be fed to a cell. These are desirable characteristics. Only saturated brine need be produced in dissolvers; there is no need to complicate the equipment or the operation with concentration control. Solution strength will not vary greatly with the temperature of the dissolving process, uncontrolled drops in temperature will not produce massive precipitation, and what precipitation occurs will be exothermic and somewhat self-correcting. Kaufmann [39] points out that NaCl is dissolved on a larger scale than any other heavy chemical and lists other desirable properties:

1. moderate to low solubility (physical properties of NaCl solutions are similar to those of water; normally only the specific gravity of 1.2 demands special attention in design);
2. lack of toxicity;
3. nonflammability;
4. general harmlessness when exposed to the body;
5. low degree of corrosiveness (dilute solutions are the most corrosive, with a maximum at about 3% NaCl; concentrated brines may be less corrosive than many grades of water);

6. nearly constant volumetric concentration over a range of temperature;
7. low caking tendency when stored under saturated brine.

Expanding on point #6, the volumetric concentration of NaCl, over the entire range of existence of saturated liquid brine, has a range of only about 4% (relative). The minimum, at about 20°C, is 317 gpl. At the boiling point, the concentration reaches its maximum of 330 gpl. In the temperature range common to brine systems, the range of concentrations is less than 1%. KCl is generally more soluble than NaCl, and its solubility is much more dependent on temperature (Figs. 7.12 and 7.18). Concentration control is more

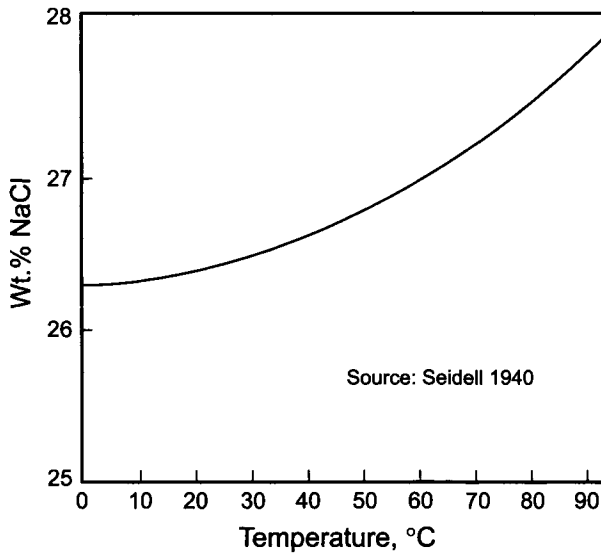


FIGURE 7.17. Effect of temperature on solubility of NaCl in water.

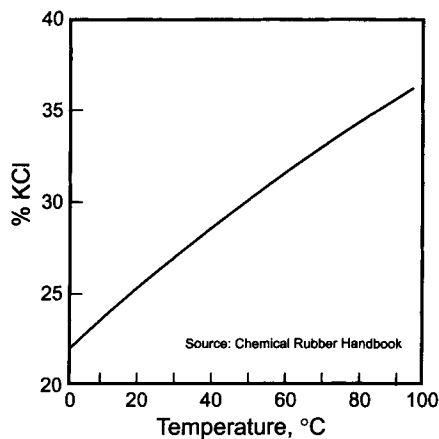


FIGURE 7.18. Effect of temperature on solubility of KCl in water.

of an issue, and saturated solutions are more likely to deposit solids at low-temperature spots. With either salt, heating the saturated solution or bypassing some of the dissolving medium around the salt dissolver so that the solution to be handled is unsaturated provides some processing safety. Heating the brine gives a more concentrated solution and perhaps more stable control. Its disadvantages are its energy consumption and the need for more apparatus.

7.2.2.2. Standard Dissolving Apparatus. Dissolvers are usually classified according to the direction of flow of the brine. In an upflow dissolver, water or dilute brine is introduced through a distributor, such as a sparger pipe, into the bottom of a vessel that contains a bed of salt. The solution becomes saturated as it rises. The saturated brine then leaves through an overflow device and is ready for further processing. In a down-flow dissolver, the direction of flow is the reverse. Some dissolvers use a combination of upflow and downflow, in which the brine is forced to flow in different directions in different parts of the dissolver. Partly because of the presence of insolubles in the salt and the need for occasional shutdown to remove sludge, many plants operate with multiple saturators.

The salt itself is broadly classified as coarse or fine; the dividing line is at a particle size of about 2 mm. Uncaked coarse salt flows freely. It stands or flows on its angle of repose and can automatically be fed into a dissolver by gravity as the lower part of a bed dissolves. Fine salt, unless exceptionally dry, tends to cake and form arches in storage hoppers. It is often fed into a dissolver in batches and stored under a cover of saturated brine. "Fine" salts include vacuum salt, evaporator salt, fine crystal rock salt, and most KCl.

It is nearly impossible to produce perfectly clear brine in an upflow dissolver. As salt dissolves, the overlying mass shifts downward in an irregular manner. The rising brine tends to develop channels through the bed, and the undissolved salt is not able to act as a filter. Another problem is the accumulation and overflow of scum containing foreign matter. Dissolved gases become less soluble as the salt concentration increases, and as these gases rise, they carry suspended matter with them by flotation.

Turbidity in the saturated brine is less of a problem in chlor-alkali production than in many other applications, because of the purification process following the dissolver. Large-scale upflow dissolving therefore is a common practice in the chlor-alkali industry. Nevertheless, turbidity is not a welcome development. Some of the particulate matter is calcium sulfate, usually the major impurity in rock salt. It will increase the concentration of sulfate ion in the treated brine, and since it is more soluble than calcium carbonate, it will add to the consumption of carbonate in the treatment process (Section 7.5.2.1B). The sulfate ion thus released becomes a problem in itself (Section 7.5.7).

The superficial velocity of the dissolving fluid at the bottom of an upflow dissolver is typically about 2.5 m hr^{-1} (say, 2–4). The depth of the salt bed usually is kept above 1.5 m. The feed brine or water enters a sparger-pipe arrangement through one or more peripheral connections. Proper design of the sparger is necessary for good flow distribution.

With fine salts of high purity, there is less carryover of insoluble impurities and a much slower buildup of undissolved matter in the dissolver itself. Cleanouts become

much less frequent, and upflow dissolvers are especially suitable in this case. Flow rates still are limited by carryover of fine particles and by the tendency to produce fissures and channels, which lead to undersaturation.

In downflow dissolvers, the brine flows through a stable bed of salt. The salt at the bottom of the vessel is exposed only to nearly saturated brine and does not dissolve or dissolves very slowly. So long as a certain height of salt remains in the vessel, therefore, it serves as a filter. The turbidity that characterizes upflow dissolvers is not present. Downflow dissolvers have been used for many years to dissolve salts that are finer than 10 or 12 mesh [23]. Purified vacuum salt is an example of a fine salt. Some fine rock salt has similar characteristics. These salts do not have stable angles of repose when covered with brine but rather tend to flow with any disturbance. Preventing the salt from flowing with the saturated brine requires the use of a porous support medium, which usually is gravel. This also provides some filtering capacity. With typical rock and solar salts, the gravel itself would be a nuisance, and various other designs have been tried but have not penetrated the chlor-alkali market to any great extent. Major deficiencies of some designs are the need for batchwise feed of salt and the accumulation of insolubles in the dissolver.

Mixed-flow dissolvers are an attempt to combine the advantages of upflow and downflow. Upflow–downflow dissolvers were conceived in order to add a filtration zone for the brine produced in an upflow mode. Problems arise when suspended solids accumulate on the filter salt and impede the flow of brine. This mode is not often found in the chlor-alkali industry. Downflow–upflow dissolvers, on the other hand, are rather commonly used. A familiar example in the industry is the highly successful Lixator™. The term, devised from “lixivate,” is a trademark of Cargill Salt Company. The *Oxford Universal Dictionary* defines lixiviation as “the action or process of separating a soluble from an insoluble substance by the percolation of water.” The basic apparatus (Fig. 7.19) consists of a cylindrical body above a conical section with a false bottom. Water or depleted brine is fed through a spray or distributor into the bed and flows to the bottom of the vessel. At the bottom is an opening in the false bottom that allows the brine to flow into the annulus between the two shells and then up to an overflow point.

Another example of salt’s favorable behavior, noted in point #7 of Section 7.2.2.1, is its ability to be stored under saturated brine. Many chlor-alkali plants take advantage of this fact. A large storage tank fitted with spargers then becomes an upflow dissolver. This is an especially useful technique in a diaphragm-cell plant. The salt recovered from the evaporators returns to the brine plant as a slurry. It is simply fed into a salt storage tank and dissolved as required by the cells. The salt storage tank becomes a buffer that allows smooth operation of the brine plant and electrolyzers while the evaporators are shut down or undergoing boilout (Section 9.3.3.3A). An incidental advantage of wet storage is the efficient utilization of space. First, the angle of repose of the salt disappears and the storage space becomes a cylinder rather than a shallow cone with its wasted space. In addition, filling the interstices of the mass of salt with saturated brine increases the NaCl-holding capacity by another 15% or so.

While wet storage has operational advantages, it imposes extra loads on the confining vessel. The mass is heavier because of the interstitial brine, and the fluidity of the contents adds a horizontal thrust on the walls. Also, when the vessel is used to accumulate

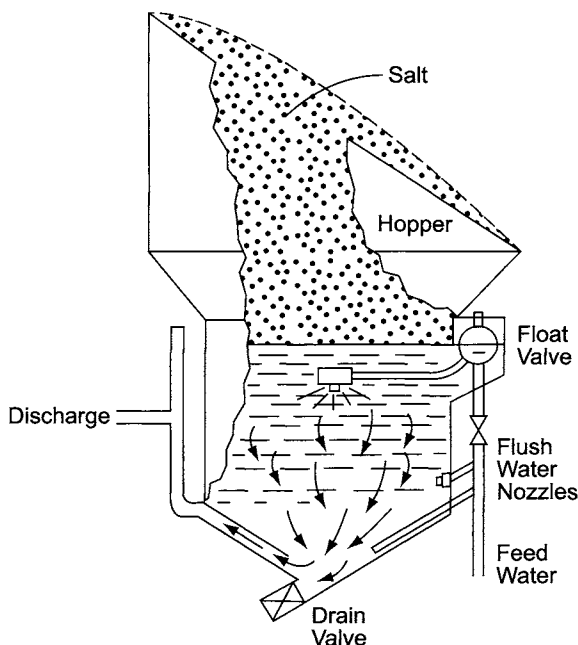


FIGURE 7.19. Downflow-upflow salt dissolver. (With permission of Cargill Salt Company.)

salt during a shutdown of the cells or brine-processing system, there may be a liquid overflow to accommodate.

7.2.2.3. Miscellaneous Dissolving Techniques. The best way to simplify dissolving apparatus is to eliminate it from the process. When large quantities of salt are stored in outdoor piles, water is often simply sprayed onto a pile to dissolve the salt. This leads to very uneven results, including uncontrolled dissolving by rainwater. Impurities can collect at the surface and partly dissolved fines in the interstices between coarser particles, forming an impervious layer. The results are the formation of channels and the production of unsaturated brine. The spray density over a large pile will be uneven. Localized dissolving will cause collapsing and avalanches in the pile. This method can not be recommended on its technical merits.

A variation on the above is a below-grade pit. This approach is sometimes used on smaller scale, and it is somewhat superior to salt-pile dissolving. The dissolving fluid can be introduced through spargers beneath the surface of the salt. A pit is also adaptable to wet-salt storage and then is less subject to some of the operating problems listed above.

Figure 7.20 shows an example of a pit dissolver. One of the two compartments can receive salt directly from the hopper car shown as the mode of delivery while the other compartment is in service as a dissolver. This drawing is part of a standardized design for capacities lower than most chlor-alkali plants require, but the basic features will be obvious.

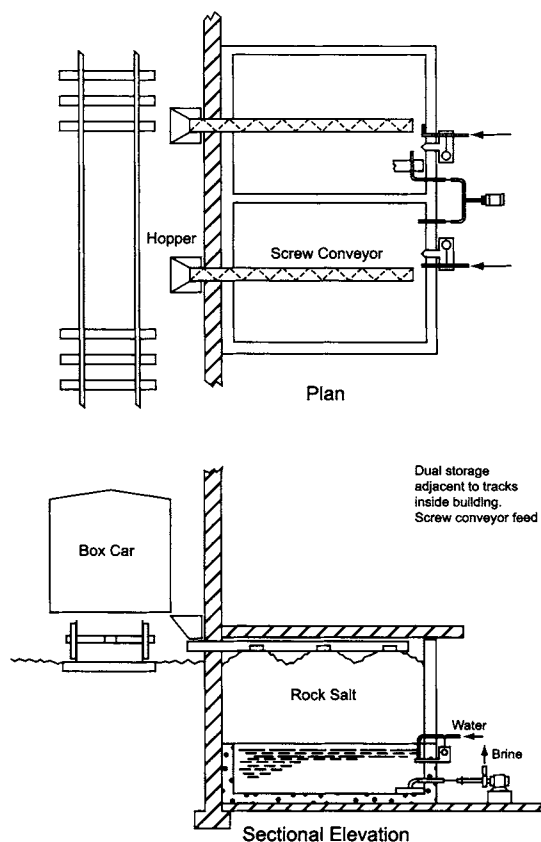


FIGURE 7.20. Typical pit dissolver. (With permission of Cargill Salt Company.)

The temperature of the saturated brine is variable when salt is dissolved outdoors. When depleted brine at the process temperature is part of the fluid used to dissolve the salt, heat loss can be a serious matter, upsetting the balance in the brine process. A steam plume from the dissolving area can be a hazard as well as a nuisance.

Conservation of heat becomes more important as the operating temperature increases. Operators of hot brine processes may use fluidized salt resaturators in which an internal cone holds a recirculating salt slurry. Fresh undersaturated brine enters the cone, and saturated brine overflows to the bottom section of the vessel for removal. The supply of salt is replenished by addition of fresh slurry near the circulating pump.

Another method is to dissolve salt in its shipping container. This is more common in KCl service. The salt is shipped in specially designed sparger cars. As the name suggests, these are equipped with internal spargers to which the operator connects a source of dissolving fluid. Section 7.1.6 pointed out that KCl as supplied to the chlor-alkali producer is already quite pure. Insolubles are less a problem than they are with NaCl. As a car empties, the concentration of the brine being produced can decrease, especially if there is no recycle. This effect must be considered in the design of the

system. It is not a factor in the more frequent case in which salt is removed from a sparger car as a slurry (Section 7.2.1.3G).

Finally, salt can be dissolved in agitated tanks. This practice is restricted to batch and small-scale processing, mostly by occasional users. It is difficult to apply the vigorous agitation necessary for efficient dissolving without promoting bypassing of undissolved salt. High-efficiency impellers should be used, with moderate speeds but with diameters equal to one third or one half of the tank diameters. Energy consumption will be at least 10 times as great as in one of the associated brine treatment tanks.

7.2.2.4. Solution Mining

7.2.2.4A. Dissolving of Salt. Soluble substances can be recovered from underground deposits by the technique of solution mining, which is widely used with both NaCl and KCl ores. Figure 7.21 shows a typical arrangement [40]. This is not different in principle from the approach used in oilfield drilling. After driving an outer ring to some depth, drillers sink a casing into the top of the deposit. The annulus is sealed with cement to establish a seal. After further drilling, a central pipe, whose length is adjustable but always greater than that of the casing, is dropped through the middle of the casing. This arrangement immediately suggests two different possible modes of operation. Water pumped into the well through the casing or the pipe dissolves salt from the deposit, and the pressure forces the resulting brine up the other channel and to the surface. In the method recommended by Deutsch [41], water enters the well through the casing. Convection of the heavier solution toward the bottom helps to increase the strength of the solution produced.

Solution mining is more effective with salt domes than with stratified deposits, and Fig. 7.21 is drawn for a domal deposit. It is the favored process for extraction of NaCl from domes, and it is also widely used with deep-lying strata, where the cost of

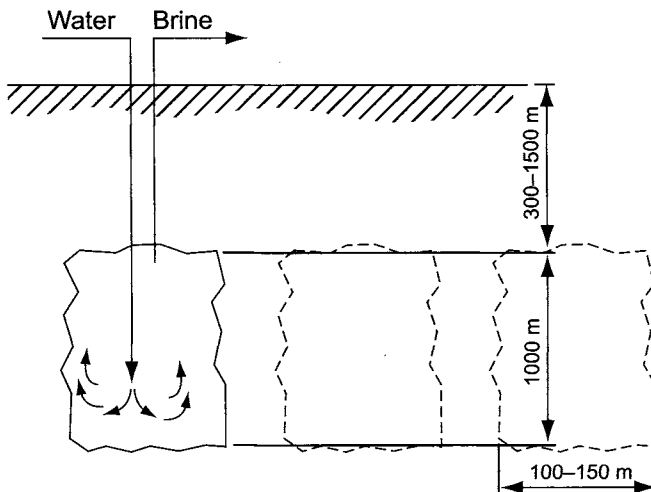


FIGURE 7.21. Solution mining from salt dome. (After Liederbach [40].)

conventional mining can be very high. The cost of a unit of NaCl as solution-mined brine from a salt dome has been estimated to be less than half that of a unit of dry-mined salt [42]. This cost advantage offers a substantial benefit to a plant able to use a brine feed, and so it favors diaphragm-cell operation. Because of this fact and the prevalence of salt domes around the Gulf of Mexico, much of the United States' chlor-alkali capacity historically has been in diaphragm-cell plants on the Gulf Coast and has been particularly resistant to penetration by membrane-cell technology.

The productivity of a well depends on the surface of salt available to the injected water. Productivity in a new well is very low, but as the cavity grows it increases to the design rate. In opening a new field, it takes some time to reach full production. This is an important consideration in the startup of a new brine/chlor-alkali complex. The rate of solution of salt increases when the flow of dissolving fluid is turbulent, but this improvement in rate may be offset by a decrease in the concentration of salt in the finished brine. When a new well is brought on line in an operating field, weak startup brine can go to a mature well for saturation, and startup is more efficient.

In salt domes, brine wells can become very large. Diameters of the cavities can be more than 100 m, and depths of some wells exceed a kilometer. Such a volume of salt would be enough to operate our reference plant for more than 30 years. Wells, when fully grown, are separated by thick walls of salt to provide structural integrity.

It has already been mentioned that stratified salt deposits are less amenable than domes to solution mining. This will become obvious from a consideration of the geometry of a stratum. Many strata are less than 20 m thick and perhaps less than ten. At the same time, they may be quite large in at least one other dimension and probably are not quite horizontal. With water and brine pipes sunk from adjacent surface locations, a cavity will not grow very large before bypassing becomes a serious problem. With stratified deposits, a group of wells is sunk and operated in parallel as a "field." Water feed pipes and brine pipes are some distance apart, as shown in Fig. 7.22. This forces flow in the long direction(s) of the salt stratum.

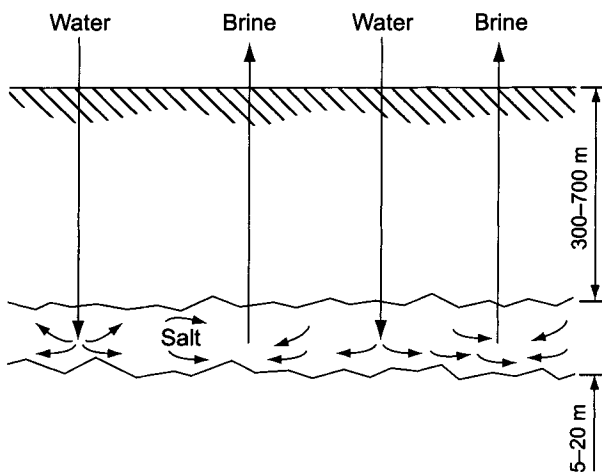


FIGURE 7.22. Solution mining from stratified deposit. (After Liederbach [40].)

Many salt deposits contain sulfides and hydrocarbon inclusions. When brine rises from the mine to the surface, noxious or hazardous gases can evolve in the pipeline or at the surface as the pressure decreases. These must be separated and disposed of safely. When temperatures in the mine are higher than those at the surface, dissolved salt may drop from solution. Process design should recognize the possibility of precipitation and accumulation of solids. In this connection, the pressure at the bottom of the well also increases the solubility of other compounds. Frear and Johnston [43] and Brandani *et al.* [44] have shown that the solubility of calcium species increases when the partial pressure of CO₂ increases. A final consideration is on rates of solution. The very long residence time in a brine well allows more of the slower-dissolving materials to enter the brine, which is generally of lower quality than brine prepared at the plant from the same salt.

Removal of salt creates the possibility of cave-ins and surface subsidence. Limited cave-ins are a fact of life in solution mining of bed deposits. The narrow deposit of salt is quickly exhausted at some points, and overlying layers of rock or anhydrite may be less stable and collapse to the floor. The rubble eventually destroys the piping or shuts off flow and causes abandonment of that section of the field. There have also been instances of surface subsidence. With dome deposits, there has been no subsidence over cavities generated by industry-approved techniques [15].

Adding salt to water until it is saturated increases the liquid volume by more than 10%. In solution mining, this expansion very closely matches the volume lost to expansion of the cavern as the salt dissolves. Volumetric flows into and out of a well therefore are nearly equal. In New York State in 1997, for example, 2.26 billion gallons of fresh water were injected and 2.25 billion gallons of brine were withdrawn [45].

7.2.2.4B. Formation of Caverns. The oldest technique in solution mining of salt is to add water through the annulus between the pipe and casing and withdraw brine through the central pipe. Convection of the denser brine toward the bottom of the well helps speed the process. However, salt dissolves much more quickly in water than in concentrated brine, and the result is a cavity much wider at the top than at lower levels. This is an unstable configuration, and some of the overburden frequently collapses. Alternative methods include bottom injection and padding of the surface of the brine. Padding, which may rely on air pressure or on a floating layer of an immiscible fluid (e.g., a hydrocarbon), prevents contact of the fresh water with the salt above the pad and allows the operator more control over the shape of the cavity as it develops.

Another result of uncontrolled addition of fresh water at the top of a deposit is poor utilization of the available salt. The abundance of salt referred to in Section 7.1.1 encouraged such wasteful practice. Closer regulation of the industry and the growing use of salt caverns for storage increased interest in regulating the shape of caverns. The measures taken improve the efficiency of operation as well as the recovery of salt from the deposit. For example, Kublanov [46], in a review of 40 years of practice in the Russian salt industry, showed how techniques have evolved from downflow dissolving to convective blending. The older method was carried out in steps at increasing depths. In the newer technique, water is added to the middle of the cavity and brine withdrawn from the bottom. The old practices resulted in development times of 1 to 2 years for new wells, rather low production rates, frequent cave-ins and breakage of columns, and

excessive consumption of the hydrocarbon oil used to seal the top of a chamber. The same practices were applied to all wells, regardless of location or the type and characteristics of a deposit. Now, development time and hydrocarbon consumption are less than half the old values, production rates are up 30–50%, and well accidents have nearly disappeared.

Different procedures apply to different types of deposit [47]. In the relatively thin layered deposits, two or more wells are drilled at no great distance apart. Mixing air with water when operation starts allows a pad to develop above the solution as it forms. This limits the upward expansion of the cavern and forces it laterally. Before long, the wells are in communication with each other. The mode of operation then changes, with water sent down one well and brine withdrawn from another. Mining begins near the planned bottom of the cavern. When the cavity reaches its planned horizontal dimensions, operation shifts to a higher level. This continues until the cavern reaches its final height.

In a domed deposit, wells more often operate singly. Sinking three concentric pipes instead of two allows the use of one annulus for the injection of oil. This forms a seal between the brine and the top of the cavity and prevents excessive dissolution of salt there. When the well is taken out of service, the intact structure is stronger and more stable. This fact helps to prevent surface subsidence.

7.2.2.4C. Use of Caverns for Storage and Waste Disposal. The use of caverns formed by dissolving salt for storage and waste disposal is a relatively new development in the long history of salt mining. The impermeability of salt deposits makes them attractive in this service. The first applications were in Canada in the 1940s [48]. Hydrocarbons were the first materials stored, branching out from liquefied petroleum gas to crude oil and natural gas. Thoms and Gehle [49] have summarized the history of the various uses of salt caverns through the year 2000. Non-hydrocarbon storage applications include compressed air, which supplies power for peak-demand shaving. Figure 7.23 shows a storage well containing a light liquid, such as a hydrocarbon. The method of operation is obvious from the drawing. Brine serves as a liquid piston; it can be injected to force the light liquid out of storage. Conversely, when more product is pumped into storage, brine is displaced and can be used or held in inventory for later withdrawal of the stored product.

Wells are also used for waste disposal. Naturally enough, the first applications were in salt-based industries like chlor-alkali and soda ash production. Salt caverns are also frequently used for disposal of oil field wastes but seldom used for toxic materials. LaGess [50] cited an early example of the disposal of brine treatment sludge in salt wells. The sludge issued as underflow from the brine clarifier (Section 7.5.3) and contained 5–10% solids, primarily CaCO_3 . It was diluted before disposal in the well. Excess treating chemicals in the sludge tended to precipitate hardness from the added water. Addition of a hold tank to allow growth on the existing particles relieved the problem of deposition in the transfer pipeline. Some of the advantages of a well as a place for disposal cited by LaGess were its definite boundaries and its lack of communication with any other space (except perhaps for a communicating well). As for lack of environmental impact, the calcium returns to its source (as the even less soluble carbonate rather than

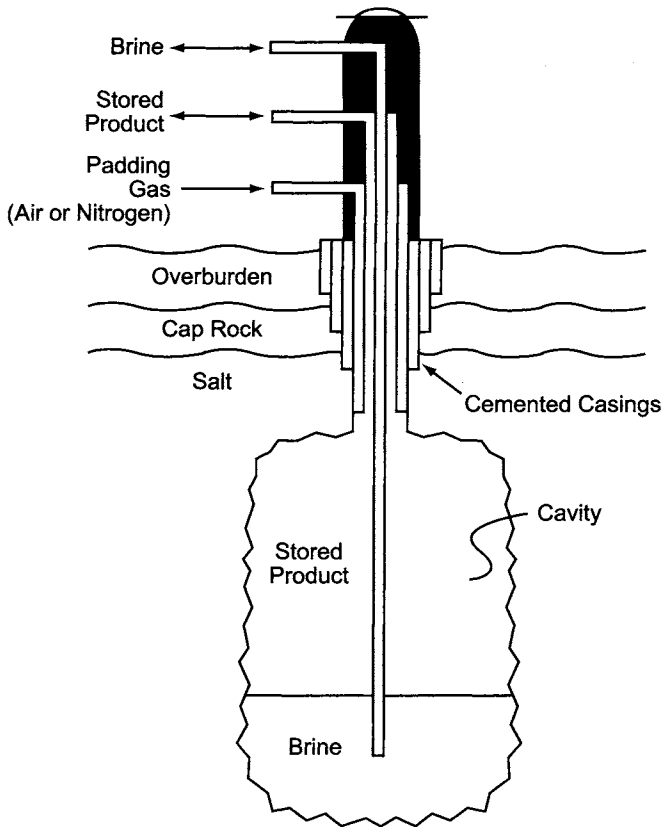


FIGURE 7.23. Use of salt cavern as a storage chamber.

sulfate), where there already is a mass of anhydrite debris. In this particular example, one solids-storage well held the residue from 15–20 brine-producing wells.

7.2.2.5. Selective Dissolving. Brine quality improves if NaCl can be dissolved selectively, leaving some of the impurities behind. Selective dissolving techniques usually are aimed at partial rejection of calcium sulfate, the major impurity in salt. These techniques can be divided into three categories:

1. control of the dissolving process
2. use of minor additives that prevent dissolution of the sulfate
3. common-ion effects

7.2.2.5A. Control of the Dissolving Process. The amount of sulfate that dissolves along with the salt depends on equilibrium and kinetics. The equilibrium solubility of sulfate is reduced at high pH and, when present as anhydrite, at high temperature, but these effects are not great enough to override other process considerations. There is more to

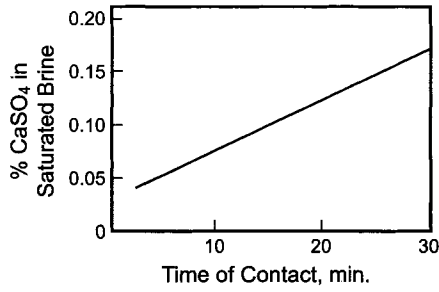


FIGURE 7.24. Rate of solution of anhydrite from rock salt.

be gained by exploiting the kinetics of the process. Calcium sulfate, at least in the form of anhydrite, dissolves much more slowly than NaCl. By controlling the contact time of the salt with the dissolving brine, it is possible to dissolve substantially all the chloride and reject most of the sulfate [51]. Figure 7.24 shows the slow increase of sulfate content when dissolving a rock salt. Many plants therefore use short-contact dissolvers [52] to obtain this effect. Under ideal conditions, a “rapid dissolver” is said to be able to reject 80–90% of the sulfate. Sutter [53] estimates the practical rejection at about 70% and recommends a contact time of about 4 min. Liederbach [40] confirms this rejection rate but recommends a contact time of 6 min. The short-contact dissolver in any event is much smaller than the conventional upflow dissolver is, but its cross-sectional area still must be large enough to prevent fluidization of the salt.

The short-contact dissolver continuously removes insolubles from the apparatus. This is a necessary part of the design of this type, but not an inherent advantage. It is also an option with many other designs. Disadvantages of the short-contact dissolver include the increased turbidity of the brine, especially if the dissolver is not followed by a settling chamber, and the small inventory of salt in the dissolving zone. The latter means that more storage volume must be supplied elsewhere and that feeding salt to the dissolver, with some designs, may become a continuous metered operation. The rate of salt feed then must be closely matched to the rate of consumption, or the surge capacity of the dissolver will soon be exhausted. Space permitting, automatic gravity feed of salt from a hopper into the dissolver can relieve these problems.

Figure 7.25 shows a typical short-contact dissolver. The conical bottom aids the removal of undissolved matter; 60° is a typical bottom angle. Water or depleted brine enters through a perforated-pipe distributor. Superficial upward velocity of the brine usually is 10–20 m hr⁻¹. Saturated brine may overflow the entire periphery or may leave through holes in the wall of the dissolving chamber. With the small dimensions of these dissolvers, velocities are much higher than in conventional large-diameter dissolvers. Some entrainment of fines is inevitable. The brine overflow usually goes to a decanter of larger diameter. Sometimes a center well is used to direct the brine downward and force it to make a 180° turn in order to leave the decanter. The cylindrical bottom leg shown in the illustration allows washing of the sludge with a small amount of water in order to reduce the amount of NaCl-saturated brine carried out with the solids.

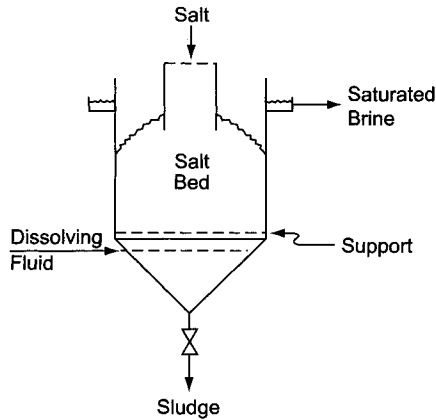


FIGURE 7.25. Short-contact dissolver.

Salt enters the top of the vessel, usually from a feeder. A coarse screen protects the dissolver from large foreign objects. A grating with large openings, covered by a woven screen, supports the salt bed. When the residues of dissolving particles become small enough, they drop through the screen and into the sludge chamber. The height of the bed is determined by the choices of brine velocity and contact time. Most frequently, it is in the range of 1–3 m.

Construction is of rubber-lined steel or other standard materials for the brine process. The small size of the dissolver often makes FRP (reinforced with PVC or CPVC) a good choice for the vessel, and the same resins can be used for internal piping. The salt-supporting grid can be carbon steel, but the thin screen should be of a more resistant material such as Monel.

The best pH for dissolving salt, all things considered, is in the range 7–9. In many systems, the stability of pH control is more important than the exact value. If there is continual fluctuation in pH, certain impurities will dissolve more freely at a particular pH and then precipitate in downstream equipment during the opposite part of the pH cycle. There are published warnings against developing too high a pH when neutralizing dechlorinated brine for recycle. Similarly, it is said, soluble magnesium species become insoluble when mixed with the alkaline brine. This effect is self-limiting. Alkalinity in the brine fed to a dissolver would act first to suppress the dissolution of magnesium compounds. Even if all the alkalinity in membrane-cell depleted brine at pH 11 caused $Mg(OH)_2$ precipitation after the dissolver, the result would be a brine stream with less than 10 ppm suspended solids. This is quite similar to brine clarifier overflow. These statements are meant to put this matter in perspective. They do not suggest that the pH of recycled brine be ignored.

7.2.2.5B. Use of Solubility Inhibitors. The dissolution of sulfate can be inhibited by addition of small quantities of certain chemicals to the dissolving water or brine. Hexametaphosphates were an early candidate for this application [54]. They function by forming insoluble coatings on the surfaces of particles of calcium sulfate and preventing

them from reaching equilibrium with the brine. In effect, they retard the dissolution of calcium. The phosphates have largely been supplanted by proprietary anionic surfactants based on alkyl benzene sulfonates (ABS). One such is marketed under the trade name SSI-200 [55]. The same product is marketed in Europe as ASR (anhydrite solubility reduction) [56]. Dosage levels are 3–30 mg L⁻¹ in the brine. The action depends on the sulfate being present as discrete particles and is enhanced if it is present as anhydrite rather than the hydrated and more easily soluble gypsum. Because of this, solubility inhibitors have been more successful with rock salts and are not recommended for use with solar salts. They can be used in a plant's salt dissolver or in caverns in solution mining. Specialized producers of brine practice the latter application on a large scale in the United States.

When the ABS type of inhibitor is used in solution mining operations in salt domes, the recommended concentration is usually about 12 ppm in the dissolving water. The material is supplied as a viscous oil and is best used without intermediate dilution. It contains free mineral acid and is correspondingly corrosive and hazardous. The remaining excess concentration in the treated brine is very low. While these inhibitors themselves are sources of sulfate in the treated brine, they are present in negligible concentrations.

SSI-200 requires a covered and vented storage tank in resistant material such as FRP. At temperatures below about 10°C, the handling system should be traced and insulated. The storage temperature usually is kept below 60°C. Hastelloy C or D and Alloy 20 are the recommended metals. After dilution, the material becomes more corrosive and requires the use of higher-nickel alloys.

Accurate low-volume metering pumps suitable for corrosive service and high viscosity (up to 3,500 cp) are necessary. For each 1,000 tpd of salt dissolved, the flowrate required to produce a concentration of 12 ppm is about 1.5 L hr⁻¹. Because of the high viscosity and high degree of dilution in the brine stream, high-pressure injection quills may be used to promote rapid dispersion.

Figure 7.26 gives an example of the effectiveness of SSI-200 when dissolving rock salt from a Texas dome. The addition of 15 ppm reduces the sulfate concentration of the solution formed by about 80%. Figure 7.27 gives a second example, at the standard inhibitor concentration of 12 ppm. This shows the general effectiveness of the product

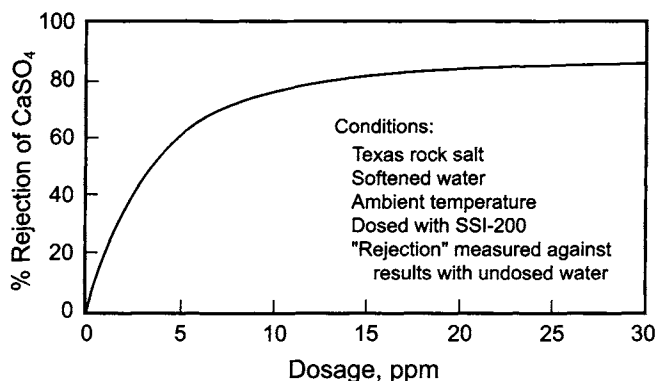


FIGURE 7.26. Effect of inhibitor dosage on sulfate rejection. (With permission of Jamestown Chemical Co.)

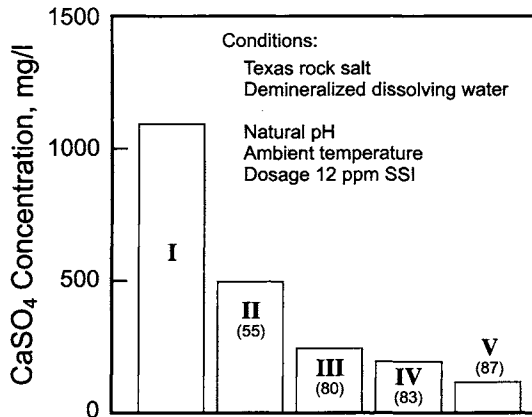


FIGURE 7.27. Rejection of calcium sulfate by inhibitor formulations. (I—no inhibitor added; II—original SSI added; III—original SSI-200 added; IV—improved blend SSI-200 added; V—optimum blend SSI-200 added.) Figures in parentheses are % inhibition vs Case I. (With permission of Jamestown Chemical Co.)

and the fact that SSI-200 is a second-generation product. There is also a possibility of improvement by special blending of the inhibitor to suit the particular salt.

Startup of a solution mining operation with solubility inhibitors or introducing inhibitors into an operation that has been on line for some time has its unique problems. Some time is required before the inhibitor can have its full effect. During this time, the sulfate content of the mined brine will be higher than desired. The use of a higher excess of inhibitor to speed up the process is of limited value [57].

7.2.2.5C. Common-Ion Effect. Sulfate can also be prevented from dissolving by the addition of the cation of a sulfate that has limited solubility. Barium and calcium are the obvious candidates, but calcium presents fewer problems in application, and its use has been demonstrated commercially [58–60]. Calcium compounds are less toxic than barium compounds. They are also cheaper on a unit basis, but their lower effectiveness can override this advantage. Santos [60] described a system in which CaCl_2 was added to the unsaturated brine flowing to the dissolver. The combined cost of CaCl_2 and Na_2CO_3 was much lower than those encountered in the equivalent precipitation processes. The cost of barium chloride, for example, is usually 50–80% higher. Santos gives comparative costs for several cases. Using his data at an operating temperature of 60°C and a sulfate ion concentration of 4.7 g L^{-1} , we find the following materials costs for a 15,000 tpy plant (ca.1992):

Process	Materials Cost, \$M per year
Calcium suppression	271
CaCl_2 precipitation	522
BaCl_2 precipitation	472

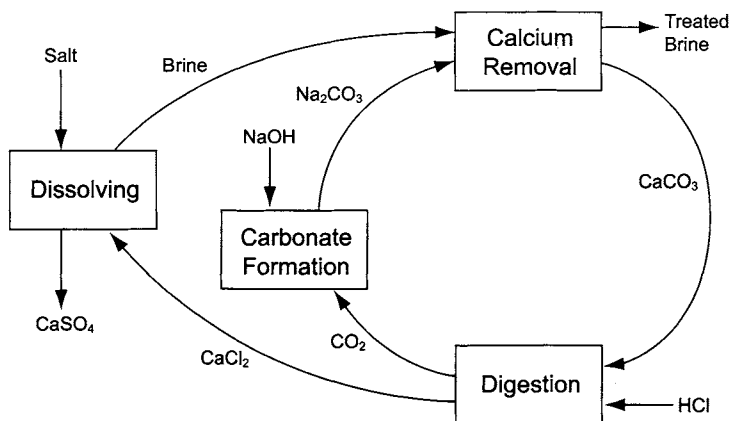


FIGURE 7.28. Closed-loop process for suppression of sulfate by calcium ion. (Reproduced with permission of Society of Chemical Industry.)

Another plant that returns brine to wells for resaturation reduced its solids waste load by 80–85% by injecting CaCl_2 solution into the returned brine [61].

Regenerating CaCl_2 from the carbonate sludge can reduce the cost of its supply to the process. This consumes HCl instead of calcium chloride. The carbonate value goes off as CO_2 . Absorption of this gas in caustic gives a closed-loop process (Fig. 7.28). This requires a purge, which under some conditions may be large, to remove the other impurities found in the brine sludge.

The suppression process is based on the same physical chemistry as precipitation, but it has several advantages. First, sulfate does not enter the brine, and no equipment is required for its later removal. We shall see in the discussion on brine treatment that this equipment often includes a very large clarifier. Second, the process tends to equilibrium from below the solubility level, not from above. Any departure from sulfate equilibrium will be in the right direction. Third, calcium precipitation tends to produce gypsum. In rock salts, sulfate is present as anhydrite, a less soluble form. The effective equilibrium is thus more favorable in the suppression process.

Calcium chloride is available commercially in several different forms. Chlor-alkali producers usually receive it as pellets, 4 to 20-mesh flakes, or solution. There is also a powdered form, but it is relatively difficult to handle and has no real advantages in our application. Pellets and flakes are available in a nearly anhydrous ($\sim 95\%$) form containing about 3% NaCl and flakes in 77% concentration, approximately the dihydrate, with about 2.5% NaCl . Flakes have an angle of repose of about 30° . Equipment design should be for about 45° .

CaCl_2 and its solutions are used as desiccants. The anhydrous solid in a scrubber can dry air to a relative humidity of 7–10% [62]. The solid forms therefore are extremely hygroscopic and can dissolve in their water of sorption. They should be stored in seal-welded equipment with gasketed openings and entrances. Carbon steel is a satisfactory material of construction and should specifically not be lined because of the abrasive nature of CaCl_2 . Rather, most designers add a corrosion allowance of about 5 mm.

Commercial solution strengths range from 25 to 45%. Solutions for use in closed systems such as a refrigeration plant often contain corrosion inhibitors. Chlor-alkali producers, for the most part, should avoid these. A 25% solution of CaCl_2 begins to freeze at -29°C . The eutectic composition is about 30%, with a freezing point of -53° . The temperature of the onset of freezing then rises rapidly with concentration, reaching 0° at about 37%. The solid form in equilibrium with solutions stronger than the eutectic composition is the hexahydrate ($\sim 51\% \text{CaCl}_2$).

Because lime is a weak base, a solution of pure CaCl_2 is acidic. The commercial form, however, contains a small amount of unreacted lime and produces solutions that are slightly alkaline. Solutions therefore are noncorrosive unless aerated. Carbon steel batch tanks or solution preparation tanks with their frequently varying levels should be lined or painted to prevent corrosion. FRP is also an acceptable material, provided that tanks are designed for the high specific gravity of the material. Carbon steel is also a satisfactory material for pumps and piping. PVC is useful up to a temperature of about 70°C .

7.3. BRINE STORAGE AND TRANSFER

In this section, we consider the need for storage of brine and the location, sizing, and design of storage tanks; the movement of brine into and through the process; and brine temperature adjustment. In choosing materials of construction for tanks, pumps, exchangers, and pipelines, it is important to consider possible contamination of the brine as well as corrosion. Certain reinforced plastics are good candidates and widely used for in-plant applications. At the large scale common to primary brine supply, however, they are not always practical, and ferrous-metal equipment is used instead.

7.3.1. Storage of Brine

Brine processing is a major part of the chlor-alkali process. Reference to Fig. 6.2 shows that none of our other subdivisions is as complex or contains as many steps. "Anyone can make chlorine but it takes a real engineer to make good brine." The large number of steps calls for a storage policy that will assist smooth operation of the plant. No two plants seem to have the same arrangement or the same needs. What is needed at the design stage in every case is a careful review of the reliability of each step in the process, leading to a decision on where and how much storage is necessary or justified. Section 11.2.1 points out that control strategy and the best storage policy are often interrelated.

Plant operators will recognize that storage tanks tend to remain full. This gives a feeling of security. Unless a plant is oversupplied with tankage, however, it may be false security. The function of intermediate storage is not to maximize the available supply to each step in a process but rather to uncouple two process steps so that disturbances are not propagated between them. Figure 7.29 illustrates the logic that should be applied to sizing a storage facility. Design usually is based on postulated shutdowns of some duration. A storage volume lies between two process units, either of which may fail. Since a failure may occur on either side of the storage element, there are two separate considerations. At normal operating level, the storage volume should allow process unit #2 to operate without input from process unit #1 for a given time. Above this level should be enough

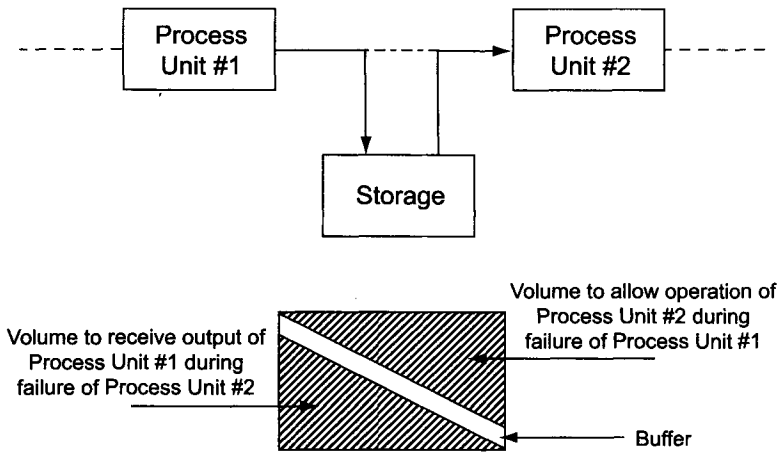


FIGURE 7.29. Analysis of storage requirement.

freeboard for the reverse situation. If process unit #2 goes down, process unit #1 then can operate and feed the storage facility for the allotted time. The inventory should be kept within a band that satisfies both needs. The fact that the shaded areas in Fig. 7.29 are equal by no means implies that the two volumes always are close to equal.

The overriding concern in a chlor-alkali plant is to keep the cells and the caustic evaporators running. There is no need to provide major storage between every two adjacent process units. Rather, the usual technique is to group units, provide large storage volumes between groups, and place smaller pump tanks that hold several minutes' flow at other locations. Process considerations influence the decision on storage volumes. The chemical treat tanks and the brine clarifier, for instance, are parts of a gravity flow sequence. Any storage between the two would serve no purpose but would rather allow the accumulation of solids. Storage of brine after the clarifier might be useful, but the arrangement of equipment limits the height of the overflow tank. A large tank would have to be placed off line and would add one or two more pumping operations to the process.

Provisions for on-site storage of the ultimate raw material, solid salt or raw brine, are highly variable. A plant with its own nearby solution mining operation may have relatively little raw brine on site. Salt storage should allow the plant to operate in spite of delays in delivery or production outages at the source. In the latter case, one presumes that there is also storage at the source, and this can be rationalized with site facilities. The minimum storage required also depends on the size of a typical shipment of salt. When salt is delivered by ship, this is frequently the determining factor. An extreme case would be a plant that receives salt infrequently or during only part of the year. Harbors in far northern locations may be closed in the winter and may force a plant to provide enclosed storage for several months' supply of salt.

The corrosiveness of brine to ferrous metals depends largely on pH and on the concentration of dissolved oxygen. When the brine is acidic, a lining or coating is usually applied to steel storage tanks. Rubber and plastic liners are used; coatings may be a simple paint or a coal-tar or a phenolic epoxy. Nonaerated, slightly alkaline brine is

relatively noncorrosive, and carbon steel is suitable. Even such a tank may have a lining applied to the parts most likely to be exposed to the air. When the level of brine varies regularly and the interface with the air moves about, the entire tank may be lined or coated.

Tank construction is not complex. The American Petroleum Institute's code API 650 is a commonly used standard, usually without a corrosion allowance. Tank bottoms have very gentle slopes, less than 1%, unless suspended solids are present. In that case, the slope may be greater and directed toward a flush or submerged drain nozzle. Where a heavy accumulation of solids is likely, tanks often have flush-bottom cleanouts. Not all tanks are covered. The likelihood of finding open tanks decreases as purity becomes greater and size of tank smaller. Where a roof exists, it is usually self-supporting.

Smaller brine tanks usually are made of FRP. At least within the process, a good grade of corrosion barrier, for example a bisphenol-type resin, is recommended. Very small quantities of brine sometimes are stored in polyolefin tanks.

7.3.2. *Transfer of Brine*

7.3.2.1. Pumping. Pumping of brine is a straightforward operation. As noted above, the corrosivity is not high, and brine is essentially an innocuous fluid. Density and viscosity are higher than those of water, and so power requirements are greater than in water service. These are not huge effects and do not complicate the basic simplicity of brine pumping.

Many different materials of construction are used. More resistant materials and those less likely to contaminate the brine are called for as pH drops, aeration increases, or the application moves closer to the cells. The most basic combination may be ductile iron casings with cast iron impellers. For in-plant service, the impellers may be upgraded to Monel. Where higher resistance is desired, high-chromium alloys (25-5 steels) appear. An example of this type is CD4MCu (27-30% Cr, 3-6% Ni, <0.04% C, <2% Mo + Cu). The ultimate metal, used frequently for pure brine feed and almost exclusively for acidified depleted brine, is titanium. Rubber-lined pumps also appear and, in the smaller sizes, FRP.

Most designers recommend double mechanical seals, usually unbalanced. Clear water is the best flushing liquid, because there is a possibility of crystallization from concentrated brine within the gland. Seal water may enter the process through the pump seals, and its quality should be chosen with that in mind. The purity of water required depends on the location of a pump within the process. In a membrane-cell plant, only the best grade of water should be used after the ion-exchange step.

7.3.2.2. Heat Exchange. At some point in the process, heat is added to the brine. Heat losses in the treating system and the thermal effect of dissolving water that is below the process temperature are responsible for this. The latter effect is absent or small in a mercury-cell plant, where the brine may actually require deliberate cooling. Shell-and-tube and plate-type exchangers both are satisfactory. At least in and around the cell room, the trend in modern plants is toward plate units. In raw and treated brine service, cupronickel tubes in carbon steel shells give robust service. In plate exchangers, stainless steel and titanium are common.

The same constructions are used for cooling brine. This occurs sometimes within the process and sometimes before long-distance transfer of brine for resaturation. In the latter case, cooling may be by interchange, this time with brine returned from the resaturation process.

Whenever untreated brine is heated, whether with steam or by interchange with hotter brine, there may be a danger of deposit of sulfates or carbonates on the heating surface. Shell-and-tube units should be designed with the appropriate fouling factor and with a facility for in-place cleaning with inhibited acid. Plate exchangers should be designed to minimize fouling, with high velocities and restrictions on plate heights. Deposits are less likely when heating by direct contact. This technique is most common in diaphragm-cell plants, specifically in brine/hydrogen interchangers. It economizes heat and keeps the chlorine that dissolves from the gas inside the main process. Section 9.2.4 contains a short discussion

In membrane-cell plants, some of the waste heat generated on the cathode side of the cells is often removed by interchanging the circulating caustic with brine. This application favors plate exchangers. With the temperatures involved and the different demands on the two sides of a plate, it is an exacting service, and Hastelloy C or a similarly resistant alloy is required.

7.3.2.3. Pipelines. This section deals only with off-site pipelines used for the long-distance transfer of brine. Some pipelines, especially among the older ones, are cast iron. Newer lines are more frequently carbon steel or even a resistant plastic.

To protect a metallic pipeline from corrosion, the brine should first be deaerated. Drawing a vacuum is the most convenient technique (Section 12.6). If the source of brine is remote, there may be no steam available to drive an ejector. A vacuum pump may then be used, or an eductor driven by brine or air. Typical operating pressures for deaeration are 10–20 kPa.

Underground steel pipelines must be protected from external as well as internal corrosion. Protective measures include wrapping the pipe with an impervious material, painting or covering it with a protective layer, and providing cathodic protection.

As more membrane-cell plants come on line, the use of dual pipelines between wells and plant will become more common. Saturated brine from the wells will be pumped to the plant and depleted brine pumped back for resaturation. When there is a high point or a substantial difference in elevation between the two sites, much of the pumping energy, at least in one direction, will be expended in lifting the brine. This creates an opportunity to use an energy-recovery turbine to assist at least one of the pumps.

The designer of brine pipelines must consider the possibility of deposition of solids. Solids may arise by settling from a slurry or suspension, by precipitation of salt as the brine cools, or by deposition of hardness compounds (with their reverse solubility characteristics) as the brine is heated.

Brine pipelines are not “long” in the sense that oil or natural gas pipelines are long. While booster stations are rare, they are not unknown. These are usually simple affairs, using a single pump provided with a bypass line containing a check valve, to allow the pipeline to function when the booster pump is out of service.

7.4. THE ROLE OF BRINE PURIFICATION

Impurities in brine affect electrode reaction kinetics, cell performance, the condition of some cell components, and product quality. Treatment of brine to remove these impurities has always been an essential and economically significant part of chlor-alkali technology. The brine system typically has accounted for 15% or more of the total capital cost of a plant and 5–7% of its operating cost. The adoption of membrane cells has made brine specifications more stringent and increased the complexity and cost of the treatment process. Brine purification therefore is vital to good electrolyzer performance. This section considers the effects of various impurities in all types of electrolyzer and the fundamentals of the techniques used for their control. Section 7.5 covers the practical details of the various brine purification operations.

7.4.1. *Composition of Salts and Brines*

The salt used by most chlor-alkali producers falls into the categories of rock salt and solar salt. The former is recovered from underground deposits by conventional mining and by solution mining, in which water or weak brine is pumped into an underground deposit to dissolve the salt. Solar salt results when saline water evaporates past the point of saturation in open ponds. Rock salt is the common supply in Europe and North America. Imported solar salt is the predominant supply in Japan and in many other parts of the world. There are other sources that are relatively minor in the industry as a whole but locally quite important. Saudi Arabia, for example, uses salt dredged from near-surface deposits found in low-lying areas.

Potassium chloride ores usually are mixed salts, and so a certain amount of refining is often a part of the KCl extraction process. As a result, the material supplied to the chlor-alkali industry usually is of higher quality than the raw NaCl. Other grades of NaCl, however, are available that have also been treated to a higher purity before sale.

With this wide variety of sources, one would expect to find great variations in the type and abundance of impurities in salt. Still, there are a number of useful generalizations. Table 7.6 shows that calcium, magnesium, and sulfate ions are the other major components of seawater and therefore the major impurities in most salts [63], and the removal or control of these constituents is a primary objective of the brine purification process. The most widespread impurity in NaCl deposits is CaSO_4 . Magnesium compounds, and to a lesser extent iron compounds, also are present in most natural salts. Oxides of silicon and aluminum are also found, as well as traces of other metals and sometimes anions such as iodide. The importance of these impurities depends greatly on the type of cell in use, and the methods used for purification of brine reflect all the above factors.

7.4.2. *Effects of Brine Impurities*

The products of the electrochemical reactions in a chlor-alkali cell are the same as the electrode products in a chlorate cell. Thus, both types of cell generate chlorine at the anode and hydrogen and hydroxyl ions at the cathode. In the chlorate cell, the products

TABLE 7.6. Some Constituents of Seawater and their Concentrations

Element	Concentration (mg L ⁻¹)
Chlorine	18980
Sodium	10561
Magnesium	1272
Sulfur	884
Calcium	400
Potassium	380
Bromine	65
Carbon	28
Strontium	13
Boron	4.6
Lithium	0.1
Iodine	0.05
Copper	0.003
Silver	0.0003
Gold	0.000006

of the electrode reactions, chlorine and hydroxyl ions, are allowed to react to form hypochlorite and, ultimately, chlorate ions. The design of chlorine cells must prevent this reaction. Diaphragm and membrane cells do so by inserting a physical barrier between the two electrodes. Mercury cells modify the cathode process from the electrolysis of water to the reduction and capture of the alkali metal ion by amalgamation, and they also remove hydrogen and caustic generation to a physically attached amalgam decomposer.

In every case, the separator, whether diaphragm, membrane, or mercury, makes the electrolytic process sensitive to impurities. Because the separators work in different ways, the effects of impurities differ among the three types of cell, each with its own requirements. Since both diaphragm and membrane cells depend on interelectrode barriers, their mechanisms of damage are similar. The impurities of most concern are the Group 2 cations, especially magnesium and calcium. Mercury cells rely on different cathode chemistry, and so a different set of impurities, primarily trace metals, is of concern. Anionic impurities are for the most part less harmful. Sulfate and chlorate concentrations, especially in mercury-cell plants, often reach high levels in brine recycle loops, to the point where they reduce the solubility of the chloride. Sulfate, especially, can also have significant effects on cell performance at lower concentrations. In older cells, high concentrations of sulfate increased the rate of wear of graphite anodes, and in diaphragm cells they can reduce the current efficiency by enhancing the generation of oxygen [64]. In membrane cells, sulfate at relatively low concentrations can destroy the membranes.

7.4.2.1. Mercury Cells

Success of the mercury cell depends on two factors:

1. high hydrogen overvoltage on the cathode, so that charge transfer of the alkali metal ion can proceed at a high current density with very little evolution of hydrogen;

2. fast (and hence with very low overvoltage) discharge of Na^+ or K^+ on mercury, which is diffusion-controlled on both sides of the amalgam–solution interface.

Amalgam formation is greatly affected if these conditions are disturbed by impurities or changes in operating conditions. In the 1950s, Angel and coworkers published a series of papers on the amalgam decomposition reaction in concentrated brine [65–67] and electrolysis at an amalgam cathode [68–70]. In their amalgam decomposition experiments, very little hydrogen was liberated from sodium amalgam in pure NaCl solution or in the presence of iron, calcium, or magnesium. A trace of vanadium catalyzed the decomposition, and the reaction rate increased with vanadium concentration. Similar effects, usually less pronounced, occurred with other metals. Foreign anions such as sulfate, bromide, iodide, fluoride, and chlorate had no deleterious effect. Certain neutral and other anionic impurities actually had some benefit by mitigating the action of vanadium. The mechanism of this seems to involve complex formation (e.g., phosphate) or the adsorption of vanadium onto colloidal particles (e.g., silica).

During electrolysis, vanadium again was extremely harmful. Concentrations less than 2 mgpl completely stopped the formation of amalgam [68]. As another example, 0.1 ppm vanadium in the brine can reduce the current efficiency by 0.7%. The fact that there are many synergistic combinations of metals puts a particular burden on the brine purification process [69]. While vanadium has pronounced effects, it is less of a practical problem now than it was at the time of the work reported here. Petrocoke was the base for the graphite used in anode manufacture and therefore the primary source of vanadium contamination. With the adoption of dimensionally stable metal anodes, vanadium contamination became a less frequent and a less serious problem.

The following classification of the effects of impurities was published by MacMullin [71]:

<i>Metallic impurities</i>	
Very harmful	V, Mo, Cr, Ti, Ta, (Mg + Fe)
Moderately harmful	Ni*, Co*, Fe*, W
Slightly harmful	Ca, Ba, Cu*, Al*, Mg*, graphite
No effect	Ag, Pb, Zn, Mn
(*known to act as a promoter)	
<i>Nonmetallic impurities</i>	
No effect	bromide, iodide, fluoride, chlorate, sulfate
Slightly beneficial	borate
Beneficial	silicate, stannate, phosphate

Table 7.7 shows MacMullin's tabulation of the data of Czernotzky [72] for the maximum allowable concentrations of several metallic impurities in the electrolysis of NaCl at 40 A dm⁻² at 80°C with a cell gas containing 0.3% H₂. The table also contains the data of Hass [73] in both NaCl and KCl brines at concentrations of 3M. There is a density factor between the bases for the two sets of data. The MacMullin/Czernotzky data are in mgpl, and Hass's are in ppm by weight. Since part of the effect of these impurities seems to stem from their interference with the amalgamation and dispersion of the alkali metal, soda and potash cells behave differently. There is also a tendency for the effects of

TABLE 7.7. Maximum Allowable Concentrations of Metallic Impurities in Mercury Cells

Impurity	MacMullin	Hass	
		NaCl	KCl
Calcium	100		
Magnesium	1		
Iron	0.3		
Titanium	0.1		
Molybdenum	0.001–0.01	0.01	0.01
Chromium	0.001–0.01	0.02	0.002
Vanadium	0.0001–0.01	0.03	0.03
Tungsten		0.09	0.01
Cobalt		0.1	0.06
Germanium		0.2	0.2
Lead		1.4	1
Antimony		6	0.6
Arsenic		6	0.8

Source: Data of MacMullin [71] and Hass [73].

impurities to be greater at higher amalgam concentrations [74]. Hass obtained his data in controlled laboratory experiments with a small mercury-drop electrode exposed to 3M solutions of NaCl or KCl. In most cases, they indicate that KCl cells are more sensitive to impurities. More recently, Colón [75] reviewed the literature and published a more extensive list, summarized in Table 7.8. The criterion used by most researchers to fix the allowable concentration of an impurity was the observed onset of hydrogen formation. This is more restrictive but less precise than Czernotsky's use of 0.3% hydrogen in the gas. Colón points out that the techniques and conditions varied widely, and so did the results. He then reports the lowest concentration limit found for each element listed without noting the experimental conditions that applied, such as the current density, the temperature, and the medium. All units in the table are in ppm, and data that appear in parentheses indicate the presence of synergistic effects. The reader should remember the inconsistencies pointed out by Colón and not regard his table as a consistent set of data.

In this table, there are examples in which NaCl cells appear to be the more sensitive. However, the data on a given element may not come from the same source for the two different electrolytes. With the variability in the reported results and the many examples of synergism, it is best to make a more careful examination of the literature, and not to rely precisely on any one table but to base conclusions on tests with the brine actually used in a plant.

Many metals other than the alkalis can amalgamate with mercury. Many of these amalgams do not completely break down in the decomposers. They are of limited solubility and eventually will build up in concentration to the point where they precipitate as mercury "butter." This interferes with the circulation of mercury and forces the operator to increase the gap between electrodes. The wider gap causes the cell voltage and power demand to increase. Removal of butter is part of the regular program with mercury cells. It can be removed physically or, sometimes, by washing with acid.

TABLE 7.8. Impurity Concentrations at Onset of Hydrogen Generation

Element	In NaCl brine	In KCl brine
Aluminum	0.1	4
Antimony	3	0.6
Arsenic	6	7.5
Beryllium	3.5	3
Calcium	10	—
Chromium	0.01	0.003
Cobalt	0.1 (0.02)	0.06
Copper	(0.02)	—
Germanium	0.07	0.15
Iron	0.1 (0.02)	—
Magnesium	1	0.04
Manganese	(2.5)	—
Molybdenum	0.01	0.01
Nickel	0.06 (0.02)	0.59
Osmium	1	—
Palladium	10	0.98
Platinum	0.01	—
Rhenium	1	—
Rhodium	1	—
Ruthenium	10	—
Tantalum	0.25	18.1
Titanium	0.007	0.05
Tungsten	0.09	0.009
Uranium	10	—
Vanadium	0.01	9
Zirconium	90	—

Source: Compiled by Colón [75].

7.4.2.2. Diaphragm Cells. We have seen that impurities in the brine can completely poison a mercury cell by altering amalgam electrochemistry. Diaphragm cells, perhaps the type most forgiving of impurities, are less susceptible to such severe damage by minute quantities of contaminants. The impurity most frequently of concern is hardness, but a cell can continue to operate at reduced efficiency even if the feed brine carries high levels of hardness. Hardness elements in the anolyte may deposit in the diaphragm as they pass through into the catholyte, resulting in a gradual increase in cell voltage. The increased hydraulic resistance of the diaphragm also tends to decrease the brine flow rate. At constant amperage, this can lead to higher conversion of the salt, with lower residual NaCl concentration and higher caustic concentration in the catholyte. The lower salt concentration permits more generation of oxygen at the anodes. The higher concentration of OH^- and the lower flow rate through the diaphragms allow more OH^- to enter the anode chamber, reducing the current efficiency of the cell and producing undesirable byproducts.

In practice, a diaphragm-cell operator varies the difference between the liquid levels in the anolyte and catholyte to keep the flow steady in the face of changes in

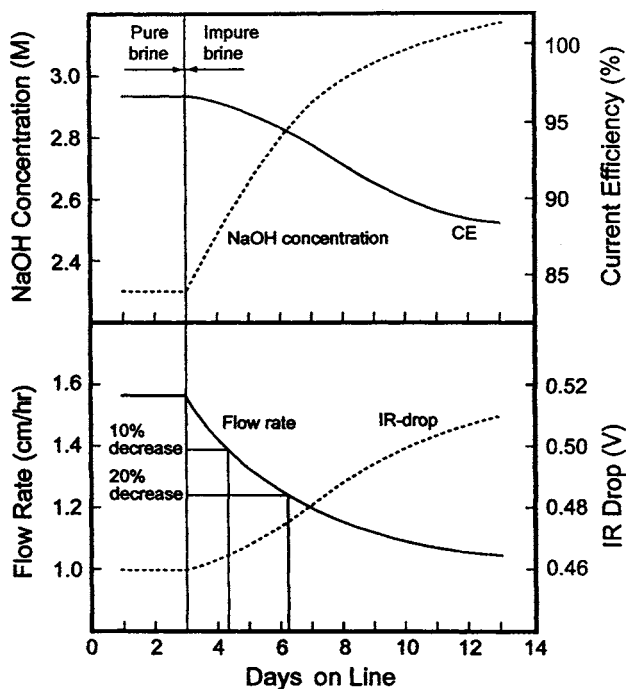


FIGURE 7.30. Effects of addition of magnesium to brine on diaphragm-cell performance; current density 10 A dm^{-2} ; Mg^{2+} concentration 100 mg L^{-1} . (Reproduced by permission of The Electrochemical Society, Inc.)

the diaphragm's hydraulic resistance. When the catholyte level becomes too low, the cell is taken out of the circuit for replacement of the diaphragm.

The transport of OH^- through the porous diaphragm is by diffusion, migration, and hydraulic flow. Diaphragm plugging affects all these factors significantly, and the operating parameters that determine cell performance change. Hine and coworkers [76] studied the effects of brine impurities on diaphragm cell performance in a laboratory cell with a modified asbestos diaphragm. Figure 7.30 shows the results obtained during the electrolysis of brine containing 100 gpl magnesium at a current density of 10 A dm^{-2} . After several days of unchanged operation with purified brine, switching to doped brine caused a decrease in anolyte flow that was due to plugging of the diaphragm. This allowed the caustic strength in the catholyte to increase. Other data showed that the IR drop increased and the current efficiency decreased. Brine doped with calcium or with other concentrations of magnesium gave similar results.

At lower concentrations, the effects of magnesium are delayed. Figure 7.31A shows the time required to produce a given effect as a function of magnesium content from 10 to 100 mgpl at three different current densities. At each current density, a logarithmic plot of time vs magnesium concentration fits a line with a slope of -1 . Such a line represents a constant amount of magnesium transported from the anolyte into the diaphragm. The damage to the diaphragm therefore is related only to the amount of magnesium that enters

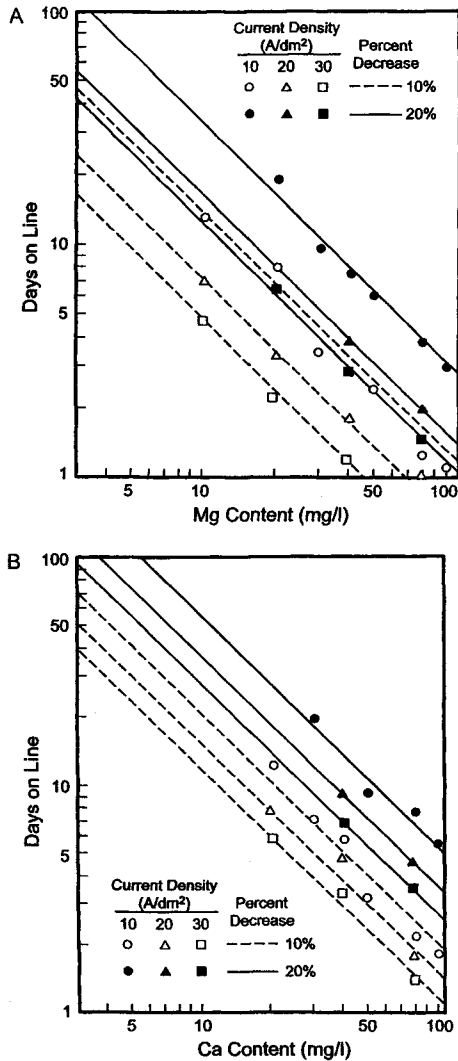


FIGURE 7.31. Effects of current density and impurity concentrations on rate of reduction of anolyte flow. (Reproduced by permission of The Electrochemical Society, Inc.)

it. Table 7.9 makes this clearer by listing the product of current density and operating time for the runs made at 10 mgpl. Only the time required at the highest current density to reduce the flow by 20% is somewhat out of line.

Figure 7.31B shows similar results for brine doped with calcium. The same effects occur, but Table 7.9 shows that the product of current density and time is higher at higher current densities. This suggests a different mechanism of plugging, with the capture of calcium by the diaphragm becoming less efficient at high flux. Figure 7.32 sheds more light on the subject. It shows the distribution of magnesium and calcium deposits in and

TABLE 7.9. Reduction of Brine Flow Rate by Deposition of Magnesium and Calcium Impurities

Impurity	Reduction in flow (%)	Current density ($A\ dm^{-2}$) (<i>i</i>)	Days on line (<i>t</i>)	<i>i</i> × <i>t</i>	
Magnesium	10	10	13.5	135	
		20	7.0	140	
		30	4.7	141	
				138.7 avg.	
	20	10	32.3	323	
		20	16.1	322	
		30	12.0	360	
				335 avg.	
	Calcium	10	10	20.5	205
20			15.2	304	
30			11.7	531	
20		10	53.0	530	
		20	36.0	720	
		30	27.0	810	

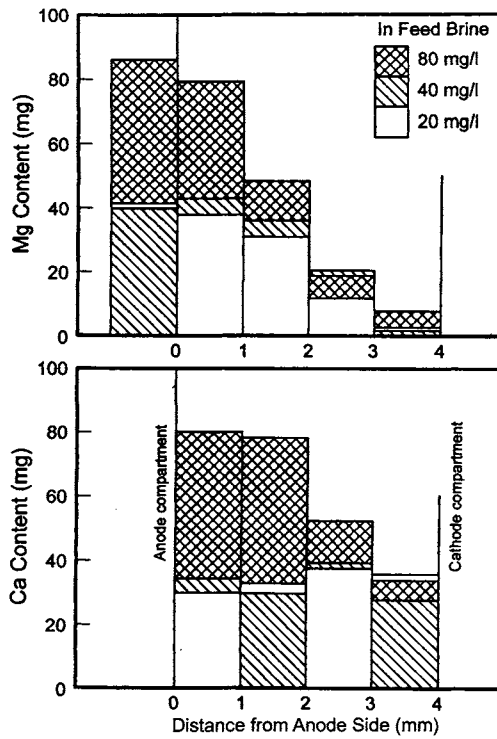


FIGURE 7.32. Distribution of magnesium and calcium precipitates in diaphragm. Diameter 50 mm; thickness 4 mm. (Reproduced by permission of The Electrochemical Society, Inc.)

on the diaphragm. Magnesium precipitates at the surface and in the anode side of the diaphragm. Calcium, on the other hand, precipitates more uniformly throughout the mat. Some fraction of it, presumably, travels through the diaphragm without being captured. This fraction should increase at higher ionic flux, accounting for the results observed in Table 7.9. The one stray point in the magnesium data suggests the same effect, or it may simply reflect experimental error.

7.4.2.3. Membrane Cells. Membrane cells are not subject to the electrode poisoning suffered by mercury cells. They are in this respect similar to diaphragm cells, but the membranes themselves are exceptionally sensitive to brine impurities [77], and brine specifications for membrane cells are more onerous. Section 4.8 discussed the structure and performance of membranes and explained the reasons for this sensitivity. Certain impurities can affect cell performance and the service life of the membranes even when present at ppb levels. Their concentrations in the brine must be rigidly controlled. When this is done successfully and ultra-pure brine is consistently available, service life can be quite long, and test cells have operated well for up to 9 years [78].

Magnesium and calcium ions combine with hydroxide and precipitate on the anode side and in the body of the membrane. Other ions, including aluminate, silicate, and sulfate, may form insoluble compounds in the membrane. These undesirables increase the IR drop through the membrane, reduce its selectivity, interfere with water transport, and lead to mechanical failure and other problems. Because high-performance membranes have composite structures, impurities may have different effects depending upon the layer of the membrane in which they deposit. The anode layer, which is the thicker and more permeable, exists to provide strength to the membrane without imposing much voltage drop. The catholyte layer is more selective and is built to reject the passage of hydroxide ions. It is less permeable and has greater resistivity. Since the catholyte layer determines the current efficiency of a membrane, deposits in that layer tend to impair the selectivity of the membrane as well as to increase its electrical resistance. Deposits in the anolyte layer tend to affect only the electrical resistance.

Magnesium and calcium behave in much the same way as they do in diaphragms, with Mg precipitating first and closer to the anode side, while Ca precipitates later and in the cathode layer. As a result, particles of $Mg(OH)_2$ tend not to interfere with selectivity and so have little effect on current efficiency. By blocking passage through the anode layer, however, they do increase the voltage drop through the membrane. $Ca(OH)_2$, on the other hand, interferes with operation of the cathode layer and so lowers the current efficiency. Nickel and iron behave like magnesium. Strontium, barium, sulfate, aluminum, and silica behave more like calcium.

Brine impurities can also affect the anode coating. Barium sulfate, for example, precipitates on or in the coating and can destroy its catalytic action. Other ions harmful to the anode coating include lead, manganese, and fluoride.

Table 7.10 summarizes the important impurities, their effects, the tolerable limits, and methods of control. Much of the table is based on a DuPont product bulletin [79] and repeats the information found in Section 4.8.6 and the Appendix to Section 4.8. In order to give a more comprehensive idea of the controls required by the chlor-alkali process, it is supplemented here with information pertaining to diaphragm and

TABLE 7.10. Brine Impurities—Sources, Effects, and Mitigation

Species	Source(s)	Action	Effect(s)	Mitigation
Hydrogen ion	Acidification of brine	At pH < 2, can convert active group on carboxylate membrane into nonconductive -COOH	Increases cell voltage; can make membrane inoperable	Limitation on acid addition rate; rapid dispersal of brine in cell
Hydroxyl ion	Chemical treatment of brine; back-migration from catholyte	Reacts with chlorine in anolyte to form undesirable byproducts in gas and liquid	Loss of anode current efficiency; lower-quality chlorine gas	Limitation on caustic addition; brine acidification; maintenance of high cathode CE; cell renewal
Alkali metal	Salt; water	Wrong alkali metal ion has little effect on electrolysis but contaminates product caustic	Lower-quality product	Selection of salt; better potash water in decomposers and ion-exchange regeneration
Magnesium	Salt	Precipitates in diaphragm or on anolyte side of membrane	Increases operating voltage; reduces diaphragm-cell current efficiency; promotes hydrogen formation on mercury cathode	Selection of salt; chemical treatment; ion exchange
Calcium	Salt; sulfate precipitation or suppression	Precipitates in diaphragm or near catholyte side of membrane	Reduces current efficiency and increases operating voltage; disrupts membrane	Selection of salt; chemical treatment; ion exchange
Strontium	Salt; impurity in barium chemical	Same as calcium, with higher concentration tolerance	Same as calcium (see above)	Selection of salt; chemical treatment; ion exchange; selection of barium salt or alternative process for sulfate control
Barium	Salt; brine treatment chemical	Same as strontium, with higher concentration tolerance; barium sulfate can damage anodes	Same as calcium, with limited effect; acts synergistically with iodine	Selection of salt; chemical treatment; ion exchange; brine purge; choice of alternative process for sulfate control

Aluminum	Salt; filter aid; transport container; atmosphere	Mostly synergistic effects ^a	<i>a</i>	pH control in dissolving and precipitation; ion exchange; choice of filter aid; choice of salt cars
Carbonate	Chemical treatment of brine	Reacts with chlorine to anolyte to form CO ₂ ; dilutes chlorine gas		Limitation of excess in treatment process; acidification and degassing of feed brine
Organics	Salt; process fluids; returned containers	Various effects on electrodes; foaming		Selection of salt; stripping, filtration, or adsorption of fluids; inspection of returned containers; some destroyed in anolyte without serious effect on cells
Silica	Salt; water; filter aid; atmosphere	Mostly synergistic effects ^b	<i>b</i>	Selection of salt; processing of water through desiccizer; selection of filter aid; covers on open equipment
Nitrogen compounds	Salt; water; drying acid; steam condensate	NCl ₃ forms from nitrogen compounds in brine		Selection of salt or of method of mining; selection or treatment of water; chlorination of brine; addition of process for safe decomposition of NCl ₃ in chlorine
Peroxide	Reducing agent; oxidation of organic residues	Damages ion-exchange resin		Selection of alternative reducing agent; treatment of dechlorinated brine with activated carbon; scavenging by other impurities in brine loop
Sulfate	Salt; reducing agent	Precipitation in membrane near cathode side; in presence of barium, deposits on anode		Many techniques available; see Section 7.5.7

TABLE 7.10. continued

Species	Source (s)	Action	Effect (s)	Mitigation
Free chlorine; hypochlorite	Reaction of chlorine in anolyte	Damages ion-exchange resin; corrodes ferrous equipment and piping; possible corrosion of diaphragm-cell evaporator; damage to membranes at shutdown; dissolves mercury	Allows hardness to break through ion-exchange beds and attack membranes; reduces life of equipment and piping; can damage evaporators and contaminate product; spreads dissolved mercury through system	Dechlorination of depleted brine; treatment of diaphragm cell liquor; automatic flushing of membrane cells upon loss of power
Chlorate	Disproportionation of hypochlorite (see above)	Damages ion-exchange resin under acidic conditions; possible corrosion of diaphragm-cell evaporator	Allows hardness to break through ion-exchange beds and attack membranes; damage to evaporators and contamination of caustic product	Brine purge; destruction in acidic brine; reduction by hydrogenation; catalytic decomposition by nickel deposited on diaphragms
Fluoride	Salt	Corrosion of titanium	Equipment damage; deactivation of anode coating	Selection of salt; brine purge
Bromide	Salt	Contamination of product chlorine	Lower-quality product; accumulation in compressor suction chiller; higher bromate concentration in bleach	Selection of salt; condensation in chlorine processing line; chlorination of brine; use of resistant membrane
Iodide	Salt	Precipitation of sodium paraperiodate (potassium salt not a problem); synergistic effects ^c	Accumulation of very finely divided solids in membrane ^c	Selection of salt; brine purge; chlorination of brine; ion exchange
Iron	Salt; water; corrosion; anticaking agent (see YPS below)	Precipitation in anolyte	Coating of membrane or diaphragm; plugging of membrane, diaphragm, or anolyte compartment	Selection of salt; treatment of water; chemical treatment of brine; ion exchange; use of noncorrosive materials

YPS (yellow prussiate of soda) $\text{Na}_4[\text{Fe}(\text{CN})_6]$	Anticaking agent in processed salt	Iron oxidized to insoluble ferric form in anolyte (see above—Iron)	See above—Iron. When primary treatment is absent, oxidized form can penetrate membrane, then precipitate	Selection of salt; salt washing
Mercury	Amalgam cells (when operated in parallel with other types of cell)	Allows spread of mercury pollution; deposits in ion-exchange resin; deposits on cathodes	Reduces capacity of ion-exchange resin for hardness; deactivates cathode coating and so increases voltage	Operation of separate brine circuits; treatment of brine to remove dissolved mercury
Nickel	Salt; cathodes; piping and equipment	Precipitates in membranes; deposits on cathodes	Increases voltage; reduces current efficiency	Brine purge; ion exchange
Mn, V, etc.	Salt; corrosion; graphite anodes	Reduction of hydrogen overvoltage on mercury cathode	Production of hydrogen at cathode—dangerous concentrations in chlorine gas	Selection of salt; selection of materials; use of metal anodes
Other heavy metals	Salt; corrosion	Same as Mn or V, with reduced effect		
Suspended solids	Salt sludge; brine treatment sludge; filter leakage; atmosphere	Plugging of equipment, membranes, ion-exchange resin, or diaphragms		Efficient coagulation and high-quality filtration; covering or siting of open equipment

Notes:

^a Aluminum precipitates as the hydroxide in near-neutral brine. It also combines with silica to form aluminum silicates and calcium aluminosilicates.

^b Silica is most dangerous in combination with other species that can form insoluble silicates. Any specification for silica presupposes that these other species (e.g., calcium and aluminum) also are under control. Because of its mechanism of transport of silica, its concentration within the membrane actually goes through a maximum (Section 4.8.5).

^c Barium iodide also can precipitate if the combination of the two elements is excessive. Some newly developed membranes have enhanced resistance to damage by iodine (Section 4.8.5). precipitates are extremely fine and a certain amount of deposit can be tolerated without deterioration of membrane performance.

mercury cells as well. The table also considers the effects of certain impurities on the composition of the chlorine gas leaving the cells. This can have important effects on the chlorine and hydrogen processing operations.

Simple mathematics helps to explain the great sensitivity of membrane cells to impurities and operating conditions. Adjusting previous calculations [80], we find that a square meter of a membrane that operates for 3 years under a current density of 4 kA m^{-2} will pass about 360 GC and move 350 tons of sodium ion and water. That square meter may weigh about 400 g, and the deposit of 1% of its weight can damage it severely. Choosing a number slightly less than 1% of its weight can damage it severely. Choosing a number slightly less than 1% of the membrane weight, we can tolerate the deposit of 3.5 g. This represents 10 ppb in the fluid that passes through the membrane. It should be no surprise to find brine specifications of the same order of magnitude.

7.4.2.4. Precipitation Patterns of Metal Hydroxides. The precipitation patterns of calcium and magnesium in diaphragm and membrane cells reflect the different solubilities of their hydroxides. By order of magnitude, their respective solubility products in water are 10^{-6} and 10^{-11} . Since anolytes are mildly acidic and catholytes very strongly basic, pH varies with position across diaphragms and membranes. $\text{Mg}(\text{OH})_2$, with its lower solubility product, precipitates at a lower pH than does $\text{Ca}(\text{OH})_2$. For this reason, magnesium precipitates are found closer to the anode side. The trend continues with strontium and barium. Their hydroxide precipitates form even closer to the cathode. Their effects on membrane cells therefore resemble those of calcium more than those of magnesium.

We can extend this logic to the case of iron. In the oxidizing atmosphere of the anolyte, the ions to consider are Fe^{3+} . With its very low solubility product (10^{-38}), $\text{Fe}(\text{OH})_3$ is quite insoluble and precipitates at a relatively low pH. Accordingly, there are many reports of $\text{Fe}(\text{OH})_3$ precipitation within the anolyte. In membrane cells, deposits can form on the anolyte face of the membrane. Iron impurities in the catholyte also can cause deposits to form on the anode side. In the catholyte, iron exists as an anion, HFeO_2^- . Like the OH^- ion, this travels through the membrane by diffusion and migration. The HFeO_2^- species oxidizes to Fe^{3+} at the anolyte/membrane interface and precipitates as $\text{Fe}(\text{OH})_3$.

Iron is therefore considered less harmful than calcium or magnesium, and its specified concentration limit in the brine is set higher. However, van der Stegen and Breuning [81] report a case in which the continued use of brine containing 200 ppb Fe adversely affected cell voltage. Understanding this phenomenon requires some knowledge of the pH profile in a cell. The pH at any section depends on the rates of transport of protons from the anolyte toward the cathode and of hydroxyl ions from the catholyte toward the anode. Ogata *et al.* [82] showed that under most conditions the pH near the anolyte surface of the membrane is between 7 and 9. This is determined in part by the type of membrane used. It also depends on operating conditions and the health of the membranes. The operating conditions change the pH profile by changing the flux of H^+ or OH^- ions. Thus, an increase in anolyte strength or acidity reduces the pH at the surface, while an increase in catholyte strength or membrane current density increases it. The state of the membrane influences the pH profile if the current efficiency changes.

A decline in current efficiency by definition is an increase in the OH^- flux. This causes the surface pH to increase.

These considerations are important to the action of iron because of its ability to form complex ions with hydroxyl. At low pH, hydrolysis is incomplete and $\text{Fe}(\text{OH})_2^{2+}$ and $\text{Fe}(\text{OH})_2^+$ exist. At high pH, ferric ion forms $\text{Fe}(\text{OH})_4^-$ (or $\text{FeO}_2^- \cdot 2\text{H}_2\text{O}$), and the solubility of iron increases. The solubility is at a minimum between pH 5 and pH 10. This range includes the normal pH at the membrane interface and explains the lack of penetration by iron. The accumulation of $\text{Fe}(\text{OH})_3$ can raise the cell voltage but does not affect the current efficiency. When the pH profile shifts to allow the interfacial value to drop below five, ions can penetrate the membrane and deposit within the membrane but closer to the anode side.

When iron is present in the brine as Fe^{2+} or Fe^{3+} , it is possible to keep its concentration in the cells under control by ion exchange. The use of high-grade purified salts containing ferrocyanide anticaking agents presents a special problem. Brines prepared from such salts, as in the case reported by van der Stegen and Breuning [81], often do not go through a chemical treatment process but rely on the ion-exchange system to remove multivalent metals. The iron, however, being present as a complex anion, flows through ion exchange and into the cells, where it oxidizes to Fe^{3+} in concentrations above the specified limit. Prior decomposition of the ferrocyanide complex and filtering of the iron hydroxide from the brine are proven technology.

7.5. THE BRINE TREATMENT PROCESS

7.5.1. Brine Specifications and Treatment Techniques

This section discusses the processes used to bring brine within the specifications imposed by the various cell technologies, as summarized in Section 4.8.6. Brine specifications depend strongly on the type of cell being used, because the effects of the various impurities, discussed in Section 7.5.2, often are specific to the type of cell. This situation is reflected in differences in the approach to brine treatment. The sections that follow describe the steps in a typical process, and these are shown in the simple diagram in Fig. 7.33, where the process steps are referred to the relevant section of the text.

Major impurities (calcium, magnesium, and other metals) are removed from solution by precipitation (Section 7.5.2). The solids are separated from the treated brine by settling (Section 7.5.3) and one or two stages of filtration (Section 7.5.4). The precipitated solids are removed from the settler for disposal, and the residual brine contains a few ppm of hardness. This is not acceptable in membrane cells. An ion-exchange process therefore follows in that case (Section 7.5.5). The fully treated brine then is ready for use in the cells but is alkaline and contains carbonate. Most plants add acid to the brine in order to improve cell operation and chlorine quality, and this is the subject of Section 7.5.6.

Other contaminants found in brine as produced include sulfate and a group of less common impurities that require treatment in some plants. Finally, brine treatment must deal with certain byproducts of cell operation that must be removed from brine recycle systems. These include dissolved chlorine (hypochlorite) and chlorate. The latter forms

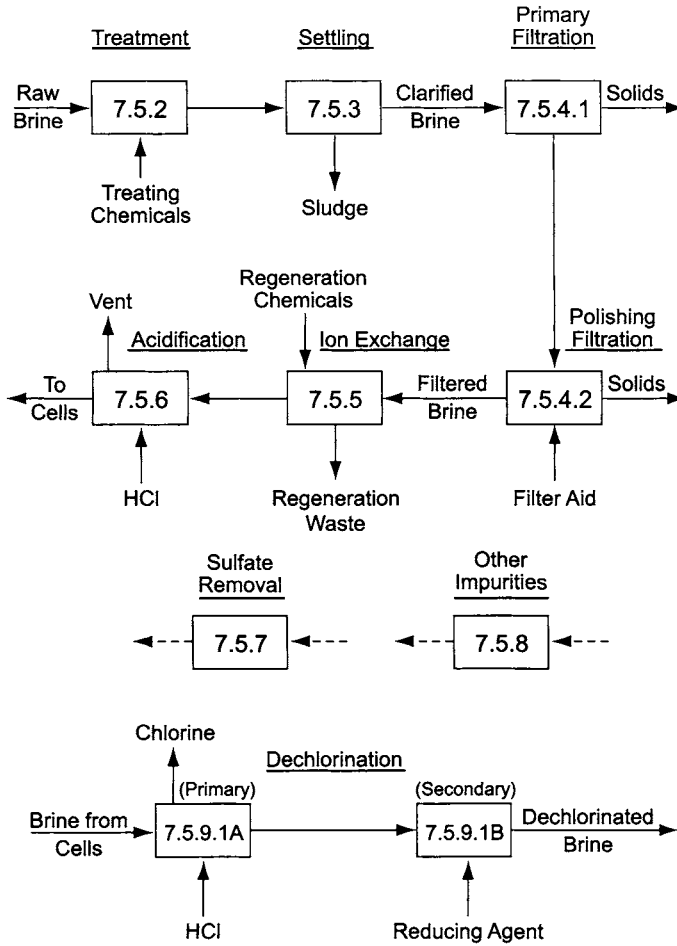


FIGURE 7.33. Guide to brine treatment processes. Basis: membrane cells; numbers in boxes correspond to sections in text.

by reaction of chlorine with any alkalinity present in the anolyte. Control of sulfate is a complex issue because of the many techniques that are available and because of the fact that it can be applied at any of several points in the process. Section 7.5.7 is dedicated to this subject. Section 7.5.8 discusses control and removal of the less common contaminants referred to above. Section 7.5.9 covers brine dechlorination and the conversion of chlorate ions back to chloride.

Each type of cell has its own requirements. Diaphragm cells are perhaps the most forgiving of impurities. While mercury cells can tolerate a higher total concentration because of their lesser sensitivity to the major impurities, they are susceptible to damage by small quantities of certain heavy metals. Membrane cells have the most exacting brine specification and are distinguished from the others by their very low hardness specification.

7.5.2. Chemical Treatment

The first step in brine purification is chemical treatment to remove certain impurities. The elements of hardness (calcium and magnesium) must be removed, along with iron and heavy metals. This is done by precipitation, adding a source of carbonate ion to remove calcium and a source of hydroxide ion to remove the other metals. Sulfate ion also can be removed by precipitation, using either calcium or barium ion. Precipitation processes cannot usefully be considered in isolation. The nature of the solids formed in this way determines how they will behave in the later processes that are designed for their physical removal. The subsections that follow therefore describe in a general way the flow behavior and settling rates of precipitated particles. Later sections of the chapter cover the details of sedimentation and filtration of the solids.

The reader who hopes to see a well-developed technical discussion of brine treatment technology that is based on first principles and explains unequivocally how a system should be designed and operated is doomed to disappointment. The following characteristics of treatment processes help to account for this situation:

1. The quality of brine/salt supplies varies over time, and in particular instantaneous values of the calcium/magnesium ratio can change quickly.
2. The quality of process water can fluctuate with the seasons or change rapidly after rainfall.
3. Outside contamination of the supply is always a possibility.
4. Particles of salt can be degraded by handling, causing variations in the output of a dissolver.
5. Close control of the process, with rapid response to variations in the feedstock, is impracticable. Real-time analytical data are hard to obtain, and the best process design creates dead time that makes simple feedback control difficult.
6. Particle formation during precipitation, which determines success in downstream processes, is a matter of surface chemistry. This is difficult to characterize in any case, and it can be profoundly altered by trace impurities. The presence of unmeasured trace impurities can cause brines with identical analyses to behave very differently in a precipitator.
7. Plant operation can introduce impurities that vary in nature and quantity. Sources are corrosion anywhere in the brine/anolyte process and foreign materials used in certain equipment (lubricants, packing, gaskets, etc.).

Careful study of the brine intended for use in a given plant can result in a nearly optimal design of the treatment process, and tests of the supply are always desirable. Considering the chlor-alkali industry as a whole, however, the extreme variations in raw material quality make it impossible to set down hard and fast rules for the design of a brine treatment plant.

7.5.2.1. Fundamentals of Precipitation. We consider “precipitation” to be the combined process of rendering a substance insoluble and forming solid particles of desirable size and shape. The latter aspect is critical, as it influences the performance of the downstream brine-purification equipment. This section discusses some basic aspects of the relevant reactions, to show that the best practices may differ with the impurity that is to be

removed. This fact is particularly important in chlor-alkali plants, where calcium and magnesium normally are precipitated together. The sequence of discussion is:

1. precipitation of $\text{Mg}(\text{OH})_2$;
2. precipitation of CaCO_3 ;
3. simultaneous precipitation of the two;
4. precipitation of sulfate ion.

7.5.2.1A. Precipitation of Magnesium Hydroxide. Since the solubility product of magnesium hydroxide in water is very small (order of magnitude 10^{-11} at room temperature), magnesium ions in brine are precipitated quite effectively by the addition of alkali:

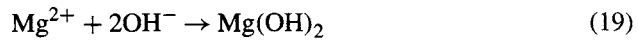


Figure 7.34 shows a pH curve for MgCl_2 titrated with NaOH in concentrated NaCl solution [83]. Addition of a very small amount of NaOH brings the combined ionic concentrations up to the solubility product of $\text{Mg}(\text{OH})_2$. Then, in the relatively flat portion of the curve at about pH 9, the pH changes slowly because the hydroxyl ion precipitates as $\text{Mg}(\text{OH})_2$ as quickly as it is added. Finally, when precipitation is complete, the pH again begins to rise rapidly.

Figure 7.35 shows sedimentation curves for magnesium hydroxide precipitated by NaOH [83]. At first, the phase boundary falls linearly with time, and the concentration of solid in the settling zone remains constant. Later, the slurry concentration begins to increase, and the settling rate declines. In the final stage, settling becomes nearly imperceptible, but the solids concentration in the settled layer continues to increase through compaction. The practical objectives in a sedimentation process are a slope in the early stages that is large in magnitude and a high concentration of solids in the fully settled material. Curve II of Fig. 7.35 is an example that shows these desirable features.

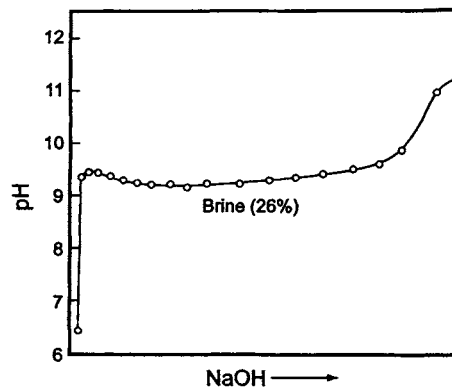
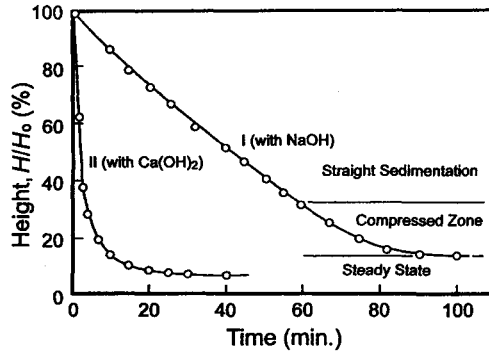
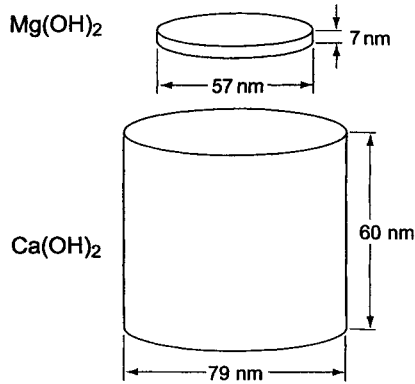


FIGURE 7.34. pH titration curve of MgCl_2 with NaOH . Temp. = 60°C , MgCl_2 conc. = 2 g L^{-1} , solution volume = 200 cm^3 .

FIGURE 7.35. $\text{Mg}(\text{OH})_2$ sedimentation curves.FIGURE 7.36. Particles of $\text{Mg}(\text{OH})_2$ precipitated by NaOH and $\text{Ca}(\text{OH})_2$.

The magnesium hydroxide precipitated by NaOH is translucent and jelly-like. The use of calcium hydroxide, on the other hand, gives a thick, white precipitate. The sedimentation rate of the latter is much higher than that of the former. Figure 7.36 shows the large difference in particle size that helps to explain this difference in the settling behavior [84].

In the chlor-alkali process, unfortunately, precipitation with calcium hydroxide is not a practical approach. NaOH or KOH , whichever is appropriate to the alkali produced in the plant, is used instead. $\text{Mg}(\text{OH})_2$ precipitates in this case are colloidal and coagulate loosely. Figure 7.37 shows the effect of agitation on their settling behavior [85]. Longer times of agitation caused lower settling rates, indicating that the precipitate is easily degraded to form finer particles. This explains the field observation that high-magnesium precipitates settle poorly and that carryover of fine particles from a clarifier can be a serious problem. Particles that have formed and settled are still fragile and tend to break up under agitation. The solid circles and dashed curve in Fig. 7.37 resulted from 15-min agitation of particles that already had been allowed to settle for 40 min. The results are essentially the same as those obtained by mild agitation of a freshly precipitated sample,

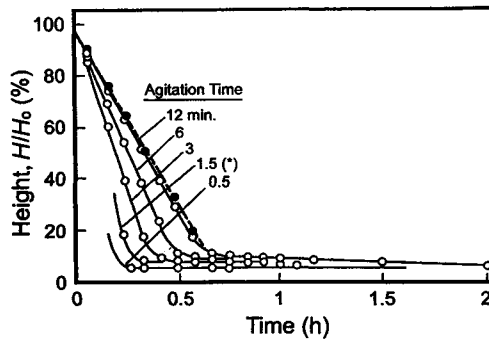


FIGURE 7.37. Effect of agitation on sedimentation curves for $Mg(OH)_2$. Temp. = $27^\circ C$, $MgCl_2$ conc. = 3.3 g L^{-1} , Alkali source = $Ca(OH)_2$. Solid circles refer to sample marked with asterisk after further agitation.

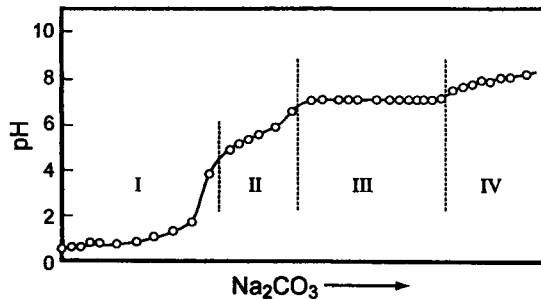


FIGURE 7.38. pH titration curve of $CaCl_2$ in saturated $NaCl$ solution. Temp. = $28^\circ C$, Na_2CO_3 conc. = $0.76M$, Solution volume = 500 cm^3 .

indicating that any growth or agglomeration of particles while settling was reversed by agitation.

Other metallic hydroxides precipitated by $NaOH$ or KOH tend to behave in the same manner as magnesium.

7.5.2.1B. Precipitation of Calcium Carbonate. At the normal temperature of the treatment process, calcium hydroxide is fairly soluble (0.1% w/w), and the addition of alkali to brine does not give a sufficiently low concentration of the calcium ion. Calcium is precipitated instead as the carbonate, according to the simple equation



Calcium carbonate has a solubility product of about 10^{-7} in slightly alkaline solutions. Figure 7.38 shows a titration curve for $CaCl_2$ in $NaCl$ solution when Na_2CO_3 was added to precipitate the calcium ion [86]. There are four distinct regions on a curve. Region I is the neutralization of acid, and Region II is the formation of bicarbonate between pH 5 and 6. In Region III, $CaCO_3$ precipitates when the pH exceeds about

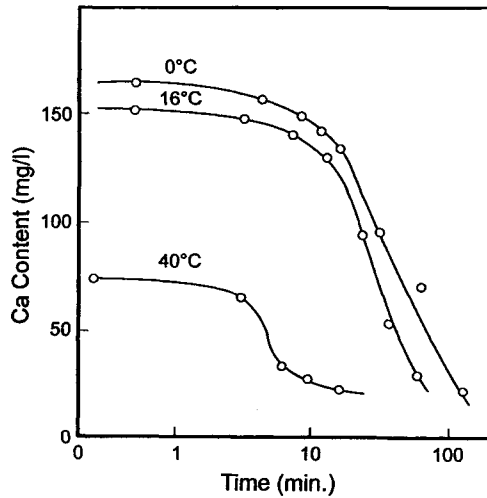


FIGURE 7.39. Effect of temperature on reaction/settling rate in calcium precipitation.

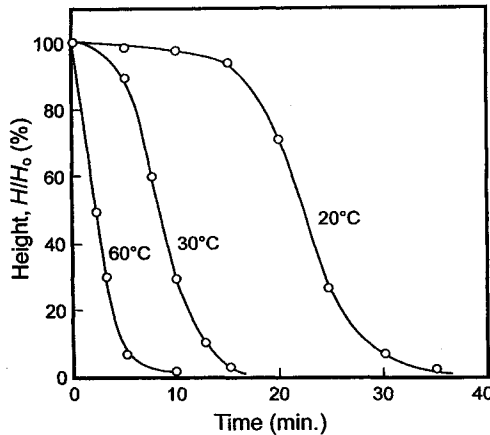


FIGURE 7.40. Sedimentation curves for CaCO_3 in saturated NaCl solution. CaCl_2 conc. = 3 g L^{-1} .

7.0. Region IV shows the increase of pH that begins when precipitation is substantially complete.

Figure 7.39 shows the effect of temperature on the reaction rate. The curves show the calcium content of the clear liquor in a cylinder as a function of time. At low temperature, there is no apparent reaction for several minutes as precipitates begin to form. At the higher temperature (40°C), reaction is much faster. These phenomena are reflected in the sedimentation curves of Fig. 7.40.

An extremely important difference between calcium and magnesium precipitates is in the quality of the particles formed and therefore in their behavior in sedimentation. Calcium carbonate precipitates in general are much denser and sturdier than magnesium

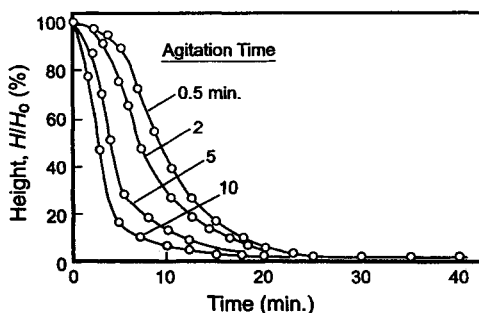


FIGURE 7.41. Effect of agitation on sedimentation of CaCO_3 .

hydroxide precipitates. Figure 7.41 shows the effect of agitation on the settling behavior of CaCO_3 . In contrast to the behavior of magnesium in Fig. 7.37, increased agitation time actually helps the rate of sedimentation. This effect indicates that the particles resist mechanical degradation and that agitation allows continued slow particle growth by promoting contact between the particles and the supersaturated solution. Therefore, given sufficient time for reaction and particle growth, solid CaCO_3 is usually much easier to remove from a suspension than the hydroxides of other metals in the brine.

As explained at the beginning of this section, it is the relatively high solubility of $\text{Ca}(\text{OH})_2$ that accounts for the use of CO_3^{2-} to precipitate calcium. However, the law of mass action tells us that the dissolved concentration of calcium would also be reduced by increasing the excess OH^- concentration and eliminating the use of CO_3^{2-} . There are several reasons not to do this, including:

1. the physical form of the precipitate; the advantages of the denser CaCO_3 particles in the solids-removal processes would be lost;
2. the effect on the solubility of certain heavier metals; the introduction to Section 7.5.8 will show that the solubility of oxygenated anionic forms of some metals increases with pH.

These disadvantages can also occur along with the use of carbonate if the excess caustic concentration is too high (say, $\text{pH} > 12$). Heavy-metal solubilities will increase, and both CaCO_3 and $\text{Ca}(\text{OH})_2$ may precipitate. Formation of the latter is a slow process that may not be complete within the bounds of the chemical treatment system. Solids then will continue to form and be deposited in other sections of the plant, leading to various operating problems. This is an example of postprecipitation, which is mentioned again in Section 7.5.2.2C.

7.5.2.1C. Simultaneous Precipitation of Calcium and Magnesium. Precipitated CaCO_3 , as explained in the preceding section, typically settles much more readily than does precipitated $\text{Mg}(\text{OH})_2$. In practice, raw brine contains both impurities and the two precipitate together. The colloidal magnesium hydroxide can in this case occlude heavy CaCO_3 precipitates. When the ratio of calcium to magnesium is sufficiently high and the precipitation process is operated correctly to produce composite particles with good characteristics, the end result is a precipitate that settles at a relatively high rate, leaving a

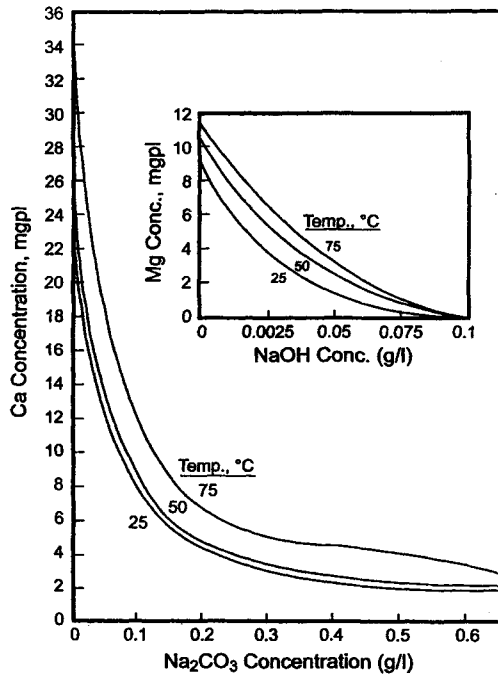


FIGURE 7.42. Residual concentrations of metals vs excess treat chemical concentrations.

clear solution behind. Excessive agitation must be avoided, or coagulation of $\text{Mg}(\text{OH})_2$ is disrupted and the rate of sedimentation becomes much lower.

Since the reactions take place in concentrated brine, the solubilities of the precipitated compounds are not the same as in water or very dilute brine. In both cases, they are “salted in”—that is, their solubilities are higher in brine than in water. Increasing the excess amounts of the reagents will reduce the residual concentrations of hardness ions. However, classical mass-action laws do not apply precisely, and this technique, at least in the case of calcium, is less effective than might be expected. Figure 7.42 shows the decline in soluble concentrations with increasing concentrations of the treating agents [87]. The easy convergence of soluble magnesium concentration to zero can be viewed with suspicion when ppm residuals are important.

7.5.2.1D. Precipitation of Sulfates. The chief anionic impurity in brines is sulfate. This can be precipitated along with the metals by adding a source of barium ion to the brine. Except for the addition of another reagent preparation system, there is no fundamental change in the brine treatment system. The new precipitate will add to the solids handling load, and because the system should be designed to operate with a very small excess of barium chemical, more time may be required to complete the precipitation reactions and to allow particle growth.

There are two sources of barium that may be used to precipitate sulfate, BaCO_3 and BaCl_2 . The chloride is usually supplied as the dihydrate, $\text{BaCl}_2 \cdot 2\text{H}_2\text{O}$. This can

be dissolved in water and added as any other solution. BaCO_3 itself is nearly insoluble and must be handled as a slurry. It works only because the solubility of BaSO_4 is even lower. The gradual dissolving of BaCO_3 to maintain a low concentration of Ba^{2+} delays the precipitation reaction even more. Besides its easier handling and metering, BaCl_2 when added to brine reacts faster. Commercial BaCl_2 has the advantage of higher purity and specifically has a lower strontium content. BaCO_3 usually has the important, if not dominant, advantage of lower cost, and it is also a source of the carbonate ion. It can precipitate both calcium and sulfate.

Calcium ions also can precipitate sulfate. Barium is quite toxic and not as readily available as calcium. Barium has the added disadvantage of attacking anode coatings and can destroy their action. Calcium compounds are cheaper on a unit cost basis, but higher excess concentrations are necessary to achieve a given residual sulfate concentration. As a result, calcium precipitation often costs more than barium precipitation [60,88]. Another disadvantage of calcium is the fact that two brine clarifiers are required. The sulfate must be precipitated first; after removal of the precipitate, calcium itself must be removed. It will be seen below that the clarifiers are large pieces of equipment that can dominate the process-plant layout.

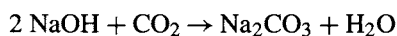
This section is included here to make the discussion of precipitation more nearly complete. There are many other techniques for the control of sulfate in brine, especially in membrane-cell plants. Because not all these come under the heading “brine treatment” and because of its importance, sulfate control is the topic of a separate section (Section 7.5.7). There, the chemistry of calcium sulfate is explored in more detail.

7.5.2.2. Plant Application of Precipitation Technology. This section begins with a discussion of the sources of the major treating chemicals. It then turns to process operating parameters, the design of the reaction tanks, the use of polymeric flocculation aids to improve particle characteristics, and some of the specific considerations necessary when using carbon dioxide gas as the source of the carbonate ion.

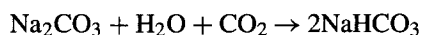
7.5.2.2A. Supply of Treating Chemicals. Carbonate solutions may be prepared from purchased solids or by the absorption on site of CO_2 from the gas phase. In order not to introduce a different kind of contamination, the cation accompanying the carbonate ion will normally be the same as that found in the alkali product of the plant. Na_2CO_3 is used in NaOH plants and K_2CO_3 in KOH plants.

The CO_2 may be purchased or found in combustion offgas. In the latter case, the extent of absorption of other components of the gas becomes important. It is also possible to absorb CO_2 directly in the carbonate reaction tank(s). This is a specialized technique, described in Section 7.5.2.2E.

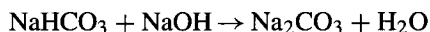
A flue gas might contain about 10% CO_2 ; gas vaporized from the liquid is of course nearly 100% CO_2 . The reaction of CO_2 with a large excess of caustic produces the carbonate:



Continued reaction with CO_2 produces bicarbonate:



This route, properly controlled, is used in the commercial production of sodium bicarbonate. When carbonate is the desired product, as in our application, bicarbonate should be avoided for two reasons. First, it reacts with caustic added later in the brine treatment process, leading to the back-formation of carbonate:



This complicates the control of the brine treatment process. Second, NaHCO_3 is less soluble than the carbonate, and its formation can allow solids to deposit. The problems of bicarbonate formation disappear when the ratio of caustic soda to CO_2 in the combined feed to the process is correctly maintained.

The reaction of CO_2 is exothermic. Standard apparatus for its absorption would be some sort of column. With a stoichiometric flow of caustic liquor through the column, and especially with pure CO_2 gas as the feed, internal temperatures may become excessive. A common practice therefore is to recirculate liquid from the bottom of the column through a cooler.

Solid soda ash is widely available and is most economically supplied in bulk. Large users often also store the solid in bulk. Operators of small chlor-alkali plants may receive and handle packaged solid.

Potassium carbonate is less widely available than its sodium counterpart. Since its manufacture is one of the chief applications of caustic potash, however, many KOH producers will have an internal supply. In years past, the reverse synthesis was practiced, the carbonate being the precursor of KOH through its reaction with hydrated lime.

Carbonates received as solids are dissolved for use in the process. K_2CO_3 is highly soluble, and there are few limitations for its use. Na_2CO_3 has a limited solubility, and more dilute solutions (<10% w/w) are used when at ambient temperatures. Commercial soda ash is supplied in several forms with various bulk densities. "Light" ash has a bulk density of 0.7–0.8. With some reprocessing at the source, a dense grade with bulk densities between 0.85 and about 1.1 can be produced. This is easier to handle and requires less storage volume.

When soda ash is received, it can be stored as a solid or as a slurry. The solid is not difficult to handle and can easily be conveyed, mechanically or pneumatically, to storage hoppers or silos. Few chlor-alkali plants justify, on the basis of rate of consumption alone, delivery by hopper car and large-volume storage. Pneumatic handling systems are then usually cheaper and more flexible. They are more easily sealed against intrusion by water, and dust control is simpler. They are best used when the delivery vehicle can be brought close to the receiving tank, and they are generally considered practical when the amount of soda ash to be handled is less than 10,000 tons a year, a number exceeded in very few chlor-alkali plants [89]. Figure 7.43 shows one of the more complicated arrangements, involving a pull–push system. This uses a collector/blow tank that alternately pulls material from the source and transfers it under pressure to the storage vessel. It can

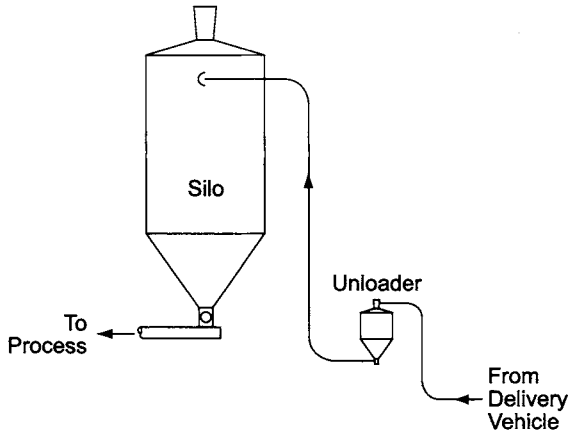


FIGURE 7.43. Pull-push conveying of soda ash.

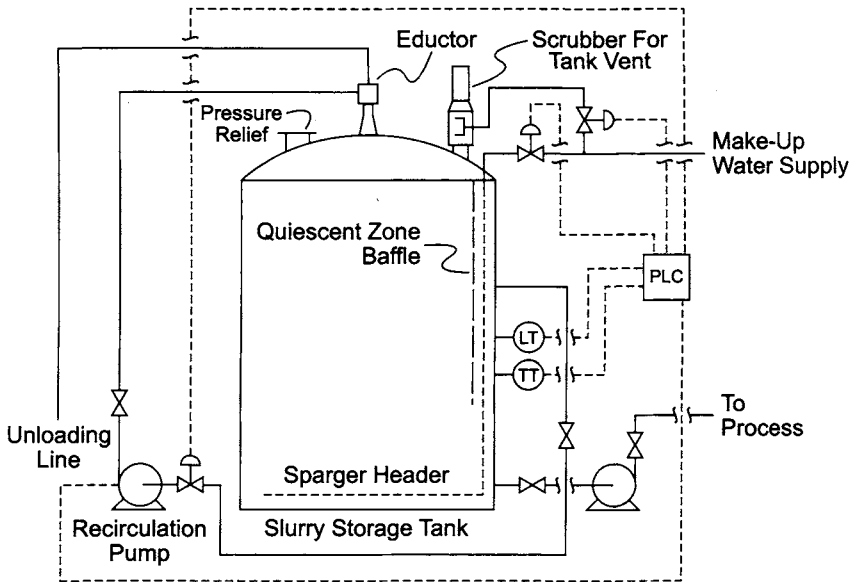


FIGURE 7.44. Storage of soda ash as slurry. (With permission of FMC Corporation.)

transport material over longer distances than simpler arrangements can, and it is included here as a general example of solids unloading.

Slurry storage is in equipment especially designed for the service. Designs and technical service are available from suppliers. Figure 7.44 shows a typical arrangement. The soda ash, unloaded pneumatically, meets a stream of water in the contactor at the top of the tank. Clear solution from behind a baffle in the tank supplies part of the stream to make the wetting of the particles more efficient. Solution transfer to the process is also from behind the baffle. A scrubber for the air used to unload the soda ash is also required.

This is mounted on top of the tank and is fed with clean, heated water. Makeup water to a slurry storage vessel enters the bed through a bottom sparger system. The water should be soft in order to avoid precipitation of hardness by the carbonate. Precipitates will foul the bed and eventually require cleanout. The pump provides recycle when the rising water fails to become saturated on a single pass.

Efficient operation of a slurry storage facility requires management of the levels of both the solid and the liquid phases in the tank. For process reasons, the depth of the bed should be sufficient to saturate fresh water. It should also meet inventory criteria. The normal liquid level and the location of the solution offtake nozzle set the maximum height of the bed. During withdrawal operations, the liquid level is constrained only by the location of the overflow. It must be returned to a lower point before accepting a new load of soda ash.

Figure 7.45 is the phase diagram for sodium carbonate and water. Three different hydrates are involved, and there are phase transitions at 32°C and 35.4°C. The solid forms of most interest are the decahydrate (washing soda) and the monohydrate. The diagram shows that the solubility of the monohydrate is nearly thermoneutral. The solubility as Na_2CO_3 is about 33% at 36°C and 31% at 80°C. The inverse solubility prevents crystallization from a solution as it cools during transfer, and soda ash storage in the slurry form is usually as the monohydrate. The temperature in the tank should remain above 43–46°C to prevent transition to the hepta- or decahydrate.

Dissolving soda ash is an exothermic process. Note that hydrate formation itself is also exothermic. This means that heat evolves even during the addition of solid material to a slurry or saturated solution.

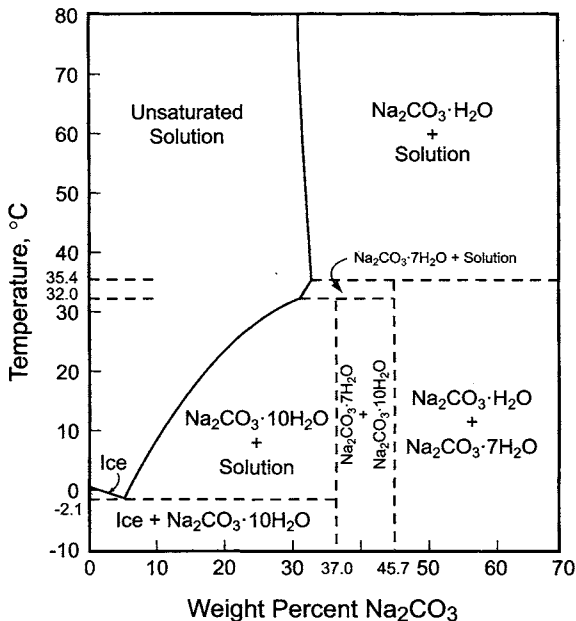


FIGURE 7.45. Sodium carbonate–water phase diagram.

Soda ash when stored in the dry form needs some protection from the atmosphere. It is slightly hygroscopic, and users must remember that the sodium oxide is not fully carbonated. Pickup of both CO_2 and water allows reversion to trona, which is the dihydrate of the sesquicarbonate, $\text{NaHCO}_3 \cdot \text{Na}_2\text{CO}_3 \cdot 2\text{H}_2\text{O}$.

Soda ash is an irritant to eyes, skin, and mucous membranes, and it is classified as a moderate health hazard. Material safety data sheets [90] contain information on protective gear and proper handling.

The source of OH^- for precipitation of magnesium and other metals, except during initial startup, usually is the alkali produced in the plant, either NaOH or KOH . The alkali may also be used for ion-exchange regeneration and scrubbing or neutralization of chlorine from process vents. Once the plant is running, there will be an ample supply of high-purity material for all these cases. The only comments to add here are on the possibilities of using lower-grade material and on special requirements for plant startup.

Where supplying hydroxide value to a process is the chief consideration, as in the treatment of brine to remove magnesium and other metals, and the full composition of the source is not important, the presence of salt in the treating solution is not a major disadvantage. In diaphragm-cell plants, therefore, the cell liquor before evaporation is frequently used instead of caustic soda. In chlorine scrubbing, cell liquor or even caustic purification waste liquor (Section 9.3.4.1) is a possible substitute. Caustic purification waste itself is too dilute for use as a scrubbing solution but can be combined with more concentrated material. This allows it to be put to some constructive use before disposal. The presence of non-caustic components will increase the volume of treating solution required as well as the total amount of dissolved solids to be disposed of from the scrubber system, and it may increase the freezing point of the used scrubber liquor to an undesirable degree. On the other hand, the cost advantages of using something short of the final product may be decisive. Along these lines, when caustic is used in a membrane-cell plant, it should be the cell product and not the evaporated grade.

Many plants will need an external supply of caustic for startup. This must cover commissioning of the cells, run-in of piping and storage systems, commissioning of ion-exchange systems, and perhaps storage of membranes or assembled electrolyzers. Any good-quality commercial material produced in the same type of cell will suffice in most cases, and very often it will be manufactured on the same site as the new plant. When the new plant uses coated cathodes, a situation that has become the standard rather than an exception for membrane cells, there may be special requirements to add to the material specification. Depending on the cell manufacturer and the type of coating used, a low iron content, for example, may be necessary. This requires more careful selection of the startup supply and caustic-handling equipment.

7.5.2.2B. Process Parameters. Figure 7.46 shows a typical chemical treatment process. Solutions of caustic and carbonate are stored in feed tanks. While direct use of Na_2CO_3 slurry is possible, this diagram is based on solution feed. There may also be a preparation tank in which carbonate solutions are made off line. The caustic solution is received from the process, preferably before evaporation in a membrane-cell plant. A separate supply of a diluted solution (20% or less) is often used, and ion-exchange regenerant solutions are another possible source of treat liquor (Section 7.5.5.2B).

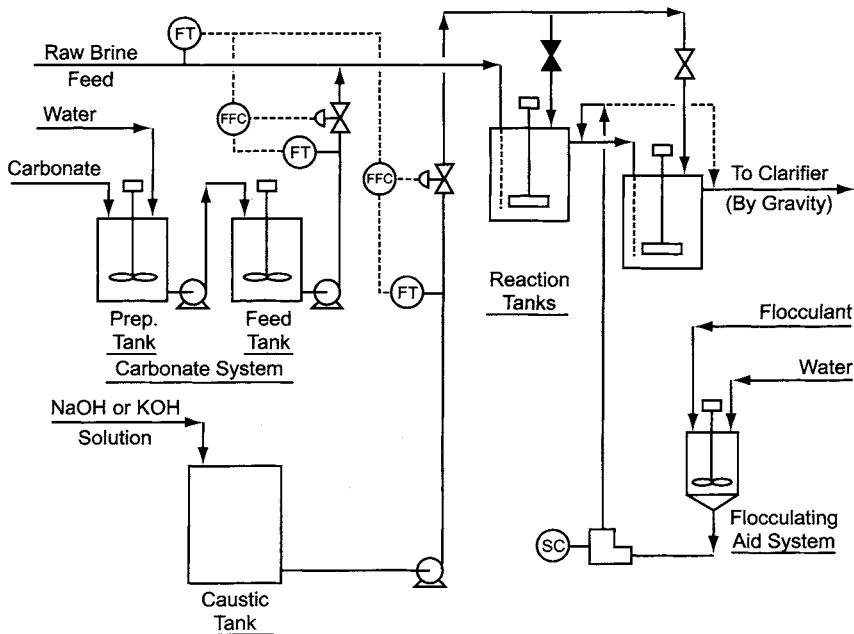


FIGURE 7.46. Flow diagram for chemical treatment process.

The treating chemicals are pumped from storage and blended with the raw brine. The reactions take place in agitated tanks. Multiple tanks, as shown in Fig. 7.46, are the industry standard. Their use reduces bypassing and allows staged addition of the reagents.

With high-quality salts, the quantities of treat chemicals needed to provide the desired excesses often are more than the amounts consumed in the precipitation reactions. The process is monitored by analysis for the reagent concentrations in the treated brine. The analytical techniques are simple, and the usual practice is to have these checks run by the plant operators. Laboratory personnel perform more exhaustive analyses as required.

While it is generally agreed that the carbonate excess should be more than the hydroxide excess, there is no firm agreement over the optimum levels. This reflects the inherent process variability referred to at the beginning of Section 7.5.2. Table 7.11 presents general recommendations from six sources; optimum levels should be determined for each plant and each brine supply. In our working examples of NaCl brine treatment, we use excess concentrations of 0.3 gpl NaOH and 0.6 gpl Na_2CO_3 . None of the sources used in the table should have strong objections to this combination.

The precipitation/particle growth reactions of Eqs. (19) and (20) do not occur with the same speed. Magnesium reacts rapidly, while calcium is slower and requires times on the order of 1 hr for completion. Magnesium also tends to form light, fluffy precipitates, while calcium gives dense, well-formed particles that tend to settle more rapidly. An important part of the art of chemical treatment of brine is the management of the structure of the particles.

When calcium/magnesium ratios are high, the structures of precipitates tend to be more favorable. Fortunately, such high ratios are common and are the rule with rock

TABLE 7.11. Recommendations for Excess Treating Chemical Concentrations

Reference	NaOH Excess	Na ₂ CO ₃ Excess
Anonymous	0.25	0.7
Eimco	0.05–0.1	0.35–0.75
Bommaraju	0.4	0.6
Liederbach	0.1–0.5	0.2–0.5
Sutter	0.1–0.3	0.15–0.5
Weston	0.3–0.5	0.5–0.8

Note: All data in grams per liter.

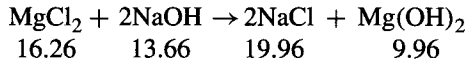
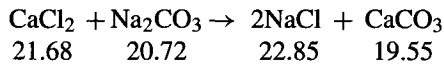
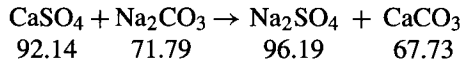
salts. Low ratios, which are more characteristic of solar salts, have more tendency to produce bulky, irregular particles that settle very slowly. When the Ca/Mg ratio is low, some operators deliberately add calcium in order to improve the settling behavior of the combined solids.

There is some controversy over the best locations for addition of the treat chemicals. One point of general agreement is that the hydroxide should not be added before the carbonate. Some technologists favor simultaneous addition of both agents at the beginning of the process. Others argue that if magnesium is precipitated at the beginning it will form its bulky floc and settling will be slow. It is better, according to this argument, to react calcium first so that the magnesium can precipitate quickly onto particles that are already formed. Later addition of OH⁻ also means less exposure to shear and less time for degradation of the Mg(OH)₂. Still another approach is to add both chemicals in two stages. This has the advantage of reducing the amount of nucleation at the beginning of the process. With fewer particles formed, average size must be greater. On the other hand, the residence time for the material added in the second stage is reduced. The design engineer's response to all these permutations and the inherent variability in some salt supplies is to add flexible hoses or a small amount of piping and a few valves to give the operator various options.

The different recommendations for addition points reflect the fact that precipitation is more art than science. Test data on the raw brine that is to be used in a plant are essential if the best design is desired. Since one objective of the precipitation process is to give solids that settle and then filter easily, testing should include those operations as well. Furthermore, changes in raw material should be made with caution. If a plant is to be designed for more than one salt, all should be tested. Laboratory test data may already exist for some salts. Operating data from another plant of known design may also be sufficient. If the salt supply to an operating plant is to be changed or supplemented with an alternative supply, test data, again, should be obtained.

Example. The treated brine flow is about 400 m³ hr⁻¹. The desired concentration of NaCl is 300 gpl. Strictly speaking, this concentration is expressed at the standard laboratory analytical temperature, not at the operating temperature. We ignore the difference here, because it is within the approximation made on the flow rate. The excess concentrations of Na₂CO₃ and NaOH, respectively, are 0.6 and 0.3 gpl, or 0.2 and 0.1% of the NaCl concentration.

The hourly flow of treated brine therefore contains $400 \times 300 = 120,000$ kg NaCl, along with 240 kg of Na_2CO_3 and 120 kg of NaOH. Since only about 45% of the NaCl is converted in each pass through the cells, $54,000 \text{ kg hr}^{-1}$ is new (untreated) salt. Using our standard salt composition, we calculate, for example, that calcium sulfate is introduced at a rate of $(17/9963) \times 54,000 = 92.14 \text{ kg hr}^{-1}$. By similar calculations, we find 21.68 kg hr^{-1} CaCl_2 and 16.26 kg hr^{-1} MgCl_2 . The insoluble impurities amount to 70.46 kg hr^{-1} . Removal of the dissolved impurities is according to these reactions:



The total requirements for Na_2CO_3 and NaOH are 333 and 134 kg hr^{-1} . Note that the carbonate consumption is more than 3.5 times the stoichiometric quantity; with NaOH, the factor approaches 10. This is a bit extreme because of the low level of impurities assumed in our salt. However, it is common for the excess quantities to exceed those theoretically required. With the solution strengths we have chosen, the total flow of treating chemical solution is about $3.6 \text{ m}^3 \text{ hr}^{-1}$ or 90 tpd. Very precise calculation should recognize the 1% increase in solution volume. With salts of lower quality, the increase in volume will become more important. The weight of solids precipitated is 97.2 kg hr^{-1} ; together with the insoluble impurities accompanying the salt, we have 167.7 kg hr^{-1} , or about 4 tpd of dry solids for disposal.

7.5.2.2C. Design of Treatment Tanks. The tanks used for precipitation must first of all be sized to give the desired total residence time. Since one of the functions of the tanks is to allow particle growth, it is not possible to give a firm criterion. Once again, test data are desirable. At typical membrane-plant operating temperatures, it can be said that most of the calcium reaction will be complete in a fairly short time (10–15 min). However, since the goal is to produce brine with less than about 10 ppm of hardness, something more than 99% removal is usually required. The reaction should have time to go nearly to completion. While the rate of course will depend on the amount of excess reagent added, many plants allow from 45 min to more than 1 hr. Inadequate design or operation of the precipitation system can have any combination of several effects:

1. incomplete removal of dissolved impurities from solution
2. excessive formation of particles too small for removal by clarifier
3. incomplete reaction/particle growth leading to postprecipitation in downstream equipment

The first two are straightforward. They will increase the load on other equipment. Failure to add enough treating chemical will leave residual dissolved hardness in the brine. This will reduce the safe operating time of the ion exchangers and perhaps increase the rate

of ionic leakage through the beds. Precipitation from the solution to form a particle of useful size, however, is not simply a matter of a chemical reaction with kinetics that could be determined. It also requires growth of that particle to a certain size above the colloidal range. Excessive amounts of fines will reduce the effectiveness of the filters. The third effect, postprecipitation, is more subtle and complex. It, too, can place demands on other systems that they are not designed to handle. It is a result of the long time scale sometimes involved in the formation of true solid particles. If precipitation conditions are less than ideal, this time will be extended. Very small particles or nuclei formed in the precipitation tanks can fail to settle in the clarifier but continue to grow very slowly and reach a size that allows them to deposit later in the process. As an example, continued precipitation into and beyond the filter system can deposit solids in the ion-exchange beds. These will act as filters with certain efficiency and capture some fraction of the particles. Any solids passing through the beds or forming later can cause problems in the cells by depositing at line restrictions and interfering with flow distribution or partially redissolving after acidification of the brine. In the latter case, the released cations can harm the membranes. The particles trapped in the ion exchangers can shorten the operating cycle by increasing the pressure drop, cause channeling in the beds and so reduce their efficiency, or redissolve in fresh brine or acid regenerant and unfavorably affect the equilibrium of the exchange or regeneration process.

Treatment tanks are constructed of FRP, an FRP composite, or lined carbon steel. Rubber or epoxy resin linings are the most common and in certain cases may be applied only to the parts of the tanks that come into contact with air or oxygenated brine. Phenolic and coal tar-based epoxies are satisfactory materials. The tanks may have open tops or be covered. Even open tanks need a structure to support their agitators, and walkways should be virtually solid in order to limit contamination. Open tanks also allow thermal shock and dilution by snow and rainfall.

Some have argued that the clarifier itself acts as a reactor with a contact time measured in hours. This is a fallacy when applied to the clarified brine portion. Most of the separation between sludge and supernatant brine takes place quickly. The solids population in the clear brine is very low, and there is little opportunity for particle growth. Any further reaction in the clarified brine therefore tends to give particles that are too small to settle.

Bypassing of some of the brine through the treatment tanks defeats their purpose. The first line of defense against this is to provide multiple tanks. Most systems have two or three. In the design of the tanks and their agitators, there should also be some effort to approach plug flow through the tanks. Vigorous agitation works against this goal, and so any agitation should be mild. Its purpose is to ensure blending and to allow contact of reagents and growing particles, not to produce great turbulence. Volumetric power input should be low, on the order of $0.03\text{--}0.15\text{ kW m}^{-3}$. There is no universal agreement among operators on the best tank geometry and agitator for the application. Many different designs are used. There are a few general principles:

1. rotational rates and tip speeds should be low (usually $<4\text{ m s}^{-1}$)
2. flat blades and radial-flow turbines are preferred to propellers
3. maximum impeller diameter is about 0.3 times tank diameter
4. dual impellers may be used, separated by about half a tank diameter

5. height-to-diameter ratios of the tanks should not be low (minimum of 1.0)
6. inlets and outlets should be separated both in height and in orientation

Some tanks are designed with horizontal baffling to create a number of layered zones and so to improve the approximation to plug flow. These may use low-speed flat-paddle agitators with diameters close to that of the tank. Liederbach [40] recommends flow into the top of a tank and out the bottom, and Sutter [53] provides sketches indicating the same approach.

With multiple tanks, flow from one to another can be through external pipelines or internal legs. The internal leg can be a pipe installed inside the tank or a baffled section incorporated into the tank wall. The latter is more complex but less disruptive of agitator flow patterns. Installing the tanks at different heights or with their overflow connections at different levels allows the brine to cascade through them under gravity flow. The last tank should overflow into the clarifier feed well. A semicircular or rectangular trough, kept open or fitted with an easily removable cover for easy cleaning, can be used to carry this last flow. FRP, properly supported, is a suitable material of construction.

Certain brines have excellent settling characteristics when treated. These include many of those produced from US Gulf Coast rock salt and brine wells. The problem of treat tank design becomes much simpler, and single-tank systems have been used effectively.

Example. With a flow of $400 \text{ m}^3 \text{ hr}^{-1}$ and a retention time of 50 min in a tank, the volume is about 333 m^3 . With $L/D = 1$, the length and diameter are nearly 7.5 m each. We allow an extra 0.5 m in height for freeboard and an overflow launder. We use two impellers on the agitator shaft, 2.25 m in diameter and about 3.5 m apart. The rotational speed is 25 rpm, giving a tip speed of 3 m s^{-1} .

7.5.2.2D. Use of Flocculating Agents. The character of the solids formed in the treatment tanks determines the efficiency of the next step in the process, brine clarification and sludge thickening. The treatment tanks are sized to promote particle growth, but many brines have unsatisfactory compositions, making it difficult to produce solids with good settling characteristics. Many plants therefore use flocculating agents to improve the situation. These are polyelectrolytes. The polymers most frequently used with chlor-alkali brines are those based on acrylamide and acrylic acid.

Probably any brine can benefit from the proper use of flocculants [53], but well-behaved brines profit little and do not justify the complication. Poorly performing brines, on the other hand, can have settling rates improved several-fold. Sutter recommends using flocculating agents when the calcium/magnesium ratio is less than two and adding them at approximately the midpoint of the treating system. When there is more than one tank, the flocculating agent is added after the carbonate and before or along with the hydroxide. As was the case with the addition of precipitants, there is controversy over the best location of the addition point. Some recommend addition of flocculant near the end of the process and even in the feedwell of the clarifier. Sometimes, a flash mixer attached to the clarifier is used for efficient dispersion. Coin [6] cites a report by Bryant [91] on tests with a brine whose Ca/Mg ratio was about 1.4. Results showed that

an acrylic polymer was much more effective than starch and that adding the polymer after 20 min reaction time was more effective than adding it to the raw brine.

Flocculant dosage rates are quite low; 2 ppm in the brine is a typical figure. Solutions are added to the brine by metering pumps, usually manually controlled. Several different agents are used successfully in the industry.

Usually, flocculating agents are received as solids or thick liquids. They are dissolved or diluted to low concentrations because the viscosity of polyelectrolyte solutions can be quite high. This can make it difficult to wet and disperse the material properly. The result of improper dispersion is the formation of lumps that dissolve extremely slowly and that are not effective in the process. A supplier reports that dilute solutions of a flocculant often give superior results and that multiple-point addition of the flocculant can improve its contact with the brine [91]. The polymers are sensitive to shear, and the agitation process must be chosen with care. Turbulence at the addition point(s) should provide good dispersion but not break the flocs.

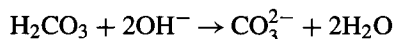
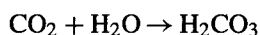
Choice of a flocculating agent requires consideration of the ionic form and the molecular weight of the polymer. The mechanism of flocculation involves the formation of bridges between particles. Longer chains are able to attach themselves to more particles, and so higher molecular weights should be more effective. The acrylamide polymers usually have molecular weights of 10 million or higher. High molecular weight aggravates the problems of dissolving and dispersing the polymer. Also, too high a concentration of flocculating agent reduces the opportunity for crosslinking and so reduces its effectiveness.

Flocculants also differ in their ionic form [92]. Polyacrylamide itself is a nonionic agent. Its monomer is usually copolymerized with another material to supply some ionic character to offset the ionic charge of the particles to be flocculated. In brine treatment, anionic materials, based on acrylic acid as comonomer, usually give better results.

The best approach is to seek and follow suppliers' recommendations on handling of their products. Suppliers' data also help in the preliminary selection of an agent, but best results usually require testing on plant brine. Previous experience with similar brines is also very valuable. Finally, the flocculant selected must not have any deleterious effects on the operation of the cells when present in a recycle brine stream. In a membrane-cell plant, preference should be given to those that have been shown to be compatible with the membranes.

When agglomerates form in brine as a result of the addition of a flocculant, they tend to trap liquid within their structure and in the irregularities on their surfaces. While clarification is enhanced, therefore, thickening may suffer. The concentration of the sludge produced in the clarifier may be reduced. The same will be true with some of the modified clarifier designs discussed in Section 7.5.3.3.

7.5.2.2E. Use of CO₂ Gas. Carbon dioxide can be used directly in brine treatment as the gas. Since hydrolysis of CO₂ tends to produce carbonic acid and therefore consumes OH⁻, the equivalent amount of hydroxide must also be added to the system:



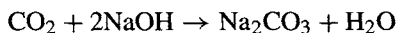
Carbon dioxide may be supplied as the liquid and then vaporized in standard apparatus for injection into the treatment tanks, or it may be recovered from a flue gas. In the latter case, the presence of impurities is an obvious concern. In a few plants, carbonate sludge is digested with acid to regenerate the CO_2 value, and this gas can also be used.

The CO_2 may be used directly in the process or may first be absorbed into a caustic solution to produce Na_2CO_3 or K_2CO_3 . In the latter case, absolute precision in stoichiometry is not necessary. While variations in composition can cause problems in process control, any deficiency in CO_2 content of the solution will result in some hydroxide value accompanying the carbonate. This is compensated for by reducing the amount of caustic solution added to the brine. If the CO_2 content is high, there will be a certain amount of bicarbonate present. This will consume OH^- when the caustic solution is added, and so the flow rate of that stream will have to be increased. This regenerates CO_3^{2-} late in the process and is more undesirable than the opposite error.

The latter situation is the same when the gas is used directly in the treatment tanks. While the absorption process is a simple one, some care is necessary to provide a good situation for mass transfer without excessive agitation of the liquor. The need to provide NaOH along with the gas also changes the mathematics of control of the excess concentration of caustic. The amount present as excess, which is the controllable portion, becomes a smaller fraction of the whole and the precision of its addition must increase.

Comparative economics of the forms of carbonate value available to a plant will determine the best choice. Providing the option to use direct CO_2 adds some flexibility to the operation and allows more variation in the caustic/chlorine ratio in the plant's output. By consuming some of the caustic, it can make possible the production of more chlorine during times when sales of caustic are slack.

Example. From the previous example, we know that our reference plant requirements are 134 kg hr^{-1} NaOH and 333 kg hr^{-1} Na_2CO_3 . If we use CO_2 gas for treatment, the reaction



shows that we need 138 kg hr^{-1} of the gas and an additional 251 kg hr^{-1} of NaOH in place of the carbonate. The total consumption of NaOH becomes 385 kg hr^{-1} , more than 9 ton per day and close to 1.2% of plant output.

The NaOH required to maintain the concentration of 0.3 gpl in the treated brine, which was about 8.5 times as great as the stoichiometric requirement, is now only 45% of that quantity. This is not low enough to cause a serious problem in controlling the excess, but part of this fortunate situation is due to the high purity of the salt being used. If we were to use a Northern US rock salt with 1.56% CaSO_4 and 0.20% MgSO_4 , the stoichiometric requirements would be about 71 kg hr^{-1} NaOH and 674 kg hr^{-1} Na_2CO_3 . *In-situ* generation of the carbonate would consume 380 kg hr^{-1} CO_2 and 690 kg hr^{-1} NaOH . The total usage of NaOH becomes 881 kg hr^{-1} , only 13.6% of which is the excess quantity. A fluctuation of 1% in the total feed rate of NaOH produces a 7.3% fluctuation in the residual excess. With a good control system and good valves, this is an acceptable situation, but the multiplication of the error is worth noting.

7.5.3. Clarification and Thickening

Clarification and thickening are two very closely related operations that come under the heading of sedimentation. Both involve the separation of a suspension of solids into a relatively clear liquid and a more concentrated suspension. The emphasis in continuous clarification is on the absence of solids in the clear liquid overflow; the emphasis in thickening is on achieving a high solids concentration in the underflow. The purpose of the clarifier in brine treatment, as the name suggests, is primarily to produce clear brine for further processing. At the same time, there is an incentive to produce a concentrated suspension of solids in order to minimize raw material losses and the costs of processing the sludge. The two goals are not incompatible, but adding to the demands on an operation always increases its cost. A clarifier/thickener, for example, is more expensive than a simple clarifier because of the greater volume required and the extra stress placed on an agitator and drive by a high solids concentration.

Figure 7.47 is a simple flowsheet of the brine clarification process. The clear liquid overflows into a pump tank and is forwarded to the brine filters. The sludge from the bottom of the clarifier is removed for disposal. Consideration of what happens during batch sedimentation will give some understanding of this continuous process. Figure 7.48 shows that when a uniformly mixed slurry placed in a container is allowed to settle, the falling particles soon reach their steady-state velocities. A clear supernatant layer quickly appears, as indicated by zone I. Particles close to the bottom gradually form a compressed layer with a higher solids content (zone III). In zone II, the particles fall at constant velocity. The concentration of solids in that zone therefore remains constant. With time, zones I and III grow at the expense of zone II. When zone II disappears, the only sedimentation occurring is the slow compression of zone III. There, the solids concentration continues to increase as the particles in the bottom layer compress one another and force more brine out of the interstices. Figure 7.49 is another depiction

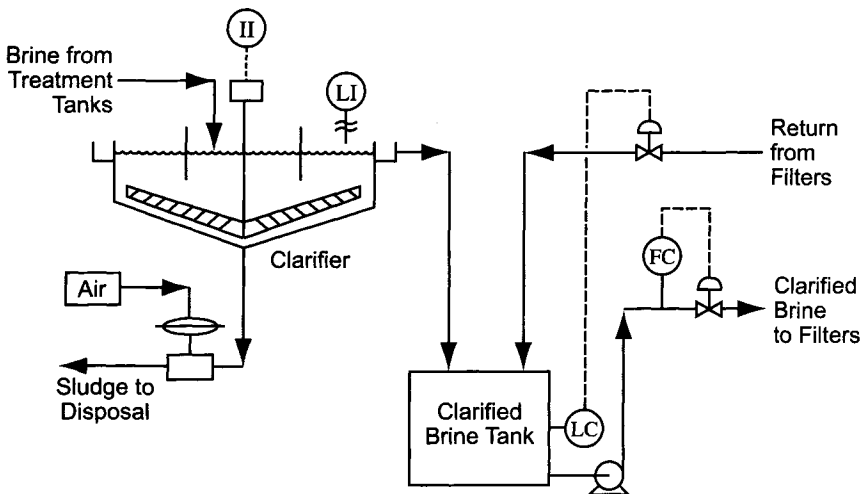


FIGURE 7.47. Flow diagram for clarification process.

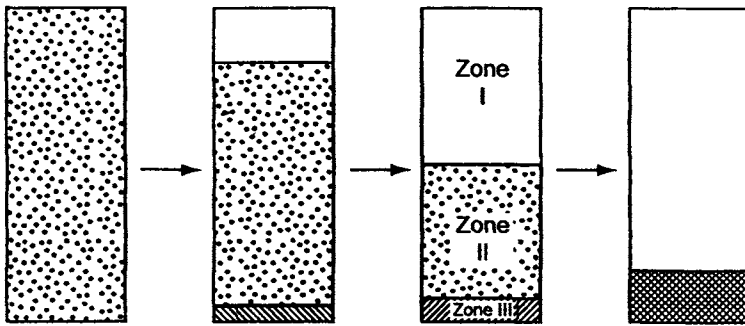


FIGURE 7.48. Batch settling of suspended solids.

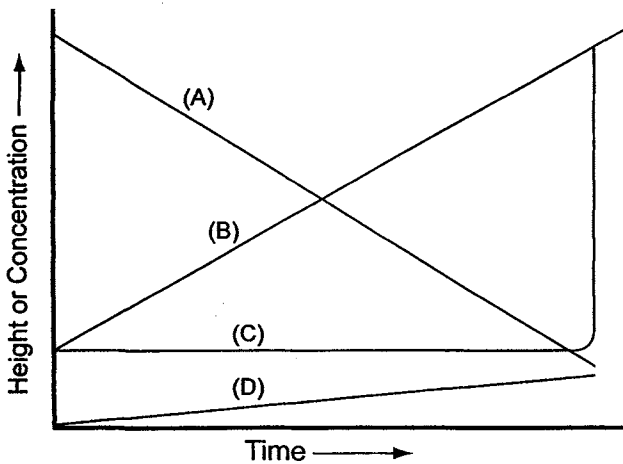


FIGURE 7.49. Zone concentrations and boundaries in batch settling. (A) Height of interface between zones I and II; (B) Concentration of zone III; (C) Concentration of zone II; and (D) Height of interface between zones II and III.

of the batch process, showing the gradual convergence of the two interfaces and the different behavior of the concentrations in zones II and III.

Real systems do not display the sharp boundaries of Fig. 7.48. One reason is that no real system is monodisperse and therefore individual particles do not all settle with the same velocity. Other reasons having to do with process control are the normal fluctuations in continuous operation and imperfect distribution of flow across the clarifier. There are also external factors that oppose the settling of particles. These include thermal convection currents that arise from nonuniform temperatures and deaeration of the brine that leads to flotation of some of the suspended matter. To allow for these effects, it is customary to apply a safety factor to the calculated area. Seifert [93], for one, recommends using an area efficiency of 50%.

Still, nearly all sedimentation processes follow in a general way the course of Figs 7.48 and 7.49. Time scales vary widely, and in the case of rapidly settling materials the existence of zone II may be quite short. The rate of settling and thus the time scale

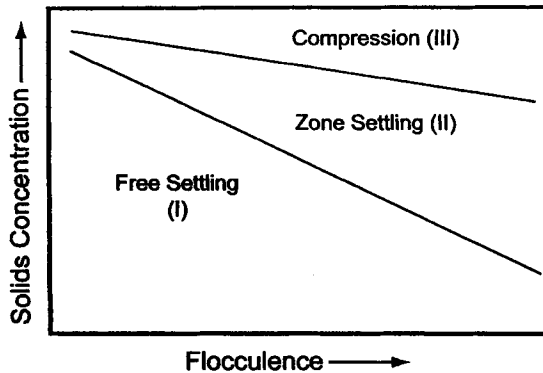


FIGURE 7.50. Settling regimes as function of particle characteristics.

depends on the characteristics of the particles. Discrete particles, such as those with well-formed crystals, have little tendency to cohere, and free settling continues even at fairly high solids concentrations. Other materials, especially organics and those with small or irregular particles of low sphericity, are more highly flocculent. They tend to form structured masses at lower concentrations and then to settle more slowly. Metal hydroxide precipitates such as $Mg(OH)_2$ are usually of this type. Figure 7.50 is a qualitative representation of the situation. The character of the solid determines its place along the abscissa. More difficult materials form loose agglomerates of irregular shape and group themselves on the right. As particles settle and the solids concentration increases, the behavior of a suspension changes. A vertical line on the figure might represent the history of the settling behavior of a given material. More flocculent materials, located farther to the right, enter the zone settling and compression regimes, where they settle more slowly, at lower concentrations. The result is a longer settling time or, in a given apparatus, poorer separation of phases.

7.5.3.1. Fundamentals of Sedimentation. The complexities of the sedimentation process appear when the solids concentration becomes high enough for particle interactions to affect settling velocities. This does not occur in the clarifying zone of the typical brine clarifier, which is similar to zone I in Fig. 7.48. We can expect design considerations there to be relatively straightforward. Ideally, the overflow will be free of suspended solids. Practically, there is a limit fixed by the smallest particle that can settle under the influence of gravity against the velocity of rising brine. The first consideration in sizing a clarifier then is to provide enough area to reduce the upward velocity of brine to a suitable value, below the settling velocity of all but the very smallest particles. Section 7.5.3.1A derives the equations that apply to this upper, or free-settling, zone.

As the solids concentration increases in the lower zones of a clarifier, the particles must settle through a suspension rather than through a clear fluid. The liquid released from the floc or displaced by a falling particle must follow a more tortuous path upward into the clear zone. The increased frictional drag reduces the rate of displacement, and the particles fall more slowly. This is the zone of hindered settling, analyzed in

Section 7.5.3.1B. It is necessary to size a thickening zone so that the upward velocity of the brine does not exceed the settling velocity (relative to brine) at any section in the lower zones.

At the bottom of the thickening zone, the particles enter the compression zone. This is equivalent to zone III in the batch test. Further settling now depends on the slow compression of the collected floc under the weight of the accumulated solids. This weight gradually squeezes the fluid out of the mass and allows it to return to the higher sections. The nature of the precipitated solids controls this process. Highly flocculent materials (to the right in Fig. 7.50) develop a structure at low concentration (about 5%). They resist dewatering and produce dilute underflow. The actual underflow concentration will also be influenced by the details of mechanical design of the unit and by the rate of withdrawal of the bottoms. While the clarification capacity depends primarily on the cross-sectional area of the confining vessel, the thickening capacity depends also on the height of the unit.

7.5.3.1A. Free Settling. Free settling occurs when there is no interaction between solid particles. This is true when the suspension is very dilute and is a good approximation to what happens in the clarification zone. The force balance on a particle falling through a fluid involves gravity, buoyancy, and friction. The net downward force is

$$F = mg - wg - F_R \quad (21)$$

where

m = mass of the particle

g = acceleration due to gravity

w = mass of fluid displaced by the particle

F_R = frictional resistance force

An expression for the frictional force appeared in Newton's *Principia*:

$$F_R = f A \rho v^2 / 2 \quad (22)$$

where

f = proportionality constant

A = representative area of the particle

ρ = density of the fluid

v = downward velocity of the particle relative to the fluid

If the particle is a sphere, the representative area can be taken as its projected area $\pi D^2/4$, and then

$$F_R = f_D \pi D^2 \rho v^2 / 8 \quad (23)$$

where

f_D = friction factor

D = diameter of particle

When the falling particle reaches its maximum, or steady-state, velocity, the net force acting on it is zero. Then we can write

$$\begin{aligned} mg - wg &= F_R \\ (\pi D^3/6)g(\rho_s - \rho) &= f_D \pi D^2 \rho v_m^2/8 \end{aligned} \quad (24)$$

where

ρ_s = density of solid particle

v_m = maximum or steady-state velocity

Dividing through by the particle volume $\pi D^3/6$, we have

$$g(\rho_s - \rho) = 3f_D \rho v_m^2/4D \quad (25)$$

The terminal velocity for falling spheres becomes

$$v_m = [4(\rho_s - \rho)gD/3\rho f_D]^{1/2} \quad (26)$$

If v_m does not exceed the upward velocity of the brine, a particle will be carried up and into the clarifier overflow.

This derivation has not considered whether the flow of the fluid around the sphere is laminar or turbulent. With no *a priori* way to evaluate f_D , Eq. (26) has no general analytical solution. In the 19th century, however, Stokes considered the restricted case of laminar flow, which prevails in brine clarifiers. He showed that the force resisting the laminar flow of a spherical particle is

$$F_R = 3\pi D\mu v \quad (27)$$

where μ is the viscosity of the surrounding fluid. Substituting this in Eq. (21) and following the procedure used above leads us to

$$g(\rho_s - \rho) = 18\mu v_m/D^2 \quad (28)$$

and

$$v_m = g(\rho_s - \rho)D^2/18\mu \quad (29)$$

Equating the right-hand sides of Eqs. (25) and (28) gives the friction factor in terms of the Reynolds number, which is defined as $Re = D\rho v_m/\mu$:

$$f_D = 24/Re \quad (30)$$

Equation (29) would appear to tell us what is required for efficient clarification. The most important term, because of its exponent, is the particle diameter. This is why it is so important to allow particles to grow during precipitation. The density of the solid particle should also be maximized. There is a fundamental limit at the true solids density, but it is possible to approach this if the process forms particles free of voids and with compact structure. Also important, although not shown in an equation developed for spherical particles, is the question of shape. Irregular particles will develop more frictional resistance and be more likely to be carried out of the clarifier by the rising flow of brine.

Equation (29) also implies that the fluid density and viscosity should be minimized. This suggests that clarification should improve at higher temperatures. One argument against this is the increasing solubility of some of the solid species (Fig. 7.42). More to the point in this development is that increased temperature, while increasing the difference in densities and reducing the frictional resistance to fall of the solids, also increases the rate of heat loss from the system. Nonuniform temperature in the clarifier results in thermal convection currents. These upset the streamline flow of solids toward the bottom of the clarifier and increase the turbidity of the overflow.

7.5.3.1B. Thickening. Since settling velocities in a thickening zone depend on the nature of the particles and the ways in which they interact, there is no way at present to predict results from first principles. The settling of masses of solid from a liquid is a complex process involving agglomeration and several possible mechanisms of compression of the agglomerates. The theories used to correlate the results obtained in thickeners go back to the work of Coe and Clevenger [94], in 1916, and of Kynch [95], in 1952.

Coe and Clevenger considered the basic material balance on a steady-state process:

$$Q_f = Q_o + Q_u \quad (31)$$

$$C_f Q_f = C_o Q_o + C_u Q_u \quad (32)$$

where Q is the flow rate of the suspension or solution, $\text{m}^3 \text{hr}^{-1}$, and C the concentration of suspended solids, kg m^{-3} of suspension, and subscripts f, o, and u denote feed, overflow, and underflow, respectively.

It is clear that the upward velocity at every level in the sedimentation zone must be no greater than the rate of sedimentation of the precipitate:

$$Q_o/A \leq R \quad (33)$$

where A is the cross-sectional area of thickener, m^2 and R the sedimentation rate, m hr^{-1} .

A stable boundary between the settling zone and the thickening zone is important for normal continuous operation; that is, the rate of introduction of solid to any section in the thickening zone must be equal to the rate of discharge of solid in the underflow (assuming essentially no solids in the overflow). In this region, the velocity of sedimentation depends

on the solids concentration, which changes with vertical position in the settler. We can write, at any position,

$$R = R_c$$

where the subscript c denotes the value of R at a particular concentration. The cross-sectional area required to permit settling at the concentration c is

$$A_c = (C_f Q_f - C Q_u) / C R_c \quad (34)$$

The Coe/Clevenger method uses experiments run on suspensions of different consistencies ranging from feed concentration to desired underflow concentration. Each solids concentration tested allows calculation of a cross-sectional area by the method described above. This calculated area will exhibit a maximum at some particular concentration, and this is the critical concentration that fixes the cross-sectional area required in the thickening zone.

The need to vary the feed concentration in the batch tests is a disadvantage of the Coe/Clevenger method especially when studying the use of a flocculant, because the average floccule size depends on the solids concentration. It will be different in each experiment. The Kynch method, on the other hand, requires only a single curve of interfacial level vs settling time, continued from the expected feed concentration until the desired final concentration is reached. Such a curve generally has two inflection points, corresponding to the boundaries between the regions in Fig. 7.50. The lower inflection point, or “compression point,” is a key value in a Kynch analysis. Sometimes, it is not easily identified on a simple plot of height vs time. It may be easier to detect on a log–log plot or on a plot of $\log(H - H_\infty)$ against time, H_∞ being the assumed or empirically determined height of settled solids after “infinite” time.

Fitch [96] points out that one fallacy in the Coe/Clevenger development is that, in a batch test, the compressed layer at the bottom continuously increases in height and has some effect on the behavior in the line settling zone above it. This fact is not accounted for in the standard calculations. Moreover, under certain conditions, clusters of solids break up into something similar to aggregative fluidization. The assumption that the settling rate depends only on concentration then breaks down. Fitch recommends the Talmadge and Fitch [97] method, also based on Kynch’s work [98]. This uses the same plots of interfacial height against settling time. The first task is to estimate the concentration at which thickening starts and the rate of settling begins to drop rapidly. The rate of settling at this critical concentration becomes the basis for sizing the clarifier. Figure 7.51 shows the graphical technique. A tangent is drawn to the batch settling curve at time zero. This is fairly easily defined, because the settling rate tends to be constant for some time from the beginning of the process. A second tangent is drawn to the curve near the end of the process. This will not be far from the horizontal. The two tangents intersect at an angle. The bisector of this angle meets the settling curve at the critical concentration C_c . The coordinates of the point are θ_c and H_c .

First, it is necessary to establish a batch settling curve that shows the height of the slurry/clear liquid interface as a function of time. Foust *et al.* [99] show how to convert this to a curve of settling rate vs concentration. The latter can then be used to calculate

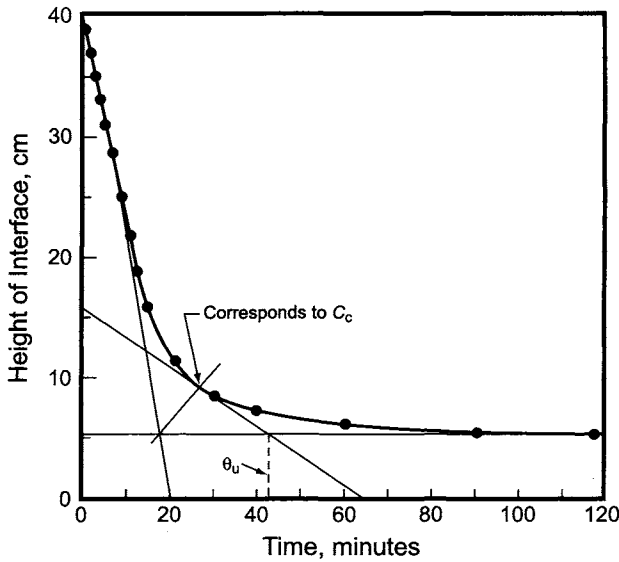


FIGURE 7.51. Talmadge and Fitch analysis of settling data.

the solids flux vs concentration. In a continuous thickener, the total flux is the settling flux determined by the batch test plus the underflow flux. The latter is a parameter chosen by the designer. The total flux reaches a minimum, F_L , at the limiting concentration C_L and is used along with the feed rate and initial concentration of the slurry to calculate the minimum acceptable cross-sectional area of the thickener.

Having established θ_c and H_c , we recognize that the mass of solids in the test cylinder remains constant, and so

$$C_o H_o = C_c H_c = C_u H_u \quad (35)$$

where

C = slurry concentration at any level

H = height of interface corresponding to C

o, c, u = initial, critical, and underflow

The designer specifies the underflow concentration. The thickening process consists in increasing the concentration of the slurry from C_c to C_u . This occurs by squeezing out brine in the volume

$$V = A(H_c - H_u) \quad (36)$$

where A is the cross-sectional area of the thickener. The time required for this to occur is $\theta_u - \theta_c$. The average volumetric flow rate, L , is then given by

$$L = V/(\theta_u - \theta_c) = A(H_c - H_u)/(\theta_u - \theta_c) \quad (37)$$

Then we have

$$\theta_u - \theta_c = A(H_c - H_u)/L \quad (38)$$

The (negative) slope of the tangent to the settling curve at the critical point is the critical velocity V_c . Construction of this tangent gives the y-intercept H_1 and we have

$$V_c = (H_1 - H_c)/\theta_c \quad (39)$$

Now the clear liquor upflow rate in a continuous thickener must be less than V_c . If it were higher, the layer of critical concentration would not be able to settle against the rising liquor. So, the flow at time θ_c , when thickening starts, is

$$L = AV_c = A(H_1 - H_c)/\theta_c \quad (40)$$

We now have two expressions for L . Equating them,

$$(H_c - H_u)/(\theta_u - \theta_c) = (H_1 - H_c)/\theta_c \quad (41)$$

Again, by a mass balance we have

$$H_u = H_o C_o / C_u \quad (42)$$

and we can then solve for the time required to reach the underflow concentration:

$$\theta_u = (H_1 - H_u)\theta_c / (H_1 - H_c) \quad (43)$$

The required area then is

$$A = L_o \theta_u / Z_o \quad (44)$$

where L_o is the volumetric rate of flow of slurry to the thickener. The value of θ_u can also be determined graphically by producing a horizontal line at height H_u and extending it to its intersection with the critical tangent. This is marked on Fig. 7.51.

Example. We consider the following data obtained in a batch settling test in a two-liter graduate [99]. The starting height at the 2,000-ml mark is 40 cm.

Time (min)	Level (ml)	Time (min)	Level (ml)
1	1,950	12	975
2	1,850	15	800
3	1,750	20	590
4	1,650	30	440
5	1,550	40	375
6	1,450	60	300
8	1,260	90	265
10	1,100	120	250

Figure 7.51 is the settling curve, in which the level data have been transformed from ml to cm. We note incidentally that the apparent rate of settling at zero time is not the maximum rate. Probably the onset of settling is delayed by initial turbulence generated by filling the cylinder or residual turbulence after agitation. The “tangent” constructed is in fact a line whose slope matches the constant-rate zone from 1 to about 7 min. The two tangents meet at about (17.5, 5.3). The angle bisector then cuts the settling curve at (27, 9.25). This point identifies the critical solids concentration C_c . In the example, it is about 4.3 times the starting concentration C_o . The tangent to the settling curve at the critical point cuts the H -axis at 15.7 cm, and this is the value of H_1 . As in previous examples, we take the flow of brine to be $420 \text{ m}^3 \text{ hr}^{-1}$. In units that match those used in the table above, this is $7,000,000 \text{ ml}$ or $\text{cm}^3 \text{ min}^{-1}$. Since the starting height is 40 cm, we have $L_o/H_o = 175,000 \text{ cm}^2 \text{ min}^{-1}$. The required area now depends on θ_u . If we set $H_u = 250 \text{ ml}$ or 5 cm, $\theta_u \approx 44 \text{ min}$, and the required area is 770 m^2 , corresponding to a diameter of 31.3 m. This matches the 30–33 m called for by arbitrarily fixing the rise rate of brine in the clarifying zone, as in the following section. This outcome can be regarded as something of a coincidence, since the size in this calculation is fixed by the designer’s choice of the underflow concentration. In reality, it can be attributed to the fact that practical choices are limited to a rather small range and the calculated size is not strongly dependent on the choice of underflow concentration. Changing the underflow concentration (and therefore the value of H_u) by 10% in this case changes the diameter of the clarifier/thickener by only 1%. The discussion of sludge removal in Section 7.5.3.2D mentions other limitations on the real concentration of the clarifier underflow.

While this method in theory gives the clarifier size from a single test, the inherent variability of the physical system and the vagaries of graphical analysis make replication worthwhile. A series of tests also will help one to optimize the extent of addition of a flocculant.

This method is easily adapted to the nonlinear plots discussed above. It is obviously empirical, and Fitch [100], writing years later, stated that there still was no satisfactory theoretical method. The designer’s best recourse is to work closely with equipment vendors and to allow a safety factor in the assumed concentration of the underflow.

Sometimes, flocculation of particles is useful by increasing the rate of sedimentation. With typical brine precipitates, the flocculants most frequently used are acrylic

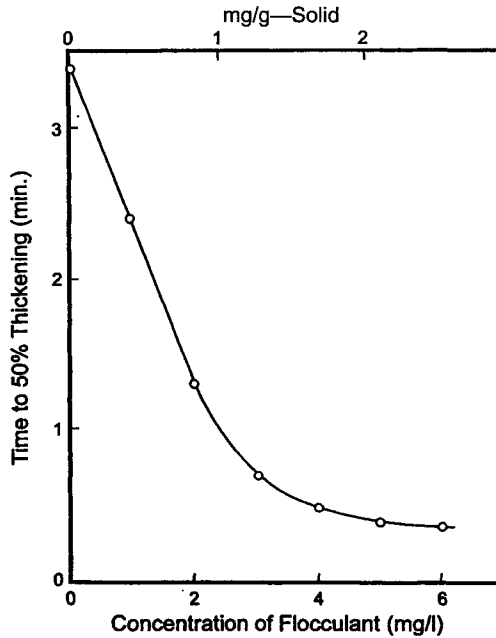


FIGURE 7.52. Effect of flocculant concentration on rate of thickening.

polymers, and their practical application is discussed in Section 7.5.2.2D. The optimum fractional coverage of particles with flocculant is said to be about 0.5 [101]. Figure 7.52 shows the effect of the addition of an anionic flocculant to saturated brine containing $\text{Mg}(\text{OH})_2$ and CaCO_3 precipitates [102]. The use of 1 mg polymer per gram of solid, or 2 mg L^{-1} of brine, decreased the time to 50% thickening by a factor of about three.

7.5.3.2. Standard Brine Clarifiers. A standard clarifier design in the chlor-alkali industry is cylindrical with a shallow conical bottom (Fig. 7.53). Brine enters the top through a circular feed well that carries it some distance down into the clarifier. Clarified brine overflows the entire periphery of the cylinder. The solids, under the influence of a slowly rotating rake, leave the center of the bottom cone as sludge.

The treated brine handled in the clarifier is alkaline and not highly corrosive. At least in diaphragm plants, carbon steel often can be used as the major material of construction. Since brine is more corrosive in the presence of oxygen, those parts near or above the water line are sometimes coated. With mercury or membrane cells, there is also the possibility of pickup of harmful elements to be considered. It is common practice to use coated walls and rubber-covered internals in these cases. When clarifiers are installed at grade level, the bottoms are frequently of concrete. This too is more characteristic of diaphragm-cell plants. Membrane cells can be damaged by pickup of such compounds as sulfates and silica.

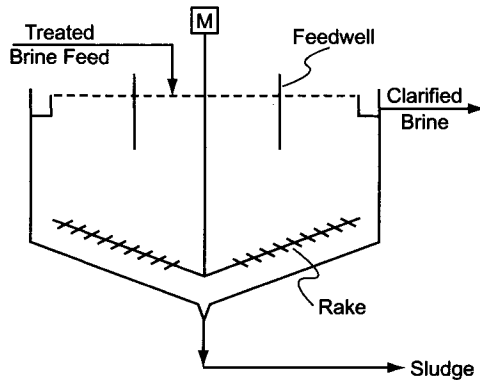


FIGURE 7.53. Standard brine clarifier/thickener.

Underwater mechanisms should be designed to the standards used for bridges and buildings. High-strength steels may be used for large spans, heavy launders, and the like [93]. FRP appears frequently in overflow channels, feedwells, baffles, and weirs.

The upward velocity of clarified brine toward the overflow is referred to as the “rise rate.” Strictly speaking, this should be the volumetric flow of only the overflowing brine through the cross-section of the clarifier vessel minus that of the feedwell. In practice, it is often taken as the total flow of brine over the area of the clarifier vessel. This approach therefore contains two errors, which are usually not large and which are always partly offsetting. The choice of a design rise rate determines the diameter of a cylindrical clarifier. Choice of the rise rate will depend on many factors, some of which are discussed below. A typical value would be 0.5 m hr^{-1} [53]. In that case, Eq. (29) predicts that particles smaller than about $15 \mu\text{m}$ in diameter will pass through the clarifier along with the brine.

Increasing the height of the sludge in the clarifier allows more time for compression and separation of liquid from the suspension. Continuing to increase the height would first become uneconomic and finally counterproductive, as the underflow would become too concentrated to flow easily. Most brine clarifiers have sidewall depths between 3.0 and 5.5 m. In a normal situation in which brine flows by gravity, the height of the clarifier affects the elevations of the treatment tanks and salt dissolvers.

7.5.3.2A. Feedwells. Figure 7.53 shows the usual arrangement in which brine is brought into the top of the clarifier near its center. This flow could produce turbulence in the clarified brine and even result in some bypassing. These effects are mitigated by installation of a center feedwell. This dissipates the velocity of the feed stream by forcing the brine to flow radially from the bottom of the well and then vertically upward through the clarifier. The velocity in the feedwell itself is not high; conditions should favor continued flocculation, not disturb it. Typical cross-sectional areas in conventional clarifiers are less than 5% of the clarifier area. Corresponding velocities are of the order of 10 m hr^{-1} , giving Reynolds numbers of 5–20,000, so that there is only mild turbulence within the feedwell.

In some feedwells, the stream is divided into halves which are introduced tangentially and in opposite directions. This destroys momentum by producing a turbulent zone where the two streams meet.

Increasing the depth of the feedwell reduces the probability of bypassing. Extending it well into the compression zone forces the brine to rise through the solid bed in order to reach the overflow. This also helps to improve the clarity of the brine produced by adding a filtering mechanism to the process.

7.5.3.2B. Overflow System Design. For best results, the flow of brine from the top of the clarifier must be smooth and evenly distributed around the periphery. This is possible only when the overflow device is level and there are no waves on the surface.

Every effort should be made to install the clarifier itself with a level top. In addition, the overflow device should have some provision for establishing a level after its installation. Sawtooth-notched weirs are used frequently. They should be built in individually adjustable sections.

With large clarifiers, there is a potential problem with the formation of waves on the surface of the clarified brine. These are caused by wind, and they can drastically upset the evenness of the overflow. The notched-weir type mentioned above gives some small protection against shallow waves. With a large open clarifier, it is good practice to add barriers to dampen these waves. Barriers might be rectangular pieces, such as planks of marine-resistant wood. When thermal insulators are floated on the surface (Section 7.5.3.4A), they also serve to dampen wave action.

A simple overflow device, such as the notched weir mentioned above, allows the top layer to overflow. This is always subject to some degree of turbulence, and it will collect a layer of foam that contains some impurities. A submerged weir overflow [53] can overcome these problems and provide some protection against surface waves. A typical design is shown in Fig. 7.54.

If the overflow rate is greater than the hydraulic capacity of the weir or launder, the clarifier will flood and no longer function properly. The capacity of a weir, being proportional to its length, increases directly with clarifier diameter. Since the phase-separating capacity, the major subject of Section 7.5.3.1, depends on the cross-sectional

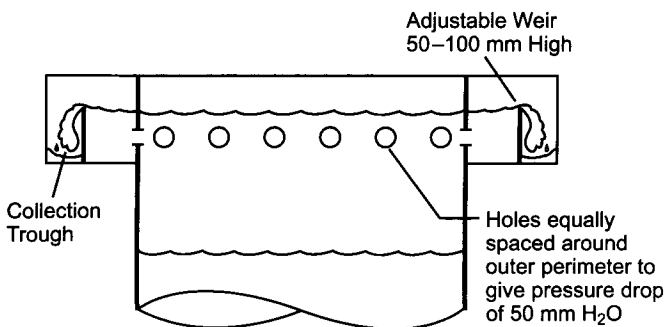


FIGURE 7.54. Submerged weir for clarifier overflow. (After Sutter [53].)

area or the square of the diameter, scaleup will eventually reach the point where flow is limited by weir capacity. Increasing the weir length available in the clarifier can offset this effect. One method is to install the overflow launder at some distance from the periphery, so that brine can overflow from both sides. This effectively doubles the weir capacity per unit of length, but it is not common practice in the chlor-alkali industry. In those cases where it might apply, there usually are other reasons for splitting the brine flow and providing more than one train.

Municipal water applications often are restricted to weir overflow rates of $3.5\text{--}15\text{ m}^3\text{ m}^{-1}\text{ hr}^{-1}$. Industrial practice is for the most part unregulated and based on higher rates. Certainly this is true of the chlor-alkali industry, where there are downstream provisions for removing the traces of suspended solids that escape the clarifier. Maximum overflow rates are usually set at $5\text{--}25\text{ m}^3\text{ m}^{-1}\text{ hr}^{-1}$. At a diameter that we shall call the critical diameter for this discussion, the criteria based on rise rate and on weir overflow rate become equal.

The flow of treated brine depends on the capacity of the plant and on the concentrations of brine into and out of the cells. It depends less strongly on other operating conditions. As a rule of thumb from our design examples, we can estimate the flow of membrane-plant treated brine in $\text{m}^3\text{ hr}^{-1}$ as 0.5 times the plant capacity in tons of chlorine per day. Using the more frequently encountered rating in terms of tpd NaOH, we estimate the diameter required to meet the criterion for weir overflow rate as

$$D_W = 0.143 T / W \quad (45)$$

where

D_W = diameter based on weir overflow, m

T = production rate, tpd NaOH

W = weir overflow rate, $\text{m}^3\text{ m}^{-1}\text{ hr}^{-1}$

The diameter required to meet the criterion for rise rate is

$$D_R = 0.757 (T/R)^{1/2} \quad (46)$$

where

D_R = diameter based on rise rate, m

R = rise rate, m hr^{-1}

The rise rate controls as long as $T R / W^2$ is less than 28.

Example. The brine flow in our reference plant is $380\text{ m}^3\text{ hr}^{-1}$. Estimating the diameter of the clarifier for a rise rate of 0.5 m hr^{-1} gives about 31 m. Estimating the diameter for a full-periphery weir overflow rate of $5\text{ m}^2\text{ hr}^{-1}$ gives 24.2 m. The parameter $T R / W^2$ is 16, well below the critical value of 28. The difference far exceeds the error in estimating the brine flow rate simply from the plant capacity. With the unit rates chosen here, the weir overflow rate would control at clarifier capacities equivalent to more than 1,400 tpd NaOH; unless design rise rates are unusually high, then, the overflow rate is unlikely to be the guiding criterion in a chlor-alkali brine clarifier.

Many clarifier designs include scum boxes that are placed at one spot along the periphery. Thin, low-speed rakes gather the scum from the surface and deliver it to the box for removal.

7.5.3.2C. Rakes and Drives. The purpose of a rake is to sweep the bottom of the clarifier and bring the collected solids to a drawoff point. Eddies that form behind a rotating rake promote the release of brine from compacted sludge. In principle, drawoff can be along the periphery or at the center of the clarifier. In chlor-alkali practice, the center is usually chosen, partially because the peripheral speed of a large rake can produce undesirable turbulence in the slurry being withdrawn. Outward raking is used most frequently in very large units, where the substantial height at the periphery makes removal of sludge easier, and in areas with high water tables, where underflow tunnels are impractical or very expensive.

Angular velocities are quite low, and so power requirements even in large units are modest. The drive motor usually is rated at no more than 0.1 kW per meter of clarifier diameter. At the same time, rakes are heavy as well as wide, and torques can be large. Heavy underflow and the accumulation of sediment or foreign objects can greatly increase the torque. Instrumentation should include high-load alarms and shutdowns. These can be activated by electrical (amperage or power) signals or by mechanical measurements of gearing or reaction forces. The drive should be able to overcome a certain amount of solids accumulation, and the normal running torque should be no more than about 25% of design. Starting torque in the presence of a blanket of sludge can be quite high, and there are various devices to reduce its maximum value. These include, for example, undervoltage starters. The installation should include a rake-lifting device with a span of perhaps half a meter. This can be operated either manually or automatically. The power required to lift the rake depends on the weight of the rake and lifting speed; typically it is only a fraction of the rake drive power. The rake should be lifted gradually until the torque returns to a more normal value. Its return to position should also be slow in order to allow the gradual removal of the accumulated solids. The rake lifter is also useful in the removal of agglomerated solids that cling to the rake structure. Raising and lowering the assembly every few hours helps to break up these masses.

Vendors' best designs show lower angular velocities at larger diameters. The rotational speed is not quite inversely proportional to the diameter, so that the peripheral speed increases slowly with diameter. A review of a number of operating units showed that the number of revolutions per hour is related to the diameter (in meters) by the equation

$$N = aD^{-0.8} \quad (47)$$

where $a = 60$ to 90 . In a 30-m clarifier, then, $N \approx 4.5$ rph, and the peripheral speed of the rake is about 0.12 m s^{-1} . It increases only slowly with diameter. In a 60-m unit, the speed called for is about 0.15 m s^{-1} . This is the outer limit of the speeds usually recommended for slow-settling precipitates, and the correlation of Eq. (47) should not be pursued to such large sizes or used as a substitute for more careful design considerations.

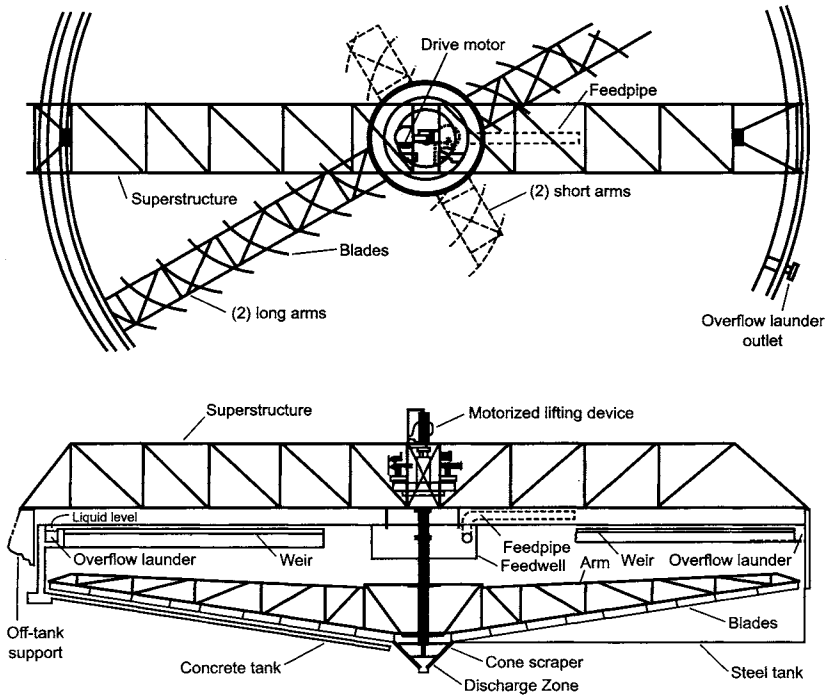


FIGURE 7.55. Bridge-supported clarifier rake. (With permission of Japan Soda Industry Association.)

Rakes and their drive mechanisms can be supported from a bridge across the clarifier or from a center column of concrete or steel. A variation on the latter uses a traction drive with the arm attached to a motorized carriage at the periphery of the tank. This is most often used on very large thickeners. Since chlor-alkali clarifiers are relatively small, bridge supports are suitable and are commonly used. These have several advantages. They transfer the support loads to the periphery of the clarifier, and they can provide easy access from the periphery to the center point. They permit simpler construction both of the rake and of the lifting device. The single drawoff point at the center of the bowl gives a more consistent underflow concentration.

Figure 7.55 shows a typical bridge-supported clarifier rake. Rakes are usually constructed from structural or tubular steel and are coated with rubber or an epoxy to avoid corrosion and brine contamination. Fasteners should be made of a resistant metal such as Monel; sometimes, titanium is used. The drive is mounted at the center, and access must be provided. Usually, a walkway is installed from some point on the periphery to the center well. Sometimes, a full-diameter walkway is provided. The drive, the rake, the center well, and the lifting mechanism are supported from the bridge structure. The rake will roughly follow the contour of the clarifier bottom, which may be flat or built with a slope of 5–15%.

7.5.3.2D. Sludge Removal. The precipitated solids must be removed from the bottom of the clarifier for disposal. Withdrawal of the sludge from the center requires a pipe to

carry the sludge beyond the wall of the clarifier. When a clarifier with conical bottom is installed at grade for cost reasons, a buried pipe or an access tunnel is required. The buried pipe, with a pump installed beyond the periphery of the clarifier, is the cheapest arrangement but also the one most difficult to maintain free of plugs. An access tunnel raises safety concerns as well as operating and maintenance complications. Elevating the clarifier means increasing the elevation of the brine treat tanks and perhaps the saturators as well, and the net effect is rather expensive. Still, this type of installation is perhaps the standard for chlorine plants. It does provide more head for gravity flow through the treatment tanks and into the brine overflow tank and transfer pumps.

Sometimes, the sludge can simply be withdrawn for disposal to a drain or a lagoon. This situation is becoming less common, as environmental regulations become stricter. Some producers with access to brine wells pump the sludge to underground disposal. This returns the hardness elements to their source. The bulk, calcium, returns as a carbonate rather than as a sulfate. The volume of solids in the sludge is very much less than the equivalent volume of salt. Therefore, one well can accept the solids from many wells of the same size. It is possible to dispose of the solids in a producing well. Since the water associated with the clarifier sludge is a small fraction of that required to dissolve salt, the sludge from a diaphragm plant can be diluted to reduce the problems of settling of the slurry and plugging of the transfer pipeline. Spillers [103] described a plant in which the sludge was diluted to 1.8% solids before pumping through 8 km of pipe to the well. The best arrangement involved injecting the dilute sludge near the bottom of the well, which allowed the suspended solids to settle, and withdrawing clear brine from the top. In a membrane-cell plant, the depleted brine flow is a substantial fraction of the feed brine flow. When returning this stream to a well for resaturation, the brine sludge is a relatively minor addition to the volume. Similarly, disposal of waste asbestos from diaphragm cells would add very little to the volume, and this procedure offers an opportunity for its convenient disposal.

Obstacles to the use of this technique may include

1. the cost of adding a return pipeline;
2. in a membrane-cell plant based on solution mining, the prior existence of a return pipeline not suitable for the slurry;
3. precipitation of hardness from the added water when it is mixed with sludge containing excess quantities of treating chemicals.

Most often, the sludge is pumped to a collection tank before going on to final disposal. Advancing-cavity pumps and diaphragm pumps operated by air or electricity are in common use, and in larger units, centrifugal slurry pumps are the norm.

If a salt contains 0.5% CaSO_4 , its treatment will generate 6 kg of CaCO_3 for every ton of chlorine produced. Even in a 1,000-tpd plant, the rate of production of 5% (w/w) sludge will be not much more than $4 \text{ m}^3 \text{ hr}^{-1}$. The very low flow rates in smaller plants using better salts make continuous removal of clarifier sludge a problem. The retention time of the sludge in the clarifier will be a number of days, and so the periodic removal of a quantity of sludge at high flow rate will not upset the process.

This is the approach usually taken. The sludge pump operates at a practical rate for a few minutes at a time. Sudden movement of the sludge in the clarifier often does not always allow the most concentrated material to flow. The compressed sludge at

the outlet begins to move, but the surrounding highly compressed material resists flow. It is easier for lower consistency material higher in the cone to flow past the thicker sludge. This is the classical problem of “ratholing” in a high-solids medium. The systems designed to handle the sludge should therefore be sized to deal with flow rates corresponding to a solids concentration well below that predicted theoretically or determined experimentally.

In some cases, much of the dilution can be avoided by pumping sludge in more frequent short pulses. Withdrawal can be matched to production, and instantaneous line velocities are high. One of the advantages of the side discharge of sludge is the simplification of sludge piping near the clarifier.

Another technique is to remove sludge continuously at a reasonable rate by pumping it to an elevated tank. This provides some clarification, with the brine overflowing to the clarifier. A conical bottom on the tank enhances thickening of the sludge, which can go to a receptacle or to further processing.

The ideal situation matches the rate of sludge withdrawal to the retention time necessary to produce the right concentration. Many plants rely on the skill of the operator to do this, using only sample taps at vertical intervals along the side of the clarifier and primitive measurement of the height of the sludge. Noninvasive instruments such as radiation gauges and sonic devices can be used to provide more precise information. Total control of the operation of a clarifier–thickener remains a difficult problem, both because of the difficulty of making reliable sludge level and density measurements and because of the very long process lag times.

Sizing and layout of a sludge-handling line should follow good practice for slurry piping. This should include arrangements for unplugging sections of the line or for quickly replacing or bypassing troublesome sections.

Example. Using the same $400 \text{ m}^3 \text{ hr}^{-1}$ forward brine flow as in previous examples, we allow 5% for recycle and reworking of backwash brine. To process $420 \text{ m}^3 \text{ hr}^{-1}$ at a rise rate of 0.5 m hr^{-1} , we require a clarifier area of 840 m^2 . The corresponding diameter is 32.7 m. The quality of our salt, if supported by test or by previous experience, should justify a higher rise rate. At 0.6 m hr^{-1} , the clarifier area becomes 700 m^2 and the diameter 29.8 m. We conclude that a standard clarifier will have a diameter of 30–33 m. The rake will operate with a tip speed of 0.12 m s^{-1} or a rotational speed of 4.6 rpm. The drive will be a 5–7.5 kW motor. The drive for the lifting mechanism will be a motor with fractional kW.

The flow from the bottom will contain 4 tpd of solids. As a 6% mud, this will have an average flow rate of $2 \text{ m}^3 \text{ hr}^{-1}$. It will contain 15 tpd salt. Section 16.5.1.3 discusses the recovery of this salt and the processing of the sludge before disposal.

7.5.3.3. Alternative Clarification Processes. The discussion so far has assumed the use of a single conventional clarifier, with a cylindrical body and conical bottom with a thickening rake, in continuous operation. In small plants, the rake may be eliminated; the use of a conical bottom for easy removal of the sludge is then very important. In very small plants, clarification may be a batch process, often in the same tanks used for chemical treatment. Very large clarifiers, on the other hand, are sometimes rectangular

rather than cylindrical in order to improve utilization of plot area. This is rarely the case in the chlor-alkali industry.

In most chlor-alkali plants, the brine clarifier will be the largest piece of process equipment in terms of plot area. There are several methods used in the industry to reduce this area. These include the use of:

1. various techniques of external solids recycle
2. solids-contact clarifiers
3. inclined-plate separators

They are listed in the order in which they depart more widely from the concepts presented above.

7.5.3.3A. Solids Recycle. Solids recycle is not simply a change in clarifier design but rather a modified technique for chemical treatment involving one of the products of the clarifier. The objective is to form larger particles, which settle more rapidly. For a given rise rate in the clarifier, there will be a cutoff diameter below which it is impossible for the particles to settle. Shifting the PSD to larger diameters will allow more particles to settle against a given rise rate. Alternatively, it will allow the use of a greater rise rate and therefore the installation of a smaller clarifier.

The formation of solid particles by crystallization or precipitation usually is divided into two phases, nucleation and growth. Anything that favors nucleation more than growth (e.g., a high level of supersaturation) will lead to small particle size. Anything that favors growth over nucleation obviously promotes larger particle size. Recycling precipitated solids to the nucleation zone is an example of the latter. Figure 7.56 shows the idea. Figure 7.56a is the standard process, or conventional solids precipitation (CSP), discussed in the sections above. With conventional solids recycle (CSR) as in Fig. 7.56b, some of the precipitate removed from the bottom of the clarifier is returned to the first reaction tank. Both precipitants are added to that tank. To the extent that precipitation continues on the recycled particles, they will grow larger and settle more easily. Effectively, this is a technique for extending the residence time of the growing particles in the treat tanks.

The results of solids recycle are enhanced when the solids first are contacted with the precipitating chemicals (Fig. 7.56c). This can take place in a relatively small tank. Possibly because of the fact that some of the precipitants cling to the solids, more precipitation then occurs on the surfaces. This technique is known as precipitant-stabilized solids recycle (PSSR).

Both solids recycle techniques allow some combination of faster rise rate, improved clarity of overflow, higher concentration of solids in the underflow, and reduced consumption of treating chemicals.

Data provided by Timmins [104] on these recycle techniques compare the results obtained with those typical of CSP (Table 7.12). The improved particle size leads to better performance in subsequent steps. Filtration becomes easier, as shown in Table 7.13 by results obtained in a recessed plate-and-frame filter.

Finally, the more efficient use of reagent chemicals with the PSSR technique allows reductions in their excess concentrations. For the same outlet brine quality, Timmins

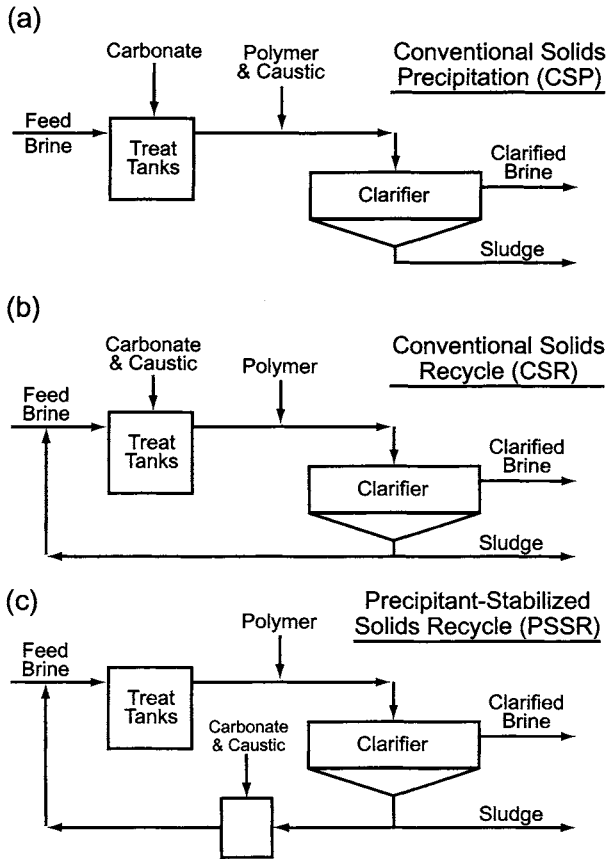


FIGURE 7.56. Solids-recycle clarification processes.

TABLE 7.12. Comparison of Clarification Processes

Parameter	CSP	CSR	PSSR
Rise rate ($m\ hr^{-1}$)	0.5–0.75	0.6–0.85	1.0–1.2
Overflow turbidity (NTU)	10–40	5–10	5–10
Underflow concentration (wt.%)	5–15	10–20	15–25

Notes:

CSP: Conventional solids precipitation.

CSR: Conventional solids recycle.

PSSR: Precipitant-stabilized solids recycle.

reported the use of concentrations of 0.3 to 0.5 gpl carbonate and 0.15 to 0.3 gpl hydroxide instead of the 0.5 to 0.8 gpl carbonate and 0.3 to 0.5 gpl hydroxide used in CSP. Others [105] have recommended excess concentrations of 0.16–0.3 gpl Na_2CO_3 and 0.08–0.16 gpl NaOH when recycling sludge to the reactors.

TABLE 7.13. Effect of Solids Recycle on Filtration Process

Parameter	CSP	CSR	PSSR
Filtration time (hr)	2–6	1–4	0.1–0.25
Wash time (hr)	4–6	2–4	0.25–0.5
Cake solids (wt.%)	50–55	50–60	55–65
Dry cake density (kg m^{-3})	800–880	880–960	960–1040

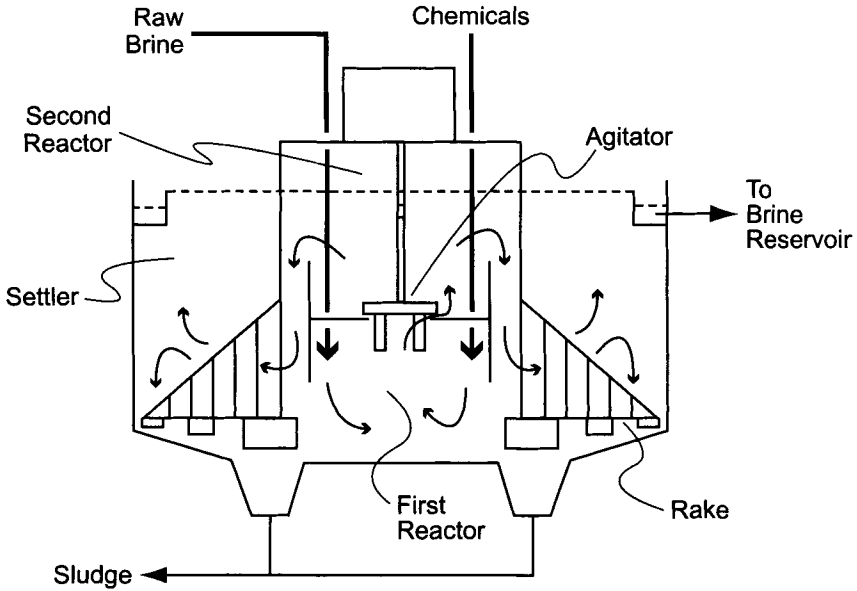


FIGURE 7.57. Typical solids-contact clarifier. (With permission of Japan Soda Industry Association.)

The organization of Fig. 7.56 shows that solids recycle techniques can be applied in modular fashion. They can be valuable in plant improvement and debottlenecking projects. Solids recycle is also useful as a temporary measure in startup of a clarifier. It helps the solids concentration in the compression zone to build up more quickly.

7.5.3.3B. Solids-Contact Reactor–Clarifiers. A solids-contact reactor–clarifier achieves enhanced solids contact within the equipment itself. It performs the operations of mixing, flocculation, and sedimentation in one vessel. A sludge blanket within the clarifier becomes a necessity. Figure 7.57 shows the internals of one type of solids-contact clarifier that employs two reaction zones [106]. Brine and treating chemicals enter the first, or lower, zone. An internal agitator pulls the mixture from the bottom of the clarifier up through a draft tube into the second reaction zone. This design promotes contact between new brine and the existing sludge from the bottom of the vessel and so enhances flocculation. Agitation must not be intense enough to break up the floc, and so a low-shear

agitator with a high pumping rate is used. Brine leaves the second reaction zone by overflowing the periphery of the central tube. Flow then is through the superstructure of the rake, with the clarified brine separating from the sludge. Inclusion of the reaction zones within the clarifier reduces the cross-sectional area for vertical flow of the brine. The extra particle growth offered by sludge contact must outweigh the higher rising velocity in order for this technique to be successful.

In many cases, the design rise rate used in a conventional clarifier can be nearly doubled in these and similar units. The tabulation below shows typical data for another type with excess chemical concentrations of $0.4 \text{ g L}^{-1} \text{ Na}_2\text{CO}_3$ and $0.04\text{--}0.05 \text{ g L}^{-1} \text{ NaOH}$ [104]. Results are best when the magnesium content of the untreated brine is low.

Mg conc., mg L^{-1}	20–50	50–150	>150
Rise rate, m hr^{-1}	1.5–1.7	1.0–1.25	0.5–0.7

The sludge concentration was 5–10%, vs 10–14% in a conventional clarifier, and the turbidity of the overflow was 10–20 turbidity units (NTU) vs 10–40.

The inherent complexity of the internals in this type of unit requires more attention during design to the problem of corrosion. Rubber and epoxy coatings are useful on major elements.

7.5.3.3C. Inclined-Plate Separators. An inclined-plate separator is comprised of a group of plates installed in parallel and at an angle of at least 45° with the horizontal. The plates are separated from each other by about 50 or 75 mm. The design takes advantage of the fact pointed out above that clarification ability is determined by separation area and not the depth of the fluid. To visualize the construction and action of an inclined-plate settler, imagine a very long and narrow rectangular settler cut along the short dimension into pieces that are raised to a certain angle, as in Fig. 7.58, and then mounted close to one

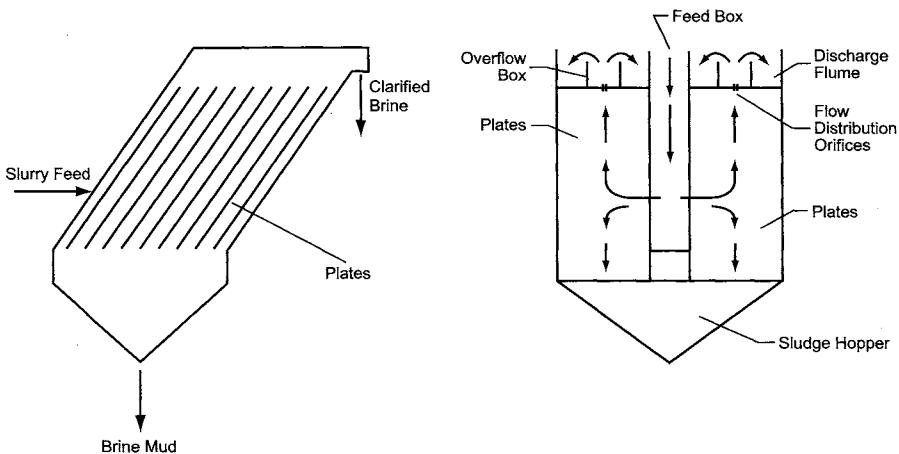


FIGURE 7.58. Inclined-plate settler.

another. Treated brine containing precipitated impurities flows to each plate, and each plate acts as a small clarifier. The effective settling area provided by an assembly is the sum of the horizontally projected areas of all the plates. This is much greater than the plot area, and so a fundamental advantage of the inclined-plate settler is its compactness. Other advantages of the small size are reductions in thermal currents and surface wave action. The reduced retention time in the apparatus is a disadvantage. It does not allow much thickening; the underflow concentration is lower than in a conventional clarifier and more variable. Also, the assembly makes the unit harder to clean. If solids accumulate on the plates, the cross-sectional area available for flow becomes smaller. The higher velocity then sweeps more solids into the clarified effluent. Some units are designed with movable plates. These swivel around fixed connections and can be adjusted to steeper angles to facilitate cleaning [107].

The feed box, which receives the chemically treated brine, is a bottomless channel of adjustable dimensions, usually mounted centrally between two groups of plates. Its length fixes the elevation at which brine is injected into the plates, usually at about one third of the height above the bottom. Its function is similar to that of the feed well in the standard clarifier. From the side, the brine enters the compartments between plates, and the clarified brine begins to separate from the brine bearing the solids. The solids fall down the plates and into a collecting hopper. The underflow thickens as it goes, but with the short residence time mentioned above, the sludge tends to be more dilute. A modification of the basic design therefore includes a sludge chamber fitted with a rake to produce more thickening action.

The clarified brine overflows the chambers through restricting orifices, which collectively act as a flow distributor. The brine then overflows a stilling section into flumes that carry it to a discharge zone. Discharge is by gravity into a collecting tank from which the brine is sent on to the rest of the process.

While inclined-plate separators are put together from a number of sub-assemblies, they are supplied as package units from one source. The sub-assemblies tend to be constructed in the vendors' standard materials. A designer or operator must review these for use in chlor-alkali brine at the process temperature.

A variation on the inclined-plate principle uses inverted triangular elements mounted above each other [108]. The fact that there are so many elements in this type of clarifier translates into a very low upward fluid velocity and a horizontal projected clarification area that is up to 20 times as great as the floor area of the unit.

Several chlor-alkali plants have used the standard inclined-plate separator, but the authors are not aware of any application of the triangular-element version.

7.5.3.4. *Miscellaneous Topics*

7.5.3.4A. *Prevention of Heat Loss.* The great size of standard clarifiers makes them prime sources of heat loss (or, infrequently, heat gain). This is a problem more of process performance than of energy consumption. The loss of heat will result in temperature gradients inside the clarifier. These gradients then are the source of convection currents, which can disrupt the settling of the particles. Most of the heat lost from an open clarifier is from the top, where a considerable amount of water vaporizes. Floating insulators, such as pieces of plastic foam placed on the surface, can reduce this loss. An alternative

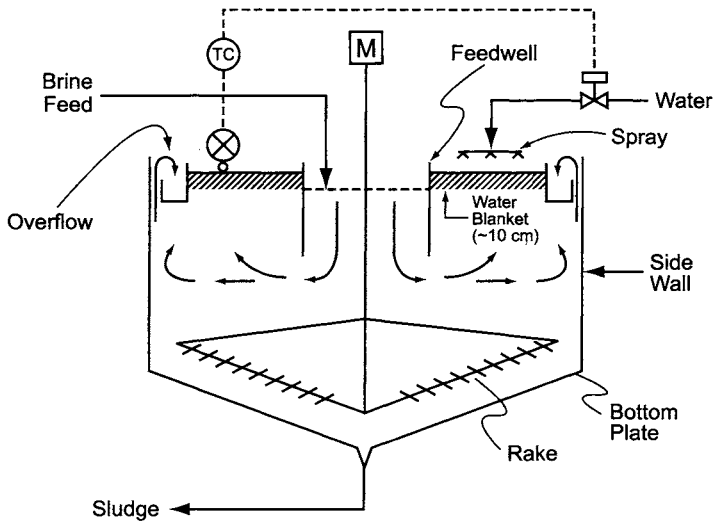


FIGURE 7.59. Insulation of clarifier by water blanket. (With permission of Japan Soda Industry Association.)

is a water blanket. Water sprayed gently onto the top of the clarifier will not mix readily with the denser brine and so will remain as an insulating layer. Figure 7.59 illustrates the concept. The water seal is about 10 cm thick. Water addition responds to a temperature controller. The clarifier can also be covered by a roof. This protects against thermal shock and dilution by rain and snow as well as evaporative and radiative heat loss and can be justified in severe climates. Insulation of the wall will also reduce heat loss. This is not a general practice; when walls are lined with rubber, there is already some insulation incidentally in place.

7.5.3.4B. Use of Centrifuges. Centrifuges are an alternative to filters in the separation of solids from brine. They appear in the sludge-handling process, handling the underflow from a clarifier. Most are simple basket-type centrifuges, and their use is more characteristic of older plants. In these older units, plain steel baskets are common. Monel would undoubtedly give better service. Monel feed and discharge chutes should be specified.

At the expense of their greater power consumption and maintenance expense, centrifuges offer higher solids concentration in the cake.

7.5.4. Filtration

The overflow from the brine clarifier is collected in a tank and then pumped to the filtration area. The clarified brine usually contains less than 50 ppm suspended solids, often as little as 10 ppm. However, clarifiers are subject to upsets and inversions, which can affect the clarity of the overflow for many hours. The filter system must be able to cope with the higher solids load, even if the operating cycle time is reduced.

Filtration is a process in which solids are removed from a liquid by passing a suspension through a porous medium that can retain the solids. The two methods of primary interest to the chlor-alkali technologist are:

1. deep-bed filtration, as in sand filters
2. cake filtration, as in leaf and candle filters

A sand filter contains a packed bed, filled with sand or other fine-particle medium, 1 or 2 m deep. It can handle a higher solids loading than the cake filters but is less efficient at retaining very fine particles. In the two-step filtration process described here, the bed filter is used in the first, or primary filtration, step. In downflow filters, the brine enters the top and then flows through the fill under pressure or by gravity. Upflow filters can be arranged for gravity flow, but the types considered here require pumping of the brine.

Membrane-cell plants, at least, also require polishing filters to remove any solids that pass through the sand filter. Their tighter specification protects the brine softening ion-exchange resin (Section 7.5.5) in the next phase of the process. Ceramic candle filters, cartridge filters, and leaf filters are most common in this application. The leaf filter depends on a filter cloth of large area and the candle filter on a number of cylindrical elements. The brine passes through the cloth, or elements, leaving the solids behind. The colloidal cake that forms is compressible and plugs readily. The normal approach is to use filter aids to improve its characteristics.

7.5.4.1. Primary Filtration. Classically, sand has been used as the medium in bed filters. While it is acceptable in most diaphragm and mercury brine processes, the possibility of dissolving small quantities of silica usually disqualifies sand from use in membrane plants. Other media such as garnet and anthracite are used instead. These have little effect on filter design, and plant conversions usually continue with the same vessels on line but the new fill substituted for sand. Typical particle sizes for both sand and anthracite are about 1 mm, but sand is, on the average, a bit smaller and contains more fines. Regardless of the fill, the apparatus still is frequently referred to as a “sand” filter.

Gravity and pressure both are used to force brine through the filters. Gravity filters give lower unit flow rates but a cheaper installation. Pressure filters achieve higher rates and more consistent results. Modern practice tends to accept the higher installed cost to obtain the advantages of pressure operation.

The next division to be made is between upflow and downflow pressure filtration. Downflow filters operate with shorter beds (about 50% of typical upflow depth). They can achieve high unit throughputs when the solids concentration is low and are most frequently chosen in such cases. Their mechanism is essentially surface filtration by the fine particles at the top of the bed.

The throughput of an upflow filter is limited by the danger of fluidization. This will disrupt the bed and allow a major increase of solids in the effluent liquid. On the other hand, upward flow allows depth filtration, in which particles can be removed from the brine anywhere in the bed. Upflow filters therefore have solids capacities two or three times as great as downflow filters, resulting in longer on-stream times. They also are more stable in the face of a clarifier upset. Some filters can tolerate up to 500 ppm solids in the feed brine while maintaining a 4-hr cycle [109].

“Mixed-media” filters use more than one type of fill. Since density and particle shape both influence fluidization during backwashing as well as the rates of settling, there is a mixture of particle sizes at any level in a bed. This gives downflow filtration some of the character of depth filtration.

While the normal solids content of clarified brine is in a range that often favors downflow filtration, the other considerations given above often result in the choice of upward flow. Both types are widely found in the chlor-alkali industry. Liederbach [40], Sutter [53], and the authors have at least a mild preference for the upflow type, which we adopt here as the standard for discussion.

The filter medium is usually graded by size. Three or four layers of different screen cuts, with the finest material on top, are common. Sand is often placed above one or two layers of gravel or pebbles. The top layer is the deepest as well as the finest. An upflow filter then has a solids capacity of 20–30 kg m⁻², compared with the 5–15 kg m⁻² obtained in downflow. The brine flow rate must be kept below about 0.3 m min⁻¹. The fluidization limit, which will depend on the size and density of the filter medium and the properties of the brine, is an absolute limit which must not be exceeded in an attempt to overcome upsets or to compensate for filter downtime. Some form of assurance that excessive flow will not occur should be part of the design.

All unit operations textbooks present methods for calculating the pressure drop during flow through uniform beds of solids. This section therefore does not address the issue in detail. Particle size and shape, along with the properties of the fluid, are the major variables. PSD is usually taken into account in defining the mean particle diameter, and the effects of shape appear in correlations for the porosity of the bed and the sphericity of the particles. In the case of brine filtration, the feed from the clarifiers can be highly variable, especially during clarifier upsets. For this reason, it is difficult to predict behavior with standard calculations, even if reliable test samples are available. Previous experience of the operator and the vendor is a more reliable guide to rating a filter. Still, it is useful to summarize the normal design procedure.

In bed filters, the deposit of solids leads to a gradual reduction in porosity and a consequent increase in pressure drop. The average porosity is directly reduced by the specific volume of the solid deposit:

$$\varepsilon = \varepsilon_0 - v_s \quad (48)$$

where

- ε = porosity of bed, i.e., fractional void volume
- ε_0 = initial porosity
- v_s = specific volume of solids deposited (m³/m³ of bed)

The specific surface of the bed increases as solids deposit:

$$S = [(1 - \varepsilon_0)S_0 + v_s S_s]/(1 - \varepsilon) \quad (49)$$

where

- S = specific surface of bed, m⁻¹ (i.e., m² of surface/m³ of bed volume)
- S_0 = specific surface of clean bed
- S_s = specific surface of deposited solids

Using these parameters with the appropriate modifications to the classical Ergun equations [110], one can, in normal cases, calculate the pressure drop in a bed [111].

Good filtration also requires proper distribution of the brine flow over the cross-section of the bed. Rather than the pipe distributor found in many other fixed-bed applications, many designs use nozzles fixed to the support plate [109]. These allow brine to pass from the bottom head up into the filtration zone. They end in a capped section with slots to permit radial flow. A screen covers the slots. These nozzles must be leveled very carefully in an upflow filter in order to achieve uniform distribution of fluid. It is particularly critical to level the nozzles to obtain even distribution of the scouring air (see below).

To maintain the best distribution and avoid disturbing the bed, variations in flow rate through a filter should be small or slow. One way to limit variation, but far from universal practice, is to control the flow at a constant rate. Variations in net throughput are then taken up by recycling excess flow back to the feed tank, which is placed on level control. This is the scheme adopted in Fig. 7.47, the clarifier flowsheet. The filters perhaps must be a bit larger to handle the increased flow.

All filters must occasionally be backwashed to remove accumulated solids. Most systems are set up to be backwashed at specified intervals. There must be at least a manual override that allows a filter to be backwashed when filtrate clarity is not up to standard or when the differential pressure is too high. Since this operation takes a filter out of service, the filter plant must be designed to operate at full process rate with at least one unit out of filtration service.

The backwash flow is always upward, and either water or brine can be used to sweep away the solids. In the case of upflow filtration, the term “backwash” then is a misnomer but is commonly used. The bed must be expanded while washing; about 30% or 40% is customary. The degree of expansion depends on the specifics of each manufacturer’s design and on the properties of the washing fluid. A denser or more viscous wash fluid will exert more drag on the particles in the bed. This should be borne in mind when considering changing the backwash fluid. When plant water is used, some adjustments may be necessary to compensate for variations in temperature. Brine is an effective backwash fluid and one that does not disturb the water balance by injecting more water into a closed brine loop. One of the advantages of upflow filtration is that it allows the use of unfiltered brine as a backwash fluid. None of the previously filtered brine then needs to be recycled through the filters, and their total operating load is somewhat reduced.

Scouring with air enhances separation of the collected particles from the filter medium. When a filter is taken out of service for backwashing, it is first drained to a level about 100 mm above the top of the bed. Blowing with air for a few minutes releases the filtered particles from the grains of filter medium. The backwash fluid then performs more efficiently. The drain–scour–backwash cycle takes 10–15 min. It is fairly common practice to repeat this cycle once or twice. This technique improves results, and its frequency can be increased if filter performance is deteriorating. Even when used infrequently, this procedure should be included in the plant operating manual and built into the control program to afford the operator easy access.

Air scouring is an intermittent operation with fairly high instantaneous demand. Superficial air flow rates (standard conditions) are between 1.0 and 1.5 m min⁻¹. The required pressure is only 0.5 or 0.7 bar, while compressed plant air is usually available

at 5–8 bar. Using this air wastes most of the energy of compression. Especially when the scouring air demand has much to do with sizing the plant air system, total cost might be reduced by installing a blower dedicated to scouring air.

Finally, the backwash containing the solids must be dealt with. After collection in a tank, the fluid can be returned to the brine treatment system. To avoid disturbing the process with sudden large flows, the collection tank should be used as a surge vessel and the fluid returned to the process at a more nearly uniform rate. It may go to the clarifier or, preferably, to a treat tank. The collecting tank often has a conical bottom to allow some of the solids to settle out. Some solid material will remain in the supernatant liquid, but continued particle growth will allow it ultimately to settle in the clarifier.

Lined carbon steel is the standard material of construction for primary pressure filter vessels. Typical linings are hard rubber, 3 or 6 mm thick, and glass-filled epoxy resins. Metallic internals tend to be Monel or titanium. Piping is FRP or a thermoplastic such as PVC wrapped with FRP for reinforcement. Internal piping, if not metal, may be of CPVC, properly supported. In larger sizes, support plates usually are of rubber-coated steel.

Most users purchase brine filters as engineered, partly prefabricated packages. Vendors supply skids containing not only the filters but also the filter media, piping, instrumentation, wiring, and some of the auxiliary equipment. At least two filters are necessary to allow operation to continue while one is being cleaned. With sufficient storage volume on both sides, it would be possible to supply two filters each with less than the design capacity of the plant. This is not the usual practice, most systems being designed to operate at full rate with one bed out of operation. Larger systems will contain more than two filters in order to keep their dimensions within the range of normal fabrication and transportation.

Example. We choose anthracite-packed beds to filter the brine in upflow. To allow operation of the filters at constant velocity, we size the beds for 5% more than the average forward flow. This gives us $420 \text{ m}^3 \text{ hr}^{-1}$, and we round this up to $425 \text{ m}^3 \text{ hr}^{-1}$ to allow for dilution by residual backwash water. We must also allow for a bed to be off line during backwash, and we provide several operating beds. The latter is in order to keep the dimensions of the beds within the limits of reasonable fabrication and transportation from the fabrication shop to the site.

To keep the superficial velocity below 18 m hr^{-1} (0.3 m min^{-1}), we need a working cross-sectional area of at least 23.6 m^2 . Providing a 50% safety factor by operating at 12 m hr^{-1} increases the area required to 35.4 m^2 . We tabulate below the internal diameters required as a function of the number of beds on line.

Beds operating	Diameter (m)
3	3.88
4	3.36
5	3.00

Diameters approaching 4 m often cause problems in transportation. The option with four beds in operation becomes attractive, and so we supply a total of five beds with nominal

diameters of 3.4 m. Each bed has a cross-sectional area of about 8.9 m^2 . The maximum solids-handling capacity mentioned in the text was 30 kg m^{-2} ; this is equivalent to about 265 kg of solids in a bed. With 50 ppm solids in the clarified brine, the filter could be on line for up to 50 hr. Even cutting this in half to avoid excessive pressure drop and to allow for clarifier upsets gives an operating time of about a day between backwashes. With four filters on line, this corresponds to a backwash approximately every 6 hr, quite a reasonable cycle. With good performance by the clarifier, a less conservative approach would require a backwash only every 8 hr, which in many plants corresponds to the length of an operating shift.

7.5.4.2. Polishing Filtration. The primary filters will be less than perfect in their removal of solids from the brine. Depending on the results desired and the type of cell used, polishing filters may be required, and in other plants they may be used without benefit of a “primary” filter. Even when using membrane cells, it is possible to do without the primary filters and rely solely on the polishing filters. However, this greatly reduces their productivity by requiring frequent regeneration. Also, polishing filters of reasonable size would not be able to cope with a clarifier upset. In all ordinary circumstances, both levels of filtration are advisable in most mercury- and membrane-cell plants. The enhanced clarity of the brine allows the operation of mercury cells at higher current densities without excessive formation of mercury butter.

Many types of filter are supplied for this sort of operation. In chlor-alkali brine treatment, the two most frequently encountered are the pressure leaf filter and the candle filter. Both types are capable of removing submicron particles and producing a filtrate with less than 1 ppm of suspended solids. A leaf filter, as the name implies, contains a number of thin, flat elements that are active on both sides. In chlor-alkali brine plants, the leaves normally are suspended vertically in a tank. The tank may be horizontal, in which case the leaves are circles or rounded squares, or vertical, in which case the leaves are approximately rectangular and of different widths.

The filtering element is a cloth (e.g., polypropylene) mounted over a metal mesh (Monel or titanium). Reinforcements are internal, and the cloth is held down by corrosion-resistant pins (e.g., titanium). Flow is through the cloth from the outside. The cloth usually has a permeability of $15\text{--}25 \text{ m air hr}^{-1} \text{ mm Hg}^{-1}$. The filtrate leaves through a bottom connection into a header.

Monel and lined carbon steel are standard materials of construction for filter vessels. Linings are similar to those used in primary filters. Figure 7.60 shows a typical vertical-tank vertical-leaf filter. The stream to be filtered enters the body of the tank. A bottom connection is shown, but there are other options. The leaves are arranged vertically, and flow is from the outside to the inside of the leaves. Filtrate collects in a pipe at the bottom; this also serves as support for the filter elements. The tank also has drain, vent, and compressed air connections. The detail shows one type of assembly that can simply be lifted from the effluent pipe. O-rings supply the seals.

A candle filter contains a number of cylindrical elements in a vertical tank, using materials of construction similar to those used in leaf filters. The elements can be built up, in modules similar to those used in mist eliminators (Section 9.1.5), or they can be “solid” cylinders made of carbon or a ceramic. The latter are porous, with walls about

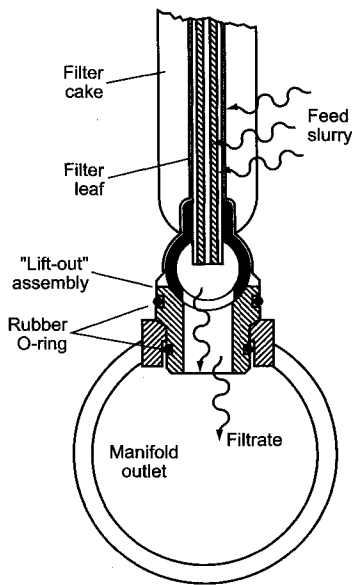
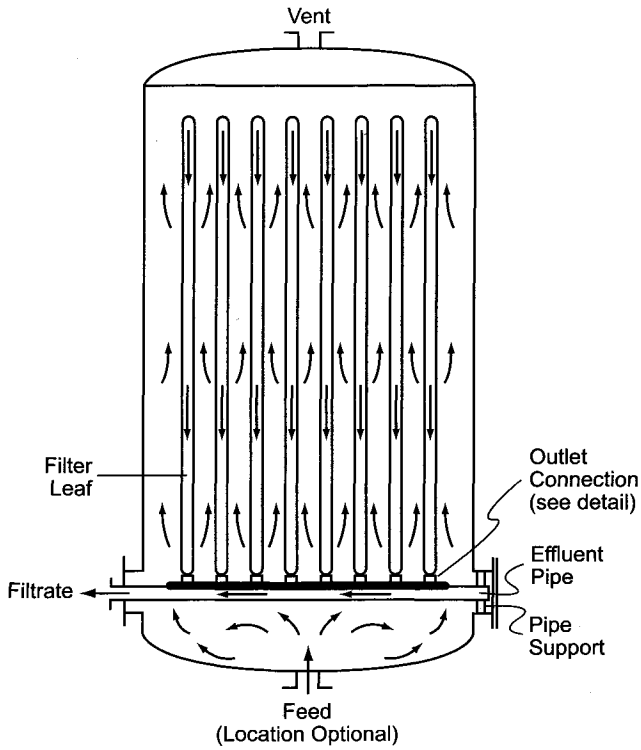


FIGURE 7.60. Pressure-leaf filter.

25 mm thick. Typical elements are 70 mm ID and 120 mm OD, in lengths up to 1.5 m. Carbon candle filters are similar to those used for many years to filter mercury-cell caustic. Candles typically have porosities of 40–45%, and their pore structure is quite uniform (average about 100 μm , maximum less than 200 μm). The latter fact helps to make backwash flow more uniform and more effective. The use of candle filters is most common in Japan, where a 1998 survey of 25 plants using two stages of filtration [112] showed that 21 used some form of bed-type filter in the first stage. Twenty of the plants reported using “ceramic” or “cartridge” filters, which we take primarily to mean candle filters, in the second stage.

Candle filters, it is argued, also have an advantage in producing brine of higher clarity. This is attributed to the fact that, under pressure, filter leaves will be slightly distorted. The cake can then develop minute cracks, allowing fine solids to pass through. The cylindrical shape of the candle filter works against this, and the elements with their great structural strength are able to maintain a good cake. Figure 7.61 illustrates this phenomenon for a typical leaf-filter screen.

In both leaf and candle filters, the cake deposits onto vertical surfaces. It should not be shocked or disturbed by sudden changes in flow rate. It is more important with polishing filters than with bed filters to maintain steady brine feed rates. The same technique of controlled flow with spillback to a feed tank is often used. The instrument diagrams of Figs. 11.6 and 11.7 illustrate this approach.

The surface of each filter element serves as a support for the deposited solids. The real filter medium is the solids themselves. Their accumulation causes the resistance to flow to increase continuously. This is the distinguishing characteristic of cake filtration. Analysis of the process requires some way to describe the changing relationship between flow rate and pressure drop. Here, we follow the method of Foust and coworkers [113].

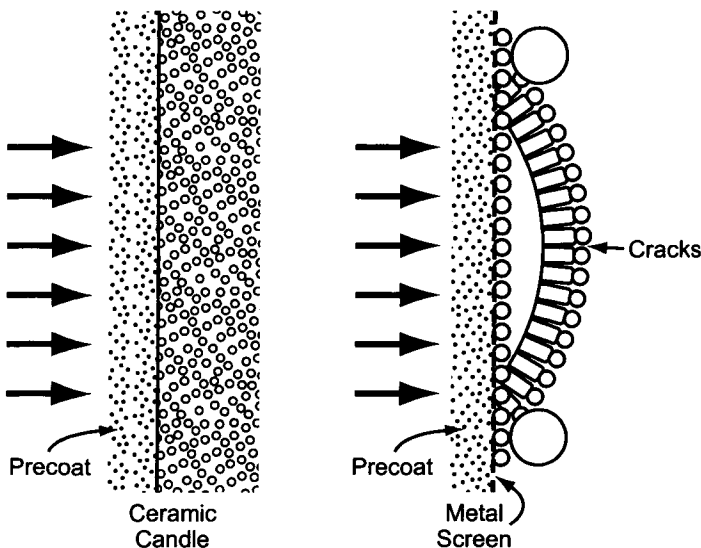


FIGURE 7.61. Distortion of filter leaf.

Flow through a filter bed or cake is usually laminar, and a form of the Carman-Kozeny equation [114] therefore applies:

$$(\Delta P g_c / L)(D_p / \rho v_s^2) \varepsilon^3 / (1 - \varepsilon) = a(1 - \varepsilon) / Re \quad (50)$$

where

ΔP = pressure drop through bed

g_c = standard acceleration due to gravity

L = length of bed (thickness of cake)

D_p = particle diameter

ρ = fluid density

v_s = average superficial velocity of fluid through bed

ε = porosity of bed (dimensionless)

a = constant

Re = Reynolds number

For laminar flow in a filter cake, this can be written as

$$\Delta P g_c / L = 180(1 - \varepsilon)^2 \mu v_s / \varepsilon^3 D_p^2 \quad (51)$$

The equation is dimensionless, and any consistent set of units can be used. The constant on the right-hand side appears with different values for different types of apparatus, but it will be assumed into an empirical quantity below. Several modifications will put Eq. (51) into a form that is easier to use. First, the equivalent diameter of the particles is that of a sphere with the same surface area per unit volume:

$$A_o / V_o = \pi D_p^2 / (\pi D_p^3 / 6) = 6 / D_p \quad (52)$$

This ratio we call the specific surface, S_o . Substituting for D_p :

$$\Delta P g_c / L = 5(1 - \varepsilon)^2 \mu v_s S_o^2 / \varepsilon^3 \quad (53)$$

This can be solved for the flow velocity, v_s . Multiplying by the filtration area A gives the total filtration rate:

$$dV / d\theta = \Delta P g_c \varepsilon^3 A / 5(1 - \varepsilon)^2 L \mu S_o^2 \quad (54)$$

where dV is the volume of filtrate produced in time $d\theta$. We have already noted that the thickness of the cake varies (increases) with time. It can be calculated from the concentration of the feed slurry and the amount of filtrate passed. The volume of solids in the cake formed by passage of a unit volume of liquid is equal to the weight of solid collected (w) divided by its density. The total volume occupied in the filter also depends on the porosity of the cake:

$$\text{Solids volume} = w / \rho_s$$

$$\text{Cake volume} = w / \rho_s (1 - \varepsilon)$$

In terms of the previous variables, we have

$$LA(1 - \varepsilon)\rho_s = w(V + \varepsilon LA) \quad (55)$$

The term εLA represents the liquid held in the filter cake. Given a long enough run, this usually becomes negligible. In that case, we can write

$$L(1 - \varepsilon) = wV/A\rho_s \quad (56)$$

Substituting this into Eq. (54) gives

$$dV/d\theta = [\varepsilon^3 \rho_s / 5S_0^2 (1 - \varepsilon)] \Delta P g_c A^2 / \mu w V \quad (57)$$

The terms grouped in brackets are all characteristics of the cake. We define the reciprocal of this group as the specific cake resistance:

$$\alpha = 5S_0^2 (1 - \varepsilon) / \varepsilon^3 \rho_s \quad (58)$$

and then

$$dV/d\theta = \Delta P g_c A^2 / \mu \alpha w V \quad (59)$$

The problem that remains is to relate ΔP and α to V and θ . In a well-behaved system, the specific cake resistance may be constant. Then, solutions of Eq. (59) usually assume that either the pressure drop or the rate of filtration is constant. In the applications of interest here, one usually operates constant-rate filtrations. Now, to relate pressure required to volume of filtrate is a simple matter, with no integration required. We have

$$\Delta P = (\mu \alpha w R / g_c A^2) V \quad (60)$$

where R is the constant rate of filtration, $dV/d\theta$.

These equations account for the resistance of the cake but not those of the piping and internals of the filter. It is customary to consider these as resistances in series and to add a constant resistance term at an appropriate point in the development, for example at Eq. (54). When this is carried through the above development, it appears as a term that must be added to the volume of the filtrate. The added resistance therefore is equivalent to passing the additional volume V_e through the filter:

$$\Delta P = (\mu \alpha w R / g_c A^2) (V + V_e) \quad (61)$$

A plot of pressure drop vs volume of filtrate then has the slope $\mu \alpha w / g_c A^2$ and the x -intercept $-V_e$.

This development is restricted to cakes of constant surface area and so is a good approximation only to the situation on a leaf filter. The variation of area with thickness is strong in a candle filter and less so in a rotary filter, where the radius of the drum normally is much greater than the thickness of the cake. These geometries require modifications

that are not presented here. The reader can derive the proper equations by relating the surface area of a cake to its thickness. Also, some design equations appear in books on unit operations, and equipment vendors publish their own versions.

The development so far is also based on constant α or on homogeneous cakes whose properties do not change with time or operating pressure. In fact, most cakes are compressible to some degree. As more fluid passes and more cake deposits, the older layers of solid are subject to frictional drag. The particles continue to move toward the filter surface and even to penetrate it, and the cake becomes denser in that direction. In other words, the cake is compressible, and the value of α varies. Significant cake compression is more likely in constant-rate filtration, where the pressure increases continuously.

This situation can be handled mathematically if α can be related to operating variables by an integrable function. Two that are in common use are

$$\alpha = \alpha_0 + b(\Delta P)^s \quad (62a)$$

$$\alpha = \alpha'_0(\Delta P)^b \quad (62b)$$

The former is limited to low or moderate pressures. The latter improperly gives $\alpha = 0$ at zero pressure drop, and so it should be used only in the range of pressure for which the constants were determined. Alternatively, α can be determined experimentally as a function of pressure, and then some form of Eq. (59) can be integrated graphically.

Since the precipitates we deal with typically are compressible and do not form permeable cakes with desirable characteristics, it is standard practice to add a filter aid. Materials such as the flocculants that are used in brine treatment are sometimes referred to as filter aids because they improve the filterability of the particles that are to be removed. In our usage, however, a filter aid is a solid material added to the process to improve the characteristics of a filter cake. It should provide a noncompressible surface that does not quickly lose its porosity as solids accumulate. Without such a material, the surface in a pressure filter would soon become blinded. The filter aid is applied to the filtering surface before flow of brine begins in order to provide a good foundation. A slurry is circulated from a tank through the filter until enough filter aid, or "precoat," has deposited.

Precoat slurries are prepared batchwise in a dedicated tank. This must have a working volume greater than that of the filter(s) to be treated along with the associated piping. An agitator is essential to keep the filter aid in suspension. Large-bladed turbines or propellers rotating at low speed are best.

The precoat should be deposited to a thickness of at least several millimeters or to a load of about $1\text{--}2 \text{ kg m}^{-2}$. A survey of commercial practice showed no firm agreement on the optimum precoat slurry concentration, but in order to ensure uniform coating of the filter surface, the slurry should be dilute, and frequently the concentration is 1% or less.

Centrifugal pumps are best for transferring precoat slurries. Low-speed pumps with open impellers will produce less degradation of the particles. The materials of construction of the pump will depend on the fluid selected as the carrier. The velocity of flow must be high enough to keep all the particles in suspension but not high enough to erode the cake as it deposits in the filter, where surface flow rates usually are between 2 and 5 m hr^{-1} . This should produce a differential pressure of about 0.15 bar , and the depositing process should take about 15 min . One of the filter feed pumps may be used as

the precoat pump if duties are compatible. When precoating is complete, the transition to duty filtration should be immediate and bumpless, in order not to disturb the precoat cake. This is more easily accomplished if the precoat batch was prepared with the same fluid that is to be filtered. Extreme temperature shocks also can disturb the applied precoat; the precoat suspension and process fluid usually should not differ by more than about 50°C.

A useful precoat is one in which the particles of filter aid, which individually may be smaller than the openings in the filter septum, have bridged these openings. This is difficult to achieve when air bubbles are attached to the particles. The entire system should therefore be designed to avoid aeration of the slurry. Low-speed agitators are used, and they must be able to operate without excessive entrainment of air while filling or emptying the tanks. Vortexes may form as the level in a tank drops, and baffles or vortex breakers should be installed if this is a problem. Elevation of the tank and sizing of the suction line should ensure that the pressure remains positive everywhere on the suction side of the pump. The return line from the filter should be taken to the bottom of the precoat tank to prevent entrainment of air.

The precoat makes it possible to obtain a clear filtrate at good rates at the start of the operating part of the cycle. After deposit of the precoat, brine usually is circulated through the filter and back to the feed tank for a short time, until its clarity is acceptable. When operation begins, the good surface presented by the precoat can then gradually become plugged with the more gelatinous precipitate. Periodic or continuous addition of a filter aid along with the feed can prevent this and help to maintain a porous surface. The filter aid in this step is designated the “admix” or “body feed.” Its function is to prevent gradual blockage of the filtering surface. Figure 7.62 shows how the measured compressibility of a cake decreases as more filter aid is used [115].

In order to form a highly permeable, stable, and incompressible cake, filter aid particles should be rigid, intricately shaped, and porous. The characteristics of the particles should allow removal of submicron solids to a level well below 1 ppm. The filter aid must also be chemically inert and insoluble. “Insoluble” here is a relative term,

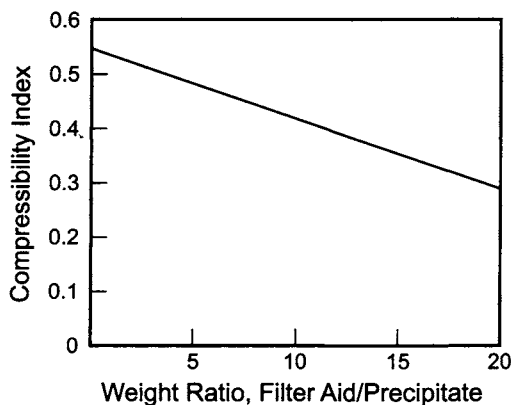


FIGURE 7.62. Effect of filter aid dosage on compressibility of cake.

and it is the slight solubility of amorphous silica in brine that disqualifies it as a filter aid in some plants.

Considerations in design of the body feed system are quite similar to those above related to the precoat. The major difference is in the rate of utilization. Body feed is added continuously at low rates. Centrifugal pumps are not appropriate in most systems; piston or diaphragm pumps are used instead. These should have variable capacity, which can be obtained by varying stroke length or speed. Filter aids also can be educted into the brine.

Because of the low rate of flow of the body feed slurry, good pipeline design includes safeguards against deposits. In any vertical lift, the velocity must be sufficient to keep the solids in suspension. This velocity varies with the choice of filter aid, but 100 m hr^{-1} is usually sufficient. There should be provision for keeping the pump operating while the filter is out of operation, and there should be flush connections on the process lines before and after the pump. When a diaphragm pump is used, the outlet should be at the bottom of the chamber. Body feed slurry concentrations are usually no higher than precoat concentrations. Often, they are lower. This allows higher line velocities and helps to keep the particles suspended.

The optimum level of addition of body feed is usually one or two parts per part of suspended solids in the brine. Since the solids concentration varies with time, some safety margin in the rate of body feed addition is a good idea. This is usually supplied by basing a constant body feed addition rate on a nominal but safe concentration of suspended solids. If the rate of addition is too low, the brine solids can plug the pores in the growing filter cake and reduce the cycle time by causing a rapid increase in operating pressure. At very low rates of addition, in fact, the use of body feed does more harm than good. It is unable to function as intended and merely adds to the solids load seen by the filter. With too much body feed, on the other hand, initial results will be deceptively good. The rate of increase of the operating pressure will be quite low. Later, however, there will be a very rapid increase, as the filter becomes prematurely full of solids.

Not all filtration applications require body feed. If there is little to be gained from its use, it becomes counterproductive as it once again reduces the holding capacity of the filter for the precipitated solids. In some applications, body feed is added directly to the liquid to be filtered, removing the need for a tank and slurry delivery system. This approach has problems of its own, including extra wear on the main pump and sometimes inadequate dispersion. It is not common in the chlor-alkali industry.

The precoat and the body feed can be the same material, or two different filter aids can be used. In the process industries in general, diatomaceous earth is the most widely used filter aid. Purified diatomaceous earth is hydrated silica in amorphous form. Its source is the fossilized external skeletons of microscopic organisms. Artificial perlite, which also is primarily silica, is a frequently used alternative. Table 7.14 shows typical chemical compositions of these materials.

Amorphous silica and the associated alumina have some solubility in alkaline brine. Figures 7.63(A) and (B) show that powders of both materials dissolve at constant rates. Figure 7.64 shows that the rates of solution increase with temperature and the alkalinity of the brine. While these effects are often accepted in those diaphragm and mercury

TABLE 7.14. Composition of Artificial Perlite and Diatomaceous Earth

Constituent	Perlite	Diatomaceous earth
SiO ₂	74.2	89.7
Al ₂ O ₃	13.1	4.8
Fe ₂ O ₃	0.8	1.9
MgO	0.07	0.7
CaO	0.28	0.8
TiO ₂	0.15	0.2
K ₂ O	4.3	
Others	7.1	1.9

All data in weight% (dry basis).

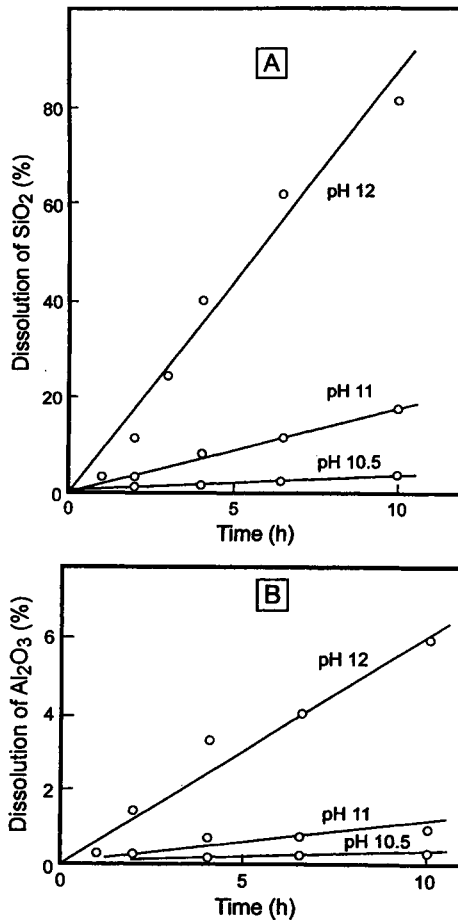


FIGURE 7.63. Dissolution of (A) SiO₂ and (B) Al₂O₃ in alkaline brine at 70°C.

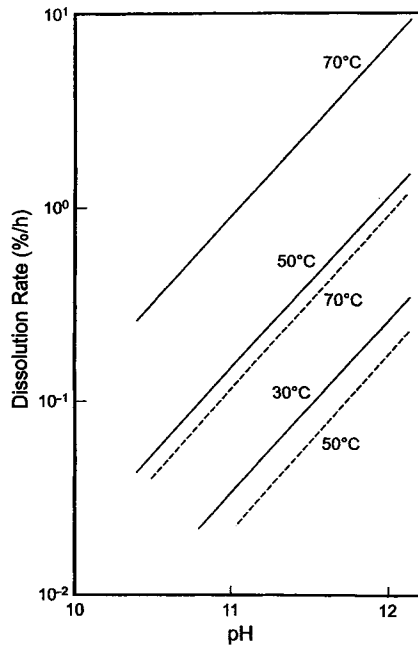


FIGURE 7.64. Al_2O_3 and SiO_2 dissolution rates as functions of pH and temperature. Al_2O_3 : dotted lines; SiO_2 : solid lines.

plants that use cake filtration, the extra sensitivity of membrane cells once again requires a change in the process. The favored substitute for siliceous filter aids is one based on α -cellulose.

Filter aids are usually supplied in bags. With their very low bulk density and fine particle size, their handling can be very dusty. Bag-handling equipment, properly vented, can alleviate the dust problem. The filter aid can be dumped directly into a mix tank or into an intermediate hopper. The advantages of the latter, more expensive, approach are that quantities larger than a single batch can be handled, reducing the frequency of the operation, and that the bag-handling equipment is exposed to a dry atmosphere. Filter aid is added from the hopper to a batch by means of a screw or a rotary valve. While more exact quantities can be transferred this way than by dumping an integral number of bags, the application of filter aids is not enough of a science for one to consider this a great advantage. A filter aid hopper and the body of a rotary valve can be in carbon steel. Since the rotor itself is subjected to a humid atmosphere above brine, a coating on the steel is useful.

Like primary filters, polishing filters must be taken off line for cleaning when flow rate deteriorates, differential pressure increases, or the body of the filter fills with solids. The emphasis in fundamental analysis of the filtration of brine is on the production of clear brine at a defined rate. The efficient removal of cake from the filter, however, is of equal importance. The removal of occluded brine from the cake for recovery or for waste minimization may also be necessary. Before cleaning, the brine inside the filter body is usually removed. This involves the use of compressed air to blow the brine back to its

feed tank. Some filters are built with a horizontal blowdown leaf to filter this material as well. This feature is more common in batch processing and does not appear to be used extensively in chlor-alkali plants.

When a cake is washed to recover liquor, the rate of flow follows the Carman equations (50) and (51). The thickness of the cake remains constant during washing. Estimation of the washing rate is then simplified but should take into account the fact that some filters adopt a “wash-through” configuration, and the washing and filtration paths are not of the same length. The characteristics of the cake should likewise be unchanged. In some cases, however, the wash fluid and the process fluid may have quite different characteristics. This complicates flow rate calculations and, perhaps more importantly, makes it more difficult to estimate the efficiency of washing. As washing begins, much of the occluded liquor moves nearly in plug flow, and the first stage of washing is a highly efficient displacement. The efficiency of later stages of washing depends largely on the relative viscosities of the filtrate and the wash liquor. A low-viscosity fluid slides more easily past the film of process fluid attached to the filter medium and does a relatively poor job of removal. Brown *et al.* [116] present data on the volume of wash fluid required to remove a given amount of filtrate as a function of average particle diameter when the viscosities of the two fluids are the same. They supplement this information with correction factors for low wash liquor viscosities and for thin cakes, in which channeling of the wash liquor is more likely. These corrections are not of great significance in the typical brine filter, but they may become more important in caustic filtration.

The washing process may be replaced or followed by a step in which air is drawn or forced through the cake. This is a case of two-phase flow with a constantly changing phase ratio. The complex calculations can be simplified by the proper assumptions if the properties of the solids are known and constant. This is seldom the case during design, and test data or approximations are necessary. The air flow during displacement usually increases rapidly as liquid is displaced, reaching a maximum essentially equal to the flow through dry cake. At least in principle, air flow can continue for some time and partially dry the cake.

After washing or air displacement, the cake may be removed by any of several mechanisms. These include sluicing (normally with water), shaking, and blowing. If cake removal is inadequate, the area effectively available for filtration in the next cycle decreases. The flow pattern through the filter medium is distorted, and the flow rate through a unit of clean area increases. The latter can cause breakthrough of solids and a shorter operating cycle.

When cake is to be removed by sluicing, a fixed nozzle is the simplest installation. However, this arrangement is less effective than a movable sluice, which may involve rotation, oscillation, or traversal. In any case, the nozzle requires a seal, and the motion complicates the problem of achieving a tight seal.

The general subject of treatment and disposal of the solids removed from the filters is covered in Section 16.5.1.4. Here, we note that there are advantages to reducing the amount of water or, especially, brine attached to the solids. Toward this end, filter cakes can be removed mechanically, by shaking or blowing with air. This avoids the dilution caused by wash water. The bottoms of the filters must then be designed to allow easy removal of this relatively dry material. Leaf filters designed for dry discharge have a shaking mechanism. This releases the bulk of the solids from the leaves. Vertical

tank filters have conical bottoms with special discharge nozzles that allow dumping to a container or removal by a screw. Horizontal tank filters usually are fitted with a conveying screw running along the bottom of the vessel. Some candle filters dislodge the solids with a pulse of compressed air. At the expense of an increased cycle time, they can also dry the cake by air blowing in order to increase the solids concentration still more.

Leaf filters usually are supplied with a sluicing mechanism. This sprays the leaves and washes away the cake. Internal piping to a sluicer usually is PVC or CPVC; metallic parts are titanium. Flow rates typically are equivalent to a face velocity of about 0.8 m hr^{-1} , with a duration of several minutes. Part of the art of design of a leaf-filter assembly is arranging the sluicing mechanism for good results. There is usually an oscillating motion to enable the whole surface of each leaf to be covered. This requires close attention because the filters are designed to minimize waste space. When the cakes reach their maximum thickness, defined by the manufacturer, there is little clearance between two cakes and little room for error in directing the sluicing liquid. The distribution of inlet brine flow should be checked closely for the same reason. Impingement of the incoming brine can wash away the cake. This causes distortion of the overall flow pattern and allows solids to leak through the cloth.

Candles can be sluiced or backwashed from the insides of the cylinders. A useful option with the cylindrical geometry is to apply a pressure pulse to dislodge the cake. With the fabric-covered version, this might be an air pulse. To avoid a sudden drop in pressure in the air header when this is done, an air tank is usually mounted on the unit. This can be filled by line pressure or by a small compressor dedicated to the service. When air is released, the pressure in the tank drops, but not so drastically as would the pressure at the end of a pipeline. With the porous carbon elements, the pressure pulse is applied to lines still filled with filtrate. This produces a sudden rush of fluid back through the elements. This so-called "flashwashing" is a very efficient form of backwash.

Candle filters usually operate with a superficial liquid velocity through the surface of an element of $2\text{--}3 \text{ m hr}^{-1}$. Precoat usage is much the same as with leaf filters, but cakes are thinner ($\sim 15 \text{ mm}$). The compressed air used to drain liquid from the filter tank can also be used to dry the filter cake. The same air at approximately the same flow rate also serves to pulse the candles. The air should be at $3\text{--}4 \text{ bar(g)}$ and, if used to dry the cake, have a dew point no higher than -20°C . In most units, the candles will be divided into groups for sequential pulsing. The air pulse rate will be equivalent to about $60 \text{ Nm}^3 \text{ hr}^{-1} \text{ m}^{-2}$ of surface. The amount of air used to drain the vessel will be about $1\text{--}1.5 \text{ Nm}^3 \text{ m}^{-2}$ of surface, and drying air consumption will be about $4\text{--}5 \text{ Nm}^3 \text{ m}^{-2}$. All these figures are highly dependent on the geometry of the equipment.

7.5.4.3. Backpulse Filtration. The polishing filters described in the preceding section rely on filter aids for efficient removal of solids. This is necessary because the pores in the filter cloths are larger than some of the solids that are to be filtered. It is necessary first to build up a surface that will retain these solids and then sometimes to continue to renew the surface to prevent its blinding with small or compressible particles. At least in principle, the operation might be simplified if the pores in a filter medium could be made reliably smaller than the suspended solids in the feed liquor and yet controlled to

avoid the formation of large numbers of channels so small that flow would be seriously impeded.

Advances in membrane technology make it possible to produce media with uniformly small openings. Solids therefore can be deposited directly upon the membrane surface, giving a clear filtrate from the start of operation, with no need to establish an impervious surface with a filter aid or the solids burden from the feed liquor. The mechanism is one of surface filtration rather than the depth filtration that occurs with conventional media [117]. If only a small amount of cake builds up, there is little if any compression of the solids, little increase in the pressure drop required to maintain a constant rate of filtration, and little difficulty in removing the deposited solids by backwashing. This is the basis of backpulse filtration. The easy and thorough removal of solids from the surface makes the downtime in each cycle very short. Figure 7.65 compares this style of operation with a conventional filter in constant-pressure mode. The effective average rate of production of a unit area of filter is higher in the backpulse mode [118].

The technique is beginning to find applications in chlor-alkali brine plants. In construction, the surface filters used in chlor-alkali applications resemble the candle filters discussed in Section 7.5.4.2. Membranes can be sintered onto supporting elements or applied as cloths held to the candles with titanium clamps. Physically modified (expanded) PTFE has the advantages of controlled pore size, great chemical resistance, and low-energy surfaces that improve the release of particles when pulsed. The candles hang from a tube sheet in a vertical vessel. The vessel may have a conical bottom, for reasons that appear below. Flow is from the outside of the candles through the tubesheet or a collecting manifold and out of the vessel. Figure 7.66 shows a thin layer of deposited solids. A backpulse of low-pressure compressed air (ca. 30 kPa) then forces filtrate back through the element and removes the solids from the membrane surface (as in “flashwashing” in the previous section). This pulse is of short duration, and the volume of liquid displaced is essentially that held inside the dome of the vessel. To make room for the pulsed liquid on the feed side of the candles, some liquid may first be drained from the shell. Usually, an air reservoir is supplied in order to help keep the line pressure constant throughout

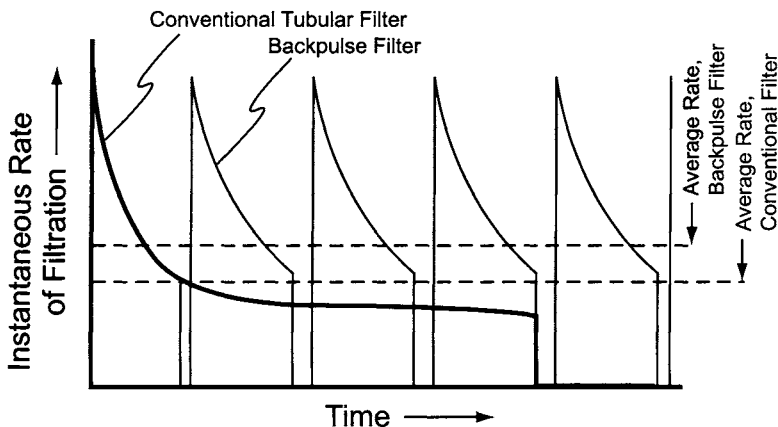


FIGURE 7.65. Operating cycles in backpulse filtration.

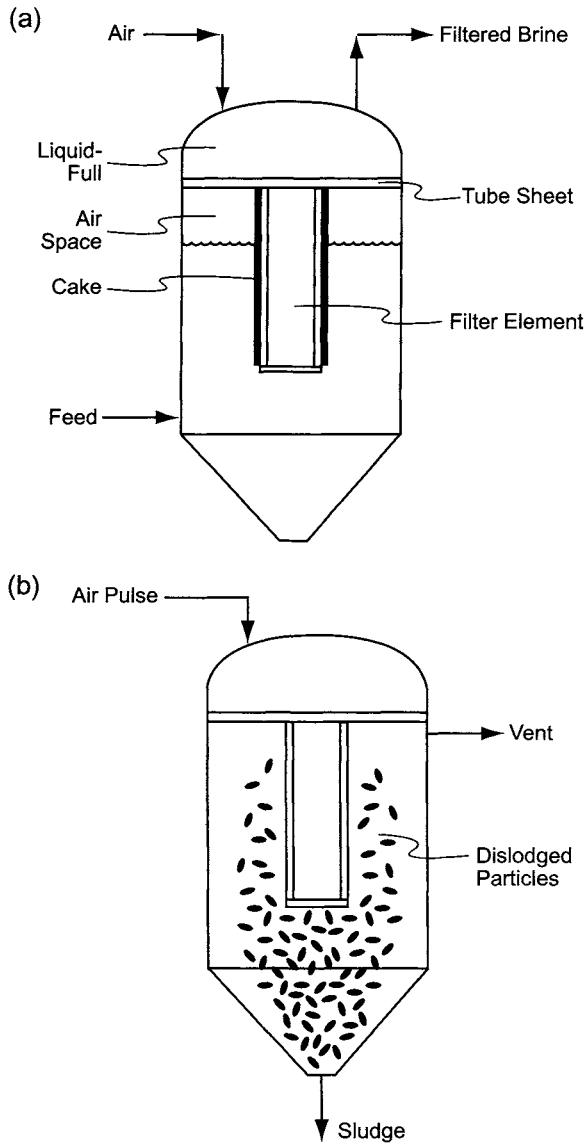


FIGURE 7.66. Typical backpulse filter operation. (a) After filtration and partial draining, and (b) Release of cake by pulse of air.

the pulse, which lasts only a few seconds. Backwash time therefore is much shorter than it is in the case of a precoated filter. In larger units, the filter elements may be grouped into sequentially pulsed registers.

The solids displaced from the surface settle through the liquid in the vessel and enter the bottom cone. This serves as a sludge collector. The sludge can be removed through a timed bottom valve after each pulse, or sludge can be accumulated through a

number of filtration–backwash cycles before discharge. Each system will have its own optimum.

At least conceptually, the potential of these filters goes far beyond replacement of the polishing filters. The ultimate achievement in the chlor-alkali brine process would be to take treated brine from the precipitation reactors and filter it directly in a single step to produce clear filtrate. This would combine the functions of the clarifier, the primary filters, and the polishing filters in a single step. Further discussion is in Section 17.3.1.

7.5.5. Ion Exchange

Properly treated and filtered brine is suitable for use in diaphragm or mercury cells. Before it can be used in membrane cells, its hardness must be reduced to ppb levels. The more rigorous specification is necessary because multivalent cations are able to travel into the membranes along with Na^+ and K^+ . Section 4.8.6 discusses the mechanisms by which these ions damage the membranes.

Early membrane cells operated at relatively low current efficiencies and were able to tolerate correspondingly higher concentrations of impurities. As membranes were improved and better results became possible, the requirements for brine purity became stricter. For a time, the addition of phosphate to the brine to sequester the hardness ions and prevent them from entering the membranes mitigated some of the effects of hardness. Finally, it became necessary to devise a process to increase the purity of the brine well beyond that obtained by chemical treatment, and ion exchange is now the standard technique. Several general reviews of the brine ion-exchange process itself are available [119–121].

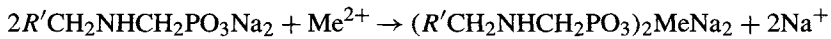
7.5.5.1. Technology and Operation. Ion exchange is defined here as the reversible exchange of ions between a solid ion-exchange material and a liquid. During this process, the solid will not undergo any permanent change in its structure. Its duty is to exchange alkali metal ions (e.g., Na^+) from its structure for alkaline earth ions (e.g., Ca^{2+}) from the solution. This is equally well a description of the duty of the ordinary water-softening resin. The important difference between water softening and brine purification lies in the composition of the fluid to be treated. Water contains low concentrations of both ions, and the selectivity of ordinary gel-type resins for calcium over sodium, while sufficient for the application, is probably less than 10. Chemically treated brine, on the other hand, contains calcium at a molarity around 10^{-4} and K^+ or Na^+ at a molarity of 4 or 5. Much higher selectivities are needed if most of the calcium is to be removed. Special resins are necessary, and so the process typically uses chelating resins having iminodiacetate or aminophosphonate end groups [120,122,123]. The typical resin in this service has a selectivity in the vicinity of 10^5 .

The resins are based on standard styrene/divinyl benzene polymers with weakly acidic functionality. The first resins developed borrowed directly from chelation (L. *chela* = *claw*) chemistry. Compounds such as ethylene diamine tetraacetic acid (EDTA) when ionized have two monovalent anionic end groups that do in fact have a claw-like structure. They have a powerful affinity for divalent cations such as calcium and magnesium. When iminodiacetate functionality is built into a polymer, it provides

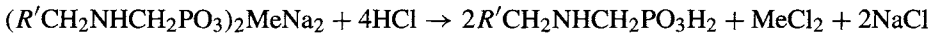
the same affinity to attract hardness ions from solution. When the first resins were used, hardness levels of a small fraction of a part per million became available. Brine hardness specifications dropped to 50 ppb, and the first true high-efficiency membranes went into commercial operation. The resins continued to improve, and other resins appeared that relied on the ability of phosphate compounds to attract calcium and magnesium. The newer aminophosphonic resins generally have better kinetics for the capture of magnesium and calcium, and so the permanent leakage of hardness through the beds is less [120]. With continuing developments in the field of ion exchange, many plants now can operate with less than 10 or 20 ppb hardness in their cell feed brine. As specialty items, the resins cost nearly 10 times as much as the mass-produced gel-type water softening resins [121].

The process takes place over fixed beds of resin. Because the resin in each bed functions in a semi-batch mode, a continuous system must have at least two beds, so that one can be taken out of service after picking up a certain amount of hardness and then be regenerated. The reaction sequence for an aminophosphonate resin in NaCl service is:

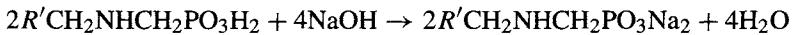
Exchange:



Regeneration:



Conversion:



“Me” refers to any bivalent metal. We can represent the normal working state of a resin as $R\text{Na}^+$, where R is either an aminophosphonic group as shown above (e.g., Duolite C-467, Purolite S-940) [124,125] or an iminodiacetic group, $R'\text{CH}_2\text{N}(\text{CH}_2\text{CO})_2(\text{ONa})_2$ (e.g., CR-10) [126]. A bivalent ion will occupy two exchange sites, so we can use the shorthand notation $R_2\text{Me}^{2+}$ for that combination. The exchange process can be described as



Since this is an equilibrium process, the apparent equilibrium constant K can be written as

$$K = [R_2\text{Me}^{2+}][\text{Na}^+]^2 / [R\text{Na}^+]^2[\text{Me}^{2+}] \quad (63)$$

where $[R_2\text{Me}^{2+}]$ and $[R\text{Na}^+]$ refer to the activities of Me^{2+} and Na^+ on the resin and $[\text{Me}^{2+}]$ and $[\text{Na}^+]$ to the activities of the ions in solution.

Recasting Eq. (63) results in:

$$\log[R_2\text{Me}^{2+}] = \log[\text{Me}^{2+}] + \log K - \log([\text{Na}^+]^2 / [R\text{Na}^+]^2) \quad (64)$$

The amount of uptake of the ion by the resin, that is, the capacity of the resin expressed in equivalents per liter of resin, is a function of the ionic concentrations in the solution.

It is sometimes assumed that the last two terms in Eq. (64) are constant. With this assumption, the resin capacity should be proportional to the activity of the bivalent ion. In brine softening, $[\text{Na}^+]$ does remain essentially constant, but $[\text{RNa}^+]$ continues to decrease as the resin takes up more of the other ion. The last term in Eq. (64) decreases as $[\text{Me}^{2+}]$ increases. The capacity of the resin for Me^{2+} therefore is less than proportional to the concentration of the ion in solution. Figure 7.67 shows generalized isothermal equilibrium data for calcium on a typical high efficiency resin [124–126]. The capacity over the fairly narrow range of typical industrial concentrations is approximately proportional to the 0.2–0.5 power of ionic concentration.

The capacity vs concentration relationships required for designing a column are determined experimentally for a given resin and for a given set of conditions (e.g., pH, temperature, composition of the matrix), using a combination of static and dynamic methods. In a static test, the resin equilibrates with the brine from which a specific ion is removed. Tests at different concentrations of the ion establish an isotherm, which is a curve showing the equilibrium amount of ion held by the resin vs the concentration of the ion in solution. This is the equilibrium capacity discussed above. The performance of a resin in plant service also depends on the rate of mass transfer. This is a function of the structure of the resin and operating conditions such as temperature, pH, and flow rate of the brine. It is established by dynamic tests that involve passing a test solution through a column packed with the resin and analyzing the effluent solution for the ion under study. A plot of the ionic concentration in the effluent vs time or volume of fluid passed will increase from nearly zero to the level in the feed. The latter point also corresponds to the equilibrium capacity.

One way of characterizing mass-transfer behavior is the concept of the transfer zone that is established. Here, one visualizes a front of brine with a certain concentration of hardness moving at uniform velocity into a fresh bed or increment of resin. The top of this resin (we assume downflow of the brine) picks up hardness and more or less quickly comes to equilibrium with the brine. In the section of bed immediately below, the concentration of hardness in the brine is depleted. The resin in this section then is less fully loaded. It continues to attract hardness ions, and the brine moves on with its hardness concentration further depleted. As we move down through the bed and continue this analysis, the concentrations of hardness continue to decrease. Finally, we reach a section at which the concentrations are indistinguishable from zero. We have established a concentration profile similar to that in Fig. 7.68.

This shows the situation in a section of the bed at a given instant. When the top of the bed reaches equilibrium with the feed brine, it picks up no more hardness. It then passes a higher solution concentration to the next section, which in turn picks up more hardness until it reaches equilibrium with the feed brine. This sequence cascades through the bed. The result is the apparent movement of the mass-transfer zone through the bed.

The sharp transitions and the linear profile in Fig. 7.68 are approximations, but they allow us to establish a “length of the transfer zone” (LTZ). This is a useful concept which at once characterizes the mass-transfer process (good mass transfer = short LTZ) and tells us what fraction of the bed’s equilibrium capacity can be utilized. When the leading edge of the mass-transfer zone reaches the bottom of the bed, breakthrough begins and the bed must be taken out of service.

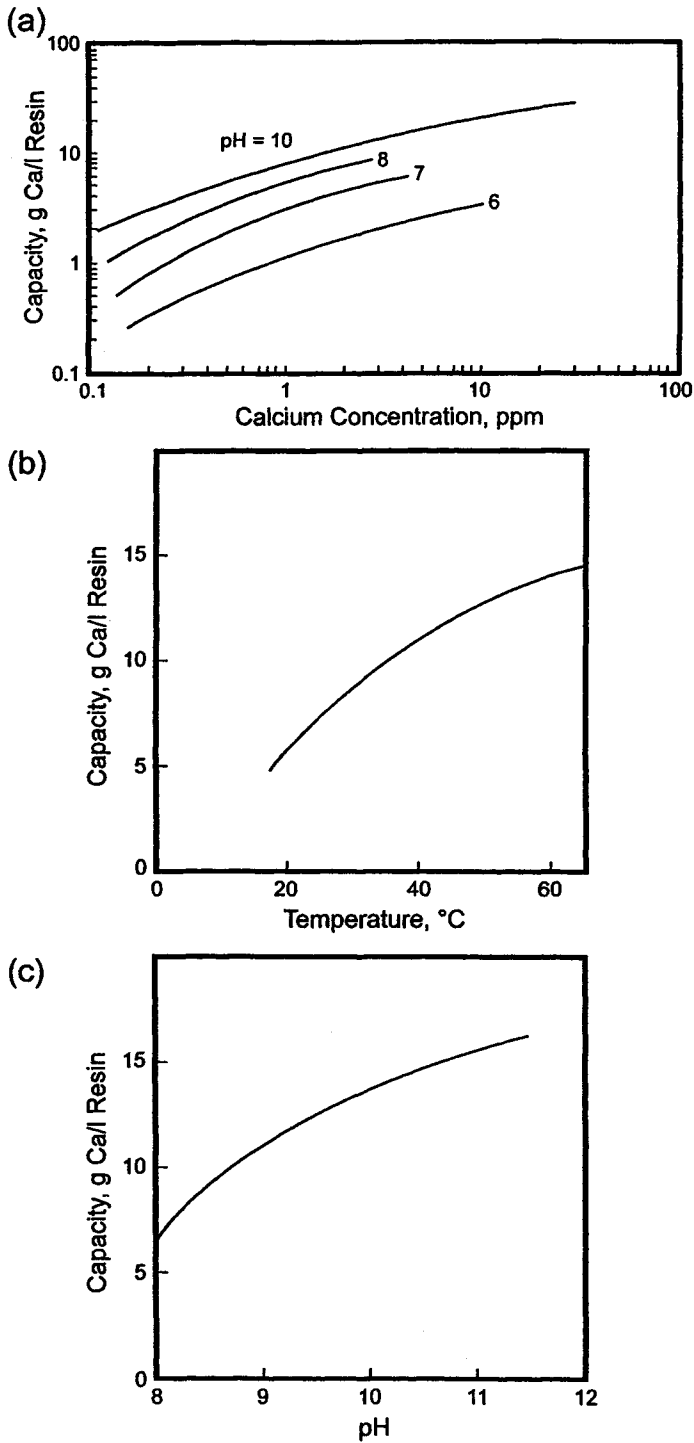


FIGURE 7.67. Capacity of Duolite C-467 ion-exchange resin for calcium as a function of (a) concentration, (b) temperature, and (c) pH. Standard conditions: brine concentration 280 g L^{-1} NaCl; temperature 70°C ; pH 10; (b) and (c) are from refs. [124,125].

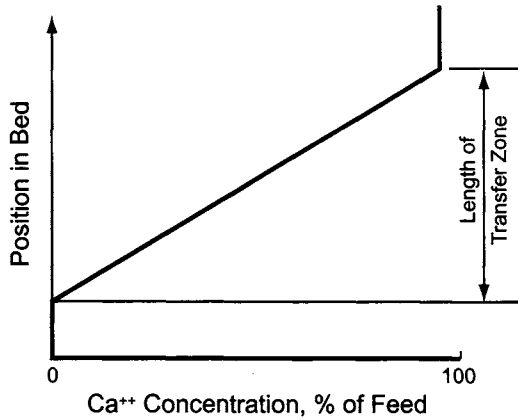


FIGURE 7.68. Transfer-zone concept.

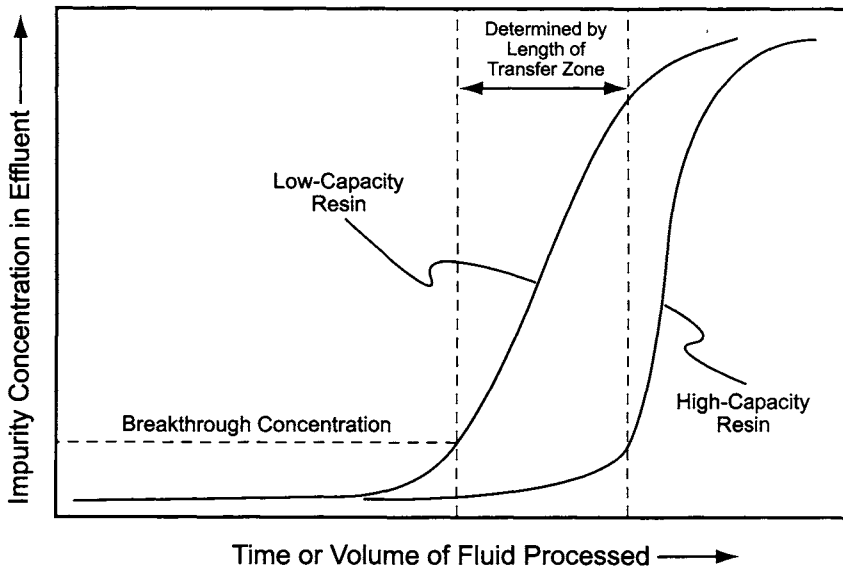


FIGURE 7.69. Ion-exchange breakthrough curves.

Figure 7.69 shows the breakthrough phenomenon directly. It gives the results of dynamic tests that were allowed to continue well beyond breakthrough. Results are good at the beginning of each run, and the effluent concentration of hardness is close to zero. At some point reflecting the dynamic capacity of the bed, the concentration begins to rise. If the runs were continued long enough, the feed and effluent concentrations would be equal. In terms of Fig. 7.68, this latter period shows the transfer zone gradually moving past the end of the resin bed.

The process variables with the greatest influence on the dynamic performance of an ion exchanger are temperature, pH, and the space velocity of the brine. Space velocity

of a fluid through a vessel is defined as the volumetric flow rate of the fluid divided by a volume representative of the capacity of the vessel. It has the units of reciprocal time. The volume chosen here is that of the bed with the resin in its sodium or potassium form. Figures 7.70 and 7.71 illustrate the effects of the primary variables. Describing these in terms of Fig. 7.68, we can say that higher temperature or pH increases the rate of mass transfer and therefore reduces the LTZ. Higher space velocity also reduces at least the mass-transfer resistances external to the resin. While the transfer rate increases, it does so less than in proportion to the flow rate, and so the distance in the bed required for a certain reduction in concentration is greater. In other words, the LTZ increases.

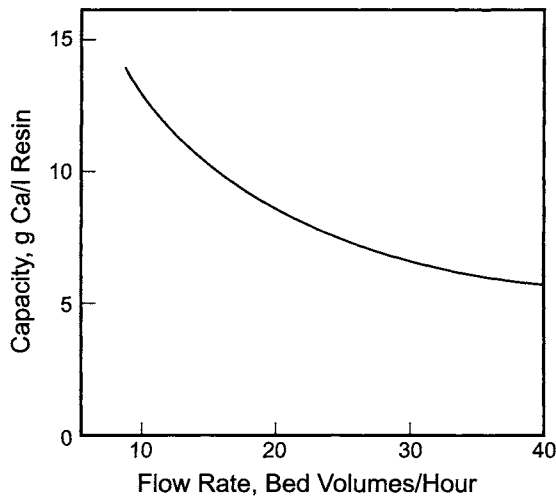


FIGURE 7.70. Variation of resin capacity with space velocity of brine.

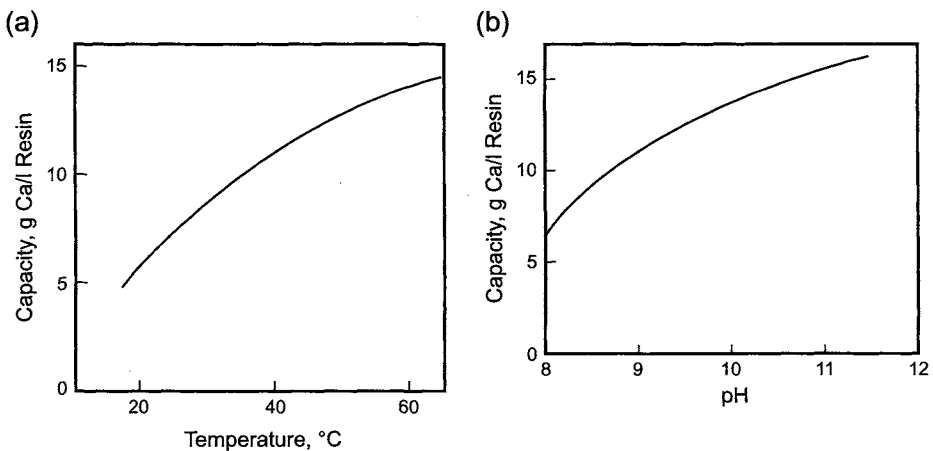


FIGURE 7.71. Effects of operating variables on capacity of resin. (a) Effect of temperature, and (b) Effect of pH.

The resin capacity increases continuously with temperature. Eventually, the effect is limited by the materials of construction and the thermal stability of the resin. The maximum service temperature of the resin will be 85°C or 90°C, and some margin should be allowed to ensure long resin life. The temperature dependence is not exponential; the rate of increase of capacity actually declines as the temperature increases.

Resins perform better on alkaline brine, and their capacity increases continuously with pH. The rate of increase becomes less at higher pH. Since brine is already alkaline from chemical treatment, there is a good match and the practical approach normally is to use the brine as it is. Not only would there be little benefit from the addition of more caustic, but residual traces of metal hydroxides might precipitate and foul the resin beds. Furthermore, at high pH, some of the residual magnesium may be colloidal. This can foul the beds or break through and be present in the cell feed brine.

The choice of space velocity is in part a classical economic balance problem. A high space velocity reduces the size and the cost of the ion-exchange installation but reduces the dynamic capacity of the resin and so increases the consumption and cost of regenerant chemicals. Reducing the height of the bed also decreases the pressure drop through the bed and therefore the pumping cost. Wolff's data [127] for a typical aminophosphonic resin (Duolite C-467) and NaCl brine flowing at 60°C show that the pressure drop per meter of bed is about

$$\Delta P = 10 - 0.25V + 0.0175V^2 \quad (65)$$

where

ΔP = pressure drop (kPa m⁻¹)

V = superficial velocity of brine (m hr⁻¹)

This is illustrative only and not suitable for design calculations. It indicates that the pressure drop in a bed 2 m high with an operating space velocity of 15 hr⁻¹ should be about 36 kPa.

Table 7.15, based on the curve in Fig. 7.70, shows the effect of design space velocity on several parameters. The first three calculated columns are normalized against a space velocity of 10 hr⁻¹, at which rate the dynamic capacity is taken to be 14 g Ca L⁻¹. The length of run is presented in real-time units in order to give a feel for the possibilities.

Calculation of the length of run assumes that the brine contains 10 ppm calcium. To avoid breakthroughs, runs are limited to 75% of the maximum capacity. The frequency

TABLE 7.15. Effect of Space Velocity on Performance of Ion Exchanger

Hourly space Velocity	Bed size	Capacity for Ca ²⁺	Regenerant consumption	Length of run (hr)
10	100	100	100	105
15	67	80	125	56
20	50	66	153	35
25	40	56	179	24
30	33	51	194	18

TABLE 7.16. Dynamic Resin Capacities for Group II Elements

Element	Concentration in solution (ppm)	Breakthrough capacity (relative)
Magnesium	1	100
Calcium	10	94
Strontium	1	62
Barium	1	25

Calculated from data of Yamaguchi *et al.* [128].

of regeneration is inversely proportional to the length of the run. Since bed volumes are smaller at high space velocities, the number of regenerations must be multiplied by bed size to get the total regenerant consumption.

The entire discussion above is in terms of calcium removal. The other alkaline earth elements must be regulated as well to meet the specifications of the membrane supplier. As the specifications in Table 4.8.8 show, strontium and barium are less harmful than magnesium and calcium. This is partly because the heavier elements are less likely to penetrate the membranes. For similar physical chemical reasons, these elements are also less susceptible to capture by ion-exchange resins. Yamaguchi *et al.* [128] published breakthrough curves for Group II ions over an iminodiacetate resin. Calculated ratios of capacities [129] are in Table 7.16. Capacity drops steadily as atomic weight increases. Dissolved magnesium is seldom a serious problem in ion-exchanger operation. Calcium normally is expected to control the design, but quite frequently strontium or barium becomes the controlling element.

The aminophosphonic resins have found wide use because of their higher operating capacities for calcium and magnesium. The resins originally developed did not always have similarly high capacities for strontium and barium. This prevented their use in some plants. Newer versions are said to show a 20% increase in operating capacity for Ca^{2+} and a doubling of the capacity for Sr^{2+} and Ba^{2+} [130].

The discussion so far has restricted itself to the exchange of a single component from the brine. When more than one ion is to be removed, the ions must compete for the available sites. If we take the combination Ca^{2+} and Sr^{2+} or Ba^{2+} as an example, we see from the sequences above that calcium is the more strongly held ion. At the start of a cycle in a fresh bed, the two ions will distribute according to their concentrations and the relative selectivity of the resin. The calcium will be absorbed more quickly and the other ion will, on the average, penetrate farther into the bed. As the cycle continues, the calcium ion that enters the bed will find most of the sites at the entrance to the bed already occupied. It will pass on to other sections of the bed, which will now be exposed to higher concentrations of Ca^{2+} and, therefore, higher ratios of $[\text{Ca}^{2+}]/[\text{Sr}^{2+}]$ or $[\text{Ca}^{2+}]/[\text{Ba}^{2+}]$. The calcium ion will begin to displace the strontium or barium ion that has already been picked up by the bed. The weakly held ion is gradually displaced by calcium, as shown in Fig. 7.72, and as a result it breaks through the bed earlier than it would in the absence of calcium. In practice, many operators find that strontium or barium governs the capacity of their systems, even when present only in low concentration. Figure 7.73 is an example of this effect. The strontium ion breaks through long before the calcium ion. This situation

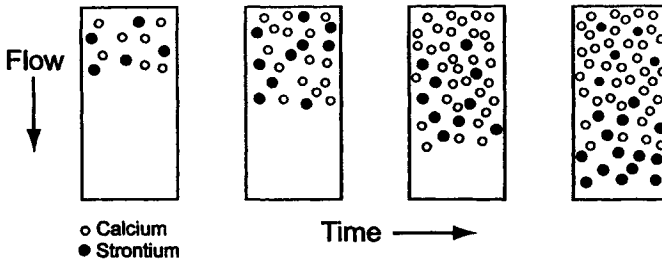


FIGURE 7.72. Displacement of strontium from resin by calcium.

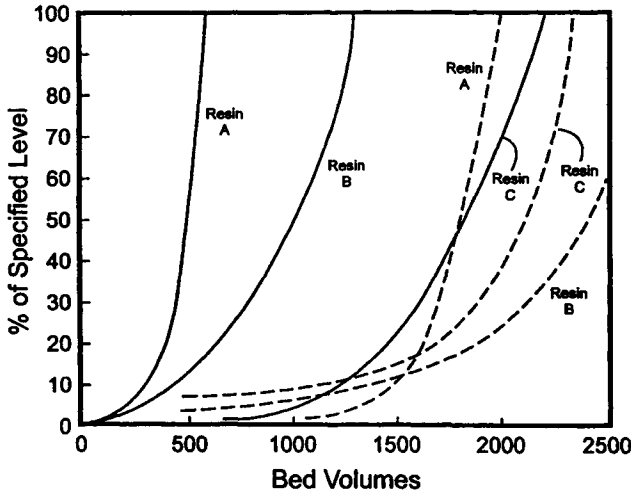


FIGURE 7.73. Simultaneous removal of strontium and calcium. Solid curves: strontium; dashed curves: calcium.

emphasizes the need for testing on the plant brine or simulation by the resin vendor as part of the design process.

It is possible to make a first estimate of the size of the columns by assuming the effects of the different ions to be additive. Thus, the required bed volume is related to the volume required for a given single element by

$$V_n/V_1 = 1 + C_2Q_1/C_1Q_2 + C_3Q_1/C_1Q_3 + \dots \tag{66}$$

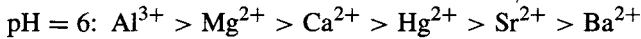
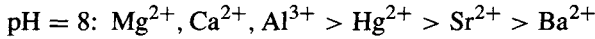
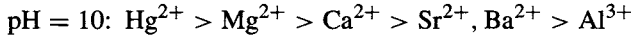
where

- V_n = bed volume required for the removal of n different elements
- V_1 = bed volume required for the removal of base element
- C_i = concentration of element i in solution
- Q_i = capacity of resin for element i

This is mathematically equivalent to assuming that when the amount of a given element that has entered the bed is $x\%$ of the bed's capacity for that element, it accounts for $x\%$

of the available sites. This contradicts the above analysis, but it has a certain degree of accuracy and serves its purpose.

We should note that the relative affinity of the various ions varies with pH:



This knowledge is essential, as the ions with lesser affinity will break through first, having been displaced by ions having greater affinities. In this respect, we might regard the ion-exchange bed as an ion chromatograph. The shifts in the list can be exploited in the process. Section 7.5.8.2, for example, discusses the use of ion exchange at lower pH to remove the aluminum ion.

The important point to be taken from this discussion is that the plant designer needs access to the full analytical history of the salt or brine supply. If data are insufficient, collection of new data should begin before or early in the process of plant design.

Another important point is that a freshly regenerated ion-exchange bed usually has a comfortable amount of excess capacity and can tolerate excursions in hardness level. In terms of the discussion in Section 10.5.3, a substantial increase in hardness level does not add greatly to the number of transfer units required in the process. As long as the bed has some residual capacity, it can produce brine of high quality. The total capacity for hardness also increases as the concentration increases in solution. While the resin holds more Ca^{2+} , however, the amount of brine that it can process falls rapidly. Doubling the concentration of calcium in the brine increases the ion-exchange capacity by about 15% but reduces the volume of brine that can be handled by more than 40%. The operator must be aware that continued use of less-pure brine saturates the resin more rapidly and requires more frequent regeneration.

7.5.5.2. Regeneration

7.5.5.2A. The Regeneration Process. Before hardness begins to break through, a bed should be taken out of service to regenerate the resin. Several steps are involved, as described below and summarized in Table 7.17. The discussion that follows considers these steps in order.

Chlorate forms in the cells by reaction of chlorine with back-migrating hydroxide ions. It circulates with the depleted brine and is present in low concentration in an ion exchanger when it is taken off line for regeneration. During regeneration of the resin with acid, there is a danger of decomposition of this chlorate to form chlorine and chlorine dioxide. These will attack the resin vigorously. Before regeneration, therefore, the brine must be displaced, and the first step in the process is a rinse with about five bed volumes of water.

Next, backwashing the bed removes fractured beads and any solids deposited by the brine. Expansion and resettling of the bed destroy channels that may have formed and reclassify the resin. Backwashing should expand the bed 50–75% for about 30 min. Depending on the temperature of the water, this requires a flow rate somewhere between

TABLE 7.17. Ion-Exchange Resin Regeneration Sequence

Operation	Fluid	Flow rate	Quantity or time	Direction
Displacement	Water	4	4–6 BV	Down
Backwash	Water	8–12	30 min	Up
Regeneration	HCl	2–6	100–200 gpl	Down
Rinse	Water	2–4	2 BV	Down
Conversion	NaOH	2–4	80–150 gpl ^a	Up
Rinse	Water	2–4	2 BV	Down
Service	Brine	10–30	Variable	Down

Notes:

^a 100–200 gpl KOH.

HCl and NaOH solutions are 4–10% by weight; quantities are g of reagent per liter of bed.

BV = bed volumes; based on density of charge in its active form.

Flow rates are in bed volumes per hour.

5 and 15 bed volumes per hour. The flow rate of water must be roughly matched to its temperature. A decrease of 20°C in water temperature will increase the degree of expansion of the bed by about 70%. With one typical resin, bed expansion data at 40°C are correlated by

$$\Delta V = 4.53(u - 1.67) \quad (67)$$

where

ΔV = volumetric bed expansion, %

u = superficial velocity of water, m hr⁻¹

With the same resin operating at lower temperatures, the following factor applies to Eq. (67):

$$F(t) = 2.8 - 0.065t + 0.0005t^2 \quad (68)$$

where t is the temperature of the water (°C).

Example. Warm water (40°C) is being used to backwash a bed of resin whose expansion characteristics follow Eq. (67). The superficial velocity is now 15 m hr⁻¹. A change in the plant utility system will reduce the temperature to 25 ± 5°C.

Presently, the expansion of the bed is 4.53(15 - 1.67) = 60.4, say, 60%. Reducing the temperature of the water to 25°C gives $F(t) = 2.8 - 1.625 + 0.3125 = 1.49$. The degree of expansion at the same linear velocity will increase by about 50%, and there will be more danger of the loss of resin. To return to the present degree of expansion, the quantity in parentheses in Eq. (67) should be reduced by the factor calculated from Eq. (68). We have

$$u - 1.67 = (15 - 1.67)/1.49$$

giving $u \approx 10.6$ m hr⁻¹, nearly a 30% reduction. With a 5°C tolerance in water temperature, $F(t)$ can vary from 1.3 to 1.7. With the flow rate adjusted for 25°C water, the changes in temperature will allow the bed expansion to vary between 53% and 69%.

Depending on the plant situation and the specific design characteristics of the vessel, this may be tolerated or offset by adjusting the backwash flow to suit the temperature.

The first objective of regeneration is to remove the hardness ions attached to the resin. In the process, sodium and potassium ions also are removed. HCl solution (3–15%) is the regenerant. The time and rate of application depend on the concentration of the solution. A typical flow rate is about four bed volumes per hour. A total dosage is specified, rather than a volume of solution. Depending on the resin, this is usually between 100 and 200 g HCl per liter of resin.

Trivalent cations are strongly attracted to the resin and resist removal by acid. When they are present in the brine in unusually high concentration, or when they gradually accumulate on the resin, the acid concentration and dosage in regeneration can be increased [131].

Before the next step in treatment of the resin, the free acid solution is rinsed from the bed with about three volumes of water. Then the resin is converted to the active (Na^+ or K^+) form by a solution of NaOH or KOH. The concentration and flow rate are similar to those used when regenerating with HCl. The total dosage in sodium service is 80–150 g NaOH per liter of resin.

Note that the quantities of acid and caustic used in regeneration are well in excess of theoretical requirements. Conversion with NaOH or KOH is more efficient than regeneration with HCl. Normal HCl usage is about 20% greater than alkali usage, and the total effluent, if mixed, will be acidic.

After conversion to the active form, the resin is ready to be put back into service. Since the bed still contains a caustic solution, another rinse with about two bed volumes of water is necessary. Finally, brine is introduced. The first solution leaving the column will be dilute and may be segregated.

All water used in the ion exchangers must be free of hardness. While demineralized water is nearly always used, soft water also meets this test. A disadvantage of soft water is that it is not possible to check the efficiency of a rinse step by a simple conductivity measurement.

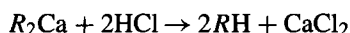
The resin is exposed to several shocks, both thermal and osmotic, in the regeneration sequence. The resins used are quite resistant to these shocks, and in fact replacement rates are only a few percent per year. One notable effect with implications in vessel design is the change in bead density between forms. The sodium form can be 35% less dense than the hydrogen form, and the bed must be free to expand while being converted. Upward flow of the caustic solution is useful from this standpoint, even as it provides a countercurrent regeneration.

The resin in its sodium form has a bead specific gravity greater than 1.1 but a bulk density of only about 0.75. The effective size of a bead is about 0.5 mm, and the PSD is fairly narrow (uniformity coefficient < 1.7). Like most ion-exchange resins, it has a great capacity for holding water (~60–65%).

7.5.5.2B. Disposal of Regeneration Effluent. The simplest way to handle regeneration effluent is to divert water and weak salt solutions to drain, collect the rest together, and neutralize the excess acid for disposal. However, from analysis of some of the data in Table 7.17, we see that regeneration will take about 5 hr and produce 15–20 bed volumes of “waste.” For each daily ton of chlorine capacity, this represents about

0.6 m³ per regeneration. If a bed is on line for 24 hr out of 30, an 800-tpd plant will have 100,000 m³ per year of spent regenerant for disposal. Even allowing for the fact that the segregation of water and weak brine reduces this volume greatly, there is a strong incentive to conserve the effluent. Some of the acid and caustic may be recycled or reused in the ion-exchange system. Little information has been published on this approach, and it is difficult to say how extensive this reuse could be.

Acid and caustic are the most expensive materials used in regeneration and also the most awkward disposal problem. Consumption of acid in the columns produces the chlorides of the bivalent metals:



These contaminate the solution containing the excess HCl and bar its use in the cells or pure brine system. It is still suitable for use in brine dechlorination. The demand in the dechlorination step is greater than the supply of acid from regeneration, so that all the acid might be disposed of by recycle. The bivalent metals simply accompany the brine in its next pass through chemical treatment, where they precipitate. For best operation of the dechlorination process, the acid supply should be of constant strength. The acid flow from regeneration is sporadic and variable in concentration. Some engineering solution to the problem of blending new and used acid is required when choosing this option.

The caustic used to convert the resin to the active form is diluted but not contaminated by its primary reaction with the resin:



It should be possible, then, to use the caustic effluent and the subsequent rinse water in the process. The equation above does not preclude blending this caustic with the cell product. Before doing so, the operator would be prudent to examine every opportunity for contamination and adopt a rigid quality control program. Another logical application is in the chemical treatment system. Again, the demand usually is sufficient to consume all the caustic from regeneration, given some means of assuring a constant concentration at the treatment tanks. A third application not so closely linked to the process is the preparation of dilute caustic for utility use. Most plants will have a facility for production of dilute (perhaps 20%) caustic that may be used for vent neutralizations as well as in the emergency vent scrubber.

7.5.5.3. Mechanical Details

7.5.5.3A. Column Internals. The analogy of brine softening to water softening does not extend to mechanical design. The systems used to soften water are not suitable for our application, where exposure conditions are quite different. More robust construction is necessary. While chemical compatibility with brine is essential, it is not the only consideration. Mechanical and thermal stability is also important. Distortion of a distributor or collecting screen, for example, can allow loss of resin or channeling of fluid.

Ion-exchange columns are quite similar to bed filters in their construction. Figure 7.74 shows a typical vessel and its connections. Since flows are upward and

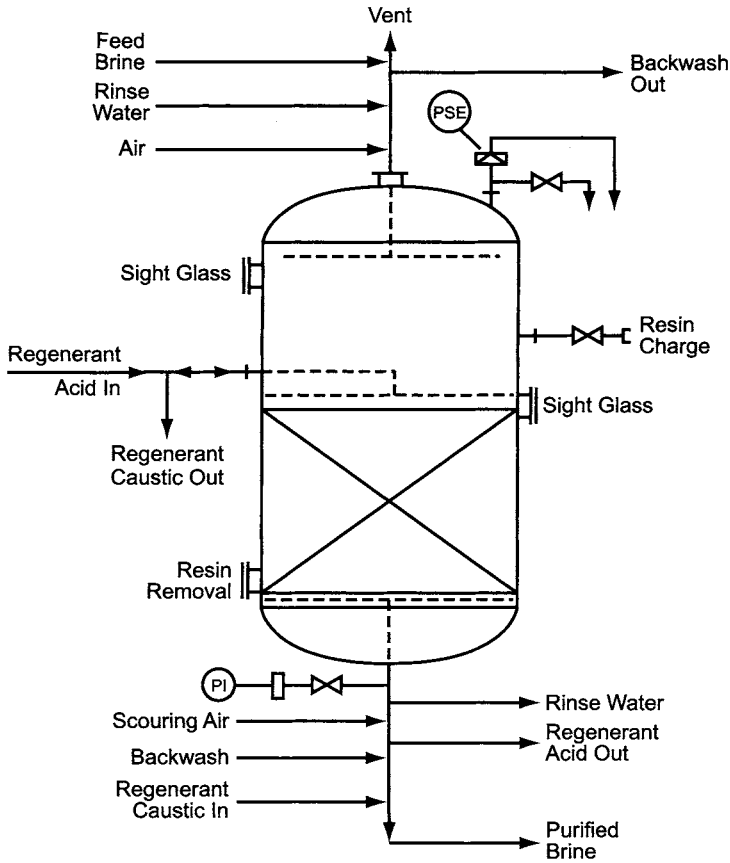


FIGURE 7.74. Arrangement of connections to ion-exchange vessel.

downward at different points in the cycle, distributors are necessary both above and below the bed. These may be designed as parallel pipes across the width of the vessel or as hub-and-lateral systems with central feed and radial distribution. To maintain the distribution of regenerant acid across the bed, it should be added within 10–30 cm of the bed level [132]. Supports, including nozzle plates and underdrains, are conventional in design and usually follow the supplier's standard practices. Subsurface washing, in which the backwash fluid is injected into the bed close to the surface, is often a feature of resin-bed design. It allows removal of deposited solids without full-scale backwashing. Because of the scrupulous filtration described above, it is not widely used in brine softening systems.

7.5.5.3B. Materials of Construction. The vessels are of carbon steel with rubber lining. Different polymers are used, sometimes in combination to give layers of differing hardness. The manufacturer, with the designer's approval, usually determines this. Tank nozzles should be lined with the same material. It is essential from this point on in the process and until depleted brine leaves the cell area that the materials in contact with the

brine contain nothing that can contaminate the brine and ultimately damage the membranes. The complete formulation of a lining material, not just the base polymer, must be reviewed.

Internals of simple shape may be rubber-coated. Other internals, such as distributors, are built of such materials as Hastelloy, titanium, and CPVC. CPVC can be used for external piping and as the piping for the flow distributors. While it is chemically acceptable, it should be verified that it contains no harmful fillers or compounding agents. PVC structurally may be an adequate substitute for CPVC in certain instances, but it is more likely to contain hardness elements in its compounding ingredients. Equipment designers should take particular care with the support of nonmetallic internals. Their distortion at process temperature and under maximum flow rates can upset flow distributions and allow resin particles to escape. Metals have the advantage in this regard.

The vessels should also have sight glasses that allow the level of the beds and the extent of expansion during backwash to be checked. Acrylic polymers are suitable here.

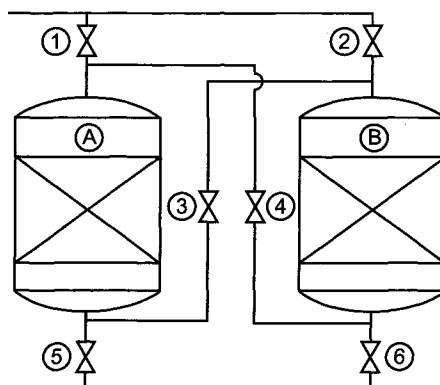
7.5.5.3C. Number of Beds. Once a basic process specification for an ion-exchange system is set, many of the mechanical details become important to commercially successful operation [133]. The first decision to be made is the number of resin beds to be installed. Since off-line time must be allowed for regeneration of the resin, the minimum number in a continuously operating commercial installation is two. Each bed then must be capable of the full process duty. In a practical system, operating time for a bed will be considerably longer than regeneration time. It is therefore possible to keep both beds on line most of the time, and this practice is to be recommended. It increases the pressure to be generated by the feed pump, but it also provides some protection against upsets in primary brine treatment, incomplete regeneration of a bed, and gradual loss in resin inventory or capacity. Figure 7.75 is a schematic of a two-bed system. The table shows the valving for both beds in operation, in different sequences, as well as for one bed in operation with the other off line.

A third bed might be considered for either of two reasons:

1. to allow some reduction in resin inventory;
2. to provide more security against breakthrough of hardness.

With three beds, two can be kept in operation at all times, barring maintenance outages. It is not essential to meet the full process duty in one bed. If hardness begins to break through the first bed in line, the second is still available to maintain outlet brine purity. The amount of resin in each bed therefore can be reduced. If we take as a limiting case cutting the volume in half, we see that the total volume of resin could be cut by up to 25%. Keeping the same linear velocity, the cross-sectional area of the beds and the freeboard height above the expanded resin volume would be the same as in the full-duty case. If the beds represent half of the straight-side height of the vessels, cutting the bed heights in half would save nothing on vessel heads or internals and 35–40% on height. The savings offered by this approach are not large in percentage terms, but in a large plant they may be considered worthwhile.

Turning to the second reason, having two full-size beds on line at all times adds to the process security. Any small breakthroughs of hardness while one bed is in regeneration in



Bed(s) On Line	Valve Position					
	1	2	3	4	5	6
A	O	X	X	X	O	X
B	X	O	X	X	X	O
AB	O	X	O	X	X	O
BA	X	O	X	O	O	X

O = Open X = Closed

FIGURE 7.75. Two-bed flow schematic.

a two-bed system may have individually imperceptible effects but eventually will affect membrane performance and life. The three-bed approach has the advantage of allowing two beds to operate at all times regardless of regeneration activity. It can be expected to reduce the number of minor breakthroughs and perhaps to prevent the occasional serious breakthrough. The value of this is hard to quantify. With the aid of the data of Table 7.15, however, we can analyze one aspect by determining the probability that, in a two-bed system, only one bed is on line at a given time.

The last column of Table 7.15 gives the length of a run as a function of the space velocity. By allowing a constant 6 hr off line for regeneration, we can calculate the percentage of time the system is left with only one bed in operation. Table 7.18 shows these percentages as a function of space velocity and converts them into the equivalent number of hours per day. Increasing the space velocity from 10 to 30 hr⁻¹ increases the average off-line time from about 1.3 to 6 hr a day. Low space velocities therefore offer more security, and this is a factor other than cost to consider when optimizing design.

The third bed, fully integrated, also gives some protection against unscheduled maintenance outages. While two-bed installations are quite common in plant practice, then, it is the authors' opinion that the addition of the third bed will improve the performance of the cells and extend the life of the membranes. When a third bed is added for security, there are two approaches to its integration into the system. In one, it is considered to be a guard bed only and is always the last bed in flow sequence. Switching and regeneration of the other two beds are fully automated, and the brine flows from them to the guard bed. The guard bed is regenerated less frequently, by operator intervention. It may be smaller than the other beds. In the other approach, all three beds are equal

TABLE 7.18. Two-Bed System—Regeneration
Off-line Time

Space velocity (hr ⁻¹)	Length of run (hr)	Off-line time (%)	Off-line time (hr day ⁻¹)
10	105	5.4	1.3
15	56	9.7	2.3
20	35	14.8	3.5
25	24	20.3	4.9
30	18	25.2	6.0

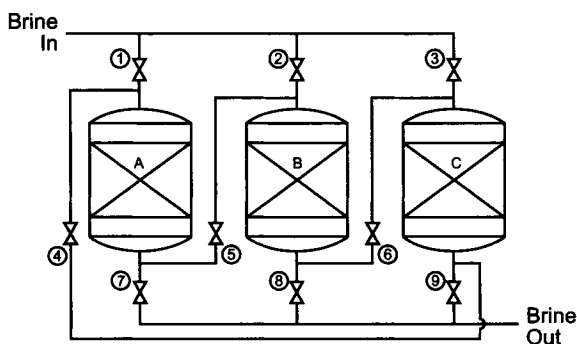


FIGURE 7.76. Three-bed "merry-go-round."

and are taken off line for regeneration in sequence. The usual arrangement (Fig. 7.76) is as a "merry-go-round." Designating the beds as A, B, and C, the brine flow sequence progresses from A-B-C to B-C-A to C-A-B and then repeats. Full flexibility to include the sequences C-B-A, B-A-C, and A-C-B is not common; as will be seen below, the complexity of the system increases for what is considered to be only a small gain.

7.5.5.3D. **Delivery of Regenerants.** Regenerants are HCl and NaOH or KOH. The concentrations used range from 3% to 15%. Dilution of the primary supplies, which are at concentrations above 30%, is necessary. This can be accomplished in several different ways. Three common approaches are

1. transfer to the process by water-powered eductors;
2. separate metering of water and concentrated solution;
3. predilution and storage at use concentration.

In the first method, demineralized water is used on eductors that draw the concentrated solutions from small storage tanks. Setting the flow of water properly and adding a variable restriction on a regenerant suction line allow the correct mixture to be sent to the beds. In the second method, concentrated regenerant is pumped to a mixer where it is combined with a metered flow of water and sent to the resin bed. A ratio controller is used to obtain the correct mixture. In the last method, regenerant solution and water are

blended and held in a tank for later use. As we move down the list of methods, we trade capital expenditure and increased operator attention for security and more efficient use of chemicals.

The usual approach to restricting the flow in the first method is to use a manual valve that can be locked into position. Once this is set at startup to give the right mixture, it theoretically need not be adjusted again. This arrangement minimizes the capital cost and is used most often in small NaOH plants. Stepwise adjustment of the restricting valve does not allow precise adjustment of the blended concentration, and any error must be on the high-concentration side. This increases the consumption of regenerant chemicals. Wear or relaxation of the valve also can permit drift. The second method improves the accuracy of blending and allows finer adjustment of concentration. Like the first, it provides no buffer between mixing and the process. There will also be a short startup period during each regeneration in which the control system is hunting and the blend is not quite correct. The third method is the high-cost approach. Its advantages are that it is the only method of the three that allows errors to be detected before use and that preparation of the blended solution is uncoupled from the regeneration process. Solutions can be made in convenient quantities at any time before use.

7.5.5.3E. Possibilities of Recontamination. The exceptional purity of softened brine raises the question of recontamination. Consider polymeric materials of construction. While the base polymer may be quite suitable for pure brine service, most fabrication involves compounding ingredients. PVC, for example, when extruded into pipe often contains large amounts of calcium carbonate (this sort of contamination is less likely with CPVC). Polypropylene often contains calcium stearate as a processing aid. Pure brine can leach hardness from such materials, and there have been cases in which they have contaminated brine. Formulations containing harmful elements should not be used in or downstream of the ion-exchange system. Suppliers may be reluctant to divulge full details of proprietary compositions, but they can be expected to certify the absence of specific harmful substances.

Contamination of brine by sample containers is a problem in itself. Laboratory results can be worse than useless if a brine sample picks up some contaminant before analysis or in some way interacts with the sample container. Cross-contamination can also destroy the purity of the treated brine. Bypassing of feed brine or partially treated brine must be avoided. If chemically treated brine contains 5 ppm of hardness, for example, bypassing of 0.1% into the product of the ion exchangers will contribute 5 ppb of hardness, a substantial fraction of the acceptable maximum. Startup lines and convenience lines increase the possibility of bypassing. The frequent switching of valves within the ion-exchange unit presents another danger. As the system becomes more complex, more valves appear which can allow partial bypassing of the process. While high-quality valves are expected to be very reliable, problems can arise with actuators and valves can reseal improperly. The latter effect might be caused by an accumulation of resin beads washed from the beds.

Perhaps more serious would be the bypassing of small quantities of regenerant solutions. The worst case would be leakage of hardness-laden HCl effluent, which has a much higher concentration than the feed brine itself, into the product brine.

Figure 7.76 showed the major process valves in a three-bed merry-go-round. Table 7.19 is a valve-position chart. The number of automatic switching valves in process service increases from 6 (in the two-bed case) to 9. The bold entries show valves that are separating fully softened brine from feed brine when all three beds are operating. In each case, there is one such valve. The same is true of a two-bed system. The time-averaged probability of complete bypassing becomes the same for every bed sequence. While the addition of more valves increases the chance of finding a leaking valve, that valve spends less time in the critical position. The sketch of the system does not show the complex valving arrangement that results when regenerant solutions, rinse water, and drains are included. Figure 7.77 is a sketch that includes this piping. The complexity is evident. During a regeneration step on any bed, the regenerant valves on the other beds are under pressure on the regenerant side. If the pressure is high enough, there is some danger of leakage of fresh regenerant into a working column. This would move the brine away from its optimum pH. Caustic would increase the probability of precipitation of hydroxides, and acid would reduce the working capacity of the resin.

At the same time, when one of the three beds is being regenerated, two valves are separating product brine from regenerant solution. During regeneration of bed B, for example, the two valves are #5 and #8. While #5 is more likely to pass regenerant

TABLE 7.19. Three-Bed Ion Exchanger—Valve Position Chart

Bed sequence	Valve positions								
	1	2	3	4	5	6	7	8	9
AB	O	x	x	x	O	x	x	O	x
ABC	O	x	x	X	O	O	x	x	O
BC	x	O	x	x	x	O	x	x	O
BCA	x	O	x	O	X	O	O	x	x
CA	x	x	O	O	x	x	O	x	x
CAB	x	x	O	O	O	X	x	O	x

Notes: O = open; x, X = closed; X = bypasses untreated brine.

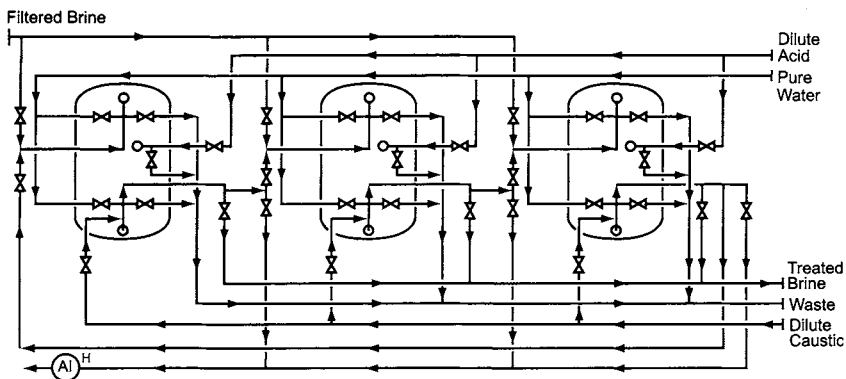


FIGURE 7.77. Three-bed piping arrangement.

TABLE 7.20. Valving Complexity in Ion-Exchange Systems

Number of beds	2	3	3
Number of flow directions	N/A	1	2
Number of switching valves	6	9	12
Number allowing bypassing			
One bed	2	2	3
Two beds	1	2	4
Three beds	N/A	1	1

because of the higher pressure level, the worst situation would be acid bypassing valve #8. This would allow a stream with very high hardness concentration to enter the product brine and jeopardize operation of the electrolyzers. The probability of this sort of contamination can be reduced by double valving or by maintaining a low back-pressure on the acid effluent.

Again, the same is true in a two-bed system. In either the two-bed or the three-bed approach, all but the brine inlet valves (one third of the total number) are in critical service at some time during each bed cycle.

In the conventional three-bed merry-go-round, it is not possible to take one bed out of service and operate the others as a normal two-bed system. This is due to the unidirectional sequencing. If bed B of Fig. 7.76 is out of service, for instance, it is possible to run the sequence CA but not the sequence AC. A two-way merry-go-round is necessary for full flexibility. This allows the three beds to run in any sequence, and it allows any two beds to run in either sequence. This convenience comes at a price (Table 7.20). The piping is more complex, and the system requires 12 process-switching valves. This compares to six in a two-bed unit and nine in a one-way merry-go-round. The potential for bypassing or cross-contamination also increases. With all three beds on line, there are now three process valves that can allow bypassing of one bed; four valves, two beds; and one valve, all three beds. The same numbers for the simpler configuration are 2, 2, and 1. Allowing the second direction of flow around the system has added one valve in the first category and two valves in the second. When two beds are operating and one is in regeneration, the two-way merry-go-round adds two valves that separate regenerant from the brine between the two operating beds and one valve that can allow raw brine to bypass ion exchange altogether.

Few plants have chosen to provide the two-way merry-go-round.

7.5.5.4. Analytical Requirements. Brine plant operators often perform control analyses for hardness after primary treatment. These are simple titrations that can be performed by a skilled operator who is not a laboratory specialist. After ion exchange, the same components must be analyzed, but the task is more daunting. The standard volumetric analysis is said to be useful down to 0.1 ppm with an accuracy of ± 0.05 ppm, which is 50% of the true value at the low end [119].

With brine, we do well to recognize two categories of analysis. One group of analyses has as its purpose the shift-by-shift guidance of the brine system operators. These

TABLE 7.21. Required Analytical Frequencies

Parameter	Frequency
Feed concentration	Continuous
Anolyte concentration	Continuous
Anolyte acidity	Continuous
Chlorate in anolyte	Once a day
Hardness (Ca + Mg)	Continuous
Strontium	Once a week
Sulfate	Once a day
Iodine	Once a week
Barium	Once a week
Aluminum	Once a week
Silica	Once a week
Catholyte concentration	Continuous
Chloride in catholyte	Once a week

should be simple and quick at the expense of the highest accuracy. Operating control analyses belong to this category. Another group has as its purpose the long-term protection of the electrolyzers. This group includes analyses that are necessarily complex and those that are intended to monitor trace components. It also includes hardness analysis of the highest accuracy. These analyses require the use of atomic absorption techniques and the attention of trained laboratory personnel. The appendix to Section 4.8 gives the type of analysis recommended for each species.

Each plant needs an analytical schedule that is followed faithfully. Each relevant analysis must be performed at a specified frequency. Since most chlor-alkali plants are built under some form of electrolyzer licensing arrangement, much of the analytical schedule is fixed by contract. In any event, the advice of suppliers of electrolyzers, membranes, and electrodes and their coatings is very important. Table 7.21 shows the recommended analyses and their frequencies for cells equipped with Nafion[®] membranes [134].

7.5.6. Acidification of Feed Brine

Acidification of brine before sending it to the electrolyzers is the standard but not universal practice. Purified brine is alkaline and contains carbonate added in excess during chemical treatment. Both OH^- and CO_3^{2-} reduce the effective anode current efficiency by consuming chlorine in the cells. The addition of HCl to the brine neutralizes the contained OH^- and decomposes the CO_3^{2-} to CO_2 and water. More chlorine is produced with no increase in electrical load. Addition of excess acid can even neutralize some of the OH^- that enters the anolyte by leakage back through diaphragms or membranes. Section 4.4.3 gives a more fundamental explanation of the effects of acid addition.

This improvement in yield may be illusory in a plant that produces its own HCl for this purpose. While more chlorine is produced in the cells, it is then consumed in HCl synthesis to allow the return of the acid to the process. In a plant without an HCl unit,

the economics depends on the price of the HCl supply. Note that at least in a membrane-cell plant, the quality of the purchased HCl must be quite high. When the costs are unfavorable, a situation not often found in large plants, a plant might elect not to acidify the feed brine.

This section discusses the technical aspects of brine acidification and considers the requirements for acid supply.

7.5.6.1. Technical Aspects of Acidification. Acidification has other benefits besides the apparent increase in current efficiency noted above [135]. Anode life may be shorter when the brine is alkaline, because of the leaching of ruthenium oxides from the coating. Another result of hydroxide ion leakage is direct electrochemical formation of oxygen at the anode (Section 6.5 and Eq. 6.9). This oxygen and the CO₂ formed from carbonate will be present in the cell gas. They will reduce the efficiency of chlorine processing. Other chapters discuss this aspect as well as the feasibility of using gas directly and without liquefaction in the production of derivatives such as ethylene dichloride (EDC). In this particular example, the presence of oxygen in the gas can affect performance of the EDC process. The benefits obtained in downstream processing are an important factor in the decision on whether or not to add acid to the brine.

Bergner's data on the effect of anolyte pH on the oxygen content of a cell gas are shown in Fig. 7.78(a). Without acidification, the oxygen content was about 2%. The data suggest that this can be reduced to almost an arbitrary level by acid addition. The curve is very nearly exponential, with each unit reduction in pH cutting the oxygen content in half. However, the extent of acidification must be limited, because an anolyte pH below two can destroy carboxylate membranes by hydrolyzing the active groups to the nonconductive -COOH form. The pH of the feed brine can be lower than two, provided that the brine is premixed with an anolyte recycle or dispersed rapidly in the cells so that regions of excessively low pH do not exist.

Figure 7.78(b) shows the oxygen content of the gas as a function of feed brine pH. Comparing this with Fig. 7.78(a) suggests:

1. operation of the cells can be safe down to a feed brine pH less than one
2. there is more scatter of the data in Fig. 7.78(b), probably reflecting the fact that the anolyte pH is the more fundamental variable
3. the curve of Fig. 7.78(b) is more gradual, and direct control of the feed brine pH, at least with occasional feedback from the anolyte pH, should be a workable process

There is a caveat attached to point #1. In a real cell room, there will be some variation in individual cell performance. Those cells with the best current efficiencies will have the least backflow of OH⁻ into the anolyte and the least capacity for neutralization of the HCl added with the brine. If there is only one point of addition of acid, aggressive treatment to counter the effects of OH⁻ in the low-efficiency cells can produce dangerously low pH values in the best cells. Acid addition must be restricted to avoid this problem. When the highest gas quality is desired, it is better to provide a number of acid addition points and increased surveillance in order to approach the ideal of individual cell control. The latest generation of membrane-cell designs (Chapter 5) takes this aspect into account.

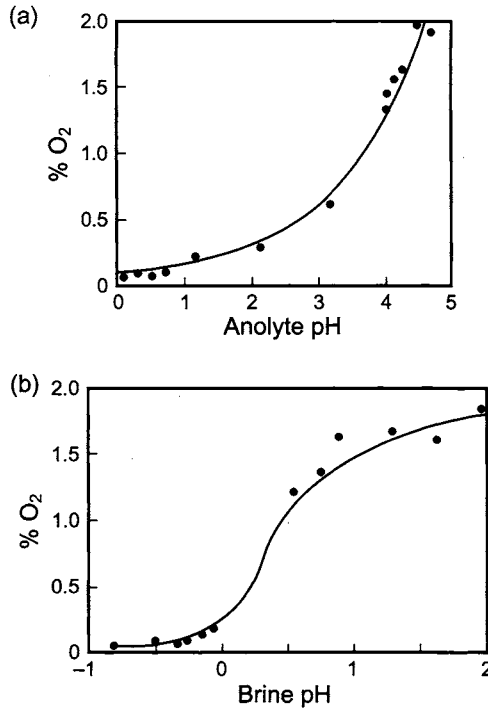


FIGURE 7.78. Oxygen production as a function of (a) anolyte or (b) brine pH.

The control philosophy should include acid flow measurement with alarms. The pH meter, in addition to high and low alarms, should have a low-pH interlock that stops the addition of acid. Some voltage monitoring systems also respond to sudden changes in cell voltages by stopping the acid flow. Finally, acid flow also should be stopped early in the cell shutdown process (Section 13.8.3.1) and whenever the rectifiers trip.

An occasional and usually sporadic problem with acidified brine is the formation of insoluble material at pH values of less than 4.5. This appears as fine particles, known as “brine rocks,” that often plug the brine rotameters. The problem can be avoided by using alkaline brine or by chlorinating the treated brine before acidification. The latter technique depends on the fact that the precursors of the brine rocks appear to be oxidized by hypochlorite in alkaline solution.

There are three particular aspects of design to consider when acid is used. These are the mixing of the acid with the brine, the possibility of precipitation of salt, and the release of carbon dioxide. Acid can be mixed with brine in an ordinary static mixer, usually made of FRP, with flow ratio measurement or a downstream pH meter controlling the rate of acid flow. If the pH is low enough first to ensure the decomposition of carbonate ion and then to neutralize some of the hydroxide back-leakage in the diaphragm and membrane cells, this is not an exacting control problem. If the brine is taken only to an intermediate pH, the excess acid will represent only a small part of the total demand, and pH control may be unstable. Figure 7.79 illustrates this by showing the calculated pH of treated brine as

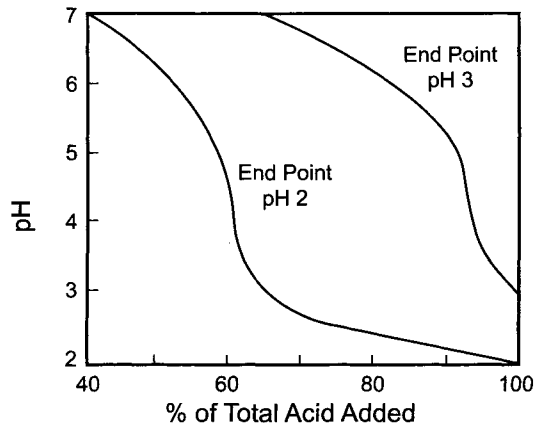


FIGURE 7.79. Development of pH during brine acidification.

a function of the normalized amount of acid added to the solution. The curve assumes starting concentrations of 0.6 gpl Na_2CO_3 and 0.3 gpl NaOH , with no other buffering. The pH is the true value; it is not corrected for salt effects to show the measured value. The purpose of the plot is to show that the conversion of bicarbonate is essentially complete at about pH 5 and that the amount of acid required to produce a low pH starts to grow rapidly only below pH 3.5. Control of the acidification process at a point between about 3.5 and 5 may be difficult. At lower levels, pH changes more slowly and control characteristics improve. We should note incidentally that reversion of sulfate to bisulfate, not considered in the calculation, begins below pH 3. This consumes acid and adds to the improvement.

The data presented in this section should be considered indicative only and not used in design. The brine used in their generation was prepared from vacuum-purified salt. Brine prepared from other grades of salt may have different characteristics.

The use of concentrated acid can present another problem. Addition of 30% HCl to nearly saturated brine can result in supersaturation. Potter and Clynne [136] studied the solubility of HCl in NaCl solution. Figure 7.80 shows some of their data at temperatures from 20°C to 100°C , as plotted by Rodermund [137]. Any tie line between two points on a curve will lie entirely within the insoluble region, and so mixing of any two solutions mutually saturated in NaCl and HCl results in some precipitation. If the brine being acidified is fully saturated and the acid is at full strength, one can expect solids to collect at the acid addition point. Some technologists recommend the use of more dilute acid for this reason. The simplest method then is to add a stream of pure water along with the acid. The heat of dilution will increase the temperature of the acid about 10°C but will have little effect on the mixed brine temperature. Most membrane-cell suppliers specify feed brine concentrations below saturation, and in that case the problem is relieved.

Once the acid and brine have been mixed, evolution of CO_2 begins. To allow this to escape, the brine should go to a vented tank. This must have disengaging space for the vapor and enough residence time for the liquid to ensure degassing. Frequently, tanks are compartmented to reduce the amount of bypassing. If the carbonate content of the brine

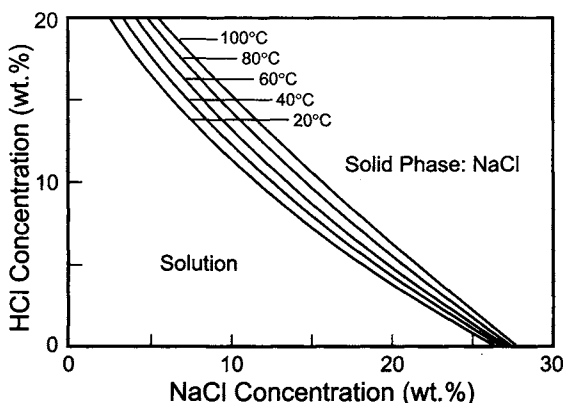
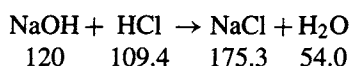
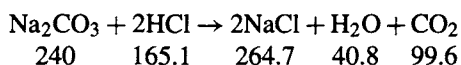


FIGURE 7.80. Mutual solubilities of HCl and NaCl in water.

is low, much of the CO_2 generated can remain dissolved with subatmospheric partial pressures. An air or nitrogen purge will reduce the partial pressure of CO_2 and assist the separation. Some plants vent the acidizing system through a small scrubber, where a countercurrent flow of brine prevents the escape of small quantities of HCl.

Example. Using the excess reagent concentrations assumed in earlier examples, a flow of $400 \text{ m}^3 \text{ hr}^{-1}$ of brine will contain 240 kg hr^{-1} of Na_2CO_3 and 120 kg hr^{-1} of NaOH. The reactions of these chemicals with HCl are:



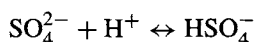
The HCl required for neutralization is 274.5 kg hr^{-1} ; as 31.5% acid, this is accompanied by 596.9 kg hr^{-1} of water. The reactions produce 440 kg hr^{-1} of NaCl.

We must add more acid if we wish to have some available in the cells. We choose a concentration of 20 mN (a nominal pH of about 1.7). In 400 m^3 , we require 8 kg mol. This is another 291.7 kg of HCl, with its accompanying 634.4 kg of water. The total requirement is then 566.2 kg hr^{-1} of HCl. This is about $1,800 \text{ kg hr}^{-1}$ or $1.55 \text{ m}^3 \text{ hr}^{-1}$ of solution. Note that the amount of excess HCl added to the brine is comparable to the stoichiometric requirement.

This is fairly aggressive treatment. The minimum case, if acidification is to be used at all, might be regarded as just enough acid to destroy the carbonate and produce a moderately low pH. Consider a pH of about 3.5, corresponding to a free HCl concentration of about 0.32 mN. The excess acid requirement drops from 291.7 kg hr^{-1} of HCl to 4.67 kg hr^{-1} , which is only 1.7% greater than the stoichiometric amount. One would then be faced with more of a control problem. This is the effect alluded to in analyzing Fig. 7.79.

This is a good opportunity to point out that throughout the brine treatment process, various small streams are being added and subtracted, and some of them produce reactions that change the amount of NaCl in solution. Careful design must consider all these effects. For the most part, we ignore them here in order not to obscure the larger points being made in these examples.

In our example, we express acid concentrations on a molar basis partly in order to avoid the complications of discussing pH and its measurement in concentrated salt solutions. Bates [138] describes the fundamental problems in measuring and even defining pH in such systems. First, a pH cell responds to activity, not to concentration. High acid concentrations also reduce the thickness of the swollen hydrous silica layer in the surface of a glass membrane. Bates also points out the lack of a unique definition of the activity of a single ionic species and the fact that establishment of a working pH scale depends on a number of assumed conventions. Still, it is the pH of the anolyte that is important, and not its total acidity [139]. The presence of sulfate in the brine, for example, provides some buffering action through the formation of the bisulfate ion:



More acid must be added to the anolyte in order to reach a given pH when sulfate is present. Other components of the solution also influence the pH. Keating [139] shows the effect of salt concentration when HCl is added to NaCl brine.

The pH defined for control purposes is usually at a reference temperature (say, 25°C) well below the cell operating temperature. On-line pH measurement requires temperature compensation. It is normally a good practice to cool the anolyte before measuring its pH in order to reduce maintenance requirements, improve the reliability, and extend the life of the instrument.

7.5.6.2. Supply of Hydrochloric Acid. Besides acidification of the cell feed brine, hydrochloric acid has two other chief uses in the process:

1. acidification of depleted brine for recycle to mercury or membrane cells (Section 7.5.9.2);
2. regeneration of the ion-exchange resin (Section 7.5.5.2).

Except for the acidification of depleted brine, the acid must be of high purity. A typical membrane-cell feed specification might call for less than 0.5 mgpl each of hardness, heavy metals, and free chlorine in the concentrated acid. The free chlorine specification is necessary to protect the ion-exchange resin from oxidation during regeneration. The water used to absorb HCl and to dilute acid to its use concentration must therefore be of high quality. Strictly speaking, there is not a need for a particular hardness specification on the acid added to the cell feed brine. The specification of about 20 ppb in the feed brine is essential; the origins of the hardness are not important so long as the overall specification is observed. A hardness specification on the acid is an operating control or a restriction on an outside supplier. It becomes more important as the practice of deep acidification grows.

Hydrochloric acid may be purchased or produced internally. It is a widely available commodity, easily obtained in good quality. HCl is available in the anhydrous form as well as in the form of aqueous acid (up to 23° Be' or about 37% HCl). The use of aqueous acid is standard in the chlor-alkali industry, and we do not discuss anhydrous HCl here. Byproduct acids are available, sometimes at lower prices, and may be suitable for use in the chlor-alkali process. Their quality should be checked carefully, and testing may be advisable before use. When HCl is produced from chlorine liquefaction tail gas, the absorbing water is the most likely source of impurities. Demineralized water is the standard source when producing acid for use in a membrane-cell chlorine plant. A certain amount of chlorine tends to be present in burner acid. This can be minimized by process control, and a small bed packed with activated carbon (Section 7.5.9.3B) is a useful safeguard. Usually only the acid intended for use in the ion-exchange system need be treated in this way.

As noted, the acid used in dechlorination of depleted brine does not have to be of the highest purity. The dechlorinated brine will circulate back through the treatment system, and any impurity that is removed there can be tolerated at a reasonable concentration in the acid. This may allow the use of byproduct acid or of some of the acidic effluent from ion exchanger regeneration.

Hydrochloric acid is an extremely hazardous material (Section 16.2.4). It is rapidly corrosive to bodily tissue and to most types of clothing. Few metals are resistant, and metallic corrosion often results in the evolution of hydrogen. Rubber-lined and FRP tanks are the most frequent choices for storage. Some rubbers are protected by a layer of rubber hydrochloride and should not be washed or used in other service as well as with HCl. Other plastics are also suitable in equipment fabrication and pipe lining. These include PTFE, PVDF, PVDC, and polypropylene. Impregnated carbon and graphite are useful at higher temperature. These do not often appear in acid distribution service in a chlor-alkali plant, except in small parts, but they are standard materials in HCl synthesis units (Section 9.1.9.2). Pumps and heat exchangers are the only common equipment items frequently found in metal. Durichlor 51, Hastelloy C, and titanium are resistant to the acid under oxidizing conditions. When no oxidants are present in the acid, zirconium and Hastelloy B are preferred. Tantalum has outstanding resistance and is a common choice for small parts and thin sections, as in instruments.

Storage tanks usually are vertical, with flat bottoms and conical or dished heads. Horizontal tanks sometimes are used when storage is under pressure or when elevation is desirable in order to allow gravity transfer. Volumes should suit the rate of usage of the acid and the logistics of its supply. As with other hazardous materials, the amount stored should be kept to a reasonable minimum. Fire retardancy and UV-light resistance are desirable in plastic tanks. Choice of the design temperature of field-lined tanks should consider the curing process, which often uses steam at atmospheric pressure.

The Chlorine Institute [140] suggests techniques for construction and testing of HCl storage tanks. Spill control might involve sumps, reservoirs, dikes, or even double-walled tanks. An exterior confinement system should include vapor control or sufficient volume for dilution and neutralization. Some storage tanks have conservation vents. The settings should minimize venting due to normal pressure fluctuations but must be consistent with the design pressure and vacuum ratings of the tank. Because of the danger of exposure to HCl vapor, external surfaces and auxiliaries such as ladders and gratings should also be corrosion-resistant. Rubber-lined steel tanks should be inspected every

2 years, inside and out. The outsides of FRP tanks should be inspected every year and the insides every 5 years. Crosslinked high-density polyethylene is a good choice for small tanks.

When HCl is purchased from outside, there will be an unloading facility. These are subject to hazardous materials regulations. In the United States, they appear in the Code of Federal Regulations, Title 49, Parts 100–199. The size and type of transport vehicle vary, as do the need for auxiliary equipment and the appropriate procedures. These must be addressed in the supplier's material safety data sheet. The user, however, is responsible for the storage facility and should pay particular attention to venting. Displacement of 100 m³ of air saturated above 32% HCl at 25–30°C will release 8 kg of HCl vapor. When acid is unloaded under air pressure, designers and operators should be aware of the hazard of a pressure surge when the supply vehicle runs empty and air flows into the storage tank unimpeded (Section 16.3).

Submerged filling of a tank is preferred, in order to avoid splashing and mist formation. As in all such arrangements, the fill pipe should have a breather hole near its top to serve as a vacuum breaker. Flat tank bottoms usually have a minimal slope to assist drainage. Some indication of liquid level in the tank should be available to the truck operator or other responsible person. The usual measuring element is a differential-pressure cell attached to the bottom of the tank through a diaphragm of tantalum or a fluoropolymer.

Most pumps in HCl service are nonmetallic. Wetted parts may be PVC, CPVC, PP, PTFE, PVDF, FRP, ceramic, or carbon. Self-priming centrifugal pumps are a standard, but diaphragm-type metering pumps also are widely used.

A bypass line on a pump discharge will ensure sufficient flow when transfer stops because a valve is closed at the receiving end of the line. This prevents shock to the pump. It is a desirable addition to many centrifugal pump systems, and it is essential with positive-displacement pumps. The pump suction nozzle on a tank should be located 50–100 mm above the floor of the tank.

The major hazard in pumping HCl is leakage. This is most likely around the pump seals, and so sealing is important, with double mechanical seals or the use of sealless pumps with magnetic drives preferred. Personnel-protection shields are appropriate, and the location of a pump should allow easy access for maintenance while minimizing the chance of exposure of workers to leaks. Pumps should also be protected from operating against a closed valve or running while dry. Tank cars or trucks with top unloading require self-priming or positive-displacement pumps. These may require vacuum protection for the tanker.

Lined steel piping is stronger and more rigid than solid plastic piping. It is therefore less susceptible to mechanical damage. The most frequently used linings are polypropylene, PTFE, and PVDF. Problems associated with lined pipe are the need for precise measurement of spool lengths and the permeability of the linings. Each spool or fitting must have a full-length vent channel with a weep hole at a flange.

FRP piping, usually of vinyl ester resin, is also widely used. Unlike lined steel pipe, it does not require painting, but outdoor installations should have a layer resistant to UV light. Other plastics used in solid piping are PVC, CPVC, PVDF, and PFA, always in Schedule 80. These materials are light and easy to install, and they have excellent resistance to exterior corrosion. They are structurally the least rigid candidates and so are most subject to mechanical damage. Piping runs require extensive support. Solid thermoplastic piping is therefore used most in small sections and in applications not

requiring structural strength (e.g., tank vents). The weakness of thermoplastic piping can in some cases be overcome by wrapping it with FRP.

Piping in transfer lines should be free of loops and pockets. Unloading connections may be flexible hose (typically 50-mm) lined with acid-resistant rubber, crosslinked polyethylene, or a fluorocarbon polymer. These hoses should not have quick disconnects. They should be inspected after every use. A sight glass on the transfer line will let the operator know when transfer is complete.

Most types of valves are satisfactory in HCl service. Quarter-turn valves are most common. Materials of construction include PTFE, CPVC, PVDF, FRP, PP, PVC, glass, and porcelain. Plug valves appear widely in HCl service, but in general they offer few technical advantages over ball valves. Butterfly valves offer low pressure drops and easy throttling, which are important in some applications. Typical construction uses ductile iron bodies with PTFE or PFA lining and discs coated with the same materials. Polypropylene is the usual choice when spacers are required to allow a disc to turn without obstruction. Heavy-duty PTFE plug valves are widely used as primary storage tank valves and on tank trailers.

7.5.7. Control of Sulfates

The major anionic impurity in most brine systems is sulfate. Control of its concentration is an issue mostly in membrane cells. In the diaphragm-cell process, sulfate passes with the rest of the anolyte into the cathode side of the cells. It can be separated from caustic soda in the evaporators and purged from the system as Glauber's salt. This is covered in Section 9.4.2.1. Mercury cells are least sensitive to sulfate. Its concentration is frequently allowed to build to the point where dissolution of calcium sulfate from the salt is inhibited. The greatest problem then caused by the sulfate is a reduction in the solubility of NaCl or KCl.

With membrane cells, there is a specification of about 7 gpl Na_2SO_4 in the depleted brine. Many different techniques are used to hold the sulfate concentration below this level. Discussion of these can be organized by dividing them into three categories [58]:

1. use of salt with low sulfate content;
2. rejection of sulfate during the salt-dissolving process;
3. removal of sulfate from the brine system.

The list is in order of decreasing elegance. The second item has already been covered under the heading of selective dissolving in Section 7.2.2.5.

7.5.7.1. Use of Low-Sulfate Salts. There is great variation in the concentrations of impurities, including sulfate, in natural salts. This should be an important part of the value analysis when choosing a raw material. Several grades of salt are purified by processing (Section 7.1.5), and some of these have attractively low sulfate contents. We discuss several forms of processed salt below.

7.5.7.1A. Vacuum Purified Salt. Brine is produced from crude salt by standard techniques and then treated chemically to remove hardness and sulfate. When this is

TABLE 7.22. Typical
Analysis—Vacuum-Purified NaCl

Component	Concentration
Dry basis	
NaCl	99.95% (w/w)
Sulfate	400 ppm
Calcium	12 ppm
Magnesium	1 ppm
Iron	1 ppm
Copper	0.04 ppm
Insolubles	50 ppm
Wet basis	
Water	2.50%

Source: Akzo Zout Chemie booklet *Electrolysis Salt (Sodium Chloride)*.

evaporated under vacuum, more purification occurs by fractional crystallization. The impurities tend to stay in solution. The slurry of purified salt is centrifuged, and the cake is washed. After drying, the salt is ready for commercial distribution. Table 7.22 shows typical analyses. Purified vacuum salt is available only at a sizeable premium, but brine prepared from it requires only ion-exchange treatment before use in membrane cells. Many chlor-alkali producers find the higher price acceptable when considering the benefits. This is especially likely with smaller plants and in the case of a producer who is not a specialist and regards the chlor-alkali plant essentially as a utility. There is also the possibility of taking advantage of scale by producing salt in quantities suitable for a number of chlorine plants [141,142].

Section 7.1.5.2 also mentioned some of the effects of salt purity on design of the brine plant. Becnel [143], in his discussion on improvements in the manufacture of purified salt, raises the possibility of production of salt directly suitable for membrane-cell operation. This could profoundly simplify the whole brine treatment plant.

7.5.7.1B. Recrystallized Salt. Section 7.1.5.3 on salt refining also mentioned the salt recrystallization process. The product is an alternative to vacuum-purified or vacuum-pan salt. To the chlor-alkali producer, the differences among all these evaporated/crystallized products come down to a value analysis of material cost vs in-plant processing cost.

7.5.7.1C. Diaphragm-Cell Evaporator Salt. The salt produced in a diaphragm-cell evaporator is also quite pure and in the industry is often referred to as chemically pure, or CP, salt. It is a valuable resource in plants that operate either mercury or membrane cells along with the diaphragm cells. Its use in the resaturation of mercury-cell depleted brine is described in Section 9.4.1. Evaporator salt is always low in hardness, but it must be treated further in order to be free of sulfate, and it may have an undesirably high concentration of silica. At certain stages during evaporation of cell liquor, a triple salt, $\text{NaCl}\cdot\text{NaOH}\cdot\text{Na}_2\text{SO}_4$, deposits. Unless this is segregated or decomposed into its

components, separation of the sulfate can not be complete. Many plants have systems for decomposition of the triple salt and removal of sulfate as Glauber's salt.

Evaporator salt, if not otherwise contaminated during its processing, could be used as a low-sulfate feed to membrane cells. However, there is a more effective method of integration in which the diaphragm cells serve as a purge for the membrane-cell brine system. Section 9.4.1 also covers this topic.

7.5.7.2. Removal of Sulfate from Brine. It is the recycle of brine around a continuous system that causes the sulfate problem. With no escape from the brine loop, any amount of sulfate in the incoming salt or brine will eventually build up to the point where the concentration specification is violated. What sulfate enters a membrane-cell brine system must therefore be removed. This means that a purge from the brine system is necessary, and the techniques used range from a simple purge of the brine itself to more elaborate schemes of precipitation or crystallization. Between these extremes are new techniques developed specifically as a response to the membrane-cell sulfate problem.

7.5.7.2A. Purge of Solution

Waste Brine. The appeal of a simple brine purge lies in its minimal capital cost and energy consumption. It serves at the same time to remove chlorate formed in the cells and trace components contributed by the salt or picked up from equipment or piping. Its disadvantages are the cost of the lost salt and any environmental problems caused by disposal of the purge stream. However, "purging" does not necessarily mean wasting the salt or releasing it to the environment. If there are alternative uses for brine that are less sensitive to the presence of sulfate, some of the brine can be diverted there and replaced with fresh brine. The extent of internal recycle is thereby decreased.

First, we shall study the simple purge of brine to determine the extent of raw material loss. Let the volume of the purge stream per unit of salt consumption be V_p and its concentration of sulfate be S_p . Then the amount of sulfate purged is $V_p S_p$. Now let the amount of sulfate accompanying a unit of NaCl or KCl in the salt be S . If we ignore the amount of sulfate passing through the membrane, a truly negligible quantity, and the amount that goes out with the brine sludge, a less justifiable but conservative assumption, we have

$$S = V_p S_p \quad (69)$$

"Sulfate" can be taken to mean either equivalent M_2SO_4 or the sulfate ion. The volume of purge required is

$$V_p = S/S_p \quad (70)$$

The concentration of NaCl or KCl in the purge is C_p . The salt lost by purging therefore is $V_p C_p$. This leads to

$$\text{Loss} = S C_p / S_p \quad (71)$$

TABLE 7.23. Salt Loss in Waste Brine Purge

Type of salt	Sulfate content, %	% of salt lost
KCl—Industrial Grade	0.16	6.5
KCl—Soluble Grade	0.012	0.5
Vacuum-purified NaCl	0.02	0.8
Washed solar salt	0.15	6.0
Rock salt 1	0.6	12 ^a
Rock salt 2	1.0	20 ^a

Note:

^a Assuming 50% rejection of CaSO₄ in dissolver.

To minimize this loss, we should where possible choose a salt with low S . This has already been discussed. Next, we look for a low value of C_p/S_p . This leads us to the depleted brine, where chloride has been consumed, but not sulfate.

Table 7.23 shows the results of applying Eq. (71) to a series of salts. The calculations assume that the sulfate content of the depleted brine is close to the specification limit and that the depleted brine is purged after proper dechlorination. In practice, much of the sulfate in a rock salt may remain undissolved, and the purging requirement is correspondingly lower. The data on rock salts in the last column are based on dissolving only 50% of the contained sulfate. The main point of the table is that the sheer volume of the stream makes purging to waste unattractive with rock salts or, at least in large plants, with solar salts. Purging becomes more practicable as the purity of the salt increases. The low purge volumes associated with most KCl and vacuum-purified NaCl make extensive processing of the waste to meet zero-discharge requirements more reasonable.

Next, we consider the possibility of purging a major part of the brine to another salt user. The outlets most likely to be available to a membrane-cell operator are other electrochemical processes.

Many chlor-alkali producers also operate chlorate plants. These are convenient receptacles for purged brine. While from the chlor-alkali plant's standpoint this is an elegant way to dispose of the sulfate problem, there are several facts working against it:

1. *Size of the chlorate plant.* It may not be possible to purge enough brine to remove the problem.
2. *Lack of a dedicated saturator.* If the purge cannot be resaturated in the chlorate plant, it may be necessary to transfer saturated brine with its higher ratio of C_p/S_p . The volume to be purged is correspondingly greater. Using a separate saturator for the purge stream can alleviate the problem.
3. *Lack of a market for chlorate solution.* Solutions usually can be sold with a certain quantity of dissolved sulfate. If a plant produces mostly solid product, there may still be problems with a sulfate specification.

The amount of sulfate that can be tolerated in a chlorate plant is inversely related to the percentage of the product sold as crystal. It is also possible to remove sulfate

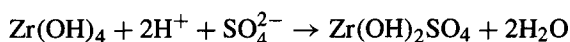
selectively in the chlorate plant by coprecipitation of Na_2SO_4 and NaClO_3 at subzero temperatures [144].

When membrane cells operate in tandem with mercury or diaphragm cells, there is an opportunity to purge sulfate by sending at least part of the depleted brine that otherwise would be recycled to the other cells. This approach is less effective with mercury cells. The water balance is extremely tight in a mercury-cell plant, and any import of water must be balanced by an export. Since export would spread the potential for mercury pollution, we reject it as an operable solution. Only mercury-cell plants with some capacity for addition of water to the brine loop, as for example a plant with a brine evaporator, could be integrated in this way.

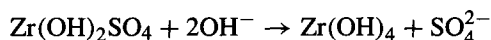
Diaphragm cells are another matter. The water load can be tolerated in the process, and the sulfate leaves with the catholyte, where there are several possibilities for its recovery or disposal. Other possibilities for integration with diaphragm cells, involving the use of evaporator salt, were mentioned above in Section 7.5.7.1C.

Concentrated Purge. New methods of sulfate control have been developed in response to the membrane-cell brine problem. These include a novel application of the familiar ion-exchange technique and a process based on the relatively new technique of nanofiltration. The processes use physical or chemical means to make a partial separation between chloride and sulfate; the problem of disposal of the sulfate remains. By concentrating the sulfate and removing most of the chloride, they may allow safe, legal, and economic disposal of the sulfate by a simple purge. In other cases, their value lies in providing a much smaller stream to be treated for the ultimate disposal of the sulfate (e.g., by precipitation).

Ion exchange. A brine purge is made selective by an ion-exchange process that selectively attracts sulfate-based ions from the solution. Reversal of the process regenerates the sulfate ions in much higher concentration relative to chloride. A commercial process developed by Kaneka Corporation and licensed through Chlorine Engineers is referred to as NDS, or the New Desulfation System. It is not the classical ion exchange with pendant groups attached to a polymeric resin. It is rather a manipulation of the favored form of an inorganic compound by changes in pH [88,145]. The ion-exchange agent is a zirconium compound. Hydrous zirconium (IV) oxide in contact with brine at $\text{pH} < 3$ converts to a sulfate form:



Because of the pH requirement, this step is most conveniently applied to the depleted brine. Later, the zirconium reverts to its original form when exposed to high pH, releasing the sulfate ion:

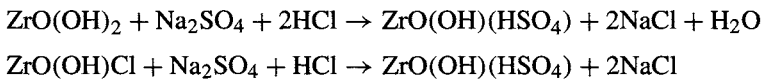


The process as first developed used a pair of slurry reactors for the two steps. In one of these, brine mixed with acid was agitated with suspended zirconium oxide. With two of the four hydroxides replaced by a sulfate, the slurry was transferred to a vacuum filter.

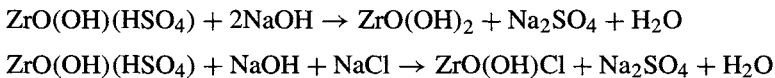
The filtrate, after polishing in a filter press, passed on to the brine process. The filter cake dropped into a second agitated slurry reactor, the desorber. Addition of caustic there raised the pH and reversed the reaction of the zirconium. This slurry was transferred to a second vacuum filter. The filtrate in this case, after polishing, became the purge stream. The cake from the second vacuum filter dropped into the first reactor to begin another cycle.

The bypassing always associated with backmixed reactors limited the efficiency of this process. In one published example, the treatment of brine containing 200 gpl NaCl and 7.5 gpl Na₂SO₄ produced a waste of 50 gpl NaCl and 15 gpl Na₂SO₄. With 85% of the sulfate removed from the treated stream, the ratio of chloride to sulfate in the purge was lower than the ratio in the feed stream by a factor of about eight. The purge stream was still quite large, since the total dissolved solids concentration was only about 25% of that in the depleted brine. The liquid effluent from the desulfation process could be nearly eliminated by precipitation of the sulfate and recycle of the liquor to the brine treatment.

A later version of the process (RNDS) is based on the use of a resin containing zirconium hydroxide in fluidized bed reactors. It removes the need for filters and filter cake handling. The sulfate-containing brine, after acidification with HCl, passes through the adsorption bed. The adsorption reactions are



Operation at high pH regenerates the bed:



As do other swing processes, this one requires two beds (or sets of beds), which cycle between service and regeneration. It offers an estimated cost reduction of 13% compared to the original NDS process [146]. It can also be adapted to the removal of silica and iodine from brine (Section 7.5.8.9).

Nanofiltration. The nanofiltration process is, along with backpulse filtration (Section 7.5.4.3), another example of the new possibilities in processing that are due to recent developments in the field of membrane technology. At conditions intermediate between those used in ultrafiltration and RO, this technology can selectively reject multivalent ions such as SO₄²⁻ while passing monovalent ions [147–149]. The process therefore can remove sulfate and other multivalent anions selectively from alkali chloride brines. Since the equivalent amount of alkali metal ions is held back by electrostatic forces, the net effect is the removal of M₂SO₄.

Table 7.24 shows where nanofiltration fits in the spectrum of specialized membrane filtration processes. The process has application regardless of the type of chlor-alkali cell in use, and it also can remove sulfate from chlorate plant liquors. The membranes used in the filters are sensitive to free chlorine. In a membrane-cell plant, therefore, the filter usually will treat a sidestream of fully dechlorinated brine. After standard filtration and,

where necessary, cooling, the brine is stored in a feed tank. From there, it is pumped at high pressure through the unit. The permeate stream, low in sulfate, returns to the main brine system. The reject can leave the brine system or pass on to another filtration stage for further recovery. In one cited example, a skid measuring 7 m × 2.5 m × 2.5 m (high) processed 3.4 m³ hr⁻¹ of brine. Utility consumption per cubic meter of brine was 3 kWhr and 4 m³ of cooling water. The sulfate rejection claimed was 80–95% in 6–8% of the original volume of brine. With 7–8 g SO₄²⁻ L⁻¹ of brine fed to the unit, the total rejection of sulfate ion was about 500 kg per day.

The filtration membranes are sensitive to fouling as well as to free chlorine. This situation is least troublesome in a membrane-cell plant, where the problem components already have been removed from the brine. In mercury-cell plant applications, an installation in the brine recycle loop should include some means of dechlorination. The usual choice is treatment with activated carbon, which is covered in Section 7.5.9.3B. The membranes are in spiral-wound modules placed in cylindrical housings and assembled as on the skid shown in Fig. 7.81. Figure 7.82 shows the construction of a modular element. The low-sulfate permeate flows through the membranes into spacer channels

TABLE 7.24. Membrane Filtration Characteristics

Technique	Cut size (nm)	Rejected species	Pressure (bars)
Microfiltration	200–400	Particulates	0.5–3
Ultrafiltration A	5–400	Bacteria, protein,	1.5–10
Ultrafiltration B	3–10	dyes, detergents	
Nanofiltration	0.5–1	Metal ions, sulfate	6–20
Reverse osmosis	<0.5	Acids, monovalent ions	10–60

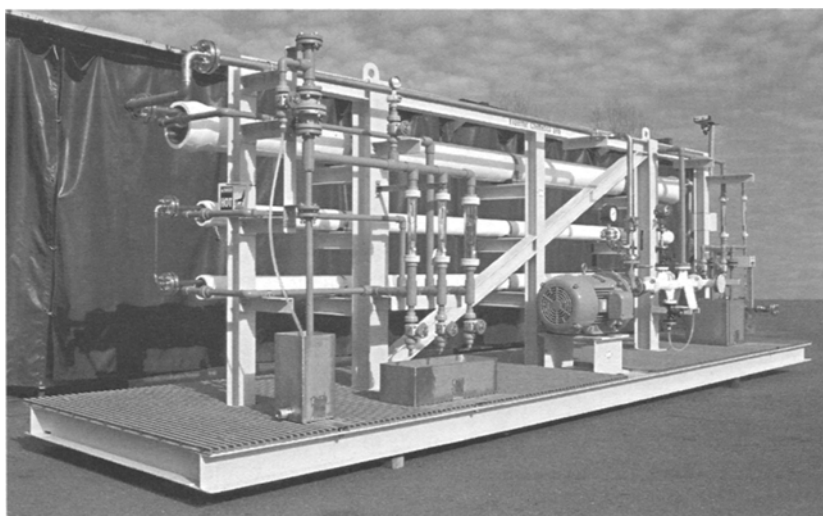


FIGURE 7.81. Nanofiltration unit for removal of sulfate. (With permission of Chemetics.)

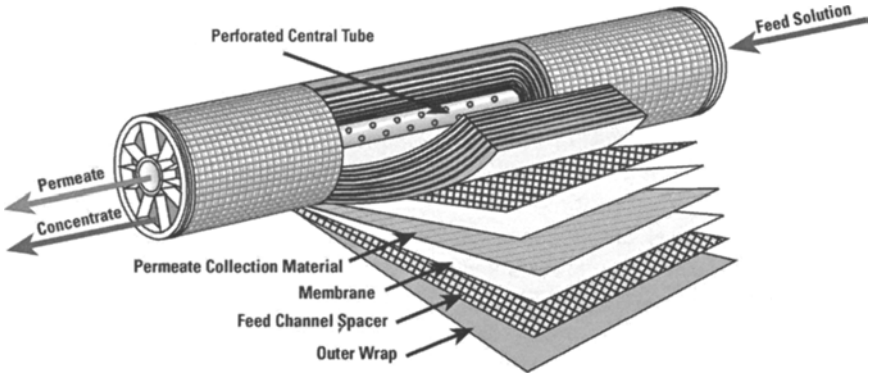


FIGURE 7.82. Construction of nanofiltration module. (With permission of Chemetics.)

TABLE 7.25. Sulfate Removal by Nanofiltration

Type of cell	Feed concentration		Permeate concentration		Reject concentration	
	NaCl	Na ₂ SO ₄	NaCl	Na ₂ SO ₄	NaCl	Na ₂ SO ₄
Membrane	200	7	200	1.5	200	85
Mercury	250	25	255	2	230	100
Diaphragm	250	25	255	2	230	100

Note: All concentrations in gpl.
 Source: Data of Kotzo *et al.* [148].

fabricated from a supporting mesh and follows the spiraling channels into a central collecting tube. The reject, high in sulfate, leaves the end of the module. Parallel installation of modules allows increased capacity, and series installation increases the recovery of brine. Since the selectivity is finite, higher recovery of NaCl always means greater leakage of the sulfate ion. This is caused by the continuous increase in the sulfate content on the feed side of the membranes—the high-sulfate reject of one module is the feed to the next module in series.

Several reports on the process indicate that typical mercury- or membrane-cell depleted brine or the CP salt wash water from a diaphragm-cell process can be concentrated to 80–100 gpl Na₂SO₄ [147,148]. The chloride concentration may remain the same as in the feed solution or actually decline to a lower level. Table 7.25 reproduces the data shown by Kotzo *et al.* [148] for the different cell technologies. The selectivity calculated from the ratios of the concentrations in the reject and the permeate is about 55 in each case. The salt lost with purge of a given amount of sulfate is reduced by a factor of about 12 in the membrane cell case and by about 4.3 in the other cases.

Chemetics is the developer and licensor of the nanofiltration process. By mid-2002, 16 units had been sold or committed [150]. Their removal capacity ranges from 18 to 360 kg hr⁻¹ of Na₂SO₄. Combined capacity is for the removal of about 1,400 kg hr⁻¹. This represents perhaps 350,000 tons per year of NaCl recovered from purge streams.

7.5.7.2B. Removal of Sulfate as a Solid. The direct purge of brine from a system is nonselective, and the major problem associated with it is the large quantities of NaCl or KCl that accompany the sulfate. The techniques of ion exchange and nanofiltration shift the ratio of sulfate to chloride but still rely on a liquid purge and so lose a certain amount of chloride. The most selective method for disposal of sulfate appears to be its removal as a solid, with a minimum amount of occluded chloride. The qualification is important. Without removal of most of the occluded chloride from a sulfate-containing sludge, much of the selectivity is lost. A 10% sludge, without removal of liquor, will carry more chloride than the concentrated purge streams discussed above. Posttreatment of sludge by filtration to a high solids concentration is necessary, and washing of the cake is desirable. The combination produces a very high selectivity.

This subsection discusses precipitation and crystallization, two unit operations that remove a component of a solution as a solid. The physical chemistry is much the same in the two operations, and so it would be well to draw a distinction between them. In precipitation, the concentration of the component in question is increased above its solubility limit. In crystallization, the bulk solubility of a component is decreased. Usually, precipitation involves the addition of one of an ion pair in order to remove the second. Addition of carbonate ion to brine, resulting in the removal of calcium, is an example. In crystallization, the conditions are changed or some of the solvent is removed, so that the amount of the component already present exceeds its solubility. Removal of salt from diaphragm-cell NaOH exemplifies both crystallization techniques. In the evaporators, removal of water increases the dissolved concentration of NaCl until it drops from solution. Cooling of the evaporated liquor before storage or shipping results in more crystallization. Flash vaporization combines the two effects in one step. As solvent is removed by vaporization, the remaining solution drops in temperature. The removal of sodium sulfate as Glauber's salt, described in the crystallization subsection, is an example.

Precipitation. Sulfate can be precipitated by either the barium or calcium ion, and both are used commercially. Turning first to barium, we note that the solubility of BaSO₄ is so low that its precipitation is the standard gravimetric technique for analysis for the sulfate ion. In a brine loop, the precipitation step could be located anywhere, but it is most convenient to combine it with the precipitation of metals in the brine treatment tanks (Section 7.5.2.2) and not to add another step to the process.

While barium is a powerful agent for the removal of sulfate, it is rather toxic and its compounds must be handled carefully. Personnel protection in the form of confinement of tanks and hoppers, the use of dust control equipment, and the wearing of respirators is essential. Because barium chemicals are regulated substances in much of the world, disposal of brine sludge becomes more of an environmental issue and usually requires some form of permit. The barium chemicals also are relatively expensive and available from fewer suppliers. There are two commercially useful sources, BaCO₃ and BaCl₂. The chloride is usually supplied as the dihydrate, BaCl₂·H₂O, which is soluble in water and can be handled as any other solution. While barium compounds are not highly corrosive, a solution of BaCl₂ is acidic and requires appropriate design and precautions. BaCO₃ is sparingly soluble and normally is handled within the process as a slurry. Besides its easier handling, BaCl₂ reacts faster when added to brine.

Finally, commercial BaCl_2 has the advantage of higher purity. The major impurity in barium chemicals is strontium, which is itself an impurity requiring control, and it is important not to create a new problem while solving an existing one. BaCl_2 usually has the lower strontium content. BaCO_3 , on the other hand, usually has the important advantage of a lower cost, and it is also a source of carbonate ion. It can precipitate both calcium and sulfate.

Membrane suppliers will place restrictions on barium concentration in the treated brine in order to prevent damage to their products. The anodes also can be a problem. Barium sulfate can deposit on the anode coating and eventually destroy it, and so the brine must also conform to the specification set by the anode supplier.

Subsequent removal of excess barium from the brine is relatively difficult (Section 7.5.5.1). When using this route for sulfate removal, therefore, the barium concentration in solution should be kept quite low. Fortunately, the specification for the sulfate ion is much more generous than those on calcium and magnesium (Section 4.8.7). By allowing sulfate to accumulate to something close to its maximum allowable concentration, the barium ion can be kept at levels near 0.1 mgpl. In this situation, the sulfate precipitation reaction may be quite slow. While this effect may be less important in coprecipitation along with magnesium and calcium, the small particles of BaSO_4 formed early in the process have enhanced solubility [35], and it is important to avoid this by allowing time for particle growth. This means that barium precipitation, if it is to be used, must be considered when designing the treatment tanks. If barium is simply added as an afterthought to provide some control over the sulfate content, the tanks may be too small and the results disappointing.

Calcium compounds are less toxic, cheaper (especially on a molar cost basis), and much more plentiful than barium compounds. On the other hand, calcium sulfate is much more soluble than barium sulfate, and higher excess concentrations of the precipitating cation are necessary to achieve a given residual sulfate concentration. As a result, calcium precipitation actually may have a higher raw material cost than barium precipitation [60,88]. Another disadvantage of calcium is the fact that two brine clarifiers are required. Calcium sulfate must be precipitated first, using an excess of calcium ion, and then removed in a settler. Normal removal of calcium ion as CaCO_3 follows. The calcium added in the first step adds to the carbonate demand, once again adding to the expense. Conventional clarifiers (Section 7.5.3.2) are large pieces of equipment that can dominate the process-plant layout, and the addition of a second unit will add significantly to the demand for real estate.

Calcium sulfate has several different crystal forms, some of which also contain sodium sulfate. The most familiar are anhydrite (CaSO_4) and gypsum ($\text{CaSO}_4 \cdot 2\text{H}_2\text{O}$). These are the forms commonly found in salt. Mixed crystals include glauberite ($\text{CaSO}_4 \cdot \text{Na}_2\text{SO}_4$), penta salt ($5\text{CaSO}_4 \cdot \text{Na}_2\text{SO}_4 \cdot 3\text{H}_2\text{O}$), and the unstable disodium salt $\text{CaSO}_4 \cdot 2\text{Na}_2\text{SO}_4 \cdot 2\text{H}_2\text{O}$.

Of the two unmixed crystals, anhydrite is usually the more stable in the presence of concentrated NaCl . However, gypsum usually forms first, and its reversion to anhydrite is slow. Of the mixed crystals, penta salt is the preferred form. In the crystallization of sulfate from NaCl brines, there are two possible solid phases to consider, gypsum and penta salt. Penta salt formation is favored at higher temperatures and at higher dissolved sulfate concentration [151]. The transition temperature between the two forms

varies from about 55°C to 80°C, but there is a wide band of metastability in which mixed crystals are formed. A successful crystallization process should be outside this band. Penta salt has been removed from NaCl brines at temperatures above 70°C, and it is also possible to precipitate glauberite by adding seed crystals to a supersaturated solution [152]. At low sulfate concentrations, gypsum can form at somewhat lower temperature, and this is the promising range for chlor-alkali application. Several plants do in fact remove sulfate by gypsum precipitation.

The amount of excess calcium required to keep the sulfate concentration within specification depends on operating conditions. Not only is CaSO_4 much more soluble than BaSO_4 in water, but there is also a salting-in effect that makes it more soluble in NaCl solutions [153]. Figure 7.83 shows solubility curves for anhydrite over the temperature range 25–100°C [154]. CaSO_4 is more soluble in depleted brine than in saturated brine.

Santos [60] studied the economics of solubility suppression and precipitation with calcium. The latter was based on the use of 100% excess. However, it is not percentage excess that matters but the concentration of free calcium ion left in solution after the precipitate forms. Figure 7.83 and the data of Madgin and Swales [155] indicate that the molarity of free Ca^{2+} should be at least 0.03–0.04. With good salts, this concentration is more than 100% in excess, and the cost per unit of sulfate removed is correspondingly higher. Santos therefore proposes this method primarily for high-sulfate salts and limits his examples accordingly.

The maxima on the curves in Fig. 7.83 are a key feature of the $\text{NaCl-CaSO}_4\text{-H}_2\text{O}$ system. While the maximum solubility of anhydrite in NaCl brine is 2.5–3 times that in pure water, the multiplying factor in saturated brine is only about 1.5. This corresponds to about 4 gpl sulfate when NaCl containing anhydrite is dissolved at 50°C. If we compare solubilities in cell feed brine and membrane-cell anolyte, we see that the volumetric solubility of CaSO_4 is much higher in the cell than in the feed brine. The higher

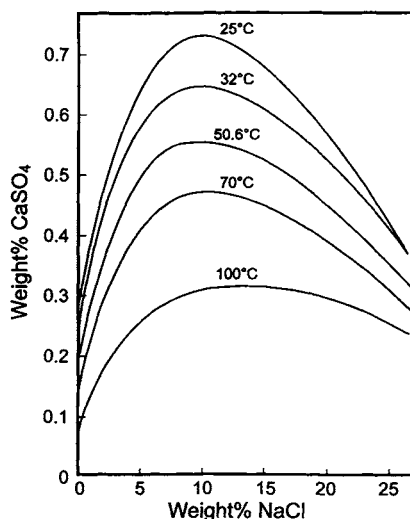


FIGURE 7.83. Solubility of anhydrite in NaCl solutions.

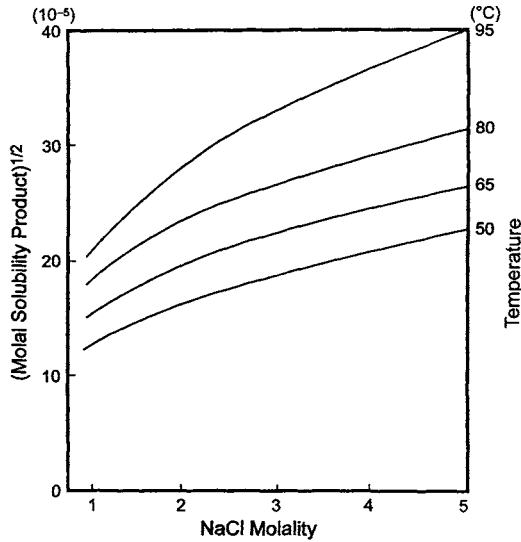


FIGURE 7.84. Solubility of BaSO₄ in NaCl solutions.

temperature and the lower NaCl concentration both contribute to the effect. In the case of BaSO₄, the enhancement is much less. Figure 7.84 shows its solubility in NaCl solutions at various temperatures [156]. Here, there is no maximum solubility, but rather a continuous increase as the brine becomes stronger in NaCl. Unlike the case of CaSO₄, the barium salt is less soluble in depleted than in saturated brine. With the unique anolyte balance of the membrane cell, this can result in deposition of BaSO₄ on the anodes.

Because the increased temperature more than offsets the effect of the reduced salt concentration, Fig. 7.84 indicates that the volumetric solubility is higher in the cell than in the feed brine. Membrane-cell operators, however, must consider another effect. The transport of water across the membranes reduces the volume of solution available. The net effect of all these factors is that feed brine saturated with BaSO₄ can become supersaturated in the cells. Figure 7.85 should make the effect clear. Point A represents feed brine saturated in BaSO₄. Point B shows that the volumetric solubility of BaSO₄ is greater in the anolyte. Line AB refers to the left-hand ordinate. The transport of water through the membranes will reduce the volume of solution by an amount represented by BC. The only real path is line AC, which shows the states of the process inside and outside the cells. The right-hand ordinate applies. The loss in total solubility allows BaSO₄ to deposit in the cells.

Keeping the barium concentration very low, as suggested above, reduces the amount of material that can deposit in the cells. If barium and sulfate ions are present at the same concentration, and if the product of their concentrations would exceed the solubility product of BaSO₄ by 23.5% in the cells, 10% of the total would drop out of solution. If the barium ion concentration were reduced relative to sulfate, and if the solubility product were exceeded by the same 23.5%, the amount of precipitation would decrease. Table 7.26 illustrates this effect. The numbers apply only to the specific degree of excess

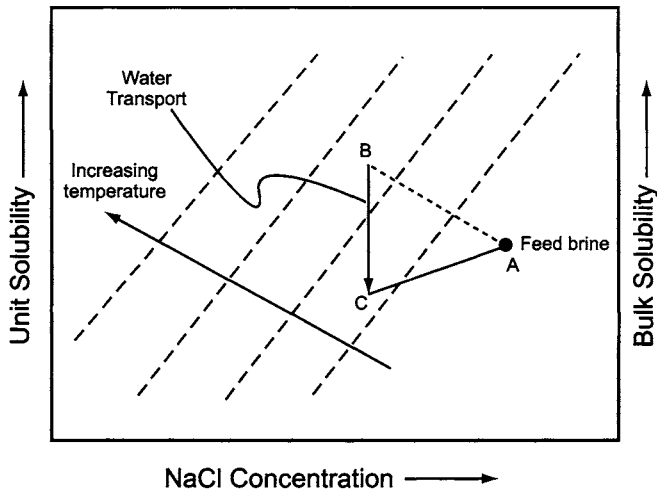
FIGURE 7.85. Precipitation of BaSO_4 in cells.

TABLE 7.26. Effect of Reduced Barium Ion Concentration on Volume of Precipitate Formed

$[\text{Ba}^{2+}]/[\text{SO}_4^{2-}]$	Precipitate volume	% Reduction
1	1	0
0.1	0.555	44.5
0.05	0.408	59.2
0.02	0.264	73.6
0.01	0.188	81.2

chosen here. The purpose of the table is to show that the problem of residual BaSO_4 is greatly mitigated at low Ba^{2+} concentration.

Returning to precipitation with Ca^{2+} , we assume that it produces crystals free of Na_2SO_4 . Above, we referred to the existence of several mixed crystals, but the conditions in a chlor-alkali brine process do not favor their formation [151]. Data on sulfate precipitation are not as plentiful as data on the more familiar hardness precipitation process, but reaction times seem to be approximately the same. Particle retention to allow growth is more important in the present case, and draft tube arrangements with feed close to a bottom agitator are common. The crystals recirculate outside the draft tube to the bottom of the vessel. The solubility in brine, considerably higher than it is in water, increases slowly with higher temperature. Fouling can occur at cold spots.

Calcium sulfate also tends to form supersaturated solutions, and its precipitates thus have a strong tendency to form scale. Pribičević [157] described a reactor into which the reagents were injected into a contact bed of gypsum crystals. This bed was held in the lower conical section of the reactor. The upper cylindrical section served as a final reactor and clarifier. Crystals of precipitated CaSO_4 fell from the upper zone into a small-diameter standpipe that carried them into a bottom leg for discharge. Cool brine

could be injected into this leg to give some countercurrent washing of the precipitated crystals.

Crystallization of Sodium Sulfate. There are two primary forms of crystalline sodium sulfate. Besides the anhydrous form, the decahydrate, or Glauber's salt, also exists. Sodium sulfate can in theory be recovered directly from aqueous solution by the evaporation of water. Removal from solutions containing NaCl is more complex. Figure 7.86 is a plot of *International Critical Tables* data on the NaCl–Na₂SO₄–H₂O system. With the coordinates used, straight lines through the origin represent simple evaporation or dilution (origin not shown on plot). The upper curve marked "S" connects mutual solubilities of sodium sulfate and sodium chloride. It is the saddle curve separating an upper field in which anhydrous Na₂SO₄ would drop from solution from a lower field in which NaCl would deposit. The straight lines between the upper curve and the x-axis are linear approximations to the isotherms connecting the mutual solubility points (curve S) with the solubility of NaCl (x-axis) at the same temperatures. The numbers along curve S are the temperatures of the various isotherms.

Figure 7.86 shows the course of a hypothetical isothermal batch evaporation of a solution represented by point A. As water is removed, the composition of the solution moves upward and to the right along the line AB. When it reaches the solubility isotherm for the temperature of the evaporation process, the solution is saturated. With realistic brine compositions such as point A, it is NaCl that drops out of solution. If evaporation continues, the composition of the residual solution moves up and to the left along the line BC. The solution becomes richer in sulfate and leaner in chloride. If the saddle curve is reached, so is the point of maximum mutual solubility. At this point, Na₂SO₄ begins to drop out of solution along with NaCl. To avoid contamination of the NaCl, the process must stop short of the saddle curve. The shape of the saddle curve means that carrying out the evaporation at lower temperatures (farther to the left) produces higher ratios of

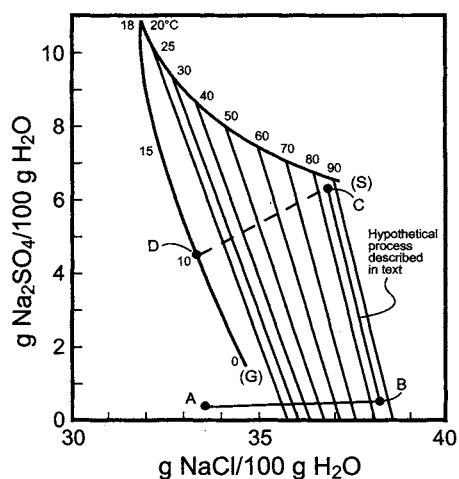


FIGURE 7.86. Mutual solubilities of NaCl and Na₂SO₄ in water.

Na_2SO_4 to residual NaCl in the liquor. These facts make it possible on the one hand to produce pure crystallized salt from a sulfate-containing brine and on the other to remove sulfate selectively from the remaining liquor.

At low temperatures, the NaCl field is bounded on the left by the curve marked "G." This is the saddle curve for solid mixtures of NaCl and Glauber's salt ($\text{Na}_2\text{SO}_4 \cdot 10\text{H}_2\text{O}$). Moving the evaporated liquor to the left side of curve G would allow some of the sulfate to drop out of solution as Glauber's salt. Under the right circumstances, this is accomplished by flash cooling the solution approximately to point D. The total amount of water removed, between flashing of vapor and crystallization of the hydrate, requires the addition of a small amount to the process in order to maintain a mass balance. A reasonable temperature for operation of a commercial Glauber's salt crystallizer is 10°C .

Example. Our starting solution is 25% NaCl and 0.373% Na_2SO_4 . In the coordinates of Fig. 7.86, the abscissa is 33.5 and the ordinate is 0.5. If we carry out the evaporation at about 82°C , the composition at the point of saturation will be 38.2 g $\text{NaCl}/100$ g water and 0.57 g $\text{Na}_2\text{SO}_4/100$ g water. We continue evaporation until the solution contains 6.5 g $\text{Na}_2\text{SO}_4/100$ g water.

We start with 152.8 units of solution. Through the course of the evaporation step, we have

	Start	At saturation	End
NaCl	38.2	38.2	3.22
Na_2SO_4	0.57	0.57	0.57
Water	114.03	100	8.78

At the saturation point, there is not yet any solids formation, and so the quantity of dissolved solids is unchanged. The amount of water remaining corresponds to the saturation composition given above. Of the total, 12.3% or 14.03 units of water have evaporated. Evaporation continues, but since it stops short of the saddle curve, no sulfate drops from solution. The residual water therefore is $0.57/0.065 = 8.78$. The remaining NaCl in solution is 36.7 g/100 g water, or $0.367 \times 8.78 \approx 3.22$. The rest of the salt, about 91.6% of the total, crystallizes during evaporation.

The solution described in the last column above goes to crystallization, where we choose a temperature of 10°C . The crystallizer mother liquor (curve G) therefore contains 33.5 g NaCl and 4.5 g Na_2SO_4 per 100 g water. If no NaCl crystallizes here, we have

	Feed	Product
NaCl	3.22	3.22
Na_2SO_4	0.57	0.43
Water	8.78	9.61

About 24% of the sulfate is removed from the system. Note that the amount of water present has increased. To prevent simultaneous crystallization of NaCl , it is necessary to add water to the process. The quantity necessary is the sum of the increase shown in

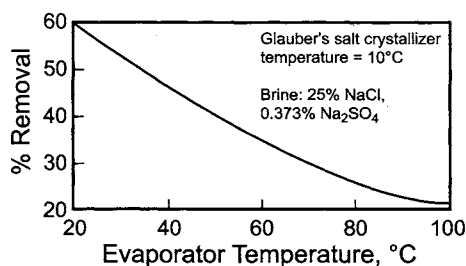


FIGURE 7.87. Efficiency of sulfate crystallization process.

the table, the amount evaporated in the crystallizer, and the amount crystallized as water of hydration.

This example ignores the entrainment of liquor with the solids removed from the system and any wash water or solution added to improve the separation. These are important questions in process design, as is the proper water balance in the crystallizer if the best results are desired. If the purpose of the Glauber's salt crystallizer is only to concentrate the sulfate purge stream, very high quality will not be as important.

With a high temperature in the NaCl crystallizer, limited amounts of sulfate can be removed, and a fairly large stream of brine would have to be treated. The efficiency would be increased if more NaCl were removed in the first crystallizer, which is possible by operating at lower temperature and moving to the left on the plot. Figure 7.87 shows the maximum possible degree of removal of sulfate in the second crystallizer as a function of operating temperature in the first.

7.5.8. Control of Other Brine Impurities

The discussion so far has been mostly in terms of the removal of calcium, magnesium, and sulfate, usually the major impurities in brine. Now it turns to other species. First, we should note that, along with calcium and magnesium, many other cationic species precipitate during primary brine treatment. Their concentrations may be reduced from the grams per liter range to the low ppm level. Those that are harmful to membrane cells include Sr^{2+} , Ba^{2+} , Mn^{2+} , Fe^{2+} , Fe^{3+} , Co^{2+} , Ni^{2+} , and Hg^{2+} . Most of these adversely affect diaphragm and mercury cells as well. Section 7.4.2.1 gives a further list of trace metals that are harmful to mercury cells. Table 7.27 lists the solubility products of a number of species that might precipitate in a brine plant. It is important to note that all these solubility products are handbook data for the species in water near room temperature. The solubility behavior in concentrated brine may be significantly different. The numbers still are useful as approximate indicators of the solubility of the various compounds in brine.

The solubility products of the hydroxides cannot be used to calculate solubilities at high pH. Bivalent positive metal ions tend to shift according to the equilibrium:

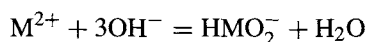


TABLE 7.27. Representative Solubility Products

Substance	Solubility product
MgCO ₃	2.6×10^{-5}
CaCO ₃	8.7×10^{-9}
SrCO ₃	1.6×10^{-9}
BaCO ₃	8.1×10^{-9}
CaSO ₄	9.1×10^{-6}
BaSO ₄	1.1×10^{-10}
Mg(OH) ₂	5.6×10^{-12}
Ca(OH) ₂	4.7×10^{-6}
Sr(OH) ₂	1×10^{-4}
Ba(OH) ₂	5×10^{-3}
Fe(OH) ₂	8.0×10^{-16}
Fe(OH) ₃	4.0×10^{-38}
Mn(OH) ₂	4.0×10^{-14}
Ni(OH) ₂	5.5×10^{-16}
Ba(IO ₃) ₂	1.5×10^{-9}
Mg ₃ (PO ₄) ₂	1.0×10^{-24}

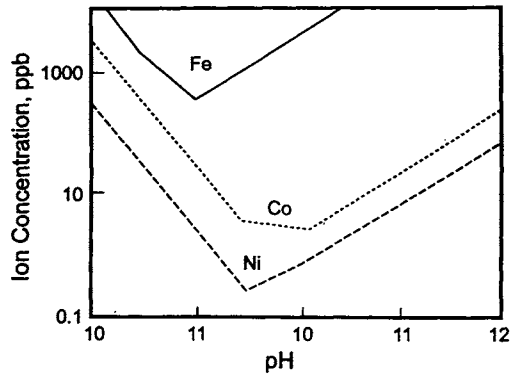


FIGURE 7.88. Solubility of iron, cobalt, and nickel as a function of pH.

With increasing alkalinity, M^{2+} becomes less soluble and HMO_2^- more soluble. Eventually, the observed solubility of the element will begin to increase with pH as the ionized metal takes the second form. Figure 7.88 shows data for iron, cobalt, and nickel at 60°C [158,159]. The logarithms of the solubilities are linear in pH. Table 7.28 gives the terms in the equations for the lines shown on Fig. 7.88 along with the terms for the equations that apply at 25°C. The equations take the form:

$$\log(\text{Solubility}) = \text{pH} - A$$

$$\text{or } \log(\text{Solubility}) = B - n(\text{pH})$$

The pH generally should be kept below 9 or 10 to minimize the solubilities of these metals.

TABLE 7.28. Logarithm of Ion Concentration in Water vs pH

Species (M)	Temperature	M ²⁺	HMO ₂ ⁻
Iron	25	13.27 - 2 pH	pH - 18.28
	60	12.49 - 2 pH	pH - 14.22
Cobalt	25	12.76 - 2 pH	pH - 16.07
	60	11.66 - 2 pH	pH - 17.98
Nickel	25	12.41 - 2 pH	pH - 17.99
	60	10.63 - 2 pH	pH - 17.98

Note: All concentrations in ML⁻¹.

The numbered subsections that follow consider impurities not amenable to satisfactory control by the standard primary treatment process. We divide the impurities dealt with here into three groups:

1. non-ionic or amphoteric:

SiO₂, Al, organics

2. cationic:

Ni, Fe, NH₃

3. anionic:

Hg, F, Br, I, NO₃

The discussion follows the above sequence.

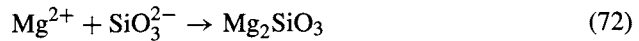
7.5.8.1. Silica. Silica is one of the secondary impurities, but it has synergistic effects in membrane cells when present along with calcium and aluminum [80]. It is difficult to remove silica from brine. The operator's best defense is prevention. Selection of salt, choice of dissolving conditions in order to reject as much silica as possible, and prevention of contamination by foreign substances are all important toward this end.

Much of the silica accompanying salt is in the form of clay or sand. Its solubility is not great, but it is possible for silica to accumulate beyond its specified limit in the brine. Other sources include brine filter beds, filter aids, sandstorms and other forms of atmospheric contamination, concrete salt storage pads, and process water. Section 7.5.4 has presented reasons for avoiding the use of sand filters and diatomaceous earth filter aids in membrane-cell plants. Anthracite and α -cellulose, respectively, are among the recommended substitutes. The other sources of silica vary greatly with locality. Atmospheric contamination can be reduced by covering salt and equipment and sometimes by

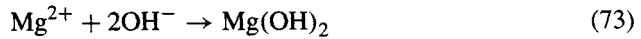
siting facilities so that the source is not upstream in the prevailing winds. When process water contains silica, a different source can be used or a silica removal unit added. Section 12.4.3.1 mentions the use of ion exchange in this service.

Silica, when present in brine, may be in either a soluble or a colloidal form. The soluble form at $\text{pH} > 10$ is HSiO_3^- or SiO_3^{2-} ; below $\text{pH} 10$, it is SiO_2 or H_2SiO_3 [160]. At $\text{pH} > 10$, silica can be removed by the addition of a soluble magnesium compound followed by NaOH addition [161]. The addition of insoluble magnesium oxide may also be used to lower the silica level, but it is not as effective as the addition of a soluble magnesium species such as the chloride. Typical data presented in Fig. 7.89 show the effect of the addition of 25 ppm Mg^{2+} to lower the silica concentration in brine from about 15 ppm to about 5 ppm. It is essential, however, to ensure a $\text{Ca} : \text{Mg}$ ratio of at least 3 : 1 during MgCl_2 addition in order to achieve good settling and filtration.

The addition of magnesium ion to a solution containing silica is the standard process for production of insoluble magnesium silicate. The equation for the formation of the metasilicate is



If we assign magnesium metasilicate a solubility product of K_2 and magnesium hydroxide as produced by the reaction



a solubility product K_1 , we have at equilibrium a residual silicate ion concentration of

$$[\text{SiO}_3^{2-}] = K_1[\text{OH}^-]^2/K_2 \quad (74)$$

As the pH increases in order to precipitate magnesium, the equilibrium solubility of silicate increases. In other words, the equilibrium concentration of the magnesium ion cannot be kept low by Eq. (73) to satisfy the demands of the downstream process and still be high to drive the reaction (72). The method outlined above therefore appears to be a nonequilibrium process that depends on the sequential precipitation of the two species.

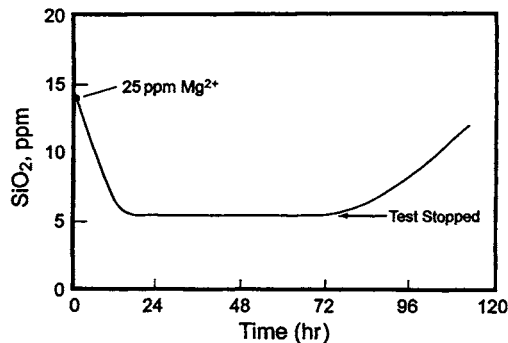


FIGURE 7.89. Effect of MgCl_2 addition on concentration of silica in filtered brine.

The magnesium silicate, once formed at high magnesium ion concentration, is probably occluded by the $Mg(OH)_2$ precipitate and is slow to redissolve.

7.5.8.2. Aluminum. Aluminum by itself is not a highly dangerous impurity, but it forms various insoluble materials in combination with calcium and silica [162]. The sources of aluminum are much the same as the sources of silica. Certain high-grade salts are shipped in aluminum containers, which also can cause contamination. Another source within the process can be the carbon used in filter media. Some of these carbons contain up to 2% Al, which leaches out when exposed to alkaline brine. Acid washing of the carbon requires copious quantities of acid to leach out the aluminum. However, carbon that has been treated with chlorine at 300–400°C is low in aluminum, and after about 48 hr of soaking and flushing with brine, less than 10 ppb Al is found in the effluent brine.

Pickup from the salt can be minimized by controlling the pH in the dissolving process. Aluminum is amphoteric, and Fig. 7.90 shows that it is present in acidic solutions as the cation Al^{3+} and in basic solutions as the anion AlO_2^- [163,164]. In neutral solutions, aluminum is present as a fairly insoluble compound $Al_2O_3 \cdot 3H_2O$ or $Al(OH)_3$. It can be precipitated as the hydroxide by addition of OH^- , but it will remain in solution above the 100 ppb limit if the pH exceeds 8.5 [165]. When salt is dissolved at low pH, the aluminum levels in raw brine are much higher than when the salt is dissolved at pH 8 or 9. The difference persists through chemical treatment to remove Ca and Mg, as shown in Table 7.29. Thus, when salt is dissolved at nearly neutral pH, the solubility of aluminum is suppressed, resulting in Al levels of 100–200 ppb after primary brine treatment.

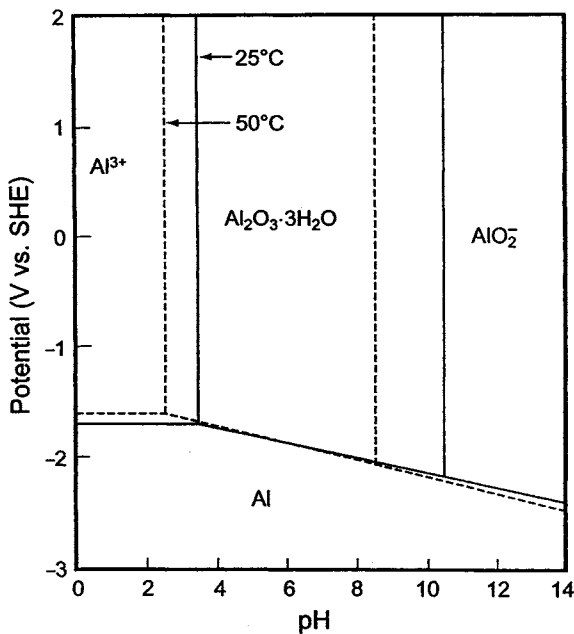


FIGURE 7.90. Potential-pH diagram for aluminum in aqueous solutions.

TABLE 7.29. Effect of pH on Aluminum Content of Brine

pH in dissolver	3	8
As dissolved	4.4 ppm	0.9 ppm
After Treatment	2.0 ppm	0.08 ppm

TABLE 7.30. Effect of pH on Ion-Exchange Capacity for Aluminum

pH	<i>k</i>	<i>b</i>
2	5.22	0.161
4	3.20	0.191
6	2.38	0.314
10	0.025	0.443

Note: Resin capacity expressed as $Q = kC^b$.

Further lowering to ppb levels can be achieved by $MgCl_2$ addition (see above for removal of silica by precipitation with Mg^{2+}). The aluminum, presumably existing as colloidal $Al(OH)_3$ or hydrated Al_2O_3 , is removed either by adsorption on the “ $Mg(OH)_2$ particles” or as a complex Mg–Al hydroxide.

Ion exchange is another technique for removal of aluminum from brine. The discussion in Section 7.5.5.1 showed that the selectivity of the chelating resins used to soften brine depends strongly on pH. We noted above that aluminum readily forms oxygen-containing anions at high pH. At the operating conditions of brine softeners, therefore, it is not removed from the brine. At low pH, where the Al^{3+} ion predominates, aluminum is held very strongly. This approach is used commercially with good success. We can approximate the equilibrium capacity of a resin for aluminum as an exponential function of the concentration of aluminum in solution. Table 7.30 shows the constants at 70°C and as functions of pH. The effect is striking, and at the expense of another pH-adjustment operation and another ion exchanger, we can remove aluminum from the brine quite effectively.

7.5.8.3. Organics. The sources of organics in the brine can be lubricants, refrigerants, paints, solvents, oils, and greases used in the plant and soot, ash, and dirt from the environment. Other sources are groundwater infiltration into the plant and reaction/corrosion products of the process materials. Also, a brine recovered from an organic chemical process will be contaminated with the species with which it has been in contact. Generally, it is difficult to characterize these compounds and even more difficult to remove them.

Certain organics will degrade the performance of chlor-alkali cells by producing foam, which increases the gas void fraction in the cells and can cause the membranes to dry out, and by blocking the active sites in the membranes, resulting in lower current efficiency. Organics also affect the catalytic activity of coated anodes and shorten their

lives. Precise information as to which organics have which specific effect is not now available in the open literature. It is reported [166] that oxygenated organics such as alcohols, ketones, and ethers reduce current efficiency up to 6% as their molecular weights increase beyond 150.

Currently available commercial technologies for removing organics from water do not all apply to removal of organics from brine. Organic-scavenging ion-exchange resins are commonly used in water treatment but cannot be used to remove organics from brine, which is the normal regenerant in such processes. RO also cannot be used because the pressure required would be more than commercial membranes can stand. Another process involving electrodialysis and ion exchange cannot be used with brine because of the generation of chlorine during the operation [167]. The effect of UV radiation or ozonation alone or in conjunction with carbon adsorption has some promise but has not been reported on a large scale.

Organics can be removed from brine to some extent by adsorption onto carbon beds [168] and by steam stripping [169]. About 80% removal of organics was observed from brine containing 15 ppm TOC for over 100 hr by an activated carbon bed at about 4 BV hr^{-1} flow rate [170]. Carbon beds are less effective with high-molecular weight organic species, because of their large size, and with highly polar compounds, because of ionic repulsion [168].

There are many adsorbents available in the market. Rohm & Haas, to name one vendor, supplies the Amberlite® class of adsorbents, which includes Amberlite XAD-4, ZAD-7, XAD-7HP, ZAD-16, and XAD-1180 [169]. These nonfunctionalized materials are reported to adsorb chlorinated solvents, herbicides, nonaromatic compounds, and aromatic species, among many others. A typical example is the use of XAD-7 to remove phenolics from brine. Another class of adsorbents is the Ambersorb® series. Ambersorb 572 is claimed to remove quaternary ammonium salts such as chloromethyl tetraethyl ammonium ions from brine [171].

7.5.8.4. Nickel and Iron. As stated earlier, iron and nickel concentrations should be in the low ppb range after primary brine treatment. However, when such treatment is not practiced, or when certain recycle streams bypass primary treatment, these metals may be present in unacceptable concentrations. One reason for contamination of the brine with these species is corrosion of mild steel or nickel-based piping or equipment, caused by the incursion of hypochlorite into the caustic or brine system.

Two possible approaches to lower the concentrations of these contaminants are precipitation as oxides or hydroxides and ion exchange. Oxides can be removed by adding NaOCl to the brine at a pH of 10–12, followed by filtration. Nickel levels as low as 5 ppb can be realized by this method. However, the practicality of instituting this scheme in an operating plant should be carefully assessed because of the possibility of corrosion and contamination of the brine by reaction of materials of construction with hypochlorite.

There are various ion-exchange resins [172,173] that can be used to remove ionic nickel and iron from brines. These include Duolite C-467, Lewatit TP-207, Purolite S-930, and Amberlite IRC-718. However, the pH of the brine must be less than about five to ensure that they are in an ionic form as Fe^{2+} or Fe^{3+} and Ni^{2+} . At higher pH,

TABLE 7.31. Removal of Nickel and Iron from Brine at 60°C

Element	Resin	Ion concentration	Capacity (mgpl)	pH
Nickel	C-467	1 ppb	10	5
	IRC-718	1 ppb	5.4	5
Iron	C-467	1 ppm	25.7	2-3
	IRC-718	1 ppm	2.4	2-3

these species exist as insoluble hydroxides. The exact pH at the transition depends on temperature and concentration, as well as the presence or absence of complexing agents. Table 7.31 shows the capacity of two resins for nickel and iron from NaCl solutions at 60°C. Both these resins are regenerable by conventional acid treatment.

7.5.8.5. Ammonia. Ammonia may be present in the molecular form or as the cation. It is discussed here among the cationic species for convenience and because some of the control techniques apply only to the ion. Ammonia compounds arise from contact of salt or brine with nitrogen bodies or through the infiltration of nitrogen-bearing groundwater. These compounds may also be present in plant water after primary treatment, especially when it is obtained from surface supplies. The major concern is not the influence of ammonium ions in the cells, but rather the formation of nitrogen trichloride. This is a highly explosive compound that will accompany the chlorine gas from the cells. It can accumulate in liquid chlorine, especially when differential condensation or vaporization takes place. Examples of these operations are compressor suction chillers and chlorine vaporizers. When NCl_3 accumulates to a certain concentration, it can detonate spontaneously. A discussion of the whole subject of nitrogen trichloride and mitigation of its hazard is in Section 9.1.11.2.

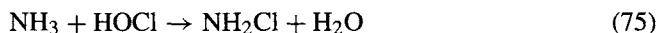
Chemical techniques for removal of ammonia include:

1. oxidation to nitrate by ozone;
2. electrochemical treatment;
3. biological oxidation;
4. formation of volatile NH_2Cl , which can be removed from solution by sparging.

Ozonation of ammonia-containing water converts NH_3 to nitrate ion [174,175]. However, ozone generation is expensive, and the treated stream is still contaminated with nitrate (Section 7.5.8.10). Fundamental work on electrochemical treatment of wastewater showed oxidation of NH_3 at $\text{pH} > 7$ [176]. The precise electrochemistry of the process was not clearly established. Removal of ammonia by biological nitrification/denitrification involves biological oxidation to nitrate followed by bacterial reduction to nitrogen [177]. The process requires large tankage and is subject to upsets. As an aside, precipitation by sodium tetraphenyl borate is a well-known analytical technique and an effective process, but the high cost of the reagent precludes its commercial use.

Of the four processes listed, only oxidation by active chlorine is practical today, and variations of this process are used widely in the chlor-alkali industry. Ammonia is partly

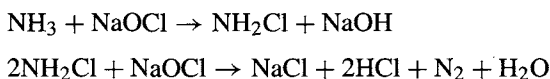
chlorinated at $\text{pH} > 9.5$ to form the very volatile monochloramine. This compound is easily removed by aeration [178]. In aqueous media, we write the active form of chlorine as HOCl:



The rate constant is given by

$$k = 6.6 \times 10^8 e^{(-1510/T)} \quad (76)$$

At 25°C , this is $4.2 \times 10^6 \text{ L mol}^{-1} \text{ s}^{-1}$ [179]. The optimal ratio of NaOCl to NH_3 is about 1.3–1.5 at 30°C at a pH of 10–12. The reaction is rapid, converting 5 ppm of ammonia to <0.1 ppm in 5–10 min. The reactions are believed to be



Reaction (75) is the first of a series of three that successively form dichloramine and nitrogen trichloride. Control of the pH allows the reaction to stop at the monochloramine stage. Section 9.1.11.2C on avoidance of NCl_3 discusses this in more detail. It also mentions that at high pH, where the hypochlorite ion is dominant, the end product can be nitrogen gas:



Bratcher [180] described a system in which hypochlorite solution was added to approximately neutral brine. This produced a two thirds reduction in the NCl_3 content of the chlorine. The ammonia N content of the brine actually was 95% lower. Incidental benefits were a 96% reduction in the ammonia N content of the hydrogen and an 86% reduction in its chloramines content.

Thus, ammonia can be removed either as NH_2Cl or as NH_3 by sparging with air or nitrogen. Whether the dominant species in solution is NH_3 or NH_4^+ depends on the pH and the temperature. This is shown by the hydrolysis reaction



NH_4^+ predominates at $\text{pH} < 7$ and NH_3 at $\text{pH} > 9$. Table 7.32 shows temperatures at which the ratio of ammonia to ammonium ion will be 80/20, 50/50, and 20/80 for various pH values. The dependence of pK on temperature can be estimated by using the equation: $\text{pK} = 0.09018 + 2730/T$ for the reaction $\text{NH}_4^+ = \text{NH}_3 + \text{H}^+$. From Table 7.32 it is clear that the amount of NH_3 present can be increased by raising either the pH or the temperature of the medium.

As alternatives to these processes, several synthetic ion-exchange resins such as Na-type Dowex HCR-S and zeolites (e.g., clinoptilolite) have been examined for their ability to remove the ammonium ion [181–185]. Clinoptilolite has limited capability

TABLE 7.32. Ammonia Equilibrium as
Function of pH

Ammonia/ammonium ratio:	Temperature (°C)		
	80/20	50/50	20/80
pH			
7	159	122	90
7.5	128	95	67
8	100	72	48
9	56	33	14

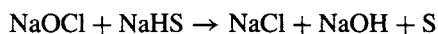
(12% of that of ion-exchange resins) and is hard to regenerate. The capacity of Dowex HCR-S was found to be proportional to the concentration of NH_4^+ in solution [186]. This is usually considered to be a characteristic of an unfavorable exchange isotherm. Adsorption of NH_3 on activated carbons also has been studied extensively [187,188]. These studies showed that only the fraction of the surface with oxygen-carbon groups was effective for NH_3 adsorption.

Ammonia can be air- or steam-stripped from aqueous solutions, steam usually being more effective than air. With high-strength industrial wastes, removal efficiencies can be more than 99% [189]. Ammonia is also removed by RO [190] and by microporous hollow fibers [191].

7.5.8.6. Mercury. Mercury in the feed brine degrades the performance of membrane cells because ionic mercury, transported through the membranes into the catholyte, is reduced to the metallic state on the cathode surface. The high overvoltage of the hydrogen evolution reaction on mercury causes the cell voltage to increase. The transport of mercury through electrolyzer membranes, fortunately, is inefficient. This results from the fact that mercury is present in anolyte as a complex anion, primarily as HgCl_4^{2-} , which must overcome electrostatic forces to reach the catholyte.

Generally, the brine is free of mercury in new membrane-cell installations. However, if a mercury plant is converted to membrane technology, it is very likely that the brine will be contaminated with mercury. Laboratory tests have shown that the concentration of mercury in the catholyte will be about 1,000-fold lower than the concentration in the anolyte, and it is usually considered that 10 ppb Hg in the catholyte has no short-term effect on voltage.

Precipitation of HgS is effective for lowering the mercury level in the brine from about 10 ppm to about 10 ppb. This is done by addition of NaHS , followed by filtration. The procedure calls for pretreatment of brine with chlorine in order to solubilize the metallic mercury and an excess of 10 ppm of NaHS to drive the reaction to completion. The excess NaHS should be removed in turn, as it may have an adverse effect on the anodes through the precipitation of elemental sulfur in the anode compartment:



Carbon impregnated with sulfur also can be used to bind mercury. A typical capacity in contact with saturated brine is 2 mg Hg/g carbon at pH 6.

A popular approach for removing ionic mercury is by ion exchange in the pH region of 6–10. One resin, IMAC-TMR, has been used in a number of plants to remove mercury from wastewater. The resin is very selective for mercury because of the formation of –SH, or mercaptan, bonds. It is used in the hydrogen form and is easily regenerated with 30–35% HCl. As the resin is easily oxidized, even by air, occasional treatment with Na₂SO₃ or NaHS is necessary to preserve the activity of the exchange sites. The capacity of the resin is independent of pH and is almost the same in KCl or NaCl solution; at 70°C, it is given by

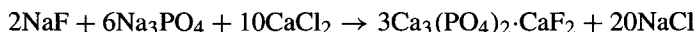
$$Q = 1.631 + 0.277 \log C \quad (77)$$

where

Q = capacity of resin, mgHg L⁻¹

C = concentration of mercury, ppm; from 0.08 to 30

7.5.8.7. *Fluoride*. Fluoride adversely affects both the anode coating and the titanium substrate. Its removal, however, is not commonly practiced in the chlorine industry. Fluoride can easily be precipitated [192,193] as an insoluble fluoroapatite, Ca₃(PO₄)₂·CaF₂, by the addition of CaCl₂ and Na₃PO₄ during primary brine treatment, followed by the addition of soda ash or caustic soda:



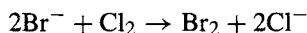
Studies [193] with chlorate cell liquors have shown that 20% excess CaCl₂ and 10% excess Na₃PO₄ are required for effective removal of fluoride ion. Further reductions can be achieved by sodium carbonate addition to remove the excess calcium ion, when the precipitated CaCO₃ removes additional amounts of fluoride, as described in Table 7.33.

TABLE 7.33. Precipitation of Fluoride from Chlorate Liquor

Reaction time (hr)	Starting concentration of F ⁻ (ppm)	[F ⁻] after treatment	
		CaCl ₂ + Na ₃ PO ₄	Na ₂ CO ₃
0.5	20	1.61	0.13
	10	0.99	0.06
	1	0.56	0.04
1.0	20	1.40	0.13
	10	0.52	0.05
	1	0.51	0.04

7.5.8.8. *Bromide*. Most salts contain small quantities of bromide. There are no documented effects of bromide on membranes, but it can adversely affect DSA electrodes. The bromine formed by electrolysis also will affect the quality of the chlorine produced. When the bromine content of the chlorine gas becomes too high, there is a need to remove it in some form somewhere in the process.

It is possible to remove the bromide ion from the brine before feeding it to the cells. The technique is the same as the one used to produce bromine commercially from chloride brines. The ion is oxidized by chlorine to form elemental bromine:



Ensuring by adjustment of the pH and control of the oxidation–reduction potential (ORP) that it is not further oxidized to bromate, the bromine is air-stripped from the solution. In commercial operation [194], this process lowers bromide levels from 50 ppm to less than 0.5 ppm. Figure 7.91 is a schematic of the process. Heating the brine to a higher temperature ($>65^\circ\text{C}$) helps to remove the low concentration of bromine; there will also be chlorine present in the offgas.

Bromine also can be removed from the chlorine gas after the cells. This is done by partial condensation in a process that also serves to chill the gas before compression. Section 9.1.6.4A on chlorine processing describes the use of compressor suction chillers to remove high boilers including bromine from the gas. It also warns of the danger of accumulation of hazardous quantities of NCl_3 .

Suction chiller bottoms usually is a waste product, and one that requires careful handling in its disposal. Recovery of bromine from the solution usually is not warranted.

Since a certain amount of bromine can be accepted in most applications of chlorine, the use of bromine-removal processes has not been widespread. However, greater scrutiny of drinking water quality has raised the issue of chlorate and bromate contamination

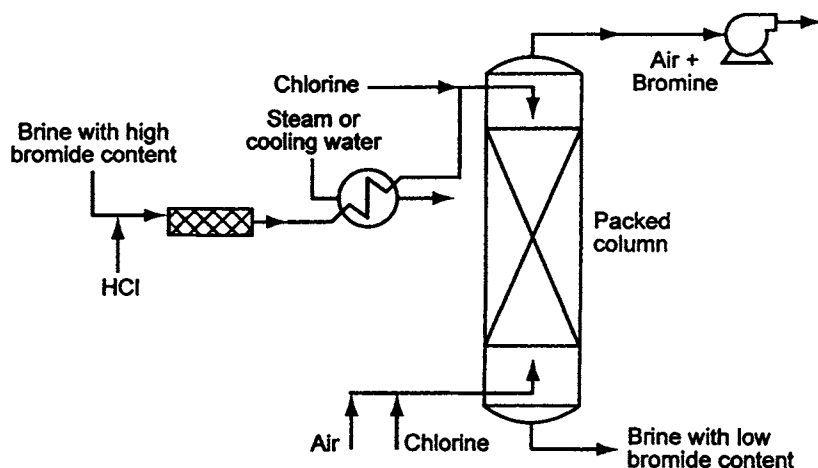


FIGURE 7.91. Process for the removal of bromide from brine. (Reproduced with permission of the Society of Chemical Industry.)

[195,196]. Chlorination of the water is the principal source of these compounds. With time, more producers may find it necessary to add bromine removal facilities to their plants.

7.5.8.9. Iodine. The iodine problem is a variable one, and in many plants it has not been of great concern. Most salts and water supplies, the most frequent sources of contamination, are relatively free of the element. High concentrations of iodide are more common in rock salts obtained from a deposit close to a petroleum or natural gas field [197]. While the iodide ion is the predominant form in salt, the Pourbaix diagram for iodine [198] shows that all forms can convert to iodate, IO_3^- , and periodate, IO_4^- , under the oxidative conditions in the anolyte chamber and the membrane. The normal practice therefore is to give brine specifications in terms of total iodine.

The stoichiometry for the formation of periodate from iodide is



A certain amount of this ion travels through the membrane, in the direction of increasing alkalinity. While most simple forms of iodate are soluble in alkaline media, there are certain insoluble species. Sodium paraperiodate, $\text{Na}_3\text{H}_2\text{IO}_6$, is a combination of two moles of sodium hydroxide with one of sodium periodate. It is quite insoluble at high pH. Accordingly, it precipitates in the catholyte layer of the membrane, reducing the current efficiency. The corresponding potassium salt is much more soluble, and so iodine is a lesser problem in KCl electrolysis.

Section 4.8 and its appendix discuss the action of iodine in more detail. It interacts with other elements to form other precipitates in either NaCl or KCl service. These precipitates include barium paraperiodate, and so there may be a synergistic effect when both barium and iodine are present in the brine. Table 4.8.8 lists commercial brine specifications for some of the common membranes [202]. The allowable concentrations of barium and iodine may be related to each other or to operating current density. Table 4.8.9 lists the adverse effects of various brine impurities. There are reports of physically distinct forms of Ba-I precipitates, with some very fine particles that form in regions away from the main current paths through the membrane [203]. These tend to have relatively little effect on membrane performance [204], and Section 4.8.8.3 also discusses the development of membranes with enhanced resistance to the effects of iodine.

While the specifications for the leading commercial membranes differ, particularly in how they consider interactions between barium and iodine, they all call for less than 0.1–0.2 ppm total I at high current densities. Barring the use of the special membranes mentioned in the preceding paragraph, the goal in the brine plant should be to achieve these levels.

Iodine is difficult to remove from brine. Techniques suggested for its removal include treatment with chlorine to oxidize the I^- ion:



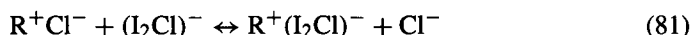
followed by aeration (as described above for the removal of bromide), conventional ion exchange of the complex I_2Cl^- ion [194], or zirconium-cycle ion exchange [146]. Carbon adsorption is another possibility [199], but the adsorptive capacity is low (~ 1 mg/g on typical activated carbon).

Iodine producers routinely use the first of these options [200,201]. It is essential that iodine not be further oxidized to IO_3^- or IO_4^- , as in Eq. (78). This oxidation is prevented by controlling the chlorine feed to keep the ORP, using a Pt/Ag/AgCl electrode, at about 900 mV. When the ORP exceeds 1,000 mV at a brine pH below 2, the chlorine will oxidize iodine to iodate.

Direct removal of iodide by ion exchange is possible. However, standard resins have capacities too low to be of practical value in chlor-alkali operations. Therefore, the approach has been first to oxidize iodide to iodine as by Eq. (79), and then to allow it to form a complex ion with chloride:



In Solvay's operation at Rosignano, Italy [194], an electrolyzer in the brine line generates enough chlorine for reactions (79) and (80). The process requires control of the pH (< 3) and the ORP. Controlling the ORP of the effluent solution by manipulating the current to the electrolyzer prevents oxidation of I_2 . The complex ion can then exchange with the chloride ion of an anionic exchanger:



where R^+ is a cationic fixed site on the resin. The process has operated commercially for more than ten years. From a starting concentration of about 3 ppm, the iodide level is held reliably below 0.2 ppm.

The reference publication does not discuss regeneration of the resin. Independent study [199] showed that the resin can be regenerated by washing with 4% NaOH or 20% NaHSO₃ and rinsing with 9% HCl or 10% brine. Standard resins tested had capacities of 1–2 g I_2 L⁻¹ of resin at an effluent iodine concentration of 0.15 ppm at 22°C and pH 2. The capacities were very low at 70°C. Thus, the iodide removal scheme involves cooling the brine and lowering its pH before ion exchange. The temperature and perhaps the pH then require adjustment before the brine enters the electrolyzers.

Recently, a novel ion-exchange material based on $ZrO(OH)_2$ has been developed by Chlorine Engineers [195]. This has been shown to remove sulfate, iodide, and silicate from brines. The advantage of this material is that one does not have to liberate iodine and capture it on a conventional ion-exchange material. Instead, the iodine liberated by the chlorination of brine can be allowed to oxidize to iodate or periodate, which is then taken up by the Zr-based oxide at pH 2 and later desorbed with caustic at pH 12 (Figs 7.92 and 7.93). Iodate is completely desorbed at 50°C but not at 25°C. Figure 7.94

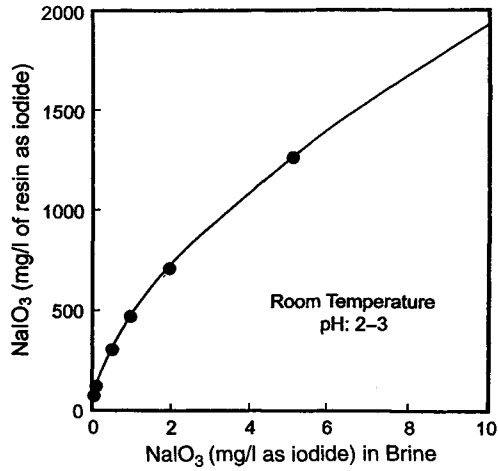


FIGURE 7.92. Adsorption isotherm for iodate on zirconium oxyhydroxide. pH = 2–3; temperature = 25°C. (Reproduced with permission of the Society of Chemical Industry.)

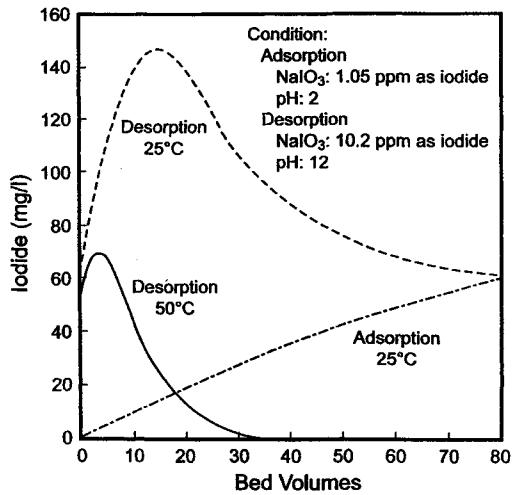
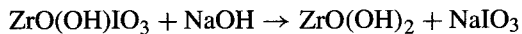
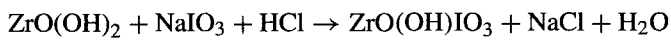


FIGURE 7.93. Influence of temperature on iodate removal by zirconium oxyhydroxide. (Reproduced with permission of the Society of Chemical Industry.)

shows adsorption isotherms for various iodine species. The reactions of iodate capture and release are:



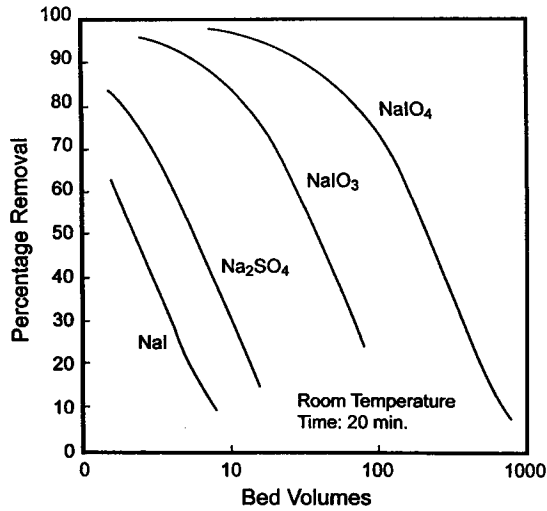


FIGURE 7.94. Adsorption behavior of various anions on zirconium oxyhydroxide. (Reproduced with permission of the Society of Chemical Industry.)

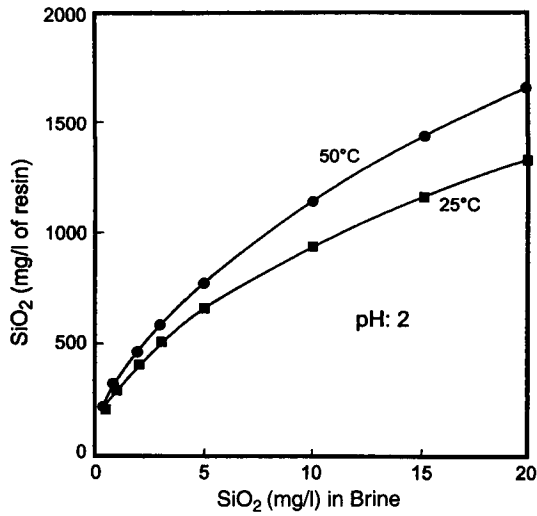


FIGURE 7.95. Isotherms for silica on zirconium oxyhydroxide. (Reproduced with permission of the Society of Chemical Industry.)

A similar mechanism is proposed for the removal of silica as shown below:

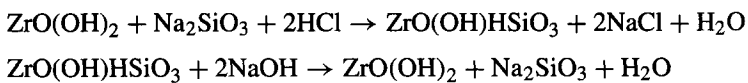


Figure 7.95 shows isotherms for the removal of silicate by zirconium oxyhydroxide.

7.5.8.10. *Nitrate.* There is some concern over the possibility of damage by nitrate ion, but there are no related citations in the open literature. Nitrate is easily reduced chemically [205–207].

7.5.9. *Removal of Dissolved Chlorine and Chlorate*

The discussion of brine purification so far has dealt with the removal of impurities that enter the plant accidentally or with the salt, the process water, or auxiliary materials. In mercury- and membrane-cell plants, the partly exhausted brine, or “depleted brine,” that leaves the cells must be recovered and resaturated for recycle to the cells. With those technologies, therefore, impurities that form or accumulate in the cells or the brine recycle loop are also important.

Depleted brine will be physically saturated with chlorine, and some chlorine will react to form hypochlorite (Section 7.5.9.1). This chlorine value represents an economic asset to be recovered and, particularly in the case of membrane cells, an intolerable contaminant in the brine treatment system. There are several approaches to this problem [208], and we cover these below. We divide them into methods aimed at recovery of the bulk of the chlorine in a useful form (primary dechlorination; Section 7.5.9.2) and those whose purpose is to reduce the active chlorine to chloride and safeguard the environment or other parts of the process (secondary dechlorination; Section 7.5.9.3). Some of the hypochlorite that forms in the anolyte will continue to react to form chlorate. This is a much less harmful impurity in the cells, and higher concentrations are tolerable. Many plants keep the chlorate concentration under control by natural or deliberate purges from the brine system (Section 7.5.7.2A). In others, it is necessary to reduce some of the chlorate ion to chloride in order to maintain control (Section 7.5.9.4).

7.5.9.1. *Solubility of Chlorine in Aqueous Systems.* Before discussing dechlorination, we consider the solubility of chlorine in water and brine. Even though the solubility of chlorine in water is not great, the system does not follow Henry’s law. The reason for this is the hydrolysis of chlorine to hydrochloric and hypochlorous acids:



This is a reversible reaction, and the HCl formed will be essentially completely ionized. At the low pH of the resulting solution, the hypochlorous acid, with a pK of about 7.5, will remain molecular. The complex ion Cl_3^- also exists:



This reaction is not favored in water, where the low concentration of the chloride ion allows the equilibrium to lie far to the left [209]. In brine, Cl_3^- is more of a factor. More chlorine can enter into combination with the ion, at least up to Cl_5^- , but only in very small amounts.

The unhydrolyzed chlorine is the species that is directly in equilibrium with the chlorine in the gas phase. If we express solubility of molecular chlorine by Henry’s law,

its concentration in solution is proportional to the partial pressure of chlorine in the gas phase. If we designate this partial pressure by P we have

$$[\text{Cl}_2] = HP \quad (84)$$

where

$[\text{Cl}_2]$ = dissolved concentration of molecular chlorine

H = solubility constant (function of temperature)

At the same time, the chlorine is in chemical equilibrium by reaction (82). The equilibrium constant is

$$K = [\text{H}^+][\text{Cl}^-][\text{HOCl}]/[\text{Cl}_2][\text{H}_2\text{O}] \quad (85)$$

More precisely, we should use activities. Assigning unit activity to water and recognizing that in the pure water/pure chlorine system the concentrations of H^+ , Cl^- , and HOCl are small and equal, we have

$$K = [\text{HOCl}]^3/HP \quad (86)$$

or

$$[\text{HOCl}] = (KHP)^{1/3} \quad (87)$$

Now the total amount of chlorine which dissolves is equal to that which remains in solution as molecular chlorine plus that which has hydrolyzed. The latter quantity is equal to the amount of hypochlorous acid formed. So we combine Eqs. (84) and (87) to obtain the total "solubility" as

$$S = HP + (KHP)^{1/3} \quad (88)$$

Dividing through by $P^{1/3}$ rectifies this equation:

$$S/P^{1/3} = (KH)^{1/3} + HP^{2/3} = a + bP^{2/3} \quad (89)$$

This is equivalent to

$$S = aP^{1/3} + bP \quad (90)$$

The constants a and b are functions of temperature and can be obtained from linear plots suggested by Eq. (89), as in Fig. 7.96. The values of a and b obtained from the solubility data in Perry's Handbook and covering temperatures from 0°C to 80°C , with pressure expressed in mmHg and solubility in milligrams per liter, are in Table 7.34. The nearest approach to the conditions used in deriving Eqs. (88) and (90) is in the dissolving of chlorine in water as it condenses from cell gas. The following example considers a typical chlorine cooler/chiller combination.

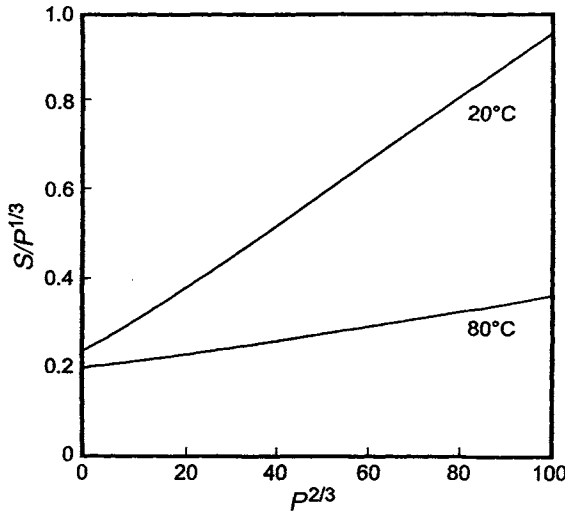


FIGURE 7.96. Linearized plots of solubility of chlorine in water. Units: pressure in mmHg, solubility in mgpl.

TABLE 7.34. Solubility Constants for Chlorine in Water

Temperature, °C	<i>a</i>	<i>b</i>	Pressure range
0	234.5	17	0–250
20	234.3	6.9	0–1000
40	229.5	3.58	0–1000
60	217.9	2.16	0–1000
80	200.7	1.514	0–1000

Note: For use with Eq. (89) or (90); *P* in mmHg, *S* in mgpl.

Example. The cell gas is cooled in stages to 40°C and then to 15°C. We take the pressures at the outlets of the exchangers to be 745 and 733 mmHg, respectively. The partial pressure of water is reduced to 55.3 mmHg, which is its vapor pressure at 40°C, in the first cooler. The uncondensed water, barring any change in the other components of the gas, would be 601.7 kg hr⁻¹. The partial pressure of chlorine after the removal of water in the cooler is 677.35 mm. Applying Eq. (88), with *a* = 229.5 and *b* = 3.58, the solubility of chlorine is

$$229.5 \times 677.35^{1/3} + 3.58 \times 677.35 = 4,440 \text{ mgpl}$$

This represents about 35.4 kg hr⁻¹ of chlorine dissolved in the water.

Since we assumed no change in the quantity of chlorine in the gas in the calculation above, the partial pressure used there is too high. Iteration is necessary, and the solution

quickly converges to

	Gas in	Gas out	Condensate
Chlorine	28,995	28,959.2	35.8
Water	8,571	598.7	7,972.3
Others	238	238.1	

If we allow for infiltration of air to a concentration of 2%, we have

	Gas in	Gas out	Condensate
Chlorine	28,995	28,960.3	34.7
Water	8,571	625.0	7,946.0
Others	766	766.1	

If at the same time, the atmospheric pressure drops and the operating pressure becomes only 730 mmHg, we have

	Gas in	Gas out	Condensate
Chlorine	28,995	28,960.9	34.1
Water	8,571	638.9	7,932.1
Others	766	766.1	

Each change allowed more water to pass through the exchanger. The presence of more inert gas, on the other hand, reduced the partial pressure of chlorine, and so the amount dissolved decreased.

Passing the cell gas through the chiller at the first set of conditions gives

	Gas in	Gas out	Condensate
Chlorine	28,959.2	28,955.5	3.69
Water	598.7	132.8	465.9
Others	238.1	238.1	

Pursuing the two variations on cooler operation, the amounts of water condensed in the chiller become 486.9 and 498.8 kg hr⁻¹, leaving 138.1 and 140.1 kg hr⁻¹ uncondensed. The amounts of chlorine dissolved are 3.74 and 3.83 kg hr⁻¹.

The last term in Eq. (88) prevents solubility from being linear with partial pressure, confirming that Henry's law does not hold for the total solubility of chlorine in water. Since that term contains the cube root of P , the amount dissolved is less than linearly dependent on the pressure. This makes it more difficult to remove chlorine from solution by reducing its partial pressure in the gas phase. Simply blowing a solution with air or reducing the total pressure above it is less effective than it

would be in the absence of hydrolysis. The usual technique for removing chlorine from an aqueous solution therefore involves the addition of HCl to reverse the hydrolysis of Eq. (82).

When HCl is added, the concentrations of the three key species no longer are equal, and under practical conditions we have

$$[\text{H}^+] \approx [\text{Cl}^-] \gg [\text{HOCl}]$$

Now

$$[\text{HOCl}] = KHP/[\text{H}^+]^2 \quad (91)$$

and Henry's law holds. The constant becomes

$$H' = (1 + K/[\text{H}^+]^2)H \quad (92)$$

Equations (91) and (92) hold only at low acid concentration. As the concentration of HCl in solution grows, more of the complex ion Cl_3^- forms (Eq. 79). This is another form of active chlorine, and its presence forces the total solubility of chlorine in aqueous HCl to go through a minimum at about 2% HCl (pH 0.2).

The solubility of chlorine in brine is less than it is in water. Equation (85) when written in terms of activities still holds, and the high activity of chloride ion makes hydrolysis less efficient and reduces the formation of HOCl. In order to maintain equilibrium, the concentration of molecular chlorine increases relative to the concentration of hydrolyzed forms. Equation (87) no longer holds, but we still have

$$[\text{H}^+] = [\text{HOCl}]$$

The analog to Eq. (90) then becomes

$$S = aP^{1/2} + bP \quad (93)$$

The equilibrium of Eq. (83) becomes more important. The Cl_3^- formed is an important part of the total solubility, but its concentration is proportional to the solubility of molecular chlorine and it does not affect the empirical form of Eq. (93).

Finally, we consider concentrated, acidified brine. The concentrations of H^+ , Cl^- , and HOCl are all different. Again, we can use Henry's law with a pseudo-coefficient H' :

$$S = H'P \quad (94)$$

Formally,

$$H' = (1 + Ka/[\text{H}^+] + k_3a_2)H \quad (95)$$

where

K = reaction equilibrium constant

H = Henry's law coefficient for dissolved Cl_2

k_3 = equilibrium constant for the formation of Cl_3^-

a_1 = activity of water

a_2 = activity of chloride ion

$a = a_1/a_2$

In terms of the hydrogen-ion concentration, this can be written at a given pressure as

$$S = a + b/[H^+] \quad (96)$$

O'Brien [208] showed representative data that gave a linear plot of solubility against the reciprocal of hydrogen-ion concentration. At constant pH, the solubility of chlorine should be proportional to its partial pressure in the gas. The data of Bott and Schulz [210] confirm this.

None of the equations above shows how solubility varies with salt concentration or temperature. Yokota [211] has published a correlation that fits the equations

$$S_1 = 10^{-5}(2.21 - 0.00398N)P \times 10^{(1000/T)} \quad (97)$$

where

S_1 = physical solubility ($\text{Cl}_2 + \text{Cl}_3^-$), mol L^{-1}

N = concentration of NaCl, g L^{-1}

P = partial pressure of chlorine, bar

T = temperature, K

$$S_2 = 0.5[X \pm \sqrt{(X^2 + 2.4 \times 10^{-6})}] \quad (98)$$

where S_2 is the combined chlorine ($\text{HOCl} + \text{OCl}^-$) in solution, mol L^{-1} . Equation (98) also covers acidified brine, where X takes on negative values. The total solubility is the sum of S_1 and S_2 .

7.5.9.2. Primary Dechlorination. The dechlorination process will have some combination of the following four objectives:

1. recovery of chlorine in a useful form;
2. reduction of rates of corrosion;
3. protection of brine-softening resins in membrane-cell plants;
4. reduction of chlorine/hypochlorite concentration in wastewater.

The last item is of interest primarily in diaphragm-cell plants. The processes used include physical and chemical dechlorination. This section discusses the physical methods.

The previous section showed that reversal of the hydrolysis of dissolved chlorine is necessary for its efficient removal from solution. The hydrolysis is partly reversed in the presence of a high chloride ion concentration. Chlorine is therefore less soluble

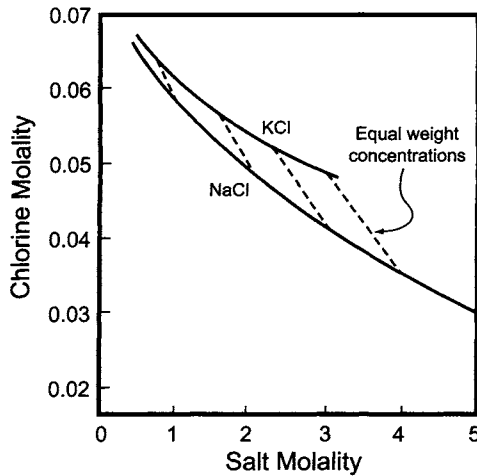


FIGURE 7.97. Solubility of chlorine in NaCl and KCl brines.

in brine than in water and less soluble in mercury-cell brine than in membrane-cell brine at the same conditions of temperature and pressure. It is inherently more soluble in KCl solutions. Figure 7.97 illustrates this. The plot, based on *International Critical Tables* data, shows the molality of dissolved chlorine as a function of the molality of the salt. In membrane-cell practice, cell brine concentrations are more nearly equal on a weight basis, so that the NaCl solutions encountered have higher molalities than the KCl solutions. As shown by the tie lines, this increases the differences. In typical membrane-cell depleted brines, chlorine is about one third more soluble in KCl solutions. Its solubility is lower in mercury-cell depleted brines, which have higher concentrations of salt. At these higher concentrations, the relative solubilities in the two types of brine continue to diverge, with the result that chlorine is about one half more soluble in KCl than in the corresponding NaCl mercury-cell brine. Hydrochloric acid, by contributing two common ions, is particularly effective in reversing the hydrolysis, and it is common practice to add HCl to the solution to be dechlorinated. In brine, HCl should be added to a pH of about 2–2.5. In water, a pH closer to 1 will be required.

With the hydrolysis reversed, the molecular chlorine can be removed from solution by reducing its partial pressure in the gas in contact with the solution. The partial pressure of chlorine over an aqueous solution is

$$P = \Pi - p_w - p_i \quad (99)$$

where

Π = total pressure on system

p_w = vapor pressure of water over brine

p_i = sum of partial pressures of other gases

A standard approach to dechlorination is to reduce the total pressure by imposing a vacuum. In Eq. (99), this reduces the term Π . Another effective method is aeration,

where the presence of air in the gas phase also reduces the partial pressure of the chlorine:

$$P = \Pi - p_w - p_{\text{air}} \quad (100)$$

where p_{air} is the partial pressure of air.

7.5.9.2A. Vacuum Dechlorination. Dechlorination with the aid of a vacuum is probably the most frequently used method. It had been the standard process in mercury-cell plants for many years and was naturally adapted to membrane cells. Any of the standard methods of producing vacuum (Section 12.6.1) will be satisfactory. Steam jets are quite acceptable as vacuum sources, since their effluent can simply join the cell gas flowing to the chlorine coolers.

With brine at or near its full process temperature, the operating pressure is reduced to about a third or a half of an atmosphere. Nearly all the chlorine in the depleted brine is recovered and can be returned to the process. The resulting brine is not suitable for return to a membrane-cell process. There is need for further dechlorination, which is the topic of Section 7.5.9.3. In a mercury-cell process, on the other hand, there actually are advantages to incomplete dechlorination. The presence of free chlorine in the brine returned to the salt dissolver, given suitable materials of construction, helps to keep mercury in solution and prevents its deposition on the brine sludge that will be removed from the process. Typical concentrations are 10–50 ppm Cl_2 . Especially given the inherently lower solubility of chlorine, conditions used to dechlorinate mercury-cell brines therefore can and should be less rigorous.

Vacuum dechlorination normally takes place in a packed column. Usually, there is little in the way of countercurrent flow; the packing serves primarily to provide surface for separation of vaporized chlorine from the liquid. While brine is introduced at the top of the column, the vacuum may be applied either at the top or at the bottom. Water will vaporize from the solution as the chlorine is released. The amount depends on the temperature and concentration of the feed brine and the depth of vacuum. The column must be sized to handle whatever vapor traffic results.

Section 12.6.3 discusses the various methods of pressure control in vacuum systems. It points out that some situations, more common with liquid-ring pumps than with steam jets, favor allowing atmospheric air to enter the process. This balances capacity and demand. The chlorine recovered here, however, may be combined with the cell gas and processed through liquefaction. In that case, the air added to the system reduces the efficiency of liquefaction (Section 9.1.7.2A). Pressure control by recycling some of the compressed vapor to the vacuum producer then would be a better method.

An option to consider is operation without pressure control. The deeper vacuum that results will release more chlorine from solution. In a membrane-cell plant, this will reduce the cost of the secondary dechlorination, which is discussed below, but the approach may not be workable in a mercury-cell plant, where higher free chlorine concentrations are desirable. More water will evaporate along with the incremental chlorine. The load on the vacuum condenser will therefore increase, but not by as much as when the addition of steam is used for pressure control. At the same time, the dechlorinated brine will become cooler. This can only help the pumping operation. The cooler brine can also

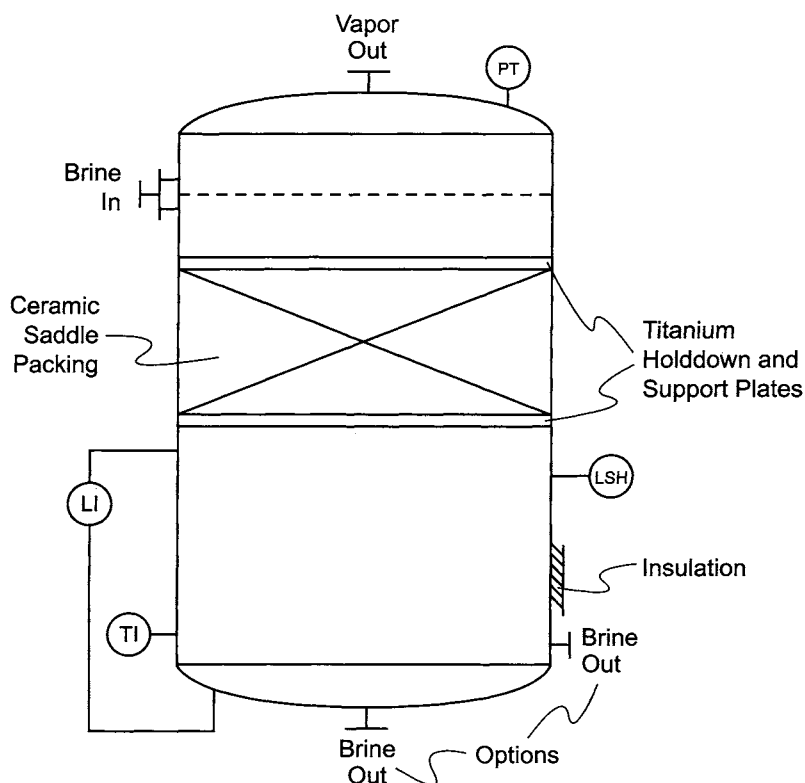


FIGURE 7.98. Packed column for vacuum dechlorination.

abstract more heat from cell-room caustic in an interchanger. In a smaller plant or one without an interchanger, on the other hand, the lower temperature adds to the load on the cell room brine preheater.

Most large vacuum dechlorination columns are constructed of rubber-lined carbon steel. They contain up to 2 m of ceramic saddle packing. The brine enters the bed through a flow distributor; weir-trough distributors fabricated of FRP or a ceramic are common. The brine may also be fed across the width of the column by an internal feed pipe. This pipe will be of a resistant plastic; it will be removable and will be inserted through a lined nozzle. Large columns may have more than one feed pipe. Packing support and hold-down plates will be of coated steel or, because of the danger of penetration of the coating by the load, titanium. Internal hardware and bolts for the various supports are of Hastelloy. Figure 7.98 is a typical example. The instrumentation shown provides temperature indication and level and pressure signals that may be used to control the process. The assumption in this drawing is that the lower section of the column serves as a liquid storage vessel. This avoids the need to add a separate tank but adds to the size of the dechlorinator and the weight that in some designs is supported in the process structure.

While the exact pressure of operation varies from plant to plant, it is normally within the operating range of a single-stage steam ejector or liquid-ring pump (Section 12.6.1). The nozzles of a jet and other parts in contact with the process fluid must be of a resistant material such as titanium. The vacuum pump is the more expensive alternative, but it has the advantages of making less noise and of adding little water to the process. The components of a liquid-ring pump may be lined steel or titanium. Some models use ceramic-coated bodies and titanium impellers. The operation of liquid-ring pumps is covered in Section 9.1.6.2C on chlorine compression.

7.5.9.2B. Air Stripping. The function of the vacuum in the preceding section is to reduce the partial pressure of chlorine vapor over the solution and so to help its release from the solution. In the alternative discussed in this section, rather than reducing P by reducing Π , one obtains the same effect by increasing the quantity to be subtracted from Π . The technique is quite simple. Acidified water or brine is pumped to the top of a column, and air is blown in at the bottom. This countercurrent arrangement has the advantage of staging the system and improving the rate of mass transfer between phases. Stripped brine from the bottom of the column flows to a collection tank that may be attached to the column. The outlet from the column must be sealed to prevent the escape of air. Typical superficial velocities of brine are about 120 m hr^{-1} .

Air stripping is a low-capital approach. Typical materials of construction are fiberglass and lined steel; packing can be ceramic or a high-strength resistant plastic. In very round terms, air stripping can be installed for a cost one third less than vacuum dechlorination. The operational disadvantages of the process are the energy consumed by compression of the air and the dilution of the recovered chlorine. The concentration of chlorine in the air leaving the column normally is less than 10% (v/v) and may be quite low. The typical liquefaction process tail gas has a higher chlorine content. Taking the product of air dechlorination to liquefaction in such a case would actually result in recovery of less liquid chlorine. This usually is decisive in large plants, and there vacuum dechlorination is the normal choice.

The gas from an air stripper can always go to a bleach plant for the recovery of the chlorine value. The production of bleach by absorption of chlorine into caustic solution is discussed in Chapters 9 and 15.

It is also possible by careful design to reduce the gas/liquid ratio and produce a richer product gas. Under these conditions, air stripping in a sieve-plate column has been a commercial process on the 100^+ -tpd scale. By providing enough theoretical plates in a column, one can keep the equilibrium and operating lines close together, reducing the air flow and thereby increasing the concentration of chlorine in the offgas. Yokota [212–216] studied the system in detail. He provided correlations for mass-transfer capacity and determined the number of plates required at different gas:liquid ratios. Figure 7.99 is a modified McCabe–Thiele diagram on a logarithmic scale. The coordinates are mole ratios (chlorine:others) rather than mole fractions. The drawing shows operating lines for three different liquid:gas ratios, corresponding to final gas-phase mole fractions, denoted by y , of 0.10, 0.25, and 0.50 chlorine. The maximum possible concentration is not much more than 50%, and Fig. 7.99 shows that there is a pinch section in a column that hinders operation above about 30% Cl_2 . The conventional air-stripping process, with

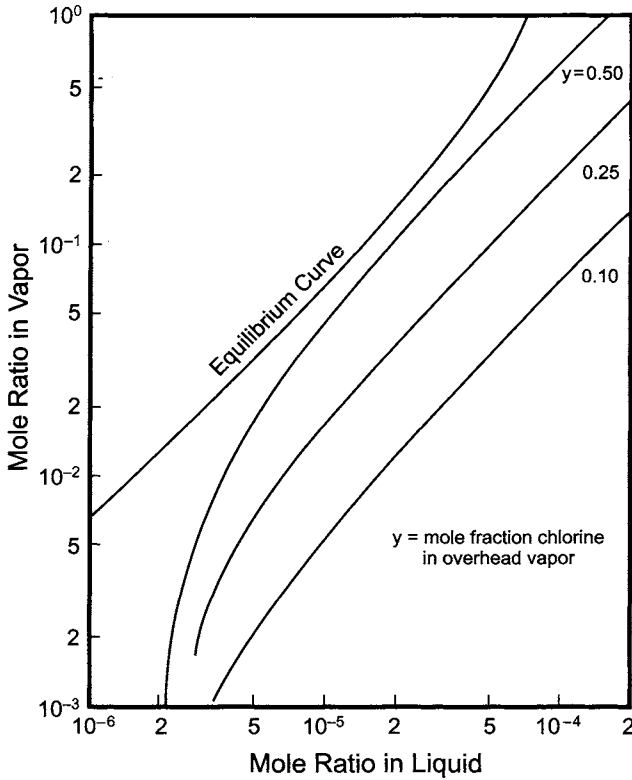


FIGURE 7.99. McCabe–Thiele diagrams for air stripping.

TABLE 7.35. Concentration of Recovered Chlorine vs Number of Plates

Number of plates	Concentration (% Cl ₂ [v/v])
2.0	10
3.0	20
4.43	30
6.83	40
16.31	50
Infinite	60

$y < 0.1$, is quite simple and does not require many plates or transfer units. Table 7.35, derived from this plot, shows the minimum number of theoretical plates required as a function of the desired chlorine concentration in the recovered gas. With restricted gas flow, the liquid : gas flow ratio then becomes unusually large, and Yokota’s work was in the range 400–6,000.

The rapid increase in the number of plates above a concentration of 30% reflects the pinch in the McCabe–Thiele diagram. The economic balance to be struck here is one

between the longer column required to keep the concentration of chlorine high and the costs associated with the higher flow of air required when using a shorter column.

The unusually small volume ratio of gas to liquid makes stripping plate efficiencies low. Yokota's model of the process assumes that liquid travels across a plate in uniform flow with no transverse mixing but that vertical mixing is perfect. He then characterizes a plate by the length of linear travel of the liquid. Correlation of the experimental data is in terms of the "length of a transfer unit." This is the distance that liquid must travel to undergo an amount of mass transfer equivalent to one transfer unit. A plate then provides a (normally fractional) number of transfer units given by

$$N = L_T/L_U \quad (101)$$

where

N = number of transfer units supplied by a plate

L_T = length of travel of liquid over a plate

L_U = length of a transfer unit

The length of a transfer unit generally decreases as gas flow rate increases. Figure 7.100 illustrates the effect, which tends to level off at a gas velocity of about 2.8 cm s^{-1} . Experimentally, L_U at that gas rate is proportional to the 0.6 power of liquid mass

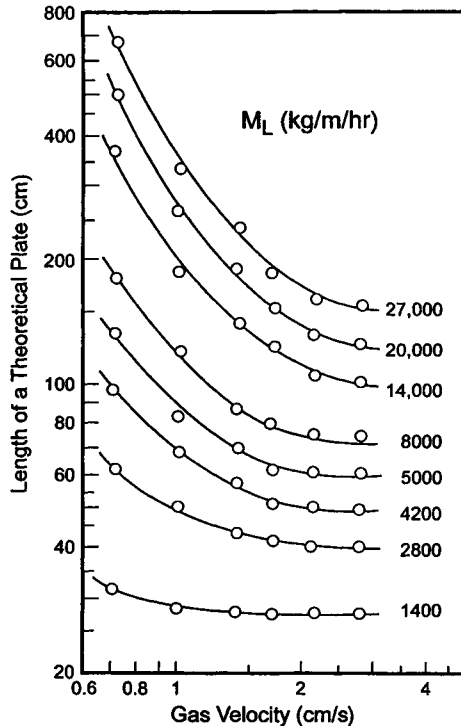


FIGURE 7.100. Lengths of transfer units in air-stripping columns.

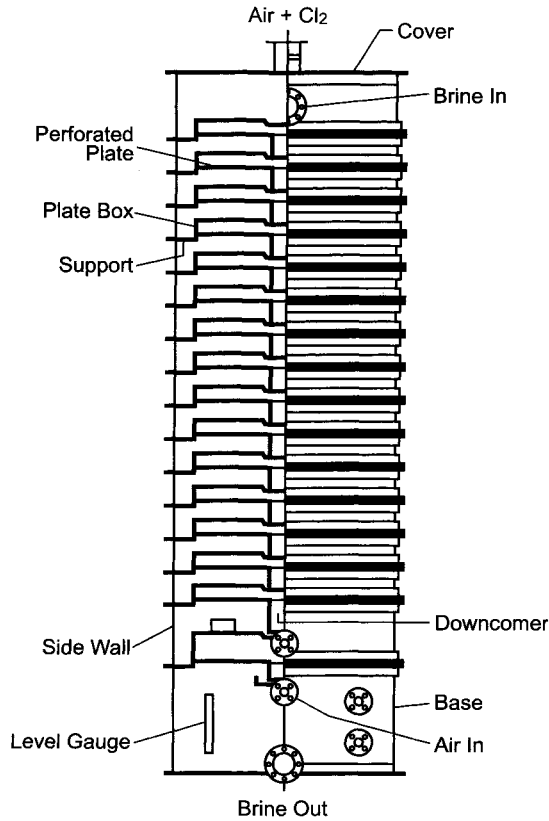


FIGURE 7.101. Plate column for air stripping.

flow rate:

$$L_U = aM_L^{0.6} \quad (102)$$

where

a = coefficient

M_L = mass flow rate of liquid ($\text{kg m}^{-1} \text{hr}^{-1}$)

With the units used on Fig. 7.100, $a \approx 0.35$. Yokota developed correction factors for other velocities and showed how to estimate the Murphree liquid-side plate efficiency for all sets of conditions.

Figure 7.101 shows a commercial tower, designed according to these principles, that has operated effectively [212]. It is about 4.5 m high, with a plate spacing of about 215 mm. PVC is the primary material of construction.

7.5.9.2C. Steam Stripping. In common with air stripping, steam stripping works in part by diluting the gas phase in the stripper. Normally, live steam is injected into the acidified

condensate recovered from a diaphragm-cell plant's gas cooling section. This has the added effect of raising the temperature of the water. The activity of dissolved chlorine becomes higher, and its tendency to vaporize increases.

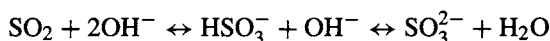
Open steam is not used to strip chlorine from brine, where the dilution it would cause is objectionable. Its application is limited to chlorine-bearing condensate, and it is therefore discussed in the Section 9.1.3.5B on chlorine cooling.

7.5.9.3. Secondary Dechlorination Free chlorine can be "destroyed" or reduced from OCl^- to Cl^- by catalysis, chemisorption on activated carbon, or addition of a chemical reducing agent. While in principle some sort of reduction could be used for the entire process of dechlorination, it would be impractical not to recover most of the chlorine as the element. The reduction or decomposition process therefore is used only as a backup measure. The process is also useful in wastewater treatment.

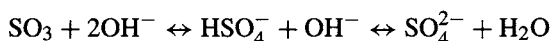
7.5.9.3A. Chemical Reduction. Most membrane-cell operators rely on a reducing agent for scrupulous removal of free chlorine. Chlorine or hypochlorite is a powerful oxidizing agent. Many other substances, therefore, can serve as reducing agents to hypochlorite and can reduce it to the more benign chloride. In this chapter, we consider only sulfur compounds and hydrogen peroxide as reducers. Both types are used in chlor-alkali plants, but the sulfur-based agents have been more common.

Use of Sulfur Compounds. These reducing agents include sulfur dioxide, sulfite, bisulfite, and thiosulfate. The first three are oxygenated forms of sulfur in the +4 valence state. They are easily oxidized, thanks to the great stability of the S^{6+} compounds, and they are widely used as dechlorinating agents throughout the chemical industry and in water treatment. It was natural to extend their use to brine dechlorination when membrane cells required addition of the secondary step. The salts derive from neutralization of sulfur dioxide. Commercial forms include sodium sulfite, Na_2SO_3 ; sodium bisulfite, NaHSO_3 ; and sodium metabisulfite, $\text{Na}_2\text{S}_2\text{O}_5$. The sulfite is available both as a solid and in a solution containing the equivalent of 23–27% SO_2 . The bisulfite, strictly speaking, is available only in solution. When dry, it reverts to its anhydride, which is the metabisulfite.

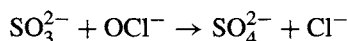
Whichever form of S^{4+} is used, the active agent will be the same. In solution, proton shifts between the different forms are rapid [217], and which form takes part in the reaction depends entirely upon the pH of the brine. Since secondary dechlorination of brine usually follows or accompanies the addition of alkali, the sulfite ion is the predominant form. Miron [218] reports that it is also the most active. The following equilibria apply:



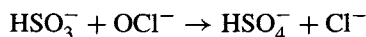
The same is true of the S^{6+} compounds:



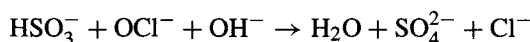
At the pH of the typical dechlorination process, the equilibrium in the latter case lies to the right, and the product of the reaction usually is the sulfate ion. The reaction between sulfite and hypochlorite ions then is simply



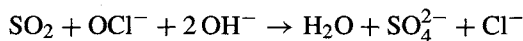
A similar reaction with bisulfite would be



Since sulfate is the normal product, the overall reaction becomes



Continuing on to SO_2 ,



Ionic strength is not important, and so rates of reaction are nearly the same in brines as in water. Sodium and potassium salts are comparable in their effects. Having made all these distinctions, from a practical standpoint the reactions are reasonably rapid and do not present a design problem.

If a reacted form of SO_2 is chosen, local availability and price will be major factors in the decision. In a price comparison of the sulfite reagents, it should be remembered that some of the apparent premium cost of sulfite or bisulfite is associated with the caustic that is combined with SO_2 . As the equations above show, SO_2 , in becoming SO_3^{2-} in alkaline brine, abstracts that same caustic from solution and loses some of its apparent advantage.

Sulfur dioxide, as the normal precursor of the others, will be the cheapest agent in bulk. However, this application represents a very minor market for SO_2 , and it may not be available at bulk prices. Furthermore, its presence raises a new set of hazards. Only the larger plants or those already using liquid SO_2 in some other application are likely to go this way. For this application, SO_2 will most probably be supplied in cylinders. Its behavior as a fluid is quite close to that of chlorine. The liquid densities are quite similar, and the vapor density of SO_2 is only about 10% lower, reflecting its lower molecular weight. Vapor pressures, however, are quite different; at normal ambient temperatures, SO_2 is about 40% as volatile as chlorine. This combined with its higher latent heat of vaporization means that SO_2 can not be withdrawn from an unheated cylinder as rapidly as can chlorine. A cylinder can be heated by placing it in a heated zone or by attaching electric strip heaters. The latter practice, unacceptable in the case of chlorine, is tolerated with thermostatic control because of the lower vapor pressure of SO_2 [219]. The vapor transfer piping also should be heated to prevent reliquefaction.

While moderate heating of an SO_2 cylinder is not likely to cause a problem of overpressure, the user should bear in mind that the cylinders are protected by fusible plugs.

SO₂ does not attack ordinary metals when dry, but it can be highly corrosive when wet. At process temperatures, stainless steels are suitable.

Sulfites and bisulfites are not considered extremely hazardous. One hazard associated with their handling derives from the possible presence of SO₂. Sodium bisulfite, with a higher ratio of SO₂ to caustic, is in equilibrium with air containing about 2% SO₂ and must therefore be regarded as more hazardous than the sulfite. Handling and storage practices established for bisulfite solutions frequently are used with sulfites as well. Solutions are stored in stainless steel or fiberglass (bisphenol resin as a minimum) tanks, which must be designed for the high specific gravity (1.3–1.35) of the solution. A common strength for supply is 38% NaHSO₃, with a freezing point of about 1.1°C. Small quantities, such as the one or two truckloads common to chlorine plants, are sometimes stored indoors or in heated enclosures. When bisulfite solution is stored outside in ambient conditions that require it to be protected from freezing, the tank must be heated. Pipelines should then be insulated and in some conditions should be electrically traced to prevent freezing. Piping may be of Schedule 80 CPVC or of Schedule 10 or 40 Type 316 stainless steel. Wetted metal parts of valves should be Type 316 SS or Alloy 20.

In the dry form, these reagents are not toxic but are irritants to the eyes, skin, and respiratory tract. Either form can react with acids or oxidizing agents to release SO₂ vapor. Again, metabisulfite is the more likely to decompose, and it should be handled with extra care. Suggested protective equipment includes boots, goggles, and gloves, along with impervious clothing. Proper venting is essential, and full-face respiratory protection is recommended when the dust concentration may be above the threshold limiting value of 5 mg m⁻³.

Since sulfur dioxide hydrolyzes after it dissolves in water, a treatment similar to that used to derive relationships for the solubility of chlorine should be useful. Using Henry's law, we set the concentration of dissolved SO₂ proportional to P , the partial pressure of SO₂ in the gas. K_1 is the equilibrium constant for the hydrolysis reaction, and the activity of water is taken as unity. In this case, we have the equations

$$[\text{SO}_2] = HP \quad (103)$$

and

$$[\text{H}_2\text{SO}_3] = K_1[\text{SO}_2] = K_1HP \quad (104)$$

for the concentrations of the molecular species in solution. Next, we have the ionization of sulfurous acid to form bisulfite:



Assigning this the equilibrium constant K_2 , we have

$$[\text{H}^+][\text{HSO}_3^-] = K_2[\text{H}_2\text{SO}_3] = K_2K_1HP \quad (106)$$

Anticipating a result from the real properties of the system, we ignore the further ionization of bisulfite to sulfite. This means that the concentrations of hydrogen and bisulfite ions are nearly equal. Now we write

$$[\text{HSO}_3^-] = (K_2 K_1 H P)^{1/2} \quad (107)$$

The total amount of SO_2 dissolved is equal to the sum of the three species SO_2 , H_2SO_3 , and HSO_3^- . So we write the solubility S as

$$S = H P + K_1 H P + (K_2 K_1 H P)^{1/2} = b P + a P^{1/2} \quad (108)$$

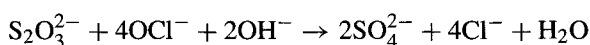
We rectify the equation by dividing through by $P^{1/2}$:

$$S/P^{1/2} = a + b P^{1/2} \quad (109)$$

The form derived fits handbook data for the solubility of SO_2 in water over reasonably wide ranges or over the entire reported range with an average relative error of about 2%. The applicable range can be extended by adding a term in $P^{1/4}$. The average relative error becomes about 0.7%. The same logic can be used to study the dissolution of SO_2 into alkaline solutions. Sulfite as well as bisulfite can be produced in such a case. The concentration of molecular SO_2 in solution will be lowered as the ionization equilibria are shifted to the right. The result is a lower vapor pressure above sulfite solutions and a reduction in emissions from their storage facilities. Johnstone, Read, and Blankmeyer [220] showed that the partial pressure of SO_2 above a solution with the pH of ordinary sodium bisulfite (4.3 at 1% concentration) is 10–12 mmHg. SO_2 pressures above sulfite solutions are very low.

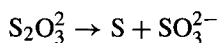
Thiosulfates also are sometimes used as reducing agents. They result from the reaction of sulfur or a polysulfide with a sulfite. Sodium thiosulfate is widely available in solid form, both anhydrous and as the pentahydrate (the photographer's "hypo"). The pentahydrate crystallizes from solutions with concentrations between 30% and 60% $\text{Na}_2\text{S}_2\text{O}_3$. The compound is quite soluble in water (33.3% at 0°C from the anhydrous form), and hypo dissolves in its water of hydration at 48°C. All forms are nontoxic under normal conditions and are used as food additives. In addition, $\text{Na}_2\text{S}_2\text{O}_3$ forms neutral solutions. While correspondingly easier to handle than NaHSO_3 , it is normally stored in similar equipment.

In the thiosulfate ion, sulfur replaces one of the sulfate oxygens [221]. The apparent valence of the sulfur therefore is the average of the +6 of sulfate and the -2 of sulfide, or +2. This would seem advantageous. In reverting to +6, this sulfur should react with twice as much chlorine as does the +4 form. The following equation shows the theoretical advantage of thiosulfate, where 1 mol accounts for 4 mol of hypochlorite:

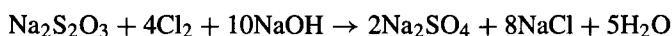
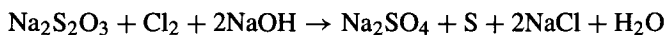
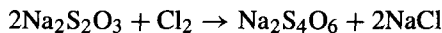


The difficulty with thiosulfate is that the acid is unstable [222] and other reactions can occur at low pH [223]. In neutral or slightly acidic solution, the thiosulfate ion

decomposes to sulfur and sulfite, a reversal of its synthesis:



As a result, there are several possible reactions with chlorine. As pH increases, the product of the reaction may be dithionite or sulfate, with or without colloidal sulfur. The stoichiometry shows that the efficiency of thiosulfate as a chlorine scavenger depends strongly on the reaction regime:



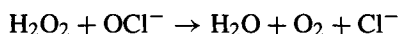
As a result, the consumption of thiosulfate is a strong function of pH. A high pH also is necessary to avoid the problem of the formation of colloidal sulfur. Over the range 4–11, the weight consumed by destruction of one weight of chlorine is as follows [224]:

pH	4.0	6.5	9.0	11.0
Na ₂ S ₂ O ₃ consumed	2.43	2.03	1.45	0.91

This exceeds the performance of sulfite on an equal-sulfur basis only at a pH above 10.5. Thiosulfate also seems to react in steps and therefore more slowly [219].

Use of Hydrogen Peroxide. The sulfur-based reducing agents are easily handled when supplied in solution and are effective in their application. The inescapable problem of their use is the formation of sulfates. Other sections cover the problems caused by high sulfate in the brine and the various methods used in its control. The cost and inconvenience of these methods precisely measure the disadvantage of sulfur-containing compounds. Hydrogen peroxide is an alternative to these compounds.

Hydrogen peroxide is one of the classical oxidizing agents, but it is weaker than hypochlorite and so can serve as a reducing agent in chlorinated brine. Its reaction with the hypochlorite ion is



This is not a completely ionic reaction and is not as rapid as the reactions of the sulfite types. Some laboratory test work to determine the rate of reaction in plant brine may be advisable.

The great advantage of hydrogen peroxide is that its use adds no new ions to the brine, and this fact has led to its use in several chlor-alkali plants. It does produce oxygen, mole for mole with the destruction of free chlorine, and this must be vented safely from the system. Furthermore, any excess peroxide is itself a contaminant. It can demonstrate its oxidizing power by damaging the ion-exchange resin. It is therefore necessary to remove this peroxide from the brine or to operate with a shortage of peroxide (i.e., an excess

of hypochlorite). Activated carbon will remove peroxide or hypochlorite, whichever is in excess, and this technique is discussed in the section on catalytic dechlorination (Section 7.5.9.3B). A plant known to one of the authors relied on organics present in the salt-dissolving system to scavenge residual peroxide.

Mannig and Scherer [225] have discussed the role of hydrogen peroxide in the chlor-alkali industry, including its use in brine dechlorination. They cover handling of the peroxide, certain other applications such as the decolorizing of caustic soda, and the requirements of a dechlorination system. In particular, they comment on process control; this is the subject of the following subsection.

Hydrogen peroxide is supplied as a water solution in several different concentrations. Anhydrous H_2O_2 is produced but seems to be used only for rocket propulsion. At any concentration, peroxide can be a hazardous material. It oxidizes nearly all organic compounds and a large number of inorganics. The heat and gas evolved in these reactions are responsible for most of the damage. H_2O_2 also decomposes slowly and spontaneously. This decomposition is catalyzed by metal ions, rough surfaces, and alkaline conditions and is accelerated at high temperatures. Among the plastics, the best materials of construction are high-density polyethylene (HDPE) and PTFE. Aluminum and some of its alloys can be used, and some suppliers of hydrogen peroxide supply standard tank designs. The chemical industry also frequently uses stainless steel. Types 304L and 316L are used, after removal of all mill scale and chemical passivation. Provision of relief of all confined peroxide is a vital part of design. This extends to the use of self-venting valves in pipelines.

Unloading should always be by pump or by gravity. Peroxide should never be transferred by pressurization with a gas. It should be handled in dedicated equipment and protected against contamination by foreign materials. Spills should be confined and promptly diluted.

Storage practice is extremely important. All surfaces catalyze decomposition, and so the vessel must be clean and smooth. Cast equipment should therefore be avoided where possible. Pumps, piping, and valves are more likely to cause decomposition, and venting is especially important in their design. Among the plastics, HDPE and PTFE are preferred and rigid PVC is also an occasional choice. Plasticized materials are not as good. HDPE is the usual recommendation. Even this is subject to stress corrosion, and so it has a limited life. With proper maintenance, it can still be an economic choice. Crosslinked material gives longer service, and UV stabilizers are essential in outdoor service (hydrogen peroxide should never be stored in bulk indoors). High-purity aluminum and the recommended stainless steels, when passivated, should last 30 years or more [226].

Storage should always be at atmospheric pressure, in tanks equipped with relief valves in addition to continuous vents. Location is important; it should be chosen to minimize the probability of contact with oxidizable or alkaline materials. Peroxide should not share dikes or impoundment areas with incompatible materials.

While it is hazardous, hydrogen peroxide is a successful product of commerce, and there are techniques for coping with the hazards [227]. Many of the safety practices recommended for peroxide apply to other hazardous materials as well. These recommendations are more emphatic than usual in the case of hydrogen peroxide and extend to greater involvement of the material supplier [228]. It is always advisable to obtain

material safety data sheets for hazardous chemicals and to consult suppliers for their advice. In the case of hydrogen peroxide, it is more of a necessity. The material supplier should inspect the facilities for unloading and storage and should review operating procedures before commissioning. Part of the management of change in an existing system should be the supplier's review of modifications. When peroxide is to be diluted with water before use, the supplier should also be asked to analyze or test a representative sample of the water.

Concentrated solutions have the obvious economic advantage of reducing shipping costs and storage volumes, and 70% H_2O_2 is a popular commercial strength. The hazards of hydrogen peroxide, however, are aggravated at high concentrations. Below 45%, the problems of reactivity and sensitivity are much relieved. With the small quantities required by most brine dechlorination applications, freight costs are not a major item on the cost sheet, and designers should consider the inherent safety of lower concentrations.

Because of its instability, hydrogen peroxide is often supplied with a stabilizer. This must be identified and checked for compatibility in the process before the peroxide is used.

Process Control. Along with selection of a chemical reducing agent and design of a system for receiving and storing it comes the problem of control of the rate of its transfer into the process. In the field of water treatment, it has been common to overfeed reducing agent to a dechlorination system in order to ensure completion of the reaction [229]. The same reference describes the successful use of a more effective control system based on monitoring of the ORP (or redox potential). This is the usual approach in the chlor-alkali industry.

The reversible potential for an oxidation–reduction reaction depends on the ratio of the activities of the oxidized and reduced states of a substance undergoing reaction. If the reduced state Red is converted to the oxidized state Ox, the potential will differ from the standard electrode potential by a quantity proportional to the logarithm of the ratio of the activities of the two states:

$$E = E^0 + (RT/nF) \ln([\text{Ox}]/[\text{Red}]) \quad (110)$$

where

E = electrode potential, V

E^0 = standard electrode potential, V

R = gas constant

T = temperature, K

n = number of electrons transferred

F = Faraday constant

$[\text{Ox}]$, $[\text{Red}]$ = activities of oxidized and reduced states

As the ratio of the two states changes, so does the electrode potential. Using an electrode similar to a pH probe, one can measure this potential and, with calibration, relate it to the ratio of, say, sulfate to sulfite ion. A high ratio will produce a high potential and indicate that all the sulfite has been consumed. A low ratio (low potential) corresponds

to a high residual concentration of sulfite. This indicates excessive feed of the reducing agent, and the controller will reduce the feed rate.

The active electrode normally is a band of platinum. The reference electrode is Ag/AgCl in a potassium chloride medium. The logarithmic form of Eq. (110) continues the analogy to pH measurement. The voltage will respond very sharply to small changes in reactant ratio near the equivalence point. Controlling a system precisely at the equivalence point can be compared to controlling a neutralization process at pH 7. Fortunately, we usually intend to operate with a certain excess of one of the reactants, where the response is less dramatic and the dynamics of control more favorable.

The maintenance requirements of an ORP-measuring system also mimic the pH system. Electrodes require the same sort of care, never being allowed to dry out and being recalibrated with some frequency. Spare calibrated electrodes should always be available, and the use of dual electrodes is not uncommon.

The system described by Martin and Kiser [229], as well as many of those in chlorine plants that are based on sulfites, is a simple in-line addition with nearby downstream measurement. This requires good mixing and rapid reaction for its success. As pointed out above, hydrogen peroxide may not react so rapidly, and some lag time may be necessary. Mannig and Scherer [225] described such a control system and presented their data on redox potential as a function of pH at two different concentrations of NaOCl (Fig. 7.102). At pH 10, the presence of 10 ppm of NaOCl shifted the potential 400 mV. This is enough to provide close control of the process. O'Brien [208] described a system in which the controller was arranged as above, with measurement close to the addition point. This was done to avoid problems with dead time in the control loop. The controller then could be reset from an ORP measurement made sufficiently far downstream that the completion of the reaction could safely be assumed. The need for such an elaboration should be determined by tests on plant brine when possible. In wastewater applications, it is common to use this technique with 15–30 min retention between the peroxide addition point and the control measurement [230].

The dependence of ORP on pH must not be overlooked. A swing of one unit in pH, according to Fig. 7.102, can change the potential at the equivalence point by 100 mV.

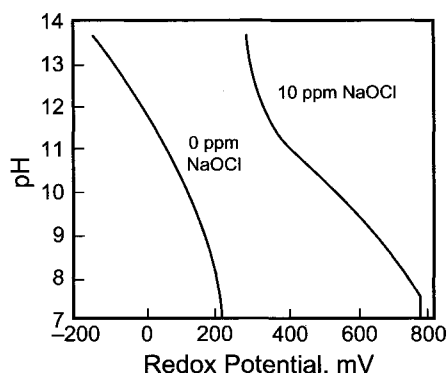


FIGURE 7.102. $\text{H}_2\text{O}_2/\text{NaOCl}$ redox potential.

This is equivalent to ± 2.5 ppm of NaOCl. Since the pH must also be adjusted after acid dechlorination, instrument engineers must ensure that the two control systems (pH and ORP) are not in conflict.

7.5.9.3B. Catalytic Decomposition.

Activated Carbon. As a special category of catalytic decomposition of species of free chlorine, we include chemisorption on activated carbon. Beds of granular activated carbon have long been used to dechlorinate water after its purification [231–233]. Because of its tendency to form surface oxides, activated carbon has the ability to abstract the oxygen generated by hydrolysis of chlorine. As an example, the reaction of HOCl can be written as:



where C^* represents an active site and C^*O a surface oxide [234]. Kinetic studies of the reaction showed that the process has an activation energy of about $10.5 \text{ kcal mol}^{-1}$ and that it is favored by low pH [235]. The pH effect is attributed to the most reactive species being HOCl, which predominates at low pH (~ 4).

The grade of carbon is an important variable. Coal- or coconut-shell types usually are preferred, with structures that are predominantly micropores and with surface areas of $700\text{--}1,200 \text{ m}^2 \text{ g}^{-1}$. Mean particle diameters are 1–2 mm. The various grades are rated by a dechlorination half-value test (DIN 19603). This determines the depth of the carbon bed that will remove half the chlorine from a flowing stream under standard test conditions. The standard test is performed on chlorinated water, and one must remember that the reaction is slower in brine than it is in water. It is best to base designs on experience or on data produced by the carbon supplier at the temperature and pH of interest.

Attractive features of a fixed bed of carbon are its lack of moving parts and the fact that during most of the operating cycle there is a substantial excess of carbon available, in the form of the unused bed. It is a more forgiving process to fluctuations in flows or operating conditions and can handle the occasional minor upset in the concentration of chlorine in the feed brine.

If the process stopped with reaction (111), a mole of carbon would be consumed for every mole of free chlorine destroyed. While some sites remain oxygenated in various forms, there is also a spontaneous partial regeneration whose stoichiometry is:



This cuts the rate of utilization of carbon in half, but the unregenerated carbon is truly consumed, and the theoretical life of a bed is still limited. The practical limitation is the gradual breakdown of the particles, which leads to disruption of the bed and high pressure drop. A conservative estimate of the capacity of a bed is the removal of $2 \text{ g Cl}_2/\text{g}$ carbon, which is only one third of the stoichiometric quantity implied by Eq. (111).

Low pH improves the kinetics of the reaction but also has its disadvantages. Chief among these probably is the fact that, under such conditions, carbon can catalyze the decomposition of chlorates. The resulting formation of gas and degradation of the carbon

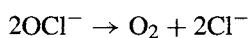
can make the process inoperable. It is better to accept the lower rates of reaction and design the system to operate on alkaline brine.

Some large water-treatment plants use upflow beds, in pulsed or moving-bed operation. In chlor-alkali brine treatment, downflow fixed beds are the rule. The columns are pressure vessels lined with hard rubber or sometimes an epoxy resin. A pressure-vacuum relief valve provides over- and under-pressure protection. This is open to the vessel but is protected from accumulations of particles by using a penetrating nozzle covered by a screen. Design principles are similar to those applied to packed bed filters or brine system ion exchangers; flow distributors and underdrains resemble those found in standard media filters [208]. The carbon is supported on a porous metal plate or screen. Dechlorinated brine flows out of the bottom of the vessel. Backwash enters at the bottom, usually through the nozzle used for brine discharge. The support assembly must be able to pass forward flow of brine and backward flow of wash water without excessive pressure drop or mechanical damage. The pressure drop through the bed depends on flow rate, solid particle size, operating temperature, and the degree of fouling of the bed. Fouling can take the form of accumulation of fine particles caused by the gradual consumption of the carbon. Flow velocities range from 5 to about 25 m hr^{-1} and depend on the grade of carbon selected. Pressure drop depends also on the grade of carbon, particle size being the major determinant.

Backwashing relieves the pressure drop by regrading the bed and sweeping away some of the finer particles. It is usually scheduled when the pressure drop reaches 2 kPa, and it should expand the bed by 20–40%. As is the case with filter or ion-exchange beds, the properties of the backwash fluid are important. Brine will have more lifting force than water, and an increase of 5°C in the temperature of the fluid can increase the amount of expansion by 20%. Backwashing requires only a few minutes and is usually necessary every week or two. It may be on a scheduled basis, or it may become necessary because of increased pressure drop or reduced effluent quality. With such a high on-line factor, it is not always necessary to provide multiple beds, as was the case with media filters and ion-exchange columns. With sufficient brine storage capacity, a single carbon bed could be taken off line, backwashed, and returned to service without disrupting the process.

If a system is designed in this way, some thought should be given to methods for removal of exhausted carbon from the vessel. If a connection is provided near the bed support plate, most of the carbon can be removed quickly and easily by flushing it out with water. There should be a space near the column where a portable container can be placed to catch the carbon. The new charge can then be loaded hydraulically. The best procedure will depend on the grade of carbon selected and so should be determined by the vendor. While some of the used carbon may remain in the vessel, a turnaround takes only a few hours. More elaborate and thorough procedures can be reserved for a scheduled plant shutdown.

Metal Catalysts. The goal in catalytic dechlorination of brine is the deoxygenation of the hypochlorite ion:



This reaction occurs slowly and spontaneously. Metals such as iron, cobalt, and nickel and their salts act as catalysts, and these are applied in various ways. Dissolved salts are used in treatment of some wastes, but they are not appropriate in process brine streams. We shall restrict this discussion to heterogeneous catalysis, where metals or salts are used in suspension and in fixed beds. The former again is of more interest in treatment of plant wastes.

We turn then to fixed-bed applications. Caldwell [236] and Hodges [237] described work with different cobalt formulations, but these are not now available commercially. A later development is a promoted nickel oxide catalyst on alumina substrate [238,239]. This was developed with destruction of strong hypochlorite solutions in mind and so is stable only under alkaline conditions. It is best applied to brine after it has been returned to alkaline pH and before resaturation.

Commercial installations of this catalyst employ a unique reactor design. An unavoidable problem with destruction of hypochlorite in a fixed bed is the release of the oxygen that is generated. In a downflow reactor, oxygen gas opposes flow of the liquid. This increases pressure drop and tends to circulate treated liquor back toward the top of the bed, where it dilutes the concentration of hypochlorite in the feed liquor and reduces the rate of dechlorination. In an upflow reactor, oxygen carries liquor through the bed. This bypassing reduces contact time of some of the liquid and reduces the conversion of hypo. To avoid these problems, the Hydecats™ reactor (Fig 7.103) uses a number of short packed sections. The liquor flows through these in series by gravity. From the bottom of one bed, it flows up through a riser to the top of the (shorter) next bed. In the treatment of strong hypochlorite solutions (e.g., vent scrubber waste), where 99.99% removal is the goal, liquid space velocities are $0.2\text{--}1\text{ hr}^{-1}$. Stitt *et al.* [239] point out that the cost of chemical treatment is proportional to the quantity of hypochlorite to be removed, while the cost of catalysis is a function of the desired fractional conversion. Thus, the cost of chemical treatment will be

$$\Gamma_{\text{chem}} = k_1 Q(C_{\text{in}} - C_{\text{out}}) \quad (113)$$

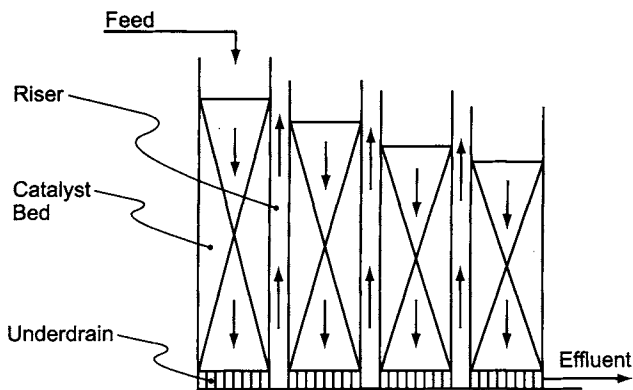


FIGURE 7.103. Proprietary system for catalytic destruction of hypochlorite.

where

- Q = volumetric flow rate
 C_{in} = hypochlorite concentration in feed
 C_{out} = hypochlorite concentration after treatment
 k_1 = proportionality constant

The cost of catalytic destruction, for a first-order process, will be

$$\Gamma_{cat} = k_2 Q \ln(C_{in}/C_{out}) \quad (114)$$

Chemical treatment is favored when a high degree of conversion is needed, or when C_{out} must be very low. Catalytic destruction becomes more practical when C_{in} is high. The process described is therefore used most often with strong waste solutions. It is also possible to optimize a process by using some combination of catalytic and chemical methods [239].

7.5.9.4. Chlorate Control Section 6.5 showed that chlorate is one of the impurities formed on the anode side of the electrolyzers as a result of back-migration of hydroxyl ions from the catholyte. Hypochlorite forms by reaction of chlorine with these ions and then disproportionates to chloride and chlorate. In diaphragm-cell operation, the chlorate accompanies the rest of the anolyte into the cathode chambers and then leaves as part of the cell liquor. The chlorate eventually leaves the plant along with the evaporated caustic solution. In membrane or mercury cells, there is no similar purge, and so the chlorate can accumulate in the circulating brine. The situation is analogous to the sulfate problem. If allowed to accumulate in the brine system, chlorate can affect the solubility of the base salt. It can also act as an oxidant of the ion-exchange resin in a membrane-cell plant and present a hazard during regeneration of the resin. Finally, it is a contaminant in the product caustic and a source of corrosion [240]. Process factors limiting chlorate concentration are the inevitable small purge from the brine system and the slow decomposition of chlorate that always takes place. However, unless all the chlorate produced is decomposed or removed somehow, its concentration will eventually exceed the specification.

The quantities of chlorate produced are not great. The rate of formation of sodium chlorate in most membrane electrolyzers is of the order of 1 or 2 kg of NaClO_3 per ton of chlorine produced. Allowable concentrations are above 10 gpl NaClO_3 . The specification then usually can be met by purging a small part of the total brine flow, and this is a popular method. Most plants that purge brine in order to control the sulfate concentration have incidentally avoided a chlorate-accumulation problem.

The actual rate of production of chlorate in a cell, while small, is quite variable. It depends on the current efficiency, the oxygen overvoltage of the anodes, and the degree of alkalinity or acidity of the feed brine. Therefore, an operator can have some influence on the rate of formation of chlorate, and this is the first line of defense against excessive accumulation:

1. Higher current efficiencies mean less production of all unintended byproducts, including chlorate. Maintaining the proper membrane environment at all

times and not allowing excessive deterioration will keep the current efficiency high.

2. At given anolyte conditions, a lower oxygen overvoltage results in less production of chlorate. The oxygen overvoltage changes along with the type of coating. This does not change the current efficiency of the cells but redistributes the products of inefficiencies. Formation of less chlorate by this method means formation of more oxygen. The technique therefore is not useful when oxygen is regarded as a more serious problem than chlorate.
3. A primary objective of deep acidification of the anolyte is reduction of the oxygen content of the chlorine gas. Since it does this by reducing the availability of hydroxyl ion in the anolyte, it also reduces the rate of production of chlorate.

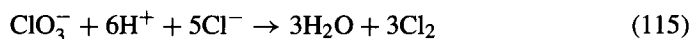
When attempts to control the formation of chlorate are not totally successful and a brine purge of the required size is undesirable, decomposition of chlorate ions by some means is necessary. It is then important to remember that only a small fraction of the chlorate present in the brine need be destroyed on each pass. This fact suggests three possible approaches:

1. low-intensity treatment of the entire depleted brine stream;
2. higher intensity treatment of a portion of the stream;
3. intermittent treatment, batch or semi-continuous, of some of the brine.

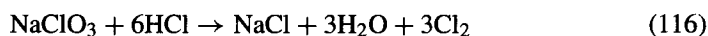
The second and third of these are the most frequent choices. A viable and common method of operation is to begin treatment to remove chlorate when the concentration is high. When the concentration reaches some selected low level, treatment stops. The chlorate concentration then increases slowly, and when it reaches a certain point, a new treatment campaign begins. Some operators favor this method, which does not require strict control at all times. This may be due to the typical unit's having substantial excess capacity.

The two subsections that follow describe several methods for reduction of chlorate ions to produce chlorine or innocuous chloride ions. The text assumes continuous operation. The first subsection deals with reduction by acidification of the brine. The second deals with other methods, including ionic reaction with a reducing agent, catalytic hydrogenation, and electrochemical reduction.

7.5.9.4A. Destruction with Hydrochloric Acid. Destruction of chlorate usually takes place in the recycle brine, where it is treated with HCl at elevated temperature ($>80^{\circ}\text{C}$). The valency of chlorine in the chlorate ion is +5. This explains the high oxidizing capacity of chlorate solutions, and it requires the oxidation of five chloride ions to produce Cl_2 . Chlorate therefore decomposes in acidic solution according to

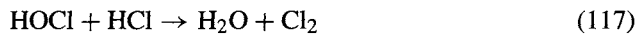


When sodium salts are involved, the stoichiometry becomes



Some decomposition of chlorate occurs whenever HCl is present in one of its solutions. Indeed, a small amount of decomposition takes place in the depleted brine when it is acidified to promote its dechlorination (Section 7.5.9.2). This mild treatment usually does not remove enough chlorate, and more vigorous treatment at higher temperature and HCl concentration becomes necessary.

We consider instead the continuous treatment of a sidestream of the brine. The most efficient process configuration couples the destruction of chlorate with dechlorination of the depleted brine. The excess HCl in the destruction reactor then becomes part of the total acid addition to the dechlorination process. Figure 7.104 is an illustration. In part (a), the base case, there is no deliberate destruction of chlorate. The acid produces a pH low enough to reverse the hydrolysis of dissolved chlorine by decomposing HOCl:



In part (b) of the drawing, the sidestream that is to be treated for removal of chlorate goes to a separate vessel. Some of the HCl to be used for acidification of the depleted brine is added to the sidestream, whose pH should be reduced to about one. The drawing

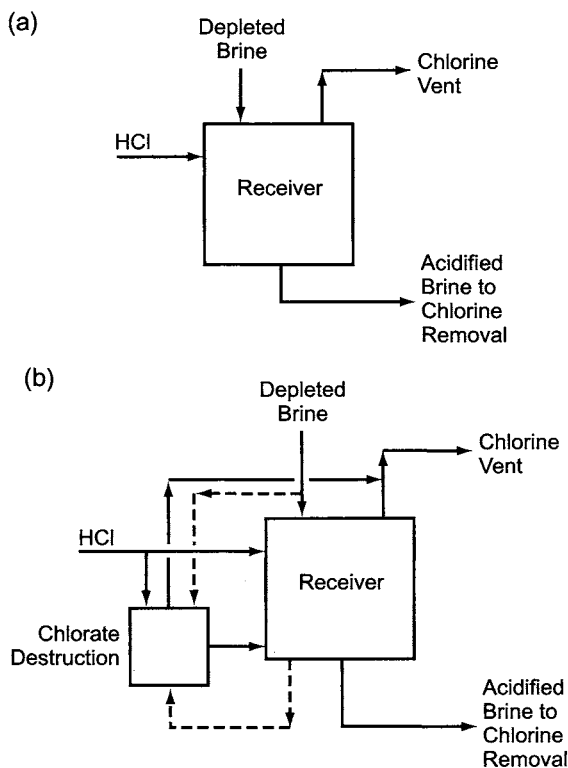


FIGURE 7.104. Treatment of sidestream for removal of chlorate. (a) Normal depleted brine flow pattern, and (b) Incorporation of chlorate destruction loop.

shows two methods (dashed lines) for withdrawal of the sidestream. In one, the depleted brine flow is split before acidification. Planning for a given excess of acid in the chlorate destruction reactor then should take into account the consumption of acid in the dechlorination reaction (117) as well as in the destruction reaction (115). The other method is more useful if acidification takes place in a tank that collects a gravity flow of depleted brine from the cells. The sidestream then is drawn or pumped from the main tank, from which the full combined stream goes off to the dechlorination column. In the end, the acid requirement of part (b) is greater than that of part (a) only by the small amount consumed in reaction (115).

The duty of the destruction reactor is to remove chlorate at the rate at which it forms in the cells. The required degree of conversion of chlorate and the volume of solution to be treated therefore are inversely related. The size of the reactor required is reduced by increasing the size of the sidestream while reducing its residence time in the reactor. This effect is limited by the practical problems of mixing the brine and preventing bypassing in the reactor, but more fundamentally by the acid balance. A low pH (~ 1) favors reaction (115), while dechlorination of brine is typically run at $\text{pH} \approx 2$. A large sidestream would require more acid than is necessary for dechlorination of all the depleted brine. A good practical compromise is to add a major part of the dechlorination acid to the sidestream. This stream therefore is at lower pH, and it can be heated and detained as necessary to remove all the chlorate formed in the previous pass through the cells. Figure 7.105 shows a schematic flowsheet with indicative control system.

Heating steam usually is not applied to a jacket on the vessel (which therefore can be non-metallic). It is possible to inject it directly into the liquid or through a sparger. Depending on the available steam pressure, it is also possible to provide some liquid

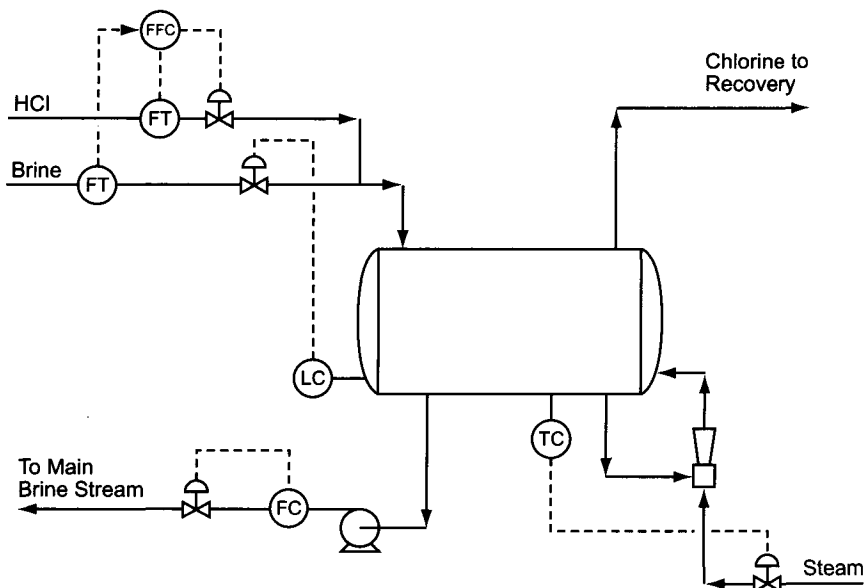
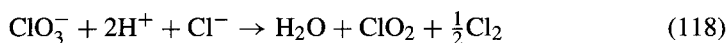


FIGURE 7.105. Flow diagram—destruction of chlorate by HCl.

circulation by means of an ejector (as shown). Failing this, a pump can provide circulation and an external exchanger the heat. Control of the brine flow through the system must be coordinated with surrounding processes. Here, it enters the tank under level control and leaves under flow control. Conceptually at least, the opposite arrangement also is useful. In the drawing, the flow of brine to the tank also is measured, in order to allow acid feed under flow ratio control.

Many plants practice this technology in some form. There are numerous references to its use in the literature, usually with few accompanying data. Mayo [241] describes a commercial operation and also points out that reaction of chlorate with acid under reducing conditions is the process used for manufacture of chlorine dioxide. While the composition of anolyte does not favor this reaction, perhaps 2–3% of the gas formed under some plant conditions is ClO_2 . The reaction involved is



Chlorine dioxide is a highly reactive and dangerous material. One of the goals in process design therefore should be the minimization of ClO_2 formation.

Both decomposition reactions involve ClO_3^- , H^+ , and Cl^- . The concentrations of these species and the temperature of the reaction are the important variables that influence the rates of both reactions. Rodermund [242] showed the effects of operating variables on the selectivity of the process. Chlorine formation by reaction (115) rather than by reaction (118) is favored by

1. higher temperature:
at 0.05M NaClO_3 , 2.6M HCl , and 4.6M NaCl , selectivities were 51% at 40°C, 62% at 60°C, and 81% at 90°C
2. lower chlorate concentration:
at 80°C, 2M NaCl , and 2.5–3M HCl , selectivities were 73% at 0.06M NaClO_3 , 79% at 0.04M, and 87% at 0.02M
3. lower acid concentration (weak effect):
at 80°C, 2M NaCl , and 0.05M NaClO_3 , selectivities were 79% at ~1.45M HCl , 78% at ~1.6M, and 76% at 2.5–3M
4. higher salt concentration (weak and mixed effect):
at 80°C and 0.05M NaClO_3 , chloride concentration had little effect when the HCl concentration was 2M. At lower acid concentration, selectivity declined with higher salt concentrations. At higher acid concentrations, which are desirable for their effect on productivity, the selectivity improved slightly as NaCl concentration increased. At 3M HCl , for example, the selectivity was 73.3% at 3M NaCl , 74.1% at 4M, and 75.5% at 5M.

Selectivity (S) is defined here as the fraction of decomposed chlorate that follows reaction (115). The mole fraction of chlorine in the dry products of decomposition is then $(1 + 5S)/(3 + 3S)$. A selectivity of 90% therefore corresponds to a 96.5% yield of chlorine.

Clearly desirable are:

1. high acid concentration, for higher reaction rates, but limited by demand of dechlorination process for acid;

2. low chlorate concentration, for higher selectivity for chlorine formation;
3. high temperature, for both effects.

A high chloride concentration generally is more desirable than reaction in a dilute solution. This is fortuitous because even the depleted brine concentration is rather high, and this is not a variable that one would choose to manipulate within the process. The tabulation above shows that the effect of increasing the chloride concentration above 3M is rather small. Other variables are more influential, and thus treatment of depleted brine is more common than treatment of concentrated brine because it is more efficiently integrated with the rest of the process.

Operating at high acid and low chlorate concentration (points #1 and #2) will reduce the fractional conversion of HCl, but within the acid requirements of a process integrated with brine dechlorination this is not a serious disadvantage. One first determines how much acid is required for brine dechlorination and chlorate destruction and then decides how to divide that acid between the two processes. Excess acid not consumed in the destruction reactor returns to the main brine loop, at the dechlorination reactor, along with the chlorate-depleted brine. This is not necessarily wasteful of acid. The amount actually consumed is fixed by the rate of generation of chlorate and by Eq. (115). The use of a large excess of acid produces a very low standing concentration of chlorate in the brine. This has no disadvantages in cell chemistry, and it makes possible the use of smaller destruction reactors. Oversizing of a reactor can limit the magnitude of the excess concentration of HCl and so reduce selectivity.

Chlorate removal in general and acidic decomposition in particular are forgiving processes. Underfeeding of acid, for example, results in an increase in chlorate concentration. With normal operation well within the specification, the change in average concentration in the brine loop will be very slow, and there will be ample time for correction. Overfeeding of acid is wasteful and also consumes more neutralizing caustic, but it is not dangerous, at least within the ability of the chlorate and chlorine removal systems to resist corrosion.

As is the case with chlorate itself, destruction of ClO_2 is an alternative or backup to the steps taken to avoid its formation. Thermal decomposition is a simple technique that has proved successful [241,242]. Heating the offgas to 100°C in a small tube packed with Raschig rings for a few minutes removes essentially all the ClO_2 . A pipeline reactor can be part of the transfer line and take up very little extra space in the plant.

7.5.9.4B. Other Methods. Other methods that may be useful for the removal of chlorate include chemical reduction, hydrogenation, and electrolysis.

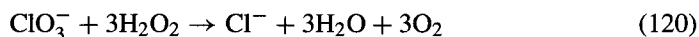
Chemical reduction can involve the same types of agent used to reduce dissolved chlorine [243]. Section 7.5.9.3A mentioned the use of sulfur-based reducing agents and hydrogen peroxide to reduce active chlorine. Using bisulfite as an example of the former, here we have the reaction



This reaction occurs only at $\text{pH} < 5$. It is rapid at $\text{pH} 1\text{--}3$ and $50\text{--}55^\circ\text{C}$, giving up to 96% removal of chlorate. The reaction is exothermic, and heats of formation indicate that the

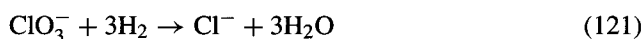
removal of 1 gpl of NaClO_3 should raise the temperature of the brine about 2°C . While it is a simple technique and easily applied, this reaction has the disadvantage of a sulfate byproduct. One part of NaClO_3 reduced in this way would produce the equivalent of four parts of Na_2SO_4 . The chlorate problem is simply transformed into a sulfate problem, which may be more harmful. This approach still may be useful when a sulfate removal system already is available, particularly when the operating cost is less than proportional to the sulfate burden.

Chlorate also is reduced by hydrogen peroxide. As is also true in chemical reduction of chlorine, this process leaves no soluble impurity:



Users of this process must take measures to avoid the accumulation of a dangerous oxygen atmosphere. The net heat effect is only about one-third as great as in reaction (119).

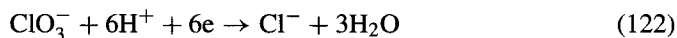
Since the key to destruction of chlorate is reduction of the chlorine from its +5 valence, hydrogenation suggests itself as another approach [194]. The reaction is quite simply



The heat of this reaction is about the same as that of reaction (119). Vaporization of water into the excess hydrogen used in the process dissipates some of the heat generated by the reaction. The net effect on the brine temperature thus depends on how much hydrogen is consumed by a unit volume of brine.

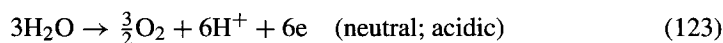
Pilot-plant results using a precious-metal catalyst show reductions of the NaClO_3 level in brine from an irregular 5 gpl to 1 gpl or less [194]. The process involves preliminary saturation of the brine under hydrogen pressure followed by passage with additional hydrogen gas through a trickle-bed reactor packed with the catalyst. While there is little commercial experience reported, this process has the advantage of not affecting the acid balance in the brine. The 80% conversion referred to above, if sustainable over time, would allow control of the chlorate level by treatment of only a small fraction of the circulating brine.

Another technique investigated in the laboratory [244] is the electrochemical reduction of chlorate from acidic ($\text{pH} \approx 2$) solution using high surface area catalyzed cathodes and oxygen-evolving DSA anodes. Chlorate is reduced at the cathode under mass-transfer-controlled conditions according to

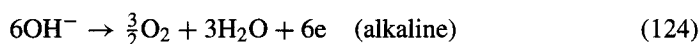


The current efficiency for this scheme is about 85% at an apparent current density of about 2 mA cm^{-2} in laboratory cells. This is a clean process that has lowered the chlorate level from 3.6 to 0.01 g L^{-1} . The process seems to have economic potential but has not been optimized for commercial application.

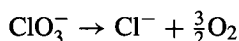
The anolyte in such a cell might be a solution of Na₂SO₄ or NaOH. The anode reaction is



or



The overall reaction is



With sulfate solution as the anolyte, the current-carrying ion is H⁺. This passes through the membrane to replace the H⁺ consumed by reaction (122). Since the current efficiency is less than 100%, there is a net accumulation of acid in the anolyte. When NaOH is used, sodium ions carry the current. This combined with reaction (124) constantly depletes the anolyte.

REFERENCES

1. M. Kurlansky, *Salt: A World History*, Walker & Co., New York (2002), p. 207.
2. B.M. Bertram, Sodium Chloride. In *Kirk-Othmer Encyclopedia of Chemical Technology*, 4th ed., vol. 22, John Wiley & Sons, Inc., New York (1997), p. 354.
3. B. Kummel, *History of the Earth*, 2nd ed., W. H. Freeman & Co., San Francisco (1970), p. 426.
4. L. Kuhns, Subterranean Salt, reprint from *Water Technology*, July–August (1978).
5. *Encyclopedia Britannica*, Salt, www.britannica.com (2002).
6. R.J. Coin, Brine Treatment, *Sixteenth Annual Electrode Corporation Chlorine/Chlorate Industry Seminar*, Cleveland, OH (2000).
7. G. Baseggio, The Composition of Sea Water and Its Concentrates, *Proceedings, Fourth International Symposium on Salt*, Cleveland, OH (1971), p. 351.
8. V.M. Venkatesh Mannar, Design of Seawater Intake Facilities for Solar Salt Plants, *Proceedings, Sixth International Symposium on Salt*, vol. II (1983), p. 289.
9. D. Butts, Maximizing Solar Evaporation through Sequential Brine Flow, *Kali91 International Potash Conference*, Hamburg (1991).
10. N.H. Swedan, *Chem. Eng. Progr.* **95**(7), 65 (1999).
11. B.S. Joshi and R.B. Bhatt, Design and Layout of Solar Salt Works, *Proceedings, Sixth International Symposium on Salt*, vol. II (1983), p. 281.
12. P.R. Bavdekar, Theory of Solar Salt Manufacture, *Symposium on Salt and Byproducts*, Bhavnagar, India (1964).
13. D.M. See, Solar Salt. In D.S. Kaufmann (ed.), *Sodium Chloride—ACS Monograph 145*, Reinhold Publishing Corp., New York (1960), p. 100.
14. R.B. Tippin and P.E. Muehlberg, Chemicals from Brine. In *Kirk-Othmer Encyclopedia of Chemical Technology*, 3rd ed., vol. 5, John Wiley & Sons, Inc., New York (1983), p. 385.
15. D. Butts, Chemicals from Brine. In *Kirk-Othmer Encyclopedia of Chemical Technology*, 4th ed., vol. 5, John Wiley & Sons, Inc., New York (1993), p. 817.
16. M. Kurlansky, *Salt: A World History*, Walker & Co., New York (2002), p. 149.
17. W.L. Badger and G.E. Seavoy, Vacuum Pan Salt. In D.S. Kaufmann (ed.), *Sodium Chloride, ACS Monograph 145*, Reinhold Publishing Corp., New York (1960), p. 206.

18. R.B. Richards, Grainer Salt. In D.S. Kaufmann (ed.), *Sodium Chloride, ACS Monograph 145*, Reinhold Publishing Corp., New York (1960), p. 262.
19. D.E. Bedford, Personal Communication (2000).
20. M. Hamada, I. Azuma, N. Imai, and H. Ono, *Proceedings, Seventh Symposium on Salt*, vol. 2, Elsevier, Amsterdam (1993), p. 59.
21. C.E. Niman, Cargill Salt Co., Personal Communication (2001).
22. T.H. Yohe, Use of Salt/Brine Evaporators in Brine-Fed Membrane Cell NaOH Plants, *30th Chlorine Institute Plant Operations Seminar*, Washington, DC (1987).
23. D. Strietelmeier, Morton Salt Co., Personal Communication (1998).
24. W.L. Badger and G.E. Seavoy, Vacuum Pan Salt. In D.S. Kaufmann (ed.), *Sodium Chloride, ACS Monograph 145*, Reinhold Publishing Corp., New York (1960), p. 211.
25. G.G. Brown and Associates, *Unit Operations*, John Wiley & Sons, Inc., New York (1950), p. 481.
26. R.B. Richards, *Chem. Eng.* **59**, 140 (1952).
27. L.J. Theilgard, *Chem. Eng. Progr.* **58**(8), 68 (1962).
28. V.A. Zandon, E.A. Schoeld, and J. McManus, Potash. In N.L. Weiss (ed.), *SME Mineral Processing Handbook*, vol. 2, Society of Mining Engineers, New York (1985), p. 22-1.
29. *Salt Storage Handbook*, Salt Institute, Alexandria, VA (1997).
30. *Sterling Salt Users Guide*, International Salt Company, Clarks Summit, PA (1981).
31. R.C. Sutter, Brine Treatment, *Fifth Annual Electrode Corporation Chlorine/Chlorate Industry Seminar*, Cleveland, OH (1989).
32. D.S. Kaufmann (ed.), *Sodium Chloride, ACS Monograph 145*, Reinhold Publishing Corp., New York (1960), p. 512.
33. D.S. Kaufmann (ed.), *Sodium Chloride, ACS Monograph 145*, Reinhold Publishing Corp., New York (1960), pp. 587-623.
34. S. Subramanian, A.S. Ganesh Kumar, and C.T. Goudar, Determine Sieve Opening from Mesh Number, reprinted in *Chemical Engineering Buyers Guide* (2000), p. 15.
35. G.N. Lewis and M. Randall, *Thermodynamics and the Free Energy of Chemical Substances*, 1st ed., McGraw-Hill Book Co., New York (1923), p. 252.
36. E.A. Avallone and T. Baumeister III (eds.), *Marks' Standard Handbook for Mechanical Engineers*, 10th ed., McGraw-Hill Book Co., New York (1996), pp. 10-35-10-55.
37. Sidney Manufacturing Co., Bucket Elevator Capacity Chart, www.sidneymanufacturing.com/capacity.htm (2002).
38. B.F. Reilly, Stearns Catalytic, Inc., Personal Communication (1983).
39. D.S. Kaufmann (ed.), *Sodium Chloride, ACS Monograph 145*, Reinhold Publishing Corp., New York (1960), pp. 282 *et seq.*
40. T.A. Liederbach, Brine Purification Systems for Chlor-Alkali Plants, *Ninth Annual Electrode Corporation Chlorine/Chlorate Industry Seminar*, Cleveland, OH (1993).
41. Z.G. Deutsch, Brine Wells and Pipelines. In D.S. Kaufmann (ed.), *Sodium Chloride, ACS Monograph 145*, Reinhold Publishing Corp., New York (1960), p. 158.
42. M.T. Halbouty, *Salt Domes, Gulf Region, United States and Mexico*, Gulf Publishing Co., Houston (1967), p. 125.
43. J.L. Frear and J. Johnston, *J. Am. Chem. Soc.* **51**, 2082 (1929).
44. V. Brandani, G. DelRe, and G. DiGiorgio, *Chem. Eng. J.* **32**, 145 (1986).
45. New York State Department of Environmental Conservation, www.dec.state.ny.us (2001).
46. A.V. Kublanov, Methods to Produce Brines from Underground Caverns in Bedded and Stock Deposits, *Solution Mining Research Institute Spring Meeting*, Orlando, FL (2001).
47. M. Slezak, Techniques in the Development of Salt Caverns for Multiple Use, *Chlorine Bicentennial Symposium*, The Electrochemical Society, Princeton, NJ (1974).
48. C.A. Bays, Use of Salt Solution Cavities for Underground Storage, *Symposium on Salt*, Northern Ohio Geological Society, Cleveland, OH (1963).
49. R.L. Thoms and R.L. Gehle, A Brief History of Salt Cavern Use, Keynote address, Salt 2000, www.solutionmining.org (2000).
50. T.F. LaGess, Disposal of Brine Treating Solids by Recycling to a Brine Well, *Chlorine Bicentennial Symposium*, The Electrochemical Society, Princeton, NJ (1974).
51. D.S. Kaufmann (ed.), *Sodium Chloride, ACS Monograph 145*, Reinhold Publishing Corp., New York (1960), p. 314.

52. H.C. Miller, *Canadian Patent* 828,062 (1969).
53. R.C. Sutter, Brine Treatment, *Seventh Annual Electrode Corporation Chlorine/Chlorate Industry Seminar*, Cleveland, OH (1991).
54. P.H. Ralston and R.R. Mitchell, *Electrochem. Technol.* **5**, 262 (1967).
55. *Sulfate Solubility Inhibitor* 2. Product data bulletin and material safety data sheets, Jamestown Chemical Corp., West Haven, CT (2002).
56. V. Sedivy, Krebs Swiss Division, Standard Messo, Personal Communication (2002).
57. R.G. Arnold, Jamestown Chemical Corp., Personal Communication (2002).
58. T.F. O'Brien, Control of Sulfates in Membrane-Cell Brine Systems. In K. Wall (ed.), *Modern Chlor-Alkali Technology*, vol. 3, Ellis Horwood, Chichester (1986), p. 326.
59. T.F. O'Brien, *U.S. Patent* 4,586,993 (1986).
60. D.A. Santos, Sulfate Control in Brine from Poor-Quality Raw Salt, *Second Nafion® Global Users Forum*, Fayetteville, NC (1993).
61. A. Damesimo, Jr., Niachlor Wastewater and Effluent Management, *39th Chlorine Institute Plant Operations Seminar*, Washington, DC (1996).
62. *Calcium Chloride*, Technical and Engineering Service Bulletin No. 16, Allied Chemical Company, Morristown, NJ (undated).
63. D.W.F. Hardie, *Electrolytic Manufacture of Chemicals from Salt*, The Chlorine Institute, Inc., New York (1975).
64. E.H. Cook and M.P. Grotheer. In T.C. Jeffrey, P.A. Danna, and H.S. Holden (eds), *Proceedings, Chlorine Bicentennial Symposium*, The Electrochemical Society, Princeton, NJ (1974), p. 374.
65. G. Angel and T. Lunden, *J. Electrochem. Soc.* **99**, 435 (1952).
66. G. Angel and R. Brannland, *J. Electrochem. Soc.* **99**, 442 (1952).
67. G. Angel, T. Lunden, and R. Brannland, *J. Electrochem. Soc.* **100**, 39 (1953).
68. G. Angel, T. Lunden, S. Dahlerus, and R. Brannland, *J. Electrochem. Soc.* **102**, 124 (1955).
69. G. Angel, T. Lunden, S. Dahlerus, and R. Brannland, *J. Electrochem. Soc.* **102**, 102 (1955).
70. G. Angel, R. Brannland, and S. Dahlerus, *J. Electrochem. Soc.* **104**, 167 (1957).
71. R.B. MacMullin, Electrolysis of Brines in Mercury Cells. In J.B. Sconce (ed.), *Chlorine, Its Manufacture, Properties, and Uses*, Robert E. Krieger Publishing Co., Huntington, NY (1972).
72. A. Czernotzky, *Acta Chim. Acad. Sci., Hungary* **18**, 167 (1959).
73. K. Hass, *Electrochem. Technol.* **5**, 246 (1967).
74. W.E. Cowley, B.Lott, and J.H. Entwisle, *Trans. Inst. Chem. Eng.* **41**, 372 (1963).
75. Z.J. Colón, Brine Impurity Effect in Mercury Cells, *Seventh Annual Electrode Corporation Chlorine/Chlorate Industry Seminar*, Cleveland, OH (1991).
76. F. Hine, M. Yasuda, and K. Fujita, *J. Electrochem. Soc.* **128**, 2314 (1981).
77. R.C. Carlson, The Effects of Brine Impurities on Dimensionally Stable Anodes, *Fourteenth Annual ELTECH Chlorine/Chlorate Industry Seminar*, Cleveland, OH (1998).
78. J.T. Keating and H.M.B. Gerner. High Current Density Operation—The Behavior of Ion Exchange Membranes in Chlor-Alkali Electrolyzers. In S. Sealey (ed.), *Modern Chlor-Alkali Technology*, vol. 7, Royal Society of Chemistry, London (1998), p. 135.
79. *Nafion® Product Information, Bulletin 97-01*, DuPont Co., Wilmington, DE (1999).
80. J.T. Keating and K.-J. Behling, Brine, Impurities, and Membrane Chlor-Alkali Cell Performance. In N.M. Prout and J.S. Moorhouse (eds), *Modern Chlor-Alkali Technology*, vol. 4, Elsevier Applied Science, London (1990), p. 125.
81. J.H.G. van der Stegen and P. Breuning, The Formation of Precipitates of Iron Ions inside Perfluorinated Membranes during Chlor-Alkali Electrolysis. In S. Sealey (ed.), *Modern Chlor-Alkali Technology*, vol. 7, Royal Society of Chemistry, London (1998), p. 123.
82. Y. Ogata, S. Uchiyama, M. Hayashi, M. Yasuda, and F. Hine, *J. Appl. Electrochem.* **20**, 555 (1990).
83. F. Hine, S. Yoshizawa, and S. Okada, *J. Chem. Soc. Jpn, Industrial Chemistry Section* **62**, 769 (1959).
84. F. Hine, T. Sugimori, S. Yoshizawa, and S. Okada, *J. Chem. Soc. Jpn, Industrial Chemistry Section* **62**, 955 (1959).
85. F. Hine, T. Sugimori, S. Yoshizawa, and S. Okada, *J. Chem. Soc. Jpn, Industrial Chemistry Section* **62**, 773 (1959).
86. F. Hine, T. Sugimori, S. Yoshizawa, and S. Okada, *J. Chem. Soc. Jpn, Industrial Chemistry Section* **62**, 778 (1959).

87. A.F. Boryachek, E.T. Gromova, and O.N. Kaluga. *Zh. Prikl. Khim*, **41**(7) 1606 (1968).
88. M.M. Silver, New Desulfation System (NDS) for Chlor-Alkali Plant, *35th Chlorine Institute Plant Operations Seminar*, New Orleans, LA (1992).
89. *FMC Soda Ash Storage Options and Technical Data*, www.fmcchemicals.com, FMC Corporation, Philadelphia, PA (2002), p. 8.
90. *Material Safety Data Sheet 497-19-8, Rev. 3*, www.fmc.com/msds/70729xup, FMC Wyoming Corp., Philadelphia, PA (2001).
91. C.T. Bryant, *Flocculant Addition—NOPCO 154*, publication information not given (1978).
92. *More than You Really Want To Know about Polymers*, Technical Information Bulletin, Tramfloc, Inc., Tempe, AZ (2001).
93. J.A. Seifert, *Chem. Eng.* **94**(14), 11 (1987).
94. H.S. Coe and G.H. Clevenger, *Trans. Am. Inst. Mining Met. Engrs.* **55**, 356 (1916).
95. G.J. Kynch, *Trans. Far. Soc.* **48**, 166 (1952).
96. E.B. Fitch, *AIChE J.* **25**, 913 (1979).
97. W.P. Talmadge and E.B. Fitch, *Ind. Eng. Chem.* **47**, 38 (1953).
98. E.B. Fitch, *Chem. Eng.* **90**(8), 83 (1971).
99. A.S. Foust, L.A. Wenzel, C.W. Clump, L. Maus, and L.B. Andersen, *Principles of Unit Operations*, 2nd ed., John Wiley & Sons, Inc., New York (1980), pp. 631–635.
100. E.B. Fitch, *AIChE J.* **39**, 27 (1993).
101. *Handbook of Chemicals for Water Treatment*, Kurita Water Industries, Ltd., Tokyo (1989), p. 188.
102. F.Hine and K.Nishiyama, *Soda to Enso (Soda and Chlorine)* **26**, 197 (1975).
103. F.W. Spillers, Brine-Treating Solids Disposal by Recycling to a Brine Well, *Proceedings, Oronzio DeNora Symposium on Chlorine Technology (Venice)*, Oronzio DeNora Impianti Elettrochimici S.p.A., Milan (1979), p. 221.
104. W.E. Timmins, Eimco Process Equipment Co., Personal Communication (1985).
105. *Soda Handbook 1998*, Japan Soda Industry Association, Tokyo (1998), p. 148.
106. *Soda Handbook 1998*, Japan Soda Industry Association, Tokyo (1998), p. 146.
107. *FlexKlear™ Inclined Plate Settlers*, product bulletin Form #TV6-05D1, Eimco Process Equipment Company, Salt Lake City, UT (2001).
108. *Delta-Stak Clarifiers*, product bulletin Form #O-111, Eimco Process Equipment Div., Baker Hughes Inc., Salt Lake City, UT (1997).
109. J.M. Dugan, Dugan Environmental Services Co., Personal Communication, (1988).
110. S. Ergun, *Chem. Eng. Progr.* **48**(2), 89 (1952).
111. A. Macías-Machín and D.J. Santana, *Chem. Eng.* **105**(9), 159 (1998).
112. *Soda Handbook 1998*, Japan Soda Industry Association, Tokyo (1998), p. 149.
113. A.S. Foust, L.A. Wenzel, C.W. Clump, L.Maus, and L.B. Andersen, *Principles of Unit Operations*, 2nd ed., John Wiley & Sons, Inc., New York (1980), pp. 667 *et seq.*
114. P.C. Carman, *J. Soc. Chem. Ind., London* **57**, 225T (1938).
115. F. Hine, Y. Yagishita, and N. Yokota, *Soda to Enso (Soda and Chlorine)* **29**, 330 (1978).
116. G.G. Brown and Associates, *Unit Operations*, John Wiley & Sons, Inc., New York (1950), p. 251.
117. M.J. Raimer, Back-Pulse Filtration using Gore-Tex® Membrane Filter Cloths. In J. Moorhouse (ed.), *Modern Chlor-Alkali Technology*, vol. 8, Blackwell Science, Oxford (2001), p. 272.
118. K.J. Julkowski, DrM Filters, Personal Communication (2003).
119. D.J. Gosser and R. J. Horvath, Ion Exchange Systems for Membrane Cell Chlor-Alkali Plants, *27th Chlorine Institute Plant Operations Seminar*, Washington, DC (1984).
120. I.F. White and T.F. O'Brien, Secondary Brine Treatment: Ion-Exchange Purification of Brine. In N.M. Prout and J.S. Moorhouse (eds), *Modern Chlor-Alkali Technology*, vol. 4, Elsevier Applied Science, London (1990), p. 271.
121. R. Szilagyi, Treatment of Brine for Membrane Cell Feed, *37th Chlorine Institute Plant Operations Seminar*, Washington, DC (1994).
122. J.-J. Wolff and R.E. Anderson, presented at AIChE meeting, Orlando, FL (1982).
123. C. Motohashi, *Soda to Enso (Soda and Chlorine)* **34**, 516 (1983); **36**, 291 (1985).
124. J.-J. Wolff, *Duolite Brine Purification*, Brochure IE-D/285, Rohm & Haas Co., Philadelphia, PA (2001).
125. *Chelation Systems*, Technical Brochure D145T, Purolite International Limited, Pontyclun, UK (2000).
126. T. Murata and J. Ungar, *Secondary Brine Purification*, Dianex Systems (1986).

127. J.-J. Wolff, *Ion-Exchange Purification of Feed Brine for Chlor-Alkali Electrolysis Cells*, Rohm & Haas Co., Philadelphia, PA (1985).
128. K. Yamaguchi, T. Ichisaka, and I. Kumagai, The Control of Brine Impurities in the Membrane Process in the Chlor-Alkali Industry, *29th Chlorine Institute Plant Operations Seminar*, Tampa, FL (1986).
129. T.F. O'Brien, Brine Supply Requirements in Plant Conversions, *46th Chlorine Institute Plant Operations Seminar*, Chicago, IL (2003).
130. Amberlite® IRC 747 Industrial Grade Chelating Resin, Preliminary Product Data Sheet IE-643 ED3, Rohm & Haas Co., Philadelphia, PA (2001).
131. Diaion CR11 Resin—General Regeneration Protocol, Mitsubishi Chemical America, White Plains, NY (1996).
132. H.C. Williford, Personal Communication (2004).
133. T.F.O'Brien, Practical Considerations in Design of Brine Ion-Exchange Systems, *2nd Nafion® Global Users Forum*, Fayetteville, NC (1993).
134. General Information on Nafion® Membrane for Electrolysis, Product Bulletin 97-0, E.I. DuPont de Nemours & Co., Inc., Fayetteville, NC (1999).
135. D. Bergner, *J. Appl. Electrochem.* **20**, 716 (1990).
136. R.W. Potter and M.A. Clynne, *J. Chem. Eng. Data* **25**, 50 (1980).
137. R. Rodermund, *Chlorate Destruction in the Brine System of a Chlor-Alkali Electrolysis Plant*, Dissertation, University of Dortmund (1983), p. 66.
138. R.G. Bates, *Determination of pH; Theory and Practice*, John Wiley & Sons, Inc., New York (1964).
139. J.T. Keating, Understanding Membrane Operating Conditions. In T.C. Wellington, (ed.), *Modern Chlor-Alkali Technology*, vol. 5, Elsevier Applied Science, London (1992), p. 69.
140. *Hydrochloric Acid Storage and Piping Systems*, Pamphlet 163, Edition 1, The Chlorine Institute, Washington, DC (2001).
141. J. Heiss, Diamond Crystal Salt Co., Personal Communication (1983).
142. L.F. Becnel, Jr., United Brine Services Co., Personal Communication (2003).
143. L.F. Becnel, Jr., Ultra-Pure Evaporated Salt for Membrane Chlor-Alkali Plants, *46th Chlorine Institute Plant Operations Seminar*, Chicago, IL (2003).
144. C. Moser, Control of Sulphate in the Production of Crystal Sodium Chlorate. In N.M. Prout and J.S. Moorhouse (eds), *Modern Chlor-Alkali Technology*, vol. 4, Elsevier Applied Science, London (1990), p. 325.
145. K. Saiki, N. Yoshida, M.M. Silver, and I. Kumagai, New Desulfation System for Chlor-Alkali Plant. In R.W. Curry, (ed.), *Modern Chlor-Alkali Technology*, vol. 4, Royal Society of Chemistry, Cambridge (1995), p. 82.
146. T. Kishi and T. Matsuoka, Process to Remove Sulfate, Iodide and Silica from Brine. In J. Moorhouse (ed.), *Modern Chlor-Alkali Technology*, vol. 8, Blackwell Science, Oxford (2001), p. 152.
147. K. Maycock, Z. Twardowski, and J. Ulan, A New Method to Remove Sodium Sulphate from Brine. In S. Sealey (ed.), *Modern Chlor-Alkali Technology*, vol. 7, Royal Society of Chemistry, Cambridge (1998), p. 214.
148. C. Kotzo, A. Barr, and F. Muret, Sulfate Removal from Brine, *43rd Chlorine Institute Plant Operations Seminar*, Houston, TX (2000).
149. J. Duffy, *Chem. Eng.* **110**(6), 35 (2003).
150. N. Eckert, Chemetics, Personal Communication (2003).
151. M.Z. Rogozovskaya and T.L. Kononchuk, *Zh. Prikl. Khim.* **54**, 1708 (1981).
152. R. Schäfer, *U.S. Patent* 4,132,759 (1979).
153. D.S. Kaufmann (ed.), *Sodium Chloride, ACS Monograph 145*, Reinhold Publishing Corp., New York (1960), p. 330.
154. C.W. Blount, *The Solubility of Anhydrite in the System CaSO₄-H₂O and CaSO₄-NaCl-H₂O and its Geological Significance*, University of California at Los Angeles, Ph.D. Dissertation 65-15, (1965), p. 182.
155. W.M. Madgin and D.A. Swales, *J. Appl. Chem.* **6**, 482 (1956).
156. C.C. Templeton, *J. Chem. Eng. Data* **5**(4), 514 (1960).
157. S. Pribičević, Brine Preparation for Chlorine Production, *Chlorine Bicentennial Symposium*, The Electrochemical Society, Princeton, NJ (1974).
158. M. Pourbaix, *Atlas of Electrochemical Equilibria in Aqueous Solutions*, Pergamon Press, New York (1966), pp. 307–342.

159. HSC chemistry software, Versions 3 and 4, Outokumpu Research Oy, Espoo (1999).
160. M. Pourbaix, *Atlas of Electrochemical Equilibria in Aqueous Solutions*, Pergamon Press, New York (1966), p. 458.
161. D.S. Novak, *U.S. Patent* 4,274,929 (1981).
162. T.C. Bissot, *Extended Abstracts*, Vol. 86-1, The Electrochemical Society meeting, Boston. The Electrochemical Society, Philadelphia, PA (1986), p. 643.
163. M. Pourbaix, *Atlas of Electrochemical Equilibria in Aqueous Solutions*, Pergamon Press, New York (1966), p. 168.
164. P.A. Brook, *Corrosion Sci.* **12**, 297 (1972).
165. F.R. Minz, HCl Electrolysis Technology for Recycling Chlorine, *Conference on Electrochemical Processing*, Glasgow (1993).
166. L.L. Burton, DuPont presentation to customers on membrane developments (2000).
167. M. Accomazzo, Ion Pure Corp., Personal Communication, PA (1991).
168. B. Parekh, *Chem. Eng.* **98**(1), 70 (1991).
169. *Amersorb Carbonaceous Adsorbents*, Technical note, Rohm & Haas Co., Philadelphia, PA (1991).
170. W.C. Ying, Personal Communication (2001).
171. J.M. Silva, *U.S. Patent* 6,214,235B1 (2001).
172. J.M. Silva, *U.S. Patent* 6,103,092 (2000).
173. *Amberlite IRC-718*, brochure, Rohm & Haas Co., Philadelphia, PA (1998).
174. W.J. Blogoslawski, C. Brown, W.W. Rhodes, and M. Broadhurst, *Proceedings, First Symposium on Ozone for Water and Wastewater Treatment*, Cleveland, OH (1975).
175. B. Wang, J. Tran, J. Yin, and G. Shi, *Ozone Sci. Eng.* **11**, 227 (1989).
176. S.H. Lin and C.L. Wu, *J. Environ. Sci. Health* **A30**(7), 1445 (1995).
177. V. Janda and J. Rudovsky, *J. Water SRT-Aqua* **43**, 120 (1994).
178. L.D. Benefield, J.F. Judkins, and B.L. Weand, *Process Chemistry for Water and Wastewater Treatment*, Prentice Hall, Englewood Cliffs, NJ (1982).
179. J.C. Morris and R.A. Isaac. In R. Jolley *et al.* (eds), *Water Chlorination*, vol. 4, Ann Arbor Science Publ., Ann Arbor, MI (1983), Chap. 2.
180. J.B. Bratcher, Nitrogen Compounds in Brine and their Fate, *43rd Chlorine Institute Plant Operations Seminar*, Houston, TX (2000).
181. A. Harahambous, E. Maliou, and M. Malamia, *Water Sci. Tech.* **25**, 139 (1992).
182. M.P. Bernal and J.M. Lopes-Real, *Bio-Resour. Technol.* **43**, 27 (1993).
183. J. Koon and W.J. Kaufman, *J. Water Pollution Control Fed.* **47**, 448 (1975).
184. M. Gespard and A. Martin, *Water Res.* **17**, 3 (1983).
185. C.W. Williford, W.J. Reynolds, and M. Quinos, *Appl. Clay Sci.* **6**, 277 (1992).
186. S.H. Lin and C.-L. Wu, *Ind. Eng. Chem. Res.* **35**, 353 (1996).
187. Th. El-Nabaraway, G.A. Fagal, and L.B. Khalil, *Adsorp. Sci. Technol.* **13**, 7 (1996).
188. A.M. Youssef, M.R. Mostafa, and E.M. Dorgham, *Bull. Soc. Chim. Fr.*, (November–December) 741 (1989).
189. G.B. Wickramanayake, S.K. Khabiri, and E.J. Voudrais, *43rd Purdue Industrial Waste Conference Proceedings*, Lewis Publications, Inc., Chelsea, MI (1989), p. 407.
190. W.V. Collentro and A.W. Collentro, *Patent Appl. US* 95-512108 (1995).
191. M.J. Semmens, D.M. Foster, and E.L. Cussler, *J. Memb. Sci.* **51**, 127 (1990).
192. S. Bruckenstein, *U.S. Patent* 4,415,282 (1979).
193. S.D. Fritts, T.V. Bommaraju, and W.W. Ruthel, *U.S. Patent* 5,215,632 (1993).
194. A. Hanneuse and L. Chiti, Improvements in Brine Quality: Removal of Bromide, Iodide and Chlorate. In S. Sealey (ed.), *Modern Chlor-Alkali Technology*, vol. 7, Royal Society of Chemistry, Cambridge (1998), p. 157.
195. T.H. Hutchinson and D.J. van Wijk, Bromate and Chlorate—Evaluation of Potential Effects in Aquatic Organisms and Derivation of Environmental Quality Standards. In S. Sealey (ed.), *Modern Chlor-Alkali Technology*, vol. 7, Royal Society of Chemistry, London (1998), p. 26.
196. ANSI/NSF 60-2001, Issue 16 (revised), Chapter 6, *Disinfection and Oxidation Chemicals*, National Science Foundation, Washington, DC (2001).
197. H. Shiroki, *U.S. Patent* 4,483,754 (1984).
198. M. Pourbaix, *Atlas of Electrochemical Equilibria in Aqueous Solutions*, Pergamon Press, New York (1966), p. 614.

199. T.V. Bommaraju, Unpublished Results (2002).
200. P.A. Lyday, Iodine and Iodine Compounds, *Ullmann's Encyclopedia of Industrial Chemistry*, **A14**, 381 (1989).
201. A. Lauterbach and G. Ober, Iodine and Iodine Compounds. In *Kirk-Othmer Encyclopedia of Chemical Technology*, 4th ed., vol. 14, John Wiley & Sons, Inc., New York (1995) p. 709.
202. Data submitted by G.M. Shannon, INEOS Chlor Ltd. (2002).
203. J.T. Keating, E.I. DuPont de Nemours & Co., Inc., Personal Communication (2004).
204. *Nafion® Technical Information Bulletin 91-08*, E.I. DuPont de Nemours & Co., Inc., Fayetteville, NC (undated).
205. D.T. Hobbs and M.A. Ebra, *Electrochemical Engineering Applications*, AIChE Symposium Series **254**, vol. 83, American Institute of Chemical Engineers, New York, NY (1987).
206. S.H. Lin and Y.L. Yen, *Environ. Technol.* **18**, 65 (1997).
207. S.H. Lin and C.L. Wu, *J. Environ. Sci. Health* **A30**(7), 1445 (1997).
208. T.F. O'Brien, Dechlorination of Brines for Membrane Cell Operation. In N.M. Prout and J.S. Moorhouse (eds), *Modern Chlor-Alkali Technology*, vol. 4, Elsevier Applied Science, London (1990), p. 251.
209. M.S. Sherrill and E.F. Izard, *J. Am. Chem. Soc.* **53**, 1667 (1931).
210. T.R. Bott and S. Schulz, *J. Appl. Chem.* **17**, 356 (1967).
211. N. Yokota, *Chem. Eng. Jpn* **22**, 476 (1958).
212. N. Yokota, Ph.D. Thesis, Kyoto University (1958).
213. N. Yokota, *Soda to Enso* (Soda and Chlorine), **9**, 495 (1958).
214. N. Yokota, *J. Inst. Chem. Engrs. (Jpn)*, **23**, 438 (1959).
215. N. Yokota, *J. Inst. Chem. Engrs. (Jpn)*, **25**, 171 (1961).
216. F. Hine and N. Yokota, Abstract No. 119, Electrochemical Society meeting, Cleveland, OH (1996).
217. S. Bengston and I. Bjerle, *Chem. Eng. Sci.* **30**, 1429 (1975).
218. R.L. Miron, Removal of Aqueous Oxygen by Chemical Means, *International Corrosion Forum*, Atlanta, GA (1979).
219. G.C. White, *Handbook of Chlorination*, Van Nostrand Reinhold, New York (1972), pp. 343–347.
220. H.F. Johnstone, H.J. Read, and H.C. Blankmeyer, *Ind. Eng. Chem.* **30**(1), 101 (1938).
221. P.J. Durrant and B. Durrant, *Introduction to Advanced Inorganic Chemistry*, John Wiley & Sons, Inc., New York (1970), p. 855.
222. M. Schmidt and G. Talsky, *Angew. Chem.* **70**, 312 (1958).
223. S.L. Bean, Thiosulfates. In *Kirk-Othmer Encyclopedia of Chemical Technology*, 4th ed., vol. 24, John Wiley & Sons, Inc., New York (1997), p. 51.
224. *Water Treatment Uses and Application—Dechlorination*. Allied Corporation product bulletin, Syracuse, NY (1985).
225. D. Mannig and G. Scherer, Hydrogen Peroxide in the Chlor-Alkali Industry, *30th Chlorine Institute Plant Operations Seminar*, Washington, DC (1987).
226. *Technical Data Sheet: Storage and Handling of Hydrogen Peroxide*, Solvay Interlox, Inc., Houston, Tx (2000).
227. *Technical Data Sheet: Materials of Construction for the Storage of Hydrogen Peroxide*, Solvay Interlox, Inc., Houston, Tx (2001).
228. J. Mackenzie, *Chem. Eng.* **97**(6), 84 (1990).
229. B.G. Martin and P. Kiser, reproduced from *Industrial Water Treatment* **26**(6) (1994).
230. G.W. Ayling and H.M. Castrantas, *Chem. Eng.* **88**(24), 79 (1981).
231. D.G. Hager and M.E. Flentje, *J. AWWA* **57**, 1440 (1965).
232. V.L. Snoeyink and M.T. Suidan. In J.D. Johnson (ed.), *Disinfection—Water and Wastewater*, Ann Arbor Science Publ., Ann Arbor, MI (1975).
233. G.M. Forster, Brine Dechlorination by Activated Carbon, *29th Chlorine Institute Plant Operations Seminar*, Tampa, FL (1986).
234. V. Magee, *Proc. Soc. Water Treatment and Examination* (England) **5**, 17 (1956).
235. M.T. Suidan, V.L. Snoeyink, and R.A. Schmitz, *Environ. Sci. Technol.* **11**, 785 (1977).
236. D.L. Caldwell, Catalytic Destruction of Hypochlorite in Chlorine Plant Effluents, Abstract No. 441, Electrochemical Society meeting, Seattle, WA (1978).
237. J.R. Hodges, K-Cat Process for Brine/Water Dechlorination, *30th Chlorine Institute Plant Operations Seminar*, Washington, DC (1987).

238. P.E.J. Abbott, M. Carlin, M.E. Fakley, M.E. Hancock, and F. King, ICI "Hydecat" Process for the Catalytic Destruction of Hypochlorite Effluent Streams. In T.C. Wellington (ed.), *Modern Chlor-Alkali Technology*, vol. 5, Elsevier Applied Science, London (1992), p. 23.
239. E.H. Stitt, F.E. Hancock, and K. Kelly, New Process Options for Hypochlorite Destruction. In J. Moorhouse (ed.), *Modern Chlor-Alkali Technology*, vol. 8, Blackwell Science, Oxford (2001), p. 315.
240. *Soda Handbook 1998*, Japan Soda Industry Association. Tokyo (1998), p. 177.
241. P.M. Mayo, Conversion of Mercury-Cell Plants to Membrane-Cell Technology, *36th Chlorine Institute Plant Operations Seminar*, Washington, DC (1993).
242. R. Rodermund, *Chlorate Destruction in the Brine System of a Chlor-Alkali Electrolysis Plant*, Dissertation, University of Dortmund (1983), pp. 58 *et seq.*
243. Y. Samejima, M. Shiga, T. Kano, and T. Kishi, *U.S. Patent* 4,643,808 (1987).
244. S. Sarangapani and T.V. Bommaraju, Unpublished Results (1999).

8

Cell-Room Design

8.1. INTRODUCTION

In their design and construction, electrochemical plants differ from ordinary chemical plants in several ways:

1. by the major importance of electrical supply and its conversion to direct current;
2. by the fact that the electrolyzers and the fluids they contain are parts of electrical circuits;
3. by the unique considerations that apply to the electrolysis area.

Bihary [1] lists the principal factors that must be considered in order to arrive at a safe and efficient cell-room design:

General design parameters

- Location of cell room
- Wind direction
- Cell line and cell room exits
- Defined cell line working zone

Instrumentation

- Process indicators and alarms
- Automatic rectifier trips
- Manual rectifier stop-buttons
- Circuit neutral point detection and alarm

Equipment and Systems

- Emergency safety equipment
- Communications system
- Fire-fighting equipment
- Eye wash stations and safety showers
- Advisory signs
- Thermal and electrical insulation and guards
- Grounding electrodes in process streams
- Personal protective equipment
- Boot and glove testing

Procedures

- Defined operating and maintenance procedures
- Extensive training
- Guidelines for work inside cell line.

While this list does not include ergonomics as a separate item, such considerations are shown to affect all parts of design.

Safety systems and protective equipment are covered in Chapter 16. The present chapter discusses buildings, electrical systems, piping, control systems, auxiliaries such as the equipment used to transport electrolyzers and their components, and the hazards associated with cell rooms.

8.2. BUILDING CONSIDERATIONS

First we consider the installation and housing of electrolyzers. We address very briefly the comparative advantages of indoor and outdoor installation of electrolyzers and then turn to the characteristics of buildings and the arrangements appropriate to the various types of cell. A description of some of the design considerations of the cell line working zone, especially those related to electrical safety, follows. Building ventilation is then considered separately, with mercury-cell installations as a special case.

8.2.1. *Outdoor vs Indoor Installation*

The natural inclination to refer to an electrolyzer installation as a “cell room” reflects the fact that most cells are located inside buildings. There are advantages to locating cells outdoors, however. Besides the obviously lower cost, these include greater opportunities for emergency escape from the area, the dissipation of minor releases of gas, and the cooler temperatures that result from unconfined ventilation. Outdoor construction makes it easier to limit ceiling concentrations of chlorine vapor and to reduce worker heat stress [2].

The chief problem with outdoor installation is the exposure to weather, especially in a cold climate. A building not only protects workers from exposure to the weather, it also shields equipment from sun, rain and snow (with their thermal shock), sand and dust storms, and corrosion. The protection offered by a building slows the natural process of deterioration of system components and helps to avoid foreign deposits that can allow short-circuiting of cell connections.

Diaphragm cells are the most amenable to outdoor installation. They have a high ratio of liquid mass to exposed surface area. This and the use of nonmetallic cell covers, and sometimes non-metallic bodies, make them less susceptible to thermal shock. At the same time, the electrode connections are more massive and less likely to be short-circuited by atmospheric deposits.

8.2.2. *Electrolyzer and Building Arrangements*

A “building” may be anything from a substantial structure with four full walls and a roof to something little more than a lean-to that provides some measure of protection from sun and rain.

In a building, floors should be designed for easy drainage of spills and wash water. They can be sloped and provided with drainage channels. Floor slopes ($\geq 2\%$) are greater than in ordinary process building design. Impervious coatings with good chemical resistance are recommended. Many plants use epoxies, silicones, or organic drying oils. Epoxy screeds, 3–6 mm thick, afford extra protection where traffic is heavy. A recent alternative, especially useful in sumps and trenches, is thermoplastic sheet stock attached to the concrete. For good service, this requires welded seams and spark testing for faults.

Concrete should not be relied upon as an electrical insulator. Reinforcing bars should be coated with, for example, epoxy resin. They should not be connected to building steel and should not be allowed to form a continuous path along the length or the width of the building. The joints between sections of precast reinforced concrete should be insulated.

Walls should be nonconductive and located to allow safe access to cell lines. If maintenance must be performed between the cells and a wall, clearances must be adequate and most of the provisions that apply between rows of cells also apply here. Grounded conductive columns must be placed far enough from anything attached to a live circuit to prevent simultaneous contact by a person, or they must be covered with good, impact-resistant insulators to a sufficient height (about 2.5 m above the floor or platform level). In many cases, full walls are not provided, but partial sidewalls give some weather protection at the operating level.

Structural steel requires protection from corrosion. Standard primers covered by polyamide or amine-cured paints are frequently used. Walkways should be nonconductive and not slippery. Fiber reinforced plastic (FRP) grating is a standard here.

Electrolyzers may be elevated or installed at grade. Diaphragm cells, with their large and deep masses of contained electrolytes, are very heavy, and their weight must be supported over a relatively small area. They are always installed at grade, perhaps supported on concrete plinths. It is customary to install mercury cells in an elevated structure. Switches and decomposers then can project or be located below the cells. Membrane cells are an intermediate case, and both arrangements exist. The more complex arrangement of intercell conductors and switching connections sometimes accounts for the installation of monopolar membrane electrolyzers at an elevation. There may be other considerations as well, and the relatively light weights of some membrane electrolyzers then make it easier to install them on an elevated structure. The ability to provide gravity rundown of electrolytes into collecting tanks without digging pits is one such consideration. This proved especially valuable in a plant on estuarial water with an inefficient sewer system that backed up during every high tide.

A cell room roof should not prevent the escape of vented hydrogen from the area. In an enclosed building, the roof is usually designed to provide gravity (natural draft) ventilation of the whole cell room (Section 8.2.3), incidentally providing a solution to this problem. The possible presence of hydrogen is an important consideration in the electrical rating and design of the building (Section 8.5.1.1).

Since the cell room is a likely source of chlorine release, it should be located with due regard to prevailing winds and ground-level wind patterns. The building and the cell lines both must have efficient escape routes and easy access to a safe haven where personnel are protected from emissions.

8.2.2.1. Diaphragm Cells. Diaphragm cells, as noted above, are installed at grade. The need for access to remove and install intercell conductors determines the spacing between

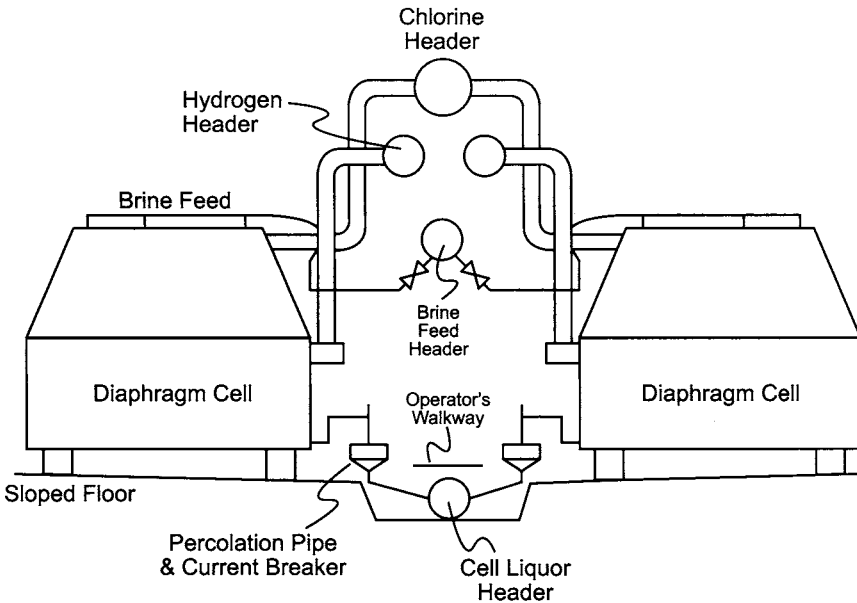


FIGURE 8.1. General arrangement—diaphragm cells.

cells. The usual piping header arrangement has the chlorine and hydrogen overhead and the brine and catholyte (or cell liquor) below. Operator access to two rows of cells is by a raised central walkway, and the header piping runs above and below this walkway. Figure 8.1 shows a typical arrangement.

It is possible to run one header for each service to cover both rows of cells. It is common practice to do this for the gases. A frequent variation, included in Fig. 8.1, is to run two separate hydrogen headers (usually carbon steel), which can serve as structural supports for the saddles that hold a single chlorine header (usually FRP). Liquid headers more frequently are installed in pairs. One reason for this is the reduction of leakage currents, which are the topic of Section 8.3.2.2.

Spaces between rows of cells must be wide enough for safe personnel access. The electrical potential between opposite cells can be quite high, and it should be impossible for operators to be in simultaneous contact with two of them. The minimum spacing is 2 m; many cell rooms provide more space. The outboard side of the cell rows is used for handling and transportation of cells. Renewal of a cell requires isolating it from the circuit, removing the conductors attaching it to adjacent cells, removing it from its berth, and transporting it to the renewal area. The reverse operations with a rebuilt cell restore the circuit to operation. There must be room for a short-circuiting switch to be placed outside the cell line. Then the designer must supply access for a cell room crane above and beside the line. It is customary to move cells into and out of the renewal area on a simple cart that is pushed or pulled by a utility vehicle.

The Glanor[®] electrolyzer is a very large bipolar diaphragm type. It has many unique features, and some of these are described in Section 5.4.1. The entire assembly, measuring

5 × 3.3 m on the base and 3.7 m high [3], is removed from its berth and transported by rail to the cell renewal area. These electrolyzers are installed in two different, mirror image, orientations. At some point in the process of removal, renewal, and reinstallation, an electrolyzer may have to be turned. The cell renewal area may include a roundtable at the end of the rail line for this purpose.

8.2.2.2. Mercury Cells. Most mercury cells are monopolar, have high current capacities, and occupy large floor areas. Cell bases are permanently installed, along with individual switches between cells. Maintenance work on a cell base requires switching the cell from the circuit and draining the mercury. The stringent safety and hygienic precautions required in the latter operation are not part of the subject of building design.

A mercury cell has a number of anodes whose length matches the width of the cell. These are individually supported and adjusted from above. They can be removed and replaced individually or in groups by an overhead crane. Space requirements between rows of mercury cells are similar to those that apply with diaphragm cells. In addition, there is a need for operator and maintenance access along the length of each cell. Most cell rooms have walkways along the length of the cells to provide this access. There is no similar requirement for maintenance access and transport beyond the cell line, because the cell body itself is not moved. The disadvantage corresponding to this is that the capacity of a cell switched out of the circuit cannot be replaced during renewal work other than by providing excess rectifier capacity and increasing the current density on the operating cells.

Mercury cells often form a U-shaped circuit with turnaround bus at the end opposite the rectifiers. Because of their geometry, it is also common practice to install a single row of cells and to provide simple return buswork from the end of the row.

The usual arrangement (Fig. 8.2) has the cells installed on the second level of a building. All piping headers and switch connections are below the cell line. This makes it possible to provide walkways and access above the cells for cranes and personnel.

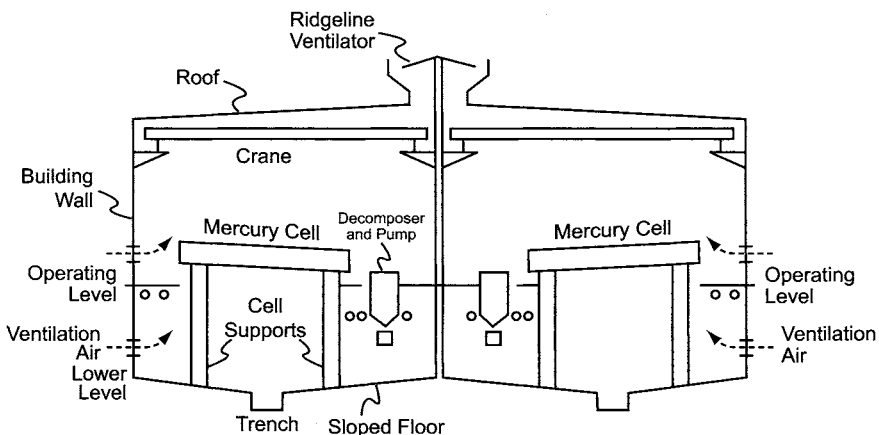


FIGURE 8.2. General arrangement—mercury cells.

In addition to piping for feed brine and the three products of electrolysis, mercury cells require a header for depleted brine. They may not require such wide maintenance access beyond the cell rows as do diaphragm cells, but there must be sufficient room for operator access and installation of piping at both ends. Brine and mercury flow across the long dimension of the cells. Feed brine enters at one end and depleted brine leaves the other. Amalgam enters the decomposer after separating from the depleted brine in the outlet end box of the electrolyzer. With some designs, a vertical decomposer and a mercury-return pump are located at the amalgam outlet. Other types of cell use horizontal decomposers, and in either case the mercury returns from the outlet end to the feed end through a conduit running the length of the cell on the underside.

Into the 1960s, wood floors were commonly used in mercury cell rooms [4]. This would now be unacceptable. Wood absorbs mercury, preventing efficient mechanical cleanup and slowly releasing the metal as vapor [5]. Other aspects of building design should also reduce the probability of accumulation of mercury and make its removal easier. For example, horizontal beams can be rounded on top and rectangular trenches can be replaced by swales with round contours [6].

8.2.2.3. Membrane Cells. Membrane electrolyzers are more diverse in their design. Some are installed at grade and some are elevated. Some are maintained in place, and some are removed whole for maintenance in a central renewal area. The large bipolar types are those most likely to have permanently installed frames from which individual components or sections are removed for repair. These require shutdown of at least some part of the electrolyzer for replacement of components. The description of the various technologies in Chapter 5 shows how the issues of maintenance turnaround time and loss of production are addressed. Some designs require space beside the electrolyzer for serial handling of components; others allow the replacement of any number of single elements, which are essentially self-contained cells.

Bipolar electrolyzers can be isolated from the alternating current (AC) side or by direct current (DC) disconnect switches and do not always require portable switches or jumper bus. While not strictly required, the latter may be used to allow one modular zone of an electrolyzer to be taken out of service while the rest stays in operation. This is in the interest of reducing the loss in production during replacement of cells. The large capacity of individual bipolar electrolyzers means that relatively few units are installed. Taking an entire electrolyzer out of production may cause a significant drop in output.

Monopolar electrolyzers, as a rule, have much smaller individual capacities than the bipolar type. Removal of one electrolyzer from a cell line then usually has only a small effect on production. The increase in working amperage of the other cells required to offset this loss is correspondingly small. We should note that certain designs, because of their switching arrangements or mounting and buswork attachment, may require the removal of two cells or electrolyzers from the live circuit. The logic otherwise prevails.

Monopolar cells require shorting switches (Section 8.4.3.1) so that individual cells can be removed and then replaced without shutting down their circuit. In very small plants, there is an argument for designing a plant without switching facilities. This saves not only the cost of the switch, but also of the building area required for maintenance

access. Along with the variety of cell designs comes a variety of switching arrangements. Switches may be located to the side of the cell row, as in the diaphragm-cell case, with the cell being raised or lowered for removal. They may also be moved by crane or transport vehicle into position above or below the cell line.

8.2.2.4. Cell Line Working Zone. Operators must perform many of their routine duties in close proximity to the cells, and many maintenance activities also take place while the circuit is energized. Many ordinary design precautions do not apply inside cell installations. The entire line, for example, cannot be enclosed and isolated as are the transformers and rectifiers. This approach would trap gases and heat and make some of the necessary manual operations impossible. There is, instead, a collection of practices that apply in what is referred to as the “cell line working zone” (CLWZ).

The CLWZ is defined in one standard [7] as “the space envelope where operation or maintenance is normally performed on or in the vicinity of exposed energized surfaces of electrolytic cell lines or their attachments.” It extends, by definition, close to 2.5 m (8 ft) above and below live surfaces of the cells or attachments and 1.1 m (3.5 ft) horizontally from the envelope just defined. It is taken not to extend through walls, roofs, floors, partitions, or the like.

The best designs keep electrical apparatus out of the cell line working zone whenever possible. Otherwise, it is possible to expose the cells to an external source of energy and bring them up to its voltage. Similarly, cell line voltages can be transmitted to systems outside the CLWZ. Mercury pumps are the prime example of equipment that, from a practical standpoint, must be placed within the zone. They must be attached to the cells or decomposers. Each pump should have an isolating transformer with a grounding screen between the primary and secondary windings.

If safety showers are present within the working zone, they should be kept at least 2 m away from cells. The showers, piping, and valves should be nonmetallic. There should be some means of containing the splash, and water should be drained immediately from the zone.

Exposed live surfaces do not in themselves present a dangerous situation. The hazard is related to current flow through the body, and that is a function of the voltage (but not of the current) on the cell line and the resistance of the path through the body. The first line of defense against dangerous contact is the excellent insulating properties of air. Clearances provide safety, and cell-room design should provide adequate spacing between elements. Slipping and tripping hazards should be eliminated. The technique of isolation of a circuit from the ground, while successful in common AC systems, is usually ineffective because leakage currents through pipes, metalwork, and conductive fluids are great enough to provide a ground. Spills inevitably occur, and conductive liquids can short out insulation and provide paths to the ground even when nonmetallic pipe is in use. Similarly, automatic ground fault protection has limited potential. If set at a level low enough to protect the body, it will not be able to handle the leakage currents. Section 8.5.1 has more information on hazards in the working zone and the rest of the cell room. Section 16.4.1 discusses personal protective equipment. The Chlorine Institute publishes a pamphlet [8] that is a good source of information and also provides a safety checklist. It is not restricted to the CLWZ.

8.2.3. Building Ventilation

The operating temperature of some electrolyzers is close to 100°C, and buswork temperatures are similar. The total amount of heat generated in a cell room by convection and radiation therefore is quite large. Besides the high temperatures of process fluids and equipment, the thermal hazards in the cell area may include prolonged exposure of personnel to high ambient temperatures. Summertime cell room temperatures in hot climates can reach 50°C. This fact is a major consideration in the decision to place a cell “room” outdoors. When the cells are placed in a building, the heat is removed by ventilation.

In some cases, as when a cell building is surrounded by other buildings, forced ventilation is necessary. In most installations, the cell building is placed to allow better natural ventilation. Gravity ventilation is a convenient, low-energy method for enclosed spaces in which there is a high rate of heat generation. In many industrial situations, the heat output occurs over a small area, and a localized ventilator is sufficient for the duty. This may be assisted by small ventilators distributed around the building. The situation in a chlorine cell room is different. Heat is generated essentially along the entire length of the building. Peaked roofs with gravity ridgeline ventilators then are common and provide instant identification of a cell room from outside the plant. A continuous ventilator running the length of the cell room is best. Desirable features are:

1. straight-line, unimpeded air flow into ventilator
2. top cover to shed rain and snow
3. bird screens
4. means to restrict flow in colder weather
5. wind resistance to match local project criteria
6. corrosion protection of hardware.

Galvanized steel, FRP, carbon steel, and aluminum are the standard materials of construction. The metals may also be coated with a polymeric film, typically polyvinylidene fluoride (PVDF). Copper, stainless steel, and other alloys formulated for weather resistance are also used. The top cover normally is adequate only for weather protection; it has no structural strength and so is suspended by attachment to the ventilator sections. The capacity of the ventilator should be set in the early stages of plant design. This may be expressed as the number of air changes in a unit time or as a volumetric rate of flow, and it should be consistent with general project criteria while at the same time meeting the specific requirements of the cell area. It would be a mistake to try to generalize and choose an appropriate number of air changes per unit time for all cell rooms. The productivity of the various cell designs and the volume of building required for a given capacity vary far too much to allow that.

The rating of a ventilator usually is in terms of linear exhaust velocity or air flow rate per square meter of ventilator area. This is a number supplied by the manufacturer. It depends strongly on temperatures and wind speed. A typical rate might give an upward air velocity of 15 m min⁻¹. In addition to or instead of dampers in the ventilator(s), the walls of the building are often supplied with adjustable louvers.

During design, calculation of the heat flux from an electrolysis unit from the laws of heat transfer would be an extremely difficult task. Designers therefore should rely on previous experience or data supplied by the cell technology supplier. In a cell room that is already operating, heat lost to the environment can be back-calculated from the

temperatures, compositions, and flowrates of the streams entering and leaving the cell room. Given a rate of heat generation and a design basis for the outside temperature, one can then calculate the air flow required to maintain a given average temperature in the cell room. When choosing this temperature, designers should consider the fact that the temperature in the working area around the cells is higher than the average. If taking credit for the heat removed by transfer to the environment through the building structure, they should also remember that the temperature at the building walls (and therefore the driving force for heat transfer) is lower than the average. Finally, the temperatures at the roof and floor levels may differ. The design engineer must consider this fact in setting a maximum allowable roof-line temperature. With the good practice of allowing an intake area at least 50% greater than the exhaust area, the temperature differential may be about 1°C per meter of height between the intake and ventilator throat [9].

Good ventilation also dissipates any release of hydrogen. Because of its great buoyancy, hydrogen is easily dispersed and tends not to accumulate to dangerous concentrations at cell level. Another reason for open-roof ventilation is the removal of hydrogen from the cell building. Cell-room areas usually are not electrically classified, but designs often use special light fittings (e.g., EX(e) grade) and prohibit electrical contacts near the roof.

In mercury-cell plants, the ventilating air itself can be a source of mercury emission. The air used to ventilate the end boxes that seal the feed and overflow at each cell is an especially rich source of mercury. Established practice now is to limit these flows and collect and treat any air that escapes the end-box system. This change alone has done much to reduce average air emissions.

Treatment of the ventilation stream for the entire building is not feasible in the usual case of gravity ventilation. While mitigation efforts have been very successful when applied to other sources, there have not been the same large reductions in the amount of mercury released with building ventilation air. This has become the primary source of emissions. Section 16.5.5.2 has more details.

8.3. ELECTRICAL SYSTEMS

The part of the electrical supply system of direct relevance to cell-room area design is that involved in the provision of direct current to the cells. This section covers the transformers, rectifiers, and buswork that handle that duty. Transformers do not provide direct current (DC), but they are included because of their intimate association with rectifiers. The transformer–rectifier installation is usually adjacent to the cell room but in a physically isolated area. Design, operation, and maintenance of these systems are all matters for specialists. This book does not discuss these subjects. Standard publications [10] cover them in detail, along with the extensive instrumentation and control systems that are necessary.

8.3.1. *Supply of Direct Current*

8.3.1.1. *Transformers.* Electricity is transmitted as alternating current (AC) largely because of the ease with which one can change its voltage. Transmission is most economical at high voltage, but lower voltages are more suitable for generation, distribution,

and use. Transformers are essentially simple devices that can change voltage from one level to another, up or down. They are highly reliable, and there is a tendency to install them and forget them. An old survey of megawatt transformers [11] showed that there were 76 failures per 10,000 transformer-years. Even with an average outage of 253 hr, the average transformer was inoperative for less than 2 hr per year. The fact that this is a very small number would be of little comfort to a plant facing an outage of a few months to rebuild a seriously damaged transformer. Transformer design and maintenance procedures therefore should follow the best industry recommendations (e.g., IEEE Standard 242). Because of the high reliability and the high cost of large transformers, it is normal practice in the chlor-alkali industry not to install major spare capacity. In other industries, such as aluminum smelting, the opposite holds true [12].

Transformers depend on the phenomenon of mutual inductance. One way to produce a current in a conductor is to move it through a magnetic field. Varying the field around a stationary conductor produces the same effect. The reciprocal effect is that when an electric current flows, it produces a magnetic field around its conductor, and an alternating current produces a field of varying strength. The changing field strength then causes an electromotive force (emf) to be generated, or *induced*, in the conductor. This is the phenomenon of self-induction. The emf is proportional to the rate of change of the field strength. For practical application, forming the conductor into a coil increases the emf. If the flux produced by each turn in the coil cuts every other turn, the resulting emf is greater in proportion to the number of turns.

If a coil such as that imagined above carries an alternating current, and if a second coil is placed alongside, a varying electromagnetic field is produced in the second coil as well as in the first. A current then flows in the second coil if it is not open-circuit. This is the phenomenon of mutual inductance, and it is the basis of the transformer.

We shall call the coil to which the alternating voltage is applied the “primary” coil and the other coil within its magnetic field the “secondary” coil. The voltage V_1 applied to the primary causes an exciting current I_0 to flow and to produce the magnetic flux ϕ , which is proportional to the number of turns in the coil. Barring losses, the same flux is present in the secondary coil. The voltage produced in the secondary, V_2 , is proportional to its own number of turns. The basic equation for an ideal transformer becomes

$$V_1/V_2 = N_1/N_2 \quad (1)$$

where V_1 and V_2 are the applied and induced voltages, respectively and, N_1 and N_2 are the numbers of turns on the primary and secondary coils.

If the secondary coil is connected to a load, a current I_2 flows in the load and a corresponding current I_1 flows in the primary coil. Since energy is conserved, the current transformation ratio is the inverse of the voltage transformation ratio:

$$I_2/I_1 = N_1/N_2 \quad (2)$$

The total supply current to the transformer is in fact $I_0 + I_1$, but I_0 normally is small enough to be ignored.

Practical transformers use cores with numerous steel laminations to transmit the magnetic field between coils. Figure 8.3 shows this schematically. Equations (1) and (2) are based on the ideal situation with no energy loss and no reactive impedance. The latter does not directly increase energy loss, but when a load current passes through the transformer it does result in the voltage at the output terminals being lower than the induced voltage V_2 . In the real case, there will also be resistance losses in primary and secondary leads and windings (copper losses) and hysteresis and eddy current losses in the core (iron losses). Iron losses tend to be constant at a given operating voltage, while copper losses vary with the square of the load current. Transformer efficiencies are nevertheless quite high. In the large units typical of chlor-alkali plants, efficiencies are greater than 98%.

Single-phase transformers can be grouped in several different ways in a three-phase system. Figure 8.4 shows the so-called Y- Δ configuration. On the Y-side (or wye side), all three coils have a common connection; they can also be shown schematically as the three legs of the letter Y. The “wye” designation is common in the United States. In certain other parts of the world, this arrangement is referred to as the “star” connection. On the delta side, there is no common connection of the three phases. Each element connects at its opposite ends to the other two elements. In the schematic representation of this arrangement, the coils are connected to form the Greek letter Δ .

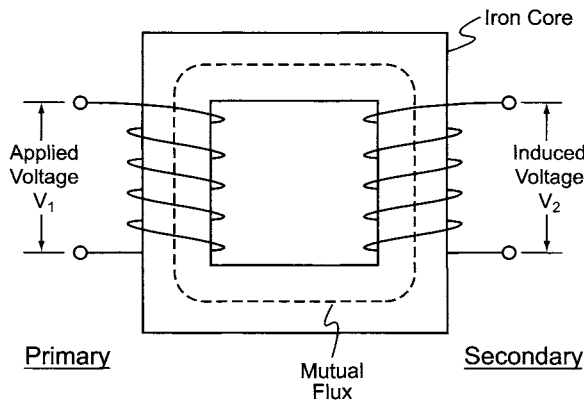


FIGURE 8.3. Simple transformer.

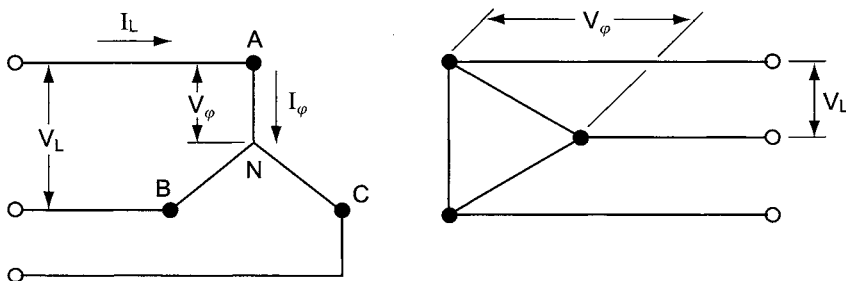


FIGURE 8.4. Wye-delta transformer configuration.

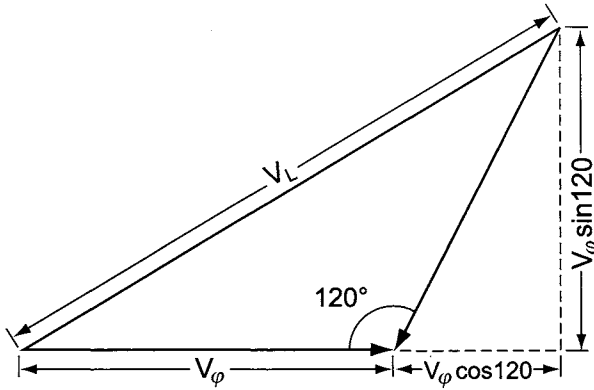


FIGURE 8.5. Vector combination of phase voltages.

In the wye arrangement, we can visualize current flowing between lines that are connected through each leg of the circuit and the common junction. Each phase current then flows from a line to the neutral point and so is equal to the line current. The voltage between two line connections is equal to the vector difference between the phase voltages (which are opposite in sign). Figure 8.5 summarizes the situation. Two equal phase voltages are separated by 120°. Each phase has the voltage V_ϕ and the resulting line voltage is V_L . The line voltage has x and y components V_x and V_y . These are the sums of the resolved components of the two phase voltages:

$$V_x = V_\phi + V_\phi \cos(120) = 1.5V_\phi$$

$$V_y = V_\phi \sin(120) = \sqrt{3}/2V_\phi$$

Combining these, we have $V_L = \sqrt{3}V_\phi$.

In the Δ -arrangement, phase voltages and line voltages are equal. Each line current is equal to the vector difference between the currents in the two phases to which the line is connected, and so in this case the line current is equal to $\sqrt{3}$ times the phase current. With either arrangement, the power output is the same for a given phase angle:

$$P = \sqrt{3}E_L I_L \cos \theta \tag{3}$$

where P is the power, E_L the line voltage, I_L the line current, and θ the phase angle between voltage and current.

The choice of either of two arrangements on both the primary and secondary gives four possibilities in a transformer. The wye–delta connection is a common one in chlor-alkali plants, as it is in many industrial installations. It is favored in step-down transformers partly because of the neutral connection that is available and the consequent relative ease of grounding the high-voltage side. For the same reason, the delta–wye hookup is common in step-up transformers.

When installing multiple transformers in parallel, one must ensure that their impedances are equal. If this is not so, sharing of the load is unequal and there will be circulating currents between adjacent transformers. These currents directly result in a loss of efficiency, which can lead to early failure, faulty power metering, and a loss in reliability. In the special case of rectifier transformers, the current in each is dictated by the rectifier control systems, but if they have been given different phase shifts to minimize harmonic distortion (Section 8.3.1.3), it is again necessary to ensure that their impedances are equal.

8.3.1.2. Rectifiers

8.3.1.2A. *Types of Element.* Rectifiers are devices that allow the passage of current in only one direction. Thermionic emission of electrons, for example, is a one-way process and was the basis for vacuum-tube diodes. The cathode must be held negative with respect to the collector in order for electrons to flow. This explains the use of the word “valve” to describe what has been known in the United States as a “tube.”

If a diode’s source of power is an alternating emf, electrons can flow during only half the cycle. A simple diode with a single-phase AC supply voltage produces a series of half-waves separated by half-cycle intervals. A three-phase signal has no periods without current flow but is still extremely choppy. Adding a second element shifted 180° in phase from the first, for example in a second wye connection with reversed polarity, fills the gaps and produces full-wave rectification.

Semiconductor rectifiers contain at least two separate materials, a P-type and an N-type silicon semiconductor, joined together and held by conductors. With an alternating voltage across this combination, normally called a silicon diode, the electrons in the N-layer and the holes in the P-layer respond by moving in opposite directions. Figure 8.6 shows that during one half of the voltage cycle, the electrons and holes move toward the junction, and current flows. In the other half of the cycle, the electrons and holes move away from the junction, and current flow is impossible.

A thyristor rectifier uses four silicon semiconductors of alternating types in a pack. Figure 8.7 shows that without some outside influence the three junctions can not simultaneously be conductive. When the cathode side is negative, two junctions are conductive, but the center, or control, junction is not. Applying a current pulse to the interior P-layer neutralizes the bias in that layer and allows current to flow through the rectifier pack.

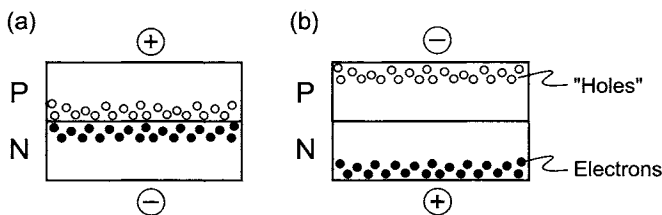


FIGURE 8.6. Operation of a silicon diode. (a) Current flows through junction. (b) No current flow.

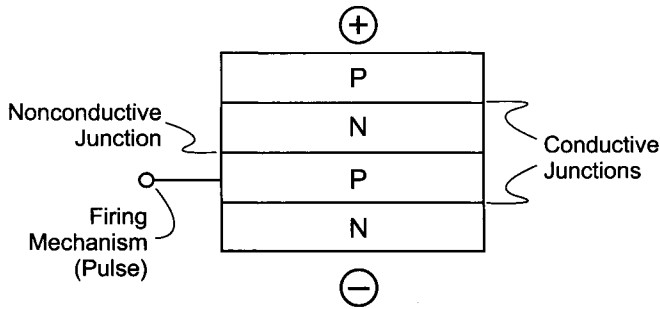


FIGURE 8.7. Operation of a thyristor rectifier.

Current flows until the voltage reverses, biasing the two outer junctions in the nonconductive mode. The time during which current flows in each cycle depends on the timing of the pulse applied to the control layer. This is designated by the point in the voltage cycle at which the firing pulse occurs. It is measured by the angular displacement of the pulse from the point of zero voltage and is referred to as the firing angle. A high firing angle means a longer delay before the control pulse is fired and therefore a shorter period of conduction, or in other words, less current flow.

8.3.1.2B. **Methods of Control.** Rectifiers are one component of a chlor-alkali plant whose design has improved greatly during the industry's history. From bulky, slow-acting, and inefficient mechanical units, through mercury-based systems, the industry has moved on to solid-state technology using silicon-based diodes and then thyristors. Most plant designers now prefer thyristors to diodes for new installations. Here, we consider both versions, but discuss only silicon rectifiers and ignore the older types.

On-load tap changers and saturable reactors control the output voltage of a diode system and hence control the current through the attached load. The saturable reactors are responsible for fine control but have limited range. Usually, they are installed in all power circuits, each one being connected to a power source that can drive it into saturation. The operator's controls effectively regulate the impedance of a reactor circuit. Zero control of the exciting current gives maximum impedance and minimum output current. Eventually, a change (say, an increase) in demand brings the tap changers into operation. When the operator calls for more current, a motor physically raises the transformer tap to the next level. The output voltage of the transformer increases, ultimately causing the DC output of the rectifier to increase. Tap changers are electromechanical devices and therefore have slower response, coarser steps, and greater maintenance needs than purely electronic devices. Unless their control systems are carefully designed, they can tend to hunt when operation is close to a limit of one of the taps. To minimize hunting problems, the control range of the saturable reactors should be equivalent to several times the size of a step in voltage by the tap changers.

The control of a thyristor unit, on the other hand, is applied to the rectifying elements themselves by varying the timing of the firing pulse. Action is much more rapid (one or two cycles, vs a number of seconds), and control is smooth over the entire range

of operation. The fast response of thyristors offers other advantages. When an operating electrolyzer is shorted out, for example, it limits the resulting momentary overcurrent in the line to a low level. Overcurrent protection during a transient short circuit is also simpler and more effective. A sudden drop in circuit impedance with a slow-acting current controller would allow a significant increase in line current. Thyristor control drops the output voltage very quickly and keeps the current within the surge limits of the rectifiers or any other preset level. Even faster response is possible with modifications to the design of thyristor-based devices. Section 17.3.2 discusses this subject.

8.3.1.2C. Other Design Considerations. A rectifier installation, whether diode- or thyristor-based, comprises a number of elements in each branch of the circuit. Normal practice is to provide redundant elements in every branch, so that failure of a single element will not reduce output. Failure of a second element will begin to overload the other devices if the total output is not reduced.

Rectifiers usually are installed, along with their transformers, in caged areas with strictly limited access. Enclosing the components protects them from dust and contaminated air. Operating inefficiencies, discussed below, generate waste heat, and so some form of cooling is necessary. Usually, the rectifying elements are supported on metallic heat sinks through which a coolant is pumped. Use of demineralized water in a closed circuit is common in modern systems, because the earlier oil cooling systems were fire hazards. Some rectifiers, usually those of small capacity, are cooled by forced circulation of air.

Special DC meters, described in Section 8.3.1.5, measure the output of the rectifiers. The control system uses this current measurement to adjust the voltage and so keep the output current constant.

The energy efficiencies of most rectifiers are less than those of transformers but still quite high. Even a small fractional loss of the power used by a cell room, however, is very expensive, and some of the basic choices made by cell-room designers influence the efficiency. Section 8.3.2.1 discusses some of these choices. In particular, that section shows that a low-amperage, high-voltage rectifier is cheaper and usually more efficient than one with the same power output but the opposite characteristics.

In a chlor-alkali plant, rectifier specifications are not set in isolation but are part of the larger question of circuit design. Rectifiers are matched with groups of cells or electrolyzers, and conversion efficiency often must be compromised in the interest of safety and an efficient cell layout. The following section discusses this further.

8.3.1.3. Rectifier Arrangement

8.3.1.3A. Current Variability and Harmonics. The function of a rectifier system is to convert a power supply received as alternating current into the direct current required by the cells. There may be a reduction in voltage through transformers prior to the rectifiers, but this is outside the scope of the present discussion. Within the rectifier system, there will be some reduction in voltage to match the varying demands of the

cell line. In the usual arrangement, the output voltage is continuously varied in order to maintain a constant current through the cells.

The rectifier(s) must do this job with high reliability, high efficiency, and minimum disruption to the external power supply. The last-named objective requires a high power factor, to avoid excessive transmission losses or burden to the supplier's kV A capacity, and an acceptably low feedback of harmonic currents into the power supply. The problem of low power factor and methods for its correction (in this case, installation of capacitor banks, dealt with in Section 8.3.2.3) are familiar subjects even to many nonelectrical engineers. The consideration of harmonic distortion of the waveform, which can cause distortions in the power grid voltages and interference with other customers' devices, is less so.

Nonlinear loads, of which electrochemical plant rectifiers are particularly troublesome examples, take current with a nonsinusoidal waveform. Analytically, one may consider that a rectifier injects currents of various harmonic frequencies (multiples of the supply frequency) into the supply system. These injected harmonic currents flow in the system impedances and so cause harmonic voltages, which are superimposed on the fundamental-frequency voltage of the power supply. From the injected harmonic currents and the harmonic impedances of the system, one can in principle calculate the extent of the harmonic voltage distortion produced by a rectifier installation. In practice, this is not so easy. The multiplicity of loads producing distortion in a given distribution system, including those outside the boundaries of the chlor-alkali plant, will have a variety of phase shifts, and it is not always clear at the design stage how the harmonic voltages due to a new load will interact with those due to existing loads. Furthermore, the supply system may have very different harmonic impedances under different system configurations, and it may have harmonic resonances that result in amplification. Harmonic voltages at remote parts of the system may become higher than the voltage at the point of connection of the distorting load.

The organization responsible for installation of the rectifier system, whether it be the operating company itself or an outside design contractor, probably will lack knowledge of the overall power supply situation. Therefore, most electric utility authorities will propose standard empirical methods for estimating the effects of a proposed new installation. In the final analysis, however, measurements must be made on the operating system. Harmonic filters can be installed to compensate for the problem, but in the real world it may later be found that these must be adjusted to cater for unforeseen conditions.

Most regulations include a limit on the total harmonic distortion voltage. The purpose of these limits is to safeguard the performance of electrical supply systems. Human safety issues are discussed in Section 8.5.1.2. Since measured AC voltages are root-mean-square values, the total harmonic voltage is the square root of the sum of the squares of the individual harmonics:

$$V_T = \sqrt{\sum_{n=2}^{\infty} V_n^2} \quad (4)$$

where V_T is the total harmonic distortion voltage and V_n the individual harmonic distortion voltages, second and higher. In practice, the summation is cut off at some reasonable value of n beyond which it is agreed there is a negligibly small contribution.

An efficient method for alleviating the generation of harmonics in the first instance is to increase the complexity of the rectifier arrangement in order to produce a more uniform current. While rectifiers produce direct current, "direct" should not be confused with "constant." A perfect diode that receives a single-phase AC voltage supply will faithfully reproduce the positive part of the voltage waveform and reject the other part (the reverse-voltage half). In the more practical case of full-wave rectification, the output voltage waveform will be successive positive halves of a sine wave, so that the rectifier produces two pulses of current from each cycle of the AC source. In the industrial case with a three-phase power supply, the rectifier therefore produces six pulses of current during each cycle. These pulses will be separated by 60° from each other. The output signal is the sum of the individual phase currents.

Because of the phase shifting and consequent overlap of the three waves, the six-pulse output is much smoother than the output of a single-phase system. In the latter, the maximum amplitude of the voltage, and hence also the current if the load is purely resistive, is 57% greater than the average. With six pulses, this difference, or current ripple, is reduced to about 4.7%. It will be obvious that further increase in the number of pulses will further reduce the current ripple.

Practically, lower current ripple results from production of more six-pulse signals, shifted in phase in order not simply to reinforce the first. This can be done by increasing the number of windings on a given rectifier transformer or by supplying multiple units. If we add a second transformer rectifier, identical to the first but phase-shifted by 30° , we will have a 12-pulse system. Replicating this once with the other units phase-shifted by $\pm 15^\circ$ or twice with the other units shifted by $\pm 10^\circ$ results in a 24- or 36-pulse system, respectively. The latter is perhaps the most complex rectifier arrangement commonly found in chlor-alkali practice. Table 8.1 gives the relative uniformity of output for the most important configurations. There is a useful reduction in current ripple in going from six to 12 pulses. There may still be a worthwhile improvement in going on to 36 pulses, but there is very little to be gained after that. This comparison is based on an ideal system in order to illustrate the principle under discussion. It is calculated assuming the supply voltage to have pure sine waves with precisely offset phase angles, perfect

TABLE 8.1. Idealized Rectifier Characteristics

Number of pulses	Amplitude ratio	
	Max./avg.	Max./min.
6	1.047	1.155
12	1.012	1.035
24	1.003	1.009
36	1.001	1.004

TABLE 8.2. AC-System Harmonic Currents in Typical Rectifiers (as Fractions of Fundamental-Frequency Component)

Number of pulses (n)	5th + 7th harmonics	$(n - 1)$ st + $(n + 1)$ st harmonics	Total distortion
6	0.207	0.207	0.215
12	0.025	0.095	0.102
18	0.030	0.018	0.036
24	0.030	0.012	0.034

transformer-rectifiers, and a purely resistive load. None of these holds perfectly in a real system.

In addition to giving a smoother DC output current, increased pulse number reduces the harmonic current injection into the AC supply system. A rectifier system with n pulses injects harmonic currents of frequency $mn \pm 1$ times the supply frequency. Thus, a six-pulse rectifier will produce no harmonic components below the fifth (it should produce the 5th, 7th, 11th, 13th, . . .). As with the DC output discussed above, the lower-frequency components are largest. Increasing the pulse number to twelve therefore greatly reduces harmonic current injection by effectively removing the fifth and seventh harmonic components.

Again, the above is a simplified and idealized picture. In a real system with imperfections in the supply voltages, the transformers, and the rectifiers, more complex rectifiers still produce lower-order “nontheoretical” harmonics at certain levels. Table 8.2 gives some typical values, as listed by Cameron [13]. Regardless of the number of pulses, some low-level fifth and seventh harmonics remain and in fact become the dominant form in the more complex units.

Regulations on harmonics usually cover both current and voltage distortion. They specify maximum total distortion and place some kind of limit on individual harmonics [14]. A third criterion relates to distortion of communications signals. Here, each harmonic current I_h is multiplied by its own defined telephone influence factor T_h . Summing all these products in the same way as the voltages in Eq. (4) gives the total distortion, designated $I * T$. The IEEE lists three categories:

Category	Description	$I * T$
I	Unlikely to cause interference	<10,000
II	Might cause interference	10,000–50,000
III	Probably will cause interference	>50,000

Cameron [13] points out that many utility standards go well beyond IEEE recommendations and seriously constrain industrial design. The compromise often reached in practice

is an after-the-fact adjustment when the real effects of the new installation become known.

If the generation of harmonics exceeds the allowable limits, filtering circuits that provide low-impedance access to harmonic sinks can reduce their magnitude. Fortunately, capacitors perform this function. Since capacitor banks are the usual solution to a low power factor, they also can give protection against harmonics. The capacitors should be arranged in several banks, each one tuned to a different harmonic frequency by means of a reactor. This sort of arrangement goes beyond the scope of this book and becomes a subject for specialists, because harmonic filters at certain frequencies can resonate with power systems and thereby increase the harmonic voltages. This situation must be avoided.

Besides the characteristic odd-numbered harmonics, some even harmonics are present in most signals. Some of their causes are: imperfections in the AC supply, including the effects of tolerances in transformer winding phase angles; commutation reactance; and incoming harmonic voltages. In rare situations, the magnitude of some even-numbered harmonics can become a problem and require special attention [15].

8.3.1.3B. Rectifiers in Circuit Design. Circuit voltage of course is not unlimited. Higher voltages are harder to contain, and problems of safety, arcing, insulation, and current leakage all multiply as voltage increases. Good practice in the chlor-alkali industry usually restricts circuit voltages to less than about 1000 V or, in some cases, 400–600 V [16]. This is somewhat arbitrary, and the aluminum industry, to choose one example, accepts higher line voltages. A survey of one manufacturer's list of 46 chlor-alkali rectifiers, large and small, showed a median voltage slightly below 300. Half the units produced between 200 and 600 V.

Monopolar electrolyzers have the advantage of great flexibility in design amperage. They can hold anywhere from a few up to (in small-electrode membrane electrolyzers) more than a hundred anodes. Varying the number of anodes and their current density gives nearly infinite flexibility from low to very high circuit amperages.

The voltage drop in each monopolar electrolyzer is equal to the voltage drop of a single cell. This depends primarily on the type of cell, the current density, and the choice of membrane or type of diaphragm. The number of electrolyzers contained in a cell line then fixes its total voltage. The design voltage must be sufficient to allow for losses in buswork and intercell connectors, the maximum current density to be used, and the deterioration with time of the components of the circuit.

Monopolar circuitry is rather straightforward. Rectifier and electrolyzer currents are easily matched, and one rectifier set serves one line of cells. A "set" may contain more than one rectifier housing. When the electrolyzers are bipolar, the rectifier arrangement is more of an issue. The basic reason for this is the low current associated with bipolar designs. The most widely used bipolar membrane electrolyzers have cross-sectional areas between 1.5 and 5 m². Even at the highest current densities used today, they are limited to loads of 10–30 kA. This is well below the range common to diaphragm-cell and typical mercury-cell loads. The low amperage presents a problem in plant conversions and requires a careful balance between circuit arrangement and cost in a new plant.

The high-voltage, low-current characteristic of bipolar electrolyzers would seem to favor the economical design of a rectifier. Limiting the circuit voltage, however, normally prevents one from installing these electrolyzers in series. This limits the power demand of a cell circuit, and the use of rectifiers with low power ratings would add to the installed cost of the system.

It is cheaper to install and operate fewer rectifiers each with higher power output. It is therefore common to install more than one bipolar electrolyzer operating in parallel off larger rectifiers. As a consequence, bipolar electrolyzers have many different rectifier arrangements. The technical ideal would be to have a separate rectifier for each electrolyzer circuit. One plant with 12 large electrolyzers in fact uses 12 rectifiers for its DC supply.

Tominaga *et al.* [17] showed several different arrangements used in other commercial plants. These are summarized below:

Number of transformers	Number of rectifiers	Number of electrolyzers
2	2	2
1	1	4
1	2	4
3	3	7

In the first three rows of the table, transformers are dedicated to particular rectifiers and rectifiers to particular electrolyzers. Thus, one transformer feeds one or two rectifiers and each rectifier in turn feeds from one to four electrolyzers. In the last row, the three transformers and rectifiers operate in parallel and their outputs come together in a common bus. Feeding the seven electrolyzers in parallel from this bus makes the electrical arrangement on the cell side equivalent to a single rectifier feeding all seven electrolyzers. A separate interesting case, not included in the table, is the use of two low-voltage rectifiers to feed an electrolyzer with a large number of cells. Here the cell stacks are electrically divided into halves with separate feeds from the rectifier output bus. The definition of what constitutes an “electrolyzer” becomes blurred, and the number of possible configurations is limited only by the bounds of ingenuity.

8.3.1.3C. Parallel Operation of Electrolyzers. While the practice of installing bipolar electrolyzers in parallel is justified on the basis of economics, one should at least realize that it has its disadvantages. Unless there is separate current control for each series of cells, there will be some mismatch between their operating currents.

Consider two electrolyzers with different voltage–current characteristics. For the operating voltage of a cell or an electrolyzer, we use the linear approximation

$$V = a + kI \quad (5)$$

where V is the cell or electrolyzer voltage, I the current (A or kA) or current density in kA m^{-2} , a the extrapolated voltage with no load current, and k a constant appropriate to units of I (the slope of the V – I curve).

We install two electrolyzers with the same operating characteristics and therefore the same initial voltage V_0 at load current I_0 . They operate in parallel on the same rectifier. We assume that one is damaged after a time and that for the two electrolyzers

$$V = a_1 + k_1 I_1 = a_2 + k_2 I_2 \quad (6)$$

Electrolyzer #1 still has the starting or "ideal" characteristics and electrolyzer #2 has suffered the damage. We also assume that the damage shows as an increase in the slope of the $V-I$ curve. In other words, $a_1 = a = a_2$ and $k_2 > k_1$. Now

$$V = a + k_1 I_1 = a + k_2 I_2 \quad (7)$$

The current through electrolyzer #1 is

$$I_1 = (V - a)/k_1 \quad (8)$$

and through electrolyzer #2 is

$$I_2 = (V - a)/k_2 \quad (9)$$

Comparing the currents in the two electrolyzers,

$$I_1 = (k_2/k_1)I_2 \quad (10)$$

The current through each electrolyzer is inversely proportional to the slope of its $V-I$ curve. This slope is the "k-factor" familiar in the chlor-alkali industry. In the authors' experience, differences of 10% in current density between electrolyzers are common in bipolar cell rooms operating in this mode. We shall return to the effects of differing current densities below. First we compare the power consumption of the above system with one that holds the two electrolyzer amperages equal.

In a real operation, the circuit voltage will be increased after one electrolyzer is damaged in order to keep the sum of I_1 and I_2 constant. If the damage to the electrolyzer has also decreased the current efficiency, currents and voltage both must be increased beyond this level if plant output is to be kept constant. First, we continue the analysis at constant current efficiency.

We denote the new amperages by I'_1 and I'_2 . The ratio of the two currents is unchanged, and so

$$I'_1 + I'_2 = 2I_0 \quad (11)$$

$$I'_1 = \kappa I'_2 \quad (12)$$

where $\kappa = k_2/k_1$.

This leads to

$$I'_1 = 2\kappa I_0/(\kappa + 1) \quad (13)$$

$$I'_2 = 2I_0/(\kappa + 1) \quad (14)$$

We still have

$$V' = a + k_1 I'_1 = a + 2\kappa k_1 I_0 / (\kappa + 1) \quad (15)$$

The DC power consumption is given by $(I'_1 + I'_2)V'$ or $2I_0V'$. This becomes

$$P' = 2aI_0 + [4\kappa/(\kappa + 1)]k_1 I_0^2 \quad (16)$$

Turning now to the other option, if the two electrolyzers were run from separate rectifiers at the same current, their operating voltages would differ, and we would have

$$V_1 = a + k_1 I_1 = a + k_1 I_0 \quad (17)$$

$$V_2 = a + k_2 I_2 = a + k_2 I_0 \quad (18)$$

The power requirements also differ:

$$P_1 = aI_0 + k_1 I_0^2 \quad (19)$$

$$P_2 = aI_0 + \kappa k_1 I_0^2 \quad (20)$$

The combined DC power consumption is

$$P = 2aI_0 + (\kappa + 1)k_1 I_0^2 \quad (21)$$

This and the expression in Eq. (16) for the power consumed in a parallel arrangement differ only in the second terms, and we have

$$P - P' = [\kappa + 1 - 4\kappa/(\kappa + 1)]k_1 I_0^2 = [(\kappa - 1)^2/(\kappa + 1)]k_1 I_0^2 \quad (22)$$

For all reasonable values of κ , the right-hand side is a small number, but it is always positive, and so $P > P'$. Operating two electrolyzers of different characteristics in parallel on the same rectifier actually consumes, at any given time, slightly less power than the same electrolyzers operating at equal currents. This is a result of letting the better electrolyzer do more of the work. If the current efficiencies are equal, running the two electrolyzers at the same voltage in fact gives the lowest possible energy consumption. Changing the distribution in either direction would move an increment of current to a higher operating voltage.

The power requirement in any of the equations above conventionally is measured in kilowatts. The amount of product made depends on the time of operation (θ), the amperage (i), the number of cells (N), the current efficiency (ξ), and the equivalent weight of the product being considered (W_e). The output is given by a constant times the product $\theta i N \xi W_e$. Amperage is denoted by i because I in our basic Eq. (5) is permitted to represent either current or current density. In a given arrangement, the two versions differ by a constant factor (the electrode or membrane area), which can be incorporated

into the constant (C). We will usually base the calculation on an interval of 1 hr, and so we can write

$$\text{Output} = CIN\xi W_e \quad (23)$$

In a given situation, N and W_e are constant. We also assume that current efficiency is independent of operating load. This is usually a good approximation over the normal operating range. Therefore, the output of the cells is proportional to the value of I . We divide the basic form of the power equation, $P = aI + kI^2$, by a constant and by I to arrive at the unit energy consumption, usually expressed as kW hr ton⁻¹ of product:

$$E = \alpha + \beta I \quad (24)$$

The discussion above assumed that only the k -factor, or the equivalent resistance of the membrane, changed. Membrane damage may also result in lower current efficiencies. We can extend the above analysis to include this effect. Keeping the linear form of Eq. (24) by assuming that current efficiency is independent of operating load, we have for the unit energy consumption by undamaged membranes

$$E_0 = \alpha_0 + \beta_0 I_0 \quad (25)$$

When one of two cells or electrolyzers is damaged, the total current must be higher to offset the loss in current efficiency. Both amperages can be expressed in terms of the starting value I_0 , and then

$$E = \alpha + \beta I_0 \quad (26)$$

with $\alpha > \alpha_0$ and $\beta > \beta_0$. Table 8.3 gives the factors α/α_0 and β/β_0 for the two operating regimes. The parameter κ is as defined above in Eq. (12); ε is the ratio of the current efficiency of the damaged electrolyzer to that obtained before the damage occurred. In all cases, $\kappa > 1$ and $\varepsilon < 1$. All factors listed in the table therefore are greater than one, and the common-current factors are greater than the common-voltage factors.

If damage to the membranes in an electrolyzer is severe, they should be replaced. In other cases, the factors in Table 8.3 are not large. The percentage differences between common-current and common-voltage operation are quite small. The purpose of the analysis reported here is to show that operation of electrolyzers with different characteristics

TABLE 8.3. Multipliers for Terms in k -Factor Equation

Operating regime	α/α_0	β/β_0
Same current	$2/(1 + \varepsilon)$	$2(\kappa + 1)/(1 + \varepsilon)^2$
Same voltage	$(\kappa + 1)/(\kappa + \varepsilon)$	$2\kappa(\kappa + 1)/(\kappa + \varepsilon)^2$

at the same voltage, while it has disadvantages, at least does not suffer from a higher overall power consumption at a given point in time.

In a large plant, even the small relative difference can represent a substantial amount of money. In our 800-tpd reference plant, for example, a difference of 0.1% corresponds to more than 500 MW hr yr⁻¹.

While our development describes a system containing only two electrolyzers, the results can be generalized to any number. The same effect could of course be obtained in the two-rectifier case by choosing currents rather than relying on a process of natural selection. The best policy depends on the effect of the operating load on the rates of deterioration of the electrolyzers. Skewing the load to favor a better electrolyzer will place more stress on its components, notably the membranes. Certainly the useful life of this electrolyzer will be shorter. Whether the operation and the working life of the damaged electrolyzer will improve enough to compensate for this loss is not a question that can be answered here. It is also important to note that, in a plant operating close to the specified maximum amperage of a performance guarantee, a high-current electrolyzer can be placed outside that limit.

8.3.1.4. Buswork Arrangement. This section will give the reader a feel for the size of the conductors required for safe handling of the cell-room current. In smaller plants, particularly in those based on bipolar electrolyzers, cables of the proper diameter can serve as conductors. Most plants use a multiplicity of bars with rectangular cross-section operating in parallel, and the following discussion is in terms of such busbars.

A good bus material must have high electrical and thermal conductivity. Other desirable properties include:

1. resistance to corrosion
2. good mechanical properties
3. resistance to fatigue
4. ease of fabrication
5. low cost and high salvage value.

The standard materials are copper and aluminum. Copper is the more frequent choice in the chlor-alkali industry, but the comparative economics shifts with time and a number of cell rooms have aluminum conductors or a mixture of copper and aluminum. Copper is chosen because of its outstandingly high electrical conductivity. Installations are more compact, and with the improvements in area productivity offered with the newest membrane cells, this aspect becomes more important. Copper can be expected to remain the favorite.

Cast copper does not have outstanding mechanical properties. Work hardening by rolling or drawing improves these properties. In sizes typical of chlor-alkali busbars, hard-drawn copper bars or strips have tensile strengths of about 2.5 tons cm⁻². Cold working destroys about 2–3% of the maximum electrical conductivity. Annealing restores this at the expense of some of the enhanced physical properties [18].

8.3.1.4A. Capacity of Busbars. Current densities through busbars are high. With copper conductor, 1,500 kA m⁻² is not rare. Even with the low resistivity of copper, this produces enough I^2R loss to raise the temperature of the metal significantly. The capacity of the

busbars therefore usually is fixed by selecting a maximum acceptable temperature rise. Given a typical cell room temperature of up to 40°C and the fact that the oxidation rate of copper begins to increase at 90°C, a typical design maximum rise is 50°C.

The rate of heat generation in a conductor is proportional to the square of the current. Both radiation and convection dissipate the heat. Compact arrangements of busbars restrict the opportunities for radiation, and convection usually is more important. Polished copper may be more attractive visually, but keeping the surface free of oxide is counterproductive. The emissivity of a polished copper surface is about 0.05; the emissivity of an oxidized surface is 10 times higher. Aluminum tends to have lower emissivities (~ 0.02), but again, heavy oxidation produces a 10-fold increase. Outside surfaces of conductors sometimes are painted to increase the emissivity even more.

Convective heat-transfer coefficients depend on the size and shape of a conductor and on the velocity of air past its surfaces. The thickness of the resistive film is less at higher air velocities. High air flow rates are clearly desirable, and so the arrangement of the busbars should not hinder that flow. This means that busbars of rectangular cross-section should be installed with the long side of the rectangle vertical. Thinness also is desirable. If the thickness of a bar is doubled, its resistance to electrical flow is cut in half. The current cannot be doubled in order to take advantage of this fact, however, because the ability to dissipate heat rises more slowly. The actual increase in capacity at a given temperature rise is only 40–45%. For this reason, multiple parallel bars are chosen over a single, thicker bar. A certain amount of thickness is desirable for strength, however, and busbars usually are at least 5 mm thick. The spacing of parallel bars involves another compromise. Wide spacing increases the rate of dissipation of heat but also increases the volume occupied by buswork and complicates its handling and installation. A practical approach is to make the space between bars essentially equal to the thickness of the bars. This makes it easy to interleave two assemblies to form a bolted or clamped joint.

The steady-state average temperature of a conductor can be obtained by calculating heat input and output as functions of temperature and then equating them. Heat input is a weak function of operating temperature; the rate of heat dissipation is a strong function. The heat generated in a conductor by a direct electrical current is

$$W = I^2 R \quad (27)$$

where W is the power in W/cm of length, I the current in amps, and R the resistance in $\Omega \text{ cm}^{-1}$.

The resistance is

$$R = \rho(1 + \alpha\theta)/A \quad (28)$$

where ρ is the electrical resistivity at ambient temperature in $\Omega \text{ cm}$, α the temperature coefficient of resistivity in $(^\circ\text{C})^{-1}$, θ the temperature difference between conductor and atmosphere in $^\circ\text{C}$, and A the cross-sectional area of conductor in cm^2 .

The energy dissipated is

$$W = hp\theta \quad (29)$$

where h is the heat-transfer coefficient in watts/ $^{\circ}\text{C}$ temperature difference/ cm^2 and p the perimeter of the conductor in cm.

By Eq. (27), the current is equal to $(W/R)^{1/2}$. We can combine Eqs. (28) and (29) at steady state to give

$$I = \sqrt{hp\theta A/\rho(1 + \alpha\theta)} \quad (30)$$

The work of Lorenz in 1881 showed that h , the coefficient for natural convection from a vertical plane, should be proportional to $(\theta/L)^{0.25}$ [19]. In Lorenz's development, these two quantities appear in the Grashof number, which also includes the square of the gas viscosity in the denominator. In our case, the increase in average viscosity as the temperature in the conductor becomes greater offsets some of the temperature effect and justifies the use of a smaller exponent, about 0.22, on the temperature differential. The use of the perimeter rather than the height of a bar in Eq. (29) reflects the fact that busbars are two-sided and not infinitely thin. The fact that practical geometry of bars does not maintain geometric similarity on scale-up and the existence of end effects mean that the flow of heat increases more rapidly with size than the equation suggests, and so the exponent on p becomes slightly less than 0.25. It also should be assigned a value of about 0.22. The heat-transfer coefficient now becomes

$$h = h'\theta^{0.22}/p^{0.22} \quad (31)$$

where h' is a proportionality constant. Equation (30) becomes

$$I = \sqrt{h'p^{0.78}\theta^{1.22}A/\rho(1 + \alpha\theta)} \quad (32)$$

From empirical observation and the properties of copper [18], the base case with a temperature rise (θ) of 50°C gives

$$I = 188.5A^{0.5}p^{0.39} \quad (33)$$

With linear dimensions in cm, Eq. (33) gives the capacity in amperes. It applies to horizontal runs of busbar. More air turbulence is developed in vertical runs, and heat-transfer coefficients therefore are higher. In a plant installation, however, horizontal runs predominate and should be the basis for design. The treatment is also limited to the case of a single conductor and assumes still air and natural convection. It should be regarded as applying only to indoor cell rooms. Outdoors, with variable winds and flow patterns, the situation becomes specialized and too complex for our level of detail.

If the specified temperature rise is between 30 and 50°C , the allowable load should be multiplied by a factor f . Two different approximations to this factor are

$$f = 0.265 + 0.019\theta - 0.000086\theta^2 \quad (34)$$

$$f = 0.1163\theta^{0.55} \quad (35)$$

When parallel bars with spacing equal to their thickness are used, the heat dissipated per unit surface is reduced. For a first estimate, the amount of current carried by a single bar can be multiplied by the factor n' :

$$n' = 0.48 + 0.68n \quad (36)$$

where n , the number of bars, is 2–5, or

$$n' = 0.78 + 0.67n - 0.01n^2 \quad (37)$$

where n is 5–10.

Five bars assembled in this way, for example, carry only 3.88 times as much current as a single bar with the same temperature rise. Ten bars carry about 1.67 times as much current as do five bars and are equivalent to 6.5 separate single bars.

Example. An electrolyzer in our reference plant carries $2.5 \times 5.5 = 13.75$ kA. We examine the possibility of carrying a slight excess, say 15,000 A, in copper bars of the following dimensions: 20×0.65 cm, 25×0.65 cm, and 30×0.95 cm. We hold the temperature rise in the bars to 45°C .

Using the average of Eqs. (34) and (35), we calculate the temperature correction factor f to be 0.945. Multiplying the result of Eq. (33) by this number, we find the capacity of a single bar 20×0.65 cm to be $0.945(188.5)(13^{0.5})(41.3^{0.39}) = 2.74$ kA. The capacities of the other shapes are 3.34 and 4.75 kA, respectively. The calculated numbers of separate bars for the three cases are 5.47, 4.50, and 3.16. We choose the smaller number of large bars. Inverting Eq. (36) to give $n = 1.47n' - 0.71$, we calculate the actual number of bars required to be 3.93 and therefore provide four. This gives a current density in the bars of 1316 kA m^{-2} .

Because of the large difference between monopolar and bipolar electrolyzer requirements, we extend this example to consider a monopolar circuit carrying 100 kA. We allow for 110 kA but permit a temperature rise of 50°C . To keep the busbar count a reasonable number, we consider larger sections. One of the many combinations that suit the application is the following:

Three stacks of seven bars each
 Dimensions 40×1.25 cm
 Total cross-section 1050 cm^2
 Current density $1,048 \text{ kA m}^{-2}$

8.3.1.4B. Copper vs Aluminum. The conductivity built into the above equations is that of standard annealed copper, referred to as "H.C." or high-conductivity copper. Other metals or other grades of copper can be substituted by inserting the proper values. The other metal of most interest is aluminum. Over the years, shortages of copper and swings in relative prices have led to the installation of aluminum bus in a number of plants. While price advantages come and go, the permanent advantage of aluminum is its light weight. Copper has more than three times the density of aluminum. Some of the relevant properties of the two metals are compared in Table 8.4. The next to

TABLE 8.4. Comparative Properties of Copper and Aluminum

Property	Copper	Aluminum
Conductivity at 20°C (% of International Annealed Copper standard) ^a	99	60.97
Resistivity at 20°C, ohm cm	1.742	2.828
Resistivity-temperature coefficient, (°C) ⁻¹	0.00393	0.00403
Density at 20°C, g ml ⁻¹	8.89	2.703
Linear coefficient of expansion, (°C) ⁻¹ × 10 ⁶	16.7	23
Resistance-temperature coefficient, ohm cm °C ⁻¹	0.0069	0.0115
ASTM tests and tolerances (section number)	B-187	B-236

^a Standard value is 0.5799 S cm⁻¹.

TABLE 8.5. Comparison of Characteristics of Copper and Aluminum Buswork

Design for	Wt. ratio, Al/Cu	Approximate %	Relative voltage drop (%)
Same shape	0.306	30	162
Temperature rise	0.43-0.44	45	111
Voltage drop	0.497	50	100

last row shows the total change of the resistance of a bar with temperature. It includes both the change in resistivity and the expansion or contraction of the bar. The disadvantage of aluminum is its higher electrical resistivity. It is about 62% more resistive than copper at 20°C, and its resistivity increases more rapidly with temperature. A given current requires more voltage to push it through an aluminum conductor of the same cross-section as a copper conductor and generates more heat inside the conductor. To carry a given current through a given shape, aluminum requires about 62% more voltage than does copper. To reduce the energy loss in aluminum bus to the same as that incurred with copper, we must increase its cross-sectional area by the same 62%. The resulting shape still weighs only half as much as the copper equivalent, but the added volume can make installation more difficult. If the voltage drops are equal, the larger aluminum bars are able to dissipate more heat and run at a lower temperature. By designing for the same temperature rise as in the copper equivalent, the aluminum conductor could therefore be made slightly smaller, incurring a greater voltage loss as the temperature increased. Table 8.5 summarizes these comparisons between copper and aluminum.

Some plants use combinations of aluminum and copper conductor. Aluminum may be used for the main bus or large sections and copper for electrolyzer connections, where it is more important to keep the components small. Prefabricated transition pieces should be used to minimize contact resistances. In these pieces, the two metals can be joined by explosion bonding.

Istas [20] described an aluminum busbar system in a mercury-cell plant. The design-basis current density for the buswork was about 900 kA m⁻²; operation was close to 800 kA m⁻². The buswork joints were clamped. Joints between aluminum and copper or steel were through 19 μm of nickel plate. Exposed aluminum surfaces were covered

with 0.4 mm of coal-tar epoxy paint. An important part of the economic justification for the use of aluminum was its easier installation. Given the geometry of a mercury cell installation, the greater volume of aluminum buswork is not the disadvantage that it might be in certain other arrangements.

8.3.1.4C. Assembly of Busbars. Energy losses occur at the joints between sections of buswork. Joints may be made by clamping, bolting, or welding strips together. Bolts are reliable and easy to use but have the disadvantage of requiring holes in the busbars. These reduce the conductive area and distort the current flow paths. Other methods disrupt the current less, but any lap joint will produce a certain amount of distortion.

The equivalent resistance of a joint comprises the actual contact resistance and that produced by spreading of the current path. Making the overlap long enough provides the extra metal that compensates for the latter. The length required is not much greater than the thickness of the busbar. The practicalities of construction ensure that the overlap is at least that long, and well-bonded lap joints actually have less resistance than a single busbar of the same length. The advantages of making the overlap more than twice the bar thickness are not great; beyond a ratio of 5 : 1, very little is to be gained.

The contact resistance between two pieces of metal depends on the quality of the surfaces and the pressure that is used to force them together. Increasing the pressure flattens out more of the microscopic irregularities on the surfaces and increases the true contact area. Beyond 20 MPa, gains are small. Beyond 40 MPa, they are inconsequential, and too much pressure on the joint can exceed the elastic limit of the material. Under high pressure and at service temperature, the metal will flow slightly. When it cools, the contact pressure will be greatly reduced and the resistance of the joint will increase. Bolted joints are particularly susceptible to this when the bolts and the bars have different thermal coefficients of expansion. From this standpoint, copper alloy bolts are superior to steel.

Clamped and bolted joints can deteriorate with time. Corrosion is one of the principal causes. Gases can penetrate joints by diffusion and liquids by capillary action. Higher operating temperatures and cycling temperatures increase the rate of deterioration. Painting the buswork or applying a thin coat of petroleum jelly to its surfaces before assembly can slow the rate of corrosion. The integrity of a joint, even in the face of corrosion, is improved by the use of special washers (e.g., Belleville washers) that spread the bonding force and cut through products of corrosion to maintain efficient line contact.

We can extend the comparison between aluminum and copper buswork to the stability of joint resistances. Aluminum flows more easily under stress than does copper, and so the problem of loss of contact pressure as buswork temperature cycles is more severe when using an aluminum bus. Aluminum oxidizes more easily and more rapidly than copper and forms an oxide with a higher resistance. Furthermore, copper oxide has a negative temperature coefficient of resistivity, so that its contribution to joint resistance actually declines as temperature increases. Aluminum oxide, like the conductors themselves, has a positive temperature coefficient. For these reasons, welded butt joints are often a better solution for aluminum busbars than clamped or bolted overlap joints.

When an electrical conductor, such as a busbar, is placed in a magnetic field, forces appear that tend to deform the circuit in such a way that the number of magnetic lines of force enclosed is increased (induction). When currents in parallel conductors are in the same direction, the force is attractive; when currents are in opposite directions, the force is repulsive. Busbar runs are usually straight and parallel. The electromagnetic force between two bars is proportional to the product of their currents. The force is small in normal operation, but it is very much larger under short-circuit conditions. It becomes the limiting stress in the design of busbar supports. The design value of the short-circuit current, which is dependent on the size of the bars and the voltage of the system, is therefore an important criterion.

The designer must consider all the forces imposed by the busbar on its supports. The supports often are insulators, which may be ceramic. These are more likely to fail in tension or shear than in compression. Therefore, their axes should not be at right angles to the force on the buswork.

Finally, it is important to consider thermal expansion when installing buswork. Combining the temperature rise allowed by design with the yearly ambient cycle, there may be a range of 70°C in buswork temperature. With copper, this represents a difference of 1.19 mm m⁻¹ of length and with aluminum, 1.68 mm m⁻¹. In a long cell room, this becomes a substantial distance. Flexible sections are sometimes used in aluminum busbar runs in order to accommodate expansion and contraction, thereby avoiding the application of high stresses to the rectifiers, cells, and busbar supports. These are prefabricated and consist of numerous thin sheets of aluminum connected in parallel between two aluminum blocks. The busbars are welded to the blocks on site.

8.3.1.4D. Intercell Connections. The main buswork runs connect lines of cells to each other and to the rectifiers. It is also necessary to provide connections between cells or electrolyzers within a row. The arrangements made to carry the load along a cell row are a vital part of the system and have much to do with building design and cell-line layout. However, they are largely beyond the control of an independent designer. Electrical connections are an integral part of electrolyzer design, and the supplier of electrolyzer technology dictates the requirements.

In monopolar circuits, a cathode of one cell must be connected to an anode in an adjacent cell. This involves a change in orientation of the connectors between the cells. The several changes in direction relieve the stresses of thermal expansion and contraction. A diaphragm cell may require connection of more than one side of a cell body (the cathodic "can") to an anode support plate at the bottom of the next. The connectors become rather massive connections that have much in common with the busbars. Mercury-cell interconnections are between the top (anode side) of one cell and the bottom (cathode side) of the next. These take the form of permanently installed connectors complete with intercell switches. Membrane cells once again are more diverse in their design. As a rule, connections are end-on to the electrodes. A fundamental limitation of monopolar membrane cells has been exposed by the trend to high (>4 kA m⁻²) cell current densities. This is the power lost by transmitting high currents through the electrodes and the complications of attaching enough intercell conductor to the edges of an electrode.

In bipolar electrolyzers, the cells are connected through the membranes and the entire faces of the electrodes. Connections between electrodes, however, do not involve the entire cross-section but normally rely on enhanced contact across some specially designed section. When an electrolyzer contains many cells and is divided into sections, intersectional connections may be in the form of transitional bus or may be similar to the supply arrangement used with undivided electrolyzers.

8.3.1.5. Current and Power Measurement. With electrical energy costs the dominant factor in chlor-alkali production economics, electrical metering is very important. On the DC side, current, voltage, and power are frequently measured. Integration of the current and power measurements over time gives the quantities of electricity (A h) and energy (W h) consumed by the circuit. On the AC side, power, power factor, and energy are often measured.

Measurement of direct currents usually is by Hall-effect devices. The Hall effect is the development of a transverse electric field across a solid material when that material carries an electric current and is in a magnetic field with a component perpendicular to the current. The electric field results in a measurable potential difference, the Hall voltage, which is directly proportional to both the current and the magnetic field. Meters usually are accurate within 0.5%, supporting a four-digit readout. Most plants can control cell current within 1%.

The physical form of a DC meter usually is a rectangular loop surrounding the current-carrying busbar. It forms a magnetic core piece with measuring elements on all four sides. The field produced by the current through the busbar generates a flux in each measuring element. Magnetic null detectors in each leg send signals to current amplifiers, which pass currents into conducting coils wound on each side of the magnetic core piece. Each coil then sets a field equal and opposite to the bus current field in order to satisfy the null detector. Summing the currents needed in the four coils produces a signal proportional to the current in the buswork.

Measurement on four sides compensates for asymmetry in the field. This can be due to off-center placement of the measuring apparatus relative to the busbar or due to an external field. Consider an external field, for example, oriented at an angle to all four sides of the magnetic core piece of the meter. This will increase the strength of the field in one or more legs of the meter and decrease it in the other(s). The sum total of the four impressed conducting-coil currents is unchanged. In normal operation of a chlor-alkali plant, the field produced by the bus current is much greater than any external field. During shutdowns or operation at low cell current, however, the presence of an external field can result in reversal of the direction of the flux in certain legs of the magnetic core piece. Not all systems are able to measure the resulting "negative" currents, and the sum becomes artificially high and fails to drop to zero even during shutdown of the rectifiers.

Measurement of the DC voltage can be achieved by use of an accurate resistive voltage divider and a high-impedance transducer. The signal from this device can then be multiplied by a signal from the DC current meter in another transducer to give a measurement of the DC power. Integration of the DC power signal gives the DC energy consumption over a period of time.

On the AC system, conventional meters can be used to determine the levels of power and power factor, and conventional tariff metering can be used to record the energy consumed over a period of time and the maximum demand. The importance of the maximum demand is discussed in Section 8.3.2.4. Power factor, discussed in Section 8.3.2.3, is a measure of the extent to which a load current is out of phase with the supply voltage.

8.3.2. *Electrical Supply Efficiency*

8.3.2.1. Rectifier Cost and Efficiency. Section 8.3.1.3, in its discussion of the effects of rectifier configuration and control on AC power requirements, showed that very small fractional differences in demand can be economically quite significant in large plants. While rectifier efficiencies are quite high, therefore, what may seem to be small differences can have a large effect on operating costs. This section discusses rectification efficiency and the importance of the operating characteristics of cell lines.

When a transformer–rectifier operates at full current but below its rated output voltage, its power efficiency declines. This is because the losses remain virtually unchanged while the power output falls proportionately with voltage. If the same transformer–rectifier operates at full voltage but below its rated output current, the reverse is true. The power efficiency increases because the resistive losses decrease with the square of the current while the power output falls only linearly. The efficiency improvement is not as great as might be expected from this statement, because the no-load (iron) losses of a transformer do not reduce at all and the rectifier losses are only partly resistive. The latter reflects the fact that semiconductor devices have fixed voltage drops in addition to their resistive losses.

In an operating a chlor-alkali cell line, it is not possible to vary current and voltage independently. The operating voltage of a cell line depends on the current. The relationship is very nearly linear (Eq. 5). The two effects discussed in the preceding paragraph therefore are offsetting. The combined effect usually produces a loss in efficiency as the operating current is reduced.

The comparisons made above considered the effects of variations in circuit load on a given rectifier. The effects of amperage and voltage ratings are also important when designing a circuit and choosing new rectifiers. One of the necessary economic balances in plant design is the optimization of electrode area. Providing less area reduces capital cost but increases operating cost by raising overvoltages at the cells and increasing resistive losses. Given a certain amount of total electrode area, monopolar cells in particular allow some extra flexibility in design. Increasing the number of electrodes in a pack increases the area provided by each electrolyzer and reduces the number of them that is required. The current flowing through a circuit increases, and the presence of fewer electrolyzers in a line reduces the voltage.

Fewer, larger electrolyzers will result in less efficient rectification. Hine [21], in a study of cell-room optimization, showed that for a particular line of rectifier models a log–log plot of efficiency loss against the rated operating voltage was linear. He derived an approximate equation for conversion efficiency in the range of interest that is

equivalent to

$$\eta = 1 - A/V \quad (38)$$

where η is the fractional conversion efficiency, V the output voltage, and A an empirical constant.

The constant A must have the units of voltage, and Eq. (38) is equivalent to a situation in which a certain number of volts is “lost” regardless of the design operating level. This is a convenient approximation in some cases, but it is one to be used with discretion. The important fact, other things being equal, is that the conversion efficiency of a rectifier improves as its design voltage increases.

For a given power output, higher operating voltages also correspond to lower capital costs. Increasing the amperage of a rectifier requires addition of more elements or at least of more conductor, at a substantial cost. Increasing the voltage requires no added conductor but perhaps only some increase in robustness or level of insulation. A low-amperage, high-voltage rectifier therefore will be cheaper and usually more efficient than one with the same power output but the opposite characteristics.

In a chlor-alkali plant, rectifier specifications are not set in isolation but are part of the larger question of circuit design. Rectifiers are matched with groups of cells or electrolyzers, and the goals of high rectification efficiency and low cost must be compromised in the interest of safety, fluctuating energy demand, and an efficient cell layout.

A certain amount of current and voltage overdesign in a rectifier–transformer usually is desirable. It allows, for example, increases in cell operating current in order to maintain production as current efficiency declines with increasing age of cell components. It also allows for any increase in line voltage required by increasing age or the addition of cells. From the point of view of return on investment, of course, operation of a transformer–rectifier well below its design point is likely to be uneconomic. Too much overdesign also may cause a rectifier–transformer to operate continuously slightly below its best efficiency and may prove to be a bad investment. This should be taken into account when considering designing an electrical system for future plant expansions. Figure 8.8 is a typical example of the decline in efficiency below design rating. The loss is modest at first and accelerates only with rather deep turndown.

In the case of rectifying elements, the total installed cost of a thyristor system is usually less than that of one based on diodes. Operating costs also are lower. Maintenance costs, as we saw in Section 8.3.1.2B, are lower because of the use of static, solid-state control devices rather than the mechanical switchgear of a tap changer. Rectification efficiency might be expected to suffer from the loss of part of the sine wave before firing, but this loss usually is comparable to the inefficiencies of the regulating transformers and the saturable reactors in a diode system.

Thyristors tend to generate more harmonic distortion than diodes. This difference is greatest when the firing angles are high (Section 8.3.1.3A). While the distortion in a thyristor-based system therefore is at least as great as the distortion caused by a diode system, the reactive power compensation that accompanies most large rectifier installations also tends to absorb some of the harmonics. Configuring the capacitance as a harmonic filter offsets some of the loss.

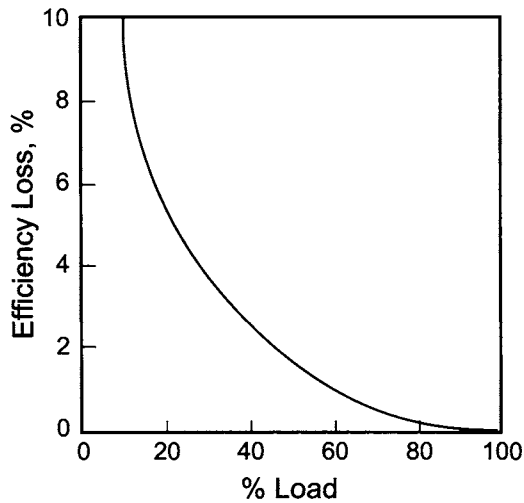


FIGURE 8.8. Loss in rectifier efficiency under partial load.

High firing angles correspond to low operating loads. The relative performance of a thyristor rectifier therefore suffers more as its output is cut back. The power factor is low and harmonic generation as a fraction of the fundamental is high. The poor power factor and harmonic distortion of thyristor and, sometimes, standard diode rectifiers have their costs. This could lead to increased future use of rectifiers using pulse-width modulated or multi-level converters. These are discussed in Section 17.3.2.

8.3.2.2. Current Leakage. A distinguishing feature of electrochemical processing is that some of the fluids can form part of an electrical circuit. The working electrolytes are chosen in part for their high electrical conductivity. As they enter or leave a cell, current will flow through any continuous path between the cell and a region of different potential. This current is lost from the process and directly affects the overall current efficiency. It also causes corrosion and can lead to extremely rapid failure of certain materials. One consideration in cell room design is the minimization of this loss, which is known as current leakage. One approach to mitigation of its effects is to install sacrificial metal probes in the electrolyte lines. These are constructed of relatively active metals, and the leakage currents gradually consume them. This renders the stray currents relatively harmless and prevents corrosion of major equipment and piping.

The amount of current leakage through a tubular column of liquid, as in a pipeline running full, is given by

$$i = kA \Delta V/L \quad (39)$$

where i is the current leakage, k the conductivity of the electrolyte, A the cross-sectional area of the tube, ΔV the potential difference between cell and target, and L the distance between cell and target.

To minimize the leakage current, this equation shows that a designer might provide some combination of the following:

1. a low-conductivity fluid
2. a low-magnitude voltage at the cell
3. a high ratio of L/A .

Considering these in turn:

1. The first approach we reject because of its effect on cell performance. We should note in passing that solutions of potassium chemicals have higher conductivities than their sodium counterparts. Prevention of current leakage is therefore somewhat more difficult in a KOH plant.
2. The total voltage across a cell line will depend on the number of cells connected in series and their operating conditions, primarily current density. The voltage at a given cell depends on its position in the cell line. At the midpoint of the circuit, barring any unwanted ground connections, the voltage relative to the ground will be close to zero. The maximum voltages, positive and negative, will be found at the ends of the cell line, and the number of cells in series determines the magnitude of these voltages. The problem of current leakage therefore is greatest at the ends of a cell line and becomes more serious as the number of cells in the line increases. The designer can reduce current leakage by forestalling ground faults and by keeping the number of cells in any one circuit low. This is one of many factors in the decision on the number of separate circuits to be provided.
3. The length/diameter ratio of the pipe or tubing determines the resistance of the current path. If this ratio is high, the current leakage will be reduced. Section 5.2.4 shows how the design of bipolar electrolyzers incorporates this strategy. The tubes which carry electrolytes into and out of the cells are small in diameter and frequently are lengthened by adding loops to their paths.

Even with very small currents in the lines connecting an electrolyte header to the cells, there will be a potential gradient along the header. With monopolar electrolyzers, the 3- or 4-V difference between adjacent cells is spread over the distance between two electrolyzers. This is not of major concern along the run of the header, but it becomes important at those points where two streams of widely different potential are brought together. Examples of this would be at the ends of headers at the rectifier end of the cell lines and at the middle of long cell rows, where headers often are brought together to reduce piping costs.

When the electrolyzers are bipolar, the potential difference between cells is exerted over the small distance between adjacent cells in the electrolyzer pack. The potential gradient along the cell row is much steeper than in the monopolar case and is of correspondingly greater concern. The safety aspects of a steep potential gradient are considered in Section 8.5.1.1.

One technique for reducing potential gradients and current leakage along headers is to pipe all electrolytes to or from the nominal neutral point of the circuit. In a U-shaped circuit, this simply means joining the two longitudinal headers serving the cell rows at the ends farther from the rectifiers. In a W-shaped circuit, it becomes more complex. The headers follow the electrical supply, as shown in Fig. 8.9. The ends of the headers are at the voltage extremes. They follow the electrical turnaround and are joined at the rectifier

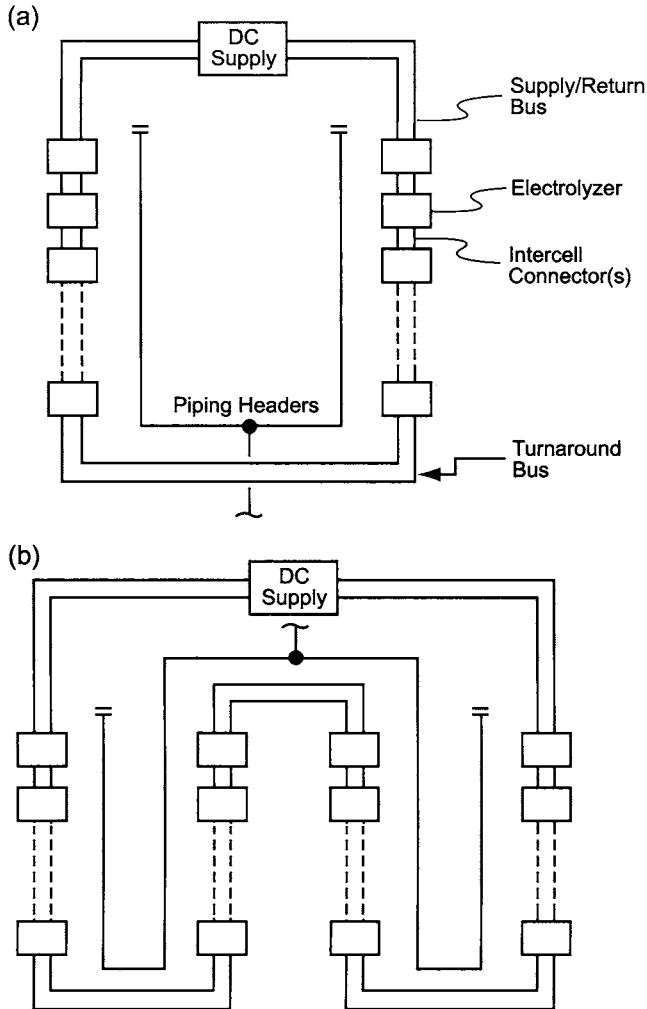


FIGURE 8.9. Cell-room piping arrangements to minimize voltage gradients. (a) U-shaped circuit. (b) W-shaped circuit.

end, at the middle of the circuit. The total length of installed piping is not significantly greater in this way, but diameters near the junctions may have to be increased. Of most concern with this arrangement is the fact that at least the gravity headers are sloped. The vertical distance between the ends of these headers and their junction is approximately twice that in a U-shaped circuit with the same aisle length.

Since current leakage through an electrolyte depends on the existence of a continuous path, another technique for the prevention of leakage currents is the use of current breakers at the cells. Their purpose is to physically break the electrolyte stream in order to interrupt the electrical path. Figure 8.10 shows the design used with some diaphragm cells. The liquor from each cell is collected in a cup (C). The demister

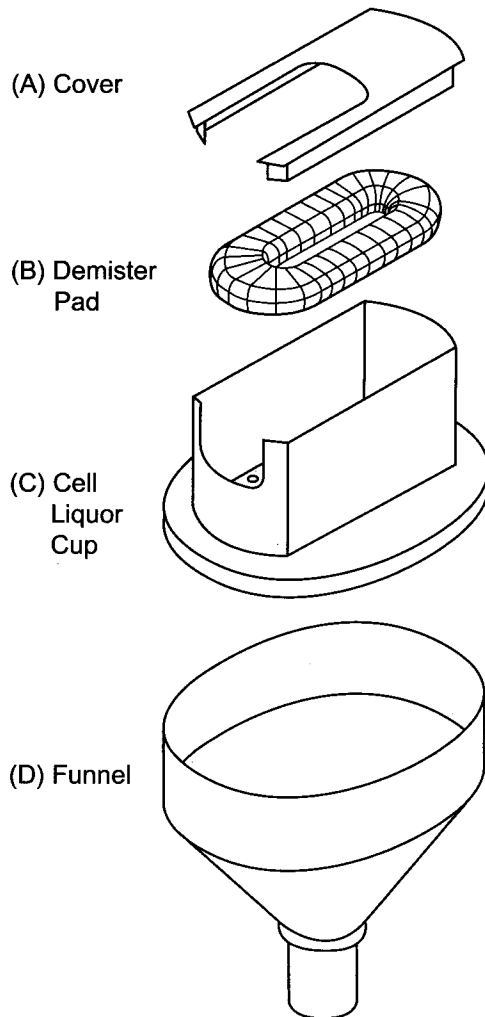


FIGURE 8.10. Diaphragm-cell current breaker. (With permission of ELTECH Systems Corporation.)

pad (B) allows vapors to escape without entrained liquid. The view of the cutaway section of the cup shows that a perforated plate restricts the flow of liquor and causes it to break up into unstable threads. Mercury-cell current breakers are in the caustic outlet from the decomposer. In a vertical unit, for example, there is a standing level of caustic above the graphite bed. The caustic leaves through a pipe attached to the wall of the vessel, located near the bottom of the caustic pool. The pipe turns upward, and the caustic overflows into a larger, concentric vertical pipe. A device at the bottom of the latter pipe breaks the stream into droplets and prevents current leakage.

8.3.2.3. Power Factor Correction. Chlor-alkali cell rooms, along with their high electrical power demands, tend to have low power factors. If uncorrected, these increase the

reactive power demand on the power supply utility. The total kV A requirement is the vector sum of the process power requirement (kW) and the reactive component (kV A_r) that results from the voltage and the current being out of phase.

Figure 8.11 illustrates the problem. The horizontal line represents the real power consumption and is assigned unit length. The vertical line is the reactive power, and its downward direction conventionally indicates that the plant's current lags the supply voltage. The hypotenuse is the apparent power, or the kV A demand on the utility. The angle between usable power and total demand is labeled φ , and its cosine is the ratio of the two quantities, or the power factor F .

While an increased kV A requirement is a direct burden on the supplier, it does not increase the kW consumption by the user. Generation and transmission losses, however, are proportional to the kV A transferred, and we saw in Section 8.3.1.1 that copper losses in transformers are proportional to the square of the kV A load. The same is true of the resistive losses in the generators, overhead lines, and cables. These losses do show up in the true power (i.e., kW) consumption of a utility supplier's system.

If the power factor is 0.85, the ratio of kV A demand to useful power is its reciprocal, 1.176. The reactive power as a fraction of useful power is given by

$$P_r/P = \tan \varphi \quad (40)$$

where P_r is the reactive power, kV A_r, P the usable process power, kW, and φ the phase angle ($= \cos^{-1} F$).

When $F = 0.85$, the reactive power is 62% as great as the useful power, quite a substantial fraction.

The cost of this inefficiency is passed on to the user by a demand charge based on total kV A or by requiring that the system be modified to achieve a minimum power factor. Since the cell room current lags the supply voltage, the addition of capacitance to the system offsets the phase shift and gives a better match. In terms of Fig. 8.12, by reducing the length of the vertical line it reduces the phase angle φ and increases its cosine. Generally, to improve the power factor from F_1 to F_2 , the amount of reactive

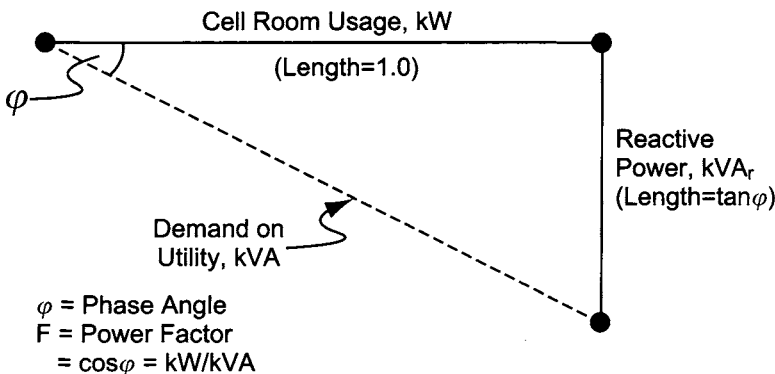


FIGURE 8.11. Influence of power factor on transmission demand.

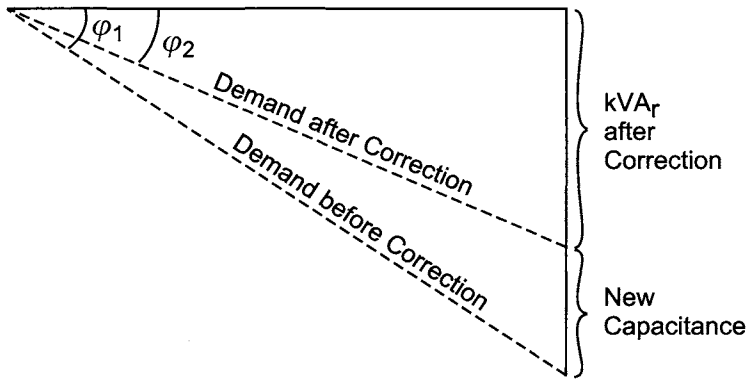


FIGURE 8.12. Effect of power-factor correction.

power to be removed or offset is given by

$$P_r = P(\tan \cos^{-1} F_1 - \tan \cos^{-1} F_2) \quad (41)$$

Example. We wish to improve a power factor from 85% (lagging) to 90%. We calculate here the rating of a capacitor system per megawatt of delivered power. The phase angle is about 31.8° ($\cos^{-1} 0.85$). We must reduce it to $\cos^{-1} 0.90 \approx 25.8^\circ$. From Eq. (41), $P_r = 1,000(\tan 31.8 - \tan 25.8) = 1,000(0.6197 - 0.4843) = 135.4 \text{ kV A}$. So, we need a capacitor installation equivalent to about 135 kV A per megawatt. The reactive power decreases from 62 to 48% of useful power, and the transmission load is 5.6% lower ($1 - 0.85/0.90$). Improvements in power factor become more expensive as we go on; especially above 90%, the capacitance required for a given amount of change increases with the power factor itself. The next 5% increase, to 95%, requires about 156 kV A MW^{-1} , an increase of about 15%. The next increment would have to be more than twice this to reach 100%, an unstable situation in any case.

In the example, it is important to note that the added capacitance, while equated to a number of kV A, is not a large power consumer. Capacitance itself does not consume energy. It stores energy during half of each cycle of the supply voltage and releases it during the other half. By being totally out of phase with the natural inductive part of the plant load, it offsets and effectively cancels out some of that inductive load. The total load seen by the utility supplier is still inductive, but less so than before correction. The load and supply are not so badly out of phase, and that statement is nothing less than the definition of an improved power factor. The only loss is due to the inefficiencies in the capacitor installation, and it is much smaller than the reduction in generation, transmission, and voltage transformation losses.

The generation of harmonics also affects the power factor by distorting the waveform. This distortion results from the combination of the higher-frequency harmonics with the fundamental frequency. A six-pulse rectifier, as pointed out in Section 8.3.1.3A, produces the 5th, 7th, 11th, 13th, . . . harmonics. These have frequencies of 250, 350, 550, 650, . . . Hz when connected to a 50-Hz supply. The output signal is the sum of the

fundamental wave plus all the harmonics. The distortion aggravates the effects of the displacement between current and voltage and contributes to an even lower power factor.

8.3.2.4. Demand Management. The previous section explained that operating power factor was one component determining the amount of transmission capacity that a utility supplier must make available to a chlor-alkali producer. Variations in operating rate are another. The user must compensate the supplier for this allocated capacity, whether or not it is consistently used. Power contracts therefore usually have a more or less complex tariff that is based not only on energy consumed but also on the maximum amount of generating capacity called on by the user. The charges based on maximum demand, as do all other components of plant cost, require management. The approach depends on the terms of the power supply contract. Smaller customers often pay a demand charge fixed at an arbitrary fraction of installed electrical capacity. In a chlor-alkali plant, typically, the contract will assess a charge based on the maximum demand (measured over a defined interval) during a billing period. The ideal would be to operate at a constant power level throughout any period while precisely meeting production goals. When the inevitable variations arise, the demand charge should be one consideration in production planning. When, for example, a change in forecast or the need to recover lost production makes a temporary increase in operating rate necessary, spreading increased production over the maximum time allowable reduces the maximum kV A demand. When plant management has some control in timing the response, there are other opportunities for controlling the demand charge. If a charge for the current billing period has already been set by a heavy output, it may be worthwhile to ignore the statement above and produce more goods earlier. The true energy consumption would be higher because of the high current density on the cells, but the incremental demand charge would be zero. Conversely, if only a few days remain in a billing period and the increased output would set a higher demand charge for that entire period, the proper decision may be to postpone the increase in production. There would be no additional demand charge in the current period, and a more reasonable schedule could be adopted in the next period.

Computer models of energy consumption and power demand are not difficult to set up. They can be very useful as planning tools. Updyke [22] discussed the subject and cited a few examples. The energy model presents quantitative data, which combined with management judgment help to determine the best course of action. In Updyke's model, for example, the cost of an additional kV A in demand was equal to the cost of 420 kW h. Allowing for an imperfect power factor, the demand charge might be equal to the cost of operating for 20 days. With such a tariff, short-term operation above a previously established maximum demand is not to be undertaken likely.

Another aspect of demand management in many plants is the daily variation of operating load. In many contracts, the power tariff reflects the time of day. Running the cells at their full capability during periods of off-peak pricing and then reducing the load when the price increases can lower the total energy cost. This mode of operation can increase certain other running costs, and in all cases some of the plant investment lies idle much of the time. These effects are obvious parts of the economic balance that will have been made to define the optimum. Constant changes in operating load can affect the long-term operation of the cells. This effect may be subtle and hard to define, but it should be considered in the sensitivity analysis of any economic evaluation.

In some locations, the price of electricity varies every few hours during the day. A good process model of cell operation makes it possible to optimize the combination of current load and other operating conditions [23].

Power supply contracts, finally, have another aspect somewhat related to demand management. When problems arise in the generating plant or on the distribution grid, the utility supplier must curtail output. Users' contracts will assign them certain priorities in these situations. Those with noninterruptible contracts will be affected least. Another task of operating company management therefore is to decide whether to invest in a premium supply contract.

8.4. CELL-ROOM AUXILIARIES

8.4.1. Piping

In the vicinity of the cells, we must add one more criterion for piping selection, that of low electrical conductivity. Attaching conductive piping to an electrolyzer certainly will increase stray current leakage and very well may create a hazard. Therefore, nonmetallic piping is favored. Once a safe length of such piping exists and carries its fluid some distance from anything in the electrical circuit, the designer may consider metals. In the hydrogen system, for example, nonmetallic risers may be joined to a metallic (carbon steel) header. Similarly, all utility connections to process lines should be through non-conductive sections. All lines carrying conductive liquids should have a solid ground connection before leaving the cell area. Section 12.7.2 discusses in a general way the connection of utility systems to the process.

The use of nonconductive piping also adds a measure of personnel protection. This can be negated by leaks of conductive fluids or by fitting the piping with valves that have metallic stems and handles.

8.4.1.1. Gases. The chlorine and hydrogen generated in the cells ultimately depend on some form of gas mover to force them through the process. Design of the piping system must cover the failure of the gas mover or any other part of the downstream process. Each gas line therefore should have some means of relief that at least allows an orderly shutdown of the cells. The appropriate sections of Chapter 9 cover these relief systems.

Both gases also contain water vapor, in amounts depending on the process and the type of cell. This also is covered in Chapter 9. The point to be made here is that the piping should contain no pockets that allow the inadvertent collection of a liquid seal. This would put a backpressure on the gas line and disrupt cell operation.

The condensate in the gas headers will be electrically conductive. Hydrogen condensate will contain dissolved caustic entrained from the catholyte. Chlorine condensate will contain entrained salt and chlorine dissolved from the gas.

8.4.1.1A. Chlorine. Choices for chlorine include titanium, lined systems, and certain plastics. Titanium is not a satisfactory material for direct connection to the cells. It would make serviceable headers, but even there its investment cost has precluded its being a common choice. Ullman [24] points out in mitigation of the cost that, especially with their

large number of connections, headers fabricated of titanium are more serviceable and more easily repaired. With proper means for removing stray currents, titanium headers have been in service for more than fifteen years with no visible wear. When the cells and headers operate under positive pressure, titanium has the added advantage that design for resistance to pressure is easier and that the headers are less subject to catastrophic failure. With these advantages, the use of titanium is growing in new plants.

Certain seamless extruded thermoplastics (e.g., CPVC) can be suitable when properly supported but are limited in size. In all but the smaller plants, they are not available in the diameters required for chlorine headers. In the past, rubber-lined piping was used, but its service life was limited and it required more flanged connections than butt-connected piping. The standard choice for chlorine headers today is still FRP.

A wide choice of base resin is available in FRP piping. Isophthalic resins are perhaps the standard in most types of industry, but the chemical industry is more likely to use bisphenol A resins for their superior corrosion resistance. Such resins are widely used in chlorine plants, but in wet chlorine itself, vinyl ester and modified resins may give better results [25]. Talbot [26] rates modified bisphenol fumarates superior to the standard resins and to vinyl esters, but finds that chlorendic acid-based resins give even better results. A commercial example of this type is Hetron 197. Notwithstanding this recommendation, today's plants frequently use vinyl ester resins.

We must emphasize that FRP piping is a composite material. It comprises layers of different composition, usually assembled by hand lay-up. The quality of the various materials and the skill of assembly are vital factors determining the success of the piping installation. Figure 8.13 shows Talbot's recommended assembly.

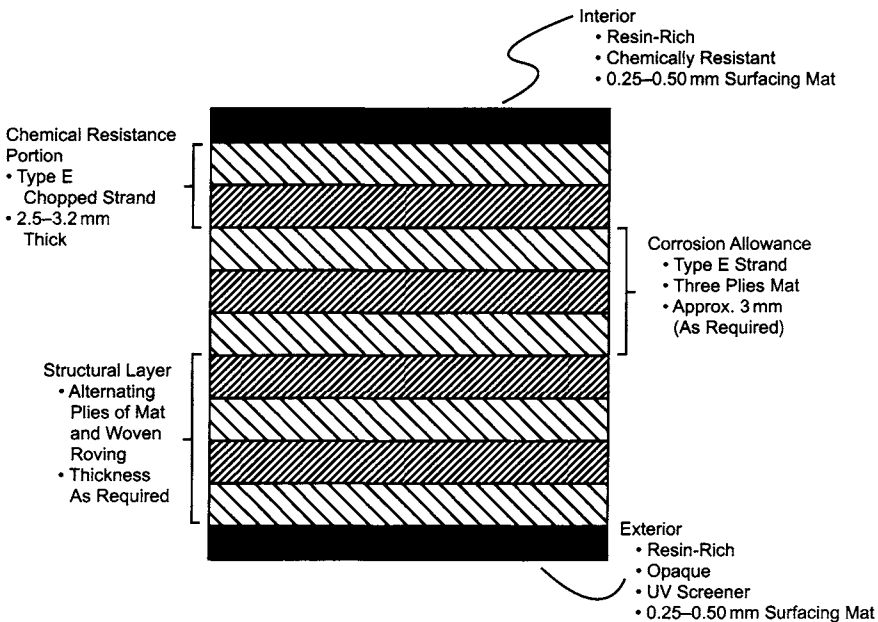


FIGURE 8.13. Buildup of typical FRP laminate for chlorine service.

The interior surface of the piping is a high resin-content mat chosen for its corrosion resistance. The differences among the various resins referred to above are felt here, and the chloro-olefin resins excel in this service. This layer is usually wrapped with two plies of standard chopped glass mat to form the corrosion barrier [27]. The hot, wet chlorine reacts with the resin-rich layer, forming a chlorinated resin sometimes referred to as "chlorine butter." Chlorine continues to penetrate the corrosion barrier for some number of years. The process is slowed by the inherent resistance of the resin and by the formation of a dense, hard butter. An important feature in chlorine piping is the addition of an additional layer of this resin (about 3 mm) for corrosion resistance.

Outside the chemically resistant layers comes the structural portion, which is designed primarily for strength. The exterior surface of the pipe, again, is rich in resin and usually is opaque. Ultraviolet (UV) screeners should be used in outdoor piping to improve its weather resistance. When chlorine has a relatively high hydrogen content, the barriers to UV and visible radiation can prevent photochemical initiation of the hydrogen-chlorine reaction.

Fiberglass-reinforced pipe has the further advantage of a smooth inner surface. Pressure drops are lower than in iron pipe of the same diameter. In a carefully fabricated and installed system, the pressure drop could be less than half that found in iron pipe. Practically, a ratio of 0.6–0.7 is more likely [28].

Since condensate forms continuously in a chlorine header, there must be provisions for removing the liquid, and there must be no pockets where the liquid could collect and form a seal.

Finally, cell room headers can be quite long, and expansion joints frequently are required. These must provide efficient seals and at the same time resist wet chlorine at cell temperatures. The inclusion of expansion joints in the main headers, which may be more than a meter in diameter, is problematical. Two desirable features of header design are simplicity and the absence of flanges. A particular problem with flanged joints in plastic piping is their weight, which complicates the problem of support. For this reason, producers may use sliding expansion joints fabricated from fluorinated polymers instead of standard metal bellows. Another report [29] describes a shrink-on bellows fabricated from FEP film with built-in convolutions. Support rings made of PFA prevent collapse under vacuum. Surface roughness of the header is taken up by applying a fluorosilicone sealant to the pipe and etching the FEP film to provide some roughness. The assembly is wrapped with EPDM elastomer applied over another coat of sealant and held in place by Monel bands.

8.4.1.1B. Hydrogen. Low-pressure hydrogen is easily handled, but designers and operators should be aware that there is always liquid in a hydrogen header. At its most innocuous, this is simply water that condenses as the gas cools. Entrained liquor from the cells can make the liquid in the pipe conductive. In a mercury-cell plant, there is the added complication of liquid mercury condensing in the lines.

Hydrogen headers should be designed to drain from known points to collecting vessels, from which the liquid can be handled properly. Design of the receiving system should recognize that entrained hydrogen gas may be released over time, and there should be some way to vent it safely.

8.4.1.2. *Electrolytes.* Their electrical conductivity makes electrolytes a special case in piping design. Stray currents will follow electrolytes regardless of the kind of piping used. Good design and layout can reduce this leakage, and several comments appear elsewhere in this book. To summarize:

1. Long connections of low diameter between cells and headers have high resistance and oppose current leakage (Section 8.3.2.2).
2. Restricting the maximum voltage in a cell line reduces the magnitude of the problem at the ends of the circuit (Section 8.3.2.2). Restricting the voltage also provides a higher degree of inherent safety (Section 16.4.2.1).
3. Provision of two liquid headers between adjacent cell rows, rather than the more compact arrangement of a single header, avoids the mixing of two streams of greatly different potential (Section 8.3.2.2).
4. Active metal targets in electrolyte headers can intercept leakage currents and prevent corrosion of piping and equipment. Leakage can also be prevented at its source by installing current breakers that actually disrupt the continuous stream of liquid (Fig. 8.10).
5. The ultimate in conservative header layout is to follow the electrical path, joining headers only at the neutral point of the circuit. Figure 8.9 shows arrangements for circuits containing two and four rows of electrolyzers. The latter is an expensive arrangement that can affect the elevation of the cells. Not many producers go to this length, but local regulations have sometimes required it.

8.4.1.2A. *Brine.* The depleted brine leaving mercury and membrane cells is saturated with chlorine. The same sorts of materials used in wet chlorine gas systems are suitable here. Brine lines generally are smaller than chlorine gas headers, and there is more scope for the use of common thermoplastics. The chlorinated types are frequently chosen. Especially at the temperatures of depleted brine, mechanical properties are also very important, and proper support is essential. The reason for the superiority of CPVC over PVC in this application may have more to do with better physical properties than with improved corrosion resistance. For added strength, these materials are often wrapped with FRP.

Laminated FRP pipe is also used in some applications. Some vendors will recommend chloroendic resins for depleted brine; some appear to have reservations over their stiffness. Vinyl esters are another candidate here, and the more highly crosslinked high-temperature grades are preferred [26].

Handling of feed brine is less demanding because of the absence of free chlorine. There is a wider choice of materials. It may be more economic to specify a cheaper construction for feed-brine lines, but it is often deemed more convenient to standardize and to use the material chosen for the depleted brine. This also reduces spare part inventories.

Both feed brine and depleted brine are subject to contamination by compounding agents and processing aids contained in plastic piping. In membrane-cell plant design, materials must be chosen with this in mind. Section 7.5.5.3 has already covered this subject in the comments on materials of construction and the possibility of recontamination.

8.4.1.2B. Catholyte. Fiberglass is generally not a suitable material for strong alkalis. The caustic soda or potash produced in membrane cells is particularly corrosive. The resistance of fiberglass to NaOH attack is actually better at concentrations of 45–50%. The most corrosive form is a solution of approximately 25% NaOH. While fiberglass may be used at low temperature and concentration, then, it does not appear in cell room piping. Many users have adopted the fiberglass composites mentioned under depleted brine. These contain a thermoplastic liner wrapped with fiberglass reinforcement. There is still the possibility of external corrosion due to leaks. Diaphragm-cell liquor, especially when the lines collecting the overflow from the cells are fitted with current breakers, often is carried in carbon steel pipe.

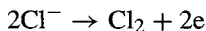
8.4.2. Cell-Room Process Control

This section describes the devices used for control of cell-room operation and considers the effects of the magnetic field associated with the high currents. Some control devices are automatic instruments, some are manually operated, and some are built into the electrolyzers.

8.4.2.1. *Control and Measuring Devices.* Section 8.3.1.5 has already mentioned some of the instrumentation associated with the cell-room power supply. Current, voltage, power, and sometimes power factor are monitored. Process monitoring around the electrolyzers themselves is not highly sophisticated, but there may be a large number of instruments. Each electrolyzer may have more than one flow indicator and several temperature indicators. Many systems, including those based on large bipolar electrolyzers with many cells mounted on a frame, include individual cell voltage scanning and alarms. Deep acidification of feed brine in order to achieve low oxygen levels in the chlorine gas (Section 7.5.6.1) can require a number of pH loops.

Operation of the electrolyzers requires control of concentrations, temperatures, pressures, and amperage. These requirements place demands on other operating variables. Pressure control is in the gas headers, outside the cell installation proper. This is discussed along with instrumentation and control systems for the entire process in Chapter 11.

The major types of cell all rely on the anode reaction



To suppress the competitive formation of oxygen, it is necessary to hold some minimum chloride ion concentration in the anolyte. Feeding excess brine to the cells maintains this concentration. The fact that the feed brine is relatively cool also limits the temperature inside the cell. Concentration control is indirect, usually through feed rate control with the rate dependent on the operating amperage. Temperature control relies on adjustment of the temperature of the feed brine as well as its flow.

Control of the flow(s) to each electrolyzer frequently is manual, with the aid of rotameters. This is especially true in monopolar installations with large numbers of electrolyzers. Monopolar diaphragm cells have essentially one chamber each for anolyte and catholyte and only one feed line (for brine). They rely on division of the feed brine

and the mixing action of the product gases to provide even flow to all the electrodes. In ELTECH's MDC™ line of cells, shown in Fig. 5.23, brine rotameters or orifices in the feed lines to the individual cells provide equal flows to all cells, and multiple feed points through the cell head distribute the flow within a cell. Mercury cells have single brine feed lines and rely on the overflow weirs provided by the inlet end boxes to distribute brine across the cells. Membrane cells have many separate chambers for both anolyte and catholyte. Two approaches to distribution of flow among all chambers are:

1. equalization of pressures at all chambers
2. addition of a device at each cell whose pressure drop dominates the hydraulic balance (e.g., an orifice).

It is of course important to control the total flow of brine and at the same time to control the flow to each electrolyzer. This is why brine header "flow control" often is in fact line pressure control (Section 11.2.2.4D). Maintaining a constant pressure in the line balances the flow into the header with the total flow to all the cells. It also allows individual electrolyzer feed rates to remain steady even through manually set valves. It is important that the cell room headers have very small pressure drops. This will cause the pressures at all control points to be essentially the same. In turn, the rates of flow to the individual electrolyzers will also be equal. Header pressure control also offers a simple way to make nearly instantaneous changes in flow to all the electrolyzers during startup, shutdown, or load changes.

The caustic recycle flow to membrane cells is metered and distributed in essentially the same way as the brine flow. Manipulation of the extent of dilution of the caustic recycle also helps to control the concentration in the cells. With mercury cells, caustic production depends on the feed of water to the decomposers. Pure water is metered to each decomposer at a rate proportional to the operating load.

Control of electrolyte flows is just one aspect of proper distribution across the entire electrode surface in the cell room. Achieving the desired total flow and the proper flow to each electrolyzer is part of process design. The steps taken to ensure good distribution internally are part of electrolyzer design, discussed in Chapter 5.

Cell design must include some means of maintaining liquid levels in the face of changing amperages and electrolyte flow rates. This involves various overflow mechanisms. Mercury and membrane cells have fixed overflow devices that hold the levels and fix the hydraulic capacities. Mercury cells depend on outlet end boxes, as shown in Fig. 5.7. Most membrane cells have overflows built into the electrode designs (Fig. 5.36). Diaphragm cells have adjustable overflows, because it is necessary to maintain levels in both the anode and the cathode chambers with a single device. Figure 8.14 shows a typical arrangement, which relies on an adjustable percolation pipe assembly. The flow through the diaphragms depends on a hydraulic gradient between the two chambers. As the diaphragm ages and loses some of its porosity, this gradient must be increased. For this reason, diaphragm cell heads are quite large and allow variations in anolyte level. Lowering the position of the overflow pipe allows the level on the cathode side to drop but keeps the level on the anode side in the desirable range. The MDC-55 (or the redesigned MDC-65), the largest cell in that series, has a sight glass nearly half a meter long (Fig. 5.23). In practice, the operator maintains the proper brine flow rate and observes the level of anolyte in the cell head. When flow through the diaphragm

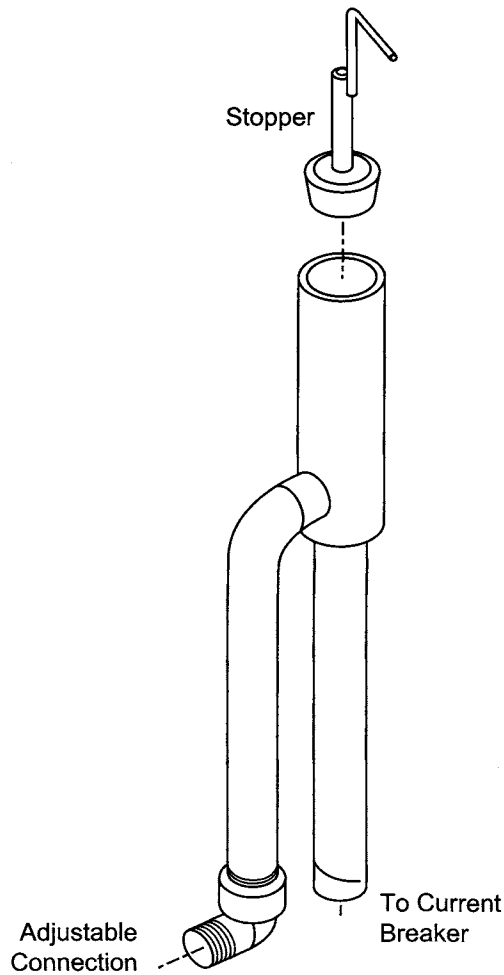


FIGURE 8.14. Adjustable overflow for diaphragm cell. (With permission of ELTECH Systems Corporation.)

decreases and that level tends to increase, the operator can lower the overflow pipe. The level of the catholyte then drops, and the increased head across the diaphragm increases the flow into the cathode chamber.

Amperage is controlled at the rectifiers. There may be several electrical circuits among the cell rows, or only one. There are several reasons why more than one circuit might be used:

1. operation can continue at a reduced rate when one circuit must be taken down for maintenance
2. the available turndown is greater, allowing more efficient operation in times of low demand
3. the voltage across a cell line is smaller, reducing insulation and protective requirements and perhaps increasing inherent safety

4. layout sometimes can be simplified
5. reuse of rectifiers after conversion to membrane cells sometimes is more efficient when output is redistributed
6. it is possible to operate different parts of the cell room at different currents.

The last item on the list may be useful if some group of cells or their auxiliaries are damaged. For example, a local failure in control or in electrolyte flow may have caused selective damage, or one group of cells may tend to operate at a substantially higher voltage than the others. The latter may result from uneven maintenance or during a general cell renewal exercise after a major incident. Long-term or frequent operation of two groups of cells at different conditions is inefficient. With a single liquor circuit each for anolyte and catholyte, the usual arrangement, the best operating conditions cannot be maintained in both groups. This problem can be overcome, at a cost, by installing a second independent loop.

Section 8.3.1.2 discusses rectifiers and Section 8.3.1.5 discusses current measurement. With high-amperage monopolar electrolyzers, more than one rectifier may be used on each circuit. Bipolar electrolyzers with their low operating amperages are not well suited to large rectifiers. This can be a problem when converting to membrane-cell operation. Sometimes, rectifier modules can be rearranged to give a better division. In other cases, multiple electrolyzers are connected to the same rectifier and the output of the rectifier is allowed to distribute itself. Because of the inevitable differences in operating characteristics, the electrolyzers will not all draw the same current. Section 8.3.1.3C considers this in some detail.

With all electrolyzers operating at the same voltage, the waste heat generated in each will be proportional to the current. The electrolyte flows required to maintain temperatures will be nearly so. A reasonable approximation to operation then is to proportion the rates of feed of brine and caustic to the currents.

8.4.2.2. Effects of Magnetic Fields. Many of the chemical services in the cell room are difficult, but they are not qualitatively different from those in the rest of the process. The distinguishing feature for cell-room instrumentation design is the presence of the electrical field.

Every current has associated with it a magnetic field that extends beyond the boundaries of the equipment. Direct current, with a steady flow in one direction, produces only static magnetic fields. The field is strongest within the cell line, and its strength depends on the amperage. Some effects can be amusing (metal objects standing on end); some are inconveniences (stopped watches, erased magnetic strips on plastic cards). Others can be more serious, and limits on the exposure of certain personnel are the subject of Section 8.5.1.2.

Cell-room magnetic fields also can influence electronic devices. The instruments chosen for the electrolysis area must be able to work in such an environment, and the quality of data transmission must be protected. A practice now finding its way into some cell rooms is the use of optical fibers to carry analog signals.

Conroy and Cameron [30] report that the components most sensitive to static magnetic fields are certain ferritic inductors. These are characteristic of some older systems, but newer PLCs, for example, appear not to be susceptible to interference. Still, behavior

in DC magnetic fields is not part of normal factory testing, and this sort of equipment should be tested on site. The field strength in the control room of a bipolar installation may be less than 50 gauss, but still the output of devices such as CRTs can be distorted. Single-color displays are the least sensitive, and liquid-crystal displays are not affected.

Cell-room currents also can have indirect effects. For example, they can destroy instrument cable screens and so influence the signals received from the instruments.

8.4.3. Cell Renewal Activities

8.4.3.1. Switching. Electrolyzers must be switched out of an active circuit before disassembly or removal from their berths. After repair or replacement, they must be physically reconnected and then switched back into service.

With a monopolar circuit, the usual technique is to employ a mobile switching device that can be brought into position adjacent to the appropriate electrolyzer. With diaphragm cells, this takes the form of a cabinet on wheels, placed in the aisle next to the cell. With membrane cells, the switch may be above, below, or beside the cell. Depending on the arrangement of intercell connectors, it may be necessary to switch two electrolyzers from the circuit, but the principle remains the same.

The switching device contains enough conductor to present a low resistance to full line current. When the switch is closed, the current is shunted away from the electrolyzer, which can then be disconnected from the surrounding cells, its piping, and its instrument wiring. Figure 8.15(a) shows the arrangement schematically.

Operation can continue indefinitely with the switch in place. Depending on its design and the amount of conductor present, water cooling may be necessary. Usually, economical operation requires prompt replacement of the removed electrolyzer. The renewal program should be organized to have a replacement available even when an electrolyzer must be removed in an emergency.

Bipolar electrolyzers also require switching. Since they usually do not operate in series, a shunting device is not necessary, and the problem of shunting across large

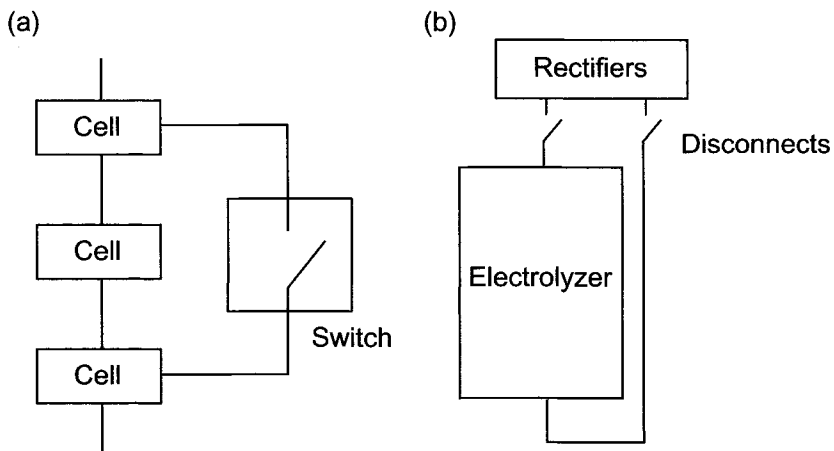


FIGURE 8.15. (a) Monopolar vs (b) bipolar switching.

voltages normally does not arise. The situation, depicted in Fig. 8.15(b), is fundamentally simpler. Standard DC disconnects are installed between the rectifier(s) and each electrolyzer. Electrolyzers served by dedicated rectifiers can be taken out of service simply by shutting down the rectifier.

Figures 3.1 and 3.2 of Chlorine Institute Pamphlet 139 [8] also show, in more detail, monopolar and bipolar switching arrangements.

8.4.3.2. Transport. Whatever type of electrolyzer is in use, cranes will be part of the transport system. Requirements vary greatly from one sort of electrolyzer to another. The most imposing requirement is in the ordinary diaphragm-cell plant, where the entire cell must be lifted and moved. An ELTECH MDC-55[®], for example, weighs about 7 tons when empty and 13 tons when full of liquor. The crane usually moves the cell from the circuit into the adjacent aisle and places it on a cart built for the purpose of transporting the cell to the renewal area, where it can be serviced or rebuilt. The replacement cell similarly is delivered near its spot in the cell line by the same sort of cart and then lifted and moved into place by the crane.

Mercury cells are far too large to be moved in a similar manner, and the analogous job for a crane is the piecemeal removal of anodes from the top of a cell.

Membrane cells again are more diverse in their design. In some cases, the crane moves entire electrolyzers. In others, notably the large bipolar electrolyzers, components or elements are the items handled.

In any of these situations, a crane is required that has access to any position within the cell line. This usually takes the form of a bridge crane that spans at least one cell line or perhaps an entire building.

Different components of a bridge crane must travel in all three directions. The bridge itself must be able to travel along the cell line to the position of any individual cell or electrolyzer. The lifting mechanism then moves on a trolley at right angles to the motion of the bridge in order to arrive directly above the object to be lifted. Finally, the hoisting apparatus travels up and down in order to gather the object in question and lift it from its position. The above discussion on the requirements presented by the three types of electrolyzer shows that the capacity of the lift and the design of the lifting rig are strongly dependent on the model of electrolyzer in use. There are few useful generalizations.

The speeds of travel are more suited to generalization. The bridge and the trolley can move at reasonable speeds, about 1 km hr^{-1} and higher. Usually, the speed is chosen to allow a complete traverse in one to a very few minutes. Speed control may be continuous. The hoisting device travels much more slowly, usually no more than 1 m min^{-1} . This allows some control of orientation of the device being lifted and prevents excessive swinging, which could lead to serious or catastrophic damage to some of the cell room components. Many hoists have two-speed controls with the lower speed only a fraction of the higher. Movement of the load near the cells then can be very slow. When the load is free of the cells and other obstructions, higher speeds may be acceptable. Hoists may also be supplied with limit switches. The lifting gear should straddle the center of gravity of the load. The design of electrolyzers usually includes proper placement of lifting lugs to facilitate this.

Bridge cranes always have access platforms (with proper safety features such as railing, etc.), but normal operation is from floor level. Typically, control is by a set of

pushbuttons mounted on a pendant attached to the crane. The crane operator must then travel with the bridge, or motion stops. Voltage on the control set should be no more than 110 V. Other means of control of crane movement include radio and nonconductive rope operators.

Cranes must have both mechanical and electrical safety features. The former should include emergency stops and fixed-position stops at the ends of the cell line. In general, Crane Institute Specification No. 49 should be followed. In fixing the electrical requirements, the designer should consider the possible presence of hydrogen in the cell room. The crane should be protected against unintentional contact with live equipment. This is most likely when the lifting mechanism is being lowered or positioned for a pickup. Insulation at the crane hooks should be considered necessary but not sufficient. Good practice includes insulation between the lifting drum or mechanism and the traveling gear.

Diaphragm-cell installations always include a cell rebuilding area separate from the cell room. It would be possible to transport cells entirely by crane, but it would also be unwieldy and very expensive. Transport by cart, as mentioned above, is the standard method. The mobility offered by this method gives great flexibility in choosing a location for the cell renewal area. The mover can be any general utility-type vehicle of sufficient capacity. Depending on the arrangement of the renewal area, the vehicle may have to be suitable for indoor use.

Within the cell renewal area, components may be handled in many different ways. Building cranes are available in some cases. In others, jib cranes move assemblies over short distances. Smaller assemblies and components are moved by monorail, cart, or hand.

The momentum of the load is an important consideration in operation of any transport device. A sudden stop to a crane will cause the suspended load to swing. Transport wagons need adequate braking capacity.

8.5. CELL-ROOM HAZARDS

Chlor-alkali plant hazards are many and varied [31], and the least familiar to most chemical-industry technologists are those associated with the cell room. Section 8.2.2.4 refers to standard rules and practices that apply in the immediate vicinity of the cell line. Chapter 16 and other sections discuss more generally the various hazards and the measures taken to overcome them. Workers must be well trained to cope with this variety, and the good safety record of the industry demonstrates the success of its training programs. Outsiders (e.g., contract maintenance personnel, equipment specialists, design engineers, plant visitors) may not be familiar with the necessary safe practices. It is important, therefore, to restrict access to parts of the plant and to provide the appropriate training or knowledgeable guides before allowing entry to such people.

8.5.1. *Electrical Hazards*

The hazards characteristic of a cell room are the electrical hazards. These carry the danger of electrocution and other damage to the human body, and they play a role in some of the thermal and explosion hazards. The thermal hazard of hot buswork has in fact been responsible for more injuries than the electrical hazard. Chlorine Institute

Pamphlet 139 [8] and a standard published by the National Fire Protection Association in the United States [32] are much more detailed than this brief presentation and also contain recommended procedures and safety checklists.

Outside the cell room itself, the transformers and rectifiers may be indoors or outdoors but always are enclosed to restrict entry to their immediate vicinities. The hazards are the high supply voltage itself, the possibility of explosion, and the risk of flash burns in case of a ground fault. The maintenance of this equipment and associated circuit breakers, switches, and relays is a subject for specialists, and other personnel should not enter the enclosures while equipment is activated.

8.5.1.1. Voltage and Shock Hazards. Inside the cell room, it is a practical necessity for operators to come into contact with live parts. Since some of the usual safety measures against electrical hazards do not apply, special codes of practice have been formulated.

It is essential that a line of cells be isolated from the ground (except perhaps at the center point of a circuit). It follows that cell-room personnel inside the working zone must also be insulated from the ground. Personal protective equipment includes insulating rubber boots and gloves. With time, these can develop faults, and it is good practice to test them regularly for defects. This can be done with a portable hand-cranked generator that develops a voltage between its terminals and allows the measurement of the resistance of any object added to form a circuit. Standard apparatus is available and can be assembled into a permanently installed tester.

Workers should also be aware that allowing other parts of the body to touch a grounded conductor while wearing boots and gloves removes one layer of protection. Designers must ensure that all routine work can be performed comfortably from a normal standing posture and without the need to stretch across any part of the electrical circuit. Kneeling, sitting, and reclining remove the protection offered by insulating boots. Any work performed in such positions requires a circuit shutdown or specific protective measures such as the use of insulating mats. Emergency work and any work requiring a number of people demand special attention to avoiding congestion. Without this attention, workers are more likely to be crowded together, too close to live surfaces or grounded implements, or working in contorted positions.

Under ideal circumstances, the potential at the center of a circuit will be zero and the magnitude of the potential at each end will be half the total. A cell line, however, is liable to ground faults, and the limiting case would be a hard ground at one end, near the rectifiers. The potential relative to the ground would be zero at this point and the full circuit voltage, above or below zero, at the other end. This situation is one reason for recommending ground fault detection for the DC circuit. System design and work practices should always consider this limiting case.

More than one level of insulation is advisable in order to keep the electrolyzers from the ground. Nonconductive supports usually comprise one level. Designers and operators must also be aware that normal operation can bring many grounded objects into the working zone. These include certain tools, jumper switches, crane hooks and cables, cell transport vehicles, instruments, piping, and utility hoses. The necessary precautions will depend on the nature and design of the object. Proper insulation is prudent but should not be considered sufficient protection. Frequent inspection or testing of insulation is a good practice. Operators should be alert for insulation that is wet or coated with electrolyte.

Another important consideration is the potential gradient along the cell line. Bipolar electrolyzers are often described as high-voltage, low-amperage items, with monopolar electrolyzers the reverse. The high voltage across bipolar electrolyzers does not necessarily translate into a high cell-room voltage. Monopolar circuits, with a sufficient number of cells in series, often run at higher voltages. It is always true, however, that the potential gradient is steeper along a bipolar electrolyzer than it is along a monopolar row. Adjacent monopolar cells, equivalent points of which are some distance apart, differ only by three or four volts. The same potential difference in a bipolar circuit occurs across a much smaller distance, the thickness of a unit in the bipolar assembly. It is possible for someone to touch two positions in a bipolar electrolyzer that are separated by a significant number of cells. The voltage across two such positions may constitute a hazard that does not exist in monopolar cell lines. There should be positive protection against the hazard, and it is usually in the form of a screen of transparent plastic.

Air is an excellent insulator and should be used as such in design. Proper spacing of items that have widely different electrical potentials is imperative. Personal protective equipment mitigates hazards and reduces the severity of accidental exposures, but it should not be relied upon as the primary defense against a hazard. Most designers provide at least 2 m between cell lines and between cells and unprotected grounded steelwork. The spacing must also allow for conductive mechanical aids, which should not be able to bridge these gaps. Since the purpose of the wide spacing is to prevent simultaneous contact with two conductors or capacitances at widely different potentials, it is also a good idea to walk single-file in aisleways and to eliminate any supporting columns in their design.

Cell rooms usually are not electrically classified. The possible release of hydrogen would be the reason for such classification, but it is present at very low pressure and dissipates rapidly and over very short distances. Proper ventilation, as discussed in Section 8.2.3, is necessary to this rapid dissipation. Hydrogen concentrations may be higher near the roof of the cell building. Many designs therefore eliminate electrical contacts at high levels and include extra protection in lighting fixtures.

A mitigating circumstance in a cell line is the fact that direct currents are less dangerous than alternating currents at the usual supply frequencies [16,33]. It takes at least four times the amperage to produce a given effect with direct current. In the dangerous range, the Chlorine Institute [8] uses a factor of seven. Very high frequency alternating currents are also "safer"; the most dangerous frequencies are in fact close to those chosen for transmission of alternating currents (there is a very broad maximum that peaks at 30–50 Hz). The high currents in a cell room do not in themselves constitute a shock or electrocution hazard. True, it is current that harms the body and can kill a person, but that current is produced by a difference in electrical potential. Potential differences occur between adjacent electrolyzers, electrolyzers in adjoining rows, and electrolyzers and the ground. Add to the cells all conductive objects in contact with them, such as buswork and intercell conductors, and there are many opportunities for accidents.

Most cell-room designs avoid the use of electrical equipment within the working zone. Mercury pumps have already been identified as a necessary exception. Mobile equipment (e.g., switches and monorails devices) frequently has air drives rather than motors. Electric motors, when used, should have isolating transformers in both the power and the control circuits.

8.5.1.2. Electromagnetic Field Hazards. Electromagnetic fields (EMFs) are present in and around cell rooms. Section 8.4.2.2 discussed the effects of magnetic fields on instruments. We must also consider possible effects on the human body. First, one must say that electrolysis area EMFs are much weaker than those shown by medical research to be dangerous and that no adverse effect on cell room workers has ever been established [34]. There is evidence that continued exposure to a steady magnetic field can lead to higher blood pressure and a lower white cell count [35]. The effects, if real, are said to be “very small” and not of any great practical effect. There has also been some public concern over the possible effects of the magnetic fields associated with high-power AC transmission lines. Many studies in various parts of the world, however, have not related any of the supposed ill effects to the fields [36]. Direct currents, as mentioned, produce primarily static magnetic fields and so are in any case less likely to have deleterious effects.

In 1991, Adams [37] reported on measurement of the fields generated by various types of cell operating between 60 and 120 kA and found that the fields were well within the limits recommended at that time. Mean levels at different elevations in all plants were between 45 and 90 G, and all 600 readings were below 200 G. The gauss (G) is the cgs unit of magnetic induction (flux density). In a field of 1 G, a conductor of unit length moving at unit velocity perpendicular to the field will experience an induced emf of one abvolt ($1 \text{ abV} = 10^{-8} \text{ V}$). The threshold limiting value (TLV), as recommended by the American Conference of Governmental Industrial Hygienists (ACGIH) in 1998, was 600 G (whole body, time-weighted average), with a ceiling value of 20,000 [37]. Given the fact that workers spend only a limited amount of time in the center of the cell circuit, the average exposure would seem to be below 10% of that allowed. One should note that all Adams’s data apply to monopolar cells.

While the data gave little reason for concern over the exposure of the general population to the field in a chlor-alkali plant, it is possible for the field to interfere with the operation of low-power electronic devices. Cardiac pacemakers are one example. The ACGIH in the same list of TLVs referred to above suggested a value of 5 G for persons with these devices. Adams reported that one company had set its own limit of 1 G. Since this is a small multiple of the normal background, the rule effectively bars those with pacemakers from approaching a cell room. While not covered specifically by these rules, there should also be special concern for those who wear or carry other medical devices such as aneurysm clips, suture staples, and prostheses. These can respond to forces produced by stronger fields, but no definite limits have been set.

Recent developments, particularly in Europe, may lead to more stringent regulations. To understand the situation, it would be well to review the characteristics and sources of the various types of field. Fields may be classified as electric or magnetic and as static or variable. Their sources are:

Field	Static	Variable
Electric	Charged conductor	Alternating voltage or current
Magnetic	Current flow in conductor	Alternating voltage or current

Static fields store energy and can influence conductors and moving charges, but they emit no radiation. Variable electric and magnetic fields are interdependent. An alternating field of one type produces an alternating field of the other type, with the same frequency. Some of the energy produced radiates away from the source. Higher frequencies have greater ratios of radiated to stored energy. The differences among the various types of EMFs require us to consider their potential health effects separately.

8.5.1.2A. **Static Fields.** A static electric field results from forces exerted at the molecular level when a conductor becomes charged. It induces a charge on an exposed person, but the field inside the body is almost zero. Except for the shock of charging or discharging, there are no known effects of static electric fields on humans or animals [37].

Static magnetic fields arise when current flows in a conductor and exert forces on moving ions in solution (as in the blood). When people move through magnetic fields, currents may be induced in blood or living tissue, in accordance with the Faraday laws of induction. This is the only postulated mechanism that might produce significant biological interaction [38]. Magnetic fields conceivably also can affect the orientation of polar molecules within the body. Theoretical studies indicate that such effects are negligible below about 10 tesla (T). A tesla being equal to 10,000 G, this is orders of magnitude greater than the strength of typical cell-room fields.

Several studies of specific postulated effects have shown no relationship with static magnetic fields:

1. leukemia mortality [34,39]
2. incidence of cancer, general mortality [40]
3. nineteen other categories of disease [39].

Slight changes in white blood cell pictures were detected in workers in electrolysis areas, but as in Marsh's work [35] quoted above, results were still within the normal range [39].

8.5.1.2B. **Time-Varying Fields.** Variable fields interact with living tissue in several ways:

Direct action	Indirect action
Absorption of energy ^a	Contact currents
Coupling to low-frequency electric fields	Medical devices
Current	
Polarization	
Reorientation of dipoles	
Coupling to magnetic fields	
Induced fields	
Circulating electric current	

^a Negligible absorption at low frequencies; no measured temperature increase below 100 kHz.

A uniform direct current will not produce a variable field, and problems would not arise. As discussed in Section 8.3.1.3A, however, cell room currents are not

uniform. Even a perfect rectifier produces a pulsating current of frequency nf , where n is the number of rectification pulses and f is the fundamental frequency of the electric supply (e.g., 50 Hz). A real device will also produce various harmonics of the fundamental frequency. Each harmonic current will produce a variable EMF. The more comprehensive regulations cover a wide range of frequencies and specify the maximum allowable flux density as a function of the frequency. Because of the higher energy content of high-frequency fields, there is an inverse relationship. Chart 4.3.2 of the Euro Chlor publication [34] shows the exposure limits published by the International Commission on Non-Ionizing Radiation Protection (ICNIRP) and five other authorities (in Europe, Great Britain, Germany, The Netherlands, and the United States). This chart is a graph showing the allowable maximum flux density as a function of frequency. There is a near consensus, with the range at a given frequency generally covering about one order of magnitude:

Frequency (Hz)	Range (mT)
1	20–100
10	1–10
100	0.1–1.5
1,000	0.01–0.5
10,000	0.01–0.2

More significant than the differences in allowable exposure levels is the use by some authorities of summation formulas. A recommendation put forward by the European Council [41] follows ICNIRP's proposal. The summation formulas are somewhat arbitrary. ICNIRP's approach [42] is to express the field strength for a relevant frequency as a fraction of the reference limit at that frequency. Thus,

$$F_{Hn} = H_n / H_{L,n} \quad (42)$$

where F is the field strength as fraction, H_n the magnetic field strength at n th frequency, and $H_{L,n}$ the magnetic field strength at n th frequency reference limit. ICNIRP's requirement then is

$$\sum F_{Hn} \leq 1 \quad (43)$$

Similarly, for variable electric fields,

$$F_{En} = E_n / E_{L,n} \quad (44)$$

$$\sum F_{En} \leq 1 \quad (45)$$

The meanings of the symbols in Eqs. (44) and (45) are analogous to those in Eqs. (42) and (43), with E referring to electrical rather than magnetic fields.

It can be seen that the ICNIRP method effectively considers that a flux density that is 50% of the allowable limit at a given frequency has used 50% of the total allowance. A second occurrence at another frequency would consume the rest of the allowance, and any field, however small, at any other frequency would then cause a violation. Dutch regulations apply the same summation formulas as ICNIRP but use different values for the reference limits. In the United Kingdom, the National Radiological Protection Board uses its own values of reference limits and also applies its own summation formula [43].

Carrying out the summation over a wide range of harmonics allows only a small fraction of any individual limit to be present. This approach effectively makes a very large reduction in allowable flux densities and field strengths. The Euro Chlor report [34] concludes that “(t)he limit concerning the multi-frequency magnetic fields will become a major problem for working places in electrolyses if the regulation is based on the ICNIRP proposals.” Measurements in a typical cell room show that what is now the routine and necessary practice of operator entry to the cell line would in many cases be prohibited.

8.5.2. Chemical and Explosion Hazards

The major chemical hazard in a cell room is the presence of chlorine, and stringent precautions must be taken to keep the concentration of chlorine gas in the air very low. The American Industrial Hygiene Association [44] publishes emergency response planning guides (ERPG) for toxic materials. Table 8.6 shows the data for chlorine based on an exposure time of 1 hr. Concentrations below 1 ppm are not a serious danger if exposure time is short. Concentrations above 20 ppm become dangerous very quickly.

One does not design a cell room to achieve a certain steady-state or 1-hr peak level of chlorine concentration in the air, nor does one attempt to establish *a priori* a tolerable exposure profile for plant personnel. Tables such as 8.6, in spite of the apparent precision of the numbers, are really qualitative or at best semi-quantitative indicators of the seriousness of a hazard. Designers of chlorine-handling plants must exercise proper care by designing to recognized industry standards, and operators must understand and observe established procedures. There is more on this subject in Section 16.2.1.

TABLE 8.6. Effects of Exposure to Chlorine for 1 hr

ERPG ^a	Level (ppm)	Definition
1	1	Very few people suffer even mild, transient health effects
2	3	Very few people suffer irreversible or other serious health effects or symptoms that could impair ability to take protective action
3	20	Very few people suffer life-threatening health effects

^aERPG, emergency response planning guide.

REFERENCES

1. D.E. Bihary, Safety in Cellroom Design, *39th Chlorine Institute Plant Operations Seminar*, Washington, DC (1996).
2. W.H. Davis, Open Cell Room Operations, *24th Chlorine Institute Plant Operations Seminar*, Houston, TX (1981).
3. G. Oliva, The Return of DeNora to Diaphragm Cell Technology with Glanor®. In *Proceedings, Oronzio de Nora Symposium on Chlorine Technology*, Venice (1979), p. 279.
4. J.H. Nichols, Ventilation in Mercury Cell Rooms, *8th Chlorine Institute Plant Operations Seminar*, New York, NY (1963).
5. J.A. Heilala, Controlling Mercury Exposure, *32nd Chlorine Institute Plant Operations Seminar*, Houston, TX (1989).
6. G.F. Gissel, Waste Water Minimization at the Vulcan Port Edwards Chlor-Alkali Facility, *39th Chlorine Institute Plant Operations Seminar*, Washington, DC (1996).
7. *Standard for Electrical Safety in Electrolytic Cell Line Working Zones*, Standard No. 463, Institute of Electrical and Electronics Engineers, New York, NY (1977).
8. *Electrical Safety in Chlor-Alkali Cell Facilities*, Pamphlet 139, Edition 3, The Chlorine Institute, Inc., Washington, DC (1998).
9. *Gravity Ventilation Systems*, www.westerncanwell.com, Western Canwell, Denison, TX (2002).
10. D.L. Beeman, ed., *Industrial Power Systems Handbook*, McGraw-Hill Book Co., New York, NY (1955).
11. W.H. Dickinson, *AIEE Trans. (App. Ind.)*, Part II **81**, 132, July (1962).
12. J.M. Lucas, Personal Communication (2002).
13. M. Cameron, *Trends in Power Factor Correction with Harmonic Filtering*, www.udgroup.com, Universal Dynamics Ltd., Vancouver (2001).
14. *Recommended Practice for Harmonic Control in Electrical Power Systems*, IEEE 519, Institute of Electrical and Electronics Engineers, New York, NY (1992).
15. P.C. Buddingh, *Even Harmonic Resonance—An Unusual Problem*, IEEE Paper No. PCIC 2002-11 (2002).
16. A.G. Forster, *IEEE Trans. Ind. Appl.* **1A-11**(6), 716 (1975).
17. Y. Tominaga, T. Kanke, K. Takagai, and T. Miyazaki, Design, Installation and Operation of Ion-Exchange Membrane Chlor-Alkali Process. In N.M. Prout and J.S. Moorhouse (eds), *Modern Chlor-Alkali Technology*, vol. 4, Elsevier Applied Science, London (1990), p. 141.
18. J.E. Harker, Catalytic International, Inc., Personal Communication (ca. 1978).
19. W.H. McAdams, *Heat Transmission*, 4th ed, McGraw-Hill Book Co., New York (1954), pp. 170–174.
20. L.J. Istas, Aluminum Intercell Bus: A Case History, *19th Chlorine Institute Plant Operations Seminar*, Montreal (1976).
21. F. Hine, *J. Electrochem. Soc.* **117**, 139 (1970).
22. L.J. Updyke, Development of Energy Models for Chlorine Plants, *28th Chlorine Institute Plant Operations Seminar*, Houston, TX (1985).
23. P.W. Masding and N.D. Browning, A Dynamic Model of a Mercury Chlorine Cell. In J. Moorhouse (ed.), *Modern Chlor-Alkali Technology*, vol. 8, Blackwell Science, Oxford (2001), p. 247.
24. A. Ullman, Cost Saving in Chlorine Plants by Benefitting from the Unique Properties of Titanium. In J. Moorhouse (ed.), *Modern Chlor-Alkali Technology*, vol. 8, Blackwell Science, Oxford (2001), p. 282.
25. *Influence of Hot/Wet Chlorine on FRP Performance*, Bulletin, Reichhold Chemicals, Inc., Research Triangle Park, NC (1986).
26. R.C. Talbot, *FRP Usage in the Chlorine Industry*, Bulletin No. 1704, Ashland Chemical Co., Columbus, OH (1988).
27. *Standard Specification for Reinforced Plastic Laminates for Self-Supporting Structures for Use in a Chemical Environment*, Standard C-582, American Society for Testing and Materials, Philadelphia, PA (1984).
28. W. Pechenik, Catalytic, Inc., Personal Communication (ca. 1980).
29. D.J. Sankey, M. Isaacs, and A. Gaines, *Chem. Processing*, p. 96, February issue (1981).
30. E. Conroy and M. Cameron, *Advances in Anode Monitoring*, www.udgroup.com, Universal Dynamics, Ltd., Vancouver (2001).
31. I.F. White, G.J. Dibble, J.E. Harker, and T.F. O'Brien, Safety Considerations in the Design of Chlor-Alkali Plants. In K. Wall (ed.), *Modern Chlor-Alkali Technology*, vol. 3, Ellis Horwood, Chichester (1986), p. 97.

32. *NFPA 70E, Standard for the Electrical Safety Requirements for Employee Work Places*, National Fire Protection Association, Quincy, MA (1995).
33. C.F. Dalziel, *IRE Trans. Med. Electron.* **PGME-5**(7), 44 (1956).
34. *Electromagnetic Fields in Chlorine Electrolyses: Effects on Health and Recommended Limits*, Health 3, 1st ed, Euro Chlor, Brussels (2001).
35. J.L. Marsh, *Health Effects of Occupational Exposure to Steady Magnetic Fields*, University of Michigan Dissertation, Ann Arbor, MI (1980).
36. R. Park, *Voodoo Science: The Road from Foolishness to Fraud*, Oxford University Press, Oxford (2000), pp. 140 *et seq.*
37. R.F. Adams, *Static Electromagnetic Fields in Chlor-Alkali Plants*, *34th Chlorine Institute Plant Operations Seminar*, Washington, DC (1991).
38. *Interaction of Static and Extremely Low Frequency Electric and Magnetic Fields with Living Systems: Health Effects and Research Needs*, World Health Organization, Geneva (1998).
39. International Commission on Non-Ionizing Radiation Protection (ICNIRP), *Health Phys.* **66**(1), 100 (1994).
40. L. Bärregard, G. Sällsten, and B. Jarvholm, *Brit. J. Ind. Med.* **47**, 99 (1990).
41. *On the Limitation of Exposure of the General Public to Electromagnetic Fields*, European Council Recommendation 519/CE, Brussels (1999).
42. International Commission on Non-Ionizing Radiation Protection (ICNIRP), *Health Phys.* **74**(4), 494 (1998).
43. *Board Statement on Restrictions on Human Exposure to Static and Time-Varying Electromagnetic Fields and Radiation*, National Radiological Protection Board (UK), Chilton, Oxon (1999).
44. *Emergency Response Planning Guidelines*, American Industrial Hygiene Association, Akron, OH (1988).

9

Product Handling

The first three sections of this chapter discuss the processing and handling of the products of electrolysis. Section 9.1, related to chlorine, comprises most of the chapter. Sections 9.2 and 9.3 then cover hydrogen and caustic soda or potash. Section 9.4 discusses applications of several byproducts that are sometimes found useful.

9.1. CHLORINE

9.1.1. Introduction

Chlorine gas from the electrolyzers is hot and nearly saturated with water. As delivered downstream, it contains various impurities that form in the cells or enter during processing. The major steps in the typical chlorine gas plant, as was shown in Fig. 6.6, are cooling, drying, compression, and liquefaction. The present section covers these steps in turn, as well as the handling of the product and of any chlorine not recovered by liquefaction.

The selection of materials of construction is very important in chlorine processing, and the requirements change greatly from one section of the process to the next. A chlorine processing plant therefore uses a wide variety of materials. In particular, there is a distinction between dry and wet chlorine. The discussion therefore starts with an overview of this important topic (Section 9.1.2).

The first step in the gas process is cooling. Direct or indirect exposure to a cooling medium brings the gas to a lower temperature. This incidentally condenses most of the water vapor. The condensate must be treated to remove dissolved chlorine before disposal or return to the electrolysis process. Section 9.1.3 discusses chlorine cooling and condensate handling.

Even at the lower temperature, the gas is too wet for many applications. In the next step, contact with concentrated sulfuric acid, usually at about 93–98% H_2SO_4 , produces a moisture content below 50 ppm (v/v). The process dilutes the acid to a concentration between 50 and 80%. This spent acid then goes to disposal or reprocessing. A lower spent acid strength reduces the consumption of acid and the amount of spent acid produced, but the final concentration must be suited to the methods used for disposal or recovery. The spent acid, like the condensate removed from the cooling section, contains dissolved

chlorine that must be removed. Section 9.1.4 discusses the problems of chlorine drying and acid handling.

There is always a certain amount of entrained liquor in the gas leaving the cells. This is in the form of a mist that has been known to survive beyond the gas coolers and into the drying system, and deposits can form in the chlorine piping and processing equipment. Also, the sulfuric acid used in the drying system is notorious as a source of mist that can interfere with the performance of downstream equipment. Mist eliminators installed both before the coolers and after the drying towers alleviate these problems. Section 9.1.5 covers this subject.

The dry gas, still at approximately atmospheric pressure, can be handled safely in mild steel equipment. Particularly with membrane cells, which can operate under some positive pressure, the gas, wet or dry, is suitable for some applications. In most cases, however, the next step will be compression. The pressure must be raised to a level sufficient for liquefaction at a reasonable temperature or for direct use as a gas in another process (e.g., the manufacture of ethylene dichloride). Operating conditions and the apparatus used for compression are highly variable and are the subject of Section 9.1.6.

Roughly half the world's chlorine is liquefied for sale or transfer to another process. Liquefaction usually involves condensation against a boiling refrigerant, in which case a mechanical refrigeration plant is required. The liquefied chlorine is stored in some quantity and is then transferred to its client process or loaded for shipment. Section 9.1.7 covers liquefaction and Section 9.1.8 the storage and handling of the liquid.

The presence of noncondensable gases in the chlorine means that liquefaction is always incomplete. These gases leave the process and carry a certain amount of chlorine with them. This "tail gas" must be treated to remove the chlorine before it can be disposed of by venting it to the atmosphere. The chlorine value can be converted to a salable product such as bleach, HCl, or FeCl_3 . It also can be recovered as elemental chlorine by absorption in a solvent followed by stripping. In some cases, it is simply absorbed in an alkaline medium and then treated for disposal. Section 9.1.9 covers the subject of tail gas handling.

The next two sections discuss protection against process hazards that are peculiar to chlorine processing. Section 9.1.10 covers emergency pressure relief both before and after the compressors. An important part of the discussion covers the design and operation of vent scrubbers to prevent the release of chlorine to the environment. Section 9.1.11 is dedicated to the explosion hazards presented by hydrogen and nitrogen trichloride. The sources of NCl_3 are discussed, as well as its fate in the process. This includes the mechanisms of accumulation and safe decomposition.

Section 9.1.12 briefly considers the handling of intermittent, nonprocess streams. These arise from the evacuation of equipment and shipping containers, purging of lines before maintenance, and similar activities.

Between the electrolyzers and the cooling plant, the gas is sometimes boosted in pressure. This improves performance and helps to reduce contamination by atmospheric air but requires special equipment. The gas will be transported in large pipes, which may have special provisions for the removal of condensate. There will also be some means of pressure relief in case of a shutdown in the gas process. This usually is in the form of a water-filled seal that vents to a caustic scrubber. The pipework conventionally is FRP. It was discussed in some detail in Section 8.4.1.1A.

9.1.2. Materials of Construction

Chlorine is a notoriously corrosive material, but that reputation is due entirely to its action in the wet state. Any gas that escapes confinement must be considered wet, and so the possibility of external corrosion is a design consideration wherever chlorine is handled. The subsections below that describe chlorine processing generally mention the materials of construction of major equipment. In addition, Euro Chlor publishes a pamphlet [1] and a spreadsheet [2] that give detailed recommendations for most systems. The former discusses the limitations and safe operating ranges of the various construction materials. The information in Table 9.1 is taken from Section 4 of the Euro Chlor pamphlet. Corrosion resistance is only one of the factors involved in the selection of materials of construction. The table therefore is a guide only and should be used only in conjunction with the information contained elsewhere in the pamphlet, this book, and technical and manufacturers' literature. The temperatures given in the table are maximum values with no safety allowance applied.

TABLE 9.1. Corrosion Resistance in Chlorine Service

Material	Conditions of service		
	Wet chlorine	Dry chlorine	
		Gas ^a	Liquid
Non-alloyed steel	N	G to 120°C	G
Stainless steels	N	G to 150°C	G
Nickel	N	G to 500°C	G
Inconel	N	G to 400–500°C	G
Monel	N	G to 350°C	G
Hastelloy C	P	G to 400–500°C	G
Aluminum	N	N	N
Copper	N	G to 150°C	G
Silver	P	G to 200°C	G
Titanium	G	N	N
Tantalum	G	G to 150°C	G
Brickwork	G	G	N
Enameled steel	G	G	N
Ebonite	G	A	N
Synthetic rubbers	A	A	N
Silicones	N	N	N
PVC	G to 60°C	G to 60°C	N
CPVC	G to 80°C	G to 80°C	N
Polyethylene	A to 30°C	A to 30°C	N
Polypropylene	A to 30°C	A to 30°C	N
PTFE	G to 200°C	G to 200°C	A
PVDF	G to 140°C	G to 140°C	N
FRP	G to 90°C	G to 90°C	N
Graphite	A	G	N

^a Less than 20 mg H₂O/kg Cl₂.

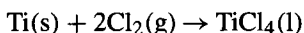
Notes: Abbreviations: G, good; A, acceptable; P, poor; N, not to be used.

Source: With permission of Euro Chlor.

The Euro Chlor spreadsheet gives the characteristics of various metals, plastics, and other materials in both dry and wet chlorine. It also lists international and specific national standards that apply to vessels, piping, flexible hoses, gaskets, and valves and their component parts.

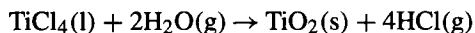
Dry chlorine reacts combustively with many metals, and each of these has a maximum service temperature that must not be exceeded. Carbon steel is generally considered serviceable up to about 120°C. Many other metals have maximum service temperatures in the 100–150°C range. Stainless steels are good up to 150–250°C, the limit depending primarily on the nickel content of the steel. Alloys with higher nickel contents can tolerate higher temperatures. Thus, Monel can be used up to about 350°C, Hastelloy C and most Inconels at 400°C and higher, and nickel itself at 500°C. Hastelloy C has the added advantage of being able to resist chlorine that contains traces of moisture, and nickel has the disadvantage of its inferior mechanical properties.

Table 9.1 shows that the corrosive behavior of chlorine depends fundamentally on its water content. Titanium is the only common metal that resists wet chlorine, and it is the nearly universal choice in sections of the process. Titanium is an active metal, and its corrosion resistance depends on the maintenance of a passivating layer of oxide on its surface. The bare metal reacts rapidly and exothermically with dry chlorine:



The product of the reaction is a liquid with some volatility (boiling point 135°C). It tends to evaporate from the surface, exposing it again to the action of chlorine, and the reaction accelerates to the point of combustion.

When the chlorine is wet, there is a second reaction:



This reaction is very fast, and the solid product forms the protective film. When there is sufficient moisture, therefore, the film forms rapidly and protects the surface from further reaction with chlorine. Section 9.1.3.5 discusses the conditions necessary to keep the film in good repair. Disappearance of the film most is frequently due to a low water content in the chlorine. The excessive dryness in turn usually results from too low a temperature, which allows some of the water to condense from the gas. When using titanium, therefore, one is in the unusual position of being more concerned with low than with high temperatures. Infrequent operations may require extra attention or special measures. Stroking a valve, for example, subjects the film on its stem to mechanical wear. Higher humidity may be necessary to counteract this. Similarly, an intermittently used wet-gas blower with titanium components may lose some of its protection when on standby, especially in cold weather. Spraying water into the gas increases humidity while reducing the temperature, providing an extra safety margin below the combustion temperature.

The materials of construction used in wet chlorine service are not required for dry chlorine and may even be unsuitable. The metal of choice in dry chlorine service usually is carbon steel. Within the chlor-alkali process, the maximum service temperature is of concern only in the compression area. Section 9.1.6 describes the design precautions

that are necessary. In some of the applications of chlorine, not described in this book, process temperatures exceed the maximum safe temperature for carbon steel, and other materials of construction become necessary. Ordinary carbon steel also has a low limiting temperature. Below about -29°C , it is subject to brittle fracture. Low-temperature grades therefore are necessary in liquefaction (Section 9.1.7) and liquid storage (Section 9.1.8) systems.

The resistance of carbon steel to corrosion by chlorine depends on a dense film of ferric chloride on the surface of the metal. Therefore, to understand the behavior of iron exposed to chlorine and the need for low moisture content, one must be familiar with the physical chemistry of FeCl_3 . The chemistry is complex because of the existence of five different hydrates. These contain 2, 2.5, 3.5, 6, and 10 molecules of water. The corrosion-resistant layer can be ferric chloride or one of its hydrates. So long as the partial pressure of water in the gas phase is lower than the vapor pressure of the relevant hydrate and the temperature is lower than its melting point, the resistant layer remains intact. If the temperature is too high, the film simply melts. If the partial pressure of water is too high, the hydrate picks up more water and can dissolve. In either case, a concentrated solution of FeCl_3 forms on the metal surface. This is a strong oxidizer as well as a strong acid and so is highly corrosive to most metals. In 45% FeCl_3 , the corrosion rate of carbon steel is $150\text{--}200\text{ mm yr}^{-1}$. Such a rate would dissolve exchanger tubing or remove a normal wall corrosion allowance within a week.

Figure 9.1 shows a phase diagram for FeCl_3 and water [3]. The hydrates correspond to the congruent points on the equilibrium curve. Figure 9.2 shows the vapor pressures of the hydrates as functions of reciprocal temperature [4]. The points marked E and T_m correspond to the eutectic and congruent points on Fig. 9.1. To avoid destruction of the protective layer, operating conditions must remain below the irregular dotted line connecting those points. Euro Chlor tests, as reported by Westen [5], verified the vapor pressures of the various hydrates and showed that the electrical resistance of the FeCl_3 deposit dropped abruptly when the partial pressure of water in chlorine gas exceeded the vapor pressure. In practice, this means that carbon steel is a suitable material of construction for gaseous chlorine with a partial pressure of water less than 1 mbar over the temperature range between -20 and 120°C . This is the range of conditions suggested by Westen, and Fig. 9.2 shows that it is conservative. Note that the pressure is equivalent to about 1000 ppm (v/v) water when the total pressure is 1 atm. Normal operation of the drying system produces a gas well below this limit (Section 9.1.4.2).

The protective film may also be disrupted by the presence of a reactive substance such as oil or grease. The system, as well as the chlorine itself, must be scrupulously dry and clean and free of reactive materials.

In liquid chlorine service, discussed in Section 9.1.7, the same equilibrium considerations apply, but there is also the danger of damaging the protective layer by erosion if velocities are too high. Accordingly, pipeline velocities should be no greater than 2 m s^{-1} and in long-distance lines no greater than 1 m s^{-1} [6]. The effects of velocity are aggravated by high water content. The data of Hammink and Westen [7] appear below. Corrosion was very slow for all velocities when the water content was below about 11 ppm H_2O .

Before the advent of titanium and fiber-reinforced plastics (FRP), such materials as stoneware, concrete, rubber, impregnated carbon, and thermosetting resins were used

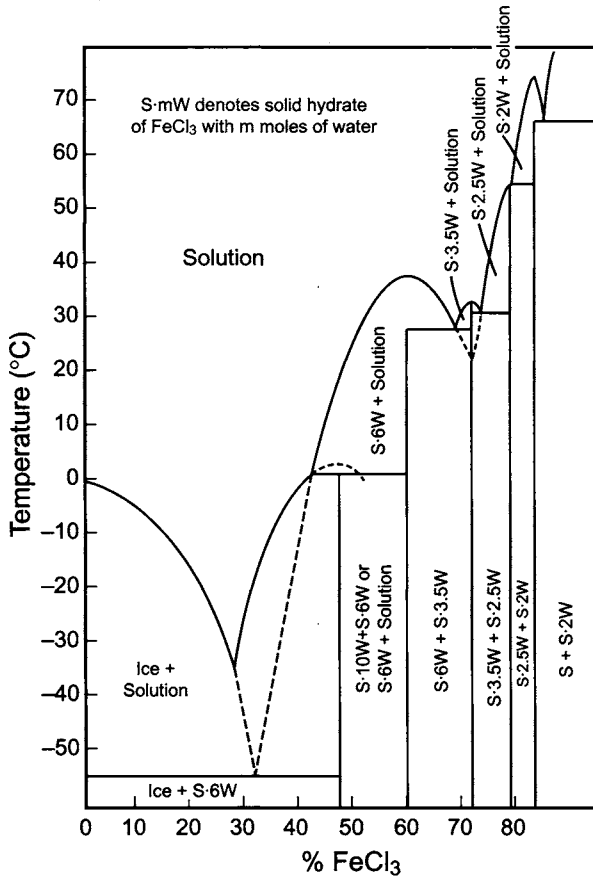


FIGURE 9.1. Phase diagram for FeCl₃-water.

Corrosion Rate of Carbon Steel Piping at 25°C, mm/yr

Water content (ppm)	Liquid velocity (m s ⁻¹)		
	0.1	1.5	2.0
19	0.3	1.0	1.6
24	0.9	1.8	2.7

widely in chlorine service. Some applications remain, but most have gradually been phased out. Nonmetallic construction is now mostly in various thermoplastics and FRP. The thermoplastics find most use in piping and small parts (Section 9.1.8.3). FRP is used in piping, notably in cell-room headers, but also has many other uses [8]. These include acidic and caustic brine piping, chlorinated brine piping, diaphragm-cell head covers, chlorinated brine tanks, chlorine scrubbers, and HCl tanks and piping.

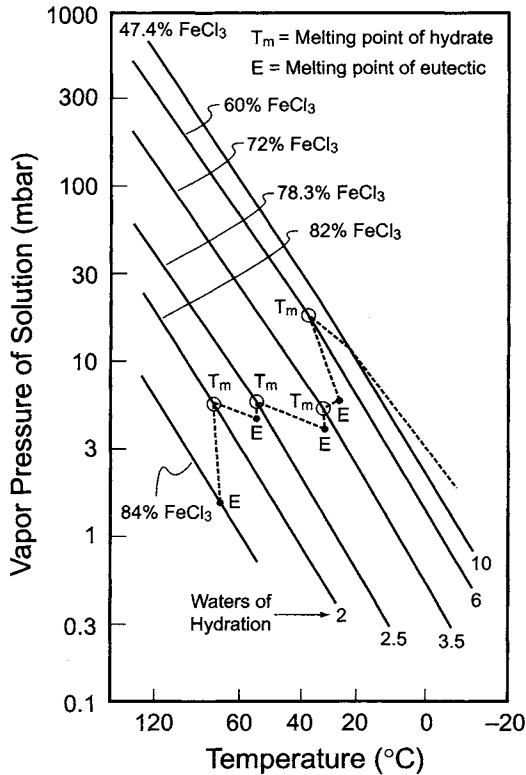


FIGURE 9.2. Vapor pressures of FeCl₃ solutions.

9.1.3. Cooling

Chlorine is produced as a hot, wet cell gas. Its temperature leaving the cells usually is greater than 85°C, and it is saturated with water at its vapor pressure over the anolyte. Nearly all applications require cooling of this gas, which causes partial condensation of the contained water vapor. Two basically different methods of cooling are in common use, based on direct and indirect contact with the coolant. These are dealt with in Sections 9.1.3.3 and 9.1.3.4. Before considering these techniques, we review methods of calculation of heat-transfer rates and the effects of simultaneous mass transfer on the heat transfer process (Sections 9.1.3.1 and 9.1.3.2).

It is important to minimize the amount of water sent to the drying process. The available cooling water temperatures in much of the world are too high to allow the operator to remove as much water as desired. Most large-plant chlorine cooling systems therefore have two exchangers in series, with the second cooled by a stream of chilled water.

9.1.3.1. Heat Transfer Calculations. Engineers are accustomed to dealing with rate coefficients and temperature differentials in their heat-transfer calculations. The heat

transferred in a differential section of an exchanger is, in terms of these quantities

$$dQ = U \Delta t dM \quad (1)$$

where

dQ = heat transferred in unit time

U = coefficient of heat transfer

Δt = temperature differential between the phases transferring heat

dM = measure of the size of a section of the apparatus

In the more familiar indirect-transfer process with a surface interposed between the two phases, dM becomes the area dA . Along a differential length dl of a tube of diameter D , for example, $dA = \pi D dl$. In indirect transfer, we usually express the rate in terms of the active volume of the apparatus, and $dM = dV$. In a cylindrical column, $dV = \pi D^2 dl/4$.

Any heat-transfer problem can be handled by working through the apparatus section by section, calculating appropriate values of U and Δt at each step. In well-behaved systems, U and Δt vary little or in mathematically tractable ways from end to end. In such systems, the coefficient U can usually be assumed constant, or an average value based on mean physical properties can be used. The engineering approach to surface exchangers then is to represent the entire process in terms of mean values:

$$Q = U_m A \Delta t_m \quad (2)$$

In a truly countercurrent system with no phase change and constant heat capacities in both fluids, the proper mean temperature differential becomes the logarithmic mean of the two terminal temperature differentials (LMTD). In Section 9.3.2.4 on caustic cooling, we rely on this approach. The literature contains standard corrections to the LMTD for configurations that do not allow true countercurrent flow, as for example in multipass shell-and-tube exchangers [9].

In a chlorine cooler, flows usually are single-pass and nearly countercurrent, but the behavior of the Δt is highly nonlinear and its mean is not calculable simply from end conditions. The composition of the gas phase also changes drastically as it passes through the cooler. This causes the heat-transfer coefficient to drop to a fraction of its value at the entrance to the cooler. This effect is discussed below in Section 9.1.3.2.

By point-to-point analysis of the process, one still can calculate mean values of U and Δt . This is in a sense an effort toward an artificial goal. The calculations give the amount of heat transferred (dQ) in each section directly, and so an exchanger can be rated or sized without ever defining the mean coefficient or temperature differential. If these quantities serve any real purpose, they are benchmarks for the experienced engineer.

The mean temperature differential (MTD), given true cocurrent or countercurrent flow, is independent of the type of apparatus and is easily calculated. A straightforward calculation gives the amount of heat that must be removed to cool the gas to any given temperature inside the exchanger. This information is often displayed in a duty curve, such as that of Fig. 9.3. This is a companion to the example given below, and it shows the temperature of the gas as a function of the percentage of the total

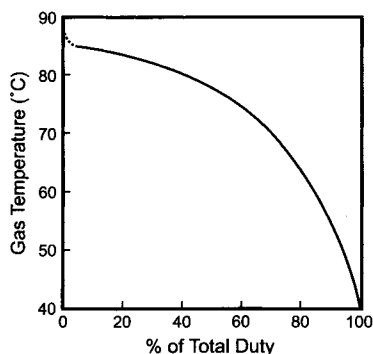


FIGURE 9.3. Heat duty curve—chlorine cooler.

duty accomplished. Equally well, absolute numbers could be used in the abscissa when considering a specific exchanger.

The inlet and outlet conditions of both streams, chlorine gas and cooling medium, are related by a simple energy balance. The total flow of coolant having been set by this overall heat balance, its temperature likewise can be calculated at any point. This provides the temperature differential as a function of the amount or percentage of heat transferred. Integration of this curve gives the MTD.

The relationship between duty and gas temperature in Fig. 9.3 is far from linear. Most of the heat removed from the gas is the latent heat of water, and the amount of water removed in equal temperature increments continuously decreases. These two facts give the duty curve its characteristic shape. The smooth continuous nature of the curve depends on the assumption that the gas and the cooling medium flow countercurrently. This is a reasonable assumption for the standard indirect chlorine cooler, which is a vertical single-pass shell-and-tube exchanger. The gas is nearly in plug flow. There is some slippage between gas and condensate, as well as some subcooling of the condensate. Neither of these has much effect on the calculations. On the water side of the exchanger, the flow advances from side to side and then from one chamber confined by baffles to the next. The assumption that the temperature of the water is a smooth function only of the vertical position is factually incorrect but is a good approximation.

In a column acting as a direct-contact cooler, there is always a certain amount of liquid recirculation caused by the opposing gas flow. The flow pattern in a packed column is tortuous, and the use of a continuous countercurrent model again is only a working approximation. The liquid on the trays tends to be backmixed, and so the liquid flow is not continuously countercurrent but rather proceeds from one more or less well-mixed volume to another. Other calculational techniques, discussed in Section 9.1.3.3, may be more appropriate to these cases.

The LMTD that appears in so many heat-transfer calculations is mathematically justified when the temperatures of both fluids are related linearly to the amount of heat transferred. It is always smaller than the arithmetic mean of the temperature differentials at the two ends of the exchanger (AMTD). The duty curve in Fig. 9.3 has a slight "tail" at the top, representing the superheat in the cell gas (the boiling point rise of the anolyte).

Except for this, the curve is everywhere above the straight line joining any two points. The true MTD in a primary chlorine cooler therefore is greater than the LMTD. In a primary cooler with a heavy condensing load, the mean Δt may be well above both the arithmetic and the logarithmic means. From data on a number of commercial designs, we can say that, roughly, the various means form a geometric progression:

$$\text{MTD/AMTD} = \text{AMTD/LMTD} \quad (3)$$

This holds with an average error of about 5%.

When a second exchanger, the chiller, is added in series, the latent heat of water is not so dominant in the exchanger duty, and the change of temperature as the process continues is more nearly linear. The various calculated mean temperature differentials are not greatly different, and a reasonable and conservative practice is to use the LMTD in exchanger calculations.

Example. The gas in our standard plant is to be cooled from 87 to 40°C, using cooling water supplied at 30°C and allowed to rise to 40°C. The temperature differentials at the ends of the cooler are 47 and 10°C. These give an arithmetic mean temperature differential of 28.5°C and a logarithmic mean of

$$\text{LMTD} = (47 - 10) / \ln(47/10) = 37 / \ln 4.7 = 23.9^\circ\text{C}$$

Cooling the gas to 40°C reduces the partial pressure of water to 55.3 mm Hg. The condensate that forms dissolves some chlorine, but we assume that the other components of the gas are not dissolved. The solubility of chlorine in water is treated in Section 7.5.9.1. The material balance on the cooler is

Material	Gas in	Gas out	Condensate
Water	8571	598.5	7,972.5
Chlorine	28,995	28,959.2	35.8
Others	238	238.1	

From handbook data on thermodynamic properties, we calculate the amount of heat transferred as 20.64 GJ hr⁻¹, or about 5.73 MW. With the assumed 10°C rise, the cooling water flow is 493,240 kg hr⁻¹.

We now have a complete heat and mass balance for the whole cooler. Similarly, we can calculate a balance between the gas inlet and the section of the cooler at which any given temperature is reached. Choosing one such point, we calculate the composition of the gas at 60°C and then the amount of heat transferred from the gas. The cooling water coming from above has already picked up the balance of the total heat. We obtain

Condensate formed	6,694.6 kg hr ⁻¹
Heat duty	16.62 GJ hr ⁻¹
Heat transferred to water	4.02 GJ hr ⁻¹
Water temperature	31.95°C
Differential temperature	28.05°C

Repeating this for other temperatures gives the data necessary to construct Fig. 9.3. Numerical integration of the equivalent temperature differential curve gives the true MTD of 35.0°C. Note that Eq. (3) predicts MTD = 34.0°C.

9.1.3.2. Simultaneous Heat and Mass Transfer. A chlorine cooler can also be considered a partial condenser for water vapor, and most of the thermal duty, as stated above, actually is the latent heat of water. Water vapor must diffuse through the noncondensable chlorine gas in order to reach a cold surface and condense. Mass transfer therefore occurs along with heat transfer. The driving force for this diffusion of water vapor is the difference in its partial pressures across the gas film. The partial pressure at the gas side of the film is that of water in the bulk gas. The partial pressure at the other side can be taken as the vapor pressure of water at the temperature of the condensate forming at the interface. More careful calculations will recognize that the liquid film is not pure water, but this fact will have only a small effect and is not pertinent to our discussion. The driving force for removal of sensible and latent heat is the temperature gradient across the condensate film.

Figure 9.4 shows that both the temperature of the gas and the concentration of water drop from their bulk values across the hypothetical gas film that forms at an interface. The interface may be at a metal tube, at the surface of a droplet of water in a spray, or at the surface of a gas bubble in contact with a stream of water. The nature of the “film” may differ mathematically depending on our standpoint; that is, whether we consider the transfer of heat or of mass. Figure 9.4 represents a particular point or cross-section in the apparatus used for cooling. The bulk quantities in the gas also decrease as it travels through the apparatus. The interfacial quantities in a typical apparatus decrease in the same direction.

Analyses of situations involving simultaneous heat and mass transfer usually depend on analogies between those processes and the transfer of momentum. The analogy between heat and momentum transfer is especially well developed and goes back to the classical work of Reynolds and Prandtl. The Reynolds analogy arose from the observation

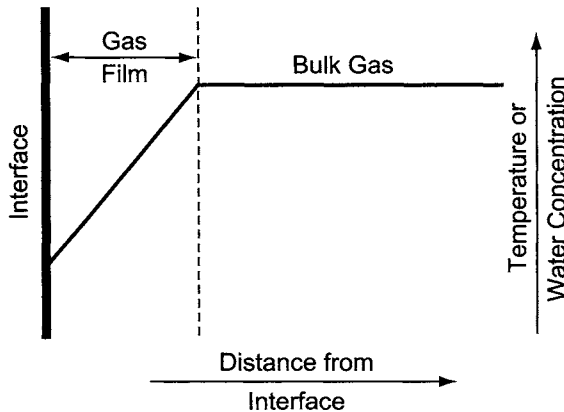


FIGURE 9.4. Gas film at interface in a chlorine cooler.

that as a fluid flows along a surface, it exchanges momentum with the film at the surface in much the same way that heat is conducted through the film between a fluid and a surface. In dimensionless terms, the Prandtl modification of this analogy is

$$h/(cG) = f/(2F_{Pr}) \quad (4)$$

where

h = film coefficient of heat transfer

c = heat capacity of the fluid

G = mass velocity of the fluid

f = friction factor

F_{Pr} = Prandtl modification factor

Any consistent set of units may be used in Eq. (4) and in the equations that follow. The original Reynolds analogy did not contain the last term, which takes the form

$$F_{Pr} = 1 - u'/u + (u'/u)(c\mu/k) \quad (5)$$

where

u' = velocity of the fluid at the edge of the laminar boundary layer

u = bulk velocity of the fluid

μ = viscosity of the fluid

k = thermal conductivity of the fluid

Again, the units must be consistent in order to render F_{Pr} dimensionless. The factor usually is quite close to one. It approaches that value as the ratio of laminar to turbulent velocity becomes small or as the Prandtl number ($c\mu/k$) approaches unity (a common occurrence with gases). The Colburn j -factor for heat transfer then is defined as

$$j_h = (h/cG)Pr^x \quad (6)$$

where Pr is the Prandtl number and the exponent x usually is taken to be $2/3$. The mass velocity G is simply the ratio of the weight flow per unit time w divided by the area available for flow, a . The film coefficient for heat transfer h can be expressed in terms of the process duty and driving force by inverting the usual rate equation to obtain

$$h = Q/A\delta t \quad (7)$$

where

Q = rate of heat transfer

A = area available for transfer of heat

δt = temperature differential driving heat transfer

For sensible heat transfer at constant specific heat, a heat balance on the process fluid gives

$$Q = wc|t_2 - t_1| \quad (8)$$

where

c = specific heat

t_1 = temperature of the process fluid in

t_2 = temperature of the process fluid out

Combining all these considerations and using a mean driving force, Δt_m , for the whole process:

$$j_h = (a/A)[|t_2 - t_1|/\Delta t_m]\text{Pr}^{2/3} \quad (9)$$

The simplest extension of this analogy to mass-transfer processes probably is in the particular case of most interest here, condensation from a wet vapor. The vapor moves along against a condensate film. As water condenses, it enters the film perpendicularly to the direction of flow and gives up its forward momentum.

The less volatile components of the vapor must diffuse through the others to reach the cold liquid film. This process is helped by a high diffusivity (k_d) and impeded by gas viscosity. The ratio μ/k_d then plays the same role in mass transfer as the ratio μ/k in heat transfer. The new ratio has the dimensions of density, and so the appropriate dimensionless quantity is the Schmidt number, $\mu/\rho k_d$. We go on to define the Colburn j -factor for diffusional transfer, by analogy to Eq. (9), as

$$j_d = (a/A)[(p_1 - p_2)/\Delta p_m]\text{Sc}^{2/3} \quad (10)$$

where

p_1 = partial pressure of the diffusing component in

p_2 = partial pressure out

Δp_m = weighted mean partial pressure differential across the film

Sc = Schmidt number

Extending the Reynolds analogy by equating the two j -factors allows us to couple the heat-transfer and mass-transfer processes [10]. Defining a gas-side mass-transfer coefficient K_G in terms of partial pressure differences according to the equation

$$dN = K_G \Delta p \, dA \quad (11)$$

where dN is the number of moles of material diffusing across differential area dA and Δp the partial pressure difference resulting in mass transfer, leads, after manipulation of the terms, to

$$K_G = h \text{Pr}^{2/3} / (\text{cp}_{\text{gf}} M_m \text{Sc}^{2/3}) \quad (12)$$

where M_m is the mean molecular weight of the gas mixture.

Equation (12) shows that the mass-transfer and heat-transfer coefficients are proportionally related through the properties of the gas. As chlorine gas cools, the water condenses and its vapor-phase concentration decreases. The mass-transfer coefficient decreases continuously. The heat-transfer coefficient follows along, and this coupled

with a decline in the driving force (concentration or temperature) causes the heat flux to drop rapidly as the process continues. Section 9.1.3.4 contains an illustration of this effect.

A secondary cooler, or chiller, takes the lean gas from the primary, and so the decline in productivity continues. The average heat flux in a commercial chlorine chiller is perhaps less than one fifth as great as the flux in the preceding cooler. It is difficult to be more precise here, because of the great variability in cooling water temperatures. A relatively high cooling water temperature will allow more water vapor to pass on into the chiller. This improves the heat-transfer coefficient in that exchanger, and it also increases temperature differentials in the first stages of the process. Justification of the secondary cooler is primarily the reduction in load in the drying system. This must be balanced against the expense and complications of the extended cooling system. A secondary cooler is more easily justified in a large plant or in one with an unfavorable cooling water temperature.

9.1.3.3. Direct Contact. The direct-contact process uses water or brine as the coolant. The elimination of the resistance of a surface between the gas and the cooling medium gives this process an advantage in thermal efficiency. This advantage applies fully only in a once-through process; if the cooling medium is recycled through a cooler, the surface barrier reappears and the thermal advantage is at least partly lost. A disadvantage of the direct-contact process is its production of a large stream of water (coolant plus condensate) that contains dissolved chlorine. As explained in Section 9.1.3.5B, this must be treated before discharge from the plant.

Any equipment used for gas-liquid contact can in principle be used to cool chlorine gas. In practice, spray columns and packed beds are most common. Beds are more expensive but, because they offer improved staging, more efficient. Ceramic ring or saddle packing is the type most often found in large units. Vessels are of rubber-lined steel or FRP construction.

Since there is no easily defined heat-transfer area in direct-contact equipment, active volume is used as a measure of its size (Section 9.1.3.1). In the case of a packed bed, for example, the volume of the bed and not the full volume of the vessel is the parameter of interest. A volumetric heat-transfer coefficient measures the efficiency of the process. At a differential section of the exchanger, we have as a variation on Eq. (1)

$$dQ = U' \Delta t dV \quad (13)$$

where

dQ = amount of heat transferred in unit time

U' = volumetric heat-transfer coefficient (e.g., $\text{kJ hr}^{-1} \text{m}^{-3}/^\circ\text{C}$)

Δt = temperature differential between gas and cooling liquid

dV = volume required for transfer of dQ

For the whole process rather than a differential slice, we use mean quantities:

$$Q = U'_{\text{av}} V \Delta t_{\text{m}} \quad (14)$$

where

- Q = total heat duty
- U'_{av} = average heat-transfer coefficient
- V = total working volume of the apparatus
- Δt_m = weighted mean temperature differential

Direct-contact apparatus is more often associated with mass-transfer processes. With this fact in mind along with the analogies among transport processes discussed in the previous section, we can expect some of the calculational techniques also to be similar. Section 10.5 discusses the basics of transport processes and the methods used for their calculation. The process duty is usually expressed as the number of theoretical stages or plates required, or as the number of transfer units. Any practicable degree of separation of components can be realized by providing a sufficient number of plates. The number required is a measure of the difficulty of the separation. Most real plates fail to meet the ideal of producing exit streams in equilibrium. Their performance then is measured by plate efficiency, and the number of actual plates required is the number of theoretical plates divided by an average plate efficiency. Along with the rate of throughput, this number determines the size of the apparatus required. In the same way, we can define a theoretical plate for heat transfer as one in which the two streams leaving the plate are in thermal equilibrium; that is, at the same temperature.

Other types of mass-transfer equipment, such as the packed bed, do not have the discrete stages defined by plates, and the concept of the transfer unit seems more appropriate. When a given component is present at different fugacities in two phases in contact, mass transfer occurs. The flux is expressed in terms of a mass-transfer coefficient, K , and a fugacity driving force:

$$N = KA(f_1 - f_2) = KA(-\Delta f) \quad (15)$$

where

- N = number of moles transferred in unit time
- A = area available for mass transfer
- $-\Delta f$ = drop in fugacity of the transferring component

Combining this rate equation with a material balance for transfer of a solute between two phases moving countercurrently in a tower gives

$$-V' dY = -L' dX = KaS dZ(f_1 - f_2) \quad (16)$$

where

- V' and L' = rates of flow of solute-free material in vapor and liquid phases, respectively
- Y and X = moles of solute/mole of solute-free material in phases V and L , respectively
- a = interfacial area between phases per unit volume of equipment
- S = cross-sectional area of the tower
- Z = height of the tower

This is equivalent to

$$- \int dY / (f_1 - f_2) = \int (KaS/V') dZ \quad (17)$$

There is obviously a similar equation that can be written in terms of X and L' . The quantity on the left is unity when the change in composition is equal to the mean driving force over an interval. This serves as the definition of a mass-transfer unit. In terms of the whole stream flow rather than on the solute-free basis used above, it becomes

$$- \int dy / (1 - y)(f_1 - f_2) = \int (KaS/V) dZ = K_m aSZ/V \quad (18)$$

where

y = mole fraction solute in phase V

V = rate of flow, including solute

K_m = mean mass-transfer coefficient

The number of transfer units (NTU) required is a measure of the difficulty of the process. It depends only on equilibrium relationships and the relative flows of the two phases. With pure cocurrent or countercurrent flow, it is independent of equipment design.

The transfer unit and theoretical plate concepts are quite similar. When equilibrium relationships and process operating lines can be reduced to simple mathematical forms, in fact, the number of transfer units and the number of theoretical plates can be related algebraically.

The efficiency of a column is measured by the height of a transfer unit (HTU) or the length of bed required to produce a unit change as defined by Eq. (17) or (18). The height of bed required, Z , then is

$$Z = (\text{HTU}) \times (\text{NTU}) \quad (19)$$

Full understanding of the transfer-unit concept requires some elaboration. If we apply the definition of Eq. (17) to the two phases in turn, the numbers of transfer units achieved in a given process are not generally the same. Consider absorption of a component from a gas. Figure 9.5 shows the concentration or fugacity profiles across the interfacial films. In terms of the mass-transfer coefficients, we write for the overall process

$$\text{Flux} = KaS dZ (f_g - f_l) \quad (20)$$

where f_g and f_l are the fugacities in gas and liquid phases. Consideration of the two films in turn gives

$$\text{Flux} = k_g aS dZ (f_g - f_i) \quad (21)$$

$$= k_l aS dZ (f_i - f_l) \quad (22)$$

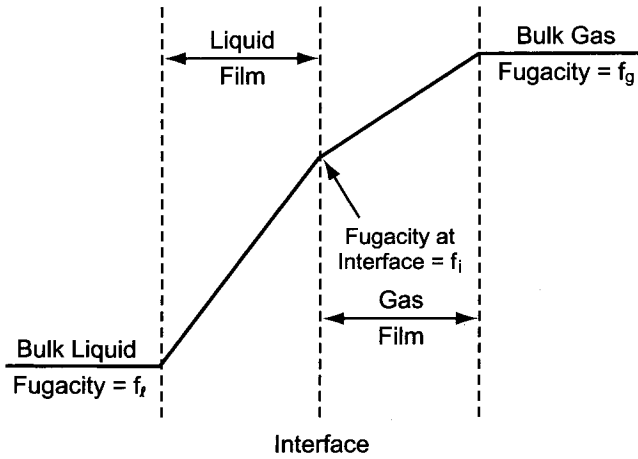


FIGURE 9.5. Fugacity profiles across interfacial films.

These two equations serve to define the mass-transfer coefficients for the gas and liquid films, k_g and k_l . Equations (20)–(22) are three different views of the same process. The right-hand sides therefore must be equal, and so

$$1/K = 1/k_g + 1/k_l \tag{23}$$

Diffusion through the gas film, by the technique used to derive Eq. (18), follows the equation

$$- \int dy/(1 - y)(f_g - f_i) = \int (k_g a S/V) dZ \tag{24}$$

We also have, in the liquid film,

$$- \int dx/(1 - x)(f_i - f_l) = \int (k_l a S/L) dZ \tag{25}$$

The overall coefficient K is the smallest of the three. In the limiting case where one of the film coefficients is much smaller than the other, K is essentially equal to the smaller of the two. We then tend to speak of a system as liquid-phase or gas-phase controlled. The same sort of relationship holds among the NTUs calculated under the different bases, and its inverse connects the heights of the various types of transfer unit. The derivations of all these relationships can be found in any textbook on diffusional operations. Suffice it to say here that we have

$$H_{og} = H_g + (mV/L)H_l \tag{26}$$

$$H_{ol} = H_l + (L/mV)H_g \tag{27}$$

$$H_{og} = (mV/L)H_{ol} \tag{28}$$

where

H_{og} = height of an overall gas-phase transfer unit (i.e., one based on total fugacity differential)

H_{ol} = height of an overall liquid-phase transfer unit

H_g = height of a gas-film transfer unit

H_l = height of a liquid-film transfer unit

V = flow rate of the liquid phase

L = flow rate of the gas phase

m = average slope of the equilibrium curve (y vs x) over an appropriate interval

Fair [11] systematized and correlated results obtained in direct-contact systems. He showed the use of both volumetric heat-transfer coefficients and the transfer-unit concept. For the case of simple heating or cooling without a phase change,

$$1/U' = 1/h'_l + 1/h'_g \quad (29)$$

where h'_l and h'_g are the liquid- and gas-side heat-transfer coefficients, respectively, and Eq. (26) applies for the height of an overall gas-phase transfer unit.

When vapor condenses, as in a chlorine cooler, these are modified to

$$1/U' = 1/h'_l + (Q_g/Q_T)(1/\alpha h'_g) \quad (30)$$

$$H_{og} = H_g + H_l(Q_T/Q_g)(Gc_g/Lc_l) \quad (31)$$

where

Q_g = sensible heat transferred to the gas phase

Q_T = total amount of heat transferred

G and L = mass velocities of the gas and liquid phases

c_g and c_l = heat capacities of the gas and liquid phases, respectively

α = quantity defined below

The factor α in Eq. (30) allows for the simultaneous transfer of mass and heat. A value greater than one indicates that mass and heat flow in the same direction, as in our case. Such values of α correspond to positive values of a process constant, C_o :

$$\alpha = C_o/(1 - e^{-C_o}) \quad (32)$$

Here,

$$C_o = Nc'_g/h'_g V_T \quad (33)$$

where

N = rate of diffusion of water in the direction of heat transfer

c'_g = gas heat capacity

h'_g = gas-phase heat-transfer coefficient

V_T = total volume of the contacting zone

The equations above give the methodology when film coefficients are known or can be estimated. When these coefficients are unknown, there is still a wealth of mass-transfer data to give diffusional transfer unit heights. This information can now be drawn on in heat-transfer problems as well. For packed beds, Fair gives

$$h'_g = (Sc_g / Pr_g)^{2/3} (c_g G / H_{g,d}) \quad (34)$$

$$h'_l = (Sc_l / Pr_l)^{2/3} (c_l L / H_{l,d}) \quad (35)$$

The physical properties of the fluids give the Schmidt and Prandtl numbers as well as the heat capacities in the last terms. Process data give the flow rates G and L . Mass-transfer data for the packing selected for the application give the values of $H_{g,d}$ and $H_{l,d}$ as functions of the other quantities. It is best to use the latest manufacturers' data to characterize packing.

The preceding paragraphs take the film-theory approach. Harriott and Wiegandt [12] used a penetration theory to correlate results:

$$h/k = C\sqrt{\rho k'/D} \quad (36)$$

where

h = heat-transfer coefficient

k = mass-transfer coefficient

ρ = density

k' = thermal conductivity

D = diffusivity

C = a constant describing the system

All quantities in Eq. (36) refer to the liquid phase, and the authors give appropriate values of the constant C .

Example. Here we consider the size of a packed column to cool chlorine cell gas from 87 to 40°C. This is the same duty as in the example of Section 9.1.3.1, which covered the duty curve and calculation of the mean temperature differential. The same data allow us to calculate the number of transfer units required. We shall assume the use of 50-mm rings (packing factor = 187 m² m⁻³).

Cooling the gas to 60°C, as in the same example, expends 80.51% of the total heat-transfer duty. The cooling water, in countercurrent flow, has therefore picked up 19.49% of the total duty. Because the condensation of water from the gas makes the temperature of the cooling water in the column slightly nonlinear with the duty, it is at 31.94°C. Repeating the calculation for a gas temperature of 58°C, we see that we have expended 83.32% of the duty and that the cooling water is at 31.66°C. This 2°C interval in gas temperature represents 83.32 – 80.51 = 2.81% of the total duty and has a mean temperature differential between gas and water of (60 – 31.94 + 58 – 31.66)/2 = 27.20°C. The NTU for this interval therefore is 2/27.2 = 0.0735. Repeating this calculation at other gas temperatures allows us to integrate the curve for the entire process and gives us 1.85 gas-phase transfer units. On the liquid side, the mass flow

is much higher and the temperature range much smaller. The number of liquid-phase transfer units therefore is only 0.314.

Sizing also requires calculation of the HTU. Figure 9.6 is a section of the familiar Eckert packed-column pressure-drop chart. First, we must calculate the parameter $(L/G)\rho_g/(\rho_l - \rho_g)$. We do this at the top, and at the bottom of the column. At the bottom, we have a gas flow of $37,804 \text{ kg hr}^{-1}$ and at the top, a water flow of $500,536 \text{ kg hr}^{-1}$. Some of the water in the gas feed condenses in the tower, giving a flow of $29,796 \text{ kg hr}^{-1}$ at the top. The condensate goes into the water stream, giving $508,544 \text{ kg hr}^{-1}$ at the bottom. The L/G ratios are 13.45 at the bottom and 16.80 at the top. The molecular weight of the gas increases from 42.4 at the bottom to 66.9 at the top. Applying the density factors, the abscissas on the Eckert plot become 0.511 and 0.861. This is a fairly broad range, and Fig. 9.6 shows its effect on ΔP . If we choose a low unit pressure drop of 0.6 mmHg m^{-1} ($0.1 \text{ in w.c. ft}^{-1}$ in the units of Fig. 9.6), the flow parameters (ordinates) at the top and bottom are about 0.0067 and 0.0048. At the bottom,

$$G^2 = 0.0067 \times 32.17 \times 0.0896 \times 61.85 / (0.9191 \times 57)$$

$$G = 0.151 \text{ lb s}^{-1} \text{ ft}^{-2} = 2,653 \text{ kg hr}^{-1} \text{ m}^{-2}$$

At the bottom, a gas mass velocity of about $2,970 \text{ kg hr}^{-1} \text{ m}^{-2}$ is acceptable. Required diameters are 4.03 m at the bottom and 3.78 m at the top.

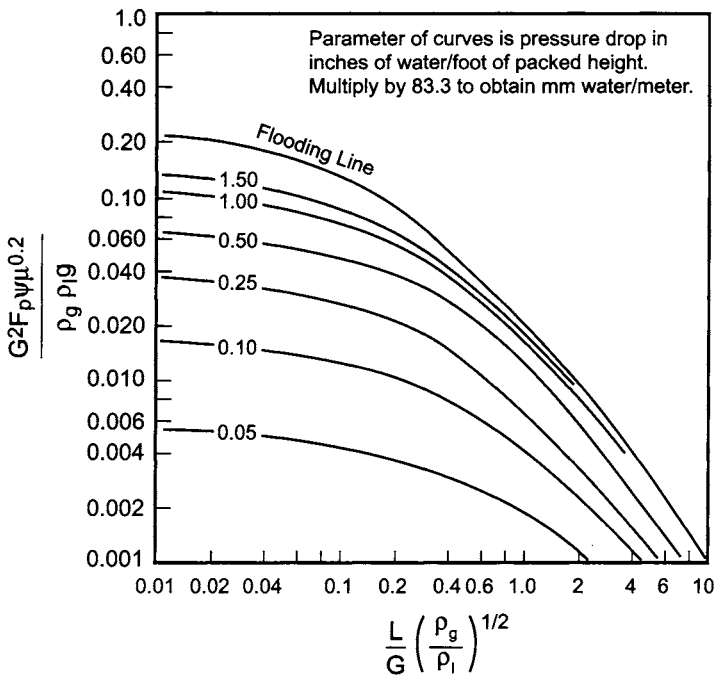


FIGURE 9.6. Pressure drops in packed beds.

Design of the cooler requires a compromise between size and pressure drop. Low gas velocity reduces the pressure drop, an important consideration in most chlorine lines, but has a two-fold effect on size. Not only does the diameter increase to accommodate the low velocity, but the HTU also increases, partly offsetting the low unit pressure drop. This two-fold effect makes it especially difficult, and dangerous, to generalize and produce rules of thumb for sizing.

The example above, with its very low pressure drop, has a HTU of about 5 m. One of the advantages of operating the cells under positive pressure would be the possibility of accepting a greater pressure drop in the coolers and so improving their transfer efficiency.

Example. We return to the preceding example to establish a more economical design. Choosing a column diameter of 3.5 m, we perform the same incremental calculations. With the new diameter, the value of G varies from 3,097 to 3,929 $\text{kg hr}^{-1} \text{m}^{-2}$. At the 60% point, we have $G = 3,389$ and $L = 51,850 \text{ kg hr}^{-1} \text{m}^{-2}$. From the amount condensed, we calculate the molecular weight of the gas to be 54.1 and the density factor on the abscissa to be about 0.044. The abscissa then is equal to 0.673. From the flow rate, the physical properties of the gas, and the packing factor, the ordinate is 0.0094. This gives us a unit pressure drop of 0.18 in $\text{H}_2\text{O ft}^{-1}$, or 0.15 kPa m^{-1} for this section of the bed. Using the method published by Fair, we estimate the height of the gas-phase transfer unit at this point in the column to be 3.85 m. We know that the interval between 60 and 62% of the duty represents 0.027 transfer units. Combining this with the HTU and the pressure drop per unit of height, we calculate the pressure drop over this portion of the bed (0.104 m) to be 0.016 kPa. Repeating this calculation for all other intervals, we obtain a packed height of 7.4 m and a pressure drop of 0.94 kPa.

Repeating the procedure with a diameter of 3 m, we encounter a pressure drop of 1.44 kPa in a packed height of 5.1 m. Allowing an increase of 53% in the pressure drop has reduced the size of the packed bed by a factor of nearly two. The heat transfer coefficients calculated from these results and the data found in the example in Section 9.1.3.1 are 8.3 $\text{MJ hr}^{-1} \text{m}^{-3}$ per degree centigrade for the larger column and 16.5 for the smaller column. The wide range makes it difficult to generalize on the heat-transfer capacity of packed columns.

The heights of a transfer unit for columns 3.0, 3.25, and 3.5 m in diameter are 2.74, 3.32, and 3.98 m respectively. While these values increase more rapidly than the diameter itself, all are reasonably close to the rule of thumb proposed by Kister [13] that $\text{HTU} \approx \text{diameter}$.

9.1.3.4. Indirect Contact. Direct contact was more popular in the past, when none of the common construction metals was resistant to chlorine. Typical materials of construction were thermosets (such as a phenolic resin reinforced with asbestos) for vessels and stoneware or glass for piping. This situation changed with improvements in fiber-reinforced plastic fabrication and the commercial advent of titanium. The indirect-contact approach has now become a standard. The typical chlorine cooler today is a single-pass vertical shell-and-tube exchanger with titanium tubes and tube sheets and a carbon steel shell (or perhaps FRP in smaller units). Construction of tube sheets may be of solid titanium, or they may be clad or explosion-bonded with titanium. The inlet channel to the primary cooler also may be of titanium; the other channels usually are of FRP.

The most frequently used configurations are based on fixed tube sheets. Under the standards of the Tubular Exchanger Manufacturers' Association (TEMA), which are illustrated in most engineering handbooks, these configurations are designated as AEL or BEM. They may be modified by bolting the inlet chlorine pipe directly to the steel shell. This is an approach that requires careful design. Tube diameters usually are about 20 or 25 mm, and the usual arrangement is triangular with a pitch of 24 to 32 mm, or 1.25 tube diameters. Outside-packed units with floating heads may replace these designs when cooling water quality is low and frequent cleaning is necessary. The tubes may then be installed with a square pitch in order to make cleaning easier. The tube thickness usually is 0.9–1.0 mm, and welding procedures vary. Seal welding of the tubes to the tube sheets is perhaps the most common approach. Similarly, there is not universal agreement on the mechanical design code. The most conservative designs follow TEMA R, the code usually specified for refinery service.

Figure 9.7 shows a temperature profile for condensation on the wall of a tube. Resistances are in the liquid film on the cooling-water side of the tube, the tube itself, a liquid condensate film, and the gas film. The relative magnitudes shown for the temperature differences are realistic. Using the mathematics associated with a heat-transfer problem, one can take the convenient if nonrigorous approach of attributing part of the process-side temperature difference to the mass transfer process and part to the heat transfer process [14]. The driving force consumed by mass transfer arises from the difference between the bulk temperature of the gas and the temperature of the condensate film. The lack of rigor in this simplification arises largely from the fact that heat transfer is also occurring here. The driving force consumed by the heat transfer is the temperature drop across the condensate film. Figure 9.8 shows a typical division of these mass-transfer and heat-transfer resistances. The important point to be noted is that the mass-transfer resistance becomes more important as condensation proceeds, and the coefficient of heat transfer continuously decreases. To illustrate the same effect, Kern [15] points out that in the condensation of steam from air the overall coefficient can drop by a factor of 100 from the inlet to the outlet.

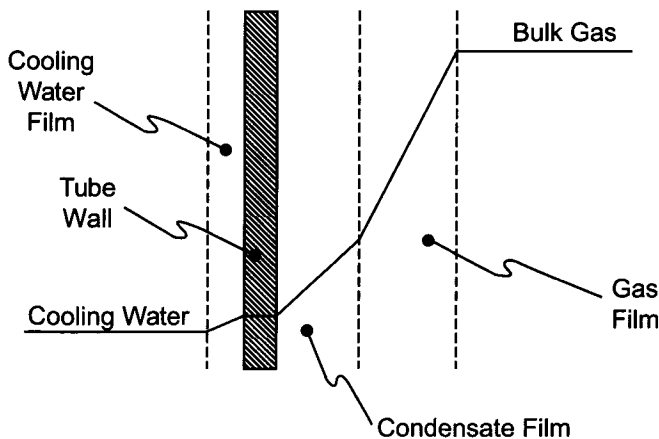


FIGURE 9.7. Temperature profiles: condensation in a tubular cooler.

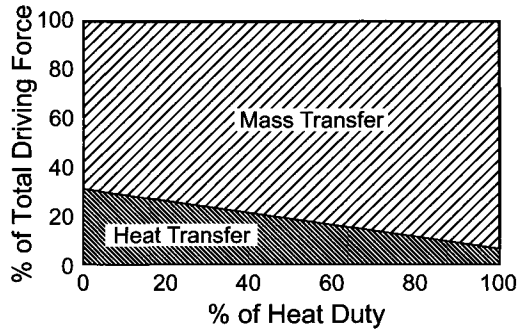


FIGURE 9.8. Division of temperature driving force in a chlorine cooler.

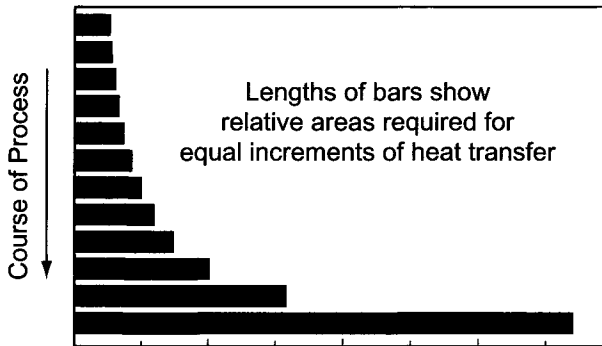


FIGURE 9.9. Areas required for equal increments of heat transfer.

The point coefficients of heat transfer decline continuously along the tube. Since the overall temperature difference is also declining, the heat flux drops off rapidly. Figure 9.9, based on subdividing a commercial design into 12 zones of equal total heat transfer, illustrates the problem. The relative area required for each increment grows slowly at first and then very rapidly toward the end of the process. This deteriorating performance is accepted by the designer because of the problems caused by water in the downstream parts of the chlorine recovery process. The next step in chlorine processing is the drying of the gas, and the standard process is based on the use of sulfuric acid to absorb the water. This acid costs money, and disposal of the weak acid produced by drying the gas is often a problem and an additional cost to the process.

As noted above, a second exchanger cooled with chilled water is often added to increase the removal of water. All the problems referred to above with increasing mass-transfer resistances occur in this second exchanger as well. Added to this problem is the fact that the gas entering the exchanger is much leaner in water. The net result is that unit heat fluxes in chlorine chillers are much lower than those in the coolers, perhaps by a factor of five or ten.

Figure 9.10 shows the behavior of the clean coefficient in a typical chlorine cooler as the gas temperature changes. As the process moves from right to left, the coefficient drops

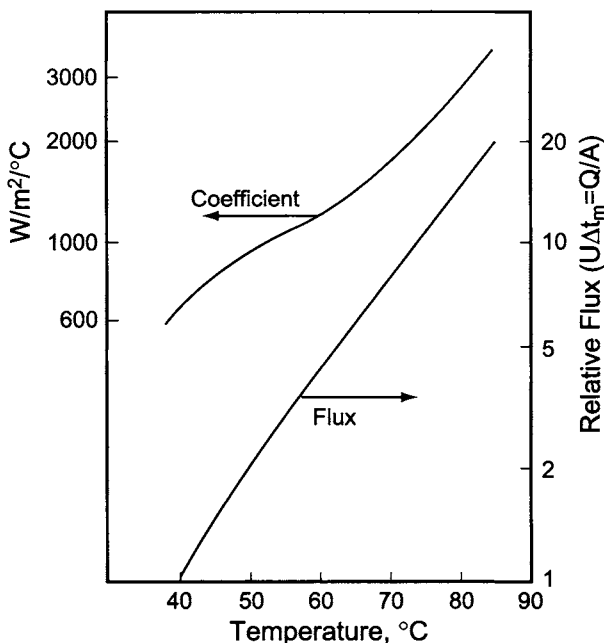


FIGURE 9.10. Effect of gas temperature on performance of chlorine cooler.

rapidly from a starting value of more than $3,000 \text{ W m}^{-2}(\text{°C})^{-1}$ to one less than 20%. Since the temperature driving force is also diminishing, we show the second line representing the unit flux. The drop is even more pronounced. Interestingly, the line is nearly straight over much of its range, with a decrease of 10°C in gas temperature reducing the flux by about 85%.

The data of Fig. 9.10 apply to clean surfaces. The addition of fouling factors would lower the heat-transfer coefficient curve and make both curves less steep. The curves also apply only to a typical exchanger with the gas nearly at atmospheric pressure. Operation at pressures above atmospheric increases the driving force for diffusion. The benefit of this increase grows as the mass-transfer process becomes more dominant. The result is that, once again, the curves become less steep.

Plate-and-frame coolers have made some inroads into this application. These will be much smaller than the typical shell-and-tube coolers, at the expense of a greater pressure drop. Titanium plates are necessary, and welded construction of the plates is highly recommended [16]. Plate-and-frame units will probably become more common as the increasing use of the newest membrane cells allows operating pressures to increase. Few units are found today in sizes above 100 tpd chlorine. Section 9.3.2.4 on caustic cooling briefly discusses the general characteristics of plate exchangers.

9.1.3.5. Limitations on Chlorine Cooling

9.1.3.5A. Minimum Gas Temperature. While the goal in cooling chlorine is to remove as much water as possible, there are fundamental limitations that must be observed.

It is not possible simply to reduce the temperature of the wet gas without limit. Chlorine forms a hydrate at atmospheric pressure below about 9.6°C, where the vapor pressure of water is 9.0 mmHg (1.2 kPa). Cooling the gas below this temperature causes solid hydrate to form and deposit in equipment and piping. Limiting the temperature of the coolant helps to avoid this situation. The chilled water used in the second stage of cooling therefore is produced at temperatures close to the freezing point of the hydrate rather than at temperatures close to the freezing point of water.

Even plant cooling water can present a seasonal problem. Winter temperatures are often low enough to make hydrate formation possible. It is then necessary to limit the temperature of the water used on the chlorine cooler. This is usually done by arranging for series use of the water in more than one service or by tempering it with a warmer stream. Often, the latter approach uses some of the water issuing from the exchanger itself, recycled to the feed point under temperature control. Cocurrent flow of gas and coolant also can reduce the probability of hydrate formation.

The use of titanium as a material of construction places another limitation on the temperature of the gas. Section 9.1.2 explained the formation of the passive titanium oxide layer on the metal surface. This depends on the presence of water in the gas to allow the hydrolysis reaction to compete successfully with chlorination of the metal. The disappearance of this layer, or failure to establish it, allows the combustive reaction of dry chlorine with titanium metal. It becomes important to define those processing conditions under which the passivating layer can not be relied upon. Work reported by Euro Chlor [17,18] showed that chlorine-cooling processes could in some cases enter the dangerous area. They recommend that the temperature should not be taken below about 13°C, where water has a vapor pressure of 11.2 mmHg. This is slightly on the conservative side of the statement of Grauman and Willey [19] that between 1.0 and 1.5% water vapor is sufficient to maintain the oxide film. Given some imprecision in temperature control, a bit of conservatism is called for.

This low-temperature combustion hazard has its implications for cold-weather shutdowns of chlorine processing systems.

9.1.3.5B. Chlorinated Condensate. An important aspect of chlorine cooling is the composition of the condensate. The water removed from the gas, or in the case of direct cooling of the cooling water as well as that condensed, will be saturated with chlorine. This water is often a process waste, and it must be made innocuous before discharge. Usually, the bulk of the chlorine is stripped from the water after adding acid to reverse its hydrolysis. The basics of dechlorination of aqueous streams were covered in the chapter on brine treatment (Section 7.5.9).

The condensate can be dechlorinated in a dedicated stripper or in a brine dechlorinator. The former is more characteristic of a diaphragm-cell plant. The latter is a unit required in a mercury- or membrane-cell plant to allow depleted brine to be recycled to the process. It can be designed to treat chlorinated condensate as well as brine, in which case there is no need for separate apparatus.

As Section 7.5.9.1 demonstrated, chlorine is more soluble in water than in brine. Its removal from condensate therefore requires more vigorous treatment. More acid is used to reverse the hydrolysis reaction, and the resulting pH may be close to one rather than in the neighborhood of two.

Stripping is usually by addition of live steam to the condensate. The condensate is pumped to the top of a stripping tower, and steam is injected into the bottom. The condensate is preheated by steam or by interchange with the dechlorinated water from the bottom of the tower. Steam can be introduced under flow control, ratioed to the condensate flow, or reset by the overhead temperature.

All metal in contact with the chlorinated water is titanium. At the temperature and pH of the stripper, Grade 2 titanium, which is an unalloyed metal and the chlorine industry's general-purpose standard, can undergo crevice corrosion. An alloyed form should be used. Molybdenum alloys (e.g., Grade 12) are serviceable down at least to pH 2. The more expensive Grade 7 (0.15–0.25% Pd) may be necessary at pH 1. This is considered the standard palladium-alloyed titanium. An alternative to consider is Grade 16, which contains only 0.04–0.08% Pd. While Grade 7 usually is produced with its Pd content close to the minimum 0.15%, it still usually costs about one third more than Grade 16.

9.1.3.5C. Chlorine Hydrate. The hydrate that forms in chlorine cooling systems is a clathrate of the formula $\text{Cl}_2 \cdot n\text{H}_2\text{O}$, where n is about seven or eight. Clathrates (*L. clathratus*, enclosed by bars of a grating) are a geometric phenomena rather than stoichiometric compounds. They appear when the presence of certain enclosed gases stabilizes the formation of crystals. In the industrial chemical world, the best-known examples are the hydrates. Chlorine hydrate has been known for many years and has played an important role in the development of the chemistry of inclusion compounds. Humphry Davy was the first to recognize that water was a component of what had been thought to be crystalline chlorine, in 1811. In 1823, Michael Faraday estimated its composition to be $\text{Cl}_2 \cdot 10\text{H}_2\text{O}$.

Chlorine forms one of the “gas hydrates” [20]. These occur in one of two different cubic forms. In the class to which chlorine belongs, crystals form with unit cells comprising 46 water molecules. Each cell contains six medium-sized and two small cages. Chlorine molecules occupy the larger cages but have difficulty entering the smaller ones. If these cages remain empty, the cell contains six chlorine molecules, and the formula of the hydrate is $\text{Cl}_2 \cdot 7.67\text{H}_2\text{O}$. Filling the small cages would give eight chlorine molecules in each cell and a formula of $\text{Cl}_2 \cdot 5.75\text{H}_2\text{O}$. Cotton and Wilkinson [21] report that about 20% of the small holes are filled, corresponding approximately to $\text{Cl}_2 \cdot 7.2\text{H}_2\text{O}$, but also give the slightly different formula $\text{Cl}_2 \cdot 7.3\text{H}_2\text{O}$. Ketelaar [22] quotes the work of Bouzat and Azinières [23] in fixing the theoretical limits and of Allen [24], who obtained $n = 7.27$.

The atmospheric-pressure hydrate formation temperature of 9.6°C quoted above is one of the constraints on operating temperatures in chlorine cooling. Later, we shall also consider the effects of chlorine hydrate in liquefaction systems (Section 9.1.7.2C). The same problem of equipment plugging may occur there, and the “melting” or decomposition of hydrate when equipment is taken out of service and allowed to warm can result in severe corrosion. International Critical Tables data for the decomposition pressure of chlorine hydrate, which extend to 16°C, fit the equation

$$P = 3.55 \times 10^{11} e^{-8817/T} \quad (37)$$

with P in kPa.

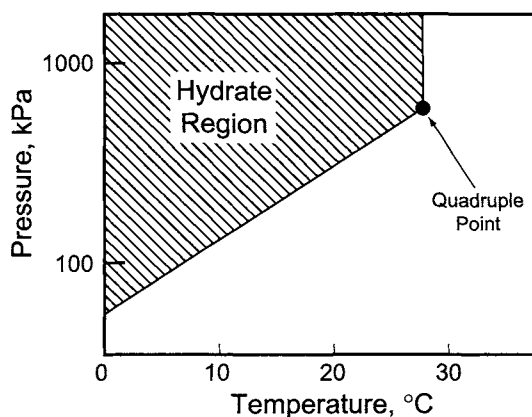


FIGURE 9.11. Region of existence of chlorine hydrate.

The quadruple point for this system is 28.7°C , where water, ice, hydrate, and vapor coexist. At higher temperatures, the hydrate does not exist. Equation (37) defines a line that separates a hydrate-formation area from a safe area. Figure 9.11 shows this line. Operation below and to the right of the curve will be free of hydrate formation.

Extrapolation of Eq. (37) to the quadruple point indicates a pressure of 7.22 atm. This is quite close to Ketelaar's extrapolated value of 7.3 and well below the vapor pressure of pure chlorine, which is 8.39 atm.

9.1.3.5D. Summarizing Flow Diagram. Some of the points made above are reflected in the flow diagram of Fig. 9.12. It takes the gas from the cells and delivers it to the drying system described in the next section. The chlorine side is deliberately quite simple. From the cells, the gas passes through a demister, the cooler, and the secondary cooler or chiller. The sections immediately above explain the two-step cooling process, and Section 9.1.5 covers the mist eliminator. Temperature and pressure measurements at each stage are not essential but allow diagnosis of problems and monitoring for excessive pressure drops.

The gas finally goes off to the drying process and the condensate to chlorine recovery. The flow of condensate from the coolers and the mist eliminator is by gravity. Each item of equipment can drain separately to the receiving vessel, which is vented back to the chlorine line after the coolers. Figure 9.12 also shows an alternative in which the three sources of condensate are piped together. The choice depends on local conditions and equipment layout. In the drawing, the demister has internal seals and the lines from the coolers have loop seals. The transfer line should be sealed on the delivery end to keep it full. One simple technique is to connect the line to the bottom of the receiving vessel. Alternatively, the condensate can go to the bottom of the vessel through a sealed dip pipe.

The chilled water flow to (or from) the second cooler is controlled in order to avoid the problems of a gas that is too cold or too dry. The only feature that requires special mention is the cooling water supply to the first cooler. The design characteristics chosen for our reference plant in Section 6.5 include a minimum cooling water supply temperature of 5°C . This is below the hydrate-formation temperature and demonstrates

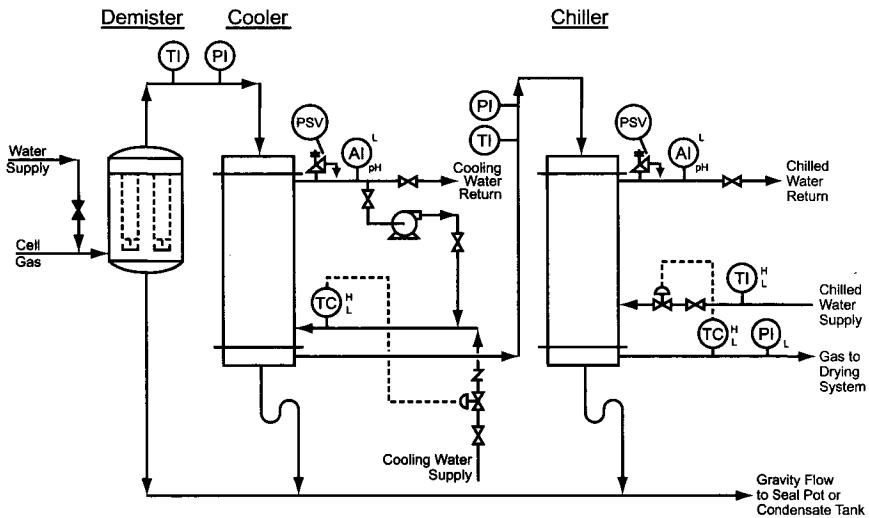


FIGURE 9.12. Flow diagram—chlorine cooling.

the point that the cooling water itself can be the source of dangerously low temperatures. One possible solution is the tempering of the supply with some of the used water. This can be achieved by a recycle pump in the water discharge line, returning water to the feed side. Two temperature controllers are necessary, one to hold the temperature of the blend that serves as the primary coolant and one to regulate the flow of cold water in order to give the desired process outlet temperature. A low-temperature alarm at the primary cooler warns of the danger of hydrate formation; a high alarm warns of inadequate cooling. The chilled water supply and the chilled gas also have high- and low-temperature alarms. Other instrumentation to note includes the thermal relief valves on the water sides of both exchangers and the pH meters. The latter detect any leakage of chlorine into the water.

9.1.4. Drying

After cooling, chlorine gas is dried by contact with concentrated sulfuric acid, a powerful desiccant over which the vapor pressure of contained water is very low. Other drying processes have been suggested from time to time, but none has had wide commercial success. The absorption of water by sulfuric acid is highly exothermic (more than 3 MJ kg^{-1}), and many combinations of feed and spent acid strengths can result in boiling if the heat is not removed. This section covers the amounts of acid required, equilibrium considerations in the process, the types of apparatus used, and the handling of the acid.

9.1.4.1. Acid Consumption. The amount of acid consumed is fixed by the process load (kg water/hr) and the concentrations of acid into and out of the drying system. A simple material balance shows the number of units of fresh concentrated acid (Q) required to

absorb 1 unit of water:

$$Q = W/(C - W) \quad (38)$$

where C is the concentration of strong acid and W the concentration of spent or waste acid.

Economics and ease of handling determine the strength of the fresh acid. Availability at low cost is usually the determining criterion. The acid strength should be at least 93%, preferably 96%, and in some plants there will be a seasonal variation. The viscosity and freezing point behavior of concentrated sulfuric acid is quite complex (see Appendix). There is a minimum of about -30°C in the freezing point curve at about 93% acid. The freezing point increases rapidly with higher concentrations, reaching 0°C at about 96% acid. This is why wintertime restrictions on acid strength are common in colder climates. At very high strength, furthermore, the mass-transfer behavior of the acid can deteriorate.

The waste acid strength depends on the method of disposal. While Eq. (38) shows that lower concentrations reduce the amount of acid consumed, there are other considerations. If the acid is to be reprocessed, its strength must be suitable for the reprocessing plant. Corrosivity, which is greater at lower concentrations, is another important factor.

Considering acid concentrations as absolute numbers, the waste concentration is more important in determining the amount of acid consumed. Differentiating Eq. (38) shows that the change in acid requirement with feed strength is

$$\partial Q/\partial C = -W/(C - W)^2 \quad (39)$$

and with spent acid strength is

$$\partial Q/\partial W = C/(C - W)^2 \quad (40)$$

The latter is larger in magnitude by the ratio of acid concentrations. Accordingly, if acid is supplied at 96% and withdrawn at 72%, Eq. (38) shows that 3 kg of fresh acid will be required to remove one kilogram of water from the gas. If the feed acid strength drops by 1% to 95%, this increases to 3.13 kg. This is a 4.3% increase in feed acid flow and a 3.3% increase in H_2SO_4 consumption. If the spent acid concentration increases by 1%, the feed acid requirement goes up to 3.174 kg, an increase of 5.8%.

9.1.4.2. Equilibrium Behavior. Equilibrium performance is determined by the vapor pressure of water over the acid and so is better at high acid concentration and low temperature. This statement does not conflict with the claimed advantages of low spent acid strength; in a three-stage system, for example, the operating concentration in the last stage is very close to the feed concentration in any case. The final concentration of water in the gas therefore is not strongly dependent on the spent acid concentration. Lower concentrations in the spent acid operate by Eq. (38) or Eq. (40) to reduce the amount of acid required. The incentive for higher feed concentrations is largely the reduction in volume handled. Increasing the feed acid concentration from 93 to 96%

reduces the amount of fresh acid required by 12.5% and the amount of 72% spent acid generated by 9%.

The temperature of the process can be kept low by cooling a circulating acid stream. Cooling the acid well below normal cooling water temperature offers no great process advantage. The equilibrium condition improves only marginally, and the mass-transfer situation can deteriorate slightly. In spite of this, chilled water still is often used as a coolant, as explained below under Acid Pumping and Cooling, in order to provide a greater temperature driving force and reduce the size of the exchanger.

With cooling and circulation of the acid around a packed bed, each stage of the process can be kept approximately isothermal. Results in each stage can be calculated from the vapor pressure of sulfuric acid, under the useful assumption that the presence of chlorine has a negligible effect on the distribution coefficient for water. For acid concentrations in increments of 5% from 50 to 95% H₂SO₄, the vapor pressure data in Perry's Handbook are accompanied by the constants for the equation $\ln p = A - B/T$. These are fitted to the tabulated data [25] over the entire range of temperature covered in the table. Not surprisingly, a better fit results when the constants are calculated for a restricted temperature range. Between 20 and 60°C, we obtain the constants given in Table 9.2. They are to be used in the equation

$$\ln p = A - B/T \quad (41)$$

with T in K and p in mmHg. Compared to the handbook values, these cut the average percentage deviation between calculated and tabulated values in half. The standard error of estimate is 6% of the measured vapor pressure.

Example. Here we calculate the vapor pressure over 78% acid at 35°C. Using Eq. (41) and the constants in Table 9.2, we calculate the logarithms of the vapor pressure at 70, 75, 80, and 85% acid. The values are 0.6997, -0.1944, -1.3254, and -2.4527, respectively.

TABLE 9.2. Vapor Pressure
Constants for Sulfuric Acid
Solutions

Wt.% H ₂ SO ₄	A	B
50	20.514	5480
55	20.429	5551
60	20.436	5682
65	20.376	5835
70	20.810	6197
75	20.750	6454
80	21.407	7005
85	21.250	7304
90	21.267	7793
95	22.645	8984

Notes: $\ln p$ (mm Hg) = $A - B/T$ (K);
for use between 20 and 60°C.

Using a four-point interpolation formula, we find a value of -0.8600 at 78% . This gives a vapor pressure of 0.423 mmHg, or 0.0564 kPa.

Example. Cell gas, joined by the chlorine recovered from the depleted brine and the condensate from the cooling process, flows through three packed towers in series, with counterflow of acid. We feed 96% acid and withdraw spent acid at 78% . By Eq. (38), the consumption of fresh acid is $78/(96-78) = 4.33$ kg per kg of water. The temperature of the gas from the chiller is 15°C , where the vapor pressure of water is 1.705 kPa. The total pressure being 97 kPa, we have $1.705/95.295 = 0.01789$ moles water per mole of dry gas. The amount of water present in the chilled gas then is 136.7 kg hr^{-1} . This requires a supply of $4.33 \times 136.7 = 592.3$ kg hr^{-1} fresh acid (568.6 kg H_2SO_4 and 23.7 kg H_2O). The spent acid contains 568.6 kg hr^{-1} H_2SO_4 and $23.7 + 136.7 = 160.4$ kg hr^{-1} H_2O .

A cooler in the recirculation line holds the temperature of the acid leaving the first stage at 35°C . From the previous example, the partial pressure of water vapor at equilibrium is 0.0564 kPa. Allowing a loss of 0.5 kPa in the tower, the total pressure now is 96.5 kPa, and we have $0.0564/96.4436 = 0.000585$ moles water per mole of dry gas. The residual water therefore amounts to 4.6 kg hr^{-1} . The amount of water absorbed is $136.7 - 4.6 = 132.1$ kg hr^{-1} . This means that the acid entering from the second tower contains $160.4 - 132.1 = 28.3$ kg H_2O per hour; its strength is 95.3% H_2SO_4 .

Continuing on these lines gives the data used in the flow diagram of Fig. 9.13. More precise calculations would reflect differences in the temperature of the acid in the various stages. Since these amount to only a few degrees, they are ignored in this calculation.

9.1.4.3. Drying Columns

9.1.4.3A. Packed Columns. Drying columns use packing, trays, or a combination of the two. Packed columns have in the past perhaps been a standard. They are robust, and their operation is simple and stable.

One disadvantage is the need for recirculation of acid. The small net flow of acid has already been mentioned and is apparent in the balance presented in Fig 9.13. Depending somewhat on the purity of the chlorine gas, the ratio of liquid to gas mass

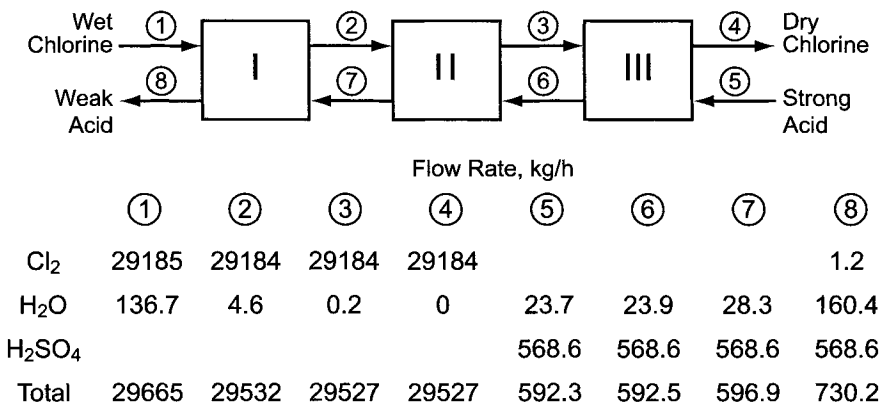


FIGURE 9.13. Chlorine drying system process flows.

flow rates (L/G) into the column without acid recycle will be about 0.015 to 0.02. One parameter used to rate the flooding behavior of packed columns is $L\varphi/G$. Here,

$$\varphi = \sqrt{\rho_g/\rho_{\text{air}}}$$

where ρ_g is the density of process gas and ρ_{air} is the density of air at standard conditions.

The value of $L\varphi/G$ will be about 0.03, far below the usual range. At any reasonable gas velocity, therefore, the net throughput of acid would be less than the minimum wetting rate of the packing. Circulation is necessary to overcome this problem. Typical mass velocities are 5–8,000 kg hr⁻¹ m⁻² for the gas phase and 15–25,000 kg hr⁻¹ m⁻² for the liquid phase. Superficial velocities then are about 35–40 m min⁻¹ for the gas and 0.15–0.20 m min⁻¹ for the liquid. These rates determine the inside diameter of a tower; when brick lining is used, the outside diameter will be 100–200 mm larger. The value of $L\varphi/G$ for most combinations will be greater than four.

Circulation of the acid largely destages the operation, and the usual design assumption is that a bed of packing represents one equilibrium stage. Normally, three stages, or three beds, are provided. Two stages can give an acceptable product, and small plants are often built this way. Most of these, however, also use acid-ring compressors (Section 9.1.6.2C), which give some extra protection. The use of only two stages will produce a marginally higher water content in the dry chlorine and greatly reduce the operating margin of the drying system.

Figure 9.13 shows the process flows in a typical three-stage arrangement. One design decision is whether to provide three separate columns or to place three beds in a single tall column. The latter approach is shown in Fig. 9.14. The reader can easily visualize the changes that occur when each bed is in a separate column. An acid-circulating pump serves each bed. By accepting some complexity in the piping, a fourth pump (not shown) can be installed as a common spare. As shown in Fig. 9.13, most of the water is removed and most of the heat is generated in the bottom section. A cooler in the circulating line removes this heat. It is possible to operate a three-stage system satisfactorily with only one cooler, accepting the small temperature rise in the last two sections. Our example, however, has a second cooler for good measure.

One advantage of the single-column construction, which may be decisive, is its smaller plot area. Use of a single shell also reduces material cost. Pressure losses at entrances and exits and in interconnecting pipe are reduced or eliminated. Offsetting disadvantages associated with the height of a column (up to 20 m) are the complications in transportation and erection and the fact that acid must be pumped at higher pressures. Since the acid reservoirs maintained in the upper stages must be designed to drain slowly upon shutdown, some inventory will be lost and the concentration profile will be upset whenever a pump stops. It then takes some time to establish a steady state when the tower is restarted. Finally, with separate columns it is possible to take advantage of the lower corrosivity in the last stage by using a cheaper material of construction.

Large towers have carbon steel shells. Brick linings, a standard in the past, are still widely used. These usually comprise two courses of acid-resistant brick held in place over a suitable protective membrane. Vinyl ester resins are suitable for the membrane and the mortar that holds the assembly together. Many systems use unlined carbon steel in the last (driest) stage. Other linings have begun to find some application; these include

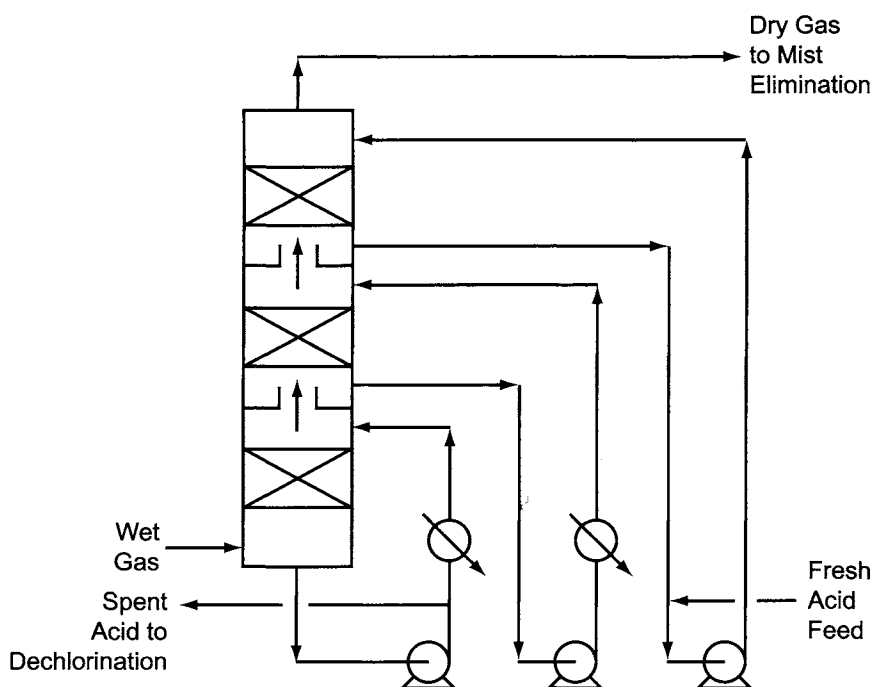


FIGURE 9.14. Three-bed acid drying column.

PVC laminates in thicknesses of 2–3 mm. Another possibility is a low-density acid-resistant block that can be combined with the same mortar and membrane used with brick linings [26]. Substituting this for brick lining can reduce the weight of a three-stage tower in a large plant by 50t or more. Because of the weight of the brick and the possibility of damage during shipping, normal practice is to apply brick linings on site. In special circumstances, towers can be shipped after lining. Handling and erection, especially of single multi-bed columns, become much more difficult.

Small towers sometimes are reinforced PVC, and there is no need for a lining. A potential problem with PVC or other nonconductive material is the accumulation of a static charge. The explosion of a set of three PVC dryers in a mercury-cell plant was attributed to static discharge in the presence of an explosive gas [27]. The root cause of the incident was the failure of the power supply to the mercury pumps, which allowed mercury to drain from the cells and uncover the steel bottoms. This led to the formation of large quantities of hydrogen. The investigators concluded that towers should be constructed of acid-proof conductive material that can be held at ground potential.

Most chlorine cell headers operate very close to atmospheric pressure. The accumulated pressure drop causes compressor suction to be under vacuum, which raises the possibility of infiltration of atmospheric air. This lowers the purity of the delivered gas and makes the liquefaction process less efficient. The front end of the gas processing train therefore should be designed for low pressure drop. To this end, the drying towers

usually are sized for the low gas velocities mentioned above and operate well below the flooding rate. Because of the high molecular weight of the gas and the high density of sulfuric acid, the mass velocities are not unusually low.

Standard packing shapes, usually saddles, are used. Many columns contain plastic packing, either polypropylene or PVDF; ceramic and chemical porcelain are also common. Plastic and ceramic supports are used, and, in carbon steel columns, stainless steel. While the pressure drop is not great (about 50 mm w.c. per bed), it could be reduced by using structured packing instead of dumped saddles. One set of data [28] on structured ceramic packing shows that the pressure drop over the packing is reduced by a factor of about four. Since a change in packing has no effect on the pressure losses at the inlet and outlet of the column or over distributor and support plates, the net saving over an entire column is reduced by about 50%.

Other advantages claimed for structured packing include better distribution, with uniform liquid films and less channeling, and less bed movement, giving a pressure drop that is more stable over time. The lower pressure drop at any given flow rate reduces energy consumption to the tune of a few thousand dollars per year in a large plant. More important, but hard to quantify, is the improvement in the composition of the gas delivered to the compressor, due to the higher pressure profile and the reduction in the amount of inleakage. The lower pressure drop and the fact that operation is well below the flooding zone also mean that in a retrofit the rate can be increased by 40% or more without exceeding the original pressure drop.

Drying columns must be able to withstand some differential pressure but should be protected from overpressure by relief valves. On the low side, they should be designed for the lowest suction pressure developed by the chlorine compressors.

9.1.4.3B. Process Control. Figure 9.15 is a basic flow diagram for the drying process, showing some of the essentials of process control. Section 11.3.2.3 describes instrumentation and control loops in more detail. In contrast to Fig. 9.14, this drawing assumes the

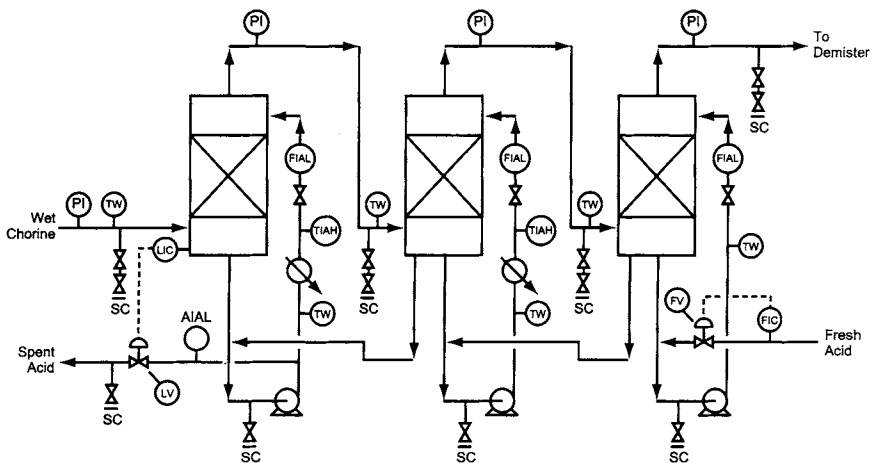


FIGURE 9.15. Flow diagram—chlorine drying.

use of three separate columns. Chlorine gas flows through the three columns in series, with measurement of pressure before and after each column. The drawing also shows thermowells and sample connections at each column. The dry gas flows on to the dry demister.

Fresh acid is supplied to the last column. Acid then flows forward under the influence of gravity. The concentration of the spent acid is usually measured by its density, and flows into and out of the system can be balanced in any of several ways. One of these is to feed fresh acid at a controlled rate and to remove spent acid under level control. This is the approach taken in Fig. 9.15. Any variation in the process will be reflected in the spent acid concentration, until the feed rate is changed to compensate. To prevent this drift, some plants feed fresh acid on outlet density (concentration) control. The feed rate varies in response to this measurement, and the acid cascades through to the first effect for removal. The holdup of acid is very large relative to its feed rate, and so spent acid concentration responds very slowly to a change in input rate. Many designers reject this approach because of the unfavorable dynamics of the long dead time. When acid flow is automatically controlled by the spent acid concentration, the reset component should be very weak.

An alternative is for the system operator to vary the acid addition set point as necessary to keep the desired spent acid concentration. Section 11.3.2.3A describes typical measuring instruments, but some systems rely on manual measurement of the concentration. There are other possibilities as well. Conceptually, at least, the spent acid can leave the first column through a lute, removing the need for level control, or it can be removed under density control with fresh feed under level control.

The rates of flow of circulating acid into the columns must be measured. Flow around a packed section usually amounts to 1.5 to 3 m³ per ton of Cl₂. The flow must be adequate rather than closely controlled. Rough manual control for occasional setting is acceptable, but the meters should have low-flow alarms. The circulating acid temperature in the first one or two stages also should be monitored, with high alarms. The drawing also shows acid sampling points in the pump suction lines.

The system for removing weak acid from the first column must be duplicated on the second if the dryers are to operate with the first column out of service. The designers may choose not to install duplicate instrumentation, but connections must be available to allow easy installation when it is needed.

9.1.4.3C. Tray Columns. With properly designed trays, there is no need to recirculate large quantities of acid in order to obtain good mass transfer. It is good practice, in the face of low acid flows, to maintain enough acid on each tray to provide good contact time. Bubble-cap or deep-seal trays are a frequent choice. Plate efficiencies are rather low, but with the small number of theoretical stages required, columns are still rather short.

The problem of heat removal remains. It is necessary to revert to heavy recirculation in the bottom sections, where most of the water is absorbed and most of the heat is generated. The recirculating section may use either trays or packing. An alternative suggested by some designers is to inject liquid chlorine into the bottom of a tower in order to cool the acid. This would require careful design and a thorough analysis of the hazards. One hazard to consider is the introduction of liquid chlorine into a new section of the plant.

With a tray column, it is relatively inexpensive to build in more equilibrium stages. It requires only extension of the column and addition of more trays. As pointed out in the discussion on equilibrium performance, this may be of limited value. The tray column has definite advantages in the costs of piping and pumping. It has a slight disadvantage in that, with most arrangements, the dry gas will be at a slightly higher temperature.

Control arrangements, with due regard to the differences in the equipment, are similar to those used with packed columns.

9.1.4.3D. Process Redundancy. A certain amount of process redundancy is usually a good thing. In the chlorine process, we can consider the cooling and drying steps together as a low-pressure gas-conditioning plant and consider ways of providing redundancy. The three-bed approach to drying has a certain amount of redundancy in itself. Operating with only two beds is practical, at least in the short term. The reader should realize that any design is a compromise and that no amount of water is “desirable.” Less-than-optimum results can be tolerated for some period of time, and the loss of one stage of drying may not justify a shutdown of the entire plant. The design of the drying system may allow operation to continue if one stage is lost, and the smaller components then should be designed for maintenance access. This approach means that the second stage may be forced into service as the “first.” The cooler on the second stage should then be designed for the process load normally seen by the first.

When two stages of chlorine cooling are supplied, the drying system sometimes is designed to operate even if the secondary cooler (or chiller) fails. The acid throughput will increase. Because the net flows are so low, this is not much of a consideration hydraulically, but the acid delivery system must have sufficient capacity for the upset condition and at the same time have enough turndown to match the minimum operating rate of the plant. The heat load on the drying system can increase substantially, and then the heat-transfer capacity will have to be markedly increased. The second-stage acid cooler will come more into play under these circumstances. To design for failure of both the secondary chlorine cooler and one stage of drying would be considered by many as carrying redundancy beyond the optimum.

Another form of redundancy is the excess capacity often built into plants with more than one processing line. If two sets of drying towers are used, for example, the capacity of each may be more than 50% of the plant design capacity. The primary justification for multiple trains usually is to enhance turndown capability or to allow continued operation even when one train must be shut down. The same approach may be taken with the cooling section. Given the sizes of chlorine gas headers, valves would be expensive and probably ineffective as shutoff devices. Many plants therefore use U- or J-shaped traps in the piping. These can be filled with water or acid to stop the gas flow and to isolate equipment for maintenance.

9.1.4.4. Acid Handling

9.1.4.4A. Characteristics of Sulfuric Acid. Besides its use in drying, sulfuric acid is the seal liquid for rotary compressors in evacuation systems and small-scale chlorine compression units (Section 9.1.6.2C). To be effective as a desiccant, it should have a concentration of at least 93% and preferably 96%. When higher strengths are used, the

lower water content is good in itself, but the freezing point and viscosity are also higher. Some plants change the strength of the acid supply with the seasons.

Standard commercial grades of acid usually are suitable. Byproduct acid is widely available commercially, and it is important for the user to know his ultimate source and to adopt the proper quality assurance program. Troublesome impurities may include heavy organics, which can form chlorine compounds that remain with the product, and nitrogen compounds, which can form nitrogen trichloride (Section 9.1.11.2A).

Sulfuric acid is a dangerous material that attacks body tissue very rapidly. Suppliers' safety data sheets will advise the standard precautions and first-aid measures. Section 16.2.5 discusses the hazards briefly.

9.1.4.4B. Handling and Unloading. Sulfuric acid is shipped in steel tank trucks and tank cars. In the United States, ICC 103-A and 103-AW tank cars are used. They are unloaded by pump or air pressure. Because acid with its specific gravity of 1.8 or more must be lifted through a dip pipe from the car or truck, self-priming pumps are preferred for the service. The car then must be vented to atmosphere to avoid the risk of pulling a vacuum and collapsing the shell. The pump suction piping should be carried no higher than necessary, in order to reduce the amount of suction lift required. An alternative to the self-priming pump is to apply a slight pressure to the tanker to begin pumping. This pressure must be applied carefully and vented off before returning the empty tanker to the supplier. When compressed air is used for unloading, the pressure must be limited to the value set by the supplier or appropriate to the particular tanker. This will usually be about two bars. If air is supplied from a plant header, the line must contain a pressure regulator and a relief valve. From the standpoint of inherent safety, pumping is preferred to unloading under applied gas pressure.

Where flexible connectors are required in unloading systems, PTFE- or FEP-lined hoses are usually chosen. Swing joints for loading and unloading arms should be ball-and-socket units with Alloy 20 balls and PTFE gaskets. Shipping, loading, and unloading of sulfuric acid often are regulated under hazardous material codes. US regulations are in Title 49 of the Code of Federal Regulations, Parts 173.249 and 272.

Unloading operations should never be left unattended. When the tanker is empty, the air pressure will drop and the sound of fluid going through the line will change. Air should continue to flow until the transfer line is empty. The air supply line then can be closed and the tanker vented carefully through a bleed valve. When all pressure has been vented, the acid discharge line can be disconnected and the outlet cap reinstalled.

High-strength acid and oleum may partially freeze in tank cars in cold weather. They can be thawed by placing the car in a heated building or by covering it with a tarpaulin and exposing it to steam. The best way to introduce steam is through a perforated pipe.

Fires and open flames should never be used around an acid tanker. Water must never be introduced into the car. Besides the violent localized evolution of heat, there is the possibility of iron corrosion, with hydrogen as a product of the reaction. There have been explosions in strong sulfuric acid systems when water was allowed to enter. Those working around a sulfuric acid system should assume that there is hydrogen present. Smoking and open lights should be banned. Hot work permits should be required for cutting or welding.

9.1.4.4C. Storage and Transfer. Concentrated sulfuric acid up to about 99% H_2SO_4 can be handled in ordinary ferrous-metal equipment. The rate of corrosion reaches a minimum at about 96%. In 93% acid at about 50°C , the rate is $0.6\text{--}0.65\text{ mm yr}^{-1}$. For a 10-year life, a corrosion allowance of 6.5 mm should be specified. Anodic protection can cut the rate of corrosion approximately in half and extend tank life, but it is not often used by chlor-alkali producers. Above 99% and 50°C , the corrosion rate of carbon steel is greater than 1.5 mm yr^{-1} , and stainless steel is often specified.

The acid can be stored in vertical or horizontal tanks. Normal good practice is to fill a tank through a submerged pipe. In a tall vertical tank, the dip pipe should be secured by a support mounted on the bottom of the tank. The end of the pipe should be at least 500 mm from the tank bottom; frequently a wear plate 10–15 mm thick is welded to the bottom to allow for erosion. This can also serve as a support for the dip pipe's guide. Top entry is preferred, under the general principle that it is well to minimize the number of bottom connections. While a side nozzle near the bottom of the shell is sometimes used, it should have an insert that is bent to direct the flow of acid away from the tank bottom.

Tank overflows are carried to grade, and vents are through goosenecks. The approach to diking or diversion of spills depends on the location of the tank and the presence of other storage tanks nearby. When a tank is connected to a vent collection system, a pressure/vacuum relief (PVR) device is required. Wetted-part materials of construction usually are Alloy 20 or a resistant plastic. The device must be set, and the relief piping designed, to operate within the tank's design pressure limits. The tank must be designed to withstand both internal and external pressures. Vertical tanks usually are designed for about $\pm 0.5\text{ kPa}$. Horizontal tanks may be designed for higher differential pressures, up to 5–10 kPa.

Other design points sometimes observed include the following:

1. Top nozzles penetrate the shell by 10–50 mm in order to avoid trickling of acid along carbon-steel plate.
2. Side-mounted nozzles similarly penetrate the shell, at least over their top 180° .
3. Internal pipes and vent and overflow nozzles are of Alloy 20 Cb-3.
4. Vertical tanks are installed on beams to allow inspection for bottom leaks.
5. Horizontal tanks are supported by steel saddles mounted on concrete piers. Top plates of the saddles are welded to the shell of the tank and span at least 120° of the circumference of the tank.

Spent acid, because of its higher water content and the presence of chlorine, is more corrosive than concentrated fresh acid. While some systems still rely on carbon steel, it is not the best choice for the service. One of the products of corrosion of steel by wet acid is hydrogen gas. Alloys and lined systems are therefore widely used. Many of the details of tank design are the same as those given above. Differences arise when a storage tank is sparged to remove dissolved chlorine (Section 9.1.4.4E).

9.1.4.4D. Pumping and Cooling. When pumping sulfuric acid, the designer must consider its density, viscosity, and tendency to corrode ferrous metals. Standard horizontal centrifugal pumps can be used to transfer acid. High-silicon iron is frequently chosen for concentrated acid. This is a brittle material, and piping connections must

be free of stress. More dilute acid, or acid containing chlorine, may require the use of rubber-lined, Alloy 20, or Hastelloy C pumps. Mechanical seals should be used in order to avoid leakage; these can be lubricated by the pumped fluid. Semi-closed impellers are the standard, and flexible connections lined with PTFE are often used at the pump connections. In the drying process itself, the rate of addition of acid will be quite small, and positive-displacement metering pumps are usually chosen for the service. These are usually constructed of one of the alloys named above or of a resistant plastic.

Circulating pumps attached to the different drying stages have different normal process duties. However, each pump must have the capability to lift concentrated acid at some rate during startup. It may be preferable to specify all pumps the same in the interest of standardization. The single-tower approach, with a substantial static head on the top-section pump, is the most likely exception. Even here, the pump body can be standardized and only the drive changed.

Acid is not pumped between columns; interstage flows are by gravity. In the single-shell column, accumulated acid overflows a weir from one stage to the next below. When separate shells are used, the arrangement of the piping provides the same effect.

Plant designers should note that the small metering pumps used for controlled addition of acid cannot fill the system quickly. Special arrangements usually are made for startups.

Carbon steel piping can be used to move concentrated acid. Many users will specify all-welded Schedule 80 pipe, at least in the smaller sizes. There will be a slow reaction between the acid and the iron in the pipe. This can result in the formation of deposits of iron sulfates. These can foul valves, and for this reason lined or alloy valves are usually specified even in a carbon-steel system. The piping should be kept full to minimize sulfation; at the same time, it should be sloped to allow efficient drainage when shut down. Hydrogen gas can also form by reaction with the pipe. The last valves in a pipeline should be vented to prevent the accumulation of hydrogen. Flanges and packing glands, if used, should be covered with shields where there is a possibility of personnel exposure.

Sulfuric acid is especially likely to corrode metal surfaces at high velocity. Carbon steel piping systems are usually designed for maximum velocities of about 1 m s^{-1} . When more resistant alloys are used (e.g., Alloy 20), velocities can be increased to about 2 m s^{-1} .

Because of the low throughput of acid and the periodic nature of transfers, the residence times in many pipelines will be quite long. Where appropriate, these lines should be protected from freezing by insulation and, where necessary, tracing.

Many plants use standard shell-and-tube exchangers to cool circulating acid. Special exchangers based on PTFE tubing are a more recent development. Heat-transfer coefficients are only about $20 \text{ W m}^{-2}(\text{°C})^{-1}$, but with low-diameter tubing, the exchangers are quite compact. Still other designs use plate exchangers. The standard plate material is Hastelloy C276, about 0.7 mm thick. Fluoroelastomer gaskets are the most common.

A special feature of plate exchangers that requires some design attention is the possible acceleration of corrosion by the flow of the acid. Keeping the acid velocity low, at a level determined by the manufacturer, protects against such corrosion but reduces the acid-side film coefficient. The cooling water velocity should be sufficiently high to

maintain the efficiency of heat transfer on that side. The combination of low acid velocity and high water velocity can result in a smaller than normal rise in temperature on the water side; this is an inefficient use of water. To correct this, many designs arrange for series flow of cooling water through more than one exchanger. With a good balance of acid and coolant flows, coefficients in the range $400\text{--}500\text{ W m}^{-2}$ per degree celsius can be obtained.

Cooling the acid well below normal cooling water temperatures offers no great process advantage. Chilled water still is frequently used as a coolant. The greater driving force for heat transfer is an advantage in the frequent case where the desired acid temperature is close to the plant cooling water temperature. Avoiding a temperature pinch provides economy in exchanger design, reducing the surface area requirement and sometimes simplifying the pass configuration in a plate exchanger. Chilled water also can relieve the need to obtain the highest coefficients by high velocity. When two stages of drying are cooled and when the header pressures permit, the chilled water consumption can be reduced with no perceptible effect on the drying process by using it on the two exchangers in series.

9.1.4.4E. Dechlorination of Spent Acid. The spent acid from the drying process frequently is a disposal problem. In some cases, it can be returned to the supplier for a credit; in others, it can be used on site as a neutralizing agent. Normally, dissolved chlorine, which is present in concentrations of 1,500–2,000 ppm, must first be removed. The usual approach is to strip the chlorine with a stream of dry air. Very frequently, air is simply blown into a storage tank or shipping container through some form of distributor until the chlorine concentration is reduced to its specified level. Sometimes, air is allowed to flow continuously into a spent acid receiving or storage tank. The chlorine-laden air can then flow to a scrubber. This approach favors the use of horizontal tanks. Spargers, which may be of CPVC or PVDF, usually run the length of the tank; their size and number depend on the diameter of the tank. When the spargers are mounted some distance from the bottom of the tank, the holes may be drilled on their undersides. Usually, the holes alternate from one side of the centerline of the pipe to the other.

Another approach is to strip the chlorine from the acid in a packed column. This should reduce the consumption of air by providing a richer off-gas. Typical liquid flow rates are close to $10,000\text{ kg hr}^{-1}\text{ m}^{-2}$ with L/G between 1.5 and 3. Ceramic saddles typically are used, in beds between 3.5 and 5 m deep. At normal scales of operation, the saddles measure 25 mm or less and result in a pressure drop of $1\text{--}2\text{ mmHg m}^{-1}$. Chlorine is least soluble in acid of 70–80% H_2SO_4 , and the waste product will have its dissolved chlorine content reduced to less than 100 or 150 ppm.

Example. In a previous example, we found that the hourly flow of spent acid from the tower contained 568.6 kg of H_2SO_4 and 160.4 kg of water. The total flow of 729 kg hr^{-1} would require a column area of about 0.073 m^2 . Allowing for $1,000\text{ kg hr}^{-1}$ would give a safety factor of 37% and provide some surge capacity. At the value of L given in the text, the area required is 0.1 m^2 and corresponds to a diameter of 350 mm. Using $L/G = 2$, we arrive at an air flow of 500 kg hr^{-1} (about $388\text{ Nm}^3\text{ hr}^{-1}$). Assuming that the air used contains 3% moisture and that the acid absorbs all the water (slightly conservative), and assuming further that the full design air flow is used but that the acid

flow is only the calculated value, the water picked up in the column is 9.4 kg hr^{-1} , and the acid is diluted slightly, from 78 to 77%.

With a packed section 5 m long and allowing for a flow distributor and an entrainment separator (mesh pad), the pressure loss is estimated to be 1.5–2 kPa. The spent acid will normally contain $1.5\text{--}2 \text{ kg hr}^{-1}$ of dissolved chlorine. Depending on the circumstances of operation and the true flow rate of the air, the concentration of chlorine in the column vent will be in the range 150–450 ppm (v/v).

Another possibility is to reduce the amount of chlorine dissolved in the spent acid as it leaves the drying system. This depends on the special ability of HCl to reverse the hydrolysis of dissolved chlorine (Section 7.5.9.1). The total solubility of chlorine in brine or in acidic solution is suppressed by the presence of any of the species on the right-hand side of Eq. (7.82). These species include H^+ and Cl^- .

In spent sulfuric acid, a certain amount of chlorine hydrolyzes according to Eq. (7.82). The addition of concentrated hydrochloric acid will reverse the reaction and release some of the chlorine from solution. One can visualize several variations on this process:

1. addition of HCl to the spent acid outside the drying column
2. addition of HCl to the drying column near the bottom or, combined with the concentrated H_2SO_4 , at the top of the column
3. addition of anhydrous HCl along with the chlorine gas.

The first two of these approaches add water to the system and dilute the spent acid. In our example, addition of 2.9 parts of 32% HCl to 100 parts of spent acid would reduce the final H_2SO_4 concentration from 78% to 75.8%. Alternatively, an increase of about 4% in the rate of feed of fresh H_2SO_4 would maintain the spent acid concentration of 78%.

The authors can cite no current application of this process. Its fundamental disadvantages are the cost of the HCl and its contamination of the sulfuric acid byproduct.

9.1.5. Mist Elimination

One of the problems associated with sulfuric acid is its tendency to form mists. The liquid particles in mists are by definition $10 \mu\text{m}$ or less in diameter, and sulfuric acid mists range down into the submicron sizes. Particles larger than about $3 \mu\text{m}$ are collected efficiently by inertial impact, but Brownian motion becomes the predominant mechanism below $1 \mu\text{m}$. Wire-mesh and other common impingement-type mist eliminators therefore lose their efficiency below 1 or $5 \mu\text{m}$.

To put the requirements of sulfuric acid demisting in perspective, the material that follows compares a wide range of typical devices. The discussion generally follows the presentation of Ziebold [29]. First, Table 9.3 shows the nominal particle diameters below which the various devices begin to lose their efficiency. The type chosen for sulfuric acid mists in chlorine is a fiber bed packed between concentric screens and suspended vertically in the gas stream. Diameters of these elements usually range from 0.2 to 0.75 m. Lengths may be up to 7.5 m. The list below compares the physical and operating characteristics of impaction and diffusion beds. The most familiar style of separator is the wire-mesh type [30], which functions by impact of the suspended particles with the demisting elements. This type therefore requires a minimum gas velocity. The list shows

TABLE 9.3. Cutoff Particle Diameters for Mist-eliminating Devices

Type	Diameter, μm
Vane separator	25
Conventional mesh pad	5
Co-knit mesh pad	3
Impaction fiber bed	1
Diffusion fiber bed	< 0.1

that the requirements of these devices are less demanding, but their ability to remove the finer particles is not adequate for our purposes.

Parameter	Impaction	Diffusion
Fiber diameter, μm	10–40	8–10
Gas velocity through bed, m s^{-1}	1–3	0.05–0.25
Pressure drop, mm w.c.	100–250	100–450
Particle size collected, μm	1–3	0.1–3

The diffusion fiber bed uses the Brownian motion of the particles to achieve high efficiency. Multiple elements, or “candles,” are the standard in all but very small plants. They are suspended from tube sheets, with flow from the outside of each element to the inside. This forward-flow arrangement has layout constraints and is the more expensive option, but it allows inspection and most maintenance work to be on the clean side of the apparatus. It also facilitates adjustment of gaskets after cold flow.

Demisters are specified to remove essentially 100% of particles above $3 \mu\text{m}$ in diameter. Removal of smaller particles depends on the type of element chosen, but in the service under discussion, it usually is specified as 99% or better. The tight construction required leads to greater pressure losses than in other types of mist eliminator. A compensating advantage is that performance improves on turndown.

Typical mist loadings in chlorine gas are $0.15\text{--}1 \text{ g m}^{-3}$. The design basis should be higher, at about 1.8 g m^{-3} , with face velocities about $2.5\text{--}8 \text{ m min}^{-1}$. Pressure drop is usually about 10–30 mbar. The packing is fiberglass, held by stainless steel mesh in a confining vessel of carbon steel. Fluoropolymer gaskets seal the candles to the tube sheet. The size and number of candles are determined by the capacity of the plant.

Figure 9.16 shows a typical flow arrangement. The fibers trap the acid mist and the liquid then trickles to the bottom of each candle. There, it must be collected and brought to a drain for removal. A liquid seal on the acid drain prevents bypassing of the chlorine gas. The tail pipes, usually of CPVC, can be sealed by maintaining a level of acid in the bottom of the vessel or each element can be sealed separately with an overflow cup attached to the bottom of the drain pipe. In the latter case, there still must

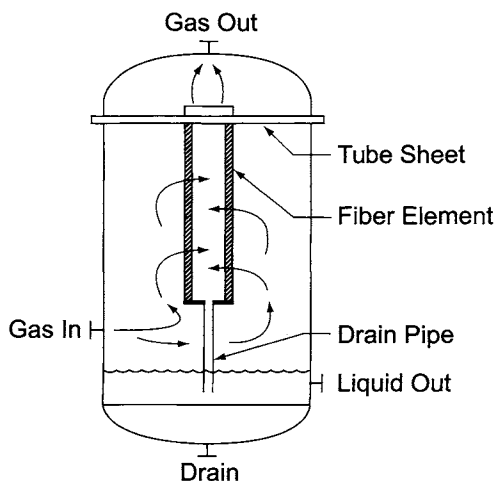


FIGURE 9.16. Typical mist eliminator element.

TABLE 9.4. Mist Eliminator Design and Operating Characteristics

Type of operation	Wet gas	Dry gas
Materials		
Elements	Glass or polyester	Glass
Mesh enclosure	FRP ^a or PVC	Stainless steel
Vessel	FRP ^a or lined	Carbon steel
Operating Characteristics		
Design mist loading (g m ⁻³)	7–10	1.5–5
Gas velocity (m s ⁻¹)	0.05–0.1	0.1
Pressure drop (mbar)	10–20	10–20
Efficiency (below 3 μm)	99–99.5%	99–99.5%

^a Minimum construction based on bisphenol-A resin.

be a positive seal at the point of removal of acid from the vessel. Withdrawal of the liquid through a pipe higher than the bottoms of the tail pipes automatically maintains a seal; this approach requires a separate small drain or cleanout at the bottom of the vessel.

The equipment used to remove the anolyte mist referred to in Section 9.1.1 is quite similar. Mist concentrations and design levels are higher than in the dry mist eliminator, by a factor of about four. A spray nozzle connected to a water supply is a useful addition at the gas inlet. This allows occasional washing of the elements.

Table 9.4 is a summary of the design characteristics of chlorine demisters [14].

9.1.6. Compression

The main process of compression raises the gas from nearly atmospheric pressure to one at which it can be processed or liquefied economically. Thermodynamically, the

compression of chlorine is quite an ordinary process. As a normal diatomic gas handled well below its critical pressure, its behavior is close to that of air and similar materials. It is the other properties of chlorine that make it a special case, and O'Brien and White [31] have summarized these in a review. Important design points are:

1. Chlorine is extremely toxic and corrosive. Releases of the gas will have serious consequences.
2. Wet chlorine is extremely corrosive to ferrous metals, which are the standard for fabrication of compressors and downstream equipment. Moisture must be effectively excluded from the process.
3. Chlorine reacts combustively with many metals at sufficiently high temperatures. The compression ratios must be limited to avoid overheating, and mechanical design should prevent dangerously hot spots.
4. Chlorine reacts with many of the common types of lubricant and can destroy their lubricating power or even cause fires. Contact between the gas and these lubricants must be avoided.
5. The dry chlorine present in the compression process will react combustively with titanium even at low temperatures. When a compressor shuts down, backflow of the gas into a titanium-based cooling system must be rigorously prevented.
6. Compression is frequently followed by liquefaction, where the efficiency of the process depends on the purity of the gas. Ingress of air or compressor seal gas will affect the results in liquefaction and therefore must be kept to a practical minimum.

9.1.6.1. Work of Compression. Section 10.4.3.1 discusses the thermodynamics of the compression process and derived the energy consumed in certain limiting cases. When operation is isothermal, for example,

$$W = RT \ln(p_2/p_1) \quad (42)$$

where

W = work expended

T = absolute temperature

p_2 = final pressure of the gas

p_1 = starting pressure

Isothermal behavior does not occur in normal compression. The process is more nearly adiabatic. With an ideal gas, we then have

$$pV^k = \text{constant} \quad (43)$$

k being the ratio of specific heat at constant pressure to that at constant volume (C_p/C_v). In this situation,

$$W = p_1 V_1 k / (k - 1) \left[(p_2/p_1)^{[(k-1)/k]} - 1 \right] \quad (44)$$

The point value of the specific heat ratio depends on the operating conditions. Over the operating range of a chlorine compressor, it decreases slightly from feed to discharge.

Section 10.4.3.1 also points out the fact that a real compression process is not quite adiabatic. Instead of Eq. (43), it follows a polytropic path in which

$$pV^n = \text{constant} \tag{45}$$

The exponent n is an empirical quantity that is greater than k and replaces it in Eq. (43). In all cases, the power consumption is greater than in the adiabatic case. Typically, $n \approx 1.45$.

Most compression processes involve more than one stage. There are two strong reasons for this. In polytropic compression of an ideal gas, the temperature rises along with the pressure. At the end points of the process,

$$T_2/T_1 = (p_2/p_1)^{(n-1)/n} \tag{46}$$

The combustive reaction of chlorine gas with metals, referred to in the introduction, makes this an especially important consideration in chlorine compression. The compression ratio in a given stage must be limited to a value fixed by the inlet temperature in order to avoid the danger of combustion.

A more mundane reason for multistage operation is the energy consumption of the process. In Fig. 9.17, the line 1-2 represents adiabatic or polytropic compression. The dashed line 1-3 shows an isothermal path. The potential reduction in the quantity of work done is the area 1-2-3. A two-stage compressor might follow the path 1-4-5-6. Line 1-4 is the first stage of compression. Line 4-5 shows that the interstage gas is cooled back to the original suction temperature, and line 5-6 is the second (adiabatic or polytropic) stage of compression. The two-stage approach requires less work than the one-stage approach, in the quantity 2-4-5-6. Note that cooling the interstage gas is an essential

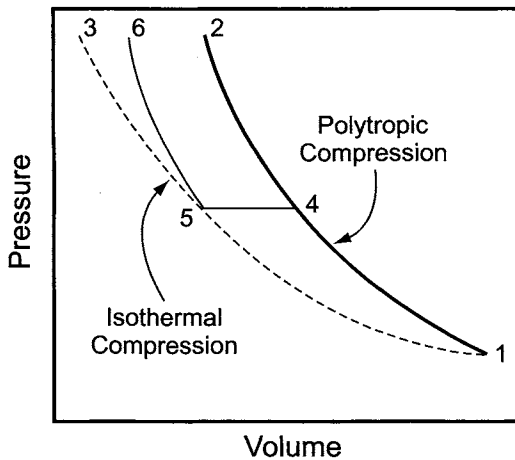


FIGURE 9.17. Energy conservation in multistage compression.

part of the process. Without gas cooling, adding the second stage will not reduce the work of compression. This justifies the tendency to refer to any number of centrifugal impellers in series as a “stage” if no intercooler separates them. Figure 9.17 ignores the pressure drop between stages of compression, which is largely due to the intercooler. In a real case, this loss will detract from the amount of energy saved by the second stage.

With this background, we turn to the equipment.

9.1.6.2. Types of Compressor. Many different types of compression machinery are used in chlorine service. Low-pressure and vacuum applications are considered elsewhere (Section 9.1.12). For compression of the main process flow, we consider centrifugal, reciprocating, and rotary liquid-ring compressors.

9.1.6.2A. Centrifugal Compressors. Centrifugal compressors are the modern standard for large plants. The capacities required in chlorine plants are well below the minimum normally considered economical for an axial-flow compressor. The machines used are constant-pressure rather than constant-volume devices. Like centrifugal pumps, they first produce high velocity in the fluid and then convert that energy into pressure energy in diffusing sections. Centrifugal machines, whether pumps or compressors, depend on impellers, which contain series of radial vanes of various shapes and curvatures, rotating inside circular casings. The fluid enters ideally at the axis of rotation and discharges from an impeller into the periphery of the casing. The impeller is the only moving part in a machine, and the pressure it develops on the fluid corresponds to the sum of the centrifugal force of rotation and the kinetic energy imparted by the vanes.

Figure 9.18 shows the velocity components at the periphery of an impeller with backward-curving vanes. The velocity of the tip of a vane is u . The velocity of the fluid is v , and the angle between these two velocities is α . The vector difference between v and u is the velocity of the fluid relative to the impeller, designated as u' . The angle between this and the vector u is $\pi - \beta$. Church [32] shows that, when a fluid enters the eye of an impeller with no prerotation, the virtual head developed is

$$H_v = uv \cos \alpha \quad (47)$$

This is the maximum head that could be developed by the impeller under the indicated operating conditions. The use of standard engineering units in Eq. (47) may require addition of a gravitational acceleration term to maintain consistency.

In Fig. 9.18, we see that

$$u = v \cos \alpha + u' \cos \beta \quad (48)$$

giving

$$H_v = u(u - u' \cos \beta) \quad (49)$$

In terms of the flow per unit peripheral area (Q), Church's development converts this to

$$H_v = u^2 - uQ/(2\pi \tan \beta) \quad (50)$$

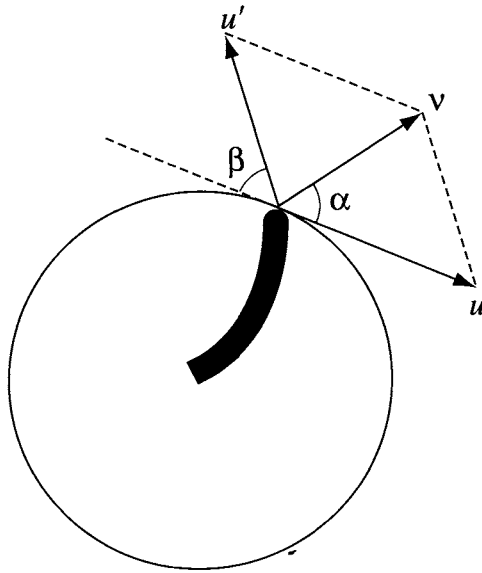


FIGURE 9.18. Centrifugal compressor operation.

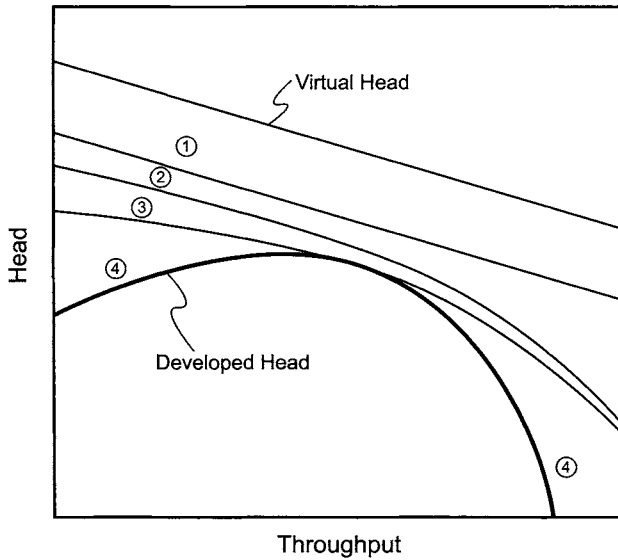


FIGURE 9.19. Deterioration of head developed by centrifugal compressor. Losses: (1) inertial effects, (2) friction, (3) leakage, (4) turbulence.

With a backward-curved impeller, the virtual head decreases continuously as the quantity pumped or compressed becomes greater. The characteristic curve of the machine, which plots the developed head against the quantity of fluid moved, then tends to have a falling characteristic, illustrated in Fig. 9.19. However, Eq. (50) represents the

ideal situation with no mechanical losses and an infinite number of vanes on the impeller. In a real case, there will be losses and there will be inertial effects in the spaces between vanes that induce flow opposite to the direction of rotation of the impeller. These effects reduce α and increase β . The virtual head becomes lower than that computed by the equations above. Mechanical, inertial, and turbulence losses are relatively more important at low flow rates. Their effects on the characteristic curve of the developed head vs throughput are more pronounced in that region. Losses due to turbulence actually decline as throughput increases toward the impeller's design point. As throughput continues to increase, turbulent losses reappear and increase rapidly. The result is a curve that contains a maximum. Design of the impeller therefore not only affects its efficiency but also determines the shape of the characteristic curve. This is an especially important fact in centrifugal compressor design, and more will be said on the subject when considering surge phenomena.

The gas is accelerated toward the periphery of the impeller by rotation. After the gas enters the diffuser section, it decelerates, and the lost kinetic energy appears as a greater pressure on the gas. Diffuser design is also important to the efficiency of the process. The gas then usually passes on to another impeller, where the action repeats.

Advantages of centrifugal compressors include:

1. high capacity in small space
2. high mechanical reliability; many operate without installed spare equipment
3. output flow can vary over a wide range with small change in head
4. smooth output; no pulsations in flow
5. no rubbing parts in flow stream
6. good mechanical efficiency (% polytropic efficiency in high 70s)
7. good match to steam turbine output; direct coupling not a problem.

Disadvantages are:

1. performance depends on molecular weight of gas
2. impeller tip speeds are very high; good rotor balance required
3. small increase in output pressure can cause serious loss in capacity
4. complex lubrication and sealing system necessary.

The dependence on molecular weight follows from the fact that pressure develops from the conversion of kinetic energy. Deceleration of a denser fluid generates a higher pressure. This fact is of enormous importance during the startup of a chlorine line. Beginning with a gas approximating air, the compressor must handle all mixtures from the starting composition up to nearly pure chlorine. An alternative with a different set of disadvantages is to allow gas from the header to bypass the compressor to the vent scrubber until the molecular weight increases to a certain point.

Performance curves for various mixtures of air and chlorine will help to guide the startup engineer. Manufacturers can frequently provide these curves. The manufacturer or the operator can also estimate the compressor's performance on various mixtures from the design curves. Lapina [33,34] describes a method that involves first changing curves of discharge pressure and power requirement versus volumetric flow into curves of polytropic head and efficiency. He also discusses the volume-ratio effects in multistage compressors and gives a criterion for judging the validity of his procedure. If any curves

are available for low-molecular weight operation, it is better to use them and to apply Lapina's method for interpolation.

Cleanliness of the gas is important. Lubricant oil must be kept out of the process stream for a variety of reasons. The air used on the compressor seals (see below) must be free of oil and particulate matter. The presence of fine particles in the gas is not as damaging in the short term as it would be in a reciprocating machine. Some users have in fact removed suction screens, preferring to deal with the occasional fine particle than with the large debris associated with a screen failure [35]. Even in the absence of solids contamination, there is a buildup on the impellers. The source is organic materials present in the cell gas. These may come from the brine or from reaction of cell components with the gas. The amount of material formed was greatly reduced by the adoption of metal anode technology. Accumulation of solids on the impellers is not a frequent cause of compressor shutdown, but removal of deposits still should be part of the routine overhaul procedure.

Performance Curves and Surge. Figure 9.20 shows the shape of a typical performance curve. Beyond a certain throughput, the curve shows that the developed pressure falls as more fluid is processed. Figure 9.19 identified some of the factors responsible for the shape of the curve. At low flow rates is the familiar "droop" of a centrifugal machine, where the impeller operation becomes inefficient and the pressure actually falls as throughput is reduced. Like a pump curve, this one applies to a given impeller operating at a given speed.

The low-flow end of the curve is dashed. This is an area of operation to avoid. At low throughput, centrifugal compressors enter the region of "surge," which is discussed below in Section 9.1.6.3 on compressor control. This is a region of dangerous mechanical instability in which the machine can be rapidly and severely damaged. We must ensure that a compressor always operates to the right of the surge point.

The shape of a performance curve depends on design of the diffuser and the impeller. The most important feature of the impeller in this regard is the angle of the vanes at the outer diameter. In chlorine service, the vanes usually are backward-leaning, as

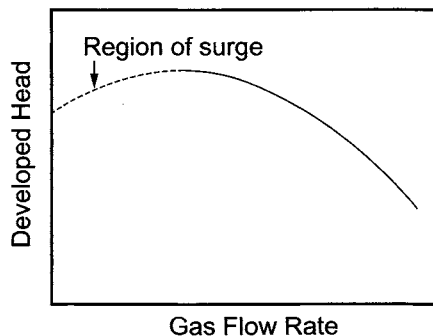


FIGURE 9.20. Centrifugal compressor performance curve.

shown in Fig. 9.18. This arrangement produces a relatively steep curve, which has two advantages:

1. better control characteristics
2. less dependence of flow rate on output pressure.

The importance of the latter lies in the reduced probability of surge. If, say, a downstream liquefaction process operates at a controlled back-pressure and the pressure increases slightly for some reason, a shallow performance curve might allow enough decrease in the flow to put the compressor into surge.

Materials of Construction. The principal materials of construction are ferrous throughout, but different grades are used for the different components. Casings usually are in cast iron or cast steel, and impellers may be in the same materials or in fabricated steel. Early designs of centrifugal compressors used riveted assembly for impellers; castings or welded constructions are preferred today. Shafts usually are of carbon steel with hardened or stainless steel sleeves at points where erosion is likely. The selection of materials for smaller components that may be subject to friction is particularly important because of the danger of combustion.

A case history will help to emphasize the importance of materials selection and the finer details of design. This concerns a fire attributed to design issues associated with a new compressor [36]. Some of the corrective actions relate to one of the minor components, the balance piston. There is a net reaction force on each impeller in a centrifugal compressor, because the outlet pressure on the discharge side works against the suction pressure at the inlet to the impeller. The sum total of these forces in a multi-impeller machine is usually too great to be withstood by an ordinary thrust bearing. The shaft therefore includes a rotating collar known as the balance piston to offset the reaction force. The balance piston is exposed to the final pressure of the gas on its upstream side. The downstream side connects by a balance line to the suction of the compressor. The pressure developed in the compressor therefore creates a thrust on the balance piston that is opposed in direction to the thrust on the impellers. Proper choice of the balance piston's diameter then largely offsets the reaction forces on the impellers and unloads the thrust bearings.

It is important to provide an efficient seal for the balance piston without allowing excessive temperatures to develop. This requires adequate clearances. Among the corrective actions taken to prevent recurrence, clearances were increased and the new balance piston was fabricated from Inconel 625, which has a much higher ignition temperature in the presence of chlorine (about 540 vs 250°C for the old carbon steel piston).

Mechanical Specifications. API 617 is a standard and widely used mechanical specification for centrifugal compressors. Since this is a generalized specification, most compressor manufacturers have their own "standard" set of exceptions. Still, it provides common ground for comparison of different offers and can be recommended as a starting point to engineers specifying part of a chlorine plant.

The high rotational speeds in a centrifugal compressor demand attention to the critical speed of the assembly, sonic velocity in the gas being compressed, and vibration of the rotor. In the normal case of a flexible-shaft machine, operating speeds should be between the first and second critical speeds. These usually differ by a factor of at least two to five or higher, and it should be possible to operate a compressor with comfortable margins on both sides.

The velocity of sound in chlorine is relatively low. At standard conditions, it is only 206 m s^{-1} (750 km hr^{-1}), less than two thirds the sonic velocity in air. While air compressors typically operate with tip speeds above 250 m s^{-1} , then, chlorine compressors are restricted to lower speeds partly in order to avoid sonic shocks.

The rotor assembly in a chlorine compressor should always be carefully balanced, and its vibration at the operating speed should be measured. A peak-to-peak vibration limit of $50 \mu\text{m}$ at low speed is common. At higher speeds above about 5,000 rpm, the vibration might be restricted to some lower value. An API specification limits the vibration amplitude to about $38 \mu\text{m}$ at 6,000 rpm. The Compressed Air and Gas Institute relates allowable vibration amplitude to the rotational speed by $\text{Amplitude (mm)} = (7.75 \text{ rpm}^{-1})^{1/2}$. Evans and Ista [35] report various criteria used in the industry, along with the fact that manufacturers in practice are more concerned with the rate of increase of vibration than in its actual value. They present a graph that is equivalent to $\text{Amplitude (mm)} = 305 \text{ rpm}^{-1}$, corresponding to a vibrational speed of about 10 mm s^{-1} .

Casings may be split horizontally or vertically. The former has advantages in maintenance, because access to the rotating element is easier. Its disadvantage lies in the increased area that must be sealed. The latter fact often leads to the use of vertically split casings. In the case of chlorine, however, required sealing pressures are not great and horizontally split casings are normally specified.

The centrifugal compressor, with its high rotational speed, is unique in requiring a speed increaser between the drive and the compressor. The chlorine process places no special demands on the gear increaser used here. Within the limits of good practice, any rugged high-quality unit will serve.

Shaft seals usually are dry ring or labyrinth units. There is no attempt to produce an absolute seal; the path for the flow of gas through the seal is long and tortuous in order to keep the flow of gas small. In chlorine service, such a seal is always padded with dry air or nitrogen at a pressure higher than that of the process gas. Flow through the innermost seal is into the process, and its presence must be accounted for in design. A number of nonsegmented seal rings are necessary, and they will be held in place by stainless steel spacers and axial springs. A buffer gas of dry air or nitrogen, supplied at 0.1–0.4 bar above the process pressure, once again is used. Most of the rings vent into the process side; in an outboard seal, a smaller number vent to the bearing side, where there will be a slight positive pressure. In a typical system, about $2\text{--}5 \text{ kg hr}^{-1}$ of air may be added to the process. The flow into the bearing chamber may be 5–10 times as high.

Figure 9.21 shows the direction of gas flows in a typical labyrinth seal. The number of chambers shown here is approximately the minimum; a real unit may be more sophisticated than the one shown. Dry air (or nitrogen) enters the outermost chambers at a positive pressure maintained above that of the inboard seal on the compressor suction by a differential pressure control valve. Flow is then either to atmosphere or into the

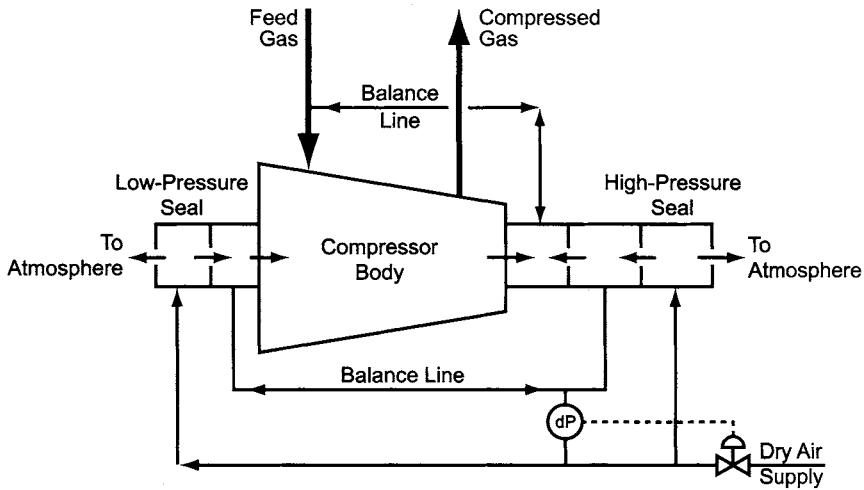


FIGURE 9.21. Air flows in compressor labyrinth seals.

next seal chamber approaching the compressor. On the suction side, flow is finally into the body of the compressor itself. On the discharge side, a balance line connects the seal chamber once removed from the compressor to the innermost seal on the suction side. The innermost chamber on the discharge is at a lower pressure, equalized with the process suction line. All gas that flows through the discharge seal toward the compressor, along with all leakage from the compressor outlet chamber, goes through this balance line and into the compressor suction.

While some gas flow is accepted through the seals, clearances are very small in order to keep it to a reasonable minimum. There is always the potential for contact friction in a seal, which means the development of a hot spot. Metal parts often are upgraded from carbon steel in order to raise the ignition temperature of chlorine. Another approach is to fabricate a seal with one member of a polymeric abradable material [37].

Lubrication is by oil supplied by an external system. The same source can be used for the compressor, the drive, and the gears. The oil system should include a spare pump. Dual filters should be supplied as a minimum. Some designs include a spare cooler and a spare filter, totally interchangeable. Oil should be on the tube side of the cooler(s), and the tubes should be of a corrosion-resistant material (e.g., cupronickel) to prevent contamination. Protection against low oil pressure should include a preliminary alarm, an automatic start of the standby pump, and ultimately a compressor shutdown. Bearings should be designed to prevent oil whip. This is a phenomenon associated with pressure-lubricated sleeve bearings and is especially likely at the high rotational speeds of centrifugal compressors. A shaft is supported by a wedge of oil, created by rotation of the shaft and shifted in the direction of rotation. At high speed, the wedge can be unstable. The oil then rotates in the bearing, a new wedge forms, and the process repeats. The result is a pronounced vibration with frequency about half that of the rotational speed of the shaft. A pressure dam bearing can counteract oil whip. A more secure approach, with somewhat higher cost, is to supply tilting-pad bearings.

9.1.6.2B. Reciprocating Compressors. Although reciprocating compressors are more energy-efficient, centrifugal machines have largely replaced them as the primary compressors in the chlorine process in large plants. Mayo [38] gives some of the reasons for this and reviews industrial experience with all common types of chlorine compressor. The chief disadvantages of reciprocating compressors are their higher maintenance requirements and their sensitivity to entrained liquid or solid. They are still used in sniff gas recovery systems and to boost the pressure between stages of liquefaction. In these applications, the disadvantages cited are less important. Suction pressures are higher, volumes are lower, and there is less chance of a problem with dirty gas.

Restrictions on frame size limit reciprocating compressors to about 200 kW operating load. API 618 is the most common general design standard for these machines. Chlorine compressors tend to have horizontal cylinders, either single- or double-acting, and to have horizontally split casings with flow in the top and out the bottom. A principal material of construction is cast iron. Because of this, a stress-free piping installation is important. Cylinders are cast iron or carbon steel, with removable liners of a resistant metal (e.g., high-nickel iron). In some applications, low-temperature steel is required. Pistons also are carbon steel, perhaps stress-relieved, with segmented carbon rings. Piston rods are stainless steel, perhaps with a hardened overlay. Small valve parts are stainless steel or high-nickel iron, and seats and guards range from cast iron to K-Monel. Cylinders and heads sometimes are water jacketed; this allows removal of some of the heat of compression. When multiple lines are needed for capacity or reliability, or when multiple stages are needed to achieve the compression ratio, it is possible to mount more than one head on a compressor frame. This, however, is not the normal practice in the chlor-alkali industry. With the proper piping arrangement, the use of only one cylinder per frame makes it possible to operate with a unit removed for maintenance.

The drive end of a compressor will be lubricated with oil. The reciprocating rod will carry oil on its surface beyond the packing box. This oil must not be allowed to come into contact with the chlorine. "Distance pieces" will prevent the oil from reaching the compression cylinder. The safest arrangement is the use of double distance pieces long enough so that no part of a piston can come into contact with both oil and chlorine. The distance pieces are closed gas-tight chambers. At the drive end, the distance piece is kept under a positive pressure of 0.1–0.5 atm by a flow of nitrogen or dry air. At the chlorine end, the distance piece is kept approximately 0.5 atm above the discharge pressure. It is isolated from the cylinder by nonlubricated carbon packing; any leakage through the cylinder packing is into the process and not to the atmosphere. The distance pieces can be vented to the compressor suction.

A reciprocating compressor can not be driven at full line speed. Rotational rates of about 500 rpm are typical; they are restricted in order to keep piston friction and wear within acceptable limits. This amount of speed reduction can be obtained with a V-belt drive through appropriately sized sheaves.

From the process standpoint, the major objection to reciprocating compressors would be their pulsating flow. Pulsation dampeners installed before and after a compressor help to rectify this. These are carbon steel vessels whose basic purpose is to provide enough volume to reduce the amplitude of the pressure pulse to a satisfactory level, usually about ± 1 –2% of the operating pressure. The pressure drop should be no more than 1% of the discharge pressure. On the suction side, the volume should be at

least five times the total displacement volume of all connected pistons. The diameters of the vessel connections should be at least twice that of the largest compressor connection. The discharge dampener will operate at high pressure but can be smaller than the suction dampener. It may be small enough to be mounted close to the compressor discharge, in which case the gas will enter the top of the shell and leave from one of the heads. There should be temperature indication at the inlet and pressure indication on the body.

Dampening vessels should have drain connections. Some are designed with baffles to make them more efficient or to achieve the same result in a smaller volume. These should be designed to permit drainage to a common point.

When there is danger of liquid entrainment in the gas fed to a compressor, a phase separator should be installed. A simple inertial/gravity separator with a tangential inlet that accelerates the fluid downward and then decelerates the gas through a 180° turn is usually all that is required.

When compressor jackets or packing glands are cooled with water, it is necessary to have a source that can tolerate higher pressure drops (1–2 bar) than called for by the typical heat exchanger. The water must not be corrosive to steel and should be filtered to a level of about 100 μm .

9.1.6.2C. Liquid-Ring Compressors. Liquid-ring compressors sealed with sulfuric acid are widely used in primary chlorine compression, especially in small plants. Figure 9.22 shows how a typical liquid-ring compressor works. The eccentrically mounted rotor circulates the liquid around inside the casing. The rotating liquid therefore moves away from and then back toward the center of the chamber. This allows gas to be drawn into the casing through inlet ports and then squeezed toward the outlet ports, where it leaves along with the liquid in two-phase flow. An approximately elliptical casing with a rotor mounted near its center will produce two suction–compression cycles with each turn of the impeller.

A rotating piston of viscous liquid is not an efficient energy-transfer device, and so the power consumption of these compressors is relatively high. Typical efficiencies are 50% and lower. A compensating advantage is that the acid absorbs most of the heat of compression, and so the process is more nearly isothermal. As Fig. 9.17 and Eqs. (42) and (44) show, this characteristic helps to offset the low efficiency by reducing the theoretical energy requirement. In addition, larger compression ratios can be achieved without danger of chlorine/metal combustion. Compression ratios of more than five are possible, and a single stage can produce normal liquefaction pressures.

The action of the liquid-ring compressor gives a certain amount of pulsation in the delivered pressure. While this is not as severe as that encountered with reciprocating compressors, it should be recognized. The acid separator attached to the compressor provides some dampening on the outlet side. Some manufacturers will recommend a minimum volume on the inlet side, which is often only a length of expanded inlet piping.

The compressor usually is of cast iron (perhaps with high nickel and molybdenum contents). The impeller may be ductile iron with an alloy steel shaft. There is usually a shaft sleeve fabricated from a more resistant alloy.

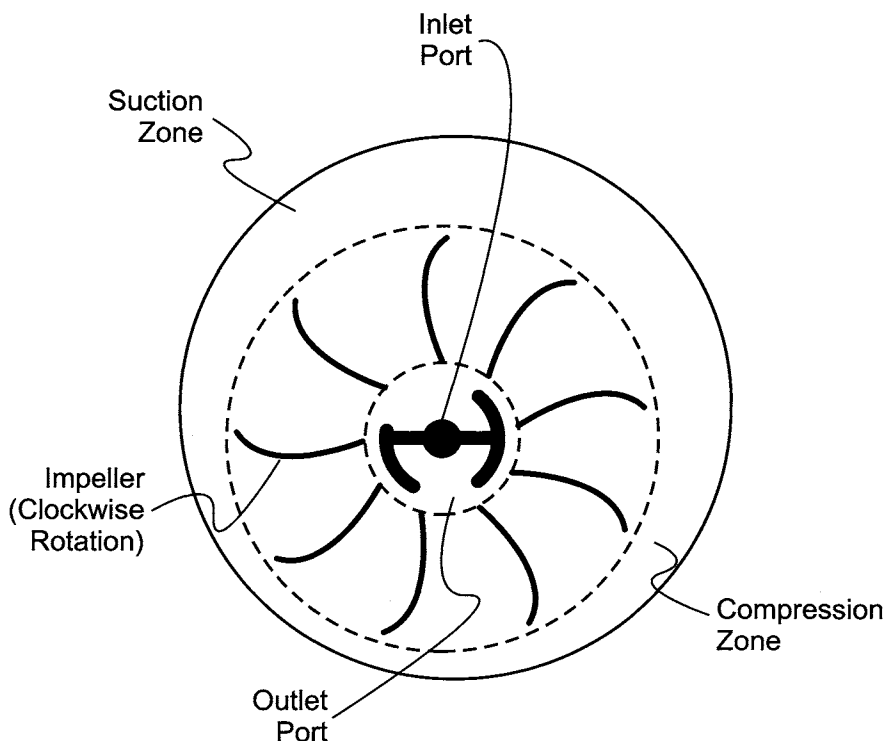


FIGURE 9.22. Operation of a liquid-ring compressor.

The gas must be separated from the acid that is pumped by the compressor. This occurs in a separating vessel on which an acid mist eliminator is mounted. The compressor and vessel may be close-coupled. They should at least be mounted close to each other, and in no case should there be a sizable increase in elevation between compressor and separator. The vessel may be horizontal or vertical, but it must provide sufficient time for the acid to settle from the gas. Carbon steel is a satisfactory material of construction, but its use depends on proper process control. The separating vessel may have a sufficient inventory of acid for the process, or a separate receiver may be supplied.

The acid collected in the separator recycles to the compressor. Depending on the arrangement, the acid is pumped or the pressure developed by the compressor forces the acid back to the suction. The circulating acid must be cooled to remove the heat of compression and to maintain a low temperature in the system. The rate of corrosion increases rapidly above about 40°C, and that should be the normal maximum permitted, with an alarm set a few degrees higher. The acid cooler can be any of the types described in Section 9.1.4.4D. Any leakage in the exchanger can not be allowed to enter the acid/chlorine side. In tubular models, the water pressure should be kept below the circulating acid pressure. If the cooling water supply pressure is not low enough to guarantee this, it should be throttled to a lower pressure or allowed to run with an open discharge. Either case may require pumping to send the

water to the return header. Plate exchangers tend to leak to the outside through the gaskets separating the plates, and with them there is less danger of water entering the process.

The mist eliminator can be internally or externally mounted. The filtering elements will be suspended candles, and the acid they capture will drain into the acid receiver. Section 9.1.5 treated the subject of removal of acid mists.

The acid concentration must be kept high to prevent corrosion. The compression system in effect acts as an additional stage of chlorine drying and continues to pick up traces of moisture. The system should be charged with acid of the highest concentration available (minimum 96%). The strength of the circulating acid should be checked regularly, and the acid should be changed when its concentration has fallen by about 2%. There should be a provision for transferring this spent acid to the drying system.

Figure 9.23 shows a flowsheet for a system using the developed pressure to transfer the acid back to the compressor. The instrumentation includes suction pressure control (by recycling compressed gas), pressure indication and high alarm on the acid separator, flow restriction on the cooling water supply, indication of differential pressure between the circulating acid and cooling water with a low alarm, and an acid flow indication with high and low alarms. The dashed lines show the insertion of an acid-circulating pump.

9.1.6.2D. Diaphragm Compressors. Diaphragm compressors effectively have a reciprocating action, but they differ mechanically from the reciprocating type described above. A diaphragm that usually moves vertically replaces the piston. It draws gas into a chamber

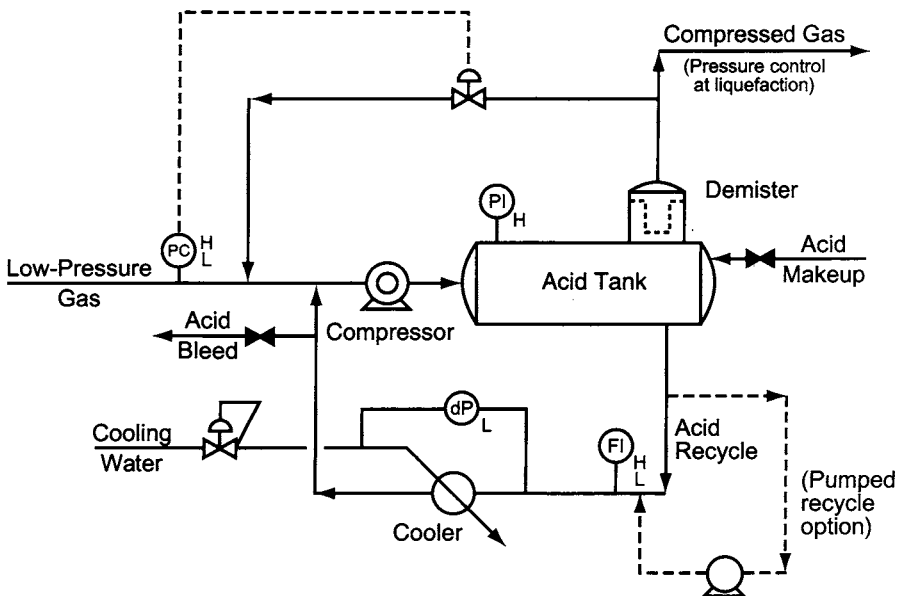


FIGURE 9.23. Flow diagram—liquid-ring compression of chlorine.

from one side and expels it from the other. As a group, diaphragm compressors are smaller and less robust than reciprocating compressors. They are not suitable in the main process.

However, diaphragm compressors can be used in chlorine service to help empty a transport container or to transfer product between storage tanks. Section 9.1.8.4A describes techniques for such transfers. One of these is to compress vapor from the tank being filled back into the tank being emptied. This increases the recovery of liquid chlorine without pumping, vaporization, or addition of an inert gas to the system. Reciprocating compressors such as those described above and diaphragm compressors are the types most frequently used. The differential pressure used to transfer chlorine usually is 2–3 bar. Sealing against the fairly high pressure involved and the potential problem of acid entrainment disqualifies liquid-ring pumps.

All the problems associated with chlorine compression apply to diaphragm compressors. They must be protected against combustion of metal parts in dry chlorine. Since the compressor head usually is carbon steel, this means a maximum temperature of about 120°C. There must be no contact between chlorine and a combustible lubricant. Double separation between the two, as was the case with reciprocating compressors, can prevent this contact. Two diaphragms with an inert intermediate fluid are standard. The oil can be a chlorinated fluorocarbon that does not react with chlorine. The space between diaphragms should have a leak detector that sounds an alarm and shuts down the compressor when either diaphragm fails.

As noted above, compressor bodies usually are carbon steel. Diaphragms are stainless steel or Monel, and cylinder valves are Monel. Preventive maintenance should include periodic replacement of diaphragms and sealing the apparatus with clean, dry air or nitrogen during its frequent idle periods.

9.1.6.3. Compressor Control

9.1.6.3A. Pressure and Surge Control. Most chlorine gas compressors have some means for controlling the suction pressure. It is essential to remember that the control systems for the compressor suction pressure and the cell gas header pressure will interact. This is one example of the peculiar demands of the chlorine process influencing the approach to control system design. Weedon [39] discusses the subject of pressure control at several points in chlor-alkali plants, and he presents detailed recommendations for systems and hardware in Chapter 11. He stresses the importance of maintaining a constant pressure on the low-pressure chlorine header. The most frequent arrangement controls cell header pressure directly with one valve. Although it responds to pressure at the cells, there are advantages in placing this valve after the drying towers and before the compressors:

1. the valve's service is less severe
2. the line size and the valve are smaller
3. the pressures in the cooling and drying systems are higher, reducing the amount of air that enters the system.

A second valve then controls compressor suction pressure by allowing gas to recycle from the discharge of the compressor. Good control maintains a constant differential

across the cellroom header control valve, keeps the compression ratio within the design limits of the compressor, and allows the compressor to stay on line during a rectifier trip by going onto full recycle.

Gas recycle wastes energy and requires that the machinery be designed for more than the net process flow. The minimum practical amount of recycle is desirable from the standpoint of process efficiency. In chlorine processing, however, safety and process stability perhaps should be given more weight than in many other applications. Most systems have a constant recycle of up to 10% of throughput.

In a plant producing liquid chlorine, the compressed gas goes next to the liquefaction system. Rather than impose a pressure drop between the processes, the gas is allowed to flow freely into liquefaction. A valve on the uncondensed gas venting from the liquefaction unit (Section 9.1.7.2) controls the pressure on both systems. When chlorine is sent to another process without liquefaction, it would be possible to withdraw it on downstream pressure control and let the compressor outlet pressure fluctuate. This approach leads to variability in the differential pressure across the compressor recycle valve. Fluctuations in this flow can cause fluctuations in the compressor suction pressure and therefore in the cellroom chlorine header. It is better to control the compressor outlet pressure itself, even at the cost of another pressure control loop at the destination. Section 11.3.2.6 describes instrumentation hardware and the problems of transferring chlorine to more than one destination.

Location of pressure-measuring points is critical. Reciprocating and liquid-ring compressors deliver pulsating flows. The pulsations are much larger in the reciprocating case. Properly sized vessels in the suction and discharge lines can dampen these pulsations. Centrifugal compressor controls, on the other hand, must be designed to prevent surge. Surge is a complex phenomenon resulting from an imbalance between radial and tangential velocities on the rotating wheel. Suffice it to say that when the net flow is too low at a given wheel speed, flow becomes unstable. When surge begins, output flow and throughput drop precipitously, allowing compressed chlorine to flow back into the compressor. Flow recovers as material "piles up" in the chamber, but then the problem can recur. This leads to a series of rapid pulsations. The frequency and amplitude of the pulsations vary with the situation. Surge can produce anything from minor damage to complete destruction of parts.

Impeller design and rotational speed determine where the onset of surge will occur. It is not possible to give precise guidelines here; they must be obtained from the compressor manufacturer for each machine. The best defense against surge is the prevention of the low flows that lead to instability. Figure 9.24 shows typical characteristic curves for a centrifugal impeller rotating at various speeds. If we move far enough to the left on any curve, surge results. The points at which this happens can be connected by a curve referred to as the surge line. As the speed of the wheel is reduced, surge occurs at lower pressures and flow rates. Dimensional analysis shows how the points on the different curves relate to each other [40]. The values of inlet flow rate divided by rotational speed and of delivered head divided by the square of rotational speed are both nearly constant.

The goal must be to remain to the right of the surge line. Given the small time scale of surge, there should be enough safety margin to overcome brief excursions in flow rate. Sufficient flow is achieved by recycling compressed gas. With a multistage compressor,

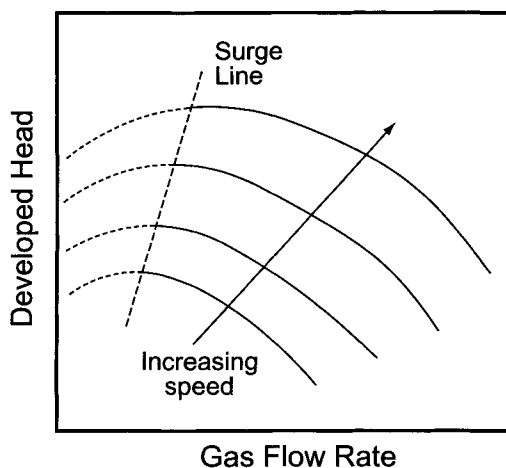


FIGURE 9.24. Centrifugal compressor characteristics at different speeds.

recycle can be from any of the stages or from the final discharge line. In this volume, we assume that the fully compressed gas from the discharge line recycles to the suction.

A surge control system will attempt to establish an operating line to the right of the surge line. Since the surge line has a positive slope, it is possible to reduce the amount of gas recycled when operating at lower speeds. There are several different approaches. When maximum efficiency and process safety are desired, the operating line will be roughly parallel to the surge line. This is characteristic of large systems with long-term variations in throughput. In such cases, the energy saved by keeping the minimum flow close to the surge flow may be significant. A second approach, with simpler instrumentation, is to establish an operating line with a slope greater than the surge line but with an intercept close to zero. This also conserves energy but increases the risk of surge at low speed. A third approach is to establish a vertical operating line. Here, the minimum total flow accepted is independent of wheel speed. This will have approximately the same flow requirement as the other methods at full speed. At lower speed, it will require more recycle and will waste energy.

The peculiarities of chlorine production offer two reasons to accept the disadvantage of the third approach. First, a profitable chlor-alkali plant is one operating near capacity or at the maximum sustainable steady rate. In most situations, load changes are infrequent, as is extended operation well below capacity. When the latter does occur, the operating line of the control algorithm can be adjusted temporarily. Second, there is an advantage in maintaining an active recycle flow at all times [39]. First of all, recycle is commonly used for suction pressure control. Second, the fact that a recycle valve is partly open and actively throttling makes it easier for that valve to respond to a rectifier trip. This increases the rate of response and helps to prevent surge in that situation. Having the compressor operating at full recycle while the cells are down then makes restarting the cells easier and smoother. Weedon therefore recommends a simple system based on a selector switch. Both the suction pressure and the total gas flow through the compressor would be monitored. The suction pressure controller normally would fix the amount of

recycle. If the total flow fell below the value set by the flow controller, the recycle valve would open farther until the desired flow was obtained.

Developments in cell and control system technology since Weedon's paper suggest possible variations. If membrane cells operate at a significant positive pressure, the cell header pressure control and compressor suction pressure control can be made less interdependent. Some variation in suction pressure can be accepted in the interest of overall process efficiency. On the control system side, computing power has advanced enormously in the past decade. Some logic can be built into the control system without compromising process dynamics.

9.1.6.3B. Capacity Control. Reciprocating compressors are constant-volume machines and in practice are run at constant speed. They tend to pump a given volume of gas from suction pressure up to a maximum pressure determined by drive capacity. Nothing in their basic operation permits capacity control. In larger plants, the use of multiple units allows some to be taken off line when the operating rate is low. Various means of unloading then can reduce the output of individual machines. In one approach, the suction is closed off and the compressor continues to run without gas feed. A variation on this holds the cylinder inlet valves open and prevents the gas from being compressed. Both, as described, are nothing more than on-off control, but it is possible to stage the response of the inlet valves to get some crude stepwise control of capacity. Smaller steps in capacity are offered by the use of clearance pockets. These are chambers built into the casing and isolated by valves. When too much gas is compressed, the clearance valves open and allow gas to be compressed into the pockets. This gas re-expands into the compressor on the suction stroke and prevents the entry of an equivalent amount of fresh low-pressure gas.

Fine adjustment of capacity depends on blowing off excess gas or recycling to the suction. Release of gas while taking the former approach obviously is not appropriate in chlorine compression.

Centrifugal compressors have head-capacity curves similar to those of the more familiar centrifugal-pump curves. Within the lower limit necessary to avoid surge and the upper limit of impeller capacity, each unit can in theory operate at any point on its curve.

Common techniques of capacity control with constant-speed machines include:

1. suction or discharge throttling
2. recycle of cooled discharge gas to suction
3. adjustment of inlet guide vanes.

In chlorine compression, suction throttling is not an option if a valve on the compressor inlet line already is being used for cell-header pressure control. Discharge throttling is the least energy-efficient approach and is seldom used. Both the other methods are used, with adjustable inlet guide vanes more likely to be supplied with larger machines. They are most effective when the gas is clean, and they usually are supplied only on the first stage of compression. In our illustrations in this volume, we assume the use of recycle of discharge gas. Compressor speed variation is another possibility. This offers higher efficiency, and Section 12.5.1 mentions recent trends in adapting variable speed

drives to other compressor applications. However, it is an expensive alternative with an electric motor drive, and the fact that surge limits must be observed even at very low net throughput limits the saving that can be achieved. If the compressor is driven by a steam turbine, however, variable-speed operation becomes more practical and is often used in combination with number (2) above. Since the net throughput in the final analysis is set at the cells, the recycle technique has the advantage of not requiring two modes of flow control to exist in series. The compressor, running on its performance curve, wastes any excess capacity. The appeal of the other methods is their avoidance of this waste, and they are often used in combination with gas recycle.

Liquid-ring compressor throughput usually is controlled with a simple gas-recycle system.

9.1.6.3C. *Protective Instrumentation.* Some compressors require an extensive list of instrumentation to avoid unsafe situations and mechanical damage to the compressors themselves. This is particularly true in the case of centrifugal machinery. A previous section discussed the most prominent example, the surge control system. Other likely sources of damage of the rotating machinery are vibration and the loss of lubrication.

Shaft position and vibration are monitored continuously during operation by eddy-current proximity probes adjusted to within 1–1.5 mm of the shaft. Radial vibration is generally not symmetrical. Ideally, vibration should be measured in more than one plane.

Lubricating oil is pumped from a reservoir to the compressor and then runs down from the machine to the tank. The tank should have level and temperature indication and a low-level alarm. The pumped oil is cooled and filtered before going to the compressors. Dual filters rated at about 10 μm are used, and a standby pump is provided. The oil must be dry, and so its reservoir is frequently blanketed with nitrogen. Some of the alarms on the oil system will be supplemented by shutdown switches in case operator action fails to prevent further departure from the control point.

When steam turbine drives are used, equipment to remove water from the oil is included. Instrumentation includes pressure gauges at the pumps; temperature indication before and after the coolers, and a high-temperature alarm after; differential and outlet pressure measurement at the filters, with a high-differential pressure alarm and a low-pressure alarm with a switch to start the idle pump; pressure indication and low-pressure alarm on the oil supply header; low-pressure alarm on the oil return; and temperature elements and high-temperature alarms on the lubricating points at the motor, gear, and compressor. Axial vibration monitors are on the outlet sides of the gear and compressor shafts. Radial monitors are on both sides of both ends of these shafts. All are equipped with prealarms and, in case of dangerously excessive movement, shutdowns. The radial vibration monitoring points may be exhibited through a common alarm. Axial vibration is indicated separately. Bearing temperatures are monitored closely. Journal and thrust bearings on both sides of the compressor and the gear increaser usually are equipped with temperature indicators.

9.1.6.4. *Cooling in Compression Systems*

9.1.6.4A. *Suction Chillers.* The ignition temperature of dry chlorine in contact with mild steel is about 250°C. A compression system is usually designed for bulk gas temperatures

well below this in order to allow for upsets and hot spots. The gas temperature is limited by limiting the compression ratio in each stage and by cooling the gas. The typical chlorine compressor therefore is a multistage device with a number of coolers attached.

Precooling of the dried gas is a common operation. Reducing the temperature of the feed gas allows higher first-stage compression ratios. Because the gas fed to the compression area from the dryers is close to normal cooling water temperature, refrigerated systems are necessary if this operation is to be of substantial value. Chlorine therefore is frequently cooled before compression by indirect contact with a refrigerant in a standard shell-and-tube exchanger or by direct contact with liquid chlorine in what is often referred to as a suction chiller.

In a suction chiller, chlorine returned from liquefaction boils at compressor suction pressure. Since this pressure is usually close to atmospheric, chlorine will boil at about -34°C , where its heat of vaporization is 288 kJ kg^{-1} . Returning 15% of the net throughput to the suction chiller can cool the gas to -30°C or lower and allow the compression ratio in the first stage to be increased by about 58%. This technique increases the flow of chlorine through the compressor by the amount of liquid vaporized. In cooling the gas, it removes no heat from the process. The heat load ultimately is transferred to the refrigeration system in liquefaction.

The typical suction chiller is a column fabricated from low-temperature carbon steel. It may use a spray, contain plates, or be packed with saddles. The liquid chlorine is brought in below the top through a distributor and allowed to fall in countercurrent flow to the gas. The top section serves as an entrainment separator to protect the compressor from droplets of liquid and usually contains a high-efficiency demister pad (about 100 mm thick). A pool of liquid is maintained in the bottom of the column, and the net accumulation is removed under level control.

The net mass velocity of chlorine through a packed suction chiller is typically $200\text{--}250\text{ tpd m}^{-2}$. Pall rings are frequently used as packing, in beds 2.5–3 m high. This makes the packing requirement $0.01\text{--}0.015\text{ m}^3$ per tpd. Carbon steel is the main material of construction, but some of the internals are stainless steel or other material with better corrosion resistance. These internals include the demister pad and sometimes support rings and packing.

If the suction chiller were simply a heat-transfer device, there would be no need to maintain a liquid flow from the bottom; the rate of liquid feed could be set strictly by thermal demand. However, the flow of liquid enables the column to serve also as a scrubber. Higher-boiling impurities are then removed in the liquid phase, and the purity of the gas going on to the compressor can be increased. Impurities commonly found in suction chiller bottoms include chlorinated organics formed by reaction of chlorine with organics in the feed brine, cell construction materials, and the corrosion-resistant layer of FRP piping; bromine formed by electrolysis of bromides in the brine; nitrogen trichloride formed by reaction of chlorine with various nitrogen-containing compounds and water. Nitrogen trichloride is a hazardous compound whose formation and control are the subjects of Section 9.1.11.2.

Some systems add a stripping section to the suction chiller. These permit the recovery of some of the chlorine that otherwise would have been in the bottoms. In doing so, they can aggravate a hazard by increasing the concentration of NCl_3 in the remaining liquid. Figure 9.25 shows extended operation with a continuous stripper.

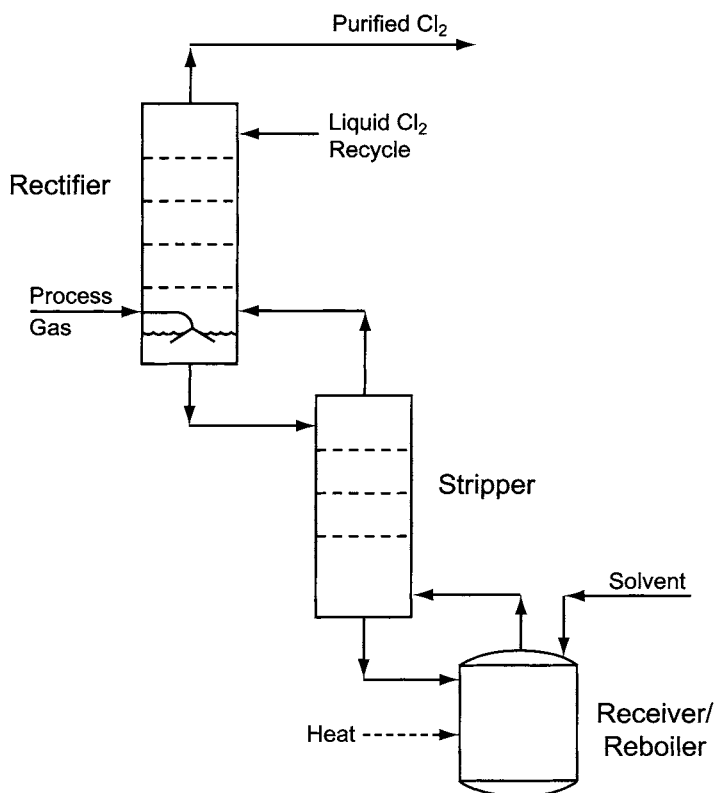
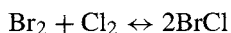


FIGURE 9.25. Suction chiller bottoms stripper.

Here, it appears as a second column. It could equally well be a smaller-diameter section attached to the main column. The bottoms product collects in a pot containing a solvent. The purpose of the solvent is to keep the concentration of NCl_3 below the hazardous level. Section 9.1.1.2 also discusses the use of the bottoms collection system to destroy NCl_3 .

Bromine scrubbed from the gas in a suction chiller is present largely as BrCl . The very existence of this compound has been somewhat controversial because the thermodynamic effects of its formation from the elements are small. Its heat of formation from the elements is only $0.7 \text{ kcal mole}^{-1}$ [41]. All six possible 1:1 interhalogen compounds of F, Cl, Br, and I, however, have been identified [42]. Of these, IF is considered unstable, and BrCl is the least stable of the remaining five [41,43]. Its freezing and boiling points are close to (very slightly below) the arithmetic means of the properties of the elements [44]. Specifically, it boils at about 5°C . The various authors referred to above give different estimates for the equilibrium constant of the reaction



but the data center on a value of about five. The practical importance of all this is that pure chlorine is marginally more difficult to recover from suction chiller bottoms.

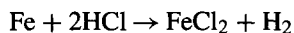
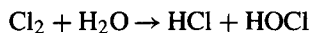
While chlorine has a vapor pressure of about 17 atm at the normal boiling point of bromine, the corresponding number at the boiling point of BrCl is only a bit more than 4 atm. About twice as many theoretical stages are required to effect a given separation of chlorine from the bromine content. The amount of bromine present in most electrolysis salt is too small for the equilibrium to be a serious limitation on chlorine recovery from the suction chiller bottoms.

The BrCl tends to decompose more to the elements as vaporization continues. It is therefore possible to recover elemental bromine. With most salts, the quantity available is too small to be attractive, and any attempt at bromine recovery will also aggravate the problems of the presence of nitrogen trichloride.

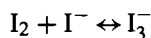
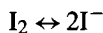
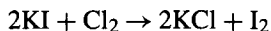
Bromine's behavior in water differs from that of chlorine. It forms a hydrate, but of a different type, with approximate composition $\text{Br}_2 \cdot 8.5\text{H}_2\text{O}$. Hydrolysis to HOBr is not favored. Dissolved bromine is present almost exclusively as Br_2 , and tabulations of physical properties often express solubility in terms of the Henry's law coefficient.

Slow corrosion of carbon steel may continue on the dry side of the process. This is due to the small residual water content of the chlorine, and so corrosion is most pronounced when water is concentrated and temperature is raised. The reboiler in a suction chiller installation therefore is a frequent source of corrosion problems, aggravating the NCl_3 hazard.

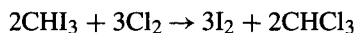
Iron reacts with both of the products of hydrolysis of chlorine:



These reactions are analogous to those involved in the production of FeCl_3 (Section 9.1.9.4). Addition of iodide salts greatly reduces the rate of corrosion [45]. This is attributed to the formation of I_3^- , which is strongly adsorbed on the surface of the iron:



When added to liquid chlorine, iodoform is an alternative source of the element:



Iodoform is reasonably soluble in the commonly used bottoms diluents. It can be added along with the diluent and replenished approximately weekly.

9.1.6.4B. *Interstage Coolers.* Even with a suction chiller as a precooler, the compression ratio will be limited to about 3.5 before cooling of the gas again becomes necessary.

In this case, the designer can consider indirect cooling with water or a refrigerant as well as direct contact with chlorine. The direct contact approach in this case suffers from the fact that the boiling point of chlorine in the cooler will be higher. Multiplying the pressure by a factor of three, for example, will increase the boiling point by nearly 30°C and reduce the cooling potential of the chlorine by a similar amount. The temperature achievable by mechanical refrigeration and indirect contact with a refrigerant or brine will not deteriorate in the same way. With the high temperature of the gas going to the cooler, furthermore, the use of cooling water in a standard shell-and-tube exchanger becomes practical. This can not reduce the temperature of the gas to the same level as a refrigerant, and the compression ratio in the next stage of compression will be smaller. The savings in refrigeration energy and capital costs, however, can make the use of water economic.

When a refrigerant is used, the heat transfer resistance on the cold side becomes negligible. Clean coefficients on the chlorine (tube) side are usually $125\text{--}150\text{ W m}^{-2}(\text{°C})^{-1}$, depending on velocity. Construction is all carbon steel.

While the pressure differential between chlorine and cooling water usually is the reverse of Section 9.1.3.4, the general comments on the hazard of leaks that permit the two fluids to mix still apply.

9.1.7. Liquefaction

9.1.7.1. The Refrigeration Process. Normally chlorine is liquefied under pressure by exposing it through a heat-transfer surface to a boiling refrigerant liquid. The choice of refrigerant and control of the pressure at which it is allowed to boil fix the cold-side temperature. The vaporized refrigerant then is compressed and condensed by exchange with plant cooling water. The condensed liquid is flashed back to the controlled lower pressure, cooling the remaining liquid to its boiling point in the chlorine liquefier. The liquid boils under the influence of the heat picked up from the condensing chlorine. This cycle continues indefinitely.

The pressure–enthalpy chart of Fig. 9.26 shows the course of a typical process. Line AC represents the boiling of the refrigerant under the influence of the process load. This takes place in the first exchanger referred to above. From the viewpoint of one following the chlorine flow, this is a liquefier. From the viewpoint of one following the refrigerant flow, and in common refrigeration industry parlance, it is an evaporator.

Segment AB of line AC, an isotherm, is the evaporation of the refrigerant. Segment BC represents superheat. Line CD represents compression, and line DG the cooling of the refrigerant. In the condenser, first the superheat is removed (segment DE) and then the refrigerant is condensed (segment EF). Segment FG represents subcooling of the liquefied refrigerant. Line GA shows the reduction in pressure from the condenser to the evaporator. Where this crosses the saturated liquid curve (point H), flashing begins. At point A, the refrigerant is partly vaporized, and the cycle begins again, with the enthalpy increasing as the refrigerant is heated by condensing chlorine.

The efficiency of refrigeration increases as the temperature of the liquid before flashing becomes lower. The process therefore is helped by subcooling the refrigerant (FG). Because only a limited amount of subcooling is possible with plant cooling water, the process normally also includes separate economizers in which some of the condensed

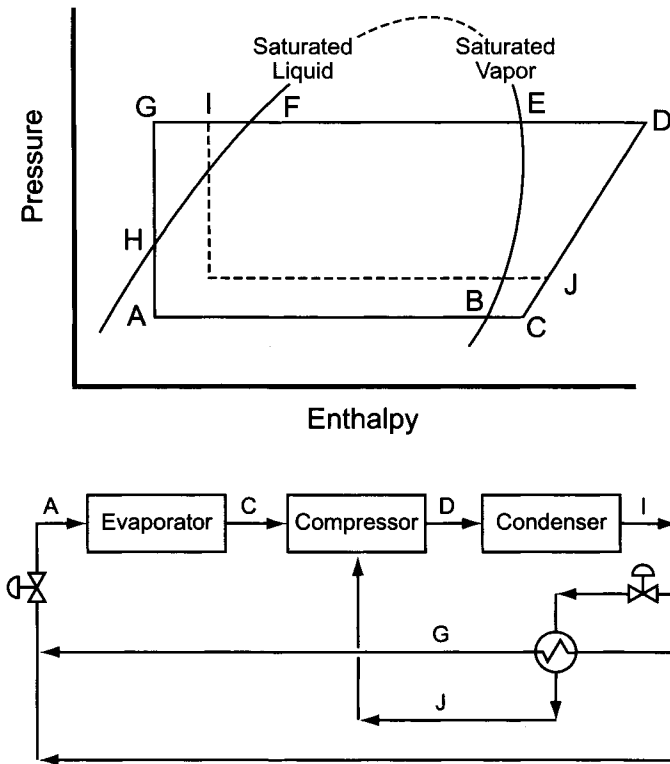


FIGURE 9.26. The refrigeration process.

refrigerant is allowed to evaporate and cool the remaining liquid. Figure 9.26 shows the use of a sidestream of liquid flashing to cool the remainder in a closed economizer. The liquid when split is at condition I. The smaller stream passes through a throttling valve and partially flashes to a lower pressure and temperature. It then warms in the economizer, becoming completely vaporized at condition J. The heat is supplied by the main stream of liquid, which in the process cools to condition G. The vapor formed in this subcooling operation is returned to the compressor at a pressure somewhat higher than that at the suction in a process known as “supercharging.” Other types of economizers are frequently used. In an open economizer, liquid simply flashes down to the pressure of a lower stage of compression. The closed economizer approach shown on the drawing is less efficient because of the temperature differential across the exchange surface. In many situations, however, it provides smoother operation.

Generally, lower-boiling refrigerants must be compressed to higher pressures if they are to be condensed by the available cooling water. The energy consumed in producing a given amount of refrigeration therefore increases as the process temperature becomes lower.

Liquefaction process design requires the choice of a combination of temperature and pressure at which chlorine can be economically condensed. There is a tradeoff

between the energy requirements of chlorine compression and refrigerant compression. This usually results in a roughly equal split of the energy between the two compressors [31].

At high enough pressure, ordinary cooling water could be used to condense chlorine. Since the vapor pressure of chlorine is about 1,000 kPa at 35°C, operating pressures of 1,200–1,600 kPa would correspond to 80% liquefaction. Most plants find it more practical to operate primary liquefiers at 300–450 kPa and to condense chlorine against a refrigerant [46]. When cold water is reliably available, perhaps in the form of seawater, it may become practical to use it for chlorine liquefaction. Once liquid chlorine has been obtained in the first stage of liquefaction, it can be used as a refrigerant in later stages. By reducing its pressure, the chlorine would be vaporized and could then be returned to its compressor for another pass through liquefaction. Given a source of sufficiently cold water, then, it becomes possible to liquefy chlorine at a reasonably low pressure without the aid of mechanical refrigeration.

9.1.7.2. The Liquefaction Process. The liquefaction process uses a combination of increased pressure and reduced temperature to condense chlorine from the gas. The first subsection below discusses the effects of the operating conditions on the amount of chlorine that condenses. In large plants and when high liquefaction efficiency is desired, there are usually two or more stages of liquefaction operating at progressively increasing severity.

Figure 9.27 is a flowsheet for the minimum case of single-stage liquefaction. The compressed gas enters the tube side of the chlorine liquefier/refrigerant evaporator. A boiling refrigerant on the shell side provides the cooling. The pressure on the refrigerant determines its boiling point and the condensing temperature of the chlorine.

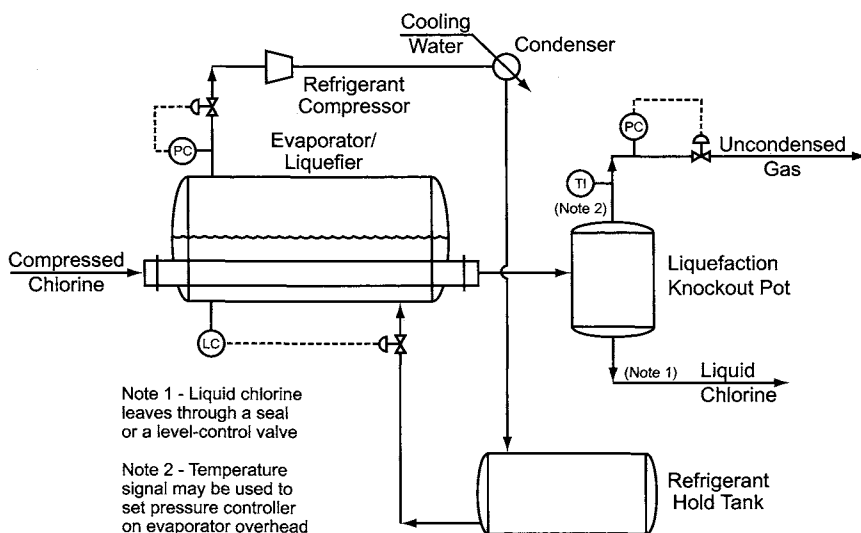


FIGURE 9.27. Basic liquefaction system.

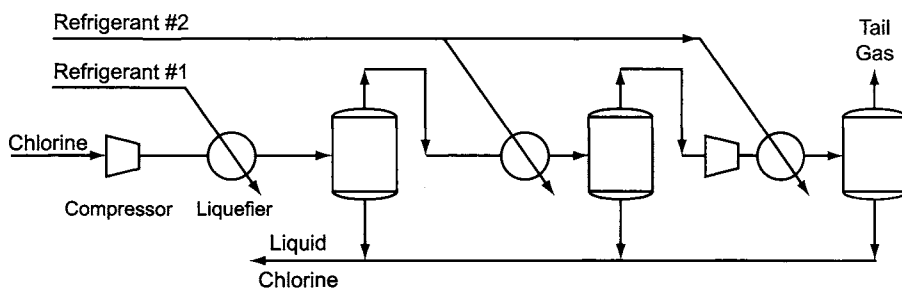


FIGURE 9.28. Three-stage liquefaction system.

The two-phase process stream goes to a receiver that also serves as a phase separator. The liquefied chlorine leaves through a bottom connection. The uncondensed gas, containing some of the chlorine along with the noncondensable impurities, goes overhead. A valve on the outlet line maintains the desired pressure on the gas in the liquefier and also serves to control the discharge pressure of the chlorine compressor. The combination of the pressure and temperature on the process side of the liquefier determines the extent to which the chlorine can condense (see Achievable Degree of Liquefaction, below).

The refrigerant vapor from the evaporator is compressed to allow it to condense against cooling water. The refrigerant loop in Fig. 9.27 is a simplified version of the process explained in Section 9.1.7.1 and shown in Fig. 9.26.

When the process as shown is not capable of condensing enough chlorine, the uncondensed vapor is taken to a second stage. More chlorine will condense if the temperature is lowered or the pressure is raised. Figure 9.27 can also represent the second stage of liquefaction. In the lower-temperature option, which does not require a second chlorine compressor, the refrigerant might be allowed to evaporate at a lower pressure. The thermodynamic properties of the refrigerant limit the range of practical operating conditions, and so it is frequently necessary to provide a second refrigeration system based on a more volatile material (see Choice of Refrigerant, below). In the higher-pressure option, the uncondensed gas from the first stage of liquefaction goes first to a compressor and then on to the second stage, and there is no need for a second refrigeration system. A particular alternative that is possible in this mode is the use of a single chlorine/refrigerant exchanger body with two sets of tubes operating at different pressures.

The process can be extended beyond two stages. While there is no fundamental limit, the practical maximum today is three stages. Most frequently, the third stage operates with both the temperature and the pressure different from those in the first stage. The second stage then can be either at a lower temperature or at a higher pressure than the first. Figure 9.28 is a schematic diagram of such a process in which the first change is in the operating temperature.

9.1.7.2A. Achievable Degree of Liquefaction. The major complication in the liquefaction of chlorine is the presence of noncondensable gases. These arise in several different

ways [31]:

1. Generation in the cells
 - (a) oxygen formed from H_2O or OH^- at anodes
 - (b) hydrogen formed at cathodic spots or leaked from catholyte chambers
 - (c) carbon dioxide formed from CO_3^{2-} in brine.
2. Air (or nitrogen) introduced into the process:
 - (a) air leakage into subatmospheric parts of process or during evacuation of equipment
 - (b) air dissolved in feed brine
 - (c) air displaced from piping and equipment after purging and during startup
 - (d) air applied to compressor labyrinth seals
 - (e) air used as a pressure pad to transfer liquid chlorine
 - (f) air added to control hydrogen content in liquefaction tail gas.

Air also may accompany chlorine removed from returned shipping containers. In this case, there may also be some contamination with the customer's process gas. This situation must be monitored and incidents dealt with individually.

The noncondensables will tend to pass through liquefaction and will carry chlorine with them at approximately its vapor pressure at the process temperature. We should note here that CO_2 is far less volatile than the other "noncondensables" considered here. More of it is likely to condense with the chlorine, and the analysis that follows here would require some modification. Assuming that all of the noncondensables pass through liquefaction and that the mole fraction of chlorine in the gas is equal to its vapor pressure divided by the total operating pressure, we have

$$L = 1 - p(1 - y)/y(1 - p) \quad (51)$$

where

L = fraction of incoming chlorine condensed

p = ratio of vapor pressure of chlorine to total pressure ($= P^0/\Pi$)

y = mole fraction of chlorine in feed gas

Efficient liquefaction results when p is low and y is close to unity. The mole fraction of chlorine is high (i.e., $y \approx 1$) when the cell gas is pure and in-process dilution is avoided. The purity of the cell gas in turn depends on the current efficiency of the cells and the state of the feed brine. Factors determining current efficiency were explained in Section 4.4. The brine, as noted above, can contribute a small amount of dissolved air, and CO_2 will form by the decomposition of carbonate. Acidification and venting of the feed brine can allow most of the CO_2 to be removed before the cells. Further dilution of the cell gas can be kept to a minimum by considering the sources listed above and taking steps to control them one by one.

There is a qualification to the last statement. When the hydrogen content of the gas is high enough, removal of chlorine by liquefaction could allow the concentration of hydrogen to exceed its lower explosive limit. It is then common practice to dilute the liquefaction gas from diaphragm and mercury cells with dry air or nitrogen to keep the hydrogen content under control. In this case, any reduction in

the amount of air from another source calls for the use of more dilution air. Except for the dictates of good practice, then, control of the incidental ingress of air is less important.

One of the advantages of membrane cells is the low hydrogen content of the cell gas. Dilution air may not be required, making the liquefaction process more efficient and the prevention of contamination by noncondensables more rewarding.

Within the liquefaction process itself, there is nothing that can be done to influence the value of y . Recovery of a given amount of chlorine as the liquid then requires a certain value of the parameter p in Eq. (51). This is the ratio of the vapor pressure of chlorine to the total operating pressure, P^0/Π . It is low when the liquefaction temperature (and therefore the vapor pressure of chlorine) is kept low and the pressure high. Either approach consumes compression energy, and the requirement increases rapidly with the severity of the process. Most of the chlorine can be recovered at conditions less extreme than those necessary to reach the desired degree of liquefaction. Liquefaction therefore is often a staged process. While Eq. (51) still holds, it must be applied to each step of an incremental process. After much of the chlorine is condensed under relatively mild conditions, the depleted gas is subjected to more vigorous liquefaction, either by compressing it or by exposing it to a lower temperature. Only a fraction of the original feed gas is exposed to the lowest value of p , and energy consumption is lower than in a single-stage process.

Example. Staging the process saves energy in both the refrigerant and the chlorine compressors. This example will consider chlorine compression only. We want to condense 98% of the chlorine from a gas whose mole fraction is 0.95. The gas is available at 90 kPa, and the liquefaction process temperature is -20°C . We rearrange Eq. (51) to $p = (1 - L)y/(1 - Ly) = (0.02)(0.95)/(1 - 0.98 \times 0.95) = 0.019/0.069 = 0.275$. Since the vapor pressure of chlorine at liquefaction temperature is 180.54 kPa, we require a total pressure of $180.54/0.275 = 656$ kPa. The compression ratio required is 7.3. Since our purpose is only to examine the energy-conservation opportunity of process staging, we ignore the problems that would arise with the high temperature of the compressed gas ($\sim 195^\circ\text{C}$) and calculate the power consumed by a single-stage compressor. Equation (44) for a unit quantity of feed gas and a polytropic constant of 1.45 is

$$W/p_1 V_1 = 3.222[(p_2/p_1)^{0.310} - 1] = 2.75$$

Now consider a two-stage liquefaction in which we compress the unit quantity of gas first to 240 kPa. The compression ratio is 2.667 and the unit power consumption $W_1/p_1 V_1$ is 1.15. We have $p = 0.752$, and Eq. (51) gives us $L = 1 - (0.05 \times 0.752)/(0.95 \times 0.248) = 0.84$. A total of 84% of the chlorine condenses. From 100 moles of gas with 95% purity, this is 79.8 moles of chlorine. Five moles of inerts accompany the remaining 15.2 moles of chlorine, giving a new mole fraction of 0.752. To complete the job of recovering 98% of the original chlorine, this gas must be brought to 656 kPa and exposed again to the liquefier temperature. Allowing for some pressure loss between stages, we now require a compression ratio of $656/225 = 2.916$. The amount of gas processed is only 20.2% of that in the first stage of compression. The power required to

compress what remains of a unit of the original gas is therefore

$$0.202 \times 3.222[(2.916^{0.310} - 1)] = 0.26$$

The power required for the two stages of compression is $(1.15 + 0.26)p_1 V_1 = 1.41 p_1 V_1$. This is approximately 49% less than the single-stage requirement. Adding more stages saves relatively little more energy but reduces compressed gas temperatures to add to the safety margin and allows more flexibility in machine design and operation.

9.1.7.2B. Choice of Refrigerant. Desirable properties of a refrigerant are:

1. no explosion potential
2. low toxicity
3. lack of corrosivity
4. no chemical reaction with chlorine
5. ease of compression
6. low cost
7. convenient range of vapor pressure at process temperatures
8. no depletion of ozone layer.

The first seven considerations account for the long dominance of chlorofluorocarbons (CFCs) in chlorine liquefaction systems. These refrigerants are outstanding in the first four points listed. The fourth is especially important in our particular case. Accidental mixing of chlorine and the refrigerant should not create a hazard. Also, generally CFCs have low specific heat ratios. This property equates to low energy consumption in compression (point #5).

Another item listed is low material cost. Replacement costs of refrigerants are very low, and only the first cost is an issue. While a low cost is always welcome, the refrigerant is a very small item in the life-cycle cost of a liquefaction plant. We should also note that energy cost depends on the efficiency of the refrigeration process. Since the coefficient of performance of a Carnot-cycle refrigerator is independent of the medium, differences among refrigerants arise only from differences in operating temperature profiles and deviations from the ideal. Given a set of process operating conditions, there is again very little to choose between any two candidates.

The seventh item on this list has to do with optimizing the temperature and pressure of liquefaction. In the liquefier, the refrigerant must boil at less than the liquefying temperature of chlorine. Its vapor pressure should be high enough to avoid subatmospheric pressure at any point. The refrigerant vapor then must be condensed at a temperature above that of the available cooling medium. Its vapor pressure at that temperature should not be so high as to create a design problem or add greatly to the cost of equipment. The ratio of these two vapor pressures will largely determine the amount of energy required to compress the refrigerant. With the variety of CFCs available, it was relatively easy to pick a refrigerant with a desirable vapor pressure range. In addition, more than one CFC could be used in a multistage system to allow cascading of temperatures. For example, a number of plants used CFC-12 in primary liquefaction and CFC-13 in a secondary or tertiary stage.

Despite their ideal in-process characteristics, the very stability of CFCs has made their use unacceptable under the eighth point in our list. When released into the atmosphere, CFCs diffuse unchanged to the ozone layer in the stratosphere, where they enter into a chain reaction that consumes large quantities of ozone. This reduces the ability of the atmosphere to shield the earth from ultraviolet radiation. One of the first actions taken under the Protocol on Substances That Alter the Ozone Layer (Montreal Protocol) was ceasing the production of most CFCs and removing them from many existing systems. The first replacements used were the hydrochlorofluorocarbons (HCFCs). HCFC-22 (CHClF_2) is an example. While not completely harmless to the ozone layer, this has an ozone depletion potential (ODP) only 5% as great as that of CFC-11 on a weight basis. Other HCFCs have higher ODPs, and as a class they are accepted only as interim replacements. Hydrofluorocarbons (HFCs) are among the classes of refrigerant that are acceptable in the long term.

While there are large fluctuations in monthly and yearly data, it is encouraging that high-altitude atmospheric observations generally show a decreasing rate of growth of the concentrations of CFCs. In a European observatory located at 3,500 m, CFCs showed no major excursions from their tropospheric background concentrations in the year 2001 [47]. This is attributed to the strong reduction in the rates of emission of CFCs. Recent increases in ozone depletion are consistent with the high degree of yearly variability. The medium- to long-term trend is to less depletion [48]. We should anticipate a leveling off of the concentrations followed by a decrease as the CFCs already present in the atmosphere diffuse away.

The growth in the concentration of the unregulated HCFC-22, on the other hand, has not abated, and its concentration more than doubled during the 1990s, from about 0.8 to 1.7×10^{15} molecules cc^{-1} . During 2000 and 2001, the concentration of HFC-134a, a new and completely anthropogenic pollutant, increased at an annual rate of 30% [47].

Projects for conversion of old plant to new refrigerants are highly individualistic. One of the very few useful generalizations that apply is that the energy consumed in compression of the refrigerant will increase. The course of each project depends on the original process design and the capabilities of the equipment. Hieger [49] describes a typical retrofit, giving some of the logic that will be important in every case. In the particular instance discussed, HFC-134a replaced CFC-12. Increasing the size and the speed of the compressor wheels and adding a larger motor offset the change in refrigerant, which would have reduced the capacity by 10–15%. Calculations for another system making the same change of refrigerants predicted a loss of only about 5% in capacity [50]. Since the replacement materials are chemically more active than CFCs, certain problems can occur if they mix with chlorine [51]. HCFC-22 and HFC-134a both can form flammable mixtures with chlorine. The approximate flammable limits at 38°C and 6.8 atm are, respectively, 30–60% and 10–40% refrigerant. HCFC-123 and chlorine seem to be nonflammable under process conditions.

In the retrofit project described above, an on-stream analyzer for chlorine in the refrigerant protected against the formation of hazardous mixtures. Flammability problems also can be avoided by physically preventing the mixing of the two fluids. Figure 9.29 shows a system in which a third fluid is interposed [52]. Chlorine condenses in the lower exchanger against the third fluid. In the upper exchanger, boiling refrigerant then cools this fluid. Connections between the two exchangers allow the transfer fluid to circulate by

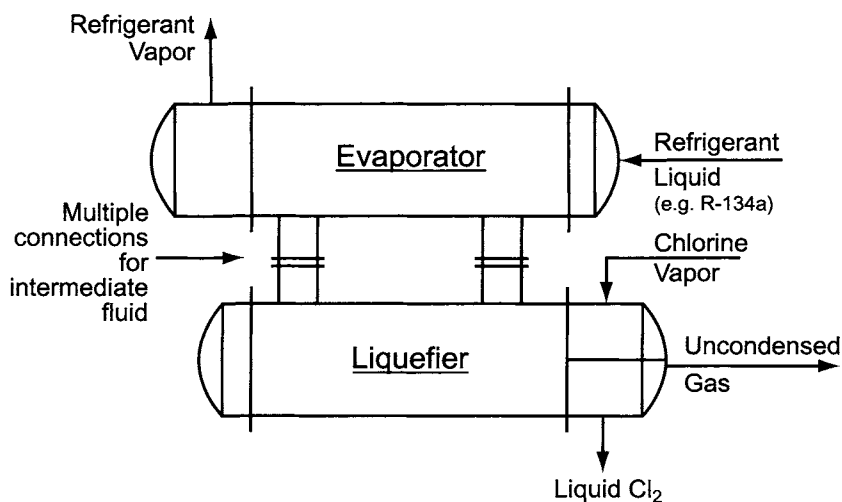


FIGURE 9.29. Use of barrier fluid in chlorine liquefaction.

natural convection. This arrangement requires a lower refrigerant temperature, because the heat of liquefaction flows first to the transfer fluid and then to the refrigerant. Each step requires its own temperature differential, and each step involves a fluid to not undergo a change in phase. The latter situation means that one film coefficient of heat transfer in each exchanger is lower than those met in conventional chlorine liquefiers. The addition of equipment and another thermal barrier increases installed cost and reduces the efficiency of the process. In estimates for a few specific cases, cost and energy consumption each increased by 5–10% [53].

Another approach to the problem is to rethink the refrigeration system and to use a refrigerant with no ODP in a central system that supplies cold brine as a utility throughout the chlor-alkali complex. Bhadsavle and Humm [50] calculated examples for a 450-tpd liquefaction plant. The base system used CFC-12 cascaded over two stages of liquefaction to obtain 99.1% recovery of liquid chlorine. The authors then calculated the effects of changing to HFC-134a, as in a retrofit. In this particular example, the original compressor was physically capable of handling the gas, but full-capacity operation required a higher rotational speed. The power requirement increased 4.6%. With the equipment models assumed, the compressor could be reused, but the motor would have to be replaced. Other examples are not so favorable and require replacement of the compressor as well. This situation points up the individual nature of retrofit projects.

Figure 9.30 shows the utility approach. The refrigerant is ammonia. Its choice is justified by:

1. its low cost
2. many years of industry experience
3. its efficiency as a refrigerant and as a heat-transfer medium
4. the ability to use a single-stage refrigerant screw compressor in place of the three-stage centrifugal machines required by the fluorocarbon refrigerants

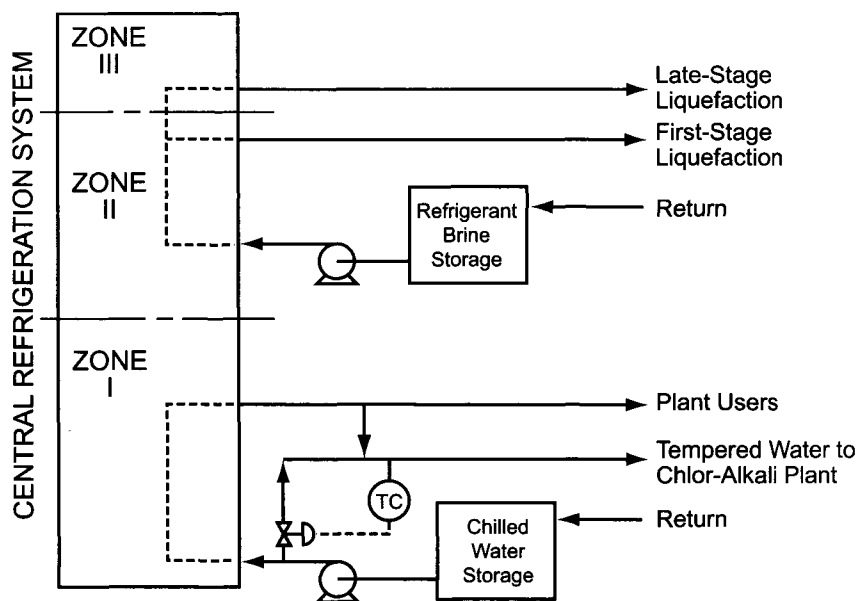


FIGURE 9.30. Utility approach to refrigerant supply.

5. the possibility of placing the refrigeration plant in a remote location to reduce the chances of personnel exposure
6. the ability to separate chlorine and ammonia in order to prevent their coming into contact.

Euro Chlor [54], however, warns against the use of ammonia as a refrigerant when there is any reasonable chance of its contaminating the chlorine. This could lead to the formation of nitrogen trichloride (Section 9.1.11.2A).

Numbers 5 and 6 above depend on use of the utility approach. Figure 9.30 shows that the refrigerant is cooling the brine rather than the process gas. The brine is then pumped as two streams (at different temperatures) to the liquefaction plant. The need for two heat-transfer operations carries the need to apply two temperature differentials, and so the primary ammonia system operates 4.5°C lower than the others. Still, the power requirement for compression is 8.5% lower than it is in the case of R-134a. Offsetting this saving are the capital costs of the system and the need to pump brine.

While other brines might be chosen, the present example uses a silicone oil with outstanding low-temperature properties. Aqueous brines are frequent choices for utility systems of the type discussed here. Leaving aside the question of service temperatures, we should note here the possibility of corrosion in these systems.

Table 9.5 summarizes the refrigeration and power requirements for the three cases studied by Bhadsavle and Humm [50]. Liquefaction pressures in all three cases were 439.2 and 432.3 kPa, and temperatures were -12.1 and -40°C . On the face of it, this approach would not seem to be justified in a conversion project, where so much of the

TABLE 9.5. Use of Central Utility Refrigeration vs Fluorocarbon Retrofit

	R-12 ^a	R-134a ^a	R-717 ^b
Stages	3	3	1
Tons required, primary	434.2	434.2	434.2
Tons required, secondary	14.2	14.2	13.4
Temperature, °C	-18	-18	-24
Speed, rpm	7,115	7,945	3,550
Power demand, kW	646	676	618.5

^aWith centrifugal compressor retrofit.

^bWith screw compressor retrofit.

existing plant can be reused. In a major project or expansion, however, its advantages might be worth considering. These include the advantages in scale offered by combining the refrigerant demand of liquefaction with those of the rest of the site.

Another aspect of Fig. 9.30 is the production of chilled water as a utility for an entire plant complex. The refrigeration system is divided into three operating levels. The warmest of these would produce chilled water directly. Sections 9.1.3.5A and 9.3.2.4 point out that the temperature of the chilled water used to cool chlorine and diaphragm-cell caustic must be restricted to prevent formation of chlorine hydrate or freezing of NaOH. A central utility system may therefore have to produce chilled water at two different temperatures. Inclusion of chilled water goes beyond Bhadsavle and Humm's suggestion but reflects the comment that will be found in Section 12.4.2.2 that it is amenable to the central utility approach. The drawing also shows a single return of brine from the process loads and a single feed to the refrigeration system. Most of the brine emerges at a temperature suited to the first stage of liquefaction, while some goes through another stage of refrigeration. This brine then goes to the second or third stage of liquefaction. The thermal efficiency would improve if the brine return was segregated and only the colder material sent to the last stage of refrigeration. The incremental expense required for this modification would require its own economic justification.

9.1.7.2C. Formation of Chlorine Hydrate. Because of the presence of traces of water in compressed chlorine, the chlorine hydrate discussed in Section 9.1.3.5 again becomes a problem. As chlorine condenses, some of the water accompanies it. Depending on the temperature, a certain amount of water is soluble in the chlorine. So long as this solubility is not exceeded, the condensate remains homogeneous and solid hydrate does not form. Below we develop an estimate of the solubility of water in liquid chlorine and show that, because of its very low solubility in chlorine and therefore its very high activity coefficient in solution, it behaves as a volatile component. The practical effect of this is that water tends to concentrate in the gas phase in most first-stage liquefiers.

When this water-enriched gas is exposed to more severe liquefaction conditions (in particular to lower temperatures) in later stages, the amount of water condensed is more likely to exceed its equilibrium solubility. Once a separate water-rich phase forms, the vapor-liquid equilibrium changes. At most liquefaction temperatures, liquid water does

not exist, and so the insoluble portion is the solid hydrate. While this is present in much smaller quantities in liquefaction than would be possible in a poorly controlled cooling process, its presence must be recognized and dealt with (see following subsection, Effects of Presence of Hydrate).

Solubility of water in chlorine. Expressing the free energy of a system in terms of partial molar quantities (chemical potentials) and comparing the result of differentiation of the whole function with an expression for the rate of change of free energy with composition leads to what is known as the Gibbs–Duhem relation [55,56]. The Gibbs–Duhem equation can be written as

$$x_1(\partial \ln \gamma_1 / \partial x_1)_{T,P} + x_2(\partial \ln \gamma_2 / \partial x_1)_{T,P} + \cdots = 0 \quad (52)$$

where x_i is the mole fraction of component i and γ_i is the activity coefficient of component i .

In a binary mixture, this becomes

$$x_1(\partial \ln \gamma_1 / \partial x_1)_T = x_2(\partial \ln \gamma_2 / \partial x_2)_T \quad (53)$$

If the logarithms of the activity coefficients of a binary system are plotted against molar composition, Eq. (53) relates the slopes at any value of the x 's. This is useful for testing the consistency of data. Such testing becomes easier if we have a systematic way to correlate and smooth data and extend them over the entire range of composition. Integrated forms of the Gibbs–Duhem relation allow us to do this. Theoretically, one reliable measurement of vapor–liquid equilibrium at any point can then be used to characterize a system.

Classical integration of Eq. (52) or (53) as it stands is not feasible, and so many approximate solutions have been derived, using various simplifying assumptions. Some of these are based on assessment of the excess free energy of mixing and some are more highly empirical. The powerful computational methods now available have allowed a number of good approximations to be made. These include the Non-Random Two-Liquid (NRTL) model and the Universal Quasi-Chemical Activity Coefficient (Uniquac) model. These methods use more parameters than the methods popular before the advent of high-speed computers, and they can estimate some of their coefficients from group contributions. They are therefore more flexible and in this sense more powerful. They are, on the other hand, in forms less convenient for our purposes. To illustrate the point to be made here, we choose one of the older methods. They include those due to Margules, van Laar, and Wilson [56]. The Wilson equation is the latest of these three and generally the most accurate, but the others have served well for many years and are easier to manipulate. To study the solubility of water in chlorine, we consider the van Laar equations for a binary mixture. For the two activity coefficients, we have

$$\ln \gamma_1 = A / (1 + Ax_1/Bx_2)^2 \quad (54)$$

$$\ln \gamma_2 = B / (1 + Bx_2/Ax_1)^2 \quad (55)$$

Substituting first $x_1 = 0$ and then $x_2 = 0$, we see that the constants A and B are the logarithms of the limiting values of the activity coefficients:

$$\ln \gamma_{1(x_1=0)} = A \quad (56)$$

$$\ln \gamma_{2(x_2=0)} = B \quad (57)$$

The $-\frac{1}{2}$ power of $\ln \gamma$ is linear in the concentration ratio of the two components. For component 1, for example,

$$1/\sqrt{\ln \gamma_1} = 1/\sqrt{A} + \left(\sqrt{A/B}\right)(x_1/x_2) \quad (58)$$

Linearizing the equation in this way makes it possible to evaluate the coefficients A and B of a binary system graphically. The scatter of the plot usually gives an indication of the quality and reliability of the data. For water in chlorine, we can simplify the equations even more. We define water as component 1 and chlorine as component 2. In the chlorine-rich phase, which holds only ppm quantities of water, we have $x_2 \approx 1$ and $x_1 \ll 1$. Now the van Laar equations are

$$\ln \gamma_1 = A/(1 + Ax_1/B)^2 \quad (59)$$

$$\ln \gamma_2 = B/(1 + B/Ax_1)^2 \quad (60)$$

In Eq. (60), x_1 is very small. Since chlorine is also highly insoluble in water, the system is not wildly unsymmetrical, and so A and B are close in magnitude. This justifies rewriting Eq. (60) as

$$\ln \gamma_2 = 0; \quad \gamma_2 = 1$$

in the chlorine-rich phase.

Now we consider water only and drop the subscripts from Eq. (59). We have

$$\ln \gamma = A/(1 + Ax/B)^2 \quad (61)$$

Expanding the quantity in parentheses but dropping the term in x^2 ,

$$\ln \gamma = A/(1 + 2Ax/B) \quad (62)$$

The expression for the reciprocal is now simpler than the general form (58):

$$1/\ln \gamma = 1/A + (2/B)x = 1/\ln \gamma_0 + (2/B)x \quad (63)$$

γ_0 being the activity coefficient of water at zero concentration. At saturation, x equals the solubility s . We have

$$1/\ln \gamma_s - 1/\ln \gamma_0 = (2/B)s \quad (64)$$

We know that s is of the order of 10^{-4} or 10^{-5} , and $2/B < 1$. The difference between the two reciprocals is therefore very small. Solving for $\ln \gamma_s$:

$$\ln \gamma_s = \ln \gamma_0 / (1 + \beta \ln \gamma_0) \quad (65)$$

Here, $\beta = 2s/B \ll 1$, in which case

$$\ln \gamma_s = \ln \gamma_0 (1 - \beta \ln \gamma_0) \quad (66)$$

For all likely values of the activity coefficient, the term in parentheses is very close to unity. Even with $\gamma = 500,000,000$, the value of $\ln \gamma$ is only 20, and the term $\beta \ln \gamma_0$ is negligible. So we have

$$\gamma_0 \approx \gamma_s \quad (67)$$

When both phases exist, liquid chlorine saturated with water is in equilibrium with liquid water saturated with chlorine. The activity of water is by definition of equilibrium the same in both phases. Considering the composition of the water-rich liquid, we see that this activity is very nearly equal to that of pure water. Setting the activity of pure water at unity, we have for the water in the chlorine-rich phase $\gamma_s s = 1$, or

$$\gamma_s = \gamma_0 = 1/s \quad (68)$$

In other words, the activity coefficient of water dissolved in chlorine is very nearly constant over the entire, but very small, soluble range. Now we go back to the fundamental equation that defines the liquid-phase activity coefficient of a component of a solution when there is ideal gas behavior:

$$\Pi y = \gamma P^0 x \quad (69)$$

where

Π = total pressure

y = mole fraction of the component in the vapor

γ = activity coefficient for the component in the liquid phase

P^0 = vapor pressure of the component

x = mole fraction of the component in the liquid

When we apply this to component #2, chlorine, we use the approximations $\gamma_2 = 1$, $x_2 = 1$, and we have, simply

$$y_2 = P_2^0 / \Pi \quad (70)$$

For water, we have

$$\Pi y_1 = \gamma_1 P_1^0 x_1 \quad (71)$$

At saturation, $x_1 = s$, and $\gamma_1 \approx 1/s$; so

$$y_1 = P_1^0/\Pi \quad (72)$$

The total pressure exerted at equilibrium, in accord with the rule of thumb for immiscible substances, is equal to the sum of the pure-component vapor pressures.

For all concentrations $x_1 < s$,

$$\Pi y_1 = P_1^0 x_1/s \quad (73)$$

The relative volatility of water with respect to chlorine therefore is

$$\alpha = (y_1/x_1)(x_2/y_2) = (P_1^0/\Pi s)(\Pi/P_2^0) = P_1^0/(P_2^0 s) \quad (74)$$

Calculated values of α are greater than four (Table 9.6, following). The physical meaning of this is that water must be recognized as a volatile component with respect to chlorine when liquefaction begins. The fraction of water condensed can be calculated from the (higher) fraction of chlorine condensed [31]. This situation holds as long as the condensate is homogeneous. Once the liquid phase becomes saturated with water, the basic assumptions made in derivation of the relative volatility no longer hold. The partial pressures of water and chlorine remain unchanged as the amount of water present increases beyond its solubility, and the apparent relative volatility begins to fall.

This development leads us to a pair of guidelines for calculating equilibria in the system:

1. the activity coefficient of water at saturation is equal to the reciprocal of its saturation concentration, and
2. the activity coefficient is equal for all concentrations of water up to and including the saturation value.

Updyke [57] performed calculations in which he assumed that, when $x_2 = s$, water exerts its full vapor pressure and that, when $x_2 < s$, the partial pressure of water in the gas is proportional to its concentration in the liquid. These working assumptions are equivalent to the guidelines developed here. Updyke then went on to show that calculations made on this basis were useful in diagnosing and identifying the solutions to problems in real liquefiers.

This somewhat roundabout approach to the problem is necessary because direct measurement of equilibrium in the chlorine–water–hydrate system at the temperatures and pressures of interest would be exceptionally difficult. Ketelaar [22] therefore made an ingenious series of individually plausible assumptions from which he estimated the vapor pressure of hydrate and its solubility in liquid chlorine. The numbered items below describe the individual steps in the reasoning process, and Fig. 9.31 shows the relative energy levels of the different states of the important species.

1. The solubility of water in liquid chlorine is taken to be equal to its solubility in CCl_4 . To justify this assumption, consider that:
 - (a) both Cl_2 and CCl_4 are essentially nonpolar (dielectric constants of 1.9 and 2.2);

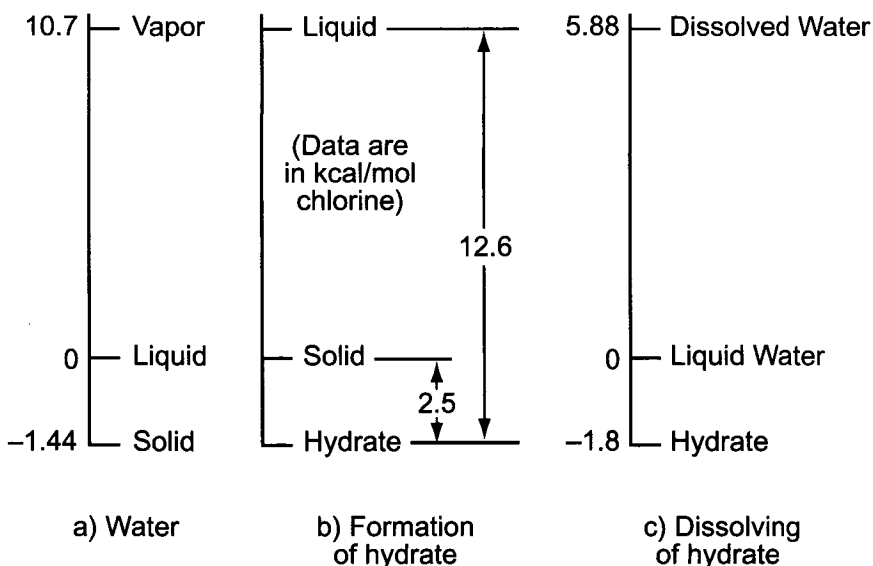
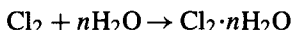


FIGURE 9.31. Energy-level diagrams—chlorine hydrate system.

(b) their solubility parameters are very nearly equal (8.5 and 8.6).

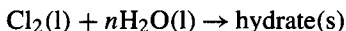
From data on the temperature dependence of the solubility of water, the enthalpy of solution of water in CCl_4 (and therefore in liquid chlorine) above the quadruple-point temperature of 28.7°C is taken to be $5.88 \text{ kcal mol}^{-1}$.

2. The difference between the enthalpies of formation of hydrate by the reaction



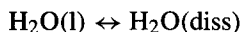
for solid and liquid water is $10.1 \text{ kcal mol}^{-1}$ of chlorine (these are based on 19th-century measurements of three-phase equilibria at 0°C and are illustrated in Fig. 9.31b). Since the heat of fusion of water is $1.44 \text{ kcal mol}^{-1}$, it follows that the hydrate contains about $10.1/1.44 = 7$ moles of water. This is compatible with the data of Section 9.1.3.5.

3. The equilibrium measurements referred to in (2) above gave a heat of reaction of $-12.6 \text{ kcal mol}^{-1}$ for

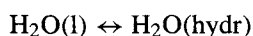


If $n = 7$ as estimated in (2), the enthalpy of formation of the hydrate from the liquids must be $(-12.6/7) = -1.8 \text{ kcal mol}^{-1}$ water. This is $0.36 \text{ kcal mol}^{-1}$ below the enthalpy of freezing of water.

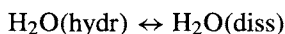
4. From (1) above, for



we have $\Delta H = 5.88$. From (3) above, for



we have $\Delta H = -1.8$. Combining these gives $\Delta H = 5.88 + 1.8 = 7.7 \text{ kcal mol}^{-1}$ for



This is the heat of solution of water from the hydrate, and it is taken as the activation energy below the quadruple point. Combined with the assumed solubility (from CCl_4 data) at that point, it gives

$$\begin{aligned}\ln X_s &= 6.056 - 3880/T \\ X_s &= 426.7e^{-3880/T}\end{aligned}$$

where X_s is the solubility of water in liquid chlorine, mole fraction, and T the temperature, $^\circ\text{K}$. This is in good agreement with the data in Chlorine Institute Pamphlet 100. Multiplying X_s by 254,000 gives the solubility in ppm (wt).

- Combining assumptions, the partial pressure of water in equilibrium with the hydrate at the quadruple point is equal to the vapor pressure of water at that temperature. The effect of temperature is then taken from an estimate of the enthalpy of sublimation. For ice, this is $12.15 \text{ kcal mol}^{-1}$. From (3) above, the same property of the hydrate is obtained by adding $0.36 \text{ kcal mol}^{-1}$. This gives 12.5, and the equation for the vapor pressure of chlorine hydrate (in atmospheres) becomes

$$\begin{aligned}\ln P &= 17.62 - 6300/T \\ P &= 4.51 \times 10^7 e^{-6300/T}\end{aligned}$$

Ketelaar's development considers only the binary system chlorine-water. It does not recognize the influence of gas-phase inerts. In the binary system, the relative volatility and the distribution coefficient are one and the same. This is not true when inerts are present.

This method therefore would indicate that the distribution coefficient and hence the mole fraction of water in the vapor phase would not be influenced by the addition of an inert gas. Consider a mixture of chlorine and water in vapor-liquid equilibrium in a closed container. By that assumption, addition of nitrogen pressure to the container would cause further vaporization of the water in order to maintain the same vapor-phase mole fraction. What happens in fact is that the vapor-phase activities of chlorine and water remain nearly unchanged. That statement properly ignores any absorption of nitrogen into the liquid and is practically equivalent to saying that, while the mole fraction of chlorine in the vapor phase decreases, its partial pressure is not affected. The equations developed here correspond to that situation.

TABLE 9.6. Distribution Coefficient of Water in Chlorine/Water Mixtures

Temperature, °C	60	40	20	0	-20	-40	-60
Coefficient α	4.11	4.11	4.11	4.12	4.18	4.32	4.58

Combining the approximations developed above with the relative volatility as defined by Eq. (74), we obtain values of α as a function of the Celsius temperature. Table 9.6 shows these for the range -60 to 60°C .

The relative volatility is quite constant at positive temperatures and probably into the first stage of a normal liquefaction system. It would seem to increase at very low temperatures, but one should bear in mind the nature of the technique used to derive these values and not place great trust in them. It is also a practical fact that at low temperatures the solubility of water is so low that the assumption of a homogeneous liquid phase probably does not hold. The best approach for calculations would seem to be to assume a constant α of 4.0–4.2.

Effects of presence of hydrate. Chlorine hydrate forms whenever operating conditions are suitable. The quadruple point referred to in Section 9.1.3.5C is that for hydrate, gas, and two liquid phases. At low temperature the water phase also freezes, and the four possible phases are gas, wet liquid chlorine, ice, and hydrate. This mixture has a quadruple point at -3°C and 244 torr.

We saw above that in the early stages of liquefaction water tends to accumulate in the gas phase. This keeps the liquid-phase concentration of water low and works against the formation of solid hydrate. In addition, the temperature is often higher in these early stages. This fact increases the solubility of water in the liquid chlorine, again discouraging hydrate formation. Hydrate accumulates more frequently in the later stages.

While solid hydrate has the potential of plugging equipment or piping, it is not a corrosion hazard during liquefaction. When an operating unit is shut down and allowed to warm, however, the presence of hydrate leads to extremely rapid corrosion. The stability of carbon steel in dry chlorine service is due to its protective layer of FeCl_3 (Section 9.1.2). Chlorinated water released from melting hydrate dissolves the FeCl_3 to produce an acidic, highly corrosive solution that dissolves more iron from the steel shell.

Condensing chlorine washes hydrate from the tubes as it forms. Since it is lighter than chlorine (density of 1.23 vs 1.5+), hydrate floats on the liquid accumulating in the shell. Unless it is removed, it can eventually restrict flow or even plug the equipment. Because the quantities involved are small, it is not rare for a chlorine liquefaction plant to operate for long periods with occasional shutdowns for cleanout.

These problems can be avoided by designing the exchanger and transfer piping to allow the hydrate to leave with the liquid chlorine. As mentioned above, most hydrate forms in the cold end of multistage systems, and combination with the warmer chlorine from other stages often allows the contained water to dissolve and form a homogeneous solution.

Chlorine often is removed from liquefiers through seal legs. Examples would be two liquefiers in series at the same nominal pressure, where a slight difference in pressure in fact exists and can be compensated for by liquid seals of different heights. These designs do not permit hydrate to escape. Updyke [57] suggests removing the liquid under level control instead of through a gravity leg and periodically dropping the level to flush out the hydrate. This would involve allowing the chlorine gas to bypass for a short time. Another approach might be to connect a pot directly beneath the liquefier with a straight pipe containing a shut-off valve. The chlorine as it condenses leaves the liquefier, carrying hydrate with it, and collects in the pot. A valve below the pot remains closed, preventing the escape of gas. Periodically, the valves above and below the pot reverse their positions. Only a small quantity of hydrate will accumulate in the pot over a short time. Properly selected valves should not interfere with flow of the suspended hydrate. As an elaboration, warmer chlorine from the preceding stage can be put into the pot to dissolve the hydrate. This technique applies only with two stages substantially at the same pressure level and when incremental liquefaction in the second stage depends on a lower temperature there.

Any attempt to automate such an operation would require strict exclusion of the possibility of passing quantities of water, in whatever form, into the liquid chlorine product system.

9.1.8. Storage and Handling of Chlorine

9.1.8.1. Reference Documents. Euro Chlor, the Japan Soda Industry Association, and The Chlorine Institute publish a large number of excellent guides to the safe handling of chlorine and related products and to the design and operation of facilities for their handling and disposal. These are prepared by groups of experienced people who are active in the industry. Designers and operators should be familiar with these publications and with the many services offered by these organizations. Many of these publications include checklists. Table 9.7 lists some of the publications consulted in preparation of this book. Most Euro Chlor documents are published by their Storage and Transport Committee and are listed according to that committee's numbering system. This is given as GEST *xx/yy*, with *xx* being the year of original publication and *yy* a sequential number. Chlorine Institute documents are issued as sequentially numbered Pamphlets. The table also gives the number and year of publication of current revisions. Below the table, the various communication addresses of these organizations are given. In this and the following sections of this chapter, we cite references by giving the identifier for the relevant publication (GEST *xx/yy* or P*zzz*) rather than by assembling a lengthy list at the end of the chapter.

The Japan Soda Industry Association also covers safety and environmental matters in Chapter 4 of its Soda Handbook [58].

9.1.8.2. Storage of Liquid Chlorine. Liquefied chlorine often drops by gravity from a knockout pot through a seal leg or a control valve into some form of storage. The "storage" may be simply a transfer tank that allows the liquid to be moved immediately

TABLE 9.7. Selected Euro Chlor and Chlorine Institute Publications

GEST #	Title	Edition	Date
<i>Euro Chlor</i>			
72/10	Pressure Storage of Liquid Chlorine	8	1993
73/17	Low Pressure Storage of Liquid Chlorine	5	1996
73/20	Code of Good Practice for Safe Transport of Bulk Liquid Chlorine by Road Tanker Vehicles	8	2001
75/43	Flexible Steel Pipes and Flexible Monel and Hastelloy Hoses for the Transfer of Dry Gaseous or Liquid Chlorine	8	2004
75/44	Articulated Arms for the Transfer of Gaseous or Liquid Chlorine	7	1997
75/45 ^a	Flexible Monel and Hastelloy Hoses for the Transfer of Dry Gaseous or Liquid Chlorine	6	1997
75/47	Chlorine Vaporizers	9	1999
76/52	Equipment for the Treatment of Gaseous Effluents Containing Chlorine	10	2001
76/55	Maximum Levels of Nitrogen Trichloride in Liquid Chlorine	10	2001
76/64	Relief Valves for Use on Dry Gas or Liquid Chlorine	4	1983
78/73	Design Principles for Installations for Off-loading of Liquid Chlorine Road and Rail Tankers and ISO-Containers	5	1997
78/74	Design Principles for Installations for Loading of Liquid Chlorine into Road and Rail Tankers and ISO-Containers	8	1997
79/79	Chlorine Transfer Compressors	3	1999
79/81	Dry Liquid Chlorine Piping Systems Located inside Producers' or Consumers' Plants	8	2001
79/82	Choice of Materials of Construction for Use in Contact with Chlorine	7	1995
79/82 (Annex)	Choice of Materials of Construction for Use in Contact with Chlorine (Spreadsheet)	1	2000
80/84	Code of Good Practice for the Commissioning of Installations for Dry Chlorine Gas and Liquid	4	1990
80/89	Code of Good Practice for Safe Transport of Liquid Chlorine by Rail Tanker	3	1981
86/128	Procedure for Homologation of Valves for Use on Liquid Chlorine Duty	1	1996
86/129	Procedure for an Independent Assessment of Valves for Use on Liquid Chlorine, Prior to Consideration for Euro Chlor Homologation	1	1996
87/130	Hazard Analysis for Chlorine Plants	7	1996
87/133	Overpressure Relief of Liquid Chlorine Installations	4	2001
89/140	Specification for Flanged Steel Globe Valves—Bellows Sealed—for Use on Liquid Chlorine	8	1997
90/150	Specification for Flanged Steel Globe Valves—Packed Gland—for Use on Liquid Chlorine	8	1997
90/151	Materials of Construction for Handling Chlorine	Paper	1990
90/154	Chlorine Hazard Properties	Paper	1990
90/158	Commissioning of Equipment for Liquid Chlorine	Paper	1990
90/159	Aspects of Transport Safety	Paper	1990
90/159B	Transport Accident Statistics	Paper	1990
90/161	Plant Safety and Quantitative Risk Assessment	Paper	1990
92/169	Guidelines for the Safe Handling and Use of Chlorine	1	1994
92/171	Personal Protective Equipment for Use with Chlorine	1	1995
92/176	Chlorine Emergency Equipment	1	1993
93/179	Emergency Intervention in Case of Chlorine Leaks	7	1996
93/194	Safe Operation	Paper	1993

TABLE 9.7. (continued)

GEST #	Title	Edition	Date
<i>Euro Chlor</i>			
93/195	Learning from Past Experience	Paper	1993
93/196	Emergency Action	Paper	1993
93/197	Storage, Loading, and Confinement of Chlorine	Paper	1993
94/215	Confinement of Units Containing Liquid Chlorine	1	1996
96/221	Protection of Road Tankers for the Carriage of Chlorine	1	1998
AP 1	Learning from Experience		1996
AP 2	Learning from Experience		1999

^a Merged with GEST 75/43.

Pamphlet	Title	Edition	Date
<i>Chlorine Institute</i>			
1	The Chlorine Manual	6	2000
5	Non-Refrigerated Liquid Chlorine Storage	6	1998
6	Piping Systems for Dry Chlorine	14	1998
9	Chlorine Vaporizing Systems	5	1997
17	Packaging Plant Safety and Operational Guidelines	3	2000
21	Nitrogen Trichloride — A Collection of Reports and Papers	4	1997
39	Maintenance Instructions for Chlorine Institute Standard Pressure Relief Devices	10	1996
41	Maintenance Instructions for Chlorine Institute Standard Safety Valves	4	1995
49	Recommended Practices for Handling Chlorine Bulk Highway Transports	8	2001
57	Emergency Shut-Off Systems for Bulk Transfer of Chlorine	3	1997
60	Chlorine Pipelines	5	2001
63	First Aid and Medical Management of Chlorine Exposures	4	1985
64	Emergency Response Plans for Chlorine Facilities	4	1995
65	Protective Clothing for Chlorine	2	1988
66	Recommended Practices for Handling Chlorine Tank Cars	3	2001
67	Safety Guidelines for the Manufacture of Chlorine	1	1979
73	Atmospheric Monitoring Equipment for Chlorine	7	2003
75	Respiratory Protection Guidelines for Chlor-Alkali Operations	2	1993
76	Guidelines for the Safe Motor Vehicular Transport of Chlorine Cylinders and Ton Containers	3	2001
78	Refrigerated Liquid Chlorine Storage	3	2000
79	Recommended Practices for Handling Chlorine Barges	2	1996
80	Recommended Practices for Handling Sodium Hydroxide Solution and Potassium Hydroxide Solution (Caustic) Barges	3	2001
83	Guidelines on Risk Analysis	1	1989
85	Recommendations for Prevention of Personnel Injuries for Chlorine Producer and User Facilities	3	1999
86	Recommendations to Chlor-Alkali Manufacturing Facilities for the Prevention of Chlorine Releases	4	2001
87	Recommended Practices for Handling Sodium Hydroxide Solution and Potassium Hydroxide Solution (Caustic) Tank Cars	2	1999
89	Chlorine Scrubbing Systems	2	1998
92	Environmental Fate and Toxicity of Mercury	1	1992
93	Pneumatically Operated Valve for Use on Chlorine Tank Cars	1	1996

(Continued)

TABLE 9.7. (continued)

Pamphlet	Title	Edition	Date
<i>Chlorine Institute</i>			
94	Sodium Hydroxide Solution and Potassium Hydroxide Solution (Caustic) Storage Equipment and Piping Systems	2	2001
95	Gaskets for Chlorine Service	3	2003
96	Sodium Hypochlorite Manual	2	2000
99	Hydrogen Chloride, Anhydrous (Non-Refrigerated)—Use, Handling and Transportation of Cylinders and Tube Trailers	1	1995
125	Guidelines: Medical surveillance and Hygiene Monitoring Practices for control of worker exposure to mercury in the Chlor-Alkali Industry	4	2003
137	Guidelines: Asbestos Handling for the Chlor-Alkali Industry	4	2000
139	Electrical Safety in Chlor-Alkali Cell Facilities	3	1998
150	Hydrochloric Acid Tank Motor Vehicle Loading/Unloading	1	1996
152	Safe Handling of Chlorine Containing Nitrogen Trichloride	1	1998
155	Water and Wastewater Operators Chlorine Handbook	1	1999
163	Hydrochloric Acid Storage and Piping Systems	1	2001
167	Learning from Experience	1	2002

Note:

- 1 The Chlorine Institute, Inc., 1300 Wilson Boulevard, Alexandria, VA 22209, USA. Telephone +1-(1)703-741-5760. Telefax +1-(1)703-741-6068. Website: <http://www.cl2.com>
- 2 Euro Chlor, Avenue E. Van Nieuwenhuysse 4, Box 2, B-1160 Brussels, Belgium. Telephone +32-(0)2-676 72 11. Telefax +32-(0)2-676 72 41. Website: <http://www.eurochlor.org>

to its final destination, or it may be a large pressure vessel whose purpose is to hold a substantial quantity of chlorine.

Arguments in favor of storage of large quantities of chlorine are those that apply to any product. Loading and shipping operations are uncoupled from product generation. Swings in plant output have no immediate effect on product loading. Product loading rates can be highly variable and can be totally stopped for some number of shifts or even days without affecting production operations. When chlorine is consumed on site, as in EDC manufacture, large storage volumes allow independent operation of the two processes and prevent disturbances from propagating back and forth. These may seem to be matters primarily of operating convenience, but in relieving stresses on the operators they also promote safety.

Arguments against large-volume storage include the economic one that extensive facilities are costly and tie up large blocks of plot area. The high cost is aggravated by the many safety precautions required when handling chlorine and by the ongoing need to deal with vapor generated in the storage tanks. Perhaps more important than the economic argument is the hazard presented by storage of liquefied chlorine. More and more handlers of chlorine are now performing hazard studies that include the “worst likely case scenario.” Section 16.4.2.5 contains more on this subject, along with one standardized definition of the worst likely case. If failure of a large chlorine storage tank or system is to be considered, it will almost always qualify as this worst case. Mitigation of such a failure, however unlikely it may be, is extremely expensive if at all practicable. The trend in chlorine plant construction and operation is now toward reduced storage volume. Indeed, some existing plants have acted to decommission some of their chlorine storage capacity.

The worst-case scenario related to a single tank can be mitigated by using a number of smaller tanks to store a given amount of liquid. This approach, however, increases the likelihood of a smaller leak by multiplying the number of accessories that accompany the tanks (GEST 72/10). On the other side of the question, the maximum size of a tank depends on capabilities in shop fabrication, stress relief, and transportation to the site.

The great majority of storage systems is located outdoors. This is especially true at large scale. Still, there are several examples of indoor storage. These are pressurized rather than refrigerated systems. The special considerations that apply to such confined storage appear below in Subsection 9.1.8.2C.

Design of the equipment and of the storage facility as a whole must satisfy all locally established codes. The designers and operators should jointly assess risks and produce the necessary studies and worst-case scenarios. Once the characteristics of a hypothetical release of chlorine are established, its effects on people, local residents as well as plant workers, must be evaluated. Euro Chlor (GEST 90/161) has published a toxicity probit (Section 16.4.3.1) that can be used in this step.

Chlorine storage tanks must be protected against overpressurization by relief devices. Most arrangements combine a frangible piece with a spring-loaded relief valve. Section 9.1.10.2 describes the systems commonly used in chlorine systems.

Avoidance of external damage to storage tanks also is important. In addition to their robust construction, tanks should be placed in a safe location or protected by barriers. Recommended minimum distances from other facilities (GEST 72/10, 73/17) include:

Public roads	25 m
Main railway lines	25 m
Plant boundaries	10 m
Other processes	
Case 1 ^a	10 m
Case 2 ^b	based on conditions
Other chlorine storage	comfortable access

^a Process without fire or explosion hazard.

^b Process with fire or explosion hazard.

Selection of the location should also consider the likelihood of damage from a fire or an explosion in a neighboring plant.

Many books and other publications are available on chemical project engineering and site design and layout. These summarize the principles involved in choosing the location of a storage area and arranging the various components. In a chlorine storage facility, consideration of toxicity is particularly important and should be a major factor in design [59,60]. Layout within storage areas, including the spacing of tanks, often follows national fire codes. These codes sometimes are inadequate for releases of toxic materials, and dispersion studies are recommended for each site. For the most accurate results, a study should be specific to site topography and should include the effects of buildings and structures. The latter can have major effects on peak concentrations after a toxic release or on the time required to reach a certain concentration at a given location [61]. Dispersion studies should also be included in emergency plans. It would make little sense, for example, to have a high probability of a rapidly toxic concentration

of chlorine somewhere along the main evacuation route. Emergency plans should have a certain amount of flexibility in order to take advantage of the information provided by chlorine monitors and real-time dispersion modeling. Where such elaborate facilities are not available, a wind direction indicator or windsock is a minimum requirement. Emergency plans require personnel training and periodic rehearsal. Training should include the proper use of protective gear, which should be stored in more than one location.

Whatever type of atmospheric monitoring system is used inside battery limits, it can be argued that the reliability of the high-level alarm is more important than the accuracy of the indication, and frequent (i.e., monthly or weekly) calibration of this feature is useful [62].

Other considerations that apply to high toxic hazard materials (HTHMs) include:

1. consider high-integrity storage tank design
2. keep storage away from flammable or explosive materials
3. if diked, separate from incompatible materials
4. consider momentum of suddenly-released fluid in designing dike wall
5. consider providing a designated dump tank to allow emptying of any one storage tank.

9.1.8.2A. Pressurized Storage. Storage tanks should be designed to the appropriate Code, using at least some of the provisions for lethal service. In the case of Section VIII of the ASME Code, Parts UW and UCS apply. Since chlorine boils when pressure is released, the minimum design temperature must be -35°C or lower. The Chlorine Institute (P5) recommends design for full vacuum and a pressure of at least 1550 kPa and also at least 120% of the maximum expected pressure. The latter quantity must include any padding gas used to transfer chlorine from the tank. Section 9.1.8.4A (Fig. 9.34) approaches this problem from the reverse viewpoint. It shows the allowable padding pressure for different assumed relief device settings. Equations (75) and (76) show the pressure and volume of gas necessary to transfer liquid at a given rate.

The size of the tank should be based on a filling density of 1.25. This gives at least 5% freeboard at 50°C and so caters to the unusually high coefficient of thermal expansion of chlorine. The tank must also retain its physical properties at low temperatures. Low-temperature carbon steels are standard. Examples are A516, Grade 70, and A612, Grade B. V-notch impact testing of the material is desirable, and vessel design should include a corrosion allowance of at least 1 mm (GEST 72/10). The Chlorine Institute recommends a corrosion allowance of 3.2 mm (P5).

Double-welded butt joints are preferred for assembly of the shell, with 100% radiography. Post-weld heat treatment is necessary. Nozzles should have full-penetration welds extending through the entire thickness of the vessel wall or nozzle wall. Most nozzle welds can be tested ultrasonically; those 250 NB and larger should be radiographed. Seams of nozzles fashioned from electric-resistance welded (ERW) piping should also be radiographed. Manways are essential. Some do double duty, for example as support for submerged pumps and various nozzles. This practice reduces the number of penetrations of the cylindrical vessel wall. In most designs, all nozzles are on top of the tank. All but pump discharge lines and dip-pipe connections then are in the vapor space. Leaks therefore are less hazardous, and the nozzles are less subject to mechanical

damage. For special reasons, nozzles sometimes may be on the side or bottom of the tank. Design and operation then must consider the increased possibility of releases of liquid chlorine. Precautions might include protective barriers, remotely operated valves, maintenance and inspection procedures, and special tank supports.

Hydrostatic testing is often necessary. Local regulations will prevail here, but this sort of testing should be kept to a minimum because of the hazards associated with residual moisture in a chlorine tank. The Chlorine Institute (P5) gives procedures for inspection and hydrostatic testing. In addition to inspection during fabrication, Euro Chlor (GEST 72/10) covers inspection and acceptance tests for the metal used in construction of storage tanks, listing applicable ISO, DIN, and Euronorm codes. European practice relies less on hydrostatic testing. Euro Chlor discourages frequent hydrostatic retesting and recommends specific procedures (GEST 80/84) to minimize corrosion. Perhaps for this reason, Euro Chlor accepts the lower corrosion allowance referred to above.

9.1.8.2B. Low-Pressure Storage. When storing liquid chlorine, the fundamental choice is between pressurized systems and refrigerated systems that operate at atmospheric or slightly elevated pressure. Storage at process pressure is cheaper and simplifies handling of the liquid. Since the pressures involved are not great, it is the more frequent choice. Its chief drawback is the increased severity of chlorine release when it occurs.

Euro Chlor (GEST 73/17) defines “low pressure” as anything up to an absolute value of 2.5 bar. This requires refrigeration and, for insulation and containment, double-walled tanks. A major advantage of storage near atmospheric pressure under refrigeration would appear to be the smaller quantity of chlorine released in a spill. When liquid chlorine escapes from a system held under pressure, there is an immediate release of vapor as the liquid flashes down to the atmospheric boiling point of -34°C . The amount flashed depends on the temperature of the chlorine in storage, but a typical number is 20%. Atmospheric-pressure storage eliminates this problem. Another advantage of atmospheric storage is that much larger vessels can be designed, and a single sphere can replace a number of pressurized storage tanks. Also, any liquid chlorine released has less momentum and is more easily contained in a defined and diked area [63].

Low-pressure storage, on the face of it, appears to have an advantage in inherent safety. However, its auxiliaries are mechanically complex and add new modes of possible failure. In this aspect the comparison is analogous to that between passive and active protective systems. Harris and Shaw [64] point out that a low-pressure system requires a source of cold liquid chlorine, a high-integrity gas handling or recompression system, and greater levels of skill or higher equipment standards. Low-pressure storage is not usually economical for capacities less than about 400 tons, and in any case, Euro Chlor (GEST 73/17) considers it inappropriate for plants that are not chlorine producers. Besides the complexity added by the refrigeration system and provisions made for its failure, the design must consider the problems due to the necessity to connect the storage system to high-pressure operations such as liquefaction. Improper operation of the connecting facilities can cause major problems very rapidly. Chlorine from a liquefaction process, for example, will be at higher pressure and perhaps higher temperature than the storage tank. Reducing its pressure can allow chlorine to flash until the bulk reaches the atmospheric pressure boiling point. Even when the chlorine is liquefied at low temperature, the reduction in pressure will allow the escape of dissolved

noncondensable gases. To avoid the release of large volumes of gas from the storage tanks, liquid chlorine should first be brought to equilibrium with that already contained in the vessel. Very slight variations in temperature can have large effects on the venting rate. In a system designed for a gassing rate of 150 kg hr^{-1} , for example, introduction of $15 \text{ m}^3 \text{ hr}^{-1}$ of chlorine that is only 1°C above the storage temperature will create vapor equal to 50% of the design load.

This aspect needs very thorough study and safety review at various stages of design. Within the safety literature, Lees [65] reports that the ICI liquefied flammable gas code considered there to be significant risk of failure of a refrigerated storage tank system but insignificant risk with a pressurized tank. Englund [66], however, considers atmospheric-pressure storage safer in the case of chlorine. He describes a system of 5,000-ton storage tanks, each mounted above a submerged concrete compartment. The compartment is large enough to receive the contents of the storage tank and is partly covered. It is also equipped with a pump for removal of rainwater and a blower system for sending vapors to a scrubber. Management controls keep the chlorine inventory to a minimum. Englund cites an example in which this arrangement prevented a hazardous release when a pump below a storage tank failed. In opposition to this, Section 9.1.8.4B points out that one of the advantages of pressurized storage is the ability to use a submerged pump in the storage tank with less risk of failure of the pump or suction piping.

Pamphlet 78 calls for the same sort of fabrication techniques recommended for pressurized storage. It also gives instructions for commissioning, inspection, and maintenance. It covers single-wall as well as double-wall tanks and horizontal as well as vertical or spherical tanks. The minimum design pressure for a single-wall tank should be about 175 kPa (25 psig). The corrosion allowance for the internal tank and connections usually is about 2 mm; this should also apply to the external vessel when one of its functions is containment.

Differential thermal expansion of the two shells is a constant problem. Design must provide for this, and the usual approach is to add expansion bellows of austenitic stainless steel. Joints are critical. All welds should be radiographed, and the assembly should be installed with due care to avoid damage to the bellows. The problem of differential thermal expansion is magnified during commissioning of a tank. Section 11.3.2.8 also mentions the special instrumentation requirements.

The minimum design temperature of the internal vessel should be -35°C ; the maximum depends on conditions when the vessel is isolated and can take into account any insulation in the annular space. The minimum design temperature precludes the use of ordinary carbon steels. The design temperatures of the external vessel depend on its purpose; if it is to provide secure containment in case of a leak, its minimum design temperature must also be -35°C .

Insulation should be designed for maximum ambient and minimum chlorine temperatures. It should be nonflammable, dry, and chemically inert to chlorine. Because a purge gas is required between the two tanks, the insulation should be a granular material. Expanded silica and diatomaceous earth are examples. The purge gas outlet should be monitored for chlorine.

9.1.8.2C. Confined Storage. Another approach that would seem to provide inherent safety is the storage of chlorine in a fully confined system. The objectives in providing

containment are to prevent or delay the release of chlorine due to a failure in storage or handling equipment and to mitigate the effects should a release occur. The Euro Chlor study of such systems (GEST 94/215) contemplates three different methods of containment:

1. full containment in a heavy bunker or underground
2. double-wall containment by “jacketing” each piece of equipment
3. light containment in a conventional building.

The heavy-bunker approach would make maintenance difficult and in many cases would require workers to don full protective equipment before entering the confined area. It is not suitable for loading/unloading systems and is largely confined to the erection of small buildings for confinement of reactors that have the potential for a sudden release of considerable energy or quantities of chlorine. The Euro Chlor conclusion is that “no credible scenario justifies (this approach) for units containing liquid chlorine.”

The double-wall approach is not uncommon in certain piping systems. Applying it to stationary equipment such as vessels, transfer equipment such as pumps and compressors, and measuring sensors raises another level of difficulty. This sort of system would be hard to design, differential expansion and contraction would be problems, monitoring and maintenance would be much more difficult, and leaks would be easy to detect but hard to locate precisely.

A light building would be of conventional construction. It would not be totally impervious and would resist only slight pressure differentials. These deficiencies are somewhat offset by the fact that the building itself provides some delay and dilution of released chlorine.

The conclusion in GEST 94/215 is that, if containment is necessary or justifiable, light containment is the preferred option.

Before deciding that containment is desirable, designers should carefully analyze the risks presented by the system and evaluate the consequences of likely accidents. This evaluation should include analysis of operating and emergency procedures and consider possible enhancements to existing safety systems. The total risk can be reduced by

1. reducing the probability of accidents
2. limiting the amount of chlorine released if an accident occurs
3. providing distance between the plant and populated areas, roads, and railways.

Several techniques can be used in any combination to limit consequences:

1. establish good emergency procedures
2. train personnel thoroughly
3. reduce the inventory of liquid chlorine in pipes and vessels
4. provide fast isolation by installing remotely controlled valves at strategic points (GEST 87/130)
5. install detectors with alarms, especially in areas not frequently visited
6. install water curtains (Section 16.4.3.2)
7. provide dump tanks or expanse tanks to allow rapid draining of some chlorine in case of a leak and to capture vapor released through pressure-relief devices
8. contain the plant.

Containment is thus one of a battery of possible techniques and should be considered as such.

In particular, the advantages and disadvantages of containment in a light building should be evaluated against those that apply to conventional outdoor storage. The list that follows is taken from Section 3 of GEST 94/215.

Outdoor storage

1. Advantages

- Visual or olfactory detection of leaks permitting early intervention
- Fast and accurate location of leaks
- Easy access permitting more efficient logistical support and greater mobility if heavy protection equipment is required
- Easier detection of substantial leaks, permitting fast intervention to limit the duration of the leak, to seal the leak, or to isolate it by manual valve(s)
- Dispersion of gaseous clouds by the wind, making intervention easier
- Easy access for inspection, operation, and maintenance

2. Disadvantages

- Very small leaks may not be noticed and may slowly increase as a result of corrosion
- More difficult for sensors to detect leaks
- Equipment requires regular maintenance to prevent external corrosion
- Dispersion of released chlorine into the atmosphere
- No recovery of discharged chlorine

3. Means of reducing disadvantages

- Regular plant patrols
- Well-prepared emergency plans
- Roof to provide shelter from bad weather
- Devices for collecting gas emissions and delivering them to an absorber
- Devices for isolating leaking parts and depressurizing or draining them
- Distance between storage tank(s) and residences
- Use of detectors between plant and any vulnerable residential area
- Use of water curtain to delay and dilute gas cloud or foam to limit the evaporation of liquid

Indoor storage

1. Advantages

- Easy and early detection by sensors of even very small leaks
- Easy collection of leaks for delivery to absorber
- Weather protection
- Possibility of increasing pressure to increase rate of transfer to users by heating the building (of limited effectiveness with insulated tanks, and rate of vaporization is also greater if a leak occurs)

- Easier clean and water-free maintenance of catch basins
 - Easier physical protection against external aggression or unfortunate intervention by unauthorized persons
2. Disadvantages
- Cost
 - Strict procedures complicating access for inspection, operation, and maintenance, increasing risk of poor detection of faults and improper maneuvers by operators
 - Lack of space for easy inspection and maintenance
 - Dangerous atmosphere as a result of even the slightest leak
 - Difficulty in locating leak when chlorine gas makes air opaque
 - Psychological barrier created by hostile environment
 - Heavy equipment required for leak intervention because of high concentration
 - ◆ difficult intervention and delayed action as a result of need to use heavy equipment in a small space
 - ◆ worsening of leak and increase in amount discharged as a result of delay
 - ◆ impossibility of machine access for handling and delivery of heavy equipment, leading to design of building to allow some dismantling to create access
 - Long time required to restore healthy atmosphere to building
 - No direct visual or oral communication with outside during intervention
3. Means of reducing disadvantages
- Local alarm indicating dangerous concentration in the building
 - Specific entry procedures
 - Well-established intervention procedures
 - Thorough training of personnel in procedures and use of protective equipment
 - Isolation systems remotely controlled from outside building
 - Optional large flow of ventilation air to speed up purification of atmosphere
 - Unit adapted to constraints of a plant in a building to facilitate entry and intervention

Building design should conform to all local codes and regulations. In particular, it should resist earthquakes. Resistance to projectiles caused by explosion is a debatable point; in particular, resistance to falling aircraft usually is not deemed worthwhile because of the extremely low probability of damage from this cause. Increased attention to the possibility of sabotage may modify these conclusions.

A catch basin should be part of the design. This will collect any spill of liquid and reduce its surface area, reducing the rate of vaporization. Buildings also may be compartmented to separate certain functions. The various functions of storage, loading and unloading, pumping, and evaporation present different degrees of hazard and may justify different design criteria. Operating equipment and valving systems, for example, may require more frequent attention than static tanks. They also occupy smaller volumes.

The design therefore might provide separate access and more intensive ventilation for certain operations.

The building, while designed to allow necessary access, should be kept small. This reduces the size of the ventilation system required or, with a given capacity, increases the intensity of the ventilation. The capacity of the system should in all cases be greater than the maximum rate of flow of chlorine that must be handled. The major criteria for design otherwise are the timely removal of chlorine to the absorption system and the rate of return to a healthy atmosphere after a release. Drawing ventilation air in at the top of the building and removing contaminated air near floor level facilitate the latter. The combined ventilation/absorption system should be designed to cope with the worst-case scenario. The maximum rate and the maximum total emission may belong to different scenarios. Sizing should reflect the facts that the building provides some dilution and that the rate of chlorine release or vaporization tends to decrease with time.

9.1.8.3. Piping Systems

9.1.8.3A. Classes and Specifications. The Chlorine Institute (P6) divides metallic piping services into six classes depending on whether liquid chlorine is or may be present and on the minimum temperature which may be encountered. Thus, Classes I, II, and III are for gas only and are rated for full vacuum and pressures up to 1,034 kPa (150 psig). Classes IV, V, and VI are suitable for liquid or liquid/gas mixtures and are rated for vacuum and 2,068 kPa (300 psig). The maximum design service temperature in all classes is 149°C. Minimum temperatures are -29°C for Classes I and IV, -46°C for Classes II and V, and -101°C for Classes III and VI.

Standard carbon steels, such as A105 and A106 Grade B are acceptable in Classes I and IV. Below -29°C, these steels become brittle, and so the other classes require low-temperature resistance. The common austenitic stainless steels are good in this regard but are subject to chloride stress-corrosion cracking, especially in the presence of moisture at ambient and higher temperatures. The choice therefore is made from the low-temperature carbon steels, with impact testing at the minimum design temperature. Even at certain temperatures above -29°C, Class V material is recommended when there is a likelihood of thermal shock or liquid hammer.

Pamphlet 6 and other industry guidelines deal with the requirements specific to chlorine service. All general good practices relating to pressure piping design, fabrication, welding, and inspection [67] should be incorporated into a piping specification.

Some plants, in certain applications, use jacketed pipe when handling liquid chlorine in order to improve its containment. Other features of Category M piping design also appear in various systems. The chlor-alkali industry as a whole has not adopted such elaborate designs. Since a single exposure to a very small quantity of chlorine does not cause irreversible harm, it is not a fixed requirement. Furthermore, Category M design would preclude the use of some of the industry's standard safety features.

While the material of construction for all classes is substantially carbon steel, the grades best suited to the different components of a piping system vary widely. Pamphlet 6 contains extensive tables of this information.

The Euro Chlor guidelines for liquid chlorine piping (GEST 79/81) recognize two temperature ranges: -10 to 120°C and -40 to 120°C. The upper limit is a maximum

service temperature, not a design temperature as in the Chlorine Institute version. The lower limits correspond fairly well to the limits for Classes II and V. There is no formal equivalent to Class VI in the Euro Chlor scheme, but there is a statement permitting temperatures lower than -40°C when impact testing is carried out at those temperatures. GEST 79/81 also contains an appendix listing French, British, German, UNI, and US standards for pipe, flanges, fittings, fasteners, plate, forged and cast parts, and welding consumables.

Neither Euro Chlor nor the Chlorine Institute encourages the use of expansion joints in liquid piping. The layout should include enough bends, loops, and offsets to take up thermal expansion and contraction and keep excessive stress off the piping and connections. Even in gas-phase piping, only Class I includes a provision for expansion joints. Metal bellows of Monel 400 or R405 or Hastelloy C or C276 are favored. Section 8.4.1.1A discusses the use of expansion joints, including those of alternative designs, in chlorine gas headers.

Velocities should be limited to 2 m s^{-1} in liquid lines and 4 m s^{-1} in gas-phase lines where entrainment is likely. More conservative design, to achieve low pressure drop or reduce the potential for erosion even further, is counterproductive when it substantially increases the liquid inventory in the piping system.

Supports for liquid piping require insulation. Wood blocks are frequently used; the wood should be selected to avoid acid corrosion of the piping. Pipe hangers are also common. Liquid chlorine piping should never hang from other piping or be used as a support for other piping. Hangers should have secondary backup to support the piping should a hanger break. The loads to be considered in designing supports include gravity (weight of piping, insulation, and contained chlorine), pressure, thermal expansion and contraction, wind, snow and ice, seismic forces, reaction forces from discharge or two-phase flow, and liquid hammer.

Nonferrous metal pipe and tubing are used mostly for flexible connections to instruments. Because of the reactivity of chlorine, the choice of material of construction is limited. Monel and copper are most widely used. Preferred grades are type B165 Monel, cold-drawn and annealed, and type B88 copper, seamless and annealed (Type K or heavier). Gasketed joints are preferred to flared fittings, and high-grade silver brazing alloys ($>44\%$ Ag, no Sn) are recommended. Certain plants use other alloys such as Hastelloy C-276 and Alloy 20.

Nonmetallic pipe and tubing can be used with chlorine gas under less demanding temperature and pressure conditions. Owing to the brittleness caused by their reaction with chlorine, hydrocarbon polymers are useful only under highly restricted conditions. Halogenated plastics are preferred, and the most difficult applications are reserved to the fluorinated polymers. Section 8.4.1.1A discussed chlorine piping in cell rooms. Table 9.8 lists the plastic materials used in chlorine gas service. Pressure is limited to 40 kPa. Screwed piping connections are sometimes used in the smaller sizes; these should all be Schedule 80. Solvent-welded piping sometimes is Schedule 40. CPVC piping is in all cases solvent-welded. Chlorinated polymers are the most widely used. Their lack of mechanical strength at high temperature and brittleness at low temperature limit their application. Particularly in the case of PVC, mechanical strength limitations are eased by reinforcement with FRP. Low-temperature limits are about -5°C for PVC and 0°C for CPVC.

TABLE 9.8. Plastics in Chlorine Gas Piping Systems

Plastic	Specification	Max. Temp., °C	Uses
PVC	ASTM D1784	54	Pipe, fittings, tube fittings, valve parts
CPVC	ASTM D1784	100	Pipe, fittings, valve parts
ABS	ASTM D3965	66	Pipe, fittings, tube fittings, valve parts
FRP	Special resins (see Chapter 8)	100	Cell covers, ductwork, cell gas headers
PE	ASTM D3350	54	Tubing, valve parts
PP		54	Tube fittings, valve parts

Plastics are sometimes used as liners in liquid chlorine piping. This application generally is restricted to the fluoropolymers. PTFE is serviceable up to 200°C, but it is permeable to chlorine at all temperatures and highly so in the upper range. Other perfluorinated types are serviceable at very low temperatures and less permeable than PTFE. PVDF is brittle below -40°C and is subject to stress cracking by Cl₂. It can be specified as “atomic chlorine resistant.” Fluoropolymers appear in valve parts, tube fittings, gaskets, packing, instrument tubing, unloading hoses, and solid piping. Their use should be approached with caution, and specification should be by a designer or supplier with direct experience in their use with chlorine.

Installation of plastic piping requires special attention to support. Problems include gradual bending due to plastic flow under the weight of the filled pipe, embrittlement by chlorine, and environmental degradation. Flexible lines require large radii of curvature to minimize stress on the plastic material.

9.1.8.3B. Valves. Selection of valves for chlorine service should be a careful and painstaking process. While many types of valve may be found suitable and safe in operation, the user should also take advantage of the screening work done by Euro Chlor and the Chlorine Institute. Euro Chlor (GEST 86/128,129) has an official procedure for homologation of valves, and those that have shown their compliance can be positively recommended. Lists of these valves have been published and are available on the Euro Chlor website. The Chlorine Institute has gathered members' experience and published tables showing which types of valve are suitable for the various piping service classes (P6). Summarizing tables are below, following brief discussions of the various types of valve that might be considered.

Globe valves provide tight shut-off in both directions without trapping liquid in cavities. Their multi-turn operation can prevent accidental or too-rapid opening and closing, and stem position gives a positive indication of valve position. However, the quarter-turn characteristic of most of the other types of valve gives an inherently more reliable stem seal. Seating can involve a PTFE insert for soft seating or Stellite hard-facing for good metal-to-metal contact. The valve stem should be blowout-proof, and special care should be taken to avoid leakage from the stuffing box. Should this occur, even at very low rates, the stem will corrode from contact with moisture in the air. Monel and Hastelloy C stems therefore give longer service than ferrous-metal stems. For best results, a bellows seal or an extended stuffing box packed with flexible graphite or PTFE should be chosen (GEST 89/140).

Ball valves also provide tight shut-off, along with less resistance to flow. The latter is especially true when full-bore valves are used. Again, blowout-proof stem design is essential, and there should be means for external adjustment of the stem seal. Fluoropolymers are the standard materials for sealing material. It is possible for a standard ball valve to trap liquid in the ball and body cavity when closed. This must have a way to relieve in the direction of higher line pressure to avoid damage by thermal expansion of the liquid. Designs include a relief hole in the ball, a passage in the body, and self-relieving seats. When one of the first two methods is used, valves must carry positive indication of intended flow direction. The valve should also carry a warning tag if it is possible to reverse the arrangement by improper assembly. Single-segmented ball valves do not trap liquid, but it is more difficult to obtain tight shut-off than it is with the conventional type. These valves therefore find their primary use as control valves.

Plug valves have the same major characteristics as ball valves but are generally harder to operate. Their design involves a balance between turning torque and shut-off capability. They usually have reduced bores and so higher flow resistance than ball valves. They also can trap liquid when closed, and the precautions listed above for ball valves apply to plug valves as well.

Butterfly valves can provide tight shut-off when soft seats are used, and their major application in chlorine service is in the larger pipe sizes. The usual design features standard adjustable packing, a wetted shaft/disc arrangement, and a one-piece soft-lip seal. Fully lined butterfly valves have lower pressure ratings and are suited only for gas applications. Fluoropolymer resin liners cover all internal surfaces. Back-up liners, not exposed to the chlorine, provide seats. Butterfly valves can provide tight shut-off with quarter-turn operation. Like the other types of valve, they should have blowout-proof stems.

Tables 9.9((a) through (c)), which follow, summarize Chlorine Institute recommendations. They are taken from Tables 4-1 through 4-7 of Pamphlet 6. Certain threaded valves are permitted in small sizes. Except for connections to transport equipment, instruments, and special process equipment, flanged valves are preferred in piping classes II, III, V, and VI. In the tables, S denotes satisfactory service, NR denotes "not recommended," and a dash denotes the lack of sufficient experience to support classification (as of December 1998).

9.1.8.3C. Gaskets. Historically, asbestos has been the nearly universal choice for gasketing under all but the most extreme conditions. It is an ideal material for the service, but with growing restrictions on the use of asbestos, other materials are now being used more widely. The Chlorine Institute has issued a test protocol for gaskets in chlorine piping systems (Appendix A of Pamphlet 95). Table 9.10 gives a recent update of available experience, with the first published results for Classes III and VI. The materials listed are considered acceptable by their historical use or have been tested according to the CI protocol for certain applications.

Hannesen [6] points out that the choice of gasket material depends on the type of flange face in use. With raised-face flanges, he names aramid fiber as a possible replacement for asbestos in dry chlorine service. With liquid chlorine, aramid should be confined by a metal envelope. With tongue-and-groove flanges, metal-reinforced

TABLE 9.9. Valves for Chlorine Service. (a) Globe valves; (b) Ball or Plug Valves; (c) Butterfly Valves.

Size, NB	End Connection	Form and Rating	CI Piping Service Class					
			I	II	III	IV	V	VI
(a) Globe valves								
To 40	Thread	Forged Class 800	S	S	NR	S	NR	NR
	Socket weld	Forged Class 800	S	S	NR	S	S	NR
All	Flange	Forged or cast Class 150/300	S	S	S	S	S	S
	Butt weld	Forged or cast Class 150/300	S	S	S	S	S	S
(b) Ball and plug valves								
To 40	Thread	Forged or cast Class 150/300	S	S	NR	S	NR	NR
All	Flange	Forged or cast Class 150/300	S	S	S	S	S	S
(c) Butterfly valves								
All	High-performance	Plate or cast* Class 150 or 300	S	S	-	S	S	-
All	Fully lined	Cast; Class 150	S	-	NR	NR	NR	NR

With permission of The Chlorine Institute, Inc.

graphite and filled PTFE may be suitable in gas service. In liquid service, aramid fiber is added to the list.

Gasket materials in wet chlorine service usually are PTFE, EPDM, or Viton. Styrene-butadiene rubber is still in service but largely has been replaced by more resistant materials. Filled and expanded PTFE products usually are preferred to virgin sheet stock because of their lower porosity and better resistance to cold flow. EPDM and Viton are used primarily with plastic or full-faced metal flanges. A standard warning with Grade 2 titanium in wet chlorine service is that crevice corrosion occurs at low pH in stagnant areas around gaskets. This was especially a problem with virgin PTFE, because of its porosity.

Wet chlorine gas, that is to say gas at low pressure, does not require tongue-and-groove flanges and can be confined by soft PVC and most of the common elastomers. Some polymeric gaskets require steel reinforcement, and some develop protective layers of chlorinated polymer.

9.1.8.4. Transfer of Liquid Chlorine

9.1.8.4A. Pressurization. The simplest way to transfer chlorine, in gas or liquid phase, is to have it flow under its own vapor pressure. This method is constrained by the temperature of the liquid, which in certain systems may vary seasonally. If transfer

TABLE 9.10. Gasket Materials for Dry Chlorine Service

Mfr	Type of Gasket	Piping service class				Test temperature, °C	
		I	II	IV	V	Min.	Max.
	Asbestos, compressed (Fed. Spec. HH-P 46E)	U	U	U	U	-73	
	Chemical lead (2-4% Sb) ^a	U	U	U	U		
	Spiral-wound Monel/PTFE	U	UK	U	UK		
	Virgin PTFE (unfilled and unexpanded)	U	U	U	U		
	Lead ^a	U	UK	U	UK		
A	Garlock Gylon 3510 ^b	U	U	U	U		
B	Duralon 9000	U	U*	U	U*	-40	121
C	GORE-TEX GR	U	UK	U	UK	-18	38
D	Inertex SQ-S	U	U	U	U	-46	16
A	Garlock Graphonic ^c	U	UK	U	UK	-18	149
E	Tex-O-Lon	U	UK	U	UK	-7	132
F	Flexitallic Sigma 500	U	UK	U	UK	-7	7
C	GORE-TEX TriGuard	U	U*	U	U*	-43	4

^a Should not be used in Class VI service

^b Tested for service in Classes III and VI up to 38°C and down to -68°C

^c Graphite with Hastelloy C276

U used or tested

UK status unknown

U* users should check for service restrictions

Note: Key to manufacturers: A, Garlock Sealing Technologies, Inc.; B, GRI Durabla Canada Ltd.; C, W. L. Gore and Associates, Inc.; D, Inertech, Inc.; E, Plastomer Products, Inc.; F, Flexitallic LLP.

Source: Adapted with permission of The Chlorine Institute, Inc. The Chlorine Institute does not approve, rate, certify, or endorse any gasket used in chlorine service. Users should refer to test results (obtained from gasket manufacturer or Chlorine Institute) before deciding on the use of a gasket.

is from the gas phase, the temperature and pressure will also depend on the extent and perhaps the rate of withdrawal. Transfer from the gas phase also allows nitrogen trichloride to concentrate in the remaining liquid. These disadvantages are overcome by adding an inert gas, under higher pressure, to the tank. Transfer then is from the liquid phase, and a vaporizer (Section 9.1.8.7) becomes necessary when a gas supply is desired. Transfer by inert gas pressure is simple and eliminates the mechanical problems of pumping or compression of chlorine. The gas is usually air and sometimes nitrogen. Section 12.5 discusses its generation and supply. Figure 9.32 shows a specially designed and prefabricated air padding system that includes compression, drying, and safety systems. It delivers about $23.8 \text{ Nm}^3 \text{ hr}^{-1}$ at 900 kPa with a dew point of -40°C or lower. The unit shown measures less than 2 m in all dimensions and has the advantage that the padding air supply is independent of all other sources. The control system maintains a minimum differential of 35 kPa between the vapor space and the delivery pressure. Power consumption at maximum pressure and rate is about 7.5 kW.

The major drawback of air padding is that, after a transfer, the operator is confronted with a vessel full of a mixture of chlorine vapor and noncondensable gas at a pressure at least 1.5–2 bar above the normal operating level (GEST 78/74). Disposal of this gas is usually by venting through a scrubber. Displacing liquid by adding chlorine gas rather

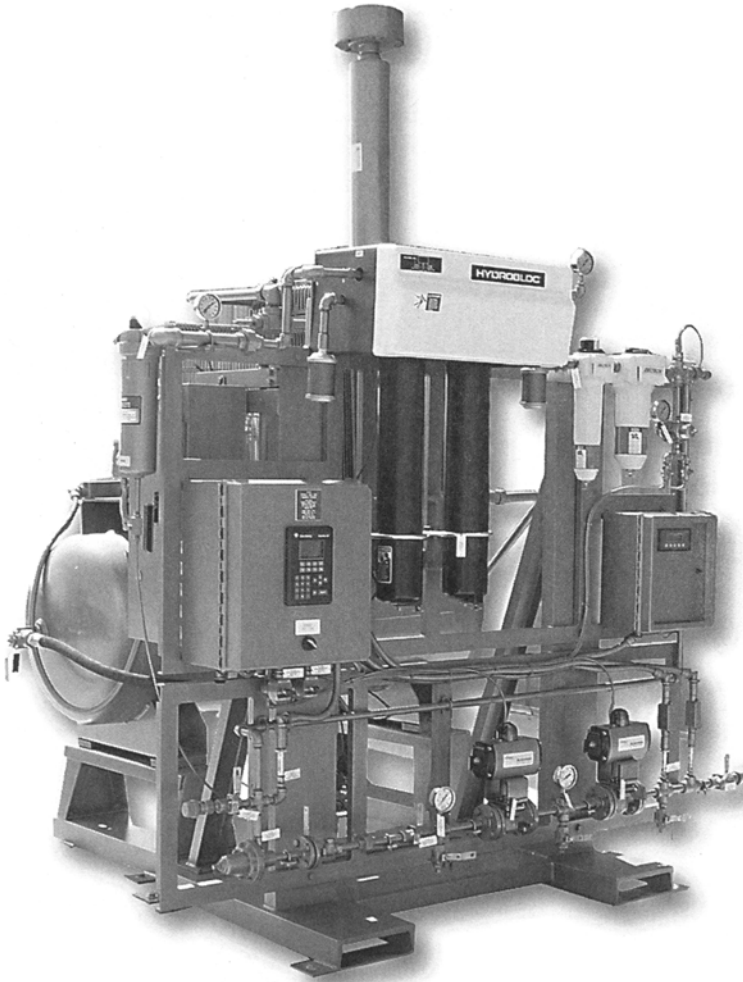


FIGURE 9.32. Packaged air padding system (with permission of Powell Fabrication and Manufacturing, Inc.).

than an inert eliminates the latter problem. The best approach technically is to raise the gas displaced from the receiving vessel to a higher pressure by compression and return it to the vessel being emptied. Compressors, described in Section 9.1.6.2, usually are of the reciprocating or diaphragm type.

Figure 9.33 shows a typical arrangement (GEST 79/79) designed to overcome the various hazards of chlorine compression. The operating temperature limitations referred to in Section 9.1.6.2 apply here as well. When the chlorine used as padding gas is already under pressure, the compression ratio usually will be low enough to avoid the hazardous region. Instrumentation deemed essential in GEST 79/79 includes pressure gauges on both sides of the compressor and a high-temperature shutdown switch on the

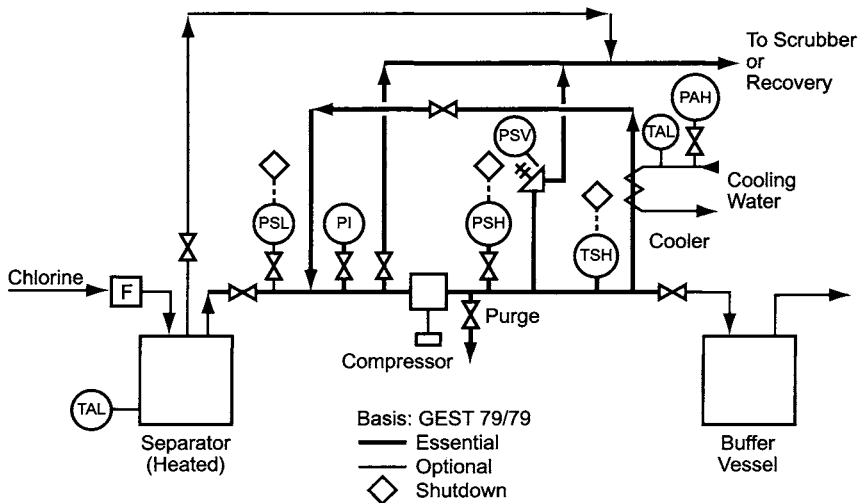


FIGURE 9.33. Chlorine transfer compressor safety systems (with permission of Euro Chlor).

outlet. The outlet pressure instrumentation should include a high-pressure shutdown. There must also be an automatic pressure relief to chlorine recovery or absorption on the outlet line and a manual vent on the inlet line. Optional features include a filter when there is any danger of the presence of solids in the chlorine supply, a low-pressure compressor shutdown switch, and a heated separation chamber. The last item is held above the boiling point of chlorine at the compressor suction pressure and is designed to vaporize entrained liquid. This too should be connected to the system vent. The bypass around the compressor permits startup of the machine. Should a bypass be required during normal operation, this line should include a cooling system. Finally, not shown on the drawing are pulsation/vibration dampeners. The need for these depends on the characteristics of the compressor.

Those using this method of transfer must ensure that no moisture enters the system and that the chlorine intended as a padding gas does not condense in the receiver. The latter could result in overfilling the vessel.

The pressure rating of a chlorine transfer tank must take into account the presence of the padding gas at its maximum pressure and the effects of thermal expansion of the liquid when the tank is closed. Conversely, the padding pressure should be chosen with the design or relieving pressure of the tank in mind. Chlorine Institute Drawing #201 shows the total pressure that can be put on a tank containing chlorine at its allowable filling density as a function of temperature. Two curves are shown, covering two different set relief pressures and assuming a maximum temperature of 105°F(40.56°C). Figure 9.34 is a modification that shows the total allowable (gauge) pressure as percent of the relieving pressure for the same two cases.

9.1.8.4B. Pumping. The major hazard in pumping is the possibility of release of liquid chlorine. To a very large extent, this drives the system design. A fundamental question is how the suction of the pump will be attached to the stock tank. As a rule, designers

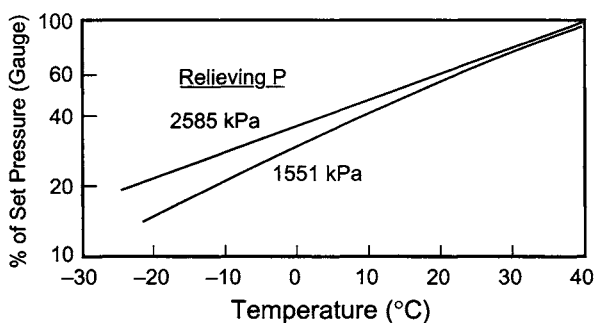


FIGURE 9.34. Allowable padding pressures on liquid chlorine.

of liquid chlorine systems avoid side and bottom connections to tanks. Top connections, being less susceptible to mechanical damage and less likely to leak or break, are usually preferred.

The ultimate simplification of the suction connection is to eliminate it with a submerged pump, and this is a very frequently used arrangement. The connection at the top of the tank then becomes a discharge line, and the pump mounting itself is another connection. These usually are grouped with others on a manway cover in order to reduce the number of penetrations of the vessel wall.

While long-shaft pumps with multiple stages usually are required, the pumping application itself is in no way extraordinary. Seal design, however, is quite specialized. Maintaining a differential pressure on the seal with dry air or nitrogen prevents leakage to the atmosphere. As in similar applications, the dew point of the sealing gas must be very low. The standard arrangement depends on a pair of differential-pressure cells, both referenced to the vessel pressure. Gas enters the outboard side through one cell. The second cell maintains a backpressure on the lower (vessel) side of the seal, so that any leakage is into the vessel. In a producing plant, seal gas then flows to the liquefiers through pressure-equalizing lines. These pumps generally offer limited turndown. Many effluent lines therefore include a pressure-relief bypass/return to the pump tank.

Another problem with submerged pumps is the amount of chlorine that cannot be removed from the tank by pumping. First, the pump and its inlet must ride some distance above the bottom of the tank. Second, suction head requirements prevent pumping down to the pump inlet level. When emptying a tank, operators must first rely on removing the last of the liquid through a dip pipe. This might be under the influence of the liquid's vapor pressure or with the aid of a dry gas pad. Complete removal of chlorine to allow maintenance or tank entry always requires evacuation or gas displacement to remove the vapor and the last traces of liquid.

The inability to remove all the chlorine in routine operation reduces the useful storage capacity of a tank and increases the minimum inventory. The latter is important when trying to reduce the consequences of the worst-case accident scenario. Installing a suction inducer to reduce the required net positive suction head or adding a pump well or "boot" to the tank can reduce the liquid heel left by a pump. The former can reduce the suction head requirement from nearly 2 m to something less than 0.5 m. The latter allows the pump to be placed below the bottom of the cylindrical portion of the tank. This adds to the complexity of the tank and may require its elevation to be

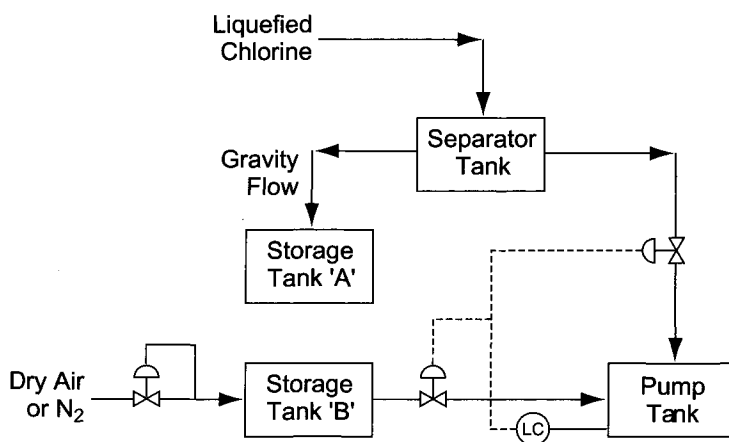


FIGURE 9.35. Use of separator tank with external pump tank.

higher. The added welding and the extra stress placed on the boot also work against this approach.

Excess flow valves are standard additions to pump discharge lines. These prevent too rapid discharge of chlorine if the line leaks or even breaks. The rising-ball design is a standard, illustrated by Chlorine Institute Drawing No. 101.

One method for external pumping from top-outlet tanks, shown in Fig. 9.35, depends on an elevated separator tank and a separate pump tank [68]. The pump tank contains a submerged pump but is considerably smaller than a storage tank. The pump shaft is correspondingly shorter. With this arrangement, the liquefaction product goes to the separator tank, from which the liquid can flow by gravity to the pump tank or a (larger) storage tank. The pump tank delivers chlorine to users by downstream control, according to demand. Liquid makeup to the pump tank is on level control, and excess production overflows from an elevated nozzle on the separator tank into the chosen storage tank. Separator, pump, and storage tanks all are equalized with the process to permit gravity flow. The separator tank must be mounted at a sufficient height above the pump tank to overcome the resistance of the level control valve. When chlorine production is less than the pumping rate, the level in the pump tank falls, and liquid must be withdrawn from storage. In order to allow this, a second storage tank is brought into play. This contains liquid chlorine held above the process pressure by a dry air or nitrogen pad. When the level in the pump tank begins to fall off, the level controller (a split-range instrument) opens a second control valve communicating with the pressurized storage tank. More chlorine enters the pump tank to meet the demand. This method still relies on gas padding, and the gas eventually must be removed from the storage system. In this case, however, the amount of gas to be handled is much less than in the standard case where the volume of gas is at least as great as the total volume of liquid chlorine transferred. To provide for continuous operation while venting, at least a third storage tank is necessary.

Another alternative to the submerged pump in the storage tank is a submerged pump in a much smaller tank connected to the large tank by a top-connected suction line [69]. This removes the necessity of taking the large storage tank out of service

for pump maintenance. It adds the disadvantages of increased plot area and the need to operate a siphon. The latter can require a high flow rate to prevent accumulation of bubbles and eventual failure. Turndown therefore is limited. This approach also can reduce investment cost when the small pump tank serves more than one storage tank. However, this latter technique complicates the piping and, more importantly, aggravates the hazard by adding a number of connections and valves.

The principal hazard of true external pumping with conventional horizontal pumps would be leakage from the seals. This is usually avoided by the use of canned pumps. These have no external seals, and leakage from the pump is eliminated so long as the body is sound. These pumps are compact and, particularly in smaller facilities, have been included in designs with bottom outlets on tanks and in confined spaces. The pumped fluid cools the pump and its bearings. Accomplishing this requires both a minimum flow through the pump itself and also a flow through the bearings and into the upper part of the pump casing.

A final variation is particularly useful with low-pressure storage in spheres or other large tanks. Using a top connection raises the problems of priming and sometimes insufficient suction head. The use of an internal eductor and recycle of some of the pump output relieves the second problem. This is a relatively low cost way to obtain the benefits of external pumping without a bottom connection. Its disadvantages include the fact that priming is still necessary and the higher operating cost associated with pumping much of the chlorine more than once.

9.1.8.5. Loading and Unloading. Loading and unloading requirements are quite similar in principle. The loading organization has several added responsibilities in checking the tankers, valves, and manways and in ensuring that neither the weight of chlorine loaded nor any applied padding pressure is excessive. Some of the other requirements may be more burdensome for a receiving organization without a sizable staff expert in chlorine safety. It is vital, however, for all safety precautions to be observed.

Recommendations for unloading and loading of road and rail tankers are contained, respectively, in GEST 78/73 and 78/74, which also provide checklists for inspection and operation. Many features are common to the two operations. For example, the location of the facility should be level, as close as practicable to the source of chlorine (loading) or the receiving equipment (unloading). It should also be well lit, adequately separated from other traffic, and accessible from at least two sides. The facility and operation should be covered in the site emergency plan.

The chlorine-containing vehicle (road or rail tanker or ISO container) should be protected from other vehicles and should be incapable of uncontrolled movement. The methods for achieving these goals depend on the type of vehicle used. Railcars can be protected by movable buffers and derauling devices or by locked switches that keep a line dedicated to chlorine transfer. On a through track, derailleurs should be placed on both sides at a distance of about 15 m. With road tankers, the barrel should move forward only; if the motive source is to be removed, drop legs should be strong enough to support a full load and should have provision for locking them into place before the connection is broken.

An outdoor location is normally preferred because of the complications associated with enclosed systems (Section 9.1.8.2C). However, a roof is a useful feature for

protection of equipment as well as protection and convenience of personnel. Access should be easy and the platform large enough for easy movement by an operator in full gear or with an air-supplied respirator. Stairs are preferred to ladders. With more than one transfer point or more than five meters between the connection and the main access point, there should also be a second exit. The loading/unloading system is best located away from danger of fire, traffic, falling objects, etc.

Piping should be of drawn (weld-free) or ERW carbon steel and should follow the recommendations of Section 9.1.8.3A. Welds should be radiographed where possible, and joints that can not be radiographed should be tested for dye penetration. The recommended pressure rating is 40 bar. The design temperature should be about -40°C , which implies the use of fine-grain weldable steels. Piping should be sized for velocities of no more than 2 m s^{-1} , and bends should have radii equal to at least 1.5 times the diameter of the pipe.

Valves should meet the design requirements given above and should conform to the practices recommended in Section 9.1.8.3b, P6, GEST 93/180 (ball valves), and GEST 89/140 and 90/150 (globe valves).

Tujague [70] suggested specific improvements beyond what has been normal practice. These include providing an enclosure for the delivery vehicle, support for the unloading hose, and design of the piping supports for seismic zone four.

Loading and unloading operations require protection against release of chlorine while the mobile container is attached to the storage system. Connection of the loading or unloading point to the vehicle should be by an articulated arm 25–50 mm in diameter. GEST 75/44 gives recommended design features. Connections to process or tankage should be through flexible hoses that conform to Appendix A of Pamphlet 6 and to GEST 75/45. These should have fail-safe automatic valves on both sides. Any sections of the liquid transfer line that can be blocked in by two closed valves should be protected by expansion chambers (Section 9.1.10.4). There should also be some means of detecting movement of the mobile container and a switch to shut the operation down before this can cause a release. Figure 9.36, based on the use of a dry padding gas to unload the vehicle, shows a typical arrangement (P57). The system should include at least two manual shutdown switches in different locations remote from the main control panel. Some installations use trip wires that break if the vehicle moves more than a certain amount. Breaking the wire breaks a circuit and causes the valves to close. In other systems, the instrument air tubing intentionally is shorter than the flexible hose used for transfer. The air supply therefore fails before a hose connection can break, again causing the valves to close. A similar arrangement that depends on an electronic signal uses a mirror mounted on the vehicle directly under a photocell. If the vehicle moves and the reflected signal disappears, the shutdown system activates.

Transfer hoses should have bursting pressures not less than five times the maximum relief device setting on the connected tank. Minimum design pressures are 2,586 kPa (375 psig) for rail or road tanker service and 2,086 kPa (300 psig) for barge service (P6). Other characteristics of metal hoses should be:

1. one continuous length, kept to a practical minimum for the installation
2. seamless or butt-welded tube of Monel 400, with annular corrugations

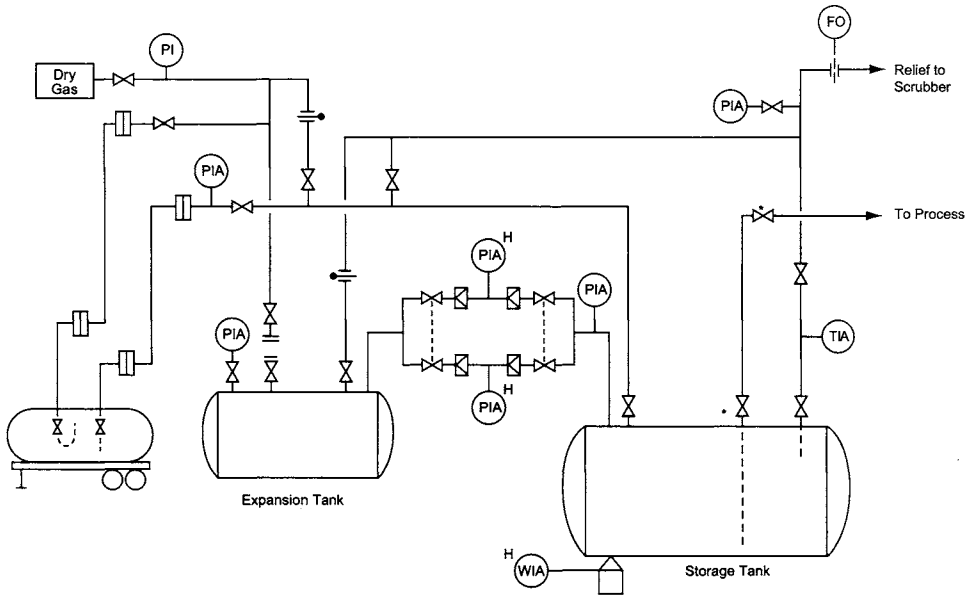


FIGURE 9.36. Air-pad unloading of chlorine (with permission of The Chlorine Institute, Inc.).

3. Schedule 80 pipe nipples permanently attached to both ends; flanges may be welded, brazed, or threaded to nipples
4. hexagonal wrench pads of steel or malleable iron with minimum width of 25 mm welded to pipe nipples or integral parts of end fittings
5. welding to proper code (Appendix A of Pamphlet 6)
6. protection by Type 304 stainless steel spiral guard or Type 302 casing for full length of hose (other means of protection acceptable if properly engineered and permanently attached to the assembly).

Nonmetallic hoses also are acceptable with the proviso that they be used only when ventilation is adequate for their degree of permeability. They should be used only at temperatures above -35°C . The same design pressures apply, along with points (1), (3), and (4) from the list above. Hoses should be of virgin PTFE. They may be of smooth bore or have annular or helical corrugations. PTFE-impregnated fiberglass can be used for reinforcement. Stainless steel reinforcement is not acceptable (GEST 78/74). A hose should also have a structural layer braid of PVDF monofilament or a structural braid of Hastelloy C-276. The braid is to be permanently attached at both ends with Monel or Hastelloy C-276 to provide a positive braid lock. Nonmetallic hoses also require chafe protection. This may take the form of a PVDF braid or a chlorosulfonated polyethylene jacket along the full length of the hose. Jackets should be pricked to allow escape of any gas that permeates the hose.

Hoses should be used only as temporary connections and should be regarded as nonrepairable. Corrosion, leakage, fraying, deformation, and ballooning or bunching of

the braid are reasons for replacing hoses. They should be inspected at least every 2 years. Inspection of metallic hoses should include visual examination and a hydrostatic test at 1.5 times the maximum pressure to which the hose is subjected in service. Proper support of the hose is essential during testing. Proper installation also is critical. Installation of any hose should be in one plane only. Compound bends induce torque and are not acceptable. The allowable bend radius of each hose should be determined by the manufacturer and indicated by tagging. The minimum bend radius should be no more than 300 mm, and there should be at least a 25-mm differential between the minimum bend radius of the outer casing and that of the inner hose. When servicing a fixed location, one end of the hose can be left in place. An idle hose should be protected against atmospheric moisture by plugging, capping, or valving of the open end. The best arrangement is to allow the hose to hang vertically when not in service. This minimizes bending stress. Often, the use of an elbow at the container connection can reduce the amount of bending required.

The discussion above follows the Chlorine Institute recommendations. Some suppliers and consumers use other types of hose successfully. The designer or user must establish that the type of hose to be used, its installation, and the operating procedures are in fact suitable for the service. Pamphlet 6 contains other details that should be reviewed before adopting transfer by flexible hose.

The Chlorine Institute (P93) also describes a pneumatically operated valve (POV) for use on chlorine tank cars. This is a dual assembly including an angle globe valve with external bellows seal and a spring-loaded ball check valve. The main features of the POV that distinguish it from the standard manual angle valve are:

1. the stem does not rotate, and packing is eliminated
2. the stem moves down to open and up to close
3. the POV can be operated from a remote location
4. the check valve does not depend on differential pressure for its seal.

The fourth item eliminates the need for the usual excess flow valve. This design lends itself to use in an automatic shutdown system and is compatible with the example described below.

Loading and unloading operations are special cases of liquid transfer, which is the subject of the preceding Section 9.1.8.4. Safety is the paramount concern. Qualified personnel should attend both operations at all times. The hazards added to those incidental to the handling of chlorine include the need to make and break connections to equipment or lines that contain chlorine and the need to secure vehicles before and after operation.

Control-panel graphics should be easy to understand, and the controls should be arranged in a way that helps the operator through the loading or unloading sequence. These precautions are observed in the tank car loading system described by Burelle and Bourgeois [71]. Many of the features are applicable to road tankers as well. This system also includes chlorine sensors immediately below the loading spot and in the surrounding area. When activated, these shut down the transfer operation and close all valves. Switches on the loading line also shut the operation down if the pressure is unusually high or low. Interlocking of the valves prevents operation in the wrong sequence. Operators must complete three levels of training and be recertified every three years.

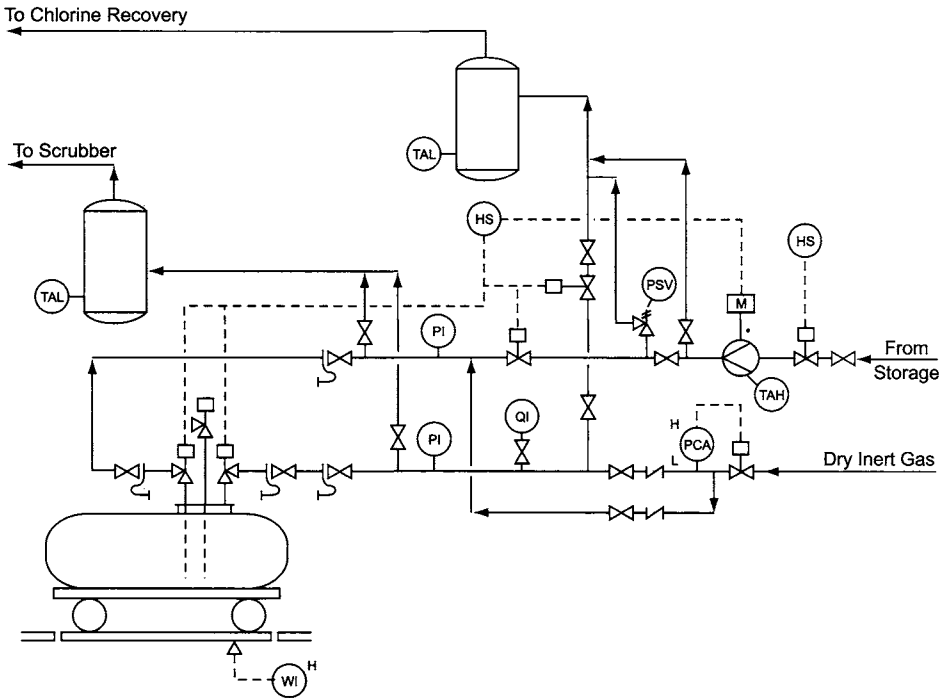


FIGURE 9.37. Chlorine tankcar loading (with permission of Euro Chlor).

Figure 9.37 shows a tank car loading operation that relies on a pump. The scheme is that of Appendix 2 of GEST 78/74. Pumping, discussed in Section 9.1.8.4B, is an option in all cases and is necessary when chlorine is stored at low pressure. The tanker itself should be on a level spot, and its lateral movement should be prevented. Lighting is important for nighttime operation and emergency situations. Emergency lighting should be provided as backup. There should also be clear indication that the tanker is in fact being filled. In Fig. 9.37, a weighing system with high alarm provides this indication. The maximum filling density of 1.25 recommended for storage tanks also applies to transport containers. The three principal methods for determining the amount of chlorine actually loaded are

1. loading into a vehicle on a weighbridge
2. weighing from storage
3. volumetric displacement from storage.

The first method is preferred, and the maximum gross weight should be based on the original tare weight of the vehicle. The second and third are acceptable only if the gross weight is checked before departure from the plant. Final precautions before shipping include leak testing, reinstallation of blank flanges, and checking of labels. Whether loading is controlled by weight or by measurement of the volume loaded, it is important to be aware of the presence of liquid chlorine in the tanker before loading begins. Unless

this is known quantitatively or the tanker is emptied on site before loading, weighing from the pump tank or loading by volume is not acceptable. In any case, emptying a container returned to the plant with residual chlorine is good practice and should be omitted only in special circumstances and with accurate knowledge of the history of the container.

The venting arrangement is an integral part of a loading or unloading system. Figure 9.37 shows a connection at the pump and two at the loading spot, near the flexible connections. Each vent line contains a trap with liquid detection to keep liquid out of the vent scrubber and chlorine recovery systems.

The organization responsible for unloading must take care to avoid the entry of moisture and the exposure of chlorine to hydrogen or other reactive materials. Inert gas, if used for pressurization, must have a dew point no higher than -40°C . The gas pressure should be 1.5–2 bar above that of the receiver and should be vented off before disconnecting. For transfer by pressurizing with compressed chlorine, the system and operating procedures should be designed to exclude moisture, and the operators should be aware of the possibility and hazard of condensing the compressed chlorine in a cold container. Most often, chlorine is unloaded into a storage facility; sometimes, it is unloaded directly into the process. The latter procedure obviously adds hazards to the operation. These should be weighed against the hazards of multiple transfers and additional equipment that are involved in intermediate storage. In all circumstances, keeping the unloading time to a minimum enhances safety.

While nitrogen gas generated from the liquid is suitable as a padding gas, the volumes required when pressurization is the primary method of transfer favor the use of compressed air. Design of an air compression system should recognize that the pressure developed by the compressor must be greater than the pressure in the vehicle, which in turn is greater than the pressure at the point of delivery. Pressure-swing regeneration of the air dryers also requires higher compressor and dryer throughput, as given by Eq. (12.7). Padding air ideally should come from an independent dedicated compressor (P49), as in Fig. 9.36 or the packaged system shown in Fig. 9.32. The air supplied for container padding should meet the requirements of Section 12.5.2.1. The quantity needed to unload a vehicle filled to the standard density of 1.25 is given approximately by

$$V = 2.4W(\Pi - P^0)/T \quad (75)$$

where

V = volume of air required, Nm^3

W = weight of chlorine unloaded, t

Π = total pressure on the vehicle, kPa

P^0 = vapor pressure of chlorine, kPa

T = temperature, K

This allows for the initial application of the pad to the vapor space as well as displacement of the liquid from the vessel. The padding gas flow rate during continuous transfer is approximately

$$Q = 2750(\Pi - P^0)/\rho T \quad (76)$$

where

Q = padding gas flow rate, $\text{Nm}^3 \text{t}^{-1}$ of liquid chlorine

Π = total pressure on the vehicle, kPa

P^0 = vapor pressure of chlorine, kPa

ρ = liquid density, kg m^{-3}

T = temperature, K

Note that about 0.4% of the amount transferred as liquid chlorine becomes vapor in the empty vessel.

Example. We wish to unload chlorine at a rate of 15 t hr^{-1} into a system held at 275 kPa (gauge). The chlorine in the tanker is at 265°K , where its vapor pressure is 170 kPa(g). We assume pressures of 400 kPa in the padded vapor space of the tanker and 450 kPa at the compressor outlet. The air flow to the tanker, by Eq. (76), is

$$\begin{aligned} Q &= 2750 (400 - 170)/(1415 \times 265) = 1.7 \text{ Nm}^3 \text{ t}^{-1} \text{ chlorine} \\ &= 25.3 \text{ Nm}^3 \text{ hr}^{-1} \end{aligned}$$

The use of the liquid temperature (265 K) to represent the vapor space as well adds a bit of conservatism. Eq. (12.7) gives the amount of dry air consumed in dryer regeneration in a pressure-swing system as about

$$P = 12,000/450 = 26.7\%$$

The compressor therefore must deliver about $25.3/0.733 = 35 \text{ Nm}^3 \text{ hr}^{-1}$ of air at 450 kPa.

The volumetric flow rate of liquid chlorine is $10.6 \text{ m}^3 \text{ hr}^{-1}$. To keep the velocity below 2 m s^{-1} , this requires a line diameter of 43 mm. Schedule 80 50-mm pipe will serve this purpose.

9.1.8.6. Transportation and Packaging. Bulk transport of chlorine may be by road, rail, or barge. Associated hazards and the methods for dealing with them vary, but in any case transportation of chlorine is closely regulated. The regulations vary from one authority to another, but national codes generally are consistent with the United Nations Recommendations on the Transport of Dangerous Goods. Regulations are aimed primarily at prevention of hazardous releases, but they also specify the labeling of containers to warn the public and inform emergency personnel of the contents. Figure 9.38 shows a typical example [72]. The placards can carry the usual hazard codes. Most of the other markings have to do with construction, testing, and the carrying capacity of the tank car. Chlorine is universally classified as a poison gas. Subsidiary classifications deal with its corrosivity and its oxidizing power. The United Nations identification for chlorine is U.N. 1017.

Common carriers bear the primary responsibility for their cargoes. However, prudence and Responsible Care[®] (Section 16.4.2.6) require a chlorine producer to be closely involved with all shipping agents and to share information and training resources. Mobile containers must be fabricated correctly to prevent or withstand damage. They require valves for loading and unloading; these are particularly susceptible

to damage, and their housing and protection are critical. Both the Chlorine Institute and Euro Chlor require valve protection. Protection should include a substantial cover, which can be a dome over externally mounted valves or a recessed housing inside the barrel. The cover should be secure in case of accident but must not damage the barrel with the forces generated in the accident. Similarly, it should not be allowed to slam closed (thus protecting both the barrel and the operator). Piping design should minimize the potential for damage by a falling cover [36]. All valves must be clearly labeled as vapor- or liquid-phase connections. Standard valves have double seals. One type, for example, provides a secondary internal closure. There are two sections:

1. an internal disc below the valve plate, with automatic closure;
2. a standard valve, remotely operated, fixed to the valve plate.

The Chlorine Institute has also cooperated in the development of a pressure relief device for chlorine transport service (Section 9.1.10.2). The Institute recommends its use on transport containers. With Euro Chlor (GEST 73/20, 80/89), pressure relief valves are “emphatically not recommended.”

Minimum design temperature is -35°C , and the design test pressure is 22 kg cm^{-2} ($\sim 2160\text{ kPa}$). The material of choice is nonalloyed fine-grain steel. In design calculations, the ultimate tensile strength at rupture (UTS) may not be assigned a value greater than $57\text{--}60\text{ kg mm}^{-2}$. The minimum elongation, expressed in percent, is $1,000/\text{UTS}$. A preferred value is $1,150/\text{UTS}$, corresponding to a value of 20% when $\text{UTS} = 57.5$. The thickness of the ends should be at least as great as that of the barrel. Only one manhole is permitted, with a diameter no larger than 500 mm. The manhole cover should contain all the other nozzles.

Chlorine transport wagons usually are not externally insulated. Such insulation, particularly if wet, can be a source of corrosion, and it impedes inspection. The standard containers therefore are double-walled vessels with insulation between the two bodies.

Releases of chlorine due to accidents en route can quickly go beyond the capabilities of train crews, drivers, and local emergency teams. Skilled help with specific training is available in the industry. The Chlorine Institute and Euro Chlor both have emergency response plans. The Chlorine Institute operates the Chlorine Emergency Plan (CHLOREP), in which teams from chlorine producers, packagers, and users are available to handle real or potential releases of chlorine. The United States and Canada provide dispatch agencies for general transportation emergencies. These agencies, the Chemical Transportation Emergency Center (CHEMTREC) in the United States and the Canadian Transport Emergency Centre (CANUTEC), will automatically activate CHLOREP.

9.1.8.6A. Rail Transport. Two aspects of importance in rail transport are the marshalling of tankers in freight yards or other handling areas and the make-up of trains. In order to avoid damage by impact, there should be no gravity shunts and no freewheeling of chlorine tankers. Some local regulations forbid the combination of chlorine and a flammable gas on the same train; some require barrier cars between chlorine and explosives, inflammables, the engine, and the brake van (GEST 80/89).

Car size depends on customer capability, rail gauge, and any restrictions on allowable axle weight. Local codes and regulations cover other aspects of design. These have

evolved over the years to take advantage of better materials and fabrication techniques. In North America, cars classified as 105A300-W or 105A500-W have been used for many years. Newer cars are being fabricated to 105J300 or 105J500 (P 66), and the older designs are being replaced. Safety systems that are emphasized include thermal protection, insulation, puncture resistance, and vertical restraint of couplers. The specification calls for at least 100 mm of prescribed insulation with a steel jacket at least 3 mm thick. P66 covers all this in detail and furnishes checklists for inspection and transfer operations.

9.1.8.6B. Road Transport. Transport by road is more common in Europe than in North America. Euro Chlor (GEST 96/221) gives design recommendations for road tankers, covering fabrication, welding, heat treatment, and inspection. Recommended appurtenances include side and rear barrel guards, side and end underrun guards, and a full rear bumper. Valves should be pneumatically operated (GEST 75/46) with facility for independent manual isolation, and they should be protected from mechanical damage. The valves should be interlocked with the parking brakes. It should be impossible to open the valves unless the brakes are set and impossible to release the brakes while any valve remains open.

GEST 73/20 sets out the procedures to follow during transportation. Particular importance should be put on the selection and training of drivers. Assignment of drivers to chlorine transport operations should not be a haphazard procedure; all drivers should be fully qualified. Medical checks are important, and each driver, in addition to the physical skills required by the types of vehicle used, should demonstrate maturity, judgment, and the ability to assume responsibility and act independently when necessary. Training should cover the properties and characteristics of chlorine; the hazards involved in loading, transportation, and unloading; the use of safety equipment; and the procedures to follow in case of an accident. Training also should cover the types of safety equipment carried on board the vehicle. In addition to that required by national highway regulations, this equipment should include respiratory protection devices, first aid and chlorine emergency equipment, and mobile phones.

The producer or shipper should supply drivers with standard accident report forms. For each journey, a route should be chosen that reduces the risks and in particular avoids areas of high population density when that is possible. Weather is another important factor, and chlorine should not be transported when weather conditions are unsuitable.

Drivers should park vehicles in safe locations, away from hazards such as falling objects and fire hazards. Should a vehicle be exposed to fire, it should be moved away as quickly as possible. Failing this, it should be cooled by a spray of water to avoid heating to the point of chlorine/steel combustion. Water, on the other hand, should never be used on a chlorine leak, because it will cause rapid corrosion. If a leak develops during transit, the vehicle should be taken to a remote spot and one of the emergency response organizations informed. The driver should on no account leave the vehicle unattended.

Drivers' pay scales should not in any way encourage violation of safety practices or short cuts around standard procedures. Vehicles should have tachographs to record speeds and distances traveled.

The Chlorine Institute (P49) gives similar advice and a list of tests and inspections. Pamphlet 49 also shows typical engineering certifications of the automatic shutoff

systems that must stop flow within twenty seconds of loss of connection to a receiver. In the United States, this is a requirement of Title 49, Code of Federal Regulations, Part 173.315 (n)(2), designated 49 CFR 173.315 (n)(2)

9.1.8.6C. Barge Transport. This book does not consider the handling of chlorine in barges, which is a specialized and relatively infrequent operation, in any detail. There is some barge traffic in North America but very little in most other parts of the world. The hazards of chlorine and the techniques involved in its handling are much the same as in transport by road or rail. They are, however, influenced by the scale of operation. Inland chlorine barges can be 60 m long and carry up to 1,200 t of chlorine in multiple tanks. Other barges can carry caustic and other products as well as chlorine. In this arrangement, chlorine tanks ride on the deck with other products stored in holds.

The Coast Guards of Canada and the United States, each with its own added requirements, regulate barge transport of chlorine (P79). There is not yet a Coast Guard-defined procedure for emergency response plans, but training is covered in 29 CFR 1910.120. This also covers emergency procedures, clean-up activities, and the use of personal protective equipment. Protective equipment is also the subject of CI Pamphlet 65 and 29 CFR 1910.132–134.

Two special characteristics are the marine hazards and the separation between the barge and the source or destination. First, all standard marine safety procedures must be added to those connected with chlorine. For instance, anyone present on the deck of a barge should wear a flotation device, except perhaps when working in an area fully protected by handrails. Second, while operations on shore and on the vessel should be closely coordinated, there should be separate individuals in charge of each location. The person in charge on the vessel will have primary authority during the transfer operation. Pamphlet 79 summarizes US Coast Guard regulations for inspection, personal protective equipment, surveillance, labeling, and emergency equipment. The last category includes acoustic underwater location devices in case a barge should sink. The Chlorine Institute deploys detectors in several locations for the industry's use.

9.1.8.6D. Accident Statistics. GEST 90/159B presents transport accident statistics in the Euro Chlor countries over the 40-year period 1950–1990. They cover transport in small containers as well as bulk transport by road and rail. Pipeline transfer and transport by barge are not common techniques in Europe. Table 9.11 summarizes the findings.

About 70% of the chlorine released in bulk transport accidents resulted from damage to valves with no internal sealing mechanism. Such valves are not acceptable under today's standards. The worst accident occurred on a crowded wharf, when a ton container slid into another and broke a bronze cap screwed into the bottom of the second container. This accounted for the fatalities noted above, and 129 persons were hospitalized for chlorine exposure. This bottom-cap arrangement also is no longer allowed.

GEST 90/159B also analyzes a number of other accidents and assesses their causes. Table 9.12 summarizes the incidents that resulted in releases of chlorine. Rail accidents involved 90 wagons in 28 derailments and 17 collisions. None resulted in punctures; there were two incidents, attributed to NCl_3 decomposition, in which barrels were distorted. Causes of derailment were shunting errors, defective switches, broken axles, and

TABLE 9.11. Euro Chlor Transport Incident Statistics 1950–1990

Transport mode	Number of incidents	Containers involved	Number of tons leaked	Largest Release, t
Rail				
No leak	50	99	–	–
Leak	17	17	21.5	15.5
Road				
No leak	18	18	–	–
Leak	5	5	15	10
Small containers				
No leak	7	39	–	–
Leak ^a	18	25	10.2	6.4

Note: ^aFour fatalities

Source: With permission of Euro Chlor

TABLE 9.12. Incidents Involving Release of Chlorine

Locus and cause	Rail tankers	Road tankers	Small containers
Valve			
Impact	2	1	1
Defective seal	7	0	2
Defective connection	8	3	0
Manhole lid			
Defective gasket	2	0	N/A
Container			
Impact puncture	0	1	5
Explosion in fire	0	0	8
Corrosion	0	0	9

Source: With permission of Euro Chlor

vandalism. Two derailments were the cause of valve damage and the release of large amounts of chlorine. Both occurred over 30 years ago, and the valves, as noted above, did not conform to modern standards.

Most road transport accidents involved vehicles going off the road; only about 25% involved collisions.

Finally, we should note that Tables 9.11 and 9.12 do not give an accurate picture of current safety performance. Most of the incidents reported occurred in the earlier years. One can expect that, when similar lists are published summarizing performance between 1990 and 2030, there will be fewer incidents to report.

9.1.8.6E. Packaging. The act of packaging of chlorine is itself a rather simple operation. The best method is to load by weight a container placed on scales. The container and its connections should be checked for leaks each time it is loaded. This can be done by charging a small amount of chlorine to a partly evacuated container and then testing the container and joints with an ammonia bottle. After testing, the container can be fully evacuated and then filled with chlorine to the proper weight. All due safety precautions

must be observed throughout the process. Mason [73] describes, among other operations, the filling of drums or ton containers. An empty drum is placed on a scale after venting or evacuation. After reading or setting the tare weight of the drum, the operator connects filling and venting hoses. The next step is pressure testing of the connections, and this is followed by filling the drum to the desired net weight. While straightforward, this procedure involves a number of operator actions and decisions. Its safety can be enhanced by computerization. Some of the steps taken by the computer are:

1. accept identification of container
2. check tare weight against recorded value and reject if in disagreement
3. calculate final gross weight and set alarms for “nearly full” and “full”
4. prompt operator to connect drum
5. verify connections made
6. start fill
7. shut down when correct weight is reached
8. prompt operator’s sequence for disconnection
9. activate emergency shutdown when unsafe condition arises

The Chlorine Institute’s Pamphlet 17 is a detailed document covering many aspects of the facilities, equipment, and techniques used in packaging chlorine. Housekeeping is a constant theme.

Pamphlet 17 covers construction of cylinders and ton containers. This essentially follows general standards; the pamphlet lists those that apply in North America. “Ton” containers may have capacity for a standard US (short) ton or a metric ton. The diameter is the same (~762 mm) in either case. The metric ton container is about 18 cm longer and 30–60 kg heavier, and it is equipped with four rather than three fusible plugs on each end.

The pamphlet also gives detailed instructions for inspection, cleaning, drying, repair, and disposal of containers. It contains illustrations of the various types of corrosion and gives criteria for rejection and condemnation of cylinders. A rejected cylinder can be repaired or rebuilt and, after certification, used again in chlorine service. A condemned cylinder must be physically destroyed and disposed of.

The Chlorine Institute provides emergency kits for repair of cylinders (Kit A) and ton containers (Kit B) and for temporary containment of leaks. Users should ensure that their containers are compatible with these kits. When a leaking cylinder cannot be repaired, it should be enclosed in a leakproof recovery vessel and returned to the supplier. CI Drawing 188 (issue 2, 1993) shows such a vessel.

Facility design also should follow Pamphlet 17 and local codes. Structures should be fire-resistant, and no flammable materials should be kept in the building unless separated from chlorine by firewalls. There should be at least two exits from each area where chlorine is stored or handled and at least two stairways or ladders at each platform. Emergency egress routes should be clearly and prominently marked and kept clear at all times. Many facilities use chlorine monitors to detect any release of chlorine (P73). Ventilation requirements are site-specific but should follow best industry practices [74]. Respiratory protective equipment should be in ample supply. This should meet all governmental requirements; it is covered in Section 16.2.1.3.

All filling stations and valving areas must be clean and dry. These are not storage areas; containers should be filled or maintained and then moved promptly. Scales and surrounding areas should be kept clean at all times. Scales require regular calibration, which is to be carefully documented. The greatest hazard is overfilling of the containers.

Storage can be indoors or outdoors. The storage area should be clearly posted. When storage is indoors, the entrance to the building also should be posted. Things to avoid when storing chlorine containers include:

1. external corrosion; cylinders should be placed on platforms rather than exposed to standing water
2. below-grade storage
3. flames and intense heat
4. falling objects
5. vehicular traffic
6. commingling with containers of other materials
7. mixing of empty with filled containers
8. entry to area or handling of containers by unauthorized persons
9. unprotected cylinder valves

The containers must be constructed to local codes, which include specifications on materials and dimensions of containers. The codes usually dictate the markings that must be stamped onto the containers. In the United States, these are in 49 CFR 178. The Chlorine Institute recommends including the tare weight in the markings.

9.1.8.7. Vaporization. Laboratories and other consumers of very small quantities of gaseous chlorine often can operate by withdrawing vapor from a cylinder. When operation is intermittent, chlorine can flow at fairly high flow rates for short periods of time. The heat of vaporization is supplied by the remaining liquid, which grows colder as the operation continues. So long as there is enough time between withdrawals, the contents can return to ambient temperature and the process can repeat. Sustainable flow rates are much lower. A ton container operating against a positive pressure of 100 kPa at an ambient temperature of 21°C can provide a bit more than 0.1 kg min⁻¹. A 68-kg cylinder can supply only one fifth this rate. For higher rates, some users connect cylinders in manifold. This technique requires caution, because it creates the hazard of flow from warm cylinders into those that are colder, overfilling them to the point at which thermal expansion during shutdown may cause too high a pressure. Deliberately heating cylinders is poor practice and should not be tolerated in any operation.

When the demand for vapor is higher, apparatus designed for this purpose becomes necessary. This section discusses design and operation of such vaporizers. Not all plants operate vaporizers, but these units still account for a large fraction of the releases of chlorine that producers and users report. Vaporization is relatively a more frequent operation among users who do not produce chlorine. In many cases, vaporization becomes a batch operation, which lacking a steady state can be more hazardous. Many incidents have resulted from overloading a scrubber system with liquid [75]. The relative lack of experience and sophistication on the part of some operators may help to account for

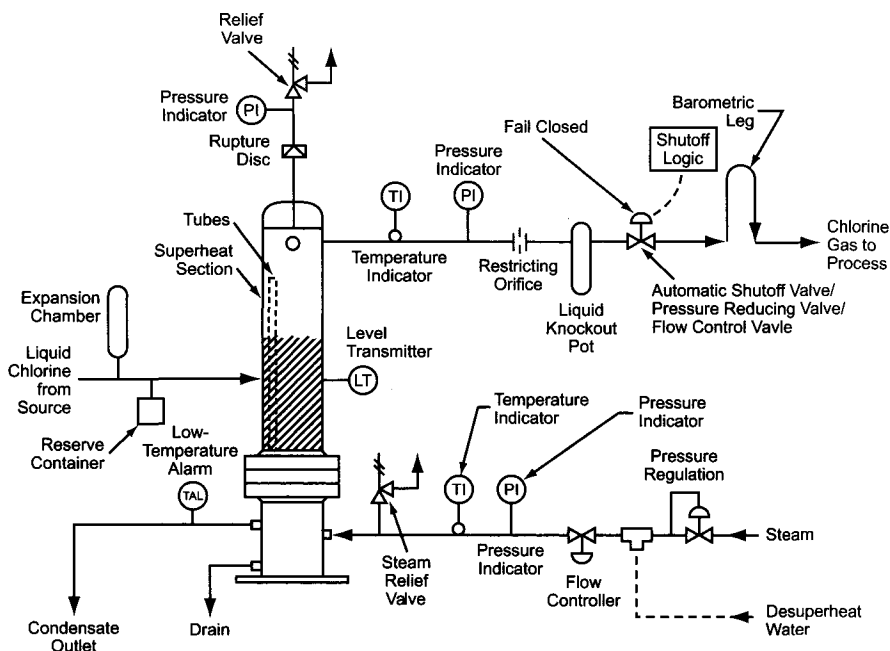


FIGURE 9.39. Chlorine vaporizer (with permission of The Chlorine Institute, Inc.).

this situation. Safety surveys, for example, sometimes show that users do not have current knowledge of the NCl_3 content of the chlorine they receive [76]. Both Euro Chlor (GEST 75/47) and the Chlorine Institute (Pamphlet 9) outline the necessary and desirable features of vaporization system design, and all operators should check their systems against these recommendations.

Vaporizer systems should be designed so that, within their heat-transfer capacity, the rate automatically adjusts to the process demand. The systems discussed here, such as the typical vaporizer in Fig. 9.39, meet this requirement. An increase in demand, for example, causes the line pressure to drop, leading to an increase in flow of liquid chlorine. The level in the vaporizer then goes up, increasing the area of active heat-transfer surface and therefore the rate of vaporization.

The vaporization of chlorine tends to be a small-scale process, usually less than 180 tpd (P9). The unit shown is a steam-heated vertical bayonet exchanger, and the drawing follows Typical Flow Schematic 3 of Pamphlet 9. This pamphlet shows a number of other arrangements, but the gas side is the same in all cases. The following paragraphs describe the functions of these devices.

The use of an overhead gas shutoff valve, as shown on this drawing, makes a pressure-relief valve necessary. A rupture disc may be placed beneath the relief valve, with some means of detecting the presence of chlorine between the two.

Pressure and temperature indicators provide useful process information and allow determination of the degree of superheat in the gas. The temperature connection may also be used as a control point (see next paragraph).

The restricting orifice and the liquid knockout pot both guard against entrainment of liquid chlorine, which might create a serious hazard in the process. The orifice, sometimes replaced by a flow control valve, limits the flow to no more than the vaporizing capacity and so helps to avoid entrainment. Other possible measures include a high-level shutdown on the vaporizer and gas temperature control or low-temperature shutdown. The knockout pot is the second line of defense.

The valve in the gas line behind the knockout pot shuts down the vaporizer when any of several hazardous events occur. The valve prevents too high a flow of gas, which should not be allowed to exceed the vaporizing capacity. This would lead to entrainment of liquid chlorine. The valve also can respond to a loss of energy input due to failure of the heating medium. With such functions, the valve should close upon loss of signal. It may also be useful to have a pressure-reducing valve in the line to stabilize the downstream pressure and incidentally to develop some superheat in the gas. When fitted with an actuator, this can also serve as the shutdown valve.

The barometric leg represents one way to prevent process material from flowing back into the vaporizer. The height of the leg should suit the density of the process fluid. When the process operates under pressure or when chlorine enters the process against a substantial head of process fluid, a barometric leg may be impractical. Other devices used include low-pressure shutdown systems, power-operated control valves, backpressure regulators, and vacuum breakers. Check valves are another possibility, but they are not widely recommended and must be used with discretion and with some assurance that they provide positive shutoff. A variation is the use of an automatic valve that shuts when the differential pressure between two points in the transfer line reverses, indicating the potential for backflow.

The feed line to the vaporizer contains an expansion chamber and a reserve container. The function of the latter is to allow continued operation while changing the source of chlorine, as for example from one cylinder to another. It is not always required. The expansion chamber is the standard apparatus protecting the line in case valves are closed at both ends (Section 9.1.10.4). Note that no valves appear in the feed line on the drawing. This allows backflow of chlorine to the source when necessary. Valves in the feed line should be strictly for purposes of isolation and maintenance. They should otherwise remain open as long as chlorine is in the vaporizer system. Pumping systems should provide a controlled constant-pressure supply to the vaporizer and should have a high-capacity bypass back to the source. The other common technique for providing delivery pressures above the vapor pressure of chlorine at storage temperature is gas padding, discussed in Section 9.1.8.4A. The gas used must be scrupulously dry and should be at the minimum pressure necessary. Those who specify vaporization systems should be aware that higher pressures increase the boiling point of chlorine in the vaporizer and may therefore reduce its capacity.

Figure 9.39 is only one of several approaches. Pamphlet 9 gives the advantages and disadvantages of several alternatives. All this is beyond the scope of this book, but the bayonet unit shown here strikes a good balance. One of the disadvantages listed is its relatively complex construction, but these units are available as high-quality engineered and fabricated units. The vertical exchanger, unless flooded, provides some superheat. While the amount of superheat is variable, the unit can be designed to meet some minimum specification. Often, there are process reasons that favor superheated vapor. Also, long

or uninsulated lines exposed to low temperature may need superheat in the gas to prevent condensation. In other cases, control elements are subject to freezing. A certain amount of superheat results simply from lowering the pressure of the chlorine after vaporization. This is limited by the danger of surging in the vaporizer when the pressure drop is too great.

Other methods for producing superheat include extending the tubes in the vaporizer and installing a separate heater. The former is compact and cheap but is technically inferior. The extended portion of the tubes must remain above the liquid level in the vaporizer in order to transfer sensible heat to the chlorine gas. This approach limits the achievable superheat, adds to the unproductive volume in the vaporizer, and makes control of the process more difficult. Control deteriorates because the low heat capacity of the gas means that a change in its temperature can represent a very small fraction of the total heat load.

When a vaporizer operates without control of the flow of steam or chlorine, the degree of superheat will be inversely related to the operating rate. In many cases, this is acceptable. When a higher level of superheat or good control of the gas temperature is necessary, external superheaters have the advantage. These allow separate and direct control of the temperature of the gas leaving the superheater. Kettle-type boilers, unlike the vertical exchangers considered here, do not provide superheat, and the second exchanger becomes a necessity rather than an option. This usually is mounted as a vertical unit on the outlet flange of the vaporizer.

Carbon steel is the standard material of construction for vaporizers. A grade appropriate to the design pressure and temperature must be used. Full-penetration welding is preferred, with all chlorine-side joints 100% radiographed. Post-weld heat treatment is necessary, and Pamphlet 9 recommends a corrosion allowance of at least 1/8" (3.2 mm).

A vaporizer is best kept close to the source of liquid chlorine. This keeps the feed line short and simple and reduces the liquid inventory in the system. The area chosen should be separate and clearly defined, with good access for emergency crews and a means of isolating the system from the rest of the plant. Siting should also minimize the probability of damage from fires and explosions in other units and from vehicles. Vehicular barriers are appropriate when the unit is close to a plant road.

High and low operating temperatures both are hazardous. In order to limit corrosion rates and reduce the probability of combustive reaction of chlorine and iron, 120°C is a recommended (P9) design temperature. Sub-zero temperatures, on the other hand, can freeze steam condensate or the water used to heat the chlorine. Chlorine boils at 0°C at 268 kPa; maintaining the pressure above this level prevents freezing due to boiling chlorine. Designers should also consider the possibility of atmospheric boiling of chlorine when pressure is released. As with chlorine storage equipment, this requires a design temperature of about -40°C and the use of low-temperature steels.

One of the hazards encountered in the operation of a vaporizer is the possible accumulation of nitrogen trichloride in the liquid phase. The hazards of nitrogen trichloride in general and the particular hazards associated with vaporizers are discussed in Section 9.1.11.2.

9.1.9. Handling of Liquefaction Tail Gas

The chlorine remaining in liquefaction tail gas is an intolerable emission. If recovered, it can be a useful economic asset, especially in the larger plants, and many processes have been considered or used for its recovery [77]. There are other sources of dilute chlorine

in most plants. These include:

1. vent gas from product loading
2. heels in returned tank cars and trucks
3. residual chlorine from chlorination reactions
4. air used to dechlorinate spent sulfuric acid
5. air used as a gas pad to transfer liquid chlorine
6. gas from evacuation of equipment and pipelines

Some smaller plants do not find it worthwhile to recover small quantities, and even in large plants it is necessary to provide a backup to any recovery process. The ultimate receptacle for residual chlorine then becomes a scrubber that removes it from the gas and converts it to the more easily handled hypochlorite. Section 9.1.10.3 discusses chlorine vent scrubbers.

The other options include enhanced recovery of elemental chlorine and its conversion to another product. We might include, under enhanced recovery, the addition of higher-severity stages to a liquefaction plant. While this is more correctly a reduction in the amount of chlorine present in the tail gas rather than its recovery, it is a viable retrofit technique and one that has been used to replace some of the older recovery plants. A unit quantity of refrigeration becomes more expensive, hydrate accumulation may be more troublesome, and some of the problems of deep liquefaction are exacerbated. These are the normal effects of extending the process, and they add nothing new to the technical discussion on liquefaction.

One technique for addition of a stage to handle relatively small amounts of gas is to compress it to a higher pressure and return it to a separate tube bundle in a liquefier that otherwise operates at lower pressure. Another option not yet in known commercial practice but which may appear in the future is to concentrate the chlorine by using gas-separation membranes [78]. The richer gas would return to a liquefier for additional recovery. This is discussed in Section 17.4.2.

Another technique is an absorption/stripping process in which the chlorine is absorbed in a solvent at high pressure and then recovered from solution by stripping at higher temperature and lower pressure. This is the subject of Section 9.1.9.1.

Several different products can be made by the reaction of chlorine in the tail gas. These include HCl (Section 9.1.9.2), bleach (Section 9.1.9.3), and ferric chloride (Section 9.1.9.4). The discussion ends with brief descriptions of other processes that have been used or considered (Section 9.1.9.5).

9.1.9.1. Absorption in Carbon Tetrachloride. Any liquid capable of dissolving chlorine could be used in an absorption/stripping process for its recovery. The ideal solvent would be one with reasonable physical properties so that it is easy to handle, of not too high a volatility, and with good solubility for chlorine without forming a highly corrosive solution or undergoing a chemical reaction that would make desorption difficult. Carbon tetrachloride was in many ways the best choice for the application.

Figure 9.40 outlines the process licensed by ELTECH Systems. Compressed gas at about 7 bar is cooled first with water and then with a refrigerant to -10 or -15°C . When this process follows a low-severity liquefaction system, this step alone can recover much of the chlorine. After removal of the liquid, the gas then passes up through an absorption column against cold CCl_4 . The noncondensable gases leave the absorption system under

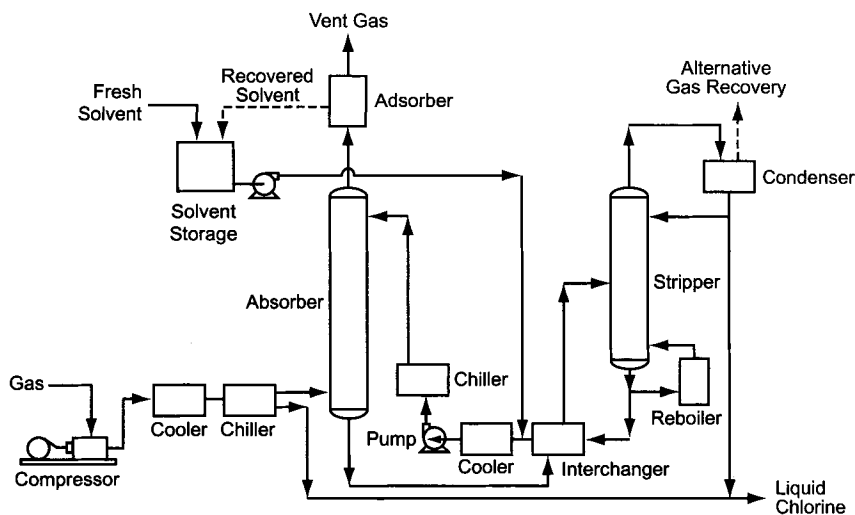


FIGURE 9.40. Recovery of chlorine from tail gas by absorption.

pressure control through the top of the column. Removal of the chlorine enriches the hydrogen in the gas, and usually this effect must be offset by adding dilution air.

The solution of chlorine in CCl_4 , now at a positive temperature, flows by its own pressure to a stripping column operating at 3–4 bar. A thermosiphon reboiler maintains the bottoms at about 130–135°C. The chlorine gas released in the stripper is scrubbed in the top section with liquid chlorine to remove traces of impurities and is then ready for use or recompression and another pass through liquefaction. The stripped solvent recycles to the absorber. The bottoms stream from the absorber and the stripper can be interchanged for heat economy. The lower part of the stripper and the tubes of its reboiler are Monel or Monel-clad. The rest of the absorber/stripper set is carbon steel.

The inert gases from the absorber are saturated with CCl_4 , which must be removed before they can be released. The standard technique for this is the use of regenerable activated carbon beds. Passing the gases through a bed in the adsorption mode removes the CCl_4 , and the adsorbed material is recovered by steaming out a bed in the recovery mode. This was a troublesome operation.

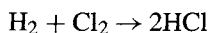
Approximate chemical and utility consumption in the recovery of a ton of chlorine was 12.5 kg CCl_4 , 600 kg steam (1,135 kPa(g)), 187 kW hr, and 67 m³ cooling water.

Several plants used this process to recover chlorine. In the Montreal Protocol of 1987, CCl_4 was listed as one of the substances whose use was to be phased out. No other solvent could be effectively substituted in existing equipment. Some of these recovery units have now been replaced by enhanced liquefaction systems, whose last stages operate at lower temperature and higher pressure than their first stages.

9.1.9.2. Production of Hydrochloric Acid. The production of HCl is an attractive option for many chlorine plants. It is a product useful to many chlorine customers and so can be a profitable part of the supplier's business. HCl can represent an upgrading

of hydrogen from fuel value and of chlorine from a depleted gas that has undergone partial liquefaction. Finally, HCl is a necessary part of many brine-treatment processes (Sections 7.5.5, 7.5.6), and there is a guaranteed internal use for a certain amount of acid. If the demand for HCl is sufficient and reliable, more chlorine than would normally be present in the tail gas can be consumed, and then the severity of the liquefaction process can be reduced.

The chemistry of HCl synthesis is simple:



The reaction is rapid and highly exothermic, producing about 22 kcal mol^{-1} HCl. The autoignition temperature is 300°C or higher, and the flame speed is about 4 m s^{-1} [79]. System design must therefore include an ignition system for startups and protection against “backfiring.” Many plants have operated with manual ignition, but modern designs include automatic ignition and sophisticated burner monitoring and control. Packed flame/explosion arresters prevent the propagation of flames beyond the limits of the synthesis system.

Figure 9.41 shows the essentials of the process. Hydrogen and chlorine enter the burner separately. In most cases in the chlor-alkali industry, chlorine is the wild stream and the flow of hydrogen is controlled to give the desired ratio. The chlorine flow may be variable, as from the end of a process. When HCl production volume is large or

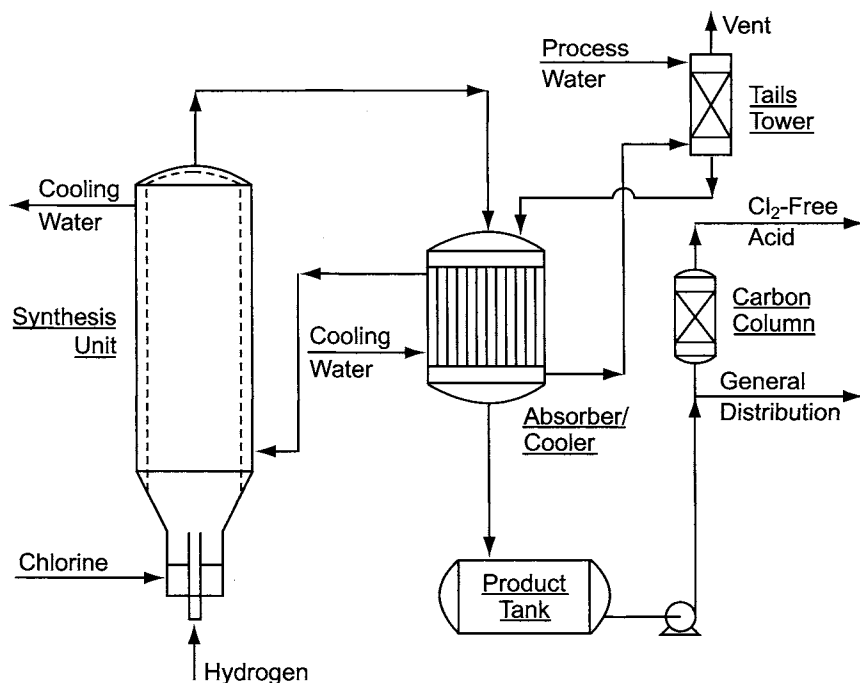


FIGURE 9.41. Hydrogen chloride synthesis process.

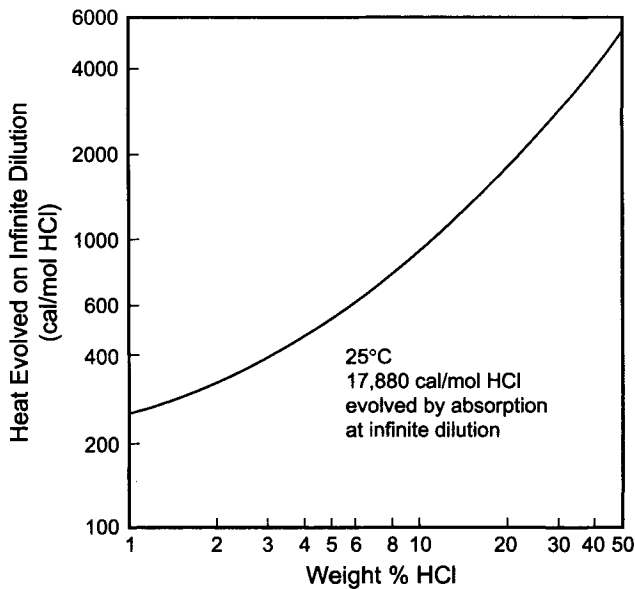


FIGURE 9.42. Heat effects in HCl absorption.

comprises a major part of plant output, chlorine may be withdrawn from a liquid supply through a vaporizer.

The synthesis unit in the flowsheet shows the upward flow of the gases. Commercial designs include both upflow and downflow. In the example shown, the gas leaves the first chamber at perhaps 1000°C and goes to a cocurrent-flow absorber/cooler. Absorption of the HCl into water releases another $12\text{--}15\text{ kcal gmol}^{-1}$ in addition to the heat of reaction. Figure 9.42 indirectly shows the heat of absorption of HCl. The plot shows the heat of dilution of HCl solution at various concentrations. The difference between the heat of absorption at infinite dilution ($17.88\text{ kcal mol}^{-1}\text{ HCl}$) and the value given by the curve is the heat of absorption of HCl gas into acid solution. When tail gas is used, the oxygen present also combines with hydrogen, producing yet another $58\text{--}68\text{ kcal gmol}^{-1}\text{ O}_2$, depending on the amount of water of combustion condensed in the process. Process and equipment design must consider the heat load, the high flame temperature ($>2,000^{\circ}\text{C}$), the corrosivity of the product, and the possibility of hydrogen-chlorine explosion (Section 9.1.11.1). The key to successful reactor design is the proper choice of materials of construction and the removal of heat as the reaction proceeds. Figure 9.41 assumes an efficient reactor design in which the combustion gases from a silica burner enter an absorption section. In the latter, an aqueous falling film of water absorbs the gas, and cooling water removes the heat. A suitable material of construction, combining corrosion resistance with high thermal conductivity, is impregnated carbon. In some designs, this is supplied as blocks that allow modular assembly of the synthesis unit. The blocks contain two sets of channels: radial passages for cooling water and shaped axial passages for the gas and absorbent. The cooling water from a block collects in a chamber at the inner or outer periphery and then passes through the next block in the opposite direction. External tie rods hold the stack of blocks together. Any type of

construction may be jacketed with steel to provide pressure resistance and protect against external impact.

Especially with the use of tail gas containing inert gases, not all the HCl may be absorbed in the synthesis/absorption column. After separation of the concentrated acid at the bottom of the column, the gas goes to a packed scrubber, the tails tower, where the absorbing water enters the process. The quality of this water must suit the specified purity of the product acid. The scrubber is elevated, and the dilute solution formed there overflows into the synthesis unit, where it acts as an absorbent. The liquid product emerges at the storage temperature; the rate of flow of process water into the system has fixed its strength.

For added security, vents from the tails tower and the product storage tank can be scrubbed with a caustic liquor. The acid solution itself will contain a small amount of dissolved chlorine. In most plant applications, as for example in the acidification of depleted brine, this is not a problem. Other uses, such as the regeneration of the brine softening resin in a membrane-cell plant, may require that this chlorine be removed. Adsorption on activated carbon is probably the simplest technique for this small-scale process, which is similar to that described in Section 7.5.9.3B.

In the standard HCl synthesis process, the flow rates of both streams are controlled. In tail gas recovery, the chlorine gas flow is usually not controlled. The tail gas flow is then metered, and the hydrogen is controlled to give the desired ratio. Operation with an excess (5–7%) of hydrogen ensures the complete reaction of chlorine. Depending on the source of chlorine, this may be enough to make the vent hazardous. In principle, either hydrogen or chlorine may be used in excess in order to ensure nearly complete reaction of the other component and to maintain reaction velocity. In practice, one would select as the excess reactant the less valuable material, the one less soluble in the product acid, the one less corrosive to the vent system, or the one less hazardous when released to the atmosphere. On each count, hydrogen would be favored. Since the hydrogen demand depends on the composition as well as the flow rate of the tail gas, the controls must compensate for any variation in the former. This can be done by maintaining an excess that is safe under reasonable circumstances or by adjusting for tail gas composition.

FRP is widely used for storage of HCl solutions. Hand layup and filament winding are suitable if the winding is not relied upon for corrosion resistance. The chopped strand usually is electrical borosilicate glass. FRP is also used as a wrapping for PVC or polypropylene. Large tanks are more likely to be rubber-lined steel. In their case, internal design should be simple and welds smooth. Some formulations require a steam cure, and this should be considered in setting the design temperature of the tank. In small tanks (<60 m³), crosslinked high-density polyethylene with heavy wall thickness is also serviceable.

Tanks are usually vertical, filled from the top, and vented at the highest point. The vent should be sized with care, especially in a receiving plant that uses compressed air unloading. The rush of air from a delivery vehicle that has just gone empty has been known to damage or destroy tanks (Section 16.3).

HCl storage should be separated from that of incompatible or reactive materials. Some form of spill containment is essential. This may be a double-walled tank, a sump, a dike, or a diversion basin. The volume provided for external containment should allow for dilution of the acid to reduce fuming.

The construction materials used for vessels are also suitable for pumps. Sealing is important, with double mechanical seals or the use of sealless pumps with magnetic drives preferred. Personnel-protection shields are appropriate, and the location of a pump should allow easy access for maintenance while minimizing the probability of exposure of personnel to any leaks. The pump should be protected against running while dry or against a closed discharge.

Lined steel piping is stronger and more rigid than the alternatives. It is therefore less susceptible to mechanical damage. The most frequently used linings are PP, TFE polymers, and PVDF. Problems associated with lined pipe are the precise requirements for spool length and the permeability of the linings. Each spool and fitting must have a full-length vent channel with a weep hole at its flange.

Other plastics used in solid piping for HCl are PVC, CPVC, PVDF, and PFA. FRP piping, usually of vinyl ester resin, also is frequently used. These materials are light and easy to install, and they have excellent resistance to external corrosion. They are also structurally the least rigid candidates and the most subject to mechanical damage. Piping runs also require extensive support. Because of the possibility of catastrophic failure, some operators prohibit the use of unreinforced solid thermoplastic pipe in HCl service. It therefore appears most often in small sections and in applications not requiring structural strength (e.g., vents). The weakness of this piping can be overcome at least to some extent by wrapping it with FRP.

Ball valves provide tight shut-off and minimum frictional resistance to flow when fully open. Steel-bodied valves are usually lined with PFA. Composite-body valves are used in FRP systems and are much lighter and easier to support. Plug valves also appear in HCl service. They offer few technical advantages over ball valves but often are cheaper. They require more torque in their operation, but this is not usually a major factor in the sizes found in a chlor-alkali plant.

Butterfly valves offer low differential pressure and easy throttling. Typical construction uses ductile iron bodies with PTFE or PFA lining. Discs are coated with the same material as are the bodies. Spacers may be necessary to allow discs to turn without obstruction; polypropylene is the usual choice of material.

The process can with modification also produce anhydrous HCl gas. Aqueous acid is produced as described above, in high concentration. The impurities in the gases pass through to the system vent. A pressurized stripper produces the anhydrous product, cooled to about -5°C at 150–350 kPa(g). The product is not bone-dry and is intended for use without further cooling or compression. The stripper bottoms stream is close to the azeotropic composition of about 20% HCl. After cooling, this is recycled to the aqueous HCl plant as an absorbent.

9.1.9.3. Production of Bleach. Production of bleaching compounds is one of the oldest applications of chlorine. These compounds include bleaching powder and sodium and calcium hypochlorites. In this section, we concentrate on sodium hypochlorite bleach. The active agent is NaOCl, in which the chlorine has a valence of +1. In reacting with a reduced species Red, it contributes oxygen to give the oxidized form Ox, with the chlorine reverting to the negative chloride ion:



Production of NaOCl is by the hydrolysis of chlorine in caustic soda solution. The reaction can be written



This is a natural application for liquefaction tail gas and other lean or intermittent chlorine vents. A bleach plant is a convenient receptacle for these streams, and so the topic is considered in this chapter. In other cases, bleach is the main product of an operation and is produced from commercial chlorine and caustic soda. A full discussion of these operations is in Section 15.3.2.

The reaction is quite exothermic, producing $1,463 \text{ kJ kg}^{-1}$ of chlorine gas. The in-process dilution of 50% NaOH to control the concentration of the product bleach can add $280\text{--}290 \text{ kJ kg}^{-1}$ to this number. Some reaction systems can operate with a liquid chlorine feed. Depending on the temperature of the liquid, this reduces the heat evolution by about 140 kJ kg^{-1} .

Prevention of hot spots and efficient removal of the heat of reaction are very important because of the thermal instability of hypochlorites. The continuing reaction of hypochlorite to form unwanted byproducts is part of the discussion of emergency vent scrubbers (Section 9.1.10.3A), where it is more of an issue. Here, we note that the production of high-quality bleach depends on a consistent supply of chlorine in the tail gas and on adequate temperature control. The absorbing solution is therefore circulated by titanium centrifugal pumps around the reactor(s) through titanium coolers, usually of the plate-and-frame type. The recirculation of liquor in itself provides turbulence in the reaction zone, and the volume of circulation determines the maximum temperature possible in the reactor. A gas feed or the vaporization of a liquid chlorine supply may also be used to promote turbulence.

The limits placed on the bleach temperature usually relate to the concentration of the product. A 6% solution of NaOCl, for example, might be limited to 30°C and a 15% solution to 20°C . Final cooling therefore is usually with chilled water. This may occur after removal from the reactor, where the retention time is short and standard cooling water may be used for temperature control. When packed-bed reactors are used, vent fans can help to overcome the gas-side pressure drop in the packing. These usually are of lined carbon steel. Epoxy linings are a frequent choice.

The percentage conversion of NaOH in a reactor is usually in the high 90s. The presence of unreacted caustic prevents overchlorination and provides product stability and process controllability. There has been a tendency to try to control the process by pH, but the best control is by redox potential, with in-line electrodes held in a fluorocarbon resin body [80].

One approach to bleach production in a chlor-alkali plant is to combine it with the emergency vent scrubber function by installing multiple towers in series. The duty of the first tower is to scrub chlorine from normal vent flows under controlled conditions. The temperature is limited to $30\text{--}40^\circ\text{C}$ by cooling a recirculating liquor stream around the tower. The flow rate is large enough to prevent excessive increase in liquor temperature in the tower. The chlorine flow assumed in setting the liquor recirculation rate is the sum

of normal flows and a reasonable maximum of intermittent flows. Typical streams in each class include:

Normal	Intermittent
Tail gas	Maintenance purges
Process/tank vents	Cell rebuilding process
Brine dechlorination	Cell startup gas
Spent H ₂ SO ₄ dechlorination	Packaging/storage vents
Dilution air	Container evacuation
End-box ventilation	

Unless liquefaction conditions are mild in order to produce a rich tail gas and a correspondingly greater quantity of bleach, the intermittent streams will probably contribute most of the design maximum chlorine load. The operating temperature therefore will vary and in the absence of intermittent flows will be lower than the specified maximum.

Various types of contacting devices used for the absorption of chlorine are discussed in Section 9.1.10.3B. Eductors are frequently used with low-pressure chlorine. Emergency vent scrubber columns usually are of lined carbon steel or a PVC/FRP composite. Internals may be rubber-coated or CPVC, and packing usually is ceramic, CPVC, or PVDF rings. Polypropylene is an alternative.

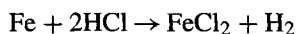
Since most other processes for the utilization of tail gas have a scrubber system as an emergency backup, a bleach plant can sometimes be installed for little incremental capital. Costs then are associated more with storage and shipping systems than with the reaction process.

The objective with batch supply of caustic will be depletion of the recirculating liquor to less than 1% NaOH. Small quantities of chlorine may pass through the first tower at maximum load, but these will be removed from the gas in the second tower. Under emergency venting conditions, the probability of breakthrough from the first tower increases, and the design maximum temperature for normal operation will be exceeded. Depending on the size and duration of the emergency vent, the quality of the batch of NaOCl will be affected.

9.1.9.4. Production of Ferric Chloride. The primary use of ferric chloride is in water and sewage treatment. It is an effective coagulant for suspended solids, making their removal by filtration much easier. The demand for FeCl₃ has increased as waste disposal regulations have become stricter. The material has a number of other uses, including photoengraving, the treatment of television tubes, and etching of printed circuit boards.

The oxidation of iron usually occurs in two steps. First, ferrous chloride forms by the reaction of the metal with hydrochloric acid, and then reaction with chlorine produces

ferric chloride. The first reaction is simply



This approach has its own practical problems, including the need to remove entrained liquor from the hydrogen and its uneven rate of generation in a semi-batch system. The amount of hydrogen generated is not great, but it is stoichiometrically equivalent to the HCl consumed. It is possible, at least in concept, to make the process nearly self-sufficient in HCl and to operate with only iron and chlorine as the major raw materials. This may be an advantage when a stand-alone ferric chloride plant is to be built. Within a chlor-alkali complex, the size of the ferric chloride plant and its location (e.g., relative to the HCl burner) determine the justification for this approach. Alternatives include using the hydrogen as fuel and simply venting it to the atmosphere.

The source of iron varies and has much to do with the quality of the finished FeCl_3 . Sometimes, particles of an iron-containing material are reacted with aqueous HCl in a column or a tank. Other plants simply use scrap iron dumped into a tank containing the HCl. FeCl_2 also forms incidentally when steel is pickled in HCl. This is probably the largest source, the mixed pickle liquor being shipped from steel mills to producers of FeCl_3 . The flow diagram of Fig. 9.43, however, assumes that both reaction steps are required.

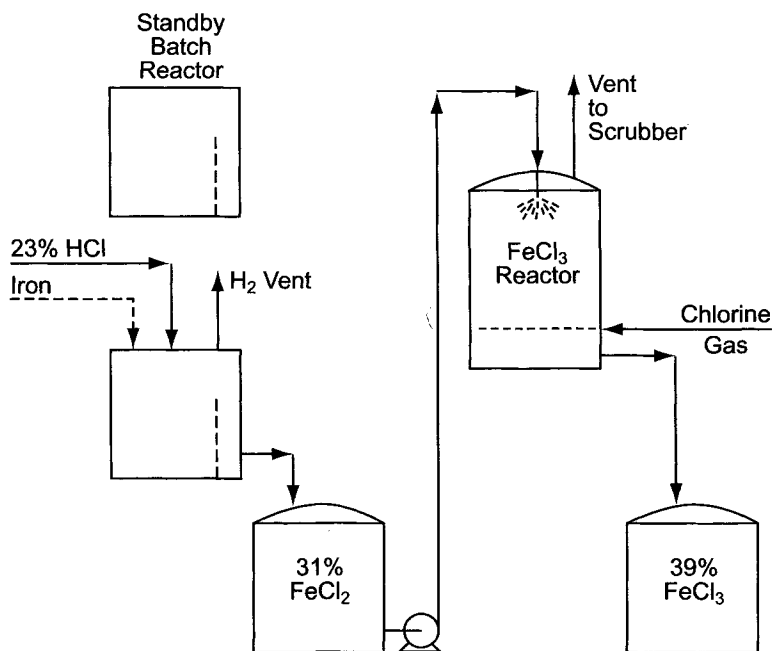
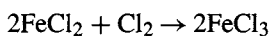


FIGURE 9.43. Ferric chloride process.

Reaction of iron with 23% HCl gives approximately a 31% solution of FeCl₂. Because of the semi-batch nature of the process, two reaction tanks are preferred. These are lined with bricks or rubber. FRP is suitable for storage of the solution, but the tanks must be able to withstand the temperature of the solution and the high specific gravity of about 1.4. Reaction of the HCl is incomplete, and the standard product may contain several percent residual acidity. With special care, this quantity can be reduced.

The fact that ferrous chloride can be produced from nearly any source of iron, including scrap metal, can be of great economic advantage. Lower grade supplies, however, give lower purity product and ultimately produce more unreacted sludge. This sludge must be treated and disposed of, usually under hazardous waste restrictions.

In the second step of the process, chlorine is absorbed by the FeCl₂ solution and reacts to form FeCl₃:



The reaction is fast [81], and the absorption process benefits from this until the ferrous ion concentration is nearly depleted. Usually, chlorine is sparged into a pool of FeCl₂ solution. The reaction tank therefore must be vented to a scrubber to prevent the release of chlorine to the atmosphere. FRP of the proper grade again is satisfactory, and again the specific gravity of the product is quite high (1.4–1.5, depending on concentration).

With no loss of water in the process, the use of 32% HCl in the first reaction would produce a mixture containing more than 50% FeCl₃, exceeding the room-temperature solubility. Commercial solutions usually contain about 39% FeCl₃, and freezing does not begin until the temperature drops below 0°C. In-process dilution would allow control of this concentration, but it seems to be standard practice instead to use a more dilute acid (about 23% HCl).

9.1.9.5. Other Processes. Silver's discussion of tail-gas recovery systems [77] covered a number of other processes. Those included here are whole-stream absorption of chlorine from cell gas, absorption of chlorine from tail gas by cold water, and adsorption. As always when hydrogen is present in the gas, protective measures are necessary when the removal of chlorine can produce a hazardous mixture.

In principle, a solvent can be used on the whole chlorine gas stream as well as on the tail gas. This can replace a conventional liquefaction system. Its advantage is that it makes possible more complete recovery than can be achieved in a liquefaction system at the same pressure and a reasonably economic temperature. It is not a process for the recovery of the chlorine value of tail gas and in that sense does not belong in this section. However, the motivation for use of this process would largely be the practical elimination of a tail-gas problem.

The process is much the same as that described in Section 9.1.9.1 but is on a much larger scale. After absorption of 99.8% of the chlorine, the remaining gas, boosted by an ejector if necessary, is scrubbed with caustic before venting. The chlorine is recovered from the solvent by steam stripping and condensation against cooling water. The stripped solvent, after cooling, returns to the absorber. The process also requires some means to prevent the loss of solvent and keep it out of the product chlorine.

Water is an inefficient solvent for chlorine (Section 7.5.9.1), but there are potential flowsheet efficiencies in some plants. A plant that uses direct-contact cooling in the main chlorine train can also absorb chlorine from the tail gas in cold water. The solution produced in this step may be used in the cooling process; in any event the absorbed chlorine is released in the steam stripper that handles the water from the cooling system. The recovered chlorine then has another pass through the recovery system, while the inert gases are vented from the tail gas absorber.

Adsorption is a frequent choice for the removal of one constituent from a gas mixture. The use of silica gel on tail gas results in recovery of about 90% of the chlorine as concentrated gas. Adsorption takes place under pressure and removal of the adsorbed chlorine takes place under vacuum.

9.1.10. Safety Devices

9.1.10.1. Low-Pressure Seals. The electrolysis of salt is nearly unaffected by the operating pressure. The generation of chlorine gas therefore stops only when the current to the cells is cut off. If the forward flow of chlorine is impeded for any reason, the pressure in the gas-processing system will rise rapidly at a rate proportional to the cell current.

Stopping electrolysis for every small upset elsewhere in the process is clearly undesirable. In order to provide a degree of redundancy to automatic shutdown devices, then, normal practice is to provide relief in the form of a water seal that allows the cell gas to vent at a rate equal to its production. The chlorine in this vent must not be allowed to enter the atmosphere. Its confinement is the subject of Section 9.1.10.3.

The water seal is installed somewhere on the low-pressure side of the chlorine process, usually between the cell room and the cooling process of Fig. 9.12. It is in communication with the process by a branch on the main chlorine header, as indicated by Fig. 9.44. The branch line terminates inside the seal vessel, slightly below the surface of a pool of water. When the pressure in the gas line exceeds the difference between the water level and the bottom of the branch line, the seal breaks and gas escapes. A source of brine can be used in place of water; consideration of the difference in density then is necessary when setting the height of the seal.

The gas cools as it passes through the main header. Under normal conditions, therefore, condensate forms. If the seal connection is at the bottom of the header, there will be a continuous small flow of water into the seal pot and out of the overflow line, and the seal will automatically be kept intact. For a more positive indication that the seal is being maintained, however, the usual practice is to add a flow of water into the seal pot. This allows a failure signal if flow stops and also helps to replenish the seal after a release of gas.

For smooth operation and in order to minimize velocity head losses, the end of the vent pipe must be level. Again to provide smooth flow, it is frequently notched or serrated.

A final consideration is the tendency of the water displaced by a gas release to fall back into the annulus created by the gas flow. This can cause pulsations, particularly when the vessel is large or the seal depth is more than a few centimeters. This phenomenon can be avoided by limiting the amount of water in the seal and allowing it to be blown away from proximity with the branch pipe when a release occurs. A central pan whose

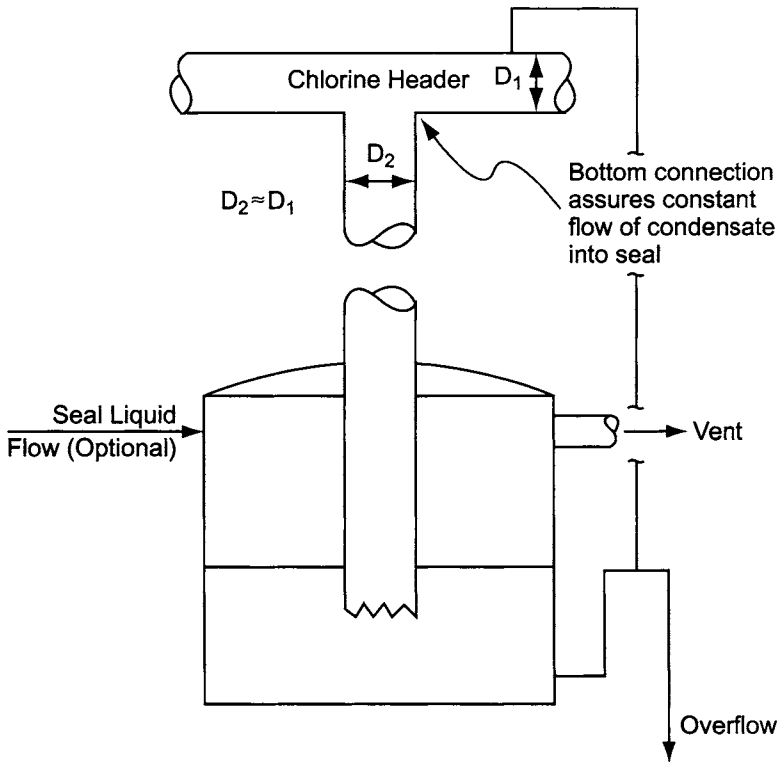


FIGURE 9.44. Chlorine seal pot connection to header.

diameter is not too much larger than that of the seal pipe, but large enough not to impede gas flow, can be supported within the vessel to accomplish this. The diameter of the pan should be small enough to allow the water to spill over when the seal blows but not so small that the annulus chokes the flow of gas.

Figure 9.45 incorporates all the desirable features listed above. The net accumulation of water overflows from a submerged outlet through a seal leg. With the arrangement shown, it is also possible to pump the water away under level control. If the central pan idea is not adopted, the overflow seal leg is positioned to maintain the proper seal depth automatically.

The fluid used to ensure that the seal is maintained can be from a service water connection or a pumped stream of condensate or brine from elsewhere in the process. In any case, the overflow from the seal pot should be treated as a chlorine-bearing liquid and dealt with appropriately. Hazard analyses sometimes reveal careless handling of this stream [76].

The seal pot vessel and its components must be chlorine-resistant. Rubber-lined and FRP construction are the most common. The vessel must be able to withstand the small pressure and vacuum which may exist in the process. Since it is connected to the chlorine header, thermal expansion and contraction of the pipe must be considered in placement and support of the seal vessel.

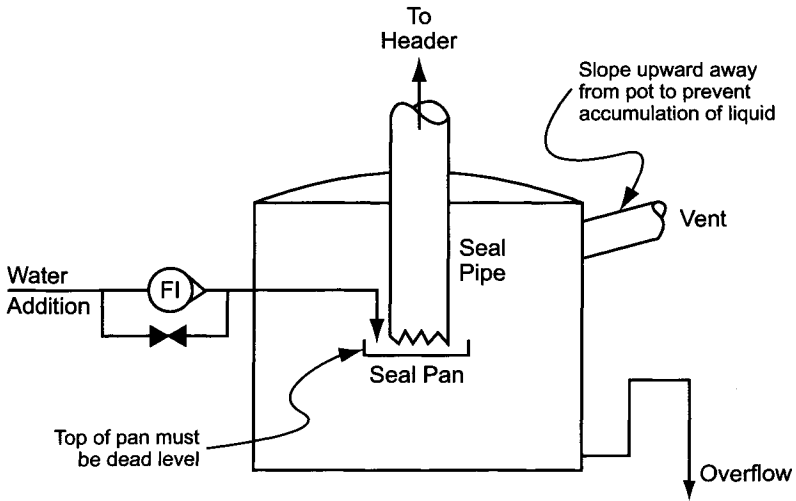


FIGURE 9.45. Chlorine seal pot design.

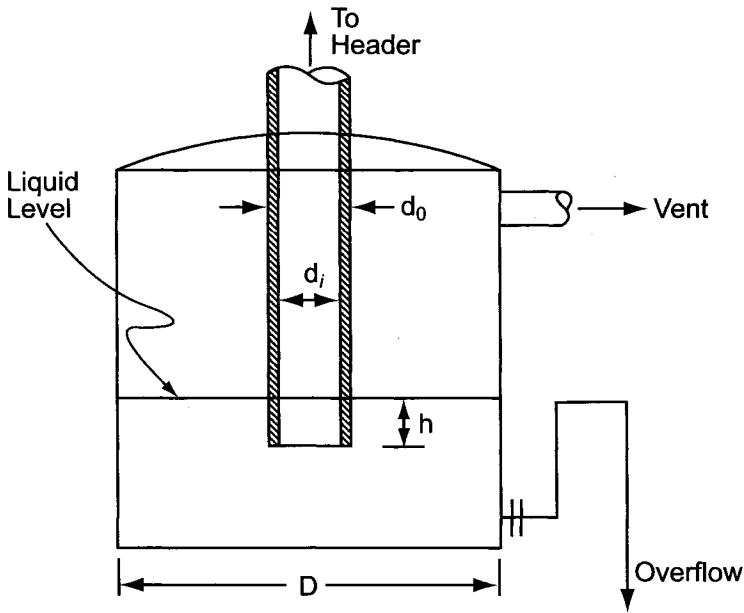


FIGURE 9.46. Simple pressure/vacuum seal.

Seal pots are also used to protect systems against vacuum. The same principle of operation applies, but practical considerations are somewhat different. This is especially important when the same apparatus is intended as a seal against both pressure and vacuum. Figure 9.46 shows the simplest arrangement, which we shall first consider as a pressure seal.

The seal pipe extends into the vessel from the chlorine header. Water flows into the vessel by condensation in the header and by deliberate addition from an outside source. The height of an overflow pipe, which may be fixed or variable, determines the level of water in the vessel. The difference in elevation between the overflow and the bottom of the seal leg is labeled h .

To analyze the operation of this seal, we distinguish between fast and slow rises in pressure. As pressure increases, water is forced out of the seal pipe and into the annulus. If the rise in pressure is slow enough, an equal volume of water leaves through the overflow pipe and the level in the pot is unchanged. The seal blows at a differential pressure equal to h . If pressure rises quickly, we may postulate a situation where water is displaced from the seal pipe without enough time to flow out of the vessel. The volume of water originally present in the seal pipe is

$$V_p = \pi d_i^2 h / 4 \quad (79)$$

where d_i is the inside diameter of the seal pipe.

The area of the annulus is

$$A_a = \pi (D^2 - d_o^2) / 4 \quad (80)$$

where D is the inside diameter of the vessel and d_o is the outside diameter of the seal pipe.

The level in the annulus increases by the ratio of the previous two expressions:

$$\Delta h = d_i^2 h / (D^2 - d_o^2) \quad (81)$$

If the wall thickness of the seal pipe can be ignored, we can call its diameter d and write

$$\Delta h / h = d^2 / (D^2 - d^2) \quad (82)$$

If the diameter of the seal pot vessel is twice the diameter of the pipe, the maximum increase in relief pressure is only one third of the set pressure. Larger vessel diameters reduce this even more.

Now we consider the same arrangement as a vacuum seal. Reversing the above procedure, we consider first the sudden imposition of a vacuum. The volume of water contained in the annulus at height h now must be moved into the seal pipe. With the same considerations, we have

$$\Delta h = (D^2 - d_o^2) h / d_i^2 \quad (83)$$

or with an infinitely thin seal pipe

$$\Delta h / h = (D^2 - d^2) / d^2 \quad (84)$$

With the same 2:1 ratio in diameters, the height of the seal at relief is four times the original setting, and pulsation is likely. Larger vessel diameters aggravate the situation.

Next we consider the slow buildup of vacuum. As water is pulled into the seal pipe from the annulus, there is time for it to be replaced. The overflow level stays the same, and the seal is maintained. The only limitation on the vacuum is the height of the chlorine header.

With the simple design we discuss here, it is difficult to have an effective two-way seal. More elaborate designs exist and are used, but more often a separate seal pot is provided for vacuum relief.

9.1.10.2. Mechanical Relief Devices. The water seals discussed above in Section 9.1.10.1 are effective only at very low differential pressures. After the compression of chlorine, and particularly in liquefaction and storage systems, more conventional relief devices, rupture discs and pressure relief valves, are used. With some fluids, there is a simple choice to be made between discs and valves. While the former are less likely to permit bypassing of small quantities of fluid, they are destroyed when they open. A release will continue even after the pressure on the system drops below the set point of the disc. Relief valves have the opposite characteristics.

Corrosive fluids are less likely candidates for the use of pressure relief valves. Whether by corrosion of the valve itself or of surrounding pipework, they often create a problem with deposits on the valve element or its seat. These deposits can prevent proper sealing and allow the slow escape of fluid. To combine the advantages of rupture discs and relief valves, the two devices can be installed in series, with the disc before the valve. Even if the valve is not precisely seated, there is no release from the system until the disc bursts. The same overpressure then also opens the valve. Once the pressure has dissipated and dropped below its set point, the valve reseats and prevents further release.

These composite relief devices introduce a hazard that must be catered for. A small leak, as through a pinhole in the disc, can raise the pressure between the disc and the valve to the normal operating level of the equipment being protected. The disc then will not rupture until the process pressure exceeds the pressure between the disc and the valve, not the atmospheric pressure, by an amount equal to the set point of the disc. This could result in catastrophic failure. Any gas that accumulates in the space between the two safety elements must be removed to prevent this.

Some devices combine the functions of disc and valve. One, the Crosby Valve Company's Style JQ pressure relief valve, was designed in collaboration with the Chlorine Institute for transportation service (Section 9.1.8.6). It has been adapted for service on pressure vessels and is widely used in North America in both types of application. The device (P39 and P41) comprises a standard spring-loaded valve and a breaking-pin assembly. The internals are protected from the chlorine by an antimony-lead diaphragm held in place by a follower in the mounting nut. The pressure on the diaphragm is transmitted by its supports to the yoke and so to the breaking pin. A typical transportation application would be a 40-mm NB valve on a tank car. There is one other standard size, 100-mm NB, suitable for barge tanks. There is also a modification to the design that allows the use of standard 300-lb flanges. Other modifications make the valve suitable for use with a closed exhaust system. The 40-mm version basically is designed to withstand about 3,100 kPa. The larger model is suitable up to 2,400 kPa. All these modifications affect the maximum pressure setting and the relieving capacity of the

valves. Breaking pin settings also can vary, and the user must evaluate the capacity of the particular combination used in each application from published data [82].

The diaphragm is not a pressure-protective device; the breaking pin serves that function. The process-side diaphragm and another one mounted at the top of the valve are there to prevent corrosion by exposure to process gas or the atmosphere. When the set pressure is exceeded, the pin breaks and the valve opens. The upper diaphragm then breaks, and chlorine escapes. When the pressure returns to a safe value, the valve closes and then functions as a standard spring-loaded relief valve until the breaking pin and diaphragms can be replaced.

Euro Chlor makes recommendations for chlorine relief valves (GEST 76/64) but does not rely on a standard design. These recommendations call for spring-loaded valves, specifically designed and constructed to resist all the static and dynamic forces to which they can be exposed. Valves must be gas-tight in the closed position at the normal operating pressure of the system under protection. A related recommendation is the use of an upstream bursting disc, designed not to interfere with the valve by material from a failed disc. The valve body, and in a general fashion all components subject to static or dynamic stress, should be of materials compatible with anhydrous chlorine and possessing adequate mechanical properties. When the protected equipment contains liquid chlorine, the materials of construction also should have adequate impact resistance at low temperature. The use of an upstream rupture disc protects the valve against deterioration due to corrosion. The valve should also be protected against the return of moisture from the vent system. A downstream protective diaphragm can achieve this, or the vent line can be purged with an inert dry gas.

Instrument engineers usually look after the sizing of relief devices, and this is a subject treated in detail in various textbooks and handbooks. The methods used for sizing often depend on national or local codes. Before choosing a size, the responsible engineer must determine the design rate of flow and the flow regime during relief. The Design Institute for Emergency Relief Systems (DIERS), among others, provides useful methods for these calculations. The design rate of flow in turn is chosen after consideration of the various scenarios that can lead to overpressure. In many cases, the design rate would be that occurring during a fire. Past practice often assumed that a fire was possible in all cases and sometimes resulted in designs that were well oversized for other relief situations. With the trend toward designing containment systems for chlorine releases, this can be counterproductive. The modern trend is to consider whether fire is a likely occurrence and to exclude it from consideration when that is justified. Euro Chlor takes the position that all tanks or systems designed to store liquid chlorine should be installed so that the intensive input of heat from any external source of radiation is avoided. GEST 76/64 then specifically recommends excluding fire as a consideration when the chlorine storage system is properly sited.

Relief devices are often installed in parallel. This arrangement allows one device to be tested or maintained while the other guards the process. Isolating valves are required for this purpose, but the designer must ensure that never are they both closed. This can be done mechanically, by linking the valve mechanisms, or administratively. The latter technique usually involves sealing the valves open or locking them open by removing their handles. Maintenance is possible when an isolating valve is closed after unlocking it; the

administrative controls must ensure that it is returned to the safe state after maintenance is finished. Three-way valves allow selection of either of two branches but are used infrequently in the chlor-alkali industry.

There must be a piping system to carry the gas relieved by opening a device to its destination. Chlorine should not under ordinary circumstances be released to the atmosphere. Two approaches are in common use. One involves direct relief to an absorption system; the other places an expansion tank between the source of gas and the absorber (GEST 87/133). The discussion of emergency vent scrubbing systems in Section 9.1.10.3C includes some of the considerations that apply to vent collection systems.

9.1.10.3. Vent Scrubbers

9.1.10.3A. Chemistry. Significant releases of chlorine from the process into the atmosphere must be prevented. To contain the inevitable discharges during upsets and equipment breakdowns, it is customary to provide an emergency vent scrubber. Its function is to destroy the chlorine before it reaches the atmosphere. Usually, the chlorine is exposed to an alkaline solution that converts it to a mixture of chloride and hypochlorite. Scrubbing solutions include diluted NaOH, diaphragm-cell liquor, caustic purification waste liquor, lime, carbonate, and alkaline hypochlorite-reducing agents. The use of cell liquor and purification waste is restricted to diaphragm-cell plants. The NaOH concentration of purification waste also is too low for it to be used without blending. Lime, carbonate, and reducing agents tend to be used more by smaller scale chlorine users than by producers, and generally in small systems. Lime may be used because of its price and availability. Carbonate is sometimes recommended for static applications to scrub a fixed quantity of chlorine, as for example cylinder lots. It has the disadvantage of CO₂ evolution. Reducing agents are much more expensive than the other scrubbing agents, but they can produce an effluent liquor free of active chlorine. Most often, the scrubbing solution is sodium hydroxide. Section 7.5.2.2A discusses possible sources. The fundamental chemical reaction is



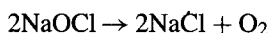
This has an exothermic heat of reaction of 1,463 kJ kg⁻¹ of chlorine gas.

Conservative design also assumes that all the water in the gas condenses in the scrubber.

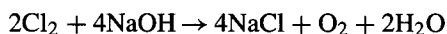
Section 9.1.9.3, on the deliberate production of bleach according to reaction (85), discusses the physical chemistry of the process and the need for careful control of the reaction conditions. In an emergency situation, good control of the temperature in the reaction zone may be absent, and side reactions are likely. One of these is the reaction of hypochlorite to chloride and chlorate:



Another is the decomposition of hypochlorite to chloride and oxygen:



High temperature and the presence of certain metal ions favor the latter reaction. Complete equations including the side reactions are:



Their heats of reaction are 2,002 and 2,272 kJ kg⁻¹ of chlorine, respectively.

Because of the side reactions and the need to maintain excess NaOH in most systems, the product of an emergency vent scrubber usually is not a saleable product. The effluent must be treated in some way before disposal (Sections 16.5.2.3 and 16.5.2.6).

9.1.10.3B. Apparatus. There are many approaches to scrubber system design and configuration. Stitt *et al.* [83] list some of the variations in design and operating philosophy:

1. caustic solution supply to the scrubber varies from once-through to recycle operation;
2. the mode of addition of fresh caustic varies from continuous to batchwise;
3. some systems provide a backup reservoir of caustic; some systems do this in effect by supplying a large batch of solution; others rely on the continuous or controlled makeup of fresh caustic.

The heart of any system is the absorption unit itself. Most common types of commercial equipment can be and have been used in this application. The advantages and disadvantages of the major categories of scrubbing equipment as given by McCollam [84] are listed in Table 9.13.

GEST 76/52, which describes various scrubbing devices, actively discourages the use of spray columns because of the danger of bypassing some of the chlorine. Otherwise, the summary of advantages and disadvantages is much the same as that in Table 9.13. One comment on venturi devices is that they are less prone than some of the other types to fouling by precipitates when the solution concentration is high. Sparger devices are also considered untrustworthy because of the possibilities of breakthrough of chlorine or backflow of NaOH. Opposing this, we should note the use of sparged tanks venting into scrubbing columns and the provision of barometric risers in suction lines which prevent backflow into the chlorine process.

Other points made by Euro Chlor include recommendations for the maximum concentrations of the various scrubbing solutions. NaOH should be prepared at a maximum strength of 20–22% in order to avoid formation of solid salt as the NaOH is replaced by NaCl and NaOCl. When a substantial amount of CO₂ is present or when the scrubber operates with a continuous flow of air, the solution should be more dilute. Diaphragm-cell liquor should be limited to 10% NaOH. In the presence of CO₂, this should be reduced to 6–8%. Milk of lime should contain 130–200 gpl CaO.

TABLE 9.13. Comparison of Types of Scrubbing Devices

Type of contactor	Advantages	Disadvantages
Spray	Low pressure drop Simple design Cheapest tower	Limited staging Nozzle plugging Performance predicted from test or experience
Packing	Large area Multistage Wide range of gas flows Performance predictable Intermediate pressure drop	Plugging possible Complete wetting of packing is necessary Intermediate pressure drop
Trays	Multistage Performance predictable Intermediate pressure drop	More expensive tower Plugging possible Trays must be filled Intermediate pressure drop
Sparger	Simplest apparatus Uses gas pressure Passive Cheap	High pressure drop Formation of mist Limited predictability
Venturi	No gas mover required Pre-engineered units	One stage only (per unit) Less effective with dilute gas Needs testing

Euro Chlor's recommended maximum temperature of the scrubbing liquor is 55°C. The Chlorine Institute does not make a specific recommendation, but the nearest equivalent round temperature of 130°F has been cited in its discussions as good practice [80].

9.1.10.3C. Collection System. Most plants will have a number of relief points connected to a scrubber system. Design of the collection and delivery piping becomes important. This differs from the situation in other chemical plants and refineries only in being relatively simple. A standard guide in much of the processing industry is API Recommended Practice 521. Chlorine plant designers should also draw on local vent system codes and regulations. "Regulations" here can include insurance requirements. Basic design data for a scrubber include carefully specified compositions and quantities for various vents and emergency systems. These specifications should include maximum and minimum concentrations, maximum flows, and indication of the presence of alkali-consuming components other than chlorine (e.g., HCl and CO₂). The gas composition both before and after scrubbing must be defined. A very important consideration in the effluent gas is its maximum possible hydrogen content and the need to add dilution air.

The collection system must be closed, with gas-tight connections. To avoid sucking the absorbent solution back into the collection system, the designer should consider providing a liquid seal. A simple technique for pressurized lines is to provide a barometric

riser on the scrubber inlet line. This line and the sparger should be designed with due regard to the time required to empty the leg of liquid and allow the passage of gas to begin and to the possibility of developing a dangerous backpressure in the vent line.

Exclusion of water from the dry-gas side of the absorption system is an important part of design. This includes protection from entry of moist gases from the scrubber itself. A small gas purge can accomplish this. Nitrogen has an advantage over dry air in being free of CO_2 , which would slowly deplete the caustic in the scrubber.

A scrubber may be called on to handle both wet and dry gases. The components and zones handling both types of gas must be constructed from material resistant to both wet and dry chlorine. This excludes all common metals. Polymeric linings can be used on vessels and external pipework. Internal piping of certain fluorinated polymers is adequate from the standpoint of corrosion, and it can be used if its support and mechanical design are adequate and if there is no problem due to porosity.

Vent absorbers are designed to receive gas, not liquid. The presence of liquid chlorine in a vent stream can disrupt flow in the scrubber, overload the system, and cause an early breakthrough. When appropriate, design should therefore include a gas/liquid separator to prevent carryover of liquid droplets. The separator should have the capacity to trap the maximum amount of liquid likely to be present and should include a temperature or level alarm to signify its presence.

Such events tend to occur in liquid transfer and vaporization operations and are therefore particularly likely in users' plants. A study by Euro Chlor showed that 14% of the safety incidents reported involved overloading of chlorine absorption systems [75]. Section 9.1.8.4 on liquid transfer describes some of the protective measures that can prevent this.

When the operation of a relief valve can release liquid chlorine or when it is necessary to limit the rate of discharge of chlorine to the receiving system, buffer tanks are useful. Those that may be subjected to liquid chlorine should have alarms that signal its presence and should be designed for low temperature. There should be provision for safe removal of the liquid after operation. Absorber design is also based on the maximum flow rate of gas at the inlet. When release rates are variable (the peak rate usually being at the start), a buffer in the system can reduce the maximum rate at the absorber.

An expanse tank is a closed vessel under no pressure or a relatively low pressure. It has its own relief system directly to the absorber and is equipped with a pressure alarm set low enough to indicate the presence of even a small amount of chlorine. The use of an expansion tank provides the buffer mentioned above. It contains some of the chlorine released and makes it possible to recover this material, reducing product loss and reactant consumption. It also can add to the complexity of accurate design. More than one source can be relieving to the expansion tank at a given time. The relief system must be large enough to handle all those sources that might relieve simultaneously. Instrumentation should be sufficient to identify the source of flow. Design must also include the case where the expansion tank is at its relief pressure. The pressure drop available across the primary relief set therefore becomes smaller. All components of the relief system must be larger on this account, and improper design can cause a system not to relieve when it should.

The increased size of components when an expansion tank is present gives the designer some incentive to offset these effects. The use of bursting discs or balanced

relief valves is one approach. Another is the more accurate calculation of the buffering action of the expansion tank, which itself can tolerate an increase in pressure when relief rates are at their highest.

The final vent from the system should be regarded as a point of possible chlorine emission. It should be at a high level and away from personnel traffic and ventilation system intakes. Particularly when the low-pressure scrubbing device is a packed bed, booster fans may be added on the tail pipe. The piping arrangement around the fans then should avoid low points that could collect liquid. As with any vent manifold, the designer of a system serving several different units should take precautions to avoid mixtures in headers that may lead to undesirable side reactions.

9.1.10.3D. Administrative Controls. Most of the time, very little happens in an emergency scrubber. Occasionally, there will be a small release of chlorine, which is easily contained. There may also be small continuous vents and perhaps a slow undetected leak. With this variability and the infrequent large release, the rate of consumption of the alkaline compound is highly variable. Since scrubbers easily can drop below an operator's attention level, most plants impose administrative controls to keep hazardous situations from developing.

When chlorine is released to a scrubber, a liquid stream containing at least enough caustic to neutralize the gas must be available to meet it. It is the product of caustic flow rate and concentration that matters. If the flow rate drops too low, or if the concentration of the solution is depleted too much, there will be a release of chlorine to the atmosphere. As a rule of thumb, if the minimum NaOH strength is taken to be 5%, the required rate of flow of scrubbing solution in tons per hour is equal to the production rate of chlorine in tons per day [85]. For concentrations other than 5% NaOH, the required flow rate is inversely proportional to the minimum strength.

Many systems rely on a batch of solution being circulated through a scrubber. Patel and Scarfe [86] describe one example, shown in Fig. 9.47. The batch must from time to time be augmented or at least partly replaced in order to keep the caustic concentration above the intended minimum. Minor episodes such as those described above can have a cumulative effect on the concentration and allow a premature breakthrough of gas. This becomes more likely when the operator is not aware of the state of the solution in the scrubber and takes no steps to replenish the caustic inventory.

It is important to note that a deficiency in either the flow rate or the concentration allows chlorine to break through. Analyzing the events that can lead to these failures shows that in many cases any one of two or more causes is sufficient to move the system closer to a failure [85]. One way to analyze this situation is to construct a "fault tree" (see Section 16.4.2.4B for example and explanation). When moving up a fault tree from one level to another and so approaching the dangerous event under analysis, events such as those above propagate through "OR-gates," in which probabilities of the events are added. When two or more failures must occur simultaneously, events propagate through "AND-gates," in which probabilities are multiplied. The latter is clearly more desirable, and the outcome of fault tree analysis often is the recommendation to create AND-gates at critical points in the tree. Addition of parallel or redundant instrumentation is one frequent approach. Another is the provision of backup columns in series with the main

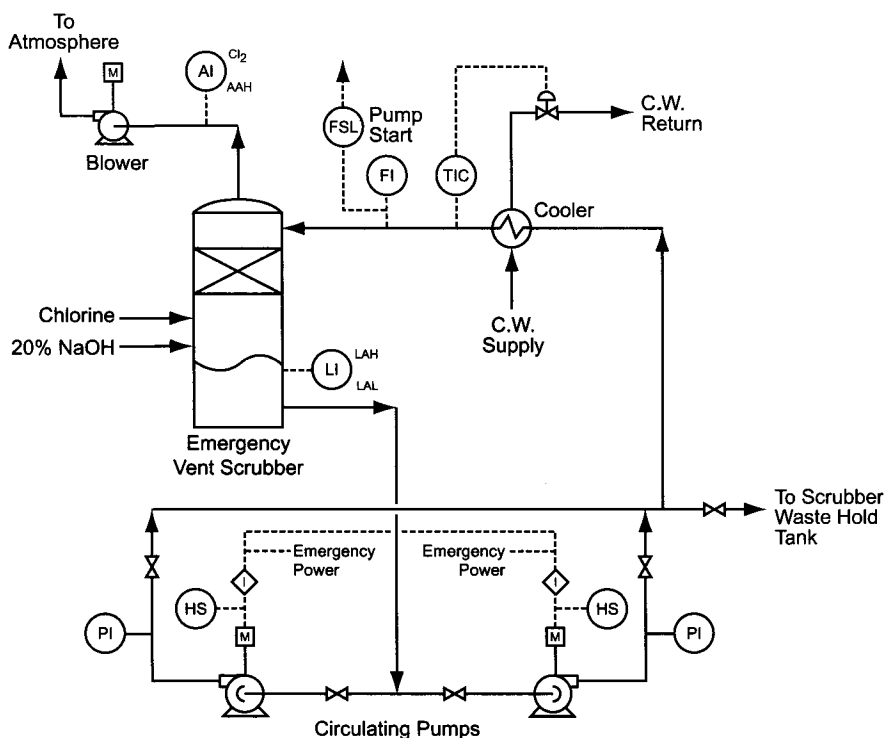


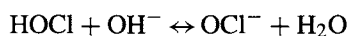
FIGURE 9.47. Example of industrial vent scrubbing system.

columns. A different sort of technique is the addition of procedural or administrative controls which force checking of equipment, operating conditions and procedures, or status of conditions (e.g., caustic concentration).

9.1.10.3E. Mass-Transfer Considerations. The earliest application of the theories of mass transfer to gas absorption did not recognize the influence of chemical reaction in the liquid phase on mass-transfer coefficients. This influence is explained in the film and penetration theories of absorption by showing that the concentration of the absorbate is depressed everywhere near the gas-liquid interface by its reaction. The interfacial concentration gradient is sharper as a result, and this increases the liquid-phase mass-transfer coefficient.

Studies of the absorption of chlorine in water had much to do with the proper development of the theory. When Vivian and Whitney [87] found apparent inconsistencies in their data on this system, they were forced to treat the results from the two absorbers separately. They resolved the inconsistencies by recognizing that the partial pressure of chlorine over a solution depends on the dissolved concentration of molecular chlorine, not on the total amount dissolved. The modern theories of absorption with chemical reaction all depend on this recognition. A review of these [88] suggests that, in the case of chlorine, the liquid phase is controlling and the two-reaction plane model of

Hikita *et al.* [89] is most suitable. This considers the consecutive reactions



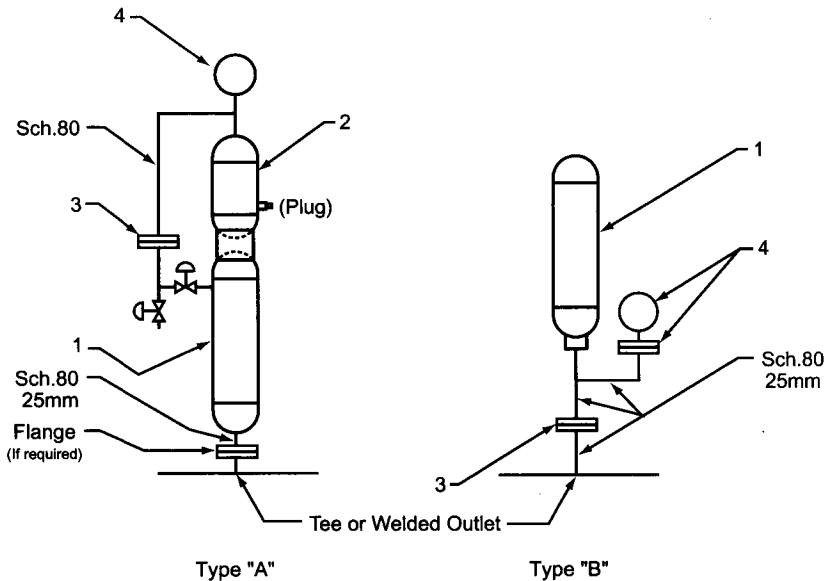
The authors show that when the first reaction is more nearly irreversible than the second and both reactions are rapid, the reactions occur at successive planes within the liquid. In this case, the first equilibrium constant is in fact greater, by a factor of about 14,000. Using this approach changes the mathematics somewhat from the single-plane model of Sherwood and Pigford [90].

Temperature is an important variable in any mass transfer process, and in an emergency situation the absorption of chlorine will be far from isothermal. With the heats of reaction given above, the temperature rise of the typical caustic soda solution in its pass through a column against chlorine at its full production rate will be about 30°C. Higher temperatures reduce the solubility of chlorine at a given partial pressure and also reduce its partial pressure by increasing the vapor pressure of water over the solution. Interestingly, if temperatures are kept low, the partial pressure of chlorine actually rises as the gas passes through the lower part of the column [91]. This increase is due to the condensation of water from the gas, and it enhances the mass-transfer process. If the temperature of the circulating caustic is allowed to increase, the chlorine partial pressure first will drop in the lower sections of the tower and then rise in the upper sections, which still are relatively cool. Ultimately, the chlorine partial pressure will decline throughout the tower. This smaller driving force combined with the less favorable absorption equilibrium produces a severe decline in mass-transfer rates and increases the probability of breakthrough.

Chlorine under pressure can be destroyed by sparging it into a tank containing an alkaline solution. The absorption process in this case also is liquid-film controlled [92].

Absorption of chlorine from weak gases, as encountered in some evacuation processes and during maintenance of piping and equipment, is a quite different process. With concentrated gases, resistance in the liquid film controls the rate of absorption. The discussion above was in those terms. With weak gases, the gas film can control. Test data [93] verify the phenomenon and show that the rate of absorption then is proportional to the concentration of chlorine in the gas. This is true in any of several absorbents tested, up to a certain gas concentration (~3.5% chlorine). A material balance limitation is a contributing factor. As the absorbent solution becomes depleted, liquid-phase effects begin to exert some control and the proportionality of the rate to the gas-phase concentration is lost. Increasing the supply of alkaline reactant can restore the situation. This can be done by increasing the rate of supply of solution or by increasing the concentration of the reactant in the solution. The absorption rate remained proportional to the strength of the gas as long as the molar ratio of alkali to chlorine supplied to the column remained above a critical value of 2.3–2.5.

9.1.10.4. Expansion Chambers. Liquid chlorine has an unusually high coefficient of expansion, ten times as great as that of water and six times as great as concentrated KCl brine. Where there is a chance of trapping liquid chlorine in a closed volume, as between



NOTES:

1. Capacity - 20% of line volume.
2. Capacity - 10% of line volume.
3. 2750 kPa relief setting suitable for many systems. Setting must not exceed system design pressure.
4. 15-mm pressure-gauge connection. Liquid-filled protective diaphragm optional.
5. Supports may be necessary but are not shown.

FIGURE 9.48. Standard chlorine expansion chambers (with permission of The Chlorine Institute, Inc.).

two valves in a pipeline, there is the possibility of generating dangerous pressures as the liquid warms and tries to expand. Standard practice therefore is to provide pressure relief to a receiver or a safe area or to install expansion chambers that take up the increase in volume. The latter are usually designed to allow up to 20% expansion of the trapped liquid. This is based on an increase in temperature from -18°C to 60°C . The design shown in Chlorine Institute drawing #136, reproduced here as Fig. 9.48, can be regarded as an industry standard.

There are two kinds of chamber. Type "A" is recommended for continuous supply pipelines and should be installed at the high point of a system. The rupture disc is set for about 2,750 kPa, and it can be changed without shutdown of the pipeline supply. The secondary chamber in such a case must be purged of chlorine and evacuated. The primary chamber can be emptied of chlorine by displacement with dry air or nitrogen. This should be done periodically as needed; the same is true of a Type "B" chamber.

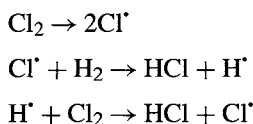
Expansion chambers should be fitted and installed in accord with Chlorine Institute Pamphlet #6. They are designed for a pressure of 3,300 kPa. Larger chambers and welded small chambers should be designed to ASME VIII. Smaller units can be fabricated from seamless drawn cylinder in accord with local regulations or from pipe and fittings as recommended by the Chlorine Institute. Fittings usually are of forged carbon steel.

Users must realize that without proper installation certain “expansion” chambers can be useless. Simply adding a chamber to a pipeline may be no more effective than adding a bulge in the line. If an empty chamber is provided, it can simply fill, along with the rest of the piping system, with liquid chlorine. More realistically, a chamber full of air at atmospheric pressure will fill until the air is compressed to line pressure. With liquid at -18°C , even at the vapor pressure of only about 200 kPa, this will mean that liquid chlorine immediately fills half the chamber and only half the vessel volume is available for expansion. The design of the Type “A” chamber attempts to avoid filling of the expansion volume by isolating it with a rupture disc. The same effect can be obtained by installing a pressurized elastic barrier [94]. The barrier may be an elastic membrane or a metal or PTFE bellows.

Gupta [95] proposed connecting multiple primary chambers to an appropriately sized secondary chamber. In this way, a relatively small number of secondary chambers would serve an entire plant. These could be thoroughly instrumented at a small expense while providing high reliability.

9.1.11. Explosion Hazards

9.1.11.1. *Hydrogen.* To the layman, probably the best-known property of hydrogen is its combustibility in air. At least as important to the chlorine technologist is the fact that hydrogen also can react explosively with chlorine even in the absence of oxygen. Because of the low energy of the Cl–Cl bond, there is always a tendency for chlorine molecules to split into a pair of free radicals. These radicals avidly seek available hydrogen to form the stable combination HCl. This is the basis for the widespread use of chlorine as a thermal catalyst for dehydrochlorination reactions. The chain reaction that results when chlorine is mixed with hydrogen can be represented by



In certain mixtures, the accumulation of energy can lead to an explosion.

Figure 9.49 is a ternary diagram of the system air– H_2 – Cl_2 showing the explosive region. The significance of the three different sets of lines is explained below. First, we remark on the lower limits represented by the two lines at the bottom of the diagram. Note that the hydrogen concentrations are nearly the same regardless of the air/chlorine ratio. Moving to the upper part of the diagram, we see that the upper limits of hydrogen concentration are higher in chlorine than in air. The explosive range of hydrogen is therefore wider in chlorine. Add to this a lower ignition energy and the graver consequences of a release of the combustion product, and mixtures of hydrogen and chlorine are much more dangerous in a process than are similar mixtures of hydrogen and air.

If hydrogen and chlorine are mixed in oxygen rather than in air, there is little change in the lower limits. The upper limits are higher, broadening the explosive range, and the ignition energies are lower. The Appendix (in Vol. V) shows this, along with the behavior of the N_2 – H_2 – Cl_2 ternary.

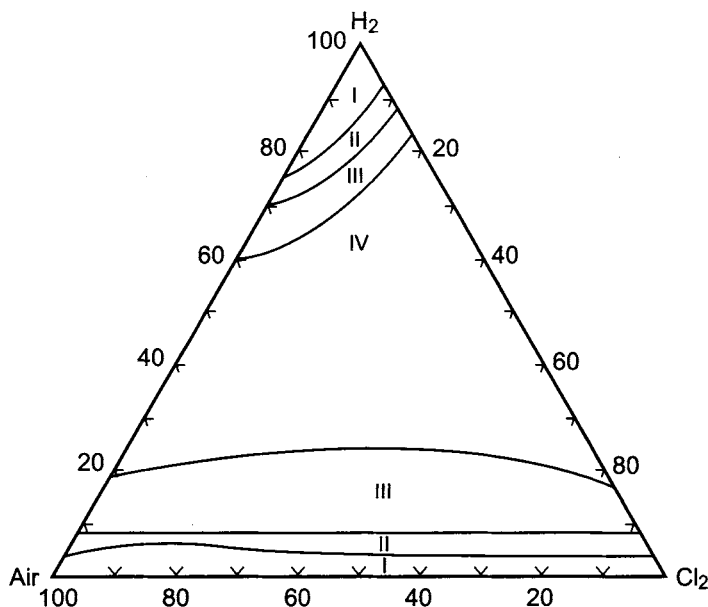


FIGURE 9.49. Explosive ranges for hydrogen-chlorine-air mixtures.

The zones in Fig. 9.49 bear numbers that characterize the behavior of the ternary system. In zone I, top or bottom, the mixture is too lean in some component to support combustion. In zone IV, detonations can occur. The other zones recognize the unusual behavior of the system, where over a fairly broad range of compositions, reaction can occur without advancing to detonation. The lines separating zone I from zone II represent ignition limits. We follow here the definition given in Member Information Report 121 of the Chlorine Institute [96]. The ignition limit is the composition of a gas which, when ignited by an adequate point source of energy such as a strong spark, will barely continue to propagate the reaction in an upward direction to the limits of the container. At the ignition limit, the process is not vigorous. It is not an explosion; the changes in temperature and pressure are quite small. At the same time, it is not a flame; no light is emitted. As the composition of the gas moves away from zone I into more dangerous areas, the reaction becomes more vigorous. At the boundaries between zones II and III, the pressure doubles from its starting level. The low-hydrogen end of Fig. 9.49 can be summarized safely and with reasonable accuracy by saying that zone II lies between 4% and 8% hydrogen for all ratios of chlorine to air. The upper boundary between zones II and III is a modification of the data of Suzuki and Fukunaga [97]. Their results generally indicated lower hydrogen concentrations at the boundary. However, their pressure-measuring system was insensitive and their apparent zone III very narrow. The curve shown in Fig. 9.49 is a somewhat arbitrary but quite reasonable adjustment made by the compilers of MIR 121. Similarly, the upper line separating zones III and IV is estimated from the measured UEL for hydrogen in chlorine. We can therefore have some reservations about the upper region of Fig. 9.49, but our main interest here is in the lower part.

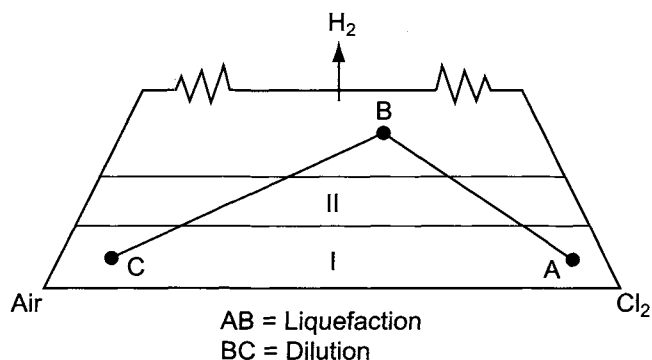


FIGURE 9.50. Principle of air dilution in the liquefaction process.

Hazardous mixtures of hydrogen and chlorine can be rendered safe by dilution. This is a technique very frequently used in chlorine recovery processes, and it was touched upon in Sections 9.1.7.2A and 9.1.9.1. As chlorine is removed from the cell gas mixture, by liquefaction or other means, the composition of the residual gas on Fig. 9.49 moves along a straight line away from the chlorine vertex. At some degree of recovery, the gas would move into the combustible zone. To prevent this, air or nitrogen is added into the gas. Figure 9.50 illustrates the principle. Starting from point A, the desired or achievable recovery of chlorine would move the mixture to point B in the explosive region. To avoid problems, air is simultaneously added at a rate sufficient to move the composition from B at least to point C and so into the safe range. One of the advantages of membrane cells is the low hydrogen content of the chlorine gas, which reduces or eliminates the need for gas dilution in liquefaction. The purpose of Fig. 9.50 is to illustrate the principle involved. It does not represent the course of the process. As said above, addition of the diluent precedes or accompanies the removal of chlorine. Only the points A and C are real.

Air is of course not the only gas that can be used for dilution. Van Diest and DeGraff [98] published curves showing that the ability to suppress hydrogen-chlorine combustion increases in the order $N_2 < HCl < CO_2 < H_2O$. As a practical matter, water is not suitable in ferrous-metal systems and HCl presents problems in separation and corrosion. CO_2 is an effective suppressant that might be used in some circumstances, but within an operating process air or nitrogen is the usual choice. Table 9.14 shows the results of some calculations of the relative effectiveness of these suppressants.

The purpose of adding dilution air to a chlorine recovery plant is to avoid the ignition hazard we discuss here. Another approach to a hazard is to mitigate or contain it. Antonov *et al.* [99] suggested that liquefier systems should be operated at hydrogen concentrations up to 8%, on the basis that the pressure multiplier would be no more than 2. P21, which incorporates much of the information from MIR 121, points out that these authors did not consider the problems associated with stationary flame fronts that could arise. Still, systems have in fact been designed and operated at hydrogen concentrations up to 16%. Keys to success here are to design for high developed pressures and to impede the development of wave fronts by installing baffles or otherwise making the geometry not conducive to the propagation of a wave.

TABLE 9.14. Amount of Diluent Gas Required to Prevent H₂-Cl₂ Combustion

Diluent	%H ₂ at ignition limit	% diluent required	Diluent volume/starting volume	Relative volume of diluent
Air	5	90	9.0	100
N ₂	7.5	85	5.7	63
HCl	9	82	4.6	51
CO ₂	13	74	2.9	32
H ₂ O	18	64	1.8	20

Note: Starting mixture 50/50 H₂/Cl₂; atmospheric pressure; 100°C.

TABLE 9.15. Effect of Temperature on Ignition Limits of Hydrogen Mixtures

Temperature of gas	%H ₂ in chlorine		%H ₂ in air		%H ₂ in oxygen	
	Lower	Upper	Lower	Upper	Lower	Upper
-60	5	90	4	69	4	96
-40	4	90.5	4	71	4	96
-20	4	91.5	4	72	4	96
0	3.5	92	4	73	4	96
20-25	3	92.3	4	75	4	96
50	3	93	3.7	76	4	96
100	3	93	3	80	4	97

Pamphlet 21 also shows that the ignition range becomes wider as temperature increases (Table 9.15) but that pressure has little effect.

9.1.11.2. Nitrogen Trichloride. Nitrogen trichloride is a very dangerous and spontaneously explosive compound. It is sensitive to light, impact, and ultrasonic radiation. The compound has a free energy of formation of +72 kcal mol⁻¹, and decomposition gives off 54.7 kcal. The explosive potential is about 30% of that of TNT. Decomposition of as little as 0.3 g cm⁻² of exposed wall area in a confined volume can overstress steel and create a very hazardous situation. Increasing that number to 1.5 g cm⁻² results in fracture [54]. The hazard therefore is less when chlorine contaminated with NCl₃ is spread in a wide pool than when it collects in a nozzle or section of piping. Further discussion of the hazardous properties of this compound is in Section 16.2.8.

NCl₃ forms in the cells by reaction of chlorine with certain nitrogen compounds, usually amines and other ammonia derivatives. Other nitrogen compounds also may act as precursors, but fully oxidized species such as the nitrates are more resistant. The most prudent approach is to assume that any nitrogen compound, given enough time in contact with free chlorine in a plant environment, can form nitrogen trichloride. NCl₃ then is able to accumulate at different points in the process, and its detonation has been responsible

for many serious incidents including a number of fatalities. It has been a major concern in the chlor-alkali industry, and Chlorine Institute Pamphlet 21 has gathered together much of the relevant literature.

Below we consider the sources and formation NCl_3 , ways to avoid its formation or accumulation, analytical procedures, and methods for removal of NCl_3 from the process.

9.1.11.2A. Sources. Precursors of NCl_3 often are in the salt supply. Nitrogen compounds may be present in the salt itself, and others may be added during its processing. This is most likely in the case of rock salts, where a common source is the ANFO explosive used to break up the beds in the mines (Section 7.1.2). The anti-caking agent frequently applied to fine salts is another source that is present in ppm concentrations. An infrequent but potentially very serious contributor is contamination of salt delivery vehicles or of auxiliary materials. In solution mining, the most likely source is the dissolving water, particularly untreated well water or surface water. A frequent source of NCl_3 precursors in surface water is agricultural runoff.

An occasional in-process source is purified NaOH , which is the upgraded version of diaphragm-cell caustic. It is produced by extracting 50% NaOH from the evaporators with ammonia (Section 9.3.4.1). It would be better to avoid the problem by using the unpurified grade for general purposes.

Calcium chloride, used in some brine systems, is sometimes a byproduct of the Solvay process for soda ash. In this case, it too may be contaminated with ammonia.

A specialized application that can result in nitrogen contamination of salt is the use of amines as separators in the recovery of KCl from mixed ores such as sylvinites (Section 7.1.6.2A).

The sulfuric acid used to dry the chlorine is also sometimes a source of ammonia compounds. Finally, the plant utilities are likely sources. Plant water that has not been thoroughly purified has many opportunities to enter the process. Examples of these opportunities are the use of impure water to prepare treatment chemical solutions, flushing water on rotating machinery seals, water recycle from waste-minimization systems, and direct-contact cooling water. Steam and its condensate are also potential sources. The culprits here usually are the amines used as corrosion inhibitors in the steam system (Section 12.3.2).

9.1.11.2B. Accumulation. Accumulation of impurities in a process usually is associated with recycle systems. However, recycle of liquid chlorine is rare, and we are more concerned here with concentration or accumulation during phase changes. Both condensation and vaporization of chlorine can concentrate NCl_3 if they are incomplete. At the normal boiling point of NCl_3 , the vapor pressure of chlorine is about 22 atm. At lower temperatures, the ratio of vapor pressures is even higher. During liquefaction, NCl_3 will drop out of the vapor in the early stages. Since the recovery of chlorine usually is rather high in a primary liquefier, the concentration factor tends to be not very great. When only a small fraction of a chlorine stream is present as the liquid, however, as in the sort of compressor suction chiller discussed in Section 9.1.6.4A, the concentration factor is higher and the hazard can become more acute. Addition of a stripping section below a suction chiller column aggravates the situation. Because

suction chiller bottoms are often removed only occasionally and batchwise, the problem of accumulation over time is added to that of concentration by vaporization. More and more NCl_3 enters the bottoms receiver with time, and the magnitude of the hazard continues to grow. This factor is offset by the steady slow decomposition of NCl_3 , discussed below. Handling of the bottoms often allows some of the chlorine to evaporate, once again concentrating the NCl_3 . This scenario is responsible for many of the most serious NCl_3 incidents. Designers and operators are well advised to scrutinize designs and procedures very carefully and to provide thorough, repetitive training to plant and laboratory personnel.

The opposite process of chlorine vaporization provides similar opportunities for concentration and accumulation. This can be a particularly acute hazard for chlorine consumers. The vaporization of a batch of liquid chlorine is essentially a process of differential distillation.

The hazard increases when chlorine is continually added to a vaporizing vessel. The concentration of NCl_3 in the unvaporized liquid can gradually increase to a dangerous level. In a continuous vaporizer, NCl_3 will reach a steady-state concentration determined by the incoming concentration and the laws of vapor-liquid equilibrium. If the liquid in the vaporizer is allowed to boil down for any reason, the concentration increases again, as in batch vaporization. Boiling down a storage tank prior to maintenance produces the same effect. A bottom purge connection on a vaporizer, in itself a possible collection point for hazardous residue, permits the vessel to be emptied without a complete boil-down.

All users of liquid chlorine should be aware of the possibility of concentration of nitrogen trichloride by partial vaporization. This should be avoided wherever possible; transfers from tankers or from storage, for example, should be made as liquid rather than as vapor. A frequent recommendation when the concentration of NCl_3 exceeds a plant standard is to dilute the chlorine with fresh material. This must be taken in the right context. Addition of chlorine in order to allow vaporization to continue can be dangerous as well as futile. If batch vaporization continues down to the same volume as that at which the fresh chlorine was added, the NCl_3 concentration in the residue will actually be higher. Addition of fresh chlorine as part of a program to flush the apparatus safely, however, is unexceptionable.

The Chlorine Institute in P152 recommends that NCl_3 concentration never be allowed to increase to more than 2%. This provides a margin below the concentration of 6% at which the rate of the exothermic decomposition begins to accelerate. Euro Chlor [54] reports that 13% is a lower limit for detonation, suggests limits similar to the CI's in processing, and publishes recommendations for maximum concentrations under various circumstances. Variables include

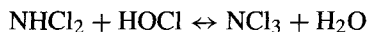
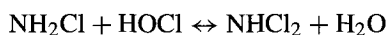
1. the size of the vessel or container (lower limits in larger vessels)
2. the frequency of monitoring (lower limits with less frequent analyses)
3. the nature of any process that takes place in the vessel (more frequent analysis when accumulation or fractionation is likely, as in a suction chiller reboiler or a vaporizer).

Users, producers, and packagers should adopt limits that suit their individual situations.

9.1.11.2C. Avoidance. Sometimes NCl_3 can be avoided by eliminating its precursors from the feeds to the process. The first step is to adopt specifications for their concentrations in raw materials and utilities. If the water used to dissolve salt presents a problem, other grades can be used or purification facilities installed. Other sources of water that can infiltrate the process can be treated the same way, and safer types of water can replace steam and condensate. Salt can be bought without anti-caking agents, and it may be possible to purchase salt mined with the help of an explosive that is free of NCl_3 precursors. A rigid analytical program can catch raw material contamination. Suppliers should be screened and made aware of the importance of preventing contamination of their materials.

Very low concentrations of NCl_3 precursors in feed materials can generate dangerous concentrations in the product chlorine. Many writers emphasize the high concentration factor that occurs when nitrogen bodies in the feed brine become NCl_3 in the chlorine. A unit weight of ammonia, to begin with, produces about seven weights of NCl_3 . Added to this is the fact that a 300 gpl NaCl feed brine is only about 15% Cl. This combined with the molecular weight change from NH_3 to NCl_3 gives a concentration factor of about 45. Going beyond this, we must recognize that not all the NaCl in the brine is converted in the cells. If we assume about a 45% conversion of NaCl with quantitative reaction of NH_3 to NCl_3 , we calculate that 1 ppm of NH_3 in the feed brine can produce 100 ppm NCl_3 in dry chlorine. However, standing concentrations of ammonia exist because conversion per pass is not quantitative. The numbers above are more interesting than realistic. One ppm of ammonia in the salt will eventually produce about 12 ppm of NCl_3 in the chlorine, and this is a more reliable way to assess the potential NCl_3 burden.

When ammonia compounds are in the brine despite preventive measures, controlled chlorination can destroy them and allow the nitrogen content to be removed by venting or sparging with air. The chlorination of ammonia proceeds in a stepwise manner [100]:



It seems senseless at first glance to try to avoid the presence of NCl_3 by adopting a procedure that leads to its formation. It is essential to limit the conversion of ammonia and to interrupt this reaction sequence before NCl_3 forms. The key here is to perform the chlorination at the correct pH. Hypochlorous acid is shown as the reactive species. As the pH drops toward the acidic region, less HOCl ionizes, and its concentration in the solution increases. For the ionization reaction



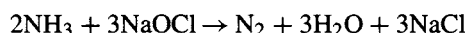
the equilibrium constant is $3.04 \times 10^{-5} e^{-2000/T}$ [101]. Table 9.16, derived from this equation, shows that the concentration of HOCl relative to the hypochlorite ion increases constantly as pH and temperature become lower (see also Fig. 4.1.2). Below pH 5, OCl^- disappears and the concentration of molecular chlorine starts to become appreciable.

TABLE 9.16. %HOCl in HOCl/OCl⁻ Mixtures

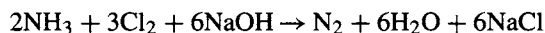
pH	Temperature, °C		
	0	40	80
9	4.8	1.9	0.94
7	83.3	66.2	48.7
5	99.8	99.5	99

These data show that when the brine remains alkaline the concentration of HOCl is not too high. At pH 8.5, the major product is chloramine, which is quite volatile and can be stripped from the brine. At pH 4.5, the major product is nitrogen trichloride. This explains the formation of NCl₃ in the cells, but acidic conditions are to be avoided when deliberately chlorinating the brine.

At even higher pH, where OCl⁻ is dominant, the decomposition byproduct, according to P152, is nitrogen:



If chlorination is by direct injection into highly alkaline brine, the overall reaction then becomes



9.1.11.2D. Detection. NCl₃ frequently is assayed by the classical Kjeldahl nitrogen test. This is time-consuming and not very sensitive at low concentrations. If samples are not kept cold, thermal decomposition will continue while they are waiting or being prepared for analysis. Reported results then will be low, and hazardous concentrations may not be detected. This has been cited as a factor in some NCl₃ incidents. More recently, Hildebrand [102] reported on the development of a chromatographic method that is both rapid and precise. The time required for analysis is about twenty minutes, instead of the 6.5 hr required for a Kjeldahl analysis. The method depends on partial (~90%) evaporation of the chlorine from a chilled sample of liquid, followed by the addition of the chromatographic eluent (methanol plus a dilute acetate buffer at pH 4) and injection into the column. The detector uses ultraviolet light. The method has been certified by ASTM (E2036-99), and one can expect it to find increasing use.

It is essential to remember that Kjeldahl analysis gives total nitrogen content. It overreports NCl₃ when other nitrogen-containing species are present. Operating limits established by previous history can not be relied on when switching from Kjeldahl analysis to a more specific test [102]. Setting new limits is a task for individual plants. If other nitrogen compounds had distorted previous analyses, it may be necessary to lower the limits.

Purchasers of chlorine may do their own analyses or may rely on the supplier's analytical history. A supplier who provides product assays and changes analytical methods as above should inform all customers of the change and its significance.

A partial review of the literature describing accidents attributed to nitrogen trichloride suggests that lack of timely recognition of an increase in NCl_3 is often a contributing factor. Many investigations after the fact find increased levels of NCl_3 in the chlorine, more nitrogen compounds in the brine, etc. Development of a speedy and reliable test, coupled with more frequent monitoring and a mechanism to call for repeat analyses and more frequent checks after one analysis has exceeded the usual range, should help to reduce the number of such incidents. To choose only one of these, we consider an incident in July 1998 that resulted in three injuries and a 2-week shutdown of an entire plant [103]. Two explosions occurred, one in a blowdown line used for periodic withdrawal from a bottoms drum and one in laboratory glassware during investigation of the causes of the incident. The latter resulted in the most serious injury. The nitrogen contamination that caused the incident eventually was traced to urea present in the soda ash used for brine treatment. This in turn arose from the supplier's blending in of a stock of imported material.

9.1.11.2E. Destruction. NCl_3 is unstable and so many possibilities exist for its safe removal from chlorine. Several plants have destroyed NCl_3 with ultraviolet light. The best frequencies are 360–478 nm [104]. Mercury-vapor lights are serviceable and are more successful with chlorine gas than with the liquid. Knoop and Santavicca [105] report that the half-life of NCl_3 exposed to a 4.5-kW lamp is about one second. UV light also catalyzes the reaction of hydrogen with chlorine to form HCl. This reaction has been used as end-of-pipe treatment to reduce the amount of chlorine in hydrogen gas. Users should be aware of this possibility before adopting the technique. Maintenance of the UV source in an operating chemical environment can be a difficult problem, and the physical arrangement of the lamps and the chlorine pipeline is a very important matter.

Some plants rely on the thermal instability of NCl_3 . Without its continuous slow disappearance, many of the reported incidents undoubtedly would have been worse. The rate of decomposition becomes useful somewhere above 50°C. Temperatures in excess of this are found in compressors, and some have installed gas holding pipes to allow the decomposition reaction to proceed. The Chlorine Institute has reprinted a 1963 paper by Ross and Bowling [106] that reports substantial reductions of NCl_3 concentration in a compressor and correlates the results with the compressor outlet temperature. Writers on the thermal decomposition of NCl_3 often state that it is a site-specific phenomenon. The kinetics of a homogeneous gas-phase reaction should be independent of site. One reason for the apparent dependence is the lack of characterization of plant systems. There seems to be a lack of confirming data and of descriptions of physical details to allow one to use published information to design a system with any confidence. Publication and discussion of plant results could contribute to alleviation of this hazard. Accurate knowledge of the various systems and the time/temperature history of the gas should then allow some correlations to be made.

However, a second reason for inconsistency is the fact that there are surface effects. These will vary greatly from site to site. Pipeline reactors, with their high ratios of surface area to volume, will be especially variable.

Euro Chlor's publication [54] contains information on rates of decomposition of NCl_3 in liquid chlorine. Figure 9.51 shows a plot of the first-order rate constant.

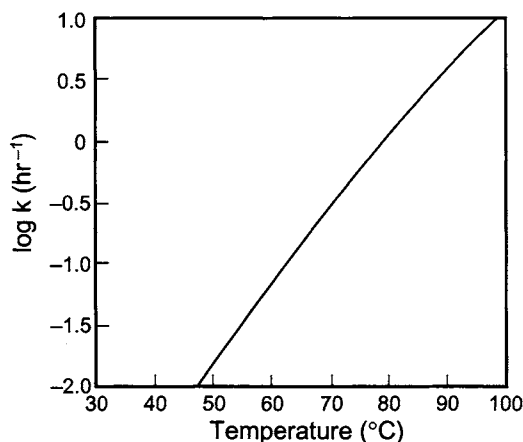


FIGURE 9.51. Rate constant for decomposition of NCl_3 in liquid chlorine (with permission of Euro Chlor).

With k in hr^{-1} and temperature in kelvin, this follows the equation

$$k = 7.46 \times 10^{19} e^{-16111/T} \quad (86)$$

There also are calculations on the decomposition that occurs in typical continuous vaporizers. A later subsection expands on this topic.

Collection of the bottoms from a compressor suction chiller (Section 9.1.6.4A) gives another opportunity for thermal decomposition. Figure 9.25 shows a typical arrangement with a collection pot. Charging this pot with a solvent allows further stripping of chlorine, and refluxing the contents of the pot causes NCl_3 to decompose at a controlled rate. Carbon tetrachloride has been the solvent of choice for many years and is still used by a number of plants. With CCl_4 being phased out, others have adopted alternatives, one of these being chloroform. Users of chloroform must remember that it has a lower boiling point than NCl_3 and that refluxing actually concentrates NCl_3 in the bottoms. The reboiler contents can not be allowed to weather or boil down excessively. One theory is that chlorination of CHCl_3 will gradually produce CCl_4 that will remain as a diluent. This of course destroys the purpose of using chloroform.

Shushunov and Pavlova [107] have published kinetics for the decomposition of NCl_3 in CCl_4 solution. Again, the reaction appears to be first-order, and the authors give 32 kcal mol^{-1} as the activation energy. The plotted data then fit the equation

$$k = 5.3 \times 10^{19} e^{-16105/T} \quad (87)$$

This is very close to Eq. (86). As we saw in Section 9.1.7.2C, the solution properties of chlorine and CCl_4 are quite similar, and this result is further confirmation of that fact.

Turning next to miscellaneous methods, several different catalysts have been suggested for treatment of the filtered dry gas. Activated carbon is the most common. Silica and alumina are other candidates, and these might be impregnated with metal to increase

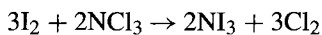
their activity. Startups with fresh beds would require careful management because of possible exotherms. This process does not seem to be in commercial use.

Iron and its compounds can also cause decomposition. The addition of metal shavings into equipment or piping can therefore reduce the NCl_3 decomposition. Because of the possibility of combustion of chlorine with iron (Section 9.1.2) as well as the higher activity of copper alloys, the use of grease-free Monel shavings would be preferred. The possible activity of iron means that wall effects are quite likely in ferrous systems. This would be a confounding factor in any effort to correlate plant experiences.

The Chlorine Institute document referred to above also mentions a number of techniques found in old patents. These include scrubbing with cold aqueous HCl and contact with dilute solutions of common reducing agents. These also seem not to have been practiced widely.

When liquid chlorine spills, its evaporation can leave a deposit of NCl_3 behind. This can detonate simply by having someone walk across it. It should always be assumed after a spill that there is a hazardous residue. A spray of an approximately 5% solution of a reducing agent followed by an inspection for any pools of NCl_3 and a final washdown with water should remove all traces.

The use of iodine-containing species to reduce suction chiller reboiler corrosion (Section 9.1.6.4A) has an added advantage. This iodine that forms reacts as below:



Decomposition of nitrogen triiodide is a relatively low-energy process without the destructive potential of NCl_3 decomposition.

Taking the use of iodoform as an example, formation of elemental iodine requires an excess of chlorine. When the excess is maintained, the addition of about 5 mg CHI_3 per liter of reboiler solvent can decompose more than 90% of the NCl_3 safely.

9.1.11.2F. Fractionation. We have referred several times to the buildup of NCl_3 concentration due to fractionation. This occurs when a small fraction of a chlorine stream condenses, as in a suction chiller reboiler, or when liquid chlorine is vaporized or is allowed to boil down in a vessel. Here, we attempt to quantify the latter situation. It is a case of simple differential distillation of a two-component mixture. We start by assuming a constant relative volatility. The Rayleigh equation [108] becomes

$$A/A_0 = (B/B_0)^\alpha \quad (88)$$

where

- A, B = moles or weights of two components in the still at any time
- A_0, B_0 = moles or weights of two components in the still at some base time
- α = relative volatility of A to B

Specifically, we can define A_0 and B_0 as the quantities present at zero time or at the beginning of vaporization. Manipulating this equation to find the ratio A/B , we obtain

$$A/B = (A_0/B_0)(B_0/B)^{1-\alpha} \quad (89)$$

$(B_0/B)^{1-\alpha}$ is a multiplying factor that relates the ratio of the two concentrations at any time to the ratio at the beginning of vaporization. Below, we refer to it as the concentration factor.

The immediate problem in analyzing this process is to determine the value of α . The first requirement is some knowledge of the vapor pressures of the two components. The physical properties of chlorine are well known. The physical properties of NCl_3 are less well known and, because of the hazards of handling this material, not easily obtained. Argade *et al.* [109] reported on the available vapor pressure data on NCl_3 , and the latest publications still refer to these same data. Vapor pressures can also be estimated from generalized methods, and the calculations of the Design Institute for Physical Property Data (DIPPR) are also widely quoted. These results were obtained using the ChemCAD program. DIPPR results do not agree with the literature data, with the two sets diverging more at low temperatures. The DIPPR vapor pressures are the higher of the two sets. They would predict lower liquid-phase concentrations of NCl_3 .

Abraham and Knoop [110] used the literature data fitted to the Antoine equation to allow extension and interpolation. They present a series of tables that show the calculated liquid and vapor concentrations of NCl_3 at various degrees of chlorine vaporization up to 99.99%. These cover starting liquid-phase concentrations between 1 and 15 ppm and temperatures between -34.5°C and -1°C . Relative volatilities of chlorine relative to NCl_3 derived from these tables are 28.5 at -34.5°C , 33 at -17.8°C , and 35.5 at -1°C . These authors also report a test in which 43% of the chlorine in a tank car was allowed to evaporate into a recovery system. Measurements before and after (data not reported) agreed better with the literature data than with the DIPPR calculations.

These data indicate that the relative volatility of chlorine increases at higher temperature. This is a surprising trend. The relative rate of increase of vapor pressure of a pure liquid with temperature is proportional to its molar heat of vaporization. In most binary mixtures, the less volatile component has the higher latent heat, and the relative volatility therefore tends to decrease as temperature increases. Argade's tabulation of physical properties [109] suggests that this should be the case here. The latent heat of vaporization of chlorine is well established, and in the temperature range considered above, it is about $4.7 \text{ kcal mol}^{-1}$. For NCl_3 , Argade *et al.* quote Apin's value of $7.58 \text{ kcal mol}^{-1}$ [111] and provide a plot showing several points calculated from this value as well as the literature data. Figure 9.52 is a reconstruction. The difficulties of working with nitrogen trichloride might justify questioning this value for the latent heat, but it is not far out of line for a compound boiling at 71°C . The modified Kistiakowsky equation for latent heats predicts a value of $7.00 \text{ kcal mol}^{-1}$, only about 8% lower. The dashed line on the figure has a slope corresponding to these expected values. Clearly, the slope of the experimental vapor pressure curve corresponds to a lower value. This slope in fact suggests that the latent heat of NCl_3 is not much different from that of chlorine, and the progression of relative volatilities in Abraham and Knoop's work corresponds to the rather small difference of about 800 cal mol^{-1} .

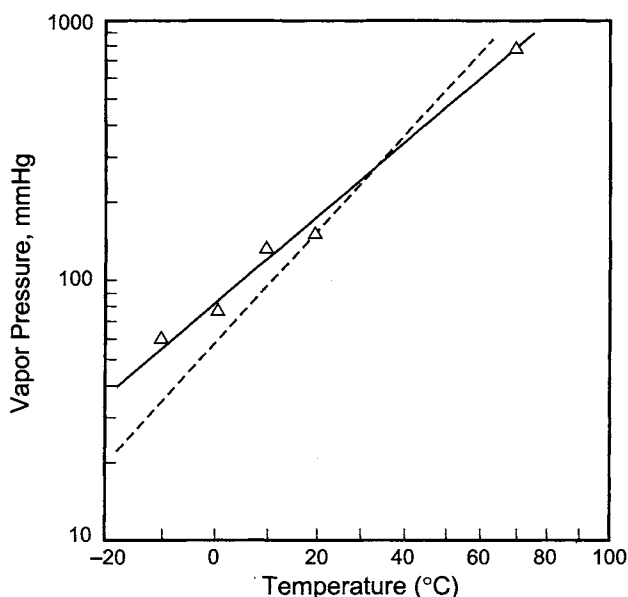


FIGURE 9.52. Vapor pressures of NCl_3 . Solid line: correlation of literature data [109]; dashed line: slope corresponding to estimated latent heat of vaporization.

The calculations described above assumed ideal vapor and liquid behavior. After choosing a model for vapor pressure data, many other workers have calculated NCl_3 accumulation in this way. For this system, one actually would expect some degree of nonideal behavior, with positive deviations. If this were true, the assumption of ideal behavior would err on the safe side, but perhaps unrealistically so. Zeller *et al.* [112] therefore collected data from an operating vaporizer by sampling both gas and liquid phases. Twelve observations at $24.5 \pm 1.3^\circ\text{C}$ gave apparent liquid-phase NCl_3 activity coefficients that ranged from 0.8 to 32. The relative volatility of chlorine to NCl_3 , based on rounded data as tabulated, ranged from 1.35 to 40. While the large range suggests measurement error or confounding factors, it is significant that Zeller *et al.* report an average γ of 13.6 with a 95% confidence interval of about 7–20. This indicates at least that there are positive deviations and that the partition of NCl_3 will be more into the vapor and less into the liquid than ideal-solution calculations would indicate. This means that the buildup of the liquid-phase concentration will be slower. The same effect occurs during the condensation of chlorine gas that contains NCl_3 . At any point during that process, less NCl_3 appears in the liquid and more in the vapor. Under this scenario, condensation and vaporization become less dangerous processes.

These two papers have pointed the way to further progress in determination of the true behavior of NCl_3 in fractionating systems. However, some of the observations are not mutually consistent. One is led to question the validity of the basic data now available.

The highest relative volatility that we have considered for Cl_2 is 40. Referring to Eq. (89) and identifying nitrogen trichloride as component A and chlorine as component B, we adopt a corresponding value of $\beta = 0.025$. The concentration factors for different degrees of vaporization of chlorine are tabulated below.

% Vaporized	B_0/B	Concentration factor
50	2	1.966
90	10	9.44
98	50	45.3
99	100	89.1
99.5	200	175.2
99.8	500	428
99.9	1,000	841
99.99	10,000	7940

Figure 9.53 shows this graphically. It also includes lines for relative volatilities of 20, 10, and 5. If chlorine is twenty times as volatile as NCl_3 ($\beta = 0.05$), for example, vaporization of 99% of the chlorine increases the concentration of NCl_3 in the heel by a factor of 79.4 rather than 89.1.

The results obtained above do not account for decomposition of NCl_3 during the process. The next subsection addresses this in typical chlorine vaporizers.

The model also assumes that vapor as it forms is immediately removed from contact with the liquid. In a real case, there is a substantial and growing amount of vapor confined along with the liquid. While new vapor forming may be in equilibrium with the liquid, the vapor that issues from the container is some mixture of new vapor and previously formed vapor. The vented material and the vapor phase in the container will, if anything, be leaner in NCl_3 than the model would suggest.

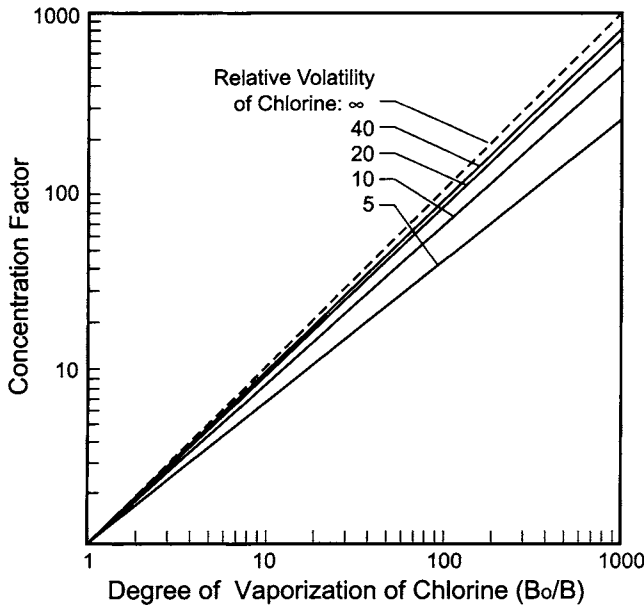


FIGURE 9.53. Concentration factors for NCl_3 during vaporization of chlorine.

There is evidence that use of the reported experimental data rather than the DIPPR equation for vapor pressure of NCl_3 and the assumption of ideal gas and liquid behavior both are conservative in their predictions of the amount of NCl_3 present in the liquid phase after vaporization. It would require basic data of higher quality than are now available to allow us to make calculations with a great degree of confidence.

While fractionation allows high boilers such as NCl_3 to accumulate, it also allows selective removal of low-boiling impurities such as oxygen. A small amount of vaporization can reduce the concentration significantly. Flashing back to lower pressures in liquefaction systems is a convenient technique [31].

9.1.11.2G. Decomposition of NCl_3 in Vaporizers. This treatment is based on the approach and information contained in Euro Chlor's GEST 76/55 [54]. Within a continuously operating vaporizer, we assume a constant volume of a uniformly mixed liquid containing only chlorine and nitrogen trichloride. The distribution coefficient for NCl_3 , or the ratio of its vapor- and liquid-phase concentrations, we label β . In the absence of any decomposition, the steady-state concentration of NCl_3 in the vapor would equal its concentration in the feed:

$$C_F = C_V \quad (90)$$

By definition of the distribution coefficient,

$$C_V = \beta C_L \quad (91)$$

Then

$$C_L = C_F/\beta \quad (92)$$

and the concentration of NCl_3 is multiplied by the factor $1/\beta$. This factor, which may be a function of temperature, fixes the maximum possible concentration to which NCl_3 can accumulate. Because of the decomposition reaction in the vaporizer, the accumulation factor will in fact be smaller.

We can calculate a new steady-state concentration in the vaporizer if we know the kinetics of the reaction. GEST 76/55 gives a plot of a first-order rate constant; this is reproduced in Fig. 9.51. The nitrogen trichloride balance including this reaction is

$$\begin{aligned} \text{rate of feed} &= \text{rate of withdrawal} + \text{rate of reaction} \\ FC_F &= FC_V + kVC_L \end{aligned} \quad (93)$$

We still have the vapor-liquid equilibrium as expressed in Eq. (91). This leads to

$$C_L = C_F/(\beta + kV/F) \quad (94)$$

V/F is the liquid retention time, τ . We can express the buildup of NCl_3 in the vaporizer by an accumulation factor, $A = C_L/C_F$. If no decomposition occurred, we would have $A_0 = 1/\beta$. The accumulation factor is smaller when we account for the reaction:

$$A = 1/(\beta + k\tau) = A_0/(1 + k\tau/\beta) \quad (95)$$

A_0 represents physical equilibrium. It places a limit on the possible accumulation of NCl_3 and is independent of vaporizer design. The term $k\tau/\beta$ in the denominator shows the influence of vaporizer design and process conditions.

GEST 76/55 analyzes the characteristics of two vaporizers, one a vertical-tube unit and the other a kettle type. The operating rate was 3 t hr^{-1} , and the liquid volumes were calculated from the physical dimensions. With vaporization at 50°C , the important parameters in the analysis made above are

$$k = 0.016 \text{ hr}^{-1}$$

$$\beta = 0.025$$

$$\tau = 0.03 \text{ hr (shell-and-tube)}$$

$$= 0.177 \text{ hr (kettle)}$$

The retention times reported in GEST 76/55 were calculated using a liquid density appropriate to a lower temperature, but this does not detract from the main point that there is little destruction of NCl_3 in the typical vaporizer. The calculated parameters lead to the results that follow:

Apparatus	$k\tau/\beta$	% destroyed	Accummulation factor
S & T	0.019	1.9	39
Kettle	0.116	10	36

Figure 9.51 shows that the rate constant is a strong function of temperature. Under the arbitrary assumptions that the liquid reaches 100°C at the walls of the tubes and that 5% of its time in the vaporizer is spent at that temperature, GEST 76/55 shows that the destruction in the smaller unit increases to 43%. We can also estimate the effect of operating at a higher temperature, say 70°C . The retention times are reduced slightly because of the lower density of the liquid, but the rate constant increases to 0.295 hr^{-1} . Now we have

Apparatus	$k\tau/\beta$	% destroyed	Accummulation factor
S & T	0.334	25	30
Kettle	1.971	64	15

This shows the importance of temperature and the fact that operation at 70°C would begin to remove useful quantities of NCl_3 (and aggravate another hazard by requiring pressures above 2 MPa). The real advantage lies not in the efficiency of destruction, which still is not impressive, but in the reduction of the accumulation factor and therefore the reduction in the magnitude of the decomposition energy hazard. It also shows that the increased retention time in a kettle reboiler is useful in minimizing the potential concentration of

NCl_3 , but one must also recognize that the total quantity of fluid present in the vessel is much greater than it is in the case of the vertical unit.

Purging liquid from the vaporizer is another method of reducing its concentration of NCl_3 . If a fraction f of the liquid feed is removed, the material balance equation (93) becomes

$$FC_F = (1 - f)FC_V + kVC_L + fFC_L \quad (96)$$

and

$$C_L = C_F / [\beta + k\tau + (1 - \beta)f] \quad (97)$$

The denominator now consists of three terms showing the effects, respectively, of vaporization, reaction, and purge. If $\beta = 0.025$, as assumed, the fraction purged would have to be very nearly that number in order to have the same effect as vaporization. In other words, a full 2.5% of the liquid would have to be removed in order to cut the accumulation factor in half. This might be acceptable in some situations, but the fact remains that, barring significant effects due to a hot surface, the volatility of NCl_3 is itself the most effective limit on its accumulation in the liquid phase. Use of a different value of β to reflect a higher vapor pressure or the existence of positive deviations in the liquid-phase activity of NCl_3 would make this fact even more striking.

9.1.12. Evacuation and Sniff Systems

Besides the liquefaction tail gas discussed in Section 9.1.9, there are several other sources of chlorine-containing vapor, most of them intermittent, which must be handled. Silver [77] gave a summary of these streams and methods for their treatment. Some streams are continuous, such as those from air-based dechlorination. Intermittent streams include

1. vent gas from loading operations
2. equipment depressurization
3. evacuation (and purging) of lines and equipment
4. cell maintenance activities
5. emergency dumps (and cleanup of spills).

This is a diverse list. The sources differ greatly in frequency, size, pressure, and quality. They sometimes are collectively referred to as “sniff” or “snift” gas and considered together.

Returned vehicles and shipping containers frequently are emptied before reuse or to allow maintenance and revalving. Once the operators have established that the chlorine is free of dangerous contaminants, they can rework it at a rate determined by the capability of the process. While the chlorine is nearly always dry and often at or above process pressure, it is a common practice to introduce it to the inlet of the chlorine dryers. Its rate of entry into the process must be limited, and Section 11.3.2.3B describes the need for control and protective systems.

The usual practice is to vent the container down to some level under its own pressure and then to continue emptying it by using an evacuation compressor. This must be done with due regard to the cautions in Section 9.1.11.2. Acid-sealed liquid-ring compressors are often used to evacuate equipment and piping for maintenance or revalving, to complete the transfer of chlorine from storage tanks, and to produce vacuum for the dechlorination of brine (Section 7.5.9.2A). Sulfuric acid is the sealing liquid when handling rich streams of chlorine. Compressor design considerations are basically as discussed in Section 9.1.6.2. As would be expected in intermittent operations, extra care is necessary to prevent contamination of the chlorine or leakage of wet air into a “dry” system on standby.

In a typical operation, chlorine flows by way of a pressure-control valve to the compressor suction knockout pot. The pressure might be held at 30–40 kPa of vacuum. Under low load, the vacuum might increase to 60–70 kPa. Makeup acid is typically 96% H_2SO_4 . The acid is discharged at 94% H_2SO_4 or higher and is sent to the chlorine drying system. After the demister, the compressed chlorine flows through a backpressure controller into the drying or vent scrubbing system. Under some circumstances, the gas might be delivered into the pressure side of the process, but operators then must be certain that the gas remains dry.

Process connections to the dry evacuation system are at the chlorine drying towers, the compressor system (coolers and compressors), liquefaction (phase separators and liquefiers), and secondary recovery systems. When an emergency spare tank exists, it is held under constant vacuum to be ready to receive chlorine as needed. The evacuation system, as its name implies, is not intended for systems under substantial pressure. These should be vented down through the process for recovery of the chlorine whenever possible. After the pressure has been reduced to a certain level, the evacuation system can take over.

Critical safety precautions associated with evacuation systems are:

1. purging and careful checking are necessary before opening any system for maintenance;
2. vessels must never be allowed to accumulate dangerous concentrations of nitrogen trichloride.

When weak chlorine is handled, as in the evacuation or purging of low-pressure pipelines, an acid seal would quickly be diluted by absorption of water from wet air. In this case, water-sealed compressors are used. Ferrous-metal construction is out of the question for this application. The materials must be suitable for use in wet chlorine service. Titanium and steel lined with titanium or a ceramic are frequently used.

There is a basic limitation on the use of water-ring vacuum pumps. The suction pressure must be greater than the vapor pressure of the sealing fluid. This is of no concern when pulling air through a system in order to sweep out residual chlorine. A frequent application for these units is in fact the boosting of chlorine-laden air to a wet scrubber.

There are process circumstances that require only modest increases in pressure. Some plants use low-pressure blowers either as boosters for the main compressors or as sources of pressure to move the gas through part of the low-pressure side of the process. Other compressors sometimes are used to transfer chlorine within the plant. We have

already mentioned the use of compressed chlorine vapor to force the transfer of liquid chlorine from a storage tank to a process or to another tank (Section 9.1.8.4A).

9.2. HYDROGEN

The major physical properties of hydrogen appear in the Appendix. Here we mention others that are important in the design of a safe system.

Hydrogen is a colorless, tasteless, odorless, and nontoxic gas [113]. It can function as a simple asphyxiant, but its greatest hazard is its explosivity. It has a wide range of explosive concentrations, 4–75% in air and 4.6–93.9% in oxygen. Its ignition temperature in air or oxygen is in the range 565–580°C. The hazard is complicated by the fact that hydrogen has a reverse Joule–Thomson coefficient, causing its temperature to increase as the gas expands. This aggravates the hazard of small leaks of hydrogen from pressurized systems.

9.2.1. Cathode Construction

Chlor-alkali cathode design, in both configuration and material of construction, is quite variable. In mercury cells, the flowing amalgam itself forms the cathodes, with current connections through the steel bottoms of the cells, over which the amalgam flows. Diaphragm cells use steel mesh, which is also the support for the diaphragms. The cell body, or “can,” is also cathodic. Membrane cells use vertical sheets, usually with perforations or engineered shapes to guide the flow of electrolyte and gas. Materials of construction include steel, special stainless steels, and nickel. Carbon steel has a relatively high electrical conductivity, but the trend in membrane cell applications is toward the more corrosion-resistant materials, and nickel generally has a higher conductivity than do the various stainless steels. Membrane-cell cathodes increasingly are supplied with active coatings that reduce the hydrogen overpotential. Coated cathodes are most common in membrane cells; diaphragm cells are a more difficult application because of their geometry and the possibility of hypochlorite attack when the cells are shut down. The latter problem is much less severe in membrane cells, but a problem still remains with reverse currents that can damage the coatings. These currents flow for a short time upon shutdown as the electrolyzers begin to act as galvanic cells. Membrane-cell plants based on coated cathodes therefore usually are equipped with polarizing rectifiers that prevent the change in polarity and consequent reverse currents.

Mercury cells and most diaphragm cells are monopolar. Commercial membrane cells are both monopolar and bipolar. Section 5.2 discusses the differences between these fundamentally different designs. Since anodes and cathodes are structurally distinct in monopolar cells, this configuration is less demanding of electrode design. Many bipolar designs, on the other hand, impose two different sets of constraints on a single assembly. In the simplest form of a bipolar electrode, this would not apply since both faces, anode and cathode, would be identical. With its other faults as an electrode (especially as an anode), graphite can be used in this way and has been in HCl electrolysis for many years. The use of graphite in chlor-alkali electrolysis, on the other hand, was abandoned with the advent of dimensionally stable metal anodes. Bipolar titanium

electrodes unfortunately are less successful, their chief problem being their performance as cathodes. This arises from the extraordinarily high diffusivity of hydrogen (especially in the atomic form), which penetrates the metallic structure. It forms titanium hydride, which is nonconductive and very brittle. The latter characteristic leads to failure of the electrode. In certain types of nonchlorine electrolyzers using bipolar titanium electrodes, the sheets were actually reversed in polarity at some point in order to extend their useful life.

Overcoming these problems was an important part of the development of bipolar membrane cells. From bonded bimetallic sheets, electrode design has advanced to more sophisticated assemblies that prevent titanium embrittlement. As designs have become more successful and as the technology has moved toward higher current densities, bipolar designs have increased their market share. Chapter 5 illustrates some of the specific designs that are now in use.

9.2.2. Uses of Hydrogen

9.2.2.1. Summary. In comparison with the principal products of the cells, hydrogen is low in value, but it can make important contributions to the economics of chlor-alkali production. This section reviews some of its uses, which include synthetic chemistry; hydrogenation; portable clean energy, as in fuel cells and welding applications; on-site production of hydrochloric acid; and fuel. Generally speaking, the higher grade applications require more intensive conditioning of the gas. In the hydrogen business generally, 90% is produced captively for refinery applications or for synthesis of ammonia or methanol. If we consider plants rated at 1,000 tpd, where the economic capacities of the three technologies may overlap, we find that a chlor-alkali plant produces about 30 tpd of hydrogen, while a methanol plant consumes 125 tpd and an ammonia plant, 175. Chlor-alkali plants therefore are not good candidates as principal suppliers of hydrogen to the major chemical consumers.

Most applications require removal of the bulk of the water and some increase in pressure. The spectrum of potential uses can be roughly divided into on-site (within the chlor-alkali plant) and off-site applications as follows:

On-site	Fuel HCl
Off-site	Chemical Refining Sale (pipeline or packaged)

On-site use is always the simpler choice, and using the gas as fuel for a boiler or furnace is the simplest of all, but financially the least rewarding. Application as a fuel, therefore, is often only as a supplement or a backup when the other outlets fail.

The most frequent synthetic use of electrolytic hydrogen is the production of HCl, which is covered in Section 9.1.9.2. This is a natural outlet for a chlor-alkali producer, who can use HCl to acidify cell feed brine or depleted brine and to regenerate ion-exchange columns. It also allows profitable use of the chlorine contained in the liquefaction tail gas. The HCl that can be consumed internally, and so the amount of

hydrogen that can be used in its production, is limited and depends on the type of cell in use. The few plants that use calcium for sulfate removal can consume more HCl if it is used to regenerate CaCl_2 from brine treatment sludge. HCl can also be produced for sale, and in some smaller plants, it is in fact a major product.

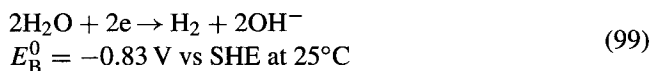
Production of HCl uses chlorine that otherwise could be recovered (at a cost) and so detracts from its net production. Where there is a reliable outlet for caustic, however, the best approach may be to increase electrolytic capacity, use HCl liberally in its in-plant applications, and reduce somewhat the severity of liquefaction. This improves the quality of the cell gas and allows more chlorine to appear in the tail gas, which is the raw material for HCl production. Both these changes reduce energy consumption in the liquefaction process. The gross production of elemental chlorine is preserved, all the benefits of acidification are obtained, and more caustic is available for use or sale.

Chemical applications of hydrogen include

1. the synthesis of ammonia and methanol
2. the saturation of multiple bonds and the conversion of nitro groups into amines (an intermediate step in the production of isocyanates)
3. nonspecific hydrogenolysis such as the hydrocracking of crude petroleum
4. refining processes such as hydrodesulfurization and reforming

While discussion of these processes is beyond our scope, hydrogen has its greatest value in this type of application. Most of these applications are growing at faster rates than the chlor-alkali industry. Refinery use of hydrogen, for example, has been growing by 5–7% per year [114]. All the processes listed require elevated pressure, and some require more extensive purification of the hydrogen. Here, compression is discussed in Section 9.2.3 and purification in Section 9.2.5.

9.2.2.2. Hydrogen Energy Economy. Electrolytic reduction of water or the hydrogen ion produces hydrogen according to reaction (98) or (99), depending on the pH of the electrolyte. In acid solution, we have



where E_{A}^0 and E_{B}^0 are the standard reversible potentials for the two reactions. These reactions occur at the cathode in

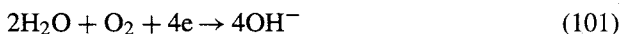
1. diaphragm-cell salt electrolysis
2. membrane-cell salt electrolysis
3. HCl electrolysis
4. electrolysis of salts to chlorates

In mercury-cell electrolysis, hydrogen also results from the reduction of the sodium ion to form amalgam followed by the external decomposition of the amalgam.

The amount of energy consumed in forming hydrogen as a product can be measured by a reverse reaction, its combustion to form water:



This reaction produces about 240 kJ mol^{-1} , equivalent to an electrode potential of 1.23 V. Adding Eqs. (99) and (100) while adjusting the stoichiometry gives



This has a standard electrode potential of +0.4 V. The difference between the potentials of Eqs (99) and (101) is the 1.23 V of Eq. (100). In a chlorine cell operating at 95% current efficiency, the difference between the two possible cathode reactions is equivalent to $980 \text{ kW hr t}^{-1} \text{ Cl}_2$.

Hydrogen is not always a desired product, and the process of last resort is its combustion to recover some of this energy. Here, we consider three ways to recover energy from hydrogen:

1. combustion in a standard burner to produce thermal energy
2. reaction with oxygen in a fuel cell to produce electrical energy
3. depolarization of cathodes to allow reaction (101) to occur directly.

Since the energy consumed by hydrogen formation is in the form of DC electricity, we should evaluate these three processes in that light.

The three techniques listed above all rely on the use of oxygen. Possible sources therefore are refined oxygen and atmospheric or enriched air. Under all ordinary circumstances, atmospheric air is the choice for simple combustion of hydrogen. In the other applications, oxygen has special advantages. While oxygen carries a substantial raw material cost and adds a new set of hazards to the process, air has its own offsetting disadvantages. Nearly 5 mol of air must be compressed and conditioned in order to provide 1 mol of oxygen to a cell. Necessary conditioning may include the removal of CO_2 , which would react with the electrolyte.

9.2.2.2A. Combustion. Combustion is the minimum-value and fallback position for the use of hydrogen. Hydrogen has a net heat of combustion of $57,800 \text{ cal mol}^{-1}$, which on a weight basis is an extraordinary $28,670 \text{ kcal kg}^{-1}$ (130 MJ kg^{-1}). The fact that it issues from the cells as a wet gas detracts from its value as a fuel, because the water in the gas acts as a heat sink. It may be worthwhile to condense some of the water by cooling the gas before sending it to a burner, and a profitable way to do this is to conserve energy by exchanging heat with another process stream, most often the brine at some stage in its treatment process.

The water content of the hydrogen is an especially important consideration in diaphragm-cell plants. Because of the low concentration of caustic in the diaphragm-cell catholyte, the vapor pressure of water is not greatly suppressed. The water content of the gas may well be more than 70%. In a hydrogen cooler that reduces the gas from the cell temperature to 40°C , about 90% of the cooling load goes into the condensation of

water vapor. In membrane-cell plants, a typical water content in the hydrogen would be 30–35%, and only about one third as much heat must be removed to cool the gas to 40°C. In mercury-cell plants, the higher caustic strength once again causes the water content to be lower. In addition to this, the common practice in mercury-cell plants is to cool the gas to some extent at each decomposer. This keeps most of the water (and nearly all of the mercury that was vaporized) within the process, and the water content in the gas header is quite low. Cooling the gas between decomposer and header requires a compact exchanger, and a special type of plate exchanger is often used. The corrugated plates are seam-welded in pairs, and the plate bundle is welded to tubes at both ends to give an assembly of parallel channels for the hydrogen. The shell is a rectangular cast-iron fabrication.

On the hydrogen side, the disadvantages of standard combustion are:

1. the capital and operating costs of preparing the hydrogen for combustion
2. the inefficiencies of combustion and energy-recovery processes
3. the low-grade application of the energy.

The last item reflects the fact that conversion of the thermal energy of combustion into the form of DC electricity, as used to produce hydrogen, is an expensive process with another set of inefficiencies. Recovery of a certain fraction of the energy as process heat therefore does not represent recovery of the same fraction of its original value.

Another practical qualification is that it is seldom attractive to use hydrogen as the only fuel even for a burner in a specialized application. The selection and engineering of burner systems that can operate with hydrogen as well as with a more conventional fuel place some restrictions on design and operation. Burner safety management systems become very important and need careful review. Most equipment suppliers have comprehensive management systems available.

9.2.2.2B. Fuel Cells. The fuel-cell application takes the hydrogen from the electrolyzers and abstracts energy by electrochemical combination with oxygen. Equations (98)–(101) still apply. The energy consumed in the brine electrolyzers by Eq. (98) or (99) is unchanged, as is the energy theoretically produced by Eq. (100). A major advantage of this process over conventional combustion is that the new energy generated by the oxidation of hydrogen does not suffer from Carnot-cycle limitations and is present in the more valuable form of direct current. Using caustic as the electrolyte in the fuel cells also gives the possible advantage of producing concentrated caustic directly at the cathodes. The anodes then would produce a more dilute liquor for recycle to the membrane electrolyzers.

Ideally, the hydrogen from the electrolytic cells would be fed directly to the fuel cells, and the electricity generated in the fuel cells would be fed directly to the electrolyzers. Space limitations aside, the addition of fuel cells to an existing electrolytic plant would then seem to be a simple retrofit. Unfortunately, the fuel-cell approach suffers from both the nonideality of the cells and the complications of delivery of the energy derived from them. Fuel cells in practical operation generate only a fraction of the theoretical voltage. As to delivery of the energy, general-purpose electrical use would involve the expense of conversion from DC to AC. The more direct use in which the fuel cells are coupled directly with the electrolyzers has not proved feasible. Figure 9.54 shows

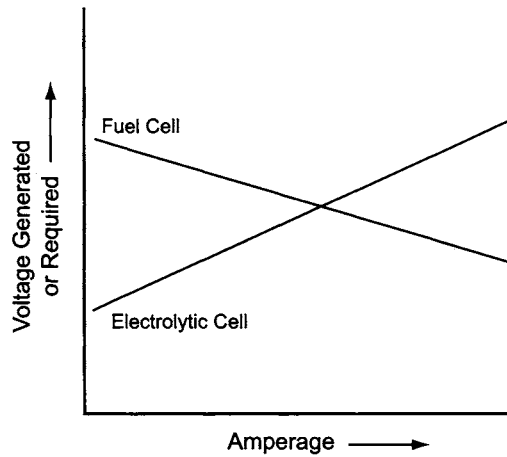


FIGURE 9.54. Opposing characteristics of fuel cells and electrolytic cells.

that one problem with this combination is that the operating curves of electrolyzers and fuel cells are incompatible. Plots of current vs voltage for the two types of apparatus have opposite slopes. As the current on a line of electrolyzers increases, for example, the applied voltage also must increase to offset growing IR losses and electrode overpotentials. If a line of fuel cells must produce a higher voltage, on the other hand, the output current decreases. It is not possible to balance the two systems at more than a single point. The problem is analogous to the one that has prevented direct energy recovery from the exothermic amalgam decomposition reaction. Second-law considerations tell us that if fuel cells are to produce the voltage required by the electrolyzers, they will not be able to generate the required amperage. As operating load increases or electrolyzer and fuel cell performance deteriorates with time, this deficiency grows.

The use of buck regulators or inverters and transformers to match output and input voltages has been suggested, but this adds another layer of cost and inefficiency [115]. Another possibility is to divide the electrolytic cells into distinct groups and to operate one or more groups with the power generated by the fuel cells. The hydrogen from the electrolyzers could be supplemented with an outside source as necessary to stabilize the output. A system for recovery of waste heat from the cells becomes necessary if economic total energy efficiency is to be achieved. Similarly, it would be possible to operate fuel cells in parallel with rectifiers to provide only a portion of the required electrolysis power.

Fuel cells must carry the costs of conditioning the two reactant gases as well as their own capital charges. Hydrogen requires transport to the anode side of the fuel cells. This is usually by rotary blower, but it also should be possible to operate membrane cells at some positive pressure and then to deliver the hydrogen without mechanical aid. The temperature and water content of the hydrogen must be considered in the overall heat and mass balance. Air and oxygen are candidates for use at the cathodes. The classical balance between cost and efficiency determines the choice. With alkaline fuel cells, the carbon dioxide in the air is of concern. It can consume the hydroxide value and contaminate the end product. It is possible to scrub the air to remove the CO_2 before

entering the fuel cells. At least some of the carbonate formed in the scrubber can be used in brine treatment. A water scrubber following the decarbonator not only reduces entrainment but also serves to humidify the air. This can be useful in preventing excessive evaporation from the cells.

Because of these practical difficulties, fuel cells in tandem with electrolyzers have not significantly penetrated the chlor-alkali industry. They have, however, begun their breakthrough into power generation. Reductions in the generation of greenhouse gases as the Kyoto Protocol takes effect will be a major driver. This trend will be helped by the advent of distributed power, in which smaller generators are placed close to the point of use in order to supplement the main power supply [116].

9.2.2.2C. Cathode Depolarization. Combustion in burners and use in fuel cells both depend on the oxidation of hydrogen already formed to reclaim some of the energy consumed in the electrolysis of brine. While not strictly a recovery process, a more elegant and possibly more effective approach would be to accomplish reaction (101) directly at the cathode. None of the equipment costs or energy losses associated with handling and reaction of the hydrogen would exist.

The oxygen-depolarized cathode (ODC), or air cathode, brings about this fundamental change in the electrode reaction. The coulombic requirement in a cell is unchanged, but the standard electrode potential is 1.23 V lower. Thermodynamically, the difference is equivalent to direct conversion of hydrogen to DC energy. The inefficiencies associated with the conversion of energy from one form to another disappear. The consumption of water in the cathode reaction is halved, and the evaporation of water into the cathode-side gas is much less. Any gas vent will still carry water of evaporation, but with any commercial form of concentrated oxygen, the flow will be less than the amount of hydrogen produced by a conventional cell. In a diaphragm-cell plant, these changes add to the evaporator load. In a membrane-cell plant, reducing the amount of dilution water added to the circulating caustic compensates for the changes. In the example of Fig. 6.9, the reduction would amount to as much as 60–65%. This either reduces the demand for high-purity dilution water or makes some of the process condensate that would be used for dilution available for other purposes. The use of air rather than oxygen as the depolarizing gas would at least double the rate of evaporation of water from the catholyte. This still does not fully offset the change in the amount of water consumed by the cathode reaction.

As is the case with fuel cells, depolarized cathodes have been considered for years but have not yet found wide commercial use in the chlor-alkali industry. Reports of work in the 1970s and 1980s [117,118] described the use of solid-polymer electrolyte systems. Microporous electrodes are necessary for electrical continuity in these cells, and the cathode reaction takes place in the interior of the gas-diffusion electrode. Operating deficiencies include the gradual penetration of gas channels by caustic solution and the possibility of bulk flow of catholyte into the gas side of the electrodes. Section 17.2.2.2 describes more recent work that addresses these deficiencies. The first commercial applications are beginning to appear.

There is a choice to be made between air and oxygen as the depolarizing medium. Oxygen is more efficient, but its cost can make cathode depolarization or the use of fuel cells unattractive. If we take as our source a standard enriched oxygen from a

pressure-swing adsorption process ($\sim 94\%$ O_2), the cost to the consumer will be about \$50 per ton. The theoretical consumption of oxygen is 0.225 t/t Cl_2 , and the oxygen cost as a percentage of the reduction in energy cost is given by

$$L = 2,250,000 X / (S P E) \quad (102)$$

where

L = lost value of energy savings, %

X = cost of oxygen, $\$ t^{-1}$

S = energy saved, $kW hr t^{-1} Cl_2$

P = cost of electric energy, $\$/MW hr$

E = conversion of the oxygen supplied, %

If $X = 50$, $S = 700$, $P = 40$, and $E = 100$, then $L = 40.2\%$. In other words, the cost of the theoretical minimum amount of oxygen alone consumes 40% of the value of the energy saved. The incomplete reaction of oxygen can make the real number substantially higher. The addition of excess oxygen, other operating costs, and a reasonable return on capital would probably make our example economically unattractive.

9.2.3. Compression

Electrolytic hydrogen is quite pure ($>99.9\%$) but has the disadvantages of being generated in relatively small quantities at low pressure with a high water content. The type of machinery used to raise the pressure of hydrogen depends on the final pressure required. The gas may be boosted through the processing train by a simple fan. Rotary blowers can generate pressures of a few tens of kilopascals. For somewhat higher pressures that allow refining and some chemical applications, water-ring compressors are a frequent choice. Section 9.1.6.2C covered the principles of these machines. In hydrogen service, the water may be supplied on a once-through basis. This removes the need for a seal-water cooler by using the equivalent cooling water directly in the machine. The water picks up entrained caustic from the gas, and this must be removed from the compressor. In a closed system, this requires blowing down the seal water. In most cases, the water condensing from the hydrogen in the compressor system will provide a natural purge. The use of gas recycle for suction pressure control adds to the total throughput and must be reflected in the design capacity. The energy efficiency of these compressors is poor, as already pointed out, but they benefit from the cooling of the gas during compression. The latter effect reduces the theoretical energy requirement below that corresponding to polytropic operation.

The construction of the compressor and its auxiliaries usually is in ferrous metals. Cast iron and ductile iron are widely used for the body of the compressor as well as for the water pumps.

Example. Using an example not related to our reference plant, consider the compression of $8,000$ cfm ($4,704$ m^3 hr^{-1}) of wet hydrogen at $40^\circ C$ from one to two atmospheres in a water-ring compressor. Since the vapor pressure of water is 55.3 mmHg, the gas holds about 695 kg hr^{-1} of water vapor. About 360 kg hr^{-1} condenses if the temperature of the compressed gas is held at $40^\circ C$. We calculate the work of isothermal compression to be 159 kW by Eq. (42) in Section 9.1.6.1. Adding 15% for recycle, we obtain 183 kW.

Using an efficiency of 35% against this basis, we would require 522 kW. A commercial installation of this description was rated at 540 kW. The waste heat generated by the machine in our calculation is $522 - 183 = 339$ kW. The latent heat of the water condensed from the gas adds 225 kW to this, giving a total cooling load of about 565 kW. At $0.088 \text{ m}^3 \text{ hr}^{-1} \text{ kW}^{-1}$, corresponding to a temperature rise of 10°C in the water, the requirement for 30°C cooling water is $50 \text{ m}^3 \text{ hr}^{-1}$. This exceeds the actual value of $42 \text{ m}^3 \text{ hr}^{-1}$. A cooling water supply temperature of 28°C would account for the difference.

For high-pressure applications, such as ammonia synthesis or packaging of hydrogen, reciprocating compressors are used. As pointed out in Section 9.1.6.2A, the performance of a centrifugal compressor depends on the molecular weight of the gas being handled. With hydrogen, the pressure developed by a given velocity head is quite small, and centrifugal compressors are not suitable. While the compression ratio for air by a single wheel might be 1.4, the most that can reasonably be achieved with hydrogen is less than 1.03.

Multistage reciprocating compressors in hydrogen service are of ferrous metal, such as cast iron. A pulsation damper, a cooler, and a water separator follow each stage. Mist eliminators will enhance the removal of water. The condensate can be removed through water traps and then discarded or returned to a hydrogen seal pot. The operator must recognize that small quantities of hydrogen are dissolved or entrained in the water and must ensure that they have a chance to escape safely. The specific heat ratio of pure hydrogen is about 1.42, and compression ratios per stage usually are limited to about 2.5.

Cylinders may be single- or double-acting, and both unloaders and clearance pockets are used for capacity control (Section 9.1.6.3B). If the compressor takes less than the full cell output of hydrogen, the excess must be vented. This can be by way of the low-pressure seal pots or by controlled venting somewhere in the compression train. This can present problems in process control. Section 11.4.2.5A describes some of the systems that have been used.

The exchangers used to cool the gas and the circulating lubricating oil are of standard construction and usually operate on plant cooling water. Compressor cylinders frequently also are jacketed and cooled. Water used in the jackets should be clean, and frequently its source is something other than plant cooling water. One must be careful not to cool the gas enough to condense water in the cylinders. At startup, it may even be necessary to heat the cylinders.

Example. We compress our reference plant hydrogen from nearly atmospheric pressure up to 3,500 kPa for delivery to a chemical process. The gas first is chilled to 20°C . The compression ratio in each stage is limited to 2.5, and the gas is cooled to 40°C after each stage of compression. Allowing for interstage pressure drops, we have

Stage	Pressure in (k Pa)	Pressure out (k Pa)	Temperature out ($^\circ\text{C}$)
1	110	260	109.7
2	250	620	142.0
3	600	1500	143.0
4	1450	3550	140.3

For a polytropic process, we use $n = 1.45$. From the physical properties of hydrogen and water, we calculate the amount of water held by the saturated gas after each cooler, and from that, the amount condensed and the total duty of each cooler:

Stage	Condensate kg hr ⁻¹	Residual water kg hr ⁻¹	Duty, kW
1	—	171.5	251.4
2	76.4	95.1	417.6
3	56.1	39.0	406.6
4	22.6	16.4	371.1

Taking the total cooling load to be 1.5 MW, we require a flow of 165 m³ hr⁻¹ of cooling water with an 8°C rise. Applying Eq. (44) from Section 9.1.6.1 successively to each of the four stages and assuming an efficiency of 75%, the compressor will consume about 1.75 MW.

Since the coldest gas enters the first stage, the outlet temperature is lowest there. It would be feasible to design for a higher compression ratio in that stage. However, the approach used here is simpler, and allowing a slightly higher volumetric flow rate (higher water content) at the compressor inlet provides for shutdowns of the hydrogen chiller.

Pressure control before and after hydrogen compressors is by standard techniques. The consumption rate is not always matched to the production rate, and some of the gas may be vented from time to time. A split-range controller managing both product hydrogen and vent valves can handle this situation. Vent system design requires careful consideration of the hazards of hydrogen (Section 9.2.6).

9.2.4. Cooling

Water is present in the hydrogen from the cells at a partial pressure equal to its vapor pressure over the caustic solution produced. The large differences in cell caustic strength therefore are reflected in the composition of the gas. Diaphragm-cell hydrogen is by far the wettest; mercury-cell hydrogen, even before the overhead coolers, is relatively quite dry (over 45% KOH, less so). Table 9.17 compares the amounts of water accompanying a unit volume of hydrogen for the different types of cell in both soda and potash production. The operating pressure is assumed to be 100 kPa, except for one special case chosen to show the effect of operation of a membrane cell in caustic soda service at modest pressure. When the gas is cooled to 40°C, Table 9.18 shows how the heat duties compare in the examples of Table 9.17 as well as in the case of diaphragm cells operating at 95 kPa.

Particularly with diaphragm cells, ambient pressure can be an important variable. The volume ratio of water to hydrogen, in terms of the vapor pressure P^0 and the ambient pressure Π is

$$r = P^0 / (\Pi - P^0) \quad (103)$$

If the vapor pressure is a large fraction of the total pressure, a small change in either one can have a large effect on the amount of water in the gas phase. Table 9.17 shows

TABLE 9.17. Water Content of Hydrogen from Cells

Type of cell	Electrolyte	Weight% caustic	Temp., °C	Vapor pressure, kPa	Volume ratio, water/H ₂	Relative volume of water
Diaphragm	NaOH ^a	11.5	95	61.5	1.597	345
Membrane	NaOH	32	89	31.66	0.463	100
Membrane	NaOH ^b	32	89	31.66	0.322	70
Mercury	NaOH	50	100	13.99	0.163	35
Mercury	NaOH	50	80	6.89	0.074	16
Membrane	KOH	30	89	42.66	0.744	160
Mercury	KOH	45	100	32.66	0.485	105
Mercury	KOH	45	80	14.46	0.169	37

Notes:

^a Also contains 14.5% NaCl.

^b Operating at 130kPa.

TABLE 9.18. Relative Heat Duties in Hydrogen Cooling

Type of cell	Electrolyte	Ambient pressure, k Pa	Operating pressure, k Pa	Relative heat duty
Diaphragm	NaOH	100	101	3.7
Diaphragm	NaOH	95	96	4.3
Membrane	NaOH	100	101	1.0
Membrane	NaOH	100	130	0.7
Mercury	NaOH	100	101	0.1
Membrane	KOH	100	101	1.7
Mercury	KOH	100	101	0.3

that this is most true in the case of the diaphragm cell. If the ambient pressure drops from 100 only to 95 kPa, the ratio of water to hydrogen rises to 1.836. For only a 5% drop in pressure, this is a 15% increase in the amount of water associated with a given amount of hydrogen. It is therefore important to design a hydrogen cooler to operate at a reasonably chosen minimum process pressure, and not simply use one related to the yearly average atmospheric pressure.

Hydrogen cooling takes place in conventional shell-and-tube exchangers or in direct-contact columns. Carbon steel is the primary material of construction for surface exchangers. As with chlorine, the cooling of hydrogen is a condensation process with continuously decreasing concentration of water. Coefficients of heat transfer and mean temperature differentials are obtained after the fact from point-by-point calculation.

Direct-contact cooling may be with water or with brine. Water frequently is applied in spray columns, and most construction is in carbon steel. Brine, being contaminated and more corrosive, more often is used with packed columns and in lined systems. In any case, pressure drop is very important on the low-pressure side of a hydrogen system, in order to minimize the infiltration of air into subatmospheric zones. In this connection, sprays that are cocurrent with gas flow can actually increase the gas pressure. At least

in membrane-cell installations, a goal usually is to maintain positive pressure from the cells through to the compressor suction.

The wide variation in the behavior of the gas from different types of cell reflects differences in operating temperatures, which also influence the chlorine cooling process. More importantly, it also reflects the large differences in water content and superheat. Figure 9.55 makes this clear with cooling curves for typical diaphragm-cell and membrane-cell hydrogen. The curve for diaphragm-cell hydrogen, with only about 5°C superheat, resembles Fig. 9.3, the curve for chlorine gas. Membrane-cell hydrogen is quite different. It is cooler to start with, and it has about 15°C superheat. The latter reflects the lowering of the vapor pressure by the higher concentration of caustic in the catholyte. The curves show that most of the heat is removed while a diaphragm-cell gas remains above 86°C. In the membrane-cell case, the 50% point is not reached until the gas is cooled to about 66°C. The mean temperature differential (MTD) in a diaphragm-cell hydrogen cooler is 60–65% greater than that in a membrane-cell hydrogen cooler with the same temperature end-point.

As was the case with primary chlorine coolers, the MTD in the diaphragm-cell case is considerably higher than the AMTD or LMTD calculated from inlet and outlet temperatures. The reasons are the same: the duty curve (Fig. 9.55) is concave downward, and the degree of superheat is small (as shown by the “tail” at the upper end of the curve). With membrane-cell hydrogen, the second of these factors is no longer true. The substantial amount of superheat distorts the curve, and much of it now is below the straight line connecting the inlet and outlet temperatures. In the particular example shown in Fig. 9.55, the true MTD is lower than the LMTD calculated from the terminal temperatures. There is too much variation in membrane-cell catholyte temperatures and concentrations to state this as a general rule.

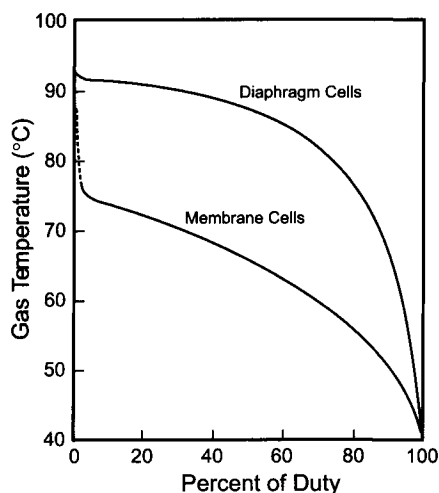


FIGURE 9.55. Heat duty curves—hydrogen cooler.

Example. The hydrogen from the membrane cells is cooled from 89°C to 40°C in a single-pass shell-and-tube exchanger. Establishing the cooling and temperature differential curves, as in the example for chlorine in Section 9.1.3.1, and integrating the latter, we find $MTD = 22.6^\circ\text{C}$. Unlike the cooling of chlorine or diaphragm-cell hydrogen, this value is less than the LMTD of 25.1°C . This is a result of the high amount of superheat (18.9°C).

Of the $3,411 \text{ kg hr}^{-1}$ of water present in the gas, $2,811 \text{ kg hr}^{-1}$ is condensed, and the heat load is $2,138 \text{ kW}$. Applying the MTD given above and using a typical heat-transfer coefficient of $875 \text{ kW m}^{-2} (\text{C}^{-1})$, we require approximately 108 m^2 of surface.

Design of hydrogen coolers must provide for a steady decrease in the heat-transfer coefficient as diffusion of the remaining water to a cold surface becomes more difficult. Because of the generally higher diffusion coefficients in hydrogen systems, the effect is less marked here than in the case of chlorine cooling.

9.2.5. Purification of Hydrogen

While cathode reactions tend to be quite efficient, low concentrations of mercury and oxygen may be objectionable. Sections 9.2.5.1 and 9.2.5.2 deal with their removal. Volatile impurities in the catholyte may also contaminate the hydrogen. This is most likely in diaphragm cells, and Section 7.5.8.5 gave an example in which the removal of ammonia from brine reduced the concentrations of chloramines and other nitrogen compounds in the hydrogen.

9.2.5.1. Removal of Mercury. Mercury is quite volatile for a metal, and its concentration in the hydrogen gas produced in a mercury cell is many times higher than the acceptable limit. The techniques used to remove the mercury can be divided into those that reduce its vapor pressure and those that reduce its concentration to even lower partial pressures. Figure 9.56 shows a typical process consisting of three steps: cooling, chilling, and adsorption. Cooling and chilling belong to the first category and adsorption to the second. The gas may also be scrubbed with an aqueous stream between the heat exchanger(s) and the adsorber. We shall see below that scrubbing may belong to either of the above categories. The objective is the reduction of the mercury content of the gas to a very low level, and the adsorption process is the most effective method for assuring this. Single-step treatment is technically feasible, but the amount of adsorbent required would be very large. The other two steps therefore may be regarded as pretreatment that reduces the load on the third step.

We have already discussed the process of hydrogen cooling in Section 9.2.4 and noted that most of the cooling occurs above the decomposers, with a separate exchanger mounted for each cell. The condensate, water, and mercury, returns to the cells. The gas in the header can be cooled further, before or after compression, and chilled water can be used to enhance the removal of mercury. The configuration of the cooling system and the thermal duties at each step depend on the characteristics of the various utilities. Using chilled water to cool the hydrogen reduces the mercury content to a relatively low level. Water at 5°C or lower can reduce the gas temperature to $7\text{--}8^\circ\text{C}$ and the mercury content to about 5 mg m^{-3} . There are several possible approaches to the

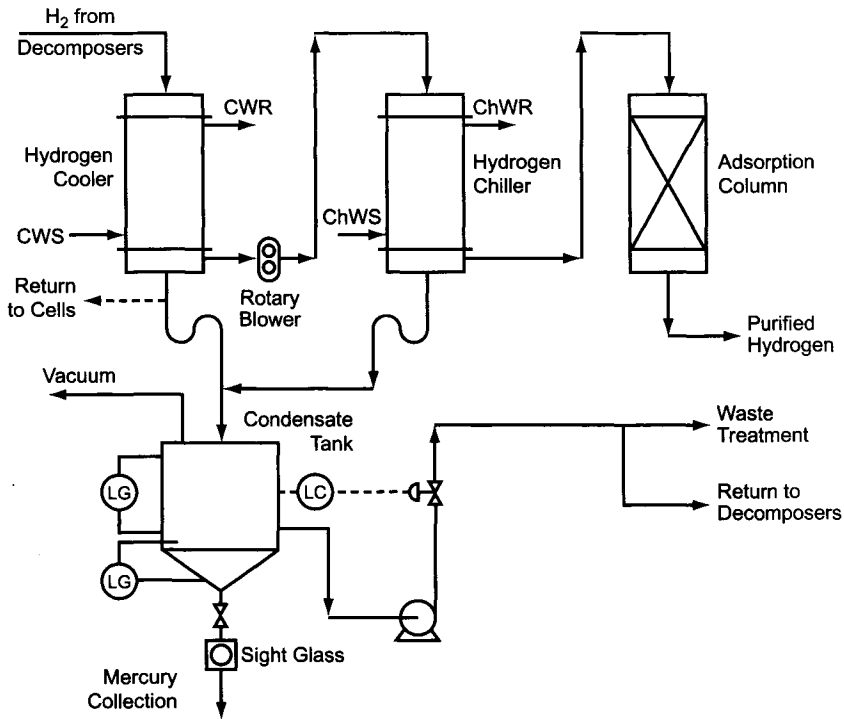


FIGURE 9.56. Removal of mercury from hydrogen.

use of chilled water:

1. Accept chilled water at a higher temperature, as produced for the purpose of cooling chlorine gas (Section 9.1.3.5A), and so allow a higher mercury concentration in the next stage of treatment.
2. Produce chilled water in the utility section of the plant at the temperature desired for hydrogen chilling, and temper the water to the chlorine system by allowing some of the return to bypass the water chiller (cf. Fig. 9.30).
3. Provide local refrigeration to control the temperatures in the hydrogen chiller and scrubber.

The hydrogen chiller resembles the chlorine coolers in its design. It is mounted vertically, with downward flow of the gas. The bottom head serves as a gas-liquid separator, and the condensate flows on to a receiver. The condensate separates into two phases, and the receiving vessel should be designed for easy removal of the metal. The water will be contaminated with mercury and so must be removed or treated carefully before being discharged (Section 16.5.5.3).

Removal of mercury by scrubbing is enhanced when the metal reacts with the scrubbing solution. Mercury in its metallic state is highly insoluble in water and has no opportunity to react. Scrubbing with pure water, unless it incidentally cools the gas, is ineffective. Certain mercuric salts, however, are more soluble, and oxidation of the

metal can allow it to dissolve. In chloride solutions that contain free chlorine, mercury not only oxidizes to the +2 state but also complexes with chloride ions. The degree of complexation depends on the concentration of Cl^- in solution. A low concentration of free chlorine is sufficient for oxidation of the mercury, and depleted brine is a convenient source. With such a high chloride content in the solution, the mercuric ion associates with close to the maximum possible number of chloride ions, which is four. The form of the ion therefore is HgCl_4^{2-} . When a gas stream containing mercury vapor is scrubbed with a brine solution containing free chlorine, the mercury will be found in solution as Na_2HgCl_4 or K_2HgCl_4 . When this mercury-laden brine returns to the cells, the reduced metal deposits onto the flowing amalgam cathode.

The scrubber should operate at essentially the same temperature as the chiller. Normal practice is to minimize fresh solution input by recirculating the scrubber liquor through a cooler, which can be on the same coolant circuit as the hydrogen chiller. Passage of the gas depletes the hypochlorite and deposits more condensate, which contributes its latent heat to the duty of the recirculation cooler. The process therefore requires replenishment of hypochlorite and removal of accumulated water. A simple approach is to provide a small continuous addition of depleted brine and to remove liquid from the bottom of the scrubber column under level control. Any hypochlorite or free chlorine carried from the scrubber must be removed from the hydrogen. A second wash column using cold water or brine serves this purpose. A small amount of reducing agent may be added to reduce hypochlorite or chlorine to chloride ion (Section 7.5.9.3A).

Finally, mercury can be adsorbed from vapor by activated carbon or molecular sieves. Again, extra measures can reduce the volatility of the adsorbed species. The low volatility and low solubility of mercuric sulfide are the basis for a number of mercury-control processes in both the liquid and the vapor phase. The metal has a high degree of affinity for sulfur and is easily captured by that element (hence the name mercaptans for organic $-\text{SH}$ compounds). The activity of an adsorbent therefore is improved by impregnating it with sulfur. This behavior is put to use by treating activated carbon with sulfur or sulfuric acid [119]. The activity of the carbon is enhanced, and hydrogen has been produced with less than $5 \mu\text{g Hg m}^{-3}$. A typical carbon contains more than 10% S and is manufactured preferably from bituminous coal [120]. When operated at about 25°C with a gas feed space velocity of 5 min^{-1} , it has capacity for as much as 20% Hg. Typical pressure drops for the bed itself are 30 mm w.c. Results are better when the gas is dry, and it is especially important to avoid condensation of water from the gas. Keeping the gas a few degrees above ambient or pre-cooler temperature normally is sufficient. The high capacity for mercury translates into long run times for the adsorbent, and on-line regeneration is not an important concern. Removal of the carbon from the bed and firing in a retort can recover nearly all the mercury for reuse.

More specialized materials also may be used. Adsorption on copper/aluminum oxide or silver/zinc oxide reduces the mercury level to less than $1 \mu\text{g m}^{-3}$ [119].

Another technique for reducing the partial pressure of mercury below its vapor pressure at line temperature is the formation of calomel. The basis for this process is the easy conversion of mercury, in the presence of excess chlorine, to calomel (mercurous chloride, Hg_2Cl_2):



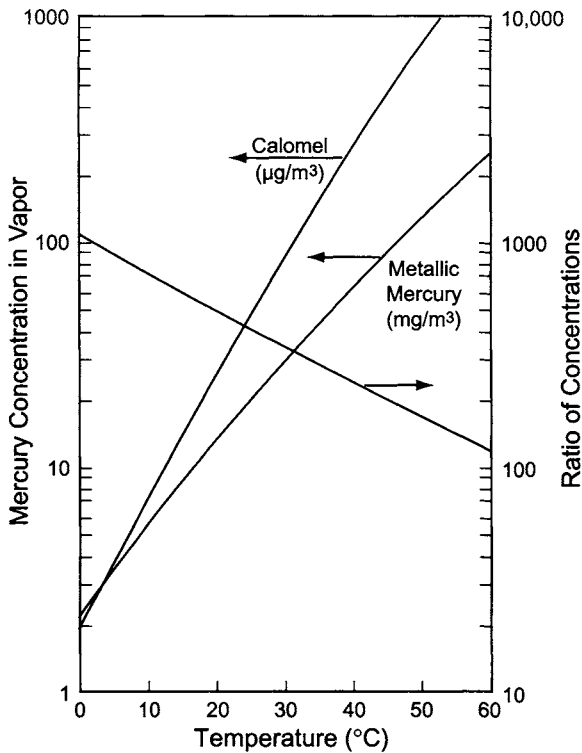


FIGURE 9.57. Reduction in mercury vapor concentration by formation of calomel.

The utility of the process lies in the fact that calomel has a much lower vapor pressure than mercury. Figure 9.57 compares the partial pressures of mercury in a gas saturated over the metal and over calomel. After calomel forms, it can be removed by allowing it to deposit on the packing in a column. Salt is one possible choice of packing; the mercury value then returns to the process when the salt is dissolved to prepare brine. The process has been applied to vent streams (hydrogen or end box ventilation air) and to hydrogen in a recovery system. When the hydrogen is to be recovered, any excess chlorine used in reaction (104) must be removed in another reactor. This process is an enhancement of hydrogen cooling but not so effective as adsorption. For this reason, it is not widely used in the most recently installed treatment systems.

9.2.5.2. Removal of Oxygen. For many of its chemical uses, hydrogen should be scrupulously free of oxygen. Small amounts are always present as a result of cell inefficiencies, air dissolved or entrained in process streams such as caustic dilution water, and infiltration and even diffusion of air into the process. This oxygen can be removed by catalytic recombination with the hydrogen. Typical catalysts are precious metal (Pt or Pd) on siliceous carriers. After compression to about 3 bar and cooling to about 40°C , the gas is passed through an oil adsorber and then over a catalyst bed. Ten seconds would be a typical

retention time. The gas then is brought to a temperature close to 0°C in one or two steps and finally passed through a drying system.

In the allied technology of electrolytic production of chlorates, cathode current efficiencies are not as good as in chlor-alkali electrolysis. Oxygen contents are higher, and the heat of oxidation is substantial. It may then be necessary to carry out the reaction in two stages with intercooling.

9.2.6. Hazards

The introduction to Section 9.2 presented some of the hazards associated with hydrogen. The most familiar of these is its flammability, and it is necessary to construct a system that is reliably free of leaks. The small molecular size and resulting high diffusivity of hydrogen make it especially likely to leak, even from a system that tests essentially gas-tight on air. The very pale or colorless flame is nearly invisible and very hard to detect. Patrolling a cell room at night is often the best way to discover small hydrogen leaks. Finally, hydrogen also has the ability to diffuse into carbon steel and cause lamination and the loss of strength. This is similar to its action on titanium [121]. Its effect on steel is attributed to its reaction with carbon, forming methane [113]. Figure 9.58 is a version of the familiar Nelson plot showing the exposure conditions that lead to hydrogen embrittlement of steel [122].

The simplest way to handle hydrogen is to vent it from the electrolysis system, and many small plants have done this. Section 8.2.2 addresses cell room design to prevent accumulations of hydrogen gas and to provide electrical safety. Venting was a more common approach in the past when profit margins generally were higher and energy costs lower than they are today. Still, there are occasions in any plant when hydrogen must be vented, and vented safely. Low-pressure systems use water seals similar to those in chlorine service (Section 9.1.10.1). These function as emergency relief devices, but at least some of them have adjustable seals that allow the hydrogen to be vented when the operator chooses. This may be during a temporary outage in the hydrogen-receiving process that does not justify shutting down the electrolyzers. Water seals become less

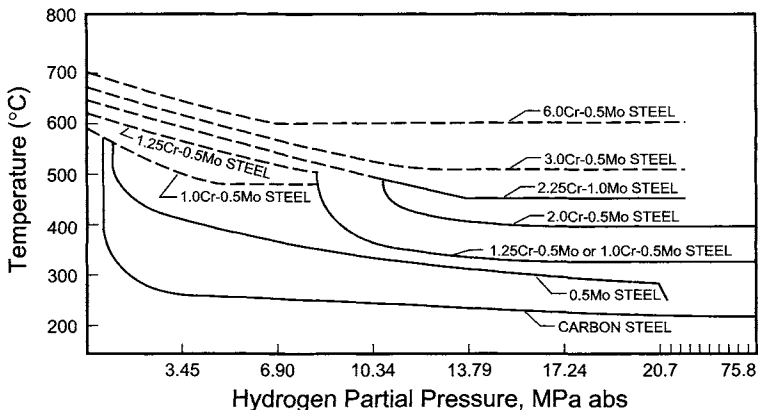


FIGURE 9.58. Operating limits for steels in hydrogen service (Nelson plot).

serviceable as operating pressure increases. Mechanical relief devices are preferred in membrane-cell lines operating under modest pressure [123], and standard pressure-control valves allow controlled venting. The different approaches to control of cell-room hydrogen systems are explored in Section 11.4.2.1.

Many plants cool their hydrogen by contact with water or brine before sending it on to compression and further processing. When a plant has two or more trains processing hydrogen, some mutual isolation of the trains is necessary. The low-pressure seal pots must be placed in line before the isolating devices. Somewhere after the compressors, the separate trains usually combine into one. This may be split again to provide redundancy in a single-use plant or to deliver hydrogen to a number of separate users. In any case, pressure relief is again necessary. When pressure is modest, as in the delivery of hydrogen to a utility plant, seal pots again may be appropriate. There usually is no reason to provide the adjustable overflow used when protecting the cell-room headers.

There is a fire hazard when hydrogen is vented, and tips of vent stacks are common scenes of fires. The top of each stack must be located in a safe location, well away from the roof of any building and in a spot where operators will not be subjected to too much radiant heat during a fire. Tops of stacks should not be constructed of a consumable material like fiberglass.

Because of the fire hazard, many vent stacks are equipped with nitrogen and steam connections. A small flow of nitrogen can maintain a nonflammable atmosphere in the stack to prevent ignition when a release of hydrogen first begins. A blast of steam can extinguish any fire that does occur at the tip, but the volume required often makes this approach impractical. Fires are especially likely when the atmosphere is disturbed. When two stacks are available, a common technique when venting during thunderstorms is to manipulate the seal levels to switch the venting point back and forth. When a fire occurs at a stack, the seal level in the other stack is dropped, and then the level in the first stack is raised to stop the flow of gas. This snuffs the fire, and a flow of steam cools the stack to prevent reignition when the stack is used again.

While lightning strikes are a likely cause of fire, they are not the only one. Corona discharge also may cause ignition. This can occur at the discharge point at any time. Installation of a NASA toroidal ring [124] is said to prevent ignition. This is a simple ring made of small (usually 25 mm) tubing and attached to the top of a stack.

Another unusual property that is of great importance in a chlor-alkali plant is the combustibility of mixtures of hydrogen and chlorine. Discussion of this hazard is in Section 9.1.11.1.

There is also the question of electrical classification of cell rooms. As noted in Section 8.5.1, most cell rooms are not classified as hazardous when the appropriate precautions for venting of hydrogen have been made. This remains an issue to be decided for each plant on its own merits.

9.3. CAUSTIC SODA AND POTASH

9.3.1. *Products of the Various Cells*

As elsewhere in this book, the term “caustic” when used alone usually refers equally to NaOH or KOH. Much more information is available in the literature on caustic soda, NaOH.

9.3.1.1. The Diaphragm Cell. Among chlor-alkali electrolyzers, the diaphragm cell is unique in not having a separate external discharge of anolyte. As with the other types of cell, brine flows into a chamber where it is exposed to the action of the anodes. The anolyte formed then flows in bulk through the diaphragm and into the cathode chamber. After electrolysis of some of the water, the catholyte leaves the cell as the only liquid-phase product.

The undischarged chloride is therefore mixed with the hydroxide formed in the cell. Because the oxygen evolution reaction becomes competitive with chlorine formation, it is not feasible to convert much more than 50% of the salt to chlorine in any cell, and the product liquor contains approximately equal amounts of chloride and hydroxide. The high concentration of chloride in the caustic liquor is the distinguishing feature and major disadvantage of the diaphragm cell.

Nearly all applications of caustic soda require separation of the chloride from the hydroxide. In sodium-brine electrolysis, fortunately, the phase equilibrium allows a rather effective separation by evaporation of the liquor. If water is removed until the concentration of NaOH approaches 50%, nearly all of the NaCl falls out of solution. After cooling, the residual concentration is about 1.0–1.1%. This removal of salt causes the concentration of NaOH to increase. The solution produced by evaporation therefore can contain somewhat less than 50% NaOH. This is discussed in some detail in Section 9.3.3.3. Dissolved salt is not acceptable in some uses of NaOH, and so there has always been a split market. Part has been reserved to a purified version of the diaphragm-cell product and to mercury-cell, and now membrane-cell, NaOH.

The KCl–KOH phase diagram is less favorable for salt/caustic separation, and so KCl is not usually electrolyzed in diaphragm cells.

9.3.1.2. The Mercury Cell. In the mercury-cell process, the anolyte, or depleted brine, is taken from the cells for processing and eventual recycle. Sodium or potassium ions in the brine are discharged by amalgamation with the flowing mercury cathode. The amalgam, which contains 0.1–0.3 wt% alkali metal, undergoes separate electrolysis in the presence of pure water. Both the amalgam itself and the water that reacts with the amalgam and forms the product solution flow into a denuder, or decomposer, which usually is packed with graphite. The amalgam and the water are in countercurrent flow. A short-circuited cell results, and NaOH or KOH forms, along with hydrogen. The concentration of the product solution is fixed by the strength of the amalgam and the ratio of its flow to that of water. The major economic advantage of the mercury cell is that it produces NaOH or KOH solution directly at commercial concentration. With the significant exception of mercury contamination, the products also are of outstandingly high purity.

The mercury cell is not limited to 50% NaOH or 45–50% KOH. It is possible to produce higher concentrations simply by reducing the flow of water to the decomposer. The lower flows can create hydraulic inefficiency. The proper statement is that by reducing the water flow, one can increase the caustic strength so long as control of the process can be maintained. Mercury-cell decomposers easily can produce 60% NaOH, and with some modification 70% [125,126]. The higher concentrations are of some value when there is a market for more concentrated solution or when anhydrous caustic is to be produced. It is also advantageous when mercury cells are to operate in parallel with membrane cells. A simple way to expand capacity by combining the operation of the two types of cell without the expense of an evaporation plant is to produce high-strength caustic in the

amalgam decomposers and blend it with the weaker membrane-cell product. With this technique, production can be expanded by making r units of caustic in membrane cells for every unit produced in mercury cells:

$$r = w_m(w_{Hg} - w_p)/w_{Hg}(w_p - w_m) \quad (105)$$

where

- r = ratio of membrane- to mercury-cell caustic produced
- w_m = weight fraction caustic in membrane-cell product
- w_{Hg} = weight fraction caustic in mercury-cell product
- w_p = weight fraction caustic in blended product

The base case in this comparison is the mercury cells operating alone and producing 50% caustic. If the mercury-cell plant produces 60% NaOH and the membrane-cell plant 30% NaOH, then, a 25% expansion with membrane cells is possible. This approach to expansion will change the economic optimum catholyte concentration in the membrane cells. Increasing this to 35% allows a 39% expansion. Combining this higher concentration with a mercury-cell product at 70% NaOH would permit a 67% expansion. Reducing the concentration of the final product also helps. Thus, a plant whose end-product is 48% NaOH or 45% KOH can be expanded to a greater degree.

Two disadvantages of this approach are the constraint on membrane-cell capacity and the fact that all the caustic can be regarded as the less marketable mercury-plant product. A larger membrane capacity can of course be installed to eliminate the first disadvantage and alleviate the second, but only at the expense of installing and operating an evaporator.

Higher concentrations from the decomposers also have disadvantages. Product handling eventually becomes more troublesome as the freezing point and viscosity (especially in the case of NaOH) increase. There is also a thermodynamic price to be paid; the electrode potential increases along with concentration, and the cells therefore consume more energy.

An alternative that overcomes some of the disadvantages of the blending approach is to use the membrane-cell caustic liquor as the aqueous feed to the amalgam decomposers. This requires closer control of the process and perhaps redesign of the decomposers [125], but it allows considerably more expansion of production and never requires handling of the product above the sales concentration. The greater expansion is a consequence of the change in the water balance. The membrane cell liquor now no longer only acts as a diluent but also provides water for hydrolysis of the amalgam and the water that evaporates from the decomposers along with the hydrogen. In the case of NaOH, about 45 kg of water are consumed by production of 100 kg of product. If the solution is 50% NaOH, another 5.7 kg of water leave with the hydrogen gas.

9.3.1.3. The Membrane Cell. The membrane cell, like the mercury cell, produces a stream of depleted brine for recycle. On the caustic side, it represents an intermediate case between the other types of cell. The caustic concentration is higher than in diaphragm-cell liquor but evaporation is still necessary. Because the flow from anolyte to catholyte is primarily by transfer of water and alkali metal ions through the membranes,

the leakage of the chloride value is much lower than in diaphragm cells. Smaller and simpler concentrating evaporators replace the large salt-crystallizing units needed in the diaphragm process.

Chloride concentrations in the catholyte are measured in tens of parts per million. These concentrations are not so low as those in the mercury cell and are of concern in certain applications. The same can be said of chlorate concentrations. The concentrations of these impurities in the product are functions of their speed of transport through the membranes relative to the speed of the cation. At lower current densities, these relative rates are higher. Moreover, at shutdown there is still a slow transfer of anions across the membranes. These effects can lead to problems in maintaining tight specifications when production is curtailed. They are particularly troublesome in the production of KOH.

The caustic concentration in a membrane cell is controlled by addition of water to a recycle caustic stream or directly into the catholyte. The optimum concentration depends primarily on the type of membrane used. Each membrane has its own characteristics, and operating concentration is chosen to give the best balance of voltage, membrane life, and current efficiency (with a view to the expense of evaporating to sales concentration). With today's high-performance membranes, the optimum concentration for NaOH is usually 30–35%. In later sections of this chapter, we use 32% as a standard. KOH is usually produced at 29–32%, depending on the type of membrane used.

Some older types of membrane were optimized at lower concentrations. There are still plants that operate with these membranes and produce caustic usually in the range 20–25%. While energy efficiency suffers in these plants, brine purity specifications may be less stringent [127].

On the other hand, there have also been efforts to develop membranes that can operate at substantially higher concentrations, ideally at 50% NaOH. These so far have not found commercial acceptance, because they usually suffer in the efficiency of their performance [128]. Still, the high-concentration membrane remains one of the industry's ultimate goals.

9.3.2. *Processing of Caustic Liquors*

Each type of chlor-alkali cell has a distinctive process for handling its caustic liquor. Mercury-cell caustic is simply filtered to remove particulates, including mercury, cooled, and stored as finished product. The only evaporation required, and that in relatively few plants, is the minor operation of concentrating some of the NaOH from 50% to about 73%. Diaphragm cells, on the other hand, are burdened with a highly complex process including evaporation combined with crystallization of NaCl. Centrifugation and filtration remove that salt from the NaOH liquor, and it is recovered as a slurry and returned to the brine system. Cooling the NaOH before storage allows another, relatively small, amount of NaCl to crystallize, and this also must be separated from the liquor. Membrane cells differ from the others by recycle of some of the product around the cells. A fairly high recycle ratio is maintained, and this stream is diluted to control the concentration in the cells and cooled to control the temperature. The net production of caustic flows forward to evaporation, cooling, and storage.

The paragraph above describes the main lines of the processes. Other processing common to all types of cell includes dilution to a concentration suitable for general

plant use, frequently about 20%, and the use of a caustic liquor to scrub chlorine from vent streams. More specialized processes include purification of diaphragm-cell NaOH to remove residual NaCl and production of anhydrous NaOH and KOH. The latter processes are described separately in Sections 9.3.4.1 and 9.3.5.

This section begins with a review of the materials of construction used in caustic service. It then turns to the common operations of pumping, cooling, and filtration before concluding with a discussion of storage, loading, and unloading. Evaporation is a major subject in its own right and appears below in Section 9.3.3.

9.3.2.1. Materials of Construction. Chapter 14 discusses the fundamentals of corrosion and should be consulted for general background. This section surveys industrial practice in caustic processing units. Caustic producers handle their materials at concentrations ranging from very dilute up to anhydrous and at temperatures ranging from below ambient up to, in the case of molten anhydrous caustic, more than 400°C. Corrosion experience with NaOH and KOH solutions varies just as widely, which accounts for the bewildering assortment of materials of construction used. The presence of salt and brine impurities in diaphragm-cell NaOH adds another variable. These inclusions tend to make caustic soda solutions more corrosive. This fact created problems during the major conversion of the Japanese industry from mercury to diaphragm cells in the 1970s [129]. With today's trend of converting diaphragm-cell plants to membrane technology, corrosivity in the caustic section generally is reduced.

Caustic soda and potash react rapidly with aluminum, zinc, tin, and copper. Many failures have been caused by use of these metals in minor components of equipment. Some of these reactions present another hazard by evolving hydrogen. The loss of zinc or aluminum can also destroy brasses and bronzes. This effect depends on the severity of the exposure; bronze is sometimes used in ambient-temperature service in utility (20–25%) caustic.

With certain other metals, caustic solutions react to form passivating films of insoluble hydroxides on the metal surfaces. Hotter, more concentrated solutions tend increasingly to react directly with the metals. As the severity of the application increases, therefore, the various metals gradually become unsuitable. KOH is at least as corrosive as NaOH, and its applications are on the whole more sensitive to contaminants.

Carbon steel is satisfactory for all concentrations at ambient temperatures. Figure 14.21 shows the influence of concentration on service temperature and indicates that stress relief extends the acceptable temperature range (area B). Some users in any case restrict the use of carbon steel with 50% NaOH to a maximum of 55°C. This limitation reflects concern for product contamination as well as for the gradually increasing rate of corrosion.

Solid caustic itself is not corrosive and it, too, is handled and stored in carbon steel equipment. It is very hygroscopic, however. Its corrosivity and the flow properties of the commercial forms are sensitive to moisture. Packages are lined and carefully sealed to prevent corrosion and product degradation.

Figure 9.59 is more comprehensive than Fig. 14.21 and divides the liquid range for all temperatures up to 200°C into four zones [130]. This is an excellent broad summary of the useful ranges of many of the materials still used in caustic service.

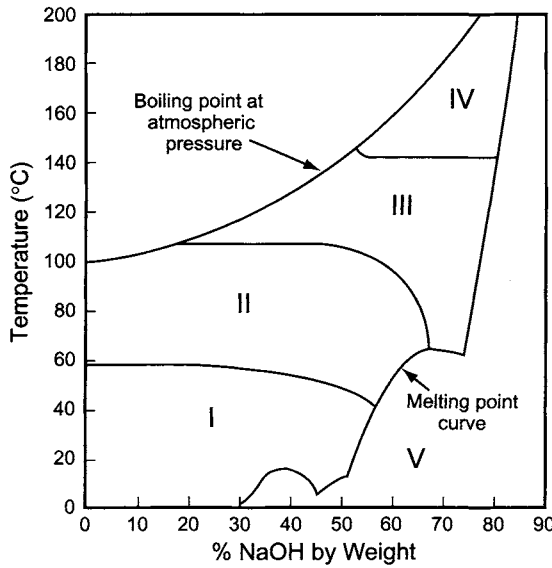


FIGURE 9.59. Materials of construction for NaOH. I. Cast iron, steel, stainless steel, copper alloys, nickel, many plastics and elastomers; II. Steel, Monel, Hastelloy B and C, Zirconium, nickel and its alloys, neoprene; III. Monel, Hastelloy, Inconel, nickel; IV. Cast iron, nickel, silver; V. Steel, stainless steel, nickel and its alloys.

TABLE 9.19. Relative Corrosion Rates of Metals in 50% NaOH

Metal	Corrosion rate
Inconel	0.8
Nickel 200	1.0
Monel	1.2
Copper-Nickel (70-30)	2.4
18-8 Stainless steel	4.2
Ni-Resist (Type 1)	8
Mild steel	33
Cast iron	38

Note: All data are based on 100-day exposure.

Alloys are preferable to carbon steel at higher temperatures, with nickel alloys the most corrosion-resistant. Table 9.19 compares the corrosion rates of various metals in 50% NaOH at 55–75°C. All rates are relative to that of nickel [131]. The first two lines of the table indicate that Inconel is slightly better than nickel itself. This is not generally true, and performance depends on the exact alloy chosen. The proper interpretation of the table is only that both these materials give excellent performance in caustic service. Section 9.3.2.2 on caustic piping systems gives more information on the practical choice of materials as a function of temperature and solution concentration.

The less resistant metals of Table 9.19 may still have some application at lower concentrations. Ni-Resist pumps, for example, are frequently used to circulate approximately

30% caustic around membrane cells. Ni-Resist is a form of cast iron with sufficient nickel to give an austenitic structure. Types 2 and 3, with higher nickel contents than the alloy in Table 9.19, are preferred in this service. Exchangers for more dilute solutions may have stainless-steel tubes or plates. The austenitic Types 304 and 316 stainless steel are useful in 50% NaOH up to about 70°C. Results beyond that point are variable, with a tendency for the metal to lose its passivation. The effect of NaCl in diaphragm-cell caustic is not always clear.

Ferritic stainless steels in general are less resistant than the austenitics and are subject to caustic cracking. Cupronickel tubes are occasionally used for low- to medium-concentration caustic at mild temperatures and with restrictions on fluid velocity. These alloys are also resistant to hot 70% NaOH, but only in the complete absence of oxidants. Monel has a number of applications, but its use can be restricted by the slow development of color due to copper contamination. It is a frequent choice for processing equipment in the salt-recovery section of the diaphragm-cell process (Sections 9.3.2.5 and 9.3.2.6).

Nickel and its alloys are the materials of choice for the most difficult duties. Only the nickel materials can meet special requirements like those found in manufacture of anhydrous caustic. They are also widely, but not universally, used in caustic evaporators. Requirements in a multiple-effect system vary from one effect to another. While nickel always gives superior performance, stainless steels can be an economic choice for parts of the system. A number of evaporators use stainless steel in part of the system, reserving nickel for the most onerous duty in the first effect.

The family of nickel alloys is large. Dillon [132] divides them into two groups: those that rely on the resistive properties of nickel itself, and those that include chromium and depend on its forming a passive film. Stainless steels have a similar chromium-passivation effect, but we do not include them here among the nickel alloys.

The chromium-free alloys include nickel itself and copper alloys such as Monel. The success of nickel in strong alkalis depends on development of a passive hydroxide film. It is fairly resistant to many acids but is unsuitable in strong oxidizing environments. The most common grades are nickel 200 and nickel 201. The former contains up to 0.1% carbon. On prolonged heating, the carbon can precipitate at temperatures as low as 315°C. Nickel 201, with a carbon content less than 0.02%, therefore is preferred at least in first-stage evaporators and in molten anhydrous caustic service.

Chromium-bearing nickel alloys may also contain iron or molybdenum. Inconel 600 is a low-iron (<10%) alloy. Its resistance is similar to that of nickel, and it is mechanically stronger. It is favored for such items as heating coils and exchanger plates. It is subject to stress cracking under severe conditions and so should be stress-relieved. Alloy 600 actually is superior to nickel in the presence of sulfur bodies. The formation of a nickel–nickel sulfide eutectic results in intergranular penetration of ordinary nickel.

Nickel and many of its alloys generally have exceptional resistance to stress-corrosion cracking [133]. In most situations, higher nickel compositions have more resistance to stress corrosion by hot 50% NaOH, but under aerated conditions, nickel-chromium alloys are superior [134].

Addition of molybdenum to nickel-chromium alloys produces grades such as Inconel 625 and Hastelloy C276. These alloys are practically unaffected by caustic up to at least 320°C [135]. Their high costs limit their application. An exception is the use of Alloy 625 in high-pressure steam expansion joints. This avoids the caustic

cracking suffered by austenitics and the chloride pitting corrosion found with Alloy 600. Hastelloy C276 is used in dual-purpose applications such as the plates in brine-caustic heat exchangers.

Some caustic evaporators also have been based on ASTM TP XM-27, a special 26-1 ferritic stainless steel [136]. This material, best known under the trade name E-Brite, is a high-chromium alloy (26% Cr, 1% Mo) with very low concentrations of inclusions such as carbon, nitrogen, and oxygen. The latter fact explains its superior resistance and workability compared to other ferritics. It can be cheaper than nickel, but heat-exchange areas are 10–15% larger, because E-Brite has a thermal conductivity only 30% as great as that of nickel. It must be used with caution in some first-effect environments, where the range of passivation is narrower and the probability of corrosion and intergranular attack greater [137]. Failures have occurred, and Schillmoller [135] attributes them to high first-effect temperatures, hot spots due to blockage of tubes by insoluble salts, and contamination of tubes with minute quantities of hydrocarbon. The last effect arises from the absorption of carbon by the metal. This disrupts the extra-low interstitial nature of the alloy and removes its advantage. Because of these problems in the field, E-Brite is no longer specified for caustic evaporators.

The deleterious effects of hot spots are well known, and they can also play a role in the damage of higher alloys, particularly when the base operating temperatures already are high and little margin for error remains. This is the case in most quadruple-effect evaporators, and causes of corrosion problems are not always easy to discover.

Even those evaporators fabricated from nickel 201 show some corrosion in the caustic environment. Corrosion of nickel is a complex phenomenon. If the passivating layer referred to above is destroyed, the resistance of the metal is much lower. Thus, caustic evaporators must be protected against the hypochlorite that might be present in diaphragm-cell liquors. Other factors that have been considered are the presence of chlorate [138] and the effects of heat flux. Yasuda *et al.* [139] show that heat flux in itself is a factor because of locally high concentrations and temperatures and because the formation and detachment of bubbles at a heated surface tend to disrupt the passivating film. Chlorates are unquestionably a factor when anhydrous caustic is produced (see Section 9.3.5.2). In that process, they are intentionally destroyed before entering the high-temperature evaporator by addition of a reducing agent. But in the standard 50% evaporator, erosion corrosion is more likely to be the cause of failure [140]. The work reported on this aspect used a rotating cylindrical electrode to produce Reynolds numbers equivalent to the velocities at various points in an evaporator system. The results correlated with practical observations and indicated that:

1. there is no discernible effect of the presence of chlorate ion
2. the presence of gaseous oxygen likewise has no effect
3. corrosion rates increase linearly with the rate of rotation of the electrode (and by implication with pipeline velocity)
4. welds corrode much more rapidly than the bulk of the metal.

The mechanism of corrosion involves oxidation of the metal to HNiO_2^- . It seems logical that this reaction might be reversed in the presence of a hydrogen donor. Hydrogen itself reduced the rate of corrosion significantly, but best results were obtained by addition of such compounds as NaBH_4 [141]. Corrosion of nickel is most likely or most severe at

the high temperatures in the first effects of quadruple-effect diaphragm-cell evaporators, where a number of plants now apply this technology to reduce their corrosion problems.

Welds and the surrounding heat-affected zones are more likely to corrode than are unstressed areas. Welding electrode 141 has been a standard with nickel. Crum and Lipscomb [142] report that NI-ROD welds are more resistant.

Because of the high cost of nickel, it is often used in clad construction. Carbon steel provides much of the structural strength, and a thinner layer of nickel is bonded to the steel. Vessels and tubesheets are often nickel-clad. Nickel plating is also used in some less-demanding applications. Plating is applied electrolytically or by means of a baked-on coating from solution application (electroless nickel). In the electrodeposition process, local thickness depends on local current density. Section 10.3 discusses some of the difficulties in obtaining uniform current density over the surface of a large or complex part. With good agitation and the right chemistry, this problem does not exist with electroless nickel [143]. Deposits are more uniform. Electroless nickel also becomes harder with heat treatment. This behavior is in contrast to that of standard forms of the metal, and it improves the wear resistance of the coating. This is of particular value in pump and valve applications.

Electroless coatings form by the reduction of nickel ions by hypophosphite (usually monobasic sodium hypophosphite, NaH_2PO_2). The treating solution contains an excess of nickel. Rates of precipitation depend on temperature and pH, and control of these variables allows control of the properties of the coating, in particular its phosphorus content [144]. The oxidized phosphorus compound releases hydrogen ions, which tend to reduce the pH of the solution. The formulation therefore usually contains acetate or citrate buffers.

High-phosphorus coatings (10–13% P) are more resistant to acids, while low-phosphorus (2–5% P) coatings are more resistant to alkalis and are therefore used in caustic service. Table 9.20 gives some comparative rates of corrosion of different coatings in caustic service. The performance of nickel 200, Type 316 stainless steel, and mild steel is also shown. Parkinson [143] quotes several examples of the successful use of electroless nickel in the chlor-alkali industry. One was on the valves of a reciprocating chlorine compressor, where steel lasted less than a year under the influence of deposits of Na_2SO_4 and FeCl_3 . EN coatings, renewed every few years, solved the problem. In another instance, a control valve in diaphragm-cell evaporator service (34% NaOH, 7% NaCl, 95°C, velocity 1.8 m s^{-1}) failed in about two weeks when fabricated in 316 SS.

TABLE 9.20. Corrosion Rates of Electroless Nickel in Caustic Solutions

Test solution	Temperature °C	1–2% EN	6–8% EN	10–11% EN	Nickel 200	316 stainless	Mild steel
40% NaOH +5% NaCl	40	0.3	0.3	0.8	2.5	6.4	36
Same	140	5.3	11.9	Failed	80	28	–
35% NaOH	93	5.3	17.8	13.2	5.1	52	94
50% NaOH	93	6.1	4.8	9.4	5.1	84	533
73% NaOH	120	2.3	7.4	Failed	5.1	333	1448

Note: All data are in $\mu\text{m}/\text{yr}$, as determined from 100-day exposure. EN, electroless nickel; “%” refers to phosphorus content of coating.

Alloy 20 lasted a few months. A 50- μm coating of low-P EN showed no deterioration in 5 years and cost only one fifth as much as a solid nickel valve.

Other materials also can be co-deposited with nickel. These include silicon carbide, which improves wear resistance, and PTFE, which provides some lubricity and reduces the tendency of process streams to erode the nickel composition [145].

There are some differences in the behavior of alloys due to the variations in caustic composition among the three cell processes. These differences occur mostly in lower-grade applications using materials less robust than nickel. Monel, for example, is subject to liquid-metal cracking by mercury and its salts. Stainless steels seem to be equally affected by diaphragm- and mercury-cell caustic, but if the caustic is consumed in some application, the residual chloride from diaphragm-cell NaOH can cause stress corrosion cracking [146].

Nonmetallics are used in caustic storage and piping systems. While caustic soda or potash can be stored in carbon steel tanks at atmospheric or slightly elevated temperatures without excessive corrosion, tanks still may be lined to prevent iron contamination. Neoprene latexes are common at temperatures up to about 80°C. Above that, halogenated butyl rubber linings are preferred. Small caustic tanks often are made of plastic. High-density polyethylene and PVC-lined FRP are used. Unlined FRP is less suitable, because caustic at most concentrations can attack both the resin and the glass reinforcement. In this regard, 50% NaOH is less corrosive than more dilute solutions [8]. This is attributed to low ionic mobility in the more viscous 50% solution. The most corrosive strength of NaOH is about 25%, and bisphenol resins generally are more resistant than vinyl esters. Design of plastic tanks must consider the high specific gravity of caustic solutions. For example, tanks should have flat bottoms and sit on flat bases that help to support the weight.

Transport vehicles are lined to prevent both corrosion and contamination. Some linings are more resistant to strong than to weak solutions, and it is important to choose a lining that will not be damaged when the vehicle is washed.

9.3.2.2. *Caustic Piping Systems*

9.3.2.2.A. *Piping.* The selection of materials of construction for metallic piping depends on the concentration and temperature of the solution. Figure 9.60 divides combinations

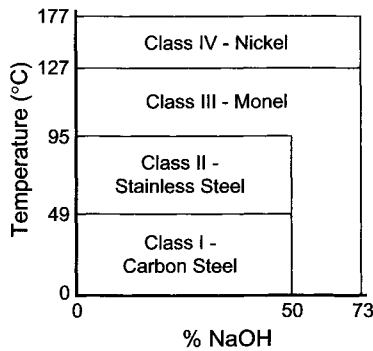


FIGURE 9.60. Piping class service limits—NaOH.

up to 73% NaOH and 350°C into four regions and shows the basic material recommended by The Chlorine Institute (P94). The boundaries reflect only the limits defined in P94; comparison with Fig. 9.59 will show that some of the combinations lie outside the liquid range. Considerations of product quality sometimes can influence the selection. Other factors are the presence or absence of contaminants in the solution, the possibility of temperature excursions, and mechanical stresses. Section 9.3.5 discusses concentrations outside the range of Fig. 9.60. All classes are rated up to 1,200 kPa.

These specifications allow the use of threaded and socket-welded connections in steel and stainless steel in sizes up to 50 mm. However, butt-welding and flanged joints are preferred in all sizes. Stainless steel and nickel threads, in particular, are subject to galling.

In carbon steel seamless Schedule 80 pipe is recommended below 50 mm in all cases and up to 50 mm when connections are threaded or socket-welded. Stainless steel usually is Type 304 or 316. Low-carbon grades have better resistance in the heat-affected zones near the welds. While Fig. 9.60 shows a wide area of application for Monel pipe, its actual use is not so broad. There are relatively few applications in Zone III, and a conservative practice is to use nickel there as well as in Zone IV. Alloy pipe should be Schedule 40 or 40S in small sizes and Schedule 10 or 10S up to 100 mm. The maximum diameter and corresponding thickness of Monel or nickel pipe are determined by the application.

Many caustic lines require insulation and heat tracing. Systems should be designed to prevent excessive surface temperatures, especially when using ferrous metal piping. Steam tracing should use standoffs to prevent direct contact of steam lines with pipe walls. High-chloride insulation material should not be applied to stainless steel piping.

Piping layout should reflect the hazardous nature of caustic and its tendency to freeze at low ambient temperature (but see Section 9.3.3.5 on KOH evaporation). Low-point traps should be avoided, and the system should be installed to allow complete drainage. Horizontal pipe loops are preferred to expansion joints. When expansion joints are required, they should be of the bellows type and of Monel or a more resistant alloy. Especially outdoors, piping should be installed in an economic fashion, avoiding dead legs and extraneous sections. At the same time, piping must have enough connections for draining, venting, hydrostatic testing, cleaning, and maintenance. When there is a complex header system carrying caustic, branches should contain block valves near the header. Because of the hazard of caustic leaks, pipes should be installed in the lower levels of pipe racks. Caustic pipes should be supported from items built for that purpose; there should be no hanging of caustic pipes from others or of other pipes from caustic pipes. Pipe supports should be chosen for the plant's seismic zone. Support intervals should be short enough to prevent sagging. Finally, all caustic piping should be clearly identified.

9.3.2.2B. Valves. Table 9.21 summarizes the application of various types of valve, according to the same four classes used for piping services in Fig. 9.60. The table has the status of a recommendation rather than a hard specification. Exceptions exist, but they should be made only after thorough testing and documentation. All practical combinations are listed, but threaded valves usually should be considered only for connection to transportation equipment, instruments, and special process equipment. Flanged valves generally are preferred.

TABLE 9.21. Valve Selection Guide for Caustic Service

Size	Connection	Form and rating	Class I	Class II	Class III	Class IV
<i>(a) Globe and gate valves</i>						
≤25	Threaded	Forged API 800; Cast ASME 150	S	S	S	S
40–50	Threaded	Forged API 800; Cast ASME 150	S	S	NR	NR
≤25	Socket welded	Forged API 800; Cast ASME 150	S	S	S	S
40–50	Socket welded	Forged API 800; Cast ASME 150	S	NR	NR	NR
All	Flanged	Forged or Cast ASME 150	S	S	S	S
<i>(b) Ball valves</i>						
≤25	Threaded	Forged or Cast ASME 150	S	S	S	SC
40–50	Threaded	Forged or Cast ASME 150	S	S	NR	NR
≤25	Socket welded	Forged or Cast ASME 150	S	S	S	SC
40–50	Socket welded	Forged or Cast ASME 150	S	NR	NR	NR
All	Flanged	Forged or Cast ASME 150	S	S	S	SC
<i>(c) Plug valves</i>						
≤25	Threaded	Forged or Cast ASME 150	S	S	S	S
40–50	Threaded	Forged or Cast ASME 150	S	S	NR	NR
≤25	Socket welded	Forged or Cast ASME 150	S	S	S	SC
40–50	Socket welded	Forged or Cast ASME 150	S	NR	NR	NR
All	Flanged	Forged or Cast ASME 150	S	S	S	S
<i>(d) Diaphragm valves</i>						
≤25	Threaded	Cast 150 psig	SC	SC	SC	SC
40–50	Threaded	Cast 150 psig	SC	SC	NR	NR
≤25	Socket welded	Cast 150 psig	SC	SC	SC	SC
40–50	Socket welded	Cast 150 psig	SC	NR	NR	NR
All	Flanged	Cast ASME 150	SC	SC	SC	SC
<i>(e) Rubber-lined butterfly valves</i>						
≥50	Wafer	Cast 150 psig	SC	SC	NR	NR
≥50	Lug	Cast 150 psig	SC	SC	NR	NR
<i>(f) Fluoropolymer-lined butterfly valves</i>						
≥50	Wafer	Cast 150 psig	SC	SC	SC	SC
≥50	Lug	Cast 150 psig	SC	SC	SC	SC
<i>(g) High-performance butterfly valves</i>						
≥50	Wafer	Cast ASME 150	S	S	S	SC
≥50	Lug	Cast ASME 150	S	S	S	SC

Note: Legend: S, satisfactory; NR, not recommended; SC, satisfactory under specific conditions, depending upon manufacturer.

Source: With permission of The Chlorine Institute, Inc.

Valve bodies for the most part are basically of the same metal as the piping. Many different types are in caustic service. Globe valves have several useful safety features. These include:

1. tight shutoff in both directions
2. no liquid trapped in cavities
3. multi-turn operation
4. positive identification of valve position.

Seals must be of high quality. Bellows seals and stuffing box designs with live-loaded packing glands are useful. Gate valves also have been used. Rising-stem types require additional maintenance. With both globe and gate valves, metal-to-metal seating with hard facing or soft seating with a fluoropolymer insert can be used.

Ball and plug valves are widely used. Their quarter-turn operation can permit inadvertent opening more easily than the multi-turn operation of other valves, but their stem seals are more reliable. Both types of valve provide tight shutoff and lower resistance to flow than globe or gate valves, and they are frequently supplied with fluoropolymer resin linings.

Butterfly and diaphragm valves are other options. Butterfly valves can be lined with an elastomer or a fluorocarbon resin. Soft-seated, high-performance valves have higher pressure ratings but allow contact of the process fluid with the metal.

All standard types of check valve are acceptable in caustic service. Springs, where used, should be Monel or Inconel.

EPDM and chlorosulfonated polyethylene are the standard elastomers for valve linings; fluoropolymers include PTFE, PFA, FEP, ETFE, and ECTFE. Gaskets and packing usually are chosen from among PTFE, graphite, graphite-filled PTFE, and asbestos (the usual cautions apply to the use of asbestos). Nonmetallic seats, sleeves, diaphragms, and seals may be of virgin or reinforced PTFE or PFA. Chlorosulfonated polyethylene is accepted in Classes I and II and EPDM in Class I.

Several cautions apply to ratings of valves. The user should discuss this situation with the manufacturer. Nickel valves may have pressure ratings that are low for their nominal design class. The pressure rating of diaphragm valves depends on size and material of construction. Fluoropolymer-lined plug valves are satisfactory only under certain conditions.

Metal parts other than the main body of a valve frequently meet higher materials standards. Except in Class IV, for example, bellows usually are of Monel 400 or 405, Hastelloy B or C, or nickel. The choice for stems, discs, balls, and tapered plugs follows the pattern below:

Alloy	Classes
316 stainless	I, II
Alloy 20	I, II
Monel	I, II, III
Hastelloy	I, II, III
Inconel	II, III
Nickel	II, III, IV

9.3.2.2C. *Instrumentation.* In-line instruments are exposed to the same conditions as process equipment and piping. Materials specifications are at least as rigorous as they are for these other systems. Instruments contain more small parts, are built to more rigorous tolerances, and often depend on their accuracy for precise and intricate movement of parts. The corrosion allowances associated with equipment and piping cannot be tolerated.

Materials such as tantalum, too expensive for widespread use in larger items, are common in instruments. The discussion of instrument materials of construction in this book is in Chapter 11, and Sections 11.5 and 11.6 in particular discuss applications in caustic service.

9.3.2.3. *Pumping.* Centrifugal pumps are the standard for caustic service, and their metallurgy follows in a general way the guidelines of Section 9.3.2.1 and the recommendations for the four piping classes of Section 9.3.2.2. Carbon steel is used at low temperatures and in many utility applications. Cast iron, being brittle, is not recommended, but ductile iron and stainless steel are frequent choices. At higher temperatures and where product contamination is an important consideration, nickel-containing alloys are used. These include Ni-Resist, Alloy 20, CD4M, Monel, Inconel, and nickel itself. In-process pumps may be stainless steel, Hastelloy, or a nickel alloy. In a cell room, stainless steel pumps may be avoided because of the possibility of iron contamination and damage to activated cathodes in the cells. For the same reason, the type of Hastelloy chosen will be Hastelloy C. Centrifugal pumps usually have open or semi-closed impellers. Rotary pumps are also used occasionally, but rarely as main process pumps.

High specific gravity, high viscosity, corrosivity, the danger of freezing, and the possibility of contamination all combine to complicate the pumping of caustic solutions. Viscosity is more of a consideration with NaOH solutions than with KOH. KOH in its higher-grade applications may be more sensitive to contamination by materials of construction. Both NaOH and KOH at 50% concentration have freezing points of about 10°C or higher, and storage and pumping systems must be designed to prevent freezing. For ease of pumping, 50% NaOH should be handled at temperatures of at least 30°C. The viscosity at 30°C is about 25 cp. Pumps therefore may require heating. Pump suction lines should be simple and short, and it may be advisable to use 45° elbows. High solution density is not a problem in itself, providing that the pump drive is sized accordingly. The freezing-point behavior of KOH solutions in the 45–50% range is quite different from that of NaOH solutions. At 45%, KOH freezes at –28°C. This eliminates the handling problems associated with a high freezing point, and KOH therefore often is supplied at the lower concentration. Even if the liquor cools extensively, there is no particular problem with viscosity.

All pumps should have wash and drain connections. In some situations, wash connections placed on the pipelines can also serve a pump. Another frequent practice is the steaming-out of lines. Designers should ensure that all materials in the pumping system can withstand the temperature.

Leakage is the major hazard when pumping caustic. It is most likely at piping joints, valves, and pump seals. Many systems use flange guards and valve covers where leaks could endanger personnel. Valves are most likely to leak at their stems. Blowout-proof

designs are preferred, and Section 9.3.2.2B discusses other aspects of valve selection. Seals may be packing glands or mechanical seals. Packing glands were quite common in the past but are being displaced because of tighter environmental standards. Table 9.22 summarizes the advantages and disadvantages of different types of containment. Double mechanical seals are perhaps the most frequently used design. Sealless pumps are used widely in special circumstances in smaller applications, and they are being used more in broader applications as designs improve and operating environmental standards.

All handling problems are aggravated by the use of 73% NaOH. All systems must be insulated, and pipelines should be traced. Handling temperatures are higher because of the high viscosity and freezing point (63°C). The selection of materials of construction reflects the temperature and concentration of the solution, in accord with Fig. 9.60. Rotary pumps become a more frequent choice with 73% NaOH.

9.3.2.4. Cooling. Mercury-cell caustic is cooled before storage or shipping. The same is true of diaphragm- and membrane-cell caustic, but it is also common to send those cell liquors directly to evaporation without cooling. Diaphragm- or membrane-cell liquor flows from the cells to collecting tanks. Section 11.5 discusses the control of this transfer. Diaphragm-cell liquor often is stored near cell operating temperature. A simple arrangement in those cases is to pump it from the collecting tanks into a line joining a liquor storage tank to an evaporator feed pump. The storage tank becomes a large capacitance in the transfer line, automatically compensating for changes in operating rates on either side. A similar effect can be obtained when cooling liquor before storage. The pressure drop taken in cooling changes the hydraulic balance and makes the simple approach mentioned above unworkable without some restriction in the transfer line to the evaporator feed pump or a change in control philosophy. Section 11.6.1.3 also addresses the use of split-range controllers to give an efficient switching system.

Standard construction for shell-and-tube exchangers includes nickel tubes and carbon steel in cooling water service on the shell side. Compact heat exchangers also are widely used in caustic service. They have found a growing market in chlor-alkali plants. Their high heat-transfer coefficients and resistance to fouling reduce the surface area required. This is especially valuable when using expensive materials such as nickel, titanium, and the Hastelloys.

While the class of compact exchangers includes spiral and lamella exchangers, the type most frequently found in the chlor-alkali industry is the plate exchanger. The spacing between plates is narrow. The resulting high fluid velocities improve the heat-transfer coefficients and discourage fouling. The flow paths also provide more nearly true countercurrent flow than do most shell-and-tube exchangers. Practical construction of the latter type frequently requires multipass arrangements that defeat attempts to provide true countercurrent flow. The ribbed or dimpled construction of the plates promotes turbulence, again improving heat transfer, and provides mechanical strength to the plates. The plates must be strong enough to control elastic deformation and to eliminate the possibility of plastic deformation.

TABLE 9.22. Caustic Pumping Applications and Seal Selection

Seal type	Advantages	Disadvantages
<i>Horizontal pumps</i>		
Single with external flush	<ul style="list-style-type: none"> Extended seal life Low seal cost Pump can be run dry if flow is lost 	<ul style="list-style-type: none"> Seal water piping required Caustic and water will intermix Freeze protection of seal water piping may be required
Double with external flush	<ul style="list-style-type: none"> Long seal life No contamination of seal water Pump can be run dry if flow is lost 	<ul style="list-style-type: none"> Seal water piping required Slightly more expensive than single seal Freeze protection of seal water piping may be required
Single with internal flush	<ul style="list-style-type: none"> No seal water required No freeze protection of seal liquid piping Simplified installation 	<ul style="list-style-type: none"> Crystallization of caustic during downtime; abrasion of seal Pump cannot be run dry More expensive than above options; faces must be more abrasion-resistant
Double with TEFC gland with air-cooled system	<ul style="list-style-type: none"> Long seal life Pump can be run dry if flow is lost Closed-loop seal system No freeze protection of seal liquid piping 	<ul style="list-style-type: none"> More expensive than other options Compressed air or nitrogen must be supplied to seal Contamination of caustic possible if seal fails
Sealless magnetic drive pump	<ul style="list-style-type: none"> No mechanical seal Zero emission No seal water required No freeze protection of seal liquid piping 	<ul style="list-style-type: none"> More expensive than standard pumps with mechanical seals Higher energy consumption Caustic must be clean Requires dry run protection
Sealless magnetic drive pump with barrier	<ul style="list-style-type: none"> Pump can be run dry 	<ul style="list-style-type: none"> Requires pressurized gas or clean liquid as barrier
<i>Vertical pumps</i>		
Sealless sump style	<ul style="list-style-type: none"> No mechanical seal No seal liquid required No freeze protection of seal liquid piping 	<ul style="list-style-type: none"> More expensive than horizontal pumps with mechanical seals Bearing flush and associated maintenance required on some models with long shafts Poor access for maintenance Motor not rigidly mounted on foundation

Source: Courtesy of Severn Trent Water Services.

Applications for coolers include caustic being transferred to storage, low-concentration solutions prepared by exothermic dilution, circulating caustic in vent scrubber systems, and full-concentration process applications. Stainless steel plates are used frequently at temperatures up to about 60°C. Nickel or one of its alloys is the

common choice at higher temperature. All plate exchangers carrying hazardous materials under pressure must be equipped with shrouds to protect personnel from any leaks of the hazardous material between plates. Aluminum is probably the most frequently used material of construction, but it is not acceptable in caustic service. Stainless steel is a frequent substitute.

We shall concentrate here on the cooling of membrane-cell catholyte and on final-product coolers. First, consider catholyte recirculation around membrane cells. The liquor, usually received from the cells at a temperature between 85 and 90°C, must be cooled sufficiently to absorb the waste heat generated by electrolysis. The amount recirculated and the temperature that must be achieved are inversely related. In a small plant, this cooling may be done in one step with plant cooling water. Depending on the specified cooling water temperature rise, the flow rates of caustic and water may be reasonably close to each other. This situation allows the use of an efficient plate configuration. In certain other applications, the cooling range of the caustic solution is much larger than the heating range of the water, and the flow rates are quite different. It becomes difficult to use the same flow and pass arrangements on both sides of the plates, and true countercurrent flow and some of the effective temperature differential are lost.

In a large plant, the designer should consider the fact that, while the caustic stream entering the cells must be cooled, the brine feed usually must be heated. This is an opportunity for economization through the interchange of heat. The flow of caustic in this case is through an interchanger to heat the brine and then through a cooler to bring it to the desired cell feed temperature. In full-load operation of most plants, the caustic carries enough excess heat for the process to operate as outlined above. The brine is brought to its required temperature without cooling all the caustic sufficiently. The fact that the caustic carries more heat than the brine requires means that its flow to the interchanger must be restricted in order not to overheat the brine. The control arrangement then is for some of the caustic to bypass the interchanger in response to a signal from the outlet brine temperature. The recombined caustic stream goes to the cooler. A caustic/brine plate interchanger is a challenge to most materials of construction. The nickel alloys favored for caustic service are not highly resistant to hot brine. The usual selection is Hastelloy C276.

Particularly with the inclusion of an interchanger, the caustic heat exchange system must have great flexibility. Figure 9.61 may help the reader to visualize the wide range of duties. Part (a) plots the required temperature of the brine and caustic fed to the electrolyzers as a function of operating load. The use of a single temperature does not distinguish between brine and caustic feeds. This simplifies the presentation and also accords with the frequent practice of maintaining approximately equal feed temperatures (Section 13.10.3.3).

The wasted voltage in the cells increases at higher operating load. More waste heat becomes available to heat the brine and caustic, and so the required feed temperature begins to decrease. The dashed lines on Fig. 9.61a show the temperatures of the caustic and brine as they enter the temperature-conditioning section. At high operating load (right-hand side), the cell feed temperature is relatively close to the brine supply temperature and far from the circulating caustic temperature. As a result, the heat content of the caustic is more than adequate to heat the brine, and the residual

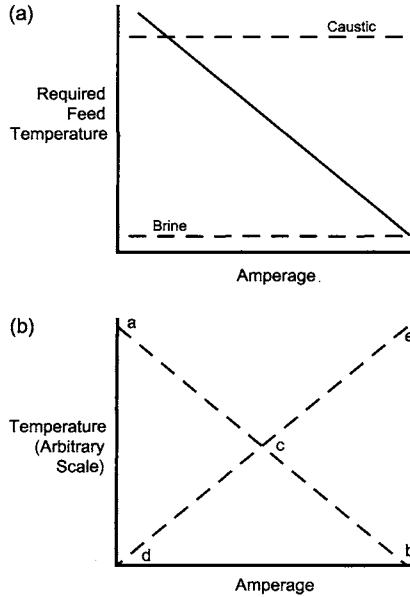


FIGURE 9.61. Feed brine and caustic heat duties.

duty to be handled by the caustic cooler is high. At slightly lower operating load, the interchanger transfers more heat in order to bring the brine up to the (higher) required temperature, and the duty of the caustic cooler becomes less. This trend continues until heating the brine reduces the temperature of the caustic to that required in the cell feed. The duty of the caustic cooler becomes zero. Beyond this point, the control algorithm of the interchanger should change in order to avoid overcooling the caustic. The heat-transfer duty of the interchanger then declines from its maximum, the duty of the caustic cooler remains zero, and it becomes necessary to add heat to the brine from another source.

Figure 9.61b illustrates the situation. Line *ab* is the same as the line shown in Fig. 9.61a. Along the segment *ac*, the caustic is cooled by the interchanger to the desired feed temperature. The brine temperature increases along segment *dc*. The interchange process must be controlled to avoid overcooling the caustic, and the brine heater must provide whatever temperature compensation is still needed. When the cell amperage is greater than that corresponding to point *c*, cooling the caustic to the desired temperature in the interchanger (segment *cb*) would result in a brine feed temperature (segment *ce*) higher than desired. Control now must shift to avoid overheating the brine, and the caustic cooler comes into operation.

Still in terms of Fig. 9.61b, we can regard triangle *acd* as the duty of the brine heater. It is largest at low amperage and decreases steadily at higher loads until it becomes zero. Triangle *bce* represents the duty of the caustic cooler, which has opposite characteristics. Below a certain load, it need not operate. Above that load, its duty increases continuously until it reaches the capacity of the exchanger. The interchanger has a totally different characteristic. Its duty is represented by triangle *bcd*. It goes through a maximum at a

certain amperage, falling off on either side. Design of the interchange system should consider the entire characteristic.

The various exchanger duties therefore have very wide ranges that depend on the condition and operating amperage of the cells. When the basis for design includes the case of a disabled interchanger, design ranges for the brine heater and caustic cooler are even wider.

A temperature element in the caustic line after the cooler controls the temperature of the feed to the cells. While the measurement of most interest is the temperature in or leaving the cells, the dynamics of control based on such temperatures would be less favorable. It is always possible, furthermore, to reset the inlet temperature from some average outlet temperature to achieve the desired result. Because the characteristics of the individual cells differ, feeding the same amount of recycle caustic to each cell will not give the same outlet temperatures, and it is hard to define what the proper average should be. Adding the fact that cells are not totally backmixed, we see that the idea of uniform cell temperature control by a single system is a snare and a delusion.

A final note on the flexibility required in the caustic cooling loop: during startup of the cells, the caustic actually must be heated. This can be done in a small exchanger provided for that service, or the cooler can be fitted with steam and condensate connections. In the case of plate exchangers, the former can be a few separate plates mounted on the same frame as the cooler. In the latter case, the demand will be much less than the exchange capacity of the cooler, and smooth removal of steam condensate may require special arrangements.

We turn next to the cooling of diaphragm-cell NaOH. The evaporation process described in Section 9.3.3.3 produces crystals of NaCl as the NaOH concentration increases. Section 9.3.2.5 below describes the use of centrifuges to remove these salt crystals. The primary centrifugate still is saturated with NaCl, and cooling it further causes more salt to precipitate. Evaporator product liquor at, say, 100°C contains 3% dissolved NaCl. Cooling it below ambient temperature removes much of the salt, giving a final product concentration of 1.0–1.1% NaCl. This removal of dissolved salt incidentally increases the concentration of NaOH in the liquor. The evaporators therefore, depending on the amount of salt removed by cooling, need produce only about a 49.5% solution. In an 800-tpd plant, the amount of salt precipitated in the coolers is more than 30 t daily. Chilled water, tempered to avoid any precipitation of NaOH, usually is necessary to reach the low residual salt levels specified. An incidental advantage of cooling to sub-ambient temperature is that it prevents slow precipitation of salt as the liquor cools in storage tanks or transport containers.

The cooling system must be designed to operate reliably even as the salt precipitates. Cooling in tanks or standard exchangers leads to uncontrolled crystallization of the salt, and some of the recovered salt often is recycled to serve as seed crystal. Some designers and operators prefer the compactness and high productivity of tubular or plate heat exchangers. Others prefer to install tanks equipped with cooling coils to make access and cleaning easier. In any case, there will be a need for occasional cleaning of the cooling surfaces. While cooling tanks require much more plot area and a structure that allows gravity flow through them in series, installing an extra tank to provide redundancy is a simple and relatively minor addition. In a series of tanks, some will be dedicated to the use of plant cooling water and others to the use of chilled water. When exchangers

are used, the same effect requires two units in series. The simplification of using chilled water only, in a single exchanger, is feasible with careful design, but is rarely economical.

The chilled caustic flows to a second set of centrifuges, also described in Section 9.3.2.5, for removal of the solid salt and then to pressure-leaf filters for final polishing. Section 9.3.2.6 discusses filtration.

9.3.2.5. Centrifugation. Monel and Type 316 stainless steel are the principal materials of construction for all caustic centrifuges. The two stages of centrifugation in a diaphragm-cell plant require different types of machinery. Evaporation produces a concentrated slurry of well-formed crystals as the feed to the first stage of recovery, which removes nearly all the suspended crystals. Pusher centrifuges are a typical choice for this duty. These are continuous units especially suited to slurries of crystals with good draining characteristics. They move the solids along by the action of a reciprocating piston (the "pusher") and require no scraping of the cake, which would be more likely to degrade the crystals. In the illustration in Fig. 9.62, feed enters on the centerline of the basket, which is a horizontal rotating cylinder. In the arrangement shown, the feed liquor travels along a tapered funnel and gradually accelerates to full speed before entering the basket. Clarified liquor flows through a screen mounted on the basket and is ready for further processing.

The pusher mechanism operates from the liquor discharge end. Typical stroke lengths are 50–70 mm with a frequency of 20–30 cycles per min. Under the influence of the pusher, the crystals move toward the feed end. There are provisions for washing them as they move. Wash liquor can be combined with product liquor or kept separate. Finally,

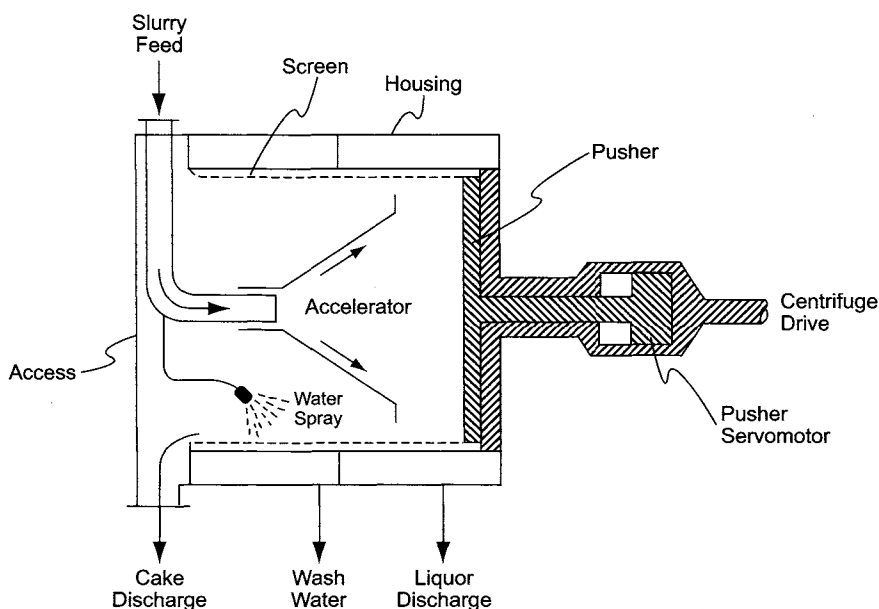


FIGURE 9.62. Pusher centrifuge.

the crystals drop at the end of the basket into a discharge pipe or chute. Section 9.3.3.3 describes the collection and recycle of this salt to the brine plant.

Cooling the liquor recovered from the pusher centrifuges, as noted in the preceding section, reduces the dissolved salt concentration from about 3% to 1%. Compared to the evaporator slurry, this is a minor and lean source of salt, in a thinner slurry and with smaller particles. Centrifugation again is the standard process for its recovery.

Solid bowl centrifuges are better adapted to this service. Figure 9.63 shows a typical unit. The working element is a horizontal rotating bowl. This is conical and tapers away from the feed end. Slurry enters the annular bowl from the central element near the large end of the cone. A conveying scroll mounted in the bowl moves the solids toward their discharge outlets at the narrow end of the cone. The scroll rotates more slowly than the bowl. Liquid flows along the flights against the motion of the scroll and through the clearances between the rotating members. The solid bowl machine also has a capability for washing the solids. Wash fluid is brought in through a central pipe into a chamber beyond the slurry feed section and enters the bowl through its own feed ports.

The salt removed in the solid bowl centrifuges is of less value than that removed in the primary (pusher) centrifuges. It usually is allowed to drop into a tank in which it is redissolved in the cell liquor and then recycled to the evaporators. The solid-bowl centrifugate still contains traces ($<0.1\%$) of very fine solid salt. The next step therefore is filtration, described below in Section 9.3.2.6. Some of the salt from the centrifuges may be used in that step.

Primary centrifugation process design is also affected by the method chosen to deal with the triple salt formed in the evaporators. In all cases, a leaching tank serves as a triple salt decomposer. One possible combination is to collect all the salt produced in the evaporators, recover the bulk of it in pusher centrifuges, and drop it into the leaching tank. The liquor in the tank, richer in sulfate, goes to sulfate recovery or disposal. The purified salt is reslurried and sent to a second set of centrifuges for final recovery. In other systems, the triple salt may be isolated from the pure salt formed in the other effects of the evaporator.

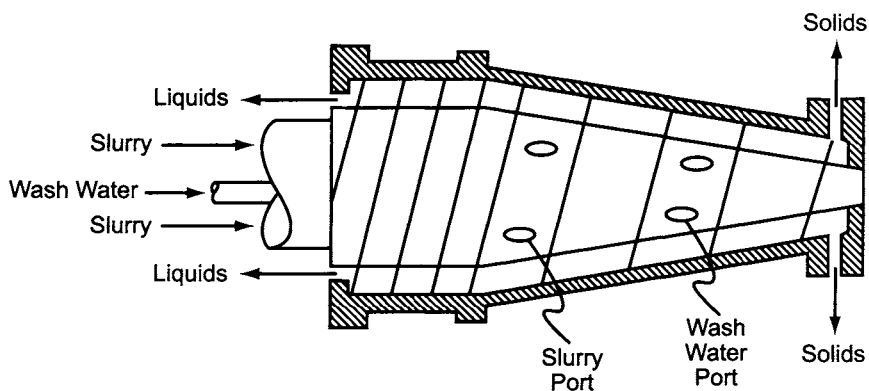


FIGURE 9.63. Solid-bowl centrifuge.

9.3.2.6. Filtration. Product solutions are sometimes filtered in order to guarantee their quality, but this is a low-level application often carried out in small cartridge filters. Filtration also is an important adjunct to centrifugation in the recovery of salt from diaphragm-cell caustic evaporators. Here, the filters follow the two steps of centrifugation described above in order to remove the fine salt that passes through the second (solid-bowl) stage. The size of the particles to be removed extends down into the submicron range, and so precoat-type pressure-leaf filters are used. This sort of filter was discussed in Section 7.5.4.2 in connection with brine purification.

The precoat usually is salt itself. Some of the slurry that ordinarily would go to the secondary centrifuges bypasses that step and goes directly to the filter that requires precoating. It is also possible to use filter feed as the precoat, but the finer salt does not work as well. When the precoat becomes blinded or the chambers filled with salt, backwashing is necessary. Fresh water, cell liquor, or unsaturated brine can be used here, and the salt, precoat as well as process load, dissolves and returns to the process. Water is the most efficient backwash fluid, but the use of brine or cell liquor prevents dilution of the process. The caustic filtrate becomes the final product and is ready for storage or shipping.

Filter bodies usually are of rubber-lined steel, with polypropylene cloths and Monel wire. Other internal parts usually also are Monel. Filtrate runs down to a tank, which also typically is rubber-lined. An agitator may provide some blending, or liquor may be recirculated by a pump. The pumped recycle may pass through a small heater in order to keep the temperature in the filtered caustic tank above the freezing point. This material is the final product; it is transferred to product storage, and its handling from this point on is the subject of Section 9.3.6.

A more specialized application is the filtration of mercury-cell liquor to remove mercury from the product. We consider two types of filter here, the candle filter using carbon tubes and the pressure-leaf filter precoated with activated carbon. The operation of candle filters also has been described in Section 7.5.4.2.

Mercury-cell caustic filters operate at higher temperatures than do other product filters. Some plants operate above 100°C. The solution, pumped under flow control or feed tank level control, leaves the filter with less than 0.5 ppm Hg, usually about 0.1. It then can be cooled before storage, usually to 40–50°C, in a plate-type exchanger.

The operation requires an agitated precoat tank and precoat handling system, similar to those described in Section 7.5.4.2. Cellulosic and diatomaceous earth filter aids similar to those used in brine filtration are common, but activated carbon is also used. Carbon sometimes is used in combination with the others, both of which have the disadvantage of partial solubility in hot caustic. One manufacturer recommends that precoat be deposited from a 2–5% slurry at a flow rate of about 1.7 m hr⁻¹ to a thickness of at least 3 mm. A bumpless transfer to on-stream operation and a temperature change of less than 50°C are recommended. Operating face velocities are 0.35–0.6 m hr⁻¹. A body feed generally is not used. Before a filter is taken off line for removal of the cake, it can be washed to recover occluded product. This is done with hot water, prepared off line and held in a storage tank or generated on line with the help of a steam–water mixer. The water should be soft. The cake then can be removed by standard methods such as backwashing, vibration, etc. Sometimes, the primary cake is not washed, but the backwash fluid is collected and refiltered through a fine cloth filter press, typically using a polypropylene cloth rated at 60 μm.

The wash liquor may contain about 20% caustic. Depending on the process duty, the solids will range from 2–4% Hg and less than 1% filter aid. At ambient to warm temperature, the resulting filtrate will have a turbidity less than 5 ppm.

Porous carbon filters for mercury usually operate at pressures up to 8 bar. The housings are nickel or nickel-coated carbon steel. The pores in the tubes have diameters less than 50 μm . Filtration face velocities range from about 0.5 to 2.0 m hr^{-1} . The content of suspended mercury is reduced from 10–30 ppm to less than 0.5 ppm. Results are better with lower velocity, lower caustic temperature, and the recycle of some of the filtrate. Many plants use multiple filtrations, perhaps with higher unit rates in the second step, and achieve lower mercury content in the effluent. Leaf filters packed with specially treated activated carbon are an alternative. These usually operate at lower temperature (60–65°C) and sometimes are used as two stages in series. The mercury concentration is reduced to 1–5 ppm in the first stage and to less than 10 ppb in the second. The spent carbon is backwashed from the filters and allowed to settle in a hold tank. The supernatant weak caustic can be used in brine treatment or pH control, and the carbon itself is stripped in a mercury furnace before disposal.

A special type of leaf filter sometimes appears in this application. The elements are horizontal discs that spin on demand to remove the dry cake. The Funda[®] filter is an example. Another special feature sometimes is “shuffling” of the cake. After the wash with hot water, the isolated filter simply sits idle for some time (1–1.5 hr). The mercury during this time penetrates the active carbon, opening the structure of the bed so that the pressure drop will be lower upon restart. This can be done several times before it is necessary to remove the carbon. This technique reduces the consumption and cost of precoat and also the volume of material that must be handled for mercury recovery.

9.3.2.7. Blending and Dilution. Caustic solutions may be blended as produced in order to promote uniformity. Users may blend other ingredients with caustic before use in a process or simply as part of a product formulation. In-tank blending requires complete top-to-bottom turnover of the batch. It is useful in damping slow changes or long-period fluctuations in product strength. It is less useful as a way of blending materials of widely different strengths or of diluting strong caustic with water. In the latter case, the mildness of the agitation can allow hot spots to develop in the tank.

The purpose of simple blending may be to compensate for fluctuations in final-product concentration or to make small adjustments in concentration before using or shipping. In-tank agitators are useful on smaller scale. The metallurgy must suit the conditions, but temperatures usually are below 50°C. Carbon steel often is suitable from the standpoint of its resistance to uniform corrosion, but stainless steel or a rubber coating may be used for better resistance to erosion corrosion or to prevent contamination of the solution by iron. Larger tanks usually rely on a pump loop or side-mounted agitators. One advantage of blending by pumping is that it can be combined with heating or cooling of the caustic. The return from a pump to the tank, when using a single return line, is best placed well away from the pump suction nozzle. The mixing effect of pumped streams also can be augmented by the use of internal mixing eductors. These should be at least as

resistant to corrosion as the caustic piping, because of the possibility of residual stresses due to fabrication. At typical storage temperatures, stainless steel is suitable; in some applications, PVC eductors are used. For best results, installation should follow normal good practice and the manufacturer's recommendations. Mixing rates are enhanced when the eductors discharge at angles above the horizontal. Entrainment rates can be three times the pumping rate, and a typical design is capable of turning over the contents of a tank in two to four hours.

There are several reasons for diluting caustic solutions before use. Consumers often dilute the conventional 45–50% material before processing. Those who receive 73% NaOH, unless the higher concentration is necessary in their processes, routinely dilute it before storage. A producing plant may require a relatively dilute solution for utility use or for the scrubbing of vent streams. A concentration frequently used is approximately 20%. In the case of NaOH, this is slightly above the eutectic concentration of 19%. Freezing points at 20% are -26°C for NaOH and -40°C for KOH. The typical membrane-cell operator also dilutes a recycle caustic stream in order to control the concentration of catholyte.

Dilution of caustic is an exothermic process. The Appendix shows the enthalpy of NaOH solutions as a function of temperature and concentration. On such a diagram with linear scales, straight lines represent simple blending processes. The steep curvature of an isotherm on each side of its minimum reflects the high heat of mixing. When two streams at the same temperature are combined, the straight line connecting the two concentrations will intersect other (higher temperature) isotherms and show the final temperature of any given blend. Combining water with 50% NaOH to produce a 20% solution, for example, produces a temperature rise of about 25°C from the evolution of about 460 kJ kg^{-1} NaOH. Dilution of more concentrated grades can produce temperatures that are quite high and solutions that are quite corrosive. For example, diluting 73% NaOH at its normal delivery temperature to a concentration of 50% will produce a temperature of about 132°C if no heat is removed. The dissolving of anhydrous NaOH also is highly exothermic and produces more than 1 MJ per kg NaOH. A 20% solution prepared this way without removal of the heat of solution will be about 90°C . A greater problem is that, during the course of batch dissolving, temperatures will be over 100°C at high concentrations of NaOH. If warm water is used, solutions in the 30–40% NaOH range actually will boil. Addition of water directly to solid caustic is quite dangerous and should never be done.

Note that one advantage of preparing utility caustic from membrane-cell product is the absence of a large exotherm. Dilution from 35% NaOH to 20% produces a temperature rise of only about 10°C . The safety hazard is small, and the process may not require cooling.

There are many techniques for diluting caustic, but perhaps the best is to blend water and a concentrated solution in an in-line mixing device, cool the dilute solution, and take the product to a tank for storage and distribution. To control the concentration of the mix, the two streams are under flow ratio control. Normally the caustic flow is controlled directly and the water flow by a ratio controller. The set point of the latter is reset by a downstream temperature-compensated density instrument. The quality of the water and the material of construction of the mixing device depend on the end use(s) of the dilute caustic. Stainless steel is perhaps the standard material of construction.

Dilute caustic for use within the main process requires water of suitable quality. Caustic intended for emergency scrubber use can use lower-grade water, with two provisos:

1. if the scrubber liquor is to be used for bleach, the water should not contain high concentrations of elements that reduce the stability of the bleach
2. in any case, heavy deposits of hardness resulting from the action of the caustic on the water can foul equipment and piping and should be avoided by choosing a better grade of water if necessary.

For cell room use, the dilution water is demineralized, and the mixing device is of nickel or a high-nickel alloy. The cell inlet concentration is controlled, while the variable of more interest is the concentration in the cells. We have the same situation that applies with temperature control, discussed above. Given a measurement of the outlet caustic concentration, again we can reset the control point at the inlet. This might be automatic or by occasional operator intervention.

The dilution water can join the circulating stream before or after the cooler. Both approaches are common in plant practice. Essential criteria are the addition of the right amount of water to maintain the mass balance and removal of the right amount of heat to maintain the energy balance. The feedback of information from cell product is necessary in any case, and it makes either approach workable.

Addition of water before the cooler gives conceptually better temperature control dynamics. Addition after the cooler gives higher temperatures on the process side of the cooler and allows removal of a given amount of heat with slightly less heat-transfer area. The lack of a strong consensus on the matter stems from the fact that the effect of addition of water on the temperature of the circulating caustic is small. While the water may be much colder than the process stream, the exothermic heat of mixing nearly offsets its cooling effect. Calculations from the standard cathode-side balance shown in Fig. 6.9 give the following changes in caustic temperature by addition of dilution water before and after the cooler at water temperatures of 20°C and 40°C:

Water temperature	Drop in process temperature, °C	
	Before cooler	After cooler
20	1.9	1.3
40	0.7	0.3

9.3.3. Evaporation

As already noted, it is possible to make caustic soda or potash directly at normal commercial concentrations in mercury cells, and in that case evaporation is unnecessary. Diaphragm-cell liquors, on the other hand, present a large evaporative load when 50% NaOH is to be produced. The evaporative load associated with membrane cells is much less, and it is at least conceivable that efficient membranes will be developed to produce commercial concentrations directly. An understanding of these differences is critical in economic comparisons of the various cell technologies. Comparisons of evaporator

economics also require an understanding of the principle of multi-effect evaporation. This is described in Section 7.1.5.2A in connection with brine evaporation. In Section 9.3.3.1 below, we apply the same considerations to caustic evaporation, with emphasis on the differences between diaphragm-cell and membrane-cell evaporators. Section 9.3.3.2 then covers some of the basics of evaporation process design. It gives a brief description of the principal types of evaporator and discusses some of the factors to consider when determining the sequence of liquor flow through the various effects of the evaporator system.

Turning from that to the various technologies, we discuss first the diaphragm cell (Section 9.3.3.3). This is limited to sodium hydroxide. The membrane cell is covered next, again with reference to sodium hydroxide (Section 9.3.3.4). Finally, we cover the differences peculiar to potassium hydroxide solutions (Section 9.3.3.5). The discussion of evaporators does not follow our usual practice of emphasizing membrane-cell technology. Because diaphragm-cell evaporators are so much more complex, it is more interesting and more instructive to discuss their design fully.

9.3.3.1. Multiple-Effect Evaporation. The discussion of brine evaporation in Section 7.1.5.2A showed how installing a number of effects and using process vapor as a source of heat reduces the amount of energy that must be added to the process. The boiling point rise (BPR) of brine solutions makes some of the available temperature potential useless as a driving force for heat transfer. This limits the number of effects and the achievable steam economy. Similar limitations exist in caustic evaporation but are much more severe.

First, the heat of evaporation of water from a solution is not the same as the latent heat of pure water. The dilution of a caustic solution being exothermic, the latent heat of vaporization out of the solution is greater. The condensation of a kilogram of water vapor against a boiling solution will therefore evaporate less than a kilogram, even without considering the fact that the latent heat of steam decreases as the pressure and temperature increase. Steam economy suffers because of this effect.

Second, the boiling point rise of caustic solutions severely limits the staging of a system. BPRs are much greater in caustic evaporation than in brine evaporation, and as a consequence less of the total available temperature differential can be used to drive the process. BPRs are affected very strongly by solution concentration and weakly by operating conditions such as pressure. Reference substance plots of thermodynamic properties use the fact that a property of one substance (e.g., a solution of NaOH of given concentration) is related very simply to the same property of a second (e.g., water). Dühring's rule, for example, states that plotting the boiling point of a solution against the boiling point of water at the same pressure results in a straight line. Engineers often use Dühring diagrams to take advantage of this simplicity. One axis then becomes the boiling point of water, which is a substitute for pressure.

Boiling-point rise data for caustic soda and caustic potash solutions are given in the Appendix.

We usually are considering in this volume a membrane-cell liquor containing 30–35% NaOH. The BPR in the feed is already 20°C and will increase along with concentration. In a triple-effect evaporator, the BPR will consume as much as 70°C of the

available temperature differential. Largely for this reason, no membrane-cell evaporator with which the authors are familiar has more than three effects. Other solutions without the large BPRs characteristic of NaOH and KOH solutions are not so constrained. Water desalination systems, for instance, may have many effects and salt evaporators typically have four or more.

Of particular interest in this work is a comparison between membrane- and diaphragm-cell caustic evaporators. Many of the latter have been or will be converted to membrane-cell duty. Since diaphragm-cell liquor has a much lower NaOH content (typically 10–12%), the initial BPR will be much lower than that in a membrane-cell system. The mathematics of concentration is such that the greatest change occurs at the end of the process. Assuming equal amounts of water to be evaporated in each stage, the progression of concentrations in various systems is shown in Table 9.23. For ease of comparison, the concentration of NaOH in diaphragm-cell liquor is expressed as that of the NaOH–water binary—the presence of NaCl is ignored. Feed concentrations are taken to be 32.0 and 13.3% in membrane-cell and diaphragm-cell liquor, respectively. It is interesting to note that in no case does the diaphragm-cell caustic concentration reach even the membrane-cell evaporator feed concentration until it suddenly leaps to 50% in the most concentrated effect. Even allowing for the presence of NaCl, the boiling point rise is much lower, stage by stage, in the diaphragm case. More of the available temperature differential therefore can be used for heat transfer, and exchanger area is more productive. Alternatively, the extra temperature differential may make the installation of a quadruple- rather than a triple-effect evaporator practical.

When membrane cells replace diaphragm cells, the unit evaporative load is greatly reduced, by a factor of 5 or 6. The steam consumption may be reduced by a similar factor. The total heat-transfer area required, by the argument made above, is not so greatly affected. This will not prevent conversion of the evaporator system but can reduce the designer's freedom.

Recompression evaporation is an alternative to the multiple-effect approach that reduces steam consumption. Section 7.1.5.2B treated both mechanical and thermal recompression. The power consumption or the motive steam usage depends on the increase in pressure that is necessary to achieve the desired condensing temperature.

TABLE 9.23. Stage-by-stage Increase in NaOH Concentration during Evaporation

Evaporator type	Intermediate concentrations (wt% NaOH)	
	Membrane	Diaphragm
Double-effect	39.0	21.0
Triple-effect	36.4	17.6
	42.1	26.0
Quadruple-effect	–	16.3
	–	21.0
	–	29.6

Note: Basis: Same amount of evaporation in each effect

This in turn is fixed largely by the boiling point rise of the solution. When the BPR is greater, more power or more motive steam is required. Recompression therefore is most likely to be justified with solutions whose BPRs are small. In the NaCl brine example, and it is true of KCl as well, a compression ratio of about two is adequate. With caustic solutions, the ratio must be at least four. Not only is the power requirement much greater, but the capital cost per unit of output also increases. Where single-stage centrifugal compressors are adequate with brine evaporators, more complex machinery would be needed to produce the compression ratio needed in a caustic evaporator. Finally, the difference in latent heats between steam and caustic solution increases the demand for fresh steam. For similar reasons, thermal recompression also becomes much less efficient in a caustic process. Caustic solutions therefore are not good candidates for recompression evaporation, and so the technique is not widely used in caustic evaporation.

9.3.3.2. *Evaporation Process Design.* Evaporator designs most often found in the chemical process industries can be divided into falling-film and circulated units. Circulated units may use either natural or forced recirculation. Figure 9.64 gives simplified sketches of several types.

In the single-pass falling-film design, feed material enters through the top of a vertical shell-and-tube unit. The feed must be efficiently distributed and directed to the walls of the tubes. As the liquor passes down the tubes, some of it vaporizes. A mixture of liquid and vapor passes from the bottoms of the tubes into a phase separator. The key feature of this design is the short time of contact of the liquor with the heat-transfer surface. Falling-film evaporators are used on food and pharmaceutical products and on other heat-sensitive materials. When the net liquor feed rate is too small to keep the heat-transfer surface wet with this design, some of the concentrated liquor is pumped along with fresh feed to the upper chamber.

Natural-circulation evaporators are thermosiphons. The difference in densities between degassed and boiling liquids is the driving force for circulation. With this style, the feed enters a lower chamber. Within the tubes, vapor forms and allows the

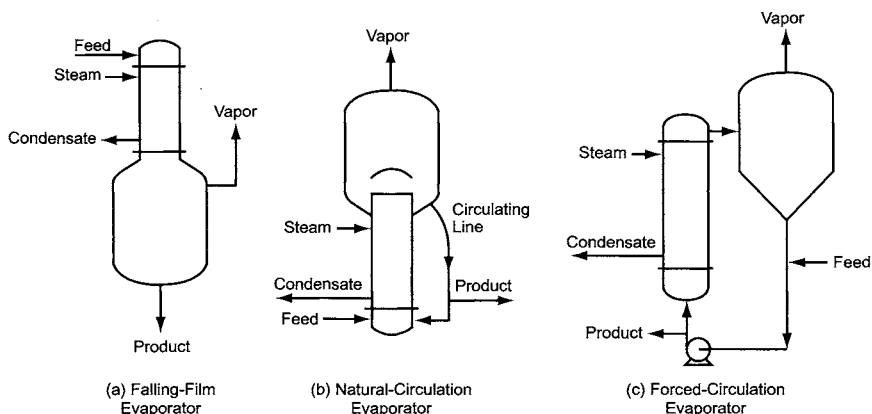


FIGURE 9.64. Principal types of evaporator design.

mixture of liquid and vapor to be forced upward. The two-phase mixture leaves the tops of the tubes and is separated. The liquid phase, denser than the mixture in the tubes, then leaves the top chamber through a pipe from which it can return to the lower chamber or be withdrawn as product. Natural-circulation evaporators are used in the processing of rayon, black liquor, low- to moderate-viscosity liquids, and nonsalting materials.

The forced-circulation design pumps liquor or slurry from the bottom of the vapor body through a horizontal or vertical tubular exchanger and back into the vapor body. It incorporates a large circulation volume. The normal intent is to maintain sufficient velocity to limit the temperature rise on each pass. When solids form during evaporation, this in turn limits both the redissolution of solids and the degree of supersaturation as the slurry re-enters the evaporator body. Low supersaturation means a low rate of nucleation and a higher average particle size, thus simplifying the job of removing salt crystals from the product liquor. Forced circulation is the standard method when solids are precipitated during evaporation and when scaling of the tubes is a likely problem. All these characteristics are especially valuable in the evaporation of diaphragm-cell liquor.

The forced-circulation design is often more expensive than some of the alternatives, and the energy consumed by the pumps must be part of any economic evaluation. At the same time, the pumps provide high heat-transfer coefficients in the exchangers, as well as the positive circulation that improves operability. In this process, pumps must have high capacities at low differential head. Axial-flow pumps as a class have the right characteristics for the duty. These are usually of single-elbow design and are mounted directly in the piping. They may hang from the piping or be spring-mounted on a base [147]. These methods allow for thermal expansion without installing expansion joints. Operating the pumps at low speed reduces attrition of the crystals and mechanical wear of the pump parts.

In forced-circulation evaporators, it is common practice to bring the recirculated liquor in below the operating liquid level in order to suppress boiling in the tubes and the circulating line. This practice can, however, reduce the efficiency of heat transfer within the vapor body itself. The emphasis in design always is on sizing the heating element and transferring enough heat into the circulating liquid. It is also necessary for the heated liquid to approach thermal equilibrium with the mass in the body of the evaporator. Rapid circulation or delivery of the heated liquid to a point where it can easily be swept into the circulating line works against this [148]. Tangential entry improves mixing within the evaporator body. A swirl breaker at the bottom nozzle helps to reduce bypassing and to avoid the problem referred to above.

Prevention of fouling has much to do with the choice of the best apparatus. The other aspects of process design should also consider fouling tendencies when choosing operating and steam temperatures, liquor velocities, possibilities of localized boiling or hot spots, solid bed densities, and rapid dispersion of liquors with fouling tendencies [149].

Besides the choice of evaporator type, evaporation process design includes selection of the number of effects to be installed. This choice is primarily a matter of a classical economic balance between the cost of supplying more effects and the benefits they offer in energy consumption. As the preceding section made clear, the number of effects in a caustic evaporator is never very great. For technical and economic reasons, diaphragm-cell evaporators usually have three or four effects and membrane-cell evaporators have two or three.

The designer also has options in the relative flow paths of liquor and vapor. The convention is to consider the flow of vapor from effect to effect as the “forward” direction and assign numbers to the effects in the sequence of that flow. There are three possibilities in a two-effect system:

1. forward feed, in which the liquor’s path from effect to effect is the same as that of the vapor
2. backward feed, in which the reverse is true (steam is supplied to what is defined as the first effect, and vapor flows from there to the second effect, while liquid feed is introduced to the second effect and partly concentrated liquor is transferred to the first)
3. parallel feed, in which fresh liquor is fed to both effects.

True parallel feed is rare in caustic soda and potash evaporation. It is more common with brine.

With more than two effects, there is also the possibility of “mixed” feed, which is neither true forward nor true backward feed. In a triple-effect system, for instance, the liquor flow might be 2–3–1.

Forward feed is often the simplest arrangement and in certain designs can eliminate the need for stage-to-stage liquor transfer pumps. The countercurrent nature of backward feed, on the other hand, sometimes allows more effective use of the temperature potential. The best choice for a given case depends also on steam conditions and the thermal condition of the feed. If the feed temperature is well below the first-effect boiling point, for example, there are thermal disadvantages in forward feed. First, the boiling point is highest in the first effect, which usually operates at the highest pressure. The feed absorbs more sensible heat before boiling, and absorbs it from the most valuable (hottest) source of heat. Second, the loss of generated vapor from the first effect is undesirable. Since this vapor is the heating medium for the second effect, less energy is available there. Less vapor then is generated for transfer to the third effect, and so the loss is propagated throughout the system.

A cold feed rather is a good candidate for backward feed. Even in a low-temperature effect, the feed may require sensible heat before it reaches its boiling point. This again reduces the amount of vapor generated. Since the vapor formed in the last effect often represents waste heat, however, it is best to take the loss in vapor production here. A hot feed has the opposite influence. A feed superheated at the operating pressure produces vapor by flashing. In the last effect, this vapor goes directly to the condenser and is a burden rather than an advantage to the process. In the first effect, it produces “free” vapor that is available to the second-effect heater.

Leaving aside the energy balance, backward feed can often improve the handling and heat-transfer properties of the process fluid. When viscosity increases significantly with concentration, it may be useful to have the most concentrated solution at the highest temperature. Usually, this is important only at the last stage of concentration, where the strength of the solution takes its largest jump (Table 9.23).

Such a situation can also favor mixed feed. The 2–3–1 arrangement used as an illustration above has the advantages of forward feed when moving liquor from the second to the third effect. By then returning the fluid to the first effect, this arrangement also keeps the final viscosity low and promotes higher heat-transfer coefficients.

The design of a multiple-effect system offers many other opportunities for the economization of heat. These include interchanging heat between various streams and flashing liquors and condensate to increase the degree of concentration or to produce more steam for use in later effects.

9.3.3.3. *Diaphragm-Cell NaOH Evaporation*

9.3.3.3A. Mechanical Design. A 50% conversion of the salt fed to a diaphragm cell will produce an approximately equimolar mixture of NaCl and NaOH. We shall use as a basis here a solution containing about 15% NaCl and 11% NaOH. Allowing for the entry of some wash water into the process, this gives an evaporative load of about six weights of water per weight of NaOH. This is a major expense to the process. The energy required for evaporation is a substantial fraction of the energy consumed in electrolysis. As noted in Section 9.3.3.1, triple- or quadruple-effect evaporators are used to reduce the amount of steam consumed.

When cell liquor is evaporated past the point of saturation, it is the NaCl that drops from solution. It is therefore possible to remove the salt even as the caustic concentration increases toward 50%. If evaporation continues until the NaOH concentration is just below 50% and the solution is cooled to 20–25°C, the residual salt concentration will be about 1%. This is the typical diaphragm-cell caustic of commerce.

The presence of solid salt as a third phase adds several considerations to process design:

1. deposition of solids in the evaporator bodies
2. transfer of solids between effects
3. control of crystal growth
4. removal and handling of solids.

Considering these in turn:

(1) The problem of solids deposition in a diaphragm-cell evaporator can be mitigated but realistically cannot be eliminated. Dissolving these deposits is an integral part of the operating procedure, and most designs provide an instantaneous capacity about 10% greater than the average to allow for it. Washing usually is by boiling water or a solution more dilute than normal in order to dissolve the salt. This process is usually referred to as a “boilout.” Boilouts are scheduled periodically. The least disruptive consists in merely adding water to normal process streams, one effect at a time. This upsets the process less than a full shutdown but is correspondingly less effective. Eventually, a shutdown with full boilout with fresh water becomes necessary. Efficient process design includes a dedicated boilout system with storage tanks and pumps. This allows controlled reuse of water and a lower total evaporative demand. Design also must allow for the periodic loss of evaporator production. This is the purpose of the extra instantaneous capacity mentioned above. Another requirement is to provide enough liquor and salt storage to isolate other steps in the caustic and brine processes from this upset.

(2) Evaporators conceivably could be operated with uniform dispersion of solids in each effect, and the solids could be transferred along with the caustic liquor. Practical construction of a crystallizing evaporator works against this, and it would be counter-productive in any case. Transferring the solids along with the liquor would expose the

solids to stepwise increases in the concentration of NaOH and decreasing concentrations of NaCl. The opposite is preferred.

Figure 9.65 is a sketch of the configuration of an evaporator designed specifically for diaphragm-cell liquor evaporation. The particular model was chosen to illustrate the mounting of a barometric condenser directly on the vapor body. It would be suitable as the last effect in its system. It is a composite of several designs. Liquor is withdrawn from a relatively quiescent zone in the bottom cone. A frequent practice is to withdraw the transfer liquor from the outlet of the circulating pump through a liquid cyclone. The clarified overflow goes on to its destination, and the concentrate returns to the evaporator or to the circulating pump suction. The solids in the evaporator body settle toward the bottom, from where they are transferred as a slurry. This design allows the liquor and the slurry to be sent in different directions. In a backward-feed evaporator, for example, the salt phase can be in forward flow. In this way, it contacts liquors with successively lower NaOH/NaCl ratios and leaves the system with a minimum of NaOH contamination. Another feature of Fig. 9.65 is the elutriation leg attached to the evaporator. The salt slurry and the feed liquor flow countercurrently in the leg. As the slurry thickens by settling, this feature helps to strip the caustic solution from the solid salt.

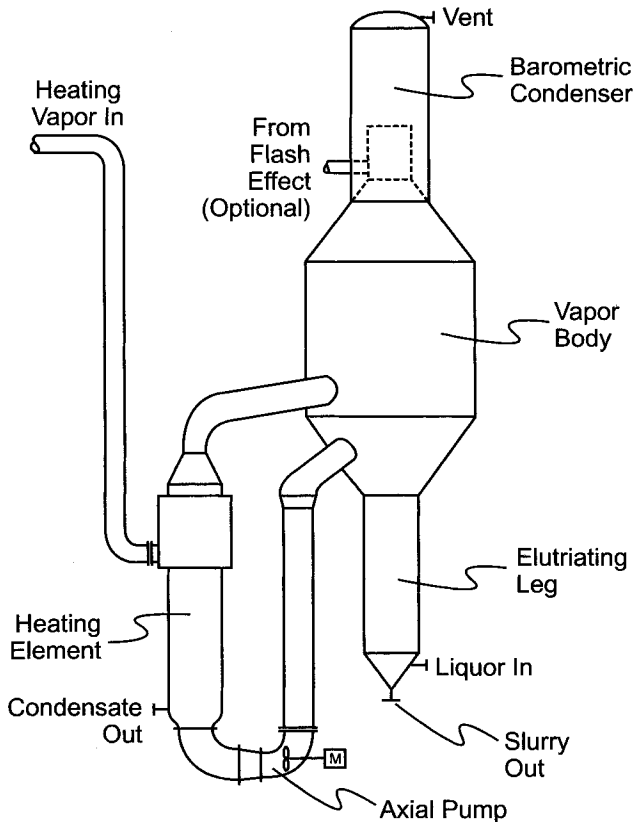


FIGURE 9.65. Typical diaphragm cell liquor evaporation effect.

(3) Some control over the growth of crystals is necessary to efficient handling of the slurry and reuse of the salt. Section 9.3.3.2 explains the advantages of a forced-circulation evaporator design in this service. The unit shown in Fig. 9.65 is an example of this type. An axial pump sends the liquor from the bottom cone through the heater. The source of heat is vapor generated in the preceding effect. The vapor duct is at the left of the drawing for emphasis. It may actually connect behind the plane of the drawing to give a more compact arrangement. The superheated liquor from the exchanger then enters the vapor body, at a slight upward angle, below the surface of the boiling liquor. Equipment and process design prevents boiling in the heater and keeps the degree of supersaturation of the hot liquor very low. The combination produces high-quality crystals. When a flash effect follows the standard evaporator bodies, it also produces solids, but in a relatively small quantity and in an uncontrolled manner. These solids may be recovered and used as seed crystal in the caustic cooling system (Section 9.3.2.4).

(4) Recovery of solid salt from the caustic liquor is primarily by centrifugation, normally in two stages. Section 9.3.2.5 has already covered this operation. Processing of the recovered salt depends on the measures taken for sulfate removal. Postponing discussion of the sulfate, we consider first the handling of the salt for reuse.

Nearly all evaporator salt is redissolved for use in chlor-alkali manufacture. Its designation as "CP" or chemically pure salt reflects its high quality. Hardness elements are largely absent, having been removed in the brine treatment process. The sulfate content may be reduced by treatment described below. On the other hand, chlorate formed in the cells and small amounts of corrosion products will have appeared.

In the diaphragm-cell process, the treated brine is less than saturated with NaCl. The recovered salt is used to saturate this stream before it flows to the cells. This consumes only a portion of the available salt. The rest also is dissolved for feed to the cells. This requires the addition of water to the process. Recovered evaporator condensate, like the salt, is soft and will add few impurities to the brine system. Since minimal amounts of hardness enter with the recovered salt and the condensate, many plants use this brine without further chemical treatment. In this case, the two functions of dissolving all the salt while resaturating the treated brine obviously can be done in a single step.

In hybrid plants that operate diaphragm cells in combination with other types, there are other options for use of the evaporator salt. One of the advantages of diaphragm cells is their ability to operate without penalty on salt supplied in the form of brine. With the other types, a brine supply presents a problem with the water balance. With mercury cells, for example, solid salt is needed to resaturate the depleted brine for recycle. Evaporator salt can fill this need, and, with the right division of production between the two types of cell, it is possible to run both types without a supply of solid salt. Several plants operate this way. With membrane cells, there are other ways to integrate the two types of cell (Section 9.4.1), but the basic idea is that the availability of salt from the evaporators again allows the combination to operate from an all-brine supply.

In any event, there is a need to bring together the salt produced and the stream requiring saturation. The usual approach is to transport the salt as a slurry to the appropriate brine system. In an all-diaphragm plant, the carrier fluid may be treated brine, evaporator condensate, or a mixture of the two. Condensate dissolves much of the salt and therefore reduces the size of the stream to be transferred. In a combined plant, the transfer fluid is the depleted and dechlorinated brine from the non-diaphragm cells.

Slurry is prepared in an agitated tank into which the centrifuged salt drops. The carrier fluid also is added to this tank, and the mixture is pumped to its destination. Crystallized salt forms a well-behaved slurry. The particles are uniform in shape and not likely to pack together to form plugs in the transfer lines. Still, the normal good practices in slurry pipeline design should be followed. Bends should be gradual, routing should be straightforward, and velocities should be high enough to prevent settling of the solids. There should be wash connections at the supply end and at other strategic points. Many plants handle the salt slurry at solids concentrations up to 25% w/w.

When some of the salt is normally transferred to membrane or mercury cells, prudent design will also allow its occasional use in the diaphragm circuit. In the membrane-cell version, this facility can be a simple branch in the slurry-transfer system. In the mercury-cell case, the use of separate tanks and transfer pumps and lines will prevent contamination of the diaphragm-cell brine system with mercury.

Under certain conditions, some of the sulfate in the cell liquor crystallizes along with the salt. This is in the form of a triple salt containing chloride, sulfate, and hydroxide. In most evaporation systems, nearly pure NaCl precipitates from the more dilute effects and triple salt from those that are more concentrated. Dissolving the high-sulfate salt along with the pure NaCl prevents the escape of the sulfate impurity from the plant. At some point, it would accumulate beyond the specified maximum level. Segregating the sulfate and purging it from the system can solve this problem, but Section 9.4.2.1 discusses a more selective process in which the sulfate is selectively redissolved and recrystallized as $\text{Na}_2\text{SO}_4 \cdot 10\text{H}_2\text{O}$, Glauber's salt. This is an item of commerce that is sometimes a useful byproduct.

9.3.3.3B. Process Arrangement. The purpose of this section is to examine the directions of material and energy flow in a typical diaphragm-cell evaporator (Figs 9.66 and 9.67). The example shown is a quadruple-effect unit with backward flow of liquor. Section 9.3.3.2 discussed some of the potential advantages of mixed feed, but this example is selected partly for the ease with which one can follow the various flows through the system. Figure 9.66 shows the flows of vapor and condensate only. This avoids much of the complexity of a complete drawing. The vapor flow is straightforward, with that generated in one effect being used to heat the next. The vapor lines are tagged with their pressure levels. The flash effect, mounted next to the first effect in order to receive its liquor, actually operates at fourth-effect pressure.

Condensate heat flow is essentially in the same direction as vapor flow. First, steam condensate and evaporator vapor condensate (the latter also variously referred to as secondary condensate and process condensate) are kept separate. Steam condensate returns to the boilers after exchanging some of its heat with process liquor. Process condensate is used as described in Section 12.4.3.2. In the drawing, condensate from each of the first three effects first passes through exchangers that heat the liquor (not shown) moving from one effect to the next higher. Variations include the use of condensate to preheat evaporator feed and the diversion of some condensate to overhead desuperheaters. As an example, the drawing shows the use of second-effect condensate to desuperheat steam and first-effect vapor.

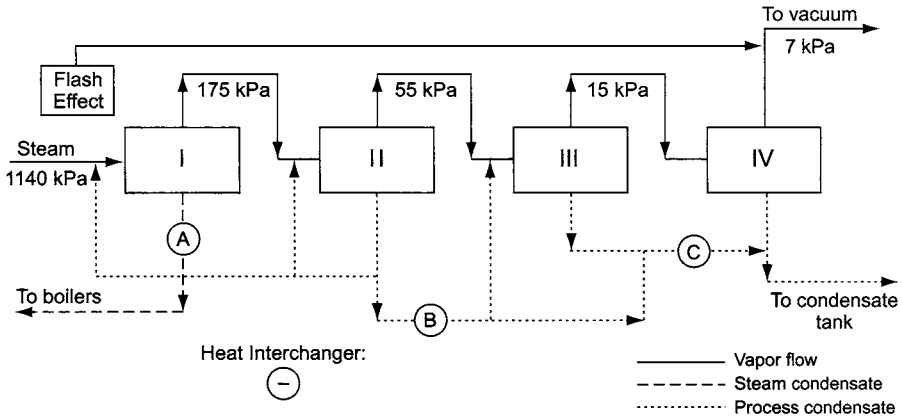


FIGURE 9.66. Diaphragm-cell caustic evaporator—vapor and condensate flows.

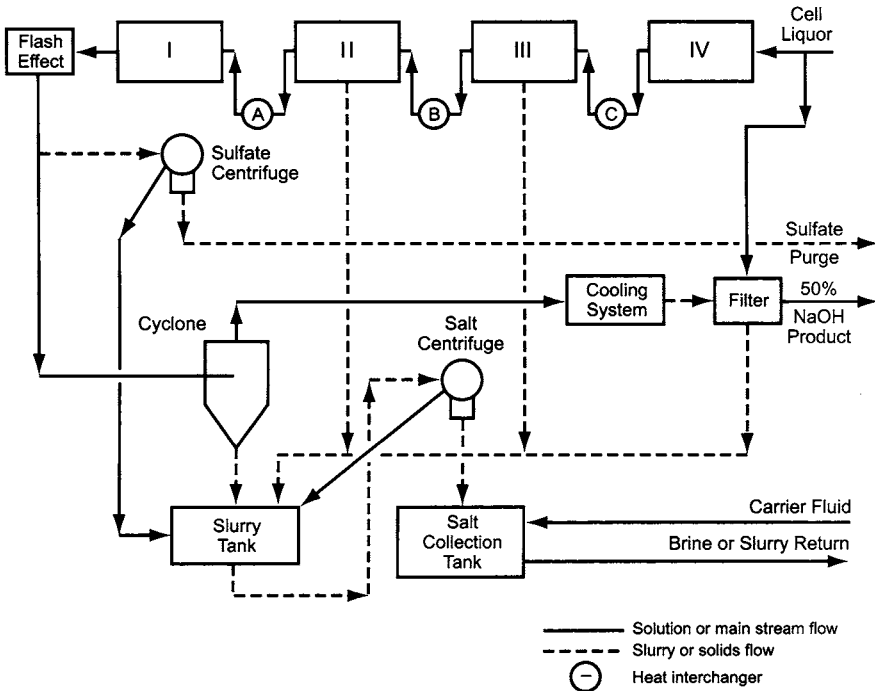


FIGURE 9.67. Diaphragm-cell caustic evaporator—solution and slurry flows.

Figure 9.67 (upper right) shows that in the example chosen the flow of cell liquor into the evaporator system splits, with a small fraction (4% in the example) going to the product filter and the rest to the fourth evaporation effect. Operating at about 7 kPa (25 torr) and heated with third-effect vapor, this effect vaporizes a bit more than 25% of the water and produces a 13.5–13.8% solution of NaOH. NaCl begins to precipitate,

forming a dilute slurry. The whole product of this effect goes on to the third effect after heat interchange with second- and third-effect condensate. Since the fourth effect produces very little in the way of solids, there are fewer constraints on equipment design, and the selection of evaporator type can vary. The other effects are conventional external forced-circulation evaporators, perhaps with elutriation legs added.

The liquor transferred to the third effect first passes through interchanger C. As Fig. 9.66 shows, a combination of second- and third-effect condensate provides the heat. The other interchangers in our example also recover heat from condensate, the sources being shown by corresponding letters in the interchangers on the two drawings. Many evaporator systems also use interchange between liquors. Another technique is to flash condensate from its operating pressure down to the pressure of another effect. This generates vapor for use in the corresponding heater.

The third effect is heated by second-effect vapor. It raises the concentration of NaOH to 18–18.5%. NaCl continues to precipitate, forming a slurry with an average solids concentration of about 13%. Relatively clear liquor from the body of the evaporator or from a cyclone fed by the third-effect circulating pump is the feed to the second effect. This design assumed the latter with a residual concentration of 2% solids. The cyclone underflow returns to the pump suction. A separate pump withdraws 25% slurry from the elutriating leg and forwards it to a tank whose operation is described below. Since circulating pumps develop little head, they may not be able to transfer liquor between effects in a backward-flow system. In place of the arrangement described above, a separate pump may be required. On the other hand, certain slurry transfers may not require pumping.

The pattern of flows holds for the second effect. It receives liquor from the third effect and is heated by vapor from the first effect. The dissolved NaOH concentration increases to about 27–28% in the second effect.

The circulating liquor in the first effect is heated with 10-bar steam. The product is 42% NaOH with about 10% suspended solids. Flashing this from the operating pressure of 175 down to 7 kPa, the fourth-effect pressure, produces a 15% slurry in 49.3% NaOH solution (b.p. 82°C). Part of the pumped stream goes to sulfate removal. The rest is split by a cyclone into a nearly clear solution and a 40% solids underflow. The underflow goes to the slurry tank. The clear stream is the final product of the evaporation section. Its dissolved NaCl concentration is about 2.5%. Product coolers deliver a solution that is 50% NaOH and 1% NaCl, with about 2.5% suspended solids. Cooling and solids removal are the subjects of Sections 9.3.2.4–9.3.2.6.

The slurry tank is a receptacle for the salt precipitated in the flasher and the first three effects. In the scheme shown in Fig. 9.67, it also receives the salt removed in the product filter. This is as a solution or slurry in cell liquor. The net production of solid salt leaves the evaporator system by way of a centrifuge that drops it into a collection tank. It can be dissolved in water or dilute brine or slurried in brine for return to the brine plant. Liquor from the centrifuge returns to the slurry tank, which usually has a conical bottom that allows it to act as a partial separator. The accumulated liquor can then be removed from the top portion of the tank as relatively dilute slurry. It returns to the evaporators.

Slurry from the second and third effects goes directly to the slurry tank. First-effect slurry requires handling of a different sort. First, it contains triple salt. This can be handled, as in Section 9.4.2.1, to produce Glauber's salt or anhydrous sodium sulfate.

It is also possible simply to purge enough of this salt to maintain the sulfate specification in the product caustic soda. The purge is more efficient when the salt is removed through a centrifuge, as shown. Second, the liquor from the first effect is on its way to final product recovery. Better phase separation is desirable here, and so the slurry passes through a set of cyclones. The emphasis is on delivery of clear liquor, and the concentrated underflow joins the other slurries in the tank.

The sidestream of first effect, or flash effect, slurry that goes to sulfate removal is centrifuged and washed if necessary for the recovery of mother liquor. The liquor and wash solution drop to the slurry tank. The collected salt, which is 15–20% Na_2SO_4 , is purged. The amount of NaCl lost, in one particular design, was about 1% of the quantity purchased. Section 9.4.2.1 describes more elaborate systems that remove sulfate more selectively.

The split of first-effect/flash-effect slurry between the main stream and the sulfate centrifuge is adjusted to maintain an acceptable standing sulfate concentration in the cells and the evaporators while removing all the fresh sulfate entering the plant. Beyond choosing slurry from the first effect, in our example there is no segregation of high- and low-sulfate evaporated salt. The design is appropriate for a plant receiving salt that contains about 0.2% CaSO_4 .

9.3.3.4. Membrane-Cell NaOH . First, assume that the product of the cells is 32% NaOH . The evaporative load per weight of NaOH in 50% product then is 1.125. The steam demand is much lower than in the diaphragm-cell process. It is important to note that the evaporative load is a strong function of cell concentration. Reducing the concentration from 35% to 30% increases the load by more than 50% when the product is to be 50% NaOH .

Evaporation of membrane-cell caustic is simple concentration, and there is no need to handle crystallized salt. With the smaller steam demand and the higher BPRs in the system, fewer effects can be justified, and Section 9.3.3.1 points out that the usual number is two or three. Very small plants may have only one effect.

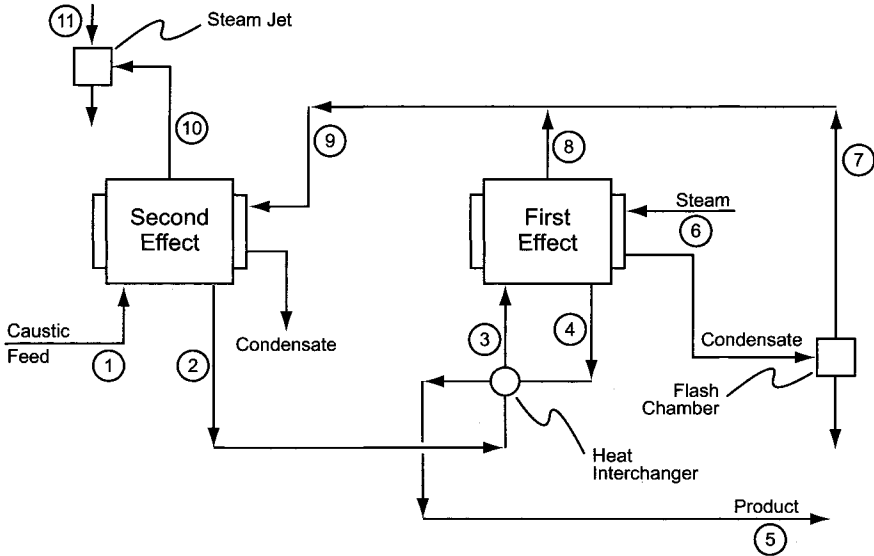
Double-effect evaporators tend to produce steam economies of 1.6–1.85 in backward-flow systems. Triple-effect steam economies are about 2.5, and flow arrangements are backward or mixed. Steam economy is variable and as a primary measure of performance may be unreliable. For example, the extent of use of steam condensate for heat interchange varies. This practice retains heat within the evaporator system and always improves the measured steam economy. The overall heat economy, however, may not improve. Recycling colder condensate to the boilers may simply transfer some of the load from the process to the utility area.

Since membrane-cell evaporators do not produce solids, forced-circulation evaporators are used less frequently. Rising-film and falling-film types appear in a number of plants. The rising-film evaporator depends on natural circulation of caustic from the bottom to the top of the tubes. Falling-film evaporators, as shown in Section 9.3.3.2, depend on pumps to lift caustic to the distribution system at the top. These units generally have better heat-transfer coefficients and less tendency to foul. Recirculated units in particular allow good control of flow to maintain a proper film on the tubes. This also permits the designer to provide more turndown capability. Liquid velocities are lower

than in rising-film evaporators, and entrainment of caustic by the vapor generated in the tubes is less of a problem.

Example. Here we consider a double-effect evaporator concentrating 35% NaOH to 50%. Figure 9.68 shows a backward-feed system using medium-pressure steam. The material balance table is based on one ton of NaOH.

The caustic feed (Stream 1), entering the second effect from the left, contains 35% NaOH and is at 90°C. A vacuum system, here in the form of a steam jet, maintains a low operating pressure. The condenser, not shown, normally is a barometric unit. With heat supplied by vapor from the first effect, the second effect produces 42% NaOH, which then goes to the steam-heated first effect. The first-effect product liquor (Stream 4) is 50% NaOH at 136°C.



Process Stream #	1	2	3	4	5	
	Caustic Feed	Intermediate Product	First-Effect Feed	First-Effect Product	Final Product	
NaOH	1000	1000	1000	1000	1000	
H ₂ O	1857	1377	1377	1000	1000	
Total	2857	2377	2377	2000	2000	
% NaOH	35	42.1	42.1	50	50	
Temp., °C	90	73	117	135	78	
Vapor Stream #	6	7	8	9	10	11
	Steam	Flash	1st Effect Vapor	Combined Vapor	2nd Effect Vapor	Ejector Steam
Flow Rate	527	83	377	460	480	22
Temp., °C	182	82	131	122	68	182
Press., kPa	760	65	65	65	7	1035

FIGURE 9.68. Double-effect membrane-cell evaporation process.

The two most common methods of energy economization are the interchange of heat between two streams and the flashing of condensate to produce steam for use in a later effect operating at lower pressure. Both methods are illustrated here. In the interchanger, the product of the first effect heats the liquor transferred from the second effect. The interchanger is specified to give a temperature approach of 5°C. This occurs on the cold side. The product therefore leaves at 78°C and may require more cooling. The 42% solution enters the first effect at 117°C. The condensate from the first effect is estimated to be at 180°C; this is a function of mechanical design as well as of the thermal properties of the system. Reducing the pressure to that in the second-effect heating element produces more vapor (Stream 7), increasing the amount available to heat the second effect by 22%.

The net result with this simple arrangement is a steam economy of about 1.62 (857 kg evaporated/527 kg steam consumed; including the estimated steam usage in the ejector drops the steam economy to 1.56). A simple single-effect evaporator with no form of economization would have a steam economy of only 0.67. The design features in our example have reduced the steam requirement by nearly 60%. The use of two effects also reduces the demand for cooling water in the final condenser. The saving here, based on vapor load, is about 44%. It is on the low side of 50% because (1) the feed material is hot and above the second-effect boiling point, and (2) flashing of condensate produces more steam for the second-effect heating element. Both situations increase the amount of vapor generated in the second effect and sent to the condenser. The absolute value of the change depends on the sort of condenser used and the policy regarding allowable water temperature rise. The use of the interchanger also reduces the amount of cooling water required by the product stream. If the product were to be cooled to 50°C for example, the cooling water usage would be reduced by a factor of about three. Assuming a 10°C rise in cooling water temperature, the saving would be about 10 m³.

The temperatures in the two effects were estimated from the boiling point data in the Appendix. The second effect operates at 7 kPa, where the boiling point of water is 38.9°C. At this pressure, 42.1% NaOH has a boiling point rise of 29.6°C. The boiling temperature of the solution therefore is 38.9 + 29.6 = 68.5°C. The first effect operates at 65 kPa. In this case, water boils at 87.2°C, and the solution concentration is 50%. The estimated BPR is 43.5°C, giving a boiling temperature of 130.7°C.

9.3.3.5. KOH Evaporation. Evaporation of KOH solutions is in all respects similar to NaOH evaporation. Many of the properties of KOH solutions are close to those of NaOH solutions at the same weight concentration. Table 9.24 compares several properties of 50% solutions; the temperature-dependent properties are listed at 40°C. Viscosity is a striking exception to the otherwise close match of properties. Handling of KOH solutions is correspondingly easier.

Because KOH produced in membrane cells often has a lower concentration than its NaOH counterpart, the evaporative load per unit of product may be higher. The final product concentration usually is either 45 or 50% KOH. The load then is 1.1–1.5 kg water per kg KOH. The lower limit is quite close to that associated with NaOH evaporation; the upper limit is about one third higher. Since KOH plant capacities are as a rule much lower, however, evaporators are physically smaller and third effects are harder to justify.

TABLE 9.24. Properties of NaOH and KOH Solutions

Property	NaOH	KOH
Boiling point, °C	143	145
Freezing point, °C	12	10
Density, kg m ⁻³	1510	1500
Specific heat	0.77	0.67
Vapor pressure, mmHg	3.5	9
Viscosity, cp	23.5	1.8

The close match of freezing points in the above table is fortuitous. The freezing-point behavior of NaOH solutions in particular is rather complex. While NaOH forms a eutectic at 47% NaOH (approximately NaOH·2.5H₂O) and there is a freezing point maximum at 39% NaOH that is actually higher than the value at 50%, the freezing point of KOH drops off rapidly with increasing dilution. The complications that accompany a positive freezing point are avoided when KOH is produced at a concentration slightly below 50%, and 45% solution is a common article of commerce.

9.3.4. Purification of Caustic

9.3.4.1. Removal of Dissolved Salt from Diaphragm-Grade NaOH. The high concentration of salt in diaphragm-cell caustic soda led to the development of a split market. The diaphragm-cell grade is not suitable for all applications and mercury-cell caustic often commanded a premium as “rayon grade.” Membrane-cell caustic has similar advantages and also can sell at a premium. Some diaphragm-cell caustic therefore is upgraded to increase its utility. Several routes are possible, including fractional crystallization of NaOH and recovery by forming an alcohol clathrate and distilling it under vacuum. The former has been practiced commercially, but because the crystals formed are NaOH·3.5H₂O, the basic product is limited to about 40% NaOH and requires further concentration.

The standard commercial process is based on extraction. Anhydrous ammonia has the ability to extract neutral and less basic salts, along with some of the water, from caustic soda. Figure 9.69 shows the process licensed by ELTECH Systems. Aqueous caustic soda and nearly anhydrous (~98%) ammonia are pumped separately to an extraction tower which operates above 3,000 kPa. A small fraction of the ammonia stream can flash through an exchanger to cool the remaining liquid. This prevents vaporization at the suction of the ammonia feed pumps. Both streams to the extractor are preheated to 60–65°C. In passing up the column, the ammonia extracts chloride, sulfate, chlorate, and some of the carbonate from the caustic. Typically, by feeding about 0.4 kg of ammonia for each kilogram of 50% caustic, 96–98% of the salt can be removed. The extract contains about 3.5% NaCl and 6.5% NaOH. The chlorate and sulfate contents depend on their levels in the caustic feed. Extraction removes a smaller fraction of the carbonate. The ammonia also is heavily diluted with water (about 2 parts H₂O/3 parts NH₃).

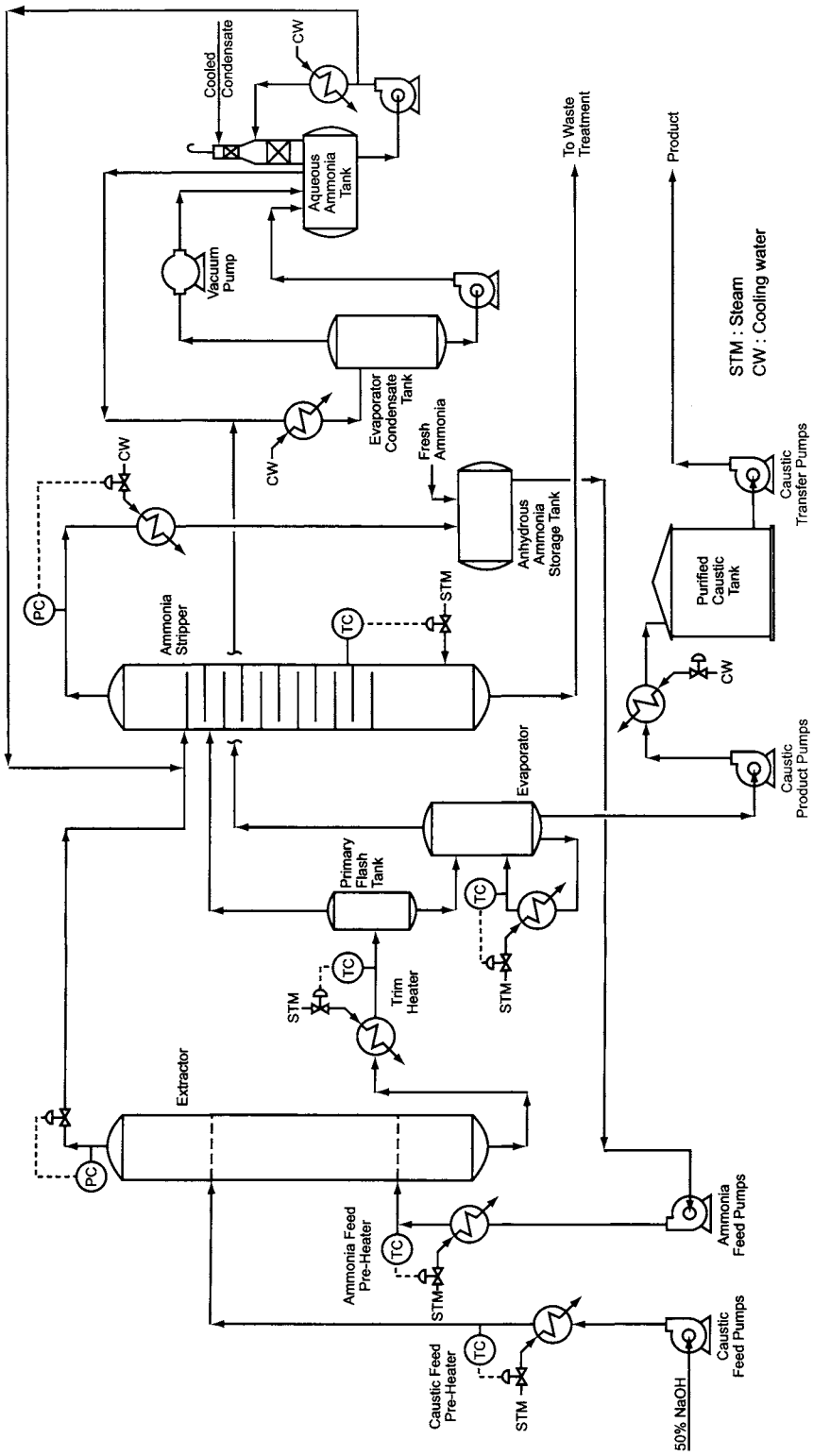


FIGURE 9.69. NaOH purification process.

The extract passes to an ammonia stripper operating at an intermediate pressure (about 1,450 kPa). Much of the ammonia flashes, and the injection of steam at the bottom of the column drives off the rest. Most of the ammonia is recovered for recycle by way of the anhydrous ammonia storage tank. At different levels in the stripper column, other ammonia-containing streams are recycled. These are identified below.

The stripper bottoms, at nearly 200°C, can be a valuable source of heat. First, it can be interchanged with a dilute ammonia stream (carrying the ammonia from the scrubber bottoms) that is being recycled to the stripper column. Then, it is flashed at a positive pressure of about 1 atm to generate some of the steam used in the feed ammonia and caustic preheaters. The resulting solution will contain 2.3–2.5% NaOH at a temperature of about 125°C. It is a waste stream from the process. In some cases, it has served as a source of OH⁻ for the chemical treatment of brine.

The caustic from the bottom of the extractor is flashed to remove most of the dissolved ammonia. Like the ammonia stripper, the primary flasher operates at the intermediate pressure of about 1,450 kPa. The flashed vapor abstracts its latent heat from the remaining liquid. A trim heater on the caustic fed to the flasher supplies the necessary heat to offset the drop in temperature that would otherwise occur. The flashed ammonia, along with some water vapor, then can go to the stripper for separation into ammonia vapor and water.

Next, the flashed caustic, which still contains about 2% ammonia, goes to an evaporator. This operates under vacuum (about 40 kPa absolute). The remaining ammonia is driven off as an approximately 15% w/w vapor, the balance being water. The condensate from the overhead exchanger is collected.

Not all the ammonia is recovered by condensation with ordinary cooling water. The remaining vapor therefore, after boosting in a vacuum pump, goes to a scrubbing column with two sections. In the first section, the vapor contacts a stream of cooled ammonia/water condensate. In the upper section, the remaining vapor contacts a cooled stream of fresh water. When all the condensate and the scrubber solution are combined, a 12–15% solution of ammonia results and collects in a storage tank. The net production of this material goes back to the stripper. This is the stream mentioned above as possibly being interchanged with the stripper bottoms.

The bottoms from the evaporator is the product of the purification plant. It will contain less than 0.05% NaCl and will be at about 125°C. It can be used in other processes or cooled for storage and shipping.

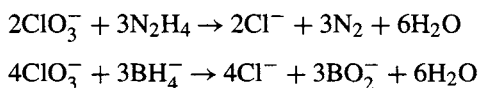
The vapor flashed from the stripper bottoms is condensed and held in a receiver that is vented to the ammonia scrubber. The condensate returns to the process.

9.3.4.2. Removal of Other Impurities. Salt is easily the impurity present in the highest concentration, and its concentration fixes the load on the extractor. Other impurities can be important in some applications of the product caustic. Color bodies, for example, contaminate some solutions. Chlorate is another contaminant whose presence may be objectionable.

As stated in the previous subsection, chlorate is successfully removed by ammonia extraction. This is an expensive process whose main objective is the removal of the much higher quantity of chloride that is present in diaphragm-cell NaOH. It is also designed

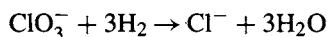
to operate on 50% NaOH solution. For both technical and economic reasons, then, it is not used to remove chlorate from membrane-cell liquor.

Other techniques can be used to supplement the extraction process or to treat higher-quality caustic, where it would be difficult to justify the high cost of an extraction/stripping plant. Most of these alternatives involve the chemical reduction of chlorate. One such process uses an oxidizable organic added to the caustic solution. Ordinary sugar is one such organic, and Section 9.3.5.2 covers its use in the production of anhydrous caustic. The presence of chlorate at high temperature and caustic concentration causes rapid corrosion of the nickel equipment, and its reduction by sucrose reduces the metal contamination of the product and extends the life of the equipment. The technique is less successful under milder conditions. Chemical reduction also is possible with classical reducing agents or hydrogen donors such as hydrazine and borohydrides:



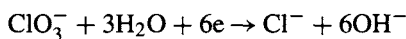
The latter is expensive.

Direct reduction with hydrogen is also possible. The chemistry is the same as that discussed in Section 7.5.9.4B:



This requires the use of a catalyst (usually a transition metal of Group VIII) at modest to high pressure and temperature. One version that has been in commercial practice for many years [150] is to use a ruthenium catalyst on carbon at 100–250°C and pressures above 5 atm.

The last method of reduction to consider is the electrochemical route. This is similar to the method described in Section 7.5.9.4B for the removal of chlorate from brine, and the overall chemistry is the same:



Development of a practical cell with efficient and stable electrodes would be necessary for commercial use of this process.

Color bodies may be metal ions or organics. Treatment with adsorbents is a conventional process, and Mannig and Scherer [151] describe the use of hydrogen peroxide as a decolorizing agent. Metal ions can also be removed electrochemically.

In diaphragm cells, it is also possible to suppress the formation of chlorate. Hypochlorite formed in the anolyte can be catalytically decomposed by additives in the diaphragms [152,153]. Impregnation of the asbestos with cobalt or nickel oxide reduces the amount of chlorate in the catholyte. The use of 1.1 kg NiO per kg asbestos lowered the chlorate level from 8 to 2 kg t⁻¹ NaOH over a period of 30 days at 95% current efficiency.

9.3.5. Solid Caustic

9.3.5.1. Solid Forms and Their Production. There is a relatively small market for solid caustic. Certain applications require the fused material, and in other cases freight savings offset the additional processing cost. We consider three forms of solid here: bulk, flaked, and prilled. KOH is seldom formed into prills.

Bulk solid, usually in drums, is made from molten caustic simply by pouring it into containers and allowing it to cool. This is the cheapest process, giving the least convenient and perhaps most hazardous form of the product. It is often removed from drums by directing a stream of water into the open tops. The drums should then be upended for greater safety. Some types of drum are simply cut away from the block of caustic, leaving a solid mass to be handled or dissolved.

Flakes result from the chilling of molten caustic containing about 2–3% water on a rotating roll. Molten material from the concentration process described in the next subsection falls by gravity into a trough or a pan and deposits onto the roll. A doctor blade scrapes the solid loose, and it breaks up into flakes between 2 and 20 mm in size. The flakes drop into a hopper and usually are packaged in specially designed multiwall bags or lined drums. The flaking drum, fabricated in low-carbon nickel, is cooled internally, usually by a water spray designed to maintain an even surface temperature. Flaking plants require equipment and area washdown systems and some means of dust control. The flaking drum is enclosed to reduce operator exposure, heat loss, and exposure of the caustic to atmospheric moisture.

Prills are made in large-diameter towers similar to those used to produce urea. Molten caustic is pumped to (an) atomizing device(s) in a tower. The molten beads thus formed are about one millimeter in diameter and are frozen by countercurrent contact with a stream of circulating air. Anhydrous caustic materials are powerful desiccants, and so it is essential to avoid sorption of moisture from the air. One approach is to keep the temperature in the tower high (e.g., 140°C) and then to take the beads through a second tower or a solids cooler outside the tower. The latter reduces the product temperature to about 50°C, and it is handled in stainless steel conveyors and elevators. Schmittinger and coauthors [154] give a flowsheet for this version of the process. The other approach to prilling is to do all the cooling with air but to keep the system dry by the continuous addition of dry air to the process.

This apparently simple process requires several tradeoffs and the balancing of variables:

1. small particles are more easily cooled but may be flung into contact with the tower walls while still molten;
2. large particles avoid the above problem and may have better flow properties when dry, but they require more time to cool even as they fall faster and spend less time in the cooling zone;
3. increasing the rate of heat transfer by providing more airflow or colder air can prevent the problems of sticky particle surfaces implied above, but too-rapid cooling can freeze the droplet surfaces prematurely. The “case hardening” that results slows the transfer of heat from the interior of the droplets. The result is sticking and agglomeration in the bottom of the tower, the downstream equipment, or the packages.

While the added processing makes prills more expensive than flakes, they have superior flow properties and are less prone to agglomeration caused by the absorption of water.

9.3.5.2. Preparation of Molten Anhydrous Material. The starting material for the production of solids usually is an approximately 50% solution from an evaporation plant. First, this must be concentrated to produce anhydrous material for one of the finishing processes described above. Optimization of design for production of solids from the cell product probably would not give 50% liquor at any stage, but no substantial integrated commercial plants are dedicated to solids, and so a liquid product must also be available for sale or transfer.

NaOH melts at 318°C and KOH at 360°C. It is theoretically possible to produce any desired concentration by evaporation. Practically, however, some water, up to several percent by weight, will remain after atmospheric evaporation. Table 9.25 shows the rapid increase of boiling point with %NaOH. The last few entries are extrapolated values based on the observation that the boiling point is linear with the logarithm of the water content [155].

“Anhydrous” NaOH is made in concentrations of 97% and up. Figure 9.70 shows the process. A nominal 97–98.5% product is made in two evaporation steps. The first is a conventional recirculated falling-film concentrator operating under vacuum. Pressure typically is about 55 torr (6.9 kPa). The outlet concentration is 60–63%. This solution goes on to the final concentrator. This, too, is a falling-film unit, operating at atmospheric pressure and heated by molten salt. The salt is a mixture of sodium and potassium nitrites and nitrates at 425–450°C. The following composition gives a melting point of 149°C:

Na	50.3%	NO ₃	63.0%
K	49.7%	NO ₂	36.9%
		OH	0.1%

The salt is circulated through a fired heater to maintain its temperature. Fuels range from hydrogen to #6 fuel oil.

The first evaporator is heated by vapor generated in the second. The feed liquor is heated by exchange with evaporator vapor and added to the recirculation line of the first evaporator. A solution of sugar (sucrose) in dilute NaOH is also added to reduce chlorate and so prevent corrosion of the nickel evaporator. The composition of the solution usually is 10–20% sugar and 1–3% NaOH.

TABLE 9.25. Boiling Points of High-concentration NaOH Solutions

% NaOH	90	95	97	98	99	99.5	99.8
BP, °C	291	328	355	377	414 ^a	451 ^a	500 ^a

Note: ^a Extrapolated value.

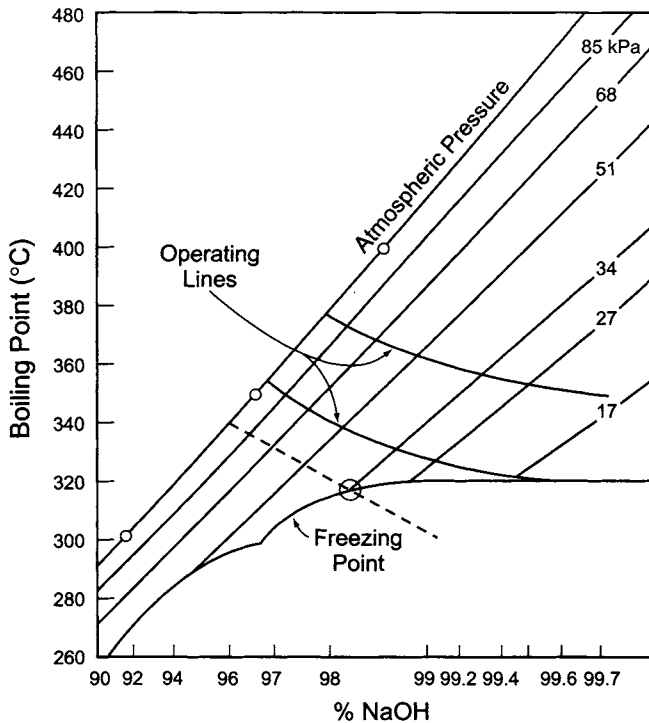


FIGURE 9.71. Course of flash evaporation of concentrated NaOH.

close to the freezing point curve. Given process heat losses and the nature of the approximations made in constructing the diagram, this is too close for comfort. With starting concentrations below 97%, the temperature at some point would drop below the freezing-point curve before the desired concentration was reached, and the process would be inoperable.

As suggested in Section 9.3.2.1, nickel is the universal choice for construction of piping and equipment handling hot anhydrous caustic. These systems require protection from stress as well as from corrosion by the hot caustic and contained chlorate. Stress can result from errors in manufacture or installation, faulty operation, or temperature cycling between ambient and the processing level. Carbon can precipitate at grain boundaries when the metal is held at temperatures above 315°C and cause intergranular stress-corrosion cracking. Nair [159] discusses failures that have been attributed to stress cracking and points out the superiority of nickel 201, with its lower carbon content, to nickel 200.

9.3.6. Caustic Product Handling

Pasquariello [160] has reviewed the requirements for efficient and safe handling of caustic and presented design considerations for storage and piping systems. Caustic soda and potash are most frequently stored in carbon steel tanks. The exterior of such tanks should

always be painted. Internal linings prevent product contamination as well as corrosion of the steel. Epoxy linings are common, and neoprene latex linings are a common feature in the chlor-alkali industry. Vertical tanks with flat bottoms and conical roofs are the standard. Smaller tanks usually have approximately equal heights and diameters, but larger tanks frequently are constrained in height by the high density of caustic solutions. Common design codes for steel tanks include API 620 and 650. The design of reinforced plastic vessels usually follows ASTM RTP-1. Horizontal tanks are sometimes used, especially when some pressure rating is required. They should be supported on concrete saddles or on steel saddles installed on concrete.

A large plant that sells all its caustic output to a diverse group of customers will need adequate storage and loading facilities and a large fleet of dedicated tankers. The latter is easily overlooked in preliminary economic evaluations. Tank cars can be leased or purchased outright. In either event, they represent a considerable cost, as the following example makes clear.

Example. As 50% solution, daily production will be 1,600 tons. This has a volume of less than $1,100 \text{ m}^3$, but to provide freeboard and a small safety margin, we shall use $1,200 \text{ m}^3$. A producer whose output is dedicated to one or a few nearby customers might require less than a day's finished product storage. The producer who is primarily a chlorine merchant with a far-flung caustic soda business will require more storage volume and an extensive fleet of delivery vehicles. Here, we shall assume that the plant has four days' worth of finished product storage.

Volume required = $4 \times 1,200 = 4,800 \text{ m}^3$. Use two tanks, each $2,400 \text{ m}^3$ liquid volume.
Tank dimensions: 17 m diameter, 12 m height (11 m to overflow = $2,497 \text{ m}^3$)
Material: carbon steel lined with neoprene latex; polyurethane insulation
Surface area: 875 m^2 exposed to air (say 900), 227 to ground (say 250).

Each tank car holds 90 tons of 50% NaOH. Approximately eighteen cars must be loaded each day. Allowing for a car turnaround of one month, the fleet must comprise about 550 cars. This number contains no specific allowance for cars that are undergoing major maintenance. Trackage should allow for 4 days' worth, or 72 cars, and should include facilities for washing as well as loading of cars.

Cell caustic at 32% will amount to 2,500 tpd with a volume of about $1,900 \text{ m}^3$. We allow for $2,000 \text{ m}^3$ liquid per day. The volume stored will depend on the policy adopted and on any provision made for storage of off-specification material.

Section 9.3.2.1 discusses materials of construction for NaOH and KOH in some detail; a short summary of their application to product tankage follows here. Carbon steel is the standard material of construction for NaOH and KOH below 50°C . Corrosion allowances of about 3 mm usually apply. Welds should be made with rods containing $\frac{1}{2}\%$ Mo. Stress relief can extend the serviceable temperature range (Fig. 14.21), but the danger of contamination of the caustic continues to increase. If temperatures may occasionally be higher or if product contamination is a major consideration, tanks are lined or coated. Rubber and thermoplastic coating systems are widely used, and some tanks are lined with metal sheets or cladding. When more resistant metals are necessary, stainless steel and nickel also appear in this service. Stainless steels offer improved

resistance to corrosion, but there is always the possibility of interior stress corrosion or exterior chloride attack. Temperature in stainless steel should be restricted to a maximum of 95°C. Nickel is suitable for all reasonable concentrations and temperatures and will not contaminate the solution. Nickel or nickel-clad construction is standard for 73% NaOH.

Suitable plastics within their temperature limitations are PVC, polyolefins, and fluorocarbons. PVC and polyolefins may be wrapped with FRP to provide strength; FRP alone is not used, because of the possibility of attack by caustic.

Tank nozzles should include an adequately sized vent and an overflow that is piped to grade. The inlet fill nozzle should be above the overflow. There should be a valve on the fill line at the nearest practical location. A location near grade usually meets the definition of "practical." The outlet line should likewise have a valve located close to the nozzle. The addition of spare nozzles should be considered for lined tanks and others that are difficult to weld after fabrication.

Storage volume should satisfy operating, maintenance, inventory, and shipping requirements. A producer's plant will usually have enough storage to hold some number of days' worth of production. A consumer's storage capacity will reflect the plant's average demand and the time required for a shipment to arrive. Often, volume is fixed at 1.5 times the size of a transport container. Large consumers will be on a regular schedule of delivery and can set their storage volume accordingly. Those who consume material continuously should have at least two tanks to provide for filling, testing, inspection, maintenance, and gauging for transfer. Multiple tanks also are common when the dimensions of a single tank would be excessive or when the use of two smaller tanks in place of a large one reduces the volume required inside a dike.

Siting of tanks should consider vehicle and personnel access and the possible exposure of personnel to leaks. Warning signs should be present, along with labeling according to local regulations. The storage area should be well lit. Even if nighttime operations are not contemplated, the design should consider emergency situations.

Most climates require heating to avoid wintertime freezing of 50% solution. Even when this is not necessary, NaOH solutions often are heated to reduce their viscosity. Tank heating may be internal or external. External heating usually is by way of pumped circulation through heat exchangers. This also provides an opportunity for blending (Section 9.3.2.7). Since it is necessary to heat only the material being pumped, the use of a preheater on the pump suction line is feasible. The reader should note that this ignores the usual advice not to add any pressure loss in suction lines. Internal heaters usually are nickel coils or bayonets served by low-pressure steam. It is important not to overheat the solution. Localized boiling on tube or coil surfaces can result if the steam pressure is too high. The primary element for temperature control should be a thermocouple at the elevation of the heater. There should be local temperature indication and a high-temperature alarm. Level instrumentation also is necessary. Again, there should be local indication. To avoid overfilling, there may be administrative controls or stepped alarms. A high-level alarm would give warning of a dangerous situation, and a high-high alarm with shutdown would stop the filling process. The shutdown signal should come from an independent switch, not from the primary level sensor.

Tanks, pipelines, and other equipment also may be traced to maintain temperatures. Offset tracing lines are recommended when the steam temperature is high enough to boil

the solution. Glass tape is a serviceable material for spacers. Steam-traced systems built of carbon steel require stress relief.

Necessary utilities include steam, air, water, and electric power. Potable water should be available for safety shower and eyewash facilities. A lower grade of water sometimes can be used for flushing. Blending operations may require water of higher purity.

Centrifugal pumps are the standard for all strengths up to 50%. Stainless steel (Type 316) is a common material of construction. In process applications, high-nickel irons (e.g., Ni-Resist) appear. Nickel again has the advantage of reducing contamination of the solution and is also used in high-temperature applications. Packing and mechanical seals both are in widespread use, although the modern trend is away from packing. Packing and double mechanical seals should be flushed with clear water. Single mechanical seals with process fluid lubrication also are used. These should be drained and flushed at every shutdown.

Spills are especially likely during loading and unloading, and spill control is an important consideration. The facilities, often in isolated locations, should be designed to contain any liquid that is discharged to the ground. Railroad ballast of necessity drains rapidly, and any spilled material can quickly penetrate the soil. Spill-containment pans will prevent the spread of hazardous or polluting materials away from the handling points [161].

A caustic merchant will also need facilities for washing returned containers. A typical system uses rotating sprays placed internally. Positioning of the sprays requires hoists and flexible loading arms. Water is pumped through the sprays to reach all parts of the car. Flow rates usually are $20\text{--}25\text{ m}^3\text{ hr}^{-1}$; the head to be developed by the pump, which may be of ductile iron, depends on the characteristics of the spray nozzle. Power requirements typically are about 12–15 kW. Warm water is much more efficient than cold water; steam–water mixers are simple means of providing heat. Experience will determine the length of the washing cycle; timers can be used to allow the operation to proceed without constant attendance. Most washing facilities include a recycle system. This requires drain collection and piping to a catchment from which the wash liquor can be pumped to a storage tank. When the liquor reaches a certain concentration, it is sent back to the process or used in the emergency scrubber system. The water used in the washing system should be suitable for the end use of the wash liquor. It should be checked for harmful impurities before use. Tankers occasionally will be returned with a heel of product. After analysis of the contents or consultation with the customer who returned the material, it can often be returned to storage. Topping up such a tanker requires careful checking and some discretion.

Caustic tank cars invariably are lined. Sometimes, there are false economies in the choice of lining. Cost cutting often leads to the use of a lining material that is less than the best or of rapid curing techniques that do not achieve high crosslink densities. Cathcart [162] reported that, in 1987 prices, the difference in costs between the cheapest and most expensive formulations surveyed was \$300 per car. Over the life of the lining (not allowing for the longer life that probably results with the better coating), the difference is less than \$0.2 per ton NaOH shipped. In application, there is a tendency to shorten curing cycles. The quality of a lining invariably benefits from thinner coats, with at least a solvent vaporization step between coats and a proper cure at the end.

The caustic shipper is well advised to invest in the quality of the lining. Using the maximum differential cost referred to above, with a modest allowance for inflation, the entire fleet of 550 cars called for in our example could have the best coating, rather than the cheapest, applied for an increment of \$200,000. If we consider that this might reduce the downtime for maintenance or increase the lifetime of a car by 1%, the size of the fleet could be reduced by five cars. The savings would be well above the \$200,000 investment in better linings.

Linings generally are more resistant to concentrated caustic than to more dilute solutions. This is of particular significance when washing tanks or tank cars. If a pool of concentrated material is diluted and then allowed to remain stagnant, a lining can be damaged more in a short time than in a long period of normal service. Finally, the linings that have been serviceable for many years in caustic service are less attractive in other applications. When tank cars are intended for multiple products, the neoprene and SBR latexes that are highly resistant to caustic products will not be chosen. A dedicated fleet of tankers, whether owned or leased, can be specified with the right lining for the service.

Example. We have assumed the use of two product storage tanks, each 17 m in diameter and 12 m high. Holding the contents at 60°C against the minimum ambient temperature of -5°C gives a differential of 65°. The heat lost from a tank is a function of the thickness of its insulation and the velocity of the wind. We allow a loss of 16 MJ hr⁻¹ from each tank. 50% NaOH boils at 140°C. To keep skin temperatures below the boiling point, the steam pressure must be limited to 265 kPa. Assume approximately 200 kPa, or a condensing temperature of 133°C. With a storage temperature of 60°C and a heat-transfer coefficient of 4,500 kJ hr⁻¹ m⁻²/°C, each square meter of exchange surface transfers 4,500 × (133-60) = 328,500 kJ hr⁻¹. The total surface requirement therefore is 16,000,000/328,500 = 48.7 m². Using nominal 3-inch diameter tubing, we require slightly more than 200 m of tubing in each storage tank.

Loading facilities should be sized on the basis of no more than twelve hours in operation per day. We therefore require a loading rate of (800 t d⁻¹)/(12 hr d⁻¹)/(0.75 t NaOH m⁻³) = 89, say, 100 m³ hr⁻¹.

Insulation and auxiliary equipment such as pumps and exchangers should be inspected along with the tanks.

Section 9.1.8.6C mentioned governmental regulations and the need to recognize marine hazards in barge transportation of chlorine. This applies as well to transport of caustic (P80). In the United States, shoreside operations are covered by 33CFR, Subchapter L, Part 126 and bargeside operations by 46CFR, Subchapter O, Part 151. Each caustic barge must carry copies of certificates of inspection and financial responsibility in a secure place. Ongoing barges must also carry an International Load Line Certificate. These certificates certify barges for the service and list any loading constraints. The load line certificate establishes the freeboard required under various circumstances and the location of the load line that is marked on each side of a vessel.

Everything in this section so far applies to cell and primary evaporator liquors. The handling of 73% NaOH solution requires extra care, and Sections 9.3.2.1 and 9.3.2.2 discuss the need to upgrade materials of construction. The freezing point of this material

is about 62°C, and tank cars and wagons that handle it have steam coils. The temperature should be restricted to 100°C.

The usual technique is to dilute the solution while unloading it. Water, added to an in-line mixer through a flow meter or a flow-ratio controller, dilutes it to the desired concentration. Both feed lines should be protected against backflow. Dilution from 73% to 50% evolves about 450 kJ kg⁻¹ NaOH. This must be removed and the final solution cooled sufficiently to prevent corrosion or contamination of the solution in the storage facility. Coolers may be shell-and-tube units with Monel tubes or plate exchangers, which for the best service have nickel plates. Temperature measurement on the streams entering and leaving the cooler is advisable. The best practice is to measure solution temperatures in and out of the cooler. Caustic pumps typically have cast iron or stainless steel bodies with stainless steel, Alloy 20, or nickel impellers.

The transfer line, which normally sees infrequent use, should be equipped with steam-out connections and should be designed accordingly. Design of the storage tank should incorporate normal standards. Appurtenances should include a bottom drain, a top fill connection, a vent, and a pump takeoff connection some distance above the floor of the tank. PTFE-lined plug valves are common in this service.

9.4. BYPRODUCT UTILIZATION

9.4.1. *Evaporator Salt*

The energy consumed in the evaporation of cell liquor to 50% NaOH is a major disadvantage of the diaphragm-cell process. The evaporation process also brings some offsetting advantages. First, the removal of water from the process makes it possible for a plant to operate with a brine feed. Most mercury- and membrane-cell plants use the more expensive solid salt or return depleted brine, at a cost, to a brine well for reconcentration. Second, the evaporation yields refined salt as a by-product.

This salt is particularly a valuable resource in plants that use more than one type of cell. Both mercury and membrane cells produce depleted brine that must be resaturated for recycle. Diaphragm-cell evaporator salt is a natural fit for this application.

Combining mercury and diaphragm cells is straightforward (Fig. 9.72). Some of the evaporator salt is used to resaturate the diaphragm-cell brine after chemical treatment. The rest is available to resaturate mercury-cell depleted brine. A given mercury-cell plant will have a certain need for salt. This fixes the minimum size of the diaphragm-cell plant required as a salt producer. Only in an ideal world would the two types of cell remain forever in perfect balance, and the plant design must accommodate any imbalances.

When diaphragm-cell production outruns the mercury cells, the excess salt can be sent to the brine resaturator that serves the diaphragm cells. In the opposite situation in which there is not enough salt for the mercury cells, it is possible to increase the salt production in the evaporators by pumping more brine through the diaphragm cells and accepting a lower conversion of NaCl. Eventually, the capacity of the brine system or the evaporators will be reached, and then there must be a curtailment in production or purchase of supplemental salt.

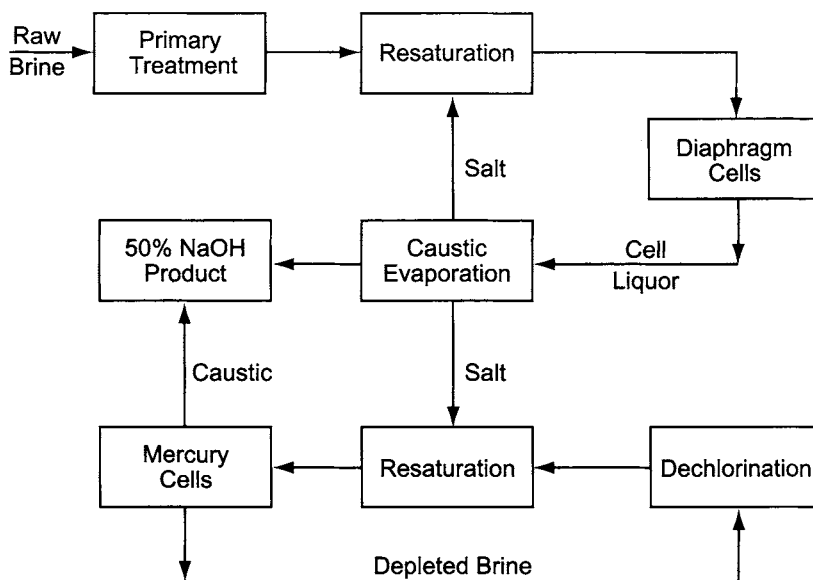


FIGURE 9.72. Integration of mercury and diaphragm cells with evaporator salt.

Plant design must also cater to the shutdown of one line of cells. If the diaphragm cells are shut down, the mercury cells can operate on stockpiled evaporator salt or purchased salt. If neither is available, the mercury cells will be forced to shut down. In the case of a mercury-cell shutdown while evaporator salt is still being produced, the salt can be stockpiled in a resaturator (see Section 7.2.2.2 for a discussion on wet storage of salt) or used to produce new brine. The latter approach probably involves curtailment of production from the diaphragm cells.

Several mercury/diaphragm hybrid plants have operated for many years. We can expect no more to be built. New mercury cells will not be installed. Any expansion at a mercury-cell site would first of all probably be based on membrane cells and second probably be an occasion for retirement of at least some of the mercury cells.

When membrane cells are to be combined with diaphragm cells, the situation is a bit different. The same approach could be taken, simply resaturating membrane-cell brine with diaphragm-cell salt and recycling the saturated brine to the membrane cells. The flowsheet then would be similar to Fig. 9.72. There is a better option [163], shown in Fig. 9.73.

The dechlorinated brine still is resaturated with evaporator salt but then is used as feed to the diaphragm cells. This approach breaks the recycle loop around the membrane cells and prevents impurities from building up in the membrane plant by recycle. This avoids damage of the membranes by the "compound X" effect in which some impurity, perhaps not originally recognized, reaches a harmful concentration. The evaporator salt may also contain recognized impurities that would accumulate in the recycle operation. The concentration of silica, for example, is not always very low in evaporator salt. It has also been suggested [164] that nickel and chromium picked up in the diaphragm-cell evaporators can damage the membrane cells.

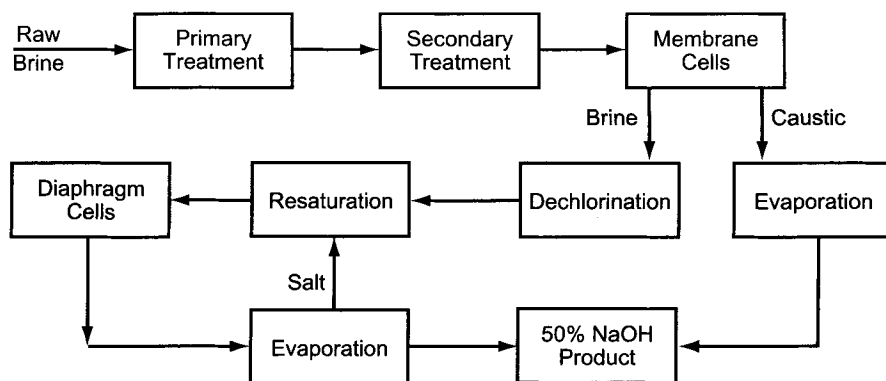


FIGURE 9.73. Integration of membrane and diaphragm cells.

If capacities are imbalanced toward the diaphragm side, some of the brine from the primary treatment must flow to the resaturator. If the membrane-cell capacity is high, some of the resaturated brine can be sent to those cells. This re-establishes the recycle loop, but the diaphragm cells remain as a gigantic purge from the brine system, and recycle accumulation of impurities still is strongly limited.

In a balanced plant, all the chemically treated brine flows through ion exchange, not just that equivalent to the membrane-cell production. This adds a cost to the process, because in a segregated operation only that brine corresponding to the membrane-cell production would be so treated. At the same time, it improves the quality of the brine fed to the diaphragm cells. This in turn improves the current efficiency of those cells, but little information is available in the literature, and it is not possible to quantify the phenomenon here.

The flowsheet of Fig. 9.73 should not be adapted to mercury–diaphragm integration because it will introduce mercury contamination into the diaphragm-cell plant.

9.4.2. Sodium Sulfate

The sulfate accompanying NaCl brine is sometimes recovered as a by-product. In the diaphragm-cell process, sulfate is available as a concentrated purge from the evaporators. In the membrane-cell process, there is no natural point of high sulfate concentration, but it is possible to isolate sodium sulfate in the brine treatment process (Section 7.5.7.2B).

9.4.2.1. Diaphragm Cells. The sulfate present in the brine passes into the catholyte and then on to the caustic evaporators. As the concentration of NaOH increases during evaporation, sulfate begins to drop out of solution as triple salt, $\text{NaCl} \cdot \text{NaOH} \cdot \text{Na}_2\text{SO}_4$. Under the proper process conditions and concentrations, this salt breaks down into its components. The result is a solution from which sodium sulfate can be crystallized as Glauber's salt. This is the decahydrate, $\text{Na}_2\text{SO}_4 \cdot 10\text{H}_2\text{O}$.

Many diaphragm plants operate triple-salt decomposers and Glauber's salt crystallizers. In some cases, this is simply an environmental measure designed to reduce

the total dissolved solids in the plant's effluent by separating the NaOH and NaCl from the sulfate. The Glauber's salt is dissolved and discarded. In other cases, the Glauber's salt is recovered for sale or on-site use. It is not a highly marketable commodity (Section 9.4.2.3). It may be easier to dispose of the anhydrous sulfate. Drying the Glauber's salt at sufficiently high temperature removes the water of hydration and leaves the anhydrous form as product.

Figure 7.86 shows equilibrium data for the system NaCl/Na₂SO₄/H₂O in connection with a description of a process for sequential crystallization of salt and sulfate from brine. The reader will recognize that the intermediate liquor in that process is similar to the liquor produced in triple salt decomposers. The same technique and operating conditions therefore apply to recovery of Glauber's salt in the present case.

Figure 9.74 shows one version of the process for removal of the sulfate from the evaporator salt. The salt falling to the leaching tank includes the triple salt formed in the evaporators. The feed may contain all the NaCl as well, or it may be just the high-sulfate salt, segregated from the pure NaCl produced in certain effects. Enough water enters the process to produce a relatively thin liquor in the leach tank, causing the triple salt to decompose.

Since the addition of water is not great enough to dissolve the salt, the leaching tank still contains a slurry, but the solid phase is now depleted in sulfate content. It is important not to dissolve too much NaCl in order to keep the Na₂SO₄ content of the liquor high. One of the pumps (left-hand side of the leaching tank) sends part of the

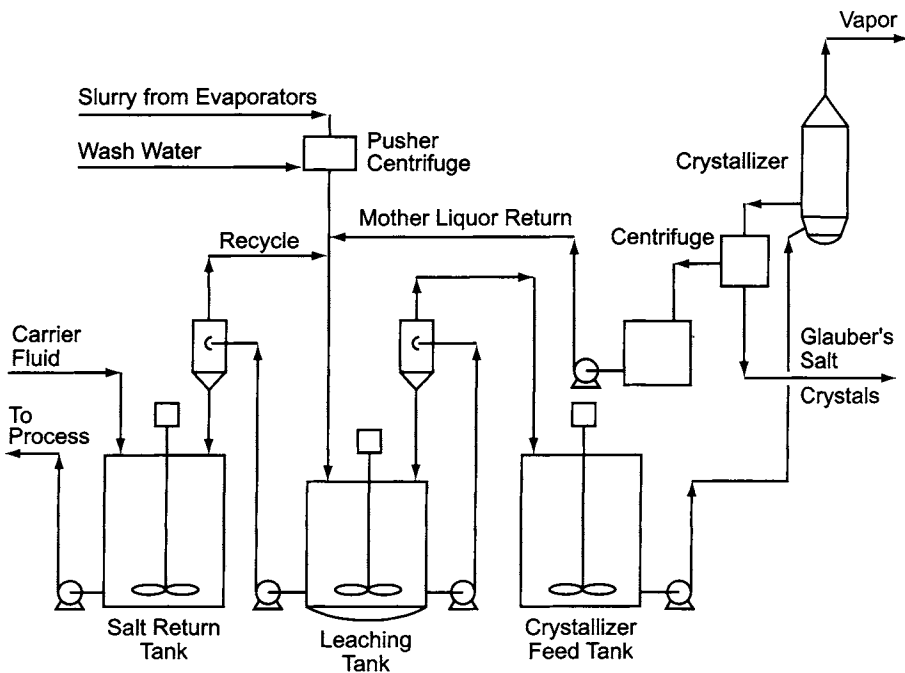


FIGURE 9.74. Crystallization of Glauber's salt.

slurry through cyclones to recover the purified salt. The overflow returns to the leaching tank while the salt with part of the sulfate removed drops into a slurry tank. From here, it goes off to the user. On the right-hand side, a second pump sends another part of the slurry through cyclones, with the concentrated underflow returning to the leaching tank. The collected liquid becomes the feed to a Glauber's salt crystallizer.

The apparatus must fit the demands of the process, and the draft tube baffle crystallizer is a frequent selection [165]. Figure 9.75 is a generic version of an evaporative type. The design features an agitator inside a central draft tube. In the illustration, the agitator is suspended from the top of the crystallizer. Some designs use underslung bottom-mounted agitators, which have the advantage of shorter shafts. The agitator is pitched to pump suspended magma up to the liquid surface. The solids concentration in the slurry usually is 25–50% apparent settled volume. With the hydrostatic head kept low, the agitator can circulate large volumes with reasonably low power consumption. A high rate of circulation limits the degree of supersaturation at the surface, which is controlled at a level some distance above the top of the draft tube. The crystals swept to the boiling surface by the agitator grow rapidly there. This leads to the production of

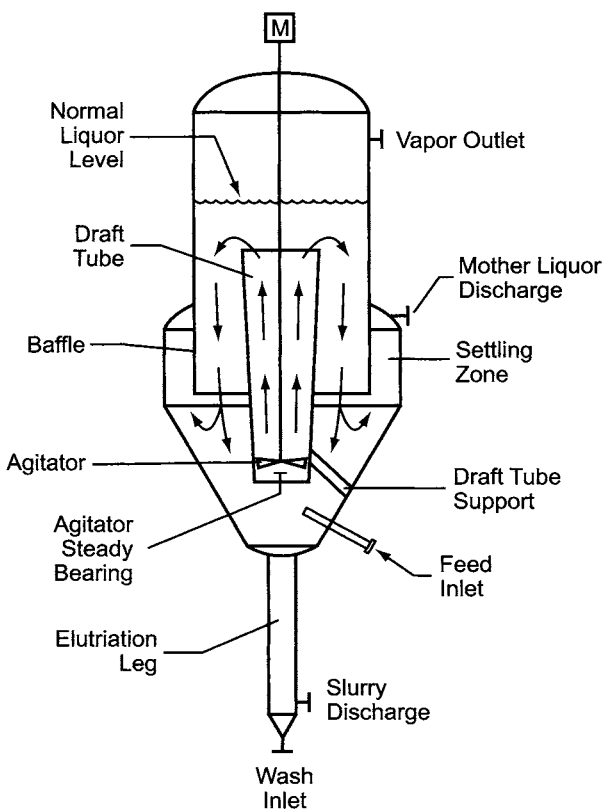


FIGURE 9.75. Draft tube baffle crystallizer.

relatively large crystals. Directing the feed liquor toward the agitator promotes its rapid dispersal and also contributes to controlled particle growth.

Recirculating crystals return to the agitator through the annulus between the draft tube and the baffle. The latter as shown here is an extension of the shell of the upper chamber. The volume between the baffle and the outer wall allows the slurry to separate. The crystals fall toward the bottom, and the clarified mother liquor overflows from the top of this section. This mother liquor can go on to further processing or return to the bottom of the crystallizer. The rate of withdrawal of mother liquor determines the clarifying efficiency behind the baffle. It can be varied to control the amount or size of fine crystals that leave the crystallizer. These crystals can redissolve in a fines killer if the circulating mother liquor is heated or if an unsaturated feed stream is introduced. The latter is the normal practice in the recovery of Glauber's salt from caustic evaporators. This action keeps the fines out of the final crystal product and makes the particle size distribution narrower.

Crystals can be withdrawn as a slurry from the bottom section. The illustration also shows the use of an elutriating leg similar in function to those described in Section 9.3.3.3. The wash liquor that enters the bottom of the leg helps to remove occluded mother liquor before the slurry leaves the vessel. Addition of the elutriating leg favors the use of the top-mounted agitator.

Supersaturation results, as noted above, from boiling in the crystallizer. Figure 7.86 shows that Glauber's salt is the stable solid phase only at reduced temperature. The system therefore runs under vacuum, provided by any standard apparatus (Section 12.6.1). Evaporation of water cools the liquor into the desired temperature range.

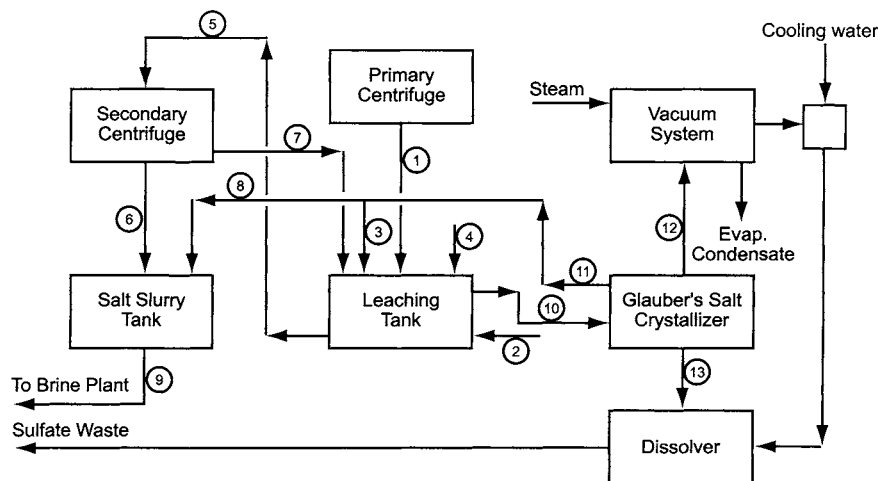
Besides the production of large crystals, draft tube baffle crystallizers have several other advantages:

1. simple process control
2. high degree of turndown possible with stable product characteristics
3. slow fouling; long operating cycles
4. easy drying of product and little caking (result of narrow particle size distribution)
5. ability to fabricate in corrosion-resistant materials

Draft tube baffle crystallizers have a broad range of application, particularly in inorganic chemistry. They are used in the recovery of KCl (Section 7.1.6.2B), other potassium salts, and sodium chlorate, as well as many other products.

Because of the normally low concentration of sulfate in the process liquors and the limited degree of recovery of Glauber's salt in the crystallizer process, the productivity is low. Figure 9.76 presents an example in which the amount of Na_2SO_4 removed is less than 1% of the total flow into the crystallizer.

Example. Washed salt from the primary centrifuge (Stream 1) drops into a leaching tank. The composition of the salt depends on the processing conditions and the amount of sulfate in the cell liquor. Here, we assume that the centrifuge cake is about 96% solids and the amount of Na_2SO_4 precipitated is 2.8% of the total solids (dry basis). This tank will export clear liquor to the Glauber's salt crystallizer and slurry to a salt recovery system, for return to the brine plant. The leach tank also receives mother liquor from the crystallizer (Stream 3) and a small amount of evaporator condensate (Stream 2) to



Example: Glauber's salt crystallizer
 Basis: 1000 kg Na₂SO₄ removed

	1 Centrifuge Salt	2 Chilled Condensate	3 ML to Leach Tank	4 Chilled Condensate	5 Leached Salt	6 Recovered Salt	7 Secondary Centrifugate
NaCl			19518		38604	537	38067
NaOH	123		516		1022	14	1008
Na ₂ SO ₄			2912		7392	103	7290
H ₂ O	2460	4837	65247	8612	117253	1630	115623
Total solution	2583	4837	88193	8612	164271	2284	161987
NaCl	59273				54632	54632	
Na ₂ SO ₄ ·10H ₂ O	3881		132		125	125	
Total stream	65737	4837	88326	8612	219029	57042	161987
Total H ₂ O	4629	4837	65321	8612	117323	1700	115623
Total Na ₂ SO ₄	1711		2970		7448	158	7290

	8 ML to Slurry Tank	9 Salt Slurry to Brine Pit.	10 Crystallizer Feed	11 Mother Liquor	12 Vapor	13 Glauber's Salt Slurry
NaCl	3637	4174	23623	23156		467
NaOH	97	111	625	613		12
Na ₂ SO ₄	542	645	4523	3454		69
H ₂ O	12160	13790	81699	77407	1463	1562
Total solution	16436	18720	110471	104629	1463	2111
NaCl		54632				
Na ₂ SO ₄ ·10H ₂ O	25	151		157		2111
Total stream	16461	73503	110471	104787	1463	4221
Total H ₂ O	12174	13874	81699	77495	1463	2742
Total Na ₂ SO ₄	553	711	4523	3523		1000

FIGURE 9.76. Glauber's salt removal process.

maintain the water balance. The evaporator system normally has a chilled source of condensate available as a utility. The leach tank is mildly agitated to promote mixing while allowing a clear liquor overflow. In the system shown, this stream does not pass through the cyclones of Fig. 9.74, while the remaining material is pumped as a 25% slurry (Stream 5) to a secondary centrifuge that produces a cake with about 96% solids (Stream 6). This drops into a tank where it meets some of the crystallizer mother liquor (Stream 8). This is another material balance requirement. This tank also receives the carrier fluid that will transfer the salt as it is pumped to the brine plant (Stream 9). Here, we assume the use of brine as the carrier but do not include it in the material balance.

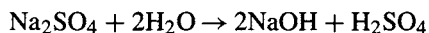
The centrifugate from the secondary centrifuge mentioned above (Stream 7) also goes to the leach tank. The overflow, joined as it leaves the tank by more chilled condensate (Stream 4), goes to a crystallizer feed tank (not shown), from where it is pumped to the Glauber's salt crystallizer (Stream 10). This is an evaporative crystallizer, operated under vacuum to remove a small fraction of the water (Stream 12). The source here is a steam jet, and the condensate from the aftercooler is in some cases combined with the main evaporator condensate. Draft-tube baffle crystallizers are common in this service, and clear mother liquor is withdrawn from behind the baffle (Stream 11, comprising Streams 3 and 8). This returns to the leach tank and the salt slurry tank, as described above. Slurry removed from the bottom of the crystallizer (Stream 13) contains the Glauber's salt that is rejected from the caustic evaporator system. The solids concentration in this slurry is taken to be 50%. This product or the anhydrous form may have some commercial application, in which case a designer might opt for a more efficient separation. In this example, we show the Glauber's salt concentrate going to a dissolving tank. It dissolves in water from the crystallizer's barometric condenser(s) and is ready for disposal. The concentration of the solution will depend on conditions in the vacuum system.

When a cyclone (not shown) is used to concentrate the Glauber's salt slurry, the overhead can be combined with the crystallizer mother liquor. "Mother liquor" at that point properly becomes a misnomer. The crystallizer process may have a number of sidestreams and recycles to improve the efficiency of the process, but these do not change the fundamental mode of operation which this example is meant to illustrate.

9.4.2.2. Membrane Cells. The bulk of the sulfate in the electrolysis circuit moves into the catholyte only in diaphragm cells. In membrane cells, it remains in the anolyte. Even when a salt contains only a modest amount of sulfate, then, it can accumulate by recycle and exceed the allowable concentration in the cells. For this reason, the many techniques of sulfate control described in Section 7.5.7 have been developed.

Some of those techniques remove sulfate from the brine in a potentially useful form. The last part of Section 7.5.7.2 describes sequential crystallization of NaCl and the sulfate from brine. As in the discussion above, the product of crystallization is Glauber's salt.

9.4.2.3. Recovery of Caustic Value. Byproduct sodium sulfate is not a readily marketable commodity. The United States alone generates more than 1.5 million tons per year, and those chlor-alkali plants which sell the material may not recover even the cost of crystallization [166]. Modified membrane cells that regenerate caustic soda and sulfuric acid by electrolysis of Na₂SO₄ solution therefore have been studied. These reverse the neutralization reaction and regenerate the acid and base:



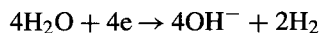
The actual course of reaction involves the electrolysis of water at both electrodes. When a solution of Na₂SO₄ is fed to the anolyte compartment, the oxidation of water occurs:



A major objective in cell construction is to have the current flow through the membrane as Na^+ , not H^+ . The latter is a potential major yield loss. Both the membrane and the anode coating must be optimized for good results.

The selectivity of the membrane process is enhanced when the sodium ion concentration in the anolyte remains high. The solution leaving the anode chamber therefore is a mixture of Na_2SO_4 and H_2SO_4 .

The familiar reduction of water occurs on the cathode side:



The quality of the NaOH formed is high, but it usually is restricted to rather low concentrations ($\sim 10\%$).

This subject is treated in more detail in Section 15.4.3, which also describes alternative arrangements such as three-compartment cells that can produce both NaOH and H_2SO_4 of high purity.

9.4.3. *Amalgam*

Alkali metal amalgams are rather exotic chemicals, and so there has always been some interest in using them in the synthesis of products more specialized than caustic soda or potash. Handling problems and the very low concentration of the alkali metal in the amalgam have prevented large-scale application. Since the advent of strict limitations on mercury discharge and the pressure to avoid its use altogether, much of the incentive has disappeared. While there still are some plants using amalgam in other syntheses, we can expect no substantial growth in this field. Our interest is mostly technical and historic.

In many of the applications of this chemistry, the identity of the cation is not important, and so we consider the use of sodium amalgam only. The classical summary of industrial amalgam chemistry is that of MacMullin [167], and we shall follow his treatment here.

Amalgams usually are classified into three types. Metals of the gallium type (Ga, Fe, Ni, Co, Mn, Cr, Al) amalgamate with difficulty and tend to be insoluble in mercury. Standard electrode potentials are more negative than those of the metals themselves, so amalgamation makes these metals less noble. The zinc type (Zn, Pb, Sn, Cu) amalgamate readily and dissolve easily in mercury. Electrode potentials of the amalgams are nearly equal to those of the metals. The sodium type (Na, K, Li, Ca) amalgams are not highly soluble in mercury, but their standard electrode potentials are less negative than those of the metals. This makes the metals less reactive in water and makes mercury-cell electrolysis possible.

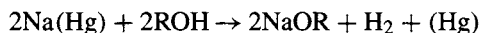
MacMullin lists possible applications of amalgams:

1. Production of free metals
 - (a) by distillation of free mercury
 - (b) by electrodeposition.
2. Production of metal alcoholates
3. Amalgam metallurgy
 - (a) separation of pure metals from their electrolytes
 - (b) reduction of metallic chlorides to produce other metals.

4. Organic reductions
 - (a) ketone to pinacone
 - (b) oxalic acid to glyoxylic acid
 - (c) quinone to hydroquinone
 - (d) nitro to azo to hydrazo aromatics.
5. Production of metal salts by reaction with element or acidic compound
 - (a) sodium sulfide from sodium and sulfur
 - (b) sodium hydrosulfite from sodium and sulfur dioxide
 - (c) sodium chlorite from sodium and chlorine dioxide
 - (d) sodium nitrite from sodium and nitrogen peroxide.

Here, we consider three examples: the production of sodium methyrate, sodium sulfide, and sodium hydrosulfite.

Alcoholates result when alcohols replace water in the decomposer reaction:



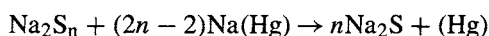
The same reaction takes place between metallic sodium and an alcohol, but that reaction can be overly vigorous, and it involves all the hazards of handling metallic sodium. The increased nobility of the metal when amalgamated was the chief attraction of the electrolytic route.

Alcohols react more sluggishly than water in a decomposer, and the rate of reaction declines as the carbon number of the alcohol increases. Except for the question of proper sizing, the decomposer design is much the same as those used for production of NaOH and KOH. Propyl alcohol is not active enough to be of any interest. Ethyl alcohol is less active than methyl alcohol, and it was in the case of sodium methyrate that this reaction had its commercial success. This compound, like any alcoholate, hydrolyzes readily to the alcohol and caustic soda, so strictly anhydrous conditions are necessary for synthesis, another reason for limited commercial production of sodium ethylate.

The decomposer product is a 5–15% solution of NaOCH₃ in methanol. The hydrogen gas from the decomposer is saturated with CH₃OH. Most of the latter is recovered in a condenser; the hydrogen is purified further in an absorber. The NaOCH₃ solution, after filtration, can then be concentrated to about 35% by evaporation under atmospheric pressure. It can be processed to a fine, white, free-flowing powder by vacuum drying. The powder requires careful handling; it is hygroscopic and slowly oxidizable, and it has a decomposition pressure of about 0.5 kPa at 20°C.

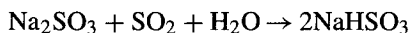
Sodium methyrate is also produced commercially by reaction of NaOH with methanol. Distillation of the byproduct water away from the reaction drives the process to completion.

Sodium amalgam can react with polysulfide solutions. Generically, some number *n* of sulfur atoms combine with two atoms of sodium and then react with amalgam to produce *n* molecules of sodium sulfide:

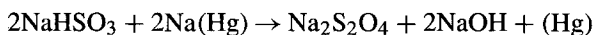


The polysulfide forms when sulfur dissolves in recycled Na₂S. The final product can be the crystalline enneahydrate (30–35% Na₂S) or a 55–60% flake. The latter derives from nominal Na₂S₄ and requires care to keep the entire system warm enough to prevent freezing. Decomposers are horizontal and arranged for cocurrent flow of the amalgam and the sulfide solution. Some versions are made more efficient by compartmentalization and the use of mild agitation in the aqueous layer in each compartment.

Sodium hydrosulfite is still a specialty product of some mercury-cell chlorine plants. As the flow diagram, Fig. 9.77, shows, the source of sulfur is SO₂. This is dissolved into a circulating Na₂SO₃ solution to form the bisulfite:



Controlling the pH at 5–7 gives a mixture in which about 80% of the contained sulfur is in the form of bisulfite. The decomposer is a stirred reactor with partial water jacket. Good agitation and temperature no higher than 40°C are essential. The reaction of amalgam with bisulfite would produce NaOH as a byproduct:



The NaOH, however, combines with some of the bisulfite to regenerate sodium sulfite. As a result, the overall stoichiometry becomes

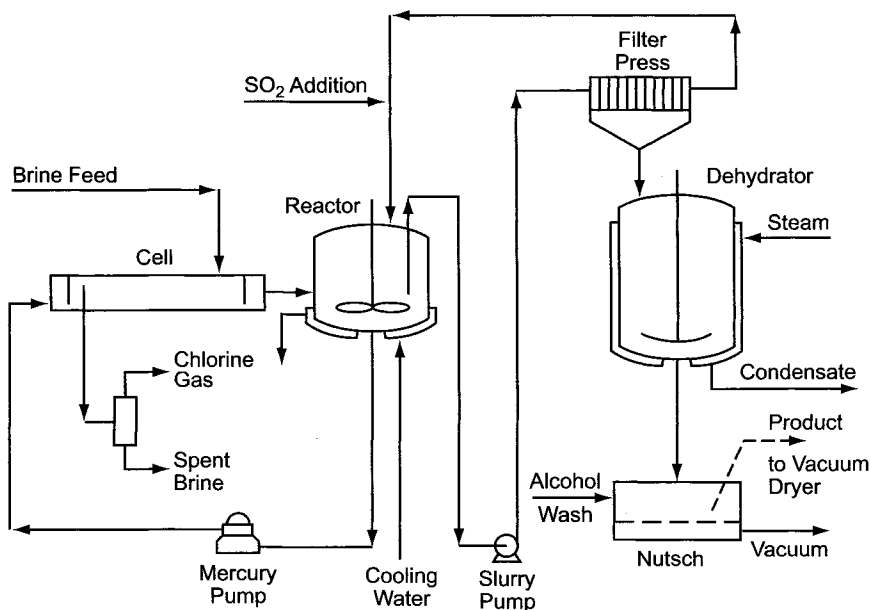
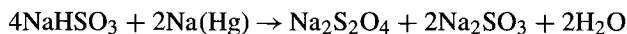


FIGURE 9.77. Production of sodium hydrosulfite using amalgam (after MacMullin [167]).

The reaction product is a slurry of crystals of $\text{Na}_2\text{S}_2\text{O}_4 \cdot 2\text{H}_2\text{O}$. The slurry is pumped through a filter press to remove the crystals. The filtrate is the sulfite solution that absorbs the SO_2 as it recycles to the amalgam decomposer. Isolation of the anhydrous product involves dehydration of the crystals at 60–65°C, filtration, washing with alcohol, and drying under vacuum. The product may contain a small amount of residual mercury. This prevents its use in some applications.

Another synthetic route to $\text{Na}_2\text{S}_2\text{O}_4$ relies on the reaction of SO_2 with zinc dust. This forms zinc hydrosulfite, and double decomposition with NaOH then yields the sodium salt.

9.4.4. Calcium Carbonate

Calcium carbonate formed during brine treatment is usually a waste product. Depending on the composition of the salt used, it may be available in large quantity (high calcium content) and reasonable purity (high calcium/magnesium ratio). As an example, an 800-tpd plant based on rock salt containing 0.5% soluble CaSO_4 will produce 1,500 tpy of CaCO_3 . In the past, a number of plants were able to sell, or transfer at no cost, much of the carbonate sludge. One of the major applications was in agricultural supplements.

Prominent markets today for fine CaCO_3 are as fillers in paper, paint, PVC, rubber, putty, cosmetics, and toothpaste and as an antacid and a calcium supplement in foods. Surface-coated grades are also produced and are more easily dispersed in organic materials. CaCO_3 is also used to coat paper, and its use as a filler has increased rapidly with the increase in alkaline papermaking. Many small precipitation plants now operate at papermill sites. Controlled precipitation of calcium carbonate allows control of crystal geometry and particle size distribution. This allows custom production with attractive properties for various markets. With the recent expansion in precipitated calcium carbonate capacity, there are fewer possibilities for disposal of the relatively low-quality material from a brine plant.

Calcium carbonate also can be decomposed into its components by calcination or into CO_2 and CaCl_2 by digestion with hydrochloric acid. The CO_2 can be absorbed into caustic solution to produce carbonate for brine treatment. If calcium is used to suppress the solubility of sulfates in raw salt, the CaCl_2 also can be recycled. The latter technique can be limited by the presence of other metallic impurities.

REFERENCES

1. *Materials of Construction for Use in Contact with Chlorine*, GEST 79/82, 7th ed., Euro Chlor, Brussels (1995).
2. *Choice of Materials of Construction for Use in Contact with Chlorine (Spreadsheet)*, GEST 79/82—Annex, 1st ed., Euro Chlor, Brussels (2000).
3. O. A. Hougen and K. M. Watson, *Chemical Process Principles*, Part One, John Wiley & Sons, Inc., New York (1952), p. 115.
4. H. Schäfer and W. Gann, *Z. Anorg. Allg. Chem.* **270**, 304 (1952).
5. P. C. Westen, The Safe Use of Steel and Titanium in Chlorine. In R. W. Curry (ed.), *Modern Chlor-Alkali Technology*, vol. 6, Royal Society of Chemistry, Cambridge (1995), p. 62.
6. K. Hannesen, Materials of Construction for Handling Chlorine, *Chlorine Safety Seminar*, Brussels (1990).

7. M. W. J. Hammink and P. C. Westen, Corrosion and Erosion of Steel in Liquid Chlorine at Different Conditions of Velocity, Water Content, and Temperature. In K. Wall (ed.), *Modern Chlor-Alkali Technology*, vol. 3, Ellis Horwood, Chichester (1986), p. 71.
8. B. G. Dixon, D. M. Longenecker, and I. R. Wilcox, *Usage of FRP for Combating Corrosion in Caustic/Chlorine Plants*, Paper No. 461-57, ICI Americas Inc., Wilmington, DE (1984).
9. D. Q. Kern, *Process Heat Transfer*, McGraw-Hill Book Co., New York (1950), pp. 828–833.
10. D. Q. Kern, *Process Heat Transfer*, McGraw-Hill Book Co., New York (1950), pp. 340 *et seq.*
11. J. R. Fair, *Chem. Eng.* **79**(12), 91 (1972).
12. P. Harriott and H. F. Wiegandt, *AIChE J.* **10**, 755 (1964).
13. H. Z. Kister, *Distillation Design*, McGraw-Hill Book Co., New York (1992).
14. T. F. O'Brien and I. F. White, Process Engineering Aspects of Chlorine Cooling and Drying. In R. W. Curry (ed.), *Modern Chlor-Alkali Technology*, vol. 6, Royal Society of Chemistry, Cambridge (1995), p. 70.
15. D. Q. Kern, *Process Heat Transfer*, McGraw-Hill Book Co., New York (1950), p. 343.
16. J. P. Kerner, Alberts and Associates, Personal Communication (ca. 1987).
17. J. A. Walkier, Chlorine Safety. In T. C. Wellington (ed.), *Modern Chlor-Alkali Technology*, vol. 5, Elsevier Applied Science, London (1992), p. 233.
18. P. C. Westen, How To Use Steel and Titanium Safely, *Third Euro Chlor Technical Seminar*, Paris (1993).
19. J. S. Grauman and B. Willey, *Chem. Eng.* **105**(8), 106 (1998).
20. F. A. Cotton and G. Wilkinson, *Advanced Inorganic Chemistry—A Comprehensive Text*, 4th ed., John Wiley and Sons, Inc., New York (1980), p. 226.
21. F. A. Cotton and G. Wilkinson, *Advanced Inorganic Chemistry—A Comprehensive Text*, 4th ed., John Wiley and Sons, Inc., New York (1980), p. 546.
22. J. A. A. Ketelaar, *Electrochem. Technol.* **5**(3–4), 143 (1967).
23. A. Bouzat and L. Azinières, *Compt. Rend.* **176**, 253; **177**, 1444 (1923).
24. K. W. Allen, *J. Chem. Soc.* **1959**, 4131 (1959).
25. C. H. Greenewalt, *Ind. Eng. Chem.* **17**, 522 (1925).
26. R. E. Moore, United Engineers and Constructors, Inc., Personal Communication (1989).
27. Y. Tabata, T. Kodama, and T. Kotoyori, *J. Hazard. Mater.* **17**(1), 47 (1987).
28. *Structured Ceramic Packing for Chlorine Drying Towers*, Bulletin No. A-100, Koch-Glitsch, Inc., Wichita, KS (2000).
29. S. A. Ziebold, *Chem. Eng.* **107**(5), 94 (2000).
30. P. S. Fabian, R. W. Cusack, P. M. Hennessey, and M. Neuman, *Chem. Eng.* **100**(11), 148 (1993).
31. T. F. O'Brien and I. F. White, Process Engineering Considerations in Chlorine Compression and Liquefaction. In S. Sealey (ed.), *Modern Chlor-Alkali Technology*, vol. 7, Royal Society of Chemistry, Cambridge (1998), p. 202.
32. A. H. Church, *Centrifugal Pumps and Blowers*, John Wiley & Sons, Inc., New York (1944).
33. R. P. Lapina, *Chem. Eng.* **96**(8), 122 (1989).
34. R. P. Lapina, *Chem. Eng.* **97**(7), 110 (1990).
35. G. R. Evans and L. J. Istant, Coexisting with the Centrifugal Compressor, *12th Chlorine Institute Plant Managers Seminar*, New York (1969).
36. *Learning from Experience*, Pamphlet 167, Edition 1, The Chlorine Institute, Inc., Alexandria, VA (2002), p. 6.
37. W. G. Hoppock, J. A. Silvaggio, Jr., and K. G. Van Bramer, Centrifugal Compressor Revamps, *Proceedings, Rotating Machinery Users Council Meeting*, Long Beach, CA (1990).
38. P. M. Mayo, Chlorine Compressors, *30th Chlorine Institute Plant Managers Seminar*, Washington, DC (1987).
39. T. A. Weedon, Jr., Pressure Control in Chlorine Plants, *Fifth Annual Electrode Corporation Chlorine/Chlorate Industry Seminar*, Cleveland, OH (1989).
40. F. G. Davis and A. B. Corripio, Dynamic Simulation of Variable-speed Centrifugal Compressors. In Instrument Society of America, *Instrumentation in the Chemical and Process Industries*, vol. 10, Research Triangle Park, NC (1974), p. 15.
41. N. V. Sidgwick, *The Chemical Elements and Their Compounds*, Oxford University Press, London (1950), pp. 1146–1150.
42. L. Miessler and D. A. Tarr, *Inorganic Chemistry*, 2nd ed., Prentice Hall, Upper Saddle River, NJ (1998), p. 268.

43. F. A. Cotton and G. Wilkinson, *Advanced Inorganic Chemistry—A Comprehensive Text*, 4th ed., John Wiley & Sons, Inc., New York (1980), p. 562.
44. T. Moeller, *Inorganic Chemistry—An Advanced Textbook*, 2nd printing, John Wiley & Sons, Inc., New York (1965), pp. 446 *et seq.*
45. C.-P. Chen, T. V. Bommaraju, and P. C. Williams, *U.S. Patent 5,639,422* (1997).
46. T. A. Liederbach, Unpublished Remarks, *Seventh Annual Electrode Corporation Chlorine/Chlorate Industry Seminar*, Cleveland, OH (1991).
47. HFSJG, *Activity Report 2001*, International Foundation High-Altitude Research Stations, www.ifjungo.ch/html/11.pdf. (2001).
48. *The Northern Hemisphere Stratosphere in the 2002/3 Winter*, European Ozone Research Coordinating Unit, University of Cambridge (2003).
49. S. Hieger, Retrofitting a Chlorine Liquefaction System to R-134a, *39th Chlorine Institute Plant Managers Seminar*, Washington, DC (1996).
50. A. Bhadsavle and W. W. Humm, A Utility Approach to Alternative Refrigerants, *CFC Refrigerant Alternative Seminar*, New Orleans, LA (1993).
51. D. O'Shaughnessey, Flammability of R134a, R22, and R123 in Chlorine, *Chlorine Institute CFC Refrigerant Alternatives Seminar*, New Orleans, LA (1993).
52. J. H. Boyette, The BOCOSI™ Chlorine Condensing System, *39th Chlorine Institute Plant Managers Seminar*, Washington, DC (1996).
53. W. W. Humm, FES, Inc., Personal Communication (1996).
54. *Maximum Levels of Nitrogen Trichloride in Liquid Chlorine*. GEST 76/55, 10th ed., Euro Chlor, Brussels (2001).
55. R. F. Strickland-Constable, General Thermodynamic Relationships, In H. W. Cremer and T. Davies (eds.), *Chemical Engineering Practice*, vol. 4, Butterworths Publications Ltd., London (1957), pp. 61–62.
56. B. G. Kyle, *Chemical and Process Thermodynamics*, 3rd ed., Prentice Hall PTR, Upper Saddle River, NJ (1999).
57. L. J. Updyke, Method for Calculating Water Distribution in a Chlorine Condensing System, *25th Chlorine Institute Plant Operations Seminar*, Atlanta, GA (1982).
58. *Soda Handbook*, Japan Soda Industry Association, Tokyo (1998), p. 423.
59. R. LeVine, *Guidelines for Safe Storage and Handling of High Toxic Hazard Materials* (prepared by team from Arthur D. Little Inc., led by P. A. Croce, from original draft), Center for Chemical Process Safety, New York, NY (1988).
60. S. M. Englund, Opportunities in the Design of Inherently Safer Chemical Plants. In *Advances in Chemical Engineering*, vol. 15, Academic Press, Inc., San Diego, CA (1990).
61. T. F. O'Brien, Beyond Hazan—The Role of Plant Safety Surveys, *39th Chlorine Institute Plant Managers Seminar*, Washington, DC (1996).
62. J. Haas, Chlorine Monitors, *30th Chlorine Institute Plant Managers Seminar*, Washington, DC (1987).
63. R. Woods, Atmospheric Chlorine Storage, *23rd Chlorine Institute Plant Managers Seminar*, New Orleans, LA (1980).
64. N. C. Harris and J. P. Shaw, European Chlorine Storage Practice, *23rd Chlorine Institute Plant Managers Seminar*, New Orleans, LA (1980).
65. F. P. Lees, *Loss Prevention in the Chemical Industries*, Butterworths, London (1980).
66. S. M. Englund, *Chem. Eng. Progr.* **87**(3), 85 (1991).
67. *Process Piping*, ASME B31.3, an ANSI Standard, The American Society of Mechanical Engineers, New York, NY (1996).
68. E. L. Sokol, Liquid Chlorine Transfer with External Pumps from Top Outlet Storage Tanks, *23rd Chlorine Institute Plant Managers Seminar*, New Orleans, LA (1980).
69. R. E. Means, Chlorine Transfer, *21st Chlorine Institute Plant Operations Seminar*, Houston, TX (1978).
70. R. Tujague, Chlorine Unloading Systems, *40th Chlorine Institute Plant Operations Seminar*, New Orleans, LA (1997).
71. J. H. Burelle and C. J. Bourgeois, Chlorine Tank Car Loading Systems—Occidental Chemical Taft, LA Facility, *40th Chlorine Institute Plant Operations Seminar*, New Orleans, LA (1997).
72. *Chlorine Tank Car Marking*, Drawing No. 167, Issue 5, The Chlorine Institute, Inc., Washington, DC (2001).

73. J. W. Mason, Design Aspects of Loading and Unloading Systems Which Can Mitigate or Eliminate Accidental Chlorine Releases. In R. W. Curry (ed.), *Modern Chlor-Alkali Technology*, vol. 6, Royal Society of Chemistry, Cambridge (1995), p. 48.
74. *Industrial Ventilation Manual: A Manual of Recommended Practices*, 22nd ed., American Conference of Governmental Industrial Hygienists, Cincinnati, OH (1995).
75. R. Papp, Chlorine Handling and Safety in the European Situation. In C. Jackson (ed.), *Modern Chlor-Alkali Technology*, vol. 2, Ellis Horwood, Chichester (1983), p. 376.
76. T. F. O'Brien, Common Factors in Hazard Analysis, *35th Chlorine Institute Plant Operations Seminar*, New Orleans, LA (1992).
77. M. M. Silver, Chlorine Tailgas and Snift Disposal Systems, *25th Chlorine Institute Plant Operations Seminar*, Atlanta, GA (1982).
78. T. F. O'Brien, The Use of Gas-Separation Membranes in Chlorine Processing. In J. Moorhouse (ed.), *Modern Chlor-Alkali Technology*, vol. 8, Blackwell Science, Oxford (2001), p. 90.
79. E. Bartholome', *Z. Elektrochem.* **54**, 3 (1950).
80. Remarks by N. C. Harris and J. A. Heilala, 2nd Chlorine Plant Operations Workshop, The Chlorine Institute, Inc., Washington, DC (1987).
81. R. L. Pigford, Course notes, University of Delaware, citing the work of Stephens and Morris (1958).
82. *Crosby Style JQ Pressure Relief Valve*, Catalog No. 306, Crosby Valve Inc., Wrentham, MA (1997).
83. E. H. Stitt, F. E. Hancock, and K. Kelly, New Process Options for Hypochlorite Destruction. In J. Moorhouse (ed.), *Modern Chlor-Alkali Technology*, vol. 8, Blackwell Science, Oxford (2001), p. 315.
84. W. D. McCollam, Chlorine Scrubbing Systems—A Discussion of CI Publication #89, *35th Chlorine Institute Plant Operations Seminar*, New Orleans, LA (1992).
85. T. F. O'Brien, Emergency Vent Scrubbing Systems—Design; Operation; Hazard Analysis, *Seventh Annual Electrode Corporation Chlorine/Chlorate Seminar*, Cleveland, OH (1991).
86. H. M. Patel and T. B. Scarfe, Safety Aspects of Niachlor Membrane Cell Plant, *31st Chlorine Institute Plant Operations Seminar*, New Orleans, LA (1988).
87. J. E. Vivian and R. P. Whitney, *Chem. Eng. Prog.* **43**, 691 (1947).
88. T. F. O'Brien and I. F. White, Design and Operation of Emergency Chlorine Absorption Systems. In T. C. Wellington (ed.), *Modern Chlor-Alkali Technology*, vol. 5, Elsevier Applied Science, London (1992), p. 239.
89. H. Hikita, S. Asai, and T. Takatsuka, *Chem. Eng. J.* **5**, 77 (1973).
90. T. K. Sherwood and R. L. Pigford, *Absorption and Extraction*, McGraw-Hill Book Co., New York (1952).
91. L. J. Updyke, Emergency Vent Scrubbers—Design Considerations, *5th Chlorine Plant Operations Workshop*, Houston, TX (1990).
92. F. Yoshida and K. Akita, *A.I.Ch.E. J.* **11**(1), 9 (1965).
93. T. A. Makhneva and P. P. Gertsen, *Zh. Prikl. Khim.* **43**(4), 766 (1970).
94. J. Boteler and D. Clucas, reprinted in *Chemical Engineering Buyers Guide* (2000), p. 10.
95. V. K. Gupta, Considerations in Design of Chlorine Expansion Chambers, in *Proceedings, Oronzio de Nora Symposium on Chlorine Technology*, Venice (1979), p. 369.
96. *Explosive Properties of Gaseous Mixtures Containing Hydrogen and Chlorine*, Member Information Report 121, Edition 1, The Chlorine Institute, Inc., Washington, DC (1977).
97. O. Suzuki and T. Fukunaga, *J. Electrochem. Soc. (Japan)* **24**, 104 (1956).
98. J. Van Diest and R. DeGraff, *Ind. Chem. Belg.* **30**(11), 1195 (1965).
99. V. N. Antonov, E. Frolov, A. I. Rozlovskii, and A. S. Maltseva, *Khim. Prom.* **3**, 205 (1974).
100. E. J. Laubusch, Water Chlorination. In J. S. Sconce (ed.), *Chlorine: Its Manufacture, Properties and Uses*, Robert E. Krieger Publishing Co., Huntington, NY (1972), p. 465.
101. B. V. Tilak and C.-P. Chen, Chlor-alkali and Chlorate Technology, in *Proceedings, R. B. MacMullin Memorial Symposium*, H. S. Burney, N. Furuya, F. Hine, and K.-I. Ota (eds.), The Electrochemical Society, Inc., Pennington, NJ (1999), p. 8.
102. D. Hildebrand, Nitrogen Trichloride Analysis and Sampling, *39th Chlorine Institute Plant Managers Seminar*, Washington, DC (1996).
103. J. Fairweather, Orica Yarraville Nitrogen Trichloride Incidents, 30 July 1998. *The Chlorine Institute Nitrogen Trichloride Workshop*, New Orleans, LA (1998).
104. C. R. Dillmore, Actual Plant Practice in the Use of Ultraviolet Light for Removal of Nitrogen Trichloride from Chlorine Gas, *7th Chlorine Institute Plant Operations Seminar*, New York, NY (1962).

105. J. F. Knoop and A. Santavicca, *The Chlorine Institute Nitrogen Trichloride Workshop*, New Orleans, LA (1998).
106. R. E. Ross and J. L. Bowling, NCl_3 Concentrations and Decomposition by Dry Compression, *Member Information Report 21*, The Chlorine Institute, Washington, DC (1988), p. 101.
107. V. A. Shushunov and L. Z. Pavlova, *Zhur. Neorg. Khim.* **2**, 2272 (1957).
108. C. S. Robinson and E. R. Gilliland, *Elements of Fractional Distillation*, 4th ed., McGraw-Hill Book Co., New York, NY (1950), p. 110.
109. S. D. Argade, E. N. Balko, D. A. Kramer, and J. F. Louvar, *Nitrogen Trichloride Control in Chlorine Manufacture*, Electrochemical Society Meeting, Seattle, WA (1978).
110. F. Abraham and J. F. Knoop, Maximum Accumulation of Nitrogen Trichloride in a Continuous-Feed Chlorine Vaporizer, *The Chlorine Institute Nitrogen Trichloride Workshop*, New Orleans, LA (1998).
111. Ya. J. Apin, *Acta Physiochim. URSS* **13**, 405 (1940).
112. R. F. Zeller, J. P. DeJac, B. B. Guildin, M. J. Korzeuk, and G. J. Garzon, Demonstrating Non-Ideal Solution Behavior of NCl_3 in Liquid Chlorine and Its Application to Chlorine Vaporizers, *Sixteenth Annual Chlorine/Chlorate Seminar*, Cleveland, OH (1999).
113. Compressed Gas Association, *Handbook of Compressed Gases*, 3d ed., Van Nostrand Reinhold, New York, NY (1990).
114. U. Herrlett, *Chem. Eng.* **109**(5), 62 (2002).
115. I. H. Warren, Energy Saving in Chlorate Production with the Use of a Fuel Cell. In C. Jackson (ed.), *Modern Chlor-Alkali Technology*, vol. 2, Ellis Horwood Limited, Chichester (1983), p. 289.
116. N. P. Chohey, *Newsfront; Chem. Eng.* **108**(7), 37 (2001).
117. E. N. Balko, SPE Hydrochloric Acid Electrolysis Cell: Performance, Cell Configuration, in *Proceedings, Oronzio DeNora Symposium on Chlorine Technology*, Venice (1979), p. 204.
118. V. H. Thomas and E. J. Rudd, Energy Savings Advances in the Chlor-alkali Industry. In C. Jackson (ed.), *Modern Chlor-Alkali Technology*, vol. 2, Ellis Horwood, Chichester (1983), p. 159.
119. P. Schmittinger, *Chlorine—Principles and Industrial Practice*, Wiley-VCH, Weinheim (2000), p. 46.
120. *Type HGR for Mercury Removal*, product bulletin, Calgon Carbon Corporation, Pittsburgh, PA (1993).
121. C. P. Dillon, *Corrosion Control in the Chemical Process Industries*, McGraw-Hill Book Co., New York, NY (1986), p. 120.
122. G. A. Nelson, *Hydrocarbon Processing* **44**(5), 185 (1965).
123. I. F. White, G. J. Dibble, J. E. Harker, and T. F. O'Brien, Safety Considerations in the Design of Chlor-alkali Plants. In K. Wall (ed.), *Modern Chlor-Alkali Technology*, vol. 3, Ellis Horwood, Chichester (1986), p. 97.
124. F. Bodurtha, *Industrial Explosion Prevention and Protection*, McGraw-Hill Book Co., New York (1980).
125. F. Hine and A. J. Acioli M., *J. Appl. Electrochem.* **22**, 699 (1992).
126. A. J. Acioli, E. F. Powell, and F. C. Viana, Production of 70% Caustic Soda Directly from Decomposer, an Effective Way to Save Energy. In T. C. Wellington (ed.), *Modern Chlor-Alkali Technology*, vol. 5, Elsevier Applied Science, London (1992), p. 199.
127. R. Coin, Brine Purification, *Sixteenth Annual Chlorine/Chlorate Seminar*, Cleveland, OH (2000).
128. D. C. Brandt, The Economics of Producing High-Strength Caustic Soda in Membrane Cells, *32nd Chlorine Institute Plant Operations Seminar*, Washington, DC (1989).
129. F. Hine and M. Okubo, *Corrosion Eng. (Japan)* **25**, 509 (1976).
130. R. K. Swandby, *Chem. Eng.* November 12, 1962, p. 186.
131. *Corrosion Resistance of Nickel and Nickel-Containing Alloys in Caustic Soda and Other Alkalies*, CEB-2, International Nickel Company, New York, NY (1973).
132. C. P. Dillon, *Corrosion Control in the Chemical Process Industries*, McGraw-Hill Book Co., New York, NY (1986), p. 113.
133. D. E. Jordan, *Stress-Corrosion Cracking of Nickel-Base Alloy Weldments*, International Institute of Welding Annual Assembly, Montreal (1990).
134. A. R. McIlree and H. T. Michels, *Corrosion* **33**(2), 60 (1977).
135. C. M. Schillmoller, *Alloy Selection for Caustic Soda Service*, NiDI Technical Series No. 10019, Nickel Development Institute, Toronto (1988).
136. A. B. Misercola, R. P. Tracy, I. A. Franson, and R. J. Knoth, The Use of E-Brite 26-1[®] Ferritic Stainless Steel in Production of Caustic Soda, *Electrochemical Society meeting*, Washington, DC (1976).
137. J. E. Houston, Evaporator Technology Corporation, Personal Communication (1983).

138. B. M. Barkel, *Accelerated Corrosion of Nickel Tubes in Caustic Evaporator Service*, CORROSION/79, Paper No. 13, Atlanta, GA (1979).
139. M. Yasuda, F. Takeya, and F. Hine, *Corrosion* **39**(10), 399 (1983).
140. T. V. Bommaraju and P. J. Orosz, Caustic Evaporator Corrosion: Causes and Remedy. In T. C. Wellington (ed.), *Modern Chlor-Alkali Technology*, vol. 5, Elsevier Applied Science, London (1992), p. 307.
141. T. V. Bommaraju, W. V. Hauck, and V. J. Lloyd, *U.S. Patent* 4,585,579 (1986).
142. J. R. Crum and W. G. Lipscomb, Performance of Nickel 200 and E-Brite 26-1 in First-Effect Caustic Environments. *CORROSION/83*, Paper No. 23 (1983).
143. R. Parkinson, *Properties and Applications of Electroless Nickel*, Technical paper 10081, Nickel Development Institute, Toronto (1997).
144. S. A. Watson, *Electroless Nickel Coatings*, Technical paper 10055, Nickel Development Institute, Toronto (1990).
145. P. Cutler, *Nickel, Nickel Everywhere*, Reprint Series No. 14,048, from *Materials World*, September 1998. Nickel Development Institute, Toronto (1998).
146. C. W. Funk and G. B. Barton, Caustic Stress Corrosion Cracking, *CORROSION* 77, Paper No. 54, National Association of Corrosion Engineers, Houston, TX (1977).
147. www.swenson-equip.com/fc-evap, *Forced-Circulation Evaporator*, Swenson Process Equipment Co., Harvey, IL (2002).
148. J. D. Kumana, *Chem. Eng. Progr.* **86**(5), 10 (1990).
149. A. Ward, Fouling of Evaporator Heat Exchangers—Causes and Cures, *Fuel/Ethanol Workshop*, Wichita, KS (1992).
150. General Electric Co., *South African Patent* 7,606,336 (1977).
151. D. Mannig and G. Scherer, Hydrogen Peroxide in the Chlor-Alkali Industry, *30th Chlorine Institute Plant Operations Seminar*, Washington, DC (1987).
152. S. G. Osborne and S. Davids, *U.S. Patent* 2,823,177 (1958).
153. L. L. Benezra, D. W. Hill, and S.-P. Tsai, *U.S. Patent* 4,055,476 (1977).
154. P. Schmittinger (ed.), *Chlorine—Principles and Industrial Practice*, Wiley-VCH, Weinheim (2000), p. 125.
155. F. C. Standiford and W. L. Badger, *Ind. Eng. Chem.* **46**(11), 2400 (1954).
156. D. J. Pye, *U.S. Patent* 2,610,105 (1952).
157. A. von Antropoff and W. Sommer, *Z. phys. Chem.* **123**, 161 (1926).
158. W. Haltenberger, Jr., *Ind. Eng. Chem.* **31**, 783 (1930).
159. P. S. Nair, *Chem. Eng.* **110**(1), 77 (2003).
160. M. Pasquariello, *Chem. Eng.* **107**(9), 77 (2000).
161. M. E. Bishop, *Chem. Eng.* **109**(5), 77 (2002).
162. W. Cathcart, Caustic Tank Car Lining, *30th Chlorine Institute Plant Operations Seminar*, Washington, DC (1987).
163. T. F. O'Brien, Considerations in the Conversion of Existing Chlor-alkali Plants to Membrane-cell Operation. In C. Jackson (ed.), *Modern Chlor-Alkali Technology*, vol. 2, Ellis Horwood, Chichester (1983), p. 190.
164. K. A. Stanley, Phased Conversion of a Diaphragm Plant to Membrane Technology. In S. Sealey (ed.), *Modern Chlor-Alkali Technology*, vol. 7, Royal Society of Chemistry, Cambridge (1998), p. 145.
165. www.swenson-equip.com/dtbxtaliz, *Draft Tube Baffle Crystallizer*, Swenson Process Equipment Co., Harvey, IL (2002).
166. M. J. Niksa, Acid/Base Recovery from Sodium Sulfate, *Fourth International Forum on Electrosynthesis in the Chemical Industry*, Fort Lauderdale, FL (1991).
167. R. B. MacMullin, *Chem. Eng. Progr.* **46**(9), 440 (1950).

10

Chemical Engineering Principles

10.1. INTRODUCTION

The purpose of this chapter is to gather in one place some of the basic considerations that apply to the engineering techniques and unit operations that are important in the chlor-alkali process. Thus, the chapter begins with a discussion of material and energy balances (Section 10.2). These are basic to all of chemical engineering and are used implicitly throughout this book. Here, we present some of the fundamentals. Section 10.3 then covers current distribution. This is uniquely important in electrochemical processing. The presentation discusses methods of predicting and determining the distribution of current in electrochemical reactors of different kinds.

Sections 10.4 and 10.5 cover some of the classical unit operations of chemical engineering. Section 10.4 covers basic fluid dynamics and the fluid-handling operations common to brine and cell gases. Section 10.5 turns to the transport operations of heat transfer, absorption, adsorption, ion exchange, distillation, and evaporation.

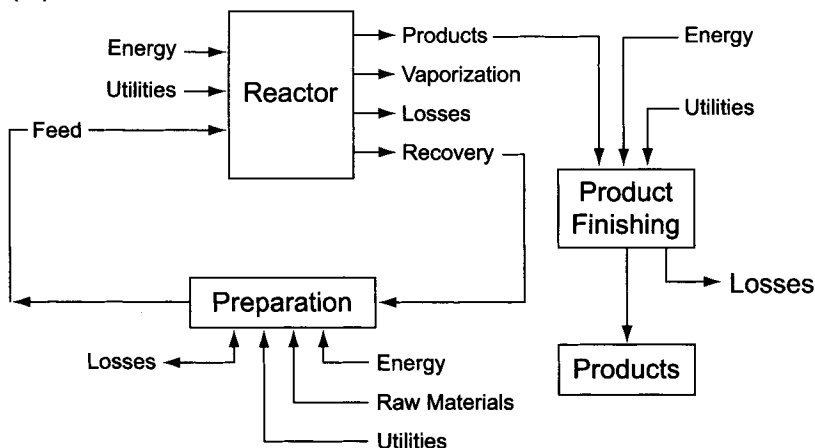
The treatment here is brief and is intended to provide general background. More detailed information is available in a wide variety of textbooks and literature review articles. This chapter does not discuss practical details of engineering and operation. These appear in the relevant sections in earlier volumes.

10.2. MATERIAL AND ENERGY BALANCE

In the chemical industry, a given raw material is typically fed to a reactor where it is processed to obtain the desired product at a finite rate and efficiency. The depleted stream is often sent back to a preparation operation to recover the unconverted raw material. The other inputs to the process, besides the materials, are utilities and energy, the sensible and latent heats of raw materials and products contributing to the energy balance. The product is separated from the effluent and is further purified in the finishing section for shipment (Fig. 10.2.1A). The energy balance for chemical processing is related to the transfer of materials in the flow diagram under discussion. Figure 10.2.1.B shows a general description of the flow of energy in and out of the reactor.

The combined flow of materials and energy in the three chlor-alkali processes shows that there is significant transfer of energy [1] between unit operations. In the case of

(A) Material Balance



(B) Energy Balance

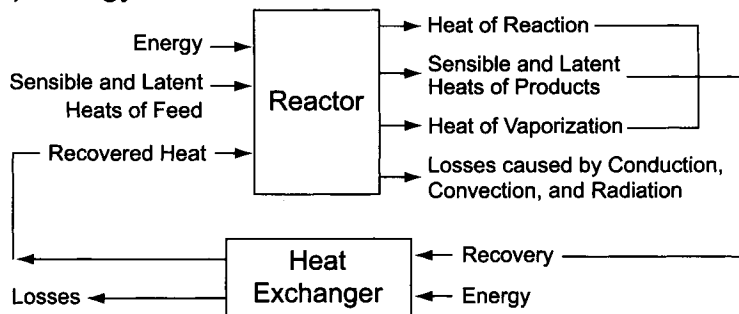


FIGURE 10.2.1. Material and energy balance around a reactor.

mercury cells, production of 1 ton of caustic requires the circulation of about 400 tons of mercury, which transfers 80–90% of the heat between the electrolyzer and the amalgam decomposer. Likewise, the brine flow is a major factor in the transfer of heat between the brine treatment process and the chlorine cell.

Since the energy balance is based on thermodynamics, we will summarize some important concepts in Section 10.2.1 before applying them to an electrochemical process in Section 10.2.2.

10.2.1. Thermodynamics

10.2.1.1. Energy Changes Caused by Chemical Reactions. The energy inflow to a system, Q , is the sum of the work done by the system, W , and the change in its internal energy, ΔU . This is the first law of thermodynamics. We may separate the electrochemical energy, nFE , from the rest of the energy inflow as illustrated in Fig. 10.2.2 (see also

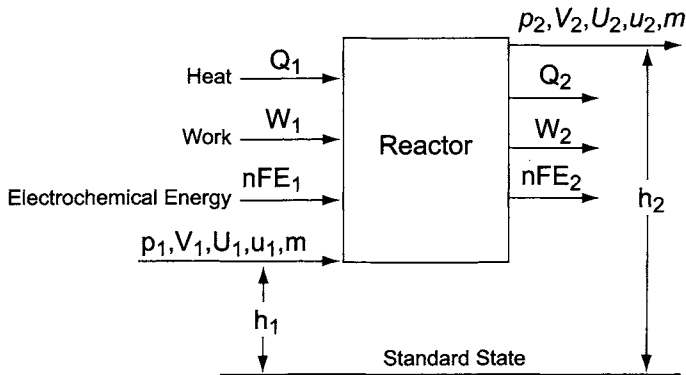


FIGURE 10.2.2. Energy balance around a continuous reactor. Q = Heat; W = Work; n = Number of electrons during charge transfer; F = Faraday's constant; E = Electrical potential; p = Pressure; V = Volume; U = Internal energy; m = Mass; u = Velocity.

Chapter 4). The inflow and outflow of the energy passing through a continuous reactor are given by Eqs. (1) and (2).

$$\text{Energy inflow} = Q_1 - W_1 - nFE_1 + h_1 \frac{g}{g_c} + p_1 V_1 + \frac{u_1^2}{2g_c} + U_1 \quad (1)$$

$$\text{Outflow energy} = -Q_2 + W_2 + nFE_2 + h_2 \frac{g}{g_c} + p_2 V_2 + \frac{u_2^2}{2g_c} + U_2 \quad (2)$$

where subscripts 1 and 2 refer to the inflow and outflow, respectively, h to height, g to acceleration due to gravity, g_c to the conversion factor for g , and

$$nFE = \text{electrochemical energy}, \quad (3)$$

$$h \frac{g}{g_c} = \text{potential energy}, \quad (4)$$

$$pV = \text{work done by pressure}, \quad (5)$$

$$\text{and } \frac{u^2}{2g_c} = \text{kinetic energy}. \quad (6)$$

Since the inflow of energy is equal to the outflow, we have:

$$Q - W - nFE = \Delta H + \frac{(h_2 - h_1)g}{g_c} + \frac{u_2^2 - u_1^2}{2g_c} \quad (7)$$

where

$$Q = Q_1 + Q_2 \quad (8)$$

$$W = W_1 + W_2 \quad (9)$$

$$E = E_1 + E_2 \quad (10)$$

$$H_i = p_i V_i + U_i \text{ (enthalpy)} \quad (11)$$

$$\Delta H = H_2 - H_1 \text{ (enthalpy change)} \quad (12)$$

10.2.1.2. Sensible Heat and Latent Heat. Since the heat inflow caused by volume change at constant pressure is equal to the enthalpy change, ΔH , the specific heat C_p is given by the equation:

$$C_p = \left(\frac{\partial H}{\partial T} \right)_p \quad (13)$$

or

$$\Delta H = \int_{T_1}^{T_2} C_p dT \quad (14)$$

The specific heat is a function of temperature and can be represented as:

$$C_p = \alpha_0 + \alpha_1 T + \alpha_2 T^2 + \alpha_3 T^3 + \dots + \alpha_{-2} T^{-2} \quad (15)$$

where the coefficients are available in standard thermodynamic data compilations.

The enthalpy change caused by the phase change of water from ice to steam through the liquid phase, for example, is given by:

$$\Delta H = \int_{T_1}^{T_m} C_p(s) dT + \lambda_m + \int_{T_m}^{T_b} C_p(l) dT + \lambda_b + \int_{T_b}^{T_2} C_p(g) dT \quad (16)$$

where λ_m = latent heat of melting, λ_b = latent heat of vaporization, (s) = solid, (l) = liquid, (g) = gas, and the subscripts: 1 = initial state, 2 = final state, m = melting point, and b = boiling point.

The integral terms in Eq. (16) are the sensible heats. The latent heats are given by the Clausius–Clapeyron equation:

$$\lambda = T(V_2 - V_1) \frac{dp_1}{dT} \quad (17)$$

where V_1 and V_2 are the molar volumes before and after the phase change respectively, and p_1 is the vapor pressure.

10.2.1.3. *Isothermal Change and Adiabatic Change.* Under isothermal conditions, the internal energy is unchanged (i.e., $\Delta U = 0$). Thus, for 1 mol of an ideal gas,

$$Q = W = RT \ln \left(\frac{V_2}{V_1} \right) = RT \ln \left(\frac{p_1}{p_2} \right) \quad (18)$$

In the case of an adiabatic change, on the other hand, there is no heat transfer, so $Q = 0$. Hence,

$$\Delta U = -W = -pV$$

Substituting the above equation and the relationships for an ideal gas

$$C_p = C_v + R \quad (19)$$

$$\gamma = C_p/C_v \quad (20)$$

into the specific heat expression at constant volume, $C_v = (\partial U/\partial T)_v$ results in:

$$\frac{T_2}{T_1} = \left(\frac{V_1}{V_2} \right)^{\gamma-1} = \left(\frac{p_2}{p_1} \right)^{(\gamma-1)/\gamma} \quad (21)$$

or

$$pV^\gamma = \text{constant} \quad (22)$$

We may consider Carnot's cycle for an ideal gas (Fig. 10.2.3). The changes from state A to state B at $T = T_1$ and from State C to State D at $T = T_2$ are isothermal, whereas changes from State B to State C and from State D to State A, are adiabatic. The overall work, W , for the cycle is:

$$W = W_{AB} + W_{BC} + W_{CD} + W_{DA} \quad (23)$$

where the subscripts represent the respective steps. Since steps BC and DA are adiabatic,

$$W_{BC} = -U_{BC} = - \int_{T_1}^{T_2} C_v dT$$

$$W_{DA} = -U_{DA} = - \int_{T_1}^{T_2} C_v dT = -W_{BC}$$

and

$$\frac{p_C}{p_D} = \frac{p_B}{p_A}$$

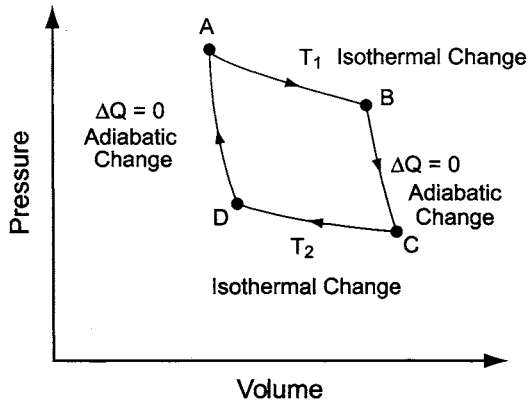


FIGURE 10.2.3. Carnot's cycle for ideal gas.

Substituting the above equations and Eq. (18) into Eq. (23) results in:

$$\begin{aligned} W &= RT_1 \ln \left(\frac{p_B}{p_A} \right) + RT_2 \ln \left(\frac{p_C}{p_D} \right) \\ &= RT_1 \ln \left(\frac{p_B}{p_A} \right) \left(1 + \frac{T_2 \ln(p_C/p_D)}{T_1 \ln(p_B/p_A)} \right) \end{aligned}$$

or

$$\frac{W}{Q_1} = 1 - \frac{T_2}{T_1} \quad (24)$$

where

$$Q_1 = W_{AB} = RT_1 \ln(p_B/p_A)$$

is the heat inflow and W is the work to the surroundings. The ratio W/Q_1 is the energy efficiency of the heat engine, which is a function of temperature but independent of the state of the surroundings. Similarly, it can be shown that $Q_1 = W_{CD}$. Therefore, with Eqs. (23) and (24), we have:

$$\frac{Q_1}{T_1} + \frac{Q_2}{T_2} = 0$$

or

$$\oint \frac{dQ(R)}{T} = 0 \quad (25)$$

Therefore, the total sum of the changes of state in a cycle is zero. In other words, since the changes of the state functions for steps AB and CD are Q_1/T_1 , and Q_2/T_2 , respectively, Eq. (25) shows that the state function Q/T of the reversible system is independent of the path. This new state function,

$$dS = \frac{dQ(R)}{T}$$

or

$$\Delta S = \int \frac{dQ(R)}{T} \quad (26)$$

is called the entropy change.

We may consider heat transfer between two rooms as shown in Fig. 10.2.4. Heat Q is transferred from the system at temperature T_1 to the surrounding at temperature T_2 , and, hence, the entropy change ΔS is

$$\Delta S = \left(\frac{Q}{T_2} - \frac{Q}{T_1} \right) = \frac{Q}{T_2} \left(1 - \frac{T_2}{T_1} \right) \quad (27)$$

The system is reversible and therefore, the work W is represented by Eq. (24). Substitution of Eq. (24) in Eq. (27) results in

$$W = T_2 \Delta S \quad (28)$$

Thus, the loss of work is the product of the entropy change ΔS and the temperature of the surroundings T_2 .

The enthalpy change caused by the phase change of water is shown by Eq. (16). Substituting Eq. (26) into Eq. (16) leads to

$$S - S_s = \int_{T_s}^{T_m} \frac{C_p(s)}{T} dT + \frac{\lambda_m}{T} + \int_{T_m}^{T_b} \frac{C_p(l)}{T} dT + \frac{\lambda_b}{T} + \int_{T_b}^T \frac{C_p(g)}{T} dT \quad (29)$$

where S_s is the entropy of the standard state and is equal to the integration constant. Consequently, S can be calculated by using this equation when S_s is known.

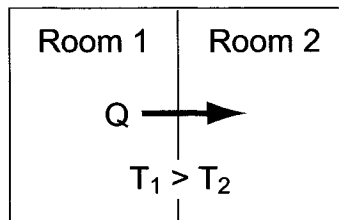


FIGURE 10.2.4. Heat transfer between rooms and entropy change.

10.2.1.4. *Free Energy and Chemical Equilibrium.* We may now recapitulate other state functions, the Helmholtz free energy A , and the Gibbs free energy G as discussed in Section 4.1.

$$A = U - TS \quad (30)$$

$$G = H - TS = U + pV - TS = A + pV \quad (31)$$

Since $dW = p dV$ and $dQ = T dS$ for a reversible system,

$$dU = dQ - dW = T dS - p dV$$

Substituting the above equation and Eq. (11) into Eqs. (30) and (31) leads to:

$$dA = dU - T dS - S dT = -[p dV - S dT] \quad (32)$$

or

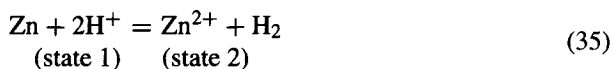
$$\Delta A = \Delta U - T \Delta S \quad (33)$$

and

$$dG = dH - T dS - S dT = V dp - S dT \quad (34)$$

Since $T \Delta S$ is the heat generated in a reversible process, $-\Delta A = -(A_2 - A_1)$ is the work of the process on the surroundings. In practice, however, the system is not ideally reversible, and hence the work to the surroundings is always smaller than $-\Delta A$. In other words, $-\Delta A$ is the maximum work of isothermal change.

With this background, we can consider an electrolytic cell containing zinc and platinum sheets in a dilute sulfuric acid solution, with the two electrodes connected with each other outside the cell. The following reaction occurs:



with the generation of 2 F of DC electricity for each mole of Zn dissolved. The reverse process may proceed if energy W is supplied from the outside. Although DC electricity is generated by a galvanic cell (Eq. 35), the work corresponding to the volume change $p \Delta V$ is not available for other use. Therefore, the maximum work capable of generating energy is

$$W_E = -\Delta A - p \Delta V = -\Delta G$$

and is equal to nFE . Consequently the maximum voltage or the electromotive force of the galvanic cell, E_F , is:

$$E_F = -\frac{\Delta G}{nF} \quad (36)$$

Since reaction (35) in the forward direction is exothermic, E_F is positive and hence, ΔG must be negative.

The Gibbs free energy change caused by temperature changes at constant pressure is given by:

$$\left(\frac{d\Delta G}{dT}\right)_p = -\Delta S = -\frac{\Delta H - \Delta G}{T} \quad (37)$$

Substituting Eq. (36) into Eq. (37), we have the Gibbs-Helmholtz equation, as well as other relationships which are useful in electrochemistry:

$$E + \frac{\Delta H}{nF} = T \frac{dE}{dT} \quad (38)$$

$$\frac{d\left(\frac{\Delta G}{T}\right)}{dT} = -\frac{\Delta H}{T^2} \quad (39)$$

and

$$\frac{d\left(\frac{\Delta G}{T}\right)}{d\left(\frac{1}{T}\right)} = \Delta H \quad (40)$$

In general, the energy changes for the chemical process,

$$\text{Initial State} \rightarrow \text{Final State} \quad (41)$$

under batch and continuous modes are represented by Eqs. (42) and (43) respectively,

$$\Delta U_R = \Sigma U_F - \Sigma U_I \quad (42)$$

$$\Delta H_R = \Sigma H_F - \Sigma H_I \quad (43)$$

where subscripts I and F denote the initial and final states, respectively. These equations constitute the Hess law of constant summation, which is another description of the first law of thermodynamics. The reaction heat ΔH_R can be calculated from these equations when the enthalpies of the two states are given. It is evident that $\Delta H_R < 0$ and $\Delta H_R > 0$ describe exothermic and endothermic reactions, respectively.

When a substance is heated to temperature T and the pressure reaches p at equilibrium, the Gibbs free energy or the chemical potential for the process can be written as:

$$\mu = G = H - TS \quad (44)$$

From the first law and the second law of thermodynamics,

$$\Delta H = Q = T \Delta S$$

it follows that:

$$\Delta\mu = \Delta H - T \Delta S = 0$$

Hence, the chemical potentials of liquid and vapor are equal to each other, that is,

$$\Sigma\mu = 0 \quad (45)$$

The chemical potential is the Gibbs free energy for 1 mol of the species under consideration, and hence it is a convenient term for the discussion of chemical processes.

Since the chemical potential of a gaseous species varies with temperature and pressure, we may define it as follows:

$$\mu = \mu^{\circ} + RT \ln f \quad (46)$$

where f is an effective pressure called the fugacity, and μ° is the standard chemical potential at $f = 1$.

These representations are also valid for liquids or solutions when the activity, a , is substituted for f :

$$\mu = \mu^{\circ} + RT \ln a \quad (47)$$

where

$$a = \gamma C \quad (48)$$

where γ is the activity coefficient and C the concentration.

By convention, γ approaches unity when the solution is infinitely dilute (i.e., $C \rightarrow 0$). When Eq. (47) is applied to the chemical equilibrium process (Eq. 41),

$$\mu_{\text{A}}^{\circ} + \mu_{\text{B}}^{\circ} + \cdots + RT \ln(a_{\text{A}} \cdot a_{\text{B}} \cdots) = \mu_{\text{C}}^{\circ} + \mu_{\text{D}}^{\circ} + \cdots + RT \ln(a_{\text{C}} \cdot a_{\text{D}} \cdots)$$

where A, B, . . . and C, D, . . . are the chemical species in the initial state and the final state, respectively. The equation shown above can be rewritten in a simple form as follows:

$$\Delta G^{\circ} = -RT \ln \frac{\Pi(a_{\text{F}})}{\Pi(a_{\text{I}})} \quad (49)$$

where

$$\begin{aligned} \Delta G^{\circ} &= \sum \mu_{\text{F}}^{\circ} - \sum \mu_{\text{I}}^{\circ} = (\mu_{\text{C}}^{\circ} + \mu_{\text{D}}^{\circ} + \cdots) - (\mu_{\text{A}}^{\circ} + \mu_{\text{B}}^{\circ} + \cdots) \\ \Pi(a_{\text{I}}) &= a_{\text{A}} \cdot a_{\text{B}} \cdots \\ \Pi(a_{\text{F}}) &= a_{\text{C}} \cdot a_{\text{D}} \cdots \end{aligned}$$

Since the equilibrium constant K is represented by

$$K = \frac{a_{\text{C}} \cdot a_{\text{D}} \cdots}{a_{\text{A}} \cdot a_{\text{B}} \cdots} = \frac{\Pi(a_{\text{F}})}{\Pi(a_{\text{I}})}$$

we have

$$\Delta G^{\circ} = -RT \ln K \quad (50)$$

10.2.2. Energy Balance in Electrochemical Processes

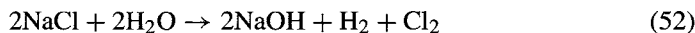
10.2.2.1. Thermodynamic Decomposition Voltage and Thermoneutral Voltage. Electricity is, of course, the primary source of energy supplied to an electrochemical reactor. It drives the reaction and heats the contents of the electrolyzer. In practice, the cell requires more electric current than that calculated by Faraday's law because some of the electricity is consumed by side reactions, resulting in current inefficiency. Also, the terminal voltage of a cell is higher than the thermodynamic voltage because of overvoltages at the electrodes and ohmic voltage drops in the electrolytes and the cell hardware.

The energy requirement for an electrolytic cell will be directly proportional to the cell voltage and inversely proportional to the cell efficiency. The factors governing the current efficiency and cell voltage are discussed in detail in Section 4.4.

The thermodynamic decomposition voltage E_{th}° is the minimum voltage required for a given electrochemical process to proceed in a given direction. It is based on the standard free energy change of the overall reaction as:

$$E_{\text{th}}^{\circ} = -\frac{\Delta G^{\circ}}{nF} \quad (51)$$

Thus, for the reaction



the ΔG° values, calculated from the free energy data [2], are noted in Table 10.2.1 along with the E_{th}° values at various temperatures. Reaction (52) is endothermic and the

TABLE 10.2.1. Free Energy and Enthalpy Change at Various Temperatures

Reaction	Temperature (°C)	$-\Delta G^{\circ}$ (kcal mol ⁻¹)	$-\Delta H^{\circ}$	E_{th}° (V)	E_{tn}°
2NaCl + 2H ₂ O → 2NaOH + H ₂ + Cl ₂	80	100.05	105.09	2.169	2.278
	90	99.91	104.81	2.166	2.272
	100	99.77	104.53	2.163	2.266
2KCl + 2H ₂ O → 2KOH + H ₂ + Cl ₂	80	100.05	105.09	2.169	2.278
	90	99.91	104.81	2.166	2.272
	100	99.77	104.67	2.163	2.269
0.5O ₂ + 2NaCl + H ₂ O → 2NaOH + Cl ₂	80	45.47	37.19	0.986	0.806
	90	45.71	36.99	0.991	0.802
	100	45.96	36.78	0.996	0.797
HCl → 0.5H ₂ + 0.5Cl ₂	25	40.02	31.35	1.36	1.74

overall heat of the reaction involved in this process is shown in Table 10.2.1. The voltage corresponding to the heat of the reaction

$$E_{\text{tn}}^{\circ} = -\frac{\Delta H}{nF} \quad (53)$$

is called the thermoneutral voltage, E_{tn}° , representing the voltage at which heat is neither lost to the surroundings nor required by the electrolytic cell.

Commercial chlor-alkali cells operate above the thermodynamic decomposition voltage in order to allow reaction (52) to proceed in the forward direction and generate the desired products. The excess voltage, constituting the overvoltages and the ohmic drops, leads to the generation of heat.

Let us now show the importance of thermoneutral voltage by comparing the E_{th}° and E_{tn}° for the electrolysis of HCl solutions. As shown in Table 10.2.1, E_{tn}° is always greater than E_{th}° because the E_{tn}° term contains the heat associated with the entropy change for the reaction $2\text{HCl} \rightarrow \text{H}_2 + \text{Cl}_2$. If a cell operates at a voltage between E_{tn}° and E_{th}° , the cell will be cooled as it dissipates the heat corresponding to the entropy change, irreversibly. On the other hand, at voltages higher than E_{tn}° , the cell is heated by the excess energy required to overcome the overvoltages and the ohmic drops and hence, must be cooled to hold at a given temperature. The amount of heat generated or absorbed by the system can be calculated as follows. The amount of heat released Q_{rev} is given as:

$$Q_{\text{rev}} = -T\Delta S = \Delta G - \Delta H \quad (54)$$

$$= nFE_{\text{th}}^{\circ} - \Delta H \quad (55)$$

The cell voltage can be written in terms of its constituents as:

$$E = E_{\text{th}}^{\circ} + \Sigma IR + \Sigma \eta \quad (56)$$

where η is the overvoltage and IR is the ohmic drop.

The irreversible heat generated Q_{irr} is given by:

$$Q_{irr} = (E - E_{th}^{\circ}) nF \tag{57}$$

Since the heat generated Q is equal to $Q_{irr} - Q_{rev}$, Q can be expressed as (from Eqs. (57) and (55)):

$$Q = nFE - \Delta H \tag{58}$$

When Q is positive, heat is released by the system, and when Q is negative, heat is absorbed by the system.

For chlor-alkali cells, following reaction (52), E_{th}° at 90°C is 2.166 V and E_{in}° is 2.272 V. In practice, the cells operate at 3.3–3.5 V. Therefore, the amount of heat generated is:

$$Q = \left[\left(\frac{100}{CE} \right) (46.099E) \right] - \Delta H \tag{59}$$

Thus, for a cell operating at a current efficiency of 96% and a cell voltage of 3.3 V, the amount of heat generated is equal to:

$$\begin{aligned} Q &= \frac{100}{96} (46.099(3.3)) - 104.81 = 158.46 - 104.81 \\ &= 53.655 \text{ kcal mol}^{-1} \text{Cl}_2 \text{ or } 0.7566 \text{ kcal g}^{-1} \text{Cl}_2 \\ &= 3165 \text{ kJ kg}^{-1} \text{Cl}_2 \end{aligned}$$

This heat is generally removed by water evaporation and radiation losses.

10.2.2.2. *Voltage and Energy Balances.* The energy requirements of chlor-alkali cells are presented in Figs 10.2.5 to 10.2.7. The area of the outer rectangle [3] represents the

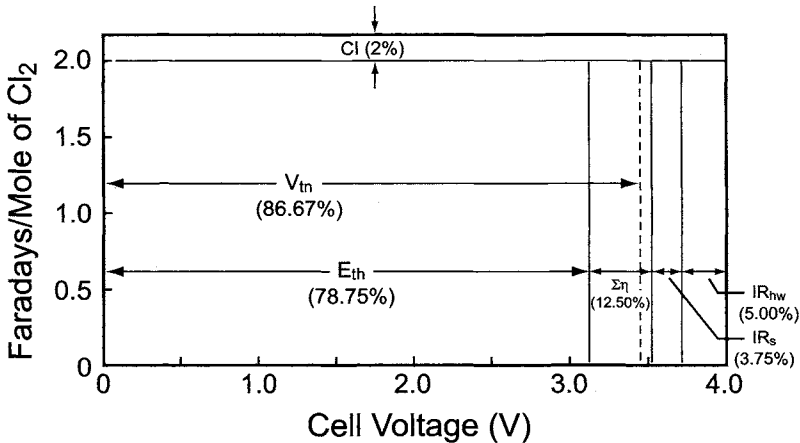


FIGURE 10.2.5. Energy distribution in an amalgam chlor-alkali cell (DeNora 24M-2) operating at 10 kA m⁻². (Energy consumption: 3,081 kW hr ton⁻¹ of Cl₂; Cell voltage: 4.0 V; Current efficiency: 98%.)

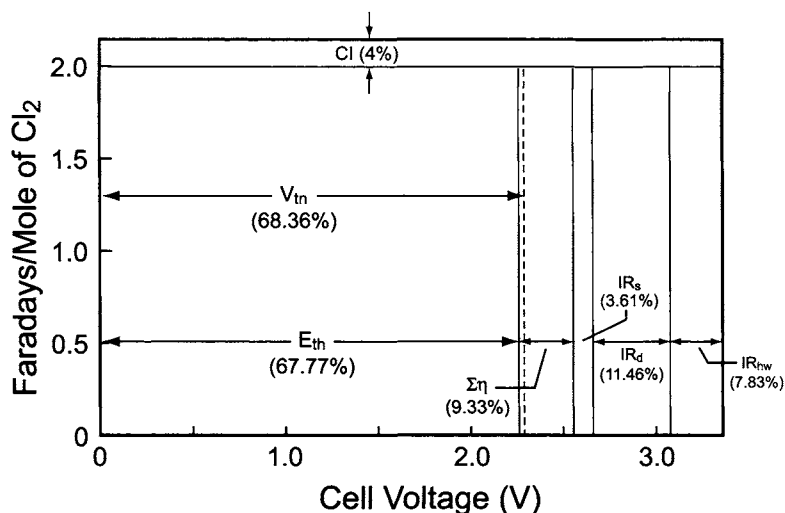


FIGURE 10.2.6. Energy distribution in a diaphragm chlor-alkali cell (ELTECH H-4/75) operating at 2.3 kA m^{-2} . (Energy consumption: $2,610 \text{ kW hr ton}^{-1}$ of Cl_2 ; Cell voltage: 3.32 V ; Current efficiency: 96% .)

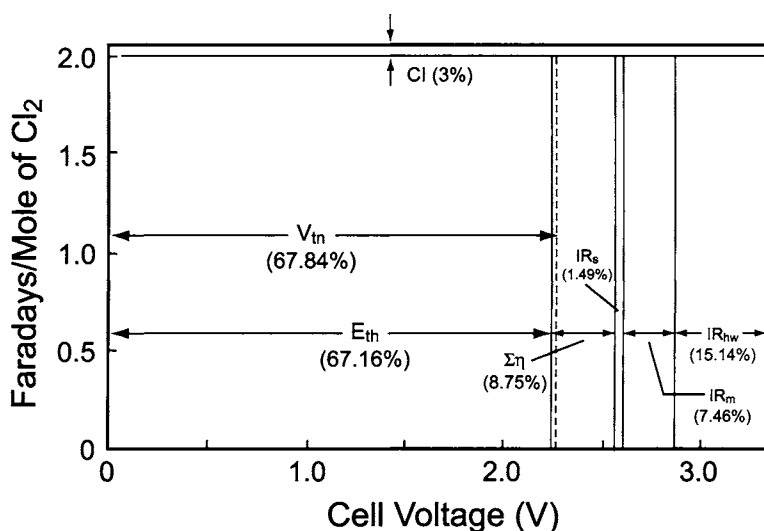


FIGURE 10.2.7. Energy distribution in a membrane chlor-alkali cell (MGC-26) operating at 5 kA m^{-2} . (Energy consumption: $2,607 \text{ kW hr ton}^{-1}$ of Cl_2 ; Cell voltage: 3.35 V ; Current efficiency: 97% .)

total energy requirement for the production of chlorine. The current inefficiencies, CI, are noted at the top of the figure and the voltage distribution is presented in terms of its components, along with the thermoneutral voltage, applicable to the given conditions. The ΔH and ΔG values for reaction (52) are noted in Table 10.2.1. The relevant data for mercury cells are calculated using the Gibbs–Helmholtz Eq. (38) with the E^0 and

dE/dt values calculated from the data in ref. [4] and the ΔG values from ref. [2]. Figure 10.2.5, depicting the overall energy profile of an amalgam-type chlorine cell, shows that part of the heat generated by the irreversible losses is effectively used to keep the cell temperature at a set value. Of course, there is still additional heat that should be removed, as is evident from Figure 10.2.5. Part of this heat is taken out of the amalgam flowing out of the electrolytic cell and hence, it is indeed possible to operate the mercury cells at the thermoneutral voltage by operating the cell at the proper temperature and current density.

The energy diagrams in Figs 10.2.6 and 10.2.7 show that in the case of the membrane and diaphragm cells, the E_{th}^o and the E_m^o are close to each other. As a result, it is almost impossible to operate them at the E_m^o , even with significant advances in the membrane technology and hardware developments.

It is interesting to note that the air depolarized cathode-based membrane cells show a E_{th}^o of 0.991 V at 90°C vs E_m^o of 0.802 V.

The thermoneutral voltage defined by Eq. (53) does not take into account the energy required to raise the temperature of the feed stream from a reference temperature of 25°C to the operating temperature of the electrolyte and to saturate the product gases with water vapor. LeRoy *et al.* [5,6] proposed a modified thermoneutral voltage V_{mtn} by considering these two heat requirements, and defined a practical thermoneutral voltage, called the thermobalance voltage, V_{tb} , for water electrolysis cells. The thermobalance voltage is defined as:

$$V_{tb} = V_{mtn} + V_{rad} + V_{conv} \quad (60)$$

where V_{rad} and V_{conv} refer to the voltage corresponding to the energy losses by radiation and convection, respectively.

V_{rad} and V_{conv} can be estimated as:

$$V_{rad} = A\epsilon\sigma(T^4 - T_a^4)10^{-3}/I \quad (61)$$

$$V_{conv} = 1.77A(T - T_a)^{1.25}10^{-3}/I \quad (62)$$

where A is the radiating area (in m^2), ϵ is the emissivity, σ is the Stefan–Boltzmann constant ($5.67 \times 10^{-8} \text{ W m}^{-2} \text{ K}^4$), T_a is the ambient temperature in K, T is the operating cell temperature in K, and I is the load in kA.

Figure 10.2.8 depicts the results of the calculations described above for water electrolysis cells [5,6]. The broken line shows the cell voltage as a function of temperature, which crosses the curve for the thermal-balance voltage at about 90°C. At temperatures lower than 90°C, the cell voltage is higher than the thermobalance voltage or the voltage corresponding to the overall requirement of heat, and hence, the cell dissipates excess heat and it must be removed. On the other hand, at temperatures higher than 90°C, the heat generation is insufficient to compensate for the total heat required for the reaction so that the cell has to be heated. Hence, the cell can be operated at about 90°C without heating or cooling.

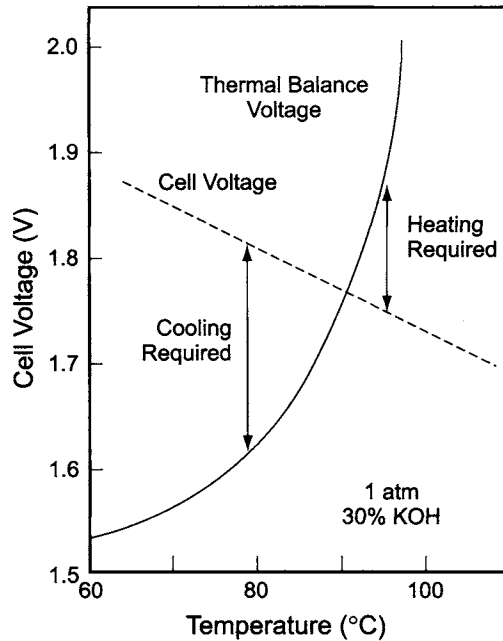


FIGURE 10.2.8. Isothermal and thermal-balance voltages of a water electrolyzer as a function of temperature at 1 atm total pressure [6]. (Reproduced by permission of The Electrochemical Society, Inc.)

The power losses arising from radiation ($V_{\text{rad}}I$) and convection ($V_{\text{conv}}I$) from Eqs. (61) and (62) are 7.9 and 5.3 mV, respectively, with $A = 3 \text{ m}^2$; $\varepsilon = 0.8$; $\sigma = 5.67 \times 10^{-8} \text{ W m}^{-2} \text{ deg}^4$; $T_a = 313 \text{ K}$ and $T = 368 \text{ K}$ at a load of 150 kA. The thermoneutral voltage of a diaphragm cell or a membrane cell would be higher by the sum of these values (i.e., 13.2 mV) than those values shown in Figs 10.2.5 and 10.2.7. Still it is difficult to realize operation of the chlor-alkali cells at the thermobalance voltage, as the ohmic and overpotential losses are too large with the present technologies.

10.2.2.3. Energy Flow Diagrams. The chlor-alkali industry, like any electrochemical operation, is energy intensive. Therefore, it is instructive to determine how the energy is distributed over the entire process. This will indicate the most profitable areas for improvement.

Development of an energy flow diagram requires a detailed knowledge of the process flow sheet with a complete material balance. From the enthalpy of formation of the input and output components, one can estimate the enthalpy change involved in a given operation, from which the energy consumed or liberated can be calculated. Such a methodology was followed [7,8] to describe the energy distribution in the mercury- and diaphragm-based chlor-alkali processes.

While the descriptions provided in these efforts are informative, they do not reflect reality in totality as the process flow sheets on which these estimates are based, start with highly optimistic descriptions of various operations. The energy flow diagram for

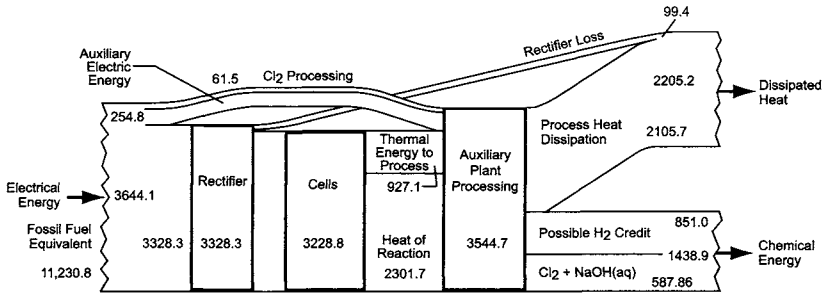


FIGURE 10.2.9. Energy flow diagram for mercury cell chlor-alkali process. (The numbers are kWh ton^{-1} of chlorine.)

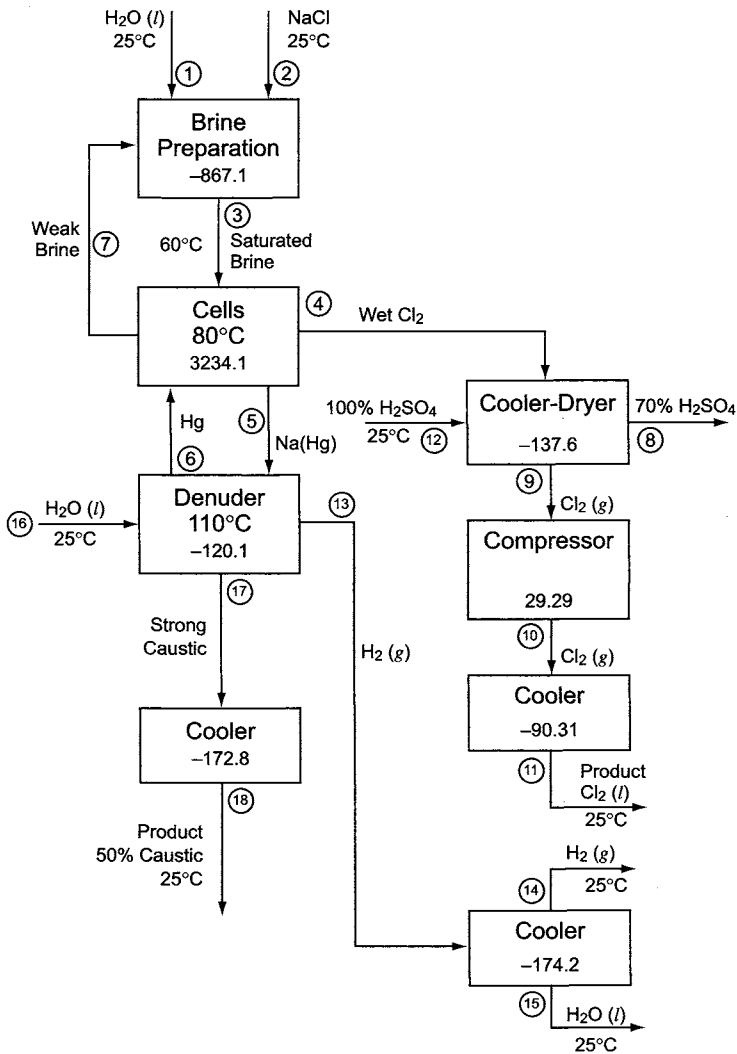


FIGURE 10.2.10. Process flowsheet for chlor-alkali mercury cell. (The numbers inside the process equipment refer to the enthalpy change in kWh ton^{-1} of chlorine.)

TABLE 10.2.2. Mass balance for Chlor-Alkali Mercury Cell Process (All mass units are kg/kg Cl₂)

Stream #	1	2	3	4	5	6	7	8	9	10	11	12	13	14	15	16	17	18
T (°C)	25	25	60	80	80	110	80	25	25	148	25		110	25	25	25	110	25
P(atm)	1.0	1.0	1.0	1.0	1.0	1.0	1.0	1.0	1.0	3.4	7.62		1.0	1.0	1.0	1.0	1.0	1.0
H ₂ O	0.15	30.59	0.15				30.44	0.15					0.133	0.008	0.125	1.754	1.12	1.12
H ₂													0.028	0.028				
NaCl		1.637	11.04				9.403											
Cl ₂				1.0					1.0	1.0	1.0							
Na					0.690	0.046												
NaOH																		1.12
Hg					459	459												1.12
H ₂ SO ₄								0.35				0.35						

a mercury-cell process is presented in Fig. 10.2.9, which is based on the flow sheet in Fig. 10.2.10 and the data in Table 10.2.2.

A general process description for mercury-cell operations is in Chapter 5 and hence, is not elaborated here. It should be noted that these energy flow diagrams do not take into consideration all the process details and can only provide a general description of the energy flows.

REFERENCES

1. F. Hine, *Electrode Processes and Electrochemical Engineering*, Plenum Press, New York (1985), p. 162.
2. *HSC Chemistry Software*, Versions 3 and 4, Outokumpu Research Oy, Espoo (1999).
3. V.A. Ettl, Electrometallurgy and Energy Crunch. In *Energy Considerations in Electrolytic Processes*, Society of Chemical Industry, London, (1980), p. 1.
4. T. Sugino and K. Aoki, *J. Electrochem. Soc., Japan* **27** (1–3), E17 (1959).
5. R.L. LeRoy, C.T. Brown, and D.J. LeRoy, *J. Electrochem. Soc.* **127**, 1954 (1980).
6. R.L. LeRoy, *J. Electrochem. Soc.* **130**, 2159 (1983).
7. T.R. Beck and R.T. Ruggeri, Energy Consumption and Efficiency of Industrial Electrochemical Processes. In H. Gerischer and C.W. Tobias (eds), *Advances in Electrochemistry and Electrochemical Engineering*, Vol. 12, John Wiley & Sons, New York (1981), p. 263.
8. Abam Engineers, Inc., *Final Report on Process Engineering and Economic Evaluations of Diaphragm and Membrane Chlorine Cell Technologies*, Contract #31-109-38-5474, Report; ANL/OEPM-80-9, Argonne National Laboratories, Argonne, IL (1980).

10.3. CURRENT DISTRIBUTION

One of the most important considerations in the design of electrochemical reactors is the distribution of current and potential in the cells. In chlor-alkali cells, nonuniform distributions can result in undesirable reactions occurring at the electrodes, corrosion of cell components during operation, and drying of membranes with localized blister formation. In electroplating operations, nonuniform current distribution leads to nonuniform plating, dendritic growth of metal, impurity deposition on the cathodes, etc. All these effects finally result in poor product quality and increased energy consumption.

The mathematical basis for calculating the potential and current distribution was established by the pioneering contributions of Kasper, Wagner, and others [1–6]. Here, we briefly address these principles and some applications related to chlor-alkali operations. The current distribution in electrochemical systems is governed by cell geometry, electrode kinetics, and mass transfer considerations. These individual contributions to current distribution are called primary, secondary and tertiary current distributions.

10.3.1. Primary Current Distribution

Primary current distribution depends only on cell geometry if the potential is uniform over the electrode, when the activation overpotential is assumed to be zero and mass-transfer effects are considered to be absent. This can be determined generally by solving the Laplace equation (1) in the bulk using either Neumann or Dirichlet boundary conditions. The Dirichlet boundary condition specifies the potential on the electrode, whereas the

Neumann boundary condition specifies flux on the surface. The solution to the Laplace equation gives the potential distribution, and differentiation of the potential distribution with respect to the chosen direction (usually orthogonal to the electrode surface) provides the primary current distribution.

Let us now consider two parallel plates maintained at potentials V_1 and V_2 , respectively (Fig. 10.3.1A). The Laplace equation may be written as:

$$\text{div grad } V = \frac{d^2 V}{dx^2} + \frac{d^2 V}{dy^2} = 0 \quad (1)$$

Assuming no end effects, the boundary conditions are:

$$V = V_1 \quad \text{at } x = 0$$

$$V = V_2 \quad \text{at } x = d$$

Solution of Eq. (1) leads to

$$V = \frac{V_0 - V_1}{d}x + V_1$$

Since

$$i = -k \text{ grad } V = k \frac{dV}{dx} \quad (2)$$

$$i = \frac{k}{d}(V_0 - V_1)$$

where k is the conductivity of the medium and i is the current density. When the electrode configuration is changed to that in Fig. 10.3.1B, as in a test cell for electroplating, named the Hull cell, it can be shown that, at a given position on the inclined cathode, the current density is proportional to the inverse of the distance between the electrodes. It should be noted that that current tends to concentrate at sharp corners. If the electrode has a saw-tooth configuration, the current density will be high at the peak and low in the valley.

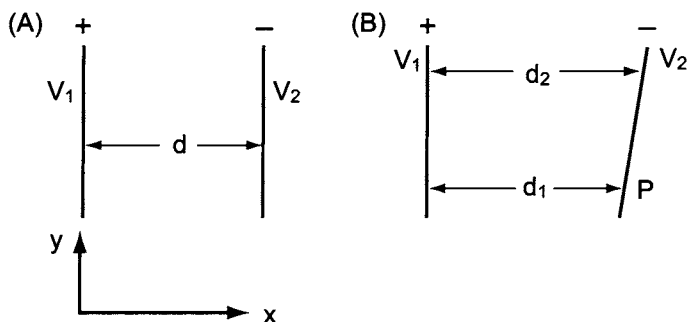


FIGURE 10.3.1. Schematic of a cell with parallel plates (A) and with an inclined cathode (B).

The examples provided above are for simple geometries. The potential distribution becomes complicated as the electrode geometry becomes more complex. Also, it is difficult to solve the Laplace equation and realize an analytical solution. This forces one to solve the problem numerically.

Let us now examine the two-dimensional field shown in Fig. 10.3.2. The Laplace equation and the boundary conditions are as follows:

$$\frac{\partial^2 V}{\partial x^2} + \frac{\partial^2 V}{\partial y^2} = 0 \quad (3)$$

$$V = 0 \quad \text{at } x = 0$$

$$V = V_0 \quad \text{at } x = a$$

$$\frac{\partial V}{\partial y} = 0 \quad \text{at } y = 0$$

and

$$\frac{\partial V}{\partial y} = 0 \quad \text{at } y = b$$

where a and b refer to the electrode distance and width of the cell, respectively. The solution of the Laplace equation, represented by a Fourier series [7], is simple when the field is unrestricted in all directions. However, in the typical case of parallel-plate electrodes in a rectangular cell, the presence of insulating walls surrounding the electrodes makes the mathematical treatment more difficult.

A two-dimensional field for electrodes of relatively simple geometry can be calculated by using a conformal transformation based on the theory of complex functions. Let us consider two complex variables, z and w , with the latter a function of z , that is,

$$z = x + jy \quad (4)$$

$$w = u + jv \quad (5)$$

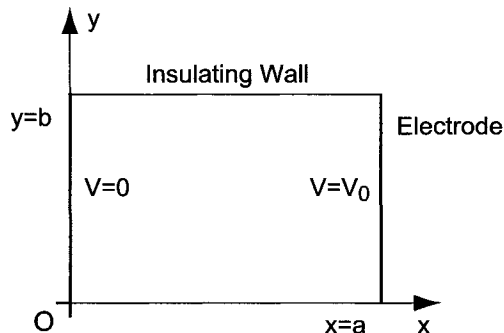


FIGURE 10.3.2. A rectangular cell with parallel flat-plate electrodes.

where j is the imaginary operator. Substituting these equations into the Laplace equation, we have:

$$\frac{\partial u}{\partial x} = \frac{\partial v}{\partial y}, \quad \frac{\partial u}{\partial y} = -\frac{\partial v}{\partial x} \quad (6)$$

$$\frac{\partial^2 u}{\partial x^2} + \frac{\partial^2 u}{\partial y^2} = \frac{\partial^2 v}{\partial x^2} + \frac{\partial^2 v}{\partial y^2} = 0 \quad (7)$$

Figure 10.3.3 shows the complex coordinates of the z - and w -planes, and the curve on the w -plane corresponds to the curve on the z -plane because w is a function of z as shown by Eq. (5). The line or figure on the z -plane is thus transformed on the w -plane conformally. The groups of lines at constant u and v may cross each other orthogonally, and the curves transformed on the z -plane are also orthogonal. In other words, the groups of lines on the z -plane correspond to the given values of u and v , illustrating the stream lines and the equipotential lines.

Let us now take Eq. (8) as an example for the conformal transformation:

$$w = \log z \quad (8)$$

or

$$u + jv = 0.5 \log(x^2 + y^2) + j \tan^{-1}(y/x) \quad (9)$$

Therefore,

$$(x^2 + y^2) = \exp(2u) \quad (10)$$

$$y/x = \tan v \quad (11)$$

Equation (10) appears as concentric circles on the x - y plane with a parameter u , while Eq. (11) represents straight lines radiating from the origin with a slope of $\tan v$ (Fig. 10.3.4). A straight line on the w -plane, $u = u_1$ for example, corresponds to a circle on the z -plane, and $v = v_1$ is related to a radial line on the z -plane. Therefore, if two electrodes are positioned at a pair of circles, the concentric circles between the two electrodes denote equipotential lines at equal intervals, and the radial lines are the flow lines of electric current. As shown in the figure, the smaller the diameter, the smaller the gap between neighboring circles, indicating that the potential gradient becomes large as the diameter decreases.

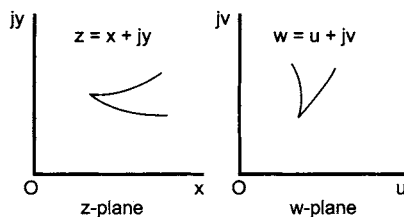


FIGURE 10.3.3. Conformal transformation between the z -plane and the w -plane.

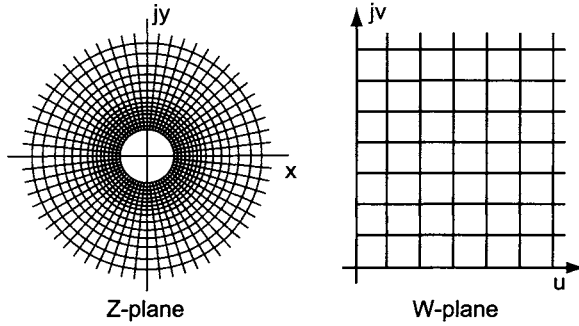


FIGURE 10.3.4. Conformal transformation with $w = \log z$.

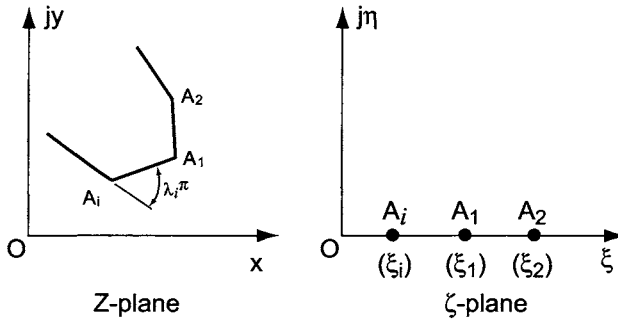


FIGURE 10.3.5. Schwarz-Christoffel transformation.

The conformal transformation is an approach to calculate complex potential fields by means of transmapping two holomorphic functions such as z and w , as described earlier. The potential field on the z -plane can be obtained if a function $w = f(z)$ is known. When the potential field is not described by a known function, it can be analyzed by the Schwarz-Christoffel transformation, which is outlined here.

The upper domain of the ξ -plane, an intermediate function or plane, in the inside of the convex polygon on the z -plane, shown in Fig. 10.3.5, is mapped by:

$$z = C_1 \int \prod_{i=1}^n (\xi - \xi_i)^{-\lambda_i} d\xi + C_2 \tag{12}$$

$$\sum_{i=1}^n \lambda_i = 2 \tag{13}$$

where C_1 and C_2 are constants, and λ_i is the external angle at point A_i of the polygon.

The relationship between z and w is:

$$z - ja = \frac{a}{\pi} (\xi - \log \xi) \tag{14}$$

$$w - jV = -\frac{V}{\pi} \log \xi \tag{15}$$

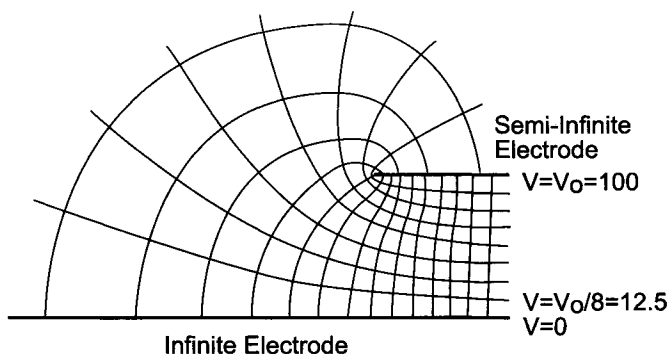


FIGURE 10.3.6. Distributions of potential and current near the semi-infinite electrode.

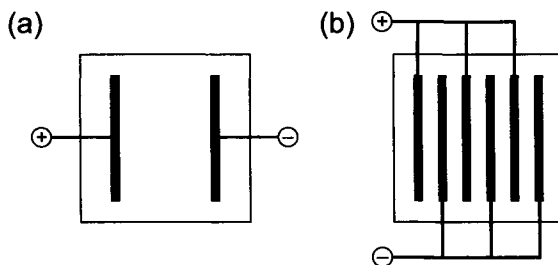


FIGURE 10.3.7. General configurations of electrolytic cells.

Figure 10.3.6 illustrates the equipotential lines and the current lines near a semi-infinite electrode. The current density is uniform on the infinite electrode (at the bottom) in the region facing the top electrode and decreases in the region where there is no electrode at the top. The potential lines concentrate at the edge of the upper electrode, indicating steep gradients and thus, large local current densities rising theoretically to infinity at the edge.

Figure 10.3.7 depicts two typical configurations of electrolytic cells: one is a rectangular cell having a pair of flat-parallel electrodes (A), and the other is a cell with multiples of electrodes (B). Hine [1] gives some examples describing the electric fields in the configurations shown in Fig. 10.3.7.

10.3.2. Secondary Current Distribution

The primary current distribution of Section 10.3.1 is influenced only by the cell geometry if the potential is uniform over the electrode surface. Secondary current distribution also takes into account electrode kinetics, which enters into the Laplace equation as a boundary condition at the electrode surface. Mass-transfer effects, however, are not considered at this level of the current distribution description.

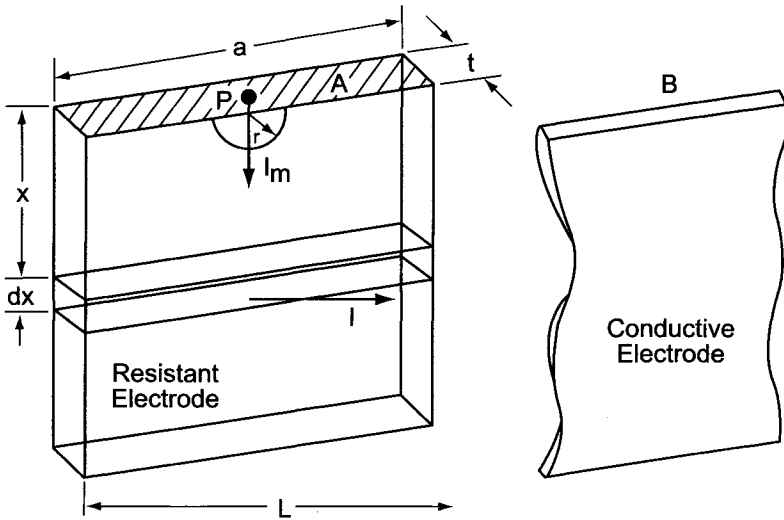


FIGURE 10.3.8. A resistant electrode in parallel with a perfectly conductive electrode.

Let us now examine the effect of overvoltage on the current distribution on a resistive, flat-plate electrode parallel to a flat counter electrode (Fig. 10.3.8). The counter electrode is assumed here to be nonpolarizable.

The overvoltage, η , as a function of the current density, i , is represented by the Tafel equation:

$$\eta = \frac{RT}{\beta F} \log \left(\frac{i}{i_0} \right) \tag{16}$$

where i_0 is the exchange current density, and β is the transfer coefficient. Equation (16) can be assumed to be linear in a limited range of current density as:

$$\eta = \eta_0 + ki \tag{17}$$

where η_0 is the value of η at $i = 0$ and k is the slope of the line with units of $\Omega \text{ cm}^2$. The differential equation describing the current flow at the working electrode can be written as:

$$i = -\frac{di_m}{dx} = \frac{V - \eta}{R_s} \tag{18}$$

where $R_s = \rho L$, ρ is the resistivity of the solution, L is the interelectrode gap, and i_m is the current passing through unit length of electrode.

From Eqs. (17) and (18), it follows that:

$$-\frac{di_m}{dx} = \frac{V - \eta_0}{R_s[1 + (k/R_s)]} \tag{19}$$

Since

$$-\frac{dV}{dx} = R_m i_m \quad (20)$$

where R_m = electric resistance of the electrode, we have,

$$\frac{d^2 i_m}{dx^2} = \left[\frac{R_m}{R_s [1 + (k/R_s)]} \right] i_m \quad (21)$$

Solving Eq. (21),

$$i_m(x) = i_m(0) e^{-\lambda_1 x} \quad (22)$$

$$\lambda_1^2 = \frac{R_m}{R_s [1 + (k/R_s)]} = \frac{R_m}{\rho L [1 + (k/\rho L)]} \quad (23)$$

$$\frac{i}{i(0)} = e^{-\lambda_1 x} \quad (24)$$

for $k > 0$.

It follows from Eq. (24) that $i/i(0)$ will be 1 when λ_1 is small or when the polarization resistance is large. The term $k/\rho L$, termed the Wagner number [1], is important in determining the effect of polarization on the current distribution. Note that when the electrode kinetics are slow, uniform current distribution prevails regardless of the shape of the electrode.

Wagner [3] examined the effect of overvoltage on the current distribution as a finite plate electrode, assuming a linear relationship between the overvoltage and the current density as:

$$V_c = E + \eta_0 + \frac{k}{\rho} \left(\frac{dV}{dn} \right) \quad (25)$$

where V_c is the cell voltage, E is the thermodynamic decomposition voltage, and n is the direction of the current.

The general solution to the Laplace equation was found to be an expression with a Fredholm integral of the second kind, presented graphically in Fig. 10.3.9. These results show that the current distribution becomes more uniform as $k/\rho a$ increases.

The Wagner number W_A can also be expressed in terms of the Tafel slope and the exchange current density i_0 as follows. The rate equation, when the backward rate is neglected, can be written as:

$$i = i_0 \exp(\eta/f) \quad (26)$$

$$f = \frac{RT}{\beta F}$$

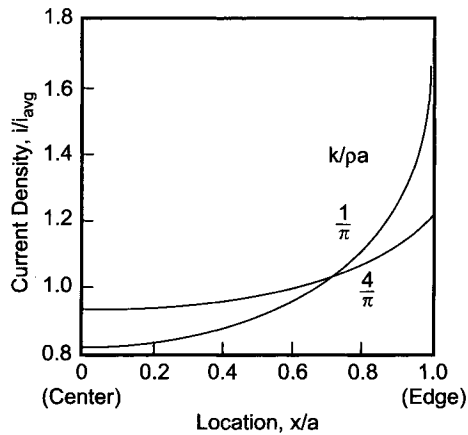


FIGURE 10.3.9. Effect of polarization on the current distribution on the electrode [3]. k = Slope of the current-voltage curve; ρ = resistivity of the solution; a = half width of the electrode.

It follows from Eq. (26) that:

$$\frac{d\eta}{di} = k = \frac{f}{i_0 \exp(\eta/f)} = \frac{f}{i} \quad (27)$$

Thus,

$$W_A = \frac{f}{i\rho L} \quad (28)$$

10.3.3. Tertiary Current Distribution

Tertiary current distribution takes into account cell geometry, electrode kinetics, and mass-transfer effects. Solutions to the tertiary current distribution are very complex, requiring the use of high-speed computation. The list of equations for simultaneous solution illustrates the complexity:

1. Momentum equation for the velocity vector components.
2. Convective diffusion equation for the concentration profile. (This requires a knowledge of the current density profile, which is not known presently.)
3. Voltage balance equation.
4. Complete electrochemical rate equation, which is an exponential relationship.
5. Laplace equation in the bulk, using the current distribution at the electrode surface.
6. Expression for the concentration overvoltage, which is logarithmic.

One has to assume a current distribution profile and solve all these equations iteratively until convergence is achieved. Fortunately, most industrial processes, specifically chlor-alkali, seek to mitigate the mass-transfer effects and therefore, in most cases, solution to

the secondary current distribution should suffice. A good electrochemical engineering design principle is to make the current distribution as uniform as possible.

10.3.4. Numerical Methods

Because of the complex geometries and the nonlinear boundary conditions involved in the current distribution problems, there are few analytical solutions. The primary concurrent distribution profiles for various geometries have been calculated and tabulated in an excellent series of papers by Kojima [8,9] and Klingert *et al.* [10]. Prentice and Tobias [11] reviewed current distribution problems solved by numerical methods in the literature. The finite difference method and the finite element method are widely used for determining current distribution profiles.

The interested reader will find details related to the computational aspects and to the various programs commercially available to solve these boundary value problems in refs [9,11,12].

10.3.5. Some Examples

A brief outline of the principles involved in the determination of the current/potential distribution between electrodes in an electrolytic medium is presented above to provide an appreciation of the concepts and to direct the reader to the proper literature. Several case studies related to the chlor-alkali industry have been performed, but the information remains proprietary with the cell technology suppliers. Nevertheless, some examples are given here to show the value of understanding the current distribution phenomena in addressing practical problems.

10.3.5.1. Vertical Electrolyzers. Diaphragm and membrane cells are generally vertical. In the case of a bipolar-type electrolyzer, electricity is supplied from both ends of the cell stack, and the current is perpendicular to the electrode surface. On the other hand, electricity is supplied to a tank-type vertical electrolyzer from the top or bottom of the electrode, and this results in ohmic voltage drops within the electrode [1,13,14].

Let us examine a flat-plate electrode at zero potential, positioned in a cell in parallel with a perfectly conductive counter electrode, as shown in Fig. 10.3.10A. The current is fed from the top end of the resistive electrode. In this case, the electrolytic current decreases gradually along the working surface from the top to the bottom because of the ohmic resistance within the electrode. The current density, $i(x)$, at the distance x from the current feed, calculated by using the equivalent circuit shown in (B), is as follows [1,13]:

$$i(x) = i_0 \exp(-\lambda x) \quad (29)$$

$$\lambda^2 = \frac{R_m}{R_s} = \frac{R_m}{\rho L} \quad (30)$$

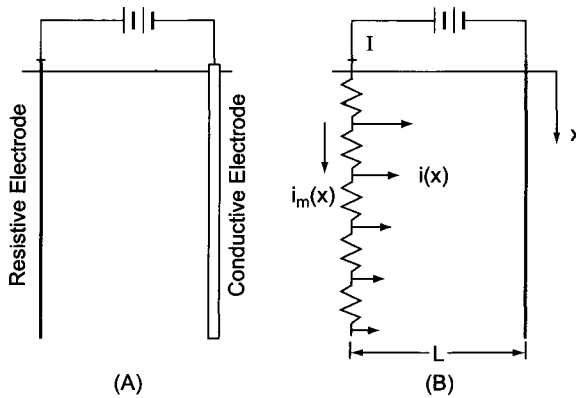


FIGURE 10.3.10. A resistant electrode in parallel with a conductive electrode (A) and the corresponding equivalent circuit (B).

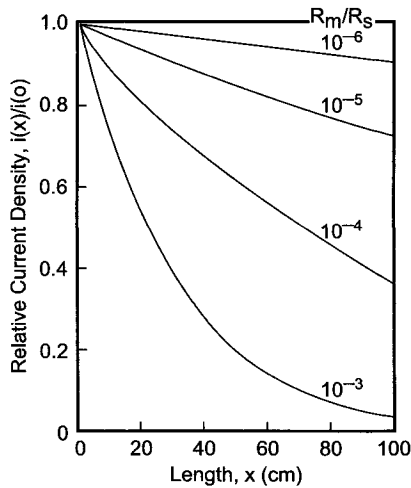


FIGURE 10.3.11. Current distribution for a resistant electrode. Current is fed from the top [13].

where

- $i(x)$ = current density, $A\ cm^{-2}$
- i_0 = current density at $x = 0$, $A\ cm^{-2}$
- R_m = electric resistance of electrode, Ω
- R_s = electric resistance of electrolyte, Ω
- ρ = electric resistivity of electrolyte, $\Omega\ cm$
- L = interelectrode gap, cm.

Figure 10.3.11 illustrates the reduced current density, $i(x)/i(0)$, as a function of x and λ . This shows the importance of choosing an electrode material with a high conductivity.

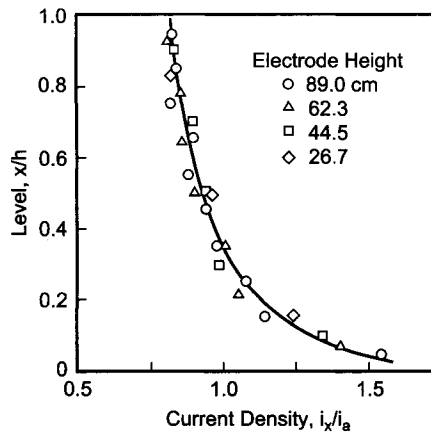


FIGURE 10.3.12. Current distribution along a vertical electrode with gas evolution.

The electrical conductivity of the gas–solution mixture is a function of the gas void fraction, ε . The larger the void fraction, the larger is the resistivity, since

$$\frac{\rho}{\rho_0} = (1 - \varepsilon)^{-3/2} \quad (31)$$

where ρ and ρ_0 are the resistivities of the gas–solution mixture and the electrolytic solution free of gas bubbles, respectively [1].

Since the gas generated ascends along the electrode, the void fraction and the resistivity of the two-phase mixture increases with height. The effect on current density is shown in Fig. 10.3.12, where the ordinate is the reduced height, the abscissa is the reduced current density, h is the electrode height, and i_0 is the average current density over the working surface of the electrode.

At the top of the cell, the gas separates from the solution and the solution free of bubbles falls to the bottom of the cell. This creates an internal circulation, thereby reducing the gas void fraction, and hence, the voltage drops in the solution. In other words, the design of the solution downcomer in the cells is of great importance for vertical cells containing gas-evolving electrodes.

10.3.5.2. Relative Disposition of Anodes and Cathodes in Diaphragm Cells. In diaphragm cells, it would be ideal if the anode and the cathode were of the same height. Failing this, it would be better if the anode were slightly taller than the cathode. Klingert *et al.* [10] have developed the primary current distribution for the geometry of L-shaped cathodes. Figure 10.3.13 shows a simplified model of the top of the cathode. α represents the brine level over the cathode, β to the distance between the anode and cathode, and B to the cathode edge.

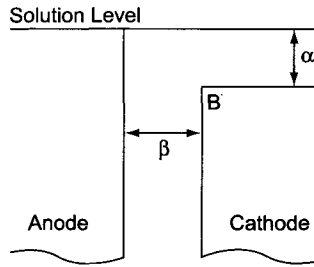


FIGURE 10.3.13. Schematic of electrodes of different heights immersed in a solution.

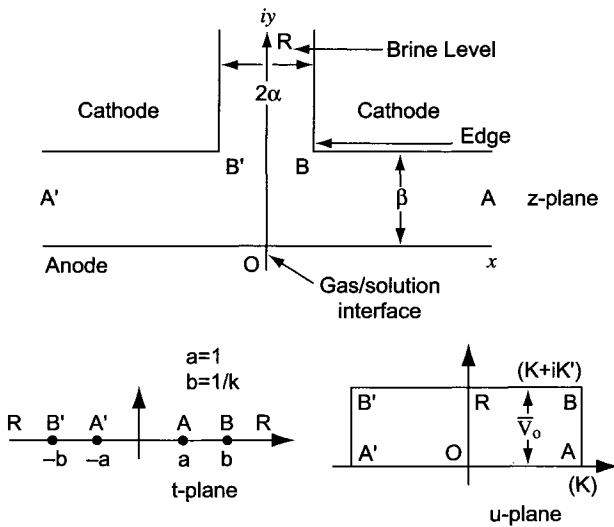


FIGURE 10.3.14. Schwarz-Christoffel transformation in the z -, t -, and u -planes.

We may examine the potential field near the cathode edge B by conformal transformation (Section 10.3.1). Figure 10.3.14 illustrates the three complex planes required for the calculations. The z -plane in Fig. 10.3.14 is turned around 90° and drawn symmetric to the y -axis for the purpose of these calculations.

The upper half of the t -plane is transformed in the z -plane conformally by the Schwarz-Christoffel mapping as follows.

$$\frac{dz}{dt} = C_1 \frac{\sqrt{t^2 - b^2}}{t^2 - a^2} \tag{32}$$

Substituting

$$t = sn u \tag{33}$$

into Eq. (32) with $a = 1$ and $b = 1/k$ and integrating it results in:

$$\begin{aligned}
 z &= C_1 \int \frac{\sqrt{sn^2 u - 1/k^2}}{sn^2 - 1} cnu \cdot dn u \, du + C_2 \\
 &= jC_1 \int dn^2 u \cdot du + C_2 = -jC_1 E(u) + C_2 \\
 u &= 0 \quad \text{at } z = 0 \quad \text{and hence } C_2 = 0 \\
 z &= -jC_1 E(u)
 \end{aligned} \tag{34}$$

Since $z = \alpha + j\beta$ and $u = K + jK'$ at point B, we have:

$$C_1 = \frac{\alpha + j\beta}{K' - E' - jE}$$

k refers to the modulus of the Jacobi elliptic function and k' is the complementary modulus. K and K' are the complete elliptic integrals of the first order, and E and E' are the complete elliptic integrals of the second order.

Substituting C_1 in Eq. (34) results in:

$$z = \frac{E(u)}{(K' - E')^2 + E^2} [\alpha(E - E' + K') + \beta(K' - E') + j\beta E] \tag{35}$$

The u -plane represents the potential plane and hence the current density on the cathode surface is represented by the equation:

$$\frac{i}{i_0} = \frac{\partial u}{\partial z} \tag{36}$$

The above relationships describe the current distribution profile on the top of the cathode finger as shown in Fig. 10.3.15. The ordinate of the figure is the local current density index on the upper surface of the cathode finger and the abscissa is the distance from the cathode edge. The current distribution varies with the ratio α/β . When the liquid level α in the catholyte goes down because of diaphragm pluggage, the top surface of the cathode is not cathodically protected and the rate of corrosion increases. Therefore, the protected area x_L on the cathode is longer when the liquid level is high. As the cathodic protection current density increases with temperature and concentration of caustic, it is desirable to maintain as high a level as is permitted by design and operational constraints.

Let us assume that a safe cathodic protection current required to protect this area is 10% of the total current density, and calculate the distances on the top of the finger from the sharp corner. These results are tabulated in Table 10.3.1. If $\beta = 1.5\text{--}1.8$ cm, and the welds are located 0.6 cm from the sharp corner, a ratio α/β of 0.25 will protect

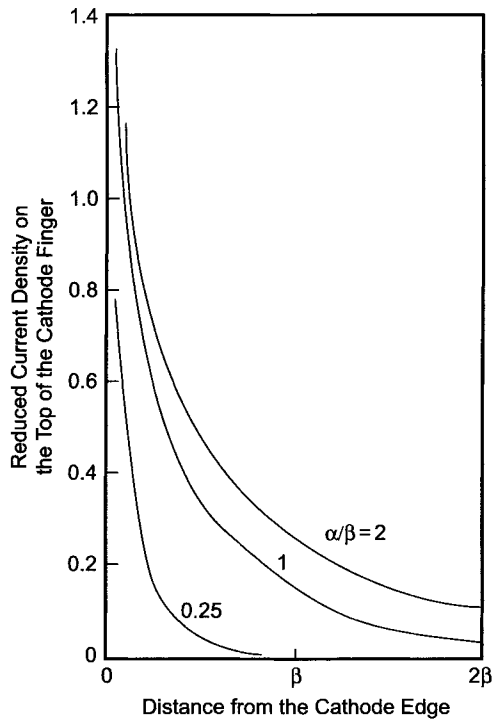


FIGURE 10.3.15. Current distribution on the upper surface of the cathode in a diaphragm cell. Reduced current density is defined as the ratio of the local current density, i , to the average current density, i_R .

TABLE 10.3.1. Critical Distances at which $i/i_R = 0.1$

α/β	Critical distance
0.25	0.33β
0.5	0.64β
1	1.42β
2	2.15β

the weld. In other words, if the anode is 6.35 mm above the top of the cathode finger, the welds will be cathodically protected.

10.3.5.3. Cathode Corrosion. One of the problems encountered with MDC-29 diaphragm cells is the severe cathode corrosion at the cell liquor/hydrogen interface near the cathode screen, which prevents deposition of good diaphragms. The primary current distribution profiles were calculated [15] using the finite difference method and the results

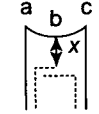
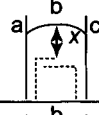
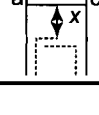
Electrode Configuration	Gap (X) (cm)	Current Density (A/m ²)		
		Location a	Location b	Location c
	3.49	0.074	0.189	0.068
	1.90	0.109	0.434	0.096
	1.59	0.124	0.543	0.105
	1.90	0.290	0.361	0.197
	1.59	0.361	0.434	0.256
	0.95	0.724	0.868	0.357
	2.70	0.132	0.240	0.118
	1.90	0.181	0.434	0.144
	1.59	0.206	0.434	0.167

FIGURE 10.3.16. Primary current distribution profiles for various cathode geometries.

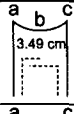
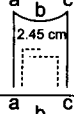
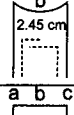
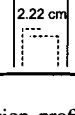
MDC Type	Current Density (A m ⁻²)	Electrode Configuration	Current Density (A/m ²)		
			Location a	Location b	Location c
29	2.17		0.074	0.189	0.068
55	2.17		0.104	0.290	0.093
55	2.25		0.107	0.299	0.096
21	1.55		0.155	0.239	0.095

FIGURE 10.3.17. Primary current distribution profiles for various MDC cathode geometries. (Cathodic protection current density = 0.099 A m⁻².)

are shown in Fig. 10.3.16. Assuming the cathodic protection current to be 0.93 kA m⁻² and the average cathode current density to be 2.17 kA m⁻², it can be seen that Case A may develop localized corrosion on the cathode screen corners. The cell configurations B and C provide better current distribution without any corrosion problems. Also, it may be noted that extending the anodes would overcome the corrosion problem, as these corrosion-prone areas will now start receiving more current and become cathodically protected. Figure 10.3.17 illustrates the current distribution in the corners for various MDC cells of ELTECH [15].

10.3.5.4. Membrane Cells. The ion-exchange membranes are supported in the cell by the anode mesh. They are normally laminated by a thin layer of carboxylate polymer

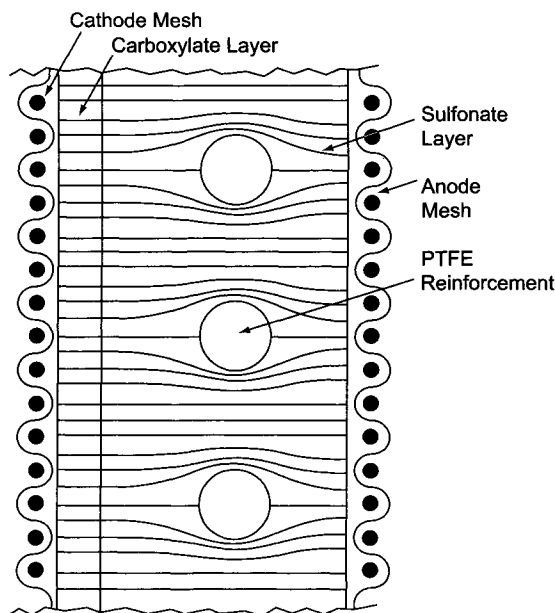


FIGURE 10.3.18. Current distribution in a zero-gap type membrane cell.

on the cathode side to prevent the transport of hydroxyl ions from the cathode compartment. The voltage drop across the membrane is small, as the highly resistive carboxylic layer is thin. In the finite-gap cells that characterized early stages of development, the cathode mesh was located far from the membrane. In the newer designs, referred to as zero-gap, the distance between the cathode and the membrane is almost zero. The electrolytic gas bubbles are liberated from the respective electrodes and dispersed in the bulk of the solution. However, gas bubbles often touch the perfluorinated membranes and tend to remain in the narrow gap between the membrane and the electrode. This causes a significant increase in the cell voltage. The membrane surface is therefore modified with a hydrophilic layer to prevent the attachment of the gas bubbles [16].

Figure 10.3.18 illustrates the structure of the electrode/membrane system where the membrane (e.g., Nafion[®] 900 Series) is reinforced by a nonconductive polytetrafluoroethylene (PTFE) fabric. Note that the current flux deforms around the PTFE reinforcement, leading to an increase in the voltage drop through the membrane. Therefore, the arrangement of the PTFE reinforcement must be optimized for mechanical strength and voltage drop.

REFERENCES

1. F. Hine, *Electrode Processes and Electrochemical Engineering*, Plenum Press, New York (1985), p. 313.
2. C. Kasper, *Trans. Electrochem. Soc.* **77**, 353, 365 (1939); **78**, 131, 147 (1940).

3. C. Wagner, *J. Electrochem. Soc.* **98**, 115 (1951).
4. J.T. Weber, *J. Electrochem. Soc.* **101**, 271 (1954); **102**, 344, 420 (1955); **103**, 64, 138 (1956).
5. F. Hine, S. Yoshizawa, and S. Okada, *J. Electrochem. Soc.* **103**, 186 (1956).
6. F. Hine, *Kogyo Kakaku Zasshi (J. Chem. Soc. Japan, Industrial Chemistry Section)* **56**, 875 (1956).
7. E.T. Whittaker and G.N. Watson, *A Course of Modern Analysis*, 4th Edition, Cambridge University Press, Cambridge (1927), p. 448.
8. K. Kojima, *Research Reports of the Faculty of Engineering, Niigata University*, **13**, 183 (1964); **14**, 117 (1965); **14**, 131 (1965).
9. R.N. Fleck, *Master's Thesis*, University of California (1964).
10. J.A. Klingert, S. Lynn, and C.W. Tobias, *Electrochim. Acta* **9**, 297 (1961).
11. G.A. Prentice and C.W. Tobias, *J. Electrochem. Soc.* **129**, 72 (1982).
12. J.S. Newman, *Electrochemical Systems*, Prentice-Hall, Englewood Cliffs, NJ (1973), p. 340.
13. S. Komagata, *Researches of the Electrotechnical Laboratory*, Ministry of Communications, Tokyo, No. 294 (1930).
14. C.W. Tobias and R. Wijsman, *J. Electrochem. Soc.* **100**, 459 (1953).
15. C.-P. Chen and T.V. Bommaraju, Investigation of Cathode Side Screen Corrosion, in 13th Annual Chlorine/Chlorate Seminar, ELTECH Systems Corporation, Cleveland, OH (1997).
16. E.I. Baucom, Nafion® Membranes for the 1990s. In T.C. Wellington (ed.), *Modern Chlor-Alkali Technology*, vol. 5, Elsevier Applied Science, London (1992), p. 131.

10.4. FLUID PROCESSING

10.4.1. Fluid Dynamics

10.4.1.1. Bernoulli's Theorem. Consider a tube in a steady-state situation as shown in Fig. 10.4.1. The masses of fluid entering the tube from the left-hand side and leaving from the right-hand side in time dt are $\rho_1 A_1 u_1 dt$ and $\rho_2 A_2 u_2 dt$, respectively, where ρ is the density of fluid, A is the cross-sectional area of the tube, and u is the flow velocity. Since the quantities of fluid passing through the sections A_1 and A_2 are equal to each other,

$$\rho_1 A_1 u_1 = \rho_2 A_2 u_2 \quad (1)$$

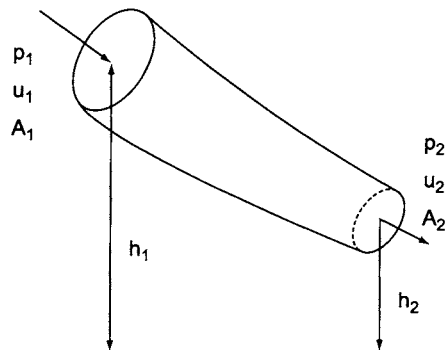


FIGURE 10.4.1. Schematic of liquid flow through a pipe.

In the case of an incompressible fluid, the density is constant in the flow tube, and

$$A_1u_1 = A_2u_2 \quad (2)$$

Equations (1) and (2) are known as the equations of continuity.

Now, we may consider gravity flow of an incompressible fluid. The kinetic energy accompanying the flow for time dt is $\frac{1}{2}(\rho A_1u_1dt)u_1^2$. The potential energy and the pressure energy are $(\rho A_1u_1dt)gh_1$ and $p_1A_1u_1dt$, respectively, where g is the acceleration due to gravity, h is the elevation, and p is the pressure. Since the total energy in the flow tube must be constant,

$$\begin{aligned} \frac{1}{2}(\rho A_1u_1 dt)u_1^2 + (\rho A_1u_1 dt)gh_1 + p_1A_1u_1 dt \\ = \frac{1}{2}(\rho A_2u_2 dt)u_2^2 + (\rho A_2u_2 dt)gh_2 + p_2A_2u_2 dt \end{aligned} \quad (3)$$

Substituting Eq. (2) into Eq. (3) leads to:

$$\frac{1}{2}\rho u_1^2 + \rho gh_1 + p_1 = \frac{1}{2}\rho u_2^2 + \rho gh_2 + p_2 \quad (4)$$

or

$$\frac{1}{2}u^2/g + p/\rho g + h = \text{constant} \quad (5)$$

When the pressure, p , is expressed in engineering units, the standard acceleration due to gravity, g_c , should be included in Eq. (5).

$$\frac{1}{2}u^2/g + pg_c/\rho g + h = \text{constant} \quad (6)$$

Since the three terms in the left-hand side of Eqs. (5) and (6) have the dimensions of height, they are respectively called the velocity head, the pressure head, and the potential head. In other words, the first term and the second term correspond to the heights of fluid required to maintain the flow velocity u at the static pressure, p .

10.4.1.2. Flow Pattern. Any fluid in contact with a wall is stagnant because of frictional forces. These are proportional to the fluid's viscosity. Although the velocity increases gradually with the distance from the wall, an internal friction still exists. When the fluid is allowed to flow along the x -axis, a velocity gradient is generated in the direction of the y -axis. The force caused by friction, f , is expressed as:

$$f = \mu A(du/dy) \quad (7)$$

where μ is the viscosity. We may now consider flow of an incompressible fluid in a straight pipe of diameter $2r_0$ at a relatively low velocity, u , with a small concentric

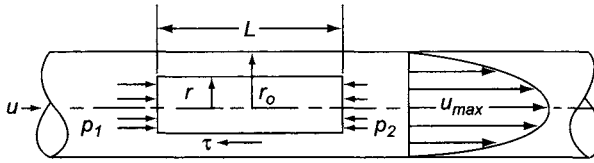


FIGURE 10.4.2. Laminar flow in a pipe (Poiseuille flow).

element of diameter $2r$ and length L as shown in Fig. 10.4.2. The friction terms on the inside surface and the outside surface of this element are:

$$f = 2\pi r L \mu (du/dr)$$

$$f + df = 2\pi r L \mu (du/dr) + d(2\pi r L \mu du/dr)$$

The force on a small ring, dr , caused by the pressure drop $(p_1 - p_2)$ is $2\pi r dr (p_1 - p_2)$, and is equal to df , that is,

$$d(2\pi r L \mu du/dr) = 2\pi r (p_1 - p_2) dr$$

or

$$L \mu d(r du/dr) = (p_1 - p_2) r dr$$

Integrating this twice, we have

$$u = -(p_1 - p_2) r^2 / 4L\mu + \text{constant}$$

Since the flow velocity at the wall is zero,

$$u = (p_1 - p_2) (r_0^2 - r^2) / 4L\mu \quad (8)$$

Hence, the maximum flow velocity at the center of pipe is given by Eq. (9).

$$u_{\max} = (p_1 - p_2) r_0^2 / 4L\mu \quad (9)$$

The volume of flow, in unit time, can now be obtained by integration as:

$$V = \int_0^{r_0} 2\pi r \cdot u \cdot dr = \frac{\pi(p_1 - p_2)}{8L\mu} r_0^4 \quad (10)$$

Also the average flow velocity u_{avg} , can be obtained by dividing Eq. (10) by the sectional area, πr_0^2 , as:

$$u_{\text{avg}} = (p_1 - p_2) D^2 / 32L\mu = u_{\max} / 2 \quad (11)$$

where D is the diameter of pipe. Equation (11) shows that the pressure drop in a laminar flow regime is proportional to the flow velocity, u_{avg} or u_{max} .

As described above, the viscosity of a fluid at relatively low velocities generates laminar flow. When the velocity exceeds a critical level, the inertial force becomes significant compared to the viscosity. This is called turbulent flow. A thorough analysis of turbulent flow is very difficult. However, it is recognized that the shearing stress is proportional to the square of the velocity gradient perpendicular to the solid/fluid interface as:

$$f = \rho L_m^2 (du/dy)^2 \tag{12}$$

where L_m is the length of mixing, which is analogous to the mean free path in the kinetic theory of gases.

The pressure drop is also proportional to the average flow velocity, as described by Eq. (13), which is known as the Fanning equation or the Darcy formula.

$$p_1 - p_2 = 4F_f(L/D) \left(u_{avg}^2/2 \right) \tag{13}$$

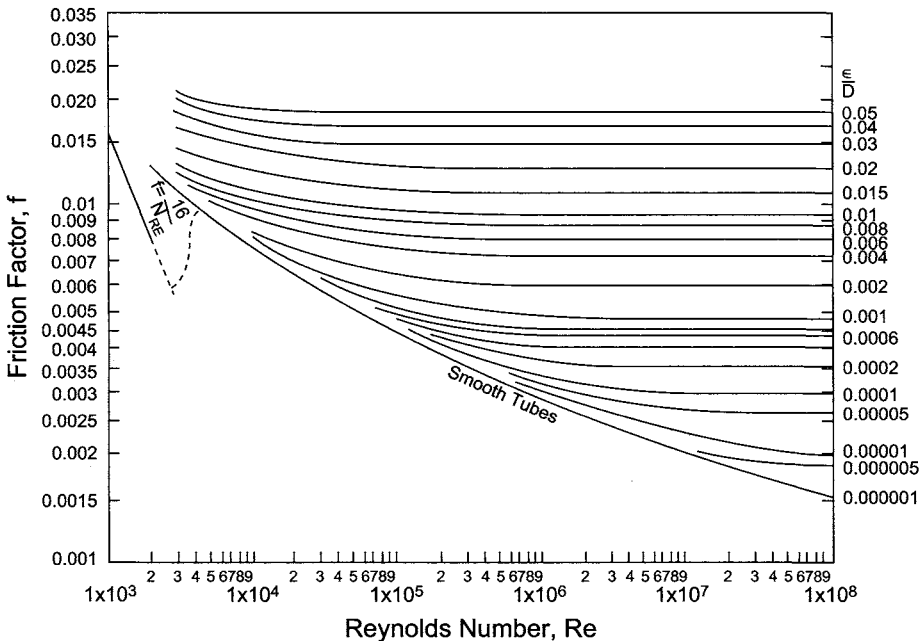


FIGURE 10.4.3. Fanning friction factor as a function of the Reynolds number [2]. ϵ refers to the surface roughness and D to the pipe diameter. (Reproduced with permission of The McGraw-Hill Companies.)

F_f in Eq. (13) is termed Fanning's friction factor. We may now extend Eq. (13) to the region of laminar flow by substituting Eq. (13) into Eq. (11). This results in:

$$F_f = 16/Re \quad (14)$$

$$Re = Du_{avg}\rho/\mu \quad (15)$$

Figure 10.4.3 shows the friction factor [1] as a function of the Reynolds number Re . It is clear that F_f is inversely proportional to Re when Re is less than 2,300. F_f deviates increasingly from Eq. (14) at high Re values. Thus the critical value or the upper limit of Re for laminar flow is about 2,000–2,300. Turbulent flow is established at Re values of higher than 4,000. In the Re range of 2,300–4,000, the flow is in the transition state. In the turbulent flow regime, the friction factor is greatly affected by the surface morphology of the solid in contact with fluid (i.e., the pipe).

Several mathematical descriptions modeling flow in a pipe under turbulent flow conditions are available along with a number of empirical equations relating F_f and Re [2].

10.4.1.3. Pressure Drop Calculations. In process industries, fluids are usually transported from one point to another by pressure differential through circular piping. The circular shape offers strength and maximum cross-sectional area per unit of wall surface.

Pressure drop calculations are essential in designing and optimizing pipelines and sizing the pumps and compressors that transport the fluids. Equations commonly used for calculating the pressure drops are discussed in this section.

10.4.1.3A. Noncompressible Fluid Flow. The Darcy formula, Eq. (13), is applicable for noncompressible liquid flow. It applies in all situations with the possible exception of a liquid pressure drop so high that the outlet pressure drops to the vapor pressure of the liquid. This condition has to be avoided by changing the pipe size, decreasing the flow rate, or forcing a back pressure. Re in Eq. (13) is calculated from Eq. (15), the flow velocity from the area of the pipe, A , and the volumetric flow rate, Q , as:

$$u_{Avg} = Q/A \quad (16)$$

The density and the viscosity data are obtained from the physical property data (see Appendix). The value of the Reynolds number will indicate whether the flow pattern is laminar, or turbulent. If the flow is laminar Eq. (14) applies. In turbulent flow, the friction factor [1] can be estimated from Fig. 10.4.3.

The frictional loss, H_L , in feet of fluid, can be calculated [3] by

$$H_L = f(L/D)(u^2/2g_c) \quad (17)$$

10.4.1.3B. Compressible Fluid Flow. Fluid flow is considered noncompressible if the pressure and temperature changes are small enough to cause insignificant changes in the

density. If the density changes more than 5 or 10%, flow is considered compressible. The pressure drop under these conditions [2] is given by

$$p_1^2 - p_2^2 = G^2(RT/M_W)[(4fL/D_H) + 2 \ln(p_1/p_2)] \quad (18)$$

where G is a mass flow rate per unit area, R is the ideal gas constant, M_W is the molecular weight of the fluid, L is the equivalent pipe length, D_H is the hydraulic diameter, and p_1 and p_2 are the pressures at the beginning and end of the pipe, respectively.

The friction-loss calculations apply to straight, uniform pipes. Valves and fittings in a pipeline disrupt flow patterns, increase turbulence, and cause additional pressure losses. Fluid-flow calculations must account for these losses. One method frequently used is to assign each valve and fitting an equivalent length of straight pipe [4]. Many textbooks and handbooks present data in the form of equivalent pipe diameters. A standard elbow, for example, may be shown as equivalent to 30 pipe diameters. In a 100-mm pipe, it is equivalent to 3 m of straight run. Addition of the equivalent lengths of all valves and fittings to the final straight run gives the equivalent length of a pipe system. The term L in Eq. (17) or (18) refers to this equivalent length. This is a simple method and is easy to apply even in hand calculations. However, it is not theoretically sound. Fittings of different sizes are not geometrically similar, and the L/D values assigned to them should really be functions of D . Therefore, an alternative method based on resistance coefficients is used [2].

10.4.1.4. Hydraulic Diameter. The flow in pipes having a circular cross section of $2r_0$ in diameter was described in earlier sections. However, piping with different geometries is used in chemical process plants. In these instances, the Fanning Eq. (13) can be employed, when the term D is replaced by the equivalent or hydraulic diameter.

$$D_H = 4A/L_W = 4R_H \quad (20)$$

where D_H is substituted for D . In Eq. (20), A refers to the sectional area of channel under consideration, L_W is the length of solid /fluid interface or wetted perimeter, and R_H is the hydraulic radius. The values of hydraulic radius for various cases are discussed in the section on "Fluid Dynamics" in ref. [2].

10.4.1.5. Pressure Drops Caused by Geometry. Hydraulic energy is dissipated by non-uniformities such as elbows and bends in a pipeline. Sudden changes of the diameter of flowing ducts, either decreases or increases in the diameter, cause entrance and exit losses. Sudden changes in cross section also increases the pressure drop. Figure 10.4.4 illustrates this effect for an expansion, where eddies form at the sharp edge behind the streamlines. Using a tapered section of pipe, or a diffuser in place of the sudden transition, can reduce the loss of energy.

10.4.1.6. Boundary Layer. The viscosity of a liquid retards its flow in the immediate vicinity of a wall. This affected region is called the boundary layer. Flow in this boundary

layer is calculated from the Navier–Stokes equation and the continuity Eqs. (21) and (22), with the proper boundary conditions.

$$\begin{aligned}\frac{\partial u_x}{\partial t} + u_x \frac{\partial u_x}{\partial x} + u_y \frac{\partial u_x}{\partial y} &= -\frac{1}{\rho} \frac{\partial \rho}{\partial x} + \nu \left(\frac{\partial^2 u_x}{\partial x^2} + \frac{\partial^2 u_x}{\partial y^2} \right) \\ \frac{\partial u_y}{\partial t} + u_x \frac{\partial u_y}{\partial x} + u_y \frac{\partial u_y}{\partial y} &= -\frac{1}{\rho} \frac{\partial \rho}{\partial y} + \nu \left(\frac{\partial^2 u_y}{\partial x^2} + \frac{\partial^2 u_y}{\partial y^2} \right)\end{aligned}\quad (21)$$

and

$$\frac{\partial u_x}{\partial x} + \frac{\partial u_y}{\partial y} = 0 \quad (22)$$

The thickness of the velocity boundary layer near a flat plate, δ_f , is a function of the Reynolds number Re and the distance x from the leading edge of the plate [5]:

$$\delta_f = 4.80x/(Re)^{1/2} \quad (23)$$

On the other hand, δ_f under turbulent flow in the pipeline [6] is:

$$\delta_f = 117r/Re^{7/8} \quad (24)$$

where r is the radius of pipe.

The mass and heat transfer in the bulk of the flow is rapid, via molecular diffusion and not by convection in the boundary layer. This results in a delay in the heat and mass transfer. Therefore, the concept and knowledge of the boundary layer are important for designing heat exchangers and any discussions of chemical processes controlled by mass transfer. In the electrochemical field, there are many processes controlled by mass transfer, mostly the diffusion of a reacting species in the vicinity of the working electrode. An example is copper deposition on the cathode from a copper sulfate solution.

The chlorine evolution reaction and the hydrogen evolution reaction at the anode and the cathode, respectively, in a chlor-alkali cell are controlled by the electrochemical and/or chemical steps rather than by mass transfer. However, the transport phenomena across the separator, either a porous diaphragm or an ion-exchange membrane, are governed by the solution flow near the surface. The disproportionation reaction of hypochlorites in a chlorate cell is diffusion-controlled process. Consequently, knowledge

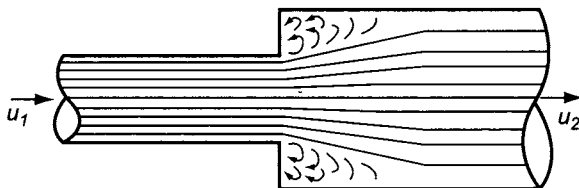


FIGURE 10.4.4. Eddy formation caused by sudden change in pipe diameter.

of the flow pattern and the boundary layer is essential for electrochemical scientists and engineers.

10.4.1.7. Two-Phase Flow [7–9]. In chlor-alkali cells, the chlorine gas and the hydrogen gas is generated at the anode and the cathode, respectively, and the gas–solution mixtures ascend along the respective electrodes. The solution may descend to the cell bottom after leaving the gas at the cell top, resulting in good circulation of electrolyte in the electrolyzer with no additional pumping, and hence efficient transfer of mass and heat in the electrochemical reactor. On the other hand, electrolytic gas increases the electric resistance of solution depending on the gas void fraction, because the gases are nonconductive. An understanding of the flow velocity is therefore essential, to decrease the gas void fraction and hence, the electrical resistance between the electrode gap.

The problem of two-phase flow has been investigated extensively in the field of chemical engineering since the 1950s. Still, the factors involved in two-phase flow are not completely clarified, as it is related to many variables such as the physical properties of the liquid and gas, the volume fraction of gas or the gas void fraction, the flow velocity, and the geometry of the space where the two-phase flow occurs.

The methods for predicting the flow pattern and the pressure drop for fully developed gas/liquid flow are complex and often the accuracy presented in these methods is not required for the pressure drop calculations involved in a chlor-alkali plant. The reader is referred to papers cited in [7–9] for a thorough discussion on two-phase flow.

When a gas and a liquid flow together, different flow patterns are developed based on the concentration of each phase and the physical properties of the fluid. The following is a description of most common flow patterns encountered in a two-phase flow.

There are seven basic flow patterns in horizontal flow. These are shown on the “map” in Fig. 10.4.5 and discussed below.

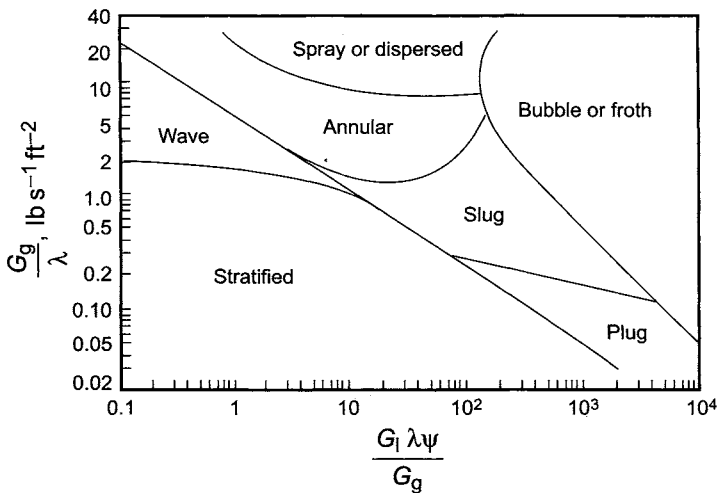


FIGURE 10.4.5. Flow patterns in cocurrent liquid–gas flow through horizontal pipes. G_g = gas mass velocity (lb s⁻¹ ft⁻²); G_1 = liquid mass velocity (lb s⁻¹ ft⁻²); μ_1 = liquid viscosity (centipoise); ρ_g = gas density (lb ft⁻³); ρ_l = liquid density (lb (cu ft)⁻¹); σ = liquid surface tension (dynes cm⁻¹); $\lambda = ((\rho_g/0.075)(\rho_l/62.3))^{1/2}$; $\psi = (73/\sigma)(\mu_1(62.3/\rho_l)^2)^{1/3}$ (from Ref. 2). (Reproduced with permission of The McGraw-Hill Companies.)

Bubble Flow. The gas flows in the form of bubbles along the upper surface of the liquid and the gas bubbles move at about the same velocity as that of the liquid. This pattern is found when there is a high liquid to gas ratio. If the bubbles are dispersed then it is called froth flow.

Plug Flow. As the gas flow rate increases, the bubbles coalesce and form a plug of gas. The plug of gas and liquid alternate along the upper part of the pipe.

Stratified Flow. The gas and liquid flow are segregated in this case, as a result the liquid flows on the bottom and the gas flows on the top of the tube with a distinct boundary.

Wave Flow. This is similar to stratified flow except that a wave is formed at the interface which continues to increase in amplitude as the gas flow is increased.

Slug Flow. As the gas flow further increases, the waves developed in the “wave-flow” are picked up by the moving gas to form a frothy slug which travels at a velocity higher than that of the liquid flow. This can cause dangerous vibrations in the equipment.

Annular Flow. In this pattern, the liquid flows on the wall like a film and gas flows in the center. A portion of the liquid is entrained in the gas as droplets.

Mist or Spray Flow. As the gas rate increases, the annular flow pattern changes to a spray or mist flow.

The flow profiles observed in vertical pipes are:

Bubble Flow. The upward flow of liquid is a continuous phase and the gas is dispersed as fine bubbles.

Slug Flow. As the gas flow increases, the gas flows as large slugs, and the slugs and the liquid flow alternately. The liquid slug contains some gas bubbles and the slug is surrounded by a laminar film. As the gas flow increases, the slug of gas length and its velocity increases.

Froth Flow. As the gas flow further increases, the slug flow pattern changes to froth.

Annular Flow. The liquid travels up the side of the wall and the gas flows in the middle of the pipe at high gas flow rates. Some liquid is entrained in the gas.

Mist Flow. As the gas flow continues to increase, the liquid film from the wall breaks off and entrains in the gas, forming a mist pattern.

References [10–12] describe the methodology for calculating the pipe size in a two-phase flow system.

10.4.2. Removal of Solids

Removal of solids from gases is important in certain processes and in protecting the environment from releases in stack gases and the like. It is less important to our topic and so is not discussed in this chapter. Removal of solids from liquids is important in caustic product processing and particularly so in the brine treatment plant. The unit operations involved are gravity sedimentation, filtration, and centrifugation. Gravity sedimentation removes solids from chemically treated brine (Section 7.5.3). The solids form as the result of addition of chemicals that precipitate ionic impurities from the solution. Since this separation is incomplete, it is necessary to follow the sedimentation operation with brine filters (Section 7.5.4). On the caustic side, polishing filtration (Section 9.3.2.6) is important, especially in mercury-cell plants. In diaphragm-cell plants, it is necessary to remove salt that precipitates in the evaporators from the caustic product. Most of this salt is removed by centrifuges (in more than one step). Removal is incomplete, and the liquor from the centrifuges must be filtered. The sludge formed during sedimentation of treated brine normally leaves the bottom of the settling apparatus as a thin slurry. Various types of filter are used in many plants to increase the solids concentration before disposal. Finally, a special case of filtration is the removal of mists from chlorine gas. There are two applications to consider here (Section 9.1.1), chlorine from the cooling system, which may still contain very fine particles entrained from the cells, and chlorine from the drying towers, which contains a sulfuric acid mist. The apparatus used in these cases normally relies on Brownian motion of particles within the separating elements. This is quite different from the mechanism of conventional filtration. Section 9.1.5 covers the subject of mist elimination.

The sedimentation operation relies on gravity to remove the denser solids from the lighter fluid phase. Settling is opposed by frictional forces between solids and liquids. The characteristics of the particles formed during precipitation, therefore, are critical in sedimentation, and this is the subject of Section 7.5.2.1. Analysis of sedimentation is straightforward when the solids can be represented by the equivalent spheres, using the Sauter mean diameter, and when their concentration is not high (Section 7.5.3.1A). The mechanism of separation becomes more complex when the concentration is high enough to allow interactions between particles. Empirical methods of calculation are then necessary. Some of the methods used are described in Section 7.5.3.1B.

Filtration involves the flow of a fluid through a porous medium. Solid particles present in the fluid entering the filter deposit onto that medium. The typical filter in a brine or caustic plant relies either on a bed of solids or on a porous cloth or cartridge for the separation. The operation becomes semi-continuous, with the filter operating until the amount of solid deposited from the fluid has sufficient effect to make its removal necessary. These filtrations, therefore, require multiple units to allow the operation to continue during the regeneration of one filter and sequence controllers to take the operation through the various steps without constant attention from the operators.

Analysis of the filtration operation is complicated by the fact that the resistance to flow changes continuously as more and more solid deposits on the filter medium.

Flow through packed beds of solids is usually analyzed by considering such characteristics as the porosity of the bed and the sphericity of the particles, and Section 7.5.4.1 shows that the analysis of a filter is helped by considering how the deposit of precipitated solids changes those characteristics. In the other filters, the solids deposit as a cake on the filter medium. The resistances of the filter cake and medium are then additive. When the resistivity, or the resistance per unit thickness, of the cake remains constant throughout operation, the specific resistance increases linearly with the amount of solid deposited. Analytical solutions for the filtration rate are then possible. In the constant-rate case, the pressure drop encountered can be expressed as a function of time (Section 7.5.4.2).

The resistivity of the cake, however, very often increases with time. Under the pressure of filtration or the friction of the fluid that continues to pass through the cake, the filtered particles continue to compact and reduce the area available for flow. Section 7.5.4.2 also describes the empirical methods that are used to characterize the compressibility of the cake. It is significant that the particles produced by precipitation from the brine are often highly compressible. At the same time, they have a tendency to become lodged in the pores of the filter medium. Filtration of these particles can become very difficult. The usual solution to this problem is the use of a filter aid. The filter aid is applied to the surface of the filter medium before introducing the brine. This is the "precoating" operation. Filter aids are selected for their desirable characteristics, and the precoat material protects the pores from penetration by filtered solids while at the same time offering little resistance to the flow. Compression of the precipitates still occurs, and so filter aid ("admix") is also added in small quantities to the brine to improve the characteristics of the cake.

Section 7.5.4.2 discusses filter aids, washing of filter cake to remove occluded liquors, removal and handling of filter cake, and the backwashing of packed bed filters to remove and recover deposited solids.

Many centrifuges are effective filters in which the separating force is intensified by the action of the machine. The major application in the chlor-alkali industry is in diaphragm-cell caustic evaporation. The salt precipitated in that operation comprises about 3% of the evaporator product. Most of this is removed by centrifuges. Section 9.3.2.5 describes the process and the use of two different types of centrifuge.

10.4.3. Compression and Liquefaction

10.4.3.1. Compression. The general equations for an ideal gas under equilibrium conditions appear in Section 10.2. Some of these are important in the study of the compression of gases:

$$dQ = dU + dW \quad (25)$$

$$dW = -p dV \quad (26)$$

$$c_p = dH/dT \quad (27)$$

$$c_v = dU/dT \quad (28)$$

$$c_p - c_v = R \quad (29)$$

We also use the ratio

$$k = c_p/c_v \quad (30)$$

Combining Eqs. (25), (26), and (28),

$$dQ = c_v dT + p dV \quad (31)$$

In an isothermal process,

$$dQ = dW = p dV \quad (32)$$

For an ideal gas $pV = RT$. Then

$$dQ = RT dV/V \quad (33)$$

Integrating from the starting volume, V_1 ,

$$W = Q = RT \ln(V/V_1) \quad (34)$$

In the adiabatic case, $Q = 0$. Then, from Eq. (31),

$$c_v \int dT/T = -R \int dV/V \quad (35)$$

$$\ln(T/T_1) = (R/c_v) \ln(V_1/V) \quad (36)$$

By Eqs. (29) and (30), $R/c_v = k - 1$. Now,

$$T/T_1 = (V/V_1)^{1-k} \quad (37)$$

This equation permits us to calculate the increase in gas temperature during adiabatic compression as a function of the compression and specific heat ratios. Again, using the ideal gas equation, we also have

$$pV^k = p_1V_1^k = \text{constant} \quad (38)$$

Since work is not a point function, the result depends on the path followed in the process, and Eq. (34) is not generally true. In the adiabatic case, the work that must be supplied over the same pressure range is

$$W = p_1 V_1 k / (k - 1) [(p_2/p_1)^{[(k-1)/k]} - 1] \quad (39)$$

For non-ideal gases, this should be multiplied by the compressibility, Z . In the case of chlorine, the error caused by omitting Z is small (and conservative). Since chlorine has a critical pressure of 77.2 bars and is infrequently compressed in its production process

beyond 10 bars, typical reduced pressures in compression are 0.01–0.1. At the inlet conditions, the reduced pressure is quite low, and Z will be about 0.98 or 0.99. When the gas is compressed, Z will be between 0.95 (low temperatures) and 0.98 (typical compressor outlet temperatures).

At typical inlet conditions, k is about 1.32–1.35. This is slightly lower than the specific heat ratio of air. Charts showing the energy required to compress air provide a modest safety factor if used to estimate the compression energy required by chlorine. The quantity $(k - 1)/k$, which appears often in compression calculations, will be about 0.25. If we designate the compression ratio as r , Eq. (39) becomes

$$W = 4RT_1(r^{0.25} - 1) \quad (40)$$

The real value of the specific heat ratio is also a function of operating conditions. Over the operating range of a chlorine compressor, the specific heat ratio decreases slightly from the feed to the discharge.

More significant is the fact that a real compression process is not quite adiabatic. Instead of Eq. (38), it follows a polytropic path in which

$$pV^n = \text{constant} \quad (41)$$

The exponent n is an empirical quantity. In all cases, the power consumption is greater than in the adiabatic case. The exponent n is always greater than k and the two are related by the polytropic efficiency η_p :

$$n = k\eta_p/[k\eta_p - (k - 1)] \quad (42)$$

With a polytropic efficiency of 75%, this reduces to $3k/(4 - k)$, which is very close to 1.5. Practical values of n for both chlorine and hydrogen appear to be about 1.45.

10.4.3.2. Liquefaction. The energy required for liquefaction is the sum of the sensible heat removed from the gas in cooling it to the liquefaction temperature and the latent heat of condensation:

$$Q = q_V + \lambda \quad (43)$$

where

Q = energy removed in liquefaction of a given quantity of gas,
 q_V = sensible heat removed to reduce temperature to point of liquefaction, and
 λ = latent heat removed at constant temperature to condense gas.

If the liquid is subcooled, another sensible heat quantity, q_L , is involved. The sensible heat of the gas at constant pressure is:

$$dq_L = c_p dt \quad (44)$$

where c_p = specific heat of gas at constant pressure.

Equation (44) and q_v in Eq. (43) can be evaluated analytically if a mathematical expression is available for the specific heat. Many of these have been published, and two frequently used equations are

$$c_p = a + bT + cT^2 \quad (45)$$

$$c_p = a + bT + c/T^2 \quad (46)$$

Equation (45), with different values for the constants, also sometimes uses Celsius temperatures. It may also be extended in some cases to include a cubic term. The last term in Eq. (46) demands the use of absolute temperature.

The latent heat of condensation is equal to the latent heat of vaporization at the same conditions. Thermodynamic equations usually are derived in terms of the vaporization process, using the latent heat of vaporization, λ . As a form of activation energy for the formation of vapor, the latent heat determines the slope of the vapor pressure curve. We have the Clausius–Clapeyron equation

$$dP^0/dT = \lambda/T(V - v) \quad (47)$$

where

P^0 = vapor pressure,

V = molar volume of gas,

v = molar volume of liquid.

When $V \gg v$, we have, with ideal gas behavior,

$$dP^0/P = (\lambda/R) dT/T^2 \quad (48)$$

Integration yields

$$\ln(P_2/P_1) = -(\lambda/R)(1/T_1 - 1/T_2) \quad (49)$$

The heat of vaporization of a substance can be obtained from its vapor pressure curve by using Eq. (49).

In practice, the gas fed to liquefaction contains some noncondensable gas. Its sensible heat must be included in Eq. (43) and we have

$$q_v = q_{C1} + q_I \quad (50)$$

where

q_{C1} = sensible heat removed from chlorine gas,

q_I = sensible heat removed from noncondensable gases.

An important factor in liquefaction system design is the effect of liquefaction temperature on the cost of removing energy. Section 9.1.7.2A points out that as the liquefaction temperature becomes lower (and the liquefaction process more effective), the cost begins to rise rapidly. The preceding Section 10.4.3.1 offers a reason for this. The actual cost is in the supply of energy to the refrigeration machinery. Consider the

cycle that the refrigerant follows. It must evaporate at some temperature below the liquefaction temperature itself. The vapor formed then must be compressed to a pressure at which it can be liquefied by plant cooling water. As the liquefaction temperature drops, the range of pressures and the compression ratio of the refrigerant compressor increase. Equation (39) shows how the power required responds to the increase in the compression ratio.

REFERENCES

1. *Kagakukikai no Riron to Keisan* (Theory and Calculation of Chemical Equipment), S. Kamei (ed.), Sangyo Tosho Publ. Co., Tokyo (1959), p. 58.
2. *Chemical Engineers Handbook*, R.H. Perry and D.W. Green (eds), 7th edition, McGraw Hill Book Co., New York (1997), pp. 6–22.
3. *Crane Catalogue 60*, Crane Company, Chicago (1960), pp. 422–430.
4. *Flow of Fluids Through Valves, Fittings and Pipes*, Technical Paper #410, Crane Company, New York, (1976).
5. F. Hine, *Electrode Processes and Electrochemical Engineering*, Plenum Press, New York (1985), p. 64.
6. *Kagakukikai no Riron to Keisan (Theory and Calculation of Chemical Equipments)*, S. Kamei (ed.), Sangyo Tosho Publ. Co., Tokyo (1959), p. 42.
7. *Chemical Engineers Handbook*, R.H. Perry, C.H. Chilton, and S.D. Kirkpatrick (eds), 5th edition, Section 5, McGraw Hill Book Co., New York (1968).
8. D.S. Scott, Properties of Cocurrent Gas-Liquid Flow, In T.B. Drew, J.W. Hoopes, Jr., and T. Vermeulen (eds), *Advances in Chemical Engineering*, vol. 4, Academic Press, New York (1963), p. 199.
9. G.W. Glovier and K. Aziz, *The Flow of Complex Mixtures in Pipes*, Robert E. Krieger Publishing Co., Huntington, NY (1977), p. 292.
10. D.Q. Kern, *Hydrocarbon Processing* **48**(10), 105 (1969).
11. W.J. Davis, *Brit. Chem. Eng.*, **8** (1963).
12. P.D. Hills, *Chem. Eng.* **90**(18), 111 (1983).

10.5. TRANSPORT OPERATIONS

Many of the operations carried out in the process industries in general and in the chlor-alkali industry in particular involve the transfer of mass or energy between phases. This section considers a few that are particularly important in chlor-alkali production.

Section 10.5.1 discusses heat transfer. Perhaps second only to fluid flow, this is the unit operation most often encountered in plant practice. Here we cover only some of the basic principles. In a chlor-alkali plant, the heat transfer process is important in the following steps:

1. heating of brine before electrolysis;
2. cooling of brine during transfer from the electrolysis area;
3. cooling of chlorine;
4. cooling of caustic to maintain temperature in the electrolyzers;
5. heating of brine or caustic to allow concentration by evaporation;
6. cooling of hydrogen to remove water and mercury vapor or heat of compression;
7. cooling of turbine exhaust from cogeneration systems.

Section 10.5.2 covers gas absorption. Absorption has been used for the recovery of chlorine from the uncondensed gas leaving a liquefaction system (Section 9.1.9.1). More highly specialized applications are the removal of water from chlorine gas by sulfuric acid (Section 9.1.4) and the absorption of chlorine in caustic solutions, either as an emergency measure (Section 9.1.10.3) or in the production of bleach solutions (Section 9.1.9.3). Absorption is necessarily a gas/liquid transfer operation. Adsorption is a similar technique involving transfer from either a gas or a liquid phase onto a solid. Section 10.5.3 covers adsorption operations. In a chlor-alkali plant, these include the drying of air in the utility Section (Section 12.4.2), miscellaneous purification steps, and the removal of traces of dissolved chlorine from depleted brine (Section 7.5.9.3B). The mechanism of ion exchange between a liquid and a solid resin differs from that in adsorption, but the mathematics of analysis and the physical arrangement of equipment are quite similar. The engineering aspects of ion exchange, therefore, are often treated along with a discussion of adsorption. Such is the case here. Important applications of ion exchange are the softening and demineralization of water (Section 12.4.3.1) and the softening of brine to the ppb levels of hardness required by membrane cells (Section 7.5.5.1). Distillation, covered in Section 10.5.4, is widely used throughout the process industries. It is less important in chlor-alkali production than it is in many industries. Examples of its use include chlorine vaporization (Section 9.1.8.7), in which the accumulation of nitrogen chloride in the liquid may create a problem, and the stripping of ammonia from aqueous solution during the purification of diaphragm-cell NaOH (Section 9.3.4.1).

The standard chemical engineering approach to estimating the rate of a transport process is to define and measure a driving force for the process, along with the physical resistances to transfer. Thus,

$$\text{Rate} = \text{Driving force/Total resistance} \quad (1)$$

In the transfer of heat by conduction, the driving force is the temperature differential between two zones. The specific resistance to conduction through a body is more frequently reported as its reciprocal, the thermal conductivity. Similarly, other transport processes are characterized by a coefficient that yields the rate when applied in Eq. (2):

$$\text{Rate} = \text{Coefficient} \times \text{Driving force} \quad (2)$$

The use of resistance has the advantage that the separate series resistances in a composite system are additive.

10.5.1. Heat Transfer

Conduction. Heat transfer takes place by conduction, convection, and radiation. Conduction is the intermolecular transfer of heat as hotter molecules pass some of their energy on to those that are colder. Pure conduction occurs only in solids and certain confined fluids. The simplest situation is the transfer of heat between parallel planar surfaces. In terms of Eq. (1), the driving force is the temperature differential between the two surfaces. The resistance is proportional to the distance between surfaces and

inversely proportional to the area available for heat transfer and the thermal conductivity of the medium. This gives

$$Q = kA \Delta t/x \quad (3)$$

where

Q = amount of heat transferred in unit time,
 k = thermal conductivity of the medium, and
 x = distance between planar surfaces.

Thermal conductivity varies slowly with temperature. In most cases, an average value can be used with very little error.

Conductive heat transfer through concentric circular surfaces is very common. Examples include tubing, piping, equipment surfaces, and insulation. Here, a logarithmic-mean cross-sectional area should be used:

$$A_{\text{avg}} = (A_2 - A_1)/\ln(A_2/A_1) \quad (4)$$

where

A_2 = area of outer surface,
 A_1 = the area of inner surface.

As the value of (A_2/A_1) approaches unity, A_{avg} approaches the arithmetic mean. When the solid comprises a number of layers, we have

$$Q = k_1 A_1 \Delta t_1/x_1 = k_2 A_2 \Delta t_2/x_2 = \dots \quad (5)$$

The individual resistances, $R_i = \Delta x_i/k_i A_i$, are additive:

$$Q = \Delta t/\Sigma R_i \quad (6)$$

Convection. Most industrial processes rely more heavily on convection for the transfer of heat. Here, the process is aided by the bulk movement of fluid. Natural convection takes place when the transfer of heat itself causes variations in the density of the fluid. The resulting flow, under the influence of gravity, transfers heat from one zone to another. When the fluid is forced into motion by an outside agency such as a pump or an agitator, we have forced convection. Most of the applications of interest here rely on forced convection.

The classical approach to analysis of this problem still relies on Eq. (1). Consider the cooling of a solid surface by a fluid. One hypothesizes a stagnant film of the fluid that possesses all the fluid-phase resistance to heat transfer. The properties of the fluid and the thickness of the film determine the magnitude of the resistance. Boundary-layer theory enables estimation of various film thicknesses, but normal engineering practice is based on the use of individual coefficients that are empirically determined. Thus, the local individual coefficient for the film at a surface is defined by the Newton relation

$$dq = h dA \Delta t \quad (7)$$

where

dq = rate of heat flow

dA = differential area under consideration

Δt = temperature differential across film

h = film coefficient of heat transfer (energy flow per unit time, area, and temperature difference)

We can compare this with Eq. (3) for conductive heat transfer. The coefficient h is analogous to k/x , the conductivity divided by the thickness of the solid. In heat-transfer calculations, we equate convection to the conduction of heat through the postulated stagnant film.

Next, we consider the common situation in which heat is transferred between fluids separated by a solid surface. We have three resistances in series, which are the two liquid films and the solid wall between them. At steady state, the rates of heat flow through the three resistances are equal. The total temperature differential then divides itself in proportion to the values of the resistances. We have

$$dq = h_h dA_h \Delta t_h = (k/x) dA_s \Delta t_s = h_c dA_c \Delta t_c$$

The terms are as defined above, and the subscripts h, s, and c refer, respectively, to the hotter film, the solid, and the colder film. We can also describe the process in terms of an overall heat transfer coefficient, U :

$$dq = U dA \Delta t$$

Here, $\Delta t = \Delta t_h + \Delta t_s + \Delta t_c$. If the surface is planar, $dA = dA_h = dA_s = dA_c$. If not, we can define U in terms of any of the individual areas. Then

$$1/U = dA/h_h dA_h = x dA/k dA_s = dA/h_c dA_c$$

In a tubular exchanger, the different areas vary with the thickness of the tube wall. Approximate work may depend on the fact that this thickness is usually a small fraction of the diameter of the tube, and that the inside and outside areas are nearly the same. Also, in many cases, one of the resistances is substantially greater than the others, which can then be ignored. Then,

$$U \approx h_L$$

where h_L is the limiting coefficient, or the reciprocal of the major resistance.

The chemical and mechanical engineering literature dealing with convective heat transfer is huge. Even to begin a summary would make this chapter unduly long. The reader is referred to engineering handbooks and the classical texts on unit operations.

Radiation. Radiation is quite different from conduction and convection. The Stefan–Boltzmann law states that radiant energy flux is proportional to the fourth power

of temperature:

$$E = \varepsilon \sigma T^4$$

where

$$\begin{aligned} \varepsilon &= \text{emissivity} \\ \sigma &= 4.88 \times 10^{-8} \text{ kcal m}^2 \text{ hr T}^4 \end{aligned}$$

The emissivity accounts for the properties of a radiating surface. An ideal radiator, or "black body," has a value of $\varepsilon = 1$. The rate of radiative heat transfer between two bodies is proportional to the difference between the fourth powers of their temperatures. In most commercial apparatus, not all the radiation from one body reaches the second. Radiation goes out in all directions, and only some of it reaches the intended receiver. The fraction that does is called the area factor or the view factor. Thus,

$$q_R = \varepsilon \sigma f_A A (T_1^4 - T_2^4)$$

where

$$\begin{aligned} q_R &= \text{heat transferred by radiation,} \\ A &= \text{area of surface, and} \\ f_A &= \text{view factor.} \end{aligned}$$

When temperature ranges are small, the usual approximation is

$$q_R = h_R A (T_1 - T_2)$$

This requires

$$h_R = \varepsilon \sigma f_A (T_1^3 + T_1^2 T_2 + T_1 T_2^2 + T_2^3)$$

If we consider a source at 200°C and an object at 80°C, a change of 1°C in source temperature changes the quantity in parentheses by 0.4%. For most practical purposes in chlor-alkali production, the above approximation is justified. In fired heaters and similar equipment, where radiation is the principal mode of heat transfer, proper calculations based on the complete equation are necessary.

Evaporation. The study of evaporation encompasses both heat transfer and special process considerations. The heat-transfer mechanism usually is convective exchange between heated tubes and a process fluid, as discussed above. There are no fundamental differences between evaporators and other heaters.

The most important process design considerations deal with efficient process design and, in particular, the practical minimization of energy consumption. Other sections that deal with evaporation (Section 9.3.3.1; Section 9.3.3.2) have covered multiple-effect and vapor-recompression evaporation. Section 9.3.3.2 also discussed evaporation process design.

10.5.2. Gas Absorption

10.5.2.1. Absorption as a Transfer Operation. Absorption is the unit operation in which a gas is brought into contact with a liquid (the solvent) that can dissolve at least one component of the gas (the solute). The process is characterized by the equilibrium relationships of all components between two phases. Henry's law, which states that solubility is proportional to partial pressure, is the simplest of these relationships:

$$c = Hp \quad (8)$$

where

c = dissolved concentration, mole fraction;

H = proportionality constant; and

p = partial pressure of component in gas phase.

Henry's law usually is valid when a substance is only sparingly soluble or when the partial pressure is very low. It then often holds true regardless of the units used to express the concentration c . In any event, the units used for H must be consistent with those of c and p .

Figure 10.5.1 shows the pressure and concentration profiles near a gas-liquid interface as a substance is absorbed. The quantities at the interface, p_i and c_i , are at equilibrium. The bulk quantities p and c are respectively higher and lower than the interfacial quantities, and the differences are the driving forces for diffusion across the interfacial films. The mass-transfer flux through the films is

$$J = D_G(p - p_i)/\delta_G = D_L(c_i - c)/\delta_L \quad (9)$$

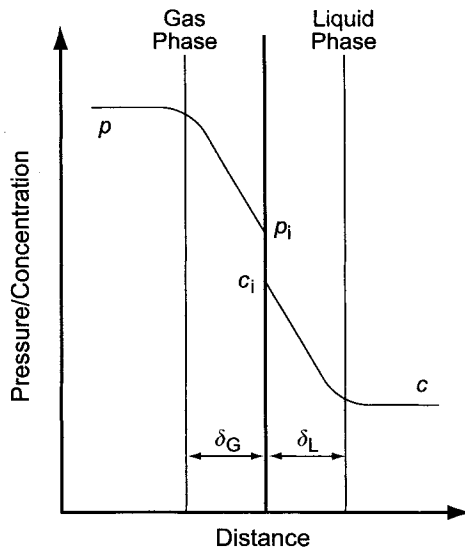


FIGURE 10.5.1. Pressure/concentration profile near the interface between gas and liquid phases.

where

J = flux, $\text{kg mol m}^{-2} \text{hr}^{-1}$

D_L = diffusivity, $\text{m}^2 \text{hr}^{-1}$

D_G = diffusivity, $\text{kg mol m}^{-1} \text{hr}^{-1} \text{atm}^{-1}$

δ = thickness of boundary layer, m

c = concentration, kg mol m^{-3}

p = partial pressure, atm

The use of the second equal sign and a single value of J is appropriate at steady state. The engineering approach relies on the use of mass-transfer coefficients:

$$k_G = D_G/\delta_G \quad (10)$$

$$k_L = D_L/\delta_L \quad (11)$$

We can define the dissolved concentration in equilibrium with the gas-phase partial pressure p as c^* . Then an overall mass-transfer coefficient K_L exists:

$$J = K_L(c^* - c) \quad (12)$$

$$1/K_L = H/k_G + 1/k_L \quad (13)$$

K_L must be smaller than either film coefficient. In the limiting case, where one film coefficient is much smaller than the other, K_L will be nearly equal to either k_G/H or k_L .

The above is the stationary two-film theory. Later developments recognized that a real process has some means of continuous agitation or renewal of the liquid surface in contact with the gas. The so-called penetration theory of gas absorption, therefore, considers the transient diffusion of a dissolved gas into a stationary liquid phase away from an interface at constant concentration. The difference between this approach and the steady-state two-film theory is that one assumes the periodic replacement of the liquid surface layer. There is no steady state, and the standard equations of diffusion hold:

$$D_A(\partial^2 A/\partial x^2) = \partial A/\partial t \quad (14)$$

where

D_A = diffusivity of substance A

A = concentration of A dissolved in liquid, molar units

x = distance in direction of diffusion, normal to interface

t = time measured from first exposure

and

$$A(0, t) = A_i$$

$$A(\infty, t) = A(x, 0) = A_o$$

The first boundary condition requires the interfacial concentration of A to be constant. In a liquid-phase controlled system, it is in equilibrium with the gas. The second requires

the initial concentration of A to be uniform throughout the liquid phase, which extends to infinity.

The solution is well known:

$$(A - A_0)/(A_i - A_0) = \operatorname{erfc}(x/\sqrt{4D_A t}) \quad (15)$$

The penetration theory then characterizes any operation or absorption apparatus by the time between replacements of the surface, or the time during which the diffusing solute “penetrates” the liquid phase. We denote this time by t_p . Differentiating Eq. (15) with respect to x gives the quantity $\partial A/\partial x$, the concentration gradient. This quantity when evaluated at the interface is the liquid-phase driving force for absorption. The instantaneous rate at time t becomes

$$R(t) = (A_i - A_0)(D_A/\pi t)^{1/2} \quad (16)$$

The average rate during the exposure of the surface is obtained by integrating $R(t)dt$ over the time interval 0 to t_p and dividing the result by t_p . The mass-transfer coefficient becomes

$$k_L = (4D_A/\pi t_p)^{1/2} \quad (17)$$

This differs from Eq. (11) by substituting a function of the penetration time for the thickness of the liquid film and by involving only the square root of the diffusivity. Figure 10.5.2 shows concentration profiles near an interface shortly after it forms. The magnitude of the interfacial concentration gradient, and therefore the liquid-phase mass-transfer coefficient, decreases rapidly. A high degree of agitation, leading to frequent surface renewal and a small value of t_p in Eq. (17), will produce a high mass-transfer coefficient.

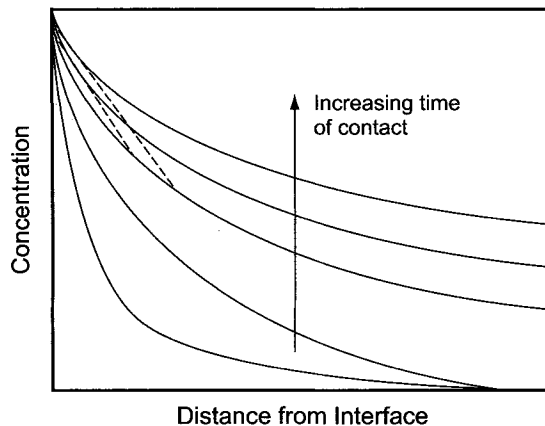


FIGURE 10.5.2. Change of concentration profile with time near the interface.

10.5.2.2. Absorption Accompanied by Chemical Reaction. When a dissolving species undergoes a reaction in the liquid phase, the concentration profiles and the mass-transfer coefficient are affected. The disappearance of the solute by reaction causes its concentration to fall more steeply across the interfacial film or penetration distance. The concentration gradient becomes steeper, and the mass-transfer coefficient becomes greater.

Figure 10.5.3 shows how the process in the liquid film of Fig. 10.5.1 is affected. As the dissolving substance A moves to the right in the boundary layer or film, a reactive component B diffuses to the left from the bulk of the liquid. We assume a rapid reaction between A and B. They will meet at some plane in the boundary layer and react with each other. The reaction plane is at some fraction x of the thickness of the film away from the interface. The equations of flux become

$$J' = D_{GA}(p_A - p_{A_i})/\delta_G = D_{LA}c_{A_i}/x\delta_L = D_{LBCB}/[(1-x)\delta_L] \quad (18)$$

The rate of transport of A through the liquid film is greater here than in Eq. (9) because there is no bulk concentration term to be subtracted from the interfacial concentration of A and because the denominator now contains the term x , which is less than unity. The value of x will be determined by the relative concentrations and diffusivities of A and B. With constant diffusivities, we define

$$\alpha = D_{LB}/D_{LA} \quad (19)$$

Following the development of Eqs. (9) through (12), we obtain

$$J' = K_L (c_A^* + \alpha c_B) \quad (20)$$

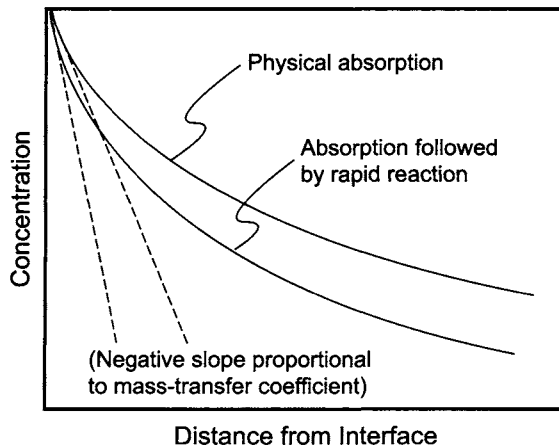


FIGURE 10.5.3. Effect of reaction on concentration profile. (Dashed lines are tangent to solid curves at y -axis.)

Comparing this to the flux without reaction, given by Eq. (12), we have

$$J^*/J = (c_A^* + \alpha c_B) / (c_A^* - c_A) = 1 + (c_A + \alpha c_B) / (c_A^* - c_A) \quad (21)$$

The last term is the extent of acceleration of gas absorption by the reaction between A and B.

Equation (21) depends only on the concentrations and diffusivities of the reactants. The reaction itself is assumed to be rapid. Slower reactions require modifications to the equations.

Equation (14) must be modified to show the disappearance of component A by reaction:

$$D_A(\partial^2 A/\partial x^2) = \partial A/\partial t + R_A \quad (22)$$

where R_A is some function of concentrations in the liquid. As an example, we take the simplest case of an irreversible first-order reaction, where

$$R_A = k_A A \quad (23)$$

Now Eq. (22) becomes

$$\partial A/\partial t = D_A(\partial^2 A/\partial x^2) - k_A A \quad (24)$$

A solution to this equation is

$$A(x, t) = k \int e^{-kt} a(x, t) dt + e^{-kt} a(x, t) \quad (25)$$

where $a(x, t)$ is a solution of the basic diffusion equation without reaction. The simplest proof of Eq. (25) is by differentiation and substitution. The advantage of this equation is that, given a reaction rate constant and a penetration time, the effect of an irreversible first-order reaction on any system already solved for the case of physical absorption is easily established.

10.5.2.3. Absorption in a Packed Column. Figure 10.5.4 shows a packed column absorber with unit cross-sectional area and height H . Gas enters the bottom of the tower and liquid absorbent enters the top. Assume that the solute in both gas and liquid is dilute, so that the volumes of carrier gas and solvent are unchanged in passing through the tower. The material balance on a differential element is

$$L dx = G dy \quad (26)$$

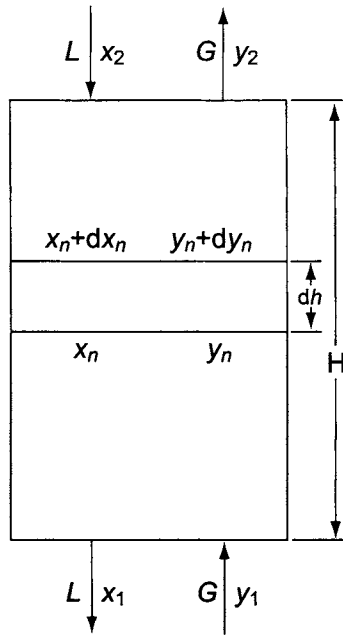


FIGURE 10.5.4. Packed tower.

where

L = flow rate of liquid, $\text{kg mol m}^{-2} \text{hr}^{-1}$

G = flow rate of gas, $\text{kg mol m}^{-2} \text{hr}^{-1}$

x = mole fraction of solute in liquid phase

y = mole fraction of solute in gas phase

For the column as a whole,

$$L(x_2 - x_1) = G(y_2 - y_1) \quad (27)$$

Figure 10.5.5 shows an equilibrium line along with operating lines for absorption and desorption. The distance between the operating line and the equilibrium line represents the driving force.

Again, we consider a volume element of height dh . Mass transfer takes place at the wetted surface of the packing, and the effective area is difficult to estimate. Consequently, it is more convenient to discuss mass-transfer coefficients for a unit volume. We denote these as K_L for the liquid phase and K_G for the gas phase in units of $\text{kg mol m}^{-3} \text{hr}^{-1}$. Combining these definitions with the material balance equations above, we have

$$L dx = K_L(x^* - x) dh \quad (28)$$

$$G dy = K_G(y - y^*) dh \quad (29)$$

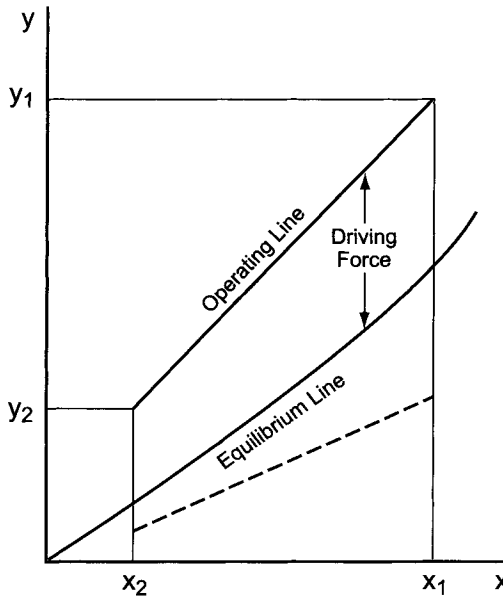


FIGURE 10.5.5. Operating line and equilibrium line of gas absorption. (Dotted line shows the operating line for gas stripping.)

where x^* and y^* are the concentrations in equilibrium with y and x , respectively. With these equations,

$$H = (L/K_L) \int dx/(x^* - x) = (G/K_G) \int dy/(y - y^*) \tag{30}$$

The quantities L/K_L and G/K_G represent the difficulty of making a change in concentration. The denominators are the mass-transfer coefficients, which describe the rates of transfer, while the numerators represent the molar flows of material, or the amounts of transfer required. The combination gives a number expressed in length, or meters. Inside each integral, the value becomes unity when the change in x or y becomes equal to the average driving force over the interval. This is a dimensionless quantity and is an intensive property that is independent of the size of the apparatus and the magnitude of the flow rates. The integrated quantity is, therefore, referred to as the number of transfer units required [1]. The numbers of transfer units on the liquid and gas sides are generally unequal:

$$N_L = \int dx/(x^* - x) \tag{31}$$

$$N_G = \int dy/(y - y^*) \tag{32}$$

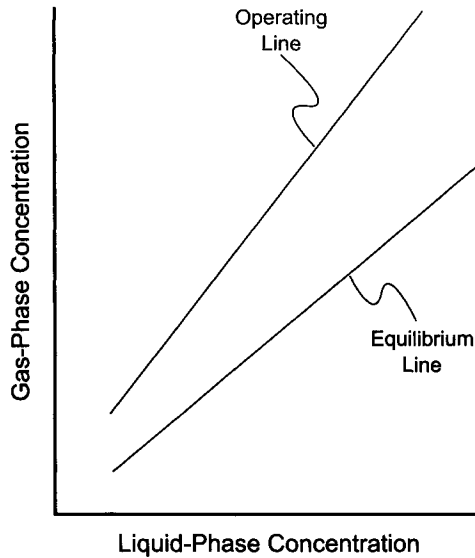


FIGURE 10.5.6. Mass-transfer operation with straight equilibrium and operating lines.

The terms L/K_L and G/K_G are the heights of column required to provide one transfer unit for the liquid and the gas phase, respectively. Multiplication of these quantities by the number of mass-transfer units called for by integration of the forms in Eqs. (31) and (32) give the height of packing required.

The course of a mass-transfer operation can also be followed graphically by establishing equilibrium and operating lines. The equilibrium line on Fig. 10.5.6 is straight in accordance with Henry's law (Eq. 8). Operating lines are established by constructing a material balance over the column. Straight lines can also represent the simplest case, as in Fig. 10.5.6. Many of the analytical solutions to absorption problems are based on the assumption of straight equilibrium and operating lines. In many real cases, this assumption fails. Figure 10.5.7 shows a more realistic case. Equilibrium lines, in particular, are often highly nonlinear. We have seen in Section 7.5.9.1 that chlorine in water is a good example of this. Graphical solutions are not affected by this nonlinearity. A practical effect is more likely to be a pinch region, as shown in the drawing, where the equilibrium and operating lines are close together. More plates or transfer units are then required to produce a given change in concentration.

10.5.3. Adsorption and Ion Exchange

10.5.3.1. Adsorption. Adsorption occurs when a fluid mixture comes into contact with a solid surface. Purification of a gas or liquid by adsorption of impurities on charcoal is a typical example. Adsorption mechanisms can be quite complex, but equilibrium can be represented by isotherms showing the amount of a given component adsorbed by a unit of solid adsorbent, which is a function of gas-phase partial pressure or liquid-phase concentration.

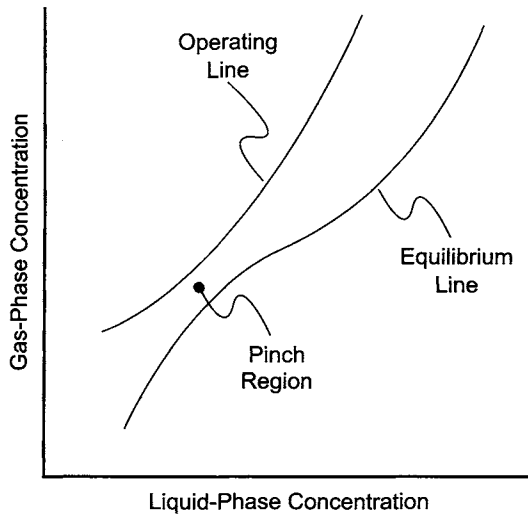


FIGURE 10.5.7. Mass-transfer operation with curved equilibrium and operating lines.

10.5.3.1A. Gas-Phase Adsorption. In the case of a gaseous mixture, the adsorption isotherm can be represented as

$$v = f(p)_T \quad (33)$$

where

v = volume of gas adsorbed by a unit weight or volume of adsorbent,
 p = partial pressure of component being adsorbed, and
 T = temperature (constant for a given isotherm).

Irving Langmuir developed an equation for adsorption on a solid surface under low pressure, where the number of adsorbate molecules present is not sufficient to cover the solid surface. At equilibrium,

$$k_1(1 - \theta)p = k_2\theta \quad (34)$$

where θ is the fraction of the surface covered by adsorbate and the two sides of the equation show the rates of adsorption and desorption, respectively. The volume of gas adsorbed (V) is proportional to the number of gas molecules on the surface:

$$V = k_3\theta \quad (35)$$

The parameters k_1 , k_2 , and k_3 all are assumed constant. Rearranging Eq. (34),

$$\theta = k_1p/(k_1p + k_2) \quad (36)$$

Then,

$$V = kp/(1 + k'p) \quad (37)$$

with

$$k = k_1 k_3 / k_2$$

$$k' = k_1 / k_2$$

The term k' is the equilibrium constant for adsorption. When k' is large, V tends to be nearly constant and not influenced by pressure. When k' is small, V is proportional to the pressure.

This isotherm can be modified to suit other conditions, such as the existence of more than one layer of adsorbed gas molecules. Alternatively, other isotherm models, usually empirical, can be used. One of these is the Freundlich isotherm,

$$V = kp^n \quad (38)$$

The simpler isotherms are used when interactions between neighboring molecules at the solid surface are relatively minor. Heats of adsorption are then as low as 5–10 kcal mol⁻¹, of the same order as the heat of vaporization. Therefore, the gas molecules are considered to be bonded physically to the surface by the van der Waals force. Other cases have heats of adsorption of 10–100 kcal mol⁻¹. Molecules dissociate to atoms and adhere to the solid surface by sharing some outer-shell electrons. This phenomenon is known as chemisorption, and it is of great importance in catalytic reactions. The adsorption of oxygen on charcoal is an example of chemisorption.

Suppose that a vessel contains L kg of adsorbent. When G kg of gas is fed to the vessel, the content of the adsorbable component in the gas decreases by $(y_1 - y_2)$. The content of the same component in the adsorbent increases by $(x_2 - x_1)$, where x and y are fractions in the adsorbent and the gas space, respectively. The material balance is

$$G(y_1 - y_2) = L(x_2 - x_1) \quad (39)$$

This gives

$$(x_1 - x_2)/(y_1 - y_2) = -G/L \quad (40)$$

Line QP on Fig. 10.5.8 represents Eq. (40). The curve represents the equilibrium for this system. Adsorption rates are generally fast, and the system reaches equilibrium rapidly. When the Freundlich isotherm applies and x_1 is zero, Eq. (40) becomes

$$G/L = ky_2^n/(y_1 - y_2) \quad (41)$$

This equation is useful in the determination of the required volume of adsorbent. Figure 10.5.8 shows only one stage. Multi-stage adsorption is common practice, then and Eq. (41) applies successively to the respective stages. Figure 10.5.9 is the graphical representation for the case in which fresh adsorbent is used in each of three stages. Note that in general the slopes of the operating lines for the different stages need not be equal.

More practically, the adsorbent is arranged in a packed column for continuous operation (Fig. 10.5.10). Sizing such a column requires us to consider the rates of mass transfer. The driving force for mass transfer is the difference in activities of the adsorbable

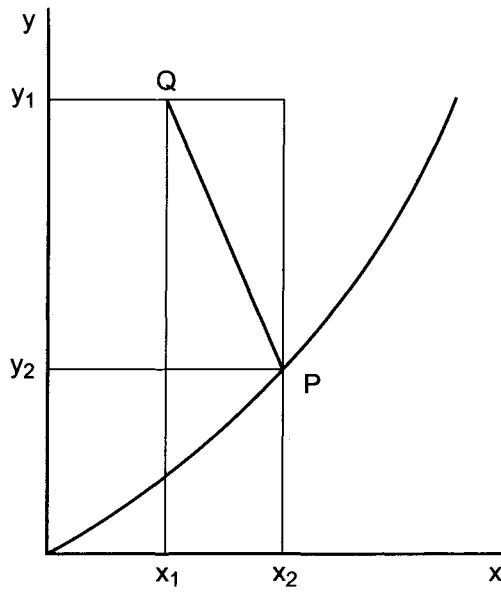


FIGURE 10.5.8. Equilibrium curve for gas adsorption.

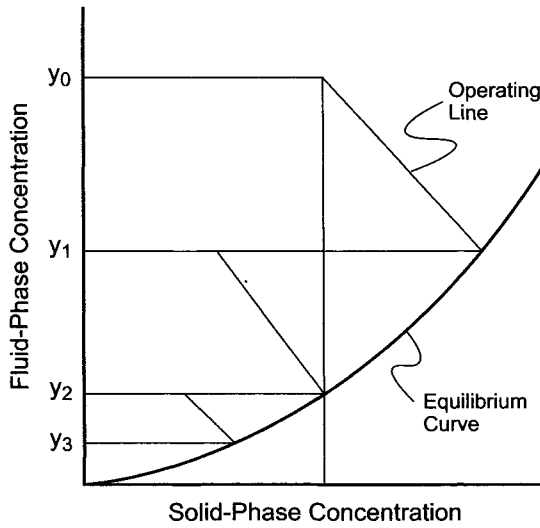


FIGURE 10.5.9. Three-stage batch adsorption operation.

component between the fluid and solid phases. The concentration in the fluid phase is y , and we denote the solid-phase activity by the fluid-phase concentration that would be in equilibrium with the adsorbate concentration. We denote this by y^* .

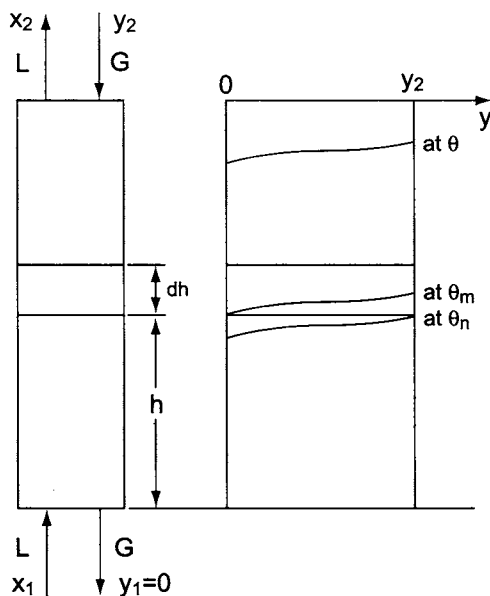


FIGURE 10.5.10. Packed column (left) and concentration profile (right) in the adsorption tower.

Now we consider a differential slice of the column in Fig. 10.5.10. The rate of flow is $G \text{ kg hr m}^{-2}$. The concentration entering the section under study is y . This changes to $y - dy$ in our differential volume. From the material balance, the amount adsorbed is $GS dy$, S being the cross-sectional area of the column. Denoting the mass-transfer coefficient by K , the rate of transfer in a unit volume is $K(y - y^*)$. Therefore, we have

$$GS dy = K S (y - y^*) dh \quad (42)$$

This reduces to

$$dh = (G/K) x dy / (y - y^*) \quad (43)$$

G/K is the height of the mass-transfer unit. Integration of the second term on the right-hand side between the limits given by the feed concentration and the desired outlet concentration gives the number of transfer units required. Multiplication of the two quantities gives the height of the column.

10.5.3.1B. Liquid-Phase Adsorption. Adsorption of both the solvent and the solute occurs when a binary liquid solution is exposed to a solid adsorbent. What one observes is the preferred adsorption of the solute. While some texts consider correction of the results for the amount of solvent adsorbed, the fraction of the total that is adsorbed is usually assumed to be negligibly small.

Liquid adsorption isotherms have many different shapes and may be quite complex. It is difficult to generalize over the whole range of possible concentrations. In dilute solutions, the common application in the chlor-alkali industry, the Freundlich isotherm frequently applies:

$$c^* = k[V(c_0 - c^*)]^n \quad (44)$$

where $V(c_0 - c^*)$ is the apparent adsorption per unit quantity of adsorbent and k and n are constants.

10.5.3.1C. Continuous Processing in Fixed Beds. There are some useful analogies between adsorption and absorption processes, and some of the techniques used to analyze absorption operations are useful here as well. Some large-scale adsorption processes depend on a moving bed of solids, and Eqs. (42) and (43) apply to these processes. After exposure to the process fluid, the adsorbent is then removed from the column and taken elsewhere for regeneration. In this case, the adsorbent plays the role of the solvent, and the analysis of transfer in the bed is quite similar to the analysis of the absorption process.

The complexities of moving and handling solids add to the cost of the operation, and so a common technique in the field of adsorption is the use of a fixed bed of solids. The process becomes unsteady-state and semicontinuous. The solids remain in place as the fluid passes through. Occasionally, operation of the bed must stop to allow removal or regeneration of the solids.

We consider this sort of operation below. The analysis applies equally well to gases and liquids. Key assumptions are that there is one strongly adsorbable component present and, at least in the illustration, that the fluid moves downward. We shall refer to the adsorbable component as the "impurity."

The upper part of Fig. 10.5.11 shows the extent of loading of the bed with adsorbate at several different times during its operation. The lower part shows the concentration of the key component in the effluent from the bed as a function of time or volume of fluid processed. At the beginning, the top layer of adsorbent removes nearly all the impurity. The rest of the column is a scavenger for trace amounts, and the concentration in the effluent is nearly zero. In the second picture of the bed, the top layer is saturated with impurity. It is in equilibrium with the feed solution. Most of the duty is then taken up by a lower section of the bed. Since this section has already had some exposure to the impurity, it has less residual capacity, and the zone of adsorption becomes longer. The concentration of impurity in the effluent is still very low. As the operation continues, more of the adsorbent becomes saturated, and the effective adsorption zone moves down through the column. The next section shows the tail of the adsorption zone as it approaches the bottom of the column. The effluent concentration begins to increase much more rapidly. This is the beginning of the phenomenon of "breakthrough." If the operation continues, the bed does not have the capacity to remove the impurity fully, and its concentration in the effluent increase more or less rapidly until the bed is totally exhausted and the feed and effluent streams have the same concentration of impurity.

The lower part of Fig. 10.5.11, the concentration–time or concentration–volume curve, is characteristic of the system, the flow rate, and the column geometry under

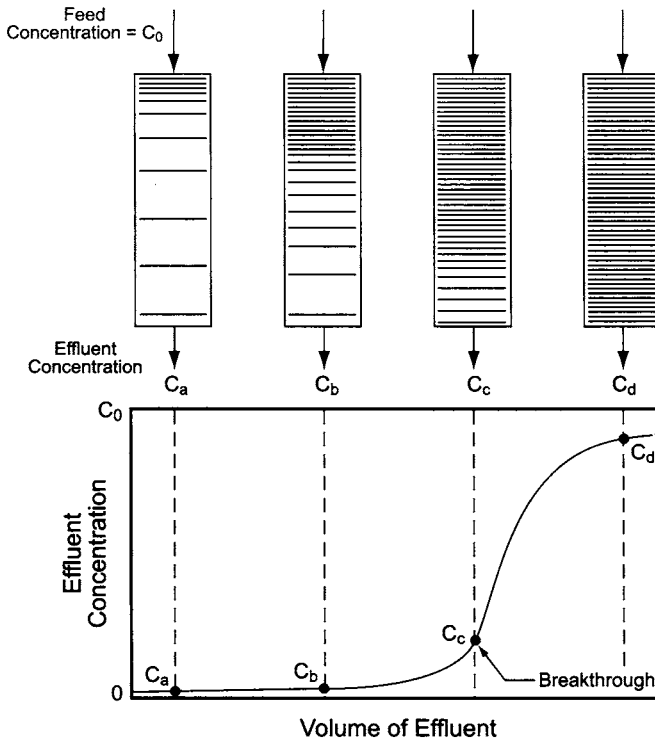


FIGURE 10.5.11. Development of the adsorption wave.

investigation. If we consider the concentrations C_c and C_d , some thought will show that an adsorption wave bounded by these values moves down through the column. The concentration profile remains fairly steady, as does the length of bed between C_c and C_d . This is referred to as the length of the transfer zone, and it is an inverse measure of the efficiency of the mass-transfer process. It fixes the length of the bed that must be subtracted if one is to avoid breakthrough. The length of the transfer zone depends on the distribution of active sites and pore structure of the adsorbent and on the velocity and transfer properties of the liquid.

10.5.3.2. Ion Exchange. Ion exchange is a reaction between two electrolytes, one of which is insoluble while the other is in solution. The insoluble electrolyte may take one of many forms, but in the applications of interest here, it will be a synthetic organic resin. The resin has one ion tightly bound as part of its structure, while the co-ion is held to it by an electrovalent bond. That ion is relatively mobile and free to exchange with the corresponding ion in the soluble electrolyte. The nature of a resin is described by the type of mobile ion present. Thus, if the anionic portion is fixed to the polymeric structure and the cationic portion can exchange with the fluid, we have a cationic, or cation-exchange resin. This is the type used in brine softening, the most important

application in the chlor-alkali industry. Water treatment depends on cation-exchange resins for simple softening and both types for complete demineralization. In the latter case, anion-exchange and cation-exchange resins are used in sequence or in mixed beds to remove essentially all ionic species from the water.

Methods of providing contact between solids and liquids are the same as those discussed under adsorption. The cation-exchange process involves the following sequential steps:

1. diffusion of the dissolved cation to the surface of a solid particle,
2. diffusion on or within the particle to an exchange site,
3. the ion-exchange reaction,
4. diffusion of the released cation to the solid/liquid interface,
5. diffusion of the released cation into the liquid phase.

In the chlor-alkali industry, fixed-bed operation is the norm, and from the engineering standpoint, an ion-exchange process closely resembles a liquid adsorption process. The same methods are used in engineering design, and so the two processes frequently are treated together in unit operations courses. In particular, the analysis of Fig. 10.5.11 and the use of the concepts of length of mass-transfer zone and length of unused bed are common in ion-exchange technology.

10.5.4. Distillation

Distillation is a process of differential vaporization of components of a liquid mixture. The tendency of a given component to vaporize is related to its vapor pressure. In an ideal solution, Raoult's law states that the partial pressure of a component in the vapor over a liquid is equal to the product of its vapor pressure and liquid-phase mole fraction:

$$p_i = P_i x_i \quad (45)$$

where

p_i = partial pressure of component i in the vapor,

P_i = vapor pressure of component i at the temperature of the system,

x_i = mole fraction of component i in the liquid.

When the liquid consists of two or more components, those with higher vapor pressures will be enriched in the vapor phase. The total pressure on the system will be the sum of the partial pressures of the various components. Thus, in an ideal system, the mole fraction of component i in the vapor space will be

$$y_i = p_i / \pi = (P_i / \pi) x_i \quad (46)$$

where π = total pressure.

Most liquid mixtures do not display ideal behavior, and then Eq. (46) does not hold. The standard engineering approach to this problem is to apply a correction factor to Eqs. (45) and (46). The correction factor is the liquid-phase activity coefficient of the

component in question. Denoting it by γ , we have

$$p_i = \gamma_i P_i x_i \quad (47)$$

$$y_i = \gamma_i p_i / \pi = (\gamma_i P_i / \pi) x_i \quad (48)$$

Applying Eq. (48) to the various components of a mixture reveals the degree of separation that occurs with partial vaporization. Assuming a binary mixture, we have

$$\begin{aligned} y_1 &= \gamma_1 p_1 / \pi = (\gamma_1 P_1 / \pi) x_1 \\ y_2 &= \gamma_2 p_2 / \pi = (\gamma_2 P_2 / \pi) x_2 \end{aligned} \quad (49)$$

or, transposed

$$\begin{aligned} y_1/x_1 &= \gamma_1 P_1 / \pi \\ y_2/x_2 &= \gamma_2 P_2 / \pi \end{aligned} \quad (50)$$

We define these ratios as the “volatility” of the component. Comparing the two components, we then have for the “relative volatility”

$$\alpha = (y_2/x_2)/(y_1/x_1) = \gamma_2 P_2 / \gamma_1 P_1 \quad (51)$$

Normally, we assign subscripts to produce $\alpha > 1$. If we consider a 50/50 mixture of two components with $\alpha = 2$, the first vapor formed will contain 66.7% of the more volatile component. Continued vaporization would be from a leaner mixture, and the concentration of the volatile material in the vapor would decrease. An equilibrium system of 50% vapor and 50% liquid thus would contain 58.6% of the more volatile component in the vapor.

With ideal solution behavior, the activity coefficients are not necessary in Eq. (51), and the relative volatility is simply the ratio of the vapor pressures. Most real systems have at least some nonideality in their behavior. It then becomes important to know the magnitude of the activity coefficients and to understand how they depend on the composition of the liquid. By necessity, the activity coefficient of a pure component is unity. The activity coefficient of a component, therefore, depends on its concentration in the liquid. The activity coefficients of the components of a mixture can be related to their chemical potentials, and there are thermodynamic requirements that govern their comparative values. The Gibbs–Duhem equation states that

$$x_1(\partial \ln \gamma_1 / \partial x_1)_{T,P} + x_2(\partial \ln \gamma_2 / \partial x_2)_{T,P} + \cdots = 0 \quad (52)$$

This relates the activity coefficient of any component of a liquid mixture to the concentrations of all components. In a binary system, Eq. (52) becomes

$$x_1(\partial \ln \gamma_1 / \partial x_1)_T = x_2(\partial \ln \gamma_2 / \partial x_2)_T \quad (53)$$

Many approximate solutions to this equation are available. Methods suitable for use in machine computation are capable of generating the necessary coefficients from the properties of the components.

One form of separation is differential distillation, in which a batch of liquid vaporizes until a certain amount is left as residue. The Rayleigh equation [2] for such an operation is

$$\ln(W/W_0) = \int_{x_0}^x dx(y - x) \quad (54)$$

where

W = weight (or moles) of mixture,

x = weight (or mole) fraction of given component in liquid,

y = weight (or mole) fraction of same component in vapor, and subscript 0 refers to starting mixture.

With no assumptions made on the relationship between x and y , this is an exact equation. Assuming that x and y are always in equilibrium and that the relative volatility of one component to the other is constant (or, more precisely, that an average value can be used with acceptable error), we have

$$A/A_0 = (B/B_0)^\alpha \quad (55)$$

This is useful in estimating the accumulation of the hazardous compound nitrogen trichloride when a batch of chlorine is allowed to vaporize.

Continuous distillations usually take place in towers containing packing or plates to promote vapor-liquid contact. With vapor and liquid in countercurrent flow through the tower, analysis usually is in terms of the number of theoretical plates required to effect the desired separation. Figure 10.5.12 illustrates the concept of a theoretical plate. The vapor and liquid leaving the plate are in physical equilibrium. Distillation calculations then depend on accurate knowledge of the equilibrium relationship. When activity

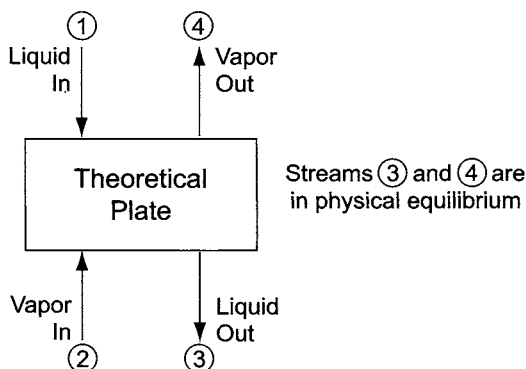


FIGURE 10.5.12. Concept of a theoretical plate.

coefficients are available or can be estimated by the Gibbs–Duhem equation, computation is straightforward but may be laborious. A number of approximate solutions to the Gibbs–Duhem equation are available and packaged for machine computation.

Chemical engineers still often rely on a simple graphical technique for preliminary estimates and to give them a feel for situations that may complicate the separation of two components. This is the McCabe–Thiele method, illustrated by Figs 10.5.13–10.5.15. The upper curve in Fig. 10.5.13 shows the vapor–liquid equilibrium conditions for the system. Its ends are joined by a 45° straight line for which $x = y$. In Fig. 10.5.14, we take as an example an operation that is to produce 95% purity at both ends of the column. The topmost line segment joining the equilibrium curve and the straight line is at $y = 0.95$. This intersects the equilibrium curve at a lower value of x . If a small amount of vapor is generated from such a liquid and then condensed, it will produce a liquid that is 95% in the more volatile component of the mixture. Because only a small amount of vapor is generated in this step, it and the liquid left behind are in equilibrium. This satisfies our definition of a theoretical plate. The first vertical line segment from the right joins the point generated as explained above to the $x = y$ line. The second horizontal segment repeats the process for a vapor of this composition. Its left end determines the composition of its equilibrium liquid. We can continue to move to the left, following the same procedure. Each step represents a theoretical plate, and we find that slightly less than seven theoretical plates will provide the desired separation. However, this is an impractical minimum. Only a differential amount of vaporization is allowed at each plate. The separation could be achieved in a column of seven theoretical plates only by operating at nearly total reflux and withdrawing very little product.

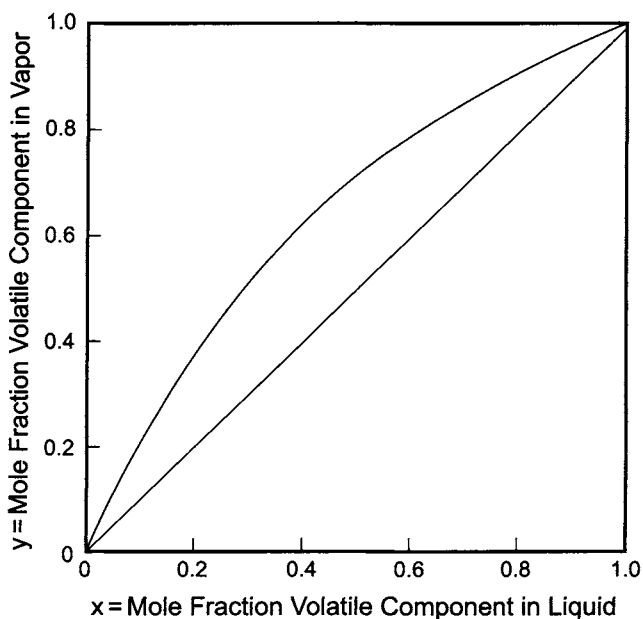


FIGURE 10.5.13. Typical vapor–liquid equilibrium curve.

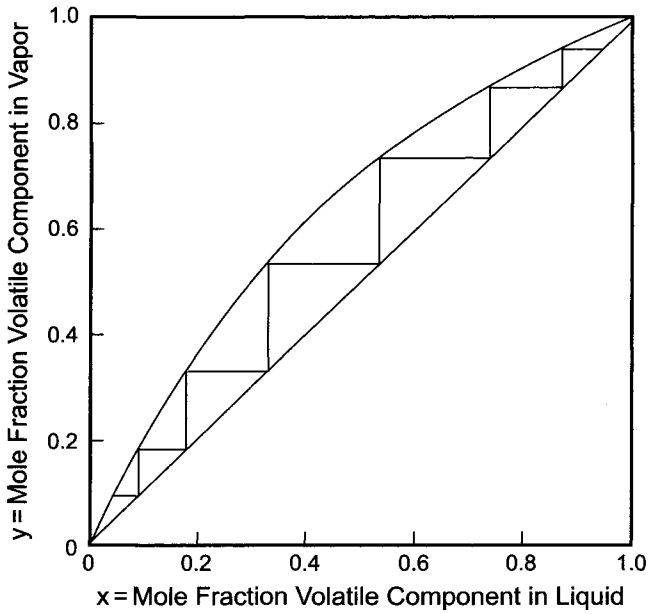


FIGURE 10.5.14. McCabe-Thiele diagram at total reflux.

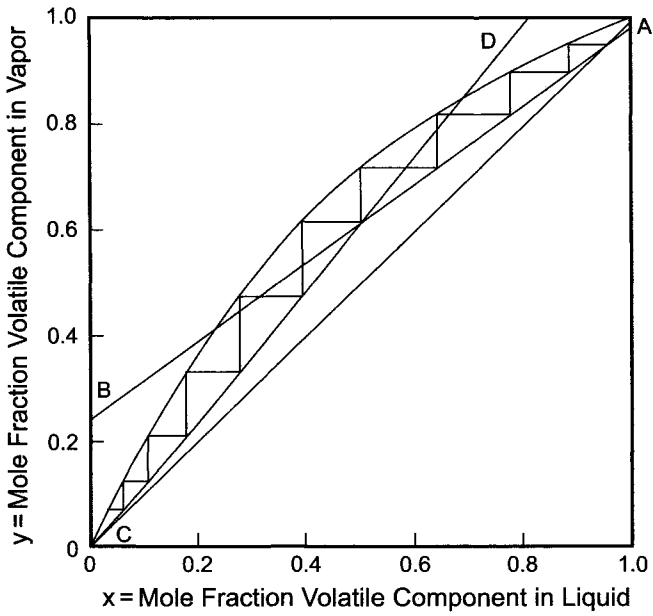


FIGURE 10.5.15. McCabe-Thiele diagram for real column with partial reflux.

In a real column with a practical rate of throughput, reflux from the top and boilup from the bottom both must be incomplete. When a significant amount of the volatile component leaves as overhead product, for example, less is available for reflux into the column. This reduces the amount of rectification available on the top tray. The 45° line no longer shows the relationship between vapor and liquid compositions in the column.

If we consider the material balance above a plate in the upper section of a column, the amount of vapor rising from the plate is equal to the amount of liquid falling from the plate above plus the amount of distillate withdrawn:

$$V_n = L_{n+1} + D \quad (56)$$

In terms of the more volatile component,

$$V_n y_n = L_{n+1} x_{n+1} + D x_D \quad (57)$$

Here, x and y refer to the concentrations of the volatile component in the indicated streams. Next,

$$y_n = (L_{n+1}/V_n)x_{n+1} + (D/V_n)x_D \quad (58)$$

or

$$y_n = [L_{n+1}/(L_{n+1} + D)]x_{n+1} + [D/(L_{n+1} + D)]x_D \quad (59)$$

The split of the overhead condensate is often referred to in terms of the reflux ratio, $R = L/D$. Then we have

$$y_n = [R/(R + 1)]x_{n+1} + x_D/(R + 1) \quad (60)$$

This is the equation of the straight line AB in Fig. 10.5.15. When R is infinite, it degenerates to $y_n = x_{n+1}$, and Fig. 10.5.14, in fact, represents the column.

There will be a similar relationship in the lower part of the column between plate compositions and the amount of bottoms leaving the column:

$$V_m y_m = L_{m+1} x_{m+1} - B x_B \quad (61)$$

$$y_m = (L_{m+1}/V_m)x_{m+1} - (B/V_m)x_B \quad (62)$$

This is another straight-line equation represented by line CD. Figure 10.5.15 shows how Eqs. (59) and (60) are used in graphical analysis. The two straight lines that these equations determine become the “operating lines” for the column. At any section of the column the vapor and liquid compositions above or below a given plate fall on one of these lines. The graphical procedure is the same as above. Stepping back and forth from equilibrium curve to operating line between the defined overhead and bottoms compositions, we find that about ten theoretical plates are necessary. Varying the slope of the operating lines will show that lower reflux and boilup ratios can be used at the

expense of adding more theoretical plates. One of the design engineer's tasks is to optimize this relationship.

The McCabe–Thiele method has the great advantage of simplicity, and it is a very useful qualitative tool in analyzing column operations. However, it is highly restricted. Nothing was said in the above derivations about heat balances inside the column. A tacit assumption in moving from Eq. (59) to Eq. (60) was that the ratio of vapor to liquid flow remains constant in the upper and in the lower section of the column. This is a fair assumption for many systems (e.g., organic homologs such as benzene and toluene). In others, there are severe deviations. Addition of feed to the column, somewhere in the center, disrupts both heat and material balances. There are various methods for dealing with these deficiencies, but exact calculations now depend on computerized analysis.

REFERENCES

1. T.H. Chilton and A.P. Colburn, *Ind. Eng. Chem.* **27**, 255 (1935).
2. C.R. Robinson and E.R. Gilliland, *Elements of Fractional Distillation*, 4th edition, McGraw-Hill Book Co., New York (1950), p. 108.

11

Instrumentation and Control Systems

11.1. INTRODUCTION

11.1.1. General

Chapters 7 through 9 have already covered the processes involved in a chlor-alkali plant, along with some of the essentials of their control. This chapter goes into the details of control systems and hardware. The discussion, where differences exist, focuses primarily on the membrane-cell process. The chlorine and hydrogen processes are essentially the same regardless of the type of cell used. Control of absolute and differential pressures is especially important in the gas systems, and so the discussion is divided primarily according to operating pressure level. Membrane cells require extremely pure brine, and some of the operations used are not necessary with the other types of cell. Otherwise, mercury-cell brine systems are for the most part very similar to those in membrane-cell plants, but they require their own special features and precautions to prevent the escape of mercury into the environment. Diaphragm cells require approximately the same treatment of new brine, but, unlike the situation with the other cells, there is no direct recycle of the anolyte. Therefore, the discussion of brine systems follows the membrane-cell process, which is the most comprehensive of the three. The caustic systems for the three manufacturing processes are very different and are discussed separately.

The individual unit operations and equipment chosen for a particular manufacturing process can vary from one plant design to another. This is especially true in the design of the brine systems, where the quality and sources of the brine vary greatly among plants. Methods for using the products or transporting them to customers also have a major influence on the design. Other factors with significant effects on control system design are the general operating philosophy of the plant's ownership and the particular design preferences of responsible engineers. It would be impossible to discuss all practical variations in process design and the resulting control systems. Thus, this chapter is restricted to a basic system design for each of the processing areas. Control engineers should be able to incorporate the changes necessary to suit individual projects.

The unit operations found in each area are discussed, covering control system design, instrument selection, and materials of construction. It is obvious that control systems engineers will have different opinions as to what controls, instruments, and materials are the best to be used for any application. The selections here emphasize simplicity of design and the use of quality equipment and materials of construction. This philosophy does not result in the lowest initial cost, but it has produced plants that are easy to start up and operate, with high onstream factors and long lives.

After a short general discussion, we cover here the major parts of the process in the sequence brine, chlorine, hydrogen, caustic liquor handling, and caustic evaporation. Small units are broken out in a series of drawings, and each drawing illustrates a particular function. Drawings illustrating given units may not show all the instrumentation that accompanies their units. They do show typical instrument hardware for the function in question. The drawings do not follow strict engineering flow diagram practice, but instrument representation and designation are conventional. Table 11.1 summarizes the grammar of designation of instrument functions.

Normal practice is to use a series of 2–4 letters to characterize each item. The first letter indicates the function under measurement or control. It is the function that matters, not the type of instrument. For example, differential pressure instruments are often used (with proper calibration) to measure the height of a level in a tank or the rate of flow of a material in a line. The designations used in these cases are L (level) and F (flow). The “succeeding letters” represent, in sequence:

1. simple readouts or passive functions;
2. output functions that actively influence the process.

An example of a simple readout is a pressure gauge. Using the first and third columns of Table 11.1, this is a pressure indicator, PI. An example of a device with a passive function is a restricting orifice placed in a line to limit the flow of a fluid without controlling it precisely. This would be designated FO. The active elements in the fourth column include such things as transmitters. If the variable is temperature, we have a TT. An example of a combination device is one that indicates the level in a tank and also manipulates other hardware to control that level—an LIC. The sequence of the letters follows the table. A control valve responding to a generated signal is designated by the single letter V. Self-actuated control valves bear the letters CV. Most control valves in the process industries will be equipped with positioners that receive control signals and then pneumatically apply the force necessary to drive the valve to the proper position. They improve response and control action. The standard followed here allows valve positioners to be included on the drawing or their presence to be assumed, with a signal shown as going directly to the valve. Here, we choose the latter, simpler option.

Finally, Table 11.1 allows the use of letters to modify those covered above. When a differential-pressure cell is used as such to measure and record the difference in pressure between two points, we modify the first letter and have a PDR. If the flow of one stream is to be held in constant ratio to that of a second while the value of the ratio is displayed, we have an FFIC.

Modifiers are also attached as required to succeeding letters. Alarms, for example, usually indicate that the value of a process variable is either too high or too low. The letters H and L modify “alarm” accordingly. Thus, a low-level alarm is an LAL. A switch that causes some action to be taken when a level is too high is an LSH. As in the case

TABLE 11.1. Instrument Identification Letters

	First letter		Succeeding letters		
	Measured or initiating variable	Modifier	Readout or passive function	Output function	Modifier
A	Analysis		Alarm		
B	Burner, combustion				
C				Control	
D		Differential			
E	Voltage		Sensor or primary element		
F	Flow rate	Ratio			
G			Glass, viewing device		
H	Hand				High
I	Current (Electrical)		Indicate		
J	Power	Scan			
K	Time, time schedule	Time rate of change		Control station	
L	Level		Light		Low
M		Momentary			Middle Intermediate
N					
O			Orifice, restriction		
P	Pressure, vacuum		Point (test) connection		
Q	Quantity	Integrate, totalize			
R	Radiation		Record		
S	Speed, frequency	Safety		Switch	
T	Temperature			Transmit	
U	Multivariable		Multifunction	Multifunction	Multifunction
V	Vibration, mechanical, analysis			Valve, damper, louver	
W	Weight, force		Well		
X	Unclassified	X-axis	Unclassified	Unclassified	Unclassified
Y	Event, state or presence	Y-axis		Relay, compute, convert	
Z	Position, dimension	Z-axis		Drive, actuator, unclassified final control element	

Source: ISA-S5.1 [1].

of the first letter, these designations apply to the state of the process. The LSH may well be activated by a low rather than a high signal.

11.1.2. Design Coordination

To achieve an efficient design, it is important that the control systems engineer work closely with the process engineer. Control systems engineers bring a different perspective with their concern for the dynamic responses of a process. They can contribute to the design by ensuring that control valves have adequate pressure drop for proper control,

reviewing the selection and size of equipment used for control, and ensuring that the process design does not result in overly complex control systems.

If the process engineer and the control systems engineer work together to satisfy the needs of both parties, the resulting plant design will benefit. The designs that appear here have had the benefit of such collaboration.

11.1.3. Control System Selection

For this basic discussion, we divide control systems into analog controls, safety systems, uninterruptible power supplies, and other digital systems.

The chlorine manufacturing process is primarily a collection of continuous operations suited to analog control. A standard distributed control system (DCS) is ideally suited to this type of process. Most DCS control software can also handle discrete logic and structured text requirements to provide all the control power necessary for any strategy. In a large plant, there should be no fewer than two operator stations, with two screens available to each station. In addition, there should be a separate “engineering” station for handling programming changes.

Certain critical safety functions require systems more reliable than a DCS, and they must be handled separately. These functions are associated, for example, with rectifiers, hydrogen compressors, and brine purging of membrane cells. In the past, redundant programmable logic controllers (PLCs) often provided the necessary reliability, but newer systems with the robustness of a standard PLC also have internal redundant logic and input checking and may also have redundant outputs.

It is standard practice to have the DCS and safety systems powered by an uninterruptible power source (UPS). Whenever the normal power supply fails, the UPS will immediately switch to its batteries, which can keep the systems powered until backup power can be applied or the process shut down. The UPS should be able to operate the control systems for at least 20 min.

A separate source may be needed to power some process pumps in the case of a general power failure. This will require a very large UPS, and so its need should be reviewed carefully.

Most chlor-alkali plants include a considerable number of packaged units with their own digital control systems. Most of these systems will need some interfacing with either the plant DCS or the safety system. Some plants will also decide to incorporate all the control functions into the DCS. It is imperative that a control specialist be involved with the individual package unit specifications to ensure that the required interfaces are completely defined and properly installed.

11.2. BRINE SYSTEMS

11.2.1. Modes of Control

Individual sections of the brine plant may be interconnected by level, pressure, or flow controllers. Some unit operations function better if they are fed by flow or pressure control systems. Whenever this is the case, a storage tank with a floating level can

eliminate the problem of simultaneous control of inventories on both sides of the point of control. A level control system to recycle brine to the tank feeding the unit, used in conjunction with total feed flow control, is another option. The various choices for each unit operation are discussed below.

11.2.2. Membrane-Cell Brine Systems

Membrane cells are used with both sodium and potassium brines. There is essentially no difference in the manufacturing process, except that KCl, with its steeper solubility curve (Fig. 7.18), tends to salt out more easily than NaCl. Raw KCl brine may also be higher in purity, thus requiring some differences in the treatment and filtering operations. The following discussions will be based on the use of solid NaCl as the principal feedstock.

11.2.2.1. Brine Saturation Systems

11.2.2.1A. Operation of Saturators. As shown in Fig. 11.1, neutralized depleted brine is fed to the saturator(s). The total rate of flow is regulated in the upstream equipment, and no automatic flow control can be applied in the saturation system itself. The feed brine should be at pH 8 or 9, but an upset in the neutralization system could allow the pH to drop well into the acidic range. Although Monel is the metal normally used for instruments in alkaline brine applications, Hastelloy C has the advantage of a greater resistance to attack by acids.

In a plant with more than one saturator, individual flow meters should be installed in each feed line to permit manual balancing of the flows. Inserted paddle-type flow meters with local indicators would be suitable for this application. Some saturator designs (Section 7.2.2.2) allow salt to fall into the vessel by gravity from an attached hopper and therefore require no instrumentation. Other systems rely on periodic additions of salt to

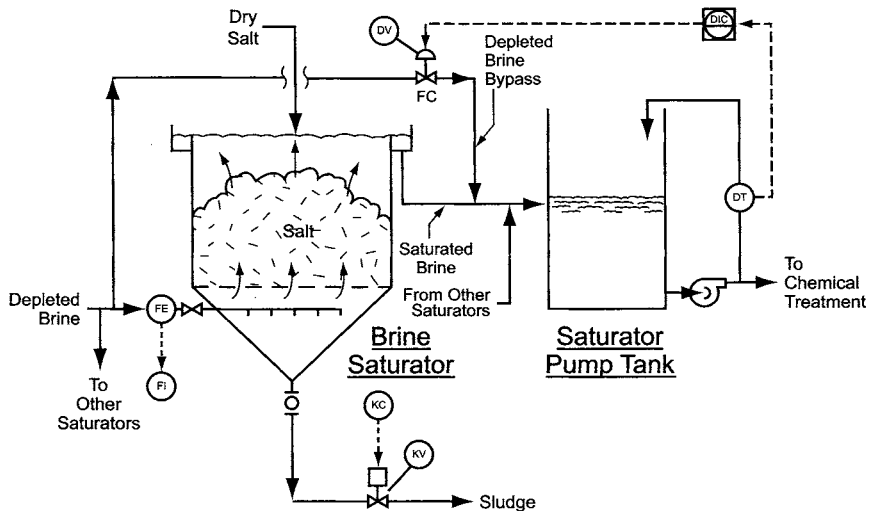


FIGURE 11.1. Brine density control.

the saturator vessel. The latter technique has implications as to the purity of the brine. Sudden introduction of a relatively large quantity of fresh salt can produce a spike in the concentration of a rapidly soluble impurity. Magnesium is the notorious example, particularly when solar salt is the feedstock (Section 7.1.5.1). Still other systems require some level of monitoring and control of the salt feed.

Insoluble matter collects in the bottom of the saturator and is frequently removed through a timed on-off valve. Air-actuated Monel knife valves are successful here, and it is possible that a pinch-style valve could be substituted. A master timer/sequencer determines when each valve is to open and close and prevents dumping of two saturators at the same time. A sight glass installed in the sludge line allows an observer to see when the stream becomes free of solids. The operators can then adjust the timers to minimize the loss of clean brine. If necessary, an air-operated sludge pump can be turned on whenever a dump valve is open.

The saturated brine from the top of a saturator flows by gravity to a pump tank. The pump tank may be a standpipe that is small in diameter but as tall as the saturator itself. The brine leaving the bed of salt in the vessel is fully saturated and would deposit salt throughout the process as its temperature dropped. Heating the brine or mixing it with some of the depleted brine produces some undersaturation and prevents this deposition. In Fig. 11.1, depleted brine bypasses around the saturators to lower the concentration in the pump tank. The brine concentration can be measured with a temperature-compensated density meter, here shown installed in a small line that spills back to the pump tank. A vibrating-tube density meter with the brine flowing through the tube is very accurate and can be obtained in materials of construction compatible with the brine. An alternative is a Coriolis mass flow meter in which the built-in density measurement is selected as the primary output. These instruments are just as accurate and less expensive. The flow of sample through either instrument must be maintained to prevent its plugging with salt. One corrective measure is to drain the brine and flush the instrument with water if the sample flow stops. Regardless of the instrument used, the brine must be well mixed with the bypass stream. The best place for measurement usually is on the discharge side of the transfer pumps.

Depending on the bypass flow rate and the minimum flow required, the control valve could be a small rubber-lined butterfly valve or an all polytetrafluoroethylene (PTFE)-lined globe valve. The sizing of this valve can be difficult, because there is very little pressure drop available. Butterfly valves should never be required to control at an open angle of less than 20°.

11.2.2.1B. Inventory Control. The membrane-cell brine process loses water with the waste streams, by transport through the membranes into the cell catholyte, and through evaporation into the chlorine produced in the cells. Even with minimization of the waste streams, there is a constant need for makeup water. This can be added to the saturator feed or directly to the pump tank. The choice of the addition point will determine the size of the bypass flow required to maintain the brine density. Addition to the pump tank is feasible only when its dilution of the brine is not excessive. One method for controlling the makeup water flow is to measure the total brine volume continuously and add water to maintain the desired amount. This is easily done because there are usually only two or

three vessels with uncontrolled levels. Figure 11.2 illustrates this approach by showing level signals from three unspecified brine tanks whose levels vary in normal operation. After conversion of levels to volumes, from function generators based on calibration data or by multiplication by a tank's cross-sectional area, addition of the signals gives the total volume. An integral-only controller provides the set point to a standard flow control loop regulating the make-up water.

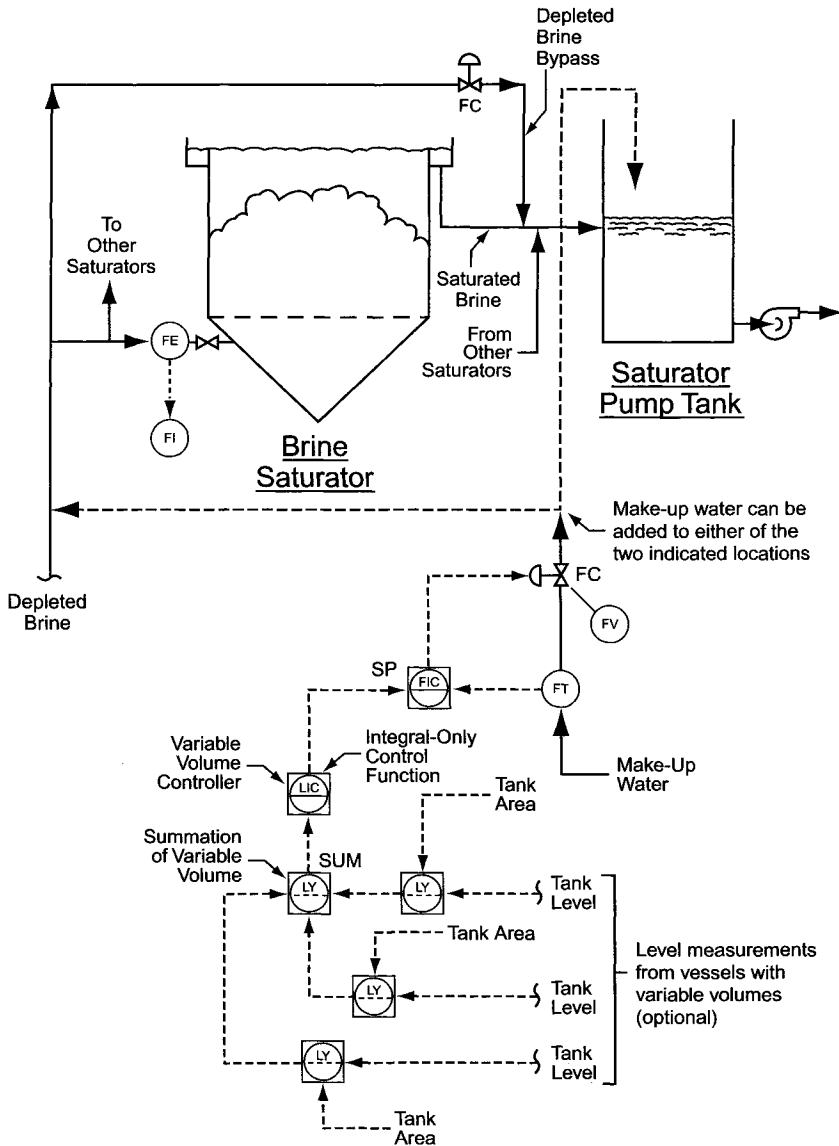


FIGURE 11.2. Makeup water to brine system.

11.2.2.1C. Pump Tank Level Control. One way to control the level in the pump tank is to throttle the stream pumped to brine treatment (Fig. 11.3a) in order to match the incoming flow. This is the simplest approach, but it results in a variable flow through the treatment tanks and clarifier. Excessive variation would be detrimental to the effectiveness of the treatment process and the settling efficiency. An alternative (Fig. 11.3b) is to control a recycle stream from the clarifier pump tank. This would then allow the use of a flow control loop to feed brine to the treatment tanks. This provides constant flow at the expense of recycle of clean brine to the treatment tanks. Depending on the design basis chosen, the tanks and the clarifier may become larger.

The control valve for the regulation of the brine flow to the treatment tanks, whether by level or by flow, can be a rubber-lined butterfly. The butterfly valve is ideally suited for this application. If a metal disc is used, it should be Monel, or by the argument made above, Hastelloy C. The recycle valve, if used, can also be a butterfly as long as the recycle flow is sufficient for the valve to be open at least 20°. A flush-type differential pressure (d/p) cell transmitter with wetted parts of Hastelloy C is an excellent choice for level measurement.

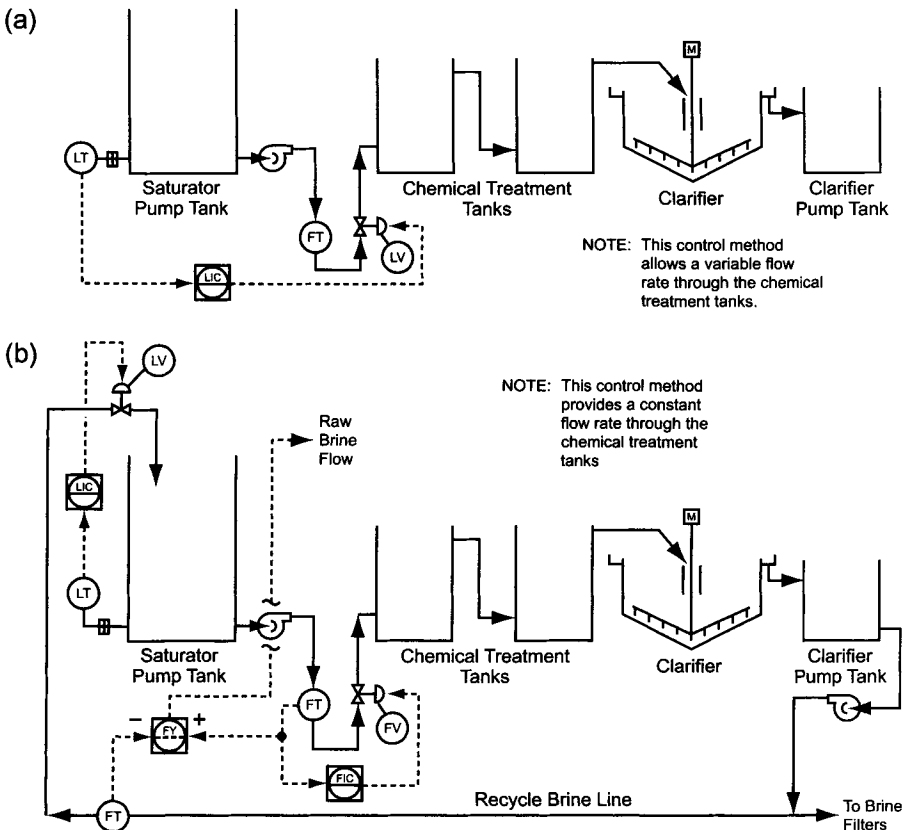


FIGURE 11.3. Saturator pump tank level control. (a) Direct control of level and (b) Flow control with recycle.

11.2.2.2. Brine Treatment Tanks and Clarifier

11.2.2.2A. Brine Treatment Tanks. Figure 11.4 shows a typical arrangement with two treatment tanks. The brine pumped from the saturator pump tank in Fig. 11.3 flows through these tanks and the clarifier by gravity. The treating agents are Na_2CO_3 and NaOH , and measurement of the raw brine flow rate allows each of them to be added under flow ratio control. Each flow rate is referred to the incoming raw brine flow. The plant operators adjust the individual ratios, based on analysis of the excess treatment chemicals that remain in the treated brine. Low residual concentrations may allow impurities to break through the treatment process. High concentrations are wasteful and can upset downstream processes.

In the drawing, the carbonate goes to the first tank and the hydroxide to the second. Section 7.5.2.2B discusses the various theories on the optimum sequence of addition of the reactants. Many plants also add a flocculating agent to the brine. Again, the point of addition varies from plant to plant. The low flow rate of this solution usually calls for addition by a metering pump. The speed or stroke of this pump may respond to flow rate (with proper damping), flow ratio, or a manual setting.

Magnetic flow meters are the preferred choice for brine feed flow measurement. If the saturator pump tank level is controlled by throttling the brine to the treatment tanks, as in Fig. 11.3a, the measurement shown in Fig. 11.4 gives the net brine flow through the system. It is used to determine the quantities of the treatment chemicals to be added. If the tank level control is through the recycle of the clarified brine, as in Fig. 11.3b, measurement of the recycle flow as well as the feed flow allows calculation of the net feed by subtraction. The resultant value can then be used to control the rates of addition of the treatment chemicals. The brine flow signal in Fig. 11.4 does not reflect the latter approach.

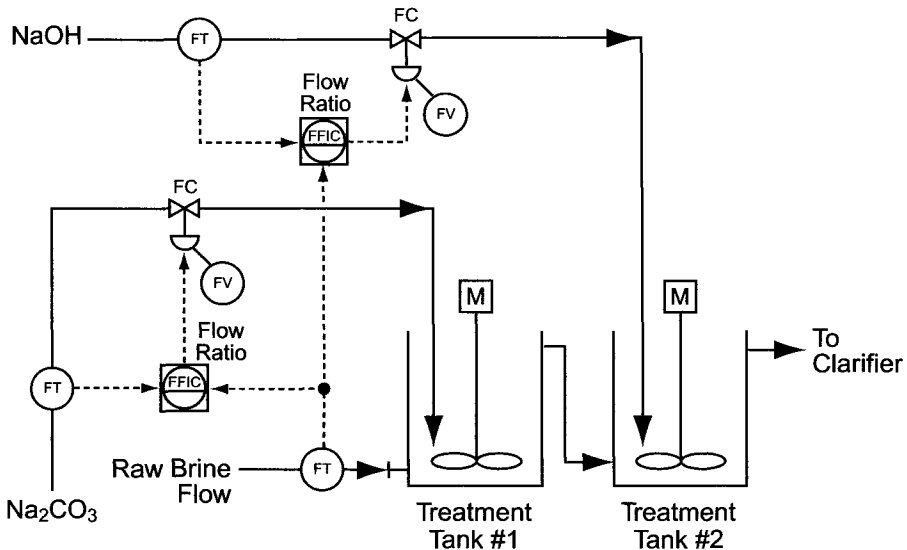


FIGURE 11.4. Brine chemical treatment tanks.

11.2.2.2B. Clarifiers. Figure 11.5 shows the clarifier side of the operation. Removal of sludge from the bottom of the clarifier is similar to its removal from the saturators (Section 11.2.2.1A). A timer determines when the pump is turned on and for how long it runs. The sight glass in the sludge line going to the pump gives proof that the slurry is moving freely. If the transfer line is flushed, the glass will also show how long it takes for the line to become clear. The operator adjusts the timer to the optimum settings.

Brine from the top of the clarifier overflows by gravity to the clarifier pump tank. A turbidity meter in this line can monitor the solids content and provide an alarm in case of an upset in the clarifier operation. Again, operation and control are similar to those discussed in connection with brine saturation. The top of the tank should be at least as high as the top of the clarifier overflow system. This provides more brine storage capacity as well as time to correct a pump failure or other simple operating problems. The normal level in the pump tank is about 50%. Level control options are as in Fig. 11.3:

1. direct control of the level
2. flow control to filters with level control by recycle of the filtered brine

Level control valves can be rubber-lined butterflies with Monel discs and shafts or completely lined butterflies. They must be sized carefully so that they can handle the maximum flow (including any recycle portion) as well as the minimum flow without having to throttle at less than 20% open. A flush diaphragm d/p cell level transmitter with Monel wetted parts is an excellent choice for this service.

Other clarifier instrumentation, not shown here, includes controls for changing the rate of rotation of the rake assembly and the angle of the rakes on the arms.

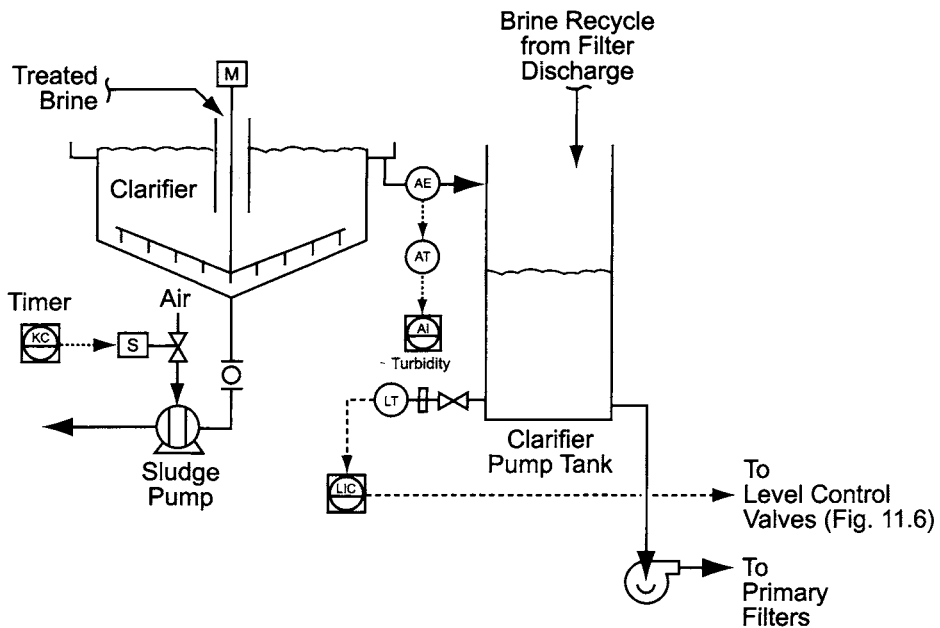


FIGURE 11.5. Brine clarifier and pump tank.

11.2.2.3. Brine Filters

11.2.2.3A. Primary Filters. Figure 11.5 shows the transfer of clarified brine to the primary filters under some form of level control. Figure 11.6 assumes flow control through the filters, to avoid any upset in their operation, coupled with a return of the excess flow to maintain the level in the clarified brine pump tank. The individual filters work best with controlled feed flows. A magnetic flow meter is used on the inlet to each filter with a butterfly valve in the outlet line. The level in the clarifier pump tank, as described above, controls the two rubber-lined control valves on the brine leaving the filters. The fail-closed valve LV-2 recycles the brine, and the fail-open valve LV-1 sends it to the polishing filter feed tank.

Flow measurement is by magnetic meters with ethylene-propylene–diene elastomer (EPDM) lining and Hastelloy C electrodes. The control valve can be a rubber-lined butterfly valve with a rubber-coated or Monel disc.

The arguments made in Sections 7.5.4.1 and 7.5.4.2 for a recycle level control were based on the characteristics of the filters. We point out here that this approach also offers advantages in precommissioning and perhaps in the quality of the control. First, in the testing phase, the filter system can be operated without the rest of the brine system running. Second, the combined demands of variable pressure drop during the filter cycle along with changes in flow rate to maintain the level in the tank can go beyond the capability of a single butterfly valve.

11.2.2.3B. Polishing Filters. Figure 11.7, showing the brine polishing filters, is quite similar to Figs. 11.3b and 11.6. The simple level control option does not appear here. Maintaining a constant flow is more important with vertical precoated elements than it is with the equipment discussed previously. Variations in flow can allow the cake to fall from the filter elements.

In this system, the feed tank level instrument controls both the recycle valve and the valve that transfers the brine to the ion-exchange system. The particular system shown here has only two filters, with flow metering in the common outlet line. More complex systems would require some modification. Hardware requirements are much the same as those already given for the primary filter system.

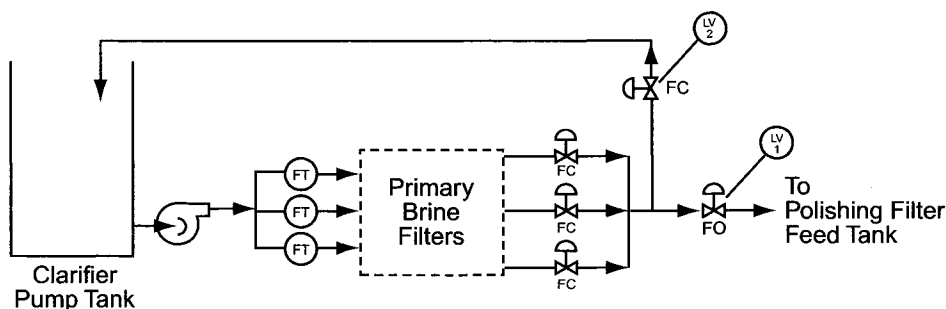


FIGURE 11.6. Primary brine filters.

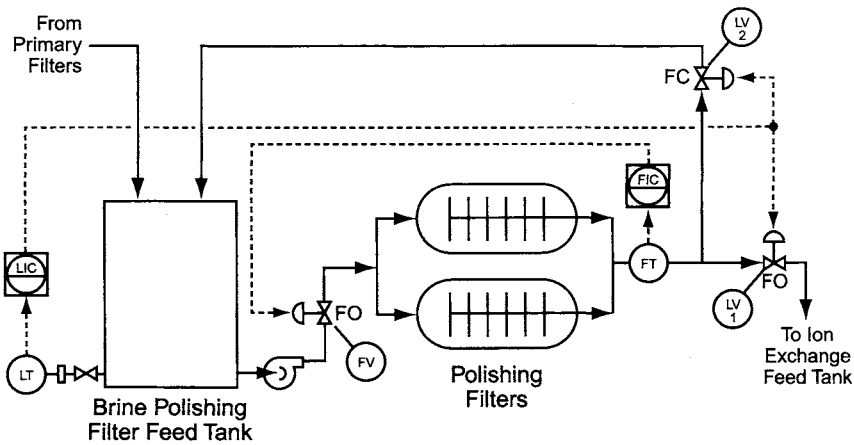


FIGURE 11.7. Brine polishing filters.

11.2.2.3C. Control System Interfaces. Figures 11.6 and 11.7 show that most operations require multiple filters. These systems, as well as the ion exchangers discussed below, operate in a cyclic manner, with each component periodically taken out of service for regeneration or redressing. Sequential controls are necessary in addition to the process line controls shown in this chapter. These are separate digital controls that are frequently supplied by the unit manufacturer in a PLC.

The sequence and lengths of the various steps in a filter cycle, discussed in Sections 7.5.4.1 and 7.5.4.2, are usually controlled by a field-mounted control system such as a PLC with an operator interface. Normally, the filter manufacturer supplies all the controls, but the plant should maintain control of part of the operation for smoother overall process operation. Items suggested for direct plant supervision are:

1. filter feed flow controllers;
2. individual filter differential pressure monitoring;
3. indication of time on line for each filter;
4. indication of quantity of brine filtered;
5. criterion for start of backwash.

Set points for the aforementioned parameters and the assignment of out-of-service filters should also be from the main control system. The local filter control system manipulates a number of on-off valves that control the operation and such actions as backwashing the filters. Full information on the status of the system should also be available through the main control system.

Hard wiring and direct digital communication are two ways to provide the interface between control systems. If the plant chooses direct digital interfacing, the packaged system software programming must be protected against improper access from the main control system.

Another alternative, which some operating companies prefer, is for all control to be through the plant's DCS.

11.2.2.4. Ion Exchange and Pure Brine Handling

11.2.2.4A. Ion-Exchange System Feed. Figure 11.8 shows the ion-exchange feed system. In it, the filtered brine storage/ion-exchange feed tank is also used as the source of backwash fluid for brine filters. The quantity involved in this operation is significant, and sizing of the tank should include about two backwash volumes.

The level in the tank is measured by a flush-mounted d/p cell with wetted parts of Monel. As one of the hold tanks with variable volume, the feed tank may also send a signal to the summation system of Fig. 11.2.

Unsupervised use of level control on the forward discharge from the tank would allow the rate of flow through the ion exchangers to vary. The sudden drop in the level after withdrawing brine to backwash a filter would cause a sudden reduction in flow, followed by a gradual increase as the level recovered. In Fig. 11.8, however, the flow rate forward from the exchangers is measured and transmitted to a selector switch that can override the ion-exchange feed tank level controller to maintain a minimum flow. As the level drops during the backwash of a filter and the controller attempts to close the valve and reduce the flow rate, the minimum flow controller takes over. After backwash, the difference between the rate of flow from the filters and the forward flow from the tank gradually refills the tank. When the level approaches the normal set point, the level controller takes over and begins to increase the flow to ion exchange. More sophisticated controllers can also communicate with the filter control system and apply logic to anticipate changes in status and smooth out the operation even more. The pumping system must also be adequate to handle all the demands. It usually involves multiple pumps.

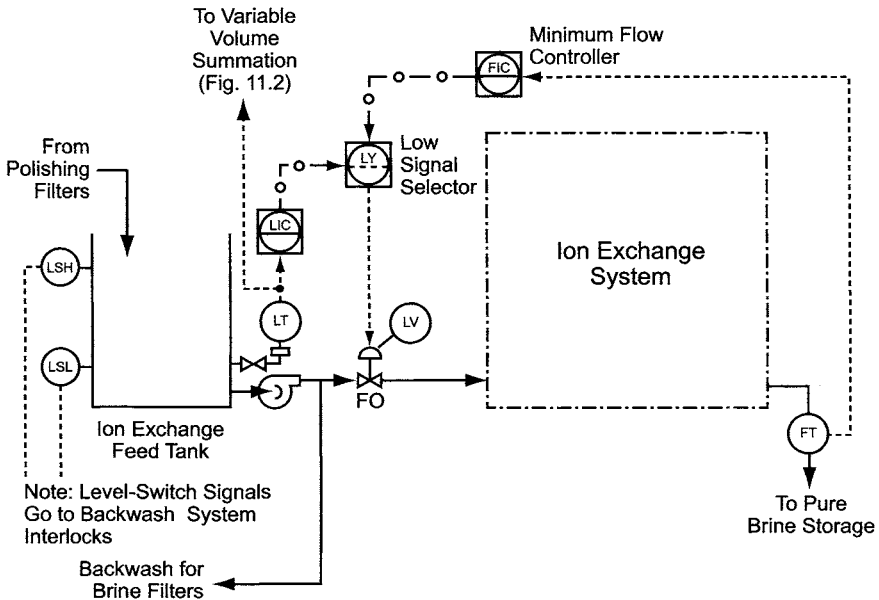


FIGURE 11.8. Ion-exchange feed tank level control.

If there are separate facilities to handle the backwash, the system described here becomes more straightforward. The complications of handling periodic large transfers then belong to the other system.

11.2.2.4B. Ion-Exchange System. There should be a hardness analyzer (range 0–50 ppb as Ca) in the ion-exchange system. This analyzer is connected through automatic sampling valves to the brine leaving each column. These valves are manipulated by the local sequence control system so that the analyzer is always monitoring the outlet of the first operating column. This provides early warning of depletion of that column. Any hardness that breaks through the first column is removed in the second column (if a second column is on line; see Section 7.5.5.3C).

Most ion-exchange systems are provided with PLC control. This should be partly integrated into the main plant control system. Section 11.2.2.3C already discussed this issue in connection with filter systems. The considerations here are essentially the same.

The skid, as supplied, usually includes small storage tanks for regeneration chemicals. They are prepared from membrane-cell product caustic, which is very pure, and from a refined source of HCl. Frequently, the HCl is the product of an on-site burner. Section 7.5.5.3D discusses various methods for the preparation and delivery of regeneration chemical solutions. Each method has its own control requirements.

Regeneration of exchange resin produces large amounts of waste solution. The simplest disposal procedure includes collection of the various streams in a large hold tank. This allows self-neutralization of the waste as caustic effluent follows the acid from an earlier step. The combined effluent from an entire regeneration sequence will be acidic. In any case, batchwise neutralization with acid or caustic is a simple procedure. Because of the quantities involved, some plants have systems in place to recover some of the regeneration waste. Sections 7.5.5.2B and 16.5.2.4 discuss this aspect.

11.2.2.4C. Pure Brine Storage. The pure brine tank (Fig. 11.9) is a large vessel intended for the storage of brine to be fed to the cells. It can also be used to flush the cells upon failure of the rectifiers if there is no separate head tank for that purpose. This feature does not appear in the drawing.

It is good practice to install another automatic hardness analyzer in the brine stream from the ion exchangers. These are complex analyzers that need experienced personnel to keep them functioning. Capital and operating costs are quite high, but analyzers have helped to prevent serious damage to membranes. The automatic analyzers should be looked upon as aids to operation and not as substitutes for proper laboratory equipment and the occasional precise measurement.

There is no control of the level in the tank of Fig. 11.9. Measurement is still desirable, and a flush-mounted d/p cell is the usual choice. Since this is a floating-level tank, the level signal can connect to the optional system of Fig. 11.2.

Another aspect of Fig. 11.9 is the acidification of the brine before storage. This is compatible with two-stage acidification before the cells. Sections 7.5.6.1 and 13.8.2.3 describe the advantages of this approach. The system shown relies on feedback pH control, with acid blended into the brine in an in-line mixer placed before the control

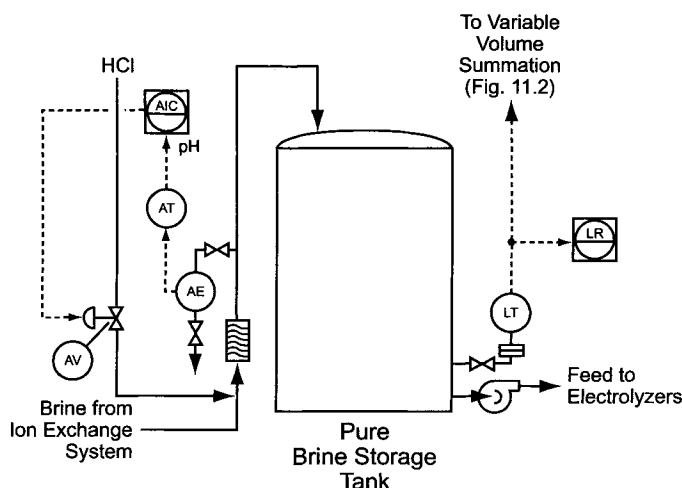
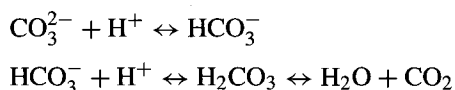


FIGURE 11.9. Pure brine storage tank.

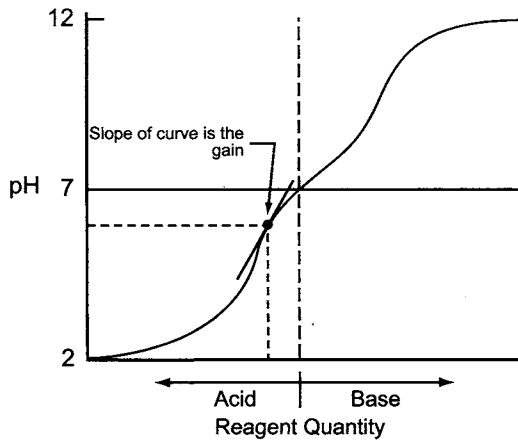
element. The HCl valve should be a fully PTFE-lined globe valve with equal percentage trim and PTFE bellows.

Figure 11.10 illustrates some of the characteristics of the recommended adaptive gain pH control system. The set point and the programmed controller response depend on the titration curve of the brine. As explained in Section 7.5.6, one objective of this preliminary acidification is the decomposition of the carbonate value in the treated brine. This takes place in two stages:



Both reactions cause inflections in a titration curve, as shown in the top part of Fig. 11.10, but the second reaction is the important one here. Its pK_a is about 6.37. At typical brine temperatures, the equivalence point is at a pH of about 5.5. Lower values are necessary to ensure complete decomposition. As the pH moves away from the equivalence point, the slope of the titration curve increases, and control becomes more difficult.

Movement along the titration curve from right to left represents the addition of acid to the brine. The fact that reaction occurs is responsible for the flattening of the curve. After enough acid has been added to complete the conversion of bicarbonate, the pH drops rapidly, and it becomes more difficult to control the process. The slope of the curve at any point is defined as the gain. Note that the calculated gain at any pH would not be affected by reversing the plot and more conventionally following the course of the titration from left to right. A second plot in Fig. 11.10 shows the measured gain as a function of pH. The third plot shows the inverse gain, defined as the reciprocal of the gain itself. Normalizing the inverse gain against its largest value provides a scale for the ordinate of the plot. This function is built into the controller as a multiplier for the primary output, as shown in the bottom part of Fig. 11.10.



Titration Curve

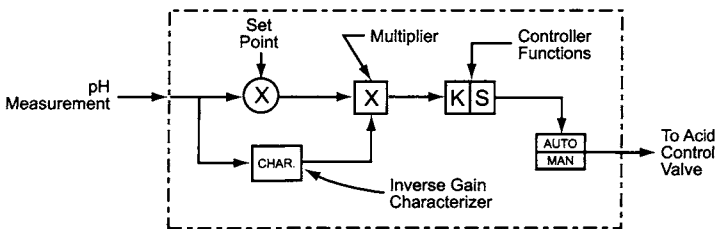
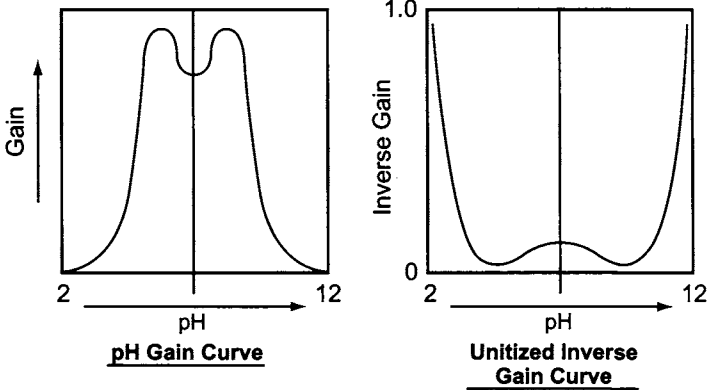


FIGURE 11.10. Adaptive gain control system.

11.2.2.4D. Brine Feed to Cell Room. Brine feed to the cell room can be by pump, by pressurized transfer from a tank at grade, or from a head tank. The discussion of Fig. 11.9 assumed the first of these, but the choice does not affect the control arrangement shown in Fig. 11.11. A head tank, or other secure system, should contain enough brine to purge the cells if the rectifiers shut down. In large cell rooms, this volume becomes quite large

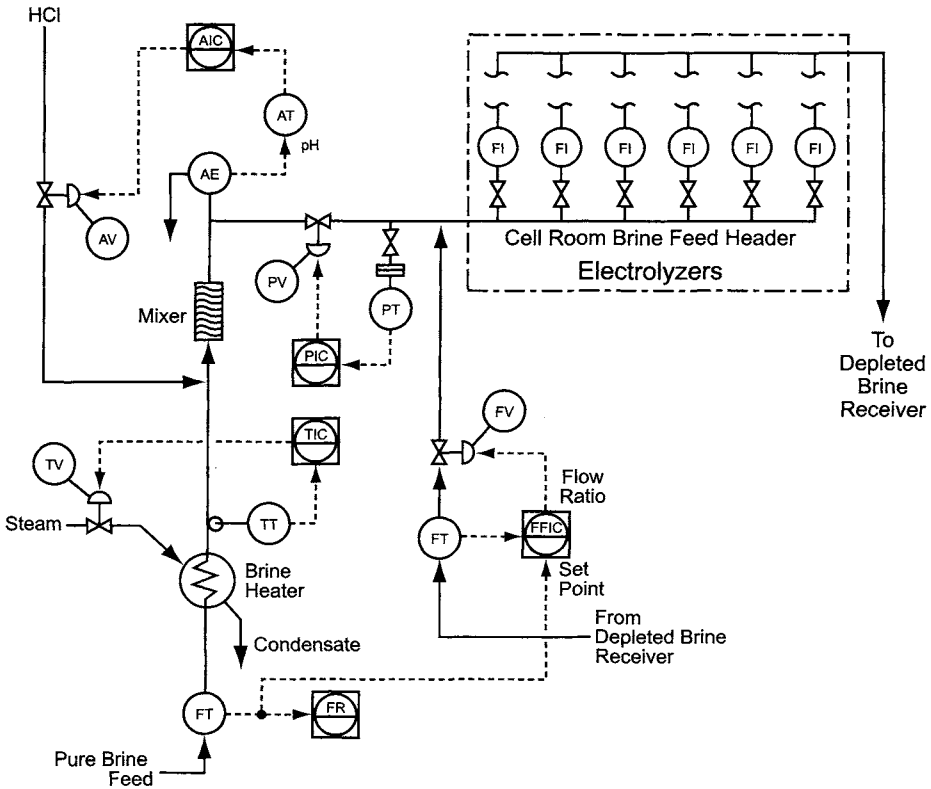


FIGURE 11.11. Electrolyzer brine feed control.

and would require a massive structure for its support. It is this aspect that can make the use of a pressurized tank attractive. Pumped brine, the other option, would require a very large UPS to power the feed pump during a general power failure.

The brine sent to the cell room is heated with low-pressure steam in a heat exchanger. The temperature is measured with a resistance temperature device (RTD) transmitter with a tantalum-sheathed flanged thermowell. The control valve is usually a fail-closed globe valve with an equal percentage characteristic. This valve should be interlocked to shut off the steam if there is no brine flow. Many plants first interchange the brine with recirculating caustic in order to conserve energy. Section 9.3.2.4 discusses this technique and considers the changes in interchanger duty as the cell room operating load varies. Brine instrument hardware for the interchanger is the same as for the heater.

A PTFE-lined magnetic flow meter measures the brine feed to the cell room. In a plant with a ratio-controlled anolyte recycle, this flow rate also can furnish the primary flow signal. The recycle anolyte stream returns to the brine feed header downstream of the pressure control valve. A PTFE-lined magnetic flow meter with platinum electrodes measures its flow. The control valve downstream of the flow meter should be a butterfly valve fully lined with PTFE. This valve should close upon rectifier failure.

An in-line pH control system is installed when the brine is to be acidified. HCl is added upstream of an inline mixer, with measurement downstream of the mixer. This is a simple case of pH control, the end point being fairly low. The process gain is also low in this case, and control is easier than in the first stage of the pH adjustment, described in the previous section. The acid valve should be a fail-closed globe valve of equal percentage characteristic with full PTFE lining and PTFE bellows. An interlock should close the acid feed valve whenever there is no brine flow or no current on the cells.

Manually operated valves with local indicators control the flow of brine to individual electrolyzers. All the electrolyzers in the circuit are fed from a common header that is maintained at a specified pressure. This approach reduces the interaction between electrolyzer feed rates when any one is adjusted. Total cell room flow can be changed by changing the header pressure. The pressure is measured by a transmitter with a capillary and diaphragm seal. Wetted parts should be tantalum or PTFE. The range is usually 0–200 kPa. The control valve, located upstream of the pressure measurement, should be a fully lined fail-open butterfly valve.

Figure 11.11 and the discussion above assume the use of monopolar electrolyzers. The cost and complexity of outfitting a large plant with the instrumentation necessary for individual cell control rule out that approach. Where there are fewer electrolyzers, as in bipolar cell rooms, there are fewer control points. The use of more automation becomes practicable. Brine flow control at each electrolyzer, for example, may become automatic. The flow can be set directly by the operators or respond to electrolyzer current. Similarly, pH control can be by individual controllers on each electrolyzer. Section 7.5.6.1 discusses the merits of various approaches. Anolyte outlet pH can be controlled, typical set points being 2.3–3.0. Adaptive gain control (Section 11.2.2.4C) is useful here.

A final consideration in the brine feed system is the need to purge the cells whenever the power supply fails or is accidentally or deliberately withdrawn. Section 13.8.3.1 discusses the need to remove acidic chlorinated brine from the cells and the factors that determine the volume required to flush the cells adequately. Given a source of brine to do this, Fig. 11.12 shows a protective system. Removal of power activates a flush timer. This, in turn, de-energizes a solenoid and opens a valve to deliver brine to the cells even when the normal feed system also has failed. The brine flushing rate is substantially the same as the normal feed rate. The brine feed control system therefore does not need resetting. After a set interval, the purge stops. The flush timer controls this interval. If the rectifiers restart before the flush timer reaches its setting, the timer stops but retains the last value. The reset timer then starts. If the rectifiers trip again before the reset device times out, the flush timer continues from where it stopped. The reset timer is reset whenever the rectifiers trip.

When power is removed from an operating cell, the spontaneous reverse reaction can occur (the “battery effect”). There will be a reverse current until the circuit is broken or the cells discharge. This can damage the cells. Cathode coatings are generally the most sensitive components. Besides flushing the anolyte chambers with clean brine, protective measures include polarizing the cells to oppose the reverse current. Many membrane-cell plants now include low-capacity rectifiers for this purpose. As implied above, these are more common in plants with coated cathodes. Some plants rely on a UPS for power to the polarizing rectifier(s).

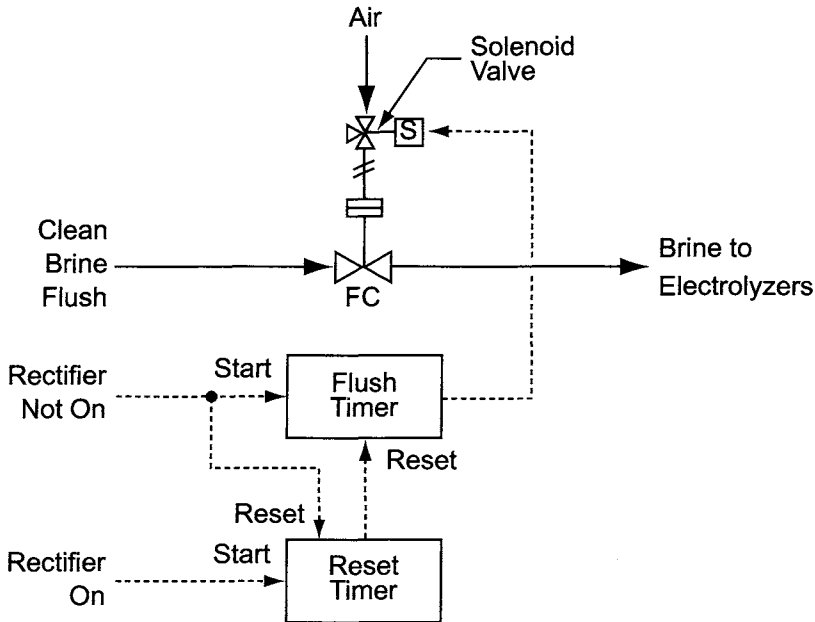


FIGURE 11.12. Clean brine purge (rectifier shutdown).

11.2.2.5. Collection and Handling of Depleted Brine

11.2.2.5A. Depleted Brine Collection. A depleted brine receiver (or anolyte tank) collects overflowing brine from the electrolyzers (Fig. 11.13). Addition of HCl releases the chlorine dissolved in the brine. By way of the depleted brine header, this vessel also receives the flushing brine when the rectifiers trip. Space constraints may prevent the use of a tank with enough freeboard to accept all the flushing brine. This situation is addressed in Section 11.2.2.5E.

It would be desirable to add the acid and measure the pH in the piping between the cell room and the depleted brine receiver. However, the header should be designed to be self-venting, and even a horizontal section before the receiver may not run full of liquid. One alternative is to design the tank with a small baffled section for pH control.

There are three destinations for the depleted brine: the brine feed header, the chlorate destruction reactor, and the brine dechlorinator. The last of these is the main process flow.

The PTFE-lined level control valve is in the line to the dechlorinator. When dechlorination is assisted by vacuum, the valve is at a low elevation in order to prevent flashing before the valve. Flashing occurs in the riser to the top of the column, and the piping must be designed accordingly.

The level transmitter at the depleted brine receiver should be a double-filled d/p cell with tantalum diaphragms.

11.2.2.5B. Chlorate Decomposition. Chlorate decomposition is the subject of Section 7.5.9.4. The decomposition reactor can take any one of many forms, as long as it provides sufficient time for the reaction. Ideally, the reacted brine should then

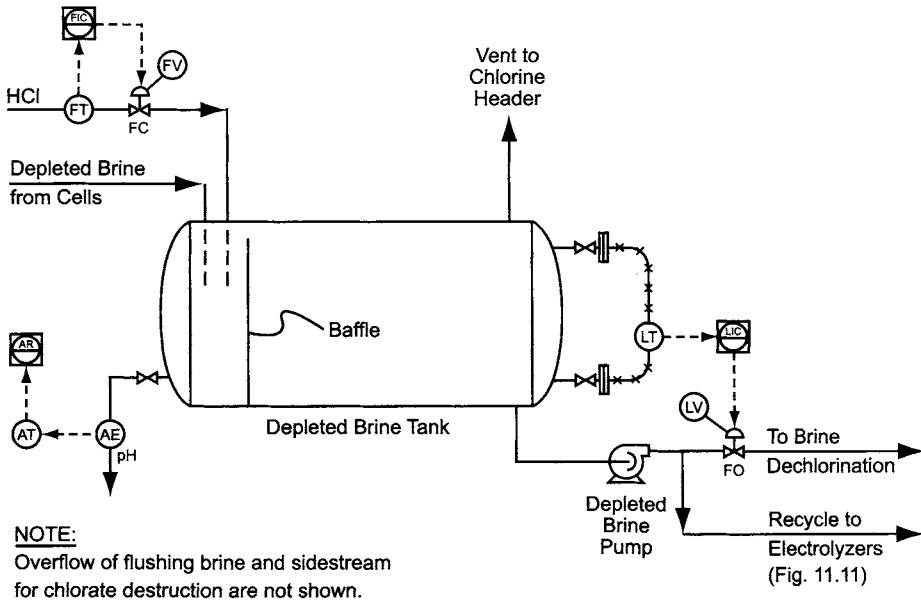


FIGURE 11.13. Depleted brine collection.

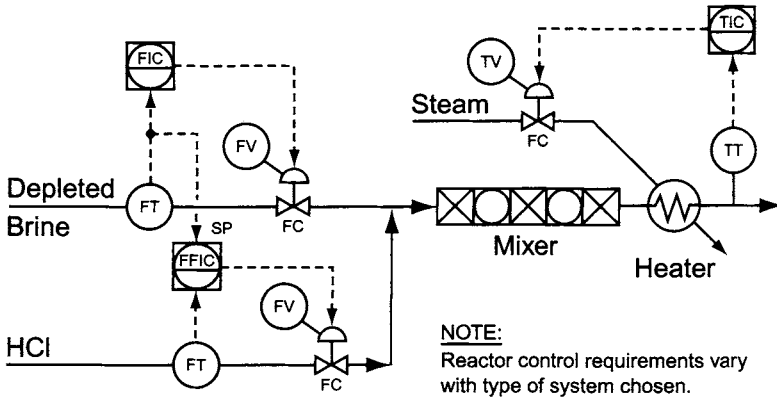


FIGURE 11.14. Brine conditioning for chlorate destruction.

return to the depleted brine receiver (anolyte tank) so that its high concentration of acid can help to release chlorine from the main brine stream and reduce the amount of fresh acid needed for dechlorination (Section 11.2.2.5C). Figure 11.14 shows a typical brine conditioning system. The brine from the chlorate reactor must be thoroughly mixed with the main depleted brine stream and the acid before pH measurement. A poor choice of location for this measurement may cause oscillations in the pH. A conventional flow control loop is used, with a PTFE-lined magnetic flow meter downstream of a fully lined control valve. The valve can be butterfly or globe, depending on its size. The signal to this valve should be interlocked with the level control signal from the depleted brine

receiver. When the depleted brine level control valve is closed, the chlorate reactor feed valve is also forced closed.

Only a small portion of the depleted brine (say, 10%) goes to the chlorate reactor, and even this might operate only part-time. Section 7.5.9.4 pointed out that more careful and more nearly continuous operation of the reactor can reduce the amount of byproduct ClO_2 formation.

Low-pressure steam is the source of heat for the brine entering the reactor. The temperature transmitter is an RTD-type sensor in a tantalum-sheathed flanged thermowell. The drawing shows a steam exchanger on a pumped feed line. The brine flow control valve is globe-style and fails closed. Section 7.5.9.4 described the use of a steam eductor as the feed mechanism. This eliminates the need for the heat exchanger. The eductor itself can be titanium or PTFE-lined.

If the chlorate reactor is a vessel, a level control loop is necessary. The transmitter should be of the flush-diaphragm type with wetted parts of tantalum. The control valve, located in the pump discharge piping, should be fully lined with PTFE. The size of the system will determine the type of valve to be used.

11.2.2.5C. Vacuum Dechlorination. Section 7.5.9.2 discussed three approaches to dechlorination. Open steam stripping applies primarily to waste water rather than brine and therefore appears more commonly in diaphragm-cell plants. Air stripping, while applied on scales up to 100 tpd of chlorine, is normally associated with small plants. Figure 11.15 assumes the use of vacuum dechlorination. Acidified dechlorinated brine is fed to a packed stripping column, shown here as mounted on a receiver.

A water-sealed corrosion-proof vacuum pump piped to the top of the dechlorination column produces a vacuum of 65–70 kPa. The pressure transmitter, with a remote tantalum diaphragm seal, should have a full vacuum range to 100 kPa(g). In this example, control is through the bleeding of atmospheric air into the vacuum line. Because of its proximity to the wet chlorine vapor, the control valve is fully lined with PTFE. Section 12.6.3 discusses other approaches to vacuum control and notes that loading with air may not be the best approach, particularly in a membrane-cell plant with chlorine liquefaction. While it is an efficient method of control and adds little to the cost or the cooling load, it reduces the efficiency of liquefaction at any given set of conditions.

Level control is critical because an unsteady level will result in varying discharge flow, which directly affects the brine neutralization control loop. The level transmitter should be a dual remote d/p cell with wetted parts of tantalum. The control valve should be a fully PTFE-lined butterfly valve in the pump discharge line. If powered by a UPS, this pump can be a source of flushing brine during a total power outage. The dechlorinated brine receiver may be elevated in order to provide more suction head to the discharge pump.

11.2.2.5D. Dechlorinated Brine Discharge System. This is the most difficult control loop in the brine system. Neutralization takes place in a static mixer. Caustic enters through an injector nozzle upstream of the mixer, and pH is measured close downstream. The starting pH of the brine is normally less than 2.0, and the end-point is between 8.0

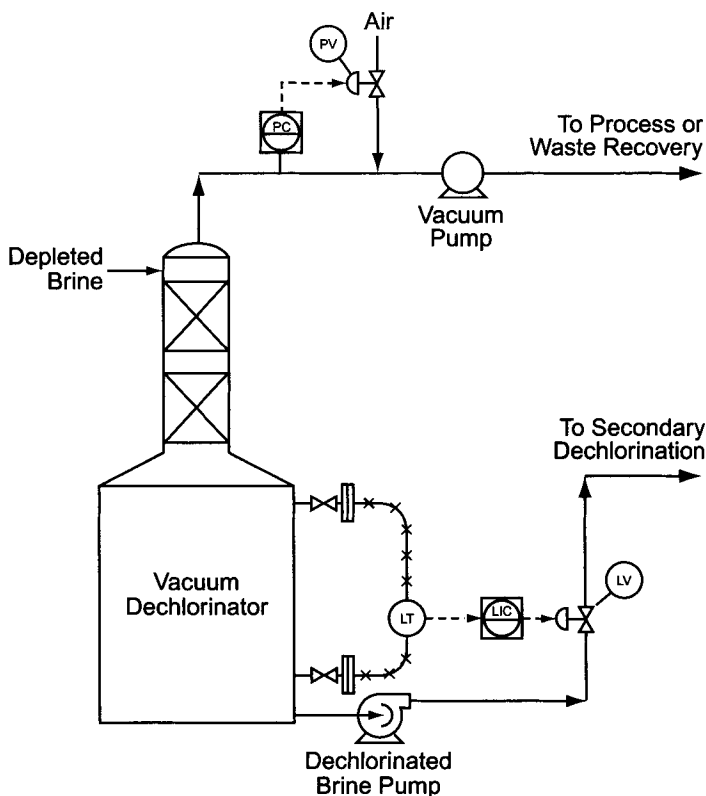


FIGURE 11.15. Brine vacuum dechlorinator.

and 9.0. Titration of typical brines shows that the amount of caustic required for a pH change of 0.1 at a set point of 8.5 is about 1/140 of the total needed. No single valve can control this with precision.

Figure 11.16 therefore shows two control valves. The first, larger valve depends on a “gap action” control arrangement. With the input signal between chosen limits, the controller of the large valve freezes its position. When the input goes outside those limits, the valve is free to move in the appropriate direction. The second valve has about 10% of the capacity of the first. It is driven by an adaptive gain controller (as in Section 11.2.2.4C) and is able to make small corrections in the caustic flow. Tuning of the pH controller follows normal practice. The gap action controller must have low gain and a high reset time so that its control action is slow. In the manual operation, the system should force the pH controller to 50% output. The manual output then controls the large valve.

After neutralization, a reducing agent is added to destroy the free chlorine not removed in the primary dechlorination step. Section 7.5.9.3A discusses this process and the various reducing agents that might be used. The drawing shows control through a conventional cascade arrangement. The control signal is based on the oxidation–reduction potential of the treated solution.

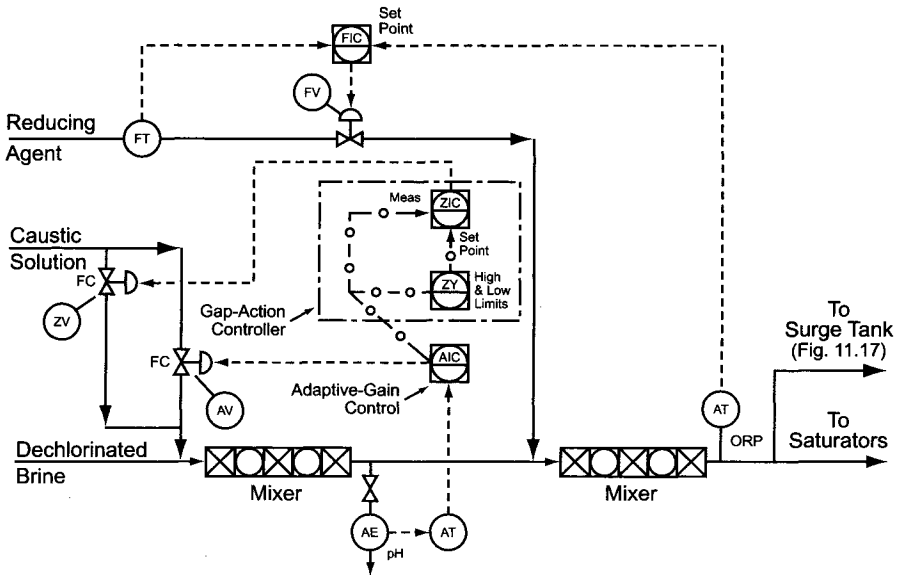


FIGURE 11.16. Dechlorinated brine neutralization and reducing agent addition.

11.2.2.5E. **Dechlorinated Brine Surge Tank.** If the depleted brine receiver cannot hold the volume required to flush the cells during the rectifier shutdown, a surge tank of sufficient volume is necessary (Fig. 11.17). The brine collected in this tank can be returned to the brine system at a controlled rate. The same tank can receive brine diverted from the process for other reasons. The diversion system shown here consists of a pair of on-off valves, one in the brine line after the neutralization system and the other in the line to the dechlorinated brine hold tank. Dechlorinated brine can be diverted into this tank manually or automatically. Reasons for automatic diversion include power failure and insufficient dechlorination.

The level transmitter should be a flush-diaphragm d/p cell with wetted parts of Hastelloy C. This is one of the vessels in the optional variable volume system (Fig. 11.2).

11.2.2.6. **Electrolyzer Area Controls.** The major control function on the brine line in the electrolyzer area is the regulation of its flow rate to individual cells. Figure 11.11 shows a number of electrolyzers attached to a brine feed header with individual flow indication. On the header is a pressure controller. With the regulating valves on the individual feed lines set, the header pressure fixes the total brine flow. Changing the set pressure will then change the flow of brine through the cell room. Good distribution of the flow among the electrolyzers depends in part on the pressure loss in the header being well less than that in each electrolyzer plus its feed line.

The system described effectively has two flow controllers in series for each electrolyzer. This would be unworkable if the flows were nearly equal. Considering first a large monopolar cell room, however, there are many branches in parallel, and flow through each branch is a small fraction of the flow through the header. Adjusting the

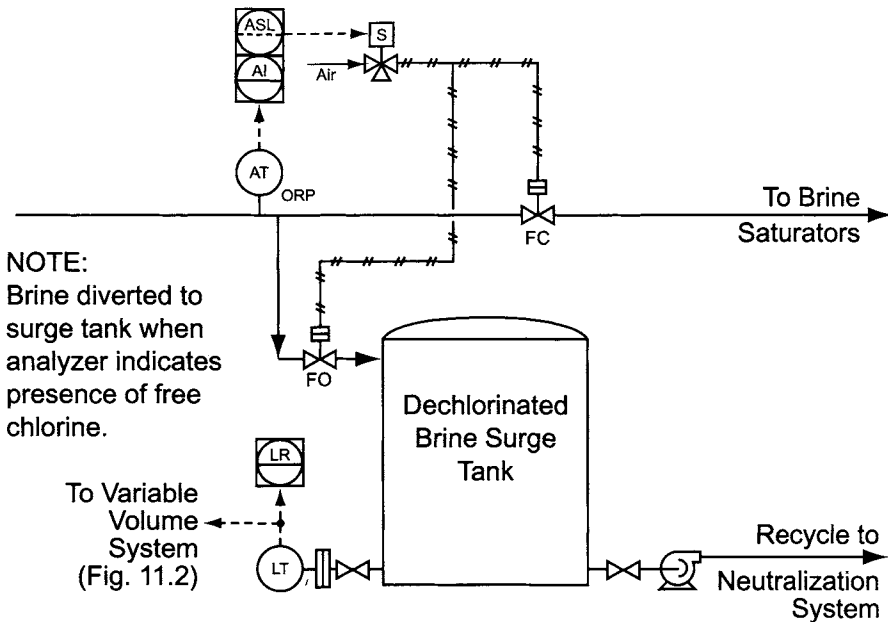


FIGURE 11.17. Dechlorinated brine surge tank.

flow rate to an individual cell by way of its manual control valve causes little disturbance to the other cells. Bipolar electrolyzers may contain many cells, and an even distribution within an electrolyzer depends on internal hardware design (Chapter 5). In a bipolar cell room with few electrolyzers or in a small monopolar cell room, adjustment of the flow in one branch off the header can begin to have a significant effect on the flows through the other branches. In these cases, designers may choose to have more than one primary flow controller.

Flows to individual electrolyzers can be adjusted by manual valves accompanied by flow indicators, and the total flow can be regulated by the brine feed header pressure controller. The latter is the first step in making global changes as, for example, when changing brine flow to suit a change in the cell room current. Because the individual flow meter/electrolyzer combinations have different nonlinearities, this change may have to be followed by trim adjustments to some of the branches.

Other control functions on the feed header include temperature and pH. The temperature control loop shown is quite straightforward. However, the cell temperature (or depleted brine temperature) is more important than the feed temperature. Therefore, the control setting must be manipulated to give the desired end result (Section 13.10.6.5). This can be done manually or by feedback of some average outlet temperature or the cell operating load.

The pH adjustment shown here is the second of two stages. It is not an essential part of a plant's control scheme. It is an option that allows the pH to be kept low in order to

reduce the formation of oxygen and hypochlorite in the cells (Section 7.5.6.1). One reason for the two-step approach is to allow degassing of the CO₂ formed by decomposition of carbonate outside the cell area. Reducing the pH in one step from the value held in the brine treatment area down to the low values necessary for oxygen control would release CO₂ in the feed line and interfere with flow patterns in the feed lines and in the cells.

11.3. CHLORINE SYSTEMS

11.3.1. Background

Chlorine gas from the cells is saturated with water vapor at 80–95°C. It may contain traces of other gases such as hydrogen, oxygen, nitrogen, and carbon dioxide. The hydrogen concentration in the cell room chlorine is usually low and well below the explosive limits but can increase rapidly to dangerous levels (Section 9.1.11.1). There have been some violent cell room explosions in the past, and small explosions that ruptured the tops of mercury cells were at one time frequent occurrences. Thus, it is prudent to make frequent analyses of the chlorine gas.

Dry chlorine is very easy to handle, to compress, and even to liquefy, while wet chlorine is very corrosive. The processing of chlorine, as pointed out in Section 9.1.1, is the conversion of wet corrosive chlorine gas into a dry noncorrosive gas or liquid.

11.3.2. Operating Systems

The handling and processing of chlorine are nearly identical for the three different types of cell. Important differences are in the cell room header pressure control and the amounts of hydrogen and oxygen contained in the gas. Pressure control requires special attention because it is necessary to maintain a constant differential between the hydrogen and chlorine gas headers that is a small fraction of the (absolute) operating pressure.

1. *Membrane process.* Cell room pressure control is probably easiest in the membrane process when operated near atmospheric pressure, because it allows the greatest pressure difference between the two headers. However, operating pressures have been rising with advances in cell design, while the specified differential pressure has remained essentially the same. This makes good differential pressure control more difficult. With a measurement range from atmospheric to an operating pressure of 35 kPa(g), for example, a transmitter would not be sensitive enough to control the header pressure with sufficient accuracy. The operation of membrane cells above this pressure, therefore, requires special control systems in order to meet the specifications for differential pressure. The narrowest span that can be calibrated into a pressure transmitter is about 2.5 kPa, or 250 mm water column (w.c.). This narrow range is needed so that each header pressure can be controlled within about 5 mm w.c. The differential pressure then can be controlled within 10 mm. With a span of 250 mm w.c., the pressure transmitter range would have to be elevated by about 3.3 m w.c., which means that the instruments would give no reading until the pressure in the headers approached that point. Section 11.3.2.1A discusses the

use of dual pressure transmitters, one to allow measurement over the full range and one to provide accurate control at the operating point.

There may be more oxygen in membrane cell chlorine than in the gas from the other processes. This can be a problem if the compressed chlorine is fed directly to chlorination processes. An offsetting advantage is that there is essentially no hydrogen in the chlorine gas.

2. *Mercury process.* Pressure control is a bit more difficult than in the low-pressure membrane-cell process but not very much different. The chlorine gas usually is very low in oxygen and hydrogen content, unless a problem in brine treatment allows some metal contaminant to produce unsafe quantities of hydrogen in the chlorine. The presence of hydrogen is most frequently a problem with mercury cells.

3. *Diaphragm process.* Control of the cell room pressures is most difficult with this system, because the chlorine and hydrogen pressures are so close to atmospheric and to each other. Both hydrogen and oxygen are present in the chlorine, but the use of modified and synthetic diaphragms has greatly reduced their concentrations.

11.3.2.1. Cell Room

11.3.2.1A. Chlorine Header Pressure Control. As pointed out above, chlorine header pressure control can be one of the most difficult control tasks, because the pressure is being controlled within a few millimeters of water column and the latitude for error is small. Each chlorine production method has its own control range and limits, but the control method is the same. The strategy, as shown in Fig. 11.18, is simple. The control valve should be a fail-closed butterfly type with a conventional disc and a positioner. Preferably, it should be located after the dry demister downstream of the drying columns (Section 9.1.5). In this location, the wetted parts of the valve can be Monel. This strategy

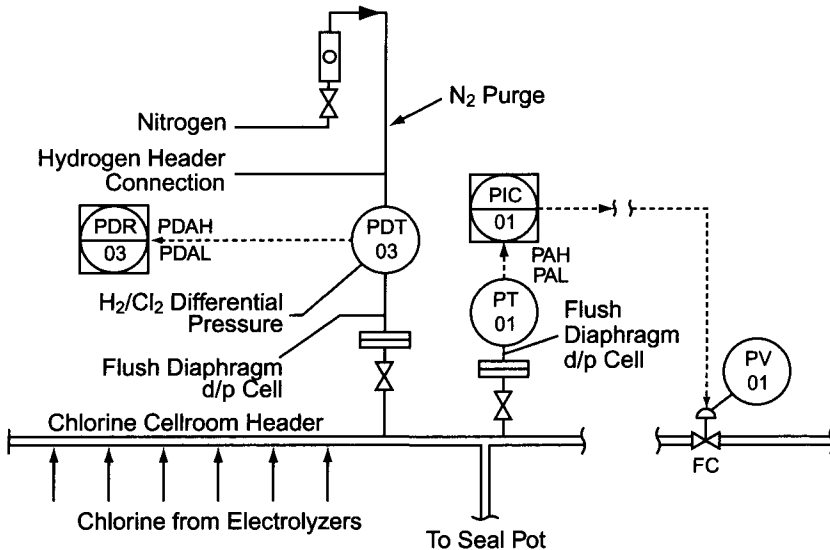


FIGURE 11.18. Chlorine header pressure control (low pressure).

requires the cooling and drying train to be designed to handle the additional pressure drop (up to 15 kPa) across the control valve. In the wet chlorine train, the valve would be larger and either be fabricated from titanium or have a PTFE-covered disc and body. Reducers between the piping and the valve must be eccentric and flat on the bottom to avoid trapping of condensate. The sizing of the butterfly must be done properly, considering the maximum and minimum flows and associated pressure drops. As with other butterfly applications discussed in this chapter, the designer must ensure that at no time will the butterfly valve be required to control at less than 20° open, where its action becomes unstable.

The transmitter can be a standard differential pressure (d/p) cell with corrosion-proof flanges or a flush-diaphragm type. Diaphragms should be tantalum. The transmitter is mounted above the chlorine header where it leaves the cell room, with the mounting arrangement and piping freely draining back into the header. The operating range of the chlorine pressure transmitter for nominally atmospheric operation might typically be -75mm to +75mm w.c. The use of slightly negative set points has been common practice. Section 11.4.2.1 discusses the pros and cons of this issue in particular regard to the hydrogen header. More recently, some membrane-cell plants have been designed to operate at 1.2–1.6 m w.c. (or even more), with set points of 1.4 or 1.5 m w.c.

The cell room header pressure controller is direct-acting with proportional and integral control modes.

Operation of the cells at even higher pressure, say 3.4–3.5 m w.c., may require dual transmitters to allow accurate control of header differential pressure. It also requires the proper startup strategy to bring the cell pressures to their normal operating values in a controlled manner. In Fig. 11.19, the wider range transmitter and controller (PT- and PIC-01), with a range down to zero, bring the operating pressure up to the desired level. Signals from the two controllers pass to a selector (PY-01) so that they can operate the one control valve. The wide-range controller should be set from a remote output station. With this arrangement, the operator can increase the pressures on both the chlorine and the hydrogen header at the same time, maintaining nearly the correct differential and taking particular care not to let the pressure differential reverse. Increases in the set points continue until the narrow-range controllers take over, close to the final pressure. The control system response charts of Fig. 11.20 show how the pressure increases gradually with the set point until reaching the operating level, where the control switches from PIC-01 to PIC-02. The ideal result is a bumpless signal to the valve, as in the bottom chart.

Since the differential pressure between the two gas headers is so important, neither gas should be considered independently of the other. This discussion, therefore, is incomplete without reading Section 11.4.2.1 on the hydrogen header.

11.3.2.1B. Chlorine Header Safety Systems. Low-pressure chlorine headers are protected from over- and under-pressures by the use of water-filled seal pots. A typical seal pot relieves at about ± 50 mm w.c. Some membrane-cell systems operate at pressures too high for effective use of a water seal and must depend upon weighted discs or an automated relieving system.

Membrane cell room chlorine headers are usually purged with air whenever there is a rectifier shutdown. The purging has two functions, removing chlorine gas from the

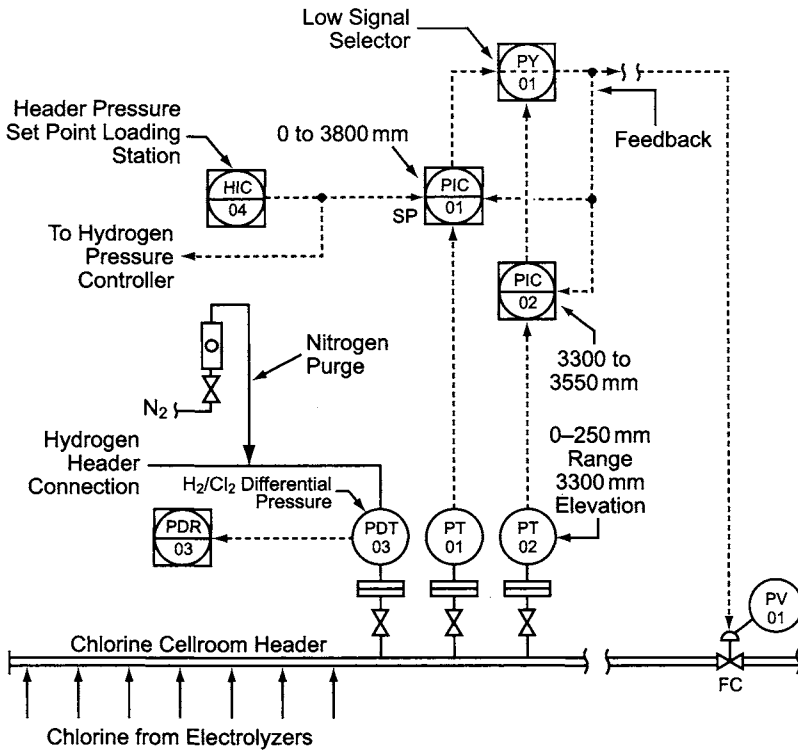


FIGURE 11.19. Chlorine header pressure control (high pressure).

header and preventing vacuum due to condensation of the water vapor. The air is purged at a constant rate for a defined period of time set on a timer. The air purge enters at the end of the header and purges through the seal pot.

The whole chlorine processing train can be upset if air enters the system through a vacuum break. If the pressure in the chlorine header is close to the point where the vacuum seal opens, the chlorine compressor should be shut down. This will prevent air from being drawn into the whole chlorine handling system.

11.3.2.1C. Local Measurements. Local measurements of wet chlorine gas pressures below 10 or 15 kPa can be made with U-tube manometers filled with water. Process connections should minimize the collection of condensate in the manometers. A simple but not foolproof technique is to make a connection in the upper half of the header and force the tubing to rise for some distance before descending to the manometer.

Bellows-type pressure gauges with 50-mm flanged diaphragm seals are useful between 15 and 100 kPa. The diaphragms should be of PTFE in order to provide sufficient flexibility for displacement of the halocarbon oil that fills the bellows pressure element. Bourdon-tube gauges with 25-mm flanged tantalum diaphragm seals, again filled with halocarbon oil, are suitable for higher pressures.

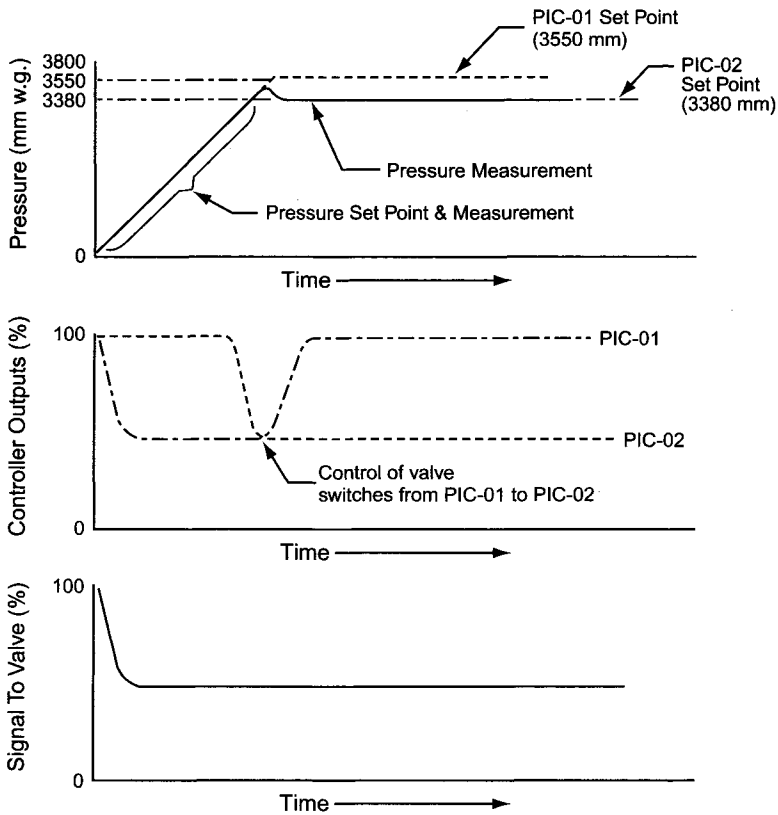


FIGURE 11.20. Chlorine pressure control system response charts.

Local measurements of wet chlorine temperature use tantalum-sheathed flanged thermowells with bimetallic dial thermometers. The insertion length should be selected to place the tip about one third of the diameter into the piping or into an elbow.

A resistance element in a flanged thermowell with a tantalum sheath measures the chlorine temperature as the header leaves the cell room. The sensing element is connected to a temperature transmitter. A typical range is 0–150°C.

11.3.2.2. Chlorine Cooling. In Fig. 11.21, wet gas from the cell room is cooled to condense most of its water vapor. This usually takes place in two separate heat exchangers (Section 9.1.3). The cooling water exchanger usually runs uncontrolled, but the temperature of the gas leaving the second cooler is controlled to avoid the problems associated with temperatures that are too low (Section 9.1.3.5A).

Chilled water is the common utility on the second chlorine cooler. It enters the exchanger through a fail-closed globe valve. The chlorine temperature is measured at the outlet by a tantalum-sheathed flanged thermowell connected to a transmitter. The temperature is typically controlled at 15°C with alarms at about 18°C and 13°C.

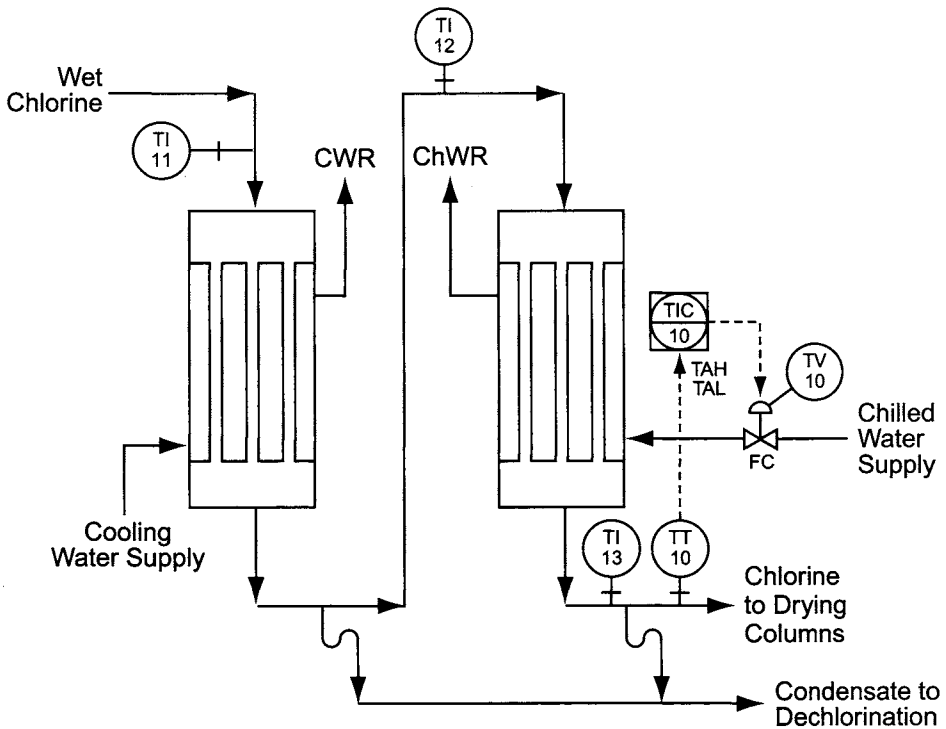


FIGURE 11.21. Chlorine cooling and chilling.

Chapter 9 also discusses the case where the cooling water temperature seasonally becomes too low. It then may be necessary to add temperature control or a temperature-limitation system to the first cooler (Fig. 9.12). Instrumentation considerations are the same as those given above.

11.3.2.3. Chlorine Drying. Chlorine drying columns commonly use direct contact with strong sulfuric acid to remove water vapor from the wet chlorine (Section 9.1.4.3A). Drying column designs vary, but they all have the same function. The chlorine enters the zone that contains the weakest acid and leaves from the zone that has the strongest acid. The feed acid may be as strong as 98% H_2SO_4 and the used or spent acid is normally at least 70% H_2SO_4 .

11.3.2.3A. Acid-Side Controls. The strong sulfuric acid feed to the drying columns (not illustrated) is by way of a flow control loop or a metering pump. Flow measurement can be with a PTFE-lined magnetic flow meter, an all-plastic vortex shedding meter, or a lined transmitting rotameter. The control valve should be a fail-closed PTFE-lined globe valve with a PTFE bellows seal on the stem. The controller is standard reverse acting with proportional and integral functions. If there are frequent production rate changes

and there is a concern regarding excessive use of strong sulfuric acid, the acid feed can be regulated by a flow-ratio controller with the electrolyzer current as the primary “flow” for the ratio. With a metering pump, control may be by way of adjustment of the stroke or operating speed, which can be calibrated against the flow rate.

Sulfuric acid enters the high-concentration end of the drying system cascade and flows from stage to stage by gravity (Section 9.1.4.3A). The weak acid usually collects in the first drying column (or bottom of a single column) for transfer to the spent acid storage tank. The rate of withdrawal here is set by a level control loop (Fig. 11.22). The level can be measured with a d/p cell that has a double capillary-filled system. The seals should have tantalum diaphragms, because the chlorine-saturated spent acid is very corrosive. The control valve should be a fail-closed PTFE-lined globe valve with a PTFE bellows sealed stem. A direct-acting proportional-plus-integral standard controller is appropriate.

The strong acid addition rate must be sufficient to reduce the moisture in the chlorine to 15 ppm or less. The control strategy outlined above, controlling the feed rate and withdrawing spent acid under level control, does not guarantee efficient use of the acid. Overfeeding acid would simply cause LV 21 in Fig. 11.22 to open wider and the concentration of the waste acid to increase. The drawing, therefore, shows a density measurement in a recycle line around the acid circulation pump. This represents the concentration of the spent acid. Using this information to adjust the rate of acid feed prevents waste. Control is indirect, with the operator maintaining the acid strength at or above design by adjusting the feed rate. Section 9.1.4.1 pointed out that the method of disposal of the spent acid plays a part in determining its acceptable concentration.

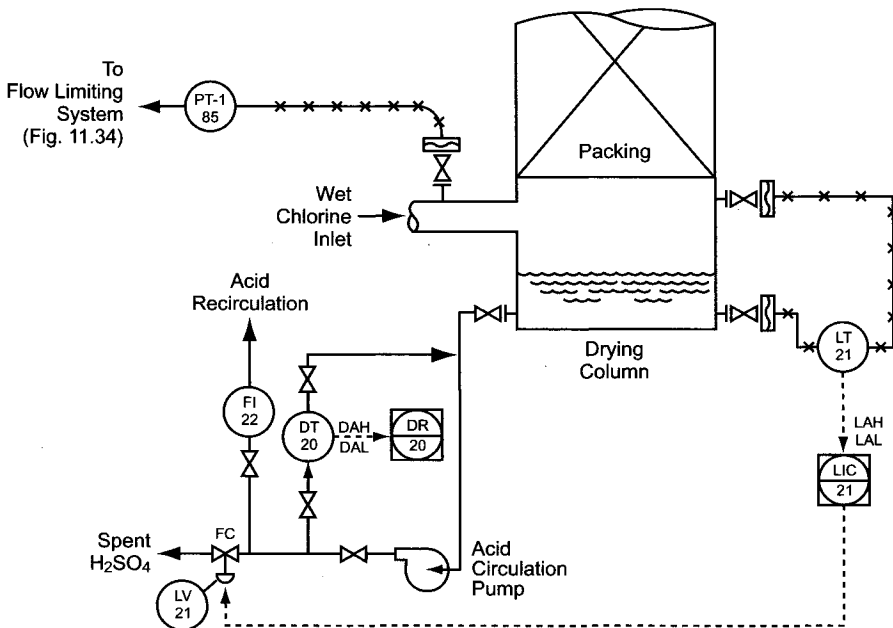


FIGURE 11.22. Chlorine drying column.

Another important consideration is the fact that the spent acid becomes very corrosive below 70% H_2SO_4 .

Conceptually, the concentration measurement could be used in closed-loop control of the rate of acid addition. With the low net flow of acid through the system, however, the dead time is quite long and may not be suited for accurate and stable control. Instead, the operator can occasionally adjust the rate of introduction of the fresh acid to keep the spent acid concentration under control.

An electrodeless conductivity instrument can measure the depleted acid concentration with reasonable accuracy in the range of 65–80%. Above 80% H_2SO_4 , inflections in the curve of conductivity vs concentration make the measurement less reliable.

11.3.2.3B. Gas-Side Instruments. The mist eliminator between the drying system and the chlorine compressors is a passive element. No controls are necessary or useful. Figure 11.23 is a conceptual depiction of the operation. The use of suspended candle demisting elements is the most common approach (Section 9.1.5). The differential pressure instrumentation is similar to that used to measure the level in the drying columns (see above), with the exception that Monel diaphragms should be sufficient. The instrument provides continuous indication and a high alarm. The drying system, likewise, has no controls on the gas side. Figure 9.15 shows that temperature and pressure instrumentation on each side is useful for monitoring the process.

If a chlorine plant handles much container (truck, tank car, barge, or cylinder) traffic, there will be a need to depressurize and evacuate these containers when customers return

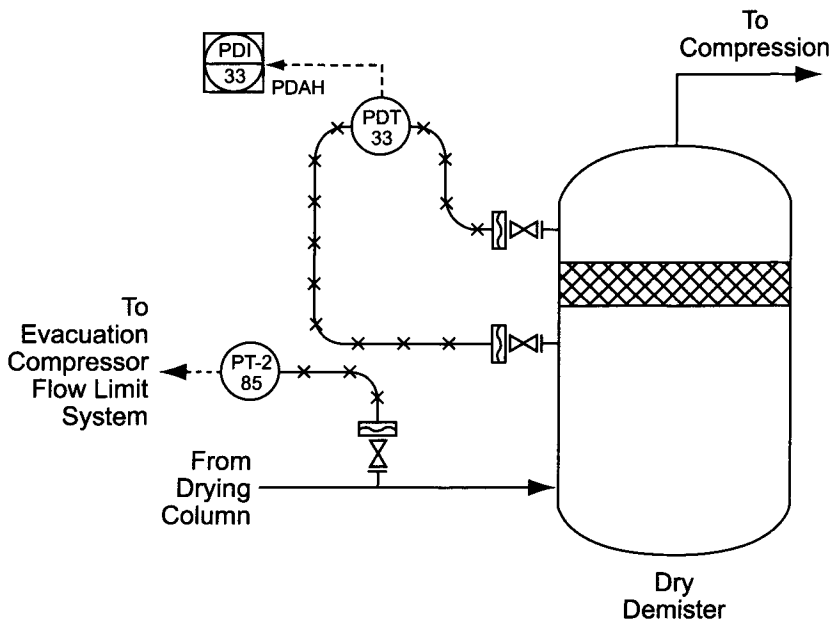


FIGURE 11.23. Chlorine drying system mist eliminator.

them. A logical place to introduce the gas recovered in this operation is at the inlet to the drying columns. Depressurization of tank cars and barges in particular can add a significant load to the drying columns. This load usually adds little to the demand for fresh acid, because the chlorine is already very dry. It does increase the pressure drop through the columns, and plant design must allow for the appropriate rate of flow. The location of the control valve exposes it to dry chlorine on the upstream side and wet chlorine on the downstream side. Section 9.1.2 showed that the choice of materials of construction for these two cases can differ widely. The best choice here is probably a normally closed fluorocarbon-lined globe valve.

The differential pressure across the drying columns provides a measure of the total gas loading. The distance between measuring points, particularly when using three separate columns, can prevent the use of a double capillary filled system. Two independent pressure transmitters with flush-mounted d/p cells are then necessary. The upstream measurement requires a tantalum diaphragm: Monel is satisfactory downstream. The downstream pressure signal is then subtracted from the upstream signal to obtain the differential pressure.

The pressure transmitter on the inlet line (Fig. 11.22) is useful when gas enters the process from a recovery system. Section 11.3.2.9 and Fig. 11.34 will cover the operation at that end.

11.3.2.4. Liquid-Ring Compressors. At this point in the process, the chlorine is dry and can be handled in steel piping and equipment without excessive corrosion, but the pressure is too low for liquefaction or use in most other processes. In this case, compression is necessary, and Section 9.1.6 describes the process and the types of equipment used. The sections that follow here discuss liquid-ring and centrifugal compressors separately.

The liquid-ring compressor has a defined compression ratio and a constant volumetric flow rate. If there is more compression capacity on line than chlorine produced, suction and discharge pressures will tend to decrease. It is sometimes argued that this situation may not be a problem and that these compressors can be run without control. In our case, upsets with rapid changes in production rate (e.g., rectifier trips) would cause the suction and discharge pressures to change significantly. This situation makes cell room header pressure control more difficult. It imposes a much higher pressure drop on the control valve as it is forced to handle a significant drop in flow.

Experience shows that providing a compressor suction pressure control system can greatly improve steady-state operation and the response of the system to an upset. It also provides a much easier startup by allowing the compressor to operate at normal conditions under full recycle before energizing the cells.

The suction pressure control system shown in Fig. 11.24 uses a fail-open recycle valve to return compressed chlorine from discharge to suction. In the common situation with multiple compressors, there is one control system, and the chlorine is piped from the common discharge header to the suction header. The control valve should have an equal percentage characteristic and should be sized to handle the total capacity of the compressors when 90% open. It should have excellent turndown in order to control small recycle flows and should be aided by a valve positioner.

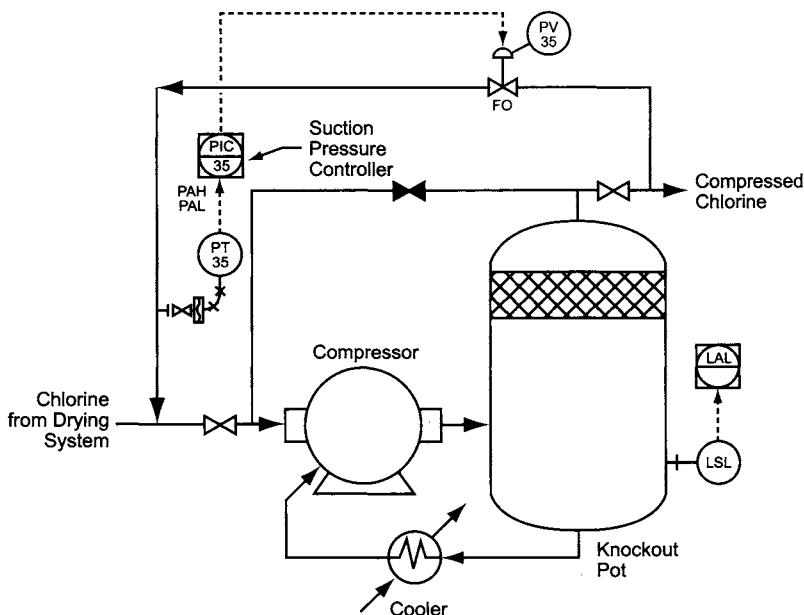


FIGURE 11.24. Suction pressure control for liquid-ring compressors.

The suction pressure transmitter can be an absolute pressure instrument with low range or a d/p cell with Monel elements. The controller should have proportional and integral modes. The control action depends on the type of transmitter used.

Losses of acid from the system should be very low, but it is prudent to monitor the level in the acid separator with some type of switch that gives a low-level alarm.

11.3.2.5. Centrifugal Compressors. Section 9.1.6.2A discussed centrifugal compressors, which are the standard in large plants, and the particular importance of surge control. Surge occurs when the total flow through any stage of a centrifugal compressor is not sufficient to maintain stability over the face of the impeller.

Too much air or nitrogen in the chlorine can also cause surge. Lower density gas cannot be compressed to the same discharge pressure as chlorine, and thus the compressor may not produce enough pressure for the gas to enter the discharge header. In the approach described below, surge control is combined with a suction pressure control system.

A suction chiller with countercurrent flow of low-pressure chlorine gas and liquefied chlorine is not essential with a centrifugal compressor, but it serves two very useful purposes. It cools the gas, making higher compression ratios possible and reducing the dependence on interstage coolers. It also scrubs impurities out of the chlorine stream that could over time damage the compressor. While removing impurities, the suction chiller also creates the possibility of accumulation of the extremely hazardous nitrogen trichloride (Section 9.1.11.2). For this reason, operation of a suction chiller is not to be undertaken lightly.

11.3.2.5A. Suction Chiller Operation. Removal of impurities scrubbed from the gas requires continuous or occasional controlled withdrawal of liquid from the bottom of the suction chiller. The existence of a liquid phase implies the use of level instrumentation and control. The controlled stream is the liquid chlorine that cools and scrubs the gas. Displacer-type transmitters with Monel internals and steel cages have been successful in this duty. Figure 11.25 assumes their use, with a reverse-acting controller with proportional and integral control functions. The valve should be a fail-closed globe valve with a 300-lb flanged body and a positioner. The stem seal can be a Monel bellows or a Hastelloy C stem with double PTFE packing.

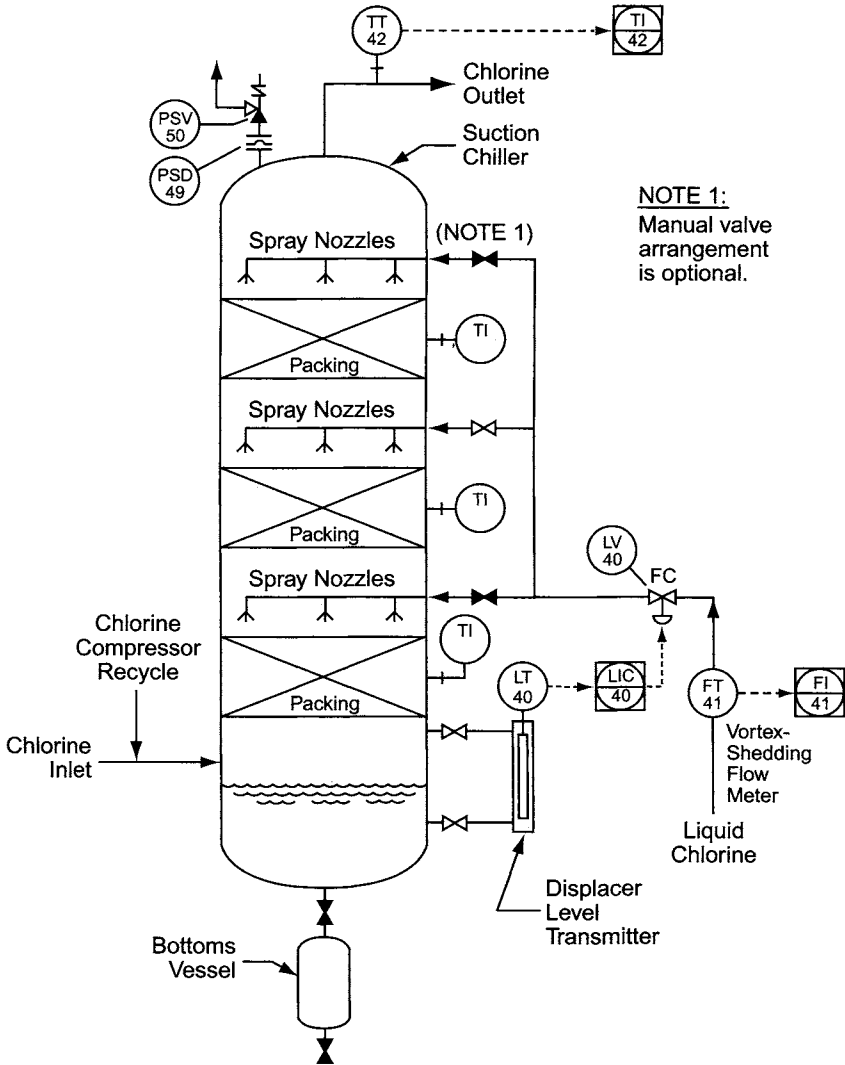


FIGURE 11.25. Compressor suction chiller level control.

It is also good practice to measure the liquid chlorine flow to the suction chiller. Control can be directly from the liquid level, as assumed above, or by flow control in cascade from the level. Vortex-shedding flow meters have given good service here.

With the simplest form of a suction chiller, the bottoms product, containing any high boilers, accumulates and is removed periodically. The bottoms vessel is charged with a solvent in order to dilute the material removed from the column. More elaborate versions and stripping columns can remove dissolved chlorine and return it to the process through the suction chiller column. Equipment arrangements and the approach to process control vary. Improper operation and the accumulation of excessive amounts of nitrogen trichloride have been responsible for a number of serious incidents, some involving fatalities. These systems must be designed and operated with great care.

Varying the addition point of the liquid can affect the temperature of the gas leaving the column. Figure 11.25 shows several nozzles along the wall of the column. Choosing a higher nozzle increases the contact time between phases and reduces the temperature of the overhead gas. Not all designs have this feature.

Figure 11.25 also shows pressure relief on the column. The normal design pressure for vessels containing liquid chlorine is 15–20 atmospheres. The suction chiller, however, is connected directly to the compressor suction, where the pressure rating is much lower. The relief system on the suction chiller must also protect the compressor. Standard construction is a reverse-buckling Monel rupture disc in combination with a safety valve having Monel internals and a PTFE O-ring seal.

11.3.2.5B. Compressor Operation. Section 11.3.2.4 reviewed the argument that a liquid-ring compressor can be run safely without a pressure controller. The same argument might be made with centrifugal compressors, but again experience shows that control of the cell room header pressure is much easier and smoother when the compressor suction pressure is controlled.

Figure 11.26 shows a system in which compressed gas recycles from the discharge, upstream of the shutoff valve, to the inlet of the suction chiller. Passing the recycled gas through the suction chiller (or other precooler) cools the gas so that the control valve can handle the full compressor capacity. The control valve is a fail-open globe valve with an equal percentage characteristic and a positioner. It should be sized to handle full compressor output when 90% open. The valve seal can be a Monel bellows or a Hastelloy C stem with double PTFE packing.

Surge flow measurements are normally made in centrifugal compressor suction lines. This is usually impractical in chlorine plants, where the suction piping is relatively large in diameter and the straight piping runs are short. It is more convenient to locate the flow meter in the compressor discharge piping before the recycle line connection. Orifices with d/p cells have been the standard for measurement of this flow, but a vortex meter with Monel or Hastelloy C wetted parts probably is technically a better choice. The latter is not affected by changes in gas density, while a d/p cell will give a reading lower than the true flow if the gas density drops.

In Fig. 11.26, the compressor flow signal goes to a direct-acting proportional-plus-integral flow controller. The controller output goes to the low selector described above.

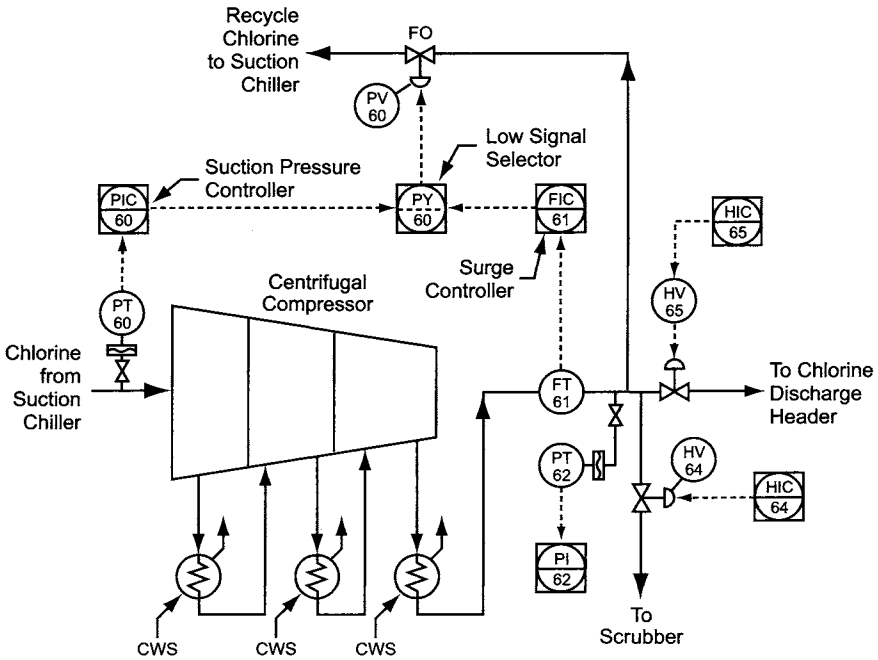


FIGURE 11.26. Centrifugal compressor suction pressure and surge control.

It is important that an output signal from the low selector also serve as external feedback to the flow controller.

The suction pressure controller, rather than the flow controller normally controls the recycle valve. However, if the compressor flow decreases to a critical point, the flow controller will take over operation of the valve and increase the flow to prevent surge. This will increase the suction pressure and in some cases can raise the cell room header pressure to the point where the seal pot opens. This would also occur if the compressor were allowed to go into surge.

In addition to the process control instrumentation described above, manufacturers of centrifugal compressors provide extensive measurement and control systems for the protection of their compressors. These cover pressure, temperature, vibration, shaft sealing, and lubrication. When these systems are included in the compressor package, the user may still want to display some of the measurements at the main control station. This can be done through digital retransmission or by providing duplicate measurements. There will also be shutdown interlocks to incorporate into the main control system. Suction pressure and surge control systems should not be incorporated into the compressor manufacturer's control and monitoring system.

11.3.2.5C. Discharge Pressure Measurement. Individual compressor discharge pressures are measured with transmitters with capillary-connected flanged Monel diaphragm seals. This pressure measurement is an important tool when bringing a compressor on line. It will indicate when the gas can be passed on to the discharge header.

In addition to the normal manual valve between a compressor and the common discharge header, there should be a fail-closed remotely actuated globe control valve with Monel trim and an equal percentage flow characteristic (HV-65 on Fig. 11.26). It should handle the full capacity of the compressor with a pressure drop of about 10 kPa. When, during startup, the pressure instrument referred to above shows that the compressed gas pressure is equal to the discharge header pressure, the operator can open this valve slowly.

Another fail-closed remotely operated control valve connects the compressor discharge to a vent scrubber (HV-64). It should have Hastelloy C trim because of its exposure to water vapor from the scrubber. Otherwise, its design characteristics are similar to those of the discharge shutoff valve discussed immediately above. During startup, this valve vents dilute gas to the high-pressure scrubber until the chlorine concentration approaches normal. In a centrifugal compressor installation, the discharge pressure will often be too low until the chlorine concentration reaches a certain point. This valve should close as the discharge shutoff valve opens.

11.3.2.6. Compressor Discharge Header Pressure Control. A plant with multiple compressors will have discharge manifolds serving groups of machines. Figure 11.27 shows the minimum case of two compressors. All the compressed chlorine is brought together for distribution to the various users. When all the chlorine is liquefied or intended for a single use, the distribution header system is very simple. Such plants need only a method to discharge excessive pressure to the high-pressure scrubber.

When the chlorine can also be sent directly as a gas to another process, to liquefaction, or to the scrubber, the distribution header becomes more complex. The control system becomes a priority selection system directing gas to the appropriate destination(s). Priorities are established by split-ranging the positioners of the various control valves. The highest priority usually is the direct user, with liquefaction next, and the scrubber as the last resort. Since the chlorine must be sent to the scrubber when instrument air fails, all valves must fail open.

The pressure transmitter, located on the discharge header, has a capillary-connected Monel diaphragm seal. It is reverse-acting, with proportional and integral control modes. Normal practice is to include both high- and low-pressure alarms.

Direct feed of compressed chlorine to another process is possible only when the quality of the chlorine meets the user's needs. The receiving process determines and controls how much chlorine is taken from the header, but another control valve is necessary at the compressor discharge header in case the user attempts to take more chlorine than is available. The liquefiers normally handle the chlorine not taken by the direct user. It has been common practice to design the liquefaction plant for full cell output, so that the cells can operate at full rate during short upsets in the user's process. This approach may be modified to suit restrictions on maximum chlorine inventory. In any case, the liquefiers should always have some chlorine gas fed to them to keep them operational and ready to handle full chlorine production should the direct user suddenly stop taking gas. In addition, a supply of liquid chlorine may be needed for a suction chiller. A bypass line around the control with a restricting orifice sized for about 10% of full capacity at the control valve drop can meet this requirement. Any chlorine not taken

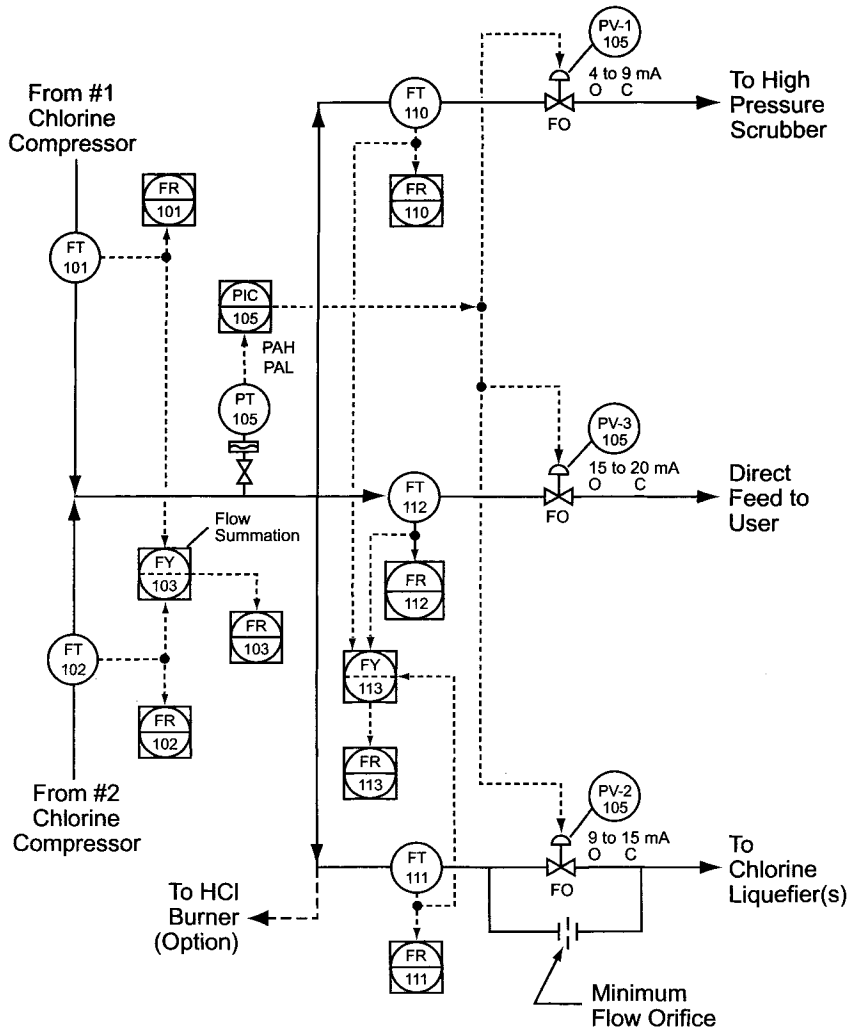


FIGURE 11.27. Compressor discharge header pressure control.

by the user and liquefiers together must go to the high-pressure emergency scrubber through the third valve.

The three valves are all built for chlorine service. Vortex meters upstream of the control valves measure and integrate the various flows. Integration of the flow to the scrubber is the least important, but given the measurement of the flow rate, it is of little added cost. A separate meter located before division of the flow can measure the total flow, or the output of the three individual meters can be added together. The valve positioners may be calibrated for ranges of 15–20 mA (direct user), 9–15 mA (liquefiers), and 4–9 mA (scrubber). The two process valves should have linear characteristics. They should be sized for full plant output when 90% open. Normally allowed pressure drops are 5–15 kPa for the direct-use valve and 20–30 kPa for the liquefier valve. The scrubber

valve can be sized for a pressure drop equal to that between the discharge header and the scrubber inlet. This should be an equal percentage valve, and, like the header shutoff valve, it should have Hastelloy C trim.

11.3.2.7. Chlorine Liquefaction. One or more liquefier units can be fed through the liquefier feed valve (Fig. 11.27). Each liquefier unit will have its own manual isolation valve. A liquefier unit comprises a complete refrigeration system, a chlorine liquefaction exchanger, and a knockout pot for vapor–liquid separation.

Removal of enough chlorine by liquefaction allows the hydrogen concentration in the remaining vapor to exceed the lower explosive limit (Section 9.1.11.1). Mercury-cell chlorine usually contains a small percentage of hydrogen, and hydrogen problems are most common with that technology. Diaphragm-cell chlorine, as a rule, contains less hydrogen, but the same problem can exist, particularly if modified diaphragms are not being used. Membrane-cell chlorine has very little hydrogen unless there is a torn membrane.

Clean dry air added to the liquefiers along with the chlorine dilutes the hydrogen and eliminates that hazard. The rate of addition of air is governed by a flow-ratio controller, with the chlorine flow to the liquefier acting as the primary flow (Fig. 11.28). The ratio to be used depends on the concentration of hydrogen in the chlorine and on the depth of liquefaction. It should be reset as required, based on the concentration of hydrogen in the tail gas from liquefaction. The control valve should fail open and have an equal percentage characteristic and a positioner. A small bypass flow of air may

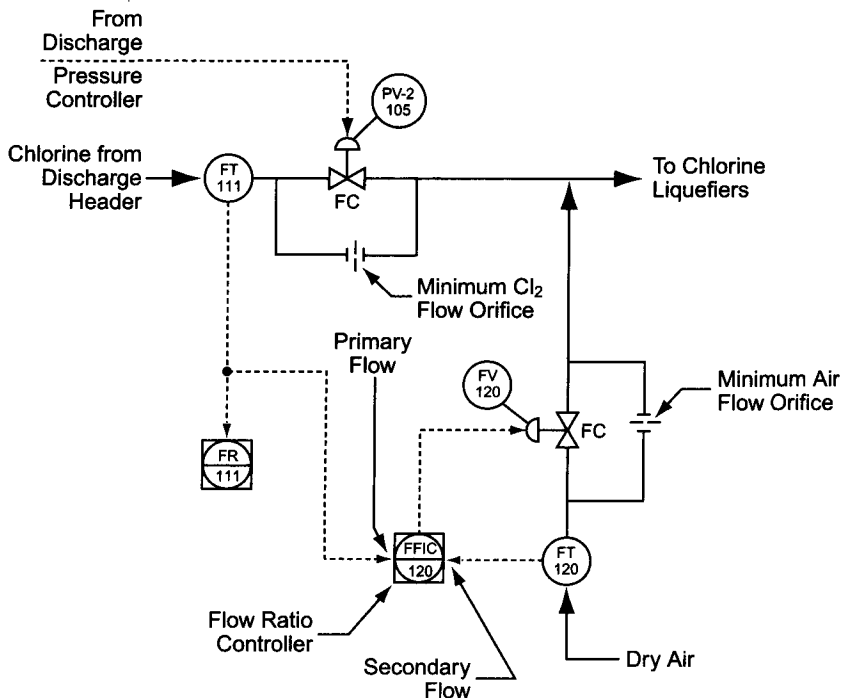


FIGURE 11.28. Dry air feed to chlorine liquefiers.

be necessary to dilute the bypassed chlorine when the flow is too small to measure accurately. Section 9.1.7.2A describes the effects of air addition on the efficiency of the liquefaction process. Multistage liquefaction will be more efficient if the dilution air is added incrementally, stage by stage. In most cases, it is not considered to be worth the added cost and complexity.

Figure 11.29 shows a liquefaction unit. As with chlorine compressors, the refrigeration systems associated with liquefaction can be supplied as completely automated packages. Within their capacity, they will automatically adjust to the amount of chlorine fed to the system. The chlorine separator temperature is used to adjust the refrigerant evaporation pressure (and therefore, its temperature). With control by PLC, the only other signals to be passed to the main control center are the alarms and the shutdown status. Refrigerant flow is balanced with process demand by control of its level in the liquefier.

The process temperature is measured in the uncondensed gas as it leaves the chlorine knockout pot or separator. This procedure is more accurate than measurement of the temperature of the liquefied chlorine, which may be subcooled. The temperature sensor in Fig. 11.29 is an RTD in a flanged Monel thermowell. The reverse-acting proportional-plus-integral controller adjusts the set point of the refrigeration chiller pressure controller.

A side connection on the knockout pot carries the liquid chlorine to storage. The tank being filled is vented back to the knockout pot to enable gravity flow. Cage-style high and low float switches monitor the level.

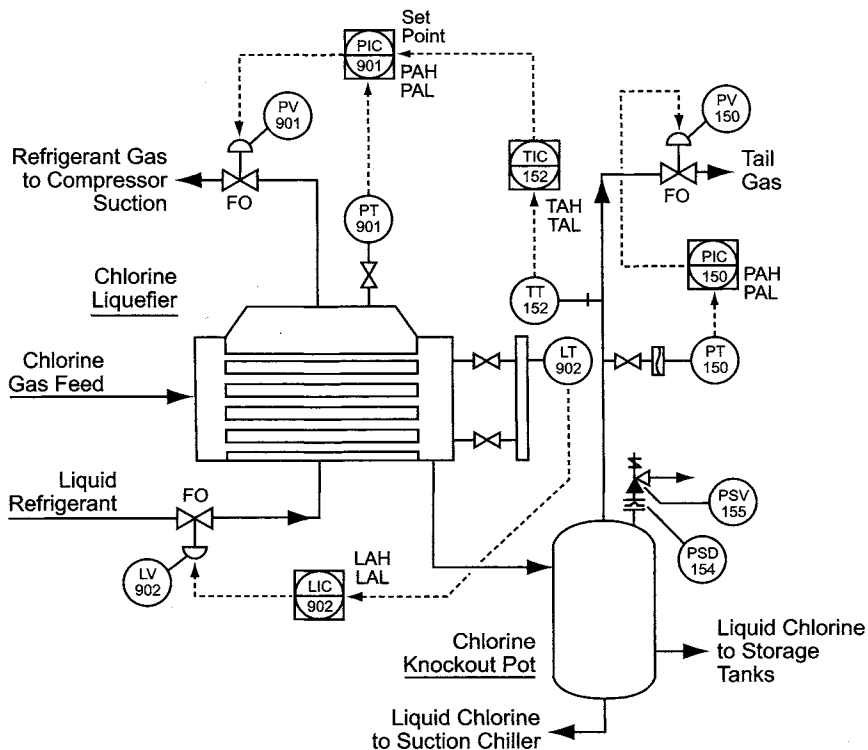


FIGURE 11.29. Chlorine liquefier temperature control.

The liquefier and knockout pot, which contain chlorine, should have 300-lb flanges, and all instruments must be rated for this pressure. A reverse-buckling Monel rupture disc coupled with a pressure safety valve with Monel internals and O-ring seal protects the vessels. This book does not discuss methods for sizing relief system components. Setting the design rate of flow requires consideration of the various events that can cause a release. Fire, when considered, usually becomes the design case. The Chlorine Institute, in its pamphlets on relief systems [2], provides equations covering this case. They are based on Compressed Gas Association standards [3]. Euro Chlor [4] specifically recommends that fire not be automatically included among the relief scenarios but be considered only when it is reasonably likely. The disadvantage of always rating for fire is that the rate obtained may be unrealistically high. This might be wasteful but would not be a hazard in a situation where the process fluid can reasonably be allowed to discharge to the atmosphere. This is not so in the case of chlorine, and the design of release-containment facilities can be as important as the design of the relief device itself. Sizing a containment system for the rate of release caused by a fire may be impracticable. Some of the options for handling chlorine emitted from storage vessels are explored in Section 9.1.10.2.

Pressure control is through a fail-open equal percentage control valve mounted in the common discharge header from the liquefier units. A transmitter with a capillary and Monel diaphragm seal measures the pressure upstream of the valve. The signal goes to a reverse-acting controller with proportional and integral control modes. This controller is set 25–30 kPa below the setting used on the discharge header controller.

11.3.2.8. Liquid Chlorine Storage Tanks. Section 9.1.8.2 discusses the various methods used to store liquid chlorine, along with the requirements for vessel design. Figure 11.30 shows a pressurized system in which the amount of chlorine present is measured by weight. There are four electronic compression load cells in this version. The drawing shows how the arrangements differ at the two ends of the tank. The swing caused by expansion and contraction of the tank must be kept less than 2.5°.

Figure 11.31 shows an arrangement used for calibration. It involves the use of a second set of calibration cells. Hydraulic jacks transfer some of the load from the measurement cells to the calibration system. This is done in a series of about five steps, leaving about 20% of the weight on the measurement cells.

When chlorine is stored under refrigeration at near-atmospheric pressure, double-wall containment is the standard. The jacket of a low-pressure vessel requires its own instrumentation. Section 9.1.8.2B discusses the design of these systems and mentions the need for a continuous air purge. Instrumentation should include a flowmeter and monitors for the humidity of the air entering the jacket and the chlorine content of the air leaving. The latter instrument will detect any leaks from the inner vessel. Because of the importance of differential thermal expansion of the storage and confining vessels, there should also be a number of wall-temperature monitors. Euro Chlor [5] and the Chlorine Institute [6] give more suggestions for instrumentation of these systems.

11.3.2.9. Chlorine Depressurization and Evacuation Compressor. Section 9.1.12 describes depressurization and evacuation of storage tanks and transport containers, and Fig. 11.32 shows the required instrumentation. In the first step, depressurization,

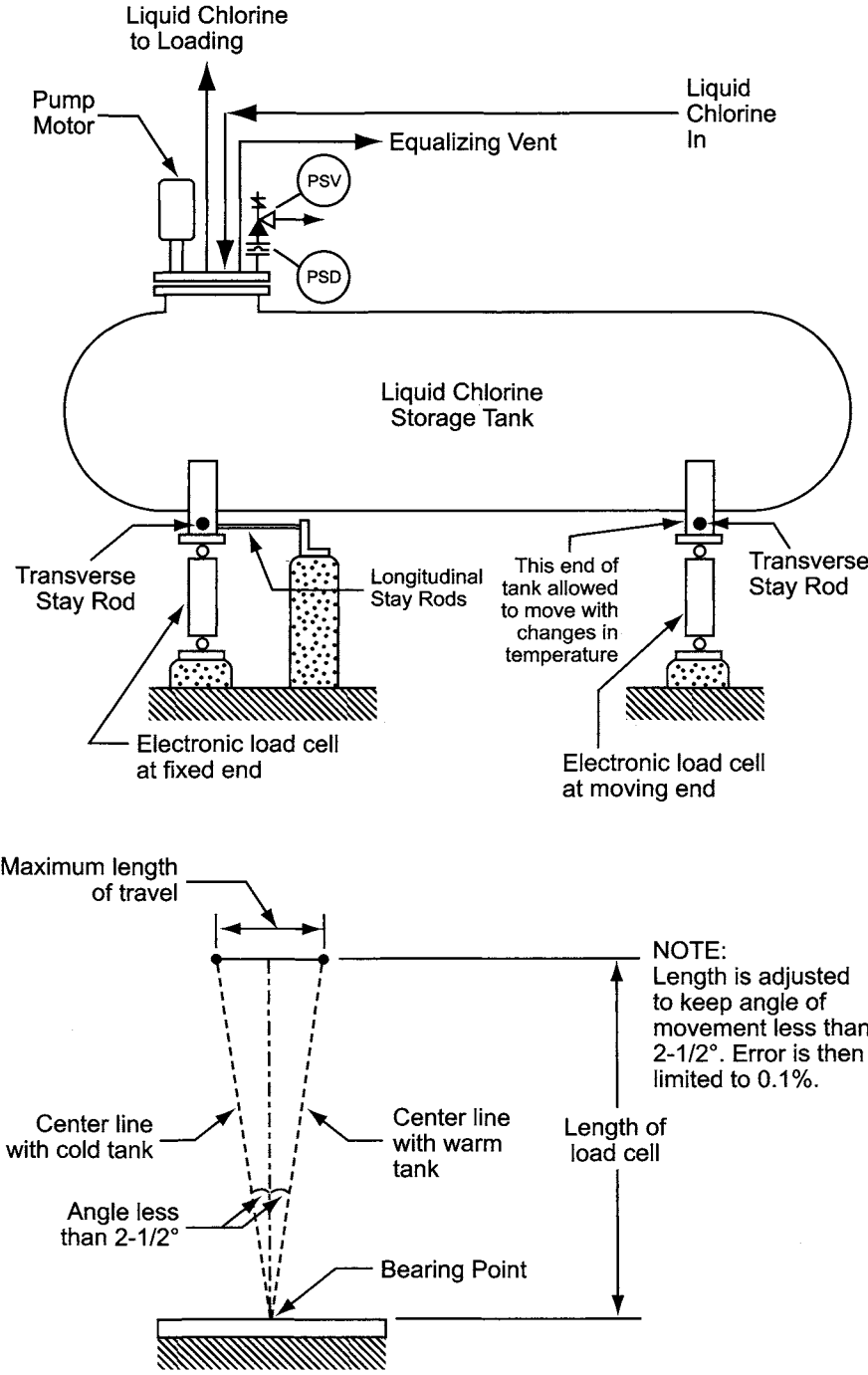


FIGURE 11.30. Liquid chlorine storage tank.

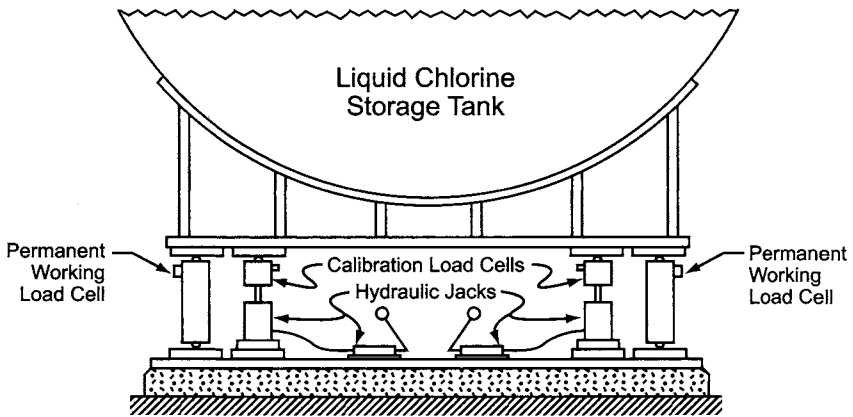


FIGURE 11.31. Calibrating liquid chlorine storage tanks.

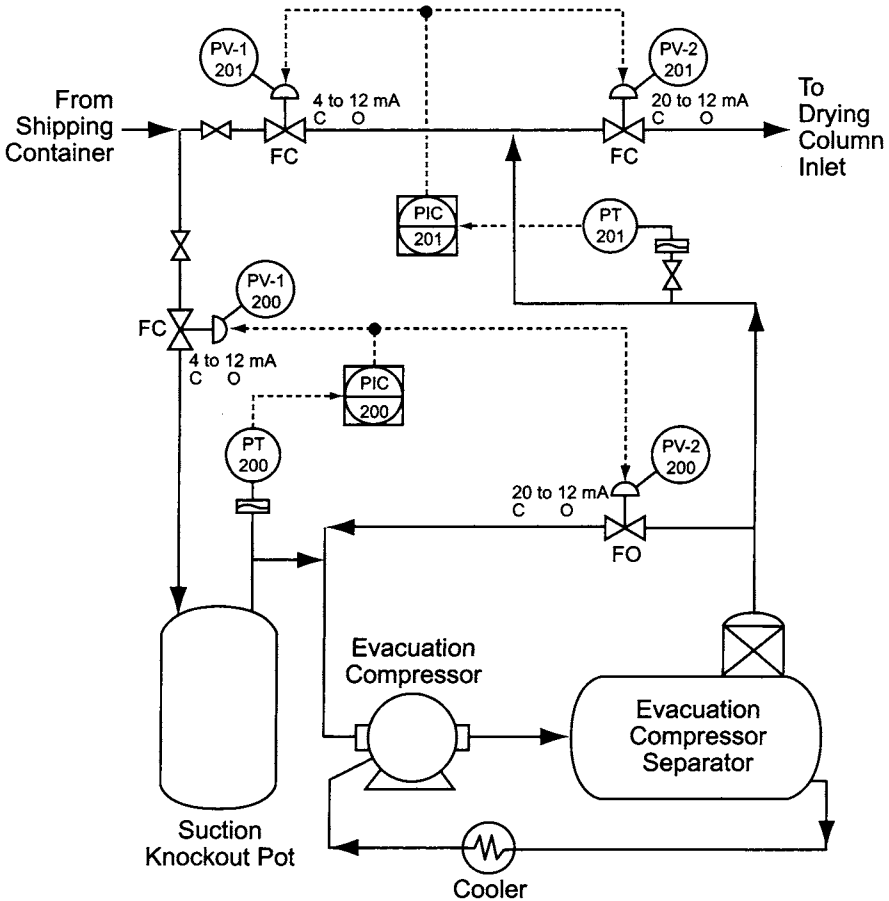
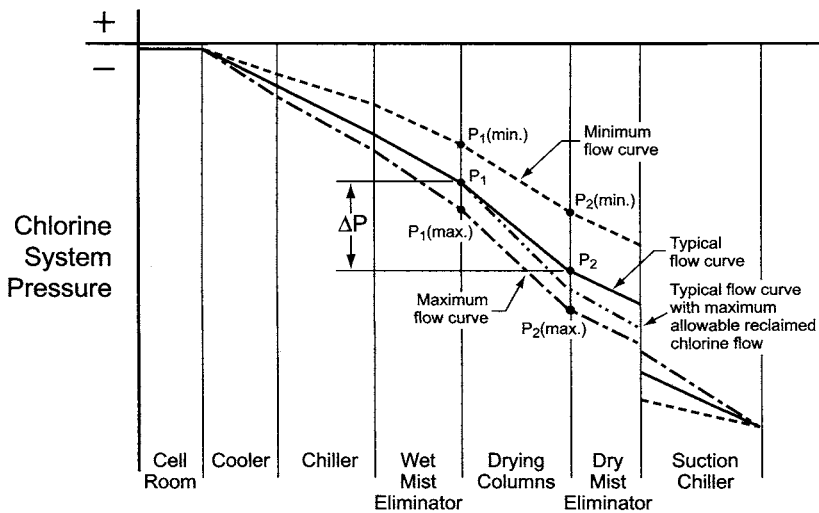


FIGURE 11.32. Depressurization/evacuation compressor system.

a vessel under pressure vents through a throttling valve (PV-1/201) into the discharge line of the evacuation compressor. This is a fail-closed 300-lb globe valve with equal percentage characteristic. It operates from a split-range direct-acting positioner. The pressure in the compressor discharge line is under control, and the second valve in the top line (PV-2/201) is wide open. As the pressure at the source drops, the first valve gradually opens to hold a pressure of 50–80 kPa in the compressor discharge line. When this valve is wide open, the evacuation compressor starts.

When the compressor first operates, the incoming pressure is well above the suction set point, and the valve upstream of the suction knockout pot (PV-1/200) must throttle the flow. As the line pressure falls, the valve continues to open. When it is wide open and can no longer hold the desired suction pressure, the compressor recycle valve (PV-2/200) must open. Finally, at some level of vacuum on the source, the system reaches its limits and can no longer pull chlorine from the container. Then comes shutdown.

A logical place for the return of the recovered chlorine is the inlet to the drying columns, where it can be reconditioned. This can add significantly to the pressure drop across the columns, and so the flow rate must be limited to stay within the design conditions. Figure 11.33 shows pressure profiles through the low-pressure chlorine processing train. The pressure drops continuously through the piping and equipment until the gas



- P_1 = Pressure at inlet to drying columns
- P_2 = Pressure at outlet of drying columns
- $P(\text{min.})$ = Pressure at minimum flow
- $P(\text{max.})$ = Pressure at maximum flow
- $\Delta P = P_1 - P_2 =$ Pressure drop across drying columns
- Break in pressure after dry mist eliminator represents control valve drop.

FIGURE 11.33. Chlorine handling system pressure profile.

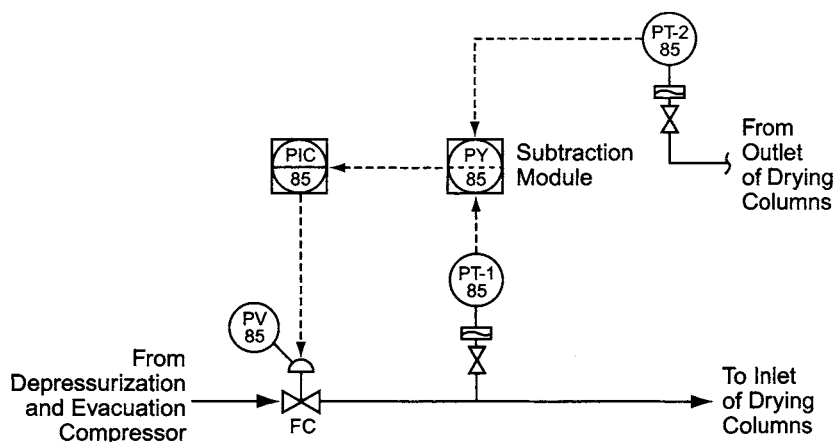


FIGURE 11.34. Reclaimed chlorine flow limiting system.

passes through the dry mist eliminator. The control valve then causes a discontinuity. Three curves show how the pressure falls more rapidly as the rate of flow increases. While the pressure at the inlet of the control valve drops, the pressure behind it must increase to maintain the downstream flow. Less pressure drop is available for the valve. Excessive flow from the evacuation system can reduce this available pressure drop to the point where the valve cannot function properly.

A control valve, therefore, is installed in the depressurization line at the drying column inlet to regulate the flow of reclaimed chlorine (Fig. 11.22). The location exposes the valve to both wet and dry chlorine. The best choice for the service is a normally closed PTFE-lined globe valve. The loading on the drying columns can be measured by differential pressure across the drying column train (Fig. 11.34). The physical distance between measuring points normally prevents the use of a double capillary system, so two independent pressure measurements are necessary. A flush-mounted d/p cell with a tantalum diaphragm can be used for the upstream pressure measurement, and a flush-mounted d/p cell with a Monel diaphragm for downstream measurement. Both transmitters need enough suppression in their calibrations so that their outputs will always be positive. The downstream pressure signal is then subtracted from the upstream signal to obtain the differential, which is the input to PIC-85.

11.4. HYDROGEN SYSTEMS

11.4.1. Introduction

The cathodes in diaphragm and membrane electrolyzers generate hydrogen gas saturated with water at 80–95°C. In mercury cells, hydrogen generation occurs in the decomposers, where temperatures may exceed 100°C. Normal practice is to cool the gas above each decomposer, and the humidity of the gas entering the collection header depends on the individual plant. The hydrogen from any type of cell can entrain some cell liquor and, in the case of mercury cells, it will also contain mercury vapor. Most chlor-alkali plants cool,

scrub, and compress this hydrogen and then use it for HCl production (Section 9.1.9.2) or as a supplemental fuel.

The explosive range of hydrogen in air is very wide (~4–74%), so air must be excluded from the system. Section 9.1.11.1 discussed the hazards of hydrogen in cell rooms, and Section 9.2.3 covered hydrogen compression systems. Low-pressure releases often are not highly dangerous because of the rapid dispersal of the gas in the air. In hydrogen processing systems, where pressures are higher and hazards aggravated, areas may be classified as Class I, Division 2, Group B.

Section 11.4.2 describes membrane-cell hydrogen systems in which the cells can operate under positive pressures to make some aspects of hydrogen handling easier and safer. Section 11.4.3 is dedicated to diaphragm-cell systems.

11.4.2. Membrane- and Mercury-Cell Hydrogen Systems

Most mercury-cell plants and low-pressure membrane-cell plants generate hydrogen at slight positive pressures, usually about 50–125 mm w.c. Mercury-cell operation tends to be in the low end of this range. Some membrane cells generate hydrogen at pressures of 50 kPa and more. Such pressures, if carried through the gas headers, may not require compressors to suit the end use of the hydrogen. Often, however, the purpose of the elevated pressure is to improve cell operation, and the pressure is let down as the gas leaves the cell room. In a mercury cell, the pressure of the hydrogen is somewhat independent of the chlorine pressure because the two gases are generated in different locations. In a membrane cell, the pressures of the two gases are closely related. Only the membrane separates them, and the differential pressure must be small and closely controlled. The hydrogen pressure must always be the higher of the two, in order to keep the membrane pressed against the anode. Differential-pressure restrictions of the various cell technologies are covered in Section 5.5.1.

11.4.2.1. Cell Room Hydrogen Header

11.4.2.1A. Operation Near Atmospheric Pressure. The simplest approach to hydrogen header control at very low pressure uses large water-sealed vents designed to maintain a fairly precise back-pressure with little or no fluctuation. Figure 11.35 shows such a vent. Section 9.1.10.1 gives design details for this type of system as a pressure-relief device with little heed to gas flow distribution. For more precise control, it is important to distribute the gas as small bubbles over a wider area of the water seal (10–20 mm deep) in order to provide minimum pressure drop and fluctuation in flow.

Problems still arise when the gas goes on to processing. It can be difficult, for example, to transfer hydrogen from a zone at low pressure to a compressor with suction throttling while maintaining good control of cell room header pressures.

The control strategy, presented in Fig. 11.35, provides smooth transfer with precise control. It must allow controlled venting as well as controlled transfer to compression, and so it requires two control valves and split-range control. The cell room header pressure is measured by a d/p cell with a Monel diaphragm. If desired, a flush-type cell can be used. It is located on top of the header as it leaves the cell room. It is important that connections to the d/p cell be freely draining.

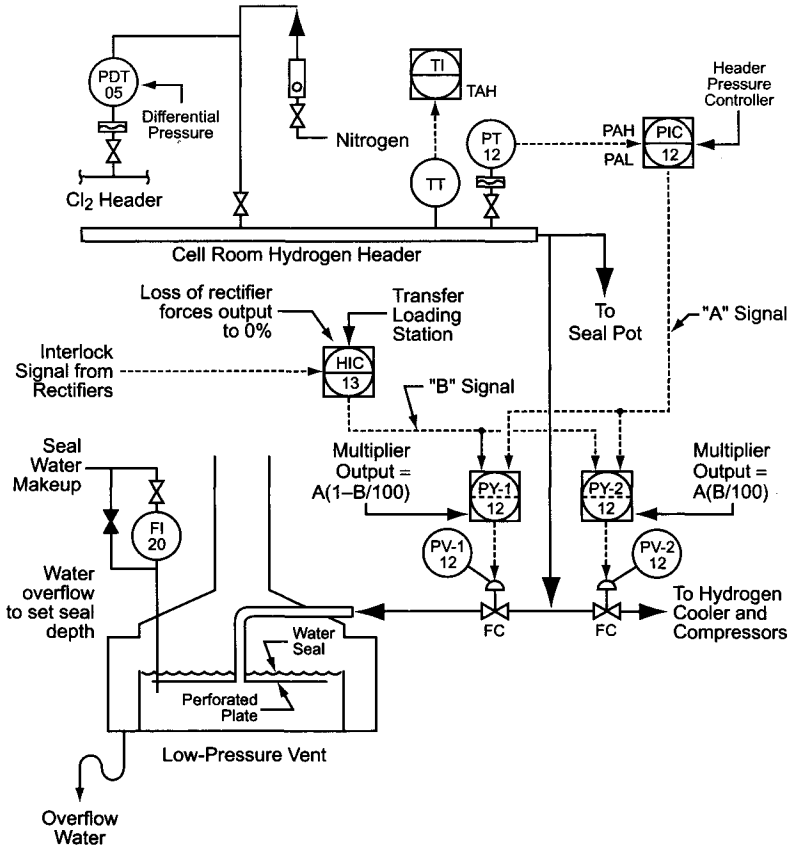


FIGURE 11.35. Hydrogen header pressure control (atmospheric pressure).

The controller is direct-acting with proportional and integral action. Split signals from the controller and from a transfer loading station go to multiplication modules with different functionalities. The setting of the transfer loading station determines the split of the hydrogen flow between the vent and the process. The signal from the pressure controller is designated *A* and that from the loading station *B*. The operator may set *B* anywhere in the range 0–100%. The multiplier associated with the low-pressure vent should have the function:

$$\text{Output} = A \times (1 - B/100) \tag{1}$$

where *A* is the output of the pressure controller and *B* is the output of the transfer loading station, %. An interlock signal forces the transfer output to zero whenever the rectifiers are off. The other multiplier should have the function:

$$\text{Output} = A \times B/100 \tag{2}$$

Figure 11.36 shows the result. The maximum controller output shown here is somewhat arbitrary. Its value will depend on operating conditions. When the transfer output *B* is

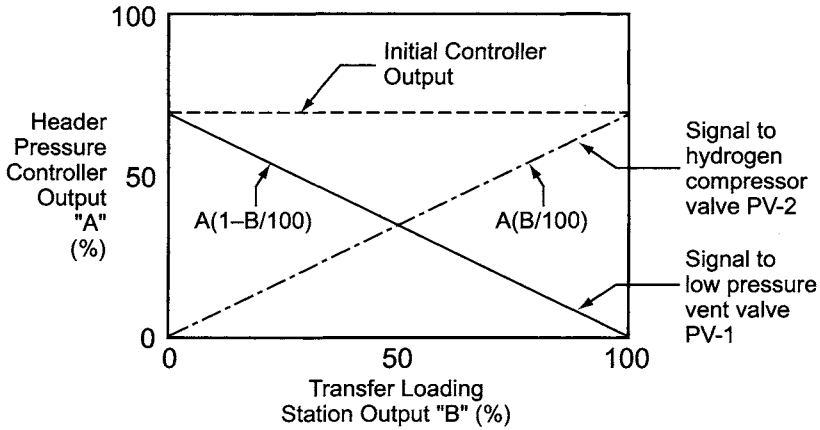


FIGURE 11.36. Diversion of hydrogen to compressors.

zero, the compressor suction valve is fully closed and the vent valve is the pressure control device. Section 11.4.2.2 covers the startup and the functioning of this arrangement when switching hydrogen from the low-pressure vent to the compressor suction.

Selection and sizing of the two control valves are critical to the success of the control strategy. Both valves must fail closed, have linear flow characteristics, have good control over the entire range to full shutoff, be sized to handle the full cell room output of wet gas, and have fairly tight seals. Cost and lack of availability preclude the use of globe valves, which would have desirable characteristics. A more economic choice is a V-ball valve with positioner modified to provide the desired linear characteristic. Both control valves should have nearly the same percentage of overcapacity.

One of the most important cell room measurements is the hydrogen to chlorine differential pressure. When both the hydrogen and chlorine header pressures are controlled separately, as assumed in Fig. 11.35, the differential pressure measurement is recorded and monitored with high and low alarms. The ideal transmitter would be of corrosion-resistant construction with each side of the cell mounted above and directly connected to one of the headers in such a way that the condensed water drains freely back into the headers. The practical compromise is a tantalum flush-mounted d/p cell connected to the chlorine header. Since the back side of the cell is unable to drain into the hydrogen header, a small nitrogen purge is used to keep the connecting tubing dry and prevent the collection of condensate.

The alternative to separate control of the header pressures is to control one pressure directly and the other through a differential pressure controller referred to the first. With this alternative, the more frequent choice is to control the chlorine pressure and the hydrogen/chlorine differential pressure. This takes advantage of better control dynamics. An argument for this approach is that it is the quality of the differential pressure control that may determine the life of the membranes, and there is only one control loop variance to deal with. In a poorly designed system, however, responses to the two control signals can be out of phase and introduce fluctuations in the pressures. In order to have a consistent approach in this presentation, we assume that the two header pressures are controlled separately and directly. Differential pressure is measured directly or computed from the outputs of the two pressure transmitters. Monitoring, alarm, and supervisory systems can be appropriate to individual applications.

The header temperature can be measured with a RTD sensing element in a flanged Type 316 SS thermowell. The transmitter should have a range of 0–250°F or 0–150°C. The transmitted measurement is recorded and monitored with a high alarm.

11.4.2.1B. Operation Under Low Positive Pressure. In addition to good control of normal operating conditions, higher pressure operation of membrane cells requires a special control strategy to bring the header pressures up to the desired level smoothly and without damaging the membranes. This goal requires coordination of the chlorine and hydrogen header pressures. Section 11.3.2.1A has already described the technique with respect to the chlorine header. There are two pressure controllers, one with a wide measurement range and one with a narrow range along with suppression of the signal below some lower limit. Figure 11.37 shows that the wide-range controller loading station controls both headers. Its signal goes directly to the chlorine header pressure controller. It reaches the hydrogen header controller through a biasing pressure relay. This keeps the pressure higher on the hydrogen side. The membranes then remain in their desired position,

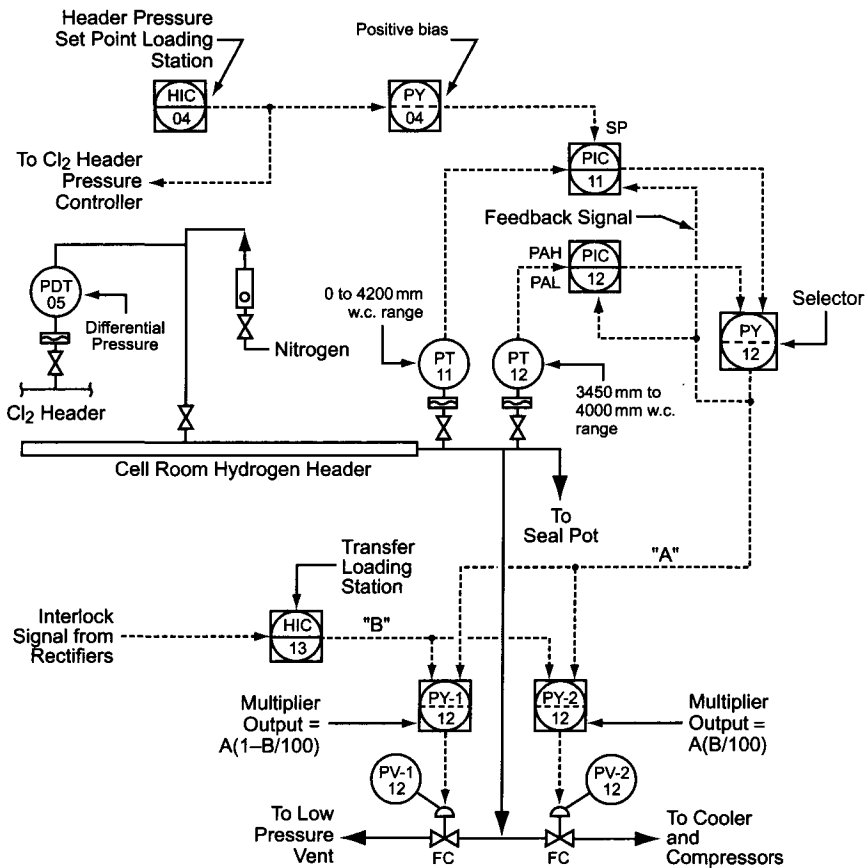


FIGURE 11.37. Hydrogen header pressure control (low pressure).

against the anodes. The biasing value selected should be appropriate to the electrolyzer technology being used.

The control signals from the two pressure controllers go to a high-signal selector switch. When the pressure set by the wide-range system reaches a certain point, then, the narrow-range system takes over control. Control response charts are in Fig. 11.38. The situation is similar to that described for the chlorine system and shown in Fig. 11.20.

The pressure control signal acts along with the signal from a transfer loading station to operate the two control valves. This is the method described in Fig. 11.35. The particular combination shown in Fig. 11.37 is appropriate for positive header pressures of about 15–35 kPa. The set points used in Figs. 11.20 and 11.38 are arbitrarily chosen near the maximum in this range and do not represent any particular electrolyzer technology.

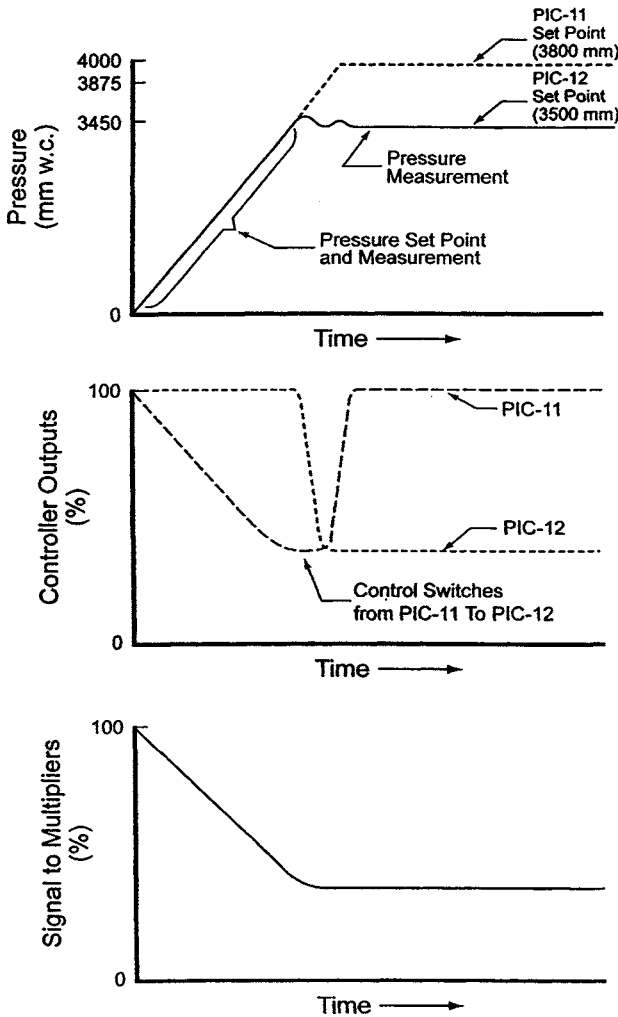


FIGURE 11.38. Hydrogen pressure control system response charts.

Higher operating pressures generally make control of the differential pressure between the two gas headers more difficult. The allowable differential pressure becomes a smaller fraction of the measured pressure. This accounts for the use of dual transmitters with different ranges in Figs. 11.19 and 11.37. Another technique to increase the accuracy of control and give more precise throttling is the use of gap-action control. Figure 11.39 is an example, and the approach is similar to that used to control the pH of dechlorinated brine (Fig. 11.16). Again, there is a loading station with a wide range that fixes the set points for both gas headers. A positive bias to the hydrogen control system fixes the differential pressure. The gap-action controller operates outside set limits (e.g., 25% and 75% of output range) and fixes the position of the larger valve. The second transmitter operates over a narrow range, and sends its signal to a second controller. The two signals are fed to a selector. In the normal control range, the narrow-range controller operates the smaller valve to maintain close control of the pressure. When this system is used, there will be a similar arrangement on the chlorine header. The smaller control valve in each header will be a globe valve with linear response. The larger valve, responding to integral control only, is shown on the drawing as a V-ball valve. A butterfly valve may be used in its place on the chlorine header.

11.4.2.1C. Safety Systems. The cell room hydrogen header should be automatically purged with nitrogen at high flow rate for a fixed time whenever the rectifiers shut down (Fig. 11.40). This ensures that condensation of water vapor does not lower the header

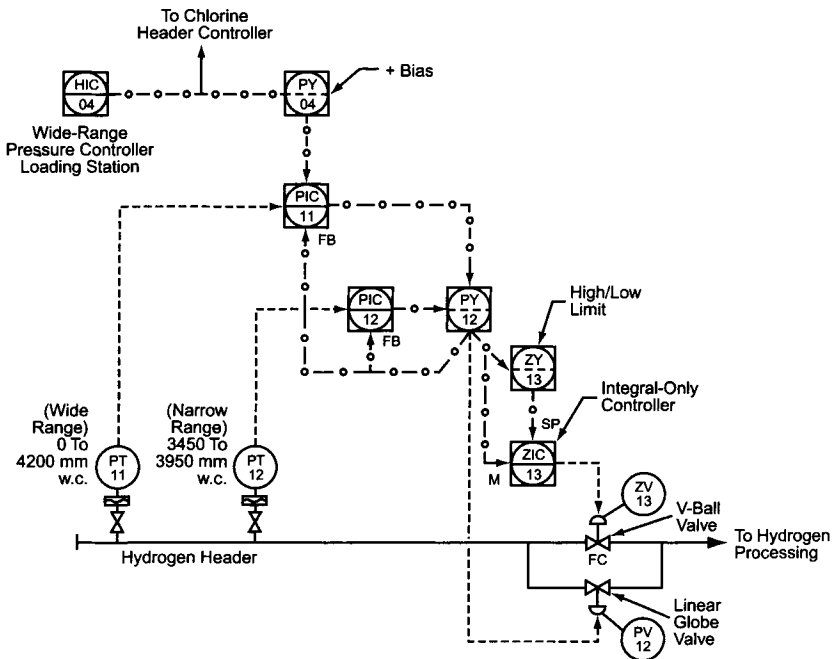


FIGURE 11.39. Low-pressure system with precise control throttling.

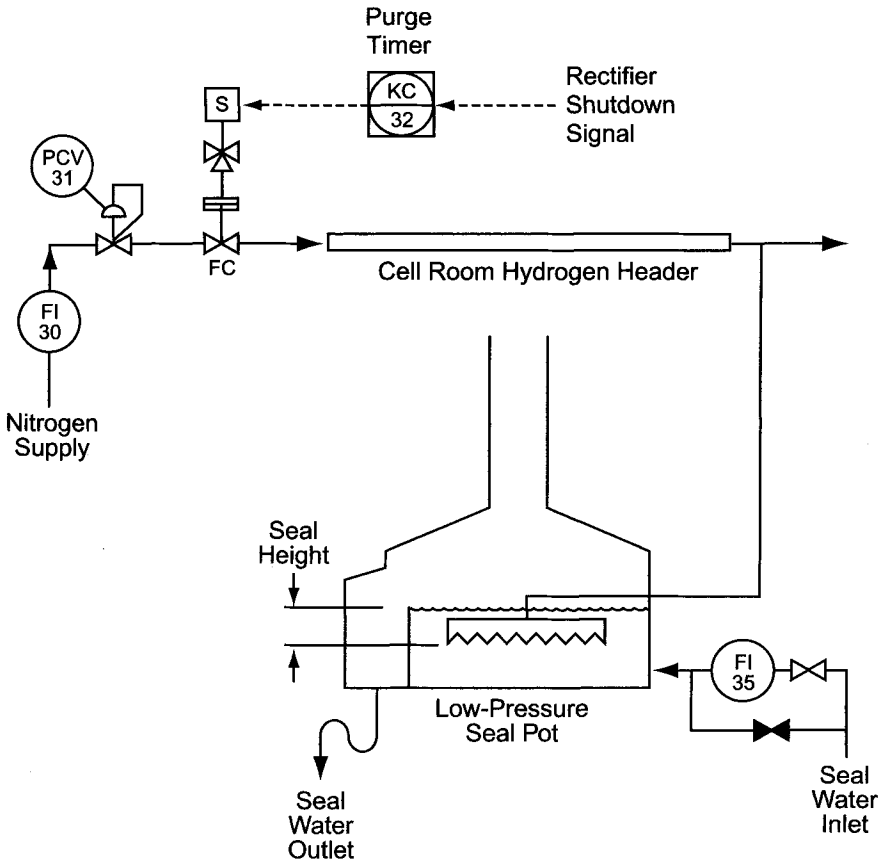


FIGURE 11.40. Purging hydrogen header and seal pot.

pressure below atmospheric and draw air into the system. Failure to exclude air has caused explosions during startup [7,8]. After the high purge rate, a pressure regulator will maintain a small positive pressure in the header. The presence of nitrogen also eliminates the hazard of mixing hydrogen and air when the rectifiers go back on line. Section 13.6.6 discusses system purge requirements in more detail.

The other principal cause of low pressure is a malfunction of the hydrogen compressor control, which could allow the header pressure to drop very quickly below atmospheric. Section 11.4.2.4 covers the relevant protective systems.

When the operating pressure is low, the cell room hydrogen header is protected from overpressure with a water set to relieve slightly above the normal operating pressure. Comparison with Fig. 11.35 shows that this is separate from the seal pot used as part of a low-pressure control system. It is the conventional type of seal pot already discussed for both chlorine and hydrogen service (Section 9.1.10.1). A small continuous flow of water, measured by rotameter and manually controlled, maintains the level of the seal. A high rate of water flow can be actuated remotely to flood the seal pot and re-establish the seal once the high pressure is relieved. High-pressure membrane systems

operate beyond the effective range of a water seal and must depend on weighted discs or an automated system for relief.

Higher pressure operation of membrane cells also complicates the header purging arrangement. The purge must take place at the operating pressure so that the hydrogen can be swept out of the header through the sealing device.

11.4.2.2. Diversion to Compressor System. Section 11.4.2.1 discussed the hydrogen header pressure control arrangement. It did not cover the mechanism for diversion of the gas to the compression system.

The control system of Fig. 11.37 contains a manual loading station with 0–100% range for transfer of hydrogen to the compressors. An interlock forces the output to zero whenever the hydrogen compressors are not running and shifts the pressure control signal to the low-pressure vent control valve. When the compressors are running, the manual loading output can be set above zero. The signal goes to the two multipliers, where it represents the “*B*” value in Eqs. (1) and (2).

The compressors are usually started on nitrogen, with 100% recycle. Increasing the output of the manual loading station causes the two multipliers to divide the pressure controller’s signal to the two control valves. At a 25% transfer output, for example, one quarter of the controller output is sent to the compressor suction control valve and three quarters to the vent control valve. The emphasis in Section 11.4.2.1A on closely related sizing of the two valves assures that the total flow through both control valves changes very little during the transfer procedure and that the transfer is smooth. Throughout the transfer, the pressure controller is in full control of the valves and will automatically make adjustments regardless of the transfer signal output. When the transfer signal is 100%, pressure control is handled completely by the compressor suction pressure control valve.

11.4.2.3. Hydrogen Cooling. The hydrogen cooler is located in the stream going to the compressors. Its purpose is to cool the gas and condense most of the associated water vapor. The cooler design can take many forms, but here we discuss direct contact between the hydrogen and water or brine. The exchanger must have a low pressure drop and provide good contact between phases. A common design uses water injected through spray nozzles (Fig. 11.41).

To remove heat from the system, water from the bottom of the column is circulated through a cooling water exchanger to the spray nozzles. The circulating water flow is measured and transmitted to the main control center. Low flow activates an alarm.

As the hydrogen cools, water condenses and accumulates in the column. The level in the bottom of the column can be measured with a d/p cell. The signal from the level transmitter goes to a direct-acting controller with proportional and integral control modes. The fail-closed control valve is in a side branch off the circulating pump discharge line.

The temperature of the hydrogen leaving the cooler is measured and transmitted to the main control center. A high-temperature alarm is necessary; a low-temperature alarm may be useful.

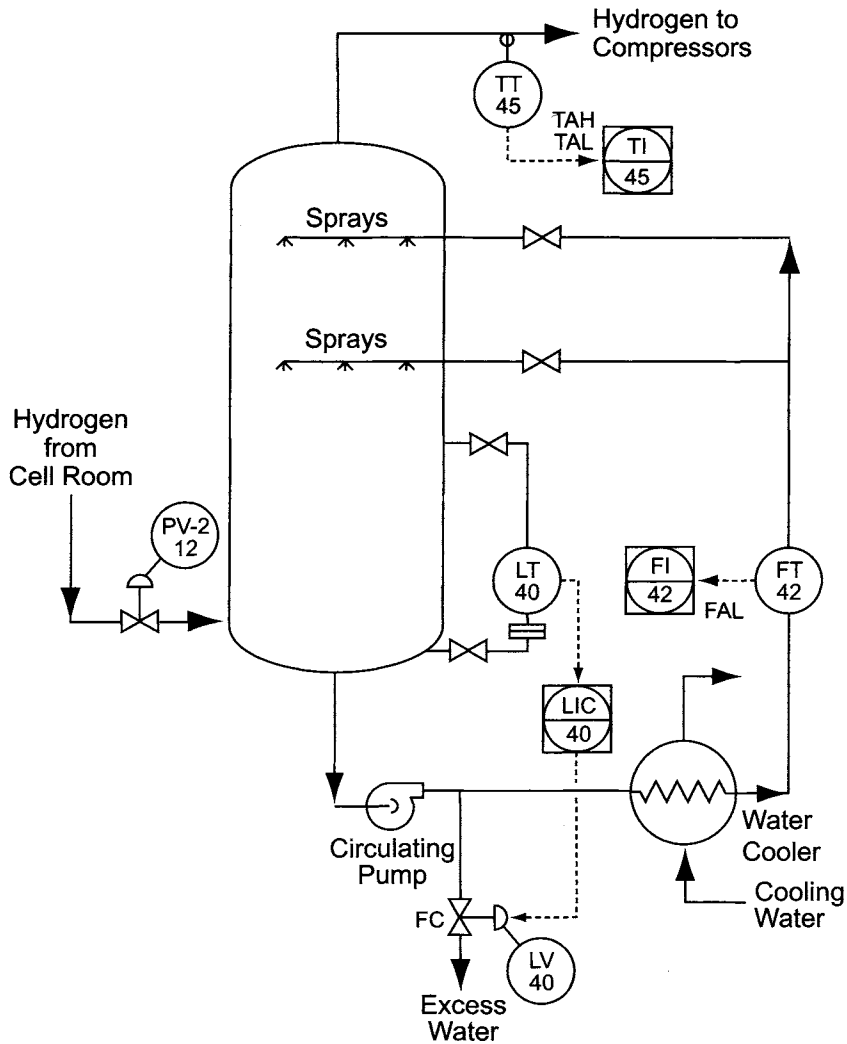


FIGURE 11.41. Direct-contact hydrogen cooling system.

11.4.2.4. Hydrogen Compression. Many applications of hydrogen are at pressures compatible with the characteristics of liquid-ring compressors (Sections 9.1.6.2C and 9.2.3). The discussion here assumes the use of this type of compressor with a discharge pressure of about 100 kPa(g). Applications at higher pressures are more specialized and may require the use of reciprocating compressors.

The suction pressure controller allows the hydrogen compressor to run on complete recycle. When there are several compressors, each should have its own controller. These maintain control by recycling compressed hydrogen to the suction.

Some designers feel that hydrogen systems should never be operated with negative suction pressures. Others argue that very modest negative pressures (typical control

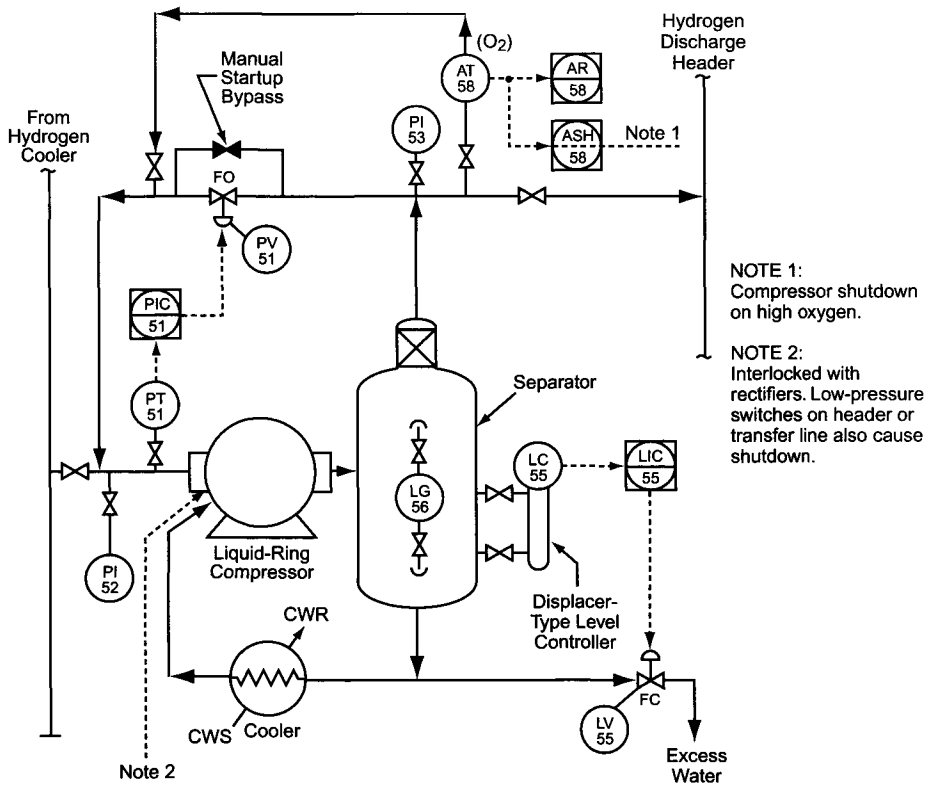


FIGURE 11.42. Hydrogen compressor system.

point -125 mm w.c.) in a small section of tightly sealed piping represents a minimal risk. In diaphragm-cell plants, compressors routinely operate at such negative pressures (Section 11.4.3). In any case, there should be protection against excessively low pressures. The compressor of Fig. 11.42, therefore, is interlocked to shut down whenever the cell current fails. Similarly, the compressor should stop whenever the suction pressure drops below a set limit for any other reason. Some number of pressure switches might be installed in the transfer system. At least one switch should be independent of control or measurement transmitters.

The suction pressure in any case is measured by a d/p cell, as shown in Fig. 11.42, and the proportional-plus-integral controller sends its output to a fail-open globe valve sized to handle the total compressor capacity at 90% of its travel. Compressors are usually a bit oversized, and this provides the additional capacity needed for the steady recycle flow.

The recycle valve usually cannot handle full flow when the system is full of nitrogen, which is much denser than hydrogen. To allow the system to start, a manual globe valve of the same size as the control valve can be added in parallel. When hydrogen feed begins, the automatic valve will begin to close as nitrogen is purged from the system. The manual valve can then be closed.

A knockout pot, or separator, mounted after the compressor removes water from the gas. Cooling of the circulating water ring means that more water condenses from the hydrogen and collects in the pot, and this must be removed from the system. The level in the pot is measured by a cage-mounted displacer-type transmitter. A direct-acting proportional-plus-integral controller commands the normally closed automatic valve. Globe valves are a good choice for this service. Handling of the excess water should be with due regard to the possibility of hydrogen entrainment.

On the compressed gas side, an analyzer gives added protection against the consequences of air intrusion. A paramagnetic analyzer is a good choice because it is sensitive primarily to oxygen. Other components of the gas are slightly diamagnetic and have the opposite response to a magnetic field. The oxygen measurement is transmitted to the main control center. The instrumentation system also provides alarm and shutdown signals. A typical range for the instrument is 0–5% O₂, with an alarm at 0.5% and compressor shutdown at 1%.

Most hydrogen systems have a spare compressor that can be interlocked with the same shutdown signals as the main compressor. In multitrain plants, interlocking of the spare compressor becomes much more complicated. It can be interlocked with any train, and so a selection is necessary when the spare compressor is to be put into service. Details are beyond the scope of this book, but the interlocking issue must be addressed.

11.4.2.5. Delivery of Compressed Hydrogen. Hydrogen compressed for use in various services must be delivered to a user or vented, and the users also must be restricted so that they cannot take too much gas. It is normal for several hydrogen compressors to discharge into a common header.

11.4.2.5A. Discharge Pressure Control. In Fig. 11.43, a standard pressure transmitter with a range to suit the process measures the pressure of the hydrogen in the discharge header. The pressure signal is transmitted to a reverse-acting proportional-plus-integral controller with split control range. The controller output goes to two fail-open control valves, a globe or V-ball valve in the line to the high-pressure vent, and a V-ball or butterfly valve in the line to the user. The high-pressure vent valve has a positioner calibrated for an input range of 4–12 mA, with the valve wide open at 4 mA. The positioner for the other valve is calibrated for 12–20 mA, and the valve is wide open at 12 mA.

When the user is not taking hydrogen, the controller throttles the vent valve to maintain the desired pressure. The control valve for the user is wide open, and the protective system at the user's end must provide closure. As the user begins to take hydrogen, the vent valve begins to close. When it is fully closed, the control valve in the line to the user starts to close to restrict the flow of hydrogen.

Note that the valve in the user's supply line acts only to restrict the flow of hydrogen to match the output of the compressors. Flow control otherwise is at the other end of the line.

In a common arrangement, the hydrogen downstream of the high-pressure vent valve can go to either of two vent stacks. The gas passes through a water seal at the bottom of the stack. If the vent from one stack catches fire, the hydrogen can be switched

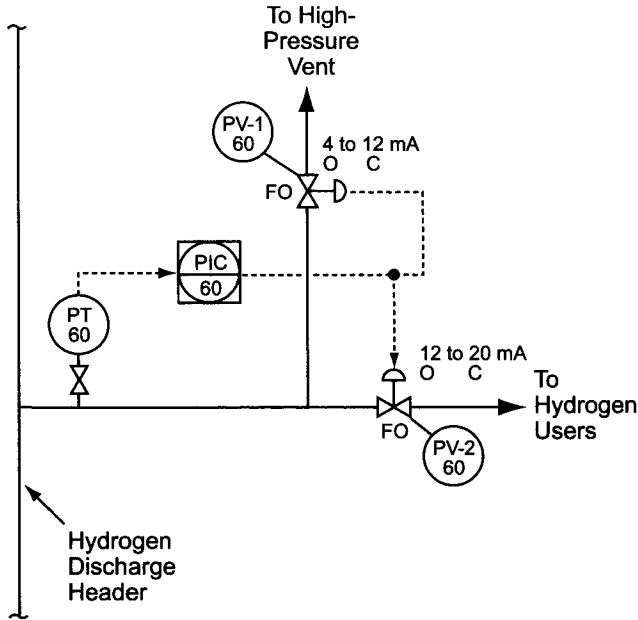


FIGURE 11.43. Hydrogen compressor discharge pressure control.

to the other stack. Each stack is supplied with the ability to inject steam in large quantities to snuff out a fire.

11.4.2.5B. Hydrogen Users Priority Control. While the discussion immediately above assumed that there was only one user of hydrogen, there are frequently several. Even with only one user, shutdown or curtailment of the offtake can force some of the hydrogen to be vented or diverted for use as fuel. The total demand by multiple hydrogen users, on the other hand, also can exceed the rate of supply. It is, therefore, the usual practice to establish user priorities by staging the hydrogen header pressure control system (Fig. 11.44).

A standard pressure transmitter is mounted on the product hydrogen header. In our case with a discharge pressure of about 100 kPa, the measurement range might be 80–120 or 85–110 kPa. The proportional band should be set to about 40%, so that the controller output changes 100% over a pressure range of 16 or 10 kPa. The manual reset should be adjusted so that with no users taking hydrogen, the controller output is 20 mA when the header pressure is slightly less than the normal hydrogen discharge pressure. As users begin to take hydrogen, the pressure drop through the valve will lower the header pressure, and the controller output will change.

Each independent user or group of users is supplied through a fail-closed linear globe valve. No more than three split-ranged control valves should be used; more complex arrangements require special control. The positioners would be calibrated for the ranges 15–20, 9–15, and 4–9 mA, with the highest range for the lowest priority user. Figure 11.44 does not take into account the requirements to vent gas or to transmit information to the users.

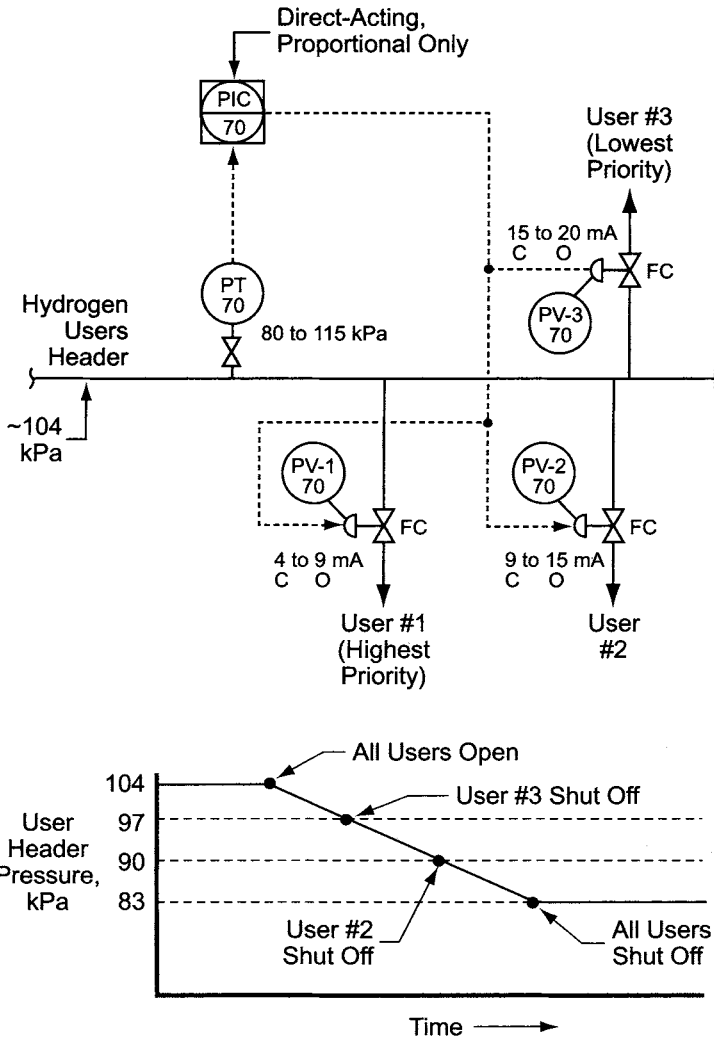


FIGURE 11.44. Hydrogen users priority selection.

After operation is established, the proportional band should be adjusted to match the pressure in the header with the hydrogen flow.

11.4.3. Diaphragm-Cell Hydrogen Systems

The differential pressure in a diaphragm cell is kept low to avoid the migration of hydrogen through the diaphragms and into the chlorine. It is also true that conventional diaphragm cells are not capable of operating under any useful positive pressure. Many cells operate at very low positive (~1–2 mm w.c.) or even negative pressure, and this increases the complexity of control.

11.4.3.1. *Cell Room.* The maximum pressure accepted in the hydrogen header does not permit use of a control valve on the low-pressure vent. A specially designed water seal (Section 11.4.2.1A) with an adjustable level is used instead. Figure 11.45 is a typical design. It can be used in conjunction with a throttling valve controlling the hydrogen going to the compressors. The control valve typically is a fail-closed V-ball valve. The pressure transmitter is a d/p cell mounted on top of the hydrogen header as it leaves the cell room. The controller is direct-acting with proportional and integral control functions.

The pressure switches produce signals as long as the operating pressure is in the safe range. If either switch detects a low pressure, no signal passes the AND gate. This causes a compressor shutdown.

The hydrogen line to the automatic seal pot contains a full-diameter U-shaped section. When the compressors are operating, this is filled with water to isolate the seal pot.

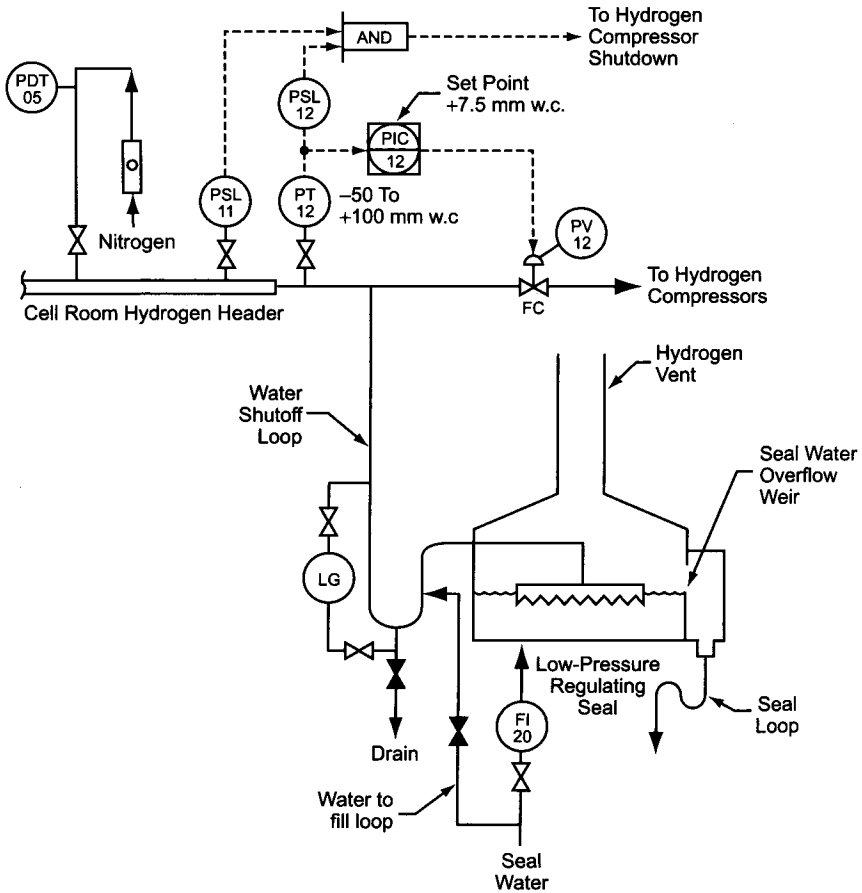


FIGURE 11.45. Diaphragm-cell hydrogen header pressure control.

11.4.3.2. Hydrogen Compressors. Except for lower instrument ranges and a lower suction pressure setting, controls here are the same as those described in Sections 11.4.2.5. The procedure for beginning transfer of hydrogen to the compressors is more complicated. With the compressor(s) operating on nitrogen under full recycle, the valve is opened slowly, allowing hydrogen to enter the compressor system. The nitrogen is purged from the system, and when about one half of the hydrogen flow has been transferred to the compressors, the cell room header pressure controller is put onto automatic. The set point is at a low value until the loop before the low-pressure seal is filled with water.

Safety interlocking is as previously described. If the compressors stop for any reason, the cell room emergency pressure seal blows and relieves the pressure until the low-pressure control vent can be put back into operation.

11.5. CAUSTIC SYSTEMS

The caustic systems for the three different methods of production are entirely different from each other and are discussed separately in this section. Evaporation is the subject of Section 11.6.

11.5.1. Mercury-Cell Caustic Systems

In the mercury cell, the alkali metal ion combines with the mercury to form an amalgam that flows by gravity into a decomposer. Here, the amalgam reacts with water to form caustic, releasing hydrogen in the process.

11.5.1.1. Decomposer Operation. Decomposers are designed to promote good contact between the amalgam and the feed water and to allow the release and collection of the hydrogen. Decomposer, amalgam, and mercury are in contact with each other and with the cathode of the cell. They all are at the same potential. After reaction of the amalgam and the water, denuded mercury from the outlet of the decomposer is pumped back to the inlet of the cell.

The concentration and quality of the caustic produced in a mercury cell depend entirely on the flow rate and quality of the water fed to the decomposer. The use of demineralized water is standard. The caustic and hydrogen produced in the decomposer are quite hot. Some of the water thus evaporates and leaves with the hydrogen gas.

Conventional instrumentation is a rotameter on the demineralized water feed, with a manual valve for adjustment of the rate. Magnetically coupled flow indicators will not work properly in the strong electrical field of the cell room. The density of the caustic solution is measured with a nickel hydrometer. The hot, strong caustic would quickly destroy a conventional glass instrument.

A slightly more automated method would be to feed the water to each rotameter from a pressure-controlled header system (Fig. 11.46). The pressure would be measured with a diaphragm seal connected to a transmitter with a filled capillary. The control valve would be a fail-open globe or V-ball valve with equal percentage characteristic. The controller would be reverse-acting with proportional and integral action. This arrangement allows

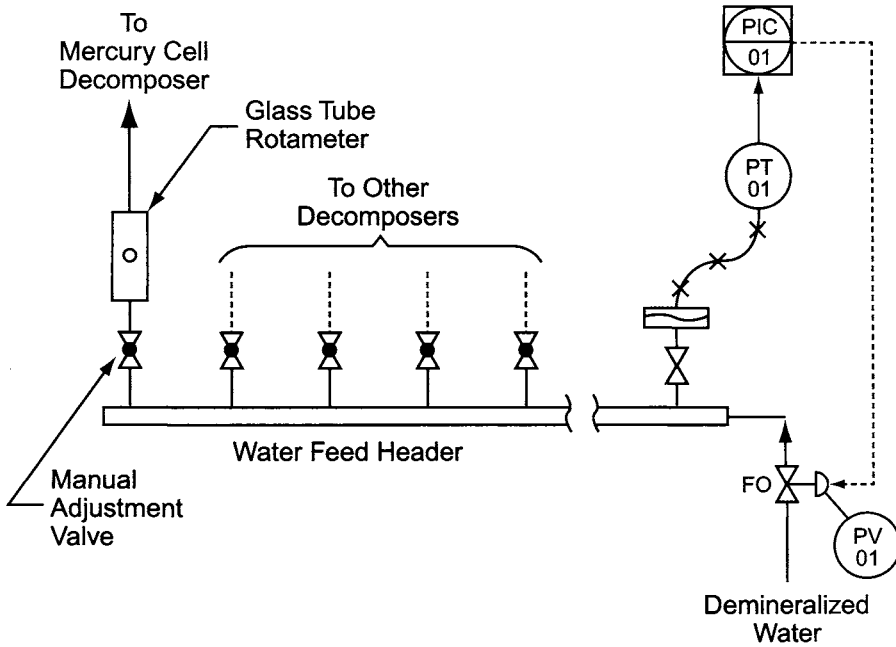


FIGURE 11.46. Water feed to amalgam decomposer.

simultaneous adjustment of the water flow to every cell by changing the pressure on the header. This is similar to the approach sometimes taken to control the cell-room brine flows (Section 11.2.2.4D). Caustic flows from the decomposers by gravity through seal loops to a collection header. The seal loops require atmospheric vents. Pressure surges in the hydrogen system can cause splashes of hot caustic from these loops.

11.5.1.2. Caustic Product Handling. The cell room collection headers carry the caustic to a pump tank from where it is transferred to storage before the filters. Figure 11.47 shows two methods of control of this operation. If the pump tank level is controlled by continuously throttling the discharge from the transfer pump, as in part (a), there is sufficient head to measure the flow with a Coriolis mass flow meter. This type of meter allows simultaneous measurement of the solution density, which represents the caustic concentration. If on-off control is used, as in part (b), there may be enough head available in the headers for the use of magnetic flow meters. These would have to be placed outside the influence of the cell-room field. In either case, caustic flow should be recorded and integrated to give the first measure of the production rate. Combination of flow and concentration signals can give the production rate directly.

Pumping must be from a redundant system with a UPS, because the collection tank usually has little extra volume and can easily overflow. A high-high level switch is normally used to activate the standby pump.

Filtration of the caustic is not discussed here. Several different types of filters are used successfully for the removal of mercury from the caustic. Each has its own

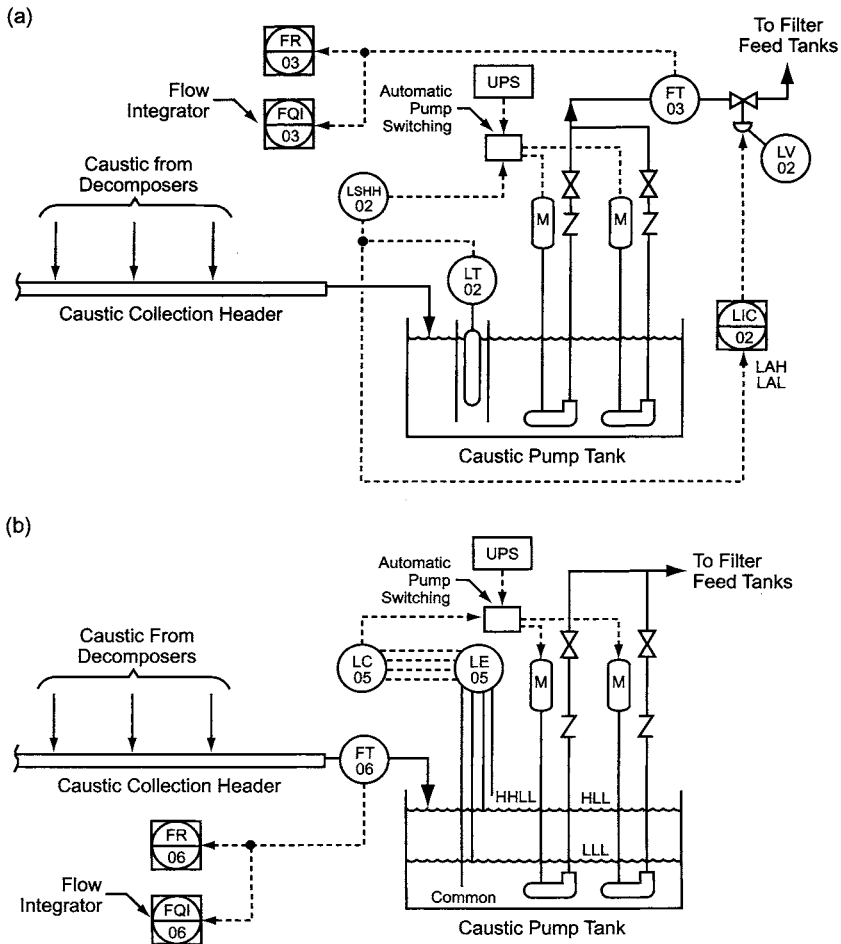


FIGURE 11.47. Operation of caustic pump tank. (a) continuous operation and (b) on-off operation.

control requirements, but most are similar to the systems used to control brine filters (Section 11.2.2.3).

Most caustic storage systems require some form of freeze protection, and the normal approach uses steam coils or bayonet heaters. The steam is regulated with a self-contained temperature control valve with a capillary system and sensing bulb in a nickel thermowell.

11.5.2. Diaphragm-Cell Caustic Systems

11.5.2.1. Diaphragm Cell Level Control. There is no external feed of fluid to the catholyte in a diaphragm cell. Partly electrolyzed brine flows through the diaphragms instead, and the resultant catholyte, containing both NaCl and NaOH, is referred to as “crude caustic” or “cell liquor.” Hydrogen evolves from the cathodes located on the inside

surfaces of the diaphragms, and it collects inside the cathode chamber above the cell liquor. Section 5.4.2 describes the conventional vertical diaphragm cell, and Figs. 5.22 and 5.23 show typical assemblies.

With only one input stream to the cell, independent control of anolyte and catholyte levels is impossible. Section 8.4.2.1 describes the mode of operation, which depends on an adjustable overflow leg for manual control of the catholyte level. The anolyte level remains above the catholyte level by an amount fixed by the flow rate and the hydraulic resistance of the diaphragm. It is this level that must be maintained safely above the top of the diaphragms.

11.5.2.2. Cell Liquor Collection Tank. Cell liquor, gathered from the individual cells into piping headers, flows by gravity to a collection tank. Since diaphragm cells customarily are installed at grade, the collection tank is normally below grade.

The control arrangement is quite similar to that used with mercury cells and shown in Fig. 11.47. The pumps can be controlled by an on-off controller set by high- and low-level switches in the tank, as in part (b) of the drawing. A technically better method, as in part (a), is to control the level with a throttling valve on the pump discharge.

The location and elevation of the collection tank will determine the type of level instrument to be used. It may be a flush diaphragm d/p cell or a nickel displacer gauge. The controller should be reverse-acting with proportional and integral functions. The control valve can be a fail-open PTFE-lined butterfly valve. It is not called on to control at nearly closed positions. Throttled level control allows the use of a magnetic flow meter to measure the flow of cell liquor to the storage tanks. In a large plant, flow rates may be too high for the use of a standard Coriolis meter.

11.5.2.3. Cell Liquor Storage Tank. The next step in the caustic process is evaporation of the cell liquor. The liquor from the collection tank may be pumped directly to the evaporators or may first be sent to storage. Here we consider the requirements of the cell liquor storage tanks. These will be rather large (Section 9.3.6), low-pressure vessels. They should be protected by combination pressure and vacuum relief devices (Fig. 11.48). Sizing should consider the worst cases of vapor release and pumpout plus condensation rate. Normally, these are set by the pumping rates in and out, but improper steaming and rapid cooling have ruined a number of vessels.

Tank level measurement relies on nickel or Monel flush diaphragm d/p cells or nickel float-type indicators. Figure 11.48 shows both types.

11.5.3. Membrane-Cell Caustic Systems

Membrane-cell caustic systems that require the dilution and recirculation of product to the cells are the most complex. Some operate with the direct addition of water, but this section is based on the more comprehensive case.

11.5.3.1. Caustic Circulation Tank. The catholyte tank, or caustic circulation tank, collects the caustic from membrane cells (Fig. 11.49). It also allows the release of entrained

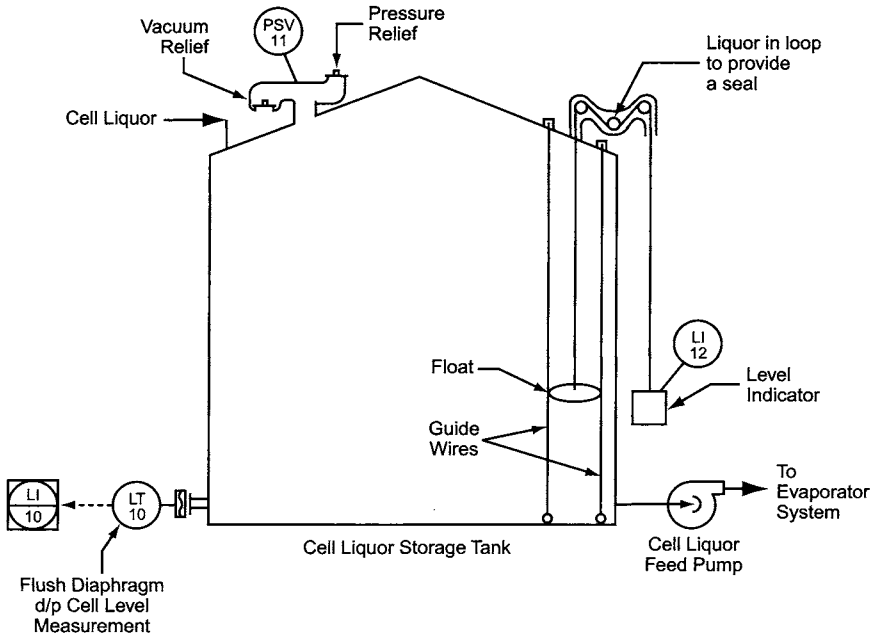


FIGURE 11.48. Diaphragm-cell liquor storage tank.

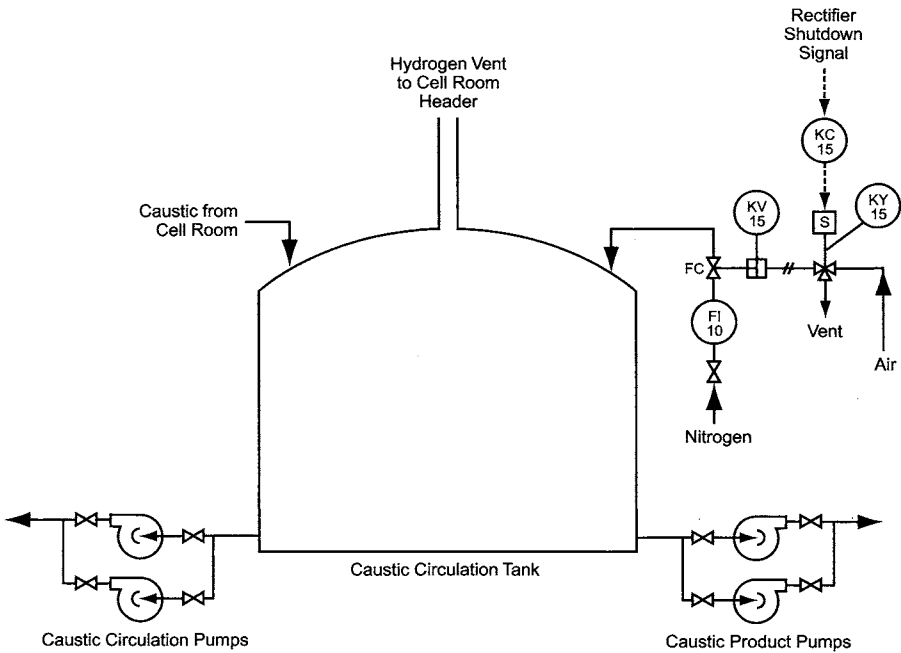


FIGURE 11.49. Membrane-cell caustic circulation tank.

hydrogen. A set of circulation pumps passes the caustic through dilution and cooling systems to the cell feed header. While many systems remove the net caustic production from the discharge of these pumps under tank level control, another option shown here is the use of a separate set of product pumps. The caustic withdrawn goes to storage or to the evaporation system.

The circulation tank operates at the pressure of the cell-room hydrogen header. When the rectifiers stop for any reason, nitrogen enters the vapor space of the tank to prevent development of an explosive environment or a vacuum due to vapor cooling. Excess gas vents through the hydrogen seal pot. The tank may be vertical, as shown, or horizontal.

11.5.3.2. Caustic Product Handling. The caustic removed from the electrolysis system may pass on through a cooler to storage tanks or directly to the evaporator system. Figure 11.50 shows the control of this transfer from the circulation tank.

Since the circulation tank rides on the hydrogen header, as in Fig. 11.49, pressure compensation is necessary for accurate measurement of the level. The level instrument uses a dual remote diaphragm seal system on a d/p cell. The lower diaphragm is connected

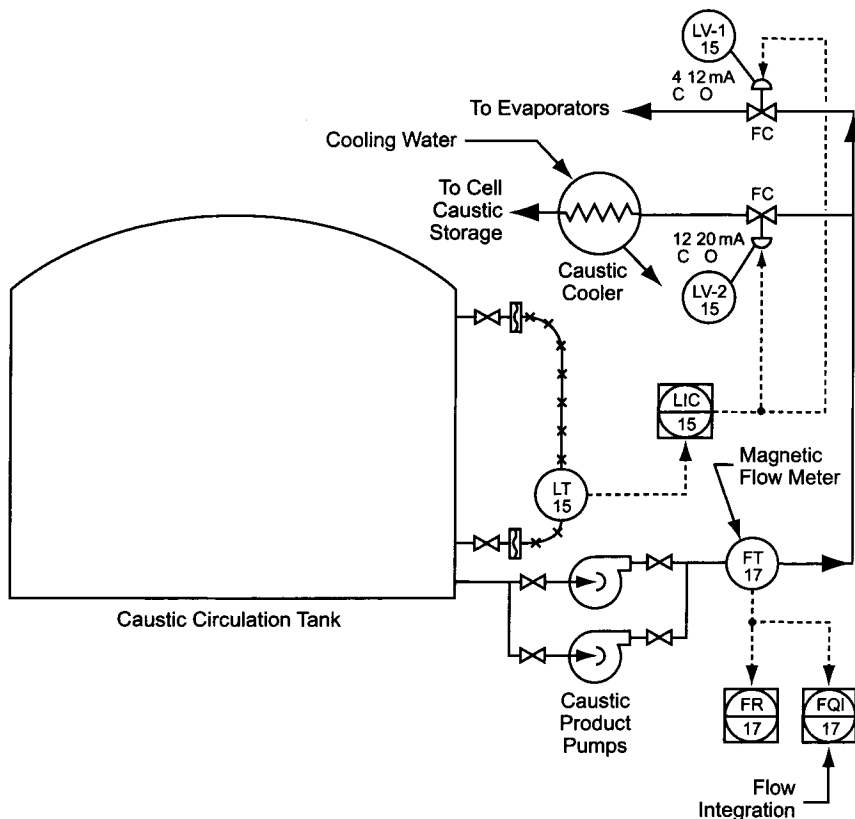


FIGURE 11.50. Transfer from caustic circulation tank.

to the tank near its bottom, and the upper diaphragm is mounted above the maximum liquid level near the top of the tank. The direct-acting controller, with proportional and integral functions, provides a split-ranged signal to two fail-closed nickel globe valves. The positioner on the valve in the line to the evaporators is calibrated for 4–12 mA. Its purpose is to restrict the flow to the evaporators if their demand becomes excessive. The positioner on the other valve is calibrated for 12–20 mA. The valve directs any caustic not taken by the evaporator to the storage tanks. The normal operating level should be low enough to allow the electrolyzers and discharge header(s) to drain without overflowing the tank.

The most common product caustic flow instrument is a PTFE-lined magnetic flow meter with nickel electrodes. The flow signal should be integrated to measure total production. A Coriolis mass flow meter, also nickel, will give more precision if desired. Two mass flow meters can be used in parallel if one is too small to handle the flow. Again, flow from the system is recorded and integrated to provide a measure of the production rate.

11.5.3.3. Recirculated Caustic Feed to Electrolyzers. Most membrane cells operate at 30–35% caustic with a slightly lower feed caustic concentration. Thus, most of the caustic collected from the cells is diluted, cooled, and recycled to the cells. The circulating pumps must continue to run in case of a power failure and so should connect to a backup power supply.

The strength of the caustic solution, as noted above, is often indicated by its density. The most successful analyzer of this type uses the vibrating U-tube principle. Figure 11.51 shows this type mounted in a small sample pipe from the discharge of the caustic circulation pumps. A small Coriolis-type mass flow meter can also be used, since a density readout is available in most models. With its reading converted to product strength, the range of the instrument should be about 5% (w/w), centered on the desired strength. The sample stream returns to the circulation tank.

Measurement of the dilution water flow is by a vortex or magnetic meter, designed not to contaminate the high-grade water required by the process. Control should be by a fail-closed globe valve, preferably all PTFE-lined, again to minimize contamination. An equal percentage flow characteristic is preferred, with the valve sized for a pressure drop of about 100 kPa. A three-way solenoid should be installed in the air line to the diaphragm. When de-energized, it will vent the diaphragm chamber and close the valve. The flow controller is reverse-acting with proportional and integral control action. Some plants use simple flow controllers that are reset manually as necessary to maintain cell product concentration. More advanced strategies rely on density control of the diluted caustic to regulate the concentration entering the electrolyzers or use the rectifier amperage signal passed through a multiplier to set the dilution water flow rate. Figure 11.51 assumes the latter. There should be some positive means of stopping the flow of water whenever the rectifiers go off line.

Section 12.7.2 will discuss techniques for connecting utilities to the process. These include methods for preventing backflow when check valves are not sufficiently reliable. Figure 11.51 assumes the use of a d/p switch set to open if the water pressure is less than 15 or 20 kPa above the caustic pressure. Opening the electrical contact cuts the power to the solenoid mounted on the control valve and forces it to close.

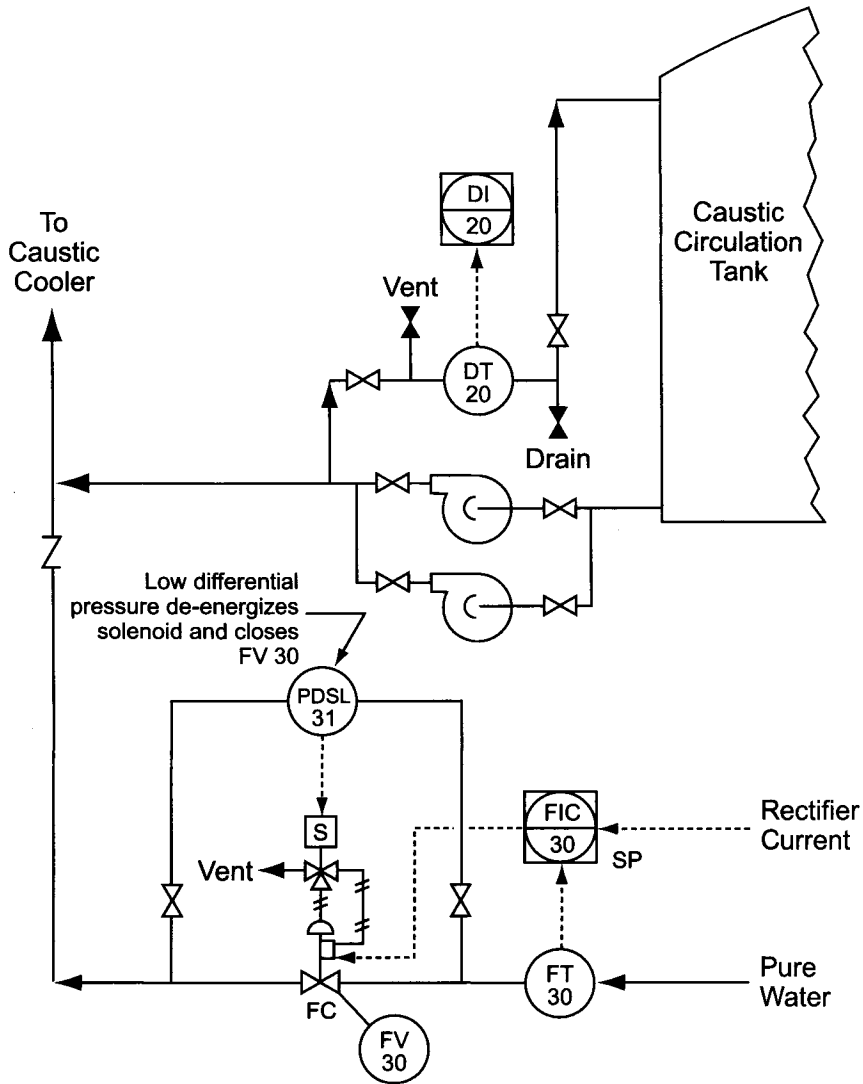


FIGURE 11.51. Concentration measurement and dilution water flow control.

Cooling the circulating caustic removes the excess heat produced in the electrolyzers. The temperature control system of Fig. 11.52 is a cascade system with the secondary control sensing the temperature of the caustic leaving the cooler. The transmitter uses a RTD sensor in a nickel thermowell. The control valve should fail open. A good turndown is necessary, and so a globe or V-ball style is suitable. The secondary portion of the cascade controller is reverse-acting with proportional and integral functions. In the drawing, its set-point signal comes from the primary transmitter measuring the caustic temperature in the header going to the caustic circulation tank. Transmitter and controller characteristics are similar to those in the secondary loop. Some plants use

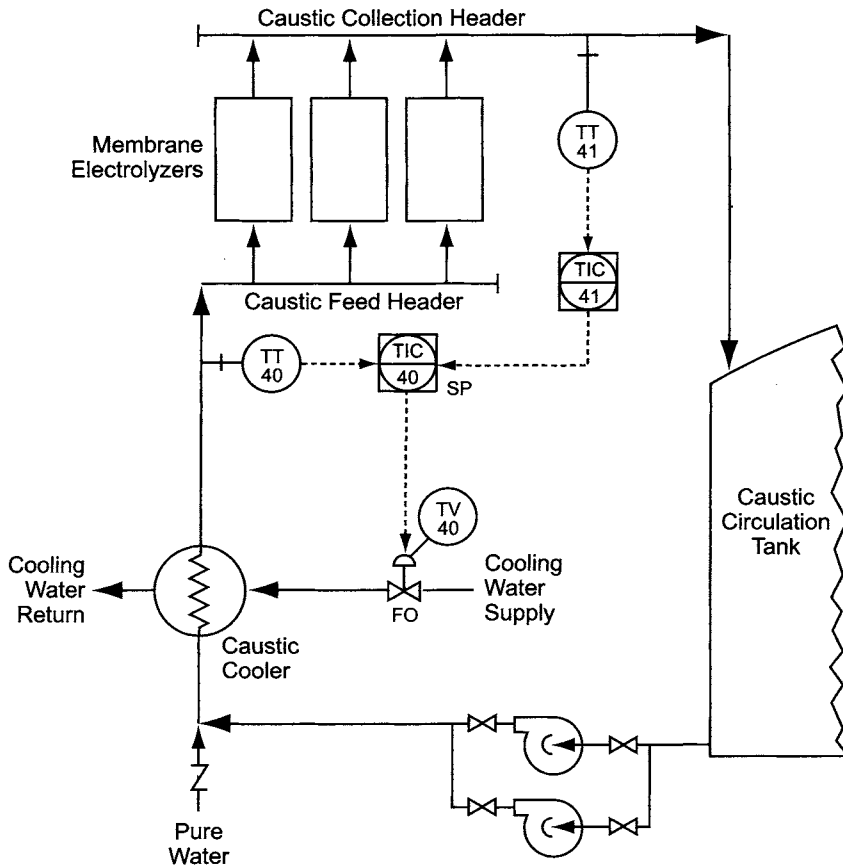


FIGURE 11.52. Circulating caustic temperature control.

an open-loop control here, with no automatic feedback from the cell exit temperature. The operators reset the temperature controller as necessary.

The caustic flow to the electrolyzer feed header is measured and monitored to ensure that there is always a flow to the cells. Magnetic flow meters are standard. The low-flow switch depicted in Fig. 11.53 starts a delay timer when it trips. After the delay set on the timer, the rectifiers will shut down. If the caustic flow recovers in time, the timer resets automatically.

Figure 11.54 shows that the feed header is controlled at a selected pressure so that adjustment of the feed rate to any one electrolyzer does not affect the other flows. The pressure is measured with a Monel or nickel diaphragm seal connected to a pressure transmitter with a capillary system. The fail-open throttling valve is an all PTFE-lined butterfly, controlled by a reverse-acting, proportional-plus-integral controller. Control of the caustic flow to individual electrolyzers is by way of hand valves and local rotameters. This is similar to the arrangement described for brine feed and shown in Fig. 11.11. Again, bipolar systems are amenable to more complete automation.

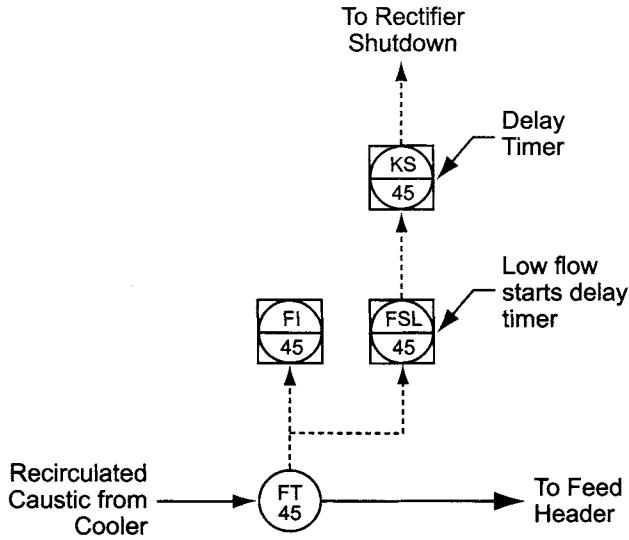


FIGURE 11.53. Circulating caustic flow monitoring.

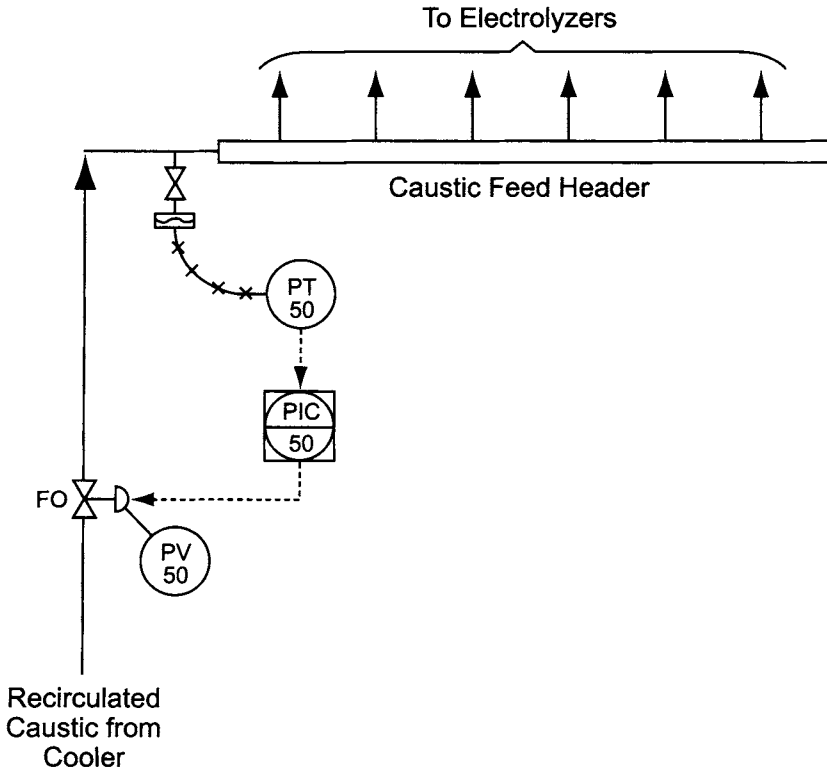


FIGURE 11.54. Circulating caustic feed header.

11.6. CAUSTIC EVAPORATION SYSTEMS

11.6.1. Membrane-Cell Caustic Evaporation

This section describes the controls for a triple-effect membrane-cell caustic evaporator. Section 9.3.3.1 explains some of the reasoning behind the selection of the number of effects and the progression of flow of caustic through the evaporators. To illustrate the control systems here, we assume backward feed of the caustic.

Multiple-effect evaporators are very complex, with many interactions among the variables. The evaporators will adjust to operate at the inlet and outlet conditions imposed on them, but intermediate conditions cannot be controlled, nor would there be any great advantage in doing so.

Membrane-cell caustic is produced at a strength of 30–35% and, compared to diaphragm-cell liquor, needs little evaporation to concentrate it to 50%. Unit size and energy considerations will determine whether two or three effects are used.

11.6.1.1. Packaged Instrumentation. Most evaporation systems are supplied by specialist companies, and many are in the form of packaged units that include instrumentation. Section 13.5.4 discusses some of the advantages and disadvantages of this approach. The customer must ensure by means of the unit specification that the instruments supplied will be of acceptable quality. Many purchasers specify types of instruments and acceptable vendors in order to conform to practice in other units on the plant. As a minimum, the purchaser should retain approval rights on all the instruments.

The type and location of the controllers also require a decision by the purchaser. Most plants will have a central DCS. Packaged units often come with their own PLCs, and Section 13.5.4 also discusses the relative merits of these two approaches. It is perhaps becoming more common for purchasers to specify that the evaporator system controls will be part of the DCS. The evaporator manufacturer then must supply information on the functional requirements of the controllers and list all necessary inputs and outputs (I/O) so that the customer can provide sufficient DCS capacity. This requires close communication between the two parties.

11.6.1.2. Production Rate Control. The primary objectives of evaporator control system design are to produce caustic at the desired rate and strength and to have a stable operation with minimum oscillations. Ideally, one would select the production rate of 50% caustic and let the steam flow and liquor feed rates be adjusted by the automatic controls to keep the evaporator system at a steady state. This is the basis of Fig. 11.55. The product is removed under flow control. Fresh feed of weak caustic and transfers between effects are under control by the level in the receiving effect. Finally, steam responds to the concentration in the first effect and so maintains the heat balance. Section 11.6.1.4 describes the details of concentration measurement. Measurement of the steam flow is necessary for evaporator calculations and diagnosis of the operating problems. This measurement may also be integrated for accounting purposes.

To prevent weak product from going to storage during startup, this arrangement requires recycle until the first-effect concentration builds up. Steam flow control would

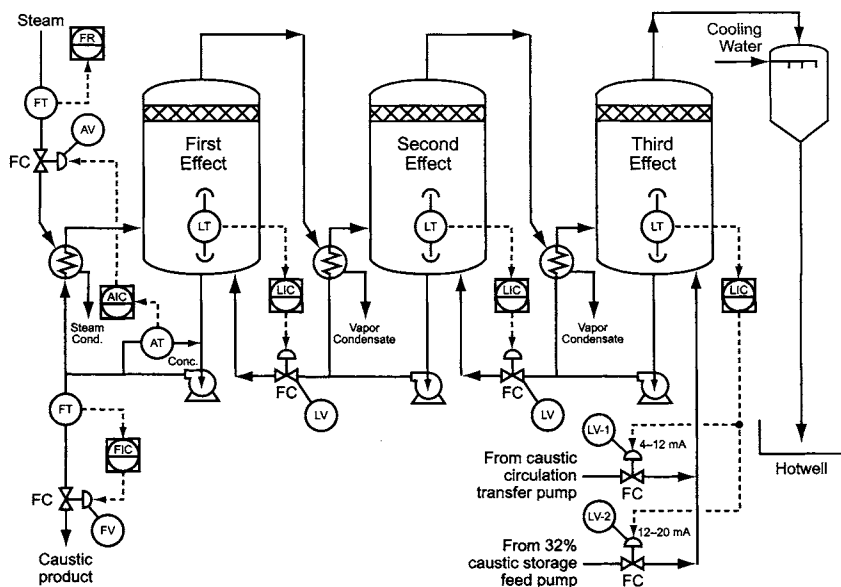


FIGURE 11.55. Evaporator control based on product flow.

be manual during this time. Even after reaching normal strength and adopting automatic operation, any correction to the product concentration would require a change in the steam flow. This would then change the concentrations in the second and third effects, leading to upsets in product concentration as the disturbances were transferred to the first effect. The result would be continuous oscillation in all variables and the deterioration of control.

Any strategy that requires the steam flow to respond to another process variable may result in poor control. This is because a change in primary steam flow affects vapor flows and liquor strengths in all effects. Process feedback from these changes causes further upsets. Given freedom of choice, the best way to control the feed to the evaporators is by controlling steam flow to the first effect, as in Fig. 11.56. The caustic feed would still respond to the level in the third effect. Transfer to the second effect would continue to respond to the level in that effect. Since the operating rate of the system is set by the steam flow (in combination with the feed concentration), the action of the level controller on the first effect changes to fix the product flow rate. Transfer from the second to the first effect then depends on the concentration measurement. While not directly controlled in this option, the product flow still is recorded and integrated. These two functions should always be part of the instrumentation system.

The steam flow should be measured with a vortex-shedding meter. The linear characteristic of such meters provides greater rangeability. A fail-closed steel globe valve with an equal percentage characteristic and a positioner should be used. The controller would be reverse-acting with proportional and integral control functions.

11.6.1.3. Weak Caustic Feed. Weak caustic flows to the third effect either directly from the cell caustic collection tank transfer pumps or from the evaporator feed pumps

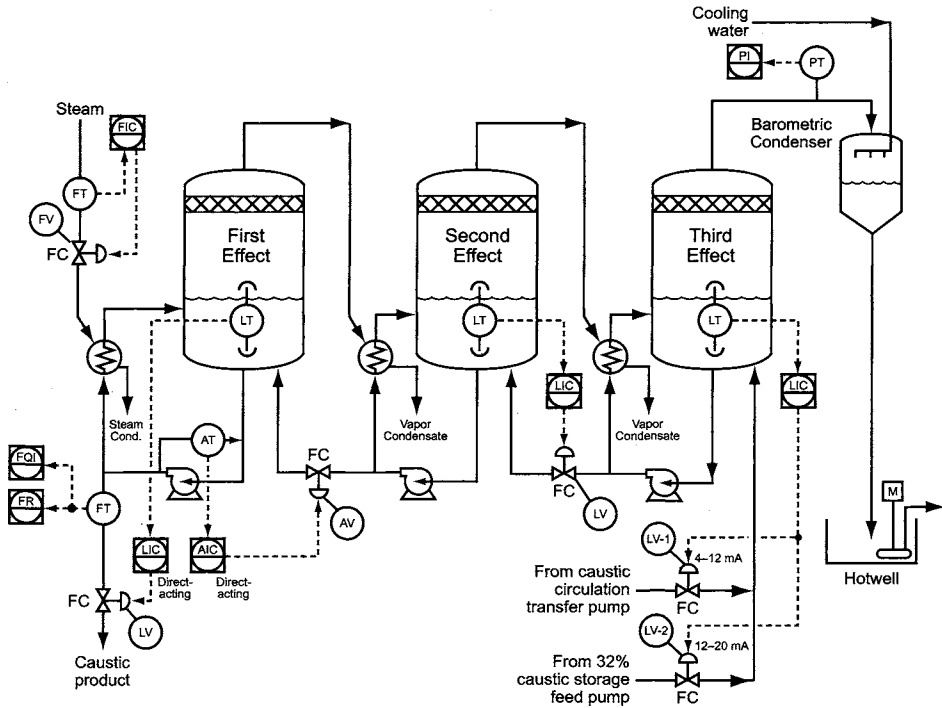


FIGURE 11.56. Evaporator control based on steam flow.

at the weak caustic storage tank. It enters the third effect under level control and is then transferred to the second effect to maintain the level in that vessel. The preferred instrumentation includes double remote flush seals connected to a d/p cell with capillary systems. The control valves are fail-closed globe or butterfly types, depending on the size required. They can be all PTFE-lined, with nickel as an alternative in the case of globe valves. The control valves should be supplied with positioners, and the controllers should be reverse-acting with proportional and integral functions.

To keep design of the caustic storage tank economic while preventing contamination of the product and corrosion of the equipment, any solution sent to the tank is cooled before entry. Figure 11.57 shows a typical arrangement. One split-range control system handles withdrawal from the collection tank in the cell room, and a second handles transfer to the evaporators. The system on the left-hand side of the drawing responds to the level in the collection tank, and the control valves are those shown in Fig. 11.50. The right-hand side responds to the level in the third effect, and the control valves are those shown in Fig. 11.55 or 11.56. For energy economy, as much liquor as possible should flow directly to the evaporators. Accordingly, the low-signal ranges of these systems direct the caustic through the valves on the top line that bypass the storage tank (LV-1/15 and LV-1/16). When the evaporator demand is low, the second of these valves begins to throttle. The first bypass valve (LV-1/15) then goes wide open, and the valve to the inlet of the storage tank (LV-2/15) opens in order to keep control of the level in

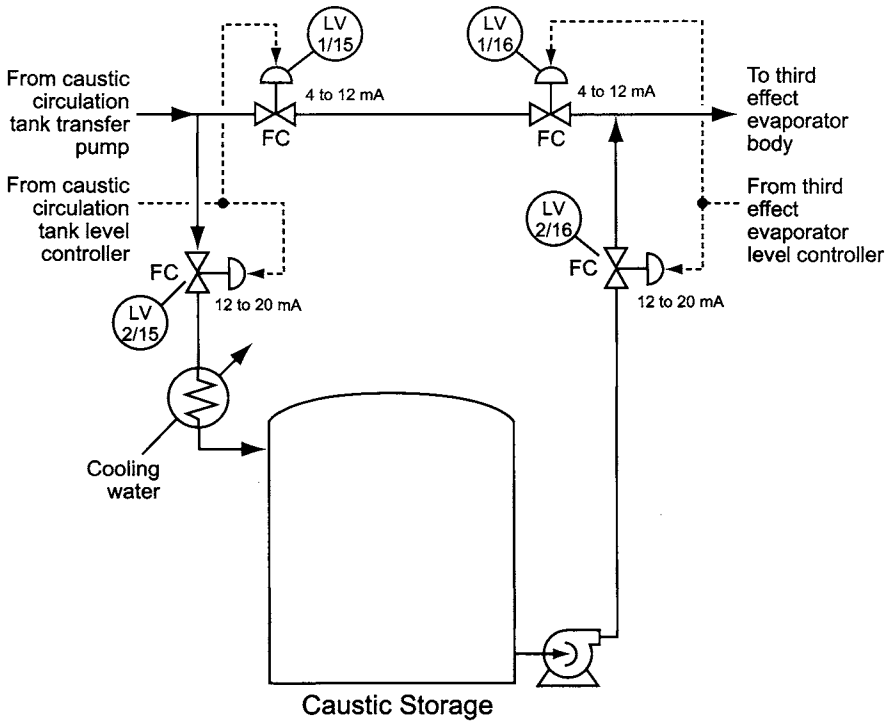


FIGURE 11.57. Caustic storage and evaporator feed control.

the cell-room tank. When the evaporator demand is high, LV-1/16 goes wide open in an attempt to maintain the level in the evaporator. However, LV-1/15 then throttles transfer from the cell-room tank in order not to deplete its level. The fourth valve (LV-2/16) then must open to allow transfer of caustic from the storage tank to the evaporator.

The flow rate to the evaporators is measured by a magnetic meter in the piping after the two streams combine. This signal should be recorded and integrated.

11.6.1.4. Product Concentration Control. Product concentration is one of the most important evaporator system control parameters. It can be determined from the solution density, as assumed in the discussion above, or the boiling point rise (BPR).

The density of a caustic solution depends on its temperature and its concentration. The density reading, therefore, must be temperature-compensated. Vibrating U-tube meters fabricated in nickel give good service. Coriolis-type mass flow meters with density readout are an alternative. It is important to keep the density instrument above the freezing point of the solution being measured. Solidification of the product can seriously damage these instruments.

The BPR is the difference between the boiling temperature of the caustic solution and the boiling (or condensing) temperature of pure water at the same pressure. It is a strong function of concentration and a weak function of operating pressure

(see Appendix). The first requirement in establishing the BPR is to measure the temperature and pressure of the boiling solution. This is done routinely and conventionally in all evaporators. The preferred method for measurement of pressure is by a diaphragm-sealed absolute pressure transmitter on the evaporator body. Now, some measurement of the boiling point of pure water is necessary. One technique, since the overhead vapor is essentially pure water, is to measure its condensing temperature in the overhead piping or in a condenser. This has been used widely, but it can be difficult to ensure that the temperature instrument is measuring the true condensing temperature at the pressure of the evaporator effect in which the vapor was generated. Present-day digital technology, however, allows direct calculation of the BPR from evaporator operating conditions. Figure 11.58 shows the logic used in such a system. The operating pressure is used to calculate the boiling point of pure water. Comparison with the actual temperature gives the actual BPR, and this determines the solution concentration. There may be a direct algorithm, or the calculation may proceed through a pressure correction

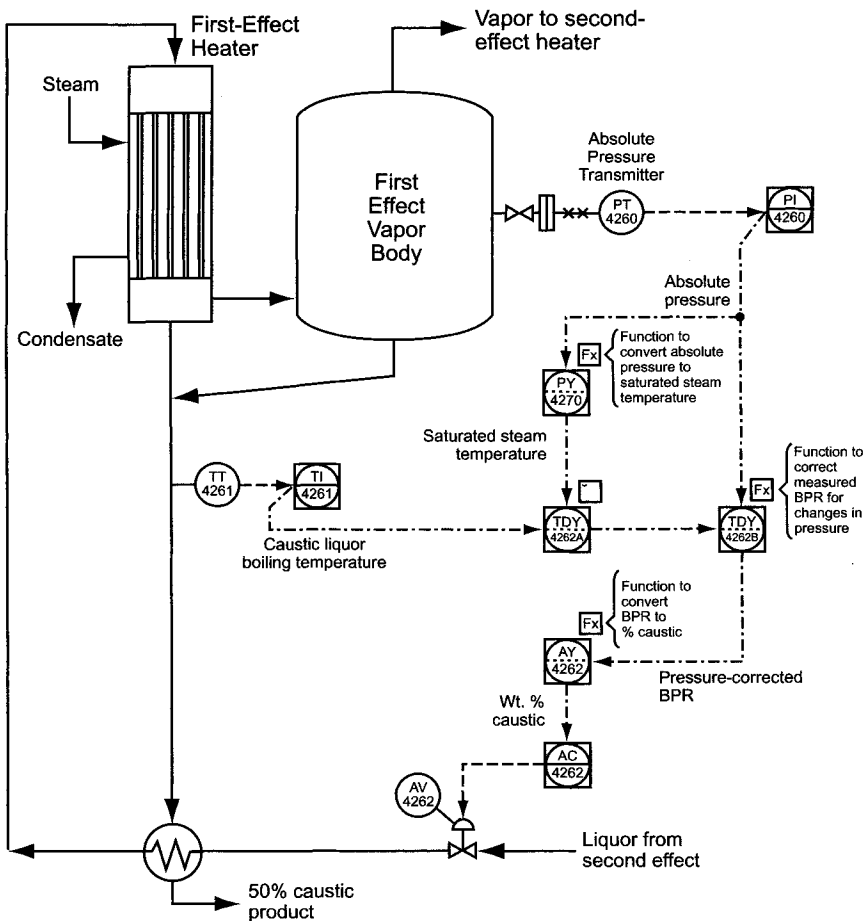


FIGURE 11.58. Caustic evaporator product concentration control.

to give the BPR at atmospheric pressure. The calculated concentration is the value sent to the controller. The drawing assumes that the controller operates on the transfer from the second to the first effect. This is the option used in Fig. 11.56.

One standard arrangement for concentration control, shown in Fig. 11.59, is to connect the controller to the product outlet valve. Level control in the first effect is then by transfer of solution from the previous liquor effect, which in our backward-flow case is the second effect. This arrangement has a particular advantage during startup because no product is allowed to leave the evaporator system until the final concentration reaches its set point. However, the concentration and level then go into oscillation very easily, as in the response chart below the drawing. The fundamental problem is that the introduction of fresh liquor is the means of adjusting both the level and the concentration. Level responds immediately and directly, but concentration lags. The problem can be resolved by reversing the concentration and level arrangements so that concentration

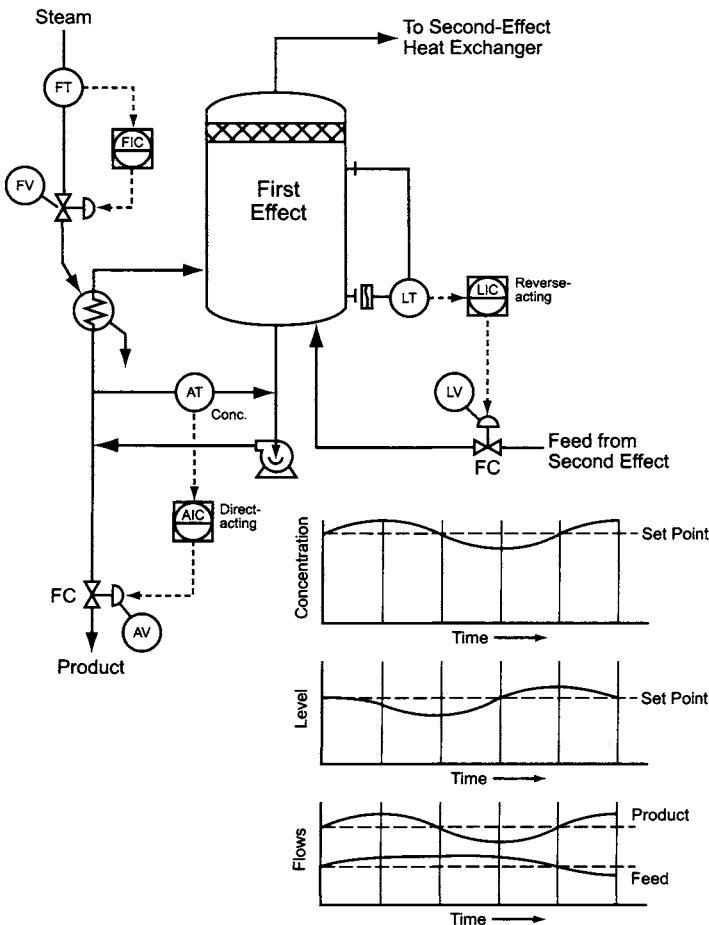


FIGURE 11.59. Concentration control by product withdrawal.

controls the dilute liquor feed valve and level controls the product discharge valve, as in Fig. 11.60. This is essentially the recommended system shown in Fig. 11.56. In this arrangement, the dilute liquor flow changes until the concentration reaches the correct value. Any accompanying change in level is corrected by changing the product outlet flow.

Since the latter arrangement is inferior during startup, a modified approach is to combine the two strategies with the use of a selector switch. One position is used for “startup” and the other for “normal operation.” Figure 11.61 shows the combination.

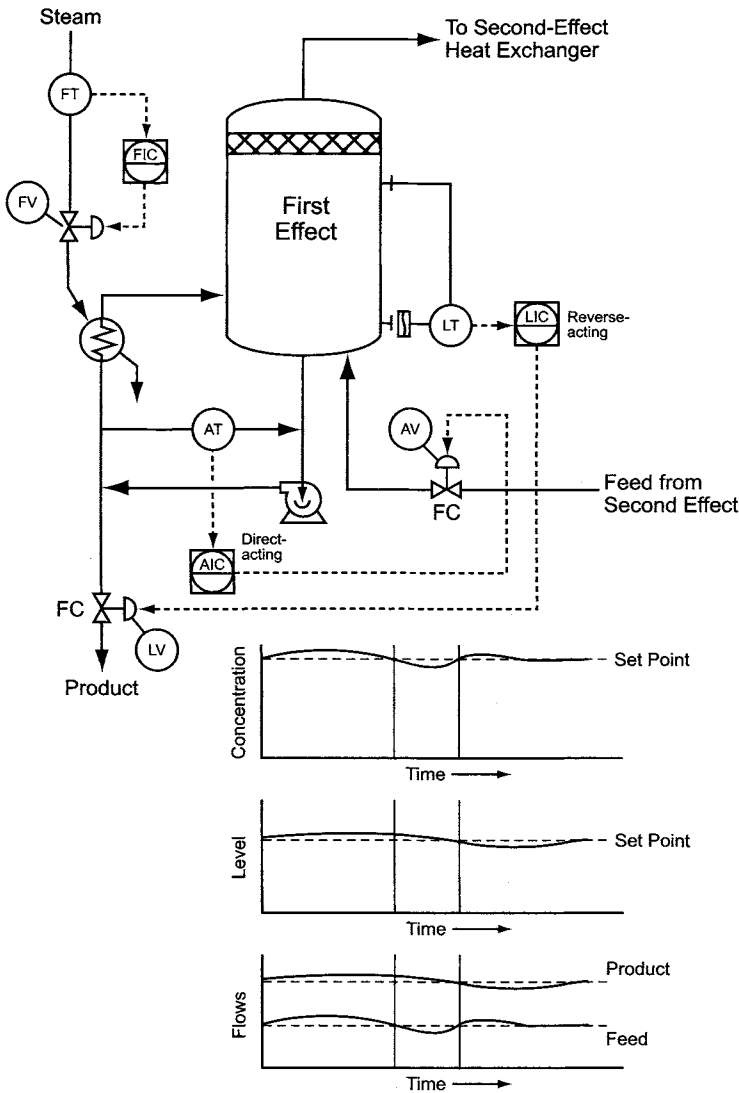


FIGURE 11.60. Concentration control by liquor feed.

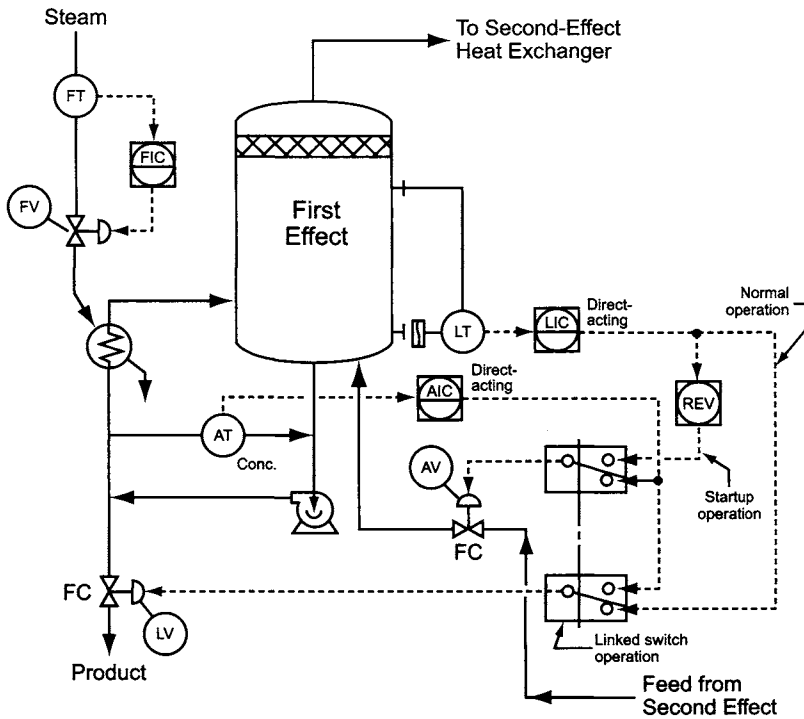


FIGURE 11.61. Concentration control for startup and normal operation.

There is a signal-reversing device between the level controller and the dilute liquor feed valve. This is necessary because the response of the valve to the control signal must change whenever the mode of operation changes. The product discharge valve responds in the same way in both modes, opening with higher signals.

11.6.2. Diaphragm-Cell Caustic Evaporation

There are two major differences between diaphragm- and membrane-cell caustic evaporation. Diaphragm-cell liquor is much lower in caustic content (and therefore consumes more steam) but contains large amounts of dissolved salt, which precipitates during the evaporation process and must be handled in slurry form. Section 9.3.3.3 covers this subject in detail.

Control system strategies are the same for both types. Diaphragm-cell evaporators may contain four effects and are more likely to have a mixed-flow configuration. Output is usually controlled by the primary steam flow, and the density control system can switch from startup to normal operation in the manner described above.

The slurry produced in the evaporators must be kept at the appropriate solids concentration to ensure its pumpability. The suspended solids content of a solution in an agitated vessel can be measured by an extended diaphragm d/p cell inserted into a 100-mm nozzle. The upper connection must be below the liquid level and purged with soft water

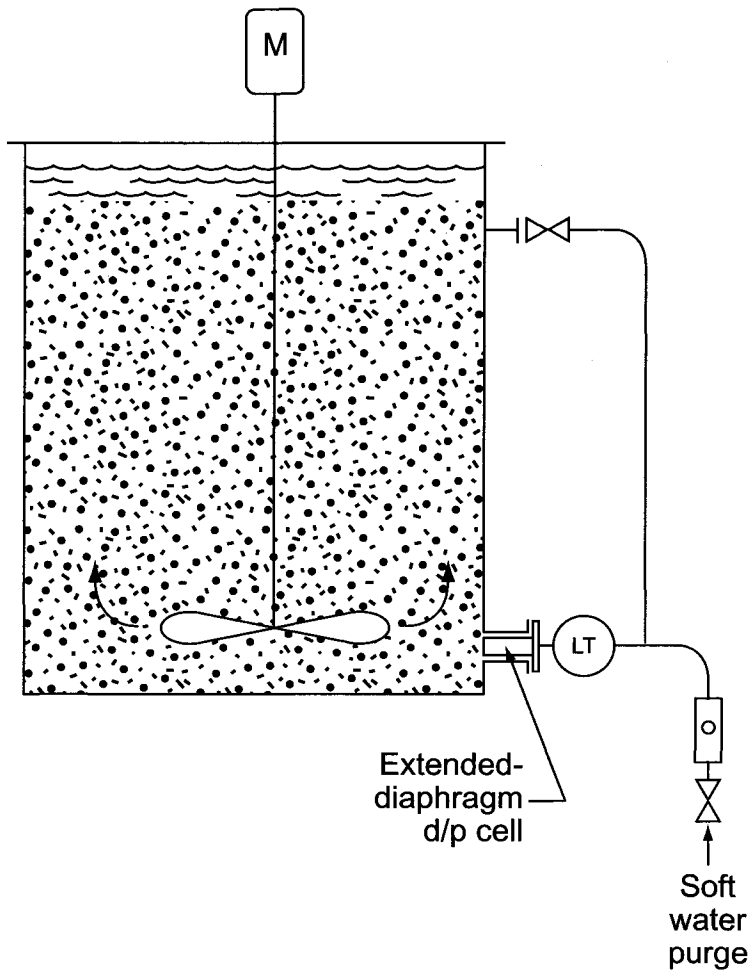


FIGURE 11.62. Slurry density measurement.

(Fig. 11.62). The differential pressure is a measure of the pseudo-density including the suspended solids.

The salt is of excellent quality. Section 9.4.1 discusses its applications.

ACKNOWLEDGMENT

This chapter was contributed by Thomas A. Weedon, Jr. In twenty-six years with the Central Engineering Department of Diamond Shamrock, he worked on many new and existing diaphragm- and mercury-cell plants. Subsequently, with his own company, Instrumentation Technology, Inc., he has worked closely with ELTECH Systems Corp. on the development of control strategies for their membrane-cell technology.

REFERENCES

1. *Instrumentation Symbols and Identification*, American National Standard ANSI/ISA-S5.1-1984 Reaffirmed, ISA, Research Triangle Park, NC (1992).
2. *Refrigerated Liquid Chlorine Storage*, Pamphlet 78, Edition 3, The Chlorine Institute, Inc., Washington, DC (2000), pp. 10, 11.
3. *Pressure Relief Device Standards—Part 3—Stationary Storage Containers for Compressed Gases*, Pamphlet CGA S-1.3, Compressed Gas Association, Arlington, VA (1995).
4. *Relief Valves for Use on Dry Gas or Liquid Chlorine*, GEST 76/64, 4th ed., Euro Chlor, Brussels (1983), p. 2.
5. *Low Pressure Storage of Liquid Chlorine*, GEST 73.17, 5th ed., Euro Chlor, Brussels (1996), pp. 11, 12.
6. *Refrigerated Liquid Chlorine Storage*, Pamphlet 78, Edition 3, The Chlorine Institute, Inc., Washington, DC (2000), pp. 8–13.
7. R.E. Kucinski and H.M.B. Gerner, Ion Exchange Membrane Plant Safety; Anode Side Mixing of Chlorine and Hydrogen. In R.W. Curry (ed.), *Modern Chlor-Alkali Technology*, vol. 6, Royal Society of Chemistry, Cambridge (1995), p. 89.
8. *Learning From Experience*, Pamphlet 167, Edition 1, The Chlorine Institute, Inc., Washington, DC (2002), p. 4.

12

Utilities

12.1. INTRODUCTION

This chapter considers the major utility systems in a chlor-alkali plant. These include electricity (Section 12.2), steam and condensate (Section 12.3), the various water systems (Section 12.4), air and nitrogen (Section 12.5), and, for convenient grouping, vacuum (Section 12.6). Finding the best basis for a discussion of utilities in a work such as this is difficult. A comprehensive description is impossible in a reasonable amount of space, and in any case it is undesirable where the emphasis is to be on chlor-alkali technology itself. Our approach is to discuss the individual utilities from the standpoint of a chlor-alkali plant operator while avoiding the complexities of such things as steam boilers.

While all utilities are essential to operation, electricity has the greatest cost impact. Still, our discussion of the incoming electrical supply here is brief. Handling and transmission of alternating current within the plant are conventional, and the reader is referred to the standard literature and equipment suppliers' publications. The distinguishing feature of chlor-alkali technology is the presence of large-scale rectification. Discussion of this aspect is more important in a work on chlor-alkali technology, and we have covered it in Chapter 8 on cell room design.

Steam is used in the largest quantities in the evaporation of caustic and, sometimes, brine. A system for the collection and reuse of steam condensate goes hand-in-hand with steam supply. In this chapter, we also consider the use of steam as a source of mechanical power. This is of growing importance as more of the industry adopts cogeneration.

The discussion of water systems includes the most basic treatment of raw water supplies to allow them to serve as plant utility water. More advanced treatment to allow higher-grade uses follows. Evaporator process condensate is included as a special grade of purified water. The most detailed discussions are those dealing with cooling water and chilled water.

Air systems include compressed air as a plant utility and refined versions for more specialized uses. These include instrument air and breathing air. Of particular significance in a chlor-alkali plant is a supply of dry air for use in the chlorine processing section. An alternative to dry air is nitrogen, which also serves as an inert gas in the hydrogen plant and sometimes in chlorine liquefaction and tail-gas handling. For convenience, we include the discussion of nitrogen in the section on air systems.

Important users of vacuum include evaporators and dechlorination systems. Lower levels of vacuum are useful in brine sludge filtration and in clearing lines and equipment for maintenance.

Utility pipelines are a special case in any plant. There is a general discussion of utility piping systems in Section 12.7. This section describes some of the features which one should provide in connections between utility supply and process piping or equipment.

12.2. ELECTRICITY

The overriding importance of electricity in chlor-alkali production stems from the huge direct-current (DC) power demand. Some of the special considerations around the conversion of power to DC and its distribution within the cell room have already been covered in Section 8.3. The primary power supply and its transformation and distribution are much the same as in any other process plant. The incoming supply is as alternating current, with 50 and 60 Hz being by far the most common frequencies. Voltages usually are in the thousands—10–30 kV being typical for small plants, but 200 kV and over applying in large plants. For supply of the rectifier transformers, the incoming supply voltage may be suitable, or it may be necessary first to transform it on site to a lower voltage. For other plant supplies, transformation to a lower supply voltage is invariably necessary.

Three-phase power is used almost exclusively as the major source of mechanical power and in plant lighting, but some single-phase circuits also exist. Most plants have a three-phase high-voltage distribution system at 2–5 kV. This is frequently used directly on large drives. For many other applications, voltage is further stepped down to 200–500 V three-phase. Low-voltage single-phase circuits usually follow local practice for domestic supplies, in the 100–250 V range. Instrument wiring, especially in intrinsically safe circuits, is a special category, with voltages below 30.

Incoming voltage and amperage are always measured. A properly connected voltmeter and ammeter can measure single-phase power. The power in a three-phase circuit can be measured by placing a single-phase wattmeter, again properly connected, in each phase and adding the readings. Comparing the result with the line voltage and current allows calculation of the power factor (PF). The same power reading results when using only two wattmeters if each is connected back to the line on the third phase. The PF can be calculated as above or without reference to the voltmeter and ammeter. The latter method uses the asymmetry of the readings of the two wattmeters. If the lower of the two readings is a fraction w of the higher, the reciprocal of the PF is given by

$$\frac{1}{\text{PF}} = \sqrt{1 + 3[(1 - w)/(1 + w)]^2} \quad (1)$$

Integration of the amperage and power readings over time gives the ampere-hour and watt-hour consumptions of the plant.

12.3. STEAM AND CONDENSATE

12.3.1. Steam Systems

Boiler design and operation are highly specialized subjects that require the attention of experts and specially trained operators. Rather than present an inadequate summary of the many factors involved, we refer the reader to suppliers of equipment and services and to the voluminous literature.

Steam is usually made available at two or more different pressures. It is the primary source of thermal energy in a chlor-alkali plant, as it is in most plants in the process industries. It also serves as a source of mechanical energy. Some of the important uses are listed below, with a general indication of the pressure level appropriate to each (L = low, M = medium, H = high).

	Pressure Level(s)
<i>Thermal Application</i>	
Brine processing	
Heating	L,M
Evaporation	L,M
Chlorine processing	
Vaporization	L
Bottoms distillation	L
Condensate stripping	L
Caustic processing	
Heating	L,M
Evaporation	M,H
Purification	M,H
Plantwide	
Tracing	L
Building heat	L
General utility	L,M
Purging (equipment and lines)	L
<i>Mechanical Application</i>	
Ejectors	M,H
Turbine drives	H
Cogeneration	H

The process requirements for steam vary widely, depending on the types of cell being used. Most mercury-cell plants are not major consumers of steam. With diaphragm and membrane cells, most of the process steam goes into the evaporation of cell liquor to concentrated caustic. Diaphragm-cell plants are therefore the largest steam consumers, and membrane-cell plants are the intermediate case. While the range is quite large, depending on supply pressure and the number of evaporator effects used, steam consumption in a diaphragm-cell plant is often about 2.5 tons per ton NaOH. In a membrane-cell plant, it might be 0.5 tons per ton NaOH. Purification of diaphragm-cell

caustic to remove dissolved salt adds even more to the steam load, while the use of a brine evaporator to avoid the need for the purchase of solid salt adds to the load in the mercury- and membrane-cell plants.

Steam pressures applied to first-effect evaporators vary from low levels up to about 2,500 kPa, the high values applying in the first effects of quadruple-effect diaphragm-cell plant evaporators. Even nickel corrodes slowly at these conditions. Section 9.3.2.1 discusses the problem.

Evaporation process design and the characteristics of caustic evaporators are covered in Section 9.3.3. The unit cost of steam is a major factor in deciding the number of effects to be used in evaporation. Costing of steam is often somewhat arbitrary, as when low-pressure exhaust steam is available or when a plant has its own cogeneration system. Reducing the consumption of cogenerated steam (Section 12.3.3) when more electrical energy must be purchased (or less sold) may save very little money.

High-pressure steam may also serve as a driver for turbines. Chlor-alkali plants, which are usually placed in areas of low electrical power cost, are less likely than most other types to justify the use of steam-turbine drives but still may use them as a backup source of power. Furthermore, one of the ways to cope with a major electrical failure is to use steam to operate critical drives until all systems are shut down or electrical power is restored. An example of a critical service is the caustic circulation pump on the emergency vent scrubber. A spare pump is always necessary, and it should have an independent source of power. One way to accomplish this is with a steam-turbine drive. Other services may also be considered critical for personnel safety or process security. The latter is especially true in a membrane-cell plant, where some systems are vital for the protection of the membranes from damage.

Trouble-free generation of steam requires water of high quality. The characteristics of boiler feed water and methods for its production are covered below in Section 12.4.3.3. This water is fed to the boiler(s) on demand. The simplest way to control the addition of water is from a level instrument in the steam drum. This approach has a certain amount of inherent instability. When (cold) water is added to the drum in response to a demand from the level controller, some of the bubbles present in the liquid will collapse. The level will go down, and the controller will call for even more water. In the opposite case, when the level rises and the water flow is reduced, more bubbles will form and the level will increase, causing the controller to call for less water. The process itself is supplying positive feedback.

The control characteristics are improved when a steam flow rate measurement is added. The water feed rate then responds to some combination of steam flow and drum level. Basing the control partly on the steam flow offsets the positive feedback and reduces fluctuations in the supply. Addition of a direct flow controller on the water feed pump output is another elaboration. This would be reset by the outlet steam flow. It provides some feedforward control, which is useful in the presence of severe load swings.

The simplest control scheme is acceptable when fluctuations in the steam rate are minor and when the ratio of water inventory in the boiler to steam production rate is high, making the system less sensitive to fluctuations in demand. The latter is more likely to be true when fire-tube boilers are used. The choice of control system depends on the individual plant characteristics. Chlor-alkali plants tend to have consistent demands for

steam, with few major unexpected changes in rate. Boiler control schemes therefore may be less elaborate than those found in other industries.

12.3.2. *Steam Condensate*

Steam condensate is a valuable resource. It has considerable thermal value and some potential uses in the process. However, intensively treated boiler feed water must replace any condensate lost from the system. Accordingly, most plants have systems to capture most of the condensate and return it to the boilers. With steam distributed at several different pressures, it is also possible to allow condensate collected at one pressure to flash down to a lower pressure and in the process form more steam at the lower pressure. Steam is often available at the evaporators well above its condensing pressure, in which case it is worthwhile to install a desuperheater. Condensate is a good source of the coolant.

Most condensate leaves the steam side of the process through steam traps. The chlor-alkali process places no special requirements on the types of trap used, and normal good industry practice should prevail here. Condensate return piping is designed for lower pressure drop than most liquid lines because of the vapor volume that would be generated as the pressure falls. This flashing complicates line sizing, and the designer should use the assistance of condensate system suppliers and their literature.

Plain carbon steel pipe is used in condensate service, but items such as pump parts, valve trim, and exchanger tubes should be copper or a copper alloy. Copper is used for tubing and bronze for pump shafts and glands.

The installation of pumps requires special care to provide enough suction head to avoid cavitation. The net suction head can disappear if a pump generates too much heat in the condensate. It is important to maintain enough flow through the pump at all times to prevent this. Minimum flow can be provided by recycle controlled by an automatic valve or by placing an orifice assembly in a recycle line. As a rule of thumb, a flow of $1 \text{ m}^3 \text{ hr}^{-1}$ is necessary for each 12 kW of input if the temperature rise is to be kept to 10°C . The recycle flow must be cooled or go into a heat sink such as a condensate hotwell or boiler feed deaerator. A simple recycle into the pump suction line is inadequate.

When condensate returns to a boiler, it may be contaminated by pipeline corrosion or with process materials. Likely sources of the latter include exchanger leakage and poorly installed process tie-ins. Carbon dioxide and oxygen are the chief causes of corrosion in steam and condensate systems. Section 12.4.3.3 discusses the treatment of boiler feed water to remove these contaminants, as well as hardness.

Hydrazine is one example of a treating agent, but any unreacted material that enters the process is possibly a precursor of nitrogen trichloride. Another is a form of sodium sulfite, a compound that is also used as a reducing agent in brine dechlorination (Section 7.5.9.3A). Since the mechanism of the reaction is different here, proceeding by way of an ion-radical, the sulfite often contains promoters [1]. These would make it less desirable as a brine-treating agent, and plants that use both grades of sulfite should keep them separated.

The presence of amines or any other nitrogen-containing residue in steam condensate restricts its use in process applications. This is especially so when these impurities enter the cells or the chlorine process and eventually form NCl_3 (Section 9.1.11.2).

12.3.3. Cogeneration Systems

The classical approach to energy supply in the process industries has been to purchase electrical energy from a utility supplier and to generate thermal energy on site by combustion of a fossil fuel. This situation arises primarily from the relative ease of transportation of the two forms of energy. Cogeneration, on the other hand, is a process in which both forms are derived from a single primary energy source. The major driving force for the adoption of cogeneration is energy economy. A heat-engine-based electrical generator, for example, rejects heat to the atmosphere if operated as a stand-alone unit. Some of the rejected heat can always be used in the thermal energy supply system without adding to the fuel requirement.

In many cases, generation of one form of energy is the principal goal, and the other form is treated as a by-product. In others, both types of energy are essential products. The smaller need then determines the design capacity of the cogeneration system, and the other form of energy must be supplemented by other means. In all real cases, the power and heat demands vary continually. The cogeneration system most probably will not be able to match all these variations. The ability to sell excess electrical power onto the local grid is an important advantage in such cases, and it has been an important factor in the justification of a number of systems. These and many other factors enter into the decision of whether a cogeneration system is the right choice for any plant [2].

Some of the important factors in selection of a cogeneration system are:

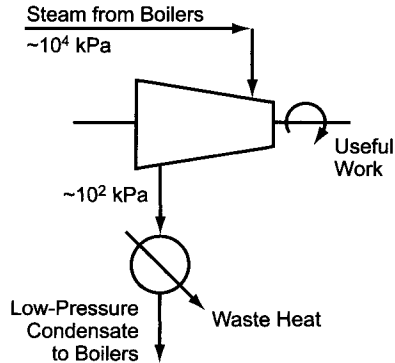
1. capacity range
2. efficiency at design point
3. efficiency at reduced load
4. heat/power ratio at design point
5. ability to vary heat/power ratio
6. ability to change fuels

Internal combustion engines, such as the diesel engine, are the primary source in some smaller units. They require clean-burning fuels with certain characteristics. Closed-cycle power systems with external firing, which are more common in chlor-alkali plant applications, can use almost any fuel.

In a simple open-cycle condensing steam turbine system, steam is raised in a boiler at high pressure ($\sim 10^4$ kPa). It is expanded through a turbine to generate power, and the low-pressure exhaust is condensed. Depending on the steam pressure, this combination gives a thermal efficiency of about 30%. Most of the loss is waste heat in the exhaust steam that is condensed. The high latent heat of water makes for an inefficient process if the heat is not abstracted in some useful way. Only in special circumstances or with special design can this heat be recovered at low pressure, and in many process plants it is lost in the cooling water system.

A more efficient arrangement from the standpoint of energy recovery is the steam cycle with extraction. Figure 12.1 compares this approach with the open cycle discussed above. Here, some of the steam is withdrawn from the turbine at a pressure suitable for process needs (say 1,000–3,000 kPa) and used as a source of heat. The rest of the steam becomes low-pressure exhaust from the turbine. The performance of this combination depends on the exact conditions chosen. Since much of the steam supplies less of its

(a) Open-Cycle Condensing Steam Turbine



(b) Steam Turbine with Extraction

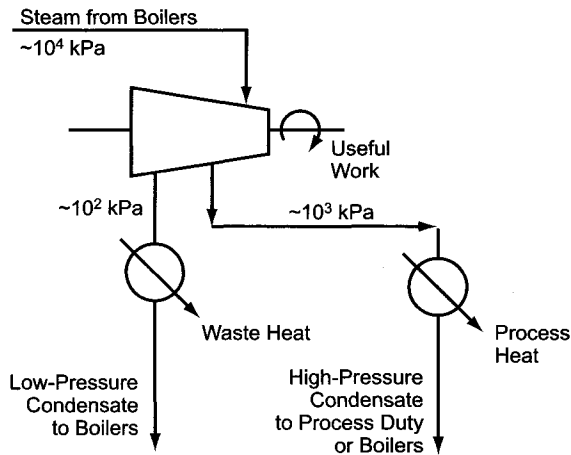


FIGURE 12.1. Comparison of turbine cycles in cogeneration systems.

pressure energy to the turbine, the power efficiency drops, perhaps to as low as 20%. Recovery of some of the thermal energy by extraction of the steam raises the total energy efficiency to 50–55%.

There are other ways to overcome some of the inefficiencies caused by the high latent heat. These include various methods for increasing the superheat of the steam. A small increase in energy content provides a large increase in thermal potential (temperature).

Gas turbines provide an alternative to steam turbines. They must be constructed of materials suitable to the high temperatures associated with combustion gases. Simple gas turbines produce efficiencies comparable to those of simple steam turbines. A combined-cycle unit that also recovers thermal energy benefits from the high temperature of the exhaust gas. Recovery of a major part of this energy, which is possible because there is not a huge latent-heat penalty, can raise the overall efficiency to as high as 80%.

An important criterion in selecting a cogeneration system for a given application is the ratio of heat to power (H/P ratio) required. The demands of a process or an operating

complex can be characterized in this way. Similarly, every turbine system can be defined by its output H/P ratio, and a cogeneration system is ideally designed to match the process demand. This can constrain the operation of a turbine to a certain range of the H/P ratio and limit its efficiency. In other words, extraction of all the available thermal energy from the gas is not practicable. Consider a heat engine with efficiency η_E :

$$\eta_E = \frac{\text{shaft work}}{\text{available heat content of fuel}}$$

In a cogeneration system, the overall efficiency, η_{OV} , is higher by an amount fixed by the H/P ratio, which is designated by R :

$$\eta_{OV} = \eta_E(1 + R) \tag{2}$$

R cannot increase without a limit. The theoretical maximum corresponding to $\eta_{OV} = 1$ is

$$R_{\max} = \frac{1}{\eta_E} - 1 = \frac{1 - \eta_E}{\eta_E} \tag{3}$$

The practical maximum corresponding to a combustor efficiency η_B is

$$R'_{\max} = \frac{\eta_B - \eta_E}{\eta_E} \tag{4}$$

where $\eta_B = \frac{\text{heat to working fluid}}{\text{available heat content of fuel}}$

Figure 12.2 shows the above relationships [3]. The limits are fundamental, and only certain combinations of heat engine efficiency and the H/P ratio are possible.

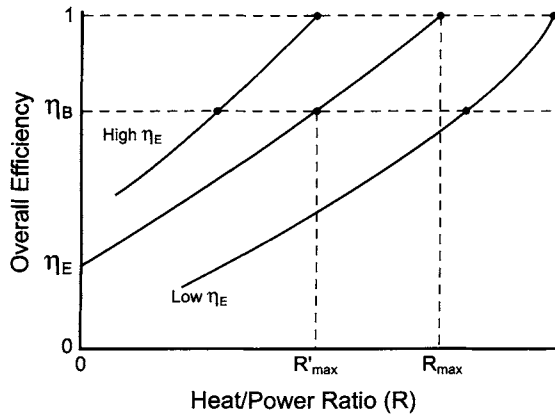


FIGURE 12.2. Operating envelope limitations in cogeneration.

The efficiency of steam turbine cogeneration systems increases relatively slowly with H/P ratio, and so these systems are more likely to be run at relatively low efficiencies. On the process side, the H/P demand of a standalone mercury- or membrane-cell chlorine plant is relatively low, and a turbine-based cogeneration system would run at a correspondingly low efficiency. Diaphragm-cell plants, with the greatest thermal-energy requirements, benefit both from the scale of operation and from a higher H/P ratio. They are the most attractive candidates for cogeneration.

In the chlor-alkali field, many cell installations are part of a larger complex, and the chlor-alkali plant demand is only part of the picture. The H/P demand is higher in an integrated operation such as an EDC, a VCM, or a PVC plant. These are the situations in which cogeneration plants are most likely to be found.

12.4. WATER SYSTEMS

Water has a myriad of applications in processing plants. Some of these, denoted by their distribution systems, are

- untreated water from sea, lake, river, or well,
- plant, process, or utility water,
- fire water,
- drinking water,
- sanitary water,
- cooling water,
- chilled water,
- soft or demineralized water,
- process condensate,
- boiler feed water.

Plants located on a body of water often use it as a source of once-through water with a minimal amount of treatment. We do not discuss these systems. The customary approach to fire protection is to provide ring mains around the various process areas, with hydrants and monitors located at intervals and at certain strategic points. There also are distribution lines within buildings and sometimes deluge systems in certain areas. These systems are not very instructive to a student of chlor-alkali technology, and they also are omitted from discussion. Drinking water and sanitary water fall into the same category.

12.4.1. Sources of Water and General Plant Use

Sources include surface waters, wells, seas and estuaries, and recovered condensate. Many plants serve all their needs with municipal water, treated to potable quality, which may be based on surface water or well water. Public water supplies usually carry a fraction of a ppm of chlorine. When used as the principal supply to a plant, these must be dechlorinated before most direct uses in the process.

Before a plant's water treatment system can be designed, a fund of analytical data is necessary. In many localities, these data are available from local authorities or neighboring plants. They should cover a period of time in order to give an idea of variability

as well as average values. Specifically, they should cover the different seasons of the year in order to show variations with the extent of rainfall, runoff of melted snow, or mixing of underground aquifers. The following data and analyses should be available, in addition to analyses for individual ions [4]:

- total dissolved solids (TDS)
- total suspended solids (TSS)
- total organic carbon (TOC)
- conductivity
- turbidity
- silt-density index (SDI)
- pH
- silica
- carbon dioxide
- chlorine (in the case of municipally treated water)
- temperature range

Local regulations governing the plant effluent will also affect the choice of water treatment processes.

The quality of natural water is extremely variable. Surface waters are generally turbid. Well waters, while clear, may have high hardness. There are also wide variations in the quality demanded by various uses. Therefore, the sort of treatment to be applied, depends both on the quality of the raw water and on the intended use.

Frenkel [5] classifies raw water supplies into several types with different characteristics (Table 12.1). Other authors propose similar classifications and often add hardness to the list of characteristics. Arden and Forrest [6] take a modular approach to treatment. Silted river water, for example, considered suitable only for irrigation, is improved by sedimentation to a quality comparable to that of most other surface waters. The clarified water then becomes suitable for crude industrial applications. Coagulation and filtration then virtually eliminate suspended solids and make the water suitable for general purposes. These include plant utility use without necessarily qualifying the water for process application. Beyond this point, the intended application determines the extent of treatment required.

The first column in Table 12.1 indicates that the turbidity of river and lake or pond water is highly variable. Rivers are especially turbid during rainy seasons or at the time

TABLE 12.1. Selected Characteristics of Natural Waters

Source	Turbidity	TSS	Color	TOC	TDS	SDI	Stability
River	H**	H*	M	M-H	L	VH	VL
Lake or large pond	L*	L*	H*	H*	L	H	VL
Well	L	L	L	M-H	L	H	M-H
Brackish	L	L	L	L-M	M-H	H	H
Sea	L-M	L	L	L-M	H**	H	H

Notes: L, low; M, moderate; H, high; V, very; TSS, total suspended solids; TOC, total organic carbon; TDS, total dissolved solids; SDI, silt-density index.

*Seasonal variation, **Highly variable.

Source: Frenkel [5].

of the spring thaw. Lakes become more turbid and can develop more color in warm weather. The other sources are more stable throughout the year. All are subject to some change. Open seawater can have moderate seasonal changes and be disturbed in stormy weather. The quality and rate of inflow of fresh water influence the characteristics of the water taken from bays and estuaries. The ability to cope with these variations is an important aspect of treatment system design.

The treatment of water is quite similar to the treatment of brine, discussed in Section 7.5, but there are certain differences in each step. The first objective is the removal of suspended solids, which would interfere in most of the subsequent steps. Preliminary clarification of highly turbid water occurs in a standard circular clarifier or in an elongated rectangular basin. This is sometimes combined with cold lime softening or with the addition of coagulants or flocculants. Coagulation differs from the process of flocculation described in Section 7.5.2.2D. It is aimed at colloids rather than at formation and growth of precipitates from dissolved species [7]. Colloidal particles, submicron in size, stay in suspension because of Brownian motion. Coagulants destabilize colloidal suspensions by overcoming the electrical repulsion between particles. The colloids, of which clay and silt are typical examples, tend to carry negative charges. The Hardy–Schulze rule states that the important ion in a coagulant is the one whose charge is opposite to that on the particles and that the power of the coagulant increases dramatically as the magnitude of the valence of the key ion increases. Multivalent cations will then be the best coagulants, and they are hundreds of times more effective than monovalent ions. Iron and aluminum salts are most frequently used, at concentrations of 10–30 ppm in the water. Ferric chloride (Section 9.1.9.4) is a widely used coagulant. The chlor-alkali producer, especially the operator of membrane cells, will find it easier to remove iron compounds in subsequent brine processing.

In removing suspended solids, clarifiers improve some of the other measures of water quality. These include color and organic content. A typical clarifier product will have less than 10 ppm suspended solids.

Filtration normally follows sedimentation. Industrial practice again resembles brine treatment (Section 7.5.4). Bed filters may contain a single medium, usually operating in a downflow mode, or several layered media. The latter usually operate in an upflow mode, with the water sequentially meeting gravel (for support), garnet, sand, and anthracite. Membrane filters are finding increased use in water treatment [5]. Microfilters can remove particles down to 0.1 μm and do not require pretreatment of the water. Ultrafilters remove particles down to 0.01 μm but frequently require pretreatment of the water. These filters can remove colloids and normal organic matter (NOM).

Filtration can be used without sedimentation, but filters have limited solids-handling capacity. Frenkel gives these rough guidelines for the choice of the primary solids-removal equipment:

TSS	Equipment
<10 ppm	Membrane filter
10–100 ppm	Media filter
>100 ppm	Clarifier

The low-solids waters become suitable for drinking and sanitary purposes after chlorination. The addition of corrosion inhibitors, and antiscalants when hardness is present, makes them usable in cooling water circuits. In-process application may require further treatment, and demineralization by ion exchange is perhaps the most common technique in chlor-alkali plant practice. There is a large literature on the technique of ion exchange, and Section 7.5.5 discusses its application to brine softening. The complexity of the system depends on the nature and concentrations of the impurities in the water. The basic ion-exchange system includes separate columns of cation- and anion-exchange resins. The exact choice of resin depends on the process duty and the nature of the water. Enhanced systems may include decarbonization by volatilization of CO_2 and a final column of mixed cationic and anionic resins. Strong-base anion resins can remove silica (Section 12.4.3.1), a property that may be useful especially to membrane-cell operators. Continuous operation requires parallel units, and acid and caustic regeneration of spent columns is necessary.

Some plants also produce their own potable water by treating a well or groundwater supply. This is not a common situation, and it is a specialized subject that will not be covered here. Most plants receive potable water from a local supplier or municipality. This water is used for drinking and sanitary use and usually in safety shower/eye wash systems. In some cases, the municipal potable water supply also serves as a general plant utility. Drinking water systems must always be kept separate from plant service systems. The method of separation is often prescribed by local regulations. Backflow preventers are a standard, but dedicated tanks that provide physical breaks are more positive and in many locations are required. These are discussed in Section 12.7.2.

12.4.2. *Water as Heat Sink*

12.4.2.1. *Cooling Water.* When a source of water of the proper quality and a reliably low temperature is available, it may be used on a once-through basis to remove process heat. This may be true of certain municipal water supplies, but they are usually too scarce or expensive for such use. It is more common to find seawater or river water in such an application.

Most chlor-alkali plants use water in a closed circuit to remove waste heat from the process. The heat is then rejected into the atmosphere by cooling the water itself by direct or indirect contact with air. Dry systems using indirect contact are useful in some situations, but the typical chlor-alkali plant uses direct contact. The nearly universal choice for this operation is the cooling tower, where heat transfer and mass transfer occur simultaneously by direct contact between phases. Sections 9.1.3.2 and 3 discuss these transfer processes in connection with the cooling of chlorine gas. The effectiveness of a cooling tower depends on the distribution of water and the means used to promote contact between the water and the air. The internal arrangements of a typical unit are discussed below.

The water cools by supplying its own latent heat of vaporization. It is therefore possible to cool the water below the dry-bulb temperature of the air supplied to the tower. The real measure of the cooling potential of the air is its wet-bulb temperature, and each tower is designed to operate at a certain inlet wet-bulb temperature.

The function of a cooling tower is, quite simply, to remove heat. However, a tower cannot be rated solely in terms of heat transfer. It will remove as much heat as the process generates even when loaded beyond design conditions. If the amount of heat to be removed increases, the tower evaporates more water to match the new rate of heat input. What changes is the temperature of the circulating water. Increases in that temperature will eventually affect process performance.

Definition of the duty of a cooling tower therefore becomes rather complex. Manufacturers' and technical literature covers the subject thoroughly. Standard thermal tests have been developed that take into account the complexities. These include ASME PTC-23 and the Cooling Technology Institute's ATC-105.

The most important specifications are the water flow rate and the range. The latter refers to the change in the temperature of the water as it passes through the tower. A specification derived from this is the "approach," which is defined as the difference between the wet-bulb temperature of the incoming air and the temperature of the outgoing water. The approach is the most influential variable determining the size of the cooling tower. Figure 12.3, a combination from several sources, shows its powerful effect.

The wet-bulb temperature used to specify the duty of a cooling tower is that which is exceeded only a certain percentage of the time during the year. In compilations of meteorological data, it is customary to list wet-bulb temperatures in this way. Frequently, these lists show data at the 1, 2.5, and 5% levels. It is important to note that, for a given location, the temperature differences between levels are not great [8]. Data for nine plants in Texas show an average difference of less than 1°C between the 1% and 5% temperatures. A commonly used basis is 2.5%. This does not mean that an exchanger, or the plant as a whole, can meet its capacity only 97.5% of the time. By superimposing the daily temperature cycle on the yearly, we would see that the design wet-bulb temperature is usually exceeded for only a few hours at a time. The thermal inertia of the cooling water system helps to dampen the effects of these temperature peaks. Furthermore, unless an exchanger operates with a narrow temperature pinch, an increase above the design water temperature will produce only a small decrease in its capacity. Usually, intentional overdesign and allowances for fouling are much greater than this decrease. Taking one commercial design at random, the authors found that an increase of 1°C in cooling water

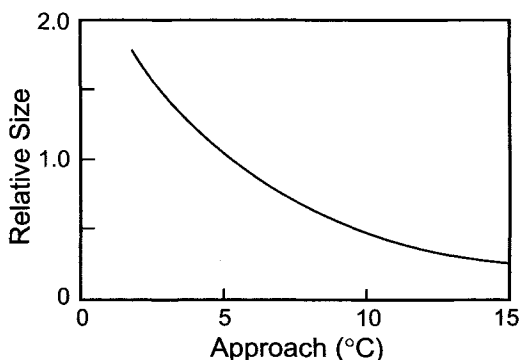


FIGURE 12.3. Influence of temperature approach on size of cooling tower.

temperature would reduce the capacity of a chlorine cooler by less than 5%. The safety factor in the amount of exchange area above that calculated to be required was 7%. The fouling factor applied to the water side of the cooler increased the amount of surface provided by 25%. Unless this exchanger is severely fouled, it should meet its design capacity even when the 97.5% wet-bulb temperature is exceeded.

When cooling water is used to cool dry chlorine, any leakage from one side of an exchanger to the other will produce a highly corrosive mixture. If water leaks into the chlorine, the effects will be more rapid and more severe. It would be better to have chlorine leaking into the water and out of the process. Therefore, the water used in an exchanger should be kept by means of a regulator at a lower pressure than the chlorine. This may require the water leaving the exchanger to be collected and pumped into the return header. A chlorine leak normally is easily detected by monitoring the conductivity of the water. Some plants located near the sea use once-through seawater as a coolant. In this case, conductivity is not sensitive to small amounts of chlorine. Oxidation–reduction potential can be used instead. The use of chlorine monitors in cooling tower fan stacks is also becoming more common. This provides a check on the other instruments and an aid in environmental reporting.

A problem specific to cooling towers is the presence of *L. pneumophila*. bacteria. The disease they carry has a high profile, and they are difficult to control with conventional biocide programs [9]. Transmission is primarily by inhalation of aerosols [10], and this is one reason to install drift eliminators (see below) and to arrange the tower so that the drift is primarily into unpopulated areas of the plant.

12.4.2.1A. Construction of Cooling Towers. Cooling towers include atmospheric spray towers, natural-draft towers, and mechanical-draft towers. The first type uses the momentum of water to draw air in cocurrent flow down through the tower. It seldom appears in chlor-alkali plants. Natural-draft towers by their nature are quite large and likewise are not common in the chlor-alkali industry. These are the large hyperbolic units associated with the power industry that are usually the first objects seen when approaching a generating plant.

Mechanical-draft cooling towers are the type most often found in the process industries. These provide their own air flow, and wind direction and velocity therefore do not greatly affect their thermal performance. They can be classified in several different ways:

1. according to the relative directions of entering air and water flows (counterflow or crossflow);
2. according to the method of producing draft or the location of the air movers (forced draft or induced draft);
3. according to the type of fill used to spread the water and increase its area of contact with the air (film or splash bar).

Counterflow, as would be expected, allows more efficient transfer of heat and mass. With the application of a modern high-efficiency fill, the counterflow tower has become the most effective and most compact type of unit [11]. It is less open in its construction than the crossflow type. This reduces the penetration of sunlight and the rate of growth of

algae. The crossflow tower, as will be seen below, has its own advantages and has been the standard in most chlor-alkali plants. It is more tolerant of suspended solids in the water and is favored by plant maintenance departments because of the relatively easy access to its internals, which include distributors, fill, structure, and drift eliminators.

Induced draft generally requires less energy to move a given amount of air and produces higher velocities through the fans ($400\text{--}800\text{ m min}^{-1}$). The latter is important in helping to reduce the amount of recirculation of warm, wet air into the tower. With induced draft, it is also easier to achieve good distribution of air over a large cross-section.

The typical fan is a multiple-bladed propeller. Tip speeds usually are held to less than 70 m s^{-1} , and vibration switches protect the fans from mechanical damage. Fan guards are essential for personnel protection. The typical induced-flow tower has a cage of heavy galvanized wire surrounding each fan. Variable-speed fans can be slowed down to regulate the air flow for low-capacity operation. With the wide range of duties encountered over the course of a year, common practice is to supply multiple units and to shut them down individually when the load is low.

Two problems associated with the air leaving a tower are drift and recirculation. “Drift” is entrained water. Massive amounts of drift would waste water. Normal drift, usually less than 2% of the circulation rate, does not affect the fresh water consumption, because greater quantities must be removed, in any case, in order to control the dissolved solids concentration. The problem with drift is that even small amounts can cause problems of fog formation, deposit of dissolved solids, and icing of surfaces. The internals of a cooling tower are designed to suppress drift. Figure 12.4 shows the presence of drift eliminators, which are baffles that allow entrained water to separate from the air. They do this by forcing sudden changes in the direction of the air flow. This allows the water impinging on the surfaces to separate from the air. It also helps to redistribute the air by creating a pressure drop. The eliminators may resemble simple baffles, being formed from wooden or plastic slats mounted in frames. Thin-walled honeycomb structures are another form that is frequently used. “Recirculation” is the reentry of discharged air into a tower. This raises the dry-bulb temperature and, more importantly, the wet-bulb

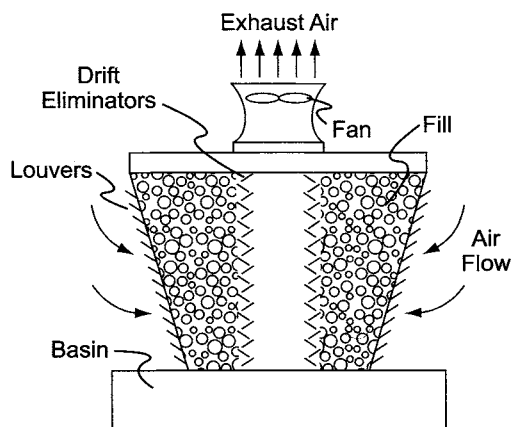


FIGURE 12.4. Induced-draft cooling tower.

temperature of the incoming air and limits the ability of the tower to cool the water. Keeping the discharge velocity of the air high, isolating the towers from other structures that can produce downdrafts, and orienting the towers to counteract the effects of prevailing winds can reduce the amount of recirculation. Occasionally, the steam plume from a tower becomes a third problem.

We take Fig. 12.4 as representative of a chlor-alkali plant cooling tower. Air enters through the sides of the tower, which are louvered. It moves under the influence of the fan mounted on top of the tower. Returning warm water enters the top through a distribution system and falls through the tower. Gravity distribution is acceptable in crossflow towers and has the advantage of requiring no pressure energy at the point of delivery. A head box is mounted above each cell of the tower, and levels can be adjusted independently. The water at the top of the tower is the most corrosive. It is warm and aerated and has a high concentration of dissolved solids. Resistant materials are required in this zone. Redwood is the favored wood, and plastics and galvanized steel are also used.

The tower sits above a basin, which serves as its foundation and also collects the cool water. The sump should be sized to allow refuse and suspended solids to settle, and it should be designed to allow on-line cleaning. Provisions might include a bottom sloped to the center, where a central pipe can carry off the settled solids, or a slope to one side, which when extended beyond the end of the tower, allows easy access for a suction hose. Concrete is the standard material of construction for cooling tower basins.

A set of pumps in a pit recirculates the cooled water. Submerged vertical pumps are standard in this service. When using multiple pumps with large capacities, it is necessary to space them properly and to design the pit to allow unimpeded access of the water flow to the suction of the pumps. The requirements of the pump vendors will fix this aspect of design. Any reverse flow through idle pumps recycles to the basin and reduces the efficiency of the process. Check valves and anti-reverse mechanisms help to prevent this.

The basin and the pit may be connected by a series of flumes. Screens constructed of fiber-reinforced plastic (FRP) or steel and mounted vertically in the flumes remove some of the suspended solids from the water. The cross-section of a flume may be small enough to allow a screen to be removed by one person. If not, some mechanical device becomes necessary. It is good practice to mount more than one screen in each channel, so that the water is still filtered when one of the screens is removed for cleaning. Flow into the flumes should be over a weir in order to retain the settled solids in the basin.

Settling and screening are a crude approach to solids separation, but they are effective in removal of trash and large particles. It may be necessary to remove finer solids as well. This can involve whole-stream filtration or filtering a sidestream and either returning it to the basin or pit or joining it with the main cooling water supply.

Clean makeup water can be introduced directly to the pump pit. Dirty water is better fed to the sump, where there is some opportunity for settling of solids. Treatment chemicals can be introduced anywhere in the system. Addition into a flume helps to mix the treating agent into the main water flow.

Wood is the standard material of construction for cooling towers. The Cooling Tower Institute publishes standards for construction from various woods and for treatment of the wood with preservatives. Almost paradoxically, fire protection is very important in cooling tower design, because the common practice of shutting down units or modular cells during times of low demand can allow wooden units to dry out. There should be a

hydrant nearby and sprinklers over and around the tower. The fan(s) should be interlocked to shut down whenever the sprinklers operate, and the startup procedure should call for starting water flow before starting the fan(s).

The trend now is away from wooden construction. With advances in fabrication techniques for plastics, preassembled plastic towers are now being used in larger size [12]. These are available in modules with ratings up to 10 GJ hr^{-1} cooling load. While they cost about 20% more than most wooden towers, they are more easily installed. Fireproofing is not necessary, and the tower blowdown contains no preservatives.

Drying of the wood should be prevented by periodically wetting the idle zone. A shutdown switch should also be available at a distance of at least 5 m from the tower. The vicinity of a cooling tower should be a no-smoking zone. All hot work and temporary wiring should be carefully supervised and checked.

12.4.2.1B. Cooling-Tower Fill. The type of medium used to subdivide the water determines the amount of interfacial area available for heat and mass transfer. This material, referred to as the "fill," usually is of one of two types, film or splash bar [11].

Film fill consists of corrugated or rippled sheets that subdivide the water and provide interfacial area. These sheets are assembled into packs that are installed vertically and stacked at offset angles. This is the more efficient of the two types of fill, but it is more difficult to install properly. Solids are more likely to deposit in the fill, and maldistribution of water is more likely.

Splash bars are less sophisticated and less effective. Staggered rows of horizontal bars form small droplets by impingement of the water. The water falling through a tower cascades from one row of splash bars to the next and so is continually subdivided. The support grids usually are of FRP. The bars themselves may be PVC, polypropylene, or wood. The plastic materials are less combustible than wood. While the effectiveness of this arrangement is less than that of the film fill, again, construction is simpler and maintenance access is much easier.

The trend in the industry is now in the direction of more efficient packing.

12.4.2.1C. Piping and Instrumentation. Cooling water piping is usually carbon steel. This fact makes it essential for the plant operator to keep up with the water treatment program. Untreated cooling water is the most corrosive form. Most plants at least add inhibitors. These vary in composition, and it is difficult to generalize other than to say that chromates, once a standard, are now seldom used, because of their toxicity.

Scaling and corrosion both are problems in cooling water piping. Calcium carbonate is the most common scalant. When sulfuric acid is used in the treatment program, this is converted to the sulfate. Calcium sulfate has less tendency to precipitate and scale the piping, but it is harder to remove when present.

Most exchangers have block valves in both cooling water connecting lines in order to allow isolation for maintenance. Improper closing of these valves with the exchanger under load will allow trapped water to heat and expand. This can damage the equipment or the piping, and some means of prevention is necessary. Most common is the addition of a thermal/pressure relief valve between the exchanger and one of the valves. This device simply opens at high pressure and allows a small amount of water to escape,

relieving the pressure. These relief valves are simple units, and in the absence of steam generation in the exchanger are quite small, usually 15–20 mm in diameter.

Each exchanger should have water-temperature instrumentation. The minimum case is a simple thermowell in the water outlet line. The most elaborate is permanently installed temperature indicators on both inlet and outlet. These instruments serve first as a means of checking the temperature profile against design and as crude indicators of the amount of water flowing. They can also be used for troubleshooting if enough information is available to construct a heat balance across the exchanger.

On the water side, particular problems are the corrosion potential of the water and the accumulation of dissolved solids.

12.4.2.1D. Concentration Effects and Blowdown. Comparison of the normal increase in cooling water temperature in the process with the latent heat of water shows that about 1–2% of the circulating water will evaporate on each pass through the tower. This must be replaced by makeup water, which brings more dissolved solids into the system. The process of treatment of the circulating water also adds dissolved solids, and one must consider the total concentration in the mixed feed water and treating solutions. Some water must then be withdrawn from the system in order to limit the dissolved solids concentration. This purge, or “blowdown,” acts along with the drift to remove both water and solids. Evaporation removes only water. The concentration factor for total dissolved solids in the recirculating water above that in the combined system makeup is

$$C = \frac{(E + L + B)}{(L + B)} \quad (5)$$

where

C = concentration factor

E = rate of evaporation

L = rate of mechanical loss of water

B = rate of blowdown

Mechanical losses include leaks, in-process applications of cooling water, and drift. To maintain a certain concentration factor, the required blowdown rate is

$$B = \frac{E}{(C - 1)} - L \quad (6)$$

The form of Eq. (6) shows that in order to maintain the concentration, the sum of B and L must be held constant. Efforts to reduce mechanical losses (L), while useful in themselves, do not always reduce the usage of water.

Many different corrosive agents can accumulate in a closed cooling water system if the concentration factor is too high. The use of inhibitors, noted above, is a standard technique. Upgrading the materials of construction also can prolong the life of equipment. Parkinson [13], for example, describes the use of a 75- μm coating of electroless nickel on cooling water pumps.

Blowdown creates a waste disposal problem and cooling towers, even aside from drift, can pollute the air. These disadvantages, combined with the growing shortage of water in parts of the world, have contributed to the beginning of a trend to dry cooling.

12.4.2.1E. Process Control. There are many different approaches to control of the cooling water treatment and blowdown process. Figure 12.5 is an example. The dissolved solids concentration is indicated by the conductivity of the water. This property is used to control the rate of blowdown. The blowdown, the evaporated water, and any system losses are replaced by makeup water, added under sump level control or through a float-operated valve. In a different approach, the rate of blowdown is made proportional to the rate of makeup water addition.

Most treating agents are fed in proportion to the makeup water flow. Analysis of the circulating water then may call for occasional changes in the ratios. The “chemical feed” of Fig. 12.5 is an example. There may be more than one such system, feeding inhibitor and other additives. The controller may adjust the speed or the stroke of the chemical feed pump. Alternatively, it may call for periodic feed of a certain volume of

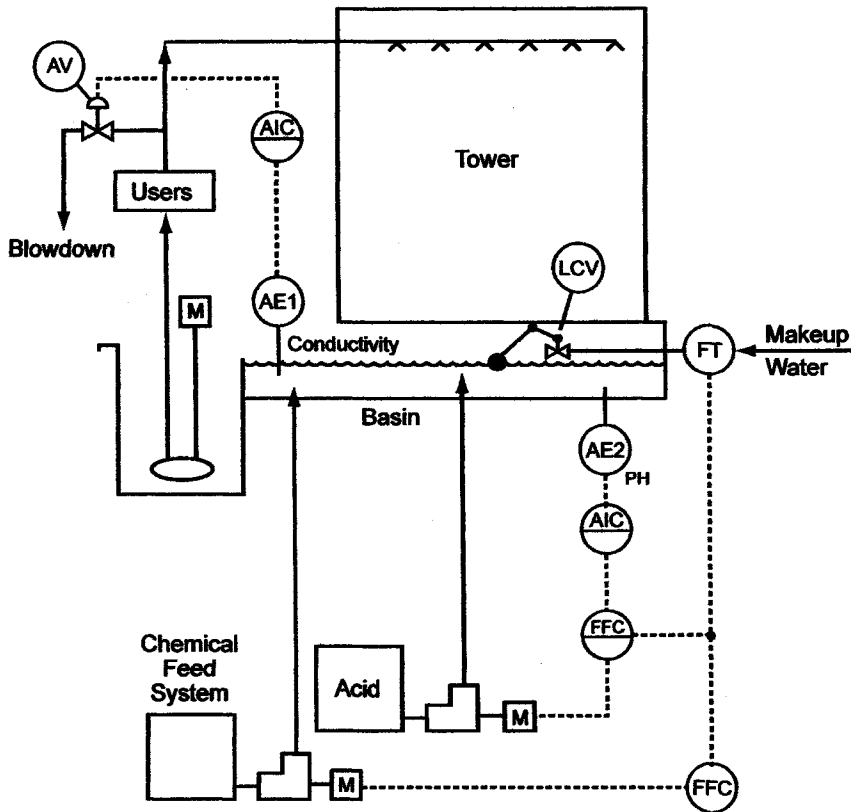


FIGURE 12.5. Cooling-tower water treatment process.

solution, with the length of the period inversely proportional to the makeup water rate. Minor ingredients may be added infrequently and manually. One technique is to charge them to a bypass tank connected to both cooling water headers and then to allow some of the supply water to flow through the tank and into the return header. Concentration control can be open- or closed-loop in nature. The control of pH is a special case that demands a proper dedicated control system. Sometimes there are two acid feed streams, with the larger proportional to the makeup water and the other responding directly to measured pH.

The treatment of cooling water is a subject for specialists. Requirements are affected by the quality of the water supply; the extent of contamination by corrosion products, process leakage, and the use of the water in direct-contact applications; and the nature and quantity of solids and gases scrubbed from the air in the cooling tower. There are extreme variations in some of these factors, and each plant will need its own treatment system and program.

12.4.2.2. Chilled Water. Chilled water is special in the sense that it may be provided not as a central utility serving a complex but rather from a unit dedicated and belonging to the chlor-alkali plant. We shall therefore consider it in more detail than we do some of the other utilities.

Its major users are the secondary chlorine cooler (or chiller) and the product caustic coolers in a diaphragm-cell plant. The latter are used to drop the final product temperature below normal cooling water temperatures in order to reduce the dissolved salt content. Other users sometimes include secondary hydrogen coolers, the sulfuric acid coolers at the drying towers, the water spray at the entrance to the wet gas demister, and acid coolers on liquid-ring pumps.

Water can be chilled at a central location by a dedicated refrigeration unit. Alternatively, refrigerant brine distributed as a general utility can be used to chill plant cooling water as and where necessary. After use, this water is sent to the cooling water return system. This becomes a standard application for a utility, and we do not consider it further.

Water chilling units in most chlor-alkali plants are not large and are usually purchased as packages. The thermal duty of a water chiller should be kept low as a matter of economy. The goal should be to approach the desired process temperatures as closely as possible through the use of cooling water. The practical limitation on this approach can be the rapidly increasing size of the primary coolers as their mean temperature differentials become smaller.

Note once more that seasonal cooling water temperatures may be lower than the minimum temperatures allowed in the chlorine and 50% NaOH processes. The plant then should operate with tempered cooling water and not with chilled water.

Chilled water supply involves a closed circuit. The water flows through a supply header, the users, and a return header to a storage/pump tank. Demineralized water is a typical source. It is added occasionally to replace water lost from the system or deliberately purged to remove contaminants such as process fluids and corrosion products. Storage tank construction is simple. The pressure is essentially atmospheric and the temperature is low. Since water is more corrosive when aerated, the tank may be blanketed, and plain carbon steel construction should be avoided. Lined steel and FRP are acceptable materials of construction.

For a given heat load, the flow of chilled water is greater than that of cooling water. This is because the temperature rise in service is restricted in order to keep the chilled water supply temperature relatively high, thereby reducing the power consumed in refrigeration.

Diaphragm-cell plants have the highest demand for chilled water. The NaOH-chilling load will be about three times as great as the chlorine-chilling load. This ratio is a function primarily of cooling water temperature. As that temperature increases, the intermediate process temperatures rise, and so the residual loads on both chillers increase. The available cooling water temperature fixes the demand. As the chlorine or caustic soda emerging from the cooling water section of the process becomes colder, the chilled water duty becomes less. As a result, water chillers seldom operate at design duty. When the annual swing in cooling water temperature is large, they may operate much of the time at a small fraction of design duty. Wide capability for turndown is very important.

Most water chillers in the chemical industry operate close to the freezing point of water in order to provide the maximum thermal potential. In our most important applications, however, there is a minimum desirable water temperature, set by the formation of chlorine hydrate, the loss of passivation of titanium surfaces in chlorine service, or the freezing of caustic soda. The water chiller can be operated at a higher outlet temperature than usual, or if colder temperatures are required somewhere, the water can be tempered for the major uses.

The duty of a chilled water system depends primarily on the cooling water temperature. Since nearly all cells operate close to atmospheric pressure and since chlorine outlet temperatures usually are 13–15°C, the end point of the chlorine chilling process is nearly constant. The starting point depends on the temperature of the gas leaving the cooler, which in turn is a function of the available cooling water temperature. Similar arguments apply to the cooling of diaphragm-cell NaOH.

Figure 12.6 shows the effect of gas temperature from the cooler on the chiller heat load. The basis is one ton of gas that is 100% chlorine (dry basis) at atmospheric pressure.

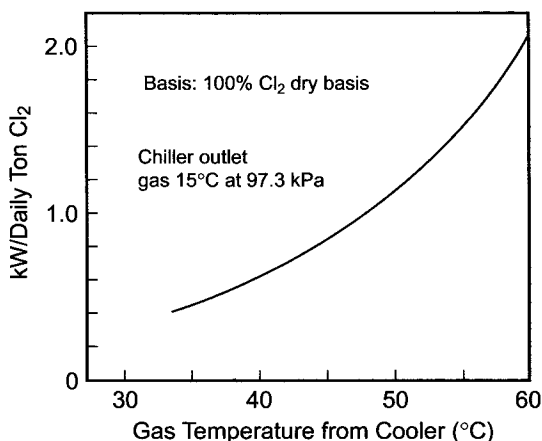


FIGURE 12.6. Thermal duty of a chlorine chiller.

The effect of gas impurities is to increase the volume of gas without changing the partial pressure of water. The latent heat component of the heat duty is therefore inversely proportional to the dry-basis mole fraction of chlorine. The same proportionality would hold for the sensible heat component if the impurities had the same average molar heat capacity as chlorine. While this is not precisely the case, the differences are small in comparison with the latent heat duty, and the assumption of constant c_p causes very little error. Figure 12.6 can, therefore, be used as a first approximation to the chiller load by dividing the indicated number by the mole fraction of chlorine.

Because cooling water is the ultimate heat sink in the water-chilling process, higher cooling water temperatures also increase the cost of refrigeration. In a mechanical system, for example, the refrigeration condenser temperature will be higher. This increases the compression ratio in the system and, therefore, the energy consumed by the compressor. Chillers use standard compressors, usually of the centrifugal or screw type. The condenser and evaporator are typical of industrial refrigeration service in their use of finned tubes formed from a copper alloy. In the operating range of 10–15°C, they consume about 70–80 kW hr GJ⁻¹.

Example. In our reference plant, the cooling water is available at 30°C and cools the chlorine gas to 40°C. We then wish to cool the gas to 15°C with chilled water. The gas leaving the cells contains, on a dry basis, 97% chlorine. We allow another 1% for entry of air. Figure 12.6 then indicates that our chilled water duty on a 100%-chlorine basis is 0.604 kW/daily ton. We therefore require $0.604/0.96 = 0.63$ kW/daily ton = 446 kW.

12.4.2.2A. Mechanical Refrigeration. Mechanical refrigeration is the most popular approach in chlor-alkali plants. The other techniques discussed below have advantages when electrical power is expensive. If that is the case, perhaps the chlor-alkali producer is in the wrong business.

Section 9.1.7.1 on chlorine liquefaction briefly describes the typical mechanical refrigeration cycle. Several different types of compressor appear in water chillers. They include reciprocating, screw, and centrifugal machines. The best choice depends very much on the suitability of a manufacturer's package details. The choice of refrigerant is not constrained by reactivity, as in the case of chlorine compression.

Since the demand for chilled water is highly seasonal, the refrigeration load is usually well below the design maximum. There is an excellent case here for multiple-stage unloading of compressors and for the installation of two partial-load machines.

12.4.2.2B. Steam-Jet Refrigeration. Under sufficient vacuum, water will boil; the latent heat of the steam formed comes from the remaining liquid, which is cooled in the process. The pressure level determines the temperature of the cooled water. One stage of eduction will accomplish the temperature reduction, but steam economy improves when several stages are used. Both the motive steam and the water vapor generated by evaporation flow to a condenser system. Most frequently, this will also be in more than one stage. Much of the load can be removed in a barometric condenser. The overall energy economy improves if a compressor and higher-pressure surface condenser follow in a later stage.

The amount of steam required to produce a given quantity of refrigeration is a function of the pressure of the supply and the condensing temperature. With steam at 7 bars and an ambient wet-bulb temperature of 25°C, about 600 kg of steam produces a gigajoule of refrigeration. As a rule of thumb, a small (say, 5 GJ) unit produces 1.6 GJ of refrigeration from 1 kW, 1 ton of steam, and 100 m³ hr⁻¹ of cooling water (10–12° rise). Note that makeup water is required continuously to replace that evaporated by the steam jets.

12.4.2.2C. Absorption Refrigeration. Water is the refrigerant in the absorption process. To allow it to evaporate and condense at the right temperatures, the whole process is under vacuum. There is no compressor between the evaporator and the condenser. Rather, the water vapor from the evaporator is picked up by absorption in a salt solution. Lithium bromide is the salt most frequently used.

The cycle includes

1. evaporation of water from LiBr solution by low-pressure steam or hot water;
2. condensation of water vapor from (1) at about 10 kPa by plant cooling water;
3. evaporation of water from (2) at about 1 kPa by exchange with the process load (circulating chilled water);
4. absorption of vapor from (3) by dilute LiBr solution, with the heat of absorption removed by plant cooling water;
5. pumping of solution from (4) to the concentrator to continue the cycle;
6. exchange of heat between concentrated LiBr from (1) and concentrator feed (5);
7. recycle of absorber solution, joined by concentrated LiBr after cooling in (6).

Containment of LiBr and maintenance of vacuum are essential. A small amount of air in the refrigeration loop can make the process inoperative. All components of the refrigeration loop may be mounted in one shell in order to reduce the potential for inleakage.

12.4.3. Purified Water

Water, after the preliminary treatment methods of Section 12.4.1, can be called “purified.” Here, we use the term to refer to the higher levels of purification in Table 12.1 or to those processes which remove dissolved contaminants. In the chlor-alkali process, the major uses of purified water are dilution of catholyte, processing of membrane-cell caustic liquor, preparation of ion-exchange system regenerants, manufacture of hydrochloric acid, acidification of brine, and, sometimes, dissolving of salt. It also serves as utility and seal water in the membrane preparation area and in certain parts of the process.

12.4.3.1. *Softened and Demineralized Water.* Ionic contaminants are removed from water by softening or demineralization. The softening process removes the hardness elements (and other multivalent cations) that are of major concern to the chlor-alkali producer. Chemical softening was the first process developed, but modern plants use a cation-resin process. Exposing water to a resin containing labile sodium ions allows the removal of divalent cations and their replacement with sodium. The chemistry is that discussed in Section 7.5.5.1. When the resin is nearly saturated with hardness ions,

contact with a concentrated solution of NaCl restores it to the sodium form and produces a waste stream. Note that softening does not reduce the total ionic loading in the water. It simply replaces some of the impurities (hardness ions) with less objectionable impurities (sodium ions). The anionic population does not change.

Demineralization is another resin-based process. It removes essentially all the ionic contamination from water. The cation resin here is in a different form and contributes hydrogen rather than sodium ions. A second resin is necessary for the removal of anions. The labile ion on this resin is OH^- . When this replaces the other anions in the water, it combines with the H^+ released by the cation-exchange resin to form water.

Silica and carbonate are special considerations in the design of demineralization systems. The carbonate content can be removed by stripping CO_2 from acidic water, rather than by using solely the ion-exchange resin for this duty. Silica is the anhydride of the weak acid H_2SiO_3 (pKs at room temperature 9.7 and 12.0). This fully ionizes only when in contact with a strong base. Removal of silica by ion exchange, therefore, requires the use of a strong-base resin. Such a resin is more expensive than the more conventional weak-base type and usually has a lower total exchange capacity. Depending on the capacity and on the desired degree of dissolved solids removal, the demineralizers can be designed in several different ways:

1. with single beds each of weak-base cation- and anion-exchange resins
2. with single beds of strong-base cation- and anion-exchange resins
3. combination (1) followed by a bed of mixed cation- and anion-exchange resins, the cation resin being of the strong-base type (this arrangement may also include a carbonate decomposer and stripper)

Regeneration of any ion-exchange bed produces a waste product. Section 16.5.2.4 covers the disposal of these streams.

12.4.3.2. Evaporator Condensate. Diaphragm- and membrane-cell plants produce useful condensate in their caustic evaporators. As the material balance of Fig. 6.9 shows, the membrane-cell evaporators produce more than enough condensate to serve the demand for dilution water in the cell room. Diaphragm-cell evaporators, with their much higher evaporative load, produce more than enough water to dissolve an incoming salt supply. Alternatively, the condensate can be used in other applications. The excess evaporative capacity can be used to restore the plant's water balance when NaCl is supplied as brine rather than as solid salt. Since a brine supply is usually cheaper than a solid salt supply, and since this option is not open to membrane or mercury cells without added expense, this feature is an economic advantage of diaphragm cells that helps to offset the expense of caustic evaporation.

Example. We consider 100 tons of cell liquor containing 11% NaOH and 15% NaCl:

	To evap.	From evap.	Vapor
NaCl	15	0.12	
NaOH	11	11.0	
H_2O	74	10.9	63.1

A generous allowance for the fresh salt required to produce 11 tons of NaOH would be $1.6 \times 11 = 17.6$ tons. The water required to produce 25% brine then is $3 \times 17.6 = 52.8$ tons. The amount of condensate recovered from the evaporator (63 tons) is about 20% more than this.

Evaporator process condensate has many potential uses:

1. utility stations in caustic area;
2. pump seals;
3. line washing;
4. evaporator wash/boilout;
5. caustic dilution;
6. soft water replacement;
7. instrument purge;
8. evaporator mesh wash;
9. centrifuge cake wash (chilled);
10. Glauber's salt crystallizer makeup (chilled).

Evaporator condensate is contaminated by entrainment of caustic. This is not a troublesome impurity in a caustic plant, and it has some positive benefits in making the water less corrosive. There is also the possibility of low-level contamination by metal ions from the processing equipment [14].

A special application of process condensate in a diaphragm-cell plant is in evaporator cleaning and boilout (Section 9.3.3.3). The salt crystallizing in the evaporators (NaCl or triple salt) continuously deposits on the surfaces of the vapor bodies and heating elements. In the latter case, it restricts circulation of liquor and can interfere with proper operation. The first symptom of a solids buildup usually is an increase in the temperature rise through the heating element. From time to time, it becomes necessary to interrupt operation in order to remove at least part of the salt deposit. The first effect usually has the heaviest deposit and requires the most frequent washing.

Depending on the extent of the buildup, there are two techniques for dissolving the deposited salt. In the less elaborate and less disruptive technique, some of the slurry is removed from one effect and replaced with water. This temporarily increases the solubility of salt in that effect. This technique, sometimes referred to as a "fly boilout," is usually the first line of attack. The more thorough complete boilout requires complete draining of an effect into a special boilout tank and replacement of the contents with water. After heating and recirculating for about an hour, the solution is dumped and replaced with slurry from the boilout tank. To conserve product and condensate, a boilout system such as that shown in Fig. 12.7 may be installed. Evaporator condensate is the normal source of water for the boilout system. For washing of small equipment or for a fly boilout of one of the evaporators, the condensate supply can be directly from its storage tank. The wash liquor then goes to the boilout water tank. This liquor can be used in either type of boilout and can be supplemented with condensate when necessary. When the boilout liquor becomes concentrated, it is transferred to the boilout collection tank, from where it is returned at a controlled rate to the evaporators.

A complete boilout is required when the simpler technique fails to restore operation for an adequate time. Maintenance shutdowns for other reasons also give opportunities

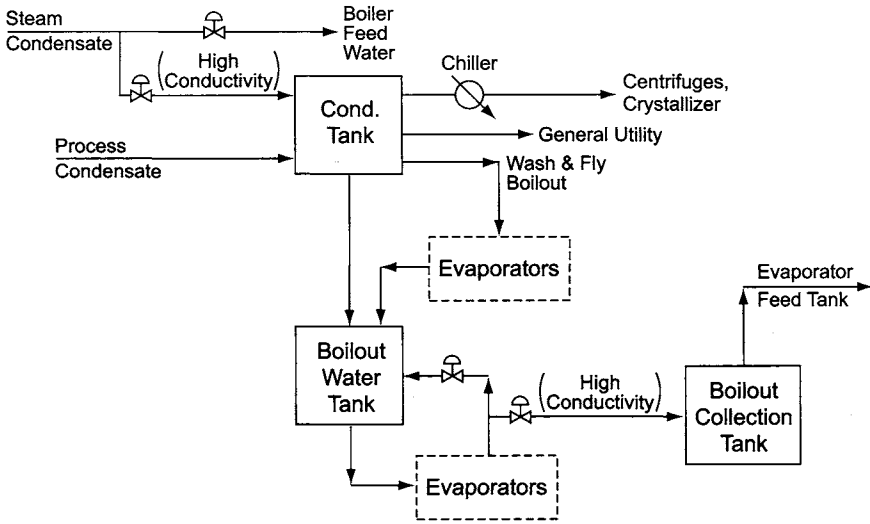


FIGURE 12.7. Diaphragm-cell evaporator boilout system.

for complete boilouts. Allowing for the operating time lost and the water added during boilouts is an important part of diaphragm-cell evaporator process design.

12.4.3.3. Boiler Feed Water. Boiler feed water is a special case of purified water. The purity required depends primarily on the operating pressure of the boilers. Arden and Forrest [6] give typical specifications for hardness and organics in boiler feed water as functions of the operating pressure of the boiler:

Pressure (atm)	Hardness (ppm)	Organics (ppm)
15	300–350	1
25	50–100	1
35	5	0.5
70	0.02	0.2
150	0.02	0.1

Hardness elements can form deposits because of the inverse solubilities of silicates and carbonates, and organics can foul surfaces or lead to corrosion. Some low-pressure systems can operate on softened water. High-pressure boilers (>6 MPa), on the other hand, require the equivalent of a three-bed demineralizer for the treatment of fresh water. To avoid the potential for contamination by regenerant chemicals, external regeneration is often chosen.

Boiler feed treatment also must remove oxygen and alkalinity from the water. Dissolved oxygen leads directly to corrosion, and it is most dangerous when corrosion takes the form of pitting. “Alkalinity” refers primarily to carbonates and bicarbonates. These

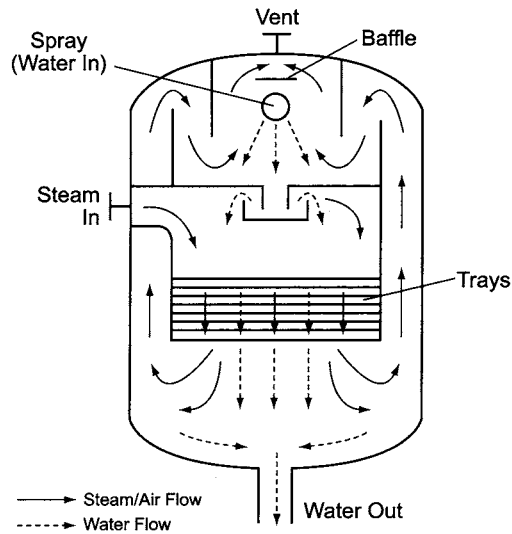


FIGURE 12.8. Condensate/feed water deaerator.

species decompose at high temperature, releasing CO_2 . As steam condenses, the CO_2 dissolves and forms the corrosive H_2CO_3 .

Stripping the water with steam in a deaerator reduces the dissolved oxygen to very low levels. Figure 12.8 shows a typical deaerator. Spray-type units are more compact and usually cheaper than tray-type units. They are also less flexible in operation, and the example chosen here therefore is a parallel-downflow tray deaerator. Counterflow units, again, are cheaper but have narrower ranges of efficient operation. In the drawing, the water to be deaerated enters the top chamber through a sparging device or a perforated distributor. The huge increase in liquid surface area makes it possible for entrained air to escape.

The water collects in a central well and overflows a weir into the tray section. Here, it falls from tray to tray, and deaeration is completed by contact with the steam. Stripped gases and any uncondensed steam leave through a top vent. The construction of the apparatus forces the steam to flow along with the deaerated water through the tray section. At the bottom, the steam separates from the water and rises through a baffled chamber to the top section, where it meets the incoming water. The deaerated water leaves through a sealed tailpipe into a collecting drum. From here, it can be pumped to the boilers. An efficient deaerator can produce water with 7 ppb of dissolved oxygen. Achieving lower levels requires chemical treatment, discussed below.

Alkalinity is removed by the methods noted in Section 12.4.3.1 for demineralized water. It may also be useful to mitigate the effects of residual CO_2 in the steam.

Strict control of purity relies on the avoidance of corrosion in the steam-distribution system and on chemical treatment of the feed water or steam condensate [15]. Treatment chemicals may include:

1. oxygen scavengers (reducing agents, including sulfites);
2. CO_2 neutralizing agents (organic amines);

3. corrosion inhibitors (film-forming amines);
4. antiscalants (sequestering agents).

Oxygen scavengers such as sulfites perform best at alkaline pH. Activators can increase their rate of reaction with oxygen 10- or 30-fold [1], but the low concentration of reducing agent and even lower concentration of oxygen keep the rate low. The scavenger needs some time to react. Furthermore, other treatment chemicals can affect the scavenger or at least its activator. The order of addition of the various chemicals therefore is important, and the best practice is to add the scavenger to the bottom of the deaerating tower or into the deaerator storage tank. The other chemicals then can be added downstream.

The neutralizing amines must be deposited throughout the steam distribution piping if they are to be effective. Each plant must have a program and usually a mixture of amines selected for varying volatilities in order to achieve good distribution.

The corrosion inhibitors operate by forming a film on pipe and equipment surfaces. The amines used in this service have higher molecular weights and so are less volatile and less soluble in water. They must be injected into steam lines, and high velocity helps their distribution.

The antiscalants include chelating agents and polymers that can disperse corrosion products and other solids that may enter the system.

Excessive use of treating chemicals not only carries the obviously higher material cost but also increases the amount of condensate blowdown that must be taken from the system to control the dissolved solids concentration.

12.5. AIR SYSTEMS

Compressed air is supplied as a utility in several different forms that for the most part are distributed separately:

1. plant or service air
2. instrument air
3. dry air
4. breathing air

For convenience, we include nitrogen, an important utility in chlor-alkali plants, with the air systems.

12.5.1. Plant or Utility Air

“Plant air” is that used as a general utility. Consumers are utility stations, flushing and purging systems, power tools, certain drives, cell room cranes, cell switches, some diaphragm pumps, and various steps in filtration and ion-exchange processes. This air is not necessarily bone dry but should be free of oil and water droplets, and it should be at a pressure sufficient to operate special tools or apparatus. It is generated by compressing atmospheric air and cooling it to condense some of the water vapor. There must be precautions against the ingress of chlorine at the compressor suction. These include selecting the location for the intake and elevating it above the likely level of chlorine

accumulation. The intake should be in a cool spot away from walls and roofs and away from or on the upwind side of vents or stacks that might introduce contamination. This discussion raises the opportunity to mention the consideration of prevailing winds in plant design. While it is always useful to know the direction of the prevailing wind, designers should recognize that at most sites the wind very frequently blows in other directions. Design must cater for these cases. The placing of an air compressor intake is a good example. In most cases, the wind alone cannot be relied on to allow an air intake anywhere in the vicinity of a potential chlorine vent.

Most uses of plant air are intermittent. Design frequently provides an intake filter, a buffer tank for compressed air, and a set of pressure switches to take the compressor on and off load. The buffer tank should be large enough to prevent excessive cycling of the compressor, and the compressor should be capable of pressures high enough above the minimum header supply pressure to provide off-line periods of reasonable length.

The above describes a standard air compression package, and many commercial models are available. Reciprocating compressors are a frequent choice, and in their case, the air buffer tank also serves as the outlet dampener. The small clearances in reciprocating machinery require better filtration than is offered by a fabric strainer at the intake point. Suction strainers on these compressors, therefore, usually are rated at about 20 mesh. Each stage of the compressor has temperature measurement and alarm. Often, cylinders are jacketed for cooling, and the system may have electric heating for use at startup. Other instrumentation measures the pressure of the gas and of the lubricating oil. The oil system includes a hold tank or sump, positive-displacement pumps, circulating piping, coolers, and filters. Pressure instrumentation on the oil system includes low-pressure alarms and an emergency shutdown when the pressure is dangerously low. Low pressure also may be used to start the spare oil pump automatically, in order to forestall shutdowns. The shells of the coolers are carbon steel or the plant's standard material. To reduce the amount of corrosion products, the tube-side construction may be based on more resistant materials such as maritime alloys.

Some applications require a high volumetric flow of air for a short time. These include purging and the use of air to displace liquid from equipment before opening or performing a cyclic operation. If a system were designed to meet their needs directly from the compressor when required, it might have a large capacity that is used infrequently. Local buffer/storage tanks can smooth these demands and help to keep the size of the air compressor within reasonable bounds. It also can pay to meet high-volume, low-pressure demands with dedicated blowers. An example cited in Section 7.5.4.1 is air scouring of bed filters before backwash.

Compressed air lines are often fitted with filters, regulators, and lubricators. These are usually installed as a set. The filter may be of standard design, to remove moisture and solids, or a coalescing filter, to remove aerosols of compressor lubricating oil. The purpose of the regulator is to adjust the pressure of the air. The lubricator injects a small amount of oil, which provides downstream lubrication. The regulator is mounted between the other two appliances so that it will handle only clean air.

A system that is not leaktight will incur the expense of replacing the lost compressed air. Leaks may be due to defective hoses, worn power tools, and faulty clamps, as well as to the more classical faults in the piping itself. A single hole 1 mm in diameter will

lose about $4 \text{ m}^3 \text{ hr}^{-1}$ of air if the line pressure is 700 kPa. The power lost is about 0.35 kW [16].

The control arrangement described above allows the pressure in the air receiver to fluctuate over a range of perhaps one bar. Because compressor drives will overheat if started and stopped too frequently, most operate in an idle mode when not compressing air. Typically, a compressor unloads when it reaches a set pressure and then continues to run unloaded for some predetermined time before shutting down. In an active system, the demand for air usually causes the compressor to cut in again before a shutdown occurs. Depending on the type of control system, an idling machine continues to consume 25–75% of full-load power. Recent developments in air compression systems use variable-speed drives on rotary screw compressors to achieve overall power savings of 20–35% [17]. By matching their output more closely to demand, these not only reduce the power consumed by off-load operation but also reduce the variation in system pressure to a small fraction of that experienced in a conventional system.

Typical distribution pressures are 550–1,000 kPa. At these levels, each kilowatt-hour used produces 5–10 Nm^3 of compressed air. Each of these requires about 100 kcal of cooling. These figures obviously vary greatly with delivery pressure, inlet air temperature, etc., but they are presented to give the reader a feel for the requirements.

Many compressors require noise attenuation. The simplest type of silencer is the absorption tube. This consists of a flanged perforated tube attached to the air line and surrounded by a larger cylindrical section. The annulus is packed with steel wool, fiberglass, or felt. The size depends on the size of the piping and the degree of attenuation required. Since the energy decays exponentially as the air travels through the tube, the decibel measurement drops off linearly with distance. The efficiency of absorption depends on the nature of the packing and the frequency of the sound. It may be necessary to consider the spectrum of sound produced by the compressor and to size the attenuator on the basis of some limiting frequency.

A sound-absorbing chamber is usually more efficient than the simple tube just described. This is a pressure vessel with diameter much greater than that of the air pipe. It is divided into two or three sections, depending on the degree of attenuation needed. Perforated pipes that are not on the centerline of flow connect these sections. The changes in direction help to deaden the sound. Other devices combine the characteristics of the two types described here.

Water will condense in the lines when air is exposed to temperatures lower than that at the compressor aftercooler. This water must be drained. At subzero temperatures, the condensate can freeze in the lines, and design must address this problem. Some plants dry all their compressed air, using the techniques of the next section, in order to mitigate these problems. In this connection, refrigerated dryers that produce dew points of about 5°C are usually considerably cheaper than desiccant dryers.

12.5.2. Purified Air

Air used in the process or in instruments and their tubing must be quite dry. In a chlor-alkali plant, maintenance work is often necessary in areas in which chlorine vapor may be present. A secure supply of uncontaminated air is then necessary, and some plants

provide a dedicated breathing air system to meet this need. This section discusses the drying of air for the former application and the purification and distribution of air for the latter.

12.5.2.1. Instrument Air and Dry Air. Instrument air and “dry air” intended for use within the chlorine processing system both must have very low dew points. A common specification level is -40°C , but the specification particularly for dry air may be lower. Modern plants meet this demand by using desiccant dryers. Drying agents include silica, alumina, and molecular sieves. The size of the desiccant beds depends on the flow rate and the inlet humidity of the air. The latter is one of the important general project criteria. The drying system sits in line after the compressor’s outlet buffer and has at least two beds of desiccant. While one operates, the other is regenerated. There are two common modes of regeneration. In one, heating the bed while sweeping it with air drives off the adsorbed water and restores the capacity of the desiccant. The regenerating air and the evaporated moisture exhaust to the atmosphere. This also can be a closed-loop regeneration, with the air or nitrogen from the bed cooled to remove water, recompressed, and reheated to provide the energy to drive off more water. Heating can be by high-pressure steam, fuel, or electricity. External heaters, on the regenerating gas line, and internal heating elements both are used. With the latter type, special care is necessary in order not to overheat some of the desiccant. The regeneration schedule includes time for heating and cooling the bed. The second mode of regeneration uses the pressure-swing technique. Some of the dry compressed air from the working bed is let down nearly to atmospheric pressure and sent to the off-line bed. The combination of low pressure and dryness gives the air a great capacity for moisture, and it is able to remove the water from the exhausted bed very efficiently. This air can be heated to supply the energy of vaporization of the adsorbed water. The supply compressor and the drying beds must be sized to handle the regenerant flow as well as the process demand. The regenerant flow depends on the outlet pressure of the working bed (pressure loss in the drying system usually is about 30 kPa). The flow can be less at higher pressure. As a first approximation, the amount of regenerant purge necessary to maintain a final dew point of -40°C is

$$\% = \frac{12,000}{P} \quad (7)$$

where

% = required recycle, % of output

P = bed outlet pressure, kPa

At a pressure of 600 kPa, for example, 20% of the air must be recycled (a 25% increase in throughput). More recycle would be necessary to maintain a lower dew point.

In any case, the operating and regeneration times are equal (a practical necessity in a two-bed system) and usually are several minutes each. Several operating systems were

found to be designed with an air space velocity in the drying columns of about 6 min^{-1} . This may vary widely. With the short running time of an individual bed, automatic switching is the normal practice.

With their similar specifications, instrument air and dry air can be generated in the same system, but they should be supplied in separate headers. There is nothing unusual about the instrument air supply in a chlor-alkali plant, and so it will not be discussed separately in this book.

Dry air is used when air is to be injected into the process anywhere on the high-pressure side or after the drying columns on the low-pressure side. When dilution of the tail gas is necessary in order to prevent accumulation of dangerous concentrations of hydrogen, the major consumer will be the liquefaction system. Other points of use include compressor seals, purging and maintenance connections, suction chiller bottoms pot connections, and anhydrous caustic processing equipment.

The immediately obvious hazard in a dry air distribution system is the entry of chlorine into the air lines during pressure reversals. Some plants use non-return valves to protect against this. The reliability of these valves is questionable, and the authors recommend the use of automatic valves that close when the differential pressure across them reverses. Figure 11.51 illustrates this technique in a different application. These valves can be used in conjunction with non-return valves when some redundancy is desired. Section 12.7.2 reviews some of the arrangements used to connect air and other utilities to process systems.

The dry air supply can be backed up by nitrogen or instrument air when the available supply of those utilities is large enough. They can also be used as backup or replacement at individual locations, subject to the caveat of Section 12.5.3.

12.5.2.2. Breathing Air. Breathing air systems should be dedicated and not integrated (except possibly at the atmospheric side) with other air systems. Oil-free compressors are necessary, with intake and outlet filters and frequently a carbon adsorber to purify the air. The air must not be bone dry. It should have enough humidity to keep a worker comfortable. The delivered air should meet the Compressed Gas Association's specification G-7.1. Electric motor drives are preferred, as they are least likely to contaminate the air intake. The compressor should have a high-temperature alarm, and the quality of the air should at least be checked frequently.

In the air distribution system, all takeoffs should be from the top of the pipe or header. Headers should slope towards their ends and should include terminal drain/blowdown valves. Connection points for hoses should be standardized throughout each plant and should carry prominent reminders to blow out the line before use.

There are two types of mask in general use—constant-flow and demand-supply. Tight-fitting constant-flow masks require about $7 \text{ Nm}^3 \text{ hr}^{-1}$ of air. The loose-fitting type requires about 50% more. Demand-type masks require up to $3 \text{ Nm}^3 \text{ hr}^{-1}$. Ventilated suits will consume $25\text{--}50 \text{ Nm}^3 \text{ hr}^{-1}$.

Breathing air is not supplied as a pipeline utility in all plants. There are many approaches to the problem of supplying emergency breathing air, each with its own set of advantages and disadvantages, as summarized in Table 16.1.

There should be no connections of breathing air to process systems. Connections to other air systems should be made only after thorough review (Section 12.7.2).

12.5.3. Nitrogen

Nitrogen is valuable for its dryness and its inertness. Both are useful in the chlorine process, and inertness is desirable in the hydrogen process. Most plants purchase nitrogen as the liquid and supply it to the processing units through a packaged vaporizer, which often remains the property of the gas supplier.

Nitrogen is much more expensive than air, and the possibility of its entering an air distribution system must be rigorously excluded because of its asphyxiant properties. It offers some advantages in compensation. Its dew point usually is lower than that of dry air, and its dryness is more reliable and not subject to desiccant bed breakthroughs. In tail gas processing, while this may not be recognized in the specifications set for hydrogen content, nitrogen is also a more effective diluent than air (Section 9.1.11.1).

12.5.4. Backup Systems

Backup supplies are always useful when a utility is lost. Spare equipment or multiple-train equipment may be used in order to keep the utility on line even if one part of the system shuts down. An alternative or supplement is to provide backup from a different utility system. The number of different air systems found in a plant provides an opportunity to do this. Moreover, nitrogen can be used to back up some of the air systems. All these tie-ins require careful review during hazard analyses. Usually, the backup supply is activated when the primary supply loses a certain amount of line pressure. If this is done by means of a single pressure regulator and the pressure is also low on the backup system, the flow may be opposite to that intended. It is essential to keep nitrogen out of an air supply to a confined, inhabited space (e.g., the instrument air supply to a control room), and it is essential to keep air out of nitrogen when it is used as an inert gas.

12.6. VACUUM SYSTEMS

For convenience, we include vacuum services among the utilities. While true utilities are supplied plantwide from a central location, vacuum producers in a chlor-alkali plant tend to be more dedicated to a single duty and installed near the point of use. Major applications in the process, keyed to the sections in which they are discussed, include:

1. brine sludge filtration (16.5.1.3)
2. brine dechlorination (7.5.9.2A)
3. chlorine system evacuation and purging (9.1.12)
4. caustic evaporation (9.3.3)
5. brine evaporation (7.1.5.2)
6. deaeration of brine (7.3.2.3)

The discussion of vapor-recompression evaporation in Section 7.1.5.2B distinguished between mechanical and thermal recompression. Vacuum systems (Section 12.6.1) can be divided in the same way between those relying on compressors and those using ejectors. Hybrid systems using both types are also quite common. Since the amount of vapor that it handles fixes the size of a vacuum producer, removal of evaporated water between

the process and the source of vacuum is a nearly universal technique in chlor-alkali plants. Removal of the condensate, which is under vacuum, requires special attention. Vapor condenser selection, arrangement, and piping, therefore, are important aspects of vacuum system design (Section 12.6.2). Methods of process control, principally a matter of maintaining the desired pressure at the process unit, depend on the type of vacuum producer being used (Section 12.6.3).

12.6.1. Sources of Vacuum

The first step in choosing a vacuum source is the definition of its duty. The process itself dictates operating conditions, but the designer must consider both startup and steady-state operation and also take into account the leakage of air into the evacuated system. An important example of the difference between startup and steady duty is the caustic evaporator. Startup requires a much greater rate but for only a short time. Common practice therefore is to supply two sources. A large source, for example a “hogging” jet, takes care of startups. A smaller parallel unit avoids the consumption of large quantities of steam or power during regular operation.

The steady-state duty includes vapors generated in the process and air that infiltrates the equipment. Estimation of the latter quantity depends on the size and arrangement of the relevant equipment and piping. Engineers will be familiar with the curves published by the Heat Exchange Institute for what are defined as “commercially tight” systems. Here, the rate of infiltration is assumed proportional to the two-thirds power of system volume. More elaborate, and one presumes more accurate, methods take account of the number, sizes, and types of fittings, valves, welds, etc. These methods and the standard factors for estimating leakage are in the publications of vacuum system vendors [18] and in process engineering textbooks [19].

The choice of apparatus normally comes down to a selection of steam jets or mechanical equipment. Important design factors include:

1. gas(es) to be handled;
2. process load (minimum and maximum);
3. air leakage;
4. allowable pump-down time;
5. range of pressures required;
6. presence of entrained solids or liquids;
7. noise.

The nature of the gases being evacuated determines the materials of construction and their molecular weight influences the duty of the vacuum producer. Items 2–4 fix the capacity. In addition to the usual overdesign factors one finds in process work, the allowance for air inleakage is often quite generous. Vacuum systems, as a rule, are well oversized for their actual duty. When the system remains tight, this has implications in process control (Section 12.6.3). Item 5 is an important differentiator among vacuum systems, and it usually determines the number of stages required. In normal chlor-alkali vacuum applications, which exhaust at essentially atmospheric pressure, the suction pressure is the determining variable. In vapor-recompression operations, the discharge pressure is equally important. Solids entrainment can affect the equipment by erosion and can

seriously reduce the capacity of a steam jet. Solids also can damage sliding-contact vacuum pumps. While the more elaborate mechanical pumps offer high efficiency and minimum pollution, they are limited to service with clean, dry gases and also suffer from the need to displace large volumes of gas at low pressure. Liquid-ring pumps are more common in chlor-alkali plants. They offer higher thermal efficiencies than steam jets and can handle higher concentrations of entrained solids or liquids. In closed-circuit systems, they also produce less pollution. Steam jets are very simple, with no moving parts, and are the cheapest systems to install. Here, we consider only liquid-ring pumps and steam jets. The Heat Exchange Institute publishes "Performance Standards for Liquid Ring Vacuum Pumps" and "Standards for Steam Jet Vacuum Systems." Members of the relevant committees [20,21] have published summaries of the major points of the then-current standards.

12.6.1.1. Liquid-Ring Pumps. Many smaller plants, in particular, compress chlorine with liquid-ring pumps. Section 9.1.6.2C discusses the mechanism of their operation, and Fig. 9.23 is a typical flowsheet. Here, we consider them as sources of vacuum.

Liquid-ring systems differ in their handling of the pumped seal liquid. Once-through systems discharge all the liquid from the gas-liquid separator into a collection system or send it to waste. This has the advantage of simplicity and is the basis for many systems that do not handle chlorine. Brine filtration is an example. It is unacceptable when discharge of the liquid presents a pollution problem. The opposite approach, full recycle of the liquid as in Fig. 9.23, minimizes discharge but involves the expense of a recycle cooler and, in many systems, a recycle pump. An intermediate approach is to provide enough fresh liquid to remove the heat of compression and maintain the process temperature, and to recycle enough to satisfy the liquid-handling capacity of the pump. This technique saves much of the liquid supply without the expense of a return pump or cooler.

There always is a net change in the quantity of water in a "closed" system. When there is a net evaporation into the compressed gas, one needs simply to arrange for makeup of fresh water. If some component of the gas being compressed is absorbed into the water, there may also be a need for blowdown to control its concentration. When there is net condensation of water, as in most applications in this volume, there is a need for a controlled purge of water into an appropriate recovery system.

Discharge piping between the vacuum pump and the separator should be as simple and as low as possible. Frequently, the two are close-coupled. If necessary, some increase in elevation above the pump discharge flange is acceptable, but this puts a backpressure on the pump and increases its power demand or reduces its capacity. With the live mechanical load and the desire to keep piping compact and even close-coupled, piping stress can be an important consideration. Careful design or the use of flexible connections is necessary.

Liquid-ring pumps require shaft seals. A simple lantern-ring arrangement appears on some models and requires a flow of cooling liquid. Recycled liquid is acceptable in this duty. However, mechanical seals are preferred in most chlorine-handling applications. Double seals with separate supplies of clean fluid are the standard.

Recycle of the sealing liquid from the receiver to the pump presents no unusual or especially difficult problems. The proper materials of construction are necessary, but

design of the recycle cooler is straightforward. The liquid may be saturated with a gas such as chlorine at separator pressure. This means that the return system, especially one without a pump, must be able to handle a certain amount of evolved gas.

The basic materials of construction of a liquid-ring pump depend on the gas being removed. In non-chlorine applications, for example brine filtration, pump bodies can be of carbon steel and water can serve as the sealing fluid. There may be some upgrading of materials, particularly in small parts and seals, because of the possibility of entrainment of process liquids. When chlorine vapor is expected to be present, as in brine dechlorination or purging of certain equipment, the combination of carbon steel and a water ring is not acceptable. We have already noted the use of sulfuric acid as the liquid ring in chlorine compression. In brine dechlorination, the amount of water vapor in the gas would consume excessive amounts of acid. Since vacuum levels are modest, a water ring is operable. The material of construction problem is solved by the use of titanium or lined materials. The combination of a titanium impeller with a ceramic-lined body has found use in brine dechlorinators.

12.6.1.2. Steam Jets and Hybrid Systems. Steam jets have the important advantage of availability in a variety of higher materials of construction. This may be a decisive factor in, for example, brine or condensate dechlorination. Their design is simple, with no moving parts, and they can be mounted in any position and in any orientation [22]. Their operation is simple, and startup and shutdown are particularly straightforward. They can handle a gas that contains condensable components. When used in chlorine service, on the other hand, they produce vapor and condensate that are contaminated with chlorine. Backflow of steam into the process system is an inherent possibility, and process design must guard against this where it is objectionable. Steam jets also are noisy and may require housing or special insulation to meet environmental standards.

The maximum compression ratio achievable by a jet usually is about 6 or 10 : 1. Practically, ratios are limited to lower values, and multistage jets are necessary in evaporation systems. While process and equipment design have much to do with the selection of the number of stages, the tabulation below is a rough guide to the absolute pressures that can be produced by two to four vacuum stages:

No. of stages	Pressure (torr)
2	5–20
3	0.5–5
4	<0.5

Figure 12.9 is a flowsheet for a system with two stages. Mechanical pumps can achieve the ratios required in chlor-alkali plants in a single stage.

Ejectors must transfer work to the low-pressure fluid, and so there is always a loss of enthalpy from the system. Expansion of the motive steam and compression of the mixed fluid are more nearly isentropic [23]. An isentropic expansion can cross the saturation curve and enter the two-phase region. This fact is an important consideration

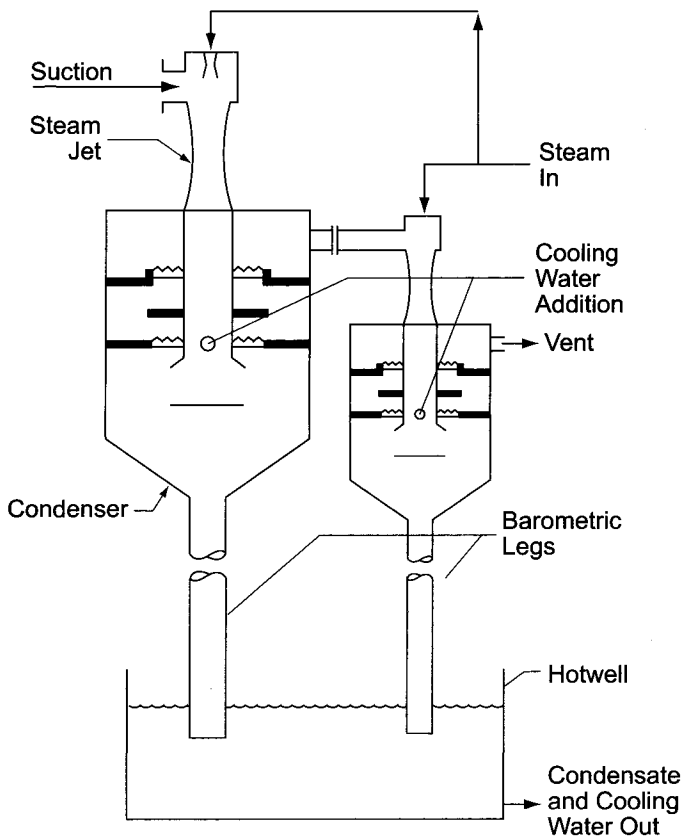


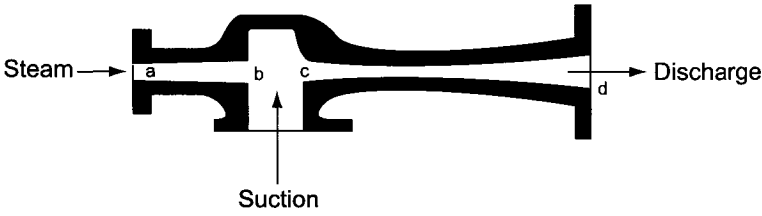
FIGURE 12.9. Two-stage steam-jet vacuum system with barometric condensers.

in the design of ejectors. The loss of enthalpy and the entrainment ratio produced, both functions of the efficiency of the jet, are important to the design of the evaporation plant.

To analyze the behavior of an ejector, we recognize three distinct stages of operation, as shown in Fig. 12.10:

1. the motive steam expands and produces work (a–b);
2. the expanded steam transfers some of its momentum to the fluid which is to be entrained (b–c);
3. deceleration of the mixed fluid in the expansion zone (the diffuser) abstracts work from the fluid and produces higher pressure (c–d).

We assign the efficiencies η_1 , η_2 , and η_3 to these regimes. The unit enthalpy of the mass M_1 of motive steam at supply conditions is H_1 . After isentropic expansion to the pressure in the nozzle, this enthalpy becomes H_2 . The steam entrains the mass M_2 of low-pressure vapor, and the unit enthalpy of the mixture at low pressure is H_3 . The mixture, of mass $M_1 + M_2$, is compressed in the diffuser and acquires the unit enthalpy H_4 at the outlet of the ejector.



Gas	Point	Flow	Pressure	Enthalpy
Motive Steam	a	M_1	P_1	H_1
Expanded Steam	b	M_1	P_2	H_2
Mixed Gas Diffuser	c	$M_1 + M_2$	P_2	H_3
Discharge	d	$M_1 + M_2$	P_3	H_4

FIGURE 12.10. Analysis of steam-jet operation.

The work produced by isentropic expansion of the motive steam would be $M_1(H_1 - H_2)$. Applying the efficiency of this step, η_1 , we have

$$W_E = \eta_1 M_1 (H_1 - H_2) \tag{8}$$

The total amount of work produced in the process also depends on the efficiency of momentum transfer, η_2 :

$$W_P = \eta_1 \eta_2 M_1 (H_1 - H_2) \tag{9}$$

The work required for isentropic compression in the diffuser would be $(M_1 + M_2)(H_4 - H_3)$. Since work is supplied at the efficiency η_3 , we have for the actual work of compression

$$W_C = \frac{(M_1 + M_2)(H_4 - H_3)}{\eta_3} \tag{10}$$

The work produced (W_P) must equal the work consumed (W_C), and so we have

$$E(H_1 - H_2) = \frac{(H_4 - H_3)(M_1 + M_2)}{M_1} \tag{11}$$

where E = combined efficiency $\eta_1 \eta_2 \eta_3$

Solving for the entrainment ratio $R_e = M_2/M_1$:

$$R_e = \frac{E(H_1 - H_2)}{(H_4 - H_3)} - 1 \tag{12}$$

Typical values of E are 0.75–0.80. Note that this is a mechanical efficiency calculated from the effectiveness of transfer of kinetic and compression energy, with the steam

discharged along with the process load as a gas. In the typical evacuation process, the steam is condensed and its latent heat wasted. The thermal efficiency of a steam-jet installation, therefore, is usually quite low.

Example. We wish to operate an evaporator at 165 kPa with condensing steam at 205 kPa. Saturated steam is available at 1,135 kPa for thermal recompression of the vapor. From the steam tables, the enthalpies in kJ kg^{-1} at the connection points are: $H_1 = 2,782$, $H_2 = 2,442$, $H_4 = 2,707$. Equation (12) also requires H_3 , which is the enthalpy at an internal point. Its estimation requires the use of the individual efficiencies described in the text. We assume $\eta_1 = 0.98$, $\eta_2 = 0.85$, and $\eta_3 = 0.95$.

H_2 is below the saturation enthalpy, and so there will be some condensation of the motive steam. First, we calculate $H_{2'}$:

$$H_1 - H_{2'} = \eta_1(H_1 - H_2) = 0.98(340) = 333.2$$

$$H_{2'} = 2,449$$

This corresponds to a steam quality of about 89%. This is the result of just the expansion of the motive steam. After it transfers momentum to the evaporator vapor, the enthalpy is lower and the quality correspondingly higher:

$$(1 - \eta_2)(H_1 - H_2) = (x_{2''} - x_{2'})\lambda = 51$$

where λ is the latent heat of vaporization ($2,220 \text{ kJ kg}^{-1}$) and $x_{2'}$ and $x_{2''}$ are the steam qualities before and after transfer of momentum. This process, therefore, raises the quality to about 91%. Isenthalpic mixing of the expanded steam with the process vapor once again increases the quality (barring entrainment of liquor from the evaporator). Since we do not yet know how much vapor is entrained by the steam, this new quantity, x_3 , requires trial-and-error calculation. Since our interest is in the method, we anticipate the result and write $x_3 = 0.95$. Applying this at the conditions of the nozzle, we have $H_3 = 2,588$. The mixture leaving the ejector has the enthalpy $H_4 = 2,707$. Now we can write

$$\begin{aligned} R_e &= E(H_1 - H_2)/(H_4 - H_3) - 1 \\ &= (0.98)(0.85)(0.95) \frac{(2,782 - 2,442)}{(2,707 - 2,588)} - 1 \\ &= 0.7913(340)/(119) - 1 = 1.26 \end{aligned}$$

Each weight of motive steam therefore entrains 1.26 weights of vapor. About 45% of the flow from the ejector nozzle is newly added steam. This number varies inversely with the enthalpy of the motive steam and directly with the compression ratio of the process vapor. The consumption of fresh steam is a fundamental limitation on the steam economy that can be achieved in thermal recompression.

The motive steam to a jet should be dry, with some superheat, and at a pressure suited to the rating of the jet. A pressure regulator in the steam line can produce some

superheat if any liquid droplets in the supply first are removed. Most jets operate in the range of 5–15 bars, but some are designed for high-pressure steam. It is most important to keep the steam dry, and designers should ensure that the lines approaching a jet are well insulated, always remembering that instrument connections can be small condensers.

When the process requires a high compression ratio, ejectors can be installed in series. The simplest arrangement for a multistage ejector system would simply feed the output of one stage to the next. The later stage therefore would have to educt the steam from the earlier stage along with the process load. In a multistage system, this can lead to large multiplication of steam flows. Once the absolute pressure is high enough to produce a dew point well above the cooling water temperature, it becomes economical to install interstage condensers. These remove condensable vapor and so reduce the load on subsequent stages. They also limit the carryover of solids and process liquids and can reduce the concentrations of corrosive substances in the vapor. An aftercondenser will have the same effects and will reduce the amount of steam exhausted to the atmosphere. We discuss types of condensers in the next section.

Steam jets operate off the kinetic energy of the motive steam and make little use of its heat content. Their thermal efficiency as a consequence is very low. As kinetic energy machines, however, their efficiency does not suffer from the large volumes of gas that must be moved when the pressure is low. At 50 torr, for example, the specific volume of saturated water vapor is about $25 \text{ m}^3 \text{ kg}^{-1}$. Displacement-type machines increase rapidly in size and begin to work very hard as suction pressure declines. Below about 10 torr, their thermal efficiencies begin to fall into the same region as those of steam jets [24]. Water-ring pumps in particular lose efficiency at deep vacuum, where the vapor pressure of the water becomes a significant fraction of the suction pressure. The comparative advantages of vacuum producers, therefore, shift with the design suction pressure. In a multistage system, this creates the opportunity to assemble a system more cost-effective than one based entirely on either pumps or jets.

Hybrid systems can combine the relatively high efficiency of steam jets at low pressure with the better performance of liquid-ring pumps at higher pressures. The steam jet(s) will be the first stage(s) in the system. After the vapor that is being exhausted has reached a sufficiently high pressure, a liquid-ring pump raises it to atmospheric pressure. Figure 12.11 shows the thermal efficiency of a hybrid system compared to those of steam jets on the one hand and a two-stage liquid-ring pump on the other. At high suction pressures, the hybrid arrangement is no more efficient than the liquid-ring system. At lower suction pressures, where the efficiency of the pump begins to fall off rapidly, the efficiency of the hybrid system declines much more slowly. In the example shown, at those suction pressures where liquid-ring pumps are not functional, the use of a pump as the final element gives a system more than three times as efficient as one based on steam-jet ejectors alone.

12.6.2. Vapor Condensers

Condensers may be indirect surface units or direct-contact barometric condensers. Surface units prevent contamination of the water used for cooling. This may be a decisive advantage when waste treatment of the cooling water is necessary. Barometric condensers usually are cheaper and are widely used in chlor-alkali applications. In a caustic

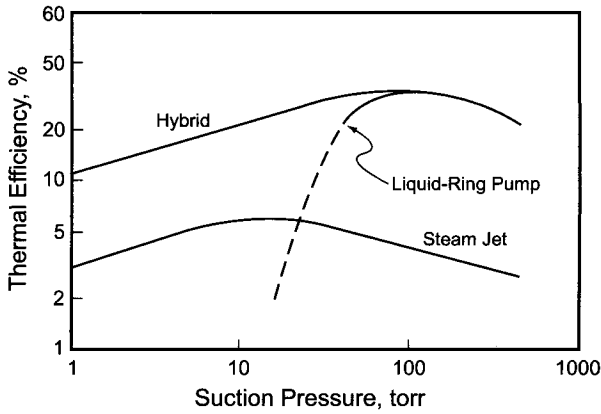


FIGURE 12.11. Relative efficiency of combination of jet and vacuum pump.

evaporator, for example, plant cooling water often is used as the cooling medium and then returned, along with water condensed in the process, to the sump of the cooling tower. With properly selected locations, this return can be by gravity. The condensed vapor becomes high-grade makeup water to the cooling tower.

An essential feature of a barometric condenser is its elevation. As Fig. 12.9 shows, the discharging water must be at atmospheric pressure at the point of overflow from the collecting vessel, or hot well. The tail pipe (or “barometric leg”) connecting the condenser and the hot well must provide enough static pressure to overcome the difference between the system pressure and the atmosphere.

The barometric condenser depicted in Fig. 12.9 is a countercurrent-flow unit. Some units operate in cocurrent flow. One of the advantages of the countercurrent arrangement is the closer approach that is possible between the temperature of the discharged water and its saturation temperature. In a well-designed unit, this can be as little as 2.5–3°C. The cooling water flow required is

$$W = \frac{Q}{t_s - t_w - t_a} \tag{13}$$

where

W = water flow, kg hr^{-1}

Q = heat duty, kcal hr^{-1}

t_s = saturation temperature of vapor, °C

t_w = inlet temperature of cooling water, °C

t_a = temperature approach, °C

Any of the common heat/mass-transfer devices can, in principle, be used to subdivide the water flow. Spray systems and baffle plates are most common.

Piping arrangements are very important [25]. Pressure drops must be very low because of the low absolute pressure on the gas side and the use of flashing gravity flow on the liquid side. Condensate piping between condensers and hotwells should have a

continuous slope of at least 45° and as few changes in direction as practicable. The tail pipe should be submerged at least 30 cm in the hotwell and should end at least 30 cm above the floor. In a very large system, the distance of the end of the tail pipe from the floor of the hotwell should also be more than half the diameter of the pipe. Vapor lines should be arranged to prevent accumulation of liquid. Because of the possible condensation of vapor, they should have no pockets, and their connections to condensers should prevent any backup of condensate or, in a direct-contact condenser, cooling water.

The height of the tail pipe should be comfortably above the equivalent height of a column of water at the highest atmospheric pressure that may be encountered. The recommendation of the Heat Exchange Institute is equivalent to about 102 mm kPa^{-1} . Finally, the size of the hotwell should conform to the length and diameter of the tail pipe, with a 50% margin in its volume. When condensate is removed by pumping from the hotwell, it should also meet the usual holdup requirements of a pump tank.

All references to water and condensate so far have assumed that they are removed at atmospheric pressure. It is also possible when desirable to remove them while still under some vacuum. This permits the use of a lower-level condenser but requires a pump of proper design for the service.

The pressure drop in vapor piping should be very low. What is considered a reasonable line loss in a pressurized system can be a substantial fraction of the absolute pressure needed at the source. Line velocities also should be limited. At typical dechlorination system pressures, a maximum of 45 m s^{-1} is desirable. With evaporators operating below 10 kPa, 55 m s^{-1} is more typical.

12.6.3. Process Control

The discussion of vacuum sources pointed out that most are well oversized for their duty. Most systems, therefore, have some form of pressure control. Control can be by throttling or, more often, by addition of a false load. Pressure control by suction throttling does not reduce the energy consumed by a jet or a liquid-ring pump with a given duty. Rather, by increasing the vacuum at the source it can increase the duty by allowing more air inleakage.

The false load added to provide control will be steam or air. The best choice for a steam-jet system is steam, which condenses in the interstage exchangers and adds very little to the loading on following stages. Air, on the other hand, passes through the system and carries uncondensed water with it. All this vapor becomes part of the load on the ejectors. The control steam can be supplied from the plant mains or, with less cost and somewhat lower effectiveness, it can recycle from the outlet of one of the jets. Air is a better choice for the false load on mechanical pumps, as it avoids any problem with condensation of water in the machinery. Liquid-ring pumps can accept either air or steam. The use of air adds less to the cooling load. In the case of brine dechlorination, however, added air accompanies the regenerated chlorine into its recovery process. When this process is liquefaction, the air reduces the efficiency of recovery, and so the use of steam is preferred.

With a liquid-ring pump, as with most mechanical systems, the most energy-efficient means of pressure control is a variable-speed drive on the pump. There is a

particular limitation in this case, however, because a certain minimum speed is necessary to keep the rotating ring of liquid intact. Another characteristic of the liquid-ring pump is that it requires a certain minimum load in order to avoid cavitation. It is not possible to run such a pump under shutoff conditions without a bleed line from the receiving vessel back to the pump casing.

An alternative already discussed for the dechlorination process is operation without pressure control (Section 7.5.9.2A). In situations where there is no harm in allowing the vacuum to go beyond that strictly required by the process, the excess capacity inherent in a vacuum producer may help a process by producing results better than design.

12.7. UTILITY PIPING AND CONNECTIONS

12.7.1. Utility Piping and Headers

Utility headers for the most part are carbon steel. Construction is conventional, and steam piping is probably the most specialized, its wall thickness and construction being functions of the pressure level. The sizes of the major headers give them great influence on the layout of pipe racks and equipment location. Sizing of utility headers differs from sizing of process lines in several ways:

1. Utility headers are more likely to be designed for later expansion, because
 - (a) increased demand may be caused by addition of new operations as well as by expansion of capacity
 - (b) modular expansions of production capacity usually are not accompanied by expansions of utility capacity in the vicinity of the process. Rather, the utility capacity is increased in the “utility area,” and the traffic in the main headers increases
 - (c) later duplication or replacement of utility headers is extremely disruptive as well as expensive. Pipe racks, unless designed for expansion, may lack both space and structural strength
2. The pressure drop per unit length of pipe is lower in utility headers, in order to keep the total system pressure drop low, because
 - (a) the value of the utility may decline along with its pressure (steam, e.g., loses some of its thermal potential when its pressure drops)
 - (b) available pressure drop through users should be reasonably constant throughout the plant
3. Utilities are more subject to variations in flow, and the maximum may be much greater than the average.
4. Certain utility water lines are subject to fouling.

Design of utility piping should consider pressure drop per unit length, total system pressure drop, and line velocity. Limiting the velocity reduces erosion and noise level. Because of item 2 above, design pressure losses tend to be quite low. Also, velocity is more likely to be the size-determining criterion in utility headers than it is in process lines. Steam velocities depend on quality and supply pressure. Typical design rates for superheated steam are from 35 up to 100 m s⁻¹. Saturated steam moves at 30–50 m s⁻¹.

Sonic velocity also is a consideration when steam is handled under vacuum, as in an evaporator. It depends on the specific heat ratio and the temperature. Using a typical value of the former, we have approximately

$$u_s = 24.4 T^{0.5} \quad (14)$$

where

u_s = sonic velocity in steam, m s^{-1}

T = temperature, K

Maximum superficial condensate velocities are about 25 m s^{-1} . In a given line, the velocity increases as the pressure drops and more liquid vaporizes. Vendors of steam traps and condensate systems can provide guidance and line-sizing charts. Water lines usually have velocities up to 3 m s^{-1} . The designer must consider water hammer as well as velocity and pressure drop. Selection of valves and their closure time becomes important. Compressed air usually is transported at $5\text{--}8 \text{ m s}^{-1}$.

12.7.2. Utility-Process Connections

When utility lines are connected to process lines or equipment, there is a danger of backflow of process material into the utility system and a danger of overpressurization of one system by the other. All connections of this kind require careful study during design and hazard analysis. Many plants review similar connections as a group and develop standard details. This standardization can include formal requirements for the number of layers of protection for each group.

The hazard to be avoided may be:

1. the process material itself (e.g., chlorine)
2. the immediate physical or chemical effects of mixing the two materials (sulfuric acid and water)
3. the especially severe consequences of contaminating the utility (potable water, breathing air, inert gas) or
4. the unsuspected presence of a utility in the wrong place (intermixing of nitrogen and certain air systems)

One way to promote reliability in the separation of two fluids is redundancy, and many of the arrangements used as utility-process connections include multiple devices. Reliability also increases with quality and with features designed to enhance the action of safety devices. An example of the latter is the use of internally force-loaded check valves (FLCVs) rather than the more conventional design.

The paragraphs that follow give some idea of the considerations that apply to certain utilities. A connection to a cell-room header may also require a length of nonconductive pipe to prevent stray voltages and currents in the utility system (Section 8.4.1).

12.7.2.1. *Potable Water.* Every plant must have a potable water supply, and many use some of that water in other applications. Small plants in particular may receive all their water from local municipal (potable) systems. It then becomes necessary to prevent the backup of water connected to process systems into the drinking water system.

There are many ways to accomplish this isolation. Combinations of check valves (FLCVs preferred) with regulators sometimes are used. These combinations must have sufficient redundancy and are better suited when the potential contaminant is not highly hazardous.

Another common isolating device is the conventional backflow preventer. Figure 12.12 shows one type. Two FLCVs provide the first level of protection, along the top of the diagram. In many water applications, this may be sufficient. As an example, consider the connection of a source of minimally treated water to a neutral brine system. While backflow is undesirable, it does not create a great hazard. In more exacting applications, as in any using potable water, the automatic dumping feature of Fig. 12.12 is added. With the normal pressure gradient from left to right, the force on both diaphragms pushes the slide to the left. This is the normal (closed) position of the valve. If the direction of the pressure gradient shifts, the force on the diaphragms now pushes to the right, and the dump valve opens.

A preferred system, which the process industries increasingly tend to use, provides a free fall or an air gap to achieve isolation. Figure 12.13 is the familiar break tank. As drawn, the water supply line does not enter the break tank. It should end at least two line diameters above the flood level of the receiver. The supply line can extend into the tank if a positive overflow is provided and the proper gap is maintained between supply and overflow. Good practice then also includes a break in the overflow pipe. The disadvantage of a break tank, especially the open type, is the loss of line head when the water is held under atmospheric pressure. This can be restored by elevating the break tank or by pumping the water from the break tank for distribution.

Some systems introduce the supply below the flood level of water in the receiver. Such a system should include a vacuum breaker mounted above the receiver to prevent siphoning back into the potable water supply.

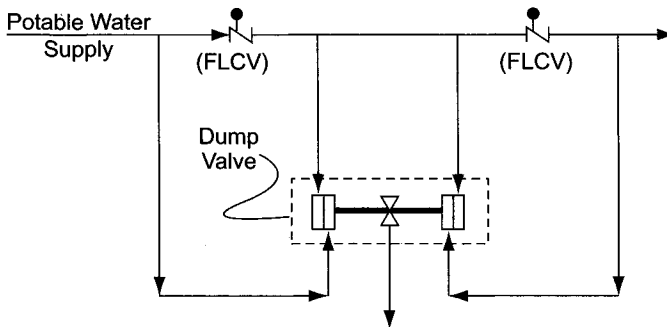


FIGURE 12.12. Typical backflow preventer.

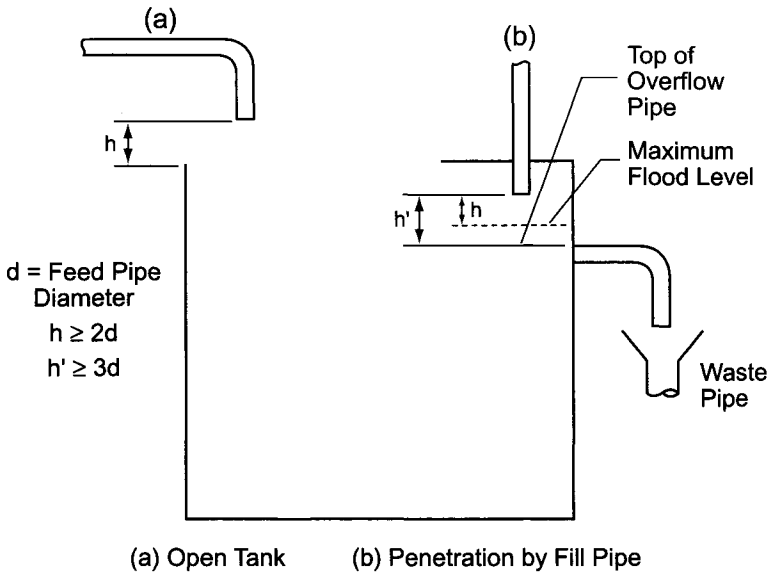


FIGURE 12.13. Potable water break tank.

12.7.2.2. Other Water. Lower grades of water require less stringent precautions. While any arrangement suitable for potable water can be used for other grades as well, simpler arrangements often are satisfactory. Multiple check valves without the automatic dumping feature of the backflow preventer were mentioned above. Manual disconnects (by way of flexible hose or pipe sleeve) are often used. They are most reliable when combined with a second level of protection, such as an FLCV on the process side of the break. Double-block-and-bleed systems are an alternative. Again, an FLCV (upstream of the bleed valve) improves the reliability.

12.7.2.3. Steam. Steam connections to process resemble ordinary water connections. Pressure usually is of more concern than contamination, and connections to process systems without adequate design pressures must include some form of pressure relief. When steam is used to purge or humidify a process system, cooling after shutdown also can produce a vacuum. Protection is then required directly on the process system.

12.7.2.4. Breathing Air. Breathing air is best not connected to the process or to a non-air utility system. It sometimes shares a compression system with another air system (e.g., instrument air). The separation between the two air systems then should be close to the source, for example, immediately after the receiving tank. Any connected lines should be fitted with check valves to prevent backflow into the common system. Design of an integrated system should include consideration of the possibility and effects of any other stream entering the breathing air system.

Pressure regulators should never be relied on as isolating devices. First, they do not always provide perfect shut-off. Second, if the pressure of the source falls below an already low downstream pressure, the regulator will remain open and allow massive backflow. A pressure regulator followed by a backpressure regulator will be more reliable.

12.7.2.5. Dry Air and Nitrogen. Dry air connections also require special attention. The dry air system exists to serve the dry chlorine end of the process, and so the problem of backflow of process material is always an important one. The connections should be chosen accordingly. In many locations, the design intent will be to have dry air enter part of the chlorine system whenever the pressure falls below a certain level. The natural approach then is to supply pressure regulators. These have the disadvantages already listed. A more secure approach is to use on-off control valves that close whenever the differential pressure across them reverses its direction.

Nitrogen may be used for the same purposes and with similar precautions. Whenever nitrogen is connected to an air system, its asphyxiation hazard requires review. If there is a possibility of infiltration into a breathing air system or release into a confined space, there must be adequate protection or abandonment of the plan to use nitrogen. An example sometimes overlooked is the use of nitrogen to back up an instrument air supply, with the possibility of use of nitrogen in a confined space behind a panel board, where there is always some amount of venting and leakage.

A similar technique, more common with air systems, is to automate the familiar double-block-and-bleed arrangement. The first step in this design might be to replace a simple check valve with a differential-pressure control valve that shuts when the pressure differential reverses. This affords two levels of protection, unless one assumes that the check valve is fundamentally untrustworthy and always allows some backleakage. Check valves can, of course, be made more reliable by proper installation and by extra measures such as force loading. An elaboration on the diagram above is to add a second valve in the line that closes when the differential pressure is too low or even negative. Finally, the space between the two in-line check valves can be vented for more positive protection.

Other elaborations might include the use of independent pressure switches rather than taking all control signals from a single transmitter. Figure 12.14 shows a typical automatic system. It also uses two block valves. The more secure arrangement has differential pressure measurement across each valve. When the pressure differential

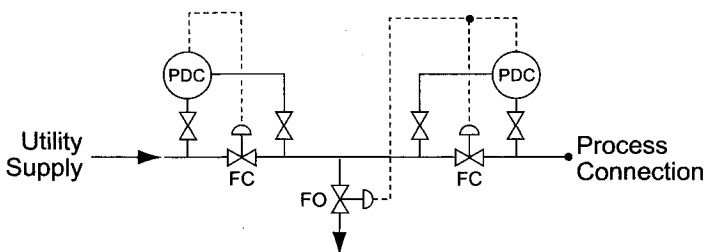


FIGURE 12.14. Automatic double-block-and-bleed system.

reverses or drops below a preset value, the valve closes and prevents flow of the utility. The downstream pressure controller also activates the bleed valve. Air failure closes the block valves and opens the bleed valve. A simpler arrangement, when the consequences of backflow are less severe, depends on a single differential pressure measurement across the assembly.

REFERENCES

1. R.L. Miron, Removal of Aqueous Oxygen by Chemical Means, *International Corrosion Forum*, Atlanta, GA (1979).
2. B.A. Garrett-Price and L.L. Fassbender, *Chem. Eng.* **94**(6), 51 (1987).
3. *Performance Envelope for Typical Steam Extraction-Condensing Turbines*, Bulletin H-37, Carrier Corp., Syracuse, NY (1973).
4. S. Siverns, C. Wilson, and J. d'Ailly, *Chem. Eng.* **107**(6), 64 (2000).
5. V.S. Frenkel, *Chem. Eng.* **109**(7), 54 (2002).
6. T.V. Arden and R.D. Forrest, *The Chemical Engineer* **1978**, 919 (1978).
7. Technical Information Bulletin, www.tramfloc.com/tf30, Tramfloc, Inc., Tempe, AZ (2004).
8. R. Burger, *Chem. Eng.* **100**(5), 100 (1993).
9. *Legionellosis Position Statement*, Cooling Tower Institute, Houston, TX (1996).
10. *Communicable Disease Management Protocol—Legionellosis*, Manitoba Public Health Department, Winnipeg (2001).
11. J. Hensley, *Chem. Eng.* **99**(2), 74 (1992).
12. Anon., *Chem. Eng.* **109**(1), 35 (2002).
13. R. Parkinson, *Properties and Applications of Electroless Nickel*. Technical paper 10081, Nickel Development Institute, Toronto (1997).
14. K.A. Stanley, Phased Conversion of a Diaphragm Plant to Membrane Technology. In S. Sealey (ed.), *Modern Chlor-Alkali Technology*, vol. 7, Royal Society of Chemistry, Cambridge (1998), p. 145.
15. M.R. Godfrey, *Chem. Eng.* **108**(10), 82 (2001).
16. K. Mangnall, *A Technical Guide to Vacuum and Pressure Producing Equipment*, Hick Hargreaves and Co. Ltd., Bolton, UK (1971), p. 110.
17. D. Hairston, *Chem. Eng.* **108**(8), 37 (2001).
18. K. Mangnall, *A Technical Guide to Vacuum and Pressure Producing Equipment*, Hick Hargreaves and Co. Ltd., Bolton, UK (1971), p. 23.
19. H.J. Sandler and E.T. Luckiewicz, *Practical Process Engineering, A Working Approach to Plant Design*, McGraw-Hill Book Co., New York (1987).
20. J. Aglitz, R.K. Bhatnagar, D.E. Bolt, and T.L. Butzbach, *Chem. Eng.* **102**(11), 132 (1995).
21. D.B. Birgenheier, T.L. Butzbach, D.E. Bolt, R.K. Bhatnagar, R.E. Ojala, and J. Aglitz, *Chem. Eng.* **102**(7), 116 (1995).
22. S.W. Croll III, *Chem. Eng.* **105**(4), 108 (1998).
23. D.Q. Kern, *Process Heat Transfer*, McGraw-Hill Book Co., New York (1950), pp. 442 *et seq.*
24. J. Ryans and D. Roper, *Process Vacuum System Design and Operation*, McGraw-Hill Book Co., New York (1986).
25. L.E. Wetzel, *Chem. Eng.* **103**(11), 104 (1996).

13

Plant Commissioning and Operation

13.1. INTRODUCTION

Commissioning is the activity whereby the installed hardware of a new plant is transformed into an operational facility. Most works on industrial chemical technology ignore the subject. However, it is an extremely important topic, and the successful startup and subsequent operation of a new plant are critically dependent on the approach taken toward its commissioning.

The commissioning and operating manuals for a chlor-alkali plant in combination with associated documents will be much thicker than these combined volumes. Only a brief discussion of the subject therefore is appropriate here. Commissioning will concern itself with every piece of equipment in the plant. Here, we will not attempt to cover minor equipment such as pumps or even major systems such as chlorine compressors and liquefaction machinery. Not a great deal concerning these items is unique to chlor-alkali plants, and there already is a substantial literature on their construction, installation, operation, and maintenance. This chapter therefore is restricted to guidelines for a commissioning approach and organization (Sections 13.2–13.4); a sequence for precommissioning, commissioning, and starting up the major systems in the plant (Sections 13.5 and 13.6); and a more detailed discussion of cell room matters (Section 13.7). The discussion is in terms of a new membrane-cell plant. Section 13.8 then discusses normal operation. This concentrates on the cell room and particularly on the necessary procedures for changing the operating load on the cells. Other subjects treated here include plant performance testing (Section 13.9), technical standards or operating specifications (Section 13.10), and performance monitoring and analytical programs (Section 13.11). Because of the unique problems that it presents, the chapter ends with a discussion of the decommissioning of mercury-cell plants (Section 13.12).

Key aspects to be highlighted are:

1. *Experienced personnel*

Because of the hazardous nature of the process and its very exacting requirements, commissioning personnel with appropriate operating experience are essential in key

areas. In those areas of the plant that handle liquid chlorine and in the cell room, where the membrane process is very sensitive to improper operation; the consequences of errors and upsets are significant delays and loss of profits.

2. *Systematic approach*

The plant should be divided into process systems, and the responsibilities for these systems should be individually assigned. Detailed consideration should be given to all precommissioning, commissioning, and operating requirements for these systems.

3. *Planning*

Consideration of the requirements for commissioning of plant equipment should begin at the outset of detailed design. It is useful to have engineering personnel with commissioning and chlor-alkali operating experience on the design team. They can ensure that proper provision is made for system commissioning. Construction planning must consider the requirements of commissioning and set priorities for services and the sequence in which systems will be commissioned. Detailed planning of all activities to be undertaken during commissioning is essential to a trouble-free startup.

4. *Operator training*

Among the prime responsibilities of the commissioning group are the compilation of operating instructions and the training of operators who will be able to operate the plant safely and competently. Depending on the type of contract, the responsibility for plant commissioning may lie with the owner/operator or with the principal contractor. In a turnkey arrangement, responsibility rests entirely with the contractor, who will furnish experienced personnel and manage this activity. At the other extreme, an operating organization with extensive experience may choose to manage commissioning directly, perhaps drawing upon the services of contractor and vendor specialists. The latter approach is more likely when a new plant is installed within an existing site (e.g., a conversion project). It then becomes important to define clearly the contractual and technical responsibilities early in project planning.

13.2. COMMISSIONING ORGANIZATION AND PLANNING

13.2.1. *Systems Approach and Personnel*

It is desirable to appoint a commissioning manager at an early stage in a project so that the manager can become fully acquainted with plant design and operational philosophy. A commissioning manager may typically be a process engineer involved in the basic design of the plant, a chlorine plant manager, or someone contracted in with experience in commissioning and operation of chlor-alkali plants.

The commissioning manager will be supported by a team of engineers who will be allocated responsibility for their own areas or systems within the plant. It is expected that people recruited for these positions will already have experience of commissioning and operating the types of equipment in their areas. The number of such engineers required for a plant incorporating liquefaction would typically be three. Most frequently, an instrument engineer will also be required.

It is convenient to divide the plant into a number of systems, with responsibility for each assigned to a particular commissioning engineer. This split generally follows the process fluids, and systems typically are:

- brine circuit,
- catholyte loop,
- caustic evaporation,
- chlorine processing,
- chlorine liquefaction,
- chlorine absorption/hypochlorite manufacture,
- hydrogen processing,
- hydrochloric acid manufacture,
- various utility systems.

In addition to the core team, extra shift coverage will be necessary in the periods immediately before and after startup. Specialists will often be brought in from proprietary equipment manufacturers to assist and advise technically on the commissioning of their items of supply. Such items may include:

- brine filters,
- brine ion exchangers,
- electrolyzers,
- caustic evaporators,
- hydrochloric acid burners,
- transformer-rectifiers,
- refrigeration units,
- chlorine compressors,
- distributed control systems.

Operator involvement should begin as soon as systems are mechanically complete and are handed over for commissioning. Not only is this a good time to learn and to acquire hands-on experience, but the operators also will be performing useful work under the direction of the commissioning engineers.

The laboratory staff also should support the commissioning effort. The demands upon analytical facilities will begin with the first introduction of chemicals to the plant. Laboratory personnel can then begin to become familiar with systems and techniques. The early establishment of routines, particularly on the brine system, is recommended.

13.2.2. Planning

A high-level commissioning plan for the entire plant should be drawn up, recognizing the order in which the systems should be commissioned and the services required by each system. It should specifically recognize those services that are needed for precommissioning and that should therefore be made available early. This plan should blend with the construction plan and determine the time line for commissioning and startup activities. It is the authors' experience that too often, inadequate planning leads to a failure to recognize the need to provide sufficient time for commissioning. Projects then fall

seriously behind schedule. This is particularly the case with modern plants provided with complex instrumentation and control.

At a lower level of detail, there will be a plan for each system and each individual item. These plans will map the sequence of commissioning and set out the requirements for bringing individual systems on stream, leading up to energizing the cells, bringing output up to full rate, and demonstrating design performance. The detailed plans should include all necessary activities, which may include among others:

- flushing and cleaning,
- inspection of vessel internals,
- pressure testing,
- punch listing,
- commissioning on air and water,
- drying,
- installation and testing of process instrumentation,
- testing and tuning of control loops,
- verification of trips and interlocks,
- requirements for vendor specialists,
- introduction of process fluids,
- initial startup,
- commissioning trials,
- performance testing.

Appointment of a commissioning planner to coordinate activities across the plant and to revise the master plan in light of the latest developments can be beneficial in large projects. The updated commissioning plan becomes the primary vehicle facilitating the commissioning manager's regular planning/progress meetings.

It is a good idea to develop checklists for the various categories of equipment and systems. These serve as control documents and, when a plant is built by a contracting firm, as forms for indicating acceptance of the various items. Thus, forms might exist for the various types of equipment, instruments, instrument panels, control hardware, civil works, structures, electrical systems, motor control centers, utilities, lighting, etc. Figure 13.1 gives a particular example created for storage tanks.

Commissioning activities offer many opportunities to collect data that will be useful later on. These data include such things as tank level calibrations, pump output pressures, pressure drops through lines and equipment, exchanger capacities, rotating equipment stability and runout, and actual utility conditions. Part of the value of this information is in the diagnosis of future operating problems. There should be specific plans in the commissioning program to acquire such data.

13.3. TRAINING

Effective training of supervisory, operating, and maintenance personnel is crucial for a smooth startup and successful on-going operation. This section covers the approach to training for a new plant in which operator experience may be limited.

Prefabricated Storage Tank Checkout

Tank Number _____ Location _____

Use _____

Manufacturer _____

Mfr's Serial Number _____

Mfr's Drawing Nos. _____

Appurtenances:

	Y/N	File #
Jacket		
Coil		
Relief device		
Insulation		
Lining		

Inspection results:

	OK	NO	N/A
General condition			
Paint/primer			
Cleanliness			
Orientation			
Leveled?			
Calibrated?			
Foundation			
Grounding			
Fire protection			
Welds			

Settlement Test Data:

Date _____

Time start/end _____

Temperature _____

Medium: Water _____

Other _____

Height _____

Test liquid _____

Overflow conn. _____

Settlement readings _____

Start _____

_____ % full _____

End _____

Instrument list: _____

Notes: _____

Comments on operation of level instrument:

The form usually has a signature block for responsible parties belonging to the manufacturer or contractor, the plant owner, and statutory authority where appropriate.

FIGURE 13.1. Sample of equipment checklist form.

Several different types of training, held in different venues, are useful. They include classroom instruction, observation of similar plants, and on-the-job training. The last of these is particularly useful for individuals or small groups being brought into an existing operation. On-the-job training also is useful, and indeed essential, in a new plant under the control of an entirely new group of operators. While startup offers opportunities for training, however, the functions are separate and should not be confused. Training

during startup and operation confirms in the most practical way what an individual has learned in earlier stages. It should never be used to justify less than complete coverage in classroom sessions.

The content and emphasis of a training program must reflect the project in question. The proceedings of one Chlorine Institute Plant Managers Seminar documents the methods used in several widely different projects [1–4]:

- expansion of diaphragm-cell plant
- expansion of membrane-cell plant, with derivatives and cogeneration
- training of new shift supervisors for existing mercury-cell plant
- chlorine packaging plant

Training programs and methods also must suit the personnel being trained. Several different groups may be identified [5]:

- managers and technical personnel
- health and safety professionals
- supervisors
- operators
- analytical staff
- maintenance personnel and skilled craftsmen
- emergency personnel
- contractors

The extent and content of training also will vary. Operators and their direct supervisors, for example, require the most extensive and specific training. While they must first have a good understanding of site programs and procedures, their specific training should concentrate on the chlor-alkali facility itself. Some of the content of a training program might be:

- process documentation (manuals, drawings, etc.)
- unit operations
- reactions
- control systems
- raw and auxiliary materials
- effluents and wastes
- equipment
- instrumentation
- safety devices
- operating procedures
- critical operating parameters
- emergency procedures
- personal safety equipment
- evacuation

Among the duties of managers and supervisory personnel are such functions as establishing methods, instructing workers, assigning tasks, maintaining process equipment, maintaining safety equipment and supplies, and direct supervision. While they

should have a broad and fundamental knowledge of the subjects covered in operator training, they should also be trained intensively in the following areas [6]:

- communication skills
- safety inspections
- accident investigation
- permit systems
- fire and electrical safety
- materials handling
- machine safeguarding
- personnel training

Certain people require more intensive training on utility or environmental systems. Besides suiting an individual's needs, training programs should:

- allow adequate time
- balance class work and hands-on training*
- provide feedback from students
- measure effectiveness of the training

Safety is always an important part of job training and especially so in a chlor-alkali plant. Trainees should be encouraged to pay close attention to the safety aspects of design and operation. One method recommended by King [7] is the use of job safety analysis (JSA). This is a formalized procedure in which analysts list the sequence of basic steps involved in a given task, consider the potential accidents that can occur, and then develop strategies and techniques of prevention. The National Safety Council of the United States [8] has developed standardized forms for JSA.

13.4. DOCUMENTATION

Required documentation is most efficiently collected in a series of manuals:

- a Plant Operating Manual
- a Plant Maintenance Manual
- an Analytical Manual

This section addresses the content of these manuals.

13.4.1. Operating Manual

An operating manual should include at least the following material [9]:

General description

Chemistry (including electrochemistry)

Raw materials, intermediates, products

Raw materials and product specifications

*Process simulators are sometimes used and can be classified as hybrids.

Battery limit conditions

Basis of design

Material balances

Operating conditions and controls

Characteristics of reactions

General nature of controls

Process variables and their effects

Technical standards (standard operating parameters)

Effects of deviations

Emergency equipment

Safety valves and rupture discs

Valve failure positions

Alarms

Trips

Monitoring systems

Protective systems

Safety circuits and logic

Personal protective equipment

Maintenance of equipment and systems

Plant operation

Commissioning instructions

First startup

Normal startups

Normal operation

Emergency operation and shutdown

Normal shutdowns

Sample log sheets

Analytical methods (list only; subject of a separate manual)

Analytical schedule

Cell handling

Assembly

Disassembly and renewal

Handling and storage of components

Transportation

Safety information

Material safety data sheets

Process safety instructions

Safety instrumentation and monitoring systems

Medical surveillance

First aid

Use and maintenance of personal protective equipment

Administrative controls

Drawings

Plot plans

General arrangements (as appropriate)

Process flow diagrams

Engineering flow diagrams (with line lists)
Instrument loop drawings
Control system functions
Interlock and trip logic diagrams
Equipment drawings/catalog cuts

Data sheets

Equipment
Instruments
Material hazards

The operating manual should also address the precommissioning and commissioning activities treated throughout this chapter. The operating manual or a separate protocol should address the procedures and methods of measurement that apply to any test run.

13.4.2. Maintenance Manual

Maintenance information should be compiled and collated for all plant equipment. This “manual” may, in fact, be a sizable collection of books. Vendors will provide specifications and maintenance requirements for equipment of their supply. There may be specific manuals for complex equipment (e.g., electrolyzers).

There should be specific written procedures for routine maintenance of process equipment and instruments. There should also be specific written instructions for isolation (piping and electrical) and decontamination of process equipment before maintenance, with particular consideration to procedures for vessel entry.

13.4.3. Analytical Manual

The analytical requirements of a chlor-alkali plant are extensive and include:

- process control—brine circuit/catholyte circuit/caustic evaporation/chlorine drying/compression and liquefaction/HCl
- operational safety—hydrogen in cell room chlorine and liquefier tail gas/moisture in dry and liquid chlorine/ NCl_3
- incoming raw materials and reagents—salt/water/ H_2SO_4 /HCl/brine treatment chemicals/reducing agents
- product quality assurance—chlorine/NaOH/KOH/HCl/hypo/others
- brine purity—see Section 13.10.4.1
- electrolyzer operational efficiency—oxygen in chlorine/chlorate and hypo in depleted brine
- effluent control

Sampling techniques should be part of the description of each analysis. Procedures should cover all relevant impurities and all important streams. Section 13.11.2 gives a detailed list of analyses and a recommended schedule. The analytical schedule should be documented in both the Operating Manual and the Analytical Manual.

13.5. GENERAL PRECOMMISSIONING

The purpose of precommissioning is to verify that all equipment is installed correctly and according to design specifications before operation or introduction of chemicals. This activity involves detailed checking of systems for completeness, compliance with mechanical flow diagrams and detailed design drawings, flushing and cleaning, pressure testing, and mechanical checks (e.g., direction of shaft rotation). Precommissioning is the time to check and test all temporary lines and tie-ins to existing systems.

This section covers some of the general aspects of precommissioning. The following section, on commissioning proper, covers the different areas of a plant individually. Some of the activities described there can properly be considered precommissioning, but this arrangement seems to give a more logical organization of the material.

A complete checklist will be of great benefit during precommissioning. This list should be developed specifically for each project. API 700, Checklist for Plant Completion, offers general guidance.

13.5.1. Flushing and Cleaning

At this stage, sensitive instruments and control valves may be absent from the system, in order to prevent damage from any debris flushed through pipework, and replaced by temporary spool pieces. Strainers should be fitted to the suction lines of pumps and certain compressors. Orifice plates should be omitted.

For initial flushing of tanks and mains to remove contamination and construction debris, an adequate supply of process water should be available. Its quality should be checked to ensure that no unacceptable contaminants are left in the system. Tanks may be washed out with hoses and then inspected through access manways.

Liquor piping should be flushed through with water, using hoses attached to appropriate flange connections. Air, nitrogen, steam, and water systems may be blown through with service fluids.

Gas header systems that are too large to fill with water should be carefully inspected visually and washed with hoses as appropriate. Smaller systems can be flushed in the normal manner if supports and structures are strong enough for the added weight of the water. Preparation of liquid chlorine piping is largely a matter of good practice as covered in Section 13.6.5, but there also are special considerations pertaining to the reactivity of chlorine and the need to dry all piping and components thoroughly [10]. Internal cleaning should be thorough and should remove all grease, scale, and rust—all of which will react with chlorine. Chemical cleaning should follow hydraulic testing but precede pneumatic testing. Inhibited acids sometimes are used to remove scale. Many prefer phosphoric acid to HCl because it is less likely to attack the metal. Materials such as hydrocarbons and lower alcohols are explosion hazards when in contact with chlorine and so are not to be used. In any event, all traces of cleaning agents should be removed. Chemical cleaning sometimes takes place in the fabricator's shop before delivery. In this case, the supplier should certify that the product contains nothing that can react with chlorine. All due safety precautions are necessary in these operations.

After erection, pressure testing (Section 13.5.2), and inspection, all chlorine piping must be thoroughly dried and kept dry. The usual procedure is to purge the piping with

dry, oil-free air or nitrogen until the dew point of the exhaust is below -40°C . Because a gas purge may not affect dead legs, applying a full vacuum for 12–24 hr may be more effective than a gas purge in removing moisture from cavities in valves and fittings. The dry system should then be brought to a slight positive pressure with dry gas and sealed off by valves and, where appropriate, blank flanges.

Spare valves and fittings must also be dry and free of reactive materials. While in storage, they should be tagged as ready for chlorine service and kept tightly sealed in impermeable plastic bags. Processing equipment for dry chlorine service must be equally clean and dry. Cleaning of equipment with complex internals may be more difficult than cleaning of straightforward pipe work. The trend toward use of aqueous cleaning agents rather than chlorinated organics complicates the task even more. Removal of organic materials is slower, and drying after cleaning is more difficult. Section 13.6.5.2 points out that the reaction of chlorine with residual materials after inadequate cleaning with aqueous systems can create a hazard.

13.5.2. Pressure Testing

The manufacturer usually sees to the testing of shop-fabricated vessels and pipework in accordance with vessel and piping design specifications. The owner's inspectors often witness these tests, which may be those required for Code certification. Further testing on site will verify that joints are leak-tight, and it is particularly valuable on systems that handle hazardous materials. Testing of site-fabricated pipework is done in place in accordance with the piping specification.

Site pressure testing may be by liquid, usually water (hydrostatic testing), or by gas, typically air, nitrogen, or steam (pneumatic testing). Hydrostatic testing is safer than pneumatic testing, because escape of the compressed test gas releases a large amount of compression energy (P - V work). Gas that is released suddenly is a hazard in itself. In addition, it may be accompanied by flying shrapnel.

Hydrostatic testing is carried out at pressures above system design pressures; pneumatic testing often is restricted to lower values. Under certain circumstances, however, hydrostatic testing may be unacceptable for technical reasons. These include:

- design and construction of the piping system making it impracticable to fill it with liquid (e.g., hydrogen and chlorine headers);
- residual test liquid cannot be sufficiently removed to avoid corrosion or hazardous interaction with process materials (e.g., electrolyzers, dry chlorine systems).

Pressure testing is a construction responsibility. It should conform to piping or equipment specifications, and the owner's or contractor's responsible engineer should witness it. The following items require special consideration before a pressure test:

- expansion bellows, which must be restrained or temporarily removed;
- pressure relief devices and pressure reducing valves, which should be removed, blocked off by slip plates, or replaced with spools;
- in-line items whose maximum cold-test pressure is less than that specified for the piping system;
- positions of control valves;

- non-return (check) valves, which must be removed and replaced by spools or have their internals removed;
- all valves other than drains and vents open;
- rotating equipment out of the test system;
- all joints visible and not covered (e.g., by insulation);
- brittle components, such as those made of glass, fully shielded or excluded from test;
- large tanks and vessels disconnected or isolated by blinds marked with visible tags.

13.5.2.1. Pneumatic Testing. In preparation for a pneumatic test, items which may be brittle (e.g., cast-iron valves) should be removed or fully shielded. Pressure then can be applied to the piping system under test and increased gradually to not more than 15% of the specified test pressure or 1.7 bar(g), whichever is less. After the first inspection for leaks, the pressure can be increased in increments of about 10% of the specified test pressure until that pressure is reached. Plastic systems are more likely to expand under pressure. Therefore, rates of pressure increase should be slower, and proof times under pressure should be longer.

No one should approach the system for close inspection or for the application of bubble-forming test solution until the pressure has been positively reduced. A 30-min test time after a pressure reduction of 20% for inspection is satisfactory in most cases. It is especially important with pneumatic testing that the work area is isolated, that no other work is performed in the area, and that only those involved in the test work are present in the area.

13.5.2.2. Hydrostatic Testing. In preparation for a hydrostatic test, the following should also be considered:

- Risk of freezing: If there is such a risk, the water temperature should be above 7°C.
- Provision of rigid support for piping normally held by springs or counterweights: This is to avoid damage due to the load imposed by the test fluid. The setting pins must not be removed from spring hangers before completion of testing and draining of the test fluid.

Process fluids may be used for hydrostatic testing in some special cases, but water is the almost universal choice. The quality of the water is an important consideration. Residues from hydrostatic testing often lead to corrosion. Chloride ions in the water are frequently a problem in apparatus or piping that is vulnerable to stress corrosion. Scrupulous removal of test water may be important for this reason or may be necessary because of interactions of water or rusted surfaces with process fluids.

A low-pressure pneumatic test often precedes hydrostatic testing as a quick and simple way to identify bad connections. The system then chosen for testing should be as large as is convenient and practicable. Some gas-processing lines and equipment may require additional support during hydrostatic testing. It is important to have the system liquid-full, and so the addition of water should be from a low point. Filling should be

at a reasonable speed, with careful venting from the high point of the system. Once a system is full, pressure can be increased in defined stages or at a steady rate. A typical program might include first inspection at 50% of the final test pressure, followed by increases in 10% increments. Again, the pressure should be reduced from the test level before starting inspection. The commissioning protocol should define the procedure for each system or item in the plant. High-quality pressure gauges of known accuracy are recommended.

The test pressure should be held for the time set out in the commissioning plan (typically 30 min) but should never be exceeded. If a leak is found, the pressure should be dropped before undertaking work to correct it. Test water normally is drained to waste; vacuum relief while draining is then essential. No repair work should be done on a system that contains process fluids.

13.5.3. *Punch Lists*

A “punch list” is a document whose purpose is to identify all instances of nonconformance to specifications or good practice for correction by the construction team. After installation of a system, it is necessary to check it for completeness and compliance with all design documentation. The approach should be methodical. Systems may be broken down into smaller units following line references and equipment item numbers. The relevant commissioning engineer should be familiar with all drawings and specifications pertaining to the part of the plant to be punch-listed. All lines should be walked and all pipes, instruments, and equipment items inspected visually.

The punch-listing process should be carried out in two stages. First, the preliminary list follows installation of equipment and pipework. Some instrumentation may still have to be installed. The final list follows completion of flushing, cleaning, pressure testing, and installation of all instruments. The following list is not exhaustive but shows some of the items that must be checked in a chlor-alkali plant.

Materials of construction

Gaskets (including absence of temporary flat-faced gaskets)

Critical elevations

Provision of condensate drains to avoid liquor locking

Provision of vents to avoid gas locking

Blanks fitted as appropriate

Pipe supports

Valves installed with correct flow direction

Correct valve types

Access to valves and field instruments

Line slopes

Adequate slope and lack of pockets in gravity-flow and free-draining lines

Proper make-up of joints

Correct installation of bellows

Orifice plate orientation

Fitting and connection of grounding electrodes

Thermowell installation in liquor spaces in two-phase lines

Provision of insulation for personnel protection
Orientation of gas pressure tapping lines to avoid condensate locking—including ΔP flow measurement devices and upper connections of level measurement devices
Lute depths
Sample point access and drainage
Lagging
Proper direction of rotation of all drives
Inclusion of temporary startup strainers
Free movement of pipe guides

The punch list should in the end discriminate between those items requiring immediate correction and those that can be taken care of after startup. The commissioning engineer should rely on his own judgment and experience as well as on design documentation to identify and highlight any potential problems found during the punch-listing process. Where significant issues arise, it is appropriate to refer them back to the design team for assistance in resolution.

13.5.4. Control Systems and Equipment Packages

The use of vendor-engineered equipment packages is a common and growing practice. It allows the contractor and plant owner to take full advantage of the expertise of firms who are particularly adept in their specialties. While some details may be beyond the absolute control of the contractor or owner, specifications for all packages should include a requirement for thorough documentation of the necessary precommissioning and commissioning activities. Packaged items often found in chlor-alkali plants include some utility systems, brine clarification systems, various types of filter, ion-exchange systems, electrolyzers, compressors, refrigeration systems for liquefaction and dedicated utilities, tail-gas handling systems (e.g., HCl synthesizers), evaporators, centrifuges, and distributed control systems. While the use of packages distributes the project engineering work among more hands, the amount of coordination that it adds to the project makes this approach of debatable cost or scheduling advantage.

Forcing all aspects of the package system design to conform to the general project criteria can be counterproductive. It foregoes many of the advantages that this approach offers. The opposite approach, in which the vendor has a totally free hand, may be attractive in a naive approach to scheduling but has its own problems. Experienced commissioning managers can attest that this can result in too much time and attention spent on debugging these units. Given the dynamics of project schedules, this always occurs when time is shortest and commissioning personnel are busiest. The best way to avoid this is to see that each unit is thoroughly checked at the factory before shipment. This is an imposition on the vendor, and so it should be emphasized in the bid documents. The final contract or purchase order should therefore contain a clear description of agreed test requirements.

It is also true that in assembling a competitive bid, a vendor may not invest in materials equal in quality to the buyer's real desires. Bid documents should therefore spell out any special requirements. Examples would include the use of certain grades of material, the identification of preferred vendors for instrumentation and control valves, and the banning of certain types of valve. Failure to cover such items in bid documents or purchase orders has caused the need to re-engineer a number of packaged units.

The control system is a good example of a package that will benefit from shop testing. Ideally, all functions should be thoroughly tested and their design calculations reviewed where appropriate. The list of functions includes displays, control actions, interlocks, alarms, shutdowns, etc. Everything that can be checked is checked using simulated signals. This precommissioning work, when completed as early as possible, leaves time for corrections and changes in a more relaxed environment. The only checking required after delivery to the field is the proper connection of the control system to the field instruments. The sources of shutdown signals must be checked for proper function as well as correct wiring (Section 13.6.2).

Packaged units have traditionally had their own programmable logic controllers (PLCs) and local control panels. This is especially true in the case of units that require extensive sequence controls for stepwise processes such as filtration and ion exchange. Many operators find it more convenient to have control supervised from a central station. From this point of view, these systems are better controlled by a distributed control system (DCS) and monitored from the control room. Some who bought systems equipped with PLCs some years ago have dispensed with the PLCs and moved control to the DCS. Many favor systems which combine local control by PLC with status and alarm signals sent to the DCS.

It is especially important to test equipment thoroughly at the factory when it is to be shipped to a remote location or into a part of the world where sophisticated help is not readily available.

13.6. SYSTEM COMMISSIONING

System commissioning begins after the completion of precommissioning work on the process and electrical systems. The boundary between precommissioning and commissioning is somewhat fluid, and normally some systems will be in the commissioning phase while others are still being precommissioned. In certain cases, there will be contractual definition of the work in each activity and a need for formal acceptance of systems as ready for commissioning.

Before startup of the electrolyzers, the process systems relating to the supply of electrolyzer feed streams (feed brine, caustic, acid, demineralized water) and to the product streams (depleted brine, product caustic, chlorine, hydrogen) must be commissioned and brought up to operational status:

1. the brine system will be fully commissioned in all respects, perhaps with the exception that the depleted brine system may not have had to deal with brine containing dissolved chlorine
2. the caustic system, including demineralized water addition, will be fully commissioned in all respects
3. the hydrogen system will have been tested and will be operational with, at minimum, the capability to vent under control, using nitrogen
4. the chlorine system will have been tested and will be operational with good pressure control, using air or nitrogen—in some cases, chlorine gas may already be available at site, allowing downstream units such as compression and liquefaction to be tested with chlorine itself

In general, this chapter describes the commissioning of a plant with brine resaturation, brine treatment, chlorine processing, and caustic evaporation. Direct operator involvement should begin at the start of the commissioning. This approach provides a good opportunity to learn and acquire hands-on experience with systems operating with water and air. The operators should carry out most of the work under direction of the commissioning engineers.

13.6.1. Commissioning Procedures

The responsible engineers should prepare detailed commissioning procedures for the individual plant systems, such as those listed in Section 13.2.1. This preparation will draw upon operating manual information as detailed above, vendor procedures, and the experience of the commissioning engineer.

These procedures should include all necessary flushing, cleaning, inspections, and tests before introduction of chemicals, resins, or packing. They should consider and detail how chemicals will be introduced into the process and the subsequent operations required to bring the system up to operational capability. Careful consideration should be given as to how all control loops will be set up and tuned, on-line process and analytical instrumentation tested and calibrated, and alarm trips and interlocks verified.

Provision should be made for testing applicable systems, wherever practicable, up to their maximum demands before cell room energization.

The subsections that follow give the outline of an approach to the commissioning of a typical membrane-cell plant with brine resaturation, primary brine treatment, secondary brine treatment, chlorine treatment, and caustic evaporation.

13.6.2. General Notes on Commissioning of Instrumentation

A group at the plant site should be responsible for the field calibration of all instruments prior to their installation. It logically is led by the responsible instrument engineer and may be organized according to plant area or may be a dedicated group responsible for all instrumentation. The group will have several objectives:

1. assuming and maintaining control of all control hardware to prevent loss or damage
2. assuring that all required material has been delivered and meets specifications
3. demonstrating that all instruments work properly and are calibrated correctly
4. checking and testing field wiring for continuity and correct installation
5. checking that the performance of cell room instruments is unlikely to be adversely affected by magnetic fields

All work on the instruments and control valves in the early stage takes place on the bench. It should be scheduled early enough to allow time for replacement of faulty items.

A number of general points relate to field testing of instrumentation for chlor-alkali plant process systems:

1. Every valve should be stroke-checked in the field from the controller or distributed control system to ensure that it is wired correctly, that its positioner is ranged correctly, that its action is smooth, and that valve action is in the correct direction (remembering that some valves are reverse-acting).
2. Valves with position sensors should be checked in the field to ensure that their indication is working correctly.
3. While temperature transmitters are checked and calibrated, sensors may not be checked directly. The operation of some, notably those on the outlets of the electrolyzers, cannot be verified by liquor circulation before startup. A common assumption is that thermocouples (T/Cs) and resistance temperature devices (RTDs) work correctly. If desired, they can be checked by a hot box, if one is available, or by immersion in a flask of hot water or other appropriate fluid. A "hot box" is a dry-heated temperature-controlled block with drilled holes to accept RTD or T/C sensors. No further calibration of the instrument is necessary after installation, and the DCS indication should be checked against a thermometer of known accuracy.
4. A key element in checking a level installation is good documentation of the calibration calculations. This will also include a dimensioned sketch of the vessel with nozzle heights and transmitter locations, showing any purges. Very often, nothing more can be checked until the actual process fluid is in the vessel. Tank level calibrations otherwise can be checked by filling with water to a suitable level that can be accurately measured (e.g., to overflow). If water is used instead of process fluid (not advisable in liquid chlorine instruments), a knowledgeable person familiar with the calculations can determine the appropriate allowance for density that is necessary with differential-pressure transmitters.
5. Density meters should be calibrated in accordance with manufacturers' recommendations.
6. pH and oxidation–reduction potential (ORP, or redox) probes should be bench-calibrated before fitting. They usually are not installed until the commissioning phase.
7. The correctness of cell voltage readings should be tested by connection of a calibration voltage source or a battery to the cables, which should temporarily be removed from the electrolyzers. The purposes of this functionality test are to check the continuity of wiring, check that electrolyzer and module connections are correct, and verify voltage readings. The DCS or voltage monitoring system indications should agree with those of a calibrated voltmeter measuring across the same field connections. A cell voltage monitoring system should undergo a thorough, witnessed test under simulated cell voltages with the common mode voltage applied before acceptance. The sources of any discrepancies should be identified and corrected. The purpose of this test is not calibration but a simple check of the wiring.

8. Instrument alarms and trips should be tested by simulation of trip conditions as far as possible during system commissioning. It is recommended in the case of trips that the function and mechanism in each case be verified by testing the system in its entirety. For example, in the case of a high-pressure rectifier trip, the system pressure should be raised to the trip value and all actions through to the circuit breaker should be observed.
9. The functionality of all control loops should be proven and all loops should be tuned as far as practicable before energization of the cells. System disturbances can be simulated by changes in flow rates or set points to facilitate tuning.
10. The functionality of relief lutes should be tested by raising the system pressure and checking the actual relief pressure against calibrated instrumentation. The ability to reseal should also be checked.
11. The functionality of automatic changeover systems on rotating equipment should be checked during water circulation.

13.6.3. Brine System

The brine system usually is one of the first major process systems to be commissioned. After precommissioning, flushing with water, and testing of the system, filling with water should begin. Demineralized water, which is necessary downstream of the brine ion exchangers, is sometimes used in much of the brine system. A large clarifier might be a notable exception. Water can be added at the make-up point to the salt dissolver. The dissolver should be filled and water pumped forward through the treatment tanks, the settler, the clarified brine storage tank, the filters, the filtered brine storage tank(s), and the brine heat exchangers. The ion-exchange system should be bypassed to the feed brine storage tank. From there, water can be pumped through feed heat exchangers and a cell room bypass to the depleted brine system and then finally through the dechlorinator and back to the salt dissolver. Once this circulating loop has been established, flow and tank level controllers can be set and tuned. Initially, the flow rate should be equivalent to the electrolyzer minimum feed rate. The rate should then be progressively raised and proven until the maximum rate is reached throughout the circuit.

The next step is to put the heat exchangers into operation, heat the circulating water, and tune the temperature controllers. The temperature at the ion exchange feed point should first be raised to about 65°C, and control should be established. With cold water in the system, it may not be possible to reach this temperature on a single pass at the maximum flowrate. The next step is to bring the electrolyzer feed brine heater into action. Careful tuning should be carried out and the ability to cycle the temperature under control established. The piping should go through a full cycle of heating and cooling to check for leaks that may develop because of expansion or contraction.

13.6.3.1. Brine Saturation and Primary Treatment. While other brine systems are being commissioned, batches of primary treatment chemicals can be prepared in accordance with process design requirements and operating instructions. Addition of salt to the dissolver can then start, and brine production begins. Addition of treatment chemicals

should commence and dosage rates should be established to achieve the correct levels of excess chemicals in the system. Operators should take care to avoid levels of alkalinity significantly above normal, because this can lead to high levels of silica and aluminum in the brine. The brine concentration should build up to about 300 gpl in the circuit, after which the dissolver should be bypassed and treatment chemical addition stopped. The quality of the brine from the settler and the filter should be monitored to ensure satisfactory performance.

Such closed-loop operation does not impose a great load on the treatment process. If it is possible to purge brine to another system, it is desirable to take up to 30% of the flow to a suitable receiver. This allows simulation of the dissolving operation, and the performance of the treatment process can be checked concurrently.

It will take some time to build up a level of mud in the clarifier. This level should be monitored in anticipation of beginning sludge removal after establishing a certain level.

13.6.3.2. Brine Filtration. When the brine circuit is under control with water under full circulation, the filtration systems can be commissioned. Both stages of filtration (Section 7.5.4) normally involve packaged units, and vendors' commissioning instructions will prevail. The vendor's representative should see to proper grading and charging of the fill in bed filters and to the installation of polishing filter elements. The owner's commissioning engineer should also inspect the installation, taking note of the integrity of filter cloths or candles and the sealing of filter elements to internal headers.

Verification of the correct sequence and proper operation of valves is normally a job for the factory when packaged units contain their own control systems. Still, a site "walk-through" is appropriate. With units assembled on site, the sequencing and correct operation of valves, position sensors, and mechanical items such as agitators and cake sluicing mechanisms should be fully tested before introducing fluid. Testing should encompass the whole cycle, with each filter run through all stages (e.g., operation, washing, blowdown, scouring, backwash or sluicing, precoating, standby).

The commissioning of a polishing filter usually involves a dilute suspension of precoat in water (Section 7.5.4.2). Continuous agitation keeps the precoat material in suspension in its preparation tank. First, the filter is filled with water, and then the precoat slurry is circulated through at a rate high enough to keep the particles suspended (settling rates in water will be greater than those in brine). The effluent should become clear in a few minutes, indicating successful precoating. The uniformity of coating of the filtering surface should be verified by draining the filter body and observing the elements, either by opening the body or examining the internals through sight glasses. The coating is likely to be thinner at the top than at the bottom. Some variation is acceptable, but there must be sufficient coating at all points to prevent breakthrough. The filter cleaning cycle should be tested in a similar fashion. Observation of the filtering surfaces after cleaning should show essentially complete removal of solids.

After successful commissioning on water, the filters should operate on brine. Once the filters are in operation, the clarity of the filtered brine should be tested. An on-line turbidimeter, if provided, can be used to verify correct operation and quality before placing the system on stream. The filtrate returns to the feed tank during this time.

The commissioning team should carefully note pressure drops, filtrate quality (clarity and hardness), and cycle times for future reference.

13.6.3.3. Brine Ion Exchange. Brine ion exchange systems remain specialty items, and vendor specialists normally assist in their commissioning. The owner should verify the action of operating and regeneration system valves before introducing fluids. The checking process should include valve positions and status indicators at the control station. The proper sequencing of valves and delay timers also must be established. Frequently, these tests can be performed in the manufacturer's shop.

Other necessary checks include the condition and assembly of column internals and the integrity of resin traps. Resin is usually added through the tops of the columns. Partial filling of a column with purified water helps the distribution of the resin and protects the internals from damage. Commissioning then includes a test of the entire sequence on demineralized water and brine. The backwash flow rate should be adjusted to suit the temperature of the water. The goal here should be to achieve the degree of bed expansion recommended by the supplier for the ionic form of the resin. When all this is satisfactory and there are no leaks in the system, chemical regeneration can be commissioned.

The regeneration process can be effectively checked and monitored by the conductivity of the effluent or by chemical titration. Sampling and measurement throughout the cycle can ensure that flow rates, regenerant concentrations, and durations of the various steps are correct. Initial rinsing of the bed should reduce the salt concentration to less than 1 gpl. Conductivity is a suitable method of analysis. Similarly, the regeneration with HCl and the later displacement of excess acid can be followed by conductivity measurement. The same is true of the steps involving caustic. Whatever method is used for analysis, the data obtained during commissioning are useful in later troubleshooting and should become part of the permanent record. It is good practice to run through several complete cycles in all bed sequences before beginning electrolysis.

The use of prefabricated skid-mounted units allows much of the necessary pretesting to be done in fabricators' shops. This is especially important with respect to the automatic valve sequencing operation [11]. When this is not convenient because the control system is not available to the skid fabricator, it becomes more important to do a thorough job of precommissioning on site. Along these lines, it may be possible to order the ion-exchange equipment early in the design process. If it can be installed soon enough, particularly in a conversion process, there will be time available for testing, adjustment, and operator training before startup of the electrolyzers.

13.6.3.4. Brine Dechlorination. Operation of the primary dechlorinator should be established next. It is not easily possible to simulate actual dechlorination. However, where vacuum dechlorination is used, it is important to establish that the vacuum and condenser systems operate properly. In the case of a conversion from mercury-cell technology, this may already be established.

The next operations to test are the pH adjustment stages. Hydrochloric acid and caustic are added at different points to lower and raise the pH of brine and to provide the acidity required for removal of dissolved chlorine from depleted brine. Instrumentation, including pH and ORP meters and controllers, should be set up, calibrated, and tuned.

Batches of reagent should be prepared and their feed systems operated to demonstrate the ability to dose and control at correct rates. Small quantities of hypochlorite solution can be injected into the anolyte tank to simulate primary dechlorinator product (~25 ppm as Cl₂) for testing of the ORP loop.

On completion of brine system commissioning, a full analysis of the feed brine should be made before startup. This analysis should include all impurities covered in the Analytical Manual.

13.6.4. Catholyte System

After flushing, the catholyte system should be drained and the catholyte recirculation tank and piping filled with demineralized water. Next comes pumped circulation through heat exchangers, flow meters, and cell room feed pipework, bypassing the electrolyzers to the return header. A circulation rate equivalent to that required for startup is appropriate but not essential. This is the time to test the catholyte system heat exchangers. The circulating stream should be heated, under control and in defined increments, to about 90°C. This continues until the highest temperature is reached and the control loop is satisfactorily tuned. Then cooling can begin, using the catholyte cooler and brine/caustic interchanger, if provided, and tuning the control loops. Again, the piping should be exposed to a full temperature cycle.

Many catholyte systems use polypropylene wrapped with fiberglass for the cell room piping. Stearates often are used as processing aids for polypropylene. Experience shows that the stearate is leached out of the polymer by the migration of unpolymerized styrene from the FRP wrapping. In operation, this leads to undesirable foaming of the caustic and sometimes to deposits that can block small-diameter feed nozzles. Another flushing operation may be necessary, and the following procedure is effective:

1. Fill system with demineralized water at pH 4–7, and circulate at 90°C for at least 36 hr. Purge water from system and replace with makeup. Check washing sample for smell of styrene, drain batch if present, and repeat procedure. Drain system completely.
2. Refill system with water and adjust pH to 9–10. Circulate at 90°C for 24 hr. Check samples for foam. If foam is visible, drain batch or purge and replace until clear.
3. After disappearance of foam, increase pH to 10–12 and circulate at 90°C for another 24 hr. Check for visible foam. Drain system and carry out visual internal checks of lines and tanks, where practical, for foam or gel-like materials.
4. Fill with caustic at approximately the design concentration and circulate at 90°C for at least 24 hr. Drain.
5. Refill system with demineralized water and circulate at 90°C with pH no higher than 10 for 2–4 hr, then drain.

If the cathodes have coatings that are sensitive to iron, step 4 gives an opportunity to check for iron pickup under near-process conditions. The main source of iron in catholyte liquors usually is ferrous metal in the circulating system. The use of these materials should have been proscribed in design, but they may be present in minor parts. The iron content should be checked every 6–8 hr during this step. Any increase should be

assessed against the specification. Because it may contain impurities or cause foaming in an evaporator, the caustic drained in step 4 usually is removed and sent to effluent disposal.

Finally, the system is filled with fresh caustic for startup. The concentration should be that of the desired cell product and the iron content should be in specification (normally less than 1 ppm). Concentrated commercial material can be added to the system and diluted with demineralized water while under circulation.

13.6.5. Chlorine System

13.6.5.1. Pre-Energization Testing. Chlorine system testing will be with air and should be as thorough as possible. Induced atmospheric air or compressed air can flow from the cell room header through the processing train all the way to the tail gas and absorption systems. Gas pressure control can be set up and tuned during this period to enable satisfactory control at cell room startup. It is important that these controls are properly tuned, because poor pressure control will lead to membrane damage. Changes in set points or in air flow rates will serve as disturbances and allow checking of the quality of the control.

The chlorine cooler(s) should be checked for pressure drop and the adequacy of temperature control. The latter is important to prevent gas temperatures that are too low. This situation would lead to formation of solid chlorine hydrate in the equipment and loss of the passivating film that protects titanium from rapid corrosion.

The acid-handling system associated with the drying towers should be commissioned and in operation before the flow of air begins. With the proper acid circulation rates established, system pressure drops can be checked and the downstream equipment protected against the introduction of moisture.

The cell room chlorine relief system pressure control should also be checked out and tuned on air at this time.

Euro Chlor's document GEST 90/158 contains guidelines for the commissioning of liquid chlorine-handling systems. This is a reprint of a paper by Hagerup Nilssen [12]. The emphasis again is on cleanliness and dryness. Equipment cleaning must eliminate materials incompatible with chlorine. Reaction of chlorine with moisture, organics, oxides, and various other materials not only directly produces corrosion but also, because of the heat generated, increases internal temperatures. This can lead to runaway reactions between chlorine and the steel components of the system. This is especially likely where there are extended surfaces, as in many of the internals found in processing equipment.

Equipment should first be inspected for compliance with specifications. This action includes checks of dimensions, internals, materials of construction, the quality of welds, and the installation of instruments and process connections. Before commissioning the liquid chlorine system, it is also necessary to have all relevant safety systems in operating order, operators trained, and operating manuals and instructions ready.

Final drying, after removal of all liquid water, is by dry air or nitrogen. Items that may have absorbed water (e.g., gaskets) should be replaced. The dryness of the gas used should be verified by dew point testing. One technique is to pressurize the apparatus with dry gas, hold for a time to allow equilibration, and then release the gas. Equipment that is free of liquid and pressurized to 7 atmospheres should be satisfactorily dry in three

or four cycles. Rusty surfaces not only may be reactive with chlorine but may also hold absorbed moisture and retard the approach to equilibrium with dry gas. It is important to identify this problem during equipment inspection.

Drying and leak testing should precede exposure of the system to chlorine. The chlorine should be introduced in small quantities, gradually increasing the amount and the concentration in the system. Each step should include testing for leaks with a bottle containing diluted (17–18%) ammonia. Once the system is dry, it should never be open to the atmosphere. During any delays in the commissioning process, all dry equipment should be maintained under a slight positive pressure with dry gas.

13.6.5.2. Commissioning of Dry Chlorine Systems. The most important aspect in commissioning of systems that handle dry chlorine is the elimination of all traces of hazardous materials from the interior of equipment and pipework. The impurities of most concern are moisture, organics (usually oils and greases), scale, and rust. It should be a primary aim of precommissioning to remove or avoid excessive surface layers of oxide, the presence of grease or solvents, and all sources of moisture. The hazards presented by these materials are made worse in items with extended surfaces. Examples include packing, filters, and mist-control elements.

Water presents the hazard of rapid corrosion; organics by reaction with chlorine can produce local hot spots and ultimately cause temperatures above the allowable maximum (Section 9.1.2), which in the case of carbon steel is usually set at 120°C. Oxide layers on the surfaces of equipment, pipes, or fittings increase the amount of water absorbed. This is an exothermic process. The increase in temperature not only increases the rate of corrosion but also can continue beyond the ignition limit.

The methods used to eliminate these undesirable materials depend on the type of system involved. The steps involved in commissioning in any case include:

1. inspection
2. cleaning
3. drying
4. leak testing
5. introduction of chlorine

The guide published by Euro Chlor [13] considers several categories of equipment:

1. large storage systems (those with manway access to their interiors)
2. smaller vessels and pipework
3. internal equipment
4. valves and control equipment

The commissioning of a large vessel usually begins with cleaning and inspection in the fabrication shop. Visual inspection for moisture, grease, rust, and scale should be repeated on site. Surface cleaning, if necessary, is usually by grit blasting. Branches that cannot be treated properly by blasting are cleaned by rotating metallic brushes. Residues are picked up by brushing or the use of aspirators. Mechanical cleaning should always be followed by another visual check. The vessel is then ready for drying, which is discussed below.

The best way to remove particulate matter from smaller vessels is to use a vacuum cleaner when there is an access opening that is large enough or to pressurize the vessel with a gas that is then released abruptly. Piping usually can be cleaned by blowing with air after removing obstructions. Air can exhaust from an open end of the pipe or from low-point drain connections. Chemical descaling, as suggested in Section 13.5.1, may also be necessary.

Grease is removed by washing. For many years, the standard practice was the use of fully chlorinated solvents such as perchloroethylene, C_2Cl_4 . The use of chlorinated solvents is becoming more restricted, and the practice of using aqueous formulations is growing. Those using the latter approach must recognize that results may not be as good and that the introduction of water to the system adds another complication. There have been incidents caused by the inefficient use of aqueous degreasers [14].

Often, cleaning of internal equipment by the same method used for the vessel itself is impractical or inefficient. It is then better to remove such equipment and treat and dry it externally. Vacuum ovens are useful for smaller parts. After cleaning, the parts should be stored away from the possible intrusion of grease or water until they are reinstalled.

When an application requires grease, it should be a chlorofluorinated type specified for chlorine service. Valves and control parts, therefore, should be checked for freedom from moisture and non-approved greases. Dried valves and parts are best stored in vapor-tight containers. Desiccants usually are placed in the containers for good measure. Chlorine pipe specifications (Section 9.1.8.3) often call for valves to be cleaned, dried, and packaged in this way, and to be delivered with the manufacturer's certification that they are ready for safe use in chlorine service. These items should not be installed until the larger systems discussed above have been cleaned and degreased.

Final drying of all equipment in dry chlorine service depends on a dry-gas (air or nitrogen) purge. Preliminary steps may include draining, wiping, and more rapid drying under the influence of superheated steam (with appropriate steps to eliminate the accumulation of condensate) or an applied vacuum. The goal in final drying is an interior gas dew point of $-40^{\circ}C$ or lower. A simple technique is alternate pressurization and venting. Bringing a system to 7 bar(a) with a dry gas three times and then venting to atmospheric pressure usually suffices. If the drying gas has a dew point of $-40^{\circ}C$, three such purges will lower the dew point in the interior from $0^{\circ}C$ to $-39^{\circ}C$ or from $20^{\circ}C$ to $-37^{\circ}C$ [13]. In either case, a dew point in the drying gas slightly lower than $-40^{\circ}C$ will produce the desired result. Use of this technique requires time for equilibration each time the system is pressurized.

In all cases, the last step should include a continuous purge with the dry gas and further checks of the dew point. Branches and connections should be flushed to ensure that no moisture is trapped in them. As parts of the dry chlorine plant are certified dry, they should be isolated with blank flanges or flanges closed with valves and allowed to sit under a slight positive pressure of the drying gas.

Leak testing involves several stages. The first is a check for sizeable leaks by a soap test under a pressure of about 4 bars or the maximum operating pressure, whichever is lower. Soap-bubble tests may not be sensitive at very low pressure, and more elaborate gas detectors then are necessary. When a system is found satisfactory in the preliminary test, it is time to introduce chlorine. This should be done at a low partial pressure, 0.1 or 0.2 bars at first, checking for leaks with an ammonia bottle. Any leak into ammonia vapor

will form a dense cloud of NH_4Cl . The pressure can be increased stepwise by addition of a dry, inert gas, checking for leaks at each step. Valves should be stroked during these tests. Finally, the concentration of chlorine in the gas phase can be increased gradually. This procedure has the advantages not only of minimizing the amount of chlorine that may escape from the system, but also of providing time and a gradually increasing the concentration to allow conditioning of steel surfaces by reaction with chlorine (Section 9.1.2).

All pneumatic testing must follow established procedures and safety guidelines (Section 13.5.2.1).

After completion of all the above, the appropriate parts of the system are ready for the introduction of liquid chlorine. Leak tests should be repeated after these sections reach steady temperature.

Commissioning of transport containers (rail cars, tank trucks, etc.) has much in common with the commissioning of process vessels. The first step is a general inspection—internal and external—for obvious flaws. The interior should be free of rust, scale, moisture, and grease. Gaskets should be suitable for chlorine service. Valves should be removed and freed of moisture and grease from the machining process. The valves should be dried and then lubricated with a grease compatible with chlorine. Drying, as in other cases, should be to a dew point of -40°C . The techniques can be similar to those used for other vessels, taking care to purge dry air through each of the valves to ensure their dryness. The first leak test should be a soap test with the container at a pressure of at least 4 bars. The second test should use a mixture of chlorine and dry gas at a lower pressure, using an ammonia bottle to detect leaks. The first fill should be with gaseous chlorine, to begin the process of conditioning the metal surfaces.

13.6.5.3. Chlorine Compression and Liquefaction. Compressors are an example of machinery used widely throughout the process industries, and so their commissioning is not covered in this chapter. Many companies will use the services of a manufacturer's representative at some point in the commissioning process. Commissioning procedures should take into account the particular features of chlorine compression noted in Section 9.1.6.

Liquefaction systems vary in their arrangement, in the number of stages used, and in the use and positioning of booster compressors. With so many combinations and the fact that they do not involve specialized process equipment, we do not consider their commissioning in any detail. There are some special considerations, however, around the refrigeration side that are worthy of some attention.

All parts that handle refrigerant must be scrupulously dry. Vacuum drying is the standard method. A dew point of -38°C corresponds to an absolute pressure of 0.1 torr. This pressure should be the final goal. Drying should take place in stages. The first stage, at about 5 torr, corresponds to a low positive dew point and therefore avoids the problem of massive ice formation. Application of heat to cold spots will speed the drying process, as will the replacement of vacuum pump oil if it becomes contaminated with water. Nitrogen is used to break the vacuum and bring the system back to a positive pressure. The second evacuation is usually at a pressure intermediate between the first and final vacuums. The exact level is not critical, but 0.5–1.0 torr is typical. Again, the

vacuum is broken with nitrogen. The process finally is repeated, reducing the system pressure to 0.1 torr.

The refrigerant normally arrives by truck or in drums or cylinders. It is best taken into the system through the receiver tank. Using the drain and vent connections to fill and vent the receiver may slow the filling process a bit, but it is the least disruptive combination. Refrigerant then flows to the condensers and other refrigerated exchangers by differential pressure. The exchangers can be under vacuum to assist the transfer. In most systems, the receiver tank is not large enough to fill the rest of the system, and recharging is necessary.

Leak test requirements for the utility, process, and refrigerant sides of the process are different. Water piping can be tested hydraulically. The test pressure is usually determined during design or by the refrigeration unit vendor. Typical pressures are 7 bar(g) or 1.5 times the normal working pressure. Leak testing on the process side should follow the directions given elsewhere for chlorine piping. Refrigerant piping should be tested with nitrogen. Again, 7 bar(g) is a typical test pressure. This usually involves removal of pressure-relief valves and their replacement with plugs. Instruments that can be isolated with valves can be tested up to their maximum allowable pressures and then valved off. Other instruments may have to be removed before applying full pressure. Testing is by soap bubbles. A second test at higher pressure uses a mixture of nitrogen and refrigerant. The test pressure may depend on whether a section is on the high- or low-pressure side of the refrigerant compressor. Testing is by way of a gas (e.g., halide) detector.

Pipelines that will handle chlorine are cleaned during construction. After sand-blasting and priming as required by specifications, lines are welded and X-rayed before erection. Construction debris is removed from the assembled lines by tapping and blowing with air. After this step, cleaned sections should be sealed with tape or plastic. Other procedures depend on the decision on hydrotesting. When omitting this step, operators or the construction crew should degrease all valves, heat exchangers, and vessels and then purge each section with dry air from top to bottom, stroking valves in order to dry all dead ends. Systems to be hydrotested must have high-point vents. They are filled with a chlorinated solvent or, increasingly more frequently as noted above, water or an aqueous solution. The major difficulty presented by hydrostatic testing then is the certain and thorough removal of water from the system.

13.6.5.4. Chlorine Storage. When it is to be stored under pressure, liquefied chlorine flows by gravity from a separator or knockout tank to a forwarding tank or to storage. In addition to the filling line, pressurized storage tanks include at least the following connections:

1. a liquid delivery line
2. a pressuring line (served by dry air or nitrogen)
3. a depressuring line (returning chlorine from the vapor space to the chlorine process)
4. an evacuation line (connected to the chlorine absorption system and to a vacuum pump that returns gas to the process)
5. a balance vent line (connected to the liquefaction process)

When starting flow to a tank, operators should ensure that the valves in the rundown header are properly oriented and that those leading to the tank in question are fully opened. They should also record the amount of chlorine already in the tank. As noted in Section 9.1.8.5, weighing the tank is the preferred method of inventory measurement.

Capturing liquid chlorine in storage tanks and then transferring it to its destination(s) is a semi-batch operation that requires more than one tank. To cover transfer of the liquid, we discuss here a pumping operation with the pump assumed to be submerged in the tank.

Starting with valves in the transfer line closed, operators must ensure that the pressure in the tank is not too high or too low. Venting the tank through the depressuring line will remove any excess pressure. Since the discharge lines from the various tanks usually are combined in a header, it is also necessary to ensure that the valves connecting other tanks to the header are closed. Valve operations here may be all manual or automated to some degree, with remote operators. The latter case will add to the task of instrument system precommissioning.

A low pressure in the system can be supplemented with dry gas. The pump will be sealed by a nitrogen purge controlled at a pressure above that of the tank itself (Section 9.1.8.4B). The standard arrangement includes a recycle line back to the storage tank. This should be at least cracked open before the pump starts. Even after the pump starts, the recycle line should be partly open in order to avoid dead-heading. Before starting liquid transfer but after development of pump pressure, the operator should check the pump shaft and the line valves with an ammonia bottle. Finally, the valves can be opened and the transfer made.

Shutdown basically follows the reverse procedure: stop pump, open recycle, close block valve, check valves with ammonia, check nitrogen seal system (which should remain in operation even when no transfer is being made).

The special requirements for transferring chlorine to shipping containers appear in Section 9.1.8.6.

Many liquid chlorine lines are fitted with expansion chambers to provide some volume for thermal expansion. The intent is to prevent dangerous increases in pressure as liquid chlorine in a static line becomes warmer. These chambers, their function, and their sizing are the subject of Section 9.1.10.4. When called for, they should be installed above the lines in question and subjected to the routines called for in the precommissioning procedures. Each chamber should be filled with dry air or an inert gas. Compression of this gas provides the buffer against expansion. Part of the commissioning documentation should be a schedule giving the appropriate pressures for all chambers.

The Euro Chlor guidelines on the commissioning of vessels [13] were referred to in Section 13.6.5.2. Chlorine Institute Pamphlet 78 [15] also discusses inspection, commissioning, and maintenance of storage tanks.

13.6.6. Hydrogen System

Before cell room startup, commissioning testing of hydrogen systems is normally limited to checking of purging and pressure control systems using nitrogen. Commissioning of downstream hydrogen-consuming systems, such as HCl synthesis, hydrogen

compression, and hydrogen burning, normally follows cell room startup, when a continuous supply of hydrogen is available.

It is critically important to ensure that purging is complete and pressure control is properly commissioned before energization of the electrolyzers. It is normal to vent hydrogen to the atmosphere at startup by means of a pressure control valve and the vent stack. This can be effectively simulated and set up using the nitrogen purge system. Nitrogen is added to the cell room hydrogen header at a predetermined rate to effect purging to remove air and to float the pressure-control valve and provide pressure control at startup. In a conventional membrane-cell plant with chlorine compression where the compressor recycle provides chlorine pressure control, the hydrogen control valve may control the differential pressure across the membranes. It is vitally important that this is properly tuned to avoid any risk of damage. Tests can take place while commissioning the chlorine system on air. Disturbances can be introduced to check control by varying set points and nitrogen flow rate. Transient over- or under-pressure conditions must always be within the acceptable range of operation to avoid opening of relief devices or operation of trips. Differential pressure should be controlled within the normal specified range.

13.6.7. Caustic Evaporation System

If the evaporation unit is required for continuous operation of the cell room, it is preferable to commission it on imported caustic prior to cell room startup. Evaporator commissioning requires

1. pressure testing
2. vacuum testing
3. operation on water
4. startup on caustic solution
5. operation on cell caustic.

Listing both 4 and 5 reflects the general practice of performing final evaporator commissioning before energizing the electrolyzers.

The startup supply of caustic can be used for step 4 after dilution. It is important to remember that dilution is exothermic. Blending of water with 50% NaOH to produce 30% NaOH results in a temperature rise of 30°C or more. The use of hard water produces solids when blended with caustic and also carries the danger of scaling of heat-transfer surfaces during commissioning runs. Water of reasonable quality, therefore, should be used during commissioning. Demineralized water is the ideal if available in sufficient quantities at reasonable cost. Steam condensate is sometimes an alternative.

In most wintertime conditions, lines handling membrane-cell product or evaporated solution require heating. The freezing points of 32 and 50% NaOH are 5°C and 12°C respectively. Freezing points vary nonlinearly with concentration, and solutions of intermediate concentrations may have higher freezing points. All KOH solutions below 48% concentration have sub-zero freezing points. Tracing with steam is one approach to line heating, and these systems also should be checked before starting operation with caustic solution. If commissioning occurs in warm weather, the tracing systems must be properly drained and closed off until they are needed.

13.6.7.1. Pressure Testing. Evaporator systems usually are supplied as packages by vendors specializing in the field. The bodies and heating elements are shop fabricated and tested. Still, a certain amount of pressure testing is advisable on site because of the possibility of minor damage in shipment. The vessels themselves can be tested with water for tightness, and the tubes in the heating elements also should be checked. Normal practice is to roll the tubes onto the sheets, and some of these may shake loose in transit.

Testing is simple but requires careful preparation. There are many connections to an evaporator system that must be closed or removed and blanked off. "Connections" can include atmospheric openings such as condenser tailpipes. The operating manual should spell out these testing procedures in detail. This phase presents an opportunity for operators to become more familiar with the arrangement of the evaporator system.

13.6.7.2. Vacuum Testing. The vacuum test should take place with water at approximately normal levels in all effects. It requires sufficient water in hotwells serving the main condenser, ejectors, and intercondensers to fill the tailpipes. To the extent possible, pumps should be isolated from the evaporator system to prevent the entry of air through their seals.

The vacuum applied to all stages should be the highest level to be used in operation. Condensers, circulating pumps, and condensate removal systems can be used to handle the water evaporated during the test. Under no circumstances should the absolute pressure go below 0.6 kPa, where evaporative cooling of the water will take the temperature to the freezing point.

When conditions are stable, the vacuum source should be shut down, and all evaporator stages should be individually isolated. Any source of major leakage (e.g., an open valve) should be identified and the problem eliminated. Rebalancing of the system may in some cases be necessary. Finally, with the system considered tight, the pressures in the various stages should be recorded for some period of time before approving the system for operation. The criteria used for this test depend on system design and vendor instructions.

13.6.7.3. Operation on Water. When the evaporator system is mechanically tight, the vacuum system is working properly, instrumentation is calibrated, and utility systems are functional, operation should begin with water as the process fluid. The operating manual for the evaporators should include detailed instructions for this phase. The sequence of operations will depend on the design of the unit (e.g., number and placement of preheaters and interchangers). Instructions may be supplied by the vendor or developed by the operating company and its contractors.

A typical sequence, once water is in the system, might include:

1. start seal water to pumps and instruments
2. start circulating pumps
3. vent heating elements
4. start water flow from feed tank
5. establish vacuum (operate hogging system first if one exists)
6. set level and flow controllers

7. establish water flow through all effects
8. circulate water and check instrumentation and controls
9. operate all pumps, including installed spares
10. establish steam supply, first draining steam lines as necessary
11. start steam flow at low rate—gradually increase to 50–60% of design
12. check for proper removal of condensate
13. purge water to prevent accumulation of impurities or deposition of solids (size of purge depends on purity of water being used)
14. continue operation
15. check operation of auxiliary systems (e.g., washing of demisting elements)
16. check accuracy of instruments
17. record data
18. reinforce training of operators

The last two items are not necessary to commissioning *per se*, but this phase and the one that follows give low-risk opportunities to record data on equipment performance that will be useful for diagnosis of operating problems later on and to sharpen training of operators with hands-on experience.

13.6.7.4. Startup on Caustic Solution. The first step is preparation of a batch of 28–32% caustic solution. This assumes use of the preferred technique of starting the evaporators before energizing the electrolyzers. The starting material can be membrane-cell caustic taken before evaporation, 50% solution diluted to suitable concentration, or solution prepared from demineralized water and solid caustic. The last-named source is not recommended. It requires due care during the dissolving operation to avoid personnel injury and excessive contamination of the solution by corrosion of the equipment in the face of the high temperatures that may be encountered.

Circulation can begin after the system is filled with solution. The next step is to start flow of water to the condensers. Then, after application of vacuum, steam flow can begin at a slow rate. During utility precommissioning, the steam lines should already have been blown out and drained of condensate.

Caustic feed begins only when all parts of the system are ready. Flow should be increased in stages up to the design rate. It will probably be necessary to have facilities to dilute the evaporated product back to feed concentration to allow enough time for proper commissioning. Operation at full rate and concentration should continue long enough to debug the system and train all operators. Operators should have an opportunity to make changes in the operation and to simulate likely problems.

Startup is an opportunity to record data on equipment performance for future reference and to check the calibrations of differential-pressure level instrumentation, which previously were based on operation with water.

13.6.7.5. Caustic Storage Systems. Storage tanks require careful inspection before use. Figure 13.1, an example of an inspection checklist, indicates some of the important items. Visual inspection will detect many faults. Welds, especially at roof and floor lines, should be tested by dye penetration or in accord with applicable codes. Ultrasonic

measurement of metal tank thickness is also a standard and useful technique. Records that include the precise locations of measured points are useful in tracking the condition of a tank over time.

Unlined carbon steel tanks are subject to atmospheric corrosion. It may be necessary to descale such a tank. After descaling, it should promptly be filled with caustic solution to passivate the surfaces. Caustic from unlined tanks generally should not be used to fill electrolyzers before startup.

Leak testing takes the form of filling a tank with water. Any settling after the tank is filled should be surveyed and documented. Insulation should not be applied until inspection and testing are complete.

Storage systems will have auxiliaries such as pumps and exchangers. Their pre-commissioning follows standard techniques, using water as the fluid. Commissioning should follow along with the storage tank(s). Concentrated caustic should not be allowed to sit stagnant in unheated lines for any long period of time.

13.6.8. Rectifier/Transformers

Work on the electrical supply and switchgear is a specialist activity and will normally be carried out by the vendor's specialist in conjunction with the client's or contractor's electrical engineer.

From the point of view of ensuring smooth and successful electrolyzer startup, it is essential that commissioning of the rectifiers and their transformers be carried out off-line. It is not considered acceptable to use the electrolyzers to commission the rectifiers. This means that low-load output tests should be carried out on site even if such a test has already been made at the factory. The commissioning engineer together with the electrolyzer vendor should always verify output polarity. An open-circuit test can demonstrate the capability of the unit to produce the design output voltage. Such tests require some care in order not to exceed the rated voltage. A short-circuit test of achievable current output is highly desirable, especially when there is to be no on-site load test. The short-circuit test can usually be carried out at rated current with a temporary shorting connection bolted across the rectifier output busbars. The permanent DC current measuring device (Section 8.3.1.5) should be included in the circuit.

A load test requires some form of temporary resistive load to be provided. The rectifier manufacturer can advise on the necessity and feasibility of such a test. Normally, for practical reasons, any load test will be limited to about 10% of rated current.

Process interlocks with the rectifier and process tripping of the rectifier should be verified. They should be proven through all stages of signal processing by actual reproduction of the process conditions, if possible, or at least by simulation and verification of the interlock or trip functionality.

13.7. ELECTROLYZER ASSEMBLY, TESTING, AND INSTALLATION

13.7.1. Membrane Handling

Manufacturers most commonly supply membranes wet, pre-treated, expanded, cut to size, and ready to use. An exception here is an alternative form of Nafion[®] supplied dry

and pre-expanded in diethylene glycol. Some technology suppliers and membrane users prefer this form of the product. These membranes require an extraction treatment after installation and before energization.

Large membrane sheets are normally rolled onto a core and sealed in plastic film. The roll, containing several sheets, is contained in a plastic tube for shipment and storage. Smaller sheets may be packed flat in stacks on plastic boards, sealed in plastic film, and contained in plastic boxes. The sheets are packaged wet after soaking in alkaline demineralized water. In order to prevent damage and drying out, they should remain sealed in their original packaging until required for use. Care must be taken in unpacking and at all stages of handling to prevent damage. Membranes must not be punctured, torn, folded, or creased before use. Handling methods should minimize any risk of damage to the membranes. After unpacking, membranes must be kept moist at all times. Soaking them in a bath of alkaline demineralized water is a convenient way to achieve this. A typical pH is 12, achieved by the addition of a small quantity of caustic to the water. The pH of the water is important for the prevention of corrosion of the cathodes during storage, after membrane fitting, and before startup.

Rolled membranes should be transferred individually to the holding tank by unrolling from the core mounted horizontally on a frame at the end of the tank (Fig. 13.2). Each sheet should be unrolled and drawn directly under water in the tank to prevent entrapment of air. This allows the membrane to settle to the bottom of the tank. A submerged roller may be useful here. Properly handled membranes can be stored indefinitely in this way. The tank filled with membranes should be covered to exclude foreign bodies. It is convenient to store the membranes in the correct orientation for fitting. For example, if they are to be fitted to a modular electrolyzer with the cathode pan facing upward, the sheets should be stored with their cathode faces down.



FIGURE 13.2. Unrolling of membranes into bath (with permission of INEOS Chlor Limited).

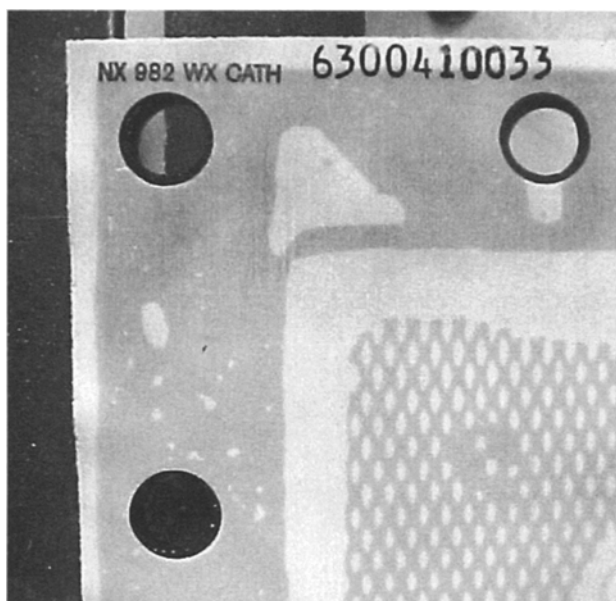


FIGURE 13.3. Typical cathode-side markings (with permission of INEOS Chlor Limited).

Figure 13.3 shows typical markings that help to prevent errors in identifying the cathode side of a membrane. Proper orientation of every one of the many sheets is of great importance.

The membranes should be allowed to equilibrate with the alkaline water in the hold tank for at least 4 hr before installation, trimming, or cutting of holes. This is because the equilibration may produce small changes in membrane dimensions. After trimming or cutting, the membranes should be returned to the tank until installation. Depending on the cell design, special jigs may be useful as guides in the trimming and cutting operation (Fig. 13.4).

Membranes from all suppliers generally can be handled in similar ways, but the user should carefully follow the detailed directions of the technology supplier or membrane manufacturer. Dry expanded membranes are a special case and require different procedures. Nafion[®] membranes designated TX have been expanded in diethylene glycol (DEG). These need no pretreatment before installation. An advantage of this type of membrane over the WX or water-expanded type is their slightly greater degree of expansion. This ensures the absence of wrinkles during operation, which is a benefit in some technologies. The membrane supplier should be asked to consult on the special procedures required to remove the DEG before startup.

13.7.2. Membrane Installation

Membrane installation details vary greatly with the type of electrolyzer. In the case of monopolar electrolyzers that can be removed from their berths for maintenance or bipolar electrolyzers containing removable single elements, membrane fitting takes place in a

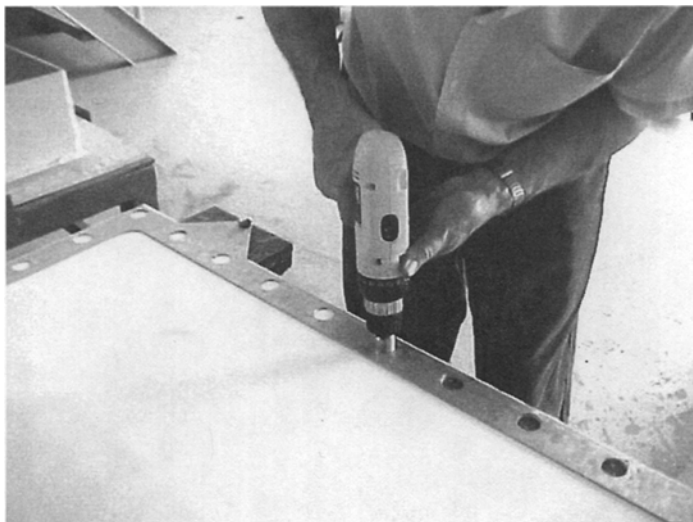


FIGURE 13.4. Cutting holes in membrane with the aid of a jig (with permission of INEOS Chlor Limited).

workshop area away from the cell room. With other large electrolyzers of the filter press type, membrane fitting takes place at the electrolyzer berth. Regardless of the electrolyzer type, the important considerations with respect to membrane fitting are:

1. Membranes of the wet-expanded type must not be allowed to dry out. Drying is much faster when the relative humidity is low. Sprays of demineralized water should be used periodically to wet membranes and electrode structures until the membranes are securely in position and the electrolyzer sealed.
2. Careful handling is necessary to prevent membrane damage. In the fitting operation specifically, dragging membranes over electrode surfaces and allowing them to snag on electrode structures are to be avoided.
3. Membranes must be correctly oriented when installed (i.e., cathode side to cathode).
4. Membranes must be flat and free of wrinkles.
5. Electrode structures must be clean and undamaged.

The membrane fitting operation provides a final opportunity for visual examination of electrode structures for damage that occurred in transit or assembly. This inspection also should check for flatness, high spots, and anything that could physically damage the membranes.

Fitting methods depend on the electrolyzer design. Some examples follow:

1. With the INEOS Chlor FM1500-type electrolyzer, which uses small sheets of membrane, the cathodes are lifted from the pack in turn, and the sheets are stapled to the gaskets on either side of the cathode (Fig. 13.5). The staples hold the sheets in position until the pack is fully assembled and compressed. In this design, the membrane is contained within the gasket to provide effective sealing.

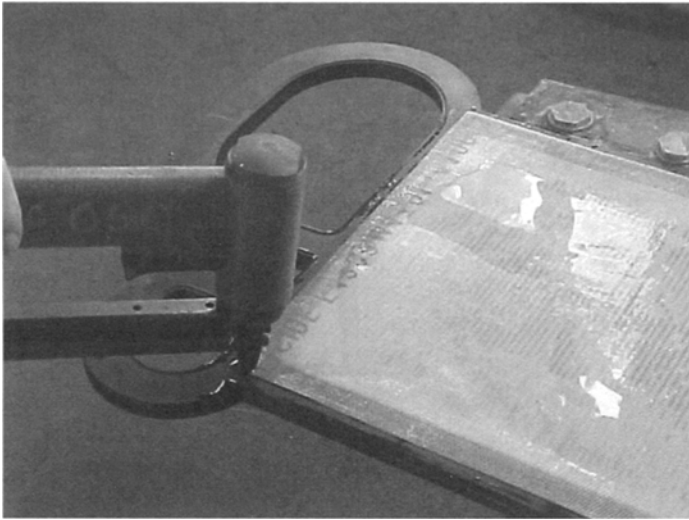


FIGURE 13.5. Attaching membrane to a small monopolar electrode (with permission of INEOS Chlor Limited).

2. In modular electrolyzers such as the Uhde single-element design, membraning takes place with the cathode pan lying horizontally, face up, on a table in the assembly area. The cathode pan is prepared with its gasket in place, and the membrane is laid on top. This is conveniently done by rolling the sheet, with precut holes, onto a roller in the holding tank, transferring it to the cathode, unrolling it and laying it from one side of the structure to the other. Alternatively, two persons can lift the sheet carefully from the bath, holding it by its four corners, and placing it flat upon the cathode. The anode pan, also with its gasket in place, is then carefully placed over the cathode pan. Standard bolts join the two electrodes together. Figure 13.6 shows the similar technique of fitting membranes to a BiChlor™ electrolyzer module. Completed modules are then fitted into the electrolyzer frame as shown in Fig. 13.7.
3. With large bipolar filter-press designs, such as Chlorine Engineers' BiTAC®, membrane fitting takes place in the cell room. The elements are assembled on the frame, and the gaskets are fitted. The elements are gathered near the moving endplate. There will be some means of moving them, one by one, starting at the fixed end (opposite the closure mechanism). Individual membrane sheets are suspended above the electrode pack and lowered into position in the gaps between adjacent anode and cathode faces. Pushing electrode structures together retains the sheets. Spraying the edges of the membranes occasionally with demineralized water will prevent their drying out before the closing of the pack. When membrane installation is complete, a mechanical or hydraulic system closes and seals the pack.

Sealing and release of membranes are also important considerations. There are two issues, prevention of leakage between membrane and gasket and the ability to remove



FIGURE 13.6. Fitting membrane to a large bipolar electrode (with permission of INEOS Chlor Limited).

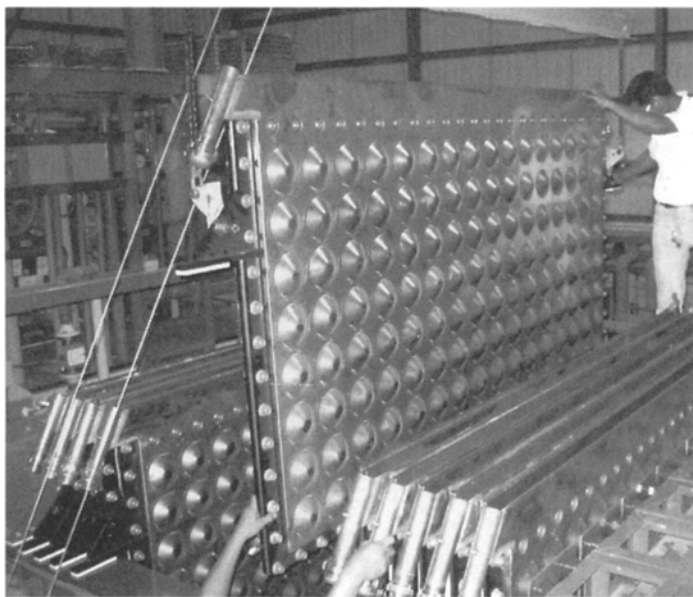


FIGURE 13.7. Fitting bipolar module into electrolyzer assembly (with permission of INEOS Chlor Limited).

membranes from gaskets for repair or replacement. Again, practices vary depending on technology, design, and type of membrane.

Achieving an effective seal is predominantly a design issue, but special assembly procedures may be required. Some jointing systems and some types of membrane require sealing agents. Designs that confine the membrane sheet within the gaskets can provide a rubber-to-rubber seal around the electrode periphery, obviating any sealing problems. In the Uhde design, sealing is effected by the use of Gore-Tex™ PTFE tape as part of the jointing system. Rubber-jointed systems may be designed with gasket profiles that provide sufficient local pressure on the membranes to give effective seals. In those designs in which the membrane protrudes from the edge of the gasket, sealing compounds are applied to joint faces to improve the seal.

The type of membrane used can also affect the sealing issue. Heavy reinforced membranes can be more difficult to seal than thinner flat designs. Also, certain membranes have sacrificial fibers in their construction. These are leached out during pretreatment to form voids that help to reduce operating voltages. These voids form channels that can provide leakage paths along which process fluids can “wick” out of the electrolyzer.

Release of membrane from the surfaces of rubber joints without damage is a consideration if one envisages patching repairs in the event of pinhole damage or if there is a possibility of disassembly to correct misalignment of membranes during cell construction. Release agents then may be applied to the surfaces of the gaskets during assembly. Silicone grease (e.g., Dow Corning 7 Compound) is a commonly used material.

13.7.3. Electrolyzer Testing

The two principal tests carried out on an assembled electrolyzer or module are:

1. membrane leak test, to ascertain that there are no membrane pinholes and that the membrane(s) is (are) properly seated across the sealing surfaces;
2. electrolyzer or module leak test, to ascertain that the unit is not leaking externally.

These tests take place soon after membrane fitting. The location may be the cell renewal workshop or the electrolyzer berth, depending on the type of electrolyzer (Section 13.7.2).

13.7.3.1. Membrane Leakage Test. The membrane leak test is conveniently carried out by pressuring one side of the membrane (usually the cathode side) with air or nitrogen at approximately 50 mbar. This can be done by attaching a gas supply line to the caustic feed connection on a module or to a suitable connection on the caustic/hydrogen side of the electrolyzer. A small valve throttles the gas flow and a manometer or diaphragm-type gauge indicates the pressure. Other connections on the caustic/hydrogen side are sealed off. The brine/chlorine side offtake connections are sealed but the feed connection is left open. Pressure is applied to the catholyte side. When it reaches 50 mbar, the valve is closed. If the membranes are in good order, the pressure will remain constant. Falling pressure indicates a leak. A tube fitted to the brine feed connection with its end submerged in a beaker of water will reveal whether the leak is internal or external. Bubbling in the

beaker indicates that there is a membrane leak or that a membrane is not properly seated. This must be investigated and corrected.

When a leak is detected after assembly or installation of an electrolyzer in its berth, it is necessary to determine which membrane is leaking. When an electrolyzer has external feed tubes to individual compartments, it is possible to disconnect the tubes and submerge their ends in a beaker of water, as above. Smaller electrolyzers with internal feed manifolds require a different approach. In the case of the FM1500, for example, testing involves the use of a standpipe to apply hydraulic pressure to the cathode side and observing leakage from the feed ports along the manifold. An endoscope is a convenient tool for this purpose.

While membranes in a newly assembled electrolyzer should not show any signs of leakage, older used membranes may be permitted a small amount of leakage [16]. A flow meter connected to the test equipment can quantify the leakage rate. In respect of membranes 1 m^2 and larger, Bergner and Hartmann [17] recommend as a safe limiting leakage rate, $20 \text{ dm}^3 \text{ hr}^{-1}$, using nitrogen gas at 50 mbar pressure. They state this to be consistent with a pore size of about 1.3 mm diameter. This is considered a good guideline in respect of testing large bipolar electrolyzers and ascertaining when to remove membranes. Clearly, prolonged operation of electrolyzers with many damaged membranes increases the operational risks. These include hydrogen/chlorine explosions in the vapor space and damage to anode coatings and, eventually, structures.

13.7.3.2. External Leakage Test. The objective of the external leakage test is to find any leaks from the assembly before starting operation with process fluids. The test involves applying pneumatic or hydraulic pressure simultaneously to both sides of the membranes.

Pneumatic tests are carried out on modules and small filter-press electrolyzers in the workshop. The pressure typically is 300–500 mbar. Equipment design should prevent overpressurization and the risk of damage to the electrodes by high differential pressure. The pressure should hold for at least 30 min after shutting off the air supply. Leaks can be identified with soapy water or a gas leak detector.

With large filter-press electrolyzers, hydraulic tests involving filling the electrolyzers with water may be more convenient.

13.7.4. Storage and Berthing

With proper precautions, electrolyzers and modules can be safely stored for some months after membrane fitting. Some precautions are:

1. feed and exit connections sealed with blank plates or plugs to prevent membrane drying
2. exterior kept dry and clean to avoid bridging of insulation between cathode and anode, with formation of a circuit for corrosion currents that attack cathode coating or substrate (can cause loss of catalytic activity and deposition of nickel in membrane)
3. electrical connections not made until ready for startup
4. feed and exit connections to individual modules or compartments on bipolar electrolyzers disconnected from headers
5. small residual volume of alkaline water in electrolyzer to maintain humidity

Smaller electrolyzers assembled in the workshop may be lifted into prepared cell room berths and installed. Piping connections can be made up (after completion of pipework testing) with slip plates inserted at the connecting flanges to prevent drying of membranes and accidental ingress of fluids.

Frames for modular electrolyzers are normally erected in cell room berths. Membrane modules from storage are placed in the frames, and the units are compressed with jacking screws to make satisfactory electrical connections between adjacent anode and cathode pans. An alternative approach, which has allowed rapid conversion of existing mercury cell rooms, is to preassemble electrode packs in their frames and lift entire units into place using a large crane.

Large filter-press designs are normally assembled in the cell room. The frame is erected and the elements placed within. Membrane fitting is carried out *in situ* as discussed in Section 13.7.2 before compressing the whole pack to seal the gaskets.

13.7.5. Record Keeping

It is vital to establish a system of record keeping in respect of the electrolyzer installation and maintenance history from the time of the initial installation.

To enable this, technology suppliers may provide appropriate database software tailored to their hardware designs. Such packages normally provide for recording both assembly and maintenance information and performance data (Section 13.11).

The purpose of such record keeping is to enable the following activities:

- monitoring of cell room maintenance requirements and costs
- monitoring and policing of warranties on components
- comparison of lifetime/performance of different types of membrane and electrode coating
- planning and budgeting of electrolyzer maintenance
- tracing of history in event of component problems

For the purpose of tracking, anodes and cathodes or bipolar elements may be stamped with serial numbers. For effective monitoring, the database system should allow the following to be recorded:

1. first startup date for each anode, cathode, and bipolar element
2. electrolyzer number and position occupied by each of these elements
3. type of membrane fitted, position, startup and removal dates
4. dates of removal for maintenance and dates of restart for each anode, cathode, and bipolar element
5. details of maintenance carried out; for example membrane change, recoating, or repair

The information stored should give the user a ready picture of the type and age of the membranes, electrodes, and coatings at all positions in an electrolyzer, along with their maintenance histories.

13.8. PLANT OPERATION

The most important considerations determining the normal operating philosophy and procedures adopted for the cell room include:

- meeting safety and health standards
- controlling operating costs
- controlling maintenance costs
- maintaining high plant productivity
- maintaining product quality

It is assumed here that design carefully considered safety, health, and environmental issues and the risks associated with the operation of the plant (e.g., processing and handling the hazardous products; operator exposure to high DC voltages). Operating and monitoring procedures are an essential part of the management of these risks.

Energy consumption is the dominant part of operating cost, and the establishment and maintenance of an energy-efficient operation are usually critical to a plant's overall economics. All personnel must fully recognize the vulnerability of membrane technology to upsets in operating conditions and in particular to brine impurities. These can cause significant losses in operating efficiency, with higher unit energy costs and reduced output. Performance losses, more often than not, are largely irreversible. Operating and monitoring procedures are necessary to detect any abnormal conditions or impurity levels in a timely manner.

Electrolyzer refurbishment is the largest item in plant maintenance cost. The mean time between refurbishments should be optimized. The need for membrane replacement is the most frequent determinant of electrolyzer operating life. Maintenance of stable current efficiency and energy consumption and avoidance of membrane damage are keys to economic cell lifetimes.

Competent personnel together with robust operating and monitoring procedures can ensure safe, efficient, and reliable operation. It is the responsibility of commissioning personnel to ensure that these requirements are in place and functional in time for startup. It is true that some refinement of operating instructions likely will result from the experience gained in startup and initial operation.

The rest of this section discusses the operation of a generic membrane-cell chlor-alkali plant. The main focus is on the operating requirements of the cell room, which are treated in some detail. Other systems are considered from the standpoint of their roles in providing raw materials or processing products from the heart of the plant, the electrolyzers.

13.8.1. Initial Plant Startup

A thorough job of commissioning will test all systems as far as is practicable before first energizing the cell room. Major systems that may not yet have operated are the electrolyzers, chlorine processing system, hydrogen gas handling, and brine dechlorination. The startup plan must recognize this and allow sufficient time for all systems to come on line and gradually reach full load. Thorough testing of control systems and

trip logic during precommissioning and commissioning activities will help to avoid an excessive number of cell room trips and shutdowns.

Analytical routines should be established and rehearsed before startup. Additional analytical staff will be necessary to handle the amount of testing required during initial startup. Only when the commissioning manager is satisfied that all necessary commissioning testing has been completed should cell room startup be attempted.

13.8.1.1. Preparation for Cell Room Energization. Electrolyzers are isolated from header systems by blanks or slip plates during commissioning of the brine, caustic, chlorine, and hydrogen systems. Immediately before startup of those systems, all blank plates should be removed, leaving only valves closed where it is appropriate to isolate electrolyzers. There should be a record of all blank plates and slip-plates and their locations. This will help to ensure that all are removed before startup.

The brine system should be fully operational, on recycle and bypassing saturation and the electrolyzers, at a rate equivalent to that required for operation at $2\text{--}3\text{ kA m}^{-2}$. The brine temperature should be about 50°C at the cell room. Concentration should be as specified for normal operation (typically 300 gpl), and quality should meet all specifications. Analytical routines for the brine system should be in full operation by this time.

Caustic, similarly, should be flowing under control around the catholyte system, through the cell room headers and the electrolyzer bypass. Again, the flow should be appropriate to a current density of $2\text{--}3\text{ kA m}^{-2}$, and the caustic temperature at the electrolyzers should be about 50°C . A concentration of 30–32% is usually satisfactory in the case of NaOH. The caustic should meet all specifications, and its concentration and iron content should be checked just before startup.

The emergency chlorine absorption system, which starts up independently, should be in full operation before energization of the cells.

Before connection to the buswork, the electrolyzers should be given a final check, covering insulation of the frame, the electrolyzers, and the buswork. There should be no debris (e.g., nuts and washers) that might compromise the integrity of the insulation. The flexible conductors or cables that join the electrolyzers to the feed bus bars should be connected only when rectifier testing is complete and immediately before energization.

Gas systems must be vented to allow the electrolyzers to be filled. It is important to keep the membrane position constant and against the anodes. Caustic, therefore, should be introduced before brine. Opening the electrolyzer caustic feed valves and closing the bypass diverts the circulating caustic flow through the electrolyzers. Brine flow through the electrolyzers should start a few minutes later. The crew should monitor brine and caustic feed rates and temperatures with the goal of achieving uniformity among the electrolyzers. With many bipolar designs, liquor flows through each compartment or module can be checked by observing the transparent feed or exit hoses. Exit temperature indication will begin to rise after the electrolyzers are full and overflowing. The brine and caustic temperatures then can be increased slowly and together to raise the electrolyzer temperatures for startup. The gentle program of temperature increase minimizes the thermal shock felt by the membranes. Feed temperatures for startup normally are about 87°C . With new membranes, it is desirable to hold at a minimum of 75°C for 1 hr to allow the membranes to equilibrate with the process fluids.

When the electrolyzers are overflowing, the gas headers can be purged. Nitrogen is used on the hydrogen header and air or nitrogen on the chlorine header. Air flow to the chlorine header may be induced with the header under slight suction from the absorption plant or the chlorine compressor or admitted under pressure from a compressed air supply. Nitrogen is used instead of air when its supply is considered more secure and when oxygen levels in the chlorine are detrimental to downstream processing. The header pressure control system should be active during purging to ensure that the recommended differential pressure is applied to the electrolyzers. The differential typically will be 10–30 mbar, with the hydrogen pressure being the higher. The hydrogen header should be positive at all times in order to avoid air ingress. After a prescribed minimum period, typically consistent with passage of up to 10 times the system volume of purge gas, the remote end of the hydrogen header should be checked for its oxygen content, which should be less than 1% v/v.

On bipolar electrolyzer circuits, once header purges have been established and the oxygen content in the hydrogen header is satisfactory, the polarization rectifier, if provided, can be started. This prevents reverse currents originating from the battery effect from causing cathode corrosion. The polarizing current, typically 10–30 A m⁻², generates oxygen at the anode and hydrogen at the cathode. It is normal to start the current at about 50°C. Higher temperatures increase the rates of corrosion and the magnitude of the reverse current.

The rate of flow of the nitrogen purge in the hydrogen header is an important process design factor. Considerations include:

1. sufficient flow rate to purge air from downstream piping and equipment in a timely manner
2. sufficient velocity at the tip(s) of the vent stack(s) to prevent burn-back in case of ignition (Section 9.2.6)
3. rapid purging of cell room headers at shutdown to prevent backflow into the electrolyzers, allowing hydrogen to diffuse through the membranes or flow through cracks and pinholes into the chlorine system (typical flow rates are 0.04–0.1 Nm³ hr⁻¹ m⁻² membrane area)

Adequate purging of the chlorine headers prevents the accumulation of dangerous quantities of hydrogen in the chlorine system. The source of hydrogen again is diffusion or leakage through the membranes. With either chlorine or hydrogen headers, there should be sufficient flow for proper operation of pressure control systems, and it is most convenient if the rates used in startups and shutdowns are essentially the same.

During preparation of the cell room, the rest of the plant must reach startup status so that there will be no delays in energization. Also, during the activities listed above, the following actions should be completed:

1. brine feeding the cell room checked for salt concentration, pH, and total hardness
2. recirculating caustic checked for concentration and iron content
3. measurement of pH of brine leaving each electrolyzer (feed pH will be 3–11, depending on whether acid is being added for CO₂ removal; exit pH will be higher because of caustic migration; excessively high exit pH indicates membrane damage)
4. brine and caustic flows to each electrolyzer maintained at proper rate for startup

13.8.1.2. Electrolyzer Energization. During the cell room startup, it is important to have facilities readily available for analysis of key process streams. Necessary measurements include brine and caustic strengths (by specific gravity), chlorine gas composition (by gas chromatograph or Orsat), brine pH, and free chlorine content of brine (by ORP).

The application of load to the electrolyzers should be made in steps, typically 0.5 kA m^{-2} at a time, with 15-min waiting periods between steps. The rate of increase at each stage will depend on the need to maintain stable control of the gas pressure control systems. The addition of water to the circulating catholyte should begin at 0.5 kA m^{-2} . The rate required is nearly linear with current density. In any event, the operating load determines the set point, which can be programmed into a DCS.

Electrolyzer exit temperatures rise as operating current is increased. Operators should adjust feed brine and caustic temperatures as the load approaches 2 kA m^{-2} in order to bring the exit temperatures under control. Design exit temperatures typically are 87°C , with an acceptable range of $80\text{--}90^\circ\text{C}$. The required feed temperatures depend on electrolyzer voltage and other technical requirements. It may be found convenient to maintain feed brine and caustic temperatures equal.

It is desirable to achieve normal on-load operating conditions, other than current density, within an hour of energization.

Increases in rectifier loads require careful monitoring of the operating voltages. The ease with which this can be done depends on the sophistication of the monitoring system provided. In monopolar cell rooms, it is normal to provide on-line voltage monitoring and rectifier trip facilities on individual electrolyzers. In bipolar cell rooms, the minimum supply may be simply a total electrolyzer trip and a Wheatstone bridge arrangement that compares voltages on the two halves of an electrolyzer. This can detect an imbalance caused by a high voltage between any pair of electrodes. Manual field measurements then are necessary for a survey of all individual anode/cathode pairs. On-line voltage monitoring of individual pairs through the DCS or a dedicated computer is very convenient and is quite common in newer plants. It can save a great deal of operator time, and the accurate and essentially simultaneous readings that it provides are helpful in troubleshooting.

In a bipolar electrolyzer, the voltages found across individual elements or anode/cathode pairs during polarization and the raising of load up to about 0.5 kA m^{-2} are useful indications of the presence of pinholes in membranes. The voltage of a cell with a membrane damaged in this way will be lower by perhaps 500 mV [18] and will increase more slowly than the voltage of a good cell. The reason for this is that a pinhole causes the level of alkalinity in the anolyte to rise, and the generation of oxygen dominates at low currents. This occurs at a lower voltage than the generation of chlorine. The relationship is time-dependent, and so voltage measurements on all elements must be concurrent to allow comparisons between individual elements. At startup, each anolyte compartment contains an accumulated stock of hydroxyl ions. The oxygen-generating reaction consumes these, causing the compartment voltages to rise, even at constant current. The increase continues until reaching equilibrium with the flow of caustic through the pinholes. Waiting for equilibrium is not a practical approach, but comparison of transients is not difficult if the voltage of every element is monitored. Voltages may be measured at several currents as load is applied. Figure 13.8 compares the startup voltage of a bipolar module with a normal, undamaged membrane

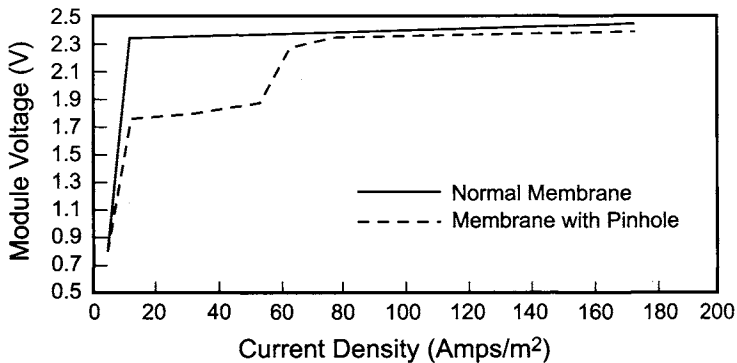


FIGURE 13.8. Startup voltage profile.

with that of a module with a pinhole. An experienced technologist should determine the level at which action should be taken. It can be said here that a module running 300 mV below the norm at 0.2 kA m^{-2} would indicate a problem requiring urgent attention.

Observation of the color of the gas in the transparent outlet hoses of a bipolar electrolyzer as the load is raised is another good indicator. The color change may be slower or less intense in those cells that are generating oxygen.

The nitrogen purge on the hydrogen header should not stop until gas generation begins. It might be discontinued at, say, 0.5 kA m^{-2} . Reduction of the nitrogen flow should be gradual and careful in order not to upset the differential pressure control.

The first two days of operation should be considered a conditioning period for the membranes and a run-in period for the rest of the plant. Caustic strength should be less than design. For example, a 32% NaOH membrane might start up at 29–31%. This concentration should be checked frequently during the startup period. It is particularly important to avoid extremes in concentration that can cause permanent damage to the membranes.

Early operation should also be at less than design current density. A typical load during this period is $2\text{--}4 \text{ kA m}^{-2}$. The load should be held stable while monitoring brine and caustic temperatures and concentrations. The differential pressure between hydrogen and chlorine should also remain stable. The rest of the chlor-alkali plant operation can also be checked for deviations and problems during this time.

Useful cell room checks that also provide base-line data for future reference include:

1. measure and record all electrolyzer and module voltages
2. sample individual electrolyzer gas streams and analyze for oxygen and hydrogen
3. measure pH of depleted brine from each electrolyzer or module
4. check current distribution
5. check voltage losses at electrical contacts

The hydrogen content of the chlorine should be less than 0.1%. If an electrolyzer shows a higher value, there is a membrane problem that should be identified and corrected. The pH of the depleted brine with new membranes but without deep acidification should be in the range 3.5–4.5. Higher values indicate leaking membranes. Since much of the caustic passing through membrane pinholes may be converted to oxygen, this indication may fail in some cases. However, an abnormally high pH always indicates that there is a problem that must be addressed.

After the stabilization period and the correction of any serious problems, the exit caustic strength can be increased and then the electrolyzer load increased in increments up to the desired level (Section 13.8.2.2).

13.8.2. Normal Cell Room Operation

13.8.2.1. General. Normal operating and monitoring routines for the individual electrolyzers, the cell room, and the associated plant are to be established and followed carefully. Process parameters should remain within the specified ranges. When upsets occur or an important parameter moves out of specification, the appropriate actions, which may include shutdown of the plant, must be taken.

It is common practice for operating personnel to carry out some of the routine analyses that require immediate attention. Most frequently, these include analysis of chlorine gas for oxygen and hydrogen, pH measurements, determination of brine and caustic strengths, primary brine treatment reagent control, brine hardness, and brine dechlorination analyses for free chlorine or reducing agent excess. Results from analyses made in the plant laboratory must be made available to operating personnel in a timely fashion to allow appropriate corrective action. The laboratory should also check the routine operator analyses on a regular basis to ensure their accuracy. This is especially important in respect of brine hardness. Special apparatus is required for precise analysis of trace elements and ppb quantities of calcium and magnesium. Real-time analyses by operators and on-line instruments are valuable for process control, but they should be checked regularly. Licensing agreements also may require periodic reporting of the more precise data.

Electrolyzer temperatures and voltages and individual bipolar cell or module voltages are primary indicators of problems and so should be closely monitored. Computer-based voltage monitoring systems offer high accuracy and automatic trending of data, and they eliminate the need for time-consuming manual readings.

Cell room feed liquor temperatures should be adjusted as necessary to keep electrolyzer outlet liquor streams at 80–90°C. At lower current densities, this will require heating of the circulating caustic; at higher current densities, it will require cooling of the caustic.

The pressure differential across the membranes should be carefully controlled in accordance with the technology supplier's requirements. Typical values are in the range 10–30 mbar. The pressure differential indicated in the control room should be checked regularly with manometers (header pressures permitting). To prevent damage to the membrane by vibration or fluttering, control should be steady, with fluctuations no more than ± 1 mbar. The pressure on the hydrogen header should at all times be positive and greater than the pressure on the chlorine header.

Section 13.11.3 discusses the frequency of monitoring and gives a typical schedule.

13.8.2.2. Changes in Electrolyzer Load. Changes in electrolyzer load should be smooth and gradual. The maximum rate of change in practice usually depends on the downstream plant and the ability to maintain good differential pressure control in the cell room. During a change in load, brine and caustic feed rates and temperatures and the rate of addition of water to the circulating caustic should vary to keep exit concentrations and temperatures within the specified ranges. This ensures that the membranes always remain in a similar ionic/temperature environment.

Incremental load changes of 0.5 kA m^{-2} or less usually allow good electrolyzer control. The procedure for an increase in load is:

1. raise the brine and caustic flow rates to those required at the higher level
2. lower the brine and caustic feed temperature set points to those required at the higher load
3. raise the water addition rate to that required at the higher load
4. begin increase in load when temperatures begin to fall, and increase at a rate that does not disturb differential pressure control

The procedure for reductions in load is:

1. raise the brine and caustic feed temperature set points to those required at the lower load
2. reduce load at a rate slow enough not to disturb differential pressure control
3. lower the water addition rate to that required at the lower load
4. lower the brine and caustic flow rates to those required at the lower load

The sequences are designed to avoid harmful excursions in concentration and temperature.

When controlling electrolyzer feed rates, water addition rate, and load from a DCS, it is convenient to ramp the load and derive the other set points from the load. A typical ramp rate might be 1 kA m^{-2} in 10 min. This technique is particularly advantageous when load variations are frequent, as in daily load shedding to avoid high power tariffs. Safe load shedding requires careful attention to control of operating variables. To minimize deterioration of the current efficiency that might result from such regular load shedding, the membrane environment should be kept nearly constant as possible. Constant brine and caustic concentrations and temperatures are best maintained by using automatic load ramping and controlling brine flow rate and caustic water addition rate automatically in response to load. The ramping rate depends on the ability to control feed temperatures and gas header pressures and to avoid uncontrolled disturbances of other plant areas. The minimum operating load depends largely on the chloride level that can be tolerated in the caustic product. Chloride concentration increases at a low load, and the increase is pronounced as the load falls below 2 kA m^{-2} . The specification may be exceeded at, say, 1.5 kA m^{-2} . Problems with chloride buildup are more likely in KOH production. Providing tankage for segregation allows the caustic produced at a low load to be blended off. It is very important to maintain good current efficiency when

shedding load. Low current efficiency also results in increasing chloride concentration in the caustic, aggravating the problem of low-load operation. It is known that load shedding, with meticulous control, can be successful down to 0.9 kA m^{-2} . More normally, the lower limit will be $1.5\text{--}2 \text{ kA m}^{-2}$.

13.8.2.3. Operation with Acidified Brine. Acidification of the feed brine improves the performance of the cells. As explained in Section 7.5.6.1, the improvement results partly from the elimination of carbonate ion, a precursor of CO_2 , and partly from neutralization of some of the hydroxyl ion that passes through the membrane from the catholyte. At the same time, overacidification is a danger, because carboxylic membranes can protonate below pH 2. The feed brine can be at a lower pH. It is the pH of the anolyte that must be limited. Since carbonate decomposes at about pH 3, the benefits of acidification come in two stages.

What one might consider the primary stage of acidification to pH 3 can be fully commissioned prior to cell room startup, and brine at pH 3 may be fed to the electrolyzers at startup and during off-load periods. It is important to allow for effective degassing (Section 7.5.6.2), which may occur in the feed brine tank or a separate degassing vessel.

Further addition of acid should begin only after establishing stable operation. As discussed above, the first 48 hr of operation will maintain a conditioning load of $2\text{--}3 \text{ kA m}^{-2}$. It is reasonable to start acid flow once the load gets to this first steady level. We should note that during the ramping up to this load, the oxygen level is always a bit high because of residual alkalinity in the anolyte. This is due to diffusion of hydroxyl ions through the off-load membranes. Acid addition may be flow controlled or flow-ratio controlled in response to the brine feed rate. When acid flow first begins, increases in rate should be slow to avoid any loss of control. The final rate will be set by the maximum allowable oxygen level in the chlorine. Requirements depend upon membrane current efficiency and the characteristics of the anode coating. The best arrangement with multiple electrolyzers is to add acid to each one separately. This permits adjustment of acid flows in response to the operating current efficiency of each electrolyzer. Some electrolyzer designs with external anolyte recirculation are well suited to acid addition in the circulating system.

The addition of acid requires continuous monitoring, with an alarm at low pH. This may also be arranged to trip the acid feed. There should also be an automatic shutoff of acid feed when the electrolyzers go off line for any reason. Without this, the reduced OH^- flux across the membrane causes the anolyte pH to fall, increasing the risk of protonation of the membranes.

Although this is not a problem at initial startup, special care must be taken where membranes of different age and current efficiency are deployed in the same electrolyzer, because measurement of the exit pH provides only an average value. The younger membranes will have a lower exit pH if their current efficiency is higher and may be more prone to damage. The rate of addition of acid then must be lower to ensure that individual anolyte compartments do not fall below pH 2. The average oxygen level, therefore, will be higher. When a plant deems it important to operate with acid addition rates close to their maximum, a frequent practice is to install trips based on rate of voltage rise.

13.8.3. Electrolyzer Shutdowns

Frequent shutdowns can have a cumulative deleterious effect on membranes and on the performance and useful life of electrode coatings. They should be avoided. If the current is interrupted for any reason, there are several actions necessary to mitigate this deterioration. Shutdown requirements and system provisions are, therefore, an important part of cell room design.

There are two types of cell room shutdown to consider:

- a normal controlled shutdown, with the load being reduced under operator control
- an emergency shutdown initiated by a process trip, a rectifier internal fault, a major power outage, or operator intervention

We also consider the shutdown of individual electrolyzers for maintenance.

13.8.3.1. Normal Shutdown. Given enough time for a planned shutdown, operators should reduce the load in the normal controlled and incremental manner until caustic cooling is no longer required. Typically, this will be at a load of 2–3 kA m⁻². With the caustic exchanger switched to heating duty (or, where there are separate exchangers, control switched from the cooler to the heater), the load should again be reduced until pressure control can no longer be maintained: Then, the rectifiers should be tripped. Where operation is at pressures significantly above atmospheric, it may be appropriate to reduce the pressure as the load is reduced in order to give better differential pressure control and avoid large transients.

The following actions, as appropriate to the particular system, should begin immediately upon interruption of cell room current:

1. start polarizing rectifier
2. start nitrogen purge of hydrogen header
3. start air or nitrogen purge of chlorine header
4. stop addition of water to caustic circulation loop
5. stop addition of acid to brine feed stream
6. stop export of caustic from catholyte system

These can in general be automated. Some plants leave polarizing rectifiers on during normal operation, in which case they are reliably available at shutdown.

Brine and caustic should continue to flow through the electrolyzers at rates at least equivalent to those required for 3 kA m⁻² operation for some time after loss of current. This keeps the electrolyzers full on both sides and flushes free chlorine from the anolyte. Flushing should last at least 30 min or until the free chlorine content of the brine leaving the cells is below 1 gpl. Appropriate measures also should be taken to prevent reverse flow of chlorine from any part of the system into the electrolyzers. If circulation continues after flushing, the brine and caustic flows should be approximately those required for operation at 2 kA m⁻². Monitoring of cell room parameters should continue at normal frequencies.

Brine and caustic temperatures should be at least 60°C while flushing the cells. This may require addition of heat to the circulating caustic. If the shutdown time is expected to be short, the temperatures may be kept above 75°C. If the shutdown will last more than

several hours or if electrolyzers are to be drained, it is better to allow the electrolyzers to cool. This reduces the rate of transfer of the chloride ion into the catholyte. Temperatures should drop to 40°C before stopping liquor flows and draining the cells. Cooling may be natural or, to speed up the process especially with large electrolyzers, forced by use of the caustic cooler. Polarization rectifiers can be shut off after the temperatures reach 50°C. Gas header purging should continue, with differential pressure control, until the polarizing current is switched off.

Water continues to flow across the membranes when the current to the cells is shut off. This transfer dilutes the circulating caustic. A certain amount of dilution is useful, and the concentration can be allowed to fall into the range used for cell startup (27–32% NaOH is desirable). From that point, addition of concentrated caustic is necessary to maintain some minimum concentration. The most convenient design would include a system for return of product caustic to the circuit from a suitably lined tank. The caustic added must have a low iron content in order not to contaminate the circulating material and adversely affect performance of the cathode coating.

When the cells are drained, it is important to hold the membranes in position against the anodes and to maintain a humid atmosphere in the cells. The following procedure accomplishes these objectives:

1. Stop circulating brine and caustic through the cell room by closing the electrolyzer feed valves and shutting down the feed pumps.
2. Ensure that hydrogen and chlorine header pressures are under control and that the differential is correct. Small header purge flows will be necessary when the electrolyzers are draining.
3. Open the feed brine drain valve to allow the anode chambers to drain.
4. After a few minutes, open the feed caustic drain valve to allow the cathode chambers to drain.
5. When draining is complete, close drain valves.
6. Stop gas header purges (not before shutting down polarizing rectifier).
7. Close all valves to and from electrolyzers in order to maintain internal humidity.

Detailed shutdown procedures vary significantly among technologies. The above should be considered general principles, and the procedures recommended by electrolyzer suppliers should be followed carefully. Some of the differences in procedures are worth highlighting here:

- not all bipolar systems use polarization rectifiers, and without them, flushing procedures are more critically important
- some suppliers or membrane manufacturers may prefer dilution of feed brine during shutdowns in order to lessen the risk of salt precipitation within the membranes
- some plants wash brine and caustic compartments with water by repeated draining and filling

Membrane performance is not unduly affected by shutdowns of long duration. Some operating companies adopt the precautionary measure of occasional refilling and circulation (using procedures as given for restart) if the cells are shut down for several weeks.

13.8.3.2. Emergency Shutdown. Emergency shutdown procedures should consider the possibility that power and instrument air may not be available. Plant design must include provisions to ensure safety and environmental protection and to prevent damage to the electrolyzers or membranes. These may include:

- emergency power supply to polarization rectifiers and critical drives (e.g., chlorine emergency absorption tower fans and circulation pumps)
- provisions for flushing electrolyzers and topping them up with brine and caustic
- uninterruptible power supply backup for DCS
- appropriate air-failure actions for critical valves

An emergency shutdown should automatically initiate all critical actions. These include those listed in the previous section. Typical minimum requirements for electrolyzers equipped with polarizing rectifiers are:

- top up anolyte and catholyte compartments to overflow
- start polarization current flow
- purge hydrogen gas header to atmosphere via relief system
- purge chlorine gas header to absorption system

Particularly if liquid nitrogen is available, the use of nitrogen rather than air for chlorine header purging may be considered more secure during power failures.

An emergency shutdown may be initiated by a process rectifier trip, the loss of incoming AC power supply, a rectifier internal fault, or operator intervention. Rectifier process trips usually include the following:

- high electrolyzer voltage
- high individual cell or module voltage
- low feed brine flow
- low feed caustic flow
- high exit caustic temperature
- high chlorine pressure
- high hydrogen pressure
- low brine feed tank level
- high anolyte tank level

When the cause of a shutdown is the loss of brine or caustic flow and when one of these flows is not available after loss of power, certain technologies require a secure supply of brine or caustic to offset the sudden loss of level in the cells. This is a consequence of escape of the gas bubbles present in both compartments of each cell. Because of the exposure of large areas of membrane to gas, the potential for transfer of hydrogen into the chlorine system is greatest during this period.

It may also be necessary to provide a secure supply of brine for adequate flushing of chlorinated brine from the anode chambers.

Once a safe state has been reached, actions can be taken to restart circulation or to allow the electrolyzers to cool and be drained. Polarization can continue for some hours without significant drop in the liquid levels in the cells. Gas header purges must remain on during polarization.

13.8.3.3. Shutdown of Individual Electrolyzers for Maintenance. In larger monopolar membrane cell rooms, individual electrolyzers may be removed by using an on-load shorting switch to bypass the current around the electrolyzer to be removed. In some small monopolar cell rooms, the entire circuit is shut down, an electrolyzer removed, and a replacement electrolyzer fitted. This practice is justified by the small loss that is sustained in production and the floor area and capital expense that are saved. Shutdowns for cell removal are infrequent, and the change can be made in about 4 hr.

Full plant shutdowns are necessary in bipolar cell rooms that contain only one electrolyzer. Since work must be carried out on the installed electrolyzer to change modules, electrodes, or membranes, downtime can be significant and is a function of the amount of work to be done and the design of the electrolyzer. Bipolar cell rooms with multiple electrolyzers may have one of several different configurations. Several electrolyzers may be fed in parallel from a common rectifier (common in mercury-cell conversions), or individual electrolyzers may be equipped with their own rectifiers (technically, the best modern practice). Electrolyzers also may be made up of a number of packs or frames arranged in electrical series. Section 8.3.1.3 discussed some of these combinations.

When each electrolyzer has its own rectifier, any one can be isolated by shutting down the rectifier and opening off-load DC breakers. With more than one electrolyzer on a rectifier, it may be necessary to lower the current on all associated electrolyzers to zero in order to open the DC breakers on the bus bars to the electrolyzer that is to be removed. An on-load DC breaker may also be used on one bus connection after the total rectifier output has been lowered to that which will apply after removal of the one electrolyzer. Opening an off-load breaker on the other bus attachment completes isolation of the electrolyzer.

Movable shunting switches can also be used on multi-pack bipolar electrolyzers to isolate one pack while allowing the others to stay in operation. This practice adds a layer of complexity to cell room design and operating procedures.

The principal shutdown requirements pertaining to individual electrolyzers are the same as those pertaining to electrolyzers in the cell room as a whole. Besides the requirements for electrical isolation, the plant design and operating procedures must give full consideration to the needs for polarization, over-pressure protection, top-up, flushing, purging, depressurization, cooling, draining, and safe isolation from process streams when individual electrolyzers are to be moved in and out of service. With the wide variations in cell room configuration and electrolyzer design, it is not appropriate to go into the subject in any detail here.

13.8.4. Normal Electrolyzer Startup

Restart of a cell room requires the same attention to detail as the initial start, but it can go more quickly. If electrolyzers have been drained, circulation should be restarted as described above. The cell temperatures for startup should be at least 75°C. Polarization can begin at about 50°C, but not until the hydrogen circuit has been purged properly.

Operation can begin, with load applied, after temperatures reach 75°C. The load can be increased steadily to about 2 kA m⁻². Monitoring of the chlorine gas for its hydrogen content should begin at this stage. After establishing normal operating conditions and

beginning to add acid to the brine to control oxygen formation, the operators can bring the load up to full operating level. As always, the rate of increase must cause no upsets in control of operating pressures, temperatures, or liquor concentrations, but the rate can be much greater than that recommended in Section 13.8.2.2 for initial startup. Ramping up the load should take 30–60 min. A typical rate of increase is 1 kA m^{-2} in 6 min. Once the membranes have been conditioned, the caustic strength can be brought up to the normal operating level.

Every startup provides an opportunity to check the membranes for pinholes by monitoring the current/voltage relationships at low loads (Section 13.8.1.2) and also to check the k-factors of electrolyzers, modules, or cells. This information is valuable in planning future maintenance and cell renewal.

13.9. PLANT PERFORMANCE TESTING

It is common practice to run a performance test in a new plant as part of or soon after startup. In many cases, it is a contractual requirement to show that guarantees have been met. These guarantees principally include:

- caustic production rate and concentration
- electrolyzer DC power consumption
- oxygen content in chlorine gas from the cell room
- hydrogen content in chlorine gas from the cell room
- chloride in caustic product from the cell room

Membrane manufacturers also normally provide a warranty on initial caustic current efficiency, which is typically 95 or 96%. This warranty is normally embedded in the energy consumption guarantee, which is based on the expected voltage performance and current efficiency.

Performance tests on particular vendor packages may also be necessary to enable acceptance of their equipment by the client or main contractor. This is typical in the case of such units as:

- filtration
- brine ion exchange
- caustic evaporation
- chlorine liquefaction refrigeration
- hypochlorite manufacturing
- rectifiers

In any event, tests provide a valuable baseline for tracking performance over time. Provisions for the performance test(s) should be part of the plant design, with procedures carefully spelled out. Startup is a very busy time, and managers should not have to divert their efforts to planning a test run. Furthermore, *ad hoc* arrangements tend to be less safe than carefully designed facilities.

The major objective of a test run will be to demonstrate that the plant can produce the required amount of product at the expected energy efficiency. The relationship between these two parameters is especially important in a chlor-alkali plant. It is usually possible

to operate above design rates simply by increasing rectifier output. The key is to be able to do this without an excessive increase in energy consumption. Because it is onerous to make a run with no variation in amperage, a test protocol should allow some leeway and define an acceptable variation in energy consumption if production exceeds the test requirement.

Energy consumption is measured in kilowatt-hours per ton of product, the “product” being either chlorine or caustic. Most operators and technology suppliers choose caustic as the basis for measurement. This choice reflects the practical difficulties of measuring chlorine production accurately and taking into account system losses that end up principally as hypochlorite or HCl. Another complication is the dependence of anolyte current efficiency on the amount of acid or alkali present in the feed brine (Section 7.5.6.1). The caustic current efficiency, for all practical purposes, depends only on the membrane efficiency. It becomes more convenient and usually more accurate to measure the production of caustic. One need only measure the amount of solution produced and analyze its caustic content. Again for convenience and accuracy, and assuming the use of membrane cells, it is best to measure the output of cell liquor. This separates the electrolyzer and evaporator test runs. These measurements make it possible to calculate the anode current efficiency from analytical data and hence, to calculate chlorine production and specific power consumption.

Other measurements might include:

Electrical

Auxiliary power consumption
Transformer-rectifier efficiencies
Power factor

Consumption of auxiliary materials

Sulfuric acid
Hydrochloric acid
Brine-treating chemicals
Regenerant chemicals

Brine area

Clarifier overflow and sludge
Filter outlet solids content, pressure drop, and operating cycle
Ion-exchange performance
 Hardness of product
 Bed life/breakthrough time
 Chemical consumption
Dissolved chlorine after primary dechlorination

Chlorine process

Dryness
Compressor energy consumption
Refrigeration system output and energy consumption
Liquefaction efficiency

Plant performance testing normally takes place soon after reaching full load and when operation of the entire plant is stable. The performance test is carried out to establish that

the plant can operate to design capacity with energy consumption and product quality in line with technology suppliers' guarantees.

A plant performance test will normally be carried out over a defined period (usually 48 hr or longer) during which the cell room will be operated steadily near the design load. To enable this, it must be established before the test that all peripheral systems are capable of steady operation at the required throughput.

In all cases of measurement, it is important that all the parties agree on the methods of determination before the performance test. This subject should be addressed in the supply contract. Measurement errors are usually to the benefit of the supplier. It is important to understand and agree on the accuracy of the measurements to be applied.

In order to determine accurately caustic soda production rate several approaches may be adopted. These are:

- Collection of caustic in a calibrated tank. This will enable volumetric production to be determined. Samples of caustic into the tank will be taken and analyzed for concentration. The mean density of the collected liquor is a function of the mean concentration and the tank temperature. The production rate can then be determined from the measured volume and the density. Caustic production is normally quoted as tons 100% NaOH or KOH. Tank calibration charts may be available. Alternatively, measurements of mean diameter may be made with due allowance for any internals. Level may be determined by dipping using a tape and plumb bob.
- In smaller plants, collection of caustic in a road tanker barrel followed by weighing on a plant weighbridge. Mean caustic concentration may be determined from averaging analyses of production at regular intervals or by sampling and analyzing the mixed contents of the tanker.
- Determination of caustic production rate using a flow meter. This is the most convenient method, but it is not always favored because of the lack of certification of calibration. The accuracy of electromagnetic flow meters and Coriolis mass flow meters is very high ($c. \pm 0.5\%$) and reliable results have been obtained consistent with other methods of measurement. Both types can be used to integrate flow. The Coriolis type is particularly advantageous, as it does not require separate density determinations.
- Indirect determination of caustic production rate may also be made from chemical analysis of cell room current efficiency and the current measurement. Several readings may be made during the course of the test and the results averaged.

In order to determine energy consumption, accurate measurement of the current is necessary. This is normally determined from shunts or Hall effect meters on the bus bars (Section 8.3.1.5). Voltages are measured at appropriate points on the bus feeding the electrolyzers, and the unit energy consumption is

$$E = \frac{VIt}{W} \quad (1)$$

where

E = energy consumption. DC kWhr t⁻¹ caustic

V = voltage across cells

I = direct current, kA

t = duration of test, hr

W = weight of 100% caustic produced, t

The leading technologies using high performance membranes typically achieve energy consumption figures of 2,050–2,200 kWhr t⁻¹ NaOH at 5 kA m⁻². Performance is often quoted at about 32% NaOH and 90°C. It is not practical to achieve exactly equal and constant temperatures on all electrolyzers, and in practice, operating temperatures may vary typically between 85–90°C. Caustic soda concentration may vary ±0.5% throughout a test. The cell voltage is directly related to temperature and caustic strength, increasing as temperature falls or caustic strength rises. Correction factors are normally applied to the test result voltage figures to make allowance for any deviation. Typically, accepted corrections are to add/subtract 9–10 mV for each degree Celsius that the operating temperature is above/below 90°C and to add/subtract 15–17 mV for each 1% in strength that the product NaOH is below/above 32%. More correctly, these corrections should vary with current density, but the size of this correction is small. The corrected voltage is used in the above formula to determine energy consumption.

Oxygen and hydrogen in chlorine will be determined by Orsat analysis or gas chromatography. Results of samples taken at intervals will be averaged.

Chloride in caustic will be measured on samples of electrolyzer product taken at intervals during the test and the results averaged.

It is important to have a period of steady operation for at least 24 hr before running a performance test. This allows the performance of the electrolyzers and major processing equipment to stabilize.

13.10. CELL ROOM OPERATING SPECIFICATIONS

13.10.1. Product Quality

The following are typical of expected or guaranteed product characteristics from membrane electrolyzers operated properly under specified conditions:

Chlorine gas (dry basis):

min. 97.5% (v/v) Cl₂

max. 0.05% (v/v) H₂

appr. 1.8% O₂ (v/v), or max. 1% with feed brine acidification

Hydrogen gas (dry basis):

min. 99.9% H₂

Sodium hydroxide solution:

typ. 32% NaOH

max. 40 ppm NaCl (solution basis)

13.10.2. Electrolyzer Voltage and Energy Consumption

Electrolyzer voltages, for all practical purposes, are linear with current density over the normal operating range. The following equation, which is similar to Eq. (8.5), applies:

$$V = V_0 + kI/A \quad (2)$$

where

V = cell voltage

V_0 = intercept voltage

k = slope of line (often referred to as “k-factor”—see Section 4.4.4.4)

I = current, kA

A = active area of membrane, m^2

The intercept voltage, V_0 , is principally the aggregate of the anode and cathode half-cell reversible potentials, the anode and cathode overpotentials, and the liquid-junction potential at the membrane (usually small). For a typical new cell with activated cathodes, V_0 is about 2.4 V. With uncoated cathodes, this increases to about 2.7 V.

The k-factor is very dependent upon the electrolyzer design and type of membrane used. Older monopolar electrolyzers using robust membranes may have a k-factor in the range 0.25–0.3, while the most modern bipolar electrolyzers using low-voltage membranes may operate with k-factors of 0.12–0.15.

It is common to quote operating voltage data normalized to a standard load. This is useful for performance trending where operating load varies. The usual method is to assume a constant E_0 and adjust the voltage according to the calculated slope, k . The current density to which data are normalized has often been 3–4 $kA\ m^{-2}$. This is useful for comparisons between plants. However, normalization to a representative load will incur less error and for modern bipolar operation at higher current density, normalization to 5 $kA\ m^{-2}$ is more appropriate.

The normalized voltage is given by the equation

$$V_2 = V_0 + (V_1 - V_0) \frac{I_2}{I_1} \quad (3)$$

where

V_2 = voltage normalized to current I_2 (current density I_2/A)

V_1 = voltage measured at operating current I_1 (current density I_1/A)

Energy consumption is related to the current efficiency as well as to the voltage:

$$E = 67,000 \frac{V}{\xi} \quad (4)$$

where

E = energy consumption, $kWhr\ t^{-1}\ NaOH$

V = operating or normalized voltage, V

ξ = NaOH current efficiency, %

If current efficiency is routinely determined for electrolyzers, energy consumption also can be trended and compared. Equation (4) relates specifically to NaOH. It is easily adapted to the case of chlorine or KOH by substituting the proper stoichiometric factor (47,770 for KOH). Section 4.4.3 contains an exhaustive discussion of the subject of current efficiency.

An excessive rise in voltage or fall in current efficiency should be investigated carefully. A very good operating plant will demonstrate a cell voltage rise of 1–2 mV per month and a current efficiency decline of less than 0.5% per year. The degree of acceptable deterioration depends to a large extent upon the energy cost. A voltage rise of 5 mV per month and a current efficiency decline of 1% per year may be considered acceptable if the energy cost is low. If deterioration rates are significantly greater, however, improvements should be sought in any case. Achieving stable voltage and efficiency, and hence stable energy consumption, depends mostly on the ability to maintain the specified operating conditions set out in this chapter and defined by the membrane and electrolyzer suppliers. Electrolyzer design, frequency of shutdowns, appropriate choice of membrane, and robustness of the electrode coatings also play a part. The rate of deterioration of current efficiency depends on the physical condition of the membranes and the rate of accumulation of impurities. Examination and analysis of a sheet of membrane by the supplier will determine the causes of deterioration and help in planning a program for remediation.

The reasons for an increase in voltage can be more complex and harder to identify. Voltage increases result most commonly from damage or poisoning of anode or cathode coatings and from effects of physical damage or impurity damage to the membranes. Organics present in the brine may also affect voltage by blanketing the anode or membrane surface or causing foaming. This list of causes is by no means exhaustive, but these are the common ones with which to start troubleshooting voltage deterioration. The current/voltage relationship discussed above is affected differently depending upon the cause of the voltage rise. Voltage rise caused by anode or cathode coating performance deterioration or damage will show as an increase in the intercept voltage E_0 . An increase in voltage resulting from membrane problems or deposition of impurity at the anode-membrane interface will show as an increase in k-factor. Foaming or problems with gas release may introduce non-linearity at higher current densities. Measurement of voltage over a range of current densities can give some pointers for further investigation. Section 4.4.4.4 discusses the k-factor and the interpretation of voltage/current plots in some detail.

13.10.3. Membrane Operating Conditions

The process conditions that determine the environment in which the membranes operate are critical to avoiding physical disruption of the polymer structure and obtaining good performance and long life. Membranes should operate at high temperature to keep their electrical conductivity high and with the right electrolyte concentrations to achieve a desirable rate of osmotic water transport and maintain the right equilibrium water content in the polymer. Table 13.1 gives typical operating conditions. These values represent averages of the conditions recommended for the various technologies. There

TABLE 13.1. Selected Membrane Operating Conditions

Parameter	Allowable range	Typical value
Feed brine concentration	270–305 gpl	300 gpl
Exit brine concentration	190–230 gpl	200 gpl
Feed brine pH	<11.6 at 23°C	
Exit brine pH	>2	2–4
Feed NaOH concentration	28–32% (w/w)	30%
Exit NaOH concentration	30–33% (w/w)	32%
Exit caustic temperature	80–90°C	87°C
Exit brine temperature	80–90°C	87°C
Differential pressure	5–30 mbar	20 mbar
Current density	1.5–6 kA m ⁻²	

are variations that depend on cell design and membrane type, and these of course take precedence over the above summary.

13.10.3.1. Brine Concentration. Membrane plant brine systems are designed to produce and handle brine at concentrations that will give satisfactory membrane performance in the long term. The exit brine concentration should protect the membranes against irreversible physical damage and the loss of current efficiency. A typical value recommended by membrane and technology suppliers is about 200 gpl NaCl. Many plants operate at higher concentrations.

As brine concentration decreases, osmotic water transport through the membrane increases. The sulfonic anolyte layer of a composite membrane carries this increased flow easily, but the carboxylic cathode layer is more resistant. Osmotic pressure therefore builds up between the layers. This causes the formation of blisters or, in the extreme, complete delamination of the membrane. A lower limit of about 170 gpl NaCl on the brine concentration protects against these problems and incidentally prevents any loss in current efficiency due to low salt concentration. The value of 200 gpl mentioned above allows for some variation between electrolyzers and their individual cells.

The feed brine concentration normally is fairly closely controlled in the brine plant. A typical operating specification is 300 gpl NaCl. Higher concentrations can lead to salting out in the electrolyzers as the system cools when off load. The proper combination of feed and exit brine concentrations gives satisfactory utilization of the salt.

With a given feed concentration, setting the flow rate to the electrolyzers according to the operating load controls the exit brine strength. The brine flow rate corresponding to any load can be programmed into a DCS. This is an effective way to keep the membrane environment under proper control. This programming should take into account the special requirements of startup, shutdown, and load changes.

13.10.3.2. Caustic Concentration. The structure of the membrane determines its optimum caustic concentration. The exact values must be set with this in mind. Excursions from the recommended range change equilibrium water content and water

and hydroxyl ion transport rates. These changes can cause irreversible damage by swelling, blistering, or solids deposition in the membranes. Composite membranes also can decarboxylate at high temperature. The maximum allowable temperature decreases at high caustic concentration, and prolonged operation of typical high-performance membranes above 35% NaOH can significantly reduce the operating life of the membrane.

Current efficiency continues to improve as the NaOH concentration rises above 30%, and it remains high at least up to 35%. However, the electrical conductivity of the membrane decreases in this range, and so the operating voltage and the internal temperature of the membrane also increase. This contributes to a shorter membrane life by accelerating decarboxylation if NaOH concentrations remain above 35% for any significant period of time. The normal operating range for many membranes therefore is 30–33% NaOH. Where the final product concentration is to be about 50%, clearly it is preferable to operate in the upper part of this range. Operating concentration targets then are normally 32–32.5%.

The exit caustic concentration is determined by the amount of water added to the recycle caustic loop or directly to the electrolyzers. At the recycle rates assumed here, the feed caustic concentration is typically 2% lower than the exit concentration.

Historically, membranes have been developed by some suppliers specifically for KOH production. Since these differ from NaOH membranes, some details will change but most of the same general phenomena occur. Since the KOH membranes are simpler in construction, they are correspondingly more resistant to the stresses of operation. The tendency now is to use higher-performance membranes that have been developed for NaOH service. Those using these membranes must remember that an important characteristic of KOH manufacture is the lower osmotic water transport through the membrane. For this reason, some membranes are more suited to KOH manufacture than others, and technology and membrane suppliers' experience should be sought if problems are to be avoided.

13.10.3.3. Operating Temperatures. High operating temperatures also decrease the voltage losses due to the resistivity of the membranes and the liquors in the electrolyzers. However, the amount of water vaporized and therefore the volume of the saturated gases produced also increase significantly. Membrane stability also decreases at high temperature, and decarboxylation becomes more likely. There is no net advantage in operating above 90°C. In practice, there will be a range of membrane ages and operating voltages in a mature cell room, and the operating temperatures of the membranes will vary somewhat. The safe range of operation is usually considered to be 80–90°C.

As noted above, the feed brine concentration is determined in the brine plant, and its feed rate is controlled to hold the desired exit brine concentration. There is a different philosophy for control of the caustic feed rate. The exit caustic concentration is determined by the amount of water added to the recycle caustic loop (or directly to the electrolyzers when there is no external recycle). The circulation rate of caustic is determined by the need for control of the temperature of the electrolyzers. At low operating loads, the caustic stream provides heating; at higher loads, it provides cooling. The crossover point depends on the operating voltage and heat losses. It is typically in the

range 2–4 kA m⁻². Some operators find from experience and modeling that the caustic and brine feed flow rates should be proportional to each other. A caustic flow 1–1.6 times the brine flow is typical. Equal rates are appropriate with new cathode coatings. Higher caustic rates are advisable with grit-blasted nickel cathodes. The ability to vary the caustic feed rate gives more flexibility in temperature control. With the rates quoted and with a brine depletion of 80–100 gpl across the electrolyzers, the difference between feed and exit caustic concentrations will be about 2%. Other operators, with certain electrolyzer designs, prefer higher caustic recycle rates. These reduce the changes in temperature and concentration across the electrolyzers and help to give a more uniform catholyte.

With the high rates of transfer of mass and energy across the membranes, it is not always practical to control caustic and brine exit temperatures independently. In practice, it has been found that satisfactory control is achieved in modern electrolyzers with the feed brine and caustic at similar temperatures. The temperatures required depend on operating voltage and typically will be 75–80°C for new electrolyzers with coated cathodes. Older electrolyzers will require lower temperatures, but they usually remain above 60°C. Electrolyzers operating at a low current density, and particularly those with coated cathodes and new membranes, require higher feed temperatures. However, feed temperatures should not exceed 90°C. The exit brine and caustic temperatures in such a case may be in the lower end of the desirable range.

The lower operating temperature limit for membranes is about 75°C. This is set in order to avoid damage by blistering. As temperatures fall, the ohmic heating due to the electrical resistance of the membrane increases. Excessive generation of heat can produce local overheating on a molecular scale, resulting in a higher internal vapor pressure, which causes the membrane to blister.

13.10.3.4. Brine pH. The pH of the brine leaving the purification section depends on the amount of excess alkalinity used in treatment. When the feed brine is alkaline, the upper limit suggested in Table 13.1 protects against rapid wear of the anode coating. The pH of the brine leaving the electrolyzers then is usually approximately 4. When acid is added to the brine to improve the quality of the cell gas, the pH of the exit brine must remain above 2 to avoid the risk of protonation of carboxylic membranes. Such damage is irreversible and results in higher voltage and, in the limit, renders the membranes nonconductive.

13.10.4. Cell Room Material Specifications

13.10.4.1. Brine Purity Specifications. Brine feed specifications depend on the specific types of membrane, anode coating, and cathode coating in use. They may vary slightly with the manufacturer, the planned operating conditions (principally current density), and the extent of the warranties provided. Table 4.8.8 gives a sampling of recommended specifications. Impurities may originate with the salt or the process water, and the required brine treatment varies widely with the nature of these sources. Section 7.5 discusses the various treatment processes.

TABLE 13.2. Specification for Hydrochloric Acid

Analysis	Specification (mgpl)
Heavy metals (incl. iron)	0.5
Hardness (as CaCO ₃)	0.5
Free chlorine	0.5
Chlorinated organics	10

Basis: 32–36% HCl

TABLE 13.3. Specification for Demineralized Water

Analysis	Specification
Chloride	1.0 ppm (w/w)
Iron	0.5 ppm (w/w)
Mercury	0.1 ppm (w/w)
Lead	0.05 ppm (w/w)
Total hardness	0.05 (as calcium)
Conductivity	5 $\mu\text{S cm}^{-1}$

13.10.4.2. Hydrochloric Acid Specification. The specification in Table 13.2 is generally applicable for electrolyzer feed brine acidification, depleted brine pH control, and ion exchanger regeneration. The contaminant levels relate to normally available commercial concentrations of 32–36% HCl. Hydrochloric acid used for brine acidification should be sufficiently dilute to prevent any risk of salting out. This aspect is covered in Section 7.5.6.1.

13.10.4.3. Demineralized Water Specification. Table 13.3 gives a typical specification for water added to the catholyte circuit and used in ion-exchange column regeneration. It may be applied to evaporator condensate as well as to demineralized water.

13.10.5. Sources and Effects of Impurities

13.10.5.1. Impurities in Brine. Control of brine impurity levels is achieved by a combination of chemical treatment plus ion exchange and an effective purge from the brine circuit. The purge may be made selective by some of the techniques discussed in Chapter 7. The qualitative effects of some of the major impurities are discussed in some detail in Chapter 4, and Table 7.10 summarizes effects and remedies. Still, a brief summary as part of this discussion does not seem out of place.

Impurities affecting membranes are generally divided into those affecting voltage (Mg, Ni, Fe) and those affecting current efficiency (Ca, Sr, Ba, Al, Si, I, SO₄). Mechanisms can be complex, and synergistic effects are not uncommon. Examples of the

latter are:

1. Ba and I, which can combine under alkaline conditions to form barium paraperiodate;
2. Ca, Al, and Si, which can form any of several precipitates, depending on the conditions in the cell and the relative concentrations of the three elements.

Suppliers' specifications for these impurities vary. This is partly a consequence of differences in membrane architecture.

Some impurities can also affect electrode performance. Those that affect anode coating life or performance include F, Fe, Mn, Pb, Ba, SO_4 , and organics. Impurities such as Hg and Pb may migrate through the membrane to affect the cathode coating. There is also evidence that iron brought in as ferrocyanide in the feed salt can affect the cathode.

13.10.5.1A. Effects of Calcium and Magnesium. Calcium and magnesium in the brine migrate into the membrane and toward the cathode under the influence of the electrostatic field. The corresponding hydroxides form inside the membrane, where they can precipitate. Calcium hydroxide precipitates within the carboxylic layer of the membrane and causes physical disruption. This layer determines the current efficiency of the membrane, and so the effect of calcium is principally upon that variable. Magnesium hydroxide, which is less soluble, precipitates at or near the surface of the sulfonic layer and causes an increase in electrolyzer voltage.

13.10.5.1B. Effects of Aluminum and Silica. There is a synergy between aluminum and silica that can lead to the formation of complex crystalline aluminosilicates within the membrane. Again, the consequence is a loss in current efficiency. Aluminum, if present in sufficient concentration, will also precipitate at the anode/membrane interface. This causes a very slight increase in voltage that can be reversed when the electrolyzer shuts down.

Problems with aluminum and silica sometimes occur when vacuum purified salt is used without primary chemical treatment. That part of the process often removes most of these secondary impurities by co-precipitation. Contamination by filter media is usually avoided by proper selection of materials (Section 7.5.4).

13.10.5.1C. Effects of Iodine. Iodide from the salt oxidizes within the membrane and anolyte compartment to iodate or periodate. In a brine resaturation circuit, there is thus a slow buildup of iodate, which can diffuse into the membrane and precipitate as crystalline paraperiodate salts. Once again, the consequence is an increase in voltage and a loss of current efficiency.

Sodium paraperiodate itself is quite insoluble. In addition, iodine interacts with barium to form the insoluble barium paraperiodate.

13.10.5.1D. Effects of Chlorate. Chlorate ion is a product of the current inefficiency reactions in the anolyte. Its accumulation can be controlled by purging or decomposition.

Membrane manufacturers recommend a maximum level of about 20 gpl NaClO_3 in the anolyte. There is a finite diffusion rate of chlorate across the membrane, resulting in contamination of the product caustic, and high levels of chlorate will reduce the solubility of salt and interfere with the determination of brine concentration by density. The authors have never encountered problems with membranes that were attributable to high chlorate concentrations.

13.10.5.1E. **Effects of Sulfate.** Excessive amounts of sulfate in the brine can lead to the precipitation of certain sulfate compounds in the carboxylic layer of the membrane. This reduces the current efficiency. Therefore, a maximum sulfate level of 8 gpl Na_2SO_4 in the feed brine is recommended. The sulfate concentration can accumulate to this level unless it is controlled by purging or by some removal process. Section 7.5.7 discusses a number of candidate processes.

13.10.5.1F. **Effects of Organics.** Some organic compounds have serious detrimental effects on anode voltage and service life. They can directly increase the rate of wear of the anode coating or blanket the coating and reduce its activity. The same effects can occur as a result of foaming caused by the organics.

Examples of possible sources are:

- lubricating oils and greases
- hydraulic fluids
- solvents used in maintenance work
- paint
- certain anticaking agents
- brine makeup water
- plant wash water
- certain flocculating agents
- salt
- airborne material
- ground water
- sealants and adhesives

Commissioning engineers, in particular, will be wary of organics, particularly if there is no analytical history or experience at the plant site.

Not all organics are harmful. For example, humic acids found in lake water and often used for brinemaking may produce some foam, but they are usually tolerated and do not appear to affect anode coatings. Similarly, short-chain volatile species are unlikely to have a serious effect on electrolyzer operation. Long-chain hydrocarbons, on the other hand, may cause serious damage.

13.10.5.1G. **Effects of Barium.** Barium sometimes is present in the salt in high enough concentration to be of concern. It is also used in some plants to precipitate sulfate ion from the brine. In the latter case, it must be used with care in order not to become a problem

in its own right. If the solubility product of BaSO_4 is exceeded, it will precipitate and scale the anode surface. The result is an essentially irreversible large increase in voltage.

The interaction of barium with iodine was mentioned in Sections 7.5.8.9 and 13.10.5.1C.

13.10.5.1H. *Effects of Nickel.* Nickel in the feed brine may deposit on the anode face of the membrane and raise the cell voltage. The sensitivity of the various membranes varies significantly in respect of nickel. Nickel is not normally present in salt, but it arises in the brine as a corrosion product. Its presence is likely in integrated plants that rely on diaphragm-cell evaporator salt or conversions of diaphragm-cell plants that use the existing evaporators to concentrate depleted membrane-cell brine.

13.10.5.1I. *Effects of Iron and Heavy Metals.* Iron and heavy metals have several objectionable effects. Manganese, lead, and iron will poison anode coatings and raise their overvoltage. Mercury and lead can pass through the membrane and poison the cathode coating, raising the overvoltage on that side of the cell. Mercury contamination usually is the result of a plant conversion. It can be prevented by disposal of heavily contaminated equipment and proper cleaning of the brine system [19]. Another cause of mercury contamination is the partial conversion or expansion that uses a common brine circuit. Some means of continuous removal of mercury may be required in this case.

Depending on the pH of the anolyte, iron precipitates on or close to the anode surface of the membrane. Under acidic conditions, it penetrates into the membrane and contributes to a rising voltage. Iron from anticaking agents has a tendency to accumulate in the anode compartment and form a brown deposit at the anode/membrane interface. Suitable means of analysis to achieve the sensitivity required are not usually deployed in a chlorine plant, and it is then necessary to make use of a specially equipped analytical laboratory.

13.10.5.1J. *Effects of Ammonia.* Many nitrogen compounds, especially ammonia and its derivatives, are converted to nitrogen trichloride in the cells. The entry of this highly explosive compound into the chlorine gas is the chief concern with nitrogen compounds, not their effects on cell performance. Section 9.1.11.2 gives a lengthy discussion of the formation of nitrogen trichloride and the management of this hazard.

13.10.5.2. Effects of Impurities in Caustic. Iron in the catholyte will plate out onto the cathode surface, and so its concentration must be kept at a low level. If the cathodes are coated, the iron deposit poisons the surface and raises the overvoltage and in turn the electrolyzer voltage. The concentration of iron is best limited by avoiding ferrous metal components in the catholyte system, using water that meets the specification of Table 13.3 to dilute the circulating caustic, and ensuring that any caustic used to fill the caustic circuit or make up the concentration during shutdowns is free of contamination.

Mercury also acts as a poison for precious metal-coated cathodes. If present in a brine circuit as a result of conversion from mercury to membrane technology, it would pass through the membranes and contaminate the cathodes. For this reason, a brine circuit

TABLE 13.4. Impurity Limits in Cell Caustic

Metal	Normal	Startup
Iron	0.7	1.0
Mercury	0.1	0.7
Lead	0.05	0.1

All data are ppm in solution.

needs to be thoroughly cleaned up during the conversion phase, or a mercury-removal resin must be employed.

Similarly, lead is a poison that will plate out on the cathode and so should be absent from the brine and the caustic. Table 13.4 gives typical recommended limits for metallic impurities. The water used to dilute the catholyte should meet the specification of Table 13.3.

13.10.5.3. Impurities in Chlorine Gas

13.10.5.3A. Hydrogen in Chlorine. The contamination of chlorine with hydrogen is the most common cause of explosions in chlorine plants. Membrane-cell plants are no exception to this statement. One feature of newer membrane cell designs—the complete flooding of the liquor chambers—reduces this hazard, but cross-contamination still occurs as a result of membrane damage. Such damage can take the form of “pinholes” or splits. Pinholes can result from

- abrasion from a membrane rubbing against a rough electrode surface as a result of instability of the pressure differential;
- puncture from a sharp electrode structure pressing against the membrane;
- blistering and degradation of the polymer resulting from incorrect operating conditions (typically occurs locally at the top of the membrane in the gas space of some electrolyzers).

Splitting of membranes usually is associated with tensile failure as a consequence of shrinkage caused by drying during off-load periods. The authors' experience is that splits occur in service because of physical damage such as that caused by a cutting knife during handling of the membrane. The cut or score opens under the stress caused by shrinkage when the membrane is exposed to process fluids.

Hydrogen in chlorine is normally about 0.02% with new membranes. This results from the normal diffusion of hydrogen. A detectable rise in the hydrogen concentration usually indicates some form of membrane damage and so should be carefully monitored. Monitoring is not normally applied on an individual cell basis, but all electrolyzers or packs should be provided with sample points. The technology supplier's advice as to the level at which action is to be taken should be followed. Investigation of levels exceeding 0.1% may be advised with a view to repair all electrolyzers. The impact of high hydrogen levels on individual electrolyzers on the overall cell room level must be considered, as this has an impact on liquefaction control. Cell room levels

above about 0.2% hydrogen will be expected to affect liquefaction efficiency and possibly result in hazardous concentrations in the tail gas if proper action is not taken (Section 9.1.7.2).

Monitoring routines should be set up to ensure that elevated levels of hydrogen in chlorine are detected in a timely manner to avoid the accumulation of explosive concentrations in the chlorine processing system. The monitoring points and frequencies for individual electrolyzers will be determined by the configuration of the cell room. The important actions are to detect significant rises in individual electrolyzers and to take timely corrective action. It is normal to use a gas chromatograph for this purpose in order to obtain the sensitivity required. In normal operation of a cell room with multiple electrolyzers connected to a common header, each such header should be checked at least every 8 hr. Any detectable rise should be traced to its source for appropriate action. Individual electrolyzers may be checked daily. In a plant with chlorine liquefaction, deployment of an on-line analyzer for hydrogen in chlorine on the liquefaction tail gas provides an additional and rapid indication of any change in the cell room.

13.10.5.3B. Oxygen in Chlorine. Oxygen in chlorine is a by-product arising from the inefficiency of the membrane that allows back-migration of hydroxyl ions into the anode compartment. These ions react with chlorine to form hypochlorous acid that is oxidized at the anode to form oxygen and chlorate. The relative amounts of these two by-products depend on the anode coating composition. In a cell operating with a good efficiency of 96%, the oxygen content of the chlorine will be in the range 1–2% (dry basis) with brine fed at pH 3–10. Excess alkalinity in the feed brine also contributes to by-product formation. Addition of HCl to the brine neutralizes hydroxyl ions, reduces the oxygen content of the chlorine gas, and improves the anode current efficiency.

Within certain limits, the desired oxygen content in the chlorine influences the choice of feed brine pH. These limits in turn depend on the type of membrane being used. The profile of pH within the membrane is such that in normal circumstances the membrane environment is alkaline. If the membrane is subjected to acidic conditions, protonation occurs. As a result, the membrane ceases to conduct and the voltage rises rapidly. The damage is irreversible but can be contained if detected quickly. Therefore, the membrane manufacturers recommend a minimum anolyte pH of 2. This is low enough in most circumstances to allow control of oxygen levels in the region of 0.5–1.0%. Data presented in Section 7.5.6.1 show that the feed pH may be less than one, particularly if the membrane current efficiency is low. In a well-mixed anode compartment, the acidic brine mixes with the bulk electrolyte so that the membrane does not see very low values of pH. The rate of mixing becomes more important as the acidity of the feed brine increases. The amount of acid required to achieve low oxygen levels also depends upon the electrode geometry and the type of coating used.

As performance deteriorates, the acid addition rate must increase to maintain the current efficiency. The exit pH should remain substantially constant and can be monitored continuously to be sure that the lower limit is not exceeded. It is not practical to adjust and monitor the pH for every membrane. Some safety margin therefore is necessary to allow for the variability within groups of membranes.

It is preferable to operate a preliminary pH control stage after ion exchange. Controlling this stage to pH 3 neutralizes any carbonate residual from primary brine treatment. Deep acidification (pH < 2) is best practiced by adding acid to feed brine on an individual electrolyzer basis. Flow ratio control may be used.

Although there may be some latitude in operation, as the membrane surface will remain alkaline because of the hydroxyl ion flux, the situation becomes more critical when hydroxide ion transfer stops at shutdown. Acid addition must then stop immediately. Additional protection may be obtained from monitoring voltage rise on electrolyzers. The rise caused by overacidification will be rapid, but rapid action to stop acid addition may obviate damage.

13.10.6. Cell Operating Conditions

13.10.6.1. Current Density. Design current density depends on electrolyzer design capability and the optimization of capital, operating, and maintenance costs. Currently, electrolyzer technologies permit operation in the range of 4.5–6.5 kA m⁻². This range is compatible with the capabilities of modern membranes in well-designed electrolyzers. This range will continue to shift upward as operating experience with new electrolyzer designs increases and as further design improvements become available.

In regions with relatively high power cost, operation at lower current densities is favored. Where power costs are low, operation at higher current densities, say 5.5 kA m⁻², is economic. Design output usually is based upon a design current density and a starting caustic current efficiency of 95–96%. Some allowance is normally made for loss of current efficiency during the membranes' lifetime, and a higher operating current may be required. In multi-electrolyzer cell rooms, some capability may also be provided to maintain design output during maintenance of an electrolyzer.

Operating flexibility down to a minimum load of 1.5 kA m⁻² is normally available. However, contamination of the caustic product by chloride ion migration across the membrane increases rapidly below 2 kA m⁻². The lower operating limit may be governed by this consideration, especially in KOH production.

13.10.6.2. Caustic Soda Concentration. Membranes are optimized during manufacture for operation within a specified range of caustic soda concentration. Excursions outside this region will change the equilibrium water and hydroxyl ion migration rates, and irreversible damage in the form of swelling or blistering may result.

Membranes will chemically degrade by decarboxylation if subjected to high temperature. This effect is reinforced at higher caustic concentrations, and membrane life can be reduced significantly by prolonged operation above 35% NaOH.

Membrane current efficiency improves as the NaOH concentration increases above 30% and is still high at 35%. However, laboratory tests show that the electrical conductivity of membranes decreases with increasing caustic concentration. This in turn leads to increases in voltage and internal temperature of the membrane due to ohmic heating.

13.10.6.3. Brine Concentration. The design basis for the brine concentration in a membrane cell is chosen according to the characteristics of the membrane to give satisfactory

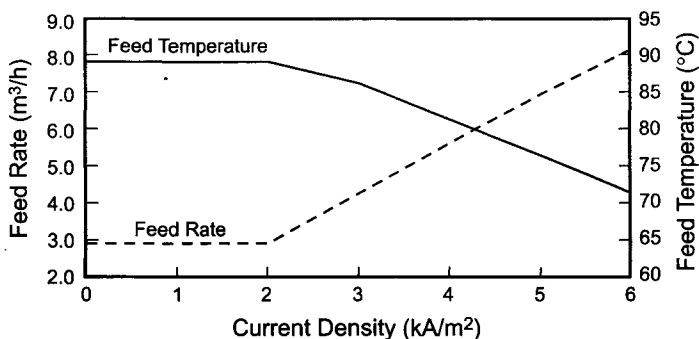


FIGURE 13.9. Electrolyzer feed rates and temperatures.

long-term performance. The exit brine concentration should be maintained in the vicinity of 200 gpl both to achieve satisfactory salt utilization and to protect the membranes against physical damage and loss of current efficiency. This target concentration allows for the variation that may occur between electrolyzers or individual cells. Low concentrations carry the serious risk of irreversible physical damage. A lower limit of 170 gpl may be specified. As the brine concentration decreases, osmotic water transport increases. The increased water flow is carried easily by the sulfonic anolyte layer but less readily by the carboxylic catholyte layer. Membranes form blisters, or in the extreme, delaminate completely, as a result of the internal buildup of osmotic pressure between layers. The effect of brine depletion on current efficiency is not great unless the exit concentration actually drops below 170 gpl.

13.10.6.4. Electrolyzer Feed Rates and Temperatures. Calculated brine and caustic feed rates for a 100-m² electrolyzer over the range of operating current density 2–6 kA m⁻² are shown in Fig. 13.9. The data are based on the following typical operating conditions:

Electrolyzer exit temperature	87°C
Brine feed concentration	300 gpl
Brine exit concentration	210 gpl
Product NaOH concentration	32.0%

The electrolyte feed temperatures corresponding to expected voltages in early membrane life also are shown in Fig. 13.9. The circulation rates and feed temperatures on the two sides of the membrane are shown as equal. In practice, the caustic circulation rate may be increased to improve cooling of the caustic. The feed temperatures also may differ from each other but should remain within about 10°C in order to maintain good control and reduce thermal shock on the membranes. The exact figures, of course, depend on electrode design and the condition of the membranes and electrodes.

The rate of demineralized water addition to the caustic circuit varies with load as shown in Fig. 13.10. Note that most of the water required by the cathode reaction together with that lost by evaporation and that required for dilution of the product passes through the membranes by electro-osmosis. The balance to be added to the circulating caustic is critical to concentration control. Calculated rates may be used for planning and startup,

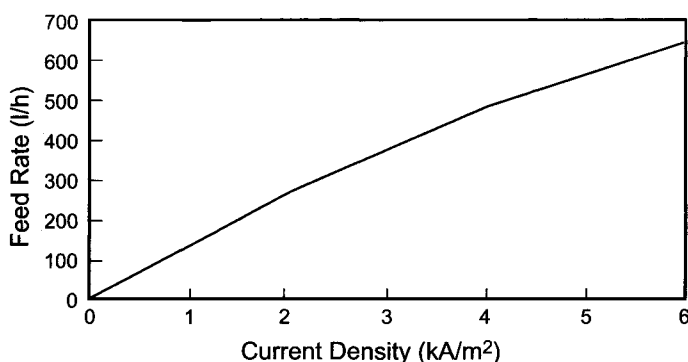


FIGURE 13.10. Water feed rate as a function of current density.

but they must be checked and verified during commissioning. As the membranes age, minor adjustments from established rates may be necessary to maintain concentration based on analysis.

Note that the relationships in Figs 13.9 and 13.10 are approximately linear over the normal operating current density range of the electrolyzers. This makes the job of modeling the behavior of the electrolyzers easier.

13.10.6.5. Operating Temperatures. To minimize voltage losses due to the resistivities of the membrane and the liquors present in a cell, it is normal practice to operate at as high a temperature as practicable. Higher temperatures bring lower voltage drops. As the temperature increases, however, the amount of water vapor and therefore the volume of saturated gas produced, increase rapidly. In addition, the stability of the membrane decreases, and decarboxylation becomes more likely. There are no net advantages to be gained by operating above 90°C. On the other hand, the lower operating temperature limit for most membranes is 75°C. This is set in order to avoid localized internal overheating due to the higher electrical resistances, which can cause blistering of membranes.

The normal range of acceptable operating temperature is 80–90°C. In a new cell room with new membranes of similar performance, it is possible to maintain temperatures on individual cells and electrolyzers within a tight band, and a typical target exit temperature would be 87°C. In an established cell room, the acceptable range provides adequate flexibility to accommodate membranes of different ages with different voltage performance.

Actual feed temperatures vary inversely with the operating load. They also will become lower as electrodes and membranes age and energy consumption increases. Typical feed temperatures on modern electrolyzers, depending on operating load, will vary from 75 to 85°C at the beginning of their life. End-of-life conditions may require feed temperatures down to about 65°C.

The circulating caustic provides the all-important temperature control for the electrolyzers. The flow rate will vary from 1–1.6 times the brine feed rate, according to design. At low loads, it is necessary to heat the caustic in order to overcome thermal and

evaporative heat losses that outweigh the heat generated by electrical resistances and overpotentials. At higher loads (typically above $2\text{--}3\text{ kA m}^{-2}$), cooling is necessary.

13.11. ROUTINE MONITORING AND ANALYSIS

The effective monitoring of process parameters and analysis of key process streams are essential to ensure process safety and maintain efficient operation with low operating and maintenance costs. The responsibility for carrying out analytical routines normally is divided between process operators and laboratory technicians. Most plants will also have a number of on-line analyzers monitoring critical parameters. Laboratory analyses to check these analyzer readings should be part of the routine. The wide use of distributed control systems with their extensive capability for recording and trending data has reduced the need for operator logsheets to some extent. All manually obtained process, analytical, and voltage data for the plant should be recorded on suitably prepared logsheets or entered into a database and retained for future reference.

It is important that responsibility for action based upon the data collected is also correctly apportioned. It will be the responsibility of the shift supervisor to take urgent decisions affecting safety and operational issues. Plant technical management should carefully review performance and trends and take advantage of the support provided by technology suppliers. The latter can review data and advise on actions to ensure optimum performance in the electrolyzer area. They may also provide data handling packages to facilitate this service.

This section outlines a typical monitoring regime, which is intended to ensure safe, efficient, and reliable operation of the cell room and associated systems. It includes a list of on-line analyzers that may be used, a suggestion for recording of operating parameters, and a consideration of the division of the analytical program between plant operators and analytical personnel.

13.11.1. Recording of Operating Parameters

Key operating parameters should be checked and logged at least every 4 hr. Data logging may be automatic, but there should also be a system that ensures that operators have checked at least the on-line analyzer outputs and the key parameters listed below:

- Circuit voltage(s)
- Circuit current(s)
- Cell room feed brine temperature
- Cell room feed brine flow rate
- Cell room feed caustic temperature
- Cell room feed caustic flow rate
- Electrolyzer feed brine temperatures
- Electrolyzer feed brine flow rates
- Cell room depleted brine temperature
- Electrolyzer depleted brine temperatures
- Electrolyzer feed caustic temperatures

Electrolyzer feed caustic flow rates
 Caustic dilution water feed rate(s)
 Cell room acid addition rate
 Electrolyzer acid addition rates
 Caustic export flow rate
 Cell room outlet caustic temperature
 Electrolyzer outlet caustic temperatures
 Chlorine header pressure
 Hydrogen header pressure
 Differential pressure between gas headers

13.11.2. Analytical Program

13.11.2.1. On-Line Analyzers. The cell room and associated areas might use on-line analyzers in the following applications:

Cell room feed brine concentration
 Cell room feed brine total hardness (Ca + Mg)
 Cell room exit brine concentration
 Cell room caustic concentration
 Product caustic concentration
 Demineralized water conductivity
 Electrolyzer exit brine pH
 Cell room exit brine pH
 Dechlorinated brine pH
 Dechlorinated brine free chlorine
 Dechlorinated brine excess reducing agent concentration (redox potential)
 Oxygen in hydrogen
 Oxygen in chlorine
 Moisture in dry chlorine
 Chlorine tail gas composition

13.11.2.2. Operator Analyses. The operator analysis schedule (Table 13.5) will depend to some extent upon the cell room configuration, the use of feed brine acidification, and the amount of analytical equipment provided. If the last item is limited, manual analysis will form a primary basis of control. If on-line instrumentation (e.g., density meters) is provided, operator analyses serve as checks on the correct functioning of the instruments. The analyses and frequencies given in the table are typical for a multi-electrolyzer bipolar cell room. The plant operators will also carry out routine analyses for process control purposes in other areas, as given in Table 13.6.

13.11.2.3. Laboratory Analyses

13.11.2.3A. Brine and Catholyte Quality. The performance of the membranes and the electrolyzer depend strongly on the quality and concentration of the liquors fed to the electrolyzer. Conformity with recommended limits set by the membrane and technology

TABLE 13.5. Frequency of Analyses by Operator (Cell Room)

Stream	Analysis	Period
Cell room feed brine	gpl NaCl or KCl	4 hr
Cell room feed brine	ppm Ca, Mg	4 hr
Electrolyzer feed brine	pH/acid concentration	8 hr
Cell room exit brine	gpl NaCl or KCl	4 hr
Electrolyzer exit brine	gpl NaCl or KCl	Daily
Electrolyzer exit brine	pH	8 hr
Cell room exit caustic	%NaOH or KOH	4 hr
Electrolyzer exit caustic	%NaOH or KOH	Daily
Cell room chlorine gas	%O ₂ , H ₂	8 hr
Electrolyzer chlorine gas	%O ₂ , H ₂	Daily

TABLE 13.6. Frequency of Analyses by Operator (Outside Area)

Stream	Analysis	Period
Drying tower acid	%H ₂ SO ₄	8 hr
Absorption tower liquor ^a	%NaOH	8 hr
Absorption tower liquor ^a	%NaOCl	8 hr
Liquefaction tail gas	%H ₂	4 hr
Reagent chemicals (e.g.: reducing agent; carbonate; barium salt; HCl; caustic)	Assay	8 hr

Note:

^aAlso after absorption tower event.

suppliers is therefore important. These suppliers will require proof that specifications are being met as part of their performance warranties. A comprehensive program of analytical measurements is therefore required.

The frequency of analysis recommended takes into account the potential loss of performance that may occur if a given component is out of specification at a typical level for a certain period of time. The analyses listed in Table 13.7 should be carried out with minimum frequencies as indicated. When an analytical history is available and results are good, many of the “weekly” items in the table can become monthly analyses.

13.11.2.3B. Product Quality. The analytical program of Table 13.7 should be extended to cover the products of the plant. Table 13.8 gives minimum requirements. Product quality control to meet customer requirements will dictate the actual analytical workload and frequencies.

13.11.3. Current Efficiency Determination

Section 4.4.3 discusses this subject exhaustively. There are many ways to calculate or approximate the current efficiency of a cell or an entire cell room. The methods vary but in principle involve determination of the amount of byproducts such as hypochlorous

TABLE 13.7. Recommended Frequencies of Laboratory Analyses

Process Stream	Analysis	Frequency
Cell room feed brine	NaCl or KCl	Daily
	Calcium	Daily
	Magnesium	Daily
	Sulfate	Daily
	Strontium	Weekly
	Barium	Weekly
	Aluminum	Weekly
	Soluble silica	Weekly
	Iron	Weekly
	Mercury	Weekly
	Total iodine	Weekly
	Nickel	Weekly
	Manganese	Weekly
	Lead	Weekly
Exit brine	NaCl or KCl	Daily
	Hypochlorite	Daily
	Chlorate	Daily
	Fluoride	Weekly
Feed caustic	Iron	Weekly
	Mercury	Weekly
	Lead	Weekly
Exit caustic	NaOH or KOH	Daily
	NaCl or KCl	Daily
Demineralized water	Conductivity	Daily

TABLE 13.8. Recommended Product Analyses

Stream	Analysis	Frequency
Product caustic	%NaOH or KOH	Daily
	ppm NaCl or KCl	Daily
Chlorine	ppm moisture	Weekly
	ppm NCl ₃	Weekly
Hypochlorite	NaOCl	Daily
Hydrochloric acid	%HCl	Daily
	Free chlorine	Daily

acid, chlorate, and oxygen formed, with appropriate allowances for the effects of feed brine acidity or alkalinity and recycle of chlorate. Simultaneous samples of feed brine, exit brine, and chlorine gas are required.

Cell room current efficiency should be determined at least twice a week. In a bipolar cell room with a relatively small number of electrolyzers, individual electrolyzer efficiencies should be measured weekly. If individual sample connections are available, the current efficiency of a single cell can be determined.

In a monopolar cell room with a large number of electrolyzers, monthly analysis is usually satisfactory. The current efficiency of a newly installed electrolyzer should be determined soon after its startup.

Section 13.9 on plant performance testing discussed measurement of the caustic current efficiency by collecting the product of the entire cell room and determining the amount of caustic produced in a measured period of time. This is time-consuming and requires special equipment or the dedication of a tank from which no product is withdrawn during the test period. It is well suited to startup periods, however, and frequently it is the basis for performance guarantee runs.

13.11.4. Voltage Monitoring

Electrolyzer and individual cell voltages provide valuable information on the condition and performance of the plant and provide early indications of things going wrong. Total electrolyzer voltage will always be continuously monitored and recorded, together with the operating current, and will normally initiate a rectifier trip if the value exceeds a specified limit. The high voltage usually indicates an operating problem, for example, loss of liquor flow. On bipolar electrolyzers, it is important to monitor individual cell voltages. The minimum requirement for safety is to monitor and compare voltages across the cells in two halves of an electrolyzer using a Wheatstone bridge circuit. This is set up to trip the rectifiers in the event of an imbalance exceeding 1 or 2 V, which may occur as a consequence of loss of brine or caustic feed to an individual cell.

An on-line computer-based system to monitor, record, and trend individual cell voltages is strongly recommended. This system may also provide a rectifier trip function if any of the voltages is too high. If there is no on-line system, individual voltages should be measured periodically. Good practice would be to make such measurements on a routine daily basis. More frequent measurements during polarization and startup to check for membrane pinholes are valuable. Voltage trends also should be monitored and compared. The cause of any sudden increase should be determined.

Normalization of cell voltage data to a standard operating load is valuable when the operating current varies (Section 13.10.2).

13.12. DECOMMISSIONING OF MERCURY-CELL PLANTS

Mercury-cell production of chlorine and alkalis is gradually being phased out. There has been substantial progress in the reduction of mercury emissions of all kinds, but these have served to delay rather than prevent the abandonment of the technology. During the 5 years ending in 2001, the combined mercury-cell capacity of Euro Chlor producers dropped from about 64% of the total to 54% [20]. Measured emissions of mercury were 1.25 g t^{-1} chlorine. This includes mercury released to the air, to water, and in products. This number represents a 74% drop in 10 years. The trend has continued, and less than half of European production is now in mercury cells [21].

The occasion for decommissioning a mercury-cell plant may be the abandonment of production or a decision to convert to membrane-cell technology. In either case, decisions also are required on the reuse of buildings, material, and equipment. In a total shutdown of a facility, site remediation will also be important.

The first major operation is removal of mercury from the cell room. Nearly all of this is recovered by draining the cells and amalgam pumping systems. The flasks that contained the mercury when first delivered are convenient receptacles. Residual liquid mercury and that adsorbed on surfaces can be recovered by washing with an alkaline peroxide solution. This solution ultimately must itself be treated to isolate mercury in a more condensed form. The same is true of other cleaning solutions and of water used for decontamination. Therefore, the aqueous treatment plant should be ready to operate at the start of decommissioning and must continue to operate beyond its completion.

Euro Chlor [22] has published methods for decontamination of the various components of a mercury-cell plant. The discussion here is based on that publication. Table 13.9, taken from Appendix 3 of the reference document, is a brief summary. Discussion of the methods referred to in the last column follows the table.

After removal of all equipment, piping, and other contaminated materials, the walls and the ceiling of the building itself can be washed with high-pressure water. All water and treating solutions used during the decontamination process must be held and then treated before release. Water used in simple washing of surfaces can in many cases be recycled to reduce the volume of effluent.

TABLE 13.9. Mercury-Cell Plant Decontamination Techniques

Material	Typical Hg content, %	Physical state	Method
Steel scrap	0.001–1	Non-homogeneous contamination	1
Decomposers			
Baffles			
H ₂ coolers			
Base plates			
Mercury pumps			
Pipework			
Rubber-lined components	Variable	Non-homogeneous contamination	2
Anode covers			
End boxes			
Side channels			
Pipework			
Graphite from decomposers	2	Porous solid	3
Carbon from caustic filters	Up to 40	Dry solid	3
Charcoal from hydrogen purification	10–20	Dry solid	3
Sludge from tanks and sumps	10–30	Wet solids	4
Sludges from drains, catch pits, etc.	2–80	Wet solids	4
Rubber/packing	Variable	Variable	5
Plastic equipment	<0.1	Solid	5
Brick work/concrete	0.01–0.1	Variable	6
Retort residues	<0.1–1	Dry porous solid	7
Miscellaneous			
Conductors	0.04	Surface contamination	1
Floor boards	0.05–0.08		5
Asphalt	1–20		6
Decomposer insulation	0.03		5
Concrete and subfloor	Variable	} Non-homogeneous contamination	6
Wood	Variable		
Soil	Variable		

With permission of Euro Chlor.

Methods of decontamination (Table 13.9):

1. Surface mercury usually is in the metallic form. Simple washing of the surface can be very effective. High-pressure water can remove mercury quickly; splash containment is necessary. Steel and rubber-lined pipework can be retorted or cleaned with HCl/Cl_2 or $\text{NaOH}/\text{H}_2\text{O}_2$. These solutions oxidize the metal to the soluble Hg^{2+} . Heavily contaminated steel will sweat mercury. Lott [19] points out that broken concrete from a cell room floor also can sweat mercury if allowed to stand overnight. Components should be stored with this in mind. Liquid droplets can be collected. The storage area should be ventilated because of evaporation of the mercury. Buswork and copper fabrications are protected by surface films and usually are not seriously contaminated with mercury. Surface washing is good practice before recycle. Copper braid or flexible strips can be more heavily contaminated and require treatment in a mercury distillation oven.
2. The lining must be removed from the metal after washing. This can be done by cryogenic shock in liquid nitrogen or by compressing the parts in a steel press and cutting them into small pieces. The steel, separated from the rubber by a magnet, is washed. The rubber is treated as chemical waste.
3. Graphite and carbon can be washed, the mercury immobilized, and the decontaminated material sent to landfill. Other methods are washing with chlorinated brine and distillation in a mercury furnace (not an option with iodine-impregnated carbon).
4. Material rich in mercury can be retorted. Post-treatment may include immobilization of the mercury and disposal in a landfill.
5. Plastics can be disposed of by standard methods after washing with water or an oxidizing solution. Reinforced plastics and thermoplastics such as PVC, PP, and the like can be washed by high-pressure water jet, with sufficient containment to prevent the spread of metallic mercury. The effectiveness of washing other materials in baths improves with the addition of detergent or acid plus free chlorine.
6. Construction materials can be washed on vibrating screens or cleaned ultrasonically.
7. Residues usually contain less than 100 ppm mercury. Their disposal depends on local regulations. Sulfur-containing materials, such as carbon and HgS sludge, can be retorted successfully by adding quicklime.

Final disposal of all materials will be governed by local regulations. The project team should identify the quantities and types of materials for disposal, set the minimum requirements for a landfill site, and consult with authorities before decommissioning begins.

A typical landfill will have an impermeable plastic liner and a thick clay barrier. The site must be monitored for leakage and emissions. Monitoring should be intensive during the disposal process. With continuing good results, it can later be reduced to a normal program, but it must continue even after the landfill is sealed.

Salt caverns can be good sites for disposal of certain wastes, but there often is resistance to their use for toxic materials and, as Section 7.2.2.4 points out, this is not a frequent practice.

Between decontamination of removed material and its disposal are transportation and storage. A storage area should be diked and drained to contain mercury-contaminated spillage. Indoor facilities should be ventilated. Watertight bags and sheets are good for small parts and local storage. There are also leakproof skips that are transportable by forklift trucks. Containers can be color coded to help identification and prevent the need for opening bags to identify their contents. Labels also are useful, and they usually are mandatory for off-site storage. Local authorities and landfill operators may have their own requirements for labeling.

Handling and transport of larger objects may be simplified by cutting them into smaller pieces. Cutting operations require all the usual safety precautions as well as protective gear to shield the workers from exposure to mercury. Cold-cutting operations are preferred, because they vaporize less mercury.

Reuse of existing facilities requires removal of contained mercury but not dismantling and detoxification of the debris. Demercurization of brine treatment systems, for example, is straightforward and sometimes quite easy to apply. This is particularly so when the brine recycle system has been operated with a low level of dissolved chlorine to prevent mercury precipitation. Lott [19] reports that such a system was drained, washed with dilute acid to remove deposits and then with dilute hypochlorite solution to solubilize mercury, and finally flushed with hot water. The residual mercury concentration was well within the specification for the new membrane cells.

Technology conversions are also opportunities to remove the hazard of mercury-contaminated soil. Generally, there are two types of contamination, uncombined metallic mercury and mercury compounds bound to the clay particles that comprise the soil [23]. Low-level nonmetallic contamination that is known not to be leachable can be taken to a secure lined (preferably double-lined) landfill. Soil contaminated with elemental mercury will require treatment. The first task is mechanical separation of the mercury from the soil burden. Section 16.5.5.1 gives a brief description of the operation of one such unit.

ACKNOWLEDGMENT

This chapter was written mostly by Gary M. Shannon, who manages technical service and plant commissioning activities for the electrochemical business of INEOS Chlor, Ltd. Coming from the technology development organization, he was involved in the commissioning of an impressively large number of plants and later also took on the technical service responsibility.

REFERENCES

1. W.L. Clark, Operator Training for an Existing Chlor-Alkali Plant, *26th Chlorine Institute Plant Managers Seminar*, New Orleans, LA (1983).
2. J.M. Boyd, Training for a Membrane-Cell Plant Operation, *26th Chlorine Institute Plant Managers Seminar*, New Orleans, LA (1983).
3. B.J. Deaton, Shift Supervisor Training for Mercury-Cell Chlor-Alkali Plant, *26th Chlorine Institute Plant Managers Seminar*, New Orleans, LA (1983).

4. J.H. Sullivan, Personnel Training in a Chlorine Packaging Plant, *26th Chlorine Institute Plant Managers Seminar*, New Orleans, LA (1983).
5. T.F. O'Brien and E.R. Luckiewicz, *Guidelines for Process Safety Fundamentals in General Plant Operations*, Center for Chemical Process Safety, New York (1995), p. 285.
6. R. King, *Safety in the Process Industries*, Butterworth-Heinemann, London (1990), p. 615.
7. R. King, *Safety in the Process Industries*, Butterworth-Heinemann, London (1990), p. 604.
8. *Accident Prevention Manual for Business and Industry: Administration and Programs*, 10th ed., National Safety Council, Itasca, IL (1995).
9. M.E. Butler, *Chem. Eng.* **100**(6), 82 (1993).
10. *Dry Liquid Chlorine Piping Systems Located inside Producers' or Consumers' Plants*, GEST 79/81, 8th ed., Euro Chlor, Brussels (2002).
11. I.F. White and T.F. O'Brien, Secondary Brine Treatment: Ion-Exchange Purification of Brine. In N.M. Prout and J.S. Moorhouse, eds., *Modern Chlor-Alkali Technology*, vol. 4, Elsevier Applied Science, London (1990), p. 271.
12. K. Hagerup Nilssen, *Commissioning of Equipment for Liquid Chlorine*, Chlorine Safety Seminar, Brussels (1990).
13. *Code of Good Practice for the Commissioning of Installations for Dry Chlorine Gas and Liquid*, GEST 80/84, 4th ed., Euro Chlor, Brussels (1990).
14. *Learning from Experience*, Pamphlet 167, Edition 1, The Chlorine Institute, Inc., Washington, DC (2002), p. 7.
15. *Refrigerated Liquid Chlorine Storage*, Pamphlet 78, Edition 3, The Chlorine Institute, Inc., Washington, DC (2000).
16. R. Kucinski, Safety in Chlor-Alkali Plant Operation with Ion-Exchange Membranes, *36th Chlorine Institute Plant Managers Seminar*, Washington, DC (1993).
17. D. Bergner and M. Hartmann, *J. Appl. Chem.* **24**, 1201 (1994).
18. K. Schneiders and B. Lüke, Safety and Economy of Membrane Cell Electrolyzers. In T.C. Wellington (ed.), *Modern Chlor-Alkali Technology*, vol. 5, Elsevier Applied Science, London (1992), p. 115.
19. B. Lott, Practical Experiences on the Conversion of Mercury Cells to Membrane Technology. In R.W. Curry (ed.), *Modern Chlor-Alkali Technology*, vol. 6, Royal Society of Chemistry, Cambridge (1995), p. 243.
20. www.eurochlor.org/chlorine/Chlorine_Industry_Re.../Environmental_performance (2002).
21. *Chlorine Industry Review 2002–2003*, Euro Chlor, Brussels (2003).
22. *Decommissioning of Mercury Chlor-Alkali Plants*, Env. Prot. 3, 2nd ed., Euro Chlor, Brussels (1999).
23. G. Thibeault, B. Cyr, Y. Denicourt, and D. Fauchet, Design, Construction, and Implementation of Pilot Unit for the Treatment of Mercury-Contaminated Soil, *36th Chlorine Institute Plant Managers Seminar*, Washington, DC (1993).

14

Corrosion

14.1. INTRODUCTION

Corrosion is a multibillion dollar worldwide problem. In the United States, corrosion is estimated [1] to occur at a rate of $14,000 \text{ kg min}^{-1}$, costing about \$200 billion per year. Incidents from corrosion may force shutdowns of chemical plants, the associated penalties in serious situations being financial loss, loss of human life, and damage to the environment. It is for these reasons that all chemical plants emphasize safety and implement safe operations by training plant personnel. Safety management extends into ensuring proper selection of materials of construction, quality control during manufacturing, fabrication, and construction, and routine maintenance during normal plant operations.

Chemical plants are designed and constructed with a variety of metals, alloys, and nonmetallic materials such as plastics. The nature and mechanism of degradation of these materials differ. Corrosion of metals and alloys in aqueous media occurs by electrochemical mechanisms, whereas the degradation of a plastic is by the penetration of chemicals into its matrix. Nevertheless, the term corrosion is used liberally to describe the oxidation of metals in aqueous solutions or gas phases and the deterioration of plastics by chemical attack.

Corrosion of metals is defined as their spontaneous deterioration by chemical interaction with the surrounding environment. It is a two-component system involving the interaction of the metal or alloy with a medium or environment. In the absence of an environment (e.g., vacuum), corrosion will not occur. Most corrosion reactions are electrochemical in nature, and for electrochemical corrosion to occur, a cell consisting of an anode, a cathode, an electrolyte, and a pathway for electron flow between the anode and the cathode is needed.

Corrosion is classified, according to the medium that the metal or alloy is exposed to (Table 14.1), as wet and dry corrosion. Corrosion of metals immersed in an aqueous medium is an example of wet corrosion, which proceeds electrochemically. Atmospheric corrosion also belongs to the class of wet corrosion, since it is caused by moisture deposited on the metal surface. Another division of wet corrosion is the degradation of metals and alloys in nonaqueous media by chemical pathways.

TABLE 14.1. Corrosion of Metals and Alloys

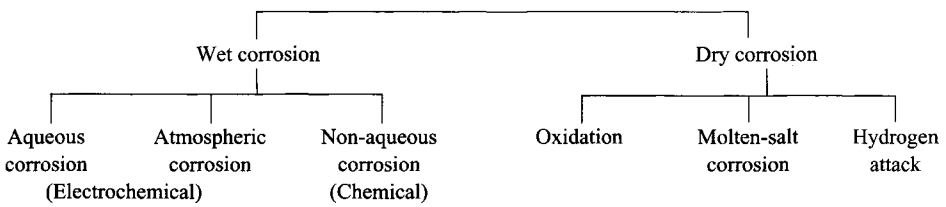
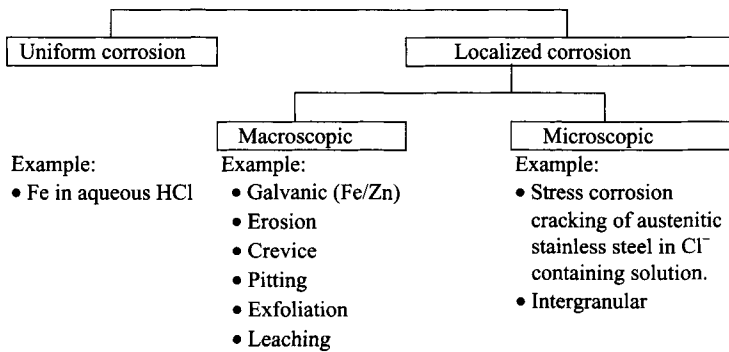


TABLE 14.2. Forms of Metallic Corrosion



Dry corrosion is classified into three types: oxidation, molten-salt corrosion, and hydrogen attack. High temperature oxidation, sulfidation, nitriding, carburization, halide attack, and others belong to the class of oxidation. The oxidation of metals and alloys in melts containing vanadium salts or oxides is an example of molten salt corrosion of metals, and proceeds electrochemically. Liquid-metal corrosion of iron and steel in mercury is a chemical process. Embrittlement of metals such as titanium by hydrogen ingress comes under the category of hydrogen attack.

Corrosion is a complex phenomenon and is classified by its appearance and uniformity or nonuniformity, which may be microscopic or macroscopic (Table 14.2). The nature of the corrodant can also be used to classify corrosion [2,3]. Most of the observed corrosion occurs as one or more of the following cases: (1) uniform or general attack, (2) galvanic or two-metal corrosion, (3) crevice corrosion, (4) pitting corrosion, (5) intergranular corrosion, (6) selective leaching or dealloying, (7) erosion corrosion, and (8) stress corrosion cracking (SCC).

The terms pitting, cracking, and erosion refer to the visual appearance of the corroded material, whereas the term crevice corrosion refers to the location of attack. Intergranular corrosion owes its name to the metallurgy of the material, and galvanic corrosion and SCC are descriptions of their failure mechanisms, while dealloying and fretting corrosion are named after the factors contributing to the failure.

Corrosion occurs not only as a result of chemical attack, but also because of mechanical stresses. Table 14.3 depicts the various forms of degradation due to mechanical factors [4].

It is important to identify the types and frequency of failures in order to address the corrosion problems in an industrial setting, as many factors can contribute to the “big failure.” Such an analysis was carried out at DuPont [5] to understand the piping and equipment failures during the period 1968–1971. The results, summarized in Table 14.4, showed that corrosion accounted for 55% of the total 685 failures, the remaining 45% being a result of mechanical problems. General corrosion contributed to 15.2% of the failures and the top five localized corrosion phenomena accounted for 32.9% of the failures. Therefore, the first task of corrosion engineering should be to survey and analyze the problems to optimize the investment against the expenses involved in the operation and maintenance of a chemical plant.

14.2. ORIGIN OF CORROSION

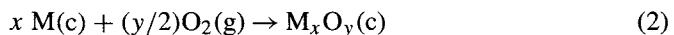
Most metals exist in nature as oxide or sulfide ores and energy is expended in extracting or winning the metals from their native state. The reverse of metal winning is corrosion, in which the metals revert to stable compounds similar to those found in nature. For corrosion to occur, as with any chemical reaction, two questions arise: (1) will a metal corrode in a given environment? and (2) how fast? The first question is answered by thermodynamics; the second by kinetics [6–8].

14.2.1. Free Energy Considerations

The free energy change of a corrosion system, ΔG , is a measure of the driving force for a reaction. This driving force at constant pressure is a function of ΔH (enthalpy), ΔS (entropy), and T (temperature).

$$\Delta G = \Delta H - T \Delta S \quad (1)$$

If ΔH is negative, heat is given off by the system to the surroundings, as in the exothermic oxidation of iron. The dissolution of metal usually yields more random, less ordered products; that is, an increase in entropy is evident. An increase in temperature contributes to a more negative second term, hence, a more negative ΔG . If ΔG is negative, the reaction is favored to go spontaneously as written. If it is positive, the reaction will not go as written (although the reverse may). If it is zero, the system is in a state of equilibrium. For the metal oxidation reaction,



where M = metal, c = crystalline, and g = gas, the free energy relationship at 25°C and 1 atm may be written as:

$$\Delta G_{\text{corr}}^0 = \Delta G_{\text{p}}^0 - \Delta G_{\text{r}}^0 \quad (3)$$

TABLE 14.3. Chemical and Mechanical Factors in Corrosion [4]

Corrosion Caused by Chemical Factors

General corrosion
Pitting corrosion
Crevice corrosion
Intergranular corrosion
Selective leaching
High temperature corrosion:
 Oxidation, Sulfidation, Nitriding, Carburizing,
 Molten salt corrosion, etc.

Degradation Caused by Mechanical Factors

Elastic deformation
Plastic deformation
Mechanical failure over the yield strength (overload)
Failure at lower than the yield strength (brittle failure)
Fatigue
High temperature creep

Failure Caused by Combination of Chemical and Mechanical Factors

Fretting corrosion
Erosion corrosion
Cavitation damage
Impingement attack
Stress corrosion cracking (SCC)
Liquid metal corrosion
Hydrogen attack
Corrosion fatigue

TABLE 14.4. Failures in Metallic Equipment and Piping in DuPont during 1968–1971 (Total number = 685)

Type of failure	Percentage
<i>Corrosion</i>	55.2
General corrosion	15.2
SCC	13.1
Pitting	7.9
Intergranular corrosion	5.6
Erosion corrosion	3.8
Weld decay	2.5
Others	7.1
<i>Mechanical failure</i>	44.8
Fatigue	14.8
Abrasion	5.4
Overload	5.4
Poor welds	4.4
Thermal cracking	3.1
Other types of cracking	3.5
Others	8.2

Note: SCC: Stress corrosion cracking.

TABLE 14.5. Free Energies of Formation ΔG_p^0 of Some Metal Oxides

Compound	ΔG_p^0 , kcal mol ⁻¹	Compound	ΔG_p^0 , kcal mol ⁻¹
Al ₂ O ₃ (α)	-376.8	ZnO	-76.1
Cr ₂ O ₃	-259.2	PbO ₂	-52.3
Fe ₃ O ₄	-242.4	NiO	-51.7
Fe ₂ O ₃	-177.1	CuO	-31.4
MgO	-136.1	Ag ₂ O	-2.6
SnO ₂	-124.2	Au ₂ O ₃ ^a	29.1

Note: ^a Does not form spontaneously.

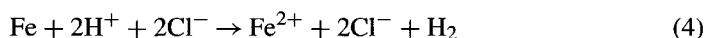
where ΔG_{corr}^0 refers to the free energy change for the corrosion (oxide formation) process, ΔG_p^0 to the free energy of formation of the products, and ΔG_r^0 to the free energy of the formation of the reactants. ΔG for any element in its normal state is zero, and hence $\Delta G_{\text{corr}}^0 = \Delta G_p^0$ of the oxide. Table 14.5 lists the ΔG_p^0 values for some oxides.

These thermodynamic values predict that aluminum has a much greater tendency to be oxidized than the other metals.

Another basis for thermodynamic prediction of corrosion reactions is the equation $\Delta G^0 = -nFE^0$, where n is the number of electrons transferred in the reaction, F is Faraday's constant (96,500 C, which is equivalent to 1 mole of electrons), and E^0 is the cell potential. A positive cell potential will lead to a negative ΔG^0 , and hence the reaction will proceed spontaneously as written in Eq. (2). As the overall cell reaction proceeds, the voltage difference between the electrodes drops as the free energies of the products and reactants approach each other. At steady state, both electrodes have the same voltage and no charge transfer occurs.

When the standard electrode potentials are listed in decreasing value as shown in Table 14.6, an electromotive series is created which has the hydrogen half-cell reaction listed at a potential of zero. These values are reduction potentials at 25°C referred to the standard hydrogen electrode (SHE). Metals listed at the top of the series are "noble" or less reactive. Metals listed below the hydrogen reaction are reactive, that is, they corrode more readily. A metal listed below another metal will displace it from a solution containing the higher metal's ions. Iron, for example, will have copper metal plated on it when placed in a copper sulfate solution. This is an iron corrosion reaction. Metals listed below hydrogen will displace the H⁺ ions from acid solutions.

Let us look at the case of iron corrosion in aqueous hydrochloric acid, by placing an iron sheet and a platinum sheet in dilute HCl solution and connecting them by a metal wire outside the solution. The overall reaction under these conditions is:



which consists of two half-cell reactions.



It is clear from Table 14.6 that the reversible potential for the hydrogen electrode process (reaction 6) is more positive than that for the iron electrode process. Therefore, the overall reaction (reaction 4) will proceed on the surface of iron immersed in dilute HCl because of the driving force arising from the potential difference between the two electrode processes. Since the two reactions proceed on the same location with opposing charge transfer, both electrodes are polarized in opposite directions to reach

TABLE 14.6. Standard Electrode Potentials at 25°C

	Electrode reaction	Standard reversible potential, volt vs SHE
Inactive	$2\text{H}_2\text{O} = \text{H}_2\text{O}_2 + 2\text{H}^+ + 2\text{e}$	1.770
	$\text{Au} = \text{Au}^+ + \text{e}$	1.680
	$\text{Au} = \text{Au}^{3+} + 3\text{e}$	1.500
	$\text{Pb}^{2+} + 2\text{H}_2\text{O} = \text{PbO}_2 + 4\text{H}^+ + 2\text{e}$	1.455
	$2\text{Cl}^- = \text{Cl}_2 + 2\text{e}$	1.359
	$2\text{H}_2\text{O} = \text{O}_2 + 4\text{H}^+ + 4\text{e}$	1.229
	$2\text{Br}^- = \text{Br}_2 + 2\text{e}$	1.065
	$\text{Pd} = \text{Pd}^{2+} + 2\text{e}$	0.987
	$\text{Ag} = \text{Ag}^+ + \text{e}$	0.799
	$2\text{Hg} = \text{Hg}_2^{2+} + 2\text{e}$	0.789
	$\text{Fe}^{2+} = \text{Fe}^{3+} + \text{e}$	0.771
	$\text{H}_2\text{O}_2 = \text{O}_2 + 2\text{H}^+ + 2\text{e}$	0.682
	$2\text{Ag} + \text{SO}_4^{2-} = \text{Ag}_2\text{SO}_4 + 2\text{e}$	0.653
	$2\text{I}^- = \text{I}_2 + 2\text{e}$	0.535
	$\text{Cu} = \text{Cu}^+ + \text{e}$	0.521
	$\text{Fe}(\text{CN})_6^{4-} = \text{Fe}(\text{CN})_6^{3-} + \text{e}$	0.360
	$\text{Cu} = \text{Cu}^{2+} + 2\text{e}$	0.337
	$\text{Ag} + \text{Cl}^- = \text{AgCl} + \text{e}$	0.222
	$\text{Cu}^+ = \text{Cu}^{2+} + \text{e}$	0.153
	$\text{H}_2 = 2\text{H}^+ + 2\text{e}$	0.000
	$\text{Pb} = \text{Pb}^{2+} + 2\text{e}$	-0.126
	$\text{Sn} = \text{Sn}^{2+} + 2\text{e}$	-0.136
	$\text{Mo} = \text{Mo}^{3+} + 3\text{e}$	-0.200
	$\text{Ni} = \text{Ni}^{2+} + 2\text{e}$	-0.250
	$\text{Co} = \text{Co}^{2+} + 2\text{e}$	-0.277
	$\text{Pb} + \text{SO}_4^{2-} = \text{PbSO}_4 + 2\text{e}$	-0.356
	$\text{Fe} = \text{Fe}^{2+} + 2\text{e}$	-0.440
	$\text{Cd} = \text{Cd}^{2+} + 2\text{e}$	-0.453
	$2\text{Nb} + 5\text{H}_2\text{O} = \text{Nb}_2\text{O}_5 + 10\text{H}^+ + 10\text{e}$	-0.650
	$\text{Cr} = \text{Cr}^{3+} + 3\text{e}$	-0.740
	$\text{Zn} = \text{Zn}^{2+} + 2\text{e}$	-0.763
	$\text{Zr} = \text{Zr}^{4+} + 4\text{e}$	-1.530
	$\text{Ti} = \text{Ti}^{3+} + 3\text{e}$	-1.630
	$\text{Al} = \text{Al}^{3+} + 3\text{e}$	-1.660
	$\text{Mg} = \text{Mg}^{2+} + 2\text{e}$	-2.370
	$\text{Na} = \text{Na}^+ + \text{e}$	-2.714
	$\text{K} = \text{K}^+ + \text{e}$	-2.925
Active	$\text{Li} = \text{Li}^+ + \text{e}$	-3.045

an intermediate value, called the mixed potential. (See Section 14.2.2 and Fig. 14.5 for additional discussion of this topic).

The potential difference between a metal and its ions in a solution can be measured with a voltmeter connected to an inert reference electrode. An electric potential exists between the anode and the cathode and has the same value as that calculated by the addition of the two half-cell reactions:

$$\Delta E^0 = E_{\text{cathode}}^0 - E_{\text{anode}}^0 \quad (7)$$

In real corrosion processes, the anodic and cathodic reactions occur randomly over the surface with regard to space and time, resulting in uniform corrosion. Oxidation and reduction occur at the same rate for the preservation of electrical neutrality of the iron. If either half-reaction stops, so does the overall reaction. These reactions will take place simultaneously on flat regions (as in uniform corrosion) in localized zones.

Pourbaix Diagrams. Another tool for predicting corrosion reactions is the Pourbaix diagram [9], which deals with thermodynamic equilibria. The pH of an electrolyte often has a profound effect on the degree and extent of corrosion. The Pourbaix diagram illustrates the dependence of the potential established between a pure metal and its ions in solution, and the pH of the electrolyte, indicating which pH–potential conditions might lead to corrosion. The Pourbaix diagram for the iron–water system is shown in Fig. 14.1, where line a represents the hydrogen reaction:

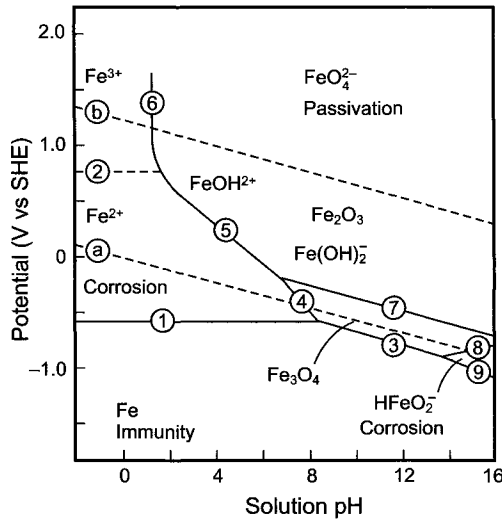


FIGURE 14.1. Potential–pH diagram for Fe–H₂O system at 25°C. The area between the lines a and b represents the thermodynamic region of the stability of water [9]. (With permission from M. POURBAIX, *Atlas of Electrochemical Equilibria in Aqueous Solutions*, NACE and CEBELCOR.)

and line **b** represents the oxygen reaction:



If the potential is moved below line **a** at a fixed pH, H_2 will evolve. Movement of the potential above line **b** will cause O_2 to evolve. Thus, the region between these two lines indicates the region of thermodynamic stability of H_2O .

The diagrams are constructed from data for reactions that are: (1) Potential dependent and pH independent, (2) pH dependent and potential independent, (3) pH and potential dependent, and (4) dependent on neither pH nor potential.

The individual lines in Fig. 14.1 are developed by assuming a reaction and calculating the dependence of potential on pH and concentration, using published free energy data. For example, line 1 refers to the equilibrium (10):



involving Fe in equilibrium with 10^{-5} M of Fe^{2+} at 25°C . The Nernst equation for this reaction is written as:

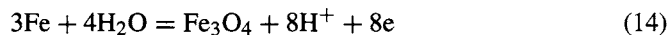
$$E_1 = E_1^0 + \frac{RT}{nF} \ln [\text{Fe}^{2+}] \quad (11)$$

$$= -0.44 + 0.0295 \log [10^{-5}] \quad (12)$$

$$= -0.555 \text{ V vs SHE} \quad (13)$$

E_1 refers to the standard electrode potential, RT/nF to the Nernst slope, n to the number of electrons involved in the charge transfer reaction, and $[\]$ to the concentration or the activity of the ions under study. Since neither H^+ nor OH^- ions are participating in reaction (10), the potential is independent of pH, as shown by line 1 in Fig. 14.1.

Line 3 represents the reaction:

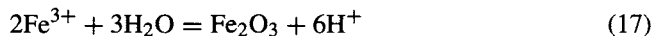


The Nernst equation for this reaction is given as:

$$E_3 = E_3^0 + \frac{RT}{F} \ln [\text{H}^+] \quad (15)$$

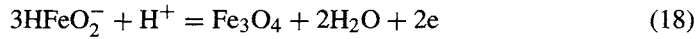
$$= E_3^0 - 0.059 \text{ pH} \quad (16)$$

Thus, the potential for reaction (14) varies with pH. At potentials higher than ca. 0.8V, Fe^{3+} is more stable than Fe^{2+} , and iron will precipitate as Fe_2O_3 .



Since reaction (17) is a chemical process, line (6) adjoining Fe^{3+} and Fe_2O_3 is independent of potential.

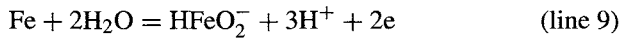
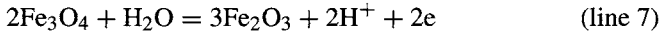
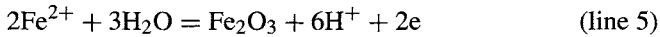
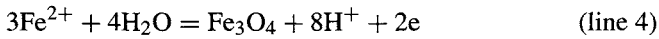
It is well known that Fe develops a corrosion resistant layer of magnetite, Fe_3O_4 , over a narrow potential range and dissolves in concentrated alkaline solutions as ferrate, which is represented by reaction (18) and line (8) in Fig. 14.1.



The Nernst equation for this reaction is:

$$E_8 = E_8^0 + 0.0295 \text{ pH} \quad (19)$$

The reactions representing the other lines in Fig. 14.1 are as follows.



The potential–pH diagrams contain an enormous amount of information describing the equilibria involving the metal and its various oxidation states, be they ionic or solid. There are three major regions in the potential–pH diagram. The first is the region of immunity. In this region, the pH is such that the potential is sufficiently negative so that metallic iron is thermodynamically stable and will not corrode. The second region is the corrosion area. In this region of pH and potential, the Fe^{2+} and Fe^{3+} ions are stable. The third region is one of passivation. The metallic form of iron does corrode but forms insoluble hydroxides or oxides such as $\text{Fe}(\text{OH})_3$ and Fe_2O_3 that prevent further dissolution. Generally, the Pourbaix diagram identifies the areas of stability of the metal–water system, and should be considered as the starting point for any corrosion study (Fig. 14.2). The predictions of the Pourbaix diagrams are shown to be in general agreement with the experimental results in Fig. 14.3 on the general corrosion of iron in flowing solutions. Figure 14.4 shows corrosion data for solutions containing small quantities of chloride, which may cause pitting.

14.2.2. Kinetics

While thermodynamics will provide a sanction for the reaction to proceed spontaneously, kinetics will dictate the rates of the electrochemical reactions. For corrosion to occur, two electrochemical reactions, an oxidation and a reduction reaction, must proceed at the same time and at the same rate to preserve the electroneutrality of the system. Thus, when iron is immersed in an acidic medium, Fe will oxidize to Fe^{2+} , the corresponding or conjugate reduction being either the discharge of H^+ to H_2 or the reduction of

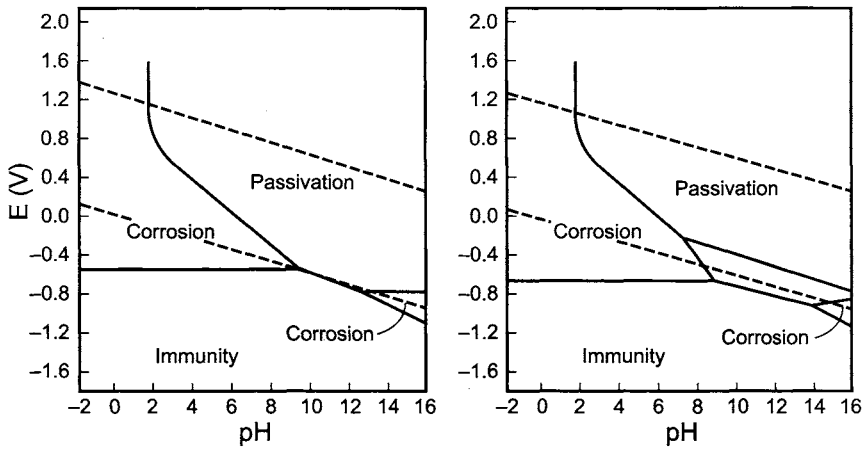


FIGURE 14.2. Theoretical conditions of corrosion, immunity, and passivation of iron. The figure on the left is based on the assumption that passivation is by a film of Fe_2O_3 and the figure on the right assumes the surface film to be Fe_2O_3 and Fe_3O_4 [9]. (With permission from M.POURBAIX, *Atlas of Electrochemical Equilibria in Aqueous Solutions*, NACE and CEBELCOR.)

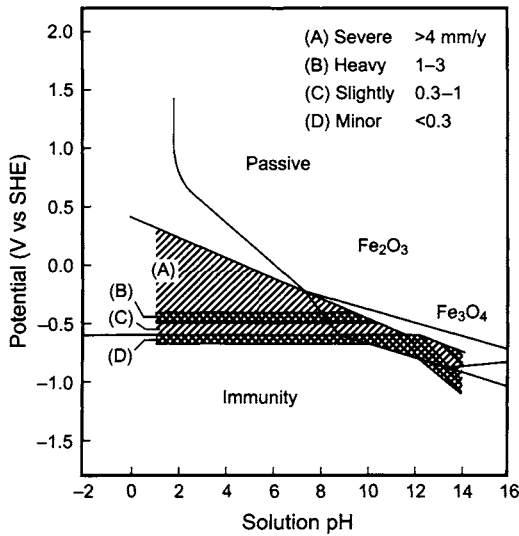


FIGURE 14.3. General corrosion of iron in flowing solutions [9]. (With permission from M.POURBAIX, *Atlas of Electrochemical Equilibria in Aqueous Solutions*, NACE and CEBELCOR.)

O_2 to H_2O as:



or



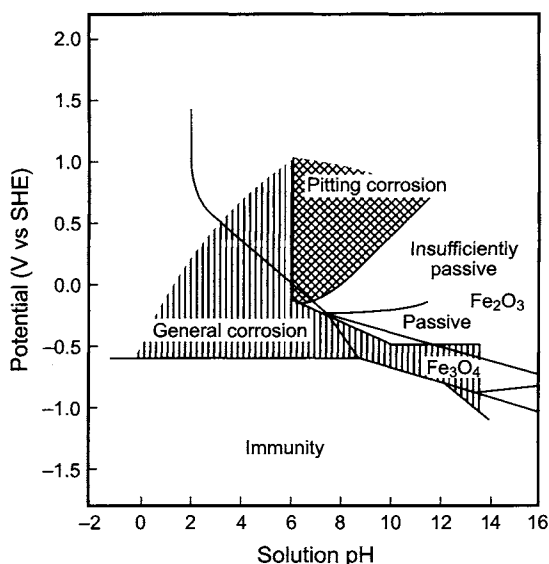


FIGURE 14.4. Corrosion of iron in solutions containing chloride ions [9]. (With permission from M.POURBAIX, *Atlas of Electrochemical Equilibria in Aqueous Solutions*, NACE and CEBELCOR.)

If reaction (21) or (22) does not occur, there will be no corrosion, since the electrons released during the oxidation of Fe cannot be consumed.

Let us now examine the case of an iron rod placed in an acidic solution of copper sulfate, when copper is deposited on the iron surface, following the dissolution of iron. This process can be described as composed of two electrochemical reactions, shown below.



The overall reaction is:



Figure 14.5 illustrates the component and overall polarization curves when iron is immersed in acidic solutions with and without Cu^{2+} . The anodic polarization curves in both solutions are almost the same (line A). The counter electrode reaction in pure solution is the hydrogen evolution reaction, whose polarization behavior is shown by line B. These curves cross each other at point P, which is the mixed potential $E_M(\text{H})$. The anodic and the cathodic overvoltages are $\eta_{\text{Fe}}(\text{H})$ and $-\eta_{\text{H}}$ respectively. The current density corresponding to $E_M(\text{H})$ is the corrosion current for iron in acid solutions, $i_{\text{corr}}(\text{H})$.

When iron is placed in a solution containing Cu^{2+} ions, copper deposits on the iron substrate at the expense of iron corrosion. Note that the reversible potential of the Fe/Fe^{2+} couple of -0.44 V is less noble than that of the reversible potential for Cu/Cu^{2+}

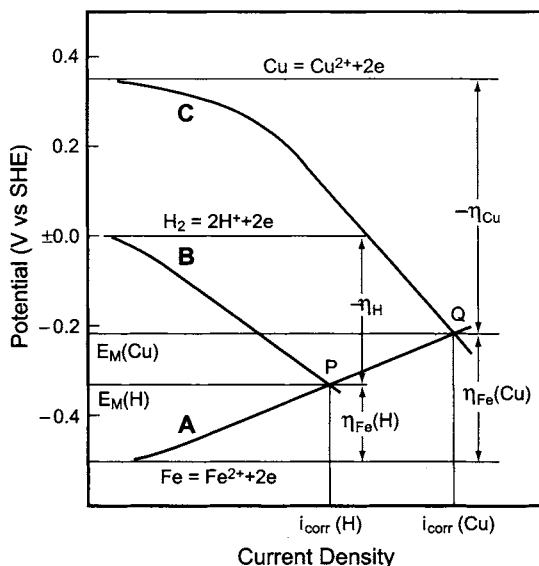


FIGURE 14.5. Polarization behavior of iron in acidic solutions with and without Cu^{2+} .

of 0.34 V, and therefore, iron and copper are polarized from their reversible potentials to a mixed potential, $E_M(\text{Cu})$ at point Q, the anodic overvoltage being $\eta_{\text{Fe}}(\text{Cu})$ and the cathodic overvoltage being $-\eta_{\text{Cu}}$. The cathodic polarization is represented by line C. The cathodic deposition of copper predominates over hydrogen evolution depending on the solution pH and the Cu^{2+} concentration. The current density corresponding to $E_M(\text{Cu})$ is the corrosion current, $i_{\text{corr}}(\text{Cu})$, which is a measure of the corrosion rate, V_{corr} . Note that the electrode reactions (23) and (24) take place on the same metal surface at a potential of E_M , which is called the mixed potential or the corrosion potential. It should also be recognized that it is impossible to measure the corrosion current directly since the current generated at the anode in this closed circuit is consumed by the conjugate electrode reaction, that is, the cathodic process.

Figures 14.6 and 14.7 depict the polarization curves of iron in weak HCl solutions, when the cathodic reaction is the hydrogen evolution reaction and when the cathodic process is the reduction of oxygen, respectively. In the former case, both the anodic and the cathodic processes are charge-transfer controlled, represented by the Tafel equation as:

$$\eta = (RT/\beta F) \ln(i/i_{\text{corr}}) \quad (26)$$

where η refers to the overvoltage and β is the transfer coefficient. X is the intersection of the extrapolated straight-line portions of RS and PQ. X represents the corrosion potential, E_M , the corresponding current being i_{corr} .

In aerated solutions, the cathodic reaction is the O_2 reduction reaction (Eq. 22). In such media, the anodic polarization curve will be the same as in acidic solutions (Fig. 14.6) in the absence of O_2 . However, the cathodic polarization curve (Fig. 14.7) has a different shape, because the reduction of O_2 is a diffusion-controlled process.

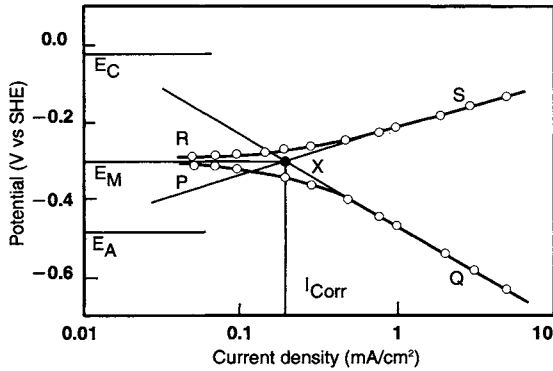


FIGURE 14.6. Polarization data for iron in weak HCl solutions.

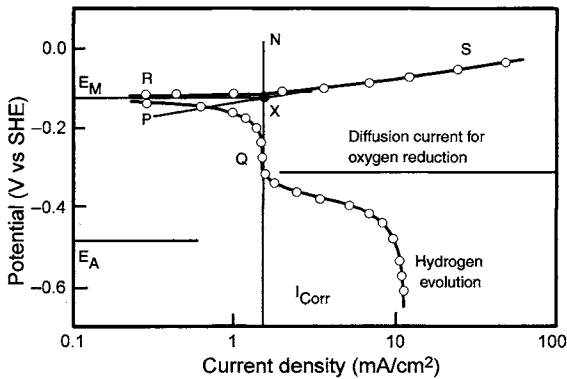


FIGURE 14.7. Polarization data for iron in aerated solutions.

The diffusion-limiting current in solutions open to air at room temperature is 0.2 to 2 mA cm⁻².

The corrosion rate in this case is the same as the diffusion-limited current for the O₂ reduction reaction. Note, however, that the corrosion potential is shifted to more positive values compared to Fig. 14.6.

When both the anodic and cathodic reactions are kinetically controlled, the corrosion rate can be obtained, in the absence of any complexities, from the slope of the current–voltage curve around the corrosion potential as:

$$i_{\text{corr}} = \frac{1}{f_A + f_C} \frac{\Delta i}{\Delta \eta} \quad (27)$$

where f_A and f_C represent the Tafel slopes for the respective anodic and cathodic processes and $\Delta i / \Delta \eta$ refers to the slope of the i vs η plot. This technique is called the linear polarization method or the polarization resistance method.

The polarization curves are not always as simple as shown in Figs. 14.6 and 14.7. Figure 14.8 illustrates the polarization behavior of a clean stainless steel (Type 446)

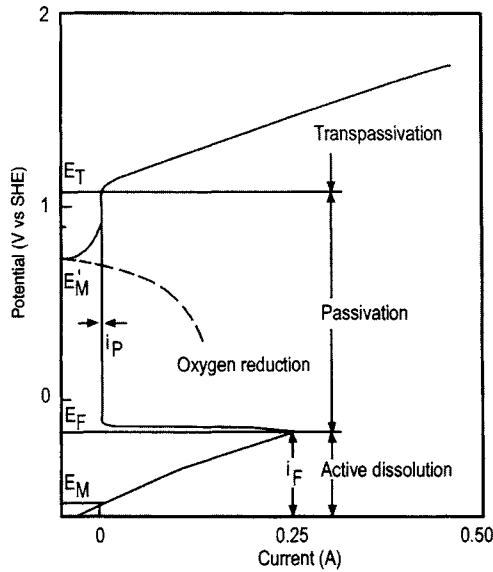


FIGURE 14.8. Anodic polarization curve for Type 446 stainless steel in 10% sulfuric acid solution at 95°C.

in deaerated sulfuric acid solutions. As a fresh specimen is made anodic, starting from E_M , the current increases because of the active dissolution of the metal. When the potential approaches a threshold value, called the Flade potential (E_F), the current decreases as a result of the formation of a thin, adherent protective oxide film, and the electrode is considered passive. Further increase in potential beyond E_T results in irregular breakdown of the passive film. Therefore more corrosion of the metal occurs. This is called transpassivation. The static potential of the metal in the presence of O_2 , E'_M , is more positive than E_M , suggesting the passivation of steel is due to the O_2 . The dotted line in Fig. 14.8 represents the cathodic polarization behavior of oxygen.

14.2.3. Corrosion Prevention

14.2.3.1. Principles. Since corrosion involves an oxidation and a reduction, we can describe the rates of these reactions, assuming kinetic control, by the electrochemical rate equations described in Section 4.2. Neglecting the backward rates of these component reactions, it can be shown that the corrosion current is a function of the exchange current densities of the anodic ($i_{o,a}$) and cathodic ($i_{o,c}$) reactions and the equilibrium potentials of the anodic (E_a) and the cathodic (E_c) processes. Assuming the transfer coefficient to be 0.5 results in

$$i_{\text{corr}} = (i_{o,a}i_{o,c})^{1/2} \exp[(F/4RT)(E_a - E_c)] \quad (28)$$

It is clear from Eq. (28) that i_{corr} can be lowered by reducing either the “ $i_{o,a} i_{o,c}$ ” term or the $(E_a - E_c)$ value. Retarding the rate of the anodic or cathodic reaction

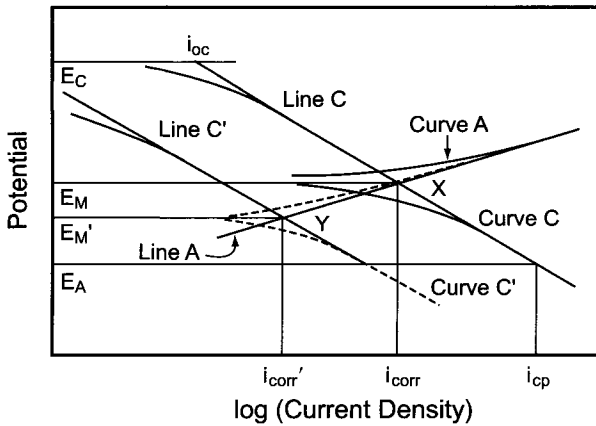


FIGURE 14.9. Schematic polarization curves illustrating the principles of cathodic protection and the influence of inhibitors.

by using inhibitors can reduce the magnitude of the exchange current densities. These inhibitors can be inorganic or organic species added to the solution or vapor-phase based and can change the polarization behavior of the anodic or cathodic reaction by lowering the exchange current density of the reaction of interest. This is called corrosion inhibition. Figure 14.9 shows the anodic and cathodic polarization curves, A and C, in the absence of any inhibitors. Curve C', representing the cathodic polarization curve in the presence of an inhibitor, shows a reduction in the corrosion rate because of the reduction in the exchange current density, i'_{oc} , by the cathodic inhibitor.

The $(E_a - E_c)$ term can be reduced by applying a cathodic current to the corroding sample so that its potential at least reaches the equilibrium potential of the anode E_a , where the corroding electrode is cathodically protected. It is necessary to apply an additional current to ensure that the potential is a few millivolts more negative than the E_a value to achieve complete protection from corrosion. Cathodic protection can be achieved by applying the current externally or by coupling the specimen of interest to sacrificial anodes of metals such as Al, Mg, Zn. These principles are illustrated in Fig. 14.9.

In a manner akin to cathodic protection, one can apply an anodic current instead, to drive the anode potential to a region where an insulating oxide film can form and protect the metal. This technique is called anodic protection.

14.2.3.2. Examples. The classical way to protect a metal surface from corrosion is to coat it with paint or a polymeric composition. Proper selection of the material and pretreatment of the surface of the substrate are necessary for good results. Many old compositions are no longer used because of environmental concerns. Use of wash primer and a second interlayer before the final painting provides good corrosion resistance—the thickness of the coating varying from about 10 μm to several millimeters depending on the need.

Metallic corrosion is also controlled by cathodic protection using sacrificial or durable anodes. The steel is polarized cathodically and hence protected from corrosion at the expense of the anodic dissolution of the less-noble metals. Corrosion protection of steel using zinc-rich paints or zinc plating (i.e., galvanizing) is based on the same mechanism. On the other hand, in the case of lead oxide paints used for painting bridges, the lead oxide layer is noble vs the steel substrate, with high hydrogen overpotential. As a result, the cathodic reaction, and hence corrosion, is suppressed.

With durable anodes, such as the DSA[®], current is applied from an external power supply to achieve cathodic protection. However, it is necessary to optimize the electrode geometry of this system to realize uniform current distribution. Cathodic protection is widely used to protect pipelines, buried steel structures, steel reinforcement in concrete, and chemical process equipment.

Anodic protection of steel can be achieved by applying a small anodic current using a less expensive metal cathode. However, it is necessary to make sure that the protective, passive film on the surface is not attacked by trace impurities such as chloride. Anodic protection of steel storage tanks for 50% NaOH is successful at a current density of 1 A m^{-2} , but it is not used with diaphragm-cell caustic because of the presence of salt.

Corrosion inhibitors are used in a wide variety of fields [10,11]. In aqueous media, oxygen scavengers are generally used to suppress corrosion caused by dissolved oxygen. These scavengers contain reducing agents such as hydrazine or sulfites. A number of ionic and nonionic inhibitors that retard corrosion either by depositing or adsorbing on the metal surface are also available. Use of corrosion inhibitors requires extensive pilot evaluation to ensure their efficiency and avoid deleterious effects on either the downstream process (by contamination) or the environment.

14.2.3.2A. Inorganic Inhibitors. The inorganic inhibitors may be classified on the basis of the role of oxygen. Inhibitors that can function without external oxygen are sometimes called passivators. These compounds include chromates and nitrates, which are readily reduced and able to oxidize the metal surface, usually iron, to form a passive oxide film. Other inorganic anions used in inhibitors include phosphates, silicates, and borates.

Tungstates and molybdates are anodic inhibitors which need oxygen to passivate a metal. However, they are not effective at high temperatures, high salt concentrations, low pH values, or low oxygen levels.

Inhibitors may also be classified in terms of their mechanism, that is, whether they function by influencing the anodic or cathodic side of the electrochemical corrosion cell. There is not always general agreement with regard to the function of a given inhibitor under given conditions of pH, oxygen content, and temperature. However, chromates, nitrates, silicates, phosphates, and borates are usually considered to be anodic inhibitors and those cations that react with the cathodically generated hydroxide to form insoluble compounds of Mg^{2+} , Cu^{2+} , Zn^{2+} , Cd^{2+} , M^{2+} , and Ni^{2+} are considered to be cathodic inhibitors. Thus, calcium polyphosphate may be viewed as a cathodic inhibitor. The differentiation is made by the direction in which the potential moves upon the addition of the inhibitor to the system. An anodic inhibitor will cause the potential to move in

the positive direction, while a cathodic inhibitor will move the potential in the negative direction, that is, toward the equilibrium potential of the anodic reaction (Fig. 14.9).

14.2.3.2B. **Organic Inhibitors.** Many organic compounds have been used as inhibitors. The effectiveness of an organic inhibitor depends on the type of bonding of the organic molecule with the metal. It is generally recognized that to be effective the compound must be adsorbed, but the type of adsorption bond varies with the configuration of the molecule. The main modes of adsorption are electrostatic adsorption, chemisorption, and π -bond (delocalized electron) adsorption. Inhibition by electrostatic adsorption is illustrated by aniline and substituted anilines, pyridine, butylamine, benzoic acid and substituted benzoic acids, and compounds such as benzenesulfonic acid.

Some of the types of compounds that function through electrostatic adsorption may also function by chemisorption. Chemisorption is most evident with nitrogen or sulfur heterocyclics. Benzotriazole and polytriazole, both effective inhibitors of copper corrosion, are believed to operate through chemisorption, as does 0.1M butylamine, which is effective in inhibiting the corrosion of iron in concentrated perchloric acid. However, the effectiveness of a given compound depends on the mechanism and operating conditions.

Corrosion inhibition by π -bond orbital interaction is exhibited by compounds such as *n*-propanol, allyl alcohol, and 2-propyne-1-ol. As the structure goes from the single bond in *n*-propanol to the double bond to the triple bond, the π -bond interaction with the metal increases, decreasing the corrosion rate of carbon steel in 2.8N HCl from several thousand to three millimeters per year. However, steric interferences may decrease the inhibitor efficiencies.

14.2.3.2C. **Vapor-Phase Inhibitors.** Vapor-phase inhibitors are volatile compounds containing one or more functional groups capable of inhibiting corrosion. The principle is to saturate the vapor surrounding the metal object with the volatile compound. The compound is adsorbed and, in the presence of atmospheric moisture, dissociates to functional groups on the surface that retard corrosion. The surface of the metal does not have to be prepared in any special way, as is the case with electroplating, and the inhibitor will function even if the surface is oxidized or rusted before application. The inhibitor will not remove the rust but will prevent further attack. Some of the effective inhibitors include: (1) amine salts with nitrous or chromic acids; (2) amine salts with carbonic, carbamic, acetic, and substituted or unsubstituted benzoic acids; (3) organic esters of nitrous, phthalic, or carbonic acids; (4) primary, secondary, and tertiary aliphatic amines; (5) cycloaliphatic and aromatic amines; (6) polymethylene amines; (7) mixtures of urea, urotropine, and ethanolamines; (8) nitrobenzene and 1-nitronaphthalene.

14.2.4. Corrosion Rates

The rate of general or uniform corrosion is expressed as weight loss per unit area and time, for example, $\text{mg dm}^{-2} \text{day}^{-1}$ (mdd), or as loss in the thickness of the sample, for example, millimeters per year (mm/y) or mils/year (mpy). These two descriptions can

TABLE 14.7. Corrosion Rate Guidelines for Selection of Materials

Rank	Uhlig ^[12] (mpy)	NACE ^[13] (mpy)	CRT ^[14] (mpy)/(mm/y)
A. Excellent	<5	<2	<2/<0.05
B. Good	5–50	<20	<20/<0.51
C. Careful		20–50	<50/<1.27
D. Inapplicable	>50	>50	>50/>1.27

be interconverted as:

$$1 \text{ mdd} = \frac{\text{density}(\text{g cm}^{-3}) \times 10^6}{365} \text{ mm/y} \quad (29)$$

$$1 \text{ mpy} = 2.5 \times 10^{-2} \text{ mm/y} \quad (30)$$

Corrosion rates can also be calculated from i_{corr} values, expressed in mA cm^{-2} by

$$\text{mpy} = \frac{128.66 \times i_{\text{corr}} \times \text{equivalent weight of the metal}}{\text{density}(\text{g cm}^{-3})} \quad (31)$$

The corrosion rate is not always constant, as it is enhanced on rough surfaces and retarded when surface oxide layers form on the metal. Therefore, it is essential that corrosion behavior be examined over a prolonged time period before selection for use in any unit operation.

Table 14.7 provides a guideline for selecting materials of construction based on their corrosion rates. This information should be weighed against the cost of the material, as a highly corrosion resistant material is not always the most economical choice. It should be cautioned that the criteria in Table 14.7 are not valid if there is localized corrosion due to pitting or SCC. In such instances, it is necessary to ensure that the chosen material is not prone to failure by the mechanisms leading to localized corrosion.

14.3. MANIFESTATIONS OF CORROSION

Corrosion appears in various forms. An understanding of these forms is essential for selection of the right materials for any given operation and to avoid simple mistakes that can lead to catastrophic corrosion failures. The ten distinct forms of corrosion discussed here are uniform corrosion, galvanic corrosion, crevice corrosion, pitting corrosion, intergranular corrosion, selective leaching or dealloying, erosion corrosion, stress corrosion, corrosion fatigue, and high-temperature corrosion.

14.3.1. Uniform or General Corrosion

This is the most common form of corrosion when metal dissolution takes place uniformly (not localized) over the entire exposed surface (e.g., rusting). Uniform corrosion can be seen in steel pipes, beams, offshore drilling platforms, heat exchanger tubes, knives, forks, and spoons.

14.3.2. Galvanic or "Two-Metal" Corrosion

Galvanic corrosion occurs when a less noble metal is in contact with a more noble metal in the same environment. The extent of corrosion depends on the:

1. positions of the metals in the EMF series
2. nature of the environment
3. polarization behavior of the metals
4. geometric relationship of the component metals.

As a general rule, when dissimilar metals are used in contact with each other and are exposed to an electrically conducting solution, combinations of metals that are as close as possible in the galvanic series should be chosen. Coupling two widely separated metals generally will produce an accelerated attack of the more active metal. Principles of electrode kinetics can be used to understand galvanic corrosion, as exemplified below.

Platinum is an inert metal and the rate of hydrogen evolution is orders of magnitude greater than that on metallic zinc (exchange current density for the hydrogen evolution reaction in 1N HCl is $\sim 10^{-3}$ A cm $^{-2}$ on Pt and $\sim 10^{-11}$ A cm $^{-2}$ on Zn in H $_2$ SO $_4$).

If a piece of platinum wire is coupled to zinc which is corroding in an air-free, acidic solution, vigorous hydrogen evolution begins on the platinum surface and the rate of zinc dissolution also increases. In terms of polarization curves (Fig. 14.10), the corrosion rate is $i_{\text{corr}}(\text{Zn})$, which is obtained as the point of intersection of the Zn dissolution and hydrogen evolution Tafel plots. The corrosion potential is represented by E_{corr} .

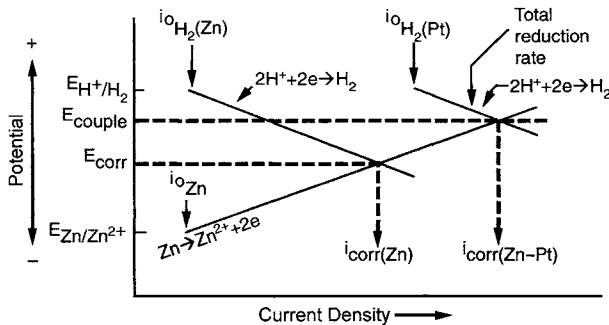


FIGURE 14.10. Effect of coupling zinc to platinum, exemplifying galvanic corrosion.

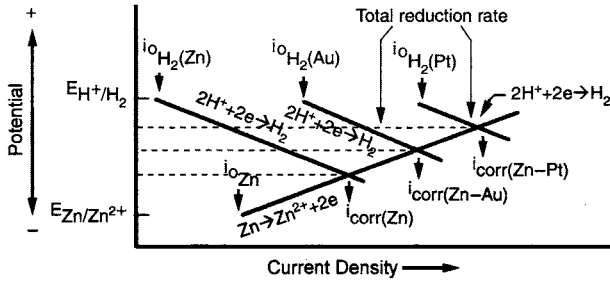


FIGURE 14.11. Comparison of zinc-platinum and zinc-gold galvanic couples.

When equal areas of Pt and Zn are coupled, the rate of hydrogen evolution is given by,

$$\begin{aligned} \text{Rate of H}_2 \text{ evolution} &= \text{Rate on the Zn surface} + \text{Rate on Pt surface} \\ &\cong \text{Rate on Pt surface} \end{aligned}$$

(since rate on the Pt surface \gg rate on Zn surface).

The corrosion rate in this coupled system is determined by the intersection of the polarization curve for H_2 evolution on Pt with the Zn dissolution curve. The corrosion current is not $i_{\text{corr}}(\text{Zn})$, and has increased many fold to $i_{\text{corr}}(\text{Zn-Pt})$. The “mixed” or corrosion potential shifts from E_{corr} to E_{couple} as shown in Fig. 14.10 (note that the corrosion potential shifts in the positive direction).

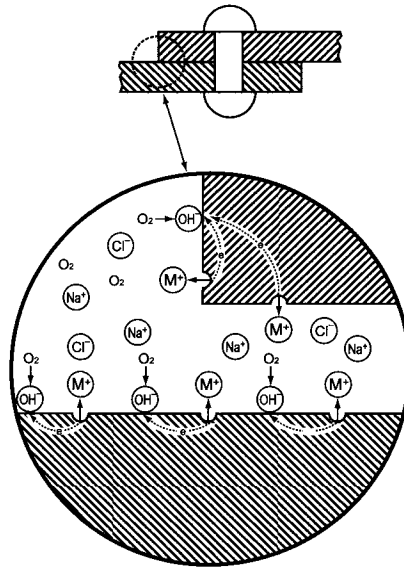
Coupling Zn to Au (of the same area) results in a decrease in the corrosion rate in comparison to the Zn-Pt couple, and the corrosion potential shifts in the negative direction. The decrease in the rate of Zn dissolution for Zn-Au compared to Zn-Pt system is not determined by the position of Au in the EMF series with respect to Pt but is due to the fact that the rate of H_2 evolution on gold is less than the rate of H_2 evolution on platinum (Fig. 14.11). In 1N HCl, the exchange current density for the H_2 evolution reaction on Pt is 10^{-3} A cm^2 vs 10^{-6} A cm^2 on Au.

Area effects in galvanic corrosion are very important. An unfavorable area ratio (e.g., large cathode and small anode) will result in corrosion rates that are 100 to 1,000 times greater than if the two areas were the same.

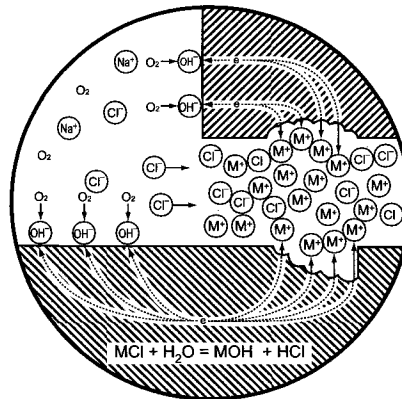
14.3.3. Crevice Corrosion

Crevice corrosion is a form of localized corrosion occurring in crevices and other shielded areas on metals exposed to a corrosive medium. It is usually observed where small volumes of stagnant solution are trapped in holes, gasket surfaces, lap joints, and crevices under bolt and rivet heads.

Differential aeration (i.e., O_2 -rich vs O_2 -starved regions) is an initial step for crevice corrosion and continued corrosion is usually due to accumulation of corrosion products inside the crevice (Fig. 14.12). The initial corrosion reactions for this case may be



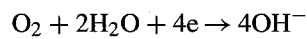
Crevice Corrosion—Initial Stage



Crevice Corrosion—Later Stage

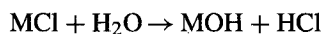
FIGURE 14.12. Schematic depicting the initial and later stages of crevice corrosion. (With permission from NACE International.)

written as:



When, in the absence of convection, the O_2 concentration inside the crevice decreases to zero, an O_2 concentration cell is set up. Metal M continues to corrode inside

the crevice while the exposed metal is protected by O_2 reduction. Corrosion inside the crevice results in an increase in M^+ ions, hence negative ions (e.g., Cl^-) migrate into the crevice to maintain electroneutrality, resulting in the formation of the metal chloride. The metal chloride hydrolyzes as:



The HCl released during the hydrolysis reaction enhances metal dissolution, and the process repeats. Thus, crevice corrosion is an autocatalytic process. Since crevice corrosion is related to the mass transport through the crevice, the size of the crevice plays a critical role. Crevice corrosion seldom occurs in wide grooves, as there is enough supply of oxygen to these areas. Figure 14.13 illustrates the crevice corrosion of a titanium heat exchanger plate covered with a synthetic rubber gasket. Damaged areas for the most part are covered with white TiO_2 .

Precipitates and suspended solids in process streams will deposit in stagnant areas (e.g., corners in vessels or bends in a pipe) and lead to corrosion of metals by the same mechanism as that involved in crevice corrosion. This is called “deposit attack.” Filtration of process fluids can prevent these problems.

Filiform corrosion found on painted materials is a type of corrosion caused by uneven transfer of dissolved oxygen. Once the solution permeates through a painted layer on an iron surface, the metal corrodes. The acidity built up during this process promotes the delamination of the paint film. Ferrous ions left behind are oxidized to ferric iron, which will precipitate as $Fe(OH)_3$.

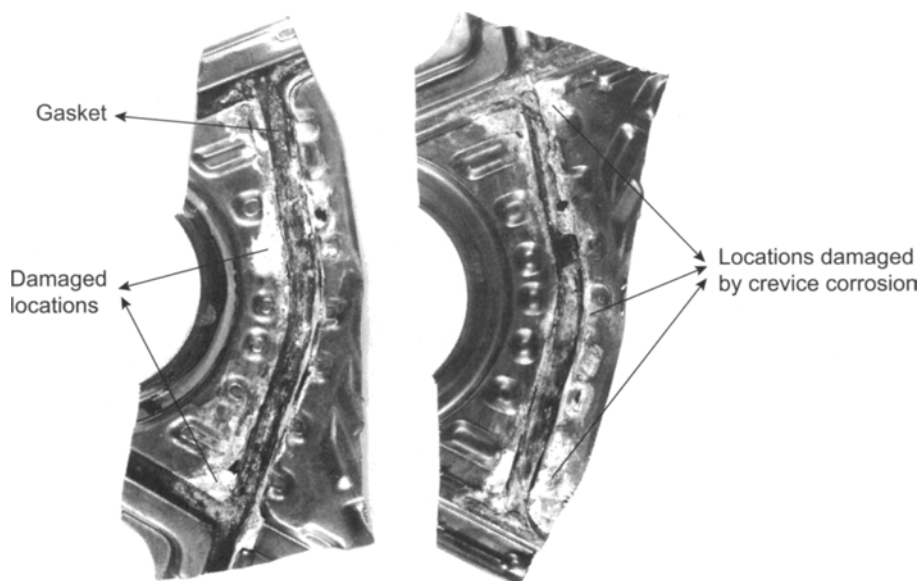


FIGURE 14.13. Crevice corrosion of titanium plate of a brine heat exchanger. (With permission from Denki Kagako Kogyo Co. (1977).)

14.3.4. Pitting Corrosion

Pitting corrosion is a dangerous form of acute localized corrosion. Localized corrosion is defined as corrosion attack on a small part of a metal surface while the remaining area is practically unattacked.

Pitting usually occurs on metals that are covered by a “passive” film, which protects them from corrosion under normal conditions. Pitting is known to occur on magnesium, aluminum, titanium, carbon steel, stainless steel, and copper. Pits develop at weak spots on the surface film and at sites where the film has been damaged.

Pitting corrosion manifests itself with the formation of holes. Equipment failures due to pitting corrosion show little or negligible weight loss, and usually the failures are quite sudden. Pitting is difficult to detect, because the holes are usually filled with corrosion products as they form. Pits usually grow in the direction of gravity and their formation is associated with a long initiation period ranging from a few months to years, depending on the metal and the medium.

The mechanism for pitting corrosion is similar to that invoked for crevice corrosion. Rapid metal dissolution in the pit area (with O_2 reduction taking place in the adjacent areas) produces an excess positive charge, which induces Cl^- ion migration, followed by H^+ ion formation due to hydrolysis, which results in further dissolution of the metal. Since the O_2 concentration in the pit is virtually zero, the pit protects the rest of the metal cathodically by sustaining O_2 reduction in the adjacent areas.

In addition to temperature, pitting corrosion is influenced by two factors:

1. *Solution Composition.* Most pitting failures have been associated with Cl^- or chlorine-containing ions such as OCl^- . Metal chloride formation and subsequent hydrolysis to generate H^+ ions is the most probable mechanism. F^- and I^- ions do not tend to induce pitting. Cations such as Cu^{2+} , Fe^{3+} , and Hg^{2+} have a marked effect on pitting. These ions do not need the presence of oxygen to promote attack, since they can participate in reduction reactions such as $Cu^{2+} + 2e^- \rightarrow Cu$ and $Fe^{3+} + e^- \rightarrow Fe^{2+}$. Copper deposition is usually associated with the pitting of aluminum.

2. *Solution Velocity.* Pitting occurs under stagnant conditions when a liquid is trapped in a part of an “inactive” pipe system. Increasing the solution velocity decreases pitting attack.

One of the techniques employed to determine whether or not a substrate is prone to pitting is an analysis of current–potential data in the given medium. Figure 14.14 shows the polarization curve of a Type 18-8 stainless steel in a slightly acidified $NiSO_4$ solution at $95^\circ C$ [15]. When it is immersed in the $NiSO_4$ solution, it is readily passivated. As the stainless steel is anodically polarized to 1 V vs the standard calomel electrode (SCE), a small amount of current flows through the system. This is the passivation current. When the anode potential increases beyond 1 V, the current increases again (curve I) as a result of transpassivation. The current–potential profile again follows curve I when the anode potential is reduced.

When a similar experiment was performed in solutions containing 0.1M $NiCl_2$, current increased at a low potential, E_R (compare curve I and curve II), indicating the breakdown of the surface film. The current fluctuated at $\sim 5 \text{ mA cm}^{-2}$ even when the potential varied from 0.3 V to 0.0 V, and then the current decreased, as indicated by

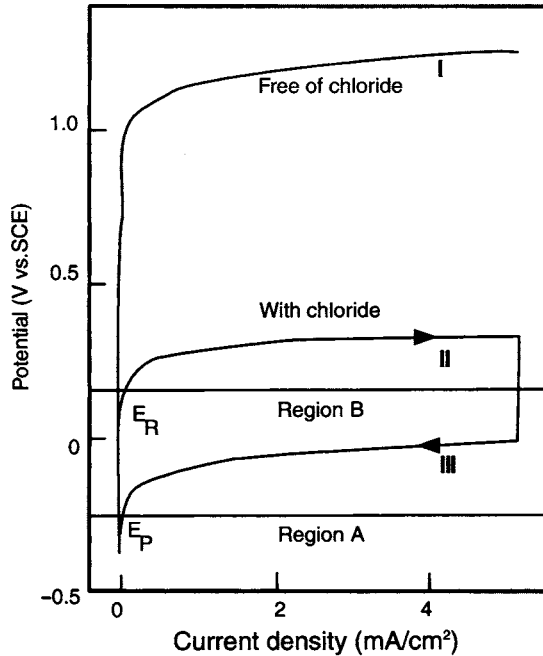


FIGURE 14.14. Anodic polarization curve of 18–8 stainless steel in acidified NiSO_4 solution at 95°C [15].

the curve III. Thus, in the potential range marked B (between E_P and E_R), the formation and the rupture of the passive film compete with each other—the passive film being attacked by the Cl^- ion. At potentials below E_P , the protection potential, the material is protected from corrosion. Note that the Cl^- ion penetrates through the oxide layer before it attacks the metal, and therefore there is an induction period before the substrate starts degrading from the anodic dissolution process.

The protection potential of Type 300 stainless steels [16] decreases as the Cl^- ion concentration increases, as shown in Fig. 14.15. As the E_P of 316 SS is more noble than that of 304 SS, it is more resistant to pitting by Cl^- ions.

14.3.5. Intergranular Corrosion

Selective corrosion in the grain boundaries of a metal or alloy without appreciable attack on the grains or crystals themselves is called intergranular corrosion. When a metal solidifies, the atoms, which are randomly distributed in the liquid state, arrange themselves in a crystalline array. Although a crystalline order is maintained in the bulk phase, there usually is a mismatch between the individual grains on the surface. These regions are called grain boundaries and constitute high-energy areas on the surface. They are generally found to be more chemically active. A preferential attack at the grain boundary can result in disintegration of the grains and lead to a rapid decrease in mechanical strength.

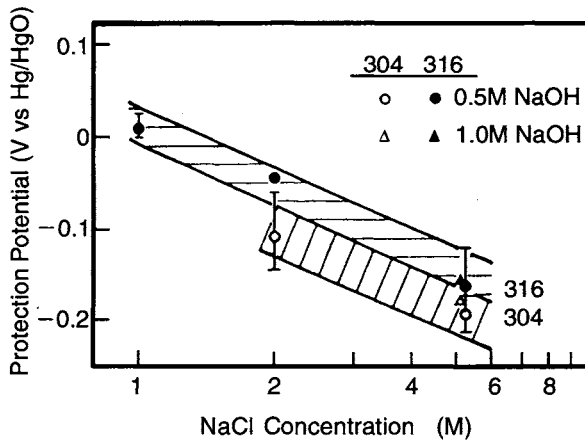


FIGURE 14.15. Protection potential of 18-8 stainless steel in mixed solutions of NaOH and NaCl at 95°C as a function of the salt concentration [16].

Intergranular corrosion can result from an enrichment or depletion of one of the alloying elements at the grain boundary. Stainless steels, chromium, and nickel-rich alloys are all susceptible to intergranular corrosion.

In stainless steels containing chromium and carbon, carbon segregates as chromium carbide at the grain boundaries, leading to the depletion of chromium around them. As a result, corrosion resistance decreases when the steel is heated. Corrosion of these heat-affected zones next to the welds is called “weld decay.”

14.3.6. Selective Leaching or Dealloying

This form of corrosion corresponds to a process where one constituent of an alloy is preferentially removed, leaving behind an altered structure. The most common example for this type of corrosion is the selective removal of zinc from brass (Cu–Zn alloys), also referred to as dezincification. Selective leaching has been observed in other alloy systems containing Al, Fe, Co, and Cr.

Dealloying is normally detectable by a color change. Brasses turn from yellow to red. Cast irons become dark from silver gray as a result of enrichment of graphite. Gray iron that has suffered such corrosion is like a “sponge” with virtually no mechanical strength.

14.3.7. Erosion Corrosion

Erosion corrosion may be defined as accelerated corrosion arising from rapid relative movement of the corrosive fluid and the metal surface. At high velocities of the corrosive fluid, mechanical wear or abrasion occurs. An increase in velocity can increase the rate of corrosion by enhancing the supply of O_2 , CO_2 , H_2S , or other constituents in the medium.

Almost all metals are susceptible to erosion corrosion. Most metals depend on protective “passivating” films to inhibit further corrosion of the underlying metal. Examples

are stainless steels, aluminum, and lead. Erosion corrosion results when protective films are damaged or worn by the velocity of the corrosive fluid. This breakdown results in an increase in the corrosion rate.

Typical systems susceptible to erosion corrosion are piping (particularly where turbulence is intensified as in bends, elbows and tees), valves, pumps, blowers, propellers, impellers, turbine blades, nozzles, ducts, and grinders. The nature and properties of surface “passivating” films are very important from the standpoint of erosion corrosion. A hard, dense, adherent, and continuous film would provide better protection than a nonadherent film. The ability for the film to “re-form” upon breakdown, is referred to as “film-repair”.

Mechanical damage of a metal surface occurs even in clear solutions when cavities are repetitively formed and destroyed or collapsed on a surface where the pressure decreases rapidly to less than the atmospheric pressure. The resulting cavitation damages the protective film on the surface, triggering further corrosion. This occurs frequently on the rear side of a pump impeller.

Copper alloys suffer from impingement attack under turbulent flow conditions, when corrosion is accelerated by solids and gas bubbles in the liquid stream. This behavior is often seen at the inlet end of a heat exchanger and is called inlet attack.

Another type of corrosion promoted by mechanical factors is fretting corrosion, which occurs on a metal surface that repeatedly touches another solid [17].

14.3.8. Stress Corrosion

Stress corrosion refers to cracking (or breakdown) of a structure due to the simultaneous presence of a tensile stress and a specific corrosive medium. During stress corrosion, the metal/alloy is virtually unattacked over most of the surface while fine cracks propagate through it. Failures due to stress corrosion cracking (SCC) occur with extreme suddenness and can have serious consequences.

The important variables affecting SCC are temperature, solution composition, metal composition, and the total stresses (residual and applied) in the metal. Residual stresses result from deformation during fabrication, unequal cooling from high temperature, and internal structural rearrangements involving volume change. Stresses induced by rivets and bolts, press and shrink fits, and dry polishing with grinders can also be classified as residual stresses. Tensile stresses at the surface, usually of a magnitude equal to the yield stress, are necessary to produce SCC.

SCC mainly occurs in two forms, intergranular and transgranular. The intergranular form corresponds to a case where the cracking follows the grain boundaries in the metal, while the transgranular type of cracking corresponds to a case where the cracks pass through the metallic grains.

Figures 14.16 and 14.17 are examples of intergranular corrosion and transgranular corrosion of stainless steels, respectively. Transgranular corrosion refers to the corrosion of the metallic grains, while intergranular corrosion refers to the corrosion in the grain boundary region. Although carbon steel is considered to be unaffected by transgranular corrosion, transgranular SCC was observed with mild steels and low alloy steels in a $H_2O-CO-CO_2$ environment [18,19].

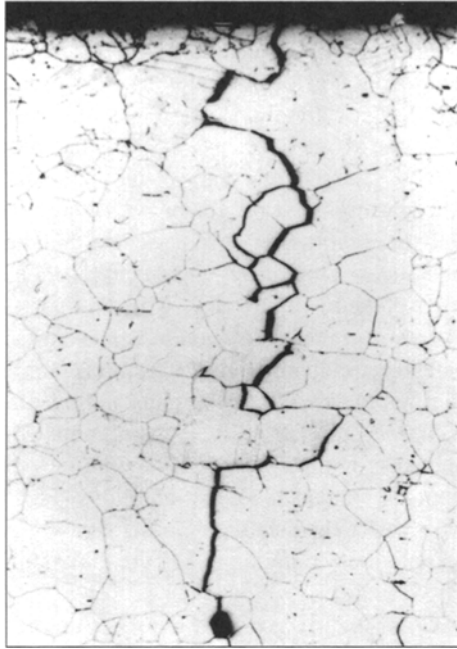


FIGURE 14.16. Intergranular corrosion of Type 347 stainless steel in polythionate solution at room temperature. (With permission from Sumitomo Metal Industries, Ltd.)

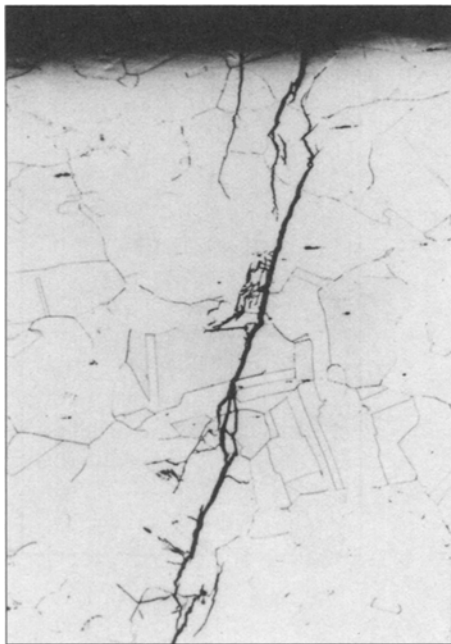


FIGURE 14.17. Transgranular corrosion of Type 304 stainless steel in 45% MgCl_2 at 154°C. (With permission from Sumitomo Metal Industries, Ltd.)

Electrochemical and mechanical factors both contribute to failure by SCC. The electrochemical nature of SCC is easily illustrated by the fact that an impressed cathodic current prevents the metal from cracking. Removing the impressed current allows the cracking to progress. Although cathodic protection is effective to mitigate the SCC, excessive polarization must be avoided to prevent hydrogen embrittlement.

SCC starts by an electrochemical mechanism. A pit, scratch, or rupture in a protective film can act as the starting point for corrosion. Anodic and cathodic areas form on the metal surface, with the weakly film-covered region and the tip of the crack acting as an anode and the oxide-covered region acting as a cathode. Once corrosion starts, the stresses tend to concentrate at the tip of the crack, which remains active. At some critical stress value, deformation results in the formation of a fresh surface (at tips where all the stresses are relieved). The electrochemical mechanism takes over on the fresh surface, building up stress at the tip of the crack. This sequence of events repeats continuously.

Austenitic stainless steels suffer from SCC in solutions containing chloride ions. Accelerated tests conducted in boiling 42% MgCl_2 solutions show the time-to-failure to be a function of the nickel content in Fe–Cr–Ni alloys (Fig. 14.18). The shadowed area represents the region where the steels are prone to SCC. Type 304 stainless steel is susceptible to SCC in solutions containing Cl^- , the maximum allowable level being ca. 0.1 mg L^{-1} .

Another cause of SCC is hydrogen embrittlement. Carbon steel fails by hydrogen embrittlement in aqueous solutions containing S, CN, As, and other impurities that prevent the recombination of adsorbed atomic hydrogen on the metal surface. Atomic hydrogen permeates through the bulk of the metal to form molecular hydrogen in the

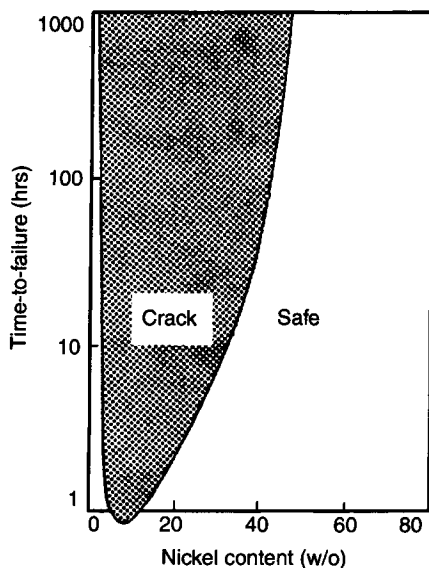


FIGURE 14.18. Time-to-failure as a function of the Ni content in Fe–Cr–Ni alloys in boiling 42% MgCl_2 solutions. (With permission from NACE International.)

voids, where the pressure increases enormously and causes the formation of blisters on the surface.

Titanium fails by hydrogen embrittlement, as it readily forms hydrides, and hence it is not used as a cathode material during electrolysis. Hydrogen also permeates into steel, where it combines with carbon (i.e., decarburization) at temperatures higher than 220°C (Fig. 9.58). This decreases mechanical strength and causes hydrogen blisters.

14.3.9. Corrosion Fatigue

Corrosion fatigue is caused by the combined action of corrosion attack and rapidly alternating tensile and compressive stresses. Corrosion fatigue can occur at low stresses in contrast to purely mechanical fatigue, which occurs only at a critical value of cyclic stress. The mechanism of corrosion fatigue involves exposure of oxide-free, cold worked metal by extraction of slip bands in the metal surface caused by cyclic stressing. The exposed metal surface becomes anodic leading to the formation of corrosion grooves, which develop to transcrystalline cracks. Corrosion fatigue can be prevented by cathodic protection or by surface hardening in the case of steels by nitriding.

14.3.10. High-Temperature Corrosion

High-temperature corrosion is the oxidation of metals in dry gas at high temperatures. It includes the chemical reaction of metals with corrosives such as sulfur dioxide, chlorine, nitrogen, hydrogen, molten salt, and liquid metal. They are called oxidation, vanadium attack, sulfidation, nitriding, carburization, halide attack, hydrogen damage, molten-salt corrosion, and others depending on the mechanism and the form of the damage.

When the oxidation of metal is controlled by diffusion of oxygen through the oxide layer on the metal surface and the chemical reaction is fast [12], the dependence of the oxide-layer thickness x with time t can be written as:

$$\frac{dx}{dt} = \frac{k'}{t} \quad (32)$$

where k' is a coefficient which contains the diffusion coefficient of oxygen in the oxide layer. With the initial condition, $x = 0$ at $t = 0$, we have

$$x = kt^{1/2}, \quad k = (2k')^{1/2} \quad (33)$$

Figure 14.19 shows an example of the weight gain of iron in air as a function of the time of oxidation. The slope of the log-log plot is 0.5, irrespective of temperature, which agrees with Eq. (33). This equation [20] is recognized as the basis of high-temperature corrosion, with some exceptions, such as the oxidation of metal covered with coarse oxide through which oxygen passes at a high rate. In this case, the thickness of the oxide is directly proportional to time:

$$x = kt \quad (34)$$

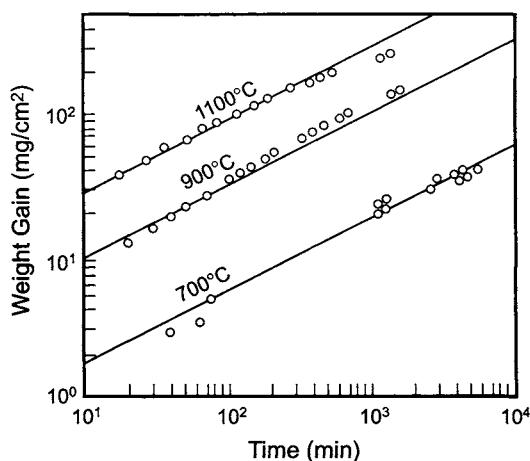


FIGURE 14.19. Weight gain vs time curves for iron in air [12]. (Reprinted with permission of John Wiley & Sons, Inc.)

The atomic ratio of oxygen to metal in the oxide layer often varies and is non-stoichiometric, and therefore it contributes to the electric conductance. When Ni^{2+} is depleted in a NiO lattice, for example, a positive hole is formed and this is called a p-type semiconductor. Cu_2O , FeO , CoO , Bi_2O_3 , and Cr_2O_3 are examples of p-type semiconductors.

On the other hand, when excess metallic ions are present in the oxide lattice of ZnO , CdO , TiO_2 , and Al_2O_3 , more electrons are needed to compensate for the imbalance of charge in the oxide. These are called n-type semiconductors.

Since the transfer of Ni^{2+} from the metal surface to the outside controls the oxidation of nickel, the addition of Cr^{3+} (a high-valence cation) requires a positive hole. This triggers the transfer of Ni^{2+} , resulting in an increased oxidation rate. On the contrary, when a low-valence cation such as Li^+ is added to NiO, Li^+ occupies the positive holes, and this results in a decreased oxidation rate. This is a description of valency control. Thus, the addition of Cr accelerates the oxidation of steel, but the Cr-enriched layers near the outside surface forms a tight oxide film, resulting in improved corrosion resistance.

Vanadium in a fuel forms various metal compounds with low melting points, and causes molten-salt corrosion of steel called vanadium attack. Another example of high temperature corrosion is sulfidation. Carbon monoxide, carbon dioxide, and hydrocarbons form metal carbides at high temperatures and this is called carburization. Nitriding involves chemical reaction of nitrogen with metal.

Liquid metal corrosion is the dissolution of solid metal into a liquid metal, when the liquid metal penetrates into the grain boundaries of the solid metal and causes intergranular corrosion.

In hot hydrogen atmospheres, carbon or carbide in the metal is reduced to hydrocarbons such as methane, and the metal structure fails by high pressures and internal stresses. Hydrogen damage depends greatly on the temperature and the pressure (see Fig. 9.58).

14.3.11. Failure of Nonmetallic Materials

14.3.11.1. Organic Materials. Degradation of organic materials is a result of chemical attack by the penetration of chemical constituents from the corrodent. The mechanisms and the phenomena depend on material composition, molecular structure, physical properties, and the operating conditions.

There are many types of degradation of organic polymers and their composites. They include sorption, swelling, crazing, cracking, blistering, decoloration, decomposition, erosion, cavitation erosion, fatigue, and environmental stress cracking.

Sorption is permeation by liquid or gas from the environment, resulting in swelling of the material. Swelling may be followed by dissolution into the solvent. This is generally not observed with cross-linked polymers. Crazing appears on the surface of polymer extrusions, caused mainly by internal stresses. Crazing may extend to cracking.

Plastics suffer from cracking by impingement. Blisters are found on painted structures and are caused by the penetration of solvent or water. Polymer-lined steels are prone to blistering, the formation of blisters being accelerated by the diffusion of water vapor when the lined surface is exposed to a hot solution. Discoloration occurs in a corrosive environment especially when the polymer is exposed to ultraviolet radiation. This is a consequence of the decomposition of the polymer and formation of double- or triple-bonded molecules. Erosion, cavitation, and fatigue are failures initiated by mechanical stresses in a corrosive medium. Polyethylene is affected by embrittlement and cracking under tensile stresses. Degradation of other organic polymers by chemical and mechanical factors is termed environmental stress cracking.

14.3.11.2. Inorganic Materials. Glass, carbon, graphite, bricks, and stoneware are sometimes used in the chemical process industries. Failure of these materials is caused by physical degradation (e.g., cracking, tipping, spalling) and chemical attack.

Glass lining (of ca. 1 mm thickness) is provided to steel to prevent it from corrosion. However, glass lining fails because of pinholes, tipping, "fish-scale," thermal shock, mechanical damage, and chemical attack.

Carbon and graphite are oxidized in aqueous solutions and by air at high temperatures. Solution and gases can penetrate into the micropores and cause physical and mechanical attack. Impregnating carbon and graphite with polymers makes them impervious, extending their useful life by 5 to 10 years.

14.4. MATERIAL SELECTION

There are several factors that must be considered in great detail when selecting materials of construction. Structural materials should offer not only corrosion resistance but also the needed mechanical strength.

General information on the suitability of metals and alloys in various environments is available in the *Corrosion Data Survey* [13], which also shows the potential of pitting, SCC, intergranular attack, and crevice corrosion associated with the given material. Figures 14.20 and 14.21 are examples of the type of information provided. *Corrosion Resistance Tables* [14] is a similar publication available in two volumes. A Carpenter

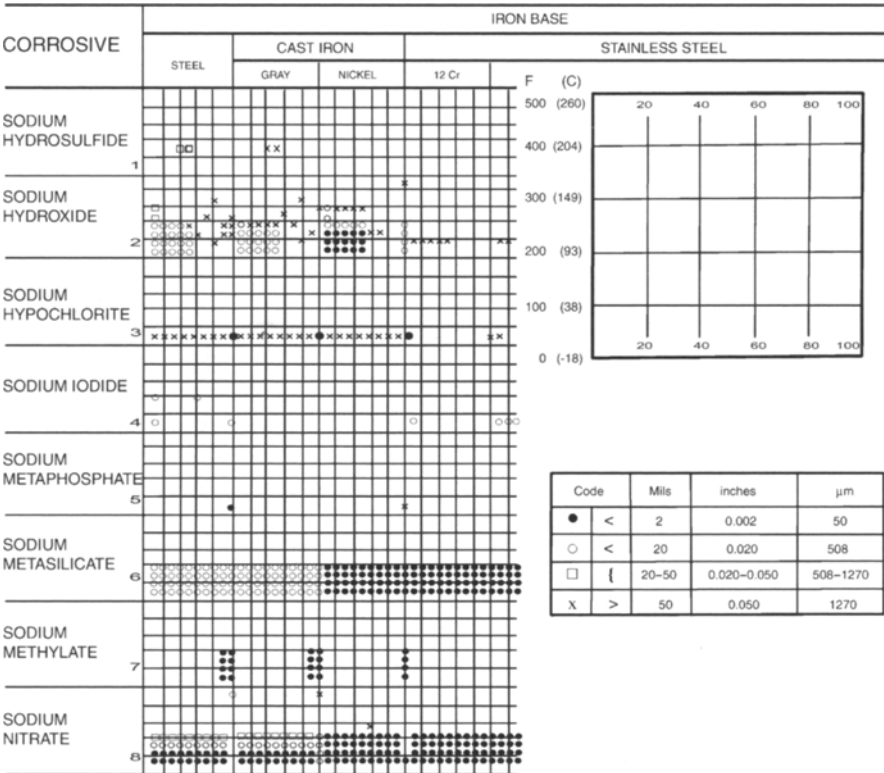


FIGURE 14.20. Typical description in corrosion data survey-metals section [13]. (With permission from NACE International.)

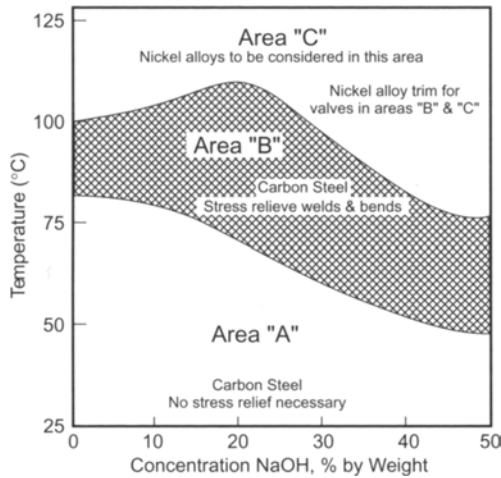


FIGURE 14.21. Corrosiveness of sodium caustic and recommended practice [13]. (With permission from NACE International.)

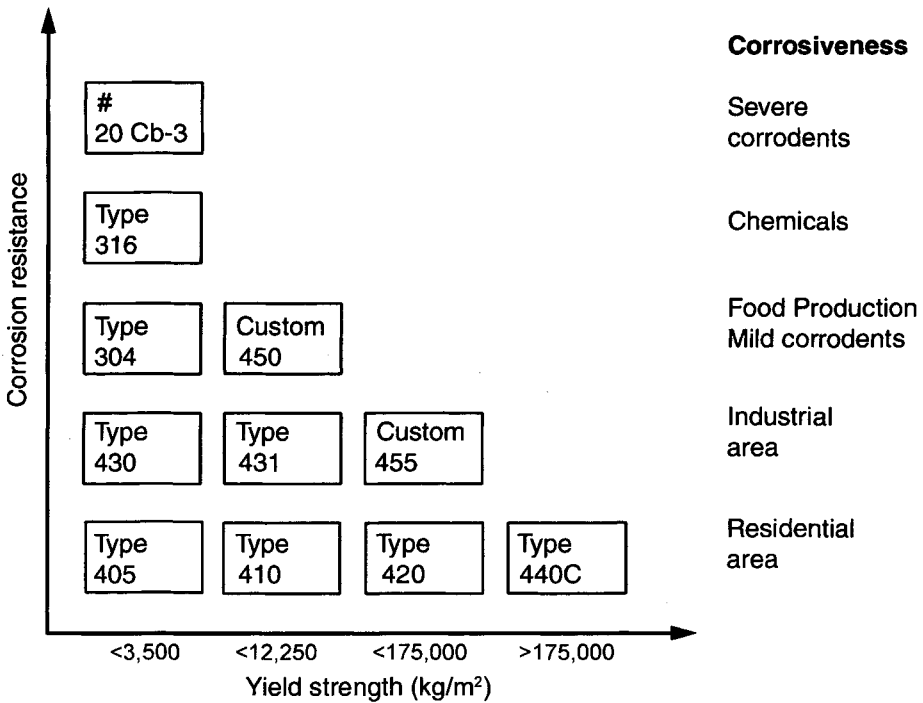


FIGURE 14.22. Classification of the corrosion resistance and mechanical strength of stainless steels of Carpenter's Selectalloy™ method [21].

brochure [21] describes various materials from the viewpoint of both corrosion resistance and mechanical strength, as shown in Fig. 14.22 for stainless steels. Thus, 316 SS can be used instead of 304 SS if the corrosion resistance of 304 SS is unacceptable. On the other hand, 430 SS is acceptable in mild environments and is cheaper. Figure 14.22 also emphasizes the need to consider mechanical strength and ease of machinability and weldability as well as corrosion resistance.

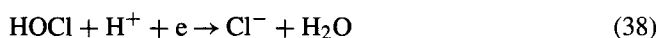
Other design and fabrication considerations that must be addressed include: (1) residual stresses in the structure, (2) heat-affected zones near welds, (3) proper geometry for fluid flow, (4) structure of the heat transfer unit and its surface, (5) use of dissimilar metals, (6) gaskets and seals, (7) air leakage, (8) fluctuation in pressure, temperature, and flow rate, and (9) the ease of maintenance and overhaul. Internal stresses generated by cold work, welding, fabrication, and installation can cause SCC. Weld zones are structurally and compositionally different from the bulk metal and may suffer localized corrosion. Sudden changes in operating pressure and flow velocity may generate erosion corrosion, impingement attack, and crevice corrosion. Nonuniform heat transfer can lead to the formation of scale, causing local increases in temperature and corrosion. Use of dissimilar metals can cause galvanic corrosion. Direct contact between such metals should be avoided by design or by insertion of insulators. However, the insulating materials, gaskets, and seals may lead to crevice corrosion. Leakage of air may

accelerate general corrosion of carbon steel, while dissolved oxygen benefits stainless steel by passivating surfaces.

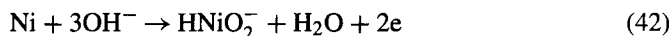
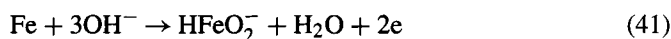
14.5. CORROSION IN CHLOR-ALKALI OPERATIONS

14.5.1. General Aspects

Irrespective of the cell technology used for producing chlorine, the materials of construction employed in a chlor-alkali plant encounter one or more of the following reactants: acid, oxygen, chlorine (gaseous or dissolved as Cl_2 , HOCl , or OCl^-), caustic, and hydrogen. All these species have the potential to degrade the materials they are exposed to. The cathodic reactions responsible for the oxidation of metals are: (1) O_2 reduction, (2) H^+ ion reduction, and (3) reduction of Cl_2 , HOCl , or OCl^- , as noted below.



Note that the metal oxidation reaction releases electrons by the reaction $\text{M} \rightarrow \text{M}^+ + \text{e}$. Iron is susceptible to oxidation by reaction (35) or (36), while Ni and stainless steels will corrode by reactions (37) to (40). Another reaction of interest in chlor-alkali operations is oxidation of Fe or Ni in alkaline media:



The extent of oxidation of transition metals in NaOH solution is a function of NaOH concentration and temperature, as will be shown later. Most of the corrosion problems observed in chlor-alkali operations are traceable to the above reactions. By properly counteracting the reactants, many commonly reported corrosion problems can be avoided.

14.5.2. Materials of Construction in Chlor-Alkali Operation

The unit processes in a commercial chlor-alkali plant can be broadly classified as follows: (1) Brine preparation and purification, (2) Electrolytic cells, (3) Cl_2 processing, (4) Caustic concentration, and (5) H_2 processing. The materials of construction in these various processes are discussed in the following sections [22–24] and in Chapters 7 and 9.

14.5.2.1. Brine Preparation and Purification. The various steps in the brine preparation and purification processes involve wide ranges of temperature, salt concentration, and pH. Each of these conditions affects the choice of materials of construction. The simplest systems may be based on carbon steel with a heavy corrosion allowance.

The pH of raw brine is generally 6.5 to 7.5. It can be pumped through carbon steel pipelines, which may be cathodically protected. Pipe bridges are protected from corrosion arising from oxygen reduction (Eqs. 35 and 36) by painting the outer surface or by cathodic protection. Underground lines may be wrapped or covered with protective material or cathodically protected. Alternatively, the piping can be rubber-lined carbon steel, fiber-reinforced polyester (FRP), vinylester, or a plastic such as PVC, PP, HDPE, fluorinated ethylene/propylene (FEP), or polytetrafluoroethylene (PTFE). Many of the same polymeric materials are used to line piping and equipment. The linings must be free of pores, or the brine will seep through and cause pitting corrosion.

Purified brine often is heated and acidified before entering the cells, the pH usually being 1–3 at temperatures up to 75–80°C. Materials must be chosen to prevent corrosion under these conditions and must not contribute harmful impurities to the brine. To avoid damage by leakage currents, steel-based pipelines are cathodically protected by properly grounded target anodes.

Heat exchangers in brine service are usually titanium or copper-nickel alloys, and pumps are made of Type 316 SS, Ni-Resist titanium, rubber-lined steel, or FRP. Storage tanks use many of the same materials employed in piping systems, the choice reflecting processing conditions and the importance of avoiding contamination.

Concrete flooring in the brine area is liable to disintegration by brine, and it is protected by coating with materials such as magnesium or zinc fluosilicate, epoxy or silicone penetrating sealers, and drying oils. Concrete surfaces exposed to mechanical wear are treated with 3- to 6-mm thick epoxy surfacing materials. Sumps and trenches employ reinforced polyester or epoxy resin systems.

14.5.2.2. Electrolysis

14.5.2.2A. Electrolytic Cells. Mercury cells are constructed with carbon steel, and the surfaces in contact with chlorine are rubber-lined. Diaphragm cells are also fabricated with carbon steel bodies and FRP or vinylester covers. The external carbon steel surfaces are usually treated with a high performance catalyzed polyamide or amine-cured painting system with 0.05–0.075-mm thick primer, 0.13–0.15-mm thick intermediate and a 0.13–0.15-mm thick finish coat, the thicknesses referring to the dry films.

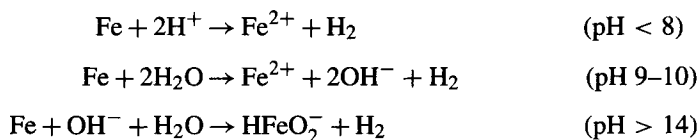
The standard materials of construction of membrane cells are titanium on the anode side and nickel on the cathode side. Painting in a manner similar to that employed for diaphragm cells protects the external surfaces of these materials.

14.5.2.2B. Cell Components. The anode material in all three chlor-alkali technologies is a titanium substrate, in the form of a mesh or a louvered structure, coated with $\text{RuO}_2 + \text{TiO}_2 + \text{IrO}_2$ or SnO_2 . The coated titanium mesh is welded to a titanium copper bar with a copper stud thread at one end to fix the anode to the anode base. The anode base has recessed holes with a copper washer or facing so that the copper anode stud makes

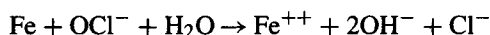
a good electrical contact. It is covered with an ethylene-propylene-diene (EPDM) blanket to prevent the anolyte from seeping to the copper base. However, because of aging of the blanket or poor assembly, the anolyte can seep through and corrode the copper facing or the washer, resulting in poor contact and higher ohmic drop. This is called ring corrosion. This is generally prevented by good housekeeping.

The cathode material is carbon steel in diaphragm cells, and nickel, often with a catalytic coating in membrane cells. As discussed in Section 4.6.6, exposure to anolyte containing active chlorine (Cl_2 , HOCl , and OCl^-) without cathodic protection is the primary reason for the corrosion of these components, unless the cathode coating is pore-free and noble metal based. Another species contributing to the corrosion of iron and nickel is the hydroxyl ion in the catholyte.

Steel cathodes in diaphragm cells are prone to corrosion when they are insufficiently cathodic during operation or when they are under open circuit conditions (e.g., during shutdowns). Corrosion under open circuit conditions is a direct consequence of (1) inherent thermodynamic instability of iron below a pH of 10 and above a pH of 14 due to the reactions,



and, (2) reaction of iron with hypochlorite as:



Corrosion rates determined under static conditions with steel coupons at 90°C at pH 4 and 11 in 300 gpl NaCl solutions in the presence of 0 to 6 gpl NaOCl, with and without sodium sulfite additions, showed (Fig. 14.23 and Table 14.8) that corrosion rates:

1. increase with increasing OCl^- concentration at pH = 4 and pH = 11,
2. increase with increasing temperature,
3. decrease with increasing pH (~50% as pH increases from 4 to 11),
4. decrease by >90% when an excess of sodium sulfite is added.

The corrosion rate of iron under these conditions can be reduced either by cathodic protection during shutdowns or by adjusting the pH of the medium to a value where iron is stable. The latter approach is commonly practiced in the chlor-alkali industry.

The corrosion rates of Fe during shutdowns can be estimated from the corrosion data in Fig. 14.23 and Table 14.8 to develop appropriate measures to reduce its extent. It is necessary to raise the pH of the anolyte and rapidly add a reducing agent to ensure minimal corrosion of the cathode.

Corrosion rates estimated for three shutdown sequences are illustrated in Fig. 14.24.

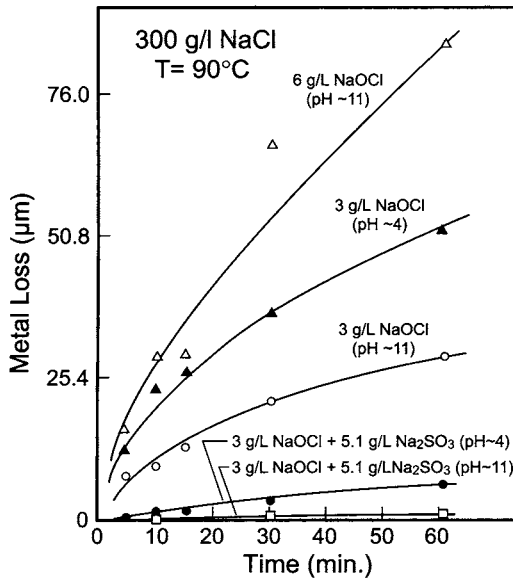


FIGURE 14.23. Corrosion rates of iron in brine solutions at pH = 4 and 11.

TABLE 14.8. Corrosion Rate of Iron in 300 gpl NaCl Solutions

Additive(s)	pH	Temperature °C	Corrosion rate (mm year ⁻¹)
0 gpl hypo	11	90	7.62×10^{-6}
1 gpl hypo	4	90	3.04×10^{-3}
3 gpl hypo	4	90	1.14×10^{-2}
1 gpl hypo	11	20	1.52×10^{-4}
1 gpl hypo	11	90	7.62×10^{-4}
3 gpl hypo	11	90	6.09×10^{-3}
6 gpl hypo	11	90	1.82×10^{-2}
3 gpl hypo + 5 gpl Na ₂ SO ₃	4	90	1.01×10^{-3}
3 gpl hypo + 5 gpl Na ₂ SO ₃	11	90	1.27×10^{-4}
6 gpl hypo + 10.2 gpl Na ₂ SO ₃	11	90	1.02×10^{-5}

14.5.2.2C. Cell Room. The cell-room environment is very corrosive because of the presence of brine, caustic, and wet chlorine, and hence the structural steel is generally protected against exposure to these corrodents. Following the preparation of the surface of the steel to a near-white metal state, it is coated first with 0.05–0.075 mm of organic zinc or polyamide epoxy primer and then with 0.13 mm of catalyzed polyamide or amine-cured paint. The siding and roofing materials are generally FRP or vinyl ester panels.

Walkways are fabricated with FRP grating. All concrete surfaces in the cell room are constructed with fusion-bonded epoxy coated steel reinforcing bars, and Type V

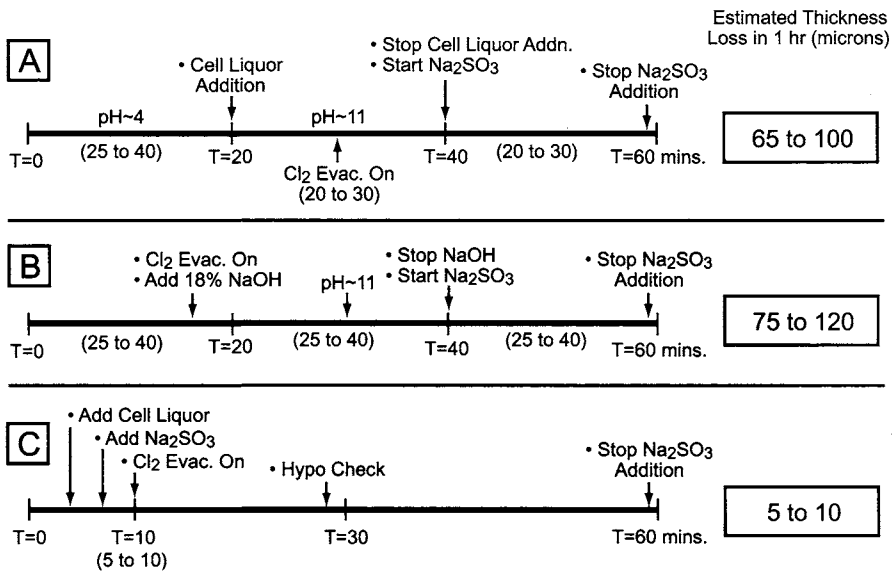


FIGURE 14.24. Shutdown schemes.

Portland cement, providing a minimum compressive strength of 30,000 kPa and sloped at 2%. Cell pedestals, equipment supports, floors, and trenches, formed of concrete, are covered with 3–6 mm thick, three-component silica or glass fabric-reinforced bisphenol A epoxy, using an aromatic amine catalyst curing system. Three-millimeter thick PVC, PP, and PE thermoplastic sheet stocks are the latest materials, which are attached to concrete structures as a permanent surface with their seams welded and spark tested, used to protect floors, equipment pads, trenches, etc. The materials of construction in the cell renewal area are the same as those used in the cell room. Corrosion in these process areas can be brought to a minimum by good housekeeping to restrict and confine the corrosive fluids.

Another important issue in any cell room is the stray or leakage currents [25] that flow through the electrolyte feed and discharge headers into grounded equipment. The leakage currents flow from the cells through a header to a reactor or tank. The current depends on the voltage difference between the electrolyte in the cells and at the target and on the resistance of the electrolyte. Depending on the polarity of the current that the metallic pipes are exposed to, one has to either anodically or cathodically protect the pipes. Anodic protection of the flanges is achieved by using concentric titanium rings coated with the DSA coating, to ensure the titanium flange area from reaching the breakdown voltage of TiO₂, which is about 11.5 V. Cathodic protection, on the other hand, is imposed by titanium blades. These require periodic replacement because of hydride formation.

Titanium is stable in chlorine-containing brine solutions. However, it is prone toward crevice corrosion in the sealing areas and gaps between welded titanium structures, as titanium can be anodically oxidized to TiO₂⁺ either from Ti or TiO₂ or to Ti³⁺, the corresponding cathodic reaction being the chlorine reduction reaction or the hydrogen

evolution reaction. This tendency of titanium [26] toward crevice corrosion, particularly in the gasketed areas, often can be avoided by the use of alloys containing Ni and Mo, the highest level of resistance is offered by alloys with Pd or Ru. These catalyze the hydrogen evolution reaction and will lower its potential to the region where TiO_2 is stable. Alternatively, the titanium surfaces can be coated with RuO_2 .

The industry standard material of construction for chlorine headers is FRP with a resin-rich inner barrier. The main polyesters used in chlorine headers are Hetron 197-3, Hetron 998/35, and Derakane 510 N. Hetron 197-3 has been popular for many years. It is being replaced by 510-N. The 197-3 resin provides the inner corrosion barrier. The outer layer is 197-3 ATP, which contains antimony to give flame retardant properties. The latter resin is replaced in the new Hetron resin FR 998/35 by a brominated vinyl ester with superior flame retardant characteristics.

The chlorine headers popular in Europe are dual laminate headers, which are preferred over FRP for environmental reasons. The dual laminate has an inner ring of less brittle PVC-C of 5-mm thickness for corrosion protection and an outer layer of 10–15 mm thickness of FRP for structural strength, the intermediate layer being 5 mm of resin-rich FRP 510N or 197-3. The outer layer contains a flame retardant and is added after the dual laminate is stress relieved. The chlorinated PVC (CPVC)/FRP dual laminate header is fabricated from CPVC tubing up to 60 cm in diameter. The dual laminate headers have a life of 8–10 years vs the 6–12 years of life of FRP, at a comparable cost.

Other materials that are available include ABS pipe P-72, supplied by Prince Rubber, and Halar wrapped with FRP. P-72 is prone to cracking at temperatures above 90°C and Halar-FRP laminate is reported to crack in chlorine gas service.

Titanium chlorine headers are used in Europe and are claimed to reduce the amount of chlorinated organics and other nonvolatile residues in gaseous and liquid chlorine. However, it suffers from crevice corrosion near the welds. The use of titanium headers for pressure operation of membrane cells is discussed in Section 8.4.1.1A.

14.5.2.3. Chlorine Systems. The choice of construction materials for chlorine service depends on equipment design and operating conditions. Figure 14.25 shows the corrosion resistance of various materials to dry chlorine, wet chlorine gas, and chlorine in aqueous solution [27].

Dry chlorine, with less than 40 ppm by weight of water, can be handled safely below 120°C in equipment made from iron, steel, stainless steels, Monel, nickel, copper, brass, bronze, or lead. Silicones, titanium, and high surface area materials such as steel wool should be avoided. Titanium ignites spontaneously in dry chlorine. Steel reacts with chlorine at an accelerated rate at high temperatures, igniting at about 250°C. Ti is passive [28] in the presence of 0.5 wt% moisture (Fig. 14.26). The presence of organic substances or rust increases the risk of steel ignition. For dry chlorine, carbon steel-Schedule 80 pipe is used in sizes up to 15-cm diameter and schedule 40 is satisfactory for large diameter pipes.

Liquid chlorine is generally stored in vessels made from non-alloyed carbon steel or cast steel. Fine grain steel, stress-relieved and subjected to Charpy impact tests for low temperature impact resistance [29], is used. Erosion of the protective layer on steel

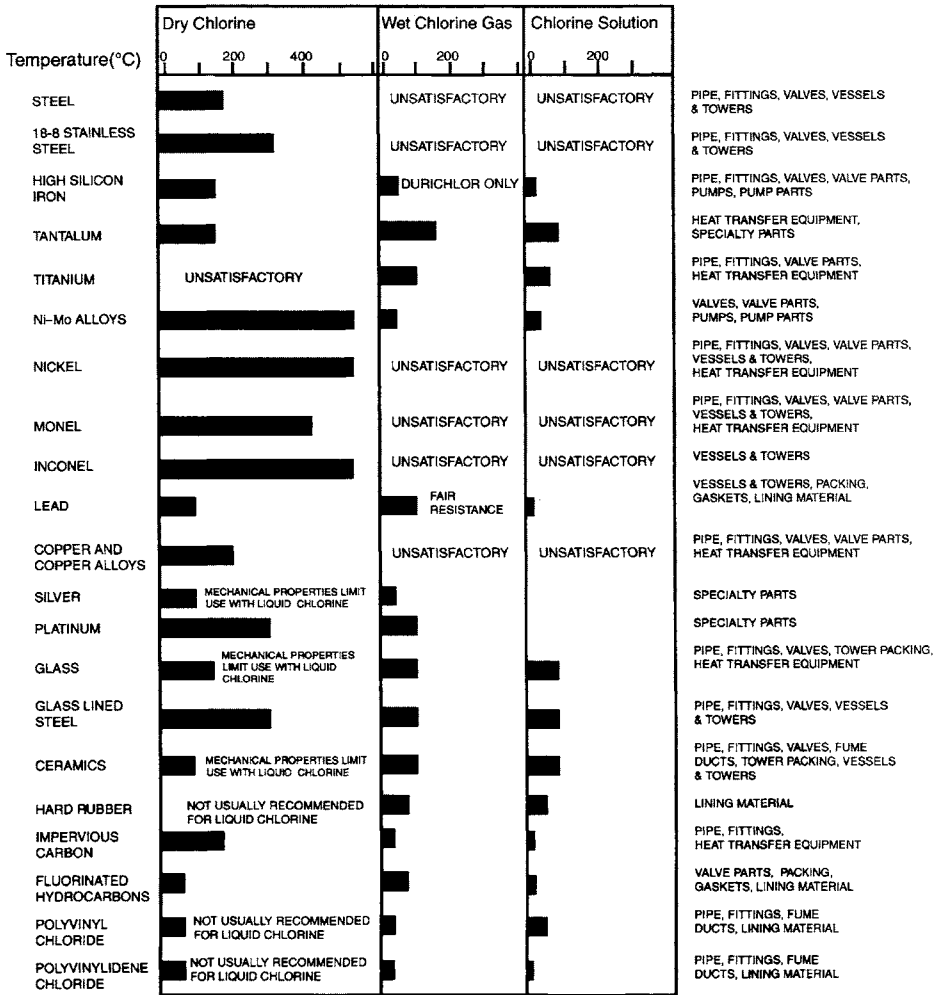


FIGURE 14.25. Corrosion resistance of structural materials to chlorine [27].

is prevented by keeping flow velocities less than 2 m s^{-1} . Organic materials, zinc, tin, aluminum, and titanium are not acceptable in dry chlorine service. Copper, silver, lead and tantalum are acceptable for some equipment.

Wet chlorine is extremely corrosive, attacking most common metals except Hastelloy C, titanium, and tantalum. Surface oxide films protect these metals from attack by the acids formed in chlorine hydrolysis. Tantalum is an ideal construction material for service with wet and dry chlorine. However it is expensive and normally used only in instruments such as transmitters, diaphragms, transducers, and thermowells. FRP is used for wet chlorine. Rubber-lined steel is also suitable for wet chlorine gas up to about 100°C . At low pressures and low temperatures, PVC, CPVC, and reinforced polyester resins are also used. Polytetrafluoroethylene (PTFE), polyvinylidene fluoride (PVDF), and polytetrafluoroethylene-hexafluoropropylene (FEP) are resistant at high temperatures. Other materials stable to moist chlorine include graphite and glass.

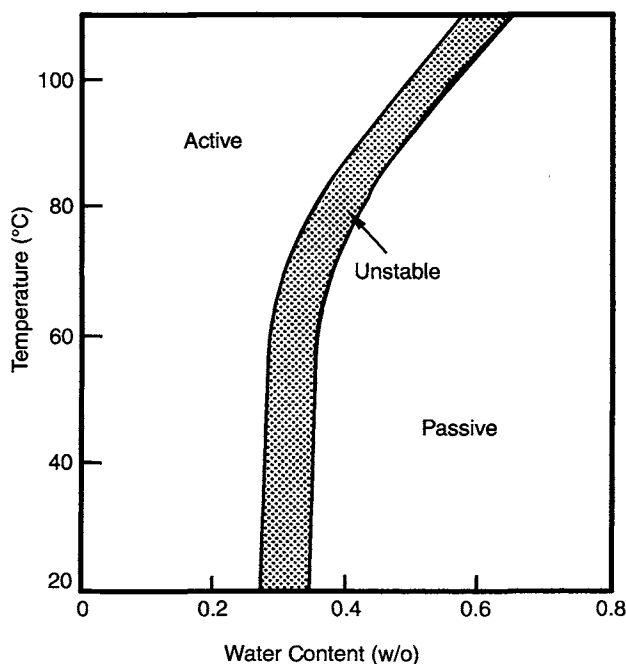
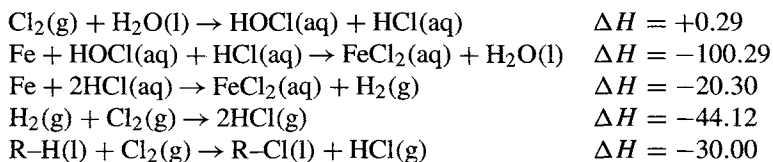


FIGURE 14.26. Water content required to passivate titanium in chlorine gas [28].

PTFE is resistant to liquid chlorine and to both wet and dry chlorine gas up to 200°C. Tantalum, Hastelloy C, PTFE, PVDF, Monel, and nickel are recommended for membranes, rupture discs, and bellows. The materials of construction for heat exchangers and tanks are generally titanium or Ti-clad, rubber-lined carbon steel, PTFE-lined carbon steel to handle wet chlorine gas or aqueous solutions containing chlorine.

Dechlorination operations are generally carried out in epoxy-coated or titanium tanks, with FRP piping and titanium pumps. Sulfuric acid drying of chlorine is usually in brick-lined towers.

It is pertinent to note here that the quantity of heat generated by the reaction of chlorine depends on the amount of moisture and organics present in the system. The enthalpy changes (kcal mol^{-1}) associated with some relevant reactions are noted below.



Simple heat balance calculations reveal that the ΔH associated with the first two reactions alone can result in excessive temperatures that can lead to combustion.

Corrosion in chlorine-handling operations is primarily a result of moisture entering the system. Therefore, it is imperative that moisture be excluded, especially if there is

TABLE 14.9. Corrosion Rates of Metals in 5 to 50% NaOH

Metal	Corrosion rate (mm/y)			
	5–10% NaOH (21°C)	10% NaOH (82°C)	15% NaOH (88°C)	30–50% NaOH (82°C)
Titanium	0.001	nil	—	
Zirconium	0.005	0.002	—	
Nickel	0.005	0.00008	0.005	0.0025
Monel	0.007	nil	0.0012	0.005
Inconel	0.001	nil	0.0007	
Mild steel	0.1	0.015	0.205	0.0925
Cast iron	—	—	0.205	0.175
Ni-Resist Type 1	—	—	0.073	
Cu–Ni–Zn (75–20–5)	—	—	—	0.0125
Copper	—	—	—	0.057
Chrome steel (14% Cr)	—	—	—	0.825

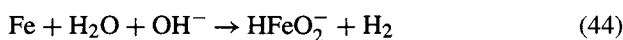
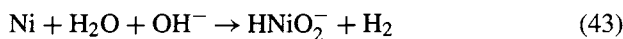
a high surface area for reaction (e.g., packings). Organics must also be removed from the metallic surfaces before admitting chlorine.

14.5.2.4. Caustic System. Table 14.9 gives data on the corrosion behavior of some metals at various concentrations of caustic [30].

Metals such as aluminum, tin, and zinc and their alloys are unstable in NaOH solutions since they spontaneously form oxyanions of the type MO_2^- , where M is Al, Sn, or Zn. Nickel, iron, and their alloys are more stable and are widely used in caustic service in the chlor-alkali industry.

Failure of Ni and Fe in caustic solutions is a consequence of:

1. Formation of anions of the type described by the following reactions:



2. Oxidation of Fe and Ni following the reduction of OCl^- or ClO_3^- ions.
3. Caustic embrittlement or SCC.

Potential–pH diagrams for Fe [31] and Ni [32] at various temperatures, presented in Figs. 14.27 and 14.28, show that these metals dissolve in highly concentrated NaOH solutions, and that the corrosion domains become larger as the temperature increases. The active dissolution of iron or nickel in NaOH is accompanied by the cathodic generation of H_2 during the corrosion process as represented by the reaction schemes (43) and (44). The hydrogen can diffuse into the metal, causing hydrogen embrittlement and SCC.

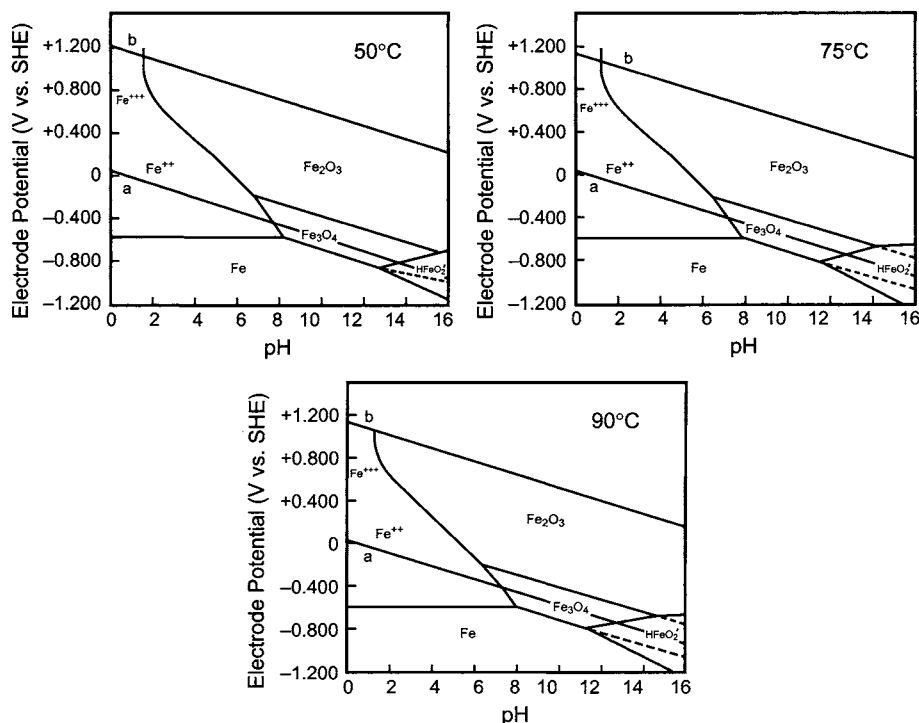


FIGURE 14.27. Potential–pH diagrams for Iron–H₂O system at elevated temperatures. Lines marked a and b represent reactions 8 and 9 respectively [31]. (With permission from Elsevier.)

Carbon Steel. Carbon steel is commonly used without danger of SCC up to 50% NaOH and 54°C. At high NaOH concentrations and temperatures, welds and stressed zones are prone to failure unless stresses are relieved. Figs. 14.29 and 14.30 show the caustic embrittling characteristics of steels and nickel alloys [33, 34].

Corrosion of steels and nickel alloys in NaOH and KOH solutions is promoted by OCl^- . Even one ppm of OCl^- in NaOH will promote the corrosion process, which leads to dendritic growth of oxides of Fe, especially in stressed areas. Such a process in membrane cells fitted with steel cathodes can lead to the puncturing of the membranes. The only way to prevent such an event is to add a reducing agent (e.g., H_2O_2 or Na_2SO_3) to remove the OCl^- during shutdowns.

The effect of chlorate on the corrosion rate of Fe was studied [34] and it was reported that iron and steel corrode in 50% NaOH at 80°C at concentrations above 1% or below 0.01%. The corrosion rate decreases rapidly at concentrations of >1% and <0.01% NaClO_3 , because of the formation of passive surface layers (Fig. 14.31). Iron and steel passivate in concentrated NaOH at noble potentials in the presence of dissolved oxygen. However, the passive film is pitted in the presence of chloride ions [35], as shown in Fig. 14.32.

One of the problems with the use of carbon steel for the storage of caustic is iron contamination. This can be avoided by protecting the tanks with nonmetallic coatings

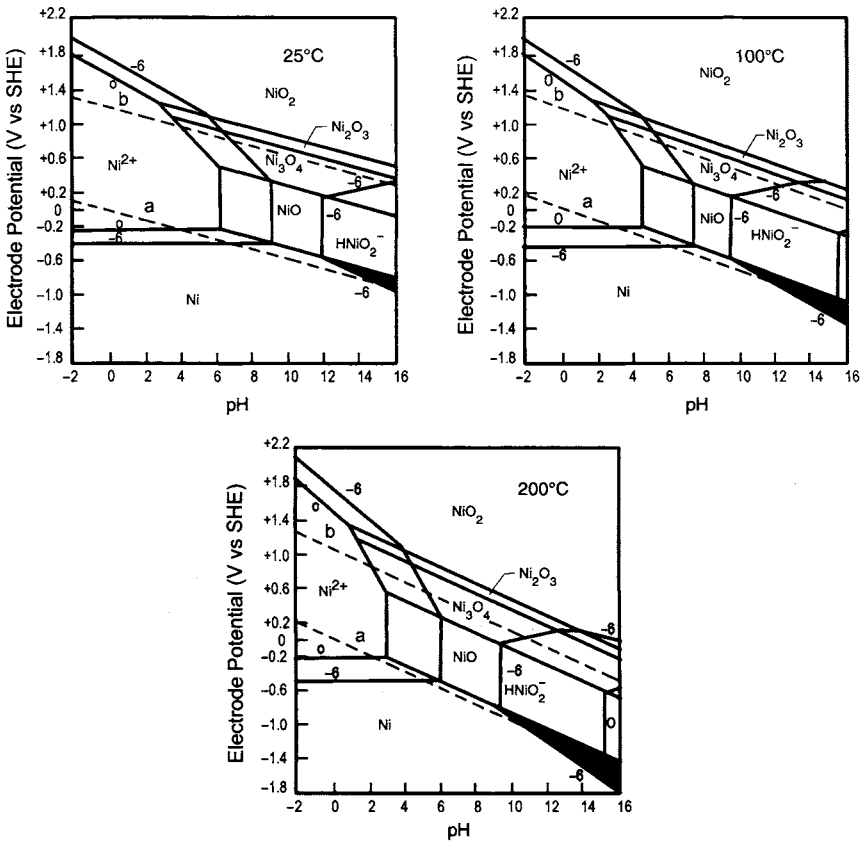


FIGURE 14.28. Potential–pH diagrams for Nickel–H₂O system at elevated temperatures. Lines marked a and b represent reactions 8 and 9, respectively. 0 and –6 refer to the logarithm of the concentration of the ionic species in moles per liter [32]. (Reproduced with permission of The Electrochemical Society, Inc.)

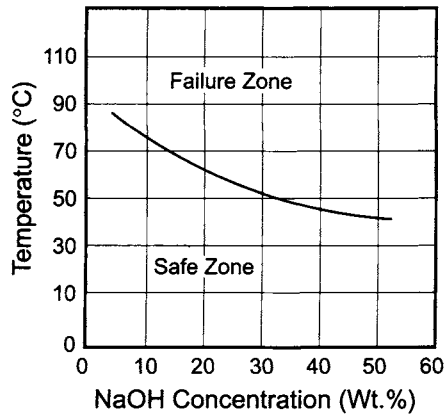


FIGURE 14.29. Temperature and NaOH concentration limits for caustic cracking of carbon steel.

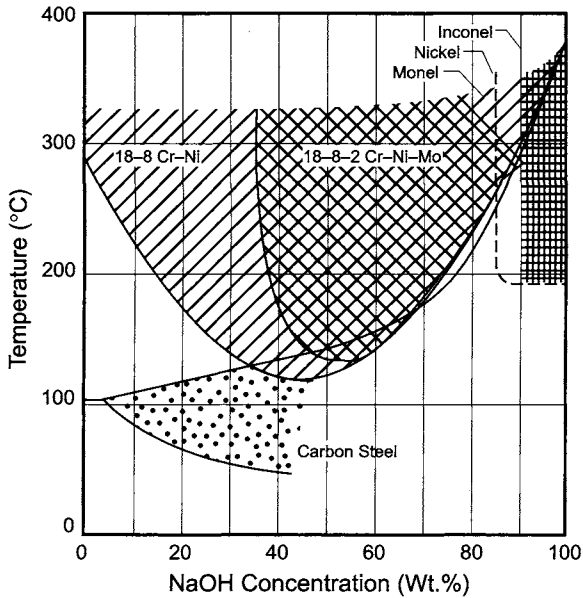


FIGURE 14.30. Regions of caustic cracking of metals and alloys. (Courtesy of M. Okubo.)

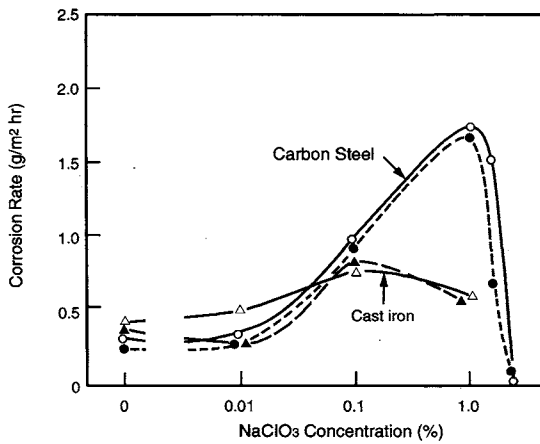


FIGURE 14.31. Effect of NaClO_3 on the corrosion rate of iron and steel at 80°C [34]. Open points: 0% NaCl ; Closed points: With 1% NaCl ; Circles: carbon steel; Triangles: Cast iron. (Courtesy of M. Okubo.)

or linings or by using nickel or stainless steel tanks. Nonmetallics useful for caustic service within their normal temperature limits include PVC, polypropylene, phenolics, PTFE, FEP, PVDF, natural rubber, neoprene, halogenated polyesters, and chlorosulfonated polyethylene.

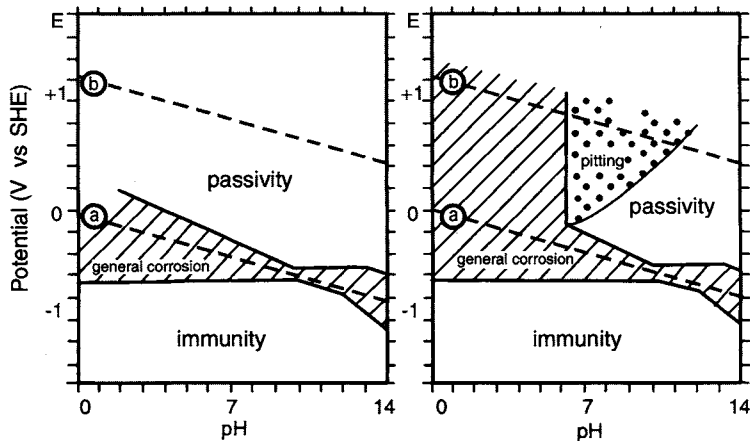


FIGURE 14.32. Pourbaix diagram of iron in aqueous solutions containing 0.01 gpl chloride [35]. (With permission of NACE International.)

Stainless Steel. A comparison of corrosion rates in hot concentrated NaOH solutions as a function of the nickel content in the alloys shows that nickel is extremely resistant to NaOH. Stainless steels are acceptable for caustic service, if the pickup of iron in caustic is acceptable. Typical corrosion rates of nickel and nickel alloys [36] are presented in Fig. 14.33. Table 14.10 depicts the typical composition of various stainless steels cited in Figs. 14.33 to 14.35.

Austenitic stainless steels show uniform corrosion and intergranular corrosion in NaOH solutions. Figures 14.34 and 14.35 illustrate the corrosion rate of materials in boiling 30% NaOH and 50% NaOH solutions, determined by weight loss measurements and linear polarization methods in hydrogen-saturated solutions [36]. These results generally show the corrosion rates to decrease with increasing nickel content in the alloy. It should be mentioned that the weight loss data obtained with 310 SS, Ni, and high Ni alloys are not reliable, as they passivate in hot 50% NaOH solutions. The reason for the high corrosion rates of Fe–Cr–Ni alloys was found to be the preferential dissolution of Fe and Cr [35–40]. Cu dissolves from Monel 400 [41, 42] and Mo from Mo-containing alloys such as Type 316 SS and alloy 825 in hot concentrated NaOH.

The corrosion behavior of nickel-based alloys was significantly influenced by the presence of oxygen or hydrogen in the solution. These materials exhibited reversible hydrogen electrode potential in hydrogen-saturated solutions. However, in oxygen-saturated solutions, they corroded by the diffusion of oxygen through the porous β -Ni(OH)₂ layer formed in the passive region on the surface.

Since austenitic stainless steels are susceptible to pitting and intergranular corrosion in the presence of chloride ions, other materials were examined for caustic service [43–47]. These include Fe–Cr alloys, which are resistant to SCC. However, these alloys are brittle and suffer from 475°C embrittlement and sigma embrittlement. A popular alloy that was examined for the caustic evaporator service was E-Brite-26-1, containing 26% Fe and 1% Mo, which exhibited performance characteristics comparable to that of

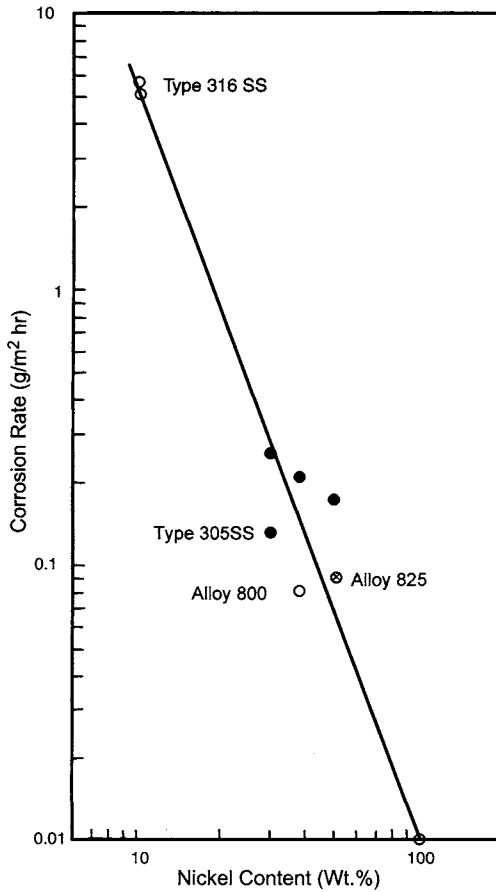


FIGURE 14.33. Corrosion rate as a function of the nickel content in alloys in boiling 40% NaOH solutions. (Data taken from [36].)

TABLE 14.10. Chemical Composition of Austenitic^a and Ferritic Stainless Steels

	Chemical composition (wt%)									
	C	Si	Mn	P	S	Ni	Cr	Mo	N	Other
AISI 304	0.06	0.54	0.81	0.031	0.002	8.48	18.91	—		
AISI 316A	0.04	0.5	1.63	0.03	0.002	13.12	16.5		2.35	
AISI 316B	0.06	0.45	1.67	0.033	0.002	12.91	16.58	2.21	—	
AISI 305J ₁	0.02	0.4	0.82	0.029	0.002	12.96	17.08	—		
Type 405	0.08						12.5	—	—	0.2 (Al)
Type 430	0.08						14–18	—	0.02	
Type 446	0.08						23–27	—	0.03	
High purity Fe–Cr	0.002						12–30	0 to 2	0.008	

^aHeat treated at 1150°C for 3 to 5 min.

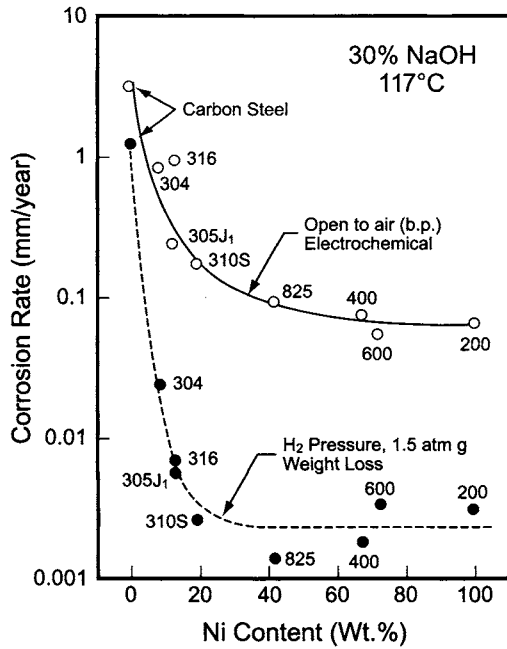


FIGURE 14.34. Corrosion rate of various materials in 30% NaOH solutions at 117°C as a function of the nickel content. Solid lines: Electrochemical technique in solutions exposed to air; Dashed line: Weight loss measurements in hydrogen-saturated solutions [36].

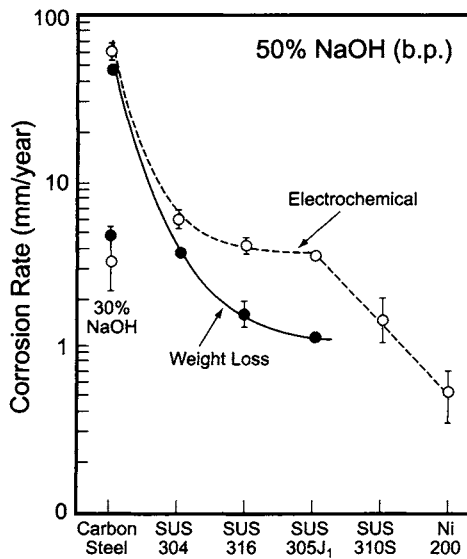


FIGURE 14.35. Comparison of weight loss data with the electrochemical results with carbon steel and austenitic stainless steels in boiling 50% NaOH solutions [36].

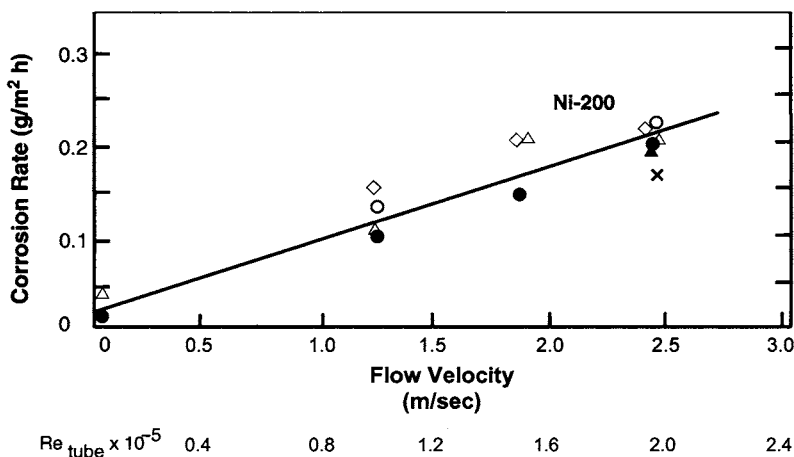


FIGURE 14.36. Corrosion rate of Nickel in 800 gpl NaOH at 158°C. ●: NaOH; ○: NaOH + ClO₃⁻; △: NaOH + solids; ▲: NaOH + ClO₃⁻ + solids; ◇: Synthetic first-effect liquor; x: Plant first-effect liquor [48]. (Reproduced with permission of The Society of Chemical Industry.)

nickel. However, it suffered from serious intergranular corrosion problems, which were attributed to changes in the metallurgy and chemistry of this material. E-Brite 26-1 is not used in new caustic evaporators.

Nickel. Nickel is the ideal material for handling caustic at all concentrations and temperatures, including molten anhydrous caustic up to 480°C. Nickel and its alloys are used for vapor bodies, piping, and heat exchangers in evaporator systems and for operations where high solution velocities are encountered (e.g., centrifugal pumps).

Thermodynamically, nickel should corrode in concentrated NaOH solutions by reaction (43). Studies [48] in 50% NaOH solutions reveal the corrosion rate of nickel to be dependent on solution velocity and temperature (Figs. 14.36 and 14.37). However, the presence of salt and chlorate in caustic has been found to have no influence on the corrosion rate of Ni-200. It has also been shown that welds and weld zones are prone to higher rates of corrosion by a factor of 10–20, depending on the nature of the weld and the methods employed to relieve stress.

The presence of hypochlorite in caustic is deleterious to nickel evaporators, forcing the oxidation of nickel to Ni(OH)₂, HNiO₂, or HNiO₂⁻. Chlorate has no influence on the corrosion rate of nickel, based on the data in Figs. 14.36 and 14.37 and the chloride–chlorate material balance around a caustic evaporator producing 50% NaOH. However, it has profound influence on nickel corrosion in anhydrous caustic concentrations. The reason for nickel corrosion in this system arises from the fact that chlorate decomposes above 250°C to chloride, releasing oxygen according to the reaction.



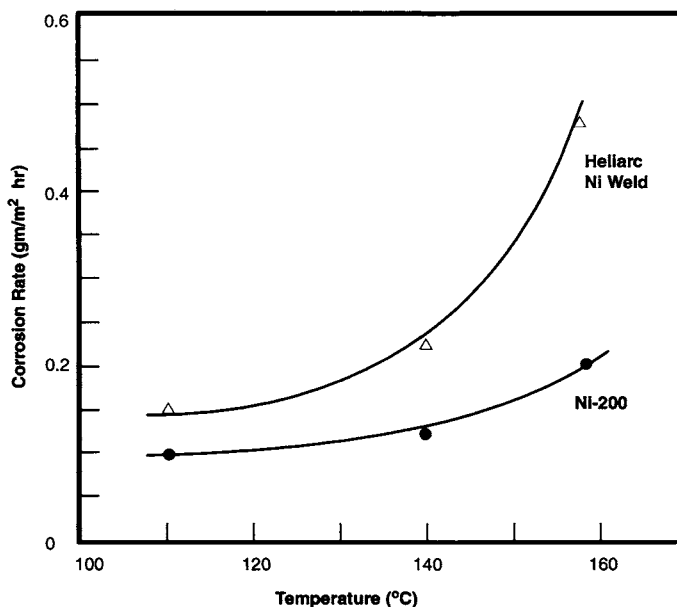
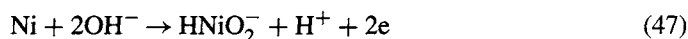


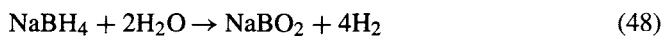
FIGURE 14.37. Effect of temperature on the corrosion rate of Ni-200 and Ni welds at a Reynolds number (for a tube) of 1.5×10^5 in 800 gpl NaOH solutions [48]. (Reproduced with permission of The Society of Chemical Industry.)

The oxidation of nickel follows as:



Chlorate corrosion in anhydrous caustic evaporator systems is prevented by decomposing chlorates with additions of sucrose or sugar [49]. The amount of sugar added with mercury-cell caustic is generally around 0.24 to 0.36 kg per dry ton of NaOH.

Corrosion of nickel in caustic evaporators can be minimized [50] by reversing the reaction (43) by providing hydrogen either directly or by adding compounds such as NaBH_4 or N_2H_4 , which decompose to provide H_2 as:



This *in situ*-generated hydrogen reverses reaction (43) thereby protecting the nickel from corrosion.

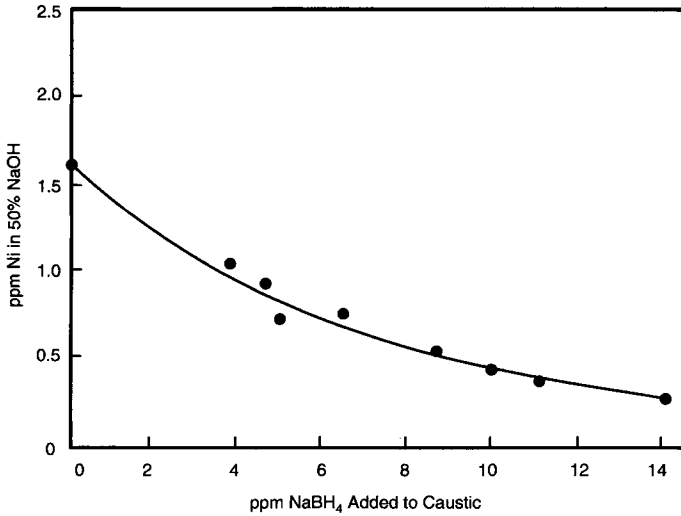


FIGURE 14.38. Variation of Ni content in 50% NaOH with the concentration of NaBH₄ [48]. (Reproduced with permission of The Society of Chemical Industry.)

TABLE 14.11. Influence of NaBH₄ on the Corrosion Rates of Materials in NaOH

	Corrosion rate (g m ⁻² hr)	
	Without additive	With additive
Ni/50% NaOH (160°C)	0.2–0.3	0.01–0.03 (5–50 ppm NaBH ₄)
Ni/50% NaOH (160°C)	0.2–0.3	0.02 (with 20–100 ppm N ₂ H ₄)
Ni/50% NaOH (160°C)	0.2–0.3	0.08 (with H ₂ fed at a constant rate)
321 SS/33% NaOH (70°C)	0.06	0.018 (with 300 ppm NaBH ₄)
316 SS/33% NaOH (70°C)	0.12	0.02 (with 300 ppm NaBH ₄)
E-Brite 26-1/50% NaOH (170°C)	0.15	0.15 (with 5–50 ppm NaBH ₄)

Plant tests show that the nickel corrosion rate can indeed be controlled very easily with addition of small amounts of NaBH₄ (Fig. 14.38). These tests also show that the NaClO₃ levels are unaltered in the presence of NaBH₄, reiterating that NaClO₃ is not causal for the corrosion of nickel in 50% NaOH solutions. The beneficial effects of NaBH₄ addition toward suppressing the corrosion of nickel and other materials are presented in Table 14.11.

This technology is currently used in most of the chlor-alkali plants in the United States and some in Europe.

Table 14.12 describes the materials of construction now used in the industry, along with the type and source of corrosion in various operations. The individual applications are discussed throughout the text, primarily in Chapters 9 through 11.

TABLE 14.12. Materials of Construction in a Chlor-Alkali Plant

Equipment	Corrosive Species/ Type of Corrosion	Material of Construction
<i>Brine Section</i>		
Vessels and tanks (i.e., salt saturators, clarifiers, chemical storage, and brine storage)	H ⁺ /General	Rubber-lined carbon steel, fiberglass reinforced polyester, spray or trowel- applied organic linings, Ti lined carbon steel, carbon steel with 3.2 mm corrosion allowance.
Pumps	H ⁺ /General	Ti, rubber-lined steel
Heat exchangers, ejectors	H ⁺ /General	Ti, Monel
Brine valves	H ⁺ /General	FRP body with rubber diaphragm, PTFE
Brine pipelines	H ⁺ /General	Cast iron, carbon steel, FRP, PVC, PP, rubber-lined steel
<i>Electrolytic Section</i>		
Cell room foundation	H ⁺ , OCl ⁻ , mechanical/ General	Concrete coated with fluosilicates of Zn or Mg, epoxy, or silicone penetrating sealers
Electrolytic cell		
Cell covers	Chlorine/General	FRP, Telene
Cell bottom	Chlorine/General	Mild steel, steel shell plasma sprayed with borides, nitrides of Ti or Ta, EPDM or neoprene covered carbon steel
Sleeves	Chlorine/General	CPVC
Seals	Chlorine/General	Neoprene, PVC, polyvinylidene fluoride
Doglegs	Chlorine/General	FRP, PTFE
Feed and return brine headers	Chlorine/General	FRP
Caustic headers	OH ⁻ /General	Ni or Ni-clad steel
Wet Cl ₂ headers	OCl ⁻ /General	FRP
Water fed to cells	H ⁺ /General	High density PE or PP
Anodes		Ti coated with TiO ₂ + noble metal oxides
Cathodes		Steel, Ni
Diaphragms		Asbestos stabilized with Teflon or Halar; non-asbestos diaphragms, ion-exchange membranes (perfluorinated)
<i>Chlorine Section</i>		
Chlorine blowers	OCl ⁻ /General	Ti or FRP
Cl ₂ gas coolers	OCl ⁻ /General	Ti tube and mild steel shell
Cl ₂ system—wet	OCl ⁻ /General	Hard rubber, PVC, PP, Ti, FRP
Drying tower	OCl ⁻ /General	FRP, carbon steel with 3.2 mm corrosion allowance and lined with asphaltic rubber or PVC membrane followed by lining with acid-resistant brick (10 cm minimum thickness) joined by corrosion-resistant silicate mortar.
Acid coolers	OCl ⁻ /General	PTFE exchanger; stainless steel or, Hastelloy plate exchangers; shell-and-tube exchangers
Pipelines	OCl ⁻ /General	FRP for wet chlorine and mild steel for dry chlorine

TABLE 14.12. *continued*

Equipment	Corrosive Species/ Type of Corrosion	Material of Construction
Trims	OCl ⁻ /General	Monel or Hastelloy
Acid pumps		Alloy 20
Mist eliminator, wet gas		FRP, glass or polyester fiber elements
Mist eliminator, dry gas		Carbon steel, glass fiber elements held in stainless steel
Cl ₂ scrubbers	OCl ⁻ /General	Brick-lined, Ti
H ₂ SO ₄ Handling		
Pumps		
Vessels	Erosion corrosion	Ni or Mo-Cu alloys (e.g., Durimet or Alloy 20)
		Carbon steel with a minimum 3.2 mm corrosion allowance, steel lined with 6.35 mm PVC-lined FRP dual laminate or PVC
		Extra heavy carbon steel, PVC-lined FRP or steel
Piping		
Valves		Alloy 20, Durimet 20, or ductile Fe plug valves with PTFE liners
<i>Caustic System</i>		
Vessels	OH ⁻ /General	Carbon steel lined with 0.5 mm of neoprene or baked-on phenolic, Ni or Ni-clad steel, 316 or 304 SS
Evaporators		Ni or Ni-clad steel
Pumps		Ni or Durimet 20
Piping		Steel or Ni or Ni-clad steel
<i>HCl Section</i>		
Vessels	H ⁺ /General	PP, FRP or rubber-lined steel
Pumps		Epoxy or rubber-lined steel, PTFE
Piping/valves		Unplasticized PVC or CPVC, rubber-lined steel
<i>Hydrogen Section</i>		
Vessels	H ₂ entry into metals/ General	Carbon steel
Compressors/blowers		Carbon steel
Piping/Valves		Fe or Fe with bronze, SS, or Ni trim

REFERENCES

1. E. Gileadi, *Electrode Kinetics for Chemists, Chemical Engineers and Material Scientists*, VCH publishers, New York (1993).
2. M.G. Fontana, *Process Industries Corrosion*, National Association of Corrosion Engineers, Houston (1975), p. 1.
3. D.H. Declerck and A.J. Patarcity, *Chem. Eng.* **93**(24), 46 (1986).
4. F. Hine, *Zairyo (J. Soc. of Mater. Sci. Japan)* **26**, 1124 (1977).
5. J.A. Collins and M.L. Monack, *Materials Performance*. **12**(6), 11 (1973).
6. H. Uhlig, *Corrosion Handbook*, John Wiley & Sons, Inc., New York (1949).
7. U.R. Evans, *An Introduction to Metallic Corrosion*, Edward Arnold Publishers, London (1963).
8. J. O'M. Bockris and A.K.N. Reddy, *Modern Electrochemistry*, Vol. 2, Plenum Press, New York (1970).
9. M. Pourbaix, *Atlas of Electrochemical Equilibria in Aqueous Solutions*, Pergamon Press, New York (1966).

10. S. Papavinasan, Corrosion Inhibitors. In R.W. Revie (ed.) *Uhlig's Corrosion Handbook*, 2nd Edition, John Wiley & Sons, Inc., New York (2000), p. 1089.
11. G. Wranglen, *An Introduction to Corrosion and Protection of Metals*, Institut For Metallskydd, Stockholm (1972).
12. H.H. Uhlig (ed.) *Corrosion Handbook*, John Wiley & Sons, Inc., New York (1969).
13. *Corrosion Data Survey, Metals Section*, 6th Edition, National Association of Corrosion Engineers, Houston (1985).
14. P.A. Schweitzer (ed.), *Corrosion Resistance Tables*, 4th Edition, Marcel Dekker, New York (1995).
15. F. Hine, *Fushoku-Kogaku No Gaiyou (Introduction to Corrosion Engineering)*, Kagaku Dojin, Kyoto (1977), p. 113.
16. F. Hine and K. Nishiyama, *Zairyo (J. Soc. of Mater. Sci., Japan)* **25**, 777 (1975).
17. M. Okubo, *Sumitomo Kagaku* **21**, 27, 135 (1971).
18. M. Kowaka and H. Nagano, *Corrosion* **24**, 427 (1968).
19. M. Kowaka and H. Nagano, *Corrosion* **32**, 395 (1976).
20. C. Wagner, *Z. Physik. Chem.* **21B**, 25 (1933).
21. *Simplifying Stainless Steel Selection with Carpenter's Selectaloy™ Method*, Brochure published by Carpenter Technology Corporation (1969).
22. B.V. Tilak and C-P. Chen, *Bull. Electrochem.* **13(b)**, 245 (1997).
23. R.W. Herbert, Selection of Appropriate Materials of Construction in the Chlor-Alkali Plant, *Fourth Annual Electrode Corporation Chlorine/Chlorate Seminar*, Chardon, OH (1987).
24. S. Krishnamurty, S. Muthukumaraswamy, and R. Thangappan, Chlor-Alkali Plant, Materials of Construction. In J.J. McKetta and W.A. Cunningham (eds), *Encyclopedia of Chemical Engineering and Design*, Marcel Dekker, New York (1987), p. 450.
25. P. Kohl and K. Lohrberg, *J. Appl. Electrochem.* **19**, 589 (1989).
26. A. Ullman, Cost Saving in Chlorine Plants by Benefiting from the Unique Properties of Titanium. In J. Moorhouse (ed.), *Modern Chlor-Alkali Technology*, vol. 8, Society of Chemical Industry, London (2001), p. 282.
27. *Chlorine—A Brochure of Olin Matheson Corporation* (1959).
28. *Titanium Design Data Book for the Chemical Processor*, Titanium Metal Corporation of America, New York (1974).
29. N.C. Horowitz, *Chem. Eng.* **88(7)**, 105 (1981).
30. T.V. Bommaraju, *Water Quality Res. J. Canada* **30**, 339 (1995).
31. V. Ashworth and P.J. Borden, *Corrosion Sci.* **10**, 709 (1970).
32. R.L. Cowan and R.W. Staehle, *J. Electrochem. Soc.* **118**, 557 (1971).
33. F. Hine and M. Okubo, *Boshoku Gijutsu (Corrosion Engineering)* **25**, 509 (1976).
34. M. Okubo and S. Tokunaga, *Soda to Enso (Soda and Chlorine)* **26**, 313 (1975).
35. M. Pourbaix, *Corrosion* **25**, 267 (1969).
36. T. Ohashi and H. Kajiyama, *Soda to Enso (Soda and Chlorine)* **26**, 307 (1975).
37. M. Yasuda, S. Tokunaga, T. Taga, and F. Hine, *Corrosion* **41**, 720 (1985).
38. Y.S. Park, A.K. Agarwal, and R.W. Staehle, *Corrosion* **35**, 333 (1979).
39. M. Yasuda, K. Fukumoto, H. Koizumi, Y. Ogata, and F. Hine, *Corrosion* **43**, 497 (1987).
40. K.H. Lee, G. Gragnoline, and D.D. MacDonald, *Corrosion* **41**, 540 (1985).
41. N.S. McIntyre, T.E. Rummery, M.G. Cook, and D. Owen, *J. Electrochem. Soc.* **123**, 1164 (1976).
42. R.D.K. Mishra, *Electrochim. Acta* **31**, 51 (1986).
43. F.K. Kies, I.A. Fromsen, and B. Coad, *Chem. Eng.* **77(6)**, 150 (1970).
44. M.A. Streicher, Austenitic and Ferritic Stainless Steels. In R.W. Revie (ed.) *Uhlig's Corrosion Handbook*, John Wiley & Sons, Inc., New York (2000), p. 601.
45. E-Brite 26-1, ASTM Grade XM-27, *Brochure of Airco Vacuum Metals*, Revised 1975.
46. J.R. Crum and W.G. Lipscomb, *Materials Perform.* **25(4)**, 9 (1986).
47. A.B. Misercola, R.P. Tracy, I.A. Franson, and R.J. Knoth, The Use of E-Brite 26-1™ Ferritic Stainless Steel in the Production of Caustic Soda, *Brochure of Airco Vacuum Metals* (1976).
48. T.V. Bommaraju and P.J. Orosz, Caustic Evaporator Corrosion: Causes and Remedy. In T.C. Wellington (ed.), *Modern Chlor-Alkali Technology*, vol. 5, Elsevier Appl. Science, New York (1992), p. 307.
49. D.J. Pye, *U.S. Patent* 2,610,105 (1952).
50. T.V. Bommaraju, W.V. Hauck, and V.J. Lloyd, *U.S. Patent* 4,585,579 (1986).

15

Alternative Processes

15.1. INTRODUCTION

Chlorine is produced not only by the electrolysis of sodium chloride solutions but also from HCl, KCl, and other metal chlorides, by both chemical and electrochemical methods. The amount of chlorine from alternative processes is about 5.9% of the total world production. In the United States, it was about 4.0% of the total in 2002 [1]. Most of this chlorine was from the electrolysis of KCl in mercury or membrane cells (Table 15.1) and from HCl. Only small amounts are produced by the electrolysis of other metal chlorides.

There is thus very little independent production of chlorine and the principal alkalis, NaOH and KOH. The inability of producers to vary the nearly constant ratio of chlorine to alkali is a constant problem to the industry. Market conditions from time to time make it important to separate some of the production. Plants dedicated to chlorine or sodium hydroxide then may appear. The processes involved in these plants also have great historical interest, and therefore most of this chapter is dedicated to them. Section 15.2 covers the production of chlorine, and Section 15.4 covers the production of caustic soda. Section 15.3 recognizes the separate importance of hypochlorites. These require the combination of chlorine with an alkali material and are not examples of the independent manufacture of the two. However, their major use is as latent sources of chlorine, and they are considered members of the “active chlorine” family [2]. Their characteristic use in sanitation or bleaching depends on the fact that the chlorine in the hypochlorite group is in the +1 oxidation state and is a strong oxidizer.

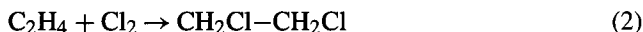
TABLE 15.1. Chlorine from Alternative Processes in 2002

Source	% of world production of 3.1 million tons	% of US production of 0.52 million tons
KCl	54.0	62.5
HCl	39.0	15.3
Metal production	6.7	20.2
Other	0.3	2.0

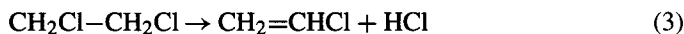
The primary alternative source of chlorine is HCl. Two reasons for this are the long history of development of technologies for the conversion of HCl to chlorine and the abundance of byproduct HCl from chlorination reactions. This abundance results from the chemistry of chlorination processes. Some organic chlorinations, such as those that produce many of the chlorinated solvents and intermediates, are substitution reactions. They produce HCl directly:



In other cases, the addition of chlorine to saturate an olefin is followed by dehydrochlorination to yield a monochlorinated olefin. This occurs in the manufacture of vinyl chloride monomer (VCM), the largest single consumer of chlorine. First, ethylene is converted to ethylene dichloride (EDC):

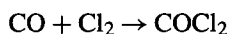


Pyrolysis of the EDC then forms VCM:

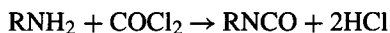


Once again, half the chlorine used in the process goes to HCl.

Another large-scale application of chlorine is the production of isocyanates. The standard process is the phosgenation of amines. Most plants produce the necessary phosgene on site, from chlorine and carbon monoxide:

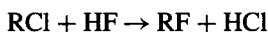


Substitution of the hydrogen atoms in the amine group then releases HCl:



The role of chlorine in isocyanate manufacture is that of a carbonyl carrier, and all the chlorine value becomes byproduct HCl.

The production of fluorocarbons is often by hydrofluorination:



Again, generation of HCl is separate from the use of chlorine in the process. Some fluorocarbon producers purchase the substrate compound, designated above as RCl. Normally, it is the product of substitution chlorination, as in Eq. (1), and most often carries more than one chlorine atom per molecule. Substitution of chlorine on the organic molecule by fluorine then may not be complete, and the net conversion of chlorine to HCl may be anywhere between 50 and 100%.

Table 15.2 shows the amount of HCl generated by various processes, along with the percentage of the chlorine used that becomes part of the product molecule [3]. The first data given for fluorocarbons pertain to the hydrofluorination process only. The starting

TABLE 15.2. Generation of HCl and Utilization of Chlorine

Product	kg HCl/kg product	% of Cl ₂ into product molecule
Vinyl chloride	0.58	50
Toluene diisocyanate	0.84	0
HCFC-22 (from CHCl ₃)	0.84	N/A
CFC-11 (from CCl ₄)	0.27	N/A
HCFC-22 (from CH ₄)	2.11	17
CFC-11 (from CH ₄)	1.33	38

TABLE 15.3. Sources of HCl in the United States

Source	% of Total
VCM	52
Solvents	17
Isocyanates	11
Fluorocarbons	6
Synthesis	7
Other	7

Note: Data are for the year 1995

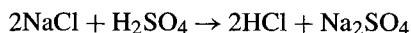
ingredients are chlorinated solvents. The second listing for those materials shows data calculated for a hydrocarbon starting material (methane in both cases).

The first column of data shows that solvents are a rich source of byproduct HCl. Production data from 1995 [3], shown in Table 15.3, indicate that they are the second-largest source in the United States. About 93% of the approximately 7 million tons of HCl is a byproduct of other operations, a typical result for the United States.

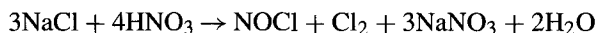
15.2. PRODUCTION OF CHLORINE WITHOUT CAUSTIC

15.2.1. Oxidation Processes

15.2.1.1. Oxidation of Salt. Salt can be decomposed by strong acids. The Mannheim process was used for many years to produce HCl and salt cake from salt and sulfuric acid:



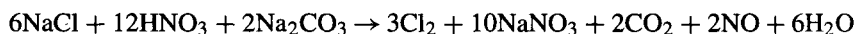
An oxidizing acid can, at the same time, oxidize the chloride to produce molecular chlorine. With nitric acid, for example,



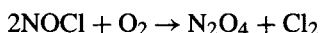
The latter process remained in operation well into the second half of the 20th century [4]. The reaction takes place between ~65% nitric acid and salt in a digester. Wet chlorine and NOCl pass overhead, while the byproduct and unreacted feed materials collect in the bottoms. The latter stream is neutralized with soda ash. After drying, the gases are condensed and separated by distillation. The NOCl can be scrubbed and neutralized by the digester bottoms according to the reaction



The overall stoichiometry becomes



Where there is use for nitrogen tetroxide, the NOCl can also be oxidized separately:



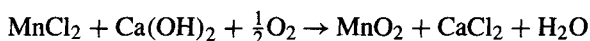
Parts of the process in effect handle *aqua regia*, and corrosion becomes a serious problem. Even allowing for the oxidation of NOCl, the process also requires about 4 tons of raw material to produce a ton of chlorine. It produces 2.4 tons of coproduct NaNO₃.

One reason for the disappearance of this process was the shift of the fertilizer market away from NaNO₃. A similar process, based on KCl and producing the more valuable KNO₃, then began operation [5].

15.2.1.2. Oxidation of HCl. Scheele first discovered chlorine through the action of hydrochloric acid on manganese dioxide:



This reaction was used in the small-scale production of chlorine. It operated under modest conditions (100–110°C), but corrosion problems were severe and the stoichiometry limited the recovery of chlorine to 50%. Practical values were 35–40%. On the positive side, the reactor gas had a high (~90%) concentration of chlorine [6]. In early operation, manganese chloride was a waste product. In 1866, Weldon achieved recycle of the manganese value by treating the chloride with lime while steaming with air or oxygen at 55–60°C:



This improved the economics, and the Weldon process operated for a time. A novel process for producing chlorine by the oxidation of hydrogen chloride with air, catalyzed by cupric chloride, then appeared:



Deacon was awarded the first patents in 1868 [7]. The Deacon process was the first vapor-phase catalytic reaction put into large-scale commercial use. While the reaction

sequence has not been described in detail, presumably cupric chloride oxidizes HCl, and the cuprous chloride thus formed reacts with oxygen to regenerate the cupric salt. The Deacon process remained the main source of chlorine until the electrolysis of sodium chloride was commercialized [8]. Chapter 2 discusses these processes and many other aspects of the history of the chlor-alkali industry.

The fundamental problem with the Deacon reaction is its reversibility. Arnold and Kobe [9] reported the thermodynamics of the reaction system, making it possible to calculate equilibrium conversions under different conditions. As an oxidation reaction, the conversion of HCl is exothermic. Therefore, lower temperatures increase the equilibrium constant but reduce the rate of reaction. Particularly in earlier versions of the catalyst, there has also been a problem with volatilization of the metal (usually copper). Reaction temperatures might range from about 450 to 650°C. Equilibrium conversions when feeding a stoichiometric amount of 95% oxygen are about 50% at 650°C and 72% at 450°C. Since conversion is not outstandingly high at any attractive temperature, the gas leaving a reactor contains substantial quantities of all the species involved in reaction (4) and is extremely corrosive. Conversion of two thirds of the HCl, a realistic example, would produce a gas equimolar in HCl, chlorine, and water. At the time of introduction of the Deacon process, the main use of the chlorine gas was in the manufacture of bleaching powder, and the low concentration of chlorine in the reactor gas was less of a problem than in higher-grade applications of chlorine.

Other equilibrium considerations include:

1. Five moles of reactant yield 4 moles of product. Therefore, increasing the pressure has a modest but favorable effect on equilibrium. This does not justify running the process under extreme pressure.
2. There is always the question of whether to use air or oxygen in a direct oxidation process. The use of oxygen speeds the reaction and improves the equilibrium by reducing the dilution of the products. At the same time, it makes the development of hot spots in the catalyst more likely and demands uniform distribution of the gas and the prevention of channeling.

Deacon worked with manganese and iron as well as copper catalysts, but copper has become the standard. Common additives include major quantities of alkali metals (to suppress vaporization of the copper) and rare earth promoters.

Figure 15.1 shows calculated equilibrium conversions and purity of chlorine as functions of the HCl/oxygen ratio at two different temperatures. It is based on the use of 95% oxygen as the feed material. Figure 15.2 shows the difference in attainable conversion between air and pure oxygen. It is based on the stoichiometric ratio of HCl to oxygen.

There have been many attempts over the years to improve the Deacon process by using alternative catalysts and by finding ways to modify the equilibrium. Certain oxygen donors, for example hydrogen peroxide, react with HCl at moderate temperatures [10]. In some cases, the temperature could be less than 60°C. The reaction may be run under vacuum or with the flow of a stripping gas in order to promote the release of chlorine. The latter approach dilutes the product chlorine. The chief problem with this type of process, and one that has prevented commercial application, is the cost of the oxygen donor.

Among the catalytic routes, the Kel-Chlor process [11–13] is one modification that has been applied commercially. The process uses hot, concentrated sulfuric acid

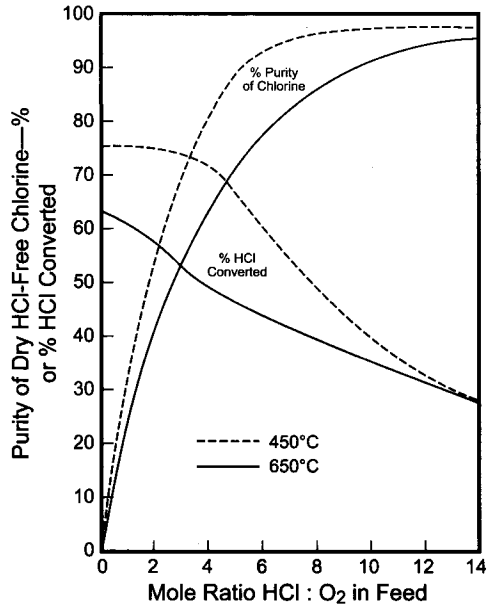


FIGURE 15.1. Equilibrium conversion and product purity in Deacon process.

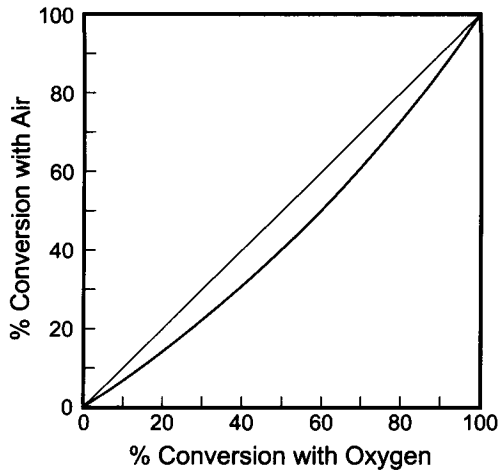
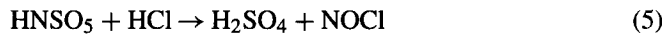
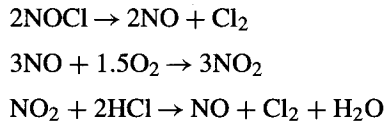


FIGURE 15.2. Conversions in Deacon process – air vs oxygen.

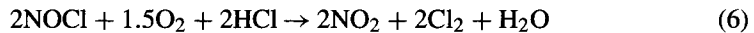
containing nitric oxide in the form of nitrosylsulfuric acid, HNSO_5 . Reaction with HCl gas then produces nitrogen oxychloride, or nitrosyl chloride, NOCl :



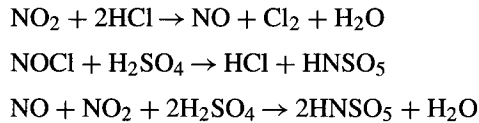
The mixed reactor gas goes to an oxidizer, where the following sequence of reactions takes place at a controlled temperature:



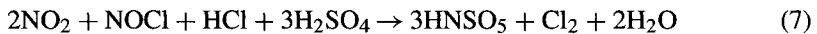
The sum of these reactions is



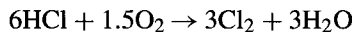
The offgas from the oxidizer goes to an absorber where sulfuric acid circulates. The nitric oxide catalyst is recovered, and other reactions complete the oxidation of HCl and regenerate nitrosylsulfuric acid:



The sum of the absorber reactions is



Adding together the reactions (5) (three times), (6), and (7),



This is Deacon process stoichiometry, but the use of the nitrogen cycle and the continued reaction of HCl in the absorber section remove the equilibrium limitation and make nearly complete recovery of the chlorine value of the HCl possible.

Figure 15.3 is a schematic of the apparatus used in the Kel-Chlor process. A unit was constructed and operated in conjunction with a fluorocarbon production in the United States. The recovered chlorine was recycled to the precursor process. The plant is no longer in operation. It is reported that corrosion problems became severe.

Other variations on the Deacon process involve modification of the catalyst. The Shell process, no longer in commercial operation, used a mixture of CuCl_2 and KCl on silica. The potassium salt, whose concentration was roughly equal to that of the copper, suppressed the volatility of the catalytic mixture. Smaller amounts of rare earth chlorides promoted the activity of the catalyst. This was a fluidized bed process that operated at 350–365°C and gave a conversion close to 80% [14].

As another example of the use of an alternative catalyst, Mitsui Toatsu Chemical Company (now Mitsui Chemical) developed the MT Chlor process for producing chlorine in a fluidized bed of a proprietary catalyst containing crystalline chromia and silica [15,16]. A plant of 30,000 tpy capacity went into operation in Kyushu, Japan, in

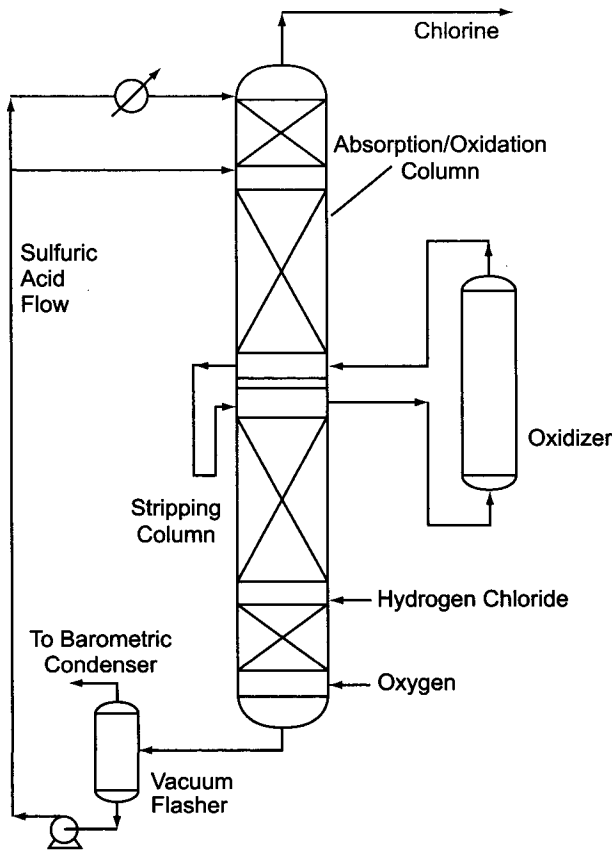
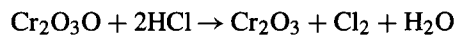
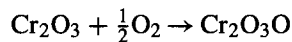


FIGURE 15.3. Kel-Chlor process diagram.

1988. The capacity was doubled in 1990. Hydrogen chloride gas and an excess of oxygen enter the reactor at 370–425°C [14]. The product gas is cooled, and residual HCl is recovered and rectified. In the reactor, chromic oxide oxidizes to $\text{Cr}_2\text{O}_3\text{O}$ and then reacts with HCl:



The overall reaction is the same as in the Deacon process. It is said that chromium oxide is not chlorinated and fused in the reactor, so that good fluidization can be maintained for a long time. The conversion per pass is greater than 75%.

Recently, Sumitomo Chemical announced the licensing of a 1,000-tpy pilot plant for reclaiming the byproduct HCl from an isocyanates plant. The process uses a fixed bed of $\text{RuO}_2/\text{TiO}_2$ catalyst. Commercial operating data are not yet available. Figure 15.4 is a generic flowsheet for this type of operation. It assumes that the HCl is available as an aqueous solution from an absorber. It is important for this solution to be as concentrated

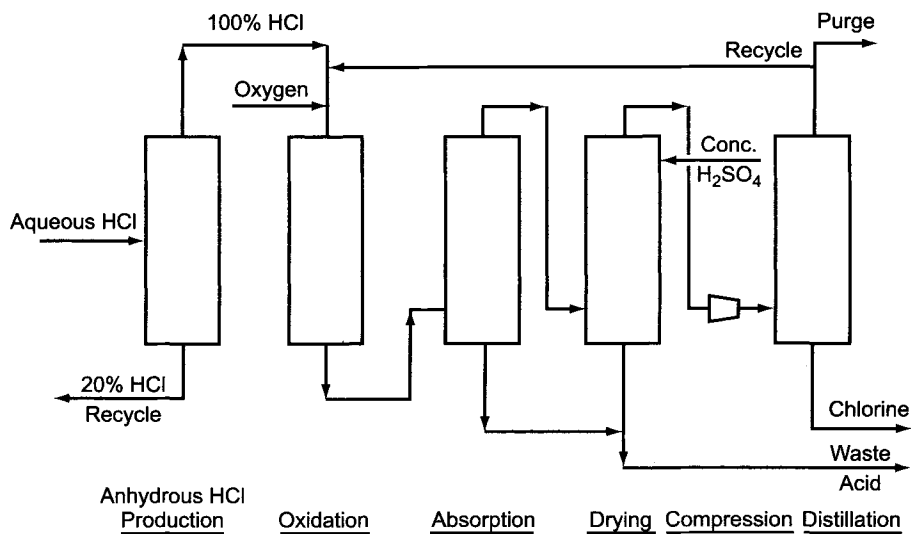
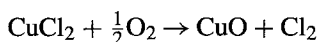
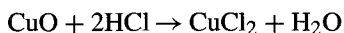


FIGURE 15.4. Generic flowsheet for catalytic oxidation.

as possible, so that the recovery of HCl in the first step of the process can be high. This step is the distillation of nearly anhydrous HCl from the azeotrope ($\sim 20\%$ HCl). The HCl gas is combined with the source of oxygen and taken to the reactor, shown here as a fixed bed. After drying with concentrated sulfuric acid, the gas is compressed and sent on to chlorine liquefaction. Depending on the operating conditions and the nature of the impurities in the gas, liquefaction may take the form of a distillation column, with chlorine as the bottoms product. Part of the overhead is a purge of a low-boiling material, such as the components of air.

In yet another modification, Minet and coworkers [14,17,18] employed two fluidized beds in series. The two steps of the process are chlorination (reaction of CuO with HCl at $200\text{--}280^\circ\text{C}$) and oxidation (reaction of CuCl_2 with oxygen at $340\text{--}380^\circ\text{C}$). Again, the sum of the two reactions is the same as Deacon chemistry:



The catalyst transfers back and forth between the two reactors, as in Fig. 15.5, and effectively carries the chlorine value from the chlorinator to the oxidizer, where it can be released as chlorine gas. For this reason, the process was dubbed the Catalytic Carrier Process. Separation of the two stages allows each to operate at its own optimum conditions, and higher conversion of HCl to Cl_2 is the result. This process has operated on a pilot scale in Spain, but no commercial operation has been reported. A study of projected economics [19] based on the optimistic assumptions of quantitative conversion of HCl vapor to chlorine and the recovery of chlorine by absorption in the prohibited solvent CCl_4 indicated that this process had advantages over certain other oxidation processes

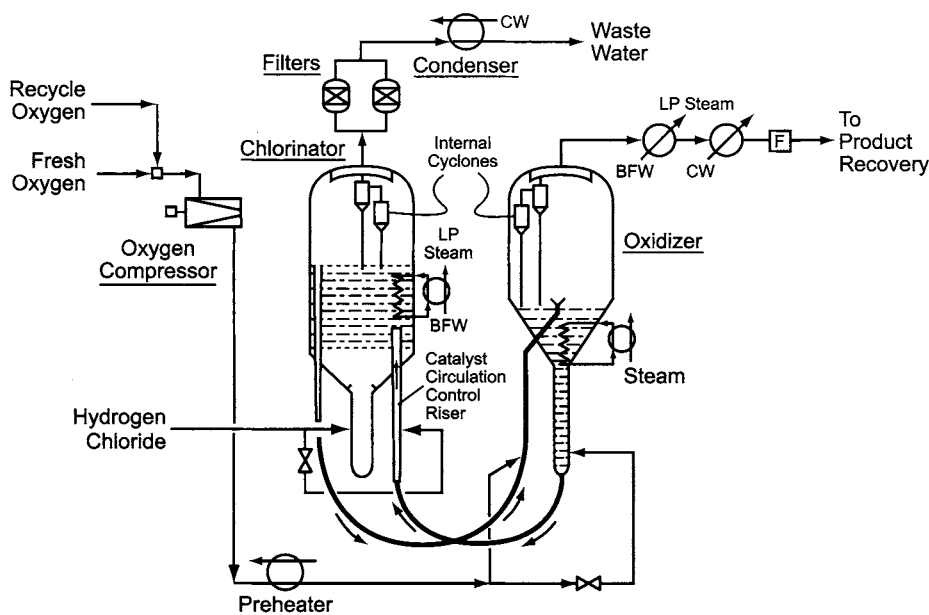
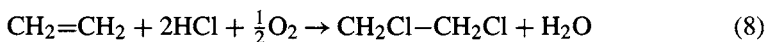


FIGURE 15.5. Catalytic Carrier Process.

and the electrolysis of aqueous acid. The study did not report the sensitivity of these assumptions.

Table 15.3 shows that vinyl chloride is the major source of byproduct HCl. This is somewhat artificial and deceptive, because most of the HCl never appears as a separate byproduct. Instead, it is consumed within the process.

Most observers believe that the oxidation of HCl first produces atomic chlorine at a high temperature. A logical step then is to carry out this oxidation in the presence of an organic molecule that is subject to chlorination. This approach takes up the chlorine as it forms, drives the conversion of HCl to completion, and produces a chlorinated molecule for application or further reaction. This process, referred to as oxychlorination or oxydehydrochlorination, is the basis for much of the world's EDC:



Without this type of process, ethylene-based VCM would be responsible for a glut of HCl. With the right combination of direct chlorination, dehydrochlorination, and oxychlorination (Eqs. 2, 3, and 8), the production and consumption of HCl can be balanced (Fig. 15.6). The theoretical requirement of chlorine is cut in half from that called for by Eqs. (2) and (3). While Fig. 15.6 shows the production of VCM with the aid of oxychlorination, it is also possible to stop with the synthesis of EDC. The HCl in this case may be the byproduct of another process. This approach has the advantage of a less volatile and less toxic product more suitable than either chlorine or VCM for export.

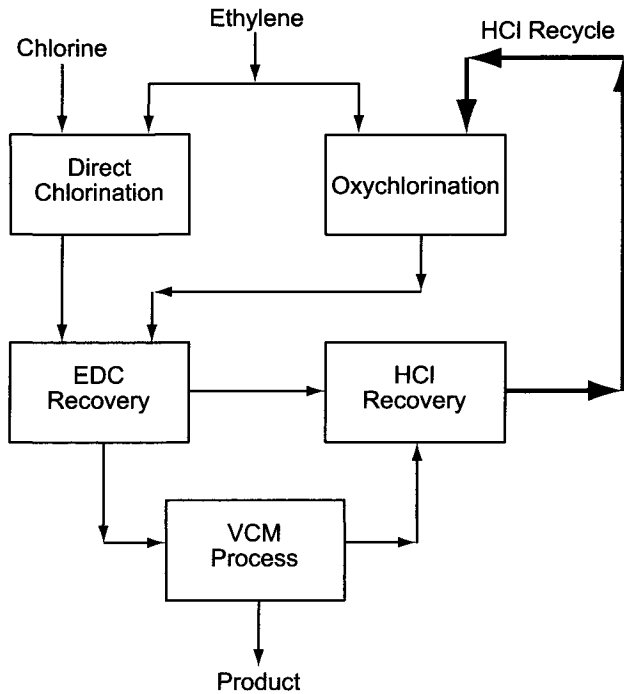
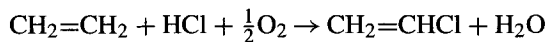


FIGURE 15.6. Concept of balanced oxychlorination.

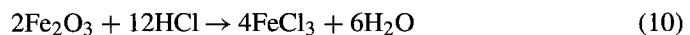
In the oxychlorination process, hydrocarbons act as chlorine acceptors and stimulate the oxidation of HCl. Consequently, oxychlorination is more efficient than the conventional process.

It is, in theory, possible to produce vinyl chloride directly from ethylene:



This is subject both to side reactions and to polychlorination through consecutive reactions, and the two-step process referred to above is the favored route.

15.2.1.3. Regenerative Oxidation. There is a group of regenerative processes in which HCl reacts with another material A to form an intermediate which then oxidizes back to compound A while releasing chlorine. The oxidation reaction usually requires the use of a catalyst or more severe conditions than the chlorination. The Grosvenor–Miller process is an example. This uses a fixed-bed reactor packed with ferric, rather than cupric, chloride. The course of reaction is



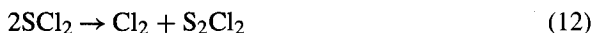
Addition of the two reactions shows the same stoichiometry as the Deacon reaction. Reaction (9) took place at 250–300°C and reaction (10) at 475–500°C. The Dow Chemical Company developed a two-stage moving-bed reactor in which Fe₂O₃ meets HCl in the upper section. FeCl₃ falls into the lower section of the tower and is converted into the oxide by hot air or oxygen. The chlorine goes to separation and purification.

The I. G. Farbenindustrie chloride melt process [8] used the same reaction paths, combining ferric and potassium chlorides to lower the melting point of the reacting mass. Dilute chlorine produced by the oxidation of FeCl₃ was recovered as a rich gas by absorption in sulfur monochloride (Eq. 11) followed by decomposition and desorption (Eq. 12):

Absorption

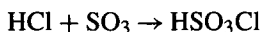


Decomposition, desorption

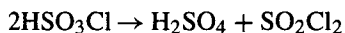


The regenerative processes, conceptually, could be made continuous by supplying multiple columns or by operating two coupled fluidized beds, as in the Catalytic Carrier Process. The distinction between “catalyzed” reactions and regenerative processes then becomes blurred.

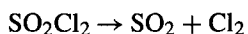
The chlorosulfonic acid process, applied to anhydrous HCl, is somewhat different, because water does not appear in the equation. The first step is the reaction of HCl with SO₃ to form the acid:



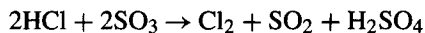
This takes place at a mild temperature, 70–100°C. The decomposition of chlorosulfonic acid requires a mercury-based catalyst and does not directly produce chlorine:



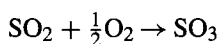
Chlorine finally results from the decomposition of sulfuryl chloride:



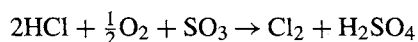
The overall stoichiometry is



The process requires some level of integration with a sulfuric acid plant if it is to be feasible. Its near-equivalence to Deacon chemistry can be shown in two steps. First, the byproduct SO₂ must return to the oxidizer in the host plant:



The combined stoichiometry becomes:



The mole of water that would have formed in the Deacon process is absorbed by the excess SO_3 .

15.2.2. *Electrochemical Methods for Producing Chlorine*

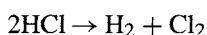
Alternative electrochemical routes to chlorine are classified as follows:

1. Electrolysis of hydrogen chloride
 - (a) Aqueous
 - (b) Anhydrous
2. Electrolysis of metal chlorides
 - (a) Indirect or cyclic processes
 - (b) Production of metals

This section discusses these routes in the order shown. Aqueous electrolysis of HCl is a commercial process that has been practiced widely. The anhydrous route is developmental but has the potential for large reductions in operating cost. The incentive for indirect electrolysis is the reduction in cathode voltage when reducing certain metals rather than hydrogen ions. The last-named process depends on the added value for its commercial success. The chief product is a metal, with chlorine as a useful byproduct. Sodium and magnesium are the examples covered in the text.

15.2.2.1. Aqueous Electrolysis of HCl. Commercial interest in HCl electrolysis did not begin until after World War II, and full-scale production began in the late 1950s [20]. A common feedstock is the byproduct acid from organic chlorinations, which may contain organic impurities that can degrade the electrodes and plug the diaphragms [21–23]. Typical impurities in the HCl are methane (which will chlorinate to CCl_4), benzene, chlorobenzenes, phenol, and chlorophenols, which intercalate in the pores of the electrode matrix, leading to its rapid deterioration. Other harmful impurities are HF, chlorofluorocarbons, and multivalent ions that can adversely affect the anode potential and lower the current efficiency. Many of the organic species can be rejected during adiabatic absorption of the HCl into boiling solution and then removed from vent gases by adsorption onto activated carbon. The exact pretreatment of the HCl depends on the nature and concentration of each impurity. Generally, organic impurities have greater effects than inorganic impurities. For example, 40–50 gpl of HF is tolerable in practice, compared with only 5 ppm of *o*-dichlorobenzene [23,24].

The electrolytic decomposition of HCl follows the overall reaction



Several cell designs have been developed and commercialized [25–27]. However, Uhde is now the only supplier of HCl electrolysis technology [21]. The electrolyzer (Fig. 15.7)

is bipolar, with graphite electrodes and PVC or PVC/PVDF diaphragms. Vertical slits are milled into the graphite plates, which are cemented in HCl-resistant plastic frames. Electrolyte feed channels are at the bottom of the frames. The gases rise up the plates and pass through ducts into collection channels in the upper part of the frames. The end plates are made of steel covered with rubber and are held together by spring-loaded tension rods. The effective surface area of an electrode is 2.5 m^2 and the current load is normally 10–12 kA.

The cells operate at 85°C or less and at about 1.9 V in the operating current density range of $4\text{--}5 \text{ kA m}^{-2}$. Therefore, the energy consumption is 1,400–1,500 kW hr $\text{ton}^{-1} \text{Cl}_2$.

The current–voltage relationship with standard electrodes and undoped electrolytes is

$$V = 2.09 + 0.115i \quad (13)$$

where

V = cell voltage,

i = current density, kA m^{-2}

Equation (13) predicts voltages higher than those quoted above. In practice, the addition of platinum salts to the catholyte reduces the cathode potential by about 0.6 V [28]. Section 4.6.3 presents some of the details.

A simplified flow diagram of the Uhde process is in Fig. 15.8. In this scheme, HCl at about 22% concentration is fed into separate catholyte and anolyte circuits. During electrolysis, the catholyte concentration falls to about 17% (sometimes higher), and the temperature increases from 65 to 80°C . The diaphragms are somewhat permeable to the electrolyte and less so to the gases. Normal practice is to hold the anode chamber at a higher pressure than the cathode chamber. This prevents leakage of hydrogen into the chlorine gas. At the same time, it permits some flow of the anolyte into the catholyte. Cathodic reduction of the chlorine dissolved in this anolyte is responsible for a 2–2.5% current inefficiency.

The anolyte and catholyte concentrations are maintained by adding more highly concentrated acid, typically 28% HCl, to the circulating streams. Both electrolytes are pumped through filters and heat exchangers to their respective head tanks. They then fall back to the electrolyzers. The concentrated acid is added to the return line between the head tanks and the cells. The heat exchangers remove the waste heat from electrolysis. They also serve as heaters when required (e.g., during startups).

With the net flow of electrolyte from the anode to the cathode side, an excess of $\sim 17\%$ acid accumulates in the catholyte. This is removed to a hold tank and then sent back to the source of HCl for reconcentration. When a byproduct gas is the source, the depleted acid acts as the solvent in an absorber. Adiabatic absorption in boiling liquid produces strong acid in the lower part of the column. The upper section removes the remaining HCl and the water vapor. The 28+% acid is cooled, purified by activated carbon treatment, adjusted in concentration as required, and pumped through a filter and a heat exchanger. It then flows to the cells by way of a gravity feed tank.

The chlorine gas from the anolyte is at $75\text{--}80^\circ\text{C}$ and is saturated with water and HCl. First, it is cooled in a surface exchanger, and the dilute acid formed by condensation

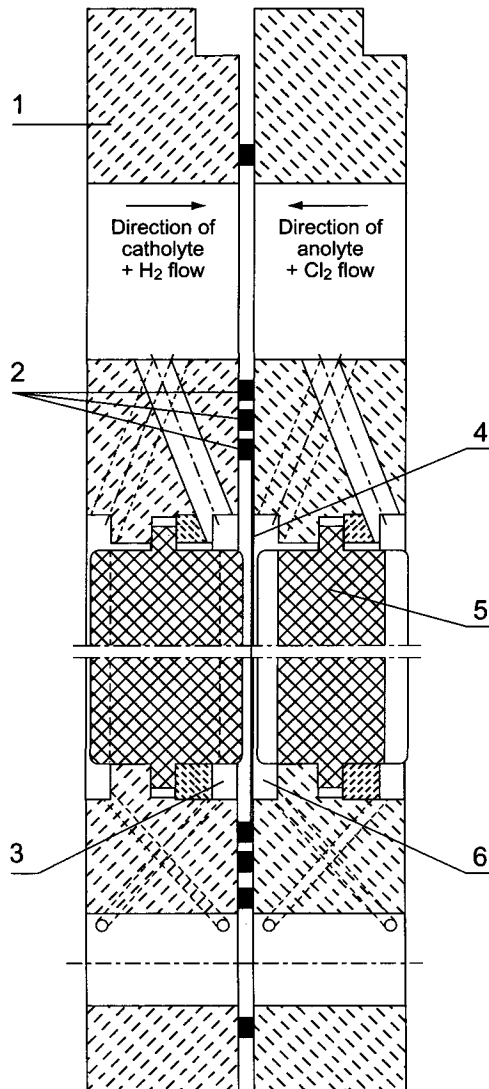


FIGURE 15.7. Cross section of an HCl electrolyzer. 1. Frame; 2. Seals; 3. Cathode side; 4. Diaphragm; 5. Graphite plates; 6. Anode side (with permission of Uhde GmbH).

collects in the anolyte tank. The cooler may be followed by a second exchanger operating on chilled water (Section 9.1.3). Next, the gas is dried to about 50 ppm (v/v) water by contact with concentrated sulfuric acid. Certain designs assume the use of a column with packing in the lower section and tunnel trays above.

Processing of the chlorine through drying, mist elimination, compression, liquefaction, and liquid handling generally follows the practices recommended in Sections 9.1.4–9.1.8. In addition, all chlorine-generating plants must have vent scrubbers to prevent the release of the gas into the atmosphere (Section 9.1.10.3). Multiple scrubbing towers installed in series are common in HCl electrolysis plants.

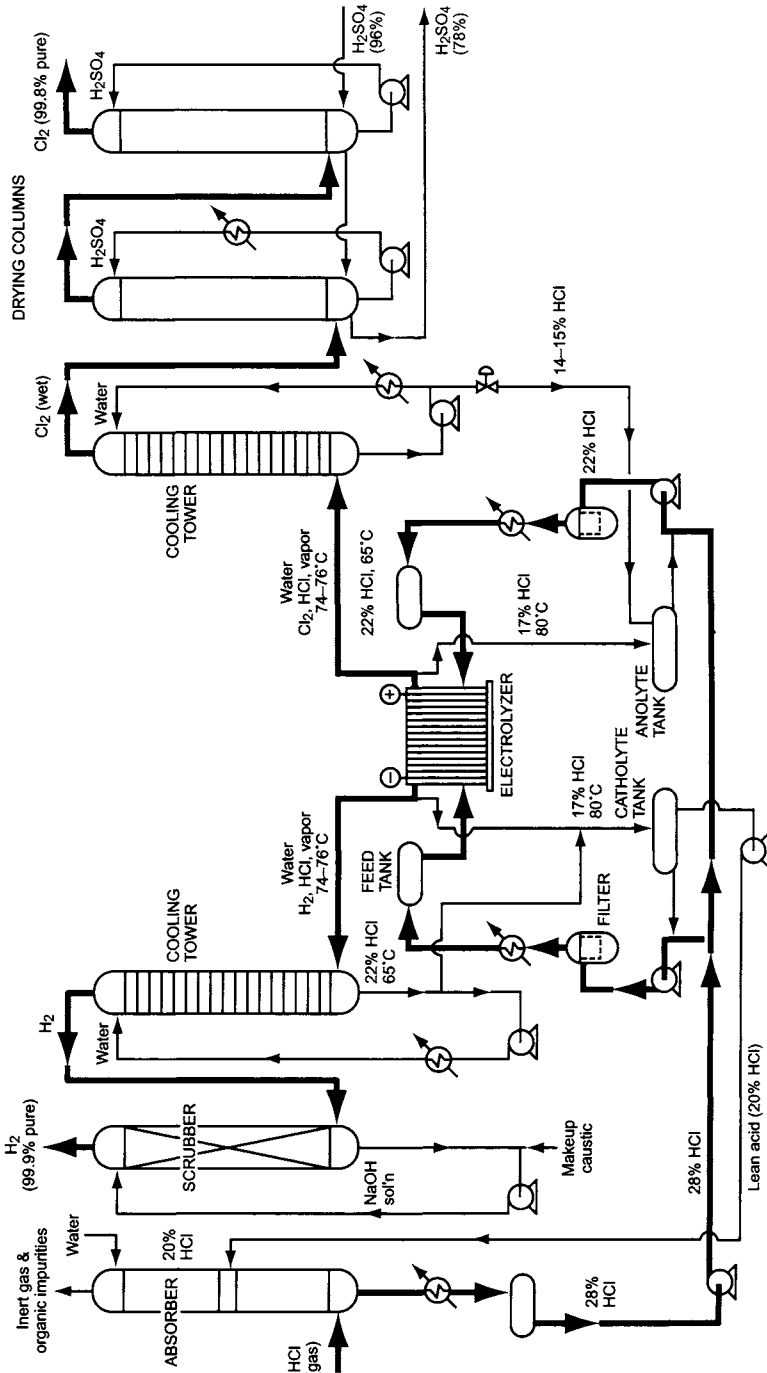


FIGURE 15.8. Flowsheet for electrolysis of hydrochloric acid.

The hydrogen generated in the cells is also saturated with water and HCl. In addition, it contains some chlorine vapor. The water and acid condense or are absorbed when the gas is cooled by direct contact with a circulating stream of dilute acid. A graphite exchanger removes the heat of condensation and absorption and maintains a steady temperature in the circulating acid. The HCl and water removed in this step go to the catholyte tank.

Scrubbing of the cooled gas with a circulating NaOH solution removes residual HCl and chlorine. A third column sometimes serves as a backup to the second in case of breakthrough. The third tower overflows to the second, where nearly all the HCl and chlorine are removed. Again, there is a cooler in the circulating line. The bleach produced in the second tower can be used elsewhere or sent to disposal. Handling of the purified hydrogen is as discussed in Sections 9.2.3 and 9.2.4.

Recent developments in cell technology include the use of ion-exchange membranes instead of diaphragms [29] and the use of oxygen-depolarized cathodes [30]. Section 11.2.2.2C discusses the latter as an alternative to the standard cathode that reduces the reversible potential by about 1.23 V. Section 17.2.2.2 identifies these cathodes as an important emerging technology. A commercial plant for production of about 24,000 tons of chlorine by electrolysis of HCl with depolarized cathodes was recently announced [31].

15.2.2.2. Vapor-Phase Electrolysis of HCl. DuPont has developed a process for generating chlorine from gaseous HCl [32–35]. This is similar to an earlier process for the vapor-phase electrolysis of water [36]. The cell includes a Nafion[®] cation-exchange membrane coated on both sides with catalysts (Fig. 15.9). Gaseous HCl is oxidized to chlorine on the anode side. The protons released there travel to the cathode side through the membrane and are reduced to hydrogen. Since the overall process does not require the absorption of HCl in water or dilute acid, the process flow diagram becomes simpler (Fig. 15.10). The anode gas goes to a drying tower containing sulfuric acid. Dry gas is compressed and then chilled to -25°C . The liquefied chlorine goes on to a purification column, which removes the HCl and residual impurities. Purified chlorine is recovered from the bottom of the column. Some of the HCl with included impurities is purged. Since there are no parasitic reactions at the anode, the current efficiency is as high as 99%. The cell voltage is less than 2.0 V at a current density of 7.5 kA m^{-2} . The operating costs for this process were estimated to be less than one third of those of the conventional HCl electrolysis process [33]. The process remains developmental, and there have been no reports of commercial application.

15.2.2.3. Indirect Electrolysis. The cathodic process in direct electrolysis of HCl has several disadvantages

1. Standard cathodes show high overvoltages.
2. Many metals have more noble thermodynamic potentials, and their reduction should occur at lower voltages (conventionally, with negative half-cell potentials).
3. The presence of gas bubbles in the catholyte increases its electrical resistivity [37]. A change in the electrode process can eliminate this effect.

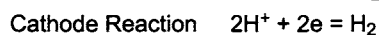
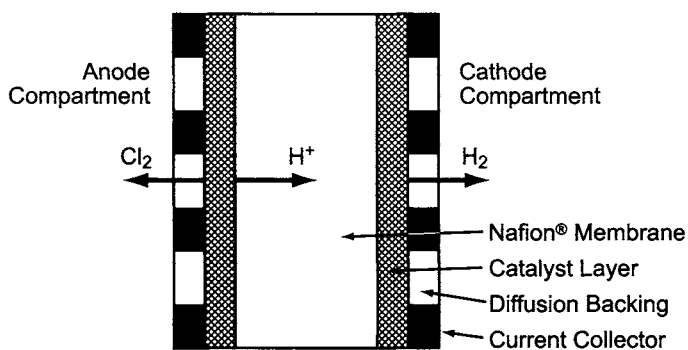


FIGURE 15.9. Electrolysis of anhydrous HCl.

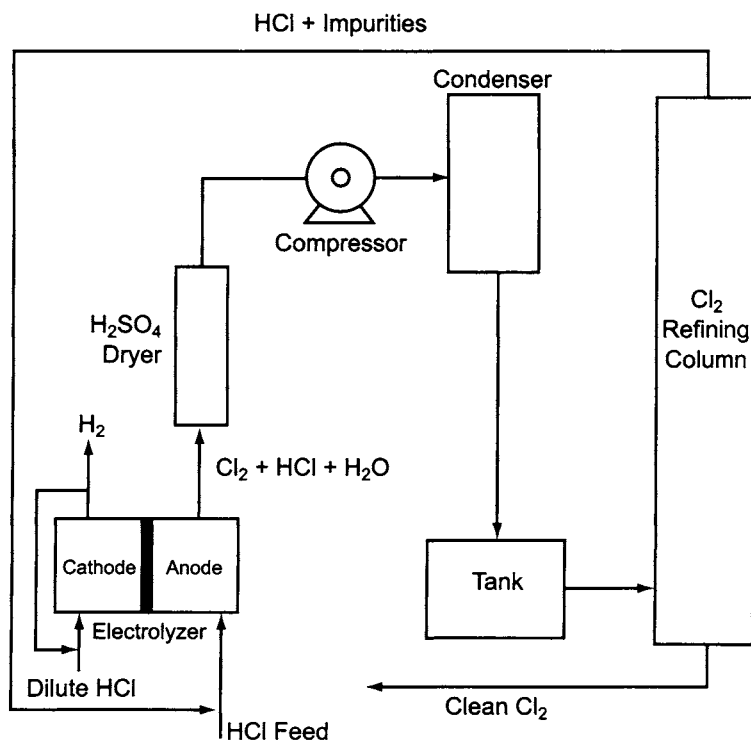
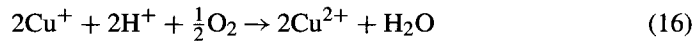


FIGURE 15.10. Process flowsheet for anhydrous HCl electrolysis.

These problems can be alleviated by electrolyzing, for example, a mixed solution of HCl and CuCl_2 [38–40]. The anode reaction is still the oxidation of chloride ion. The cathode reaction becomes the reduction of the cupric ion to cuprous:



Regeneration of the cupric ion is necessary to keep the process operating. Therefore, the spent catholyte goes to an oxidizer for reaction with air or oxygen:



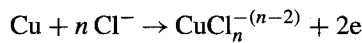
The sum of the reactions (14)–(16) yields the same chemistry as the Deacon process.

The water that forms in the oxidizer must be removed from the process to maintain a balance. The nitrogen or excess oxygen passing through the reactor helps to strip the water from the reacting mass.

This approach to the conversion of HCl is known as the Westvaco process. The slow oxidation of cuprous chloride is its major disadvantage. Increasing the temperature to speed up the reaction also increases the vaporization of HCl and water.

Hine and coworkers studied this electrolysis with oxygen-depolarized graphite cathodes [41]. This combination is known as the “Kyoto cell,” and it operates with either air or oxygen supplied to the cathode compartment. The reactions are the same as in the Westvaco process, but the oxidation of cuprous chloride takes place in the cell rather than in an external reactor.

Hine and Yamakawa [42,43] investigated the kinetics and mechanism of the processes in the cathode chamber. They first conducted EMF measurements with a copper electrode in HCl solutions containing various concentrations of cupric chloride and assumed the reaction



The Nernst equation for the reversible potential of this reaction is

$$E = E^\circ + (RT/2F) \ln (a_{\text{Cu}}/a_{\text{Cl}}) \quad (17)$$

where the activities are those of the cupric and chloride ions. The slope of a curve showing E against $\ln (a_{\text{Cl}})$ is

$$dE/d(\ln a_{\text{Cl}}) = nRT/2F \quad (18)$$

The experimental data showed that $n = 3$.

The same authors also studied the polarization behavior of a rotating-disc electrode and the chronopotentiometry of a graphite disc electrode. Figure 15.11 illustrates the situation in the vicinity of the cathode. A cupric chloride ion, CuCl_3^- , moves to the cathode through its diffusion layer (Step 1) and is electrochemically reduced to CuCl_3^{2-} (Step 2).

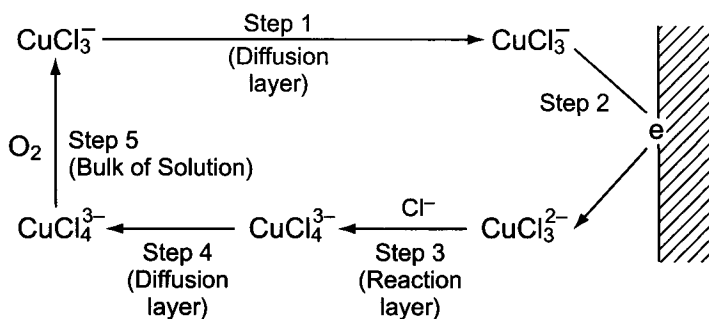
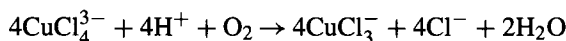


FIGURE 15.11. Cyclic reactions in the vicinity of Kyoto cell cathode.

Since the tetrachloride complex is more stable, CuCl_3^{2-} converts to CuCl_4^{3-} in the reaction layer at the electrode surface (Step 3). The complex ion transfers to the bulk of the solution through its diffusion layer (Step 4), and dissolved oxygen in the bulk oxidizes the cuprous form to cupric (Step 5). Since the chemical reactions of Steps 2, 3, and 5 are fast, the two diffusion processes, Steps 1 and 4, determine the rate of the process. At low current densities, Step 4 is rate-determining. Both diffusion steps contribute to the resistance at high current densities.

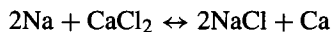
The oxidation of cuprous chloride ion with oxygen in the bulk of the solution (Step 5):



is also controlled by diffusion of dissolved oxygen.

15.2.2.4. Molten Salt Electrolysis

15.2.2.4A. Production of Sodium. Elemental sodium is produced along with chlorine by the electrolysis of fused NaCl – CaCl_2 mixtures [44–46]. The most popular of the many cell designs, and one still in commercial use, has been the Downs cell. Separate paths of development have led to several different versions, all referred to under the Downs name. Figure 15.12 [47] shows one of these. It operates at 580–600°C on a mixture of 42% NaCl and 58% CaCl_2 . The CaCl_2 lowers the melting point of the batch, reduces the solubility of Na in the bath, and leads to the formation of metallic calcium according to the equilibrium reaction



The cathode product therefore contains about 5% calcium, which precipitates in the cooler pipes. The deposited calcium is scraped off and falls into the bath, where it helps to reverse the above reaction. Filtration of the metallic sodium at 110°C removes the calcium and reduces its concentration in the product to less than 0.04%.

The cell has a large dome covering the anodes, cathodes, and diaphragm. Within the large dome, there are four chlorine collection chambers which come together in

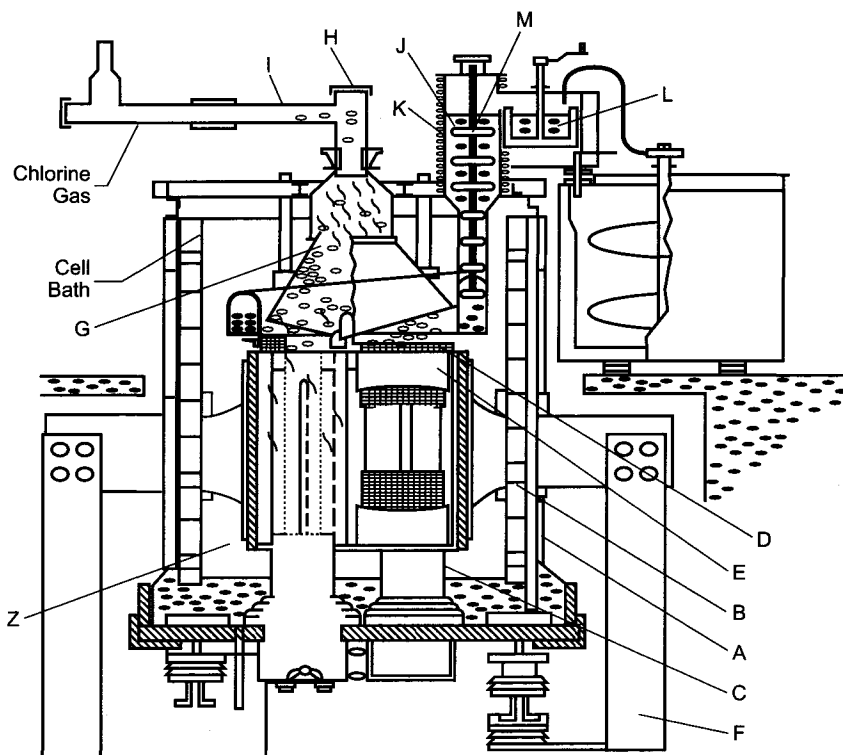


FIGURE 15.12. Downs cell. A. Steel shell containing fused bath; B. Fire-brick lining; C. One of four cylindrical anodes projecting upward from the base of the cell, each surrounded by D, an iron gauze diaphragm, and E, a steel cathode. The four cathodes are joined to form a single unit supported on cathode arms projecting through the cell walls and connected to F, the cathode bus bar. The diaphragms are suspended from G, the collector assembly that is supported from steel beams spanning the cell top. H. Nickel dome; I. Chlorine line; J. Metallic sodium; K. Riser pipe; L. Receiver; M. Scraper. Dark circles represent metallic sodium and open circles represent gaseous chlorine. (With permission from John Wiley & Sons, Inc.)

the middle. The electrolyte is outside the large dome, in region Z. This arrangement prevents the recombination of chlorine and sodium. The collector unit is a complex setup that collects the products of electrolysis in separate chambers as they rise through the molten bath.

The anode is made of cylindrical graphite, built from graphite blocks and inserted through the center of the cell bottom. Iron-gauze diaphragms surround the anode. They hang from an inverted trough that also collects the sodium metal. Chlorine rises from the anode into a brick-lined nickel dome, H, in the center of the cell. The cylindrical cathodes, also made of steel, are located at the side. The body of the cell is made of iron, which may be coated with ceramic material or clay. The molten sodium rises in a vertical pipe, K, collects in an inverted trough, and overflows into a collecting pot. It is then drained into storage tanks at 120°C. After filtration, it is cast into bricks weighing about 4 kg each.

The Downs cell was modified in the 1940s by incorporating four anodes in a square pattern, each anode having its own diaphragm and cathode [44]. This increased the

TABLE 15.4. Operating Characteristics of Downs Cells

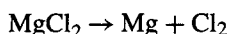
Parameter	Country of manufacture		
	UK	US	Germany
Bath temperature, °C	565–595	580–600	585–595
Load, kA	25–35	43–45	24–32
Cell voltage, V	7	7	5.7–6.0
Current density (cathode), kA m ⁻²	9.8	11–12	9.8
Current efficiency, %	75–80	85–90	78
Cell life, days	500–700	600–800	300–350
Diaphragm life, days	20–100	50–90	20–30

capacity of the cell without altering its outside dimensions. The cell operating life is determined by the rate of wear of the graphite anodes. Carbon gradually oxidizes to CO and CO₂. The use of electrically conducting ceramic anodes coated with noble metal oxides (e.g., IrO₂) extends the life of the cell [48]. In recent years, DuPont has made a number of changes to the basic design. This information remains proprietary.

Table 15.4 describes the operating characteristics of various Downs-type cells [49].

15.2.2.4B. Production of Magnesium. Another example of the coproduction of chlorine and a metal is the electrolysis of magnesium chloride [50]. Cell designs and methods of preparation of the raw material vary because of the wide variety of sources. These include seawater, natural brines, magnesium-rich brines, magnesite (MgCO₃), carnallite (MgCl₂·KCl·6H₂O), and dolomite (MgCO₃·CaCO₃).

Molten MgCl₂ can be prepared by the carbochlorination of MgCO₃ ores or Mg(OH)₂ at 700–800°C. The thermodynamic decomposition voltage for the reaction



is 2.5 V. The minimum energy consumption is 5.5 kW hr kg⁻¹ of metal.

The Dow process, formerly operated in Freeport, Texas, used seawater as the source of magnesium. In this process, Mg(OH)₂ is precipitated, dried, and then treated with HCl to form MgCl₂. After removal of calcium as CaSO₄, the purified material is concentrated to produce granules containing about 70% MgCl₂. This is the only process to use MgCl₂ that is not anhydrous. As a consequence, the cells operate at a low voltage (2.6–2.7 V). Current efficiencies are between 75 and 90%, and the DC energy consumption is about 7 kW hr kg⁻¹ Mg.

The cell is made of steel with cathodes welded to the tub-like container. The cylindrical graphite anodes are independently suspended and inserted through the cell's refractory covers. This arrangement allows adjustment of the anode–cathode gap as the graphite oxidizes in the aqueous medium. The magnesium collects in its chamber in front of the cell and is periodically withdrawn for further processing.



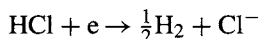
FIGURE 15.13. The Norsk Hydro cell. A. Refractory material; B. Graphite anode; C. Steel cathode; D. Refractory cover; E. Metal outlet; F. Metal; G. Partition wall; H: Electrolyte flow; I. Electrolyte level; J. Chlorine outlet. (With permission from John Wiley & Sons, Inc.)

The Norsk Hydro process, in contrast to the Dow process, uses anhydrous MgCl_2 . The cells, in use since 1978, are brick-lined and have two separate chambers, one for electrolysis and one for collection of the metal (Fig. 15.13). Cooled graphite anode plates enter the cell from the top, and steel cathode plates enter from the back of the cell wall. Chlorine collects in a central pipe in the anode compartment. The circulation of electrolyte parallel to the electrodes brings the metal to a collection chamber, from which it is extracted by vacuum. This type of cell operates at $700\text{--}720^\circ\text{C}$, and the energy consumption is $12\text{--}14\text{ kW hr kg}^{-1}\text{ Mg}$. While the latter is higher than the energy consumption in the Dow process, the anhydrous electrolyte has the advantage of being less corrosive.

A magnesium facility in Rowley, Utah, owned by Magcorp, uses brine from the Great Salt Lake. This contains about 0.4% Mg, four times as high as the concentration in ocean water. The feed salt is produced by solar evaporation (Section 7.1.3) and then treated to remove CaSO_4 , KCl , and NaCl . Evaporation of the resulting solution and spray drying produce a powder containing 4% H_2O , 4% MgO , and other salts. Treatment of the powder with chlorine removes MgO , water, bromide, sulfate, and heavy metals. The cells are similar to the Norsk Hydro type, described above.

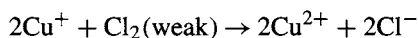
15.2.2.5. Related Processes. Schroeder [51] investigated the electrolysis of a mixed solution of HCl and NiCl_2 with graphite electrodes. He obtained chlorine at the anode and electrodeposited nickel at the cathode. The process calls for interruption of electrolysis when the nickel deposit reaches a certain thickness, followed by dissolving of the nickel in an oxygenated solution of HCl . The intermittent nature of the process works against its practical application.

Ding and Winnick [52] studied the recovery of chlorine from a molten LiCl–KCl eutectic. The usual oxidation of the chloride ion takes place at the anode. The cathode generates hydrogen gas from anhydrous HCl, at the same time replacing the chloride ion:

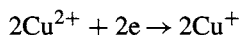


The thermodynamic decomposition voltage at 400°C is about 1 V.

Hine and coworkers [53,54] used a depolarized cathode with an HCl cell to recover chlorine from dilute waste gas. The gas, fed to the cathode compartment, oxidizes cuprous chloride in the bulk of the solution:



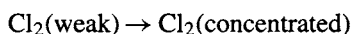
The cupric ion is reduced to cuprous at the cathode:



At the anode,



The net reaction in the cell is



The decomposition voltage for the process is low, as with the Kyoto cell (Section 15.2.2.3). A possible application for this approach is the recovery of chlorine from liquefaction tail gas and other dilute streams.

15.3. PRODUCTION OF HYPOCHLORITE

The processes covered in this section do not produce elemental chlorine, nor are they truly sources of chlorine without caustic. Rather, they combine the two products to produce hypochlorites. Since these are valuable principally as sources of active chlorine and leave very little accompanying free caustic, they are treated in this chapter.

Hypochlorites are direct substitutes for chlorine in such applications as bleaching and disinfecting. Their use removes the need to handle or store liquid chlorine at the processing facility, except as it is needed for hypochlorite generation. On-site production from salt or brine removes even that need.

Bleaching compounds are rated by their available chlorine content. This is a number that expresses the bleaching capacity of a substance as a percentage of the capacity of an equal weight of chlorine. Because of the change in the valence of chlorine from +1 to –1 during the process, the hypochlorite group has the same bleaching capacity as a mole of Cl₂. Sodium hypochlorite therefore contains 95.2% available chlorine and calcium

hypochlorite, 99.2%. Other compounds, even those that do not function by contributing hypochlorite groups, are rated in the same way. Thus, chlorine dioxide, which is useful in pulp bleaching, has 263% available chlorine. This number is 5/2 times the ratio of the molecular weights of Cl_2 and ClO_2 . The factor of five represents the ability of the chlorine atom to accept five electrons in changing its oxidation state from +4 to -1.

It is estimated that 3–5% of the total production of chlorine in advanced countries goes into the treatment of drinking water and sewage. Another major market historically has been in the pulp and paper industry, where chlorine bleaching was a widespread practice. Virtual loss of this market has greatly reduced the use of chlorinated bleaching chemicals. Now, the global use of sodium hypochlorite should begin to increase along with population growth, the growing shortage of water resources, the increase in per capita water consumption, and many other factors.

Most hypochlorite production is in the form of the sodium compound, which will be the focus of our discussion. There will also be a short note on calcium hypochlorite (Section 15.3.4). Figure 15.14 shows a typical flowsheet for production of NaOCl solution [55]. We note here that the compound is more properly designated NaClO . Industry practice, however, favors the form NaOCl .

15.3.1. Electrochemical Production of Hypochlorite

15.3.1.1. On-Site Production. Section 9.1.9.3 already discussed the formation of NaOCl when chlorine is exposed to NaOH solution. This section discusses its electrochemical production at the point of use.

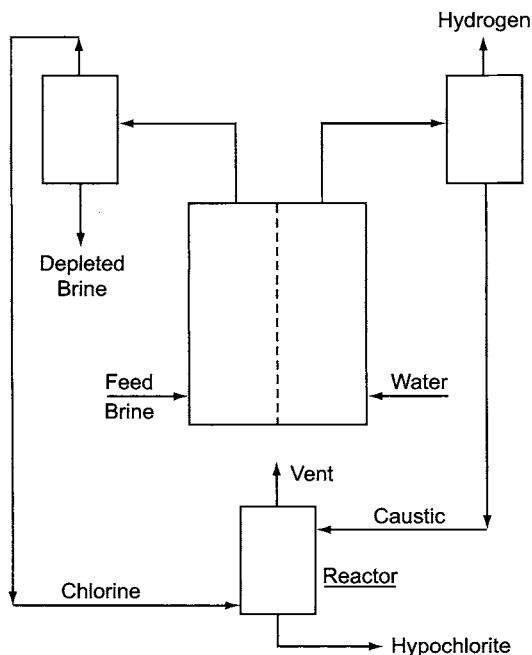


FIGURE 15.14. Flowsheet for electrolytic production of bleach.

Relatively large consumers of NaOCl often produce it from delivered liquid chlorine and caustic soda solutions. The hazards and public concerns associated with shipment of these chemicals remain. Although NaOCl solution is safer than liquid chlorine and caustic soda solution, its large-volume storage is undesirable because of its gradual decomposition, especially during hot weather. This situation favors on-site production from salt over centralized production and shipment of the solution.

15.3.1.1A. Use of Membrane Cells. Ionics, Inc., pioneered the on-site electrochemical generation of full-strength hypochlorite solution [56]. The Ionics system comprises membrane cells, gas-liquid separators, a hypochlorite generator, and auxiliaries.

Purified NaCl solution and water enter the anode compartment and the cathode compartment, respectively, of a conventional bipolar membrane electrolyzer. The anolyte and the catholyte flow to their respective gas-liquid separators. The chlorine gas and the NaOH solution then join in the reactor to form NaOCl solution. Depleted brine from the chlorine separator returns to the brine section for resaturation. Hydrogen from its separator is normally mixed with a large amount of air before discharging to the atmosphere. The operating conditions for the Ionics cell and similar systems are as follows:

Current density	20–50 A dm ⁻²
Cell voltage	3.5–4.0 V
Temperature	80–90°C
Current efficiency	80–90%

Figure 15.15 illustrates the processing of chlorine and caustic soda from the cells.

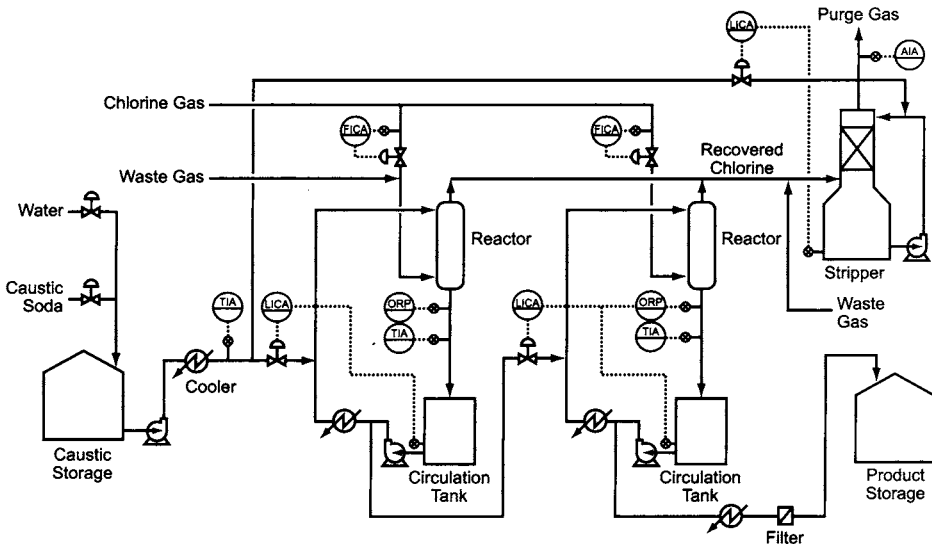
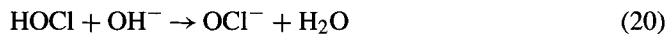
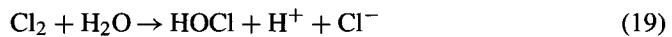


FIGURE 15.15. Flowsheet for producing sodium hypochlorite. (Reproduced with permission of Japan Soda Industry Association.)

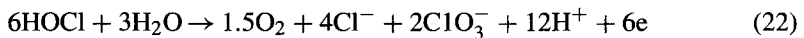
15.3.1.1B. Use of Undivided Cells. Electrolytic production of hypochlorite in undivided cells is a traditional process [57–59]. Such cells are still used because of their simplicity and low cost. Chlorination has long been recognized as the most effective procedure for disinfection of drinking water and wastewater. Large quantities of liquid chlorine have been used in water treatment, but the use of hypochlorite has increased since the 1940s because of its easy handling and relative lack of hazard [60]. Bennett [61] described a large installation with an equivalent chlorine capacity of about 2.3 t day^{-1} that was used to treat water in Houston.

The electrochemical reactions at the anode and the cathode are the same as in chlor-alkali cells, but the chlorine generated at the anode combines with caustic in solution to form hypochlorous acid or hypochlorite:



The hydrolysis of dissolved chlorine keeps the solution pH in the range 7–9.

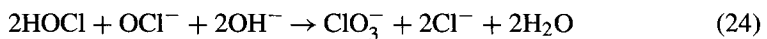
Besides the main reactions shown above, many side reactions take place in the cell. Because of the relatively high pH, oxygen evolution and chlorate formation may occur at the anode:



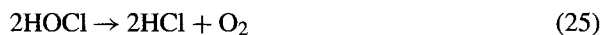
On the other hand, hypochlorite ions in the bulk of the solution diffuse to the cathode, where they are easily reduced to chloride:



In the bulk of the solution, disproportionation also proceeds, especially at high temperatures:



Other losses include the decomposition of hypochlorous acid:



and the release of dissolved chlorine to the atmosphere. These side processes constitute the current inefficiency of the overall process. To minimize them, Brockmann [57] recommended:

1. low temperature
2. high NaCl concentration
3. neutral solution

4. platinum-plated electrodes
5. high current density
6. no stirring
7. addition of potassium dichromate

With the exception of the last, these proposals are still valid today. Chromates deposit on the cathode surface and retard the cathodic reduction of hypochlorite.

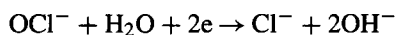
The rate of oxygen evolution is lower at high NaCl concentrations. However, recycling the electrolytic solution to the undivided cell is cumbersome, and so the utilization of NaCl decreases. Modern processes use relatively dilute NaCl solutions to improve the utilization of the salt. Many electrolyzers use platinized titanium or DSA electrodes. Operation at high current densities increase the yield because the rates of the loss reactions (24) and (25) are independent of current density. Finally, agitation of the solution promotes undesirable mass transport of OCl^- to the electrodes.

Some of the characteristics listed above favor the use of seawater as a feedstock. There are several applications for the product of seawater electrolysis. First, it is a low-level bleach and disinfectant, making it useful as a utility-type water- and sewage-treating agent. It is also useful in marine sanitation and as an algacide in seawater evaporation plants. Power stations at coastal locations also operate on-site seawater electrochlorination of cooling water [62]. In this case, magnesium and calcium deposit on cathode surfaces as the oxyhydroxides. These have the useful effect of retarding the reduction of hypochlorite. On the other hand, thick deposits increase the operating voltage. Occasional cleaning with acid or so-called reverse electrolysis, in which the direction of the current is reversed for a short time, helps to remove such scale.

15.3.1.2. Electrodes and Electrode Processes. Most electrolyzers in this service are bipolar. Carbon or graphite was the material of choice in earlier designs [57,58]. While these materials are resistant to concentrated NaCl under anodic polarization, they are less resistant to dilute solutions because of the increased rate of generation of oxygen. Carbon steel also has been used as a cathode. Because the hydrogen overvoltage is low, iron and steel are not cathodically protected and therefore corrode at the working potential and when a cell is shut down. Ferrous ions oxidize and precipitate on the anode surface as ferric oxyhydroxide. To avoid these problems, modern electrolyzers use stainless steels, nickel alloys, and titanium. Platinum plating on titanium substrates prevents hydrogen embrittlement and also reduces the hydrogen overvoltage.

One of the authors (FH) experienced heavy corrosion of a platinized anode in a seawater electrolyzer in winter, caused by the deposition of chlorine hydrate. He concluded that the cell must operate at temperatures above 8–10°C.

The efficiency of hypochlorite generation depends on the rate of its reduction at the cathode, which is a diffusion-controlled process. The reaction is



The main reaction at the cathode, hydrogen evolution, is activation-controlled. The total cell current, i , includes the current participating in the hydrogen evolution

reaction (HER), i_H , and the current consumed by hypochlorite reduction, i_R . The current efficiency then is

$$\xi = i_H / (i_H + i_R) \quad (26)$$

or

$$\xi = 1 / (1 + i_R / i_H) = 1 / (1 + r)$$

The last equation uses r , the ratio of unproductive to productive current. This parameter can be shown to be

$$r = n F C D / \delta i_o e^{k\eta} \quad (27)$$

where

- n = number of electrons involved in the hypochlorite reduction reaction
- F = Faraday constant
- C = concentration of hypochlorite ion
- D = diffusion coefficient of hypochlorite ion
- δ = diffusion layer thickness
- i_o = exchange current density for the HER
- k = constant at a given temperature on a given electrode surface
- η = overvoltage for the HER

The combination CD/δ is a measure of the ease of reducing hypochlorite. For best results, it must be kept small. A low concentration of hypochlorite and a thick diffusion layer are preferred. Hence, Brockmann's "no stirring" and the use of low flow rates through the cell are normal practices. High current densities improve the current efficiency because the rate of the desired reaction increases in proportion, while the rate of hypochlorite destruction increases only as the diffusion layer becomes thinner. The hydrogen bubbles generated at the cathode agitate the solution and reduce the thickness of the diffusion layer. Krstajic *et al.* [63] showed that

$$\delta = a / i_H^m \quad (28)$$

where a and m are constants. They estimated m to be 0.5.

The limiting current density for hypochlorite reduction is

$$i_R = 2 F C D / \delta \quad (29)$$

Substituting Eqs. (28) and (29) into Eq. (26) gives the quadratic

$$\xi^2 - (K C^2 / i + 2) \xi + 1 = 0 \quad (30)$$

where $K = (2FD/a)^2$

Rudolf and coworkers [64,65] represented the current loss, ξ' , as a function of two dimensionless factors, P and Q :

$$\xi' = \xi'(P, Q) \quad (31)$$

Here, P is related to the concentration of hypochlorite ion in the bulk of the solution and Q to its rate of mass transfer towards the cathode surface:

$$P = \text{OCl}^- \text{ concentration} / \text{Cl}^- \text{ concentration}$$

$$Q = \text{limiting current density for OCl}^- / \text{total current density}$$

This work showed that ξ' increased monotonically with increasing Q . The relationship between ξ' and P was more complex. When Q was large, the current inefficiency ξ' was large and a weak function of P . In agreement with the points made above, the conclusion was that a cell should operate at high current density and therefore a high degree of conversion.

15.3.2. Chemical Production of Hypochlorite

Powell Fabrication and Manufacturing, Inc., a prominent supplier of bleach plants and other chlorine processing equipment, supplied a number of sponsored papers and internally published documents [66], and much of this section is based on that information.

15.3.2.1. The Process. When a good local market exists for bleach, the demand usually can exceed the quantities that can be made from normal tail gas and may justify the installation of plants dedicated to bleach production. This section will show that such units also can produce bleach of superior quality. They will be small in capacity, at least relative to chlorine plants. They may be considered specialty bleach producers, and one of their important functions may be packaging bleach for customers.

The typical dedicated plant purchases liquid chlorine and 50% NaOH from a manufacturer. The process, however, can operate (with suitable modifications) either on liquid or on gas. When chlorine is available as the liquid, there are advantages in using it directly in that form. This eliminates the expense of a vaporizer and reduces the cooling load by absorbing about 16% of the heat of reaction.

Section 9.1.10.3A described the chemistry of the reaction and the routes of decomposition of the primary product. With proper control of the process, the decomposition reactions can largely be avoided. Reaction of chlorine with 50% NaOH would far exceed the limits of solubility and product stability, and so an essential part of the process is the addition of water to control the product concentration. The quality of this dilution water largely determines the quality of the final product. With a 50% NaOH feedstock, more than half the process input will be dilution water whenever the final product contains less than 16% NaOCl.

Section 9.1.9.3 mentioned the production of NaOCl from liquefaction plant tail gas. This is an opportunistic approach to converting a hazardous waste into a useful product. The main objective usually remains the safe disposal of the uncondensed

chlorine. While there is a possibility of some control over the process and the amount of hypochlorite produced, the output still is constrained by the needs of the liquefaction plant. Section 9.1.10.3B reviewed some typical equipment configurations that combine chlorine recovery with the functions of an emergency vent scrubber. Packed columns are a widely used example. The packed column is well suited for the complete removal of chlorine from a vent stream. It is less suited for the efficient manufacture of quality bleach. Some of the problems are:

1. A column is an efficient chlorine removal device when the caustic concentration is high, but high excess caustic concentrations are unsatisfactory for the production of bleach.
2. Restricting the caustic concentration to improve the quality of bleach can make a scrubber system uneconomically large or unreliable in an emergency, where the available caustic may be insufficient to prevent a breakthrough of chlorine gas.
3. The use of a reactor as an emergency scrubbing device subjects it to unpredictable large demands that can destroy process control.
4. Scrubbing column process conditions are nonuniform (in time and in space), promoting corrosion and the development of hot spots.
5. The caustic in a column is not isothermal because its temperature increases as it passes through the column. This leads to undesirable side-effects such as the increased production of chlorate.
6. Nonuniformity of temperature is pronounced on a microscale, because of the low degree of turbulence in the liquid and gas films in a packed column.

Augmented designs and special techniques can help offset some of these disadvantages [67]. One technique is to operate the scrubber with a safe excess of caustic and postchlorinate the liquor under more controlled conditions [66]. The latter step allows controlled reduction of the residual NaOH concentration into the desired range. Some system designs rely on multiple columns operating in series. This allows staging of the caustic concentration. Normal chlorine vents are then handled by a column operating at low NaOH concentration. Sudden increases in chlorine flow and emergency releases can still be handled by a later column in which the NaOH concentration is higher. A problem that remains with any tower operating with little NaOH present is the danger of overchlorination. Continued absorption of chlorine in such a case reduces the pH of the solution. This sometimes causes decomposition of the hypochlorite in solution, with the release of chlorine and formation of foam that overflows the system [68].

Reactor efficiency improves when reactant flows become more turbulent. Section 9.1.10.3E showed that the absorption process can be either liquid- or gas-film controlled, depending on process conditions and reactant stream compositions. The controlling regime probably changes during the course of the reaction of a gas bubble, and so it is important to provide turbulence in both phases. A reactor based on high-velocity circulation of the reacting liquid phase, with injection of gas at a point of high turbulence, will be much more efficient than a packed column. Figure 15.16 is a photograph of a unit of this type designed specifically for hypochlorite manufacture. Capacities range up to 150 tpd chlorine equivalent. This design can produce solution concentrations of 3–16.5% from chlorine in any of several forms—liquid, dry gas, wet gas, or dilute gas. The NaOH

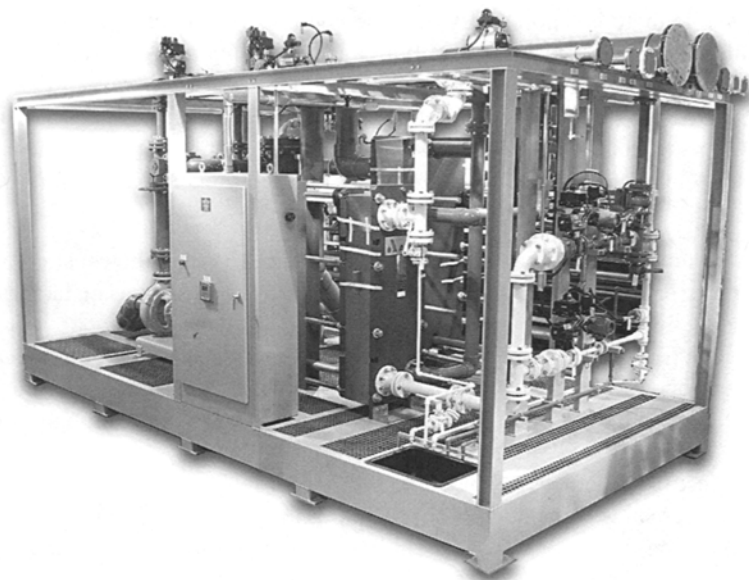


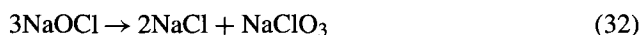
FIGURE 15.16. Packaged bleach plant. (With permission of Powell Fabrication and Manufacturing, Inc.)

concentration can be anywhere from the minimum required to give the desired product strength up to 50%. Use of the more concentrated form requires the addition of dilution water. This is combined with the caustic soda stream before the reactor. The good mixing and control available in these units are said to result in lower chlorate concentrations in the product and to allow the NaOH excess to be reduced from 1% to 0.2–0.3%.

Flow controllers set the rates of both streams, one being under flow-ratio control. In principle, either caustic soda or dilution water can be the master stream, with the other following it to maintain the ratio. Blending is controlled by a feedforward system, ultimately reset by the product concentration or density. Feedback from caustic concentration measurement (usually by density) could be used for final adjustment, but the concentration of the hypochlorite solution is the more important variable. The simple flow-ratio controller mentioned here can be replaced by a multi-stream version that allows use of other streams in addition to the principal 50% NaOH and dilution water. A cooler downstream of the mixing point removes the heat of dilution. The standard design is a titanium plate exchanger, which can also provide turbulence to complete the mixing process. Chlorine joins the diluted caustic in the reactor. Its rate of addition is controlled by an oxidation–reduction potential (ORP) instrument. The reaction mass recirculates from a collection tank around the system to reduce the increase of temperature across the reactor and to promote turbulence. The net production is removed from the tank, normally under level control.

15.3.2.2. Decomposition of Sodium Hypochlorite. Hypochlorites are unstable, and all systems for their production or application must be designed accordingly. Decomposition

can follow one of two pathways. The more likely is



At the high concentrations of commercial bleach solutions, this is a true second-order reaction. The rate of dissociation can be expressed by

$$\text{Rate} = k[\text{OCI}^-]^2 \quad (33)$$

From extensive data gathered by the American Water Works Association (AWWA), Gordon and Adam [69] have created a predictive modeling program for the calculation of bleach strength and chlorate concentration during storage. While Eq. (33) tracks the concentration of hypochlorite over time for a given starting solution, calculations for different solutions fail when it is assumed that k depends only on temperature. It in fact also depends on the ionic strength of the solution. This means that the rate constant for decomposition increases along with the starting concentration. The apparent order of reaction in such a partial comparison is greater than two. Doubling the starting concentration then increases the rate of decomposition not by a factor of four, as required by a second-order reaction with constant k , but often by a factor of about five.

One of the practical effects of this situation is that the extent of formation of chlorate is greater in strong solutions. Because of the effect of ionic strength, a strong solution may actually decompose to a given lower strength more rapidly than a weaker one. It will certainly contain a significantly higher concentration of chlorate after the reaction.

Thus, more dilute solutions will have longer shelf lives and higher purity than highly concentrated solutions. They obviously require larger storage facilities and would have greater transportation costs. A sensible and practical compromise is to ship concentrated solutions and dilute them at the customer's site (using high-grade water). Those who dilute bleach should be aware that it may be necessary to adjust the alkalinity after dilution.

Good storage and handling practices will prolong the useful life of a bleach solution. These practices include the use of proper materials of construction, discussed below. Low temperature and avoidance of sunlight are other examples of good practices. Chilling the bleach to maintain a low temperature is one possible approach. This is done by some handlers, but many do not find a justification for this expense. Smaller containers (e.g., totes and drums) can be stored indoors, out of the sun and in air-conditioned surroundings. Outdoor storage tanks can be opaque and located in a shaded area. In general, those who handle bleach solutions should not:

1. store very high-concentration bleach
2. add new bleach to an existing heel in a storage tank
3. ship over long distances in hot weather
4. store for long times before delivery or use

Similarly, purchase contracts should include a requirement for the timely delivery of material [66].

The second pathway for decomposition evolves oxygen:



Under most normal conditions, this is a secondary but possibly troublesome reaction. The presence of free oxygen is a problem in itself, but the reaction also has several mechanical effects. It can cause gas-locking when the reaction continues in a pump that is idle. The pump may then run dry, accelerating mechanical wear and increasing the maintenance burden. The gas can accumulate in instruments and piping systems that are not well vented. This can cause malfunctioning of instruments and gas-locking of the pipes. The accumulation of oxygen in valves can lead to minor explosions and blowouts. This is a problem similar to one described in the handling of hydrogen peroxide (Section 7.5.9.3A), and the solution is similar. Valves should be vented on the high-pressure side. Ball valves, which are commonly used in hypochlorite service, can have holes drilled in the balls on the upstream side. This makes it necessary to identify the direction of flow on the valve itself to ensure proper installation.

Decomposition is accelerated by sunlight, low pH, and the presence of heavy metals. Avoidance of sunlight is a factor in the design of storage facilities and product containers. The problem of decomposition at excessively low pH was mentioned above in connection with packed-column performance. The effects of metals vary. Iron, for example, is not a particularly strong catalyst for decomposition, but concentrations of more than 1 ppm produce discoloration. Certain other metals are stronger catalysts. Nickel and copper are frequently encountered examples, and their specifications normally are set at 50 ppb. Gordon *et al.* [70] have reported on the effects of various metals. The order of their activity is $\text{Ni} > \text{Co} > \text{Cu} > \text{Fe} > \text{Mn} > \text{Hg}$ [71].

Caustic soda is a likely source of nickel from the corrosion of the evaporators (Section 9.3.2.1). The nickel content of 50% NaOH can be reduced by addition of a corrosion inhibitor to the evaporation process (Section 9.3.4.2). Nickel can be avoided in integrated on-site production of hypochlorite by using less-concentrated NaOH from membrane cells, without evaporation.

Other metals commonly found in bleach solutions include calcium, magnesium, and iron. These also arise in the process [72]. The principal source of calcium and magnesium is the process dilution water. Iron accompanies the caustic, and its concentration depends on the type of cell being used. Diaphragm-cell liquor typically contains 0.5–0.6 ppm. Further corrosion and concentration by evaporation increase the level of iron to about 3 ppm in 50% NaOH. Mercury- and membrane-cell caustic solutions generally have lower iron contents. Transportation in lined steel carriers and processing (e.g., dilution) and storage in carbon steel at the user's site can increase the concentration of iron. The concentration will be highest in storage tank bottoms.

Most metals are present in bleach largely as very fine suspended solids or colloids. Section 15.3.2.4 describes a filtration process and shows the typical results. A simple laboratory test for bleach quality uses the timed vacuum filtration of a fixed volume of solution through a 0.8 μm filter [73].

Removal of metals improves the appearance of the bleach and reduces the rate of decomposition dramatically. The shelf life therefore improves. By removing the residues formed by impurities, filtration also makes it possible to use lower-quality materials in

the process. In particular, a lower grade of water can be accepted. Use of an aqueous waste stream reduces the volume of effluent from the process. Such an arrangement can require the use of a multistream blending system with some logic capacity. All these advantages may help to offset the cost of the filtration plant.

When the rate of decomposition of bleach is reduced, achieving the desired product strength at the point of use does not require as large a safety margin in the concentration of the product from the reactor. This results in a direct savings in raw material consumption. The improved yield also saves raw materials, as does the ability to reduce the excess caustic concentration. With chlorine and caustic priced at \$550 per ecu, the combined effect of the three factors just enumerated is about $\$10 \text{ m}^{-3}$ of 16% bleach [66].

15.3.2.3. Materials of Construction. Preventing contamination of process materials is one criterion in the selection of materials of construction. With hypochlorite solutions, it is especially important. The presence of contaminants in a solution is itself objectionable. Section 15.3.2.2 discussed the fact that certain contaminants also catalyze the decomposition of hypochlorite, reducing the useful life of the product and even creating process hazards and mechanical difficulties.

The choice of metals is highly restricted. The only metals found satisfactory and in wide use are titanium, tantalum, and precious metals. Of these, only titanium is used in quantity for the construction of equipment. Its application is straightforward, and commercially pure metal (Grade 2) is satisfactory without alloying. The other metals listed above are used primarily in instruments and other small items. The ban on the large majority of metals extends to their use in auxiliary systems. Copper, for example, is used in many industrial water systems. It should not be used with bleach dilution water, however, because of its catalysis of hypochlorite decomposition reactions.

Other metals may be used in certain applications and under less aggressive conditions (low temperature, high pH, low concentration) [74]. They include Alloy 20 and the silicon cast irons, especially in pumps. Alloys such as Hastelloy C and Chlorimet 3 show good resistance in some solutions.

Given the cost of titanium, hypochlorite handling systems usually are constructed from nonmetallic materials. The most widely used materials are halogenated polymers, polyethylene, and fiber-reinforced plastics (FRP). They often appear as linings on metal substrates, and PVC wrapped with FRP is also quite common. Polymeric systems in outdoor use should have ultraviolet (UV) light barriers.

The most serviceable material for centrifugal hypochlorite pumps is titanium. The major deterrent to its use is its cost. Other pump materials may be lined with fluoropolymers (PTFE, ETFE). Diaphragm pumps usually have polytetrafluoroethylene (PTFE) or elastomer (preferably Viton) diaphragms. FRP pumps are generally not used.

The same types of material can be used in piping. Titanium piping will be Schedule 10, maximum. It may be used in long welded runs with properly designed expansion joints. Most piping, again, is nonmetallic. PVC is common at pressures below 3.5 bar. It should be Schedule 80, and line velocities should not exceed 2 m s^{-1} . PVC can also be wrapped with FRP. FRP piping can be used without a liner, but results are often poor because of the difficulty of designing a sound system. Lined metallic piping

is also very common. Several different lining materials are acceptable. PTFE-lined pipe is more expensive than most, but it gives excellent service over a long life.

Valves, for the most part, follow the piping material selection. Because of the importance of reducing stresses on storage tanks, the valve nearest the tank on a given line should be of very high quality. Except on small valves, gear drives are advisable. Most types of valves are acceptable. A typical selection is a lined steel plug, ball, or butterfly valve. Seals and gaskets are usually fluoropolymers. The physical structure of a gasket should match the torque requirement of its application.

The economic design of high-quality tanks for storing hypochlorite solutions has been a long-standing problem [75]. Titanium would be an excellent material of construction, but only at a very high cost. Rubber-lined carbon steel has been widely used in both horizontal and vertical tanks. Fiber-reinforced polymers are attractive candidates, but results often have been unsatisfactory. Vinylester resins (e.g., Derakane 411) are preferred, and polyester resins also may be satisfactory. Those with high chemical resistance are best, and bisphenol A resins, for example, are preferred to those based on isophthalic acid.

Many of the failures of FRP tanks in hypochlorite service stem from inadequate mechanical design [75,76]. The presence of a highly corrosive chemical aggravates any problems due to poor design. For example, any penetration of the corrosion barrier in a standard filament-wound tank allows hypochlorite to follow the continuous strands of glass, which are applied on a bias, along and around the entire tank. This can cause early catastrophic failure. The use of hand layup or rotational molding instead of filament winding can relieve this problem.

Another common experience is leakage from flat-bottomed tanks. Prevention requires special attention to the design and fabrication of the bottom knuckle. Gates [76] points out that while the tensile properties of FRP approach those of alloys, the modulus of elasticity is only about 3% of that of steel. Therefore, flat-bottomed vessels should not be subjected to pressure or vacuum.

The thickness of the corrosion barrier should not be included in structural calculations. This principle apparently is often ignored, leading to early failure. Because exposure to sunlight increases the rate of decomposition of hypochlorite, good practices include the use of UV stabilizers and storage whenever possible in a shaded location.

Benzoyl peroxide-dimethyl aniline (BPO-DMA) is a superior resin curing system. The more common systems are based on methyl ethyl ketone peroxide and cobalt naphthenate. We have already discussed (Section 15.3.2.2) the disadvantages of exposure of hypochlorite solutions to cobalt. It is one of the most powerful decomposition catalysts [71], and it has been used for dehypochlorination of process streams and wastewater (Section 7.5.9.3B). Some users of FRP tanks avoid the more difficult fabrication techniques required with a BPO-DMA cure, arguing that likely fabrication defects more than outweigh the advantages. The highest quality, however, results when these difficulties are overcome and the cobalt is eliminated. There is also some evidence [77] that, in general, the use of thixotropic agents in the formulation makes the composite less resistant chemically.

Because of some of the problems with FRP vessels, cross-linked polyethylene (XLPE) is sometimes specified for hypochlorite service. The long-term stability of this material, however, may be inadequate under certain conditions [78]. Rotationally molded

XLPE tanks have a high rate of failure in hot-weather locations. Many of the failures have been in swimming-pool applications. The failures were attributed to a combination of elevated temperatures, stress, the evolution of reactive oxygen, and frequent refilling with fresh concentrated bleach (which keeps the rate of oxygen generation high).

Particularly in the case of unfiltered solutions, designers should allow for sedimentation during storage. The normal discharge nozzle should be some distance above the floor of the tank (with another nozzle at the bottom to allow complete draining, removal of sediment, and occasional cleaning). Conical bottoms facilitate the removal of sediment from smaller tanks.

The design of transfer piping includes proper sizing and routing. If unloading lines contain low points that cannot be drained, new material can be contaminated by partly decomposed solutions from a previous delivery.

15.3.2.4. Bleach Filtration. The discussion of brine treatment in Section 7.5 covered the characteristics of the particles formed by chemical precipitation and the types of filter used to remove them. As that discussion would indicate, the particles found in bleach solutions are not easy to filter. Filter aids are necessary, and pressure-leaf filters are commonly used. Figure 15.17 shows a typical skid-mounted unit. Pumps and bleach filter bodies and plates should be titanium. Nonmetallic components are PVC or PTFE. Other components of the system (e.g., filter aid tanks) may be FRP. Filter aids should be diatomaceous earth or Perlite (Section 7.5.4.2).

Typically, pressure filtration will reduce copper and nickel concentrations below or close to the limits of detection, respectively, about 5 and 10 $\mu\text{g L}^{-1}$. Residual iron normally is 0.2–0.3 ppm [66]. Final disposal of the solids can be by one of the methods

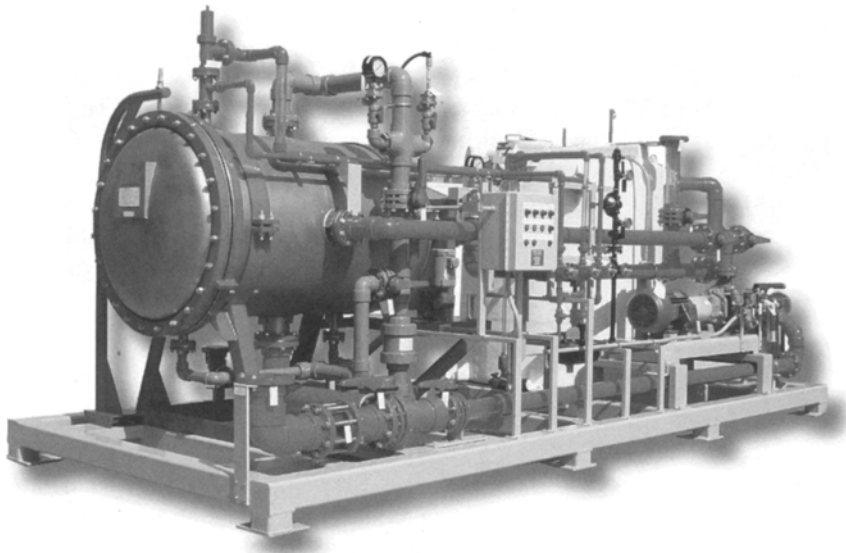


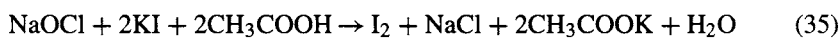
FIGURE 15.17. Bleach filter. (With permission of Powell Fabrication and Manufacturing, Inc.)

discussed in Section 7.5.4.2. In particular, the filter can be backwashed and the resulting slurry taken to a dry-cake pressure filter.

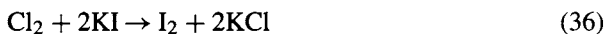
Filtration normally is the last step in the process, before product storage. One of its advantages is that, by removing contaminants picked up at any stage of the process, it provides a corrective mechanism [79]. It compensates for some deficiencies in design and operation. In particular, by removing metals from the bleach, it reduces the amount of oxygen generated by reaction (34). Filtration also makes it more feasible to produce quality bleach from relatively impure diaphragm-cell caustic. This grade often has advantages in price and availability.

15.3.2.5. Analyses and Specifications. The discussion above stressed the instability of hypochlorite solutions. Therefore, accurate analysis requires proper sampling and careful handling. Sample containers must be free of the many substances that react with the hypochlorite group or catalyze its decomposition. Samples then should not be subjected to high temperature or UV light. If prompt analysis is not possible, samples should be kept under refrigeration.

The strength of a hypochlorite solution is usually expressed in terms of available chlorine. As explained above, "available chlorine" refers to the amount of chlorine that has the same oxidizing power as the active agent found in a given solution. In analysis by the starch-iodide test, for example, we have



A mole of chlorine also oxidizes two moles of KI:



A mole of hypochlorite therefore has the same oxidizing power as a mole of chlorine.

A hypochlorite assay can be done on a weight or a volume basis. The standard laboratory analysis usually involves pipetting an approximate volume into a weighing bottle. The resulting analysis, based on the reduction by thiosulfate of the iodine formed in reaction (35), would be in terms of weight % available chlorine or weight % NaOCl. The analysis might also be expressed as gpl available chlorine or "trade percent" available chlorine. The latter is a hybrid weight/volume measurement that represents the number of grams of available chlorine contained in 100 ml of solution. Therefore,

$$\begin{aligned} \text{Trade percent available chlorine} &= \text{weight/volume}\% = \text{gpl}/10 \\ &= (\text{weight}\%) \times (\text{specific gravity}) \end{aligned}$$

A simpler and more rapid but less accurate assay can be made from the specific gravity of the bleach solution. For best results, this requires knowledge of the excess caustic concentration. The presence of excess caustic soda increases the specific gravity by a small but significant amount. Chlorine Institute Pamphlet 96 [80] gives some physical properties. It indicates that, at 20°C, the specific gravity of NaOCl solutions derived

from chlorine and NaOH is approximately

$$G_o = 1.002786 + 0.013547 T - 6.14063 \times 10^{-5} T^2 \quad (37)$$

where

G_o = specific gravity of solution with no excess NaOH

T = trade percent available chlorine

The presence of excess NaOH increases the specific gravity:

$$G = G_o + 0.00135 X \quad (38)$$

where

G = specific gravity of solution

X = excess NaOH concentration, gpl

The coefficients of the linear terms in Eqs. (37) and (38) show that the addition of a small quantity of NaOH has roughly the same effect as the same increase in the concentration of available chlorine. An excess of 0.5% NaOH (~6 gpl) in 16% bleach produces the same specific gravity as a 16.6% stoichiometric solution, a difference of about 4% in assay.

Example. A solution of 15% (trade) NaOCl and the equivalent amount of NaCl should have a specific gravity of $1.002786 + 15 \times 0.013547 - 225 \times 6.14063 \times 10^{-5} = 1.192$. To determine the assay from the gravity measurement, it would be more convenient to invert Eq. (37). Suppose the gravity is 1.21. We use the equation $(1 - t)^2 = 1 - 1.3384 (G_o - 1.002786)$, where $t = T/110.3$. This gives $(1 - t)^2 = 0.722$. Finally, $T = 16.53\%$. If the solution contains excess NaOH, Eq. (38) also comes into play. With 5 gpl NaOH, we have $(1 - t)^2 = 1 - 1.3384 (1.21 - 1.002786 - 5 \times 0.00135)$, and $T = 15.95\%$.

The pH of the product solution ranges from about 12 to 13. A frequently specified minimum NaOH concentration is 0.3%, corresponding to pH 11.86. Addition of NaOH beyond pH 13 (~4.0 gpl) is counterproductive. It provides little added stabilization but increases the ionic strength of the solution and therefore the rate of decomposition to chlorate. It is important to remember when consulting old tables of specific gravity as a function of hypochlorite strength that the old practice was to use a higher excess caustic concentration, say, 0.7 or 0.8%. With improvements in quality over the years, the specified minimum caustic excess has decreased. Tables based on old solutions will show higher gravities than would be found with today's products. Conversely, a given gravity will indicate less than the true strength of a bleach solution.

A typical specification for sodium chlorate in bleach is 1,500 mgpl. It cannot practically be removed from a solution but must be controlled by proper reaction and handling. Production at lower temperature, lower final product strength, and the proper pH limits the in-process formation of chlorate. The use of high-purity ingredients also contributes to this. Finally, prompt use of the product limits its gradual deterioration by reactions (32) and (34).

Na_2CO_3 may enter the process along with the NaOH or may form by reaction of NaOH with atmospheric CO_2 . Also, in some cases the reaction product may be back-treated with CO_2 in order to reduce the excess NaOH concentration. The reason for

this is that, while caustic protects the product from decomposition, it also reduces its activity as a bleach. The Na_2CO_3 may itself provide some stability, but it can also cause precipitation of certain elements or gather suspended solids into larger particles that can settle and deposit in equipment, piping, and instrumentation.

One of the results of contamination of bleach with transition metals is the accumulation of oxygen in pipelines and storage tanks. This has become a safety issue for suppliers and utilities. Many utilities have revised their specifications for transition metal ions in bleach into the ppb range. This requires more sensitivity and precision in analytical methods. Pham [81] has studied a number of methods and reported results obtained by chloroform extraction colorimetry and ion chromatography. The latter is the preferred analytical method.

The specifications for chlorate and bromate ion concentrations have become more important [82,83], particularly with the increased use of hypochlorite solutions as a substitute for liquid chlorine in the treatment of potable water. Some authorities will limit the fraction of permissible impurity contributed by the disinfecting agent, and in some situations this will require the selective use of high-purity hypochlorite.

15.3.2.6. Safety. Because of the presence of active chlorine and the possibility of evolution of elemental chlorine, hypochlorite solutions are highly corrosive and toxic. No one should be allowed to handle these substances without thorough training. Plant systems should be carefully designed, using the proper materials of construction (Section 15.3.2.3), and in particular should rigidly exclude the possibility of accidental contact with excess acid.

In addition to normal plant requirements (e.g., hard hats), personal protective equipment should include, as a minimum, chemical splash goggles and rubber gloves and boots. Some operations may require a full face shield, a chemically resistant suit, or a respirator. Safety showers and eyewash facilities should also be in the operating or handling area.

Handling outside battery limits is also important. This encompasses storage, loading, and unloading. Spill containment is an important consideration in all these operations. The *Sodium Hypochlorite Manual* [80], published by the Chlorine Institute, is a comprehensive source of information. In addition to general safety information on bleach solutions of commercial and household strength, it discusses the principles of handling, storage, and transport. It considers large-scale bulk systems and, in particular, the special aspects of non-bulk packaging and shipping.

15.3.3. Miscellaneous Applications

Development of small but sophisticated systems for electrochemical generation of hypochlorite from very dilute solutions of NaCl is of present interest. In recent years, electrochemical synthesis of extra-pure sodium hypochlorite solutions for medical use has received growing attention [84,85]. The electrolytic solution is an isotonic physiological salt solution containing 0.89% NaCl . Another application is the disinfection of drinking water that contains only 10–100 mg NaCl per liter [86,87]. Reviews of on-site generation of hypochlorite for water treatment and of the sterilization of water and wastewater include those of Michalek and Leitz [56] and, more recently, Scott [88].

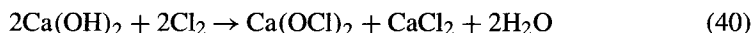
15.3.4. Calcium Hypochlorite

The entire discussion of hypochlorites so far has been in terms of NaOCl. Another product in frequent use is calcium hypochlorite, $\text{Ca}(\text{OCl})_2$. This has many of the characteristics of NaOCl, but it is an approximately neutral compound and its low solubility makes it possible to produce a granular material with a higher available chlorine content.

In the chemical production of sodium hypochlorite, we had

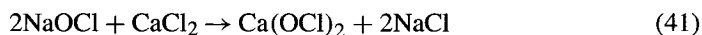


The fundamental reaction of chlorine with lime is entirely analogous:

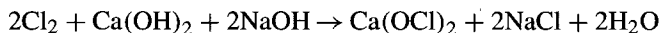


In the latter case, the insoluble hypochlorite drops from the solution, leaving the CaCl_2 behind.

It is possible to recover this residual calcium value as well. Recovery depends on the parallel production of NaOCl according to reaction (39). Double decomposition of NaOCl and CaCl_2 yields more product:



The sum of reactions (39), (40), and (41) is



Ideally, all the calcium used in the reaction becomes part of the product, while the waste product contains the sodium value.

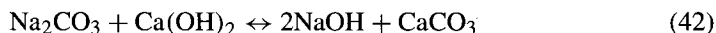
Calcium hypochlorite is isolated from solution as mixed crystal whose composition depends on the purity of the lime and on process conditions. It is recovered by filtration and dried with hot air to give a solid containing typically 65–70% available chlorine. Careful handling and process control minimize mechanical and thermal degradation of the product.

Weaker products result from simple chlorination of lime slurry or solution, and up to 35% available chlorine can be achieved in bleaching powder. This is of declining industrial importance.

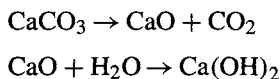
15.4. PRODUCTION OF CAUSTIC WITHOUT CHLORINE

15.4.1. Causticization of Soda Ash

In a process older than the electrochemical route, NaOH is produced by the causticization of soda ash. This is an equilibrium reaction between a solution of carbonate and solid hydrated lime:



Calcination of recovered byproduct CaCO_3 produces quicklime, and slaking then regenerates hydrated lime for recycle:



With the increase in demand for chlorine, the electrolytic route displaced this process. Several plants were built more recently in expectation of a long-term imbalance in the markets for caustic soda and chlorine. If this should come to pass, one may expect to see the construction of more chemical caustic plants.

The classical equilibrium constant for Eq. (42) would be written as

$$K = [\text{OH}^-]^2 / [\text{CO}_3^{2-}] \quad (43)$$

Since the calcium compounds have low solubilities, we can write their solubility products as

$$[\text{Ca}^{2+}][\text{CO}_3^{2-}] = K_1 \quad (44)$$

$$[\text{Ca}^{2+}][\text{OH}^-]^2 = K_2 \quad (45)$$

From Eqs. (44) and (45), we have

$$K_2/K_1 = [\text{OH}^-]^2 / [\text{CO}_3^{2-}] = K \quad (46)$$

The success of the process depends on the fact that the solubility product of lime (K_2) is much higher than that of limestone (K_1). Therefore, the value of K is high, and equilibrium conversions in turn can be rather high.

The forward reaction is driven by the carbonate concentration and the reverse reaction by the square of the hydroxyl concentration. The use of dilute solutions therefore favors the production of NaOH . A 10% solution of Na_2CO_3 , for example, has an equilibrium conversion of 96–97% when dry lime is added, while a 15% solution gives 91% and produces 2.5–3 times as much soluble carbonate residue. Too high a solution concentration also makes possible the production of a double salt of sodium and calcium rather than the desired CaCO_3 . On the other hand, low solution concentrations, while favoring equilibrium conversion, increase equipment sizes and in particular, increase the evaporative load per unit of product.

The reaction is nearly thermoneutral ($\Delta H = -2100 \text{ cal mol}^{-1}$), and so temperature has little effect on equilibrium. High temperature increases the rate of reaction and the rate at which CaCO_3 settles from the reaction product. The reaction therefore takes place at atmospheric pressure and close to the boiling point.

One version of the process involves:

1. Reaction of carbonate solution with lime slurry in agitated tanks. The lime gradually converts to limestone. For best results, several reactors are used, and the slurry cascades through them continuously.

2. Separation of the solids, primarily CaCO_3 , from the caustic solution. Primary separation is in a thickener that produces NaOH solution in the overflow and a suspension of solids in the caustic liquor in the underflow. The solids go to a second set of thickeners for washing with hot water and recycle filtrate (from step #3). The overflow, a dilute caustic solution, is used to prepare the process feed solution.
3. Filtration of the underflow from the second thickener. The filtrate, as noted, returns to step #2. The CaCO_3 returns to the trona plant (see below) or, in a dedicated caustic plant, to a lime kiln and slaker in order to prepare the calcium value for reuse. The second thickener overflow can also be used in the lime slaker.
4. Evaporation of the caustic solution from the first thickener (step #2) to final product concentration. In the production of 50% NaOH, the residual calcium salt drops from solution. This evaporation therefore is analogous to that of diaphragm-cell liquor (Section 9.3.3.3), but with a lower solids burden.

Reaction and phase separation can also be batchwise in a single vessel. This of course has a low productivity and would be practical, if at all, only at small scale. Some very old plants operated this way. The use of solutions recovered from previous batches as wash liquors improves process efficiency.

Paper mills may use this chemistry to recover caustic value, but large-scale chemical caustic production is usually integrated with sodium carbonate. The world's largest source of the latter now is natural trona, which is the dihydrate of the sesquicarbonate ($\text{Na}_2\text{CO}_3 \cdot \text{NaHCO}_3 \cdot 2\text{H}_2\text{O}$). By far the largest source is in Wyoming, in the western United States. There are also substantial deposits in Kenya. The Kenyan ore is contaminated with fluoride, and so another purification step is necessary in the process.

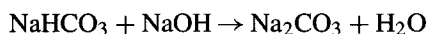
Processing of trona involves recrystallization to remove impurities and calcination to convert the bicarbonate portion to carbonate. There are two versions in commercial use. The older, or sesquicarbonate, process first hot-leaches the crushed ore to extract the mineral. This is followed by clarification, evaporation, and cooling. The refined trona is then calcined to form soda ash. The newer, or monohydrate, process first roasts the crushed ore to form a crude carbonate. This is dissolved and the solution evaporated to crystallize the monohydrate, $\text{Na}_2\text{CO}_3 \cdot \text{H}_2\text{O}$. Mild calcination then yields the anhydrous soda ash.

The monohydrate process is more energy-efficient. Because of the low solubility of trona, the dissolving and clarification steps in the sesquicarbonate process both are at a high temperature. The solution is more corrosive. The major disadvantage of the monohydrate process is the contamination of the carbonate solution with organics and minerals such as silicates. This makes a purge of the crystallizer mother liquor necessary. Its size depends on the extent of contamination.

As a matter of interest, we note that a relatively minor source of sodium carbonate is the solar evaporation of natural brines (cf. Section 7.1.3). Recovery from a concentrated solution is by carbonation with CO_2 . The precipitated bicarbonate is filtered and calcined to give the final product.

Mechanical mining of trona is similar to that of coal or salt (Section 7.1.2). Solution mining (Section 7.2.2.4) is an alternative. Because of the low solubility of the bicarbonate, the dissolving fluid is a dilute solution of NaOH. This converts the bicarbonate portion

of trona into the more soluble carbonate:



Production of a 30% solution of Na_2CO_3 theoretically requires about a 6% solution of NaOH .

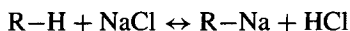
15.4.2. Salt Splitting by Ion Exchange

Various ion-exchange resins are capable of removing chloride and alkali metal ions from solution, and so conceptually it is possible to produce HCl and NaOH or KOH by this route. The practical problems easily foreseen with such a process include:

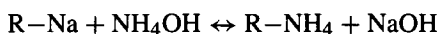
1. the selectivity of the ion-exchange medium for M^+ and Cl^- ions
2. the efficiency of regeneration
3. dilution of process materials in the course of an ion-exchange/regeneration cycle
4. disposal of used regeneration solutions
5. the stability of the ion-exchange medium
6. the disparity between market demands for HCl and NaOH

Nayak [89] reported work on a process that would remove most of the technical problems listed above, at least in the case of NaOH . The resin cycle includes:

1. exchange of Na^+ for H^+



2. exchange of NH_4^+ for Na^+



3. deammoniation of the resin



Absorption of ammonia in water makes it is ready for reuse in the second exchange step and closes the cycle.

The decomposition in step (3) requires a temperature of 400–500°C. This precludes the use of organic resins, and so Nayak used zeolites. Even so, conventional forms with Si/Al ratios less than 2 are not thermally stable under these conditions. High-ratio zeolites, such as ZSM-5, are preferred. Since ion exchange takes place at the Al sites, the capacities of these resins are rather low.

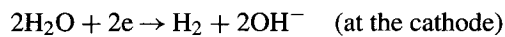
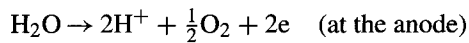
Nayak did not demonstrate an integrated process. Rather, he studied the three steps individually, in the batch mode, and proposed a continuous process involving moving beds of resin in series. Obstacles to commercialization include:

1. development costs
2. lack of market for stoichiometric quantities of HCl

3. low capacity of resin, particularly in step (1)
4. possible contamination of product solutions because of incomplete conversion of reactants

15.4.3. Electrochemical Methods

The electrolysis of sodium sulfate is a much-studied process for production of caustic soda without chlorine. When Na_2SO_4 electrolyzes in a divided cell, oxygen and hydrogen form at the anode and cathode, leaving H^+ and OH^- in the respective compartments. Dilute solutions of sulfuric acid and caustic soda form by the reactions



The overall reaction is the electrochemical decomposition of water.

With a porous diaphragm, it is difficult to achieve efficient separation of the acidic anolyte from the alkaline catholyte. The result is a significant loss of current efficiency. Also, the choice of a diaphragm resistant to both sulfuric acid and caustic soda and the selection of an anode stable in sulfuric acid solution are limited. These difficulties have retarded the development of sodium sulfate electrolysis.

Grube [90] was probably the first to study sulfate electrolysis in diaphragm and mercury cells. He used a porcelain diaphragm and a platinum–iridium anode in a vertical diaphragm cell and an asbestos diaphragm, deposited with barium sulfate paste, in a horizontal cell. The products were 3N H_2SO_4 and 3N NaOH , both containing Na_2SO_4 , at 0.6 kA m^{-2} and about 80% current efficiency. The cell voltage was high ($\sim 5 \text{ V}$).

Grube's horizontal mercury cell more closely resembled the standard salt electrolyzers and had an asbestos diaphragm between the electrodes in order to isolate the amalgam cathode from sulfuric acid. This cell produced pure caustic soda free of chloride ions from its amalgam decomposer. However, voltage and energy consumption still was high ($\sim 4,000 \text{ kW hr t}^{-1} \text{ NaOH}$).

The availability of perfluorinated membranes and DSA anodes has led to new developments in the electrochemical splitting of Na_2SO_4 . The anode for the oxygen evolution reaction is a DSA with iridium replacing at least some of the ruthenium in the oxide layers because of the greater resistance of IrO_2 to acidic solutions. In some cases, especially those involving high current density, Ta_2O_5 replaces the TiO_2 .

These anodes are used extensively in electrogalvanizing, tin electroplating, electrochemical production of copper foil for printed circuit boards, and electrowinning of copper and zinc [91–95]. The application of oxide-coated anodes to sodium sulfate electrolysis so far is small and is not a major driver of electrode development programs. However, environmental concerns associated with byproduct or waste sodium sulfate, along with possible imbalances in the demand for chlorine and caustic soda are enough to maintain interest in the technique.

Figure 15.18 shows that there are two types of membrane cells used to split Na_2SO_4 . In a cell divided by a cation-exchange membrane (A), purified and concentrated Na_2SO_4 solution is fed to the anode compartment. Oxygen is generated at the anode,

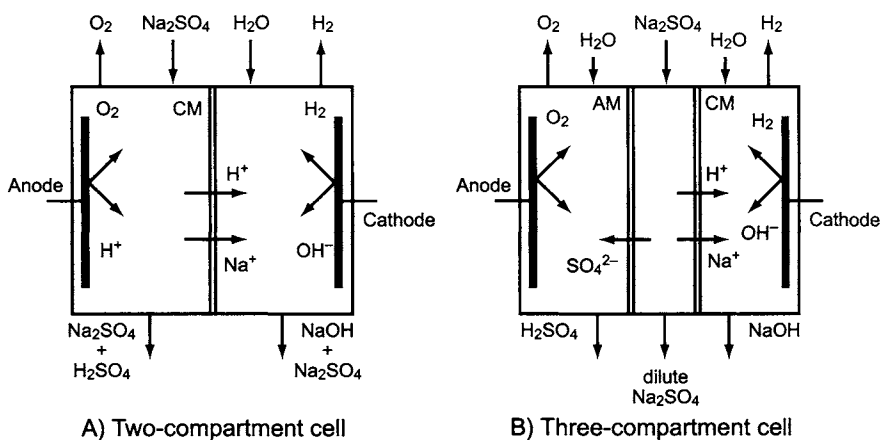


FIGURE 15.18. Electrolyzers for splitting sodium sulfate. AM: Anion-exchange membrane; CM: Cation-exchange membrane.

leaving H^+ ions. Sodium ions pass through the membrane into the cathode compartment. Hydrogen is generated at the cathode, along with NaOH . Some H^+ also passes through the membrane. It neutralizes some of the OH^- , reducing the current efficiency and the yield of NaOH . The catholyte is a usable form of caustic soda. The anolyte is a mixed solution of H_2SO_4 and Na_2SO_4 , which may or may not have a practical application. In the second cell design (B), concentrated Na_2SO_4 solution enters a central compartment between anionic- and cationic-exchange membranes. The electrode reactions, as in the two-compartment cell, are oxygen and hydrogen evolution. In this case, sodium ions again pass through the cationic membrane into the cathode chamber. This is a case of electrodialysis rather than electrolysis. The sulfate ions permeate the anionic membrane into the anode compartment. Theoretically, this cell can produce pure H_2SO_4 and NaOH solutions. The depleted sulfate from the central compartment recycles to the brine treatment process. Unfortunately, versatile and robust anion-exchange membranes comparable to the cation-exchange membranes used in chlor-alkali cells are not available. Consequently, most research and development efforts have been devoted to the electrolytic process using membranes such as Nafion[®] [96–103]. It would seem that this process requires further development in its application to solutions generated in chlorine plants. Development of a durable anion-exchange membrane would provide more process options and increase the probability of commercial success.

Because of the high thermodynamic decomposition voltage and the oxygen overvoltage, high energy consumption is characteristic of sulfate electrolysis. Substitution of a hydrogen-depolarized anode for the conventional type could reduce the cell voltage and hence the energy consumption [104].

DeNora Permelec S.p.A. has developed an electrolyzer (trade name Hydrina) with such an anode [104,105]. The first application has been the production of NaOH from Na_2CO_3 . The cell has three compartments, separated by a cation-exchange membrane on the cathode side and a porous diaphragm on the anode side (Fig. 15.19). The hydrogen generated at the cathode goes to the depolarized anode. Water is fed to the cathode

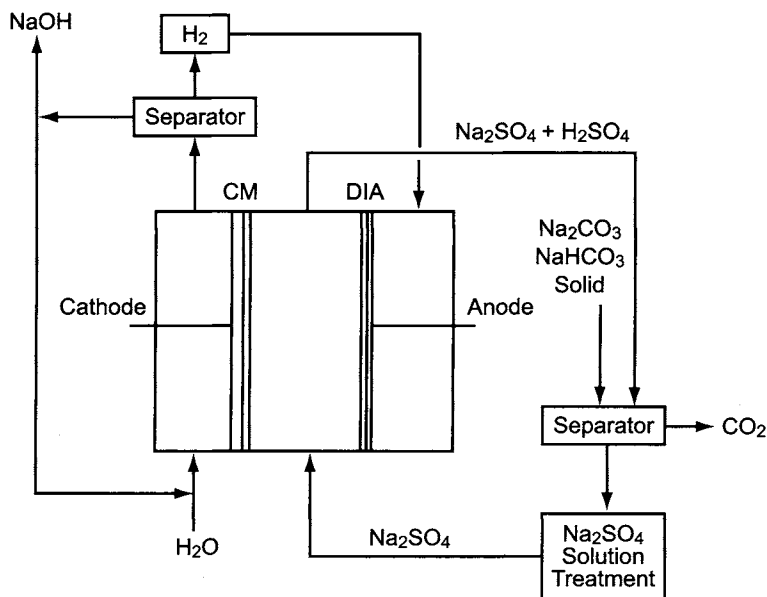
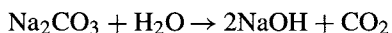


FIGURE 15.19. Electrochemical production of caustic soda from sodium carbonate/bicarbonate using Hydrina™ electrolyzer CM: Cation-exchange membrane; DIA: Diaphragm.

compartment, and caustic soda is recovered. The electrolyte fed to the central compartment is a solution of sodium sulfate. The mixed anolyte (Na_2SO_4 and H_2SO_4) goes to a reactor/separator for reaction with solid sodium carbonate or bicarbonate. This regenerates sodium sulfate for recycle to the cell. The overall reaction becomes



A second Hydrina process involves recovery and recycle of caustic soda and a mixed solution of Na_2SO_4 and H_2SO_4 . This is similar to the two-compartment cell of Fig. 15.18, but it uses the hydrogen-depolarized anode instead of the conventional type. A third version uses a three-compartment cell with the hydrogen anode [106,107]. Saturated Na_2SO_4 enters the central compartment, and water is added to the electrode compartments. The products are sulfuric acid and caustic soda of high purity.

Another technology involves the electrochemical splitting of sodium sulfate to form caustic soda and ammonium sulfate [102]. The addition of ammonia to the anolyte of a three-compartment cell forms ammonium sulfate, and the low acidity of the anolyte reduces the back-migration of H^+ from the anode compartment.

Thus, the development of durable anodes and versatile ion-exchange membranes has opened an opportunity for commercialization of sodium sulfate and electro dialysis. Various electrolyzers, processes, and applications have been proposed to handle byproduct sodium sulfate from various industries. Developers include ELTECH Systems Corporation [96] and Aquatech™ Systems [108]. An estimated capital cost for treating 100,000 tpy of Na_2SO_4 is \$200–250 MM [109].

REFERENCES

1. M. Blackburn, CMAI, Personal Communication (2002).
2. W.H. Sheltmire, Chlorinated Bleaches and Sanitizing Agents. In J.S. Sconce (ed.), *Chlorine: Its Manufacture, Properties, and Uses*, ACS Monograph 154 Robert E. Krieger Publishing Co., Huntington, NY (1972), p. 512.
3. T.F. O'Brien, *Regenerating Chlorine from Waste HCl*, Chloralkali Industry Update and Forecast, Consulting Resources Corp. conference, Philadelphia, PA (1996).
4. M.F. Fogler, The Salt Process for Chlorine Manufacture. In J.S. Sconce (ed.), *Chlorine: Its Manufacture, Properties, and Uses*, ACS Monograph 154, Robert E. Krieger Publishing Co., Huntington, NY (1972), p. 235.
5. C.P. Van Dijk, *Chem. Econ. Eng. Rev.* **4**(12), 42 (1972).
6. O. Lange (ed.), *Blüchers Auskunftsbuch für die chemische Industrie*, Walter de Gruyter and Co., Berlin (1926).
7. H. Deacon, *U.S. Patent* 85,370 (1868).
8. A. Redniss, HCl Oxidation Processes. In J.S. Sconce (ed.), *Chlorine: Its Manufacture, Properties, and Uses*, ACS Monograph 154, Robert E. Krieger Publishing Co., Huntington, NY (1972), p. 250.
9. C.W. Arnold and K.A. Kobe, *Chem. Eng. Progr.* **48**(6), 293 (1952).
10. H. Klebe, A. Meffert, and A. Longenfeld, *German Patent* 1,963,946 (1974).
11. C.P. Van Dijk and W.C. Schreiner, *Chem. Eng. Progr.* **69**(4), 57 (1973).
12. L.E. Bostwick, *Chem. Eng.* **83**(21), 86 (1976).
13. W.C. Schreiner, A.E. Cover, W.D. Hunter, C.P. Van Dijk, and H.S. Jongenberger, *Hydrocarbon Proc.* **53**(11), 151 (1974).
14. H.Y. Pan, R.G. Minet, S.W. Benson, and T.T. Tsotsis, *Ind. Eng. Chem. Res.* **33**, 2996 (1994).
15. H. Itoh, Y. Kono, M. Aijoka, S. Takesaka, and M. Katzita, *U.S. Patent* 4,803,065 (1989).
16. T. Kiyoura, Y. Kogure, T. Nagayama, and K. Kanaya, *U.S. Patent* 4,822,589 (1989).
17. R.G. Minet, S.W. Benson, and T.T. Tsotsis, *U.S. Patent* 4,994,256 (1991).
18. R.G. Minet, T.T. Tsotsis, and M. Mortensen, Economic and Environmental Aspects for a 60,000-ton per Year Plant for Chlorine Recovery from Hydrogen Chloride, *Ninth Large Plants Symposium*, Antwerp (1995).
19. V. Wong and S.H. Wang, *Chlorine from Hydrogen Chloride by the Carrier Catalyst Process*, PEP Review 94-1-3, SRI International, Inc., Menlo Park, CA (1995).
20. F.M. Berkey, Electrolysis of Hydrochloric Acid Solutions. In J.S. Sconce (ed.), *Chlorine: Its Manufacture, Properties and Uses*, ACS Monograph 154, Robert E. Krieger Publishing Co., Huntington, NY (1972), p. 200.
21. *Chlorine and Hydrogen from Acid by Electrolysis*, technical brochure, Krupp Uhde, Dortmund (1993).
22. F.B. Grosselfinger, *Chem. Eng.* **71**(19), 172 (1964).
23. S. Payer and W. Strewé. In T.C. Jeffrey, P.A. Danna, and H.S. Holden (eds) *Proceedings, Chlorine Bicentennial Symposium*, The Electrochemical Society, Princeton, NJ (1974), p. 257.
24. F. Hine, *Electrode Processes and Electrochemical Engineering*, Plenum Press, New York (1985), p. 129.
25. P. Gallone and G. Messner, *Electrochem. Technol.* **3**, 321 (1965).
26. W.C. Gardiner, *Chem. Eng.* **54**(1), 100 (1947).
27. H. Isfort and W.J. Stockmans. In M.M. Silver and E.M. Spore (eds), *Advances in the Chlor-Alkali and Chlorate Industry, Proceedings*, vol. 84-11, The Electrochemical Society, Princeton, NJ (1984), p. 259.
28. F. Hine, *Electrode Processes and Electrochemical Engineering*, Plenum Press, New York (1985), p. 87.
29. K. Schneiders and C. Herwig, Recycle of HCl to Chlorine, *38th Chlorine Institute Plant Operations Seminar*, Houston, TX (1995).
30. F. Federico, G.N. Martelli, and D. Pinter, Gas-Diffusion Electrodes for Chlorine-Related Technologies. In J. Moorhouse (ed.), *Modern Chlor-Alkali Technology*, vol. 8, Blackwell Science, Oxford (2001), p. 114.
31. *Chemical Week*, 10 March 2004, p. 22.
32. D.J. Eames and J. Newman, *J. Electrochem. Soc.* **142**, 3619 (1995).
33. J.A. Trainham and F.J. Freire, *Fifth World Congress of Chemical Engineering* (1996).
34. S. Motupally, D.T. Mah, F.J. Freire, and J.W. Weidner, *Interface* **7**(2), 32 (1998).
35. J.A. Trainham, C.G. Law, Jr., J.S. Newman, K.B. Keating, and D.J. Eames, *U.S. Patent* 5,411,641 (1995).

36. B.V. Tilak, P.W.T. Lu, J.E. Colman, and S. Srinivasan. In J. O'M. Bockris, B.E. Conway, E. Yeager, and R.E. White (eds), *Comprehensive Treatise on Electrochemistry*, vol. 2, Plenum Press, New York (1981), p. 1.
37. F. Hine, *Electrode Processes and Electrochemical Engineering*, Plenum Press, New York (1985), p. 87.
38. F.S. Low, *U.S. Patent* 2,486,766 (1949).
39. F.S. Low, *U.S. Patent* 2,470,073 (1949).
40. C.P. Roberts, *Chem. Eng. Progr.* **46**(9), 456 (1950).
41. F. Hine, S. Yoshizawa, K. Yamakawa, and Y. Nakane, *Electrochem. Technol.* **4**, 555 (1966).
42. F. Hine and K. Yamakawa, *Electrochim. Acta* **13**, 2119 (1968).
43. F. Hine and K. Yamakawa, *Electrochim. Acta* **15**, 769 (1970).
44. C.L. Mantell, *Electrochemical Engineering*, McGraw-Hill Book Co., New York (1960).
45. C.H. Lemke and V.H. Markant, *Kirk-Othmer Encyclopedia of Chemical Technology*, 4th edition, vol. 22, John Wiley & Sons, Inc., New York (1997), p. 134.
46. M. Sittig, *Sodium: Its Manufacture, Properties and Uses*, Reinhold Publishing Corp., New York (1956).
47. J.C. Downs, *Brit. Patent* 238,956 (1924).
48. T. Minani and S. Soda, *U.S. Patent* 4,192,794 (1980).
49. D.W.F. Hardie, *Ind. Chemist* **30**, 161 (1954).
50. D.A. Kramer, *Kirk-Othmer Encyclopedia of Chemical Technology*, electronic version, John Wiley & Sons, Inc., New York (2003).
51. D.W. Schroeder, *Ind. Eng. Chem. Proc. Des. and Devt.* **1**(2), 141 (1962).
52. Y. Ding and J. Winnick, *J. Appl. Electrochem.* **26**, 143 (1996).
53. F. Hine and M. Yasuda, *J. Electrochem. Soc.* **119**, 1057 (1972).
54. F. Hine, M. Yasuda, and M. Higuchi. In T.C. Jeffrey, P.A. Danna, and H.S. Holden (eds), *Proceedings, Chlorine Bicentennial Symposium*, The Electrochemical Society, Princeton, NJ (1974), p.278.
55. *Soda Handbook 1998*, Japan Soda Industry Association, Tokyo (1998), p. 365.
56. S.A. Michalek and F.B. Leitz, *J. Water Pollution Control* **44**, 1697 (1972).
57. C.J. Brockmann, *Electrochemistry*, D. Van Nostrand, New York (1931), p. 216.
58. C.L. Mantell, *Industrial Electrochemistry*, McGraw-Hill Book Co., New York (1960), p. 372.
59. C.L. Mantell, *Industrial Electrochemistry*, McGraw-Hill Book Co., New York (1960), p. 296.
60. E.J. Laubusch, Water Chlorination. In J.S. Sconce (ed.), *Chlorine: Its Manufacture, Properties and Uses*, ACS Monograph 154, Reinhold Publishing Corp., New York (1972), p. 457.
61. J.E. Bennett, *Chem. Eng. Progr.* **70** (12), 60 (1974).
62. B. Case and W.E. Heaton, Cooling Water Electrolysis at Coastal Power Stations. In *Local Generation and Use of Chlorine and Hypochlorite*, Society of Chemical Industry, London (1980).
63. N. Krstajic, V. Nakic, and M. Spasojevic, *J. Appl. Electrochem.* **17**, 77 (1987).
64. M. Rudolf, I. Rousar, and J. Krysa, *Electrochim. Acta* **40**, 169 (1995).
65. M. Rudolf, I. Rousar, and J. Krysa, *J. Appl. Electrochem.* **25**, 155 (1995).
66. Package assembled by Powell Fabrication and Manufacturing, Inc. from internal sources and related papers for authors' use (2003).
67. T.F. O'Brien, Emergency Vent Scrubbing Systems—Design; Operation; Hazard Analysis, *Seventh Annual Electrode Corporation Chlorine/Chlorate Seminar*, Cleveland, OH (1991).
68. L.J. Updyke, Emergency Vent Scrubbers, *5th Chlorine Plant Operations Workshop*, Houston, TX (1990).
69. G. Gordon and L. Adam, *Minimizing Chlorate Ion Formation in Drinking Water when Hypochlorite is the Chlorinating Agent*, published by AWWA Research Foundation; undated, supplied by Powell Fabrication and Manufacturing, Inc., (2003).
70. G. Gordon, L. Adam, and B. Bubnis, *J. AWWA* **87**(6), 97 (1995).
71. C.E. Redemann, *The Chemistry of Hypochlorous Acid and the Hypochlorites with Applications to Bleaching and Bleachmaking*, 2nd edition, Purex Corp. (1970).
72. T.V. Bommaraju, *Water Quality Res. J. Canada* **30**, 339 (1995).
73. B. Bubnis, *Suspended-Solids Quality Test for Bleach by Vacuum Filtration*, Novachem Laboratories, Oxford, OH (2001).
74. J.K. Nelson, Materials of Construction for Alkalies and Hypochlorites. In B.J. Moniz and W.I. Pollock (eds), *Process Industries Corrosion*, National Association of Corrosion Engineers, Houston, TX (1986), p. 297.
75. *FRP Storage Tanks for Sodium Hypochlorite*, Powell Fabrication and Manufacturing, Inc., St. Louis, MI (2003).

76. J.J. Gates, AnCor Plastics, Personal Communication (1989).
77. *Factors Affecting Performance of FRP in Sodium Hypochlorite Environments*, revised and updated from presentation to 25th Annual Technical Conference of the Reinforced Plastics/Composites Division of the Society of the Plastics Industry, Inc., in 1970, Reichhold Chemicals, Inc., Research Triangle Park, NC (1990).
78. H.F. Wachob, F. McGarry, and G.H. Abell, *The Effect of Sodium Hypochlorite on the Long-Term Performance of Rotationally Molded XLPE Storage Tanks*; undated, supplied by Powell Fabrication and Manufacturing, Inc., (2003).
79. G. Gordon and B. Bubnis, Bleach Stability and Filtration, *AWWA Water Technology Conference*, Boston, MA (1996).
80. *Sodium Hypochlorite Manual*, Pamphlet 96, Edition 2, Rev. 1, The Chlorine Institute, Inc., Washington, DC (2000).
81. H.A. Pham, *A Comparison of Methods for Determining the Concentration of Transition Metal Ions in Liquid Bleach*, thesis, Miami University, Oxford, OH (1997).
82. *ANSI/NSF 60/2001*, Issue 16, NSF International, Ann Arbor, MI (2001).
83. T.H. Hutchinson and D.J. Van Wijk, Bromate and Chlorate—Evaluation of Potential Effects in Aquatic Organisms and Derivation of Environmental Quality Standards. In S. Sealey (ed.), *Modern Chlor-Alkali Technology*, vol. 7, Royal Society of Chemistry, Cambridge (1998), p. 26.
84. V.A. Grinberg, A.M. Shundin, E.K. Tuseeva, D.P. Aleksandrova, Yu.B. Khokhryakov, V.I. Sergienko, and A.K. Mantynov, *Russian J. Electrochem.* **33**, 577 (1997).
85. V.A. Grinberg, A.M. Shundin, and E.K. Tuseeva, *Russian J. Electrochem.* **34**, 1079 (1998).
86. A. Kraft, M. Stadelmann, M. Blaschke, D. Kreysig, B. Sandt, F. Schröder, and J. Rennau, *J. Appl. Electrochem.* **29**, 861 (1999).
87. A. Kraft, M. Stadelmann, M. Blaschke, D. Kreysig, B. Sandt, F. Schröder, and J. Rennau, *J. Appl. Electrochem.* **29**, 895 (1999).
88. K. Scott, *Electrochemical Processes for Clean Technology*, Royal Society of Chemistry, Cambridge (1995), p. 189.
89. V.S. Nayak, *Ind. Eng. Chem. Res.* **35**, 3808 (1996).
90. H.G. Grube, *Z. Electrochem.* **44**, 640 (1938).
91. M. Yamashita, F. Hine, and S. Yoshizawa, *Denki Kagaku (J. Electrochem. Soc. Japan)* **32**, 366 (1964).
92. M. Yamashita, F. Hine, and S. Yoshizawa, *Denki Kagaku (J. Electrochem. Soc. Japan)* **30**, 562 (1962).
93. W.N. Brooks, D.A. Denton, and N.M. Sammes. In F. Hine, B.V. Tilak, J.M. Fenton, and J.D. Lisius (eds), *Process Performance of Electrodes for Industrial Electrochemical Processes*, **PV 89–10**, The Electrochemical Society, Pennington, NJ (1989), p. 39.
94. C.G. Ferron and P.F. DUBY. In F. Hine, B.V. Tilak, J.M. Fenton, and J.D. Lisius (eds), *Process Performance of Electrodes for Industrial Electrochemical Processes*, **PV 89–10**, The Electrochemical Society, Pennington, NJ (1989), p. 259.
95. G.N. Marteni, R. Ornelas, and G. Faita, *Electrochim. Acta* **39**, 1551 (1994).
96. M.J. Niksa, Acid/Base Recovery from Sodium Sulfate, *Fifth International Forum on Electrolysis*, Clearwater, FL (1990).
97. A.D. Martin, Electrodialysis—A Means for Recovery of Sodium Hydroxide from Sodium-Containing Process Streams, *Fifth International Forum on Electrolysis*, Clearwater, FL (1990).
98. J. Jörissen and K.H. Simmrock, *J. Appl. Electrochem.* **21**, 869 (1991).
99. G. Faita, Caustic Soda without Chlorine Production, *Seventh International Forum on Electrolysis*, Clearwater, FL (1993).
100. A.D. Martin. In T.C. Jeffrey, K. Ota, J. Fenton, and H. Kawamoto (eds), *Chlor-Alkali and Chlorate Production, and New Mathematical and Computational Methods in Electrochemical Engineering*, **PV 93–14**, The Electrochemical Society, Princeton, NJ (1993), p. 65.
101. A.D. Martin and D.H. Mann, *Electrohydrolysis of Sodium Sulfate*, Special publication, Royal Society of Chemistry, Cambridge (1995), p. 274.
102. J.P. Gender, D. Hartsough, and J. Thompson. In J. Newman and R.C. White (eds), *Proceedings, Douglas N. Bennion Memorial Symposium, Topics in Electrochemical Engineering*, **PV 94–22**, The Electrochemical Society, Pennington, NJ (1994), p. 457.
103. M. Rakib, Ph. Mocotaguy, Ph. Viers, E. Petit, and G. Durand, *J. Appl. Electrochem.* **39**, 1439 (1999).

104. S. Holze, J. Jörissen, C. Pischen, and H. Kalvelege, *Chem. Eng. Technol.* **17**, 382 (1994).
105. *Hydrind™ Membrane Electrolyzers*, Brochure, DeNora Permelec S.p.A., Milan (1993).
106. D. Pletcher, D. Genders, N.L. Weinberg, and E.F. Spiegel, *U.S. Patent* 5,246,551 (1993).
107. J.S. Thompson and D. Genders, *U.S. Patent* 5,098,332 (1992).
108. K.N. Mani, Aquatech Systems, Inc., Personal Communication (1995).
109. T.V. Bommaraju, Unpublished Results (1998).

16

Environmental Safety and Industrial Hygiene

16.1. GENERAL INTRODUCTION

Safety considerations are inseparable from the principles of good design and operation and so have been a constant theme in our discussion of the chlor-alkali process. The preceding chapters deal with the practical details of direct protection of personnel in the workplace. They refer frequently to the programs and publications of various organizations with special interest in industrial safety. Other publications [1,2] also discuss operating safety and provide guidance in design and operation. In this chapter, we consider safety more generally and also provide more quantitative information on hazard levels. To put those hazards in perspective and show the degree of success the industry has had in coping with them, consider the following [3]:

1. In 40 years of production, transport, and use in Western Europe, the number of fatalities caused by exposure to chlorine is equal to the number of road fatalities on a typical weekend in Belgium
2. A chlorine plant worker faces the following relative risks of accidental death

At work	1
At home	5
In an automobile	11

These are calculated from Van Diest's data [3] on the arbitrary assumption of 45 hr spent at work, 110 hr at home, and 13 hr in an automobile. In the 1930s, 11 fatalities occurred in the industry per million tons of chlorine produced worldwide. By the 1980s, it had dropped to 0.15 (0.04 in the Euro Chlor (EC) countries). The 1.5 fatal accidents suffered in 10^8 exposure hours compare favorably to 3 in the chemical industry as a whole and 5 in all manufacturing industry.

After discussing the hazards associated with various materials and process conditions in Sections 16.2 and 16.3, this chapter turns to the prevention and the mitigation

of accidents (Section 16.4). Personal protective equipment (PPE) and administrative programs are both covered. There is an emphasis on process safety management (PSM) and hazard analysis programs. Finally, we discuss methods to reduce the effects of the release of chlorine. The chapter closes with a discussion of waste minimization and disposal (Section 16.5). While this covers all the principal wastes from a chlor-alkali plant, it concentrates on those containing mercury.

There are many ways in which toxic materials may act to harm the body and several ways in which they may be enabled to do harm. The latter include contact, ingestion, and inhalation. A given material can present a hazard by all three routes (hydrochloric acid is an example), but more frequently one route predominates. Materials such as sulfuric acid and caustic soda or potash are corrosive to tissue and are primarily contact hazards. The familiar major episodes with mercury are due to ingestion. Chlorine and asbestos are primarily inhalation hazards.

An ingested or inhaled material usually requires a bodily process to spread throughout the system or to reach an organ where it accumulates. At the same time, some is eliminated from the body or rendered harmless. It is therefore possible to establish safe limits for most materials below which conversion and elimination prevent dangerous accumulation. These limits appear throughout the literature and on material safety data sheets (MSDS). Contact hazards, on the other hand, usually act locally and immediately. These hazards can be mitigated by dilution, but this reduces the usefulness of most materials and is not a practical approach in a production area.

Ingestion hazards are not a major issue in the workplace. Rarely does someone drink from a beaker of sulfuric acid. There is a first line of defense against inhalation hazards. Their concentrations in the environment can for the most part be kept below dangerous levels. PPE is the second line, used in case of release or infrequent work in a hazardous situation (e.g., opening of equipment or pipelines). Complete protection against contact hazards requires absolute prohibition. Methods for achieving this include confinement of the hazard, good work practices, and the use of protective equipment.

With its many references to safety regulations and supervisory agencies, this chapter is especially rich in abbreviations and acronyms. A glossary of some of these terms is included at the end of the chapter.

16.2. MATERIALS HAZARDS

The subsections that follow cover the hazards associated with the various materials used and produced in a chlor-alkali plant. These include chlorine, hypochlorites, caustic soda and potash, hydrogen, hydrochloric acid, sulfuric acid, mercury, asbestos, nitrogen trichloride, and miscellaneous materials.

Exposure limits for toxic materials in the atmosphere often appear as Threshold Limiting Values (TLVs) or their equivalents. TLVs are not official or consensus standards [4], and their publishers advise against adopting them as a matter of course. They should be viewed as one source of data, fixed without regard to cost-benefit analysis or

the practicability of measurement. Several different measures exist:

TLV-TWA	Time-weighted average
TLV-STEL	Short-time exposure limit
TLV-C	Ceiling

The TWA is set assuming a 7–8-hr working day and a 40–45-hr working week and is usually based on atmospheric conditions of 25°C and 760 mmHg. The STEL allows excursions above the TWA. Regulations in the United States allow up to four excursions a day of no more than 15 min each, with at least an hour between excursions. The STEL is set to prevent (1) intolerable irritation, (2) chronic or irreversible tissue change, and (3) narcosis sufficient to promote accidents, impair self-rescue from a hazardous area, or reduce work efficiency. The ceiling concentration is just that; no excursions of any duration above TLV-C are permitted.

TLVs are set by various competent authorities and may vary from one part of the world to the next. A toxic material may be assigned only one or any combination of the three parameters defined. With the shortage of data involving human exposure to these materials, the process of arriving at a TLV is highly judgmental. In any event, specific values of TLV do not become reliable design parameters. Design engineers follow evolving standards and good practices to arrive at a safe design, always keeping in mind the fact that TLVs are usually set for normally healthy individuals. A diverse work force of any size will have individual members who are more sensitive than the average to various kinds of exposure.

16.2.1. Chlorine and Hypochlorites

The corrosiveness of wet chlorine is due to its hydrolysis to hydrochloric and hypochlorous acids. The latter has its own corrosive properties. The combination of the two acids is therefore more potent than HCl alone, and some of the corrosive properties remain after neutralization and the formation of the free hypochlorite ion. Hypochlorites, when contacted with strong acid, also revert to molecular chlorine, which is easily released from solution. Hypochlorites, therefore, must be treated as potentially very toxic, with special precautions to prevent their exposure to acids.

There is copious literature on the toxic effects of chlorine, not reviewed here. This includes direct studies of toxicity, calculations of the spread and consequences of the releases of gas, and accounts of some of the major accidents and other incidents that have occurred.

16.2.1.1. *Nature of the Hazard.* Standard hazard ratings for chlorine are:

Health	3
Flammability	0
Reactivity	1

These ratings follow the National Fire Protection Association (NFPA; USA) Standard 704, which designates the severity of each of these hazards on a 0–4 scale. The health rating, for example, corresponds to “extreme danger.” These ratings appear on familiar labels applied to containers, storage tanks, operating equipment, and enclosed storage areas. The numbers are placed on the four corners of a diamond and are often color-coded for instant identification (e.g., the health hazard is on a blue background). While chlorine is not a fire hazard in itself, it reacts violently with many materials and can cause fires. Proper care in handling and storage in isolation from these materials control this hazard. Chlorine is a strong oxidizer, and its reaction with other materials can also generate dangerous byproducts. The major concern with chlorine, however, is its rating as an extremely dangerous health hazard. It irritates mucous membranes, the respiratory tract, and the eyes. Inhalation produces coughing, burning, vomiting, chest pain, headache, anxiety, and feelings of suffocation. It can permanently damage bodily membranes, and its ultimate action on the lungs is to produce pulmonary edema and death. The effects can be related to its concentration [5]:

0.2–0.5 ppm	No toxic long-term effect
1–3 ppm	Odor; irritation of eyes and nose
5–8 ppm	Throat, eye, and mucous membrane irritation
30 ppm	Intense coughing fits
34–51 ppm	Lethal in 1–1.5 hr
40–60 ppm	30–60 min without effective respiration can cause bronchitis, bronchopneumonia, or edema
100 ppm	May be lethal after 50 min
430 ppm	Lowest level known to be lethal in 30 min
1,000 ppm	May be fatal with a few deep breaths

Chlorine is not an insidious hazard. Its maximum allowable concentration is more than 10 times its odor threshold [6]. This is a relatively high ratio. The ratio for ammonia, for example, is less than five and for toluene, less than one. The odor threshold and the level at which the presence of chlorine becomes intolerable depend not only on the individual but also on a host of other variables. Notwithstanding this complexity, the World Health Organization (WHO) reports that it is generally accepted that chlorine, when present at undetectable levels, has no effect on human reflexes [7].

The WHO report also summarizes a number of studies on industrial workers exposed to chlorine. While the pattern is a bit confusing, the conclusion from any study that included a control group is that there are no chronic effects that can properly be attributed to chlorine.

16.2.1.2. Monitoring for Exposure to Chlorine. Medical surveillance of workers for the effects of exposure to chlorine is valuable, but real-time field monitoring is more proactive. Area monitoring to discover and track leaks has already been mentioned as

a useful technique. The topic in this section is the individual monitoring of workers for exposure to chlorine. The best approach for personal monitoring is full-period sampling, and EC [8] lists a number of lightweight electrochemical sensors that can be worn by employees. These generally have data-logging functions and software that can download the data for recording and analysis. The sensors usually operate under constant voltage and respond to chlorine that permeates a plastic membrane into a liquid electrolyte. This mechanism makes the instruments sensitive to other halogens and to gases such as HCl, HF, and ClO₂.

There must be a clear definition of what is to be considered dangerous or unacceptable. EC's approach is to use short-term exposure data and to compare them to the STEL, which it defines as the maximum acceptable TWA concentration over a 15-min period. The anticipated value, somewhat conservative, is 0.5 ppm. At the time of publication of this standard, various national exposure limits were between 0.5 and 1.0 ppm, averaged over an 8-hr day, with STELs most frequently at 1.0 ppm.

The reliability of a database is enhanced and the administrative burden eased by grouping workers who have similar duties or who work in proximity to each other. Each of these Similar Exposure Groups (SEGs) will have a certain exposure profile. Health and safety analysts then can use pooled exposure data to determine the probability that a member of any given SEG has encountered a particular risk. Once an adequate database is available and a clear frequency distribution emerges, EC recommends the following:

1. if the probability of the atmospheric concentration of chlorine exceeding the STEL is less than 0.1% and if it can be shown that the data are representative for the long term, further measurements are unnecessary;
2. if the probability of exceeding the STEL lies between 0.1% and 5%, exposure is acceptable but monitoring must continue, with repeat measurements at defined intervals;
3. if the probability of exceeding the STEL is greater than 5%, exposure is unacceptable, and control measures are necessary.

The threshold value of 5% probability of exceeding the STEL follows the recommendation of Annex D of the European Standard EN 689.

Title 29 of the Code of Federal Regulations (CFR; USA) defines the employee exposure as that which would occur in the absence of respiratory protection. One line of defense in any activity in which there is a relatively high probability of exposure to high concentrations of atmospheric chlorine is to require the use of respirators (Section 16.4.1).

16.2.1.3. Protective Equipment. Section 16.4.1 discusses safety equipment in general and gives some guidelines for the use of PPE when exposure to chlorine is possible. The first line of defense against exposure to chlorine gas is the ubiquitous mouthpiece respirator. No one should be present on a chlorine plant or chlorine-using facility without one of these. However, their function is strictly to permit escape from a contaminated area. When someone must work in an area where chlorine gas may be present, some way of supplying uncontaminated air is necessary. The work may be standard maintenance

TABLE 16.1. Characteristics of Respiratory Equipment

Type of respirator	Classification	Characteristics
Self-contained breathing apparatus (SCBA)	Atmosphere-supplying	Highest level of protection against airborne contaminants and oxygen deficiency. Highest level of protection under strenuous work conditions
Positive-pressure supplied-air respirator ^a (SAR)	Atmosphere-supplying	Less bulky and heavy than SCBA. Weighs less than 2.5 kg ^b Enables longer work periods than SCBA
Air-purifying respirator	Air-purifying	Enhanced mobility. Lighter than SCBA. Weighs less than 1 kg ^c Air supply from cylinder. Highest level of protection
Open-circuit SCBA	Entry-and-escape	Air supply from cylinder. Highest level of protection. Heavier than closed-circuit type. Shorter operating time
	Escape only	Weighs less than 5 kg. Provides only 5–15 min of protection

Notes:^a Also called air-line respirator.^b Add 5 kg if escape SCBA is provided.^c Without power unit.

or it may be connected with an emergency. The fundamental decision to be made here is whether to use a self-contained breathing apparatus (SCBA) or to rely on an external supply. Table 16.1 summarizes a comparison of several types of apparatus [9].

The basic deficiencies of a SCBA are its limited supply of air and the need for the worker to carry a bulky, heavy weight (typically 15 kg). The use of an air-line respirator attached to a compressed air line seems to remove these problems. However, the supplied-air respirator (SAR) has several deficiencies of its own:

1. possible damage to the supply hose
2. kinking or snagging of the hose, reducing the rate of supply of air
3. loss of pressure at the source
4. still some reduction in mobility
5. need to retrace steps in order to leave an area

Because of its limitations, the SAR is not recommended for use in situations that can be immediately dangerous to life or health without some other protection to allow escape as the last resort.

16.2.1.4. Environmental Fate of Chlorine. Most of the chlorine released to the atmosphere reacts to form HCl. This returns to the earth as acid rain and must be accounted for in evaluating that phenomenon. The HCl concentration in rain in the United States typically is 0.15–0.2 µgpl [10]. Using the higher number, one calculates that, in a year of average precipitation [11], the city of Chicago receives about 100 kg of HCl. The total chlorine acid rain burden is less than 1% of that due to SO₂, but it is still a factor in the corrosion of buildings, etc. [12].

16.2.2. *Caustic Soda and Potash*

Caustic soda and potash are classified as corrosive materials. While they are generally regarded as stable, they rapidly attack and destroy leather, wool, and aluminum, zinc, tin, and their alloys. Reaction with the metals can produce hydrogen and create an explosion hazard. Neutralization with strong acids is highly exothermic, and so is dilution. In all forms of storage, caustic materials should be kept separate from acids.

The major hazard with caustic solutions is bodily contact [13]. Both NaOH and KOH are very strong alkalis and are corrosive to human tissue. A concentration of 1 mg m^{-3} of NaOH in the air, as mist or dust, can cause mild watering of the eyes. A concentration of 2 mg m^{-3} is taken as an average or a ceiling exposure limit. The National Institute of Occupational Safety and Health (NIOSH) now lists 10 mg m^{-3} as immediately dangerous to life or health (changed from 250 mg m^{-3} c.1995). Those who work with these materials must also be alert to delayed symptoms, as minor contact may not produce immediate effects.

The use of PPE depends on the sorts of operation undertaken [14]. Equipment is sometimes covered by regulation (e.g., in the United States, CFR Title 29, Parts 1910.132–134 and 262). Typical items are hard hats, splash goggles, full-face shields, rubber boots and gloves, etc. Note that because of its reactivity, leather is not suitable for footwear. Contact of leather with caustic solutions can be an insidious hazard, as the reaction is slow and its effects may not be seen for some time.

Training is a vital part of the safety program for those exposed to caustic. It should meet all regulatory requirements and cover all aspects necessary for each job involved. Plant programs must also include reporting procedures for all incidents and an emergency response procedure.

Mercury-cell caustic carries the incidental hazard of its mercury content. The hazards of mercury are the subject of Section 16.2.6. Filtration of caustic to remove mercury is part of the subject of Section 9.3.2.6. With proper handling, the mercury content of filtered caustic is quite low, and according to the Environmental Protection Agency (EPA) of the United States [15], all the mercury in NaOH and KOH solutions amounts to less than 0.2% of the total anthropogenic release.

16.2.3. *Hydrogen*

The major hazard with hydrogen is its wide explosive range in air. Section 9.1.11.1 pointed out that hydrogen also forms explosive mixtures with chlorine and discussed measures to control this hazard.

Other than being a simple asphyxiant, hydrogen does not present a personal hazard. Therefore, it is not discussed further in this section.

16.2.4. *Hydrochloric Acid*

The term “hydrochloric acid” properly refers to aqueous solutions of hydrogen chloride, and the material is sometimes referred to as muriatic acid. Certain plants produce the anhydrous form for sale. Otherwise, it is not a frequent hazard in the chlor-alkali industry and so is not considered here.

Hydrochloric acid is a strong acid that reacts readily with metals and their oxides, many organics, and alkaline materials. Its dilution is quite exothermic, and the partial pressure of HCl vapor over concentrated solutions is substantial and produces an inhalation hazard. The acid reacts rapidly with bodily tissue, and prevention of contact with any part of the body is essential. Short exposure to the skin can cause severe burns, and contact with the eyes causes lachrymation and severe irritation of the cornea. This can result in permanent impairment or loss of vision. The ceiling concentration of HCl in the air is usually set at 5 ppm. A 32% solution of HCl at 30°C exerts a partial pressure of about 50 mm Hg, giving a concentration of more than 13,000 times as large as the TLV-C just mentioned. Confinement of vents, including those from storage tanks that hold concentrated acid, is necessary.

Grossel [16] discusses the safe handling of HCl solutions. Grossel [17] and Gallant [18] describe proper techniques for pumping and transferring toxic liquids and for training operators in these techniques. Section 7.5.6.2 describes in some detail the requirements for HCl used in the acidification of brine. It also discusses materials of construction and the design of handling facilities.

16.2.5. Sulfuric Acid

The major hazard associated with sulfuric acid is its rapid destruction of bodily tissue. Protective equipment is essential. The types and extent of protective equipment depend on the activity that is undertaken. Supplier data sheets should be used to specify the gear used in each operation involving sulfuric acid. Grossel [19] also covers this subject. Section 9.1.4.4 discusses the precautions necessary when handling sulfuric acid.

Secondary hazards are the breathing of acid mists and the possibility of fire caused by reaction of the acid. The ease with which sulfuric acid forms mists and the types of apparatus used to control them have already been mentioned in Section 9.1.5. The threshold limit has been set at 1 mg m^{-3} . Most people easily recognize mists of this concentration. Concentrations of 5 mg m^{-3} are highly unpleasant and are detected immediately. The acid itself is nonflammable, but contact with a strong acid can lead to ignition of combustible materials. The acid also reacts with many metals to release hydrogen gas.

Oleum, which is found infrequently in chlor-alkali plants, is an enriched form of sulfuric acid containing free SO_3 . It is characterized by its SO_3 concentration or referred to as “X% acid” with $X > 100$. It has all the hazards of H_2SO_4 in addition to that of an objectionable vapor concentration of SO_3 .

Sulfuric acid must also be handled as a waste product from the drying columns. The hazard of dissolved chlorine appears while all the hazards mentioned above remain.

16.2.6. Mercury

The toxicity of mercury has long been recognized, and the most widely known example is the syndrome found among felt workers, primarily in the 19th century. This became famous through Carroll’s Mad Hatter. Early scientific workers made extensive use of mercury. Being unaware of its hazards, they were often quite careless in their handling of the metal. Isaac Newton’s breakdown in the 1690s has been attributed to mercury

poisoning (traces of mercury were detected in his hair), and it has been suggested that Michael Faraday's health problems were also due to mercury exposure [20,21]. While direct exposure to mercury vapor was responsible for these problems, more recent serious incidents have involved ingestion of organomercury compounds. An example is the Minamata Bay experience in Japan, which was the result of the accumulation of 5–20 ppm of mercury in seafood [22]. A major source was the dumping of a mercury-based catalyst used in the production of acetaldehyde. An outbreak in Iraq in 1972 resulted from eating bread made from seed wheat treated with a methyl mercury fungicide.

In the 1970s, high levels of mercury were found in fish taken from Lake St. Clair, which lies between the United States and Canada. Chlorine plants that dumped depleted brine into the waterways were among the contributors. Before these incidents, many assumed that the very low solubility of mercury meant that it would have great difficulty entering the food chain. However, it can be assimilated by certain water-borne bacteria and converted into methyl mercury and its compounds. Eventually, mercury appears in the fatty tissue of fish, concentrated more than 1,000 times. It continues to concentrate as it works its way through the food chain. In a recent development, the EPA adopted a new criterion for water quality based on the level found in fish. The level of 0.3 ppm is equivalent to 7 ng L^{-1} in the water, a 7-fold reduction from the previous standard. This is said to be the first standard based on accumulation of a substance in marine life rather than on its concentration in the water [23].

16.2.6.1. Mechanisms. Mercury is a ubiquitous pollutant with many sources, both anthropogenic and natural. Natural emissions to the atmosphere, as reported by the WHO, are an estimated 2,700–6,000 tons/year [24]. Human actions contribute another 2,000–3,000 tons/year. Mercury, in its various forms, is also highly persistent and is a bioaccumulator. The Chlorine Institute (CI) [25] has published an extensive review of its sources and its toxicology. EC [26] has adopted a code of practice to control the exposure of workers to mercury.

There are two primary reasons for concern over human exposure:

1. direct exposure of workers to the metal and its vapor
2. bioaccumulation of mercury and exposure of the public to ingestion of organomercury compounds with foods

The body will absorb about 90% of the elemental mercury in inhaled air. Corresponding to its unique status among metals of being a liquid at subambient temperature, mercury has a relatively high vapor pressure. At 30°C, it is 0.0028 mm Hg. The equilibrium concentration of the vapor in air thus is about 3.5 ppm or 28 mg m^{-3} . Based on lowest observed adverse effect levels (LOAELs), the WHO's estimated guideline for the concentration of mercury in air was $1 \text{ } \mu\text{g m}^{-3}$, less than 0.5% of the equilibrium concentration above the metal. Accepted values of the TLV-TWA are more than another order of magnitude lower, at 0.025 or 0.05 mg m^{-3} . The smaller of these represents a partial pressure more than 1,000 times smaller than the vapor pressure. Good ventilation in a mercury-handling facility is essential, and Section 16.5.5.2 will refer to recent improvements in the containment of mercury vapor.

On a grand scale, mercury released into the atmosphere can be the cause of elevated concentrations in bodies of water. Most of it is scrubbed from the air by rainfall. In a 1990 report, this route accounted for about one third of the total pollution of water by mercury [27].

The toxic effects of mercury depend on its chemical state. The organomercury compounds that form through biological action are generally toxic and have been responsible for the most notorious incidents leading to restrictions on chlor-alkali plant operations. Their efficient absorption by the body makes them more dangerous. Most methyl mercury compounds, for example, are nearly completely absorbed in the gastrointestinal tract. Most of it accumulates in the brain. In aqueous solutions, mercuric ions are the toxic species. In contrast to the organic forms, only about 10% of ingested inorganic mercury is absorbed, and that accumulates in the kidneys. The nervous system is the most sensitive part of the body to acute exposure to very high concentrations of mercury, which can cause loss of memory, insomnia, irritability, excessive shyness, and emotional instability [26].

The danger of inhaled mercury vapor (elemental or metallic mercury) is in its ability to penetrate the brain by way of the bloodstream. There, it disrupts the metabolic processes. The liver and kidneys are other major organs of deposition. Furthermore, mercury is retained in the body and eliminated very slowly. Rates of elimination vary with the organ involved. Significant levels can remain in the brain, for example, many years after exposure has stopped [26].

The metal can also be absorbed in some quantity through the skin. Allergic contact dermatitis is possible, but rare. Mercury is classified neither as a carcinogen [28] nor as a reprotoxin [29], but it can cross the placenta and the fetal blood/brain barrier. Pregnant and nursing mothers should undergo a risk assessment before working with mercury [30].

Table 16.2 [31] summarizes the exposure of a hypothetical average person to the three principal forms of mercury. The largest numbers are associated with dental amalgam and the eating of fish. While estimates of the intake of mercury vapor from dental fillings show rather extreme variations [31,32], they are said to account for 90–99%

TABLE 16.2. Retention of Mercury by an Average Person^a

Source	Form of mercury		
	Elemental	Inorganic	Organic
Atmosphere	30–160 ^b	0	0
Drinking water	0	5	0
Food: fish	0	60	2300
Food: non-fish	0	0	?
Dental amalgam	3–17,000 ^c	0	0

All data in ng/day.

^a Weight = 70 kg; retention of mercury from various sources estimated to be: elemental, 80%; inorganic, 10%; organic, 95%

^b Extremes are typical of rural and urban environments, respectively.

^c Estimate of Olsson and Bergman [32] shows only 2000 ng/day.

of the total exposure to the element. While intake from the atmosphere then appears to be relatively minor, and most of that source is a product of natural release, there is no case for less vigilance in control of industrial emissions. Much of the mercury released into the air returns dissolved in precipitation, finally to be converted into methylmercuric compounds by marine life. The concentration factor for methylmercury (fish tissue/water) is 10–100,000 [33].

16.2.6.2. In-Plant Surveillance. A good medical surveillance program will include pre-employment examinations of all employees and periodic checkups. Those whose duties are most likely to expose them to mercury should be tested at least annually. Medical surveillance should be supplemented by analyses of plant products, emissions, and effluents and by an environmental monitoring program. Employee monitoring may be on a personal basis or by way of atmospheric measurements.

The level of mercury in the blood is a good indicator of short-term effects. It is a useful tool when a severe exposure is suspected. Mercury in urine tracks long-term exposure more accurately and reflects the average kidney burden over a period of 2–4 months. The test is noninvasive and has become the industry standard. Analysis is based on spot samples. There are known to be diurnal variations, and the concentration of the urine itself is a factor in the level of mercury. While the diurnal variations are a small part of the total variance of the procedure, they are easily and conveniently eliminated by standardizing the time of day for collecting samples. External contamination also is avoided by taking samples at the beginning of a shift or, after showering, at the end. Variations in urine concentration are offset by normalizing the mercury analysis against creatinine. This is a component of urine that is taken as an indicator of the total dissolved concentration. The criteria for action are:

$\mu\text{g Hg/g creatinine}$	Action
<50	None
50–100	Review employee work practices and use of PPE
>100	Remove employee from exposure until level is below 75 and confirmed by second week's sample

An annual average below about 35 for an SEG should produce a minimum number of cases above 50 $\mu\text{g Hg/g creatinine}$. Mercury levels are sometimes high because of dental amalgam. This is a fact to keep in mind and to investigate if certain workers consistently show abnormally high levels.

16.2.6.2A. Area Monitoring. Monitors should be distributed throughout the workplace, with one measuring point for every 200–400 m^2 of floor area. They should be concentrated in the locations where workers spend most of their time. The sample points should

be at breathing level. There will be diurnal variations in concentration due to temperature, work patterns, etc. Therefore, best results require periodic measurements at intervals to reflect the entire day. Analytical data of vapor concentration usually have an approximately lognormal distribution. Use of the geometric mean is satisfactory for a small number of samples (<30). The simplest record will show what percentage of the results is below the accepted standard, with 95% usually deemed acceptable (see Chlorine, Section 16.2.1.2). It is also useful to record percentages above and below other levels (e.g., 0.3 or 0.5 and 2.0 or 3.0 times the standard) to discover any trends. The desirable frequency of sampling depends on the level of contamination. If concentrations are 0.1–0.5 times the standard, an interval of one or two months is acceptable. If concentrations are 0.5–1.0 times the standard, measurements should be made every one or two weeks.

16.2.6.2B. Personal Monitoring. While exposure to materials such as chlorine and caustic is “self-reminding” because of their rapid effects on the body, exposure to mercury is not [34]. Effective personal monitoring therefore is essential. As with chlorine, monitoring a plant population for exposure to mercury can be more effective if the workers are divided into SEGs. Individuals from each group should be selected for monitoring. The goal should be 90% confidence of selecting at least one individual from the highest 10% in the exposure level in each group. This means monitoring all members of a small group or 36% from a group of 50 [35]. Sampling should cover all periods of the working day, with representative frequencies. The detectors require sampling pumps. These should be calibrated with a flowmeter before and after sampling. The sampling device, mounted vertically and face downward, can be worn on a shoulder, on a lapel, or elsewhere in the breathing zone. Sampling heads must be sealed until required. After opening the seal, the subject should turn on the pump and note the time. The reverse applies at the end of the sampling period. The frequency of measurement, again, depends on the results.

16.2.6.3. Hygiene and Protective Equipment. When a good surveillance program is in place, good working practices and routine precautions against exposure to mercury should be sufficient. Ambient levels of mercury vapor should be quite low and in any event, closely monitored. Respiratory protection should be necessary only when workers engage in activities such as maintenance that requires opening cells or decomposers. Respirators are then called for, and their frequency and time in use should be recorded.

Mercury can be absorbed on clothing and on the body. The best approach is to issue work clothing for use in the cell area and to provide changerooms between “clean” and “contaminated” areas. Workers should shower after each shift. The most secure arrangement is for work clothes to be laundered on site. Sometimes, outside services are used with special measures to segregate plant workers’ clothing. Workers should be aware of the possible accumulation of mercury on small personal items such as billfolds, combs, and watches. Long hair is likely to absorb more mercury. While not all sites enforce restrictions on hair length and facial hair, Heilala [34] points out that workers should be made aware of their own responsibility for good hygiene.

Food and smoking materials should be kept out of the cell area. Lunch facilities should be physically removed from the area, and workers should leave their work gloves behind and wash their hands before eating. Fingernails require special attention.

The cell room and laboratory facilities should be inspected routinely for spills or accumulations of mercury metal. These should be picked up promptly and disposed of with the plant's mercury waste or taken in secure containers to the mercury-recovery facility.

Stricter environmental standards and improved protective measures have reduced the level of exposure of workers in the chlor-alkali industry. In the 1960s, the mean level of mercury in the urine of Swedish mercury-cell workers was 100–140 $\mu\text{g L}^{-1}$ and the peak level 300 $\mu\text{g L}^{-1}$. In 1990, the mean value was 30 $\mu\text{g L}^{-1}$ and the peak value 120 [36].

16.2.7. Asbestos

Inhalation of asbestos fibers can lead to diseases such as lung cancer, asbestosis, and mesothelioma. The last-named is a cancer of the lung and bowels apparently caused only by asbestos [37]. Asbestosis is a fibrosis that attacks the lung after long or severe exposure. Since lung damage is the primary effect of exposure to asbestos, it is not surprising that the risk is greater for smokers. While "asbestos" is a generic term applying to a number of hydrated mineral silicates, more than 90% of that produced is chrysotile, or white asbestos. This is a magnesium silicate of the formula $3\text{MgO}\cdot 2\text{SiO}_2\cdot \text{H}_2\text{O}$. Chrysotile is preponderantly the type used in cell diaphragms. Blue asbestos, or crocidolite, seems the most dangerous. Its formula is $\text{Na}_2\text{O}\cdot \text{Fe}_2\text{O}_3\cdot 3\text{FeO}\cdot 8\text{SiO}_2$, and it is not used in chlor-alkali diaphragms.

The toxicity of asbestos is related to its physical state, not just to its chemical composition. The size and shape of particles determine how far they penetrate the respiratory tract and whether they stay there. Diameters in the submicron range allow particles to enter the smallest branches of the respiratory system. The dimensions regarded as most dangerous are diameters between 0.0625 and 1.0 μm and lengths in the vicinity of 15 μm [38]. Chrysotile has diameters of 0.1–3 μm and lengths of 0.1–60 μm , very much in the hazardous range. Romine [39] has reviewed the properties of these and other types of asbestos. He also discussed the history of the use of asbestos, the legislative status and enforced TLVs in various parts of the world, and the safety measures appropriate to chlor-alkali plants. He shows that the hazardous range of particle sizes depends on the specific disease under discussion. Mesothelioma, for example, is favored by smaller particle sizes. The worst particles are those less than 0.1 μm in diameter with lengths down to 5 μm .

The Occupational Safety and Health Administration (OSHA) standard for exposure to asbestos defines a "fiber" as one at least 5 μm long with a length/diameter ratio of at least 3.0. The TLV-TWA is 0.1 fibers/cc of air; the excursion limit for a 30-min sampling period is 1.0. The standard, published in 29 CFR 1910.1001 specifies sampling methods and frequencies as well as the analytical procedure (NIOSH Method 7400). Some countries allow higher concentrations of fiber. In Brazil, Canada, and Mexico, for example, the TLV is 2 fibers/ml. In the European Union, the TLV is 0.6 fibers/ml (0.25 in Germany), with an action level of 0.2.

All chlor-alkali producers should have a surveillance and monitoring program. Given the long latency period of asbestos-related diseases, employers should retain monitoring and medical records for longer than normal periods. The tabulation below shows the normal lag after the first exposure for death rates to become mathematically significant and the number of years required for death rates to reach their peaks.

Disease	Time to reach significant rate (yr)	Time to reach peak rate (yr)
Lung cancer	10–14	30–35
Asbestosis	15–20	40–45
Mesothelioma	20	45+

There is regulatory pressure to continue to reduce the use of asbestos. The chlor-alkali industry has been exempted from outright prohibition in many countries. In others, the use of asbestos in diaphragm cells has been banned. One should expect that the pressure will increase to eliminate asbestos. Most of the diaphragm-cell plants in Europe will in fact soon have been retired or converted to membranes or synthetic, non-asbestos membranes [40].

Handling of dry asbestos is a chlorine producer's most hazardous operation [41]. It begins when the material arrives at the plant, and everyone involved should wear proper respirators and protective clothing. Those who unload asbestos and move it to its storage spot should be very careful not to damage the bags. The storage area should be enclosed, with restricted access, and dedicated to asbestos. Some asbestos-handling areas are held at negative pressure. Cleanliness is essential. Any accumulation of asbestos should be removed immediately. This can be done by washing it into a collection system or by picking it up with a vacuum cleaner equipped with a high-efficiency filter. In the latter case, the filter and the bag containing the waste should be placed in a sealed, impervious container for disposal. Damaged bags should be enclosed in strong asbestos bags until taken to the depositing area for use.

While the storage area is ideally away from normal traffic patterns, the route from the storage area to the depositing area should be simple, short, and unencumbered. The asbestos-handling system should be enclosed and vented to a vacuum system with a high-efficiency dust collector. Bags should be fully cut and emptied with a minimum of shaking. This should be done only in a vented system. Empty bags should be folded over the cut and placed in a closed container. When the full contents of a bag are not required, the partially empty bag is best left inside the enclosed area for use in a later batch.

Diaphragm repair sometimes requires a worker to handle small quantities of dry asbestos. The technique of "doping" calls for addition of a slurry of asbestos to the anode compartment of a cell. Where there is substantial damage to a portion of the diaphragm, the flow rate will be high and the added asbestos will be attracted to the damaged area. Slurry preparation (addition of dry asbestos to brine, perhaps with the help of a wetting agent) should be in a ventilated hood to prevent exposure to the dry powder, and the slurry should be handled carefully in a covered vessel.

Asbestos removal for diaphragm replacement is usually by hydroblasting. The slurry thus formed can be collected in a sump. There is little hazard in the slurry-handling operation as long as the asbestos stays wet. Dewatering of the slurry by screening or filtering gives a compact mass of wet asbestos, which after collection in a bag or drum and proper sealing is ready for off-site disposal. It is best to collect the water and use it again in the blasting process. Any asbestos that flies from the containment area or collects on building or equipment surfaces should be collected while wet.

16.2.8. Nitrogen Trichloride

Section 9.1.11.2 gives a detailed discussion on nitrogen trichloride. The CI [42] discusses the hazards of NCl_3 and the safe handling of chlorine that contains it. Table 16.3 lists some of its physical properties. The most striking properties are the large positive standard heat and free energy of formation. These account for the instability of the compound and its tendency to decompose spontaneously and energetically. Once decomposition begins, the exothermic heat of reaction causes it to propagate very rapidly and move on to detonation.

NCl_3 is much less volatile than chlorine, and so it tends to accumulate in suction chiller bottoms (Section 9.1.6.4A) and in chlorine vaporizers (Section 9.1.8.7) or other vessels from which chlorine is withdrawn as vapor. One method for its removal as a waste from suction chillers has been the dilution of the bottoms with a chlorinated organic. The standard choice for this duty has been carbon tetrachloride. With the use of this solvent restricted under the Montreal protocol, other materials have been suggested as replacements. Chloroform is one possibility, but it is important to note that it (b.p. $\sim 61^\circ\text{C}$) is more volatile than nitrogen trichloride. Section 17.4.2 outlines problems that can arise with replacement solvents. Section 9.1.11.2E discusses alternative processes for the safe destruction of NCl_3 .

TABLE 16.3. Properties of Nitrogen Trichloride

Property	Value or description
Physical appearance	Pale yellow oil
Odor	Pungent (attacks eyes and throat)
Molecular weight	120.4
Melting point	-40°C
Boiling point	71°C
Density at 20°C	1.65 g ml^{-1}
Heat of formation (in CCl_4)	$54.7 \text{ kcal mol}^{-1}$
Entropy of formation	45 e.u. (est.)
Free energy of formation (in CCl_4)	72 kcal mol^{-1}
Heat of vaporization	$7.58 \text{ kcal mol}^{-1}$
Solubility	Soluble in chlorinated organics; practically insoluble in water
Vapor pressure at 0°C	80 mm Hg

Source: Argade *et al.* [43]

16.2.9. Other Materials

Many of the other materials used in a chlor-alkali plant present some kind of hazard. A brief discussion of some of these follows. Much more detail is available in the suppliers' MSDS and other literature.

Salt. As a major component of the human body, salt has no toxic properties to speak of. Since it is somewhat hygroscopic, dry salt can be an irritant to tissue, and spills of salt can create tripping hazards and lead to the corrosion of metallic equipment and structures. Therefore, salt should be confined when handled and removed when spilled.

Sulfate Solubility Inhibitor. The major ingredient in the inhibitor described in Section 7.2.2.5B is a sulfonate produced from H_2SO_4 . The product has a low pH (<2) and is corrosive to tissue. It should be handled in the same manner as sulfuric acid. It is highly viscous, and so it is difficult to remove it from the skin.

Sodium Carbonate and Carbon Dioxide. Carbonates are possible sources of CO_2 (see below), and the alkali metal carbonates are hazardous in their own right. Soda ash is rated as a moderate health hazard. It is irritating to the eyes upon contact, and continuous contact can irritate the skin. When the dry material is handled, some dust becomes airborne, and its inhalation irritates the respiratory tract. Pneumatic transfer requires effective filtration of exhaust air. Manual handling requires good mechanical ventilation of the work area and the use of protective equipment to minimize contact.

CO_2 is not highly toxic, but it is an asphyxiant. Because it is heavier than air, there is a danger of its accumulation at low points when it is accidentally released or deliberately generated and vented (Sections 7.2.2.5C, 7.5.6.1).

Calcium Chloride. Calcium chloride is an irritant. Its hygroscopicity and the exothermic nature of water absorption aggravate the hazard of the solid form. The heat of solution of the anhydrous material given in the *International Critical Tables* is 162.2 cal g^{-1} , and a particle in contact with the body can quickly become hot. The heat of solution of the dihydrate, even on a dry basis, is much lower (73.3 cal g^{-1} hydrate, or 90.5 cal g^{-1} CaCl_2). The high heats of solution also suggest that CaCl_2 should not be dissolved in hot water.

Because CaCl_2 has a low degree of oral toxicity, ingestion is not a serious plant hazard. Handling precautions are routine and should follow the supplier's MSDS. Users should be aware that contact with calcium chloride can stiffen leather shoes and clothing, thereby destroying their protective properties.

Barium Chemicals. The barium chemicals of interest here are classified as Category 1, acute hazards [44]. They can cause severe abdominal and muscular effects, including transient paralysis and fatal paralysis of the respiratory muscles. The TLV-TWA is 0.5 mg m^{-3} as Ba. Both barium chloride and barium carbonate carry the following NFPA ratings:

Health	2
Fire	0
Reactivity	0

They are characterized as hazardous wastes and are regulated substances. Their use in the brine process forms BaSO_4 . This material forms because of its extremely low solubility, and process wastes may therefore contain less than the allowable level of soluble barium [44,45]. Disposal then becomes a matter of good practice and local regulation.

Barium chemicals are ingestion and inhalation hazards. There is little danger of penetration of intact skin or of chronic effects from skin contact. It is necessary to maintain good hygiene, use respiratory protection, and follow good dust-control practices.

Flocculating Agents. Flocculants are not generally highly hazardous, and the active agents of some types are used in certain consumer products. Handling should still include all precautions specified on the MSDS supplied by the manufacturer of each compound.

Filter Aids. The types of filter aid described in Section 7.5.4.2 are rather innocuous materials. The principal hazard is inhalation of dust, and dust control is the most important protective measure.

Ion-Exchange Resins. Ion-exchange resins are slightly toxic and present a slight fire hazard. The latter is mitigated by the normally high water content of the resins. They should not be exposed to strong oxidants or to temperatures above 220°C , where decomposition occurs. The normal maximum storage temperature of 50°C is specified to assure their activity. Resins are also irritating to the eyes. If spilled, they make a floor slippery and so become physical hazards.

Reducing Agents. The sulfur-based reducing agents described in Section 7.5.9.3A are irritating to the eyes, skin, and mucous membranes. They also present a breathing hazard in the form of a mist or SO_2 vapor. TLVs for mists generally are about 5 mg m^{-3} . The TLV-TWA for SO_2 in the air is 2 ppm, and the STEL is 5 ppm. Temperatures above ambient aggravate the problems, and all of these materials should be kept away from heat and contact with acids.

Section 7.5.9.3A also discussed the process hazards of hydrogen peroxide in some detail. Its bodily effects result from its strong irritant properties, which can blister the skin and damage the eyes if it is not removed quickly. The vapor from decomposition, a mixture of oxygen and H_2O_2 , is highly irritating to mucous membranes. The exothermic decomposition of hydrogen peroxide can create a thermal hazard when spilled on clothing. Clothing brought into contact with this material should be changed or washed with water. Ingestion of hydrogen peroxide is particularly dangerous. Catalase enzyme decomposes H_2O_2 rapidly, and the high volume of vapor generated can distend organs and cause internal bleeding.

Activated Carbon. The primary use of activated carbon is in the dechlorination of brine, but it also sometimes serves as a filter medium, most frequently in mercury-cell caustic service. In any case, consumption after the initial charge is small.

Carbon is a fairly innocuous material. The small particle size (0.5–5 mm) can make it rather dusty. Therefore, handling should be confined, and operators should have respiratory protection when making transfers.

Some grades of activated carbon are impregnated with other materials to enhance their activities in certain processes. This treatment often makes the material more hazardous. Again, the user should consult the literature and the supplier's MSDS for specific information.

Membranes. Membranes are extremely stable chemically, as evidenced by their long service life in the hostile environment of a cell. However, the polymers can decompose thermally above 150°C, releasing HF, COF₂, and organic fluorine compounds. They should be stored in a dry, clean place at cool to moderate temperatures.

Contamination of smoking materials with membrane dust or scraps can result in decomposition and, when the byproducts are inhaled, lead to "fume fever" associated with the products of degradation of fluorinated polymers.

Refrigerants. Fluorocarbon refrigerants are standard materials in chlor-alkali applications. They are inert and not toxic. Principal hazards are the low temperatures encountered and the asphyxiating property of the gases. Those using other refrigerants (ammonia and hydrocarbons are examples) must provide for their particular hazards in design and operation.

The major concern with fluorocarbon refrigerants is not personnel hazards but their ozone depletion potential. Many types that were popular in the past are now banned by the Montreal Protocol or successor agreements (Section 9.1.7.2B). Handling and disposal of refrigerants with the potential for depleting the stratospheric ozone layer require special care.

Transformer Oils. Transformer oils are complex mixtures of hydrocarbons, and their decomposition can produce a wide variety of lower molecular weight compounds. The products of a decomposition induced by a fault in a transformer can give some clue as to the nature of the fault. Given the impossibility of an internal examination of an operating transformer system, this is valuable diagnostic information.

The results of a fault depend on the distribution of energy and temperature in the neighborhood of the fault and on the time for which the oil is exposed to a thermal or electrical stress. Higher severities produce more hydrogen and more unsaturated gases. Lower energy faults produce smaller amounts of unsaturated compounds in general. Therefore, lower temperature decomposition produces primarily methane and hydrogen, with traces of ethane. Higher temperatures (>500°C) give more hydrogen than methane, and ethylene begins to appear. Somewhere above 750°C, there will be more ethylene than ethane. High-intensity arcing gives rise to very high localized temperatures and to the formation of acetylene. The thermal decomposition of oil-immersed cellulosic insulation generates carbon oxides. These byproducts accumulate in the gas space above the oil and equilibrate with the liquid. The composition of gas found dissolved in the transformer oil or in the gas space above the oil will therefore provide some clue to the nature of the fault(s) in the transformer system.

The concentrations of the various decomposition products in or above the oil depend on their rates of escape from the system as well as on their rates of formation. Ratios of concentrations therefore are more instructive than the absolute values themselves. The Institution of Electrical and Electronics Engineers (IEEE) Standard C57.104 [46]

describes the logic and presents flow charts used by different authors to arrive at a diagnosis from the analytical data.

Lubricants. A plant may use many different lubricants in various applications. Each may have its own inherent hazards, as identified on the suppliers' MSDS. There are also hazards related to the conditions under which they are used (temperature, mechanical stress, etc.). Chemical compatibility with the process is also a major consideration. While all lubricants may be chosen properly in this regard, there have been failures caused by improper substitutions. Substitutions of one lubricant for another should never be made without careful study, and there should be precautions against accidental substitutions.

16.3. PROCESS HAZARDS

We must consider process hazards as well as material hazards. Among these we have temperature (high or low), pressure, high voltage, exposed live electrical parts, and magnetic fields. The temperatures and pressures involved in chlor-alkali processing are not unusual, and standard precautions serve to control these hazards. Several points relating to inherent safety are still worth noting in this regard:

1. The trend toward deeper liquefaction sometimes involves temperatures that are quite low and perhaps should be considered unusual. These call for proper care and insulation, along with more attention to confinement of the refrigerant when it warms.
2. Higher pressures can increase the likelihood of a chlorine release.
3. The low temperature of liquid chlorine is an important factor in the choice of materials of construction.
4. The low temperature also requires design pressures well above normal operating levels in order to allow for warming. The high coefficient of expansion of liquid chlorine also requires special consideration.
5. Buswork, while not insulated, is quite hot. Contract workers and other outsiders, especially, do not always recognize this fact.
6. In addition to high temperatures of process fluids and equipment, thermal hazards in the cell area may include prolonged exposure to high ambient temperatures.

The electrical hazards of AC supply and distribution also are those faced in industry in general. We may consider the hazards from the primary supply through the area transformers as conventional. The DC side and the magnetic fields associated with high current are more characteristic of chlor-alkali production. These are discussed in Section 8.5.1.

Many liquids are off-loaded into storage tanks by applying air pressure to a delivery vehicle. These may include caustic, sulfuric acid, hydrochloric acid, and certain auxiliary chemicals. The compressed air may be generated on the receiving site, or the delivery vehicle may be equipped with a compressor. A particular hazard of this type of operation is the surge of air that can occur when the last liquid has been removed from the vehicle. If the receiving vessel has a small vent nozzle and a low pressure rating, its design

can be very quickly exceeded. An Industry Warning published jointly by the EPA and OSHA [47] describes the failure of a HCl storage tank from this cause. The tank had a volume of about 22 m³, and it released about 18 m³ of 31% HCl. Modeling of the pressure in the tank showed that the design pressure was exceeded in less than a second after completion of liquid delivery. With a 50-mm vent line, dangerous pressures capable of bursting the tank would develop in 10–30 s. Use of a 100-mm vent would limit the pressure to about 10 kPa. The presence of a scrubber on the vent line imposes a pressure drop and aggravates the situation.

EPA/OSHA recommendations included:

1. standard operating procedures
2. hazard analysis during design, before operation, and when making changes to equipment
3. maintenance of environmental control systems to ensure reliability

Design options to relieve the hazard include:

1. minimize air pressure used for transfer
2. size vent system for air surge
3. restrict air flow by partially closing a valve in the transfer line as soon as the delivery vehicle is empty of liquid
4. add pressure sensor to receiving tank and close inlet or open vent to atmosphere when pressure becomes too high
5. avoid use of passive scrubber in which vent air enters a pool of liquid
6. use a tank designed to withstand pressure
7. transfer by pump rather than by air pressure

We include electricity among the process hazards. Many ordinary electrical design precautions do not apply inside cell installations. The entire line, for example, cannot be enclosed and isolated as are the transformers and rectifiers. This approach would trap gases and heat and make many necessary manual operations impossible. The technique of isolation of a circuit from ground, while successful in common AC systems, is usually ineffective because leakage currents through pipes, metalwork, and conductive fluids are great enough to provide a ground. Similarly, automatic ground fault protection has a limited value. If set low enough to protect the body, it will not be able to handle leakage currents.

The practices described in Chapter 8 are designed to overcome electrical hazards. Air being an excellent insulator, clearances between live equipment and potential grounds provide safety.

Within the cell room, electrical components also present thermal hazards. Section 8.3.1.4A showed that busbars, for example, are designed to operate at temperatures up to 90°C and higher. The ambient temperature can be quite high and is limited by the rate of ventilation. Good ventilation is an important part of building design. It also serves to remove any hydrogen that escapes from the cells or piping.

Because of the unusual working demands in the cell area, it is not common practice to classify cell rooms electrically, but this should be a separate decision for each project. In particular, the design of light fittings and any other electrical apparatus near the roof should be reviewed. Air drives may be preferred to motors for mobile equipment, and isolating transformers should be present in both power and control circuits when electrical devices are chosen.

While much of the piping in cell rooms is nonmetallic, the fluids may be conductive and may still be at some voltage after leaving the cell line. The piping itself will provide insulation for personnel protection, but the use of metallic valve bodies and handles should be reviewed.

In the long run, spills of process fluids are nearly inevitable. These create slipping hazards and can also short out insulation. Cell room housekeeping is therefore very important. Floor gratings, besides being nonconductive, should also have nonslip properties. FRP and timber have been widely used. The former is the material of choice in most modern cell rooms.

16.4. PREVENTION AND MITIGATION

16.4.1. Safety Equipment

PPE is the gear worn or carried on a plant to protect workers and visitors from injury due to chemical or environmental exposure. It should not be considered the primary defense against plant hazards. Its purpose is to supplement other means (physical or administrative) of hazard avoidance. There are both governmental regulations and industry standards that are useful in formulating a PPE program. In the United States, OSHA publishes regulations in 29 CFR 1910. Important subsections include:

132	General Requirements
133	Eye and Face Protection
134	Respiratory Protection
135	Head Protection
136	Foot Protection
137	Electrical Protective Devices
195	Noise Exposure

The CI [48,49] and EC [50] also publish guidelines. The CI suggests standard outfits for various tasks that can be divided into three categories each for chlorine and caustic. The equipment appropriate for each category is

Chlorine exposure

Category I	No specialized PPE
Category II	Full-face air-purifying respirator Gloves for thermal protection (when handling liquid)
Category III	SCBA or air-line respirator Gloves for thermal protection (when handling liquid)

Caustic exposure

Category I	Face shield and chemical splash goggles Chemical protective gloves
Category II	Category I and chemical protection for the head and neck
Category III	Chemical protection for the head and neck Face shield and chemical splash goggles Chemical protective suit Chemical protective boots or overshoes Chemical protective gloves sealed at the sleeve

Typical activities for which these apply are:

Chlorine

1. *Sampling*—when demonstrated that vapor concentration remains within TLVs, Category I; when concentration may exceed a TLV but will remain within the capability of a respirator, Category II; otherwise, Category III
2. *Initial line break*—when demonstrated that vapor concentration will remain within the capability of a respirator, Category II; otherwise, Category III
3. *Loading/unloading*—given a system for purging, evacuation, and verification of the pipelines and hoses used for loading or unloading, together with sound operating and maintenance procedures and the use of well-trained employees, same as Sampling

Caustic

1. *Sampling* Category I
 2. *Line break* Category III
 3. *Loading* Remotely operated systems, Category II when in vicinity of connection point and no special PPE elsewhere; if not remotely operated, Category III
 4. *Unloading* Category III
-

Emergency situations may require the use of more PPE. Most procedures should be predetermined and written. A foreseeable emergency is not the time for improvisation by untrained personnel. While the idea of added layers of protection may be appealing, they often add to operator discomfort and impede mobility. Their net effect can be negative.

The EC guidelines describe the selection, use, and maintenance of breathing apparatus in some detail. There is a shorter discussion of full protective clothing for use in chlorine atmospheres.

Training in the proper use, maintenance, and decontamination is important with all forms of PPE. Specifics vary with the type of equipment, its manufacturer, and sometimes model numbers. The reader is referred to specific manufacturers' literature on this subject. Portable safety equipment, along with emergency tools and maintenance supplies, should be available at all times in a vehicle that can approach any part of the plant. EC [51] publishes a detailed list of recommended items.

16.4.2. Safety-Oriented Programs

The programs described in this section cover the entire range of activities from preliminary design of a plant through its construction and operation to the safe delivery and use

of the products of the plant. Most of the programs are tools for continuous improvement. Documentation is therefore an important part of the process, and certain aspects are mandatory. Safety management documentation should be reviewed and revised at least every 5 years [52], with a yearly review to determine whether accumulated changes have affected the “safe operating envelope” of the plant.

16.4.2.1. Inherent Safety in Design. The pursuit of what appear to be improvements in process efficiency and productivity can lead to the choice of systems or operating conditions that add new hazards to a plant or increase the potential consequences of existing hazards. The design stage of a project offers an opportunity to remove or mitigate some of these hazards and to provide an inherently safer plant [53–55]. Some of the techniques used to do this, with examples cited throughout this text, are:

1. use less-hazardous material (lower concentration hydrogen peroxide)
2. reduce inventory (smaller chlorine storage facility)
3. use less severe process conditions (low-intensity liquefaction, or elimination of liquefaction, when chlorine can be processed on site as the gas; limitation of cell-room voltage)
4. use fail-safe redundant safeguards (independent switches or transmitters for alarms or shutdowns)
5. use passive rather than active protection systems (emergency release of chlorine, when under pressure, to static tank of caustic)
6. use corrosion-proof materials to lessen accelerated corrosion by upsets or need for inspection (high-temperature alloys for possible touch points in chlorine compressors; alloys that exceed normal specifications in parts of brine system that may become acidic during excursions)
7. minimize piping carrying high toxic hazardous materials outside area limits
8. review design and operation according to established schedule and before making modifications

None of these measures necessarily removes a hazard. The intention is always to reduce the magnitude of a hazard and the consequences of an accident. The value of each technique depends on the other protective measures taken, and its application is a matter of judgment.

16.4.2.2. Process Safety Management. Nearly all chlor-alkali manufacturers practice some kind of PSM program. In most locations, there are industry codes or governmental regulations to follow. Other chapters in this work describe various PSM procedures where appropriate. In order to bring the various aspects of PSM together in one place, we record here some of the generalizations that apply to all phases. We follow the explanatory material attached to the OSHA document, Compliance Guidelines and Recommendations for Process Safety Management (29 CFR 1910.119, Appendix C). The main body of the same document contains the regulations that apply to each of the activities noted below. Some of the items treated here are covered in more detail in the subsections that follow.

PSM is the proactive identification, evaluation, and mitigation or prevention of chemical releases that could occur as a result of failures in processes, procedures, or equipment. Appendix C referred to above covers 14 topics:

1. Introduction to Process Safety Management
2. Employee Involvement in Process Safety Management
3. Process Safety Information
4. Process Hazard Analysis
5. Operating Procedures and Practices
6. Employee Training
7. Contractors
8. Pre-Startup Safety
9. Mechanical Integrity
10. Nonroutine Work Authorizations
11. Management of Change
12. Investigation of Incidents
13. Emergency Preparedness
14. Compliance Audits.

Taking these in turn:

1. The regulation defines the major objective of PSM of highly hazardous chemicals as the prevention of unwanted releases, especially into locations where people would be exposed to serious hazards. There is a need for a systematic approach to evaluating the whole process. The introduction specifically mentions reduced inventories as one approach to control.

2. Employees must be consulted in the development and implementation of the PSM program. The relevant sections of the underlying legislation also require training employees with respect to processes, procedures, and equipment. They must be kept current and specifically informed of the results of incident investigations (#12).

3. Safety information should cover materials, equipment, and technology. Safety data on raw materials, process intermediates, and final products should cover fire and explosion hazards, reactivity hazards, safety and health hazards to workers, and corrosion and erosion effects on process and auxiliary equipment. MSDS should form part of the background for this information. Technology information, with the aid of design drawings, block diagrams, and sketches, should establish the basis for design (e.g., by reference to the various codes and standards used in design) and set limits on operating conditions. This information becomes a resource for contractors, emergency planners, insurers, enforcement officials, and those performing hazard analyses (#4) or preparing operating procedures (#5) and training programs (#6).

4. Part 1910.119 presents the objectives of hazard analysis and some of the considerations that determine the choice of techniques. The material presented below in Section 16.4.2.4 is consistent with this discussion. The type of hazard analysis chosen should be appropriate to the complexity of the process studies, and there should be a system to ensure prompt action on the findings of the study.

5. Written operating procedures must be specific and detailed. They must include applicable information on safety and be understandable, accurate, and current. The last requirement forces their inclusion in the management of change (#11). They are also

an important part of employee training (#6). They should cover startup, shutdown, and emergencies as well as times of normal operation. Subject matter should include the tasks to be done by various operators, the operating conditions to be maintained, the methods and frequencies of taking samples, the safety and health precautions to be observed, and the responsibilities of supervision. Laboratory procedures and safety information should be documented in a similar fashion in the appropriate detail.

6. All employees, including maintenance and contract workers, must adequately understand the hazards of the chemicals and processes with which they work. Other subsections of Part 1910 cover training requirements (e.g., Hazcom regulations, Part 1910.1200). The employer has the responsibility of identifying those who require training and determining what subjects need to be covered in that training. A good training program will have quantitative goals and provisions for periodic evaluation and reassessment. Appendix C of the *Guidelines* gives examples of some of the techniques that might be used.

7. Employers who use contract employees in and around hazardous processes have the responsibility of choosing contractors with the proper skills and monitoring their performance. Contractors should be screened for safety performance in other work, skill in the required tasks, and knowledge of the process or types of systems on which they will work. It is sometimes useful for an employer to include contract employees in existing training programs. Contractor employees often perform specialized and hazardous tasks. Examples are nonroutine repairs and entry into confined spaces. It is therefore important to control their activities. A permit or work authorization system is a useful vehicle toward this end.

8. A process hazard analysis (#4) is a useful part of preparation for startup. Chapter 13 discusses some of the precommissioning activities appropriate to a new chlor-alkali plant. For restart of an existing plant, requirements vary with the extent of the changes that might have occurred during the shutdown. Except for changes in kind, management of change (#11) procedures apply. When there have been changes, the employer must see to the revision of all applicable documents. Depending on the nature and magnitude of the change, retraining may also be appropriate.

9. Section 16.4.2.3 discusses mechanical integrity in more detail. A necessary part of PSM is the review of existing maintenance programs. These should be parts of an ongoing mechanical integrity program rather than “breakdown” maintenance activities that are entirely reactive.

10. Work outside the normal routine needs special management control. This requires formal procedures, carefully followed, for such things as confined space entry, hot work, and line breaking and equipment opening. The procedures should cover the activities of operators, plant maintenance workers, contractors, and any others who may become involved. Written documents should spell out responsibilities, approval mechanisms, tagout procedures, and methods for verification of proper completion.

11. The standard defines the types of “change” that require management. Basically, it refers to changes in technology, equipment, and instrumentation. Any modification other than a replacement in kind comes under this regulation, which requires identification and review before implementation of the change. The change, its impact on operation, and all review procedures must be documented and become part of the permanent record. The standard specifically covers temporary changes, which have been

responsible for a number of catastrophic incidents, and requires time limits to be placed on their existence. Removal of a temporary facility also requires review of the new final configuration or assurance that the system has been returned to its original state. Again, some changes will require retraining of certain personnel.

12. Employers should have trained inhouse teams for investigation of unusual incidents. These include accidents and “near misses” that could have had harmful consequences. The objective of an incident investigation is to learn from experience, and this requires publication and dissemination of a clear report of the findings. Multidisciplinary teams are better able to gather and analyze the facts of an event. The knowledge of employees who work in the area where an incident occurred is a substantial asset. They should be consulted, interviewed, or made part of the investigating team.

13. Emergencies arise when primary and secondary lines of defense fail to contain a hazard. The most likely or most hazardous incidents are identifiable for each type of plant. This allows effective preplanning for many identifiable incidents. A chlorine handler, for example, must consider what actions to take if chlorine gas is released. Some of the requirements for in-plant response are included in Part 1910.120, and the Hazcom regulations (#6) also apply. Under this heading, an employer must establish specific programs, identify and train responders, and make all proper arrangements for outside help. Employers also need to decide on the number and nature of lines of defense to provide. A minimum requirement is the publishing and dissemination of an emergency action plan for the entire facility in question. It should provide for a warning system, an evacuation plan that may include alternatives that depend on circumstances (e.g., location of a release, direction of wind), and the establishment of safe havens. OSHA discourages the use of control centers as safe havens.

14. Compliance audits are necessary after establishing and documenting a PSM program. They are best performed by knowledgeable, trained individuals or teams. The auditors should verify the implementation of the PSM plan and evaluate its effectiveness. Key elements in a successful auditing program are planning, staffing, conducting the audit, evaluation, preparation of an action plan, follow-up, and documentation.

16.4.2.3. Mechanical Integrity. The concept of mechanical integrity refers to the ability of an item or a system to contain hazardous materials safely. Establishing mechanical integrity requires:

1. proper design, in order for the system to be able to withstand all likely service conditions
2. installation and construction in accordance with design and all relevant codes and good practices
3. correct maintenance, to prevent overly rapid deterioration
4. safe operating practices, to avoid errors that can overcome the safeguards designed into the system

The elements of a preventive program should include these actions:

1. identification of equipment and instrumentation: categorization and listing of items needing special or heightened attention
2. testing and inspection: documentation, acceptance criteria, frequency of testing, adherence to codes and standards (American Society for Testing and Materials

[ASTM], American Petroleum Institute [API], NFPA, Factory Mutual [FM], American Society of Mechanical Engineers [ASME], American National Standards Institute [ANSI], CI, EC), including non-equipment items such as criteria for inspection of foundations and supports, anchor bolts, pipe hangers, guy wires, grounding connections, nozzles and sprinklers, insulation, protective coatings, external surfaces of vessels, insulation, etc.

3. developing maintenance standards: procedures, training, establishing mean time to failure for instruments and equipment parts
4. compiling and using manufacturers' information: maintenance, rates and consequences of failures

Mechanical integrity becomes an especially important consideration in a chlor-alkali plant, where the products are not only dangerous but also present a variety of hazards. Most producers now have some form of mechanical integrity program as part of their PSM initiative. Such initiatives are frequently government-mandated and may cover the following.

1. mechanical systems:
 - (a) pressure vessels and storage tanks
 - (b) piping systems
 - (c) relief and vent systems
 - (d) emergency shutdown systems
 - (e) controls
 - (f) pumps (and by extension, compressors);
2. written procedures
3. maintenance training
4. inspection and testing
5. equipment deficiencies
6. quality assurance

Equipment deficiencies that are outside acceptable limits are to be corrected before the equipment is used or in a safe and timely manner when necessary steps are taken to assure safe operation until repairs can be made.

Quality assurance, it will be seen, is critical to establishing mechanical integrity. The OSHA rule covering PSM states that "the quality assurance program is an essential part of the mechanical integrity program and will help to maintain the primary and secondary lines of defense. . ." These "lines of defense" are the protective systems and procedures that one adopts to prevent hazardous releases. They might include:

1. Primary measures:
 - (a) operate process as designed in order to keep hazards confined
 - (b) maintain all systems in good repair
 - (c) control all releases by using scrubbers, flares, and surge systems;
2. Secondary measures:
 - (a) fire protection systems (sprinkler, spray/deluge, monitor gun)
 - (b) dikes
 - (c) drainage/diversion systems
 - (d) other systems.

The last category extends the definition of the “system” to auxiliaries and those features of design that help to mitigate the effects of a release rather than contain the material in question. The work by Harris [56] on chlorine storage systems is an example.

The quality assurance program should verify that proper materials of construction are used throughout. It can involve field inspection, examination of mill or supervisory board certificates, and, especially in the case of equipment handling liquid chlorine, review of impact test results. The program should extend to verifying that fabrication and inspection techniques were proper.

Other matter for the mechanical integrity program includes:

1. documentation:
 - (a) as-built drawings
 - (b) equipment design drawings, calculations, certificates
2. installation of equipment:
 - (a) quality of materials, including gaskets, packing, bolts, valves, lubricants, welding materials, etc.
 - (b) quality of craftsmen
 - (c) welding procedures and certification of welders
3. installation of safety devices:
 - (a) procedures (e.g., measuring torque on rupture disc bolts; applying uniform torque to flange bolts)
 - (b) inspection
4. design and installation of rotating equipment seals

One aid to a mechanical integrity program can be positive materials identification (PMI) of critical components. This is a process of verification that materials of construction of an object are in fact what were called for in design or specification. A recent investigation by the Chemical Safety and Hazard Investigation Board in the United States [57] shows the value of PMI. The Board found that the failure of a transfer hose that led to the release of 22 tons of chlorine was due to the use of Type 316L stainless steel for the structural braid, rather than the Hastelloy C-276 that had been specified. A PMI program somewhere in the chain of supply might have prevented this incident.

16.4.2.4. Hazard Analysis. Recognizing that no plant can be perfectly safe, modern safety engineering has turned to techniques for the formal or quantitative assessment of risk [58]. Many techniques for formal analysis now exist [59,60]. They differ widely in scope and intention, and the Center for Chemical Process Safety [59] tabulates for each of them:

1. the purpose of the method
2. when to use it
3. the type of results to expect
4. the nature of the results, and whether they are qualitative or quantitative
5. the data required for a successful analysis
6. staffing requirements
7. the time required for a study
8. an estimate of the total cost

API Recommended Practice 750 also treats the subject of hazard control and management. Harris [61] considers the general topic of hazard assessment in the chlor-alkali industry.

Many governments and other regulatory bodies now require some form of hazard analysis either before a new plant is built or as part of the ongoing requirements for operating permits. The system used in the United States is typical and has been adopted in other areas. This is OSHA's PSM rule, which formed the basis for Section 16.4.2.2. At the time of design, engineers would do well to adopt some of these methods as well as to be alert for opportunities to improve the inherent safety of the plant (Section 16.4.2.1).

Table 16.4 lists some of the more popular analytical methods and summarizes their characteristics. "What-If" analysis, sometimes aided by a checklist, and Hazop analysis are widely used in design and operation. Sellers [62] points out the value of the checklists provided in the CI pamphlets in this regard.

Failure Modes and Effects Analysis and Fault Tree Analysis (FTA) are used less widely than Hazop but sometimes allow more comprehensive and quantitative analysis of certain situations. Table 16.4 lists these techniques and their applications at different stages in the hazard evaluation process. No one technique is efficient or even useful at

TABLE 16.4. Hazard Evaluation Procedures

Category	Methods	Applications
Preliminary	Checklists	Identify hazards
	Safety review Preliminary hazard analysis	Identify deviations from good practice ^a
Detailed	"What-If"	Identify hazards
	Hazop	Identify accident-initiating events
	FMECA	Estimate "worst-case" consequences ^b
Specialized or quantitative	FTA	Estimate probabilities of initiating events ^c
	ETA	Identify opportunities to reduce probabilities ^c
	Cause/consequence analysis	Identify sequences of events
		Estimate probabilities and consequences
		Identify opportunities to reduce probabilities and consequences
	Quantitative hazard evaluation	

Notes:

^aExcept PrHA.

^bIndirect with Hazop.

^cExcept ETA

Hazop = Hazard and Operability Study; FMECA = Failure Modes, Effects, and Criticality Analysis; FTA = Fault Tree Analysis; ETA = Event Tree Analysis; PrHA = Preliminary Hazard Analysis.

every stage, and the analyst must first define the purpose of an exercise before committing substantial resources.

Most plants now favor software-based safety systems over the older hardware-dominated approach. These systems were adopted piecemeal, with the result that practices vary widely between companies and even between plants within a company. Now, the International Electrotechnical Commission (IEC) has adopted and published a generic standard, IEC 61508, that brings together much of the published material and provides a framework for its coordination [63].

Much of the process industry already follows the standard ISA-S84.01. This conforms to IEC 61508 but does not cover the early activities that precede the formal risk analysis. In this sense, IEC 61508 is more comprehensive. A common standard in Europe has been DIN 19250. This is an application-independent standard that covers identification and classification of risks. System design then requires the use of other DIN standards. Again, IEC 61508 combines the relevant parts of the various standards.

It must be emphasized that with the advent of quantitative hazard analysis, most designers are seeking very low probabilities of failure. Mean intervals of 10,000 years between failures of a system are quite common goals. Intuitive judgment and the wisdom gained through experience begin to fail against such criteria.

In quantitative analysis, one way to reduce the residual risk in a system is to increase the frequency of proof testing. This reduces the probability of random failure by detecting flaws that have already developed and by reducing the probability of development of a new flaw in the interval between the proof test and a possible real event. Requiring more testing is an imposition on a plant operating crew that may appear senseless when many tests have been made on a system that “never” fails in practice. Training and educational programs should make the reasons for added safety devices and more frequent proof testing clear. There are systems that have always appeared safe that have had redundant elements added. Because there have been no problems in these systems, there is a temptation not to give high priority to maintaining reliable operation of all its elements.

16.4.2.4A. Hazard and Operability Study (Hazop). Here we discuss only Hazop and FTA in any detail. The first of these has become a standard tool in the industry. In fact, “Hazop” has nearly degenerated into a generic term and is often applied incorrectly to other types of analysis. Johnson and Leverenz [64] define it as follows: “A hazard and operability study is a hazard analysis method in which a review team systematically identifies deviations in one part of an operation at a time, then examines each deviation’s possible causes and consequences to identify previously unrecognized hazards and to develop action items where risk reduction is warranted.” Designers may apply some form of Hazop several times during a project. It is an integral part of periodic reviews. Its purpose, as defined above and set out in Table 16.4, is the identification of hazards in order to take measures to mitigate them. It is a detailed and a relatively expensive process. A team of technical and operating people with a good knowledge of the process is required. Part of the strength of Hazop is in the variety of viewpoints brought to bear and the brainstorming atmosphere.

TABLE 16.5. Hazop Guide Words and Meanings

Guide word	Meaning	
No	Negation of design intent	
Less	Quantitative decrease	
More	Quantitative increase	
Part Of	Qualitative decrease	
As Well As	Qualitative increase	
Reverse	Logical opposite of intent	
Other Than	Complete substitution	
Substitutions	For	When Concerning
Sooner, Later	Other Than	Time
Where Else	Other Than	Position; Source; Destination
Higher, Lower	More, Less	Process variable; Elevation

Hazop is a formalized technique. The team considers selected study points, or nodes, one by one and applies a series of key words to uncover hazards. Table 16.5 lists the standard key words. When considering the flow of a material, for example, this list requires the analysts to consider the possibility and effects of loss of flow, insufficient flow, excessive flow, the wrong composition or wrong material, etc.

There has been a rapid increase in the number of hazard analyses performed in the industry. This is due to the general recognition of their value, industry initiatives such as Responsible Care[®] (Section 16.4.2.6), and governmental regulation. The use of Hazop has grown more than most other methods because of (1) the power of team review, (2) the suitability of the method to the analysis of process systems, and (3) the natural development of accident scenarios from Hazop study results.

As an example of the product of a Hazop study, we consider the production of sodium hypochlorite by continuously reacting chlorine with a solution of caustic soda. The node chosen for study is the point at which the caustic solution enters the process. The variable being studied is flow. Table 16.6 shows the results. This is adapted from the example on Chapter 4, page 45 of Ref. [59]. The first key word applied is “No.” If no caustic enters the reactor, there will be an excess of chlorine, and the hazard produced will be the release of chlorine from the system into the atmosphere. The table identifies possible causes and suggests remedial action. Some of the other key words are then considered in sequence, with similar entries. Note that some key words (in this case “More”) will not identify another hazard but may suggest operability problems that also require action. Other situations may require further study. These are noted for action and assigned to some member(s) of the team. While all items in Table 16.6 have suggested actions listed, this is not essential. The purpose of the Hazop study by the full team is to identify hazards but not necessarily to provide solutions. Time is better spent on completing the assigned task than on engineering solutions to a few of the problems raised.

16.4.2.4B. Fault Tree Analysis. FTA complements Hazop. It does not identify hazards; rather it identifies and analyzes the causes of a known hazard. Designers may use FTA

TABLE 16.6. Example of Hazop Output—Hypochlorite Production

Node: Caustic feed point Parameter: Flow				
Guide word	Deviation	Consequences	Causes	Suggested action
No	No flow	Excess chlorine in reactor Release of gas to atmosphere	(1) Caustic valve fails closed (2) Caustic supply exhausted (3) Pipe ruptured or plugged	Automatic closure of chlorine feed valve upon loss of caustic flow
Less	Less flow	Excess chlorine in reactor Release of gas to atmosphere, with amount released related to quantitative reduction in supply ^a	(1) Caustic valve partly closed (2) Partial plug, or leak from pipe	Automatic closure of chlorine feed valve upon reduced flow from caustic supply; set point determined by calculation ^a
More	More flow	Excess NaOH in reactor Off-specification operation but not a hazard	—	Operability issue to be addressed separately
Part of	Normal flow rate, but at low concentration of NaOH	Excess chlorine in reactor. Release of gas to atmosphere, with amount released related to quantitative reduction in supply ^a	(1) Delivery of wrong grade (2) Error in dilution	Check batch of caustic after preparation. Monitor strength of continuously blended caustic

Note:

^a Member(s) of team assigned to calculate toxic hazard vs reduction in rate of flow or concentration of solution.

for a thorough analysis of a recognized serious hazard. The technique is probably used more frequently to study existing or generic systems.

Starting from the event chosen for study, the analysts define those events that are possibly immediate causes. Listing these events forms the beginning of the fault tree diagram, which shows the causes linked to the event under study. Figure 16.1 shows part of a fault tree for the escape of chlorine from an emergency vent scrubber [65]. The model is the type of system described by Patel and Scarfe [66]. Contributing events are easily identified as too high a flow of chlorine and an inadequate supply of caustic. Equally important in the analysis is the relationship between the contributing events. The hazardous event may require both contributing events to occur simultaneously, or it may follow on from either one individually. Our specific case is an example of the latter. We return to this aspect below.

Next, the analysts consider each of the contributing events in turn and identify the sub-events that lead to them. Regarding an inadequate flow of caustic, we see that it can result from a solution flow rate less than that specified or from too low a concentration of reactant. This process of analysis continues to lower and lower levels until all the base causes are identified. Figure 16.1 is a simplified version of the result. The appearance of the diagram shows why we speak of a fault “tree.” Note that only one side of the tree is shown. In practice, the other side would also require development.

The symbols in the lines connecting the various events define the type of relationship between the sub-events. At each step of the tree, either one of the two causes is sufficient for us to move up to the next level of the tree. The “gate” through which we pass therefore is the OR gate. The symbol that appears in Fig. 16.1 is that used in logic diagrams to show an OR gate.

One of the advantages of the fault tree method is its adaptability to mathematical analysis. The probabilities of the basic events at the bottom of the tree must be known or estimated. Analysis then moves up the tree with the aid of Boolean algebra. We are interested in two possible relationships between events leading to a step up the tree. First, either of the two events may suffice. Chlorine escapes when its rate of flow is too high OR the rate of supply of NaOH is too low. Either failure causes a gas release even if the

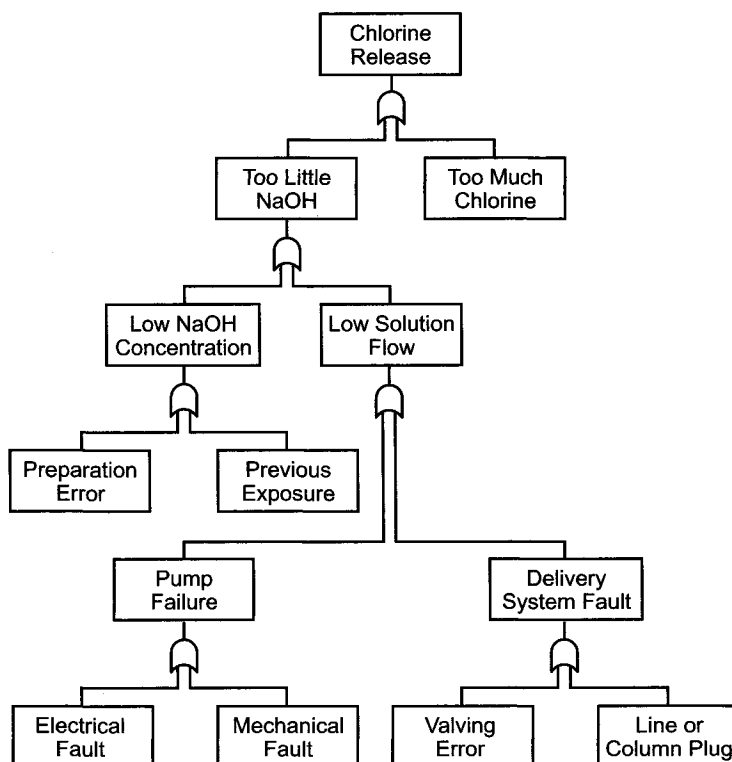


FIGURE 16.1. Partial fault tree for vent scrubber.

other does not occur. On the diagram, therefore, the two sub-events are joined through an OR gate. In other situations, when two or more events must occur simultaneously or sequentially, AND gates appear. A very common example is a system with a spare pump that should start automatically when the first pump fails to deliver sufficient flow. Mathematically, the difference between the two types of gate is the addition (OR) or multiplication (AND) of probabilities. The probability of two events A and B occurring together is the probability of one event multiplied by the conditional probability of the second. Thus:

$$P_2 = P_A \times P_{BA} = P_B \times P_{AB} \quad (1)$$

When two events are independent, conditional probabilities are equal to the probabilities of the relevant events, and

$$P_2 = P_A \times P_B \quad (2)$$

The probability of either event occurring, when the two are independent, is

$$P_1 = P_A + P_B - P_A P_B \quad (3)$$

The logical operators AND and OR reproduce these results. Table 16.7 is a truth table for both relationships. Each row represents some combination of the two events. The AND column mimics Eq. (2) and the OR column follows Eq. (3). The advantage of the AND relationship, which eliminates two of the three hazardous OR combinations, is obvious.

The probability calculations recognize differences between active and passive systems. An “active” system is one whose failure generates a demand on the protective system. Most continuously operating equipment is in this category, and failure normally becomes obvious very quickly. The failure of a “passive” system, on the other hand, is not obvious until a demand (incident or proof test) is placed on it. Some components have both active and passive character. Many instruments are good examples. Transmitters generally provide continuous or frequent output and might be considered active. Gradual deterioration in the performance of measuring elements may not be obvious, and these might be considered passive. Another variation that requires special treatment is the sequential AND gate. Here, one system must already have failed before the failure of a second produces a hazardous event (e.g., failure of the mechanism of a relief valve followed by excessive pressure on the protected system). These differences in treatment

TABLE 16.7. Boolean Truth Table

A	B	AND	OR
1	1	1	1
1	0	0	1
0	1	0	1
0	0	0	0

and method of calculation for various types of gate do not affect the basic logic presented above.

One of the deficiencies in the FTA in our example is that the logic of the method as presented assumes that variables are discrete. Flows are either adequate or inadequate. Concentrations are either high enough or too low. In fact, flow and concentration are continuous variables. It is possible for both quantities to drop off, producing a hazard when neither one is low enough to cause a problem on its own. This makes the example used here less than ideal for the FTA. Realistic calculation of probabilities, for instance, is not feasible. The approach, however, has been useful in real cases in a more qualitative way. Construction of fault trees for similar systems revealed a number of initiating events that were able to move up the tree through nothing but OR gates.

The example used above is not typical of the applications of the FTA. Complex and interrelated systems, such as intricate safety systems that involve redundancy, elaborate logic, and multiple layers of safety are more typical, but it would be unwieldy to try to describe such a system here. The FTA is often misapplied, and Minton and Johnson [67] have summarized the most frequent errors.

16.4.2.5. Toxic Gas Release Modeling. A form of consequence analysis performed by a growing number of operations is the study of the dispersion of released gases into the atmosphere. This is most often used to determine the possible effects of a hypothetical accident. One can calculate a concentration profile at any time, or the concentration at any distance from the source as a function of time, if given the following information:

1. the amount of material released, instantaneously or over a period of time at a given rate
2. the location (especially the height) of the release
3. the direction and speed of the wind
4. the state of the atmosphere

The last item reveals where and for how long concentrations that are deemed hazardous can prevail. To characterize the state of the atmosphere, environmental personnel most often use a series of defined stability classes. The definitions go back to the work of Pasquill [68] and Gifford [69] in 1961. Their "F stability" is a stable atmospheric condition in which vertical turbulent mixing is suppressed by a sub-adiabatic temperature profile; in other words, an inversion. The "adiabatic lapse rate," the limiting condition for spontaneous vertical mixing, is about $-10^{\circ}\text{C km}^{-1}$. If the negative temperature gradient with altitude is smaller in magnitude, the atmosphere fails to "turn over." This minimizes the turbulent dispersion and allows a plume of released gas to cohere and to move downwind with a minimum of dilution.

Some dispersion studies are responses to regulations. It is becoming more common to require inclusion of a "worst-case" scenario for toxic releases in licensing applications and other plant reports. One definition of "worst case" is the release of the largest inventory of toxic material over a 10-min period with a 1.5 m s^{-1} wind and stability F. The use of F stability is the most conservative assumption. Some regulations allow the use of a more unstable Pasquill class when F stability is a very rare phenomenon. Each class has built into the dispersion model a set of values for horizontal and vertical

standard deviations that fix the calculated spread of the Gaussian plume. The more unstable models predict more rapid dispersion. While they may not be suitable for worst-case scenarios, these models are important in real-time modeling. They provide less drastic but more realistic projections. A moderately unstable atmosphere (“D stability”) is assigned a horizontal dispersion coefficient twice as great as a stable atmosphere. Greater instability, or “A stability,” increases the horizontal dispersion coefficient by another factor of 3. The vertical dispersion coefficients increase even more as the atmosphere becomes less stable. The applied factors are not constant but vary with conditions. The end result is that downwind centerline concentrations may be reduced by factors greater than 100 in progressing from F to A stability.

Choice of the stability class allows relatively easy manual calculation, and many of the results are available in the form of standard charts [70]. This is a simplified approach to a complex phenomenon, and modern computing power makes it possible to take into account variations in wind velocity, terrain, and gas density. Many specialized models and commercial systems are now available [71], and some are used in plants for real-time modeling. Near-field variability remains a difficult problem, and inclusion of features of the terrain and the presence of obstacles such as buildings can have a major influence on the calculated spread of a plume and on the predicted consequences of a release [72].

The ability to model the spread of gases considerably denser than air is particularly interesting to chlorine processors. Relative degrees of atmospheric stability have less effect on the dispersion of heavy gases. Some of the specific characteristics of chlorine also modify the phenomenon of dispersion [73]. Ice tends to form near the release point, for example. There is also the possibility of entrainment of liquid chlorine by the formation of mist or by a choking flow that produces a two-phase mixture. The latter leads to rainout and revaporization of liquid at some distance from the source.

16.4.2.6. Responsible Care®. The typical producer or large consumer of chlorine has a good knowledge of the hazards involved in its handling and provides the proper equipment and training to ensure a good safety record. Some customers and intermediaries are less well informed and equipped. These groups can benefit from more active involvement of those in the chlorine business. This involvement is one of the objectives and obligations of Responsible Care®. Responsible Care is a program whose aim is to promote safety throughout the life cycle of a chemical. It considers development, production, distribution, use, final consumption, and disposal [74]. Signatories to the program commit themselves to communication and cooperation among raw material suppliers, producers, shippers, packagers, users, regulators, and the public. The Canadian Chemical Producers Association established the first program in 1984, and the movement now covers more than 40 countries. It is essentially a voluntary program, but many agencies and associations now encourage or require their members to have Responsible Care programs in place. These include the Japan Soda Industry Association (JSIA), the CI, and EC.

The guiding principles of Responsible Care [75] require subscribers to:

1. seek and incorporate community input regarding products and operations
2. provide chemicals that can be manufactured, transported, used, and disposed of safely

3. make health, safety, the environment, and resource conservation critical considerations for all new and existing products and processes
4. provide information on health or environmental risks and pursue protective measures for employees, the public, and other key stakeholders
5. work with customers, carriers, suppliers, and distributors to foster the safe use, transportation, and disposal of chemicals
6. operate facilities in a manner that protects the environment and the health and safety of employees and the public
7. support education and research on the health, safety, and environmental effects of products and processes
8. work with others to resolve problems associated with past handling and disposal practices
9. lead in the development of responsible laws, regulations, and standards to safeguard the community, workplace, and environment
10. practice Responsible Care by encouraging and assisting others to do the same

The specific requirements were originally gathered into a series of Codes of Management Practice. A Code dealing with security has since been added. This has attracted great attention and accounted for a major part of the recent effort put into this program. It is an active subject in industry conferences [76], and a growing list of publications is available for guidance [77].

Responsible Care has been basically a voluntary program, with members setting their own goals and responsible for their own evaluations. One result was great variability in programs, in public involvement, and in the self-assessed measurement of success. At this writing, the fundamental approach to Responsible Care is being modified. The changes are in the direction of requiring more uniformity in the programs adopted by subscribers and providing new metrics to evaluate the success of the program. Monitoring will be by third parties.

16.4.2.7. Training. Good training programs are essential to safe operation of production facilities, and many regulatory bodies publish minimum requirements [78]. The content of a training program should take into account the needs of different audiences, and testing for comprehension should be an important part. Audiences may include:

1. managers and supervisors
2. plant operators
3. maintenance personnel
4. service personnel
5. technical personnel
6. outside contractors
7. emergency response personnel
8. participants in PSM exercises

Section 13.3 discussed training as part of the commissioning process. Safety should also be a prominent feature of any training program. After the startup of a plant, the extent and frequency of training will depend on the composition of the workforce and the frequency of changes in duties. All new employees should receive general training

on hazards, duties, and company policies. All new and reassigned employees should receive job-specific training, and the programs should be monitored and revised when necessary [79]. There is extensive literature on the subject, which is too specialized for inclusion here. Compilations and general guides are readily available [80]. The many documents published by industry associations will be useful, and the members of these associations freely share information on their successful programs.

There are many publications on training programs, including the two references immediately above, and many training aids are available in the form of seminars, printed material, tapes and films, training kits, and computer software.

The principles covered in this work and the procedures published by EC, the CI, and the JSIA also can be used as material for training programs. While much of it is written for chlor-alkali producers, the basic ideas can be extended to plants that consume rather than produce these materials.

16.4.3. Mitigation of Effects of Release of Chlorine

Here we turn to mitigation of the effects of any releases of chlorine after they occur. We consider first release as vapor, whether from a system handling chlorine gas or from a liquid-phase leak, and then the release of relatively large quantities as the liquid. Small leaks sometimes can be dealt with by emergency intervention. Techniques are highly individualized and are not discussed here. The reader is referred instead to EC's GEST 93/179.

16.4.3.1. Release as Vapor. Section 16.2.1 discussed the allowable concentrations of chlorine vapor in the workplace. The values presented are very low and are tolerable on a more or less routine basis without endangering the health of workers. This section turns to higher concentrations that may be present under emergency conditions. Withers and Lees [81] suggest as a probit for the toxicity of chlorine:

$$Y = -8.29 + 0.92 \ln(C^2t) \quad (4)$$

where

Y = the probit

C = the lethal concentration of chlorine in air, ppm (v/v)

t = the time of exposure, min

The probit is an arbitrary mathematical construct. It is a random variable with a normal distribution, assigned a mean value of 5.0 and a standard deviation of 1.0 [82]. Substituting a value of 5.0 for the probit in Eq. (4) gives the concentration-time relationship for the median case. This is designated by LC_{50} , the dose that is lethal to half the population. We have $\ln(C^2t) = 14.446$, or $C^2t = 1,878,000$. This gives, for example, a 30-min LC_{50} of 250 ppm. The advantages of the probit are that it relates lethality to exposure over a wide range of values and allows some estimation of the fraction of the population affected by a given concentration. The LC_{10} , for example, is removed from the mean by 1.28 standard deviations, and so the value of the probit

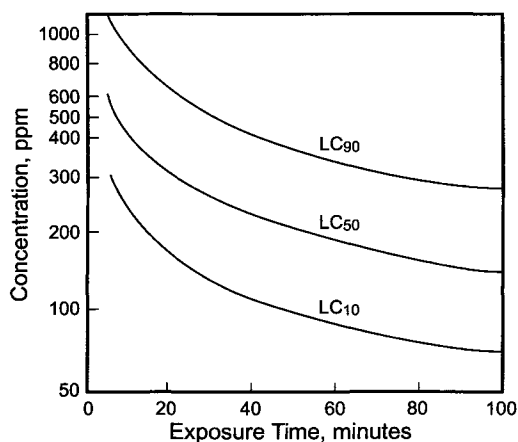


FIGURE 16.2. Time-concentration behavior of toxicity of chlorine.

is 3.72, and $\ln(C^2t) = 13.054$. The 30-min value of LC_{10} is 125 ppm. Other time intervals correspond to other concentrations, and Fig. 16.2 is an example.

The form of Eq. (4) and the shape of the curves in Fig. 16.2 show that there is not a single "toxic dose." In other words, the product $C \times t$ is not constant. Higher concentrations of chlorine are more dangerous than the assumption of a toxic dose would indicate. This seems to be a widespread if not a general phenomenon. When the independent variable in the probit equation is expressed as $C^n t$, the exponent normally is greater than 1.0. Lees [83] gives an approximate value of 2.75 for both ammonia and chlorine.

Harris [84] warns against placing too much faith in the accuracy of the probit over the full range. It would be most helpful to use Eq. (4) to estimate what concentrations are toxic to a smaller fraction, say 1% or less, of the population, but the values even at the 10% and 90% levels are questionable. The difference between the concentration exponent of 2 used in Eq. (4) and the value of 2.75 used by Lees illustrates the problem.

Combining the probit with gas-cloud dispersion calculations (Section 16.4.2.5) is an approach to consequence analysis. Again, users should be aware of all the assumptions behind such a model and have a healthy suspicion of the precision of the results. The generalized dispersion calculations referred to above may not adequately reflect the effect of gravity on dense gases like chlorine. A chlorine gas cloud tends to stay close to the ground. Here, it usually meets more obstacles and always feels more ground friction. This speeds up the dispersion process and reduces the downwind penetration of hazardous concentrations. On the other hand, it increases the lateral spread of the cloud. This can increase the width of the hazardous area, especially near the release point. Gravity also keeps more of the cloud at a breathable height. Another aspect not covered by generalized methods is the possibility of aerosol formation in a two-phase release. The total amount of chlorine present in a cloud may be more than that calculated. Depending on the size of the particles formed, there may be gradual rainout as the cloud travels, followed by

vaporization at ground level. This was already alluded to in Section 16.4.2.5. Very small particles may remain with the cloud and gradually vaporize.

Most public disaster plans include some scheme for evacuation of a plant and part of its surrounding area. Given the speed with which a chlorine cloud moves downwind, such schemes are of doubtful value in many instances. A better approach may be to take shelter in a building with doors and windows closed and air circulators idle until the cloud has passed.

16.4.3.2. Release as Liquid. Liquid chlorine itself is easily contained if it spills. The greater hazard lies in its vaporization, and the preceding discussion on vapor releases applies to liquid releases as well. There are two stages of vaporization to consider, immediate flashing to the atmospheric boiling point and slower continuous vaporization from an unconfined pool. The first mechanism pertains to chlorine that was held under pressure above the atmospheric boiling point of -34°C . Liquid, when released, will boil under its own sensible heat until its temperature drops to the boiling point. This vaporization is nearly instantaneous. Figure 16.3 shows the calculated percentage vaporization as a function of storage temperature. Another curve with a different ordinate scale shows the saturation pressure corresponding to that temperature. Working backward from the storage pressure will give a conservative estimate of the amount of vapor generated. Note that at most primary liquefaction temperatures, about 10% of a chlorine spill will vaporize immediately. When chlorine held at warm ambient temperature spills, this increases to 20–25%. Given a favorable mass-transfer situation, such as being spread into a wide pool and subjected to a wind, the liquid can become subcooled. Figure 16.3 also shows that cooling to -50°C increases the quantity of chlorine vaporized by 4.5–5% of the amount spilled.

After flash vaporization, or from the start if chlorine spills from a system at atmospheric pressure, the pool begins to evaporate. Since the liquid has no sensible heat to contribute, an outside source of heat is required to produce vapor. Therefore, the

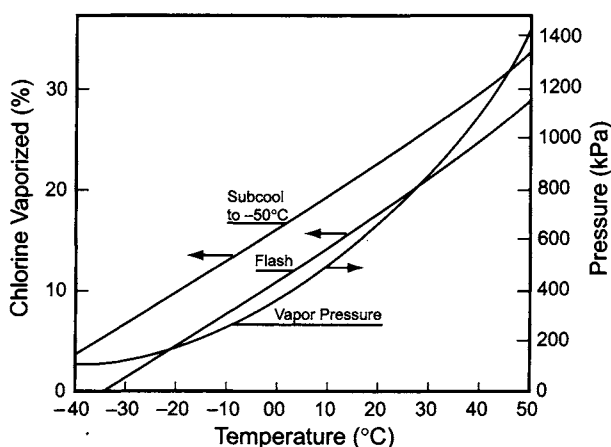


FIGURE 16.3. Instantaneous vaporization of chlorine spill.

substrate in the collection zone should be impervious. If chlorine is able to percolate, for example into sandy soil or a surface covering of gravel, the area of solid in contact with chlorine increases markedly. This increases the rate of heat input and thus the rate of vaporization of chlorine. Similarly, there are advantages to using materials with poor heat-transfer properties in the collection area. At the same time, these materials should have low porosity, again in order to reduce the surface area in contact with the chlorine.

If a chlorine storage tank is simply diked, a low wall may be sufficient for containment, but the area available for vaporization of chlorine and for transfer of heat to the chlorine from the air and the ground will be relatively very high. Better control of the vaporization process results when the floor under the storage tank is sloped and the liquid is collected into a deeper sump of smaller area. Dike walls should always be vertical or nearly so in order to prevent spillover of chlorine due to wave action or its initial momentum.

A collecting sump can be designed with a small area exposed to the atmosphere. This reduces the rate of mass transfer (i.e., the rate of formation of vapor). It also provides an opportunity to apply a cover and vent the sump to an absorption device. Figure 16.4 shows some of the design practices that contribute to mitigation of the results of a spill of a volatile liquid.

Another technique for control of the vaporization of liquids is the application of foam. This provides a barrier between the surface of the liquid and the atmosphere, and its intent is the reduction of heat- and mass-transfer rates. Those considering the use of foam should have a clear understanding of the physics involved. Harris [56] points out two basic facts:

1. The application of aqueous foam to a pool of chlorine adds heat to the liquid mass. As the foam collapses, the contained water drains and contributes sensible heat to the colder chlorine. The water will also freeze or react with the chlorine

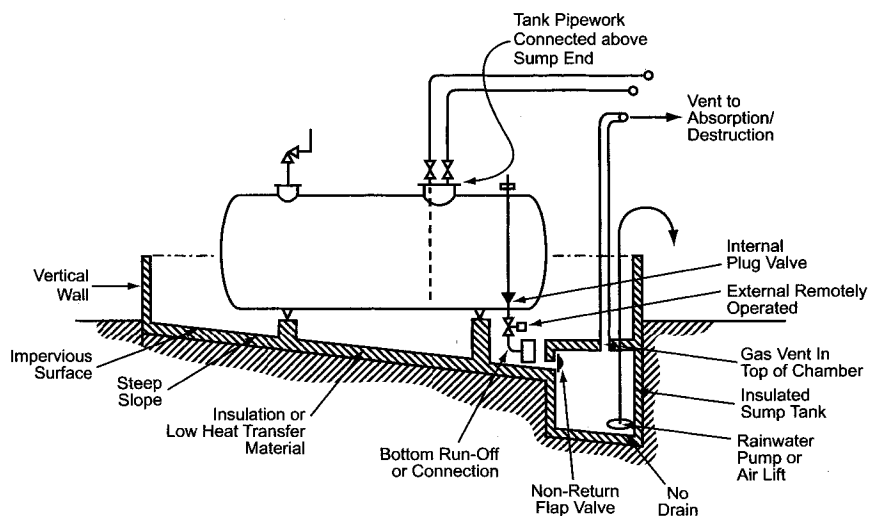


FIGURE 16.4. Possible containment features for liquid chlorine storage.

to form the hydrate (Section 9.1.3.5). Both these processes are exothermic. The heat supplied by the application of the foam will cause a certain amount of chlorine to vaporize.

2. The best methods of treatment of flammable and nonflammable spills may be quite different. Part-time emergency workers, such as those in local fire departments, do not always understand this. It is the responsibility of the chlorine manufacturer or user to see to it that these people have some training in the proper response to a chlorine spill and do not automatically apply a foam when it is not called for.

A foam can break down with time or be carried away by the wind. Repeated applications may be necessary. The ideal foam will have a high expansion factor, to keep the water content low, but not too high a factor, to make it less likely to be carried away. For a foam to be effective, it must prevent more vaporization that is due to other causes than it creates by its own action. It can do this only by preventing the influx of heat from the atmosphere. Accordingly, there is no case for the use of foam on a chlorine spill indoors in any case or outdoors on a cold, still night. An alternative to foam is a plastic sheet large enough to cover the surface of the collected liquid.

Another technique for mitigation of the consequences of the release of a volatile liquid is the control of the vapor by a water spray or curtain. For example, large quantities of water have been effective in capturing pressurized, superheated HF after sudden release from a container [85,86]. Neutralizing agents added to the water were of little value, and fire monitors appeared to be as efficient as spraying systems. HF is highly soluble in water, and this fact accounts for its efficient removal from the gas cloud. The first thing to understand about the use of a water curtain in our case is that it is not a technique for dissolving chlorine. The solubility of chlorine is too low (Section 7.5.9.1) and the mass-transfer process is too inefficient. A water curtain is a barrier on one or more sides of a vapor cloud and a source of energy for dispersal of the vapor. Any absorption of chlorine provides very slight mitigation of the original hazard but also creates a cleanup problem. Anyone planning to use a water curtain for containment within a plant therefore must plan carefully for drainage and collection of the water. It is also important to avoid spraying water onto a leak, especially in a ferrous metal system. This can increase the rate of corrosion dramatically and aggravate the problem.

Thomerson and Billings [87] describe field tests in which chlorine was released at up to 70 kg min^{-1} from three 1-ton containers. Typical wind velocities were about 9 m s^{-1} . Relative humidity was very low, the test site being located in the Nevada desert. It is noteworthy that the temperature of the spilled liquid stabilized at about -50°C , well below the boiling point of -34°C . The wind subcooled the liquid, which was collected in a well-insulated pan, and approximately 50% of the chlorine vaporized during a test. The use of downwind water sprays in these tests reduced the concentration of chlorine in the air by an average of 31%. This was attributed to the induction of dilution air by transfer of momentum from the spray. As noted above, the spray also forced the vapor cloud lower, so that the concentration of chlorine at 1.5 m elevation was actually higher for a distance of 230 m from the point of release. In these tests, portable fire water monitors performed relatively poorly.

16.4.3.3. Quantitative Risk Assessment. Previous sections in this chapter dealt with the identification, measurement, and mitigation of hazards in a chlor-alkali plant. Plant safety and Responsible Care programs define the objectives of continuous improvement in safety performance. The discussion of mitigation immediately above naturally leads on to the larger question of the most direct and cost-effective approach to this improvement.

Quantitative risk assessment, based on the techniques presented here, is finding increased use in the guidance of these efforts. The risks presented to workers and plant neighbors by a chlorine release, for example, can be evaluated by combining:

1. preliminary hazard analysis (PrHA) to identify the most likely sources
2. Hazop to identify likely scenarios
3. FTA to determine potential incidents and their probabilities
4. estimation of the size of a release
5. maps and population density data to determine how many people may be at risk
6. gas-release modeling to establish time-concentration behavior over the affected area
7. probit analysis to assess the potential for fatalities

The major objective of quantitative risk assessment is to determine the magnitude of a specific risk and the sum total of foreseeable risks to an individual worker and to the population at large. Staying with our example of a release of chlorine, one should be able to identify the probability of exposure to a certain concentration or use all the information available along with an agreed probit to determine the expected frequency of fatal accidents. On a larger scale, quantitative risk assessment also allows an analyst to determine a frequency distribution of incidents leading to the various numbers of fatalities. The latter is usually presented in a plot of calculated frequency (f) against the number of prompt fatalities (N).

For quantitative risk assessment to be useful, there must be recognized criteria for judging hazards. The criteria given in EC's GEST 90/161 [88] start from consideration of natural mortality. The minimum level, for 10–15-year olds, is about 10^{-4} /year. The policy adopted requires that an activity should not increase the background risk by more than 1%. The upper bound of acceptable individual risk is therefore 10^{-6} /year. An increase of 0.01% in risk is considered negligible. This corresponds to 10^{-8} /year. The definition of individual risk set by the government of The Netherlands is the expected frequency with which a hypothetical person permanently located out-of-doors at a given distance from the hazardous source would be killed. The real risk to an individual will generally be significantly lower, because this definition allows no reduction for successful escape from the hazard.

There must also be a risk criterion for hazards with potentially large societal impact. Here, incidents in which 10 or more people are killed with calculated frequencies of 10^{-5} /year or higher are deemed unacceptable. A reduction of the expected frequency by a factor of 100 again allows the risk to be considered negligible. The seriousness of a risk is taken to be proportional to the square of the number of people involved. Figure 16.5 summarizes these criteria.

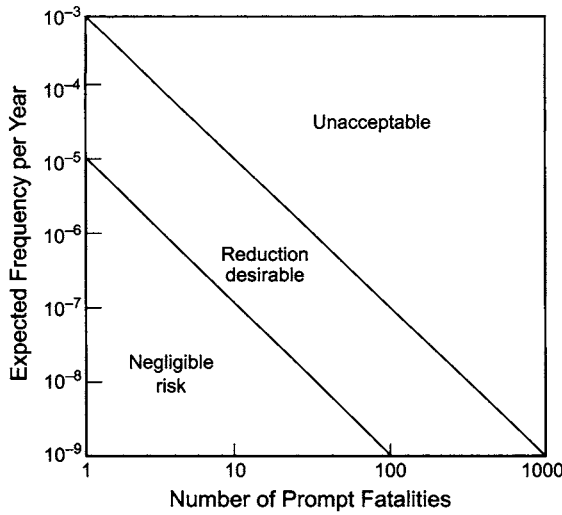


FIGURE 16.5. Criteria for group risk.

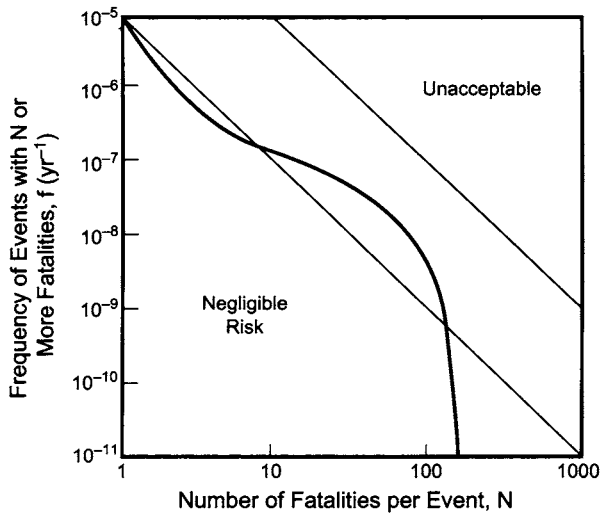


FIGURE 16.6. Typical group risk f - N curve.

Figure 16.6 shows the f - N curve generated by a risk analysis for one site [83]. The lines of Fig. 16.5 are superimposed. These show that the risk is at all points below the acceptable level. It is in fact always less than 10% of the acceptable level, and the overall rating would be that this is a low-risk operation. In the range $N = 5$ –150, the risk is above that considered negligible. To the extent that one can choose, continued efforts at improvement might concentrate in this area.

16.5. WASTE MINIMIZATION AND DISPOSAL

The amount and nature of wastes generated in a chlor-alkali operation depend on the technology practiced and the condition and methods of operation of the plant. Disposal practices will depend on the wastes generated and on local regulations or plant objectives regarding their disposal. This section gives a brief discussion of disposal problems and practices for certain wastes. For convenience, we group these as solid, liquid, and gas depending on their state in the process. Mercury-bearing wastes are a special case and are treated in a separate section. While not a "waste," retired brine caverns are an ongoing environmental issue, and a brief discussion of the most likely problems also appears in this section.

16.5.1. Solids

16.5.1.1. Membranes. Membranes are generally inert and contain no hazardous material. They are considered safe to handle, and only the most basic precautions, such as avoiding prolonged contact with the skin, are necessary. There are no serious problems with liquid or gaseous discharge, and we comment here only on disposal of the membranes themselves.

Membranes to be removed from the cells will be wet and swollen with electrolytes and should be handled accordingly. Rinsing and soaking relieve this particular hazard. Used membranes can be sent to a sanitary landfill. Another possible method of disposal is incineration. Off-gases must then be scrubbed with an alkaline medium to prevent the escape of HF and other corrosive or toxic gases.

Scrap produced by trimming sheets of membrane to size should be disposed of in a similar fashion.

16.5.1.2. Asbestos

16.5.1.2A. Air Emissions. Inhalation of airborne particles is the major concern with asbestos. The measures taken to confine solid and waterborne asbestos are intended primarily to prevent its later escape as dry fibers into the atmosphere.

There is also the possibility of direct discharge to the atmosphere whenever asbestos is handled. Final handling of the dry material and application of diaphragms take place in enclosed, ventilated areas. Workers in those areas wear respirators for protection. Access regulations, negative pressures in operating areas, and filters on air discharges prevent the escape of asbestos into the surroundings. Much of the handling of asbestos from its arrival on the plant to its delivery to the depositing facility is often in closed containers to prevent its escape. Any spills that occur should be collected promptly before they are dispersed and become airborne.

16.5.1.2B. Water Effluent. Most chlor-alkali asbestos waste is first produced as a suspension in water. Spent diaphragms typically are removed from cathodes by a water spray. Especially in the case of modified diaphragms, the water supply may be at high pressure, and splashing is severe. Facility design must first of all confine the discharge and then collect the water and wet asbestos in a defined area or sump. Wash water used

to remove spills and asbestos flyings from floors and walls can be collected in the same way. The momentum of a stream of wash water can disperse dry asbestos before it is sufficiently wet. Therefore, this operation requires some care.

Primary separation of the mass of asbestos can be by settling in the sump. Final cleanup of water discharge is by filtration. Much of the water can be reused, reducing the volume to be discharged.

The concentrated asbestos slurry also can be filtered to a concentration suitable for collection in secure packages for disposal. Wet, filtered asbestos is much easier to handle and less likely to escape than dry asbestos. It is therefore less hazardous. Wet asbestos, however, has the unfortunate tendency to become dry asbestos, and so it should be collected and packaged promptly.

16.5.1.2C. **Solid Waste.** Regulations for the disposal of asbestos vary with locality but usually involve sealing the wastes in impermeable containers for final disposal by a licensed agent.

Some producers prefer to use disposable clothing for employees handling asbestos. The clothing should be considered contaminated, and then wrapped and disposed of as asbestos waste.

16.5.1.3. *Brine Sludges.* Here we consider the undissolved or precipitated solids that must be removed from salt dissolvers and brine clarifiers. The amount of solids left behind in the salt dissolvers depends greatly on both the composition of the salt and the method of operation of the dissolving process. Table 7.2 gives representative figures for the amount of residue left by salts of different quality. The solids are primarily sand, clays, atmospheric deposits, soil picked up while handling the solid salt, and calcium sulfate that did not dissolve. The last-named contaminant is selectively left behind, especially in those dissolvers that limit the time of contact between the salt and the dissolving water. It may also be selectively rejected by special inhibitors or by the addition of calcium ions to the dissolving fluid. All these techniques of selective dissolving are discussed in Section 7.2.2.5. The great mass of this particular sludge is nonhazardous, and its disposal often does not pose a regulatory problem. Unless the dissolvers are designed for continual removal of the undissolved solids, shutdowns are required, and removing the solids from the vessels can be a very messy operation. This is one reason for confining the area at the bottom of the dissolvers, so that the remnants of the sludge that are hard to pick up cleanly can be contained and later collected by sweeping, scraping, or flushing with water into a sump.

Clarifier sludge is removed continually from the bottom of the clarifier cone (Section 7.5.3.2D). Its composition is quite different from that of saturator sludge, consisting mainly of carbonates and hydroxides of the precipitated metals. Like the saturator sludge, it is usually nonhazardous, and disposal is not complicated. When barium is used to precipitate sulfate, and in those rare cases where barium is found in considerable quantity in the salt or brine, the sludge requires characterization before it can be sent to a landfill. Traces of other heavy metals may also restrict methods of disposal.

The reference to the material in the sludges as nonhazardous applies only to membrane- and diaphragm-cell plants. In a mercury-cell plant, the sludges will contain

mercury dissolved in the occluded solutions and possibly also as precipitated solids. The latter problem can be relieved by maintaining a certain level of free chlorine in the depleted brine that is recycled to the dissolvers for reconcentration (Section 7.5.9.2A). This keeps the mercury oxidized to the soluble form HgCl_4^{2-} . The recovered sludge still must be rinsed to remove the occluded brine, and with it the dissolved mercury. The sludge also can be treated to remove mercury before disposal.

16.5.1.4. Filter Solids. There are several different kinds of filtration operation in chlor-alkali plants. Every case requires a separate decision on how to dispose of the solids removed from the filter. In this discussion, we do not consider the problem of occluded mercury in filter solids. The special problems of mercury-contaminated solids are discussed in Section 16.5.5.1.

Some minor operations and some utility-polishing filters have very low solids loads, which may not be recovered separately. Rather, the filter element may be discarded along with the solids. These seldom present a serious toxic hazard. Good practice may require rinsing of these elements before disposal to remove traces of process fluids. Otherwise, it may be the safe and acceptable disposal of the filter elements themselves that governs the procedure.

Brine polishing filters (Section 7.5.4.2) usually employ solid filter aids, which become part of the disposal problem. Their most obvious effect is to add to the volume of solids requiring disposal. Since most filter aids are cellulosic or siliceous, again the toxic hazard is quite low. The operator handling these wastes, however, should be familiar with their detailed analyses, because trace contaminants (e.g., metals in the filter aids) may need special attention. The filtered solids are of approximately the same composition as the clarifier sludges discussed in Section 16.5.1.3.

Both steps in the brine filtration process usually rely on backwashing or sluicing to remove the filtered solids. This is done to keep the productivity of the filter installation high and to avoid the handling of messy pastes and sludges. The practice in some plants has been to take these backwash streams to a settling chamber or pond and to let the solids gradually settle out of the liquor. After removal of the supernatant liquor, the resulting muds can be scooped or dredged for removal from the site or even allowed to accumulate in a designated area. Removal to an offsite landfill is now becoming more common, and this usually requires production of a mass with a high solids content. This leads to another filtration operation in which the recovered solids are delivered as a slurry. Belt filters and rotary vacuum filters appear in this duty. The filtrate, which may still contain suspended solids, returns to the brine treatment process. Commonly, the final filters are elevated to allow the cake to drop directly into containers or vehicles for removal from the site.

Another method for disposal of brine-system solids, although much less frequently used, is to send them to an operating or retired brine well for underground disposal. Section 7.2.2.4C discusses this option.

16.5.1.5. Miscellaneous Solids. Miscellaneous solids include auxiliary materials used in the process, small parts being replaced, packages and wrappings, and everyday trash. Carbon, other adsorbents, filter aids, and ion-exchange resins used to treat water and

brine are examples of materials removed from the process. Consumable parts include valves, gaskets, packings, cell renewal material, etc. Materials in these two categories should be rinsed or washed to remove process materials. All miscellaneous solids should then be disposed of properly, according to their respective properties. Segregation of the various types can simplify the procedures.

Anything exposed to mercury during its use will require special handling and perhaps decontamination (Section 13.12).

16.5.2. Liquids

16.5.2.1. Spent Sulfuric Acid. The sulfuric acid used to dry chlorine gas becomes a waste product. The discussion in Section 9.1.4.1 shows that the quantity of waste acid generated is inversely related to the difference between the concentrations of feed acid and waste acid. Production of a more dilute waste acid means generation of less waste product. This is constrained by the ability of the drying system to produce chlorine gas of satisfactory quality, the increasing corrosivity of the chlorine-containing acid, and the method of disposal of the waste acid.

Possible means of disposal include:

1. productive use as a neutralizing agent for alkaline waste streams
2. dechlorination of waste condensate from a chlorine cooling system
3. return to the sulfuric acid supplier for disposal or reconstitution
4. neutralization by alkaline material for disposal

In any of these cases, prior removal of dissolved chlorine from the spent acid is desirable, and this is the subject of Section 9.1.4.4E. Method (4) appears on the list above as well as method (1) because the amount of acid generated may exceed the local demand for neutralization of alkaline waste. This situation depends on a plantwide balance and is not constrained to the battery limits of the chlor-alkali unit. Use of the acid as a dechlorinating agent, as in number (2), is limited to situations in which the treated condensate is not returned to the brine process (e.g., diaphragm-cell plants). The presence of sulfates in the stripped product makes it unsuitable for recycling. Many producers favor option number (3), when it is available. The supplier's ability to handle the material may dictate the concentration of the spent acid.

16.5.2.2. Process Condensates. Many operations produce condensed water from process fluids. These may arise from cooling process gases (chlorine and hydrogen) or from condensation of vapors produced in evaporation or crystallization operations (salt, sulfate, or caustic). Selective reuse of the condensate streams in the process reduces the volume, and especially the total dissolved solids load, for disposal.

We shall treat handling of these condensates in a mercury-cell plant as a special case in Section 16.5.5.3. In the other technologies, with the exception of chlorinated condensate, the condensed streams usually present no severe hazard, and their disposal is relatively simple. Contamination with caustic or salts is usually through entrainment from an evaporating system. Unless there is an accidental massive entrainment, the dissolved solid content of these streams can usually be kept within reasonable bounds.

Disposal is safe and can be kept within permissible limits by managing the degree of entrainment with standard devices.

Caustic is the most valuable as well as the most hazardous of the latter group of contaminants. Most plants have more or less elaborate schemes for recovery of caustic evaporator condensate and its use in the process. This is especially true in diaphragm-cell plants with their high evaporative load, and the reuse of evaporator process condensate is the subject of Section 12.4.3.2. Hydrogen gas will also carry a certain amount of caustic entrained from the cells. Much of this is removed in cooling the gas.

While the solubility of hydrogen in aqueous solutions is very low, there is still the possibility of some entrainment of gas when condensate forms. This is usually not a large quantity, but it should be considered whenever the condensate is held in a closed system.

Chlorinated condensate arises in the chlorine cooling system and must be stripped before disposal and even before reuse in the process. A secondary dechlorination may be necessary if the water is to be discarded or transferred to another operating unit.

Condensation may take place by transfer of hot gas with a process stream, by indirect cooling through a heat-exchange surface, or by direct contact with a coolant. In the first instance, condensed material is kept within the process and is not an immediate disposal problem. When removed by indirect cooling, condensates are at full strength and are most easily gathered for treatment. Direct-cooling systems, as for instance in barometric condensers attached to evaporation systems, produce low-level contamination of cooling water. The immediate result is usually a slight increase in the dissolved content of the cooling water. This requires a higher rate of blowdown of water from the cooling water system (Section 12.4.2.1D).

16.5.2.3. Caustic. Dilute solutions of caustic that are free of process contaminants can return to the process. They can be used to dilute caustic product for brine treatment or for general utility application. In membrane- and diaphragm-cell plants, they can be blended at a controlled rate with evaporator feed. In mercury-cell plants, they can similarly be used as part of the decomposer water feed.

In some cases, it will be necessary to dispose of caustic wastes outside the chlor-alkali production area. Local regulations and permits then govern their final disposal. The waste should always be neutralized before discharging to a stream or a sewer. Dilution also may be necessary when the caustic concentration is high. Strong alkalis can interfere with bacterial activity in wastewater and sewage treatment plants. Those in charge of a receiving facility should be notified promptly whenever there is an accidental spill of caustic.

Chlorine scrubber waste solutions are a special case here. The controlled reaction of chlorine and caustic soda produces commercial bleach solutions. A loss of strict control of the reaction conditions allows the hypochlorite produced by the primary reaction to degrade (Section 9.1.10.3A). In an emergency scrubber, total capture of chlorine that is released unpredictably and at highly variable rates is a more urgent goal than is the preservation of the hypochlorite. The liquor may then become a waste product. It should be considered a hypochlorite waste and treated as in Section 16.5.2.6.

16.5.2.4. Ion-Exchange Regenerants. Section 7.5.5.2B shows that each regeneration of an ion-exchange bed creates about 0.6 m^3 of effluent/daily ton of chlorine capacity. This is a large total volume of high dissolved solids concentration. The reference section therefore discusses ways to reuse much of the acid and caustic value somewhere in the process, and this should be one goal in design.

With proper design and monitoring, it is possible to segregate objectionable effluents from nearly pure water (the average electrolyte concentration in the streams listed in Table 7.17 is only 1.3%). This would reduce the volume requiring treatment but not the true pollution load. The simplest approach to reducing the amount of hazardous material is to allow the effluent to equalize somewhere. Self-neutralization then removes most of the HCl and NaOH. Table 7.17 shows that conversion of the resin back to its sodium form is more efficient than regeneration with HCl. The equalized effluent therefore is acidic. All the residual NaOH should be converted to NaCl, along with about 90% of the HCl. The combined effluent has a concentration of about 1%, consisting of 0.20% HCl, 0.07% CaCl_2 , and 0.78% NaCl. This produces a calculated pH of 1.0–1.5. In all normal cases, then, discarded waste from regeneration requires neutralization by an alkaline material. Using the same basis as above, neutralization would require up to 1.5 kg NaOH/t Cl_2 and produce a stream with 1.1–1.2% total dissolved solids.

16.5.2.5. Utility System Blowdown. The generation of plant utilities also produces wastes that require proper treatment and disposal. Here we consider three categories:

1. Water treatment
2. Steam condensate
3. Cooling water

All of these utilities are discussed in Chapter 12. Their wastes, described below, usually do not present new or different problems of waste disposal, but they do require the proper facilities and management.

The water treatment process, which may not be necessary in some plants and not connected with the chlor-alkali operation in others, may remove suspended solids, dissolved solids (primarily hardness elements), color bodies, and other organics. Suspended solids may be removed directly by sedimentation or with the aid of coagulants. Dissolved impurities are usually removed by precipitation with chemical treating agents. The solids generated are removed by sedimentation and filtration, often with the use of filter aids. All these additives increase the volume of waste. Control measures are quite similar to those used with similar process wastes.

In some plants, further treatment of the water is required. The generation of boiler feed water to raise steam for the process nearly always requires more treatment, notably by ion exchange. This operation produces its own waste when regeneration of the resin is necessary.

Steam condensate may be contaminated in the process, and it usually contains some level of treating chemicals that include corrosion inhibitors, neutralizing agents, and oxygen scavengers.

Cooling water makeup normally is not highly treated water, and so it adds to the dissolved solids disposal burden. It also contains treating chemicals such as corrosion

inhibitors, neutralizing agents, etc. Equation (12.6) relates the volume of blowdown required to the acceptable concentration factor (effluent/makeup) for dissolved solids and the characteristics of the cooling tower operation.

16.5.2.6. Hypochlorites. Hypochlorites are not highly stable compounds. One of the problems faced by bleach producers is their tendency to decompose spontaneously:



This instability can be put to good use in the handling of waste solutions. A simple holding pond, especially one subject to strong sunlight, can substantially reduce the hypochlorite content of a solution. The disadvantages of this approach are the lack of operator control of the decomposition process, the large plot area required, and the odors (in this case, usually not unpleasant) that arise from open ponds.

Various metals catalyze reaction (5). Homogeneous catalysis by dissolved salts, such as nickel sulfate, is useful in the treatment of plant wastes. The higher rate of reaction makes treatment in vessels of reasonable size feasible. These catalysts would not be applicable to streams, such as depleted brine, that recycle to the process. Instead, over the years, there have been attempts to produce heterogeneous catalysts for use in fixed beds. These rely on catalytically active metals such as cobalt and nickel. Section 7.5.9.3B discusses the process and apparatus now used commercially with a nickel catalyst [89].

16.5.2.7. Refrigerant. While some chlor-alkali plants may still be using refrigerants with high ozone-depletion potential, we assume that they are few and gradually disappearing and that no new plants will use such refrigerants. Therefore, the extra measures required for containment are not discussed here.

There is no situation in which it is desirable to remove a refrigerant from its confining system during operation. An efficient system will contain a purge unit designed to remove accumulating moisture and noncondensable gases. This should be carefully designed to prevent escape of a refrigerant with the purged gases. The refrigerant should instead be condensed and returned to the system.

Refrigerant losses can occur when charging a supply, during operation, and during maintenance shutdowns. Keeping the refrigerant confined during operation is a matter of proper design and installation. All joints must be made and kept tight. Occasional checking for leaks will help to prevent losses. Maintenance may require removing the refrigerant charge from a machine. Every installation should have a pump-out compressor that can be used on any one of the parallel refrigeration systems. The compressor should be able to remove essentially all the refrigerant from the unit being shut down and transfer it to a holding tank or to one of the parallel units.

16.5.3. Vapors and Gases

Well-operated membrane- and diaphragm-cell plants should not have serious problems with gas releases. Some plants, generally small in capacity, deliberately release hydrogen

into the atmosphere. Proper dilution and dispersal keep the concentration of hydrogen everywhere well below the lower explosive limit. Otherwise, hydrogen is not a dangerous substance and does not create an air pollution hazard. Gaseous chlorine can escape when there is a process upset or when it is incompletely liquefied or reacted in the plant. As described in other sections of the book, there are extensive facilities to prevent its escape into the atmosphere. Fugitive emissions of chlorine are another issue [90]. These can arise from any point in the chlorine-handling process, whether the fluid is liquid or gas. Leakage is more severe when liquid chlorine is present at the fault. Even under the same pressure, a liquid-phase leak will release much more chlorine than will a gas-phase leak. Under one typical set of conditions, there is a factor of 16 between the two cases in the rates of release [91]. At low pressure and in the absence of flashing within the orifice, this factor becomes greater (~ 25). Every joint and every valve are potential sources of emission. In addition to the normal maintenance programs, there should be occasional surveys to identify points of leakage. Identified sources can then be assigned maintenance priorities.

16.5.4. Retired Brine Caverns

Section 7.2.2.4 discussed the production of brine by solution mining. Eventually, each solution-mining site will go out of operation and must be secured. Conversion into a waste storage facility is a different case, not treated here.

Usually, addition of a sealant to the mineshaft isolates the retired cavern and allows it to be abandoned. However, there are several processes that continue underground. These must be considered in planning for abandonment and probably will require monitoring for some time [92]. First, salt will continue to creep into the hollow space created by mining. Second, there usually is transfer of heat from the salt to the brine in the cavern. Both these processes tend to increase the internal pressure. The first process is most pronounced in the first 10 years; the second can continue for decades. In either case, the rate of pressure increase is greatest at the start and gradually decreases. An example in the reference report showed that pressure in one well increased from essentially atmospheric up to about 2.6 MPa in 2 years. The increase in pressure is partly offset by leakage through the seal and permeation into the salt. Both are undesirable, especially the second. The salt becomes much more permeable when the internal pressure reaches the point where it closely matches the stresses in the salt formation. This must be avoided to prevent spread of the fluid. The first measure is to leave the well uncapped for as long as is reasonably possible. Next, the increase in pressure can be mitigated by occasional withdrawal of fluid from the cavern.

16.5.5. Mercury-Containing Wastes

The typical mercury-cell chlor-alkali plant has elaborate facilities for containment of mercury within the process area and for removing it from discharged streams. The amount of mercury released into the environment by chlor-alkali producers has been decreasing steadily, partly because of the emphasis on its control and partly because of the downward trend in mercury-cell production. During the five years ending in 2001, for example, the mercury-cell capacity of EC producers dropped from 64% of the

installed total to 54% [93]. Since then, European mercury-cell production has, for the first time, dropped below 50% of the total [40]. Measured releases of mercury in 2001 were 1.25 g t^{-1} chlorine. This includes emissions to the air or water and mercury contained in products. It represents a 74% drop in the total over 10 years. A perennial problem with the analysis of mercury-release data has been the poor accountability usually achieved in global material balances. Purchases have consistently been several times higher than measured releases. In the United States in 1996, for example, the chlor-alkali industry identified 35 tons of released mercury. Total purchases for the same year were 136 tons [94]. The latter figure will vary from year to year because it is only a small part of the total chlor-alkali inventory of about 3,000 tons. A running average of 150 tons purchased per year indicates that the inventory, nearly all of it in-process, is about 20 times the yearly reported consumption.

Regulatory pressure to reduce mercury emissions, meanwhile, increases continually. There is a new trend to regulate the effects of mercury rather than its concentration in plant effluents or in receiving systems. In this regard, Section 16.2.6 mentioned the use of the concentration in fish rather than in the body of water in which they reside. In the United States, the EPA wants to regulate the overall use of mercury and reduce its “intentional” use by 50% of 1995 levels by 2006 [95]. Goals are to limit the impact of mercury from abandoned mines and ongoing mining activities, reduce air emissions, limit the use of mercury as a global commodity, and develop water discharge limits that take deposition from the air into account.

The retirement of mercury-cell plants has created a new issue, the disposal of their mercury inventory. This has been considered a “waste” by some. However, mercury remains a useful commodity and automatically regarding it as a hazardous waste may be counterproductive [96]. Handling of mercury is an issue that requires an accepted societal policy. The metal is available from strategic reserves, retired or converted cell rooms, and reclamation processes. Total stocks worldwide are estimated roughly to be 25–50,000 tons [97]. The gradual run-down of mercury inventory before retiring a plant is not a useful technique. The opposite approach, increasing the amount of mercury in the cells, has in fact been used in older plants to improve cell performance and reduce the loss of mercury to the environment [98].

Worldwide demand still requires the production of virgin elemental mercury. In some countries, however, availability from the sources mentioned above exceeds demand. It would seem better to withdraw mercury from such a stock than to continue to produce metal from ore and thus to add to the world’s inventory. Such an approach has already been agreed upon between the EC and a Spanish mine [99,100]. In the years from 2001 to 2003, 920 tons were transferred from idle plants to the mine, replacing that much new production. Along the same lines, Sznoppek and Goonan [94] point out the ease with which metallic mercury can be reclaimed from defunct plants and recycled for use elsewhere.

Section 16.2.6 discusses the toxicity of mercury and matters of industrial hygiene. This section is concerned only with the methods that are used to reduce the amount of mercury released into the environment. The subsections that follow describe some of the techniques used in treating solids, gases, and liquids as they leave the process. It is always preferable, however, to control the release of undesirable material within the process. Section 9.2.5.1 described techniques for removal of mercury from hydrogen

as the gas is prepared for delivery. Section 9.3.2.6 described the removal of mercury from product caustic by filtration. In the case of hydrogen, mercury condensed from the gas can be returned directly to the electrolyzer system. Hydrogen is also often scrubbed with brine containing free chlorine. This is discussed below. Mechanical changes and modified procedures may also be considered in-process controls. These are commonly used by mercury-cell operators in their abatement programs, and some of the techniques are discussed below.

16.5.5.1. Mercury-Contaminated Solids. Many plants have recovery facilities that include a retort for vaporizing mercury in order to recover it from inert solids. This is useful for treating small items or small lots of material that are to be removed from the area. Examples include gaskets, decomposer packing, etc. Some wastes, such as the decomposer packing, can be pretreated to remove most of the mercury beforehand. Mercury butter, or thick mercury, is another source that yields mercury by vaporization. This is recovered from cells periodically, and stable operation of the cells with high-quality brine can minimize its formation [101].

Section 13.12 treats the special subject of decommissioning of mercury-cell plants. It tabulates the methods that might be used to reclaim mercury from various types of waste or render it less likely to escape into the environment. It includes the disposal of large parts such as cells and contaminated structural elements [102].

Large-scale handling of solids is also necessary in site-reclamation projects. Thibeault *et al.* [103] discuss the handling and treatment of contaminated soil. The separation in their unit was primarily mechanical. Classification to remove rocks followed by shredding of the soil and then attrition with water in a cement mixer released much of the mercury for collection and storage. The process continued with screening, centrifugation in hydrocyclones, and flotation. The clean soil from the flotation cells was agglomerated, dewatered, and filtered before disposal in a secure landfill. The treatment of about 9,000 tons of soil yielded 650 kg of recovered mercury.

In operating plants, brine and water treatment sludges are the major sources of solid waste that is contaminated with mercury. Maintaining a slight concentration of hypochlorite in the circulating brine has already been mentioned as a way to prevent deposition of mercury in brine-treatment sludge. Similarly, hypochlorite solutions can dissolve residual mercury that is present in low concentration in brine sludge or oxidize and dissolve mercury that is present in high concentration as a precipitated compound in water-treatment sludge. The clean sludge, after testing to ensure compliance with regulations, can be removed from the producing site. The dissolved mercury, present as HgCl_4^{2-} , can, in many cases, be recycled directly into the brine system. With additional processing, it can also be reduced to reusable metallic mercury by contact with the appropriate metal (e.g., powdered iron) [104].

16.5.5.2. Air Emissions. In an early study of methods for plantwide mercury control, Hine and coworkers [101] recognized at the outset that control of emissions in the cell room ventilating air would be the most difficult task. This situation is due to the diversity of possible sources and the difficulty of treatment of the air. The use of gravity ventilation in cell rooms (Section 8.2.3) makes such treatment impracticable. Likewise, it is not

feasible to reduce the flow of ventilation air below a certain point. Abatement therefore requires measures to eliminate sources of mercury vapor, to contain them where possible, and to treat air emissions at their source. Among the first actions in an old plant, accordingly, was the removal of accumulated mercury from the floor and other surfaces in the building. Mercury subdivides very easily and gathers in cracks and small depressions in surfaces. It then proceeds to vaporize slowly into the cell room air. The floor in a cell building therefore should be whole, smooth, and properly sloped to collect any spilled mercury.

Improved control of sources can be as simple as providing covers for end boxes and caustic outlets from decomposers. A vacuum system can then collect vapors from these locations for treatment as described below. A typical vacuum in the collecting header is 100–150 mm H₂O. Equalizing orifices at pickup points and the eduction of a small amount of fresh air at each point stabilize the pressures and prevent the accumulation of hydrogen in dangerous concentrations.

Similarly, cells can be sealed temporarily with covers whenever they are opened. Cooling a cell to room temperature before opening also reduces the initial surge of vapor. A more elaborate measure was the replacement or modification of mercury pumps to provide sealless “canned” pumps. Along with the use of properly annealed piping and caulking with a urethane polymer to close any pinholes, this reduced emissions from the mercury recycle system.

Vaporization of mercury into end box ventilating air has been one of the larger sources of pollution. Establishing control of this air flow has made possible probably the greatest single reduction in air emissions. In many plants, air flows had gradually increased more than necessary. In others, gradual deterioration of seals and increases in open dimensions as a result of maintenance activities were responsible for these higher air flows. The last factor can be offset by upgrading the end boxes. It is also possible, through improved design, to provide seals that make the use of ventilation air minimal or unnecessary [105]. Section 5.3.1 shows some of the new designs intended to prevent the release of mercury.

Several processes are available for removing vaporized mercury from gases. Here we discuss:

1. cooling (condensation of mercury)
2. gas scrubbing
3. adsorption

These are the same techniques used to treat hydrogen from the cells. Section 9.2.5.1 discusses them individually.

The simplest process, and one that is highly effective in treating hydrogen from the decomposers, is cooling. Figure 9.57 shows the saturation concentration of mercury vapor in a gas at atmospheric pressure as a function of temperature. A typical result would be reduction of the mercury vapor concentration to 20–50 mg m⁻³. This is far above the acceptable limit, but it greatly reduces the load on a subsequent process.

Section 9.2.5.1 also mentions the removal of mercury from hydrogen by scrubbing with chlorinated brine or water. The same process can be used to scrub air, as from cell end boxes, when enough differential pressure is available to operate a column with some degree of efficiency. The chlorine in the scrubbing liquor oxidizes the mercury, which

then forms soluble complex ions. In brine, which was assumed to be the scrubbing agent for hydrogen, the predominant ion is HgCl_4^{2-} . When the chloride concentration is low, as in some wastewater streams that might be used to scrub air, the coordination number of the complex ion decreases. With a chloride ion activity of about 0.1 (3–3.5 gpl), the average coordination number is three. In more dilute solutions (<1 gpl Cl^-), mercuric ions form HgCl_2 , while the mercurous form is present as the insoluble Hg_2Cl_2 .

The treated carbons that remove mercury from hydrogen are also effective with air. Operating conditions are similar. The higher density of air causes the pressure drop through a typical column to be higher (about 80 mm w.c. vs 30 mm with hydrogen). Alternatively, a larger column can offer lower gas velocities and therefore reduced pressure drops.

Fugitive emissions are a continuing problem for the usual process reasons and also because of the frequent need for operator intervention and opening of equipment. With better control over process conditions and more rigorous end-of-pipe treatment of controlled vents, the concern over fugitive emissions increased in relative importance. Various techniques can reduce the amount of mercury that vaporizes while equipment is open. Reducing the frequency of openings accomplishes the same thing in a more elegant fashion. Careful attention to the design of cell components and operation combines these approaches and offers the possibility of achieving the next significant reduction in mercury vapor emissions [105].

16.5.5.3. Mercury in Wastewater. The last category to consider is the release of mercury in plant wastewater. We have already discussed the fact that very little water leaves the anolyte circuit naturally. This is one reason that the typical mercury-cell plant operates on purchased solid salt. Since most plants collect wash waters and some rainwater, there must be a steady purge. In-process sources include brine purges, cell end boxes, seal water, condensates, water treatment systems, and cleaning of equipment, piping, and buildings. Frequent cleaning is an important part of mercury control. Removal of droplets of mercury from the cell room floor, for example, reduces the amount of their vaporization. Eventually, however, a program of washing equipment and floors becomes counterproductive. In their zeal to collect any unknown spills of mercury as soon as possible, many plants wash floors, for example, frequently and thoroughly. As a result, control of the total volume of liquid in the brine circuit becomes more difficult. Gissel [106] describes a program that was undertaken specifically to reduce the volume of water effluent. Over a period of time and in two different stages, the total effluent volume was reduced by nearly 60% to less than $1 \text{ m}^3 \text{ t}^{-1} \text{ Cl}_2$ without deleterious effect. The reduced volume contributed to the reduction of mercury in the final discharge. Schmittinger [107] reports that a waste water rate of $0.3\text{--}1.0 \text{ m}^3 \text{ t}^{-1} \text{ Cl}_2$ is achievable.

The mercury recovered from wastewater may be in any of three forms:

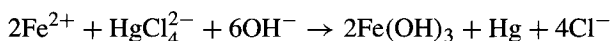
1. metallic mercury
2. precipitated mercury compound
3. dissolved mercury compound

1. *Metallic mercury.* Since mercury is so insoluble, simply equalizing flows and allowing some time for settling will recover a large fraction of the metal. This recovery can be enhanced by treating waste streams to ensure the reduction of mercury compounds to the metal. Sodium borohydride and hydrazine are typical reducing agents. After gravity

settling, residual mercury is removed by filtration. Pressure filtration with activated carbon as the filter aid is the standard process. The filter cake is washed and dried before removal. Final recovery of the metal from the carbon is by vaporization in a mercury still. Some mercury will remain dissolved in the filtrate. This can be recovered by the process described below (#3).

2. *Precipitates.* Mercuric sulfide is highly insoluble. In fact, its solubility is so low that there is some spread in reported values of the solubility product, but all are in the general region of 10^{-50} . Precipitation with sulfide or a sulfur-containing compound therefore is a common technique. The solids are removed by filtration. Again, mercury can form anionic complexes with sulfur, and so overtreatment with a sulfide solution can be counterproductive.

There are several other groups of insoluble mercury compounds. One plant that included a fluorocarbons unit adopted a different approach to mercury control [108]. The waste HCl from fluorocarbon production was shipped several hundred kilometers to a steel mill for use in pickle liquor. The trucks that carried the waste acid then returned empty. The solution adopted was to fill some of the returned trucks with waste pickle liquor, which is strong in FeCl_2 . This was available at a very low cost and nearly zero incremental freight expense. Combining it with chloride-containing wastewater that had been made alkaline produced the reaction:

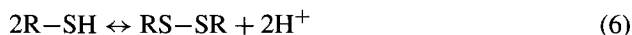


Coprecipitation of ferric hydroxide helped the mercury to settle more rapidly. The first approach, at the beginning of the recognized mercury crisis, was to hold the solids in a lagoon.

3. *Dissolved mercury.* Ion exchange is one of the favored processes for removing dissolved mercury from waste water or brine. The mercury is in its anionic complex form. Again, the process is enhanced by the affinity of $-\text{SH}$ groups for mercury. A commonly used resin contains more than 1.2 g.eq L^{-1} of thiol groups. In contact with 1 mg Hg L^{-1} (in the form of HgCl_4^{2-}), it holds more than 60 g Hg L^{-1} . With a solution space velocity of about 10 hr^{-1} , it reduces the mercury content of wastewater well below 5 ppb. Performance is reported to be essentially independent of pH and salt concentration.

The first step in the treatment process usually is the chlorination of the solution to ensure oxidation of all the mercury. This may be carried out at pH 3 to avoid the precipitation of iron. After filtration to remove undissolved mercury and hydroxides of other metals, the effluent goes on to final treatment. In order to protect the easily oxidized thiol groups, reduction of free chlorine is necessary. This is usually done in two steps, chemical treatment with a reducing agent and chemisorption on activated carbon (both in Section 7.5.9.3). The reducing agent in mercury-removal plants is commonly an S^{4+} -based species.

The regenerating agent for the resin is concentrated HCl. In spite of the process precautions, there is always some oxidation of the resin. In the presence of an oxidizer, the thiol groups split off protons and form sulfide linkages:



Continued reaction, which is irreversible, forms oxidized sulfur compounds. After regeneration, the resin is occasionally treated with a rejuvenating solution (e.g., alkaline NaHS) to reverse reaction (6).

The mercury removed from the wastewater is dissolved in the regenerating acid. It can return to the cells by way of the brine system.

GLOSSARY

ANSI	American National Standards Institute
API	American Petroleum Institute
ASME	American Society of Mechanical Engineers
ASTM	American Society for Testing and Materials
CFR	Code of Federal Regulations
CI	The Chlorine Institute
EC	Euro Chlor
EPA	Environmental Protection Agency (USA)
ETA	Event Tree Analysis
FM	Factory Mutual (insurers)
FMECA	Failure Modes, Effects, and Criticality Analysis
FTA	Fault Tree Analysis
Hazan	Hazard Analysis
Hazop	Hazards and Operability Review (also HAZOP, Hazops)
ICC	Interstate Commerce Commission
IEC	International Electrotechnical Commission
IEEE	Institution of Electrical and Electronics Engineers
JSIA	Japan Soda Industry Association
LOAEL	Lowest Observed Adverse Effects Level
MSDS	Material Safety Data Sheet(s)
NFPA	National Fire Protection Association
NIOSH	National Institute of Occupational Safety and Health
NOAEL	No Observed Adverse Effects Level
OSHA	Occupational Safety and Health Administration
PMI	Positive Material Identification
PPE	Personal Protective Equipment
PrHA	Preliminary Hazard Analysis
PSM	Process Safety Management
SAR	Supplied-Air Respirator
SCBA	Self-Contained Breathing Apparatus
SEG	Similar Exposure Group
STEL	Short-Term Exposure Limit (in conjunction with TLV)
TLV	Threshold Limiting Value
TWA	Time-Weighted Average (in conjunction with TLV)
WHO	World Health Organization

REFERENCES

General reference, prepublication: *Guidelines—Medical Surveillance and Hygiene Monitoring Practices for Control of Worker Exposure to Mercury in the Chlor-Alkali Industry*, Chlorine Institute Pamphlet 125, Edition 4—Draft 5. Presented at Chlorine Institute Annual Meeting, Chicago (2003).

1. I.F. White, G.J. Dibble, J.E. Harker, and T.F. O'Brien, Safety considerations in the design of chlor-alkali plants. In K. Wall (ed.), *Modern Chlor-Alkali Technology*, vol. 3, Ellis Horwood, Chichester (1986), p. 97.
2. I.F. White, Chloralkali Plants—Designing for Safety, *Institution of Mechanical Engineers Seminar on Essential Tools for Designing Safe and Reliable Plant*, London (1993).
3. J. Van Diest, Euro Chlor Commitment to Safer Handling of Chlorine. In R.W. Curry (ed.), *Modern Chlor-Alkali Technology*, vol. 6, Royal Society of Chemistry, Cambridge (1995), p. 21.
4. *Statement of Position Regarding the TLVs[®] and BEIs[®]*, American Conference of Governmental Industrial Hygienists, Cincinnati, OH (2002).
5. *Chlorine (Liquid or Gas)*, Occidental Chemical Corporation, Material Safety Data Sheet M35410, Dallas, TX (1999).
6. T.R. Robbins and R. Manley, *Chem. Eng.* **109**(2), 5 (2002).
7. *Environmental Health Criteria 21. Chlorine and Hydrogen Chloride*, World Health Organization, Geneva (1982).
8. *Code of Practice: Monitoring Chlorine Exposure to Workers*, Health 4, 1st ed., Euro Chlor, Brussels (2000).
9. T.F. O'Brien and E.R. Luckiewicz, *Guidelines for Process Safety Fundamentals in General Plant Operations*, Center for Chemical Process Safety, New York (1995), p. 237.
10. *Interim Assessment: The Causes and Formation of Acid Deposition*, vol. 4, National Acid Precipitation Assessment Program, Washington, DC (1987).
11. E.A. Pearce and C.G. Smith, *Fodor's World Weather Guide*, Random House, New York (1998), p. 387.
12. T.E. Graeder and R. McGill, *Environ. Sci. Technol.* **20**, 1093 (1986).
13. M. Pasquariello, *Chem. Eng.* **107**(9), 78 (2000).
14. *Personal Protective Equipment for Chlorine and Sodium Hydroxide*, Pamphlet 65, Edition 3, The Chlorine Institute, Inc., Washington, DC (1995).
15. *Mercury Study Report to Congress*, EPA-452-R-97-003, vol. 1, Environmental Protection Agency, Washington, DC (1997), pp. 3–6.
16. S.S. Grossel, *Chem. Eng.* **105**(12), 104 (1998).
17. S.S. Grossel, *Chem. Eng.* **97**(4), 110 (1990).
18. R.W. Gallant, *Chem. Eng.* **97**(4), 116 (1990).
19. S.S. Grossel, *Chem. Eng.* **105**(7), 89 (1998).
20. J.F. O'Brien, *Bull. Hist. Chem.* **11**, 47 (1990).
21. J.F. O'Brien, *Famous Mad Hatters*, American Chemical Society tour lecture, Philadelphia, PA (2003).
22. S.E. Manahan, *Environmental Chemistry*, 5th ed., Lewis Publishers, Inc., Chelsea, MI (1990).
23. Anon., *Chem. Eng.* **108**(2), Government and Business section (2001).
24. Mercury, in *Air Quality Guidelines*, 2nd ed., World Health Organization Regional Office for Europe, Copenhagen (2000), chapter 6.9, p. 1.
25. *Environmental Fate and Toxicity of Mercury*, Pamphlet 92, Edition 1, The Chlorine Institute, Inc., Washington, DC (1992).
26. *Code of Practice: Control of Worker Exposure to Mercury in the Chlor-Alkali Industry*, Health 2, 4th ed., Euro Chlor, Brussels (1997).
27. J.O. Nriagu, *Environment* **32**(7), 7 (1990).
28. IARC Monographs on the Evaluation of Carcinogenic Risks to Humans **58**, 239 (1993).
29. A.S. Rowland, D.D. Baird, C.R. Weinberg, D.L. Shore, C.M. Shy, and A.J. Wilcox, *Occupational and Environmental Medicine* **51**/1, 28 (1994).
30. Council Directive 92/85/EEC, European Council, Brussels (1992).
31. Mercury. In *Air Quality Guidelines*, 2nd ed., World Health Organization Regional Office for Europe, Copenhagen (2000), chapter 6.9, p. 4.

32. S. Olsson and M. Bergman, *J. Dental Res.* **71**, 414 (1992).
33. *Methylmercury*, Environmental Health Criteria #101, World Health Organization, Geneva (1990).
34. J.A. Heilala, Controlling Mercury Exposure, *24th Chlorine Institute Plant Managers Seminar*, Houston, TX (1981).
35. *Occupational Exposure Sampling Strategy Manual*, Publication No. 77-173, National Institute of Occupational Safety and Health, Washington, DC (1977).
36. G. Sällsten, L. Bärregard, and B. Jarvholm, *Ann. Occup. Hyg.* **34**(2), 205 (1990).
37. F.P. Lees, *Loss Prevention in the Chemical Industries—Hazard Identification, Assessment and Control*, vol. 1, Butterworths, London (1980), p. 649.
38. T.F. Florkiewicz and L.C. Curlin, Polyramix® Diaphragm—A Commercial Reality. In T.C. Wellington (ed.), *Modern Chlor-Alkali Technology*, vol. 5, Elsevier Applied Science, London (1992), p. 209.
39. R. Romine, Asbestos Issues Update, *Fifteenth Annual ELTECH Chlorine/Chlorate Seminar*, Cleveland, OH (1999). Revision of 1997 presentation.
40. *Chlorine Industry Review 2002–2003*, Euro Chlor, Brussels (2003).
41. *Guidelines: Asbestos Handling for the Chlor-Alkali Industry*, Pamphlet 137, Edition 4, The Chlorine Institute, Inc., Washington, DC (2000).
42. *Safe Handling of Chlorine Containing Nitrogen Trichloride*, Pamphlet 152, Edition 1, The Chlorine Institute, Inc., Washington, DC (1998).
43. S.D. Argade, E.N. Balko, D.A. Kramer, and J.F. Louvar, *Nitrogen Trichloride Control in Chlorine Manufacture*, Abstract 438, Electrochemical Society Meeting, Seattle, WA (1978).
44. *Material Safety Data Sheet No. 42*, www.chemicalproductscorp.com. Chemical Products Corporation, Cartersville, GA (2001).
45. T.F. O'Brien, Control of Sulfates in Membrane-Cell Brine Systems. In K. Wall (ed.), *Modern Chlor-Alkali Technology*, vol. 3, Ellis Horwood, Chichester (1986), p. 326.
46. *IEEE Guide for the Interpretation of Gases Generated in Oil-Immersed Transformers*, Standard C57.104, Institution of Electrical and Electronic Engineers, New York, NY (1991).
47. www.epa.gov/ceppo/pubs/surpass.pdf, Industry Warning, Environmental Protection Agency and Occupational Safety and Health Administration, Washington, DC (1997).
48. *Respiratory Protection Guidelines for Chlor-Alkali Operations*, Pamphlet 75, Edition 1, The Chlorine Institute, Inc., Washington, DC (1982).
49. *Personal Protective Clothing for Chlorine and Sodium Hydroxide*, Pamphlet 65, Edition 3, The Chlorine Institute, Inc., Washington, DC (1995).
50. *Personal Protective Equipment for Use with Chlorine*, GEST 92/171, 1st ed., Euro Chlor, Brussels. (1995).
51. *Chlorine Emergency Equipment*, GEST 92/176, 1st ed., Euro Chlor, Brussels (1993).
52. R.S. Jasniecki, *Chem. Eng.* **108**(8), 2001.
53. T.A. Kletz, *What You Don't Have, Can't Leak*, Jubilee Lecture, Chemistry and Industry (1978).
54. T.A. Kletz, *Cheaper, Safer Plants, or Wealth and Safety at Work*, Institution of Chemical Engineers, Rugby (1984).
55. S.M. Englund, Opportunities in the Design of Inherently Safer Chemical Plants. In *Advances in Chemical Engineering*, vol. 15, Academic Press, Inc., San Diego, CA (1990), p. 73.
56. N.C. Harris, Mitigation of Accidental Chlorine Releases, *30th Chlorine Institute Plant Managers Seminar*, Washington, DC (1987).
57. *Chlorine Transfer Hose Failure*, Safety Advisory No 2002-01-SA, U.S. Chemical Safety and Hazard Investigation Board, Washington, DC (2002).
58. T.A. Kletz, *Hazop and Hazan—Identifying and Assessing Process Industry Hazards*, 3rd ed., Institution of Chemical Engineers, Rugby (1992).
59. *Guidelines for Hazard Evaluation Procedures*, Center for Chemical Process Safety, New York (1992).
60. P.D. Fletcher, Hazard Assessment, *Hazardous Material Seminar*, Monterrey (1992).
61. N.C. Harris, Hazard Assessment in the Chlor-Alkali Industry. In M.O. Coulter (ed.), *Modern Chlor-Alkali Technology*, Ellis Horwood, Chichester (1980), p. 279.
62. G. Sellers, Using the Chlorine Institute Pamphlet Checklists, *46th Chlorine Institute Plant Operations Seminar*, Chicago, IL (2003).
63. B. Lytollis, *Chem. Eng.* **109**(11), 50 (2002).
64. R.W. Johnson and F.W. Leverenz, Jr., *HAZOPS Today*, AIChE Loss Prevention Symposium, New Orleans, LA (1992).

65. T.F. O'Brien, Emergency Vent Scrubbing Systems—Design; Operation; Hazard Analysis, *Seventh Annual Electrode Corporation Chlorine/Chlorate Seminar*, Cleveland, OH (1991).
66. H.M. Patel and T.B. Scarfe, Safety Aspects of Niachlor Membrane Plant, *31st Chlorine Institute Plant Operations Seminar*, New Orleans, LA (1988).
67. L.A. Minton and R.W. Johnson, *Fault Tree Faults*, International Conference on Hazard Identification and Risk Analysis, Orlando, FL (1992).
68. F. Pasquill, *Met. Mag.* **90**, 33 (1961).
69. F.A. Gifford, *Nuclear Safety* **2**(4), 47 (1961).
70. P. Tobia, S. Khajehnajafi, and C. Brackbill, Estimating the Area Affected by a Chlorine Release, *40th Chlorine Institute Plant Operations Seminar*, New Orleans, LA (1997).
71. R. Turpin, G. DeAngelis, P. Groulx, K. Ocheski, and M. Gemelli, *Air Plume Modeling . . . Planning or Diagnostic Tool*, www.ofcm.gov/atdworkshop/proceedings/session/campagna.pdf (2002).
72. T.F. O'Brien, Beyond Hazan, *39th Chlorine Institute Plant Operations Seminar*, Washington, DC (1996).
73. J. Woodward, Recent Developments which Improve the Accuracy of Hazard Zone Predictions for a Chlorine Release, *40th Chlorine Institute Plant Managers Seminar*, New Orleans, LA (1997).
74. *Responsible Care Report 2001*, The Japan Responsible Care Council, Tokyo (2001).
75. www.socma.com/ResponsibleCare (2004).
76. P. Anastasio, Security Vulnerability Assessment Application, *46th Chlorine Institute Plant Operations Seminar*, Chicago, IL (2003).
77. Center for Chemical Process Safety, *Guidelines for Analyzing and Managing the Security Vulnerabilities of Fixed Chemical Sites*, CCPS, New York (2002).
78. *Training Requirements in OSHA Standards and Training Guidelines*, Occupational Safety and Health Administration, Washington, DC (2000).
79. R. King, *Safety in the Process Industries*, Butterworth-Heinemann, London (1990), p. 598.
80. *Accident Prevention Manual for Business and Industry: Administration and Programs*, 10th ed., National Safety Council, Itasca, IL (1992).
81. R.J.M. Withers and F.P. Lees, *J. Haz. Matls.* **12**, 283 (1985).
82. D.J. Finney, *Probit Analysis*, Cambridge University Press, London (1971).
83. F.P. Lees, *Loss Prevention in the Chemical Industries—Hazard Identification, Assessment, and Control*, vol. 1, Butterworths, London (1980), pp. 651–652.
84. N.C. Harris, *Guidelines on Risk Analysis*, Pamphlet 83, Edition 1, The Chlorine Institute, Inc., Washington, DC (1989).
85. K.W. Schatz and R.P. Koopman, Water Spray Mitigation of Hydrofluoric Acid Releases, *AIChE Conference*, Philadelphia, PA (1989).
86. R.L. Van Zele and R. Diener, *Hydrocarbon Proc.* **69**, 6 (1990).
87. J.R. Thomerson and D.E. Billings, Chlorine Vapor Suppression Tests D.O.E. Nevada Test Site. In T.C. Wellington (ed.), *Modern Chlor-Alkali Technology*, vol. 5, Elsevier Applied Science, London (1992), p. 223.
88. R. Vis Van Heemst, *Plant Safety and Quantitative Risk Assessment*, GEST 90/161, Euro Chlor, Brussels (1990).
89. P.E.J. Abbott, M. Carlin, M.E. Fakley, M.E. Hancock, and F. King, ICI “Hydecate” Process for the Catalytic Destruction of Hypochlorite in Effluent Streams. In T.C. Wellington (ed.), *Modern Chlor-Alkali Technology*, vol. 5, Elsevier Applied Science, London (1992), p. 23.
90. P.A. Ross, Chlorine Fugitive Emissions Study, *34th Chlorine Institute Plant Operations Seminar*, Washington, DC (1991).
91. *Guidance Note for Chlorine Installations on Technical Aspects of the Safety Case Report Required by Control of Industrial Major Accident Hazard (CIMAH) Regulations*, Appendix VI, ICI Chlor-Chemicals (1991).
92. J.L. Ratigan, *Summary Report. The Solution Mining Research Institute Cavern Sealing and Abandonment Program. 1996 through 2002*. Research Project Report No. 2002-3-SMRI, Solution Mining Research Institute, Encinitas, CA (2003).
93. www.eurochlor.org/chlorine/Chlorine_Industry_Re.../Environmental...performance.htm, Euro Chlor, Brussels (2001).
94. J.L. Sznoppek and T.G. Goonan, *The Materials Flow of Mercury in the Economies of the United States and the World*, Circular 1197, U.S. Geological Survey, Denver, CO (2000).

95. *The RT Review* 10(4), 4. Published by RT Environmental Services, King of Prussia, PA (2002).
96. A.E. Dungan, *Chlor-Alkali Industry Principles concerning the Retirement of Mercury*, The Chlorine Institute, Inc., Washington, DC (2002).
97. A.E. Dungan, *10th Mercury Issues Workshop*, Chlorine Institute Annual Meeting, Chicago, IL (2003).
98. G. Sellers, *10th Mercury Issues Workshop*, Chlorine Institute Annual Meeting, Chicago, IL (2003).
99. B.S. Gilliatt, *Mercury Issues in Europe, 10th Mercury Issues Workshop*, Chlorine Institute Annual Meeting, Chicago, IL (2003).
100. B.S. Gilliatt, *Mercury and the European Chlor-Alkali Industry, 11th Mercury Issues Workshop*, Chlorine Institute Annual Meeting, Houston, TX (2004).
101. F. Hine, N. Yokota, and T. Takasaki, *Intern. Chem. Eng.* 17(1), 1 (1977).
102. *Decommissioning of Mercury Chlor-Alkali Plants*, Env. Prot. 3, 2nd ed., Euro Chlor, Brussels (1999).
103. G. Thibeault, M. Cyr, Y. Denicourt, and D. Faucher, *Design, Construction, and Implementation of Pilot Unit for the Treatment of Mercury-Contaminated Soil, 36th Chlorine Institute Plant Managers Seminar*, Washington, DC (1993).
104. J. Selby and L.G. Twidwell, *The Recovery and Recycle of Mercury from Chlor-Alkali Plant Wastewater Sludge*, www.udgroup.com/library/p83, Universal Dynamics Ltd., Vancouver (2001).
105. D. Francis, *Cell Room Technology Enhancements to Reduce Mercury Emissions*, Chlorine Institute conference, New Orleans, LA (2001).
106. G.F. Gissel, *Waste Water Minimization at the Vulcan Port Edwards Chlor-Alkali Facility, 39th Chlorine Institute Plant Managers Seminar*, Washington, DC (1996).
107. P. Schmittinger, *Chlorine: Principles and Industrial Practice*, Wiley-VCH, Weinheim (2000), p. 47.
108. T.F. O'Brien, *Control of Mercury Release from a Chlorine Plant, Southwest Missouri State University Lecture Series*, Springfield, MO (1971).

17

Future Developments

17.1. INTRODUCTION

Chapter 2 recounts some of the history of chlor-alkali technology and production. While very important industrially, the process is an old one and, as one of the few examples of large-scale electrochemical production, somewhat outside the mainstream of chemical research and development. The industry is part of the commodity chemical business and has often faced difficult economic problems. All this seems a recipe for technological stagnation. However, the past few decades have seen two major developments that have had profound effects on the technology and economics of production. These are the introduction of metal anodes and the partial substitution of membrane technology for the older diaphragm and mercury technologies. The first of these was made possible by the development of durable, low-voltage coatings that could be applied to titanium. Metal anodes offered many advantages over graphite. Furthermore, direct replacement of graphite by metal anodes of essentially the same dimensions was also rather a simple matter. The changeout therefore was rapid. Membrane technology, on the other hand, required extensive changes in the process. Except for the “membrane-bag” cells, which were a compromise approach, these changes included new electrolyzers. This is quite an expensive proposition, and the energy economy of the membrane cell has not in itself justified wholesale conversion. When a producer has the opportunity to expand conversion, new facilities are easier to justify, but the economic state of the industry has, for the most part, been only fair or poor. The conversion to membrane technology has therefore been slow, and only very recently has the membrane process approached the total installed capacities of the other technologies.

Improvements in membrane technology still continue. Any discussion of future developments must assume that conversion to this technology will be almost total. There is now a new generation of cell designs capable of operating at higher current densities than previous versions. This has created a trend toward bipolar technology. Changes are underway in the processing of brine and of products, and in the distribution of power and the design of cathodes.

This chapter discusses likely changes in methods of cell operation (Section 17.2), auxiliary operations such as brine filtration and power supply (Section 17.3), and methods of handling chlorine (Section 17.4). The last section (17.5) speculates on improved

electrode characteristics and on the process improvements that might follow if cells were operated under substantial positive pressure.

17.2. CELL OPERATION

The introduction referred to the ability of newer membrane cells to operate at higher current densities. Section 17.2.1 treats this subject briefly.

Section 9.2.2.2 discussed alternatives for use or recovery of the hydrogen produced in the cells. Two methods of integration with electrolysis are suppression of hydrogen formation by oxygen-depolarized cathodes and the use of the hydrogen in fuel cells to generate power. These methods would compete with the combustion of hydrogen to generate thermal energy, as in raising steam. The three processes are thermodynamically equivalent. Oxygen-depolarized cathodes contribute to the efficiency of the process by reducing the operating voltage of a cell, and so they would be applied directly in new electrolyzers or as retrofits to existing electrolyzers. Fuel cells would be intended for external generation of recoverable energy, and they would be an adjunct to electrolytic cell lines. The two processes are treated below in Section 17.2.2. Section 9.2.2.2B also discussed some of the practical problems of application. Neither of these technologies has yet had a major impact on the chlor-alkali industry. However, further optimization of conventional membrane-cell design offers little in the way of reducing energy consumption, and these two options are an area of research that may lead to the next major improvement.

17.2.1. Increased Current Density

For some years, the current density of membrane cells was limited to about 4 kA m^{-2} . This was fixed in part by the limited capability of composite membranes to pass high current without undue loss of operating life or performance. Each element of a composite membrane has its own characteristics for transport of the various species that pass through the membrane. The imbalances in transport rates grow as current density increases and create internal stresses that can eventually damage the membrane. With limitations placed on the membranes, cell hardware could be designed for current densities in the same range. With recent improvements, it has become possible to operate at higher current densities. At the same time, the resistivity of membranes has decreased, reducing the voltage penalty of operation at an increased current density. This shifts the economic optimum in the direction of a higher current density [1]. Many plants report operation at 5 or 6 kA m^{-2} , and cell hardware is being designed for 8 kA m^{-2} and more. This change, as explained in Chapter 5, favors bipolar electrolyzer designs over monopolar. The reason for this is the increasing difficulty and expense of providing enough conductor to carry current between the edges of the individual cells and the next elements in the monopolar cell line.

The higher current densities involve the expenditure of more energy than would be required if cell loads were kept lower. At lower amperage, the advances in membrane cell design and construction would be seen in lower power costs, but the user would forego the potentially lower capital cost. The direction in which the industry is now moving is

reminiscent of the developments in mercury-cell technology. Collins and Entwisle [2] reported on the evolution of the mercury cell over the course of nearly 100 years. Changes in the unit energy consumption at plant operating conditions were modest. Changes in cell configuration and operating current density were large. Cell areas increased by a factor of 30–40 and the slopes of cell bottoms by a factor of 10. Operating k -factors were lowered by a factor of 10–20. In other words, the industry’s response to economic reality was primarily to use the improvements in technology to increase the productivity of the cells rather than to reduce their energy consumption. One reason for this is probably the influence of the decomposition potential on the mathematics of cell improvement. On a plot of operating voltage vs current density, assume a constant intercept but a reduction in k -factor (the slope of the line). Fig. 17.1 illustrates the situation. The starting point is V_1 and I_1 on the upper curve. If the k -factor improves to give the lower curve, the limiting choices are to maintain the amperage and reduce the voltage to V_2 and to increase the amperage to I_2 while holding the original voltage. Consider the latter situation first. The original operating characteristic shows that

$$V_1 = a + k_1 I_1 \tag{1}$$

When the k -factor decreases from k_1 to k_2 ,

$$V_1 = a + k_2 I_2 \tag{2}$$

Setting $\kappa = k_1/k_2$, we have

$$I_2/I_1 = \kappa \tag{3}$$

The available increase in operating amperage is inversely proportional to the decrease in the k -factor. With the 10-fold improvement in the mercury-cell k -factor referred to above,

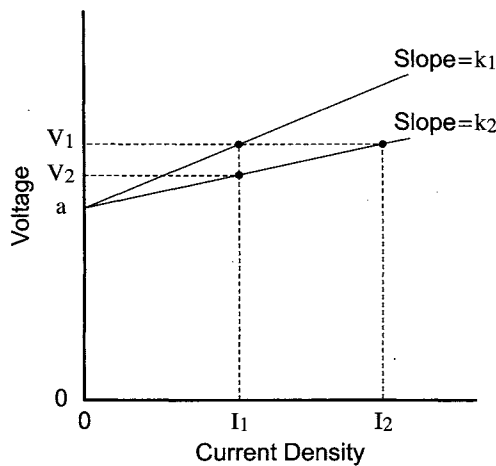


FIGURE 17.1. Options with reduced k -factor.

productivity could be improved by a factor of 10 without increasing the cell voltage. In the real case, nonlinearity might limit the increase, but there were also improvements in electrode overvoltages that would tend to permit higher amperages.

Now if the improved k -factor were used instead to reduce energy consumption, we would move to a different operating point:

$$V_2 = a + k_2 I_1 \quad (4)$$

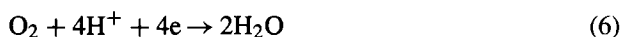
Combining this with Eq. (1) and the definition of κ , we have

$$V_2 = (1/\kappa)V_1 + (1 - 1/\kappa)a \quad (5)$$

Eliminating the second term on the right-hand side of Eq. (5) would give an improvement proportional to the reduction in the k -factor. This would be analogous to Eq. (3). Since $\kappa > 1$, the second term is positive and increases V_2 . Its existence means that the improvement in voltage is less than proportional to the k -factor change, and the departure increases as a becomes greater in proportion to the voltage V_2 . The changes that a reduced k -factor allows in operating voltage or energy consumption are, therefore, less impressive than the possible changes in operating amperage, and this may help to explain the trends noted above.

17.2.2. Depolarized Cathodes and Fuel Cells

17.2.2.1. Overview. The electrochemistry of oxygen is directly relevant to fuel-cell technology [3,4]. Reduction of oxygen takes place in both acidic and alkaline aqueous solutions:



The standard potential of reaction (6), which takes place in acid solutions, is 1.23 V vs. standard hydrogen electrode (SHE). Reaction (7), in alkaline solutions, has a potential of 0.40 V vs. SHE. Both reactions are 1.23 V positive to the reversible potential of the hydrogen evolution reaction (HER) in the respective media. Therefore, the theoretical decomposition voltages of certain electrochemical processes can be reduced by 1.23 V if an oxygen-consuming cathode is substituted for the conventional hydrogen-evolving type. Examples of these processes [5] are:

1. metal-air primary and secondary cells
2. diaphragm- and membrane-type chlor-alkali cells
3. amalgam decomposers
4. HCl electrolyzers
5. chlorate cells
6. perchlorate cells
7. oxygen concentrators

In a chlor-alkali cell, this reduction in voltage would translate into an energy saving of more than 900 kW hr t^{-1} of chlorine.

17.2.2.2. Oxygen-Depolarized Cathodes for Chlor-Alkali Cells. The reversible potential for the oxygen reduction reaction in alkaline solution (Eq. 7) is positive as measured against the SHE. However, the oxygen cathode exhibits large overvoltages under the operating conditions of chlor-alkali cells. These are due to the low rate constant of reaction (7) and low concentrations of dissolved oxygen near the cathode. Overcoming these factors required the development of high-surface area electrodes to promote the rate of oxygen reduction, which takes place in a three-phase region in a porous matrix. Figure 17.2 is a schematic of a membrane cell operating with an oxygen-depolarized cathode, also termed a “gas-diffusion electrode” (GDE).

The anode reaction is the same as in a conventional chlor-alkali cell, and anode-side components can be used without modification. At the cathode, oxygen is reduced to OH^- ions, which combine with the sodium or potassium ions that travel through the membrane to form the alkali product. The oxygen consumed in this reaction enters the air-cathode compartment either as water-saturated oxygen or as air. The advantages of the oxygen reduction reaction include avoidance of costly downstream treatment of hydrogen and absence of the gas void fraction in the catholyte, resulting in a smaller ohmic drop in the cell. When air is the source of oxygen, however, this scheme requires a high-performance scrubbing system to remove all carbon dioxide from the air in order to protect the cathode from the accumulation of sodium carbonate and consequent premature failure.

Modern discussions of the development and demonstration of air cathodes for chlorine production date back at least to 1979. LaConti [6] described the principles of operation, with an emphasis on fuel-cell applications. Coker [7] disclosed the operation

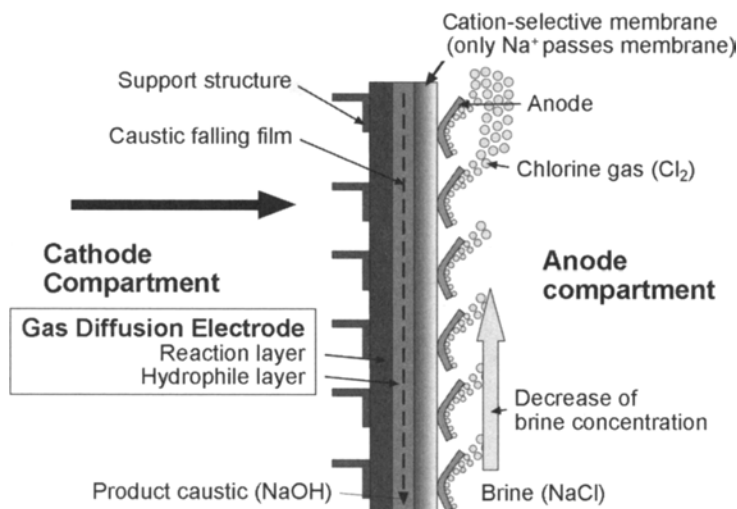


FIGURE 17.2. Membrane cell with gas-diffusion electrode. (With permission of Uhde GmbH.)

of a cell using solid polymer electrolyte technology. This cell achieved a reduction of 0.6–0.8 V at 3 kA m^{-2} . Case Western Reserve University and Diamond Shamrock Corporation [7–9] then developed a pilot chlorine cell employing an air cathode. The cathode operated at a potential of 600 mV vs. the reversible hydrogen electrode (RHE) in the same solution at 3.1 kA m^{-2} . This is 0.85 V less than a hydrogen-evolving cathode at the same current density. The cell operated at about 2.1 V; the energy consumption was $1,450 \text{ kW hr t}^{-1}$ of NaOH. The first attempted industrial application (in an HCl electrolyzer) used first-generation membranes and solid-polymer electrolytes [10]. Problems with stability and performance of the cathodes prevented their wide adoption. These technologies were not actively developed at the time, as they would have been too expensive to commercialize at prevailing US power costs.

The Japan Soda Industry Association (JSIA) began further development of oxygen cathodes in 1994 [11]. Their focus was on development of cathode materials, the structure of the oxygen cathode, life testing in cells of various types and sizes, and scale-up procedures.

In this work, a porous carbon cathode doped with a platinum catalyst was found to be active for the oxygen reduction reaction in a laboratory cell, but its activity deteriorated after 350 days because of oxidation of carbon by the intermediates generated during the oxygen reduction reaction [12]. The JSIA then developed a cathode material activated with silver that has the same voltage characteristics as a Pt-coated cathode. The cathode material consists of a porous nickel support, coated with hydrophobic and hydrophilic carbon layers, which is activated with a silver catalyst at a loading of about 3 mg cm^{-2} [13–16]. A laboratory cell ($10 \times 10 \text{ cm}^2$) with a silver-activated cathode, operating at 3.0 kA m^{-2} in 32% NaOH at 80°C , ran at constant voltage for over 1,100 days. A conventional Pt-loaded cathode, for comparison, lasted 350 days [17]. Table 17.1 provides an example of the voltage balance of a cell with an oxygen cathode containing a silver catalyst [18]. A liquid-permeable oxygen cathode for a zero-gap cell also has been investigated [19], and its configuration is shown in Fig. 17.3. A test cell operated for more than 3 years at 2.0 V at 3 kA m^{-2} and 90°C .

TABLE 17.1. Component Voltages of an Air-Cathode Cell

Component	Voltage
Decomposition voltage	1.02
Cathode overvoltage	0.46
Anode overvoltage	0.06
Ohmic drop across membrane	0.28
Ohmic drop across cathode	0.06
Others	0.08
Total cell voltage	1.96

Note: Cathode: Ag-loaded oxygen cathode. Cell height: 120 cm. Anode: DSA. Membrane: Flemion 893. Catholyte gap: 2 mm. Anolyte: 200–210 gpl NaCl. Catholyte: 32–33% NaOH. Current density: 3 kA m^{-2} . Temperature: 87°C .

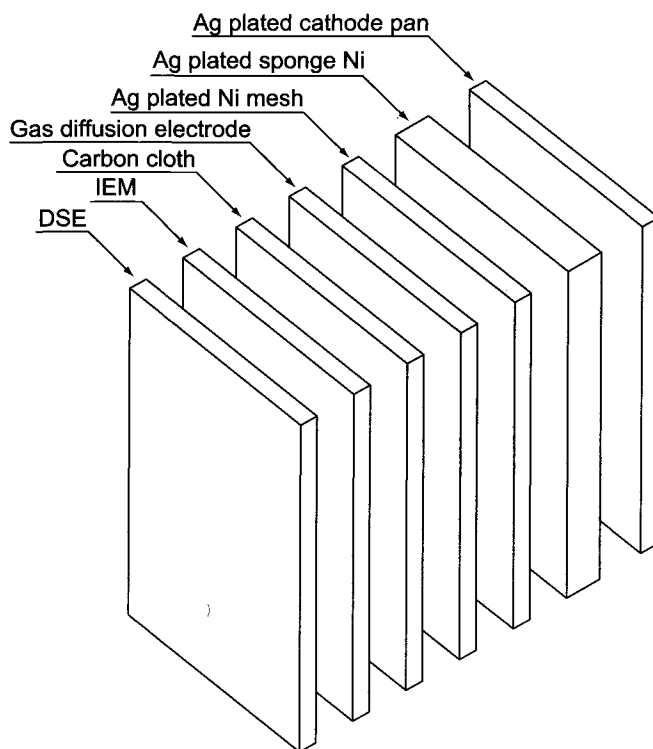


FIGURE 17.3. Liquid-permeable cathode. (With permission of Uhde GmbH.)

Even more recently, European work has led to significant advances in the scaleup of air cathodes, with pilot electrolyzers operating at less than 2.5 V at a current density of 6 kA m^{-2} [20]. With full-sized cathodes, there is a fundamental issue of adjusting the local differential pressure between the caustic and the oxygen compartment on the other side of the electrode. Because of the porous nature of the GDE, a pressure balance across the electrode must be established in order to avoid excessive flow from one side to the other. As shown in Fig. 17.4, there is a restricted range of differential pressure within which the electrode works properly. This new set of constraints has required new developments in electrode structure and fabrication [21].

Because of the different densities of the fluids, the local differential pressure is a function of height and can be made small either of two ways. The first involves splitting the cathode compartment into several horizontal compartments, called gas pockets, in which the height of each sub-compartment limits the hydrostatic pressure of the caustic to a tolerable value. The lean caustic flows through the pockets successively, by overflowing from one pocket to the next one below. This gas-pocket principle (Fig. 17.5) is being tested by the Bayer AG group [22]. A second approach to the problem is the falling-film principle (Fig. 17.6), initiated by the Hoechst group in the 1980s [23–24] but presently continued by Uhde [25]. The idea here is to decrease the hydrostatic pressure

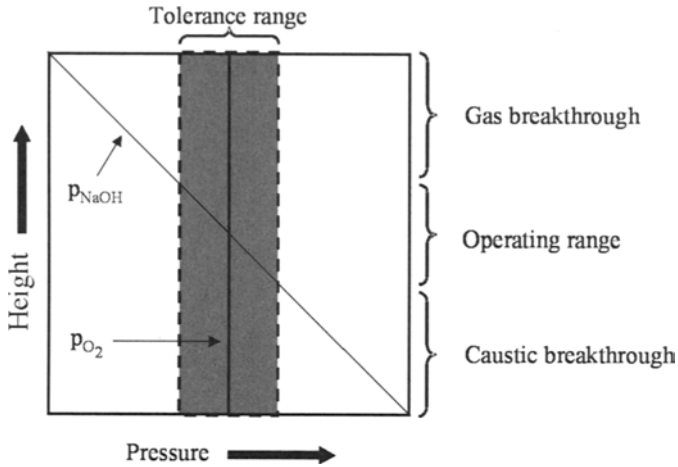


FIGURE 17.4. Differential pressure over a porous GDE-type electrode. (With permission of Uhde GmbH.)

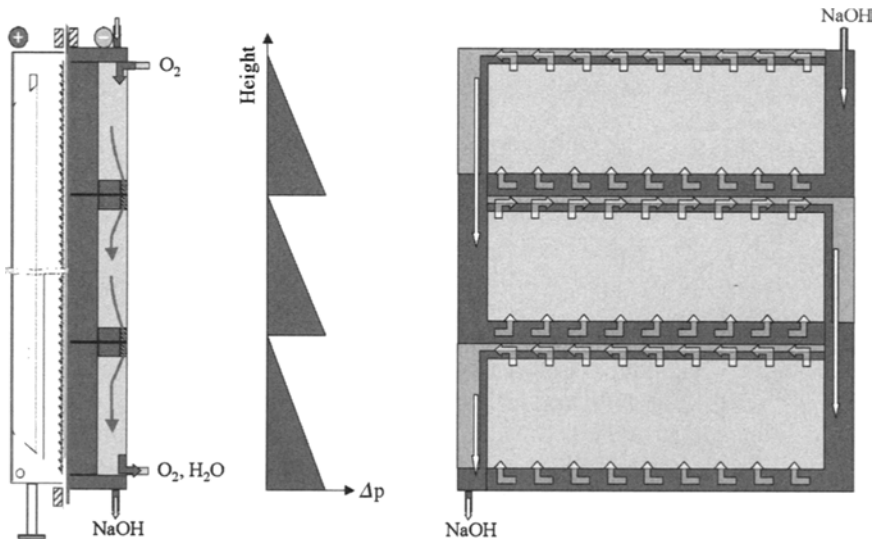


FIGURE 17.5. Gas-pocket-type GDE element. (With permission of Uhde GmbH.)

of the caustic by establishing a falling film of caustic between the electrode and the membrane. This is realized by creating a hydrophilic layer between the anode and cathode. This design ensures a constant gap between the GDE and the membrane. Because of electroosmotic water transport from the anolyte, the caustic flow increases from the top to the bottom of the cell. Design of the hydrophilic layer must prevent too high a flow in order to avoid flooding of the GDE and breakthrough of caustic into the oxygen compartment.

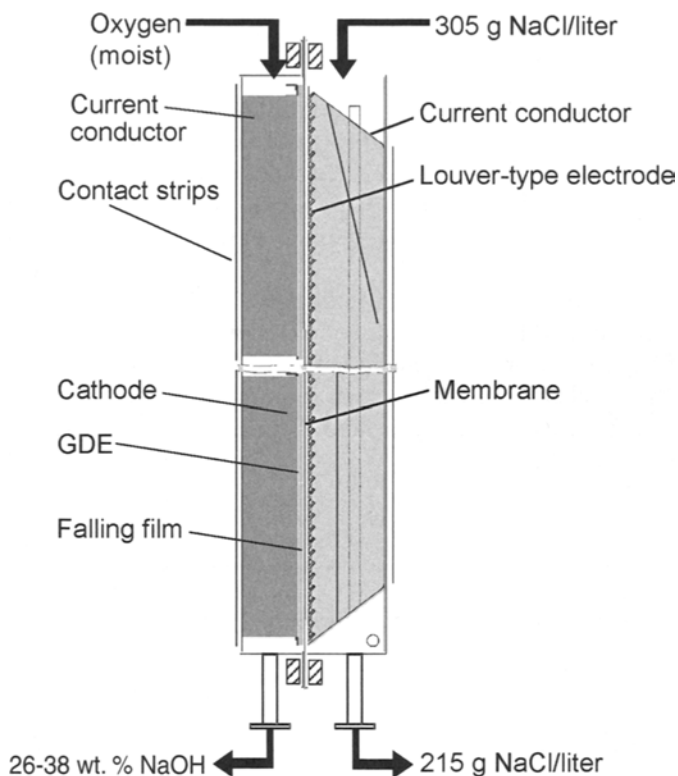
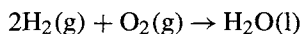


FIGURE 17.6. Falling-film type GDE element. (With permission of Uhde GmbH.)

Commercial operation of a plant for the electrolysis of HCl using depolarized cathodes is now underway [26]. There are plans to expand the capacity to 20,000 tons per year of chlorine.

17.2.2.3. Fuel Cells. A hydrogen fuel cell is an electrochemical system in which the free-energy change of the reaction:



is converted into electrical energy. Fuel cells have several advantages over more conventional energy-conversion processes, the primary one being the lack of Carnot limitations. High energy efficiencies can be achieved with the fuel cell operating not only as an energy-producing device but also as a source of heat (via ohmic and overpotential losses). Other advantages include:

1. simpler operation than other energy-conversion devices
2. clean, quiet operation
3. operation over wide temperature ranges

4. siting flexibility, because of modularity in design
5. ability to operate with a variety of fuels

Development of fuel cells accelerated with the energy crisis of the 1970s. The fuels used most frequently are hydrogen, hydrocarbons, and alcohols. Normally, hydrogen is not a primary fuel but is produced from the others and used primarily in low-temperature cells. Table 17.2 describes the characteristics of the most important types, and Table 17.3 summarizes their current status [27]. Figure 17.7 shows their potential–current density behavior [28].

The PEMFC (see Table 17.2 for identification) has the greatest potential to reach high power densities. DMFCs suffer from the high activation potential of the cathodic reduction of oxygen and anodic oxidation of methanol. MCFCs operate at 650°C and SOFCs at 1000°C, their electrolytes being, respectively, molten carbonates and solid metal oxides. Their activation overpotentials are small, but ohmic overpotentials at the

TABLE 17.2. Essential Characteristics of Fuel Cells

Type of cell ^a	PEMFC	DMFC	AFC	PAFC	MCFC	SOFC
Electrolyte	Membrane	Membrane	KOH (8–12N)	H ₃ PO ₄	Carbonate (Li,Na,K) 650°C	ZrO ₂ –Y ₂ O ₃
Temperature	50–90°C	50–90°C	50–250°C	180–200°C		750–1050°C
Charge carrier	H ⁺	H ⁺	OH ⁻	H ⁺	CO ₃ ²⁻	
Electrocatalyst	Pt, Pt alloy	Pt–Ru anode; Pt or Pt alloy cathode	Pt, Pt alloy, or Ni/NiO _x , anode; Au, Au alloy, or Ag cathode	Pt anode, Pt–Co–Cr cathode	Ni/LiNiO _x	Ni anode, Sr-doped LaMnO ₃ cathode
Fuel	H ₂	CH ₃ OH	H ₂	H ₂ (reformed)		
Poisons	10 ppm CO	Adsorbed intermedi- ates	CO, CO ₂	1% CO; 50 ppm H ₂ S	0.5 ppm H ₂ S	1 ppm H ₂ S
Applications	3, 4, 5, 7, 8	3, 4	7, 9	1, 2, 3	1, 2	1, 2, 6

Note: ^a“FC” in all types denotes “fuel cell.” PEM: proton exchange membrane; DM: direct methanol; A: alkaline; PA: phosphoric acid; MC: molten carbonate; SO: solid oxide.

Key to applications: 1—power generation; 2—cogeneration; 3—transportation; 4—portable; 5—residential; 6—hybrids with gas turbines; 7—space; 8—defense; 9—regenerative energy storage coupled with renewable energy system (wind, photovoltaic, etc.).

TABLE 17.3. Status of Fuel Cell Technologies

Type of cell	kW	Fuel efficiency %	kW m ⁻²	Life, k hr	Cost, \$ kW ⁻¹
PEMFC	0.1–200	40–50	5–10	10–100	50–2,000
DMFC	0.1–10	30–45	0.5–2	1–10	1,000
AFC	20–100	65	2.5–4	3–10	1,000
PAFC	20–10,000	40–45	2–3	30–40	200–3,000
MCFC	100–5,000	50–55	1.5–3	10–40	1,250
SOFC	25–5,000	50–60	2–4	8–40	1,500

Note: See footnote to Table 17.2 for identifications.

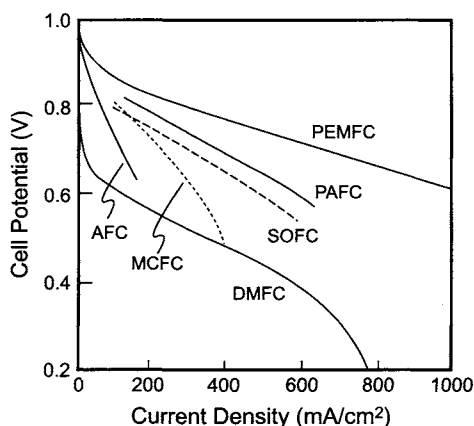


FIGURE 17.7. Cell voltage vs current density for typical fuel cells. (Courtesy of Dr. S. Srinivasan.)

oxygen electrode appear to decrease the output voltages. Both DMFCs and PEMFCs use perfluorosulfonic acid membranes. These membranes dehydrate above 100°C. PAFCs use concentrated phosphoric acid as the electrolyte. The operating temperature is chosen to maximize the conductivity. The operating temperature of an AFC depends on the concentration of KOH chosen as the electrolyte.

Fuel cells are no longer a laboratory curiosity. Self-contained stationary power plants generating from several hundred kilowatts up to 1–2 MW have operated for a number of years. Tests are underway worldwide, and R&D efforts are aimed at reducing costs to match the competing technologies. Hydrogen-based fuel cells for automobiles are also in an advanced stage of development. There is already a pilot project in place in Japan [29] with a number of refueling stations around Tokyo. Some of the goals of this program are to have 50,000 fuel cell vehicles on the road by 2010 and 5 million by 2020.

The driving force for the development of fuel cells is primarily their potential use in power generation. In the chlor-alkali industry, the greatest interest in fuel cells is in their integration with the electrolysis plant. Fuel cells producing power from the hydrogen generated in the electrolytic cells would represent an upgrade for many plants that now use their hydrogen as fuel in steam boilers. Therefore, development work within the industry has concentrated on fuel cells amenable to this application.

There is a growing literature on fuel cell applications. This includes a number of useful general summaries [30–32].

17.2.3. Membranes

17.2.3.1. High Caustic Concentration. Early membranes operated at low caustic concentrations, and a number of commercial plants have produced NaOH at about 20%. Today's membranes operate at 30–35% NaOH. This has been the situation for many years now. There have been attempts to develop membranes that operate efficiently at higher caustic concentrations, but none has had wide commercial application. One goal in this development work must be a membrane that can produce commercial caustic

(48–50% NaOH) directly in the cell. This would eliminate the need for evaporation. The savings are obvious, but one should note that the energy required for electrolysis must increase at high concentrations. The reversible potential in 50% NaOH is about 0.15 V greater than it is in 33% NaOH. This alone adds more than 100 kW hr t^{-1} to the DC energy consumption.

Brandt [33] reviewed the technology available in 1989 and concluded that high-strength operation was uneconomical. A cost structure in which steam carried a higher value than electricity would favor this approach, but there were more examples of the opposite situation where electricity carried an unusually high premium.

Still, one may expect continued developments in membrane technology, and the future may see more plants without evaporation systems. We should note that it is not essential to produce full-strength caustic directly in the cells. The heat contained in the liquor can be used in an isenthalpic flash under vacuum to remove some of the water from the solution.

17.2.3.2. Impurity-Resistant Membranes. Section 4.8 discusses two fundamental issues related to membranes, the possibility of achieving nearly 100% current efficiency and the development of impurity-resistant membranes. Total rejection of the hydroxyl ion by the membrane is possible if the only anode reaction is the discharge of the chloride ion. However, if oxygen evolution, which is favored thermodynamically, also takes place, the principle of electroneutrality makes it impossible for the membrane to exclude the back-migration of the hydroxyl ion.

All membrane manufacturers have research programs in these areas, and some of the concepts are being field tested. We have already referred to membranes that are resistant to the effects of iodine (Section 4.8.5). Asahi Glass has developed AG 8020 that has operated for over a year in the presence of iodide without a loss of efficiency [34]. Asahi Kasei's F-4401 was reported immune to iodide for 2 years [35]. DuPont's NE2010 is reported to have significantly enhanced resistance to nickel, silica, and iodide in plant environments for over 3 years [36].

While none of the membrane suppliers has provided technical details on the composition or structure of these membranes, we can expect interest to remain high and to bring about more developments.

17.3. AUXILIARY OPERATIONS

The important supplies to the cells from outside the electrolysis area are brine and electrical energy. The most basic operations in brine treatment are those of precipitating impurities and removing the resulting suspended particles. New filters are available that give improved performance (Section 9.4.4.3) and offer the promise of one-step removal of suspended solids. Section 17.3.1 describes these.

When it comes to rectification of an electrical signal for supply of direct current to the cells, thyristors are generally the preferred devices (Section 10.3.1.2). One of their deficiencies is a low power factor, particularly when operating well below the design current. New devices for reconfiguring DC signals (DC choppers) can overcome this

problem, and their use seems particularly attractive when combined with inexpensive, uncontrolled diode rectifiers. Section 17.3.2 discusses this subject.

17.3.1. Back-Pulse Filtration

General membrane technology, like the ion-exchange membrane technology that applies to electrolysis, is a rapidly advancing field. If we also look at non-ionic membranes as filters, in the very broadest sense, many new applications are becoming practical. An important example of membrane technology throughout industry, and in its own right as a source of potable water, is reverse osmosis (RO). This functions by applying to a solution, usually a source of contaminated water, a pressure greater than its osmotic pressure. The differential pressure forces purified water to flow from the solution through the membrane. Drinking water can be recovered from brackish water or seawater, and RO now competes in large commercial systems with processes based on the vaporization of water from solutions. Many plants also produce process utility water from raw supplies. Recyclable solutions can also be recovered from plant wastes, leaving a smaller volume of concentrated waste for treatment or disposal. RO is a more powerful technique than the allied process of ultrafiltration (UF), which removes very fine particles but not solutes. Section 7.5.7.2A also introduced the application of nanofiltration for the removal of certain dissolved solids from brine.

What all of these have in common is their ability to remove or separate species on the basis of size. UF can remove fine particles and colloids; RO can remove all ionic species from water; nanofiltration, being an intermediate process, actually distinguishes between ions of different size. It is the ability to manufacture materials not only with very fine pores but also with closely controlled pore size and narrow pore size distribution that has made all these processes commercially feasible. Table 7.24 shows the spectrum of applications. Nanofiltration is the newest application in the chlor-alkali field. We can expect the number of membrane-based installations to continue to grow.

The great appeal of membrane filtration in brine processing is in the ordinary filtration of suspended solids resulting from chemical treatment of the raw brine. Sections 7.5.3 and 7.5.4 describe clarification of the brine by gravity settling followed by two stages of filtration to remove the residual solids from the clarifier overflow. This is a complex and expensive process, sometimes prone to operating upsets, with the apparently simple objective of removing precipitated impurities. Ideally, one would prefer a more straightforward approach in which a single process unit would accomplish the goal.

Preventing this is the characteristic problem with equipment that necessarily becomes fouled or somehow deactivated during operation. The considerable length of time required for regeneration makes it necessary to allow for a nonoperating unit that is in the regenerative mode. The service time in most commercially attractive processes is comfortably more than the regeneration time, and under reasonable circumstances regeneration is complete and the regenerated unit ready for reuse when called upon. Chlor-alkali brine filters (Section 7.5.4) and ion exchangers (Section 7.5.5) fall into this category.

When the regeneration time becomes a very small fraction of the operating time, a different approach becomes possible. A slight increase in design capability and enough storage to accommodate the downtime allow one to avoid the cost of a standby unit and

design a system with operating units only. Carbon-bed secondary dechlorination units (Section 7.5.9.3B) are an example of this approach.

Now consider the filtration process. Typical “sand” filters (Section 7.5.4.1) cannot produce brine of membrane-cell quality. The use of some type of cake filter is normally considered necessary as a polishing step (Section 7.5.4.2). Because the pores in the typical filter are not uniformly smaller than all the particles suspended in the brine, filter aids become necessary. These provide a better surface for filtration and reduce the compressibility of the filter cake.

The root cause of all these complications is the incompatibility between the particles and the filtering surface. Some of the particles are quite small, and the sizes of the openings in the normal filtering medium are quite variable. The particle-size distribution of the solids overlaps with the hole-size distribution of the filtering medium, and the finest particles are not captured. To provide a standard medium with a maximum opening small enough to capture all the particles is an impractical goal. The permeability of the medium would be very low and the pressure drop very high. Pressure drop and surface tension effects would rapidly get out of hand with such small openings. This situation is relieved when the openings in the filter medium become more uniform. Ultimately, one could achieve high porosity, and thus high productivity, in a unit that was able to remove the finest particles.

Raimer [37] has described such a unit. His filter medium is a membrane of expanded polytetrafluoroethylene (e-PTFE). This provides a high open area with very fine openings in the cloth. The fine structure provides true surface filtration. The particles removed from the fluid stay on the surface and do not penetrate the structure of the cloth. This is in contrast to the standard filter, where the nonuniform surface and relatively large openings allow penetration and, until a good filter cake is established, leakage of solids. Therefore, the membrane filter does not normally require precoating and is able to produce clear filtrate almost immediately, without the need to recycle filtrate until clarity improves.

The preferred arrangement is filter candles suspended from a tube sheet in a vertical pressure vessel. The operating cycle comprises filling the tank, filtration, removal of filtered solids from the surface (the back pulse), settling of the solids, and discharge. The vessel is first filled with pretreated brine to a preset level. Flow then begins, from the outside of the filter candles. The operation is usually at a constant flow rate, with operating pressure increasing as solids deposit on the candles. The filtration step continues until a timer or a differential pressure switch intervenes. The backwashing step that follows is the distinguishing feature of these filters. The facts that the solids have not penetrated the filter cloth and that the low-energy PTFE surface releases them readily make it possible to remove the deposit quickly and easily. First, some of the unfiltered brine is drained from the “dirty side” below the tube sheet. This provides room for expansion. After the vessel is vented, a pulse of low-pressure air (0.3 bar) enters the dome and forces filtrate back down through the filter elements. This expands the cloth, cracks the cake, and releases the solids. It then takes some time for the solids to settle into the lower chamber of the filter vessel. This chamber is usually a conical section below the slurry feed point. It can collect solids for some number of filtration cycles, so that it is not necessary to drain the vessel every time.

Backpulse filtration is applicable to all the main electrolytic processes [38], and it has begun to find wide use in the chlor-alkali industry. This trend should continue.

17.3.2. DC Power Supply

Section 8.3.1.2A covered the various types of rectifying devices that have been used and mentioned that thyristors are the type favored in modern chlor-alkali plants. Section 8.3.1.3A then showed that thyristors tend to generate more harmonic distortion than diodes. This difference is greatest when the firing angles are high, which corresponds to greater turndown in output. Thyristor-based rectifiers therefore suffer from low power factors and even greater generation of harmonics at low operating rates.

The distortion of the output waveform in a thyristor-based system is therefore at least as great as the distortion caused by a diode system. Fortunately, the reactive power compensation that accompanies most large rectifier installations also tends to absorb some of the harmonics. Configuring the added capacitance as a harmonic filter therefore offsets some of the loss.

Still, the poor power factor and harmonic distortion of thyristor and, sometimes, standard diode rectifiers do have their costs. This situation could lead to future use of rectifiers that use pulse-width modulated or multi-level converters. More recent semiconductor devices such as gate turn-off thyristors (GTOs), insulated gate bipolar transistors (IGBTs), and integrated gate commutated thyristors (IGCTs) have resulted in major changes in other fields of electrical engineering (e.g., in variable-speed drives).

As rectifying elements, these devices offer more modes of control than do the older types. The standard diode is a passive device that passes current only (but always) when exposed to voltage of a certain polarity. It filters out the negative components of an AC supply. The standard thyristor rectifier, in contrast, passes no current until it is activated. Current flow continues until the voltage is removed or the polarity is reversed. In the next cycle of current, the device must be activated again. The newer semiconductor devices can also be "turned off," opening more possibilities for management of the output. They can be used, for example, to modulate a DC waveform. This is the basis of the so-called DC chopper rectifier. Direct current signals with reasonable characteristics can be altered to fit the requirements of a cell line. Because of this characteristic, an efficient combination for rectifying an AC signal is an unregulated diode rectifier followed by a DC chopper. The combination relieves the problems with power factors and harmonics are relieved.

Choppers may not yet be competitive economically with thyristors and diodes for new high-power rectifiers. In projects involving modifications to existing rectifiers in good condition, however, the situation changes. The existing rectifiers may have the wrong voltage and current ratings for the proposed new duty (e.g., a chlor-alkali replacement line). The use of enhanced semiconductor devices in a DC-to-DC converter, or a DC chopper, may then be economically sound [39]. An (existing) diode rectifier is used to convert AC to DC without control, followed by conversion to a higher or lower voltage DC supply by the DC chopper. The result is a system with high efficiency, high power factor, and much less generation of harmonics. The combination discussed here might retain its high power factor down to about 15% of design kW load. A typical thyristor might have a power factor of only 80% when operating at a 50% of design load.

Another advantage of thyristors over simple diodes is their faster control action. This gives more protection against transient surges in current. Control still requires completion of an electrical cycle before the supply can be interrupted. Response time is measured in tens of milliseconds. Therefore, thyristors are not able to eliminate very

rapid transients and so allow them to propagate until the next commutation. Chopper devices with their turn-off feature can be interrupted even during an electrical cycle. The higher switching frequency that is possible with choppers permits extremely fast shutdowns. The time required typically is about 50 μ s.

Popp and Tomas [40] made a direct comparison of the performance of standard thyristors and choppers. The application chosen for study was a graphite furnace. This is a difficult application, with the load impedance subject to very sudden changes. The fast response of the chopper system met the requirements of the furnace with less dynamic deviation than did the thyristor system. The chopper also provided a constant power factor, easier control of harmonics, and less ripple.

17.4. CHLORINE PROCESSING

17.4.1. Integrated Production of Ethylene Dichloride

With PVC consuming higher percentages of the chlorine made, production of ethylene dichloride (EDC) has become the major outlet. More and more, the production of chlorine and EDC has become integrated, and this has certain advantages [41]. One such derives from the increasing importance of EDC as an item of commerce. Chlorine can be produced where power costs are low, and it can be conveniently and safely exported in the form of EDC for conversion to vinyl chloride monomer (VCM) and PVC. A major process advantage is the ability to use gaseous chlorine directly, without the expense of liquefaction.

Section 9.1.7.2A discussed the steadily increasing difficulty of recovering more chlorine from process gas by liquefaction. Each increment of chlorine condensed requires more severe conditions than the previous one. This is caused by the presence of noncondensables. As chlorine condenses, the total partial pressure of the noncondensables increases and that of chlorine drops. Continuing liquefaction then, according to Eq. (9.51), demands some combination of higher pressure and lower temperature. Section 9.1.9.1 explained the shift away from final recovery by absorption to higher severity liquefaction, where the marginal effect is greatest. This increases the incentive to use some of the chlorine directly as gas.

A disadvantage of separating EDC and VCM production geographically is that balanced oxychlorination (Section 15.2.1.2) with consumption of the byproduct HCl is no longer possible (or at least requires more complex arrangements). The HCl is released at the site that produces VCM, where the EDC is decomposed. The acid can no longer easily be recycled to the ethylene chlorination process, and some other outlet must be found.

17.4.2. Chlorine Recovery

The discussion of liquefaction of chlorine (Section 9.1.7.2B) also pointed out that new systems operate on refrigerants other than the CFCs that were the industry standard for many years. Many existing systems have also been converted to the newer materials. HCFCs, such as R-22, have much lower ozone depletion potentials than the CFCs but

are themselves subject to phaseout as newer types are developed. Ahmed [42] points out that many refrigerant users adopt the alternative of changing their manufacturing processes to eliminate or reduce the amount or levels of refrigeration required. With the move to enhanced liquefaction and the removal of CCl_4 absorption systems from operation, the trend in the chlorine industry has been counter to this. Therefore, there is a growing potential for the introduction of new processes.

The use of other types of separation processes reduces the need for high-severity liquefaction and so reduces the energy consumed in that process. Absorption is such a process, and the advent of a process based on a solvent other than CCl_4 would be a positive development here. We have already discussed the use of chloroform. This is a simple replacement that requires little change in operation. One of its drawbacks is the fact that it is more volatile than NCl_3 , making it possible for the solvent to evaporate or weather away from the hazardous compound. Other solvents with higher boiling points have also been considered. These require higher operating temperatures and tend to increase the heat load on a continuously operating system. Simple retrofits are no longer possible. Other problems also may arise when considering solvents that are not fully saturated and chlorinated. For example, both the unsaturated perchloroethylene and the hydrogenated EDC can form C_2Cl_6 when exposed to chlorine in the plant. This compound has a high melting point, subliming at 185°C , and can deposit in the equipment. The tabulation that follows gives a qualitative comparison of the problems encountered with solvents of different volatilities.

Boiling point	Ease of retrofit	Vent losses	Possibility of NCl_3 accumulation	Reboiler temperature	Reboiler heat load
Low	High	High	High	Low	High
High	Low	Low	Low	High	Low

Silver [43] reviewed a number of other processes for application to plant tail gas. More recently, gas-diffusion membranes have found a number of applications in process industries [44]. They have not been applied commercially to chlorine recovery, but Lokhandwala *et al.* [45] have published the results of laboratory investigations. O'Brien [46] studied the possibility of applying these results to the upgrading of chlorine gas for EDC production and to the use of membranes as an adjunct to a liquefaction process. For very high recovery, the latter included a third stage of liquefaction, with the offgas sent through membrane permeators and the recovered gas compressed for recycle to the third stage. This promises to save energy in the final stage and to eliminate the need for operation at very low temperature. The latter effect reduces the concentration of dissolved inerts at any given degree of recovery of chlorine.

A promising approach to selective recovery of chlorine from the inerts in the vent gas is to electrochemically reduce chlorine to chloride at the cathode and oxidize the ion to chlorine at the anode. The selectivity arises because of the fast kinetics of the chlorine reduction reaction compared to that of the oxygen and carbon dioxide reduction

reactions. This cell will operate at a low voltage because of the small overpotentials for the chlorine reduction and chloride oxidation reactions on noble metal surfaces.

Laboratory studies have shown the viability of the concept [47,48], but commercial tests have yet to demonstrate the practicality of this approach.

17.5. SPECULATIONS

17.5.1. *Improved Electrodes*

Beer's development of the dimensionally stable anode revolutionized the industry with its energy savings and the ability to operate economically at high current densities (now $>5 \text{ kA m}^{-2}$ with membrane cells and $>10 \text{ kA m}^{-2}$ with mercury cells). Motivated by the success of DSA anodes, there has been significant activity to continue improvement of the anodes, develop activated cathode coatings for diaphragm and membrane cells, and understand the electrocatalytic factors in the hydrogen and chlorine evolution processes. It would seem that developments in the following areas would lead to greater energy savings and ease of operation.

1. *Low-oxygen anodes.* Presently, anodes generate 1–2% oxygen, and this can be reduced at low anolyte pH (≥ 2). It is theoretically possible to reduce the amount of oxygen generated at a pH of 3–4, without addition of acid to the feed brine, if the exchange current density for the oxygen-evolution reaction can be suppressed by proper selection of the anode catalyst (Section 4.5). This is not an easy task, as our present understanding of electrocatalysis does not permit accurate prediction of catalytic behavior. Fundamental study in this field may allow us to achieve this goal in the future.

2. *Impurity-resistant activated cathodes.* As discussed in Section 4.6, the strategy to reduce sensitivity to impurities has been to provide enough surface area that the deposited or adsorbed impurities do not affect the HER. If the coating had sites that would negate the effects of these impurities, it would be possible to operate high-surface area cathodes for long periods without the effects of poisoning.

3. *Hypochlorite-resistant cathodes.* Commercialization of activated cathodes for diaphragm cells has been hampered because hypochlorite corrodes steel under open-circuit conditions (Section 4.6). In the process, the coating spalls off or loses its activity. Development of resistant coatings for steel or other substrates could render the cathode immune during shutdowns.

The three improvements noted here are ideals that are not easily reached. One may argue that the problems fundamentally are not completely solvable. However, the tools for addressing the problems may become available as our knowledge base expands.

17.5.2. *Operation under Pressure*

In their design, membrane electrolyzers are, in general, more amenable than the other types to pressure operation. Certain types of membrane cell routinely run under modest pressure, but even in this case, most plants drop the pressure to nearly atmospheric before processing the gases. Conventional design of the wet end of a chlorine train and

the operating/monitoring philosophy of a cell room today are very much oriented toward atmospheric pressure operation. There is good reason for this, and while the purpose of this section is to consider the positive aspects of pressure, it would be well to list some of its disadvantages.

In the gas processing plant, the various techniques named below might be replaced by other, more attractive options. The advantages to be gained are still reasonably predictable and well founded. While most membrane cells now operate close to atmospheric pressure, it is also true that some are designed to withstand certain amounts of pressure. Most of the components, moreover, are easily adapted to pressure operation. An arbitrary goal of 10 atm is beyond the limits of any design known to the authors. However, there is no fundamental reason to restrict the design to very low pressures, and the level chosen here remains arbitrary. We shall regard mechanical design for pressure operation as a problem that would be solved when the incentive appeared. In and around the cells, however, there are several fundamental problems that would need attention:

1. Simultaneously maintaining essentially equal pressures along both chlorine and hydrogen headers, keeping the differential pressure across membranes at currently specified levels, and operating cells at high pressure may be impracticable. Adding gas pressure controllers and valves at each electrolyzer would relieve the need to make header pressure drop negligible. This would be an expensive proposition, especially in a monopolar circuit. An offsetting advantage would be the ability to use smaller headers (titanium in the case of chlorine), thus reducing the inventory of gases.

2. Membranes must be held against the anodes and not allowed to flutter. The latter requirement is one reason for the tight specification on differential pressure. With good support in a cell operating under substantial pressure, it might be possible to maintain membrane position without excessive flutter by allowing a greater differential pressure. At the same time, one would have to avoid excessive distortion of the membrane and gradual deformation by extrusion of the membrane through the holes in the anode structure while at the same time not developing a framework that interrupted the ionic current through the membrane. These aspects of cell design might prove to be the most difficult adjustments necessary to successful pressure operation.

3. The amount of chlorine dissolved in the anolyte would increase. This, presumably, would increase the amount transferred through the membranes. Changes in operating conditions could offset this effect to some degree.

Operation under pressure would seriously aggravate the consequences of a chlorine leak in the cell room. Outdoor construction or the use of some of the practices associated with contained storage systems (Section 9.1.8.2C) would help to relieve the hazard. In any event, there would have to be a complete rethinking of many operating practices as well as major revisions in design.

Changing the operating philosophy would be one of the great obstacles to adopting pressure operation. Pressure also appears to detract from the inherent safety of the process. Still, it is interesting to speculate on the effects and potential benefits of running the process under substantial positive pressure. The following subsections describe some of the process advantages. These improvements can in themselves provide some inherent safety, and so a careful balance of the pros and cons would be necessary.

Among the first benefits seen in a change to higher pressure is the ability to transfer the gases from the cells through their processing trains without falling below atmospheric pressure and creating the potential for infiltration of air. The energy consumed in processing the gases will be lower, and there is special significance in an increase that allows elimination of a processing step.

As pressure goes up, we can identify several opportunities for simplification:

1. Some plants use low-pressure boosting fans to assist flow through the chlorine and hydrogen handling systems; these would be eliminated.
2. Chlorine is often used in low-pressure processes in which cell gas would be a satisfactory feed. The first substantial goal in raising the pressure would then be to allow these processes to be run with uncompressed chlorine. This might be taken directly from the cells or after cooling or drying.
3. Continuing increases in pressure allow other steps to be eliminated or at least simplified. The rest of this section considers some of these opportunities.
4. Keeping pressure drops small is an important consideration in the design of standard chlorine cooling and drying systems. In a pressurized system, it would be less, and this fact, along with the lower volumetric flow rates, would allow the use of much smaller piping and equipment.

Pressures today are limited to tens of kilopascals. This section speculates on other advantages that would become available if the operating pressure were increased well beyond this range. In order to be specific, we assume a pressure of about 10 atm, or 1 MPa.

17.5.2.1. Cell Operation. Operation under pressure would cause substantial changes in behavior of the cells. The reversible potential would increase to match the higher energy content of the products, partly offsetting some of the advantages to be described below.

The partial volumes of the gases generated in the cells would be inversely proportional to the pressure. The partial pressure of water vapor, given the same temperature and electrolyte composition, would be unchanged. The amount of water vaporized with the gas, therefore, would be lower. This fact changes the material balance on the electrolytes. The vaporization of less water from the catholyte would mean that less dilution water is required on that side. Because the vapor pressure of the membrane-cell catholyte is low, the amount of water vaporized into the hydrogen is not great in any case, and the reduction in dilution water requirement is of the order of 10% or less. The anolyte has a higher vapor pressure, and so the changes are greater on that side. Raising the pressure by a factor of 10, for example, would reduce vaporization by up to 95%. This effectively keeps more water in the anolyte, and so a greater volume of feed brine would be required to maintain the salt concentration in the anolyte. The increase might be 6–8%, and all this would become part of the depleted brine recycle.

The change in gas bubble volume would affect the electrical conductivity of the electrolytes. While the volume generated would be lower by a calculable amount, the bubble size and the quantity retained within the cell cannot be predicted with great precision. We can speculate on the change in conductivity by using the data presented by MacMullin in Sconce's work [49]. First, the effect of bubble volume on resistivity is

given by the Bruggemann equation [50]:

$$\rho/\rho_0 = (1 - \varepsilon)^{-1.5} \quad (8)$$

where

ρ = resistivity of two-phase mixture

ρ_0 = resistivity of liquid phase

ε = void fraction

In the range of interest for membrane cells, this is approximately

$$\rho/\rho_0 = 1 + 1.5\varepsilon + 2\varepsilon^2 \quad (9)$$

Sconce illustrates a number of mercury-cell anodes ranging from flat horizontal plates to anodes with large numbers of grooves and holes. The value of ε ranged from 0.06 to 0.25 [51]. While the latter would produce a large change in resistivity (>50%), a flat horizontal plate is not a realistic model for a membrane cell. If we consider instead a range of 6–12% voids, the increase in resistivity due to gas bubbles becomes 10–23%. Reducing the void fraction by a factor of 10 changes these figures to 1–2%. Electrolyte resistances, therefore, would decrease by 9–17% from their present values. This change could be used to reduce the energy consumption or it could be used to increase the operating current while maintaining the same voltage. Section 17.2.1 suggests that most users would choose the latter course. The value of the change would depend on the spacing between the electrodes. In a membrane-gap cell, then, the reduction in voltage might be quite small. On the other hand, the change would reduce the penalty of finite-gap operation and perhaps offer more flexibility in designing improved cells.

Operation under pressure would also allow the cells to operate at higher temperatures. This would reduce the operating voltage, but it also has several disadvantages. It would:

1. offset the advantages of the lower bubble volume and the lower water content of the gases
2. increase the corrosivity of the electrolytes
3. add to the stress on the membranes and the components that seal the cell compartments

17.5.2.2. Chlorine Cooling. The vapor pressures of the electrolytes are essentially unaffected by total operating pressure. Therefore, the molar concentration of water vapor in the gases leaving the cells is inversely proportional to the total pressure. A given concentration of water then corresponds to a higher partial pressure, allowing a higher temperature in the cooling system. Table 17.4 shows the gas temperatures required to reach the same residual water content as that in a gas cooled to 15°C at atmospheric pressure.

Continuously increasing the pressure at the chlorine coolers first gradually reduces the number of plants that require a chilled water system. Beyond about 2.3 atm, the acceptable temperature exceeds the quadruple-point temperature of the chlorine hydrate

TABLE 17.4. Temperature–Pressure Combinations for Equal Water Content in Gas

Pressure, atm	Temperature, °C
1	15.0
2	26.3
2.3	28.7 ^a
3	33.3
5	42.8
10	56.7

Note: ^aQuadruple-point temperature.

TABLE 17.5. Maximum Reduction in Water Content Outside Hydrate-Formation Zone

Temperature, °C	Decomposition pressure, atm	Vapor pressure of water	Relative VP	Relative mole fraction	% Reduction in water content
9.6	1	8.965	0.660	0.660	34
15	1.8	12.79	1	0.556	44
20	3	17.535	1.371	0.457	54
28.7	7.2	29.525	2.308	0.321	68

Note: Base case: 15°C, 1 atm. Vapor pressures are in mm Hg.

system. The hydrate can no longer exist, and the problems caused by its plugging lines and equipment disappear.

We can also take advantage of the pressure by reducing the temperature below those given in Table 17.4. The concentration of water will then be below that at an atmospheric dew point of 15°C. We can strive for the maximum removal of water consistent with no hydrate formation. Table 17.5 lists several data on hydrate decomposition pressure along with the vapor pressure of water at the corresponding temperatures, the resulting equilibrium mole fraction of water vapor, and the ratios of the last two quantities to those that apply at 15°C and 1 atm pressure. The last column is the approximate reduction in water loading of a given quantity of chlorine. Note that these calculations assume operation at the highest allowable pressure. At a temperature of 20°C, for example, where the decomposition pressure is 3.0 atm, we can operate at any pressure up to that level without forming hydrate. The vapor pressure of water is about 37% higher than it is at 15°C. With a 2-fold increase in operating pressure, the vapor-phase mole fraction of chlorine is only 46% as great as in our standard case.

There is still the question of protection of titanium surfaces by the passivating oxide layer. Section 9.1.3.5A discussed the need to maintain a certain minimum partial pressure of water vapor in order not to destroy this film. Under positive pressure, the partial pressure of chlorine will be higher. Available data on the effects of water and chlorine do not tell us whether the same partial pressure of water vapor will suffice or whether something more nearly approaching the same ratio of water to chlorine is

necessary. The argument that passivation occurs when the formation of TiO_2 competes successfully with chlorination of the bare metal [52] suggests that, at least below some critical pressure, the ratio of partial pressures is important. This would limit one's ability to reduce the water concentration without losing passivation. This is an area of research that is necessary before adopting pressure operation.

The purpose of cooling chlorine at this point in the conventional process is largely to remove most of the accompanying water. One of the speculations on chlorine drying, discussed below, would make it possible to eliminate this step and replace it with a liquid-phase cooler.

17.5.2.3. Chlorine Drying. The drying process also benefits from higher pressure. The best approach here depends partly on the method of operation chosen in the cooling system. The same principles apply. The higher partial pressure of water vapor at a given mole fraction increases the amount of water that sulfuric acid can hold against a gas of a given composition. Conversely, operating at a given acid concentration can reduce the mole fraction of water in the dry chlorine. The latter offers more processing safety, and a certain amount of reduction in water content can always be recommended.

Results equivalent to those available at atmospheric pressure can be achieved with lower acid concentrations. This fact can give the chlorine plant operator a wider choice. Less-concentrated feed acid might be used; for example, 93% H_2SO_4 becomes a sound choice. The concentration of the spent acid can also be lower, provided that its increased corrosivity is acceptable. A wider spread between feed and waste acid concentrations reduces the consumption of acid and the amount of waste generated. Equation (9.38) gives the relationship.

Higher pressures also allow us to consider other drying agents. Brine is a candidate. The partial pressure of water in the gas from a typical membrane cell is 50 or 60 kPa. Cooling the gas to 15°C reduces this to about 2 kPa. At atmospheric pressure, these numbers are very close to the concentration of water in mol%. The vapor pressure of 25% NaCl solution at 60°C is about 15 kPa; at 40°C , it is about 5.7 kPa. At a total pressure of 1 MPa, the concentration of water in a gas at equilibrium with 25% NaCl brine will therefore be about 1.5% at 60°C and 0.6% at 40°C , in either case lower than the water content of chlorine chilled at atmospheric pressure. Contact of the gas with brine could replace the entire gas cooling system and most of the duty of the drying system. The latent heat of the condensing water, in the case shown in Fig. 6.10, would heat the feed brine about 12°C . In some cases, this would be merely a useful interchange of energy and add to the thermal efficiency of the process. In other cases, removal of the heat is necessary for process reasons (e.g., to keep the temperature of the brine low and to remove more water from the gas). This heat would be removed in a liquid (circulating brine) rather than a gas cooler, under more favorable heat-transfer conditions. There would be no danger of hydrate formation. The system could be designed to avoid the use of titanium wherever dry chlorine is present. When the brine temperature in the dryer is low for the sake of process efficiency, reheating may be necessary. Note also that the vapor pressure of KCl brine is about 3% higher than that of NaCl brine, and so it would be a slightly less efficient drying agent.

Condensation of water from the gas will dilute the brine. However, membrane cells usually are fed with unsaturated brine. In any case, increasing the concentration of the brine in the treating system by about 0.7% easily offsets the amount of dilution.

Sulfuric acid drying still might follow this step in order to reach very low moisture contents. The amount of acid required, however, would be much less than in today's typical plant. Handling and disposal of the waste acid generated in the plant would be much easier.

17.5.2.4. Chlorine Compression and Liquefaction. At the pressures considered above, primary compression could be eliminated. Alternatively, the gas could be compressed further and then liquefied at a higher temperature. Probably, the first choice would be to carry out at least some liquefaction at line pressure. Boosting for secondary or tertiary liquefaction would then be easier.

Section 9.1.7.2 discussed the balance between the operating temperature and pressure that is required in liquefaction process design. Increasing the pressure on the gas allows continuous reduction in the level of refrigeration required to obtain a given result. The value of high pressure also becomes a step function when it permits the use of a different coolant. Air or plant cooling water could be regarded as the ultimate in low cost. Suppose that the cooling water available could reduce the temperature of the gas to 40°C. Table 17.6 shows the attainable degree of liquefaction of chlorine as a function of operating pressure.

The results in Table 17.6 were calculated using Eq. (9.51). Further increases in pressure would probably not be economical and in any case would invalidate the assumption of ideal gas behavior that is part of the derivation of the equation. Unless an unusually cold source is available, cooling water will not produce what is normally considered efficient liquefaction. Section 9.1.7.1 points out the possibility of using cooling water to produce some liquefaction and then producing lower gas temperatures by the autorefrigeration of boiling chlorine. This appears to be a sound approach compared to liquefaction under extreme pressure.

As a final note, the conditions imagined so far for electrolysis are not very far removed from the vapor pressure curve of chlorine. By reducing the temperature in the

TABLE 17.6. Liquefaction of Chlorine as a Function of Pressure

Operating pressure, kPa	% Liquefaction
1200	40.8
1300	70.7
1500	85.4
2000	93.5
2500	95.9
3000	96.9

Note: 95% (v/v) chlorine in feed gas. Final temperature: 40°C.

cells, one could produce liquid chlorine directly, eliminating any need for large compression and liquefaction systems. At 1 MPa, a temperature in the range 30–40°C would be below the boiling point of chlorine and safely above the quadruple-point temperature of chlorine hydrate. The liquid chlorine would form a two-phase mixture with the electrolyte, placing a new set of demands on cell design. There would also be some new features in chlorine processing. First, there would have to be assurance that the final product contained no occluded electrolyte. The chlorine would contain dissolved water at a concentration matching its activity in the electrolyte. As Section 9.1.7.2C demonstrated, this water could be removed in the overhead vapor from a stripping process. Wet gas could be recycled to electrolysis. The pressure lost in stripping and recycle could be offset by compressing the stripped vapor or pumping the liquid chlorine into the stripper.

Hart [53] demonstrated some of these concepts in a batch operation of a specially designed cell. The cathodic process was the deposition of a metal (e.g., zinc).

REFERENCES

1. R. Keller, Economic Optimization of Industrial Electrochemical Processes. In R. Alkire and T. Beck (eds.), *Tutorial Lectures in Electrochemical Engineering and Technology*, AIChE Symposium Series 204, vol. 7, American Institute of Chemical Engineers (1981), p. 15.
2. J.H. Collins and J.H. Entwisle, Development and Operation of High-Current Density Mercury Cells. In M.O. Coulter (ed.), *Modern Chlor-Alkali Technology*, Ellis Horwood, Chichester (1980).
3. J.P. Hoare, *The Electrochemistry of Oxygen*, Interscience Publishers, New York (1968).
4. M.R. Tarasevich, A. Sadkowsky, and E. Yeager, Oxygen Electrochemistry. In B.E. Conway, J.O'M. Bockris, E. Yeager, S.U.M. Khan, and R.E. White (eds.), *Comprehensive Treatise on Electrochemistry*, vol. 7, Plenum Press, New York (1983), p. 301.
5. E. Yeager, Oxygen Electrodes for Industrial Electrolysis and Electrochemical Power Generation. In U. Landau, E. Yeager, and D. Kortan (eds.), *Electrochemistry in Industry*, Plenum Press, New York (1980), p. 29.
6. A.B. LaConti, Introduction to SPE Cell Technology, *Proceedings, Oronzio DeNora Symposium: Chlorine Technology*, Venice (1979), p. 94.
7. T.G. Coker, SPE Brine Electrolyzers, *Proceedings, Oronzio DeNora Symposium: Chlorine Technology*, Venice (1979), p. 128.
8. E. Yeager, Presentation to Japan Soda Industry Association (translation), *Soda to Enso (Soda and Chlorine)* **31**, 147 (1980).
9. V.H. Thomas and E.J. Rudd, Energy Savings Advances in the Chlor-Alkali Industry. In C. Jackson (ed.), *Modern Chlor-Alkali Technology*, vol. 2, Ellis Horwood, Chichester (1983), p. 159.
10. E.N. Balko, SPE Hydrochloric Acid Electrolysis Cells: Performance, Cell Configuration, *Proceedings Oronzio DeNora Symposium: Chlorine Technology*, Venice (1979), p. 204.
11. H. Aikawa, *Soda to Enso (Soda and Chlorine)* **45**, 85 (1994).
12. A. Sakata, M. Kato, K. Hayashi, H. Aikawa, and K. Saiki, Long Term Performance of Gas Diffusion Electrodes in Laboratory Cells. In H.S. Burney, N. Furuya, F. Hine, and K.-I. Ota (eds.), *Chlor-Alkali and Chlorate Technology: R.B. MacMullin Symposium*, Proc. vol. **99-21**, The Electrochemical Society, Pennington, NJ (1999), p. 223.
13. A. Uchimura, H. Aikawa, K. Saiki, A. Sakata, and N. Furuya, Gas Diffusion Electrode Using Porous Nickel. In J.W. Van Zee, P.C. Foller, T.F. Fuller, and F. Hine (eds.), *Advances in Mathematical Modelling and Simulation of Electrochemical Processes and Oxygen Depolarized Cathodes and Activated Cathodes for Chlor-Alkali and Chlorate Processes*, Proc. vol. **98-10**, The Electrochemical Society, Pennington, NJ (1998), p. 220.

14. N. Furuya, H. Syojaku, H. Aikawa, and O. Ichinose, Ag Based Oxygen Cathodes for Chlor-Alkali Membrane Cells. In J.W. Van Zee, P.C. Foller, T.F. Fuller, and F. Hine (eds.), *Advances in Mathematical Modelling and Simulation of Electrochemical Processes and Oxygen Depolarized Cathodes and Activated Cathodes for Chlor-Alkali and Chlorate Processes*, Proc. vol. **98-10**, The Electrochemical Society, Pennington, NJ (1998), p. 243.
15. N. Furuya and H. Aikawa, A Study of the Gas Diffusion Electrodes for Chlor-Alkali Membrane Cells. In H.S. Burney, N. Furuya, F. Hine, and K.-I. Ota (eds.), *Chlor-Alkali and Chlorate Technology: R.B. MacMullin Symposium*, Proc. vol. **99-21**, The Electrochemical Society, Pennington, NJ (1999), p. 180.
16. O. Ichinose, H. Aikawa, T. Watanabe, and A. Uchimura, Pilot Cell Scale Manufacture of the Gas Diffusion Electrode. In H.S. Burney, N. Furuya, F. Hine, and K.-I. Ota (eds.), *Chlor-Alkali and Chlorate Technology: R.B. MacMullin Symposium*, Proc. vol. **99-21**, The Electrochemical Society, Pennington, NJ (1999), p. 216.
17. H. Aikawa, *Chlor-Alkali Technology Seminar*, Japan Soda Industry Association, Tokyo (1999).
18. K. Saiki, A. Sakata, H. Aikawa, and N. Furuya, Reduction in Power Consumption of Chlor-Alkali Membrane Cell Using Oxygen Depolarized Cathode. In H.S. Burney, N. Furuya, F. Hine, and K.-I. Ota (eds.), *Chlor-Alkali and Chlorate Technology: R.B. MacMullin Symposium*, Proc. vol. **99-21**, The Electrochemical Society, Pennington, NJ (1999), p. 188.
19. S. Nakamatsu, N. Furuya, K. Saiki, H. Aikawa, and A. Sakata, Liquid-Permeable Gas Diffusion Electrode for Chlor-Alkali Membrane Cell. In H.S. Burney, N. Furuya, F. Hine, and K.-I. Ota (eds.), *Chlor-Alkali and Chlorate Technology: R.B. MacMullin Symposium*, Proc. vol. **99-21**, The Electrochemical Society, Pennington, NJ (1999), p. 196.
20. F. Gestermann and A. Ottaviani, Chlorine Production with Oxygen-Depolarized Cathodes on an Industrial Scale. In J. Moorhouse (ed.), *Modern Chlor-Alkali Technology*, vol. 8, Blackwell Science, Oxford (2001), p. 49.
21. F. Federico, G.N. Martelli, and D. Pinter, Gas-Diffusion Electrodes for Chlorine-Related (Production) Technologies. In J. Moorhouse (ed.), *Modern Chlor-Alkali Technology*, vol. 8, Blackwell Science, Oxford (2001), p. 114.
22. K. Schneiders, A. Zimmermann, and G. Henßen, Membranelektrolyse—Innovation für die chlor-alkali-Industrie, *Forum Thyssen-Krupp*, Dortmund (2001).
23. *German Patents EP-PA0150017* (1984); *EP0150018* (1985).
24. K.-H. Tetzlaff and W. Wendel, *Chem. Ing. Tech.* **60**, 563 (1988).
25. *German Patent DE 19715429 A1* (1998).
26. *Chemical Week*, 10 March 2004, p. 22.
27. C. Iamy, J.-M. Leger, and S. Srinivasan, Direct Methanol Fuel Cells: From Electrochemist's Dream to a Twenty-First Century Emerging Technology. In J.O'M. Bockris, B.E. Conway, and R.E. White (eds.), *Modern Electrochemistry*, vol. 34, Plenum Publishers, New York (2001), p. 53.
28. S. Srinivasan, L. Krishnan, A.B. Bocarsly, K.-L. Hsueh, C.-C. Lai, and A. Peng, Fuel Cells vs Competing Technologies, *First International Fuel Cell Science, Engineering and Technology Conference*, Rochester, NY (2003).
29. *Japan Hydrogen and Fuel Cell Demonstration Project*, www.jhfc.jp (2004).
30. A.J. Appleby and F.R. Foulkes, *Fuel Cell Handbook*, Van Nostrand Reinhold, New York (1989).
31. EG&G Services, Parsons Inc., *Fuel Cell Handbook*, 5th ed., U.S. Department of Fossil Energy, Washington, DC (2000).
32. *Fuel Cell Technology Handbook*, G. Hoogers (ed.), CRC Press, Boca Raton, FL (2003).
33. D.C. Brandt, The Economics of Producing High-Strength Caustic Soda in Membrane Cells, *32nd Chlorine Institute Plant Managers Seminar*, Washington, DC (1989).
34. T. Shimohira, T. Kimura, T. Uchibori, and H. Takeda, Advanced Cell Technology with Flemion[®] Membranes and the Azec[®] Bipolar Electrolyzer. In J. Moorhouse (ed.), *Modern Chlor-Alkali Technology*, vol. 8, Blackwell Science, Oxford (2001), p. 237.
35. H. Obanawa, Effects of Brine Impurities and Blisters on Membrane Service Life, *Sixteenth Annual Electrode Corporation Chlorine/Chlorate Seminar*, Cleveland, OH (2000).
36. C. Bricker, *Membrane Development Review*, DuPont presentation to customers (2001).
37. M.J. Raimer, Back-Pulse Filtration using Gore-Tex[®] Filter Cloths. In J. Moorhouse (ed.), *Modern Chlor-Alkali Technology*, vol. 8, Blackwell Science, Oxford (2001), p. 272.

38. P.H. Sears, Chlorine Solutions LLC, Personal Communication (2003).
39. P. Buddingh and S. Hagemoen, New Life for Old Power Rectifiers, *44th Chlorine Institute Plant Managers Seminar*, New Orleans, LA (2001).
40. A.S. Popp and M. Tomas, Comparison of Thyristor vs Chopper Rectifiers in a Common Application, IEEE Paper #PCIC-2000-13, *Petroleum and Chemical Industry Technical Conference*, San Antonio, TX (2000).
41. I.F. White and R.L. Sandel, Ethylene Dichloride—Part of the Chlor-Alkali Plant? In J. Moorhouse (ed.), *Modern Chlor-Alkali Technology*, vol. 8, Blackwell Science, Oxford (2001), p. 260.
42. K. Ahmed, *Technological Development and Pollution Abatement. A Study of How Enterprises Are Finding Alternatives to Chlorofluorocarbons*, Technical Paper No. 271, World Bank, Washington, DC (1995).
43. M.M. Silver, Chlorine Tail Gas and Snift Disposal Systems, *25th Chlorine Institute Plant Managers Seminar*, Atlanta, GA (1982).
44. R.W. Baker, J. Kaschemekat, and J.G. Wijmans, *CHEMTECH* **26**, 36 (1996).
45. K.A. Lokhandwala, S. Segelke, P. Nguyen, R.W. Baker, T.T. Su, and I. A. Pinnau, *Ind. Eng. Chem. Res.* **38**, 3606 (1999).
46. T.F. O'Brien, Chlorine Processing Beyond the Millennium—The Use of Gas-Separation Membranes. In J. Moorhouse (ed.), *Modern Chlor-Alkali Technology*, vol. 8, Blackwell Science, Oxford (2001), p. 90.
47. S. Sarangapani and T.V. Bommaraju, *U.S. Patent* 6,203,692B1 (2001).
48. S. Sarangapani, D. Gage, and T.V. Bommaraju, Electrochemical Purification of Chlorine from Chlor-Alkali Tail Gas, *2002 NSF Design Service and Manufacturing Grantees and Research Conference*, San Juan, PR (2002).
49. R.B. MacMullin, Electrolysis of Brines in Mercury Cells. In J.W. Sconce (ed.), *Chlorine: Its Manufacture, Properties and Uses*, ACS Monograph 154, Robert E. Krieger Publishing Co., Huntington, NY (1972), p. 163.
50. R.M. De La Rue and C.W. Tobias, *J. Electrochem. Soc.* **106**, 827 (1959).
51. S. Okada, S. Yoshizawa, F. Hine, and Z. Takehara, *J. Electrochem. Soc. Jpn* **26**, 165 (1958).
52. P.C. Westen, The Safe Use of Steel and Titanium in Chlorine. In R.W. Curry (ed.), *Modern Chlor-Alkali Technology*, vol. 6, Royal Society of Chemistry, Cambridge (1995), p. 62.
53. T.G. Hart, *U.S. Patent* 4,086,393 (1978).

Appendix

A. UNIVERSAL CONSTANTS

Avogadro's constant	N_A	$6.022 \times 10^{23} \text{ mol}^{-1}$
Faraday's constant	F	$96,485 \text{ C g-eq}^{-1}$ $26,801 \text{ Ahr g-eq}^{-1}$
Gas constant	R	$23,060 \text{ cal V}^{-1} \text{ g-eq}^{-1}$ $8.3145 \text{ J mol}^{-1} \text{ K}^{-1}$ $1.987 \text{ cal mol}^{-1} \text{ K}^{-1}$ $1.987 \text{ BTU lb-mol}^{-1} \text{ }^\circ\text{R}^{-1}$ $0.08206 \text{ m}^3 \text{ atm kg-mol}^{-1} \text{ K}^{-1}$ $0.730 \text{ ft}^3 \text{ atm lb-mol}^{-1} \text{ }^\circ\text{R}^{-1}$
Gravity acceleration	g_c	9.807 m s^{-2} $1.27 \times 10^8 \text{ m hr}^{-2}$ 32.2 ft s^{-2} $4.17 \times 10^8 \text{ ft hr}^{-2}$
Standard molar volume of ideal gas at 0°C and 760 mmHg		$22.41 \text{ m}^3 \text{ kg-mol}^{-1}$

B. CONVERSION FACTORS

Length

m	cm	mm	in.	ft
1	100	1000	39.37	3.281
0.01	1	10	0.3937	0.03281
0.001	0.1	1	0.03937	0.003281
0.0254	2.54	25.4	1	0.08333
0.3048	30.48	304.8	12	1

1 mile = 1,760 yards = 5,280 ft; $1 \mu\text{m} = 10^{-4} \text{ cm}$; 1 Angstrom = 10^{-8} cm .

Area

m ²	cm ²	in ²	ft ²	acre
1	1×10^4	1.550×10^3	10.76	2.471×10^{-4}
1×10^{-4}	1	0.155	1.076×10^{-3}	2.471×10^{-8}
6.452×10^{-4}	6.452	1	6.944×10^{-3}	1.594×10^{-7}
9.29×10^{-2}	9.29×10^2	1.44×10^2	1	2.296×10^{-5}
4.047×10^3	4.047×10^7	6.273×10^6	4.3560×10^4	1

1 are = 100 m², 1 hectare = 100 ares.

Volume

m ³	L	ft ³	US gallon
1	1000	35.31	264.2
0.001	1	0.03531	0.2642
0.028232	28.32	1	7.481
0.003785	3.785	0.1337	1

1 British gallon = 1.201 US gallons, 1 ft³ = 1728 in.³;
1 barrel (petroleum) = 42 US gallons.

Weight

kg	g	lb	metric ton	US ton	UK ton
1	1×10^3	2.205	1×10^{-3}	1.102×10^{-3}	9.824×10^{-4}
1×10^{-3}	1	2.205×10^{-3}	1×10^{-6}	1.102×10^{-6}	9.842×10^{-7}
0.4536	4.536×10^2	1	4.536×10^{-4}	5×10^{-4}	4.464×10^{-4}
1×10^3	1×10^6	2.205×10^3	1	1.102	0.9842
9.072×10^2	9.072×10^5	2×10^3	0.9072	1	0.8929
1.016×10^3	1.016×10^6	2.24×10^3	1.016	1.12	1

1 pound = 16 ounces.

Density

g cm^{-3}	$\text{kg m}^{-3} = \text{gL}^{-1}$	lb ft^{-3}	lb/US gal
1	1000	62.43	8.345
0.001	1	0.06243	0.008345
0.01602	16.02	1	0.1337
0.1198	119.8	7.481	1

Power

kW	kg m s^{-1}	lb ft s^{-1}	HP	kcal hr^{-1}	BTU hr^{-1}
1	1.02×10^2	7.376×10^2	1.341	8.604×10^2	3.415×10^3
9.807×10^{-3}	1	7.233	1.315×10^{-2}	8.438	33.49
1.356×10^{-3}	0.1383	1	1.82×10^{-3}	1.167	4.63
0.7457	76.04	5.50×10^2	1	6.419×10^2	2.547×10^3
1.162×10^{-3}	0.1185	0.8569	1.559×10^{-3}	1	3.967
2.929×10^{-4}	2.989×10^{-2}	0.216	3.929×10^{-4}	0.2521	1

1 kW = $1,000 \text{ J s}^{-1}$, HP = horsepower.

Energy

Joule	kgf m	$\text{lb}_f \text{ ft}$	kWhr	HP hr	L atm	kcal	BTU
1	0.102	0.7376	2.778×10^{-7}	3.725×10^{-7}	9.869×10^{-3}	2.390×10^{-4}	9.486×10^{-4}
9.807	1	7.233	2.724×10^{-6}	3.653×10^{-6}	9.678×10^{-2}	2.344×10^{-3}	9.302×10^{-3}
1.356	0.1383	1	3.766×10^{-7}	5.051×10^{-7}	1.338×10^{-2}	3.241×10^{-4}	1.286×10^{-3}
3.6×10^6	3.671×10^5	2.655×10^6	1	1.341	3.553×10^4	8.605×10^2	3.415×10^3
2.685×10^6	2.738×10^5	1.980×10^6	0.7457	1	2.649×10^4	6.417×10^2	2.547×10^3
1.013×10^2	10.33	74.73	2.815×10^{-5}	3.774×10^{-5}	1	2.422×10^{-2}	9.612×10^{-2}
4.183×10^3	4.266×10^2	3.086×10^3	1.162×10^{-3}	1.558×10^{-3}	41.29	1	3.968
1.054×10^3	1.075×10^2	7.775×10^2	2.928×10^{-4}	3.927×10^{-4}	10.4	0.252	1

Thermal conductivity

$\text{kcal m}^{-1} \text{ hr}^{-1} \text{ }^\circ\text{C}^{-1}$	$\text{cal cm}^{-1} \text{ s}^{-1} \text{ }^\circ\text{C}^{-1}$	$\text{BTU ft}^{-1} \text{ hr}^{-1} \text{ }^\circ\text{F}^{-1}$	$\text{BTU in}^{-1} \text{ hr}^{-1} \text{ }^\circ\text{F}^{-1}$
1	2.778×10^{-3}	0.672	5.600×10^{-2}
360	1	2.419×10^2	20.16
1.488	4.136×10^{-3}	1	8.333×10^{-2}
17.86	4.960×10^{-2}	12	1

Pressure

bar	$\text{kg}_f \text{ m}^{-2}$	$\text{lb}_f \text{ in.}^{-2}$	atm	10^3 mm Hg	$10^3 \text{ mm H}_2\text{O}$	kPa
1	1.02	14.5	0.9869	0.75	10.21	100
0.9807	1	14.22	0.9678	0.7355	10.01	98.07
0.06895	0.07031	1	0.06804	0.05171	0.7037	6.895
1.013	1.033	14.7	1	0.76	10.34	101.3
1.333	1.36	19.34	1.316	1	13.61	133.3
0.03386	0.03453	0.4912	0.00342	0.0254	0.3456	3.386
0.09798	0.09991	1.421	0.0967	0.07349	1	9.798
0.002489	0.002538	0.0361	0.002456	0.001867	0.0254	0.2489

1 bar = 1 megadyne cm^{-2} , 1 megadyne = 10^6 dyne, 1 mm Hg = 1 Torr.

Viscosity

Poise	Centipoise (mPa s) ^a	$\text{kg m}^{-1} \text{ s}^{-1}$ (Pa s)	$\text{kg m}^{-1} \text{ hr}^{-1}$	$\text{lb ft}^{-1} \text{ s}^{-1}$	$\text{lb ft}^{-1} \text{ hr}^{-1}$
1	100	0.1	360	6.720×10^{-2}	2.419×10^2
0.01	1	1×10^{-3}	3.6	6.720×10^{-4}	2.419
10	1×10^3	1	3.600×10^3	6.720×10^{-1}	2.419×10^3
2.778×10^{-3}	0.2778	2.778×10^{-4}	1	1.867×10^{-4}	0.672
14.88	1.488×10^3	1.488	5.357×10^3	1	3600
4.134×10^{-3}	0.4134	4.134×10^{-4}	1.488	2.778×10^{-4}	1

Note:

^amPa = milli-Pascal.

Heat transfer coefficient

kcal m ⁻² hr ⁻¹ °C ⁻¹	cal cm ⁻² s ⁻¹ °C ⁻¹	BTU ft ⁻² hr ⁻¹ °F ⁻¹
1	2.778 × 10 ⁻⁵	0.2048
3.6 × 10 ⁴	1	7.374 × 10 ³
4.882	1.3562 × 10 ⁻⁴	1

Current density

mA cm ⁻²	A dm ⁻²	kA m ⁻²	A in ⁻²	A ft ⁻²
1	0.1	0.01	0.00694	0.9294
10	1	0.1	0.0645	9.2937
100	10	1	0.645	92.937
155	15.5	1.55	1	144.05
1.076	0.1076	0.01076	6.94 × 10 ⁻³	1

C. DIMENSIONLESS GROUPS

Arrhenius number	$\frac{E}{RT}$	Peclet number	$\frac{v\rho cL}{k}$
Biot number	$\frac{hL}{k}$	Poiseuille number	$\frac{g_c d^2 (-dp/dL)}{\mu v}$
Condensation group	$\frac{h}{k} \left(\frac{v^2}{a}\right)^{1/3}; \frac{h}{k} \left(\frac{v^2}{g}\right)^{1/3}$	Prandtl number	$\frac{c\mu}{k}$
Euler number	$\frac{g_c p}{\rho v^2}$	Reynolds number	$\frac{\rho v L}{\mu} = \frac{vL}{\nu}$
Fanning friction factor	$\frac{g_c d \Delta P}{2\rho v^2 L}$	Schmidt number	$\frac{\mu}{\rho D}$
Fourier number	$\frac{kc}{\rho c L^2}$	Sherwood number	$\frac{k_c L}{D}$
Froude number	$\frac{v^2}{gL}$	Stanton number	$\frac{h}{cv\rho}$
Gay-Lussac number	$\frac{1}{\beta \Delta T}$	Stokes number	$\frac{\mu t}{\rho L^2}$
Grashof number	$\frac{L^3 \rho^2 \beta g \Delta T}{\mu^2}$	Thiele number	$\frac{\rho v^2 L}{\sigma}$
Hatta number	$\frac{\gamma_H}{\tanh \gamma_H}^a$	Thring radiation number	$\frac{\rho cv}{seT^3}$
MacMullin number	$\frac{\rho_n}{\rho_o} = \frac{\tau}{\varepsilon}$	Wagner number	$\frac{k_p}{\rho_o L}$
Nusselt number	$\frac{hd}{k}$	Weber number	$\frac{\rho v^2 L}{\sigma}$

Note:

$$^a \gamma_H = \frac{\sqrt{k_T D}}{k_c}$$

D. NOMENCLATURE IN APPENDIX C

a	Acceleration
c	Specific heat
c_p	Specific heat at constant temperature
D	Diffusivity
d	Diameter
E	Activation energy
e	Emissivity
F_R	Force
g	Acceleration of gravity
g_c	Newton's law conversion factor
h	Heat transfer coefficient
k	Thermal conductivity
k_c	Mass transfer coefficient (liquid film)
k_p	Slope of potential-current density curve
k_r	Reaction rate constant (first-order)
L	Specific length
p	Pressure
R	Gas constant
s	Stefan-Boltzmann constant
T	Temperature
t	Time
u	Reaction rate
v	Linear velocity
β	Coefficient of bulk expansion
Δ	Difference
ε	Porosity
μ	Viscosity
ν	Kinematic viscosity
ρ	Density
ρ_n	Resistivity of electrolytic solution with nonconductive suspensions
ρ_o	Resistivity of electrolytic solution free of nonconductive suspensions
σ	Surface tension
τ	Tortuosity of porous medium

E. CORRELATIONS

Sodium chloride

1. Solubility of NaCl in water

$$\text{Wt}\% = 26.2516 - 0.001235t + 4.8755 \times 10^{-5}t^2$$

where

$$t = ^\circ\text{F}$$

2. Solubility of NaCl in NaOH

$$S = 0.009c^2 - 0.895c + 0.0003125t^2 + 22.95$$

where

S = wt% of NaCl

t = temperature, 20–60°C

c = NaOH concentration from 35% to 50%

3. Vapor pressure lowering

$$20^\circ\text{C}: y = 0.4718x + 0.01714x^2$$

$$100^\circ\text{C}: y = 0.4508x + 0.0196x^2$$

where

y = % reduction

x = wt% salt (0–27%)

4. Enthalpy

$$H = 111.3611 + 0.274305c - 0.0076797c^2 \\ + 0.999216t - 0.0131122ct + 1.77404 \times 10^{-4}c^2t$$

where

H = Enthalpy (kcal kg⁻¹)

c = wt% NaCl

t = °C

5. Density

$$\text{Specific Gravity} = Q + Rc + Sc^2$$

where

$$Q = 1.0004075 - 0.71687895 \times 10^{-5}t - 0.51792075 \times 10^{-5}t^2 \\ + 0.1054032 \times 10^{-7}t^3$$

$$R = 0.0074569085 - 0.2960572 \times 10^{-4}t + 0.30564225 \times 10^{-6}t^2 \\ - 0.934493315 \times 10^{-9}t^3$$

$$S = 0.18372605 \times 10^{-4} + 0.42360185 \times 10^{-6}t - 0.51483125 \times 10^{-8}t^2 \\ + 0.1794537 \times 10^{-10}t^3$$

c = wt% NaCl

t = °C

Potassium chloride

1. Solubility in water

$$S = 27.8054 + 0.30925t - 0.00211584t^2$$

where

S = solubility (g/100 g·H₂O)

t = temperature (°C)

2. Vapor pressure lowering

$$y = 0.3723x + 0.0091x^2$$

where

y = % reduction of vapor pressure (solution in water)

x = wt% salt (0–37%)

3. Specific heat of solutions

$$c_p = 0.974 - 0.01P$$

where

c_p = specific heat

P = wt% salt

4. Density of solutions

$$\rho = 1.0016 - 3.525 \times 10^{-4}t - 1.625 \times 10^{-6}t^2 + 5.833 \times 10^{-3}P \\ + 3.006 \times 10^{-5}P^2 + 4.5 \times 10^{-7}tP$$

Sodium hydroxide

$$\text{Specific Gravity} = Q + Rc + Sc^2 + Tc^3$$

where

$$Q = 1.00224925 - 0.116831975 \times 10^{-3}t - 0.3210971 \times 10^{-5}t^2$$

$$R = 0.01148599 - 0.319841025 \times 10^{-4}t + 0.21510285 \times 10^{-6}t^2$$

$$S = 0.19658565 \times 10^{-5} + 0.761527825 \times 10^{-6}t - 0.61560685 \times 10^{-8}t^2$$

$$T = -0.334691125 \times 10^{-6} - 0.7552771 \times 10^{-8}t + 0.661632323 \times 10^{-10}t^2$$

c = wt% NaOH

t = °C

Potassium hydroxide

$$\text{Specific heat at } 18^\circ\text{C} = 1 - 1.648 \times 10^{-3}c + 5.1574 \times 10^{-6}c^2 - 8.5826 \times 10^{-9}c^3$$

where

$$c = \text{g/l KOH}$$

Chlorine

1. Vapor pressure

$$\log P = 31.9142 - 1811.8011/T - 10.989096 \log T + 0.00732037T$$

where

$$P = \text{atm}; T = \text{K}$$

2. Vapor pressure of liquid chlorine (at liquefaction temperatures)

$$\text{Vapor pressure (kPa)} = (100.403898 - 0.07629155t - 0.0009227t^2) \exp \left[9.596 - \frac{3726.9}{1.8t + 491.8} - \frac{175088.4}{(1.8t + 491.8)^2} \right]$$

where

$$t = ^\circ\text{C}$$

3. Density of liquid chlorine

$$\rho = 573 + 1060.6083Y - 160.418Y^2 + 837.08192Y^3 - 247.20716Y^4$$

where

$$\rho = \text{kg m}^{-3}$$

$$Y = (1 - T_r)^{1/3}$$

T_r = reduced temperature

4. Viscosity of liquid chlorine

$$\ln(\mu_1) = -2.64947 + \frac{484.686}{t + 285.3845}$$

where

$$\mu_1 = \text{mPa s (or centipoises)}$$

$$t = ^\circ\text{C}$$

5. Thermal conductivity of liquid chlorine

$$k = 0.2458 - 3.094 \times 10^{-4}T - 4.053 \times 10^{-7}T^2$$

where

k = thermal conductivity $\text{W m}^{-1}\text{K}^{-1}$

T = temperature (K)

6. Specific heat of gaseous chlorine

$$c_p = 0.605770219 - 4.6076698 \times 10^{-5}T - 41.8722507/T + 2408.76803/T^2$$

where

c_p = specific heat

T = temperature (K)

7. Viscosity of chlorine gas

$$\ln(\mu_g) = -2.40357 - \frac{1117.90}{t + 565.833}$$

where

μ_g = Viscosity mPa s (or centipoises)

$t = ^\circ\text{C}$

8. Thermal conductivity of gaseous chlorine

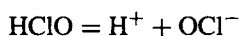
$$\ln k = -2.7230 - 1004.4/(T + 202.68)$$

where

k = thermal conductivity $\text{W m}^{-1}\text{K}^{-1}$

T = temperature (K)

9. Dissociation constant of hypochlorous acid



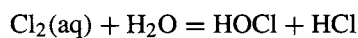
$$K = \frac{[\text{H}^+][\text{OCl}^-]}{\text{HOCl}}$$

where

$$K = 3.7508 \times 10^{-6} \exp\left(\frac{-1450.6}{T}\right)$$

T = temperature (K)

10. Hydrolysis constant of chlorine



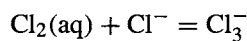
$$K = \frac{[\text{HOCl}][\text{HCl}]}{[\text{Cl}_2(\text{aq})]}$$

where

$$K = 11.625 \exp\left(\frac{-3085.44}{T}\right)$$

T = temperature (K)

11. Equilibrium constant of trichloride ion



$$K = \frac{[\text{Cl}_3^-]}{[\text{Cl}_2(\text{aq})][\text{Cl}^-]}$$

where

$$K = 6.4498 \times 10^{-3} \exp\left(\frac{1030.87}{T}\right)$$

T = temperature (K)

NaOH + NaCl solutions

1. Density

$$\begin{aligned} \rho = & 1.00686 + 0.01147527C_{\text{NaOH}} - 0.1722033 \times 10^{-4}C_{\text{NaOH}}^2 \\ & - 0.3585138 \times 10^{-3}t - 0.2143812 \times 10^{-5}t^2 \\ & + 0.007550802C_{\text{NaCl}} \end{aligned}$$

where

$$\begin{aligned} \rho &= \text{Density, g ml}^{-1} \\ C_{\text{NaOH}} &= \text{wt\% NaOH (0-65 wt\%)} \\ C_{\text{NaCl}} &= \text{wt\% NaCl (0-28 wt\%)} \\ t &= \text{°C (0-130)} \end{aligned}$$

F. SODIUM CHLORIDE

TABLE F1. Specific Gravity of NaCl Solutions

Bé (15°C)	Specific gravity	NaCl wt%	Solution g l ⁻¹	NaCl g l ⁻¹	H ₂ O g l ⁻¹
2.0	1.01405	1.938	1013.167	19.635	993.532
3.0	1.02123	2.929	1020.333	29.886	990.447
4.0	1.02850	3.932	1027.600	40.405	987.198
5.0	1.03589	4.951	1034.981	51.242	983.739
6.0	1.04338	5.962	1042.464	62.152	980.312
7.0	1.05098	6.987	1050.062	73.368	976.694
8.0	1.05869	8.024	1057.760	84.875	972.885
8.5	1.06259	8.549	1061.653	90.761	970.892
9.0	1.06651	9.078	1065.574	96.773	968.841
9.5	1.07046	9.611	1069.525	102.792	966.733
10.0	1.07446	10.145	1073.518	108.908	964.610
10.5	1.07847	10.672	1077.527	114.994	962.533
11.0	1.08251	11.202	1081.563	121.157	960.406
11.5	1.08659	11.738	1085.644	127.433	958.211
12.0	1.09069	12.275	1089.738	133.765	955.973
12.5	1.09483	12.818	1093.876	140.213	953.663
13.0	1.09900	13.365	1098.043	146.753	951.290
13.5	1.10320	13.916	1102.238	153.387	948.851
14.0	1.10743	14.471	1106.463	160.116	946.347
14.5	1.11170	15.030	1110.730	166.943	943.787
15.0	1.11600	15.573	1115.026	173.643	941.383
15.5	1.12033	16.120	1119.351	180.439	938.912
16.0	1.12470	16.672	1123.720	187.347	936.373
16.5	1.12910	17.227	1128.118	194.341	933.777
17.0	1.13353	17.786	1132.544	201.434	931.110
17.5	1.13801	18.351	1137.013	208.653	928.360
18.0	1.14251	18.919	1141.511	215.962	925.549
18.5	1.14706	19.493	1146.053	223.400	922.653
19.0	1.15163	20.068	1150.623	230.907	919.716
19.5	1.15625	20.628	1155.237	238.302	916.935
20.0	1.16089	21.192	1159.879	245.802	914.077
20.5	1.16558	21.761	1164.565	253.421	911.144
21.0	1.17032	22.335	1169.294	261.162	908.132
21.5	1.17508	22.912	1174.052	268.999	905.053
22.0	1.17988	23.496	1178.852	276.983	901.869
22.5	1.18472	24.082	1183.682	285.054	898.628
23.0	1.18961	24.676	1188.570	293.292	895.278
23.5	1.19453	25.259	1193.486	301.463	892.023
24.0	1.19949	25.829	1198.445	309.546	888.899
24.5	1.20450	26.415	1203.448	317.891	885.557

(With permission from Japan Soda Industry Association)

TABLE F2. Specific Heat of NaCl Solutions

%	-10°C	0°C	10°C	20°C	30°C
0		1.0082	1.0058	0.9996	0.9991
5		0.9343	0.9367	0.9391	0.9413
10		0.8813	0.8858	0.8894	0.8921
15	0.8340	0.8400	0.8448	0.8483	0.8507
16	0.8273	0.8330	0.8376	0.8409	0.8433
17	0.8206	0.8261	0.8307	0.8340	0.8362
18	0.8144	0.8199	0.8242	0.8273	0.8292
19	0.8084	0.8137	0.8178	0.8206	0.8225
20	0.8029	0.8080	0.8118	0.8144	0.8158
21	0.7974	0.8022	0.8060	0.8084	0.8096
22	0.7927	0.7972	0.8006	0.8025	0.8034
23	0.7879	0.7920	0.7951	0.7970	0.7979
24	0.7834	0.7872	0.7898	0.7915	0.7922
25	0.7791	0.7826	0.7850	0.7865	0.7867

(With permission from Japan Soda Industry Association)

TABLE F3. Surface Tension of NaCl Solutions in dyne cm^{-1}

%	0°C	10°C	20°C	30°C
0	75.64 ± 0.1	74.22 ± 0.05	72.75 ± 0.05	71.18 ± 0.05
2.84	76.46 ± 0.3	75.04 ± 0.15	73.57 ± 0.1	72.00 ± 0.15
5.52	77.28 ± 0.3	75.86 ± 0.15	74.39 ± 0.1	72.82 ± 0.15
10.47	78.92 ± 0.3	77.50 ± 0.2	76.03 ± 0.15	74.46 ± 0.2
14.92	80.54 ± 0.3	78.12 ± 0.25	77.65 ± 0.15	76.08 ± 0.25
18.95		80.76 ± 0.25	79.29 ± 0.2	77.72 ± 0.25
22.62		82.39 ± 0.25	80.92 ± 0.25	79.35 ± 0.25
25.97		84.02 ± 0.25	82.55 ± 0.25	80.98 ± 0.25

(With permission from Japan Soda Industry Association)

TABLE F4. Activity (α), Coefficient of Osmotic Pressure (Φ), and Mean Activity Coefficient (γ_{\pm}) of NaCl Solutions

m	α	Φ	$\log \gamma_{\pm}$
0.1	0.99665	0.9324	-0.1088
0.2	0.99336	0.9245	-0.1339
0.3	0.99009	0.9215	-0.1489
0.4	0.98682	0.9203	-0.1594
0.5	0.98355	0.9209	-0.1668
0.6	0.98025	0.9230	-0.1722
0.7	0.97692	0.9257	-0.1760
0.8	0.97359	0.9288	-0.1789
0.9	0.97023	0.9320	-0.1810
1.0	0.96686	0.9355	-0.1825
1.2	0.96010	0.9428	-0.1842
1.4	0.95320	0.9513	-0.1841
1.6	0.94610	0.9616	-0.1822
1.8	0.93890	0.9723	-0.1792
2.0	0.93160	0.9833	-0.1755
2.2	0.92420	0.9948	-0.1709
2.4	0.91660	1.0068	-0.1656
2.6	0.90890	1.0192	-0.1598
2.8	0.90110	1.0321	-0.1534
3.0	0.89320	1.0453	-0.1465
3.2	0.88510	1.0587	-0.1302
3.4	0.87690	1.0725	-0.1316
3.6	0.86860	1.0867	-0.1234
3.8	0.86060	1.1013	-0.1148
4.0	0.85150	1.1158	-0.1061
4.2	0.84280	1.1306	-0.0971
4.4	0.83390	1.1456	-0.0878
4.6	0.82500	1.1608	-0.0782
4.8	0.81600	1.1761	-0.0685
5.0	0.80680	1.1916	-0.0585
5.2	0.79760	1.2072	-0.0483
5.4	0.78830	1.2229	-0.0380
5.6	0.77880	1.2389	-0.0274
5.8	0.76930	1.2548	-0.0167
6.0	0.75980	1.2706	-0.0060

Note: $\ln \alpha = -(v m W/1000)\Phi$

where v = stoichiometric number of ions generated from one mole of electrolyte, W = mass of water in g mol^{-1} , and m = concentration in molality (mol kg^{-1} water). (Based on the vapor pressure of 23.753 mm Hg of pure water at 25°C.) (With permission from Japan Soda Industry Association)

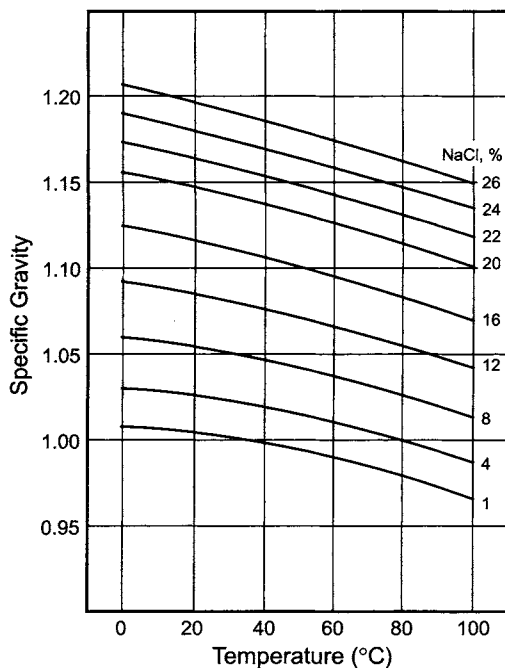


FIGURE F1. Specific gravity of NaCl solutions. (Data from International Critical Tables, Vol. 3, p. 79, McGraw-Hill, Book Co., New York (1928).)

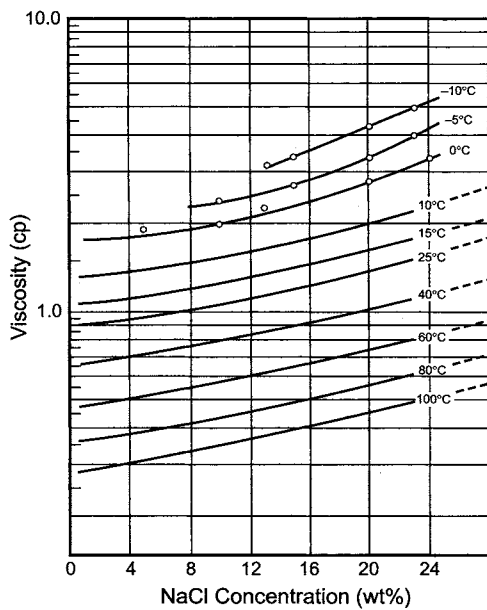


FIGURE F2. Viscosity of NaCl solutions. (Data from Mellor's "Comprehensive Treatise of Inorganic and Theoretical Chemistry," Vol. II, supplement II, p. 845, Longman (1961); open circles from Kaufmann's "Sodium Chloride," p. 622, Reinhold Publishing Corp., New York (1960).)

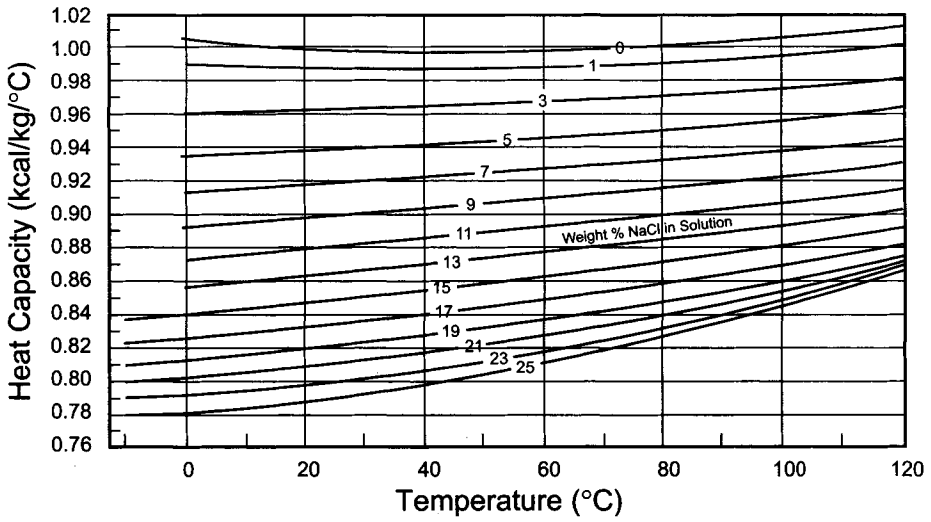


FIGURE F3. Heat capacity of NaCl solutions. (Data from International Critical Tables, Vol. II, p. 328 (1927), Vol. V, p. 115 (1929), McGraw-Hill Book Co., New York and M. Randall and F.D. Rossini, *J. Amer. Chem. Soc.* **51**, 323 (1929).)

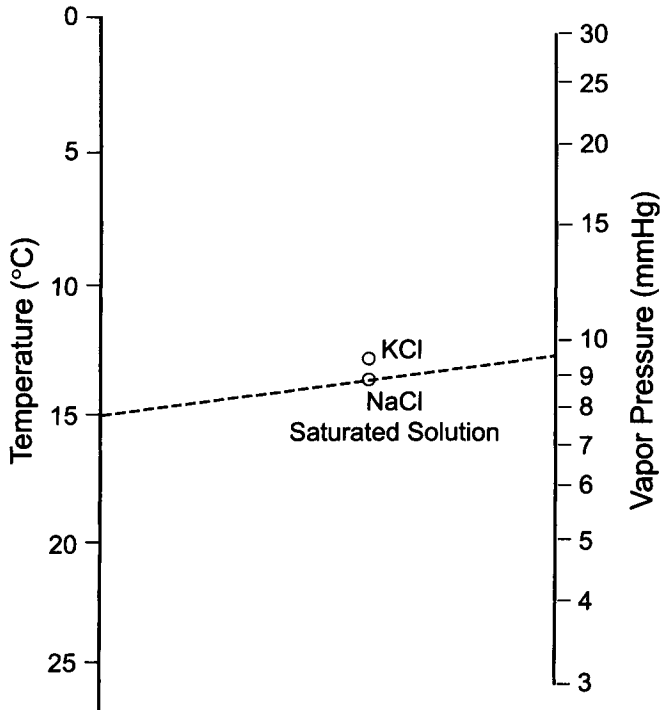


FIGURE F4. Vapor pressure of NaCl and KCl solutions. (Courtesy of Japan Soda Industry Association.)

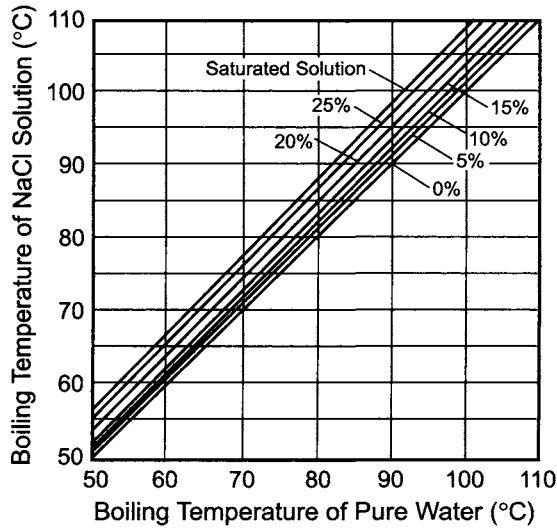


FIGURE F5. Dühring diagram of NaCl solutions. (Courtesy of Japan Soda Industry Association.)

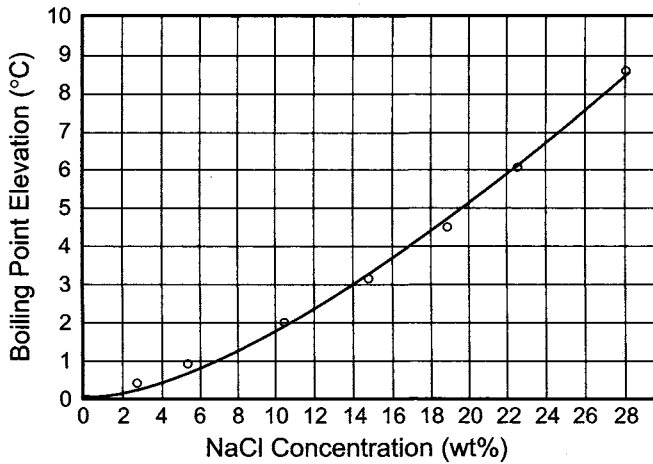


FIGURE F6. Boiling point elevation of NaCl solutions at atmospheric pressure. (Data from International Critical Tables, Vol. III, p. 326, McGraw-Hill Book Co., New York (1928).)

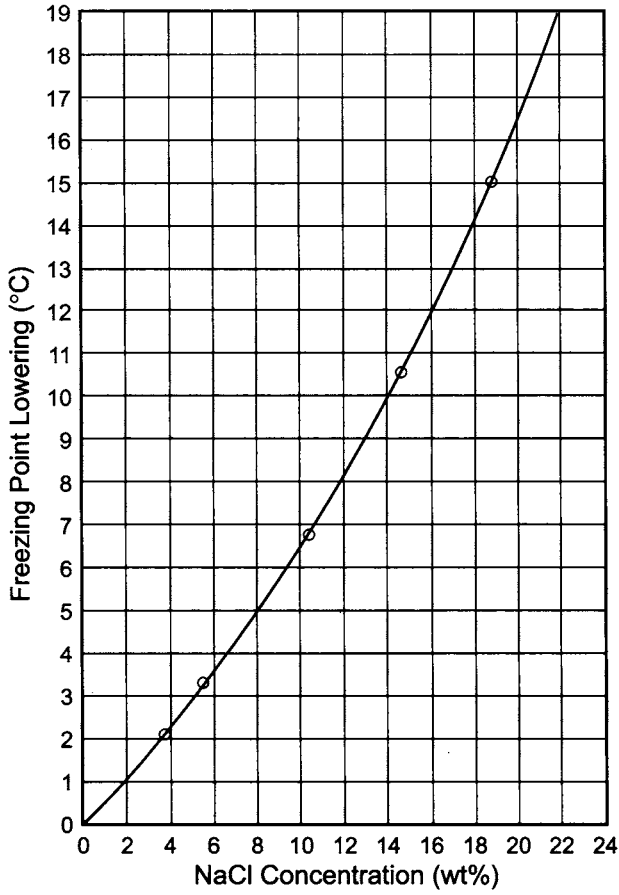


FIGURE F7. Freezing point lowering of NaCl solutions. (Data from International Critical Tables, Vol. IV, p. 258, McGraw-Hill Book Co., New York (1929).)

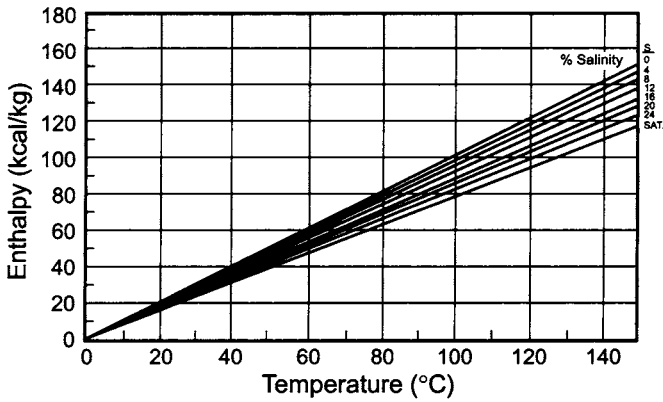


FIGURE F8. Enthalpy of NaCl solutions. (Data from G. Fabry, *Acta Tech. Acad. Sci. Hung.* **14**, 313 (1956).)

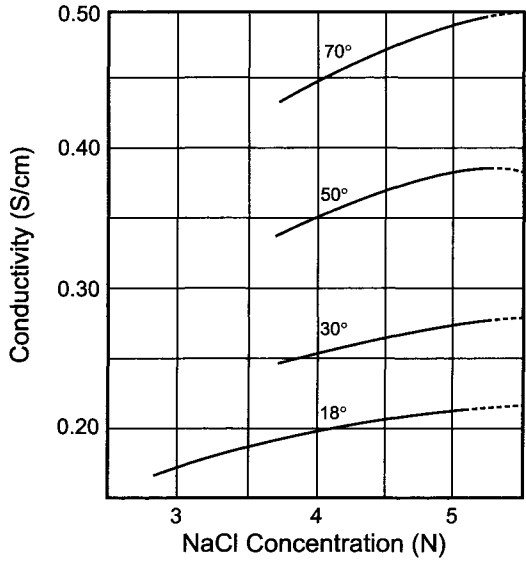


FIGURE F9. Conductivity of NaCl solutions. (Courtesy of Japan Soda Industry Association.)

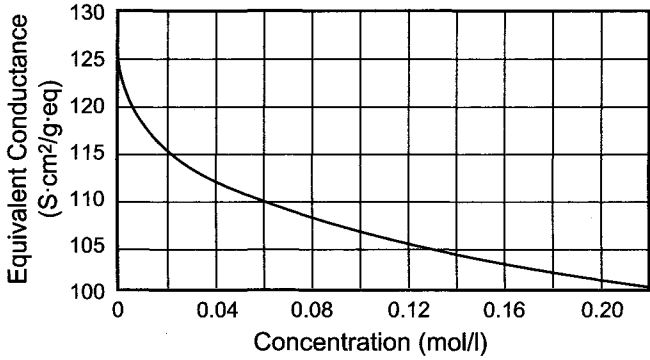


FIGURE F10. Equivalent conductance of NaCl solutions at 25°C. Shedlovsky's equation $(\lambda + \sigma\sqrt{c}) / (1 - \theta\sqrt{c}) = \lambda_0 + B_1c + B_2c^2$ ($\lambda_0 = 126.29$; $B_1 = 95.7478$; $B_2 = -65.6364$; $\sigma = 59.78$; $\theta = 0.2273$). (F. Hine, *Electrode Processes and Electrochemical Engineering*, pp. 81–82, Plenum Press, New York (1985).)

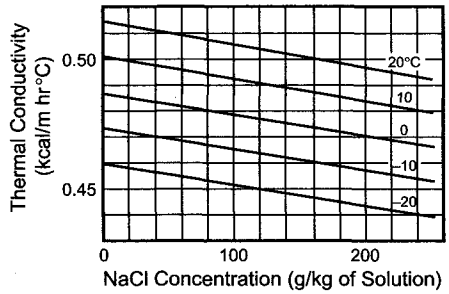


FIGURE F11. Thermal conductivity of NaCl solutions. (Courtesy of Japan Soda Industry Association.)

G. POTASSIUM CHLORIDE

TABLE G1. Density of Solutions of KCl

% KCl	Temperature, °C						
	0	20	25	40	60	80	100
2	1.01335	1.01103	1.00997	1.00471	0.9956	0.9842	0.9708
4	1.02690	1.02391	1.02255	1.01727	1.0080	0.9966	0.9834
6	1.04055	1.03690	1.03544	1.02995	1.0206	1.0092	0.9960
8	1.05431	1.05003	1.04847	1.04278	1.0333	1.0219	1.0088
10	1.06820	1.06332	1.06167	1.05578	1.0461	1.0347	1.0218
12	1.08222	1.07679	1.07506	1.06897	1.0592	1.0478	1.0350
14	1.09638	1.09046	1.08865	1.08237	1.0725	1.0611	1.0483
16	1.11068	1.10434	1.10245	1.09600	1.0861	1.0746	1.0619
18	1.12513	1.11845	1.11647	1.10987	1.0998	1.0884	1.0757
20	1.13973	1.13280	1.13072	1.12399	1.1138	1.1024	1.0897
22	1.15449	1.14740	1.14521	1.13836	1.1281	1.1166	1.1040
24		1.16226	1.15995	1.15299	1.1425	1.1311	1.1185
26			1.17495	1.16788	1.1573	1.1458	1.1333
28				1.18304	1.1723	1.1609	1.1483

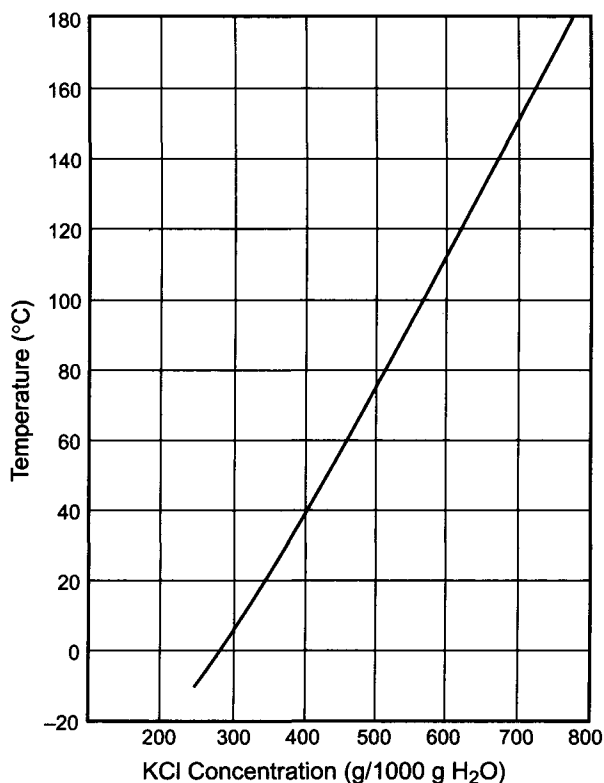


FIGURE G1. Solubility of KCl in water. (Data from International Critical Tables, Vol. IV, p. 239, McGraw-Hill Book Co., New York (1929))

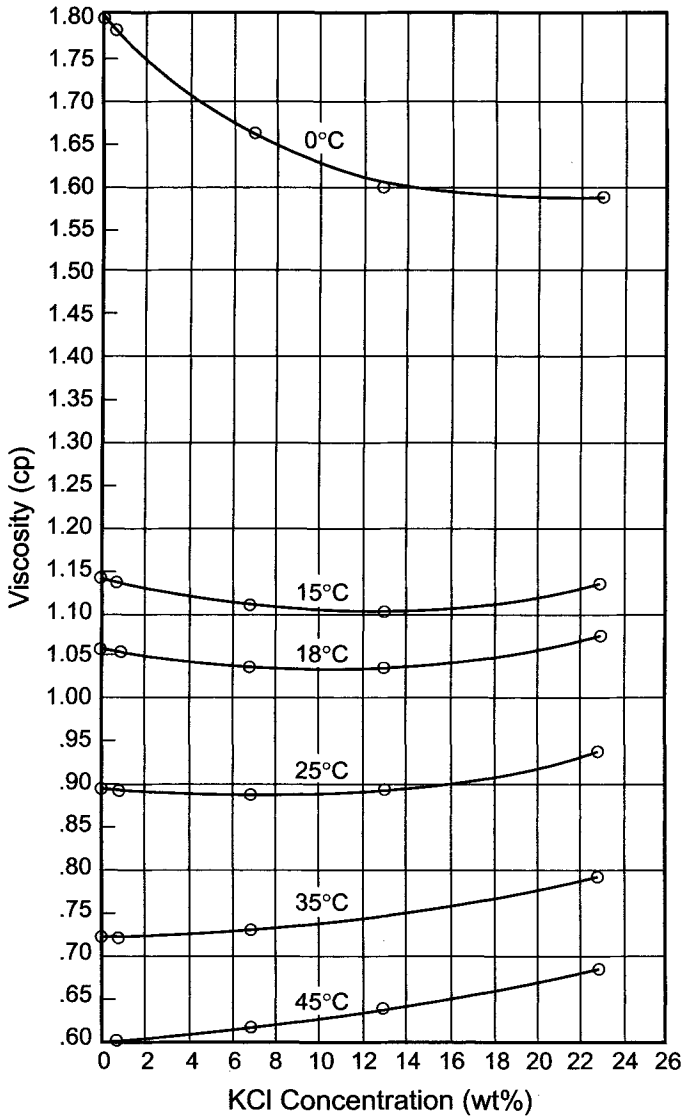


FIGURE G2. Viscosity of KCl solutions. (Data from International Critical Tables, Vol. V, p. 17, McGraw-Hill Book Co., New York (1929).)

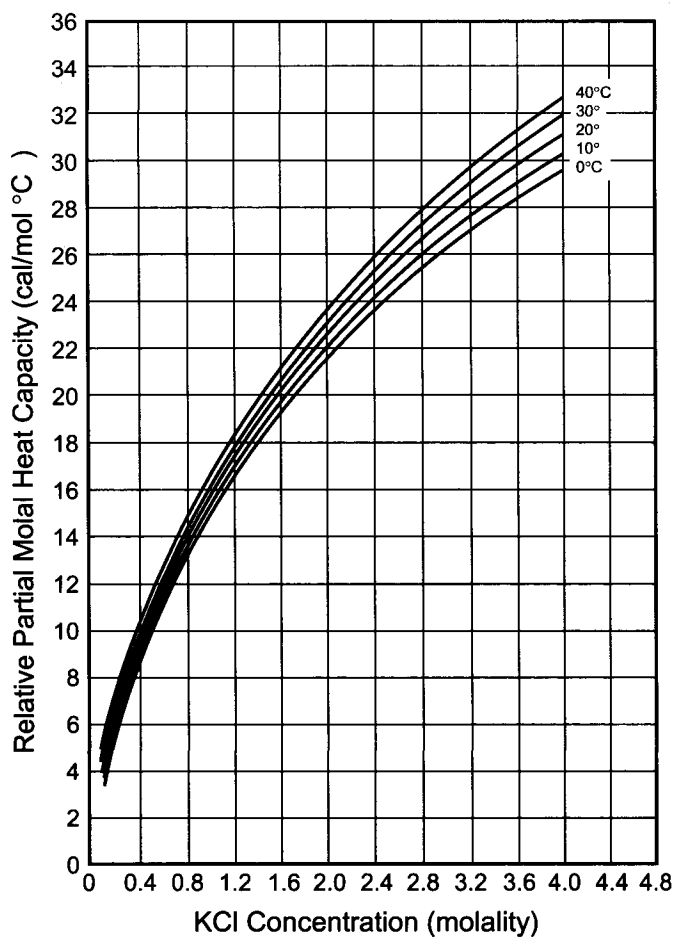


FIGURE G3. Relative partial molal heat capacity of solute in KCl solutions. (Data from R. Parsons, *Handbook of Electrochemical Constants*, Academic Press Inc., New York (1959), p. 43.)

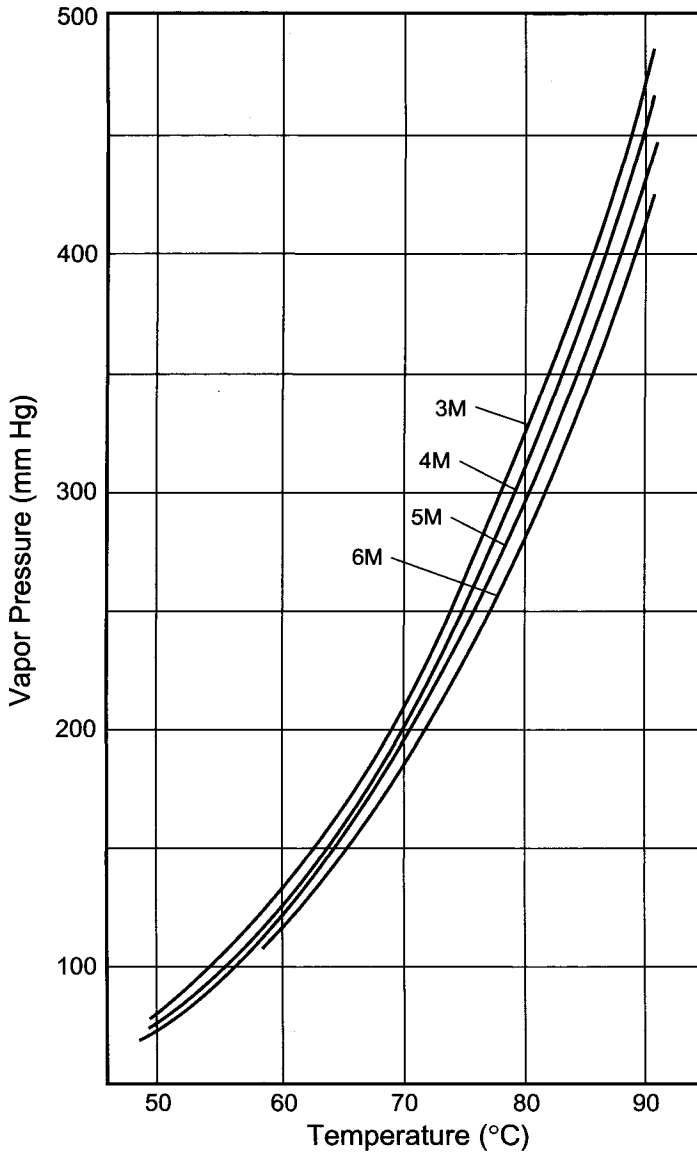


FIGURE G4. Vapor pressure of KCl solutions.

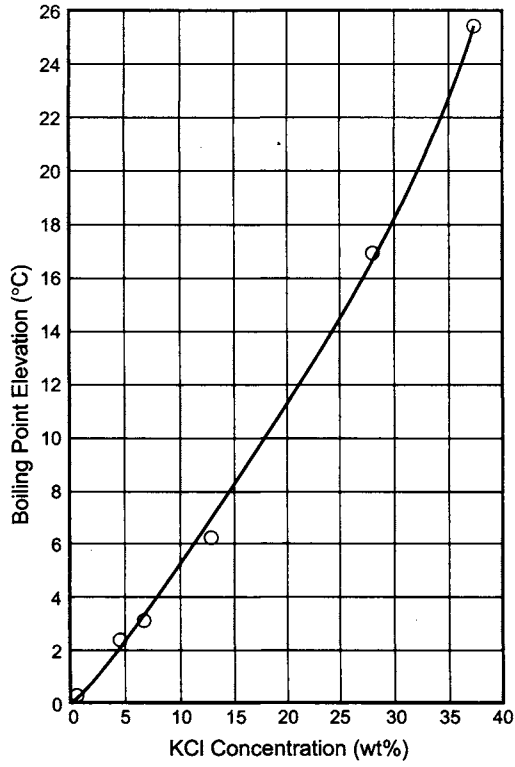


FIGURE G5. Boiling point elevation of KCl solutions. (Data from International Critical Tables, Vol. III, p. 326, McGraw-Hill Book Co., New York (1928).)

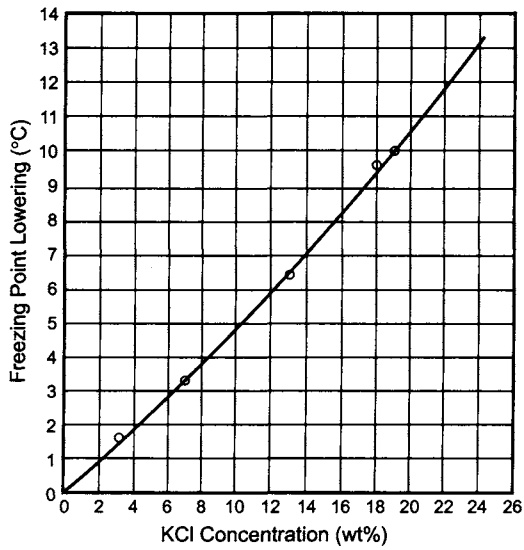


FIGURE G6. Freezing point lowering of KCl solutions. (Data from International Critical Tables, Vol. IV, p. 259, McGraw-Hill Book Co., New York (1929).)

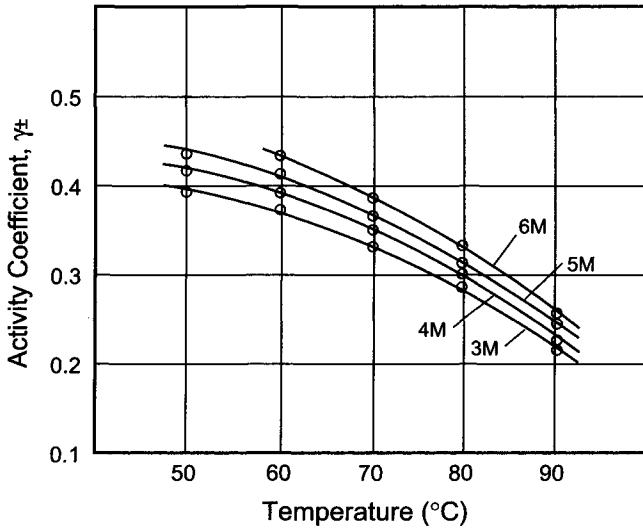


FIGURE G7. Mean activity coefficient of KCl in solution.

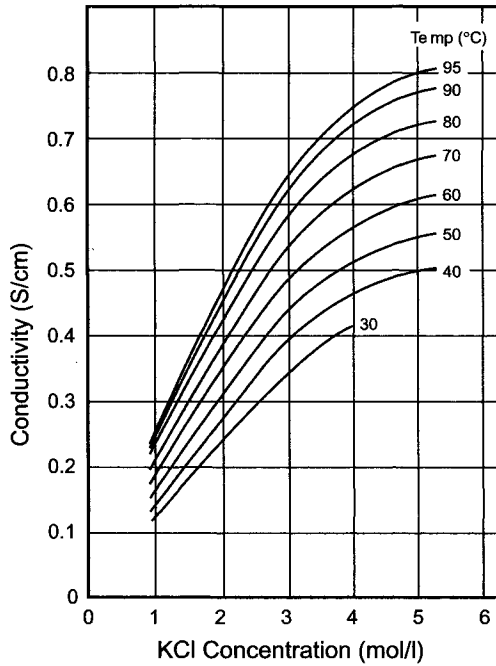


FIGURE G8. Conductivity of KCl solutions. (F. Hine, *Electrode Processes and Electrochemical Engineering*, p. 79, Plenum Press, New York (1985).)

H. SODIUM HYDROXIDE

Physical Properties of Sodium Hydroxide

Property	Value
CAS registry number	[1310-73-2]
Molecular weight	39.998
Specific gravity at 20°C	2.130
Melting point, °C	318
Boiling point, °C at 101.3 kPa	1388
Specific heat, J g ⁻¹ °C ⁻¹ at 20°C	1.48
Refractive index at 589.4 nm	
320°C	1.433
420°C	1.421
Latent heat of fusion, J g ⁻¹	167.4
Lattice energy, kJ mol ⁻¹	737.2
Entropy, J mol ⁻¹ K ⁻¹ at 25°C and 101.3 kPa	64.45
Heat of formation, kJ mol ⁻¹	
α form	422.46
β form	426.60
Heat of transition from α form to β form, J g ⁻¹	103.3
Transition temperature, °C	299.6
Free energy of formation, kJ mol ⁻¹ at 25°C and 101.3 kPa	-379.5

TABLE H1. Specific Gravity of NaOH Solutions

$d^{15/4}$	Bé	NaOH %	NaOH g l ⁻¹	$d^{15/4}$	Bé	NaOH %	NaOH g l ⁻¹
1.007	1	0.59	6.0	1.220	26	19.65	239.7
1.014	2	1.20	12.0	1.231	27	20.60	253.6
1.022	3	1.85	18.9	1.241	28	21.55	267.4
1.029	4	2.50	25.7	1.252	29	22.50	281.7
1.036	5	3.15	32.6	1.263	30	23.50	296.8
1.045	6	3.79	39.9	1.274	31	24.48	311.9
1.052	7	4.56	47.3	1.285	32	25.50	327.7
1.060	8	5.20	55.0	1.297	33	26.58	344.7
1.067	9	5.86	62.5	1.308	34	27.65	361.7
1.075	10	6.58	70.7	1.320	35	28.83	380.4
1.083	11	7.30	79.1	1.332	36	30.00	399.6
1.091	12	8.07	88.0	1.345	37	31.20	419.6
1.100	13	8.78	96.6	1.357	38	32.50	441.0
1.108	14	9.50	105.3	1.370	39	33.73	462.1
1.116	15	10.30	114.9	1.383	40	35.00	484.1
1.125	16	11.06	124.4	1.397	41	36.36	507.9
1.134	17	11.90	134.9	1.410	42	37.65	530.9
1.142	18	12.69	145.0	1.424	43	39.06	556.2
1.152	19	13.50	155.5	1.438	44	40.47	582.0
1.162	20	14.35	166.7	1.453	45	42.02	610.6
1.171	21	15.15	177.4	1.468	46	43.58	639.8
1.180	22	16.00	188.8	1.483	47	45.16	669.7
1.190	23	16.91	201.2	1.498	48	46.73	700.0
1.200	24	17.81	213.7	1.514	49	48.41	732.9
1.210	25	18.71	226.4	1.530	50	50.10	766.5

(With permission from Japan Soda Industry Association)

TABLE H2. Heat of Solution of Caustic Soda

% NaOH	Water/mole NaOH	Cal g ⁻¹ NaOH
0.44	500	253.3
0.55	400	253.4
1.10	200	253.7
2.17	100	254.7
4.25	50	256.7
8.16	25	257.1
14.13	13.5	261.2
19.79	9	256.8
24.08	7	254.4
30.75	5	232.9
42.53	3	179.8

TABLE H3. Heat of Dilution of NaOH Solutions

wt% NaOH	kcal kg ⁻¹ NaOH	kcal kg ⁻¹ of solution
0	0	0
2	0.649	0.0129
4	-1.122	-0.0455
6	-2.629	-0.1578
8	-3.932	-0.3146
10	-4.730	-0.4730
12	-5.021	-0.5995
14	-4.757	-0.6655
16	-4.037	-0.6435
18	-2.744	-0.4935
20	-0.825	-0.1655
22	1.804	0.3965
24	5.208	1.248
26	9.427	2.453
28	14.536	4.070
30	20.537	6.160
32	27.483	8.790
34	35.227	11.968
36	43.796	15.763
38	53.075	20.168
40	62.810	25.129
42	72.985	30.679
44	83.435	36.718
46	93.885	43.186
48	104.335	50.072

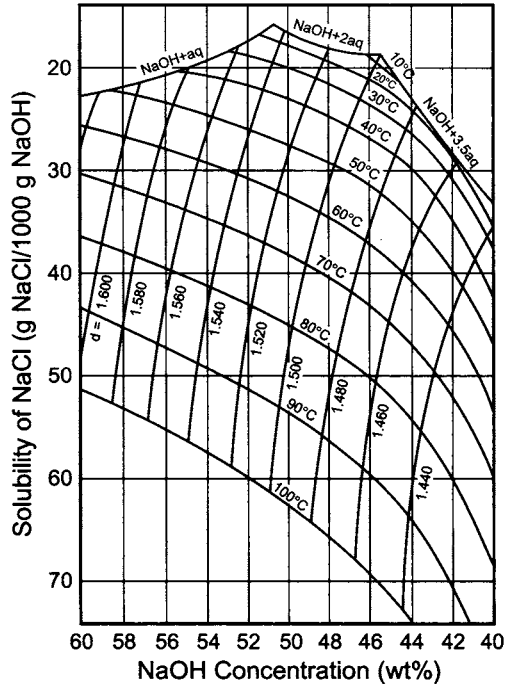


FIGURE H1. Solubility of NaCl in NaOH solutions. (Courtesy of Japan Soda Industry Association.)

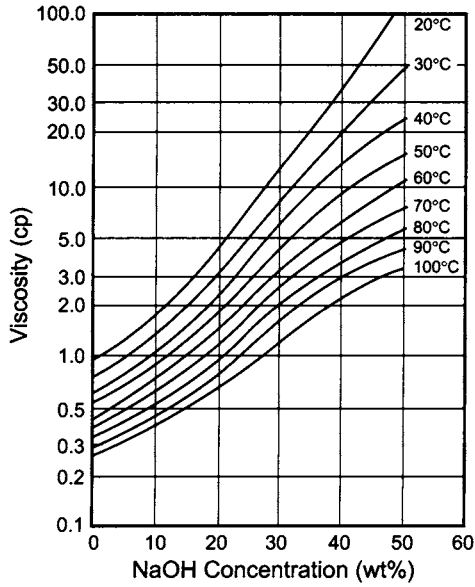


FIGURE H2. Viscosity of NaOH solutions. (Courtesy of Japan Soda Industry Association.)

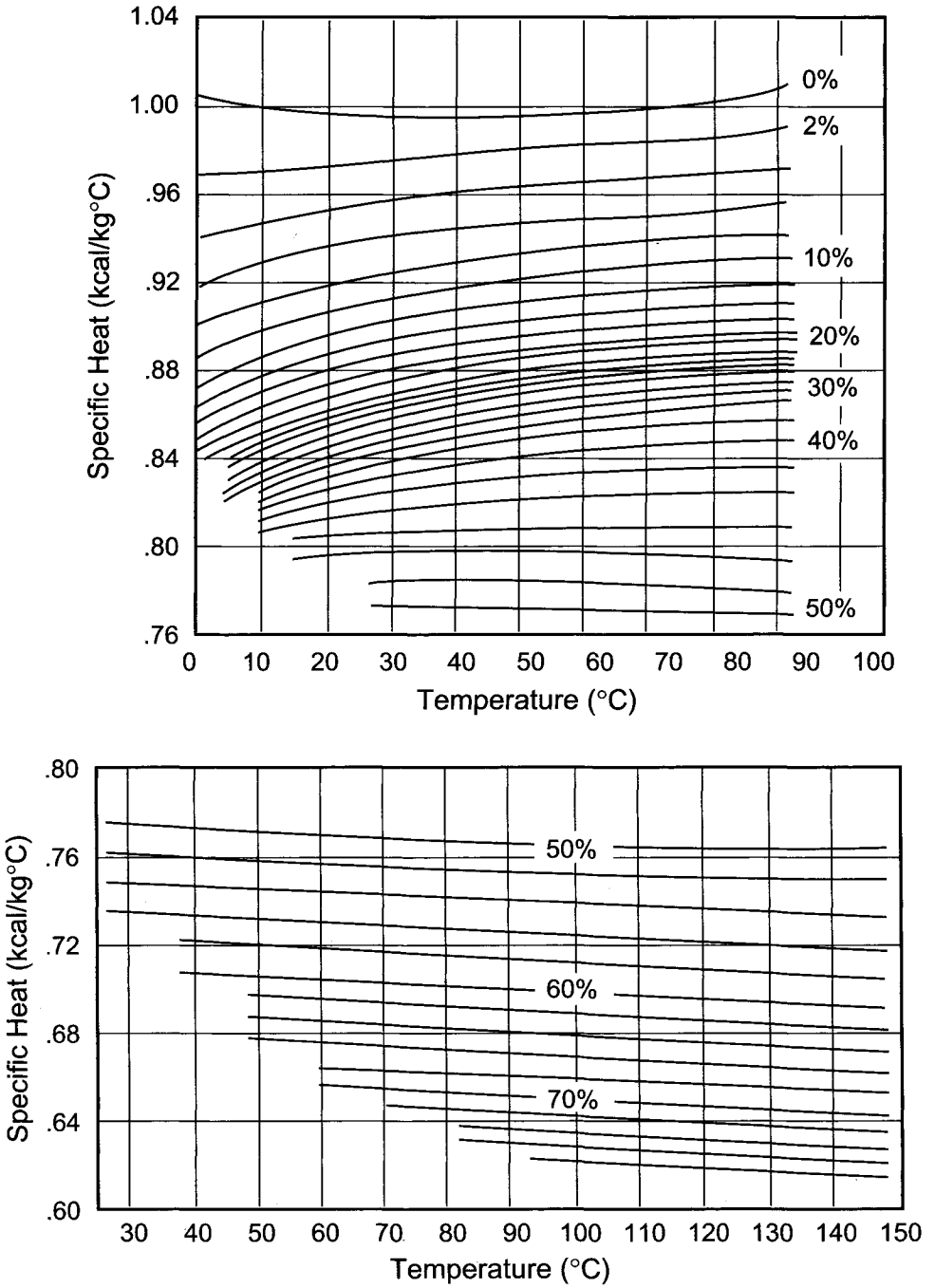


FIGURE H3. Specific heat of NaOH solutions. (Courtesy of Japan Soda Industry Association.)

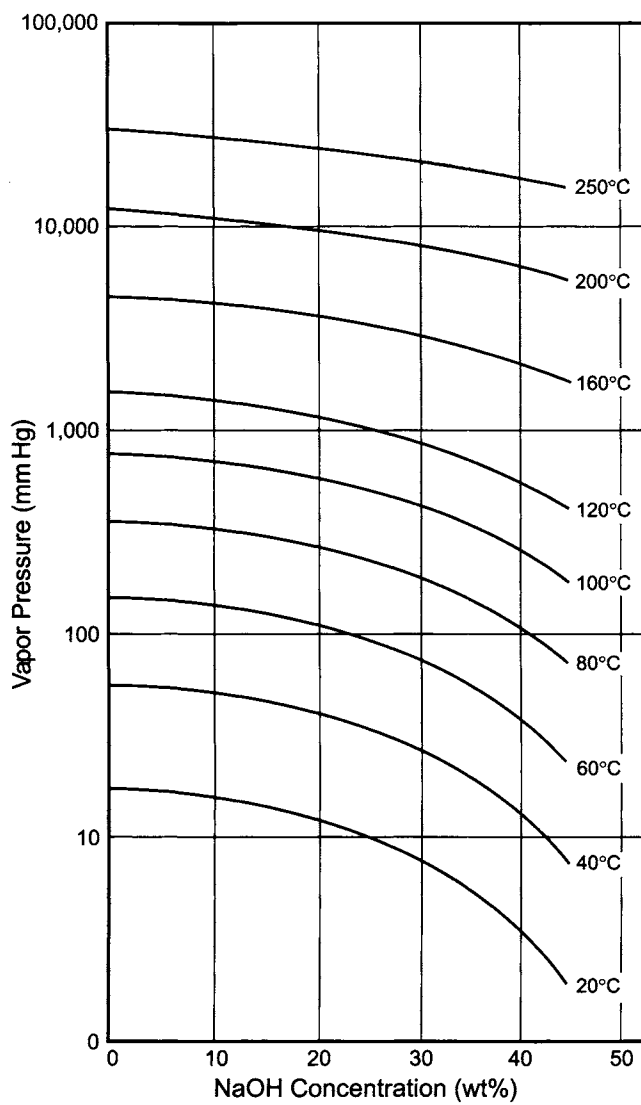


FIGURE H4. Vapor pressure of NaOH solutions. (Data from International Critical Tables, Vol. II, p. 370, McGraw-Hill Book Co., New York (1927).)

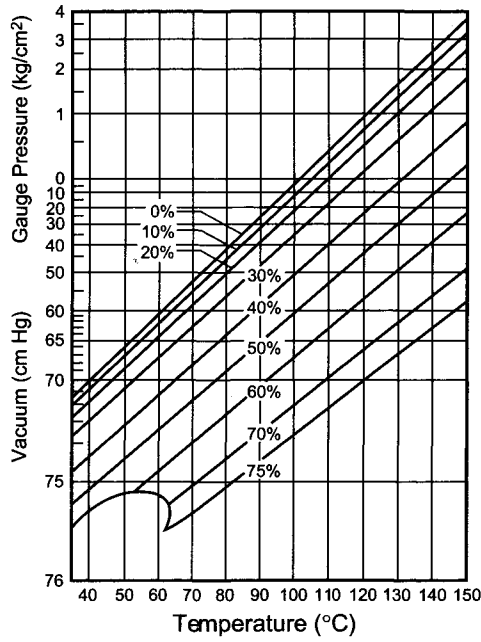


FIGURE H5. Boiling point of NaOH solutions. (Courtesy of Japan Soda Industry Association.)

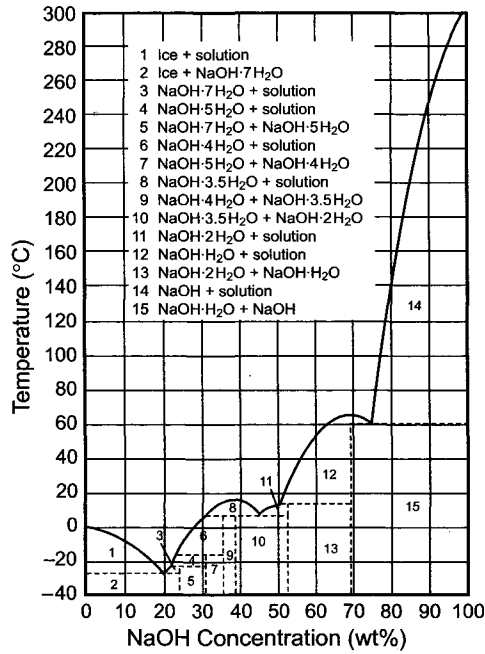


FIGURE H6. Phase diagram of caustic soda. (Courtesy of Japan Soda Industry Association.)

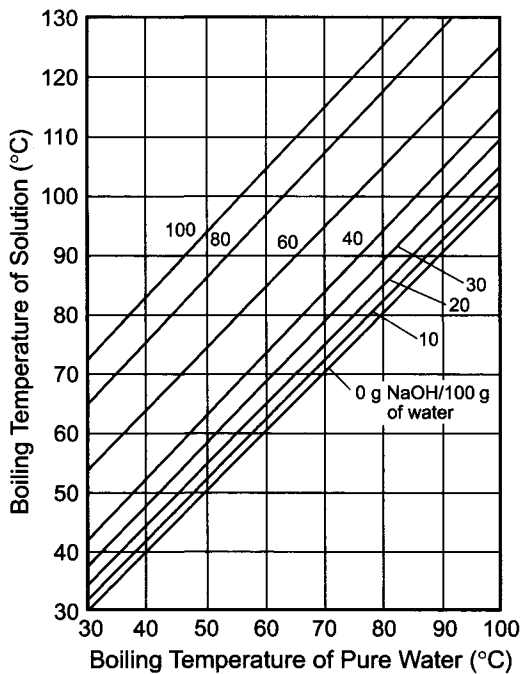


FIGURE H7. Dühring diagram of NaOH solutions. (Courtesy of Japan Soda Industry Association.)

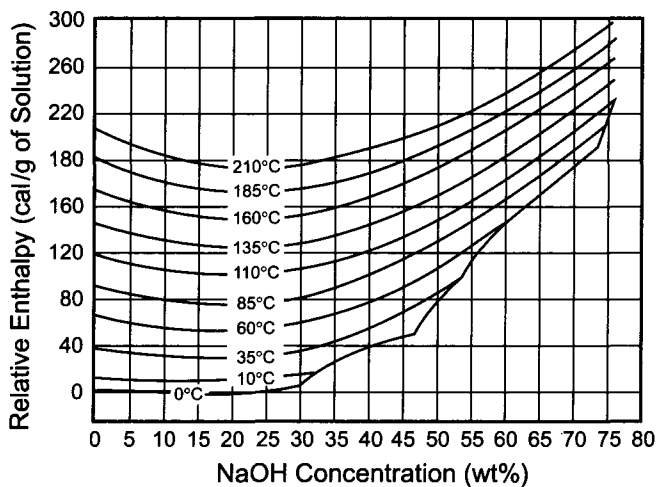


FIGURE H8. Enthalpy of NaOH solutions.

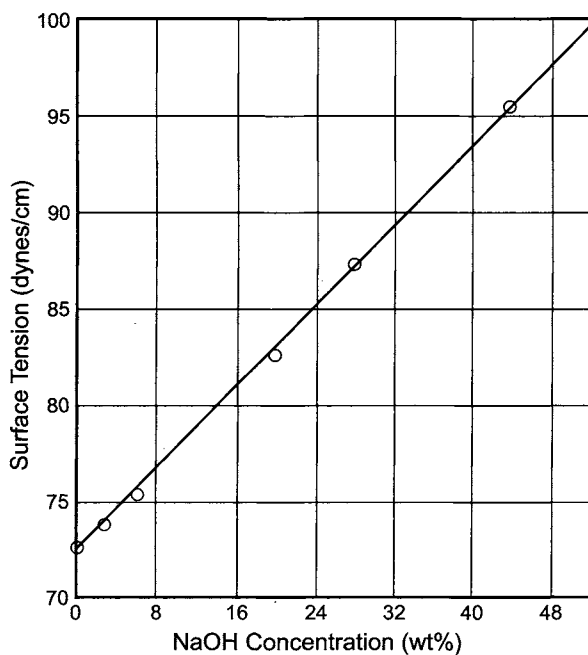


FIGURE H9. Surface tension of NaOH solutions. (Data from International Critical Tables, Vol. IV, p. 465, McGraw-Hill Book Co., New York (1929); surface tension of water at 18°C = 72.58 dynes cm⁻¹.)

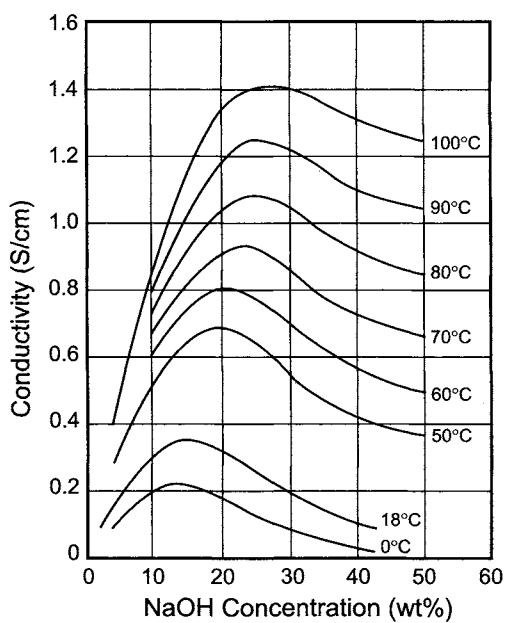


FIGURE H10. Conductivity of NaOH solutions. (F. Hine, *Electrode Processes and Electrochemical Engineering*, p. 75, Plenum Press, New York (1985).)

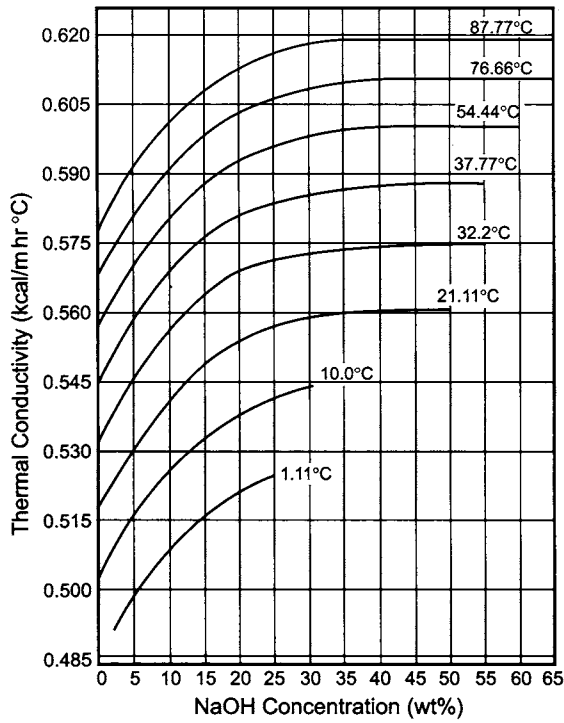


FIGURE H11. Thermal conductivity of NaOH solutions. (From Hooker Chemical Corporation's Technical Bulletin "Caustic Soda," p. 40 (1954).)

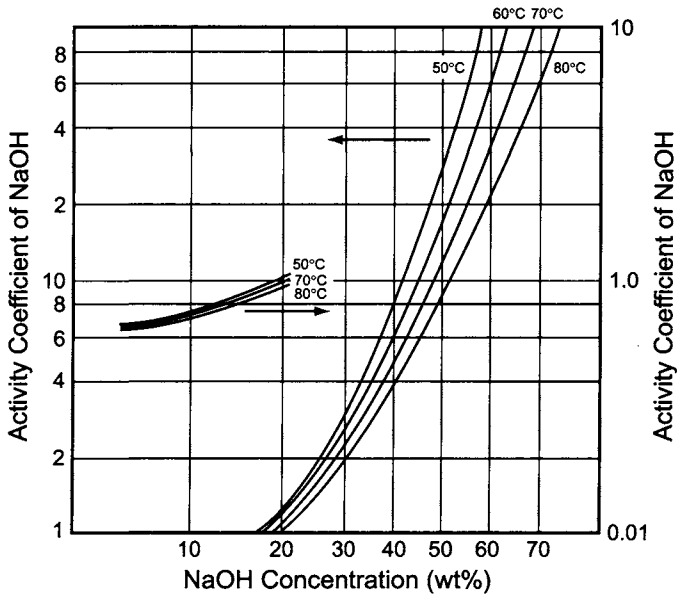
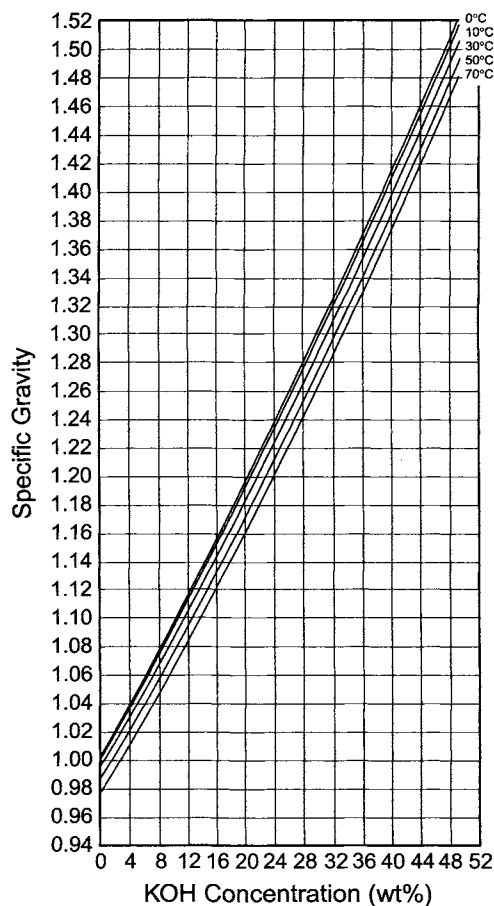


FIGURE H12. Activity coefficient of NaOH in solution. (From G. Akerlof and G. Kegeles, *J. Amer. Chem. Soc.* **62**, 620 (1940).)

I. POTASSIUM HYDROXIDE

TABLE II. Thermal Conductivity of Potassium Hydroxide Solutions

Wt% KOH	Heat conductivity at $t^{\circ}\text{C}$ ($\text{kcal m}^{-1} \text{hr}^{-1} \text{ }^{\circ}\text{C}^{-1}$)								
	0	10	20	30	40	50	60	70	80
0	0.486	0.501	0.515	0.528	0.540	0.551	0.561	0.570	0.578
10	0.490	0.505	0.519	0.532	0.544	0.555	0.565	0.574	0.582
20	0.486	0.501	0.515	0.528	0.540	0.551	0.561	0.570	0.578
30	0.473	0.488	0.502	0.515	0.527	0.538	0.548	0.557	0.565
40	0.456	0.471	0.485	0.498	0.510	0.521	0.531	0.540	0.548
50	0.432	0.447	0.461	0.474	0.486	0.497	0.507	0.516	0.524

FIGURE II. Specific gravity of KOH solutions. (G. Akerlof and P. Bender, *J. Amer. Chem. Soc.* **63**, 1088 (1941).)

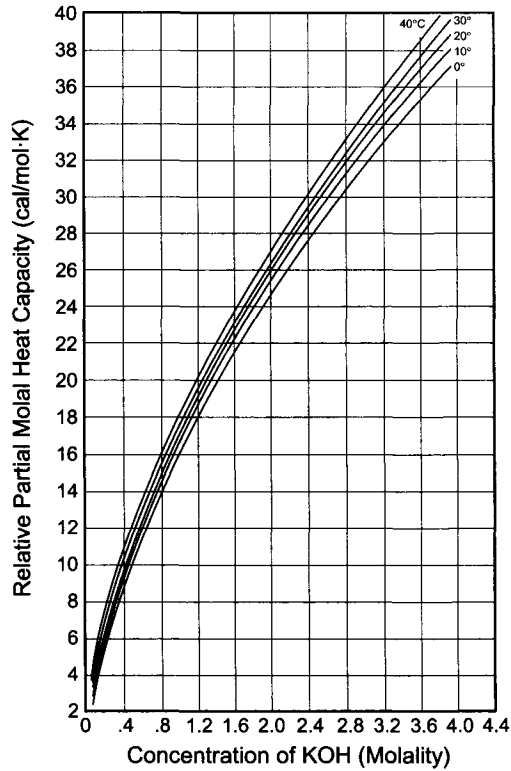


FIGURE I2. Relative partial molal heat capacity of solute in KOH solutions. (Data from R. Parsons, *Handbook of Electrochemical Constants*, Academic Press Inc., New York (1959), p. 43.)

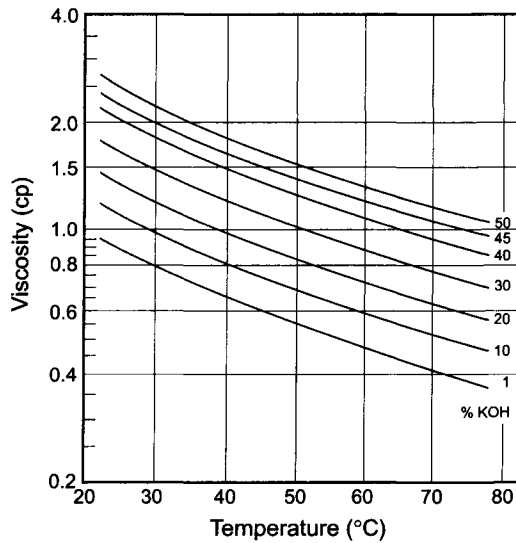


FIGURE I3. Viscosity of KOH solutions. (Data from International Critical Tables, Vol. V, p. 17, McGraw-Hill Book Co., New York (1929).)

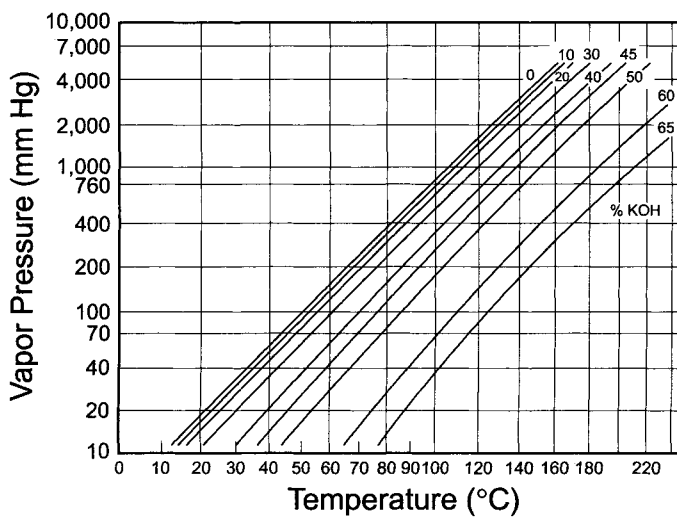


FIGURE I4. Vapor pressure of KOH solutions. (From *International Critical Tables of Numerical Data: Physics, Chemistry and Technology*, McGraw-Hill Book Co. (1923–1933).)

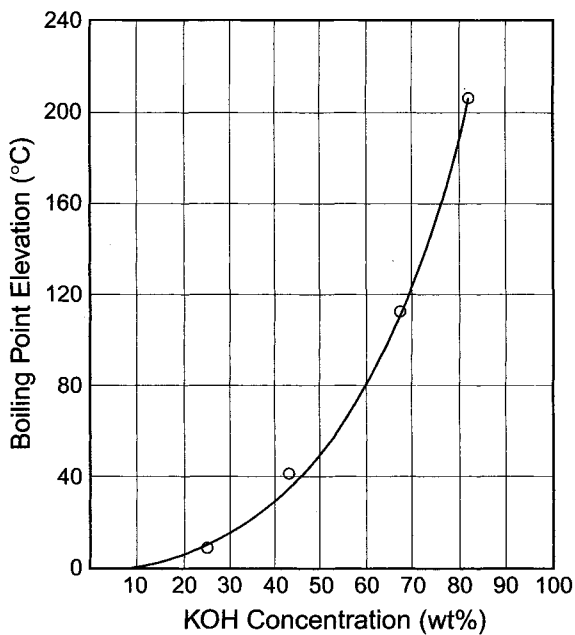


FIGURE I5. Boiling point elevation of KOH solutions. (Data from *International Critical Tables*, Vol. III, p. 326, McGraw-Hill Book Co., New York (1928).)

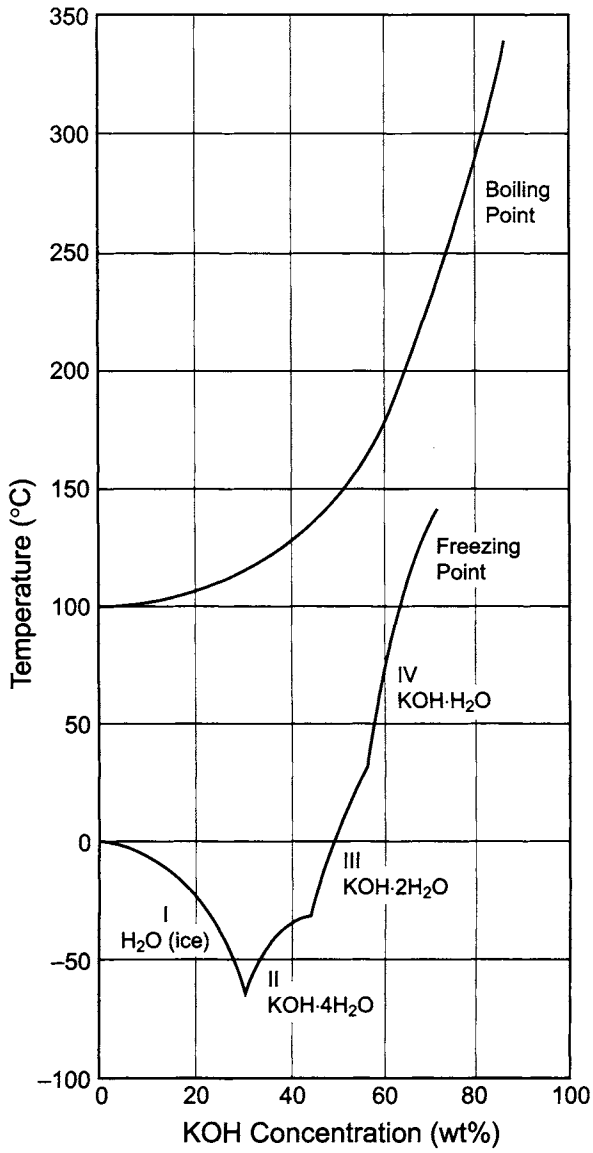


FIGURE I6. Plot of boiling and freezing points of KOH-water system.

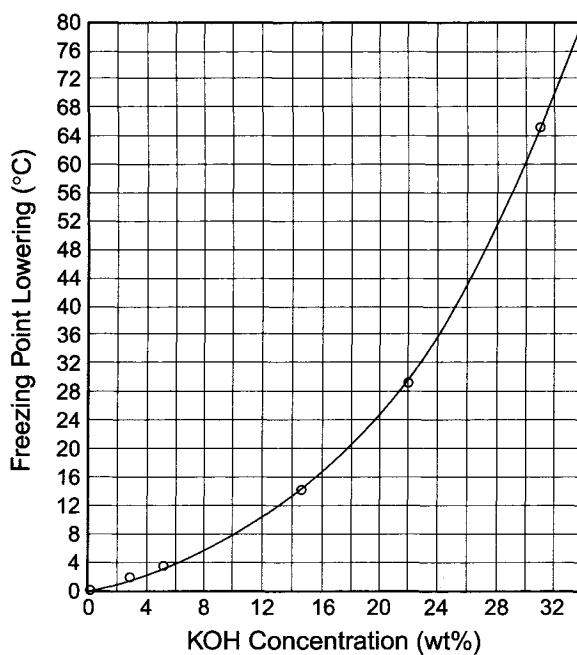


FIGURE I7. Freezing point lowering of KOH solutions. (Data from International Critical Tables, Vol. IV, p. 259, McGraw-Hill Book Co., New York (1929).)

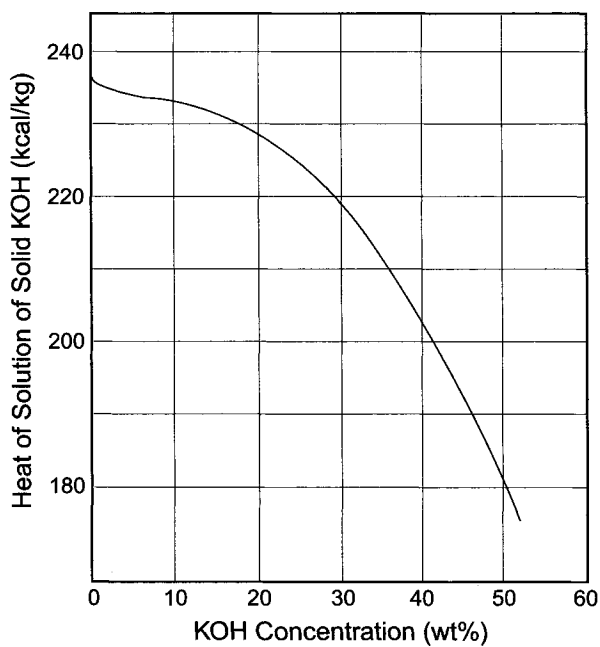


FIGURE I8. Heat of solution of KOH. (F.D. Rossini *et al.*, *Selected Values of Chemical Thermodynamic Properties*, p. 93, U.S. Government Printing Office, Washington, DC (1952).)

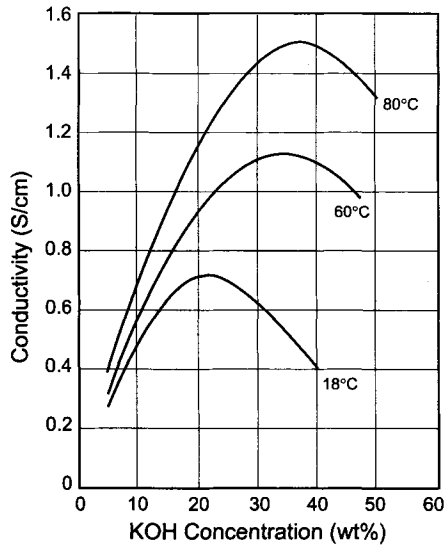


FIGURE I9. Conductivity of KOH solutions. (F. Hine, *Electrode Processes and Electrochemical Engineering*, p. 76, Plenum Press, New York (1985).)

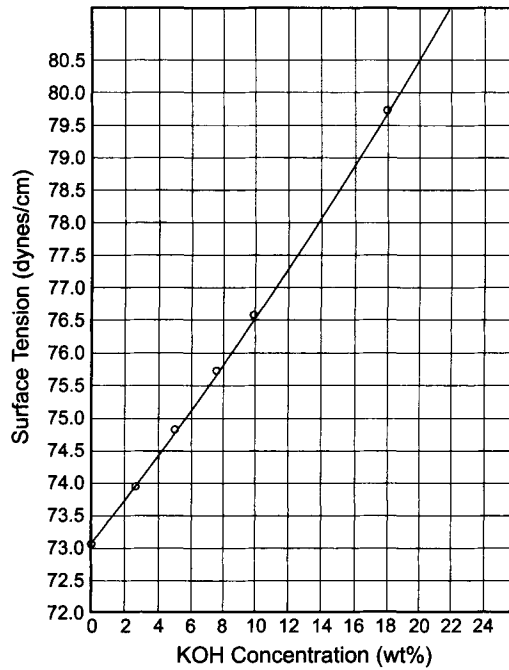


FIGURE I10. Surface tension of KOH solutions at 18°C. (Data from *International Critical Tables*, Vol. IV, p. 466, McGraw-Hill Book Co., New York (1929).)

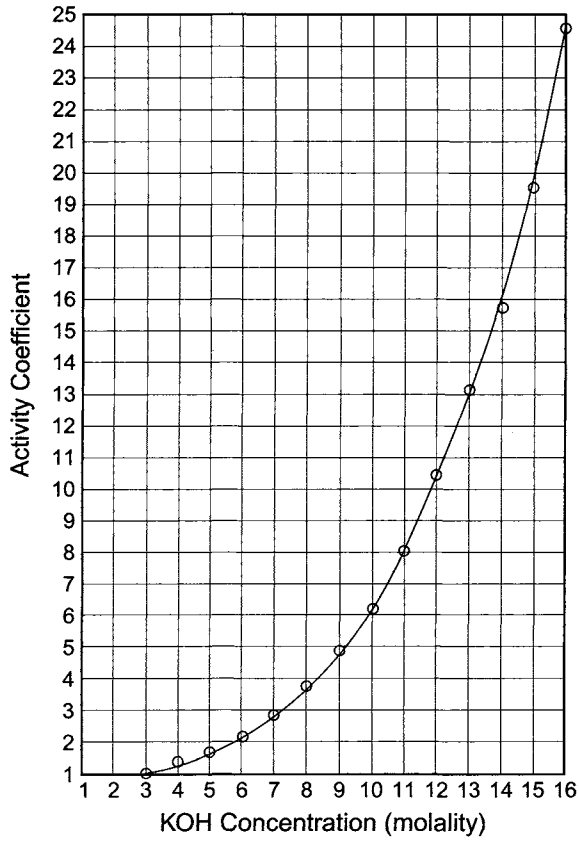


FIGURE I11. Stoichiometric mean molal activity coefficient of KOH solutions at 25°C. (Data from R. Parsons, *Handbook of Electrochemical Constants*, Academic Press Inc., New York (1959), pp. 22, 28.)

J. CHLORINE

Physical Properties of Chlorine

Property	Value
CAS Registry number	[7782-50-5]
Atomic number	17
Atomic weight	35.453
Stable isotope abundance, atom%	
³⁵ Cl	75.53
³⁷ Cl	24.47
Electronic configuration in ground state	[Ne]3s ² 3p ⁵
Melting point, °C	-100.98
Boiling point at 101.3 kPa (°C)	-33.97
Gas density relative to air	2.48
Critical density, kg m ⁻³	573
Critical pressure, kPa	7977
Critical volume, m ³ kg ⁻¹	0.001745
Critical temperature, °C	143.75
Critical compressibility	0.284777
Gas density, kg m ⁻³ at °C and 101.3 kPa	3.213
Gas viscosity, mPa s at 20°C	0.0134
Liquid viscosity, mPa s at 20°C	0.346
Gas thermal conductivity at 20°C, W m ⁻¹ K ⁻¹	0.00866
Liquid thermal conductivity at 20°C, W m ⁻¹ K ⁻¹	0.120
Latent heat of vaporization, kJ kg ⁻¹	287.75
Latent heat of fusion, kJ kg ⁻¹	90.33
Heat of dissociation, kJ mol ⁻¹	2.3944
Heat of hydration of Cl ⁻ , kJ mol ⁻¹	405.7
Standard electrode potential, V	1.359
Electron affinity, eV	3.77
Ionization energies, eV	13.01, 23.80, 39.90, 53.30, 67.80, 96.60, 114.20
Specific heat at constant pressure	0.481
Specific heat at constant volume	0.357
Specific magnetic susceptibility at 20°C, m ³ kg ⁻¹	-7.4 × 10 ⁻⁹
Electrical conductivity of liquid at -70°C (ohm ⁻¹ cm ⁻¹)	10 ⁻¹⁶
Dielectric constant at °C (wavelengths > 10 m)	1.97

TABLE J1. Thermodynamic Properties of Saturated Chlorine

Temp. (°C)	Absolute pressure (kPa)	Volume (m ³ kg ⁻¹)		Enthalpy (kJ kg ⁻¹)			Entropy (kJ kg ⁻¹ K ⁻¹)		
		Liquid	Vapor	Liquid	Vaporization	Vapor	Liquid	Vaporization	Vapor
-90	3.5785	0.00058670	5.9925	182.46	318.96	501.43	1.5688	1.7414	3.3102
-85	5.3042	0.00059088	4.1511	187.58	316.02	503.60	1.5963	1.6795	3.2759
-80	7.6791	0.00059517	2.9417	192.64	313.13	505.78	1.6229	1.6211	3.2440
-75	10.879	0.00059955	2.1283	197.66	310.29	507.95	1.6485	1.5658	3.2144
-70	15.111	0.00060403	1.5694	202.64	307.48	510.12	1.6733	1.5135	3.1868
-65	20.610	0.00060863	1.1775	207.58	304.70	512.29	1.6973	1.4638	3.1611
-60	27.642	0.00061334	0.89779	212.49	301.95	514.44	1.7206	1.4165	3.1371
-55	36.502	0.00061816	0.69460	217.38	299.20	516.58	1.7432	1.3714	3.1147
-50	47.517	0.00062311	0.54470	222.25	296.46	518.71	1.7652	1.3284	3.0937
-45	61.041	0.00062820	0.43249	227.10	293.71	520.81	1.7867	1.2873	3.0740
-40	77.456	0.00063341	0.34736	231.94	290.95	522.89	1.8077	1.2478	3.0555
-35	97.171	0.00063877	0.28194	236.78	288.17	524.95	1.8281	1.2100	3.0381
-34.05	101.32	0.00063981	0.27129	237.69	287.64	525.34	1.8320	1.2079	3.0349
-30	120.61	0.00064429	0.23109	241.61	285.37	526.98	1.8481	1.1735	3.0217
-25	148.25	0.00064996	0.19113	246.44	282.53	528.97	1.8677	1.1385	3.0062
-20	180.54	0.00065580	0.15940	251.28	279.65	530.93	1.8869	1.1046	2.9916
-15	218.00	0.00066182	0.13396	256.12	276.72	532.85	1.9058	1.0719	2.9777
-10	261.13	0.00066802	0.11339	260.97	273.74	534.72	1.9243	1.0402	2.9645
-5	310.45	0.00067442	0.096617	265.83	270.70	536.54	1.9424	1.0095	2.9519
0	366.53	0.00068104	0.082826	270.71	267.60	538.31	1.9603	0.97965	2.9400
5	429.90	0.00068788	0.071406	275.60	264.42	540.02	1.9779	0.95061	2.9285
10	501.14	0.00069496	0.061882	280.51	261.16	541.67	1.9952	0.92231	2.9175
15	580.83	0.00070229	0.053888	285.44	257.81	543.26	2.0123	0.89469	2.9070
20	669.55	0.00070990	0.047136	290.39	254.37	544.77	2.0291	0.86769	2.8968
25	767.92	0.00071781	0.041400	295.38	250.82	546.20	2.0457	0.84123	2.8870
30	876.53	0.00072603	0.036499	300.39	247.16	547.56	2.0621	0.81528	2.8774
35	996.02	0.00073460	0.032290	305.45	243.37	548.82	2.0784	0.78976	2.8681
40	1127.0	0.00074354	0.028657	310.54	239.44	549.99	2.0945	0.76461	2.8591
45	1270.1	0.00075288	0.025506	315.68	235.37	551.06	2.1104	0.73979	2.8502
50	1426.0	0.00076267	0.022760	320.88	231.13	552.01	2.1262	0.71522	2.8415
55	1595.5	0.00077294	0.020358	326.14	226.71	552.85	2.1420	0.69085	2.8329
60	1779.0	0.00078376	0.018246	331.47	222.09	553.56	2.1577	0.66661	2.8243
65	1977.4	0.00079517	0.016383	336.88	217.24	554.13	2.1733	0.64243	2.8158
70	2191.4	0.00080725	0.014732	342.39	212.15	554.55	2.1890	0.61823	2.8072
75	2421.6	0.00082008	0.013263	348.01	206.78	554.80	2.2047	0.59394	2.7987
80	2668.9	0.00083376	0.011952	353.75	201.10	554.86	2.2205	0.56944	2.7900
85	2934.0	0.00084842	0.010777	359.64	195.07	554.72	2.2364	0.54465	2.7811
90	3217.7	0.00086421	0.0097201	365.70	188.64	554.35	2.2526	0.51944	2.7720
95	3520.8	0.00088134	0.0087645	371.96	181.74	553.71	2.2689	0.49366	2.7626
100	3844.2	0.00090006	0.0078972	378.45	174.32	552.77	2.2857	0.46714	2.7528
105	4188.8	0.00092071	0.0071062	385.21	166.26	551.48	2.3028	0.43967	2.7425
110	4555.3	0.00094378	0.0063808	392.30	157.46	549.76	2.3206	0.41095	2.7315
115	4944.9	0.00086995	0.0057111	399.80	147.73	547.54	2.3390	0.38060	2.7196
120	5358.4	0.0010003	0.0050871	407.81	136.84	544.66	2.3585	0.34807	2.7066
125	5796.9	0.0010365	0.0044986	416.48	124.43	540.91	2.3793	0.31251	2.6918
130	6261.4	0.0010820	0.0039324	426.08	109.84	535.92	2.4020	0.27244	2.6744
135	6753.1	0.0011440	0.0033671	437.13	91.755	528.89	2.4279	0.22480	2.6527
140	7273.1	0.0012467	0.0027471	451.19	66.265	517.45	2.4606	0.16038	2.6210
144	7710.9	0.0017455	0.0017455	483.27	00.000	483.27	2.5364	0.00000	2.5364

TABLE J2. Equilibrium Constant K for the
Reaction $\text{Cl}_2(\text{g}) = \text{Cl}_2(\text{aq})$

Temperature ($^{\circ}\text{C}$)	K from ref. [1]	K from ref. [2]
10	0.116	
15	0.0935	
20	0.0775	
25	0.0623	0.0553
40		0.0356
60		0.0229
80		0.0171

[1] R.P. Whitney and J.E. Vivian, *Ind. Eng. Chem.* **33**, 741 (1941).

[2] A. Cerquetti *et al.*, *J. Electroanal. Chem.* **20**, 411 (1969).

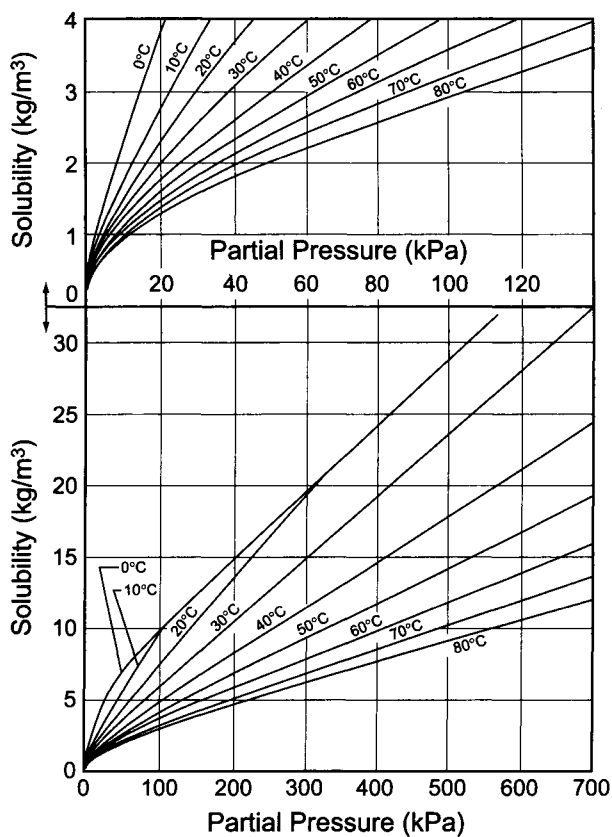


FIGURE J1. Solubility of chlorine in water. (F.W. Adams and R.G. Edmonds, *Ind. Eng. Chem.* **29**, 447 (1937).)

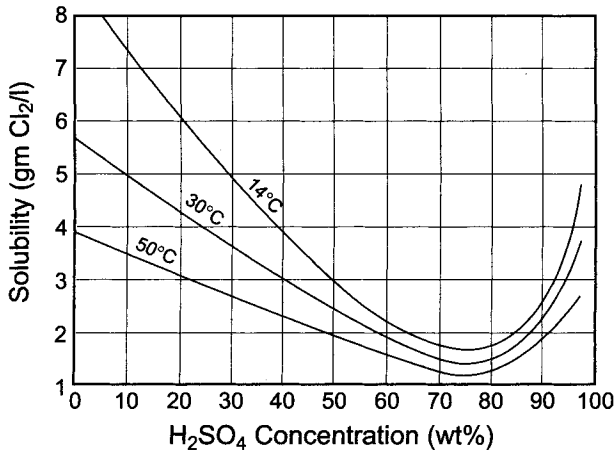


FIGURE J2. Solubility of chlorine in aqueous H₂SO₄ at 1 atm. (Data from International Critical Tables, Vol. III, p. 256, McGraw-Hill Book Co., New York (1928).)

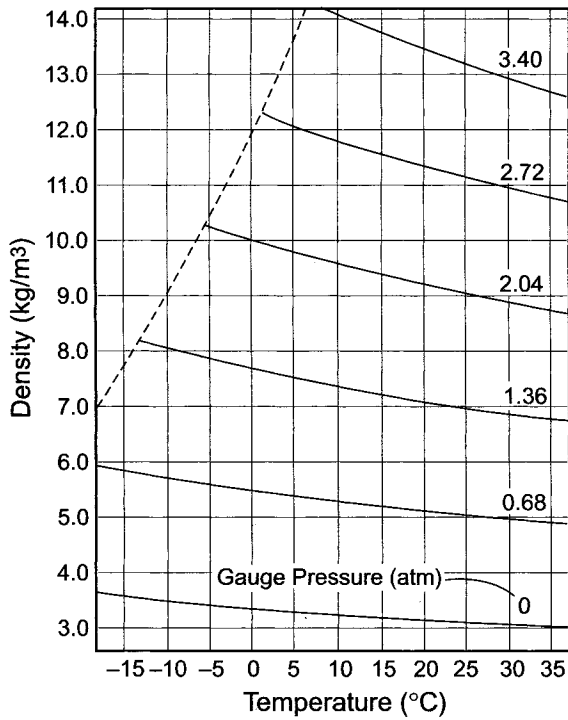


FIGURE J3. Density of chlorine gas. (Data from A.S. Ross and O. Maas, *Can. J. Res.* **18**, section B, 55 (1940).)

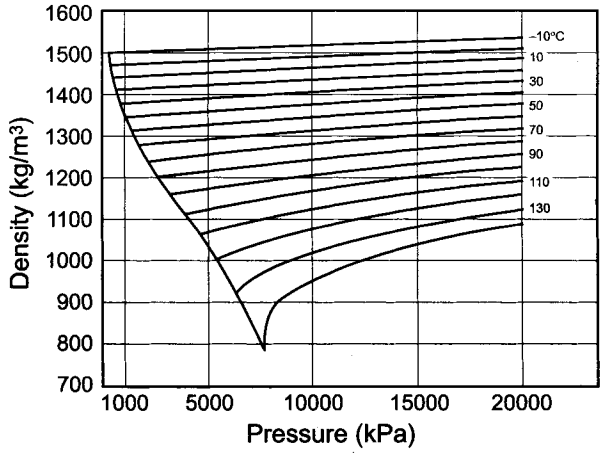


FIGURE J4. Density of liquid chlorine. (H. Wagenbreth, PTB—Mitteilungen, **78**(2), 91 (1968).)

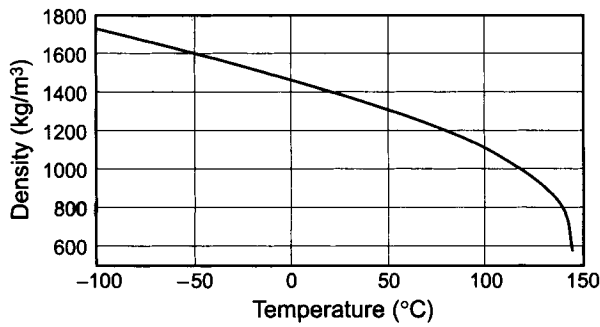


FIGURE J5. Density of saturated liquid chlorine. (R.M. Kapoor and J.J. Martin, *Thermodynamic Properties of Chlorine*, Engineering Research Institute, University of Michigan, Ann Arbor, MI (1957).)

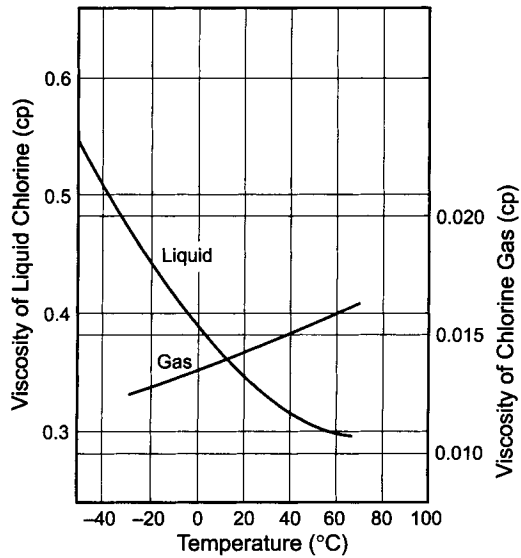


FIGURE J6. Viscosity of liquid chlorine and chlorine gas. (Courtesy of Japan Soda Industry Association.)

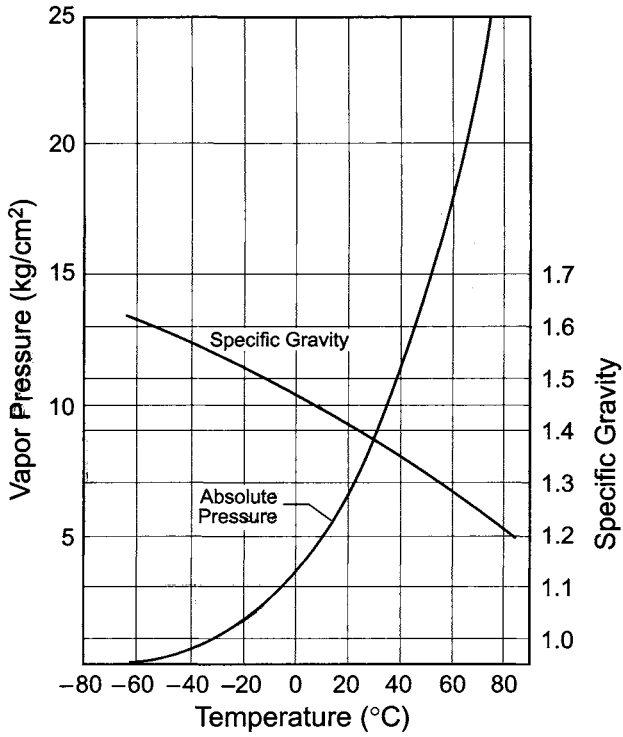


FIGURE J7. Vapor pressure and specific gravity of liquid chlorine. (Courtesy of Japan Soda Industry Association.)

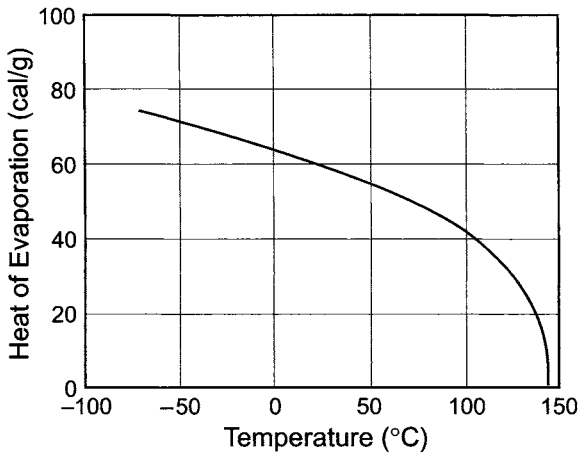


FIGURE J8. Heat of evaporation of liquid chlorine. (Courtesy of Japan Soda Industry Association.)

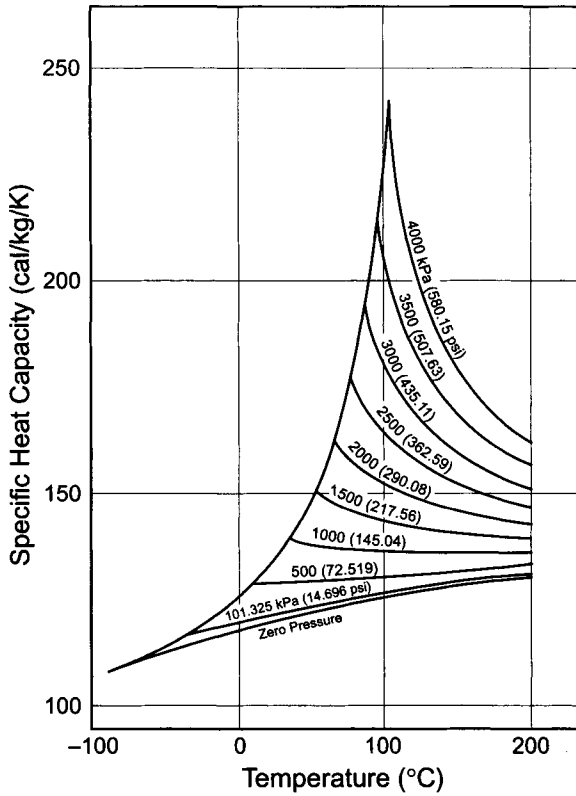


FIGURE J9. Specific heat capacity of chlorine gas at constant pressure. (R.M. Kapoor and J.J. Martin, *Thermodynamic Properties of Chlorine*, Engineering Research Institute, University of Michigan, Ann Arbor, MI (1957).)

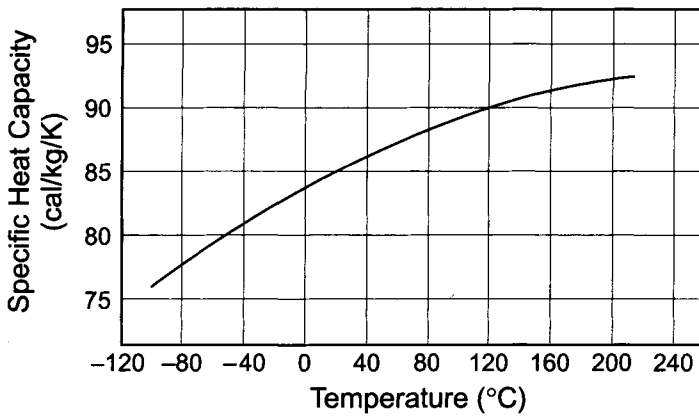


FIGURE J10. Specific heat capacity of chlorine gas at constant volume (ideal gas state). (R.M. Kapoor and J.J. Martin, *Thermodynamic Properties of Chlorine*, Engineering Research Institute, University of Michigan, Ann Arbor, MI (1957).)

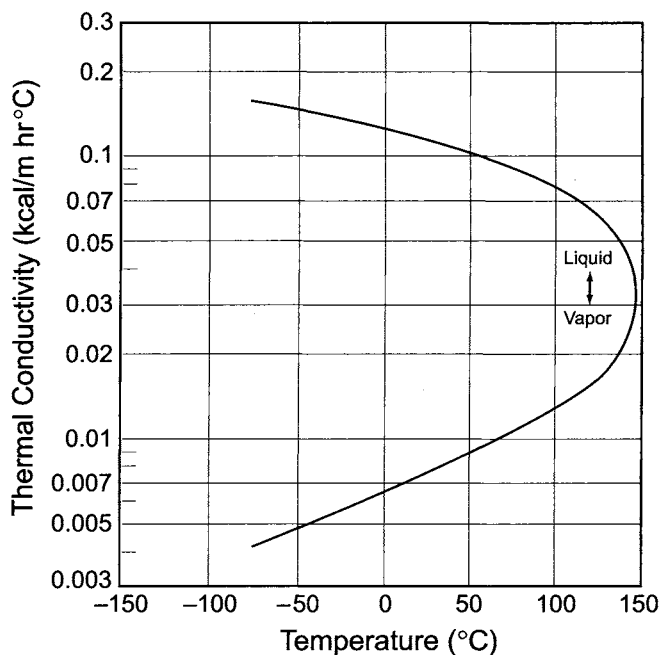


FIGURE J11. Thermal conductivity of chlorine gas and liquid. (C.Y. Ho, R.W. Powell, and P.E. Liley, *J. Phys. Chem. Ref. Data* 3 (Suppl. 1), 226 (1974).)

K. HYDROGEN

TABLE K1. Physical Properties of Gaseous Hydrogen at 101.3 kPa

Property	Value
Density at 0°C, (mol cm ⁻³) × 10 ³	0.04460
Compressibility factor at 0°C	1.00042
Adiabatic compressibility at 300 K, MPa ⁻¹	7.03
Coefficient of volume expansion at 300 K, K ⁻¹	0.00333
C _p at 0°C, J mol ⁻¹ K ⁻¹	28.59
C _v at 0°C, J mol ⁻¹ K ⁻¹	20.30
Enthalpy at 0°C, J mol ⁻¹	7749.2
Internal energy at 0°C, J mol ⁻¹	5477.1
Entropy at 0°C	139.59
Velocity of sound at 0°C, m s ⁻¹	1246
Viscosity at 0°C, cp	0.00834
Thermal conductivity at 0°C, mW cm ⁻¹ K ⁻¹	1.740
Dielectric constant at 0°C	1.000271
Isothermal compressibility at 300 K, MPa ⁻¹	-9.86
Self-diffusion coefficient at 0°C, cm ² s ⁻¹	1.285
Gas diffusivity in water at 25°C, cm ² s ⁻¹	4.8 × 10 ⁻⁵
Heat of dissociation at 25°C, kJ mol ⁻¹	435.881

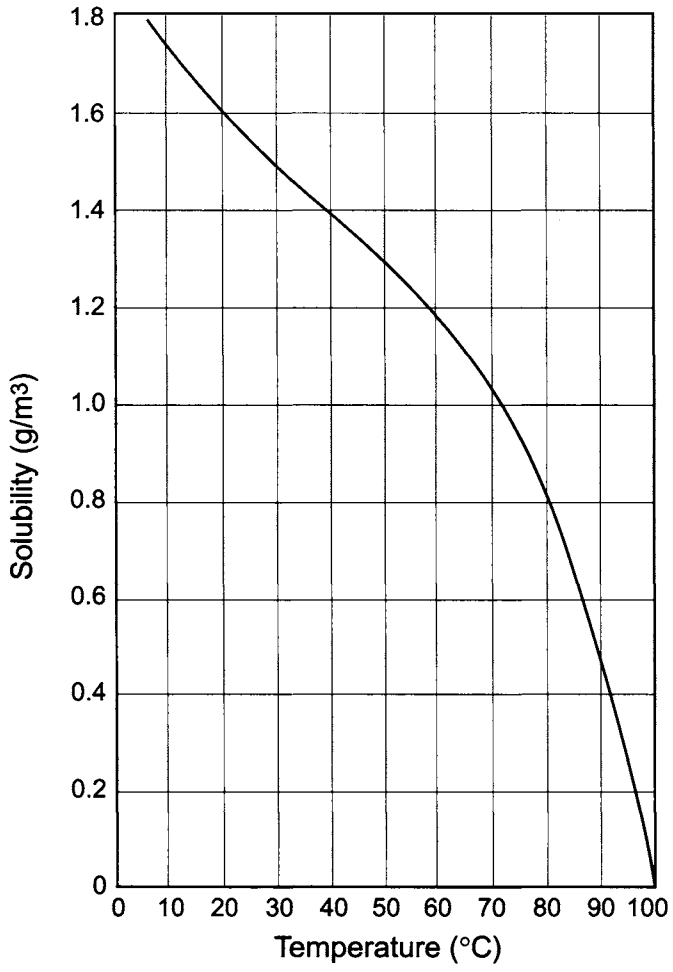


FIGURE K1. Solubility of hydrogen in water at 1 atm.

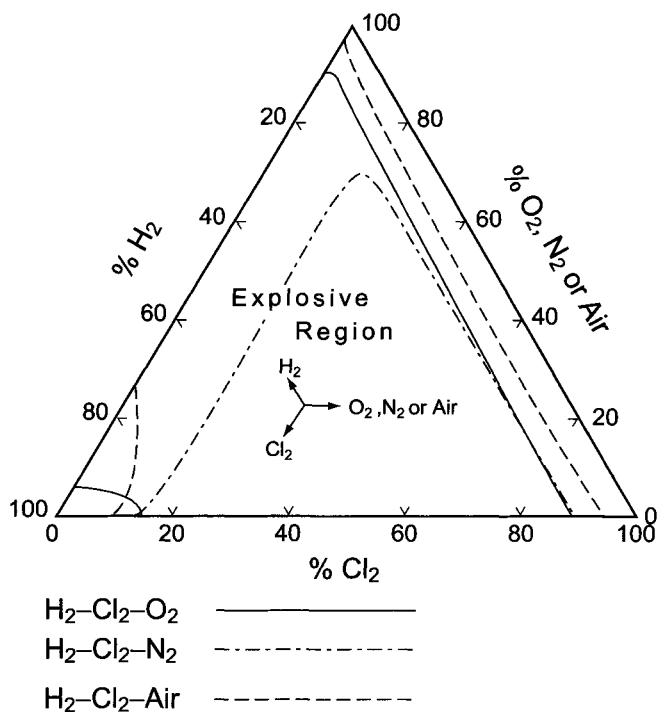


FIGURE K2. Explosive limits for H₂-Cl₂-O₂⁽¹⁾, H₂-Cl₂-N₂⁽¹⁾, and H₂-Cl₂-air⁽²⁾ mixtures.
 Notes: (1) R.B. MacMullin, *Electrolysis of Brines in Mercury Cells*. In J. Sconce (ed.), *Chlorine*, ACS monograph 154, Reinhold Publishing Co., New York (1962), p. 127. (2) *Soda Handbook*, p. 723, Japan Soda Industry Association, Tokyo (1998).

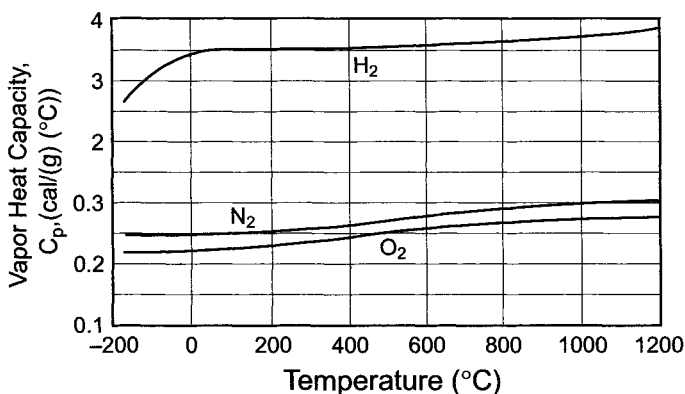


FIGURE K3. Vapor heat capacity of hydrogen, nitrogen, and oxygen. (From C.L. Yaws, *Physical Properties, A Guide to the Physical, Thermodynamic and Transport Data of Industrially Important Chemical Compounds*, McGraw-Hill Publishing Co., New York (1977).)

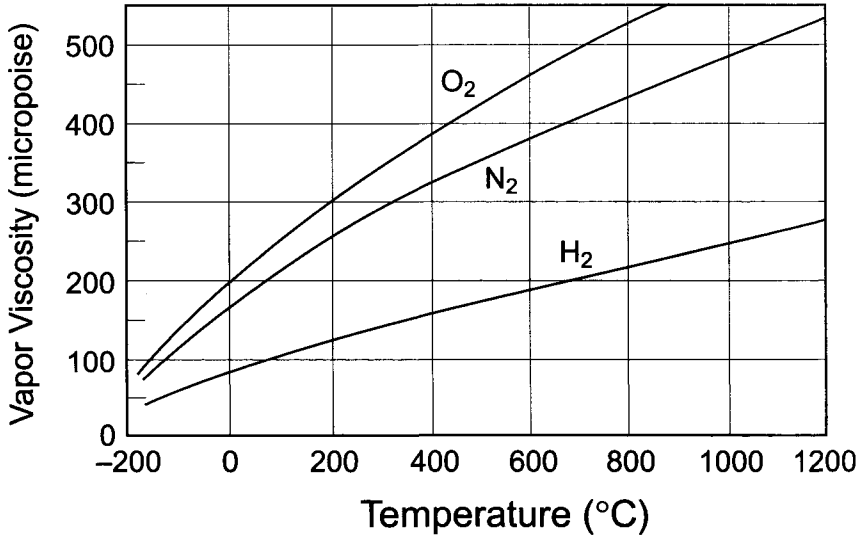


FIGURE K4. Vapor viscosity of hydrogen, nitrogen, and oxygen. (From C.L. Yaws, *Physical Properties, A Guide to the Physical, Thermodynamic and Transport Data of Industrially Important Chemical Compounds*, McGraw-Hill Publishing Co., New York (1977).)

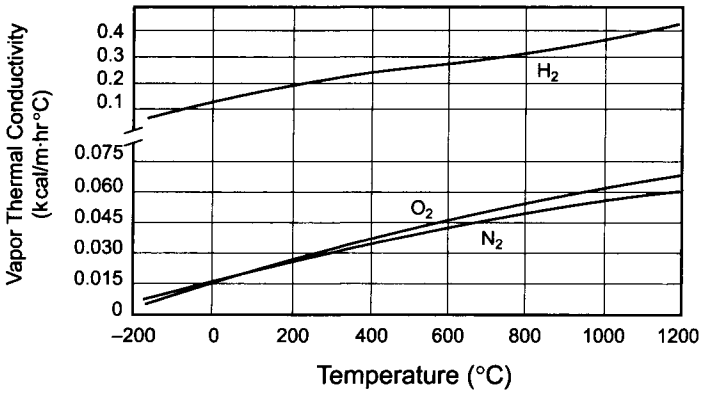


FIGURE K5. Vapor thermal conductivity of hydrogen, nitrogen, and oxygen. (From C.L. Yaws, *Physical Properties, A Guide to the Physical, Thermodynamic and Transport Data of Industrially Important Chemical Compounds*, McGraw-Hill Publishing Co., New York (1977).)

L. SULFURIC ACID

TABLE L1. Density of Solutions of H₂SO₄

% H ₂ SO ₄	Temperature, °C						
	0	20	25	40	60	80	100
5	1.0364	1.0317	1.0300	1.0240	1.0140	1.0022	0.9888
10	1.0735	1.0661	1.0640	1.0570	1.0460	1.0338	1.0204
15	1.1116	1.1020	1.0994	1.0914	1.0798	1.0671	1.0537
20	1.1510	1.1394	1.1365	1.1275	1.1153	1.1021	1.0855
25	1.1914	1.1783	1.1750	1.1653	1.1523	1.1388	1.1250
30	1.2326	1.2185	1.2150	1.2046	1.1909	1.1771	1.1630
35	1.2746	1.2599	1.2563	1.2454	1.2311	1.2169	1.2027
40	1.3179	1.3028	1.2991	1.2880	1.2732	1.2589	1.2446
45	1.3630	1.3476	1.3437	1.3325	1.3177	1.3029	1.2886
50	1.4110	1.3951	1.3911	1.3795	1.3644	1.3494	1.3348
55	1.4619	1.4453	1.4412	1.4293	1.4137	1.3984	1.3834
60	1.5154	1.4983	1.4940	1.4816	1.4656	1.4497	1.4344
65	1.5714	1.5533	1.5490	1.5361	1.5195	1.5031	1.4873
70	1.6293	1.6105	1.6059	1.5925	1.5753	1.5582	1.5417
75	1.6888	1.6692	1.6644	1.6503	1.6322	1.6142	1.5966
80	1.7482	1.7272	1.7221	1.7069	1.6873	1.6680	1.6493
85	1.8009	1.7786	1.7732	1.7571	1.7364	1.7161	1.6966
90	1.8361	1.8144	1.8091	1.7933	1.7729	1.7525	1.7331
95	1.8544	1.8337	1.8286	1.8137	1.7944		
96	1.8560	1.8355	1.8305	1.8157	1.7965		
97	1.8569	1.8364	1.8314	1.8166	1.7977		
98	1.8567	1.8361	1.8310	1.8163	1.7976		
99	1.8551	1.8342	1.8292	1.8145	1.7958		
100	1.8517	1.8305	1.8255	1.8107	1.7922		

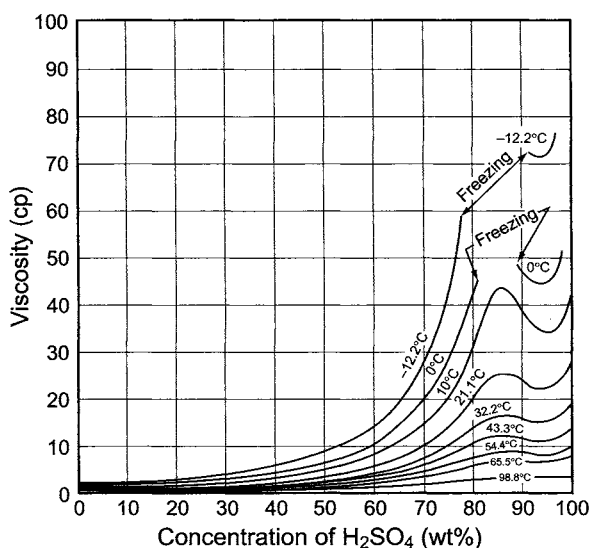


FIGURE L1. Viscosity of sulfuric acid solutions. (Data from Bright *et al.*, *J. Soc. Chem. Ind.*, **65**, 385 (1946); *International Critical Tables*, Vol. 5, pp. 11–13, McGraw-Hill Book Co., New York (1929); *Z. Physik. Chem. Neue Folge*, **3**, 52 (1955).)

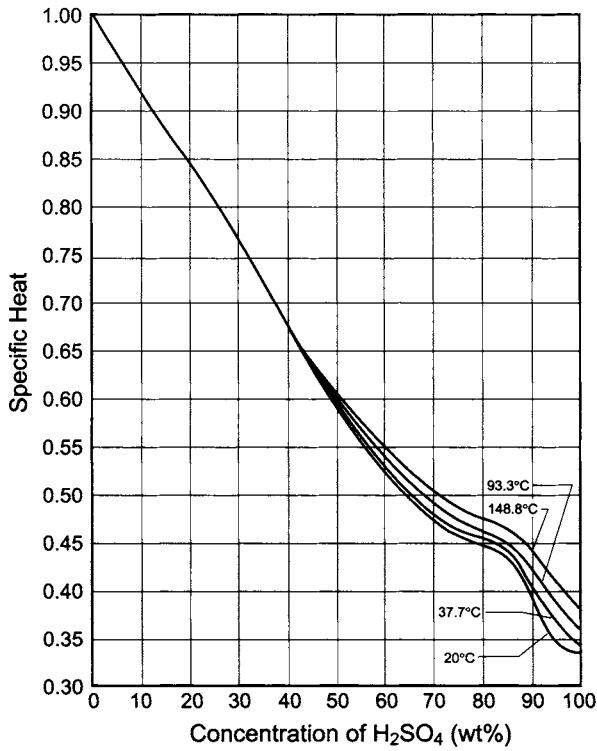


FIGURE L2. Specific heat of sulfuric acid solutions. (Socilik, *Z. Physik. Chem. Neue Folge*, **158A**, 305 (1932); Perry, *Chemical Engineers' Handbook*, 3rd ed., p. 234, McGraw-Hill, New York (1950).)

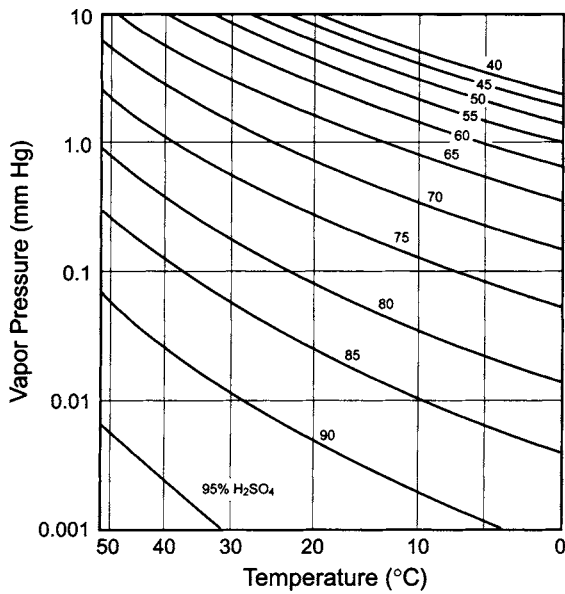


FIGURE L3. Vapor pressure of sulfuric acid solutions.

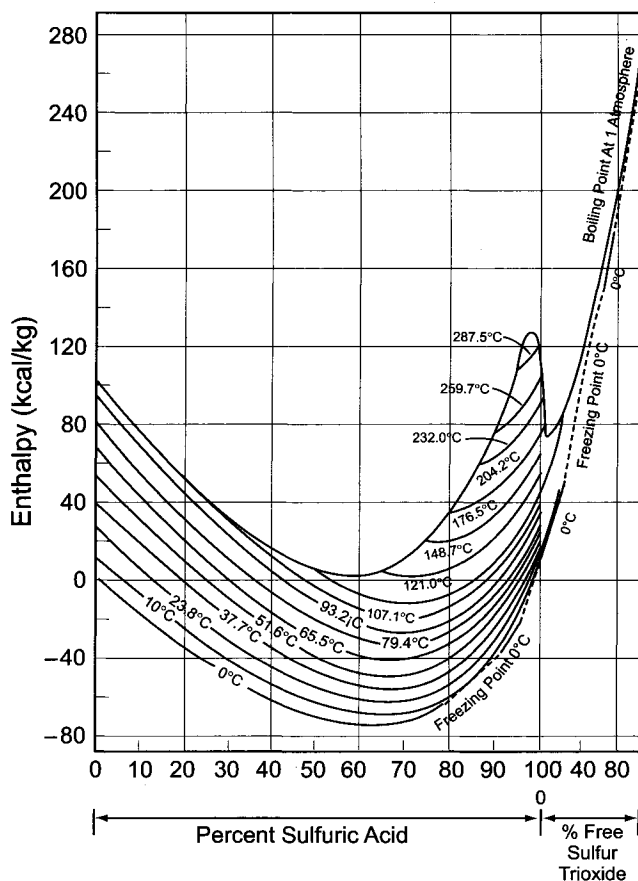


FIGURE L4. Enthalpy of sulfuric acid solutions. (Data from Broughton, *Chem. Metall.*, **52**(4), 123 (1945); Miles *et al.*, *Trans. Faraday. Soc.*, **40**, 281 (1944); Morgen, *Ind. Eng. Chem*, **34**, 571 (1942); Ross, *Ind. Eng. Prog.*, **48**, 314 (1952).)

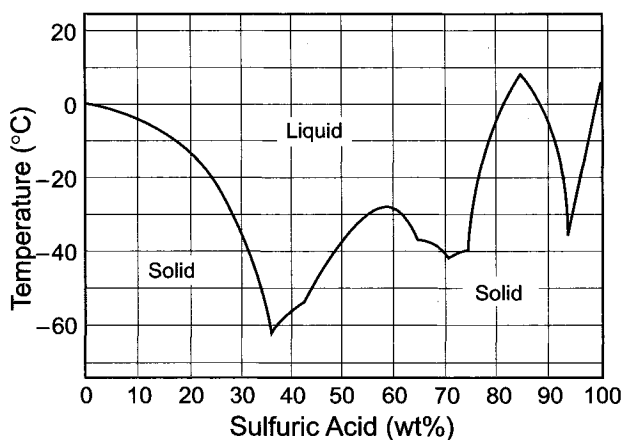


FIGURE L5. Freezing point of sulfuric acid solutions. (From C. Gable, H.F. Betz, and S.H. Morgan, *J. Amer. Chem. Soc.*, **72**, 1445 (1950).)

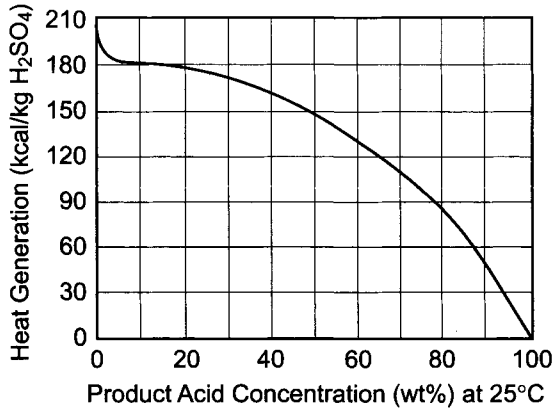


FIGURE L6. Heat generation when water is added to sulfuric acid solutions.

M. HYDROCHLORIC ACID

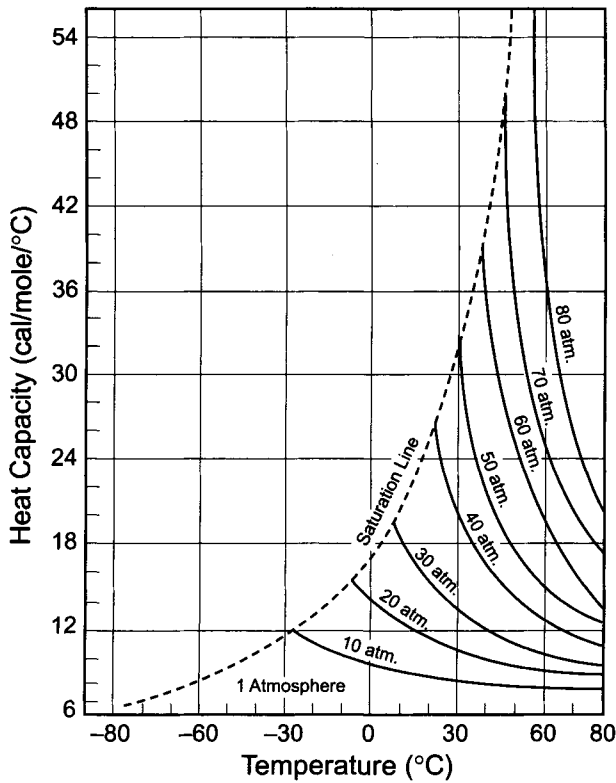


FIGURE M1. Heat capacity of anhydrous hydrogen chloride gas.

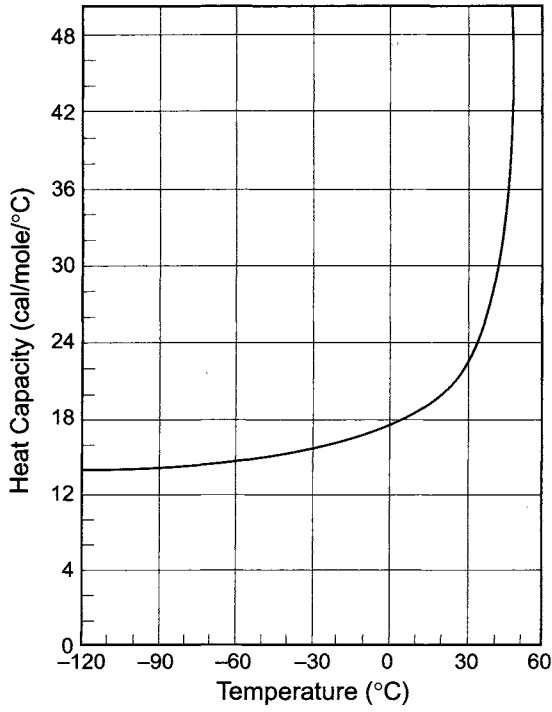


FIGURE M2. Heat capacity of anhydrous liquid hydrogen chloride.

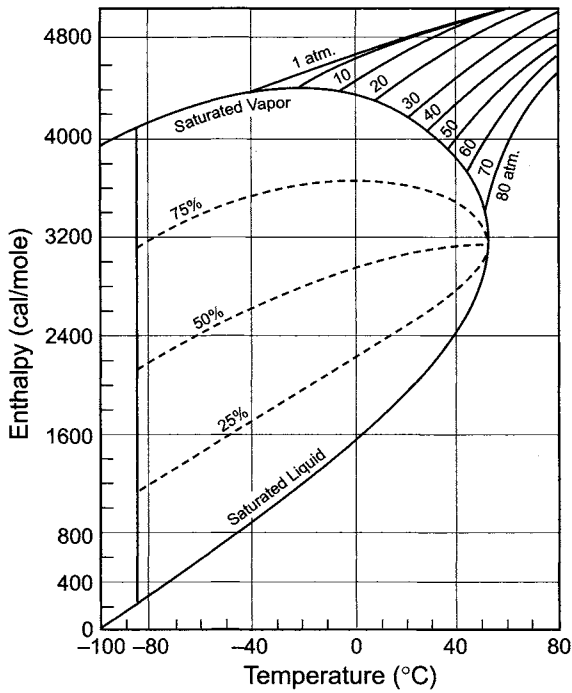


FIGURE M3. Enthalpy of anhydrous hydrogen chloride.

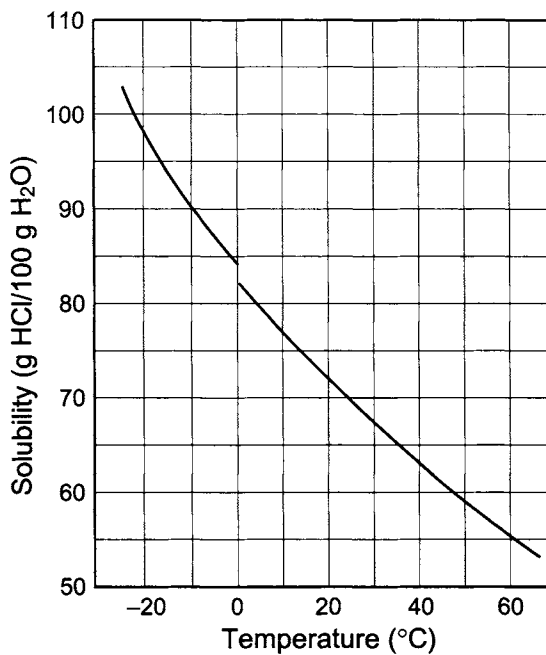


FIGURE M4. Solubility of HCl in water. (Data quoted from Seidell's *Solubilities*, Vol. 1, 4th ed., W.F. Linke (ed.), p. 1108, *Amer. Chem. Soc.*, Washington, DC (1958).)

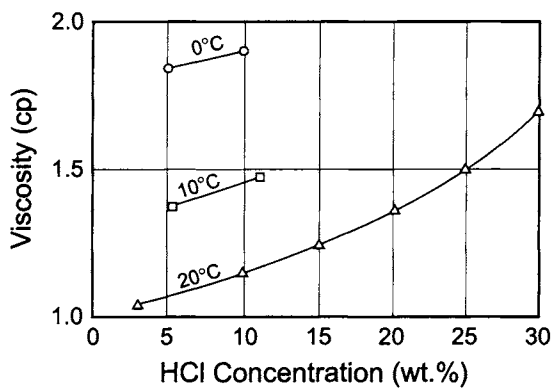


FIGURE M5. Viscosity of hydrochloric acid solutions. (Courtesy of Japan Soda Industry Association.)

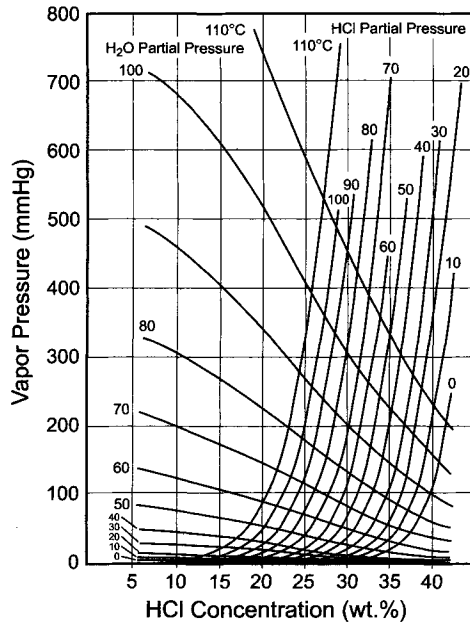


FIGURE M6. Partial pressure of HCl and water over HCl solutions. (Courtesy of Japan Soda Industry Association.)

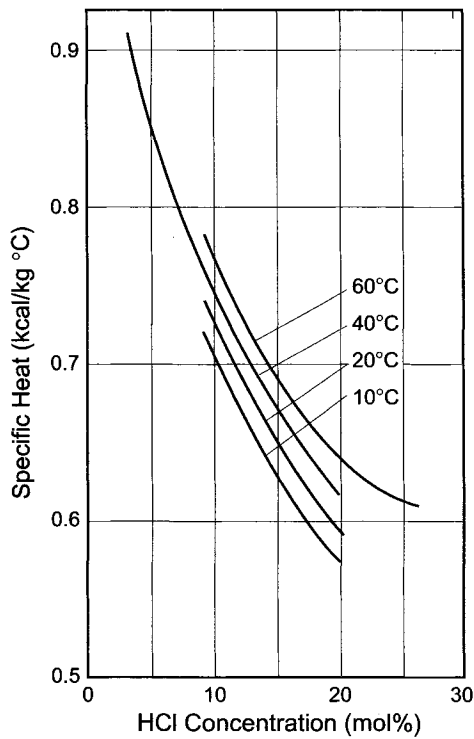


FIGURE M7. Specific heat of hydrochloric acid. (Courtesy of Japan Soda Industry Association.)

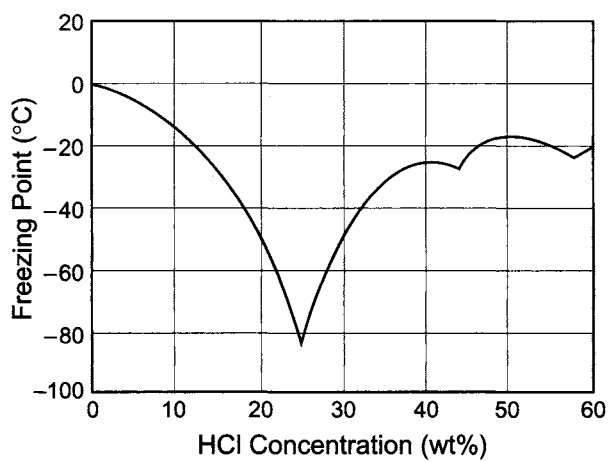
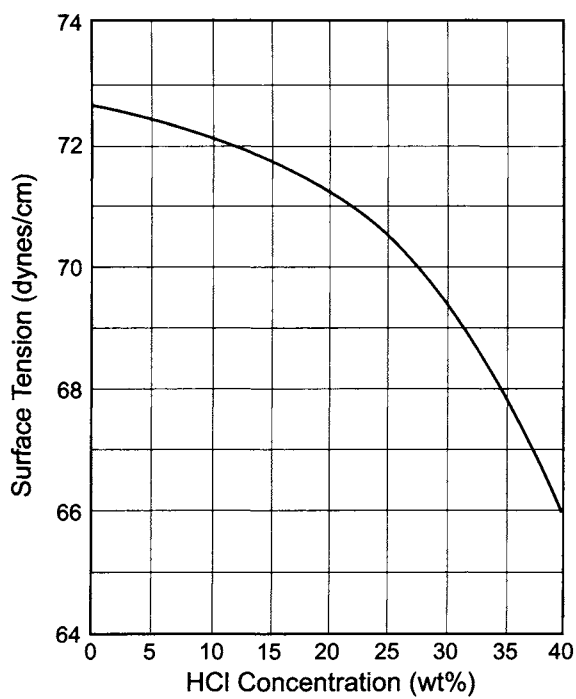


FIGURE M8. Freezing point of HCl solutions.

FIGURE M9. Surface tension of HCl solutions at 20°C. (From N.A. Lange, *Handbook of Chemistry*, 9th ed., p. 1652.)

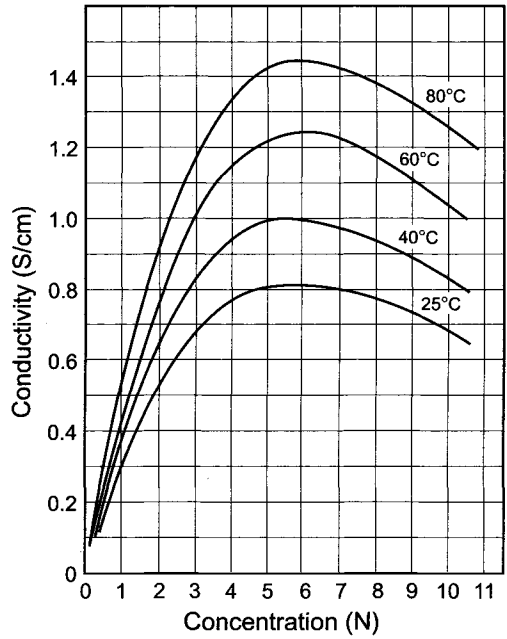


FIGURE M10. Conductivity of HCl solutions. (F. Hine, *Electrode Processes and Electrochemical Engineering*, p. 74, Plenum Press, New York (1985).).

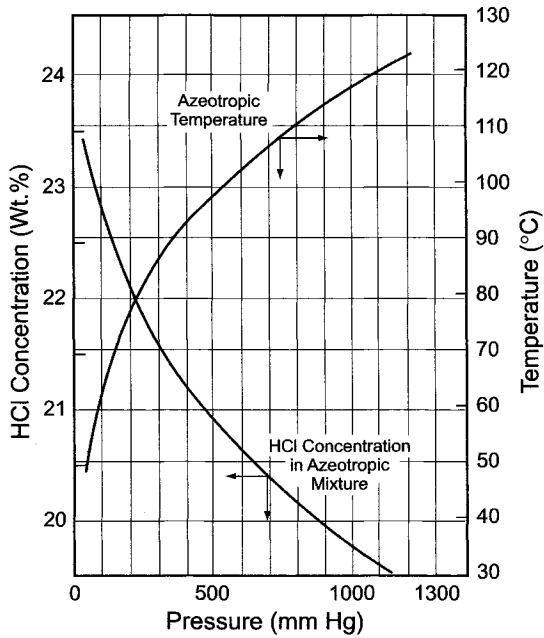


FIGURE M11. HCl concentration and temperature of azeotropic mixture of HCl and H₂O. (Courtesy of Japan Soda Industry Association.)

N. NaOH + NaCl MIXTURES

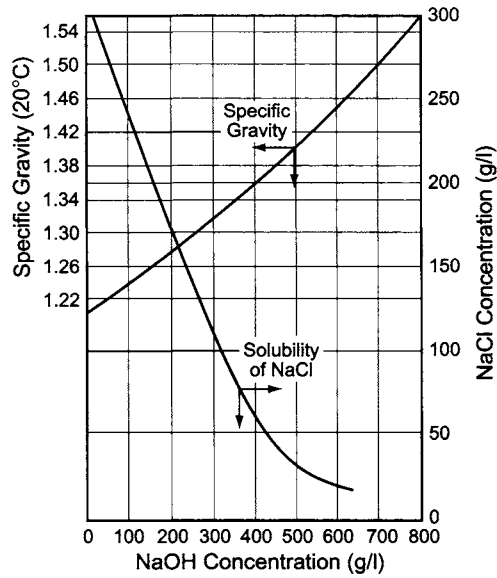


FIGURE N1. Specific gravity of saturated NaOH–NaCl solutions. (Courtesy of Japan Soda Industry Association.)

O. BLEACH

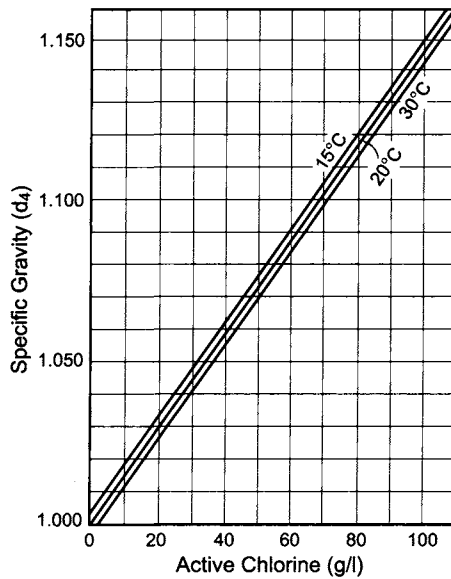


FIGURE O1. Specific gravity of bleach solutions. (Courtesy of Japan Soda Industry Association.)

P. SODIUM CARBONATE

TABLE P1. Specific Gravity of Sodium Carbonate Solutions

Na ₂ CO ₃ %	Na ₂ CO ₃ ·10H ₂ O %	<i>d</i> ^{20/4}	<i>d</i> ^{25/4}	Na ₂ CO ₃ g l ⁻¹ (20°C)	Na ₂ CO ₃ %	<i>d</i> ^{30/4}
1	2.7	1.0086	1.0073	10.09	14	1.1417
2	5.4	1.0190	1.0176	20.39	15	1.1520
3	8.1	1.0294	1.0278	30.88	16	1.1636
4	10.8	1.0398	1.0381	41.59	17	1.1747
5	13.5	1.0502	1.0484	52.51	18	1.1859
6	16.2	1.0606	1.0588	63.64	19	1.1972
7	18.9	1.0711	1.0692	74.98	20	1.2086
8	21.6	1.0816	1.0797	86.53	21	1.2201
9	23.3	1.0922	1.0902	98.20	22	1.2317
10	27.0	1.1029	1.1008	110.30	23	1.2434
11	29.7	1.1136	1.1115	122.50	24	1.2552
12	32.4	1.1244	1.1223	137.90	25	1.2671
13	35.1	1.1354	1.1332	147.60	26	1.2790
14	37.8	1.1463	1.1442	160.50	27	1.2910
					28	1.3031
					29	1.3152
					30	1.3274

(with permission from Japan Soda Industry Association)

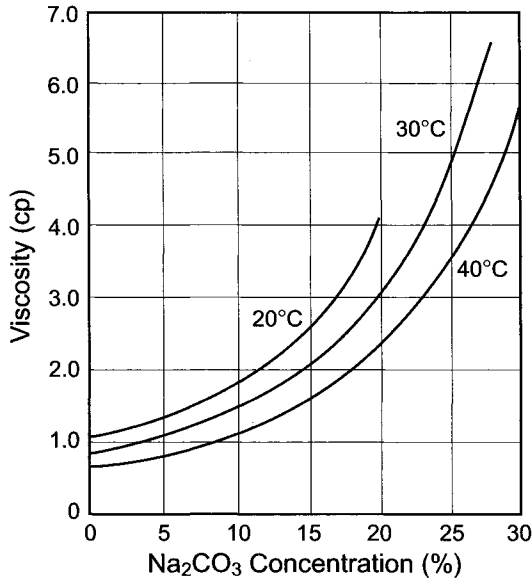


FIGURE P1. Viscosity of sodium carbonate solutions. (Courtesy of Japan Soda Industry Association.)

Q. WATER

TABLE Q1. pH of Pure Water at Various Temperatures

Temperature, °C	pH	Temperature, °C	pH	Temperature, °C	pH
0	7.44	120	5.91	240	5.71
20	7.04	140	5.80	260	5.72
40	6.63	160	5.76	280	5.80
60	6.40	180	5.72	300	5.82
80	6.20	200	5.70		
100	6.02	220	5.70		

(With permission from Japan Soda Industry Association)

TABLE Q2. Water Vapor Pressure in mm Hg

	Temperature (°C)									
	0.0	0.1	0.2	0.3	0.4	0.5	0.6	0.7	0.8	0.9
0	4.579	4.613	4.647	4.681	4.715	4.750	4.785	4.820	4.855	4.890
1	4.926	4.962	4.998	5.034	5.070	5.107	5.144	5.181	5.219	5.256
2	5.294	5.332	5.370	5.408	5.447	5.486	5.525	5.565	5.605	5.645
3	5.685	5.725	5.766	5.807	5.848	5.889	5.931	5.973	6.015	6.058
4	6.101	6.144	6.187	6.230	6.274	6.318	6.363	6.048	6.453	6.498
5	6.543	6.589	6.635	6.681	6.728	6.775	6.822	6.869	6.917	6.965
6	7.013	7.062	7.111	7.160	7.209	7.259	7.309	7.360	7.411	7.462
7	7.513	7.565	7.617	7.669	7.722	7.775	7.828	7.882	7.936	7.990
8	8.045	8.100	8.155	8.211	8.267	8.323	8.380	8.437	8.494	8.551
9	8.609	8.668	8.727	8.786	8.845	8.905	8.965	9.025	9.086	9.147
10	9.209	9.271	9.333	9.395	9.458	9.521	9.585	9.649	9.714	9.779
11	9.844	9.910	9.976	10.042	10.109	10.176	10.244	12.312	10.380	10.449
12	10.518	10.588	10.658	10.728	10.799	10.870	10.941	11.013	11.085	11.158
13	11.231	11.305	11.379	11.453	11.528	11.604	11.680	11.756	11.833	11.910
14	11.987	12.065	12.144	12.223	12.302	12.382	12.462	12.543	12.624	12.706
15	12.788	12.870	12.953	13.037	13.121	13.205	13.290	13.375	13.461	13.547
16	13.634	13.721	13.809	13.898	13.987	14.076	14.166	14.256	14.347	14.438
17	14.530	14.622	14.715	14.809	14.903	14.997	15.092	15.188	15.284	15.380
18	15.477	15.575	15.673	15.772	15.871	15.971	16.071	16.171	16.272	16.374
19	16.477	16.581	16.685	16.789	16.894	16.999	17.105	17.212	17.319	17.427
20	17.535	17.644	17.753	17.863	17.974	18.085	18.197	18.309	18.422	18.536
21	18.650	18.765	18.880	18.996	19.113	19.231	19.349	19.468	19.587	19.707
22	19.827	19.948	20.070	20.193	20.316	20.440	20.565	20.690	20.815	20.941
23	21.068	21.196	21.324	21.453	21.583	21.714	21.845	21.977	22.110	22.243
24	22.377	22.512	22.648	22.785	22.922	23.060	23.198	23.337	23.476	23.616
25	23.756	23.897	24.039	24.182	24.326	24.471	24.617	24.764	24.912	25.060
26	25.209	25.359	25.509	25.660	25.812	25.964	26.117	26.271	26.426	26.582
27	26.739	26.897	27.055	27.214	27.374	27.535	27.696	27.858	28.021	28.185
28	28.349	28.514	28.680	28.847	29.015	29.184	29.354	29.525	29.697	29.870
29	30.043	30.217	30.392	30.568	30.745	30.923	31.102	31.281	31.461	31.642
30	31.824	32.007	32.191	32.376	32.561	32.747	32.934	33.122	33.312	33.503

(continued)

TABLE Q2. continued

	Temperature (°C)									
	0.0	0.1	0.2	0.3	0.4	0.5	0.6	0.7	0.8	0.9
31	33.695	33.888	34.082	34.276	34.471	34.667	34.864	35.062	35.261	35.462
32	35.663	35.865	36.068	36.272	36.477	36.683	36.891	37.099	37.308	37.518
33	37.729	37.942	38.155	38.369	38.584	38.801	39.018	39.237	39.457	39.677
34	39.898	40.121	40.344	40.569	40.796	41.023	41.251	41.480	41.710	41.942
35	42.175	42.409	42.644	42.880	43.117	43.355	43.595	43.836	44.078	44.320
36	44.563	44.808	45.054	45.301	45.549	45.799	46.050	46.302	46.556	46.811
37	47.067	47.324	47.582	47.841	48.102	48.364	48.627	48.891	49.157	49.424
38	49.692	49.961	50.231	50.202	50.774	51.048	51.323	51.600	51.879	52.160
39	54.442	52.725	53.009	53.294	53.580	53.867	54.156	54.446	54.737	55.030
40	55.324	55.61	55.91	56.21	56.51	56.81	57.11	57.41	57.72	58.03
41	58.34	58.65	58.96	59.27	59.58	59.90	60.22	60.54	60.86	61.18
42	61.50	61.82	62.14	62.47	62.80	63.13	63.46	63.79	64.12	64.46
43	64.80	65.14	65.48	65.82	66.16	66.51	66.86	67.21	67.56	67.91
44	68.26	68.61	68.97	69.33	69.69	70.05	70.41	70.77	71.14	71.51
45	71.88	72.25	72.62	72.99	73.36	73.74	74.12	74.50	74.88	75.26
46	75.65	76.04	76.43	76.82	77.21	77.60	78.00	78.40	78.80	79.20
47	79.60	80.00	80.41	80.82	81.23	81.64	82.05	82.46	82.87	83.29
48	83.71	84.13	84.56	84.99	85.42	85.85	86.28	86.71	87.14	87.58
49	88.02	88.46	88.90	89.34	89.79	90.24	90.69	91.14	91.59	92.05
50	92.51	92.97	93.43	93.89	94.36	94.82	95.29	95.77	96.24	96.72
51	97.20	97.68	98.16	98.64	99.13	99.62	100.11	100.60	101.10	101.59
52	102.09	102.59	103.10	103.60	104.11	104.62	105.13	105.64	106.16	106.68
53	107.20	107.72	108.24	108.76	109.29	109.82	110.35	110.89	111.43	111.97
54	112.51	113.05	113.59	114.14	114.69	115.24	115.80	116.36	116.92	117.48
55	118.04	118.60	119.16	119.73	120.31	120.89	121.47	122.05	122.63	123.21
56	123.80	124.40	124.99	125.58	126.18	126.78	127.38	127.99	128.60	129.21
57	129.82	130.44	131.06	131.68	132.30	132.92	133.55	134.18	134.81	135.45
58	136.08	136.72	137.36	138.01	138.66	139.31	139.96	140.62	141.28	141.94
59	142.60	143.27	143.94	144.61	145.28	145.96	146.64	147.32	148.00	148.69
60	149.38	150.07	150.77	151.47	152.17	152.87	153.58	154.29	155.00	155.71
61	156.43	157.15	157.87	158.59	159.32	160.06	160.80	161.58	162.28	163.02
62	163.77	164.52	165.27	166.02	166.78	167.54	168.30	169.07	169.84	170.61
63	171.38	172.16	172.94	173.73	174.52	175.31	176.10	176.90	177.70	178.50
64	179.31	180.11	180.92	181.74	182.56	183.38	184.20	185.03	185.86	186.70
65	187.54	188.38	189.22	190.06	190.91	191.77	192.63	193.49	194.35	195.42
66	196.09	196.96	197.84	198.72	199.60	200.48	201.37	202.26	203.16	204.06
67	204.96	205.87	206.78	207.69	208.61	209.53	210.45	211.37	212.30	213.23
68	214.17	215.11	216.06	217.01	217.96	218.91	219.87	220.83	221.79	222.76
69	223.73	224.71	225.69	226.67	227.66	228.65	229.65	230.65	231.65	232.65
70	233.7	234.7	235.7	236.7	237.8	238.8	239.8	240.9	241.9	242.9
71	243.9	245.0	246.0	247.1	248.1	249.2	250.3	251.4	252.4	253.5
72	254.6	255.7	256.8	257.9	259.0	260.1	261.2	262.3	263.5	264.6
73	265.7	266.8	268.0	269.1	270.3	271.4	272.6	273.7	274.9	276.0
74	277.2	278.4	279.5	280.7	281.9	283.1	284.3	285.5	286.7	287.9
75	289.1	290.3	291.5	292.8	294.0	295.2	296.5	297.7	298.9	300.2
76	301.4	302.7	303.9	305.2	306.5	307.7	309.0	310.3	311.6	312.9
77	314.1	315.4	316.7	318.0	319.3	320.7	322.0	323.3	324.7	326.0

(continued)

TABLE Q2. continued

	Temperature (°C)									
	0.0	0.1	0.2	0.3	0.4	0.5	0.6	0.7	0.8	0.9
78	327.3	328.7	330.0	331.4	332.7	334.1	335.5	336.8	338.2	339.6
79	341.0	342.4	343.8	345.2	346.6	348.0	349.4	350.8	352.2	353.7
80	355.1	356.5	358.0	359.4	360.9	362.4	363.8	365.3	366.8	368.3
81	369.7	371.2	372.7	374.2	376.7	377.3	379.8	380.3	381.8	383.4
82	384.9	386.4	388.0	389.5	391.1	392.7	394.2	395.8	397.4	399.0
83	400.6	402.2	403.8	405.4	407.0	408.6	410.3	411.9	413.5	415.2
84	416.8	418.4	420.1	421.7	423.4	425.1	426.8	428.5	430.2	431.9
85	433.6	435.3	437.0	438.7	440.5	442.2	443.9	445.7	447.4	439.2
86	450.9	452.6	454.4	456.2	458.0	459.7	461.5	463.3	465.1	466.9
87	468.7	470.5	472.3	474.1	476.0	477.8	479.7	481.5	483.4	485.2
88	487.1	489.0	490.9	492.7	494.6	496.5	498.4	500.3	502.3	504.2
89	506.1	508.0	510.0	511.9	513.9	515.9	517.8	519.8	521.8	522.8
90	525.76	527.76	529.77	531.78	533.80	535.82	537.86	539.90	541.95	544.00
91	546.05	548.11	550.18	552.26	554.35	556.44	558.53	560.64	562.75	564.87
92	566.99	569.12	571.26	573.40	575.55	577.71	579.87	582.04	584.22	586.41
93	588.60	590.80	593.00	595.21	597.43	599.66	601.89	604.13	606.38	608.64
94	610.90	613.17	615.44	617.72	620.01	622.31	624.61	626.92	629.24	631.57
95	633.90	636.24	638.59	640.94	643.30	645.67	648.05	650.43	652.82	655.22
96	657.62	660.03	662.45	664.88	667.31	669.75	672.20	674.66	677.12	679.59
97	682.07	684.55	687.04	689.54	692.05	694.57	697.10	699.63	702.17	704.71
98	707.27	709.83	712.40	714.98	717.56	720.15	722.75	725.36	727.98	730.61
99	733.24	735.88	738.53	741.18	743.85	746.52	749.20	751.89	754.58	757.29
100	760.00	762.72	765.45	768.19	770.93	773.68	776.44	779.22	782.00	784.78
101	787.57	790.37	793.18	796.00	798.82	801.66	804.50	807.35	810.21	813.08

R. MISCELLANEOUS

TABLE R1. Solubility of Barium Salts in
g/100 g H₂O

Temperature, °C	BaCl ₂ ·2H ₂ O	BaCO ₃	BaSO ₄
0	23.8		0.00115
8.8		0.0016	
10	25.0		0.002
18		0.0022	
20	26.3		0.0024
25	27.1		0.00223
30	27.7	0.0014	0.00285
40	28.9		
50			0.00336
60	31.6		
80	34.3		
100	37.5		0.0039

TABLE R2. Solubility of Calcium Sulfate in NaCl Solution

Specific gravity	NaCl (g/100 cc)	CaSO ₄ (g/100 cc)
0.9998	0.000	0.212
1.0644	9.115	0.666
1.0981	14.399	0.718
1.1012	14.834	0.716
1.1196	17.650	0.712
1.1488	22.876	0.670
1.1707	26.417	0.650
1.2034	32.049	0.572

(With permission from Japan Soda Industry Association)

TABLE R3. Equivalent Conductance of Ions in Solutions of Infinite Dilution

Cations	0°C	25°C	100°C	Anions	0°C	25°C	100°C
H ⁺ (H ₂ O)	225.0	349.7	637	OH ⁻	105	200	446
Li ⁺	19.1	38.68	120	F ⁻		55.6	
Na ⁺	25.85	50.1	150	Cl ⁻	41.4	76.3	207
K ⁺	40.3	73.5	200	ClO ₃ ⁻	36	64	172
Rb ⁺	43.5	76.4		ClO ₄ ⁻	37.3	68	179
Cs ⁺	44	76.8	200	Br ⁻	43.1	78.3	
NH ₄ ⁺	40.3	73.7	184.3	BrO ₃ ⁻	31	56	155
(1/2)Mg ²⁺	28.5	53.06	170	I ⁻	42	76.8	
(1/2)Ca ²⁺	30.8	59.50	187	IO ₃ ⁻	21	41	127
(1/2)Ba ²⁺	33.6	63.7	200	IO ₄ ⁻		55.6	
(1/3)Ce ³⁺		67		(1/2)SO ₄ ²⁻	41	79.8	256
(1/3)Cr ³⁺		67		NO ₃ ⁻	40.2	71.42	189
(1/2)Mn ²⁺	27	53.5		H ₂ PO ₄ ⁻		36	
(1/2)Fe ²⁺	28	53.5		(1/2)HPO ₄ ²⁻		57	
(1/3)Fe ³⁺		68		HCO ₃ ⁻		44.5	
(1/2)Co ²⁺	28	54		(1/2)CO ₃ ²⁻	36	72	
(1/2)Ni ²⁺	28	54		CN ⁻		78	
(1/2)Cu ²⁺	28	56		(1/2)CrO ₄ ²⁻	42	85	
Ag ⁺	33	61.9	180	(1/2)MoO ₄ ²⁻		74.5	
(1/2)Zn ²⁺	28	53.5		MnO ₄ ⁻	36	62.8	
(1/2)Cd ²⁺	28	54		CH ₃ COO ⁻	20	41	130
Tl ⁺	43.3	74.9		HCOO ⁻		47 at 18°C	
(1/2)Pb ²⁺	37.5	70		(1/2)C ₂ O ₄ ²⁻		63 at 18°C	

Source: From F. Hine, *Electrode Processes and Electrochemical Engineering*, Plenum Press, New York (1985), p. 77.

TABLE R4. Ion Hydration Energy and Number of Waters of Hydration

	Hydration energy (kcal/g ion)	Number of waters of hydration
H ⁺	255	4
Li ⁺	131	6
Na ⁺	97	4
K ⁺	77	2-3
Rb ⁺	73	2
Ag ⁺		3-4
Mg ²⁺		9-13
Ca ²⁺		8-10
Ba ²⁺		6-8
Zn ²⁺		11-13
Fe ²⁺		11-13
Cu ²⁺		11-13
Cd ²⁺		10-12
Pb ²⁺		5-7
F ⁻	123	5
Cl ⁻	83	3
Br ⁻	73	2
I ⁻	63	0-1
ClO ₄ ⁻		0
NO ₃ ⁻		2

Source: From F. Hine, *Electrode Processes and Electrochemical Engineering*, Plenum Press, New York (1985), p. 194.

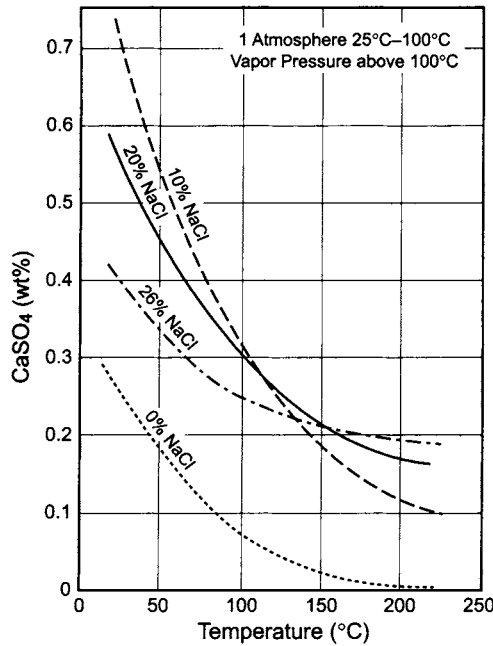


FIGURE R1. Solubility of CaSO₄ in brines.

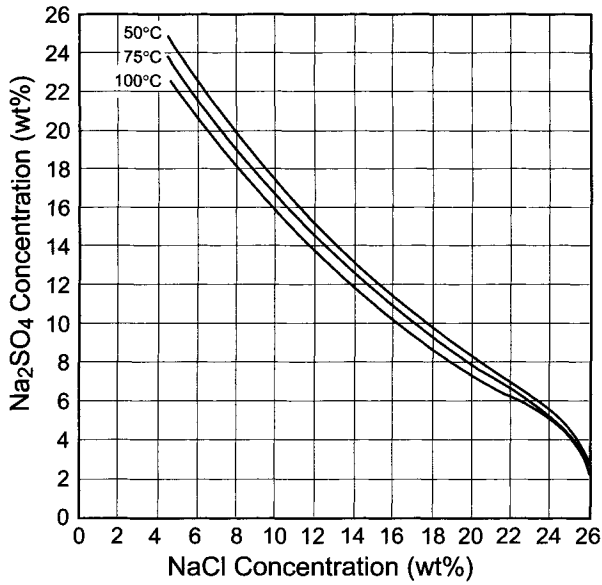


FIGURE R2. NaCl-Na₂SO₄-H₂O system at various temperatures.

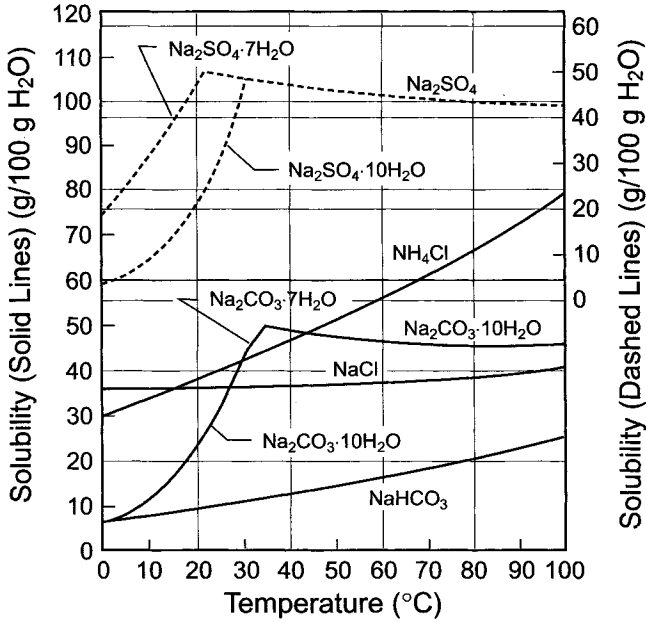


FIGURE R3. Solubility of sodium chloride, sodium carbonate, sodium bicarbonate, sodium sulfate, and ammonium chloride. (Courtesy of Japan Soda Industry Association.)

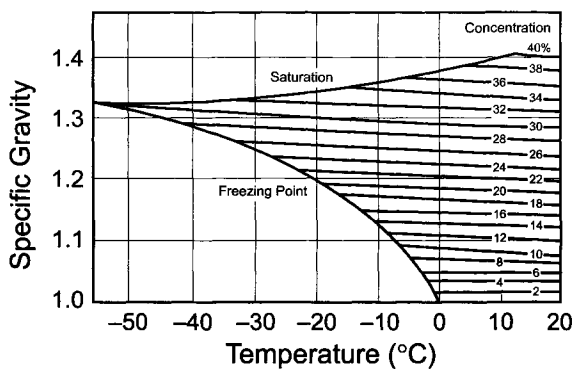


FIGURE R4. Specific gravity of calcium chloride solutions. (Courtesy of Japan Soda Industry Association.)

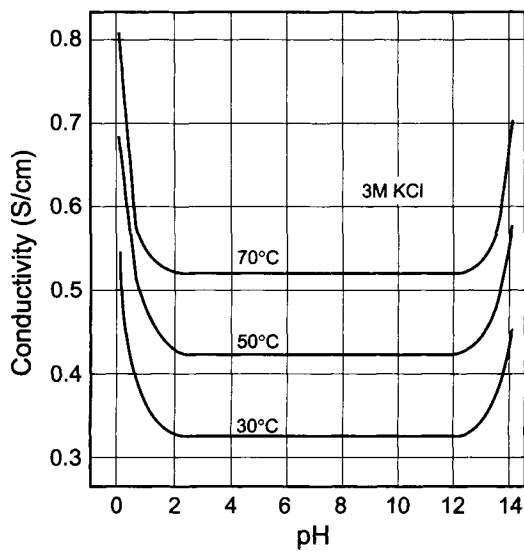


FIGURE R5. Conductivity vs pH of 3M KCl at constant temperature. (F. Hine, *Electrode Processes and Electrochemical Engineering*, p. 80, Plenum Press, New York (1985).)

Index

A

- Absorption, 1070
 - gas absorption, 885
 - of chlorine
 - in aqueous systems, 665
 - in caustic solution, 901, 1378
 - in organic solvents
 - in CCl_4 , 885
 - in others, 1479
 - packed column, 1067
 - penetration theory, 1068
- AC impedance, 147
- Aciplex[®] membranes, 307, 361
- Activated complex, 95
- Activated cathodes (*see* cathodes), 241, 244, 251, 252
- Active chlorine, 1349, 1386
- Activity coefficient, 1022
 - potassium chloride, 1515
 - potassium hydroxide, 1531
 - sodium amalgam, 86
 - sodium chloride, 1504
 - sodium hydroxide, 1524
- Adaptive gain pH control system, 1103, 1110
- Adiabatic change, 1017
- Adiabatic compression, 1058, 1059
- Adsorbable organic halogens (AOX), 59,72
- Adsorption, 1074
 - adsorption isotherms, 1075
 - followed by chemical reaction, 1070
 - continuous operation, 1079
 - gas-phase adsorption, 1075
 - liquid-phase adsorption, 1078
- Advanced Diaphragm Cell Technology (ADCT[®]), 410
- Air systems, 1196
 - breathing air, 1200
 - dry air, 1199
 - instrument air, 1199
 - plant air, 1196
 - purified air, 1198
- Alkali-related chemicals
 - inorganic, 15
 - organic, 14
- Alkaline fuel cell, 1472
- Alternative processes, 1349
 - caustic soda, 1389
 - chlorine, 1351
 - hypochlorite, 1372
- Aluminum busbar, 731
- Amalgam, sodium
 - activity coefficient, 86
 - amalgam butter, 194
 - decomposition, 375, 378, 404, 447, 1149
 - electrode process, 85, 114
- Amalgam cell (*see* mercury cells)
- Amalgam process (*see* mercury cells)
- Analysis of process streams, 1287
- Analytical manual, 1225
- Annular flow (*see* flow patterns), 1055
- Angel curve, 287
- Anode adjustment system, 403
- Anodes (*see* coated anodes), 211
- Anodic protection, 1309
- Anticaking additive, 499
- Asahi Chemical Industries, *see* Asahi Kasei
- Asahi Glass membrane cells (AZEC[®] cell), 432
- Asahi Kasei membrane cells, 428
- Asbestos, 272, 296
- Asbestos diaphragm, 21, 272, 291
- Asbestos waste, 1413, 1445
- Atomic force microscopy, 150
- Avogadro's number, 164
- Azeotropic mixtures ($\text{HCl} + \text{H}_2\text{O}$), 1551

B

- Backflow preventer, 1213
- Back-pulse filtration (*see* filtration), 603, 1475
- Barometric condenser, 1208
- Barium salts, 1556

- Beer, H.B., 24, 212
- Bell jar cell, 271
- Beneficiation of KCl, 489
- Bernoulli's theorem, 1048
- Berthing and storage of membrane cells, 1254
- BiChlor[®] cell, 435
- Billiter cell, 21, 22
- Bipolar membrane cell, 27, 33, 388, 405, 413
- Bipolar diaphragm cell
- Dow cell, 405
 - Glanor cell, 405
- BiTAC[®] cell, 431
- Black body, 1066
- Bleach, 11, 191, 890, 1372
- chemical production, 1378
 - decomposition, 1381
 - electrochemical production, 1373
 - filtration, 1385
 - materials of construction, 1383
 - specifications and analyses, 1386
- Blind current losses, 179, 193
- Bode plot/AC impedance, 150
- Boiler feed water, 1194
- Boiling points of solutions
- potassium chloride, 1514
 - potassium hydroxide, 1527, 1528
 - sodium chloride, 1507
 - sodium hydroxide, 990, 1521
- Boiling point rise (BPR), 483, 969
- Boilout of diaphragm-cell evaporators, 1193
- Boltzman's constant, 95
- Boolean algebra/truth table, 1433, 1434
- Boundary layer, 1053
- Breakdown/rupture potential, 1318
- Breakthrough/adsorption columns, 1079
- Breathing air, 1200, 1214
- Brine (NaCl or KCl solution)
- preparation, 495, 509
 - composition of salt and brine, 529
 - dissolving processes, 509, 1093, 1234
 - delivery of salt, 501
 - selective dissolving, 519
 - solution mining (*see* sulfate control), 515
 - standard dissolvers, 511
 - processing, 447
 - depleted brine
 - collection, 1107
 - dechlorination, 1109
 - destruction of chlorate, 1107
 - concentrated brine
 - circulation around cells, 447, 449
 - concentrations in cells, 1092, 1274
 - evaporation, 473, 480
 - feed to cells, 1104, 1111
 - heating and cooling, 527
 - pipelines, 528
 - pumping, 527
 - pure brine storage, 1101
 - reverse osmosis, 472, 478
 - storage, 525, 1094, 1102
 - evaporation, 480
 - materials of construction, 486
 - mechanical vapor-recompression, 484
 - multiple-effect evaporation, 481
 - thermal vapor recompression, 486
 - vapor-recompression evaporation, 484
 - quality
 - anodes, 227, 354
 - cathodes, 263, 354
 - chemical analysis, 625
 - frequency, 626
 - composition of brine, 529
 - diaphragms, 294,
 - diaphragm cells, 294, 533
 - impurities (*see* effects of brine impurities)
 - aluminum, 653
 - ammonia, 656
 - bromide, 660
 - fluoride, 659
 - iodine, 661
 - mercury, 658
 - nickel and iron, 655
 - nitrate, 665
 - organics, 654
 - silica/silicates, 651
 - sulfate (*see* sulfate control), 634
 - ion-exchange membranes, 353, 337, 341, 342, 348, 354, 537
 - membrane cells, 341, 342, 348, 354, 537
 - mercury cells, 194, 195, 530, 531
 - saturation (*see* brine preparation, dissolving systems)
 - specifications, 194, 294, 341, 531, 543, 1277
 - diaphragm cells, 294, 533
 - membrane cells, 341, 342, 348, 354, 537, 1277
 - mercury cells, 194, 195, 531
 - treatment, 43, 444, 465, 529, 545, 1097, 1234
 - acidification, 626
 - supply of HCl, 631
 - technical aspects, 627
 - clarification, (*also see* clarifiers/thickeners), 444, 564, 1097, 1234
 - filtration, 587, 1099, 1235
 - ion exchange, 446, 606, 1236
 - pH control, 1105, 1109, 1276
 - precipitation, 545
 - floculation, 561
 - process parameters, 556
 - treating chemical supply, 552
 - treating tank design, 559, 1097, 1234
 - thickening (*see* clarification)

- waste disposal
 - brine caverns, 1452
 - filter cakes, 1457
 - removal of mercury, 1456
 - sludges, 1446
 - Brine caverns, 517, 1452
 - Brine dechlorination (*see* dechlorination)
 - Bruggemann's equation (*see* bubble effect), 276, 1483
 - Bubble effect (*see* Bruggemann's equation), 201, 1483
 - Bubble flow (*see* flow patterns), 1055
 - Building arrangement (cell room), 706
 - Building ventilation, 712
 - gravity ventilators, 712
 - Busbar installation, 728
 - aluminum, 731
 - arrangement, 728
 - assembly, 733
 - capacity, 728
 - comparison, aluminum and copper, 731
 - copper, 731
 - electromagnetic force, 734
 - internal cell connections, 734
 - Butler-Volmer equation, 97
 - Bypass current (*see* parasitic current), 391
 - Byproduct salt (*see* salt), 476
 - Byproducts, 884, 995
 - amalgam, 1003
 - bleach, 890
 - byproduct handling, 990
 - calcium carbonate, 1006
 - evaporator (CP) salt, 995
 - ferric chloride, 892
 - hydrochloric acid, 886, 1350
 - sodium sulfate (Glauber's salt), 997
- C**
- Caking (*see* salt), 492, 499
 - Calcium sulfate, 1557
 - Calomel electrode, 92
 - Carnot cycle, 1017, 1471
 - Castner, H.Y., 30
 - Catalytic Carrier Process, 1357, 1360
 - Catalytic decomposition (*see* dechlorination), 686
 - Cathode depolarization, 933
 - Cathode design, 23, 24, 927
 - Cathodes (*see* activated cathodes), 241, 265
 - amalgam cathode, 85, 114
 - cathode design, 23, 927
 - composition/preparation, 251
 - cost/performance, 246
 - deactivation/stability, 248, 263
 - depolarization, 933, 1372, 1466
 - effects of shutdowns, 263, 300
 - electrocatalytic activity, 246
 - insitu activation, 259
 - low overvoltage cathodes, 244
 - Ni-based alloy cathodes, 252, 256, 257
 - oxide-coated cathodes, 258
 - Raney Ni cathode, 252
 - sulfide-coated cathodes, 259
 - Cathodic protection, 1309
 - Catholyte quality, 1287
 - Catholyte system commissioning, 1237
 - Caustic evaporation, 452, 968, 1159
 - boiling point rise (BPR), 969
 - commissioning, 1244
 - control systems, 1159
 - feed rate control, 1160
 - packaged instrumentation, 1159
 - product concentration control, 1162
 - production rate control, 1159
 - diaphragm-cell caustic, 974
 - boilout and cleaning, 1193
 - mechanical design, 974
 - quadruple-effect example, 977
 - KOH evaporation, 982
 - membrane-cell caustic, 980
 - double-effect heat and mass balance, 981
 - multiple-effect evaporation, 969
 - process design, 971
 - types of evaporator, 971
 - liquor flow paths, 973
 - Caustic liquor processing, 947, 1152, 1204
 - blending, 966
 - centrifugation, 963
 - pusher centrifuge, 963
 - solid-bowl centrifuge, 964
 - circulation, 1152, 1155
 - collection and storage, 1152
 - concentration in cells, 1274
 - cooling, 958
 - membrane-cell catholyte, 960
 - range of duties, 961
 - diaphragm-cell liquor, 962
 - dilution, 966
 - evaporation (*see* caustic evaporation), 968, 1204
 - filtration, 965
 - materials of construction, 948
 - piping, 953
 - pumping, 957
 - purification, 983, 986
 - valves, 954
 - Caustic soda/potash, 11, 15, 41, 944
 - product handling, 990, 1150, 1154
 - anhydrous, 988
 - boiling points, 990
 - diaphragm-cell caustic, 945

- Caustic soda/potash *Contd.*
 market/price, 58, 65
 materials of construction, 948
 membrane-cell caustic, 946
 mercury-cell caustic, 945
 processing, 11, 14, 41, 451
 product handling, 990, 1150, 1154
 purification, 983
 removal of chlorate, 986
 removal of metal ions, 986
 removal of salt by extraction, 983
 simultaneous production of NaOH and KOH, 448
 solid products (bulk, flake, prill), 987
- Caustic soda, production without chlorine, 1389
 causticization of soda ash, 1389
 electrochemical methods, 1393
 salt splitting, 1392
- Caustic waste liquor, 985, 1407, 1449
 Causticization of soda ash, 1389
 Cavitation damage (*see* corrosion), 1320
 Cell line working zone, 711
 Cell performance, 224, 456
 Cell renewal, 753
 switching, 753
 transport of electrolyzers, 754
- Cell resistance (*see* cell voltage), 127
 Cell room systems design, 458, 745
 building ventilation, 712
 cell-to-cell variation, 463
 floor, roof, rows, walls, walkways, 707
 process control
 concentrations, 462
 pressure, 461
 temperature, 462
- Cell voltage and its components, 195, 200, 1272
 diaphragm cells, 206
 membrane cells, 206
 mercury cells, 206
- Centrifugal compressors, 1122
 Centrifuges, 1058
 Chemical hazards, 761
 Chemical potential, 77, 78, 1022
 Chemical supply (brine treatment)
 carbon dioxide, 552
 carbonates, 553
 hydroxides, 556
- Chilled water, 1188
 absorption refrigeration, 1191
 mechanical refrigeration, 1190
 steam-jet refrigeration, 1190
 thermal duty in chlorine cooling, 1189
- Chlor-alkali industry
 Brazil, 60
 Canada, 59
 China, 65
 Eastern Europe, 64
 India, 65
 Japan, 64
 Korea, 65
 Mexico, 60
 Middle East, 64
 Taiwan, 65
 United States, 52
 Western Europe, 60
 world, 47
- Chlorate decomposition, 118, 665, 689, 1107
 destruction by HCl, 690
 destruction by reducing agents, 694
 miscellaneous methods of destruction, 695
 suppression of ClO₂ formation, 693
- Chlorate formation, 167, 191
 Chlorinated condensate, 789
 Chlorinated ethanes and methanes, 55
 Chlorination, 68
 Chlorine-based chemicals, 4, 11
 Chlorine butter, 747
 Chlorine, depressurization and evacuation of equipment, 1130
 Chlorine dioxide, 693
 Chlorine electrode process, 81, 109, 220
 Chlorine Emergency Plan (CHLOREP), 876
 Chlorine gas quality, 923, 1271
 Chlorine hazards, 1403, 1438
 environmental fate, 1406
 liquid form, 1440
 mitigation of effects of release, 1438
 monitoring for exposure, 1404
 protective equipment, 1405
 risk assessment, 1443
 toxicity, 1439
 vapor form, 1438
- Chlorine header pressure, 1114
 Chlorine header safety, 1115
 Chlorine hydrate, 790, 839
 composition, 790
 effects in liquefaction systems, 846
 in liquefaction systems, 839
 region of existence, 791
- Chlorine processing, 40, 450, 765, 923, 1113, 1239
 absorption, 885
 applications, 4, 55, 57
 commissioning of systems (*see* under process step)
 dry systems, 1239
 pre-energization testing, 1238
 compression, 807, 1121, 1241, 1486
 centrifugal compressors, 810
 materials of construction, 814
 mechanical specifications, 814
 performance curve, 813, 823
 surge, 813

- control, 821, 1122
 - protective systems, 825
 - pressure, 821, 1114, 1125
 - discharge pressure, 1125, 1126
 - surge, 821, 1126
 - throughput, 824
- diaphragm compressor, 820
- energy consumption, 808
- evacuation, 925
- liquid-ring compressor, 818, 1121
- reciprocating compressor, 817
- cooling, 771, 825, 1117
 - chilled water, thermal duty, 1189
 - chlorinated condensate, 789
 - compressor interstage coolers, 828
 - direct contact, 771, 778, 826
 - effect of gas temperature, 788
 - flow diagram, 792
 - heat duty curve, 773
 - heat transfer calculations, 771
 - AMTD, 773, 938
 - LMTD, 772, 938
 - indirect, 771, 785, 829
 - pressure operation, 1483
 - simultaneous heat and mass transfer, 775
 - transfer unit concept, 780
 - transport process analogies, 776
- density, 1499, 1535, 1536
- dissociation constant, 1500
- drying, 792, 1118, 1485
 - acid consumption, 792
 - drying columns, 795
 - packed columns, 795
 - process control, 798
 - tray columns, 799
 - equilibrium behavior, 793
 - flow diagram, 798
 - pressure operation, 1485
 - process control, 1118
 - process redundancy, 800
- equilibrium constant, 1501, 1534
- evacuation of lines and equipment, 925
- history, 2
- hydrolysis constant, 1501
- liquefaction, 829, 1128, 1241, 1486
 - achievable degree of, 832
 - commissioning, 1241
 - control, 1128
 - addition of dry air, 1128
 - process control, 1129
 - hydrate, formation of, 839
 - liquefaction process, 831
 - noncondensables, 833
 - partition of water, 843
 - refrigerants, 835
 - refrigeration process, 829
 - tail gas, 885
 - use of barrier fluid, 836
 - utility approach to refrigeration, 837
 - without gas compression, 1486
- materials of construction, 767
 - reaction with titanium, 768
 - wet vs. dry chlorine, 768
- oxygen in chlorine, 833, 923
- physical properties, 1532
- solubility, 1534, 1535
- specific heat, 1500, 1538
- thermal conductivity, 1500, 1539
- thermodynamic properties, 1533
- transfer – *see* chlorine storage and handling
- vapor pressure, 1499, 1537
- viscosity, 1500, 1536
- Chlorine production, 37, 398, 405, 413
- Chlorine, production without caustic
 - electrochemical processes, 1361
 - aqueous electrolysis of HCl, 1361
 - indirect electrolyses, 1365
 - molten-salt electrolysis, 1368
 - vapor-phase electrolysis of HCl, 1365
 - oxidation processes, 1351
 - oxidation of HCl, 1352
 - oxidation of salt, 1351
 - regenerative oxidation processes, 1359
- Chlorine recovery, 1479
- Chlorine storage and handling, 847, 856, 1242
 - confined storage, 854
 - expansion chambers, 907
 - gaskets, 861
 - liquid chlorine, 847, 862
 - low-pressure seals, 895
 - low-pressure storage, 853
 - mechanical relief devices, 899
 - pipng systems, 858
 - pressurized storage, 852
 - reference documents, 847
 - safety devices, 895
 - transfer, 862
 - pressurization, 862
 - air required for, 873
 - with air, 863
 - with chlorine, 864
 - pumping, 865
 - valves, 860, 883
 - vaporization, 881
 - vent scrubbers (*see* scrubbers, chlorine), 901
 - water seal, 895
- Chlorine transportation and packaging, 874
 - accident statistics, 878
 - barge transport, 878
 - Chlorine Emergency Plan (CHLOREP), 876
 - labeling of transport containers, 875

- Chlorine transportation and packaging *Contd.*
 loading and unloading, 868
 system requirements, 868
 tankcar loading system, 872
 transfer hoses, 869
 packaging, 879
 pumping, 865
 rail transport, 876
 road transport, 877
 unloading by air pad, 870
- Chlorobenzene, 56
- Chlorofluorocarbons, 7, 9, 56, 835
- Chrysotile (*see* asbestos), 272, 296
- Clarification and thickening, 552, 564, 1057, 1058
 free settling, 567
 thickening, 569
- Clarifiers/thickeners, 574, 581
 centrifuges, 587
 feedwells, 575
 heat loss, 586
 inclined-plate separators, 585
 overflow systems, 576
 rakes, 578
 sludge removal, 579
 solid contact reactors, 584
 solids recycle, 582
 standard brine clarifiers, 574
- Clausius-Clapeyron equation, 1016, 1061
- Cleaning and flushing (precommissioning), 1226
- Coated anodes, 212
 chlorine evolution reaction, 110, 220
 composition/preparation, 236
 cost, 235
 degradation/failure, 224, 227, 231
 dimensionally stable anodes (DSA[®]), 212
 electrochemical behavior, 217
 impurity effects, 227
 lifetime, 235
 physical properties and morphology, 214, 215
 preparation, 237
 rejuvenation/recoating, 232
 structure, 232
- Coated cathodes (*see* cathodes), 251
- Cogeneration, 1174
 combined-cycle operation, 1175
 heat/power ratio, 1175
- Colburn *j*-factor, 776
- Cole-Cole plot (*see* AC impedance), 149
- Combustion of hydrogen, 930
- Commercial considerations/membrane cells, 424
- Commissioning (*see* precommissioning), 1217, 1231
 brine system, 1234
 dechlorination, 1236
 filtration, 1235
 ion exchange, 1236
 catholyte system, 1237
 caustic evaporation system, 1244
 caustic storage systems, 1246
 chlorine system, 1238
 compression and liquefaction, 1241
 dry systems, 1239
 storage, 1242
 control systems, 1230
 documentation, 1223
 equipment checklists, 1220
 hydrogen system, 1243
 instrumentation, 1232
 organization, 1218
 planning, 1219
 rectifier/transformers, 1247
 training, 1220
- Common-ion effect, 523
- Compressibility, 1059
- Compressible fluid flow, 1052
- Compression, 807, 934, 1060
 adiabatic compression, 1059
 chlorine (*see* chlorine compression), 807, 1121
 hydrogen (*see* hydrogen systems), 934, 1143
 isothermal compression, 1060
 polytropic compression, 1060
- Condensate
 evaporator (or process), 455, 981, 1192
 steam, 1173
- Conductive heat transfer, 1063
- Conductivity, electrical
 diaphragms, 156
 electrolytic solutions, 155
 equivalent conductance, 153, 290
 hydrochloric acid, 1551
 measurements, 150, 203
 membranes, 157
 molar conductivity, 153
 potassium chloride, 1515, 1560
 potassium hydroxide, 1530
 sodium chloride, 1509
 sodium hydroxide, 1523
 specific conductivity, 150
- Conformal transformation/mapping, 1033
- Control system interface, 1100
- Control system selection, 1092
- Convection, 1064
- Conversion factors, 1491
 area, 1492
 current density, 1495
 density, 1493
 energy, 1493
 heat transfer coefficients, 1495
 length, 1491
 power, 1493
 pressure, 1494
 thermal conductivity, 1494

- viscosity, 1494
 - volume, 1492
 - weight, 1492
 - Conveying (*see* salt transfer)
 - Cooling towers, 1181
 - blowdown, 1186
 - concentration factor, 1186
 - construction, 1182
 - instrumentation, 1185
 - pipng, 1185
 - process control, 1187
 - tower fill, 1185
 - Copper busbar
 - capacity, 728
 - comparison with aluminum, 731
 - Copper losses (*see* transformer), 715
 - Corrosion
 - chlor-alkali industry, 1328
 - classification, 1295
 - diaphragm cell cathode, 242, 248, 1046, 1330, 1331
 - Corrosion current/corrosion rate, 1306, 1311
 - Corrosion data survey, 1325
 - Corrosion fatigue, 1323
 - Corrosion inhibition, 1309
 - inorganic inhibitors, 1310
 - organic inhibitors, 1311
 - vapor-phase inhibitors, 1311
 - Corrosion potential, 1306
 - Corrosion prevention, 1308, 1344
 - brine area, 1329
 - caustic system, 1336
 - cell room, 1331
 - chlorine system, 1333
 - electrolyzer, 1329
 - Cost analysis, 388
 - Crevice corrosion, 1314
 - Crystallization
 - potassium chloride, 490
 - sodium chloride, recrystallization of, 487
 - sodium sulfate, 647
 - solar salt, 470
 - Current breakers, 740
 - Current density/reaction rate, 95
 - Current distribution, 1031
 - calculation methods, 1040
 - diaphragm cell, 1042
 - gas-generating electrode, 1042
 - membrane cell, 1046
 - primary current distribution, 1031
 - secondary current distribution, 1036
 - tertiary current distribution, 1039
 - vertical electrolyzers, 1040
 - Current efficiency, 165, 168, 207
 - chlorine, 167, 168
 - diaphragm cell, 179
 - hydrogen, 207
 - membrane cell, 176
 - mercury cell, 182
 - oxygen, 188
 - plant measurement of, 1288
 - sodium hydroxide, 165, 167, 168, 173
 - Current inefficiency (*see* current efficiency), 174, 185, 457
 - Current interruption technique, 134
 - Current leakage, 391, 397, 398, 738
 - pipng header arrangements, 740
 - Current measurement, 735
 - Cyclic voltammetry, 142
- ## D
- Darcy equation, 274, 1051
 - DC power supply (*see* rectifier/transformer)
 - Deacon process, 17, 1352
 - Deactivation (*see* failure/degradation)
 - Deaeration of boiler feedwater, 1195
 - Dealloying by selective leaching, 1319
 - Dechlorination of brine, 447, 448, 665
 - aeration, 671, 674
 - mass transfer, 676
 - plate column for, 677
 - catalytic decomposition, 686
 - on activated carbon, 686
 - on metal catalysts, 688
 - chemical reduction, 678
 - chlorine recovery, 665
 - Hydecats[®] reactor, 688
 - length of transfer unit, 676
 - McCabe-Thiele diagram, 674
 - primary dechlorination, 670
 - process control, 684
 - secondary dechlorination, 678
 - use of hydrogen peroxide, 682
 - use of sulfur compounds, 678
 - forms of supply, 678, 680, 681
 - steam stripping, 677
 - system control, 1109
 - vacuum dechlorination, 672
 - packed column for, 673
 - Dechlorination of spent sulfuric acid, 804
 - Decommissioning of mercury cell plants, 1290
 - Decomposition voltage, 89, 127, 1023
 - diaphragm cell, 196
 - membrane cell, 196
 - mercury cell, 198
 - Degradation (*see* failure)
 - inorganic materials of construction, 1325
 - organic materials of construction, 1325

- DeNora cells
 diaphragm cells (Glanor[®] cell), 405
 mercury cells, 400
 runner anode, 401
- Density
 chlorine, 1499, 1535, 1536
 potassium chloride, 1498, 1510
 sodium chloride, 1497
 sodium hydroxide, 1498
 NaCl + NaOH, 1501
- Depolarized cathodes, 933, 1027, 1372, 1467
- Deposit attack, 1316
- Deposited diaphragms (*see* diaphragms), 295
- Design coordination of control systems, 1091
- Dezincification, 1319
- Diamond cell, 23, 26
- Diaphragms, 271
 asbestos diaphragms, 25, 272, 291
 deposition, 296
 dimensionally stable diaphragms, 25
 effects of shutdowns, 300
 HAPP, 291
 mass transfer in, 274, 279
 modeling, 281, 286
 non-asbestos diaphragms, 293
 Polyramix[®], 26, 293, 294, 410
 porosity, 157, 276
 retrofit, 34
 SM-1, 291
 SM-2, 291
 SM-3, 291
 Tephram[®], 294
 tortuosity, 157, 276
 voltage drop, 289
- Diaphragm cells/process, 18, 405, 408, 446
 cell efficiency, 179
 decomposition voltage, 196
- Diaphragm cell level control, 1151
- Differential capacitance, 137
- Differential pressure (*d/p*) transmitter, 1096
- Diffusion current, 105
- Diffusion equation, 1068
- Diffusion layer, 115, 141
- Dilution of caustic liquor, 966
- Dimensionally stable anodes (DSA[®]), 24, 212
- Dimensionally stable diaphragm, 25
- Dimensionless groups, 1495
- Diode rectifiers, 717, 1477
- Dioxins, 73
- Direct methanol fuel cell (DMFC), 1472
- Dirichlet boundary condition, 1032
- Discharge step (*see* electrode process), 99, 110
- Distillation, 1081
- Distributed control system, 1092, 1231
- Dissociation constant
 chlorine, 1501
 water, 85
- Donnan potential, 315
- Dow cells
 diaphragm cell, 27, 405
 magnesium cell, 1370
- Downs cell, 1368
- Dry air system, 1199
- Dühring diagrams
 NaCl/water, 1507
 NaOH/water, 1522
- ## E
- Eckert chart (*see* pressure drop in packed column), 784
- Effects of brine impurities, 352, 354, 529, 537, 1277
 aluminum, 369
 ammonia, 656
 analytical methods, 352, 365
 anodes, 227
 barium, 227, 346, 367
 bromide, 660
 calcium, 342, 365, 534, 537
 cations, 342
 coated cathodes, 227
 control methods, 365
 diaphragm cell, 533
 fluoride, 227
 iodide, 346, 368, 661
 magnesium, 342, 366, 534
 membrane cell, 341, 365, 537
 mercury, 658
 mercury cell, 530
 nickel, iron, 227, 368
 nitrate, 665
 organics, 654
 silica, 345
 strontium, 367
 sulfate, 343
- Effects of caustic impurities, 1280
- Ejectors, 1202, 1204
- Electric power supply, 713, 1170
 demand management, 744
 energy efficiency, 736
 phase angle/power factor, 741
- Electrical hazards in cell rooms, 755
- Electrical metering, 735
- Electrocatalysis, 107
- Electrochemical processes (*see* electrode processes)
- Electrochemical reaction rate (*see* reaction rate)
- Electrochemical techniques
 non-steady state techniques, 142
 polarization measurements, 128
 steady state techniques, 128

- Electrochemical unit (ECU), 47, 166
- Electrode processes
- amalgam electrode, 85
 - chlorate reduction, 118
 - chlorine electrode, 81, 110
 - Horiuti-Heyrovsky mechanism, 99
 - hydrogen electrode, 83, 99, 107
 - hypochlorite reduction, 118
 - kinetics, 95
 - mass-transfer controlled process, 104
 - oxygen electrode, 122, 186
- Electrodialysis (*see* seawater), 478
- Electrolysis of hydrochloric acid, 1361, 1365
- Electrolysis of molten magnesium chloride, 1370
- Electrolysis of molten sodium chloride-calcium chloride mixtures, 1368
- Electrolysis of sodium sulfate, 1393
- Electrolyzer area (*see* cell room design)
- Electrolyzer assembly, 1247, 1253
- external leakage test, 1254
 - membrane handling, 1247
 - membrane installation, 1249
 - membrane leakage test, 1253
 - record keeping, 1255
 - storage and berthing of electrolyzers, 1254
- Electrolyzer installation, 707
- diaphragm cells, 707
 - membrane cells, 710
 - mercury cells, 709
- Electrolyzer shutdown, 1264
- emergency, 1266
 - maintenance, 1267
 - normal, 1264
- Electrolyzer startup, 1267
- Electrolyzer (cell) voltage, 195, 1272
- Electromagnetic field, 734, 758
- effects on busbars, 734
 - proposed limits for exposure to variable fields, 759
 - threshold limiting value, 758
- Electromotive force, 77, 377, 1021
- Electronegativity, 111
- Electroosmosis, 332
- Elemental chlorine free (ECF) bleaching, 57
- ELTECH cells, 432
- Embrittlement/alloys, 1340
- 475°C embrittlement, 1340
 - sigma embrittlement, 1340
- Emergency response planning guide (ERPG), 761
- Emissivity/radiation, 1066
- End uses of chlorine and caustic soda, 4, 11, 14
- Energy balance (*see* voltage balance), 1013, 1025
- electrochemical process, 1023, 1025
- Energy consumption in chlorine production, 163, 165, 1270
- diaphragm cells, 413
 - from hydrochloric acid, 1362
 - membrane cells, 415, 1270
 - mercury cells, 399, 448
 - theoretical coefficients, 166
- Energy consumption in magnesium production, 1370
- Energy consumption in sodium production, 1370
- Energy flow/reactor, 1014
- Energy flow diagrams, 1028
- Energy losses in DC systems
- current leakage, 738
 - rectifier efficiency, 736
- Enthalpy, 75, 1019
- Environmental considerations, 66
- chlorinated solvents, 72
 - chlorination, 68
 - chlorine derivatives, 70
 - chlorine-based pesticide, 68
 - EDC/VCM/PVC, 67
 - inorganic chemicals, 72
 - organic chemicals, 55
 - phosgene, 68
 - propylene chlorohydrin, 67
- Equilibrium constant, 1023, 1501, 1534
- Equilibrium potential (*see* reversible potential)
- Equipotential lines, 1036
- Equivalent conductance, 153, 289, 1509, 1557
- Equivalent weight, 308
- Erosion corrosion, 1319
- Error analysis, 209
- Ethylene dichloride (EDC/VCM/PVC), 4, 1350, 1478
- Evacuation systems, chlorine, 925
- Evaporated salt, 995
- Evaporation of brine (*see* brine evaporation), 480
- Evaporation of caustic solutions (*see* caustic evaporation), 968
- Exchange current density, 97, 99
- Explosion hazards, 909
- evacuation, 925
 - hydrogen, 909, 943
 - control with diluent gases, 911
 - nitrogen trichloride, 912
- Explosive limits (H₂ and Cl₂ in O₂, N₂, air), 909, 1541
- ## F
- Failure/degradation
- coated anodes, 224, 227, 231
 - coated cathodes, 263
 - ion exchange membranes, 341, 350
- Fanning equation, 274, 1051
- Faradaic resistance, 98

- Faraday constant, 77, 165
 Faraday's law, 164
 Fault tree analysis, 1429, 1431
 Feedwater (to boilers), 1194
 Ferric chloride, 769, 892
 physical chemistry of hydrates, 769
 production from liquefaction tail gas, 892
 Filiform corrosion, 1316
 Filter aids, 444, 597
 admix (body feed), 598
 cellulosic, 601
 composition, 600
 diatomaceous earth, 599
 handling of, 601
 perlite, 599
 precoat, 597
 solubility in brine, 599
 Filtration, 444, 587, 1057, 1475
 backwash, 590, 602
 bed filters, 589
 brine, 587, 1099, 1235
 cake compressibility, 597
 cake filtration, 594
 cake removal, 602
 cake washing, 602
 candle filters, 588, 592
 cartridge filters, 588
 caustic, 965
 ceramic filters, 594
 leaf filters, 588, 592, 594
 medium, 588
 mixed-media filters, 589
 polishing filters, 592, 601
 primary filtration, 588
 sand filters, 588
 Finger-type cells, 23, 405
 First law of thermodynamics, 1014
 Fixed bed/continuous
 operation, 1079
 Flade potential, 141, 1308
 Flat plate cells, 388
 Flemion[®], 34, 360
 Flocculating agents, 561
 Flotation of KCl ores, 489
 Flow patterns
 gas/liquid mixture, 1055
 pipe, 1049
 Fluid dynamics, 1048
 Fluid flow
 compressible fluid, 1052
 flow patterns, 1049, 1055
 noncompressible fluid, 1052
 Fluorocarbons, 835, 1350
 FM21-SP[®] cell, 433
 475°C embrittlement of alloys, 1340
 Free energy, 75, 1020, 1297
 Gibbs free energy, 1021
 Freezing point of solutions
 hydrochloric acid, 1550
 potassium chloride, 1514
 potassium hydroxide, 1528, 1529
 sodium chloride, 1508
 Fretting corrosion, 1320
 Freundlich isotherm, 1076
 Friction factor, 1052
 Froth flow (*see* flow patterns), 1055
 Fuel cells, 931, 1466, 1471
 alkaline fuel cell (AFC), 1472
 direct methanol fuel cell (DMFC), 1472
 molten carbonate fuel cell (MCFC), 1472
 phosphoric acid fuel cell (PAFC), 1472
 proton exchange membrane fuel cell (PEMFC), 1472
 solid oxide fuel cell (SOFC), 1472
 Fugacity (*see* activity), 779, 1022
 Future developments, 1463
- ## G
- Galvanic cell, 89
 Galvanic corrosion, 1313
 Gas absorption, 1067
 penetration theory, 1068
 two-film theory, 1068
 Gas diffusion electrodes, 1467
 Gas-liquid interface, 1067
 Gas-phase adsorption, 1075
 Gas turbines in cogeneration, 1174
 Gas void fraction in cells, 201, 1483
 Gate turn-off thyristor, 1477
 General corrosion, 1313
 Gibbs-Duhem equation, 840, 1082
 approximate solutions, 840
 Gibbs free energy, 77, 1021
 Gibbs-Helmholtz equation, 1021
 Glanor[®] cell, 27, 405
 Glauber's salt (sodium sulfate decahydrate), 647, 997
 Global warming potential, 70
 Glossary, 1458
 Glycerin, 56
 Grain boundary, 1318
 Graphite anodes, 24, 211
 Graphite packings, 386
 Greenhouse gas, 72
 Griesheim Elektron cell, 18
 Grosvenor-Miller process, 1359
- ## H
- Hagen-Poiseuille flow theory, 274
 Hardy-Schulze rule, 1179

- Hargreaves-Bird cell, 19
- Hazards, 755, 1402, 1419
 - cell room, 755
 - chemical, 761
 - electrical, 755
 - electromagnetic, 758
 - explosion, 761, 909, 912, 925
 - hydrogen, 943
 - materials, 1402
 - mechanical, 1402
 - process, 1419
- Hazard analysis, 1428
 - hazard and operability study (HAZOP), 1430, 1443
 - fault tree analysis, 1431
- Hazard protection and mitigation, 1421
 - chlorine release, 1438
 - hazard analysis, 1428
 - inherent safety, 1423
 - mechanical integrity, 1426
 - process design, 1423
 - process safety management (PSM), 1423
 - Responsible Care[®], 1436
 - safety equipment, 1421
 - safety-oriented programs, 1422
 - training, 1437
- Hazard rating, 1403
- Heat-affected zone, 1319
- Heat capacity
 - hydrochloric acid, 1546, 1547
 - hydrogen, 1541
 - H₂, N₂, O₂, 1541, 1542
 - sodium chloride solution, 1506
- Heat content (*see* enthalpy), 75, 1016
- Heat of dilution (NaOH), 1517
- Heat of solution (NaOH), 1517
- Heat/power ratio in cogeneration, 1175
- Heat transfer, 1063
 - chlorine cooler, 771
 - conduction, 1063
 - convection, 1064
 - evaporation, 1066
 - in brine, 1027
 - Newton's law, 1064
 - radiation, 1065
- Heat transfer duty curves
 - chlorine cooler, 773, 787
 - hydrogen cooler, 938
- Height of transfer unit (*see* chlorine cooler), 380, 780
- Henry's law, 681, 1067
- Hess's law, 1021
- High-performance membranes, 355
- High-temperature corrosion, 1323
 - liquid metal corrosion, 1324
 - molten salt corrosion, 1324
 - nitriding, 1324
 - oxidation, 1324
 - sulfidation, 1324
 - vanadium attack, 1324
- History of chlor-alkali industry, 17, 28, 31
- Hooker cell, 23, 26
- Horiuti-Heyrovsky mechanism, 99
- Hydecatal[®] reactor, 688
- Hydration energy, 1558
- Hydraulic length, 277
- Hydraulic radius/diameter, 275, 1053
- Hydrazine, 1173, 1344
- Hydrina[®] process, 1394
- Hydrochloric acid, 886, 909, 1350, 1407, 1546
 - azeotropic mixtures (HCl + H₂O), 1551
 - byproduct, 1350
 - conductivity, 1551
 - electrolysis (*see* HCl electrolysis), 1361
 - enthalpy, 1547
 - freezing point, 1550
 - from tail gas
 - synthesis of HCl, 886
 - heat effects in absorption, 888
 - hazards, 1407
 - heat capacity, 1546, 1547
 - partial pressure, 1549
 - solubility, 1548
 - specific heat, 1549
 - surface tension, 1550
 - viscosity, 1548
- Hydrochloric acid electrolysis, 1361
 - aqueous solution electrolysis, 1361
 - indirect electrolysis, 1365
 - Kyoto process, 1367
 - Uhde process, 1362
 - vapor phase electrolysis, 1365
 - Westvaco process, 1367
- Hydrochloric acid oxidation process, 1352
 - Catalytic Carrier Process, 1357, 1360
 - Deacon process, 1352
 - Kel-Chlor process, 1353
 - MT Chlor process, 1355
 - regenerative oxidation, 1352
 - Weldon process, 1352
- Hydrochlorofluorocarbons (HCFC), 836
- Hydrodynamics, 1048
- Hydrofluorocarbons (HFC), 836
- Hydrogen electrode reaction, 83, 97, 99, 107, 261
- Hydrogen header control, 1135
 - atmospheric pressure operation, 1135
 - positive pressure operation, 1138
 - safety systems, 1140
- Hydrogen peroxide
 - as decolorizing agent, 986
 - handling of, 683
 - in dechlorination, 682

Hydrogen purge, 1140
 Hydrogen purification, 939
 removal of mercury, 939
 as calomel, 941
 by activated carbon, 939
 removal of oxygen, 942
 Hydrogen systems, 909, 927, 1134
 combustion, 930
 commissioning, 1243
 compression, 934, 1143
 control
 compressed hydrogen distribution, 1146
 compressor discharge pressure, 1145
 diaphragm cell systems, 1147
 cooling, 936
 energy economy, 929
 explosion hazard, 943
 fuel cell, 931
 hazards, 909, 943, 1407
 embrittlement of steel, 943, 1322
 explosion, 909, 943
 fire, 944
 physical properties, 1539
 processing, 40, 451
 solubility, 1540
 uses, 928
 Hydrogen damage, 244, 1324
 Hydrolysis constant (*see* chlorine), 1501
 Hydrostatic test (*see* precommissioning), 1227
 Hydroxide precipitates, 542
 Hypochlorites, 1372, 1403, 1451
 analyses, 1386
 calcium hypochlorite, 1389
 chemical production, 1378
 decomposition, 1380
 electrochemical production, 1373
 electrode processes, 1376
 membrane cell process, 1374
 on-site production, 1373
 undivided cells, 1375
 filtration, 1385
 hazards, 1403
 materials of construction, 1383
 miscellaneous applications, 1388
 reduction (*see* dechlorination), 118
 safety, 1388
 specifications, 1386
 wastes, 1451

I

Impedance spectroscopy, 147
 Impingement attack, 1320
 Impurity effects, membrane cells, 538
 Impurity-resistant membranes, 1474

Incompressible fluid flow, 1052
 Indoor vs outdoor cell rooms, 706
 Industrial hygiene, 1401
 INEOS cells, 433
 Inhibitors (*see* corrosion inhibition), 1309
 Instrument air, 1199
 Instrumentation commissioning, 1232
 Instrumentation system design, 1089
 design coordination, 1091
 nomenclature, 1090
 selection of control systems, 1092
 Insulated gate bipolar thyristor, 1477
 Integrated gate commutated thyristor, 1477
 Integrated production of EDC, 1478
 Interface, control systems, 1100
 Intergranular corrosion, 1318, 1320
 Internal energy, 75
 International Commission on Non-Ionizing
 Radiation Protection (ICNIRP), 760
 Ion exchange, 606, 1080, 1236
 basic principles, 606
 breakthrough curve, 610
 brine, 606, 1236
 capacity, 312, 607
 chemical analysis, 625
 commissioning, 1236
 effects of operating variables, 611
 ion exchange system control, 1102
 mechanical details, 618
 column internals, 618
 delivery of regenerants, 622
 materials of construction, 619
 number of beds, 620
 merry-go-round operation, 622
 recontamination of brine, 623
 regeneration effluent, 617, 1450
 regeneration sequence, 616
 required bed volume for multiple species, 614
 simultaneous removal of two species, 613
 space velocity, 612
 Ion-exchange membranes, 306, 355, 421, 1445,
 1473
 Aciplex[®], 307
 anion transport, 333
 bilayered membrane, 307, 355
 blistering, 348, 350, 359
 brine quality, 353
 conductivity, 316
 damage to, 343, 350
 diffusivity in, 320
 electroosmosis, 332
 equivalent weight (EW), 308, 312
 Flemion[®], 307
 handling, 1247
 high-performance membranes, 355
 impurity effects, 337, 341, 354
 impurity-resistant membranes, 1474

- installation, 1249
- ion exchange capacity, 312
- leakage test, 1253
- Nafion[®], 307
- network model, 309
- operating conditions, 1273
- osmotic pressure, 332
- perfluorinated membranes, 306
- perfluorocarboxylate, 307, 355
- perfluorosulfonate, 307, 355
- performance, 341
- pH/NaOH concentration profile, 342
- physicochemical properties, 310
- reinforcement, 358, 362
- selectivity, 313
- structure, 308, 355
- tears, 350
- water content/uptake, 310, 317
- water transport, 333
- Ion-exchange resin bed
 - length of transfer zone, 608
 - multi-bed system, 620
- Ion hydration energy/waters of hydration, 1558
- Iron losses (*see* transformers), 715
- Isentropic expansion and compression, 809, 1058, 1206
- Isocyanates, 1350
- Isothermal change, 1017
- Isothermal compression, 1060

K

- Kel-Chlor process, 1353
- Kellner, K., 30
- k-factor/volt-ampere curve, 206, 725, 1465
- Kinetics/reaction kinetics, 95, 1303
- Kinetic parameters
 - chlorine electrode process, 111, 120, 201
 - hydrogen electrode process, 201, 247
 - oxygen electrode process, 120, 124, 201
- Kirchoff's law, 395
- Krebskosmo cell, 403

L

- Laboratory control analyses, 1287
- Laminar flow, 1050
- Langmuir adsorption isotherm, 107, 1075
- Laplace equation, 396, 1032
- Latent heat, 1016, 1060
- Leakage test for membranes, 1253
- Leakage current (*see* parasitic current)
- LeBlanc process, 17

- Length of transfer zone, 676
- LeSueur diaphragm cell, 20
- Lime-soda process, 35
- Limiting current density, 105
- Linear polarization method, 1307
- Liquefaction (*see* chlorine processing)
- Liquid-phase adsorption, 1078
- Liquid-ring compressor control, 1121
- Liquid-ring pump, 818, 1203
- Liquid wastes, 1448
 - caustic, 1449
 - hypochlorite, 1451
 - ion exchange regenerants, 1450
 - process condensate, 1448
 - refrigerant, 1451
 - sulfuric acid, 1448
 - utility system blowdown, 1450
- Local measurements in cell rooms, 1116
- Localized corrosion, 1296, 1314
- Logarithmic mean sectional area, 1064
- Low-pressure storage of chlorine, 853
- Lowest observed adverse effect level (LOAEL), 1409
- Luggin-Haber probe, 132

M

- MacMullin number, 156, 205, 277, 286, 301
- Magnesium chloride electrolysis, 1370
 - Dow process, 1370
 - Norsk Hydro process, 1371
- Magnetic field, 734, 758
- Maintenance manual, 1225
- Makeup water control in brine system, 1095
- Marsh cell, 23
- Mass balance
 - membrane cells, 453
 - anode side, 456
 - cathode side, 456
 - reactor, 168, 1013
- Mass transfer
 - diaphragm, 279
 - membrane, 323
 - modeling, 281
- Mass transfer coefficient, 779, 1068
- Mass transfer controlled process, 104
- Material hazards, 1402
 - asbestos, 1413
 - caustic soda and potash, 1407
 - chlorine and hypochlorites, 1403
 - hydrochloric acid, 1407
 - hydrogen, 1407
 - mercury, 1408
 - miscellaneous materials, 1416
 - nitrogen trichloride, 1415
 - sulfuric acid, 1408

- Material safety data sheet (MSDS), 1402
- Material specifications in cell room, 1276
- brine purity, 1276
 - demineralized water, 1277
 - hydrochloric acid, 1277
- Materials of construction
- brine, 527, 619, 1329
 - brine evaporator, 486
 - calcium chloride, 524
 - caustic system, 948, 1336
 - cell components, 1329
 - cells, 1329
 - cell room, 1331
 - chlor-alkali plant, 1346
 - chlorine system, 767, 814, 858, 1333
 - hydrochloric acid, 633
 - hydrogen peroxide, 683
 - hypochlorite system, 1383
 - potassium chloride, 492
 - steels in hydrogen service, 943
 - sulfuric acid, 801, 802
- McCabe-Thiele diagram, 674, 1084
- Mechanical factors/corrosion, 1297
- Mechanical integrity, 1426
- Mechanical pressure relief (*see* chlorine), 899
- Mechanical vapor recompression, 484
- steam economy, 485
- Membranes (*see* ion-exchange membranes), 421, 1445, 1473
- Membrane cells/processes, 31, 39, 413, 426, 448
- Asahi Glass cells, 432
 - Asahi Kasei cells, 428
 - caustic system, 946, 1152
 - Chlorine Engineers cells, 429
 - current efficiency, 176
 - decomposition voltage, 196
 - ELTECH cells, 432
 - hydrogen system control, 1135
 - INEOS cells, 433
 - Uhde cells, 436
- Membrane filtration, 604
- Mercury cells, 28, 38, 398, 447
- caustic system, 945, 1149
 - control, 1149
 - in tandem with membrane cells, 945
 - current deficiency, 182
 - decommissioning, 1290
 - decomposition voltage, 198
 - hydrogen system control, 1135
- Mercury-containing waste, 1452
- air emissions, 1454
 - solids, 1454
 - waste water, 1456
- Mercury rocking cell, 31
- Mercury toxicology, 1408
- hygiene, 1412
 - mechanisms, 1409
 - medical surveillance, 1411
 - monitoring, 1411
 - protective equipment, 1412
- Merry-go-round system (*see* ion exchange), 622
- Metal catalysts in dechlorination, 687
- Migration of ions (*see* mass transfer), 281, 333
- Mist elimination (*see* chlorine), 1120
- Mist elimination (*see* sulfuric acid), 805
- Mist flow (*see* flow patterns), 1055
- Mitigation of chlorine release, 1404, 1438
- Mixed gases
- explosive limits, 1541
 - heat capacity, 1541, 1542
 - thermal conductivity, 1542
- Mixed potential, 1301, 1305, 1306
- Modeling (*see* bypass current), 394
- Modified asbestos diaphragm, 26, 290
- Molten carbonate fuel cell (MCFC), 1472
- Molten salt electrolysis, 1368
- production of magnesium, 1370
 - production of sodium, 1368
- Monitoring of plant operation, 1286
- analytical program, 1287
 - current efficiency determination, 1288
 - operating data, 1286
 - voltage monitoring, 1290
- Monopolar cells, 33, 388
- MT Chlor process, 1355
- Multiple-effect evaporation, 481
- steam economy, 482
- Multistage ejectors, 1208
- N**
- Nafion[®] membranes, 33, 307, 362, 364
- Nanofiltration (*see* sulfate control), 639, 1475
- operating results, 640
 - module construction, 641
- National Institute of Occupational Safety and Health (NIOSH), 1407
- Navier-Stokes equation, 1054
- Nelson diagram (*see* hydrogen damage), 943
- Nernst equation, 78, 1302
- Nernst-Planck equation, 333
- Network model (*see* perfluorinated membrane), 309
- Neumann boundary conditions, 1032
- New Desulfation System (NDS), 638
- Newton's equation/heat transfer, 1064
- Nickel in caustic service, 949, 950, 1343
- Nitrogen, 1201, 1215
- Nitrogen trichloride, 826, 912, 1415
- accumulation, 826, 913, 920
 - avoidance, 915
 - decomposition in vaporizers, 923

decomposition rate, 917
 destruction, 917, 923
 detection, 916
 fractionation, 919
 sources, 913
 vapor pressure, 920
 Nonasbestos diaphragms, 25, 293
 Nonmetallic materials, 1325
 Non-Random Two-Liquid Model (NRTL), 840
 Nonsteady state technique, 142
 (*see* electrochemical techniques)
 Norsk Hydro process for magnesium
 production, 1371
 Number of transfer units (NTU), 380
 air stripper, 676
 chlorine cooler, 780
 gas absorption, 1071
 Nyquist plot (*see* AC impedance method), 149

O

Occupational Safety and Health Administration
 (OSHA), 1413
 Ohmic drop, 201
 Olin mercury cells, 403
 On-line analyzers, 1287
 On-the-job training, 1221
 Operating conditions in membrane cells, 346,
 1273
 brine concentration, 1274, 1283
 brine pH, 1276
 caustic concentration, 1274, 1283
 current density, 1283
 electrolyzer feed rates, 1284
 recording, 1286
 temperatures, 1275, 1284, 1285
 Operating manual, 1223
 Operating parameters, recording of, 1286
 Operating specifications, cell room, 1271
 Operating variables (membrane cells), 458
 Operation under pressure, 1480
 advantages and disadvantages, 1481
 cell operation, 1482
 chlorine compression and liquefaction, 1486
 chlorine cooling, 1483
 chlorine drying, 1485
 Operator analyses, 1287
 Organic inhibitors, 1311
 Organic materials of construction, 1325
 Osmotic pressure, 332
 Outhenin-Chalandre cell, 20
 Overview of chlor-alkali industry, 37
 Overvoltage (overpotential), 97
 Oxidation states of chlorine, 81, 1349
 Oxide-coated anodes (*see* coated anodes), 212
 Oxychlorination, 1358

Oxygen cathodes, 122, 933, 1027, 1466
 Oxygen content in cell gas, 186, 188, 923
 Oxygen evolution processes, 116, 186, 191
 Ozone depletion potential (ODP), 70, 836

P

Packaged instrumentation, 1159
 Packed column/gas absorption, 1071
 Parasitic current, 391, 738, 1332
 measurement, 397
 minimization, 398
 modeling/equivalent circuit, 395
 Paris Marine Commission (PARCOM), 60
 Particle size distribution (PSD), 491, 496
 Passivation, 1308
 Peclet number, 302
 Penetration theory of gas
 absorption, 1068
 Perfluorinated membranes, 306, 355
 (*see* ion-exchange membranes)
 Performance
 anode, 224, 235
 cathode, 244, 265
 electrolyzers, 399, 413, 415
 membranes, 341
 Permeability of porous media, 278
 Personal protective equipment, 1402, 1421
 Pesticides, 56, 68
 pH control in brine system, 1103
 pH profile in membranes, 342
 Phase angle/power factor, 150, 720,
 735, 741, 744 (*see* electric power
 management)
 Phase diagrams
 FeCl₃-H₂O system, 770
 Na₂CO₃-H₂O system, 555
 NaCl-H₂O system, 500
 NaCl-Na₂SO₄-H₂O system, 647
 NaOH-H₂O system, 1521
 Phosgene, 68
 Phosphoric acid fuel cell (PAFC), 1472
 Physical properties
 barium salts
 solubility, 1556
 bleach
 specific gravity, 1552
 calcium chloride
 specific gravity of solutions, 1560
 calcium sulfate
 solubility, 1557, 1558
 chlorine
 density, 1499, 1535, 1536
 general properties, 1532
 latent heat of vaporization, 1537
 solubility, 1534, 1535

Physical properties *Contd.*chlorine *Contd.*

- specific heat, 1500, 1538
- thermal conductivity, 1500, 1539
- thermodynamic properties, 1533
- vapor pressure, 1499, 1537
- viscosity, 1500, 1536

hydrochloric acid

- azeotropic mixtures of HCl + H₂O, 1551
- conductivity, 1551
- enthalpy, 1547
- freezing point, 1550
- heat capacity, 1546, 1547
- partial pressure, 1549
- solubility, 1548
- specific heat, 1549
- surface tension, 1550
- viscosity, 1548

hydrogen

- explosive limits, 1541
- general properties, 1539
- heat capacity, 1541
- solubility, 1540
- thermal conductivity, 1542
- viscosity, 1542

nitrogen trichloride

- general properties, 1415
- vapor pressure, 920

potassium carbonate solutions

- specific gravity, 1553
- viscosity, 1553

potassium chloride solutions

- activity coefficient, 1515
- boiling point, 1514
- conductivity, 1515
- density, 1498, 1510
- freezing point, 1514
- heat capacity, 1512
- solubility, 490, 1510
- specific heat, 1498
- vapor pressure, 1513
- viscosity, 1511

potassium hydroxide solutions

- activity coefficient, 1531
- boiling point, 1527, 1528
- conductivity, 1530
- freezing point, 1528, 1529
- heat capacity, 1526
- heat of solution, 1529
- specific gravity, 1525
- specific heat, 1499
- thermal conductivity, 1524, 1525
- vapor pressure, 1527
- viscosity, 1526

sodium amalgam

- activity coefficient, 86
- equilibrium potentials, 199

sodium carbonate solutions

- specific gravity, 1553
- viscosity, 1553

sodium chloride

- activity coefficient, 1504
- angle of repose, 494
- boiling point, 1507
- conductivity, 1509
- density, 1497
- density (NaCl + NaOH), 1501
- Dühring diagram, 1507
- enthalpy, 1497, 1508
- equivalent conductance, 1509
- freezing point, 1508
- general properties, 496
- heat capacity, 1506
- osmotic pressure, 1504
- specific heat, 1503
- solubility, 490, 509, 1496, 1497
- solubility (NaCl + NaOH), 1518
- specific gravity, 1502, 1505
- surface tension, 1503
- thermal conductivity, 1509
- uniformity coefficient, 496
- vapor pressure, 1497, 1506
- viscosity, 1505

sodium hydroxide

- activity coefficient, 1524
- boiling point, 1521
- conductivity, 1523
- density, 1498
- Dühring diagram, 1522
- enthalpy, 1522
- general properties, 1516
- heat of dilution, 1517
- heat of solution, 1517
- phase diagram, 1521
- solubility (NaCl + NaOH), 1518
- specific gravity, 1516
- specific heat, 1519
- surface tension, 1523
- thermal conductivity, 1524
- vapor pressure, 152
- viscosity, 1518

sodium sulfate

- solubility, 647

water

- pH, 1554
- vapor pressure, 1554

Piping materials

- brine system, 748
- catholyte system, 749
- chlorine system, 745
 - FRP laminates, 746
- hydrogen system, 747

Pitting corrosion, 1317

Planck's constant, 95

- Plant air, 1196
- Plant operation, 1263
 - brine acidification, 1263
 - initial startup, 1256
 - electrolyzer startup and shutdown, 1264, 1267
 - load changes, 1262
 - normal operation, 1261
- Plant performance test, 1268
- Plug flow (*see* flow patterns), 1055
- Pneumatic test (*see* precommissioning), 1228
- Polarization curve, 128, 137, 1305
- Polarization measurements, 128, 137
 - galvanostatic, 137
 - potentiostatic, 137
- Polarization resistance method, 1307
- Polycarbonate, 56
- Polyramix[®] diaphragms, 26, 293, 294, 410
- Polytropic compression, 1060
- Polyvinyl chloride (PVC), 49, 55
- Porosity of diaphragms, 205, 275, 276
- Positive materials identification), 1428
- Postprecipitation (*see* precipitation)
- Potassium carbonate solutions, 1553
 - specific gravity, 1553
 - viscosity, 1553
- Potassium chloride, 487, 1498, 1510
 - activity coefficient, 1515
 - beneficiation, 489
 - boiling point, 1514
 - caking, 499
 - conductivity, 1515
 - crystallization, 490
 - density, 1498, 1510
 - flotation, 489
 - freezing point, 1514
 - heat capacity, 1512
 - materials of construction, 492
 - particle size distribution, 491, 496
 - solubility, 490, 1510
 - sources, 487
 - specific heat, 1498
 - storage, 492
 - sylvinite, 488
 - vapor pressure, 1513
 - viscosity, 1511
- Potassium hydroxide solutions, 15,
 - 1499, 1525
 - activity coefficient, 1531
 - boiling point, 1527, 1528
 - conductivity, 1530
 - freezing point, 1528, 1529
 - heat of solution, 1529
 - heat capacity, 1526
 - specific gravity, 1525
 - specific heat, 1499
 - thermal conductivity, 1524, 1525
 - vapor pressure, 1527
 - viscosity, 1526
- Potential sweep method, 142
- Pourbaix diagrams, 1301
- Power factor/phase angle, 741
 - improvement with capacitors, 742
- Power measurement, 735
- PPG/DeNora Glanor[®] cell, 405
- Prandtl number, 776
- Precipitation of brine impurities, 545, 1058 (*see* clarification and thickening)
 - calcium carbonate, 548
 - chemicals supply, 552
 - concentrations of precipitants, 557
 - effects of Ca:Mg ratio, 558
 - magnesium hydroxide, 546
 - postprecipitation, 550, 560
 - simultaneous precipitation of Ca and Mg, 550
 - sulfate-calcium, 551
 - sources of barium ion, 551
 - calcium vs barium, 552
 - use of CO₂ gas, 562
- Precipitation patterns of hydroxides, 542
- Precoat (*see* filtration)
- Precommissioning (*see* commissioning), 1226
 - control systems, 1230
 - flushing and cleaning, 1226
 - packaged equipment, 1230
 - pressure testing, 1227
 - punch lists, 1229
- Preparation
 - coated anodes, 212
 - deposited diaphragms, 295
- Pressure drop
 - compressible flow, 1052
 - noncompressible flow, 1052
- Pressurized electrolysis, 1481
- Pressurized storage (*see* chlorine storage), 852
- Primary dechlorination (*see* dechlorination), 670
- Primary filtration (*see* filtration), 588
- Primary current distribution, 1031
- Process control, 459, 749
 - brine clarifier, 1098
 - brine concentration, 1094
 - brine feed to cells, 1104
 - brine filters, 1099
 - brine pump tank level, 1096
 - brine purge, 1106, 1109, 1111
 - brine saturation system, 1093
 - brine system inventory, 1094
 - brine treatment tanks, 1097
 - cell room, 749, 1111, 1114
 - control and measuring devices, 749
 - effects of magnetic field, 752
 - header pressure control and safety systems, 1114
 - chlorine compressor, 821, 1125

Process control *Contd.*
 chlorine drying, 798, 1118
 dechlorination system, 1109
 evaporator production rate, 1159
 hydrogen discharge pressure, 1135, 1138, 1145
 ion exchange process, 1101
 makeup water to brine system, 1095
 pH control in brine system, 1103
 Process hazards, 1419
 Process safety management (PSM), 1423
 Process/utility connections, 1212
 Product quality
 chlorate in caustic, 191, 985, 989
 diaphragm cell caustic, 41, 983, 986
 membrane cell caustic, 339, 986
 oxygen in chlorine, 186, 923
 Product recovery
 caustic soda, 451
 chlorine, 449
 hydrogen, 451
 Production capacity/demand, 47, 52
 Programmable logic controller (PLC), 1092
 Propylene chorohydrin, 67
 Protection potential, 1318
 Protective equipment, 1405, 1421 (*also see* under relevant hazards)
 Proton exchange membrane fuel cell (PEMFC), 1472
 Pseudocapacitance, 143
 Purification of products
 caustic, 983
 hydrogen, 939
 Purified air, 1198
 Purified water, 1191
 boiler feedwater, 1194
 deaeration, 1195
 demineralized water, 1191
 evaporator condensate, 1192
 oxygen scavengers, 1196
 soft water, 1191

R

Radiation, 1065
 Rake (*see* clarifier)
 Raney nickel cathode, 252
 Raoult's law, 1081
 Rapid dissolving (*see* selective dissolving, short-contact dissolver)
 Rate constant, 95
 Rate-controlling step, 101, 110
 Reaction kinetics, 95, 1303
 Reaction rate/current density, 95
 Rebuilding of cells – *see* cell renewal
 Record of operating parameters, 1286

Recovery of chlorine (*see* dechlorination), 670
 Rectifier/transformer, 717, 1247, 1477
 arrangement, 719, 723
 control, 718
 design considerations, 719
 diode rectifiers, 717
 distortion, 722
 electrical efficiency, 736
 harmonics, 720
 alleviation, 721
 interference with communications, 722
 multi-pulse system, 721
 operation in parallel, 724
 semiconductor rectifiers, 717
 thyristor rectifiers, 717
 uncontrolled diode plus DC chopper, 1477
 Reference electrodes, 92, 129
 calomel electrode, 92, 130
 copper-cupric sulfate electrode, 132
 hydrogen electrode, 92, 129
 mercury-based electrodes, 130
 silver-silver chloride electrode, 93, 132
 Refrigerants, 835, 1451
 ammonia, 837
 chlorofluorocarbons (CFC), 835
 chlorohydrofluorocarbons (HCFC), 836
 flammability in chlorine, 836
 hydrofluorocarbons (HFC), 836
 Regeneration (*see* ion exchange), 615, 1450
 Relative volatility, 1082
 Resaturation (*see* salt dissolving), 509, 511, 513
 Resistivity (*see* conductivity)
 Responsible Care[®], 67, 874, 1431, 1436
 Retired brine caverns, 1452
 Reverse osmosis, 472, 1475
 Reversible potentials, 81
 amalgam electrode, 200
 chlorine electrode, 197
 hydrogen electrode, 197
 Reynolds number, 115, 141, 275, 1052
 Risk analysis, 1443
 Rotating electrodes, 141
 Rupture/breakdown potential, 1318

S

Safety devices in chlorine lines, 895
 mechanical relief, 899
 pressure/vacuum seal, 897
 water seal, 895
 Safety equipment, 1402, 1421
 Safety management, 1256, 1402
 Safety-oriented programs, 1422
 Salt (*see* sodium chloride)
 brine, 466
 byproduct salt, 476

- caking, 492, 499
- crystallization, 470, 487
- dissolving, 509, 511, 513
- evaporator salt (CP salt), 995
- freezing, 500
- halite, 488
- handling, 495
- inland sources, 475
- mining, mechanical, 466, 467
- mining, solution, 515
 - from domes, 515
 - from stratified deposits, 516
 - particle size distribution (PSD), 496
 - refining, 478
 - rock salt, 466
 - selective dissolving, 519
 - sources, 465
 - solar salt, 469
 - solubility, 509, 1496, 1497
 - storage, 492
 - transfer, 501
 - vacuum pan salt, 475
 - vacuum purified, 480
 - washing, 478
- Salt dissolvers, 512
- Salt domes, 467
- Salt mine engineering, 469
- Salt splitting, 1392
- Salt transport
 - belt conveyors, 501
 - bucket elevators, 503
 - conveyor drive systems, 507
 - feeders, 507
 - pneumatic conveyors, 508
 - screw conveyors, 504
 - slurry transfer, 508
- Sand filter, 588
- Scanning tunneling microscopy, 150
- Scheele, C.W., 2
- Schmidt number, 777
- Schwartz-Christoffel transformation, 1035
- Screen sizes, 498
- Scrubbers/chlorine, 901
 - administrative control, 905
 - apparatus, 902
 - chemistry, 901
 - collection systems, 903
 - mass transfer in, 906
- Sea salt (*see* solar salt)
- Seawater (*see* brine)
 - composition of, 470
 - electrodialysis of, 478
- Secondary current distribution, 1036
- Secondary dechlorination (*see* dechlorination), 678
- Sedimentation (*see* precipitation), 566, 1057
- Selective dissolving, 519
 - common-ion effect, 523
 - supply of CaCl_2 , 524
 - control of process, 519
 - short-contact dissolver, 520
 - solubility inhibitors, 521
- Selective leaching/dealloying, 1319
- Self-contained breathing apparatus (SCBA), 1406
- Sensible heat, 1016, 1060
- Shunt current/parasitic current, 391, 738, 1332
- Shutdown
 - effect on anodes, 228, 231
 - effect on cathodes, 248, 263
 - effect on diaphragms, 300
 - effect on membranes, 351
 - effect on product quality, 251, 336
 - for maintenance, 1267
 - in emergency, 1266
 - normal, 1264
- Sigma embrittlement, 1340
- Silica (*see* brine impurities), 651
- Silver-silver chloride electrode, 93
- Similar exposure groups (SEG), 1405, 1411
- Simultaneous precipitation of Ca and Mg, 550
- Slug flow (*see* flow patterns), 1055
- Soda ash, causticization of, 1389
- Sodium, production of, 1368
- Sodium amalgam (*see* amalgam)
- Sodium chloride, 1496, 1502
 - activity coefficient, 1504
 - angle of repose, 494
 - boiling point, 1507
 - conductivity, 1509
 - density, 1497
 - density ($\text{NaCl} + \text{NaOH}$), 1501
 - Dühring diagram, 1507
 - enthalpy, 1497, 1508
 - equivalent conductance, 1509
 - freezing point, 1508
 - heat capacity, 1506
 - osmotic pressure, 1504
 - physical properties, 496
 - solubility, 490, 509, 1496, 1497
 - solubility ($\text{NaCl} + \text{NaOH}$), 1518
 - specific gravity, 1502, 1505
 - specific heat, 1503
 - surface tension, 1503
 - thermal conductivity, 1509
 - uniformity coefficient, 496
 - vapor pressure, 1497, 1506
 - viscosity, 1505
 - wet storage, 512
- Sodium hydroxide, 1516
 - activity coefficient, 1524
 - boiling point, 1521
 - conductivity, 1523

- Sodium hydroxide *Contd.*
 density, 1498
 Dühring diagram, 1522
 enthalpy, 1522
 heat of dilution, 1517
 heat of solution, 1517
 phase diagram, 1521
 physical properties, 1516
 solubility (NaCl + NaOH), 1518
 specific gravity, 1516
 specific heat, 1519
 surface tension, 1523
 thermal conductivity, 1524
 vapor pressure, 1520
 viscosity, 1518
- Sodium hypochlorite
 (*see* hypochlorites), 1378
- Sodium sulfate (Glauber's salt), 647, 997
- Sodium sulfate electrolysis, 1393
- Solar salt, 469
 energy efficiency in production, 475
 evaporation of seawater, 473
 fractional crystallization of, 471
 inland sources, 475
 percolation of brine, 474
 pond management, 471
 seawater intake, 472
 structure of particle, 478
- Solid waste, 1445
 asbestos, 1445
 brine sludges, 1446
 filter solids, 1447
 membranes, 1445
 miscellaneous solids, 1447
- Solid oxide fuel cell (SOFC), 1472
- Solid polymer electrolyte (SPE), 1467
- Solid caustic, production of, 987
- Solid removal, 1057
- Solubility
 BaSO₄, 645
 CaSO₄, 644, 1557, 1558
 crystalline forms of, 643
 HCl, 629, 1548
 KCl, 490, 1498
 NaCl, 490, 1496, 1497
 Na₂SO₄, 647
 NaCl + NaOH mixed solutions, 1518
 NaCl-BaSO₄-H₂O system, 645
 NaCl-CaSO₄-H₂O system, 644
 NaCl-Na₂SO₄-H₂O system, 1559
 barium salts, 1556
 chlorine, 208, 665, 671, 1534, 1535
 in acid solution, 669
 in brine, 669, 671
 in water, 665
 hydrogen, 1540
 sulfur compounds, 678
 various salts, 1559
- Solubility inhibitor, 521
- Solubility products, 650
- Solvay process, 17
- Specific heat, 1016, 1060, 1498, 1499, 1500, 1503, 1519, 1538, 1544, 1549
- Spray flow (*see* flow patterns), 1055
- Specific gravity
 bleach, 1552
 calcium chloride solution, 1560
 hydrochloric acid, 1552
 sodium chloride, 1502, 1505
 sodium hydroxide, 1516
- Specific heat
 chlorine, 1500, 1538
 hydrochloric acid, 1549
 sodium hydroxide, 1519
- Standard electrode potential, 79, 1300
- Standard hydrogen electrode (SHE), 83, 92
- Star connection in transformers, 715
- Startup, 1256, 1267
- Steam cycle in cogeneration, 1174
- Steam jets, 1203
- Steam systems, 1171
 steam, 1171
 steam condensate, 1173
 treatment chemicals, 1173
- Steam turbines, 1174
- Stefan-Boltzmann law, 1066
- Stoichiometric coefficient (number), 77, 107
- Storage and berthing of
 membrane cells, 1254
- Storage of solid raw materials
 potassium chloride, 492
 soda ash, 553
 sodium chloride, 492
- Storage policy, brine, 525
- Stratified flow (*see* flow patterns), 1055
- Stray current (*see* parasitic current)
- Stress corrosion cracking (SCC), 1320 (*see* materials of construction, corrosion prevention)
- Sulfate control, 634
 crystallization, 647
 Glauber's salt, 647
 low-sulfate salt, 634
 chemically pure (CP), 635
 vacuum-purified, 634
- New Desulfation System (NDS), 638
 removal from brine
 ion exchange, 638
 nanofiltration, 639
 precipitation, 642
 purge, 636
 removal from salt, 636

Sulfate ratio, 177
Sulfur compounds (*see* dechlorination), 678
Sulfuric acid, 1118, 1408, 1448, 1543
 density, 1543
 enthalpy, 1545
 freezing point, 1545
 hazards, 1408, 1448
 heat generation, 1546
 specific heat, 1544
 vapor pressure, 1544
 viscosity, 1543
Supplied-air respirator, 1406
Surface analysis, 150
Surface coverage, 97
Surface tension
 hydrochloric acid, 1550
 sodium chloride, 1503
 sodium hydroxide, 1523
Symmetry factor, 96

T

Tafel equation and Tafel slope, 98
Tafel step, 99
Tail gas from chlorine liquefaction, 884
 recovery of chlorine, 884
 as bleach, 890
 as ferric chloride, 892
 by absorption/desorption, 885
 by synthesis of HCl, 886
 miscellaneous processes, 894
Temkin adsorption isotherm, 100
Tephram[®] diaphragms, 26, 294
Tertiary current distribution, 1039
Theoretical plate/distillation, 1083
Thermal conductivity
 H₂, N₂, O₂, 1542
 chlorine, 1500, 1539
 sodium chloride, 1509
 sodium hydroxide, 1524
Thermal vapor recompression, 486
Thermobalance voltage, 1027
Thermodynamic properties/chlorine, 1533
Thermodynamics, 75, 1014, 1297
 first law, 1014
Thermonutral voltage, 1023
Thickening (*see* clarification)
Threshold limiting values (TLV), 1402,
 1405, 1458 (*see* under relevant
 materials)
Thyristors (*see* rectifiers), 1477
Time-to-failure of membranes, 343
Toxic gas release modeling, 1435
Tortuosity, 157, 276
Total chlorine free (TCF) bleaching, 57

Townsend cell, 22
Training of personnel, 1220, 1427
Transfer hoses for liquid chlorine, 869
Transformers, 713, 1247
 commissioning, 1247
 copper losses, 715
 iron losses, 715
 phase voltage, 716
 principle of operation, 714
 star connection, 715
 Y- Δ configuration, 715
Transgranular corrosion, 1320
Transpassivation, 1308
Transport number, 106
Trihalomethanes, 57
Trona, 1391
Turbulent flow, 1052, 1055
Two-film theory of mass transfer, 1068
Two-metal corrosion, 1313
Two-phase flow, 1055

U

Uhde cells
 membrane cells, 436
 mercury cells, 402
Ultrafiltration, 1475
Uniform general corrosion, 1313
Uniformity coefficient, 496
Uninterruptible power supply (UPS), 1092
Universal constants, 1491
Universal Quasi-Chemical Activity Coefficient
 Model (UNIQUAC), 840
U.S. chlor-alkali industry, 52
Utility piping systems, 1211
 breathing air, 1214
 dry air and nitrogen, 1215
 steam, 1214
 utility/process connections, 1212
 water, 1212, 1214
Utility-process connections, 1212
Utility systems, 1169
 backup systems, 1201
Utility system blowdown, 1450

V

Vacuum systems, 1201
 hybrid systems, 1208
 liquid-ring pumps, 1203
 process control, 1210
 sources, 1202
 stream jets, 1204
 vapor condensers, 1208

Vapor release from process, 1438
Vapor phase electrolysis of
 HCl, 1365
Vapor phase inhibitors, 1311
Vapor pressure
 chlorine, 1499, 1536
 ferric chloride hydrates, 769
 potassium chloride, 1498
 sodium chloride, 1497, 1506
 sodium hydroxide, 1520
Vapor recompression
 evaporation, 484
Vaporization of chlorine, 881
Ventilation, 712
Vertical electrolyzers, 1040
View factor/radiation, 1066
Vinyl chloride monomer
 (VCM), 4, 67
Vinylidene chloride, 56
Viscosity
 chlorine, 1499, 1536
 hydrochloric acid, 1548
 sodium chloride, 1505
 sodium hydroxide, 1518
Volatility, 1082
Volcano plots, 109
Volmer step, 99

Voltage balance, 1013, 1025
Voltage monitoring, 1290

W

Wagner number, 1038
Waste disposal, 518, 1445
Water balance in membrane cells, 444
Water systems, 1177
 chilled water, 1188
 cooling water, 1180
 purified water, 1191
 sources and their quality, 1177
 treatment, 1179
Water transport in membranes, 333
Water transport coefficient, 460
Wave flow (*see* flow patterns), 1055
Weld decay, 1319
Westvaco process, 1367
Wheatstone bridge, 153

Y

Y- Δ configuration, 715